

# ORGANOMETALLICS

Volume 14, Number 6, June 1995

© Copyright 1995  
American Chemical Society

## Communications

### ( $\eta^6$ -Polyarene) $Mn(CO)_3^+$ Complexes as Manganese Tricarbonyl Transfer Reagents. A Convenient and General Synthetic Route to (Arene) $Mn(CO)_3^+$ Complexes

Shouheng Sun, Lee K. Yeung, and Dwight A. Sweigart\*

Department of Chemistry, Brown University, Providence, Rhode Island 02912

Tae-Young Lee, Su Seong Lee, and Young K. Chung\*

Department of Chemistry, Seoul National University, Seoul 151-742, Korea

Susan R. Switzer and Robert D. Pike\*

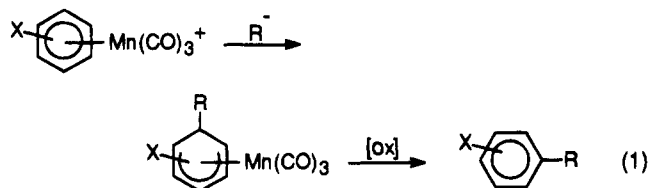
Department of Chemistry, College of William and Mary, Williamsburg, Virginia 23187

Received March 22, 1995<sup>®</sup>

**Summary:** (Polyarene) $Mn(CO)_3^+$  complexes containing naphthalene-type ligands can be readily synthesized in high yield. These complexes function as efficient manganese tricarbonyl transfer (MTT) reagents by rapidly and cleanly transferring the  $Mn(CO)_3^+$  moiety to other arenes upon warming in dichloromethane.

The activation of arenes by coordination to transition metals provides a useful synthetic route to functionalized arenes and cyclohexadienes. The manganese-mediated functionalization of arenes is particularly attractive in this regard because the relevant complexes, (arene) $Mn(CO)_3^+$ , are known to undergo high-yield regio- and stereoselective attack by a very wide range of nucleophiles.<sup>1</sup> The resultant cyclohexadienyl com-

plexes readily liberate the functionalized arene upon oxidative removal of the metal, as shown in eq 1. Alternatively, cyclohexadienes can be generated by reactivation of the cyclohexadienyl complexes with  $NO^+$ , followed by a second nucleophilic addition.<sup>1d,2</sup>



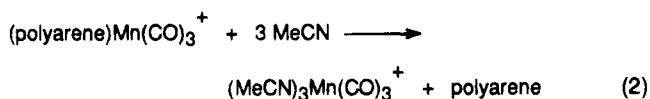
Three synthetic methods have been reported for the coordination of arenes to the  $Mn(CO)_3^+$  moiety: (1) heating  $Mn(CO)_5Br$  and the arene in the presence of  $AlCl_3$ , (2) treating a  $CH_2Cl_2$  solution of  $Mn(CO)_5Br$  with

<sup>®</sup> Abstract published in *Advance ACS Abstracts*, May 1, 1995.  
(1) (a) Pauson, P. L.; Segal, J. A. *J. Chem. Soc., Dalton Trans.* **1975**, 1677, 1683. (b) Kane-Maguire, L. A. P.; Honig, E. D.; Sweigart, D. A. *Chem. Rev.* **1984**, *84*, 525. (c) Chung, Y. K.; Williard, P. G.; Sweigart, D. A. *Organometallics* **1982**, *1*, 1053. (d) Pike, R. D.; Sweigart, D. A. *Synlett* **1990**, 563. (e) Krow, G. R.; Miles, W. H.; Smiley, P. M.; Lester, W. S.; Kim, Y. J. *J. Org. Chem.* **1992**, *57*, 4040. (f) Pearson, A. J.; Shin, H. *Tetrahedron* **1992**, *48*, 7527. (g) Chung, T.-M.; Chung, Y. K. *Organometallics* **1992**, *11*, 2822. (h) Lee, S.; Chung, Y. K.; Yoon, T.-S.; Shin, W. *Organometallics* **1993**, *12*, 2873. (i) Woo, K.; Carpenter, G. B.; Sweigart, D. A. *Inorg. Chim. Acta* **1994**, *220*, 297.

(2) (a) Chung, Y. K.; Sweigart, D. A.; Connelly, N. G.; Sheridan, J. B. *J. Am. Chem. Soc.* **1985**, *107*, 2388. (b) Pike, R. D.; Ryan, W. J.; Carpenter, G. B.; Sweigart, D. A. *J. Am. Chem. Soc.* **1989**, *111*, 8535. (c) Miles, W. H.; Brinkman, H. R. *Tetrahedron Lett.* **1992**, *33*, 589. (d) Lee, T.-Y.; Kang, Y. K.; Chung, Y. K.; Pike, R. D.; Sweigart, D. A. *Inorg. Chim. Acta* **1993**, *214*, 125.

a Ag(I) salt and then adding the arene and warming, and (3) heating  $\text{Mn}_2(\text{CO})_{10}$  and the arene in trifluoroacetic anhydride (TFAA) and strong acid.<sup>3</sup> A rather large number of monocyclic arenes have been coordinated by these methods. However, attempts to coordinate polycyclic arenes such as naphthalene produced at best a trace of the desired complex, along with varying amounts of partially hydrogenated product.<sup>3,4</sup> For example, attempted synthesis of (naphthalene) $\text{Mn}(\text{CO})_3^+$  by method 1 gave instead (tetralin) $\text{Mn}(\text{CO})_3^+$ .

Herein we report that method 2 is, in fact, capable of giving good yields with polycyclic arenes, provided all reagents are thoroughly dried and contact with donor solvents is avoided (*vide infra*). Thus, compounds 1–6 were readily prepared in good yield and found to be stable in the solid state.<sup>5</sup> They were also found to provide an excellent vehicle for polyarene functionalization by nucleophilic addition to the coordinated ring; these reactions as well as the chemistry of the monoanions of 1–5, obtained by two-electron reduction, will be reported in a future communication. The naphthalene-type ligands in 1–6 as well as the  $\eta^6$ -heterocyclic ligands in 7–9<sup>3,6</sup> were observed to undergo ready displacement by donor solvents. Equation 2 shows the reaction with



acetonitrile; some half-lives in  $\text{CH}_2\text{Cl}_2$  containing 1.0 M MeCN are given in Table 1. It can be seen that the naphthalene-type complexes in particular are extremely reactive. It is possible to compare this reactivity to that previously reported<sup>7</sup> for the analogous reaction of (toluene) $\text{Mn}(\text{CO})_3^+$  (10) with MeCN. In sharp contrast to the behavior of the polyarene complexes 1–9, the toluene complex is calculated to have a half-life of ca. 4

(3) Jackson, J. D.; Villa, S. J.; Bacon, D. S.; Pike, R. D. *Organometallics* **1994**, *13*, 3972 and references therein.

(4) Stobart, S. R.; Zaworotko, M. J. *J. Chem. Soc., Chem. Commun.* **1984**, 1700.

(5) For the synthesis of 1–9, it is important that all glassware, solvents, and chemicals be carefully dried. Complexes 1–7 were made typically as follows:  $\text{Mn}(\text{CO})_5\text{Br}$  (1.0 g) and  $\text{AgBF}_4$  (1.1 equiv) were dissolved in 50 mL of  $\text{CH}_2\text{Cl}_2$  and refluxed for 1 h under  $\text{N}_2$  in the dark. The polyarene (2–4 equiv) in 10 mL of  $\text{CH}_2\text{Cl}_2$  was then added and the reaction mixture refluxed overnight. After it was cooled to room temperature, the solution was filtered through Celite and concentrated to ca. 20 mL *in vacuo* and the product precipitated with diethyl ether. The yellow [(arene) $\text{Mn}(\text{CO})_3\text{BF}_4$ ] salts were washed repeatedly with ether and dried *in vacuo*. Complex 9 was synthesized by the TFAA method, as previously described for 8.<sup>3</sup> The new polyarene complexes were thoroughly characterized by IR ( $\nu_{\text{CO}}$  2073  $\pm$  7, 2017  $\pm$  5  $\text{cm}^{-1}$ ) and  $^1\text{H}$  NMR, which showed the absence of any free polyarene. The coordination of the metal to a terminal ring in 1 was confirmed by X-ray crystallography.<sup>11</sup>  $^1\text{H}$  NMR ( $\text{CD}_2\text{Cl}_2$ ): 1,  $\delta$  8.76 (d,  $J$  = 9 Hz,  $\text{H}^5$ ), 8.25 (d,  $J$  = 9 Hz,  $\text{H}^6$ ), 8.18–7.96 (m,  $\text{H}^{6,7,9,10}$ ), 7.72 (d,  $J$  = 9 Hz,  $\text{H}^4$ ), 7.29 (d,  $J$  = 6 Hz,  $\text{H}^1$ ), 6.80 (m,  $\text{H}^{2,3}$ ); 2,  $\delta$  8.06 (s,  $\text{H}^{5-8}$ ), 7.50–7.35 (m,  $\text{H}^{1,4}$ ), 6.80–6.65 (m,  $\text{H}^{2,3}$ ); 3,  $\delta$  8.11–7.41 (m,  $\text{H}^{4-8}$ ), 6.76 (m,  $\text{H}^3$ ), 6.55 (d,  $J$  = 5 Hz,  $\text{H}^2$ ), 2.97 (s, Me); 4,  $\delta$  8.25–8.10 (m,  $\text{H}^{5-8}$ ), 6.22 (s,  $\text{H}^{2,3}$ ), 2.95 (s, Me<sup>1,4</sup>); 5,  $\delta$  7.81 (d,  $J$  = 9 Hz,  $\text{H}^5$ ), 7.44 (d,  $J$  = 9 Hz,  $\text{H}^6$ ), 7.37–7.26 (m,  $\text{H}^{4,8}$ ), 7.08 (s,  $\text{H}^1$ ), 6.02 (d,  $J$  = 6 Hz,  $\text{H}^3$ ), 4.15 (s,  $\text{OMe}^2$ ), 4.04 (s,  $\text{OMe}^7$ ); 6,  $\delta$  8.07 (m,  $\text{H}^6$ ), 7.90–7.75 (m,  $\text{H}^{5,7}$ ), 7.17 (d,  $J$  = 7 Hz,  $\text{H}^4$ ), 6.75 (m,  $\text{H}^3$ ), 6.58 (d,  $J$  = 6 Hz,  $\text{H}^2$ ), 3.90–3.60 (m,  $\text{H}^{9,10}$ ); 9,  $\delta$  (in  $\text{CD}_2\text{COCD}_2$ ) 8.53 (2,  $J$  = 7.8 Hz,  $\text{H}^8$ ), 8.17 (d,  $J$  = 6.6 Hz,  $\text{H}^1$ ), 7.93 (m,  $\text{H}^{5,6}$ ), 7.70 (t,  $J$  = 6.9 Hz,  $\text{H}^7$ ), 7.68 (d,  $J$  = 7.0 Hz,  $\text{H}^4$ ), 7.09 (t,  $J$  = 6.6 Hz,  $\text{H}^3$ ), 6.66 (t,  $J$  = 6.4 Hz,  $\text{H}^2$ ). Complexes 7 and 8 have been previously reported.<sup>3,6</sup> Satisfactory elemental analysis was obtained for the new complexes 1–6 and 9.

(6) Lee, S. S.; Chung, Y. K.; Lee, S. W. *J. Organomet. Chem.*, submitted for publication.

(7) Kane-Maguire, L. A. P.; Sweigart, D. A. *Inorg. Chem.* **1979**, *18*, 700.

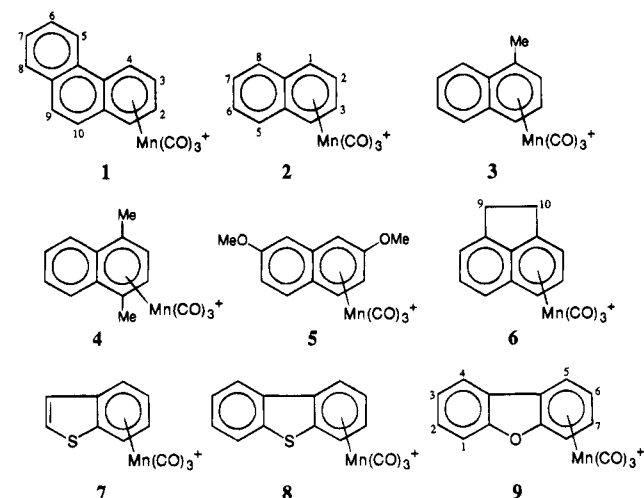


**Figure 1.** Manganese complexes investigated (the counterion was  $\text{BF}_4^-$  in all cases).

**Table 1.** Yield and Reactivity Data for Complexes 1–9

	1	2	3	4	5	6	7	8	9
synthetic methods	Ag(I)	Ag(I)	Ag(I)	Ag(I)	Ag(I)	Ag(I)	Ag(I)	TFAA	TFAA
% yield	69	86	90 <sup>a</sup>	89 <sup>a</sup>	77	87	87	89	76
half-life for eq 2, min <sup>b</sup>	50	~1			16	2.2	55	250	260

<sup>a</sup> Product consists of a mixture with the metal coordinated to either the methylated or unsubstituted ring (ratio 1:1 for 3 and 4:1 for 4). <sup>b</sup> At 25 °C in dichloromethane containing 1.0 M MeCN.

years! This reactivity difference most likely is due to easier  $\eta^6 \rightarrow \eta^4$  ring slippage for 1–9, which accompanies associative attack by MeCN at the metal. A similar interpretation has been presented to explain the rate of arene displacement by P-donor nucleophiles from (arene) $\text{Cr}(\text{CO})_3$  complexes, which also follows the reactivity order arene = naphthalene > phenanthrene >>> benzene.<sup>8</sup> The important reactivity factor is the change in resonance energy ( $\Delta\text{RE}$ ) upon the  $\eta^6 \rightarrow \eta^4$  ring slippage.  $\Delta\text{RE}$  follows the order benzene (84 kJ) > phenanthrene (59 kJ) > naphthalene (44 kJ).<sup>8</sup> With the rough assumption that changes in  $\Delta\text{RE}$  alone determine the relative reactivity of 1, 2, and 10, the half-life order is predicted to be 10 > 1 > 2 (20 000:1:0.0025). This approximates the data in Table 1 (40 000:1:~0.02).

The ease with which complexes 1–9 undergo arene displacement by donor solvents suggested to us that they may be effective at transferring the  $\text{Mn}(\text{CO})_3^+$  moiety to other arenes; i.e., they may function as manganese tricarbonyl transfer (MTT) reagents.<sup>9</sup> Indeed, it was found that simply heating complexes 1–9 in dichloromethane containing a modest excess of any of a number of arenes led to clean substitution, as illustrated by eq 3 for complex 6. The time of heating and reaction yields are given in Table 2.<sup>10</sup> Not surprisingly, the ease of manganese tricarbonyl transfer from 1–9 to an arene correlates with the rate of reaction with MeCN (Table 1). Thus, MTT from 8 and 9 generally required more than 10 h (at 70 °C), while 2 reacted within 1 h (at 40 °C). With respect to yield and time of

(8) Zhang, S.; Shen, J. K.; Basolo, F.; Ju, T. D.; Lang, R. F.; Kiss, G.; Hoff, C. D. *Organometallics* **1994**, *13*, 3692.

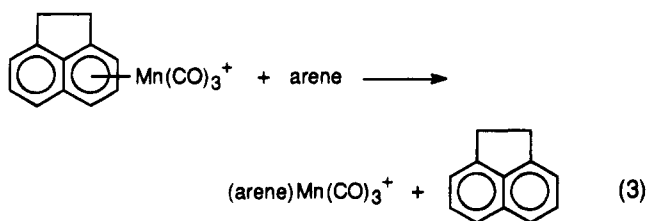
(9) In analogy, (naphthalene) $\text{Cr}(\text{CO})_3$  and (*N*-methylpyrrole) $\text{Cr}(\text{CO})_3$  are known to function as chromium tricarbonyl transfer reagents.<sup>12,13</sup>



**Table 2. Percent Yields for Manganese Tricarbonyl Transfer from Complexes 1–9 to Various Arenes in Analogy to eq 3<sup>a</sup>**

arene	1	2	3	4	5	6	7	8	9
C <sub>6</sub> H <sub>6</sub>	87 (3)	87 (1)	91 (4)	93 (1)	81 (3)	90 (1)	60 (17)		
C <sub>6</sub> Me <sub>6</sub>	77 (3)	70 (0.5) <sup>b</sup>	99 (4)	88 (1)	93 (3)	83 (1)	88 (10) <sup>c</sup>		
C <sub>6</sub> Et <sub>6</sub>	30 (5)			20 (6)	49 (6)	40 (5)			
1,3,5-C <sub>6</sub> H <sub>3</sub> Me <sub>3</sub>	92 (3)	89 (1)	96 (4)	94 (1)	88 (3)	92 (1)	80 (10)		
1,2,4,5-C <sub>6</sub> H <sub>2</sub> Me <sub>4</sub>								58 (24)	56 (20)
C <sub>6</sub> H <sub>5</sub> CH <sub>2</sub> CHMe <sub>2</sub>								45 (16)	43 (22)
C <sub>6</sub> H <sub>5</sub> CMe <sub>3</sub>		93 (1)	87 (3)				90 (8)		
C <sub>6</sub> H <sub>5</sub> SiMe <sub>3</sub>		86 (1)	74 (3)				57 (10) <sup>c</sup>		
<i>t</i> -C <sub>6</sub> H <sub>5</sub> CH=CHC <sub>6</sub> H <sub>5</sub>						91 (2)			
<i>t</i> -C <sub>6</sub> H <sub>5</sub> CH=CHMe						88 (1)		47 (16)	44 (6)
C <sub>6</sub> H <sub>5</sub> C(Me)=CH <sub>2</sub>		82 (1)	75 (4)				75 (10)		
C <sub>6</sub> H <sub>5</sub> NMe <sub>2</sub>	58 (3)	50 (0.5) <sup>b</sup>		70 (1)	89 (3)	80 (1)		56 (21) <sup>b</sup>	42 (17) <sup>b</sup>
C <sub>6</sub> H <sub>5</sub> OH	88 (3)	54 (1)	79 (4)	87 (1)	76 (3)	84 (1)	62 (10)	71 (20)	66 (18)
1,4-C <sub>6</sub> H <sub>4</sub> (Me)(OMe)								69 (17)	73 (17)
1,4-C <sub>6</sub> H <sub>4</sub> (OH)(CMe <sub>3</sub> )		71 (1)	98 (4)				31 (10) <sup>c</sup>		
1,3,5-C <sub>6</sub> H <sub>3</sub> (OMe) <sub>3</sub>	82 (2)			91 (1)	69 (3)	91 (1)		77 (17)	66 (18)
indole	80 (3)			96 (1)		94 (1)		86 (15)	
2-naphthol		81 (1)							
2-methoxytetralin		93 (1)	81 (4)				70 (10)		
phenylsilatrane		90 (1)	93 (4)				98 (10) <sup>c</sup>		
estrone 3-methyl ether	49 (2)			72 (2)					

<sup>a</sup> The reaction times (h) are given in parentheses. All yields refer to isolated products. Unless noted otherwise, the reaction temperature was 70 °C for complexes 1, 4–6, 8, and 9 and 40 °C for 2, 3, and 7. The number of equivalents of free arene used in the exchange reactions was as follows for each complex: 1, 4–6 (1.5 equiv); 2, 3 (2 equiv); 8, 9 (5 equiv); 7 (10 equiv). <sup>b</sup> Reaction conditions were 70 °C and 1.5 equiv of free arene. <sup>c</sup> Five equivalents of free arene used.



reaction, any of the naphthalene-type complexes are excellent transfer reagents. However, when the cost of the precursor polyarene and the ease of complexation to Mn(CO)<sub>3</sub><sup>+</sup> are considered, the  $\alpha$ -methylnaphthalene and acenaphthene complexes (3 and 6) are perhaps the preferred MTT reagents. The important point to note is that the synthesis of (arene)Mn(CO)<sub>3</sub><sup>+</sup> complexes via MTT reagents constitutes an exceptionally mild procedure and can be utilized to coordinate arenes that fail

(10) The arene exchange reactions, as in eq 3, were performed as follows: under N<sub>2</sub>, the complex (1–9; 0.2 g) was dissolved in ca. 25 mL of CH<sub>2</sub>Cl<sub>2</sub> and the arene added in modest excess (Table 2). At this stage the reaction solution was either refluxed (40 °C) or sealed in a pressure bottle and heated to 70 °C for the times indicated in Table 2. In order to determine appropriate reaction times, initial synthetic runs were followed by IR. The product and reactant have similar IR spectra in the  $\nu_{CO}$  region, but the differences are sufficient so that the reactant is easily distinguished as a shoulder (or separate peak) on the product IR bands. After IR spectra showed no trace of the starting complex 1–9, the reaction mixture was cooled, concentrated, and filtered through Celite (if necessary). Diethyl ether was used to precipitate the product, which was washed with ether and dried *in vacuo*. <sup>1</sup>H NMR (and IR) indicated that the products were very pure. Satisfactory elemental analyses were obtained for all previously unreported [(arene)Mn(CO)<sub>3</sub>]BF<sub>4</sub> complexes obtained by this procedure.

to react satisfactorily by the other available methods (*vide supra*) due to the presence of sensitive functional groups or other reasons.

In summary, we have shown that (polyarene)Mn(CO)<sub>3</sub><sup>+</sup> complexes can be synthesized in good yield and that they are effective general reagents for the transfer of the Mn(CO)<sub>3</sub><sup>+</sup> moiety to arenes. Indeed, it is even possible to transfer Mn(CO)<sub>3</sub><sup>+</sup> to naphthalene-type complexes to obtain naphthalenes with a manganese carbonyl unit attached to each ring on the same side.<sup>11</sup>

**Acknowledgment.** This work was supported by grants from the National Science Foundation (CHE-9400800 and INT-9312709), the Korea Science and Engineering Foundation (No. 93-0500-02-01-3 and the Korean-USA Cooperative Science Program), the Thomas F. and Kate Miller Jeffress Memorial Trust, and the donors of the Petroleum Research Fund, administered by the American Chemical Society (PRF No. 26521-GB1).

**Supplementary Material Available:** Text and a table giving characterization data for the compounds prepared in this paper (4 pages). Ordering information is given on any current masthead page.

OM950213A

(11) Sun, S.; Dullaghan, C. A.; Carpenter, G. B.; Sweigart, D. A. To be submitted for publication.

(12) Kündig, E. P.; Perret, C.; Spichiger, S.; Bernardinelli, G. *J. Organomet. Chem.* **1985**, *286*, 183.

(13) Goti, A.; Semmelhack, M. F. *J. Organomet. Chem.* **1994**, *470*, C4.

# Ruthenium-Mediated Hydrogenation of Carbon Dioxide by $\text{NaBH}_4$ via the Formation of the Formate Complex $\text{C}_5\text{Me}_5\text{Ru}(\text{PCy}_3)(\eta^2\text{-OCHO})$

Chae S. Yi\* and Nianhong Liu

Department of Chemistry, Marquette University, Milwaukee, Wisconsin 53233

Received January 13, 1995<sup>§</sup>

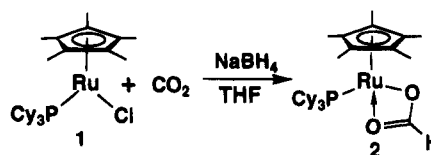
**Summary:** Reaction of  $\text{C}_5\text{Me}_5\text{Ru}(\text{PCy}_3)\text{Cl}$  (**1**) with 1–2 atm of carbon dioxide in the presence of  $\text{NaBH}_4$  initially gave the new formate complex  $\text{C}_5\text{Me}_5\text{Ru}(\text{PCy}_3)(\eta^2\text{-OCHO})$  (**2**). The complex **2** in the reaction mixture was gradually converted into formic acid and the previously known  $\text{C}_5\text{Me}_5\text{Ru}(\text{PCy}_3)(\text{CO})\text{H}$  (**3**). Deuterium labeling experiments suggest that the acid proton of formic acid came from the solvent. A possible mechanism of the formation of **2** and subsequent formation of formic acid is discussed.

Remarkable progress has been made in the transformation of carbon dioxide employing organometallic catalysts in recent years.<sup>1,2</sup> A few notable recent examples include Nicholas's rhodium-catalyzed hydrogenation of carbon dioxide,<sup>2a</sup> Kubiak's electrocatalytic reduction of carbon dioxide in a nickel cluster,<sup>2b</sup> and Noyori's  $(\text{PMe}_3)_4\text{RuH}_2$ -catalyzed formation of formic acid in supercritical  $\text{CO}_2$  medium.<sup>2c</sup> To get some understanding of the mechanisms involving the reactions of transition-metal complexes with carbon dioxide, we have been investigating the reactions of ruthenium complexes with carbon dioxide, and herein we report a mild hydrogenation reaction of carbon dioxide using the organoruthenium complex  $\text{C}_5\text{Me}_5\text{Ru}(\text{PCy}_3)\text{Cl}$  (**1**)<sup>3</sup> and  $\text{NaBH}_4$ .

Our initial plan was to prepare a coordinatively unsaturated ruthenium hydride species of the type  $\text{C}_5\text{Me}_5\text{Ru}(\text{PCy}_3)(\text{H})$  and use it as a precursor for the carbon dioxide reaction. Several preliminary attempts to generate  $\text{C}_5\text{Me}_5\text{Ru}(\text{PCy}_3)(\text{H})$  from the reactions of **1** with

hydride reagents, however, gave disparate results. Reaction of **1** with  $\text{LiAlH}_4$  exclusively gave the previously known trihydride complex  $\text{C}_5\text{Me}_5\text{Ru}(\text{PCy}_3)(\text{H})_3$ , whereas reaction with  $\text{LiBH}_4$  gave both the borohydride species  $\text{C}_5\text{Me}_5\text{Ru}(\text{PCy}_3)(\mu\text{-H})_2\text{BH}_2$  and  $\text{C}_5\text{Me}_5\text{Ru}(\text{PCy}_3)(\text{H})_3$ .<sup>4</sup> No apparent reaction was observed in the reaction of **1** with  $\text{NaBH}_4$ , and none of these hydride complexes were reactive toward carbon dioxide under our reaction conditions.

Surprisingly, however, when **1** was treated with carbon dioxide in the presence of  $\text{NaBH}_4$ , a new species was observed by NMR. In a sealed NMR tube, a mixture of carbon dioxide (1–2 atm), **1** (10 mg, 0.0368 mmol), and 5 equiv of  $\text{NaBH}_4$  (7 mg, 0.184 mmol) in  $\text{THF-}d_8$  was vigorously shaken at room temperature for 1–2 h. The deep blue solution turned red-brown, and a set of new resonances appeared which was subsequently characterized as the new formate complex  $\text{C}_5\text{Me}_5\text{Ru}(\text{PCy}_3)(\eta^2\text{-OCHO})$  (**2**).<sup>5</sup> The  $^1\text{H}$  NMR of **2** exhib-



ited a downfield-shifted formate hydrogen signal at  $\delta$  8.50, which became a doublet when  $^{13}\text{CO}_2$  was employed ( $J_{\text{CH}} = 209.6$  Hz). The formate carbon resonance at  $\delta$  164.1 (d,  $^3J_{\text{PC}} = 3.7$  Hz) and the characteristic formate IR stretching frequencies ( $\nu_{\text{OCO}(\text{asym})} = 1618$  and  $\nu_{\text{OCO}(\text{sym})} = 1452$   $\text{cm}^{-1}$ ) were also consistent with the  $\eta^2$ -formate geometry.<sup>6</sup> On a preparative scale, complex **2** was isolated as a brown-red solid in approximately 80% yield, but we were not able to obtain an analytically pure complex due to its thermal instability. Several attempts to synthesize **2** independently from the reaction of **1** with  $\text{NaO}_2\text{CH}$  were unsuccessful.

The initially formed **2** in a sealed NMR tube in  $\text{THF-}d_8$  was further converted to a mixture of the previously known carbonyl hydride  $\text{C}_5\text{Me}_5\text{Ru}(\text{PCy}_3)(\text{CO})\text{H}$  (**3**)<sup>7</sup> and formic acid in approximately a 1:2 ratio. In the  $^1\text{H}$  NMR, a set of new peaks at  $\delta$  11.34 ( $\text{HCO}_2\text{H}$ ) and  $\delta$  7.90 ( $\text{HCO}_2\text{H}$ ) due to formic acid appeared at the expense of

<sup>§</sup> Abstract published in *Advance ACS Abstracts*, May 1, 1995.

(1) For recent reviews, see: (a) Behr, A. *Carbon Dioxide Activation by Metal Complexes*; VCH: New York, 1988. (b) Darensbourg, D. J.; Kudarowski, R. A. *Adv. Organomet. Chem.* **1983**, *22*, 129. (c) Sneed, R. P. A. In *Comprehensive Organometallic Chemistry*; Wilkinson, G., Stone, F. G. A., Eds.; Pergamon Press: New York, 1982; Vol. 8. (d) Braunstein, P.; Matt, D.; Nobel, D. *Chem. Rev.* **1988**, *88*, 747. (e) *Catalytic Activation of Carbon Dioxide*; Ayers, W. M., Ed.; ACS Symposium Series 363; American Chemical Society: Washington, DC, 1988. (f) Denise, B.; Sneed, R. P. A. *CHEMTECH* **1982**, *12*, 108. For recent selected transition-metal carbon dioxide complexes, see: (g) Calabrese, J. C.; Heerskovitz, T.; Kinney, J. B. *J. Am. Chem. Soc.* **1983**, *105*, 5914. (h) Alvarez, R.; Carmona, E.; Marin, J. M.; Poveda, M. L.; Gutierrez-Puebla, E.; Monge, A. *J. Am. Chem. Soc.* **1986**, *108*, 2286. (i) Fu, P.-F.; Khan, M. A.; Nicholas, K. M. *J. Am. Chem. Soc.* **1992**, *114*, 6579. (j) Komiya, S.; Akita, M.; Kasuga, N.; Hirano, M.; Fukuoka, A. *J. Chem. Soc., Chem. Commun.* **1994**, 1115. (k) Fu, P.-F.; Fazlur-Rahman, A. K.; Nicholas, K. M. *Organometallics* **1994**, *13*, 413. (l) Sakamoto, M.; Shimizu, I.; Yamamoto, A. *Organometallics* **1994**, *13*, 407. (m) Pinkes, J. R.; Steffey, B. D.; Vites, J. C.; Cutler, A. R. *Organometallics* **1994**, *13*, 21. (n) Gibson, D. H.; Ye, M.; Richardson, J. F.; Mashuta, M. S. *Organometallics* **1994**, *13*, 4559.

(2) (a) Tsai, J.-C.; Nicholas, K. M. *J. Am. Chem. Soc.* **1992**, *114*, 5117. (b) Morgenstern, D. A.; Wittig, R. E.; Fanwick, P. E.; Kubiak, C. P. *J. Am. Chem. Soc.* **1993**, *115*, 6470. (c) Jessop, P. G.; Ikariya, T.; Noyori, R. *Nature* **1994**, *368*, 231. (d) Jessop, P. G.; Hsiao, Y.; Ikariya, T.; Noyori, R. *J. Am. Chem. Soc.* **1994**, *116*, 8851.

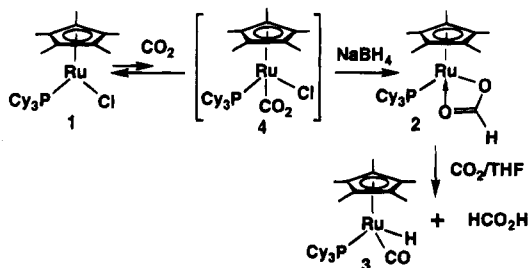
(3) (a) Campion, B. K.; Heyn, R. H.; Tilley, T. D. *J. Chem. Soc., Chem. Commun.* **1988**, 278. (b) Campion, B. K.; Heyn, R. H.; Tilley, T. D. *J. Am. Chem. Soc.* **1988**, *110*, 7558. (c) Luo, L.; Nolan, S. P.; Fagan, P. J. *Organometallics* **1993**, *12*, 4305.

(4) (a) Suzuki, H.; Lee, D. H.; Oshima, N.; Moro-oka, Y. *Organometallics* **1987**, *6*, 1569. (b) Lee, D. H.; Suzuki, H.; Moro-oka, Y. *J. Organomet. Chem.* **1987**, *330*, C20.

(5) For **2**:  $^1\text{H}$  NMR ( $\text{C}_6\text{D}_6$ , 300 MHz)  $\delta$  8.50 (s,  $\text{O}_2\text{CH}$ ), 1.76 (s,  $\text{C}_5\text{Me}_5$ ), 1–2 (m,  $\text{PCy}_3$ );  $^{13}\text{C}\{^1\text{H}\}$  NMR ( $\text{C}_6\text{D}_6$ , 75 MHz)  $\delta$  164.1 (d,  $^3J_{\text{CP}} = 3.7$  Hz,  $\text{O}_2\text{CH}$ ), 88.2 ( $\text{C}_5\text{Me}_5$ ), 31.2, 28.2, 27.4, and 26.4 ( $\text{PCy}_3$ ), 11.7 ( $\text{C}_5\text{Me}_5$ );  $^{31}\text{P}$  NMR ( $\text{C}_6\text{D}_6$ , 121.6 MHz)  $\delta$  54.6 ( $\text{PCy}_3$ ); IR ( $\text{C}_6\text{H}_6$ ) 1618 (s,  $\nu_{\text{OCO}(\text{asym})}$ ), 1452 (s,  $\nu_{\text{OCO}(\text{sym})}$ )  $\text{cm}^{-1}$ .

(6) (a) Nakamoto, K. *Infrared and Raman Spectra of Inorganic and Coordination Compounds*, 4th ed.; Wiley: New York, 1986. (b) Silverstein, R. M.; Bassler, G. C.; Morrill, T. C. *Spectrometric Identification of Organic Compounds*, 5th ed.; Wiley: New York, 1991.

the resonances of **2**. The formate hydrogen peak at  $\delta$  7.90 became a doublet ( $J_{\text{CH}} = 210.3$  Hz) when  $^{13}\text{CO}_2$  (99%, Cambridge Isotopes) was employed in the reaction, indicating its attachment to formic acid. Eventually after 5 h, all formic acid was decomposed to  $\text{NaO}_2\text{CH}$ , **3**, and other unidentified species. In a preparative reaction, complex **3** was isolated as a pale white solid in 85% yield based on **1**. The choice of solvent appeared to be important to the success of the reaction; similar reactions in MeOH led to the exclusive formation of the trihydride complex  $\text{C}_5\text{Me}_5\text{Ru}(\text{PCy}_3)(\text{H})_3$ , while no reaction was observed in  $\text{Et}_2\text{O}$  or  $\text{CH}_2\text{Cl}_2$ .



The apparent lack of reactions between **1** and  $\text{NaO}_2\text{CH}$  indicates that the possible formation of complex **2** from the reaction of **1** with a preformed formate ion is not likely.<sup>8</sup> The fact that complex **1** is unreactive toward  $\text{NaBH}_4$  in the absence of carbon dioxide suggests that carbon dioxide was pre-coordinated to **1** before the hydrogenolysis of chloride.<sup>9</sup> These results are consistent with a reversible pre-coordination of carbon dioxide to **1** to produce the  $18 e^-$  intermediate **4** and subsequent reduction by  $\text{NaBH}_4$  to give the more stable formate complex **2**.<sup>10</sup> Although carbon dioxide is a labile ligand and, therefore, the concentration of the intermediate **4** should be quite low at relatively low pressures of carbon dioxide, the pre-coordination of carbon dioxide to **1** would reduce the  $\pi$ -bonding interactions between the ruthenium and the chloride, making the chloride ligand more susceptible to the  $\text{NaBH}_4$  reduction. Further intramolecular insertion of carbon dioxide would give the formate complex **2**. Carbon dioxide insertion into the transition-metal-hydride bond has been well documented.<sup>1a,b</sup> Also, a reversible carbon dioxide insertion into  $\text{Ru}(\text{PR}_3)_4\text{H}_2$  ( $\text{R} = \text{Ph}, \text{Me}$ ) has been previously reported.<sup>11</sup>

The detailed reaction mechanism of the conversion from **2** to **3** and formic acid is not yet clearly understood. In a preliminary experiment, initially formed **2** and formic acid were extensively deuterated at the formate hydrogen when  $\text{NaBD}_4$  in THF was employed in the reaction, but the hydride of **3** contained approximately 50% deuterium as estimated by NMR. Similarly, when the reaction was carried out with  $\text{NaBH}_4$  in  $\text{THF-}d_8$ , the acid proton of formic acid contained nearly 70% deuterium. These results suggest that the possible source of the acid proton of formic acid is from the solvent and not from  $\text{NaBH}_4$  and that the substantial deuterium scrambling may have occurred during the subsequent formation of formic acid and **3**. Wilkinson previously proposed a mechanism involving proton transfer from a coordinated THF to a coordinated hydroxy ligand.<sup>12</sup>

In summary, the formation of formic acid from the hydrogenation of carbon dioxide using the coordinatively unsaturated ruthenium complex **1** and  $\text{NaBH}_4$  has been described. Preliminary studies indicated that the pre-coordination of carbon dioxide to the complex **1** promoted the hydrogenolysis of chloride ligand to give the formate complex **2**, and the subsequent decomposition of **2** led to the formation of formic acid and **3**. Studies on the scope and the detailed reaction mechanism involving the complex **1** are currently being pursued.

The detailed reaction mechanism of the conversion from **2** to **3** and formic acid is not yet clearly understood. In a preliminary experiment, initially formed **2** and formic acid were extensively deuterated at the formate hydrogen when  $\text{NaBD}_4$  in THF was employed in the reaction, but the hydride of **3** contained approximately 50% deuterium as estimated by NMR. Similarly, when the reaction was carried out with  $\text{NaBH}_4$  in  $\text{THF-}d_8$ , the acid proton of formic acid contained nearly 70% deuterium. These results suggest that the possible source of the acid proton of formic acid is from the solvent and not from  $\text{NaBH}_4$  and that the substantial deuterium scrambling may have occurred during the subsequent formation of formic acid and **3**. Wilkinson previously proposed a mechanism involving proton transfer from a coordinated THF to a coordinated hydroxy ligand.<sup>12</sup>

**Acknowledgment.** Financial support from Marquette University is gratefully acknowledged.

OM950025K

(7) Complex **3** was previously prepared from the reaction of **1** with CO followed by  $\text{NaBH}_4$  reduction: Arliguie, T.; Border, C.; Chaudret, B.; Devillers, J.; Poilblanc, R. *Organometallics* **1989**, *8*, 1308. Spectral data for **3**:  $^1\text{H}$  NMR ( $\text{C}_6\text{D}_6$ , 300 MHz)  $\delta$  1.98 (s,  $\text{C}_5\text{Me}_5$ ), 1–2 (m,  $\text{PCy}_3$ ), –11.90 (d,  $J_{\text{PH}} = 33.8$  Hz, Ru–H);  $^{13}\text{C}\{^1\text{H}\}$  NMR ( $\text{C}_6\text{D}_6$ , 75 MHz)  $\delta$  210.4 (d,  $J_{\text{CP}} = 18.3$  Hz, CO), 95.1 ( $\text{C}_5\text{Me}_5$ ), 38.3, 30.8, and 28.1 ( $\text{PCy}_3$ ), 12.1 ( $\text{C}_5\text{Me}_5$ );  $^{31}\text{P}$  NMR ( $\text{C}_6\text{D}_6$ , 121.6 MHz)  $\delta$  75.0 ( $J_{\text{CP}} = 18.3$  Hz,  $\text{PCy}_3$ ); IR ( $\text{C}_6\text{H}_6$ ) 1892 (s)  $\text{cm}^{-1}$ ; FAB MS  $\text{M}^+$  at  $m/z$  545.

(8) The reaction of  $\text{NaBH}_4$  with  $\text{CO}_2$  (5 atm) in  $\text{THF-}d_8$  did not produce any detectable amount of  $\text{NaO}_2\text{CH}$  even in the presence of  $\text{AlCl}_3$ .

(9) Reference 3a described the reversible formation of the adduct  $\text{C}_5\text{Me}_5\text{Ru}(\text{PCy}_3)(\text{CH}_2=\text{CH}_2)(\text{Cl})$  from the reaction of **1** with  $\text{CH}_2=\text{CH}_2$ . In support of the mechanism, we also found that the reaction of **1** with  $\text{CH}_2=\text{CH}_2$  in the presence of  $\text{NaBH}_4$  gave  $\text{C}_5\text{Me}_5\text{Ru}(\text{PCy}_3)(\text{CH}_2=\text{CH}_2)(\text{H})$ , which may have formed in a fashion similar to that in **2**.

(10) Another possible mechanism involves  $\text{NaBH}_4$  reduction of **1** in the first step to generate the reactive  $\text{C}_5\text{Me}_5\text{Ru}(\text{PCy}_3)(\text{H})$ , which then inserts carbon dioxide to give **2**. Although we cannot rule out this mechanism, the apparent lack of reactivity of  $\text{NaBH}_4$  toward **1** in the absence of carbon dioxide and the general tendency of forming a stable and unreactive  $\text{C}_5\text{Me}_5\text{Ru}(\text{PCy}_3)(\text{H})_3$  suggest that this route is unlikely. Also, as a reviewer pointed out, carbon dioxide could react first with  $\text{NaBH}_4$  to form a formate ion, which would then react with **1** to form **2**. The facts that complex **1** did not react with  $\text{NaO}_2\text{CH}$  and that we did not observe any evidence of reaction between carbon dioxide and  $\text{NaBH}_4$  in the absence of **1** suggest that this route also seems unlikely.

(11) (a) Komiya, S.; Yamamoto, A. *J. Organomet. Chem.* **1972**, *46*, C58. (b) Kolomnikov, I. S.; Gusev, A. I.; Aleksandrov, G. G.; Lobeeva, T. S.; Struchkov, Y. T.; Vol'pin, M. E. *J. Organomet. Chem.* **1973**, *59*, 349.

(12) Chaudret, B. N.; Cole-Hamilton, D. J.; Nohr, R. S.; Wilkinson, G. *J. Chem. Soc., Dalton Trans.* **1977**, 1546.

# Synthesis of the First Redox-Active Organometallic Polymers Containing Cyclosiloxanes as Frameworks

Carmen M. Casado,<sup>†</sup> Isabel Cuadrado,<sup>\*,†</sup> Moisés Morán,<sup>†</sup> Beatriz Alonso,<sup>†</sup> Francisco Lobete,<sup>†</sup> and José Losada<sup>‡</sup>

Departamento de Química Inorgánica, Facultad de Ciencias, Universidad Autónoma de Madrid, Cantoblanco 28049-Madrid, Spain, and Departamento de Ingeniería Química Industrial, Escuela Técnica Superior de Ingenieros Industriales, Universidad Politécnica de Madrid, 28006-Madrid, Spain

Received February 23, 1995<sup>®</sup>

**Summary:** A new class of ferrocenyl and permethylferrocenyl polymers **2** and **3**, containing a cyclotetrasiloxane in the backbone, has been prepared via hydrosilylation reactions. The synthesis of the tetranuclear model 1,3,5,7-tetrakis(ferrocenylethyl)-1,3,5,7-tetramethylcyclotetrasiloxane (**1**) is also reported. The different nature of the cyclopentadienyl ring substituents was found to have influence on the electrochemical behavior of solutions and of electrode surfaces modified with electrodeposited films of these polymers.

Macromolecular systems containing organometallic units are of increasing interest as a result of their unique properties.<sup>1</sup> Ferrocenyl-based polymers<sup>2</sup> are useful materials for modification of electrodes, as electrochemical biosensors,<sup>3</sup> and as nonlinear optical systems.<sup>2c</sup> As a part of our ongoing studies on the chemistry of silicon-containing organometallic compounds, we recently synthesized new classes of macromolecules containing ferrocenyl moieties together with polyhedral octasilsesquioxanes,<sup>4</sup> linear siloxanes,<sup>5</sup> or organosilicon dendrimers.<sup>6</sup> Now we have extended our studies to systems that contain cyclosiloxanes as frameworks of silicon atoms. Due to their stereochemical properties, organometallic-substituted cyclosiloxanes are potential candidates as sterically controlled multifunctional catalyst systems. Although several examples of metallobonded-substituted cyclosiloxanes have been

reported,<sup>7</sup> no examples of organometallic polymers with siloxane rings in the backbone are known. We report herein preliminary results on the synthesis, characterization, and redox properties of cyclotetrasiloxanes in which the silicon atoms of the rings are attached to ferrocenyl or octamethylferrocenyl units through a two-carbon linkage. While polymers containing ferrocenyl moieties in the backbone or as pendant substituents are numerous, polymers constructed from permethylferrocene monomers have been relatively unexplored.<sup>8,9,10a</sup> As a result of the enhanced donor properties of the permethylated cyclopentadienyl rings, electrode surfaces functionalized with redox-active polymethylferrocenyl derivatives promise to be of importance in electrocatalysis; for instance, electrode surfaces modified with a pentamethyl ferrocene derivative can be used as sensors for cytochrome *c*.<sup>10</sup>

The hydrosilylation of 1,3,5,7-tetramethylcyclotetrasiloxane with 4 equiv of vinylferrocene, in the presence of Karstedt catalyst (bis(divinyltetramethyldisiloxane)-platinum(0) in xylene) was performed in toluene solution at 20 °C (Scheme 1). From <sup>1</sup>H NMR and IR analysis of the reaction mixture it was established that complete reaction of the SiH functionalities was easily achieved in 4 h.<sup>11</sup> After column chromatography on silica gel using a 1/3 mixture of dichloromethane and *n*-hexane as eluent, the tetranuclear compound **1** was isolated as an orange viscous oil in 92% yield. Treatment with hexane affords a yellow solid.<sup>12</sup> Obviously, the mild conditions under which **1** can be cleanly formed are of importance for its successful preparation, and in addition siloxane ring degradation cannot occur as a side reaction.<sup>13</sup> The structure of the tetranuclear **1** was straightforwardly established on the basis of multinuclear (<sup>1</sup>H, <sup>13</sup>C, <sup>29</sup>Si) NMR data, IR spectroscopy, mass

<sup>†</sup> Universidad Autónoma de Madrid.

<sup>‡</sup> Universidad Politécnica de Madrid.

<sup>®</sup> Abstract published in *Advance ACS Abstracts*, May 1, 1995.

(1) (a) *Inorganic and Organometallic Polymers II: Advanced Materials and Intermediates*; Wisian-Neilson, P., Allcock, H. R., Wynne, K. J., Eds.; ACS Symposium Series 572; American Chemical Society: Washington, DC, 1994. (b) *Inorganic and Metal-Containing Polymeric Materials*; Sheats, J. E., Carraher, C. E., Jr., Pittman, C. U., Jr., Zeldin, M., Currell, B., Eds.; Plenum Press: New York, 1990. (c) *Inorganic Polymers*; Mark, J. E., Allcock, H. R., West, R., Eds.; Prentice-Hall: Englewood Cliffs, NJ, 1992. (d) *Contemporary Polymer Chemistry*, 2nd ed.; Allcock, H. R., Lampe, F. W., Eds.; Prentice-Hall: Englewood Cliffs, NJ, 1990. (e) Allcock, H. R. *Adv. Mater.* **1994**, *6*, 106.

(2) Recent reviews of the main areas of research on ferrocenes include the following: (a) *Ferrocenes*; Togni, A., Hayashi, T., Eds.; VCH: Weinheim, Germany, 1995. See also: (b) Foucher, D. A.; Ziembinski, R.; Rulkens, R.; Nelson, J.; Manners, I. In ref 1a, Chapter 33. (c) Wright, M. E.; Cochran, B. B.; Toplikar, E. G.; Lackritz, H. S.; Kerney, J. T., In ref 1a, Chapter 34.

(3) See for example: (a) Ikeda, S.; Oyama, N. *Anal. Chem.* **1993**, *65*, 1910. (b) Hale, P. D.; Lee, H. S.; Okamoto, Y. *Anal. Lett.* **1993**, *26*, 1. (c) Hale, P. D.; Boguslavsky, L. I.; Inagaki, T.; Karan, H. I.; Lee, H. S.; Skotheim, T. A.; Okamoto, Y. *Anal. Chem.* **1991**, *63*, 677. (d) Hale, P. D.; Lan, H. L.; Boguslavsky, L. I.; Karan, H. I.; Okamoto, Y.; Skotheim, T. A. *Anal. Chim. Acta* **1991**, *251*, 121. (e) Hale, P. D.; Inagaki, T.; Karan, H. I.; Okamoto, Y.; Skotheim, T. A. *J. Am. Chem. Soc.* **1989**, *111*, 3482.

(4) Morán, M.; Casado, C. M.; Cuadrado, I.; Losada, J. *Organometallics* **1993**, *12*, 4237.

(5) Casado, C. M.; Morán, M.; Losada, J.; Cuadrado, I. *Inorg. Chem.* **1995**, *34*, 1668.

(6) Alonso, B.; Cuadrado, I.; Morán, M.; Losada, J. *J. Chem. Soc., Chem. Commun.* **1994**, 2575.

(7) (a) Harrod, J. F.; Pelletier, E. *Organometallics* **1984**, *3*, 1064, 1070. (b) Harrod, J. F.; Shaver, A.; Tucka, A. *Organometallics* **1985**, *4*, 2166.

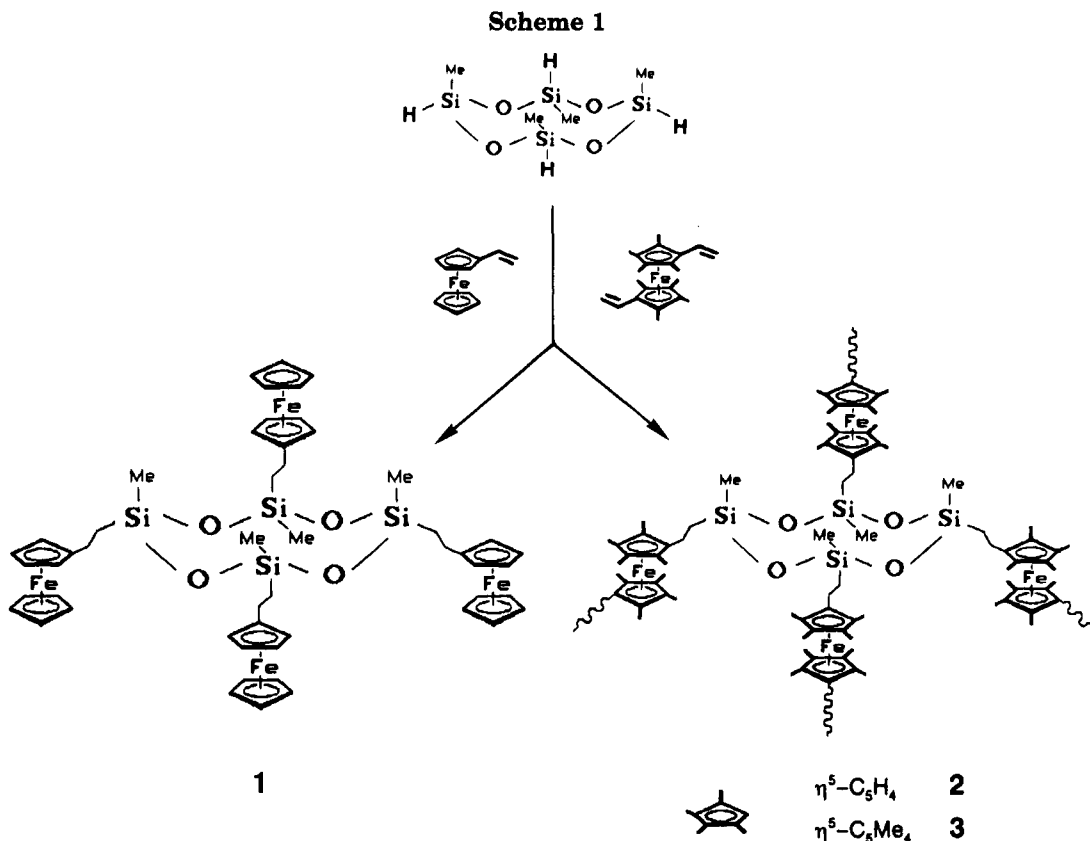
(8) Although several examples of functionally substituted octamethylferrocenyl derivatives have been reported,<sup>9,10a</sup> to the best of our knowledge the first octamethylated ferrocene polymer was prepared in our laboratory.<sup>4</sup>

(9) See for example: (a) Pudelski, J. K.; Callstrom, M. R. *Organometallics* **1994**, *13*, 3095. (b) Ogasa, M.; Mallin, D. T.; Macomber, D. W.; Rausch, M. D.; Rogers, R. D.; Rollins, A. N. *J. Organomet. Chem.* **1991**, *405*, 41. (c) Gibson, C. P.; Bem, D. S.; Falloon, S. B.; Cortopassi, J. E. In *Inorganic and Metal-Containing Polymeric Materials*; Sheats, J. E., Carraher, C. E., Jr., Pittman, C. U., Jr., Zeldin, M., Currell, B., Eds.; Plenum Press: New York, 1990; p 127.

(10) (a) Chaofeng, Z.; Wrighton, M. S. *J. Am. Chem. Soc.* **1990**, *112*, 7578. (b) Chao, S.; Robbins, J. L.; Wrighton, M. S. *J. Am. Chem. Soc.* **1983**, *105*, 181.

(11) The  $\nu(\text{SiH})$  frequency of 1,3,5,7-tetramethylcyclotetrasiloxane suggests that the electronic environment about the reacting silicon centers is suitable for hydrosilylations. See: Stein, J.; Lewis, L. N.; Smith, K. A.; Lettko, K. X. *J. Inorg. Organomet. Polym.* **1991**, *1*, 325.

(12) Attempts to isolate **1** as a crystalline solid have been unsuccessful so far, probably because it is a mixture of geometric isomers.



spectrometry, and microanalysis.<sup>14</sup> Of particular relevance was the presence in the  $^1\text{H}$  NMR spectrum of several resonances in the Si-CH<sub>3</sub> region, which indicates the existence of four geometric isomers.<sup>15</sup> The  $^{29}\text{Si}$  NMR spectrum of **1** (in  $\text{CDCl}_3$ ) consists of a singlet resonance at  $-20.14$  ppm, which is within the range expected for a D-type silicon atom in a cyclic tetrasiloxane<sup>16</sup> and which agrees with a totally substituted structure. Likewise, an additional definitive spectral evidence of the incorporation of the four ferrocenyl units to the cyclotetrasiloxane ring in **1** was the mass spectrum, which shows the molecular ion  $\text{M}^+$  as the base peak at  $m/z$  1088, together with some informative peaks assignable to reasonable fragmentation products.

In order to synthesize novel three-dimensional polymers, containing skeletal ferrocenyl units together with cyclosiloxane frameworks, hydrosilylation reactions of 1,3,5,7-tetramethylcyclotetrasiloxane with either 1,1'-divinylferrocene or 1,1'-divinyloctamethylferrocene have been explored.<sup>17</sup> Not surprisingly, the reaction with the octamethylated monomer was less successful since, in

spite of using more forcing conditions, a lower degree of SiH functionalization was obtained. This is due to the steric hindrance effect imposed by the methyl groups. Polymers **2** and **3** were purified by repeated precipitations from  $\text{CH}_2\text{Cl}_2$  solutions by addition to a large volume of  $\text{CH}_3\text{CN}$ . **2** was isolated as a brown shiny solid and **3** as a yellow-brown material.<sup>18</sup> NMR spectra of polymers **2** and **3** show broad resonances in the expected regions. The  $^1\text{H}$  NMR spectrum of **3** shows, in addition, resonances corresponding to trace quantities of unreacted vinyl and SiH groups. Consis-

(13) Ring opening in cyclic siloxanes occurs in the presence of anionic or cationic initiators. See for example: (a) Chojnowsky, J. In *Siloxane Polymers*; Clarson, S. J., Semlyen, J. A., Eds.; Prentice-Hall: Englewood Cliffs, NJ, 1993; p 1. (b) Saam, J. C. In *Silicon-Based Polymer Science*; Zeigler, J. M., Gordon Fearon, F. W., Eds.; Advances in Chemistry Series 224; American Chemical Society: Washington, DC, 1990.

(14) Selected spectroscopic and analytical data for **1** are as follows.  $^1\text{H}$  NMR (300 MHz,  $\text{CDCl}_3$ ):  $\delta$  4.12–4.06 (m, ferrocenyl protons), 2.44 (m,  $\text{C}_5\text{H}_4\text{CH}_2$ ), 0.90 (m,  $\text{SiCH}_2$ ), 0.19 (m,  $\text{SiCH}_3$ ).  $^{13}\text{C}\{^1\text{H}\}$  NMR (75.43 MHz,  $\text{CDCl}_3$ ):  $\delta$  91.90 ( $\text{C}_5\text{H}_4$ ), 68.40 ( $\text{C}_5\text{H}_5$ ), 67.54 and 67.01 ( $\text{CH}_2\text{H}_4$ ), 22.64 ( $\text{C}_5\text{H}_4\text{CH}_2$ ), 18.40 ( $\text{SiCH}_2$ ),  $-0.49$  ( $\text{SiCH}_3$ ).  $^{29}\text{Si}\{^1\text{H}\}$  NMR (59.3 MHz,  $\text{CDCl}_3$ , 0.015 M  $\text{Cr}(\text{acac})_3$ ):  $\delta$   $-20.14$  ppm. MS (FAB;  $m/z$  (%)): 1088 ( $\text{M}^+$ , 100), 213 ( $[\{\eta^5\text{-C}_5\text{H}_5\}\text{Fe}\{\eta^5\text{-C}_5\text{H}_4\text{CH}_2\text{CH}_2\}]^+$ , 10.69), 199 ( $[\{\eta^5\text{-C}_5\text{H}_5\}\text{Fe}\{\eta^5\text{-C}_5\text{H}_4\text{CH}_2\}]^+$ , 15.16), 121 ( $[\{\eta^5\text{-C}_5\text{H}_5\}\text{Fe}]^+$ , 16.07). Anal. Calcd for  $\text{Si}_4\text{O}_4\text{C}_{52}\text{H}_{64}\text{Fe}_4$ : C, 57.36; H, 5.92. Found: C, 57.41; H, 5.97.

(15) The use of the Si-CH<sub>3</sub> resonances in the  $^1\text{H}$  NMR spectrum of **1** for investigation of its isomeric composition will be reported in the full paper.

(16) Williams, E. A. In *The Chemistry of Organic Silicon Compounds*; Patai, S., Rappoport, Z., Eds.; Wiley: New York, 1989; Part 1, p 511.

(17) Synthesis and spectral data for polymers **2** and **3**: 2.5 equiv of 1,1'-divinylferrocene (**2**) (or 1,1'-divinyloctamethylferrocene (**3**)) was added to a toluene solution (20 mL) containing 10  $\mu\text{L}$  of a 3–3.5% solution of Karstedt's catalyst in xylene. The mixture was stirred at room temperature for approximately 1 h. A gentle stream of air was blown through the solution for a few seconds. A solution of 1,3,5,7-tetramethylcyclotetrasiloxane (0.54 g, 2.25 mmol) in dry toluene (20 mL) was added dropwise. The reaction mixture was heated to 75  $^\circ\text{C}$ . In the synthesis of **2**, after 30 h, FTIR spectra of the reaction mixture showed quantitative loss of the Si-H stretch. However for **3** after 90 h at 75  $^\circ\text{C}$  the reaction was not yet completed. A 10% excess of 1,1'-divinyloctamethylferrocene was added, and the reaction mixture was heated to 90  $^\circ\text{C}$  and stirred for an additional 8 h, but IR analysis did not show further reduction of the Si-H absorption. After removal of the solvent both polymers were purified by successive reprecipitations from  $\text{CH}_2\text{Cl}_2$  into  $\text{CH}_3\text{CN}$ . In both cases primarily light brown materials insoluble in  $\text{CH}_2\text{Cl}_2$  and  $\text{CH}_3\text{CN}$  were separated, and subsequently a light brown solid (**2**) (yellow-brown for **3**) insoluble in  $\text{CH}_3\text{CN}$  was also isolated: yields 70–83%. The following characterization data correspond to the fractions soluble in  $\text{CH}_2\text{Cl}_2$ . Key data for **2** was as follows.  $^1\text{H}$  NMR (300 MHz,  $\text{C}_6\text{D}_6$ ):  $\delta$  4.24 (br, ferrocenyl protons), 2.68 (br,  $\text{C}_5\text{H}_4\text{CH}_2$ ), 1.14 (br,  $\text{SiCH}_2$ ), 0.25 (br,  $\text{SiCH}_3$ ).  $^{13}\text{C}\{^1\text{H}\}$  NMR (75.43 MHz,  $\text{CDCl}_3$ ):  $\delta$  91.88 and 68.57 (ferrocenyl carbons), 23.38 ( $\text{C}_5\text{H}_4\text{CH}_2$ ), 19.38 ( $\text{SiCH}_2$ ), 0.26 ( $\text{SiCH}_3$ ).  $^{29}\text{Si}\{^1\text{H}\}$  NMR (59.3 MHz,  $\text{CDCl}_3$ ):  $\delta$   $-20.31$  ppm. Anal. Calcd for  $[\text{Si}_4\text{O}_4\text{C}_{32}\text{H}_{44}\text{Fe}_2]_n$ : C, 53.63; H, 6.19. Found: C, 50.33; H, 5.75.  $M_n$  (VPO, THF):  $2.3 \times 10^4$ . Key data for **3** are as follows. IR (KBr,  $\text{cm}^{-1}$ ): 2158  $\nu(\text{SiH})$ , 1624  $\nu(\text{C}=\text{C})$ .  $^1\text{H}$  NMR (300 MHz,  $\text{CDCl}_3$ ):  $\delta$  6.35 (dd,  $\text{CH}=\text{CH}_2$ ), 5.28–5.22 (m,  $\text{CH}=\text{CH}_2$ ), 5.21 (br,  $\text{SiH}$ ), 2.17 (br,  $\text{C}_5(\text{CH}_3)_4\text{CH}_2$ ), 1.71 (br,  $\text{C}_5(\text{CH}_3)_4$ ), 0.55 (br,  $\text{SiCH}_2$ ), 0.14 (br,  $\text{SiCH}_3$ ).  $^{29}\text{Si}\{^1\text{H}\}$  NMR (59.3 MHz,  $\text{CDCl}_3$ ):  $\delta$   $-21.12$  ppm. Anal. Calcd for  $[\text{Si}_4\text{O}_4\text{C}_{48}\text{H}_{76}\text{Fe}_2]_n$ : C, 61.25; H, 8.15. Found: C, 60.14; H, 7.78.  $M_n$  (VPO, THF):  $1.9 \times 10^4$ .

(18) Wide-angle X-ray scattering (WAXS) studies of both polymers are in progress in order to analyze their morphology.

tent with this, weak absorptions at 2158 and 1624  $\text{cm}^{-1}$  in the IR (KBr) spectrum of the polymer with permethylated ferrocenyl units are also observed. The  $^{29}\text{Si}$  NMR spectra of both polymers **2** and **3** are nearly identical with that of the tetranuclear model **1** and consist of a single resonance corresponding to D-type silicon atoms. For **3** this resonance appears slightly shifted to high field. Polymers **2** and **3** appear to be stable to the atmosphere and form amber free-standing films when cast from THF solutions. The thermal behavior of both polymers was analyzed by thermogravimetric analysis (ramp rate 10  $^{\circ}\text{C}/\text{min}$ , under a nitrogen atmosphere) and indicates that the major decomposition occurs between 480 and 600  $^{\circ}\text{C}$  for **2** and between 230 and 575  $^{\circ}\text{C}$  for **3**.

The electrochemical properties of compounds **1**–**3** have been studied. The cyclic voltammogram of each compound dissolved in  $\text{CH}_2\text{Cl}_2$  with 0.1 M TBAH exhibited a single reversible oxidation wave.<sup>19</sup> The determination of the number of electrons transferred in the oxidation of **1** was effected by coulometry (Pt mesh, in  $\text{CH}_2\text{Cl}_2$ ), resulting in the removal of 4.0 e/molecule. Differential pulse voltammetry measurements (DPV) give only one wave, suggesting that the oxidations of the four ferrocenyl units in **1** occur at the same potential. Therefore, in **1** the ferrocenyl units are noninteracting redox centers. The blue tetranuclear ferrocenium cation  $[\mathbf{1}]^{4+}[\text{PF}_6]^{-4}$  was synthesized by either controlled-potential electrolysis or chemical oxidation with  $\text{NOPF}_6$ , in  $\text{CH}_2\text{Cl}_2$  at room temperature.

It is worth noting that, for both polymers **2** and **3**, an increase in the peak current upon continuous scanning in  $\text{CH}_2\text{Cl}_2$  was observed in the cyclic voltammograms, which indicates that the formation of an electroactive polymer film occurs on the electrode surface. In this way, platinum electrodes modified with electrodeposited films of these polymers were prepared.<sup>20,21</sup> Their voltammetric responses were found to be clearly different (Figure 1), and this must be related to the nature of the substituents on the cyclopentadienyl rings. Electrodeposited films of **2** show a well-defined, very sharp oxidation–reduction wave, with a linear relationship of peak current with potential sweep rate  $\nu$ , typical of surface-confined redox couples<sup>22</sup> (Figure 1A). In contrast, the surface redox wave observed for electrodes modified with films of the permethylated polymer **3** is broader and shows diffusional features (Figure 1B). In

(19) Cyclic voltammetric data (vs saturated calomel electrode, SCE), in  $\text{CH}_2\text{Cl}_2$  with 0.1 M  $\text{NBu}_4\text{PF}_6$  (TBAH): for **1**,  $E_{1/2} = +0.35$  V; for **2**,  $E_{1/2} = +0.33$  V; for **3**,  $E_{1/2} = +0.005$  V. For details of the electrochemical equipment, see refs 4 and 5.

(20) Platinum-disk electrodes ( $A = 0.070, 0.017$   $\text{cm}^2$ ) were modified with electrodeposited films of **2** and **3** by scanning the potential at 50 or 100  $\text{mV}/\text{s}$  between the appropriate potential limits, in degassed  $\text{CH}_2\text{Cl}_2$  solutions of the polymers with TBAH; subsequently the electrodes thus coated were rinsed with  $\text{CH}_2\text{Cl}_2$  to remove any adhering solution and dried in air. The polymer films were characterized by cyclic voltammetry in fresh  $\text{CH}_3\text{CN}$  containing only supporting electrolyte. The surface coverage of the polymer films ( $\Gamma$ ,  $\text{mol}/\text{cm}^2$ ) is determined by integrating the area under the oxidation wave. The amount of the electroactive material deposited on the electrode surface can be controlled by the number of scans.

(21) The electrochemistry of electrodes modified with related silicon-ferrocenyl and siloxane-ferrocenyl polymers has been reported: (a) Nguyen, M. T.; Diaz, A. F.; Dement'ev, V. V.; Pannell, K. H. *Chem. Mater.* **1994**, *6*, 952. (b) Inagaki, T.; Lee, H. S.; Skotheim, T. A.; Okamoto, Y. *J. Chem. Soc., Chem. Commun.* **1989**, 1181. (c) See also refs 4 and 5.

(22) (a) Abruña, H. D. In *Electroresponsive Molecular and Polymeric Systems*; Skotheim, T. A., Ed.; Dekker: New York, 1988; Vol 1, p 97. (b) Murray, R. W. In *Molecular Design of Electrode Surfaces*; Murray, R. W., Ed.; Techniques of Chemistry XXII; Wiley: New York, 1992; p 1.

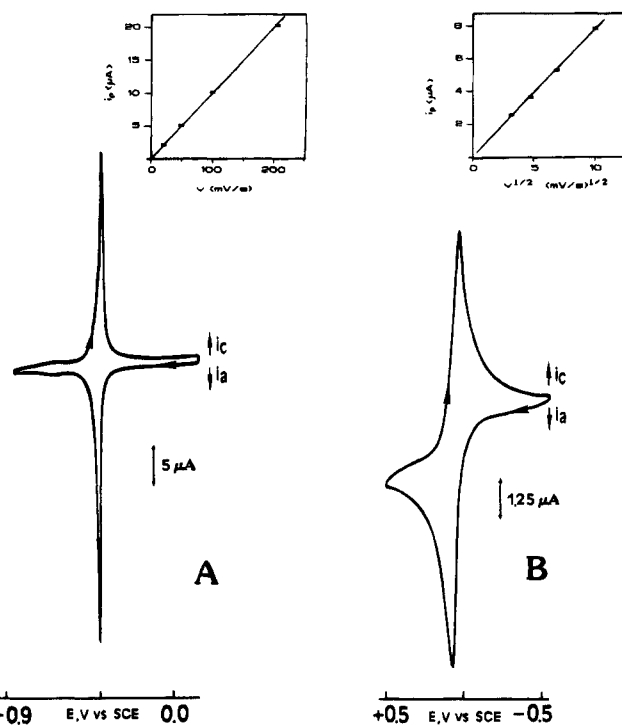


**Figure 1.** Cyclic voltammograms, measured in  $\text{CH}_3\text{CN}/0.1$  M TBAH, of Pt-disk electrodes modified with electrodeposited films of (A) polymer **2** ( $\Gamma = 1.46 \times 10^{-8}$   $\text{mol}/\text{cm}^2$ ) and (B) polymer **3** ( $\Gamma = 7.11 \times 10^{-8}$   $\text{mol}/\text{cm}^2$ ). The scan rate was 100  $\text{mV}/\text{s}$ .

addition, at scan rates between 10 and 300  $\text{mV}/\text{s}$ , the peak current increases linearly with the square root of the sweep rate  $\nu^{1/2}$ , which suggests that in this case the charge transport through the film is limited by the electrolyte diffusion into the polymer film. The anodic and cathodic wave shapes of films of **2** are extremely narrow, and values of the full width at half-maximum,  $\Delta E_{\text{FWHM}} \approx 5$  mV, are measured at a scan rate of 20  $\text{mV}/\text{s}$ , which reflect attractive interactions among the ferrocene sites and suggest a phase transition.<sup>22</sup> For the broader voltammetric peaks of films of **3**, a  $\Delta E_{\text{FWHM}}$  value of about 125 mV was measured at the same scan rate, which indicates repulsive interactions.<sup>22</sup> On the other hand, a formal potential value of  $E_{1/2} = +0.05$  V vs SCE was found for films of polymer **3**, which is nearly identical with the formal potential of the polymer in solution. This potential is considerably more negative than that of films of the nonmethylated ferrocenyl polymer **2** ( $E_{1/2} = +0.35$  V vs SCE), and this is the result of the strong electron-donating effect of the eight methyl groups on the ferrocene rings. To our knowledge, this represents the first example of electrode surfaces derivatized with an octamethylated polymer. The Pt electrodes derivatized with films of both **2** and **3** in either organic or aqueous electrolyte solutions are completely stable and do not show loss of electroactivity with use.

Further detailed studies directed toward understanding the relation between the structure and the redox properties of these polymers and related ferrocene-containing siloxane materials are in progress.

**Acknowledgment.** We thank the Dirección General de Investigación Científica y Técnica (Grant No. PB-93-0287) for financial support of this research.

OM9501440

# Generation of Dinuclear Tartrate-Bridged Dicationic Titanocene Complexes

Wolf Spaether, Gerhard Erker,\* and Mathias Rump

Organisch-Chemisches Institut der Universität Münster,  
Corrensstrasse 40, D-48149 Münster, Germany

Carl Krüger and Jörg Kuhnigk

Max-Planck-Institut für Kohlenforschung, Kaiser-Wilhelm-Platz 1,  
D-45470 Mülheim a.d. Ruhr, Germany

Received January 26, 1995<sup>®</sup>

**Summary:** The  $[(\mu\text{-tartrato})(\text{Cp}_2\text{TiCH}_3)_2]$  complexes **2**, derived from the reaction between dimethyl and dibutyl tartrate, respectively, with dimethyltitanocene, react with tris(pentafluorophenyl)borane to give the monocations  $[(\mu\text{-tartrato})(\text{Cp}_2\text{Ti})(\text{Cp}_2\text{TiCH}_3)]^+$  and subsequently the dications  $[(\mu\text{-tartrato})(\text{Cp}_2\text{Ti})_2]^{2+}$ . In dichloromethane solution in both cases internal ester coordination is observed, leading to mixtures of five- and six-membered ring product isomers.

Tartrate-based chelating phosphane donor ligands are easily available in great variety, and their application in organometallic chemistry and catalysis is legion. It is amazing that almost nothing is known about their potential electrophilic counterparts. Chiral bis Lewis acids are almost unknown, although they might open up very interesting new ways of activating a wide variety of organic substrates toward selective nucleophilic attack.<sup>1</sup> Therefore, it should be attractive to start searching for effective ways of generating such chiral ligand bridged bis-electrophilic systems. The first examples of this development are presented in this paper.

It is well-known that dimethylzirconocene and related reagents react with 1,*n*-diols with evolution of 2 molar equiv of methane and the formation of cyclic systems that often dimerize, exhibiting two strong Zr–O bonds per monomeric unit.<sup>2</sup> We have shown that dialkyl tartrates react in this way with  $\text{Cp}_2\text{Zr}(\text{CH}_3)_2$  to form dimetallatricyclic tartrato–zirconocene complexes that equilibrate with 10-membered dimetalla monocyclic tartrato–zirconocene complexes.<sup>3</sup> We have now treated

dimethyltitanocene with dimethyl and dibutyl tartrate, respectively, and observed that this reaction very selectively proceeds with the liberation of only 1 equiv of methane per titanium. In each case a dinuclear tartrato-bridged bis(titanocene) complex of the composition  $[(\text{Cp}_2\text{TiCH}_3)\text{OCH}(\text{CO}_2\text{R})\text{CH}(\text{CO}_2\text{R})\text{O}(\text{Cp}_2\text{TiCH}_3)]$  is obtained in high yield.

In a typical experiment  $\text{Cp}_2\text{Ti}(\text{CH}_3)_2$  (**1**) is treated with 0.5 molar equiv of (+)-(2*R*,3*R*)-dimethyl tartrate for 3 days at 40 °C in an ether/dichloromethane mixture. The product crystallizes from the reaction mixture at 5 °C overnight. Recrystallization from ether/dichloromethane (1:1) gives the  $(\mu\text{-tartrato})\text{bis}(\text{methyltitanocene})$  complex **2a** in 79% yield: mp 164 °C (DSC),  $[\alpha]_D^{25} = -81.5^\circ$  ( $c = 0.2$ ,  $\text{CH}_2\text{Cl}_2$ ). The compound exhibits uncoordinated symmetry-equivalent ester groups (IR (KBr)  $\tilde{\nu} = 1749\text{ cm}^{-1}$  (C=O); <sup>13</sup>C NMR ( $\text{CDCl}_3$ )  $\delta$  172.3 (–CO<sub>2</sub>CH<sub>3</sub>)). In solution the chiral complex **2a** behaves as *C*<sub>2</sub> symmetric. It exhibits a single <sup>1</sup>H/<sup>13</sup>C NMR methyl ester ( $\delta$  3.67/51.6) and TiCH<sub>3</sub> resonance ( $\delta$  0.52/35.0). The tartrate methine proton resonance is a singlet at  $\delta$  4.90 (<sup>13</sup>C NMR ( $\text{CDCl}_3$ )  $\delta$  88.5 (–CH–OTi)). The two titanocene units are symmetry equivalent; each contains a pair of diastereotopic Cp ligands which give rise to a 1:1 intensity pair of <sup>1</sup>H/<sup>13</sup>C NMR signals at  $\delta$  5.86, 5.95/112.2, 112.7.<sup>4</sup>

The reaction of  $\text{Cp}_2\text{Ti}(\text{CH}_3)_2$  (**1**) with (+)-(2*R*,3*R*)-dibutyl tartrate proceeds analogously. The corresponding dinuclear  $(\mu\text{-dibutyl tartrato})\text{bis}(\text{methyltitanocene})$  complex **2b** was characterized by X-ray diffraction.<sup>5</sup> In the crystal the dinuclear compound **2b** is close to *C*<sub>2</sub> symmetric. The titanium centers are each pseudotetrahedrally coordinated to two Cp rings (average Ti–C(Cp) distance 2.41 Å), a methyl group ( $d(\text{Ti1}–\text{C33}) = 2.17(1)\text{ Å}$ ,  $d(\text{Ti2}–\text{C34}) = 2.18(1)\text{ Å}$ ) and the tartrate oxygen. The Ti–O bonds are very short ( $d(\text{Ti2}–\text{O2}) = 1.862(6)\text{ Å}$ ,  $d(\text{Ti1}–\text{O1}) = 1.835(6)\text{ Å}$ ), and the bond angles at the tartrato oxygen centers are very large ( $\text{Ti1}–\text{O1}–\text{C26} = 152.5(6)^\circ$ ,  $\text{Ti2}–\text{O2}–\text{C27} = 150.1(5)^\circ$ ).

(4) **2b**: 1.40 g (76%) isolated; mp 88 °C (DSC);  $[\alpha]_D^{25} = -82.5^\circ$  ( $c = 0.2$ ,  $\text{CH}_2\text{Cl}_2$ ); Anal. Calcd for  $\text{C}_{34}\text{H}_{46}\text{O}_6\text{Ti}_2$  (646.5): C, 63.16; H, 7.17. Found: C, 63.46; H, 6.92. IR (KBr)  $\tilde{\nu}$  1710  $\text{cm}^{-1}$  (C=O); <sup>1</sup>H/<sup>13</sup>C NMR ( $\text{CDCl}_3$ )  $\delta$  0.53/34.9 (Ti–CH<sub>3</sub>), 4.92/88.8 (–CHO[Ti]), 5.86, 5.96/112.1, 112.6 (Cp), 172.1 (C=O).

(5) X-ray crystal structure analysis of **2b**:  $\text{C}_{34}\text{H}_{46}\text{O}_6\text{Ti}_2$  (646.5), crystal size 0.18 × 0.28 × 0.25 mm,  $a = 10.530(1)\text{ Å}$ ,  $b = 10.103(1)\text{ Å}$ ,  $c = 15.551(1)\text{ Å}$ ,  $\beta = 95.32(1)^\circ$ ,  $V = 1647.3\text{ Å}^3$ ,  $T = 293\text{ K}$ ,  $d_{\text{calcd}} = 1.30\text{ g cm}^{-3}$ ,  $\mu = 5.19\text{ cm}^{-1}$ ,  $F(000) = 684\text{ e}$ ,  $Z = 2$ , monoclinic, space group *P*<sub>2</sub><sub>1</sub> (No. 4), Enraf-Nonius CAD4 diffractometer,  $\lambda = 0.71069\text{ Å}$ , data measured  $[\pm h, +k, +l]$ ,  $(\sin \theta)/\lambda_{\text{max}} = 0.65\text{ Å}^{-1}$ , 3966 independent and 3234 observed reflections, 308 refined parameters,  $R = 0.080$ ,  $R_w = 0.090$ , programs used SHELX 86, SHELX 93, ORTEP.

<sup>®</sup> Abstract published in *Advance ACS Abstracts*, May 1, 1995.

(1) For examples of achiral chelating bis Lewis acids see: Beauchamp, A. L.; Olivier, M. J.; Wuest, J. D.; Zacharie, B. *J. Am. Chem. Soc.* **1986**, *108*, 73; *Organometallics* **1987**, *6*, 153. Wuest, J. D.; Zacharie, B. *J. Am. Chem. Soc.* **1987**, *109*, 4714. Bachand, B.; Wuest, J. D. *Organometallics* **1991**, *10*, 2015. Sharma, V.; Simard, M.; Wuest, J. D. *J. Am. Chem. Soc.* **1992**, *114*, 7931. Simard, M.; Vaugeois, J.; Wuest, J. D. *J. Am. Chem. Soc.* **1993**, *115*, 370. Katz, H. E. *Organometallics* **1987**, *6*, 1134. Adams, R. D.; Chen, G.; Chen, L.; Wu, W.; Yin, J. *J. Am. Chem. Soc.* **1991**, *113*, 9406. Bach, T.; Fox, D. N. A.; Reetz, M. T. *J. Chem. Soc., Chem. Commun.* **1992**, 1634. Jacobsen, S.; Pitzer, R. J. *J. Am. Chem. Soc.* **1993**, *115*, 11216. See also: Boyle, T. J.; Eilerts, N. W.; Heppert, J. A.; Takusagawa, F. *Organometallics* **1994**, *13*, 2218.

(2) Erker, G.; Noe, R. *J. Chem. Soc., Dalton Trans.* **1991**, 685. Stephan, D. W. *Organometallics* **1990**, *9*, 2718; **1991**, *10*, 2037. Nadasdi, T. T.; Stephan, D. W. *Organometallics* **1992**, *11*, 116. Gau, H.-M.; Chen, C.-A.; Chang, S.-J.; Shih, W.-E.; Yang, T.-K.; Jong, T.-T.; Chien, M.-J. *Organometallics* **1993**, *12*, 1314. See also references cited in these articles.

(3) Erker, G.; Dehnicke, S.; Rump, M.; Krüger, C.; Werner, S.; Nolte, M. *Angew. Chem.* **1991**, *103*, 1371; *Angew. Chem., Int. Ed. Engl.* **1991**, *30*, 1349. Erker, G. In *Selective Reactions of Metal-Activated Molecules*; Werner, H., Ed.; Vieweg: Braunschweig, Germany, 1992; p 33. Erker, G.; Rump, M.; Krüger, C.; Nolte, M. *Inorg. Chim. Acta* **1992**, *198*, 679.



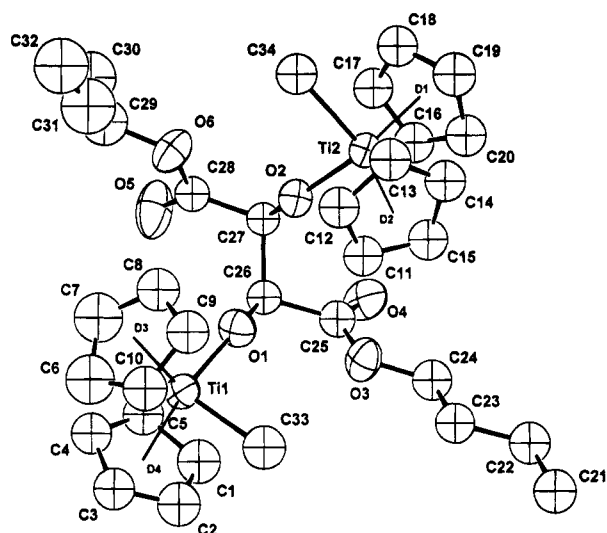
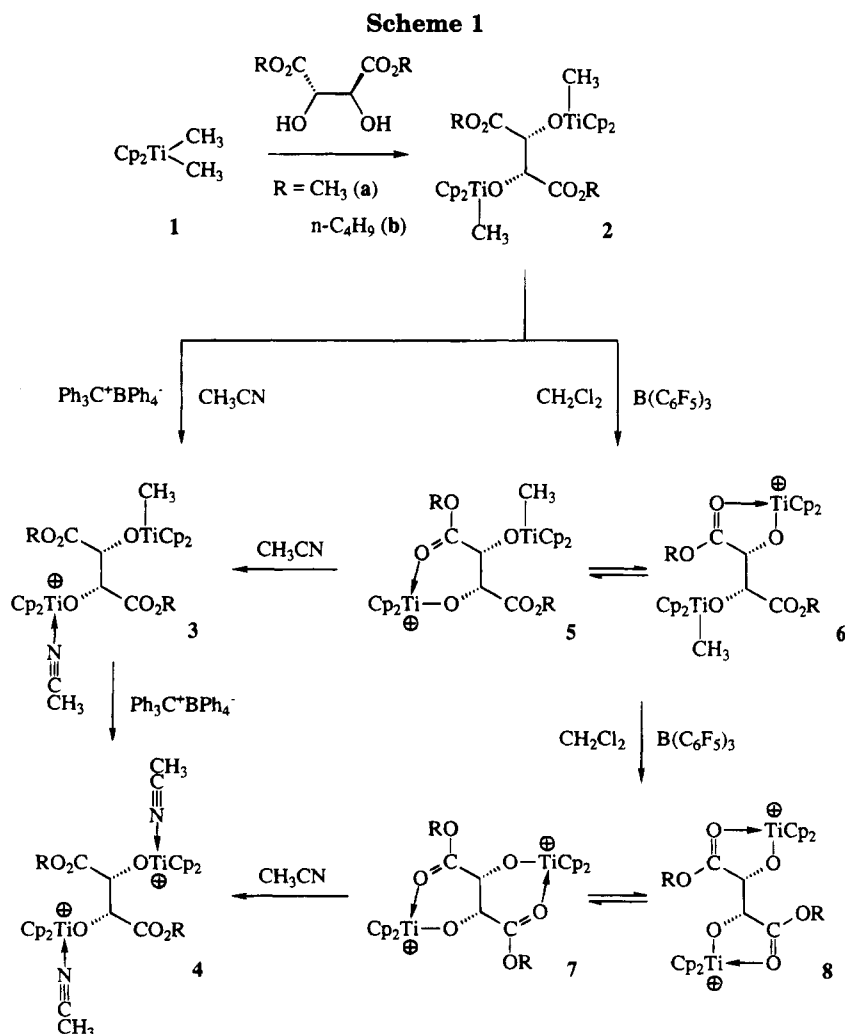


**Figure 1.** View of the molecular geometry of **2b**.

This brings the  $\text{Cp}_2\text{TiCH}_3$  groups far away from the central C26–C27 (1.54(1) Å) core of the molecule. Overall the  $-\text{O}-(\text{TiCp}_2\text{CH}_3)$  moieties behave as sterically small substituents at the central tartrate framework. Therefore, the more bulky *n*-butyl ester substituents are found almost anti-periplanar arranged (dihedral angle C25–C26–C27–C28 = 162.9°), whereas the  $-\text{O}-(\text{Ti})$  groups are found nearly in a gauche orientation (dihedral angle O1–C26–C27–O2 = 54.3°).

Three methods were tested in order to convert the dinuclear ( $\mu$ -tartrato)bis(methyltitanocene) complexes **2** into the corresponding dication. The reaction of **2b** with the mild Brønsted acid  $[\text{HNBU}_3]^+[\text{BPh}_4]^-$  in acetonitrile proceeds very slowly at room temperature. After 3 days the monocation **3b** (see below) can be detected by NMR but there is still some of the starting material **2b** left. In contrast, the *n*-butyl tartrato complex (**2b**) reacts rapidly with trityl tetraphenylborate. Under the same conditions (20 °C, acetonitrile) the reaction is complete within less than 10 min. The monocation **3b** can be detected spectroscopically in the reaction of **2b** with  $[\text{Ph}_3\text{C}]^+[\text{BPh}_4]^-$  in a 1:1 molar ratio in  $\text{CD}_3\text{CN}$  (final product ratio **2b**:**3b**:**4b** = 1:1.3:0.6). The monocation **3b** exhibits three  $^1\text{H}$  NMR Cp signals at 5.94, 6.00, and 6.44 in a 5:5:10 intensity ratio ( $^{13}\text{C}$  NMR resonances at  $\delta$  113.3, 113.5, and 119.2). The tartrato methine protons give rise to an AX pattern at  $\delta$  5.09 and 5.48 ( $^3J = 1.8$  Hz;  $^{13}\text{C}$  NMR:  $\delta$  89.7, 92.9), and there is a single  $^1\text{H}/^{13}\text{C}$  NMR Ti–CH<sub>3</sub> resonance at  $\delta$  0.58/36.2.

Reaction of **2b** with 2 molar equiv of trityl tetraphenylborate gives the ( $\mu$ -dibutyl tartrato)bis(titanocene) dication **4b**. In  $\text{CD}_3\text{CN}$  it exhibits a single  $^1\text{H}/^{13}\text{C}$  NMR Cp resonance at  $\delta$  6.47/119.2 aside from a methine CH singlet at  $\delta$  5.67/92.7 at room temperature. One would expect pairs of diastereotopic Cp ligands in the dication **4**, provided that each titanium atom has only one acetonitrile ligand coordinated to it in a pseudotetra-





hedral geometry, whereas pairs of homotopic Cp ligands would result from coordination of two nitrile ligands to the lateral positions of each titanocene group (i.e. having the tartrate  $-O-R$  group placed between them in the Cp-Ti-Cp bisecting  $\sigma$ -ligand plane). Lowering the monitoring temperature has revealed that complex **4b** exhibits dynamic NMR spectra even in  $CD_3CN$  solution. When the temperature is lowered, the  $^1H$  NMR Cp resonance rapidly broadens and complex **4b** exhibits signals of diastereotopic Cp groups in the  $^1H$  NMR spectrum in  $CD_3CN$  at 258 K, i.e. under conditions where the exchange of coordinated acetonitrile has become slow on the NMR time scale. This spectral symmetry behavior is as expected for pseudotetrahedral mono(acetonitrile) metallocene cation centers.<sup>6,7</sup>

The ( $\mu$ -tartrato)bis(titanocene) mono- and dications were also generated in a donor-ligand-free environment using tris(pentafluorophenyl)borane in methylene chloride solvent as the methyl anion abstracting reagent.<sup>8</sup> In this case we have observed that the adjacent ester carbonyl groups serve as intramolecular donor ligands for the stabilization of the highly electrophilic titanocene cation centers. Treatment of **2a** with 2 molar equiv of  $B(C_6F_5)_3$  in  $[D_2]$ dichloromethane at room temperature cleanly gives  $[(Cp_2Ti)_2(\mu-OCH(CO_2CH_3)CH(CO_2CH_3)-O)]^{2+}[H_3CB(C_6F_5)_3]^{-2}$ . The dication has two possibilities for internal ester carbonyl coordination, giving rise to the formation of five- or six-membered ring systems. Both are favorable. Consequently we observe the two isomeric dications **7a** and **8a** in a ratio of 2:1 (see Scheme 1). The internal ester coordination is evident from the IR spectrum exhibiting two strong bands at  $\tilde{\nu}$  1636 and 1629  $cm^{-1}$  for the mixture in dichloromethane. The major dicationic isomer shows  $^1H/^{13}C$  NMR reso-

nances at  $\delta$  4.17/59.7 (OCH<sub>3</sub>), 6.34/89.7 ( $-CHO[Ti]$ ), 6.63, 6.79/123.0, 124.9 (Cp), and 181.8 (C=O) ( $Ar_3B-CH_3^-$  signal at  $\delta$  0.54/11.0), whereas the corresponding signals of the minor isomer appear at  $\delta$  4.08/58.1 (OCH<sub>3</sub>), 5.67/81.0 ( $-CHO[Ti]$ ), 6.72, 6.89/121.7, 123.0 (Cp), and 176.6 (C=O). Addition of excess acetonitrile breaks the internal ester coordination, and we observe the typical signals of the more stable acetonitrile-coordinated dication (see above, albeit with a slightly changed anion). The ( $\mu$ -dibutyl tartrato)bis(titanocene) dication behaves analogously: in the absence of external donor ligands two internally stabilized dications are observed in a 10:3 ratio.<sup>9</sup>

This study shows that tartrate-bridged bis(titanocene) dications can readily be formed from very easily available precursors. Whether these dication systems (and their more electrophilic zirconocene and hafnocene analogues) can be used as chiral chelating bis electrophiles<sup>1</sup> is currently under active investigation in our laboratory.

**Acknowledgment.** Financial support from the Fonds der Chemischen Industrie and the Alfred Krupp von Bohlen und Halbach-Stiftung is gratefully acknowledged.

**Supplementary Material Available:** Details of the X-ray crystal structure analysis of **2b**, with listings of bond lengths and angles, positional parameters, and thermal parameters, and text giving experimental details and characterization data for the products (23 pages). Ordering information is given on any current masthead page.

OM9500681

(9) Treatment of **2a** and **2b** each with 1 molar equiv of  $B(C_6F_5)_3$  gives the corresponding monocations quite selectively. Two isomers are observed in each case by  $^1H/^{13}C$  NMR in  $[D_2]$ dichloromethane at 273 K (a: 10/2 ratio): **5a**, **6a**, major isomer  $\delta$  0.48/36.2 (TiCH<sub>3</sub>), 3.82, 3.93/52.6, 56.2 (OCH<sub>3</sub>), 5.10 and 5.40 ( $^3J = 1.9$  Hz)/82.3, 87.8 ( $-CHO[Ti]$ ), 6.04, 6.08, 6.44, 6.67/113.4, 113.8, 119.8, 121.7 (Cp), 169.3 and 178.2 (C=O); **5a**, **6a**, minor isomer  $\delta$  0.59/35.5 (TiCH<sub>3</sub>), 3.75, 4.10/58.1 (OCH<sub>3</sub>) (one methoxy not observed), 5.20 and 5.73 ( $^3J = 4.0$  Hz)/87.3, 92.6 ( $-CHO[Ti]$ ), 6.00, 6.58, 6.74 (one Cp not observed)/113.0, 113.4, 121.2, 124.2 (Cp), 171.0 and 184.5 (C=O); **5b**, **6b**, (b: two isomers in a 1.65:1 ratio at 273 K) major isomer  $\delta$  0.60/36.2 (Ti-CH<sub>3</sub>), 5.11 and 5.37 ( $^3J = 2.0$  Hz)/82.5, 88.0 ( $-CHO[Ti]$ ), 6.05, 6.09, 6.44, 6.66/113.4, 113.8, 119.8, 121.7 (Cp), 168.9 and 178.0 (C=O); **5b**, **6b**, minor isomer  $\delta$  0.63/35.6 (Ti-CH<sub>3</sub>), 4.98 and 5.62 ( $^3J = 3.0$  Hz)/88.0, 92.7 ( $-CHO[Ti]$ ), 6.02, 6.06, 6.57, 6.73, 113.0, 113.4, 121.5, 124.0 (Cp), 171.0 and 184.5 (C=O). Addition of excess acetonitrile in both cases converts the monocations **5/6** to their ligand-stabilized counterparts **3**.  $^1H/^{13}C$  NMR in  $CD_2Cl_2$  at 300 K: **7b**, **8b**, major isomer  $\delta$  0.92, 1.35, 1.75, 4.58/13.3, 18.9, 30.3, 74.8 ( $-C_4H_9$ ), 6.39/90.1 ( $-CHO[Ti]$ ), 6.71, 6.89/122.8, 124.8 (Cp), 182.2 (C=O); **7b**, **8b**, minor isomer  $\delta$  5.68/81.1 ( $-CHO[Ti]$ ), 6.63, 6.79/121.6, 122.9 (Cp), 177.2 (C=O); B-CH<sub>3</sub> at  $\delta$  0.55/11.0.

(6) Jordan, R. F. *Adv. Organomet. Chem.* **1991**, *32*, 325 and references cited therein. For the description of examples exhibiting a similar dynamic behavior see e.g.: Alelyunas, Y. W.; Baenziger, N. C.; Bradley, P. K.; Jordan, R. F. *Organometallics* **1994**, *13*, 148.

(7) The ( $\mu$ -dimethyl tartrato)bis(titanocene) system shows the same behavior. Monocation **3a**:  $^1H/^{13}C$  NMR in  $CD_3CN$  (300 K)  $\delta$  0.57/36.2 (TiCH<sub>3</sub>), 3.74, 3.75/53.3 (OCH<sub>3</sub>), 5.10, 5.49 ( $^3J = 1.9$  Hz)/92.7 ( $-CHO[Ti]$ ), 5.95 (5H), 6.01 (5H), 6.45 (10H)/113.5, 113.7, 119.0 (Cp); dication **4a** (300 K)  $\delta$  3.83/53.3 (OCH<sub>3</sub>), 5.68/92.7 ( $-CH-O[Ti]$ ), 6.47/119.3 (Cp). At 258 K the  $^1H$  NMR Cp signal of **4a** is split into two signals at  $\delta$  6.41 and 6.46.

(8) Yang, X.; Stern, C. L.; Marks, T. J. *J. Am. Chem. Soc.* **1991**, *113*, 3623; *Angew. Chem.* **1992**, *104*, 1406; *Angew. Chem., Int. Ed. Engl.* **1992**, *31*, 1375; *J. Am. Chem. Soc.* **1994**, *116*, 10015. Pellecchia, C.; Immirzi, A.; Grassi, A.; Zambelli, A. *Organometallics* **1993**, *12*, 4473. Bochmann, M.; Lancaster, S. J.; Hursthouse, M. B.; Abdul Malik, K. M. *Organometallics* **1994**, *13*, 2235. Review: Bochmann, M. *Angew. Chem.* **1992**, *104*, 1206; *Angew. Chem., Int. Ed. Engl.* **1992**, *31*, 1181.

# Aromatic Silylation of (Trimethylgermyl)benzene by Gaseous $\text{Me}_3\text{Si}^+$ Ions via $\text{Me}_3\text{Ge}^+$ Displacement

Barbara Chiavarino, Maria Elisa Crestoni, and Simonetta Fornarini\*

Dipartimento di Studi di Chimica e Tecnologia delle Sostanze Biologicamente Attive, Università di Roma "La Sapienza", P.le A. Moro 5, I-00185 Roma, Italy

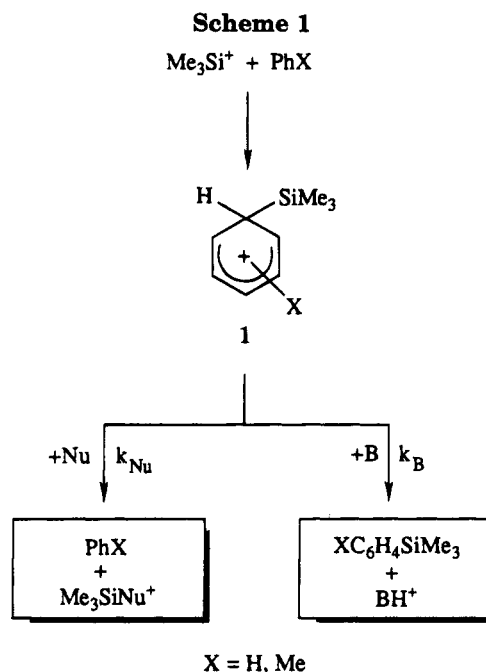
Received January 4, 1995<sup>®</sup>

**Summary:** Silylated aromatic products have been obtained from the  $\text{Me}_3\text{Si}^+$  reaction with  $\text{XC}_6\text{H}_4\text{GeMe}_3$  ( $\text{X} = \text{H}, \text{Me}$ ).

The study of positively charged or positively polarized " $\text{R}_3\text{Si}^+$ " species is rapidly expanding. One reason for the increasing interest is the opportunities it provides for comparing the behavior of cationic silicon species with that of their carbon analogues. Despite the proximity of Si and C in the same group, the differences in their chemical behavior are probably more striking than the similarities. One such case is provided by the long-established Friedel-Crafts alkylation chemistry of aromatic compounds, which is not paralleled by a silylation counterpart.<sup>1</sup> In fact, it has been reported only recently that benzene and toluene can be silylated by  $\text{R}_3\text{SiCl}$  under  $\text{AlCl}_3$  catalysis in the presence of sterically hindered tertiary amines.<sup>2</sup> The presence of the latter bases is necessary to obtain silylated products from benzene and toluene, namely, aromatic substitution products where  $\text{R}_3\text{Si}^+$  has formally displaced a ring proton. In all cases, such products are recovered only in minute yields, unless the silylation is performed on highly activated  $\pi$ -systems such as ferrocene.<sup>3</sup>

High-pressure gas-phase studies performed with the radiolytic technique<sup>4</sup> have been instrumental for the understanding of the mechanisms involved in the conversion of a  $\text{R}_3\text{Si}^+$ /arene reactant pair to silylated aromatic products.<sup>5</sup> In fact, the use of highly basic hindered amines was reported in the first successful example of electrophilic silylation of benzene and toluene by gaseous  $\text{Me}_3\text{Si}^+$  ions with excellent radiolytic yields. The role of the amine is illustrated in Scheme 1. The nitrogen base B affects the conversion of the intermediate  $\sigma$ -complex 1 to neutral products ( $k_B$ ).<sup>6</sup> At the same time, the nitrogen atom, especially if sterically encumbered, does not behave as an efficient nucleophile toward silicon. Nucleophilic attack at silicon ( $k_{\text{Nu}}$ ) is the preferred pathway of oxygen-containing nucleophiles ( $\text{Nu} = \text{H}_2\text{O}, \text{MeOH}, \text{etc.}$ ), on account of the remarkable affinity of  $\text{R}_3\text{Si}^+$  for oxygen.<sup>5c,7</sup> It is note-

worthy that the competition between deprotonation and desilylation involves the  $\sigma$ -complex 1, which displays no tendency to isomerize by 1,2-H shifts<sup>8</sup> due to the enhanced basicity of the silylated carbon.<sup>9</sup> Such stability towards isomerization represents a further difference from the analogous intermediate from the reaction of C-electrophiles such as  $\text{Me}_3\text{C}^+$ .<sup>10</sup> In the context of Scheme 1, it is obvious that no silylated aromatics are formed in the absence of a suitable amine, either in the gas-phase under radiolytic conditions ( $\text{Nu} = \text{trace oxygen nucleophiles}$ ) or in solution ( $\text{Nu} = \text{halogen and/or oxygen-containing solvents and catalysts}$ ). We now report the formation of silylated products without resorting to the addition of amines. We made use of the well-known observation of increasing rate of protolytic cleavage of  $\text{Ph-YR}'_3$  ( $\text{R}' = \text{Me}, \text{Et}$ ) for  $\text{Y} = \text{Ge}$  compared to  $\text{Y} = \text{Si}$ .<sup>11</sup>  $\text{PhGeMe}_3$  as the reactant substrate for radiolysis<sup>14</sup> results in the recovery of substantial yield of  $\text{PhSiMe}_3$  (Table 1) from the neat



<sup>®</sup> Abstract published in *Advance ACS Abstracts*, April 15, 1995.

(1) Häbich, D.; Effenberger, F. *Synthesis* **1979**, 841.  
 (2) Olah, G. A.; Bach, T.; Prakash, G. K. S. *J. Org. Chem.* **1989**, *54*, 3770.  
 (3) Olah, G. A.; Bach, T.; Prakash, G. K. S. *New J. Chem.* **1991**, *15*, 571. (b) Sollott, G. P.; Peterson, W. R. *J. Am. Chem. Soc.* **1967**, *89*, 5054. (c) Simchen, G.; Frick, U. *Synthesis* **1984**, 929.  
 (4) Cacace, F. *Acc. Chem. Res.* **1988**, *21*, 215.  
 (5) (a) Cacace, F.; Crestoni, M. E.; Fornarini, S.; Gabrielli, R. *Int. J. Mass Spectrom. Ion Processes* **1988**, *84*, 17. (b) Fornarini, S. *J. Org. Chem.* **1988**, *53*, 1314. (c) Wojtyniak, A. C. M.; Stone, J. A. *Int. J. Mass Spectrom. Ion Processes* **1986**, *74*, 59. (d) Stone, J. M.; Stone, J. A. *Int. J. Mass Spectrom. Ion Processes* **1991**, *109*, 247. (e) Li, X.; Stone, J. A. *Can. J. Chem.* **1992**, *70*, 2070.  
 (6) The [areneSiMe<sub>3</sub><sup>+</sup>] addition complex is highly thermodynamically favored (ref 5c) over the reactant pair under typical conditions of radiolytic experiments.

(7) Lew, C. S. Q.; McClelland, R. A. *J. Am. Chem. Soc.* **1993**, *115*, 11516.

(8) Crestoni, M. E.; Fornarini, S. *Angew. Chem., Int. Ed. Engl.* **1994**, *33*, 1094.

(9) (a) Schleyer, P. v. R.; Buzek, P.; Müller, T.; Apeloig, Y.; Siel, H.-U. *Angew. Chem., Int. Ed. Engl.* **1993**, *32*, 1471. (b) Cacace, F.; Crestoni, M. E.; de Petris, G.; Fornarini, S.; Grandinetti, F. *Can. J. Chem.* **1988**, *66*, 3099.

(10) Cacace, F.; Crestoni, M. E.; Fornarini, S. *J. Am. Chem. Soc.* **1992**, *114*, 6776.

(11) (a) Eaborn, C. *J. Organomet. Chem.* **1975**, *100*, 43. (b) Seyferth, D.; White, D. L. *J. Am. Chem. Soc.* **1972**, *94*, 3132.

(12) Niiranen, J. T.; Gutman, D. *J. Phys. Chem.* **1993**, *97*, 4106.

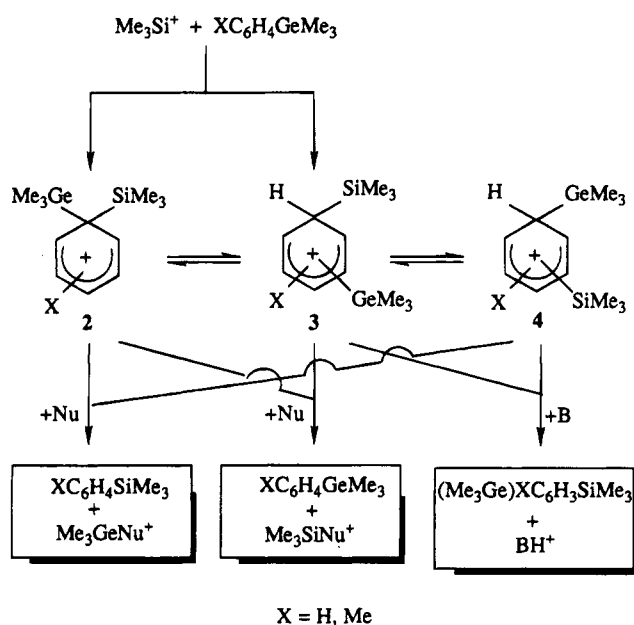
(13) Ausloos, P.; Lias, S. G.; Gorden, R., Jr. *J. Chem. Phys.* **1963**, *39*, 3341.

**Table 1. Silylated Products from the Reaction of Gaseous  $\text{Me}_3\text{Si}^+$  Ions with Aryltrimethylgermanes ( $\text{XC}_6\text{H}_4\text{GeMe}_3$ ; X = H, *o*-Me, *m*-Me, *p*-Me)**

system composition (Torr) <sup>a</sup>		relative yields of products (%) <sup>b</sup>		
substrate	c-C <sub>5</sub> H <sub>10</sub> NH	$\text{XC}_6\text{H}_4\text{SiMe}_3$	$\text{XC}_6\text{H}_3(\text{GeMe}_3)\text{SiMe}_3$	abs yields (%) <sup>c</sup>
X = H, 1.7		100 (X = H)		50
X = H, 1.7	1.2	78 (X = H)	22 <sup>d</sup>	57
X = <i>o</i> -Me, 1.6		100 (X = <i>o</i> -Me)		36
X = <i>o</i> -Me, 1.9	1.4	68 (X = <i>o</i> -Me)	32 <sup>e</sup>	19
X = <i>m</i> -Me, 1.7		100 (X = <i>m</i> -Me)		22
X = <i>m</i> -Me, 1.9	1.2	100 (X = <i>m</i> -Me)		9
X = <i>p</i> -Me, 1.8		100 (X = <i>p</i> -Me)		12
X = <i>p</i> -Me, 2.1	1.3	100 (X = <i>p</i> -Me)		6

<sup>a</sup> The bulk gas was a 30:1  $\text{CH}_4/\text{Me}_4\text{Si}$  mixture at 650 Torr, to which 10 Torr of  $\text{O}_2$  were added as  $\text{Me}_3\text{Si}^+$  radical scavenger.<sup>12</sup> <sup>b</sup> Standard deviation ca. 2%. <sup>c</sup> The absolute yields expressed as  $G_{+M}$  range from 0.025 to 0.16  $\mu\text{mol J}^{-1}$  ( $\mu\text{mol}$  products formed per unit of absorbed energy). The percent absolute yields (standard deviation ca. 10%) are relative to the  $G_{+M}$  value (0.28  $\mu\text{mol J}^{-1}$ )<sup>13</sup> of  $\text{CH}_5^+/\text{C}_2\text{H}_5^+$  ions produced by  $\gamma$ -radiolysis of  $\text{CH}_4$ , which are precursors to the reactant  $\text{Me}_3\text{Si}^+$  ions.<sup>5</sup> The relatively low values are accounted for by: (i) the presence of trace oxygen nucleophiles (see  $k_{\text{Nu}}$  step in Scheme 1); (ii) the added piperidine, which reacts by addition and proton transfer both with  $\text{Me}_3\text{Si}^+$  and with the  $\text{CH}_5^+/\text{C}_2\text{H}_5^+$  precursor ions; (iii) the reaction of  $\text{Me}_3\text{Si}^+$  with  $\text{XC}_6\text{H}_4\text{GeMe}_3$  to yield (in part)  $\text{XC}_6\text{H}_4\text{GeMe}_2^+$  and ensuing products of nucleophilic capture. <sup>d</sup> Two isomers: *m*- $\text{Me}_3\text{GeC}_6\text{H}_4\text{SiMe}_3$  (37%) and *p*- $\text{Me}_3\text{GeC}_6\text{H}_4\text{SiMe}_3$  (63%). <sup>e</sup> Two isomers: 1-Me-2- $\text{Me}_3\text{Ge-4-Me}_3\text{Si-C}_6\text{H}_3$  (92%) and 1-Me-2- $\text{Me}_3\text{Ge-5-Me}_3\text{Si-C}_6\text{H}_3$  (8%).

$\text{CH}_4/\text{Me}_4\text{Si}$  mixture where  $\text{Me}_3\text{Si}^+$  ions are formed.<sup>5a,b</sup> Thus, the presence of an amine is no longer required for the formation of silylation products. It is, however, still required for the formation of silylated products retaining the original  $\text{Me}_3\text{Ge}$  group. In the presence of added piperidine, not only is the silyl-degermylated product ( $\text{PhSiMe}_3$ ) formed, but also silylated products ( $\text{Me}_3\text{GeC}_6\text{H}_4\text{SiMe}_3$ ). Scheme 2 provides a mechanism which may account for their formation, with  $\sigma$ -complexes **2**, **3**, and **4** envisioned as reaction intermediates.<sup>15</sup> Two channels may lead to silyl-degermylated products. In one, an ipso-addition complex **2** is formed; the decomposition of **2** via degermylation rather than desilylation may be accounted for by the easier nucleophilically assisted loss of  $\text{Me}_3\text{Ge}$ . Alternatively, the  $\sigma$ -complex intermediate **3** may undergo H-shifts to the  $\text{Me}_3\text{Ge}$ -substituted carbon to yield **4**. In the first case the progress to products is driven by the higher mobility of  $\text{Me}_3\text{Ge}$  with respect to  $\text{Me}_3\text{Si}$  under conditions of nucleophilic catalysis, in the second by the enhanced basicity conferred by  $\text{Me}_3\text{Ge}$  to the adjacent ring carbon, again as compared to the similar effect exerted by  $\text{Me}_3\text{Si}$ .<sup>9</sup> An approach to discriminate between these two possibilities was devised by introducing a methyl group in the ortho, meta, or para position with respect to the

**Scheme 2**

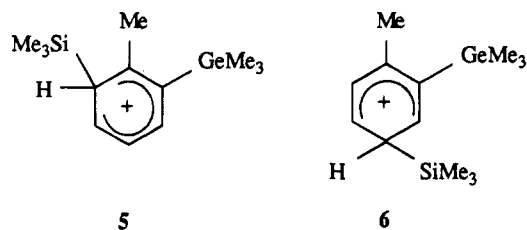
(14) Gaseous samples for the radiolytic experiments reported in Table 1 were prepared as follows. The substrate ( $\text{XC}_6\text{H}_4\text{GeMe}_3$ ) and base (piperidine) were weighed into breakable glass ampoules and introduced into 135-mL Pyrex vessels which were thoroughly outgassed and filled with the gaseous components ( $\text{CH}_4/\text{O}_2/\text{Me}_4\text{Si}$ ), using standard vacuum line techniques. Once the vessels were sealed off, the ampoules were broken, allowing their contents to diffuse. The homogeneous gaseous systems were irradiated at 40 °C into a  $^{60}\text{Co}$  220 Gammacell (Nuclear Canada Ltd) to a total dose of  $1 \times 10^4$  Gy delivered at the dose rate of  $2 \times 10^4$  Gy  $\text{h}^{-1}$ . The radiolytic product mixture was recovered by introducing a measured volume of an ethyl acetate solution of internal standard ( $\text{PhCH}_2\text{SiMe}_3$ ) through a gastight septum and submitting the vessel to repeated freeze-thaw cycles from liquid nitrogen temperature to room temperature. The resulting solution was analyzed by GLC-MS on a Hewlett-Packard 5890 gas chromatograph in series with a HP 5970B mass selective detector, using a 50-m long, 0.20-mm i.d. fused silica column, coated with a 0.5- $\mu\text{m}$  cross-linked methylsilicone film (HP PONA column). The products were identified by their retention times and mass spectra, checked against authentic standard compounds. Yields were determined from the ratio of the integrated elution peaks of the products over those of the internal standard, checked against an appropriate calibration curve.

(15) Both experimental evidence (refs 5a,b, 8) and theoretical calculations (ref 9a) point to a  $\sigma$ -complex structure for gaseous [arene $\text{SiMe}_3^+$ ] adducts. On the basis of the evidence presently available, it cannot, however, be excluded that species **2** may represent a transition state toward a possibly favored [PhSiMe<sub>3</sub>-GeMe<sub>3</sub>]<sup>+</sup>  $\pi$ -com-

$\text{Me}_3\text{Ge}$  group. The methyl group has been chosen to label the aromatic ring positions because of its known reluctance to undergo migration within arenium ions.<sup>16</sup> At the same time, the methyl group does not become a preferred reaction site for electrophilic attack, such as it is for a fluorine substituent. The reaction of *o*-, *m*-, and *p*- $\text{MeC}_6\text{H}_4\text{GeMe}_3$  yields the products shown in Table 1. In all cases, the added  $\text{Me}_3\text{Si}$  group retains the positional relationship of the original  $\text{Me}_3\text{Ge}$  group, suggesting that species **2** lies on the reaction coordinate for the formation of silyl-degermylated products. The formation of *p*- $\text{MeC}_6\text{H}_4\text{SiMe}_3$  from *p*- $\text{MeC}_6\text{H}_4\text{GeMe}_3$  necessarily implies a type **2** intermediate. The same does not strictly hold for the *o*- and *m*- $\text{MeC}_6\text{H}_4\text{SiMe}_3$  products, which may conceivably arise from attack of  $\text{Me}_3\text{Si}^+$  either at the germlyl-substituted or the unsubstituted carbons. Nevertheless, the latter possibility should be disfavored in view of the known outcome of the reaction of  $\text{Me}_3\text{Si}^+$  with toluene. The absence of *o*-substituted products from the silylation of toluene

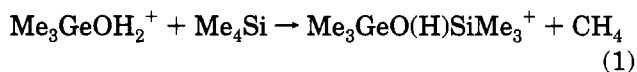
(16) Koptug, V. A. In *Contemporary Problems in Carbonium Ion Chemistry III*; Rees, C. W., Ed.; Springer-Verlag: Berlin, 1984, and references therein.

makes the exclusive formation of species **5** highly unlikely compared to isomer **6**. Thus, the highly regioselective formation of *o*-MeC<sub>6</sub>H<sub>4</sub>SiMe<sub>3</sub> from *o*-MeC<sub>6</sub>H<sub>4</sub>-GeMe<sub>3</sub> also points to the intermediacy of **2** rather than to formation of **3**, followed by isomerization to **4** and final degermylation.



The above arguments are supported by the finding of substantial amounts of a silylated product formally derived from the deprotonation of **6** in the presence of piperidine. The formation of silylated products, both from PhGeMe<sub>3</sub> and from *o*-MeC<sub>6</sub>H<sub>4</sub>GeMe<sub>3</sub>, in the presence of piperidine shows that species **3** plays a role in the overall reaction, produced either by direct silylation at an unsubstituted carbon or by isomerization of **2**. Deprotonation of **3** obviously requires the presence of a base to compete with the nucleophilic desilylation route. On the other hand, isomerization of **3** by a hydrogen shift to yield **4** does not appear to occur to any significant extent, as it would yield silyl-degermylation products which do not retain the original Me<sub>3</sub>Ge/Me relationship, in contrast to the experimental finding.

The silyl-degermylation products are accompanied by Me<sub>3</sub>SiOGeMe<sub>3</sub>, which originates from traces of H<sub>2</sub>O in the radiolytic system. The protonated germanol (Me<sub>3</sub>-GeNu<sup>+</sup> = Me<sub>3</sub>GeOH<sub>2</sub><sup>+</sup>) initially formed may further react with Me<sub>4</sub>Si (eq 1) according to a process previously described in mass spectrometric studies.<sup>5c,17</sup>



In conclusion, gaseous Me<sub>3</sub>Si<sup>+</sup> ions are found to promote silyl-degermylation of XC<sub>6</sub>H<sub>4</sub>GeMe<sub>3</sub> (X = H, Me) compounds in the absence of any added amine. The process appears to be highly regioselective. Me<sub>3</sub>Si<sup>+</sup> attack at unsubstituted ring carbons may also occur, followed by deprotonation to yield silyl-dehydrogenation products. Their relative yields will be governed both by electronic and steric factors affecting the Me<sub>3</sub>Si<sup>+</sup> addition and by factors such as steric hindrance affecting the deprotonation to final neutral products. Further work is in progress to elucidate the reaction mechanisms.

**Acknowledgment.** The authors are grateful to Professor Fulvio Cacace for valuable discussions and acknowledge the Italian Ministero dell'Università e della Ricerca Scientifica for financial support.

OM950006A

(17) Stone, J. A.; Wytenburg, W. J. *Can. J. Chem.* **1987**, *65*, 2146.

# Synthesis, Structure, and Olefin Polymerization Activity of Vanadium(V) Catalysts Stabilized by Imido and Hydrotris(pyrazolyl)borato Ligands

Sylvie Scheuer, Jean Fischer, and Jacky Kress\*

Laboratoire de Chimie des Métaux de Transition et de Catalyse, URA au CNRS 424, Université Louis Pasteur, Institut Le Bel, 4, rue Blaise Pascal, 67000 Strasbourg, France

Received February 8, 1995\*

**Summary:** The complexes  $TpV(N-t-Bu)Cl_2$  (**3**),  $Tp^*V(N-t-Bu)Cl_2$  (**4**),  $TpV(NAr)Cl_2$  (**5**), and  $Tp^*V(NAr)Cl_2$  (**6**) ( $Tp = HBPz_3$ ,  $Pz = \text{pyrazolyl}$ ;  $Tp^* = HBPz^*_3$ ,  $Pz^* = 3,5\text{-dimethylpyrazolyl}$ ;  $Ar = 2,6\text{-}i\text{-Pr}_2\text{-C}_6\text{H}_3$ ), as well as a series of derivatives of these compounds, were synthesized and analyzed by  $^1H$  and  $^{51}V$  NMR spectroscopy. The crystal and molecular structures of **3** and **6** (shown) were determined by X-ray crystallography. The polymerization of ethylene and propylene, in the presence of **6** and methylalumoxane, is described.

Transition metals of groups 3, 4, and 5 build numerous complexes catalyzing the homogeneous Ziegler–Natta polymerization of olefins.<sup>1</sup> The most active catalysts derived from the first two groups are  $d^0$  metallocene hydrides, alkyls, and halides.<sup>2</sup> On the other hand, vanadium-based catalysts generally show configurations  $d^2$  or  $d^3$ ;  $d^0$  vanadium complexes have frequently been used as catalysts but were readily reduced to lower oxidation states on addition of cocatalysts.<sup>3</sup> It has not been excluded, however, that vanadium(V) complexes would also be effective catalysts if they could be stabilized in their high oxidation state. Recent studies seem to give some support to such an assumption.<sup>4</sup>

In this contribution, we describe the synthesis and characterization of vanadium(V) compounds possessing imido and hydrotris(pyrazolyl)borato ligands. These complexes catalyze, in the presence of methylalumoxane (MAO), the polymerization of ethylene and propylene at room temperature. Such ligands are well-known as stabilizing high-oxidation-state transition-metal complexes.<sup>5</sup> Furthermore, their analogy with cyclopentadienyl ligands results in an isolobal relationship be-

tween these vanadium complexes and the highly active metallocene catalysts of group 4.<sup>5,6</sup> Hydrotris(pyrazolyl)borato complexes of vanadium(V) are rare,<sup>7</sup> and only one imido derivative has been reported recently,<sup>7c</sup> in the course of our study.

Treatment of  $VOCl_3$  with 1 equiv of  $t\text{-BuNCO}$  or  $ArNCO$  ( $Ar = 2,6\text{-}i\text{-Pr}_2\text{-C}_6\text{H}_3$ ) in refluxing octane led to  $V(N-t-Bu)Cl_3$  (**1**) and  $V(NAr)Cl_3$  (**2**), respectively. **1** and **2** react with 1 equiv of  $KTp$  ( $Tp = HBPz_3$ ,  $Pz = \text{pyrazolyl}$ ) or  $KTp^*$  ( $Tp^* = HBPz^*_3$ ,  $Pz^* = 3,5\text{-dimethylpyrazolyl}$ ) in methylene chloride or toluene to produce the complexes  $TpV(N-t-Bu)Cl_2$  (**3**),  $Tp^*V(N-t-Bu)Cl_2$  (**4**),<sup>7c</sup>  $TpV(NAr)Cl_2$  (**5**), and  $Tp^*V(NAr)Cl_2$  (**6**) in good yields.<sup>11</sup> These bright black solids are crystalline, insensitive to water and oxygen, and thermally stable up to 110 °C in toluene solution.

The structures of **3** (Figure 1) and **6** (Figure 2) have been determined by single-crystal X-ray diffraction studies.<sup>12–14</sup> Complex **3** consists of monomeric units containing a facially coordinating tridentate  $Tp$  ligand, as well as one imido and two chloro ligands. The

(6) (a) Pez, G. P.; Armor, J. N. In *Advances in Organometallic Chemistry*; Stone, F. G. A., West, R., Eds.; Academic Press, New York, 1981; Vol. 19, p 1. (b) Sundermeyer, J.; Runge, D. *Angew. Chem., Int. Ed. Engl.* **1994**, *33*, 1255. (c) Williams, D. N.; Mitchell, J. P.; Poole, A. D.; Siemeling, U.; Clegg, W.; Hockless, D. C. R.; O'Neil, P. A.; Gibson, V. C. *J. Chem. Soc., Dalton Trans.* **1992**, 739. (d) Dyer, P. W.; Gibson, V. C.; Howard, J. A. K.; Whittle, B.; Wilson, C. *J. Chem. Soc., Chem. Commun.* **1992**, 1666. (e) McCleverty, J. A.; *Chem. Soc. Rev.* **1983**, *12*, 331.

(7) (a) Holmes, S.; Carrano, C. J. *Inorg. Chem.* **1991**, *30*, 1231. (b) Carrano, C. J.; Mohan, M.; Holmes, S. M.; de la Rosa, R.; Butler, A.; Charnock, J. M.; Garner, C. D. *Inorg. Chem.* **1994**, *33*, 646. (c) Sundermeyer, J.; Putterlik, J.; Foth, M.; Field, J. S.; Ramesar, N. *Chem. Ber.* **1994**, *127*, 1201.

(8) (a) Preuss, F.; Towae, W. Z. *Naturforsch.* **1981**, *36B*, 1130. (b) Hills, A.; Hughes, D. L.; Leigh, G. J.; Prieto-Alcon, R. *J. Chem. Soc., Dalton Trans.* **1993**, 3609.

(9) Buijink, J.-K. F.; Teuben, J. H.; Kooijman, H.; Spek, A. L. *Organometallics* **1994**, *13*, 2922.

(10) Addition of THF to **2** yields  $V(NAr)Cl_3 \cdot THF$  as a brown powder:  $^1H$  NMR ( $C_6D_6$ )  $\delta$  6.87 (d, 2H,  $NAr H_m$ ), 6.76 (t, 1H,  $NAr H_p$ ), 4.71 (sept, 2H,  $CHMe_2$ ), 4.12 (m, 4H,  $OCH_2CH_2$ ), 1.46 (m, 4H,  $OCH_2CH_2$ ), 1.30 (d, 12H,  $CHMe_2$ ). Addition of bpy to **2** yields  $V(NAr)Cl_3 \cdot bpy$  as an orange air-stable powder:  $^1H$  NMR ( $CD_2Cl_2$ )  $\delta$  9.65, 8.90 (d, d; 1H, 1H; bpy H-6 and H-6'); 8.31, 8.28 (d, d; 1H, 1H; bpy H-3 and H-3'); 8.17, 8.13 (t, t; 1H, 1H; bpy H-4 and H-4'); 7.66, 7.54 (t, t; 1H, 1H; 1H; bpy H-5 and H-5'); 7.25 (d, 2H,  $NAr H_m$ ), 7.08 (t, 1H,  $NAr H_p$ ), 5.02 (sept, 2H,  $CHMe_2$ ), 1.39 (d, 12H,  $CHMe_2$ );  $^{51}V$  NMR ( $C_6D_6$ )  $\delta$  380 (s,  $\Delta\nu_{1/2} = 2000$  Hz). Anal. Calcd for  $C_{22}H_{25}N_3Cl_3V$ : C, 54.04; H, 5.22; N, 8.60. Found: C, 54.20; H, 5.11; N, 8.28.

(11) Procedure for **3**: A suspension of  $KTp$  (330 mg, 1.31 mmol) in  $CH_2Cl_2$  (45 mL) was added under nitrogen to an orange solution of **1** (300 mg, 1.31 mmol) in  $CH_2Cl_2$  (60 mL). The mixture turned olive green; it was stirred for 1 h and filtered and the solvent removed under vacuum to yield 240 mg of product as a green powder (50%). This was subjected to Florisil column chromatography using methylene chloride as an eluant. Removal of the eluant under vacuum and washing with hexane left pure product as a black crystalline solid. Anal. Calcd for  $C_{13}H_{19}N_7Cl_2V$ : C, 38.46; H, 4.72; N, 24.15. Found: C, 38.69; H, 4.64; N, 24.12. Compounds **4–6** were obtained, purified, and analyzed similarly.

\* Abstract published in *Advance ACS Abstracts*, April 15, 1995.

(1) (a) Kaminski, W.; Sinn, H., Eds. *Transition Metals and Organometallics as Catalysts for Olefin Polymerization*; Springer: New York, 1988. (b) Quirk, R. P., Ed. *Transition Metal Catalyzed Polymerizations: Ziegler-Natta and Metathesis Polymerizations*; Cambridge University Press: Cambridge, U.K., 1988.

(2) (a) Watson, P. L.; Parshall, W. *Acc. Chem. Res.* **1985**, *18*, 51. (b) Burger, B. J.; Thompson, M. E.; Cotter, W. D.; Bercaw, J. E. *J. Am. Chem. Soc.* **1990**, *112*, 1566. (c) Coughlin, E. B.; Bercaw, J. E. *J. Am. Chem. Soc.* **1992**, *114*, 7606. (d) Sinn, H.; Kaminski, W. *Adv. Organomet. Chem.* **1980**, *18*, 137. (e) Kaminski, W.; Steiger, R. *Polyhedron* **1988**, *7*, 2375. (f) Jordan, R. F. *Adv. Organomet. Chem.* **1991**, *32*, 325.

(3) (a) Henrici-Olivé, G.; Olivé, S. *Angew. Chem., Int. Ed. Engl.* **1971**, *10*, 776. (b) Christman, D. L. *J. Polym. Sci., Polym. Chem. Ed.* **1972**, *10*, 471. (c) Mortimer, G. A. *J. Appl. Polym. Sci.* **1976**, *20*, 55. (d) Zambelli, A.; Allegra, G. *Macromolecules* **1980**, *13*, 42. (e) Jiao, S.; Yu, D. *Polym. J.* **1985**, *17*, 899.

(4) (a) Feher, F. J.; Blanski, R. L. *J. Am. Chem. Soc.* **1992**, *114*, 5886. (b) Feher, F. J.; Blanski, R. L. *Organometallics* **1993**, *12*, 958.

(5) (a) Nugent, W. A.; Mayer, J. M. *Metal-Ligand Multiple Bonds*; Wiley-Interscience: New York, 1988. (b) Trofimenko, S. *Chem. Rev.* **1993**, *93*, 943. (c) Gamble, A. S.; Boncella, J. M. *Organometallics* **1993**, *12*, 2814. (d) Eagle, A. A.; Young, C. G.; Tienkink, E. R. T. *Organometallics* **1992**, *11*, 2934.

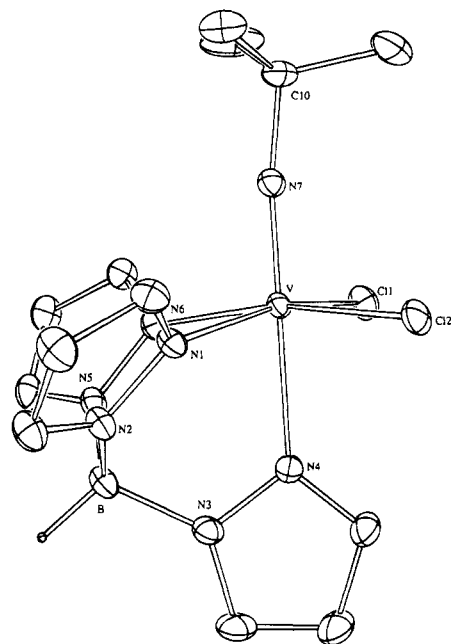


**Figure 1.** ORTEP diagram of compound **3** showing 30% probability thermal ellipsoids and the atom-labeling scheme. Hydrogen atoms, except B–H, are omitted. Selected bond distances (Å): V–Cl(1) = 2.2941(8), V–Cl(2) = 2.2843(7), V–N(1) = 2.098(2), V–N(4) = 2.207(2), V–N(6) = 2.097(2), V–N(7) = 1.638(2). Selected bond angles (deg): V–N(7)–C(10) = 172.2, Cl(1)–V–Cl(2) = 98.24(3), Cl(1)–V–N(1) = 165.43(6), Cl(1)–V–N(4) = 85.12(6), Cl(1)–V–N(6) = 89.58(6), Cl(1)–V–N(7) = 94.22(7), Cl(2)–V–N(1) = 89.25(6), Cl(2)–V–N(4) = 86.56(6), Cl(2)–V–N(6) = 166.29(6), Cl(2)–V–N(7) = 93.82(7), N(1)–V–N(4) = 82.86(8), N(1)–V–N(6) = 80.80(8), N(1)–V–N(7) = 97.75(9), N(4)–V–N(6) = 82.89(8), N(4)–V–N(7) = 179.28(9), N(6)–V–N(7) = 96.83(9).

octahedral geometry about vanadium is slightly distorted. In particular, the three N–V–N angles within the TpV fragment are as usual less than 90°, as a result of the chelate nature of the Tp ligand. On the other hand, the Cl(1)–V–Cl(2) angle is equal to 98.24(3)°. The four ligands *cis* to the imido group are all bent away from this ligand, so that the V atom is shifted out of the least-squares plane defined by Cl(1), Cl(2), N(1), and N(6), toward N(7), by 0.2117(4) Å. Among the *trans* bond angles, only N(4)–V–N(7) is nearly linear.

Comparison of the vanadium–ligand bond distances with those of related complexes affords some insight into electronic effects in **3**. The V–N(7) and the two V–Cl bond lengths are slightly higher than the corresponding

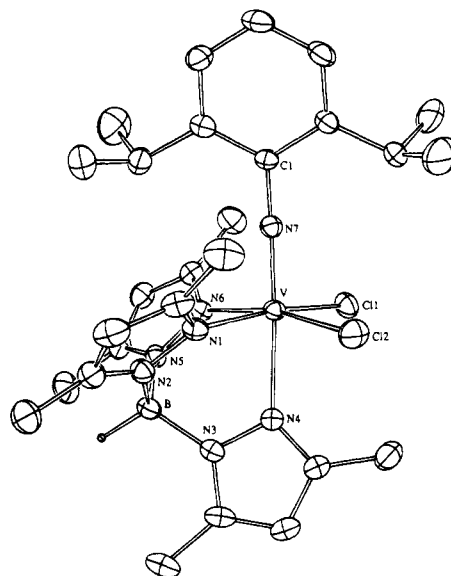


**Figure 2.** ORTEP diagram of compound **6** showing 50% probability thermal ellipsoids and the atom-labeling scheme. Hydrogen atoms, except B–H, are omitted. Selected bond distances (Å): V–Cl(1) = 2.304(1), V–Cl(2) = 2.292(1), V–N(1) = 2.111(4), V–N(4) = 2.236(4), V–N(6) = 2.093(4), V–N(7) = 1.693(4). Selected bond angles (deg): V–N(7)–C(1) = 173.7(3), Cl(1)–V–Cl(2) = 95.43(6), Cl(1)–V–N(1) = 170.0(1), Cl(1)–V–N(4) = 86.9(1), Cl(1)–V–N(6) = 89.0(1), Cl(1)–V–N(7) = 96.3(1), Cl(2)–V–N(1) = 89.3(1), Cl(2)–V–N(4) = 85.4(1), Cl(2)–V–N(6) = 167.6(1), Cl(2)–V–N(7) = 95.8(1), N(1)–V–N(4) = 84.8(1), N(1)–V–N(6) = 84.7(1), N(1)–V–N(7) = 91.9(2), N(4)–V–N(6) = 83.2(1), N(4)–V–N(7) = 176.5(2), N(6)–V–N(7) = 95.3(2).

values in the hexacoordinate chloro-bridged chains of  $[V(N-t-Bu)Cl_3]_n$  (1.62 and 2.22 Å)<sup>15</sup> and in the analogous cyclopentadienyl complex  $CpV(N-t-Bu)Cl_2$  (1.59 and 2.245 Å),<sup>16</sup> illustrating the better electron-donating ability of the Tp ligand with respect to chloro and Cp ligands. The vanadium–imido bond length, together with the large V–N(7)–C(10) bond angle of 172.2(2)°, is still characteristic, however, of strong  $\pi$  donation from N to V. The vanadium–pyrazolyl bond *trans* to the imido ligand is, as expected, significantly longer than the two bonds *trans* to the chloro ligands. The three distances are smaller than the corresponding values in  $TpVOCl(O-t-Bu)$ ,<sup>7b</sup> suggesting that Tp is more strongly bound to vanadium in **3**.

The molecular structure of **6** (Figure 2) is analogous to that of **3**. The octahedral geometry is slightly less distorted: the vanadium center, for instance, is shifted by only 0.1871(3) Å out of the least-squares plane defined by Cl(1), Cl(2), N(1), and N(6). The phenyl plane of the imido ligand lies in the symmetry plane of the molecule. One of its isopropyl substituents is thus inserted between two pyrazolyl rings of the Tp\* ligand, while the other is capping the two Cl ligands. The V–Cl bonds are only 0.01 Å longer than in **3**, probably reflecting, however, the slightly stronger electron-donor character of Tp\* with respect to Tp.

The <sup>1</sup>H NMR spectra of complexes **3**–**6**<sup>17</sup> are in agreement with the molecular structures described above. In particular, the two pyrazolyl rings *trans* to

(12) Single crystals were grown in air by slow diffusion of pentane into dichloromethane solutions of the compounds. Crystal data were obtained at room temperature using an Enraf-Nonius CAD4F (**3**) or MACH3 (**6**) diffractometer with Mo K $\alpha$  graphite-monochromated radiation ( $\lambda = 0.7107$  Å). The scan widths (deg) in the  $\theta/2\theta$  mode used were  $\Delta\theta = 1.05 + 0.34 \tan \theta$  (**3**) or  $0.76 + 0.34 \tan \theta$  (**6**). A total of 3730 *hkl* (**3**) or 3559  $\pm hkl$  (**6**) reflections were recorded within  $2^\circ < \theta < 24^\circ$  (**3**) or  $26^\circ$  (**6**), and 2329 (**3**) or 2391 (**6**) reflections having  $I > 3\sigma(I)$  were used for determining and refining the structure. The structures were determined using the heavy-atom method and refined using full-matrix least squares to  $R(F) = 0.029$  (**3**) or 0.033 (**6**) and  $R_w(F) = 0.043$  (**3** and **6**). Absorption corrections derived from the  $\psi$  scans of four reflections were applied. The Enraf-Nonius Molenvax package was used for all calculations.

(13) Crystal data for **3**:  $C_{13}H_{19}BN_7Cl_2V$ ,  $M_r = 406.0$ , orthorhombic, space group  $Pbca$ ,  $a = 15.582(4)$  Å,  $b = 18.700(5)$  Å,  $c = 12.975(3)$  Å,  $V = 3780.5$  Å<sup>3</sup>,  $Z = 8$ ,  $D_{calc} = 1.427$  g cm<sup>-3</sup>,  $\mu = 8.022$  cm<sup>-1</sup>.

(14) Crystal data for **6**:  $C_{27}H_{39}BN_7Cl_2V$ ,  $M_r = 594.3$ , monoclinic, space group  $Cc$ ,  $a = 17.802(5)$  Å,  $b = 9.610(2)$  Å,  $c = 19.361(5)$  Å,  $\beta = 115.14(2)^\circ$ ,  $V = 2998.7$  Å<sup>3</sup>,  $Z = 4$ ,  $D_{calc} = 1.316$  g cm<sup>-3</sup>,  $\mu = 5.273$  cm<sup>-1</sup>.

(15) Massa, W.; Wocadlo, S.; Lotz, S.; Dehnicke, K. *Z. Anorg. Allg. Chem.* **1990**, 587, 79.

(16) Preuss, F.; Becker, H.; Häusler, H.-J. *Z. Naturforsch.* **1987**, 42B, 881.

the chloro ligands are equivalent and are clearly distinguished from the third pyrazolyl ring *trans* to the imido ligand, for the Tp as well as for the Tp\* complexes. In **5**, the two  $-\text{CHMe}_2$  substituents of the  $=\text{NAr}$  group give rise to one doublet (12H) and one septuplet (2H), showing that the Ar group is probably rotating freely about the  $=\text{N}-\text{Ar}$  bond axis. In **6**, this process is hindered by the presence of the 3-Me substituents of the two pyrazolyl ligands *cis* to the imido ligand, resulting in the observation of two nonequivalent *i*-Pr substituents, as expected from the solid-state structure. The spectrum of **6** is not modified at 110 °C, showing that the barrier to rotation about the  $=\text{N}-\text{Ar}$  bond axis is greater than 19 kcal mol<sup>-1</sup>.<sup>18</sup>

Complexes **3–6** show broad unresolved <sup>51</sup>V NMR signals ( $\Delta\nu_{1/2} = 1500\text{--}2900$  Hz),<sup>19</sup> as expected from the presence of four nitrogen atoms bound to vanadium. Both  $\delta$  and  $\Delta\nu_{1/2}$  values are larger for the NAr derivatives than for the *N-t*-Bu ones, and for the Tp\* derivatives than for the Tp ones. Notably also, the signals of compounds **3**, **4** and **5**, **6** show up at much lower fields than those of the corresponding cyclopentadienyl complexes CpV(*N-t*-Bu)Cl<sub>2</sub><sup>16</sup> and CpV(NAr)Cl<sub>2</sub>,<sup>9</sup> respectively.

Further derivatives were obtained by substitution of the chloro ligands in **3–6**. For instance, reaction of **4** with 1 equiv of LiOMe, LiO-*t*-Bu, or AgCF<sub>3</sub>SO<sub>3</sub> led respectively to complexes Tp\*V(*N-t*-Bu)(OMe)Cl (**7**), Tp\*V(*N-t*-Bu)(O-Bu)Cl (**8**), and Tp\*V(*N-t*-Bu)(CF<sub>3</sub>SO<sub>3</sub>)Cl (**9**), which were characterized by <sup>1</sup>H NMR spectroscopy.<sup>20</sup> In these compounds, the three pyrazolyl groups of Tp\* are nonequivalent and the metal center is chiral. Disubstitution can occur as well, leading for instance to Tp\*V(*N-t*-Bu)(CF<sub>3</sub>SO<sub>3</sub>)<sub>2</sub> (**10**).<sup>20</sup> In contrast with their dichloro precursor, these compounds are air-sensitive. Further, they could not be obtained free of the oxo-amido complex Tp\*VO(NH-*t*-Bu)Cl (**11**)<sup>20</sup> in variable and often non-negligible amounts. **11** was synthesized free of any other complex by reaction of **4** with Ag<sub>2</sub>CO<sub>3</sub>.<sup>20</sup> Given that also *n*-Bu<sub>4</sub>NOH (in methanol) converts **4** into **11** and that hydrolysis of compounds **7–9** does not yield **11**, we suggest that **11** results from hydroxylation<sup>21</sup> of **4** into Tp\*V(*N-t*-Bu)(OH)Cl, followed by rapid hydrogen

transfer from O to N. Chloride exchange in **11**, on addition of 1 equiv of SnBr<sub>4</sub> or AgCF<sub>3</sub>SO<sub>3</sub>, leads to Tp\*VO(NH-*t*-Bu)X (X = Br (**12**), CF<sub>3</sub>SO<sub>3</sub> (**13**)).<sup>20</sup>

Preliminary experiments show that the above complexes can, in the presence of MAO, catalyze the polymerization of ethylene and propylene at room temperature. In toluene solution, **6** polymerized ethylene at atmospheric pressure with an activity of at least 14 kg mol<sup>-1</sup> h<sup>-1</sup>.<sup>22</sup> The polymer was a white powder with  $M_w = 47\,000$  and  $M_w/M_n = 3.0$ , as established by GPC analysis in 1,2,4-trichlorobenzene (140 °C). Propylene polymerized as well to a viscous oil, when exposed under pressure (7 bar) to a solution of **6** and MAO in toluene.<sup>23</sup> The minimum activity was estimated at 1 kg mol<sup>-1</sup> h<sup>-1</sup> bar<sup>-1</sup>. The resulting polymer was essentially atactic, exhibiting however a slight excess of *r* diads, according to <sup>13</sup>C NMR spectroscopy,<sup>24</sup> and consisted of regioregular chains of low molecular weight ( $M_w = 3800$ ,  $M_w/M_n = 2.0$ ). The observation of isopropyl groups as major chain ends is consistent with 1–2 insertions of propylene into chain-initiating V–Me and chain-carrying V–C bonds.

Further studies on these catalyst systems, including on the nature of the active species produced on addition of MAO to the vanadium complexes,<sup>25</sup> are in progress and will be reported separately.

**Acknowledgment.** We thank Prof. J. A. Osborn and the CNRS for supporting this work, Mrs. N. Kyritsakas and Dr. A. De Cian for solving the X-ray structures, and Dr. D. Constantin (Enichem polymères France SA, Mazingarbe, France) and Dr. L. Reibel (CRM, Strasbourg, France) for the GPC measurements.

**Supplementary Material Available:** Tables of crystal data, positional and thermal parameters, and bond distances and angles for **3** and **6**; IR data for **3–6**; <sup>1</sup>H NMR spectra for **7–13**, preparation and characterization of **11** (21 pages). Ordering information is given on any current masthead page.

OM950101J

(21) The OH<sup>-</sup> function would be generated by reaction of the initial reactants with water.

(22) Experimental procedure: A solution of **6** (10 mg,  $1.68 \times 10^{-5}$  mol) in toluene (10 mL) was placed under an atmosphere of ethylene (1 bar). MAO (11.26 mL of a 10% solution in toluene, Schering, ca. 1000 equiv) was added at room temperature and ethylene bubbled through the resultant orange solution for 105 min. The reaction was quenched by addition of acidified (5 mL aqueous HCl) methanol (35 mL). The white precipitate thus formed was collected by filtration, washed with methanol, dried in vacuo (25 °C, 12 h), and weighed (402 mg). Its polyethylene nature was verified by elemental analysis, IR, and <sup>13</sup>C NMR.

(23) Experimental procedure: **6** (10 mg,  $1.68 \times 10^{-5}$  mol) was placed in a stainless steel autoclave, and MAO (11.26 mL of a 10% solution in toluene, Schering, ca. 1000 equiv) was added at room temperature under nitrogen. After ca. 5 min, propylene was introduced into the reactor and the pressure maintained at 7 bar for 3 h. After the excess propylene was vented, the reaction mixture was poured into MeOH–HCl (35 mL). The toluene fraction was decanted, and the volatiles were evaporated under vacuum (25 °C, 12 h), yielding an oily residue of oligomeric polypropylene (320 mg), as shown by IR, <sup>1</sup>H and <sup>13</sup>C NMR (C<sub>2</sub>D<sub>2</sub>Cl<sub>4</sub>, 125 °C), and GPC (THF).

(24) Ewen, J. A. *J. Am. Chem. Soc.* **1984**, *106*, 6355.

(25) At the present stage, we cannot conclude that the polymerization reactions are actually catalyzed by vanadium(V) species.

(17) <sup>1</sup>H NMR spectrum for **3** (CD<sub>2</sub>Cl<sub>2</sub>):  $\delta$  7.96, 7.89, 7.72, 7.62 (d, d, d, 2H, 1H, 2H, 1H); <sup>3</sup>J<sub>HH</sub> = 2.2 Hz, Pz H-3 and H-5); 6.30, 6.21 (t, t, 2H, 1H); <sup>3</sup>J<sub>HH</sub> = 2.2; Pz H-4); 1.64 (s, 9H, N-*t*-Bu). <sup>1</sup>H NMR spectrum for **4** (CD<sub>2</sub>Cl<sub>2</sub>):  $\delta$  5.89, 5.76 (s, s; 2H, 1H; Pz\* H-4); 2.60, 2.40, 2.38, 2.37 (s, s, s, s; 6H, 6H, 3H, 3H; Pz\* Me-3 and Me-5); 1.83 (s, 9H, N-*t*-Bu). <sup>1</sup>H NMR spectrum for **5** (CDCl<sub>3</sub>):  $\delta$  8.05, 7.82, 7.76, 7.57 (d, d, d, d; 1H, 2H, 2H, 1H); <sup>3</sup>J<sub>HH</sub> = 2.2 Hz; Pz H-3 and H-5); 7.11 (d, 2H, <sup>3</sup>J<sub>HH</sub> = 7.8, NAr H<sub>m</sub>); 6.98 (t, 1H, <sup>3</sup>J<sub>HH</sub> = 7.8, NAr H<sub>p</sub>); 6.24, 6.18 (t, t; 2H, 1H); <sup>3</sup>J<sub>HH</sub> = 2.2; Pz H-4); 4.13 (sept, 2H, <sup>3</sup>J<sub>HH</sub> = 6.8, CHMe<sub>2</sub>); 1.14 (d, 12H, <sup>3</sup>J<sub>HH</sub> = 6.8, CHMe<sub>2</sub>). <sup>1</sup>H NMR spectrum for **6** (CDCl<sub>3</sub>):  $\delta$  7.25 (dd, 1H, <sup>3</sup>J<sub>HH</sub> = 7.4 Hz, <sup>4</sup>J<sub>HH</sub> = 1.5, NAr H<sub>m</sub>); 6.95 (dd, 1H, <sup>3</sup>J<sub>HH</sub> = 7.4, <sup>3</sup>J<sub>HH</sub> = 7.8, NAr H<sub>p</sub>); 6.89 (dd, 1H, <sup>3</sup>J<sub>HH</sub> = 7.8, <sup>4</sup>J<sub>HH</sub> = 1.5, NAr H<sub>m</sub>); 5.82, 5.70 (s, s; 2H, 1H; Pz\* H-4); 5.73, 2.81 (sept, sept; 1H, 1H); <sup>3</sup>J<sub>HH</sub> = 6.8, CHMe<sub>2</sub>); 2.67, 2.45, 2.33, 2.29 (s, s, s, s; 3H, 6H, 3H, 6H; Pz\* Me-3 and Me-5); 1.58, 0.75 (d, d; 6H, 6H); <sup>3</sup>J<sub>HH</sub> = 6.8, CHMe<sub>2</sub>).

(18) Gunther, H. *NMR Spektroskopie*; G. Thieme Verlag: Stuttgart, Germany, 1973.

(19) <sup>51</sup>V NMR spectra (C<sub>6</sub>D<sub>6</sub>): **3**,  $\delta$  -140 (s,  $\Delta\nu_{1/2} = 1500$  Hz); **4**,  $\delta$  -75 (s,  $\Delta\nu_{1/2} = 1800$  Hz); **5**,  $\delta$  240 (s,  $\Delta\nu_{1/2} = 2600$  Hz); **6**,  $\delta$  250 (s,  $\Delta\nu_{1/2} = 2900$  Hz).

(20) The <sup>1</sup>H NMR spectra for **7–13** and details of the preparation and characterization of **11** can be found in the supplementary material.

## Chemistry of Organosilicon Compounds. 314. Preparation of (Pentamethyldisilanyl)lithium and Two Isomers of (Heptamethyltrisilanyl)lithium. Structural Characterization of $(\text{CH}_3)_5\text{Si}_2\text{Li}$

Akira Sekiguchi, Masato Nanjo, Chizuko Kabuto, and Hideki Sakurai

*Organometallics*, 1995, 14 (6), 2630-2632 • DOI: 10.1021/om00006a007 • Publication Date (Web): 01 May 2002

Downloaded from <http://pubs.acs.org> on March 9, 2009

### More About This Article

---

The permalink <http://dx.doi.org/10.1021/om00006a007> provides access to:

- Links to articles and content related to this article
- Copyright permission to reproduce figures and/or text from this article





# Preparation of (Pentamethyldisilanyl)lithium and Two Isomers of (Heptamethyltrisilanyl)lithium. Structural Characterization of (CH<sub>3</sub>)<sub>5</sub>Si<sub>2</sub>Li<sup>1</sup>

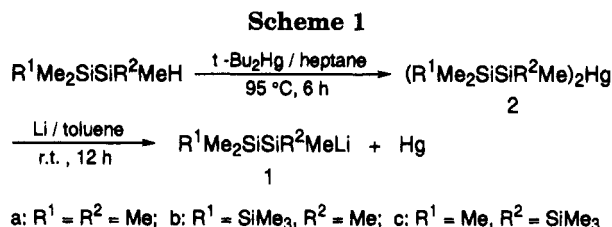
Akira Sekiguchi,\* Masato Nanjo, Chizuko Kabuto, and Hideki Sakurai\*<sup>†</sup>

Department of Chemistry and Organosilicon Research Laboratory, Faculty of Science, Tohoku University, Aoba-ku, Sendai 980-77, Japan

Received January 18, 1995<sup>®</sup>

**Summary:** (Pentamethyldisilanyl)lithium (Me<sub>3</sub>SiSiMe<sub>2</sub>-Li, **1a**) and two isomers of (heptamethyltrisilanyl)lithium (Me[Me<sub>2</sub>Si]<sub>2</sub>SiMe<sub>2</sub>Li, **1b**; Me[Me<sub>3</sub>Si]<sub>2</sub>SiLi, **1c**) were prepared and isolated as highly inflammable colorless crystals by the reaction of the corresponding bis-(oligosilanyl)mercury species and lithium in toluene. The tetrameric structure of silyllithium **1a** was established by X-ray diffraction. The reaction of **1a** with chlorosilanes gave the expected substitution product quantitatively in hexane, whereas an electron-transfer reaction occurred with benzyl chloride to form decamethyltetrasilane and bibenzyl.

Silyl anions are useful in some applications not only in organosilicon chemistry but also in organic synthesis.<sup>2</sup> Gilman pioneered the preparation of phenyl-substituted silyl anions,<sup>3</sup> and later trialkylsilyl anions were introduced.<sup>4</sup> More recently, alkoxy,<sup>5</sup> and amino-substituted<sup>6</sup> silyl anions have been reported.<sup>7</sup> Despite the large number of these reports on monosilyl anions, (pentamethyldisilanyl)lithium (Me<sub>3</sub>SiSiMe<sub>2</sub>Li, **1a**), the simplest oligosilyllithium with an Si–Si bond, had



never been isolated and characterized, although its formation as a byproduct in the course of the preparation of (trimethylsilyl)lithium (Me<sub>3</sub>SiLi)<sup>4i</sup> from hexamethyldisilane and methyl lithium has been noted.<sup>8</sup> Silyl anions readily undergo scrambling and redistribution reactions, presumably by electron-transfer reactions.<sup>9</sup> We report herein the first successful isolation and full characterization of (pentamethyldisilanyl)- and two isomeric (heptamethyltrisilanyl)lithium compounds, together with the crystal structure of **1a** and its reactions.

For the preparation of (pentamethyldisilanyl)lithium (**1a**), we have adopted a strategy based on the lithium–mercury exchange reaction.<sup>10</sup> Thus, bis(pentamethyldisilanyl)mercury (**2a**)<sup>11</sup> was subjected to the Li–Hg exchange reaction with excess lithium metal in toluene to give colorless crystals of **1a** that could be recrystallized from pentane at 0 °C. Like most other organolithium compounds, **1a** was highly inflammable in air (Scheme 1).<sup>12</sup>

(Pentamethyldisilanyl)lithium (**1a**) is tetrameric in the solid state, as determined by X-ray diffraction.<sup>13</sup> The crystal structure of **1a** possesses a crystallographic 2-fold axis, the ORTEP drawing of **1a** being shown in

(8) (a) Hudrlik, P. F.; Waugh, M. A.; Hudrlik, A. M. *J. Organomet. Chem.* **1984**, *271*, 69. (b) Hudrlik, P. F.; Hudrlik, A. M.; Yimenu, T.; Waugh, M. A.; Nagendrappa, G. *Tetrahedron* **1988**, *44*, 3791. (c) Gong, L.; Leung-Toung, R.; Tidwell, T. T. *J. Org. Chem.* **1990**, *55*, 3634. (d) Nadler, E. B.; Rappoport, Z. *Tetrahedron Lett.* **1990**, *31*, 555. Matyjaszewski et al. reported the spectroscopic observation of PhMe<sub>2</sub>SiSiMe<sub>2</sub>Li as a mixture with PhMe<sub>2</sub>SiLi in THF: (e) Ruehl, K. E.; Davis, M. E.; Matyjaszewski, K. *Organometallics* **1992**, *11*, 788. Allred et al. have reported the preparation of Si<sub>6</sub>Me<sub>11</sub><sup>–</sup> anions: (f) Allred, A. L.; Smart, R. T.; Van Beek, D. A., Jr. *Organometallics* **1992**, *11*, 4225. (9) (a) Carberry, E.; West, R. *J. Am. Chem. Soc.* **1969**, *91*, 5440. (b) Sakurai, H.; Okada, A. *J. Organomet. Chem.* **1972**, *35*, C13. (10) Et<sub>2</sub>Ge<sub>2</sub>Li has been prepared by the reaction of (Et<sub>2</sub>Ge)<sub>2</sub>Hg and Li. Bravo-Zhivotovskii, D. A.; Pigaev, S. D.; Vyazankina, O. A.; Vyazankin, N. S. *Izv. Akad. Nauk SSSR, Ser. Khim.* **1984**, 2414; *Chem. Abstr.* **1985**, *102*, 132171.

(11) Compound **2a** was prepared as an air- and light-sensitive yellow oil by heating a mixture of pentamethyldisilane and di-*tert*-butylmercury in heptane at 95 °C for 6 h: <sup>1</sup>H NMR (C<sub>6</sub>D<sub>6</sub>, δ) 0.21 (s, 18 H), 0.41 (s, 12 H); <sup>13</sup>C NMR (C<sub>6</sub>D<sub>6</sub>, δ) –0.14, 0.64; <sup>29</sup>Si NMR (C<sub>6</sub>D<sub>6</sub>, δ) –5.74, 34.9.

(12) Compound **1a**: <sup>1</sup>H NMR (C<sub>7</sub>D<sub>8</sub>, δ) 0.22 (s, 9 H), 0.33 (s, 6 H); <sup>13</sup>C NMR (C<sub>7</sub>D<sub>8</sub>, δ) –2.51, –0.56; <sup>29</sup>Si NMR (C<sub>7</sub>D<sub>8</sub>, δ) –79.6 to –81.4 (m), –12.4; <sup>6</sup>Li NMR (C<sub>7</sub>D<sub>8</sub>, δ) 2.11; <sup>1</sup>H NMR (THF-*d*<sub>6</sub>, δ) –0.17 (s, 9 H), –0.04 (s, 6 H); <sup>13</sup>C NMR (THF-*d*<sub>6</sub>, δ) –0.15, 1.31; <sup>29</sup>Si NMR (THF-*d*<sub>6</sub>, 180 K, δ) –74.9 (t, *J* = 18.8 Hz), –10.6; <sup>6</sup>Li NMR (THF-*d*<sub>6</sub>, δ) 0.58.

<sup>†</sup> Current address: Department of Industrial Chemistry, Faculty of Science and Technology, Science University of Tokyo, Noda, Chiba 278, Japan.

<sup>®</sup> Abstract published in *Advance ACS Abstracts*, May 1, 1995.

(1) Chemistry of Organosilicon Compounds. 314.

(2) (a) Fleming, I. In *Comprehensive Organic Chemistry*; Barton, D., Ollis, W. D., Eds.; Pergamon Press: Oxford, U.K., 1979; Vol. 3, pp 664–669. (b) Lambert, J. B.; Schulz, W. J., Jr. In *The Chemistry of Organic Silicon Compounds*; Patai, S., Rappoport, Z., Eds.; Wiley: Chichester, U.K., 1989; pp 1007–1010.

(3) Gilman, H.; Lichtenwalter, G. D. *J. Am. Chem. Soc.* **1958**, *80*, 608.

(4) Et<sub>3</sub>SiLi: (a) Vyazankin, N. S.; Razuvaev, G. A.; Gladyshev, E. N.; Korneva, S. P. *J. Organomet. Chem.* **1967**, *7*, 353. (b) Vyazankin, N. S.; Gladyshev, E. N.; Korneva, S. P.; Razuvaev, G. A. *Zh. Obshch. Khim.* **1966**, *36*, 2025; *Chem. Abstr.* **1967**, *66*, 76050. (c) Vyazankin, N. S.; Gladyshev, E. N.; Arkhangel'skaya, E. A.; Razuvaev, G. A.; Korneva, S. P. *Izv. Akad. Nauk SSSR, Ser. Khim.* **1968**, 2081; *Chem. Abstr.* **1969**, *70*, 334. Me<sub>3</sub>SiNa: (d) Sakurai, H.; Okada, A.; Kira, M.; Yonezawa, K. *Tetrahedron Lett.* **1971**, 1511. (e) Sakurai, H.; Okada, A.; Umino, H.; Kira, M. *J. Am. Chem. Soc.* **1973**, *95*, 955. (f) Sakurai, H.; Kondo, F. *J. Organomet. Chem.* **1975**, *92*, C46. Me<sub>3</sub>SiK: (g) Sakurai, H.; Kira, M.; Umino, H. *Chem. Lett.* **1977**, 1265. Me<sub>3</sub>SiLi: (h) Hengge, E.; Holtschmidt, N. *Monatsh. Chem.* **1968**, *99*, 340. (i) Still, W. C. *J. Org. Chem.* **1976**, *41*, 3063.

(5) Watanabe, H.; Higuchi, K.; Goto, T.; Muraoka, T.; Inose, J.; Kageyama, M.; Iizuka, Y.; Nozaki, M.; Nagai, Y. *J. Organomet. Chem.* **1981**, *218*, 27.

(6) Tamao, K.; Kawachi, A.; Ito, Y. *J. Am. Chem. Soc.* **1992**, *114*, 3989.

(7) Theoretical studies on silyl anions: (a) Hopkinson, A. C.; Lien, M. H. *Tetrahedron* **1981**, *37*, 1105. (b) Magnusson, E. *Tetrahedron* **1985**, *41*, 2945. (c) Schleyer, P. v. R.; Clark, T. *J. Chem. Soc., Chem. Commun.* **1986**, 1371. (d) Schleyer, P. v. R.; Reed, A. E. *J. Am. Chem. Soc.* **1988**, *110*, 4453. (e) Hopkinson, A. C.; Rodriguez, C. F. *Can. J. Chem.* **1990**, *68*, 1309. NMR studies on silyl anions: (f) Olah, G. A.; Hunadi, R. *J. Am. Chem. Soc.* **1980**, *102*, 6989. (g) Buncel, E.; Venkatachalam, T. K.; Eliasson, B.; Edlund, U. *J. Am. Chem. Soc.* **1985**, *107*, 303. (h) Edlund, U.; Lejon, T.; Venkatachalam, T. K.; Buncel, E. *J. Am. Chem. Soc.* **1985**, *107*, 6408. (i) Edlund, U.; Lejon, T.; Pyykkö, P.; Venkatachalam, T. K.; Buncel, E. *J. Am. Chem. Soc.* **1987**, *109*, 5982.

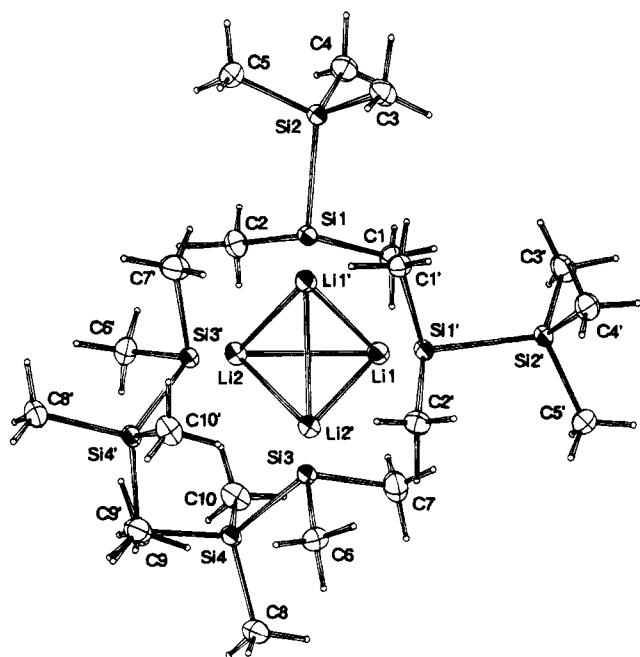


**Figure 1.** ORTEP drawing of **1a**. Selected bond lengths (Å): Li1–Li2: 2.749(7), Li1–Li1' = 2.795(7), Li1–Li2' = 2.783(7), Li2–Li1' = 2.783(7), Li2–Li2' = 2.819(8), Li1'–Li2' = 2.749(7), Si1–Li1 = 2.662(4), Si1–Li2 = 2.683(6), Si1–Li1' = 2.687(5), Si3–Li1 = 2.715(6), Si3–Li2 = 2.700(6), Si3–Li2' = 2.650(5), Si1–Si2 = 2.348(0), Si1–C1 = 1.944(2), Si1–C2 = 1.919(4), Si3–Si4 = 2.344(0), Si3–C6 = 1.944(4), Si3–C7 = 1.928(4). Selected bond angles (deg): Si2–Si1–C1 = 101.9(1), Si2–Si1–C2 = 103.6(1), C1–Si1–C2 = 102.5(1), Si4–Si3–C6 = 101.8(1), Si4–Si3–C7 = 102.6(1), C6–Si3–C7 = 101.6(1).

Figure 1. The lithium atoms are arranged such that a tetrahedron with an average Li–Li distance of 2.780 Å is defined.<sup>14</sup> The Li–Li distance of the framework is somewhat longer than that of typical alkyl lithium tetramers (Li–Li = 2.55–2.56 Å).<sup>15</sup> Substitution of carbon in tetrameric alkyl lithium with silicon should lead to expansion of the lithium core due to the increased Li–Si bond length compared to that of Li–C. The pentamethyl-disilanyl group caps each face of the tetrahedron with the three nearly equal Li–Si distances of 2.683 Å (average). The equal length of the Li–Si bonds implies that each silicon participates equally in bonding to the three lithium atoms. The C–Si bond distance of 1.934 Å (av) is considerably longer than the normal one (1.88 Å). However, the Si–Si distance of 2.346 Å (av) is quite normal, suggesting no dative bonding exists as observed for (tris(trimethylsilyl)silyl)-

(13) A single crystal (0.4 × 0.3 × 0.25 mm) of **1a** was sealed in a glass capillary tube for data collection. Diffraction data were collected at 200 K on a Rigaku Denki AFC-5R diffractometer with a rotating anode (45 kV, 200 mA) with graphite-monochromatized Mo K $\alpha$  radiation ( $\lambda = 0.71069$  Å). A total of 3852 reflections with  $2\theta = 3$ –62° were collected. Crystal data: molecular formula  $\text{Si}_5\text{C}_{20}\text{H}_{60}\text{Li}_4$ ,  $M_r = 553.2$ , orthorhombic;  $a = 9.354(2)$  Å,  $b = 17.998(4)$  Å,  $c = 22.881(5)$  Å,  $V = 3852.1(16)$  Å<sup>3</sup>, space group  $Aba2$ ,  $Z = 4$ ,  $D_c = 0.954$  g/cm<sup>3</sup>. The final  $R$  factor was 0.033 ( $R_w = 0.035$ ) for 2769 reflections with  $F_o > 3\sigma(F_o)$ .

(14) The hexameric structure of  $(\text{LiSiMe}_3)_6$ , found by X-ray diffraction, was reported; see: (a) Schaaf, T. F.; Butler, W.; Glick, M. D.; Oliver, J. P. *J. Am. Chem. Soc.* **1974**, *96*, 7593. (b) Ilsley, W. H.; Schaaf, T. F.; Glick, M. D.; Oliver, J. P. *J. Am. Chem. Soc.* **1980**, *102*, 3769.

(15) (a) Dietrich, H. *Acta Crystallogr.* **1963**, *16*, 681. (b) Weiss, E.; Lucken, E. A. C. *J. Organomet. Chem.* **1964**, *2*, 197. (c) Weiss, E.; Hencken, G. *J. Organomet. Chem.* **1970**, *21*, 265. (d) Dietrich, H. *J. Organomet. Chem.* **1981**, *205*, 291. (e) Weiss, E.; Lambertsen, T.; Schubert, B.; Cockcroft, J. K.; Wiedenmann, A. *Chem. Ber.* **1990**, *123*, 79.

**Table 1.** Reaction of  $\text{Me}_3\text{SiSiMe}_2\text{Li}$  (**1a**) with Electrophiles<sup>a</sup>

reagent	products	yield (%) <sup>b</sup>
D <sub>2</sub> O	Me <sub>5</sub> Si <sub>2</sub> D	100
Me <sub>3</sub> SiCl	Me(SiMe <sub>2</sub> ) <sub>3</sub> Me	100
Me <sub>2</sub> SiCl <sub>2</sub>	Me(SiMe <sub>2</sub> ) <sub>5</sub> Me	100
Cl(SiMe <sub>2</sub> ) <sub>6</sub> Cl	Me(SiMe <sub>2</sub> ) <sub>10</sub> Me	100
PhCH <sub>2</sub> Cl	PhCH <sub>2</sub> Si <sub>2</sub> Me <sub>5</sub>	42
	Me(SiMe <sub>2</sub> ) <sub>4</sub> Me	36
	PhCH <sub>2</sub> CH <sub>2</sub> Ph	42
O <sub>2</sub>	Me <sub>5</sub> Si <sub>2</sub> H	31
	(Me <sub>5</sub> Si <sub>2</sub> ) <sub>2</sub> O	18
	Me(SiMe <sub>2</sub> ) <sub>4</sub> Me	19

<sup>a</sup> Aliquots of a stock solution of **1a** (ca. 0.1 M) in hexane were used for the reactions. <sup>b</sup> Determined by GLC.

lithium.<sup>16</sup> Of particular interest is the fact that the angles about silicon are significantly contracted, the sum of the angles being only 307.0°. The Si–Si bond distance of **1a** is in close agreement with the calculated value of 2.393 Å for H<sub>3</sub>SiSiH<sub>2</sub><sup>−</sup> at the 6-31G\* level.<sup>17</sup> In addition, the calculation shows significant contraction of the angles about silicon (95° for H–Si–H).

The unique structural feature of **1a** is also elucidated by its NMR spectra. The <sup>29</sup>Si NMR resonance of the silicon attached to lithium was observed at −74.9 ppm as a triplet signal with equal intensities ( $J(^6\text{Li}-^{29}\text{Si}) = 18.8$  Hz) in THF-*d*<sub>8</sub> at 180 K.<sup>12</sup> Thus, the silicon atom is coupled only to one lithium atom, indicating that **1a** is monomeric in THF.<sup>18</sup> Unusually small values of other coupling constants,  $J(^{29}\text{Si}-^{29}\text{Si}) = 19.1$  Hz and  $J(^{13}\text{C}-^{29}\text{Si}) = 9.5$  Hz, suggest localization of the negative charge on the silicon atom attached to the lithium. In hydrocarbon solvents such as toluene and benzene, the <sup>29</sup>Si NMR spectrum differs from that in THF, appearing at −79.6 to −81.4 ppm as an unresolved multiplet in toluene-*d*<sub>8</sub>.<sup>12</sup> These results suggest that **1a** is aggregated in hydrocarbons, and a tetrameric structure may be involved. Due to the lesser ionic and more covalent character of the species in toluene than in the case for THF, the coupling constants  $J(^{29}\text{Si}-^{29}\text{Si}) = 43.2$  Hz and  $J(^{13}\text{C}-^{29}\text{Si}) = 15.9$  Hz are much larger than those in THF.

By the same procedure, two isomeric (heptamethyl-trisilanyl)lithiums, **1b** and **1c**, were prepared (Scheme 1).<sup>19</sup> As the anionic silicon centers are substituted by the trimethylsilyl group, a major contribution of stabilizing the ionic character comes from the trimethylsilyl groups, which is indicated by the lack of scalar coupling between silicon and lithium. Thus, the <sup>29</sup>Si NMR spectrum of **1c** showed a singlet signal at −133.8 ppm in THF-*d*<sub>8</sub> at 180 K. Like **1a**, however, **1b** showed the triplet signal at −62.7 ppm ( $J = 18.6$  Hz) in THF-*d*<sub>8</sub> at 180 K.

(16) The Si–Si bond distances of  $\{[\text{LiSi}(\text{SiMe}_3)_3]_2\cdot 3\text{DME}\}$  and  $(\text{Me}_3\text{Si})_3\text{SiLi}(\text{THF})_3$ , determined by X-ray diffraction methods, were reported to be 2.342 and 2.330–2.331 Å: (a) Becker, G.; Hartmann, H.-M.; Münch, A.; Riffel, H. *Z. Anorg. Allg. Chem.* **1985**, *530*, 29. (b) Heine, A.; Herbst-Irmer, R.; Sheldrick, G. M.; Stalke, D. *Inorg. Chem.* **1993**, *32*, 2694. (c) Dias, H. V. R.; Olmstead, M. M.; Ruhlandt-Senge, K.; Power, P. P. *J. Organomet. Chem.* **1993**, *462*, 1.

(17) Damewood, J. R., Jr.; Hadad, C. M. *J. Phys. Chem.* **1988**, *92*, 33.

(18) Other factors to be considered are the slow exchange of Li under the conditions of the NMR study and steric bulkiness due to an extra SiMe<sub>2</sub> unit.

(19) **1b**: <sup>1</sup>H NMR (C<sub>7</sub>D<sub>8</sub>,  $\delta$ ) 0.36 (s, 6 H), 0.18 (s, 6 H), 0.15 (s, 9 H); <sup>7</sup>Li NMR (C<sub>7</sub>D<sub>8</sub>,  $\delta$ ) 2.21; <sup>13</sup>C NMR (C<sub>7</sub>D<sub>8</sub>,  $\delta$ ) −0.49, −1.21, −4.19; <sup>29</sup>Si NMR (C<sub>7</sub>D<sub>8</sub>,  $\delta$ ) −14.2, −40.4, −73.5 (m). **1c**: <sup>1</sup>H NMR (C<sub>7</sub>D<sub>8</sub>,  $\delta$ ) 0.36 (s, 3 H), 0.27 (s, 36 H); <sup>7</sup>Li NMR (C<sub>7</sub>D<sub>8</sub>,  $\delta$ ) 2.18; <sup>13</sup>C NMR (C<sub>7</sub>D<sub>8</sub>,  $\delta$ ) 2.8, −1.6; <sup>29</sup>Si NMR (C<sub>7</sub>D<sub>8</sub>,  $\delta$ ) −8.3, −137 (m).

The present X-ray and NMR data for **1a–c** suggest that the delocalization of the negative charge is much smaller than for the carbanions due to the Si–Si distance being longer than that of Si–C.<sup>20</sup> As a result, the oligosilanyl anions exhibit high reactivity owing to the substantial localization of the negative charge. On reaction of **1a** with chlorosilanes, substitution reactions occurred even in hexane to give the corresponding oligosilanes quantitatively, whereas an electron-transfer reaction occurred with benzyl chloride to result in the formation of decamethyltetrasilane and bibenzyl (Table 1). In these reactions, no dodecamethylcyclohexasilane formed; thus, no scrambling reaction occurred.

---

(20) It is known that  $(\text{Me}_3\text{Si})_3\text{SiLi}$  is a stable silyl anion: Gilman, H.; Smith, C. L. *J. Organomet. Chem.* **1968**, *14*, 91.

Further applications of (oligosilanyl)lithium species in organosilicon synthesis will be reported soon.<sup>21</sup>

**Acknowledgment.** We are grateful for the financial support of the Ministry of Education, Science and Culture of Japan (Specially Promoted Research No. 02102004 and the Grant-in-Aid for Scientific Research on Priority Area of Reactive Organometallics No. 05236102). M.N. thanks the Japan Society for Promotion of Science for the Fellowship for Japan Junior Scientists.

**Supplementary Material Available:** Text giving details of the X-ray experiment, figures giving additional views, and tables of atomic parameters, anisotropic temperature factors, and distances and angles for **1a** (8 pages). Ordering information is given on any current masthead page.

OM950035L

---

(21) Sekiguchi, A.; Nanjo, M.; Kabuto, C.; Sakurai, H. *J. Am. Chem. Soc.*, in press.

## Articles

**Living Polymerization of Ethylene Catalyzed by Diene Complexes of Niobium and Tantalum,  $M(\eta^5\text{-C}_5\text{Me}_5)(\eta^4\text{-diene})\text{X}_2$  and  $M(\eta^5\text{-C}_5\text{Me}_5)(\eta^4\text{-diene})_2$  ( $M = \text{Nb}$  and  $\text{Ta}$ ), in the Presence of Methylaluminoxane**

Kazushi Mashima,<sup>\*,†</sup> Shinjiro Fujikawa,<sup>‡</sup> Yoshiyuki Tanaka,<sup>‡</sup> Hisao Urata,<sup>§</sup>  
Toshiyuki Oshiki,<sup>§</sup> Eiji Tanaka,<sup>§</sup> and Akira Nakamura<sup>\*,‡,||</sup>

*Department of Chemistry, Faculty of Engineering Science, Osaka University, Toyonaka, Osaka 560, Japan, Department of Macromolecular Science, Faculty of Science, Osaka University, Toyonaka, Osaka 560, Japan, and Mitsubishi Chemical Corporation, Yokohama Research Center, Aoba-ku, Yokohama, Kanagawa 227, Japan*

Received September 9, 1994<sup>®</sup>

Catalyst systems of  $\text{MX}_2(\eta^5\text{-C}_5\text{R}_5)(\eta^4\text{-diene})$  ( $M = \text{Nb}$  and  $\text{Ta}$ ;  $R = \text{H}$  and  $\text{CH}_3$ ;  $X = \text{Cl}$  and  $\text{CH}_3$ ) in a combination of methylaluminoxane (MAO) are the precursors of the living polymerization of ethylene. Mono-diene complexes  $\text{MCl}_2(\eta^5\text{-C}_5\text{R}_5)(\eta^4\text{-diene})$  [ $M = \text{Nb}$ ,  $R = \text{CH}_3$  (**1**);  $M = \text{Ta}$ ,  $R = \text{CH}_3$  (**2**);  $M = \text{Ta}$ ,  $R = \text{H}$  (**3**);  $M = \text{Nb}$ ,  $R = \text{H}$  (**4**); diene = buta-1,3-diene (**a**), isoprene (**b**), 2,3-dimethylbuta-1,3-diene (**c**)] were prepared by the reaction of  $\text{MCl}_4(\eta^5\text{-C}_5\text{R}_5)$  with 2 equiv of the methylated allyl Grignard reagents in THF. Reaction of **2** and **3** with  $\text{MeMgI}$  afforded dimethyl complexes,  $\text{Ta}(\eta^5\text{-C}_5\text{R}_5)(\eta^4\text{-1,3-butadiene})\text{Me}_2$  [ $R = \text{CH}_3$  (**5**);  $R = \text{H}$  (**6**)], respectively. The polymerization of ethylene catalyzed by **1**/MAO, **2**/MAO, and **5**/MAO at low temperature ( $-20^\circ\text{C}$ ) gave polyethylene with very narrow polydispersities ( $M_w/M_n$  as low as 1.05). The niobium complexes are superior to the tantalum complexes in terms of the catalyst activity and the polydispersity. When the ligand was Cp instead of Cp\*, the catalyst activity of **3** for the polymerization of ethylene at  $-20^\circ\text{C}$  increased but the polydispersity of the obtained polyethylene broadened ( $M_w/M_n = 1.40$ ). Protolytic reaction of **5b** with 1 equiv of TfOH produces  $\text{TaCp}^*(\eta^4\text{-isoprene})(\text{CH}_3)(\text{OSO}_2\text{CF}_3)$  (**7**), whose structure is determined by single-crystal X-ray diffraction. Compound **7** crystallizes in the orthorhombic space group  $P2_12_12_1$  (No. 19) with  $a = 13.388(6) \text{ \AA}$ ,  $b = 16.196(4) \text{ \AA}$ ,  $c = 9.214(4) \text{ \AA}$ ,  $Z = 4$ ,  $V = 1998(1) \text{ \AA}^3$ ,  $D_{\text{calcd}} = 1.823 \text{ g/mL}$ , and  $R = 0.041$  based on 2191 reflections. The molecular structure shows that **7** is not a cationic complex. The tantalum atom is in a chiral center surrounded by four different ligands:  $\eta^1$ -triflate,  $\eta^5\text{-Cp}^*$ ,  $\eta^4$ -isoprene, and methyl. A cationic species derived from **5b** and  $\text{B}(\text{C}_6\text{F}_5)_3$  was detected by  $^1\text{H}$  NMR spectroscopy and found to be active in ethylene polymerization. A system of one of the bis-diene complexes of the type  $\text{M}(\eta^5\text{-C}_5\text{R}_5)(\eta^4\text{-2,3-dimethyl-1,3-butadiene})_2$  [ $M = \text{Nb}$ ,  $R = \text{H}$  (**8**);  $M = \text{Nb}$ ,  $R = \text{CH}_3$  (**9**);  $M = \text{Ta}$ ,  $R = \text{CH}_3$  (**10**)] in the presence of a large excess of MAO was also found to be an active catalyst for the polymerization of ethylene.

### Introduction

Polymerization of  $\alpha$ -olefins is one of the most important industrial processes. The catalyst system of group 4 metallocenes and methylaluminoxane (MAO) has been actively investigated in view of its homogeneous process and high ability to control the stereoregularity of polymerization.<sup>1–4</sup> Recent developments of organome-

tallic chemistry proved cationic 14-electron group 4 metallocenes to be catalytically active species without the cocatalyst MAO.<sup>5,6</sup> Moreover, isoelectronic neutral group 3 or lanthanide metallocene hydrides or alkyls have been found to be catalysts for olefin polymerization.<sup>7,8</sup> On the other hand, the catalyst system based on group 5 metallocene/MAO, e.g.,  $\text{TaCl}_2\text{Cp}_2$  and  $\text{NbCl}_2$ -

<sup>†</sup> Faculty of Engineering Science, Osaka University.

<sup>‡</sup> Faculty of Science, Osaka University.

<sup>§</sup> Mitsubishi Chemical Co.

<sup>||</sup> 1993–1994, Coordination Chemistry Laboratories, Institute for Molecular Science, Okazaki 444, Japan.

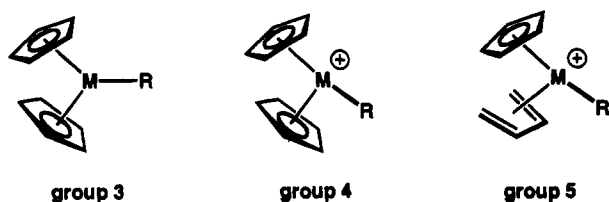
<sup>®</sup> Abstract published in *Advance ACS Abstracts*, April 15, 1995.

(1) Reviews: (a) Sinn, H.; Kaminsky, W. *Adv. Organomet. Chem.* **1980**, *18*, 99. (b) Pino, P. *Angew. Chem., Int. Ed. Engl.* **1980**, *19*, 857. (c) Quirk, R. P., Ed. *Transition Metal Catalyzed Polymerizations; Ziegler-Natta and Metathesis Polymerizations*; Cambridge University Press: Cambridge, **1988**. (d) Kaminsky, W.; Steiger, R. *Polyhedron* **1988**, *7*, 2375.

(2) Kaminsky, W.; Külper, K.; Brintzinger, H. H.; Wild, F. R. W. P. *Angew. Chem., Int. Ed. Engl.* **1985**, *24*, 507. Ewen, J. A.; Jones, R. L.; Razavi, A.; Ferrara, J. D. *J. Am. Chem. Soc.* **1988**, *110*, 6255.

(3) Recent examples of metallocene catalysis of group 4 metals: (a) Erker, G.; Nolte, R.; Aul, R.; Wilker, S.; Krüger, C.; Noe, R. *J. Am. Chem. Soc.* **1991**, *113*, 7594. (b) Mise, T.; Kageyama, A.; Miya, S.; Yamazaki, H. *Chem. Lett.* **1991**, 1525. (c) Resconi, L.; Piemontesi, F.; Franciscano, G.; Abis, L.; Fiorani, T. *J. Am. Chem. Soc.* **1992**, *114*, 1025. (d) Erker, G.; Temme, B. *J. Am. Chem. Soc.* **1992**, *114*, 4004. (e) Erker, G. *Pure Appl. Chem.* **1992**, *64*, 393. (f) Erker, G.; Fritze, C. *Angew. Chem., Int. Ed. Engl.* **1992**, *31*, 199. (g) Resconi, L.; Abis, L.; Franciscano, G. *Macromolecules* **1992**, *25*, 6818. (h) Razavi, A.; Atwood, J. L. *J. Am. Chem. Soc.* **1993**, *115*, 7529.

Chart 1



$\text{Cp}_2$ , was found to have no activity, although the Ziegler–Natta catalysts based on vanadium have been reported to be active for the polymerization of  $\alpha$ -olefins.<sup>9,10</sup> While studying diene complexes of niobium and tantalum, we noticed that the fragments of  $\text{MCp}(1,3\text{-diene})$  ( $M = \text{Nb}$  and  $\text{Ta}$ ) are isoelectronic to those of  $\text{MCp}_2$  ( $M = \text{Zr}$  and  $\text{Hf}$ ).<sup>11–15</sup> This prompted us to investigate the capability of the diene complexes of niobium and tantalum as catalyst precursors for olefin polymerization. To make the idea clear, 14-electron isoelectronic species for group 3, 4, and 5 metals are schematically shown in Chart 1. Here we report that the systems of  $\text{MX}_2(\eta^5\text{-C}_5\text{R}_5)(\eta^4\text{-diene})$  ( $M = \text{Nb}$  and  $\text{Ta}$ ;  $R = \text{H}$  and  $\text{CH}_3$ ;  $X = \text{Cl}$  and  $\text{CH}_3$ ,  $X_2 = 1,3\text{-diene}$ ) in the presence of an excess of MAO are new catalyst precursors for the living polymerization of ethylene and that the narrowest polydispersity ( $M_w/M_n$  as low as 1.05) for polyethylene has been accomplished.<sup>16</sup>

## Results and Discussion

**Preparation of Diene Complexes of Niobium and Tantalum.** First of all we prepared mono-diene complexes of niobium and tantalum,  $\text{MCl}_2(\eta^5\text{-C}_5\text{R}_5)(\eta^4\text{-diene})$  ( $M = \text{Nb}$  and  $\text{Ta}$ ;  $R = \text{H}$  and  $\text{Me}$ ; diene = buta-1,3-diene, isoprene, 2,3-dimethylbuta-1,3-diene), as catalyst precursors. These complexes have been previously synthesized by the reaction of  $\text{M}(\eta^5\text{-C}_5\text{R}_5)\text{Cl}_4$  with the corresponding 1,3-diene compounds of magnesium.<sup>11</sup> The methylated allyl Grignard reagents can be used for the preparation of mono-diene complexes 1–4.<sup>12</sup> Reaction of  $\text{NbCl}_4\text{Cp}^*$  in THF with 2 equiv of 2-methyl-2-butenyl Grignard in ether resulted in the formation of a deep green solution. Evaporation of all volatiles and the following extraction and recrystallization from hexane solution afforded  $\text{NbCl}_2\text{Cp}^*(\eta^4\text{-isoprene})$  (**1b**) as light green crystals in 35% yield. Two processes proposed to account for the formation of **1b** are invoked: (1) a hydrogen abstraction from a prenyl moiety of an initially formed bis-prenyl species, affording allyl-hydride–diene species and (2) the successive reductive elimination of hydride and allyl to give 2-methylbutenes. Formation of diene complexes from allyl and homoallyl complexes has been reported in the case of actinoids and early transition metals such as  $\text{Cp}^*_2\text{Th}(\eta^4\text{-buta-1,3-diene})$ ,<sup>17</sup>  $\text{Cp}^*\text{M}(\eta^4\text{-1,3-diene})(\text{allyl})$ ,<sup>18</sup>  $\text{Cp}^*\text{Zr}(\eta^4\text{-1,3-diene})(\text{CH}_2\text{PPh}_2)$ .<sup>19</sup> Similarly, **1a** and **1c** were prepared in 4% and 22% yields, respectively. Analogous deriva-

(4) Recent examples of ansa-type metallocene catalysis of group 4 metals: Collins, S.; Gauthier, W. J.; Holden, D. A.; Kuntz, B. A.; Taylor, N. J.; Ward, D. G. *Organometallics* **1991**, *10*, 2061. Chien, J. C. W.; Tsai, W.-M.; Rausch, M. D. *J. Am. Chem. Soc.* **1991**, *113*, 8570. Chien, J. C. W.; Llinas, G. H.; Rausch, M. D.; Lin, G.-Y.; Winter, H. H.; Atwood, J. L.; Bott, S. G. *J. Am. Chem. Soc.* **1991**, *113*, 8569. Lee, I.-M.; Gauthier, W. J.; Ball, J. M.; Iyengar, B.; Collins, S. *Organometallics* **1992**, *11*, 2115. Spaleck, W.; Antberg, M.; Rohrmann, J.; Winter, A.; Bachmann, B.; Kiprof, P.; Behm, J.; Herrmann, W. A. *Angew. Chem., Int. Ed. Engl.* **1992**, *31*, 1347. Llinas, G. H.; Dong, S.-H.; Mallin, D. T.; Rausch, M. D.; Lin, Y.-G.; Winter, H. H.; Chien, J. C. W. *Macromolecules* **1992**, *25*, 1242. Erker, G.; Wilker, S.; Krüger, C.; Goddard, R. J. *Am. Chem. Soc.* **1992**, *114*, 10983. Rieger, B. *J. Organomet. Chem.* **1992**, *428*, C33. Banu, G. N.; Newmark, R. A.; Cheng, H. N.; Llinas, G. H.; Chien, J. C. W. *Macromolecules* **1992**, *25*, 7400. Mengele, W.; Diebold, J.; Troll, C.; Röhl, W.; Brintzinger, H.-H. *Organometallics* **1993**, *12*, 1931. Giardello, M. A.; Eisen, M. S.; Stern, C. L.; Marks, T. J. *J. Am. Chem. Soc.* **1993**, *115*, 3326. Razavi, A.; Atwood, J. L. *J. Organomet. Chem.* **1993**, *459*, 117. Coates, G. W.; Waymouth, R. M. *J. Am. Chem. Soc.* **1993**, *115*, 91. Alt, H. G.; Milius, W.; Palackal, S. J. *J. Organomet. Chem.* **1994**, *472*, 113. Spaleck, W.; Küber, F.; Winter, A.; Rohrmann, J.; Bachmann, B.; Antberg, M.; Dolle, V.; Paulus, E. F. *Organometallics* **1994**, *13*, 954.

(5) Reviews: (a) Jordan, R. F.; Bradley, P. K.; LaPointe, R. E.; Taylor, D. F. *New J. Chem.* **1990**, *14*, 499. (b) Jordan, R. F. *Adv. Organomet. Chem.* **1991**, *32*, 325 and references cited therein.

(6) Recent examples of cationic metallocenes of group 4 metals: (a) Alelyunas, Y. W.; Jordan, R. F.; Echols, S. F.; Borkowsky, S. L.; Bradley, P. K. *Organometallics* **1991**, *10*, 1406. (b) Eisch, J. J.; Caldwell, K. R.; Werner, S.; Krüger, C. *Organometallics* **1991**, *10*, 3417. (c) Amorose, D. M.; Lee, R. A.; Petersen, J. L. *Organometallics* **1991**, *10*, 2191. (d) Yang, X.; Stern, C. L.; Marks, T. J. *J. Am. Chem. Soc.* **1991**, *113*, 3623. (e) Hlatky, G. G.; Eckman, R. R.; Turner, H. W. *Organometallics* **1992**, *11*, 1413. (f) Eshuis, J. J. W.; Tan, Y. Y.; Meetsma, A.; Teuben, J. H.; Renkema, J.; Evens, G. G. *Organometallics* **1992**, *11*, 3623. (g) Sishita, C.; Hathorn, R. M.; Marks, T. J. *J. Am. Chem. Soc.* **1992**, *114*, 1112. (h) Kesti, M. R.; Coates, G. W.; Waymouth, R. M. *J. Am. Chem. Soc.* **1992**, *114*, 9679. (i) Bochmann, M.; Lancaster, S. J. *J. Organomet. Chem.* **1992**, *434*, C1. (j) Crowther, D. J.; Borkowsky, S. L.; Swenson, D.; Meyer, T. Y.; Jordan, R. F. *Organometallics* **1993**, *12*, 2897. (k) Bochmann, M.; Lancaster, S. J. *Organometallics* **1993**, *12*, 633. (l) Chien, J. C. W.; Song, W.; Rausch, M. *Macromolecules* **1993**, *26*, 3239. (m) Eisch, J. J.; Pombrink, S. I.; Zheng, G.-X. *Organometallics* **1993**, *12*, 3856. (n) Bochmann, M.; Lancaster, S. J. *Makromol. Chem., Rapid Commun.* **1993**, *14*, 807. (o) Guo, Z.; Swenson, D. C.; Jordan, R. F. *Organometallics* **1994**, *13*, 1424. (p) Bochmann, M.; Lancaster, S. J.; Hursthouse, M. B.; Malik, K. M. A. *Organometallics* **1994**, *13*, 2235. (q) Yang, X.; Stern, C. L.; Marks, T. J. *J. Am. Chem. Soc.* **1994**, *116*, 10015 and references cited therein.

(7) (a) Watson, P. L. *J. Am. Chem. Soc.* **1982**, *104*, 337. (b) Watson, P. L.; Parshall, G. W. *Acc. Chem. Res.* **1985**, *18*, 51. (c) Jeske, G.; Lauke, H.; Mauermann, H.; Swepston, P. N.; Schumann, H.; Marks, T. J. *J. Am. Chem. Soc.* **1985**, *107*, 8091. (d) Burger, B. J.; Thompson, M. E.; Cotter, W. D.; Bercaw, J. E. *J. Am. Chem. Soc.* **1990**, *112*, 1566. (e) Coughlin, E. B.; Bercaw, J. E. *J. Am. Chem. Soc.* **1992**, *114*, 7606. (f) Yasuda, H.; Yamamoto, H.; Yokota, K.; Miyake, S.; Nakamura, A. *J. Am. Chem. Soc.* **1992**, *114*, 4908. (g) Hajela, S.; Bercaw, J. E. *Organometallics* **1994**, *13*, 1147.

(8) Lin, Z.; Le Marechal, J.-F.; Sabat, M.; Marks, T. J. *J. Am. Chem. Soc.* **1987**, *109*, 4127. Yang, X.; Stern, C. L.; Marks, T. J. *Organometallics* **1991**, *10*, 840.

(9) Doi, Y.; Tokuhiko, N.; Suzuki, S.; Soga, K. *Makromol. Chem., Rapid Commun.* **1987**, *8*, 285. Doi, Y.; Suzuki, S.; Soga, K. *Macromolecules* **1986**, *19*, 2896.

(10) Feher, F. J.; Walzer, J. F.; Blanski, R. L. *J. Am. Chem. Soc.* **1991**, *113*, 3618. Feher, F. J.; Blanski, R. L. *J. Am. Chem. Soc.* **1992**, *114*, 5886 and references cited therein.

(11) (a) Yasuda, H.; Tatsumi, K.; Okamoto, T.; Mashima, K.; Lee, K.; Nakamura, A.; Kai, Y.; Kanehisa, N.; Kasai, N. *J. Am. Chem. Soc.* **1985**, *107*, 2410. (b) Okamoto, T.; Yasuda, H.; Nakamura, A.; Kai, Y.; Kanehisa, N.; Kasai, N. *J. Am. Chem. Soc.* **1988**, *110*, 5008. (c) Okamoto, T.; Yasuda, H.; Nakamura, A.; Kai, Y.; Kanehisa, N.; Kasai, N. *Organometallics* **1988**, *7*, 2266.

(12) Mashima, K.; Yamanaka, Y.; Fujikawa, S.; Yasuda, H.; Nakamura, A. *J. Organomet. Chem.* **1992**, *428*, C5.

(13) Herberich, G. E.; Englert, U.; Linn, K.; Ross, P.; Runsink, J. *Chem. Ber.* **1991**, *124*, 975. Herberich, G. E.; Englert, U.; Roos, P. *Chem. Ber.* **1991**, *124*, 2663. Melendez, E.; Arif, A. M.; Rheingold, A. L.; Ernst, R. D. *J. Am. Chem. Soc.* **1988**, *110*, 8703.

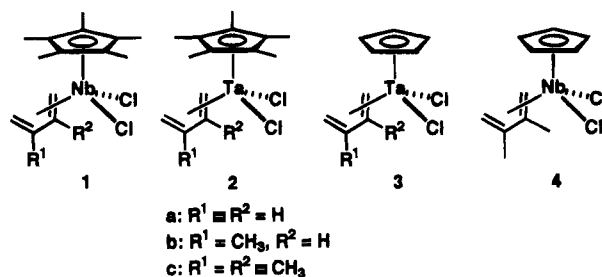
(14) Metallocene-like fragments: Siriwardane, U.; Zhang, H.; Hosmane, N. S. *J. Am. Chem. Soc.* **1990**, *112*, 9637. Williams, D. S.; Schofield, M. H.; Anhaus, J. T.; Schrock, R. R. *J. Am. Chem. Soc.* **1990**, *112*, 6728. Crowther, D. J.; Baenziger, N. C.; Jordan, R. F. *J. Am. Chem. Soc.* **1991**, *113*, 1455. Poole, A. D.; Gibson, V. C.; Clegg, W. J. *Chem. Soc., Chem. Commun.* **1992**, 237. Uhrhammer, R.; Crowther, D. J.; Olson, J. D.; Swenson, D. C.; Jordan, R. F. *Organometallics* **1992**, *11*, 3098. Dyer, P. W.; Gibson, V. C.; Howard, J. A. K.; Whittle, B.; Wilson, C. J. *Chem. Soc., Chem. Commun.* **1992**, 1666. Cockcroft, J. K.; Gibson, V. C.; Howard, J. A. K.; Poole, A. D.; Siemeling, U.; Wilson, C. J. *Chem. Soc., Chem. Commun.* **1992**, 1668. Siemeling, U.; Gibson, V. C. *J. Chem. Soc., Chem. Commun.* **1992**, 1670. Bazan, G. C.; Schaefer, W. P.; Bercaw, J. E. *Organometallics* **1993**, *12*, 2126. Schmidt, S.; Sundermeyer, J. *J. Organomet. Chem.* **1994**, *472*, 127.

(15) Gibson, V. C. *J. Chem. Soc., Dalton Trans.* **1994**, 1607.

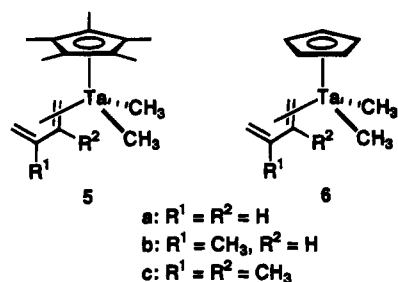
(16) (a) Mashima, K.; Fujikawa, S.; Nakamura, A. *J. Am. Chem. Soc.* **1993**, *115*, 10990. (b) Mashima, K.; Fujikawa, S.; Urata, H.; Tanaka, E.; Nakamura, A. *J. Chem. Soc., Chem. Commun.* **1994**, 1623.

(17) Smith, G. M.; Suzuki, H.; Sonnenberger, D. C.; Day, V. C.; Marks, T. J. *Organometallics* **1986**, *5*, 549.

tives 2–4 of niobium and tantalum were also prepared by the similar reactions.

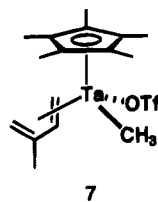


Dimethyl complexes of tantalum 5a–c, 6a, and 6c were prepared as follows. Treatment of 2a–c with 2 equiv of MeMgI afforded 5a–c in 32–50% yields as purple crystals. Complexes 6a and 6c were prepared by the successive reactions of TaCl<sub>4</sub>Cp with 2 equiv of the corresponding methylated allyl Grignard reagents and 2 equiv of MeMgI in THF.



The dimethyl complex of niobium derived from 1c was thermally unstable and decomposed gradually at room temperature. The formation of carbene complex in the course of decomposition was revealed by a trapped reaction with benzophenone, affording 1,1-diphenylethylene in modest yield (detected by <sup>1</sup>H NMR), which corresponds to the reactivity of Cp<sub>2</sub>TiMe<sub>2</sub>.<sup>20</sup>

The complex 5b reacts with 1 equiv of TfOH in toluene at ambient temperature to generate a compound TaCp\*( $\eta^4$ -isoprene)(OSO<sub>2</sub>CF<sub>3</sub>)Me (7) with elimination of



1 equiv of methane. Characterization of the product by NMR (<sup>1</sup>H and <sup>13</sup>C) spectroscopy indicated that simple substitution of one methyl group by the triflate ligand

(18) Zwijneburg, A.; van Oven, H. O.; Groenenboom, C. J.; de Liefde Meijer, H. J. *J. Organomet. Chem.* **1975**, *94*, 23. Blenkins, J.; de Liefde Meijer, H. J.; Teuben, J. H. *J. Organomet. Chem.* **1981**, *218*, 383. Alcock, N. W.; Toogood, G. E.; Wallbridge, M. G. H. *Acta Crystallogr.* **1984**, *C40*, 598. Booth, B. L.; Ofunne, G. C.; Stacey, C.; Tait, P. J. *J. Organomet. Chem.* **1986**, *315*, 143. Klapötke, T.; Köpf, H.; Gourik, P. *J. Chem. Soc., Dalton Trans.* **1988**, 1529. Sontag, C.; Berke, H.; Sarter, C.; Erker, G. *Helv. Chim. Acta* **1989**, *72*, 1676. Prins, T. J.; Hauger, B. E.; Vance, P. J.; Wemple, M. E.; Kort, D. A.; O'Brinen, J. P.; Silver, M. E.; Huffman, J. C. *Organometallics* **1991**, *10*, 979.

(19) Vance, P. J.; Prins, T. J.; Hauger, B. E.; Silver, M. E.; Wemple, M. E.; Pederson, L. M.; Kort, D. A.; Kannisto, M. R.; Geerligs, S. J.; Kelly, R. S.; McCandless, J. J.; Huffman, J. C.; Peters, D. G. *Organometallics* **1991**, *10*, 917.

(20) Petasis, N. A.; Fu, D.-K. *J. Am. Chem. Soc.* **1993**, *115*, 7208 and references cited therein.

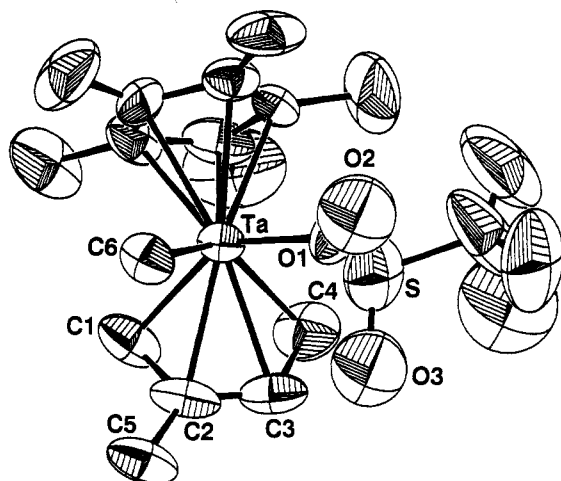


Figure 1. ORTEP drawing of (*R*)-7 with numbering scheme. Hydrogen atoms are omitted for clarity.

Table 1. Selected Bond Distances and Angles for (*R*)-7

Ta–O1	2.097(9)	Ta–C1	2.20(1)
Ta–C2	2.39(1)	Ta–C3	2.41(2)
Ta–C4	2.22(2)	Ta–C6	2.21(1)
C1–C2	1.44(2)	C2–C3	1.36(3)
C2–C5	1.53(2)	C3–C4	1.45(2)
Ta–CP <sup>a</sup>	2.105		
O1–Ta–C1	140.2(5)	O1–Ta–C4	83.2(5)
O1–Ta–C6	84.8(4)	C1–Ta–C4	75.8(6)
Ta–O1–S	144.1(6)	C1–Ta–C6	86.5(5)
C4–Ta–C6	134.6(6)		
CP–Ta–O1	108.9	CP–Ta–C6	111.3
CP–Ta–C1	110.5	CP–Ta–C4	114.1

<sup>a</sup> CP is the centroid of the cyclopentadienyl carbons.

had taken place. In the <sup>1</sup>H NMR spectrum of 7, one set of signals assignable to a monomethyl compound was observed, indicating that one of the two nonequivalent methyl groups had been selectively replaced by TfO anion. Crystals of 7 suitable for an X-ray diffraction study were grown from a concentrated hexane–toluene solution. The result of this analysis confirmed that the triflate coordinated to tantalum in the  $\eta^1$ -mode and at the less hindered site, resulting in the formation of a chiral molecule; one of the enantiomers (*R*)-7, is shown in Figure 1. Some pertinent bond distances and angles are listed in Table 1. In (*R*)-7, the isoprene ligand is coordinated to tantalum in a *supine* fashion.<sup>21</sup> The bonding parameters for the isoprene and the pentamethylcyclopentadienyl ligands are unexceptional. The Ta–C(6) distance of 2.21(1) Å lies in the range observed for the Ta–C(sp<sup>3</sup>) distances, TaCp\*( $\eta^2$ -benzyl)Me<sub>2</sub> [2.169(6) and 2.181(6) Å],<sup>22</sup> TaCp\*[(CH<sub>2</sub>)<sub>2</sub>P(Ph)<sub>2</sub>]Me<sub>2</sub> [2.230(16) and 2.198(17) Å],<sup>23</sup> and TaCp<sub>2</sub>(=CH<sub>2</sub>)Me [2.246(12) Å].<sup>24</sup>

When B(C<sub>6</sub>F<sub>5</sub>)<sub>3</sub> was added to 5b in toluene at room temperature, the purple color of the solution turned to yellow. This is the same color with the catalyst system

(21) The terms *supine* and *prone* have been already used in many of the papers on similar diene complexes. The definition has been given in ref 11.

(22) McLain, S. J.; Schrock, R. R.; Sharp, P. R.; Churchill, M. R.; Youngs, W. J. *J. Am. Chem. Soc.* **1979**, *101*, 263. Churchill, M. R.; Youngs, W. J. *Inorg. Chem.* **1979**, *18*, 1697.

(23) Gómez, M.; Jimenez, G.; Royo, P.; Pelinghelli, M. A.; Tiripicchio, A. *J. Organomet. Chem.* **1992**, *439*, 309.

(24) Guggenberger, J. L.; Schrock, R. R. *J. Am. Chem. Soc.* **1975**, *97*, 6578.

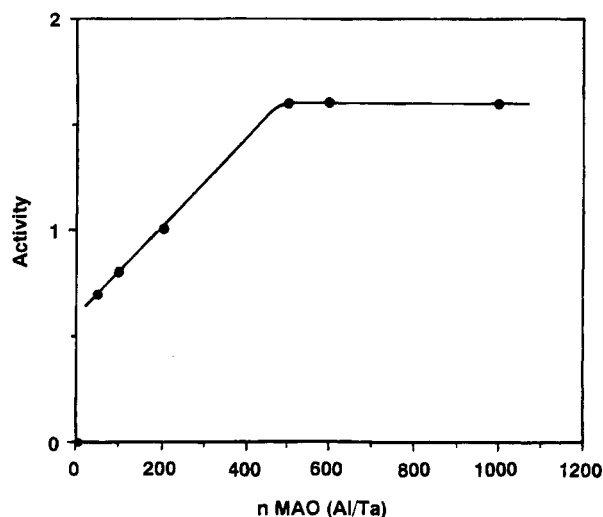
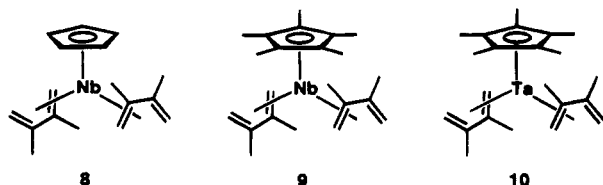


**Figure 2.** Plot of activity ( $\text{kg atm}^{-1} \text{h}^{-1} (\text{mol of Ta})^{-1}$ ) vs amount of methylaluminoxane (Al per Ta) for the polymerization of ethylene (atmospheric pressure) catalyzed by **2b** (1.44 mM) in toluene for a period of 6 h at 20 °C.

for ethylene polymerization (*vide infra*). Monitoring the reaction by  $^1\text{H}$  NMR in benzene- $d_6$  indicated new signals due to  $\text{Cp}^*$  and isoprene, and a broad singlet at  $\delta -0.56$  ppm was assignable to both methyl protons of cationic  $\text{Ta-CH}_3$  and anionic  $\text{B-CH}_3$ . Marks *et al.* reported NMR line broadening of the signals assignable to methyl groups of a cationic complex such as  $[\text{ZrCp}_2(\text{CH}_3)]\text{-}[(\text{CH}_3)\text{B}(\text{C}_6\text{F}_5)_3]$ .<sup>6d</sup> The broadening indicates an exchange of the methyl groups between zirconium and boron. These cationic complexes were too unstable thermally to be isolated. When they were generated in situ, they were found to be catalytically active for the polymerization of ethylene without MAO. The activity of the polymerization by using the catalyst system composed of **5a** and  $\text{B}(\text{C}_6\text{F}_5)_3$  was  $1.38 \text{ kg atm}^{-1} \text{h}^{-1} (\text{mol of Ta})^{-1}$ . In the presence of  $\text{AlEt}_3$ , this catalyst system showed activity of  $8.12 \text{ kg atm}^{-1} \text{h}^{-1} (\text{mol of Ta})^{-1}$ , which is in sharp contrast to the absence of any activity on the combination of **5a** and  $\text{AlEt}_3$ . Thus, the 14-electron cationic species should be responsible for the polymerization of ethylene (*vide infra*).

Bis(2,3-dimethylbuta-1,3-diene) complexes of niobium (**8** and **9**) and tantalum (**10**) were prepared by the reaction of  $\text{MCl}_4(\eta^5\text{-C}_5\text{R}_5)$  with 2 equiv of  $\text{Mg}(2,3\text{-dimethylbuta-1,3-diene)}$  in THF according to the literature.<sup>11a,b</sup>



**Polymerization of Ethylene.** Mono-diene complexes of niobium and tantalum,  $\text{MX}_2(\eta^5\text{-C}_5\text{R}_5)(\eta^4\text{-diene})$ , are active catalyst precursors for the polymerization of ethylene. At first we estimated how much MAO per each catalyst precursor is needed to achieve high activity for the polymerization. Figure 2 shows the plot of activity for the polymerization of ethylene by a catalyst system of complex **2b** in the presence of variable amounts of MAO at 20 °C. As more than 500 equiv of

**Table 2.** Polymerization of Ethylene Catalyzed by Tantalum-diene Complexes/MAO<sup>a</sup>

run no.	complex	temp (°C)	activity $\text{kg h}^{-1} (\text{mol of Ta})^{-1}$	$M_n/10^4$ <sup>c</sup>	$M_w/M_n$ <sup>c</sup>
1	<b>2a</b>	20	5.93	2.03	2.04
2	<b>2a</b>	-20	1.51	2.03	1.16
3	<b>2b</b>	20	1.90	1.15	1.63
4	<b>3a</b>	20	0.52		
5	<b>3a</b>	-20	7.07	8.18	1.40
6	<b>3a</b>	-40	4.29	4.29	1.32
7	<b>3a</b>	-60	0.94	1.68	1.11
8	<b>3b</b>	20	0.88		
9	<b>3c</b>	20	3.77		
10	<b>5a</b>	20	4.48	2.04	2.06
11	<b>5a</b>	-20	1.18	2.55	1.08
12	<b>5a</b>	-40	0.73	0.86	1.10
13	<b>5b</b>	20	1.61	1.23	1.65
14	<b>5c</b>	20	5.69	1.20	2.09
15	<b>6a</b>	20	0.37		
16	<b>6a</b>	-20	5.47	8.74	1.51

<sup>a</sup> Polymerization reactions were carried out in toluene ( $1.44 \times 10^{-3} \text{ M}$  of  $[\text{Ta}]$ ) in the presence of MAO (500 equiv) for 6 h. <sup>b</sup> Polymer has methanol-insoluble parts. <sup>c</sup> GPC analysis.

**Table 3.** Polymerization of Ethylene Catalyzed by Niobium-Diene Complexes/MAO<sup>a</sup>

run no.	complex	temp (°C)	activity ( $\text{kg h}^{-1} (\text{mol of Nb})^{-1}$ ) <sup>b</sup>	$M_n/10^4$ <sup>c</sup>	$M_w/M_n$ <sup>c</sup>
1	<b>1a</b>	20	38.70	8.29	1.30
4	<b>1a</b>	0	14.50	4.95	1.07
7	<b>1a</b>	-20	10.65	2.36	1.05
2	<b>1b</b>	20	19.22	3.95	1.16
5	<b>1b</b>	0	6.94	2.22	1.07
8	<b>1b</b>	-20	1.02	0.51	1.09
3	<b>1c</b>	20	35.23	10.54	1.18
6	<b>1c</b>	0	21.87	8.16	1.08
9	<b>1c</b>	-20	12.71	4.10	1.05
10	<b>4<sup>d</sup></b>	20	6.89		

<sup>a</sup> Polymerization reactions were carried out in toluene ( $1.44 \times 10^{-3} \text{ M}$  of  $[\text{Nb}]$ ) in the presence of MAO (500 equiv) for a period of 1 h. <sup>b</sup> Polymer has methanol-insoluble parts. <sup>c</sup> GPC analysis. <sup>d</sup> Reaction time, 3 h.

MAO does not increase the activity of the polymerization, we used 500 equiv of MAO for all the polymerization of ethylene. This amount of MAO is less than that generally used for conventional group 4 metallocene systems.

When mono-diene complexes of niobium and tantalum reacted with 500 equiv of MAO in toluene, the color of the solution turned to pale yellow, which corresponded to the color of the mixture of **5b** and  $\text{B}(\text{C}_6\text{F}_5)_3$  (*vide supra*). After the introduction of ethylene (atmospheric pressure), the resulting solution was stirred at ambient temperature. After the prescribed reaction time, an  $\text{HCl-MeOH}$  mixture was added to terminate the polymerization. The data of activity and GPC analysis for the obtained polyethylene are summarized in Tables 2 and 3.

As shown in Table 2, dichloro and dimethyl complexes having  $\text{TaCp}^*(\eta^4\text{-1,3-diene})$  moieties, **2** and **5**, have almost the same catalyst property, indicating that the same catalytically active species are formed. Methylaluminoxane acts as both the methylation reagent and the ligand exchange partner between aluminum and tantalum, resulting in the formation of cationic species.

The catalytic activity depends on the steric and electronic effects of ligands, *i.e.*, cyclopentadienyl and diene ligands. Plots of the catalyst activity by using tantalum-butadiene complexes bearing a Cp (**3a**) or a  $\text{Cp}^*$  (**5a**) ligand in the presence of MAO versus reaction



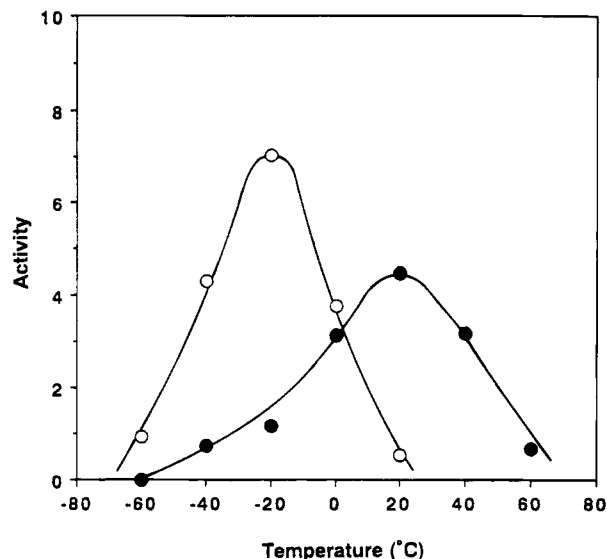


**Figure 3.** Plots for the catalyst activity ( $\text{kg atm}^{-1} \text{h}^{-1} (\text{mol of metal})^{-1}$ ) of the diene complexes of tantalum bearing Cp (**3a**) or Cp\* (**5a**) at variable temperature ( $^{\circ}\text{C}$ ) in toluene; ○ for **3a**, and ● for **5a**.

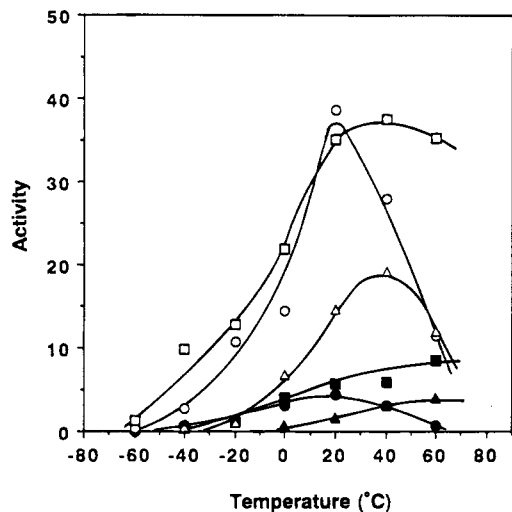


**Figure 4.** Plots for catalyst activity ( $\text{kg atm}^{-1} \text{h}^{-1} (\text{mol of metal})^{-1}$ ) of the diene complexes of niobium and tantalum bearing Cp\* at variable temperature ( $^{\circ}\text{C}$ ) in toluene; ○ for **1a**, Δ for **1b**, □ or **1c**, ● for **5a**, ▲ for **5b**, and ■ for **5c**.

temperature are shown in Figure 3. Activity of **3a** for the ethylene polymerization has a maximum of activity at lower temperature ( $-20^{\circ}\text{C}$ ) than that ( $20^{\circ}\text{C}$ ) of **5a**. This is attributed to the thermal instability of the cationic species derived from **3**. Methyl substitution on the coordinated diene also controls the catalyst activity for the polymerization of ethylene. Figure 4 indicates that both tantalum complexes **5a** and **5c** have comparable catalyst activity, while the isoprene complex **5b** is less active. For niobium complexes **1**, a similar tendency has been observed. Thus, the diene coordination is essential to have the same activity for the polymerization. The presence of one diene at the tantalum center of the catalytically active species was further supported by the observed fact that only very low activity for the ethylene polymerization was found in a system of  $\text{TaCl}_4\text{Cp}^*$  and MAO.

At  $-20^{\circ}\text{C}$ , the polymerization of ethylene catalyzed by butadiene complexes such as **1a**, **2a**, **3a**, **5a**, and **6a** in the presence of an excess of MAO gave polyethylene

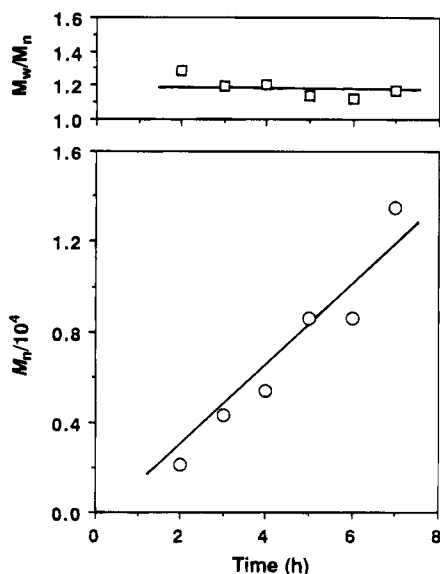


**Figure 5.** A time-conversion plot for the catalyst activity ( $\text{kg atm}^{-1} \text{h}^{-1} (\text{mol of Ta})^{-1}$ ) for the ethylene polymerization by using **5a** (1.44 mM in toluene) as catalyst precursor at  $-20^{\circ}\text{C}$ . The values  $M_w/M_n$  were determined by GPC analyses.

with narrow polydispersities ( $M_w/M_n = 1.05\text{--}1.51$ ), suggesting the character of the living polymerization. So far the narrow polydispersities for polyethylene have been reported for the following homogeneous catalysts:  $(\text{Cp}^*_2\text{LuH})_2$  ( $M_w/M_n = 1.37$ ),<sup>7c</sup>  $[\text{Cp}^*\text{Cr}(\text{thf})_2\text{Me}]^+$  ( $M_w/M_n = 1.63$ ),<sup>25a-c</sup>  $\text{Cp}^*\text{Cr}(\text{thf})(\text{CH}_2\text{Ph})_2$  ( $M_w/M_n = 1.41$ ),<sup>25d</sup>  $[\text{Cp}^*\text{Co}(\text{P}(\text{OMe})_3)(\text{CH}_2\text{CH}_2\text{Me})]^+$  ( $M_w/M_n = 1.17$ ),<sup>26</sup>  $[\text{C}_n\text{-Rh}(\text{Me})(\text{OH})(\text{OH}_2)]^+$  ( $C_n = 1,4,7\text{-trimethyl-1,4,7-triazacyclononane}$ ) ( $M_w/M_n = 1.6$ ).<sup>27</sup> Thus we plotted the time-molecular weight ( $M_n$ ) relationship for polyethylene catalyzed by **5a**/MAO to show an essentially linear relation, and the values of  $M_w/M_n$  for each polyethylene formed indicate rather narrow polydispersities and thus clearly the living nature of polymerization (Figure 5). In the conventional systems composed of  $\text{MCl}_2\text{Cp}_2$  ( $M = \text{Zr}$  and  $\text{Hf}$ ) and MAO, zirconocene is superior to hafnocene in the activity. In our case, the niobium complexes are superior to the corresponding tantalum complexes as the catalyst precursors, as shown in Figure 4. Moreover, the polyethylene obtained by catalysts **1a** and **1c** at  $-20^{\circ}\text{C}$  has the narrowest polydispersity ( $M_w/M_n = 1.05$ ) found to date.

We also found that bis-diene complexes **8–10** were the active catalyst precursors for the polymerization of ethylene (Table 4), whose activities were compared with those of the corresponding mono-diene complexes, indicating that mono-diene and bis-diene complexes gave the similar catalytically active species. We have already revealed the two different coordination modes (*supine* and *prone*) of diene ligands in **8–10**.<sup>11,21</sup> The diene coordinated in the *supine* fashion has more  $\sigma$ -character than the *prone* one,<sup>11c</sup> and the complex underwent

(25) (a) Thomas, B. J.; Theopold, K. H. *J. Am. Chem. Soc.* **1988**, *110*, 5902. (b) Theopold, K. H. *Acc. Chem. Res.* **1990**, *23*, 263. (c) Thomas, B. J.; Noh, S. K.; Sculte, G. K.; Sendlinger, S. C.; Theopold, K. H. *J. Am. Chem. Soc.* **1991**, *113*, 893. (d) Bhandari, G.; Kim, Y.; McFarland, J. M.; Rheingold, A. L.; Theopold, K. H. *Organometallics* **1995**, *14*, 738.

(26) Brookhart, M.; Grant, B.; Volpe, A. F., Jr. *Organometallics* **1992**, *11*, 3920.

(27) Wang, L.; Lu, R. S.; Bau, R.; Flood, T. C. *J. Am. Chem. Soc.* **1993**, *115*, 6999.



**Table 4. Polymerization of Ethylene Catalyzed by Bis-Diene Complexes/MAO<sup>a</sup>**

run no.	complex	time (h)	temp (°C)	activity (kg h <sup>-1</sup> (mol of metal) <sup>-1</sup> ) <sup>b</sup>	$M_n/10^4$ <sup>c</sup>	$M_w/M_n$ <sup>c</sup>
1	8	1	20	9.03	16.86	2.24
2	8	1	0	17.03	31.80	2.94
3	8	1	-20	7.55	27.14	4.13
4	9	1	20	24.65	3.07	1.18
5	9	1	0	21.95	2.82	1.13
6	9	1	-20	12.48	1.42	1.06
7	10	6	20	3.39	0.40	2.00
8	10	6	0	1.44	0.96	1.30
9	10	6	-20	0.26	0.54	1.09

<sup>a</sup> Polymerization reactions were carried out in toluene (1.44 × 10<sup>-3</sup> M of [metal]) in the presence of MAO (500 equiv). <sup>b</sup> Polymer was methanol-insoluble parts. <sup>c</sup> GPC analysis.

selective ligand exchange reaction at the *prone* diene ligand with the methyl group on aluminum of MAO to generate a 14-electron catalytically active species similar to that obtained from the mono-diene complexes and MAO. The catalyst efficiency can be estimated by using the  $M_n$  and  $M_w/M_n$  values of the polyethylene thus obtained. When **1c** and **9** were used for this purpose, complex **9** (catalyst efficiency 78–92%) is threefold as effective as complex **1c** (catalyst efficiency 27–34%). Thus, the bis-diene complexes are superior to the mono-diene complexes as the catalyst presursors for ethylene polymerization, which might be attributed to the stability of the diene aluminum species generated by the ligand exchange reaction.<sup>28</sup> In the catalyst systems obtained by combination of **10** with B(C<sub>6</sub>F<sub>5</sub>)<sub>3</sub>, with or without alkylaluminum such as AlEt<sub>3</sub>, the color of the solution is different from that found for mono-diene complex and no catalytic activity is observed. This might be attributed to the ability of aluminum to abstract the diene unit and to provide the required alkyl group.

## Conclusions

We have shown that the mono-diene complexes of niobium and tantalum can be easily prepared by the reaction of MCl<sub>4</sub>(η<sup>5</sup>-C<sub>5</sub>R<sub>5</sub>) with methylated allyl Grignard reagents. These mono-diene and bis-diene complexes of niobium and tantalum with a combination of MAO are active catalyst precursors for the polymerization of ethylene. At -20 °C, the living polymerization afforded the polyethylene with the narrowest polydispersity ( $M_w/M_n$  as low as 1.05) observed heretofore. The combination of dimethyl complex **5a** with B(C<sub>6</sub>F<sub>5</sub>)<sub>3</sub> afforded 14 electron cationic species which are also active for the polymerization of ethylene.

## Experimental Section

**General.** All manipulations involving air- and moisture-sensitive organometallic compounds were carried out by the use of the standard Schlenk technique under argon atmosphere. Toluene and benzene were purified by distillation under argon after drying over sodium benzophenone ketyl. THF was dried over sodium benzophenone ketyl and then dried over Na/K alloy. MAO (prepared by the method of the reaction of trimethylaluminum with hydrated CuSO<sub>4</sub>) was purchased as a toluene solution from Toso-Akzo Co. Ethylene was purchased from Seitetsu-Kagaku Co.

Nuclear magnetic resonance [<sup>1</sup>H (400 and 270 MHz), <sup>13</sup>C (100 and 68 MHz)] spectra were measured on JEOL JNM-GX400 and JEOL EX-270 spectrometers. Other spectra were recorded by the use of the following instruments: IR, Hitachi 295 and Horiba FT-300; low- and high-resolution mass spectra, JEOL D300 (70 eV); GPC analyses, Waters 150C equipped with a column TSK-GMH-6 (2 ft × 2) eluted with 1,2,4-trichlorobenzene at 135 °C. GPC columns were calibrated against commercially available polystyrene standards (Polymer Laboratories Ltd.) which ranged in molecular weight from 500 to 1.11 × 10<sup>6</sup> MW. Elemental analyses were performed at Elemental Analysis Center, Faculty of Science, Osaka University. Melting points of all complexes were measured in sealed tubes and were not corrected, and those of polyethylene were measured by DSC analysis (Seiko I & E SSC580DS).

**Preparation of NbCl<sub>4</sub>Cp\*(η<sup>4</sup>-isoprene) (1b).** To a solution of NbCl<sub>4</sub>Cp\* (0.62 g, 1.67 mmol) in THF (25 mL) cooled at -78 °C was added a solution of (2-methyl-2-butenyl)magnesium chloride (3.17 mmol) in ether (6.5 mL) via syringe. The reaction mixture was stirred for a period of 2 h at 20 °C. All volatiles were removed under reduced pressure. The resulting residue was extracted by hot hexane (60 mL). The combined extract was concentrated and then cooled at -20 °C overnight to afford **1b** as light green crystals in 35% yield. The <sup>1</sup>H NMR (C<sub>6</sub>D<sub>6</sub>) spectrum was superimposable to that of the literature.<sup>11b</sup> Similarly, complexes **1a** and **1c** were prepared in 4% and 22% yield, respectively.

**Preparation of TaCl<sub>2</sub>Cp\*(η<sup>4</sup>-butadiene) (2a).** To a solution of TaCl<sub>4</sub>Cp\* (0.786 g, 1.72 mmol) in THF (30 mL) cooled at -78 °C was added a solution of 2-butenylmagnesium chloride (3.46 mmol) in ether (4.7 mL) via syringe. The reaction mixture was stirred for 4 h at 20 °C. All volatiles were removed under reduced pressure. The resulting residue was extracted with hot hexane (50 mL) at 50 °C. The combined extract was concentrated and then cooled at -20 °C overnight to afford **2a** as purple crystals in 37% yield. The <sup>1</sup>H NMR (C<sub>6</sub>D<sub>6</sub>) spectrum was superimposable to that of the literature.<sup>11a</sup>

Similarly, complexes **2b** and **2c** were prepared in 72% and 45% yield, respectively.

**Preparation of TaCl<sub>2</sub>Cp(η<sup>4</sup>-isoprene) (3b).** To a solution of TaCl<sub>4</sub>Cp (1.41 g, 3.61 mmol) in THF (50 mL) and HMPA (1.0 mL) was added dropwise (2-methyl-2-butenyl)magnesium chloride (6.50 mmol) in ether (13.2 mL) at -78 °C. After the reaction mixture was stirred at -20 °C for 2 h, all volatiles were removed and the resulting residue was extracted with hot hexane (2 × 60 mL) at 50 °C. Recrystallization from a mixture of toluene and hexane at -20 °C afforded **3b** as blue-purple crystals in 18% yield. The <sup>1</sup>H NMR (C<sub>6</sub>D<sub>6</sub>) spectrum was superimposable to that of the literature.<sup>11a</sup>

Similarly, complexes **3a** and **3c** were prepared in 8% and 26% yield, respectively.

**Preparation of NbCl<sub>4</sub>Cp(η<sup>4</sup>-2,3-dimethylbutadiene) (4).** To a solution of NbCl<sub>4</sub>Cp (0.536 g, 1.79 mmol) in a suspension of THF (30 mL) was added dropwise (2,3-dimethyl-2-butenyl)magnesium chloride (3.40 mmol) in ether (3.8 mL) at -78 °C. Precipitated magnesium salts were removed by centrifugal separation. After the reaction mixture was stirred at 20 °C overnight, all volatiles were removed. The resulting residue was extracted with hexane (8 × 50 mL). Recrystallization from hexane at -20 °C afforded complex **4** as green crystals in 20% yield. The <sup>1</sup>H NMR (C<sub>6</sub>D<sub>6</sub>) spectrum was superimposable to that of the literature.<sup>11b</sup>

**Preparation of TaCp\*(η<sup>4</sup>-butadiene)Me<sub>2</sub> (5a).** To a solution of **2a** (0.535 g, 1.21 mmol) in THF (50 mL) cooled at -78 °C was added a solution of MeMgI (2.42 mmol) in ether (2.3 mL) via syringe. The reaction mixture was stirred for 17 h at 20 °C. Precipitated magnesium salts were removed by centrifugal separation, and then all volatiles were removed under reduced pressure. The resulting residue was extracted with hexane (50 mL, four times). The combined extract was concentrated and then cooled at -20 °C overnight to afford

**5a** as dark-violet crystals in 32% yield, mp 162–164 °C (decomp).  $^1\text{H NMR}$  ( $\text{C}_6\text{D}_6$ ):  $\delta$  -1.08 (m,  $\text{H}^1_{\text{anti}}$  and  $\text{H}^4_{\text{anti}}$ ), -0.43 (s, Ta-CH<sub>3</sub>), 0.09 (m,  $\text{H}^1_{\text{syn}}$  and  $\text{H}^4_{\text{syn}}$ ), 1.81 (s, C<sub>5</sub>Me<sub>5</sub>), 6.98 (m, H<sup>2</sup> and H<sup>3</sup>).  $^{13}\text{C NMR}$  ( $\text{C}_6\text{D}_6$ ):  $\delta$  11.3 (C<sub>5</sub>Me<sub>5</sub>,  $J_{\text{C-H}} = 127$  Hz), 40.0 (Ta-CH<sub>3</sub>,  $J_{\text{C-H}} = 117$  Hz), 56.5 (C<sup>1</sup> and C<sup>4</sup>,  $J_{\text{C-H}} = 147$  Hz), 117.0 (C<sup>2</sup> and C<sup>3</sup>,  $J_{\text{C-H}} = 165$  Hz), 119.2 (C<sub>5</sub>Me<sub>5</sub>). Anal. Calcd for C<sub>16</sub>H<sub>27</sub>Ta: C, 48.00; H, 6.80. Found: C, 47.49; H, 6.89. Mass spectrum for  $^{181}\text{Ta}$   $m/z = 400$  (M<sup>+</sup>).

Similarly, complexes **5b** and **5c** were prepared in 50% and 47% yield, respectively. **5b**: mp 87–91 °C (decomp).  $^1\text{H NMR}$  ( $\text{C}_6\text{D}_6$ ):  $\delta$  -1.24 (m,  $\text{H}^1_{\text{anti}}$ ), -0.60 and -0.49 (s, Ta-CH<sub>3</sub>), -1.03 (m,  $\text{H}^4_{\text{anti}}$ ), -0.35 (m,  $\text{H}^1_{\text{syn}}$ ), 0.17 (m,  $\text{H}^4_{\text{syn}}$ ), 1.83 (s, C<sub>5</sub>Me<sub>5</sub>), 2.66 (s, CH<sub>3</sub>), 6.60 (m, H<sup>3</sup>).  $^{13}\text{C NMR}$  ( $\text{C}_6\text{D}_6$ ):  $\delta$  11.3 (C<sub>5</sub>Me<sub>5</sub>,  $J_{\text{C-H}} = 127$  Hz), 23.3 (CH<sub>3</sub>,  $J_{\text{C-H}} = 126$  Hz), 37.4 and 46.9 (Ta-CH<sub>3</sub>,  $J_{\text{C-H}} = 118, 128$  Hz), 58.0 (C<sup>1</sup>,  $J_{\text{C-H}} = 139$  Hz), 59.7 (C<sup>4</sup>,  $J_{\text{C-H}} = 146$  Hz), 114.0 (C<sup>3</sup>,  $J_{\text{C-H}} = 159$  Hz), 118.9 (C<sub>5</sub>Me<sub>5</sub>), 122.3 (C<sup>2</sup>). Anal. Calcd for C<sub>17</sub>H<sub>29</sub>Ta: C, 49.28; H, 7.16. Found: C, 48.94; H, 7.03. Mass spectrum for  $^{181}\text{Ta}$   $m/z = 414$  (M<sup>+</sup>).

**5c**: mp 92–94 °C (decomp).  $^1\text{H NMR}$  ( $\text{C}_6\text{D}_6$ ):  $\delta$  -1.08 (m,  $\text{H}^1_{\text{anti}}$  and  $\text{H}^4_{\text{anti}}$ ), -0.68 (s, Ta-CH<sub>3</sub>), -0.22 (m,  $\text{H}^1_{\text{syn}}$  and  $\text{H}^4_{\text{syn}}$ ), 1.84 (s, C<sub>5</sub>Me<sub>5</sub>), 2.51 (s, CH<sub>3</sub>).  $^{13}\text{C NMR}$  ( $\text{C}_6\text{D}_6$ ):  $\delta$  11.3 (C<sub>5</sub>Me<sub>5</sub>,  $J_{\text{C-H}} = 127$  Hz), 20.3 (CH<sub>3</sub>,  $J_{\text{C-H}} = 126$  Hz), 44.3 (Ta-CH<sub>3</sub>,  $J_{\text{C-H}} = 118$  Hz), 63.7 (C<sup>1</sup> and C<sup>4</sup>,  $J_{\text{C-H}} = 145$  Hz), 116.9 (C<sup>2</sup> and C<sup>3</sup>), 118.5 (C<sub>5</sub>Me<sub>5</sub>). Anal. Calcd for C<sub>18</sub>H<sub>31</sub>Ta: C, 50.47; H, 7.29. Found: C, 50.34; H, 7.36. Mass spectrum for  $^{181}\text{Ta}$   $m/z = 428$  (M<sup>+</sup>).

**Preparation of TaCp( $\eta^4$ -butadiene)Me<sub>2</sub> (6a).** To a solution of TaCl<sub>4</sub>Cp (2.07 g, 5.33 mmol) in a mixture of THF (60 mL) and HMPA (0.79 mL) was added Mg(butadiene)(thf)<sub>2</sub> (0.82 g, 5.33 mmol) suspended in THF (4.35 mL) at -78 °C. After the reaction mixture was stirred at -20 °C for 2 h, 2 equiv of MeMgI was added and then the mixture was stirred at room temperature overnight. All volatiles were removed, and the resulting residue was extracted with hexane (4 × 60 mL). Recrystallization from a mixture of toluene and hexane at -20 °C afforded complex **6a** as blue-purple crystals in 33% yield, mp 146–148 °C (decomp).  $^1\text{H NMR}$  ( $\text{C}_6\text{D}_6$ ):  $\delta$  -0.80 (m,  $\text{H}^1_{\text{anti}}$  and  $\text{H}^4_{\text{anti}}$ ), -0.25 (s, Ta-CH<sub>3</sub>), 0.25 (m,  $\text{H}^1_{\text{syn}}$  and  $\text{H}^4_{\text{syn}}$ ), 5.95 (s, Cp), 6.92 (m, H<sup>2</sup> and H<sup>3</sup>).  $^{13}\text{C NMR}$  ( $\text{C}_6\text{D}_6$ ):  $\delta$  38.0 (Ta-CH<sub>3</sub>,  $J_{\text{C-H}} = 119$  Hz), 51.9 (C<sup>1</sup>,  $J_{\text{C-H}} = 148$  Hz), 110.6 (C<sub>5</sub>H<sub>5</sub>,  $J_{\text{C-H}} = 176$  Hz), 116.8 (C<sup>2</sup>,  $J_{\text{C-H}} = 167$  Hz). Mass spectrum for  $^{181}\text{Ta}$   $m/z = 330$  (M<sup>+</sup>).

**Preparation of TaCp( $\eta^4$ -2,3-dimethylbutadiene)Me<sub>2</sub> (6c).** To a solution of TaCl<sub>4</sub>Cp (1.20 g, 3.09 mmol) in a mixture of THF (50 mL) and HMPA (0.46 mL, 3.09 mmol) was added 2,3-dimethyl-2-butenylmagnesium chloride (5.69 mmol) in ether (6.7 mL) via syringe at -78 °C. After the reaction mixture was stirred at 20 °C for 4 h, the reaction solution was cooled at -78 °C, 2 equiv of MeMgI was added, and then the mixture was stirred at room temperature overnight. All volatiles were removed, and the resulting residue was extracted with hexane (4 × 60 mL). Recrystallization from hexane at -20 °C afforded complex **6c** as dark-violet crystals in 7% yield, mp 84–85 °C (decomp).  $^1\text{H NMR}$  ( $\text{C}_6\text{D}_6$ ):  $\delta$  -0.76 (m,  $\text{H}^1_{\text{anti}}$  and  $\text{H}^4_{\text{anti}}$ ,  $J_{\text{gem}} = 5.3$  Hz), -0.52 (s, Ta-CH<sub>3</sub>), -0.08 (m,  $\text{H}^1_{\text{syn}}$  and  $\text{H}^4_{\text{syn}}$ ), 6.92 (m, CH<sub>3</sub>), 5.97 (s, Cp).  $^{13}\text{C NMR}$  ( $\text{C}_6\text{D}_6$ ):  $\delta$  20.1 (CH<sub>3</sub>,  $J_{\text{C-H}} = 118$  Hz), 42.4 (Ta-CH<sub>3</sub>,  $J_{\text{C-H}} = 125$  Hz), 58.6 (C<sup>1</sup>,  $J_{\text{C-H}} = 144$  Hz), 110.1 (C<sub>5</sub>H<sub>5</sub>,  $J_{\text{C-H}} = 176$  Hz), 117.2 (C<sup>2</sup>). Mass spectrum for  $^{181}\text{Ta}$   $m/z = 358$  (M<sup>+</sup>).

**Preparation of TaCp\*( $\eta^4$ -isoprene)(OSO<sub>2</sub>CF<sub>3</sub>)Me (7).** To a solution of **2b** (0.572 g, 1.38 mmol) in toluene (40 mL) cooled at -78 °C was added a solution of CF<sub>3</sub>SO<sub>3</sub>H (1.38 mmol) in toluene (5.1 mL) via syringe. The reaction mixture was stirred for 1 h at 20 °C. All volatiles were removed under reduced pressure. Recrystallization from a mixture of hexane and toluene at -20 °C afforded complex **11** as red-violet crystals in 39% yield, mp 134–136 °C (decomp).  $^1\text{H NMR}$  (THF-*d*<sub>8</sub>):  $\delta$  -0.77 (d,  $\text{H}^1_{\text{anti}}$ ,  $J_{\text{gem}} = 8.7$  Hz), -0.48 (d,  $\text{H}^1_{\text{syn}}$ ), -0.12 (t,  $\text{H}^4_{\text{anti}}$ ,  $J_{\text{gem}} = 7.7$  Hz), 0.08 (s, Ta-CH<sub>3</sub>), 1.14 (t,  $\text{H}^4_{\text{syn}}$ ,  $J_{\text{cis}} = 8.0$  Hz), 2.12 (s, C<sub>5</sub>Me<sub>5</sub>), 2.45 (s, CH<sub>3</sub>), 6.33 (t, H<sup>3</sup>,  $J_{\text{trans}} = 7.5$  Hz).  $^{13}\text{C NMR}$  (THF-*d*<sub>8</sub>):  $\delta$  11.3 (C<sub>5</sub>Me<sub>5</sub>,  $J_{\text{C-H}} = 128$  Hz), 23.7 (CH<sub>3</sub>,  $J_{\text{C-H}} = 128$  Hz), 47.4 (Ta-CH<sub>3</sub>,  $J_{\text{C-H}} = 120$  Hz), 59.9

Table 5. Crystallographic Data for 7

formula	C <sub>17</sub> H <sub>26</sub> O <sub>3</sub> F <sub>3</sub> STa
fw	548.39
cryst syst	orthorhombic
space group	P2 <sub>1</sub> 2 <sub>1</sub> 2 <sub>1</sub>
<i>a</i> , Å	13.388(6)
<i>b</i> , Å	16.196(4)
<i>c</i> , Å	9.214(4)
<i>Z</i>	4
<i>V</i> , Å <sup>3</sup>	1998(1)
<i>d</i> <sub>calcd</sub> , g cm <sup>-3</sup>	1.823
cryst size, mm <sup>3</sup>	0.6 × 0.2 × 0.2
abs coeff, cm <sup>-1</sup>	55.74
scan mode	$\omega$ -2 $\theta$
temp, °C	23
scan speed, deg min <sup>-1</sup>	8
scan width, deg	1.15 + 0.35 tan $\theta$
2 $\theta$ <sub>max</sub> , deg	60.1
no. of data collected	3308
no. of unique data ( $I > 3\sigma(I)$ )	2191
no. of variables	211
<i>R</i>	0.041
<i>R</i> <sub>w</sub>	0.044
GO <sub>F</sub>	1.51
$\Delta$ , e Å <sup>-3</sup>	1.12 (max), -0.99 (min)

(C<sup>4</sup>,  $J_{\text{C-H}} = 148$  Hz), 70.6 (C<sup>1</sup>,  $J_{\text{C-H}} = 146$  Hz), 113.8 (C<sup>3</sup>,  $J_{\text{C-H}} = 161$  Hz), 119.6 (CF<sub>3</sub>,  $J_{\text{C-F}} = 321$  Hz), 123.8 (C<sub>5</sub>Me<sub>5</sub>), 133.0 (C<sup>2</sup>). Anal. Calcd for C<sub>17</sub>H<sub>26</sub>F<sub>3</sub>O<sub>3</sub>STa: C, 37.23; H, 4.78. Found: C, 36.25; H, 4.70. Mass spectrum for  $^{181}\text{Ta}$   $m/z = 548$  (M<sup>+</sup>).

**X-ray Structure Determination of 7.** The X-ray study was carried out by using a Rigaku AFC-5R automatic diffractometer. Intensity data were obtained by  $\omega$ -2 $\theta$  scans with Mo K $\alpha$  radiation ( $\lambda = 0.71069$ ). Lattice parameters were obtained by a least-squares analysis of 25 reflections scattered in reciprocal space, obtained from the automatic centering routine. Intensities of three standard reflections were monitored after every 100 data points. Background was measured before and after each peak. The solution and refinement of the structure were carried out on a VAX computer using the TEXSAN package that includes subroutines for direct method (Patterson), difference Fourier maps, full-matrix least-squares refinements, and distance and angle calculations. The data were corrected for Lorentz and polarization effects. Absorption correction was made by the standard method using the azimuthal scan of a reflection near 90°.

The solution and refinement of the structure were performed with the TEXAN program package. The position of tantalum atom was determined by a Patterson map. Subsequent least-squares refinements (full-matrix) and difference Fourier maps revealed the remaining non-hydrogen atoms. Hydrogen atoms bonded to the carbon atoms were placed in calculated positions and were not refined. All non-hydrogen atoms were refined anisotropically. The crystal data and data collection parameters are summarized in Table 5. Final positional parameters of non-hydrogen atoms are given in Table 6.

**Polymerization of Ethylene Catalyzed by Mono-Diene Complexes. General Procedure.** To a solution of **2b** (12.1 mg,  $2.66 \times 10^{-5}$  mol) in toluene (18.5 mL) was added MAO (500 equiv) via syringe at -78 °C. The color of the solution immediately changed from dark violet to yellow. After the catalyst mixture was stirred at 20 °C for 10 min, ethylene (atmospheric pressure) was introduced. After 6 h at 20 °C, the polymerization of ethylene was quenched by the addition of HCl-MeOH, and the activity was found to be 1.90 kg h<sup>-1</sup> (mol of Ta)<sup>-1</sup>.

**Polymerization of Ethylene Catalyzed by TaCl<sub>4</sub>Cp\* in the Presence of MAO.** To TaCl<sub>4</sub>Cp\* (12.2 mg,  $2.66 \times 10^{-5}$  mol) suspended in toluene (18.5 mL) was added MAO (500 equiv) via syringe. After the catalyst mixture was stirred at room temperature for 10 min, ethylene (atmospheric pressure) was introduced. After 6 h at room temperature, the polymerization was quenched by the addition of HCl-MeOH, and the activity was found to be  $7.89 \times 10^{-2}$  kg h<sup>-1</sup> (mol of Ta)<sup>-1</sup>.

Table 6. Atomic Positional Parameters for 7

atom	<i>x</i>	<i>y</i>	<i>z</i>	<i>B</i> <sub>eq</sub>
Ta	0.07917(4)	0.15042(3)	0.84829(5)	3.45(2)
S	-0.0728(4)	0.0447(4)	1.0811(5)	8.2(3)
F1	-0.224(1)	-0.047(1)	1.126(2)	13(1)
F2	-0.159(2)	-0.064(1)	0.926(2)	19(2)
F3	-0.232(2)	0.055(1)	0.960(2)	19.3(7)
O1	-0.0245(6)	0.0694(6)	0.942(1)	4.8(4)
O2	-0.022(1)	-0.026(1)	1.152(2)	15.6(6)
O3	-0.108(1)	0.110(1)	1.167(2)	13.9(5)
C1	0.124(1)	0.2808(8)	0.857(2)	5.7(7)
C2	0.047(1)	0.2798(8)	0.965(2)	5.8(8)
C3	-0.044(1)	0.248(1)	0.931(2)	5.8(8)
C4	-0.057(1)	0.219(1)	0.783(2)	7(1)
C5	0.072(2)	0.3101(9)	1.118(2)	6.7(8)
C6	0.162(1)	0.1351(8)	1.054(2)	4.8(7)
C7	-0.173(3)	-0.021(2)	1.020(3)	13(2)
C11	0.223(1)	0.082(1)	0.748(2)	5.1(7)
C12	0.142(1)	0.0255(8)	0.739(2)	4.8(7)
C13	0.076(1)	0.0596(8)	0.642(2)	5.0(6)
C14	0.113(1)	0.133(1)	0.594(1)	5.8(8)
C15	0.204(1)	0.1486(9)	0.656(2)	5.5(6)
C16	0.318(1)	0.060(2)	0.841(2)	10(1)
C17	0.134(1)	-0.0563(9)	0.814(2)	8(1)
C18	-0.020(2)	0.023(2)	0.588(3)	13(2)
C19	0.075(3)	0.188(2)	0.477(2)	13(2)
C20	0.280(2)	0.216(1)	0.629(2)	11(1)

**Polymerization of Ethylene by Bis-Diene Complexes.**

**General Procedure.** To a solution of NbCp\*(2,3-dimethyl-1,3-butadiene)<sub>2</sub> (**9**) (5.2 mg, 1.33 × 10<sup>-6</sup> mol) in toluene (9.3 mL) was added MAO (500 equiv) via syringe at -78 °C. The color of the solution immediately changed from brownish yellow to yellow. After the catalyst mixture was stirred at 20 °C for 10 min, ethylene (atmospheric pressure) was introduced. After 1 h at 20 °C, polymerization was quenched by the addition of HCl-MeOH, and the activity was found to be 24.65 kg h<sup>-1</sup> (mol of Nb)<sup>-1</sup>. Gel permeation chromatography (GPC) analysis of this sample showed that the molecular weight (*M<sub>n</sub>*) and the molecular weight distribution (*M<sub>w</sub>*/*M<sub>n</sub>*) were 3.07 × 10<sup>4</sup> and 1.18, respectively.

**Attempted Preparation of a Cationic Tantalum Complex.** The reaction of **5b** with B(C<sub>6</sub>F<sub>5</sub>)<sub>3</sub> at room temperature resulted in the formation of a yellow solution of cationic organometallic species, which was characterized only by <sup>1</sup>H NMR since the cationic complexes were too unstable thermally to be isolated. <sup>1</sup>H NMR (C<sub>6</sub>D<sub>6</sub>): δ -1.27 (1H, d, H<sup>1</sup><sub>anti</sub>, *J* = 6.9 Hz), -1.06 (1H, t, H<sup>4</sup><sub>anti</sub>, *J* = 7.1 Hz), -0.56 (6H, brs, CH<sub>3</sub>), -0.08 (1H, d, H<sup>1</sup><sub>syn</sub>), 0.39 (1H, t, H<sup>4</sup><sub>syn</sub>), 1.79 (15H, s, C<sub>5</sub>Me<sub>5</sub>), 2.61 (3H, s, CH<sub>3</sub>), 6.52 (1H, t, H<sup>3</sup>).

**Polymerization of Ethylene Catalyzed by in Situ Mixture of 5a and B(C<sub>6</sub>F<sub>5</sub>)<sub>3</sub>.** To a solution of **5a** (7.8 mg, 0.019 mmol) in toluene (7.4 mL) was added dropwise a solution of B(C<sub>6</sub>F<sub>5</sub>)<sub>3</sub> (9.7 mg, 0.019 mmol) in toluene via syringe at 20 °C, and then atmospheric pressure of ethylene was introduced. After 1 h, polymerization was quenched by the addition of 1 N HCl and the activity was found to be 1.38 kg h<sup>-1</sup> (mol of Ta)<sup>-1</sup>.

Similarly, polymerization of ethylene was carried out by a system of **5a** (3.7 mg, 0.0092 mmol) with B(C<sub>6</sub>F<sub>5</sub>)<sub>3</sub> (1 equiv, 4.7 mg, 0.0092 mmol) and AlEt<sub>3</sub> (10 equiv, 10.5 mg, 0.092 mmol) to show an activity of 8.12 kg h<sup>-1</sup> (mol of Ta)<sup>-1</sup>, while a system of **5a** (7.2 mg, 0.018 mmol) and AlEt<sub>3</sub> (10 equiv, 20.6 mg, 0.18 mmol) had no activity at all.

**Acknowledgment.** The author (AN) is grateful for financial support from the Ministry of Education, Science and Culture of Japan (Specially Promoted Research No. 06101004).

**Supplementary Material Available:** GPC analyses of polyethylene for Figure 4 and tables of X-ray data for **7** (10 pages). This material is contained in many libraries on microfiche, immediately follows this article in the microfilm version of the journal, and can be ordered from the ACS: see any current masthead page for ordering information.

OM9407114

# Synthesis and Characterization of ( $\beta$ -Diketonate)(7-*tert*-butoxynorbornadiene)copper(I) Compounds, a Series of New Copper CVD Precursors

Kai-Ming Chi,\* Hung-Chang Hou, and Pao-Ts'un Hung

Department of Chemistry, National Chung Cheng University, Ming-Hsiung, Chia-Yi, Taiwan, Republic of China

Shie-Ming Peng\* and Gene-Hsiang Lee

Department of Chemistry, National Taiwan University, Taipei, Taiwan, Republic of China

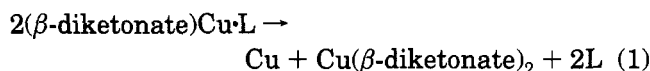
Received November 21, 1994<sup>®</sup>

Organocopper compounds of the general formula ( $\beta$ -diketonate)Cu(7-*t*-BuO-NBD) where 7-*t*-BuO-NBD = 7-*tert*-butoxynorbornadiene and  $\beta$ -diketonate = 1,1,1,5,5,5-hexafluoro-2,4-pentanedionate (1), 1,1,1-trifluoro-2,4-pentanedionate (2), 2,4-pentanedionate (3), 4,4,4-trifluoro-1-(2-thienyl)-1,3-butanedionate (4), 4,4,4-trifluoro-1-phenyl-1,3-butanedionate (5), and 2,2-dimethyl-6,6,7,7,8,8,8-heptafluoro-3,5-octanedionate (6) were prepared by reaction of CuCl with Na( $\beta$ -diketonate) in the presence of 7-*t*-BuO-NBD. All compounds were characterized by elemental analyses and <sup>1</sup>H, <sup>13</sup>C, and <sup>19</sup>F NMR, IR, and mass spectra. Single-crystal structures of compounds 1, 4, and 5 were determined by X-ray diffraction analyses that showed mononuclear copper species with coordination of a chelating  $\beta$ -diketonate ligand through two oxygen atoms and the 7-*t*-BuO-NBD through one C=C double bond and an oxygen atom in the solid state. Variable-temperature <sup>1</sup>H NMR spectral data of compound 2 in the solution are consistent with this structural nature. Hot-wall chemical vapor deposition experiments revealed that compound 1 is suitable as a precursor to deposit copper films in the temperature range 200–260 °C. Crystallographic data for compounds 1, 4, and 5: (hfac)Cu(7-*t*-BuO-NBD) (1) crystallizes in monoclinic system, space group  $P2_1/c$ ,  $a = 8.923(1)$  Å,  $b = 19.558(4)$  Å,  $c = 10.495(3)$  Å,  $\beta = 90.45(2)^\circ$ ,  $V = 1831.3(7)$  Å<sup>3</sup>,  $Z = 4$ . (Ttfac)-Cu(7-*t*-BuO-NBD) (4) crystallizes in monoclinic system, space group  $P2_1/n$ ,  $a = 10.689(6)$  Å,  $b = 9.712(4)$  Å,  $c = 19.323(4)$  Å,  $\beta = 97.22(3)^\circ$ ,  $V = 1990.2(15)$  Å<sup>3</sup>,  $Z = 4$ . (Btfac)Cu(7-*t*-BuO-NBD) (5) crystallizes in triclinic system, space group  $P\bar{1}$ ,  $a = 9.617(1)$  Å,  $b = 9.894(4)$  Å,  $c = 11.322(2)$  Å,  $\alpha = 104.57(2)^\circ$ ,  $\beta = 95.50(1)^\circ$ ,  $\gamma = 104.76(3)^\circ$ ,  $V = 993.4(5)$  Å<sup>3</sup>,  $Z = 2$ .

## Introduction

Metal-organic chemical vapor deposition (MOCVD) of metals has a large number of important applications in the electronics and coatings industries.<sup>1</sup> For instance, CVD of aluminum<sup>2</sup> and tungsten<sup>3</sup> thin films are commonly used to deposit interconnect layers in microelectronic devices. The use of copper(I) compounds as precursors of chemical vapor deposition of copper attracts much research interest as the result of potential applications in the microelectronic industry.<sup>4–8</sup> Lewis base-stabilized ( $\beta$ -diketonate)copper(I) complexes receive the most attention because they deposit highly

pure copper films via the disproportionation reaction of eq 1. Although such complexes have been known for



about 30 years,<sup>9</sup> relatively little structural information is available.<sup>8b,10–12</sup> Therefore, it is valuable to systematically investigate the structural properties of these compounds to provide insight into their volatility,

(4) ( $\eta^5\text{-C}_5\text{H}_5$ )Cu(PR<sub>3</sub>) as MOCVD precursors: (a) Dupuy, C. G.; Beach, D. B.; Hurst, J. E. Jr.; Jasinski, J. M. *Chem. Mater.* **1989**, *1*, 16. (b) Beach, D. B.; LeGroues, F. A.; Hu, C.-K. *Chem. Mater.* **1990**, *2*, 216. (c) Hampden-Smith, M. J.; Kotas, T. T.; Paffett, M.; Farr, J. D.; Shin, H. K. *Chem. Mater.* **1990**, *2*, 636.

(5) (*t*-BuOCu)<sub>4</sub> as MOCVD precursor: (a) Jeffries, P. M.; Girolami, G. S. *Chem. Mater.* **1989**, *1*, 8. (b) Jeffries, P. M.; Dubois, L. H.; Girolami, G. S. *Chem. Mater.* **1992**, *4*, 1169.

(6) ( $\beta$ -diketonate)Cu(PR<sub>3</sub>) as MOCVD precursors: (a) Shin, H.-K.; Chi, K.-M.; Hampden-Smith, M. J.; Kotas, T. T.; Farr, J. D.; Paffett, M. *Adv. Mater.* **1991**, *3*, 246. (b) Shin, H. K.; Chi, K. M.; Hampden-Smith, M. J.; Kotas, T. T.; Farr, J. D.; Paffett, M. *Chem. Mater.* **1992**, *4*, 788.

(7) ( $\beta$ -diketonate)Cu(alkene) as MOCVD precursors: (a) Reynolds, S. K.; Smart, C. J.; Baran, E. F.; Baum, T. H.; Larson, C. E.; Brock, P. *J. Appl. Phys. Lett.* **1991**, *59*, 2332. (b) Jain, A.; Chi, K.-M.; Hampden-Smith, M. J.; Kotas, T. T.; Paffett, M.; Farr, J. D. *J. Mater. Res.* **1992**, *7*, 261. (c) Norman, J. A. T.; Muratore, B. A.; Dyer, P. N.; Robert, D. A.; Hochberg, A. K. *J. Phys. (Paris)* **1991**, *IV*, C2/271. (d) Jain, A.; Chi, K.-M.; Hampden-Smith, M. J.; Kotas, T. T. *J. Electrochem. Soc.* **1993**, *140*, 1434.

\* Author to whom correspondence should be addressed.

<sup>®</sup> Abstract published in *Advance ACS Abstracts*, April 15, 1995.

(1) (a) Sherman, A. *Chemical Vapor Deposition for Microelectronics: Principles, Technology, and Applications*; Noyes Publications: Park Ridge, NJ, 1987. (b) Hess, D. W.; Jensen, K. F. *Microelectronics Processing, Chemical Engineering Aspects*; American Chemical Society: Washington, D. C., 1989.

(2) (a) Broadbent, E. K.; Ramiller, C. L. *J. Electrochem. Soc.* **1984**, *131*, 1427. (b) Green, M. L.; Levy, R. A. *J. Electrochem. Soc.* **1985**, *132*, 1243.

(3) (a) Levy, R. A.; Green, M. L.; Gallagher, R. K. *J. Electrochem. Soc.* **1984**, *131*, 2175. (b) Bent, B. E.; Nuzzo, R. G.; Dubois, L. H. *J. Am. Chem. Soc.* **1989**, *111*, 1634. (c) Beach, D. B.; Blum, S. E.; LeGroues, F. K. *J. Vac. Sci. Technol.* **1989**, *A7*, 3117. (d) Gross, M. E.; Dubois, L. H.; Nuzzo, R. G.; Cheung, K. P. *Mat. Res. Soc. Symp. Proc.* **1991**, *204*, 383. (e) Dubois, L. H.; Zegarski, B. R.; Gross, M. E.; Nuzzo, R. G. *Surface Sci.* **1991**, *244*, 89.

stability, and reactivity, especially in relation with CVD. Here, we report the syntheses and characterizations of a series of new ( $\beta$ -diketonate)Cu(alkene) complexes with coordination number 4, in which alkene = 7-*tert*-butoxynorbornadiene (7-*t*-BuO-NBD) and  $\beta$ -diketonate = 1,1,1,5,5,5-hexafluoro-2,4-pentanedionate (hfac) (1), 1,1,1-trifluoro-2,4-pentanedionate (tfac) (2), 2,4-pentanedionate (acac) (3), 4,4,4-trifluoro-1-(2-thienyl)-1,3-butanedionate (Ttfac) (4), 4,4,4-trifluoro-1-phenyl-1,3-butanedionate (Btfac) (5), and 2,2-dimethyl-6,6,7,7,8,8,8-heptafluoro-3,5-octanedionate (fod) (6), variable-temperature  $^1\text{H}$  NMR spectroscopic studies of the title compounds, single-crystal structures of compounds 1, 4, and 5, and the results of hot-wall CVD experiments with compound 1 as a precursor.

## Experimental Section

**General Procedures and Starting Materials.** All operations were performed under an atmosphere of nitrogen purified by passage through columns of activated BASF catalyst and molecular sieves and using standard Schlenk techniques<sup>13</sup> in conjunction with a double manifold vacuum line. All hydrocarbon and ethereal solvents were dried and distilled from sodium benzophenone ketyl at atmospheric pressure before use. Copper(I) chloride, sodium hydride, 1,1,1,5,5,5-hexafluoro-2,4-pentanedione, 1,1,1-trifluoro-2,4-pentanedione, 2,4-pentanedione, 4,4,4-trifluoro-1-(2-thienyl)-1,3-butanedione, 4,4,4-trifluoro-1-phenyl-1,3-butanedione, and 2,2-dimethyl-6,6,7,7,8,8,8-heptafluoro-3,5-octanedione (Aldrich Chemical Co.) were used without further purification. The sodium salts of the  $\beta$ -diketonates<sup>10b</sup> and the diene 7-*tert*-butoxynorbornadiene<sup>14</sup> were prepared by the methods previously described in the literature. Elemental analyses and mass spectral analyses were made at National Science Council Southern Instrument Center (Department of Chemistry, National Cheng Kung University). NMR data were recorded on a Varian Gemini-200 NMR spectrometer by using the protio impurities of deuterated solvents as references for the  $^1\text{H}$  NMR and the  $^{13}\text{C}$  signals of the solvents as references for  $^{13}\text{C}$  NMR spectroscopies.  $^{19}\text{F}$  NMR spectra were externally referred to  $\text{CFCl}_3$ . Infrared data were recorded on a Perkin-Elmer Model 16 PC FTIR spectrophotometer. Melting points were measured in sealed capillaries on a Thomas-Hoover Unimelt instrument without calibration.

**Synthesis and Characterization of ( $\beta$ -Diketonate)Cu(7-*t*-BuO-NBD).** a. (hfac)Cu(7-*t*-BuO-NBD) (1). Addition of 7-*t*-BuO-NBD (6.2 mL, 32.3 mmol) to a 250-mL Schlenk flask containing a solution of CuCl (3.21 g, 32.3 mmol) in diethyl ether (50 mL) gave a white slurry solution. A solution of Na(hfac) (7.52 g, 32.7 mmol) in  $\text{Et}_2\text{O}$  (50 mL) was transferred into the reaction flask with stirring, and the reaction mixture turned yellow immediately. The mixture was stirred for 4 h

at room temperature. The volatile components were removed *in vacuo* (0.1 Torr), and hexane (80 mL) was added to dissolve the product. After filtration and removal of hexane, a yellow powder was obtained. Recrystallization of the compound from hexane (10 mL) at 0 °C afforded yellow, crystalline (hfac)Cu(7-*t*-BuO-NBD) (10.2 g, 73% yield).

Anal. Calcd for  $\text{C}_{16}\text{H}_{17}\text{O}_3\text{F}_6\text{Cu}$ : C, 44.19; H, 3.94. Found: C, 44.31; H, 3.93.

NMR data ( $\text{C}_6\text{D}_6$ , 18 °C):  $^1\text{H}$   $\delta$  6.27 (s, 1H, CH on hfac), 6.04 (m, 2H, noncoordinated CH=CH on 7-*t*-BuO-NBD), 5.02 (br, s, 2H, coordinated CH=CH on 7-*t*-BuO-NBD), 3.31 (br, s, 1H, bridge H on 7-*t*-BuO-NBD), 2.93 (br, s, 2H, bridgehead H on 7-*t*-BuO-NBD), 0.85 (s, 9H,  $\text{C}(\text{CH}_3)_3$  on 7-*t*-BuO-NBD) ppm;  $^{13}\text{C}\{^1\text{H}\}$   $\delta$  178.3 (q,  $J_{\text{FC}} = 33.7$  Hz,  $\text{CF}_3\text{CO}$  on hfac), 139.6 (s, noncoordinated CH=CH on 7-*t*-BuO-NBD), 119.3 (q,  $J_{\text{FC}} = 284.5$  Hz,  $\text{CF}_3$  on hfac), 101.9 (s, coordinated CH=CH on 7-*t*-BuO-NBD), 92.7 (s, bridge C on 7-*t*-BuO-NBD), 90.1 (s, CH on hfac), 76.8 (s,  $(\text{CH}_3)_3\text{C}$  on 7-*t*-BuO-NBD), 56.0 (s, bridgehead C on 7-*t*-BuO-NBD), 28.2 (s,  $(\text{CH}_3)_3\text{C}$  on 7-*t*-BuO-NBD) ppm;  $^{19}\text{F}\{^1\text{H}\}$   $\delta$  -76.3 (s) ppm.

IR data (KBr disk): 3764 (w), 2986 (w), 1644 (s), 1574 (m), 1540 (m), 1488 (s), 1387 (m), 1262 (s), 1194 (s), 1144 (s), 1084 (s), 898 (w), 800 (m), 676 (m), 586 (w)  $\text{cm}^{-1}$ .

Mass spectral data (FAB<sup>+</sup>,  $m/z$ ): 434, 34.5 [Cu(hfac)(7-*t*-BuO-NBD)]<sup>+</sup>; 378, 81.8 [Cu(hfac)(7-HO-NBD)]<sup>+</sup>; 227, 39.4 [Cu(7-*t*-BuO-NBD)]<sup>+</sup>; 171, 23.8 [Cu(7-HO-NBD)]<sup>+</sup>; 139, 100 [CF<sub>3</sub>C(O)CHC(O)H]<sup>+</sup>; 107, 50.2 [(7-O-NBD)]<sup>+</sup>; 91, 62.7 [C<sub>7</sub>H<sub>7</sub>]<sup>+</sup>; 77, 47.5 [C<sub>6</sub>H<sub>5</sub>]<sup>+</sup>; 63, 17.9 [Cu]<sup>+</sup>; 57, 50.3 [C<sub>4</sub>H<sub>9</sub>]<sup>+</sup>.

Mp: 105 °C, sublimation temperature: 75 °C/0.1 Torr.

b. (tfac)Cu(7-*t*-BuO-NBD) (2). Pale yellow, crystalline (tfac)Cu(7-*t*-BuO-NBD) was prepared in 60% yield with a procedure analogous to that of synthesis of compound 1.

Anal. Calcd for  $\text{C}_{16}\text{H}_{20}\text{O}_3\text{F}_3\text{Cu}$ : C, 50.46; H, 5.29. Found: C, 50.16; H, 5.28.

NMR data ( $\text{C}_6\text{D}_6$ , 18 °C):  $^1\text{H}$   $\delta$  6.09 (m, 2H, noncoordinated CH=CH on 7-*t*-BuO-NBD), 5.77 (s, 1H, CH on tfac), 4.96 (br, s, 2H, coordinated CH=CH on 7-*t*-BuO-NBD), 3.40 (br, s, 1H, bridge H on 7-*t*-BuO-NBD), 3.05 (br, s, 2H, bridgehead H on 7-*t*-BuO-NBD), 1.75 (s, 3H, CH<sub>3</sub> on tfac), 0.99 (s, 9H,  $\text{C}(\text{CH}_3)_3$  on 7-*t*-BuO-NBD) ppm;  $^{13}\text{C}\{^1\text{H}\}$   $\delta$  197.9 (s,  $\text{CH}_3\text{CO}$  on tfac), 171.4 (q,  $J_{\text{FC}} = 31.0$  Hz,  $\text{CF}_3\text{CO}$  on tfac), 139.8 (s, noncoordinated CH=CH on 7-*t*-BuO-NBD), 120.8 (q,  $J_{\text{FC}} = 284.1$  Hz,  $\text{CF}_3$  on tfac), 97.4 (s, coordinated CH=CH on 7-*t*-BuO-NBD), 95.3 (s, CH on tfac), 92.2 (s, bridge C on 7-*t*-BuO-NBD), 76.5 (s,  $(\text{CH}_3)_3\text{C}$  on 7-*t*-BuO-NBD), 55.9 (s, bridgehead C on 7-*t*-BuO-NBD), 29.6 (s, CH<sub>3</sub> on tfac), 28.5 (s,  $(\text{CH}_3)_3\text{C}$  on 7-*t*-BuO-NBD) ppm;  $^{19}\text{F}\{^1\text{H}\}$   $\delta$  -75.4 (s) ppm.

IR data (KBr disc): 3764 (w), 2980 (w), 1628 (s), 1518 (s), 1497 (m), 1360 (w), 1298 (s), 1233 (m), 1182 (s), 1136 (s), 1084 (s), 886 (w), 774 (w), 700 (w), 582 (w)  $\text{cm}^{-1}$ .

Mass spectral data (FAB<sup>+</sup>,  $m/z$ ): 380, 51.2 [Cu(tfac)(7-*t*-BuO-NBD)]<sup>+</sup>; 324, 83.8 [Cu(tfac)(7-HO-NBD)]<sup>+</sup>; 227, 83.6 [Cu(7-*t*-BuO-NBD)]<sup>+</sup>; 216, 12.1 [Cu(tfac)]<sup>+</sup>; 171, 50.5 [Cu(7-HO-NBD)]<sup>+</sup>; 141, 23.0 [Cu(C<sub>6</sub>H<sub>6</sub>)]<sup>+</sup>; 107, 22.0 [(7-O-NBD)]<sup>+</sup>; 92, 39.3 [NBD]<sup>+</sup>; 91, 100 [C<sub>7</sub>H<sub>7</sub>]<sup>+</sup>; 79, 10.7 [C<sub>6</sub>H<sub>7</sub>]<sup>+</sup>; 63, 15.2 [Cu]<sup>+</sup>; 57, 51.2 [C<sub>4</sub>H<sub>9</sub>]<sup>+</sup>.

Mp: 110 °C dec, sublimation temperature: 75 °C/0.1 Torr.

c. (acac)Cu(7-*t*-BuO-NBD) (3). White, crystalline (acac)Cu(7-*t*-BuO-NBD) was prepared in 47% yield following a procedure similar to that of synthesis of compound 1 except that THF was used as the solvent for reaction.

Anal. Calcd for  $\text{C}_{16}\text{H}_{23}\text{O}_3\text{Cu}$ : C, 58.79; H, 7.09. Found: C, 58.40; H, 7.14.

NMR data ( $\text{C}_6\text{D}_6$ , 18 °C):  $^1\text{H}$   $\delta$  6.14 (br, s, 2H, noncoordinated CH=CH on 7-*t*-BuO-NBD), 5.36 (s, 1H, CH on acac), 4.88 (br, s, 2H, coordinated CH=CH on 7-*t*-BuO-NBD), 3.47 (br, s, 1H, bridge H on 7-*t*-BuO-NBD), 3.16 (br, s, 2H, bridgehead H on 7-*t*-BuO-NBD), 1.94 (s, 6H, CH<sub>3</sub> on acac), 1.09 (s, 9H,  $\text{C}(\text{CH}_3)_3$  on 7-*t*-BuO-NBD) ppm;  $^{13}\text{C}\{^1\text{H}\}$   $\delta$  190.3 (s, CO on acac), 139.9 (s, noncoordinated CH=CH on 7-*t*-BuO-NBD), 100.0 (s, CH on acac), 93.3 (s, coordinated CH=CH on 7-*t*-BuO-NBD), 91.6 (s, bridge C on 7-*t*-BuO-NBD), 76.1 (s,  $(\text{CH}_3)_3\text{C}$  on

(8) ( $\beta$ -diketonate)Cu(alkyne) as MOCVD precursors: (a) Jain, A.; Chi, K.-M.; Kodas, T. T.; Hampden-Smith, M. J.; Farr, J. D.; Paffett, M. *Chem. Mater.* **1991**, *3*, 995. (b) Baum, T. H.; Larson, C. E. *Chem. Mater.* **1992**, *4*, 365.

(9) Nast, R.; Lepel, W.-H. *Chem. Ber.* **1969**, *102*, 3224.

(10) (a) Anderson, W. A.; Carty, A. J.; Palenik, G. J.; Schreiber, G. *Can. J. Chem.* **1971**, *49*, 761. (b) Shin, H.-K.; Chi, K. M.; Farkas, J.; Hampden-Smith, M. J.; Kodas, T. T.; Duesler, E. N. *Inorg. Chem.* **1992**, *31*, 424. (c) Chi, K. M.; Corbitt, T. S.; Hampden-Smith, M. J.; Kodas, T. T.; Duesler, E. N. *J. Organomet. Chem.* **1993**, *449*, 181.

(11) (a) Doyle, G.; Eriksen, K. A.; Van Engen, D. *Organometallics* **1985**, *4*, 830. (b) Chi, K. M.; Shin, H.-K.; Hampden-Smith, M. J.; Kodas, T. T.; Duesler, E. N. *Polyhedron* **1991**, *10*, 2293. (c) Kumar, R.; Fronczek, F. R.; Mavreick, A. W.; Lai, W. G.; Griffin, G. F. *Chem. Mater.* **1992**, *4*, 577.

(12) Chi, K. M.; Shin, H.-K.; Hampden-Smith, M. J.; Kodas, T. T.; Duesler, E. N. *Inorg. Chem.* **1991**, *30*, 424.

(13) Shriver, D. F.; Drezden, M. A. *The Manipulation of Air-Sensitive Compounds*, 2nd ed.; Wiley: New York, 1986.

(14) Story, P. R.; Fahrenholtz, S. R. *Organic Syntheses*; Wiley: New York, 1973; Collect. Vol. V, p 151.

7-*t*-BuO-NBD), 55.8 (s, bridgehead C on 7-*t*-BuO-NBD), 28.9 (s, CH<sub>3</sub> on acac), 28.7 (s, (CH<sub>3</sub>)<sub>3</sub>C on 7-*t*-BuO-NBD) ppm.

IR data (KBr disk): 3083 (w), 2976 (w), 1596 (s), 1514 (s), 1462 (m), 1406 (s), 1363 (m), 1320 (w), 1272 (w), 1232 (m), 1188 (m), 1090 (s), 1016 (m), 936 (w), 890 (w), 672 (m), 702 (m), 572 (w) cm<sup>-1</sup>.

Mass spectral data (EI<sup>+</sup>, *m/z*): 326, 10.7 [Cu(acac)(7-*t*-BuO-NBD)]<sup>+</sup>; 270, 7.4 [Cu(acac)(7-HO-NBD)]<sup>+</sup>; 261, 10.3 [Cu(acac)<sub>2</sub>]<sup>+</sup>; 163, 13.0 [HCu(acac)]<sup>+</sup>; 147, 9.1 [Cu(C<sub>4</sub>H<sub>9</sub>O<sub>2</sub>)]<sup>+</sup>; 108, 31.1 [(7-HO-NBD)]<sup>+</sup>; 107, 18.8 [(7-O-NBD)]<sup>+</sup>; 91, 79.0 [C<sub>7</sub>H<sub>7</sub>]<sup>+</sup>; 85, 15.9 [(C<sub>4</sub>H<sub>9</sub>O<sub>2</sub>)]<sup>+</sup>; 79, 50.9 [C<sub>6</sub>H<sub>5</sub>]<sup>+</sup>; 78, 19.6 [C<sub>6</sub>H<sub>6</sub>]<sup>+</sup>; 63, 6.3 [Cu]<sup>+</sup>; 57, 100 [C<sub>4</sub>H<sub>9</sub>]<sup>+</sup>.

Mp: 115 °C dec, sublimation temperature: 90 °C/0.1 Torr.

**d. (Ttfac)Cu(7-*t*-BuO-NBD) (4).** Yellow, crystalline (Ttfac)Cu(7-*t*-BuO-NBD) was prepared in 66% yield by using a procedure analogous to that of the synthesis of compound 1.

Anal. Calcd for C<sub>19</sub>H<sub>20</sub>O<sub>3</sub>F<sub>3</sub>CuS: C, 50.83; H, 4.49. Found: C, 50.62; H, 4.47.

NMR data (C<sub>6</sub>D<sub>6</sub>, 18 °C): <sup>1</sup>H δ 7.26 (d, 1H, *J* = 3.2 Hz, thienyl *H* on Ttfac), 6.85 (d, 1H, *J* = 4.8 Hz, thienyl *H* on Ttfac), 6.53 (m, 1H, thienyl *H* on Ttfac), 6.51 (s, 1H, methine CH on Ttfac), 6.09 (br, s, 2H, noncoordinated CH=CH on 7-*t*-BuO-NBD), 4.99 (br, s, 2H, coordinated CH=CH on 7-*t*-BuO-NBD), 3.39 (br, s, 1H, bridge *H* on 7-*t*-BuO-NBD), 3.06 (br, s, 2H, bridgehead *H* on 7-*t*-BuO-NBD), 0.97 (s, 9H, C(CH<sub>3</sub>)<sub>3</sub> on 7-*t*-BuO-NBD) ppm. <sup>13</sup>C{<sup>1</sup>H} δ 183.0 (s, CO on Ttfac), 172.5 (q, *J*<sub>FC</sub> = 32 Hz, CF<sub>3</sub>CO on Ttfac), 146.8 (s, thienyl C on Ttfac), 139.6 (s, noncoordinated CH=CH on 7-*t*-BuO-NBD) 132.7 (s, thienyl C on Ttfac), 130.5 (s, thienyl C on Ttfac), 120.8 (q, *J*<sub>FC</sub> = 284 Hz, CF<sub>3</sub> on Ttfac), 98.2 (s, coordinated CH=CH on 7-*t*-BuO-NBD), 92.3 (s, bridge C on 7-*t*-BuO-NBD), 91.5 (s, methine CH on Ttfac), 76.5 (s, (CH<sub>3</sub>)<sub>3</sub>C on 7-*t*-BuO-NBD), 55.9 (s, bridgehead C on 7-*t*-BuO-NBD), 28.5 (s, (CH<sub>3</sub>)<sub>3</sub>C on 7-*t*-BuO-NBD) ppm; <sup>19</sup>F{<sup>1</sup>H} δ -75.3 (s) ppm.

IR data (KBr disk): 3752 (w), 2976 (w), 1602 (s), 1536 (s), 1516 (m), 1464 (m), 1412 (m), 1354 (m), 1304 (s), 1232 (m), 1172 (s), 1144 (s), 1080 (s), 1036 (w), 930 (w), 888 (w), 782 (m), 728 (w), 688 (m), 668 (w), 584 (w) cm<sup>-1</sup>.

Mass spectral data (FAB<sup>+</sup>, *m/z*): 568, 12.2 [Cu<sub>2</sub>(Ttfac)<sub>2</sub>]<sup>+</sup>; 448, 34.1 [Cu(Ttfac)(7-*t*-BuO-NBD)]<sup>+</sup>; 392, 85.2 [Cu(Ttfac)(7-HO-NBD)]<sup>+</sup>; 285, 24.5 [HCu(Ttfac)]<sup>+</sup>; 227, 67.3 [Cu(7-*t*-BuO-NBD)]<sup>+</sup>; 171, 39.2 [Cu(7-HO-NBD)]<sup>+</sup>; 141, 18.0 [Cu(C<sub>6</sub>H<sub>6</sub>)]<sup>+</sup>; 111, 21.8 [C<sub>5</sub>H<sub>3</sub>OS]<sup>+</sup>; 107, 18.8 [(7-O-NBD)]<sup>+</sup>; 92, 26.2 [NBD]<sup>+</sup>; 91, 100 [C<sub>7</sub>H<sub>7</sub>]<sup>+</sup>; 63, 7.0 [Cu]<sup>+</sup>; 57, 24.8 [C<sub>4</sub>H<sub>9</sub>]<sup>+</sup>.

Mp: 115 °C dec, sublimation temperature: 90 °C/0.1 Torr.

**e. (Btfac)Cu(7-*t*-BuO-NBD) (5).** Yellow, crystalline (Btfac)Cu(7-*t*-BuO-NBD) was prepared in 63% yield by using a procedure analogous to that of synthesis of compound 1.

Anal. Calcd for C<sub>21</sub>H<sub>22</sub>O<sub>3</sub>F<sub>3</sub>Cu: C, 56.94; H, 5.01. Found: C, 56.94; H, 5.02.

NMR data (C<sub>6</sub>D<sub>6</sub>, 18 °C): <sup>1</sup>H δ 7.86 (m, 2H, phenyl *H* on Btfac), 7.07 (m, 3H, phenyl *H* on Btfac), 6.59 (s, 1H, methine CH on Btfac), 6.16 (br, s, 2H, noncoordinated CH=CH on 7-*t*-BuO-NBD), 5.03 (br, s, 2H, coordinated CH=CH on 7-*t*-BuO-NBD), 3.43 (br, s, 1H, bridge *H* on 7-*t*-BuO-NBD), 3.12 (br, s, 2H, bridgehead *H* on 7-*t*-BuO-NBD), 0.96 (s, 9H, C(CH<sub>3</sub>)<sub>3</sub> on 7-*t*-BuO-NBD) ppm; <sup>13</sup>C{<sup>1</sup>H} δ 189.9 (s, C<sub>6</sub>H<sub>5</sub>CO on Btfac), 173.0 (q, *J*<sub>FC</sub> = 32.0 Hz, CF<sub>3</sub>CO on Btfac), 140.4 (s, phenyl C on Btfac), 139.8 (s, noncoordinated CH=CH on 7-*t*-BuO-NBD), 132.6 (s, phenyl C on Btfac), 121.3 (q, *J*<sub>FC</sub> = 284.3 Hz, CF<sub>3</sub> on Btfac), 97.9 (s, coordinated CH=CH on 7-*t*-BuO-NBD), 92.3 (s, methine CH on Btfac), 92.0 (s, bridge C on 7-*t*-BuO-NBD), 76.6 (s, (CH<sub>3</sub>)<sub>3</sub>C on 7-*t*-BuO-NBD), 56.0 (s, bridgehead C on 7-*t*-BuO-NBD), 28.5 (s, (CH<sub>3</sub>)<sub>3</sub>C on 7-*t*-BuO-NBD) ppm; <sup>19</sup>F{<sup>1</sup>H} δ -75.2 (s) ppm.

IR data (KBr disk): 3752 (w), 2982 (w), 1612 (s), 1587 (m), 1540 (m), 1482 (m), 1377 (w), 1292 (s), 1257 (m), 1178 (s), 1152 (s), 1088 (m), 898 (w), 764 (w), 686 (w), 658 (w), 596 (w) cm<sup>-1</sup>.

Mass spectral data (FAB<sup>+</sup>, *m/z*): 720, 12.4 [Cu<sub>2</sub>(Btfac)<sub>2</sub>(7-*t*-BuO-NBD)]<sup>+</sup>; 442, 59.6 [Cu(Btfac)(7-*t*-BuO-NBD)]<sup>+</sup>; 386, 100 [Cu(Btfac)(7-HO-NBD)]<sup>+</sup>; 279, 51.4 [HCu(Btfac)]<sup>+</sup>; 227, 87.2 [Cu(7-*t*-BuO-NBD)]<sup>+</sup>; 216, 12.5 [HBtfac]<sup>+</sup>; 171, 41.1 [Cu(7-

HO-NBD)]<sup>+</sup>; 141, 15.2 [Cu(C<sub>6</sub>H<sub>6</sub>)]<sup>+</sup>; 107, 15.5 [(7-O-NBD)]<sup>+</sup>; 92, 12.9 [NBD]<sup>+</sup>; 91, 83.3 [C<sub>7</sub>H<sub>7</sub>]<sup>+</sup>; 77, 9.5 [C<sub>6</sub>H<sub>5</sub>]<sup>+</sup>; 63, 4.6 [Cu]<sup>+</sup>; 57, 17.6 [C<sub>4</sub>H<sub>9</sub>]<sup>+</sup>.

Mp: 116 °C, sublimation temperature: 90 °C/0.12 Torr.

**f. (fod)Cu(7-*t*-BuO-NBD) (6).** Yellow, crystalline (fod)Cu(7-*t*-BuO-NBD) was prepared in 53% with a procedure analogous to that for compound 1.

Anal. Calcd for C<sub>21</sub>H<sub>26</sub>O<sub>3</sub>F<sub>7</sub>Cu: C, 48.23; H, 5.01. Found: C, 48.10; H, 5.04.

NMR data (C<sub>6</sub>D<sub>6</sub>, 18 °C): <sup>1</sup>H δ 6.15 (s, 1H, CH on fod), 6.10 (br, s, 2H, noncoordinated CH=CH on 7-*t*-BuO-NBD), 4.93 (br, s, 2H, coordinated CH=CH on 7-*t*-BuO-NBD), 3.39 (br, s, 1H, bridge *H* on 7-*t*-BuO-NBD), 3.03 (br, s, 2H, bridgehead *H* on 7-*t*-BuO-NBD), 1.10 (s, 9H, C(CH<sub>3</sub>)<sub>3</sub> on fod), 0.97 (s, 9H, C(CH<sub>3</sub>)<sub>3</sub> on 7-*t*-BuO-NBD) ppm; <sup>13</sup>C{<sup>1</sup>H} δ 206.1 (s, (CH<sub>3</sub>)<sub>3</sub>CCO on fod), 172.9 (t, *J*<sub>FC</sub> = 22.6 Hz, CF<sub>2</sub>CO on fod), 139.8 (s, noncoordinated CH=CH on 7-*t*-BuO-NBD), 123.0–104.9 (m, CF<sub>2</sub>CF<sub>2</sub>CF<sub>3</sub> on fod), 97.5 (s, coordinated CH=CH on 7-*t*-BuO-NBD), 92.4 (s, CH on fod), 92.1 (s, bridge C on 7-*t*-BuO-NBD), 76.4 (s, (CH<sub>3</sub>)<sub>3</sub>C on 7-*t*-BuO-NBD), 55.9 (s, bridgehead C on 7-*t*-BuO-NBD), 43.0 (s, C(CH<sub>3</sub>)<sub>3</sub> on fod), 28.6 (s, C(CH<sub>3</sub>)<sub>3</sub> on fod), 28.5 (s, C(CH<sub>3</sub>)<sub>3</sub> on 7-*t*-BuO-NBD) ppm; <sup>19</sup>F{<sup>1</sup>H} δ -80.5 (s), -119.0 (s), -126.2 (s) ppm.

IR data (KBr disk): 2986 (m), 1627 (s), 1581 (m), 1511 (m), 1480 (s), 1401 (w), 1355 (m), 1231 (s), 1198 (s), 1125 (m), 1083 (s), 1028 (w), 918 (w), 793 (w), 697 (m), cm<sup>-1</sup>.

Mass spectral data (EI<sup>+</sup>, *m/z*): 522, 2.3 [Cu(fod)(7-*t*-BuO-NBD)]<sup>+</sup>; 466, 3.1 [Cu(fod)(7-HO-NBD)]<sup>+</sup>; 359, 4.9 [HCu(fod)]<sup>+</sup>; 301, 15.7 [Cu(C<sub>3</sub>F<sub>7</sub>C(O)CH-C(O))]<sup>+</sup>; 239, 13.7 [C<sub>3</sub>F<sub>7</sub>C(O)CHC(O)]<sup>+</sup>; 227, 10.0 [Cu(7-*t*-BuO-NBD)]<sup>+</sup>; 171, 7.4 [Cu(7-HO-NBD)]<sup>+</sup>; 149, 7.6 [(7-(CH<sub>3</sub>)<sub>2</sub>CO-NBD)]<sup>+</sup>; 141, 5.4 [Cu(C<sub>6</sub>H<sub>6</sub>)]<sup>+</sup>; 108, 37.1 [(7-HO-NBD)]<sup>+</sup>; 107, 27.6 [(7-O-NBD)]<sup>+</sup>; 92, 11.6 [NBD]<sup>+</sup>; 91, 97.0 [C<sub>7</sub>H<sub>7</sub>]<sup>+</sup>; 79, 63.8 [C<sub>6</sub>H<sub>7</sub>]<sup>+</sup>; 78, 21.0 [C<sub>6</sub>H<sub>6</sub>]<sup>+</sup>; 77, 27.1 [C<sub>6</sub>H<sub>5</sub>]<sup>+</sup>; 69, 24.4 [CF<sub>3</sub>]<sup>+</sup>; 63, 11.3 [Cu]<sup>+</sup>; 57, 100 [C<sub>4</sub>H<sub>9</sub>]<sup>+</sup>.

Mp: 115 °C dec, sublimation temperature: 85 °C/0.1 Torr.

**X-ray Single-Crystal Structural Determination.** Three examples of the title compounds were characterized structurally in the solid state by single-crystal X-ray diffraction. All diffraction data were collected on an Enraf-Nonius CAD-4 diffractometer with monochromated Mo Kα radiation (λ = 0.709 30 Å) using Θ/2Θ scan mode. Crystal, collection, and refinement data are summarized in Table 1.

**a. (hfac)Cu(7-*t*-BuO-NBD) (1).** Bright yellow crystals of (hfac)Cu(7-*t*-BuO-NBD) were grown by crystallization from hexane solution at -20 °C, and a single crystal of dimensions 0.40 × 0.50 × 0.50 mm<sup>3</sup> was selected for X-ray analysis. Cell parameters were determined from a fit of 25 reflections (23.40 < 2Θ < 27.60 °). All data were corrected for Lorentz and polarization effects and for effects of absorption. A total of 3228 reflections was collected, but only 2586 unique reflections with *I* > 2σ(*I*) were used for structural solution and refinement. The structure was solved by the heavy-atom method and refined by full-matrix least-squares methods based on *F* values. All non-hydrogen atoms were refined with anisotropic thermal parameters. The atomic scattering factors were taken from *International Tables for X-ray Crystallography*.<sup>15</sup> The final agreement factors are *R*<sub>F</sub> = 0.042, *R*<sub>w</sub> = 0.042 with *w* = 1/σ<sup>2</sup>(*F*).

**b. (Ttfac)Cu(7-*t*-BuO-NBD) (4).** Light yellow crystals of (Ttfac)Cu(7-*t*-BuO-NBD) were grown by crystallization from hexane solution at -20 °C and a single crystal of dimensions 0.50 × 0.50 × 0.70 mm<sup>3</sup> was selected for X-ray analysis. Cell parameters were determined from a fit of 25 reflections (19.42 < 2Θ < 25.38°). All data were corrected for Lorentz and polarization effects and for effects of absorption. A total of 3495 reflections was collected, but only 2481 unique reflections with *I* > 2σ(*I*) were used for structural solution and refinement. The structure was solved by the heavy-atom method and

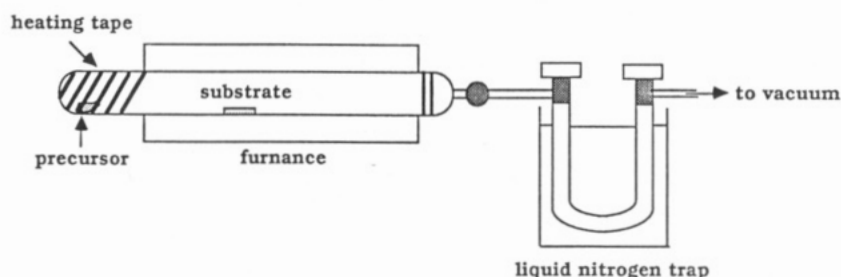
(15) *International Tables for X-ray Crystallography*; Kynoch Press: Birmingham, U.K., 1974; Vol. IV.



**Table 1. Summary of Crystallographic Data for Compounds 1, 4, and 5**

compd	1	4	5
emp form.	C <sub>16</sub> H <sub>16</sub> O <sub>3</sub> CuF <sub>6</sub>	C <sub>19</sub> H <sub>20</sub> O <sub>3</sub> CuF <sub>3</sub> S	C <sub>21</sub> H <sub>22</sub> O <sub>3</sub> CuF <sub>3</sub>
form. wt	434.84	448.96	442.94
cryst size (mm <sup>3</sup> )	0.40 × 0.50 × 0.50	0.50 × 0.50 × 0.70	0.35 × 0.50 × 0.65
space grp	monoclinic; <i>P</i> 2 <sub>1</sub> / <i>c</i>	monoclinic; <i>P</i> 2 <sub>1</sub> / <i>n</i>	triclinic <i>P</i> $\bar{1}$
<i>a</i> (Å)	8.9227(12)	10.689(6)	9.6174(13)
<i>b</i> (Å)	19.558(4)	9.712(4)	9.894(4)
<i>c</i> (Å)	10.495(3)	19.323(4)	11.3223(19)
$\alpha$ (°)			104.574(24)
$\beta$ (°)	90.450(17)	97.22(3)	95.501(12)
$\gamma$ (°)			104.76(3)
<i>V</i> (Å <sup>3</sup> )	1831.3(7)	1990.2(15)	993.4(5)
<i>Z</i>	4	4	2
<i>d</i> (calcd) (g/cm <sup>3</sup> )	1.577	1.498	1.481
$\lambda$ (Å)		0.70930	
<i>T</i> (K)		298.00	
<i>F</i> (000)	880	922	457
2 $\theta$ range (deg)	23.40–27.60	19.42–25.38	18.92–30.48
scan type		$\theta/2\theta$	
scan speed (deg/min)		2.06–8.24	
scan width		2(0.70 + 0.35 tan $\theta$ )	
2 $\theta_{max}$		50	
$\mu$ (cm <sup>-1</sup> )	12.623	12.412	11.446
transmission	0.864; 1.000	0.882; 1.000	0.892; 1.000
index ranges	-10 < <i>h</i> < 10 0 < <i>k</i> < 23 0 < <i>l</i> < 12	-12 < <i>h</i> < 12 0 < <i>k</i> < 11 0 < <i>l</i> < 22	-11 < <i>h</i> < 10 0 < <i>k</i> < 11 -13 < <i>l</i> < 13
<i>R</i> <sub>F</sub> ; <i>R</i> <sub>w</sub> <sup>a</sup>	0.042; 0.042	0.051; 0.052	0.035; 0.035
goodness-of-fit <sup>b</sup>	3.47	2.47	2.25
weights scheme		1/ $\sigma^2(F_o)$	
refine. prog.		NRCVAX	
no. of atoms	43	47	50
no. of params refined	268	245	254
largest $\Delta\sigma$	0.0299	0.0255	0.0216

<sup>a</sup>  $R_F = \sum(F_o - F_c)/\sum F_o$ .  $R_w = (\sum[w(F_o - F_c)^2]/\sum(wF_o^2))^{1/2}$ . <sup>b</sup> Goodness-of-fit =  $(\sum[w(F_o - F_c)^2]/(\text{no. of reflections} - \text{no. of parameters}))^{1/2}$ .

**Figure 1.** Schematic plot of hot-wall CVD reactor.

refined by full-matrix least-squares methods based on *F* values. All non-hydrogen atoms were refined with anisotropic thermal parameters. The atomic scattering factors were taken from *International Tables for X-ray Crystallography*.<sup>15</sup> The final agreement factors are  $R_F = 0.051$ ,  $R_w = 0.052$  with  $w = 1/\sigma^2(F)$ .

**c. (Btfac)Cu(7-*t*-BuO-NBD) (5).** Yellow crystals of (Btfac)Cu(7-*t*-BuO-NBD) were grown by crystallization from hexane solution at -20 °C, and a single crystal of dimensions 0.35 × 0.50 × 0.65 mm<sup>3</sup> was selected for X-ray analysis. Cell parameters were determined from a fit of 25 reflections (18.92 < 2 $\theta$  < 30.48°). All data were corrected for Lorentz and polarization effects and for effects of absorption. A total of 3499 reflections was collected, but only 2940 unique reflections with  $I > 2\sigma(I)$  were used for structural solution and refinement. The structure was solved by the heavy-atom method and refined by full-matrix least-squares based on *F* values. All non-hydrogen atoms were refined by full-matrix least-squares based on *F* values. All non-hydrogen atoms were refined with anisotropic thermal parameters. The atomic scattering factors were taken from *International Tables for X-ray Crystallography*.<sup>15</sup> The final agreement factors are  $R_F = 0.035$ ,  $R_w = 0.035$  with  $w = 1/\sigma^2(F)$ .

**Chemical Vapor Deposition of Copper Films from Compound 1.** CVD experiments were conducted in the hot-

wall reactor shown in Figure 1. Substrates of two types, Si (100) wafers coated with 1000 Å of Pt and with 2000 Å of thermally grown SiO<sub>2</sub>, were used. The substrates, typically 1.5 cm × 1.5 cm<sup>2</sup>, were cleaned with deionized water, acetone, and 1,1,1-trichloroethane and then heated to 100 °C for 20 min before use. The CVD reactor was charged with (hfac)Cu(7-*t*-BuO-NBD) (approximately 0.5 g) and a substrate in a glovebox with nitrogen atmosphere for each experiment. The assembled reactor was attached to a U-trap that was cooled with liquid N<sub>2</sub> and connected to a vacuum line. While the system was evacuated (0.1 Torr), the deposition zone was preheated with a furnace for 1 h to attain the deposition temperature and the precursor remained at room temperature. The precursor was then warmed to 80 °C with a heating tape to transfer into the deposition zone and deposition was continued until all precursor had evaporated. Deposition was undertaken over a temperature range 140–260 °C at 30 °C intervals. No carrier gas was used in these experiments. Film resistivities were measured with a four-point probe.

## Results and Discussion

**1. Synthesis of ( $\beta$ -Diketonate)Cu(7-*t*-BuO-NBD) Complexes.** The title compounds were prepared from reactions of CuCl with the corresponding  $\beta$ -diketonate

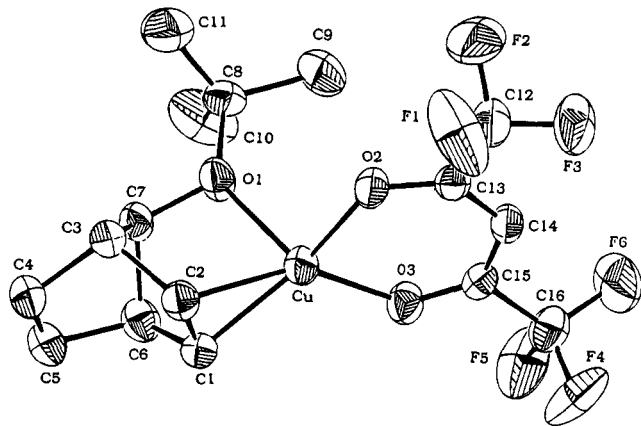


Figure 2. ORTEP drawing of (hfac)Cu(7-*t*-BuO-NBD) (1).

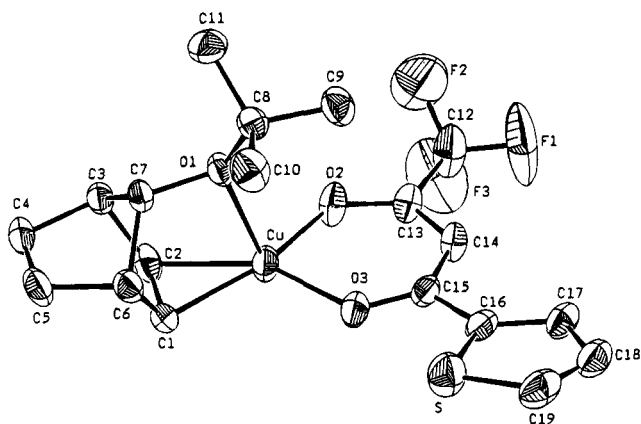
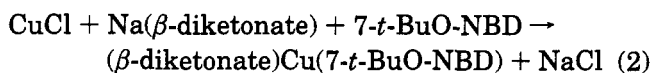


Figure 3. ORTEP drawing of (Ttfac)Cu(7-*t*-BuO-NBD) (4).

salts of sodium in the presence of 7-*t*-BuO-NBD according to eq 2. The reactions were carried out in ethereal



solutions at room temperature, and products were isolated on extraction with hexane and removal of volatile species *in vacuo*. A similar method was used to prepare analogous complexes of 1,5-cyclooctadiene (1,5-COD).<sup>11b</sup> These compounds are yellow to white solids that can be sublimed at temperatures above 75 °C under a reduced pressure (about 0.1 Torr). They are thermally robust and moderately sensitive to air and moisture. All compounds gave satisfactory elemental analyses and were characterized by solution <sup>1</sup>H, <sup>13</sup>C, and <sup>19</sup>F NMR, IR, and mass spectroscopic methods.

**2. Single-Crystal Structural Determination of Compounds 1, 4, and 5.** The molecular structures of (hfac)Cu(7-*t*-BuO-NBD) (1), (Ttfac)Cu(7-*t*-BuO-NBD) (4), and (Btfac)Cu(7-*t*-BuO-NBD) (5) were determined in the solid state by single-crystal X-ray diffraction analyses. ORTEP diagrams showing the atomic labeling scheme of these molecules are presented in Figures 2–4. The crystal, collection, and refinement data are summarized in Table 1; selected bond lengths and bond angles are given in Tables 2 and 3. Unlike the dinuclear norbornadiene derivative, [(hfac)Cu]<sub>2</sub>(norbornadiene),<sup>11a</sup> these compounds are mononuclear and the central copper atom is coordinated by the chelating  $\beta$ -diketonate ligand through two oxygen atoms and the 7-*t*-BuO-NBD through one C=C double bond and an oxygen atom. The same coordination mode for the 7-*t*-BuO-NBD ligand is

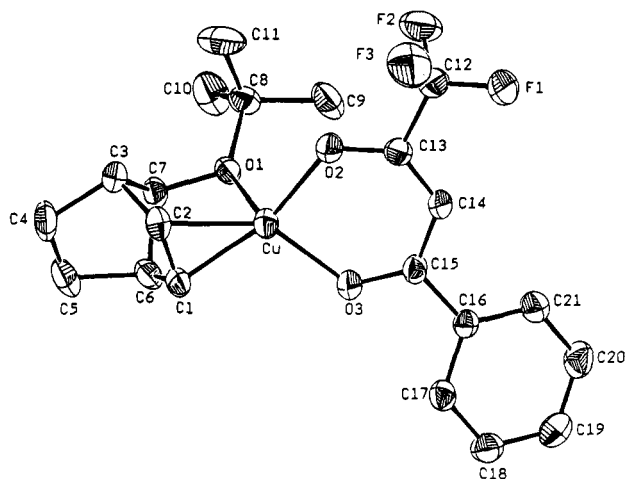


Figure 4. ORTEP drawing of (Btfac)Cu(7-*t*-BuO-NBD) (5).

Table 2. Selected Bond Lengths (Å) for Compounds 1, 4, and 5

compd	1	4	5
Cu–O(1)	2.249(2)	2.344(3)	2.365(2)
Cu–O(2)	1.976(2)	1.943(3)	1.953(2)
Cu–O(3)	1.988(2)	1.962(3)	1.966(2)
Cu–C(1)	2.011(3)	1.991(5)	1.987(3)
Cu–C(2)	2.029(3)	2.014(4)	2.033(3)
C(1)–C(2)	1.346(5)	1.359(8)	1.354(4)
C(4)–C(5)	1.294(6)	1.299(8)	1.311(6)

Table 3. Selected Bond Angles (deg) for Compounds 1, 4, and 5

compd	1	4	5
O(1)–Cu–O(2)	105.4(1)	104.2(1)	101.8(1)
O(1)–Cu–O(3)	109.2(1)	99.7(1)	104.4(1)
O(1)–Cu–C(1)	81.6(1)	81.8(2)	80.5(1)
O(1)–Cu–C(2)	81.2(1)	79.8(2)	81.3(1)
O(2)–Cu–O(3)	93.3(1)	95.2(1)	94.0(1)
O(2)–Cu–C(1)	152.7(1)	153.6(2)	159.3(1)
O(2)–Cu–C(2)	115.0(1)	115.2(2)	120.2(1)
O(3)–Cu–C(1)	109.5(1)	109.4(2)	105.4(1)
O(3)–Cu–C(2)	146.6(1)	149.0(2)	143.8(1)
C(1)–Cu–C(2)	38.9(2)	39.7(2)	39.3(1)
Cu–O(1)–C(7)	99.6(2)	97.1(2)	96.3(1)
Cu–C(1)–C(2)	71.3(2)	71.1(3)	72.2(2)
Cu–C(2)–C(1)	69.8(2)	69.3(3)	68.5(2)

reported in the structure of (7-*t*-BuO-NBD)<sub>2</sub>Mo(CO)<sub>2</sub>.<sup>16</sup> The bond distances and angles within the  $\beta$ -diketonate ligand are similar to those of other  $\beta$ -diketonate copper(I) complexes according to previous reports.<sup>10–12</sup> The coordination geometry about copper is best described as a highly distorted tetrahedron that resembles that of (hfac)Cu(1,5-COD).<sup>11b</sup> The atoms O(2), O(3), C(1), and C(2) are mutually coplanar, and the copper atom lies slightly (for example, 0.091 Å for compound 1) above the plane. The O(1) atom occupies the fourth coordination site with a relatively weak interaction to copper atom (Cu–O(1) distance = 2.249(2), 2.344(3), and 2.365(2) Å for compounds 1, 4, and 5, respectively) compared with bonding between copper and oxygens of  $\beta$ -diketonate ligands in the same molecule (Cu–O(2), Cu–O(3) bond distances are 1.94–1.99 Å for compounds 1, 4, and 5), and with Cu–O bonding in the molecule (*t*-BuOCu)<sub>4</sub> (average bond length is 1.85 Å).<sup>17</sup> Thus, the structures are best described as “3 + 1” coordination of the copper center also observed in the molecular struc-

(16) Chow, T. J.; Chao, Y.-S.; Liu, L.-K. *J. Am. Chem. Soc.* **1987**, *109*, 797.

(17) Greiser, T.; Weiss, E. *Chem. Ber.* **1976**, *109*, 3142.



**Table 4. Chemical Shifts<sup>a</sup> of Olefinic <sup>1</sup>H and <sup>13</sup>C NMR Resonances for 7-*t*-BuO-NBD and Compounds 1–6**

compd	$\delta$ ( $\Delta\delta^b$ ) (ppm)			
	<sup>1</sup> H		<sup>13</sup> C	
7- <i>t</i> -BuO-NBD	6.54	6.56	137.9	140.6
<b>1</b>	5.02 (-1.52)	6.04 (-0.52)	101.9 (-36.0)	139.6 (-1.0)
<b>2</b>	4.96 (-1.58)	6.09 (-0.47)	97.4 (-40.5)	139.8 (-0.8)
<b>3</b>	4.88 (-1.66)	6.14 (-0.42)	93.3 (-44.6)	139.9 (-0.7)
<b>4</b>	4.99 (-1.55)	6.09 (-0.47)	98.2 (-39.7)	139.6 (-1.0)
<b>5</b>	5.03 (-1.51)	6.16 (-0.40)	97.9 (-40.0)	139.8 (-0.8)
<b>6</b>	4.93 (-1.61)	6.10 (-0.46)	97.5 (-40.4)	139.8 (-0.8)

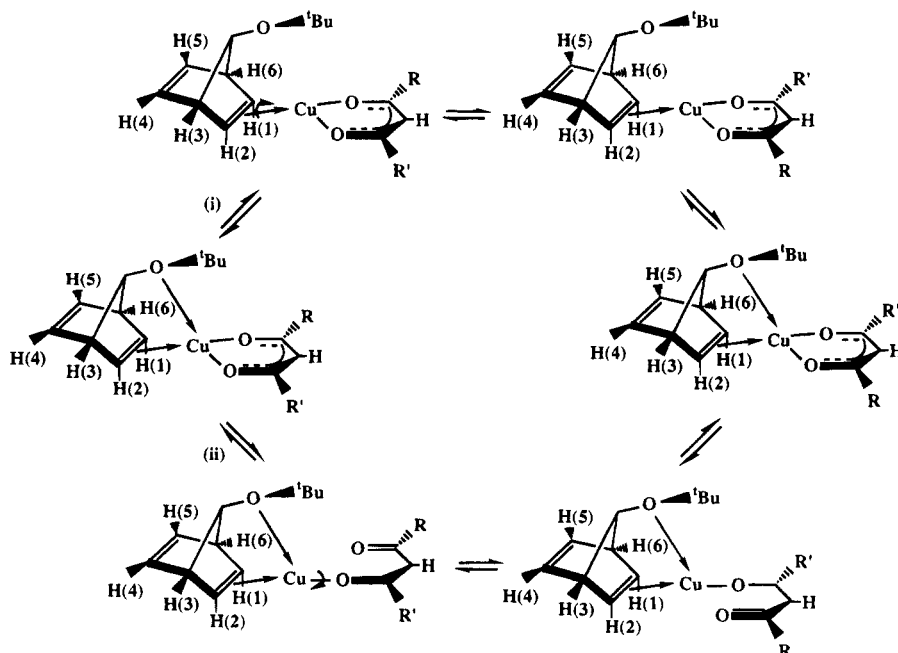
<sup>a</sup> In C<sub>6</sub>D<sub>6</sub>. <sup>b</sup>  $\Delta\delta = \delta_{\beta\text{-diketonate compd}} - \delta_{7\text{-}t\text{-BuO-NBD}}$ .

ture of (hfac)Cu(1,5-COD).<sup>11b</sup> Because hfac ligand possesses two electron-withdrawing CF<sub>3</sub> substituents, bond distances between copper and oxygen atoms of  $\beta$ -diketonate in compound **1** are longer than those in compounds **4** and **5**. To compensate for the electron deficiency on the copper center, donation of more electron density from O(1) to Cu, which resulted in a shorter (approximately 0.1 Å) Cu–O(1) bond in compound **1** than in compounds **4** and **5**, was observed. The longer bonds of the coordinated olefins (C(1)–C(2) = 1.346(5), 1.359(8), and 1.354(4) Å for compounds **1**, **4**, and **5**, respectively) than those of the noncoordinated olefins (C(4)–C(5) = 1.294(6), 1.299(8), and 1.311(6) Å for compounds **1**, **4**, and **5**, respectively) indicate the existence of  $\pi$ -backbonding between alkene and copper centers in these compounds (see below). No other distances and angles within the 7-*t*-BuO-NBD are exceptional.

**3. NMR Spectroscopic Studies of ( $\beta$ -Diketonate)Cu(7-*t*-BuO-NBD) Complexes.** The integrated <sup>1</sup>H and <sup>13</sup>C NMR spectra of the title compounds are consistent with the empirical formula ( $\beta$ -diketonate)-Cu(7-*t*-BuO-NBD) and exhibit olefinic resonances of the two types presented in Table 4. Both resonances have smaller chemical shifts than those of free 7-*t*-BuO-NBD. The signal at higher field is associated with the coor-

ordinated olefinic <sup>1</sup>H or <sup>13</sup>C and the other is attributed to the noncoordinated olefin. Comparisons of <sup>1</sup>H and <sup>13</sup>C chemical shifts for the free alkene and the alkene coordinating to the Cu(I) center were used to evaluate the relative contributions of  $\pi$  and  $\sigma$  bonding in the complexes.<sup>18,19</sup> Variations of chemical shifts ( $\Delta\delta$ ) of olefinic protons and carbons for compounds **1–6** are listed in Table 4 and are much larger than those for other ( $\beta$ -diketonate)(alkene)Cu(I) compounds that were found to be between +0.02 and –0.74 ppm and between –8.14 and –29.04 ppm for <sup>1</sup>H and <sup>13</sup>C signals, respectively.<sup>18</sup> This feature implies the existence of relatively stronger  $\pi$ -backbonding between alkene and copper center in the title compounds. Shieldings of both coordinated olefinic <sup>1</sup>H and <sup>13</sup>C nuclei of these compounds follow the increasing order of **3** > **2** > **1** in agreement with electron donor capabilities of  $\beta$ -diketonate ligands.

On the basis of the solid-state structures of compounds **4** and **5**, those containing an asymmetrically substituted  $\beta$ -diketonate ligand (R  $\neq$  R', see Scheme 1) are expected to exhibit bridgehead [H(3), H(6)], coordinated olefinic [H(1), H(2)], and noncoordinated olefinic [H(4), H(5)] proton NMR signals of two types. This structural feature is consistent with the variable-temperature <sup>1</sup>H NMR spectra of compound **2** in CD<sub>2</sub>Cl<sub>2</sub> solution are shown in Figure 5. The room-temperature NMR spectrum exhibits single bridgehead, coordinated olefinic, and noncoordinated olefinic proton signals at  $\delta$  3.37, 5.21, and 6.52 ppm, respectively, probably resulting from rapid dynamic rearrangement of the molecule in solution. Upon cooling, bridgehead and coordinated olefinic proton resonances decoalesced each into two signals of equal intensity. The activation barrier  $\Delta G^\ddagger$  of dynamic rearrangement was estimated to be  $11.7 \pm 0.5$  kcal·mol<sup>-1</sup> from the coalescence temperature (about 241 K,  $\Delta\nu = 16.3$  Hz) of bridgehead protons. However, only one broad noncoordinated olefinic proton resonance was observed in these spectra even at a temperature of 203 K. Similar variable-

**Scheme 1**

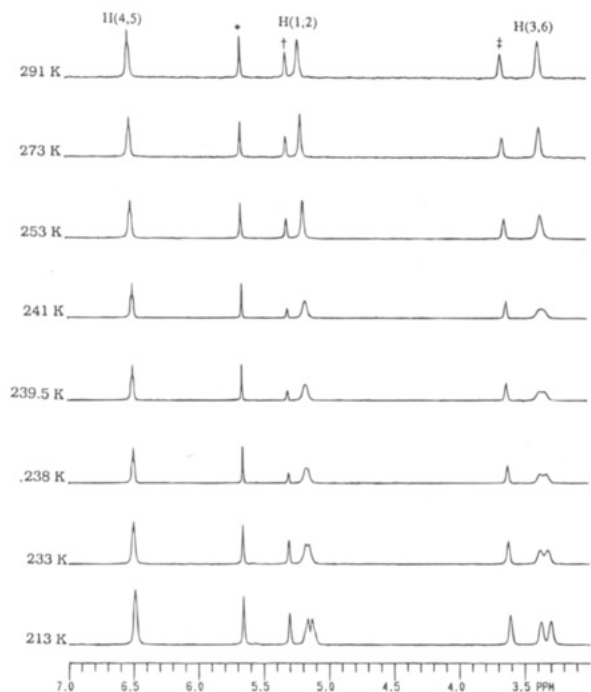
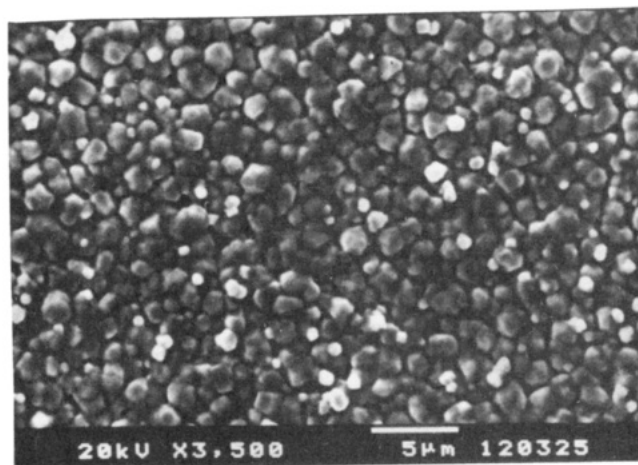


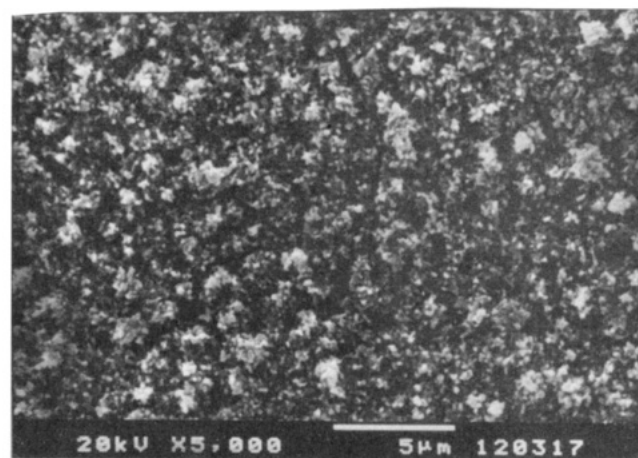
**Figure 5.** Variable-temperature  $^1\text{H}$  NMR spectra of  $(\text{tfac})\text{Cu}(7\text{-}t\text{-BuO-NBD})$  (\*,  $\text{CD}_2\text{Cl}_2$ ; †, methine H on tfac; and ‡, bridge H on 7-*t*-BuO-NBD).

temperature NMR measurements (down to 203 K) of compounds 4–6 were made, but the low-temperature limiting spectra were not attained. Two plausible routes to undergo the dynamic rearrangement are proposed in Scheme 1: (i) rotation of the  $\text{Cu}(\beta\text{-diketonate})$  moiety about the  $\text{Cu}$ –olefin bond and (ii) rotation of the  $\text{Cu}(7\text{-}t\text{-BuO-NBD})$  moiety about the bond between  $\text{Cu}$  and one O atom of the  $\beta\text{-diketonate}$  ligand. Both routes involve cleavage of the  $\text{Cu}$ –O bond. On the basis of the structures of compounds 1, 4, and 5 in the solid state, the bonds between  $\text{Cu}$  and O of 7-*t*-BuO-NBD are more labile than those between  $\text{Cu}$  and O of the  $\beta\text{-diketonate}$  in the title compounds. Exchange between the free  $\beta\text{-diketonate}$  anion with the coordinated  $\beta\text{-diketonate}$  of compound 2 has also been examined. Addition of  $\text{Na}(\text{tfac})$  to a  $\text{CD}_2\text{Cl}_2$  solution of  $(\text{tfac})\text{Cu}(7\text{-}t\text{-BuO-NBD})$  resulted in no exchange with coordinated tfac ligand on the  $^1\text{H}$  NMR time scale at 303 K. Thus, it appears that molecules of compound 2 can undergo rearrangement via the rotation of  $\text{Cu}(\beta\text{-diketonate})$  moiety about the  $\text{Cu}$ –olefin bond.

**4. Chemical Vapor Deposition of Copper from  $(\text{hfac})\text{Cu}(7\text{-}t\text{-BuO-NBD})$ .** Chemical vapor deposition experiments in the hot-wall system were carried out with  $(\text{hfac})\text{Cu}(7\text{-}t\text{-BuO-NBD})$  as precursor over the deposition temperature range 140–260 °C. The precursor was sublimed at 80 °C under reduced pressure (0.1 Torr) and was transferred through the deposition zone. Durations of deposition were 60–90 min, and the film thicknesses were 1.5–3.5  $\mu\text{m}$ . Continuous copper films with a metallic color and resistivities less than 6  $\mu\Omega\text{-cm}$  were deposited on both  $\text{SiO}_2$ - and Pt-coated substrates at deposition temperatures above 200 °C. Hence, the



(a) 230 °C



(b) 140 °C

**Figure 6.** Scanning electron micrographs of copper films deposited from  $(\text{hfac})\text{Cu}(7\text{-}t\text{-BuO-NBD})$  at (a) 230 °C and (b) 140 °C.

$\text{Cu}(\text{I})$  precursor may undergo disproportionation to form  $\text{Cu}$  metal and greenish-blue  $\text{Cu}(\text{hfac})_2$  which was observed on the cool end of the CVD reactor. The same mechanism was proposed for the CVD reactions with other  $\beta\text{-diketonate}$  complexes of copper(I) as precursors by Hampden-Smith.<sup>6–8</sup> All copper films had good adhesion according to the Scotch tape test. The surface morphology of the films was determined with SEM; a typical example deposited on a Pt-coated Si substrate at 230 °C appears in Figure 6a. The films deposited at temperatures above 200 °C consist of continuous grains similar to those in previous reports.<sup>6–8,10c</sup> The grain size increases with increasing deposition temperature. X-ray diffraction analyses of these films show the existence of crystalline material. A diffraction pattern of a film deposited on a  $\text{SiO}_2$ -coated substrate at 200 °C (Figure 7) corresponds to cubic copper.

Films deposited at the temperatures below 170 °C have a dark red color that is distinct from that of films deposited at temperatures >200 °C. It is possible that these films contain significant amount of impurities that result in larger resistivities (>1000  $\mu\Omega\text{-cm}$ ). These films have a morphology (Figure 6b) apparently distinct from those deposited at higher temperatures, which indicates

(18) Baum, T. H.; Larson, C. E.; May, G. J. *Organomet. Chem.* **1993**, *425*, 189.

(19) (a) Salomon, R. G.; Kochi, J. K. *J. Am. Chem. Soc.* **1973**, *95*, 1889. (b) Salomon, R. G.; Kochi, J. K. *J. Organomet. Chem.* **1974**, *64*, 135.

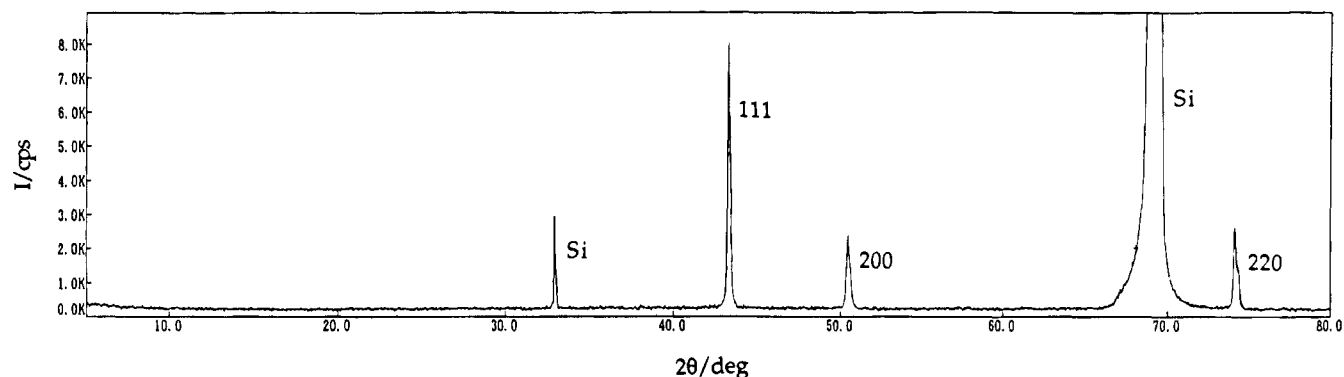


**Figure 7.** XRD pattern of a film deposited on a SiO<sub>2</sub>-coated substrate at 200 °C.

a different composition. Although all title compounds are volatile, compounds **2–6** exhibited insufficient thermal stability at sublimation temperatures to allow CVD experiments.

In conclusion, we prepared new copper(I) complexes of the general formula ( $\beta$ -diketonate)Cu(7-*t*-BuO-NBD). All compounds were characterized by analytical and spectral methods. Structural properties of three compounds were determined by single-crystal X-ray diffraction analyses. <sup>1</sup>H NMR spectra of all compounds in solution at varied temperatures indicated rapid rearrangements of these flexible molecules. CVD experiments using (hfac)Cu(7-*t*-BuO-NBD) as precursor demonstrated deposition of pure copper films at temperatures above 200 °C.

**Acknowledgment.** We thank Professor S. P. Wang of Department of Chemistry, National Cheng Kung University, for discussion of the NMR data, Dr. S.-G. Shyu of Institute of Chemistry, Academia Sinica, for obtaining SEM data, and the National Science Council of the Republic of China (NSC 82-0208-M-194-025) for support of this work.

**Supplementary Material Available:** Crystallographic data for compounds **1**, **4**, and **5**, including tables of crystal data, atomic coordinates, bond distances and angles, anisotropic thermal parameters (30 pages). Ordering information is given on any current masthead page.

OM940886D

# Novel Synthetic Route to Vinylidenerhodium(I) and -iridium(I) Complexes Using Vinyl Chlorides as Substrates<sup>†,1</sup>

Justin Wolf, Raimund W. Lass, Matthias Manger, and Helmut Werner\*

Institut für Anorganische Chemie der Universität Würzburg,  
Am Hubland, D-97074 Würzburg, Germany

Received January 18, 1995<sup>©</sup>

The bis(triisopropylphosphine)rhodium(I) and -iridium(I) compounds  $[\text{RhCl}(\text{PiPr}_3)_2]_n$  (**1**) and  $[\text{IrCl}(\text{C}_8\text{H}_{14})(\text{PiPr}_3)_2]$  (**2**) react with 2 equiv of  $\text{RR}'\text{C}=\text{CHCl}$  and 2 equiv of Na in benzene at room temperature to give the vinylidene complexes *trans*- $[\text{MCl}(\text{C}=\text{C}=\text{CRR}')(\text{PiPr}_3)_2]$  (**3–7**) in moderate to good yields. From **2**,  $\text{Ph}_2\text{C}=\text{CHCl}$ , and Na, the alkyne derivative *trans*- $[\text{IrCl}(\text{PhC}\equiv\text{CPh})(\text{PiPr}_3)_2]$  (**8**) is obtained as the main product. Preliminary studies aimed to elucidate the mechanism of the reaction indicate that from  $\text{RR}'\text{C}=\text{CHCl}$  and Na a vinyl radical  $\text{RR}'\text{C}=\text{CH}^\cdot$  is possibly formed which, depending on the substituents R and R', either reacts to give the alkyne  $\text{RC}\equiv\text{CR}'$ , initiates polymerization, or attacks the metal center of the starting material, to give the metal vinylidenes.

Whereas numerous vinylidene transition-metal complexes of general composition  $[\text{M}(\text{C}=\text{C}=\text{CRR}')\text{L}_n]$  with R = H and R' = alkyl or aryl are known, only a few examples of corresponding uncharged derivatives where both substituents R and R' are alkyl or aryl have been described in the literature.<sup>2</sup> Recently, Schubert and Groenen have shown that cyclopentadienylmanganese and (arene)chromium complexes of the type  $[(\text{ring})\text{M}(\text{C}=\text{C}=\text{CR}_2)(\text{CO})\text{L}]$  (R = Me, Ph; L = CO,  $\text{PR}_3$ ) can be prepared from cyclopentadienyl- or arene-metal precursors and  $\text{R}_2\text{C}=\text{C}(\text{SiMe}_3)\text{Cl}$ ,<sup>3</sup> but this route could not be extended to  $d^8$  systems of the cobalt or nickel subgroup. Attempts to use olefins  $\text{R}_2\text{C}=\text{CHCl}$  for the preparation of these complexes and instead of  $\text{Me}_3\text{SiCl}$  to eliminate HCl remained unsuccessful.<sup>4</sup> Following our work on the synthesis of silyl- and stannyl-substituted vinylidenerhodium compounds *trans*- $[\text{RhCl}(\text{C}=\text{C}(\text{SiR}_3)\text{R}')(\text{PiPr}_3)_2]$  and *trans*- $[\text{RhCl}(\text{C}=\text{C}(\text{SnPh}_3)\text{R}')(\text{PiPr}_3)_2]$  (R' = alkyl or aryl),<sup>5</sup> we wish to report here that related complexes *trans*- $[\text{MCl}(\text{C}=\text{C}=\text{CRR}')(\text{PiPr}_3)_2]$  for M = Rh and Ir are accessible on a route using vinyl chlorides and alkaline metals as substrates. This novel procedure illustrates that not only terminal alkynes  $\text{HC}\equiv\text{CR}$  and their silyl or stannyl derivatives  $\text{R}_3\text{EC}=\text{CR}'$  (E = Si, Sn) but also chloro-substituted olefins without  $\text{SiMe}_3$  as a further substituent can provide an entry into the chemistry of transition-metal vinylidenes.

## Results and Discussion

The starting materials **1** and **2** (the latter generated in situ from  $[\text{IrCl}(\text{C}_8\text{H}_{14})_2]_2$  and  $\text{PiPr}_3$ )<sup>6</sup> which have already been used for the preparation of *trans*- $[\text{MCl}(\text{C}=\text{C}=\text{CHR})(\text{PiPr}_3)_2]$  (M = Rh,<sup>7</sup> Ir<sup>8</sup>) react with  $\text{Me}_2\text{C}=\text{CHCl}$  and sodium sand (average diameter of the particles 1 mm) in benzene at room temperature to give **3** and **4** in 50–55% yield (Scheme 1). Both compounds are red-violet crystalline solids which are only slightly air-sensitive and thermally stable to about 100 °C. Related derivatives **5–7** are obtained in less satisfying yield (20–30%) and, like **3** and **4**, have been characterized by elemental analysis and NMR spectroscopy. The most typical features are (1) the low-field signals in the <sup>13</sup>C NMR spectra at  $\delta = 260\text{--}300$  and  $105\text{--}130$  which in analogy to previously obtained data are assigned to the  $\alpha\text{-C}$  and  $\beta\text{-C}$  vinylidene carbon atoms<sup>7,8</sup> and (2) the single <sup>31</sup>P NMR resonance (singlet for **4** and **7** and doublet for **3**, **5**, and **6**) indicating that the phosphine ligands are in *trans*-disposition.

With regard to the mechanism of formation of the vinylidene complexes **3–7** from the starting materials **1** and **2** and vinyl chlorides  $\text{RR}'\text{C}=\text{CHCl}$  in the presence of Na, we note that the ratio of metal vinylidenes to side products considerably depends (1) on the vinyl substituents R and R', (2) on the amount of sodium used, and (3) on the concentration of the reactants. As far as the influence of the substituents is concerned, the best yield of vinylidene complex has been obtained for R = R' =  $\text{CH}_3$ . In contrast, if R and R' is  $\text{C}_6\text{H}_5$  (and M = Ir), the yield of *trans*- $[\text{MCl}(\text{C}=\text{C}=\text{CPh}_2)(\text{PiPr}_3)_2]$  is rather low

<sup>†</sup> Dedicated to Professor Karl-Heinz Thiele on the occasion of his 65th birthday.

<sup>©</sup> Abstract published in *Advance ACS Abstracts*, April 15, 1995.  
(1) Vinylidene Transition-Metal Complexes. 37. For part 36, see: Kukla, F.; Werner, H. *Inorg. Chim. Acta*, in press.

(2) Reviews: (a) Bruce, M. I.; Swincer, A. G. *Adv. Organomet. Chem.* **1983**, *22*, 59–128. (b) Bruce, M. I. *Chem. Rev.* **1991**, *91*, 197–257. (c) Antonova, A. B.; Johansson, A. A. *Usp. Khim.* **1989**, *58*, 1197–1230. (d) Werner, H. *Angew. Chem.* **1990**, *102*, 1109–1121; *Angew. Chem., Int. Ed. Engl.* **1990**, *29*, 1077–1089.

(3) (a) Schubert, U.; Groenen, J. *Organometallics* **1987**, *6*, 2458–2459. (b) Schubert, U.; Groenen, J. *Chem. Ber.* **1989**, *122*, 1237–1245.

(4) Groenen, J. Dissertation, Universität Würzburg, 1989.

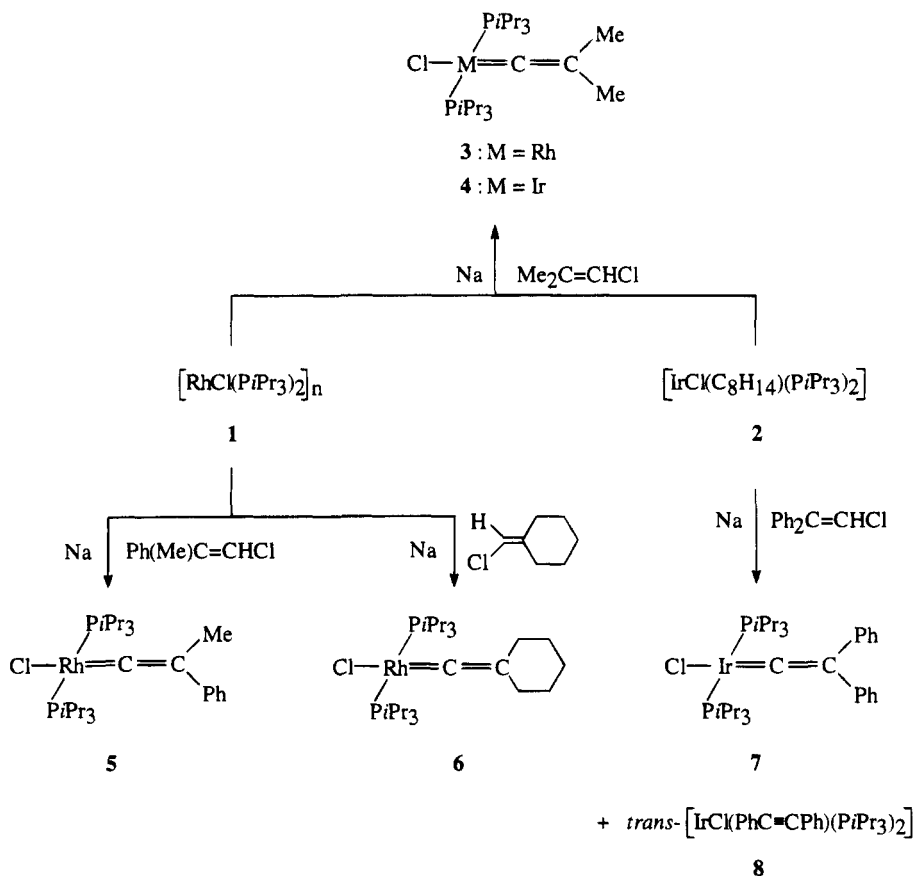
(5) (a) Schneider, D.; Werner, H. *Angew. Chem.* **1991**, *103*, 710–712; *Angew. Chem., Int. Ed. Engl.* **1991**, *30*, 700–702. (b) Werner, H.; Baum, M.; Schneider, D.; Windmüller, B. *Organometallics* **1994**, *13*, 1089–1097. (c) Baum, M.; Windmüller, B.; Werner, H. *Z. Naturforsch., B: Anorg. Chem., Org. Chem.* **1994**, *49*, 859–869. (d) Baum, M.; Mahr, N.; Werner, H. *Chem. Ber.* **1994**, *127*, 1877–1886.

(6) Schulz, M. Diploma Thesis, Universität Würzburg, 1988.

(7) (a) Werner, H.; Garcia Alonso, F. J.; Otto, H.; Wolf, J. Z. *Naturforsch., B: Anorg. Chem., Org. Chem.* **1988**, *43*, 722–726. (b) Werner, H.; Brekau, U. Z. *Naturforsch., B: Anorg. Chem., Org. Chem.* **1989**, *44*, 1438–1446. (c) Werner, H.; Rappert, T.; Wolf, J. *Isr. J. Chem.* **1990**, *30*, 377–384. (d) Rappert, T.; Nürnberg, O.; Mahr, N.; Wolf, J.; Werner, H. *Organometallics* **1992**, *11*, 4156–4164. (e) Werner, H.; Rappert, T. *Organometallics* **1993**, *12*, 1359–1364.

(8) (a) Höhn, A.; Otto, H.; Dzialis, M.; Werner, H. *J. Chem. Soc., Chem. Commun.* **1987**, 852–854. (b) Höhn, A.; Werner, H. *J. Organomet. Chem.* **1990**, *382*, 255–272. (c) Werner, H.; Höhn, A.; Schulz, M. *J. Chem. Soc., Dalton Trans.* **1991**, 777–781.

Scheme 1



since among the reaction products the isomeric alkyne compound **8** dominates. The formation of **8** is not surprising because it has been proven by us that one of the products of the reaction of  $\text{Ph}_2\text{C}=\text{CHCl}$  with Na is  $\text{PhC}\equiv\text{CPh}$  which reacts with **2** by ligand displacement to yield **8**.<sup>9</sup>

The influence of the amount of vinyl chloride and sodium on the product ratio has been investigated in the synthesis of **4**. We found that in order to obtain a yield of 50–55% it is necessary to use 2 equiv of  $\text{Me}_2\text{C}=\text{CHCl}$  and 2 equiv of Na. If more vinyl chloride is employed, the rate of the reaction increases but not the yield of vinylidene complex **4**. If more sodium is used, the yield of **4** decreases significantly, while after chromatographic workup among the iridium-containing products the carbonyl compound *trans*- $[\text{IrCl}(\text{CO})(\text{PiPr}_3)_2]$ <sup>10</sup> dominates.

Besides the ratio  $2:\text{Me}_2\text{C}=\text{CHCl}:\text{Na}$ , the concentration of the reactants also seems to be important for the preferred formation of **4**. Originally, we expected that a higher yield of the vinylidene complex could be obtained if dilute solutions of the starting materials **2** and  $\text{Me}_2\text{C}=\text{CHCl}$  were used. However, instead of **4** the amount of the side products increased. Our hypothesis is that the vinyl radical  $\text{Me}_2\text{C}=\text{CH}\cdot$ , generated from  $\text{Me}_2\text{C}=\text{CHCl}$  and Na, attacks the metal center of **2** to give the paramagnetic iridium(II) species  $[\text{IrCl}(\text{CH}=\text{CMe}_2)(\text{PiPr}_3)_2]$  as an intermediate which reacts with a second vinyl radical to yield **4** and isobutene. We

finally note that to use potassium instead of sodium does not effect the rate of formation and the yield of **4** and that potassium-graphite preferentially gives  $[\text{IrH}_2\text{Cl}(\text{PiPr}_3)_2]$ .<sup>11</sup>

In summary, we have established a new route to vinylidenerhodium and iridium complexes *trans*- $[\text{MCl}(\text{C}=\text{CRR}')(\text{PiPr}_3)_2]$  based on the formal elimination of HCl from vinyl chlorides  $\text{RR}'\text{C}=\text{CHCl}$ . We are presently trying to extend our methodology to other transition-metal compounds and other olefinic substrates and will report on these efforts in the near future.

### Experimental Section

All experiments were carried out under an atmosphere of argon using Schlenk tube techniques. The starting materials **1**<sup>1b</sup> and  $[\text{IrCl}(\text{C}_8\text{H}_{14})_2]_2$ <sup>12</sup> were prepared as described in the literature. Melting points were determined by DTA. For the interpretation of the NMR spectra, the following abbreviations were used: s, singlet; d, doublet; t, triplet; vt, virtual triplet; m, multiplet.

**Preparation of *trans*- $[\text{RhCl}(\text{C}=\text{CMe}_2)(\text{PiPr}_3)_2]$  (**3**).** A solution of **1** (70 mg, 0.15 mmol for  $n = 1$ ) in 10 mL of benzene was treated with sodium sand (9.1 mg, 0.40 mmol) and  $\text{Me}_2\text{C}=\text{CHCl}$  (90.6 mg, 1.00 mmol). After the reaction mixture was vigorously stirred for 3 h, the solvent was removed in vacuo. The residue was extracted twice with 5 mL of hexane, and the solution was chromatographed on  $\text{Al}_2\text{O}_3$  (neutral, activity grade V). With hexane, a violet fraction was eluted

(11) (a) Hietkamp, S.; Stufkens, D. J.; Vrieze, K. *J. Organomet. Chem.* **1978**, *152*, 347–357. (b) Werner, H.; Wolf, J.; Höhn, A. *J. Organomet. Chem.* **1985**, *287*, 395–407. (c) Werner, H.; Höhn, A.; Dziallas, M. *Angew. Chem.* **1986**, *98*, 1112–1114; *Angew. Chem., Int. Ed. Engl.* **1986**, *25*, 1090–1092.

(12) van der Ent, A.; Onderdelinden, A. L. *Inorg. Synth.* **1973**, *14*, 92–95.

(9) Werner, H.; Höhn, A. *J. Organomet. Chem.* **1984**, *272*, 105–113.

(10) (a) Strohmeier, W.; Onoda, T. *Z. Naturforsch., B: Anorg. Chem., Org. Chem.* **1968**, *23*, 1377–1379. (b) Werner, H.; Höhn, A. *Z. Naturforsch., B: Anorg. Chem., Org. Chem.* **1984**, *39*, 1505–1509.

which was concentrated in vacuo to ca. 5 mL and then stored at  $-78^{\circ}\text{C}$ . Violet crystals precipitated which were filtered out, washed with small quantities of pentane ( $-40^{\circ}\text{C}$ ), and dried: yield 40 mg (52%); mp  $134^{\circ}\text{C}$  dec. Anal. Calcd for  $\text{C}_{22}\text{H}_{48}\text{ClP}_2\text{Rh}$ : C, 51.52; H, 9.43. Found: C, 51.52; H, 9.74. IR (KBr):  $\nu(\text{C}=\text{C})$   $1680\text{ cm}^{-1}$ .  $^1\text{H}$  NMR (200 MHz,  $\text{C}_6\text{D}_6$ ):  $\delta$  2.65 (m,  $\text{PCHCH}_3$ ), 1.69 [dt,  $J(\text{RhH}) = 0.6$ ,  $J(\text{PH}) = 2.3$  Hz,  $=\text{C}(\text{CH}_3)_2$ ], 1.29 [dvt,  $N = 13.3$ ,  $J(\text{HH}) = 6.2$  Hz,  $\text{PCHCH}_3$ ].  $^{13}\text{C}$  NMR (50.3 MHz,  $\text{C}_6\text{D}_6$ ):  $\delta$  293.16 [dt,  $J(\text{RhC}) = 57.1$ ,  $J(\text{PC}) = 16.7$  Hz,  $\text{Rh}=\text{C}=\text{C}$ ], 105.58 [dt,  $J(\text{RhC}) = 15.8$ ,  $J(\text{PC}) = 5.9$  Hz,  $\text{Rh}=\text{C}=\text{C}$ ], 23.54 (vt,  $N = 19.4$  Hz,  $\text{PCHCH}_3$ ), 20.29 (s,  $\text{PCHCH}_3$ ), 6.56 [s,  $=\text{C}(\text{CH}_3)_2$ ].  $^{31}\text{P}$  NMR (81.0 MHz,  $\text{CDCl}_3$ ):  $\delta$  42.48 [d,  $J(\text{RhP}) = 136.1$  Hz].

**Preparation of *trans*-[IrCl(=C=CMe<sub>2</sub>)(PiPr<sub>3</sub>)<sub>2</sub>] (4).** A suspension of [IrCl(C<sub>6</sub>H<sub>14</sub>)<sub>2</sub>]<sub>2</sub> (100 mg, 0.11 mmol) in 10 mL of benzene was treated first with PiPr<sub>3</sub> (72.0 mg, 0.45 mmol) and then with sodium sand (10.4 mg, 0.45 mmol) and Me<sub>2</sub>C=CHCl (90.6 mg, 1.00 mmol). The reaction mixture was vigorously stirred for 5 h at room temperature and was then worked up as described for **3**. Red-violet crystals were obtained: yield 72 mg (54%); mp  $169^{\circ}\text{C}$ . Anal. Calcd for  $\text{C}_{22}\text{H}_{48}\text{ClIrP}_2$ : C, 43.88; H, 8.03. Found: C, 43.46; H, 8.29. IR (KBr):  $\nu(\text{C}=\text{C})$   $1705\text{ cm}^{-1}$ .  $^1\text{H}$  NMR (200 MHz,  $\text{CDCl}_3$ ):  $\delta$  2.78 (m,  $\text{PCHCH}_3$ ), 2.14 [t,  $J(\text{PH}) = 2.2$  Hz,  $=\text{C}(\text{CH}_3)_2$ ], 1.29 [dvt,  $N = 13.4$ ,  $J(\text{HH}) = 6.3$  Hz,  $\text{PCHCH}_3$ ].  $^{13}\text{C}$  NMR (50.3 MHz,  $\text{C}_6\text{D}_6$ ):  $\delta$  226.31 [t,  $J(\text{PC}) = 13.2$  Hz,  $\text{Ir}=\text{C}=\text{C}$ ], 103.67 [t,  $J(\text{PC}) = 3.9$  Hz,  $\text{Ir}=\text{C}=\text{C}$ ], 22.78 (vt,  $N = 26.1$  Hz,  $\text{PCHCH}_3$ ), 20.12 (s,  $\text{PCHCH}_3$ ),  $-0.81$  [t,  $J(\text{PC}) = 1.7$  Hz,  $=\text{C}(\text{CH}_3)_2$ ].  $^{31}\text{P}$  NMR (81.0 MHz,  $\text{CDCl}_3$ ):  $\delta$  30.41 (s).

**Preparation of *trans*-[RhCl(=C=(Me)Ph)(PiPr<sub>3</sub>)<sub>2</sub>] (5).** A solution of **1** (93 mg, 0.20 mmol for  $n = 1$ ) in 7 mL of benzene was treated with sodium sand (10.7 mg, 0.47 mmol) and Ph(Me)C=CHCl (145  $\mu\text{L}$ , 0.94 mmol). After the reaction mixture was vigorously stirred for 6 h, the solvent was removed in vacuo. The residue was extracted with 30 mL of pentane, and the extract was concentrated to ca. 3 mL and then chromatographed on Al<sub>2</sub>O<sub>3</sub> (neutral, activity grade III). With hexane/ether (5:1) first yellow and then violet fractions were eluted, the latter of which was brought to dryness in vacuo. The residue was dissolved in 2 mL of pentane, and after the solution was stored at  $-78^{\circ}\text{C}$  for 18 h, violet crystals were formed. They were filtered out, washed with small quantities of pentane ( $-40^{\circ}\text{C}$ ), and dried: yield 28 mg (24%); mp  $119^{\circ}\text{C}$  dec. Anal. Calcd for  $\text{C}_{27}\text{H}_{50}\text{ClP}_2\text{Rh}$ : C, 56.40; H, 8.77. Found: C, 56.73; H, 8.63. MS (70 eV),  $m/z$ : 576 ( $\text{M}^+$  for  $^{37}\text{Cl}$ ), 574 ( $\text{M}^+$  for  $^{35}\text{Cl}$ ). IR (KBr):  $\nu(\text{C}=\text{C})$   $1648\text{ cm}^{-1}$ .  $^1\text{H}$  NMR (200 MHz,  $\text{C}_6\text{D}_6$ ):  $\delta$  7.37 [d,  $J(\text{HH}) = 7.3$  Hz, *ortho*-H of  $\text{C}_6\text{H}_5$ ], 7.19 [t,  $J(\text{HH}) = 7.3$  Hz, *meta*-H of  $\text{C}_6\text{H}_5$ ], 6.89 [t,  $J(\text{HH}) = 7.3$  Hz, *para*-H of  $\text{C}_6\text{H}_5$ ], 2.59 (m,  $\text{PCHCH}_3$ ), 2.06 [t,  $J(\text{PH}) = 2.1$  Hz,  $=\text{CCH}_3$ ], 1.26 [dvt,  $N = 13.5$ ,  $J(\text{HH}) = 6.6$  Hz,  $\text{PCHCH}_3$ ].  $^{13}\text{C}$  NMR (100.6 MHz,  $\text{CDCl}_3$ ):  $\delta$  299.34 [dt,  $J(\text{RhC}) = 59.4$ ,  $J(\text{PC}) = 16.4$  Hz,  $\text{Rh}=\text{C}=\text{C}$ ], 128.59 (s, *ipso*-C of  $\text{C}_6\text{H}_5$ ), 127.69, 124.37 and 123.97 (all s,  $\text{C}_6\text{H}_5$ ), 114.73 [dt,  $J(\text{RhC}) = 14.1$ ,  $J(\text{PC}) = 7.0$  Hz,  $\text{Rh}=\text{C}=\text{C}$ ], 23.94 (vt,  $N = 19.7$  Hz,  $\text{PCHCH}_3$ ), 20.25 (s,  $\text{PCHCH}_3$ ), 3.36 (s,  $=\text{CCH}_3$ ).  $^{31}\text{P}$  NMR (81.0 MHz,  $\text{C}_6\text{D}_6$ ):  $\delta$  43.24 [d,  $J(\text{RhP}) = 135.2$  Hz].

**Preparation of *trans*-[RhCl(=C=CCH<sub>2</sub>(CH<sub>2</sub>)<sub>3</sub>CH<sub>2</sub>)-(PiPr<sub>3</sub>)<sub>2</sub>] (6).** A solution of **1** (132 mg, 0.28 mmol for  $n = 1$ ) in 7 mL of benzene was treated with sodium sand (15 mg, 0.65 mmol) and 1-(chloromethylene)cyclohexane (130  $\mu\text{L}$ , 1.2 mmol). After the reaction mixture was vigorously stirred for 2.5 h at room temperature, the solvent was removed and the residue extracted twice with 15 mL of benzene each. The extract was evaporated in vacuo and the residue dissolved in 3 mL of hexane. The further workup procedure was the same as described for **5**. Red-violet crystals were obtained: yield 46 mg (29%); mp  $126^{\circ}\text{C}$  dec. Anal. Calcd for  $\text{C}_{25}\text{H}_{52}\text{ClP}_2\text{Rh}$ : C, 54.30; H, 9.48. Found: C, 54.32; H, 9.31. MS (70 eV),  $m/z$ : 554 ( $\text{M}^+$  for  $^{37}\text{Cl}$ ), 552 ( $\text{M}^+$  for  $^{35}\text{Cl}$ ). IR (KBr):  $\nu(\text{C}=\text{C})$   $1687\text{ cm}^{-1}$ .  $^1\text{H}$  NMR (200 MHz,  $\text{CDCl}_3$ ):  $\delta$  2.68 (m,  $\text{PCHCH}_3$ ), 2.27 (m, br,  $=\text{CCH}_2(\text{CH}_2)_3\text{CH}_2$ ), 1.30 [dvt,  $N = 13.3$ ,  $J(\text{HH}) = 6.2$  Hz,  $\text{PCHCH}_3$ ]; the signal of the  $(\text{CH}_2)_3$  protons is probably covered by the signals of the PiPr<sub>3</sub> protons.  $^{13}\text{C}$  NMR (100.6 MHz,  $\text{CDCl}_3$ ):  $\delta$  290.88 [dt,  $J(\text{RhC}) = 59.7$ ,  $J(\text{PC}) = 16.4$  Hz,  $\text{Rh}=\text{C}=\text{C}$ ], 110.73 [dt,  $J(\text{RhC}) = 16.1$ ,  $J(\text{PC}) = 6.4$  Hz,  $\text{Rh}=\text{C}=\text{C}$ ], 25.98 and 25.77 [both s,  $(\text{CH}_2)_3$ ], 23.07 (vt,  $N = 19.3$  Hz,  $\text{PCHCH}_3$ ), 20.02 (s,  $\text{PCHCH}_3$ ), 17.38 [t,  $J(\text{PC}) = 1.9$  Hz,  $=\text{CCH}_2(\text{CH}_2)_3\text{CH}_2$ ].  $^{31}\text{P}$  NMR (81.0 MHz,  $\text{CDCl}_3$ ):  $\delta$  42.07 [d,  $J(\text{RhP}) = 135.2$  Hz].

**Preparation of *trans*-[IrCl(=C=CPh<sub>2</sub>)(PiPr<sub>3</sub>)<sub>2</sub>] (7).** A suspension of [IrCl(C<sub>6</sub>H<sub>14</sub>)<sub>2</sub>]<sub>2</sub> (100 mg, 0.11 mmol) in 10 mL of benzene was treated first with PiPr<sub>3</sub> (72.0 mg, 0.45 mmol) and then with sodium sand (10.4 mg, 0.45 mmol) and Ph<sub>2</sub>C=CHCl (142 mg, 0.66 mmol). After the reaction mixture was vigorously stirred for 6 h at room temperature, the solvent was removed and the residue extracted twice with 5 mL of hexane each. Chromatography on Al<sub>2</sub>O<sub>3</sub> (neutral, activity grade V) with hexane gave first a yellow fraction (containing complex **8**) and then a blue fraction which was worked up as described for **3**. Dark-blue crystals were obtained: yield 27 mg (17%); mp  $108^{\circ}\text{C}$ . Anal. Calcd for  $\text{C}_{32}\text{H}_{52}\text{ClIrP}_2$ : C, 52.92; H, 7.22. Found: C, 53.23; H, 7.40. IR (KBr):  $\nu(\text{C}=\text{C})$   $1620, 1580\text{ cm}^{-1}$ .  $^1\text{H}$  NMR (200 MHz,  $\text{CDCl}_3$ ):  $\delta$  7.32, 7.20 and 6.97 (all m,  $\text{C}_6\text{H}_5$ ), 2.73 (m,  $\text{PCHCH}_3$ ), 1.25 [dvt,  $N = 13.7$ ,  $J(\text{HH}) = 6.6$  Hz,  $\text{PCHCH}_3$ ].  $^{13}\text{C}$  NMR (50.3 MHz,  $\text{CDCl}_3$ ):  $\delta$  263.03 [t,  $J(\text{PC}) = 12.1$  Hz,  $\text{Ir}=\text{C}=\text{C}$ ], 123.90 [t,  $J(\text{PC}) = 3.0$  Hz,  $\text{Ir}=\text{C}=\text{C}$ ], 128.11, 127.82, 124.90 and 122.00 (all s,  $\text{C}_6\text{H}_5$ ), 23.86 (vt,  $N = 26.4$  Hz,  $\text{PCHCH}_3$ ), 20.05 (s,  $\text{PCHCH}_3$ ).  $^{31}\text{P}$  NMR (81.0 MHz,  $\text{CDCl}_3$ ):  $\delta$  30.41 (s). Complex **8** (yield 110 mg, 68%) was identified spectroscopically ( $^1\text{H}$ ,  $^{31}\text{P}$  NMR) by comparison with an authentic sample.

**Acknowledgment.** We thank the Volkswagen Stiftung and the Fonds der Chemischen Industrie for financial support and Degussa AG for various gifts of chemicals. We also gratefully acknowledge support by Mrs. I. Geiter (experimental assistance), Mrs. U. Neumann and Mr. C. P. Kneis (elemental analysis), Mrs. R. Schedl (DTA), and Dr. G. Lange and Mr. F. Dadrach (mass spectra).

OM9500331

# Gas-Phase Chemistry of the Silaformamide Ion

Joseph A. Hankin,<sup>†</sup> Michèle Krempp,<sup>†</sup> and Robert Damrauer<sup>\*,‡</sup>

Departments of Chemistry, University of Colorado at Boulder, Boulder, Colorado 80309, and  
University of Colorado at Denver, Denver, Colorado 80217-3364

Received March 23, 1995<sup>®</sup>

The anion  $[\text{HSi}(\text{O})\text{NH}]^-$  (**2**) has been produced in the source region of a tandem flowing afterglow selected ion flow tube from phenylsilane, amide, and water and mass-selected for further study. Its connectivity has been established from studies of its formation from deuterated reactants and by chemical reactivity studies with  $\text{CO}_2$ ,  $\text{COS}$ , and  $\text{CS}_2$ . A variety of alcohols undergo interesting reactions with **2**. In particular, reactions with fluoro alcohols are considered in terms of the energy content of the complex formed when a proton is transferred from a fluoroalcohol to **2**. A series of anions related to **2** have been studied by *ab initio* methods. For a number of these, the silylene anion form is more stable than its isomer (e.g.  $[\text{Si}(\text{O})\text{NH}_2]^-$  (**1**) is more stable than  $[\text{HSi}(\text{O})\text{NH}]^-$  (**2**)). Computational energies suggest that Si-H deprotonation of  $\text{HSi}(\text{X})\text{Y}$  (for X = O, NH,  $\text{CH}_2$ ) when Y =  $\text{NH}_2$ ,  $\text{CH}_3$  is favored over deprotonation at N-H or C-H, while O-H deprotonation is favored when Y = OH. Charge density computations of a variety of neutrals and anions reveal the dominant effect of silicon in determining charge density. The acidity ( $\Delta G_{\text{acid}}$ ) of silaformamide has been estimated by bracketing methods to be between 350 and 355 kcal mol<sup>-1</sup>.

## Introduction

Low-valent silicon-containing compounds continue to attract a great deal of attention in both experimental<sup>1-3</sup> and computational studies.<sup>4,5</sup> Neutral unsaturated species having silicon-carbon, silicon-silicon, silicon-oxygen, silicon-nitrogen, and silicon-phosphorus double bonds are generally stable if substituted by sterically demanding groups. Our understanding of such species has markedly increased in recent years, although it hardly compares with our understanding of analogous carbon species.

Using flowing afterglow selected ion flow tube (FA-SIFT) techniques, we have studied the ion-molecule reaction chemistry of anions closely related to the following low-valent silicon-containing molecules:  $(\text{CH}_3)_2\text{Si}$ ,<sup>6</sup>  $(\text{CH}_3)_2\text{Si}=\text{CH}_2$ ,<sup>7</sup>  $\text{Si}=\text{CH}_2$ ,<sup>8</sup>  $\text{H}_2\text{Si}=\text{O}$ ,<sup>9</sup>  $\text{CH}_3\text{SiHO}$ ,<sup>10</sup>  $\text{CH}_3\text{OSiHO}$ ,<sup>10</sup>  $\text{H}_2\text{SiS}$ ,<sup>11</sup> and  $\text{HSiNH}_2$ .<sup>11</sup> FA-SIFT studies are particularly suited to the indirect study of such compounds, since closely related, simple silicon-containing anions can be often be prepared in the gas phase, even though their conjugate acids would be expected to be exceptionally reactive in either the gas or condensed

phase. In studying the reaction chemistry of simple anions unencumbered by bulky substituents in the gas phase, we can explore not only the reactivity of such anions but also, by indirect means, the properties of their corresponding conjugate acids as well.<sup>1</sup>

The flowing afterglow selected ion flow tube technique allows the selection of ions from complex reaction mixtures.<sup>8-11</sup> Because reaction chemistry studies occur under single-collision conditions, stoichiometric relationships can be determined. In addition, we can measure reaction rates and detect multiple reaction pathways. In favorable cases, thermochemical properties such as heats of formation of anions and their corresponding conjugate acids, electron affinities of corresponding radicals, and gas-phase acidities of the conjugate acids can be determined as well.<sup>1,9</sup> In relating the chemistry of anions and their conjugate acid species, it is important to realize that the structure of the acid is not always known. For example, the conjugate acid of the anionic species containing two hydrogens, one silicon, and one carbon (designated  $[\text{H}_2\text{Si,C}]^-$ : see the note at the end of this paragraph) could be  $\text{HC}\equiv\text{SiH}$ ,  $\text{H}_2\text{C}=\text{Si}$ , or  $\text{C}=\text{SiH}_2$ . When we study the reactions of  $[\text{H}_2\text{Si,C}]^-$  with acids, we are often uncertain of the structure of the reaction product unless other information is available.<sup>11</sup> Linking our experimental studies with computational work carried out both by other workers and by us has proven advantageous in sorting out structural questions for such species.<sup>9,11-13</sup> (General formulations such as  $[\text{H}_2\text{Si,C}]^-$  and  $[\text{H}_2\text{Si,C}]^-$  will be used for compounds and anions whose compositions are known but whose structures are not. When the structure is known, the connectivity of its atoms will be clearly designated. For example, the  $[\text{H}_2\text{CSi}]^-$  formulation indicates that two hydrogens are bound to carbon which is bonded to silicon. Similarly,  $[\text{HSiO}]^-$  repre-

<sup>†</sup> University of Colorado at Boulder.

<sup>‡</sup> University of Colorado at Denver.

<sup>®</sup> Abstract published in *Advance ACS Abstracts*, May 15, 1995.

(1) Damrauer, R.; Hankin, J. A. *Chem. Rev.*, in press.

(2) Raabe, G.; Michl, J. In *The Chemistry of Functional Groups*; Patai, S., Rappoport, Z., Eds.; Wiley: New York, 1989; pp 1015-1142.

(3) Iraqi, M.; Schwarz, H. *Chem. Phys. Lett.* **1993**, *205*, 183-186.

(4) Apeloig, Y. In *The Chemistry of Functional Groups*; Patai, S., Rappoport, Z., Eds.; Wiley: New York, 1989; pp 57-225.

(5) Baldrige, K. K.; Boatz, J. A.; Koseki, S.; Gordon, M. S. *Annu. Rev. Phys. Chem.* **1987**, *38*, 211-252.

(6) Damrauer, R.; DePuy, C. H.; Davidson, I. M. T.; Hughes, K. J. *Organometallics* **1986**, *5*, 2054-2057.

(7) Damrauer, R.; DePuy, C. H.; Davidson, I. M. T.; Hughes, K. J. *Organometallics* **1986**, *5*, 2050-2054.

(8) Damrauer, R.; DePuy, C. H.; Barlow, S. E.; Gronert, S. *J. Am. Chem. Soc.* **1988**, *110*, 2005-2006.

(9) Gronert, S.; O'Hair, R. A. J.; Prodnuk, S.; Sülzle, D.; Damrauer, R.; DePuy, C. H. *J. Am. Chem. Soc.* **1990**, *112*, 997-1003.

(10) Damrauer, R.; Krempp, M. *Organometallics* **1990**, *9*, 999-1004.

(11) Damrauer, R.; Krempp, M.; O'Hair, R. A. J. *J. Am. Chem. Soc.* **1993**, *115*, 1998-2005.

(12) Schmidt, M. W.; Gordon, M. S. *J. Am. Chem. Soc.* **1991**, *113*, 5244-5248.

(13) Shimizu, H.; Gordon, M. S.; Damrauer, R.; O'Hair, R. A. J. *Organometallics*, in press.

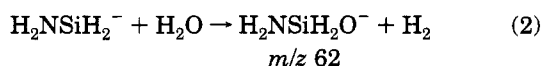
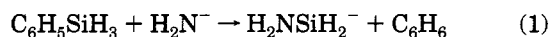


sents a typical anion where the negative charge location is unknown but the connectivity is known.  $\text{HSiO}^-$  indicates known connectivity with negative charge localization on oxygen.)

In this paper we describe experimental and computational studies on  $[\text{H}_2\text{Si}_2\text{N}_2\text{O}]^-$  and related species. The work on the structure and reactivity of this anion and its conjugate acid further probes the relationship between low-valent silicon analogs of important carbon compounds, in this case between the silaformamide and formamide. Of particular interest is the potential ambident behavior of this anion. We have studied very few species of this type in our previous work.

## Experimental Section

**Instrumental Details.** All experiments were carried out at room temperature in the flowing afterglow selected ion flow tube (FA-SIFT). Although this instrument has been described in detail previously,<sup>14</sup> a brief summary of its operation in these experiments is appropriate for readers who are not familiar with the technique. The FA-SIFT consists of four sections: a flow tube for ion preparation (A), an ion separation and purification region (B), a second flow tube for studying the chemical reactions of the ions selected (C), and finally an ion detection region (D). In the first flow tube (A), for example, ions such as  $\text{H}_2\text{N}^-$  (prepared by electron impact of  $\text{NH}_3$ ) are entrained in a rapidly flowing helium stream (0.3 Torr). In this study, phenylsilane and water are added downstream through a movable inlet producing the  $m/z$  62 ion by a complex series of reactions that are summarized by eqs 1 and 2.



At the end of the first flow tube the ions are sampled through a 2 mm orifice into the ion separation region (B), and the helium and other neutrals are removed by pumping while the ions are focused into a quadrupole mass filter by a series of electrostatic lenses. This SIFT quadrupole can be tuned to inject  $\text{H}_2\text{NSiH}_2\text{O}^-$  ( $m/z$  62) into the second flow tube (C), where it is again entrained in helium (0.5 Torr). Ions so injected typically undergo thermalizing collisions with helium before reaction and subsequent detection. At the end of the second flow tube the requisite ion is sampled through a 0.5 mm orifice and detected by an electron multiplier. To inject ions from the low-pressure ( $10^{-6}$  Torr) region of the SIFT quadrupole into the higher pressure region of the second flow tube, they must be extracted by an electrical potential. While this potential imparts kinetic energy to the ions, they are generally relaxed by multiple collisions with the helium buffer gas. However, when this potential is made sufficiently high, some ions can be induced to undergo collisionally induced dissociation (CID) to form new ions.<sup>9</sup> The  $m/z$  62 ion produced above is such an ion and is transformed into an ion of  $m/z$  60 as summarized in eq 3.

(14) Van Doren, J. M.; Barlow, S. E.; Depuy, C. H.; Bierbaum, V. M. *Int. J. Mass Spectrom. Ion Processes* **1987**, *81*, 85–100.

(15) Chesnavich, W. J.; Su, T.; Bowers, M. T. *J. Chem. Phys.* **1980**, *72*, 2641–2655.

(16) Frisch, M. J.; Head-Gordon, M.; Trucks, G. W.; Foresman, J. B.; Schlegel, H. B.; Raghavachari, K.; Robb, M.; Binkley, J. S.; Gonzalez, C.; Defrees, D. J.; Fox, D. J.; Whiteside, R. A.; Seeger, R.; Melius, C. F.; Baker, J.; Martin, R. L.; Kahn, L. R.; Stewart, J. J. P.; Topiol, S.; Pople, J. A. Gaussian 90; Gaussian, Inc., Pittsburgh, PA, 1990.

(17) Frisch, M. J.; Trucks, G. W.; Head-Gordon, M.; Gill, P. M. W.; Wong, M. W.; Foresman, J. B.; Johnson, B. G.; Schlegel, H. B.; Robb, M. A.; Replogle, E. S.; Gomperts, R.; Andres, J. L.; Raghavachari, K.; Binkley, J. S.; Gonzalez, C.; Martin, R. L.; Fox, D. J.; Defrees, D. J.; Baker, J.; Stewart, J. J. P.; Pople, J. A. Gaussian 92; Gaussian, Inc., Pittsburgh, PA, 1992.



We have also prepared the  $m/z$  60 ion directly in the first flow tube without a separate CID step. Thus,  $[\text{H}_2\text{Si}_2\text{N}_2\text{O}]^-$  ( $m/z$  60) can be directly extracted from a mixture of  $\text{NH}_2^-$ ,  $\text{C}_6\text{H}_5\text{SiH}_3$ , and  $\text{H}_2\text{O}$ . The direct route has been used in most of the studies reported here. The connectivity of the silaformamide anion was established by deuteration studies using both  $\text{ND}_2^-$  and  $\text{D}_2\text{O}$  in eqs 1 and 2. These experiments will be fully discussed in the Results and Discussion.

All reactions were studied at 300 K at a helium buffer gas pressure of 0.5 Torr and a flow of  $\sim 225$  STP  $\text{cm}^3 \text{ s}^{-1}$ . Branching ratios were determined as a function of reaction distance and are reported as extrapolations to zero reaction distance to eliminate any effects of differential diffusion among the ions and of secondary reactions. Branching ratios were also corrected for mass discrimination in the detection region by directly measuring the detector response as a function of ion current at the nose cone orifice. Rate coefficients were determined under pseudo-first-order conditions by monitoring the reactant ion density as a function of reaction distance (which is proportional to time) using a measured flow of the neutral reagent. Reported values are the average of three measurements using different reagent flows and are reproducible to within 10%. Reaction efficiencies have been calculated from ion–neutral collision rates using the variational transition state theory model of Bowers and co-workers.<sup>15</sup>

Gases were obtained from commercial sources and were of the following purities: He (99.995%),  $\text{NH}_3$  (99.99%),  $\text{CO}_2$  (99.5%), and COS (97.7%). Other reagents also were obtained from commercial sources. The helium buffer gas was passed through a liquid-nitrogen-cooled molecular sieve trap before entering the flow tubes.

**Computational Details.** *Ab initio* calculations were carried out with the Gaussian 90 and 92 programs.<sup>16,17</sup> Molecular geometries were optimized using closed-shell restricted-Hartree–Fock (RHF) self-consistent-field (SCF) calculations at the MP2/6-31+G(d,p) level. The structures determined in this manner were verified to be minima by analytically calculating and then diagonalizing the matrix of energy second derivatives (hessian). The hessian is positive definite in all cases dis-

(18) Bader, R. F. W. *Acc. Chem. Res.* **1985**, *18*, 9–15.

(19) Wiberg, K. B.; Bader, R. F. W.; Lau, C. D. H. *J. Am. Chem. Soc.* **1987**, *109*, 985–1001.

(20) Wiberg, K. B.; Bader, R. F. W.; Lau, C. D. H. *J. Am. Chem. Soc.* **1987**, *109*, 1001–1012.

(21) Curtiss, L. A.; Raghavachari, K.; Trucks, G. W.; Pople, J. A. *J. Chem. Phys.* **1991**, *94*, 7221. This paper indicates that “for 125 energies the average absolute deviation at the G2 level is 1.21 kcal/mol compared to 1.53 kcal/mol for the G1 level”. It is not clear how accurately G2 deals with compounds containing first- versus second-row elements. The  $\pm 3$  kcal  $\text{mol}^{-1}$  range given in the paper is the commonly accepted range for G2 level computations (Gordon, M. S., personal communication).

(22) Damrauer, R.; Krempp, M. *Organometallics* **1995**, *14*, 170–176.

(23) Bartmess, J. E. *Mass Spectrom. Rev.* **1989**, *8*, 297–343.

(24) Schmidt, M. W.; Gordon, M. S. *J. Am. Chem. Soc.* **1991**, *113*, 5244–5248.

(25) Froelicher, S. W.; Freiser, B. S.; Squires, R. R. *J. Am. Chem. Soc.* **1984**, *106*, 6863–6864.

(26) We use “delocalized” and “silylene” to denote in a simple way a grouping of species. We do not mean to imply that delocalized means a delocalized anion any more than we mean that silylene is actually a neutral silylene.

(27) Sulfur over oxygen ring closure is observed in all the studies of low-valent silicon anions that we have carried out. These studies are best summarized in ref 1.

(28) Bartmess, J. E.; Kiplinger, J. P. *J. Org. Chem.* **1986**, *51*, 2173–2176.

(29) Brickhouse, M. D.; Squires, R. R. *J. Phys. Org. Chem.* **1989**, *2*, 389–409.

(30) Freriks, I. L.; de Koning, L. J.; Nibbering, N. M. M. *J. Am. Chem. Soc.* **1991**, *113*, 9119–9124.

(31) Freriks, I. L.; de Koning, L. J.; Nibbering, N. M. M. *Int. J. Mass Spectrom. Ion Processes* **1992**, *117*, 345–356.

(32) Freriks, I. L. Reactivity of Ambident Anions in the Gas Phase. Dissertation, University of Amsterdam, Dec 1992.

(33) Wladkowski, B. D.; Wilbur, J. L.; Zhong, M.; Brauman, J. I. *J. Am. Chem. Soc.* **1993**, *115*, 8833–8834.

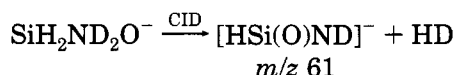
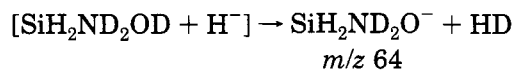
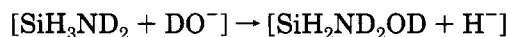
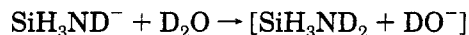
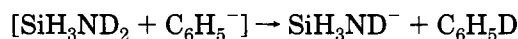
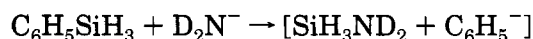
cussed here. The energies typically were determined using the 6-311++G(d,p) basis set with full fourth-order perturbation theory (MP4). The computational results are presented in Table 3 and are uncorrected. Zero-point corrections are reported as well. We have also carried out both charge density analyses using Bader's atoms in molecules methodology<sup>18-20</sup> and several G2<sup>21</sup> computations to be discussed later.

## Results and Discussion

The experimental and computational studies carried out in this work on silaformamide are presented in the following sections. These sections parallel the experimental approach we have actually undertaken in that they consider the preparation and characterization of the silaformamide anion followed by studies of its reactivity with a variety of different reagents. Computational work is also presented to provide a fuller understanding of the silaformamide anion and a number of closely related anions. Finally, the gas-phase acidity of silaformamide is considered in the context of both experimental bracketing studies of the silaformamide anion and computational studies of several isomers of silaformamide.

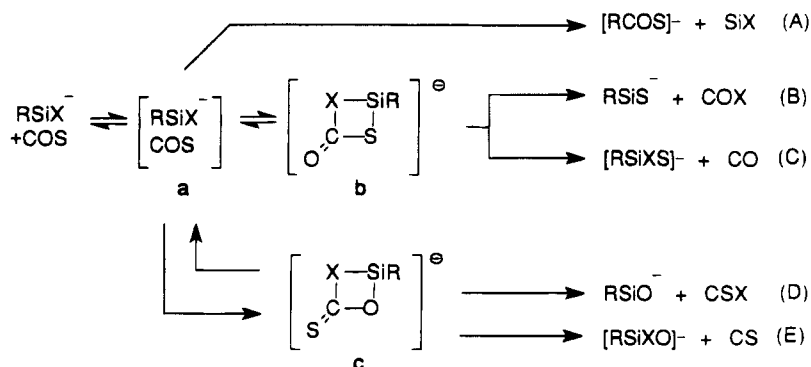
**Connectivity of [H<sub>2</sub>SiN,O]<sup>-</sup>.** The [H<sub>2</sub>SiN,O]<sup>-</sup> ion that has been produced in the source flow tube by reaction of amide, phenylsilane, and water (see Experimental Section) can be cleanly mass selected (*m/z* 60), allowing the study of its reaction chemistry in the second flow tube. Although computational studies to be discussed later establish that [Si(O)NH<sub>2</sub>]<sup>-</sup> (**1**) is more stable than [HSi(O)NH]<sup>-</sup> (**2**), they tell us nothing about the identity of the experimentally produced anion. Deuteration and reactivity studies, however, suggest a connectivity for this anion [HSi(O)NH]<sup>-</sup> (**2**). Equations 1 and 2 indicate that the *m/z* 62 anion, H<sub>2</sub>NSiH<sub>2</sub>O<sup>-</sup>, is formed in the source, a result which is based on earlier work exploring the reaction chemistry of silamides, particularly H<sub>3</sub>SiNH<sup>-</sup>, with deuterated alcohols and D<sub>2</sub>O.<sup>22</sup> Collision-induced dissociation (CID) of the *m/z* 62 ion in the source produces *m/z* 60 as well. When water is replaced by D<sub>2</sub>O and H<sub>2</sub>N<sup>-</sup> by D<sub>2</sub>N<sup>-</sup>, anions with *m/z* 64 and 61 are produced, suggesting the formation of [D<sub>2</sub>NSiH<sub>2</sub>O]<sup>-</sup> (*m/z* 64) and the CID product [HSi(O)ND]<sup>-</sup> (*m/z* 61). Scheme 1 provides a mechanistic rationale for the production of these anions. If D<sub>2</sub>O and H<sub>2</sub>N<sup>-</sup> react with C<sub>6</sub>H<sub>5</sub>SiH<sub>3</sub> in the source, the monodeuterated anion [HDNSiH<sub>2</sub>(O)]<sup>-</sup> (*m/z* 63) is obtained. Its CID gives two anionic products with *m/z* 61 and 60 in a 2:1 ratio, indicating that H<sub>2</sub> loss is favored over HD loss under these CID conditions.

## Scheme 1

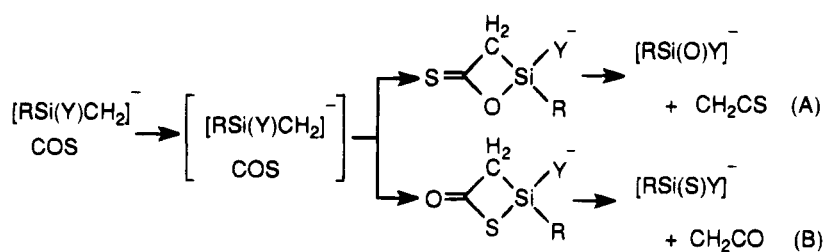


**Reaction Chemistry Studies. General Considerations.** Reaction chemistry studies of low-valent silicon-containing anions have established reactivity patterns that are similar for various, quite different anions.<sup>8,9,11</sup> Many of these reactions are believed to occur through cyclic intermediates, particularly for reactions with CO<sub>2</sub>, COS, and CS<sub>2</sub>. Scheme 2 for the reaction between [RSiX]<sup>-</sup> and COS illustrates many of the general features of the reaction pathways we have observed for such reactions. Ion-molecule reactions are initiated by the ion-dipole attraction between an ion such as [RSiX]<sup>-</sup> and the dipole of a neutral molecule such as COS (giving **a**). The attractive forces are typically quite large (~15–20 kcal/mol).<sup>23</sup> Reaction occurs when the initially formed ion-dipole complex **a** is transformed into products. Depending on R, two major reaction patterns have been observed. One involves hydride transfer to COS (path A);<sup>9</sup> the other involves formation of cyclic intermediates **b** and **c** (or possibly three-membered-ring analogs<sup>13</sup>), which can dissociate as shown in pathways B–E. Cyclic intermediates analogous to **b** and **c** have been proposed in the reactions of [HCSi]<sup>-</sup>, [HSiO]<sup>-</sup>, [CH<sub>3</sub>OSiO]<sup>-</sup>, [CH<sub>3</sub>SiO]<sup>-</sup>, [HSiS]<sup>-</sup>, and [HSiNH]<sup>-</sup>.<sup>8-11</sup> Both isotope labeling<sup>9</sup> and computational studies<sup>13,24</sup> have clearly established that such intermediates occur in reactions of this type. A recent detailed computational study of the potential energy surface of the [HSiO]<sup>-</sup> reaction with CO<sub>2</sub> has suggested the intermediacy of a four-membered-ring species as an intermediate for oxygen exchange and a three-membered intermediate leading to [HSiO<sub>2</sub>]<sup>-</sup> plus CO.<sup>13</sup>

## Scheme 2<sup>a</sup>



<sup>a</sup> For R = H and X = O, R = CH<sub>3</sub>O and X = O, R = CH<sub>3</sub> and X = O, R = H and X = S, and R = H and X = NH.

Scheme 3<sup>a</sup>

<sup>a</sup> For R = CH<sub>3</sub> and Y = O, R = H and Y = O, and R = CH<sub>3</sub> and Y = CH<sub>2</sub>.

Table 1. Important Reactions and Rate Data for Anion 2

reactant	products	branching ratio	rate coeff, in cm <sup>3</sup> (molecule) <sup>-1</sup> s <sup>-1</sup> (efficiency) <sup>a</sup>
CO <sub>2</sub>	[HSiO <sub>2</sub> ] <sup>-</sup> + HNCO	44	2.08 × 10 <sup>-11</sup> (0.26)
	adduct	16	
	[NCO] <sup>-</sup> + H <sub>2</sub> SiO <sub>2</sub>	15	
	[HSiO <sub>3</sub> ] <sup>-</sup> + HNC	13	
	[C <sub>2</sub> Si <sub>2</sub> O <sub>3</sub> N] <sup>-</sup> + H <sub>2</sub>	8	
	[Si <sub>2</sub> H <sub>2</sub> O <sub>2</sub> N] <sup>-</sup> + CO	4	
CS <sub>2</sub>	[NCS] <sup>-</sup> + HSi(O)SH	83	very slow: av of 7 measurements ~4 × 10 <sup>-12</sup> (very small)
	[HS] <sup>-</sup> + HSi(O)NCS	9	
COS	[Si <sub>2</sub> H <sub>2</sub> N <sub>2</sub> O <sub>2</sub> S] <sup>-</sup> + CS	8	1.36 × 10 <sup>-10</sup> (0.10)
	[HSi(O)S] <sup>-</sup> + HNCO	62	
CH <sub>2</sub> FCH <sub>2</sub> OH	[HSi(S)NH] <sup>-</sup> + CO <sub>2</sub>	38	1.11 × 10 <sup>-9</sup> (0.50)
	F <sup>-</sup> + [C <sub>2</sub> Si <sub>2</sub> H <sub>7</sub> N <sub>2</sub> O <sub>2</sub> ]	59	
	[C <sub>2</sub> Si <sub>2</sub> H <sub>6</sub> N <sub>2</sub> O <sub>2</sub> ] <sup>-</sup> + HF	24	
	[HSi(NH <sub>2</sub> )(F)O] <sup>-</sup> + C <sub>2</sub> H <sub>4</sub> O	10	
	[C <sub>2</sub> Si <sub>2</sub> H <sub>5</sub> N <sub>2</sub> O <sub>2</sub> F] <sup>-</sup> + H <sub>2</sub>	4	
	[CH <sub>2</sub> =CHO] <sup>-</sup> + [Si <sub>2</sub> H <sub>4</sub> N <sub>2</sub> O <sub>2</sub> F]	3	
CHF <sub>2</sub> CH <sub>2</sub> OH	[C <sub>2</sub> Si <sub>2</sub> H <sub>5</sub> N <sub>2</sub> O <sub>2</sub> F] <sup>-</sup> + HF	43	7.38 × 10 <sup>-10</sup> (0.38)
	[CHF=CHO] <sup>-</sup> + [Si <sub>2</sub> H <sub>4</sub> N <sub>2</sub> O <sub>2</sub> F]	30	
	F <sup>-</sup> + [C <sub>2</sub> Si <sub>2</sub> H <sub>7</sub> N <sub>2</sub> O <sub>2</sub> F]	10	
	[HSi(NH <sub>2</sub> )(F)O] <sup>-</sup> + C <sub>2</sub> H <sub>3</sub> FO	10	
	adduct	7	
CF <sub>3</sub> CH <sub>2</sub> OH	[C <sub>2</sub> Si <sub>2</sub> H <sub>4</sub> N <sub>2</sub> O <sub>2</sub> F <sub>2</sub> ] <sup>-</sup> + HF	40	1.77 × 10 <sup>-9</sup> (0.88)
	[CF <sub>2</sub> =CHO] <sup>-</sup> + [Si <sub>2</sub> H <sub>4</sub> N <sub>2</sub> O <sub>2</sub> F]	29	
	[HSi(NH <sub>2</sub> )(F)O] <sup>-</sup> + C <sub>2</sub> H <sub>2</sub> F <sub>2</sub> O	20	
	adduct	6	
	[CF <sub>3</sub> CH <sub>2</sub> O] <sup>-</sup> + [Si <sub>2</sub> H <sub>3</sub> N <sub>2</sub> O]	5	
CF <sub>3</sub> CD <sub>2</sub> OD	[C <sub>2</sub> Si <sub>2</sub> H <sub>2</sub> D <sub>2</sub> N <sub>2</sub> O <sub>2</sub> F <sub>2</sub> ] <sup>-</sup> + DF	33	1.14 × 10 <sup>-9</sup>
	[CF <sub>2</sub> =CDO] <sup>-</sup> + [Si <sub>2</sub> H <sub>2</sub> D <sub>2</sub> N <sub>2</sub> O <sub>2</sub> F]	52	
	[HSi(NHD)(F)O] <sup>-</sup> + C <sub>2</sub> D <sub>2</sub> F <sub>2</sub> O	5	
	adduct	4	
	[CF <sub>3</sub> CD <sub>2</sub> O] <sup>-</sup> + [Si <sub>2</sub> D <sub>3</sub> N <sub>2</sub> O]	6	
CH <sub>3</sub> OH	adduct		
	adduct + CH <sub>3</sub> OH		
CH <sub>3</sub> CH <sub>2</sub> OH	[HSi(OH)(NH <sub>2</sub> )O] <sup>-</sup> + CH <sub>2</sub> =CH <sub>2</sub>		
	adduct		
CH <sub>3</sub> CH <sub>2</sub> CH <sub>2</sub> OH	[HSi(OH)(NH <sub>2</sub> )O] <sup>-</sup> + CH <sub>3</sub> CH=CH <sub>2</sub>		
	adduct		
(CH <sub>3</sub> ) <sub>2</sub> CHOH	[HSi(OH)(NH <sub>2</sub> )O] <sup>-</sup> + CH <sub>3</sub> CH=CH <sub>2</sub>		
	adduct		
CH <sub>3</sub> CH <sub>2</sub> CH <sub>2</sub> CH <sub>2</sub> OH	[HSi(OH)(NH <sub>2</sub> )O] <sup>-</sup> + CH <sub>3</sub> CH <sub>2</sub> CH=CH <sub>2</sub>		
	adduct		
(CH <sub>3</sub> ) <sub>3</sub> COH	[HSi(OH)(NH <sub>2</sub> )O] <sup>-</sup> + (CH <sub>3</sub> ) <sub>2</sub> C=CH <sub>2</sub>		
	adduct		
(CH <sub>3</sub> ) <sub>3</sub> CCH <sub>2</sub> OH	[HSi(OH)(NH <sub>2</sub> )O] <sup>-</sup> + (CH <sub>3</sub> ) <sub>2</sub> C=CH <sub>2</sub>		
	adduct		

<sup>a</sup> The efficiencies (given in parentheses) are the ratios of the experimental to the computed rate coefficients. The latter are obtained as  $k_L$  (Langevin) or  $k_{\text{var}}$  (variational), depending on whether the reactant has a permanent dipole moment. References to their calculation are given in ref 15.

Potentially ambident anions such as [HSi(O)CH<sub>2</sub>]<sup>-</sup> and [CH<sub>3</sub>Si(O)CH<sub>2</sub>]<sup>-</sup> react exclusively at their CH<sub>2</sub> site with CO<sub>2</sub>, COS, and CS<sub>2</sub> (Scheme 3). Although such reactions have not been studied in nearly the detail as those just discussed,<sup>7,25</sup> the reactivity of such "delocalized" anions<sup>26</sup> differs from that of the localized species outlined by Scheme 2. Even in the two "delocalized" cases where silicon bears an oxygen, there is no evidence of ambident reactivity for the anions.

**Reaction Chemistry of [HSi(O)NH]<sup>-</sup> (2).** Although anion 2 reacts with standard neutral reagents such as CO<sub>2</sub>, CS<sub>2</sub>, and COS by pathways that are analogous to those of many silicon-containing anions, its reactions with alcohols, particularly fluorinated ethanols, are more complicated (Table 1). The standard neutral and alcohol reactions will be discussed separately.

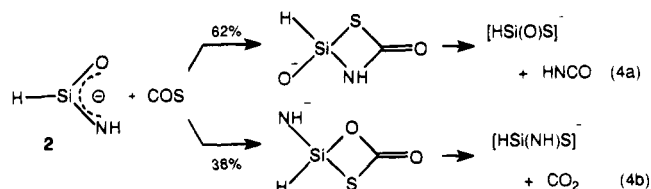
**Reactions of [HSi(O)NH]<sup>-</sup> (2) and CO<sub>2</sub>, CS<sub>2</sub>, and**

Table 2. Product of Reaction of  $[\text{HSi}(\text{O})\text{NH}]^-$  (**2**) with  $\text{CFXYCH}_2\text{OH}^a$ 

anionic product (keyed to Scheme 4)	yield with 2-fluoroethanol (X = Y = H), %	yield with 2,2-difluoroethanol (X = H, Y = F), %	yield with 2,2,2-trifluoroethanol (X = Y = F)
adduct (A → B)	0	7	6
$\text{CFXYCH}_2\text{O}^-$	0	0	6
$\text{F}^-$ (A → D → E)	59	10	0
$\text{HSi}(\text{F})(\text{NH}_2)\text{O}^-$ (A → D → F)	10	10	20
$[\text{XYC}=\text{CHO}]^-$ (A → D → G → H)	3	30	29
[adduct - HF] $^-$ (A → D → G → I)	24	43	40
[adduct - H <sub>2</sub> ] $^-$	4	0	0

<sup>a</sup> X = Y = H for 2-fluoroethanol; X = H, Y = F for 2,2-difluoroethanol; X = Y = F for 2,2,2-trifluoroethanol.

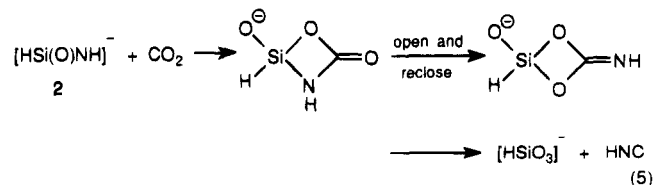
**COS.** We suggest that anion **2** displays ambident reactivity in its reaction with COS (Table 1). Equation 4 gives a possible course for these reactions. In the more



favorable channel given by eq 4a, **2** reacts at its nitrogen end, while in eq 4b it reacts at oxygen. In both cases subsequent four-membered-ring formation takes place through sulfur ring closure, despite the possibility of the COS oxygen closing the ring.<sup>27</sup> There are now several silicon anion reactions with COS in which preferential sulfur ring closure has been observed.<sup>1,11,22</sup>

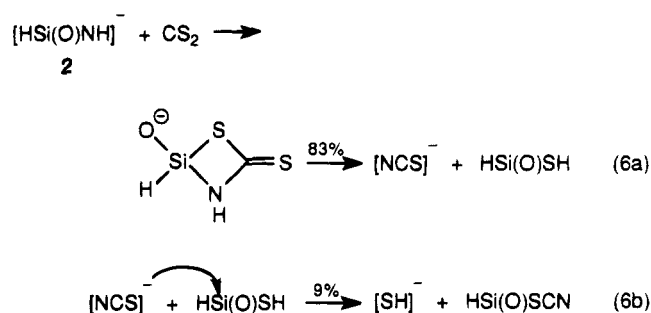
This represents the first example of ambident behavior in a low-valent silicon anion of which we are aware, although other non-silicon-containing ambident species have been observed in the gas phase.<sup>28–33</sup> In particular, ambident behavior in formamide and other imidate anions has been studied by Nibbering and co-workers.<sup>30–32</sup>

The reactions of **2** with  $\text{CO}_2$  and  $\text{CS}_2$  are somewhat more complex (Table 1). They give no evidence of its ambident character, although in the  $\text{CO}_2$  reaction it is masked by the probable reversible loss of  $\text{CO}_2$ . Six products are detected with  $\text{CO}_2$ , including an adduct (16%) and three other products that arise from four-membered intermediates analogous to those just discussed. These amount to 79% of the reaction. In addition, we observe 13% of  $[\text{HSiO}_3]^-$  plus  $[\text{H,C,N}]$  and 8% of  $[\text{C,Si,N,O}_3]^-$  plus  $\text{H}_2$ . Although eq 5 illustrates a



reasonable pathway for  $[\text{HSiO}_3]^-$  formation, we are less certain about the path leading to the 8% product. It seems likely that  $\text{H}_2$  forms from initial loss of hydride followed by proton abstraction, but that could occur from more than one intermediate in the  $\text{CO}_2$  reaction.

Equation 6 shows the pathways that lead to 92% of the products in the reaction of **2** and  $\text{CS}_2$ . There is ambiguity about whether the other channel leading to  $[\text{H}_2\text{Si,N,O,S}]^-$  plus CS (8%) derives from the four-membered intermediate shown in eq 6 or the related "ambident" intermediate that would form if **2** reacted at its oxygen end.

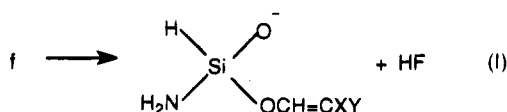
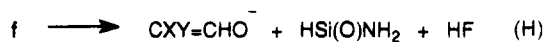
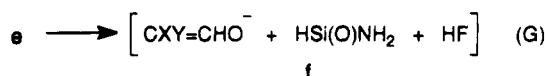
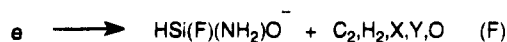
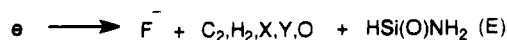
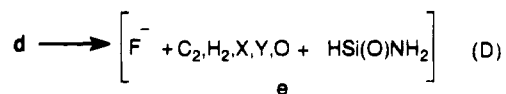
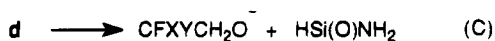
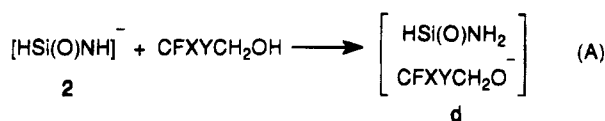


The rate coefficients of the reactions of **2** and  $\text{CO}_2$  and  $\text{COS}$  are 0.21 and  $1.4 \times 10^{-10} \text{ cm}^3 \text{ s}^{-1} (\text{molecule})^{-1}$ , respectively. The rate coefficient for reaction with  $\text{CS}_2$  is considerably smaller (approximately  $4 \times 10^{-12} \text{ cm}^3 \text{ s}^{-1} (\text{molecule})^{-1}$ ). The efficiencies of reaction for  $\text{CO}_2$  and  $\text{COS}$  are 0.26 and 0.10, with that for  $\text{CS}_2$  being considerably smaller.<sup>11</sup> Previously reported efficiencies of low-valent silicon-containing anions reacting with  $\text{CO}_2$ ,  $\text{CS}_2$ , and  $\text{COS}$  indicate that oxygen and nitrogen reactive sites react with similar efficiencies while the sulfur species have somewhat attenuated reactivity:  $[\text{HSiO}]^-$  (0.38, 0.55, and 0.20);<sup>9</sup>  $[\text{HSiNH}]^-$  (0.41, 0.35, and 0.24);<sup>11</sup>  $[\text{HSiS}]^-$  (0.043, 0.016, and 0.008).<sup>11</sup> The data presented for **2**, while showing similar reactivity with  $\text{CO}_2$  and  $\text{COS}$ , indicate that it is even less reactive with  $\text{CS}_2$  than are the other low-valent species.

**Reactions of  $[\text{HSi}(\text{O})\text{NH}]^-$  (**2**) and Fluorinated Ethanol.** Several products are observed for the reactions of **2** with 2-fluoroethanol, 2,2-difluoroethanol, and 2,2,2-trifluoroethanol with the product distribution depending dramatically on the particular fluoroethanol (Tables 1 and 2). Two striking features of these reactions are the decrease in the amount of fluoride and the increase in the product that has the  $m/z$  value for an adduct minus HF as the fluoroethanols become more acidic. For 2-fluoroethanol, for example, fluoride totals 59% of the ionic products while the adduct minus HF anion is observed in 24% yield. For 2,2,2-trifluoroethanol, in contrast, fluoride is not observed and the adduct minus HF anion totals 40%. In Scheme 4, we present a general formulation of the pathways of the fluorinated ethanol. Although speculative, it offers the reader a sense of how the observed products might arise. Scheme 4 forms the basis of a discussion of how they might vary with fluoroethanol structure.

Complex **d** formed in A is central to Scheme 4. Its formation is endergonic for 2-fluoroethanol ( $\Delta G_{\text{acid}} = 364 \text{ kcal mol}^{-1}$ ) and 2,2-difluoroethanol ( $\Delta G_{\text{acid}} = 359 \text{ kcal mol}^{-1}$ ) and nearly thermoneutral for 2,2,2-trifluoroethanol ( $\Delta G_{\text{acid}} = 354 \text{ kcal/mol}$ )<sup>34</sup> (see subsequent discussion on the acidity of silaformamide, in which it is estimated to be between 350 and 355  $\text{kcal mol}^{-1}$ ). The formation of such complexes is driven by ion-dipole attraction,<sup>23</sup> which leads to a gradation of energy

Scheme 4

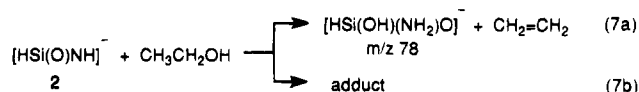


contents from the "cooler" 2-fluoroethanol complex to a "hotter" one for 2,2,2-trifluoroethanol. The cooler complex formed from 2-fluoroethanol is expected to yield products that involve less interaction between its two components, 2-fluoroethoxide and silaformamide. As a result, the major pathway for 2-fluoroethanol produces fluoride (A → D → E in Scheme 4; 59%) by the collapse of 2-fluoroethoxide by internal ("intramolecular") reaction in the cool complex. Since the neutral components in typical flowing afterglow experiments cannot be identified, they are generally inferred by mechanistic analysis based on thermochemical considerations and reactivity precedents. In reaction E of Scheme 4, we have formulated one neutral product as HSi(O)NH<sub>2</sub>. The other, which would arise from 2-fluoroethoxide in complex **d**, would have a [C<sub>2</sub>H<sub>4</sub>O] composition. It could be acetaldehyde, its enol, or ethylene oxide, although acetaldehyde is the most stable thermodynamically.<sup>34</sup>

In complexes with a higher energy content such as those formed from 2,2-difluoroethanol and 2,2,2-trifluoroethanol, the corresponding fluoroethoxide ions are expected to be increasingly diverted from similar internal reaction pathways to ones where the complex members interact. The pathway A → D → G → I in Scheme 4, for example, involves further reaction of fluoride with neutral [C<sub>2</sub>H<sub>2</sub>X<sub>2</sub>YO]. As one goes from 2-fluoroethanol to 2,2-difluoroethanol to 2,2,2-trifluoroethanol, the amount of fluoride (A → D → E) decreases from 59 to 10 to 0% and the amount of adduct minus

HF (A → D → G → I) increases from 24 to 43 to 40%. All the other products reported in Table 2 (with the exception of the minor products in the bottom line) increase as **d** and/or **e** become hotter. The products are also consistent with the increasing likelihood that the complexes will fly apart (A → C) or undergo further reaction with increasing energy. Finally, studies with CF<sub>3</sub>CD<sub>2</sub>OD are consistent with the mechanistic scheme presented.

**Reactivity of [HSi(O)NH]<sup>-</sup> (2) and Aliphatic Alcohols.** The interesting and complicated reactions of fluorinated alcohols lead us to comment briefly on the reactions of **2** and aliphatic alcohols. These have proved difficult to study because of large signal losses that we are unable to explain. Nevertheless, the qualitative nature of aliphatic alcohol reactivity can be obtained from the data presented in Table 1 for the reactions of **2** and CH<sub>3</sub>OH, CH<sub>3</sub>CH<sub>2</sub>OH, CH<sub>3</sub>CH<sub>2</sub>CH<sub>2</sub>OH, (CH<sub>3</sub>)<sub>2</sub>CHOH, CH<sub>3</sub>CH<sub>2</sub>CH<sub>2</sub>CH<sub>2</sub>OH, (CH<sub>3</sub>)<sub>3</sub>COH, and (CH<sub>3</sub>)<sub>3</sub>CCH<sub>2</sub>OH. The most interesting feature of these reactions is that aliphatic alcohols having β-hydrogens undergo an elimination reaction that is not observed with fluorinated alcohols. Thus, all of the aliphatic alcohols having a β-hydrogen give an *m/z* 78 anion, as indicated in eq 7a for ethanol. Neither CH<sub>3</sub>OH nor (CH<sub>3</sub>)<sub>3</sub>CCH<sub>2</sub>OH



undergoes elimination, but they, like all the alcohols, give adducts with **2** (eq 7b) as well as secondary products that are alcohol-adduct clusters. Attempts to unequivocally establish the β-elimination pathway by labeling studies with deuterated ethanols have been thwarted not only by the signal loss problem mentioned but also by the appearance of a product inconsistent with simple β-elimination. Thus, CH<sub>3</sub>CD<sub>2</sub>OH and CD<sub>3</sub>-CD<sub>2</sub>OD react to give HSi(OH)(NH<sub>2</sub>)O<sup>-</sup> (*m/z* 78) and HSi(OD)(NHD)O<sup>-</sup> (*m/z* 80), as might be expected in a simple β-elimination. On the other hand, CD<sub>3</sub>CH<sub>2</sub>OH and CH<sub>3</sub>CH<sub>2</sub>OD, which would be expected to give only *m/z* 79 by β-elimination, actually yield mixtures containing both *m/z* 78 and 79, even when special precautions were undertaken to dry the deuterated alcohols. Together, the labeling studies and the lack of an elimination product channel for CH<sub>3</sub>OH and (CH<sub>3</sub>)<sub>3</sub>CCH<sub>2</sub>OH indicate the occurrence of a β-elimination process, even though the labeling experiments suggest that other processes are at work as well.

#### Computational Energies of Anionic Species.

Computational studies have been carried out to (1) help elucidate the structure and reactivity of **2** and to (2) examine the factors controlling the relative stability of the "silylene" versus "delocalized" forms of a series of anions related to **1** and **2**. We have undertaken *ab initio* studies of silylene and delocalized anions<sup>26</sup> derived from HSi(X)Y, varying X from O to NH<sub>2</sub> and Y from OH to NH<sub>2</sub> to CH<sub>3</sub>. Thus, **1** and **2** are the silylene and delocalized anions obtained by removing a proton from Si-H and the Y group, in this case NH<sub>2</sub>, respectively. The other anions that have been studied are [Si(O)OH]<sup>-</sup> (**3**), [HSi(O)O]<sup>-</sup> (**4**), [Si(O)CH<sub>3</sub>]<sup>-</sup> (**5**), [HSi(O)CH<sub>2</sub>]<sup>-</sup> (**6**), [Si(NH)OH]<sup>-</sup> (**7**), [Si(NH)NH<sub>2</sub>]<sup>-</sup> (**8**), [HSi(NH)NH]<sup>-</sup> (**9**), [Si(NH)CH<sub>3</sub>]<sup>-</sup> (**10**), [HSi(NH)CH<sub>2</sub>]<sup>-</sup> (**11**), [Si(CH<sub>2</sub>)OH]<sup>-</sup>

(34) Lias, S. G.; Bartmess, J. E.; Liebman, J. F.; Holmes, J. L.; Levin, R. D.; Mallard, W. G. *J. Phys. Chem. Ref. Data, Suppl.* **1988**, *17* (Supplement 1). This is the primary source for gas-phase acidity data. Unless otherwise specified, all gas-phase acidities used in this paper come from this source.

**Table 3. Energies of Important Species Obtained by *ab Initio* Computational Methods**

	MP4(SDTQ)/6-311++G(d,p)// MP2/6-31+G(d,p) (hartree)	diff at MP4 level (kcal mol <sup>-1</sup> )	zero-point correction	important geom value <sup>a</sup>
HSi(O)NH <sub>2</sub> (16)	-420.590 24 (G2 = -420.710 35) <sup>21</sup>	0	0.038 76	Si-O 1.55 Si-N 1.69 Si-H 1.47 N-H 1.01 O-Si-N 127.0 O-Si-H 126.0 N-Si-H 107.1 Si-N-H 122.8 Si-N-H 123.4 H-N-H 113.7
Si(OH)NH <sub>2</sub> (18)	-420.581 14	5.71	0.040 32	O-Si 1.69 O-H 0.966 Si-N 1.74 N-H 1.01 Si-O-H 122.0 O-Si-N 102.0 Si-N-H 127.9 Si-N-H 120.6 H-N-H 111.5
HSi(OH)NH (19)	-420.565 20	15.7	0.037 07	O-H 0.966 O-Si 1.66 Si-N 1.60 Si-H 1.45 N-H 1.01 H-O-Si 118.2 O-Si-N 135.6 O-Si-H 104.8 N-Si-H 120.0 Si-N-H 130.9
[Si(O)NH <sub>2</sub> ] <sup>-</sup> (1)	-420.022 19 (G2 = -420.153 71) <sup>21</sup>	0	0.027 69	O-Si 1.60 Si-N 1.80 N-H 1.02 N-H 1.01 O-Si-N 108.1 Si-N-H 122.4 Si-N-H 122.9 H-N-H 113.4
[HSi(O)NH] <sup>-</sup> (2)	-420.013 38 (G2 = -420.151 61) <sup>21</sup>	5.53	0.025 21	O-Si 1.58 Si-N 1.65 Si-H 1.49 N-H 1.02 O-Si-N 138.1 O-Si-H 114.4 N-Si-H 107.6 Si-N-H 115.6
[HSiO <sub>2</sub> ] <sup>-</sup> (4)	-439.904 76	0	0.014 18	Si-O 1.58 Si-H 1.50 H-Si-O 111.9 O-Si-O 136.2
[Si(O)OH] <sup>-</sup> (4) (cis)	-439.899 45	3.33	0.016 22	Si-O 1.60 Si-O 1.76 (OH) O-H 0.973 O-Si-O 107.8 Si-O-H 105.5
[Si(O)CH <sub>3</sub> ] <sup>-</sup> (5)	-403.956 29	0	0.038 00	Si-O 1.60 Si-C 1.98 C-H 1.10 O-Si-C 107.7 Si-C-H 111.7 Si-C-H 109.9 H-C-H 109.2 H-C-H 106.9
[HSi(O)CH <sub>2</sub> ] <sup>-</sup> (6)	-403.945 17	6.98	0.035 33	Si-O 1.58 Si-C 1.74 Si-H 1.50 C-H 1.08 C-H 1.09 O-Si-H 116.0 O-Si-C 134.3 H-Si-C 109.7 Si-C-H 125.0 Si-C-H 119.1 H-C-H 115.9
[HSi(NH)O] <sup>-</sup> (same as 2)	-420.013 38	0	0.025 21	see 2 above
[Si(NH)OH] <sup>-</sup> (7)	-419.998 50	9.33		N-H 1.02 N-Si 1.67 Si-O 1.75 O-H 0.97

Table 3 (Continued)

	MP4(SDTQ)/6-311++G(d,p)// MP2/6-31+G(d,p) (hartree)	diff at MP4 level (kcal mol <sup>-1</sup> )	zero-point correction	important geom value <sup>a</sup>
HSi(O)NH <sub>2</sub> ( <b>16</b> )				H-N-Si 109.8 N-Si-O 105.2 Si-O-H 106.8
[Si(NH)NH <sub>2</sub> ] ( <b>8</b> ) (trans)	-400.129 78	0	0.039 24	N-H 1.02 Si-N 1.68 Si-N 1.79 (NH <sub>2</sub> ) N-H 1.01 (NH <sub>2</sub> ) N-H 1.02 (NH <sub>2</sub> )
[HSi(NH)NH] <sup>-</sup> ( <b>9</b> )	-400.119 68	6.34	0.036 00	N-H 1.02 Si-N 1.66 Si-H 1.48 Si-N-H 116.3 H-Si-N 109.0 N-Si-N 141.9
[Si(NH)CH <sub>3</sub> ] <sup>-</sup> ( <b>10</b> )	-384.070 11	0	0.049 93	Si-N 1.69 Si-C 1.95 N-H 1.02 C-H 1.08 C-H 1.09 H-N-Si 109.9 N-Si-C 101.5 Si-C-H 109.4 Si-C-H 111.1 H-C-H 109.2 H-C-H 109.8
[HSi(NH)CH <sub>2</sub> ] <sup>-</sup> ( <b>11</b> )	-384.051 40	11.7	0.045 99	Si-N 1.66 Si-C 1.75 Si-H 1.49 N-H 1.02 C-H 1.08 C-H 1.09 H-N-Si 115.2 N-Si-H 110.5 N-Si-C 138.3 H-Si-C 111.2 Si-C-H 124.9 Si-C-H 119.6 H-C-H 115.5
[HSi(CH <sub>2</sub> )O] <sup>-</sup> (same as <b>6</b> )	-403.945 17	0	0.035 32	see <b>6</b> above
[Si(CH <sub>2</sub> )OH] <sup>-</sup> ( <b>12</b> )	-403.933 24	7.48	0.037 38	C-H 1.10 Si-C 1.77 C-H 1.09 Si-O 1.77 O-H 0.969 H-C-Si 126.4 H-C-H 113.4 Si-C-H 120.2 C-Si-O 104.1 Si-O-H 109.9
[Si(CH <sub>2</sub> )NH <sub>2</sub> ] <sup>-</sup> ( <b>13</b> )	-384.062 21	0	0.049 77	Si-N 1.82 Si-C 1.77 N-H 1.01 N-H 1.02 C-H 1.09 H-N-Si 118.5 N-Si-C 103.3 Si-C-H 109.4 H-N-H 110.2 Si-C-H 120.3 Si-C-H 125.8 H-C-H 113.8
[HSi(CH <sub>2</sub> )NH] <sup>-</sup> (same as <b>11</b> )	-384.051 39	6.79	0.045 99	see <b>11</b> above
[Si(CH <sub>2</sub> )CH <sub>3</sub> ] <sup>-</sup> ( <b>14</b> )	-368.010 22	0	0.060 92	C-H 1.09 (CH <sub>2</sub> ) Si-C 1.78 (CH <sub>2</sub> ) Si-C 1.97 (CH <sub>3</sub> ) C-H 1.10 (CH <sub>3</sub> ) H-C-H 113.6 (CH <sub>2</sub> ) H-C-Si 124.5 (CH <sub>2</sub> ) H-C-Si 121.9 (CH <sub>2</sub> ) C-Si-C 100.9 Si-C-H 111.7 (CH <sub>3</sub> ) Si-C-H 111.0 (CH <sub>3</sub> ) H-C-H 108.2 (CH <sub>3</sub> ) H-C-H 106.6 (CH <sub>3</sub> )



Table 3 (Continued)

	MP4(SDTQ)/6-311++G(d,p)// MP2/6-31+G(d,p) (hartree)	diff at MP4 level (kcal mol <sup>-1</sup> )	zero-point correction	important geom value <sup>a</sup>
[HSi(CH <sub>2</sub> )CH <sub>2</sub> ] <sup>-</sup> (15)	-367.983 92	16.5	0.055 73	Si-C 1.75 Si-H 1.49 C-H 1.08 H-C-Si 124.5 H-C-Si 120.0 C-Si-H 112.5 C-Si-C 135.0 H-Si-C 112.5 H-C-H 115.5

<sup>a</sup> From MP2/6-31+G(d,p) optimizations; distances in Å and angles in deg.

Table 4. Gas-Phase Acidities of Important Low-Valent Species

compd	$\Delta G_{\text{acid}}^{\circ}$ (kcal mol <sup>-1</sup> )	bracketing acid		ref	$\Delta G_{\text{acid}}^{\circ}$ of C analog (kcal mol <sup>-1</sup> )	ref
		anion abstracts H <sup>+</sup>	anion does not abstract H <sup>+</sup>			
HSi(O)NH <sub>2</sub>	350-355	see text	see text	this work	353	34
H <sub>2</sub> SiO	356 ± 8	CH <sub>3</sub> NO <sub>2</sub>	CH <sub>3</sub> C(O)CH <sub>3</sub>	9	386	34
CH <sub>3</sub> Si(O)CH <sub>3</sub>	356 ± 4	CF <sub>3</sub> CH <sub>2</sub> OH	CH <sub>3</sub> CHO	10	362	34
CH <sub>2</sub> =Si(CH <sub>3</sub> )CH <sub>2</sub> -H	~374	see ref	see ref	6	383	34

(12), [HSi(CH<sub>2</sub>)O]<sup>-</sup> (6), [Si(CH<sub>2</sub>)NH<sub>2</sub>]<sup>-</sup> (13), [HSi(CH<sub>2</sub>)NH]<sup>-</sup> (11), [Si(CH<sub>2</sub>)CH<sub>3</sub>]<sup>-</sup> (14), and HSi(CH<sub>2</sub>)CH<sub>2</sub>]<sup>-</sup> (15) (Table 3).

Calculated energies at the MP4(SDTQ)/6-311++G(d,p)//MP2/6-31+G(d,p) level indicate that the silylene isomer **1** is 5.53 kcal mol<sup>-1</sup> more stable than **2**. At the more highly correlated QCISD(T)/6-31+G(d,p)//MP2(full)/6-31+G(d,p) level, this energy gap increases to 7.5 kcal mol<sup>-1</sup>, suggesting that the qualitative result that silylene **1** is more stable than **2** is unlikely to change, even at better theoretical levels. We have also included the G2 energies<sup>21</sup> of **1**, **2**, and **16** in Table 3. These results will be discussed in the next section.

Among the other anions studied, the most stable anions result from Si-H deprotonation of HSi(O)CH<sub>3</sub>, HSi(NH)NH<sub>2</sub>, HSi(NH)CH<sub>3</sub>, HSi(CH<sub>2</sub>)NH<sub>2</sub>, and HSi(CH<sub>2</sub>)CH<sub>3</sub>, not from deprotonation at NH<sub>2</sub> or CH<sub>3</sub>. In contrast, the delocalized HSi(X)O<sup>-</sup> species, where X = O, NH<sub>2</sub>, and CH<sub>2</sub>, are the most stable anions from HSi(O)OH, HSi(NH)OH, and HSi(CH<sub>2</sub>)OH. Thus, deprotonation of HSi(X)OH, HSi(X)NH<sub>2</sub>, and HSi(X)CH<sub>3</sub>, where X = O, NH, and CH<sub>2</sub>, is favored at Si-H for the NH<sub>2</sub> and CH<sub>3</sub> species but at O-H for the three OH compounds. This suggests that electronegativity effects are controlling the site of deprotonation and that all three HSi(X)O<sup>-</sup> anions are favored over their silylene isomers because the negative charge is best accommodated by the more electronegative oxygen.

To examine the reactivity of anion **2** from another perspective, we have carried out charge density analyses of several species from wave functions generated at the MP2/6-31+G(d,p) level using Bader's theory of atoms in molecules.<sup>18-20</sup> Charge densities for the neutral silaformamide **16**, the anions **1-15**, and the precursor anion [H<sub>2</sub>Si(O)NH<sub>2</sub>]<sup>-</sup> (**17**) are given in Figure 1. All of these species show the dominance of their electropositive silicon atom, no matter what other substitution pattern they possess. Thus, hydrogen, oxygen, nitrogen, and carbon atoms bonded to silicon are negatively charged. The nearly equal charges on oxygen and nitrogen in anion **2** suggest a simple explanation for its ambident behavior. Interestingly, **2**, **16**, and the precursor anion **17** have similar electron densities on silicon, hydrogen, oxygen, and nitrogen despite their very different structures. There are, of course, more subtle features of the charge densities. Precursor anion

**17**, which has four electronegative substituents attached to silicon, balances the positive and negative charges differently than the neutral **16**; nevertheless, their similarities are more striking than any subtle differences. In contrast with this are the different charges on silicon in the various anions. Thus **1**, **3**, **5**, **7**, **8**, **10**, **12**, **13**, and **14**, which in a formal valence bond sense are silylene anions having negative charge localized on silicon, have greatly attenuated positive charges compared to species such as **2**, **4**, **6**, **9**, **11**, and **15**. Important structural parameters for the computed anions are also given in Table 3.

**Gas-Phase Acidity Studies.** The gas-phase acidity of the parent of [HSi(O)NH]<sup>-</sup> (**2**) has been difficult to bracket because no sharp demarcation has been observed with a variety of reference acids. For example, while CF<sub>3</sub>CH<sub>2</sub>OH ( $\Delta G_{\text{acid}} = 354$  kcal mol<sup>-1</sup>)<sup>34</sup> is consistently deprotonated by **2** to a small extent (6%), other more acidic acids either are deprotonated to only a very small extent (e.g. CH<sub>3</sub>SH with  $\Delta G_{\text{acid}} = 351$  kcal mol<sup>-1</sup>) or not at all (e.g. *N*-methylformamide with  $\Delta G_{\text{acid}} = 353$  kcal mol<sup>-1</sup>). (Since gas-phase acidities are always endothermic, larger values of  $\Delta H_{\text{acid}}$  correspond to weaker acids.) Still other reference acids such as pyrrole ( $\Delta G_{\text{acid}} = 351$  kcal mol<sup>-1</sup>), CD<sub>3</sub>NO<sub>2</sub> ( $\Delta G_{\text{acid}} \approx 350$  kcal mol<sup>-1</sup>)<sup>34,35</sup> and (CH<sub>3</sub>)<sub>3</sub>CSH ( $\Delta G_{\text{acid}} = 346$  kcal mol<sup>-1</sup>) deprotonate more extensively, but by no means exclusively (never more than about 20% deprotonation). These results suggest that the acidity of silaformamide is between 350 and 355 kcal mol<sup>-1</sup>. We have used the G2 method<sup>21</sup> to estimate the acidity of silaformamide computationally, obtaining a  $\Delta G_{\text{acid}}$  at 298.15 K of 345 kcal mol<sup>-1</sup>.<sup>36</sup> This result is consistent with the experimental range we have reported, given the lack of a sharp bracketing demarcation. The G2 energy values have uncertainties of less than ±3 kcal/mol.<sup>21</sup>

The acidities corresponding to three other low-valent silicon-containing anions whose carbon analogs are known are presented in Table 4. In presenting the data

(35) The  $\Delta G_{\text{acid}}$  value for CH<sub>3</sub>NO<sub>2</sub> is 349.7 kcal mol<sup>-1</sup>. Deuteration effects on acidity are fairly small, leading to slightly weaker acids. See ref 34 for examples.

(36) Thermal corrections (to 298.15 K) to the G2 results reported in Table 3 were carried out as follows. Contributions of 3.08, 0.889, and 3.38 kcal mol<sup>-1</sup> were used as temperature corrections of the internal energy of **2**, H<sup>+</sup>, and **16**, respectively. The enthalpy change at 298.15 K was obtained by adding a  $\Delta PV$  value of 0.59 kcal mol<sup>-1</sup> ( $\Delta nRT$ ). We estimated the  $T\Delta S$  value to be 7 kcal mol<sup>-1</sup> to obtain  $\Delta G_{\text{acid}}$ .

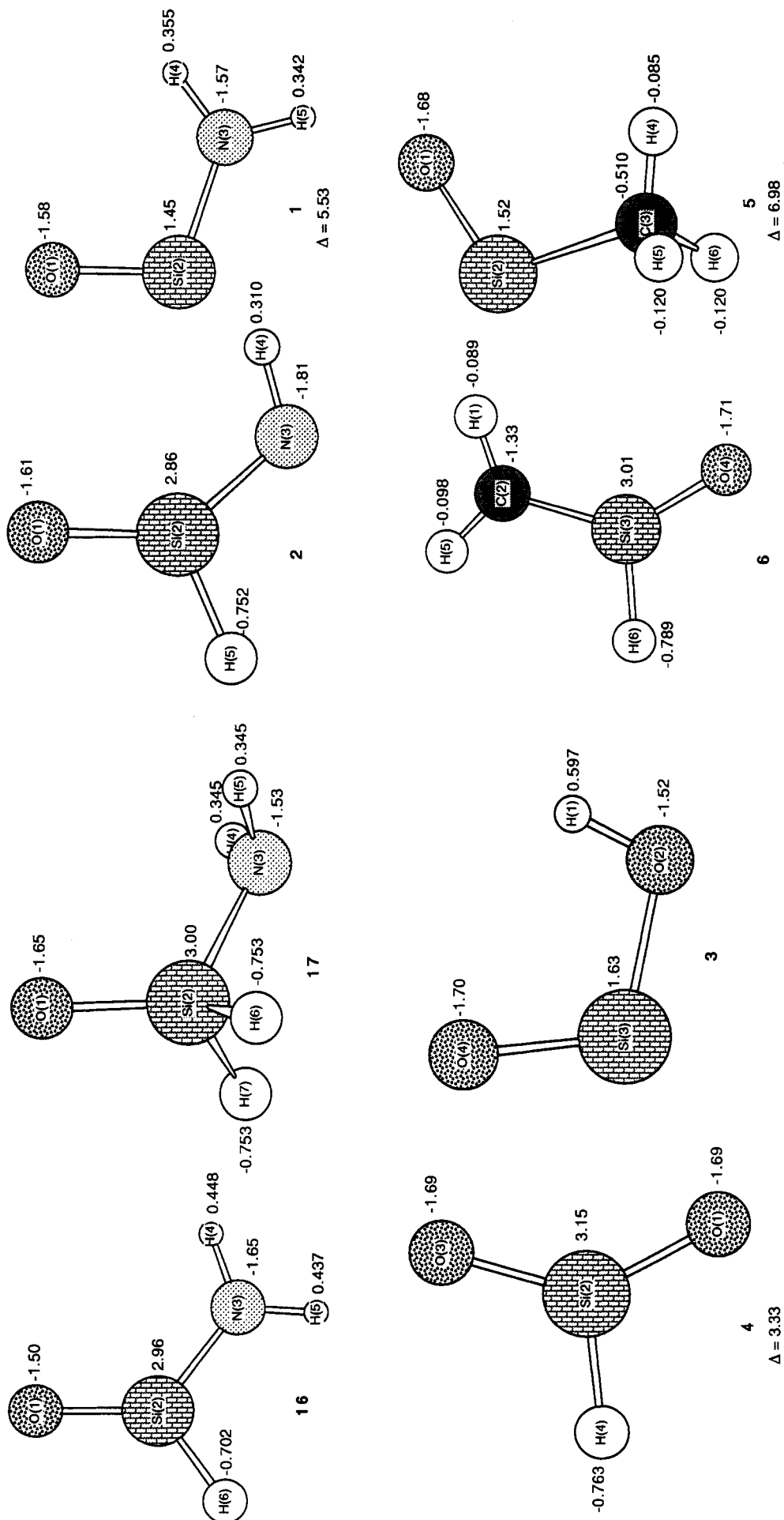
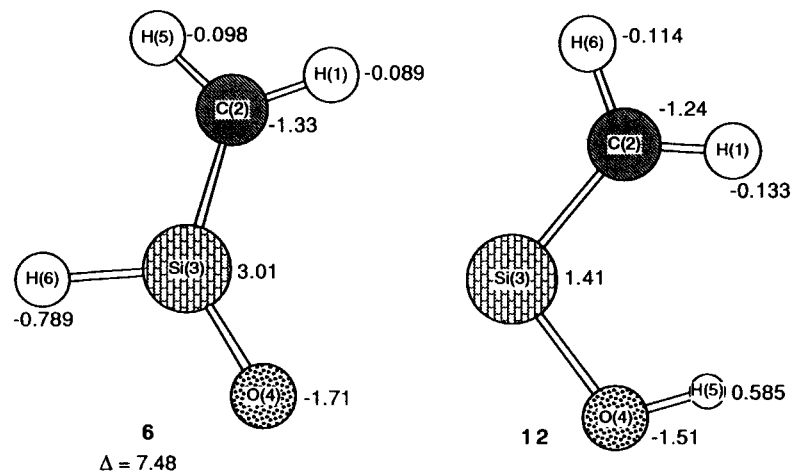
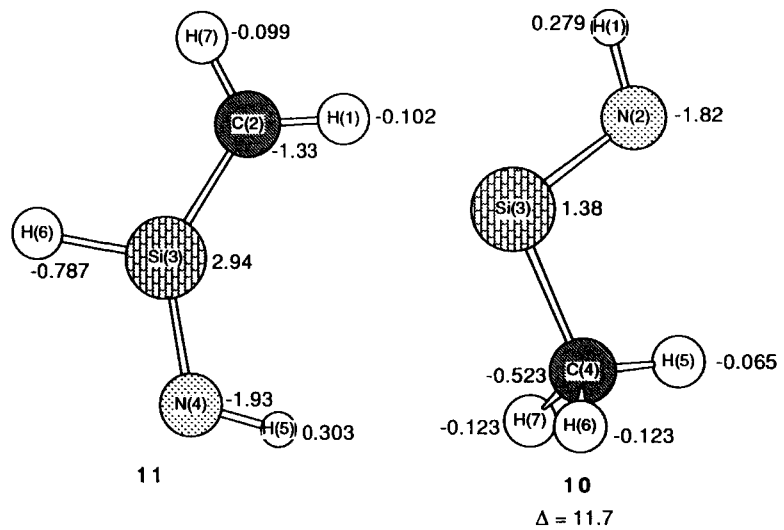
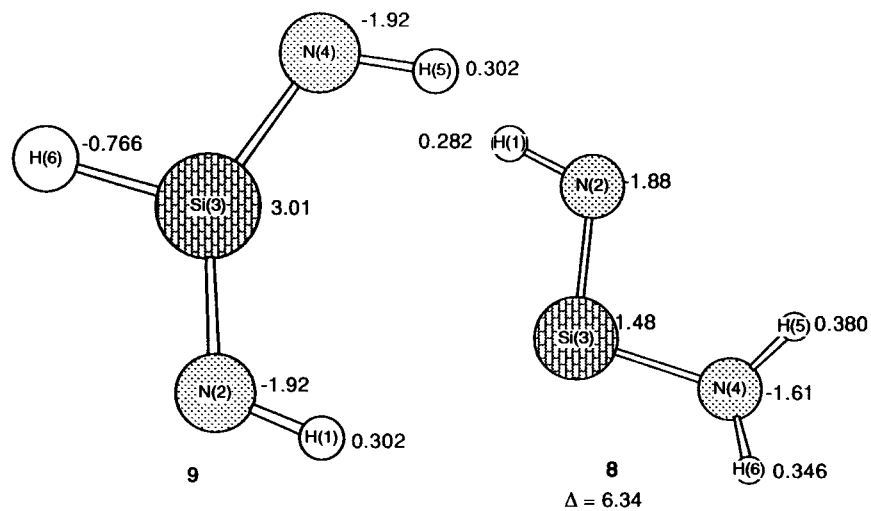
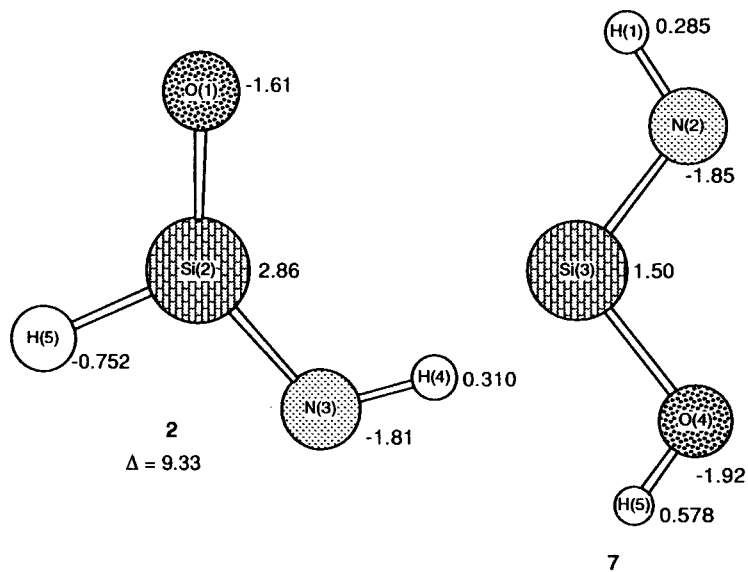
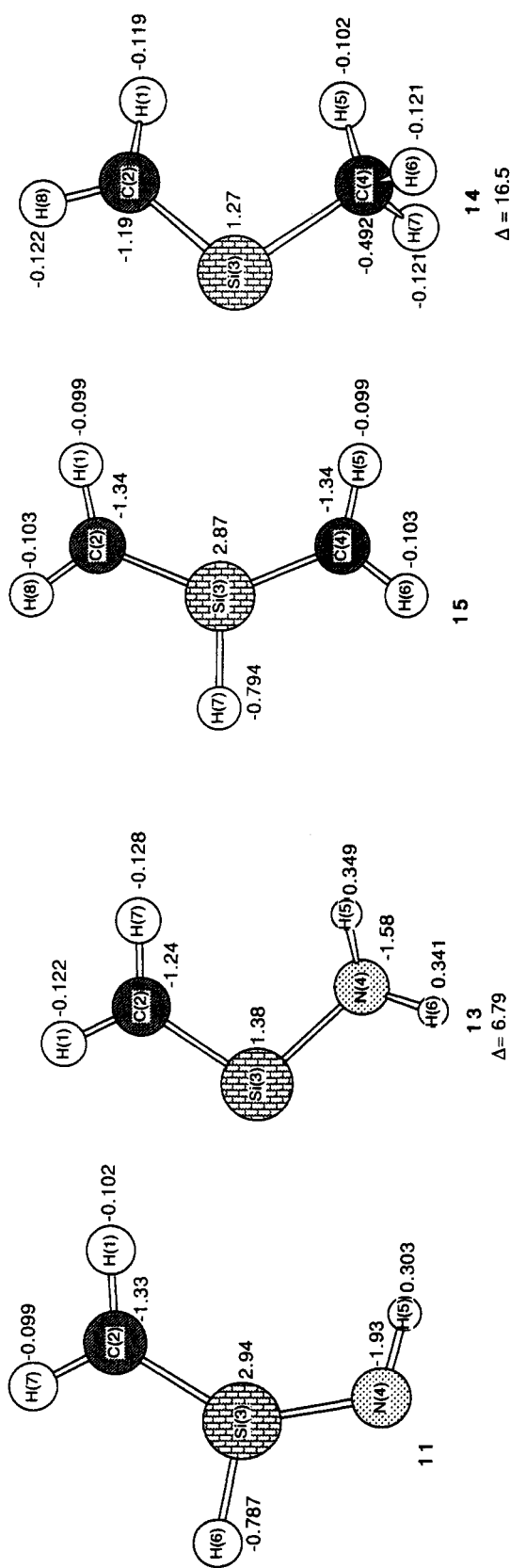


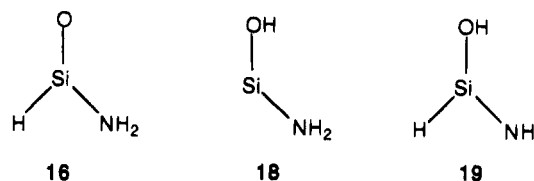
Figure 1. (see caption on p 2663)





**Figure 1.** Charge densities of anions and neutrals and energy differences of pairs of anion isomers. The  $\Delta$  value (kcal mol<sup>-1</sup>) is the energy difference between each pair of isomers and is placed under the isomer of lower energy.

in Table 4, we use the convention adopted earlier for the protonated parent species of an anion that might have more than one isomeric structure, namely that the protonated species is given as the most stable of the isomeric species as determined by computational studies.<sup>1,11</sup> This convention was adopted primarily for the sake of simplicity and does not imply that protonation necessarily occurs to give the most stable isomer. In the case of [HSi(O)NH]<sup>-</sup> (**2**), we refer to computations we have carried out on the three [H<sub>3</sub>Si,N,O] compounds studied at the MP4(SDTQ)/6-311++G(d,p)/MP2/6-31+G(d,p) level of theory (Table 3). The silaformamide isomer **16** is 5.71 kcal mol<sup>-1</sup> more stable than silylene **18** and 15.7 kcal mol<sup>-1</sup> more stable than silanimine **19**. These



computations show an interesting parallel to those of the [H<sub>2</sub>Si,O] isomers, in which H<sub>2</sub>SiO is more stable than HSiOH by 2.7 kcal mol<sup>-1</sup>, but only at the highly correlated MP4/MC-311G(d,p) level.<sup>9,37</sup> Similarly, structure **16** is the most stable isomer only at the MP4 level.<sup>38</sup> A related recent *ab initio* study of [H<sub>3</sub>Si,N,O] by Marshall indicates that **16** is the most stable of several other isomers, including **19**, studied at the MP4/6-311G(d,p)/MP2/6-31G(d) level.<sup>39</sup> Thus, of a number of [H<sub>3</sub>Si,N,O] isomers, silaformamide **16** is the most stable, and as the result of our convention, its acidity is listed in Table 4.

**Summary.** Studies of [HSi(O)NH]<sup>-</sup> (**2**) in a tandem flowing afterglow selected ion flow tube have focused on determining its structure and chemical reactivity with a variety of neutral reagents. Related *ab initio* computations probed the stability of **2** and its isomer [Si(O)NH<sub>2</sub>]<sup>-</sup> (**1**) as well as eight other related anionic isomer pairs. The silylene anion isomers are the most stable for Si-H deprotonation of HSi(X)Y (for X = O, NH, and CH<sub>2</sub> and Y = NH<sub>2</sub> and CH<sub>3</sub>). However, O-H deprotonation is favored when X = O, NH, and CH<sub>2</sub> and Y = OH. Charge density computations have also been carried out on a large number of neutrals and anions. Silaformamide has a  $\Delta G_{\text{acid}}$  value estimated to be between 350 and 355 kcal mol<sup>-1</sup>.

**Acknowledgment.** We wish to acknowledge the financial support of the National Science Foundation (Grant Nos. CHE-8921522 and 9223037) and the donors of the Petroleum Research Fund, administered by the American Chemical Society. We thank Professor Christopher Hadad (The Ohio State University) for providing extensive help and considerable insight in our charge density studies. Professor Mark S. Gordon provided help in explaining the *ab initio* silylene anion trends, for which we express our appreciation.

OM950215V

(37) Gordon, M. S.; Pederson, L. A. *J. Phys. Chem.* **1990**, *94*, 5527-5530.

(38) The MP2/6-31+G(d,p)/MP2/6-31+G(d,p) energies for **16**, **18**, and **19** are -420.475 34, -420.480 40, and -420.448 27 hartree.

(39) Marshall, P. *Chem. Phys. Lett.* **1993**, *201*, 493-498.

# Potential Energy Surface of the Reaction of the Silaformyl Anion and CO<sub>2</sub>

Hideaki Shimizu and Mark S. Gordon\*

Department of Chemistry, Iowa State University, Ames, Iowa 50011-3111

Robert Damrauer

Department of Chemistry, University of Colorado at Denver, P.O. Box 1733364, Denver, Colorado 80217-3364

Richard A. J. O'Hair<sup>†</sup>

Department of Chemistry and Biochemistry, University of Colorado at Boulder, Boulder, Colorado 80309-0215

Received March 15, 1995<sup>⊗</sup>

The potential energy surface (PES) for the reaction of the silaformyl anion (HSiO<sup>-</sup>) with CO<sub>2</sub> was studied in detail using *ab initio* electronic structure theory. The calculated PES, using fourth-order perturbation theory (MP4) energies with the 6-311++G(d,p) basis set, obtained at MP2/6-31++G(d,p) geometries, shows that there are two important (low-energy) paths leading to different products, SiO + HCO<sub>2</sub><sup>-</sup> and HSiO<sub>2</sub><sup>-</sup> + CO<sub>2</sub>. There are, in addition, two paths that correspond to oxygen exchanges. All four of these paths lie below the initial reactants, HSiO<sup>-</sup> + CO<sub>2</sub>. The calculated potential energy surface is in good agreement with the available experimental data.

## Introduction

The reactions of HSiO<sup>-</sup> with CO<sub>2</sub>, COS, CS<sub>2</sub>, and SO<sub>2</sub> have recently been studied by flowing afterglow experiments.<sup>1</sup> On the basis of analyses using isotopic substitutions, these four reaction systems have been proposed to have similar reaction mechanisms. The proposed mechanisms typically invoke four-membered rings that may be intermediate complexes or transition states. Similar reaction schemes may also apply to other analogous ion–molecule reactions, such as those involving HSiS<sup>-</sup> and HSiNH<sup>-</sup>.<sup>2</sup>

The purpose of the current study is to use accurate electronic structure theory methods to analyze the detailed potential energy surface (PES) for a prototypical HSiO<sup>-</sup> ion–molecule reaction, in order to gain some insight into the mechanism. We chose HSiO<sup>-</sup> + CO<sub>2</sub> as a representative system. A similar set of calculations on the reaction of HSiO<sup>-</sup> with COS are in progress.<sup>3</sup>

Experimentally, HSiO<sup>-</sup> reacts with CO<sub>2</sub> to produce HCO<sub>2</sub><sup>-</sup> + SiO and HSiO<sub>2</sub><sup>-</sup> + CO with a branching ratio of 0.45:0.55. The use of isotopically substituted HSi<sup>18</sup>O<sup>-</sup> has established that oxygen atoms from HSiO<sup>-</sup> and CO<sub>2</sub> undergo partial exchange. The proposed reaction mechanism shown in Scheme 1, including the central role played by a four-membered-ring structure, is consistent with all of these observations. A similar four-membered

ring was proposed<sup>4</sup> for the reaction of silaacetylide anion (HCSi<sup>-</sup>) with CO<sub>2</sub> and was verified to be an intermediate in the metathesis reactions for those two species.<sup>5</sup> The simplified mechanism proposed in Scheme 1 also involves an extrusion reaction, in which CO is eliminated from the four-membered ring. Possible competing mechanisms<sup>1</sup> include the formation of intermediate three-membered ring species. The calculations described here must account for the relative energetics of the possible competing reactions, as well as the relative stabilities of the proposed cyclic intermediates.

## Computational Methods

All geometries were optimized with second-order perturbation theory (MP2)<sup>6</sup> using the 6-31++G(d,p)<sup>7</sup> basis set. In the MP2 optimizations, no core orbitals were frozen. For all stationary points the analytic Hessian was calculated and diagonalized to confirm that they are minima (positive definite) or transition states (only one vibrational mode with an imaginary frequency). For preliminary Hartree–Fock (HF)/6-31G(d) optimized transition states, the minimum energy

(4) Damrauer, R.; DePuy, C. H.; Barlow, S. E.; Gronert, S. *J. Am. Chem. Soc.* **1988**, *110*, 2005–2006.

(5) Schmidt, M. W.; Grodon, M. S. *J. Am. Chem. Soc.* **1991**, *113*, 5224–5248.

(6) Møller, C.; Plesset, M. S. *Phys. Rev.* **1934**, *46*, 618. Krishnan, R.; Frisch, M. J.; Pople, J. A. *J. Chem. Phys.* **1980**, *72*, 4244.

(7) (a) H: Ditchfield, R.; Hehre, W. J.; Pople, J. A. *J. Chem. Phys.* **1971**, *54*, 724–728. (b) C, O: Hehre, W. J.; Ditchfield, R.; Pople, J. A. *J. Chem. Phys.* **1972**, *56*, 2257–2261. (c) Si: Gordon, M. S. *Chem. Phys. Lett.* **1980**, *76*, 163–168. (d) Standard polarizations were used. H (p = 1.1), C (d = 0.8), O (d = 0.8), Si (d = 0.395). (e) Standard diffuse functions were used: H (s = 0.0360), C (l = 0.0438), O (l = 0.0845), and Si (l = 0.0331), where l means an sp shell. See: Clark, T.; Chandrasekhar, J.; Spitznagel, G. W.; Schleyer, P. v. R. *J. Comput. Chem.* **1983**, *4*, 294–301.

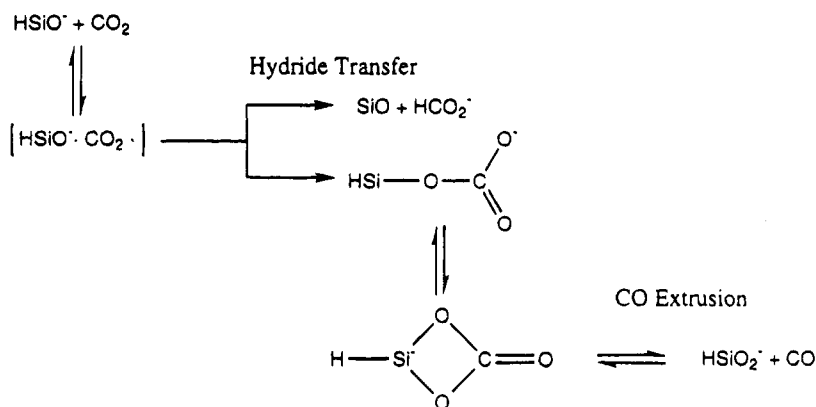
<sup>†</sup> Current address: Department of Chemistry, Kansas State University, Manhattan, KS 66506.

<sup>⊗</sup> Abstract published in *Advance ACS Abstracts*, May 1, 1995.

(1) Gronert, S.; O'Hair, R. A. J.; Prodnuk, S.; Sülzle, D.; Damrauer, R.; DePuy, C. H. *J. Am. Chem. Soc.* **1990**, *112*, 997–1003.

(2) Damrauer, R.; Krempf, M.; O'Hair, R. A. J. *J. Am. Chem. Soc.* **1993**, *115*, 1998.

(3) The MP2/6-31++G(d,p) potential energy surface of the HSiO<sup>-</sup> + COS system is under investigation by R. A. J. O'Hair.

Scheme 1. Proposed Reaction Paths for HSiO<sup>-</sup> + CO<sub>2</sub>

paths<sup>8</sup> were followed to verify the minima connected by the transition state.

The final energies, determined at the MP2/6-31++G(d,p) geometries, were obtained with fourth-order perturbation theory (MP4SDTQ) using the larger 6-311++G(d,p) basis set.<sup>9</sup> This energy is denoted as MP4SDTQ/6-311++G(d,p)//MP2-(full)/6-31++G(d,p). The energy differences corrected with MP2 zero-point energies thus correspond to the enthalpy differences at absolute zero,  $\Delta H^\circ(0)$ . Energy differences discussed in the remainder of the text refer to this highest level of theory.

The Bader atoms in molecules analysis (AIM) was used to interpret the bonding.<sup>10</sup> According to this model, a saddle point in the electron density between two atoms (referred to as a "bond critical point") is taken as an indication that a chemical bond connects those two atoms. The electron density  $\rho_c$  at the bond critical point reflects the relative bond strength for a given pair of atom types (e.g., C-C), and the bond critical point is closer to the less electronegative atom of the two atoms in the bond.

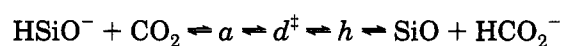
The majority of the calculations reported here were performed using Gaussian92,<sup>11</sup> following preliminary restricted Hartree-Fock (RHF) geometry optimizations with GAMESS.<sup>12</sup> Some MP2 geometry optimizations were performed using CADPAC4.2.<sup>13</sup>

## Results and Discussion

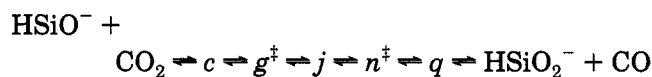
**1. Preliminary Considerations.** The MP2/6-31++G(d,p) geometries for all of the stationary points found on the potential energy surface are summarized in Figure 1, and schematics for the reaction mechanism are presented in Figure 2 and Scheme 2. The total, zero-point, and relative energetics are summarized in Table 1. The main reaction channels, as illustrated in

Figure 2 and Scheme 2, are (transition states are indicated with a superscript ‡)

## 1. hydride transfer

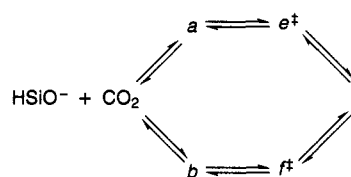


## 2. oxygen transfer



## 3. oxygen exchange

## (a) four-membered-ring intermediate

(b)  $h \rightleftharpoons k^\ddagger \rightleftharpoons h$ 

Note that intermediate *h* and transition state *k* are both lower in energy than HSiO<sup>-</sup> + CO<sub>2</sub>, so that this simple oxygen exchange reaction may occur with the energy available from the reactants. This is consistent with the experimental conclusions, noted earlier, based on isotopic substitutions. Similarly, intermediates *a*, *b*, and *i* and the transition states connecting them to each other (*e*, *f*) are all lower in energy than the separated reactants. Therefore, all of these species in the oxygen exchange cycle are accessible with the energy available from the reactants. As shown in Figure 2, all species in the hydride transfer and oxygen transfer routes are also lower in energy than the separated reactants. Thus, from the perspective of the potential energy surface all three routes summarized above are energetically feasible.

There are in addition two stationary points (*l*, *m*) that lie above the initial reactants, HSiO<sup>-</sup> + CO<sub>2</sub>. Structure *l* is a transition state that leads from the four-membered-ring intermediate *i* to a cyclic carbene *o*. Saddle point *m* connects *i* with the complex *q* that leads to CO extrusion. The high barriers (Table 1) predicted for *l* (62.7 kcal·mol<sup>-1</sup>) and *m* (21.0 kcal·mol<sup>-1</sup>) suggest that CO production from the four-membered ring is unlikely.

(8) (a) Garrett, B. C.; Redmon, M. J.; Steckler, R.; Truhlar, D. G.; Baldrige, K. K.; Bartol, D.; Schmidt, M. W.; Gordon, M. S. *J. Phys. Chem.* **1988**, *92*, 1476-1488. (b) Gonzales, C.; Schlegel, H. B. *J. Phys. Chem.* **1990**, *94*, 5523-5527. (c) Gonzales, C.; Schlegel, H. B. *J. Chem. Phys.* **1991**, *95*, 5853-5860.

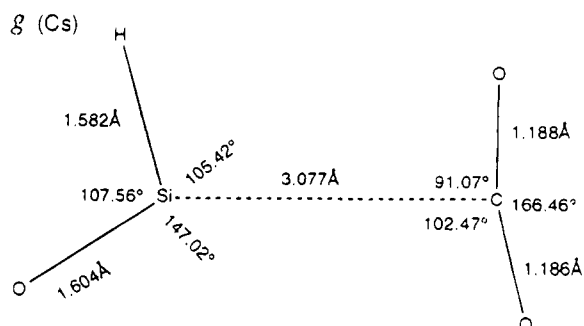
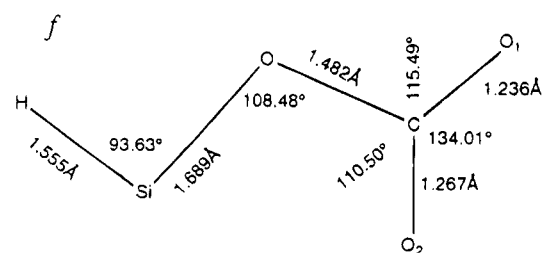
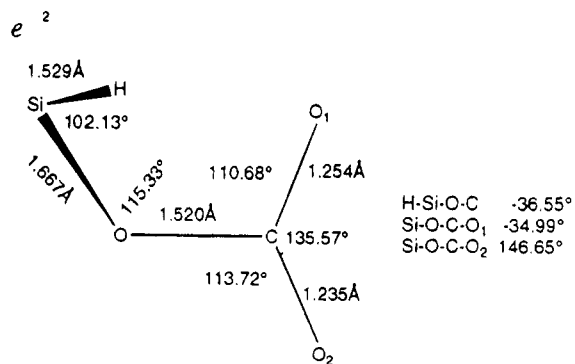
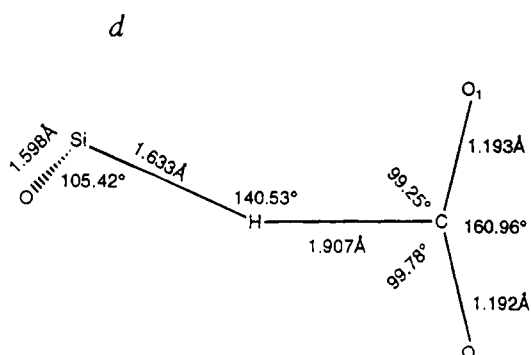
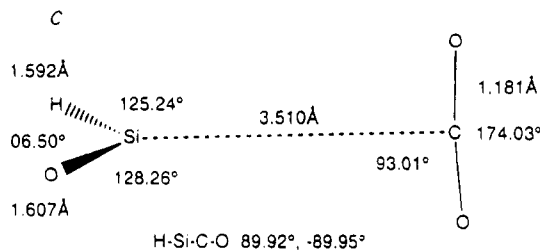
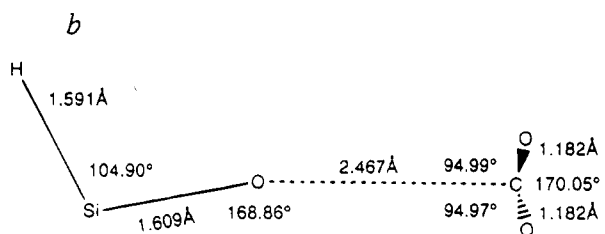
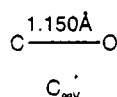
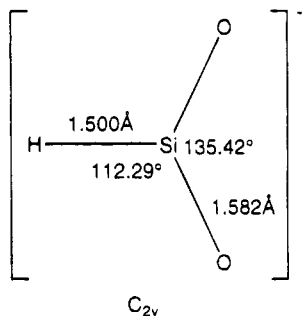
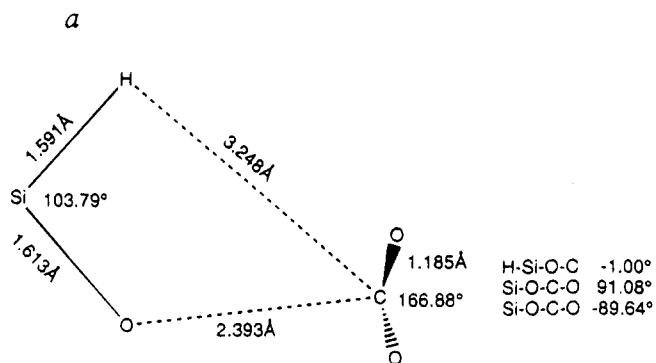
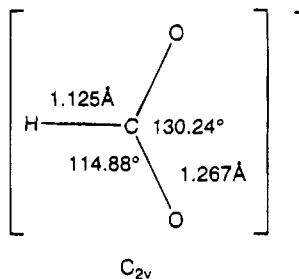
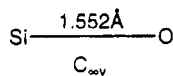
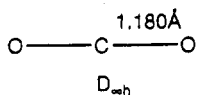
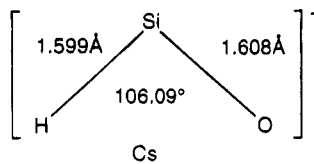
(9) Krishnan, R.; Binkley, J. S.; Seeger, R.; Pople, J. A. *J. Chem. Phys.* **1980**, *72*, 650-654.

(10) Bader, R. F. W. *Acc. Chem. Rev.* **1985**, *18*, 9.

(11) Frisch, M. J.; Trucks, G. W.; Head-Gordon, M.; Gill, P. M. W.; Wong, M. W.; Foresman, J. B.; Johnson, B. G.; Schlegel, H. B.; Robb, M. A.; Replogle, E. S.; Gomperts, R.; Andres, J. L.; Raghavachari, K.; Binkley, J. S.; Gonzalez, C.; Martin, R. L.; Fox, D. J.; Defrees, D. J.; Baker, J.; Stewart, J. J. P.; Pople, J. A. Gaussian 92; Gaussian Inc., Pittsburgh, PA, 1992.

(12) GAMESS (General Atomic and Molecular Electronic Structure System): Schmidt, M. W.; Baldrige, K. K.; Boatz, J. A.; Elbert, S. T.; Gordon, M. S.; Jensen, J. H.; Koseki, S.; Matsunaga, N.; Nguyen, K. A.; Su, S.; Windus, T. L.; Dupuis, M.; Montgomery, J. A. *J. Comput. Chem.* **1993**, *14*, 1347-1363.

(13) Amos, R. D.; Rice, J. E. CADPAC: Cambridge Analytic Derivatives Package, issue 4.2, 1989.





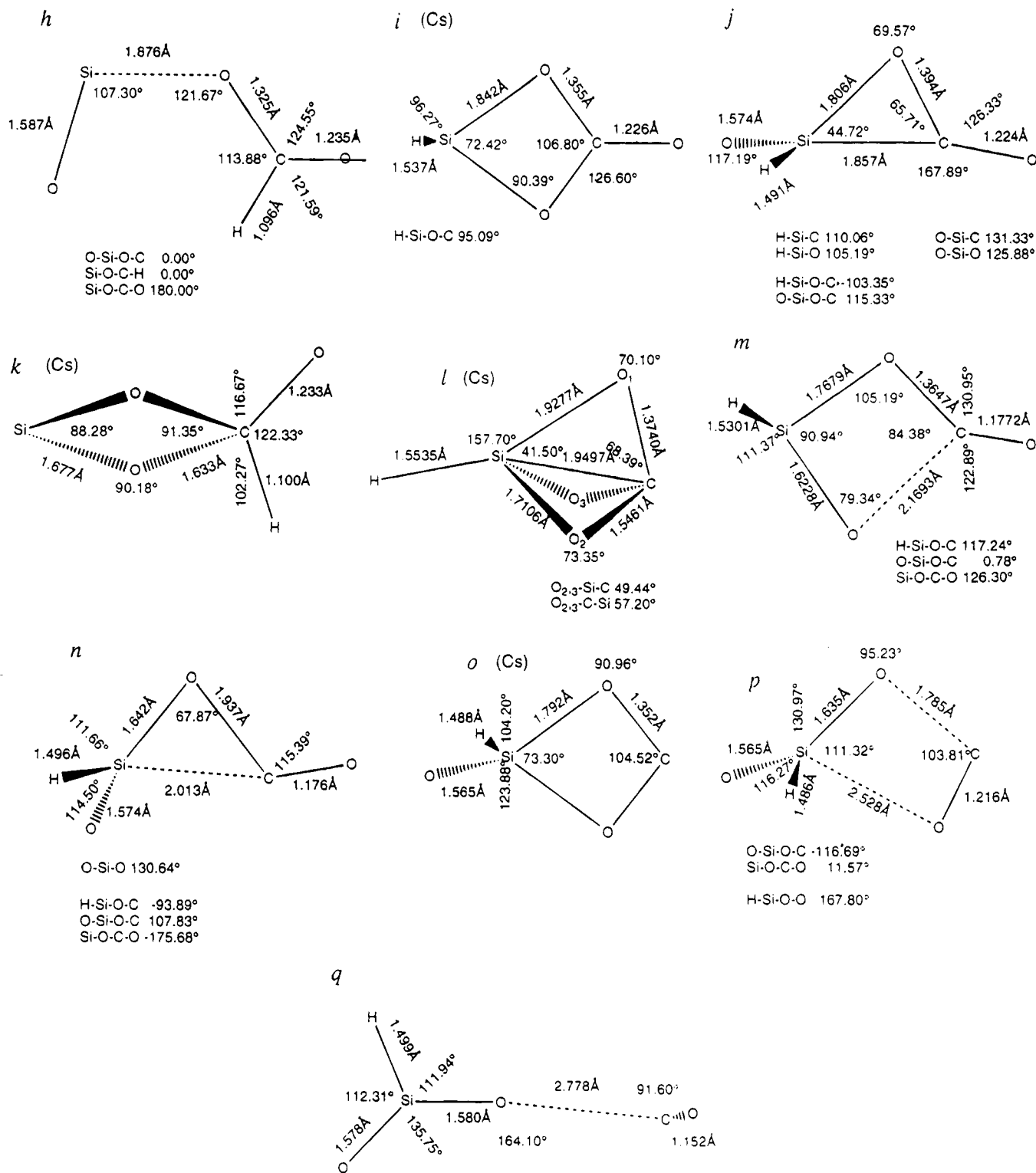
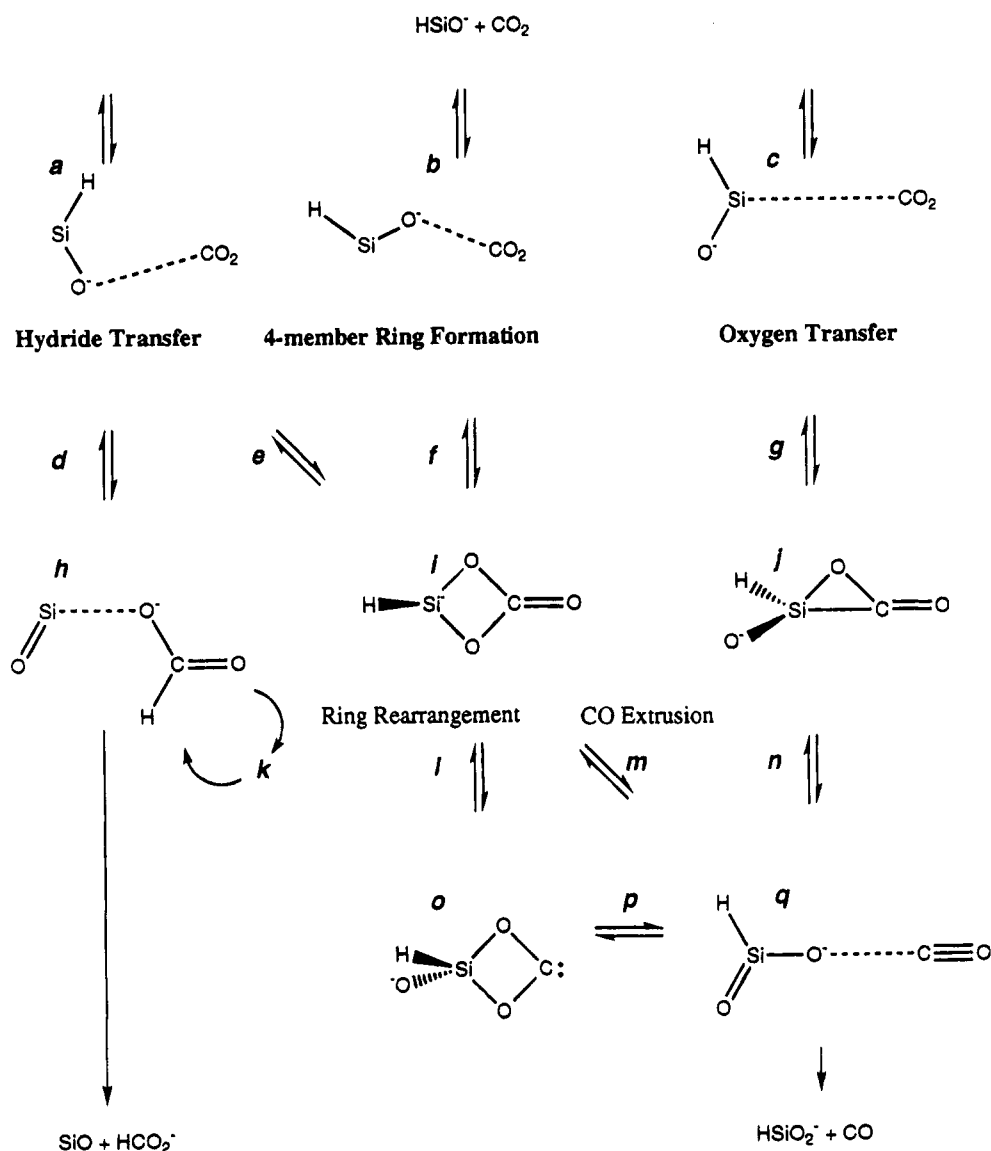


Figure 1. MP2 optimized geometries.

**2. Energetics. Hydride Transfer.** As shown in Table 1, all stationary points on the hydride transfer reaction path (see also Scheme 2 and Figure 2) lie below the reactants  $\text{HSiO}^- + \text{CO}_2$ . The initial ion-molecule complex *a* is  $8.9 \text{ kcal}\cdot\text{mol}^{-1}$  downhill. This complex *a* may follow two competing paths, hydride transfer via transition state *d* to form complex *h*, and four-membered-ring formation (*i* via transition state *e*). The energy of the hydride transfer transition state (*d*) is predicted to be only  $0.7 \text{ kcal}\cdot\text{mol}^{-1}$  lower than the transition state (*e*) that leads to four-membered-ring formation. Complex *h* has the lowest energy on the potential energy

surface, lying  $35.4 \text{ kcal}\cdot\text{mol}^{-1}$  below the initial reactants. No intervening barrier has been found between *h* and the final products,  $\text{HCO}_2^- + \text{SiO}$ . The energy of  $\text{HCO}_2^- + \text{SiO}$  is slightly higher than that of the hydride transfer transition state (*d*), but these products are still  $\sim 4 \text{ kcal}\cdot\text{mol}^{-1}$  below the reactants. Since this entire segment of the reaction surface is lower than the initial reactants in energy, all species are energetically accessible.

**Oxygen Transfer.** Complex *c* is a few  $\text{kcal}\cdot\text{mol}^{-1}$  less stable than the other two ion-molecule complexes (*a*, *b*). The barrier at transition state *g*, that separates *c*

Scheme 2. Calculated Reaction Paths for  $\text{HSiO}^- + \text{CO}_2^a$ 

<sup>a</sup> Labels adjacent to arrows refer to transition states.

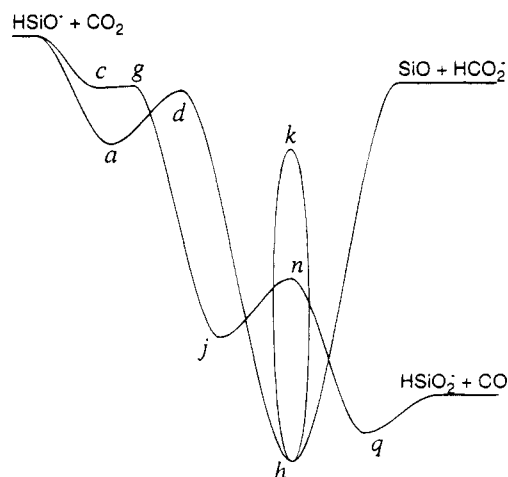


**Figure 2.** Schematic potential surface ([MP4SDTQ/6-311++G(d,p)//MPS(full)/6-31++G(d,p)] level).

from the three-membered ring *j*, is very small ( $0.1 \text{ kcal}\cdot\text{mol}^{-1}$ ); therefore, this transition state may well disappear at higher levels of theory. Such an occurrence would result in the direct formation of the three-membered ring from the separated reactants. The

energy of the three-membered ring *j* is similar to that of the four-membered ring *i*. Both structures are about  $25 \text{ kcal}\cdot\text{mol}^{-1}$  below  $\text{HSiO}^- + \text{CO}_2$ . The ring scission reaction via transition state *n*, in which the three-membered ring opens to form a complex (*q*) between  $\text{HSiO}_2^-$  and CO, has a small ( $5.0 \text{ kcal}\cdot\text{mol}^{-1}$ ) barrier. The ion-molecule complex (*q*) in the exit channel is  $8.0 \text{ kcal}\cdot\text{mol}^{-1}$  lower in energy than the three-membered ring, and the final products  $\text{HSiO}_2^- + \text{CO}$  are only  $3.2 \text{ kcal}\cdot\text{mol}^{-1}$  above *q*. There is apparently no barrier to decomposition from *q*. As noted for the hydride transfer path, all stationary points on the oxygen transfer path are also lower in energy than the initial reactants. Therefore, the observed branching ratio for the two paths must be determined by the detailed dynamics of the reaction.

**Four-Membered-Ring Formation.** There are two routes<sup>14</sup> to the four-membered ring *i*, starting from the

(14) In each route, at the MP2/6-31++G(d,p) level of theory, there is an additional transition state and minimum (between *a*, *e* or *b*, *f*). In each case, these additional stationary points disappear (that is, the transition state falls below the minimum in energy) at the MP4/6-311++G(d,p) level of theory; these stationary points are likely to be artifacts and are therefore not discussed in the text.

Table 1. Energetics of the HSiO<sup>-</sup> + CO<sub>2</sub> Reaction Network

	MP2(full)/6-31++G(d,p)/MP2(full)/6-31++G(d,p)			MP4SDTQ(fc)/6-311++G(d,p)/MP2(full)/6-31++G(d,p)	
	E/hartree	ZPE/kcal·mol <sup>-1</sup>	ΔH(0)/kcal·mol <sup>-1</sup>	E/hartree	ΔH(0)/kcal·mol <sup>-1</sup>
HSiO <sup>-</sup> + CO <sub>2</sub>	-552.783 97	12.2	0.0	-552.959 76	0.0
<i>a</i>	-552.799 76	12.9	-9.1	-552.975 15	-8.9
<i>b</i>	-552.798 41	12.7	-8.5	-552.973 33	-7.9
<i>c</i>	-552.791 23	12.5	-4.2	-552.967 09	-4.2
<i>d</i>	-552.790 97	12.5	-4.0	-552.967 55	-4.5
<i>e</i>	-552.799 01	14.2	-7.4	-552.969 03	-3.8
<i>f</i>	-552.798 82	14.0	-7.5	-552.968 01	-3.4
<i>g</i>	-552.791 18	12.4	-4.3	-552.966 69	-4.1
<i>h</i>	-552.861 38	16.6	-44.2	-553.023 26	-35.4
<i>i</i>	-552.842 39	15.5	-33.3	-553.007 56	-26.6
<i>j</i>	-552.841 67	14.8	-33.6	-553.003 74	-25.0
<i>k</i>	-552.819 87	16.3	-18.4	-552.981 20	-9.3
<i>l</i>	-552.700 56	12.2	52.4	-552.859 95	62.7
<i>m</i>	-552.757 81	13.4	17.6	-552.928 16	21.1
<i>n</i>	-552.827 77	13.5	-26.1	-552.993 73	-20.0
<i>o</i>	-552.839 80	14.8	-32.4	-552.999 44	-22.2
<i>p</i>	-552.812 44	13.2	-16.8	-552.976 75	-9.6
<i>q</i>	-552.845 67	12.4	-38.5	-553.012 75	-33.0
SiO + HCO <sub>2</sub> <sup>-</sup>	-552.799 73	14.5	-7.6	-552.969 63	-3.9
HSiO <sub>2</sub> <sup>-</sup> + CO	-552.839 12	11.9	-34.9	-553.006 84	-29.8

ion-molecule complexes *a* and *b*. These complexes are nearly isoenergetic, as are the corresponding transition states *e* and *f*. The barrier heights that lead from complexes *a* and *b* to the four-membered ring are 4–5 kcal·mol<sup>-1</sup>, and the ring is 26.6 kcal·mol<sup>-1</sup> below HSiO<sup>-</sup> + CO<sub>2</sub>. Once this ring has been formed, it can rearrange to form the cyclic carbene *o* or extrude a CO via complex *q*. As noted earlier, each of these last two processes involves a large barrier (at *l* and *m*, respectively); thus, these reactions are not likely to occur, except at high temperature. A more energetically accessible route to CO production has already been discussed.

**3. Structure and Bonding.** The geometries for the structures discussed in this work are summarized in Figure 1, and the imaginary normal modes for the saddle-point structures are shown in Figure 3. As noted earlier, each minimum energy path, starting from the direction indicated by the imaginary frequency at the transition state, was traced to the connecting reactants and products (at the Hartree-Fock level of theory) to verify that these compounds do indeed connect.

It is interesting to compare the three HSiO<sup>-</sup>-CO<sub>2</sub> complexes (*a*, *b*, and *c*) using the molecular electrostatic potential map (MEP map) of HSiO<sup>-</sup> shown in Figure 4. The MEP map exhibits three negative maxima, indicated by "a", "b", or "c" on the figure. These maxima correspond to the points of interaction with CO<sub>2</sub>, resulting in structures *a*, *b*, and *c*. Moreover, the ion-molecule distances, as measured by the Si-C or O-C distance, correlate with the magnitude of the potential, the ion-molecule interaction increasing in the order *c* < *b* < *a*. According to the Mulliken population analysis, there is only nominal charge transfer from HSiO<sup>-</sup> to CO<sub>2</sub>: 0.059, 0.051, and 0.044 for *a*, *b*, and *c*, respectively. These results suggest that initial formation of the ion-molecule complexes is mainly based on electrostatic interactions and that the internal electronic structure of each fragment remains essentially unchanged upon complex formation, except for a slight bending of the O-C-O angle.

The structure of transition state *d* is closer to that of *a* than to that of *h*. This is consistent with the

Hammond Postulate,<sup>15</sup> since *h* is much lower in energy than *a*. The C-O length in *d* is not much different from that in isolated CO<sub>2</sub>, and the Si-H length is only 0.02 Å longer than that in *a*. The electron densities  $\rho_c$  at the bond critical points are shown in Figure 5, for *a*, *d*, and *h*. The weak C<sub>3</sub>O<sub>2</sub> bond in complex *a* and the weak C<sub>3</sub>H<sub>4</sub> bond in transition state *d* are apparent from the relatively small values for  $\rho_c$  in these bonds.  $\rho_c$  is also small for the Si<sub>1</sub>-O<sub>5</sub> bond in *h*.

In the intermediate *h*, Si is connected to an oxygen (O<sub>5</sub>) that originally was in the CO<sub>2</sub> molecule, with a Si-O<sub>5</sub> distance of 1.88 Å. Though this is quite long for an Si-O single bond, it is shorter than the analogous distances found in the complexes *a*, *b*, and *c*. The C-O<sub>5</sub> distance of 1.32 Å may be compared with the C-O<sub>6</sub> distance of 1.22 Å. These distances suggest that O<sub>5</sub> forms partial bonds with both Si and C, and this is supported by the large electron densities at the bond critical points (Figure 5). For example,  $\rho_c$  for Si<sub>1</sub>-O<sub>5</sub> in *h* is about 50% of that for Si<sub>1</sub>-O<sub>2</sub>, a nominal double bond. In contrast, the very weak C<sub>3</sub>O<sub>2</sub> bond in complex *a* has a  $\rho_c$  value which is only 5% of that for C<sub>3</sub>O<sub>5</sub>.

A plot of the total density for the three-membered-ring species *j* is shown in Figure 6. As expected for a strained ring, the Si-C bond path is bent. As has been illustrated for neutral analogs,<sup>16</sup> the C-O and Si-O bond paths are less bent than the Si-C bond path. Upon dissociation of C-O, Si-C stays weakly bound up to the transition state *n*, while the C-O distance changes from 1.39 to 1.94 Å. The product *q* is an ion-molecule complex connecting HSiO<sub>2</sub><sup>-</sup> and CO. The geometries of both fragments in *q* are very similar to those in the product molecules.

The transition states (*e* and *f*) that lead to the formation of the four-membered ring *i* from *a* and *b*, respectively, differ mainly in their H-Si-O-C torsional angles (Figure 1). In both *e* and *f*, the Si-O distance is slightly longer than a normal Si-O single-bond length, and the internal C-O distance is about 0.1 Å longer

(15) Hammond, G. S. *J. Am. Chem. Soc.* **1955**, *77*, 334.

(16) (a) Boatz, J. A.; Gordon, M. S. *J. Phys. Chem.* **1989**, *93*, 3025.  
(b) Boatz, J. A.; Gordon, M. S.; Sita, L. R. *J. Phys. Chem.* **1990**, *94*, 5488–5493.

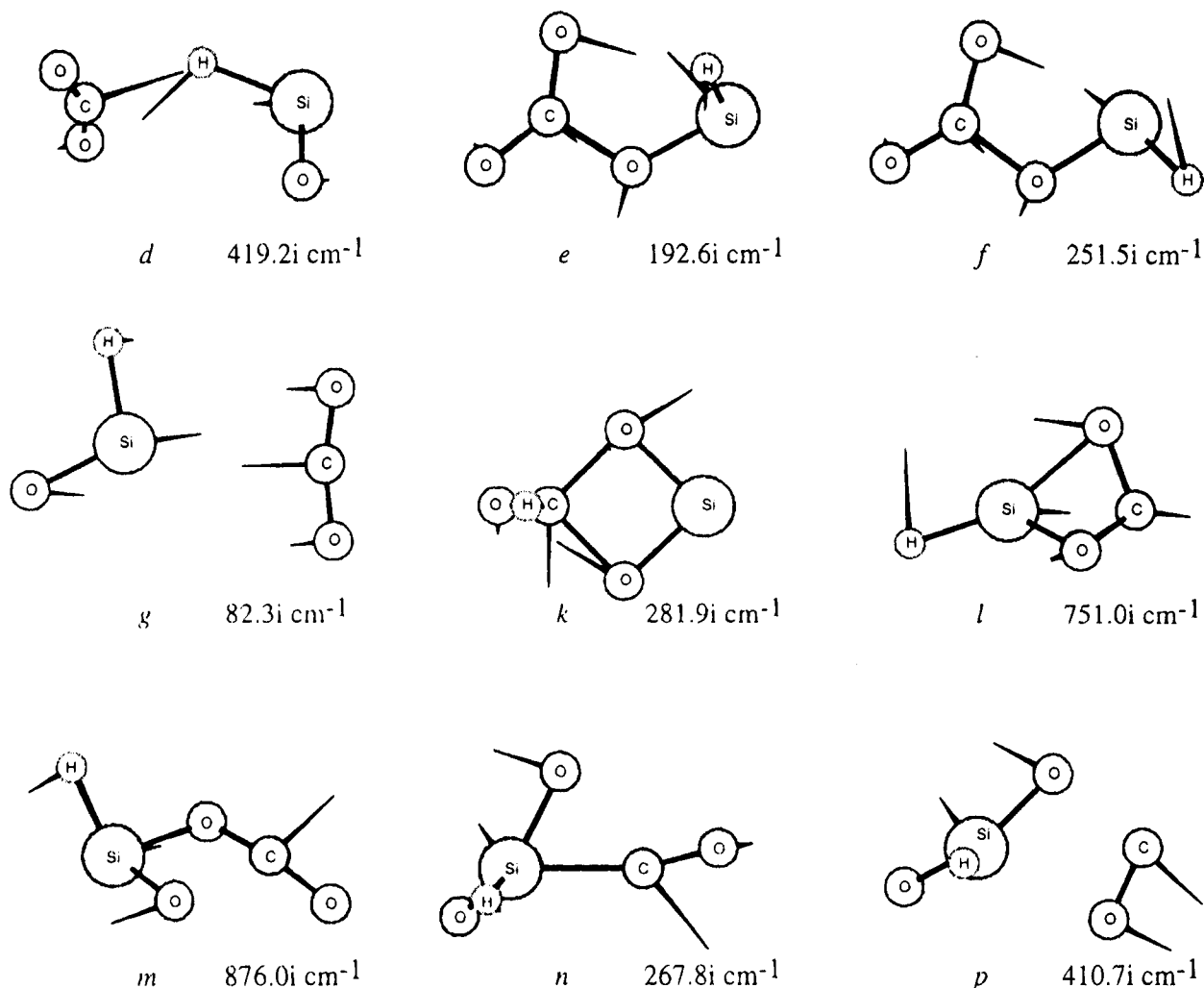


**Figure 3.** Reaction mode of each transition state.

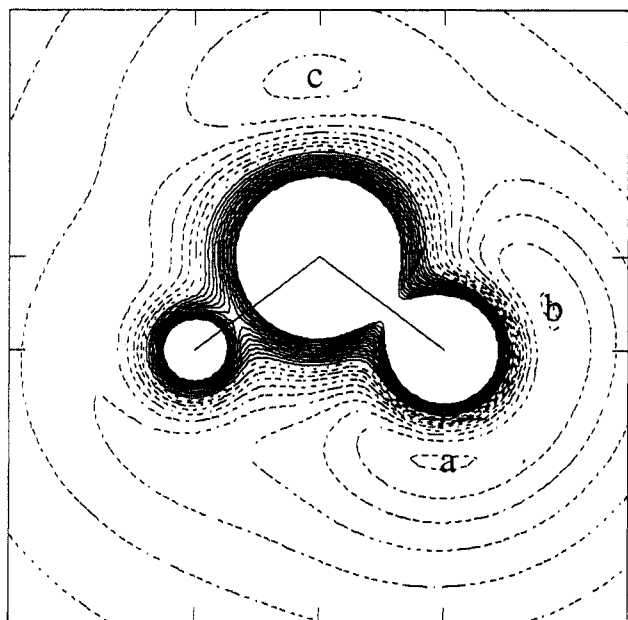


**Figure 4.** Molecular electrostatic potential of  $\text{HSiO}^-$  (electrostatic potential was calculated for a +0.001 test charge, and spacings between lines are  $20 \text{ kcal}\cdot\text{mol}^{-1}$ ): (solid line) positive; (widely spaced dotted line) zero; (dashed line) negative.

than a normal C–O single bond. Although the four-membered ring *i* is  $26.6 \text{ kcal}\cdot\text{mol}^{-1}$  below  $\text{HSiO}^- + \text{CO}_2$

and therefore has a relatively stable structure, its Si–O bonds are quite long ( $1.84 \text{ \AA}$ ).

At transition state *m*, connecting *i* with the  $\text{HSiO}_2^-$ –CO complex *q*, one C–O bond is elongated to  $2.17 \text{ \AA}$ , while the other stays at roughly a single-bond length. One of the Si–O bonds is  $1.65 \text{ \AA}$ , and the other is  $1.70 \text{ \AA}$ . While a normal single Si–O bond is very strong and the extrusion reaction is actually exothermic, at the initial stage of the reaction there apparently is not enough energetic gain from shortening the Si–O bonds to compensate for the C–O bond breaking. As a result, there is a large  $47.7 \text{ kcal}\cdot\text{mol}^{-1}$  barrier for this process.

### Conclusion

The potential energy surface for the reaction system of  $\text{HSiO}^- + \text{CO}_2$  has been explored in detail. In general, this surface has many characteristics that are typical for ion–molecule reactions. Strong electrostatic interactions between the ion and the neutral substrate lead to the formation of ion–molecule complexes that may be bound by as much as  $10\text{--}30 \text{ kcal}\cdot\text{mol}^{-1}$ . Once formed, these ion–molecule complexes may rearrange through intramolecular isomerizations to more stable structures, leading eventually to dissociation into final products. The ultimate fate of these compounds depends on two factors: the initial energy available to the reacting species and the heights of any barriers to the rearrangements of the ion–molecule complex. If, as in

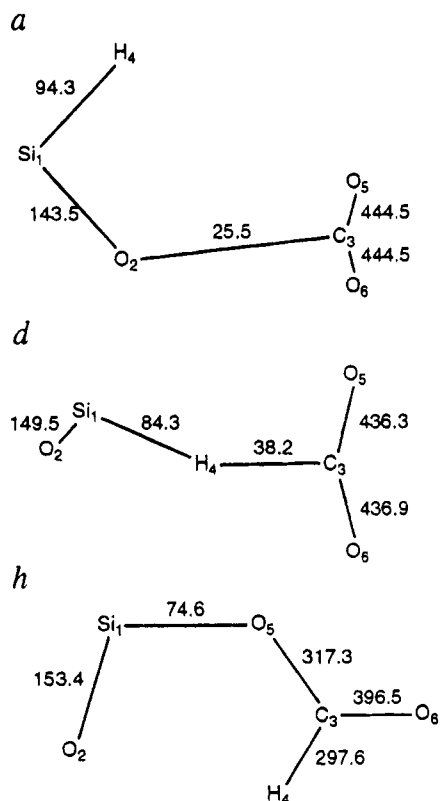


**Figure 5.** Electron density on the bond critical points at the stationary points along the hydride transfer (units are milli(atomic units)).

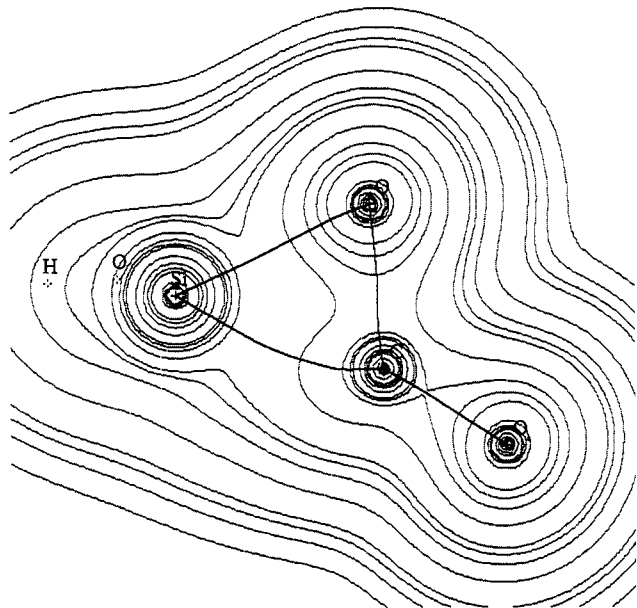


**Figure 6.** Electron density and bond path of *j*. Bond paths are denoted by dark lines between atomic centers.

the experiments related to the calculations presented here, only thermal energies are available, any significant barriers will be insurmountable. When the neutral species have highly polar bonds, as in the case here, it is likely that relatively stable cyclic intermediates will form.

The potential surface described in this work is in good agreement with the experimental results. The main path leading to  $\text{HSiO}_2^- + \text{CO}$  is oxygen extraction by  $\text{HSiO}^-$  via a three-membered-ring intermediate. The reaction that produces  $\text{HCO}_2^- + \text{SiO}$  is the single hydride transfer. All stationary points (intermediates and transition states) on both paths are lower in energy than the initial reactants; therefore, both reactions can take place easily. Exploration of the reaction dynamics would be required to understand the observed branching ratio. The formation of a four-membered-ring intermediate does not play an important role in determining the final products, because there is a large ( $18 \text{ kcal mol}^{-1}$ ) barrier to CO extrusion from this intermediate. Instead, the four-membered ring acts as a oxygen exchange intermediate.

This paper once again highlights the importance of carrying out accurate *ab initio* calculations to gain mechanistic insights into the gas-phase ion-molecule reactions of low-valent silicon species. Just as a previous theoretical<sup>15</sup> paper revealed a plausible new channel for the reaction of  $\text{HCSi}^-$  with COS, this paper sheds new light on the reaction of  $\text{HSiO}^-$  with  $\text{CO}_2$ . In particular, this paper demonstrates that the originally proposed mechanism needs some revision. Although the four-membered-ring intermediate *i* is a key intermediate in the oxygen scrambling process, contrary to the original hypothesis, extrusion of CO from this intermediate is not energetically favored. Instead, the three-membered-ring intermediate *j*, which can be formed either directly from the reactants or indirectly via the four-membered-ring intermediate, undergoes facile loss of CO to form the observed products. Thus, the observed partial scrambling process for the loss of CO is likely to involve the following process (Scheme 2):  $\text{HSiO}^- + \text{CO}_2 \rightarrow b \rightarrow [f^\ddagger] \rightarrow i \rightarrow [f^\ddagger] \rightarrow b \rightarrow c \rightarrow [g^\ddagger] \rightarrow i \rightarrow [n^\ddagger] \rightarrow q \rightarrow \text{HSiO}_2^- + \text{CO}$ . Oxygen exchange in the hydride transfer reaction is equally fascinating, occurring via two competing processes. The first process also occurs via the four-membered-ring intermediate:  $\text{HSiO}^- + \text{CO}_2 \rightarrow a$  or  $b \rightarrow [e^\ddagger \text{ or } f^\ddagger] \rightarrow i \rightarrow [e^\ddagger] \rightarrow a \rightarrow [d^\ddagger] \rightarrow h \rightarrow \text{HCO}_2^- + \text{SiO}$ . A novel second exchange process, occurring within the product ion molecule complex *h*, has been revealed in this study:  $\text{HSiO}^- + \text{CO}_2 \rightarrow a \rightarrow [d^\ddagger] \rightarrow h \rightarrow [k^\ddagger] \rightarrow h \rightarrow \text{HCO}_2^- + \text{SiO}$ . Without modeling the dynamics of these competing processes, it is impossible to determine which dominates the observed oxygen exchange.

**Acknowledgment.** This work was supported by grants from the Air Force Office of Scientific Research (Grant No. 93-0105 (M.S.G.)) and the National Science Foundation (Grant Nos. CHE-8921522 (R.D.), 9223037 (R.D.), and 9313717 (M.S.G.)). The calculations were performed on IBM RS/6000 workstations generously provided by Iowa State University. We thank Dr. Mike Schmidt for fruitful discussions.

OM9501992

# Rate Constants and Arrhenius Parameters for the Reaction of Acyl Radicals with Bu<sub>3</sub>SnH and (Me<sub>3</sub>Si)<sub>3</sub>SiH

C. Chatgililoglu,<sup>\*1</sup> C. Ferreri,<sup>2</sup> M. Lucarini,<sup>3</sup> P. Pedrielli,<sup>3</sup> and G. F. Pedulli<sup>3</sup>

*I.Co.C.E.A., Consiglio Nazionale delle Ricerche, Via P. Gobetti 101, 40129 Bologna, Italy, Dipartimento di Chimica Organica e Biologica, Università di Napoli "Federico II", Via Mezzocannone 16, 80134 Napoli, Italy, and Dipartimento di Chimica Organica "A. Mangini", Università di Bologna, Via S. Donato 15, 40127 Bologna, Italy*

Received January 3, 1995<sup>®</sup>

The kinetics of hydrogen abstraction from Bu<sub>3</sub>SnH and (Me<sub>3</sub>Si)<sub>3</sub>SiH by a variety of acyl radicals have been studied in nonpolar solvents over a range of temperatures by using competing decarbonylation reactions. The relative preexponential factors are essentially independent of the nature of the acyl radical and of the hydride; i.e.  $\log(A_d/A_{MH}) \cong 4.8$ . On the other hand, the relative activation energies, i.e.  $E_d - E_{MH}$ , decrease by ca. 2 kcal mol<sup>-1</sup> on going from primary to secondary and also on going from secondary to tertiary substituents at the carbonyl moiety for a particular hydride. As one goes from Bu<sub>3</sub>SnH to (Me<sub>3</sub>Si)<sub>3</sub>SiH for a particular acyl radical, the  $E_d - E_{MH}$  also decreases by ca. 2 kcal mol<sup>-1</sup>. Combining our relative kinetic data with the gas-phase Arrhenius parameters for the propanoyl radical decarbonylation allows for the evaluation of the absolute Arrhenius expressions for the reactions of acyl radicals with Bu<sub>3</sub>SnH and (Me<sub>3</sub>Si)<sub>3</sub>SiH and for the decarbonylation of secondary and tertiary acyl radicals. Rate constants at 80 °C for the reactions of (Me<sub>3</sub>-Si)<sub>3</sub>Si<sup>•</sup> and Bu<sub>3</sub>Sn<sup>•</sup> radicals with acyl derivatives have also been estimated.

## Introduction

In recent years free-radical reactions have proven to be valuable in synthetic organic chemistry, due to their selectivity and the mild conditions required.<sup>4</sup> In particular, the reduction of several functional groups and the formation of new carbon-carbon bonds have successfully been accomplished. Tri-*n*-butyltin hydride<sup>5</sup> and tris(trimethylsilyl)silane<sup>6</sup> are the most widely used reagents for these procedures, which utilize radical chain reactions.

For a synthetically useful radical chain reaction the intermediates must be *disciplined*. The concept of discipline in free-radical reactions is strictly connected with the kinetic information in each individual step, although upon first consideration, the importance of kinetic knowledge might be less apparent in planning a synthetic strategy. Thus, for the design of new radical reactions one is faced with the problem of simultaneously occurring carbon-centered radicals which must have different duties. Therefore, it is of considerable importance to know how rapidly different classes of carbon-centered radicals abstract hydrogen from different hydrides.<sup>7</sup>

In 1981 and 1991, rate constants and Arrhenius parameters for the reaction of some carbon-centered

radicals with Bu<sub>3</sub>SnH<sup>8</sup> and (Me<sub>3</sub>Si)<sub>3</sub>SiH<sup>9</sup> (henceforth (TMS)<sub>3</sub>SiH) were determined. The numerous citations of the former article over the last decade undoubtedly indicate the importance of these widely used data in understanding and programming free-radical reactions.<sup>4,6,7</sup> Furthermore, rate constants and Arrhenius parameters for the reaction of benzyl radicals with Bu<sub>3</sub>SnH<sup>10,11</sup> as well as absolute rate constants for hydrogen transfer reactions of the perfluoro-*n*-heptyl radical with Bu<sub>3</sub>SnH and (TMS)<sub>3</sub>SiH have also been determined.<sup>13</sup>

Acyl radicals are very important intermediates in chemical synthesis, as demonstrated by the large number of related papers which have appeared in the last

(8) Chatgililoglu, C.; Ingold, K. U.; Scaiano, J. C. *J. Am. Chem. Soc.* **1981**, *103*, 7739.

(9) Chatgililoglu, C.; Dickhaut, J.; Giese, B. *J. Org. Chem.* **1991**, *56*, 6399.

(10) Franz, J. A.; Suleman, N. K.; Alnajjar, M. S. *J. Org. Chem.* **1986**, *51*, 19.

(11) Rate constants and Arrhenius parameters for the reaction of phenyl, vinyl, cyclopropyl, and neopentyl radicals with Bu<sub>3</sub>SnH using the corresponding acyl peroxides with light as the source of radical formation have also been reported.<sup>12</sup> However, recent measurements on the decarboxylation processes indicated that some of these data are not reliable.<sup>7</sup>

(12) Johnston, L. J.; Luszytk, J.; Wayner, D. D. M.; Abeywickreyma, A. N.; Beckwith, A. L. J.; Scaiano, J. C.; Ingold, K. U. *J. Am. Chem. Soc.* **1985**, *107*, 4594.

(13) (a) Rong, X. X.; Pan, H.-Q.; Dolbier, W. R., Jr.; Smart, B. E. *J. Am. Chem. Soc.* **1994**, *116*, 4521. (b) Avila, D. V.; Ingold, K. U.; Luszytk, J.; Dolbier, W. R. Jr.; Pan, H.-Q.; Muir, M. *J. Am. Chem. Soc.* **1994**, *116*, 99.

(14) Acyl radical chemistry is an extremely active field at present. For some recent examples, see: (a) Penn, J. H.; Liu, F. *J. Org. Chem.* **1994**, *59*, 2608. (b) Chen, L.; Gill, B.; Pattenden, G. *Tetrahedron Lett.* **1994**, *35*, 2593. (c) Mendenhall, G. D.; Protasiewicz, J. D.; Brown, C. E.; Ingold, K. U.; Luszytk, J. *J. Am. Chem. Soc.* **1994**, *116*, 1718. (d) Ryu, I.; Yamazaki, H.; Ogawa, A.; Kambe, N.; Sonoda, N. *J. Am. Chem. Soc.* **1993**, *115*, 1187 and references cited therein. (e) Ryu, I.; Hasegawa, M.; Kurihara, A.; Ogawa, A.; Tsunoi, S.; Sonoda, N. *Synlett* **1993**, 143. (f) Boger, D. L.; Mathvink, R. J. *J. Org. Chem.* **1992**, *57*, 1429 and references cited therein. (g) Bachi, M. D.; Bosch, E. *J. Org. Chem.* **1992**, *57*, 4696 and references cited therein. (h) Chen, C.; Crich, D.; Papadatos, A. *J. Am. Chem. Soc.* **1992**, *114*, 8313 and references cited therein.

<sup>®</sup> Abstract published in *Advance ACS Abstracts*, April 1, 1995.

(1) Consiglio Nazionale delle Ricerche.

(2) Università di Napoli.

(3) Università di Bologna.

(4) For example, see: (a) Curran, D. P. *Synthesis* **1988**, 417, 489. (b) Jasperse, C. P.; Curran, D. P.; Fevig, T. L. *Chem. Rev.* **1991**, *91*, 1237. (c) Curran, D. P. In *Comprehensive Organic Synthesis*; Trost, B. M., Fleming, I., Eds.; Pergamon Press: Oxford, U.K., 1991; Vol. 4, Chapters 1 and 2. (d) Motherwell, W. B.; Crich, D. *Free Radical Chain Reactions in Organic Synthesis*; Academic Press: London, 1992.

(5) Neumann, W. P. *Synthesis* **1987**, 665.

(6) (a) Chatgililoglu, C. *Acc. Chem. Res.* **1992**, *25*, 188. (b) Chatgililoglu, C. *Chem. Rev.*, in press.

(7) For a recent review, see: Newcomb, M. *Tetrahedron* **1993**, *49*, 1151.

few years.<sup>14</sup> However, not much is known as to how rapidly this class of carbon-centered radicals abstracts hydrogen from various hydrogen donors. To our knowledge, the only previously reported rate constants are limited to the reaction of a benzoyl radical with benzenethiol<sup>15,16</sup> and to our preliminary report of the present work.<sup>17</sup> In order to overcome this gap of information, we have used competing decarbonylation reactions as timing devices (free-radical clocks<sup>7,18</sup>) to investigate the rates of primary, secondary, and tertiary acyl radicals as a function of temperature with the above common reducing agents.

## Results and Discussion

**Reduction of  $RC(O)Cl$  and  $RC(O)SePh$  by  $Bu_3SnH$  and  $(TMS)_3SiH$ .** Tri-*n*-butyltin hydride reacts spontaneously at ambient temperature with acid chlorides,  $RC(O)Cl$ , to form  $Bu_3SnCl$ ,  $RCHO$ ,  $RC(O)OCH_2R$ , and a number of minor products.<sup>19</sup> Luszytk et al.<sup>20</sup> have shown, in disagreement with earlier conclusions,<sup>21</sup> that free radicals are not involved in such a spontaneous reaction. When free radicals are deliberately generated in the system, the nature of the products may be changed.<sup>22</sup> In fact, the reproducibility of the product distribution for the radical-initiated reactions is relatively poor, the reason probably being that the free-radical process and the spontaneous reaction occur together.

Phenyl selenoesters, readily available from the corresponding carboxylic acids,<sup>23</sup> have been reported by Pfenninger et al.<sup>24</sup> to undergo reduction to the corresponding aldehydes and/or alkanes in the presence of  $Bu_3SnH$ . This methodology has successfully been applied to the synthesis of elaborate molecules *via* cyclization of intermediate acyl radicals.<sup>14b,f,25</sup> On the other hand, it has been shown that no spontaneous reaction occurs between acyl chlorides and  $(TMS)_3SiH$  under similar conditions and that, in the presence of a free-radical initiator, a reaction takes place to give aldehydes and/or alkanes depending on the reaction conditions.<sup>26</sup>

(15) Neville, A. G.; Brown, C. E.; Rayner, D. M.; Luszytk, J.; Ingold, K. U. *J. Am. Chem. Soc.* **1991**, *113*, 1869.

(16) Recently the reaction of propanoyl radical with tri-*n*-butyltin deuteride has also been measured by using time-resolved infrared spectroscopy and found to be  $3.0 \times 10^8 \text{ M}^{-1} \text{ s}^{-1}$  at 296K (Brown, C. E.; Neville, A. G.; Rayner, D. M.; Ingold, K. U.; Luszytk, J. *Aust. J. Chem.* **1995**, *48*, 363). We thank Dr. J. Luszytk for kindly informing us of his article prior to publication.

(17) Chatgililoglu, C.; Lucarini, M. *Tetrahedron Lett.* **1995**, *36*, 1299. (In this communication, *tert*-butylbenzene should be read as toluene.)

(18) Griller, D.; Ingold, K. U. *Acc. Chem. Res.* **1990**, *13*, 317.

(19) For reviews, see: (a) Kupchik, E. J. In *Organotin Compounds*; Sawyer, A. K., Ed.; Marcel Dekker: New York, 1971; Vol. 1, pp 28–33. (b) Kuivila, H. G. *Synthesis* **1970**, 499.

(20) (a) Luszytk, J.; Luszytk, E.; Maillard, B.; Ingold, K. U. *J. Am. Chem. Soc.* **1984**, *106*, 2923. (b) Luszytk, J.; Luszytk, E.; Maillard, B.; Lunazzi, L.; Ingold, K. U. *J. Am. Chem. Soc.* **1983**, *105*, 4475.

(21) (a) Kuivila, H. G.; Walsh, E. J., Jr. *J. Am. Chem. Soc.* **1966**, *88*, 571. (b) Walsh, E. J., Jr.; Kuivila, H. G. *J. Am. Chem. Soc.* **1966**, *88*, 576.

(22) Walsh, E. J., Jr.; Stoneberg, R. L.; Yorke, H.; Kuivila, H. G. *J. Org. Chem.* **1969**, *34*, 1156.

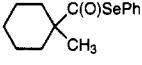
(23) (a) Grieco, P. A.; Jaw, J. Y.; Claremon, D. A.; Nicolaou, K. C. *J. Org. Chem.* **1981**, *46*, 1215. (b) Nicolaou, K. C.; Claremon, D. A.; Barnette, W. E. *J. Am. Chem. Soc.* **1979**, *101*, 3704.

(24) Pfenninger, J.; Heuberger, C.; Graf, W. *Helv. Chim. Acta* **1980**, *63*, 2328.

(25) (a) Batty, D.; Crich, D. *Tetrahedron Lett.* **1992**, *33*, 875. (b) Batty, D.; Crich, D.; Fortt, S. M. *J. Chem. Soc., Perkin Trans. 1* **1990**, 2875. (c) Batty, D.; Crich, D. *Synthesis* **1990**, 273.

(26) Ballestri, M.; Chatgililoglu, C.; Cardi, N.; Sommazzi, A. *Tetrahedron Lett.* **1992**, *33*, 1787.

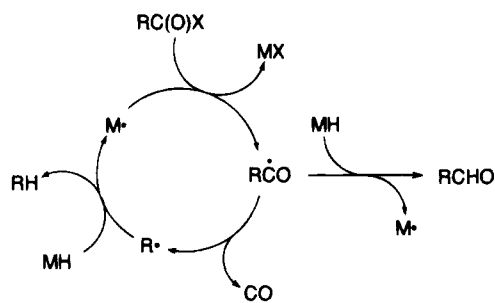
**Table 1. Reaction of Phenyl Selenoester Derivatives with  $(TMS)_3SiH^a$**

$RC(O)SePh$	yield of RH, <sup>b</sup> %	yield of $RC(O)H$ , <sup>b</sup> %
$CH_3(CH_2)_9CH_2C(O)SePh$	35	40
$CH_3CH_2CH_2CH_2CH_2CH_2CH_2CH_2C(O)SePh$	75	7
	79	<1

<sup>a</sup> Reactions initiated by UV irradiation at 50 °C in toluene.

<sup>b</sup> Yields by GC analysis based on formation of RH or  $RC(O)H$ .

### Scheme 1



X = Cl, SePh and MH =  $Bu_3SnH$ ,  $(TMS)_3SiH$

Table 1 summarizes product ratios and yields for the reduction of primary, secondary, and tertiary acyl selenides with  $(TMS)_3SiH$  under free-radical conditions.<sup>27</sup> The decrease of aldehyde formation through the primary, secondary and tertiary substituted series, under the same conditions, indicates that a decarbonylation of acyl radicals takes place.<sup>28</sup> The mechanism that we conceived for the reduction of acyl selenides is outlined in Scheme 1, and it is similar to those proposed for the reduction of acid chlorides with  $(TMS)_3SiH$ <sup>26</sup> and acyl selenides with  $Bu_3SnH$ .<sup>24</sup> That is, silyl or stannyl radicals, initially generated by a small amount of initiator, replace the phenylseleno group (or abstract a chlorine atom in the case of an acyl chloride with  $(TMS)_3SiH$ ) to form an acyl radical intermediate which undergoes either an intermolecular hydrogen abstraction, giving the aldehyde, or an  $\alpha$ -scission, to form an alkyl radical. Hydrogen abstraction from the hydrides by  $R\cdot$  regenerates the silyl or stannyl radicals, thus completing the cycle of these chain reactions.

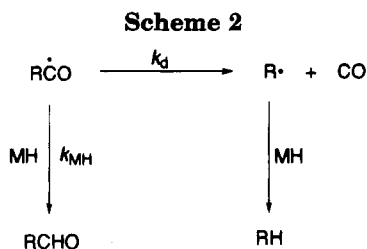
**Rate Constants for the Formation of Acyl Radicals.** The relative reactivity of  $(TMS)_3Si\cdot$  toward *t*-BuCl and *t*-BuC(O)Cl has been reported to be  $k_{RC(O)Cl}/k_{RCl} = 0.6$  at 80 °C.<sup>26</sup>

The photolytically initiated competition between  $CH_3(CH_2)_{11}C(O)Cl$  and  $CH_3(CH_2)_{11}C(O)SePh$  toward  $(TMS)_3Si\cdot$  indicates that the PhSe removal is much faster than chlorine abstraction. A value of  $k_{RC(O)Cl}/k_{RC(O)SePh} =$

(27) In the reaction of decanoyl chloride,  $RC(O)Cl$ , with  $(TMS)_3SiH$  the formation of the corresponding ester  $RCH_2OC(O)R$ , derived from the hydrosilylation of the decanal followed by spontaneous reaction with acid chloride, has also been observed.<sup>26</sup> With the analogous phenylseleno derivative, the hydrosilylation of aldehyde is unimportant, probably because the PhSe group removal by silyl radicals is much faster than the addition of silyl radicals to the carbonyl moiety of aldehyde.<sup>9</sup> It is also worth mentioning that the silyl ethers, obtained from the hydrosilylation of dodecanal, which react spontaneously with acid chlorides, do not react with phenyl selenoesters under the same conditions.

(28) Fischer, H.; Paul, H. *Acc. Chem. Res.* **1987**, *20*, 200 and references cited therein.





0.0031 at 80 °C was determined from the loss of starting materials under second-order conditions.<sup>7</sup> In a similar experiment, the relative reactivity of Bu<sub>3</sub>Sn<sup>•</sup> toward *t*-BuBr and CH<sub>3</sub>(CH<sub>2</sub>)<sub>11</sub>C(O)SePh was obtained by a thermally initiated reaction between the tin hydride and the two substrates. A value of  $k_{\text{RBu}}/k_{\text{RC(O)SePh}} = 12.5$  at 80 °C was determined.

The absolute rate constants for the reactions at room temperature of (TMS)<sub>3</sub>Si<sup>•</sup> with *t*-BuCl<sup>29</sup> and of Bu<sub>3</sub>Sn<sup>•</sup> with *t*-BuBr<sup>30</sup> are  $4.0 \times 10^5$  and  $1.7 \times 10^8$  M<sup>-1</sup> s<sup>-1</sup>, respectively. Assuming  $\log(A/M^{-1} \text{ s}^{-1}) = 8.7$  for these halogen abstraction reactions, we estimate the rate constants for the reactions at 80 °C of (TMS)<sub>3</sub>Si<sup>•</sup> with RC(O)Cl, of (TMS)<sub>3</sub>Si<sup>•</sup> with RC(O)SePh, and of Bu<sub>3</sub>Sn<sup>•</sup> with RC(O)SePh to be  $7 \times 10^5$ ,  $2 \times 10^8$ , and  $2 \times 10^8$  M<sup>-1</sup> s<sup>-1</sup>, respectively.

**Kinetics for the Reaction of Acyl Radicals with Bu<sub>3</sub>SnH and (TMS)<sub>3</sub>SiH.** An indirect procedure for measuring the rate constant of a radical–molecule reaction involves competition between this process and a unimolecular path of the radical (free-radical clocks<sup>7,18</sup>). In our case, a rate constant for H atom abstraction from a hydride (MH) by an acyl radical can be obtained, providing that conditions can be found in which the intermediate acyl radical is partitioned between the two reaction channels (Scheme 2), that is, reaction with the hydride (MH) and decarbonylation. By measuring the relative yields of RC(O)H and RH and applying one of the following methods, one is able to calculate the rate constant ratio, i.e.  $k_d/k_{\text{MH}}$ .

**Method A.** If the hydride concentration changes appreciably during the course of the reaction (bimolecular process under second-order conditions), the following relation holds:

$$[\text{RCHO}]/[\text{RH}] = \frac{1}{[\text{RH}]\{[\text{MH}]_0 + k_d/k_{\text{MH}}\}\{1 - e^{-k_{\text{MH}}/k_d[\text{RH}]}\} - 1} \quad (1)$$

**Method B.** If the hydride concentration remains essentially constant under the experimental conditions (bimolecular process under pseudo-first-order conditions), the above relation can be simplified as follows:

$$k_d/k_{\text{MH}} = ([\text{RH}]/[\text{RCHO}])[\text{MH}]_0 \quad (2)$$

To generate the desired acyl radical, acid chlorides or phenyl selenoesters have been used with (TMS)<sub>3</sub>SiH and phenyl selenoesters with Bu<sub>3</sub>SnH. Thus, the acyl radicals 1–3 are formed as intermediates in the reduction of the corresponding acyl derivatives.

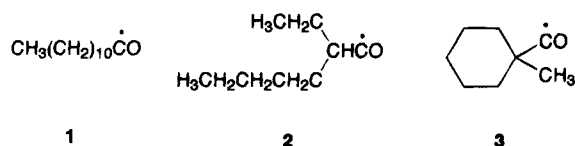


**Table 2. Competitive Kinetic Data for the Reactions of Acyl Radicals with the Two Hydrides and Their Decarbonylation**

acyl radical	hydride	T/K <sup>a</sup>	log A <sub>d</sub> /A <sub>MH</sub>	E <sub>d</sub> - E <sub>MH</sub> , kcal mol <sup>-1</sup>	k <sub>d</sub> /k <sub>MH</sub> at 296 K, M
1	(TMS) <sub>3</sub> SiH	323–433	4.89 ± 0.68	9.19 ± 1.14	0.013
2	(TMS) <sub>3</sub> SiH	294–353	4.63 ± 0.38	6.53 ± 0.54	0.644
3	(TMS) <sub>3</sub> SiH	273–353	4.80 ± 0.40	4.55 ± 0.58	27.594
1	Bu <sub>3</sub> SnH	353–423	4.87 ± 0.45	11.10 ± 0.79	0.00047
2	Bu <sub>3</sub> SnH	313–368	4.78 ± 0.24	8.54 ± 0.38	0.030
3	Bu <sub>3</sub> SnH	273–373	4.99 ± 0.28	6.64 ± 0.41	1.224

<sup>a</sup> Range of temperature employed.

The quantities of RCHO, RH, and MH were obtained by GC analysis, following the thermally or photolytically initiated radical reaction, and by using an internal standard. The ratio [RCHO]/[RH] varied in the expected manner with a change in the hydride concentration. Only data obtained at low conversion levels were employed in order to avoid any undesired processes. Mean values of  $k_d/k_{\text{MH}}$  were obtained at different hydride concentrations (generally four) according to eq 1 or 2. In a few cases, in which the hydride concentration had to be kept constant (for example, when the reaction was performed in pure hydride), the obtained value was the average of several different experiments. The detailed results of the individual experiments are available in the supplementary material. Analysis of these data (Figure 1) yielded the Arrhenius expressions for  $k_d/k_{\text{MH}}$  which are listed in Table 2. It is worth pointing out that for the reaction of acyl radical 2 with (TMS)<sub>3</sub>SiH (at 50 °C) for which both acid chloride and phenyl selenoester were employed, the obtained  $k_d/k_{\text{MH}}$  values were  $1.52 \pm 0.29$  and  $1.42 \pm 0.17$ , respectively. This reconfirms the similarities in the reaction mechanism for the two substrates.

When the data in Table 2 for the (TMS)<sub>3</sub>SiH and Bu<sub>3</sub>SnH series are compared, the  $k_d/k_{\text{SiH}}$  and  $k_d/k_{\text{SnH}}$  values increase at room temperature ca. 50-fold on going from primary to secondary and also on going from secondary to tertiary substituents at the carbonyl moiety. Since the  $\log(A_d/A_{\text{MH}})$  values are essentially the same in the silane and in the tin hydride series, this increase must be due to the E<sub>d</sub> - E<sub>MH</sub> term. This behavior is in agreement with the well-known properties of acyl radicals, which on one hand show rates of decarbonylation highly dependent on the degree of stabilization of the resulting alkyl radical<sup>28</sup> and on the other, being σ-type radicals, are expected to exhibit very similar reactivities in their intermolecular reactions.<sup>31</sup> Consequently, we conclude that the hydrogen donation from a specific hydride toward RCO radicals is essentially independent of the nature of the alkyl substituent R.

When the data in Table 2 are compared between (TMS)<sub>3</sub>SiH and Bu<sub>3</sub>SnH, the three calculated values of  $k_{\text{SnH}}/k_{\text{SiH}}$  prove to be similar. Thus, at room temperature, an acyl radical abstracts a hydrogen from Bu<sub>3</sub>SnH ca. 25 times faster than from (TMS)<sub>3</sub>SiH, this value being almost independent of the composition of the carbon substituent at the carbonyl moiety. The silane is a notably less reactive hydrogen donor than the tin

(29) Chatgililoglu, C.; Griller, D.; Lesage, M. *J. Org. Chem.* **1989**, *54*, 2492.

(30) Ingold, K. U.; Luszytyk, J.; Scaiano, J. C. *J. Am. Chem. Soc.* **1984**, *106*, 343.

(31) (a) Davies, A. G.; Sutcliffe, R. *J. Chem. Soc., Perkin Trans. 2* **1980**, 819; **1982**, 1483. (b) Paul, H.; Fischer, H. *Helv. Chim. Acta* **1973**, *56*, 1575.

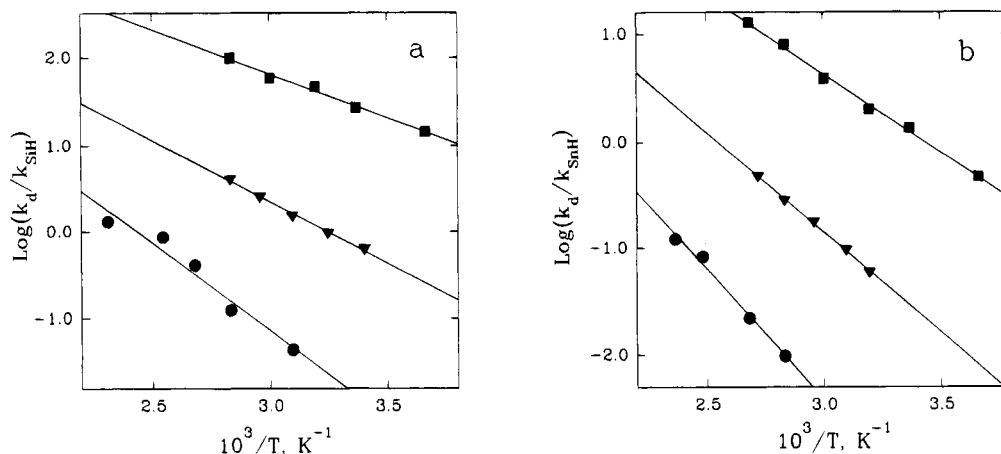


**Figure 1.** Arrhenius plots for  $k_d/k_H$  ratios obtained at various temperatures for the reaction of acyl radicals 1 (●), 2 (▼), and 3 (■) with  $(TMS)_3SiH$  (a) and  $Bu_3SnH$  (b).

hydride, presumably because the Si–H bond is ca. 5 kcal mol<sup>-1</sup> stronger than the Sn–H bond.<sup>6,32</sup> This difference in bond strength manifests itself in the enthalpy of activation, which is larger for  $(TMS)_3SiH$  than for  $Bu_3SnH$ . On the basis of the facts that (i)  $\log(A_d/A_{SnH})$  and  $\log(A_d/A_{SiH})$  can be considered as the same and (ii)  $E_{SiH} - E_{SnH} \approx 2$  kcal mol<sup>-1</sup> is independent of the nature of acyl radical, the following relation holds:

$$\log(k_{SnH}/k_{SiH}) = 437/T \quad (3)$$

which suggests that when the temperature is increased, the gap between  $k_{SnH}$  and  $k_{SiH}$  will decrease. For example at 20, 65, and 150 °C an RCO radical abstracts a hydrogen from  $Bu_3SnH$  ca. 30, 20, and 10 times faster than from  $(TMS)_3SiH$ , respectively.

A few measurements were also made for the rate constants for deuterium abstraction from  $Bu_3SnD$  by radical 2 and from  $(TMS)_3SiD$  by radical 1. At 80 °C,  $k_d/k_{SnD} = 0.980 \pm 0.035$  and  $k_d/k_{SiD} = 0.521 \pm 0.052$  were obtained. Detailed results of these experiments are also available in the supplementary material. These values together with the corresponding data calculated from the Arrhenius expressions in Table 2 yield  $k_{SnH}/k_{SnD} = 3.16$  and  $k_{SiH}/k_{SiD} = 3.25$  at 80 °C. The deuterium kinetic isotope effects found in this work are slightly higher than those reported for the reaction at the same temperature of primary alkyl radicals with  $Bu_3SnH$  and  $(TMS)_3SiH$ , i.e. 2.1 and 2.3, respectively.<sup>8,9</sup>

Relative rate constants and Arrhenius parameters in Table 2 can be converted to absolute rate constants and Arrhenius parameters for hydrogen abstraction from  $Bu_3SnH$  and  $(TMS)_3SiH$  via the absolute kinetic data for the decarbonylation reactions. Although kinetic data for such unimolecular processes are numerous,<sup>28,33</sup> the choice is not an easy one. For example, the reported frequency factor for the endothermic decarbonylation scatters between  $10^{11}$  and  $4 \times 10^{14}$  s<sup>-1</sup>.<sup>28</sup> A value close to  $10^{13}$  s<sup>-1</sup> is expected for a decomposition reaction.<sup>34</sup> The Arrhenius expression obtained by averaging the

data for the decarbonylation of the  $CH_3CH_2\dot{C}O$  radical in the gas phase has been considered (eq 4)<sup>35</sup>

$$\log(k_d/s^{-1}) = 13.1 - 14.6/\vartheta \quad (4)$$

where  $\vartheta = 2.3RT$  kcal mol<sup>-1</sup>. However, it has been shown that the rate constant for the decarbonylation of the pivaloyl and phenylacetyl radicals decreases with increasing solvent polarity,<sup>38</sup> i.e., there is a 4-fold decrease from *n*-hexane ( $8.3 \times 10^5$  s<sup>-1</sup>) to acetonitrile ( $1.9 \times 10^5$  s<sup>-1</sup>) for the pivaloyl radical.<sup>38a</sup>

With the due precautions, therefore, combinations of the Arrhenius expressions for  $k_d/k_{SiH}$  and  $k_d/k_{SnH}$  from primary acyl radicals (Table 2) with eq 4 yield the relationships

$$\log(k_{SiH}/M^{-1} s^{-1}) = 8.2 - 5.4/\vartheta \quad (5)$$

$$\log(k_{SnH}/M^{-1} s^{-1}) = 8.2 - 3.5/\vartheta \quad (6)$$

where  $\vartheta = 2.3RT$  kcal mol<sup>-1</sup>. As we mentioned above, eqs 5 and 6 should be independent of the composition of the carbon substituent at the carbonyl moiety. Examination of the rate constants at 23 °C, i.e.,  $k_{SiH} = 1.6 \times 10^4$  M<sup>-1</sup> s<sup>-1</sup> and  $k_{SnH} = 4.1 \times 10^5$  M<sup>-1</sup> s<sup>-1</sup>, indicates that  $(TMS)_3SiH$  is 10–20 times and  $Bu_3SnH$  3–6 times less reactive with acyl radicals than with alkyl radicals.<sup>8,9</sup> Furthermore, the  $k_{SnH}$  value is in good agreement with  $k_{SnD} = 3.0 \times 10^5$  M<sup>-1</sup> s<sup>-1</sup>, measured directly by laser flash photolytic techniques in *n*-hexane.<sup>16</sup>

Combination of eqs 5 and 6 with the kinetic data in Table 2 yields the Arrhenius parameters for the decarbonylation of secondary and tertiary substituted acyl radicals (Table 3). The decarbonylation of secondary and tertiary acyl radicals has previously been studied, and the Arrhenius parameters are subject to large errors due to uncertainties in the estimation procedure.<sup>39,40</sup> Although the  $\log(A/s^{-1})$  values scatter be-

(36) Watkins, K. W.; Thompson, W. W. *Int. J. Chem. Kinet.* **1973**, *5*, 791.

(37) Kerr, J. A.; Lloyd, A. C. *Trans. Faraday Soc.* **1967**, *63*, 2480.

(32) Kanabus-Kaminska, J. M.; Hawari, J. A.; Griller, D.; Chatgililoglu, C. *J. Am. Chem. Soc.* **1997**, *119*, 5267.

(33) Vollenweider, J.-K.; Paul, H. *Int. J. Chem. Kinet.* **1986**, *18*, 791.

(34) Benson, S. W. *Thermochemical Kinetics*, 2nd ed.; Wiley: New York, 1976.

(35) The temperature-dependent functions for decarbonylation of  $CH_3CH_2\dot{C}O$  radicals in the gas phase are as follows:<sup>36,37</sup>  $\log(k_d/s^{-1}) = 12.8 - 14.4/\vartheta$  and  $\log(k_d/s^{-1}) = 13.3 - 14.7/\vartheta$ , where  $\vartheta = 2.3RT$  kcal mol<sup>-1</sup>.

(38) (a) Tsentelovich, Y. P.; Fischer, H. *J. Chem. Soc., Perkin Trans. 2* **1994**, 729. (b) Corens, F. L.; Scaiano, J. C. *J. Am. Chem. Soc.* **1993**, *115*, 5204. (c) Lunazzi, L.; Ingold, K. U.; Scaiano, J. C. *J. Phys. Chem.* **1983**, *87*, 529.

(39) For the decarbonylation of  $Me_2CH\dot{C}O$  radical, see the following. (a) Gas phase: Cadman, C.; Dorwell, C.; Trotman-Dickenson, A. F.; White, A. J. *J. Chem. Soc. A* **1970**, 2371. (b) Liquid phase: Lipscher, J.; Fischer, H. *J. Phys. Chem.* **1984**, *88*, 2555.

**Table 3. Arrhenius Parameters for the Decarbonylation of Acyl Radicals**

acyl radical	$\log(A_d/s^{-1})$	$E_d$ , kcal mol <sup>-1</sup>	$k_d$ at 296 K, s <sup>-1</sup>
1	13.1	14.6	$2.1 \times 10^2$
2	13.0	12.0	$1.4 \times 10^4$
3	13.1	10.0	$5.2 \times 10^5$

tween 11.9 and 14.0, it is gratifying to see an average value of 13.1. Furthermore, the calculated  $k_d = 5.2 \times 10^5 \text{ s}^{-1}$  at 23 °C for the tertiary acyl radical (Table 3) is in excellent agreement with the recent value of the pivaloyl decarbonylation ( $k_d = 6.7 \times 10^5 \text{ s}^{-1}$  at 23 °C in *n*-hexane as a solvent) obtained by time-resolved infrared spectroscopy.<sup>16</sup> Taking into consideration the observed solvent effect in the rate of decarbonylation of pivaloyl and phenylacetyl radicals,<sup>38</sup> we are suggesting that the Arrhenius parameters reported in Table 3 are the best available data at present and should be used either in gas-phase or in nonpolar solvents.

### Experimental Section

**Materials.** Phenyl selenoesters were prepared by reacting an appropriate carboxylic acid with *N*-phenylselenophthalimide.<sup>23</sup> (TMS)<sub>3</sub>SiD was synthesized by reduction of the corresponding chloride with LiAlD<sub>4</sub>.<sup>41</sup> All other compounds used in this work were commercially available and, where necessary, were purified by standard methods.

**General Procedure for the Reduction of Phenyl Selenoesters (Table 1).** A solution containing the appropriate

phenyl selenoester (0.1 M) and (TMS)<sub>3</sub>SiH (2 equiv) in toluene (500 μL total volume) was photolyzed at 50 °C for ca. 0.5 h and then analyzed by GC. Yields were quantified by GC using decane or undecane as an internal standard.

#### General Procedure for the Kinetic Measurements.

**Method A.** Di-*tert*-butyl peroxide and an internal GC standard were added to a solution of a ca. 1:1 ratio of a known amount of tin hydride (from 0.1 to 0.15 M) and phenyl selenoester. The resulting solutions were degassed, sealed under argon in Pyrex ampules, and heated to the appropriate temperature.

**Method B.** A solution of the acyl derivative, the appropriate hydride (in a ratio of ca. 1:20), and an internal GC standard in toluene, *tert*-butylbenzene, or *n*-hexane was degassed and sealed under argon in Pyrex ampules. The reaction mixture was either photolyzed or thermolyzed at the appropriate temperature. Di-*tert*-butyl peroxide was used as the radical initiator when necessary.

The products of the reactions were analyzed by GC using a 30 m × 0.53 mm HP-5 column with temperature programming from 40 to 250 °C using a HP Series II chromatograph. The products of interest were identified by comparison of their retention times with authentic materials. For additional information on specific experimental conditions, see the tables in the supplementary material.

**Acknowledgment.** We are grateful to Mr. Marco Ballestri for some technical assistance. Financial support from the Progetto Strategico del CNR "Tecnologie Chimiche Innovative" is gratefully acknowledged.

**Supplementary Material Available:** Tables 4–13, giving detailed product ratio kinetic data (7 pages). Ordering information is given on any current masthead page.

OM950005I

(40) For the decarbonylation of Me<sub>3</sub>CĊO radical in the liquid phase, see: (a) Schuh, H.; Hamilton, E. J., Jr.; Paul, H.; Fischer, H. *Helv. Chim. Acta* **1974**, *57*, 2011. (b) Reference 33.

(41) Bürger, H.; Kilian, W. *J. Organomet. Chem.* **1969**, *18*, 299.

**Palladium-Assisted Formation of Carbon–Carbon Bonds.  
3.<sup>1</sup> Study of Reactions of Bis{ $\eta^2$ -(2,3,4-trimethoxy-6-acetylphenyl-C,O)}bis( $\mu$ -chloro)dipalladium(II) with Symmetrical and Unsymmetrical Internal Alkynes. A Stoichiometric Route to Highly Functionalized Spirocyclic and Benzofulvene Compounds. Isolation of a  $\pi$ -Allylic Palladium Intermediate. X-ray Structure of 10-(1-Hydroxyethyl)-6,7-dimethoxy-1,2,3,4-tetraphenylspiro[4.5]1,3,6,9-decatetraen-8-one**

José Vicente,<sup>\*,†</sup> José-Antonio Abad,<sup>\*</sup> and Juan Gil-Rubio

*Grupo de Química Organometálica, Departamento de Química Inorgánica, Universidad de Murcia, Apto. 4021, Murcia, 30071 Spain*

Peter G. Jones

*Institut für Anorganische und Analytische Chemie, Technische Universität Braunschweig, Postfach 3329, 38023 Braunschweig, Germany*

Received December 28, 1994<sup>®</sup>

The reactions of bis{ $\eta^2$ -(2,3,4-trimethoxy-6-acetylphenyl-C,O)}bis( $\mu$ -chloro)dipalladium(II) (**1**) with different internal alkynes ArC $\equiv$ CR, Ar = aryl and R = aryl or CO<sub>2</sub>R', result in the selective formation of spirocyclic organic compounds. Thus, **1** reacts with diphenyl- or bis(4-tolyl)acetylene giving 10-acetyl-6,7-dimethoxy-1,2,3,4-tetraphenylspiro[4.5]1,3,6,9-decatetraen-8-one (**2**) or 10-acetyl-6,7-dimethoxy-1,2,3,4-tetrakis(4-tolyl)spiro[4.5]1,3,6,9-decatetraen-8-one (**3**), respectively. Among unsymmetrical alkynes, ethyl 2-phenylpropionate gives the head-to-tail isomer 10-acetyl-2,4-bis(carboxyethyl)-6,7-dimethoxy-1,3-diphenylspiro[4.5]1,3,6,9-decatetraen-8-one (**4**) as the only isomer whereas methyl 2-phenylpropionate gives 10-acetyl-2,4-bis(carboxymethyl)-6,7-dimethoxy-1,3-diphenylspiro[4.5]1,3,6,9-decatetraen-8-one (**5a**) as the major isomer and a small amount of a head-to-head or tail-to-tail isomer (**5b**), the ratio **5a**/**5b** being 5/1. When these reactions are carried out with unsymmetrical diarylalkynes, Ar = Ph, R = 4-nitrophenyl or 4-methoxyphenyl, a moderate or no regioselectivity toward the head-to-tail spiro product is observed. The molar ratios of this isomer to the head-to-head and to the tail-to-tail isomers are, respectively, 4/1/1 or 2/1/1. When one of the substituents is an alkyl group, for example R = Me, the benzofulvene 5,6,7-trimethoxy-3-methyl-2-phenyl-1-methylene-1*H*-indene (2-PhBzf) (**9**) is obtained along with the mixture of spiro compounds (head-to-tail (**8a**)/head-to-head or tail-to-tail (**8b**) = 7/1; **8b**/**9** = 8/1.5). Dialkylacetylenes react with **1** giving benzofulvenes (Bzf). Thus, **1** reacts with dimethyl- or *tert*-butylmethylacetylene giving 2-MeBzf (**10**) or 2-*t*BuBzf (**11**). The reaction of **1** with diethylacetylene gives both isomers *E*- and *Z*-5,6,7-trimethoxy-3-methyl-2-ethyl-1-ethylidene-1*H*-indene, (*E*)-**12** and (*Z*)-**12** (2.6/1). In the reaction of **1** with diphenylacetylene, an organopalladium intermediate can be isolated, which reacts with 2,2'-bipyridine and thallium(I) trifluoromethylsulfonate giving the ( $\pi$ -allyl)palladium complex,  $\eta^3$ -{10-acetyl-6,7,8-trimethoxy-1,2,3,4-tetraphenylspiro[4.5]1,3,6-decatetraen-8-enyl}(2,2'-bipyridine)palladium(II) trifluoromethylsulfonate (**13**), the structure of which has previously been reported. Reduction of **2** with Na[BH<sub>4</sub>] gives 10-(1-hydroxyethyl)-6,7-dimethoxy-1,2,3,4-tetraphenylspiro[4.5]1,3,6,9-decatetraen-8-one (**14**), the structure of which has been determined by diffraction at -130 °C. It crystallizes in *P*2<sub>1</sub>2<sub>1</sub> with *a* = 10.635(3) Å, *b* = 13.199(4) Å, *c* = 20.643(7) Å and *R* = 0.063). The structure consists of two ring systems, 2,3,4,5-tetraphenylcyclopenta-2,4-diene and 2,3-dimethoxy-6-(1-hydroxyethyl)-cyclohexa-2,5-dien-4-one, with a common spiro carbon atom.

### Introduction

The formation of the spiro framework, which forms part of a great number of natural products, usually

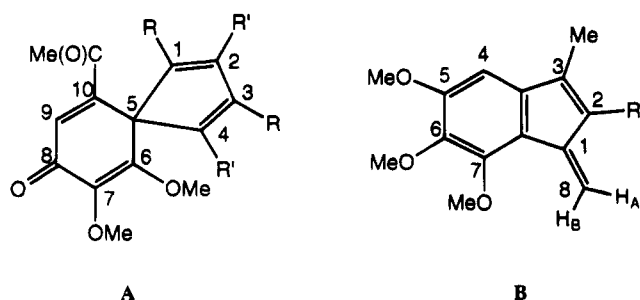
requires specially designed organic molecules as starting materials and multistep processes.<sup>2</sup> Some palladium-catalyzed reactions generating spirocycles have recently

<sup>†</sup> E-mail: JVS@FCU.UM.ES.

<sup>®</sup> Abstract published in *Advance ACS Abstracts*, May 1, 1995.

(1) (a) Part 2: Vicente, J.; Abad, J. A.; Gil-Rubio, J.; Jones, P. G. *Inorg. Chim. Acta* **1994**, *222*, 1. (b) Part 1: Vicente, J.; Abad, J. A.; Gil-Rubio, J. *J. Organomet. Chem.* **1992**, *436*, C9.

Chart 1



been reported, involving intramolecular nucleophilic attack on alkenes mediated by ( $\pi$ -allyl)palladium complexes<sup>3</sup> or by intramolecular Heck-type cyclization reactions.<sup>4</sup> Reactions of alkynes and alkenes or arenes, catalyzed by palladium compounds, also give spiro compounds.<sup>2,5</sup> Insertion reactions of alkynes into palladium aryl bonds lead, in a few cases, stoichiometrically to spiro compounds.<sup>6</sup>

Fulvenes are interesting compounds because of their usefulness as synthetic precursors.<sup>7</sup> For example, fulvenes have served as key intermediates in the total synthesis of naturally occurring products *d,l*-hirsutene and *d,l*- $\Delta$ -capnellene.<sup>8</sup> The synthesis of a benzofulvene and its conversion to a spiro compound are key steps in the synthesis of fredericamycin A, a key compound for the chemotherapy of human cancers.<sup>9</sup> A family of benzofulvenes (2-methyl-3,5,6,7,8-pentasubstituted-1*H*-indenenes; see **B** in Chart 1) have been patented as useful antiinflammatory agents having antipyretic and analgesic activity.<sup>10</sup> Benzofulvenes have been obtained by different methods: (i) acid-catalyzed cycloisomerizations from tetraarylbutatrienes, *o*-bis(phenylethynyl)benzenes, or tetra- or triphenylbutenyne or by reaction of (ii) sodium indenide with 1-chloroalkyl acetates, (iii) indenenes with ketenes, (iv) indenones with malonodini-

trile in the presence of NaOEt, etc.<sup>11</sup> Most of these methods do not lead to 1-methylene-1*H*-indenenes but to 8-substituted benzofulvenes (see **B** in Chart 1). Only a few transition metal-mediated fulvene syntheses have been reported.<sup>5b,6a,12</sup> Fulvenes are also interesting ligands in organometallic chemistry.<sup>13</sup>

We wish to report here on the reactions of the cyclopalladated complex **1** (see Scheme 1) with a variety of symmetrical and unsymmetrical internal alkynes, affording highly functionalized spirocyclic or benzofulvene compounds. All benzofulvene compounds have in common a 5,6,7-trimethoxy substitution on the benzo moiety (see **B** in Chart 1). This grouping is present in organic molecules of pharmaceutical interest, for example the antileukemic lactones steganacin and steganangin,<sup>14</sup> the antibacterial agent trimethoprim,<sup>15</sup> or the cytotoxic colchicine.<sup>16</sup> Some of these results have been published in preliminary form.<sup>1a</sup>

## Experimental Section

Infrared spectra were recorded on a Perkin-Elmer 16F PC spectrometer (except those of compounds **2**, **4**, and **12**, Perkin-Elmer 1430) using mineral oil mulls between polyethylene sheets. NMR spectra were recorded on a Bruker AC-200 or a Varian XL-300 spectrometer and referenced to internal SiMe<sub>4</sub> (<sup>1</sup>H) or CDCl<sub>3</sub> (<sup>13</sup>C,  $\delta$  77.1). Conductivities were measured with a Phillips 9501 conductimeter. Melting points were determined on a Reichert apparatus and are uncorrected. C, H, N, and S analyses were carried out with a Carlo Erba EA 1108 microanalyzer. The relative positions of the methoxy and keto groups of spirocyclic compounds and the structures of benzofulvene compounds are proposed according to NOE studies. NOE enhancements are corrected for partial saturation of

(2) Kong, K. C.; Cheng, C. H. *Organometallics* **1992**, *11*, 1972 and references therein.

(3) Godleski, S. A.; Valpey, R. S. *J. Org. Chem.* **1982**, *47*, 381. Stanton, S. A.; Felman, S. W.; Parkhurst, C. S.; Godleski, S. A. *J. Am. Chem. Soc.* **1983**, *105*, 1964. Godleski, S. A.; Heacock, D. J.; Meinhart, J. D.; Wallendaal, S. V. *J. Org. Chem.* **1983**, *48*, 2101. Anderson, P. G.; Nilsson, Y. I. M.; Bäckvall, J. E. *Tetrahedron* **1994**, *50*, 559. Brown, R. D.; Godfrey, P. D.; McNaughton, D.; Pierlot, A. P. *J. Am. Chem. Soc.* **1988**, *110*, 2329. Easley, D. A.; McLeod, D.; Miller, J. A.; Quayle, P. *Tetrahedron Lett.* **1992**, *33*, 409. Grigg, R.; Sridharan, V.; Stevenson, P.; Sukirthalingam, S. *Tetrahedron* **1989**, *45*, 3557.

(4) Wu, G. Z.; Lamaty, F.; Negishi, E. I. *J. Org. Chem.* **1989**, *54*, 2507. Ashimori, A.; Overman, L. E. *J. Org. Chem.* **1992**, *57*, 4571. Katz, T. J.; Gilbert, A. M.; Huttenloch, M. E.; Min-Min, G.; Britzinger, H. H. *Tetrahedron Lett.* **1993**, *34*, 3551.

(5) (a) Trost, B. M.; Shi, Y. *J. Am. Chem. Soc.* **1991**, *113*, 701. (b) Lee, G. C. M.; Tobias, B.; Holmes, J. M.; Harcourt, D. A.; Garst, M. E. *J. Am. Chem. Soc.* **1990**, *112*, 9330. (c) Tao, W.; Silverberg, L. J.; Rheingold, A. L.; Heck, R. F. *Organometallics* **1989**, *8*, 2550. (d) Abelman, M. M.; Overman, L. E. *J. Am. Chem. Soc.* **1988**, *110*, 2328. (e) Grigg, R.; Fretwell, P.; Meerholtz, C.; Sridharan, V. *Tetrahedron* **1994**, *50*, 359.

(6) (a) Pfeffer, M.; Sutter, J.-P.; Rottevel, M. A.; De Cian, A.; Fischer, J. *Tetrahedron*, **1992**, *48*, 2427. (b) Dupont, J.; Pfeffer, M.; Theurel, L.; Rottevel, M. A. *New J. Chem.* **1991**, *15*, 551.

(7) Paquette, L. A. In *Comprehensive Organic Chemistry*; Trost, B. M., Fleming, I., Eds.; Pergamon Press: Oxford, U.K., 1991; Vol. 5, p 626. Bergmann, E. D. *Chem. Rev.* **1968**, *68*, 41.

(8) Stone, K. J.; Little, R. D. *J. Org. Chem.* **1984**, *49*, 1849 and references therein.

(9) Kelly, T. R.; Bell, S. H.; Ohashi, N.; Armstrong-Chong, R. J. *J. Am. Chem. Soc.* **1988**, *110*, 6471.

(10) Pfister, K.; Sletzing, M.; Hinkley, D. F. Brit. Pat. 1,345,628 (*Chem. Abstr.* **1974**, *80*, 133112).

(11) Brand, K.; Krucke-Amelung, D. *Chem. Ber.* **1939**, *72*, 1036. Whitlock, H. W., Jr.; Sandwick, P. E.; Overman, L. E.; Reichardt, P. I. *J. Org. Chem.* **1969**, *34*, 879. Neuenschwander, M.; Vögeli, R.; Fahrni, H.-P.; Lehmann, H.; Ruder, J.-P. *Helv. Chim. Acta* **1977**, *60*, 1073. Galin, F. Z.; Ignatyuk, V. K.; Lakeev, S. N.; Rakhimov, R. G.; Sultanova, V. S.; Tolstikov, G. A. *Zh. Org. Khim.* **1989**, *25*, 103 (*Chem. Abstr.* **1989**, *111*, 133743b). Marcuzzi, F.; Azzena, U.; Melloni, G. *J. Chem. Soc., Perkin Trans.* **1993**, 2957. Yukhnovski, I. N.; Ivanov, Ch.; Vladovska, I. C. *R. Acad. Bulg. Sci.* **1967**, *20*, 449 (*Chem. Abstr.* **1968**, *68*, 59343w).

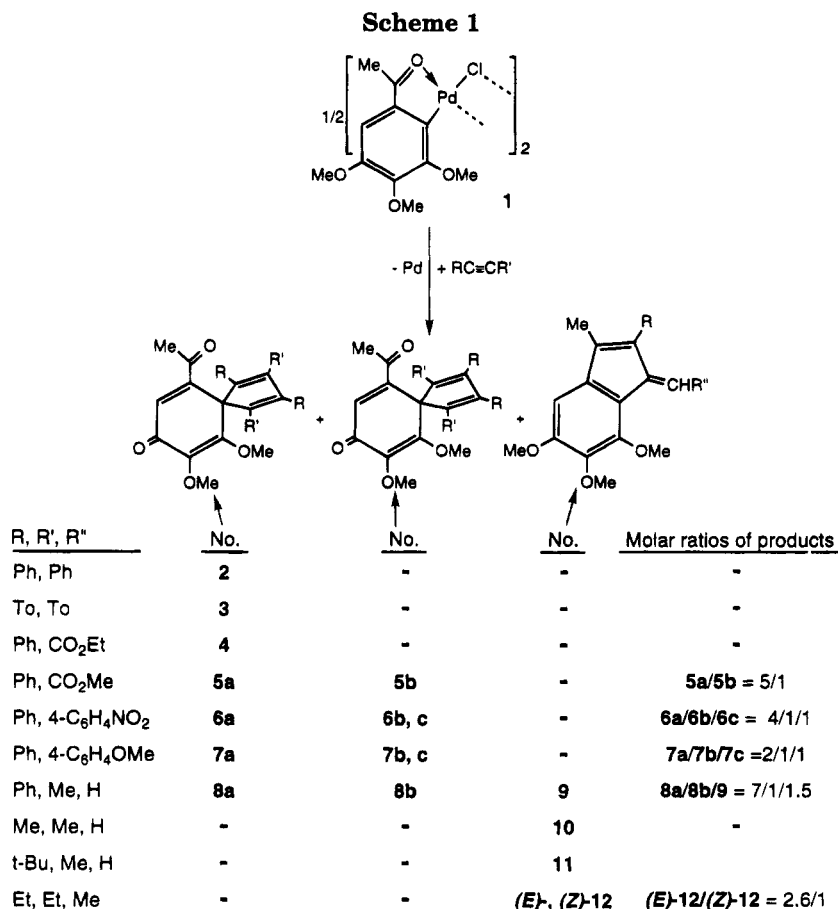
(12) Blomquist, A. T.; Maitlis, P. M. *J. Am. Chem. Soc.* **1962**, *84*, 2329. Silverberg, L. J.; Wu, G.; Rheingold, A. L.; Heck, R. F. *J. Organomet. Chem.* **1991**, *409*, 411 and references therein.

(13) See for example: Luinstra, G. A.; Teuben, J. H. *J. Am. Chem. Soc.* **1992**, *114*, 3361. Sinnema, P. J.; Meetsma, A.; Teuben, J. H. *Organometallics* **1993**, *12*, 184. Downton, P. A.; Sayer, B. G.; McGlinchey, M. J. *Organometallics* **1992**, *11*, 3281. Hashimoto, H.; Tobita, H.; Ogino, H. *Organometallics* **1993**, *12*, 2182. Klahn, A. H.; Moore, M. H.; Perutz, R. N. *J. Chem. Soc., Chem. Commun.* **1992**, 1699. Kreiter, C. G.; Klaus, L. *J. Organomet. Chem.* **1993**, *454*, 199. Kovac, S.; Rapic, V.; Filipovic-Marinic, N. *J. Organomet. Chem.* **1993**, *448*, 181. Vondrak, T.; Mach, K.; Varga, V.; Terpstra, A. *J. Organomet. Chem.* **1992**, *425*, 27. Nagashima, H.; Fukahori, T.; Aoki, K.; Itoh, K. *J. Am. Chem. Soc.* **1993**, *115*, 10430. Hoard, D. W.; Sharp, P. R. *Inorg. Chem.* **1993**, *32*, 612. Luinstra, G. A.; Teuben, J. H. *Organometallics* **1992**, *11*, 1793. Suzuki, H.; Kakigano, T.; Fukui, H.; Tanaka, M.; Morooka, Y. *J. Organomet. Chem.* **1994**, *473*, 295. Rau, D.; Behrens, U. *J. Organomet. Chem.* **1993**, *454*, 151. Troyanov, S. I.; Mach, K.; Varga, V. *Organometallics* **1993**, *12*, 3387. Callan, B.; Cox, M. G.; Mccabe, A.; Manning, A. R.; Sayal, P.; Soye, P.; Wade, S. C.; Stephens, F. S.; Mcardle, P.; Cunningham, D. *J. Organomet. Chem.* **1994**, *466*, 185. Cloke, F. G. N.; Hitchcock, P. B.; Joseph, S. C. P. *J. Chem. Soc., Chem. Commun.* **1994**, 1207. Herges, R.; Reif, W. *Chem. Ber.* **1994**, *127*, 1143.

(14) Ziegler, F. E.; Chliwner, I.; Fowler, K. W.; Kanfer, S. J.; Kuo, S. J.; Sinha, N. D. *J. Am. Chem. Soc.* **1980**, *102*, 790. Tomioka, K.; Ishiguro, T.; Mizuguchi, H.; Komeshima, N.; Koga, K.; Tsukagoshi, S.; Tsuruo, T.; Tashiro, T.; Tanida, S.; Kishi, T. *J. Med. Chem.* **1991**, *34*, 54 and references therein.

(15) Chan, J. H.; Roth, B. *J. Med. Chem.* **1991**, *34*, 550 and references therein.

(16) Ringel, I.; Jaffe, D.; Alerhand, S.; Boye, O.; Muzafar, A.; Bossi, A. *J. Med. Chem.* **1991**, *34*, 3334.



irradiated signals.<sup>17</sup> Some signals in the NMR spectra have been assigned with the help of COSY, DEPT, and GATEDEC techniques.

Solvents were purified as follows: acetone, distilled from KMnO<sub>4</sub>; diethyl ether, distilled from sodium-benzophenone; CH<sub>2</sub>Cl<sub>2</sub>, distilled from P<sub>2</sub>O<sub>5</sub> and then from Na<sub>2</sub>CO<sub>3</sub>; hexane, distilled from CaCl<sub>2</sub>. Complex 1 was prepared as described previously.<sup>18</sup> Diphenylacetylene, ethyl phenylpropiolate, phenylmethylacetylene (Janssen), methyl phenylpropiolate, 4,4'-dimethyl-2-pentyne (Lancaster), 2-butyne (Fluka), and 3-hexyne (Merck) were used as received. Bis(4-tolyl)acetylene,<sup>19</sup> (4-nitrophenyl)phenylacetylene,<sup>20</sup> and (4-methoxyphenyl)phenylacetylene,<sup>21</sup> were prepared as described previously. The reactions were carried out at room temperature and without precautions to exclude atmospheric moisture unless otherwise stated. Chromatographic separations were performed using preparative-scale TLC plates prepared by us with commercial 60-mesh silica gel and were visualized with 254 and 365 nm UV light. Chart 1 shows the numbering of the organic compounds prepared.

**Synthesis of 2.** General Procedure for the Preparation of Spirocyclic Compounds. Complex 1 (203 mg, 0.29 mmol) and diphenylacetylene (210 mg, 1.18 mmol) were reacted in dichloromethane at room temperature for 52 h. The mixture was filtered over Celite and the solution evaporated to dryness. Most of the crude material proved to be 2 (by <sup>1</sup>H NMR). It was chromatographed over silica gel; elution with mixtures of *n*-hexane/diethyl ether gave a yellow solution from which

pure, yellow 2 was obtained by evaporation of the solvent. Yield: 207 mg, 65%. An analytical pure sample of 2 can be obtained by crystallization from diethyl ether/hexane. Mp: 159–61 °C. IR:  $\nu(\text{C}=\text{O})$  1687, 1644 cm<sup>-1</sup>. <sup>1</sup>H NMR (300 MHz, CDCl<sub>3</sub>,  $\delta$ ): 7.14–7.07, 6.98–6.92 (m, 4 C<sub>6</sub>H<sub>5</sub>, 20 H), 6.73 (s, H<sub>9</sub>, 1 H), 4.03 (s, MeO, 3 H), 3.44 (s, MeO, 3 H), 2.10 (s, MeCO, 3 H). <sup>13</sup>C{<sup>1</sup>H} NMR (75 MHz, CDCl<sub>3</sub>,  $\delta$ ): 197.2 (CH<sub>3</sub>CO), 184.1 (C8), 167.1, 149.6, 149.0, 141.3, 141.2, 135.1, 134.4, 133.7 (C9), 129.9, 128.9, 128.1, 127.8, 127.4, 127.1, 68.9 (C5), 61.5 (MeO), 60.5 (MeO), 28.8 (MeCO). Mass spectrum: *m/z* (% abundance) 550 (M<sup>+</sup>, 64), 215 (16), 178 (17), 167 (13), 165 (28), 115 (35), 105 (PhCO<sup>+</sup>, 100), 91 (C<sub>7</sub>H<sub>7</sub><sup>+</sup>, 31), 77 (Ph<sup>+</sup>, 46). Anal. Calc for C<sub>38</sub>H<sub>30</sub>O<sub>4</sub>: C, 82.89; H, 5.49. Found: C, 82.57; H, 5.45.

**Synthesis of 3.** 3 was prepared similarly from 1 (120 mg, 0.17 mmol) and bis(4-tolyl)acetylene (ToC≡CTo, 141 mg, 0.68 mmol). Reaction time: 68 h. The resulting mixture was extracted with diethyl ether and chromatographed over silica gel using 1:1 diethyl ether/*n*-hexane. The solvent was removed to give 105 mg of yellow compound 3, 51%. An analytical sample was obtained from diethyl ether/*n*-hexane. Mp: 86–88 °C. IR:  $\nu(\text{C}=\text{O})$  1694, 1650 cm<sup>-1</sup>. <sup>1</sup>H NMR (200 MHz, CDCl<sub>3</sub>,  $\delta$ ): 6.92–6.80 (m, C<sub>6</sub>H<sub>4</sub>, 16 H), 6.68 (s, H<sub>9</sub>, 1 H), 3.98 (s, MeO, 3 H), 3.47 (s, MeO, 3 H), 2.24 (s, MeC<sub>6</sub>H<sub>4</sub>, 6 H), 2.21 (s, MeC<sub>6</sub>H<sub>4</sub>, 6 H), 2.10 (s, MeCO, 3 H). <sup>13</sup>C{<sup>1</sup>H} NMR (50 MHz, CDCl<sub>3</sub>,  $\delta$ ): 197.2 (CH<sub>3</sub>CO), 184.21 (C8), 162.0, 150.4, 148.9, 141.3, 140.5, 136.4, 136.5, 133.2 (C9), 132.5, 131.7, 129.5, 128.8, 128.7, 128.5, 68.8 (C5), 61.2 (MeO), 60.4 (MeO), 28.8 (MeCO), 21.3 (MeC<sub>6</sub>H<sub>4</sub>), 21.2 (MeC<sub>6</sub>H<sub>4</sub>). Mass spectrum: *m/z* (% abundance) 606 (M<sup>+</sup>, 13), 206 (11), 195 (11), 183 (12), 178 (17), 119 (MeC<sub>6</sub>H<sub>4</sub>CO<sup>+</sup>, 100), 105 (23), 91 (55). Anal. Calc for C<sub>42</sub>H<sub>38</sub>O<sub>4</sub>: C, 83.14; H, 6.31. Found: C, 83.19; H, 6.72.

**Synthesis of 4.** 4 was similarly prepared from 1 (153 mg, 0.22 mmol) and ethyl 3-phenylpropiolate (160 mg, 0.92 mmol). Reaction time: 65 h. The resulting mixture was extracted with diethyl ether and chromatographed over silica gel using dichloromethane, giving an orange solution that was chromatographed over silica gel using 1:1 acetone/*n*-hexane. The

(17) Neuhaus, D.; Williamson, M. P. *The Nuclear Overhauser Effect in Structural and Conformational Analysis*; VCH: New York, 1989.

(18) Vicente, J.; Abad, J. A.; Gil-Rubio, J.; Jones, P. G.; Bembenek, E. *Organometallics* **1993**, *12*, 4151.

(19) Cope, A. C.; Smith, D. S.; Cotter, R. J. *Org. Synth.* **1954**, *34*, 42.

(20) Okuro, K.; Furuue, M.; Enna, M.; Miura, M.; Nomura, M. *J. Org. Chem.* **1993**, *58*, 4716.

(21) Sonogashira, K.; Tohda, Y.; Hagihara, N. *Tetrahedron Lett.* **1975**, 4467.

solvent was removed to give **4** as an orange oil. Yield: 182 mg, 76%. A crystalline sample could be obtained from diethyl ether/*n*-hexane after 10 days in the fridge. Mp: 97 °C. IR:  $\nu(\text{C}=\text{O})$  1720–1680 (br), 1650 (br)  $\text{cm}^{-1}$ .  $^1\text{H}$  NMR (200 MHz,  $\text{CDCl}_3$ ,  $\delta$ ): 7.37, 7.29–7.26, 7.25–7.11 (m, 2  $\text{C}_6\text{H}_5$ , 10 H), 6.88 (s, H9, 1 H), 4.04 (s, MeO, 3 H), 4.0–3.8 (two overlapping quadruplets, 2  $\text{CH}_2$ , 4 H), 3.70 (s, MeO, 3 H), 2.31 (s, MeCO, 3 H), 0.93 (t,  $\text{CH}_2\text{Me}$ , 3 H,  $^3J_{\text{HH}} = 7$  Hz), 0.75 (t,  $\text{CH}_2\text{Me}$ , 3 H,  $^3J_{\text{HH}} = 7$  Hz).  $^{13}\text{C}\{^1\text{H}\}$  NMR (50 MHz,  $\text{CDCl}_3$ ,  $\delta$ ): 196.4 (MeCO), 184.0 (C8), 163.7 (COOEt), 162.0 (COOEt), 159.3, 158.7, 155.5, 146.1, 141.8, 140.6, 135.7 (C9), 134.8, 132.6, 129.1, 128.7, 128.2, 127.9, 127.7, 127.5, 127.4, 66.9 (C5), 61.9 (MeO), 60.7 (CH<sub>2</sub>), 60.4 (MeO), 60.2 (CH<sub>2</sub>), 27.8 (MeCO), 13.7 (CH<sub>2</sub>Me), 13.4 (CH<sub>2</sub>Me). Mass spectrum:  $m/z$  (% abundance) 543 ( $\text{M}^+ + 1$ , 2.6), 239 (20), 189 (14), 149 (21), 129 (18), 105 (100), 91 (30). Anal. Calc for  $\text{C}_{32}\text{H}_{30}\text{O}_8$ : C, 70.84; H, 5.57. Found: C, 70.66; H, 5.69.

**Synthesis of 5a,b.** These compounds were similarly prepared from **1** (101 mg, 0.14 mmol) and methyl 3-phenylpropionate (114 mg, 0.71 mmol). Reaction time: 96 h. The resulting mixture was extracted with diethyl ether and chromatographed over silica gel using 2:1 diethyl ether/*n*-hexane. A pale yellow band ( $R_f$  0.3–0.5) was collected. The solvent was removed to give a mixture of head-to-tail compound **5a** with a head-to-head or tail-to-tail isomer **5b** (**5a/5b** = 5/1). Yield: 70 mg, 49%.  $^1\text{H}$  NMR of the mixture (200 MHz,  $\text{CDCl}_3$ ,  $\delta$ ): 7.41–7.08 (m, Ph, 10 H), 6.90 (s, H9 of **5a**, 1 H), 6.76 (s, H9 of **5b**, 1 H), 4.05 (s, MeO of **5b**, 3 H), 4.03 (s, MeO of **5a**, 3 H), 3.70 (s, MeO2C of **5b**, 6 H), 3.69 (s, MeO of **5a**, 3 H), 3.53 (s, MeO of **5b**, 3 H), 3.47 (s, MeO of **5a**, 3 H), 3.40 (s, MeO of **5a**, 3 H), 2.30 (s, MeCO of **5a**, 3 H), 2.15 (s, MeCO of **5b**, 3 H).  $^{13}\text{C}\{^1\text{H}\}$  NMR (50 MHz,  $\text{CDCl}_3$ ,  $\delta$ ): 196.4, 196.0 (MeCO), 184.0, 183.4 (C8), 164.6, 164.5, 162.5 (COOMe), 136.0, 135.8 (C9), 129.3, 129.0, 128.4, 128.3, 128.3, 127.8, 127.7, 127.6, 127.5 (CH, Ph), 66.8, 65.8 (C5), 61.9, 61.7, 60.6, 60.5, 52.1, 51.7, 51.3 (MeO), 27.8 (2 MeCO). Anal. Calc for  $\text{C}_{30}\text{H}_{26}\text{O}_8$ : C, 70.03; H, 5.09. Found: C, 69.64; H, 5.39.

The mixture of **5a** and **5b** was chromatographed over silica gel with 1:3 acetone/hexane, giving a yellow oil, 43 mg, 30% of pure yellow **5a**. IR (KBr):  $\nu(\text{C}=\text{O})$  1728(br), 1698, 1652  $\text{cm}^{-1}$ .  $^1\text{H}$  NMR (200 MHz,  $\text{CDCl}_3$ ,  $\delta$ ): 7.41–7.08 (m, Ph, 10 H), 6.90 (s, H9, 1 H), 4.03 (s, MeO, 3 H), 3.69 (s, MeO, 3 H), 3.47 (s, MeO, 3 H), 3.40 (s, MeO, 3 H), 2.30 (s, MeCO, 3 H).  $^{13}\text{C}\{^1\text{H}\}$  NMR (50 MHz,  $\text{CDCl}_3$ ,  $\delta$ ): 196.4 (MeCO), 184.0 (C8), 164.5 (COOMe), 162.5 (COOMe), 159.2, 158.6, 155.3, 145.9, 141.7, 140.5, 135.8 (C9), 134.4, 132.5, 132.4, 129.3, 128.4, 128.3, 127.8, 127.7, 127.5, 66.8 (C5), 61.9, 60.5, 51.7, 51.3 (MeO), 27.8 (MeCO). Mass spectrum:  $m/z$  (% abundance) 514 ( $\text{M}^+$ , 100), 483 (23), 443 (25), 427 (20), 423 (14), 239 (17), 105 (10), 59 ( $\text{CO}_2\text{Me}^+$ , 45). Anal. Calc for  $\text{C}_{30}\text{H}_{26}\text{O}_8$ : C, 70.03; H, 5.09. Found: C, 69.74; H, 5.04.

**Synthesis of 6a–c.** These compounds were similarly prepared from **1** (100 mg, 0.14 mmol) and (4-nitrophenyl)phenylacetylene (159 mg, 0.71 mmol). Reaction time: 52 h. The resulting mixture was extracted with diethyl ether and chromatographed over silica gel using 1:1 diethyl ether/*n*-hexane to obtain a mixture of three isomers (head-to-tail **6a**, head-to-head or tail-to-tail **6c,b**) (**6a/6b/6c**: 4/1/1). Yield: 107 mg, 60%. Pure samples of each isomer were obtained by further chromatography (silica gel, 2:3 acetone/hexane). Yields: **6a**, 48 mg, 27%; **6b**, 19 mg, 11%; **6c**, 15 mg, 8%. Yellow crystalline samples can be obtained from diethyl ether/*n*-hexane.

**6a.** Mp: 110–112 °C. IR:  $\nu(\text{C}=\text{O})$  1694, 1650  $\text{cm}^{-1}$ ;  $\nu(\text{NO}_2)$  1518, 1344  $\text{cm}^{-1}$ .  $^1\text{H}$  NMR (300 MHz,  $\text{CDCl}_3$ ,  $\delta$ ): 7.97 (d,  $\text{C}_6\text{H}_4\text{-NO}_2$ , 2 H,  $J_{\text{HH}} = 9$  Hz), 7.95 (d,  $\text{C}_6\text{H}_4\text{-NO}_2$ , 2 H,  $J_{\text{HH}} = 8$  Hz), 7.23–6.87 (m, Ph, 14 H), 6.85 (s, H9, 1 H), 4.07 (s, MeO, 3 H), 3.52 (s, MeO, 3 H), 2.18 (s, MeCO, 3 H).  $^{13}\text{C}\{^1\text{H}\}$  NMR (50 MHz,  $\text{CDCl}_3$ ,  $\delta$ ): 196.8 (MeCO), 183.4 (C8), 159.8, 150.6, 147.3, 146.8, 146.7, 146.6, 146.2, 141.4, 141.3, 140.9, 139.8, 135.2, 133.8, 132.9, 130.7, 129.4, 129.3, 128.7, 128.6, 128.5, 128.3, 123.4, 123.1, 68.6 (C5), 61.7 (MeO), 60.6 (MeO), 28.4 (MeCO).

Mass spectrum:  $m/z$  (% abundance) 640 ( $\text{M}^+$ , 100), 569 (16), 389 (38), 387 (53), 374 (29), 363 (29), 326 (33), 324 (25), 314 (31), 313 (75), 311 (26), 300 (28), 265 (30), 150 ( $4\text{-NO}_2\text{C}_6\text{H}_4\text{-CO}^+$ , 25), 105 (95), 91 (26). Anal. Calc for  $\text{C}_{38}\text{H}_{28}\text{N}_2\text{O}_8$ : C, 71.24; H, 4.41; N, 4.39. Found: C, 71.08; H, 4.83; N, 4.18.

**6b.** Mp: 178–180 °C. IR:  $\nu(\text{C}=\text{O})$  1688, 1652  $\text{cm}^{-1}$ ;  $\nu(\text{NO}_2)$  1514, 1344  $\text{cm}^{-1}$ .  $^1\text{H}$  NMR (300 MHz,  $\text{CDCl}_3$ ,  $\delta$ ): 7.99 (d,  $\text{C}_6\text{H}_4\text{-NO}_2$ , 4 H,  $J_{\text{HH}} = 8$  Hz), 7.27–7.10 (m, Ph, 10 H), 6.93 (d,  $\text{C}_6\text{H}_4\text{-NO}_2$  groups, 4 H,  $J_{\text{HH}} = 8$  Hz), 6.84 (s, H9, 1 H), 4.05 (s, MeO, 3 H), 3.57 (s, MeO, 3 H), 2.18 (s, MeCO, 3 H).  $^{13}\text{C}\{^1\text{H}\}$  NMR (75 MHz,  $\text{CDCl}_3$ ,  $\delta$ ): 196.7 (CH<sub>3</sub>CO), 183.2 (C8), 159.7, 151.7, 147.9, 146.8, 141.3, 140.9, 140.5, 134.8, 133.8, 129.6, 129.5, 128.4, 128.2, 123.6, 68.0 (C5), 61.9 (MeO), 60.8 (MeO), 28.7 (MeCO). Mass spectrum:  $m/z$  (% abundance) 640 ( $\text{M}^+$ , 23), 387 (23), 313 (49), 265 (31), 165 (25), 150 ( $4\text{-NO}_2\text{C}_6\text{H}_4\text{CO}^+$ , 46), 105 (100), 104 (24), 91 (27), 77 (63). Anal. Calc for  $\text{C}_{38}\text{H}_{28}\text{N}_2\text{O}_8$ : C, 71.24; H, 4.41; N, 4.39. Found: C, 70.61; H, 4.30; N, 4.46.

**6c.** Mp: 234–236 °C. IR:  $\nu(\text{C}=\text{O})$  1690, 1650  $\text{cm}^{-1}$ ;  $\nu(\text{NO}_2)$  1514, 1344  $\text{cm}^{-1}$ .  $^1\text{H}$  NMR (300 MHz,  $\text{CDCl}_3$ ,  $\delta$ ): 7.99 (d,  $\text{C}_6\text{H}_4\text{-NO}_2$ , 4 H,  $J_{\text{HH}} = 7$  Hz), 7.22–7.06 (m, Ph, 10 H), 6.88 (d,  $\text{C}_6\text{H}_4\text{-NO}_2$ , 4 H,  $J_{\text{HH}} = 7$  Hz), 6.84 (s, H9, 1 H), 4.08 (s, MeO, 3 H), 3.48 (s, MeO, 3 H), 2.16 (s, MeCO, 3 H).  $^{13}\text{C}\{^1\text{H}\}$  NMR (75 MHz,  $\text{CDCl}_3$ ,  $\delta$ ): 197.1 (CH<sub>3</sub>CO), 183.7 (C8), 160.0, 147.0, 146.9, 145.6, 145.5, 141.6, 141.3, 135.7, 133.2, 130.7, 128.7, 128.6, 128.5, 123.5, 69.4 (C5), 61.8 (MeO), 60.7 (MeO), 28.4 (MeCO). Mass spectrum:  $m/z$  (% abundance) 640 ( $\text{M}^+$ , 5), 387 (6), 313 (15), 300 (5), 239 (6), 213 (8), 200 (12), 194 (13), 187 (14), 165 (11), 150 ( $4\text{-NO}_2\text{C}_6\text{H}_4\text{CO}^+$ , 14), 105 (100), 91 (14), 77 (30). Anal. Calc for  $\text{C}_{38}\text{H}_{28}\text{N}_2\text{O}_8$ : C, 71.24; H, 4.41; N, 4.39. Found: C, 71.49; H, 4.38; N, 4.54.

**Synthesis of 7a–c.** These were similarly prepared from **1** (140 mg, 0.20 mmol) and (4-methoxyphenyl)phenylacetylene (208 mg, 1.00 mmol). Reaction time: 102 h. The crude product was extracted with diethyl ether and chromatographed over silica gel using 2:1 diethyl ether/*n*-hexane to give an orange solid which is a 2:1:1 mixture of three isomers (head-to-tail **7a**, head-to-head **7b**, and tail-to-tail **7c**, respectively). Attempts to separate them gave mixtures of two or three isomers in different proportions. Yield: 133 mg, 54%. IR:  $\nu(\text{C}=\text{O})$  1694, 1650 (br)  $\text{cm}^{-1}$ . The assignment of the  $^1\text{H}$  NMR resonances for the different isomers is based on spectra of samples enriched in each isomer.  $^1\text{H}$  NMR (200 MHz,  $\text{CDCl}_3$ ,  $\delta$ ): **7a**, 7.13–7.07, 7.00–6.82 (m, Ph +  $\text{C}_6\text{H}_4\text{OMe}$ , 14 H), 6.71 (s, H9, 1 H), 6.62 (2 d, H3 of  $\text{C}_6\text{H}_4\text{OMe}$ , 4 H,  $J_{\text{HH}} = 13$  Hz), 4.00 (s, MeO, 3 H), 3.71 (s,  $\text{C}_6\text{H}_4\text{OMe}$ , 3 H), 3.70 (s,  $\text{C}_6\text{H}_4\text{OMe}$ , 3 H), 3.46 (s, MeO, 3 H), 2.10 (s, MeCO, 3 H); **7b** or **7c**, 7.12–7.08, 7.00–6.93 (m, Ph, 10 H), 6.89 (d, H3 of  $\text{C}_6\text{H}_4\text{OMe}$ , 4 H,  $J_{\text{HH}} = 13$  Hz), 6.71 (s, H9, 1 H), 6.62 (d, H2 of  $\text{C}_6\text{H}_4\text{OMe}$ , 4 H,  $J_{\text{HH}} = 13$  Hz), 4.00 (s, MeO, 3 H), 3.71 (s,  $\text{C}_6\text{H}_4\text{OMe}$ , 6 H), 3.49 (s, MeO, 3 H), 2.12 (s, MeCO, 3 H); **7c** or **7b**, 7.12–7.09, 6.98–6.93 (m, Ph, 10 H), 6.86 (d, H3 of  $p\text{-C}_6\text{H}_4\text{OMe}$ , 4 H,  $J_{\text{HH}} = 13$  Hz), 6.70 (s, H9, 1 H), 6.65 (d, H2 of  $\text{C}_6\text{H}_4\text{OMe}$ , 4 H,  $J_{\text{HH}} = 13$  Hz), 4.00 (s, MeO, 3 H), 3.73 (s,  $\text{C}_6\text{H}_4\text{OMe}$ , 6 H), 3.43 (s, MeO, 3 H), 2.08 (s, MeCO, 3 H).  $^{13}\text{C}\{^1\text{H}\}$  NMR (50 MHz,  $\text{CDCl}_3$ ,  $\delta$ ): 197.33, 197.30, 197.28 (MeCO), 184.19, 184.16, 184.12 (C8), 133.37, 133.29, 133.23 (C9), 68.9, 68.8, 68.7 (C5), 61.4 (3 MeO), 60.5 (3 MeO), 55.1 (3  $\text{C}_6\text{H}_4\text{OMe}$ ), 28.88, 28.85, 28.81 (MeCO). Mass spectrum:  $m/z$  (% abundance) 610 ( $\text{M}^+$ , 100), 539 (12), 636 (6), 327 (8), 313 (6), 300 (5), 289 (5), 135 ( $4\text{-MeOC}_6\text{H}_4\text{CO}^+$ , 9), 105 ( $\text{PhCO}^+$ , 3). Anal. Calc for  $\text{C}_{40}\text{H}_{34}\text{O}_6$ : C, 78.67; H, 5.61. Found: C, 78.62; H, 5.71.

**Synthesis of 8a,b and 9.** Complex **1** (180 mg, 0.26 mmol) and phenylmethylacetylene (119 mg, 1.02 mmol) were reacted similarly for 96 h. The resulting mixture was extracted with diethyl ether and evaporated to dryness. The  $^1\text{H}$  NMR of the residue showed the presence in the mixture of the head-to-tail spiro compound **8a** as the major component, mixed with small amounts of a head-to-head or tail-to-tail isomer **8b**, and the benzofulvene **9** (**8a/8b/9**: 7/1/1.5) along with other indeterminate minor components. The presence of these compounds was also confirmed by GC–MS analysis of the mixture.



It was chromatographed (silica gel, 1:1 diethyl ether/*n*-hexane), giving first a pale yellow band and second an orange-yellow band. The pale yellow solution was dried over MgSO<sub>4</sub> and evaporated to give **9**. Yield: 24 mg, 15%. Mp: 100–101 °C. IR:  $\delta(\text{CH}_2)$  (out of plane, overtone) 1822 cm<sup>-1</sup>;  $\nu(\text{C}=\text{C})$  1598, 1578 cm<sup>-1</sup>. <sup>1</sup>H NMR (300 MHz, CDCl<sub>3</sub>,  $\delta$ ): 7.43–7.29 (m, Ph, 5H), 6.68 (s, H<sub>4</sub>, 1 H), 6.41 (s, H<sub>B</sub>, 1 H), 5.59 (s, H<sub>A</sub>, 1 H), 4.02 (s, MeO<sub>7</sub>, 3 H), 3.95 (s, MeO<sub>5</sub>, 3 H), 3.90 (s, MeO<sub>6</sub>, 3H), 2.13 (s, Me<sub>3</sub>, 3 H). <sup>13</sup>C{<sup>1</sup>H} NMR (50 MHz, CDCl<sub>3</sub>,  $\delta$ ): 154.1, 150.2, 146.0, 140.6, 140.3, 138.0, 137.0, 134.8, 130.4, 128.0, 126.9, 119.2, 115.7 (CH<sub>2</sub>), 99.2 (C<sub>4</sub>), 61.2 (MeO), 60.2 (MeO), 56.4 (MeO), 11.4 (Me<sub>3</sub>). Mass spectrum:  $m/z$  (% abundance) 308 (M<sup>+</sup>, 100), 294 (15), 293 (M<sup>+</sup> - CH<sub>3</sub>, 72), 265 (5), 235 (12), 179 (7), 178 (8). Anal. Calc for C<sub>20</sub>H<sub>20</sub>O<sub>3</sub>: C, 77.90; H, 6.54. Found: C, 77.45; H, 6.95.

Evaporation of the orange-yellow solution gave an orange oil composed of an inseparable mixture of two isomeric spiro compounds. Yield: 37 mg, 17%. IR (KBr):  $\nu(\text{C}=\text{O})$  1698, 1650 cm<sup>-1</sup>. <sup>1</sup>H NMR (300 MHz, CDCl<sub>3</sub>,  $\delta$ ): 7.47–7.12 (m, Ph), 6.66 (s, H<sub>9</sub> of **8a**, 1 H), 6.56 (s, H<sub>9</sub> of **8b**, 1 H), 3.98 (s, MeO of **8a**, 3H), 3.95 (s, MeO of **8b**, 3H), 3.74 (s, MeO of **8a**, 3H), 3.51 (s, MeO of **8b**, 3H), 2.14 (s, MeCO of **8a**, 3H), 2.08 (s, 2Me of **8b**, 6H), 2.05 (s, MeCO of **8b**), 1.95 (s, Me of **8a**, 3H), 1.67 (s, Me of **8a**, 3H). <sup>13</sup>C{<sup>1</sup>H} NMR (75 MHz, CDCl<sub>3</sub>,  $\delta$ ): 197.5, 197.4 (MeCO carbons of **8a** and **8b**), 184.4, 184.2 (C<sub>8</sub>), 132.9, 132.0 (C<sub>9</sub>), 68.5, 68.4 (C<sub>5</sub>), 61.5, 61.2, 60.7, 60.4 (MeO), 29.2, 29.1 (MeCO), 14.5, 13.4, 11.3 (Me). GC-MS [ $m/z$  (% abundance)]: **8a**, 426 (M<sup>+</sup>, 100), 393 (100), 355 (13), 265 (17), 253 (15), 252 (24), 239 (12); **8b**, 426 (M<sup>+</sup>, 100), 383 (12), 355 (16), 265 (9), 253 (8), 252 (11). Anal. Calc for C<sub>28</sub>H<sub>26</sub>O<sub>4</sub>: C, 78.85; H, 6.14. Found: C, 78.42; H, 6.39.

**Synthesis of 10.** 2-Butyne (approximately 0.03 mL, 0.38 mmol) was added to a suspension of compound **1** (120 mg, 0.17 mmol) in dichloromethane. The mixture was heated at 80 °C over a period of 23 h in a closed glass tube. The resulting mixture was filtered over Celite and concentrated. A <sup>1</sup>H-NMR showed that most of this mixture was the benzofulvene **10**. It was chromatographed on an alumina column using 1:1 diethyl ether/*n*-hexane. The first pale yellow band was taken. The solution was dried over MgSO<sub>4</sub>, and the solvent was removed to give a pale yellow oil. Yield: 21 mg, 25%. A yellow crystalline sample was obtained from diethyl ether/*n*-hexane. Mp: 71–73 °C. IR:  $\delta(\text{CH}_2)$  (out of plane, overtone) 1826 cm<sup>-1</sup>;  $\nu(\text{C}=\text{C})$  1600, 1578 cm<sup>-1</sup>. <sup>1</sup>H NMR (200 MHz, CDCl<sub>3</sub>,  $\delta$ ): 6.53 (s, H<sub>4</sub>, 1 H), 6.22 (s, H<sub>B</sub>, 1 H), 5.65 (s, H<sub>A</sub>, 1 H), 3.97 (s, MeO<sub>7</sub>, 3 H), 3.92 (s, MeO<sub>5</sub>, 3 H), 3.86 (s, MeO<sub>6</sub>, 3 H), 2.04 (s, Me<sub>3</sub>, 3 H), 2.03 (s, Me<sub>2</sub>, 3 H). <sup>13</sup>C{<sup>1</sup>H} NMR (50 MHz, CDCl<sub>3</sub>,  $\delta$ ): 153.9, 149.9, 147.0, 141.2, 140.0, 135.6, 132.5, 119.2, 112.0 (CH<sub>2</sub>), 98.7 (C<sub>4</sub>), 61.2 (MeO), 60.2 (MeO), 56.4 (MeO), 10.6 (Me), 9.7 (Me). Mass spectrum:  $m/z$  (% abundance) 246 (M<sup>+</sup>, 58), 231 (M<sup>+</sup> - CH<sub>3</sub>, 45), 173 (39), 149 (77), 115 (32), 91 (45). Anal. Calc for C<sub>15</sub>H<sub>18</sub>O<sub>3</sub>: C, 73.15; H, 7.37. Found: C, 72.96; H, 7.85.

**Synthesis of 11.** *tert*-Butylmethylacetylene (68 mg, 0.71 mmol) was added to a suspension of compound **1** (100 mg, 0.14 mmol) in dichloromethane. The suspension was stirred at room temperature until compound **1** dissolved completely. The dark red solution was heated at 80 °C over a period of 24 h in a closed glass tube. The resulting mixture was filtered over Celite and concentrated. The <sup>1</sup>H NMR spectrum of the mixture showed the signals of **11** and another unidentified compound. Diethyl ether was added, precipitating a brown compound whose <sup>1</sup>H NMR is that of the pure unidentified compound. The solution was chromatographed over silica gel using 1:2 diethyl ether/*n*-hexane. The first pale yellow band was taken. The solvent was removed under reduced pressure to give a pale yellow oil. Yield: 31 mg, 38%. IR:  $\delta(\text{CH}_2)$  (out of plane, overtone) 1834 cm<sup>-1</sup>;  $\nu(\text{C}=\text{C})$  1598, 1560 cm<sup>-1</sup>. <sup>1</sup>H NMR (300 MHz, CDCl<sub>3</sub>,  $\delta$ ): 6.61 (s, H<sub>B</sub>, 1 H), 6.57 (s, H<sub>4</sub>, 1 H), 6.05 (s, H<sub>A</sub>, 1 H), 3.96 (s, MeO<sub>7</sub>, 3 H), 3.91 (s, MeO<sub>5</sub>, 3 H), 3.85 (s, MeO<sub>6</sub>, 3 H), 2.26 (s, Me<sub>3</sub>, 3 H), 1.48 (s, *t*-Bu, 9 H). <sup>13</sup>C{<sup>1</sup>H} NMR (50 MHz, CDCl<sub>3</sub>,  $\delta$ ): 153.5, 149.9, 145.9, 142.4,

141.2, 140.5, 134.6, 119.9, 116.7 (CH<sub>2</sub>), 98.7 (C<sub>4</sub>), 61.2 (MeO), 60.1 (MeO), 56.4 (MeO), 35.5 (quaternary carbon of *t*-Bu) 33.0 (Me of *t*-Bu), 13.3 (Me<sub>3</sub>). Mass spectrum:  $m/z$  (% abundance) 288 (M<sup>+</sup>, 53), 274 (20), 273 (100), 258 (17), 243 (20), 77 (12), 57 (11). Anal. Calc for C<sub>18</sub>H<sub>24</sub>O<sub>3</sub>: C, 74.97; H, 8.39. Found: C, 74.84; H, 8.56.

**Synthesis of (E)-12 and (Z)-12.** Diethylacetylene (70 mg, 0.85 mmol) was added to a suspension of compound **1** (120 mg, 0.17 mmol) in dichloromethane. The suspension was stirred at room temperature until compound **1** dissolved completely. The brown solution was heated at 80 °C over a period of 25 h in a closed glass tube. The resulting mixture was filtered over Celite, and the solvent was evaporated. The residue was extracted with *n*-pentane. The orange solution was chromatographed over silica gel using 1:2 diethyl ether/*n*-hexane. The first pale yellow band was taken. The solvent was removed under reduced pressure to give a pale yellow oil that is a 2.6/1 mixture of (*E*)-**12** and (*Z*)-**12**. Yield: 30 mg, 32%. IR (KBr):  $\nu(\text{C}=\text{C})$  1630, 1598, 1574 cm<sup>-1</sup>. <sup>1</sup>H NMR (300 MHz, CDCl<sub>3</sub>,  $\delta$ ): 7.19 (q, H<sub>8</sub> of *E* isomer, 1 H, <sup>3</sup>J<sub>HH</sub> = 8 Hz), 6.55 (s, H<sub>4</sub> of *E* and *Z* isomers, 1 H), 6.25 (q, H<sub>8</sub> of *Z* isomer, 1 H, <sup>3</sup>J<sub>HH</sub> = 8 Hz), 3.94 (s, MeO of *E* isomer, 3 H), 3.92 (s, MeO of *Z* isomer, 3 H), 3.91 (s, MeO of *E* isomer, 3 H), 3.87, 3.86 (2 s, MeO of *Z* isomer, 6 H), 3.85 (s, MeO of *E* isomer, 3 H), 2.68 (q, CH<sub>2</sub> of *E* isomer, 2 H, <sup>3</sup>J<sub>HH</sub> = 8 Hz), 2.49 (q, CH<sub>2</sub> of *Z* isomer, 2 H, <sup>3</sup>J<sub>HH</sub> = 8 Hz), 2.42 (d, Me<sub>8</sub> of *Z* isomer, 3 H, <sup>3</sup>J<sub>HH</sub> = 8 Hz), 2.23 (d, Me<sub>8</sub> of *E* isomer, 3 H, <sup>3</sup>J<sub>HH</sub> = 8 Hz), 2.06 (s, Me<sub>3</sub> of *E* isomer, 3 H), 2.03 (s, Me<sub>3</sub> of *Z* isomer, 3 H), 1.14 (t, CH<sub>2</sub>CH<sub>3</sub> of *E* isomer, <sup>3</sup>J<sub>HH</sub> = 8 Hz, 3 H), 1.08 (t, CH<sub>2</sub>CH<sub>3</sub> of *Z* isomer, <sup>3</sup>J<sub>HH</sub> = 8 Hz). <sup>13</sup>C{<sup>1</sup>H} NMR (50 MHz, CDCl<sub>3</sub>,  $\delta$ ): 153.6, 152.7, 149.6, 149.3, 142.4, 140.8, 140.3, 140.0, 139.3, 139.2, 138.8, 138.3, 135.8, 130.6 (quaternary carbons), 128.5, 127.2 (ethylenic CH), 120.4, 119.1 (quaternary carbons), 98.4, 98.3 (C<sub>4</sub>), 61.20, 61.17, 61.0, 60.1, 56.4, 56.3 (MeO), 20.6, 18.3 (CH<sub>2</sub>), 16.8, 15.6, 15.2, 14.9 (Me<sub>3</sub> and ethylenic Me), 10.3, 10.1 (CH<sub>2</sub>CH<sub>3</sub>). GC-MS [ $m/z$  (% abundance)]: *E* isomer, 274 (M<sup>+</sup>, 80), 260 (17), 259 (100), 230 (13), 229 (17), 201 (12), 128 (15), 115 (16); *Z* isomer, 274 (M<sup>+</sup>, 71), 260 (21), 259 (100), 230 (11), 229 (20), 201 (14), 129 (11), 128 (18), 115 (18). Anal. Calc for C<sub>17</sub>H<sub>22</sub>O<sub>3</sub>: C, 74.42; H, 8.08. Found: C, 74.25; H, 8.34.

**Synthesis of the Organometallic Spirocyclic Complexes C and 13.** Complex **1** (170 mg, 0.24 mmol) and diphenylacetylene (173 mg, 0.97 mmol) were reacted in dichloromethane (15 mL) at ca. -10 °C for 2.5 h. The mixture was filtered over Celite, the resulting solution was concentrated to ca. 2 mL, and *n*-pentane was added, precipitating the brown intermediate **C** (266 mg). A sample of **C** (100 mg) was reacted with 2,2'-bipyridine (39 mg, 0.25 mmol) in acetone (15 mL) for 20 min. The precipitated yellow solid was washed with acetone and diethyl ether, dried, and reacted with Ti(CF<sub>3</sub>SO<sub>3</sub>)<sub>3</sub> (88 mg, 0.25 mmol) in acetone (15 mL) for 30 min. The suspension was filtered over Celite. The solution was evaporated and the residue recrystallized twice from dichloromethane/*n*-hexane giving yellow **13** (83 mg, 18% from **1**). Mp: 194 °C dec.  $\Lambda_m$  (acetone): 120  $\Omega^{-1}$  cm<sup>2</sup> mol<sup>-1</sup>. Anal. Calc for C<sub>50</sub>H<sub>41</sub>N<sub>2</sub>F<sub>3</sub>O<sub>7</sub>PdS: C, 61.45; H, 4.23; N, 2.87. Found: C, 62.74; H, 4.57; N, 3.45. Our efforts to improve these analytical data failed because of tenacious solvents (as seen by NMR and in the crystal structure determination). IR:  $\nu(\text{C}=\text{O})$  1671, 1626 cm<sup>-1</sup>. <sup>1</sup>H NMR (200 MHz, CDCl<sub>3</sub>,  $\delta$ ): 8.5–6.3 (several multiplets, bpy, 4 Ph, H<sub>9</sub>, 29 H), 4.04 (s, MeO, 3 H), 3.80 (s, MeO, 3 H), 3.70 (s, MeO, 3 H), 2.39 (s, MeCO, 3 H). <sup>13</sup>C{<sup>1</sup>H} NMR (50 MHz, CDCl<sub>3</sub>,  $\delta$ ): 198.9 (C=O), 154.2, 152.7, 149.4, 148.4, 147.7, 147.1, 141.2, 140.7, 139.2, 135.8, 135.7, 134.6, 134.5, 130.0, 129.5, 129.3, 128.0, 127.8, 127.6, 127.3, 126.9, 126.5, 126.3, 123.8, 122.8, 70.7 (C<sub>5</sub>), 61.5, 61.2, 57.2 (MeO), 27.0 (MeCO). Single crystals of **13** were obtained by liquid diffusion of cyclohexane into a solution of **13** in 1,2-dichloroethane. The crystal structure of **13**·C<sub>2</sub>H<sub>4</sub>Cl<sub>2</sub> has been published.<sup>1a</sup>

**Synthesis of 14.** Sodium borohydride (54 mg, 1.43 mmol) was added to a suspension of compound **2** (125 mg, 0.23 mmol) in methanol over 1 h. The mixture was then stirred over 30



**Table 1. Atomic Coordinates ( $\times 10^4$ ) and Equivalent Isotropic Displacement Parameters ( $\text{\AA}^2 \times 10^3$ ) of **14****

	<i>x</i>	<i>y</i>	<i>z</i>	<i>U</i> (eq) <sup>a</sup>
C(1)	5736(3)	4597(2)	6376.2(15)	25.1(7)
C(2)	6940(3)	4097(2)	6597(2)	27.8(7)
C(3)	7104(3)	3763(3)	7198(2)	33.4(8)
C(4)	6049(4)	3707(4)	7648(2)	52.1(11)
C(5)	4857(3)	4168(3)	7447(2)	39.5(9)
C(6)	4697(3)	4610(2)	6880.1(15)	26.8(7)
C(7)	5183(3)	4177(3)	5740.9(15)	27.1(7)
C(8)	5150(3)	4928(3)	5296.1(15)	27.1(7)
C(9)	5716(3)	5862(3)	5570.3(15)	25.6(7)
C(10)	6068(3)	5686(2)	6187.1(15)	24.4(7)
C(11)	9059(4)	3869(4)	6184(2)	62.2(14)
C(12)	8832(4)	4152(4)	7842(2)	51.6(11)
C(13)	3486(3)	5171(3)	6712(2)	32.3(8)
C(14)	2375(3)	4526(3)	6805(2)	34.6(8)
C(21)	4641(3)	3144(3)	5702.8(15)	30.1(7)
C(22)	5263(4)	2322(3)	5972(2)	39.4(9)
C(23)	4748(4)	1342(3)	5933(2)	47.9(10)
C(24)	3622(4)	1200(3)	5620(2)	51.6(11)
C(25)	3002(4)	2008(3)	5351(2)	45.7(10)
C(26)	3499(3)	2969(3)	5394(2)	34.9(8)
C(31)	4564(3)	4897(3)	4646.7(15)	29.0(7)
C(32)	4840(4)	4138(3)	4202(2)	40.5(9)
C(33)	4200(4)	4090(4)	3622(2)	56.8(12)
C(34)	3282(4)	4778(4)	3482(2)	63.3(13)
C(35)	3019(4)	5548(4)	3904(2)	52.6(11)
C(36)	3654(3)	5604(3)	4487(2)	36.7(8)
C(41)	5875(3)	6811(3)	5205.5(14)	26.4(7)
C(42)	5366(3)	7713(3)	5433(2)	34.3(8)
C(43)	5491(4)	8595(3)	5081(2)	44.7(10)
C(44)	6138(4)	8598(3)	4500(2)	46.8(10)
C(45)	6677(4)	7707(3)	4277(2)	43.8(10)
C(46)	6534(3)	6825(3)	4623(2)	34.6(8)
C(51)	6889(3)	6302(2)	6619.4(15)	26.4(7)
C(52)	8050(4)	6615(3)	6389(2)	41.7(9)
C(53)	8903(4)	7085(3)	6793(2)	50.9(11)
C(54)	8598(4)	7267(3)	7435(2)	40.5(9)
C(55)	7445(4)	6968(3)	7662(2)	41.9(9)
C(56)	6591(3)	6491(3)	7261(2)	35.1(8)
O(1)	7769(2)	4121(2)	6103.7(11)	36.8(6)
O(2)	8244(2)	3410(2)	7428.3(13)	42.8(7)
O(3)	6164(3)	3301(4)	8175(2)	108(2)
O(4)	3324(3)	6038(2)	7144.6(15)	57.6(8)

<sup>a</sup> *U*(eq) is defined as one-third of the trace of the orthogonalized  $U_{ij}$  tensor.

min. The resulting pale yellow solution was evaporated, and 1:1 dichloromethane/water was added. The mixture is stirred over 20 min, decanted, and extracted with dichloromethane (2  $\times$  10 mL). The extract was washed with water, dried with anhydrous  $\text{MgSO}_4$ , and evaporated to yield compound **14**. Yield: 89 mg, 70%. Colorless crystals of **14** can be obtained from dichloromethane/hexane. IR:  $\nu(\text{OH})$  3426  $\text{cm}^{-1}$ ;  $\nu(\text{C}=\text{O})$  1652  $\text{cm}^{-1}$ .  $^1\text{H}$  NMR (200 MHz,  $\text{CDCl}_3$ ,  $\delta$ ): 7.17–6.80 (m, Ph, 20 H), 6.61 (s, H<sub>9</sub>, 1 H), 4.23 (q, CHOH, 1 H,  $^3J_{\text{HH}} = 10$  Hz), 3.72 (s, MeO, 3 H), 3.40 (s, MeO, 3 H), 1.28 (d, Me, 3 H,  $^3J_{\text{HH}} = 10$  Hz). Single crystals of **14** were obtained by liquid diffusion of hexane and a solution of **14** in dichloromethane.

**X-ray Structure Determination of 14.** *Crystal Data:*  $\text{C}_{38}\text{H}_{32}\text{O}_4$ , orthorhombic,  $P2_12_12_1$ ,  $a = 10.635(3)$   $\text{\AA}$ ,  $b = 13.199(4)$   $\text{\AA}$ ,  $c = 20.643(7)$   $\text{\AA}$ ,  $U = 2898$   $\text{\AA}^3$ ,  $Z = 4$ ,  $D_x = 1.267$   $\text{Mg m}^{-3}$ ,  $F(000) = 1168$ ,  $\mu(\text{Mo K}\alpha) = 0.08$   $\text{mm}^{-1}$ ,  $T = -130$   $^\circ\text{C}$ . A colorless block ca.  $0.55 \times 0.5 \times 0.45$  mm was mounted on a glass fiber in inert oil and transferred to the cold gas stream of the diffractometer (Stoe STADI-4 with Siemens LT-2 low-temperature attachment). A total of 5487 reflections were collected to  $2\theta$  50 $^\circ$ , of which 5115 were independent ( $R_{\text{int}} = 0.030$ ). Cell constants were refined from  $\pm\omega$  values of 60 reflections in the range  $2\theta$  20–23 $^\circ$ .

**Structure Solution and Refinement.** The structure was solved by direct methods and refined on  $F^2$  (program SHELXL-93, G. M. Sheldrick, Univ. of Göttingen). Hydrogen atoms were included using a riding model or as rigid methyl groups.

**Table 2. Selected Bond Lengths ( $\text{\AA}$ ) and Angles (deg) of **14****

C(1)–C(2)	1.510(5)	C(1)–C(6)	1.518(4)
C(1)–C(10)	1.531(4)	C(1)–C(7)	1.541(4)
C(2)–C(3)	1.330(5)	C(2)–O(1)	1.347(4)
C(3)–O(2)	1.383(4)	C(3)–C(4)	1.459(5)
C(4)–O(3)	1.219(5)	C(4)–C(5)	1.466(6)
C(5)–C(6)	1.318(5)	C(6)–C(13)	1.525(5)
C(7)–C(8)	1.352(5)	C(7)–C(21)	1.481(5)
C(8)–C(31)	1.479(4)	C(8)–C(9)	1.484(5)
C(9)–C(10)	1.347(4)	C(9)–C(41)	1.471(5)
C(13)–O(4)	1.462(4)		
C(2)–C(1)–C(6)	114.6(3)	C(2)–C(1)–C(10)	106.9(3)
C(6)–C(1)–C(10)	109.4(3)	C(2)–C(1)–C(7)	115.0(3)
C(6)–C(1)–C(7)	108.0(3)	C(10)–C(1)–C(7)	102.1(3)
O(3)–C(4)–C(3)	120.8(4)	O(3)–C(4)–C(5)	121.5(4)
C(3)–C(4)–C(5)	117.6(3)	C(8)–C(7)–C(21)	128.9(3)
C(8)–C(7)–C(1)	108.9(3)	C(21)–C(7)–C(1)	121.7(3)
C(7)–C(8)–C(31)	127.3(3)	C(7)–C(8)–C(9)	109.9(3)
C(31)–C(8)–C(9)	122.6(3)	C(10)–C(9)–C(41)	126.8(3)
C(10)–C(9)–C(8)	109.3(3)	C(41)–C(9)–C(8)	124.0(3)
C(9)–C(10)–C(51)	129.4(3)	C(9)–C(10)–C(1)	109.8(3)
C(51)–C(10)–C(1)	119.7(3)	O(4)–C(13)–C(14)	106.3(3)
O(4)–C(13)–C(6)	109.9(3)	C(14)–C(13)–C(6)	111.6(3)
C(2)–O(1)–C(11)	122.6(3)	C(3)–O(2)–C(12)	110.7(3)

The oxygen atom O(3) displays high displacement parameters and may be disordered. The absolute structure was not determined. The final  $wR(F^2)$  was 0.157 for all reflections, with a conventional  $R(F)$  of 0.063, for 383 parameters and 413 restraints.  $S = 1.06$ ; maximum  $\Delta\rho$  0.1, maximum  $\Delta\rho$  0.4 e  $\text{\AA}^{-3}$ . Final atomic coordinates are given in Table 1, with selected bond lengths and angles in Table 2.

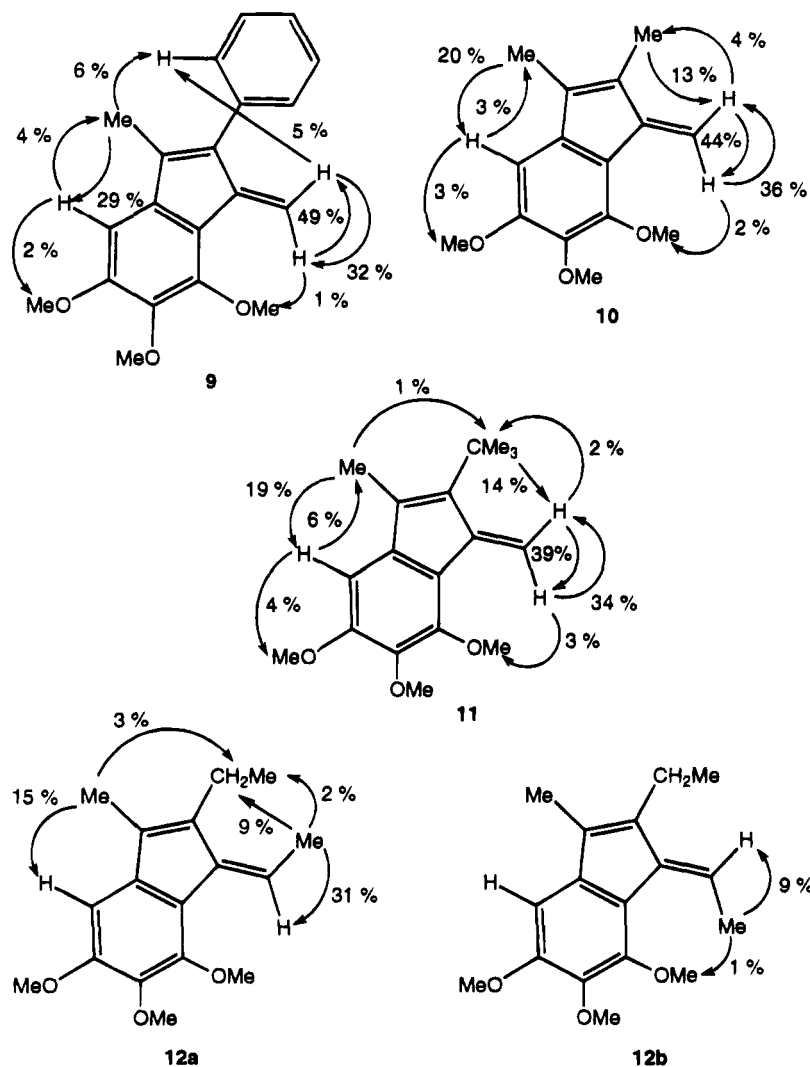
## Results

**Synthesis of Spirocyclic Compounds 2–8 and Benzofulvene 9.** The reaction of the cyclopalladated complex **1** with symmetric alkynes such as diphenylacetylene and bis(4-tolyl)acetylene, at room temperature, gives metallic palladium and the spirocyclic compounds **2** and **3** (Scheme 1,  $\text{To} = p\text{-tolyl}$ ). Other symmetric alkynes  $\text{R}_2\text{C}_2$  ( $\text{R} = \text{Me}_3\text{Si}$ ,  $\text{ClCH}_2$ ,  $\text{MeOCH}_2$ ,  $\text{CO}_2\text{Me}$ ) give intractable mixtures. Terminal alkynes  $\text{RC}_2\text{H}$  ( $\text{R} = t\text{Bu}$ ,  $n\text{Bu}$ ,  $\text{Ph}$ ,  $\text{CO}_2\text{Et}$ ) behave similarly, as has often been observed in their reactions with other cyclopalladated complexes.<sup>22</sup>

We have also tested reactions of **1** with unsymmetric alkynes such as ethyl 3-phenylpropiolate. In this case, complete selectivity in favor of the head-to-tail spiro compound is observed, since **4** is virtually the only product present in the crude material obtained after removal of the metallic palladium and the reaction solvent. A high to moderate regioselectivity, with respect to the formation of the head-to-tail isomers, with methyl 3-phenylpropiolate and (4-nitrophenyl)phenylacetylene have been observed. The molar ratios head-

(22) (a) Maassarani, F.; Pfeffer, M.; Le Borgne, G. *Organometallics* **1987**, *6*, 2043. (b) Dupont, J.; Pfeffer, M. *J. Organomet. Chem.* **1987**, *321*, C13. (c) Wu, G.; Rheingold, A. L.; Geib, S. J.; Heck, R. F. *Organometallics* **1987**, *6*, 1941. (d) Wu, G.; Rheingold, A. L.; Geib, S. J.; Heck, R. F. *Organometallics* **1987**, *6*, 2386. (e) Maassarani, F.; Pfeffer, M.; Spencer, J.; Wehman, E. *J. Organomet. Chem.* **1994**, *466*, 265. (f) Dupont, J.; Rottevel, M. A.; Pfeffer, M.; De Cian, A.; Fischer, J. *Organometallics* **1989**, *8*, 1116. (g) Maassarani, F.; Pfeffer, M.; Le Borgne, G. *Organometallics* **1987**, *6*, 2029. (h) Maassarani, F.; Pfeffer, M.; Le Borgne, G. *Organometallics* **1990**, *9*, 3003. (i) Dupont, J.; Pfeffer, M.; Daran, J. C.; Gauteron, J. *J. Chem. Soc., Dalton Trans.* **1988**, 2421. (j) Pfeffer, M.; Sutter, J.-P.; De Cian, A.; Fischer, J. *Organometallics* **1993**, *12*, 1167. (k) Pfeffer, M.; Rottevel, M. A.; Le Borgne, G.; Fischer, J. *J. Org. Chem.* **1992**, *57*, 2147. (l) Pfeffer, M. *Recl. Trav. Chim. Pays-Bas* **1990**, *109*, 567. (m) Beydoun, N.; Pfeffer, M.; DeCian, A.; Fischer, J. *Organometallics* **1991**, *10*, 3693.

Chart 2



to-tail/head-to-head or tail-to-tail are, respectively, 5/1 and 4/1 (see Scheme 1). However, (4-methoxyphenyl)-phenylacetylene gives the 2:1:1 mixture expected for an unselective double insertion of the alkyne.

The presence of an alkyl group in the alkyne changes the chemoselectivity of the process. Thus, in the case of 1-phenylpropyne, 5,6,7-trimethoxy-3-methyl-2-phenyl-1-methylene-1*H*-indene (2-PhBzf) (**9**) is obtained along with a mixture of two spiro compounds (head-to-tail (**8a**)/head-to-head or tail-to-tail (**8b**)/**9** = 7/1/1.5). The nature of **9** was known by separate preparation using another method (see below).

After chromatography of the corresponding mixtures, **5a**, **6a**, and **9** could be isolated and characterized. Although isomers **6b** and **6c** could also be isolated, their NMR data do not indicate which is the head-to-head or the tail-to-tail isomer. From mixtures **7a** + **7b** + **7c** or **8a** + **8b** only different enriched samples of the head-to-tail isomer could be obtained. NMR data of these enriched mixtures allowed us to assign the resonances corresponding to the isomers **7a**, **8a**, and **8b**.

All reactions proceed rapidly to give dark red or brown solutions from the suspensions containing **1**. However, formation of palladium is a slow process at room temperature. We have tried to follow the course of the reaction by TLC, but its completion is difficult to ascertain. Sometimes, reaction times shorter than

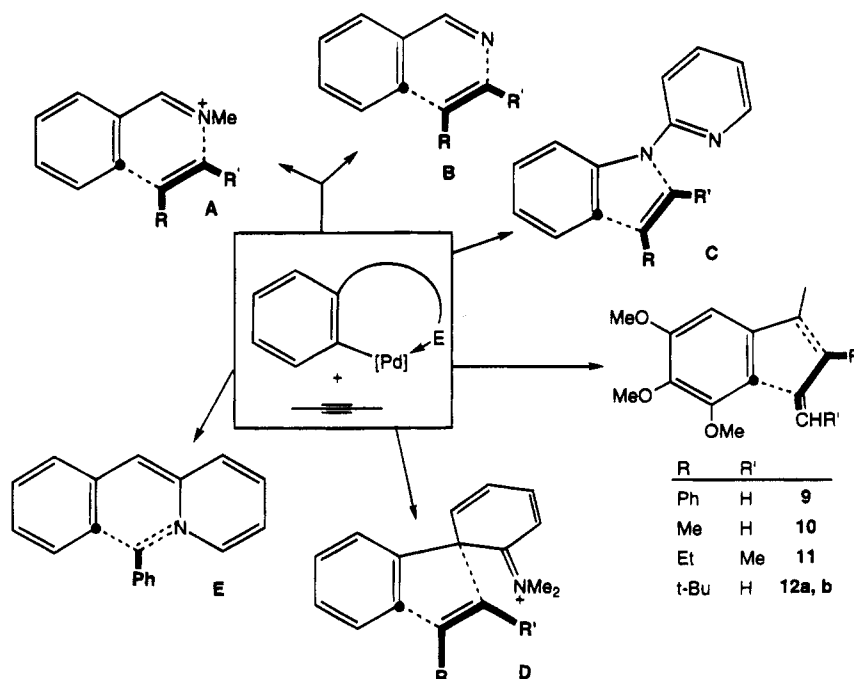
indicated in the Experimental Section gave products that still contained palladium.

**Synthesis of Benzofulvene Derivatives 10–12.** Only benzofulvenes could be isolated from reactions of **1** with dialkylacetylenes. However, whereas 2-butyne selectively affords the benzofulvene 2-MeBzf (**10**) (see Scheme 1), *tert*-butylmethyl- or diethylacetylene gives 2-*t*BuBzf (**11**) or a mixture of both isomers *E*- and *Z*-5,6,7-trimethoxy-3-methyl-2-ethyl-1-ethylidene-1*H*-indene, (*E*)-**12** and (*Z*)-**12** (2.6/1) (see Scheme 1 and Chart 2), along with minor amounts of unidentified products. In the case of the reaction of **1** with *tert*-butylmethylacetylene the byproduct (**X**) seems to be the result of a monoinsertion process. The molar ratio **11**/**X** was 3.5 (by NMR).

All reactions of **1** with dialkylacetylenes are even slower than those with those alkynes giving spiro compounds. It is for this reason that reactions leading to **10–12** were carried out at 80 °C.

## Discussion

A noteworthy feature of our results is the high chemoselectivity observed, depending on the nature of the R and R' groups of the alkynes. Thus, almost quantitative formation of the spiro compounds **2–7** is achieved when R is an aryl group and R' is an aryl or

**Scheme 2. Reactions of Cyclopalladated Compounds with Alkynes Giving Cycloadducts with One Alkyne Molecule<sup>a</sup>**


<sup>a</sup> The new bonds are indicated by dashed lines, the carbon atom originally palladated, C<sub>Pd</sub>, is represented by ●, and the acetylene molecule or moiety is drawn bold.

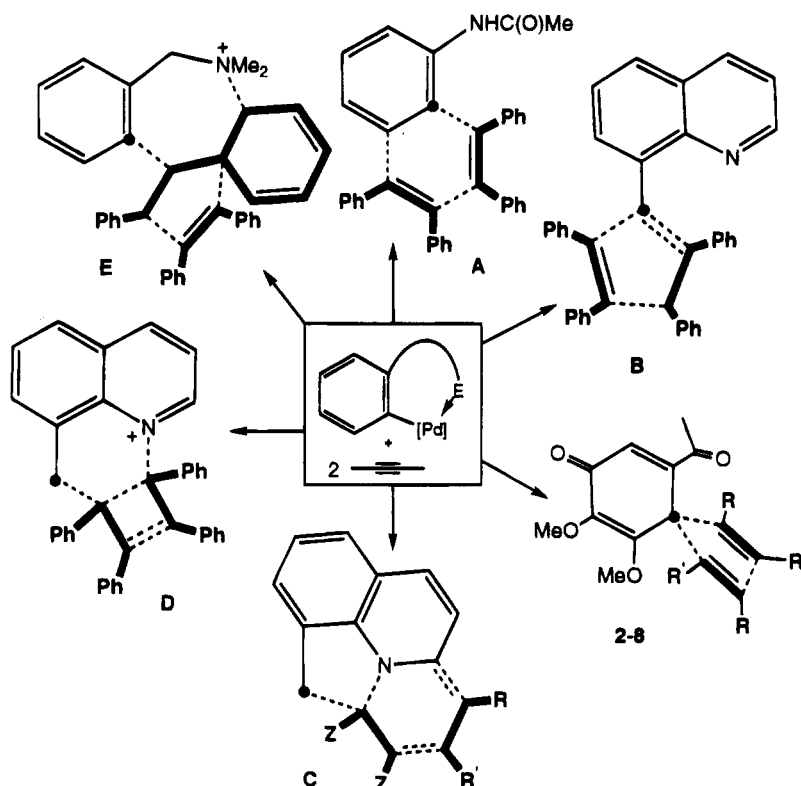
alkylcarboxylate group, whereas when both groups are alkyl the main component of the mixture is a benzofulvene. This dependence is clearly shown by the fact that the mixed alkyne 1-phenylpropyne gives spiro compounds **8** and the benzofulvene **9**. Also remarkable are the high regioselectivities in favor of the head-to-tail spiro isomer in most cases and of the benzofulvene isomer containing the exocyclic alkene function in the position shown in Scheme 1 for **9**–**12**. Finally, also significant are the demethylation of the trimethoxy substituent *para* to the position originally occupied by the palladium atom, giving a keto group, and that all demetalation reactions giving spiro compounds were performed at room temperature in contrast to previous studies at high temperatures.

The formation of the spiro compounds, although not unexpected according to the catalytic processes mentioned above,<sup>2–5</sup> is a rare result in terms of the previous studies on reactions of alkynes and cyclometallated palladium complexes.<sup>6,22</sup> Thus, most of these reactions give rise, after depalladation, to different families of compounds. The most numerous is that resulting from cycloaddition of one molecule of the alkyne to the depalladated moiety. Generally, the cycle is closed between the two atoms initially bonded to the palladium atom, C<sub>Pd</sub>, and the donor atom in the group E (N or S; see Scheme 2) giving cationic heterocycles (see **A** in Scheme 2).<sup>6b,22a–e,g,h</sup> In some cases, one or two of the substituents of the E group are lost during the process and neutral heterocycles are obtained (see **B** in Scheme 2). Less frequently the cycle involves a nitrogen or carbon atom of the chain that links C<sub>Pd</sub> and E (see **C** and **D** and our compounds **9**–**12** in Scheme 2).<sup>1b,6b,22e</sup> Compound **E** can be considered as the result of the cycloaddition of the PhC≡ fragment of the alkyne PhC≡CCO<sub>2</sub>Et between the C<sub>Pd</sub> and N atoms.<sup>22h</sup> Although compounds **9**–**12** resemble the case of compound

**D**, because the cycles involve a carbon atom of the C<sub>Pd</sub>–E chain, they are however the only examples in which the donor atom in the E group (O) is lost and, in addition, the alkyne is deprotonated. A second group of products can be considered as built through coupling of C<sub>Pd</sub> and a monoradical formed by a cyclization process between two or three molecules of the alkyne.<sup>5c,6a,22c,i,j</sup> In a third group of compounds two molecules of alkyne form (i) one cycle containing C<sub>Pd</sub> (compounds **2**–**8** and **B**<sup>22j</sup> in Scheme 3) or containing C<sub>Pd</sub> and its *ortho* carbon atom [see **A**<sup>5c,6b,22c,f,i</sup> in Scheme 3] to give naphthalene derivatives or (ii) two cycles involving C<sub>Pd</sub> and E (see **C**–**E**<sup>6a,22g,k</sup> in Scheme 3). Compounds **2**–**8** are unique among all the above products because they are the only ones in which C<sub>Pd</sub> is a spiro atom. This is, however, the normal result in the palladium-catalyzed synthesis of spiro compounds from alkenes and alkynes where there is not a donor atom to give metallacyclic intermediates.<sup>2–5</sup> Our results can be compared with the palladium-catalyzed reaction of *ortho*-iodoanisole with 3-hexyne to give a conjugated polyene compound.<sup>5c</sup> Therefore, it is probable that the weak donor ability of the carbonyl group was, in part, responsible for the unusual result. Reaction of diphenylacetylene with the only C,O palladacycle we are aware of (group E = NH-COMe) gave a spirocyclic ( $\pi$ -allyl)palladium complex of the same structure we propose as intermediate in our reactions (see below and Scheme 4, compound **C**). However, thermal decomposition of this complex led to a naphthalene compound (see **A** in Scheme 3). The different result could be due to the different temperature used for the depalladation reaction.<sup>22i</sup>

**Reaction Pathway.** Scheme 4 shows our proposed pathway for the synthesis of spiro compounds. Formation of mono- (**A**) and di-inserted (**B**) compounds as intermediates in reactions of cyclopalladated complexes and alkynes is well documented.<sup>22</sup> The same spiro

**Scheme 3. Reactions of Cyclopalladated Compounds with Alkynes Giving Products That Can Be Considered As Built through Cyclization of Two Molecules of the Alkyne and  $C_{Pd}^a$**



<sup>a</sup> The new bonds are indicated by dashed lines, the carbon atom originally palladated,  $C_{Pd}$ , is represented by ●, and the alkyne molecules are drawn bold.

compounds and unreacted **1** were obtained when a 1:1 molar ratio was used, because formation of the mono-inserted compound is the rate-determining step.<sup>23</sup> The doubly inserted species would undergo a ring contraction, leading to a spirocyclic junction at the formerly palladium-bonded aryl carbon,  $C_{Pd}$ , and the  $PdCl^+$  moiety would migrate to occupy the other position *ortho* to the acetyl substituent. Coordination to the adjacent double bond would give a  $\pi$ -allylic compound **C**. Similar compounds have been proposed as intermediates after the double insertion of an alkyne into a palladacyclic compound,<sup>5c,6b,22a,f</sup> and in one case, such an intermediate has been characterized by an X-ray diffraction study [see **A** ( $R = Ph$ ) in Scheme 5].<sup>22a</sup> However, after depalladation, they give undetermined<sup>22a</sup> or nonspirocyclic compounds (see Scheme 5).<sup>5c,6b,22c,f</sup>

When the reaction forming **2** ( $R = Ph$  in Scheme 4) is carried out in dichloromethane at  $-10^\circ C$ , no depalladation occurs, and an organopalladium compound can be isolated. If the reaction is conducted in acetone at room temperature, the same compound precipitates; if it is dissolved in dichloromethane it decomposes at room temperature giving metallic palladium and compound **2**, which indicates that it is an intermediate in the formation of **2**. Its instability has prevented its characterization, but we propose it to be intermediate **C** (Scheme 4) because it reacts with 2,2'-bipyridine (bpy) and  $Tl(CF_3SO_3)$  to give the cationic derivative **13**, which was fully characterized and its structure determined by an X-ray diffraction study.<sup>1a</sup> We formulate **C** as a dimer because the IR spectrum shows that the oxygen of the

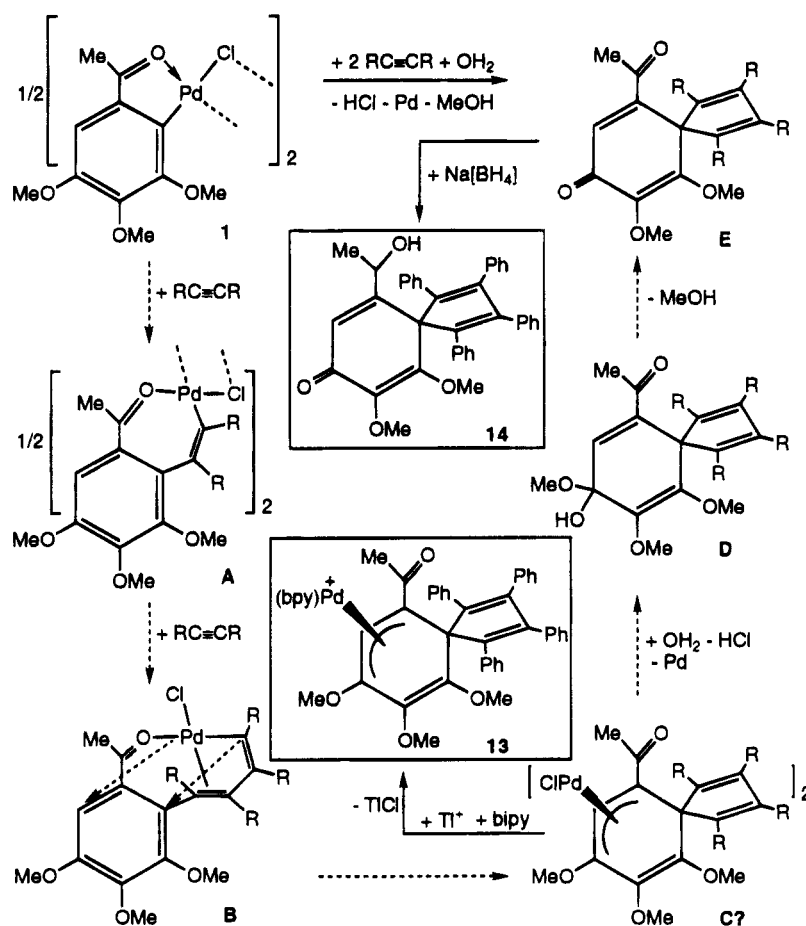
carbonyl group is not bonded to palladium. As mentioned above, a dimeric palladium complex of the same structural type was isolated from the reaction of diphenylacetylene and the product of cyclopalladation of acetanilide.<sup>22i</sup> Formation of the keto group and depalladation are assumed to occur through reaction of **C** with adventitious water, leading to intermediate **D**, which would decompose to give the spiro compound **E**. In fact, when the reaction with diphenylacetylene is carried out using freshly distilled dichloromethane, slow decomposition is initially observed but rapidly stops. The resulting solution remains unaltered, but addition of water gives **2**.

Although we have used an excess of the alkyne, the benzofulvenes **9–12** are the result of a monoinsertion reaction. We assume formation of the same intermediate **A** as in the case of the spiro compounds (see Scheme 6). The second insertion, when both substituents are alkyl groups, must, if it occurs, be much slower than the very slow depalladation process that gives **10–12**. The presence of one aryl group in the alkyne molecule, such as in phenylmethylacetylene, favors the double insertion process giving mainly spiro compounds **8a,b**.

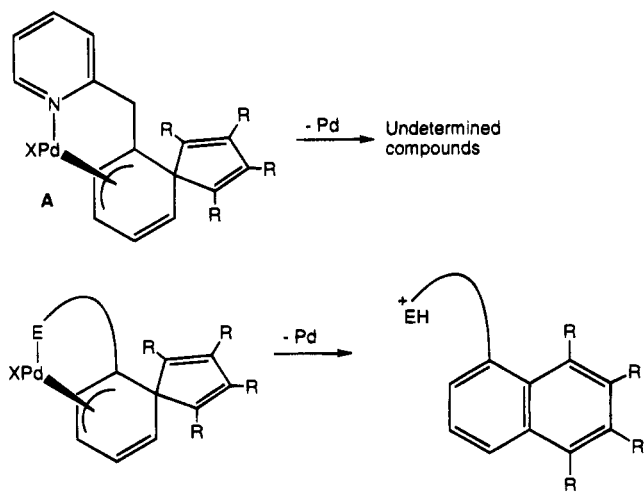
The mono-insertion of an unsymmetrical alkyne without electron-withdrawing substituents into an aryl-Pd<sup>22a,e</sup> or -Mn<sup>24</sup> bond seems to be under steric control. The regioisomer obtained is that in which the least bulky substituent becomes adjacent to  $C_{Pd}$  (see **D** in Scheme 2,  $R = Me$ ,  $R' = tBu$ ) or  $C_{Mn}$ , respectively. In our case, the syntheses of **9** and **11** are new examples

(23) Ryabov, A. D.; van Eldick, R.; Le Borgne, G.; Pfeffer, M. *Organometallics* **1993**, *12*, 1386.

(24) Liebeskind, L. S.; Gasdaska, J. R.; McCallum, J. S.; Tremont, S. J. *J. Org. Chem.* **1989**, *54*, 669.

**Scheme 4. Proposed Pathway (Dashed Arrow) for the Synthesis of Spiro Compounds and Syntheses of Compounds 13 and 14**


Scheme 5



of this rule. The contrary effect is observed in the mono-insertion reaction of alkynes into a Cl-Pd bond.<sup>25</sup>

From intermediate **A** (see Scheme 6) we assume formation of the aquo complex **B** that, after depalladation, gives the indenol **C**. We have proposed a similar pathway to account for the synthesis of indenols from alkynes with an ortho-palladated aromatic aldehyde.<sup>1b</sup> Formation of an acidic medium in the depalladation process **B** → **C** can catalyze the 1,4-allylic dehydration of the indenol **C** to give benzofulvenes **9–12**. In fact,

indenols of the type **C** are the final products of reactions between ortho-manganated methyl aryl ketones with alkynes probably because an acidic medium is not formed.<sup>24</sup> We have independently prepared all the indenols **C**<sup>26</sup> and shown that addition of a catalytic amount of HO<sub>3</sub>SCF<sub>3</sub> or HCl gives **9–12**.

The observed high to moderate regioselectivity in the synthesis of spiro compounds **4–6** and **8** also represents a difference from most reactions between alkynes and cyclopalladated compounds. Thus, while the insertion of the first molecule of an unsymmetric alkyne can be regioselective<sup>22a,b,e,g,m</sup> or not,<sup>6b</sup> the second one rarely is.<sup>22i</sup> Regiospecific mono- or di-insertions are observed only for certain cyclopalladated complexes, mainly when one of the substituents is Ph and the other one an electron-withdrawing group (CO<sub>2</sub>R, CHO, *p*-tolylSO<sub>2</sub>). The mono-insertion process occurs in such way that the carbon bearing the more electron-withdrawing group is bonded to C<sub>Pd</sub>.<sup>22a,b,e,g,m</sup> In the only example we know in which a regiospecific double insertion occurs the head-to-tail isomer is obtained.<sup>22i</sup> This means that, when the double insertion reaction is regiospecific, the second insertion follows the same rule than the first. Because the steric requirements of Ph and CO<sub>2</sub>R are comparable, these insertion processes seem, therefore, to be under electronic control. In our case, the expected results are obtained; *i.e.*, when the reaction has some regioselectivity, the more abundant isomer is the head-to-tail one. According to the above arguments, in the case of **8**, the

(25) Kelley, E.; Maitlis, P. M. *J. Chem. Soc., Dalton Trans.* **1979**, 167.

(26) To be published.

## Scheme 6. Proposed Pathway (Dashed Arrow) for the Synthesis of 9–12

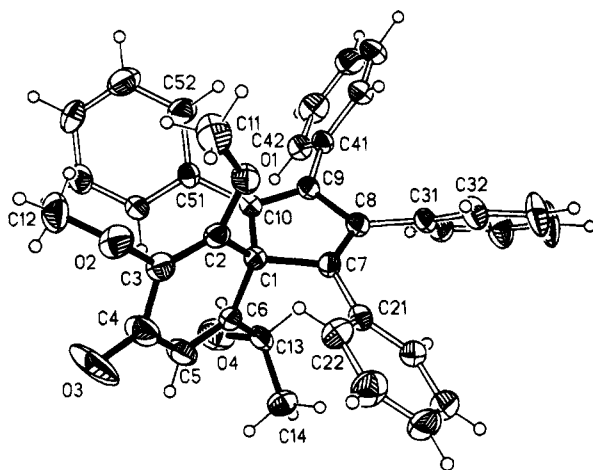
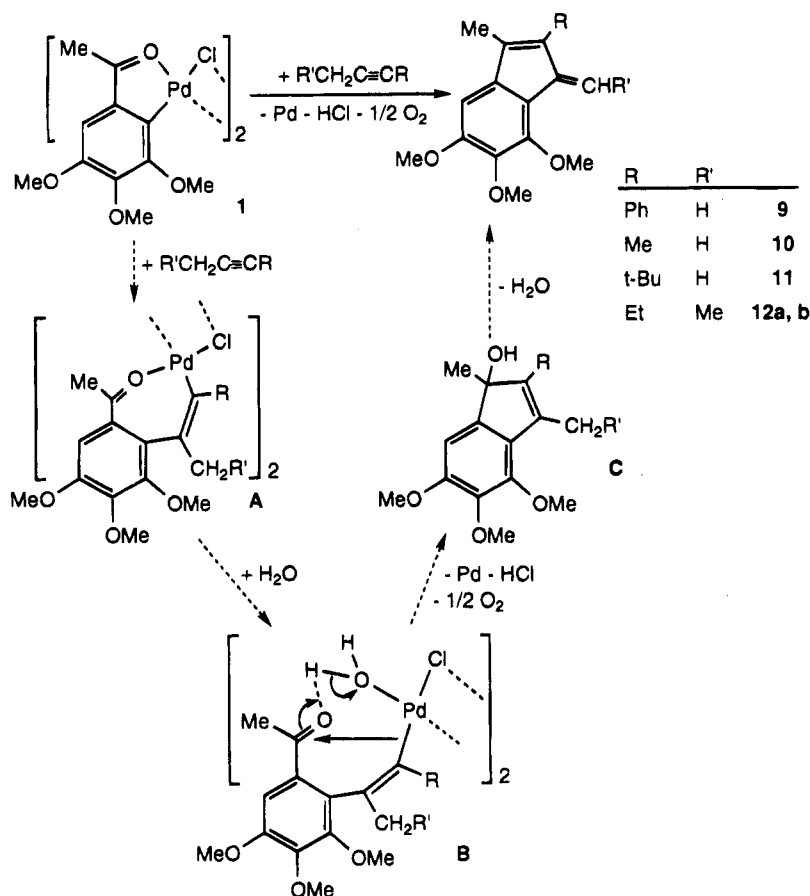


Figure 1. Structure of compound 14.

steric and/or the electronic control of both insertions account for the high regioselective formation of **8a**. The electronic control of the double insertion reactions is well illustrated by comparing the results of reactions leading to **6** and **7**.

As far as we are aware there is only one reported spiro compound having the spiro[4.5]decatetraenone skeleton.<sup>27</sup>

**Structural Studies.** Our efforts to grow single crystals of the spirocyclic compounds failed; nevertheless, the structure of the alcohol **14** (Figure 1), obtained (see Scheme 4) through the selective reduction with Na[BH<sub>4</sub>] of the 10-acetyl group in **2**, proves, along with the

analytical and spectroscopic data, the structure of **2**. The observed absence of NOE between the hydrogen bonded to the carbon 9 (see **A** in Chart 1) and the MeO groups in **2** also points to that formulation; however, the absence of NOE is not conclusive. The determination of the structure<sup>1a</sup> of the intermediate derivative **13** shows that the 8-methoxy group is involved in the allylic system and, hence, it is reasonable to assume that this group would be demethylated, according to our pathway proposal, to give **2**. The structures of the other spirocyclic compounds can be proposed by analogy, since their <sup>1</sup>H and <sup>13</sup>C NMR spectra show that their relevant signals, *i.e.* those corresponding to the 9-CH, 8-CO, and the spiro C, appear in similar positions. When several regioisomers are obtained, it is very easy to distinguish the head-to-tail one by <sup>13</sup>C NMR.

The structures of the benzofulvenes **9–12** have been proposed by NOE experiments (see Chart 2).

**Structure of 14.** The structure of **14** (see Figure 1 and Tables 1 and 2) consists of two ring systems, 2,3,4,5-tetraphenylcyclopenta-2,4-diene and 2,3-dimethoxy,6-(1-hydroxyethyl)-cyclohexa-2,5-dien-4-one, with a common spiro carbon atom C(1) (see Figure 1). With the exception of C(13)–O(4) [1.462(4) Å] and of C(3)–O(2) [1.383(4) Å], which are longer than the mean value reported for secondary alcohols (1.432 Å)<sup>28</sup> and in enol esters (C=C–O–, 1.354 Å),<sup>28</sup> respectively, the bond lengths are normal. Thus, the C=C bond distances in the five-membered ring [1.347(4) and 1.352(5) Å] are consistent with the mean value found in other cyclo-

(27) Kende, A. S.; Hebeisen, P. *Tetrahedron Lett.* **1985**, *26*, 3769.

(28) Allen, F. H.; Kennard, O.; Watson, D. G.; Brammer, L.; Orpen, A. G.; Taylor, R. *J. Chem. Soc., Perkin Trans. 2* **1987**, S1.

penta-1,3-dienes (1.341 Å<sup>28</sup>) and those in the six-membered ring [1.330(5) and 1.318(5) Å] with the mean value reported for cyclohexa-2,5-dien-1-ones (1.329 Å<sup>28</sup>). Similarly, C–C bond distances involving the carbon C(4) [1.459(5), 1.466(6) Å] or the spiro carbon C(1) [1.510(5)–1.541(4) Å] and C(8)–C(9) [1.484(5) Å] are in agreement with mean values found in other C=C–C(O)–C=C (1.456 Å),<sup>28</sup> R<sub>3</sub>C–C=C (1.522 Å),<sup>28</sup> and C=C–C=C (1.455 Å)<sup>28</sup> moieties, respectively. The intermolecular contact O4–H4···O3 (1 – *x*, 0.5 + *y*, 1.5 – *z*) [O···O = 3.11(1) Å, O–H···O = 156(1)°] may indicate weak hydrogen bonding.

### Conclusions

The reactions of complex **1** with different internal alkynes have proved useful for the synthesis, with moderate to good yields, of several organic spirocyclic or benzofulvene compounds, depending on the nature of the alkyne substituents. When at least one of these substituents is an aryl group, high chemoselectivities in favor of spiro compounds are obtained. High or moderate regioselectivities are observed in most cases

for the head-to-tail spiro isomer that results from the insertion of two molecules of alkyne. When both substituents are alkyl groups, benzofulvenes (25–38% yield) can be isolated. The isolation and X-ray structure determination of the  $\pi$ -allylic palladium intermediate **13** and of **14** (see Figure 1), a derivative of the spiro compound **2**, has allowed us to propose the structures of the spirocycles and a reasonable pathway for their formation.

**Acknowledgment.** We thank the Dirección General de Investigación Científica y Técnica (PB92-0982-C) and the Fonds der Chemischen Industrie for financial support. J.G.-R. is grateful for a grant from the Ministerio de Educación y Ciencia (Spain).

**Supplementary Material Available:** Tables of H positional and thermal parameters, X-ray data collection parameters, bond distances and angles, and anisotropic thermal parameters (4 pages). Ordering information is given on any current masthead page.

OM940990V

# Comparison of the Properties of Polymethyl-1,1'-diheteroferrocenes of the Group 15 Elements

Arthur J. Ashe, III,\* Saleem Al-Ahmad, Steffen Pilotek, and Dhananjay B. Puranik

Department of Chemistry, The University of Michigan, Ann Arbor, Michigan 48109

Christoph Elschenbroich\* and Andreas Behrendt

Fachbereich Chemie der Philipps-Universität, D-35032 Marburg, Germany

Received January 31, 1995<sup>⊗</sup>

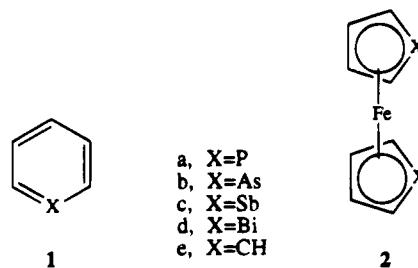
2,2',5,5'-Tetramethyl-1,1'-diheteroferrocenes,  $(C_4H_2-\alpha-Me_2X)_2Fe$ , and 2,2',3,3',4,4',5,5'-octamethyl-1,1'-diheteroferrocenes,  $(C_4Me_4X)_2Fe$ , where X = P, As, Sb, and Bi, have been prepared from the reactions of the corresponding 1-phenylheteroles with lithium followed by  $FeCl_2$ . The redox chemistry has been explored using cyclic voltammetry. The redox  $E_{1/2}(0/+)$  values of both series of diheteroferrocenes correlate well with the ionization potentials of the free atoms X = P, As, Sb, and Bi. The 3,3',4,4'-tetramethyl-1,1'-diheteroferrocenes  $(C_4H_2-\beta-Me_2X)_2Fe$ , where X = P, As, and Sb, have been prepared in a similar manner. These compounds undergo electrophilic isotopic exchange of the ring hydrogen atoms on treatment with trifluoroacetic acid- $d_1$  at rates that increase with the atomic number of the heteroatom.

## Introduction

The heterobenzenes of the group 15 elements (**1a–d**) comprise a series in which elements of an entire column of the periodic table have been incorporated into aromatic rings.<sup>1–3</sup> The comparison of the properties of **1a–d** has been particularly valuable for the study of aromaticity and  $\pi$ -bonding between carbon and the heavier main group elements. However the heterobenzene series has two important limitations: only arsa-benzene (**1b**) has a true aromatic chemistry,<sup>4</sup> while stibabenzene (**1c**) and particularly bismabenzene (**1d**) are so labile that their study is difficult.<sup>5</sup>

The group 15 element diheteroferrocenes (**2a–d**) form a similar series. We have undertaken a study of diheteroferrocenes to supplement our work on the heterobenzenes and in the hope that compounds **2a–d** might circumvent the shortcomings of the heterobenzene series. Derivatives of **2a**,<sup>6</sup> **2b**,<sup>7</sup> **2c**,<sup>8,7d</sup> and **2d**<sup>8c,9</sup> have been reported. We now report on details of the

preparation of polymethyl diheteroferrocenes, their electrochemistry, and electrophilic substitution reactions.



## Results and Discussion

**Synthesis.** The group 15 element 1,1'-diheteroferrocenes can be prepared generally from the corresponding 1-phenylheteroles (**3**, **4**, **6**, **10**). The reaction of a 1-phenylheterole with lithium metal in THF gives phenyllithium and the lithium heterocyclopentadienide (Scheme 1). Subsequent addition of  $NH_3$  to remove the phenyllithium followed by treatment with  $FeCl_2$  affords the desired 1,1'-diheteroferrocene in 30%–70% yield.<sup>6–9</sup>

1-Phenyl-2,5-dimethylheteroles (**4b–d**) were converted to the corresponding 2,2',5,5'-tetramethyl-1,1'-diheteroferrocenes (**5b**,<sup>7a</sup> **5c**,<sup>8a,b</sup> and **5d**<sup>9</sup>) via Scheme 1 as described in the literature. Similarly the readily available 1-phenyl-2,5-dimethylphosphole (**4a**)<sup>10</sup> was converted to 2,2',5,5'-tetramethyl-1,1'-diphosphaferrocene (**5a**), which had not previously been described. 1-Phenyl-2,3,4,5-tetramethylheteroles (**6a–d**) were prepared via an adapted Fagan–Nugent heterole synthe-

<sup>⊗</sup> Abstract published in *Advance ACS Abstracts*, May 1, 1995.

(1) Ashe, A. J., III. *Acc. Chem. Res.* **1978**, *11*, 153.  
(2) Ashe, A. J., III. *Top. Curr. Chem.* **1982**, *105*, 125.  
(3) Märkl, G. *Chem. Unserer Zeit.* **1982**, *16*, 139.  
(4) Ashe, A. J., III; Chan, W.-T.; Smith, T. W.; Taba, K. M. *J. Org. Chem.* **1981**, *46*, 881.  
(5) Ashe, A. J., III; Diephouse, T. R.; El-Sheikh, M. Y. *J. Am. Chem. Soc.* **1982**, *104*, 5693.  
(6) (a) de Lauzon, G.; Deschamps, B.; Fischer, J.; Mathey, F.; Mitschler, A. *J. Am. Chem. Soc.* **1980**, *102*, 994. (b) Mathey, F. *Nouv. J. Chim.* **1987**, *11*, 585. (c) Nief, F.; Mathey, F.; Ricard, L.; Robert, F. *Organometallics* **1988**, *7*, 921.  
(7) (a) Thiollet, G.; Mathey, F.; Poilblanc, R. *Inorg. Chim. Acta* **1979**, *32*, L67. (b) Chiche, L.; Galy, J.; Thiollet, G.; Mathey, F. *Acta Crystallogr.* **1980**, *B36*, 1344. (c) Ashe, A. J., III; Mahmoud, S.; Elschenbroich, C.; Wünsch, M. *Angew. Chem., Int. Ed. Engl.* **1987**, *26*, 229. (d) Ashe, A. J., III; Kampf, J. W.; Pilotek, S.; Rousseau, R. *Organometallics* **1994**, *13*, 4067.  
(8) (a) Ashe, A. J., III; Diephouse, T. R. *J. Organomet. Chem.* **1980**, *202*, C95. (b) Ashe, A. J., III; Diephouse, T. R.; Kampf, J. W.; Al-Taweel, S. M. *Organometallics* **1991**, *10*, 2068. (c) Ashe, A. J., III; Kampf, J. W.; Al-Taweel, S. M. *Organometallics* **1992**, *11*, 1491.

(9) Ashe, A. J., III; Kampf, J. W.; Puranik, D. B.; Al-Taweel, S. M. *Organometallics* **1992**, *11*, 2743.

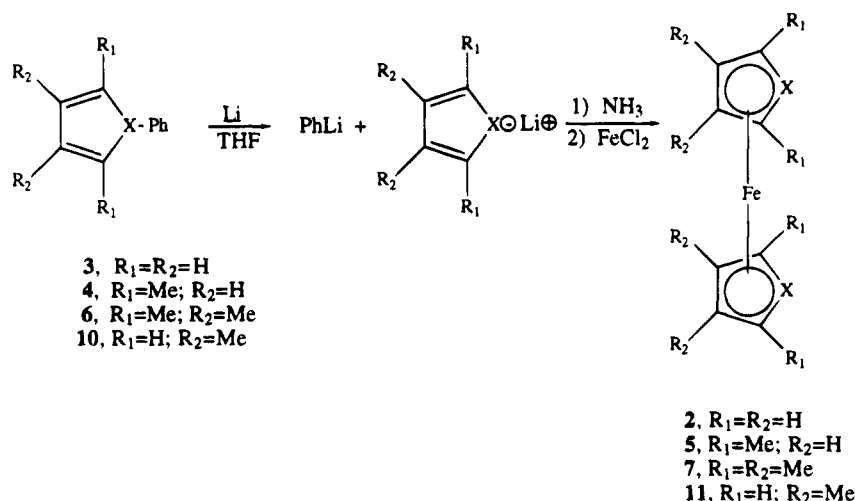
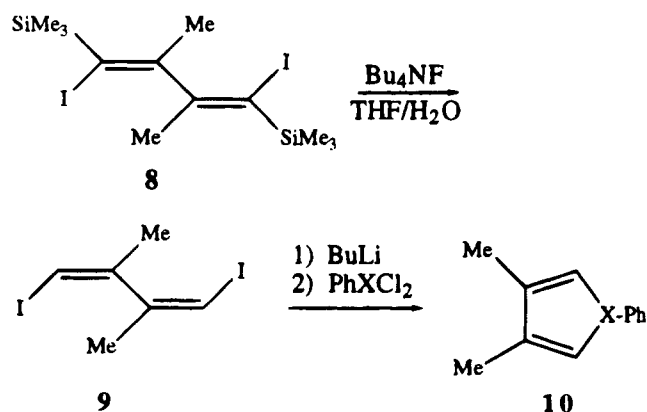
(10) Märkl, G.; Hauptmann, H. *Tetrahedron Lett.* **1968**, 3257.



**Table 1.**  $^{13}\text{C}$  NMR (and  $^1\text{H}$  NMR in Parentheses) Chemical Shift Values of the Polymethyl-1,1'-diheteroferrocenes

compd	$\alpha$ -CH	$\alpha$ -Me	$\beta$ -CH	$\beta$ -Me	ref
$(\text{C}_4\text{H}_2\text{-}\alpha\text{-Me}_2\text{X})_2\text{Fe}$					
<b>5a</b> , X = P	97.9 <sup>a</sup> (-)	16.3 <sup>a</sup> (1.80) <sup>b</sup>	84.4 <sup>a</sup> (4.90) <sup>b</sup>		this work
<b>5b</b> , X = As	108.6 (-)	19.0 (1.90)	86.5 (5.12)		7a and this work
<b>5c</b> , X = Sb	113.6 (-)	23.0 (1.84)	93.5 (5.63)		8b
<b>5d</b> , X = Bi <sup>c</sup>	n.o. <sup>e</sup> (-)	29.1 (2.17)	109.6 (7.15)		9
$(\text{C}_4\text{Me}_4\text{X})_2\text{Fe}$					
<b>7a</b> , X = P <sup>c</sup>	94.0 <sup>e</sup> (-)	14.1 <sup>e</sup> (1.63) <sup>f</sup>	95.1 <sup>e</sup> (-) <sup>f</sup>	12.7 <sup>e</sup> (1.96)	6c
<b>7b</b> , X = As <sup>c</sup>	103.8 (-)	17.0 (1.73) <sup>d</sup>	97.2 (-)	13.9 (1.67) <sup>d</sup>	7d
<b>7c</b> , X = Sb <sup>c</sup>	105.6 (-)	20.9 (1.65) <sup>d</sup>	103.9 (-)	14.8 (1.50) <sup>d</sup>	7d
<b>7d</b> , X = Bi <sup>c</sup>	n.o. <sup>g</sup> (-)	26.1 (1.50) <sup>d</sup>	117.9 (-)	18.9 (1.86) <sup>d</sup>	this work
$(\text{C}_4\text{H}_2\text{-}\beta\text{-Me}_2\text{X})_2\text{Fe}$					
<b>11a</b> , X = P	82.1 <sup>h</sup> (3.71) <sup>i</sup>		97.5 <sup>h</sup> (-)	16.1 <sup>h</sup> (2.11)	6
<b>11b</b> , X = As	89.8 (4.32)		98.5 (-)	16.8 (2.05)	this work
<b>11c</b> , X = Sb	86.4 (3.90)		104.8 (-)	18.4 (2.01)	this work

<sup>a</sup>  $^1J_{\text{PC}} = 59.6$  Hz,  $^2J_{\text{PCH}} = 21.6$  Hz,  $^2J_{\text{PC}} = 0$  Hz. <sup>b</sup>  $^3J_{\text{PCH}_3} = 9.2$  Hz,  $^3J_{\text{PCH}} = 4.2$  Hz. <sup>c</sup> Solvent is  $\text{C}_6\text{D}_6$ . For all other compounds the solvent is  $\text{CDCl}_3$ . <sup>d</sup> Relative assignment of  $\alpha$  and  $\beta$  positions uncertain. <sup>e</sup>  $^2J_{\text{PCH}_3} = 24.4$  Hz,  $^1J_{\text{PC}} = 55.2$  Hz,  $^2J_{\text{PC}} = ^3J_{\text{PCH}_3} = 0$  Hz. <sup>f</sup>  $^3J_{\text{PCH}_3} = 9.4$  Hz. <sup>g</sup> n.o. = not observed. <sup>h</sup>  $^1J_{\text{PC}} = 61.6$  Hz,  $^2J_{\text{PC}} = 7.5$  Hz. <sup>i</sup>  $^2J_{\text{PCH}} = 36$  Hz.

**Scheme 1****Scheme 2**

sis.<sup>11</sup> We have previously reported on the preparation of **7b**<sup>7d</sup> and **7c**,<sup>7d</sup> while **7a** has been reported by Mathey and co-workers.<sup>6c</sup> Octamethyldibismaferrocene (**7d**) could be prepared from **6d** in a similar manner.

1-Phenyl-3,4-dimethylphosphole (**10a**) is readily available via the McCormack reaction.<sup>12</sup> The Mathey group converted **10a** to **11a**, which has been investigated in

detail.<sup>6</sup> There are no prior syntheses of the heavier heteroles **10b** and **10c**. We find that diiodide **8**<sup>8c</sup> is easily stereospecifically desilylated with  $\text{Bu}_4\text{NF}/\text{H}_2\text{O}$  to afford **9** in 86% yield. Lithiation of **9** with butyllithium followed by reaction with dichlorophenylphosphine affords **10a** in 82% yield (see Scheme 2). Arsole **10b** and stibole **10c** were prepared in the same manner using dichlorophenylarsine and dichlorophenylstibine, respectively. Alternatively we have prepared stibole **10c** by the desilylation of 2,5-bis(trimethylsilyl)-3,4-dimethylphenylstibole.<sup>8c</sup> Unfortunately, we have not been able to prepare useful quantities of bismole **10d**. Conversion of **10a-c** to the 3,3',4,4'-tetramethyl-1,1'-diheteroferrocenes (**11a-c**) takes place in good yield.  $^1\text{H}$  NMR and  $^{13}\text{C}$  NMR spectral parameters of polymethyl-1,1'-diheteroferrocenes are summarized in Table 1.

**Redox Behavior of 5 and 7.** We have explored the redox chemistry of the complete series **5a-d** and **7a-d** in dimethoxyethane at  $-45^\circ\text{C}$  using cyclic voltammetry. Since the redox behavior in the two series was completely analogous, we have decided against examining series **11**. Mathey and co-workers have previously studied **11a** and **2a**<sup>13</sup> under slightly different conditions, while we have previously reported on the redox behavior of **2b**.<sup>7c</sup>

(11) Fagan, P. J.; Nugent, W. A. *J. Am. Chem. Soc.* **1988**, *110*, 2310. Fagan, P. J.; Nugent, W. A.; Calabrese, J. C. *J. Am. Chem. Soc.* **1994**, *116*, 1880.

(12) Breque, A.; Mathey, F.; Savignac, P. *Synthesis* **1981**, 983.

(13) Lemoine, P.; Gross, M.; Braunstein, P.; Mathey, F.; Deschamps, B.; Nelson, J. H. *Organometallics* **1984**, *3*, 1303.

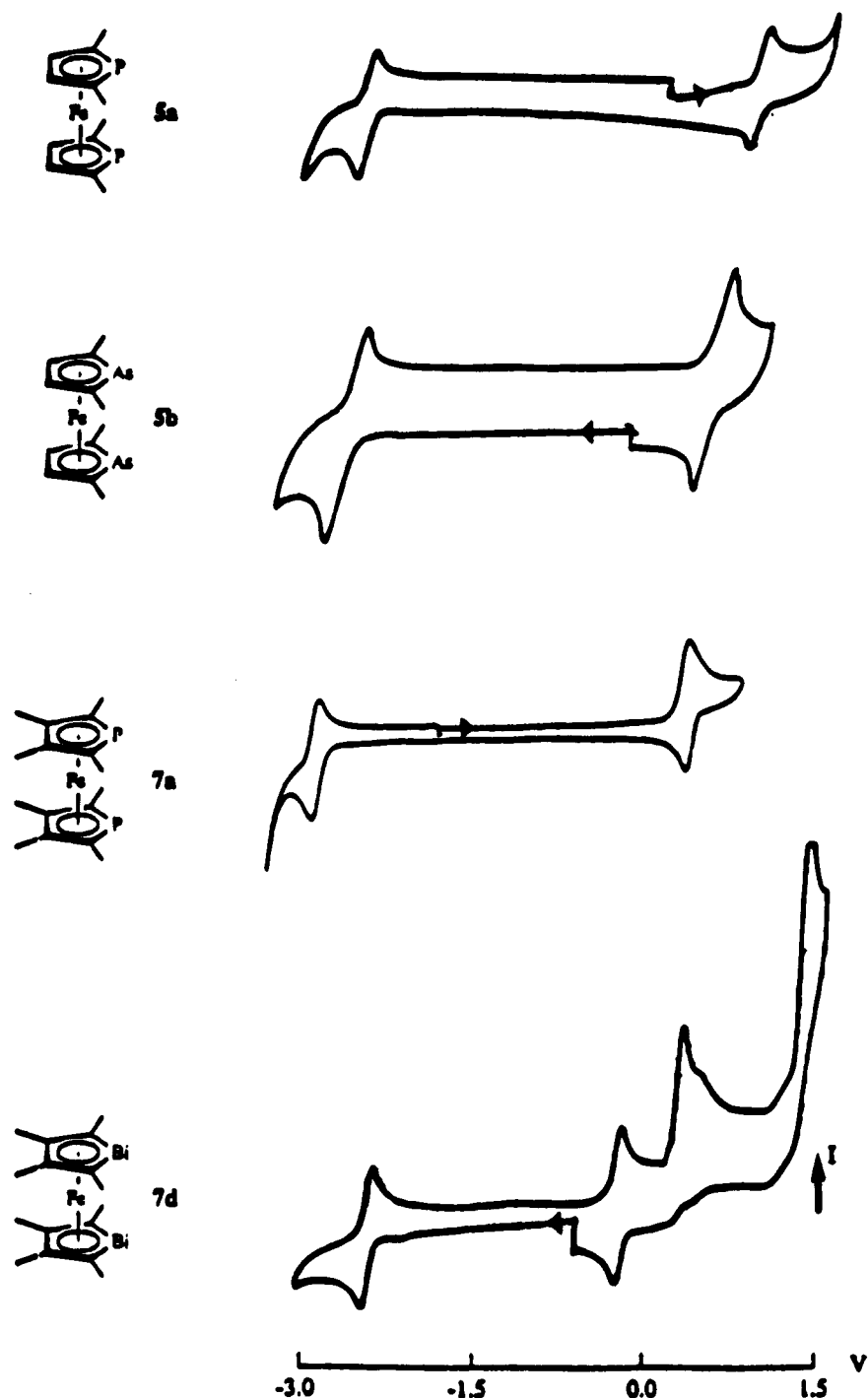


**Figure 1.** CV scans of  $(C_4H_2-\alpha-Me_2P)_2Fe$  (**5a**),  $(C_4H_2-\alpha-Me_2As)_2Fe$  (**5b**),  $(C_4Me_4P)_2Fe$  (**7a**), and  $(C_4Me_4Bi)_2Fe$  (**7d**) in DME/0.1 M  $Bu_4NClO_4$  at glassy carbon.  $T = -40^\circ C$ ,  $\nu = 100$  mV/s.

Like ferrocene,<sup>14</sup> the series of diheteroferrocenes **5** and **7** undergo one-electron oxidation ( $0/+$ ) to their radical cations and one-electron reduction ( $0/-$ ) to their radical anions. The ( $0/+$ ) redox processes are quasi-reversible, while the ( $0/-$ ) redox processes are irreversible. Representative traces are shown in Figure 1, while the data are summarized in Table 2.

In each series (**5** and **7**) the potentials  $E_{1/2}$  pertaining to the couples ( $0/-$ ) show monotonic anodic shifts, the potentials  $E_{1/2}(+/0)$  display cathodic shifts as the heteroatom increases in atomic number. Thus, it is easier to both oxidize and reduce the heavier diheterofer-

rocenes. This is synonymous with a decrease of the HOMO/LUMO gap, a gradation which is familiar from the free heterobenzenes.<sup>15</sup> The trends in the oxidations are interpreted more readily and will therefore be discussed first.

For oxidation, the cathodic shifts are nearly equivalent in both the tetramethyl (**5**) and the octamethyl (**7**) series. For the tetramethyl series, the shifts are  $P \rightarrow As$ , 144 mV;  $As \rightarrow Sb$ , 285 mV; and  $Sb \rightarrow Bi$ , 263 mV, while in the octamethyl series they are  $P \rightarrow As$ , 160 mV;  $As \rightarrow Sb$ , 264 mV; and  $Sb \rightarrow Bi$ , 274 mV. Since the

(14) Gubin, S. P. *Pure Appl. Chem.* **1970**, *23*, 463.

(15) Burrow, P. D.; Ashe, A. J., III; Belville, D. J.; Jordan, K. D. *J. Am. Chem. Soc.* **1982**, *104*, 425.

**Table 2. Cyclic Voltammetry Data for Various Redox Processes of the Complexes (C<sub>4</sub>H<sub>4</sub>X)<sub>2</sub>Fe, (C<sub>4</sub>H<sub>2</sub>-α-Me<sub>2</sub>X)<sub>2</sub>Fe, and (C<sub>4</sub>Me<sub>4</sub>X)<sub>2</sub>Fe<sup>a</sup>**

		$E_{1/2}(0/-)/V^b$	$\Delta E_p/mV^b$	$r^c$	$E_{1/2}(0/+)/V^b$	$\Delta E_p/mV^b$	$r^c$	$E_{pa}/V^d$
(C <sub>4</sub> H <sub>4</sub> X) <sub>2</sub> Fe	<b>2a</b>				[0.882]			
	<b>2b</b>	-2.190 <sub>r</sub>		0.98	0.730 <sub>r</sub>		1.0	
	<b>2c</b>				[0.453]			
	<b>2d</b>				[0.190]			
(C <sub>4</sub> H <sub>2</sub> -α-Me <sub>2</sub> X) <sub>2</sub> Fe	<b>5a</b>	-2.352 <sub>r</sub>	54	0.73	0.722 <sub>r</sub>	55	1.0	1.516
	<b>5b</b>	-2.258 <sub>r</sub>	57	0.79	0.578 <sub>r</sub>	56	1.0	1.089
	<b>5c</b>	-2.036 <sub>r</sub>	51	0.82	0.293 <sub>r</sub>	58	1.0	0.547
	<b>5d</b>	-2.004 <sub>r</sub>	76	0.83	0.030 <sub>r</sub>	75	1.0	0.344
(C <sub>4</sub> Me <sub>4</sub> X) <sub>2</sub> Fe	<b>7a</b>	-2.507 <sub>r</sub>	78	0.85	0.565 <sub>r</sub>	77	1.0	>1.6
	<b>7b</b>	-2.381 <sub>r</sub>	57	0.74	0.405 <sub>r</sub>	75	1.0	1.151
	<b>7c</b>	-2.176 <sub>r</sub>	66	0.86	0.141 <sub>r</sub>	76	1.0	0.607
	<b>7d</b>	-2.140 <sub>r</sub>	58	0.87	-0.133 <sub>r</sub>	58	1.0	0.35

<sup>a</sup> In DME/(n-Bu)<sub>4</sub>NClO<sub>4</sub> (0.1 M) at glassy carbon vs SCE,  $T = -40$  °C,  $v = 100$  mV s<sup>-1</sup>, values in square brackets are estimated. Abbreviations: *r*, reversible. <sup>b</sup>  $E_{1/2} = 1/2(E_{pa} + E_{pc})$ ;  $\Delta E_p = E_{pa} - E_{pc}$ . <sup>c</sup>  $t = i_{pa}/i_{pc}$ . <sup>d</sup> Peak potential of an irreversible wave.

magnitude of the atom shifts are independent of the degree of methyl substitution, it is likely that the same atom shifts apply to the unsubstituted diheteroferrocenes (**2**). Using the measured oxidation of **2b**, we predict that the as yet unknown unsubstituted 1,1'-distibaferrocene (**2c**) and 1,1'-dibismaferrocene (**2d**) will have  $E_{1/2}(0/+) = 0.450$  and  $0.190$  mV, respectively. The predicted value for 1,1'-diphosphaferrocene (**2a**),  $E_{1/2}(0/+) = 0.882$  mV, differs from the experimental value of  $E_{1/2}(0/+) = 0.780$  mV found by the Mathey group using different conditions.<sup>13</sup> We note that their value for  $E_{1/2}(0/+) of ferrocene (0.400 mV) and our value (0.490 mV) differ by virtually the same magnitude.$

MO treatments of the diheteroferrocenes indicate that the HOMO is effectively an Fe(*d*<sub>z<sup>2</sup>) orbital.<sup>7d,16</sup> Variation in the  $E_{1/2}(0/+)$  values in the diheteroferrocenes series should measure the ability of the heterocyclopentadienyl ligands, and hence the heteroatoms themselves, to donate electron density to Fe. We associate atom electron donation with the ionization potential (IP) of the atom. Indeed the ionization potentials of the free atoms (P, As, Sb, and Bi) correlate very well with  $E_{1/2}(0/+)$  values of series **5** and **7**. In Figure 2 we plot  $E_{1/2}(0/+)$  of **5** and **7** with the IP(X) of the free atoms X = P, As, Sb, and Bi (<sup>4</sup>S<sub>3/2</sub> → <sup>3</sup>P<sub>0</sub>): P, 11.0 eV; As, 9.81 eV; Sb, 8.64 eV; and Bi, 7.29 eV<sup>17</sup> as independent variables. The least-squares fit yields</sub>

$$E_{1/2}(0/+) (\mathbf{5}) = 0.219(\text{IP}) - 1.758v \quad (1)$$

$$R = 0.999$$

and

$$E_{1/2}(0/+) (\mathbf{7}) = 0.192(\text{IP}) - 1.519v \quad (2)$$

$$R = 0.995$$

As has previously been found for **2a**<sup>13</sup> and **2b**,<sup>7c</sup> the diphosphaferrocenes and the diarsaferrocenes are harder to oxidize than are the corresponding substituted ferrocenes (see Table 2). The distibaferrocenes have nearly the same  $E_{1/2}(0/+)$  as the ferrocenes, while only dibismaferrocenes are easier to oxidize. Thus the P and As heterocyclopentadienyl groups are more effective at withdrawing electron density from Fe in **2**, **5**, and **7** than

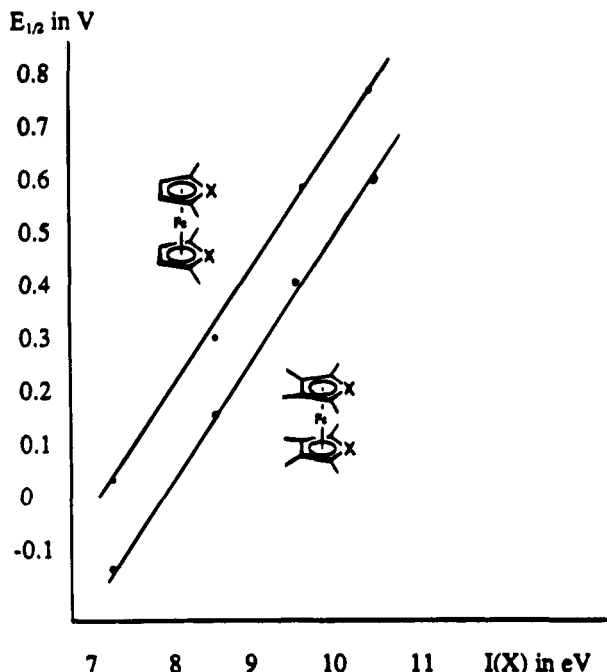


**Figure 2.** Regressions of the  $E_{1/2}(0/+)$  of the 2,2',5,5'-tetramethyl-1,1'-diheteroferrocenes, (C<sub>4</sub>H<sub>2</sub>-α-Me<sub>2</sub>X)<sub>2</sub>Fe (**5**) (top line) and the 2,2',3,3',4,4',5,5'-octamethyl-1,1'-diheteroferrocenes, (C<sub>4</sub>Me<sub>4</sub>X)<sub>2</sub>Fe (**7**) (bottom line) on the atomic ionization energies  $I(X)$  of the free atoms X = P, As, Sb, and Bi.

are the corresponding substituted cyclopentadienyl rings of ferrocenes. A similar conclusion was reached in a comparison of the redox behavior of bis( $\eta^6$ -heterobenzene) metal complexes (E = P, As) with those of the **1a** and **1b**.<sup>7c,18</sup> It may seem paradoxical that replacement of C by atoms with lower Pauling electronegativities results in raising the  $E_{1/2}(0/+)$  values. However, evidence from MCD of the closely related heterobenzenes (**1**) has shown that the effective  $\pi$ -electronegativities of P, As, and perhaps Sb are greater than C.<sup>19</sup>

The average difference in  $E_{1/2}(0/+)$  between the pairs of diheteroferrocenes which differ by four methyl groups (**2b**–**5b**, **5b**–**7b**, **5c**–**7c**, and **5d**–**7d**) is 0.162 V or 40.5 mV/methyl group. Thus each methyl group enhances

(16) (a) Kostic, N. M.; Fenske, R. F. *Organometallics* **1983**, *2*, 1008. (b) Guimon, C.; Gonbeau, D.; Pfister-Guillouzo, G.; de Lauzon, G.; Mathey, F. *Chem. Phys. Lett.* **1984**, *104*, 560. (c) Su, M.-D.; Chu, S.-Y. *J. Phys. Chem.* **1989**, *93*, 6043.

(17) Moore-Sitterley, C. E. *Natl. Bur. Stand. Circ.* **1949**, *1*, 1952, 2; **1958**, 3.

(18) Elschenbroich, Ch.; Nowotny, M.; Metz, B.; Massa, W.; Graulich, J.; Biehler, K.; Sauer, W. *Angew. Chem., Int. Ed. Engl.* **1991**, *30*, 547. (b) Elschenbroich, Ch.; Bär, F.; Bilger, E.; Mahrwald, D.; Nowotny, M.; Metz, B. *Organometallics* **1993**, *12*, 3373.

(19) Waluk, J.; Klein, H.-P.; Ashe, A. J., III; Michl, J. *Organometallics* **1989**, *8*, 2804.

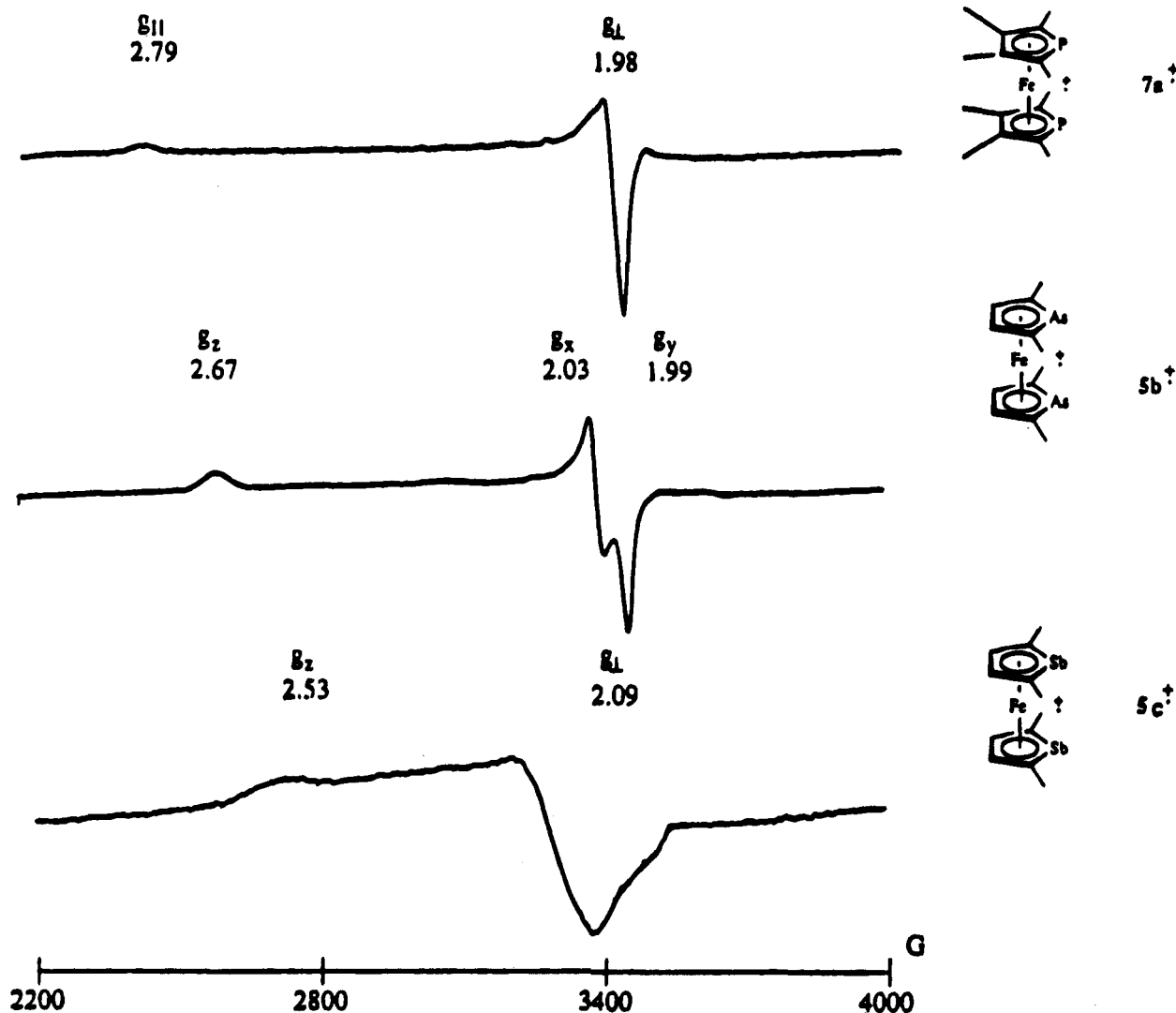


**Figure 3.** EPR spectra of the radical cations  $7a^{+\bullet}$ ,  $5b^{+\bullet}$ , and  $5c^{+\bullet}$  obtained from the neutral precursors by means of oxidation with  $AgBF_4$  in 1,2-dichloroethane at 100 K.

the oxidation by 40.5 mV. This value is somewhat smaller than the 47 mV/methyl group found for metallocenes.<sup>20</sup>

The trends in the  $E_{1/2}(0/-)$  redox values match those of  $E_{1/2}(0/+)$  in only a qualitative way. The heavier diheteroferrocenes are easier to reduce. However, the magnitude of the shifts are not constant between the tetramethyl and the octamethyl series. The qualitative MO treatments suggest that the LUMO's into which the extra electron must be placed in the radical anion have a metal-ligand character.<sup>7d,16</sup> The exact mix between ligand and metal may change in the series. If so we would not expect to see a simple trend in the values of  $E_{1/2}(0/-)$ . Indeed no simple trend is obvious to us.

**EPR Spectroscopy.** We have attempted to observe products of oxidation of **5** and **7** using EPR spectroscopy. The stability of ferrocenium ions is strongly dependent on the medium, and the decomposition to solvated Fe(III) has led to a controversy during early EPR studies of the ferrocenium ion.<sup>21</sup> Prins' original data<sup>21a</sup> are now

generally accepted. The group 15 diheteroferrocenium ions are even less stable in solution.<sup>13</sup> They were generated as soluble salts through oxidation of the parent neutral complexes with  $AgBF_4$  in 1,2-dichloroethane. During this manipulation, the solution turns violet and a precipitate forms. No EPR signals are observed for the supernatant solution at ambient temperature. The low-temperature EPR spectra of  $7a^{+\bullet}$ ,  $5b^{+\bullet}$  and  $5c^{+\bullet}$  are shown in Figure 3. Two trends are discernible: with increasing atomic number of the heteroatom, the  $g$  anisotropy ( $\Delta g = g_{\parallel} - g_{\perp}$ ) of the diheteroferrocenium radical cations decreases and the difference between the components  $g_x$  and  $g_y$  of  $g_{\perp}$  increases. The latter effect may be rationalized by the increase in interannular interaction between the heteroatoms which creates a barrier to ring rotation, favoring the eclipsed cis conformation for **5b** and **5c**.<sup>7d,16</sup> In this static situation,  $g_x$  and  $g_y$  must differ. Contrarily, for  $7a^{+\bullet}$  free ring rotation averages  $g_x$  and  $g_y$  leading to the observation of a single value  $g_{\perp}$ . The diminishing anisotropy  $\Delta g(2e^{+\bullet}) \gg \Delta g(7a^{+\bullet}) > \Delta g(5b^{+\bullet}) > \Delta g(5c^{+\bullet})$  correlates with the extent of perturbation introduced by the heteroatoms. For the ferrocenium ion  $2e^{+\bullet}$  the very large deviation of  $g_{\parallel}$  and  $g_{\perp}$  from the free spin value is attributed to the degeneracy of the ground state  $^2E_{2g}$ -

(20) Sabbatini, M. M.; Cesarotti, E. *Inorg. Chim. Acta* **1977**, *24*, L9.

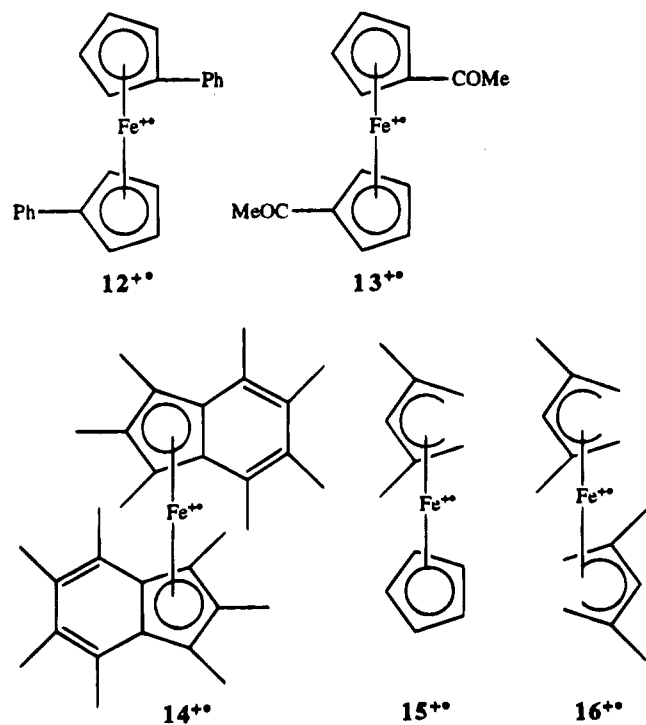
(21) (a) Prins, R. *Mol. Phys.* **1970**, *19*, 603. (b) Horsfield, A.; Wassermann, A. *J. Chem. Soc., Dalton Trans.* **1972**, 187. (c) Warren, K. D. *Struct. Bonding* **1976**, *27*, 45. (d) Ammeter, J. H. *J. Magn. Res.* **1978**, *30*, 299.

**Table 3.** *g*-Factor Anisotropies for Selected Ferrocenium, Diheteroferrocenium, and Related Ions

compd	$g^1, g_{  }$	$g^2$	$g_{\perp}$	$g^3$	EPR (25 °C fluid solution)
<b>2e<sup>+</sup></b> <sup>a</sup>	4.35		1.26		—
<b>12<sup>+</sup></b> <sup>a</sup>	3.98		1.58		—
<b>13<sup>+</sup></b> <sup>a</sup>	2.62		1.76		—
<b>21<sup>+</sup></b> <sup>b</sup>	2.93		2.15		—
<b>7a<sup>+</sup></b> <sup>c</sup>	2.79 <sup>d</sup>		1.98 <sup>d</sup>		—
<b>5b<sup>+</sup></b> <sup>c</sup>	2.67	2.03	(2.01) <sup>e</sup>	1.99	—
<b>5c<sup>+</sup></b> <sup>c</sup>	2.53		2.09		—
<b>15<sup>+</sup></b> <sup>e</sup>	2.225	2.103	(2.051) <sup>f</sup>	2.002	+
<b>16<sup>+</sup></b> <sup>e</sup>	2.182	2.069	(2.043) <sup>f</sup>	2.016	+

<sup>a</sup> Reference 21a. <sup>b</sup> Reference 22. <sup>c</sup> This work. <sup>d</sup> For (C<sub>6</sub>H<sub>2</sub>–βMe<sub>2</sub>P)<sub>2</sub>Fe<sup>+</sup> (**11a<sup>+</sup>**) the values  $g_{||} = 2.72$  and  $g_{\perp} = 1.99$  have been obtained previously. Reference 13. <sup>e</sup> Reference 23. <sup>f</sup> Average:  $g_{\perp} = 1/2(g_x + g_y)$ .

[( $a_{1g}$ )<sup>2</sup>( $e_{2g}$ )<sup>3</sup>],  $\Delta g$  being strongly dependent on variations in the molecular environment.<sup>21d</sup> Since peripheral substitution at **2e<sup>+</sup>** raises orbital degeneracy, the anisotropy  $\Delta g$  changes inversely proportional to the degree of perturbation. Radical cations **2e<sup>+</sup>**, **12<sup>+</sup>**, **13<sup>+</sup>**, **14<sup>+</sup>**, **15<sup>+</sup>**, and **16<sup>+</sup>** can be viewed as an ordered series



of ferrocenium ions with increasing degree of perturbation. Table 3 presents the *g* factor anisotropy for this series and for diheteroferrocenium ions **7a<sup>+</sup>**, **5b<sup>+</sup>**, and **5c<sup>+</sup>**. It is seen that the perturbation inflicted by inclusion of a group 15 heteroatom into the  $\eta^5$ -perimeter lies between those caused by condensation of benzene rings to the sandwich unit and by opening the  $\pi$ -bonded perimeter. Along the series depicted in Table 3 a change in ground state symmetry from  ${}^2E_{2g}[(a_{1g})^2(e_{2g})^3]$  to  ${}^2A_1[(e_{2g})^4(a_{1g})]$  occurs, the latter having been assigned to **14<sup>+</sup>** on the basis of photoelectron spectroscopy<sup>22</sup> and to **16<sup>+</sup>** by means of INDO calculations.<sup>23</sup> Thus, as

(22) O'Hare, D.; Green, J. C.; Marder, T.; Collins, S.; Stringer, G.; Kakkar, A. K.; Kaltsoyannis, N.; Kuhn, A.; Lewis, R.; Mehnert, C.; Scott, P.; Kurmoo, M.; Pugh, S. *Organometallics* **1992**, *11*, 48.

(23) Elschenbroich, Ch.; Bilger, E.; Ernst, R. D.; Wilson, D. R.; Kralik, M. S. *Organometallics* **1985**, *4*, 2068.

inferred from EPR, the ground state of the group 15 heteroferrocenium cations should also be  ${}^2A_1$  with the single occupancy of an iron  $3d_{z^2}$  orbital. Predominantly Fe  $3d_{z^2}$  quality of the HOMO for diphosphaferrocene had also been deduced from quantum chemical calculations of the Fenske–Hall type and the extended Hückel and MS X $\alpha$  varieties.<sup>16</sup> The decrease in symmetry from  $D_{5h}$  in ferrocene to  $C_{2v}$  for the diheteroferrocenes (in their cis-eclipsed conformation) allows for mixing of  $3d_{z^2}$  with  $3d_{x^2-y^2}$  and with ligand orbitals. Therefore, the calculation of the *g* tensor for a diheteroferrocene would be a formidable task. Even if this could be accomplished, comparison with experiment would suffer from the absence of a single-crystal EPR study of magnetically dilute material.

**Electrophilic Aromatic Substitution.** 1,1'-Diphosphaferrocene (**2a**)<sup>6a</sup> and 1,1'-diarsaferrocene (**2b**)<sup>7c</sup> undergo electrophilic aromatic substitution at the position  $\alpha$  to the heteroatoms. 3,3',4,4'-Tetramethyl-1,1'-distibaferrocene (**11c**) is the first example of a stibaferrocene with this (presumed) more reactive position available. Thus it is of considerable interest to examine the aromatic chemistry of the series **11a–c** (Scheme 3).

Mathey has found that acetylation of **11a** using acetyl chloride and aluminum chloride affords a monoacetyl product **17a** or a mixture of diastereomeric diacetyl products **18a** and **19a**.<sup>6a</sup> We find that 3,3',4,4'-tetramethyl-1,1'-diarsaferrocene **11b** reacts in an identical manner. Acetylation of **11b** with 1 equiv of acetyl chloride gives **17b** in 54% yield. Acetylation of **11b** with an excess of acetyl chloride gives a mixture of diacetyl products in the ratio of 3:5. It is possible to separate the meso and racemic products **18b** and **19b** by chromatography, but their spectra do not allow a structural assignment.

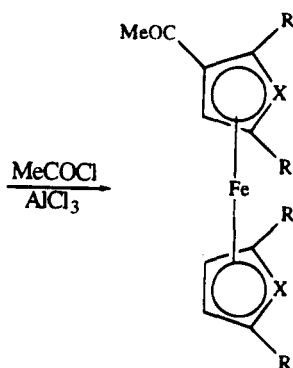
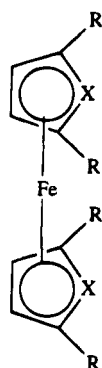
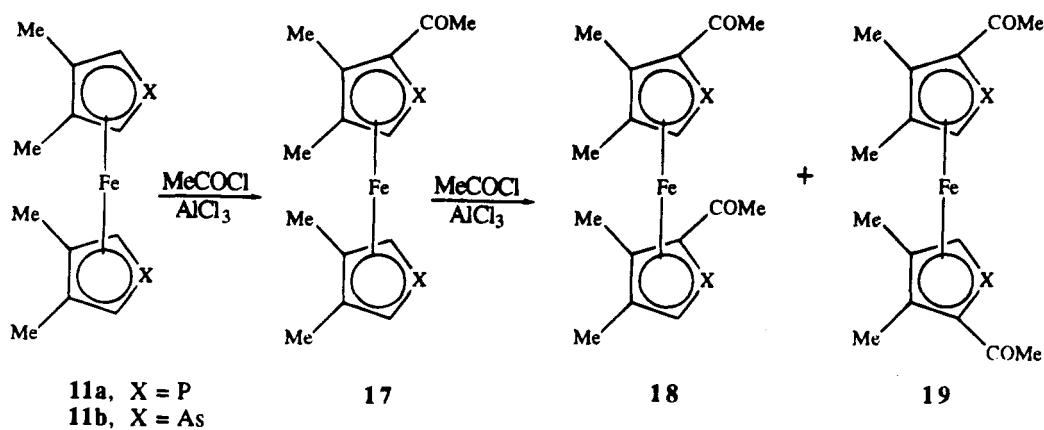
If the reactive  $\alpha$  positions of 1,1'-diphosphaferrocenes are blocked, substitution can still take place at the  $\beta$ -position. Thus acetylation of 2,2',5,5'-tetraphenyldiphosphaferrocene **20a** gives 3-acetyl derivative **21a** as well as phenyl-substituted product **22**.<sup>24</sup> In the same manner we find that acetylation of **5b** gives the 3-acetyl product **23b**.

Unfortunately, treatment of either **11c** or **5c** with acetyl chloride, under the conditions which acetylated **11b**, led to formation of an intractable precipitate and complete destruction of the distibaferrocene.

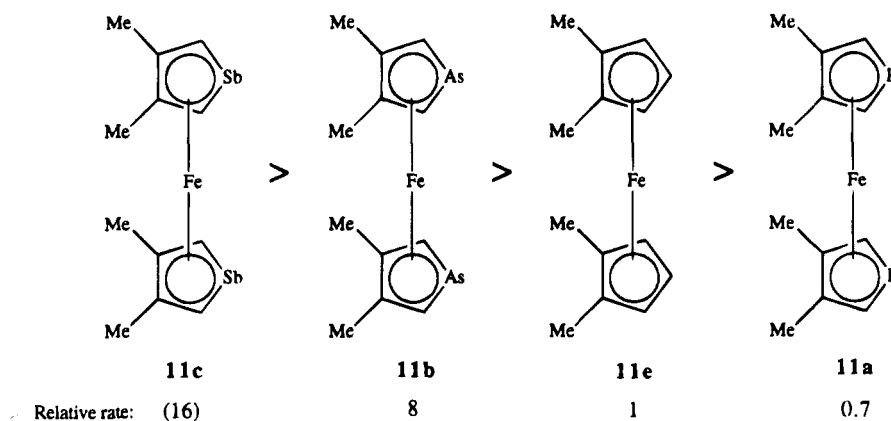
Since acetylation of distibaferrocene **11c** failed, we decided to study the simpler acid catalyzed H/D exchange of **11a–c**. Treating either **11a** or **11b** with trifluoroacetic acid- $d_1$  at  $-22$  °C led to immediate exchange of all four  $\alpha$ -protons as indicated by the  ${}^1\text{H}$  NMR spectra and mass spectra of the reisolated diheteroferrocene. Similar reaction of **11c** with trifluoroacetic acid- $d_1$  at  $-22$  °C led to the immediate formation of an intractable precipitate. However a solution of **11c** in 0.1 M trifluoroacetic acid- $d_1$  in toluene is stable at  $-22$  °C. Warming this solution to 0 °C leads to slow fading of red color of **11c** concurrently with the formation of precipitate. Yet reisolation of the distibaferrocene from solutions held at  $-20$  °C for 20 min showed that **11c** had incorporated deuterium. Deuteration of **11c** is the first example of any electrophilic substitution for an antimony–carbon heteroaromatic.

(24) Roberts, R. M. G.; Wells, A. S. *Inorg. Chim. Acta* **1987**, *130*, 93.

## Scheme 3



## Scheme 4. Relative Rates of H/D Exchange



It is of interest to compare the relative rates of H/D exchange of 11a–c, and the corresponding 1,1',2,2'-tetramethylferrocene (11e).<sup>25</sup> Solutions of pairs of compounds 11a, 11b, and 11e in methylene chloride were added to trifluoroacetic acid-*d*<sub>1</sub> at –22 °C. Because of the great lability of 11c, the relative rates were determined in toluene containing trifluoroacetic acid-*d*<sub>1</sub>. Thus the relative rate of exchange of 11c is only qualitatively comparable. The relative rates of exchange are summarized in Scheme 4.

The rates of acid-catalyzed H/D exchange in substituted ferrocenes have been found to correlate with their oxidation potentials.<sup>26</sup> This correlation is plausibly

explained by noting that protonation (deuteration) of ferrocene (2e) to form intermediate 24e<sup>27</sup> effectively removes electron density from the iron-bound system as does actual oxidation to 2e<sup>+</sup> (see Scheme 5).<sup>28</sup>

Qualitatively the diheteroferrocenes 11a–c fit this pattern since the more easily oxidized diarsaferrocene and distibaferrocene undergo H/D exchange faster than the diposphaferrocene. However, diarsaferrocene 11b and distibaferrocene 11c undergo H/D exchange faster

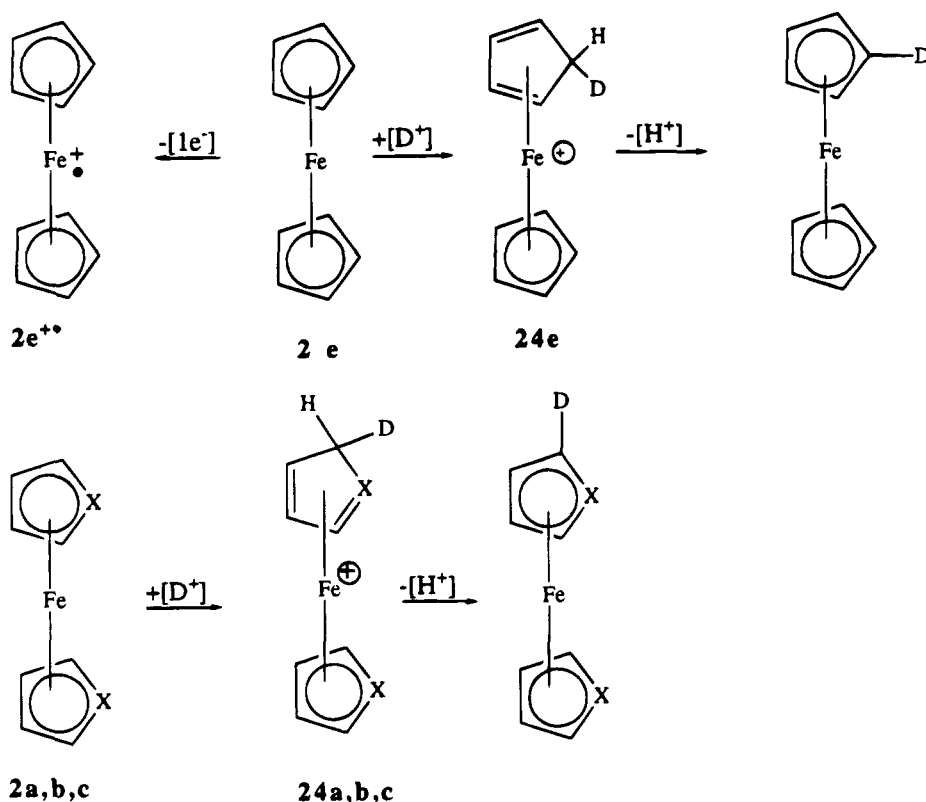
(26) Setkina, V. N.; Kursanov, D. N. *Russ. Chem. Rev.* **1968**, *37*, 737.

(27) Iron–electrophile complexes may also be intermediates. For a recent discussion, see: Cunningham, A. F., Jr. *Organometallics* **1994**, *13*, 2480.

(28) However, see: McKee, M. L. *J. Am. Chem. Soc.* **1993**, *115*, 2818.

(25) Miller, L. L.; Valentine, J. R. *J. Am. Chem. Soc.* **1988**, *110*, 3982.

Scheme 5



than the corresponding ferrocene (**11e**), even though diarsaferrocenes are harder to oxidize than ferrocenes, while distibaferrocenes have  $E_{1/2}(0/+)$  values comparable with those of ferrocenes. Thus, other factors must be involved.

We note that the formation of intermediate **24** from the diheteroferrocene involves the loss of delocalized bonding of the heterocyclopentadienyl group. A lower delocalization energy should correspond to a higher rate of H/D exchange. Recent experimental results from a gas phase acidity study indicate that the delocalization energy of the phospholyl anion ( $C_4H_4P^-$ ) is comparable with that of  $C_5H_5^-$  but the arsoly anion ( $C_4H_4As^-$ ) has a smaller delocalization energy.<sup>29</sup> Although there are neither experimental data nor calculations on  $C_4H_4Sb^-$ , the general trend toward weaker  $\pi$ -bonding for the heavier main group elements,<sup>2,3</sup> suggests that its delocalization energy would be smaller than that of  $C_4H_4As^-$ . Therefore the higher rates of H/D exchange of **11b** and **11c** are consistent with lower delocalization energies of the heavier heterocyclopentadienyl systems.

### Experimental Section

**General Remarks.** All reactions were carried out under an atmosphere of argon. Solvents were dried by using standard procedures. The mass spectra were determined by using a VG-70-S spectrometer, while the NMR spectra were obtained by using either a Bruker WH-360 or AM-300 spectrometer on solutions in  $CDCl_3$  or  $C_6D_6$ . The  $^1H$  and  $^{13}C$  NMR spectra were calibrated by using signals from the solvents referenced to  $Me_4Si$ . The combustion analyses were determined by the Analytical Services of the Department of Chemistry, University of Michigan. Cyclic voltammetry was performed with electrochemical equipment from AMEL (Mi-

lano) consisting of a model 552 potentiostat, model 568 function generator, model 563 multipurpose unit, Nicolet model 3091 storage oscilloscope, and Kipp and Zonen model BD 90x/y recorder. The electrochemical cell was operated under an atmosphere of argon, with glassy carbon, platinum rod, and saturated calomel (SCE) serving as working, counter, and reference electrodes, respectively. For temperature control, the cell was immersed in a thermostated cooling bath.

**Materials.** Trifluoroacetic acid- $d_1$  was prepared by mixing 1 equiv of deuterium oxide with trifluoroacetic anhydride. Dichlorophenylarsine,<sup>30</sup> dichlorophenylstibine,<sup>31</sup> and diiodophenylbismuthine<sup>32</sup> were prepared by standard methods. Compounds **5b**,<sup>7a</sup> **5c**,<sup>8a,b</sup> **5d**,<sup>9</sup> **7a**,<sup>6c</sup> **7b**,<sup>7d</sup> **7c**,<sup>7d</sup> **11a**,<sup>6</sup> and **11e**<sup>25</sup> were prepared by routes reported in the literature. Properties were consistent with those originally reported. All other materials are available commercially.

**(1Z,3Z)-1,4-Diido-2,3-dimethyl-1,3-butadiene (9).**<sup>33</sup> A solution of (1Z,3Z)-1,4-bis(trimethylsilyl)-1,4-diido-2,3-dimethyl-1,3-butadiene (1.5 g, 3.1 mmol) in 10 mL of THF was treated with 7 mL of a 1.0 M solution of tetrabutylammonium fluoride in THF containing 5%  $H_2O$  with stirring at 0 °C. Stirring was continued at 0 °C for 20 min, after which 10 mL of water was added and the resulting mixture was extracted with 50 mL of hexane. The extracts were dried over anhydrous  $MgSO_4$ . Removal of the solvent under vacuum left 0.9 g (86%) of white crystals, mp 34 °C.  $^1H$  NMR ( $CDCl_3$ ):  $\delta$  1.96 (d,  $J = 1.5$  Hz, 2H), 6.05 (q,  $J = 1.5$  Hz, 6H).  $^{13}C$  NMR ( $CDCl_3$ ):  $\delta$  21.7, 74.9, 150.1. MS (EI) exact mass: calcd for  $C_6H_8I_2$ ,  $m/z$  333.8716; found,  $m/z$  333.8723.

**1-Phenyl-3,4-dimethylstibole (10c).** (a) 1-Phenyl-2,5-bis(trimethylsilyl)-3,4-dimethylstibole (0.5 g, 1.2 mmol) was added to 10 mL of a 1.0 M solution of tetrabutylammonium fluoride in THF containing 5%  $H_2O$ . The solution was then heated to

(30) Barker, R. L.; Booth, E.; Jones, W. E.; Millidge, A. F.; Woodward, F. N. *J. Soc. Chem. Ind.* **1949**, 68, 289.

(31) Nunn, M.; Sowerby, D. B.; Wesolek, D. M. *J. Organomet. Chem.* **1983**, 251, C45.

(32) Wilkinson, J. F.; Challenger, F. *J. Chem. Soc.* **1924**, 125, 854.

(33) The procedure was originated by Mr. Jack Waas of the University of Michigan in 1994.

(29) Sunderlin, L. S.; Panu, D.; Puranik, D. B.; Ashe, A. J., III; Squires, R. R. *Organometallics* **1994**, 13, 4732.

80 °C for 6 h. After cooling to 25 °C, 10 mL of water was added and the resulting mixture was extracted with hexane (3 × 30 mL). The combined extracts were washed with dilute aqueous HCl and then water. After drying over anhydrous MgSO<sub>4</sub> the solvent was removed under reduced pressure, affording 0.24 g (73%) of **10c** as a yellow oil. (b) A solution of 2.5 N butyllithium in hexane (1.5 mL, 3.75 mmol) was added dropwise to a solution of (1Z,3Z)-1,4-diiodo-2,3-dimethyl-1,3-butadiene (0.61 g, 1.8 mmol) in 50 mL of ether at -78 °C with stirring. Stirring was continued for 90 min at -78 °C, after which the solution was allowed to warm to 25 °C. After stirring an additional 20 min at 25 °C the solution was recooled to -78 °C and then added to a solution of dichlorophenylstibine (0.5 g, 1.9 mmol) in 20 mL of ether at -78 °C. The color changed to yellow on addition. After stirring at -78 °C for 90 min, the mixture was allowed to warm to 25 °C. The solvent was removed under vacuum, and the residue was extracted with hexane. Removal of the solvent from the extract gave 0.39 g (77%) of product as a yellow oil. <sup>1</sup>H NMR (CDCl<sub>3</sub>): δ 2.06 (s, 6H), 6.84 (s, 2H), 7.21–7.32 (m, 5H). <sup>13</sup>C NMR (CDCl<sub>3</sub>): δ 22.5 (CH<sub>3</sub>), 135.5, 157.5 (vinyl C), 135.8, 133.3, 128.5, 128.3 (C<sub>6</sub>H<sub>5</sub>). MS (EI) exact mass: calcd for C<sub>12</sub>H<sub>13</sub>-<sup>121</sup>Sb, *m/z* 278.0055; found *m/z* 278.0052.

**1-Phenyl-3,4-dimethylphosphole (10a).** In a similar manner the reaction of (1Z,3Z)-1,4-diiodo-2,3-dimethyl-1,3-butadiene (1.08 g, 3.2 mmol) with 2.6 mL of 2.5 M solution of butyllithium in hexane, followed by the reaction with dichlorophenylphosphine (0.58 g, 3.2 mmol) afforded 0.5 g (82%) of **10a**. The <sup>1</sup>H NMR spectrum of **10a** prepared in this manner is identical to that reported.<sup>12</sup>

**1-Phenyl-3,4-dimethylarsole (10b).** In the same manner as procedure b above, the reaction of (1Z,3Z)-1,4-diiodo-2,3-dimethyl-1,3-butadiene (0.81 g, 2.4 mmol) with 2.5 N butyllithium in hexane (1.9 mL, 4.8 mmol), followed by the reaction of dichlorophenylarsine (0.54 g, 2.4 mmol) afforded 1-phenyl-3,4-dimethylarsole (0.45 g, 40%) as a yellow oil. <sup>1</sup>H NMR (CDCl<sub>3</sub>): δ 2.07 (s, 6H), 6.65 (s, 2H), 7.32–7.21 (m, 5H). <sup>13</sup>C NMR (CDCl<sub>3</sub>): δ 18.9 (CH<sub>3</sub>), 150.8 (vinyl C), 136 (vinyl C), 134.6, 133.0, 128.3, 128.2 (C<sub>6</sub>H<sub>5</sub>). MS (EI) exact mass: calcd for C<sub>12</sub>H<sub>13</sub>As, *m/z* 232.0233; found, *m/z* 232.0240.

**3,3',4,4'-Tetramethyl-1,1'-distibaferrocene (11c).** An excess (0.5 g) of lithium wire cut into small pieces was added to a solution of 1-phenyl-3,4-dimethylstibole (0.59 g, 2.1 mmol) in 20 mL of THF at 25 °C. The color changed to dark red while stirring was continued for 12 h. The solution was decanted from the excess lithium and cooled to -78 °C. Ammonia gas was passed through the solution for 5 min, after which the solution was allowed to warm to 25 °C. The mixture was recooled to -78 °C and cannulated into a suspension of FeCl<sub>2</sub> (0.13 g, 1.05 mmol) in 20 mL of THF at -78 °C. The mixture was allowed to warm to 25 °C and then was stirred for 12 h. The solvent was removed leaving a red residue, which was extracted with hexane (3 × 30 mL). The combined extracts were cooled to -78 °C, affording 0.15 g (31%) of a red crystalline product, mp 295 °C. (decomp). <sup>1</sup>H NMR (C<sub>6</sub>D<sub>6</sub>): δ 1.80 (s, 6H), 3.80 (s, 2H). Anal. Calcd for C<sub>12</sub>H<sub>16</sub>FeSb<sub>2</sub>: C, 31.35; H, 3.51. Found: C, 31.75; H, 3.50. MS (EI) exact mass: calcd for C<sub>12</sub>H<sub>16</sub><sup>56</sup>Fe<sup>121</sup>Sb<sub>2</sub>, *m/z* 457.8678; found, *m/z* 457.8673.

**2,2',5,5'-Tetramethyl-1,1'-diphosphaferrocene (5a).** In a similar manner, the reaction of 1-phenyl-2,5-dimethylphosphole (0.60 g, 3.2 mmol) with 0.4 g of lithium metal followed by the reaction with FeCl<sub>2</sub> (0.20 g, 1.6 mmol) afforded 0.14 g (32%) of **5a** as a red-orange oil. MS (EI) exact mass: calcd for C<sub>12</sub>H<sub>16</sub><sup>56</sup>FeP<sub>2</sub>, *m/z* 278.0077; found, *m/z* 278.0098.

**3,3',4,4'-Tetramethyl-1,1'-diarsaferrocene (11b).** In a similar manner, reaction of 3,4-dimethyl-1-phenylarsole (0.42 g, 2.02 mmol) with Li wire (0.5 g) followed by reaction with FeCl<sub>2</sub> (0.12 g, 1.0 mmol) afforded 0.13 g (35% yield) of **11b** as a red crystalline solid, mp 305 °C (decomp). Anal. Calcd for C<sub>12</sub>H<sub>16</sub>As<sub>2</sub>Fe: C, 39.38; H, 4.41. Found: C, 39.47; H, 4.31. <sup>1</sup>H

NMR (C<sub>6</sub>D<sub>6</sub>): δ 2.05 (s, 6H), 4.32 (s, 2H). MS (EI) exact mass: calcd for C<sub>12</sub>H<sub>16</sub>As<sub>2</sub><sup>56</sup>Fe, *m/z* 365.9033; found, *m/z* 365.9033.

**2,2',3,3',4,4',5,5'-Octamethyl-1,1'-dibismaferrocene (7d).** In a similar manner, the reaction of 1-phenyl-2,3,4,5-tetramethylbismole (0.80 g, 2.2 mmol) with 0.5 g of lithium metal at -10 °C followed by reaction with FeCl<sub>2</sub> (0.14 g, 1.1 mmol) at 0 °C afforded a 2:1 mixture of **7d** and 2,2',3,3',4,4',5,5'-octamethyl-1,1'-bibismole.<sup>34</sup> After removal of solvent from this mixture, the residue was extracted at 0 °C first with 60 mL of pentane and then with 20 mL of toluene. After filtration and cooling to -78 °C for 12 h, 60 mg (9%) of the bibismole were isolated from the pentane fraction. The <sup>1</sup>H and <sup>13</sup>C NMR spectra of this material were identical to that reported.<sup>9</sup> On cooling to -78 °C, the toluene extracts furnished 150 mg (21%) of **7d** as shiny black needles, which decomposed on heating above 100 °C. <sup>1</sup>H NMR (C<sub>6</sub>D<sub>6</sub>): δ 1.50 (s, 12H), 1.86 (s, 12H). MS (EI) exact mass: calcd for C<sub>16</sub>H<sub>24</sub>Bi<sub>2</sub><sup>56</sup>Fe, *m/z* 690.0835; found, *m/z* 690.0799.

**3-Acetyl-2,2',5,5'-tetramethyl-1,1'-diarsaferrocene (23b).** A solution of 2,2',5,5'-tetramethyl-1,1'-diarsaferrocene (85 mg, 0.23 mmol) in 2 mL of methylene chloride was added dropwise with stirring to a mixture of aluminum chloride (70 mg, 0.46 mmol) and acetyl chloride (36 mg, 0.46 mmol) in 5 mL of methylene chloride at 25 °C. The mixture was heated to reflux for 5 h, after which time it was added to 50 mL of ice water. The organic layer was separated, washed with 30 mL of saturated aqueous NaHCO<sub>3</sub>, and dried over anhydrous calcium chloride. The solvent was removed under reduced pressure leaving a red residue, which was purified by column chromatography on activated silica gel. The unreacted starting material was eluted with toluene, while the product was eluted with acetonitrile/toluene (1:9, v/v). The product (20 mg, 21%) was isolated as dark red crystals, mp 54–55 °C. <sup>1</sup>H NMR (C<sub>6</sub>D<sub>6</sub>): δ 1.49 (s, 3H), 1.58 (s, 3H), 1.67 (s, 3H), 1.81 (s, 3H), 2.15 (s, 3H), 4.37 (d, *J* = 4 Hz, 1H), 4.88 (d, *J* = 4 Hz, 1H), 5.57 (s, 1H). MS (EI): 408 (M<sup>+</sup> for C<sub>13</sub>H<sub>18</sub>As<sub>2</sub><sup>56</sup>FeO). IR (CDCl<sub>3</sub>): 1650 cm<sup>-1</sup>.

**2-Acetyl-3,3',4,4'-tetramethyl-1,1'-diarsaferrocene (17b).**<sup>35</sup> A solution of 3,3',4,4'-tetramethyl-1,1'-diarsaferrocene (50 mg, 0.13 mmol) in 5 mL of methylene chloride was added dropwise with stirring to a mixture of aluminum chloride (20 mg, 0.15 mmol) and acetyl chloride (13 mg, 0.16 mmol) in 10 mL of methylene chloride at 0 °C. The reaction mixture was allowed to stir at 25 °C for 4 h, after which time it was added to 10 mL of ice water. The organic layer was separated, washed with 10 mL of saturated aqueous NaHCO<sub>3</sub>, and dried over anhydrous sodium sulfate. Removal of solvent left an orange red residue, which was subjected to column chromatography on silica gel. The unreacted starting material was eluted with hexane, while the product was eluted with benzene, affording 30 mg (54%) orange red crystals of **17b**, mp 79 °C. Anal. Calcd for C<sub>14</sub>H<sub>18</sub>As<sub>2</sub>FeO: C, 41.21; H, 4.45. Found: C, 41.65; H, 4.38. <sup>1</sup>H NMR (CDCl<sub>3</sub>): δ 1.97 (s, 3H), 2.00 (s, 3H), 2.07 (s, 3H), 2.20 (s, 3H), 2.31 (s, 3H), 4.14 (d, *J* = 2 Hz, 1H), 4.19 (d, *J* = 2 Hz, 1H), 4.45 (s, 1H). <sup>13</sup>C NMR (CDCl<sub>3</sub>): δ 14.8, 15.2, 15.8, 16.7, 32.2, 90.6, 90.7, 91.1, 96.9, 97.1, 100.0, 100.7, 104.4, 205.7. MS (EI) exact mass: calcd for C<sub>14</sub>H<sub>18</sub>As<sub>2</sub><sup>56</sup>FeO, *m/z* 407.9139, found, *m/z* 407.9141. IR (KBr): 1650 cm<sup>-1</sup> (s).

**2,2'-Diacyl-3,3',4,4'-tetramethyl-1,1'-diarsaferrocenes (18b, 19b).** In the same manner as above, the reaction of 3,3',4,4'-tetramethyl-1,1'-diarsaferrocene (50 mg, 0.13 mmol) with AlCl<sub>3</sub> (40 mg, 0.31 mmol) and acetyl chloride (25 mg, 0.32 mmol) in 15 mL of methylene chloride for 12 h gave a product, which was subjected to column chromatography on silica gel. Elution with hexane gave traces of **12b** while product **18b** was eluted with a mixture of benzene/methylene

(34) Spence, R. E. v. H.; Hsu, D. P.; Buchwald, S. L. *Organometallics* **1992**, *11*, 3492.

(35) This procedure was originated by Dr. T. R. Diephouse. Ph.D. Thesis, University of Michigan, 1981.



chloride (1:1). Evaporation of solvent left 20 mg (34%) of **18b** as red crystals, mp 121 °C. Anal. Calcd for  $C_{16}H_{20}As_2FeO_2$ : C, 42.79; H, 4.49. Found: C, 42.87; H, 4.48.  $^1H$  NMR ( $CDCl_3$ ):  $\delta$  2.01 (s, 6H), 2.18 (s, 6H), 2.19 (s, 6H), 4.22 (s, 2H).  $^{13}C$  NMR ( $CDCl_3$ ):  $\delta$  13.8, 15.6, 32.2, 92.4, 98.0, 98.2, 106.9, 205.1. IR (KBr): 1559, 1644  $cm^{-1}$ . MS (EI) exact mass: calcd for  $C_{16}H_{20}As_2^{56}FeO_2$ ,  $m/z$  449.9245; found,  $m/z$  449.9239. Elution with methylene chloride/benzene (3:1) afforded after evaporation of solvent 12 mg (20%) of **19b** as orange red crystals, mp 124 °C.  $^1H$  NMR ( $CDCl_3$ ):  $\delta$  2.01 (s, 6H), 2.04 (s, 6H), 2.19 (s, 12H), 4.68 (s, 2H).  $^{13}C$  NMR ( $CDCl_3$ ):  $\delta$  13.7, 14.1, 32.3, 93.7, 98.6, 99.9, 105.4. MS (EI) exact mass: calcd for  $C_{16}H_{20}As_2^{56}FeO_2$ ,  $m/z$  449.9245; found,  $m/z$  449.9240.

**Relative Rates of Deuteriation of 11a, 11b, and 11e.** Solutions containing 0.01 mmol of each of two components (A and B) in 200  $\mu L$  of  $CH_2Cl_2$  were cooled to  $-22$  °C and added via a syringe to 500  $\mu L$  of trifluoroacetic acid- $d_1$  with stirring at  $-22$  °C. After an interval of time the solutions were added to an excess of aqueous  $NaHCO_3$  containing  $NaBH_4$ . The resulting mixture was extracted with hexane, and the extracts were dried over anhydrous  $Na_2SO_4$ . Removal of solvent under reduced pressure left a residue, which was extracted with  $C_6D_6$ . These solutions were checked by  $^1H$  NMR spectroscopy. Analysis by GC/MS allowed determination of relative concentration of  $d_0$ ,  $d_1$ ,  $d_2$ , etc. for each component. Corrections were made for isotopes  $^{13}C$  and  $^{57}Fe$ .

The initial concentrations of undeuterated compounds ( $A_0$ ,  $B_0$ ) were assumed equal to the sum of  $d_0$ ,  $d_1$ ,  $d_2$ , etc., while  $A_t$  and  $B_t$  were the measured concentration of the  $d_0$  component. The ratio of the first-order rate constants ( $k_A/k_B$ ) was found by using the equations

$$A_t = A_0 e^{-k_A t} \quad (3)$$

$$B_t = B_0 e^{-k_B t} \quad (4)$$

$$k_A/k_B = \ln(A_0/A_t) - \ln(B_0/B_t) \quad (5)$$

Three determinations were made for each pair of compounds. The same general method was used to evaluate the relative rates of **11c** and **11b** except that the solvent was 2.0 mL of toluene containing 7  $\mu L$  of trifluoroacetic acid- $d_1$ .

**Acknowledgment.** Support for work by the National Science Foundation (Grant No. CHE-9224967), Deutsche Forschungsgemeinschaft (Grant No. E1 62/7-2), and Fonds der Chemischen Industrie is gratefully acknowledged. We also acknowledge a NATO grant which has aided the collaboration.

OM950080T

# Imido/Oxo Exchange between Osmium and Tantalum as a Route to Os(NAr)<sub>2</sub>R<sub>2</sub> and OsO(NAr)R<sub>2</sub> Complexes (NAr = N-2,6-*i*-Pr<sub>2</sub>C<sub>6</sub>H<sub>3</sub>; R = CH<sub>2</sub>CMe<sub>3</sub>, CH<sub>2</sub>CMe<sub>2</sub>Ph, CH<sub>2</sub>SiMe<sub>3</sub>) and Attempts To Induce α-Hydrogen Abstraction To Give Alkylidene Complexes

Anne M. LaPointe, Richard R. Schrock,\* and W. M. Davis

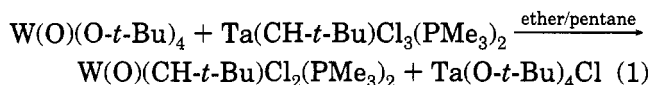
Department of Chemistry, Massachusetts Institute of Technology,  
Cambridge, Massachusetts 02139

Received January 11, 1995<sup>®</sup>

OsO<sub>2</sub>R<sub>2</sub> (R = CH<sub>2</sub>-*t*-Bu, CH<sub>2</sub>CMe<sub>2</sub>Ph) or [OsO<sub>2</sub>(CH<sub>2</sub>SiMe<sub>3</sub>)<sub>2</sub>]<sub>n</sub> reacts with 1 or 2 equiv of Ta(NAr)(O-*t*-Bu)<sub>3</sub> (NAr = N-2,6-*i*-Pr<sub>2</sub>C<sub>6</sub>H<sub>3</sub>) to form complexes of the type OsO(NAr)R<sub>2</sub> or Os(NAr)<sub>2</sub>R<sub>2</sub>. OsO(NAr)(CH<sub>2</sub>-*t*-Bu)<sub>2</sub> reacts with 2 equiv of HCl or Me<sub>3</sub>SiI in CH<sub>2</sub>Cl<sub>2</sub> or DME to form Os(NAr)(CH<sub>2</sub>-*t*-Bu)<sub>2</sub>Cl<sub>2</sub> or Os(NAr)(CH<sub>2</sub>-*t*-Bu)<sub>2</sub>I<sub>2</sub>, respectively, or with SiMe<sub>3</sub>X in CH<sub>2</sub>-Cl<sub>2</sub> to form green, crystalline Os(NAr)(CH<sub>2</sub>-*t*-Bu)<sub>2</sub>(OSiMe<sub>3</sub>)(X) (X = Cl, OTf). An X-ray structure of Os(NAr)(CH<sub>2</sub>-*t*-Bu)<sub>2</sub>(OSiMe<sub>3</sub>)(OTf) showed it to be an approximate square pyramid with a neopentyl group in the apical position. The reaction of OsO(NAr)(CH<sub>2</sub>-*t*-Bu)<sub>2</sub> with 2 equiv of trimethylaluminum in pentane yields red *trans*-Os(NAr)(CH<sub>2</sub>-*t*-Bu)<sub>2</sub>-(CH<sub>3</sub>)<sub>2</sub>. None of the Os(VI) dineopentyl complexes shows any evidence for controlled α-hydrogen abstraction reactions.

## Introduction

A "Wittig-like" reaction between a metal oxo complex and an alkylidene source has been an attractive potential method of preparing alkylidene complexes for approximately two decades. For example, the reaction shown in eq 1



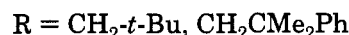
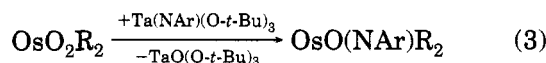
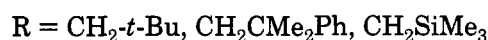
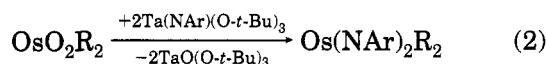
was an attempt to exchange the oxo and alkylidene ligands.<sup>1</sup> However, in this case the oxo ligand is the only one that does *not* exchange between tungsten and tantalum. In contrast, we recently found that tantalum alkylidene complexes are well-behaved "Wittig" reagents toward osmium oxo complexes.<sup>2,3</sup> For example, OsO<sub>2</sub>(CH<sub>2</sub>-*t*-Bu)<sub>2</sub> reacts with 2 equiv of Ta(CH-*t*-Bu)(CH<sub>2</sub>-*t*-Bu)<sub>3</sub> in pentane to yield insoluble [TaO(CH<sub>2</sub>-*t*-Bu)]<sub>n</sub> and *syn,anti*-Os(CH-*t*-Bu)<sub>2</sub>(CH<sub>2</sub>-*t*-Bu)<sub>2</sub>. We believe this to be the first example of a Wittig-like reaction involving a metal oxo species. The other examples of reactions in which covalently doubly bound ligands exchange between metals are imido/oxo exchange between d<sup>0</sup> tungsten and molybdenum complexes<sup>4</sup> or between OsO<sub>4</sub> and phosphinimines<sup>5</sup> or molybdenum imido complexes.<sup>6</sup>

We became interested in the possibility that osmium imido complexes of the type Os(NAr)<sub>2</sub>R<sub>2</sub> could be prepared by exchange reactions between Os=O and Ta=NR. Os(NAr)<sub>2</sub>R<sub>2</sub> (NAr = N-2,6-*i*-Pr<sub>2</sub>C<sub>6</sub>H<sub>3</sub>) complexes were first synthesized via a route that began with Os(NAr)<sub>3</sub>,<sup>7</sup>

but these syntheses are relatively long and proceed in low yield. Monoimido Os(VI) complexes, particularly imido-alkylidene complexes of Os(VI), would also be of interest. In this paper we describe some imido/oxo exchange reactions that yield mono- or bis(imido) complexes of Os(VI) and attempts to form imido-alkylidene complexes by α-hydrogen abstraction reactions.

## Results

OsO<sub>2</sub>R<sub>2</sub> complexes (R = CH<sub>2</sub>-*t*-Bu<sup>8</sup> or CH<sub>2</sub>CMe<sub>2</sub>Ph<sup>2</sup>) or [OsO<sub>2</sub>(CH<sub>2</sub>SiMe<sub>3</sub>)<sub>2</sub>]<sub>n</sub><sup>2</sup> react readily with 2 equiv of Ta(NAr)(O-*t*-Bu)<sub>3</sub> in pentane or toluene to form Os(NAr)<sub>2</sub>R<sub>2</sub> complexes in 50–70% yield (eq 2). TaO(O-*t*-Bu)<sub>3</sub> is removed by passing the reaction mixture through silica gel. This convergent route is relatively efficient, since it requires only two steps involving osmium (starting with [PPh<sub>4</sub>]<sub>2</sub>[OsO<sub>2</sub>Cl<sub>4</sub>]) and proceeds in approximately 40% yield overall (based on osmium). Ta(NAr)(O-*t*-Bu)<sub>3</sub> is readily synthesized in 10–20 g quantities from readily available Ta(NAr)Cl<sub>3</sub>(dimethoxyethane)<sup>9</sup> and 3 equiv of LiO-*t*-Bu in THF. If only 1 equiv of Ta(NAr)(O-*t*-Bu)<sub>3</sub> is added to OsO<sub>2</sub>R<sub>2</sub> (R = CH<sub>2</sub>-*t*-Bu, CH<sub>2</sub>CMe<sub>2</sub>Ph) in THF, then purple OsO(NAr)R<sub>2</sub> is isolated in 60–70% yield (eq 3).



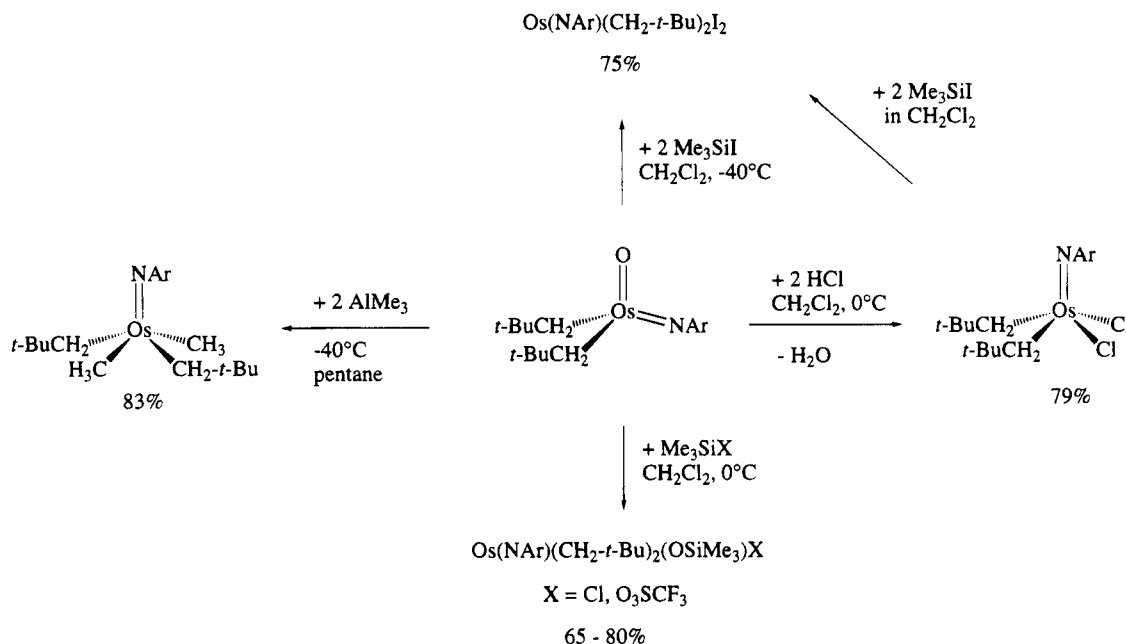
If [OsO<sub>2</sub>(CH<sub>2</sub>SiMe<sub>3</sub>)<sub>2</sub>]<sub>n</sub> is treated with 1 equiv of Ta-

(7) Schofield, M. H.; Kee, T. P.; Anhaus, J. T.; Schrock, R. R.; Johnson, K. H.; Davis, W. M. *Inorg. Chem.* **1991**, *30*, 3595.

(8) Marshman, R. W.; Bigham, W. S.; Wilson, S. R.; Shapley, P. A. *Organometallics* **1990**, *9*, 1341.

(9) Chao, Y.-W.; Wexler, P. A.; Wigley, D. E. *Inorg. Chem.* **1989**, *28*, 3860.

<sup>®</sup> Abstract published in *Advance ACS Abstracts*, April 15, 1995.  
(1) Wengrovius, J. H.; Schrock, R. R. *Organometallics* **1982**, *1*, 148.  
(2) LaPointe, A. M.; Schrock, R. R.; Davis, W. M. *J. Am. Chem. Soc.*, in press.  
(3) LaPointe, A. M.; Schrock, R. R. *Organometallics* **1993**, *13*, 3379.  
(4) Jolly, M.; Mitchell, J. P.; Gibson, V. C. *J. Chem. Soc., Dalton Trans.* **1992**, 1331.  
(5) Chong, A. O.; Oshima, K.; Sharpless, K. B. *J. Am. Chem. Soc.* **1977**, *99*, 3420.  
(6) Robbins Wolf, J.; Bazan, G. C.; Schrock, R. R. *Inorg. Chem.* **1993**, *32*, 4155.

Scheme 1. Reactions of OsO(NAr)(CH<sub>2</sub>-*t*-Bu)<sub>2</sub>

(NAr)(O-*t*-Bu)<sub>3</sub> in THF at -40 °C, a mixture of OsO(NAr)(CH<sub>2</sub>SiMe<sub>3</sub>)<sub>2</sub> and Os(NAr)<sub>2</sub>(CH<sub>2</sub>SiMe<sub>3</sub>)<sub>2</sub> is formed. (Since [OsO<sub>2</sub>(CH<sub>2</sub>SiMe<sub>3</sub>)<sub>2</sub>]<sub>n</sub> is not a monomer in solution, the first imido/oxo exchange with the oligomeric complex is likely to be slower than the subsequent exchange reaction between monomeric OsO(NAr)(CH<sub>2</sub>SiMe<sub>3</sub>)<sub>2</sub> and Ta(NAr)(O-*t*-Bu)<sub>3</sub>.) OsO(NAr)<sub>2</sub> complexes probably are structurally analogous to distorted-tetrahedral OsO(N-*t*-Bu)(mesityl)<sub>2</sub>, which was synthesized in 5% yield from OsO<sub>3</sub>(N-*t*-Bu) and dimesitylmagnesium.<sup>10</sup>

Coordinating solvents such as THF significantly slow the rate of imido/oxo exchange, presumably by blocking sites for ligand transfer, most likely primarily on the more electron-poor tantalum center. For example, the reaction between OsO(NAr)(CH<sub>2</sub>-*t*-Bu)<sub>2</sub> and Ta(NAr)(O-*t*-Bu)<sub>3</sub> in toluene-*d*<sub>8</sub> was essentially complete after a few minutes at -40 °C, while no reaction was observed in THF-*d*<sub>8</sub> until the sample was warmed to 35 °C. Unfortunately, reliable kinetic data for the exchange reaction could not be obtained by NMR methods due to overlapping resonances. The kinetics of imido/oxo exchange between Mo(NAr)<sub>2</sub>(O-*t*-Bu)<sub>2</sub> and MoO<sub>2</sub>(O-*t*-Bu)<sub>2</sub> were found to be consistent with a bimolecular mechanism.<sup>4</sup> It seems likely that the exchange reactions described here proceed in a related manner.

OsO(NAr)(CH<sub>2</sub>-*t*-Bu)<sub>2</sub> reacts with 2 equiv of HCl in DME to yield yellow Os(NAr)(CH<sub>2</sub>-*t*-Bu)<sub>2</sub>Cl<sub>2</sub> in 79% yield, while red, crystalline Os(NAr)(CH<sub>2</sub>-*t*-Bu)<sub>2</sub>I<sub>2</sub> is formed in the reaction between Os(NAr)(CH<sub>2</sub>-*t*-Bu)<sub>2</sub>Cl<sub>2</sub> and 2 equiv of Me<sub>3</sub>SiI in CH<sub>2</sub>Cl<sub>2</sub> or by treating OsO(NAr)(CH<sub>2</sub>-*t*-Bu)<sub>2</sub> with 2 equiv of Me<sub>3</sub>SiI in CH<sub>2</sub>Cl<sub>2</sub> or DME (Scheme 1). The neopentyl methylene protons are diastereotopic by proton NMR in Os(NAr)(CH<sub>2</sub>-*t*-Bu)<sub>2</sub>X<sub>2</sub> complexes. We think the most likely structure for Os(NAr)(CH<sub>2</sub>-*t*-Bu)<sub>2</sub>X<sub>2</sub> is a square pyramid with a *cis* orientation of the neopentyl groups on the basis of the

approximately square-pyramidal structure observed for Os(NMe)(CH<sub>2</sub>SiMe<sub>3</sub>)<sub>4</sub>.<sup>11</sup>

The reaction of OsO(NAr)(CH<sub>2</sub>-*t*-Bu)<sub>2</sub> and Me<sub>3</sub>SiCl or Me<sub>3</sub>SiOTf in dichloromethane yields green, crystalline Os(NAr)(CH<sub>2</sub>-*t*-Bu)<sub>2</sub>(OSiMe<sub>3</sub>)Cl or Os(NAr)(CH<sub>2</sub>-*t*-Bu)<sub>2</sub>(OSiMe<sub>3</sub>)(OTf), respectively (Scheme 1). Proton NMR data for these complexes (in C<sub>6</sub>D<sub>6</sub>) suggest that the two *tert*-butyl groups of the neopentyl ligands are equivalent on the NMR time scale, although the methylene protons are diastereotopic. The resonances for Os(NAr)(CH<sub>2</sub>-*t*-Bu)<sub>2</sub>(OSiMe<sub>3</sub>)(OTf) are broadened at 25 °C in C<sub>6</sub>D<sub>6</sub>, while those for Os(NAr)(CH<sub>2</sub>-*t*-Bu)<sub>2</sub>(OSiMe<sub>3</sub>)Cl are relatively sharp at 25 °C in C<sub>6</sub>D<sub>6</sub>. Variable-temperature studies were not pursued.

An X-ray study of Os(NAr)(CH<sub>2</sub>-*t*-Bu)<sub>2</sub>(OSiMe<sub>3</sub>)(OTf) showed it to be approximately a square pyramid in the solid state (Figure 1) with one of the neopentyl groups in the apical position (O(1)-Os-C(11) = 92.8(3)°, O(4)-Os-C(11) = 109.2(3)°, N-Os-C(11) = 95.8(3)°, C(11)-Os-C(12) = 90.4(3)°, O(1)-Os-C(12) = 172.0(3)°, and N-Os-O(4) = 153.6(3)°; Table 1). The Os-O(4) (1.832(5) Å), Os-C(11) (2.097(8) Å), Os-C(12) (2.083(9) Å), and Os=N (1.689(6) Å) bonds are all relatively short, consistent with covalent bonds to a metal in a relatively high oxidation state and with a relatively low coordination number and possibly also indicative of significant  $\pi$  bonding between osmium and lone pairs on the alkoxide (Os-O(4)-Si = 147.6(4)°) or on nitrogen (Os-N-C(1) = 166.7(6)°). The Os-O(1) distance (2.326(6) Å) is consistent with a considerably weaker, ionic bond, as one would expect for a triflate ligand. In solution the neopentyl groups must become equivalent on the NMR time scale in an intermediate that does not have a plane of symmetry through the methylene carbon atoms.

OsO(NAr)(CH<sub>2</sub>-*t*-Bu)<sub>2</sub> reacts cleanly with 2 equiv of AlMe<sub>3</sub> in pentane to yield red Os(NAr)(CH<sub>2</sub>-*t*-Bu)<sub>2</sub>(CH<sub>3</sub>)<sub>2</sub> in 80% yield (Scheme 1). The pure product is readily isolated after passing the reaction mixture through

(10) Stavropoulos, P.; Edwards, P.; Behling, T.; Wilkinson, G.; Motevalli, M.; Hursthouse, M. B. *J. Chem. Soc., Dalton Trans.* **1987**, 169.

(11) Marshman, R. W.; Shapley, P. A. *J. Am. Chem. Soc.* **1990**, *112*, 8369.

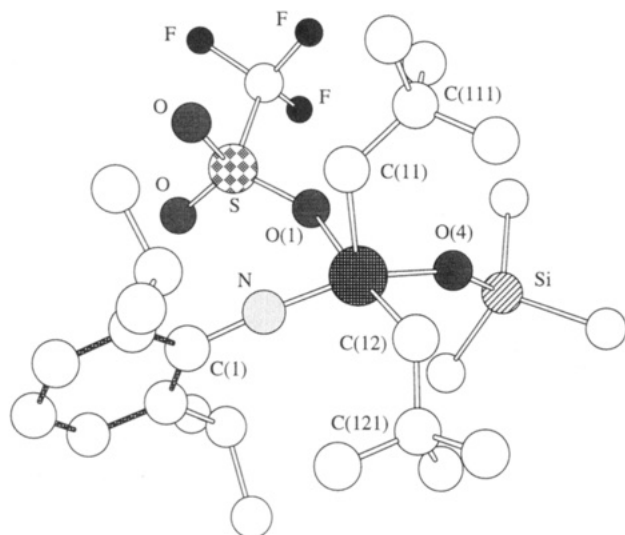


**Figure 1.** Chem 3D drawing of the structure of  $\text{Os}(\text{N}-2,6-i\text{-Pr}_2\text{C}_6\text{H}_3)(\text{CH}_2\text{CMe}_3)_2(\text{OSiMe}_3)(\text{O}_3\text{SCF}_3)$ .

**Table 1. Important Distances (Å) and Angles (deg) in  $\text{Os}(\text{N}-2,6-i\text{-Pr}_2\text{C}_6\text{H}_3)(\text{CH}_2\text{CMe}_3)_2(\text{OSiMe}_3)(\text{O}_3\text{SCF}_3)$**

Distances			
Os–O(1)	2.326(6)	Os–C(12)	2.083(9)
Os–O(4)	1.832(5)	Os–N	1.689(6)
Os–C(11)	2.097(8)		
Angles			
Os–N–C(1)	166.7(6)	O(1)–Os–C(11)	92.8(3)
Os–O(1)–S	131.4(4)	O(1)–Os–C(12)	172.0(3)
Os–C(11)–C(111)	120.0(5)	O(1)–Os–O(4)	80.4(2)
Os–C(12)–C(121)	122.1(6)	O(4)–Os–C(11)	109.2(3)
Os–O(4)–Si	147.6(4)	O(4)–Os–C(12)	91.7(3)
N–Os–O(1)	90.3(3)	C(11)–Os–C(12)	90.4(3)
N–Os–O(4)	153.6(3)	N–Os–C(12)	96.7(3)
N–Os–C(11)	95.8(3)		

silica gel. Proton NMR reveals that the complex is highly symmetric in solution, with equivalent methyl and *tert*-butyl groups. All four methylene protons of the neopentyl groups are also equivalent, suggesting that on the NMR time scale the complex is a square pyramid with a *trans* orientation of the neopentyl ligands or an analogous trigonal bipyramid. The high symmetry of the molecule, the  $^1\text{H}$  chemical shift of the methyl protons (3.40 ppm), the elemental analysis, and its stability to silica gel suggest that it is *not* a trimethylaluminum adduct, i.e., " $\text{Os}(\text{OAlMe}_3)(\text{NAr})(\text{CH}_2\text{-}t\text{-Bu})_2$ ". There is also precedent in the form of structurally characterized square-pyramidal  $\text{Os}(\text{NMe})(\text{CH}_2\text{SiMe}_3)_4$ .<sup>11</sup>

We hoped that  $\text{Os}(\text{NAr})(\text{CH}_2\text{-}t\text{-Bu})_2\text{X}_2$  ( $\text{X} = \text{Cl}, \text{I}$ ) or  $\text{Os}(\text{NAr})(\text{CH}_2\text{-}t\text{-Bu})_2(\text{OSiMe}_3)\text{X}$  ( $\text{X} = \text{Cl}, \text{OTf}$ ) would undergo intramolecular  $\alpha$ -hydrogen abstraction reactions to form imido-alkylidene complexes, " $\text{Os}(\text{NAr})(\text{CH-}t\text{-Bu})\text{X}_2$ " and " $\text{Os}(\text{NAr})(\text{CH-}t\text{-Bu})(\text{OSiMe}_3)\text{X}$ ", respectively, which would be  $d^2$  analogs of  $d^0$  molybdenum and tungsten imido-alkylidene complexes such as  $\text{M}(\text{NAr})(\text{CH-}t\text{-Bu})(\text{dimethoxyethane})\text{Cl}_2$  or  $\text{M}(\text{NAr})(\text{CH-}t\text{-Bu})(\text{OR})_2$ .<sup>12</sup> Dehydrohalogenation of  $\text{Os}(\text{NAr})(\text{CH}_2\text{-}t\text{-Bu})_2\text{X}_2$  to form " $\text{Os}(\text{NAr})(\text{CH-}t\text{-Bu})(\text{CH}_2\text{-}t\text{-Bu})\text{X}$ " is another possible route to imido-alkylidene complexes of  $\text{Os}(\text{VI})$ , although we have found in related  $\text{Os}(\text{VI})$  systems that removing an  $\alpha$ -proton from neopentyl ligands is relatively difficult.<sup>2</sup>

Addition of excess pyridine to a toluene solution of  $\text{Os}(\text{NAr})(\text{CH}_2\text{-}t\text{-Bu})_2(\text{OSiMe}_3)(\text{OTf})$  yields a precipitate

of green  $\text{Os}(\text{NAr})(\text{CH}_2\text{-}t\text{-Bu})_2(\text{py})(\text{OSiMe}_3)(\text{OTf})$  in 80% yield. In  $\text{CDCl}_3$  at 25 °C, the isopropyl and pyridine peaks of  $\text{Os}(\text{NAr})(\text{CH}_2\text{-}t\text{-Bu})_2(\text{py})(\text{OSiMe}_3)(\text{OTf})$  are extremely broad, and the resonances associated with the neopentyl methylene protons could not be located. No evidence for  $\alpha$ -hydrogen abstraction reactions in  $\text{Os}(\text{NAr})(\text{CH}_2\text{-}t\text{-Bu})_2(\text{py})(\text{OSiMe}_3)(\text{OTf})$  is observed, even when a  $\text{CDCl}_3$  solution was heated for 1 h at 70 °C.

$\text{Os}(\text{NAr})(\text{CH}_2\text{-}t\text{-Bu})_2(\text{OSiMe}_3)(\text{Cl})$  does not react with pyridine in  $\text{C}_6\text{D}_6$  at 25 °C. Likewise, no reaction was observed when pyridine was added to  $\text{C}_6\text{D}_6$  or  $\text{CD}_2\text{Cl}_2$  solutions of  $\text{Os}(\text{NAr})(\text{CH}_2\text{-}t\text{-Bu})_2\text{X}_2$  ( $\text{X} = \text{Cl}, \text{I}$ ) or when  $\text{Os}(\text{NAr})(\text{CH}_2\text{-}t\text{-Bu})_2\text{X}_2$  was dissolved in pyridine- $d_5$ , and no reaction was observed when these solutions were heated or photolyzed with a medium-pressure mercury lamp in  $\text{CD}_2\text{Cl}_2$  or  $\text{C}_6\text{D}_6$  at 25 °C. Reactions between  $\text{Os}(\text{NAr})(\text{CH}_2\text{-}t\text{-Bu})_2\text{X}_2$  ( $\text{X} = \text{Cl}, \text{I}$ ) or  $\text{Os}(\text{NAr})(\text{CH}_2\text{-}t\text{-Bu})_2(\text{OSiMe}_3)\text{X}$  ( $\text{X} = \text{Cl}, \text{OTf}$ ) and trimethylphosphine in  $\text{C}_6\text{D}_6$  or  $\text{CD}_2\text{Cl}_2$  gave neopentane, but no metal-containing products could be identified.

Attempts to isolate " $\text{Os}(\text{NAr})(\text{CH-}t\text{-Bu})(\text{CH}_2\text{-}t\text{-Bu})_2$ " by treating  $\text{OsO}(\text{NAr})\text{R}_2$  with a variety of tantalum alkylidene complexes were unsuccessful. These attempts included reactions between  $\text{OsO}(\text{NAr})(\text{CH}_2\text{-}t\text{-Bu})_2$  and  $\text{Ta}(\text{CH-}t\text{-Bu})(\text{CH}_2\text{-}t\text{-Bu})_3$  or  $\text{Ta}(\text{CH-}t\text{-Bu})(\text{O-}t\text{-Bu})_3$  in pentane, or in pentane to which THF or pyridine had been added. Reactions between  $\text{OsO}(\text{NAr})(\text{CH}_2\text{CMe}_2\text{Ph})_2$  and  $\text{Ta}(\text{CH-}t\text{-Bu})(\text{CH}_2\text{-}t\text{-Bu})_3$  also failed to yield any tractable products.

## Discussion

In either alkylidene/oxo or imido/oxo exchange reactions, the ancillary ligands on tantalum and osmium must be chosen with care in order to avoid a circumstance in which (i) the ancillary ligands *can* exchange from one one metal to another and do *not* have a strong preference to bind to only osmium or to only tantalum. Bulky alkyl groups (on either tantalum or osmium) are advantageous since they are unlikely to exchange readily. Alkoxides are also suitable ancillary ligands when bound to tantalum, since they are likely to remain bound to the more oxophilic metal. Some evidence in support of that conclusion is the reaction of  $\text{OsO}(\text{OCH}_2\text{-CH}_2\text{O})_2(\text{py})_2$  with 1 equiv of  $\text{Ta}(\text{NAr})(\text{O-}t\text{-Bu})_3$  in THF to give  $\text{Os}(\text{NAr})_3$ <sup>7</sup> as the only osmium-containing product. As expected, halides readily transfer from tantalum to osmium. For example,  $\text{OsO}_2(\text{CH}_2\text{-}t\text{-Bu})_2$  reacts slowly with 1 equiv of  $\text{Ta}(\text{NAr})(\text{dimethoxyethane})\text{Cl}_3$  in  $\text{C}_6\text{D}_6$  to give  $\text{Os}(\text{NAr})(\text{CH}_2\text{-}t\text{-Bu})_2\text{Cl}_2$ ;  $\text{OsO}(\text{NAr})(\text{CH}_2\text{-}t\text{-Bu})_2$  is not observed by  $^1\text{H}$  NMR.

It is interesting to note that  $\text{OsO}(\text{NAr})(\text{CH}_2\text{-}t\text{-Bu})_2$  exhibits enhanced reactivity of the oxo relative to the arylimido group, as evidenced by the selective syntheses of  $\text{Os}(\text{NAr})(\text{CH}_2\text{-}t\text{-Bu})_2\text{X}_2$  and  $\text{Os}(\text{NAr})(\text{CH}_2\text{-}t\text{-Bu})_2\text{Me}_2$ . In contrast,  $\text{OsO}_2(\text{CH}_2\text{-}t\text{-Bu})_2$  does not react with  $\text{HCl}$ ,  $\text{Me}_3\text{SiCl}$ , or triflic acid in DME.<sup>13</sup> Interestingly, Shapley observed that  $\text{OsO}(\text{CH}_2\text{SiMe}_3)_4$  does not react readily with  $\text{HCl}$ , while both  $\text{Os}(\text{NMe})(\text{CH}_2\text{SiMe}_3)_4$  and  $[\text{Os}(\text{N})(\text{CH}_2\text{SiMe}_3)_4]^-$  do.<sup>11</sup> We speculate that the imido group in  $\text{OsO}(\text{NAr})(\text{CH}_2\text{-}t\text{-Bu})_2$  is kinetically a poorer base than the oxo group, as a consequence of its being a better  $\pi$  donor to the metal than the oxo group. The

(12) Feldman, J.; Schrock, R. R. *Prog. Inorg. Chem.* **1991**, *39*, 1.

(13) LaPointe, A. Ph.D. Thesis, Massachusetts Institute of Technology, 1994.

arylimido group is also a "protecting group" during alkylation reactions. For instance,  $\text{OsO}(\text{NAr})(\text{CH}_2\text{-}t\text{-Bu})_2$  reacts with 2 equiv of  $\text{AlMe}_3$  to form  $\text{Os}(\text{NAr})(\text{CH}_2\text{-}t\text{-Bu})_2(\text{CH}_3)_2$  with no net reduction, but  $\text{OsO}_2(\text{CH}_2\text{-}t\text{-Bu})_2$  is reduced under identical conditions, forming  $[\text{Os}(\text{CH}_2\text{-}t\text{-Bu})_2(\text{CH}_3)]_2$ .<sup>2</sup> The technique of using an imido ligand as a protecting group toward reduction is a key feature of the high-yield synthesis of imido-alkylidene complexes of tungsten and molybdenum.<sup>12</sup>

The fact that the  $\text{Os}(\text{NAr})(\text{CH}_2\text{-}t\text{-Bu})_2\text{X}_2$  ( $\text{X} = \text{Cl}, \text{I}$ ) complexes show no evidence of undergoing  $\alpha$ -hydrogen abstraction reactions in the presence of coordinating ligands is consistent with our previous observations concerning the resistance of  $\text{Os}(\text{VI})$  neopentyl complexes toward  $\alpha$ -abstraction reactions.<sup>2,3</sup> We found that  $\text{Os}(\text{VI})$  complexes require at least two metal–ligand  $\pi$  bonds in order to be stable, and that circumstance is already fulfilled in  $\text{Os}(\text{NAr})(\text{CH}_2\text{-}t\text{-Bu})_2\text{X}_2$  if the imido ligand is pseudo triply bound to the metal. We also found that a neopentyl group is much more reluctant to undergo an  $\alpha$ -hydrogen abstraction reaction than a neopentylidene ligand, a tendency that has been known now for some time.<sup>14</sup> Today one would say that  $\alpha$ -agostic<sup>15</sup> interactions, which are presumed to be required for  $\alpha$ -abstraction reactions, are much less favorable in alkyl ligands than in alkylidene ligands in similar circumstances.

It is interesting to note that no reaction is observed between  $\text{OsO}_2(\text{CH}_2\text{-}t\text{-Bu})_2$  and  $\text{Mo}(\text{NAr})_2(\text{O-}t\text{-Bu})_2$  in  $\text{C}_6\text{D}_6$ , even at 70 °C, although  $\text{OsO}_4$  reacts readily with  $\text{Mo}(\text{NAr})_2(\text{O-}t\text{-Bu})_2$ .<sup>6</sup> Therefore, it appears that a more oxophilic metal (tantalum) is required for imido/oxo exchange reactions involving  $\text{Os}(\text{VI})$ , while molybdenum is sufficiently oxophilic in reactions involving  $\text{OsO}_4$ . This trend parallels that observed in alkylidene/oxo exchange reactions involving  $\text{OsO}_2\text{R}_2$ .<sup>2,3</sup>

In conclusion, we have demonstrated that imido/oxo exchange between tantalum and osmium(VI) is a viable means of synthesizing a variety of  $\text{Os}(\text{VI})$  mono- and bis(imido) complexes. Unfortunately, osmium imido-alkylidene complexes have not yet been synthesized by analogous methods or by  $\alpha$ -abstraction in imido-neopentyl complexes of  $\text{Os}(\text{VI})$ . We might speculate that other imido complexes of later transition metals perhaps can be synthesized by employing tantalum imido complexes as imido transfer agents, if the appropriate later metal oxo complexes can be prepared. Alternatively, exchange of alkoxide ligands for imido ligands may be a route to imido complexes of the later transition metals, if the appropriate later metal alkoxide complexes can be prepared.

## Experimental Section

General procedures are described elsewhere.<sup>2</sup>  $\text{Ta}(\text{NAr})\text{Cl}_3$ - (dimethoxyethane) was prepared as described in the literature.<sup>9</sup>  $\text{OsO}_2\text{R}_2$  complexes were prepared from  $[\text{PPh}_4]_2[\text{OsO}_2\text{Cl}_4]$  and  $\text{ZnR}_2$  in  $\text{CH}_2\text{Cl}_2$ .<sup>2,3</sup> Trimethylchlorosilane, trimethylsilyl triflate, and trimethyliodosilane were purchased from Aldrich and used without further purification. Lithium *tert*-butoxide was purchased from Strem. Silica gel was typically 70–230 mesh (Aldrich) or 230–400 mesh (Bodman).

(14) Schrock, R. R. In *Reactions of Coordinated Ligands*; Braterman, P. R. Ed.; Plenum: New York, 1986.

(15) Brookhart, M.; Green, M. L. H. *J. Organomet. Chem.* **1983**, *250*, 395.

**$\text{Ta}(\text{NAr})(\text{O-}t\text{-Bu})_3$ .** A slurry of  $\text{Ta}(\text{NAr})\text{Cl}_3(\text{DME})$  (5.27 g, 9.5 mmol;  $\text{NAr} = \text{N-2,6-i-Pr}_2\text{C}_6\text{H}_3$ ) in 50 mL of THF was cooled to  $-40$  °C. Solid  $\text{LiO-}t\text{-Bu}$  (2.30 g, 28.8 mmol) was added, and the mixture was warmed to room temperature and stirred for 3 h. THF was removed in vacuo from the pale yellow reaction mixture, leaving a beige solid which was extracted with pentane (40 mL). The extracts were filtered through Celite, and pentane was then removed in vacuo from the filtrate. A waxy beige solid was isolated and recrystallized from pentane at  $-40$  °C to give two crops of colorless crystals of  $\text{Ta}(\text{NAr})(\text{O-}t\text{-Bu})_3$ ; yield 2.79 g (51%). The high solubility of  $\text{Ta}(\text{NAr})(\text{O-}t\text{-Bu})_3$  in nonpolar solvents such as pentane is believed to contribute to the relatively low isolated yield. However, the crude material obtained upon extraction with pentane is pure by  $^1\text{H}$  NMR and can be used in exchange reactions without complications:  $^1\text{H}$  NMR ( $\text{C}_6\text{D}_6$ )  $\delta$  7.17 (br s, 2, Ar), 6.92 (t, 1, Ar), 4.22 (sept, 2,  $\text{CHMe}_2$ ), 1.36 (d, 12,  $\text{CHMe}_2$ ), 1.28 (s, 27,  $\text{OCMe}_3$ );  $^{13}\text{C}$  NMR ( $\text{C}_6\text{D}_6$ )  $\delta$  152.1, 143.1, 122.4, 121.8, 80.0 ( $\text{OCMe}_3$ ), 32.3 ( $\text{OCMe}_3$ ), 27.6 ( $\text{CHMe}_2$ ), 24.4 ( $\text{CHMe}_2$ ). Anal. Calcd for  $\text{TaC}_{24}\text{H}_{44}\text{NO}_3$ : C, 50.08; H, 7.70; N, 2.43. Found: C, 50.13; H, 7.96; N, 2.41.

**$\text{Os}(\text{NAr})_2(\text{CH}_2\text{-}t\text{-Bu})_2$ .**  $\text{OsO}_2(\text{CH}_2\text{-}t\text{-Bu})_2$  (77 mg, 0.21 mmol) was dissolved in 5 mL of pentane, and the solution was cooled to  $-40$  °C. Solid  $\text{Ta}(\text{NAr})(\text{O-}t\text{-Bu})_3$  was added, and the mixture immediately became orange-green. The mixture was warmed to room temperature and was stirred for 1 h. It was then filtered through silica gel in order to remove  $\text{TaO}(\text{O-}t\text{-Bu})_3$ . The solvent was removed in vacuo from the filtrate to leave orange, crystalline  $\text{Os}(\text{NAr})_2(\text{CH}_2\text{-}t\text{-Bu})_2$  (80 mg, 57%). NMR data match those reported.<sup>7</sup>

**$\text{Os}(\text{NAr})_2(\text{CH}_2\text{CMe}_2\text{Ph})_2$ .**  $\text{Os}(\text{NAr})_2(\text{CH}_2\text{CMe}_2\text{Ph})_2$  was prepared from  $\text{OsO}_2(\text{CH}_2\text{CMe}_2\text{Ph})_2$  in a manner similar to that described for  $\text{Os}(\text{NAr})_2(\text{CH}_2\text{-}t\text{-Bu})_2$ , except toluene was used as the solvent:  $^1\text{H}$  NMR ( $\text{C}_6\text{D}_6$ )  $\delta$  7.4–6.8 (m, 16 total,  $\text{Ph} + \text{NAr}$ ), 4.63 (s, 4,  $\text{CH}_2\text{CMe}_2\text{Ph}$ ), 3.62 (sept, 4,  $\text{CHMe}_2$ ), 1.44 (s, 12,  $\text{CMe}_2\text{Ph}$ ), 1.28 (d, 24,  $\text{CHMe}_2\text{Ph}$ );  $^{13}\text{C}$  NMR ( $\text{C}_6\text{D}_6$ )  $\delta$  154.3, 151.1, 145.2, 126.9, 126.0, 125.7, 123.3 (one aryl carbon resonance is apparently obscured by the solvent resonance), 44.4 ( $\text{CMe}_2\text{Ph}$ ), 31.7 ( $\text{CMe}_2\text{Ph}$ ), 29.0 ( $\text{CHMe}_2$ ), 24.1 ( $\text{CHMe}_2$ ). Anal. Calcd for  $\text{OsC}_{44}\text{H}_{60}\text{N}_2$ : C, 65.47; H, 7.49; N, 3.47. Found: C, 65.40; H, 7.66; N, 3.51.

**$\text{Os}(\text{NAr})_2(\text{CH}_2\text{SiMe}_3)_2$ .**  $\text{Os}(\text{NAr})_2(\text{CH}_2\text{SiMe}_3)_2$  was prepared from  $[\text{OsO}_2(\text{CH}_2\text{SiMe}_3)_2]_n$  and 2 equiv of  $\text{Ta}(\text{NAr})(\text{O-}t\text{-Bu})_3$  (per Os) in a manner identical with that used to prepare  $\text{Os}(\text{NAr})_2(\text{CH}_2\text{-}t\text{-Bu})_2$ ; yield 60%. NMR data match those reported.<sup>7</sup>

**$\text{Os}(\text{O})(\text{NAr})(\text{CH}_2\text{-}t\text{-Bu})_2$ .**  $\text{OsO}_2(\text{CH}_2\text{-}t\text{-Bu})_2$  (105 mg, 0.288 mmol) was dissolved in 10 mL of THF, and the solution was cooled to  $-40$  °C. A prechilled solution of  $\text{Ta}(\text{NAr})(\text{O-}t\text{-Bu})_3$  (170 mg, 0.300 mmol) in THF was then added dropwise. The mixture became purple-red as it was warmed to room temperature or to 22 °C. After 1 h the mixture was passed through silica gel in order to remove  $\text{Ta}(\text{O})(\text{O-}t\text{-Bu})_3$ , and the resulting filtrate was reduced to dryness in vacuo. The purple solid was extracted into pentane (2 mL) and recrystallized at  $-40$  °C: yield 98 mg (65%);  $^1\text{H}$  NMR ( $\text{C}_6\text{D}_6$ )  $\delta$  7.20 (t, 1, Ar), 6.86 (d, 2, Ar), 4.52 (d, 2,  $J_{\text{HH}} = 12$  Hz,  $\text{CH}_a\text{H}_b\text{-}t\text{-Bu}$ ), 4.21 (d, 2,  $J_{\text{HH}} = 12$ ,  $\text{CH}_a\text{H}_b\text{-}t\text{-Bu}$ ), 3.66 (sept, 2,  $\text{CHMe}_2$ ), 1.21 (d, 12,  $J_{\text{HH}} = 7$ ,  $\text{CHMe}_2$ ), 1.15 (s, 18,  $\text{CH}_2\text{-}t\text{-Bu}$ );  $^{13}\text{C}$  NMR ( $\text{C}_6\text{D}_6$ )  $\delta$  152.2 ( $\text{C}_i$ ), 144.9 ( $\text{C}_o$ ), 129.4 ( $\text{C}_p$ ), 123.6 ( $\text{C}_m$ ), 35.6 ( $\text{CH}_2\text{CMe}_3$ ), 32.1 ( $\text{CMe}_3$ ), 30.5 ( $\text{CH}_2\text{-}t\text{-Bu}$ ), 29.1 ( $\text{CHMe}_2$ ), 23.3 ( $\text{CHMe}_2$ ); IR (Nujol)  $925$   $\text{cm}^{-1}$  ( $\text{Os}=\text{O}$ ). Anal. Calcd for  $\text{OsC}_{22}\text{H}_{39}\text{NO}$ : C, 50.45; H, 7.51; N, 2.67. Found: C, 50.37; H, 7.40; N, 2.50.

**$\text{OsO}(\text{NAr})(\text{CH}_2\text{CMe}_2\text{Ph})_2$ .**  $\text{OsO}(\text{NAr})(\text{CH}_2\text{CMe}_2\text{Ph})_2$  was prepared from  $\text{OsO}_2(\text{CH}_2\text{CMe}_2\text{Ph})_2$  and  $\text{Ta}(\text{NAr})(\text{O-}t\text{-Bu})_3$  in a manner identical with that described for  $\text{OsO}(\text{NAr})(\text{CH}_2\text{-}t\text{-Bu})_2$ :  $^1\text{H}$  NMR ( $\text{C}_6\text{D}_6$ )  $\delta$  6.8–7.4 (m, 13 total,  $\text{Ph} + \text{NAr}$ ), 4.69 (d, 2,  $\text{CH}_a\text{H}_b$ ,  $J_{\text{HH}} = 12$  Hz), 4.50 (d, 2,  $\text{CH}_a\text{H}_b$ ,  $J_{\text{HH}} = 12$ ), 3.23 (sept, 2,  $\text{CHMe}_2$ ), 1.49, 1.44 (s, 6 each,  $\text{CMe}_2\text{Ph}$ ), 1.12 (d, 12,  $\text{CHMe}_2$ ); IR (Nujol)  $928$   $\text{cm}^{-1}$  ( $\text{Os}=\text{O}$ ).

**$\text{Os}(\text{NAr})(\text{CH}_2\text{-}t\text{-Bu})_2\text{Cl}_2$ .**  $\text{Os}(\text{NAr})(\text{O})(\text{CH}_2\text{-}t\text{-Bu})_2$  (132 mg, 0.25 mmol) was dissolved in 5 mL of DME, and the solution

was cooled to 0 °C. A 1.0 M solution of HCl in ether (1.0 mL, 1.0 mmol) was added to the stirred solution by syringe; the reaction mixture became yellow-brown. The solution was warmed to room temperature and was stirred for 1 h. DME was removed in vacuo, and the yellow-brown solid was extracted with pentane (10 mL). The volume of the solution was reduced to 1 mL in vacuo, and the solution was cooled to -40 °C. Yellow-green prisms formed and were collected and dried in vacuo: yield 115 mg (79%);  $^1\text{H NMR}$  ( $\text{CD}_2\text{Cl}_2$ )  $\delta$  8.90 (d, 2,  $J_{\text{HH}} = 12$  Hz,  $\text{CH}_a\text{H}_b\text{-}t\text{-Bu}$ ), 7.95 (t, 1, Ar), 7.08 (d, 2, Ar), 6.78 (d, 2,  $J_{\text{HH}} = 12$ ,  $\text{CH}_a\text{H}_b\text{-}t\text{-Bu}$ ), 2.98 (sept, 2,  $\text{CHMe}_2$ ), 1.28 (d, 12,  $\text{CHMe}_2$ ), 1.10 (s, 18,  $t\text{-Bu}$ );  $^{13}\text{C NMR}$  ( $\text{CDCl}_3$ )  $\delta$  153.5, 145.4, 132.7, 126.5 (Ar), 57.0 ( $\text{CH}_2\text{-}t\text{-Bu}$ ), 41.4 ( $\text{CMe}_3$ ), 32.8 ( $\text{CMe}_3$ ), 32.2 ( $\text{CHMe}_2$ ), 23.9 ( $\text{CHMe}_2$ ). Anal. Calcd for  $\text{OsC}_{25}\text{H}_{39}\text{NCl}_2$ : C, 45.66; H, 6.79; N, 2.42. Found: C, 45.88; H, 7.07; N, 2.29.

**Os(NAr)(CH<sub>2</sub>-*t*-Bu)<sub>2</sub>I<sub>2</sub>.** OsO(NAr)(CH<sub>2</sub>-*t*-Bu)<sub>2</sub> (60 mg, 0.115 mmol) was dissolved in 3 mL of dichloromethane, and the solution was cooled to -40 °C. Me<sub>3</sub>SiI (34  $\mu\text{L}$ , 0.24 mmol) was added. The solution became red immediately. After it was warmed to room temperature, the solution was stirred for 1.5 h. Dichloromethane was removed in vacuo, and the resulting red oily solid was extracted with pentane (10 mL). The extract was filtered, and the volume of the filtrate was reduced to 2 mL and cooled to -40 °C. Dark red crystals formed after several days and were collected and dried in vacuo: yield 66 mg (75%);  $^1\text{H NMR}$  (toluene-*d*<sub>3</sub>)  $\delta$  9.29 (d, 2,  $J_{\text{CH}} = 12$  Hz,  $\text{CH}_a\text{H}_b\text{-}t\text{-Bu}$ ), 7.25 (t, 1, Ar), 7.21 (d, 2,  $J_{\text{CH}} = 12$ ,  $\text{CH}_a\text{H}_b\text{-}t\text{-Bu}$ ), 6.46 (d, 2, Ar), 3.05 (sept, 2,  $\text{CHMe}_2$ ), 1.11 (d, 12,  $\text{CHMe}_2$ ), 1.09 (s, 9,  $t\text{-Bu}$ );  $^{13}\text{C NMR}$  (toluene-*d*<sub>3</sub>) 153.0, 141.6, 130.6, 126.0 (Ar), 63.3 ( $\text{CH}_2\text{-}t\text{-Bu}$ ), 38.8 ( $\text{CMe}_3$ ), 33.6 ( $\text{CMe}_3$ ), 31.7 ( $\text{CHMe}_2$ ), 23.1 ( $\text{CHMe}_2$ ). Anal. Calcd for  $\text{OsC}_{25}\text{H}_{39}\text{NI}_2$ : C, 34.70; H, 5.14; N, 1.84. Found: C, 34.69; H, 5.14; N, 2.01.

**Os(NAr)(CH<sub>2</sub>-*t*-Bu)<sub>2</sub>(OSiMe<sub>3</sub>)Cl.** OsO(NAr)(CH<sub>2</sub>-*t*-Bu)<sub>2</sub> (81 mg, 0.15 mmol) was dissolved in 5 mL of dichloromethane, and the solution was chilled to -40 °C. Trimethylchlorosilane (25  $\mu\text{L}$ , 0.19 mmol) was added, and the resulting green solution was warmed to 25 °C and stirred for 1 h. Dichloromethane was removed in vacuo, and the resulting green solid was recrystallized from ether/pentane at -40 °C. Dark green prisms were collected and dried in vacuo: yield 64 mg in two crops (66%);  $^1\text{H NMR}$  ( $\text{C}_6\text{D}_6$ )  $\delta$  7.14 (t, 1, Ar), 6.60 (d, 2, Ar), 6.31 (d, 2,  $\text{CH}_a\text{H}_b\text{-}t\text{-Bu}$ ), 5.15 (d, 2,  $\text{CH}_a\text{H}_b\text{-}t\text{-Bu}$ ), 3.5 (sept, 2,  $\text{CHMe}_2$ ), 1.30 (s, 18,  $t\text{-Bu}$ ), 1.18 (d, 12,  $\text{CHMe}_2$ ), 0.47 (s, 9, OSiMe<sub>3</sub>);  $^{13}\text{C NMR}$  ( $\text{C}_6\text{D}_6$ )  $\delta$  153.1, 146.3, 130.4, 125.6 (Ar), 50.5 ( $\text{CH}_2\text{-}t\text{-Bu}$ ), 39.3 ( $\text{CHMe}_2$ ), 32.5 ( $\text{CMe}_3$ ), 30.8 ( $\text{CMe}_3$ ), 24.0 ( $\text{CHMe}_2$ ), 2.9 (SiMe<sub>3</sub>). Anal. Calcd for  $\text{OsC}_{25}\text{H}_{48}\text{NClOSi}$ : C, 47.48; H, 7.65; N, 2.21. Found: C, 47.42; H, 7.65; N, 2.17.

**Os(NAr)(CH<sub>2</sub>-*t*-Bu)<sub>2</sub>(OSiMe<sub>3</sub>)(OTf).** OsO(NAr)(CH<sub>2</sub>-*t*-Bu)<sub>2</sub> (108 mg, 0.21 mmol) was dissolved in 5 mL of dichloromethane, and the solution was chilled to -40 °C. Trimethylsilyl triflate (42  $\mu\text{L}$ , 0.21 mmol) was added, and the resulting green solution was warmed to 25 °C and stirred for 1 h. Dichloromethane was removed in vacuo, and the resulting olive green solid was washed with pentane and dried in

vacuo: yield 121 mg (77%);  $^1\text{H NMR}$  ( $\text{C}_6\text{D}_6$ )  $\delta$  7.5 (br d, 2,  $\text{CH}_a\text{H}_b\text{-}t\text{-Bu}$ ), 7.14 (t, 1, Ar), 6.62 (d, 2, Ar), 5.8 (br d, 2,  $\text{CH}_a\text{H}_b\text{-}t\text{-Bu}$ ), 3.25 (br m, 2,  $\text{CHMe}_2$ ), 1.27 (d, 12,  $\text{CHMe}_2$ ), 1.13 (s, 18,  $t\text{-Bu}$ ), 0.33 (s, 9, OSiMe<sub>3</sub>);  $^{13}\text{C NMR}$  ( $\text{CDCl}_3$ )  $\delta$  153.8, 146.7, 132.0, 125.3 (Ar), 43 (br,  $\text{CH}_2\text{-}t\text{-Bu}$ ), 40.0 ( $\text{CMe}_3$ ), 31.9 ( $\text{CMe}_3$ ), 31.3 ( $\text{CHMe}_2$ ), 23.8 ( $\text{CHMe}_2$ ), 2.3 (OSiMe<sub>3</sub>). Anal. Calcd for  $\text{OsC}_{26}\text{H}_{48}\text{NF}_3\text{O}_4\text{SiS}$ : C, 41.86; H, 6.49; N, 1.88. Found: C, 41.59; H, 6.90; N, 1.90.

**Os(NAr)(CH<sub>2</sub>-*t*-Bu)<sub>2</sub>(py)(OSiMe<sub>3</sub>)(OTf).** Os(NAr)(CH<sub>2</sub>-*t*-Bu)<sub>2</sub>(py)(OSiMe<sub>3</sub>)(OTf) was prepared in 80% yield by adding excess pyridine to a toluene solution of Os(NAr)(CH<sub>2</sub>-*t*-Bu)<sub>2</sub>(OSiMe<sub>3</sub>)(OTf). The resulting green precipitate was washed with pentane and dried in vacuo:  $^1\text{H NMR}$  ( $\text{CDCl}_3$ )  $\delta$  8.6 (br d, 2, py), 8.15 (t, 1, Ar), 7.75 (br t + d, 3, py), 3.0 (br,  $\text{CHMe}_2$ ), 1.15 (br, 12,  $\text{CHMe}_2$ ), 1.00 (s, 18,  $t\text{-Bu}$ ), 0.38 (s, 9, SiMe<sub>3</sub>), the methylene protons could not be located;  $^{13}\text{C NMR}$  ( $\text{CDCl}_3$ )  $\delta$  152.5, 147.1, 141.7, 129.3, 128.4, 126.7, 125.5 (py + Ar), 46 (br,  $\text{CH}_2\text{-}t\text{-Bu}$ ), 39 (br,  $\text{CMe}_3$ ), 32.0 ( $\text{CMe}_3$ ), 31.3 ( $\text{CHMe}_2$ ), 23.6 ( $\text{CHMe}_2$ ), 2.7 (SiMe<sub>3</sub>).

**Os(NAr)(CH<sub>3</sub>)<sub>2</sub>(CH<sub>2</sub>-*t*-Bu)<sub>2</sub>.** Os(NAr)(O)(CH<sub>2</sub>-*t*-Bu)<sub>2</sub> (55 mg, 0.105 mmol) was dissolved in 5 mL of pentane, and the solution was chilled to -40 °C. A solution of trimethylaluminum in hexane (0.24 mmol) was added. The reaction mixture became red and then orange as it was warmed to room temperature. After 30 min, the solution was filtered, the volatile components were removed in vacuo, and the residue was dissolved in pentane and the resulting solution was passed through silica gel. The solvent was removed in vacuo to give an orange crystalline solid: yield 47 mg (83%);  $^1\text{H NMR}$  ( $\text{C}_6\text{D}_6$ )  $\delta$  7.01 (t, 1, Ar), 6.72 (d, 2, Ar), 3.63 (s, 4,  $\text{CH}_2\text{-}t\text{-Bu}$ ), 3.40 (s, 6,  $\text{CH}_3$ ), 3.31 (sept, 4,  $\text{CHMe}_2$ ), 1.27 (s, 18,  $\text{CH}_2\text{-}t\text{-Bu}$ ), 1.12 (d, 12,  $J_{\text{HH}} = 7$  Hz,  $\text{CHMe}_2$ );  $^{13}\text{C NMR}$  ( $\text{C}_6\text{D}_6$ )  $\delta$  146.4 (C<sub>1</sub>), 142.5 (C<sub>2</sub>), 127.0 (C<sub>3</sub>), 124.5 (C<sub>m</sub>), 74.2 ( $\text{CH}_2\text{-}t\text{-Bu}$ ), 40.7 ( $\text{CH}_3$ ), 40.4 ( $\text{CH}_2\text{CMe}_3$ ), 34.1 ( $\text{CH}_2\text{CMe}_3$ ), 29.0 ( $\text{CHMe}_2$ ), 23.8 ( $\text{CHMe}_2$ ). Anal. Calcd for  $\text{OsC}_{24}\text{H}_{45}\text{N}$ : C, 53.60; H, 8.43; N, 2.60. Found: C, 53.92; H, 8.79; N, 2.56.

**X-ray Study of Os(NAr)(CH<sub>2</sub>-*t*-Bu)<sub>2</sub>(OSiMe<sub>3</sub>)(OTf).** The space group was found to be  $P\bar{1}$  with  $a = 9.785$  Å,  $b = 10.126$  Å,  $c = 18.712$  Å,  $\alpha = 97.79^\circ$ ,  $\beta = 95.72^\circ$ ,  $\gamma = 114.61^\circ$ ,  $V = 1645$  Å<sup>3</sup>,  $Z = 2$ ,  $fw = 746.01$ , and  $D_{\text{calcd}} = 1.506$  g/cm<sup>3</sup>. Details can be found in the supplementary material.

**Acknowledgment.** R.R.S. thanks the National Science Foundation (Grant CHE 91 22827) for research support.

**Supplementary Material Available:** Text giving experimental details for the X-ray study of Os(NAr)(CH<sub>2</sub>-*t*-Bu)<sub>2</sub>(OSiMe<sub>3</sub>)(OTf), an ORTEP drawing, and tables of final coordinates and final thermal parameters (11 pages). This material is contained in many libraries on microfiche, immediately follows this article in the microfilm version of the journal, and can be ordered from the ACS; see any current masthead page for information.

OM950019O



# Reactions of H(PhMeSi)<sub>x</sub>H (x = 2, 3, 4) with Triflic Acid: Competitive Cleavage and Rearrangement Processes

Joyce Y. Corey,\* Dennis M. Kraichely, Jean L. Huhmann,  
Janet Braddock-Wilking, and Anna Lindeberg

Department of Chemistry, University of Missouri—St. Louis, St. Louis, Missouri 63121

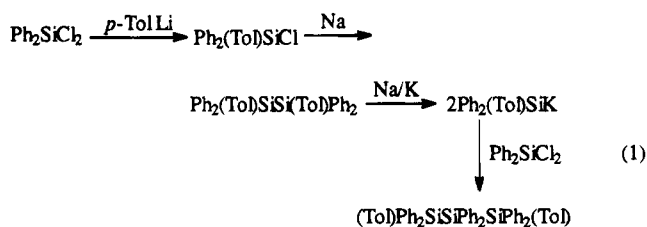
Received November 29, 1994<sup>®</sup>

The removal of phenyl groups in H(PhRSi)<sub>x</sub>H (R = Me, x = 2, 3, 4; R = Ph, x = 2) with 1 to x equiv of triflic acid, HOTf, was examined in hexane, toluene, and methylene chloride. The resulting triflate-substituted oligomers were not isolated but reacted with Grignard reagents or LiAlH<sub>4</sub> to provide air and moisture stable products, which were purified by preparative gas chromatography and characterized by <sup>1</sup>H, <sup>13</sup>C, and <sup>29</sup>Si NMR spectroscopy. From H(PhRSi)<sub>2</sub>H and 1 equiv of HOTf, disilanes such as HPhMeSiSiMe<sub>2</sub>H, HPhMeSiSiMeH<sub>2</sub>, and HPh<sub>2</sub>SiSiPhMeSiH were produced in modest yields. Treatment of H(PhMeSi)<sub>3</sub>H with 1 equiv of HOTf in CH<sub>2</sub>Cl<sub>2</sub> followed by MeMgBr provided HPhMeSiSiPhMeSiMe<sub>2</sub>H and HPhMeSiMe<sub>2</sub>SiPhMeH as mixtures of diastereomers and revealed the competitive cleavage of internal vs terminal SiPh groups by HOTf. Similarly, quenching of (TfO)Ph<sub>2</sub>Me<sub>3</sub>Si<sub>3</sub>H<sub>2</sub> with LiAlH<sub>4</sub> provided two isomers of Ph<sub>2</sub>Me<sub>3</sub>Si<sub>3</sub>H<sub>3</sub>, which could be separated prior to spectroscopic characterization. The reaction of H(PhMeSi)<sub>3</sub>H with 2 equiv of HOTf in CH<sub>2</sub>Cl<sub>2</sub> followed by MeMgBr resulted in the isolation of PhMe<sub>5</sub>Si<sub>3</sub>H<sub>2</sub> as two isomers, both with terminal SiH groups. Reactions of H(PhMeSi)<sub>3</sub>H with 3 equiv of HOTf followed by RMgX also revealed the formation of two isomers, which were assigned the structures H(RMeSi)<sub>3</sub>H and HRMeSiSiMeHSiMeR<sub>2</sub> based on spectroscopic data. The results of the reactions of the trisilane with 2 and 3 equiv of triflic acid are unexpected and require a rearrangement of a group from a terminal silicon to the internal silicon which can be rationalized through a cationic intermediate. The reactions of H(PhMeSi)<sub>4</sub>H with HOTf appear to follow the trend established in the reactions of the trisilanes.

## Introduction

The development of silicon oligomer chemistry requires new methods of synthesis not only for the generation of specific chains but also for the ability to manipulate functional groups on the chain without silicon–silicon bond cleavage. The usual reaction employed to form a silicon–silicon bond involves a Wurtz-type coupling of chlorosilanes which are often commercially available. However, condensation of RR'SiCl<sub>2</sub> provides either or both cyclopolysilanes and linear polysilane.<sup>1</sup> A one-step synthesis of a chain from a monosilane which still provides functional groups at various positions in the chain would be ideal, but there are few suitable precursors. The reaction of Na or K with SiH<sub>4</sub> provides MSi<sub>n</sub>H<sub>2n+1</sub> (M = Na, K; n = 1–4)<sup>2</sup> but is not a practical method for providing easily handled oligomers. Transition metal promoted dehydrocoupling of secondary silanes, RR'SiH<sub>2</sub> provides mixtures of small oligomers H(RR'Si)<sub>x</sub>H (mainly x = 2, 3) and is most effective when one of the substituents at silicon is an aryl group.<sup>3</sup> A preliminary report also describes the formation of short oligomers, H(PhMeSi)<sub>x</sub>H from the electrolysis of PhMeSiH<sub>2</sub> on a 1 mmol scale.<sup>4</sup>

Silicon oligomers are formed usually by indirect routes that involve the condensation of halosilanes with alkali metals or magnesium or involve the condensation of a silyllithium or its equivalent with a halosilane. Examples of this methodology are demonstrated in the synthesis of the trisilane shown in the sequence in eq 1.<sup>5</sup> In general this method leads to organic “saturated”



systems, R<sub>x</sub>R'<sub>y</sub>Si<sub>n</sub> (x + y = n + 2) and is employed for the synthesis of disilanes and trisilanes. More recently, an electrochemical synthesis has been utilized to form disilanes through pentasilanes from chlorosilanes.<sup>6</sup> The electrochemical synthesis was also used to generate unsymmetrically substituted disilanes such as Ph<sub>2</sub>MeSiSiMe<sub>3</sub> as well as to couple chlorodisilanes in high yields, both of which are more difficult to perform under Wurtz coupling conditions. For example, the condensa-

<sup>®</sup> Abstract published in *Advance ACS Abstracts*, May 1, 1995.

(1) West, R. In *The Chemistry of Organic Silicon Compounds*; Patai, S., Rappoport, Z., Eds.; Wiley Interscience: New York, 1989; Part 2, Chapter 19.

(2) Feher, F.; Krancher, M.; Feher, M. *Z. Anorg. Allg. Chem.* **1991**, *606*, 7–16.

(3) (a) Corey, J. Y.; Zhu, X.-H.; Bedard, T. C.; Lange, L. D. *Organometallics* **1991**, *10*, 924–930. (b) Corey, J. Y.; Zhu, X.-H. *Organometallics* **1992**, *11*, 672–683.

(4) Kimata, Y.; Suzuki, H.; Satoh, S.; Kuriyama, A. *Chem. Lett.* **1994**, 1163–1164.

(5) (a) Breed, L. W.; Wiley, J. C. *J. Polym. Sci.* **1976**, *14*, 83–92. (b) Hassler, K. *Monatsh. Chem.* **1988**, *119*, 1051–1056.

(6) (a) Biran, C.; Bordeau, P. P.; Léger, M. P.; Dunoguès, J. J. *Organomet. Chem.* **1990**, *382*, C17–C20. (b) Kunai, A.; Kawakami, T.; Toyoda, E.; Ishikawa, M. *Organometallics* **1991**, *10*, 893–895. (c) Kunai, A.; Kawakami, T.; Toyoda, E.; Ishikawa, M. *Organometallics* **1991**, *10*, 2001–2003.

tion of PhMe<sub>2</sub>SiSiMe<sub>2</sub>Cl with Li gave a mixture of Ph-(Me<sub>2</sub>Si)<sub>x</sub>Ph (x = 1, 3, 4, 5).<sup>7</sup> Currently the most reliable route to larger oligomers involves ring-opening of a cyclopolysilane which provides oligomers with terminal functional groups, X(RR'Si)<sub>x</sub>X but is of practical use only for the range x = 4–6. An example is given in eq 2.<sup>8</sup>



Only when functional groups are present can the chemistry of a molecule be developed. In silicon oligomer chemistry one of the most exploited "functional groups" for building new systems is actually a phenyl substituent which may be removed by electrophilic cleavage usually without degradation of the silicon chain. Substitution of activating groups on the phenyl ring can direct cleavage to a specific aryl group. Reaction of the trisilane in the sequence in eq 1 with AlBr<sub>3</sub>/HBr, resulted in the specific removal of the *p*-Tol groups to give Br(Ph<sub>2</sub>Si)<sub>3</sub>Br.<sup>9</sup> A similar tactic was recently employed for the synthesis of the tetrasilane Br<sub>2</sub>-HSiSiPh<sub>2</sub>SiPh<sub>2</sub>SiHBr<sub>2</sub> from [Mes<sub>2</sub>HSiSiPh<sub>2</sub>]<sub>2</sub> (Mes = mesityl).<sup>10</sup> Triflic acid (HOTf) may be more selective in removal of phenyl groups since the replacement of one phenyl substituent at a silicon center with a triflate group deactivates that center toward additional substitution. Thus, the reaction of Ph<sub>3</sub>Si<sub>3</sub> with 2 equiv of HOTf produced only TfO(Ph<sub>2</sub>Si)<sub>3</sub>OTf and in 90% yield.<sup>11</sup> Deactivation has been shown in the rates of removal of the second phenyl group in PhMe<sub>2</sub>Si(SiMe<sub>2</sub>)<sub>x</sub>SiMe<sub>2</sub>Ph and in Me<sub>2</sub>SiPh<sub>2</sub>.<sup>7,12</sup> In no example has there been reported removal of an internal SiPh in a trisilane such as Ph<sub>3</sub>SiSiPh<sub>2</sub>SiPhMe<sub>2</sub> where 1 equiv of HOTf provides Ph<sub>3</sub>SiSiPh<sub>2</sub>SiMe<sub>2</sub>(OTf) and 2 equiv of HOTf produces (TfO)Ph<sub>2</sub>SiSiPh<sub>2</sub>SiMe<sub>2</sub>(OTf).<sup>10,13</sup>

The dehydrocoupling of the monosilane PhMeSiH<sub>2</sub> in the presence of the hydrogen acceptor cyclooctene promoted by the precatalyst combination Cp<sub>2</sub>TiCl<sub>2</sub>/nBuLi<sup>3b</sup> provides mixtures of oligomers H(PhMeSi)<sub>x</sub>H (x = 2–4) which contain two types of functional groups: SiH and SiPh. Thus, these easily prepared oligomers may be used as starting materials for the production of new oligomers. This report will focus on the isolation and characterization of the products and product mixtures that are obtained when HOTf is used to remove phenyl groups in H(PhMeSi)<sub>x</sub>H oligomers. In contrast to our expectations, the results of these experiments demonstrated both competitive cleavage of internal and terminal SiPh bonds as well as a new rearrangement of groups on the silicon chain.<sup>14</sup>

## Results

**Preparation of Oligomers.** Although the isolation and characterization of the disilane through the tet-

**Table 1. Condensation of PhRSiH<sub>2</sub>/C<sub>8</sub>H<sub>14</sub> Promoted by Cp<sub>2</sub>TiCl<sub>2</sub>/nBuLi**

PhRSiH <sub>2</sub> R	conditions temp/time	x in H(PhMeSi) <sub>x</sub> H <sup>c</sup>			
		2	3	4	5
Me <sup>a</sup>	25 °C/24 h	1	0.39	0.01	
	25 °C/96 h	1	2.0	0.23	
Me <sup>a</sup>	20 °C/22 h; 90 °C/9 h	1	3.4	1.4	0.12
	85 °C/30 h	1	3.2	2.7	0.31
Ph <sup>b</sup>	110 °C/20 h	1			

<sup>a</sup> Reactions run in toluene, PhMeSiH<sub>2</sub> (20 mL)/C<sub>8</sub>H<sub>14</sub> (20 mL)/CH<sub>2</sub>C<sub>6</sub>H<sub>5</sub> (10 mL); Si/Ti ~30–50/1. At times shown ≥75% of the starting material has been consumed. See Experimental Section for reaction details. <sup>b</sup> Ph<sub>2</sub>SiH<sub>2</sub> (12 mL)/C<sub>8</sub>H<sub>14</sub> (8 mL)/CH<sub>2</sub>C<sub>6</sub>H<sub>5</sub> (8 mL). <sup>c</sup> Uncorrected GC data normalized to the disilane. See Experimental Section for isolation of the oligomers.

rasilane of H(PhMeSi)<sub>x</sub>H have been reported previously from the condensation of PhMeSiH<sub>2</sub> with the catalyst Cp<sub>2</sub>ZrCl<sub>2</sub>/nBuLi, the reactions were carried out on a small scale.<sup>3a</sup> For the purposes of this study, multigram quantities of each oligomer were required and it was desirable to develop conditions that would favor one of the chain lengths over the others. For this goal, the condensation of mixtures of secondary silanes and cyclooctene in the presence Cp<sub>2</sub>TiCl<sub>2</sub>/nBuLi was selected since reaction of PhMeSiH<sub>2</sub> occurs at room temperature and will thus provide more flexibility in the variation of reaction conditions.<sup>15</sup> When reactions were run at room temperature, the disilane was the major product after 1 day, and for longer periods or at higher temperatures the trisilane became the major product. Table 1 summarizes the distribution of oligomer products as a function of the conditions for both PhMeSiH<sub>2</sub> and Ph<sub>2</sub>SiH<sub>2</sub>. The reaction of PhMeSiH<sub>2</sub> at room temperature provides disilane as the predominant product after 1 day. Continued reaction at room temperature slowly converts the disilane to a mixture in which the trisilane predominates. Heating reaction mixtures produces trisilane at a faster rate, but tetrasilane appears in significant quantities. However, even with longer periods of time at higher temperatures, a maximum yield of about 35% of the tetrasilane is obtained from the oligomer mixtures. Dehydrocoupling of Ph<sub>2</sub>SiH<sub>2</sub> provides a clean conversion to H(Ph<sub>2</sub>Si)<sub>2</sub>H in 75% yield without the siloxane by-product usually found in samples prepared from the reaction of Ph<sub>2</sub>SiHCl with Mg.<sup>16</sup>

**H(PhRSi)<sub>2</sub>H (R = Me, Ph) with 1 and 2 Equiv of Triflic Acid.** The reactions of the disilane were carried out in toluene or methylene chloride with 1 or 2 equiv of acid per mole of disilane. The triflates were not isolated, and reaction mixtures were quenched with solutions of excess Grignard reagent or LiAlH<sub>4</sub> (LAH). After aqueous workup all volatile material was distilled under vacuum and the components in the reaction mixture determined by GC and GCMS. In most cases, a single major product was obtained and redistillation provided material of sufficient purity for spectroscopic studies. In some cases, preparative gas chromatography was required to remove residual impurities in order to obtain samples suitable for chemical analysis. The overall sequence for reaction of H(PhMeSi)<sub>2</sub>H with 1 and

(7) Ruehl, K. E.; Matyjaszewski, K. *J. Organomet. Chem.* **1991**, *410*, 1–12.

(8) Jarvie, A. W. P.; Winkler, H. J. S.; Peterson, D. J.; Gilman, H. *J. Am. Chem. Soc.* **1961**, *83*, 1921–1924.

(9) Hassler, K.; Poeschl, M. *J. Organomet. Chem.* **1990**, *385*, 201–206.

(10) Stüger, H. *J. Organomet. Chem.* **1993**, *458*, 1–7.

(11) Uhlig, W. *Chem. Ber.* **1992**, *125*, 47–53.

(12) Matyjaszewski, K.; Chen, Y. L. *J. Organomet. Chem.* **1988**, *340*, 7–12.

(13) Uhlig, W. *J. Organomet. Chem.* **1991**, *421*, 189–197.

(14) A preliminary report of this work has appeared. Corey, J. Y.; Kraichely, D. M.; Huhmann, J. L.; Braddock-Wilking, J. *Organometallics* **1994**, *13*, 3408–3410.

(15) The only other example of the room temperature condensation of a secondary silane involves the reaction of PhMeSiH<sub>2</sub> with CpCp\*Zr[Si(SiMe<sub>3</sub>)<sub>3</sub>]Me, but reactions were slow and run on a small scale. Imori, T.; Woo, H.-G.; Walzer, J. F.; Tilley, T. D. *Chem. Mater.* **1993**, *5*, 1487–92.

(16) Stuedel, W.; Gilman, H. *J. Am. Chem. Soc.* **1961**, *83*, 6129–6132.



**Table 2. Reaction of H(PhRSi)<sub>2</sub>H (R = Me, Ph) with 1 and 2 Equiv of HOTf Followed by Quenching with RMgX or LiAlH<sub>4</sub>**

H(PhRSi) <sub>2</sub> H R	SiPh/ HOTf <sup>a</sup>	conditions solvent <sup>b</sup> /temp	quenching agent	products (GC%)		distilled wt (g) (theoretical) <sup>c</sup>
				major	minor	
Me	2/1	A/−40 °C	MeMgBr	HPhMeSiSiMe <sub>2</sub> H (99)	PhMe <sub>4</sub> Si <sub>2</sub> H (1)	0.95 (2.13)
	2/1	A/0 °C	LiAlH <sub>4</sub>	HPhMeSiSiMe <sub>2</sub> H (99)		0.65 (1.67)
Ph	4/1	B/0 °C	MeMgBr	HPh <sub>2</sub> SiSiPhMeH (96)		0.64 (1.25)
	4/1	A/0 °C	MeMgBr	HPh <sub>2</sub> SiSiPhMeH (77)	H(PhMeSi) <sub>2</sub> H (3) Ph <sub>2</sub> Me <sub>3</sub> Si <sub>2</sub> H(18) <sup>d</sup>	1.25 (2.23)
Me	4/1.1	A/−40 °C	MeMgBr	HPh <sub>2</sub> SiSiPhMeH (80)	H(PhMeSi) <sub>2</sub> H (20)	1.95 (2.57)
	2/2	B/−20 °C	PhMgBr	H(PhMeSi) <sub>2</sub> H (89)	C <sub>6</sub> H <sub>5</sub> −C <sub>6</sub> H <sub>5</sub> (4.1) <sup>e</sup> 3 components (7.2) <sup>f</sup>	0.59 (0.99)
Ph	4/2	A/−20 °C	PhMgBr	H(PhMeSi) <sub>2</sub> H (97)	C <sub>6</sub> H <sub>5</sub> −C <sub>6</sub> H <sub>5</sub> (3) <sup>e</sup>	0.67 (1.04)
		A/−20 °C	BuMgCl	H(BuMeSi) <sub>2</sub> H (90)	2 components (10) <sup>f</sup>	0.41 (1.02)
		B/−20 °C	MeMgBr	H(PhMeSi) <sub>2</sub> H (90)	2 components (10) <sup>f</sup>	0.43 (0.93)
		A/−40 °C	MeMgBr	H(PhMeSi) <sub>2</sub> H (97)	Ph <sub>2</sub> MeSiH (2)	1.06 (1.36)

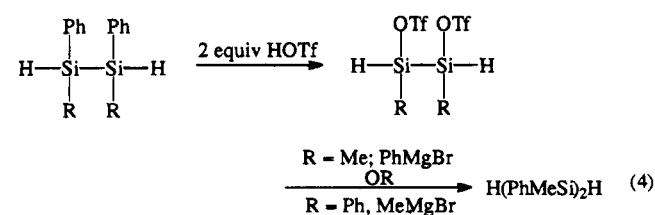
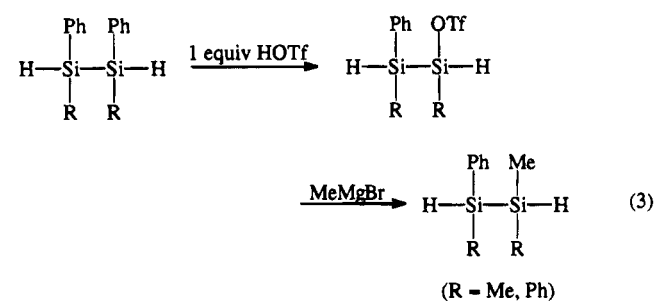
<sup>a</sup> Ratio of total moles of SiPh bonds in oligomer to number of moles of HOTf. <sup>b</sup> Solvent key: A = CH<sub>2</sub>Cl<sub>2</sub>; B = CH<sub>3</sub>C<sub>6</sub>H<sub>5</sub>. <sup>c</sup> Based on conversion to major product. <sup>d</sup> Sum of 2 isomers. <sup>e</sup> Biphenyl is present in samples of PhMgBr solution. <sup>f</sup> Components not identified.

**Table 3. Reaction of H(PhMeSi)<sub>3</sub>H with 1 to 3 Equiv of HOTf followed by quenching with RMgX or RLi**

run no.	H(PhMeSi) <sub>n</sub> H n (%) <sup>a</sup>	Si/HOTf <sup>b</sup>	conditions solvent <sup>c</sup> /temp	quenching agent	products (GC%)		distilled wt (g) (theoretical) <sup>d</sup>
					major	minor	
1	3 (>99)	1/0.33	A/−40 °C	MeMgBr	Ph <sub>2</sub> Me <sub>4</sub> Si <sub>3</sub> H <sub>2</sub> (78) (two isomers)	PhMe <sub>5</sub> Si <sub>3</sub> H <sub>2</sub> (13) Ph <sub>3</sub> Me <sub>3</sub> Si <sub>3</sub> H <sub>2</sub> (3)	1.63 (2.17)
2	3 (83) <sup>e</sup>	1/0.33	B/0 °C	LiAlH <sub>4</sub>	Ph <sub>2</sub> Me <sub>3</sub> Si <sub>3</sub> H <sub>3</sub> (83) (two isomers)	PhMe <sub>3</sub> Si <sub>3</sub> H <sub>4</sub> (4) <sup>f</sup>	1.10 (1.92)
3	3 (95); 4 (4)	1/0.67	A/−40 °C	MeMgBr	PhMe <sub>5</sub> Si <sub>3</sub> H <sub>2</sub> (97) (two isomers)	Ph <sub>2</sub> Me <sub>4</sub> Si <sub>3</sub> H <sub>2</sub> (3)	0.68 (1.52)
4	3 (78); 2 (5); 4 (5)	1/1	A/−20 °C	PhMgBr	H(PhMeSi) <sub>3</sub> H (89)	H(PhMeSi) <sub>2</sub> H (2)	0.75 (1.20)
5	3 (95); 2 (2); 4 (1)	1/1	B/0 °C	PhMgBr	Ph <sub>3</sub> Me <sub>3</sub> Si <sub>3</sub> H <sub>2</sub> (75) (two isomers)		0.41 (1.05)
6	3 (65); 2 (3); 4 (32)	1/1	C/0 °C	BuLi	Bu <sub>3</sub> Me <sub>3</sub> Si <sub>3</sub> H <sub>2</sub> (46) (two isomers)	Bu <sub>x</sub> Me <sub>x</sub> Si <sub>x</sub> H <sub>2</sub> x = 2 (5); 4 (20); <sup>f</sup> 5 (7) <sup>g,h</sup>	0.96 (1.65)
7	3 (94); 4 (3)	1/1	B/0 °C	BuLi	Bu <sub>3</sub> Me <sub>3</sub> Si <sub>3</sub> H <sub>2</sub> (65) (two isomers)	Bu <sub>2</sub> Me <sub>3</sub> Si <sub>3</sub> H <sub>3</sub> (9.2) Bu <sub>4</sub> Me <sub>3</sub> Si <sub>3</sub> H (6.5) Bu <sub>3</sub> Me <sub>2</sub> Si <sub>3</sub> H (4.8)	1.24 (1.84)
8	3 (82); 2 (5); 4 (6)	1/1	B/−40 °C	BuLi	PhBu <sub>2</sub> Me <sub>3</sub> Si <sub>3</sub> H <sub>2</sub> (74)	H(BuMeSi) <sub>3</sub> H (5)	0.93 (1.73)
9	3 (>99)	1/1	A/−40 °C	BuMgCl	PhBu <sub>2</sub> Me <sub>3</sub> Si <sub>3</sub> H <sub>2</sub> (67)	Bu <sub>3</sub> Me <sub>3</sub> Si <sub>3</sub> H <sub>2</sub> (33)	0.58 (1.58)

<sup>a</sup> Percentage from uncorrected GC data. <sup>b</sup> Ratio of SiPh/HOTf. <sup>c</sup> Solvent key: A = CH<sub>2</sub>Cl<sub>2</sub>; B = C<sub>6</sub>H<sub>5</sub>CH<sub>3</sub>; C = n-C<sub>6</sub>H<sub>14</sub>. Temperature listed is temperature for addition of HOTf and for quenching reaction. <sup>d</sup> Based on conversion to major product. <sup>e</sup> Ph<sub>2</sub>Me<sub>2</sub>Si<sub>2</sub>H(C<sub>7</sub>H<sub>11</sub>) (17%); hydrosilylation product of norbornene used to promote oligomer formation. <sup>f</sup> PhMe<sub>2</sub>(C<sub>7</sub>H<sub>11</sub>)Si<sub>2</sub>H (11%; 2 isomers). <sup>g</sup> Three isomers. <sup>h</sup> Starting pentasilane not observed in GC trace.

2 equiv of HOTf is summarized in eqs 3 and 4, respectively. Typical results of these reactions are



summarized in Table 2. Although the major component obtained from the isolated, volatile material was that expected from the sequence in eqs 3 and 4, the mass recovery in all cases was low and usually varied from

about 30% to 75%. The nature of the nondistilled material was not determined. The major product is produced more cleanly in reactions run below 0 °C and in CH<sub>2</sub>Cl<sub>2</sub>. This is particularly the case for reactions run with 2 equiv of HOTf compared to those with 1 equiv of the acid.

**Reaction of H(PhMeSi)<sub>3</sub>H with Triflic Acid.** The trisilane was treated with 1, 2, and 3 equiv of triflic acid followed by quenching with Grignard reagents in the manner described for the disilane. The results are summarized in Table 3. Although one major product of composition Ph<sub>2</sub>Me<sub>4</sub>Si<sub>3</sub>H<sub>2</sub> was expected when the trisilane was treated with 1 equiv of HOTf followed by MeMgBr (run 1, Table 3) there are actually two products with this composition. Likewise, the reaction of the trisilane with 2 equiv of HOTf followed by quenching with MeMgBr produced two isomers of PhMe<sub>5</sub>Si<sub>3</sub>H<sub>2</sub> (run 2, Table 3). When 3 equiv of HOTf are added to H(PhMeSi)<sub>3</sub>H at low temperatures (−40 °C; runs 7 and 8) followed by treatment with RM (R = Ph, Bu; M = Li, MgBr), PhR<sub>2</sub>Me<sub>3</sub>Si<sub>3</sub>H<sub>2</sub> is the major product, but at higher temperatures the major product contains two isomers of R<sub>3</sub>Me<sub>3</sub>Si<sub>3</sub>H<sub>2</sub> (R = Ph, Bu; runs 4, 5, and 6). In all cases, the reaction mixtures contained several minor components, particularly for the experiments performed in either hexane or toluene solvents, and, in addition, mass recovery was usually below 65%. The

formation of isomeric products was independent of the commercial source of triflic acid and occurred with HOTf from freshly opened sealed glass ampules and when either freshly distilled or "aged" triflic acid was used. The yields of distilled trisilane products were sometimes lower in distilled samples of triflic acid that had been stored over a drying agent in the freezer for periods of time prior to use.

### Discussion

In this study, the reactions of oligomers of the type  $H(\text{PhMeSi})_x\text{H}$  ( $x = 2, 3$ ) with 1 to  $x$  equiv of triflic acid were conducted in hexanes, toluene, or methylene chloride at temperatures ranging from below  $-40^\circ\text{C}$  to room temperature. The triflates that were produced were neither isolated nor characterized in solution but were converted to products that were air and moisture stable by reaction with Grignard reagents or with LAH. All volatile material was removed from the product mixture, the composition of the major components was determined by GCMS, and, when possible, assignments for the minor components were attempted; such data are included in Tables 2 and 3. More by-products were observed in reactions that were conducted in hexanes, therefore the bulk of the investigation concentrated on results obtained in toluene and methylene chloride. In reactions of the trisilanes, the major products were obtained as a mixture of structural isomers in contrast to the expectation of one product on the basis of literature precedence. Therefore, an important aspect of the study became the characterization of the isomeric mixtures, which, in most cases could not be separated. Purification was achieved either by several redistillations or by preparative gas chromatography to obtain material suitable for spectroscopic and chemical analysis. Spectroscopic data ( $^1\text{H}$ ,  $^{13}\text{C}$ , and  $^{29}\text{Si}$ ) were usually collected in both  $\text{C}_6\text{D}_6$  and  $\text{CDCl}_3$  as the chemical shift values, particularly for the Si-H resonances, were influenced by the solvent. Samples of the silicon oligomers begin to decompose in  $\text{CDCl}_3$  after about 2 days and therefore data are reported only for freshly prepared solutions.

In the discussion that follows the focus is on  $^1\text{H}$  NMR data for SiH and SiMe regions since the aryl region was not useful in distinguishing structural features of the new oligomers. The  $^3J_{\text{CHSiH}}$  coupling constants were utilized to distinguish which signals in the SiMe region of the  $^1\text{H}$  NMR spectra corresponded to multiplets associated with HSiMe units. In some cases, COSY experiments were required to determine the coupling of an SiH multiplet with the appropriate SiMe resonance(s).

**Characterization of Disilane Products.** The reaction of  $H(\text{PhRSi})_2\text{H}$  with 1 equiv of triflic acid should provide the intermediate triflate,  $\text{HPhRSiSi}(\text{OTf})\text{RH}$  ( $\text{R} = \text{Me}, \text{Ph}$ ) from which disilanes with different sets of substituents at each silicon center can be obtained, in principle, by standard silicon substitution chemistry. In this study, the triflates were quenched with  $\text{MeMgBr}$  to give  $\text{HPhMeSiSiMe}_2\text{H}$  and  $\text{HPh}_2\text{SiSiPhMeH}$  or with LAH to provide  $\text{HPhMeSiSiMeH}_2$ . The disilanes  $\text{HPhMeSiSiMe}_2\text{H}$  and  $\text{HPh}_2\text{SiSiPhMeH}$  have previously been reported in about 50% yield from the Na cross-coupling condensation of  $\text{HMePhSiCl}$  with  $\text{HMe}_2\text{SiCl}$  and  $\text{HPh}_2\text{SiCl}$ , respectively.<sup>17</sup> The preparation of  $\text{HPh}$

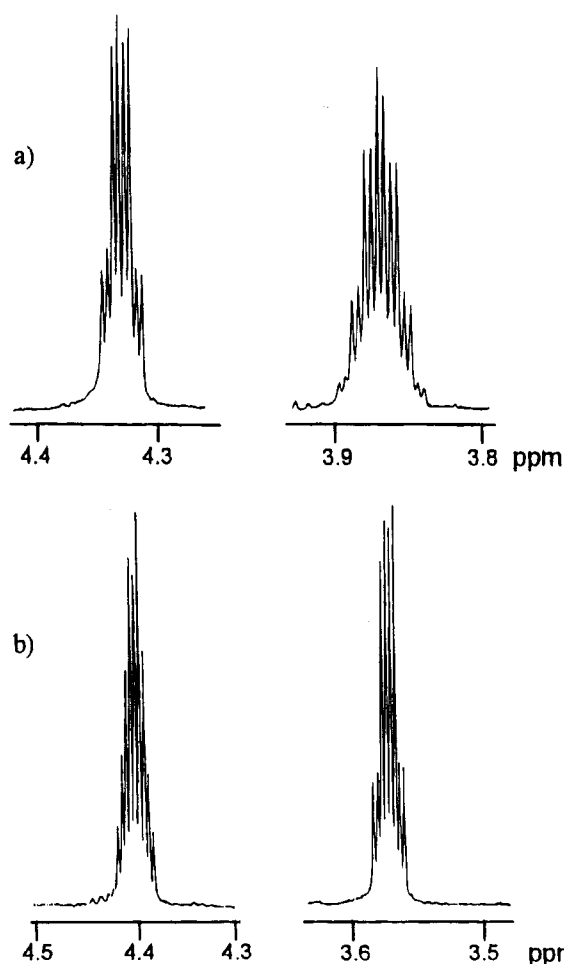


**Figure 1.**  $^1\text{H}$  NMR (500 MHz,  $\text{CDCl}_3$ ) for the SiH region: (a)  $\text{HPhMeSiSiMe}_2\text{H}$ ; (b)  $\text{HPhMeSiSiMeH}_2$ .

$\text{MeSiSiMeH}_2$  required the condensation of  $\text{MeH}_2\text{SiOTf}$  with  $\text{Ph}_2\text{MeSiLi}$  followed by reaction of the  $\text{Ph}_2\text{MeSiSiMeH}_2$  produced with 1 equiv of HOTf and subsequent reduction of the isolated  $(\text{TfO})\text{PhMeSiSiMeH}_2$  with LAH.<sup>18</sup>

One of the most useful spectroscopic characteristics of the disilanes involves the  $^1\text{H}$  NMR data of the SiH region. In a 1,2-dihydrodisilane of the type  $\text{HR}^1\text{R}^2\text{SiSiR}^3\text{R}^4\text{H}$  there are two distinctly separated SiH regions and the effect of the SiH-SiH coupling of 2.5 Hz is directly observed as illustrated in the expanded view of the SiH region of Figure 1. The spectrum of  $\text{H}_a\text{PhMeSiSiMe}_2\text{H}_b$  exhibits a quartet of doublets for  $\text{H}_a$  and a septet of doublets for  $\text{H}_b$ . In contrast to the quartet of doublets observed for the SiMe<sub>2</sub> unit, the quartet of triplets for  $\text{H}_a$  in  $\text{H}_a\text{PhMeSiSiMeH}_2$  was not completely resolved as a result of the overlap of the triplets of the inner lines of the quartet.

When  $\text{H}(\text{PhMeSi})_2\text{H}$  is treated with 2 equiv of HOTf followed by  $\text{PhMgBr}$ , the starting disilane is regenerated as the major product and exhibits the same spectroscopic properties as  $\text{H}(\text{PhMeSi})_2\text{H}$  produced from dehydrocoupling. Although the overall mass recovery was similar in reactions run in toluene and in  $\text{CH}_2\text{Cl}_2$  the

(17) Gerval, P.; Frainnet, E.; Lain, G.; Moulines, F. *Bull. Soc. Chim. Fr.* **1974**, 1548-1552.

(18) Uhlig, W. Z. *Anorg. Allg. Chem.* **1993**, 619, 1479-1482. The  $^1\text{H}$  NMR ( $\delta$ ;  $\text{CDCl}_3$ ) data for  $\text{H}_2\text{MeSiSiPhMeH}$  are reported at 0.09 (t,  $\text{H}_2\text{SiMe}$ ), 0.21 (d,  $\text{HPhMe}$ ), 3.60 (dq,  $\text{H}_2\text{SiMe}$ ), and 3.64 (m,  $\text{HSiPhMe}$ ).

latter solvent tends to produce fewer by-products. When the ditriflate  $\text{H}[\text{Me}(\text{OTf})\text{Si}]_2\text{H}$  was treated with  $\text{BuMgCl}$ ,  $\text{H}(\text{BuMeSi})_2\text{H}$  was isolated in modest yields. Alkylated disilanes of the type  $\text{H}(\text{RR}'\text{Si})_2\text{H}$  are not easily prepared by dehydrocoupling of  $\text{RR}'\text{SiH}_2$ ,<sup>3b</sup> but  $\text{H}(\text{BuMeSi})_2\text{H}$  has been prepared from the Na coupling of  $\text{BuMeSiHCl}$ .<sup>19</sup>

**Characterization of Trisilane Products.** The reactions of  $\text{H}(\text{PhMeSi})_3\text{H}$  with 1, 2, or 3 equivalents of HOTf followed an unexpected course. When  $(\text{TfO})\text{Ph}_2\text{Me}_3\text{Si}_3\text{H}_2$  was quenched with  $\text{MeMgBr}$ , two isomers of  $\text{Ph}_2\text{Me}_4\text{Si}_3\text{H}_2$  were obtained which could not be separated but could be removed from the minor components by preparative gas chromatography. The  $^1\text{H}$  NMR spectrum ( $\text{C}_6\text{D}_6$ ) of the mixture exhibited three distinct SiH multiplets centered at 4.17, 4.58, and 4.73 ppm. The quartet centered at 4.73 ppm and the septet at 4.17 ppm are present in a 1:1 ratio and thus are consistent with the trisilane  $\text{HPhMeSi}(\text{SiPhMe})\text{SiMe}_2\text{H}$  (major isomer) which would result from removal of a terminal phenyl group and replacement of the triflate with a Me group. The multiplet (two quartets overlap to form a quintet in  $\text{C}_6\text{D}_6$ ; two resolved quartets in  $\text{CDCl}_3$ ) centered at 4.58 ppm suggests a trisilane that has terminal silicon centers with the same substituents and is assigned to  $\text{HPhMeSi}(\text{SiMe}_2)\text{SiMePhH}$ , the isomer that would result from cleavage of the internal phenyl group. The ratio of major to minor isomer was 2.7:1. The Me region of the  $^1\text{H}$  NMR spectrum is more complicated. If all signals are observed in the Me region for the mixture of  $\text{H}^a\text{PhMe}^a\text{SiSiSiPhMe}^b\text{SiMe}^c\text{H}^c$  and  $\text{H}^d\text{PhMe}^d\text{SiSiMe}^e\text{SiPhMe}^d\text{H}^d$  there would be 2 doublets for  $\text{Me}^a$ , 2 singlets for  $\text{Me}^b$  and 4 doublets for  $\text{Me}^c$  (diastereotopic Me groups) in addition to 2 doublets for  $\text{Me}^d$  and 2 singlets for  $\text{Me}^e$  (diastereotopic Me groups). All of these resonances are observed as illustrated in Figure 1a (see also Experimental Section). The coupling of  $\text{H}^a$  with  $\text{Me}^a$ ,  $\text{H}^c$  with  $\text{Me}^c$ , and  $\text{H}^d$  with  $\text{Me}^d$  was verified by COSY experiments. In a similar fashion, when  $(\text{TfO})\text{Ph}_2\text{Me}_3\text{Si}_3\text{H}_2$  was quenched with  $\text{LiAlH}_4$ , two isomers of  $\text{Ph}_2\text{Me}_3\text{Si}_3\text{H}_3$  were obtained in a 2.6:1 ratio and could be separated by preparative gas chromatography. The  $^1\text{H}$  NMR spectrum ( $\text{C}_6\text{D}_6$ ) of the major isomer,  $\text{H}_a\text{PhMe}_a\text{SiSiPhMe}_b\text{SiMe}_c\text{H}_b\text{H}_b'$  (Figure 2b), exhibits 2 multiplets in the SiH region, a quartet at 4.71 ppm ( $\text{SiH}_a$ ), and a multiplet at 3.87 ppm ( $\text{SiH}_b\text{H}_b'$ ; diastereotopic protons would generate a total of 4 quartets for the 2 diastereomers) in a 1:2 ratio. The resonances for  $\text{Me}_c$  for the two diastereomers are coincident and observed as an apparent triplet (centered at  $\delta = 0.04$ ) but  $\text{Me}_a$  and  $\text{Me}_b$  exhibit 2 doublets ( $\delta = 0.40, 0.43$ ) and 2 singlets ( $\delta = 0.441, 0.445$ ), respectively. The SiH resonances of the minor isomer,  $\text{H}_a\text{PhMe}_a\text{SiSiMeH}_b\text{SiPhMeH}_a$  (4 diastereomers: 2 *meso* and 2 *dl* forms), are observed as unresolved multiplets centered at 3.76 ( $\text{H}_b$ ) and 4.67 ( $\text{H}_a$ ) in a 1:2 ratio. If all SiMe resonances were observed there would be 6 doublets associated with the  $\text{MeSiPhH}_a$  unit and 4 doublets associated with the  $\text{MeSiH}_b$  unit. However, there are 4 discernible doublets for  $\text{MeSiPhH}_a$  (centered at  $\delta = 0.34$ ; coupling to  $\text{H}_a$  was verified by a COSY experiment) and at least 3 doublets for  $\text{MeSiH}_b$  ( $\delta = 0.15$ ; Figure 1c). As the number of diastereomers increases the possibility of coincidence of resonances increases and it is not possible to determine whether

all diastereomers are present on the basis of the  $^1\text{H}$  NMR data.

When  $\text{H}(\text{PhMeSi})_3\text{H}$  was treated with 2 equiv of HOTf followed by  $\text{MeMgBr}$ , both GC and GCMS data appear to support formation of a single isomer of  $\text{PhMe}_5\text{Si}_3\text{H}_2$ . However, after purification by preparative gas chromatography, the  $^1\text{H}$  NMR spectrum revealed that a minor isomer was present. The major isomer,  $\text{PhMe}_a\text{Si}(\text{SiMe}_b\text{Me}_b'\text{H})_2$ , exhibited a clean septet at  $\delta = 4.18$  ( $\text{HMe}_2\text{Si}$ ), a singlet for  $\text{Me}_a$  ( $\delta = 0.43$ ) and 2 resonances at  $\delta 0.16$  and  $0.18$  for  $\text{Me}_b$  and  $\text{Me}_b'$  (diastereotopic Me groups). The resonances for the minor isomer,  $\text{H}_a\text{SiPhMe}_a\text{SiMe}_b\text{Me}_b'\text{Si}(\text{Me}_c)_2\text{H}_b$  include multiplets at  $\delta 4.59$  ( $\text{SiH}_a$ ) and  $4.02$  ( $\text{SiH}_b$ ) in addition to a doublet for  $\text{Me}_a$  and an apparent triplet assigned to  $\text{SiMe}_b\text{Me}_b'$  ( $\delta = 0.09$ ; signals due to  $\text{Si}(\text{Me}_c)_2$  appear to overlap with the  $\text{SiMe}_2\text{H}$  resonances of the major isomer that are centered at  $0.18$  ppm). The ratio of the major to the minor isomers is 13:1 for reactions conducted at low temperature but decrease to a value of about 6:1 when the temperature is increased.

In the reactions of  $\text{H}(\text{PhMeSi})_3\text{H}$  with 3 equiv of HOTf conducted in toluene or hexane at room temperature followed by addition of  $\text{PhMgBr}$  a mixture of two isomers of  $\text{Ph}_3\text{Me}_3\text{Si}_3\text{H}_2$  was obtained. The spectroscopic properties of the major isomer were consistent with starting trisilane. The minor isomer exhibited SiH multiplets centered at  $\delta = 4.4$  and  $3.6$  ( $\text{CDCl}_3$ ) and 2 SiMe singlets ( $\delta = 0.57$  and  $0.59$ ). The upfield SiH resonance supports an internal  $\text{HSiMe}$  unit and the singlets suggest a Me group that is not coupled to an SiH. The structure of  $\text{HPhMeSiSiMeHSiPh}_2\text{Me}$  is consistent with the observed NMR data. The  $\text{Ph}_3\text{Me}_3\text{Si}_3\text{H}_2$  mixtures could not be suitably purified; thus, confirmation of the formation of two different triflates was developed from quenching  $(\text{TfO})_3\text{Me}_3\text{Si}_3\text{H}_2$  solutions with  $\text{BuMgBr}$  to give two isomers of  $\text{Bu}_3\text{Me}_3\text{Si}_3\text{H}_2$ . The SiH region of the proton spectrum ( $\text{CDCl}_3$ ) exhibited a sextet at  $\delta = 3.68$  consistent with  $\text{H}(\text{BuMeSi})_3\text{H}$  and two multiplets at  $\delta = 3.16$  and  $3.77$  for the minor isomer. The Si-Me resonances of the 3 diastereomers (2 *meso* forms and one *dl* form) of the major isomer are coincident and exhibit a singlet and a doublet at  $\delta = 0.14$  and  $0.13$  respectively. The Me groups for the minor isomer appear as a singlet ( $\delta = 0.085$ ) and as two doublets ( $\delta = 0.16$  and  $0.17$ ) both with a  $^3J_{\text{CHSiH}}$  coupling of 4.5 Hz. The resonances of the Bu groups of the two isomers overlap between 0.8 and 1.5 ppm and were not useful in assignment of the structure. The  $^1\text{H}$  NMR data combined with the  $^{29}\text{Si}$  data (discussed in a later section) are consistent with an assignment of the second isomer as  $\text{HBuMeSiSiMeHSiBu}_2\text{Me}$ . The ratio of  $\text{H}(\text{BuMeSi})_3\text{H}$  to  $\text{HBuMeSiSiMeHSiBu}_2\text{Me}$  varied between 1:1 and 2:1.

When reactions of  $\text{H}(\text{PhMeSi})_3\text{H}$  are conducted at low temperatures in  $\text{CH}_2\text{Cl}_2$  with 3 equiv of HOTf, cleavage of the last phenyl group was sufficiently slow that, when the reaction mixture was quenched with  $\text{BuMgBr}$ ,  $\text{PhBu}_2\text{Me}_3\text{Si}_3\text{H}_2$  was obtained (see Table 3). The major product was  $\text{HBuMeSiSiPhMeSiBuMeH}$  (2 *meso* and 2 *dl* pairs are possible; Figure 1d), which exhibits an unresolved SiH multiplet at  $\delta = 4.16$  in addition to singlets at  $\delta = 0.530, 0.525$ , and  $0.520$  (ratio 1:2:1) for the internal SiMe group and 2 doublets of equal intensity at  $\delta = 0.24$  and  $0.22$  ( $^3J_{\text{CHSiH}} = 4.6$ ) for the

(19) Trefonas, P., III; West, R.; Miller, R. D. *J. Am. Chem. Soc.* **1985**, *107*, 2737-2742.

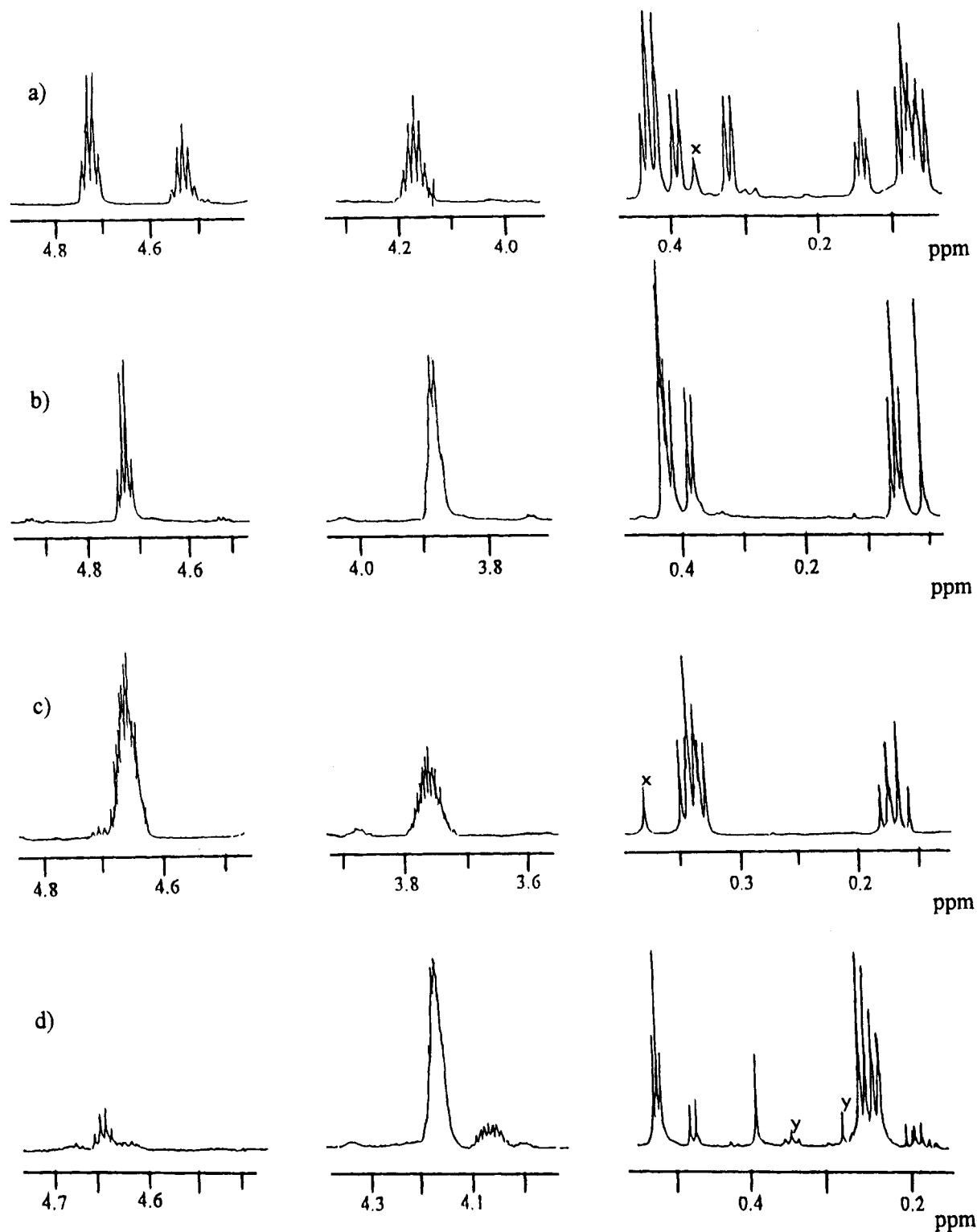


**Figure 2.**  $^1\text{H}$  NMR (500 MHz,  $\text{C}_6\text{D}_6$ ) data for SiH and SiMe regions for selected trisilanes ( $x = \text{H}_2\text{O}$ ;  $y = \text{impurity peaks}$ ): (a) mixture of  $\text{HPhMeSiSiPhMeSiMe}_2\text{H}$  and  $\text{HPhMeSiSiMe}_2\text{SiPhMeH}$ ; (b)  $\text{HPhMeSiSiPhMeSiMeH}_2$ ; (c)  $\text{HPhMeSiSiHMeSiPhMeH}$ ; (d) mixture of  $\text{HBuMeSiSiPhMeSiBuMeH}$  and  $\text{HBuMeSiSiBuMeSiPhMeH}$ . See text and Experimental Section for assignments.

terminal SiMe groups. If two of the internal SiMe resonances of the four diastereomers overlap, then the 1:2:1 ratio of the singlets near 0.52 ppm suggest that the diastereomers are present in equal quantities. When the reaction was run at higher temperatures a second isomer is produced, which has been tentatively assigned the structure  $\text{HBuMeSiSiBuMeSiPhMeH}$  on the basis of two SiH multiplets centered at  $\delta = 4.67$  (quartet for  $\text{SiPhMeH}$ ) and 4.04 [septet (overlapping

sextets) for  $\text{SiBuMeH}$ ], an SiMe doublet at 0.48 ppm for the  $\text{SiPhMeH}$  unit, and 4 SiMe doublets between 0.17 and 0.14 ppm assigned to the terminal  $\text{SiBuMeH}$ . The internal SiMe resonances overlap with the SiMe doublets of the major isomer.

**Characterization of Oligomer Products by  $^{29}\text{Si}$  NMR Spectroscopy.** The  $^{29}\text{Si}$  NMR data are provided in Table 4. Unlike the  $^1\text{H}$  NMR data,  $^{29}\text{Si}$  NMR chemical shifts in these oligomers do not seem to be

**Table 4.**  $^{29}\text{Si}$  NMR Assignments for Silicon Oligomers

compd	HPhMeSi	H <sub>2</sub> MeSi	HMe <sub>2</sub> Si	HPh <sub>2</sub> Si	PhMeSi	Me <sub>2</sub> Si	HBuMeSi	BuMeSi	SiMeH	SiR <sub>2</sub> Me
HPhMeSiSiMeH <sub>2</sub> <sup>a</sup>	-36.54	-66.27								
HPhMeSiSiMe <sub>2</sub> H <sup>a</sup>	-36.01		-39.46							
HPhMeSiSiMePhH <sup>a,b,c</sup>	-36.37									
	-36.80									
HPh <sub>2</sub> SiSiMePhH <sup>a</sup>	-37.71			-32.97						
HPh <sub>2</sub> SiSiPh <sub>2</sub> H <sup>a</sup>				-34.97						
HBuMeSiSiMeBuH <sup>a,c</sup>							-33.1			
HPhMeSi(SiPhMe)SiPhMeH <sup>a,d</sup>	-34.06				-45.78					
	-34.07				-45.92					
	-34.13				-46.11					
	-34.20									
HPhMeSi(SiHMe)SiPh <sub>2</sub> Me <sup>e,f</sup>	-34.09 <sup>g</sup>								-73.62	-17.72 (Ph)
									-73.80	-17.74 (Ph)
HPhMeSi(SiPhMe)SiMe <sub>2</sub> H <sup>a,f</sup>	-33.30		-36.68		-45.45					
	-33.37		-36.82		-45.57					
HPhMeSi(SiMe <sub>2</sub> )SiMePhH <sup>a,c</sup>	-34.14					-47.22				
	-34.15					-47.23				
HPhMeSi(SiPhMe)SiMeH <sub>2</sub> <sup>e,f</sup>	-33.94	-64.44			-45.07					
		-64.77			-45.26					
HPhMeSi(SiMeH)SiPhMeH <sup>e,h</sup>	-33.56								-73.27	
	-33.62								-73.38	
	-33.72								-73.50	
	-33.83									
HMe <sub>2</sub> Si(SiMePh)SiMe <sub>2</sub> H <sup>a</sup>			-37.20		-45.47					
HMe <sub>2</sub> Si(SiMe <sub>2</sub> )SiPhMeH <sup>e</sup>	-33.14		-36.14			-47.15				
HBuMeSi(SiBuMe)SiMeBuH <sup>a,d</sup>							-33.06	-44.42		
							-33.09	-44.45		
							-33.10	-44.48		
							-33.12			
HBuMeSi(SiMeH)SiBu <sub>2</sub> Me <sup>a,f</sup>							-32.16		-76.49	-9.95 (Bu)
							-32.54		-77.18	-10.01 (Bu)
HBuMeSi(SiPhMe)SiMeBuH <sup>e,h</sup>					-46.12 <sup>a</sup>		-32.62 <sup>a</sup>			
					-46.21 <sup>e</sup>		-32.65 <sup>e</sup>			
					-46.23 <sup>e</sup>		-32.71 <sup>e</sup>			
							-32.75 <sup>e</sup>			

<sup>a</sup> CDCl<sub>3</sub>. <sup>b</sup> From dehydrocoupling. <sup>c</sup> Two diastereomers (1 *meso* + 1 *dl*). <sup>d</sup> Three diastereomers (2 *meso* and 1 *dl*). <sup>e</sup> C<sub>6</sub>D<sub>6</sub>. <sup>f</sup> Two diastereomers (2 *dl* forms). <sup>g</sup> The second signal overlaps with the major isomer. <sup>h</sup> Four diastereomers (2 *meso* and 2 *dl*).

influenced in any significant way by solvent.<sup>14</sup> The data in Table 4 are organized by the nature of the silicon unit and demonstrate the similarities for the same unit in different compounds. As an example, the range of the  $^{29}\text{Si}$  chemical shift values for the terminal HPhMeSi group in seven trisilanes and also for the internal PhMeSi unit present in five trisilanes was about 1 ppm. In the two types of trisilanes, H(RMeSi)<sub>3</sub>H (R = Ph, Bu), the  $^{29}\text{Si}$  chemical shift difference between HRMeSi (terminal) and RMeSi (internal) was about 10 ppm but the value of the chemical shift was not particularly sensitive to the R group (in this case, Ph vs Bu) although a terminal HMe<sub>2</sub>Si may be distinguished from HRMeSi (R = Ph, Bu).

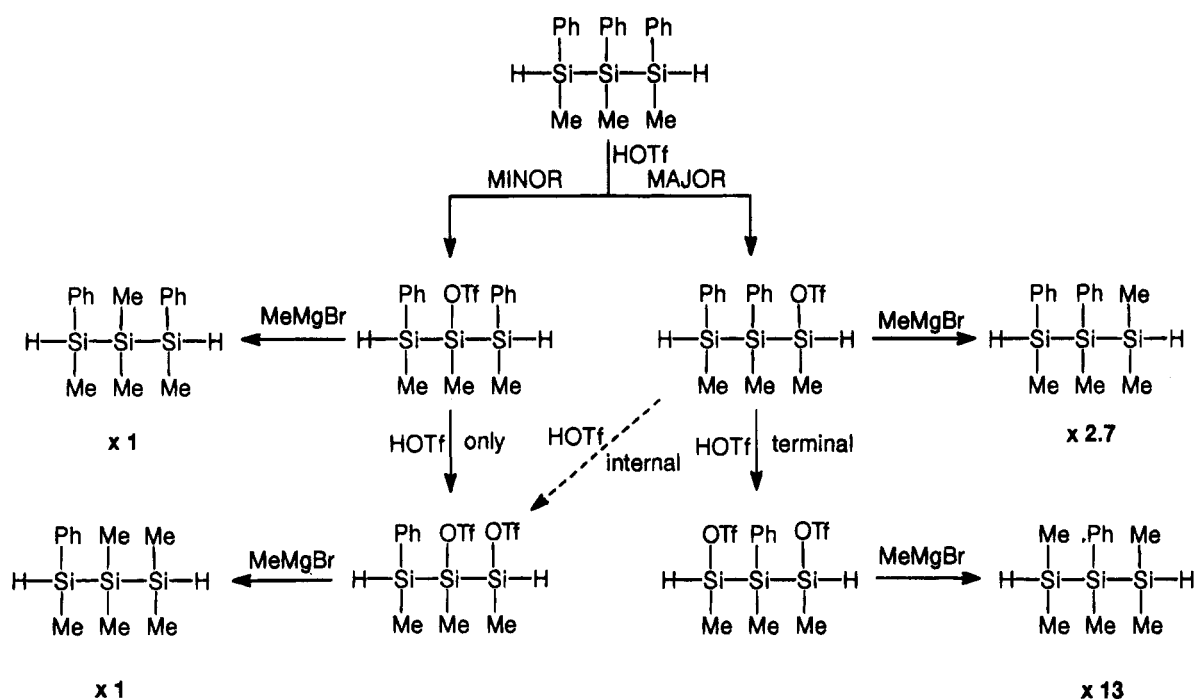
A key point revealed by the  $^{29}\text{Si}$  data was support for the number of diastereomers present. Seven of the oligomers in Table 4 should be present as a mixture of two diastereomers. The two disilanes, HPhMeSiSiMePhH and HBuMeSiSiMeBuH, would be formed as a mixture of *meso* and *dl* forms and should give rise to one  $^{29}\text{Si}$  signal for each diastereomer. Similarly, the trisilane HPhMeSiSiMe<sub>2</sub>SiMePhH should be present as two diastereomers (*meso* and *dl*) but would exhibit two  $^{29}\text{Si}$  signals for each diastereomer since there are two types of silicon centers. The trisilanes HPhMeSiSiHMeSiR<sub>2</sub>Me (R = Ph, Bu) and HPhMeSiPhMeSiMeRH (R = Me, H) should exist as mixtures of two chiral diastereomers, and since each of the silicon centers is uniquely substituted there should be three  $^{29}\text{Si}$  signals for each of the two diastereomers. The number of signals corresponds to that expected except for HBuMeSiSiMeBuH, where only one of the two  $^{29}\text{Si}$  resonances

was observed. In the remaining trisilanes the number of diastereomers increases. For the case of H(RMeSi)<sub>3</sub>H (R = Ph, Bu) there are three diastereomers (two *meso* forms and one *dl* form) and seven  $^{29}\text{Si}$  resonances are predicted (four for the terminal Si and three for the internal Si). All seven are observed for each of the two systems (R = Ph, Bu). Thus, the  $^{29}\text{Si}$  data support a mixture of diastereomers for H(BuMeSi)<sub>3</sub>H although the Si-Me <sup>1</sup>H resonances coincide for the three diastereomers. In the two examples HPhMeSiSiMeHSiMePhH and HBuMeSiSiPhMeSiMeBuH, there should be four diastereomers (two *meso* forms and two *dl* forms) with a total of 10 signals. For HPhMeSiSiMeHSiMePhH, seven of the 10 are observed and for HBuMeSiSiPhMeSiMeBuH, five of the 10 are observed. Although it is possible that a nonstatistical mixture of diastereomers was produced, it is likely that the differences in chemical shifts of all four diastereomers is too small to be resolved. The remaining six examples in Table 4 contain either no chiral centers or one chiral center, and therefore only one signal is observed for each of the unique silicon centers.

Another important observation from the  $^{29}\text{Si}$  data was the support for the assignment of the structure of the minor isomer produced in the reaction of H(PhMeSi)<sub>3</sub>H with 3 equiv of HOTf. The presence of an SiH in an internal position results in an upfield shift of the  $^{29}\text{Si}$  resonance by  $\geq 40$  ppm compared to the terminal position in HMe<sub>2</sub>SiSMeHSiMe<sub>2</sub>H.<sup>20</sup> A similar trend was

(20) Schenzel, K.; Hassler, K. *Spectrochim. Acta* **1994**, *50A*, 127-138.

**Scheme 1. Summary of the Reaction of  $H(\text{PhMeSi})_3\text{H}$  with 1 and 2 Equiv of HOTf Followed by Quenching with MeMgBr**



demonstrated in the minor isomer,  $\text{HPhMeSiSiMeH-SiPhMeH}$ , produced from  $H(\text{PhMeSi})_3\text{H}$  and 1 equiv of HOTf after quenching with LAH. In this case, the minor isomer was separated from the major isomer prior to characterization. The minor isomer  $\text{HRMeSiSiMeH-SiR}_2\text{Me}$ , produced from reaction of  $H(\text{PhMeSi})_3\text{H}$  and 3 equiv of HOTf, had to be determined in the mixture but could easily be identified by the upfield shift for the central silicon.

**Competitive Cleavage of Si-Ph and Rearrangement.** Although the yields in the reactions of the disilanes  $H(\text{PhRSi})_2\text{H}$  ( $R = \text{Me, Ph}$ ) are not particularly high, the reactions follow the patterns described in the literature by Uhlig<sup>13,18</sup> and Matyjaszewski.<sup>7,12</sup> The phenyl groups were cleaved in preference to SiH, and in the case of  $H(\text{Ph}_2\text{Si})_2\text{H}$  one phenyl group from each silicon center was removed on treatment with 2 equiv of HOTf, as determined from quenching with MeMgBr. There was no evidence for the formation of  $\text{HPh}_2\text{-SiSiMe}_2\text{H}$ .

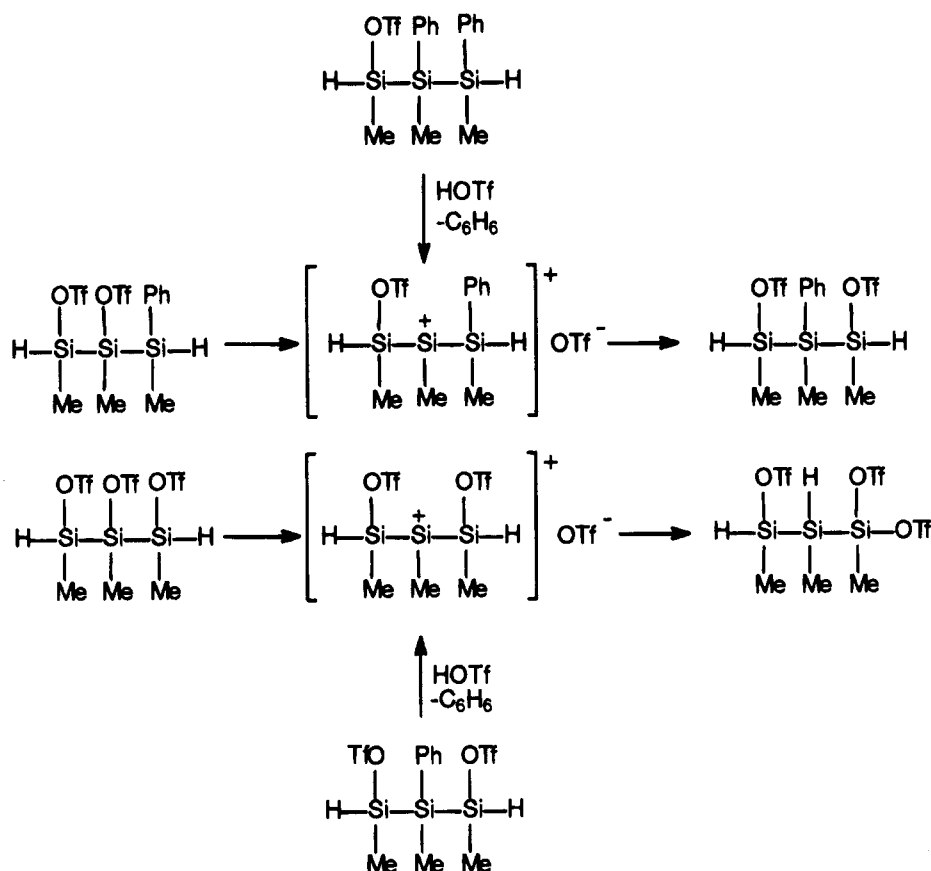
However, the results with trisilanes, which are summarized in Scheme 1, differ from those reported in the literature. Only the cleavage of terminal SiPh groups occurred when  $\text{Ph}_3\text{SiSiPh}_2\text{SiPhR}_2$  ( $R = \text{Ph, Me}$ )<sup>18</sup> was treated with either 1 or 2 equiv of HOTf. When 1 equiv of HOTf was added to  $H(\text{PhMeSi})_3\text{H}$  followed by a quenching agent, two structural isomers of  $\text{Ph}_2\text{Me}_3\text{-RSi}_3\text{H}_2$  ( $R = \text{Me, H}$ ) were obtained. In the case of  $\text{Ph}_2\text{-Me}_3\text{Si}_3\text{H}_3$ , the two isomers could be separated and thus the characterization did not have to depend on assignment of resonances in the mixture (compare Figure 1a to 1b and 1c). In order to demonstrate that cleavage of internal Si-Ph groups competed with terminal Si-Ph group cleavage it was necessary to prepare the labeled trisilane  $\text{HPh}_D\text{MeSiSiPhMeSiPh}_D\text{MeH}$  ( $\text{Ph}_D = \text{C}_6\text{D}_5$ ). By monitoring the reaction of the labeled trisilane with 1 equiv of HOTf by  $^1\text{H}$  NMR spectroscopy it could be

demonstrated that both  $\text{C}_6\text{H}_5$  and  $\text{C}_6\text{D}_5$  were removed in approximately a 1:2.6 ratio, which corresponds closely to the ratio of 1:2.7 observed for the  $\text{Ph}_2\text{Me}_4\text{Si}_3\text{H}_2$  products produced on quenching with MeMgBr (see Scheme 1).<sup>14</sup>

The reaction of  $H(\text{PhMeSi})_3\text{H}$  with a second equivalent of HOTf also resulted in the formation of products that were structural isomers. However, in this case, the ratio of the isomers of  $\text{PhMe}_5\text{Si}_3\text{H}_2$  did not correspond to that which would be expected on the basis of the observed ratio between the isomers of  $\text{Ph}_2\text{Me}_4\text{Si}_3\text{H}_2$  produced from 1 equiv of HOTf (see Scheme 1). Since the minor isomer  $\text{HPhMeSiSi(OTf)MeSiMePhH}$  can only react by cleavage of a terminal SiPh and the major isomer  $\text{HPhMeSiSiPhMeSi(OTf)MeH}$  could react by removal of either a terminal or an internal SiPh, with the former expected to dominate, the two bistriflates,  $\text{Ph(TfO)}_2\text{Me}_3\text{Si}_3\text{H}_2$ , should be observed in a ratio near or less than 2.7:1. Instead, the ratio of  $\text{HMe}_2\text{-SiSiPhMeSiMe}_2\text{H}$  to  $\text{HMePhSiSiMe}_2\text{SiMe}_2\text{H}$  is 13:1. When  $H(\text{PhMeSi})_3\text{H}$  is treated with 3 equiv of HOTf, two structural isomers were produced on quenching with  $\text{RMgX}$ . The spectroscopic data unequivocally demonstrate that one of the isomers was  $\text{H(RMeSi)}_3\text{H}$ , which corresponds to the sequence in the starting trisilane, and that the second isomer contained SiH bonds on adjacent silicon centers, i.e.,  $\text{HRMeSiSiHMe-SiR}_2\text{Me}$ . Formation of this latter product requires that a rearrangement of some type take place. The results of the reactions observed with both 2 and 3 equiv of HOTf can be rationalized through a similar cationic intermediate as shown in Scheme 2. Whether the rearrangement occurs at the point of the protodesilylation of the Si-Ph or from ionization of a bound triflate has not yet been determined. In Scheme 2, loss of a triflate from the internal silicon results in migration of either a phenyl or a hydride from a terminal silicon and suggests a migratory aptitude of  $\text{Ph} > \text{H} \gg \text{Me}$ . Loss

(21) Horwitz, C.; Corey, J. Y. Unpublished work.

## Scheme 2. Proposed Rearrangement of Silicon Triflates through a Cationic Intermediate



of triflate from a terminal silicon to produce a cationic center would require that a Me group migrate from an internal silicon, and this must be quite slow compared to the migrations that were actually observed. A concerted rearrangement of triflate and a phenyl (or hydride) between two adjacent silicon centers cannot be eliminated on the basis of data obtained thus far, nor can some type of process assisted by triflic acid be eliminated.

Rearrangement also occurs in the reactions of  $\text{H}(\text{PhMeSi})_x\text{H}$ . Unfortunately, purification of the reaction products by preparative gas chromatography has not been successful when there are two or more Ph substituents remaining in the products, that is, for tetrasilanes such as  $\text{Ph}_2\text{Me}_6\text{Si}_4\text{H}_2$  or  $\text{Ph}_3\text{Me}_5\text{Si}_4\text{H}_2$ . Reaction of  $\text{H}(\text{PhMeSi})_4\text{H}$  with 1 equiv of HOTf followed by  $\text{MeMgBr}$  clearly gives two isomeric products of composition  $\text{Ph}_3\text{Me}_5\text{Si}_4\text{H}_2$  indicating competitive cleavage of terminal vs internal SiPh substituents with the former dominating.<sup>21</sup> The reaction of a mixture of  $\text{H}(\text{PhMeSi})_x\text{H}$  (approximately 1:1 trisilane to tetrasilane) with 1 equiv of HOTf per Si-Ph at 0 °C in toluene followed by quenching with  $\text{MeMgBr}$  resulted in the isolation of a mixture of  $\text{PhMe}_5\text{Si}_3\text{H}_2$  and  $\text{PhMe}_7\text{Si}_4\text{H}_2$ . The trisilane was present as two isomers (major/minor = 11:1 as determined by  $^1\text{H}$  NMR spectroscopy). However, the tetrasilane, after purification by preparative gas chromatography, appears to be a single isomer  $\text{H}_a(\text{Me}_a)_2\text{-SiSiPhMe}_b\text{Si}(\text{Me}_c)_2\text{Si}(\text{Me}_d)_2\text{H}_d$  with SiH resonances at  $\delta = 4.05$  (septet,  $\text{H}_d$ ) and 4.57 (septet,  $\text{H}_a$ ) as well as SiMe resonances at  $\delta = 0.48$  (s,  $\text{Me}_b$ ), 0.24 and 0.25 (two s,  $\text{Me}_c$ ), 0.19 and 0.20 (two d,  $\text{Me}_a$ ), and 0.08 (d,  $\text{Me}_d$ ). The assignments for the two  $\text{HMe}_2\text{Si}$  units were verified by a COSY experiment. The integrated ratio of  $\text{Me}_a$ :

$\text{Me}_b$ : $\text{Me}_c$ : $\text{Me}_d$  is 2:1:2:2. Attempts to resolve the types of isomers produced from  $\text{H}(\text{PhMeSi})_4\text{H}$  with 4 equiv of HOTf in hexane followed by quenching with BuLi revealed the formation of three isomers of  $\text{Bu}_4\text{Me}_4\text{-Si}_4\text{H}_2$  in a ratio of  $\sim 7:3:1$ . The  $^1\text{NMR}$  spectrum of the mixture was too complex to interpret, and attempts to purify and/or separate the isomers were unsuccessful. However, these preliminary data indicate that the tetrasilane chemistry parallels that observed for the trisilane.

**Summary.** The reactions of  $\text{H}(\text{PhMeSi})_x\text{H}$  with triflic acid have demonstrated that cleavage of internal phenyl substituents competes with the cleavage of terminal phenyl groups in contrast to the observations previously reported for the trisilanes  $\text{Ph}_3\text{SiSiPh}_2\text{SiPhR}_2$  ( $\text{R} = \text{Me}, \text{Ph}$ ).<sup>11,13</sup> Thus, phenyl cleavage by HOTf may not be as selective as suggested by earlier reports, and results may be a function of the structure of the system. The rearrangements that were observed for the trisilanes in this study also suggest that removal of phenyl groups in longer chains (or polymers) by electrophilic reagents could lead to changes in the pattern of substituents at adjacent silicon centers.

The focus of this report has been on the characterization of silicon oligomers that are produced as mixtures of diastereomers. The presence of the diastereomers was evident in most cases from the complexity of the  $^1\text{H}$  NMR data for the Si-Me region. For the disilanes and most of the trisilanes  $^{29}\text{Si}$  NMR data have also provided unique support for the presence of these diastereomers.

The development of silicon oligomer chemistry requires new methods to generate chains but also reliable synthetic procedures that will allow the conversion of

one silicon oligomer to another oligomer. The investigation reported here demonstrates the ready production of oligomers of the type  $H(\text{PhMeSi})_x\text{H}$  from a monomeric starting material. However, it has also demonstrated that although the reactions of the phenyl substituents of the oligomers with triflic acid may be simple to execute, the product mixtures obtained may be more complex than anticipated. The yields of distillable products in most reactions varied only from about 30 to 75%. The nature of the nonvolatile products was not determined. Although the reactions of  $H(\text{PhMeSi})_x\text{H}$  ( $x = 3, 4$ ) with HOTf are accompanied by competitive cleavage of phenyl substituents and migration of groups between silicon centers, it may be possible to control or suppress such side reactions at lower temperatures. An unanswered question concerns whether the rearrangement process is unique to a triflate substituent. To resolve this question requires future investigations of other protic reagents for removal of Si-Ph groups. As a *synthetic* method the two-step route to new silicon oligomers reported here may be less attractive as a consequence of the observed rearrangement reactions. It may, nonetheless, provide an entry into a study of the factors that influence the formation and reaction of cationic silicon centers.

That groups will migrate from a silicon center to an adjacent positively charged metal center has been demonstrated for  $[\text{Cp}^*(\text{L})\text{IrSiR}_3]^+\text{OTf}^-$  (L = tertiary phosphine) where  $\text{Cp}^*(\text{L})\text{Ir}(\text{R})\text{SiR}_2\text{OTf}$  was the observed product.<sup>22</sup> In this case, the migratory aptitude appears to be  $\text{R} = \text{H} > \text{R} = \text{Ph} > \text{R} = \text{Me}$ . Whether silicon cations are responsible for the rearranged products formed from the silyl triflates generated in this study or whether some other process results in the migration of groups between silicon centers will only be determined by future studies.

## Experimental Section

**General Experimental Considerations.** All reactions unless otherwise noted were carried out under an atmosphere of dry nitrogen or argon with standard Schlenk techniques. Solvents were dried before use: ether (Na/benzophenone); toluene ( $\text{CaH}_2$ );  $\text{CH}_2\text{Cl}_2$  ( $\text{P}_2\text{O}_5$  after pretreatment with sulfuric acid and drying over  $\text{CaH}_2$ ). All glassware was dried in an oven at 110–120 °C prior to use. Commercial reagents nBuLi (in hexanes), BuMgCl (in ether), MeMgBr (in ether), PhMgBr (ether), and  $\text{LiAlH}_4 \cdot 2\text{THF}$  (toluene) were used as supplied, and the commercial HOTf was distilled. The  $\text{PhMeSiH}_2$ <sup>23a</sup> and  $\text{Ph}_2\text{SiH}_2$ <sup>23b</sup> were prepared by reduction of the commercial chlorides with  $\text{LiAlH}_4$ . The individual oligomers of  $H(\text{PhMeSi})_x\text{H}$  ( $x = 2, 3, 4$ ) have been previously characterized.<sup>3a</sup>

<sup>1</sup>H and <sup>13</sup>C NMR data were recorded on either an XL-300 Varian spectrometer equipped with a four-nucleus probe or a Bruker ARX500 equipped with either an inverse probe or a broad band probe. <sup>29</sup>Si NMR data were recorded on the Bruker ARX500 spectrometer (99.36 MHz) using the INEPTD (with a <sup>1</sup>H refocusing pulse) or DEPT pulse sequences and are referenced to internal TMS. The <sup>29</sup>Si data are summarized for all compounds in Table 4. For <sup>1</sup>H and <sup>13</sup>C data, the characteristic solvent peaks were used as internal reference unless otherwise specified. Mass spectral data were collected at 70 eV on a Hewlett-Packard model 5988A GC/MS instru-

ment equipped with an RTE-A data system, and gas chromatographic separations were performed in a split injection mode using a 12.5-m (HP-1) capillary column. The GC data were collected on a Shimadzu GC-14A gas chromatograph on a DB5 capillary column (20 m × 0.25 mm, 0.25 μm film; J&W) at a helium flow rate of 4 mL/min and a temperature programming of 60–320 °C (20 °C/min). The injection and detection temperatures were 275 and 350 °C, respectively, and the output was recorded on a Shimadzu CR601 integrator. Other than the parent ion, all peaks in the mass spectrum are reported that are >10% of the base peak and are uncorrected. Preparative gas chromatography was performed on a Varian Model 705 with columns specified for the individual compounds.

Chemical analyses were performed by Schwarzkopf Microanalytical Laboratory or Galbraith Laboratories.

**$H(\text{PhMeSi})_x\text{H}$ .** A mixture of cyclooctene (20 mL), toluene (10 mL), and  $\text{Cp}_2\text{TiCl}_2$  (0.654 g, 2.6 mmol) was cooled in an ice bath and degassed for several minutes. nBuLi (2.8 mL, 2.1 M nBuLi) was added, and the solution turned almost black. After 5 min at 0 °C,  $\text{PhMeSiH}_2$  (20 mL, 0.15 mol) was injected. The solution was stirred for 5 days, after which hexane was added. After the slurry was filtered through celite and the volatiles were removed, the residual oil was distilled to give  $H(\text{PhMeSi})_2\text{H}$  (bp 100–135 °C/0.3 mmHg; 4.8 g, 99% by GC) and  $H(\text{PhMeSi})_3\text{H}$  (bp 150–190 °C/0.3 mmHg; 9.3 g, 96% by GC); additional components are  $H(\text{PhMeSi})_2\text{H}$  (1%) and  $H(\text{PhMeSi})_4\text{H}$  (2%). Spectroscopic characteristics are identical to published data.<sup>3a</sup>

A similar reaction of  $\text{PhMeSiH}_2$  (11.7 g, 95.9 mmol) with  $\text{Cp}_2\text{TiCl}_2$  (0.310 g, 1.24 mmol), nBuLi (1.1 mL, 2.5 M) in toluene (5 mL), and *cis*-cyclooctene (10 mL) for 42 h at room temperature provided  $H(\text{PhMeSi})_2\text{H}$  (bp 110–115 °C/0.1 mmHg; 6.9 g, 95% by GC).

When  $\text{PhMeSiH}_2$  (18 g, 160 mmol) was heated with  $\text{Cp}_2\text{TiCl}_2$  (0.694 g, 2.78 mmol), nBuLi (2.2 mL, 2.5 M) in toluene (20 mL), and *cis*-cyclooctene (18 mL) for 16 h at 82 °C, first fraction (bp 150–195 °C/0.3 mmHg; 10.4 g,  $H(\text{PhMeSi})_x\text{H}$ ,  $x = 3$  (83%), 4 (17%)) and second fraction (bp 200–245 °C/0.15 mmHg; 4.6 g,  $H(\text{PhMeSi})_x\text{H}$ ,  $x = 3$  (6.6%), 4 (88%), 5 (5.3%)) were obtained. Redistillation provided samples that were >95%  $H(\text{PhMeSi})_x\text{H}$ .

**$\text{HPh}_2\text{SiSiPh}_2\text{H}$ .** A mixture of cyclooctene (5.0 mL) and toluene (5.0 mL) was cooled with an ice bath, and nitrogen was bubbled through the mixture for 5 min. A sample of  $\text{Cp}_2\text{TiCl}_2$  (0.163 g, 0.665 mmol) was added followed by nBuLi (0.55 mL of 2.5 M) to give a dark brown solution. After  $\text{Ph}_2\text{SiH}_2$  (8.00 g, 43.5 mmol) was added the mixture was heated in an oil bath at 90 °C for 17 h. Hexanes were added to the cooled mixture, and the resultant slurry was filtered. Removal of the volatiles and distillation of the residue provided a fraction, bp 160–200 °C/0.10 mmHg, which solidified (6.25 g, 78%; 98% by GC). Recrystallization of a sample (0.23 g from absolute ethanol) provided white crystalline  $\text{HPh}_2\text{SiSiPh}_2\text{H}$ , mp 84.9–85.4 °C (lit.<sup>16</sup> mp 79–80 °C) (0.14 g). Mass spectrum [*m/e* (relative intensities)]: 366 ( $\text{P}^+$ , 2.8), 259 ( $\text{Ph}_3\text{Si}^+$ , 100), 183 ( $\text{Ph}_2\text{SiH}^+$ , 46), 181, 105 ( $\text{PhSi}^+$ , 31).

**$\text{HPhMeSiSiMe}_2\text{H}$  from Reaction of  $H(\text{PhMeSi})_2\text{H}$  with HOTf Followed by MeMgBr.** A solution of  $H(\text{PhMeSi})_x\text{H}$  [ $x = 2$  (93%); 3 (3.3%)] (2.86 g) in  $\text{CH}_2\text{Cl}_2$  (28 mL) was cooled to –40 °C before addition of HOTf (1.05 mL, 11.9 mmol). The solution was warmed to –10 °C over 30 min and was then stirred at 0 °C for 30 min. After recooling the reaction mixture to –40 °C, a solution of MeMgBr in ether (4.8 mL, 3.0 M) was slowly added. The mixture was warmed to room temperature and was stirred overnight. After aqueous workup, the organic layer was dried over  $\text{Na}_2\text{SO}_4$  and the volatiles removed. Distillation of the residue up to 102 °C/26 mmHg gave  $\text{HPhMeSiSiMe}_2\text{H}$  (0.946 g, 99% by GC) [lit.<sup>17</sup> 96 °C/25 mmHg]. <sup>1</sup>H NMR ( $\delta$  (J, Hz);  $\text{CDCl}_3$ , 500 MHz): 0.21 (d,  $\text{Me}_2\text{SiH}$ ,  $^3J_{\text{SiHCH}} = 4.5, 6.5$ ), 0.47 (d,  $\text{MePhSiH}$ ,  $^3J_{\text{SiHCH}} = 4.6, 2.8$ ), 3.87 (septet of d,  $\text{HSiMe}_2$ ,  $^3J_{\text{SiHCH}} = 4.5$ ,  $^3J_{\text{SiSHH}} = 2.2, 0.8$ ), 4.32 (q of d,

(22) Burger, P.; Bergman, R. G. *J. Am. Chem. Soc.* **1993**, *115*, 10462–10463.

(23) (a) Zakharkin, L. I. *Izv. Akad. Nauk SSSR* **1960**, 2244–45. (b) Benkesser, R. A.; Landesman, H.; Foster, D. J. *J. Am. Chem. Soc.* **1952**, *74*, 648–850.



$\text{HSiPhMe}$ ,  $^3J_{\text{SiHCH}} = 4.6$ ,  $^3J_{\text{SiHSiH}} = 2.3$ , 0.8).  $^{13}\text{C}$  NMR ( $\delta$ ;  $\text{CDCl}_3$ , 75.4 MHz) 134.60, 128.70, 127.81, 127.73 (arom), -6.13 ( $\text{HSiPhMe}$ ), -7.47 ( $\text{HSiMe}_2$ ). Mass spectrum [ $m/e$  (relative intensities)]: 180 ( $\text{P}^+$ , 5.9), 135 ( $\text{PhMe}_2\text{Si}^+$ , 100), 121 ( $\text{PhMeSiH}^+$ , 45), 105 ( $\text{PhSi}^+$ , 35).

Preparative gas chromatography (15% SE30, 20 ft by  $1/4$  in.) provided a purified sample.  $^1\text{H}$  NMR ( $\delta$ ;  $\text{C}_6\text{D}_6$ , 500 MHz; in part): 0.09 (d,  $\text{Me}_2\text{SiH}$ , 6.2), 0.34 (d,  $\text{MePhSiH}$ , 3.0), 4.06 (septet of d,  $\text{HSiMe}_2$ , 0.93), 4.52 (q of d,  $\text{HSiPhMe}$ , 0.92). Anal. Calcd. for  $\text{C}_9\text{H}_{16}\text{Si}_2$ : C, 59.92; H, 8.94. Found: C, 59.14; H, 8.49.

**HPhMeSiSiMeH<sub>2</sub>**. An aliquot of HOTf (0.61 mL, 6.9 mmol) was injected dropwise into a cooled (0 °C) solution of HPhMeSiSiMePhH (1.67 g, 6.90 mmol) in toluene (40 mL). The reaction mixture was warmed to room temperature and was stirred for 1 h. The clear solution was then cooled to 0 °C, an aliquot of  $\text{LiAlH}_4 \cdot 2\text{THF}$  (8.6 mL, 1.0 M in toluene) was slowly added, and the resulting milky solution was stirred at room temperature overnight. Water and hexanes were added, the organic layer was separated and dried over  $\text{Na}_2\text{SO}_4$ , and the solvents were removed under vacuum. Distillable material was removed up to 120 °C/0.1 mmHg, and the resultant oil was redistilled at 26–28 °C/0.01 mmHg [lit.<sup>18</sup> bp, 73–75 °C/10 mmHg] to provide HPhMeSiSiMeH<sub>2</sub> (0.65 g, 99% by GC, 57% yield).  $^1\text{H}$  NMR ( $\delta$  ( $J$ , Hz);  $\text{CDCl}_3$ , 500 MHz): 0.21 (t,  $\text{CH}_3\text{SiH}_2$ , 3.3), 0.51 (d,  $\text{CH}_3\text{PhSiH}$ , 3.7), 3.59 (q of d,  $^3J_{\text{SiHCH}} = 4.9$ ;  $^3J_{\text{SiHSiH}} = 2.5$ ,  $\text{H}_2\text{SiMe}$ , 1.3), 4.42 {9-line multiplet (overlapping q of t),  $^3J_{\text{SiHCH}} = 4.7$ ;  $^3J_{\text{SiHSiH}} = 2.4$ ,  $\text{HSiPhMe}$ , 0.67}.  $^{13}\text{C}$  NMR ( $\delta$ ;  $\text{CDCl}_3$ , 75.4 MHz): -134.64, 128.99, 127.94 (arom), -6.66 ( $\text{HSiPhCH}_3$ ), -11.71 ( $\text{H}_2\text{SiCH}_3$ ). Mass spectrum [ $m/e$  (relative intensities)]: 166 ( $\text{P}^+$ , 13), 121 ( $\text{PhMeSiH}^+$ , 100), 105 ( $\text{PhSi}^+$ , 27).

**HPh<sub>2</sub>SiSiMePhH from Reaction of H(Ph<sub>2</sub>Si)<sub>2</sub>H with HOTf Followed by MeMgBr.** To a solution of HPh<sub>2</sub>SiSiPh<sub>2</sub>H (1.5g, 4.1 mmol) in toluene (8 mL) which had been cooled to 0 °C was added HOTf (0.36 mL, 4.1 mmol). After 45 min, a solution of MeMgBr (1.4 mL, 3.0 M) was added and the mixture was stirred for 1 h. After aqueous workup and removal of the volatiles, the residue was distilled to give a fraction, bp 130–160 °C/0.1 mmHg, which contained HPh<sub>2</sub>SiSiPhMeH (79%) and 4 additional minor components by GC. After removal of materials with bp up to 140 °C/0.1 mmHg, the residue contained HPh<sub>2</sub>SiSiPhMeH (0.64 g, 96% by GC) [Lit.<sup>18</sup> 168 °C/1 mmHg].  $^1\text{H}$  NMR ( $\delta$  ( $J$ , Hz);  $\text{CDCl}_3$ , 300 MHz): 0.54 (d,  $^3J_{\text{CHSiH}} = 4.6$ ,  $\text{CH}_3\text{SiPhH}$ ), 4.66 (q of d,  $^3J_{\text{CHSiH}} = 4.5$ ,  $^3J_{\text{SiHSiH}} = 2.4$ ,  $\text{HSiPhMe}$ ), 5.04 (d,  $^3J_{\text{SiHSiH}} = 2.4$ ,  $\text{HSiPh}_2$ ), 7.3–7.5 (m, Arom).  $^{13}\text{C}$  NMR ( $\delta$ ;  $\text{CDCl}_3$ , 300 MHz): 135.71, 134.93, 134.85, 129.19, 129.01, 127.97, 127.93, 127.83, -6.96. Mass spectrum [ $m/e$  (relative intensities)]: 304 ( $\text{P}^+$ , 4.7), 259 ( $\text{Ph}_3\text{Si}^+$ , 56), 197 ( $\{\text{P}-\text{PhSiH}_2\}^+$ , 100), 183 ( $\{\text{P}-\text{PhMe}_2\text{Si}\}^+$ , 51), 181 ( $\{\text{P}-\text{PhMe}_2\text{Si}-\text{H}_2\}^+$ , 37), 121 ( $\{\text{PhMeSiH}\}^+$ , 14).

In a second run, a slurry of HPh<sub>2</sub>SiSiPh<sub>2</sub>H (3.06 g, 8.36 mmol) in  $\text{CH}_2\text{Cl}_2$  (14 mL) was treated at -40 to -45 °C with HOTf (0.75 mL, 8.5 mmol) for 45 min, followed by addition of MeMgBr (3.5 mL, 3.0 M) and  $\text{Et}_2\text{O}$  (14 mL), whereupon a clear solution was obtained. After aqueous workup and removal of the volatiles, a fraction (2.12 g, bp 140–180/0.1 mmHg, was obtained [HPh<sub>2</sub>SiSiPhMeH (79%) and HPh<sub>2</sub>SiSiPh<sub>2</sub>H (21%)].

In an additional run, a slurry of HPh<sub>2</sub>SiSiPh<sub>2</sub>H (3.1 g, 8.5 mmol) in  $\text{CH}_2\text{Cl}_2$  (14 mL) at -42 °C was treated with HOTf (1.4 g, 9.3 mmol) and the solution was warmed to -10 °C over 30 min, after which time it was stirred at 0 °C for 40 min. The reaction was quenched with MeMgBr (11 mmol) and after the usual workup provided an oil, bp 140–160 °C/0.1 mmHg, 1.95 g, which contained HPh<sub>2</sub>SiSiPhMeH (80%) and HPhMeSiSiMePhH (20%).

Attempts to prepare a purified sample by preparative gas chromatography with several different columns were unsuccessful.

**HPhMeSiSiMePhH from Reaction of H(PhMeSi)<sub>2</sub>H with HOTf Followed by PhMgBr.** A solution of H(PhMeSi)<sub>2</sub>H [1.04 g, 8.67 mmol PhMeSi,  $x = 2$  (92%); 3 (3%)] in

$\text{CH}_2\text{Cl}_2$  (10 mL) was cooled to -20 °C before adding, dropwise, HOTf (distilled, 0.76 mL). After 30 min at -20 °C, the cold bath was removed and the homogeneous pale yellow solution was stirred for an additional 30 min. After removal of  $\text{CH}_2\text{Cl}_2$  under vacuum, ether (10 mL) was added and the mixture cooled to -20 °C before addition of PhMgBr (3.7 mL, 3.0 M). After 20 min, the cold bath was removed and the solution was stirred for 19 h. After aqueous workup and removal of the volatiles, the residue was distilled to give H(PhMeSi)<sub>2</sub>H, bp up to 104 °C/0.1 mmHg (0.67 g, 97% by GC; 3% biphenyl).  $^1\text{H}$  NMR ( $\delta$ ;  $\text{CDCl}_3$ , 500 MHz, in part), 0.45 (d, SiMe), 4.42 (m, SiH). Mass spectrum [ $m/e$  (relative intensity)]: 242 ( $\text{P}^+$ , 4.0%).

**HBuMeSiSiMeBuH from Reaction of H(PhMeSi)<sub>2</sub>H with 2 Equiv of HOTf Followed by BuMgBr.** To a solution of H(PhMeSi)<sub>2</sub>H [1.2 g, 10 mmol of PhMeSi,  $x = 2$  (92%), 3 (3.3%)] in  $\text{CH}_2\text{Cl}_2$  (12 mL) that had been cooled to -20 °C was added HOTf (0.90 mL, 10 mmol) dropwise. The homogeneous solution was stirred for 30 min at -20 °C and then 30 min at room temperature. After recooling the mixture to -20 °C,  $\text{Et}_2\text{O}$  (12 mL) and then BuMgCl (6.5 mL, 2.0 M) were added, and the mixture was stirred for 30 min at this temperature and then overnight at room temperature. After aqueous workup the oil obtained from the organic layer was distilled to give HBuMeSiSiMeBuH, bp up to 104 °C/0.1 mmHg (0.41 g, 90% by GC). Redistillation provided a fraction, bp 50–60 °C/0.1 mmHg, 0.16 g, that showed <1% impurities by GC [lit.<sup>19</sup> 40 °C/0.2 mm].  $^1\text{H}$  NMR ( $\delta$  ( $J$ , Hz);  $\text{CDCl}_3$ , 500 MHz): 0.13, 0.12 (2 d,  $^3J_{\text{CHSiH}} = 4.6$ ,  $\text{CH}_3\text{SiBu}$ ), 0.70 (m,  $\text{RCH}_2\text{SiMe}$ ), 0.87 (t,  $\text{CH}_3(\text{CH}_2)_3\text{SiMe}$ , 1.33 (m,  $\text{RCH}_2\text{CH}_2\text{CH}_2\text{Si}$ ), 3.63 (overlapping multiplets, HSi).  $^{13}\text{C}$  NMR ( $\delta$ ;  $\text{CDCl}_3$ , 75.4 MHz): 28.72, 28.51, 26.80, 26.34, 13.89, 13.84, 12.28, 11.98, 11.91, -7.40. Mass spectrum [ $m/e$  (relative intensities)]: 202 ( $\text{P}^+$ , 9.5), 100 ( $\text{BuMeSi}^+$ , 31), 89 ( $\text{Me}_2\text{Si}_2\text{H}_3^+$ , 29), 85 ( $\text{BuSi}^+$ , 27), 72 (100), 59 (66). Anal. Calcd for  $\text{C}_{10}\text{H}_{26}\text{Si}_2$ : C, 59.37; H, 12.85. Found: C, 57.48; H, 12.71.

**HPhMeSiSiMePhH from Reaction of H(Ph<sub>2</sub>Si)<sub>2</sub>H with 2 Equiv of HOTf Followed by MeMgBr.** A solution of H(Ph<sub>2</sub>Si)<sub>2</sub>H (2.05 g, 5.6 mmol) in  $\text{CH}_2\text{Cl}_2$  (15 mL) was cooled to -45 °C before dropwise addition of HOTf (1.0 mL). The solution was maintained between -45 and -30 °C for 1 h before the addition at -45 °C of ether (10 mL) and MeMgBr (4.5 mL, 3.0 M). The solution was allowed to warm to room temperature and was stirred for an additional 1 h. After aqueous workup and removal of the volatiles from the organic layer, the residue was distilled to give H(PhMeSi)<sub>2</sub>H, bp up to 120 °C/0.1 mmHg (1.06 g, 97% by GC). Spectroscopic data were identical to those obtained for HPhMeSiSiMePhH produced from dehydrocoupling reactions.

The reaction of H(Ph<sub>2</sub>Si)<sub>2</sub>H (1.41 g, 3.85 mmol) and HOTf (0.68 mL) was conducted in toluene (10 mL) for 20 min at -20 °C followed by 30 min at room temperature. The resultant heterogeneous solution was cooled to -20 °C before addition of MeMgBr (3.1 mL, 3.0 M). The reaction mixture was stirred overnight before aqueous workup and distillation provided H(PhMeSi)<sub>2</sub>H (0.434 g, 90% by GC).

**Isomers of Ph<sub>2</sub>Me<sub>4</sub>Si<sub>3</sub>H<sub>2</sub> from Reaction of H(PhMeSi)<sub>3</sub>H with 1 Equiv of HOTf Followed by MeMgBr** (Table 3, Run 1). A solution of H(PhMeSi)<sub>3</sub>H (2.63 g, 21.9 mmol of PhMeSi) in  $\text{CH}_2\text{Cl}_2$  (26 mL) was cooled to -40 °C before dropwise addition of HOTf (0.65 mL, 7.3 mmol). The mixture was kept between -40 and -30 °C for 60 min. After the solution was recooled to -40 °C, ether (10 mL) and MeMgBr (2.9 mL, 3.0 M) were added and the mixture was allowed to warm to room temperature and was stirred overnight. After aqueous workup and removal of solvents, distillation up to 200 °C/0.1 mmHg gave an oil (1.63 g) which contained a mixture of Ph<sub>2</sub>Me<sub>4</sub>Si<sub>3</sub>H<sub>2</sub> (78%), PhMe<sub>5</sub>Si<sub>3</sub>H<sub>2</sub> (13%), Ph<sub>3</sub>Me<sub>3</sub>Si<sub>3</sub>H<sub>2</sub> (3%), and 4 additional components between 1 and 2% each. Redistillation provided a center cut, bp 90–98 °C/0.05 mmHg [0.23 g, as a mixture of two isomers of Ph<sub>2</sub>Me<sub>4</sub>Si<sub>3</sub>H<sub>2</sub> (97% by GC)].

The isomers were assigned to mixtures of diastereomers of H(PhMeSi)<sub>a</sub>(PhMeSi)<sub>b</sub>(SiMe<sub>2</sub>)<sub>c</sub>H and H(PhMeSi)<sub>d</sub>(SiMe<sub>2</sub>)<sub>e</sub>(Si-

$\text{MePh}_d\text{H}$ .  $^1\text{H}$  NMR ( $\delta$  (J, Hz);  $\text{CDCl}_3$ , 500 MHz): 0.10, 0.12, 0.13 [3 doublets,  $^3J_{\text{CHSiH}} = 4.6$  (av), ( $\text{Me}_2\text{SiH}$ )<sub>c</sub>], 0.17 [apparent triplet, ( $\text{Me}_2\text{Si}$ )<sub>e</sub>], 0.38 [d,  $^3J_{\text{CHSiH}} = 4.7$ , ( $\text{MeSiPhH}$ )<sub>d</sub>], 0.44 [d,  $^3J_{\text{CHSiH}} = 4.5$ , ( $\text{MeSiPhH}$ )<sub>a</sub>], 0.45, 0.46 [2s, ( $\text{MeSiPhH}$ )<sub>a</sub>], 0.49 [d,  $^3J_{\text{CHSiH}} = 4.5$ , ( $\text{MeSiPhH}$ )<sub>a</sub>], 3.90 [overlapping septets,  $^3J_{\text{CHSiH}} = 4.5$ , ( $\text{HSiMe}_2$ )<sub>c</sub>], 4.32 [quintet, (2 overlapping quartets), ( $\text{HSiPhMe}$ )<sub>d</sub>], 4.47 [q,  $^3J_{\text{CHSiH}} = 4.5$ , ( $\text{HPhMeSi}$ )<sub>a</sub>], 7.2–7.5 (m, arom). Ratio of  $H(\text{PhMeSi})(\text{PhMeSi})\text{SiMe}_2\text{H}$  to  $H(\text{PhMeSi})(\text{SiMe}_2)(\text{SiPhMe})\text{H}$  = 2.7/1.  $^{13}\text{C}$  NMR ( $\delta$ ;  $\text{CDCl}_3$ , 75.4 MHz, TMS): 134.65, 134.54, 128.72, 128.60, 128.18, 127.56 (arom), -5.71, -5.78, -5.64, -5.96, -6.95, -7.32, -7.94, -7.97 (SiMe). Mass spectrum [ $m/e$  (relative intensities)] major isomer: 300 ( $\text{P}^+$ , 5.3), 241 ( $\{\text{P} - \text{Me}_2\text{SiH}\}^+$ , 28), 240 ( $\{\text{P} - \text{Me}_2\text{SiH}_2\}^+$ , 12), 225 (15), 197 ( $\text{Ph}_2\text{MeSi}^+$ , 54), 179 ( $\text{PhMeSiH}^+$ , 44), 178 ( $\{\text{P} - \text{PhMeSiH}_2\}^+$ , 55), 164 ( $\{\text{P} - \text{PhMe}_2\text{SiH}\}^+$ , 75), 163 (48), 135 ( $\text{PhMe}_2\text{Si}^+$ , 100), 121 ( $\text{PhMeSiH}^+$ , 37), 105 ( $\text{PhSi}^+$ , 86). Minor isomer: 300 (4.0), 197 (21), 179 (65), 178 (100), 177 (20), 164 (39), 163 (53), 135 (79) 121 (24), 105 (40), 102 (19).

An analytical sample of a mixture of the  $\text{Ph}_2\text{Me}_3\text{Si}_3\text{H}_2$  isomers was obtained by preparative gas chromatography (5% SE30; 10 ft  $\times$  3/8 in. column).  $^1\text{H}$  NMR ( $\delta$ ;  $\text{C}_6\text{D}_6$ , 500 MHz; isomer mixture, in part): 0.09, 0.10, 0.11, 0.12 [four d,  $^3J_{\text{CHSiH}} = 4.6$  Hz, ( $\text{Me}_2\text{SiH}$ )<sub>c</sub>], 0.17 [apparent triplet, ( $\text{Me}_2\text{Si}$ )<sub>e</sub>], 0.34 [d,  $^3J_{\text{CHSiH}} = 4.6$ , ( $\text{MeSiPhH}$ )<sub>d</sub>], 0.40 [d,  $^3J_{\text{CHSiH}} = 4.6$ , ( $\text{MeSiPhH}$ )<sub>a</sub>], 0.44, 0.43 [two s, ( $\text{MeSiPhH}$ )<sub>a</sub>], 0.44 [d, ( $\text{MeSiPhH}$ )<sub>d</sub>], 4.17 [septet, ( $\text{HSiMe}_2$ )<sub>c</sub>], 4.58 [quintet, (2 overlapping quartets), ( $\text{HSiPhMe}$ )<sub>d</sub>], 4.73 [q, ( $\text{HPhMeSi}$ )<sub>a</sub>]. Anal. Calcd for  $\text{C}_{16}\text{H}_{24}\text{Si}_3$ : C, 63.92; H, 8.05. Found: C, 63.50; H, 8.31.

**Isomers of  $\text{Ph}_2\text{Me}_3\text{Si}_3\text{H}_3$  from Reaction of  $H(\text{PhMeSi})_3\text{H}$  with 1 Equiv of HOTf and Quenching with  $\text{LiAlH}_4$ .** To a solution of  $H(\text{PhMeSi})_3\text{H}$  [2.93 g, containing  $\text{HPhMeSiSiPhMe}$  ( $\text{C}_7\text{H}_{11}$ ) (17%)] in toluene (20 mL) cooled to 0 °C was added HOTf (0.71 mL 8.0 mmol). The reaction mixture was warmed to room temperature and was stirred for three hours. The clear solution was then cooled to 0 °C, and  $\text{LiAlH}_4 \cdot 2\text{THF}$  (8.10 mL, 1.0 M in toluene) was injected slowly. The resulting cloudy solution was stirred at room temperature for 15 h, after which time water and hexanes were added, the organic layer was separated and dried over  $\text{Na}_2\text{SO}_4$ , and the volatiles were removed under vacuum. The resulting cloudy oil was distilled to give a clear, colorless oil, bp 80–100 °C/0.05 mmHg, 1.10 g. Analysis (GC) of the oil showed the presence of the following components (determined by GCMS):  $\text{Ph}_2\text{Me}_3\text{Si}_3\text{H}_3$  (two isomers, 83%),  $\text{PhMe}_2(\text{C}_7\text{H}_{11})\text{Si}_2\text{H}_2$  (two isomers, 11%), and  $\text{PhMe}_3\text{Si}_3\text{H}_4$  (3.9%).

The two isomers,  $\text{HPhMeSiSiPhMeSiMeH}_2$  (major) and  $\text{HPhMeSiSiMeHSiPhMeH}$  (minor) were separated by preparative gas chromatography (5% SE30; 10 ft  $\times$  3/8 in. column).  $^1\text{H}$  NMR ( $\delta$  (J, Hz);  $\text{C}_6\text{D}_6$ , 500 MHz, major isomer, in part): 0.04 (t,  $\text{MeSiH}_2$ ,  $^3J_{\text{SiHCH}} = 4.9$ ), 0.40, 0.43 (d,  $^3J_{\text{CHSiH}} = 4.6$ ,  $\text{PhCH}_3\text{-SiH}$ ), 0.441, 0.445 (s,  $\text{PhCH}_3\text{Si}$ ), 3.87 (m,  $\text{MeSiH}_2$ ), 4.72 (q,  $^3J_{\text{CHSiH}} = 4.6$ ,  $\text{PhMeSiH}$ ).  $^{13}\text{C}$  NMR ( $\delta$ ;  $\text{C}_6\text{D}_6$ , 125.7 MHz, TMS, in part): -7.32, -7.38, -7.53, -11.68. Mass spectrum [ $m/e$  (relative intensities)]: 286 ( $\text{P}^+$ , 4.8), 241 ( $\{\text{P} - \text{MeSiH}_3\}^+$ , 46), 197 ( $\text{Ph}_2\text{MeSi}^+$ , 64), 164 ( $\{\text{P} - \text{PhMeSiH}_2\}^+$ , 94), 149 ( $\text{PhSi}_2\text{-MeH}^+$ , 22), 135 ( $\text{PhMe}_2\text{Si}^+$ , 54), 121 ( $\text{PhMeSiH}^+$ , 44), 105 ( $\text{PhSi}^+$ , 100).  $^1\text{H}$  NMR ( $\delta$ ;  $\text{C}_6\text{D}_6$ , 500 MHz, minor isomer, in part): 0.15 (overlapping d,  $\text{MeSiH}$ , 2.5), 0.34 (overlapping d,  $\text{PhMeSiH}$ , 5.9), 3.76 (m,  $\text{MeSiH}$ , 1.2), 4.67 (m,  $\text{PhMeSiH}$ , 2.4).  $^{13}\text{C}$  NMR ( $\delta$ ;  $\text{C}_6\text{D}_6$ , 125.7 MHz, in part): -6.39, -6.41, -6.58, -6.59 ( $\text{CH}_3\text{PhSiH}$ ), -11.86, -11.94, -12.03 ( $\text{CH}_3\text{SiH}$ ). Mass spectrum [ $m/e$  (relative intensities)], minor isomer: 286 ( $\text{P}^+$ , 2.6), 197 ( $\text{Ph}_2\text{MeSi}^+$ , 31), 164 ( $\{\text{P} - \text{PhMeSiH}_2\}^+$ , 100), 149 ( $\text{PhSi}_2\text{MeH}^+$ , 52), 135 ( $\text{PhMe}_2\text{Si}^+$ , 51), 121 ( $\text{PhMeSiH}^+$ , 65), 105 ( $\text{PhSi}^+$ , 78). The ratio of the isomers is 2.7:1 from integration of the SiH region in the  $^1\text{H}$  NMR spectrum. Anal. Calcd for  $\text{C}_{15}\text{H}_{22}\text{Si}_3$ : C, 62.91; H, 7.75. Found: C, 62.67; H, 7.78.

**Preparation of  $\text{PhMeSi}(\text{SiMe}_2\text{H})_2$**  (Table 3, run 2). To a solution of  $H(\text{PhMeSi})_x\text{H}$  [2.31 g, 19.3 mmol of  $\text{PhMeSi}$ ,  $x = 3$  (95%); 4 (4%)] in  $\text{CH}_2\text{Cl}_2$  (23 mL) that had been cooled to -40 °C was added, dropwise, HOTf (1.1 mL), and the reaction

mixture was stirred for 1 h at temperatures between -40 and -30 °C. A small amount of oil was present. Ether (10 mL) and then  $\text{MeMgBr}$  (5.1 mL, 3.0 M) were added at a bath temperature of -40 °C. The clear colorless solution was stirred overnight before aqueous workup. After removal of the volatiles, the residual oil was distilled up to 120 °C/0.05 mmHg to give  $\text{HMe}_2\text{SiSiPhMeSiMe}_2\text{H}$  (0.68 g, 97% by GC; additional component  $\text{Ph}_2\text{Me}_4\text{Si}_3\text{H}_2$ ).  $^1\text{H}$  NMR ( $\delta$  (J, Hz);  $\text{CDCl}_3$ , 500 MHz): 0.21 (d,  $^3J_{\text{SiHCH}} = 4.5$ ,  $\text{Me}_2\text{SiH}$ ), 0.23 (d,  $^3J_{\text{SiHCH}} = 4.4$ ,  $\text{Me}_2\text{SiH}$ ), 0.48 (s,  $\text{MeSiPh}$ ), 3.93 (septet,  $^3J_{\text{SiHCH}} = 4.5$ ,  $\text{HSiMe}_2$ ), 7.28–7.48 (m, arom).  $^{13}\text{C}$  NMR ( $\delta$ ;  $\text{CDCl}_3$ , 75.4 MHz): 134.57, 128.09, 127.80 (arom), -5.62, -8.12 ( $\text{MeSi}$ ). Mass spectrum [ $m/e$  (relative intensities)]: 238 ( $\text{P}^+$ , 5.7), 179 ( $\{\text{P} - \text{Me}_2\text{SiH}\}^+$ , 46), 178 ( $\{\text{P} - \text{Me}_2\text{SiH}_2\}^+$ , 32), 177 (19), 163 ( $\text{PhSi}_2\text{Me}_2^+$ , 37), 135 ( $\text{PhMe}_2\text{Si}^+$ , 100), 121 ( $\text{PhMeSiH}^+$ , 16), 116 ( $\text{Me}_4\text{Si}_2^+$ , 15), 105 ( $\text{PhSi}^+$ , 44), 102 ( $\text{Me}_3\text{Si}_2\text{H}^+$ , 52). A minor isomer,  $\text{HPhMeSiSiMe}_2\text{SiMe}_2\text{H}$ , was also present as evidenced by multiplets in the  $^1\text{H}$  NMR ( $\delta$ ;  $\text{CDCl}_3$ , 500 MHz): 0.12 ( $\text{HMe}_2\text{-Si}$ ), 0.48 ( $\text{HMePhSi}$ ), 3.76 ( $\text{HMe}_2\text{Si}$ ) and 4.35 ( $\text{HPhMeSi}$ ).

A purified sample was obtained by preparative gas chromatography (15% SE30, 20 ft  $\times$  1/4 in.; 20% OV-25, 18 ft  $\times$  1/4 in.).  $^1\text{H}$  NMR ( $\delta$ ;  $\text{C}_6\text{D}_6$ , 500 MHz, major isomer): 0.16, 0.18 (two d,  $\text{HMe}_2\text{Si}$ ), 0.43 (s,  $\text{MePhSi}$ ), 4.18 (septuplet,  $\text{HMe}_2\text{Si}$ ). Minor isomer: 0.09 (pseudo t,  $\text{Me}_2\text{Si}$ ), 0.41 (d,  $\text{HPhMeSi}$ ), 4.02 (septet,  $\text{HMe}_2\text{Si}$ ), 4.59 (q,  $\text{HPhMeSi}$ ). Ratio of SiH (major)/SiH (minor) = 13. Anal. Calcd for  $\text{C}_{11}\text{H}_{22}\text{Si}_3$ : C, 55.38; H, 9.30. Found: C, 54.79; H, 9.00.

In one experiment conducted in  $\text{CH}_2\text{Cl}_2$  below -35 °C the ratio of major/minor isomers of  $\text{PhMe}_5\text{Si}_3\text{H}_2$  produced was 6. The  $^{29}\text{Si}$  NMR spectrum in  $\text{C}_6\text{D}_6$  showed additional weak resonances at -33.14 ( $\text{HPhMeSi}$ ), -36.14 ( $\text{HMe}_2\text{Si}$ ), and -47.15 ( $\text{Me}_2\text{Si}$ ).

**Formation of  $H(\text{PhMeSi})_3\text{H}$  from Reaction of  $H(\text{PhMeSi})_x\text{H}$  with  $x$  Equiv of HOTf followed by  $\text{PhMgBr}$ .** (a)  $\text{CH}_2\text{Cl}_2$  Solvent (Table 3, run 3). To a solution of  $H(\text{PhMeSi})_x\text{H}$  [1.20 g, 10 mmol of  $\text{PhMeSi}$ ,  $x = 2$  (5%), 3 (78%), and 4 (5%)] in  $\text{CH}_2\text{Cl}_2$  (12 mL) which had been cooled to -20 °C was added, dropwise, HOTf (0.88 mL, 10 mmol). The solution was stirred for 30 min to give a clear solution that contained a small quantity of a brown oil. The mixture was stirred an additional 30 min at room temperature and recooled to -20 °C before addition of  $\text{PhMgBr}$  (4.3 mL, 3.0 M). After 20 h at room temperature, aqueous workup provided an oil after removal of the volatiles. Distillation up to 198 °C/0.1 mmHg provided  $H(\text{PhMeSi})_3\text{H}$  [0.75 g, 89% by GC; minor component,  $\text{HPhMeSiSiMePhH}$  (4%)]. Redistillation removed material with bp up to 185 °C/0.1 mm Hg to give a residue of  $H(\text{PhMeSi})_3\text{H}$  (0.31 g, 100% by GC). Spectroscopic data ( $^1\text{H}$  and  $^{29}\text{Si}$ ) were identical to those previously reported.

(b) Toluene Solvent (Table 3, run 4). A solution of  $H(\text{PhMeSi})_x\text{H}$  [1.05 g, 8.75 mmol of  $\text{PhMeSi}$ ,  $x = 2$  (1.5%), 3 (95%), 4 (1%)] in toluene (10 mL) was cooled to 0 °C before addition of HOTf (0.78 mL, 8.8 mmol). The solution was stirred at 0 °C for 30 min and then at room temperature for 30 min. The homogeneous red-brown solution was recooled to 0 °C before addition of  $\text{Et}_2\text{O}$  (10 mL) and  $\text{PhMgBr}$  (3.8 mL, 3.2 M). The resultant heterogenous mixture was stirred at 0 °C for 30 min and then at room temperature for 75 min before aqueous workup. Distillation of the oil obtained from the organic layer provided a fraction, bp 145–215 °C/0.1 mmHg, 0.41 g. Redistillation provided a purified sample of a mixture of two structural isomers of  $\text{Ph}_3\text{Me}_3\text{Si}_3\text{H}_2$  [0.13 g, bp 150–160/0.2 mmHg, 84% by GC] in a ratio of 1.6(isomer A):1(isomer B). Isomer A has the same retention time as  $H(\text{PhMeSi})_3\text{H}$  produced from the dehydrocoupling reaction of  $\text{PhMeSiH}_2$ . Isomer B has been assigned the structure  $(\text{MePh}_2\text{Si})_2(\text{SiMeH})_2(\text{SiPhMeH})_2$ .  $^1\text{H}$  NMR ( $\delta$  (J, Hz);  $\text{CDCl}_3$ , 300 MHz, in part): 0.16, 0.20 [two d,  $^3J_{\text{CHSiH}} = 5.2$  Hz, ( $\text{MeSiH}$ )<sub>b</sub>], 0.28, 0.29 [two d,  $^3J_{\text{CHSiH}} = 4.6$ , ( $\text{MeSiPhH}$ )<sub>c</sub>], 0.32–0.40 [4d and 3s,  $\text{MeSiPh}$ , isomer A]<sup>3a</sup>, 0.57, 0.59 [two s, ( $\text{MeSiPh}_2$ )<sub>a</sub>], 3.62 [m, ( $\text{SiMeH}$ )<sub>b</sub>], 4.37–4.45 [overlapping multiplets,  $\text{HSiPhMe}$  (both isomers)]. Mass spectrum [ $m/e$  (relative intensities)], isomer B: 362 ( $\text{P}^+$ ,

1.9), 241 ( $\{P - \text{PhMeSiH}\}^+$ , 17), 240 ( $\{P - \text{PhMeSiH}_2\}^+$ , 32), 225 ( $\{P - \text{PhMeSiH}_2 - \text{Me}\}^+$ , 24), 197 ( $\{P - \text{PhMe}_2\text{Si}_2\text{H}_2\}^+$ , 100), 195 (16), 164 ( $\text{PhMe}_2\text{Si}_2\text{H}^+$ , 57), 163 ( $\text{PhMe}_2\text{Si}_2^+$ , 14), 149 ( $\text{PhMeSi}_2\text{H}^+$ , 10), 135 ( $\text{PhMe}_2\text{Si}^+$ , 23), 121 ( $\text{PhMeSiH}^+$ , 18), 105 ( $\text{PhSi}^+$ , 43).

**Reaction of H(PhMeSi)<sub>x</sub>H with *x* Equiv of HOTf Followed by BuM (M = Li or MgCl): Isolation of Bu<sub>x</sub>Me<sub>x</sub>Si<sub>x</sub>H<sub>2</sub> (*x* = 3, 4).** (a) Hexane Solvent (Table 3, run 5). To a solution of H(PhMeSi)<sub>x</sub>H [1.98 g, 16.5 mmol of PhMeSi; 0.80 g of *x* = 3 and 1.18 g of nondistilled condensation product with *x* = 4 and 5] in hexane (3 mL) at 0 °C was added HOTf (1.5 mL, 16 mmol). After 1 h at 0 °C a two-phase mixture was present. Ether (10 mL) and nBuLi (6.6 mL, 2.5 M) were added, and the solution was stirred for 1 h before aqueous workup. Distillation of the residue up to 160 °C/25 mmHg removed a small quantity of material (0.11 g) which was not investigated further. Vacuum distillation provided two fractions, bp 100–140 °C/0.1 mmHg [0.51 g, Bu<sub>3</sub>Me<sub>3</sub>Si<sub>3</sub>H<sub>2</sub> (71%; 2 isomers) and Bu<sub>4</sub>Me<sub>4</sub>Si<sub>4</sub>H<sub>2</sub> (22%; 3 isomers)] and bp 160–200 °C/0.1 mmHg [0.34 g, Bu<sub>4</sub>Si<sub>4</sub>Si<sub>4</sub>H<sub>2</sub> (44%; 3 isomers) and Bu<sub>5</sub>Me<sub>5</sub>Si<sub>5</sub>H<sub>2</sub> (55%; 3 isomers)].

Redistillation of the trisilane/tetrasilane mixture provided an oil, bp 100–110 °C/0.05 mmHg [0.35 g, Bu<sub>3</sub>Me<sub>3</sub>Si<sub>3</sub>H<sub>2</sub> (90%) and Bu<sub>4</sub>Me<sub>4</sub>Si<sub>4</sub>H<sub>2</sub> (4%)]. The two isomers of the trisilane have been assigned the structures (HBuMeSi)<sub>a</sub>(SiBuMe)<sub>b</sub>(SiBuMeH)<sub>a</sub> and (HBuMeSi)<sub>c</sub>(SiMeH)<sub>d</sub>(SiBu<sub>2</sub>Me)<sub>e</sub>. <sup>1</sup>H NMR ( $\delta$  (*J*, Hz); CDCl<sub>3</sub>, 500 MHz, in part): 0.085 [s, (MeBu<sub>2</sub>Si)<sub>a</sub>], 0.13 [d, <sup>3</sup>J<sub>CHSiH</sub> = 4.6, (MeSiBuH)<sub>a</sub>], 0.14 [s, (MeSiBu)<sub>b</sub>], 0.16, 0.17 [two d, <sup>3</sup>J<sub>CHSiH</sub> = 4.5, (MeSiH)<sub>a</sub> + (MeSiBuH)<sub>c</sub>], 3.16 [overlapping multiplets, (HSiMe)<sub>d</sub>], 3.68 [sextet, <sup>3</sup>J<sub>CHSiH</sub> = 4.6, (HSiBuMe)<sub>a</sub>], 3.77 [overlapping multiplets, (HSiBuMe)<sub>c</sub>]. The ratio of Me<sub>a</sub>/Me<sub>b</sub>/Me<sub>e</sub> = 1:1:1, and the isomers are present in approximately a 1:1 ratio. The presence of two structural isomers is also indicated by 2 multiplets centered at 0.6 and 0.8 for RCH<sub>2</sub>-SiMe. <sup>13</sup>C ( $\delta$ ; CDCl<sub>3</sub>, 300 MHz, SiMe region only): -4.13, -4.16, -6.42, -6.82, -7.37, -7.44, -11.58, -11.80. Mass spectrum [*m/e* (relative intensities)]: 302 (P<sup>+</sup>, 1.8), 200 ( $\{P - \text{BuMeSiH}_2\}^+$ , 78), 145 (BuMe<sub>2</sub>Si<sub>2</sub>H<sub>2</sub><sup>+</sup>, 80), 144 (BuMe<sub>2</sub>Si<sub>2</sub>H<sup>+</sup>, 100), 133 (Me<sub>3</sub>Si<sub>3</sub>H<sub>3</sub><sup>+</sup>, 43), 117 (18), 115 (BuSiH<sub>2</sub><sup>+</sup>, 19), 113 (BuSi<sup>+</sup>, 18), 103 (54), 101 (BuMeSiH<sup>+</sup>, 18). Mass spectrum [*m/e* (relative intensities)]: 302 (P<sup>+</sup>, 1.7), 157 (Bu<sub>2</sub>MeSi<sup>+</sup>, 36), 144 (BuMe<sub>2</sub>Si<sub>2</sub>H<sup>+</sup>, 94), 133 (30), 113 (14), 101 (BuMeSiH<sup>+</sup>, 100).

Redistillation of the second fraction provided an oil, bp 132–150 °C/0.05 mmHg [0.16 g, Bu<sub>4</sub>Me<sub>4</sub>Si<sub>4</sub>H<sub>2</sub> (73%, 3 isomers) and presumed Bu<sub>5</sub>Me<sub>5</sub>Si<sub>5</sub>H<sub>2</sub> (20%, 3 isomers)]. An additional distillation provided a fraction, bp 110–120 °C/0.05 mmHg enriched in tetrasilane (87 mg, 97% by GC; the GC ratio of the three isomers is 7.3:3.2:1). <sup>1</sup>H NMR ( $\delta$ ; CDCl<sub>3</sub>, 500 MHz, in part) 0.06, 0.08 (two s, MeSi), 0.12–0.18 (overlapping multiplets and singlets, MeSi), 3.23, (2 overlapping quartets, HSi), 3.26 (broad, overlapping multiplets, HSi), 3.54 (broad overlapping multiplets, HSi), 3.69 (6-line multiplet, HSi), 3.80 (broad, overlapping multiplets, HSi), 3.87 (pentet, HSi). Mass spectrum [*m/e* (relative intensities)]: 402 (P<sup>+</sup>, 2.5), 301 ( $\{P - \text{BuMeSiH}\}^+$ , 16), 300 ( $\{P - \text{BuMeSiH}_2\}^+$ , 20), 245 ( $\{P - \text{Bu}_2\text{MeSi}\}^+$ , 49), 244 ( $\{P - \text{Bu}_2\text{MeSiH}\}^+$ , 52), 189 (BuMe<sub>3</sub>Si<sub>3</sub>H<sub>3</sub><sup>+</sup>, 86), 188 (BuMe<sub>3</sub>Si<sub>3</sub>H<sub>2</sub><sup>+</sup>, 49), 177 (41), 145 (BuMe<sub>2</sub>Si<sub>2</sub>H<sub>2</sub><sup>+</sup>, 44), 144 (BuMe<sub>2</sub>Si<sub>2</sub>H<sup>+</sup>, 65), 143 (Bu<sub>2</sub>Si<sub>2</sub>H<sup>+</sup>, 21), 133 (Me<sub>3</sub>Si<sub>3</sub>H<sub>3</sub><sup>+</sup>, 100), 132 (Me<sub>3</sub>Si<sub>3</sub>H<sub>3</sub><sup>-</sup>, 49), 131 (35), 117 (19), 115 (29), 113 (24), 103 (30), 101 (37). Mass spectrum [*m/e* (relative intensities)]: 402 (P<sup>+</sup>, 0.7), 244 (100), 189 (38), 188 (96), 177 (32), 145 (20), 144 (16), 143 (13), 133 (60), 132 (88), 128 (34), 115 (17), 113 (17), 103 (17), 101 (42). Only two isomers were observed under the GCMS conditions.

(b) Toluene Solvent. A solution of H(PhMeSi)<sub>x</sub>H [1.57 g, 13 mmol of PhMeSi; *x* = 3 (30%); 4 (70%)] in toluene was cooled to 0 °C, and HOTf (1.1 mL, 13 mmol) was added. The ice bath was removed after 5 min, and the solution was stirred an additional 80 min before recooling to 0 °C and addition of nBuLi (2.4 M, 5.5 mL). After 80 min, aqueous workup provided an oil. Distillation gave a colorless oil, bp 100–160 °C/0.1 mmHg, 1.01 g. The oil contained Bu<sub>3</sub>Me<sub>3</sub>Si<sub>3</sub>H<sub>2</sub> (22%,

2 isomers), PhBu<sub>2</sub>Me<sub>3</sub>Si<sub>3</sub>H<sub>2</sub> (4%), Bu<sub>4</sub>Me<sub>4</sub>Si<sub>4</sub>H<sub>2</sub> (49%, 2 isomers), and PhBu<sub>3</sub>Me<sub>4</sub>Si<sub>4</sub>H<sub>2</sub> (17%).

Redistillation of the product mixture provided a fraction, bp 100–115 °C/0.05 mmHg, 0.311 g, which was redistilled to provide a colorless oil, bp 90–95 °C/0.05 mmHg, 0.22 g [Bu<sub>3</sub>Me<sub>3</sub>Si<sub>3</sub>H<sub>2</sub> (94%) and an impurity (6%)]. Preparative gas chromatography (5% SE30, 10 ft × 3/8 in.) provided a purified sample. <sup>1</sup>H NMR ( $\delta$ ; C<sub>6</sub>D<sub>6</sub>, 500 MHz, in part): 3.60 [m, (SiMeH)<sub>d</sub>], 4.07 [sextet, (HBuMeSi)<sub>a</sub>], 4.14 [m, (HBuMeSi)<sub>c</sub>]. The ratio of H(BuMeSi)<sub>3</sub>H to HBuMeSi(SiMeH)SiBu<sub>2</sub>Me is 6.2:1. Anal. Calcd C<sub>15</sub>H<sub>38</sub>Si<sub>3</sub>: C, 59.36; H, 12.67. Found: C, 58.74; H, 12.33.

A second fraction, bp 120–140 °C/0.10 mmHg, 0.53 g, was redistilled to provide Bu<sub>4</sub>Me<sub>4</sub>Si<sub>4</sub>H<sub>2</sub>, bp 120–135 °C/0.10 mmHg, with <1% impurities (GC). The sample could not be purified by preparative gas chromatography.

(c) Toluene Solvent (Table 3, run 6). A solution of H(PhMeSi)<sub>x</sub>H [2.21, 18.4 mmol of PhMeSi; *x* = 3 (94%); 4 (2.6%)] in toluene (22 mL) was cooled to 0 °C before HOTf (2.71 g, 18.0 mmol) was slowly added. The solution was stirred for 30 min at 0 °C and 30 min at room temperature before quenching with nBuLi (17 mL, 1.25 M). After the usual workup, distillation provided an oil, bp up to 95 °C/0.05 mmHg, 1.24 g.

In another experiment (Table 3, run 7) a solution of H(PhMeSi)<sub>x</sub>H [2.08 g, 17.3 mmol PhMeSi; *x* = 2 (5%); 3 (82%); 4 (6%)] in toluene (21 mL) was cooled to -45 °C before HOTf (2.5 g, 17 mmol) was added dropwise over a 15 min period. After completion of the addition the mixture was stirred at -45 °C for 45 min during which time an oil separated. Ether (5 mL) was added, the oil dissolved, and the solution was stirred an additional 45 min before quenching with nBuLi (10.8 mL, 1.6 M). After workup, distillation provided an oil, bp up to 160 °C/0.1 mmHg, 0.93 g.

In a third experiment (Table 3, run 8) a solution of H(PhMeSi)<sub>x</sub>H [1.90 g, 15.8 mmol of PhMeSi; *x* = 3 (>99%)] in CH<sub>2</sub>Cl<sub>2</sub> (13 mL) was cooled to -45 °C before addition of HOTf (2.4 g, 16 mmol). The solution was kept below -35 °C for 1 h before quenching with BuMgBr (10 mL, 2.0 M). After workup, distillation provided an oil, bp 105–120 °C/0.1 mmHg, 0.58 g.

**HBuMeSiSiPhMeSiMeBuH from Reaction of H(PhMeSi)<sub>3</sub>H with HOTf.** (a) CH<sub>2</sub>Cl<sub>2</sub> Solvent. To a solution of H(PhMeSi)<sub>3</sub>H [2.87 g, 24 mmol of PhMeSi; *x* = 3 (97%), 4 (3%)] in CH<sub>2</sub>Cl<sub>2</sub> (28 mL) which had been cooled to -45 °C was added HOTf (2.1 mL, 24 mmol). The solution was kept below -35 °C for 60 min before addition of Et<sub>2</sub>O (10 mL) and BuMgCl (2.0 M, 14.4 mL). After 15 min, the cold bath was removed and the mixture was stirred for 3 h before aqueous workup. The residual oil was distilled, and the fraction, bp up to 155 °C/0.05 mmHg, 0.56 g, contained Bu<sub>3</sub>Me<sub>3</sub>Si<sub>3</sub>H<sub>2</sub> (61%) and PhBu<sub>2</sub>Me<sub>3</sub>Si<sub>3</sub>H<sub>2</sub> (27%) and several minor impurities (<2% each). Preparative gas chromatography provided a purified sample of PhBu<sub>2</sub>Me<sub>3</sub>Si<sub>3</sub>H<sub>2</sub> as one isomer assigned the structure HBuMeSiSiPhMeSiMeBuH. <sup>1</sup>H NMR ( $\delta$  (*J*, Hz), C<sub>6</sub>D<sub>6</sub>, 500 MHz, TMS, major isomer, in part): 0.22, 0.24 (two d, <sup>3</sup>J<sub>CHSiH</sub> = 4.6, BuCH<sub>2</sub>SiH), 0.520, 0.525, 0.530 (three s, 1:2:1 ratio, PhSiCH<sub>3</sub>), 0.7–0.9 (overlapping multiplets, CH<sub>3</sub>CH<sub>2</sub>CH<sub>2</sub>CH<sub>2</sub>-SiMe), 1.2–1.4 (overlapping multiplets, CH<sub>3</sub>CH<sub>2</sub>CH<sub>2</sub>CH<sub>2</sub>-SiMe), 4.16 (m, BuMeSiH). <sup>13</sup>C NMR ( $\delta$ ; C<sub>6</sub>D<sub>6</sub>, 125.7 MHz, TMS, in part): 28.58, 28.53, 26.49, 26.45, 13.90, 13.88, 11.86 (CH<sub>3</sub>CH<sub>2</sub>CH<sub>2</sub>CH<sub>2</sub>SiMe), -7.40, -7.49, -7.58, -7.59 (CH<sub>3</sub>-SiBu). Mass spectrum [*m/e* (relative intensities)]: 322 (P<sup>+</sup>, 2.7), 220 ( $\{P - \text{BuMeSiH}_2\}^+$ , 18), 177 (17), 165 ( $\{P - \text{Bu}_2\text{MeSi}\}^+$ , 100), 164 ( $\{P - \text{Bu}_2\text{MeSiH}\}^+$ , 51), 163 (PhMe<sub>2</sub>Si<sub>2</sub><sup>+</sup>, 25), 149 (PhMeSi<sub>2</sub>H<sup>+</sup>, 16), 144 (BuMe<sub>2</sub>Si<sub>2</sub>H<sup>+</sup>, 42), 135 (PhMe<sub>2</sub>Si<sup>+</sup>, 43), 121 (PhMeSiH<sup>+</sup>, 63), 105 (PhSi<sup>+</sup>, 40). <sup>1</sup>H NMR ( $\delta$  (*J*, Hz); CDCl<sub>3</sub>, 500 MHz): 0.17, 0.20 (two d, CH<sub>3</sub>SiBu, <sup>3</sup>J<sub>CHSiH</sub> = 4.5 Hz), 0.50 (s, CH<sub>3</sub>SiPh), 3.85 (sextet, HSiBuMe, <sup>3</sup>J<sub>CHSiH</sub> = 4.5), 7.3–7.6 (m, arom). <sup>13</sup>C NMR ( $\delta$ ; CDCl<sub>3</sub>, 75.4 MHz): 134.58, 128.48, 127.98, 127.73, 28.33, 26.26, 13.78, 11.62, -7.34, -7.51. <sup>29</sup>Si NMR ( $\delta$ ; CDCl<sub>3</sub>, 500 MHz): -32.62, -46.17.

(b) Toluene Solvent. To a solution of H(PhMeSi)<sub>x</sub>H (1.87 g, 16 mmol PhMeSi; *x* = 2 (7.9%), 3 (89%), 4 (2.6%) in 20 mL of

toluene which had been cooled to 0 °C was added HOTf (1.2 mL, 14 mmol). After 5 min, the ice bath was removed and the solution was stirred for 90 min. The mixture was cooled to 0 °C,  $\text{BuMgCl}$  (2.0 M, 11 mL) was added, and the slurry was stirred for 90 min. Aqueous workup provided an oil, which was distilled to give a fraction, bp 95–135 °C/0.1 mmHg, 1.35 g [ $\text{Bu}_3\text{Me}_3\text{Si}_3\text{H}_2$  (13%) and  $\text{PhBu}_2\text{Me}_3\text{Si}_3\text{H}_2$  (60%)]. Redistillation provided a fraction, bp 100–105 °C/0.1 mmHg, 0.49 g [ $\text{Bu}_3\text{Me}_3\text{Si}_3\text{H}_2$  (28%) and  $\text{PhBu}_2\text{Me}_3\text{Si}_3\text{H}_2$  (35%)] and a second fraction, bp 110–118 °C/0.1 mmHg, 0.73 g [ $\text{Bu}_3\text{Me}_3\text{Si}_3\text{H}_2$  (9%) and  $\text{PhBu}_2\text{Me}_3\text{Si}_3\text{H}_2$  (88%)]. Preparative gas chromatography provided a purified sample of  $\text{PhBu}_2\text{Me}_3\text{Si}_3\text{H}_2$  as a mixture of  $\text{HBuMeSiSiPhMeSiBuMeH}$  (isomer A, with spectroscopic characteristics identical to those described in the previous paragraph) and  $\text{HPhMeSiSiBuMeSiBuMeH}$  (isomer B). Ratio of A/B = 14.  $^1\text{H}$  NMR ( $\delta$ (J, Hz);  $\text{C}_6\text{D}_6$ , 500 MHz, isomer B, in part): 0.14, 0.156, 0.158, 0.17 (four d,  $^3J_{\text{CHSiH}} = 4.5$ ,  $\text{BuCH}_2\text{-SiH}$ ), 0.24, 0.23 [two s (overlap the doublets of isomer A),  $\text{BuSiCH}_3$ ], 0.48 (d,  $^3J_{\text{CHSiH}} = 4.5$ ,  $\text{HPhSiCH}_3$ ), 4.04 (septet,  $^3J_{\text{CHSiH}} = 4.5$ ,  $\text{BuMeSiH}$ ), 4.67 (q,  $^3J_{\text{CHSiH}} = 4.5$ ). Anal. Calcd  $\text{C}_{17}\text{H}_{34}\text{Si}_3$ : C, 63.32; H, 10.64. Found: C, 62.42; H, 10.41.

**Reaction of  $H(\text{PhMeSi})_x\text{H}$  with  $x$  Equiv of HOTf and Quenching with  $\text{MeMgBr}$ .** To a solution of  $H(\text{PhMeSi})_x\text{H}$  [2.35 g, 19.6 mmol  $\text{PhMeSi}$ ;  $x = 3$  (55%), 4 (45%)] in 20 mL toluene which had been cooled to 0 °C was added HOTf (1.7 mL, 19 mmol), and the mixture was stirred for 100 min before addition of  $\text{MeMgBr}$  (3.0 M, 6.5 mL). The reaction mixture was stirred overnight before aqueous workup. Distillation of the oil after removal of volatiles provided a fraction, bp 100–160 °C/25 mmHg, 0.88 g which contained  $\text{H}(\text{Me}_2\text{Si})_4\text{H}$  (9.4%),  $\text{PhMe}_5\text{Si}_3\text{H}_2$  (23%),  $\text{PhMe}_7\text{Si}_4\text{H}_2$  (59%),  $\text{PhMe}_8\text{Si}_4\text{H}$  (5.3%), and unknown components (3.1%). A second fraction, bp 130–160 °C/0.1 mmHg, 0.16 g, contained  $\text{PhMe}_7\text{Si}_4\text{H}_2$  (69%) and 3 additional minor components.

Preparative gas chromatography (5% SE30, 10 ft  $\times$   $\frac{3}{8}$  in.) provided  $\text{PhMe}_5\text{Si}_3\text{H}_2$  as a mixture of isomers,  $\text{HMe}_2\text{SiSiPhMeSiMe}_2\text{H}$  and  $\text{HPhMeSiSiMe}_2\text{SiMe}_2\text{H}$  in an 11:1 ratio (integration of SiH region). The tetrasilane  $\text{PhMe}_7\text{Si}_4\text{H}_2$  was isolated as a single isomer which was assigned the structure  $(\text{HMe}_2\text{Si})_a(\text{SiPhMe})_b(\text{SiMe}_2)_c(\text{SiMe}_2\text{H})_d$ .  $^1\text{H}$  NMR ( $\delta$ (J, Hz);  $\text{C}_6\text{D}_6$ , 500 MHz, in part): 0.08 [d,  $^3J_{\text{CHSiH}} = 4.4$ ,  $(\text{HSiMe}_2)_d$ ], 0.19, 0.20 [d,  $^3J_{\text{CHSiH}} = 4.67$ ,  $(\text{HSiMe}_2)_a$ ], 0.24, 0.25 [s,  $(\text{SiMe}_2)_c$ ], 0.48 [s,  $\text{SiPhMe}$ ], 4.05 [septet,  $(\text{HMe}_2\text{Si})_d$ ], 4.21 [septet,  $(\text{HMe}_2\text{-Si})_a$ ].  $^{13}\text{C}$  NMR ( $\delta$ ;  $\text{C}_6\text{D}_6$ , 300 MHz, in part): -5.10, -5.20, -5.55, -5.61, -7.57. Anal. Calcd for  $\text{C}_{13}\text{H}_{28}\text{Si}_4$ : C, 52.68; H, 9.53. Found: C, 50.64; H, 9.22. Mass spectrum [ $m/e$  (relative intensities)]: 296 (P<sup>+</sup>, 5), 237 [ $\{\text{P} - \text{Me}_2\text{SiH}\}^+$ , 39], 236 [ $\{\text{P} - \text{Me}_2\text{SiH}_2\}^+$ , 22], 179 [ $\{\text{P} - \text{Me}_4\text{Si}_2\text{H}\}^+$ , 27], 177 (36), 163 ( $\text{PhMe}_2\text{Si}_2^+$ , 41), 160 [ $\{\text{P} - \text{PhMe}_2\text{SiH}\}^+$ , 100], 135 ( $\text{PhMe}_2\text{Si}^+$ , 66), 116 ( $\text{Me}_4\text{-Si}_2^+$ , 57), 105 ( $\text{PhSi}^+$ , 22).

**Acknowledgment** is made to the donors of the Petroleum Research Fund, administered by the American Chemical Society, to the National Science Foundation (CHE-9213688), to the Research Board of the University of Missouri, and to a UM–St. Louis Research Award for support of this work. D.M.K. was supported by a Brunngraber Fellowship and the NSF-REU program. We wish to thank Dr. M. Singh for assistance in conducting the preparative gas chromatography separations and Dr. J. Chickos for discussions concerning the stereochemistry of the oligomers.

OM9409130

**$\mu_2\text{-}\eta^2\text{:}\eta^1\text{-Benzylidene(diphenylphosphino)maleic Anhydride Mediated } \text{PMe}_3 \text{ Addition to the Tricobalt}$**

**Cluster  $\text{Co}_3(\text{CO})_6[\mu_2\text{-}\eta^2\text{:}\eta^1\text{-C(Ph)C=C(PPh}_2\text{)C(O)OC(O)}](\mu_2\text{-PPh}_2)$ . Structure and Redox Properties of the Arachno Cluster**

**$\text{Co}_3(\text{CO})_4(\text{PMe}_3)_2[\mu_2\text{-}\eta^2\text{:}\eta^1\text{-C(Ph)C=C(PPh}_2\text{)C(O)OC(O)}](\mu_2\text{-PPh}_2)$**

Kaiyuan Yang, Simon G. Bott,\* and Michael G. Richmond\*

*Center for Organometallic Research and Education, Department of Chemistry, University of North Texas, Denton, Texas 76203*

Received January 18, 1995<sup>⊗</sup>

The reaction of  $\text{PMe}_3$  (2.5 equiv) with the tricobalt arachno cluster  $\text{Co}_3(\text{CO})_6[\mu_2\text{-}\eta^2\text{:}\eta^1\text{-C(Ph)C=C(PPh}_2\text{)C(O)OC(O)}](\mu_2\text{-PPh}_2)$  (**1**) at room temperature proceeds rapidly to give the disubstituted arachno cluster  $\text{Co}_3(\text{CO})_4(\text{PMe}_3)_2[\mu_2\text{-}\eta^2\text{:}\eta^1\text{-C(Ph)C=C(PPh}_2\text{)C(O)OC(O)}](\mu_2\text{-PPh}_2)$  (**4**) in a stepwise process via the known clusters  $\text{Co}_3(\text{CO})_5(\mu_2\text{-CO})(\text{PMe}_3)[\mu_2\text{-}\eta^2\text{:}\eta^1\text{-C(Ph)C=C(PPh}_2\text{)C(O)OC(O)}](\mu_2\text{-PPh}_2)$  (**2**) and  $\text{Co}_3(\text{CO})_5(\text{PMe}_3)[\mu_2\text{-}\eta^2\text{:}\eta^1\text{-C(Ph)C=C(PPh}_2\text{)C(O)OC(O)}](\mu_2\text{-PPh}_2)$  (**3**). Independent experiments using cluster **2** show that CO loss occurs in preference to  $\text{PMe}_3$  substitution, giving cluster **3** first, and it is cluster **3** that reacts rapidly with added  $\text{PMe}_3$  to afford the disubstituted cluster  $\text{Co}_3(\text{CO})_4(\text{PMe}_3)_2[\mu_2\text{-}\eta^2\text{:}\eta^1\text{-C(Ph)C=C(PPh}_2\text{)C(O)OC(O)}](\mu_2\text{-PPh}_2)$ . The kinetics for the reaction between  $\text{Co}_3(\text{CO})_5(\text{PMe}_3)[\mu_2\text{-}\eta^2\text{:}\eta^1\text{-C(Ph)C=C(PPh}_2\text{)C(O)OC(O)}](\mu_2\text{-PPh}_2)$  and  $\text{PMe}_3$  have been measured in  $\text{CH}_2\text{Cl}_2$  by UV–vis spectroscopy. On the basis of the second-order rate constants and the activation parameters ( $\Delta H^\ddagger = 11.9 \pm 0.6 \text{ kcal mol}^{-1}$  and  $\Delta S^\ddagger = -20 \pm 2 \text{ eu}$ ), an associative reaction that involves  $\text{PMe}_3$  addition to cluster **3** is supported. Cluster **4** has been isolated and characterized in solution by IR and NMR ( $^{31}\text{P}$  and  $^{13}\text{C}$ ) spectroscopy and in the solid state by X-ray diffraction analysis.

$\text{Co}_3(\text{CO})_4(\text{PMe}_3)_2[\mu_2\text{-}\eta^2\text{:}\eta^1\text{-C(Ph)C=C(PPh}_2\text{)C(O)OC(O)}](\mu_2\text{-PPh}_2)$  crystallizes in the monoclinic space group  $P2_1/n$ :  $a = 11.0047(8) \text{ \AA}$ ,  $b = 19.558(2) \text{ \AA}$ ,  $c = 17.683(1) \text{ \AA}$ ,  $\beta = 94.947(6)^\circ$ ,  $V = 4664.4(6) \text{ \AA}^3$ ,  $Z = 4$ ,  $d_{\text{calc}} = 1.419 \text{ g cm}^{-3}$ ;  $R = 0.0453$ ,  $R_w = 0.0489$  for 3795 observed reflections. The solid-state structure of **4** indicates that the second  $\text{PMe}_3$  ligand adds to the cobalt center that is substituted by the maleic anhydride  $\pi$  bond. The electrochemical properties of cluster **4** were examined by cyclic voltammetry in  $\text{CH}_2\text{Cl}_2$  solvent. Two diffusion-controlled, one-electron redox responses at  $E_{1/2} = 0.30 \text{ V}$  and  $E_{1/2} = -1.06 \text{ V}$  were observed in addition to an irreversible reduction at  $E_p^c = -1.87 \text{ V}$ , with the first two processes assignable to the  $0/1+$  and  $0/1-$  redox couples, respectively. The importance of the  $\mu_2\text{-}\eta^2\text{:}\eta^1\text{-benzylidene(diphenylphosphino)maleic anhydride}$  ligand in cluster **3** in directing the site of  $\text{PMe}_3$  ligand addition is discussed in terms of an associative  $\text{PMe}_3$  process that is coupled with a dissociation of the maleic anhydride moiety from the cobalt center in **3**.

### Introduction

The ligand substitution chemistry of polynuclear metal clusters remains an intensely studied field, in part because of the myriad pathways that are available for the replacement of the cluster-bound ligand, which is usually a CO group, by an incoming ligand.<sup>1</sup> The vast majority of the cluster substitution reactions proceed by a pathway(s) involving a dissociative, associative, or

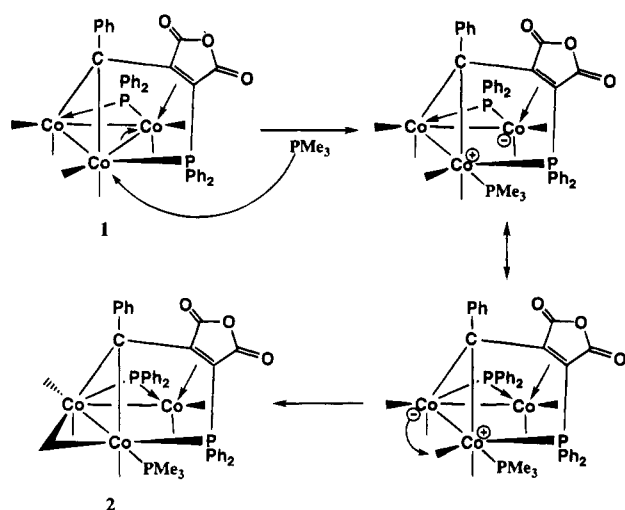
cluster fragmentation sequence.<sup>2</sup> In 1979, Huttner and co-workers provided the first experimental data dealing with a ligand addition to a metal cluster that was accompanied by metal-metal bond cleavage.<sup>3</sup> Since that

(2) (a) Richmond, M. G.; Kochi, J. K. *Inorg. Chem.* **1986**, *25*, 1334 and references therein. (b) Don, M.-J.; Richmond, M. G.; Watson, W. H.; Nagl, A. *J. Organomet. Chem.* **1989**, *372*, 417. (c) Poë, A. J.; Farrar, A. J.; Zheng, Y. *J. Am. Chem. Soc.* **1992**, *114*, 5146. (d) Shen, J.-K.; Basolo, F. *Organometallics* **1993**, *12*, 2942. (e) Dahlinger, K.; Falcone, F.; Poë, A. J. *Inorg. Chem.* **1986**, *25*, 2654. (f) Atwood, J. D.; Wovkulich, M. J.; Sonnenberger, D. C. *Acc. Chem. Res.* **1983**, *16*, 350 and references therein. (g) Shojaie, R.; Atwood, J. D. *Inorg. Chem.* **1987**, *26*, 2199; **1988**, *27*, 2558. (h) Taube, D. J.; Ford, P. C. *Organometallics* **1986**, *5*, 99. (i) Darensbourg, D. J.; Incorvia, M. J. *Inorg. Chem.* **1980**, *19*, 2585. (j) Darensbourg, D. J.; Peterson, B. S.; Schmidt, R. E., Jr. *Organometallics* **1982**, *1*, 306.

<sup>⊗</sup> Abstract published in *Advance ACS Abstracts*, May 1, 1995.

(1) (a) Darensbourg, D. J. In *The Chemistry of Metal Cluster Complexes*; Shriver, D. F., Kaesz, H. D., Adams, R. D., Eds.; VCH Publishers: New York, 1990; Chapter 4. (b) Muettterties, E. L.; Burch, R. R.; Stolzenberg, A. M. *Annu. Rev. Phys. Chem.* **1982**, *33*, 89.

Scheme 1

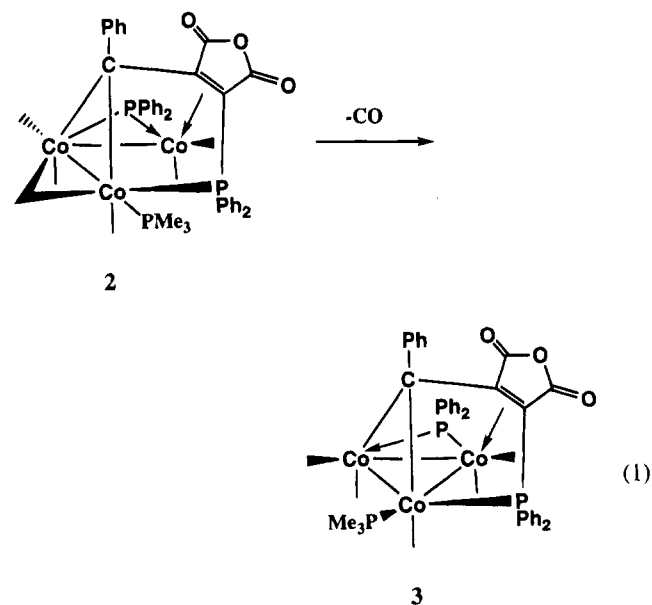


time, other reports of ligand substitution reactions involving polyhedral cluster expansion have been published,<sup>4</sup> with the polyhedral opening being successfully rationalized, in many cases, through the use of electron-topology rules.<sup>5</sup>

We have recently published our results concerning the  $\text{PMe}_3$  ligand substitution in the tricobalt cluster  $\text{Co}_3(\text{CO})_6[\mu_2\text{-}\eta^2\text{-}\eta^1\text{-C(Ph)C=C(PPh}_2\text{)C(O)OC(O)}](\mu_2\text{-PPh}_2)$  (**1**; where the  $\mu_2, \eta^2, \eta^1$  descriptors refer to the coordination mode adopted by the benzylidene, maleic anhydride, and phosphine groups, respectively, of the six-electron benzylidene(diphenylphosphino)maleic anhydride ligand).<sup>6,7</sup> Of interest in this reaction is the first step that leads to the unexpected regioselective addition of the  $\text{PMe}_3$  ligand to the phosphine-substituted cobalt center in **1**, as shown in Scheme 1. The first intermediate zwitterionic cluster in Scheme 1 illustrates the importance of polar metal-metal scission in cluster substitution reactions that possess a strongly electron-withdrawing functionality, a concept first put forward by Johnson for carbonyl ligand substitution in  $\text{M}_3(\text{CO})_{12}$  (where  $\text{M} = \text{Fe, Ru, Os}$ ).<sup>8</sup> In the case of cluster **1**, the maleic anhydride moiety assists in directing the site of  $\text{PMe}_3$  attack by helping to stabilize the developing anionic charge on the adjacent cobalt center. The observed polyhedral changes are consistent within the context of polyhedral skeletal electron pair (PSEP) theory, which supports the arachno  $\rightarrow$  hypho structural expansion.

The monosubstituted cluster **2** is stable at low temperature but readily loses CO at elevated temperatures,

coupled with re-formation of the Co-Co bond, to ultimately afford the simple substitution product  $\text{Co}_3(\text{CO})_5(\text{PMe}_3)[\mu_2\text{-}\eta^2\text{-}\eta^1\text{-C(Ph)C=C(PPh}_2\text{)C(O)OC(O)}](\mu_2\text{-PPh}_2)$  (**3**) at room temperature. Equation 1 depicts this transformation.



Accordingly, we wished to examine the reaction between cluster **3** and additional  $\text{PMe}_3$  to see if Co-Co bond heterolysis could again be achieved. However, what we observed was the rapid substitution of CO by  $\text{PMe}_3$  at the maleic anhydride-substituted cobalt center. Herein, we report our results on the substitution chemistry of cluster **3**, which gives the new cluster  $\text{Co}_3(\text{CO})_4(\text{PMe}_3)_2[\mu_2\text{-}\eta^2\text{-}\eta^1\text{-C(Ph)C=C(PPh}_2\text{)C(O)OC(O)}](\mu_2\text{-PPh}_2)$  (**4**). The solution and solid-state structures of

$\text{Co}_3(\text{CO})_4(\text{PMe}_3)_2[\mu_2\text{-}\eta^2\text{-}\eta^1\text{-C(Ph)C=C(PPh}_2\text{)C(O)OC(O)}](\mu_2\text{-PPh}_2)$  have been determined by spectroscopic methods (IR and NMR) and X-ray crystallography. The electrochemical properties of cluster **4** have been explored by cyclic voltammetry at a platinum electrode in  $\text{CH}_2\text{Cl}_2$  and are discussed relative to the redox properties of the related diphosphine-substituted clusters  $\text{PhCCO}_3(\text{CO})_7\text{P}_2$ . A plausible substitution mechanism outlining the role of a coordinatively flexible maleic anhydride ligand in controlling the site of ligand attack in cluster **3** and supported by kinetic measurements is presented.

## Results and Discussion

### I. Synthesis and Spectroscopic Characterization of $\text{Co}_3(\text{CO})_4(\text{PMe}_3)_2[\mu_2\text{-}\eta^2\text{-}\eta^1\text{-C(Ph)C=C(PPh}_2\text{)C(O)OC(O)}](\mu_2\text{-PPh}_2)$ (**4**).

The reaction of the monosubstituted arachno cluster  $\text{Co}_3(\text{CO})_5(\text{PMe}_3)[\mu_2\text{-}\eta^2\text{-}\eta^1\text{-C(Ph)C=C(PPh}_2\text{)C(O)OC(O)}](\mu_2\text{-PPh}_2)$  with 1.2 mol equiv of  $\text{PMe}_3$  in  $\text{CH}_2\text{Cl}_2$  proceeds rapidly at room temperature to give the new cluster  $\text{Co}_3(\text{CO})_4(\text{PMe}_3)_2[\mu_2\text{-}\eta^2\text{-}\eta^1\text{-C(Ph)C=C(PPh}_2\text{)C(O)OC(O)}](\mu_2\text{-PPh}_2)$  as the sole observable product by IR and TLC analyses. Alternatively, cluster **4** may also be synthesized by starting with either the

(3) Huttner, G.; Schneider, J.; Müller, H.-D.; Mohr, G.; von Seyerl, J.; Wohlfahrt, L. *Angew. Chem., Int. Ed. Engl.* **1979**, *18*, 76.

(4) (a) Vahrenkamp, H. *Adv. Organomet. Chem.* **1983**, *22*, 169. (b) Adams, R. D.; Yang, L.-W. *J. Am. Chem. Soc.* **1983**, *105*, 235. (c) Knoll, K.; Huttner, G.; Zsolnai, L.; Jibril, I.; Wasjucionek, M. *J. Organomet. Chem.* **1985**, *294*, 91. (d) Schneider, J.; Minelli, M.; Huttner, G. *J. Organomet. Chem.* **1985**, *294*, 75. (e) Planalp, R. P.; Vahrenkamp, H. *Organometallics* **1987**, *6*, 492. (f) Huttner, G. *Angew. Chem., Int. Ed. Engl.* **1987**, *26*, 743. (g) Curtis, M. D.; Curnow, O. J. *Organometallics* **1994**, *13*, 2489. (h) Richmond, M. G.; Kochi, J. K. *Inorg. Chem.* **1987**, *26*, 541.

(5) (a) Wade, K. In *Transition Metal Clusters*; Johnson, B. F. G., Ed.; Wiley: New York, 1980, Chapter 3. (b) Wade, K. *Adv. Inorg. Chem. Radiochem.* **1976**, *18*, 1. (c) Mingos, D. M. P. *Acc. Chem. Res.* **1984**, *17*, 311. (d) Mingos, D. M. P.; Wales, D. J. *Introduction to Cluster Chemistry*; Prentice-Hall: New York, 1990.

(6) Yang, K.; Bott, S. G.; Richmond, M. G. *Organometallics* **1995**, *14*, 919.

(7) Yang, K.; Smith, J. M.; Bott, S. G.; Richmond, M. G. *Organometallics* **1993**, *12*, 4779.

(8) Johnson, B. F. G. *Inorg. Chim. Acta* **1986**, *115*, L39.

**Table 1. Observed Rate Constants for the Disappearance of  $\text{Co}_3(\text{CO})_5(\text{PMe}_3)[\mu_2-\eta^2:\eta^1-\text{C}(\text{Ph})\text{C}=\text{C}(\text{PPh}_2)\text{C}(\text{O})\text{OC}(\text{O})](\mu_2-\text{PPh}_2)$  (**3**) in the Presence of  $\text{PMe}_3^a$**

entry no.	temp, °C	$10^4[\text{PMe}_3], \text{M}$	$10^4 k_{\text{obsd}}, \text{s}^{-1}$
1	15.1	15.6	$3.5 \pm 0.01$
2	15.1	31.3	$9.4 \pm 0.2$
3	15.1	46.9	$12.5 \pm 0.3$
4	15.1	62.5	$20.7 \pm 0.9$
5	23.3	15.6	$10.5 \pm 0.04$
6	23.3	31.3	$18.8 \pm 0.2$
7	23.3	31.3	$16.6 \pm 0.9^b$
8	23.3	46.9	$30.4 \pm 0.9$
9	23.3	62.5	$39.1 \pm 1.0$
10	28.3	15.6	$14.5 \pm 0.2$
11	28.3	31.3	$33.8 \pm 0.7$
12	28.3	46.9	$44.7 \pm 1.1$
13	28.3	62.5	$56.4 \pm 2.1$
14	33.3	15.6	$19.4 \pm 0.3$
15	33.3	31.3	$40.5 \pm 4.9$
16	33.3	46.9	$60.4 \pm 13.2$
17	33.3	62.5	$73.2 \pm 1.9$

<sup>a</sup> From  $8.10 \times 10^{-5} \text{ M Co}_3(\text{CO})_5(\text{PMe}_3)[\mu_2-\eta^2:\eta^1-\text{C}(\text{Ph})\text{C}=\text{C}(\text{PPh}_2)\text{C}(\text{O})\text{OC}(\text{O})](\mu_2-\text{PPh}_2)$  in  $\text{CH}_2\text{Cl}_2$  by following the decrease absorbance of the UV-vis band at 374 nm. <sup>b</sup> In the presence of 1 atm of CO.

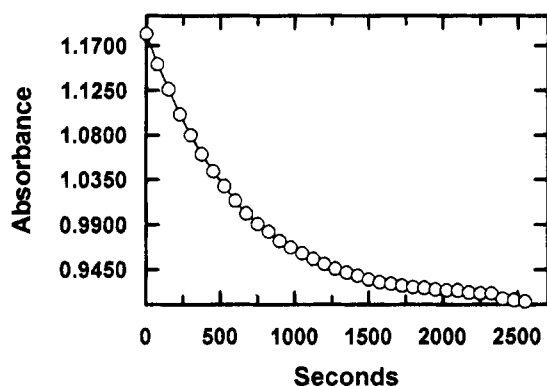


**Figure 1.** Plot of  $A_\infty - A_t$  for the reaction of  $\text{Co}_3(\text{CO})_5(\text{PMe}_3)[\mu_2-\eta^2:\eta^1-\text{C}(\text{Ph})\text{C}=\text{C}(\text{PPh}_2)\text{C}(\text{O})\text{OC}(\text{O})](\mu_2-\text{PPh}_2)$  with  $\text{PMe}_3$  at 23.3 °C (entry 6, Table 1) showing the raw data (○) and the experimentally fitted (—) curve.

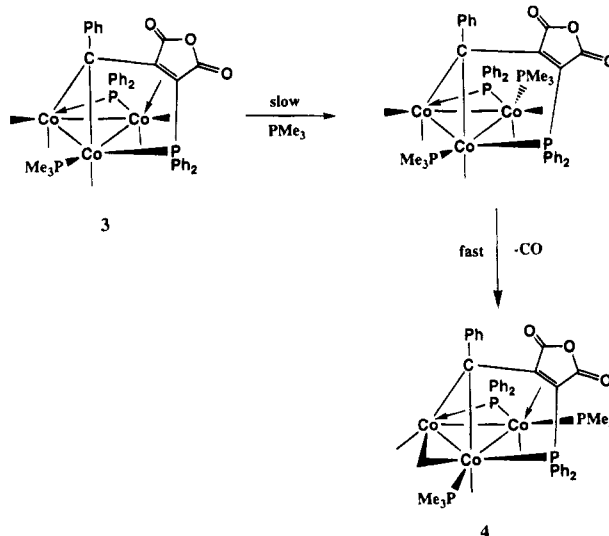
parent cluster  $\text{Co}_3(\text{CO})_6[\mu_2-\eta^2:\eta^1-\text{C}(\text{Ph})\text{C}=\text{C}(\text{PPh}_2)\text{C}(\text{O})\text{OC}(\text{O})](\mu_2-\text{PPh}_2)$  or the monosubstituted hypho cluster  $\text{Co}_3(\text{CO})_5(\mu_2-\text{CO})(\text{PMe}_3)[\mu_2-\eta^2:\eta^1-\text{C}(\text{Ph})\text{C}=\text{C}(\text{PPh}_2)\text{C}(\text{O})\text{OC}(\text{O})](\mu_2-\text{PPh}_2)$  and a slight excess of  $\text{PMe}_3$ , as these reactions eventually give cluster **3**, which is the direct precursor to **4**. The reaction leading to **4** is sensitive to the temperature at which the reaction is conducted. Whereas the parent cluster **1** reacts with excess  $\text{PMe}_3$  below 0 °C to yield the hypho cluster **2**, clusters **2** and **3** are substitutionally inert under these conditions.

The rates of the reaction for **3** to **4** in  $\text{CH}_2\text{Cl}_2$  in the presence of a measured excess of  $\text{PMe}_3$  were monitored by UV-vis spectroscopy by following the decrease in the absorption of the 374 nm band belonging to **3**. The reaction followed first-order kinetics for at least 5 half-lives over the temperature range 15–33 °C, as evidenced by the linear plots of  $\ln(A_\infty - A_t)$  vs time, from which the rate constants quoted in Table 1 were obtained. Figure 1 shows a sample plot of the raw absorbance data at 374 nm as a function of time. Plots of the pseudo-

**Table 2. Second-Order Rate Constants for the Reaction between  $\text{Co}_3(\text{CO})_5(\text{PMe}_3)[\mu_2-\eta^2:\eta^1-\text{C}(\text{Ph})\text{C}=\text{C}(\text{PPh}_2)\text{C}(\text{O})\text{OC}(\text{O})](\mu_2-\text{PPh}_2)$  (**3**) and  $\text{PMe}_3$**

temp, °C	$10^2 k_2, \text{M}^{-1} \text{s}^{-1}$	temp, °C	$10^2 k_2, \text{M}^{-1} \text{s}^{-1}$
15.1	$35.0 \pm 4.3$	28.3	$87.4 \pm 8.6$
23.3	$62.3 \pm 2.9$	33.3	$116.0 \pm 8.7$

**Scheme 2**



first-order rate constants ( $k_{\text{obsd}}$ ) as a function of  $\text{PMe}_3$  concentration (not shown) were found to be linear and gave intercepts of zero within experimental error; the slopes of these plots afforded the second-order rate constants given in Table 2. The activation parameters of  $\Delta H^\ddagger = 11.9 \pm 0.6 \text{ kcal mol}^{-1}$  and  $\Delta S^\ddagger = -20 \pm 2 \text{ eu}$  fully support an associative mechanism that obeys the rate law<sup>1a,9</sup>

$$\text{rate} = k_2[\text{Co}_3(\text{CO})_5(\text{PMe}_3)[\mu_2-\eta^2:\eta^1-\text{C}(\text{Ph})\text{C}=\text{C}(\text{PPh}_2)\text{C}(\text{O})\text{OC}(\text{O})](\mu_2-\text{PPh}_2)][\text{PMe}_3]$$

We have also examined the effect of CO on this reaction. Entry 7, which represents the reaction conducted under 1 atm of CO, is, for all purposes, identical with the reaction run under argon (entry 6). Taken collectively, this leads us to propose a mechanism whereby the incoming  $\text{PMe}_3$  ligand displaces the alkene-coordinated bond in **3**, affording the putative cluster  $\text{Co}_3(\text{CO})_5(\text{PMe}_3)_2[\mu_2-\eta^2:\eta^1-\text{C}(\text{Ph})\text{C}=\text{C}(\text{PPh}_2)\text{C}(\text{O})\text{OC}(\text{O})](\mu_2-\text{PPh}_2)$ , whose maleic anhydride moiety then rapidly ejects CO by an associative coordination of the alkene moiety. Scheme 2 illustrates the course of this reaction, starting with cluster **3**.

Cluster **4** was isolated routinely in yields of 50–65% as a green-black solid by chromatography over silica gel using  $\text{CH}_2\text{Cl}_2$  as the eluant. The FT-IR spectrum of **4** in  $\text{CH}_2\text{Cl}_2$  exhibits two terminal carbonyl bands at 1992 (sh) and 1978 (vs) along with an absorption at 1865 (m)  $\text{cm}^{-1}$ , which we ascribe to the semibringing CO ligand that spans the benzylidene-bridged Co–Co bond in the X-ray structure of **4** (vide infra). A strong  $\nu(\text{CO})$  band at 1871  $\text{cm}^{-1}$  in the solid-state IR spectrum (KBr) of **4** further strengthens this assignment as that of a semibringing ligand.<sup>10</sup> The maleic anhydride moiety is

(9) Atwood, J. D. *Inorganic and Organometallic Reaction Mechanisms*; Brooks/Cole Publishing: Monterey, CA, 1985.

(10) Cotton, F. A. *Prog. Inorg. Chem.* **1976**, *21*, 1.



**Table 3. X-ray Crystallographic Data and Processing Parameters for  $\text{Co}_3(\text{CO})_4(\text{PMe}_3)_2[\mu_2\text{-}\eta^2\text{-}\eta^1\text{-C}(\text{Ph})\text{C}=\text{C}(\text{PPh}_2)\text{C}(\text{O})\text{OC}(\text{O})](\mu_2\text{-PPh}_2)$  (4)**

space group	$P2_1/n$
$a$ , Å	11.0047(8)
$b$ , Å	19.558(2)
$c$ , Å	17.683(1)
$\beta$ , deg	94.947(6)
$V$ , Å <sup>3</sup>	4664.4(6)
mol formula	$\text{C}_{45}\text{H}_{43}\text{Co}_3\text{O}_7\text{P}_4$
fw	996.54
formula units per cell ( $Z$ )	4
$\rho$ , g cm <sup>-3</sup>	1.419
abs coeff ( $\mu$ ), cm <sup>-1</sup>	12.33
$\lambda$ (Mo K $\alpha$ ), Å	0.710 73
collec range, deg	$2.0 \leq 2\theta \leq 44.0$
temp, °C	24
max scan time, s	120
scan speed range, deg min <sup>-1</sup>	0.67–8.0
total no. of data colld	6253
no. of indep data, $I > 3\sigma(I)$	3795
$R$	0.0453
$R_w$	0.0489
GOF	0.94
weights	$[0.04F^2 + (\sigma F)^2]^{-1}$

ascertained by the presence of  $\nu(\text{CO})$  bands at 1791 (m) and 1728 (m)  $\text{cm}^{-1}$ , whose frequency and intensity are consistent with related compounds of this genre.<sup>6,7,11</sup> Cluster 4 exhibits four <sup>31</sup>P NMR resonances, as a result of inequivalent phosphine groups. The resonance observed at  $\delta$  172.9 in the <sup>31</sup>P{<sup>1</sup>H} NMR spectrum of 4, which was recorded in THF at -97 °C, may be confidently assigned to the  $\mu_2$ -phosphido group, on the basis of the chemical shift data reported for clusters 1–3 and related systems.<sup>6,7,12</sup> The remaining three <sup>31</sup>P resonances at  $\delta$  7.2, 0.9 ( $J_{\text{P-P}} = 100.6$  Hz), and -10.5 ( $J_{\text{P-P}} = 100.6$  Hz) are tentatively assigned to the  $\text{Ph}_2\text{P}$ (maleic anhydride) and  $\text{PMe}_3$  groups, respectively. The assignment of these last two phosphorus resonances is strengthened by the X-ray structure of 4, which displays trans  $\text{PMe}_3$  groups that are situated on adjacent cobalt centers. The <sup>13</sup>C{<sup>1</sup>H} NMR spectrum of <sup>13</sup>CO-enriched 4 exhibited three carbonyl resonances at  $\delta$  224.0 ( $J_{\text{C-P}} = 25.5$  Hz), 207.4, and 206.7 in an integral ratio of 1:1:2, respectively. While no attempt has been made to assign these last two carbonyl resonances to specific groups, the first resonance is highly suggestive of a semibridging CO group, as was observed in the solid-state structure of 4.

**II. X-ray Crystallographic Results.** The molecular structure of 4 was determined by X-ray diffraction analysis. Cluster 4 exists as discrete molecules in the unit cell with no unusually short inter- or intramolecular contacts. The X-ray data collection and processing parameters for 4 are given in Table 3, and the final fractional coordinates are listed in Table 4.

The ORTEP diagram in Figure 2 shows the molecular structure of cluster 4 and establishes the disposition of the ancillary  $\text{PMe}_3$  ligands about the cluster polyhedron and the arachno nature (7 SEP) of this cluster. Table 5 contains selected bond distances and angles for 4. The Co–Co bonds are disparate in length, ranging from 2.422(1) to 2.832(1) Å, with the longest Co–Co bond

**Table 4. Positional Parameters for the Non-Hydrogen Atoms in  $\text{Co}_3(\text{CO})_4(\text{PMe}_3)_2[\mu_2\text{-}\eta^2\text{-}\eta^1\text{-C}(\text{Ph})\text{C}=\text{C}(\text{PPh}_2)\text{C}(\text{O})\text{OC}(\text{O})](\mu_2\text{-PPh}_2)$  (4) with Estimated Standard Deviations in Parentheses<sup>a</sup>**

atom	$x$	$y$	$z$	$B$ , Å <sup>2</sup>
Co(1)	0.98841(8)	0.18816(5)	0.25954(4)	2.95(2)
Co(2)	1.00280(9)	0.07004(5)	0.20679(5)	3.40(2)
Co(3)	1.19085(8)	0.09797(5)	0.26958(4)	2.87(2)
P(1)	1.1779(2)	0.1505(1)	0.35979(9)	3.18(4)
P(2)	0.9439(2)	0.1620(1)	0.15959(9)	3.61(4)
P(3)	0.8319(2)	0.2616(1)	0.2682(1)	4.13(5)
P(4)	1.3509(2)	0.0289(1)	0.2947(1)	4.20(5)
O(1)	1.1373(5)	0.3088(3)	0.2483(3)	5.3(1)
O(2)	0.8520(7)	-0.0425(4)	0.1590(4)	9.9(2)
O(3)	1.2018(5)	0.0409(3)	0.1359(3)	6.2(2)
O(4)	1.3432(5)	0.1877(3)	0.2032(3)	6.2(1)
O(12)	0.9313(5)	0.1970(3)	0.4389(2)	5.7(1)
O(13)	0.8201(4)	0.1260(3)	0.3741(2)	4.6(1)
O(14)	0.7611(5)	0.0454(3)	0.3036(3)	5.5(1)
C(1)	1.0838(7)	0.2596(4)	0.2529(3)	3.6(2)
C(2)	0.9082(8)	0.0040(5)	0.1796(4)	5.6(2)
C(3)	1.1380(8)	0.0572(4)	0.1726(4)	4.5(2)
C(4)	1.2829(7)	0.1544(4)	0.2305(4)	3.9(2)
C(11)	1.0146(6)	0.1508(4)	0.3487(3)	3.3(2)
C(12)	0.9262(7)	0.1640(4)	0.3922(3)	4.0(2)
C(14)	0.8396(6)	0.0818(4)	0.3254(4)	3.8(2)
C(15)	0.9669(6)	0.0927(4)	0.3106(3)	2.9(1)
C(16)	1.0455(6)	0.0407(4)	0.2893(3)	3.0(1)
C(17)	1.0410(6)	-0.0313(4)	0.3090(3)	3.2(2)
C(18)	0.9869(7)	-0.0514(4)	0.3608(4)	3.9(2)
C(19)	0.9867(8)	-0.1190(4)	0.3797(4)	4.9(2)
C(20)	1.0419(8)	-0.1678(4)	0.3472(4)	5.0(2)
C(21)	1.0908(7)	-0.1501(4)	0.2942(4)	4.4(2)
C(22)	1.0906(7)	-0.0827(4)	0.2758(3)	3.9(2)
C(31)	0.6778(8)	0.2325(5)	0.2728(5)	6.3(2)
C(32)	0.8117(8)	0.3252(4)	0.2074(4)	5.3(2)
C(33)	0.8556(9)	0.3183(5)	0.3349(4)	6.8(3)
C(41)	1.3501(8)	-0.0349(5)	0.3552(4)	5.6(2)
C(42)	1.4839(8)	0.0776(5)	0.3240(5)	7.2(3)
C(43)	1.4069(9)	-0.0182(5)	0.2327(5)	7.5(3)
C(111)	1.2245(6)	0.1098(4)	0.4344(3)	3.6(1)*
C(112)	1.1608(8)	0.0553(5)	0.4536(4)	5.5(2)*
C(113)	1.1989(9)	0.0183(5)	0.5067(4)	6.1(2)*
C(114)	1.297(1)	0.0386(6)	0.5411(5)	7.1(3)*
C(115)	1.365(1)	0.0922(6)	0.5250(6)	9.0(3)*
C(116)	1.3277(9)	0.1296(5)	0.4706(5)	6.5(2)*
C(117)	1.2370(7)	0.2373(4)	0.3738(3)	3.5(1)*
C(118)	1.3502(7)	0.2535(4)	0.3572(4)	4.8(2)*
C(119)	1.4002(8)	0.3188(5)	0.3687(4)	5.8(2)*
C(120)	1.3333(9)	0.3650(5)	0.3962(5)	6.4(2)*
C(121)	1.2219(8)	0.3511(5)	0.4122(4)	6.1(2)*
C(122)	1.1719(7)	0.2861(4)	0.4020(4)	4.8(2)*
C(211)	1.0309(7)	0.1985(4)	0.1005(3)	4.0(2)*
C(212)	1.0800(8)	0.2631(5)	0.1029(4)	5.9(2)*
C(213)	1.151(1)	0.2859(6)	0.0570(5)	7.2(3)*
C(214)	1.171(1)	0.2447(6)	0.0110(5)	7.6(3)*
C(215)	1.123(1)	0.1814(6)	0.0062(5)	7.7(3)*
C(216)	1.0519(9)	0.1576(5)	0.0518(5)	6.5(2)*
C(217)	0.7863(7)	0.1679(4)	0.1238(4)	4.6(2)*
C(218)	0.7499(8)	0.2148(5)	0.0773(4)	5.6(2)*
C(219)	0.6257(9)	0.2177(5)	0.0531(5)	6.2(2)*
C(220)	0.5470(9)	0.1760(5)	0.0738(5)	6.8(2)*
C(221)	0.576(1)	0.1291(6)	0.1190(5)	7.7(3)*
C(222)	0.7003(8)	0.1261(5)	0.1450(4)	5.9(2)*

<sup>a</sup> Starred values denote atoms refined isotropically. Anisotropically refined atoms are given in the form of the isotropic equivalent displacement parameter, defined as  $\frac{1}{3}[a^2B(1,1) + b^2B(2,2) + c^2B(3,3) + ab(\cos \gamma)B(1,2) + ac(\cos \beta)B(1,3) + bc(\cos \alpha)B(2,3)]$ .

belonging to the  $\text{PMe}_3$ -substituted Co(1)–Co(3) vector. This elongated Co(1)–Co(3) bond is presumed to result from unfavorable steric interactions and/or a trans influence that originates from the two trans  $\text{PMe}_3$  groups. The introduction of the first  $\text{PMe}_3$  ligand in cluster 3 leads to a 0.083 Å increase in the Co(1)–Co(3) bond relative to the parent cluster 1. Coordination of

(11) Yang, K.; Bott, S. G.; Richmond, M. G. *Organometallics* 1994, 13, 3767, 3788.

(12) Don, M.-J.; Richmond, M. G. *Inorg. Chem.* 1991, 30, 1703 and references therein.



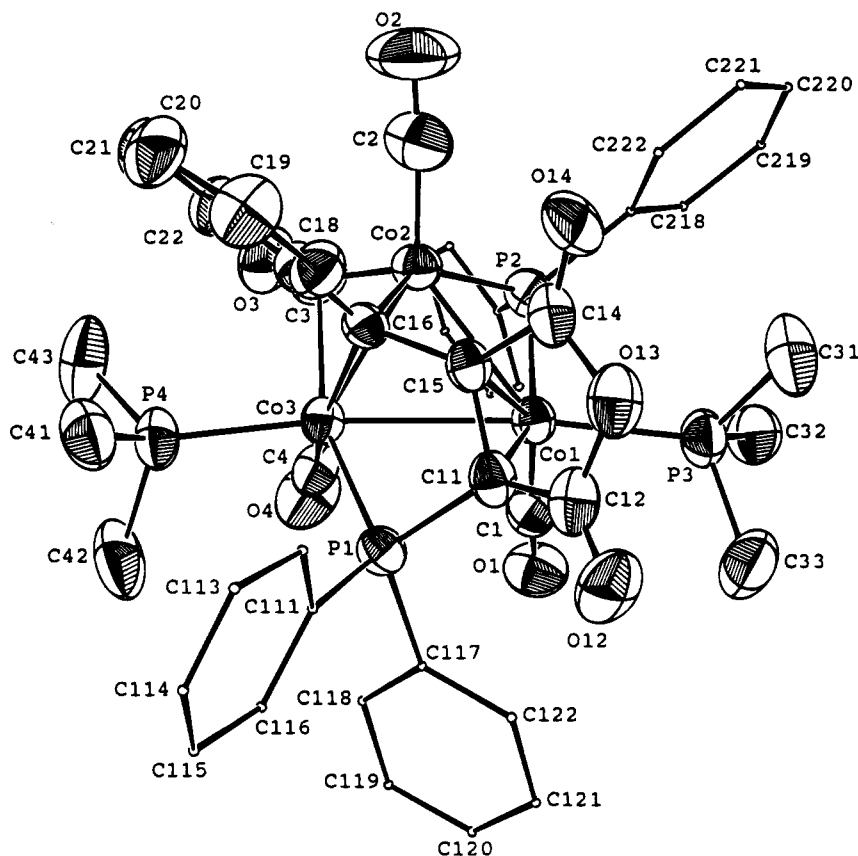


**Figure 2.** ORTEP diagram of the non-hydrogen atoms of  $\text{Co}_3(\text{CO})_4(\text{PMe}_3)_2[\mu_2\text{-}\eta^2\text{-}\eta^1\text{-C(Ph)C=C(PPh}_2\text{)C(O)OC(O)}]_2(\mu_2\text{-PPh}_2)$  showing the thermal ellipsoids at the 50% probability level.

a second  $\text{PMe}_3$  ligand as one goes from **3** to **4** lengthens this same bond by 0.053 Å. Similar ligand-induced bond length alterations have been observed by us in other structurally characterized cobalt clusters.<sup>13</sup>

The two  $\mu_2$ -benzylidene-Co bond distances of 1.900(7) and 2.035(7) Å and the terminal Co-CO distances that range from 1.725(9) to 1.775(8) Å are in close agreement with the  $\mu_3$ -benzylidyne-Co and Co-CO distances, respectively, reported for the nonacarbonyl cluster  $\text{PhCCo}_3(\text{CO})_9$ .<sup>14</sup> The semibridging interaction between Co(3) and the C(3)O(3) group bound to Co(2) is confirmed by the observed 2.278(8) Å bond length and the distinctly nonlinear bond angles of 128.3(6) and 159.1(7)° exhibited by the Co(3)-C(3)-O(3) and Co(2)-C(3)-O(3) groups.<sup>10,15</sup> The bond distances and angles exhibited by the Co- $\text{PMe}_3$  and the  $\mu_2\text{-}\eta^2\text{-}\eta^1$ -benzylidene-(diphenylphosphino)maleic anhydride ligands are unexceptional and require no comment.

Unequal Co-phosphido bond lengths are observed in **4**, and interestingly enough, when these Co-phosphido bonds in **4** are viewed by using a conventional electron-counting formalism, the shorter Co(2)-P(2) bond of 2.139(2) Å corresponds to the donor-acceptor (2e) bond while the longer covalent (1e) Co(1)-P(1) bond displays a length of 2.241(2) Å. This trend appears to serve as a reliable indicator as to the coordination mode exhib-

ited by the Co-phosphido bond in parent cluster **1** and its relatives that have been structurally characterized to date, as is summarized in Table 6 for clusters **1-4**.

**III. Cyclic Voltammetry Data.** The cyclic voltammetry studies were conducted at a platinum electrode in  $\text{CH}_2\text{Cl}_2$  containing 0.2 M TBAP as the supporting electrolyte. Figure 3 shows the room-temperature cyclic voltammogram of **4** at a scan rate of 0.1  $\text{V s}^{-1}$ . Two well-defined, diffusion-controlled redox responses are observed at  $E_{1/2} = 0.30$  V and  $E_{1/2} = -1.06$  V, along with an irreversible reduction (not shown) at  $E_p^c = -1.87$  V. The first two redox responses are readily assignable to the 0/1+ and 0/1- redox couples. These two redox couples represent fully reversible, one-electron processes, on the basis of the measured peak current ratios of unity and plots of the current function ( $I_p$ ) vs the square root of the scan rate, which were found to be linear over the scan range of 0.1-1.0  $\text{V s}^{-1}$ .<sup>16</sup> Calibration of the peak currents against ferrocene recorded under analogous conditions and application of Walden's rule confirmed the one-electron nature of each couple.<sup>16b</sup>

The reduction potential recorded for cluster **4** is in good agreement with the electrochemical data reported for the disubstituted clusters  $\text{PhCCo}_3(\text{CO})_7\text{P}_2$  (where  $\text{P}_2$  = two monodentate ligands or one bidentate ligand).<sup>17</sup>

(13) (a) Schulman, C. L.; Richmond, M. G.; Watson, W. H.; Nagl, A. *J. Organomet. Chem.* **1989**, *368*, 367. (b) Richmond, M. G.; Kochi, J. K. *Organometallics* **1987**, *6*, 254.

(14) (a) Colbran, S. B.; Robinson, B. H.; Simpson, J. *Acta Crystallogr. Sect. C* **1986**, *42*, 972. (b) Ahlgrén, M.; Pakkanen, T. T.; Tahvanainen, I. *J. Organomet. Chem.* **1987**, *323*, 91.

(15) Horwitz, C. P.; Shriver, D. F. *Adv. Organomet. Chem.* **1984**, *23*, 219.

(16) (a) Rieger, P. H. *Electrochemistry*; Chapman & Hall: New York, 1994. (b) Bard, A. J.; Faulkner, L. R. *Electrochemical Methods*; Wiley: New York, 1980.

(17) (a) Watson, W. H.; Nagl, A.; Hwang, S.; Richmond, M. G. *J. Organomet. Chem.* **1993**, *445*, 163. (b) Yang, K.; Bott, S. G.; Richmond, M. G. *J. Organomet. Chem.* **1993**, *454*, 273. (c) Downard, A. J.; Robinson, B. H.; Simpson, J. *Organometallics* **1986**, *5*, 1122, 1132, 1140. (d) Hinkelmann, K.; Heinze, J.; Schacht, H.-T.; Field, J. S.; Vahrenkamp, H. *J. Am. Chem. Soc.* **1989**, *111*, 5078.

**Table 5. Selected Bond Distances (Å) and Angles (deg) in  $\text{Co}_3(\text{CO})_4(\text{PMe}_3)_2[\mu_2-\eta^2:\eta^1-\text{C}(\text{Ph})\text{C}=\text{C}(\text{PPh}_2)\text{C}(\text{O})\text{OC}(\text{O})](\mu_2-\text{PPh}_2)$  (**4**)<sup>a</sup>**

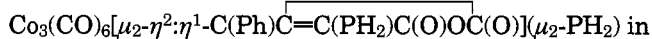
$\text{C}(\text{Ph})\text{C}=\text{C}(\text{PPh}_2)\text{C}(\text{O})\text{OC}(\text{O})](\mu_2-\text{PPh}_2)$ ( <b>4</b> ) <sup>a</sup>			
Bond Distances			
Co(1)–Co(2)	2.592(1)	Co(1)–Co(3)	2.832(1)
Co(2)–Co(3)	2.422(1)	Co(1)–P(2)	2.241(2)
Co(1)–P(3)	2.265(2)	Co(1)–C(1)	1.762(7)
Co(1)–C(11)	2.068(7)	Co(1)–C(15)	2.198(7)
Co(2)–P(2)	2.139(2)	Co(2)–C(2)	1.725(9)
Co(2)–C(3)	1.750(9)	Co(2)–C(16)	1.900(7)
Co(3)–P(1)	2.235(2)	Co(3)–P(4)	2.242(2)
Co(3)–C(3)	2.278(8)	Co(3)–C(4)	1.775(8)
Co(3)–C(16)	2.035(7)	P(1)–C(11)	1.788(7)
P(1)–C(111)	1.836(7)	P(1)–C(117)	1.832(7)
P(2)–C(211)	1.827(8)	P(2)–C(217)	1.830(8)
P(3)–C(31)	1.802(9)	P(3)–C(32)	1.813(9)
P(3)–C(33)	1.83(1)	P(4)–C(41)	1.815(9)
P(4)–C(42)	1.806(9)	P(4)–C(43)	1.80(1)
O(1)–C(1)	1.138(9)	O(2)–C(2)	1.16(1)
O(3)–C(3)	1.16(1)	O(4)–C(4)	1.14(1)
O(12)–C(12)	1.201(9)	O(13)–C(12)	1.405(9)
O(13)–C(14)	1.402(9)	O(14)–C(14)	1.180(9)
C(11)–C(12)	1.45(1)	C(11)–C(15)	1.47(1)
C(14)–C(15)	1.48(1)	C(15)–C(16)	1.44(1)
Bond Angles			
Co(2)–Co(1)–Co(3)	52.81(3)	Co(1)–Co(2)–Co(3)	68.68(4)
Co(1)–Co(3)–Co(2)	58.51(4)	Co(1)–Co(2)–C(16)	82.5(2)
Co(1)–Co(3)–P(4)	170.33(8)	Co(1)–Co(3)–C(16)	74.3(2)
Co(2)–Co(3)–P(4)	127.28(7)	P(1)–Co(3)–P(4)	100.48(8)
P(4)–Co(3)–C(3)	97.7(2)	P(4)–Co(3)–C(4)	91.1(2)
P(4)–Co(3)–C(16)	103.4(2)	C(4)–Co(3)–C(16)	160.8(3)
Co(3)–P(1)–C(11)	92.2(2)	Co(1)–P(2)–Co(2)	72.53(7)
Co(1)–C(1)–O(1)	174.6(7)	Co(2)–C(2)–O(2)	174.6(7)
Co(2)–C(3)–Co(3)	72.6(3)	Co(2)–C(3)–O(3)	159.1(7)
Co(3)–C(3)–O(3)	128.3(6)	Co(3)–C(4)–O(4)	176.2(7)
Co(1)–C(11)–P(1)	99.7(3)	Co(1)–C(11)–C(12)	120.9(5)
Co(1)–C(11)–C(15)	74.6(4)	P(1)–C(11)–C(12)	130.2(5)
P(1)–C(11)–C(15)	111.6(5)	C(12)–C(11)–C(15)	106.4(6)
O(12)–C(12)–O(13)	119.1(7)	O(12)–C(12)–C(11)	132.3(7)
O(13)–C(12)–C(11)	108.5(6)	O(13)–C(14)–O(14)	120.8(7)
O(13)–C(14)–C(15)	107.3(6)	O(14)–C(14)–C(15)	131.8(7)
Co(1)–C(15)–C(11)	65.1(4)	Co(2)–C(16)–Co(3)	75.9(3)
C(15)–C(16)–C(17)	122.8(6)		

<sup>a</sup> Numbers in parentheses are estimated standard deviations in the least significant digits.

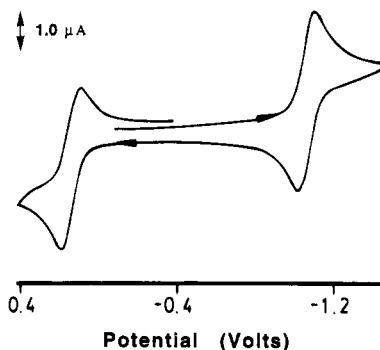
**Table 6. Bond-Length Comparisons of the Asymmetric Cobalt–Phosphido Moiety in Clusters 1–4**

cluster	donor–acceptor (2e) bond, Å	covalent (1e) bond, Å	ref
1	2.129(3)	2.264(3)	7
2	2.129(7)	2.188(6)	6
3	2.135(3)	2.253(3)	6
4	2.139(2)	2.241(2)	this work

This suggests that the LUMO in **4** is best described as an antibonding Co–Co orbital, with little or no contribution from the  $\mu_2-\eta^2:\eta^1$ -benzylidene(diphenylphosphino)maleic anhydride ligand. This stands in contrast to compounds that are substituted with an intact 2,3-bis(diphenylphosphino)maleic anhydride (bma) ligand, where it has been shown that the initial reduction occurs over a potential range of  $-0.5$  to  $-0.8$  V and at the  $\pi^*$  orbital that is localized on the bma ligand.<sup>11,18</sup> To verify this premise, we have carried out preliminary extended Hückel calculations on the model compound



(18) (a) Yang, K.; Bott, S. G.; Richmond, M. G. *Organometallics* **1995**, *14*, 2387. (b) Tyler, D. R. *Acc. Chem. Res.* **1991**, *24*, 325 and references therein. (c) Mao, F.; Tyler, D. R.; Bruce, M. R. M.; Bruce, A. E.; Rieger, A. L.; Rieger, P. H. *J. Am. Chem. Soc.* **1992**, *114*, 6418. (d) Fenske, D.; Becher, H. *J. Chem. Ber.* **1974**, *107*, 117; **1975**, *108*, 2115. (e) Becher, H. J.; Bensmann, W.; Fenske, D. *Chem. Ber.* **1977**, *110*, 315.

**Figure 3.** Cathodic scan cyclic voltammogram of  $\text{Co}_3(\text{CO})_4(\text{PMe}_3)_2[\mu_2-\eta^2:\eta^1-\text{C}(\text{Ph})\text{C}=\text{C}(\text{PPh}_2)\text{C}(\text{O})\text{OC}(\text{O})](\mu_2-\text{PPh}_2)$  (ca.  $10^{-3}$  M) in  $\text{CH}_2\text{Cl}_2$  containing 0.2 M TBAP at  $0.1$  V  $\text{s}^{-1}$ .

order to explore the nature of the LUMO in this genre of cluster. Our MO results indicate that the LUMO corresponds to an antibonding  $a_2$  orbital that involves the three cobalt atoms, the nature of which is consistent with the MO data published by Hoffmann on ligand-capped  $\text{M}_3\text{L}_9$  clusters.<sup>19</sup>

## Conclusions

The reaction of  $\text{Co}_3(\text{CO})_5(\text{PMe}_3)[\mu_2-\eta^2:\eta^1-\text{C}(\text{Ph})\text{C}=\text{C}(\text{PPh}_2)\text{C}(\text{O})\text{OC}(\text{O})](\mu_2-\text{PPh}_2)$  with added  $\text{PMe}_3$  proceeds to give the bis(phosphine) cluster  $\text{Co}_3(\text{CO})_4(\text{PMe}_3)_2[\mu_2-\eta^2:\eta^1-\text{C}(\text{Ph})\text{C}=\text{C}(\text{PPh}_2)\text{C}(\text{O})\text{OC}(\text{O})](\mu_2-\text{PPh}_2)$ , as a result of a regioselective addition of  $\text{PMe}_3$  to the maleic anhydride substituted cobalt center in **3**. The observed second-order kinetics and activation parameters support this contention. The X-ray structure of **4** confirms the site of  $\text{PMe}_3$  addition in **3**. Cyclic voltammetry data indicate the existence of accessible oxidation (0/1+) and reduction (0/1-) couples, with the nature of the latter redox couple being best described as an antibonding metal-based  $a_2$  orbital.

## Experimental Section

**General Considerations.** The  $\text{PhCCo}_3(\text{CO})_5$ <sup>20</sup> and the bma ligand<sup>21</sup> that were used in the synthesis of  $\text{Co}_3(\text{CO})_5(\text{PMe}_3)[\mu_2-\eta^2:\eta^1-\text{C}(\text{Ph})\text{C}=\text{C}(\text{PPh}_2)\text{C}(\text{O})\text{OC}(\text{O})](\mu_2-\text{PPh}_2)$ <sup>6</sup> were prepared according to literature procedures, while  $\text{PMe}_3$  was synthesized from  $\text{P}(\text{O}Ph)_3$  and  $\text{MeMgI}$ .<sup>22</sup> The solvents THF,  $\text{Bu}_2\text{O}$ , pentane, and benzene used in these studies were distilled from sodium/benzophenone ketyl under argon.  $\text{CH}_2\text{Cl}_2$  was distilled similarly from  $\text{CaH}_2$ . All distilled solvents were handled under argon using Schlenk techniques, and when not in use they were stored in Schlenk vessels equipped with Teflon stopcocks.<sup>23</sup> The  $^{13}\text{CO}$  (99%) used in the synthesis of  $^{13}\text{CO}$ -enriched **4** was purchased from Isotec, Inc. The tetra-*n*-butylammonium perchlorate (TBAP; *Caution!* strong oxidant) was obtained from Johnson Matthey Electronics and recrystallized from ethyl acetate/petroleum ether and dried for

(19) Schilling, B. E. R.; Hoffmann, R. *J. Am. Chem. Soc.* **1979**, *101*, 3456.

(20) Nestle, M. O.; Hallgren, J. E.; Seyferth, D. *Inorg. Synth.* **1980**, *20*, 226.

(21) Mao, F.; Philbin, C. E.; Weakley, T. J. R.; Tyler, D. R. *Organometallics* **1990**, *9*, 1510.

(22) Luetkens, M. L., Jr.; Sattelberger, A. P.; Murray, H. H.; Basil, J. D.; Fackler, J. P., Jr. *Inorg. Chem.* **1989**, *26*, 7.

(23) Shriner, D. F. *The Manipulation of Air-Sensitive Compounds*; McGraw-Hill: New York, 1969.

up to 48 h prior to use. The microanalysis was performed by Atlantic Microlab, Norcross, GA.

All infrared spectra were recorded on a Nicolet 20SXB FT-IR spectrometer. Room-temperature spectra were recorded in 0.1 mm NaCl cells, while low-temperature IR spectra were recorded by using a Specac Model P/N 21.000 variable-temperature cell equipped with inner and outer CaF<sub>2</sub> windows. Dry ice/acetone was employed as the coolant, and the cell temperature was measured with the aid of a copper–constantan thermocouple. The <sup>13</sup>C (75 MHz) and the <sup>31</sup>P (121 MHz) NMR spectra were recorded on a Varian 300-VXR spectrometer. All <sup>31</sup>P chemical shifts are reported relative to external H<sub>3</sub>PO<sub>4</sub> (85%), taken to have δ 0. Positive chemical shifts represent resonances that are to low field of the external standard.

**Synthesis of Co<sub>3</sub>(CO)<sub>4</sub>(PMe<sub>3</sub>)<sub>2</sub>[μ<sub>2</sub>-η<sup>2</sup>:η<sup>1</sup>-C(Ph)C=C(PPh<sub>2</sub>)-C(O)OC(O)](μ<sub>2</sub>-PPh<sub>2</sub>).** To a Schlenk tube containing 0.1 g (0.11 mmol) of Co<sub>3</sub>(CO)<sub>5</sub>(PMe<sub>3</sub>)<sub>2</sub>[μ<sub>2</sub>-η<sup>2</sup>:η<sup>1</sup>-C(Ph)C=C(PPh<sub>2</sub>)-C(O)OC(O)](μ<sub>2</sub>-PPh<sub>2</sub>) in 20 mL of CH<sub>2</sub>Cl<sub>2</sub> at room temperature was added 1.5 equiv of PMe<sub>3</sub> (0.34 mL of a 0.48 M solution of PMe<sub>3</sub> in CH<sub>2</sub>Cl<sub>2</sub>). The reaction mixture was stirred for 1.0 h, followed by IR and TLC examination, which revealed the complete conversion to the desired bis(phosphine) cluster **4**. The product was subsequently isolated by chromatography over silica gel using CH<sub>2</sub>Cl<sub>2</sub> as the eluant. The analytical sample was recrystallized from a benzene solution containing **4** that had been layered with pentane. Yield: 0.058 g (53%). IR (CH<sub>2</sub>Cl<sub>2</sub>): ν(CO) 1992 (sh), 1978 (vs), 1865 (m), 1791 (m, asym bma C=O), 1728 (m, sym bma C=O) cm<sup>-1</sup>. <sup>31</sup>P{<sup>1</sup>H} NMR (THF, 176 K): δ 172.9 (μ<sub>2</sub>-PPh<sub>2</sub>), 7.2 [Ph<sub>2</sub>P(maleic anhydride)], 0.9 (PMe<sub>3</sub>, J<sub>P-P</sub> = 100.6 Hz), -10.5 (PMe<sub>3</sub>, J<sub>P-P</sub> = 100.6 Hz). <sup>13</sup>C{<sup>1</sup>H} NMR (THF, 176 K): δ 224.0 (semibridging CO, J<sub>C-P</sub> = 25.5 Hz), 207.4 (1CO), 206.7 (2CO). Anal. Calcd (found) for C<sub>45</sub>H<sub>43</sub>Co<sub>3</sub>O<sub>7</sub>P<sub>4</sub>·1/2C<sub>6</sub>H<sub>6</sub>: C, 55.67 (55.29); H, 4.48 (4.76).

**X-ray Diffraction Structure of Co<sub>3</sub>(CO)<sub>4</sub>(PMe<sub>3</sub>)<sub>2</sub>[μ<sub>2</sub>-η<sup>2</sup>:η<sup>1</sup>-C(Ph)C=C(PPh<sub>2</sub>)-C(O)OC(O)](μ<sub>2</sub>-PPh<sub>2</sub>).** Single crystals for X-ray diffraction analysis were grown from a CH<sub>2</sub>Cl<sub>2</sub> solution of **4** that had been layered with pentane. A suitable black crystal, of dimensions 0.25 × 0.27 × 0.30 mm<sup>3</sup>, was chosen and sealed inside a Lindemann capillary, followed by mounting on the goniometer of an Enraf-Nonius CAD-4 diffractometer that employed Mo Kα radiation. Cell constants were obtained from a least-squares refinement of 25 reflections with 2θ > 30°. Intensity data in the range 2.0 ≤ 2θ ≤ 44.0° were collected at room temperature using the ω-scan technique in the variable-scan speed mode and were corrected for Lorentz, polarization, and absorption (DIFABS). Three reflections (600; 0,10,0; 0,0,10) were measured after every 3600 s of exposure time in order to monitor crystal decay (<1%). The structure was solved by SHELX-86, which enabled all of the non-hydrogen atoms to be located in the difference Fourier

maps. With the exception of the phenyl groups associated with the phosphorus atoms, all non-hydrogen atoms were refined anisotropically. Refinement converged at R = 0.0453 and R<sub>w</sub> = 0.0489 for 3795 unique reflections with I > 3σ(I).

**Electrochemical Studies.** Cyclic voltammograms were obtained with a PAR Model 273 potentiostat/galvanostat, with all CV experiments carried out by using positive feedback circuitry to compensate for iR drop. The airtight cyclic voltammetry cell was of homemade design and employed a three-electrode configuration. All electrochemical experiments employed platinum disks as the working and auxiliary electrodes. The reference electrode in all experiments consisted of a silver-wire quasi-reference electrode, with all potential data reported relative to the formal potential of the Cp\*<sub>2</sub>Fe/Cp\*<sub>2</sub>Fe<sup>+</sup> (internally added) redox couple, taken to have E<sub>1/2</sub> = -0.23 V.<sup>24</sup> The Cp\*<sub>2</sub>Fe/Cp\*<sub>2</sub>Fe<sup>+</sup> potential used as an offset value in these studies was obtained from a CV experiment using ferrocene as a reference.

**Kinetic Studies.** All kinetic studies were carried out under pseudo-first-order conditions with concentrations of PMe<sub>3</sub> being at least 20 times greater than that of cluster **3**. The reactions were monitored spectrophotometrically by using a Hewlett-Packard 8452A UV-vis spectrometer equipped with a variable-temperature cell. The extent of the reaction was determined by following the UV-vis changes in the 374 nm band of **3** for at least 5 half-lives. A VWR refrigerated constant temperature circulator was used to maintain a constant temperature, to within ±0.2 °C. Plots of ln(A<sub>∞</sub> - A<sub>t</sub>) vs time were linear and gave the pseudo-first-order rate constants (k<sub>obsd</sub>) shown in Table 1. The second-order rate constants displayed in Table 2 were obtained from plots of k<sub>obsd</sub> vs [PMe<sub>3</sub>], while the activation parameters were calculated by using the Eyring equation.<sup>25</sup>

**Acknowledgment.** We are grateful for financial support from the Robert A. Welch Foundation (Grant B-1202-SGB and B-1039-MGR) and the UNT Faculty Research Program.

**Supplementary Material Available:** Textual presentations of the crystallographic experimental details and listings of crystallographic data, bond distances, bond angles, and hydrogen positional and thermal parameters for Co<sub>3</sub>(CO)<sub>4</sub>(PMe<sub>3</sub>)<sub>2</sub>[μ<sub>2</sub>-η<sup>2</sup>:η<sup>1</sup>-C(Ph)C=C(PPh<sub>2</sub>)-C(O)OC(O)](μ<sub>2</sub>-PPh<sub>2</sub>) (15 pages). Ordering information is given on any current masthead page.

OM9500376

(24) Ryan, M. F.; Richardson, D. E.; Lichtenberger, D. L.; Gruhn, N. E. *Organometallics* **1994**, *13*, 1190.

(25) Carpenter, B. K. *Determination of Organic Reaction Mechanisms*; Wiley-Interscience: New York, 1984.

# Ligand-Induced C,C Coupling and C,C Bond Breaking in Diarylfulvene Complexes of Cobalt(0)

Hans-Friedrich Klein,<sup>\*,†</sup> Emmanuel Auer,<sup>†</sup> Thomas Jung,<sup>†</sup> and Caroline Röhr<sup>‡</sup>

Institut für Anorganische Chemie der Technischen Hochschule Darmstadt, Petersenstrasse 18, 64287 Darmstadt, FRG, and Hochschulstrasse 10, 64289 Darmstadt, FRG

Received August 25, 1994<sup>®</sup>

6,6-Diarylpentafulvenes upon coordination by odd-electron (trimethylphosphine)cobalt(0) moieties undergo a reductive C,C coupling reaction in the 1-position of the C<sub>5</sub> ring, forming dinuclear ( $\eta^3$ -allyl)cobalt(I) compounds. The C,C coupling is reversed under ambient conditions by reaction of the metal with carbon monoxide. Even-electron methyl- or phenyl-(trimethylphosphine)cobalt(I) moieties accommodate 6,6-diarylfulvenes as  $\eta^4$ -diene ligands in mononuclear complexes.

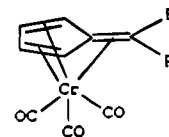
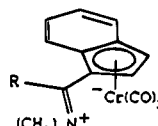
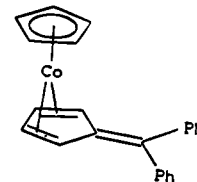
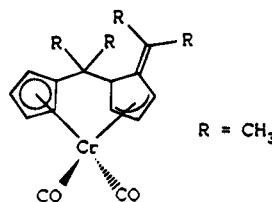
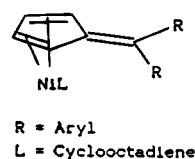
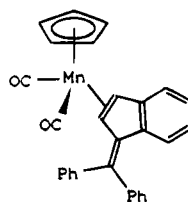
## Introduction

Coordination of olefins by zerovalent cobalt (d<sup>9</sup>) supported by three trimethylphosphine ligands is observed in molecular complexes that attain 17 metal valence electrons and can be regarded as stable radicals<sup>1</sup> under ambient conditions. Formally replacing the olefin and one of the phosphines, nonconjugated diolefins may be introduced as chelating ligands without altering the paramagnetic valence state,<sup>2</sup> while azulene upon coordination is reduced by two (trimethylphosphine)cobalt units to form a dinuclear cobalt(I) complex containing the  $\eta^5$ : $\eta^3$ - azulene dianion.<sup>3</sup>

We have been investigating substitution reactions of mononuclear cobalt(0) complexes using pentafulvenes as electron-accepting  $\pi$  ligands. These gave unexpected products containing transformed hydrocarbon ligands. We report here on a new C,C-coupling mode via radical reactions in the ligand periphery that is initiated by the odd-electron metal center and can be reversed by admitting carbon monoxide.

When coordinated to a single transition metal, pentafulvenes may act as  $\eta^2$ -olefin,<sup>4</sup>  $\eta^3$ -allyl,<sup>5</sup>  $\eta^4$ -diene,<sup>6</sup>  $\eta^5$ -cyclopentadienyl,<sup>7</sup> or  $\eta^6$ -triene<sup>8</sup> ligands (Chart 1), while in dinuclear complexes a still greater variety of coordination modes has been observed.<sup>9</sup> Radical anion intermediates have been suggested<sup>10</sup> for some of these pentafulvene transformations.

## Chart 1



R = Phenyl

## Experimental Section

**General Procedures and Materials.** Standard vacuum techniques were used in manipulations of volatile and air-sensitive materials.<sup>11</sup> Literature procedures were followed in the syntheses of Co(olefin)(PMe<sub>3</sub>)<sub>3</sub>,<sup>12</sup> CoCH<sub>3</sub>(PMe<sub>3</sub>)<sub>4</sub>,<sup>13</sup> 6-(4-methylphenyl)-6-phenylfulvene,<sup>14</sup> 6,6-diphenylfulvene,<sup>15</sup> 6,6-bis(4-methylphenyl)fulvene,<sup>16</sup> 6,6-bis(4-chlorophenyl)fulvene,<sup>17</sup> 6,6-bis(4-methoxyphenyl)fulvene,<sup>18</sup> 6,6-bis(4-(dimethylamino)-

(10) Rinehart, K. L.; Frerichs, A. K.; Kittle, P. A.; Westman, L. F.; Gustavson, D. H.; Pruel, R. L.; McMahon, J. E. *J. Am. Chem. Soc.* **1960**, *82*, 4111.

(11) Klein, H.-F.; Mager, M.; Flörke, U.; Haupt, H.-J.; Breza, M.; Boca, R. *Organometallics* **1992**, *11*, 2912.

(12) Klein, H.-F.; Lull, G.; Rodenhäuser, B.; Cordier, G.; Paulus, H. *Z. Naturforsch.* **1988**, *43B*, 1256.

(13) Klein, H.-F.; Karsch, H. H. *Chem. Ber.* **1983**, *108*, 944.

(14) Konovalow, A. I.; Yarkowa, E. G.; Salikhov, I. S.; Izmailowa, R. G. *Zh. Org. Chem.* **1967**, *3*, 1319.

(15) (a) Jeffery, J.; Probitts, E. J.; Mawby, R. J. *J. Chem. Soc., Dalton Trans.* **1984**, 2423. (b) Day, J. H. *Chem. Rev.* **1953**, *53*, 167. (c) Probitts, E. J.; Mawby, R. J. *J. Organomet. Chem.* **1986**, *310*, 121.

<sup>†</sup> TH Darmstadt, Petersenstrasse 18, 64287 Darmstadt, FRG.

<sup>‡</sup> TH Darmstadt, Hochschulstrasse 10, 64289 Darmstadt, FRG.

<sup>®</sup> Abstract published in *Advance ACS Abstracts*, May 1, 1995.

(1) Klein, H.-F.; Lull, G.; Rodenhäuser, B.; Cordier, G.; Paulus, H. *Z. Naturforsch.* **1988**, *B43*, 1256.

(2) (a) Klein, H.-F.; Gross, J.; Witty, H.; Neugebauer, D. *Z. Naturforsch.* **1984**, *B39*, 643. (b) Klein, H.-F.; Fabry, L.; Witty, H.; Schubert, U.; Lueken, H.; Stamm, U. *Inorg. Chem.* **1985**, *24*, 683.

(3) Klein, H.-F.; Hammerschmitt, B.; Lull, G.; Flörke, U.; Haupt, H.-J. *Inorg. Chim. Acta* **1994**, *218*, 143.

(4) Edelmann, F.; Jens, K. J.; Behrens, U. *Chem. Ber.* **1984**, *117*, 344.

(5) Edelmann, F.; Wormsbächer, B.; Behrens, U. *Chem. Ber.* **1978**, *111*, 817.

(6) Rau, D.; Behrens, U. *J. Organomet. Chem.* **1990**, *397*, 219.

(7) Jeffery, J.; Probitts, E. J.; Mawby, R. J. *J. Chem. Soc., Dalton Trans.* **1984**, 2423.

(8) (a) Fischer, E. O.; Semmlinger, W. *Naturwissenschaften* **1961**, *48*, 535. (b) Cooper, R. L.; Fischer, E. O.; Semmlinger, W. *J. Organomet. Chem.* **1967**, *9*, 333.

(9) (a) Toefke, S.; Haupt, E. T. K.; Behrens, U. *Chem. Ber.* **1986**, *119*, 96. (b) Behrens, U.; Weiss, E. *J. Organomet. Chem.* **1975**, *96*, 399.

phenyl)fulvene,<sup>18</sup> 6-(dimethylamino)fulvene,<sup>19</sup> and triphenylphosphonium cyclopentadienide.<sup>20</sup> Methods of characterization have been described elsewhere.<sup>21</sup> For air-sensitive compounds elemental analyses correct within 1% were regarded to be tolerable.

**Preparations. Synthesis of [(1-3- $\eta$ ): (1'-3'- $\eta$ )-4,4'-Bis(diphenylmethylidene)-5,5'-dihydrofulvalene]hexakis(trimethylphosphine)dicobalt(I) (1).** To a solution of Co(c-C<sub>5</sub>H<sub>5</sub>)(PMe<sub>3</sub>)<sub>3</sub> (640 mg, 1.80 mmol) in 70 mL of pentane at 0 °C was added dropwise 6,6-diphenylfulvene (410 mg, 1.78 mmol) in 70 mL of pentane. After 2 h at 20 °C the red solution was filtered and the volume reduced to 40 mL. At -20 °C 780 mg of dark red shining crystals was isolated (75%); dec pt >140 °C. Anal. Calcd for C<sub>54</sub>H<sub>82</sub>Co<sub>2</sub>P<sub>6</sub> (1035.0): C, 62.72; H, 8.00. Found: C, 63.34; H, 8.40. <sup>1</sup>H NMR (300 MHz, THF-d<sub>8</sub>): 305 K,  $\delta$ (PCH<sub>3</sub>) 0.95 (s, 54 H),  $\delta$ (H-5,H-5') 2.30 (s, 2 H),  $\delta$ (H-1,H-1',H-3,H-3') 3.13 (s, 4 H),  $\delta$ (H-2,H-2') 4.35 (s, 2 H),  $\delta$ (C<sub>6</sub>H<sub>5</sub>) 6.75-7.30 (m, 20 H); 193 K,  $\delta$ (PCH<sub>3</sub>) 0.95 (s, 54 H),  $\delta$ (H-5,H-5') 2.30 (s, 2 H),  $\delta$ (H-1,H-1',H-3,H-3') 2.99 (s, 2 H) and 3.13 (s, 2 H);  $\delta$ (H-2,H-2') 4.35 (s, 2 H),  $\delta$ (C<sub>6</sub>H<sub>5</sub>) 6.75-7.30 (m, 20 H). <sup>13</sup>C NMR (75 MHz, THF-d<sub>8</sub>, 297 K):  $\delta$ (C-5,C-5') 15.7,  $\delta$ (PCH<sub>3</sub>) 22.7,  $\delta$ (C-1,C-1',C-2,C-2',C-3,C-3') 48.3, 52.0, 55.6, and 66.2,  $\delta$ (C<sub>aromat</sub>) 116.5, 123.2, 125.3, 126.3, 128.4, 128.5, 129.5, 130.2, and 132.2,  $\delta$ (C<sub>quart</sub>) 146.8, 149.6, and 155.8.

**Synthesis of [(1-3- $\eta$ ): (1'-3'- $\eta$ )-4,4'-Bis[(4-methylphenyl)methylidene]-5,5'-dihydrofulvalene]hexakis(trimethylphosphine)dicobalt(I) (2).** Solutions of Co(c-C<sub>5</sub>H<sub>5</sub>)(PMe<sub>3</sub>)<sub>3</sub> (680 mg, 1.91 mmol) in 60 mL of pentane and of 6-(4-methylphenyl)-6-phenylfulvene (460 mg, 1.89 mmol) in 80 mL of pentane were combined dropwise at 20 °C to give a dark red solution. After 4 h this was filtered and the volume was reduced to 50 mL in vacuo. At -20 °C 800 mg of small dark red sticks with shiny surfaces were obtained (70%); mp 122-124 °C dec. Anal. Calcd for C<sub>55</sub>H<sub>86</sub>Co<sub>2</sub>P<sub>6</sub> (1062.3): C, 63.31; H, 8.16; P, 17.49. Found: C, 63.78; H, 8.36; P, 17.88. <sup>1</sup>H NMR (300 MHz, THF-d<sub>8</sub>, 297 K):  $\delta$ (PCH<sub>3</sub>) 0.85 (s, 54 H),  $\delta$ (H-5,H-5') and 1.35 (s, 2 H),  $\delta$ (CH<sub>3</sub>) 2.24 (s, 6 H),  $\delta$ (H-1,H-1',H-3,H-3') 3.00 (m, 4 H),  $\delta$ (H-2,H-2') 4.21 (s, 2 H),  $\delta$ (C<sub>6</sub>H<sub>5</sub>,C<sub>6</sub>H<sub>4</sub>) 6.75-7.22 (m, 18 H). <sup>13</sup>C NMR (75 MHz, THF-d<sub>8</sub>, 297 K):  $\delta$ (CCH<sub>3</sub>) 14.4,  $\delta$ (C-5,C-5') 21.3,  $\delta$ (PCH<sub>3</sub>) 22.6,  $\delta$ (C-1,C-1',C-2,C-2',C-3,C-3') 48.5, 51.8, 58.2, 66.1, and 66.8,  $\delta$ (C<sub>aromat</sub>) 123.0, 125.1, 128.4, 128.9, 129.1, 129.4, 129.9, and 132.1,  $\delta$ (C<sub>quart</sub>) 143.2, 144.0, 146.5, 149.5, and 155.5.

A sample recrystallized from ether was used for X-ray diffraction.

**Preparation of [(1-3- $\eta$ ): (1'-3'- $\eta$ )-4,4'-Bis[bis(4-methylphenyl)methylidene]-5,5'-dihydrofulvalene]hexakis(trimethylphosphine)dicobalt(I) (3).** Co(c-C<sub>5</sub>H<sub>5</sub>)(PMe<sub>3</sub>)<sub>3</sub> (710 mg, 2.00 mmol) in 60 mL of ether at 20 °C was combined with 6,6'-bis(4-methylphenyl)fulvene (570 mg, 1.98 mmol) in 100 mL of ether. The solution turned dark red, and 30 min later after filtering, the volume was reduced to 30 mL. At -20 °C a dark red solid was precipitated (which was also obtained from pentane or toluene solutions): yield 740 mg (68%); dec pt >150 °C. Anal. Calcd for C<sub>55</sub>H<sub>90</sub>Co<sub>2</sub>P<sub>6</sub> (1091.0): C, 63.79; H, 8.31; P, 17.03. Found: C, 62.85; 8.79; P, 17.30. <sup>1</sup>H NMR (300 MHz, THF-d<sub>8</sub>, 297 K):  $\delta$ (PCH<sub>3</sub>) 0.85 (s, 54 H),  $\delta$ (H-5,H-5') 2.08 (s, 2 H),  $\delta$ (CCH<sub>3</sub>) 2.30 (s, 12 H),  $\delta$ (H-1,H-1',H-3,H-3') 3.22 (s, 4 H),  $\delta$ (H-2,H-2') 4.30 (s, 2 H),  $\delta$ (C<sub>6</sub>H<sub>4</sub>) 6.94-7.28 (m, 16 H).

**Preparation of [(1-3- $\eta$ ): (1'-3'- $\eta$ )-4,4'-Bis[bis(4-chlorophenyl)methylidene]-5,5'-dihydrofulvalene]hexakis(t-**

**rimethylphosphine)dicobalt(I) (4).** Co(C<sub>2</sub>H<sub>4</sub>)(PMe<sub>3</sub>)<sub>3</sub> (830 mg, 2.63 mmol) in 40 mL of pentane and 6,6'-bis(4-chlorophenyl)fulvene (590 mg, 1.97 mmol) in 80 mL of pentane were combined at -70 °C. Within 5 min the mixture turned red. After this mixture was warmed to 20 °C and filtered, the volume was reduced to 60 mL in vacuo, affording 1200 mg of a dark red solid (85%); dec pt >120 °C. Anal. Calcd for C<sub>54</sub>H<sub>78</sub>Cl<sub>4</sub>Co<sub>2</sub>P<sub>6</sub> (1172.1): C, 55.90; H, 7.15; P, 15.49. Found: C, 55.33; H, 6.70; P, 15.86. <sup>1</sup>H NMR (300 MHz, THF-d<sub>8</sub>, 297 K):  $\delta$ (PCH<sub>3</sub>) 0.85 (s(broad)), 54 H),  $\delta$ (H-5,H-5') 2.26 (s, 2 H),  $\delta$ (H-1,H-1',H-3,H-3') 3.18 (s, 2 H) and 3.21 (s, 2 H),  $\delta$ (H-2,H-2') 4.45 (s, 2 H),  $\delta$ (C<sub>6</sub>H<sub>4</sub>) 6.90-7.55 (m, 16 H).

**Preparation of [(1-3- $\eta$ ): (1'-3'- $\eta$ )-4,4'-Bis[bis(4-methoxyphenyl)methylidene]-5,5'-dihydrofulvalene]hexakis(trimethylphosphine)dicobalt(I) (5).** Co(C<sub>2</sub>H<sub>4</sub>)(PMe<sub>3</sub>)<sub>3</sub> (750 mg, 2.38 mmol) in 150 mL of ether at -70 °C was combined with 6,6-bis(4-methoxyphenyl)fulvene (670 mg, 2.31 mmol). The mixture was warmed to form a red-brown solution. After 3 h at 20 °C a slight turbidity was removed by filtration, and the volume of the solution was reduced to 40 mL. At -20 °C dark red rods were obtained that after drying in vacuo gave 780 mg of a red powder (75%); dec pt >140 °C. Anal. Calcd for C<sub>56</sub>H<sub>90</sub>Co<sub>2</sub>O<sub>4</sub>P<sub>6</sub> (1155.0): C, 60.30; H, 7.85; P, 16.08. Found: C, 60.11; H, 8.10; P, 15.19. <sup>1</sup>H NMR (300 MHz, THF-d<sub>8</sub>, 297 K):  $\delta$ (PCH<sub>3</sub>) 0.90 (s, 54 H),  $\delta$ (H-5,H-5') 2.25 (s, 2 H),  $\delta$ (NCH<sub>3</sub>) 2.71 (s, 12 H) and 2.79 (s, 12 H),  $\delta$ (H-1,H-1',H-3,H-3') 3.05 (s, 2 H) and 3.25 (s, 2 H),  $\delta$ (H-2,H-2') 4.10 (s, 2 H),  $\delta$ (C<sub>6</sub>H<sub>4</sub>) 6.55-7.03 (m, 16 H).

**Preparation of [(1-3- $\eta$ ): (1'-3'- $\eta$ )-4,4'-Bis[bis(4-(dimethylamino)phenyl)methylidene]-5,5'-dihydrofulvalene]hexakis(trimethylphosphine)dicobalt(I) (6).** To a solution of Co(C<sub>2</sub>H<sub>4</sub>)(PMe<sub>3</sub>)<sub>3</sub> (520 mg, 1.65 mmol) in 40 mL of ether was added at 20 °C 6,6-bis(4-(dimethylamino)phenyl)fulvene (500 mg, 1.58 mmol) in 100 mL of ether. Within 30 min the mixture formed a dark red solution. After 6 h this was filtered and the volume reduced to 80 mL. At 20 °C 760 mg of dark red cubic rods with shiny surfaces was formed (80%); dec pt >185 °C. Anal. Calcd for C<sub>62</sub>H<sub>102</sub>Co<sub>2</sub>N<sub>4</sub>P<sub>6</sub> (1207.6): C, 61.68; H, 8.45; P, 15.39. Found: C, 61.77; H, 8.61; P, 14.92. <sup>1</sup>H NMR (300 MHz, THF-d<sub>8</sub>, 297 K):  $\delta$ (PCH<sub>3</sub>) 0.90 (s, 54 H),  $\delta$ (H-5,H-5') 2.25 (s(broad), 2 H),  $\delta$ (NCH<sub>3</sub>) 2.71 (s, 6 H) and 2.79 (s, 6 H),  $\delta$ (H-1,H-1',H-3,H-3') 3.05 (s, 2 H) and 3.25 (s, 2 H),  $\delta$ (H-2,H-2') 4.10 (s, 2 H),  $\delta$ (C<sub>6</sub>H<sub>4</sub>) 6.79 (m, 16 H).

**Attempted Reactions with 6-(Dimethylamino)fulvene and Triphenylphosphonium Cyclopentadienide.** (a) Solutions of Co(C<sub>2</sub>H<sub>4</sub>)(PMe<sub>3</sub>)<sub>3</sub> (950 mg, 3.01 mmol) in 80 mL of toluene were combined with mole equivalent amounts of the fulvenes at 20 °C, respectively. Heating the mixture to reflux for 3 h had no effect. Both fulvenes were recovered by crystallization in 81% and 92% yields, respectively.

(b) Solutions of CoCH<sub>3</sub>(PMe<sub>3</sub>)<sub>4</sub> (500 mg, 1.32 mmol) in 50 mL of toluene were treated likewise, giving 86% and 95% of unchanged fulvene, respectively.

**Preparation of [(1-4- $\eta$ )-6,6-Diphenylfulvene]methylbis(trimethylphosphine)cobalt(I) (7).** CoMe(PMe<sub>3</sub>)<sub>4</sub> (340 mg, 0.90 mmol) in 100 mL of pentane at -70 °C was combined with 6,6-diphenylfulvene (200 mg, 0.87 mmol). The mixture was warmed to become a red solution. After 6 h at 20 °C filtration and crystallization from a volume of 40 mL at 0 °C afforded 390 mg of dark red-black shining crystals (98%); mp 105-106 °C. Anal. Calcd for C<sub>25</sub>H<sub>35</sub>CoP<sub>2</sub> (456.4): C, 65.79; H, 7.72; Co, 12.91. Found: C, 64.91; H, 7.79; Co, 13.21. <sup>1</sup>H NMR (300 MHz, THF-d<sub>8</sub>, 297 K):  $\delta$ (CoCH<sub>3</sub>) -0.40 (s, 3 H),  $\delta$ (PCH<sub>3</sub>) 1.14 (s, 18 H),  $\delta$ (H-2/3) 4.15 (s, 2 H),  $\delta$ (H-1/4) 5.05 (s, 2 H),  $\delta$ (C<sub>6</sub>H<sub>5</sub>) 7.05-7.43 (m, 10 H). <sup>13</sup>C NMR (75 MHz, THF-d<sub>8</sub>, 297 K):  $\delta$ (CoCH<sub>3</sub>) -20.9,  $\delta$ (PCH<sub>3</sub>) 18.1,  $\delta$ (C-1/4,C-2/3) 66.1 and 84.3,  $\delta$ (C-5) 96.8,  $\delta$ (C<sub>6</sub>H<sub>5</sub>) 122.0, 128.2, and 130.0,  $\delta$ (C<sub>quart</sub>) 142.5 and 146.6.

**Preparation of [(1-4- $\eta$ )-6,6-Bis(4-methylphenyl)fulvene]methylbis(trimethylphosphine)cobalt(I) (8).** CoMe(PMe<sub>3</sub>)<sub>4</sub> (650 mg, 1.72 mmol) in 40 mL of pentane and 6,6-bis(4-methylphenyl)fulvene (420 mg, 1.63 mmol) in 100 mL

(16) (a) Alper, H.; Laycock, D. E. *Synthesis* **1980**, 799. (b) Fuson, R. C.; Bakker, G. R.; Vittimberga, B. *J. Am. Chem. Soc.* **1959**, *81*, 264.

(17) (a) Kresze, G.; Rau, S.; Sabelus, G.; Goetz, H. *Justus Liebigs Ann. Chem.* **1961**, *648*, 51, 57. (b) Friedrichsen, W.; Oeser, H. G. *Justus Liebigs Ann. Chem.* **1978**, 1139.

(18) Rau, D.; Behrens, U. *J. Organomet. Chem.* **1990**, *397*, 219.

(19) Hafner, K.; Vöpel, K. H.; Ploss, G.; König, C. *Justus Liebigs Ann. Chem.* **1963**, *661*, 52.

(20) Ramirez, F.; Levy, S. *J. Am. Chem. Soc.* **1957**, *79*, 67.

(21) Klein, H.-F.; Bickelhaupt, A.; Hammerschmitt, B.; Flörke, U.; Haupt, H.-J. *Organometallics* **1994**, *13*, 2944.

of pentane were combined at 0 °C to give a dark red solution which after 1 h at 20 °C was filtered and reduced to 60 mL in vacuo. Crystallization at 6 °C gave 550 mg of deep red cubic rods with shiny surfaces (68%, not optimized); mp 139–139.5 °C. Anal. Calcd for  $C_{27}H_{39}CoP_2$  (484.5): C, 66.94; H, 8.11; Co, 12.16. Found: C, 66.97; H, 8.25; Co, 12.18.  $^1H$  NMR (300 MHz, THF- $d_8$ , 297 K):  $\delta(CoCH_3)$  -0.65 (t, 3 H,  $^3J(PH) = 9.4$  Hz),  $\delta(PCH_3)$  1.22 (d, 18 H,  $^2J(PH) = 7.2$  Hz),  $\delta(CCH_3)$  2.39 (s, 6 H),  $\delta(H-2,H-3)$  4.15 (s, 2 H),  $\delta(H-1,H-4)$  5.01 (s, 2 H),  $\delta(C_6H_4)$  6.95 (m, 8 H).  $^{13}C$  NMR (75 MHz, THF- $d_8$ , 297 K):  $\delta(CoCH_3)$  -22.5,  $\delta(PCH_3)$  18.2,  $\delta(C-1/4,C-2/3)$  61.7, 84.4,  $\delta(C_6H_4)$  129.0 and 130.0,  $\delta(C_{quart})$  132.1, 142.6, 143.8.

**Preparation of [(1-4- $\eta$ )-6-(4-Methylphenyl)-6-phenylfulvene]methylbis(trimethylphosphine)cobalt(I) (9).**  $CoMe(PMe_3)_4$  (550 mg, 1.45 mmol) in 50 mL of pentane and 6-(4-methylphenyl)-6-phenylfulvene (340 mg, 1.40 mmol) in 70 mL of pentane were combined at 20 °C to give a deep red solution. After 3 h filtration and crystallization from a volume of 40 mL at -20 °C afforded 480 mg of dark red plates (72%); mp 112–113 °C. Anal. Calcd for  $C_{26}H_{37}CoP_2$  (470.5): C, 66.38; H, 7.92; Co, 12.52. Found: C, 66.25; H, 8.15; Co, 11.85.  $^1H$  NMR (300 MHz, THF- $d_8$ , 297 K):  $\delta(CoCH_3)$  -0.62 (t, 3 H,  $^3J(PH) = 10.3$  Hz),  $\delta(PCH_3)$  1.21 (d, 18 H,  $^2J(PH) = 6.9$  Hz),  $\delta(CCH_3)$  2.20 (s, 3 H),  $\delta(H-2/3)$  3.83 (s, 1 H) and 3.91 (s, 1 H),  $\delta(H-1/4)$  4.81 (s, 2 H),  $\delta(C_6H_5/4)$  6.84–7.16 (m, 9 H).  $^{13}C$  NMR (75 MHz, THF- $d_8$ , 297 K):  $\delta(CoCH_3)$  -22.6,  $\delta(PCH_3)$  18.2,  $\delta(C-1/2/3/4)$  61.5, 62.6, 84.4, and 84.5;  $\delta(C_6H_5/4)$  123.0, 128.2, 129.1, 129.9, 130.3, and 132.4;  $\delta(C_{quart})$  142.7, 143.8, and 146.7.

**Preparation of [(1-4- $\eta$ )-6,6-Bis(4-chlorophenyl)fulvene]methylbis(trimethylphosphine)cobalt(I) (10).**  $CoMe(PMe_3)_4$  (520 mg, 1.37 mmol) in 140 mL of pentane at -70 °C was combined with 6,6-bis(4-chlorophenyl)fulvene (390 mg, 1.30 mmol) and allowed to warm up under stirring. After 1 h at 20 °C the red solution was filtered and the volume reduced to 30 mL in vacuo. At -20 °C 650 mg of small dark red sticks was obtained (93%); mp 155–156 °C. Anal. Calcd for  $C_{25}H_{33}Cl_2CoP_2$  (524.7): C, 57.17; H, 6.29; P, 11.81. Found: C, 56.92; H, 6.65; P, 11.59.  $^1H$  NMR (300 MHz, THF- $d_8$ , 297 K):  $\delta(CoCH_3)$  -0.50 (t, 3 H,  $^3J(PH) = 9.3$  Hz),  $\delta(PCH_3)$  1.21 (d, 18 H,  $^2J(PH) = 6.1$  Hz),  $\delta(H-2/3)$  3.92 (s, 2 H),  $\delta(H-1/4)$  4.82 (s, 2 H),  $\delta(C_6H_4)$  7.10 (m, 8 H).  $^{13}C$  NMR (75 MHz, THF- $d_8$ , 297 K):  $\delta(CoCH_3)$  -25.3,  $\delta(PCH_3)$  18.0,  $\delta(C-1/2/3/4)$  62.9, and 84.5,  $\delta(C-5)$  88.6,  $\delta(C_6H_4)$  128.6 and 131.2,  $\delta(CCl)$  193.2 and 195.2.

**Preparation of [(1-4- $\eta$ )-6,6-Bis(4-methoxyphenyl)fulvene]methylbis(trimethylphosphine)cobalt(I) (11).**  $CoMe(PMe_3)_4$  (600 mg, 1.58 mmol) in 50 mL of pentane and 6,6-bis(4-methoxyphenyl)fulvene (440 mg, 1.50 mmol) in 80 mL of pentane were combined at 20 °C. After 15 min a dark red solid started depositing, and after 4 h of stirring the volume of the mixture was reduced to 70 mL. The solid was filtered and washed with 30 mL of fresh pentane. Extraction of the solid with 80 mL of ether and crystallization from a volume of 30 mL at -20 °C afforded 720 mg of dark red shining crystals (90%); mp 146–148 °C. Anal. Calcd for  $C_{27}H_{39}CoO_2P_2$  (516.5): C, 62.79; H, 7.61; Co, 11.41. Found: C, 61.90; H, 7.80; Co, 11.72.  $^1H$  NMR (300 MHz, THF- $d_8$ , 297 K):  $\delta(CoCH_3)$  -0.60 (t, 3 H,  $^3J(PH) = 10.2$  Hz),  $\delta(PCH_3)$  1.22 (d, 18 H,  $^2J(PH) = 8.2$  Hz),  $\delta(OCH_3)$  3.70 (s, 6 H),  $\delta(H-2/3)$  3.77 (s, 2 H),  $\delta(H-1/4)$  4.86 (s, 2 H),  $\delta(C_6H_4)$  123.8 and 130.8,  $\delta(C_{quart})$  139.2 and 156.8.

**Preparation of [(1-4- $\eta$ )-6,6-Bis(4-(dimethylamino)phenyl)fulvene]methylbis(trimethylphosphine)cobalt(I) (12).**  $CoMe(PMe_3)_4$  (350 mg, 0.92 mmol) in 50 mL of ether and 6,6-bis(4-(dimethylamino)phenyl)fulvene (280 mg, 0.89 mmol) in 100 mL of ether were combined at 20 °C to give a red solution. After 2 h filtration and crystallization from a volume of 40 mL at -20 °C afforded 420 mg of dark red shining crystals (73%, not optimized); mp 165–166 °C. Anal. Calcd for  $C_{29}H_{45}CoN_2P_2$  (542.5): C, 64.20; H, 8.36; N, 5.16. Found: C, 64.28; H, 8.30; N, 5.19.  $^1H$  NMR (300 MHz, THF- $d_8$ , 297 K):  $\delta(CoCH_3)$  -0.68 (t, 3 H,  $^3J(PH) = 9.8$  Hz),  $\delta(PCH_3)$  1.15 (s, 18 H),  $\delta(NCH_3)$  2.85 (s, 12 H),  $\delta(H-2/3)$  3.80 (s, 2 H),  $\delta(H-1/4)$  4.80

(s, 2 H),  $\delta(C_6H_4)$  6.80 (m, 8 H).  $^{13}C$  NMR (75 MHz, THF- $d_8$ , 297 K):  $\delta(CoCH_3)$  -23.2,  $\delta(PCH_3)$  16.4,  $\delta(NCH_3)$  39.2,  $\delta(C-1/2/3/4)$  59.4 and 82.6,  $\delta(C_6H_4)$  111.4 and 128.8,  $\delta(C_{quart})$  138.8, 140.0, and 146.0.

**Preparation of [(1-4- $\eta$ )-6,6-Diphenylfulvene]phenylbis(trimethylphosphine)cobalt(I) (13).**  $CoPh(PMe_3)_4$  (910 mg, 2.07 mmol) in 40 mL of pentane and diphenylfulvene (450 mg, 1.95 mmol) in 60 mL of pentane were combined at -70 °C. The mixture was warmed up to -30 °C and within 2 h formed a deep red solution. Filtering and concentrating to a volume of 40 mL followed by cooling to -40 °C afforded 550 mg of dark red shining crystals (53%, not optimized); dec pt >95 °C. Anal. Calcd for  $C_{30}H_{37}CoP_2$  (518.5): C, 69.40; H, 7.19; Co, 11.36. Found: C, 69.90; H, 7.75; Co, 11.48.  $^1H$  NMR (60 MHz, THF- $d_8$ , 297 K):  $\delta(PCH_3)$  0.9 (s, 18 H),  $\delta(H-2/3)$  3.8 (s, 2 H),  $\delta(H-1/4)$  4.8 (s, 2 H),  $\delta(CoC_6H_5)$  6.3–6.5 (m, 5 H),  $\delta(CC_6H_5)$  7.2–6.7 (m, 10 H).

**Preparation of [(1-4- $\eta$ )-6-(4-Methylphenyl)-6-phenylfulvene]phenylbis(trimethylphosphine)cobalt(I) (14).**  $CoPh(PMe_3)_4$  (590 mg, 1.34 mmol) in 30 mL of pentane and 6-(4-methylphenyl)-6-phenylfulvene (3220 mg, 1.30 mmol) in 100 mL of pentane were combined at -70 °C. Warming to -40 °C gave a deep red solution which after 3 h was filtered and reduced to a volume of 50 mL. At -50 °C 360 mg of dark red shining crystals was obtained (51%, not optimized); dec pt >85 °C. Anal. Calcd for  $C_{31}H_{39}CoP_2$  (532.6): C, 69.91; H, 7.38; P, 11.64. Found: C, 69.79; H, 7.25; P, 11.58.  $^1H$  NMR (60 MHz, THF- $d_8$ , 297 K):  $\delta(PCH_3)$  0.9 (s, 18 H),  $\delta(H-2/3)$  4.0 (s, 2 H),  $\delta(H-1/4)$  4.6 (s, 2 H),  $\delta(CoC_6H_5)$  6.1–6.4 (m, 5 H),  $\delta(C_6H_5/4)$  6.8–7.3 (m, 9 H).

**Preparation of [(1-4- $\eta$ )-6,6-Bis(4-chlorophenyl)fulvene]phenylbis(trimethylphosphine)cobalt(I) (15).**  $CoPh(PMe_3)_4$  (500 mg, 1.14 mmol) in 40 mL of pentane and 6,6-bis(4-chlorophenyl)fulvene (300 mg, 1.00 mmol) in 60 mL of pentane were combined at -70 °C and when warmed to -50 °C formed a deep red solution. After 2 h filtration and crystallization at -70 °C from a volume of 30 mL gave 270 mg of dark red shining crystals (43%, not optimized); dec pt >90 °C. Anal. Calcd for  $C_{30}H_{35}Cl_2CoP_2$  (587.4): C, 61.34; H, 6.00; P, 10.54. Found: C, 61.34; H, 6.26; P, 10.20.  $^1H$  NMR (300 MHz, THF- $d_8$ , 243 K):  $\delta(PCH_3)$  1.23 (d, 18 H,  $^2J(PH) = 6.9$  Hz),  $\delta(H-2/3)$  4.04 (s, 2 H),  $\delta(H-1/4)$  5.14 (s, 2 H),  $\delta(CoC_6H_5)$  6.67–6.78 (m, 5 H),  $\delta(C_6H_4)$  7.10–7.38 (m, 8 H).

**Preparation of [(1-4- $\eta$ )-6,6-Bis(4-methoxyphenyl)fulvene]phenylbis(trimethylphosphine)cobalt(I) (16).**  $CoPh(PMe_3)_4$  (390 mg, 0.89 mmol) in 40 mL of pentane and 6,6-bis(4-methoxyphenyl)fulvene (260 mg, 0.88 mmol) in 60 mL of pentane were combined at -70 °C and warmed up to 20 °C. After 2 h the deep red solution was filtered. Crystallization from a volume of 30 mL at -20 °C gave 290 mg of small dark red cubes (57%); dec pt >110 °C. Anal. Calcd for  $C_{32}H_{41}CoO_2P_2$  (578.5): C, 66.44; H, 7.10; P, 10.70. Found: C, 66.22; H, 7.58; P, 10.54.

**Preparation of [(1-4- $\eta$ )-6,6-Bis(4-(dimethylamino)phenyl)fulvene]phenylbis(trimethylphosphine)cobalt(I) (17).**  $CoPh(PMe_3)_4$  (410 mg, 0.93 mmol) in 80 mL of ether and 6,6-bis(4-(dimethylamino)phenyl)fulvene (290 mg, 0.93 mmol) in 100 mL of ether were combined at -70 °C. After the mixture was stirred for 3 h at -30 °C, a dark red solution was formed that was filtered and reduced to a volume of 30 mL. Crystallization at -40 °C gave 360 mg of small dark red sticks (65%); dec pt >90 °C. Anal. Calcd for  $C_{30}H_{35}CoN_2P_2$  (587.4): C, 67.48; H, 7.77; P, 10.25. Found: C, 67.56; H, 8.28; P, 10.43.  $^1H$  NMR (300 MHz, THF- $d_8$ , 213 K):  $\delta(PCH_3)$  1.22 (s, 18 H),  $\delta(NCH_3)$  2.85 (s, 12 H),  $\delta(H-2/3)$  3.93 (s, 2 H),  $\delta(H-1/4)$  5.12 (s, 2 H),  $\delta(CoC_6H_5)$  6.56–6.68 (m, 5 H),  $\delta(C_6H_4)$  7.04–7.34 (m, 8 H).

**Reaction of 1 with Carbon Monoxide.** Complex 1 (320 mg, 0.31 mmol) in 120 mL of ether at 20 °C was stirred under 1 bar of CO for 18 h. The deep red solution changed to orange.

**Table 1. Crystal Data and Refinement Details for 2 and 8**

	2	8
formula	C <sub>60</sub> H <sub>91</sub> Co <sub>2</sub> OP <sub>6</sub>	C <sub>27</sub> H <sub>39</sub> CoP <sub>2</sub>
fw	1132.0	484.5
crystal size, mm	0.22 × 0.19 × 0.14	0.25 × 0.25 × 0.22
cryst syst	triclinic	triclinic
space group	<i>P</i> $\bar{1}$	<i>P</i> $\bar{1}$
<i>a</i> , Å	19.432(8)	8.639(2)
<i>b</i> , Å	15.155(6)	12.205(3)
<i>c</i> , Å	14.609(5)	13.626(5)
$\alpha$ , deg	63.611(10)	74.82(2)
$\beta$ , deg	66.240(10)	73.19(2)
$\gamma$ , deg	61.169(10)	77.1(2)
<i>V</i> , Å <sup>3</sup>	3275.8(22)	1307.5(7)
<i>Z</i>	2	2
<i>T</i> , K	293(2)	293(2)
<i>D</i> <sub>calc</sub> , g cm <sup>-3</sup>	1.148	1.230
$\lambda$ (Mo K $\alpha$ ), Å	0.710 73	0.710 73
$\mu$ , mm <sup>-1</sup>	0.687	0.790
scan mode	$\theta/2\theta$	$\theta/2\theta$
<i>F</i> (000)	1206	516
2 $\theta$ limits, deg	5–40	5–56
<i>hkl</i> range	–20 to 20; –15 +16; 0–16	–10 to 11; –15 +15; 0, 17
no. of rflns colld	6427	6288
no. of indep rflns	6104	6035
<i>R</i> <sub>int</sub>	0.0461	0.0265
abs cor	Lp, empirical	$\psi$ scans
min/max transmissn		0.892/0.813
no. of params	530	281
R1 ( <i>I</i> > 2 $\sigma$ ( <i>I</i> ))	0.0981	0.0461
wR2	0.2520	0.0944
GOF	1.060	0.954

All volatile material was removed in vacuo, and the orange residue was extracted with 40 mL of pentane. From a volume of 20 mL at –20 °C 110 mg of light red crystals was obtained that was identified as 6,6-diphenylfulvene by <sup>1</sup>H NMR (77% yield); mp 78–78.5 °C. The mother liquor contained tetracarbonyltetrakis(trimethylphosphine)dicobalt(0)<sup>12</sup> (IR).

**Reaction of 7 with Carbon Monoxide.** Complex 7 (710 mg, 1.56 mmol) in 150 mL of ether was stirred under 1 bar of CO at 20 °C. An orange solution was obtained after 1 h, which after 3 h was worked up as described for 1. A total of 310 mg of 6,6-diphenylfulvene was isolated, and the mother liquor was shown to contain Co(COCH<sub>3</sub>)(CO)<sub>2</sub>(PMe<sub>3</sub>)<sub>2</sub><sup>12</sup> (IR).

**X-ray Crystallography.** The determination of the X-ray structures of 2 and 8 was carried out using single crystals sealed in capillaries under argon. Data for 2 were collected on a Philips PW1100 diffractometer, while for 8 a Nicolet R3m/V diffractometer was used.

Crystal data and a summary of structure refinements are collected in Table 1; atomic positional parameters for 2 are given in Tables 2 and 3 and those for 8 in Tables 4 and 5. The structure of 2 was solved by direct methods using SHELXS-86<sup>22</sup> and refined on *F*<sup>2</sup> by full-matrix least-squares techniques using SHELXL-93<sup>23</sup> with all data corrected for absorptions by DIFABS.<sup>24</sup> Cobalt, phosphorus, and non-methyl carbon atoms were refined anisotropically and all methyl groups isotropically with H atoms fixed in idealized positions. A solvating ether molecule could be located but not fully refined due to insufficient crystal quality. The structure of 8 was solved and refined using the SHELXTL-PLUS routine.<sup>25</sup> All non-hydrogen atoms were refined isotropically with hydrogen atoms fixed in calculated positions.<sup>26</sup>

(22) Sheldrick, G. M. *Acta Crystallogr.* **1990**, *A46*, 467.

(23) Sheldrick, G. M. SHELXL-93; University of Göttingen, 1993.

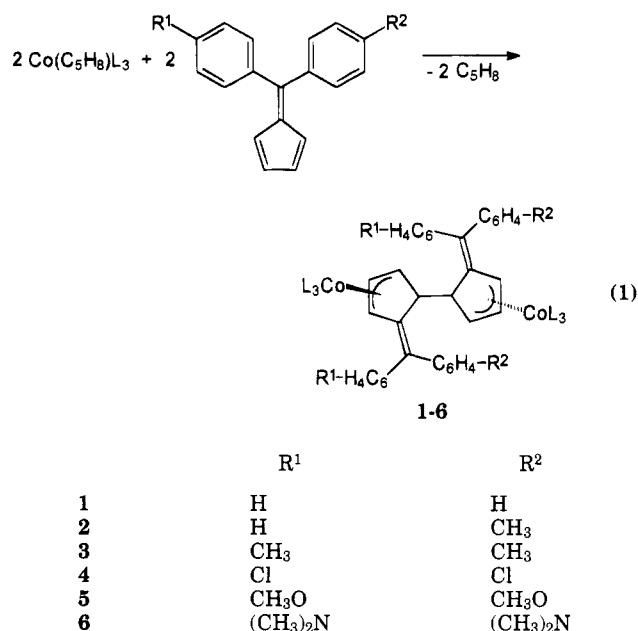
(24) Walker, N.; Stuart, D. *Acta Crystallogr.* **1983**, *A39*, 158.

(25) Sheldrick, G. M. SHELXTL-PLUS Structure Determination Software Programs; Siemens Analytical X-ray Instruments Inc.: Madison, WI, 1990.

(26) The X-ray crystallography study of 8 was kindly carried out by U. Flercke and H.-J. Haupt, University of Paderborn, Paderborn, FRG.

## Results and Discussion

**Preparations.** Combining the (cyclopentene)cobalt(0) complex Co(C<sub>5</sub>H<sub>8</sub>)(PMe<sub>3</sub>)<sub>3</sub> and a 6,6-diarylfulvene compound (eq 1) in pentane either at 20 °C or at –70 °C immediately gives a red solution (except for 6 which is slowly formed). Dark red crystals of 1, 2, 4, and 6 are



obtained that are stable in air for a few minutes, while in solution oxidative degradation is complete within seconds. Complex 3 was deposited from pentane or ether solutions as a dark red solid and on careful cooling did not form larger crystals. Complex 5 formed large crystals from ether that on drying in vacuo were transformed into a red powder.

Both solids are air-sensitive. Solid compounds 1–6 are slightly soluble in pentane and progressively better soluble in ether, THF, and toluene. A slow reaction is observed with acetone, and fast decomposition occurs in chlorinated or protic solvents.

**IR and NMR Spectra.** Infrared spectra of 1–6 contain all bands characteristic for coordinated trimethylphosphine, while the fingerprint of the hydrocarbon ligand does not clearly indicate the type of metal coordination.

The <sup>1</sup>H NMR spectrum of 1 is representative of those for complexes 1–6. There are neither unusual shifts nor line broadenings that could be connected with a paramagnetic valence state. All proton resonances are observed where expected for a diamagnetic complex. When the temperature is lowered, one of the signals (305 K: 3.13 ppm, 2 H) splits into two singlets at 3.13 ppm (1 H) and 2.99 ppm (1 H), which are assigned to the terminal allyl protons. The central allyl proton resonates at 4.31 ppm, and the fourth proton of the C<sub>5</sub> ring experiences a high-field shift to 2.30 ppm by transformation of this ring atom into an sp<sup>3</sup>-C atom. The same pattern of <sup>1</sup>H NMR signals is observed in the spectra of complexes 2–6, but there is no coincidence of allyl proton signals at 305 K.

The spectra indicate dimerization of the (fulvene)cobalt(0) complex via C,C coupling to give a diamagnetic dicobalt(I) compound. Proof was obtained by a single-crystal X-ray study.



**Table 2. Atomic Coordinates ( $\times 10^4$ ) and Equivalent Isotropic Displacement Parameters ( $\text{\AA}^2 \times 10^3$ ) for **2**<sup>a</sup>**

atom	x	y	z	U(eq)
Co(1)	1747(1)	1460(2)	6858(2)	39(1)
Co(2)	2673(1)	3815(2)	8999(2)	43(1)
P(1)	1698(2)	-106(3)	7451(3)	57(1)
P(2)	513(2)	2410(3)	6722(4)	76(1)
P(3)	2445(2)	1557(3)	5232(3)	61(1)
P(4)	3241(2)	2527(3)	10234(3)	65(1)
P(5)	1872(2)	5011(3)	9788(3)	70(1)
P(6)	3649(2)	4411(3)	7953(3)	66(1)
C(1)	2716(6)	2495(9)	6820(8)	34(3)
C(2)	1830(7)	2623(10)	7134(10)	45(3)
C(3)	1712(7)	1754(11)	8043(10)	48(3)
C(4)	2450(7)	915(9)	7918(9)	44(3)
C(5)	3134(7)	1287(9)	7292(8)	37(3)
C(6)	3917(7)	701(9)	7249(9)	39(3)
C(7)	4600(4)	1098(6)	6666(7)	43(3)
C(8)	5208(5)	659(6)	7188(6)	56(4)
C(9)	5871(4)	968(8)	6716(8)	68(4)
C(10)	5926(4)	1717(8)	5723(8)	71(4)
C(11)	5319(6)	2156(6)	5201(6)	65(4)
C(12)	4656(4)	1846(7)	5672(6)	56(4)
C(13)	4165(5)	-467(5)	7829(8)	47(3)
C(14)	3924(5)	-856(8)	8919(7)	61(4)
C(15)	4127(6)	-1941(9)	9418(7)	82(5)
C(16)	4571(7)	-2637(6)	8827(11)	92(5)
C(17)	4813(5)	-2248(7)	7738(10)	78(5)
C(18)	4610(5)	-1163(8)	7239(6)	64(4)
C(19A)	6667(16)	2019(20)	5282(20)	79(8)
C(19B)	4683(26)	-3701(35)	9377(34)	93(13)
C(20A)	1301(16)	-518(20)	6766(22)	76(9)
C(20B)	1055(28)	-474(35)	7158(40)	41(13)
C(21A)	1346(18)	-627(22)	8897(21)	70(8)
C(21B)	964(31)	-329(38)	8818(37)	52(13)
C(22A)	2668(12)	-1250(16)	7462(18)	71(6)
C(22B)	2790(38)	-1088(50)	6886(56)	92(21)
C(23A)	-46(11)	2154(15)	6193(15)	61(5)
C(23B)	-152(31)	3297(54)	7423(57)	74(15)
C(23C)	45(23)	3800(30)	6590(41)	97(11)
C(24A)	341(36)	3808(44)	5766(58)	71(16)
C(24B)	551(36)	3663(46)	5264(50)	122(22)
C(25A)	-162(21)	2686(38)	7938(33)	64(10)
C(25B)	-332(23)	2061(33)	8209(30)	74(11)
C(26A)	2702(22)	2729(26)	4228(25)	74(9)
C(26B)	2216(22)	3002(26)	4348(26)	78(10)
C(27A)	3514(15)	940(22)	4838(21)	79(8)

<sup>a</sup>  $U(\text{eq})$  is defined as one-third of the trace of the orthogonalized  $U_{ij}$  tensor.

**Molecular Structure of 2.** The triclinic cell of **2** contains two enantiomers; the molecule adopting an *S,S* configuration is shown in Figure 1. In the molecular unit each of the two tris(trimethylphosphine)cobalt fragments is coordinated to an  $\eta^3$ -allyl function of a hydrocarbon ligand that appears as a dimer of the pentafulvene and has become a methyldene-substituted dihydrofulvalene derivative. In spite of identical metal coordination the bond connecting the halves of the molecule does not contain a center of symmetry, possibly reflecting the centrosymmetric point group. Rather, the molecules of **2** adopt  $C_1$  symmetry because the  $C_5$  rings are twisted in a helical manner and are forced into a staggered conformation with respect to each other. This is best illustrated by a view perpendicular to the CoCo vector (Figure 1). The shortest distances between atoms C(2)-C(5) and C(30)-C(33) are 3.2-3.5 Å, excluding bonds between the rings.

As a result of  $\eta^3$ -allyl coordination the fulvene  $C_5$  rings are not planar and double and single C,C bonds do not alternate any longer. Only the formerly exocyclic C=C bond is still present (C(5)-C(6) = 1.33(2) Å, C(33)-C(34)

**Table 3. Selected Bond Lengths (Å) and Angles (deg) for 2**

Co(1)-C(3)	1.937(11)	Co(1)-C(2)	2.062(11)
Co(1)-C(4)	2.102(11)	Co(1)-P(2)	2.158(5)
Co(1)-P(1)	2.173(4)	Co(1)-P(3)	2.189(5)
Co(2)-C(31)	1.933(11)	Co(2)-C(30)	2.065(11)
Co(2)-C(32)	2.101(11)	Co(2)-P(4)	2.163(5)
Co(2)-P(5)	2.174(5)	Co(2)-P(6)	2.199(5)
Co(1)-C(2)	1.53(2)	C(1)-C(5)	1.54(2)
C(1)-C(29)	1.58(2)	C(2)-C(3)	1.43(2)
C(3)-C(4)	1.39(2)	C(4)-C(5)	1.49(2)
C(5)-C(6)	1.33(2)	C(6)-C(13)	1.50(2)
C(6)-C(7)	1.50(2)	C(29)-C(30)	1.48(2)
C(29)-C(33)	1.53(2)	C(30)-C(31)	1.45(2)
C(31)-C(32)	1.42(2)	C(32)-C(33)	1.45(2)
C(33)-C(34)	1.34(2)	C(34)-C(35)	1.51(2)
C(34)-C(41)	1.50(2)		
P(2)-Co(1)-P(1)	99.2(2)	P(2)-Co(1)-P(3)	104.0(2)
P(1)-Co(1)-P(3)	101.7(2)	P(4)-Co(2)-P(5)	101.2(2)
P(4)-Co(2)-P(6)	101.9(2)	P(5)-Co(2)-P(6)	102.4(2)
C(2)-C(1)-C(5)	101.9(9)	C(2)-C(1)-C(29)	112.2(9)
C(5)-C(1)-C(29)	111.6(8)	C(3)-C(2)-C(1)	108.8(10)
C(4)-C(3)-C(2)	103.8(10)	C(3)-C(4)-C(5)	112.0(10)
C(6)-C(5)-C(4)	126.4(10)	C(6)-C(5)-C(1)	129.6(10)
C(4)-C(5)-C(1)	103.8(9)	C(5)-C(6)-C(13)	119.0(10)
C(5)-C(6)-C(7)	125.9(10)	C(13)-C(6)-C(7)	115.1(9)
C(8)-C(7)-C(6)	115.3(7)	C(12)-C(7)-C(6)	124.7(7)
C(14)-C(13)-C(6)	122.0(8)	C(18)-C(13)-C(6)	117.9(8)
C(30)-C(29)-C(33)	101.4(9)	C(30)-C(29)-C(1)	115.1(8)
C(33)-C(29)-C(1)	112.8(9)	C(31)-C(30)-C(29)	111.0(9)
C(32)-C(31)-C(30)	100.4(10)	C(31)-C(32)-C(33)	113.0(10)
C(34)-C(33)-C(32)	127.3(10)	C(34)-C(33)-C(29)	127.7(10)
C(32)-C(33)-C(29)	104.7(9)	C(33)-C(34)-C(35)	127.2(10)
C(33)-C(34)-C(41)	119.7(10)	C(35)-C(34)-C(41)	113.1(10)

**Table 4. Atomic Coordinates ( $\times 10^4$ ) and Equivalent Isotropic Displacement Parameters ( $\text{\AA}^2 \times 10^3$ ) for **8****

atom	x	y	z	U(eq)
Co(1)	2393(1)	971(1)	2315(1)	33(1)
P(1)	4957(1)	72(1)	2147(1)	40(1)
P(2)	2518(1)	2388(1)	2953(1)	44(1)
C(1)	1000(4)	-194(3)	3603(2)	40(1)
C(2)	96(4)	877(3)	3235(3)	43(1)
C(3)	130(4)	970(3)	2177(3)	43(1)
C(4)	1079(4)	-55(3)	1899(2)	40(1)
C(5)	1321(3)	-915(3)	2841(2)	35(1)
C(6)	1754(4)	-2094(3)	2953(2)	36(1)
C(7)	2160(4)	-2883(3)	3897(2)	36(1)
C(8)	1820(4)	-4018(3)	4200(3)	46(1)
C(9)	2200(4)	-4777(3)	5082(3)	50(1)
C(10)	2936(4)	-4477(3)	5727(3)	48(1)
C(11)	3294(4)	-3366(3)	5429(3)	50(1)
C(12)	2919(4)	-2591(3)	4549(2)	44(1)
C(13)	3344(5)	-5324(3)	6682(3)	69(1)
C(14)	1788(4)	-2611(2)	2070(2)	36(1)
C(15)	459(4)	-2419(3)	1643(3)	50(1)
C(16)	478(4)	-2913(3)	839(3)	53(1)
C(17)	1839(4)	-3627(3)	416(2)	43(1)
C(18)	3177(4)	-3827(3)	840(3)	44(1)
C(19)	3157(4)	-3339(3)	1651(2)	41(1)
C(20)	1882(5)	-4175(3)	-467(3)	60(1)
C(21)	5890(5)	-167(4)	3250(3)	63(1)
C(22)	6529(4)	736(4)	1073(3)	65(1)
C(23)	5427(4)	-1370(3)	1909(3)	57(1)
C(31)	961(5)	3650(3)	2723(3)	69(1)
C(32)	2259(6)	2083(4)	4370(3)	77(1)
C(33)	4342(5)	3085(3)	2479(3)	67(1)
C(41)	2864(4)	2036(3)	883(2)	52(1)

= 1.34(2) Å). C-C bonds connecting the atoms C(1)-C(2), C(1)-C(5), C(29)-C(30), and C(29)-C(33) and in particular bond angles at C(1) and C(29) show values characteristic for  $sp^3$ -C atoms. Both  $C_5$  rings are connected by a rather long bond (C(1)-C(29) = 1.58(2) Å). Surprisingly this can be opened by simply introduc-



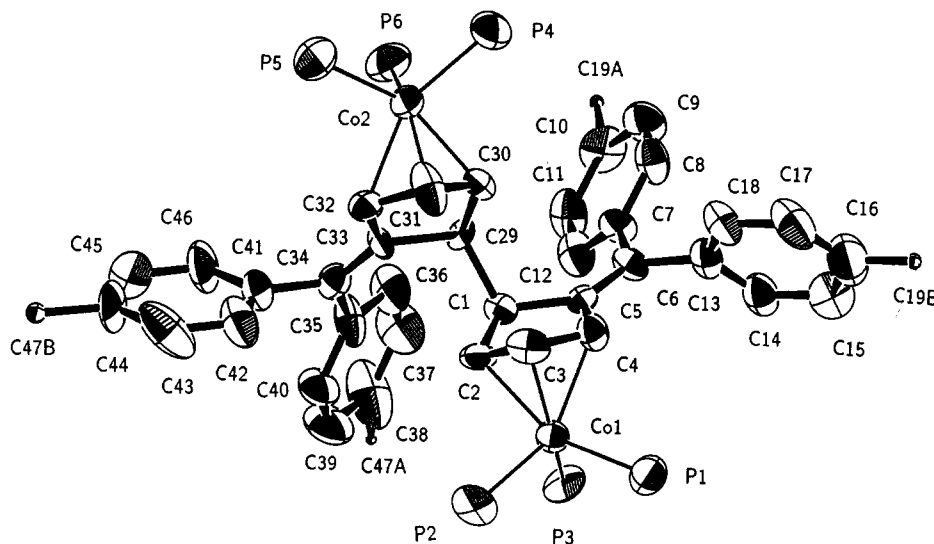
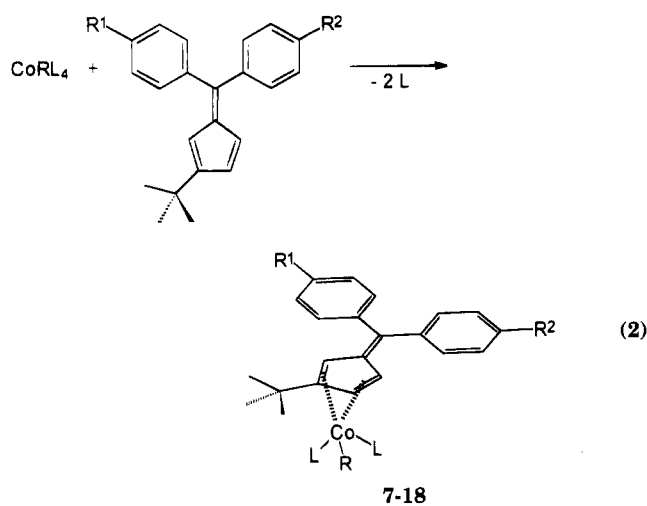


**Figure 1.** Molecular structure of **2** (ORTEP plot). Hydrogen atoms and phosphorus methyl groups (showing rotational disorder) are omitted for clarity. The 4-methylphenyl and phenyl groups show pairwise statistical disorder.

ing carbon monoxide ligands at the metal (see carbonylation of **1** below).

**$\eta^4$ -Fulvene Complexes of Cobalt(I).** Methyltetraakis(trimethylphosphine)cobalt and its  $\sigma$  phenyl analogue react with the same range of diarylfulvenes in pentane solution, liberating two phosphine ligands (eq 2). In the synthesis of phenylcobalt complexes, temper-



	R	R <sup>1</sup>	R <sup>2</sup>
<b>7</b>	CH <sub>3</sub>	H	H
<b>8</b>	CH <sub>3</sub>	H	CH <sub>3</sub>
<b>9</b>	CH <sub>3</sub>	CH <sub>3</sub>	CH <sub>3</sub>
<b>10</b>	CH <sub>3</sub>	Cl	Cl
<b>11</b>	CH <sub>3</sub>	CH <sub>3</sub> O	CH <sub>3</sub> O
<b>12</b>	CH <sub>3</sub>	(CH <sub>3</sub> ) <sub>2</sub> N	(CH <sub>3</sub> ) <sub>2</sub> N
<b>13</b>	C <sub>6</sub> H <sub>5</sub>	H	H
<b>14</b>	C <sub>6</sub> H <sub>5</sub>	H	CH <sub>3</sub>
<b>15</b>	C <sub>6</sub> H <sub>5</sub>	CH <sub>3</sub>	CH <sub>3</sub>
<b>16</b>	C <sub>6</sub> H <sub>5</sub>	Cl	Cl
<b>17</b>	C <sub>6</sub> H <sub>5</sub>	CH <sub>3</sub> O	CH <sub>3</sub> O
<b>18</b>	C <sub>6</sub> H <sub>5</sub>	(CH <sub>3</sub> ) <sub>2</sub> N	(CH <sub>3</sub> ) <sub>2</sub> N

atures below  $-30\text{ }^\circ\text{C}$  provide better yields, and solutions of compounds **13–17** on standing at  $20\text{ }^\circ\text{C}$  slowly decompose, forming *inter alia* biphenyl, elemental co-

**Table 5.** Selected Bond Lengths (Å) and Angles (deg) for **8**

Co–P(1)	2.1705(11)	Co–P(2)	2.2187(11)
Co–C(1)	2.177(3)	Co–C(2)	2.026(3)
Co–C(3)	2.016(3)	Co–C(4)	2.136(3)
Co–C(5)	2.517(3)	Co–C(41)	2.016(3)
C(1)–C(2)	1.410(4)	C(2)–C(3)	1.406(4)
C(3)–C(4)	1.415(4)	C(4)–C(5)	1.457(4)
C(1)–C(5)	1.465(4)	C(5)–C(6)	1.382(4)
C(6)–C(7)	1.464(4)	C(6)–C(14)	1.494(4)
P(1)–Co–P(2)	100.08(4)	C(1)–Co–P(1)	103.71(9)
C(1)–Co–P(2)	106.22(9)	C(2)–Co–P(1)	142.34(10)
C(2)–Co–P(2)	89.84(10)	C(3)–Co–P(1)	146.82(10)
C(3)–Co–P(2)	113.03(10)	C(4)–Co–P(1)	107.13(9)
C(4)–Co–P(2)	152.43(9)	C(5)–Co–P(1)	91.55(7)
C(5)–Co–P(2)	141.63(7)	C(41)–Co–P(1)	94.02(11)
C(41)–Co–P(2)	87.13(11)	C(41)–Co–C(1)	155.26(14)
C(41)–Co–C(2)	122.90(14)	C(41)–Co–C(3)	89.77(14)
C(41)–Co–C(4)	94.22(13)	C(41)–Co–C(5)	128.67(13)
C(1)–C(2)–C(3)	108.6(3)	C(2)–C(3)–C(4)	106.7(3)
C(3)–C(4)–C(5)	109.9(3)	C(4)–C(5)–C(1)	101.6(3)
C(1)–C(5)–C(6)	130.6(3)	C(4)–C(5)–C(6)	127.8(3)
C(5)–C(6)–C(7)	124.1(3)	C(5)–C(6)–C(14)	118.6(3)

balt, and fulvene. The dark red crystals of compounds **13–17** are extremely air-sensitive, in contrast to their methyl analogues, which are stable in air for several hours. Likewise, complexes **7–12** can be grown as dark red crystals with black shining surfaces. Their solubilities closely resemble those of their counterparts **1–6**. As complex **12** is precipitated from pentane and proved difficult to recrystallize, a synthesis in ether or THF solvent is preferred.

The IR spectra of complexes **7–12** display strong bands between  $1180$  and  $1140\text{ cm}^{-1}$  which are assigned to  $\nu(\text{C}=\text{C})$  stretches of endocyclic double bonds with a characteristic bathochromic coordination shift.<sup>11</sup>

In the  $^1\text{H}$  NMR spectra high-field shifts for C<sub>5</sub>-ring protons H(1)–H(4) of 1.5–3.0 ppm confirm the presence of coordinated C=C bonds. P,H couplings of PMe<sub>3</sub> and CoMe resonances display an angular dependence expected for (ax,eq) diene coordination in a trigonal-bipyramidal geometry. This was verified by a single-crystal X-ray study of **8**.

**Molecular Structure of 8.** The triclinic unit cell of **8** contains two molecules of the same conformation

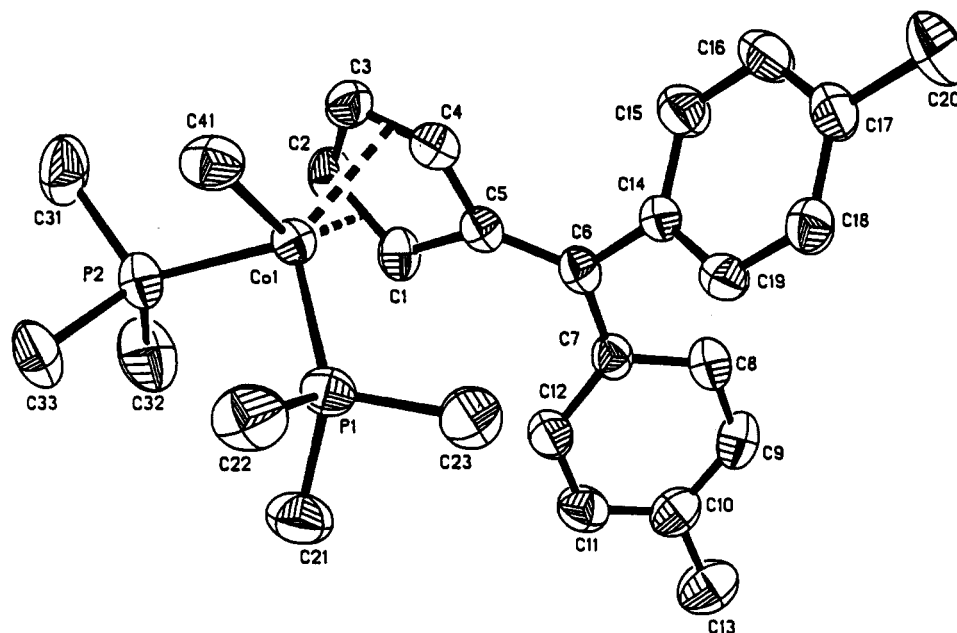


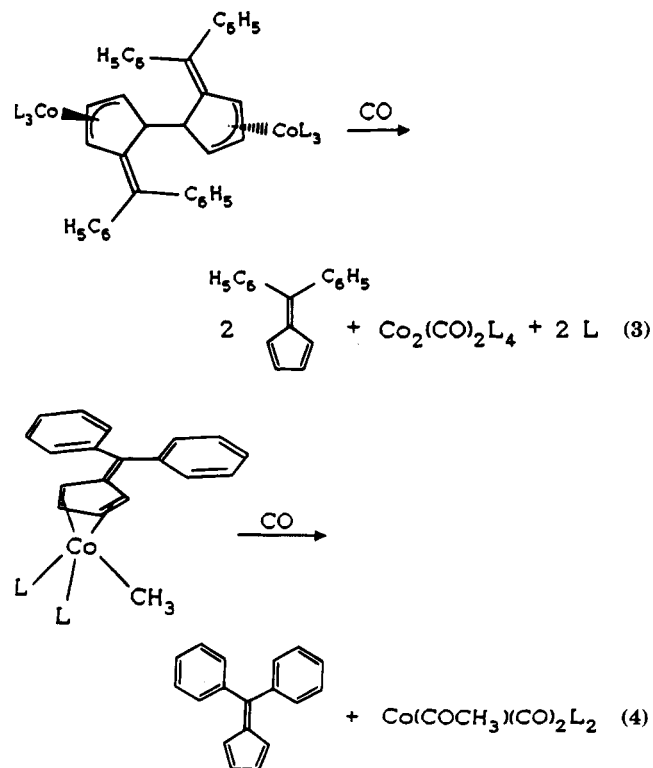
**Figure 2.** Molecular structure of **7** (ORTEP plot).

(Figure 2). In the mononuclear complex a  $\text{CoMe}(\text{PMe}_3)_2$  group is  $\eta^4$ -coordinated to the endocyclic  $\text{C}=\text{C}$  bonds of the pentafulvene. The fifth atom of the  $\text{C}_5$  ring is held at a nonbonding distance ( $\text{C}(5)\text{--Co} = 2.517(3)$  Å) and is bent out of the plane  $\text{C}(1)\text{C}(2)\text{C}(3)\text{C}(4)$  and away from the metal at an angle of  $19.8^\circ$  with respect to that plane. Bond distances and angles are as expected and, for instance, closely resemble the structure of a cyclopentadienylcobalt(I) complex containing a diarylfulvene ligand.<sup>27</sup>

If we define the atoms  $\text{C}(41)$ ,  $\text{P}(1)$ , and  $\text{P}(2)$  and the midpoints of the bonds  $\text{C}(1)\text{--C}(2)$  and  $\text{C}(3)\text{--C}(4)$  as ligand positions, the geometry around the cobalt is trigonal bipyramidal.  $\text{P}(1)$ ,  $\text{P}(2)$ , and the midpoint  $\text{C}(3)\text{--C}(4)$ , occupy equatorial positions, and the  $\text{CoMe}$  group is in one of the axial positions. Certainly in the other axial position the midpoint  $\text{C}(1)\text{--C}(2)$  deviates from an ideal trigonal-bipyramidal geometry by an angle of  $45.4^\circ$ , which is due to the rigid geometry of the fulvene ring. Bond lengths and angles are thus as expected for  $\sigma$ -methyl, trimethylphosphine, and diene coordination.

**Reactions of 1 and 7 with CO.** In order to learn how ligand properties are affected by other strong  $\pi$ -acceptor ligands, carbonylation reactions under ambient conditions have been conducted with the representative complexes **1** and **7**. In ether solutions under 1 bar of CO both reactions proceed within a few hours as indicated by the orange color of free fulvene (eqs 3 and 4).

From both solutions 6,6-diphenylfulvene is crystallized in almost quantitative yield. The cobalt is transformed into a well-known derivative<sup>[13]</sup> of  $\text{Co}_2(\text{CO})_8$ . The formal reduction of cobalt in complex **1** is balanced by the oxidative C,C cleavage of the dihydrofulvalene system. Carbonylation of **7** smoothly transforms the methylcobalt moiety into the expected acetylcobalt(I) compound.<sup>13</sup> No carbonylcobalt compound containing a hydrocarbon ligand was obtained.



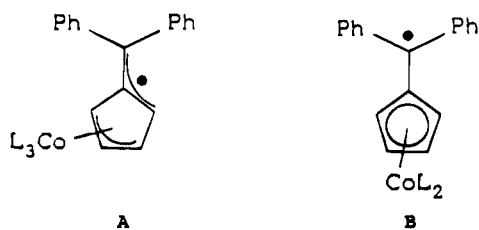
### Conclusion

Ligand substitution reactions in  $d^9$  (trimethylphosphine)cobalt complexes involving 6,6-diarylfulvenes induce spin-spin interactions of two metals and result in C,C coupling reactions between two fulvene  $\text{C}_5$  rings. While there are numerous reports on reactions of (trimethylphosphine)cobalt complexes with isolated, conjugated, or cumulated  $\text{C}=\text{C}$  functions providing  $\pi$ -coordinated paramagnetic metal systems without indicating transfer of electron density from the cobalt onto the  $\pi$ -ligands,<sup>1,2,28</sup> using fulvene ligands substantial delocalization of unpaired electron density from the metal onto the  $\pi$ -perimeter of the cross-conjugated system is observed for the first time. Single-electron

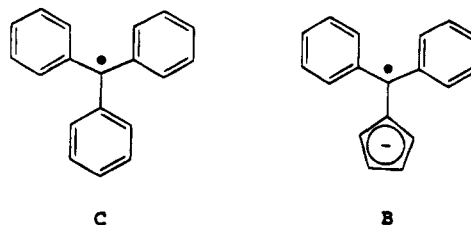
(27) Wade, H.; Pritzko, H. *Acta Crystallogr.* **1991**, *C47*, 2061.

transfer appears to be the key step, which is followed by reductive dimerization and coordination of the oxidized metal species. This reaction sequence is reversed by simply admitting carbonyl ligands to the metal.

Radical intermediates A and B can be envisaged to take part in the regioselective C,C-coupling reaction between the two C(4) positions. The C(6) position in a



radical dimerization reaction would be subject to steric hindrance similar to that of the triphenylmethyl radical C (B is shown without the metal in this representation).



Pentafulvenes appear to be ideal reactants that can activate the unpaired electron of zerovalent cobalt for metal-controlled radical reactions in the periphery of the hydrocarbon ligand. The absence of carbonyl ligands is essential.

**Acknowledgment.** Financial support of this work by the *Deutsche Forschungsgemeinschaft* and *Fonds der Chemischen Industrie* is gratefully acknowledged.

**Supplementary Material Available:** Tables of bond lengths and angles, anisotropic displacement parameters, and atomic coordinates for compounds **2** and **8** (19 pages). Ordering information is given on any current masthead page.

OM940683P

(28) (a) Agnes, G.; Bassi, W.; Benedicenti, C.; Intrito, R.; Calcaterra, M.; Santini, G. *J. Organomet. Chem.* **1977**, *129*, 401. (b) Woode, K. A.; Bart, J. C. J.; Calcaterra, M.; Agnes, G. *Organometallics* **1983**, *2*, 627. (c) Klein, H.-F.; Ellrich, K.; Lamac, S.; Lull, G.; Zsolnai, L.; Huttner, G. *Z. Naturforsch.* **1985**, *B40*, 1377. (d) Klein, H.-F.; Helwig, M.; Koch, U.; Tadic, M.; Krüger, C.; Hofmann, P. *Z. Naturforsch.* **1988**, *B43*, 1427.

**Iridium(III)- and Rhodium(III)-Promoted Binuclear C–H Bond Activation of  $\pi$ -Complexed Platinum(0) Ethylene and Phenylacetylene and Formation of Heterobimetallic Complexes. X-ray Crystal Structures of**  
 $[(\eta^5\text{-C}_5\text{Me}_5)(\text{PMe}_3)\text{Ir}(\mu\text{-H})(\mu\text{-}\eta^2\text{:}\eta^1\text{-CH}_2\text{=CH})\text{Pt}(\text{PPh}_3)_2]^{2+}\text{[}^{-}\text{OSO}_2\text{CF}_3\text{]}_2$  and  
 $[(\eta^5\text{-C}_5\text{Me}_5)(\text{PMe}_3)\text{Rh}(\mu\text{-H})(\mu\text{-}\eta^2\text{:}\eta^1\text{-PhC}\equiv\text{C})\text{Pt}(\text{PPh}_3)_2]^{2+}\text{[}^{-}\text{OSO}_2\text{CF}_3\text{]}_2^\dagger$

Danh H. Cao, Peter J. Stang,\* and Atta M. Arif\*

*Department of Chemistry, The University of Utah, Salt Lake City, Utah 84112*

*Received January 23, 1995*<sup>®</sup>

Reactions of  $[(\eta^5\text{-C}_5\text{Me}_5)(\text{PMe}_3)\text{Ir}(\text{OSO}_2\text{CF}_3)_2]$ , **1**, and  $[(\eta^5\text{-C}_5\text{Me}_5)(\text{PMe}_3)\text{Rh}(\text{OSO}_2\text{CF}_3)_2]$ , **2**, with  $[(\text{PPh}_3)_2\text{Pt}(\pi\text{-CH}_2\text{=CH}_2)]$ , **3**, and  $[(\text{PPh}_3)_2\text{Pt}(\pi\text{-HC}\equiv\text{CPh})]$ , **4**, affords the complexes  $[(\eta^5\text{-C}_5\text{Me}_5)(\text{PMe}_3)\text{M}(\mu\text{-H})(\mu\text{-}\eta^2\text{:}\eta^1\text{-CH}_2\text{=CH})\text{Pt}(\text{PPh}_3)_2]^{2+}\text{[}^{-}\text{OSO}_2\text{CF}_3\text{]}_2$  (M: Ir, **5**; Rh, **6**) and  $[(\eta^5\text{-C}_5\text{Me}_5)(\text{PMe}_3)\text{M}(\mu\text{-H})(\mu\text{-}\eta^2\text{:}\eta^1\text{-PhC}\equiv\text{C})\text{Pt}(\text{PPh}_3)_2]^{2+}\text{[}^{-}\text{OSO}_2\text{CF}_3\text{]}_2$  (M: Ir, **7**; Rh, **8**). The formation of the Ir–Pt (**5**; **7**) and Rh–Pt (**6**; **8**) heterobimetallic complexes was promoted by C–H bond activation at ambient temperatures in  $\text{CH}_2\text{Cl}_2$ . These complexes have been fully characterized by NMR spectroscopy; particularly distinct are the upfield chemical shifts of the  $\mu$ -hydrido ligand between the two metallic centers. The structures of **5** and **8** have been determined by X-ray crystallographic analysis. Crystallographic data with Mo K $\alpha$  radiation ( $\lambda = 0.70930 \text{ \AA}$ ): **5**,  $\text{PtIrC}_{54}\text{H}_{60}\text{P}_3\text{S}_2\text{O}_6\text{F}_6\text{Cl}_2$ , monoclinic, space group  $P2_1/n$ ,  $a = 14.053(2) \text{ \AA}$ ,  $b = 20.725(8) \text{ \AA}$ ,  $c = 20.509(5) \text{ \AA}$ ,  $\beta = 103.80(1)^\circ$ ,  $Z = 4$ ,  $R = 0.0419$ ; **8**,  $\text{PtRhC}_{59}\text{H}_{60}\text{P}_3\text{S}_2\text{O}_6\text{F}_6$ , monoclinic, space group  $P2_1/n$ ,  $a = 14.455(4) \text{ \AA}$ ,  $b = 18.575(3) \text{ \AA}$ ,  $c = 22.626(4) \text{ \AA}$ ,  $\beta = 104.54(2)^\circ$ ,  $Z = 4$ ,  $R = 0.0337$ .

### Introduction

One of the most intriguing goals of organometallic chemistry has been the use of transition-metal complexes to “activate” carbon–hydrogen bonds.<sup>1,2</sup> Understanding C–H bond activation should help to develop methods for the conversion of simple compounds into more complex functionalized compounds.

We recently described the mild intermolecular insertion of a platinum(0) metal center into C–H bonds activated by an Ir(I) species, leading to stable bridging hydrido, olefinic, Ir–Pt complexes.<sup>3</sup> It is generally accepted that preactivation of ethylenes, acetylenes, and arenes is a necessary step prior to C–H bond oxidative

addition. Utilization of the platinum ethylene  $\text{Pt}(\text{H}_2\text{C=CH}_2)(\text{PPh}_3)_2$ , **3**, provided the precoordinated Lewis base metal complex to the  $\pi$ -system generally needed, resulting in facile C–H oxidative addition to the platinum metal center. Furthermore, triflate ligands have long been recognized as labile leaving groups and have been utilized for many organometallic transformations.<sup>4</sup> Therefore, it seemed likely that a transition-metal triflate complex, a Lewis acid, should be susceptible to a nucleophilic attack by a metal nucleophile such as  $\text{Pt}(\text{H}_2\text{C=CH}_2)(\text{PPh}_3)_2$ , **3**. Indeed, reaction of a variety of Ir(I)–triflate complexes, *trans*-Ir(OTf)(CO)(PR<sub>3</sub>)<sub>2</sub>, with the Pt(0)–ethylene complex resulted in C–H bond activation of the precomplexed olefin and formation of heterobimetallic Ir–Pt complexes.<sup>3</sup>

We next wished to examine (a) the possibility of C–H activation of a precomplexed ethylene with an Ir(III) species, (b) the feasibility of analogous C–H olefin activation by a Rh(III) species,<sup>5</sup> and (c) extension to activation of a precomplexed alkyne. In this paper, we report the results of the above investigations along with single-crystal molecular structures of two of the resulting heterobimetallic complexes.

### Results and Discussion

#### Synthesis of $(\eta^5\text{-C}_5\text{Me}_5)(\text{PMe}_3)\text{Ir}(\text{OSO}_2\text{CF}_3)_2$ and Interaction with $(\text{PPh}_3)_2\text{Pt}(\pi\text{-CH}_2\text{=CH}_2)$ . The start-

<sup>†</sup> Dedicated to Professor Jack Halpern on the occasion of his 70th birthday.

<sup>®</sup> Abstract published in *Advance ACS Abstracts*, May 1, 1995.

(1) For recent reviews see: Davies, J. A.; Watson, P. L.; Liebman, J. F.; Greenberg, A. *Selective Hydrocarbon Activation*; VCH Publishers, Inc.: New York, 1990. Hill, C. L. *Activation and Functionalization of Alkanes*; Wiley: New York, 1989.

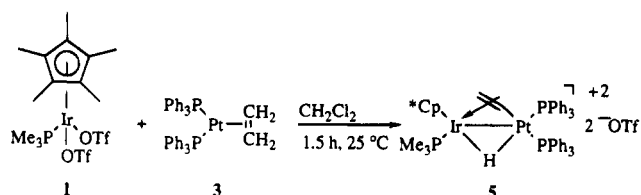
(2) Inter alia: (a) Schulz, M.; Werner, H. *Organometallics* **1992**, *11*, 2790. (b) Antwi-Nsiah, F.; Cowie, M. *Ibid.* **1992**, *11*, 3157. (c) Casey, C. P.; Rutter, E. W., Jr. *J. Am. Chem. Soc.* **1989**, *111*, 8917. (d) Bergman, R. G.; Stoutland, P. O. *J. Am. Chem. Soc.* **1988**, *110*, 5732. (e) McGhee, W. D.; Hollander, F. J.; Bergman, R. G. *J. Am. Chem. Soc.* **1988**, *110*, 8428. (f) Brainard, R. L.; Nutt, W. R.; Lee, T. R.; Whitesides, G. M. *Organometallics* **1988**, *7*, 2379. (g) Adams, R. D.; Babin, J. E. *J. Am. Chem. Soc.* **1987**, *109*, 6872. (h) Silvestre, J.; Calhorda, M. J.; Hoffman, R. Stoutland, P. O.; Bergman, R. G. *Organometallics* **1986**, *5*, 1841. (i) Stoutland, P. O.; Bergman, R. G. *J. Am. Chem. Soc.* **1985**, *107*, 4581. (j) Berry, D. H.; Eisenberg, R. *J. Am. Chem. Soc.* **1985**, *107*, 7181. (k) McGhee, W. D.; Bergman, R. G. *J. Am. Chem. Soc.* **1985**, *107*, 3388. (l) Bergman, R. G.; Seidler, P. F.; Wenzel, T. T. *J. Am. Chem. Soc.* **1985**, *107*, 4358. (m) Fryzuk, M. D.; Jones, T.; Einstein, F. W. B. *Organometallics* **1984**, *3*, 185. (n) Jones, W. D.; Feher, F. J. *J. Am. Chem. Soc.* **1984**, *106*, 1650.

(3) (a) Stang, P. J.; Huang, Y.-H.; Arif, A. M. *Organometallics* **1992**, *11*, 845. (b) Huang, Y.-H.; Stang, P. J.; Arif, A. M. *J. Am. Chem. Soc.* **1990**, *112*, 5648.

(4) Lawrance, G. A. *Chem. Rev.* **1986**, *86*, 17.

(5) Preliminary results have appeared in a communication: Stang, P. J.; Cao, D. H. *Organometallics* **1993**, *12*, 996.

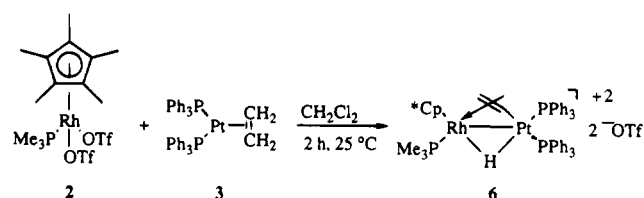
Scheme 1



ing Ir(III)–bis(triflate) complex was obtained by exchange of the two chlorides in  $(\eta^5\text{-C}_5\text{Me}_5)(\text{PMe}_3)\text{Ir}(\text{Cl})_2$  with the trifluoromethanesulfonate (triflate) ligands using excess AgOTf in  $\text{CH}_2\text{Cl}_2$  at room temperature for 45 min. Workup by filtration and  $\text{Et}_2\text{O}$  precipitation from  $\text{CH}_2\text{Cl}_2$ , afforded  $(\eta^5\text{-C}_5\text{Me}_5)(\text{PMe}_3)\text{Ir}(\text{OSO}_2\text{CF}_3)_2$ , **1**, as an analytically pure, orange, microcrystalline solid in 92% yield. Ir(III)–bis(triflate) complex **1** is thermally stable and can be stored for long periods of time under a nitrogen or argon atmosphere. However, upon exposure to atmospheric moisture, rapid decomposition was observed. This complex was characterized by IR and NMR ( $^1\text{H}$ ,  $^{13}\text{C}\{^1\text{H}\}$ ,  $^{31}\text{P}\{^1\text{H}\}$ ,  $^{19}\text{F}$ ) spectroscopy and by microanalysis. The high lability of the triflate ligands provides a Lewis metal center that is susceptible to nucleophilic attack by a metal nucleophile.

It is known that ethylene is evolved during certain reactions<sup>7</sup> of the complex  $\text{Pt}(\text{CH}_2=\text{CH}_2)(\text{PPh}_3)_2$  with various Lewis metal centers. It was therefore interesting to investigate the possible formation of a direct metal–metal bond via a nucleophilic attack of the Ir(III) metal center by  $\text{Pt}(\text{CH}_2=\text{CH}_2)(\text{PPh}_3)_2$ . Mixing of **1** with **3**, at room temperature in  $\text{CH}_2\text{Cl}_2$  (Scheme 1), within 2 h leads instead to the formation of  $[(\eta^5\text{-C}_5\text{Me}_5)(\text{PMe}_3)\text{Ir}(\mu\text{-H})(\mu\text{-}\eta^2\text{-}\eta^1\text{-CH}_2=\text{CH})\text{Pt}(\text{PPh}_3)_2]^{2+}[\text{OSO}_2\text{CF}_3]_2$ , **5**, a light yellow solid in 90% isolated yield. Complex **5** is air and heat stable and is highly soluble in various organic solvents such as  $\text{CH}_2\text{Cl}_2$ ,  $\text{CH}_3\text{NO}_2$ , and  $\text{CHCl}_3$  but insoluble in hexane and diethyl ether. The structure of complex **5** was assigned on the following grounds. The  $^{31}\text{P}\{^1\text{H}\}$  NMR spectrum displays three distinct chemical shifts, two of which are downfield at 17.2 and 8.06 ppm, with large platinum satellites,  $J_{\text{Pt-P}} = 2402$  and 4167 Hz, respectively, while the third is upfield with no observable platinum satellites. Thus the two downfield doublets, with mutual phosphorus–phosphorus couplings,  $J_{\text{P-P}} = 19.6$  Hz, along with the strong  $J_{\text{Pt-P}}$  couplings, are assigned to the two triphenylphosphines attached to the platinum metal center. The third  $^{31}\text{P}\{^1\text{H}\}$  chemical shift at  $-36$  ppm has a small phosphorus–phosphorus coupling of 3.8 Hz and, therefore, was assigned to the trimethylphosphine attached to the iridium metal center.  $^1\text{H}$  NMR spectrum displays the vinylic resonances at  $\delta$  4.66–4.31 and

Scheme 2



3.87–3.76 as multiplets. The  $\text{Cp}^*$  protons are shifted slightly downfield from the starting Ir(III)–bis(triflate) complex, whereas the trimethylphosphine proton signal remains virtually the same at 1.7 ppm as a doublet with  $J_{\text{H-P}} = 11$  Hz. Most diagnostic of the proposed structure is the high upfield chemical shift of the bridging hydride moiety of  $-13.6$  to  $-15.4$  ppm as a multiplet. This chemical shift is in good accord with that seen for other bimetallic bridging hydride systems.<sup>8</sup> In the  $^{13}\text{C}\{^1\text{H}\}$  NMR spectrum, the bridging ethylene signals are observed at 142 and 61 ppm, respectively.

**Synthesis of  $(\eta^5\text{-C}_5\text{Me}_5)(\text{PMe}_3)\text{Rh}(\text{OSO}_2\text{CF}_3)_2$  and Interaction with  $(\text{PPh}_3)_2\text{Pt}(\pi\text{-CH}_2=\text{CH}_2)$ .** Preparation of  $(\eta^5\text{-C}_5\text{Me}_5)(\text{PMe}_3)\text{Rh}(\text{OSO}_2\text{CF}_3)_2$ , **2**, is analogous to that of **1** by reacting  $(\eta^5\text{-C}_5\text{Me}_5)(\text{PMe}_3)\text{Rh}(\text{Cl})_2$  with AgOTf in  $\text{CH}_2\text{Cl}_2$ ; after workup **2** is obtained as an analytically pure, bright-orange, microcrystalline solid in 90% yield. Rh(III)–bis(triflate) **2** is also thermally stable but decomposes rapidly when exposed to atmospheric moisture.

$(\eta^5\text{-C}_5\text{Me}_5)(\text{PMe}_3)\text{Rh}(\text{OSO}_2\text{CF}_3)_2$ , **2**, was reacted with  $(\text{PPh}_3)_2\text{Pt}(\pi\text{-CH}_2=\text{CH}_2)$ , **3**, at room temperature in  $\text{CH}_2\text{Cl}_2$ , Scheme 2, to give a single product **6**. Complex **6** was characterized by IR and NMR ( $^1\text{H}$ ,  $^{13}\text{C}\{^1\text{H}\}$ ,  $^{31}\text{P}\{^1\text{H}\}$ ,  $^{19}\text{F}$ ) spectroscopy and by microanalysis. The  $^{31}\text{P}\{^1\text{H}\}$  NMR spectrum, which contains, as expected, three distinct signals at 18.8, 15.9, and 8.97 ppm, has not only phosphorus–phosphorus couplings,  $J_{\text{P-P}} = 6.9\text{--}20$  Hz, and platinum–phosphorus couplings,  $J_{\text{Pt-P}} = 43\text{--}3829$  Hz, but also rhodium–phosphorus couplings,  $J_{\text{Rh-P}} = 3.5\text{--}118$  Hz. This pattern of rhodium–phosphorus coupling is good evidence for ligand–metal interaction, thus further supporting the proposed structures. Furthermore, in the  $^{13}\text{C}\{^1\text{H}\}$  NMR spectrum the bridging ethylene signals are observed at 162 and 76 ppm, for the  $\sigma$ - and  $\pi$ -bonded carbons, respectively. In the  $^1\text{H}$  NMR spectrum of **6**, the diagnostic upfield multiplet can be observed centered at  $\delta$   $-12$  accompanied by the corresponding  $^{195}\text{Pt}$  satellites,  $J_{\text{Pt-H}} = 541$  Hz. In addition, in the IR spectrum of **6**, the observation of stretching frequencies at 1260 (s), 1150 (m), and 1030 (s)  $\text{cm}^{-1}$  is consistent with the presence of ionic triflate groups.<sup>4</sup>

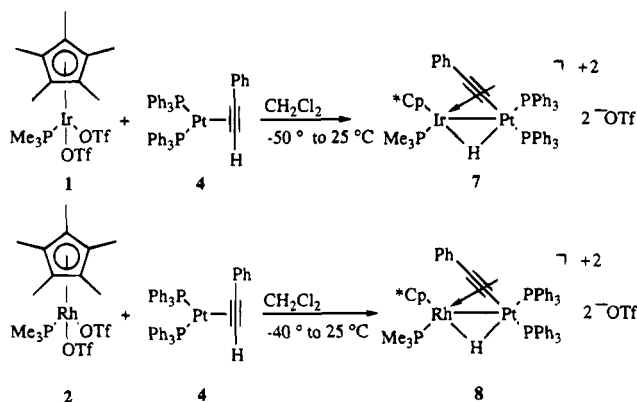
**Reaction of  $(\eta^5\text{-C}_5\text{Me}_5)(\text{PMe}_3)\text{M}(\text{OSO}_2\text{CF}_3)_2$  (M = Ir, Rh) with  $(\text{PPh}_3)_2\text{Pt}(\pi\text{-HC}\equiv\text{CPh})$ .** We have demonstrated that both Ir(III) bis(triflate) **1** and Rh(III) bis(triflate) **2** undergo nucleophilic attack by the Pt(olefin) Lewis base to form a binuclear product via C–H olefinic activation. This prompted us to investigate acetylenic

(6) (a) Isobe, K.; Bailey, P. M.; Maitlis, P. M. *J. Chem. Soc., Dalton Trans.* **1981**, 2003. (b) Kang, J. W.; Moseley, K.; Maitlis, P. M. *J. Am. Chem. Soc.* **1969**, *91*, 5970.

(7) (a) Mirkin, C. A.; Geoffroy, G. L.; Macklin, P. D.; Rheingold, A. L. *Inorg. Chim. Acta* **1990**, *170*, 11. (b) Hartley, F. R. In *Comprehensive Organometallic Chemistry*; Wilkinson, G., Stone, F. G. A., Eds.; Pergamon Press: Oxford, U.K., 1982; Chapter 39. (c) Khandelwal, B. L.; Gupta, S. K.; Kundu, K. *Inorg. Chim. Acta* **1990**, *178*, 35. (d) Stang, P. J.; Kowalski, M. H.; Schiavelli, M. D.; Longford, D. *J. Am. Chem. Soc.* **1989**, *111*, 3347. (e) Powell, J.; Sawyer, J. F.; Stainer, M. V. R. *Inorg. Chem.* **1989**, *28*, 4461. (f) Rossell, O.; Seco, M.; Torra, I. *J. Chem. Soc., Dalton Trans.* **1986**, 1011. (g) Kermodé, N. J.; Lappert, M. F. *J. Chem. Soc., Chem. Commun.* **1981**, 698. (h) Farrugia, L. J.; Howard, J. A. K.; Mitrprachachon, P.; Stone, F. G. A.; Woodward, P. *J. Chem. Soc., Dalton Trans.* **1981**, 155. (i) Eaborn, C.; Pidcock, A.; Steele, B. R. *J. Chem. Soc., Dalton Trans.* **1976**, 767. (j) Akhtar, M.; Clark, H. C. *J. Organomet. Chem.* **1970**, *22*, 233.

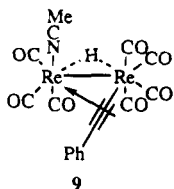
(8) (a) Top, S.; Gunn, M.; Jaouen, G.; Vaissermann, J.; Daran, J. C.; McGlinchey, M. J. *Organometallics* **1992**, *11*, 1201. (b) Powell, J.; Fuchs, E.; Gregg, M. R.; Phillips, J.; Stainer, M. V. R. *Organometallics* **1990**, *9*, 387. (c) Blum, T.; Braunstein, P. *Organometallics* **1989**, *8*, 2497. (d) Albinati, A.; Lehner, H.; Venanzi, L. M.; Wolfer, M. *Inorg. Chem.* **1987**, *26*, 3933. (e) Bars, O.; Braunstein, P.; Geoffroy, G. L.; Metz, B. *Organometallics* **1986**, *5*, 2021. (f) Jans, J.; Naegeli, R.; Venanzi, L. M. *J. Organomet. Chem.* **1983**, *247*, C37. (g) Pregosin, P. S. *Coord. Chem. Rev.* **1982**, *44*, 247.

Scheme 3



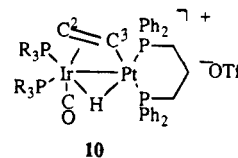
C–H bond activation. A stable and well-known alkyne system is the  $\text{Pt}(\pi\text{-phenylacetylene})$  complex. Initially the same conditions were applied to the reaction of  $(\eta^5\text{-C}_5\text{Me}_5)(\text{PMe}_3)\text{Ir}(\text{OSO}_2\text{CF}_3)_2$ , **1**, with  $(\text{PPh}_3)_2\text{Pt}(\pi\text{-HC}\equiv\text{CPh})$ , **4**, as those for the formation of the Ir–Pt(olefin) bimetallic **5**. However, this did not produce a clean single Ir–Pt(acetylenic) bimetallic complex **7**. The best way to obtain good yields of **7** was to add  $(\text{PPh}_3)_2\text{Pt}(\pi\text{-HC}\equiv\text{CPh})$ , **4**, at low temperature ( $-50^\circ\text{C}$ ) to a  $\text{CH}_2\text{Cl}_2$  solution of **1**, followed by slow warming to room temperature. When formed in a preparative-scale experiment, the heterobinuclear bridging hydrido complex  $[(\eta^5\text{-C}_5\text{Me}_5)(\text{PMe}_3)\text{Ir}(\mu\text{-H})(\mu\text{-}\eta^2\text{-}\eta^1\text{-PhC}\equiv\text{C})\text{Pt}(\text{PPh}_3)_2]^{2+}[\text{OTf}^-]_2$ , **7**, was isolated in 51% yield as an analytically pure, light-brown solid (Scheme 3).

In the  $^1\text{H}$  NMR spectrum, an upfield chemical shift is the most diagnostic spectroscopic evidence for the presence of a bridging hydride moiety of the heterobinuclear complex **7**, centered at  $-12.1$  ppm with  $J_{\text{Pt-H}} = 501$  Hz. The  $^{31}\text{P}\{^1\text{H}\}$  NMR spectrum of **7** also displays three distinct signals at 17.7 ppm with  $J_{\text{Pt-P}} = 3093$  Hz,  $J_{\text{P-P}} = 23.2$  Hz, at 7.34 ppm with  $J_{\text{Pt-P}} = 3523$  Hz,  $J_{\text{P-P}} = 23.2$  Hz,  $J_{\text{P-P}} = 2.4$  Hz, and at  $-28.1$  ppm with  $J_{\text{Pt-P}} = 15.3$  Hz,  $J_{\text{P-P}} = 2.4$  Hz. On the basis of their large platinum satellite couplings, the chemical shifts observed at 17.7 and 7.34 ppm were assigned to the phosphorus nuclei attached to the platinum metal center, while the signal for the trimethylphosphine was assigned to the upfield chemical shift at  $-28.1$  ppm, since it did not contain a significant platinum satellite coupling. In the  $^{13}\text{C}\{^1\text{H}\}$  NMR spectrum the acetylenic signals are at 131 and 120 ppm for the  $\sigma$ - and  $\pi$ -bonded carbons, respectively. The spectral data for **7** compare favorably with those for the related complex **9** reported by Top and co-workers.<sup>8a</sup> Especially notable is the  $^1\text{H}$  NMR absorption observed for compound **9** at  $-11.5$  ppm, compared to  $-12.1$  ppm for compound **7**; moreover, the  $^{13}\text{C}\{^1\text{H}\}$  NMR absorption of  $\text{M}-\text{C}\equiv\text{C}$  is at 101.8 ppm for **9** and at 119.5 ppm for **7**.

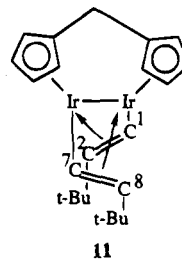


In analogy to the reaction of  $(\eta^5\text{-C}_5\text{Me}_5)(\text{PMe}_3)\text{Ir}(\text{OSO}_2\text{CF}_3)_2$ , **1**, with  $(\text{PPh}_3)_2\text{Pt}(\pi\text{-HC}\equiv\text{CPh})$ , **4**, the interaction of the rhodium analogue  $(\eta^5\text{-C}_5\text{Me}_5)(\text{PMe}_3)\text{Rh}(\text{OSO}_2\text{CF}_3)_2$ , **2**, with **4** results in an 58% yield of the related adduct  $[(\eta^5\text{-C}_5\text{Me}_5)(\text{PMe}_3)\text{Rh}(\mu\text{-H})(\mu\text{-}\eta^2\text{-}\eta^1\text{-PhC}\equiv\text{C})\text{Pt}(\text{PPh}_3)_2]^{2+}[\text{OTf}^-]_2$ , **8**, as a red microcrystalline solid (Scheme 3). This complex was also characterized by IR and NMR ( $^1\text{H}$ ,  $^{13}\text{C}\{^1\text{H}\}$ ,  $^{31}\text{P}\{^1\text{H}\}$ ,  $^{19}\text{F}$ ) spectroscopy and by microanalysis as summarized in the Experimental Section.

**X-ray Structures of 5 and 8.** A definitive structural assignment for the heterobimetallics Ir–Pt, **5**, and Rh–Pt, **8**, was obtained by single-crystal X-ray crystallography. The numbering diagrams and ORTEP representations are shown in Figures 1 and 2. X-ray data are summarized in Table 1. The important bond distances and angles are given in Table 2, whereas the atomic coordinates are summarized in Tables 3 and 4. As can be seen from Figures 1 and 2, the Ir–Pt and Rh–Pt metal centers are bridged by a hydride ligand. The H1,  $\mu$ -hydride ligand, for complex **8** was located by the difference Fourier method and refined with fixed thermal parameters, while for complex **5**, H1 the location of was calculated and added to the final structure factor calculations. The existence of an iridium–platinum bond is indicated by the bond distance of 2.8362(6) Å, which is slightly shorter than the value of 2.8393(12) Å found for an unbridged Ir–Ir bond distance.<sup>9</sup> However in comparison to that of structure **10** previously reported



by Stang and co-workers,<sup>3a</sup> this Ir(III)–Pt bond length is slightly longer than the Ir(I)–Pt bond distance of 2.7484(2) Å. The Ir–C1, Ir–C2, and Pt–C1 distances are 2.15(1), 2.24(1), and 2.01(1) Å, respectively. The Pt–C1 bond distance is very close to the analogous bond distance of Pt–C3 = 2.014(4) Å in **10**. Whereas a slight difference is observed in a comparison of the Ir–olefin bond distances of **5**, where Ir–C2 is 2.24(1) Å and Ir–C1 is 2.15(1) Å, while in **10**, Ir–C2 is 2.197(4) Å and Ir–C3 is 2.168(4) Å. An interesting structural feature in complex **5** is the C1–C2 distance of 1.38(2) Å, which is indicative of a nearly normal C=C double bond. This is surprising since an  $\eta^2$ -type bonding typically reduces the double-bond character, thereby lengthening the olefin bond to a distance between that of a C–C single and C=C double bond, as observed with complex **10**, where the C=C double-bond distance was found to be 1.415(6) Å. However, this C1–C2 distance of complex **5** correlates well with structure **11**, which has an Ir–Ir



metal center  $\sigma$ - and  $\pi$ -bonded to a vinylic bridging unit,

(9) Einstein, F. W. B.; Jones, R. H.; Zhang, X.; Yan, X.; Nagelkerke, R.; Sutton, D. *J. Chem. Soc., Chem. Commun.* **1989**, 1424.

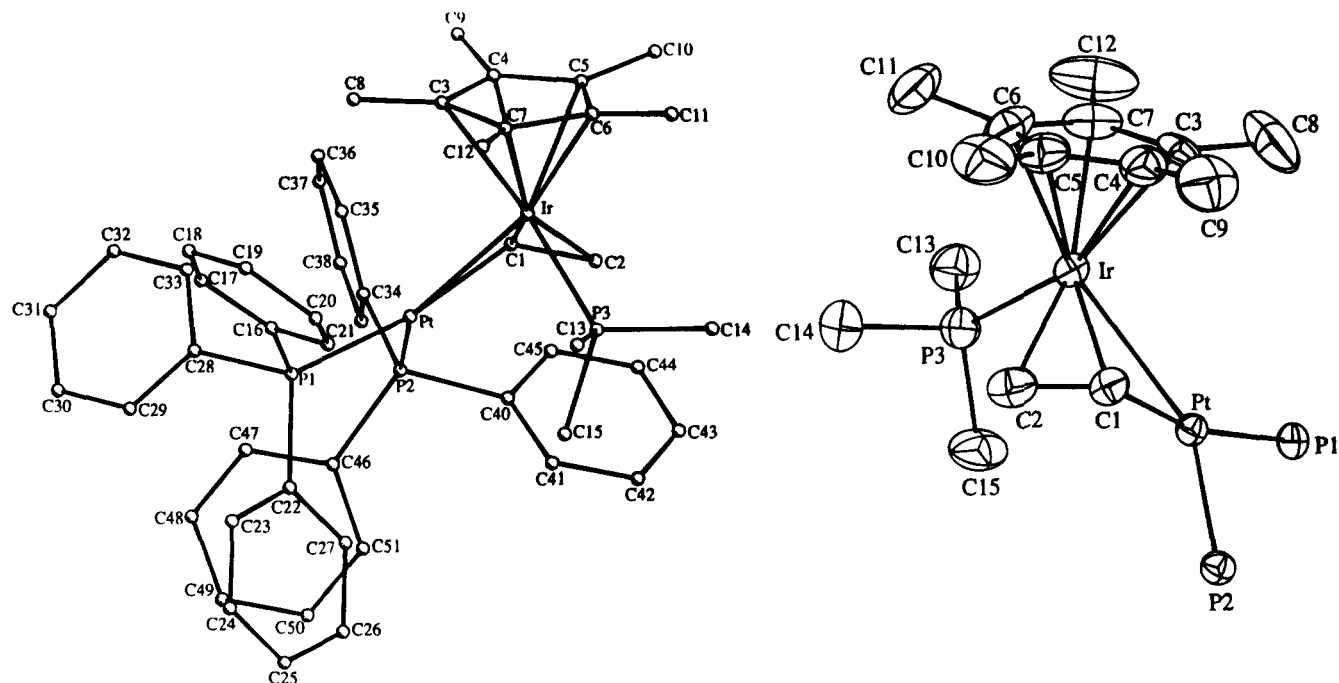


**Figure 1.** Two views of the structure of **5**: (left) numbering diagram (hydrogen atoms omitted for clarity); (right) ORTEP representation (both triflates,  $\mu$ -hydride ligand, and phenyl rings of the  $\text{PPh}_3$  groups, including all hydrogen atoms, omitted for clarity).

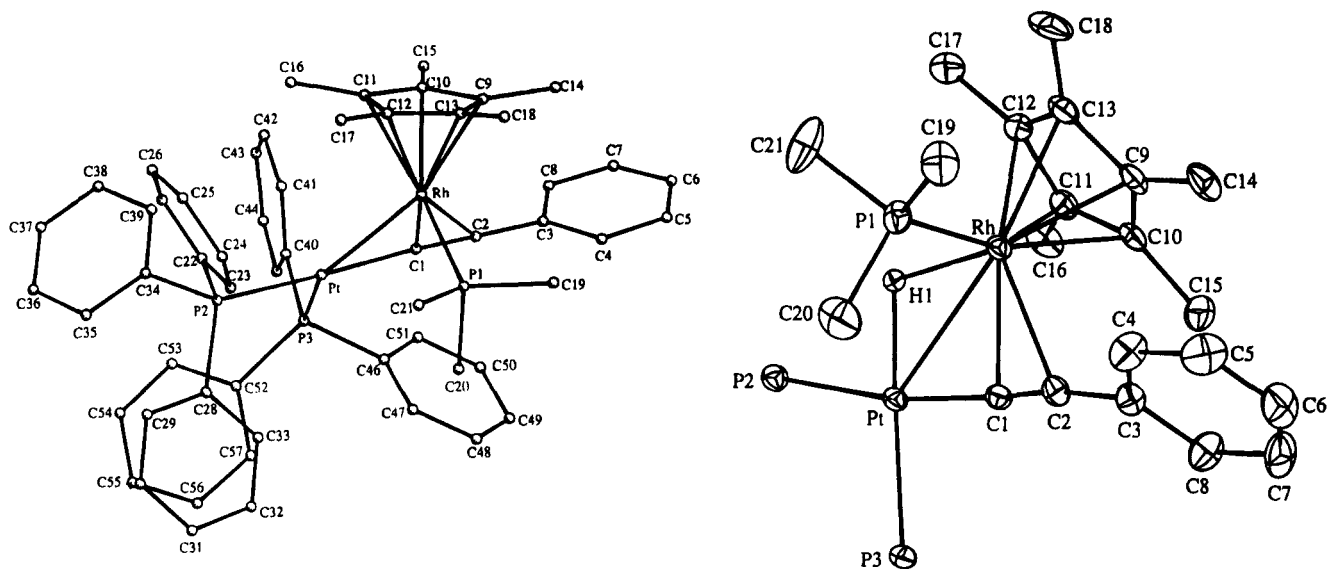


**Figure 2.** Two views of the structure of **8**: (left) numbering diagram (hydrogen atoms omitted for clarity); (right) ORTEP representation (both triflates, phenyl rings of the  $\text{PPh}_3$  groups, and hydrogen atoms other than the  $\mu$ -hydride ligand omitted for clarity).

with a C1–C2 bond distance of 1.40(1) Å and a C7–C8 bond length of 1.42(1) Å.<sup>10</sup> A similar structural feature is also observed for complex **8**, where the C1–C2 bond distance of 1.21(1) Å closely resembles that of an unperturbed C≡C triple bond, whereas a lengthening of between a C=C double and a C≡C triple bond was predicted. These structural data suggest that the  $\eta^2$  binding of Ir(III) to the olefin and of Rh(III) to the acetylene is weaker, and this is supported by the observed longer bond distances of M–C1 and M–C2, relative to the literature data for the Ir(I)–Pt analogue, **10**.<sup>3a</sup>

## Conclusion

The interaction, under mild conditions, of the respective ( $\eta^5$ -C<sub>5</sub>Me<sub>5</sub>)Ir(PMe<sub>3</sub>)(OTf)<sub>2</sub>, **1**, and ( $\eta^5$ -C<sub>5</sub>Me<sub>5</sub>)Rh(PMe<sub>3</sub>)(OTf)<sub>2</sub>, **2**, species with [(PPh<sub>3</sub>)<sub>2</sub>Pt( $\pi$ -CH<sub>2</sub>=CH<sub>2</sub>)], **3**, and [(PPh<sub>3</sub>)<sub>2</sub>Pt( $\pi$ -HC≡CPh)], **4**, results in an olefinic and acetylenic C–H bond activation and the facile formation of novel heterobimetallic Ir–Pt, **5** and **7**, and Rh–Pt, **6** and **8**, complexes. X-ray diffraction of complexes **5** and **8**, unambiguously established their structures as uniquely bridged Ir–Pt and Rh–Pt complexes. These complexes form via an intermolecular, irreversible transition metal olefin and acetylene C–H bond activation of a precomplexed alkene and alkyne. Moreover, complexes **5**–**8** are new members of the select

(10) Nessel, A.; Nurnberg, O.; Wolf, J.; Werner, H. *Angew. Chem., Int. Ed. Engl.* **1991**, *30*, 1006.

**Table 1. Crystallographic Data for  $[(\eta^5\text{-C}_5\text{Me}_5)(\text{PMe}_3)\text{Ir}(\mu\text{-H})(\mu\text{-}\eta^2\text{:}\eta^1\text{-CH}_2\text{=CH)Pt}(\text{PPh}_3)_2]^{2+}[\text{-OSO}_2\text{CF}_3]_2$ , 5, and  $[(\eta^5\text{-C}_5\text{Me}_5)(\text{PMe}_3)\text{Rh}(\mu\text{-H})(\mu\text{-}\eta^2\text{:}\eta^1\text{-PhC}\equiv\text{C)Pt}(\text{PPh}_3)_2]^{2+}[\text{-OSO}_2\text{CF}_3]_2$ , 8**

	5	8
molecular formula	PtIrC <sub>54</sub> H <sub>60</sub> P <sub>3</sub> S <sub>2</sub> O <sub>6</sub> F <sub>6</sub> Cl <sub>2</sub>	PtRhC <sub>59</sub> H <sub>60</sub> P <sub>3</sub> S <sub>2</sub> O <sub>6</sub> F <sub>6</sub>
formula weight	1534.313	1434.168
space group	$P2_1/n$	$P2_1/n$
space group no.	14	14
crystal system	monoclinic	monoclinic
a (Å)	14.053(2)	14.455(4)
b (Å)	20.725(8)	18.575(3)
c (Å)	20.509(5)	22.626(4)
$\beta$ (deg)	103.80(1)	104.54(2)
V (Å <sup>3</sup> )	5800.99	5880.42
Z	4	4
$D_{\text{calc}}$ (g cm <sup>-3</sup> )	1.754	1.620
crystal dimensions (mm)	0.33 × 0.28 × 0.19	0.28 × 0.25 × 0.25
absorption coeff (cm <sup>-1</sup> )	50.178	28.914
radiation, $\lambda$ (Å)	Mo, 0.70930	Mo, 0.709 30
no. of unique reflections	6778	9520
2 $\theta$ range (deg)	4.00–50.00	4.00–48.00
scan technique	$\theta/2\theta$	$\theta/2\theta$
scan width (deg)	0.8000 + 0.3400 tan $\theta$	0.8000 + 0.3400 tan $\theta$
data rejected if I	<3.00 $\sigma$ (I)	<3.00 $\sigma$ (I)
no. of observations	6774	6323
no. of variables	677	707
data to parameter ratio	10.006	8.943
shift to error ratio	0.011	0.002
error in an observn of unit weight	0.9028	0.5231
R ( $R_w$ )	0.0419 (0.0501)	0.0337 (0.0372)

**Table 2. Relevant Bond Distances (Å) and Angles (deg) for Compounds 5 and 8<sup>a</sup>**

Compound 5			
Ir-Pt	2.8362(6)	Pt-P1	2.335(3)
Ir-C1	2.15(1)	Pt-P2	2.272(3)
Ir-C2	2.24(1)	Pt-C1	2.01(1)
Ir-P3	2.318(4)	C1-C2	1.38(2)
C1-Ir-C2	36.6(5)	Ir-C2-C1	68.0(8)
C1-Ir-P3	106.9(4)	P1-Pt-C1	166.4(4)
C2-Ir-P3	81.9(5)	P2-Pt-C1	88.9(4)
Pt-Ir-C1	45.1(3)	P1-Pt-P2	103.0(2)
Pt-Ir-C2	72.3(4)	Ir-Pt-P1	119.62(8)
Pt-Ir-P3	94.6(1)	Ir-Pt-P2	137.28(7)
Ir-C1-C2	75.4(8)	Ir-Pt-C1	49.1(3)
Ir-C1-Pt	85.8(5)	Pt-C1-C2	125(1)
Compound 8			
Rh-Pt	2.8265(8)	Pt-P2	2.309(3)
Rh-C1	2.18(1)	Pt-P3	2.306(3)
Rh-C2	2.54(1)	Pt-C1	1.99(1)
Rh-P1	2.320(3)	C1-C2	1.21(1)
C1-Rh-C2	28.4(3)	P2-Pt-C1	171.2(3)
C1-Rh-P1	94.3(3)	P3-Pt-C1	88.4(3)
C2-Rh-P1	91.0(3)	P2-Pt-P3	100.4(1)
Pt-Rh-C1	44.6(3)	Rh-Pt-P2	121.25(7)
Pt-Rh-C2	72.8(2)	Rh-Pt-P3	137.85(7)
Pt-Rh-P1	93.22(8)	Rh-Pt-C1	50.2(3)
Rh-C1-C2	92.6(8)	Pt-C1-C2	173.9(9)
Rh-C1-Pt	85.3(4)	Rh-C2-C3	128.4(7)
Rh-C2-C1	59.0(6)	C1-C2-C3	171(1)

<sup>a</sup> Numbers in parentheses are estimated standard deviations in the least significant digits.

family of rare Ir-Pt<sup>3,11</sup> and Rh-Pt<sup>11a,12</sup> heterobimetallic complexes.

## Experimental Section

**General Methods.** All reactions were conducted under a dry nitrogen atmosphere using Schlenk techniques, unless

(11) (a) Stang, P. J.; Huang, Y.-H.; Arif, A. M. *Organometallics* **1992**, *11*, 231. (b) Albinati, A.; Emge, T. J.; Koetzle, T. F.; Meille, S. V.; Musco, A.; Venanzi, L. M. *Inorg. Chem.* **1986**, *25*, 4821. (c) Markham, D. P.; Shaw, B. L.; Thornton-Pett, M. *J. Chem. Soc., Chem. Commun.* **1987**, 1005.

otherwise noted. IR spectra were recorded on a Mattson Polaris FT-IR spectrophotometer and NMR spectra were recorded on a Varian XL-300 spectrometer. <sup>1</sup>H NMR spectra were recorded at 300 MHz, and all chemical shifts ( $\delta$ ) are reported in ppm relative to tetramethylsilane (Me<sub>4</sub>Si) as an internal standard or the proton resonance resulting from incomplete deuteration of the NMR solvent: CDCl<sub>3</sub> (7.24 ppm), C<sub>6</sub>D<sub>6</sub> (7.15 ppm), CD<sub>2</sub>Cl<sub>2</sub> (5.32 ppm), or CD<sub>3</sub>NO<sub>2</sub> (4.33 ppm). <sup>13</sup>C NMR spectra were recorded at 75 MHz, and all chemical shifts ( $\delta$ ) are reported in ppm relative to the carbon resonance of the deuterated NMR solvent: CDCl<sub>3</sub> (77.0 ppm), CD<sub>3</sub>NO<sub>2</sub> (62.8 ppm), or CD<sub>2</sub>Cl<sub>2</sub> (53.8 ppm). <sup>31</sup>P NMR spectra were recorded at 121 MHz, and all chemical shifts ( $\delta$ ) are reported in ppm relative to external 85% H<sub>3</sub>PO<sub>4</sub> at 0.00 ppm. <sup>19</sup>F NMR spectra were recorded at 282 MHz, and all chemical shifts are reported relative to external CFCl<sub>3</sub> at 0.00 ppm. Microanalyses were performed by Atlantic Microlab Inc., Norcross, GA. Melting points were obtained with a Mel-Temp capillary melting point apparatus and were not corrected.

**Materials.** Solvents were purified as follows: CH<sub>3</sub>NO<sub>2</sub>, CH<sub>2</sub>Cl<sub>2</sub>, CHCl<sub>3</sub>, C<sub>6</sub>H<sub>6</sub>, PhCH<sub>3</sub>, and hexanes were purified by literature procedures<sup>13</sup> and were distilled over CaH<sub>2</sub>; Et<sub>2</sub>O and THF were purified by literature procedures<sup>13</sup> and were distilled over Na/benzophenone; CH<sub>3</sub>CN and CD<sub>3</sub>NO<sub>2</sub> were distilled over CaH<sub>2</sub>; CDCl<sub>3</sub>, CD<sub>2</sub>Cl<sub>2</sub>, and C<sub>6</sub>D<sub>6</sub> were vacuum-transferred from CaH<sub>2</sub>. All solvents were freeze-thaw-pump degassed three times before use.

All commercial reagents were ACS reagent grade and were obtained as follows: IrCl<sub>3</sub>·3H<sub>2</sub>O (Johnson-Matthey), RhCl<sub>3</sub>·H<sub>2</sub>O (Johnson-Matthey), 1.0 M PMe<sub>3</sub> in toluene (Aldrich), 37% formaldehyde (Mallinckrodt), dimethylformamide (Mallinckrodt), NH<sub>2</sub>NH<sub>2</sub>·H<sub>2</sub>O (Baker), NaBH<sub>4</sub> (Morton Thiokol), NaH (Aldrich), pentamethylcyclopentadiene (Aldrich), PtCl<sub>2</sub> (Aldrich), ethylene (Matheson), CO (Matheson), and Ar (Liquid Air) were all used as received; silver trifluoromethanesulfonate (Aldrich) was used as received, and PPh<sub>3</sub> (Aldrich) was recrystallized from hexanes and dried under vacuum. ( $\eta^5$ -C<sub>5</sub>-

(12) (a) Schiavo, S. L.; Rotondo, E.; Bruno, G.; Faraone, F. *Organometallics* **1991**, *10*, 1613. (b) Carr, S. W.; Pringle, P. G.; Shaw, B. L. *J. Organomet. Chem.* **1988**, *341*, 543. (c) Balch, A. L.; Guimerans, R. R.; Linehan, J.; Olmstead, M. M.; Oram, D. E. *Organometallics* **1985**, *4*, 1445. (d) Farr, J. P.; Olmstead, M. M.; Wood, F. E.; Balch, A. L. *J. Am. Chem. Soc.* **1983**, *105*, 792.

(13) Perrin, D. D.; Armarego, W. L. F. *Purification of Laboratory Chemicals*; Pergamon Press: Oxford, U.K., 1988.



Table 3. Positional Parameters and Estimated Standard Deviations<sup>a</sup> for Compound 5

atom	x	y	z	B (Å <sup>2</sup> )	atom	x	y	z	B (Å <sup>2</sup> )
Pt	0.33183(3)	0.15077(2)	0.19099(2)	2.585(7)	C22	0.1182(8)	0.2295(5)	0.2177(5)	3.3(2)
Ir	0.51013(3)	0.21636(2)	0.19458(2)	3.053(8)	C23	0.0447(9)	0.2759(7)	0.2033(6)	4.4(3)
P1	0.1832(2)	0.2054(1)	0.1553(1)	2.92(6)	C24	-0.0074(9)	0.2931(7)	0.2500(7)	5.3(3)
P2	0.2849(2)	0.0519(1)	0.2197(1)	2.81(6)	C25	0.014(1)	0.2628(8)	0.3119(8)	6.0(4)
P3	0.5147(3)	0.2680(2)	0.2956(2)	4.69(8)	C26	0.088(1)	0.2170(8)	0.3287(6)	5.6(3)
S1	0.7738(4)	-0.1290(3)	0.4881(2)	8.8(2)	C27	0.1401(9)	0.2013(6)	0.2802(6)	4.3(3)
S2	0.2749(5)	0.0555(4)	0.8888(4)	8.9(2)	C28	0.0977(8)	0.1618(6)	0.0905(6)	3.5(2)
O1	0.749(1)	-0.1043(8)	0.4216(6)	9.9(5)	C29	-0.002(1)	0.1576(7)	0.0877(7)	5.4(3)
O2	0.8659(9)	-0.162(1)	0.5025(7)	12.0(6)	C30	-0.065(1)	0.1224(8)	0.0385(8)	6.3(4)
O3	0.756(1)	-0.0921(9)	0.5389(7)	13.9(5)	C31	-0.029(1)	0.0916(8)	-0.0092(8)	6.9(4)
O4	0.202(1)	0.0874(8)	0.846(1)	11.8(5)	C32	0.069(1)	0.0951(7)	-0.0083(7)	5.6(4)
O5	0.264(2)	-0.0120(8)	0.887(1)	13.8(7)	C33	0.1344(9)	0.1303(6)	0.0417(6)	4.1(3)
O6	0.311(2)	0.085(1)	0.9570(8)	14.0(7)	C34	0.2879(8)	-0.0119(6)	0.1591(5)	3.3(2)
F1	0.5986(9)	-0.1724(8)	0.4693(8)	11.1(5)	C35	0.3138(8)	0.0002(6)	0.0997(6)	3.7(3)
F2	0.698(1)	-0.2361(8)	0.4400(8)	13.9(5)	C36	0.3190(9)	-0.0504(7)	0.0571(6)	4.7(3)
F3	0.700(1)	-0.2224(8)	0.5429(7)	13.5(5)	C37	0.3022(9)	-0.1127(6)	0.0749(6)	4.8(3)
F4	0.452(1)	0.035(1)	0.906(2)	14(1)	C38	0.2754(9)	-0.1244(6)	0.1332(7)	4.6(3)
F5	0.420(2)	0.110(1)	0.860(2)	13.2(7)	C39	0.2671(9)	-0.0745(6)	0.1757(6)	4.1(3)
F6	0.361(2)	0.050(2)	0.797(1)	15(1)	C40	0.3735(8)	0.0275(5)	0.2951(5)	3.1(2)
C1	0.4702(8)	0.1177(6)	0.2064(6)	3.5(2)	C41	0.3831(9)	0.0635(6)	0.3550(6)	4.3(3)
C2	0.5449(9)	0.1302(6)	0.2623(7)	4.7(3)	C42	0.458(1)	0.0490(7)	0.4113(6)	5.2(3)
C3	0.4907(8)	0.2417(6)	0.0842(5)	3.7(2)	C43	0.522(1)	-0.0000(8)	0.4087(7)	5.7(4)
C4	0.555(1)	0.1911(7)	0.0989(6)	5.3(3)	C44	0.516(1)	-0.0348(7)	0.3515(7)	5.2(3)
C5	0.6390(9)	0.2069(7)	0.1504(7)	5.1(3)	C45	0.4407(9)	-0.0204(7)	0.2942(6)	4.4(3)
C6	0.634(1)	0.2714(8)	0.1723(8)	5.9(4)	C46	0.1629(8)	0.0401(5)	0.2364(5)	3.3(2)
C7	0.541(1)	0.2963(7)	0.1308(7)	5.7(3)	C47	0.0838(9)	0.0307(6)	0.1805(7)	4.5(3)
C8	0.405(1)	0.253(1)	0.0331(8)	9.7(6)	C48	-0.008(1)	0.0228(8)	0.1889(8)	5.8(4)
C9	0.540(1)	0.1302(9)	0.0580(8)	8.4(5)	C49	-0.0260(9)	0.0247(7)	0.2518(9)	6.1(4)
C10	0.727(1)	0.164(1)	0.1756(9)	8.5(5)	C50	0.051(1)	0.0340(7)	0.3071(7)	5.8(3)
C11	0.715(1)	0.309(1)	0.2142(9)	8.9(5)	C51	0.1449(9)	0.0422(6)	0.2997(7)	4.7(3)
C12	0.512(1)	0.3660(8)	0.1259(9)	10.1(5)	C52	0.691(1)	-0.1947(8)	0.4849(8)	6.1(4)
C13	0.492(1)	0.3535(7)	0.2901(7)	5.9(4)	C53	0.382(2)	0.062(1)	0.863(2)	10.4(7)
C14	0.629(1)	0.2606(9)	0.3581(8)	6.6(4)	S2'	0.296(1)	0.1061(8)	0.8901(8)	7.5(4)*
C15	0.422(1)	0.2406(8)	0.3387(7)	6.7(4)	C53'	0.410(3)	0.025(2)	0.841(2)	10(1)*
C16	0.1943(8)	0.2817(6)	0.1151(6)	3.7(3)	C11	0.329(3)	0.386(2)	0.879(2)	10(1)*
C17	0.152(1)	0.2960(7)	0.0488(6)	5.0(3)	O4'	0.355(3)	0.155(2)	0.877(2)	12(1)*
C18	0.161(1)	0.3571(7)	0.0231(7)	6.1(4)	C54'	0.353(4)	0.442(3)	0.916(3)	10(1)*
C19	0.210(1)	0.4047(7)	0.0619(7)	6.1(4)	C54	0.282(4)	0.453(3)	0.882(3)	10(2)*
C20	0.251(1)	0.3926(6)	0.1294(7)	5.2(3)	C12	0.416(4)	0.466(3)	0.957(3)	9(1)*
C21	0.2440(9)	0.3313(6)	0.1535(6)	4.4(3)					

<sup>a</sup> Starred values are for atoms refined isotropically. Anisotropically refined atoms are given in the form of the isotropic equivalent displacement parameter defined as  $(4/3)[a^2B(1,1) + b^2B(2,2) + c^2B(3,3) + ab(\cos \gamma)B(1,2) + ac(\cos \beta)B(1,3) + bc(\cos \alpha)B(2,3)]$ .

$\text{Me}_5\text{M}(\text{P}(\text{CH}_3)_3)(\text{OTf})_2$  complexes (**1**, M = Ir; **2**, M = Rh) were available from previous work of Stang and co-workers.<sup>11a</sup> The precursors  $(\eta^5\text{-C}_5\text{Me}_5)\text{M}(\text{P}(\text{CH}_3)_3)(\text{Cl})_2$  and  $[(\eta^5\text{-C}_5\text{Me}_5)\text{M}(\text{Cl})_2]_2$  (M = Ir, Rh), along with  $\text{Pt}(\text{CH}_2=\text{CH}_2)(\text{PPh}_3)_2$ , **3**, and  $\text{Pt}(\text{PhC}\equiv\text{CH})(\text{PPh}_3)_2$ , **4**, were prepared according to literature methods.<sup>6a,b,14,15</sup>

**Preparation of  $[(\eta^5\text{-C}_5\text{Me}_5)(\text{P}(\text{CH}_3)_3)\text{Ir}(\mu\text{-H})(\mu\text{-}\eta^1\text{-CH}_2=\text{CH})\text{Pt}(\text{PPh}_3)_2]^{2+}[\text{OTf}]_2$  (**5**).** A 100-mL Schlenk flask equipped with a stir bar was charged with 0.151 g (0.215 mmol) of  $(\eta^5\text{-C}_5\text{Me}_5)\text{Ir}(\text{P}(\text{CH}_3)_3)(\text{OTf})_2$ , **1**, 0.164 g (0.219 mmol) of  $\text{Pt}(\text{PPh}_3)_2(\text{CH}_2=\text{CH}_2)_2$ , **3**, and distilled, degassed  $\text{CH}_2\text{Cl}_2$  *via* syringe (25 mL). The resulting yellow solution was allowed to stir under nitrogen for 1.5 h at 25 °C. The reaction mixture was then filtered under nitrogen using a Whatman 934-AH glass microfiber. Diethyl ether was added to the filtrate, resulting in the formation of a light yellow precipitate. The solid was collected and washed with diethyl ether (ca. 20 mL). Drying *in vacuo* afforded 0.279 g (90%) of an air-stable, light yellow product. Recrystallization from  $\text{CH}_2\text{Cl}_2$ /hexane afforded analytically pure product **5**: mp 220–221 °C dec; <sup>1</sup>H NMR ( $\text{CD}_2\text{Cl}_2$ ) 7.48–7.95 (m, 30 H,  $\text{C}_6\text{H}_5$ ), 6.84 (b m, 1 H,  $\text{CHHCH}$ ), 4.66–4.31 (m, 1 H, <sup>3</sup>J<sub>H-P</sub> = 12.4 Hz, <sup>3</sup>J<sub>H-Pt</sub> = 84 Hz,  $\text{CHHCH}$ ), 3.87–3.76 (m, 1 H,  $\text{CHHCH}$ ), 1.85 (d, 15 H, <sup>4</sup>J<sub>H-P</sub> = 2.2 Hz,  $\text{C}_5\text{Me}_5$ ), 1.74 (d, 9 H, <sup>2</sup>J<sub>H-P</sub> = 10.9 Hz,  $\text{P}(\text{CH}_3)_3$ ), -13.6 to -15.4 (m, 1 H, <sup>1</sup>J<sub>H-Pt</sub> = 450 Hz,  $\mu\text{-H}$ ), <sup>13</sup>C{<sup>1</sup>H} NMR ( $\text{CD}_2\text{Cl}_2$ ) 142.2 (d, <sup>1</sup>J<sub>C-Pt</sub> = 84.2 Hz,  $\text{CH}_2\text{CH}$ ), 134.0–129.2 (m, phenyl carbons), 121.3 (q, <sup>1</sup>J<sub>C-F</sub> = 320 Hz,  $\text{CF}_3\text{SO}_3$ ), 102.6 (s,  $\text{C}_5\text{Me}_5$ ), 60.7 (s,

$\text{CH}_2\text{CH}$ ), 19.2 (d, <sup>1</sup>J<sub>C-P</sub> = 42.2 Hz,  $\text{P}(\text{CH}_3)_3$ ), 10.1 (s,  $\text{C}_5\text{Me}_5$ ); <sup>31</sup>P{<sup>1</sup>H} NMR ( $\text{CD}_2\text{Cl}_2$ ) 17.2 (d, <sup>2</sup>J<sub>P-P</sub> = 19.6 Hz, <sup>195</sup>Pt satellites, <sup>1</sup>J<sub>P-Pt</sub> = 2402 Hz,  $\text{Pt}-\text{P}(\text{C}_6\text{H}_5)_3$ ), 8.06 (dd, <sup>2</sup>J<sub>P-P</sub> = 19.6 Hz, <sup>3</sup>J<sub>P-P</sub> = 3.80 Hz, <sup>195</sup>Pt satellites, <sup>1</sup>J<sub>P-Pt</sub> = 4167 Hz,  $\text{Pt}-\text{P}(\text{C}_6\text{H}_5)_3$ ), -36.1 (d, <sup>3</sup>J<sub>P-P</sub> = 3.80 Hz,  $\text{Ir}-\text{P}(\text{CH}_3)_3$ ); <sup>19</sup>F NMR ( $\text{CD}_2\text{Cl}_2$ ) -76.6 (s, 2  $\text{CF}_3\text{SO}_3$ ). Anal. Calcd for  $\text{C}_{53}\text{H}_{55}\text{P}_3\text{S}_2\text{O}_6\text{F}_6\text{IrPt}\cdot\text{CH}_2\text{Cl}_2$ : C, 42.27; H, 3.94; S, 4.18. Found: C, 42.43; H, 3.90; S, 4.23.

**Preparation of  $[(\eta^5\text{-C}_5\text{Me}_5)(\text{P}(\text{CH}_3)_3)\text{Rh}(\mu\text{-H})(\mu\text{-}\eta^1\text{-CH}_2=\text{CH})\text{Pt}(\text{PPh}_3)_2]^{2+}[\text{OTf}]_2$  (**6**).** A 100-mL Schlenk flask equipped with a stir bar was charged with 0.190 g (0.310 mmol) of  $(\eta^5\text{-C}_5\text{Me}_5)\text{Rh}(\text{P}(\text{CH}_3)_3)(\text{OTf})_2$ , **2**, 0.232 g (0.310 mmol) of  $\text{Pt}(\text{PPh}_3)_2(\text{CH}_2=\text{CH}_2)_2$ , **3**, and distilled, degassed  $\text{CH}_2\text{Cl}_2$  *via* syringe (25 mL). The resulting yellow solution was allowed to stir for 2 h at 25 °C. The reaction mixture was then filtered under nitrogen using a Whatman 934-AH glass microfiber. Cyclohexane was added to the filtrate, resulting in the formation of a yellow precipitate. The solid was collected and washed with cyclohexane (ca. 10 mL) and diethyl ether (ca. 20 mL). Drying *in vacuo* afforded 0.302 g (72%) of an air-stable, yellow solid **6**. Recrystallization from  $\text{CH}_2\text{Cl}_2$ /hexane afforded analytically pure product: mp 195–197 °C dec; <sup>1</sup>H NMR ( $\text{CD}_2\text{Cl}_2$ ) 7.47–7.18 (m, 30 H,  $\text{C}_6\text{H}_5$ ), 4.62–4.26 (m, 1 H, <sup>3</sup>J<sub>H-P</sub> = 10.9 Hz, <sup>3</sup>J<sub>H-Pt</sub> = 84 Hz,  $\text{CHHCH}$ ), 3.87–3.76 (m, 1 H,  $\text{CHHCH}$ ), 1.77 (d, 15 H, <sup>4</sup>J<sub>H-P</sub> = 3.3 Hz,  $\text{C}_5\text{Me}_5$ ), 1.62 (d, 9 H, <sup>2</sup>J<sub>H-P</sub> = 10.9 Hz,  $\text{P}(\text{CH}_3)_3$ ), -11.2 to -13.0 (m, 1 H, <sup>1</sup>J<sub>H-Rh</sub> = 64 Hz, <sup>1</sup>J<sub>H-Pt</sub> = 541 Hz,  $\mu\text{-H}$ ); <sup>13</sup>C{<sup>1</sup>H} NMR ( $\text{CD}_2\text{Cl}_2$ ) 163.1–161.8 (m,  $\text{CH}_2\text{CH}$ ), 134.0–129.2 (m, phenyl carbons), 121.2 (q, <sup>1</sup>J<sub>C-F</sub> = 320 Hz,  $\text{CF}_3\text{SO}_3$ ), 107.5 (d, <sup>1</sup>J<sub>C-Rh</sub> = 5 Hz,  $\text{C}_5\text{Me}_5$ ), 75.7 (d, <sup>1</sup>J<sub>C-Rh</sub> = 7.3 Hz,  $\text{H}_2\text{CCH}$ ), 18.7 (d, <sup>1</sup>J<sub>C-P</sub> =

(14) Blake, D. M.; Roundhill, D. M. *Inorg. Synth.* **1978**, *18*, 120.

(15) (a) Allen, A. D.; Cook, C. D. *Can. J. Chem.* **1964**, *42*, 1063. (b) Koie, Y.; Shinoda, S.; Saito, Y. *J. Chem. Soc., Dalton Trans.* **1981**, 1082.

Table 4. Positional Parameters and Estimated Standard Deviations<sup>a</sup> for Compound 8

atom	x	y	z	B (Å <sup>2</sup> )	atom	x	y	z	B (Å <sup>2</sup> )
Pt	0.29400(2)	0.23220(2)	0.14322(1)	2.427(5)	C21	0.3880(9)	0.4588(6)	0.1932(5)	8.2(3)
Rh	0.46897(4)	0.30091(3)	0.14451(2)	2.59(1)	C22	0.1589(5)	0.3556(4)	0.0384(4)	3.6(2)
P1	0.4561(1)	0.3805(1)	0.2211(1)	3.72(5)	C23	0.1730(6)	0.4232(5)	0.0657(4)	4.7(2)
P2	0.1503(1)	0.2776(1)	0.08660(8)	2.92(4)	C24	0.1830(7)	0.4832(5)	0.0320(5)	6.1(3)
P3	0.2435(1)	0.1250(1)	0.17586(9)	3.16(4)	C25	0.1764(7)	0.4762(6)	-0.0300(5)	6.5(3)
S1	0.3051(2)	0.0745(2)	0.8546(1)	6.17(7)	C26	0.1618(7)	0.4104(6)	-0.0574(4)	6.0(2)
S2	0.7109(3)	0.3073(2)	-1.0189(2)	12.0(1)	C27	0.1526(6)	0.3492(5)	-0.0234(4)	4.8(2)
O1	0.2726(5)	0.1270(5)	0.8901(4)	8.9(2)	C28	0.0732(5)	0.3118(4)	0.1329(3)	3.3(2)
O2	0.2923(5)	0.0902(5)	0.7901(3)	8.9(3)	C29	-0.0146(5)	0.3442(5)	0.1063(4)	4.1(2)
O3	0.2819(6)	0.0026(5)	0.8665(4)	9.8(3)	C30	-0.0710(5)	0.3680(5)	0.1426(4)	4.8(2)
O4	0.7979(6)	0.3244(7)	-1.0239(4)	12.2(3)	C31	-0.0416(6)	0.3639(5)	0.2055(4)	5.7(2)
O5	0.6762(8)	0.2430(5)	-1.0020(4)	15.4(3)	C32	0.0462(6)	0.3348(6)	0.2315(4)	5.5(2)
O6	0.6624(8)	0.3774(6)	-0.9929(5)	20.9(3)	C33	0.1035(5)	0.3081(5)	0.1959(4)	3.9(2)
F1	0.4745(4)	0.0332(5)	0.8524(3)	10.7(2)	C34	0.0833(5)	0.2128(4)	0.0325(3)	3.4(2)
F2	0.4597(5)	0.0636(6)	0.9411(3)	11.8(3)	C35	-0.0152(6)	0.2025(5)	0.0221(4)	5.1(2)
F3	0.4646(5)	0.1421(5)	0.8751(4)	12.7(3)	C36	-0.0607(7)	0.1520(6)	-0.0198(5)	6.7(3)
F4	0.6446(6)	0.3853(5)	-1.1142(4)	11.3(3)	C37	-0.0089(8)	0.1106(6)	-0.0505(5)	6.6(3)
F5	0.6571(8)	0.2649(6)	-1.1207(4)	17.9(3)	C38	0.0874(7)	0.1201(6)	-0.0416(4)	5.8(2)
F6	0.5403(6)	0.3214(8)	-1.0879(5)	18.0(4)	C39	0.1341(6)	0.1708(5)	-0.0000(4)	4.3(2)
C1	0.4263(5)	0.2073(4)	0.1893(3)	2.8(1)	C40	0.2687(5)	0.0496(4)	0.1317(4)	3.5(2)
C2	0.5065(5)	0.1979(4)	0.2205(3)	3.3(2)	C41	0.3093(6)	0.0606(5)	0.0830(4)	5.1(2)
C3	0.5991(5)	0.1744(4)	0.2570(3)	3.6(2)	C42	0.3255(7)	0.0027(6)	0.0485(5)	6.2(3)
C4	0.6572(6)	0.2198(5)	0.2994(4)	5.1(2)	C43	0.3054(7)	-0.0657(6)	0.0641(5)	6.5(3)
C5	0.7490(7)	0.1978(6)	0.3296(5)	6.8(3)	C44	0.2664(6)	-0.0774(5)	0.1124(5)	5.5(2)
C6	0.7806(7)	0.1302(6)	0.3189(5)	6.7(3)	C45	0.2477(6)	-0.0196(5)	0.1459(4)	4.7(2)
C7	0.7234(7)	0.0850(6)	0.2793(5)	6.4(3)	C46	0.3126(5)	0.1091(5)	0.2542(4)	4.0(2)
C8	0.6325(7)	0.1072(5)	0.2478(4)	5.0(2)	C47	0.3128(6)	0.1625(6)	0.2976(4)	5.1(2)
C9	0.6093(5)	0.2931(5)	0.1237(3)	3.7(2)	C48	0.3682(6)	0.1559(6)	0.3570(4)	6.0(3)
C10	0.5461(4)	0.2426(4)	0.0851(3)	3.1(1)	C49	0.4223(7)	0.0949(7)	0.3731(4)	6.8(3)
C11	0.4706(5)	0.2810(4)	0.0479(3)	3.3(2)	C50	0.4244(8)	0.0442(7)	0.3308(5)	7.2(3)
C12	0.4840(5)	0.3566(4)	0.0636(3)	3.6(2)	C51	0.3706(6)	0.0502(5)	0.2716(4)	5.4(2)
C13	0.5714(5)	0.3640(4)	0.1092(4)	3.9(2)	C52	0.1175(5)	0.1125(4)	0.1762(4)	3.6(2)
C14	0.7048(5)	0.2759(6)	0.1648(4)	5.3(2)	C53	0.0548(6)	0.0814(5)	0.1267(4)	5.2(2)
C15	0.5643(6)	0.1634(5)	0.0831(4)	5.0(2)	C54	-0.0417(6)	0.0753(6)	0.1257(5)	6.3(3)
C16	0.3929(6)	0.2507(5)	-0.0032(4)	5.0(2)	C55	-0.0750(6)	0.1007(6)	0.1731(5)	6.8(3)
C17	0.4241(6)	0.4168(5)	0.0303(4)	5.3(2)	C56	-0.0125(6)	0.1309(6)	0.2225(5)	7.1(3)
C18	0.6212(7)	0.4334(5)	0.1294(5)	6.3(2)	C57	0.0834(6)	0.1370(5)	0.2254(4)	5.3(2)
C19	0.5640(7)	0.4155(6)	0.2706(5)	6.4(3)	C58	0.4310(7)	0.0782(7)	0.8823(5)	7.6(3)
C20	0.3952(8)	0.3446(6)	0.2750(5)	7.5(3)	C59	0.6235(6)	0.3466(8)	-1.0766(4)	12.4(3)

<sup>a</sup> Anisotropically refined atoms are given in the form of the isotropic equivalent displacement parameter defined as  $(4/3)[a^2B(1,1) + b^2B(2,2) + c^2B(3,3) + ab(\cos \gamma)B(1,2) + ac(\cos \beta)B(1,3) + bc(\cos \alpha)B(2,3)]$ .

35.1 Hz,  $P(\text{CH}_3)_3$ , 10.6 (s,  $\text{C}_5\text{Me}_5$ );  $^{31}\text{P}\{^1\text{H}\}$  NMR ( $\text{CD}_2\text{Cl}_2$ ) 18.8 (dd,  $^2J_{\text{P-P}} = 20.0$  Hz,  $^2J_{\text{P-Rh}} = 3.50$  Hz,  $^{195}\text{Pt}$  satellites,  $^1J_{\text{P-Pt}} = 2300$  Hz,  $\text{Pt-P}(\text{C}_6\text{H}_5)_3$ , 15.9 (m,  $^2J_{\text{P-P}} = 20.0$  Hz,  $^3J_{\text{P-P}} = 6.90$  Hz,  $^2J_{\text{P-Rh}} = 5.40$  Hz,  $^{195}\text{Pt}$  satellites,  $^1J_{\text{P-Pt}} = 3829$  Hz,  $\text{Pt-P}(\text{C}_6\text{H}_5)_3$ , 8.97 (dd,  $^2J_{\text{P-P}} = 6.90$  Hz,  $^1J_{\text{P-Rh}} = 118$  Hz,  $^{195}\text{Pt}$  satellites,  $^2J_{\text{P-Pt}} = 42.9$  Hz,  $\text{Rh-P}(\text{CH}_3)_3$ );  $^{19}\text{F}$  NMR ( $\text{CD}_2\text{Cl}_2$ ) -76.7 (s, 2  $\text{CF}_3\text{SO}_3$ ). Anal. Calcd for  $\text{C}_{53}\text{H}_{58}\text{P}_3\text{S}_2\text{O}_6\text{F}_6\text{RhPt-CH}_2\text{Cl}_2$ : C, 44.89; H, 4.19; S, 4.44. Found: C, 45.00; H, 4.15; S, 4.40.

**Preparation of  $[(\eta^5\text{-C}_5\text{Me}_5)(\text{P}(\text{CH}_3)_3)\text{Ir}(\mu\text{-H})(\mu\text{-}\eta^2\text{:}\eta^1\text{-PhC}\equiv\text{C})\text{Pt}(\text{PPh}_3)_2]^{2+}[\text{OTf}^-]_2$  (7).** A 50-mL Schlenk flask equipped with a stir bar was charged with 0.074 g (0.106 mmol) of  $(\eta^5\text{-C}_5\text{Me}_5)\text{Ir}(\text{P}(\text{CH}_3)_3)(\text{OTf})_2$ , **1**, and distilled, degassed  $\text{CH}_2\text{Cl}_2$  (25 mL). The yellow solution was cooled to  $-50$  °C, and 0.087 g (0.106 mmol) of  $\text{Pt}(\text{PhC}\equiv\text{CH})(\text{PPh}_3)_2$ , **4**, dissolved in  $\text{CH}_2\text{Cl}_2$  (ca. 5 mL) was then added dropwise *via* syringe over a period of 2 h. The reaction mixture was allowed to slowly warm to 25 °C with stirring for 12 h, during which time a color change from bright yellow to dark brown was noted. Diethyl ether was then added (ca. 200 mL), resulting in the formation of a sticky brown residue. The crude product was collected using a medium-porosity glass frit and was washed successively with diethyl ether. Drying *in vacuo* afforded 0.083 g (51%) of an air-stable, light-brown product. Recrystallization by slow diffusion from  $\text{CH}_2\text{Cl}_2$ /ether gave analytically pure product **7**: mp 199–201 °C dec;  $^1\text{H}$  NMR ( $\text{CD}_2\text{Cl}_2$ ) 7.66–6.99 (m, 35 H,  $\text{C}_6\text{H}_5$ ), 1.79 (d, 15 H,  $^4J_{\text{H-P}} = 1.5$  Hz,  $\text{C}_5\text{Me}_5$ ), 1.74 (d, 9 H,  $^2J_{\text{H-P}} = 10.9$  Hz,  $\text{P}(\text{CH}_3)_3$ ), -11.3 to -13.2 (m, 1 H,  $^1J_{\text{H-Pt}} = 501$  Hz,  $\mu\text{-H}$ );  $^{13}\text{C}\{^1\text{H}\}$  NMR ( $\text{CD}_2\text{Cl}_2$ ) 135.1–129.2 (m, phenyl carbons), 131.2 (s, PhCC), 121.4 (q,  $^1J_{\text{C-F}} = 319$  Hz,  $\text{CF}_3\text{SO}_3$ ), 119.5 (s, PhCC), 100.5 (d,  $^2J_{\text{C-P}} = 2.3$  Hz,  $\text{C}_5\text{Me}_5$ ), 19.4 (d,  $^1J_{\text{C-P}}$

= 2.3 Hz,  $\text{P}(\text{CH}_3)_3$ , 10.2 (s,  $\text{C}_5\text{Me}_5$ );  $^{31}\text{P}\{^1\text{H}\}$  NMR ( $\text{CD}_2\text{Cl}_2$ ) 17.7 (d,  $^2J_{\text{P-P}} = 23.2$  Hz,  $^{195}\text{Pt}$  satellites,  $^1J_{\text{P-Pt}} = 3093$  Hz,  $\text{Pt-P}(\text{C}_6\text{H}_5)_3$ , 7.34 (dd,  $^2J_{\text{P-P}} = 23.2$  Hz,  $^3J_{\text{P-P}} = 2.4$  Hz,  $^{195}\text{Pt}$  satellites,  $^1J_{\text{P-Pt}} = 3523$  Hz,  $\text{Pt-P}(\text{C}_6\text{H}_5)_3$ , -28.1 (d,  $^3J_{\text{P-P}} = 2.4$  Hz,  $^{195}\text{Pt}$  satellites,  $^2J_{\text{P-Pt}} = 15.3$  Hz,  $\text{Ir-P}(\text{CH}_3)_3$ );  $^{19}\text{F}$  NMR ( $\text{CD}_2\text{Cl}_2$ ) -76.9 (s, 2  $\text{CF}_3\text{SO}_3$ ). Anal. Calcd for  $\text{C}_{59}\text{H}_{60}\text{P}_3\text{S}_2\text{O}_6\text{F}_6\text{IrPt}$ : C, 46.52; H, 3.97; S, 4.21. Found: C, 46.43; H, 3.99; S, 4.31.

**Preparation of  $[(\eta^5\text{-C}_5\text{Me}_5)(\text{P}(\text{CH}_3)_3)\text{Rh}(\mu\text{-H})(\mu\text{-}\eta^2\text{:}\eta^1\text{-PhC}\equiv\text{C})\text{Pt}(\text{PPh}_3)_2]^{2+}[\text{OTf}^-]_2$  (8).** A 50-mL Schlenk flask equipped with a stir bar was charged with 0.048 g (0.078 mmol) of  $(\eta^5\text{-C}_5\text{Me}_5)\text{Rh}(\text{P}(\text{CH}_3)_3)(\text{OTf})_2$ , **2**, and distilled, degassed  $\text{CH}_2\text{Cl}_2$  (20 mL). The yellow reaction mixture was cooled to  $-40$  °C, and 0.087 g (0.106 mmol) of  $\text{Pt}(\text{PhC}\equiv\text{CH})(\text{PPh}_3)_2$ , **4**, dissolved in  $\text{CH}_2\text{Cl}_2$  (ca. 5 mL) was added dropwise *via* syringe over a period of 2 h. The reaction mixture was allowed to slowly warm to 25 °C, with stirring for an additional 12 h, at which time a color change from cloudy yellow to deep red was noted. Diethyl ether was then added (ca. 150 mL), resulting in the formation of a red residue, which was collected and washed successively with diethyl ether (ca. 50 mL). Drying *in vacuo* afforded 0.065 g (58%) of an air-stable, red product **8**: mp 217–218 °C dec;  $^1\text{H}$  NMR ( $\text{CD}_2\text{Cl}_2$ ) 7.55–6.94 (m, 35 H,  $\text{C}_6\text{H}_5$ ), 1.62 (d, 15 H,  $^4J_{\text{H-P}} = 2.9$  Hz,  $\text{C}_5\text{Me}_5$ ), 1.58 (d, 9 H,  $^2J_{\text{H-P}} = 11.2$  Hz,  $\text{P}(\text{CH}_3)_3$ ), -9.07 to -11.4 (m, 1 H,  $^1J_{\text{H-Rh}} = 79.4$  Hz,  $^1J_{\text{H-Pt}} = 588$  Hz,  $\mu\text{-H}$ );  $^{13}\text{C}\{^1\text{H}\}$  NMR ( $\text{CD}_2\text{Cl}_2$ ) 134.4–129.2 (m, phenyl carbons), 121.3 (q,  $^1J_{\text{C-F}} = 319$  Hz,  $\text{CF}_3\text{SO}_3$ ), 118.9 (s, PhCC), 106.0 (dd,  $^1J_{\text{C-Rh}} = 2.4$  Hz,  $^2J_{\text{C-P}} = 6.1$  Hz,  $\text{C}_5\text{Me}_5$ ), 18.3 (d,  $^1J_{\text{C-P}} = 33.0$  Hz,  $\text{P}(\text{CH}_3)_3$ ), 10.5 (s,  $\text{C}_5\text{Me}_5$ );  $^{31}\text{P}\{^1\text{H}\}$  NMR ( $\text{CD}_2\text{Cl}_2$ ) 17.9 (dd,  $^2J_{\text{P-P}} = 21.6$  Hz,  $^2J_{\text{P-Rh}} = 4.3$  Hz,  $^{195}\text{Pt}$  satellites,  $^1J_{\text{P-Pt}} = 2941$  Hz,  $\text{Pt-P}(\text{C}_6\text{H}_5)_3$ , 16.2

(m,  $^2J_{P-P} = 21.6$  Hz,  $^3J_{P-P} = 6.4$  Hz,  $^2J_{P-Rh} = 5.5$  Hz,  $^{195}\text{Pt}$  satellites,  $^1J_{P-Pt} = 3226$  Hz,  $\text{Pt}-P(\text{C}_6\text{H}_5)_3$ ), 5.72 (dd,  $^3J_{P-P} = 6.4$  Hz,  $^1J_{P-Rh} = 135$  Hz,  $^{195}\text{Pt}$  satellites,  $^2J_{P-Pt} = 30.1$  Hz,  $\text{Rh}-P(\text{CH}_3)_3$ );  $^{19}\text{F}$  NMR ( $\text{CD}_2\text{Cl}_2$ )  $-77.1$  (s, 2  $\text{CF}_3\text{SO}_3$ ). Anal. Calcd for  $\text{C}_{59}\text{H}_{60}\text{P}_3\text{S}_2\text{O}_6\text{F}_6\text{RhPt}$ : C, 49.41; H, 4.22; S, 4.47. Found: C, 49.52; H, 4.26; S, 4.57.

**X-ray Crystallographic Analyses of 5 and 8.** X-ray-quality crystals were grown by slow vapor diffusion of  $\text{Et}_2\text{O}$  into a  $\text{CH}_2\text{Cl}_2$  solution of **5** and **8** at  $25^\circ\text{C}$ . A yellow crystal,  $0.33$  mm  $\times$   $0.28$  mm  $\times$   $0.19$  mm, **5**, and a red crystal,  $0.28$  mm  $\times$   $0.25$  mm  $\times$   $0.25$  mm, **8**, was glued onto a glass fiber and mounted for data collection on a CAD4 Diffractometer. The unit cell parameters were obtained by a least-squares refinement of 25 centered reflections in the range  $20 < 2\theta < 30^\circ$ . The space group was determined from systematic absences ( $h0l$ ,  $h + l = 2n$ ;  $0k0$ ,  $k = 2n$ ) and subsequent least-squares refinement. The data were collected by the  $\theta$ - $2\theta$  scan technique, with variable scanning rate, using monochromatic Mo radiation. A total of 6778 unique reflections were measured in the range  $4.0 < 2\theta < 50^\circ\text{C}$ , of which 6774 were considered observed, and a total of 9520 unique reflections were measured in the range  $4.0 < 2\theta < 48^\circ$ , of which 6323 were considered observed; i.e.,  $I > 3\sigma(I)$ , for crystals **5** and **8**, respectively. Standard reflections showed no decay for either crystals during data collection. Lorentz and polarization corrections and an empirical absorption correction based upon a series of  $\psi$  scans were applied to the data. Intensities of equivalent reflections were averaged.

The structures were solved by the standard heavy-atom techniques with the SDP/VAX package. Non-hydrogen atoms were refined with anisotropic thermal parameters. There is a disordered solvent molecule of  $\text{CH}_2\text{Cl}_2$  in the lattice and some disorder being exhibited by one of the triflate anion molecules for crystal **5**. All hydrogen atoms were calculated and added to the structure factor calculations, except for the hydride. Scattering factors and  $\Delta f'$  and  $\Delta f''$  values were taken from the literature.<sup>16</sup>

**Acknowledgment.** We thank the NSF (Grant CHE-9101767) for financial support and Johnson-Matthey, Inc., for the generous loan of  $\text{IrCl}_3 \cdot x\text{H}_2\text{O}$ ,  $\text{RhCl}_3 \cdot x\text{H}_2\text{O}$ , and  $\text{K}_2\text{PtCl}_4$ .

**Supplementary Material Available:** For compounds **5** and **8**, listings of calculated positional parameters for the hydrogen atoms, anisotropic displacement parameters, and extended bond lengths, bond angles, and torsion angles (38 pages). Ordering information is given on any current mast-head page.

OM950049R

---

(16) Chromer, D. T.; Waber, J. T. In *International Tables for X-ray Crystallography*; Ibers, J. A., Hamilton, W. C., Eds.; Kynoch Press: Birmingham, England, 1974; Table 2.3.1.

# Stability in Solution of (Chloromethyl)palladium(II) Complexes: X-ray Structures of *trans*-Bis(triphenylphosphine)chloro(chloromethyl)palladium(II) and -platinum(II) and Comparison of the Relative Stabilities of Analogous Palladium and Platinum Chloromethyl Complexes Containing Phosphine Ligands

Robert McCrindle,\* George Ferguson,\* Alan J. McAlees, Gilles J. Arsenault, Anuradha Gupta, and Michael C. Jennings

Guelph-Waterloo Centre for Graduate Work in Chemistry, Guelph Campus, Department of Chemistry and Biochemistry, University of Guelph, Guelph, Ontario, Canada N1G 2W1

Received January 27, 1995<sup>⊗</sup>

The stabilities to storage in CDCl<sub>3</sub> solution (both in the absence and presence of air) of a series of chloro(chloromethyl)palladium(II) complexes of neutral olefinic, sulfide, amine, and phosphine ligands have been investigated. The decomposition rates and types of products formed depend upon the nature of the ligands. Three types of reactions involving the CH<sub>2</sub>Cl moiety were found: (i) oxidation to formaldehyde, (ii) formation of ylide complexes, and (iii) coupling to ethene and propene. Since the phosphine complex *trans*-[(Ph<sub>3</sub>P)<sub>2</sub>Pd(CH<sub>2</sub>Cl)Cl] (**9**) proved to be much more stable to storage in solution than its Pt analogue (**17**), we have compared their X-ray structures. Crystals of **9** (C<sub>37</sub>H<sub>32</sub>Cl<sub>2</sub>P<sub>2</sub>Pd) are monoclinic, space group *P*2<sub>1</sub>/*n*, with 4 molecules in a cell of dimensions *a* = 12.361(5) Å, *b* = 22.714(4) Å, *c* = 12.328(4) Å, and β = 111.36(3)°. Compound **17** (C<sub>37</sub>H<sub>32</sub>Cl<sub>2</sub>P<sub>2</sub>Pt) is isomorphous with **9**, with cell dimensions *a* = 12.332(2) Å, *b* = 22.784(3) Å, *c* = 12.344(1) Å, and β = 111.32(1)°. Both structures were refined by full-matrix least-squares calculations on *F*; the final *R* values are 0.024 for both structures (for 5763 and 6621 reflections, respectively). The possibility that differences in the M–CH<sub>2</sub>–Cl distances in **9** and **17** may reflect their relative tendencies to form carbene complexes by heterolysis of the CH<sub>2</sub>–Cl bond is discussed.

## Introduction

α-Halogenomethyl derivatives of transition metals have attracted widespread interest, in particular as synthetic intermediates and potential precursors of a wide range of organometallic compounds.<sup>1</sup> A number of these α-halogenomethyl derivatives have been described as being labile, tending to decompose to the related halogenometal complex.<sup>2</sup> While the fate of the CH<sub>2</sub> moiety was often not investigated, some workers have reported the formation of ethene and, in several cases, polymethylene was identified as a major product.<sup>3</sup> In a recent paper<sup>3b</sup> we reported the results of an investigation of the stability of both mono- and bis-(chloromethyl)platinum(II) complexes. In this work we have shown that in chloroform solution (a) bis(chloromethyl) bis(phosphine) derivatives are stable but decompose cleanly to the corresponding dichlorides plus ethene when the polarity of the medium is increased by adding hexafluoro-2-propanol; (b) mono(chloromethyl) *cis*-bis(phosphine) derivatives are stable under

similar conditions, and (c) the related *trans* mono-(chloromethyl) derivatives are stable in very dry chloroform but decompose in the presence of traces of water to the corresponding hydrides plus formaldehyde. The present paper deals with the behavior of (chloromethyl)palladium(II) complexes under similar conditions. Where structural similarities warrant comparison there are some sharp contrasts. Thus, for example, apart from our lack of success so far in even preparing bis-(chloromethyl) complexes of palladium, *trans*-bis(phosphine) complexes of (chloromethyl)palladium(II) are considerably more stable than their platinum counterparts while the opposite is true for the corresponding *cis* derivatives.

## Results

[Pd(CH<sub>2</sub>Cl)Cl(COD)] (**1**) (COD = 1,5-cyclooctadiene) (Chart 1) was prepared<sup>4</sup> by treatment of solutions of [PdCl<sub>2</sub>(COD)] with a small excess of diazomethane. Yields of **1** in excess of 90% were obtained when the products formed were chromatographed immediately, whereas when reaction mixtures were stored overnight in the refrigerator before chromatography, recoveries

\* To whom correspondence should be addressed. E-mail addresses: mcrindle@chembio.uoguelph.ca; ferguson@chembio.uoguelph.ca.

<sup>⊗</sup> Abstract published in *Advance ACS Abstracts*, April 15, 1995.

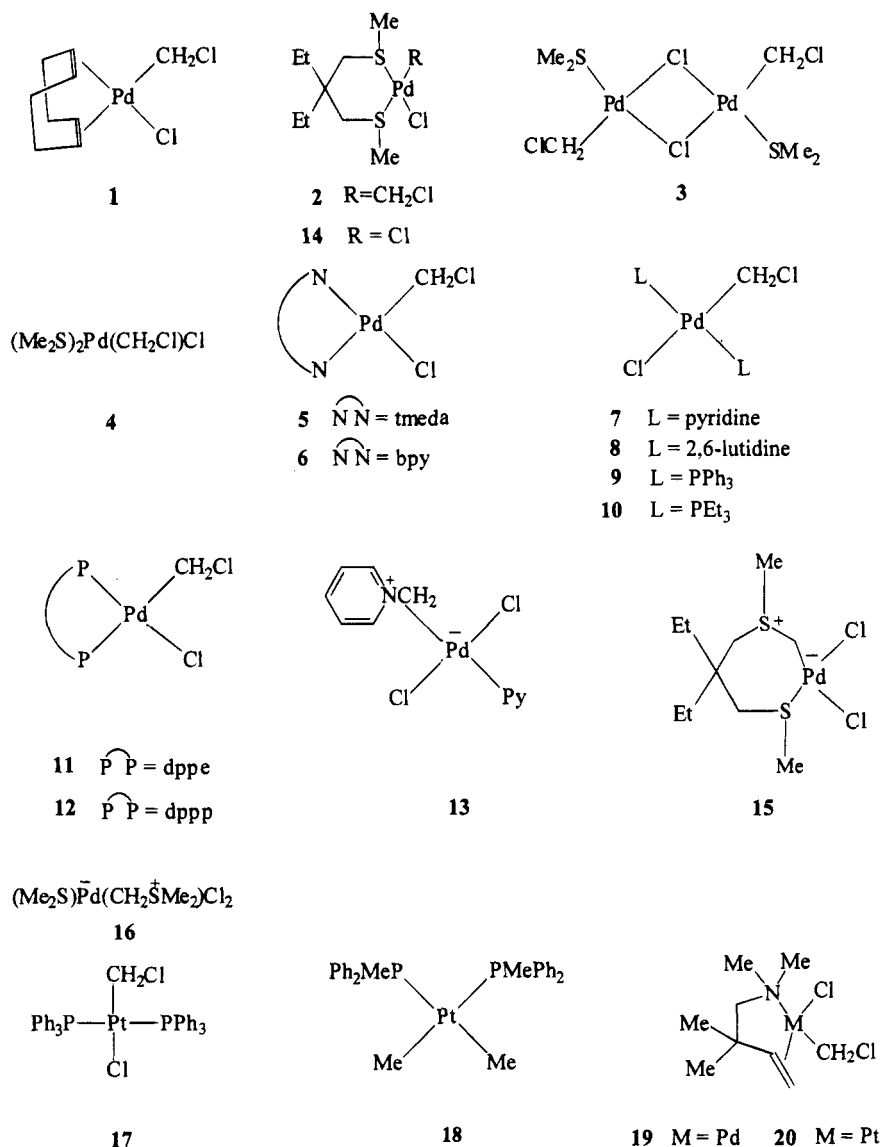
(1) See for example: Friedrich, H. B.; Moss, J. R. *J. Organomet. Chem.* **1993**, 453, 85–95 and references therein.

(2) While little appears to be known about the decomposition pathways available to monoalkylpalladium(II) complexes which cannot undergo β-hydrogen abstraction, both radical and ionic pathways have been found for thermal decomposition in some cases: Gretz, E.; Sen, A. *J. Am. Chem. Soc.* **1986**, 108, 6038–6039.

(3) For leading references see: (a) Hubbard, J. L.; McVicar, W. K. *J. Organomet. Chem.* **1992**, 429, 369–378. (b) McCrindle, R.; Arsenault, G. J.; Gupta, A.; Hampden-Smith, M. J.; Rice, R. E.; McAlees, A. *J. Chem. Soc., Dalton Trans.* **1991**, 949–954.

(4) McCrindle, R.; Arsenault, G. J.; Farwaha, R.; McAlees, A. J.; Sneddon, D. W. *J. Chem. Soc., Dalton Trans.* **1989**, 761–766.

Chart 1



usually dropped to below 30%. After purification, **1**, which is quite stable to storage as the solid in the refrigerator under air, was used<sup>4</sup> to produce the other complexes (**2–12**) by ligand displacement. The product (**7**), from reaction of **1** with pyridine, sometimes contained a small quantity of a second component which proved to be the ylide complex (**13**). The dimeric complex (**3**)<sup>5</sup> was isolated upon reaction of **1** with excess dimethyl sulfide.

Generally, the stability of the complexes was determined for samples stored in the dark<sup>6</sup> at room temperature in CDCl<sub>3</sub> solution. Complexes containing olefin, sulfur, nitrogen and phosphorus donor ligands are dealt with in that order.

<sup>1</sup>H NMR spectra of solutions of [Pd(CH<sub>2</sub>Cl)Cl(COD)] (**1**) showed no sign of deterioration of the solute during several weeks of storage, even under air.

(5) The stereochemistry shown in the chloromethyl complex **3** is suggested on the basis of analogy with that found in the related methyl complex: Byers, P. K.; Carty, A. J.; Englehardt, L. M.; White, A. H. *J. Chem. Soc., Dalton Trans.* **1986**, 1731–1734.

(6) We have not investigated the effect of exposure of these solutions to light. However, we have observed that such exposure makes no qualitative difference in the case of the chelating sulfide complex **2** but does induce reaction in the otherwise stable *trans*-bis(phosphine) complexes **9** and **10** under air.

In contrast to **1**, purified samples of the chelating bis-(sulfide) complex chloro(chloromethyl)(4,4-diethyl-2,6-dithiaheptane)palladium(II) (**2**) decomposed largely to the corresponding dichloro complex **14** during 2 days in solution when given free access to air. When these decompositions were allowed to proceed under an atmosphere of air in sealed NMR tubes, <sup>1</sup>H signals attributable<sup>3b</sup> to monomeric and oligomeric formaldehyde species gradually replaced the resonance arising from the PdCH<sub>2</sub>Cl moiety over a period of about 1 week. The presence of formaldehyde in these solutions was confirmed by its isolation as the 2,4-dinitrophenylhydrazone derivative. The <sup>1</sup>H NMR spectra obtained in these sealed tube experiments revealed the presence of a Pd-containing product other than **14**. The identity of this complex became clear when the stability of **2** was monitored by <sup>1</sup>H NMR spectroscopy for solutions which had been sealed under vacuum after several freeze/pump/thaw cycles. Under these conditions, **2** decomposed much more slowly (with about 60% surviving after 1 month) to give a single product, the sulfur ylide complex **15**.<sup>7</sup> The dimeric dimethyl sulfide complex **3** showed no change in solution under vacuum over 2 weeks, but under air, the slow growth of <sup>1</sup>H NMR peaks

ascribable to both formaldehyde and  $[(\text{Me}_2\text{S})\text{PdCl}_2]_2^8$  was observed. When excess dimethyl sulfide was added in small increments to a solution of **3**, the  $^1\text{H}$  NMR signal at  $\delta$  3.78 ascribable to the  $\text{CH}_2\text{Cl}$  moiety broadened and moved upfield finally resharping to give a singlet at  $\delta$  3.53 attributable to monomeric species **4**. On sitting under air, very slow oxidation to give formaldehyde occurred. However, the  $^1\text{H}$  NMR spectrum of the solution after 3 weeks indicated that the major product was the ylidic species **16** (singlets at  $\delta$  2.13, 2.85, and 2.88). At this stage, the consumption of **4** was essentially complete and the spectrum showed additional singlets at  $\delta$  2.25, 2.39, and 2.60 ascribable to the dimer  $[(\text{Me}_2\text{S})\text{PdCl}_2]_2$ ,<sup>8</sup>  $[(\text{Me}_2\text{S})_2\text{PdCl}_2]$ ,<sup>9</sup> and, possibly, dimethyl sulfoxide, respectively.

The complexes **5** and **6** derived from the chelating diamines *N,N,N',N'*-tetramethylethylenediamine and 2,2'-bipyridine showed no evidence of decomposition after 2 weeks in  $\text{CDCl}_3$  under vacuum. However, under air, the development of peaks arising from formaldehyde was evident immediately after preparation of the solutions and the greater part of the starting complexes reacted over a few days to give the corresponding dichloro complexes. The pyridine and 2,6-lutidine complexes **7** and **8**, in which the nitrogen donors are *trans*, are also stable in  $\text{CDCl}_3$  under vacuum. Under air, the former behaved in a similar fashion to the *cis*-diamine complexes **5** and **6** while the lutidine complex proved to be stable under the same conditions. In the presence of excess pyridine, **7** rearranges cleanly, upon standing under vacuum, into the ylide complex **13**.<sup>10</sup>

The complexes **11** and **12** of the chelating diphosphine ligands 1,2-bis(diphenylphosphino)ethane and 1,3-bis(diphenylphosphino)propane both decompose very slowly under vacuum in  $\text{CDCl}_3$ . Signs of reaction are detectable within 1 week, but complete disappearance of substrate required several months. Monitoring by  $^{31}\text{P}$  NMR spectroscopy showed only peaks corresponding to the substrates and the derived dichlorides. The fate of the chloromethyl moiety in both cases was revealed by the  $^1\text{H}$  NMR spectra which showed the growth of peaks ascribable to mainly ethene, propene, and methyl chloride. The relative amount of methyl chloride formed varied from sample to sample (*cf.* footnote 32), while the concentration of propene relative to ethene was enhanced when higher initial amounts of substrate were used. Under air, this slow route of decomposition was accompanied by similarly slow oxidation to formaldehyde and the dichloro complexes. In contrast, the *trans*-bis(triphenyl)- and *trans*-bis(triethyl)phosphine complexes **9** and **10** survived prolonged storage under vacuum or air<sup>6</sup> even when the solvent was not dried prior to use.

The contrasting behavior of the palladium and the previously studied<sup>3b</sup> platinum phosphine complexes led us to conduct a detailed comparison of the molecular

**Table 1. Summary of Crystal Data, Data Collection, Structure Solution, and Refinement Details**

	9	17
	(a) Crystal Data	
empirical formula	$\text{C}_{37}\text{H}_{32}\text{Cl}_2\text{P}_2\text{Pd}$	$\text{C}_{37}\text{H}_{32}\text{Cl}_2\text{P}_2\text{Pt}$
molar mass	715.92	804.61
color, habit	pale yellow, needle	colorless, needle
cryst size, mm	$0.39 \times 0.29 \times 0.25$	$0.42 \times 0.30 \times 0.18$
cryst system	monoclinic	monoclinic
<i>a</i> , Å	12.361(5)	12.332(2)
<i>b</i> , Å	22.714(4)	22.784(3)
<i>c</i> , Å	12.328(4)	12.344(1)
$\beta$ , °	111.36(3)	111.32(1)
<i>V</i> , Å <sup>3</sup>	3224(3)	3231(1)
space group	$P2_1/n$	$P2_1/n$
<i>Z</i>	4	4
molecular symmetry	none	none
<i>F</i> (000)	1456	1584
<i>d</i> <sub>calc</sub> , g cm <sup>-3</sup>	1.48	1.65
$\mu$ , cm <sup>-1</sup>	8.57	46.8
	(b) Data Acquisition <sup>a</sup>	
temp, K	294	294
unit-cell reflns	25 (10–13)	25 (10–22)
( $\theta$ -range, deg)		
max $\theta$ for reflns, deg	54.0	60.0
<i>hkl</i> range of reflns	0 to 15, 0 to 28, –15 to 15	0 to 17, 0 to 32, –17 to 17
variation in $\int$		
std reflns	no decay	no decay
reflcs measd	7702	7705
unique reflns	6992	6621
<i>R</i> <sub>int</sub>	0.017	0.017
reflcs with <i>I</i> > 3 $\sigma$ ( <i>I</i> )	5763	6621
abs corr type	Gaussian	Gaussian
	integration	integration
min, max abs corr	0.7232, 0.8460	0.2659, 0.4570
	(c) Structure Solution and Refinement <sup>b</sup>	
refinement on	<i>F</i>	<i>F</i>
solution method	Patterson	coords from <b>9</b>
H-atom treatment	riding, C–H = 0.95 Å	riding, C–H = 0.95 Å
no. of variables in L.S.	379	379
<i>k</i> in $w = 1/(\sigma^2 F_o + kF_o^2)$	0.0008	0.0008
<i>R</i> , <i>R</i> <sub>w</sub> , <i>gof</i>	0.024, 0.037, 1.53	0.024, 0.030, 1.10
density range in final	–0.35, 0.41	–0.80, 1.09
$\Delta$ -map, e Å <sup>-3</sup>	(adjacent Pd)	(adjacent Pt)
final shift/error ratio	0.00	0.00

<sup>a</sup> Data collection on an Enraf Nonius CAD4 diffractometer with graphite-monochromated Mo K $\alpha$  radiation ( $\lambda$  0.7107 Å). <sup>b</sup> Calculations were done on a PDP-11 computer system with the SDP-Plus system of programs.

structures of *trans*-bis(triphenylphosphine)chloro-(chloromethyl)palladium(II) (**9**) and its platinum analogue (**17**) by X-ray crystallography. Crystals of **9** and **17** suitable for diffraction studies were both obtained by adding the stoichiometric amount of triphenylphosphine to  $[(\text{COD})\text{M}(\text{CH}_2\text{Cl})\text{Cl}]$  (*M* = Pd or Pt) in a minimum amount of dichloromethane. The crystals of **9** and **17** proved to be isomorphous, and details of the cell data, data collection, structure solution, and refinement parameters are summarized in Table 1. A view of the structure of palladium complex **9**, along with our numbering scheme, is shown in Figure 1; as the structures are isomorphous, the corresponding view for the Pt isomer **17** is essentially identical. Principal dimensions are listed in Table 2. In both cases the metal atom and the four immediately attached atoms lie in essentially a single plane. The main deviations from a formal square planar arrangement involve the P–M–C and P–M–Cl angles, which are, respectively, greater than and less than 90°.

(7) We have previously reported the preparation of the platinum analogue of this complex: McCrindle, R.; Arsenaute, G. J.; Farwaha R. *J. Organomet. Chem.* **1985**, *296*, C51–C53.

(8) Goggin, P. L.; Goodfellow, R. J.; Haddock, S. R.; Reed, F. J. S.; Smith, J. G.; Thomas, K. M. *J. Chem. Soc., Dalton Trans.* **1972**, 1904–1909.

(9) Tubino, M.; Merbach, A. E. *Inorg. Chim. Acta* **1983**, *71*, 149–153.

(10) The  $^1\text{H}$  NMR parameters found for the pyridine residues in **13** are very similar to those reported for the analogous platinum complex: Hanks, T. W.; Ekeland, R. A.; Emerson, K.; Larsen, R. D.; Jennings, P. W. *Organometallics* **1987**, *6*, 28–32.

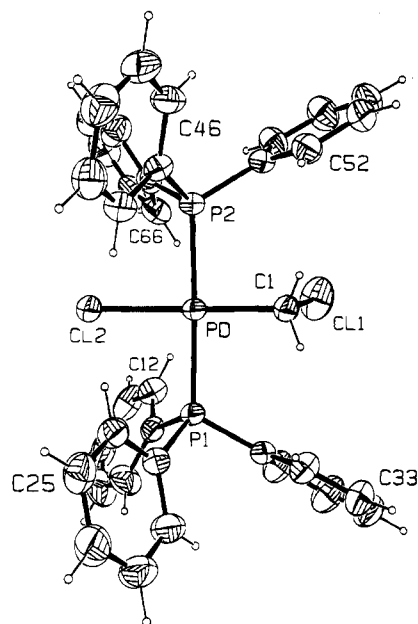


**Figure 1.** View of **9** with an indication of the numbering scheme. Phenyl ring C atoms are labeled C*i*1–C*i*6 (*i* = 1–6). Thermal ellipsoids are drawn at the 50% probability level.

**Table 2. Summary of Principal Dimensions (Å, deg) in Cl–M(PPh<sub>3</sub>)<sub>2</sub>–CH<sub>2</sub>Cl**

bond	M =		angle	M =	
	Pd ( <b>9</b> )	Pt ( <b>17</b> )		Pd ( <b>9</b> )	Pt ( <b>17</b> )
M–Cl2	2.402(1)	2.410(1)	Cl2–M–P1	89.04(2)	88.22(3)
M–P1	2.337(1)	2.310(1)	Cl2–M–P2	88.67(2)	87.94(3)
M–P2	2.329(1)	2.308(1)	Cl2–M–C1	178.87(7)	179.2(1)
⟨M–P⟩	2.333(4)	2.309(1)	P1–M–P2	177.59(2)	176.08(3)
M–C1	2.031(2)	2.031(3)	P1–M–C1	91.86(6)	92.2(1)
C1–C11	1.767(2)	1.799(3)	P2–M–C1	90.44(6)	91.6(1)
P1–C11	1.819(2)	1.822(3)	M–C1–C11	110.79(9)	112.1(1)
P1–C21	1.826(2)	1.822(2)	⟨M–P–C⟩	114.4(39)	114.3(33)
P1–C31	1.825(2)	1.825(3)	⟨C–P–C⟩	104.2(24)	104.2(24)
P2–C41	1.824(2)	1.828(3)			
P2–C51	1.828(2)	1.830(3)			
P2–C61	1.815(2)	1.814(3)			
⟨P–C⟩	1.823(4)	1.824(5)			

## Discussion

**Comparison of X-ray Structures.** A potentially important reaction pathway for (halomethyl)metal complexes involves dissociation of halide ion and formation of a reactive carbene species. It is well-known<sup>11</sup> that, for compounds of analogous structure, platinum is better able than palladium to stabilize a carbene substituent. It has been concluded that this is mainly due to the superior capability of platinum to engage in back-donation of d-electrons to the carbene fragment. We have compared the structures of **9** and **17**, to determine if the expected easier formation of a carbene from the latter is reflected in the relative dimensions of the M–CH<sub>2</sub>Cl fragments.

There are very few reported instances<sup>12–14</sup> where the X-ray structures of analogous organopalladium(II) and

-platinum(II) complexes have been determined. Where comparisons have been made, it has been concluded<sup>12,15</sup> that, in general, Pt–P bond lengths are shorter than Pd–P bond lengths but Pt–C bond lengths are longer than Pd–C bond lengths. In **9** and **17**, we do observe that the Pt–P bond lengths [ $\langle\text{Pt–P}\rangle = 2.309(1)$  Å] are shorter than the Pd–P bond lengths [ $\langle\text{Pd–P}\rangle = 2.333(4)$  Å]. However, the Pt–C and Pd–C bond lengths are identical [2.031(3) vs 2.031(2) Å] in the two complexes. This might be taken to indicate that the Pt–C bond is relatively short and, combined with the observation that the C–Cl bond is longer in the platinum complex than in the palladium one [1.799(3) vs 1.767(2) Å], could be interpreted as implying an enhanced contribution of the ionic form (M=CH<sub>2</sub>)<sup>+</sup>Cl<sup>–</sup> to the ground state structure of the platinum complex, **17**. Comparison of the Rh–C bond lengths found in [RhCl(CH<sub>2</sub>Cl)(Me<sub>2</sub>PCH<sub>2</sub>CH<sub>2</sub>PM<sub>2</sub>)<sub>2</sub>]Cl [2.161(2) Å] and [RhCl(I)(CH<sub>2</sub>I)(CO)(PET<sub>3</sub>)<sub>2</sub>] [2.080(6) Å] led<sup>16</sup> to the suggestion that a carbenic resonance form may make a greater contribution to the structure of the latter. The relatively long C–Cl bond length in **17** finds a parallel in the lability<sup>17</sup> of the C–F bonds in *trans*-[PtH(CF<sub>3</sub>)(PPh<sub>3</sub>)<sub>2</sub>], which gives difluorocarbene species when treated with acids.

The metal–carbon bond length, on its own, is not a useful indicator of the degree of back-bonding from the metal. It is affected *inter alia* by the electronegativities of the other substituents on the carbon atom<sup>18</sup> (increasing electronegativity results in a shortening of the M–C bond length) and the nature of the other ligands present (both steric and electronic effects). In a comparison of the complexes *cis*-M(CH<sub>3</sub>)<sub>2</sub>(MePPh<sub>2</sub>)<sub>2</sub> [M = Pt (**18**) or Pd], it was suggested<sup>12b</sup> that steric interactions between P and C result in a longer M–C bond in **18** because the M–P bonds are shorter in this case. Since the Pt–P bonds in **17** are longer (see above) than those in **18** [ $\langle\text{Pt–P}\rangle = 2.285(2)$  Å], a closer approach of the carbon ligand may be possible in the former, resulting in an M–C bond length which happens to match that found in its Pd analogue (**9**). Indeed, the results of calculations have been taken<sup>12b</sup> to suggest that, if only electronic factors were involved, Pd–C and Pt–C bonds should be of very similar lengths. Clearer evidence for a contribution from back-bonding might be obtained by comparison of complexes in which this type of steric effect is reduced. Such is the case for the chelating olefinic amine complexes **19** and **20**.<sup>13</sup> Here, the Pt–C bond [2.016(11) Å] in **20** may even be shorter than the Pd–C bond [2.039(8) Å] in **19**. The C–Cl bonds in the two complexes are, however, about the same length [1.753(11) Å for **20** vs 1.743(10) Å for **19**].

**Decomposition Reactions.** [Pd(CH<sub>2</sub>Cl)Cl(COD)] (**1**) is more stable than the corresponding methyl

(14) (a) McCrindle, R.; Ferguson, G.; McAlees, A. J.; Parvez, M.; Roberts, P. *J. Chem. Soc., Dalton Trans.* **1982**, 1699–1708. (b) Del Fra, A.; Zanotti, G.; Bombieri, G.; Ros, R. *Inorg. Chim. Acta* **1979**, *36*, 121–125.

(15) Cavell, K. J.; Jin, H.; Skelton, B. W.; White, A. H. *J. Chem. Soc., Dalton Trans.* **1993**, 1973–1978.

(16) Gash, R. C.; Cole-Hamilton, D. J.; Whyman, R.; Barnes, J. C.; Simpson, M. C. *J. Chem. Soc., Dalton Trans.* **1994**, 1963–1969.

(17) Michelin, R. A.; Ros, R.; Guadalupi, G.; Bombieri, G.; Benetollo, F.; Chapuis, G. *Inorg. Chem.* **1989**, *28*, 840–846.

(18) See, for example: Bardi, R.; Piazzesi, A. M. *Inorg. Chim. Acta* **1981**, *47*, 249–254.

(11) Wada, M.; Koyama, Y.; Sameshima, K. *J. Organomet. Chem.* **1981**, *209*, 115–121.

(12) (a) Wisner, J. M.; Bartczak, T. J.; Ibers, J. A. *Organometallics* **1986**, *5*, 2044–2050. (b) Wisner, J. M.; Bartczak, T. J.; Ibers, J. A.; Low, J. J.; Goddard W. A. *J. Am. Chem. Soc.* **1986**, *108*, 347–348.

(13) (a) McCrindle, R.; Ferguson, G.; Arsenaull, G. J.; McAlees, A. J.; Ruhl, B. L.; Sneddon, D. W. *Organometallics* **1986**, *5*, 1171–1178. (b) Ferguson, G.; Ruhl, B. L. *Acta Crystallogr. C* **1984**, *40*, 2020–2022.



analogue.<sup>4,19</sup> This may be explained if decomposition of the latter involves migration of the alkyl group onto a coordinated olefin as demonstrated<sup>20</sup> for the pentafluorophenyl analogue. This type of migration is expected to be less favorable for the chloromethyl group. The *trans*-bis(phosphine) derivatives **9** and **10** are also very stable, as has been found by others<sup>21</sup> for similar complexes.

For the remaining complexes examined in this study, three distinct modes of apparently spontaneous reaction involving the chloromethyl group have been observed, namely, (i) replacement of halogen by ligand, (ii) oxidation to formaldehyde, and (iii) coupling to give ethene and propene. These reactions are discussed below.

**(i) Replacement.** Nucleophilic replacement of the halogen in (halomethyl)metal derivatives has been reported<sup>22</sup> for a wide range of transition metals and nucleophiles. In the present study, the only complex that suffers an apparently spontaneous reaction of this nature is the chelating bis(sulfide) complex **2**. The conversion of **2** into the ylide **15** may be envisaged to involve initial cleavage of the Pd-S bond *trans* to C followed by intramolecular attack of this S atom on the chloromethyl moiety. The coordination site vacated by the sulfur ligand may be occupied initially by e.g. solvent, ubiquitous water, or bridging chloride. Failure of the chelating amine and phosphine ligand complexes to behave similarly can then be rationalized on the basis of the lower lability of Pd-N and Pd-P bonds *vs* Pd-S bonds. Conversion of the pyridine complex **7** into the ylide **13** requires the presence of excess pyridine. This conversion could proceed *via* direct external nucleophilic attack of pyridine at carbon or by migration of a pyridine molecule within a five-coordinate species. Formation of ylide complexes by mechanisms of these types has been discussed by several authors.<sup>22e,23</sup>

**(ii) Oxidation to Formaldehyde.** While alkyl derivatives of palladium are generally prepared under inert atmosphere conditions and can usually be handled under air as solids, there appears to have been no systematic study of their stability under air in solution. However, in a recent publication,<sup>24</sup> it is reported that certain methyl-, benzyl-, and arylpalladium(II) complexes containing planar bidentate nitrogen ligands are stable for several days in chloroform at 20 °C in air. This contrasts with our observations for several of the chloromethyl derivatives, in particular the bipyridine complex **6**. Reports have appeared of light-induced

reactions of certain organopalladium derivatives with oxygen,<sup>25</sup> and recently there has been considerable interest in the generation of oxygenated products by reaction of organopalladium complexes with both organic and inorganic peroxides.<sup>26</sup>

In the case of the compounds studied here, formaldehyde appears to be the only, or at least major, organic product of oxidation. The relative reactivities of the complexes suggest that oxygenation is accelerated by increasing electron density at the metal center, with the sulfide and amine complexes [other than the lutidine derivative **8**] being the most reactive and the olefin and phosphine complexes the least reactive. A similar observation has been made for the oxidation of organopalladium derivatives with *tert*-butyl hydroperoxide.<sup>26a</sup> The stability of the lutidine derivative may indicate that access of the oxidizing species to the metal is necessary for reaction to proceed.

**(iii) Formation of Ethene and Propene.** This coupling was only observed for the *cis* phosphine complexes and, to our knowledge,<sup>27</sup> is the first instance in which ethene (and propene) has been identified as a major product from the decomposition of a mono-(chloromethyl) derivative of a transition metal. We have considered three basic possibilities [(a)-(c) below] for the generation of ethene, but none appear to be entirely satisfactory. (a) Examples of ethene production *via* dimerization of carbene species have been known for almost 30 years.<sup>28</sup> A similar process could be envisaged in the present case proceeding *via* initial ionization of the C-Cl bond. However, the platinum analogues, which would be expected to undergo this type of ionization more readily (see above), are stable under the same conditions. Thus, unless such platinum carbenes do not couple readily,<sup>29</sup> this mechanism seems unlikely. (b) Disproportionation to give bis(chloromethyl) complexes followed by decomposition of the latter could generate ethene. However, this would require that the intermediate bis(chloromethyl) complexes decompose more readily than the platinum analogues which are stable<sup>3b</sup> under the conditions employed in the present study. The latter do decompose cleanly to give ethene in polar media, and we have suggested that this involves initial generation of cationic carbene species. Such a route seems less likely for palladium. (c) Carbon-carbon coupling could be achieved *via* oxidative addition of one molecule of the PdCH<sub>2</sub>Cl complex to another molecule of the same complex<sup>30</sup> (see Scheme 1). The resulting adduct could conceivably undergo either reductive elimination, to give a  $\beta$ -chloroethyl palladium species, or

(19) Rudler-Chauvin, M.; Rudler, H. *J. Organomet. Chem.* **1977**, *134*, 115-119.

(20) Albeniz, A. C.; Espinet, P.; Jeannin, Y.; Piloche-Levisalles, M.; Mann, B. E. *J. Am. Chem. Soc.* **1990**, *112*, 6594-6600.

(21) (a) Leoni, P. *Organometallics* **1993**, *12*, 2432-2434. (b) Huser, M.; Youinou, M. T.; Osborn, J. A. *Angew. Chem., Int. Ed. Engl.* **1989**, *28*, 1386-1388.

(22) For leading references see: (a) Reference 1. (b) Hubbard, J. L.; McVicar, W. K. *J. Organomet. Chem.* **1992**, *429*, 369-378. (c) Friedrich, H. B.; Moss, J. R. *Adv. Organomet. Chem.* **1991**, *33*, 235-290. (d) Hoover, J. F.; Stryker, J. M. *J. Am. Chem. Soc.* **1990**, *112*, 464-465. (e) Werner, H.; Wilfried P.; Feser, R.; Zolk, R.; Thometzek, P. *Chem. Ber.* **1985**, *118*, 261-274.

(23) See for example: (a) Alcock, N. W.; Pringle, P. G.; Bergamini, P.; Sostero, S.; Traverso O. *J. Chem. Soc., Dalton Trans.* **1990**, 1553-1556. (b) Marder, T. B.; Fultz, W. C.; Calabrese, J. C.; Harlow, R. L.; Milstein, D. *J. Chem. Soc., Chem. Commun.* **1987**, 1543-1545. (c) Engelter, C.; Moss, J. R.; Nassimbeni, L. R.; Niven, M. L.; Reid, G.; Spiers, J. C. *J. Organomet. Chem.* **1986**, *315*, 255-268. (d) Werner, H.; Hofmann, L.; Feser, R.; Paul, W. *J. Organomet. Chem.* **1985**, *281*, 317-347.

(24) van Asselt, R.; Vrieze, K.; Elsevier, C. J. *J. Organomet. Chem.* **1994**, *480*, 27-40.

(25) (a) Vicente, J.; Areas, A.; Bautista, D.; Shul'pin, G. B. *J. Chem. Soc., Dalton Trans.* **1994**, 1505-1509. (b) Muzart, J.; Riahi, A. *Organometallics* **1992**, *11*, 3478-3481.

(26) For leading references see: (a) Alsters, P. L.; Teunissen, H. T.; Boersma, J.; Spek, A. L.; van Koten, G. *Organometallics* **1993**, *12*, 4691-4696. (b) Alsters, P. L.; Boersma, J.; van Koten, G. *Organometallics* **1993**, *12*, 1629-1638.

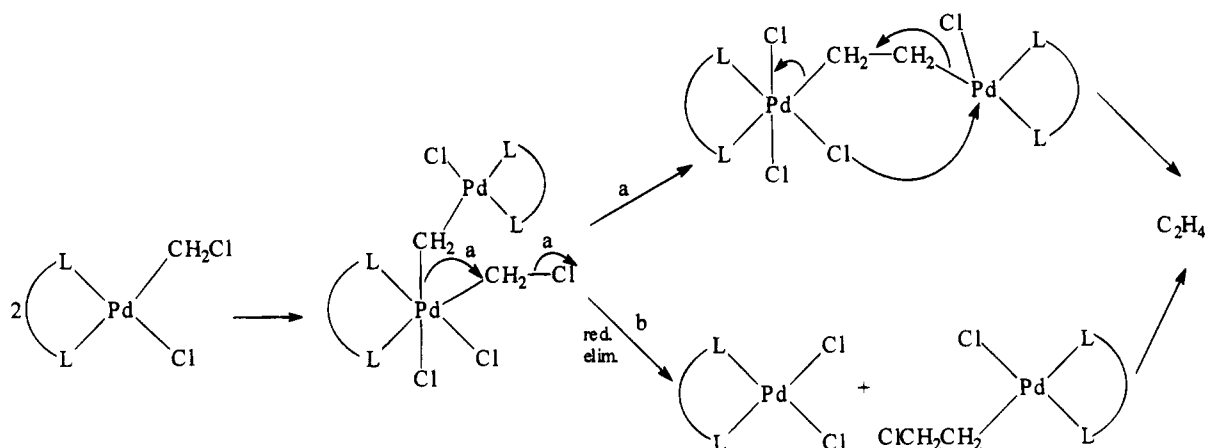
(27) Ethylene was suggested to be the likely product from decomposition of *trans*-[(*n*-Bu<sub>3</sub>P)<sub>2</sub>Pt(CH<sub>2</sub>Cl)Cl] (Young, G. B.; Whitesides, G. M. *J. Am. Chem. Soc.* **1978**, *100*, 5808-5815.). However later studies<sup>3b</sup> indicate that formaldehyde was probably generated from the CH<sub>2</sub>Cl fragment.

(28) For leading references see: (a) Hayes, J. C.; Jernakoff, P.; Miller, G. A.; Cooper, N. *J. Pure Appl. Chem.* **1984**, *56*, 25-33. (b) Merrifield, J. H.; Lin, G.-Y.; Kiel, W. A.; Gladysz, J. A. *J. Am. Chem. Soc.* **1983**, *105*, 5811-5819.

(29) It has been reported that the labile molybdenum methyldiene [(*n*-C<sub>5</sub>H<sub>5</sub>)Mo(CO)<sub>2</sub>(PPh<sub>3</sub>)<sub>2</sub>(=CH<sub>2</sub>)]<sup>+</sup>CF<sub>3</sub>SO<sub>3</sub><sup>-</sup> couples at >ca. -70 °C and the tungsten analogue at >ca. -20 °C. Kegley, S. E.; Brookhart, M.; Husk, G. R. *Organometallics* **1982**, *1*, 760-762.



Scheme 1



rearrangement to a 1,2-dipalladioethane species, both of which would be expected to decompose with release of ethene. If such a mechanism is operative, it is perhaps surprising that the bipyridine complex **6**, even on prolonged storage, gives no detectable ethene although the chelating nitrogen ligand is expected<sup>31</sup> to facilitate oxidative addition reactions relative to the chelating phosphines. Overall, however, this mechanism may be the mostly likely of the three possibilities discussed.

Propene is presumably formed by reaction of ethene with the palladium chloromethyl complexes **11** and **12** via olefin coordination, chloromethyl group migration to give a ( $\gamma$ -chloropropyl)palladium complex,  $\beta$ -hydride elimination/readdition, and finally  $\beta$ -chloride elimination.

### Experimental Section

Unless indicated otherwise, <sup>1</sup>H NMR and <sup>31</sup>P NMR spectra were acquired using CDCl<sub>3</sub> solutions (residual proton resonance at  $\delta$  7.24 as reference and phosphorus resonance of triphenylphosphine in CDCl<sub>3</sub> at  $\delta$  -5.3 as external reference, respectively). Immediately prior to use, CDCl<sub>3</sub> was passed through a short plug of anhydrous potassium carbonate. Elemental analyses were determined by Galbraith Laboratories, Inc., Knoxville, TN, or Guelph Chemical Laboratories Ltd., Guelph, Ont, Canada. Analytical and preparative-scale thin layer chromatography (TLC) were performed on Kieselgel G (Merck). Silica gel for flash chromatography (Fisher, 230–425 mesh) was used for short column cleanup of reaction mixtures.

**Preparation of the Complexes.** The complexes were prepared from [Pd(CH<sub>2</sub>Cl)Cl(COD)] (**1**) in essentially quantitative yield by ligand exchange and were purified by preparative TLC and/or crystallization unless otherwise noted. The (COD) complex **1** was obtained as described<sup>4</sup> earlier except that the treatment with diazomethane was carried out at ice-bath temperature, solvent was evaporated at low temperature (rapid darkening of the reaction mixture), and the resulting material was passed through a short plug of silica gel in dichloromethane to give a clear yellow solution.

**Stabilities of the Complexes.** In general, the stabilities of the complexes (0.01–0.05 mmol) were monitored by <sup>1</sup>H and,

where appropriate, by <sup>31</sup>P NMR spectroscopy for solutions in CDCl<sub>3</sub> in 5 mm tubes which were kept at ambient temperature in the dark.

**Complexes containing Sulfur Ligands.** (a) **Chloro-(chloromethyl)(4,4-diethyl-2,6-dithiaheptane)palladium(II)**<sup>4</sup> (**2**). (i) This complex, when stored in solution in a tube protected only by a plastic cap, decomposed relatively cleanly to the corresponding dichloro complex<sup>4</sup> (**14**) during 2 days. (ii) When the sample was stored in a sealed tube under air, decomposition to the dichloro complex occurred more slowly. When decomposition was complete (ca. 1 week), the <sup>1</sup>H NMR spectrum also showed signals attributable<sup>3b</sup> to monomeric and oligomeric formaldehyde species and a minor amount of a second palladium-containing complex (**15**). In one case, the resulting solution was treated with excess ethanolic 2,4-dinitrophenylhydrazine reagent and the resulting formaldehyde derivative isolated and identified, as described<sup>3b</sup> previously. (iii) When solutions of **2** were sealed under vacuum after several freeze/pump/thaw cycles, slow decomposition to the sulfur ylide complex **15** (ca. 40% after 1 month; added D<sub>2</sub>O had no detectable effect) was observed. Preparative TLC (dichloromethane/methanol, 97:3) of the mixture gave pure *dichloro[(2,2-diethyl-4-thia-1-pentyl)methylsulfonium methylidene-C,S]palladium(II)*, mp 144–147 °C (from methanol/dichloromethane/hexane): <sup>1</sup>H NMR (CDCl<sub>3</sub>/CD<sub>3</sub>OD, 200 MHz)  $\delta$  0.93 (t,  $J_{H-H} = 7.3$  Hz, 3 H, Me-C), 0.95 (t,  $J_{H-H} = 7.3$  Hz, 3 H, Me-C), 1.59 (q,  $J_{H-H} = 7.3$  Hz, 2 H, CH<sub>2</sub>-C), 1.65 (q,  $J_{H-H} = 7.3$  Hz, 2 H, CH<sub>2</sub>-C), 2.60 (s, 3 H, Me-S), 2.62 (d,  $J_{H-H} = 13$  Hz, 1 H, CH<sub>2</sub>-S), 2.68 (d,  $J_{H-H} = 13$  Hz, 1 H, CH<sub>2</sub>-S), 2.78 (d,  $J_{H-H} = 11.5$  Hz, 1 H, CH<sub>2</sub>-S), 2.97 (s, 3 H, Me-S), 3.49 (d,  $J_{H-H} = 11.5$  Hz, 1 H, CH<sub>2</sub>-S), 3.52 (brs, 2 H, CH<sub>2</sub>-S). Anal. Calcd for C<sub>10</sub>H<sub>22</sub>Cl<sub>2</sub>PdS<sub>2</sub>: C, 31.31; H, 5.79. Found: C, 31.32; H, 5.81.

(b) **Complexes of Dimethyl Sulfide.** The (COD) complex **1** (33 mg, 0.11 mmol) was reacted with dimethyl sulfide (45  $\mu$ L, 0.62 mmol) in dichloromethane (2 mL), and the solvent was then evaporated in a stream of nitrogen. The resulting yellow solid was crystallized from dichloromethane/pentane to give *bis(chloromethyl)bis(dimethyl sulfide)bis( $\mu$ -chloro)dipalladium(II)* (**3**): <sup>1</sup>H NMR (CDCl<sub>3</sub>, 200 MHz)  $\delta$  2.47 (s, 12 H, Me's), 3.78 (s, 4 H, CH<sub>2</sub>'s). Anal. Calcd for C<sub>6</sub>H<sub>16</sub>Cl<sub>4</sub>Pd<sub>2</sub>S<sub>4</sub>: C, 14.22; H, 3.18. Found: C, 14.19; H, 2.96. (i) When solutions of **3** were sealed under air, <sup>1</sup>H NMR peaks ascribable to formaldehyde and [Cl<sub>2</sub>PdSMe<sub>2</sub>]<sub>2</sub> slowly increased in intensity over several weeks. (ii) Over a period of 2 weeks, no change was observed in the <sup>1</sup>H NMR spectrum of solutions of **3** which had been sealed under vacuum.

Excess dimethyl sulfide was added in small increments to a solution of the dimeric species **3**. The final solution showed singlets in its <sup>1</sup>H NMR spectrum (CDCl<sub>3</sub>, 200 MHz) at  $\delta$  2.26

(30) Formation of stable adducts of this type has been reported for reaction of Me<sub>2</sub>Pt(bipy) (bipy = 2,2'-bipyridine) with (chloromethyl)gold(I) and (chloromethyl)mercury(II) derivatives, the metal (Au or Hg) having a strong activating effect on the C–Cl bond in these reactions: Arsenault, G. J.; Crespo, M.; Puddephatt, R. J. *Organometallics* **1987**, *6*, 2255–2256.

(31) (a) van Asselt, R.; Rijnberg, E.; Elsevier, C. J. *Organometallics* **1994**, *13*, 706–720. (b) Canty, A. J. *Acc. Chem. Res.* **1992**, *25*, 83–90.

(br) and 3.53. This solution was then allowed to sit under air (some evaporative loss of dimethyl sulfide and of formaldehyde occurs) for 3 weeks with occasional topping of solvent. By this time, the singlet at  $\delta$  3.53 was no longer detectable and the spectrum contained singlets at  $\delta$  2.13 (br), 2.25, 2.39, 2.60, 2.85, and 2.88. In spectra run during the first few days a weak singlet at  $\delta$  9.70 arising from formaldehyde was present.

**Complexes Containing Nitrogen Ligands.** (a) **Chloro(chloromethyl)(*N,N,N',N'*-tetramethylethylenediamine)-palladium(II)<sup>4</sup> (5).** (i) A <sup>1</sup>H NMR spectrum of a solution of **5** that had been protected by a plastic cap contained signals for only the dichloro analogue of **5** after 4 days. (ii) When the previous experiment was repeated with a solution that had been sealed under air, the rate of decomposition was reduced and <sup>1</sup>H NMR signals attributable to formaldehyde were present. (iii) Complex **5** showed no evidence of decomposition after two weeks in CDCl<sub>3</sub> under vacuum.

(b) **Chloro(chloromethyl)(2,2'-bipyridine)palladium(II) (6).** Reaction of [Pd(CH<sub>2</sub>Cl)Cl(COD)] (50.1 mg, 0.17 mmol) in dichloromethane (0.5 mL) with 2,2'-bipyridine (29.0 mg, 0.19 mmol) in the same solvent (1 mL) under N<sub>2</sub> gave an immediate crystalline precipitate. The supernatant was removed by syringe, and the crystals were washed with fresh dichloromethane and dried *in vacuo* to give *chloro(chloromethyl)(2,2'-bipyridine)palladium(II) (6)*: <sup>1</sup>H NMR (CDCl<sub>3</sub>, 400 MHz)  $\delta$  4.05 (s, 2 H, CH<sub>2</sub>), 7.49 (m, 1 H, aryl), 7.61 (m, 1 H, aryl), 7.97 (m, 2 H, aryl), 8.05 (m, 2 H, aryl), 8.90 (m, 1 H, aryl), 9.20 (m, 1 H, aryl). Anal. Calcd for C<sub>11</sub>H<sub>10</sub>Cl<sub>2</sub>N<sub>2</sub>Pd: C, 38.02; H, 2.90; N, 8.06. Found: C, 37.97; H, 2.63; N, 7.82. Because of the very low solubility of **6** in CDCl<sub>3</sub>, decomposition studies were carried out in 10 mm NMR tubes. (i) A <sup>1</sup>H NMR spectrum of a solution of **6** that had been stored under air for 5 days contained signals attributable to only the related dichloro complex and to formaldehyde species. (ii) A similar solution that had been sealed under vacuum showed no new <sup>1</sup>H NMR signals after 2 weeks. Even after 1 year no signals attributable to ethene or propene could be detected.<sup>32</sup>

(c) **trans-Chloro(chloromethyl)bis(pyridine)palladium(II) (7).** Pyridine (20  $\mu$ L, 0.25 mmol) was added to a solution of [Pd(CH<sub>2</sub>Cl)Cl(COD)] (30 mg, 0.10 mmol) in dichloromethane (1 mL) under nitrogen. After 5 min pentane was added and the resulting off-white precipitate was washed with pentane and dried *in vacuo* to give *trans-chloro(chloromethyl)bis(pyridine)palladium(II) (7)*: <sup>1</sup>H NMR (CDCl<sub>3</sub>, 200 MHz)  $\delta$  3.49 (s, 2 H, CH<sub>2</sub>), 7.38 (m, 4 H, aryl), 7.79 (m, 2 H, aryl), 8.97 (m, 4 H, aryl). Anal. Calcd for C<sub>11</sub>H<sub>12</sub>Cl<sub>2</sub>N<sub>2</sub>Pd: C, 37.80; H, 3.46; N, 8.01. Found: C, 37.85; H, 3.27; N, 7.65. This material contained a trace of the ylide complex **13** (see below). (i) When kept in CDCl<sub>3</sub> under air, ca. 50% of **7** was converted into the dichloride in 5 days. (ii) A solution of **7** was unchanged after 16 days under vacuum. (iii) When **7** (15 mg, 0.043 mmol) and pyridine (3  $\mu$ L, 0.038 mmol) were kept in CDCl<sub>3</sub> under vacuum for 16 days, the magnitude of the resonances for free pyridine remained unchanged in the <sup>1</sup>H NMR spectra but the signals for **7** were replaced by those<sup>10</sup> for **13**: <sup>1</sup>H NMR (CDCl<sub>3</sub>, 200 MHz)  $\delta$  4.99 (s, 2 H, CH<sub>2</sub>), 7.27 (m, 2 H, aryl), 7.63 (m, 3 H, aryl), 8.10 (m, 1 H, aryl), 8.84 (m, 2 H, aryl), 9.07 (m, 2 H, aryl).

(d) **trans-Chloro(chloromethyl)bis(2,6-lutidine)palladium(II) (8).** 2,6-Lutidine (50  $\mu$ L, 0.43 mmol) was added to a solution of [Pd(CH<sub>2</sub>Cl)Cl(COD)] (30 mg, 0.10 mmol) in dichloromethane (0.5 mL) under nitrogen. Upon standing overnight, a crystalline solid was deposited. The supernatant was removed, and the solid was washed with pentane and dried *in vacuo* to give *trans-chloro(chloromethyl)bis(2,6-lutidine)palladium(II) (8)*: <sup>1</sup>H NMR (CDCl<sub>3</sub>, 200 MHz)  $\delta$  3.32

(s, 2 H, CH<sub>2</sub>), 3.39 (s, 12 H, Me's), 7.13 (m, 4 H, aryl), 7.55 (m, 2 H, aryl). Anal. Calcd for C<sub>15</sub>H<sub>20</sub>Cl<sub>2</sub>N<sub>2</sub>Pd: C, 44.41; H, 4.97; N, 6.91. Found: C, 44.44; H, 4.62; N, 6.67. A <sup>1</sup>H NMR spectrum of a solution of **8** in CDCl<sub>3</sub> kept under air for 6 days was essentially identical to one run initially.

**Complexes Containing Phosphine Ligands.** (a) **[1,2-Bis(diphenylphosphino)ethane]chloro(chloromethyl)-palladium(II) (11)<sup>4</sup> and [1,3-Bis(diphenylphosphino)propane]chloro(chloromethyl)palladium(II) (12)<sup>4</sup>** These complexes exhibited very similar decomposition behavior. Because of the low solubilities of **11** and **12** and the even lower solubilities of the corresponding dichloro complexes, sealed tube reactions were performed with undissolved material present and the tubes were agitated at intervals. (i) <sup>1</sup>H and <sup>31</sup>P NMR spectra of solutions containing **11** or **12** which had been kept under air showed essentially complete decomposition to the dichlorides within 1 month. (ii) <sup>1</sup>H NMR spectra of similar solutions which had been sealed under air contained resonances attributable to formaldehyde species. (iii) When solutions containing **11** or **12** were sealed under vacuum and their decomposition monitored by <sup>31</sup>P NMR, gradual decomposition to the corresponding dichlorides was observed and was complete within 4 months. <sup>1</sup>H NMR spectra of the solutions after decomposition contained strong signals attributable to ethene ( $\delta$  5.38), propene [ $\delta$  1.71 (m, 3 H, Me), 4.95 (m, 2 H, CH<sub>2</sub>), 5.82 (m, 1 H, CH)], and methyl chloride ( $\delta$  3.02). Taken together, these were estimated<sup>3b</sup> to account for 70–80% of the initial CH<sub>2</sub>Cl moiety. The <sup>1</sup>H NMR spectra also showed numerous much weaker resonances which might be attributable to oligomeric products.

(b) **trans-Bis(triethylphosphine)chloro(chloromethyl)-palladium(II) (10).** Et<sub>3</sub>P. AgI (258 mg, 0.732 mmol) in dichloromethane (3 mL) was added to a solution of [Pd(CH<sub>2</sub>Cl)Cl(COD)] (110 mg, 0.366 mmol) in the same solvent (1 mL). Silver iodide precipitated immediately and was filtered off and washed with dichloromethane. The residue resulting from evaporation of solvent from the combined filtrates *in vacuo* was purified by preparative TLC (dichloromethane) and crystallization from pentane at –78 °C to give very pale yellow crystals of *trans-bis(triethylphosphine)chloro(chloromethyl)-palladium(II) (10)*: <sup>1</sup>H NMR (C<sub>6</sub>D<sub>6</sub>, 400 MHz)  $\delta$  0.97 (m, 18 H, Me's), 1.72 (m, 12 H, CH<sub>2</sub>-P), 3.58 (t, *J*<sub>P-H</sub> = 8.9 Hz, 2 H, CH<sub>2</sub>-Cl); <sup>31</sup>P NMR (C<sub>6</sub>D<sub>6</sub>, 161.9 MHz)  $\delta$  18.3. Anal. Calcd for C<sub>13</sub>H<sub>32</sub>Cl<sub>2</sub>P<sub>2</sub>Pd.0.2C<sub>5</sub>H<sub>12</sub>: C, 38.03; H, 7.84. Found: C, 38.28; H, 7.31. (i) <sup>1</sup>H and <sup>31</sup>P NMR spectra of solutions of **10** in C<sub>6</sub>D<sub>6</sub> or CDCl<sub>3</sub>, sealed under air, when acquired after 8 months, were essentially identical to those obtained initially. (ii) A similar result to that just described was obtained when a sample of **10** in C<sub>6</sub>D<sub>6</sub> was sealed under vacuum and stored for three years.

(c) **trans-Bis(triphenylphosphine)chloro(chloromethyl)-palladium(II) (9).** Triphenylphosphine (89.2 mg, 0.340 mmol) in dichloromethane (3 mL) was added to a solution of [Pd(CH<sub>2</sub>Cl)Cl(COD)] (81.0 mg, 0.170 mmol) in the same solvent. The solution was reduced to a volume of ca. 1 mL, and hexane was added. The resulting pale yellow solid was recovered, washed with hexane, and purified by crystallization from dichloromethane–hexane to give crystals of *trans-bis(triphenylphosphine)chloro(chloromethyl)palladium(II) (9)*: <sup>1</sup>H NMR (CDCl<sub>3</sub>, 400 MHz)  $\delta$  2.97 (t, *J*<sub>P-H</sub> = 9.4 Hz, 2 H, CH<sub>2</sub>-Cl) 7.42 (m, 18 H, Ar), 7.77 (m, 12 H, Ar); <sup>31</sup>P NMR (C<sub>6</sub>D<sub>6</sub>, 161.9 MHz)  $\delta$  27.8. Crystals suitable for X-ray studies were deposited from a solution obtained by dissolving the stoichiometric quantity of triphenylphosphine in a solution of [Pd(CH<sub>2</sub>Cl)Cl(COD)] in the minimum volume of dichloromethane. (i) <sup>1</sup>H and <sup>31</sup>P NMR spectra of solutions of **9** which were covered only by plastic caps did not change appreciably when run from time to time over a period of 1 month, as long as the solutions were protected from light. (ii) When a solution of **9** was sealed under vacuum, <sup>1</sup>H and <sup>31</sup>P NMR spectra acquired after 3 years were essentially identical to those obtained initially.

(32) A signal at  $\delta$  3.02 was apparent in a spectrum run at this time and is attributable to CH<sub>3</sub>Cl arising from cleavage of the CH<sub>2</sub>Cl moiety by acid produced from traces of water in the solvent.

**Crystal Structure Analyses.** The crystals of **9** and **17**<sup>33</sup> proved to be isomorphous, and details of the cell data, data collection, structure solution, and refinement parameters are summarized in Table 1.

A view of the Cl-Pd(PPh<sub>3</sub>)<sub>2</sub>-CH<sub>2</sub>-Cl structure (**9**) with our numbering scheme is in Figure 1; as the structures are isomorphous, the corresponding view for the Pt isomer **17** is essentially identical. Principal dimensions are listed in Table 2.

---

(33) McCrimble, R.; Arsenault, G. J.; Farwaha, R.; Hampden-Smith, M. J.; Rice, R. E.; McAlees A. J. *J. Chem. Soc., Dalton Trans.* **1988**, 1773-1780.

**Acknowledgment.** We thank the NSERC, Canada, for financial support.

**Supplementary Material Available:** Tables of positional and thermal parameters, bond distances and angles, and anisotropic thermal parameters and figures showing the crystal shapes (15 pages). Ordering information is given on any current masthead page.

OM9500735

# Synthesis and Photophysics of Luminescent Rhenium(I) Acetylides—Precursors for Organometallic Rigid-Rod Materials. X-ray Crystal Structures of [Re(<sup>t</sup>Bu<sub>2</sub>bpy)(CO)<sub>3</sub>(<sup>t</sup>BuC≡C)] and [Re(<sup>t</sup>Bu<sub>2</sub>bpy)(CO)<sub>3</sub>Cl]

Vivian Wing-Wah Yam,\* Victor Chor-Yue Lau, and Kung-Kai Cheung

Department of Chemistry, The University of Hong Kong, Pokfulam Road, Hong Kong

Received November 29, 1994<sup>⊗</sup>

A series of rhenium(I) diimine acetylide complexes [Re(<sup>t</sup>Bu<sub>2</sub>bpy)(CO)<sub>3</sub>(RC≡C)] (R = <sup>t</sup>Bu (**2**), Me<sub>3</sub>Si (**3**), Ph (**4**)) have been synthesized and shown to exhibit rich photoluminescent behavior at room temperature. The X-ray crystal structures of [Re(<sup>t</sup>Bu<sub>2</sub>bpy)(CO)<sub>3</sub>(<sup>t</sup>BuC≡C)] and its precursor complex [Re(<sup>t</sup>Bu<sub>2</sub>bpy)(CO)<sub>3</sub>Cl] have also been determined. Both **1** and **2** crystallize in the monoclinic space group *P*2<sub>1</sub>/*n* with *a* = 16.814(1) Å, *b* = 12.195(1) Å, *c* = 22.599(2) Å, and β = 100.87(1)° for **1** and *a* = 11.116(1) Å, *b* = 13.128(1) Å, *c* = 18.328(2) Å, and β = 94.49(1)° for **2**.

## Introduction

The study of metal-to-ligand charge transfer (MLCT) excited states has attracted enormous attention over the past few decades. The most extensively studied system is the d<sup>6</sup> metal polypyridine complexes of Ru(II) and Re(I), some of which have been widely used as building blocks for synthesizing redox-active and luminescent supramolecular metal complexes.<sup>1</sup> With our recent interest in the photophysical studies of mononuclear and polynuclear organometallic systems,<sup>2</sup> in particular the acetylide complexes,<sup>2c–g</sup> a program was initiated to investigate the possibility of incorporating acetylide moieties into the MLCT excited states. We believe that the introduction of these good σ-donor ligands would render the metal center more electron rich, with the additional advantage of raising the energy of the d–d states which would improve the population of the MLCT state.<sup>2b</sup> In addition, acetylides are ideal moieties for the synthesis of rigid-rod organometallics, in particular with the increasing attention on materials having nonlinear optical and/or liquid crystalline properties.<sup>3,4</sup> In this paper, we report on the synthesis and photophysics of

a series of rhenium(I) diimine acetylides. The X-ray crystal structures of [Re(<sup>t</sup>Bu<sub>2</sub>bpy)(CO)<sub>3</sub>(<sup>t</sup>BuC≡C)] and its precursor complex [Re(<sup>t</sup>Bu<sub>2</sub>bpy)(CO)<sub>3</sub>Cl] are also described.

## Experimental Section

**Materials and Reagents.** [Re(CO)<sub>5</sub>Cl] was obtained from Strem Chemicals, Inc. Phenylacetylene and 3,3-dimethylbut-1-yne were obtained from Aldrich Chemical Co. (Trimethylsilyl)acetylene was purchased from Lancaster Synthesis Ltd. Tetrahydrofuran was distilled over sodium benzophenone ketyl. All other solvents were purified and distilled using standard procedures before use.<sup>5</sup> All other reagents were of analytical grade and were used as received.

**Syntheses of Rhenium Complexes.** All reactions were carried out in the dark under anaerobic and anhydrous conditions using standard Schlenk techniques.

**[Re(<sup>t</sup>Bu<sub>2</sub>bpy)(CO)<sub>3</sub>Cl] (**1**).** This was synthesized by a literature procedure.<sup>6</sup> <sup>1</sup>H NMR (270 MHz, acetone-*d*<sub>6</sub>, 298 K, relative to TMS): δ 1.4 (s, 18H, <sup>t</sup>Bu), 7.6 (dd, 2H, 5- and 5'-pyridyl H's), 8.1 (d, 2H, 3- and 3'-pyridyl H's), 9.0 (d, 2H, 6- and 6'-pyridyl H's). IR (Nujol mull, cm<sup>-1</sup>): ν(CO) 2021, 1921, 1910, 1889. Positive FAB-MS: ion clusters at *m/z* 574 {M}<sup>+</sup>, 539 {M – Cl}<sup>+</sup>. UV–vis (THF, 298 K; λ/nm (ε/(dm<sup>3</sup> mol<sup>-1</sup> cm<sup>-1</sup>)): 292 sh (22 090), 314 sh (8270), 384 (3905).

**[Re(<sup>t</sup>Bu<sub>2</sub>bpy)(CO)<sub>3</sub>(<sup>t</sup>BuC≡C)] (**2**).** A solution of complex **1** (100 mg, 0.174 mmol) in THF (10 mL) was treated at –40 °C with a solution of <sup>t</sup>BuC≡CLi (0.575 mmol) in THF (10 mL), prepared *in situ* from <sup>t</sup>BuC≡CH and <sup>n</sup>BuLi, under an inert atmosphere of nitrogen, followed by stirring at room temperature for 24 h. Water was then added to destroy the unreacted <sup>t</sup>BuC≡CLi. The product was extracted with a THF/diethyl ether mixture, dried over anhydrous magnesium sulfate, and filtered and the filtrate was reduced in volume and purified by column chromatography on silica gel using petroleum ether–diethyl ether (1/1 v/v) as eluent. The first band, containing the unreacted acetylene, was discarded, and the second band is the required product. Subsequent recrystallization from a diethyl ether–*n*-hexane mixture gave orange crystals of **2** (yield 49 mg, 45%). <sup>1</sup>H NMR (270 MHz, acetone-*d*<sub>6</sub>, 298 K, relative to TMS): δ 0.7, (s, 9H, <sup>t</sup>BuC≡C), 1.4 (s,

\* Abstract published in *Advance ACS Abstracts*, May 1, 1995.

(1) Balzani, V.; Scandola, F. *Supramolecular Photochemistry*; Ellis Horwood: Chichester, U.K., 1991. Kalyanasundaram, K. *Photochemistry of Polypyridine and Porphyrin Complexes*; Academic Press: London, 1992. Horváth, O.; Stevenson, K. L. *Charge Transfer Photochemistry of Coordination Compounds*; VCH: New York, 1993.

(2) (a) Yam, V. W. W.; Tam, K. K.; Lai, T. F. *J. Chem. Soc., Dalton Trans.* **1993**, 651. (b) Yam, V. W. W.; Choi, S. W. K.; Lai, T. F.; Lee, W. K. *J. Chem. Soc., Dalton Trans.* **1993**, 1001. (c) Yam, V. W. W.; Chan, L. P.; Lai, T. F. *Organometallics* **1993**, *12*, 2197. (d) Yam, V. W. W.; Lee, W. K.; Lai, T. F. *Organometallics* **1993**, *12*, 2383. (e) Yam, V. W. W.; Chan, L. P.; Lai, T. F. *J. Chem. Soc., Dalton Trans.* **1993**, 2075. (f) Yam, V. W. W.; Lee, W. K.; Yeung, P. K. Y.; Phillips, D. *J. Phys. Chem.* **1994**, *98*, 7545. (g) Müller, T. E.; Choi, S. W. K.; Mingos, D. M. P.; Murphy, D.; Williams, D. J.; Yam, V. W. W. *J. Organomet. Chem.* **1994**, *484*, 209. (h) Yam, V. W. W.; Choi, S. W. K. *J. Chem. Soc., Dalton Trans.* **1994**, 2057. (i) Yam, V. W. W.; Lee, V. W. M.; Cheung, K. K. *J. Chem. Soc., Chem. Commun.* **1994**, 2075.

(3) Marder, S. R.; Sohn, J. E.; Stucky, G. D., Eds. *Materials for Nonlinear Optics: Chemical Perspectives*; ACS Symposium Series 455; American Chemical Society: Washington, DC, 1991. Bruce, D. W.; O'Hare, D., Eds. *Inorganic Materials*; Wiley: Chichester, U.K., 1992.

(4) Weidmann, T.; Weinrich, V.; Wagner, B.; Robl, C.; Beck, W. *Chem. Ber.* **1991**, *124*, 1363. Jia, G.; Puddephatt, R. J.; Vittal, J. J.; Payne, N. C. *Organometallics* **1993**, *12*, 263. Khan, M. S.; Kakkar, A. K.; Ingham, S. L.; Raithby, P. R.; Lewis, J.; Spencer, B.; Wittmann, F.; Friend, R. H. *J. Organomet. Chem.* **1994**, *472*, 247.

(5) Perrin, D. D.; Armarego, W. L. F.; Perrin, D. R. *Purification of Laboratory Chemicals*, 2nd ed.; Pergamon: Oxford, U.K., 1980.

(6) Wrighton, M. S.; Morse, D. L. *J. Am. Chem. Soc.* **1974**, *96*, 998. Wrighton, M. S.; Morse, D. L.; Pdungsap, L. *J. Am. Chem. Soc.* **1975**, *97*, 2073.

**Table 1. Crystal and Structure Determination Data for 1**

formula	ReClO <sub>3</sub> N <sub>2</sub> C <sub>21</sub> H <sub>24</sub>
fw	574.09
T, K	298
a, Å	16.814(1)
b, Å	12.195(1)
c, Å	22.599(2)
β, deg	100.87(1)
V, Å <sup>3</sup>	4550.7(6)
cryst syst	monoclinic
space group	P2 <sub>1</sub> /n
Z	8
F(000)	2240
D <sub>c</sub> , g cm <sup>-3</sup>	1.544
cryst dimens, mm	0.20 × 0.20 × 0.50
λ, Å (graphite monochromated, Mo Kα)	0.710 69
μ, cm <sup>-1</sup>	46.45
transmissn factors	0.419–1.000
collection range, deg	2θ <sub>max</sub> = 45 (h, 0–18; k, 0–13; l: –23 to +23)
scan mode and scan speed, deg min <sup>-1</sup>	ω–2θ; 16.0
scan width, deg	1.42 + 0.35 tan θ
no. of data collected	6555
no. of unique data	6306
no. of data used in refinement, m	4933
no. of parameters refined, p	505
R <sup>a</sup>	0.027
R <sub>w</sub> <sup>a</sup>	0.034
goodness of fit, S	2.15
max shift, (Δ/σ) <sub>max</sub>	0.03
residual extrema in final diff map	+0.68, –1.17

<sup>a</sup>  $w = 4F_o^2/\sigma^2(F_o^2)$ , where  $\sigma^2(F_o^2) = \sigma^2(I) + (0.011F_o^2)^2$  with  $I \geq 3\sigma(I)$ .

18H, <sup>t</sup>Bu), 7.7 (dd, 2H, 5- and 5'-pyridyl H's), 8.7 (d, 2H, 3- and 3'-pyridyl H's), 8.9 (d, 2H, 6- and 6'-pyridyl H's). IR (Nujol mull, cm<sup>-1</sup>): ν(C≡C) 2088, ν(CO) 2003, 1907, 1881. Positive FAB-MS: ion clusters at *m/z* 619 {M}<sup>+</sup>, 591 {M – CO}<sup>+</sup>, 563 {M – 2CO}<sup>+</sup>, 538 {M – <sup>t</sup>BuC≡C}<sup>+</sup>. UV–vis (λ/nm (ε/(dm<sup>3</sup> mol<sup>-1</sup> cm<sup>-1</sup>)): in THF at 298 K, 300 sh (20 765), 328 sh (3040), 421 (3480); in MeOH at 298 K, 275 sh (10 610), 292 (12 940), 391 (2370); in Me<sub>2</sub>CO at 298 K, 402 (3510); in CH<sub>2</sub>Cl<sub>2</sub> at 298 K, 297 (15 500), 410 (2500); in PhMe at 298 K, 301 (17 630), 439 (2740).

**[Re(<sup>t</sup>Bu<sub>2</sub>bpy)(CO)<sub>3</sub>(Me<sub>3</sub>SiC≡C)] (3).** The procedure is similar to that described for the preparation of **2**, except (trimethylsilyl)acetylene was used in place of 3,3-dimethylbut-1-yne to give orange crystals of **3** (44 mg, 40%). <sup>1</sup>H NMR (270 MHz, acetone-*d*<sub>6</sub>, 298 K): δ –0.3 (s, 9H, Me<sub>3</sub>Si–), 1.5 (s, 18H, <sup>t</sup>Bu), 7.8 (dd, 2H, 5- and 5'-pyridyl H's), 8.7 (d, 2H, 3- and 3'-pyridyl H's), 8.9 (d, 2H, 6- and 6'-pyridyl H's). IR (Nujol mull, cm<sup>-1</sup>): ν(C≡C) 2036, ν(CO) 2003, 1907, 1887. UV–vis (THF, 298 K; λ/nm (ε/(dm<sup>3</sup> mol<sup>-1</sup> cm<sup>-1</sup>)): 296 sh (21 060), 406 (3550). Anal. Calcd for C<sub>26</sub>H<sub>33</sub>N<sub>2</sub>O<sub>3</sub>SiRe: C, 49.11; H, 5.23; N, 4.41. Found: C, 49.46; H, 4.95; N, 4.58.

**[Re(<sup>t</sup>Bu<sub>2</sub>bpy)(CO)<sub>3</sub>(PhC≡C)] (4).** The procedure is similar to that described for the preparation of **2**, except phenylacetylene was used in place of 3,3-dimethylbut-1-yne to give orange crystals of **4** (46 mg, 40%). <sup>1</sup>H NMR (270 MHz, acetone-*d*<sub>6</sub>, 298 K, relative to TMS): δ 1.4 (s, 18H, <sup>t</sup>Bu), 6.7–7.0 (m, 5H, PhC≡C), 7.8 (dd, 2H, 5- and 5'-pyridyl H's), 8.8 (d, 2H, 3- and 3'-pyridyl H's), 9.0 (d, 2H, 6- and 6'-pyridyl H's). IR (Nujol mull, cm<sup>-1</sup>): ν(C≡C) 2094, ν(CO) 2001, 1912, 1899, 1890, 1867. UV–vis (THF, 298 K; λ/nm (ε/(dm<sup>3</sup> mol<sup>-1</sup> cm<sup>-1</sup>)): 325 sh (11 550), 419 (3485). Anal. Calcd for C<sub>29</sub>H<sub>29</sub>N<sub>2</sub>O<sub>3</sub>Re. 1/6 C<sub>6</sub>H<sub>14</sub>: C, 55.09; H, 4.79; N, 4.28. Found: C, 55.27; H, 4.47; N, 4.45.

**Physical Measurements and Instrumentation.** UV–visible spectra were obtained on a Milton Roy Spectronic 3000 diode array spectrophotometer, IR spectra were obtained as Nujol mulls on a Bio-Rad FTS-7 Fourier-transform infrared spectrophotometer (4000–400 cm<sup>-1</sup>), and steady-state excitation and emission spectra were obtained on a Spex Fluorolog

**Table 2. Crystal and Structure Determination Data for 2**

formula	ReO <sub>3</sub> N <sub>2</sub> C <sub>27</sub> H <sub>33</sub>
fw	619.78
T, K	298
a, Å	11.116(1)
b, Å	13.128(1)
c, Å	18.328(2)
β, deg	94.49(1)
V, Å <sup>3</sup>	2666.4(4)
cryst syst	monoclinic
space group	P2 <sub>1</sub> /n
Z	4
F(000)	1232
D <sub>c</sub> , g cm <sup>-3</sup>	1.544
cryst dimens, mm	0.10 × 0.15 × 0.20
λ, Å (graphite monochromated, Mo Kα)	0.710 69
μ, cm <sup>-1</sup>	46.45
transmissn factors	0.697–1.000
collection range, deg	2θ <sub>max</sub> = 50 (h, 0–13; k, 0–15; l: –21 to +21)
scan mode and scan speed, deg min <sup>-1</sup>	ω–2θ; 16.0
scan width, deg	1.31 + 0.35 tan θ
no. of data collected	5207
no. of unique data	4939
no. of data used in refinement, m	3049
no. of params refined, p	298
R <sup>a</sup>	0.027
R <sub>w</sub> <sup>a</sup>	0.025
goodness of fit, S	1.63
max shift, (Δ/σ) <sub>max</sub>	0.01
residual extrema in final diff map	+0.71, –0.53

<sup>a</sup>  $w = 4F_o^2/\sigma^2(F_o^2)$ , where  $\sigma^2(F_o^2) = \sigma^2(I) + (0.001F_o^2)^2$  with  $I \geq 3\sigma(I)$ .

111 spectrofluorometer. Low-temperature (77 K) spectra were recorded by using an optical Dewar sample holder. <sup>1</sup>H NMR spectra were recorded on a JEOL JNM-GSX270 Fourier-transform NMR spectrometer with chemical shifts reported relative to TMS. Positive ion FAB mass spectra were recorded on a Finnigan MAT95 mass spectrometer. Elemental analyses of the new complexes were performed by Butterworth Laboratories Ltd.

Luminescence quantum yields, φ, were measured at room temperature by the Parker-Rees method using [Ru(bpy)<sub>3</sub>]<sup>2+</sup> as a standard.<sup>7</sup> Emission-lifetime measurements were performed using a conventional laser system. The excitation source was the 355-nm output (third harmonic) of a Quanta-Ray Q-switched DCR-3 pulsed Nd-YAG laser (10 Hz, G-resonator). Luminescence decay signals were recorded on a Tektronix Model 2430 digital oscilloscope and analyzed using a program for exponential fits. All solutions for photophysical studies were prepared under vacuum in a 10-cm<sup>3</sup> round-bottom flask equipped with a side arm 1-cm fluorescence cuvette and sealed from the atmosphere by a Kontes quick-release Teflon stopper. Solutions were rigorously degassed with no fewer than four freeze–pump–thaw cycles.

**Crystal Structure Determination.** Crystals of **1** and **2** were obtained by slow evaporation of their solutions in a diethyl ether/hexane mixture. Diffraction data for **1** and **2** were measured at 25 °C on a Rigaku AFC7R diffractometer with graphite-monochromatized Mo Kα radiation (λ = 0.710 69 Å). Three standard reflections measured after every 300 reflections showed no decay. The intensity data were corrected for Lorentz, polarization, and absorption effects. The empirical absorption corrections were based on azimuthal (ψ) scans of five strong reflections. In **1**, there are two independent molecules per asymmetric unit. Crystal and structure determination data for **1** and **2** are summarized in Tables 1 and 2,

(7) van Houten, J.; Watts, R. J. *J. Am. Chem. Soc.* **1976**, *98*, 4853. Parker, C. A.; Rees, W. T. *Analyst (London)* **1962**, *87*, 83. Demas, J. N.; Crosby, G. A. *J. Phys. Chem.* **1971**, *75*, 991.

**Table 3. Fractional Coordinates and Thermal Parameters<sup>a</sup> for Non-Hydrogen Atoms and Their Esd's for 1**

atom	x	y	z	$B_{\text{eq}}, \text{\AA}^2$
Re(1)	0.21789(2)	0.13871(3)	0.33592(1)	3.125(7)
Re(2)	-0.43394(2)	0.19985(3)	-0.13675(2)	3.783(9)
Cl(1)	0.0863(1)	0.2238(2)	0.29197(9)	4.47(5)
Cl(2)	-0.3548(1)	0.0679(2)	-0.0664(1)	5.04(6)
O(1)	0.2246(4)	0.2870(5)	0.4468(3)	6.3(2)
O(2)	0.3134(4)	0.3052(5)	0.2741(3)	6.1(2)
O(3)	0.3759(4)	0.0288(6)	0.3949(3)	8.1(2)
O(4)	-0.2925(4)	0.3619(6)	-0.1188(4)	9.6(3)
O(5)	-0.3725(4)	0.1172(6)	-0.2476(3)	6.7(2)
O(6)	-0.5338(4)	0.3693(6)	-0.2175(3)	7.5(2)
N(1)	0.1890(3)	0.0292(5)	0.2592(3)	3.1(1)
N(2)	0.1373(3)	0.0156(5)	0.3612(3)	3.2(1)
N(3)	-0.5329(3)	0.0839(5)	-0.1395(3)	3.5(2)
N(4)	-0.4872(3)	0.2387(5)	-0.0590(3)	3.5(2)
C(1)	0.2245(4)	0.2322(7)	0.4059(4)	4.0(2)
C(2)	0.2788(5)	0.2443(8)	0.2985(4)	4.5(2)
C(3)	0.3156(5)	0.0679(7)	0.3715(4)	4.6(2)
C(4)	0.2224(4)	0.0303(6)	0.2098(4)	3.6(2)
C(5)	0.1930(4)	-0.0287(6)	0.1585(3)	3.7(2)
C(6)	0.1246(4)	-0.0939(6)	0.1555(3)	3.5(2)
C(7)	0.0915(4)	-0.0982(6)	0.2080(3)	3.3(2)
C(8)	0.1237(4)	-0.0391(6)	0.2579(3)	3.1(2)
C(9)	0.0938(4)	-0.0433(6)	0.3161(3)	3.2(2)
C(10)	0.0274(4)	-0.1038(6)	0.3240(3)	3.7(2)
C(11)	0.0035(4)	-0.1067(6)	0.3795(3)	3.5(2)
C(12)	0.0521(5)	-0.0508(7)	0.4257(3)	4.5(2)
C(13)	0.1164(5)	0.0094(7)	0.4157(3)	4.2(2)
C(14)	0.0846(5)	-0.1566(7)	0.0997(4)	4.3(2)
C(15)	0.1289(6)	-0.1387(9)	0.0473(4)	7.0(3)
C(16)	0.0863(5)	-0.2792(8)	0.1143(4)	5.9(3)
C(17)	-0.0023(5)	-0.1183(8)	0.0809(4)	5.5(2)
C(18)	-0.0721(5)	-0.1699(7)	0.3876(4)	4.8(2)
C(19)	-0.0553(6)	-0.2924(9)	0.3819(5)	7.4(3)
C(20)	-0.1427(5)	-0.1343(9)	0.3391(4)	6.2(3)
C(21)	-0.0957(6)	-0.1479(9)	0.4483(4)	7.1(3)
C(22)	-0.3451(6)	0.3014(7)	-0.1254(5)	5.9(3)
C(23)	-0.3942(5)	0.1482(7)	-0.2050(4)	4.8(2)
C(24)	-0.4985(5)	0.3044(7)	-0.1870(4)	4.5(2)
C(25)	-0.5566(5)	0.0094(7)	-0.1827(4)	4.4(2)
C(26)	-0.6208(5)	-0.0574(7)	-0.1844(4)	4.8(2)
C(27)	-0.6666(4)	-0.0533(6)	-0.1390(4)	4.0(2)
C(28)	-0.6409(4)	0.0221(6)	-0.0933(3)	3.6(2)
C(29)	-0.5754(4)	0.0883(6)	-0.0940(3)	3.1(2)
C(30)	-0.5480(4)	0.1737(6)	-0.0477(3)	3.0(2)
C(31)	-0.5824(4)	0.1908(6)	0.0027(3)	3.4(2)
C(32)	-0.5579(4)	0.2758(6)	0.0426(3)	3.3(2)
C(33)	-0.4955(5)	0.3403(6)	0.0296(4)	4.4(2)
C(34)	-0.4616(5)	0.3203(7)	-0.0197(4)	4.5(2)
C(35)	-0.7425(5)	-0.1250(8)	-0.1415(5)	5.5(3)
C(36)	-0.7185(9)	-0.230(1)	-0.114(1)	23.8(10)
C(37)	-0.7837(9)	-0.147(2)	-0.2041(7)	19.0(8)
C(38)	-0.7986(8)	-0.077(1)	-0.1051(9)	18.3(7)
C(39)	-0.5971(5)	0.3005(7)	0.0969(4)	4.7(2)
C(40)	-0.6531(9)	0.214(1)	0.1096(6)	10.6(5)
C(41)	-0.650(1)	0.400(1)	0.0808(8)	16.3(7)
C(42)	-0.5351(9)	0.322(2)	0.1509(6)	21.5(9)

$$^a B_{\text{eq}} = \frac{8}{3}\pi^2(U_{11}(aa^*)^2 + U_{22}(bb^*)^2 + U_{33}(cc^*)^2 + 2U_{12}aa^*bb^* \cos \gamma + 2U_{13}aa^*cc^* \cos \beta + 2U_{23}bb^*cc^* \cos \alpha).$$

respectively. The space group was determined from systematic absences and the solution of the structure by heavy-atom Patterson methods and expanded using Fourier techniques<sup>13</sup> and refinement by full-matrix least squares using the MSC-Crystal Structure Package TEXSAN on a Silicon Graphics Indy computer. All non-hydrogen atoms were refined anisotropically. Hydrogen atoms at calculated positions with thermal parameters equal to 1.3 times that of the attached carbon atoms were not refined. The final agreement factors for **1** and **2** are given in Tables 1 and 2, respectively. The final atomic coordinates and thermal parameters of the non-hydrogen atoms of **1** and **2** are collected in Tables 3 and 4, respectively. The atomic coordinates of the hydrogen atoms are given in Tables SI and SVI (supplementary material).

**Table 4. Fractional Coordinates and Thermal Parameters<sup>a</sup> for Non-Hydrogen Atoms and Their Esd's for 2**

atom	x	y	z	$B_{\text{eq}}, \text{\AA}^2$
Re(1)	0.15654(3)	0.12277(3)	0.17065(1)	3.615(6)
O(1)	-0.0683(5)	0.0951(5)	0.0624(3)	7.0(2)
O(2)	0.2745(5)	-0.0535(4)	0.0932(3)	6.1(2)
O(3)	0.2486(6)	0.2770(5)	0.0624(3)	6.8(2)
N(1)	0.0742(5)	0.0350(4)	0.2554(3)	3.2(1)
N(2)	0.0661(5)	0.2330(4)	0.2368(3)	3.2(1)
C(1)	0.0143(7)	0.1049(6)	0.1042(4)	4.6(2)
C(2)	0.2321(7)	0.0136(6)	0.1220(4)	4.2(2)
C(3)	0.2171(7)	0.2160(6)	0.1028(4)	4.7(2)
C(4)	0.3074(5)	0.1428(5)	0.2510(3)	2.9(1)
C(5)	0.3787(7)	0.1518(5)	0.2970(4)	4.7(2)
C(6)	0.4719(8)	0.1615(6)	0.3652(4)	5.4(2)
C(7)	0.4664(10)	0.0667(8)	0.4135(5)	8.8(3)
C(8)	0.447(1)	0.2541(8)	0.4103(6)	11.7(4)
C(9)	0.6012(8)	0.1695(8)	0.3418(5)	7.6(3)
C(10)	0.0832(6)	-0.0669(5)	0.2955(4)	3.9(2)
C(11)	0.0216(6)	-0.1200(5)	0.3152(3)	4.0(2)
C(12)	-0.0530(6)	-0.0692(5)	0.3593(4)	3.5(2)
C(13)	-0.0609(6)	0.0353(5)	0.3510(3)	3.4(2)
C(14)	0.0037(6)	0.0861(5)	0.3001(3)	3.0(1)
C(15)	-0.0002(6)	0.1968(5)	0.2897(3)	3.0(1)
C(16)	-0.0640(6)	0.2623(5)	0.3323(3)	3.4(2)
C(17)	-0.0615(5)	0.3670(5)	0.3224(3)	3.3(1)
C(18)	0.0099(6)	0.4017(5)	0.2693(4)	3.9(2)
C(19)	0.0709(6)	0.3349(5)	0.2282(4)	4.1(2)
C(20)	-0.1264(7)	-0.1281(6)	0.4125(4)	4.7(2)
C(21)	-0.0457(8)	-0.1967(6)	0.4611(4)	6.2(2)
C(22)	-0.2193(9)	-0.1929(8)	0.3680(5)	9.2(3)
C(23)	-0.188(1)	-0.0570(7)	0.4625(6)	10.7(4)
C(24)	-0.1358(6)	0.4399(5)	0.3647(4)	3.6(2)
C(25)	-0.0621(8)	0.5337(7)	0.3900(5)	7.7(3)
C(26)	-0.2408(8)	0.4757(8)	0.3140(4)	7.3(3)
C(27)	-0.1825(8)	0.3920(6)	0.4311(4)	6.4(2)

$$^a B_{\text{eq}} = \frac{8}{3}\pi^2(U_{11}(aa^*)^2 + U_{22}(bb^*)^2 + U_{33}(cc^*)^2 + 2U_{12}aa^*bb^* \cos \gamma + 2U_{13}aa^*cc^* \cos \beta + 2U_{23}bb^*cc^* \cos \alpha).$$

## Results and Discussion

Analogous to the preparation of the related [Re(CO)<sub>5</sub>(RC≡C)] compounds,<sup>8</sup> reaction of [Re(<sup>t</sup>Bu<sub>2</sub>bpy)(CO)<sub>3</sub>Cl] (**1**) with RC≡C<sub>2</sub>Li in anhydrous THF at -40 °C under an inert atmosphere of nitrogen, followed by stirring at room temperature for 24 h, gave [Re(<sup>t</sup>Bu<sub>2</sub>bpy)(CO)<sub>3</sub>(RC≡C)], which was purified by column chromatography on silica gel using petroleum ether–diethyl ether (1/1 v/v) as eluent. Subsequent recrystallization from a diethyl ether–*n*-hexane mixture gave crystals of [Re(<sup>t</sup>Bu<sub>2</sub>bpy)(CO)<sub>3</sub>(RC≡C)] in good yield (R = <sup>t</sup>Bu (**2**), Me<sub>3</sub>Si (**3**), Ph (**4**)). All the newly synthesized compounds gave satisfactory elemental analyses and have been characterized by IR, positive FAB-MS, and <sup>1</sup>H NMR spectroscopy. Compounds **1** and **2** have also been characterized by X-ray crystallography.

Figures 1 and 2 depict the perspective drawing of compounds **1** and **2** with atomic numbering. Selected bond distances and angles are listed in Tables 5 and 6. Both of them show a slightly distorted octahedral geometry with the three carbonyl ligands arranged in a facial fashion. There are two independent molecules per asymmetric unit in **1**. Similar findings have been observed in related rhenium(I) systems.<sup>6,9</sup> In both compounds **1** and **2**, the N–Re–N bond angles are less than 90°, as required by the bite distance exerted by

(8) Bruce, M. I.; Harbourne, D. A.; Waugh, F.; Stone, F. G. A. *J. Chem. Soc. A* **1968**, 356. Koridze, A. A.; Zdanovich, V. I.; Kizas, O. A.; Yanovsky, A. I.; Struchkov, Yu. T. *J. Organomet. Chem.* **1994**, *464*, 197.

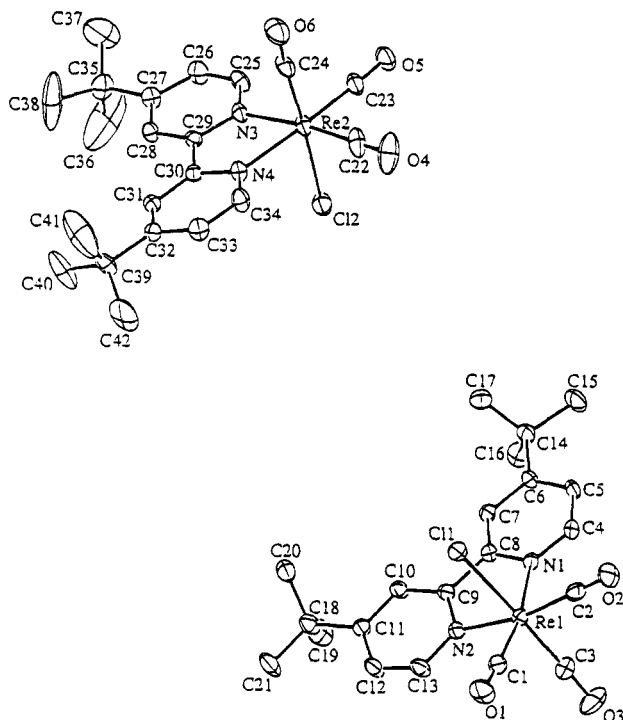


**Figure 1.** Perspective drawing of compound **1** with the atomic numbering scheme. Hydrogen atoms have been omitted for clarity. Thermal ellipsoids are shown at the 50% probability level.

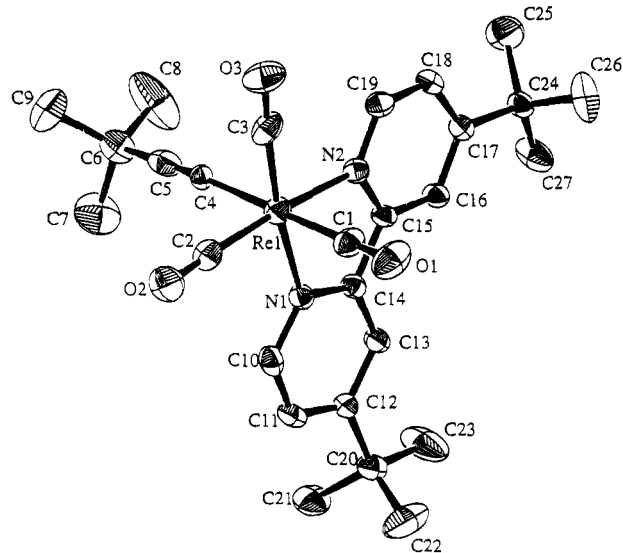


**Figure 2.** Perspective drawing of compound **2** with the atomic numbering scheme. Hydrogen atoms have been omitted for clarity. Thermal ellipsoids are shown at the 50% probability level.

the steric demand of the chelating bipyridyl ligand. In **2**, the Re–C(<sup>t</sup>Bu) bond is longer than the Re–CO bonds as expected for a Re–C(sp<sup>3</sup>) versus Re–C(sp) bond. The C≡C bond distance in the *tert*-butylacetylide moiety is typical of terminal acetylides.

The electronic absorption spectra of compounds **1–4** all show an intense absorption band at *ca.* 380–430 nm in THF, tentatively assigned as the  $d\pi(\text{Re}) \rightarrow \pi^*(\text{tBu}_2\text{bpy})$  MLCT transition (Table 7).<sup>10</sup> The red shift in

**Table 5.** Selected Bond Distances (Å) and Bond Angles (deg) for Compound **1**

Re(1)–C(1)	1.935(9)	Re(1)–C(2)	1.935(9)
Re(1)–C(3)	1.896(8)	Re(1)–Cl(1)	2.476(2)
Re(1)–N(1)	2.169(6)	Re(1)–N(2)	2.170(5)
Re(2)–C(22)	1.92(1)	Re(2)–C(23)	1.901(9)
Re(2)–C(24)	1.904(9)	Re(2)–Cl(2)	2.467(2)
Re(2)–N(3)	2.175(6)	Re(2)–N(4)	2.169(6)
C(1)–O(1)	1.141(9)	C(2)–O(2)	1.148(9)
C(3)–O(3)	1.154(9)	C(22)–O(4)	1.14(1)
C(23)–O(5)	1.156(9)	C(24)–O(6)	1.140(9)
C(1)–Re(1)–N(1)	170.1(3)	C(2)–Re(1)–N(2)	169.5(3)
C(3)–Re(1)–Cl(1)	176.9(3)	C(1)–Re(1)–Cl(1)	89.4(2)
C(2)–Re(1)–Cl(1)	93.0(2)	N(1)–Re(1)–Cl(1)	83.6(1)
N(2)–Re(1)–Cl(1)	80.8(2)	Re(1)–C(1)–O(1)	176.7(7)
Re(1)–C(2)–O(2)	177.2(7)	Re(1)–C(3)–O(3)	176.9(8)
N(1)–Re(1)–N(2)	74.2(2)	C(22)–Re(2)–N(3)	174.1(4)
C(23)–Re(2)–N(4)	172.6(3)	C(24)–Re(2)–Cl(2)	176.3(3)
C(22)–Re(2)–Cl(2)	91.3(3)	C(23)–Re(2)–Cl(2)	94.4(3)
N(3)–Re(2)–Cl(2)	84.9(2)	N(4)–Re(2)–Cl(2)	82.9(2)
Re(2)–C(22)–O(4)	179.7(9)	Re(2)–C(23)–O(5)	177.8(8)
Re(2)–C(24)–O(6)	176.8(8)	N(3)–Re(2)–N(4)	74.6(2)

**Table 6.** Selected Bond Distances (Å) and Bond Angles (deg) for Compound **2**

Re(1)–C(1)	1.933(8)	Re(1)–C(2)	1.917(8)
Re(1)–C(3)	1.905(8)	Re(1)–N(1)	2.192(5)
Re(1)–N(2)	2.183(5)	Re(1)–C(4)	2.159(6)
C(1)–O(1)	1.156(8)	C(2)–O(2)	1.146(8)
C(3)–O(3)	1.162(8)	C(4)–C(5)	1.118(9)
C(1)–Re(1)–C(4)	176.0(3)	C(2)–Re(1)–N(2)	172.7(3)
C(3)–Re(1)–N(1)	171.6(3)	Re(1)–C(4)–C(5)	174.1(6)
N(1)–Re(1)–N(2)	73.7(2)	C(2)–Re(1)–C(4)	93.6(3)
C(3)–Re(1)–C(4)	94.1(3)	N(1)–Re(1)–C(4)	85.7(2)
N(2)–Re(1)–C(4)	84.7(2)	Re(1)–C(1)–O(1)	177.5(6)
Re(1)–C(2)–O(2)	178.0(7)	Re(1)–C(3)–O(3)	175.9(7)

**Table 7.** Photophysical Data for Compounds **1–4**

compd	medium (T/K)	MLCT		
		abs band/nm	emission $\lambda_{em}/\text{nm}$ ( $\tau_0/\mu\text{s}$ )	quantum yield <sup>b</sup> $\Phi_{em}$
<b>1</b>	tetrahydrofuran (298)	<b>384</b>	624 (0.06)	0.006
	solid (298)		547 (0.90)	
	solid (77)		510	
<b>2<sup>a</sup></b>	methanol (298)	<b>391</b>	690	
	acetone (298)	<b>402</b>	690	
	dichloromethane (298)	<b>410</b>	640	
	tetrahydrofuran (298)	<b>421</b>	700 (0.13)	<0.001
	toluene (298)	<b>439</b>	690	
	hexane (298)	<b>464</b>	not measd	
	solid (298)		610 (0.11)	
solid (77)		610		
<b>3</b>	tetrahydrofuran (298)	<b>406</b>	670 (0.25)	0.001
	solid (298)		610 (0.35)	
	solid (77)		600	
<b>4</b>	tetrahydrofuran (298)	<b>419</b>	688 (0.20)	0.001
	solid (298)		600 (0.24)	
	solid (77)		585	

<sup>a</sup> The solvents used for the recording of the UV/vis spectra are arranged in order of decreasing polarity. <sup>b</sup> Quantum yield was measured at room temperature using  $[\text{Ru}(2,2'\text{-bipyridine})_3]^{2+}$  as a standard.<sup>7</sup>

MLCT absorption energies of Re–C≡CR in compounds **2–4** compared to Re–Cl in **1** is consistent with the  $\sigma$ -donating ability of the acetylide being stronger than that of the chloro moiety. Similar findings have been observed in Re(I)–alkyl complexes.<sup>11</sup> The MLCT nature

(9) Horn, E.; Snow, M. R. *Aust. J. Chem.* **1980**, *33*, 2369. Tikkanen, W.; Kaska, W. C.; Moya, S.; Layman, T.; Kane, R. *Inorg. Chim. Acta* **1983**, *76*, L29. Calabrese, J. C.; Tam, W. *Chem. Phys. Lett.* **1987**, *133*, 244.

(10) Fredericks, S. M.; Luong, J. C.; Wrighton, M. S. *J. Am. Chem. Soc.* **1979**, *101*, 7415. Caspar, J. V.; Meyer, T. J. *J. Phys. Chem.* **1983**, *87*, 952. Tapolsky, G.; Duesing, R.; Meyer, T. J. *Inorg. Chem.* **1990**, *29*, 2285. Lin, R.; Fu, Y.; Brock, C. P.; Guarr, T. F. *Inorg. Chem.* **1992**, *31*, 4346.

of the low-energy absorption band has been further confirmed by solvatochromic studies. The red shift in absorption energies from methanol ( $\lambda$  391 nm) to *n*-hexane ( $\lambda$  464 nm) in order of decreasing polarity is in accordance with the charge-transfer nature of the transition.<sup>12</sup> Excitation of **2–4** in the solid state or in fluid solutions at room temperature results in strong orange-red luminescence, red-shifted relative to that of **1**. This again is consistent with the good  $\sigma$ -donor ability of the acetylide moiety, which would render the rhenium center more electron rich and hence lower the MLCT transition energy. Unlike the Re(I)-alkyl or aryl complexes which emit only at low temperature,<sup>11</sup> **2–4** represent the first examples of organorhenium(I) exhibiting room-temperature luminescence in solution. It is interesting to note that compounds **2–4** are reasonably stable toward Re–C bond homolysis, as reflected by no apparent UV–visible spectral changes upon steady-state irradiation using a conventional light source ( $\lambda > 330$  nm) for more than 12 h, though irradiation with a strong laser source ( $\lambda$  355 nm) did

produce spectral changes. This finding is quite different from the extremely efficient bond homolysis reaction observed for the alkyl and aryl counterparts,<sup>11</sup> suggesting that the interstate crossing from  $d\pi(\text{Re}) \rightarrow \pi^*(\text{tBu}_2\text{bpy})$  to  $\sigma_b(\text{Re}-\text{C}) \rightarrow \pi^*(\text{tBu}_2\text{bpy})$  is not very efficient in **2–4**.

It is interesting to note that **3** is a good precursor for the synthesis of acetylide-bridged organometallics, since the trimethylsilyl group is a good leaving group. Work is in progress to design and isolate these luminescent rigid-rod organometallics. Preliminary work also shows that a related binuclear  $[\{\text{Re}(\text{CO})_3(\text{phen})\}_2(\text{L})]^{2+}$  complex (L = 1,4-bis(4-pyridyl)butadiyne) exhibits interesting photoluminescent behavior (solid state:  $\lambda_{\text{em}} = 610$  nm,  $\tau_0 = 0.6 \mu\text{s}$ ).

**Acknowledgment.** V.W.W.Y. acknowledges financial support from the Research Grants Council and The University of Hong Kong. V.C.Y.L. acknowledges the receipt of a Croucher Studentship administered by the Croucher Foundation.

**Supplementary Material Available:** Hydrogen coordinates and thermal parameters (Tables SI and SVI), general displacement parameter expressions,  $U$  (Tables SII and SVII), all bond distances involving non-hydrogen atoms (Tables SIII and SVIII), and all bond angles involving non-hydrogen atoms (Tables SIV and SIX) for **1** and **2**, respectively (17 pages). Ordering information is given on any current masthead page.

OM940909O

(11) Lucia, L. A.; Burton, R. D.; Schanze, K. S. *Inorg. Chim. Acta* **1993**, *208*, 103. Stufkens, D. J.; van Outersterp, J. W. M.; Oskam, A.; Rossenaar, B. D.; Stor, G. J. *Coord. Chem. Rev.* **1994**, *132*, 147.

(12) Giordano, P. J.; Wrighton, M. S. *J. Am. Chem. Soc.* **1979**, *101*, 2888. Sullivan, B. P. *J. Phys. Chem.* **1989**, *93*, 24. Dominey, R. N.; Hauser, B.; Hubbard, J.; Dunham, J. *Inorg. Chem.* **1991**, *30*, 4754.

(13) PATTY and DIRDIF92: Beurskens, P. T.; Admiraal, G.; Beursken, G.; Bosman, W. P.; Garcia-Granda, S.; Gould, R. O.; Smits, J. M. M.; Smykalla, C. The DIRDIF program system; Technical Report of the Crystallography Laboratory; University of Nijmegen, The Netherlands, 1992.



# Synthesis, Structure, and Fluxional Behavior of a Dihydrosilane Bearing an Aryldiamine Pincer Ligand

Francis Carre, Claude Chuit, Robert J. P. Corriu,\* Ahmad Mehdi, and Catherine Reye

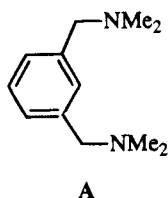
Laboratoire "Hétérochimie et Aminoacides" CNRS, URA 1097, Université Montpellier II, Sciences et Techniques du Languedoc, Place E. Bataillon, 34095 Montpellier Cedex 5, France

Received February 2, 1995<sup>®</sup>

1,4-Bis({2,6-bis[(dimethylamino)methyl]phenyl}dihydrosilyl)benzene (**1**) was prepared by treatment of the 1,4-bis(trihydrosilyl)benzene with 2 mol equiv of {2,6-bis[(dimethylamino)methyl]phenyl}lithium. The X-ray crystal structure of **1** shows the hexacoordination of the silicon atom, with a geometry corresponding to a bicapped tetrahedron. Furthermore, the two chelating amino groups are in cis disposition to each other. Dynamic solution NMR studies have been carried out. Of the two interpretations considered, only one is consistent with the solid state structure.

## Introduction

Molecular structures of dihydrosilanes in which pentacoordination is achieved by intramolecular ring closure of a chelating group are known.<sup>1</sup> In all of these structures the geometry around the silicon atom is that of a somewhat distorted trigonal bipyramid in which the donor atom occupies an axial site and the hydrogen atoms the equatorial sites. When two chelating ligands are coordinated to the silicon center, a [4 + 2] type coordination is observed around the silicon atom.<sup>2,3</sup> Interestingly, the geometry of these compounds<sup>2,3</sup> is not octahedral but corresponds to a bicapped tetrahedron, the two nitrogen atoms being cis to each other. Another possibility of bis chelation on a silicon center could originate from using the aryldiamine pincer ligand **A**



introduced by van Koten.<sup>4</sup> To illustrate this purpose, we have prepared the bis(dihydrosilyl)benzene **1** with two identical silicon centers, from which crystals available for an X-ray structure analysis have been obtained. We report in this paper the synthesis, structural characterization, and dynamic NMR behavior of this compound.

**Table 1. Summary of Crystal Data, Intensity Measurements, and Refinement**

formula	C <sub>30</sub> H <sub>46</sub> N <sub>4</sub> Si <sub>2</sub>
cryst syst	monoclinic
space group	P2 <sub>1</sub> /c
a, Å	9.655(2)
b, Å	12.630(2)
c, Å	12.550(3)
β, deg	99.29(2)
V, Å <sup>3</sup>	1510.2 <sup>a</sup>
mol wt	518.9
Z	2
d <sub>calcd</sub> , g cm <sup>-3</sup>	1.141 <sup>a</sup>
d <sub>measd</sub> , g cm <sup>-3</sup>	1.10(2) <sup>b</sup>
cryst size, mm <sup>3</sup>	0.24 × 0.35 × 0.70
cryst color	colorless
recryst solvent	CH <sub>2</sub> Cl <sub>2</sub>
mp, °C	131–33
method of data collectn	ω/θ
radiation (graphite-monochromated)	Mo Kα
μ, cm <sup>-1</sup>	1.366
2θ limits, deg	4–48
no. of unique reflns	2258
no. of obsd reflns	1726
final no. of variables	95
R	0.038
R <sub>w</sub>	0.045
residual electron density	0.25

<sup>a</sup> Measured at -100 °C. <sup>b</sup> Measured at 27 °C.

## Results and Discussion

**Synthesis and Solid State Structure of 1.** Reduction of 1,4-bis(trimethoxysilyl)benzene<sup>5</sup> by LiAlH<sub>4</sub> results in the formation of the corresponding 1,4-bis(trihydrosilyl)benzene **2**. The 1:2 molar reaction of **2** with {2,6-bis[(dimethylamino)methyl]phenyl}lithium affords **1** in 60% yield (see Scheme 1). Translucent crystals were grown from a CH<sub>2</sub>Cl<sub>2</sub> solution cooled to -10 °C. The ORTEP drawing is displayed in Figure 1, and selected bond distances and angles are listed in Table 3. Figure 1 showed that the molecule is centrosymmetric. On each silicon atom the lone pairs of both NMe<sub>2</sub> groups were directed toward the silicon center, but the bis chelation is not symmetrical, the N(2)Me<sub>2</sub> group being opposite to the SiH(2) bonds [N(2)–Si–H(2) = 169.4°] while the N(1)Me<sub>2</sub> group is

(5) Corriu, R. J. P.; Moreau, J. J. E.; Thepot, P.; Wong Chi Man, M. *Chem. Mater.* **1992**, *4*, 1217.

<sup>®</sup> Abstract published in *Advance ACS Abstracts*, May 1, 1995.

(1) (a) Blake, A. J.; Ebsworth, E. A. V.; Welch, A. J. *Acta Crystallogr., Sect. C* **1984**, *40*, 895. (b) Brelière, C.; Carré, F.; Corriu, R. J. P.; Poirier, M.; Royo, G. *Organometallics* **1986**, *5*, 388. (c) Boyer, J.; Brelière, C.; Carré, F.; Corriu, R. J. P.; Kpton, A.; Poirier, M.; Royo, G.; Young, J. C. *J. Chem. Soc., Dalton Trans.* **1989**, 43.

(2) Brelière, C.; Carré, F.; Corriu, R. J. P.; Poirier, M.; Royo, G.; Zwecker, J. *Organometallics* **1989**, *8*, 1831.

(3) Carré, F.; Cerveau, G.; Chuit, C.; Corriu, R. J. P.; Reye, C. *New J. Chem.* **1992**, *16*, 63.

(4) van Koten, G. *Pure Appl. Chem.* **1989**, *61*, 1681; **1990**, *62*, 1155. Jastrzebski, J. T. B. H.; van Koten, G. *Adv. Organomet. Chem.* **1993**, *35*, 241.

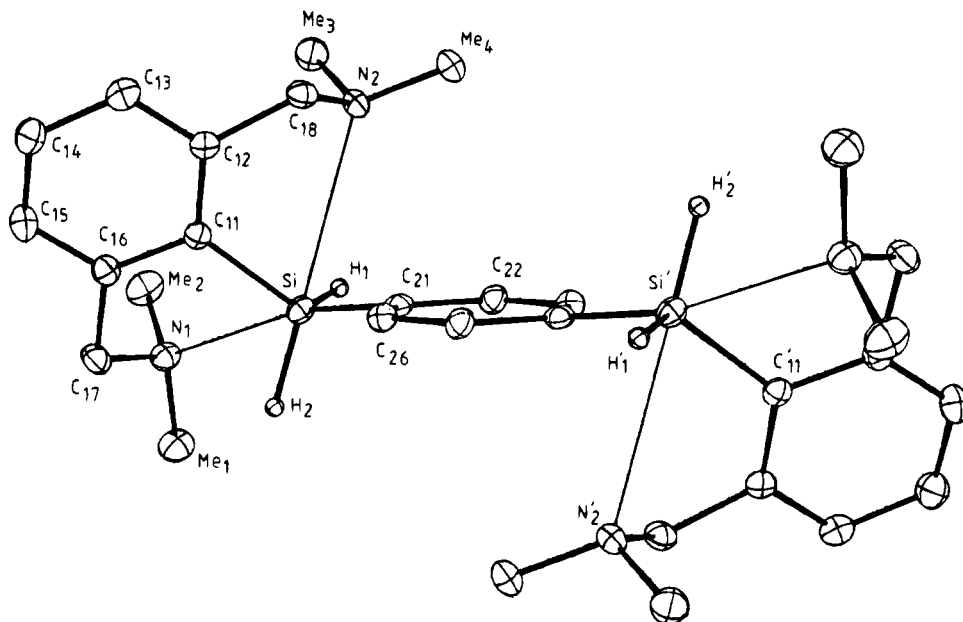


**Figure 1.** ORTEP drawing of the molecular structure of silicate **1** showing the numbering scheme. The thermal ellipsoids and spheres are at the 30% probability level.

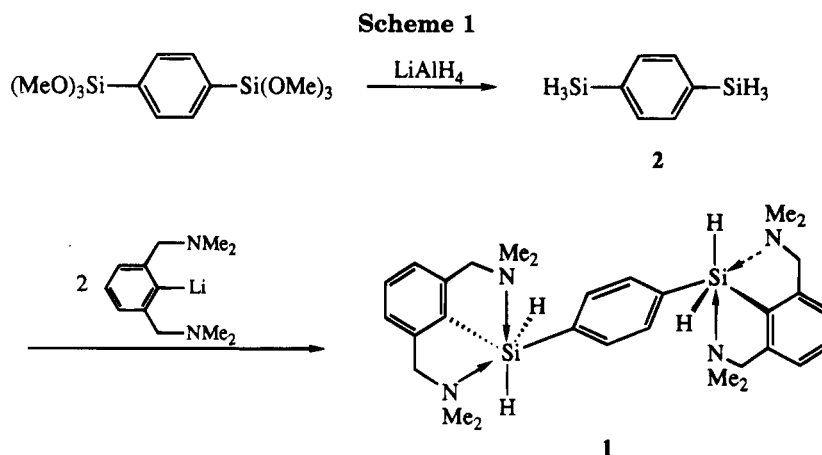


**Table 2.** Fractional Atomic Coordinates ( $\times 10^4$ )

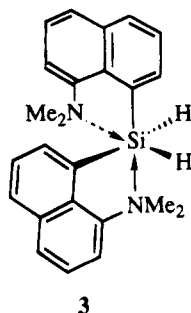
atom	<i>x/a</i>	<i>y/b</i>	<i>z/c</i>
Si	3106.3(6)	41.5(4)	1567.1(4)
C11	3098(2)	833(1)	2839(2)
C12	1978(2)	827(1)	3435(1)
C13	1968(2)	1511(2)	4290(2)
C14	3070(2)	2213(2)	4594(2)
C15	4214(2)	2191(2)	4062(2)
C16	4234(2)	1508(2)	3199(2)
C17	5514(2)	1463(2)	2646(2)
N1	5809(2)	369(1)	2397(1)
Me1	6768(2)	305(2)	1608(2)
Me2	6344(3)	-239(2)	3364(2)
C18	786(2)	40(2)	3183(2)
N2	1296(2)	-1016(1)	2993(2)
Me3	2140(3)	-1448(2)	3966(2)
Me4	106(2)	-1714(2)	2616(2)
C21	1308(2)	6(1)	722(2)
C22	775(2)	-916(1)	185(2)
C26	492(2)	918(1)	512(2)
H1	3620(18)	-1025(16)	1715(15)
H2	3762(18)	684(15)	862(15)

trans to the Si-C(21) bond [N(1)-Si-C(21) angle = 166.8°]. Furthermore, the Si...N(2) distance (3.008 Å) is 12% longer than the Si...N(1) bond (2.681 Å), both distances being below the sum of the van der Waals radii (3.5 Å)<sup>6</sup> of silicon and nitrogen atoms. The same observation has been previously made for compound **3**,<sup>2</sup>

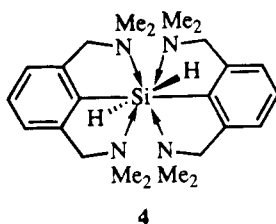
**Table 3.** Interatomic Distances (Å) and Main Bond Angles (deg)

Si-C11	1.884(2)	C11-C12	1.411(3)
Si-C21	1.883(2)	C12-C13	1.379(3)
Si-H1	1.44(2)	C13-C14	1.390(3)
Si-H2	1.42(2)	C14-C15	1.380(3)
Si...N1	2.681(2)	C15-C16	1.388(3)
Si...N2	3.008(2)	C16-C11	1.405(3)
N1-C17	1.456(3)	C12-C18	1.514(3)
N1-Me1	1.464(3)	C16-C17	1.512(3)
N1-Me2	1.459(3)	C21-C22	1.401(3)
N2-C18	1.455(3)	C21-C26	1.397(3)
N2-Me3	1.460(3)	C26-C22	1.384(3)
N2-Me4	1.465(3)		
C11-Si-C21	111.1(1)	C11-C12-C18	120.9(2)
C11-Si-H1	115.9(7)	C13-C12-C18	118.3(2)
C11-Si-H2	106.7(8)	C11-C16-C17	118.9(2)
C21-Si-H1	108.5(7)	C15-C16-C17	119.8(2)
C21-Si-H2	97.2(7)	C16-C17-N1	109.7(2)
H1-Si-H2	116(1)	C12-C18-N2	111.7(2)
N1...Si-C21	166.8(1)	C17-N1...Si	91.0(1)
N2...Si-H2	169.4(7)	C18-N2...Si	86.3(1)
N1...Si...N2	117.4(1)	Si-C21-C22	121.7(1)
Si-C11-C12	123.7(1)	Si-C21-C26	121.8(1)
Si-C11-C16	119.0(1)	C22-C21-C26	116.2(2)
C12-C11-C16	117.2(2)		

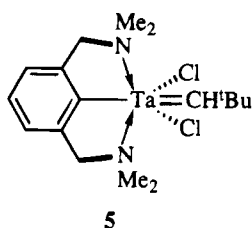
in which the Si...N distance opposite to the Si-H bond is also longer (2.80 Å) than that trans to the Si-C bond (2.61 Å), in spite of the rigidity of the 8-(dimethylamino)-



naphthyl group. Furthermore, it is noteworthy that the tetrahedral geometry of the silicon atom is maintained (Table 3). Two faces of the tetrahedron are capped by two NMe<sub>2</sub> groups so that compound **1** is [4 + 2] coordinated. Another interesting aspect of this structure is the cis disposition of the two nitrogen donor atoms of the ligand [the N(1)–Si–N(2) angle being 117.4°]. This situation was previously observed for the [4 + 4] coordinate silicon compound **4**,<sup>7</sup> in which the



N(1)–Si–N(2) angle is 116.7°. It is noteworthy that in most octahedral organometallic complexes of the late transition metals the ligand **A** adopts meridional coordination with N–M–N angles of typically 161–163°,<sup>8</sup> with the exception of the tantalum compound **5**,<sup>9</sup> in



which the N(1)–Ta–N(2) angle is 118.63 (1)°.

**NMR Spectroscopy of 1 in Solution and in the Solid State.** The <sup>29</sup>Si NMR chemical shift of **1** is –51.3 ppm in solution and –49.6 ppm in the solid state. Since these resonances are upfield of those for Ph<sub>2</sub>SiH<sub>2</sub><sup>10</sup> (δ –33.8 ppm) and for the pentacoordinated silicon compound **6**<sup>1c</sup> (δ –47.25 ppm), it can be concluded that the silicon atom is at least pentacoordinated. Furthermore the <sup>29</sup>Si NMR shift of **1** is not temperature-dependent throughout the temperature range studied (293–173 K

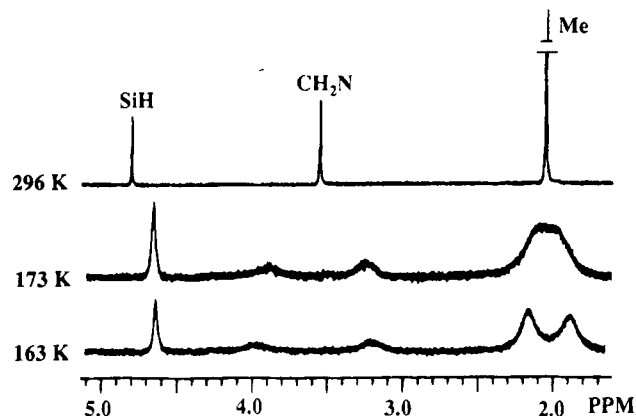


**Figure 2.** <sup>1</sup>H NMR spectra (250 MHz) of **1** from CD<sub>2</sub>Cl<sub>2</sub>/Freon.

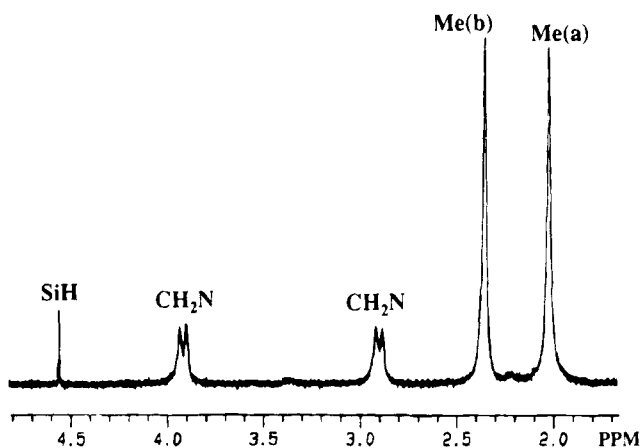
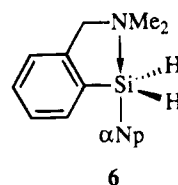


**Figure 3.** <sup>1</sup>H NMR spectrum (360 MHz) of **1** at 180 K from CD<sub>2</sub>Cl<sub>2</sub>.



from CD<sub>2</sub>Cl<sub>2</sub>). The <sup>1</sup>H NMR spectrum of **1** in solution (250 MHz, CDCl<sub>3</sub>) displays at room temperature a single resonance for all the methyl groups and a single resonance for all the methylene protons. A singlet is also observed for the SiH<sub>2</sub> protons. Lowering the temperature of the NMR sample resulted in broadening and decoalescence of the NMe<sub>2</sub> and methylene signals (Figure 2). At 180 K (360 MHz, CD<sub>2</sub>Cl<sub>2</sub>) the <sup>1</sup>H NMR spectrum of **1** exhibited two single resonances for the dimethylamino groups and an AX pattern for the benzylic protons (Figure 3), the SiH<sub>2</sub> protons being a singlet.

We assume that the <sup>1</sup>H NMR spectrum of **1** at 180 K indicates the hexacoordination of the silicon atom. Indeed, if only one NMe<sub>2</sub> group were coordinated at the silicon atom (on the NMR time scale), we would observe two singlets for the benzylic protons and two singlets for the methyl groups (if we consider that the two SiH bonds are in equatorial positions as is always observed<sup>1</sup>). Hexacoordination of the silicon atom has also been revealed by the X-ray structure analysis of **1**.

Nevertheless, the <sup>1</sup>H NMR spectrum of **1** at 180 K cannot be explained by the static arrangement (on the NMR time scale) around the Si atom found in the solid

(6) Bondi, A. J. *Phys. Chem.* **1964**, *68*, 441.

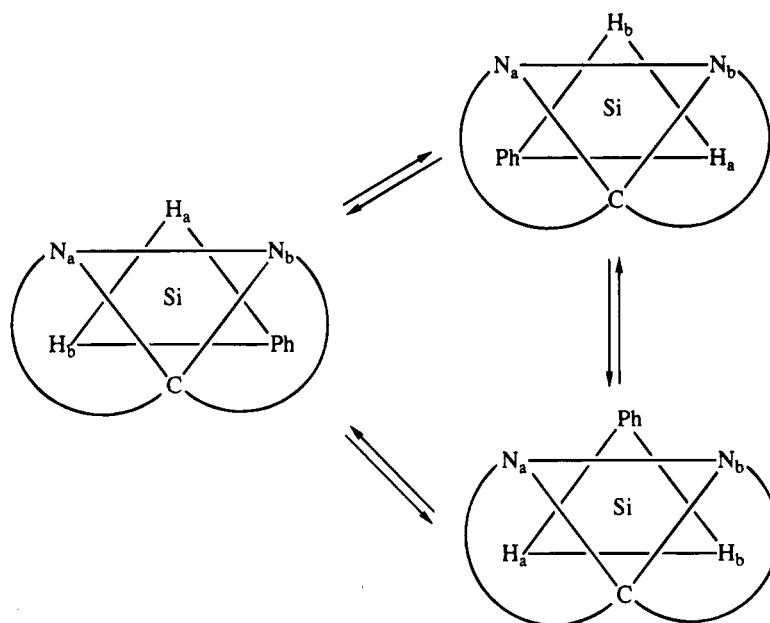
(7) Carré, F.; Chuit, C.; Corriu, R. J. P.; Mehdi, A.; Reyé, C. *Angew. Chem.* **1994**, *106*, 1152; *Angew. Chem., Int. Ed. Engl.* **1994**, *33*, 1097.

(8) Abbenhuis, H. C. L.; Feiken, N.; Grove, D. M.; Jastrzebski, J. T. B. H.; Kooijman, H.; van der Slijs, P.; Smeets, W. J. J.; Speck, A. L.; van Koten, G. *J. Am. Chem. Soc.* **1992**, *114*, 9773.

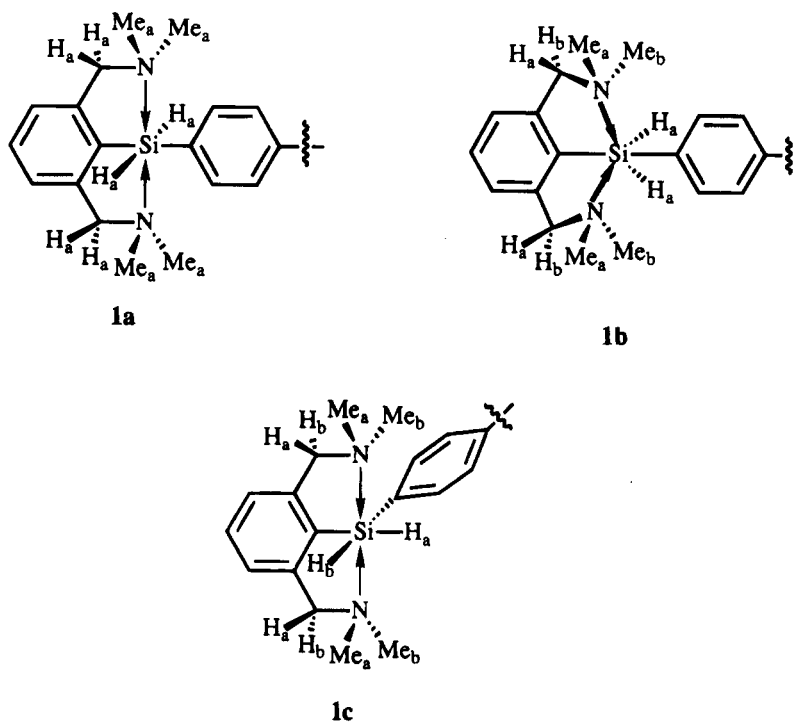
(9) (a) Therheijden, J.; van Koten, G.; De Booys, J. L.; Ubbels, H. J. C.; Stam, C. H. *Organometallics* **1983**, *2*, 1882. (b) Grove, D. M.; van Koten, G.; Mul, W. P.; van der Zeijden, A. A. H.; Terheijden, J. *Organometallics* **1986**, *5*, 322. (c) van der Zeijden, A. A. H.; van Koten, G.; Luijk, R.; Vrieze, K.; Slob, C.; Krabbendam, H.; Speck, A. L. *Inorg. Chem.* **1988**, *27*, 1014.

(10) Kintzinger, J. P.; Marsmann, H. In *NMR Basic Principles and Progress*; Diehl, P., Fluck, E., Kosfeld, R., Eds.; Springer-Verlag: New York, 1981.

Scheme 2



Scheme 3



state. Indeed, with such a dissymmetric geometry at silicon, the  $^1\text{H}$  NMR spectrum should display four signals for the two  $\text{NMe}_2$  units, two AB (or AX) systems for the benzylic protons, and one AB system for the  $\text{SiH}_2$  protons, which is not the case. To explain the  $^1\text{H}$  NMR spectrum of **1**, we propose two interpretations. The first is that in solution the molecule adopts the same dissymmetric geometry as in the solid state, but at this temperature it undergoes a nondissociative limited isomerization process such as a Bailer twist (Scheme 2) with a  $\Delta G^\ddagger$  too weak to be measured under the experimental conditions employed (360 MHz). This limited process would explain the presence of an AB system for the benzylic protons instead of the two expected in the fixed geometry. The second interpretation that can be put forward is that the molecule adopts

in solution a geometry in which the two  $\text{CH}_2\text{NMe}_2$  units are magnetically equivalent, this being a situation different from that found in the solid state. We have represented in Scheme 3 the three possible arrangements of this type.

The low-temperature  $^1\text{H}$  NMR spectrum of **1** is not consistent with the molecular geometry **1a**, in which all the benzylic protons and all the methyl groups are equivalent. The geometry **1c** in which the  $\text{SiH}_2$  protons are different can also be ruled out.

The  $^1\text{H}$  NMR data of **1** can only be explained by the geometry **1b**, the two  $\text{CH}_2\text{NMe}_2$  units being equivalent as is also the case for the  $\text{SiH}_2$  protons. In each  $\text{CH}_2\text{NMe}_2$  unit, the benzylic protons are different as are the Me groups, which is consistent with the low-temperature NMR spectrum of **1**. When the temperature is

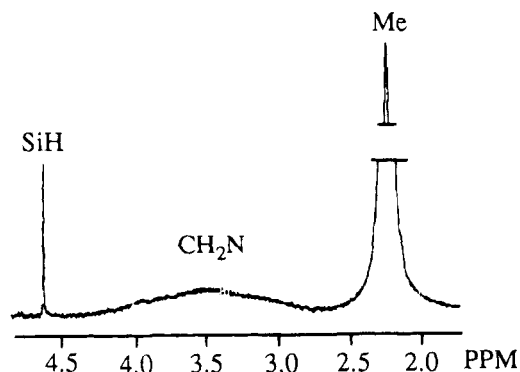
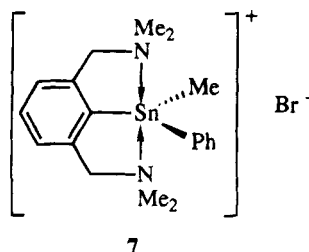


**Figure 4.**  $^1\text{H}$  NMR spectrum (360 MHz) of **1** at 250 K from  $\text{CD}_2\text{Cl}_2$ .

raised, the resonances of the  $\text{NMe}_2$  groups and of the methylene protons coalesce at different rates. The coalescence of  $\text{NMe}_2$  groups is shown in Figure 2 (173 K, 250 MHz), and that of methylene protons is shown in Figure 4 (250 K, 360 MHz). This indicates that the respective protons become isochronous as a result of two different processes: the magnetic equivalence of Me groups at room temperature is interpreted in terms of a dynamic coordination process involving the two  $\text{NMe}_2$  units whereby fast exchange (on the NMR time scale) of one unit by the other occurs. The  $\Delta G^\ddagger$  for this process (173 K, 250 MHz) was estimated to be  $35 \text{ kJ mol}^{-1}$  from the coalescence temperature of the methyl protons. To explain the equivalence of the benzylic protons at room temperature, we have to assume that, during this dissociative process, there is concomitant rotation of the chelating ligand around the Si-C bond. A similar explanation has been proposed by van Koten et al. to explain the  $^1\text{H}$  NMR behavior of compound **7**.<sup>11</sup> An estimation of the  $\Delta G^\ddagger$  of this second process was calculated from the coalescence temperature (250 K, 360 MHz) for the benzylic protons ( $\Delta G^\ddagger = 48 \text{ kJ mol}^{-1}$ ).



**7**

The  $^{13}\text{C}$  NMR spectrum of **1** at room temperature shows in solution (Figure 5a) a single resonance for the benzylic carbons and a single resonance for the methyl groups. These are consistent with the  $^1\text{H}$  NMR spectrum of **1** at the same temperature. The solid state  $^{13}\text{C}$  NMR spectrum shows two resonances for the benzylic carbons (Figure 5b) and a broad resonance for the methyl groups. If we consider that the broad signal corresponds to the juxtaposition of several signals, this spectrum is consistent with the solid state structure for which four Me signals and two benzyl signals are expected.

In conclusion, the hexacoordination of the silicon atom has been shown for compound **1** both in the solid state as well as in solution. Two hypotheses have been put

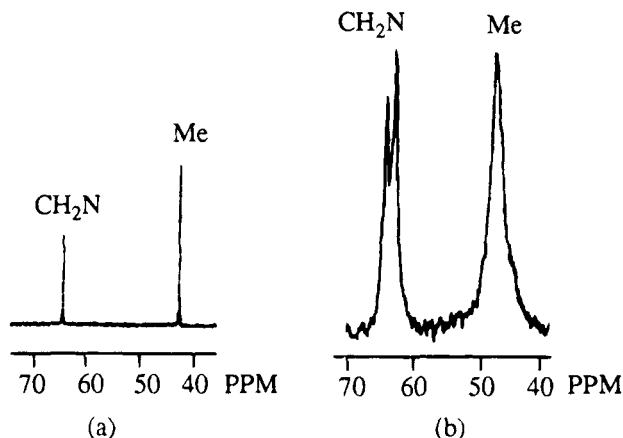


**Figure 5.**  $^{13}\text{C}$  NMR spectra of **1** in solution (a) and in the solid state (b).

forward to explain the low temperature NMR spectra. One supposes that the geometry of **1** in solution is different from that in the solid state, but this is not consistent with the concept of Dunitz et al.<sup>13</sup> The other explanation, which is consistent with the latter concept, supposes that the geometry in solution is the same as in the solid state and that the compound undergoes at this temperature an easy, nondissociative limited isomerization process.

## Experimental Section

All of the reactions were performed under a dry argon atmosphere using standard Schlenk techniques.  $^1\text{H}$ ,  $^{13}\text{C}$ , and  $^{29}\text{Si}$  NMR spectra were obtained using Bruker WP-200-SY, Bruker 250 AC, or Bruker WM-360-WB spectrometers. Solid state NMR spectra were recorded on a Bruker AM-300 spectrometer.  $^1\text{H}$ ,  $^{13}\text{C}$ , and  $^{29}\text{Si}$  chemical shifts were reported relative to  $\text{Me}_4\text{Si}$ . Elementary analysis were performed by the Centre de Microanalyse du CNRS.

**1,4-Bis(trihydrosilyl)benzene (2).** A 7.15 g amount ( $2.25 \times 10^{-2}$  mol) of 1,4-bis(trimethoxysilyl)benzene<sup>5</sup> in 30 mL of  $\text{Et}_2\text{O}$  was added dropwise at room temperature to a suspension of 2.56 g ( $6.74 \times 10^{-2}$  mol) of  $\text{LiAlH}_4$  in 80 mL of  $\text{Et}_2\text{O}$ . The mixture was stirred at room temperature overnight. Ether and the reaction product were removed under vacuum and trapped in liquid nitrogen. After distillation of ether at atmospheric pressure, 2.16 g of a colorless oil was obtained (68% yield). *Caution! The 1,4-bis(trihydrosilyl)benzene was not distilled in order to avoid a possible explosion.*  $^1\text{H}$  NMR ( $\delta$  in  $\text{CCl}_4$ ): 4.18 (s, 6H, SiH<sub>3</sub>), 7.55 (s, 4H, Ar).  $^{29}\text{Si}$  NMR ( $\text{CDCl}_3$ ): -61.5.

**1,4-Bis({2,6-bis((dimethylamino)methyl)phenyl}-dihydrosilyl)benzene (1).** A 30.5 mmol amount of the {2,6-bis((dimethylamino)methyl)phenyl}lithium derivative in 50 mL of  $\text{Et}_2\text{O}$  was added dropwise at  $0^\circ\text{C}$  to 2.1 g (15.2 mmol) of 1,4-bis(trihydrosilyl)benzene in 50 mL of  $\text{Et}_2\text{O}$ . The reaction mixture was stirred at room temperature overnight. Then 0.27 mL of  $\text{H}_2\text{O}$  was added to hydrolyze LiH; after removal of the solvent, the residue was taken up again in 25 mL of  $\text{CH}_2\text{Cl}_2$ . The precipitate of LiOH was filtered through Celite, and then the solvent was removed under vacuum to give 4.7 g (9.12 mmol, 60% yield) of **1** as transparent crystals: mp  $131\text{--}133^\circ\text{C}$ .  $^{29}\text{Si}$  NMR: (39.76 MHz,  $\text{CDCl}_3$ ,  $25^\circ\text{C}$ )  $-51.4$  (t,  $^1J_{\text{Si,H}} = 194 \text{ Hz}$ ); (59.63 MHz, solid state, {H})  $-49.6$  (s); (49.69 MHz,  $\text{CD}_2\text{Cl}_2$ , Freon,  $-110^\circ\text{C}$ )  $-52.3$  (t,  $^1J_{\text{Si,H}} = 194 \text{ Hz}$ ).  $^1\text{H}$  NMR: (360 MHz,  $\text{CD}_2\text{Cl}_2$ ,  $25^\circ\text{C}$ ) 2.24 (s, 24H,  $\text{NCH}_3$ ), 3.48 (s, 8H,  $\text{CH}_2\text{N}$ ), 4.60 (s, 4H,  $\text{SiH}_2$ ), 7.04–7.27 (2m, 6H, Ar), 7.57

(11) van Koten, G.; Jastrzebski, J. T. B. H.; Noltes, J. G.; Speck, A. L.; Schoone, J. C. *J. Organomet. Chem.* **1978**, *148*, 233.

(12) Boyer, J.; Corriu, R. J. P.; Kpton, A.; Mazhar, M.; Poirier, M.; Royo, G. *J. Organomet. Chem.* **1986**, *301*, 131.

(13) Britton, D.; Dunitz, J. D. *J. Am. Chem. Soc.* **1981**, *103*, 2971.

(s, 4H, Ar); (360 MHz, CD<sub>2</sub>Cl<sub>2</sub>, -93 °C) 1.99 (s, 12H, NCH<sub>3</sub>), 2.34 (s, 12H, NCH<sub>3</sub>), 2.90 (d, 4H, <sup>2</sup>J<sub>(H,H)</sub> = 12.9 Hz, CH<sub>2</sub>N), 3.89 (d, 4H, <sup>2</sup>J<sub>(H,H)</sub> = 12.9 Hz, CH<sub>2</sub>N), 4.55 (s, 4H, SiH<sub>2</sub>), 7.11 (d, 4H, <sup>3</sup>J<sub>(H,H)</sub> = 6.8 Hz, Ar), 7.24 (t, 2H, <sup>3</sup>J<sub>(H,H)</sub> = 6.8 Hz, Ar), 7.57 (s, 4H, Ar). <sup>13</sup>C NMR: (62.90 MHz, CDCl<sub>3</sub>, {H}) 43.95 (NCH<sub>3</sub>), 64.13 (CH<sub>2</sub>N), 127.27, 128.80, 132.50, 132.65, 135.87, 147.88 (Ar); (75.47 MHz, solid state, {H}) 45.65 (broad signal, NCH<sub>3</sub>), 64.53, 66.21 (CH<sub>2</sub>N), 126.85, 128.25, 129.94, 132.80, 133.73, 141.22, 143.04, 144.87, 147.64, 149.21 (Ar). IR (KBr): 2114.1, 2156.6 (SiH). MS (IE, 70 eV): *m/z* = 517 (M)<sup>+</sup>, 37; 501 ((M - Me + 2H)<sup>+</sup>, 72); 58 ((CH<sub>2</sub>=NMe<sub>2</sub>)<sup>+</sup>, 100). Anal. Calcd for C<sub>30</sub>H<sub>46</sub>N<sub>4</sub>Si<sub>2</sub>: C, 69.49; H, 8.88; N, 10.81. Found: C, 69.49; H, 8.88; N, 10.73.

**Crystal Structure of Compound 1. Crystal Preparation.** Crystals of compound **1** were grown by slowly cooling to -10 °C a dichloromethane solution in a nitrogen atmosphere. Colorless elongated prisms were obtained. A small block of dimensions 0.24 × 0.40 × 0.60 mm<sup>3</sup> was sealed inside a capillary and mounted on a Nonius CAD 4 automated diffractometer at 173 K.

**X-ray Data Collection.** Data were collected with graphite-monochromated Mo K $\alpha$  radiation ( $\lambda$  = 0.710 69 Å). Lattice constants (Table 1) come from a least-squares refinement of 21 reflections obtained in the range 27 < 2 $\theta$  < 72. The intensities of three standard reflections were monitored at intervals of 60 min; no significant change in these intensities occurred during data collection. The systematic absences were uniquely defining the space group *P*<sub>21</sub>/*c*, with *z* = 2. The structure amplitudes were obtained after the usual Lorentz and polarization reduction. Only the reflections having  $\sigma(F)/F$  < 0.23 were considered to be observed. The absorption corrections were neglected.

**Structure Determination and Refinement.** Direct meth-

ods (SHELXS-86 program<sup>14</sup>) succeeded in locating the whole set of non-hydrogen atoms through a single calculation. After four cycles of least-squares refinement with isotropic thermal parameters for all atoms, the hydrogen atoms were positioned by calculation (SHELX-76 program<sup>15</sup>). The hydrogen atoms on silicon were located in a difference Fourier synthesis and refined with isotropic thermal parameters, while all non-hydrogen atoms were refined anisotropically. Since convergence was difficult to obtain, the thermal parameters of the carbon atoms were kept fixed in the last stages of the refinement. Refinement converged to the final *R* value of 0.038.

The final atomic coordinates are listed in Table 2. The labeling scheme is given in Figure 1; a stereoview is provided with Figure 2. Individual bond lengths and main bond angles are listed in Table 3. Full lists of the bond angles (Table 4), the anisotropic thermal parameters (Table 5), and the calculated hydrogen atom coordinates (Table 6) are available as supplementary material.

**Supplementary Material Available:** A full list of the bond angles for compound **1** (Table 4), along with a list of anisotropic parameters for all non-hydrogen atoms (Table 5), and a list of calculated hydrogen atom coordinates (Table 6) (3 pages). Ordering information is given on any current masthead page.

OM950086I

(14) Sheldrick, G. M. *SHELXS-86, A Program for Crystal Structure Solution*; Institut für Anorganische Chemie der Universität: Göttingen, Germany, 1986.

(15) Sheldrick, G. M. *SHELX-76, A Program for Crystal Structure Determination*; University of Cambridge: Cambridge, England, 1976.

# Reaction of Aminocarbene Complexes of Chromium with Alkynes. 5. Influence of the Ring Size on the Product Distribution. Formation of Pyrroles from Pyrrolidine and Its Derivative-Substituted Carbene Complexes

Andrée Parlier, Michèle Rudler, Henri Rudler,\* Régis Goumont, Jean-Claude Daran, and Jacqueline Vaissermann

Laboratoire de Chimie Organique, URA 408, and Laboratoire de Chimie des Métaux de Transition URA 608, Université Pierre et Marie Curie, 4 place Jussieu, 75252 Paris Cedex 5, France

Received July 22, 1994<sup>®</sup>

A series of aminocarbene complexes of chromium derived from piperidine (**1**), hexa- and heptamethyleneimine (**4**) and (**8**), pyrrolidine (**13a-d**,  $R_1 = \text{Me, H, Ph, thienyl}$ ), perhydroindole (**21**), thiazolidine (**24a,b**,  $R_1 = \text{Me, Ph}$ ), pyrroline (**30a,b**), and azetidines (**33a-e** and **36**) have been synthesized and subjected to alkyne insertion reactions. Aminocarbene complex **24a-E** has been fully characterized by X-ray structure analysis. Crystal data for **24a-E**:  $\text{C}_{10}\text{H}_9\text{O}_5\text{NSCr}$ , monoclinic, space group  $P2_1/n$ ,  $a = 8.3011(9) \text{ \AA}$ ,  $b = 11.949(1) \text{ \AA}$ ,  $c = 13.101(2) \text{ \AA}$ ,  $\beta = 95.74(1)^\circ$ ,  $V = 1293(1) \text{ \AA}^3$ ,  $d_{\text{calcd}} = 1.41 \text{ g cm}^{-3}$ ,  $Z = 4$ . Whereas complex **1** reacted with diphenylacetylene to give first the ylide complex **2**, the thermolysis of which led to the bridgehead lactam **3**, complexes **4**, and **8** gave directly the expected bridgehead lactams **6** and **11**. The structure of **3** has been determined by X-ray diffraction. Crystal data for **3**:  $\text{C}_{27}\text{H}_{25}\text{ON}$ , monoclinic, space group  $P2_1/c$ ,  $a = 10.080(4) \text{ \AA}$ ,  $b = 11.727(3) \text{ \AA}$ ,  $c = 18.014(6) \text{ \AA}$ ,  $\beta = 102.40(3)^\circ$ ,  $V = 2080(14) \text{ \AA}^3$ ,  $d_{\text{calcd}} = 1.21 \text{ g cm}^{-3}$ ,  $Z = 4$ . In contrast to **1**, **4**, and **8**, all of the new carbene complexes derived from five-membered cycloamines except **24b** gave pyrrole derivatives as the result of the alkyne/CO insertion followed by migration of an alkyl chain from nitrogen to the carbon atom of the inserted carbonyl group and loss of its oxygen atom. The structures of **14a**, the  $\text{Cr}(\text{CO})_3$  complex of **15a**, and **22** could be unambiguously established by X-ray crystallography. Crystal data for **15**:  $\text{C}_{24}\text{H}_{21}\text{O}_3\text{NCr}$ , triclinic, space group  $P1$ ,  $a = 6.918(1) \text{ \AA}$ ,  $b = 10.057(1) \text{ \AA}$ ,  $c = 15.193(2) \text{ \AA}$ ,  $\alpha = 72.410(9)^\circ$ ,  $\beta = 84.99(1)^\circ$ ,  $\gamma = 84.66(3)^\circ$ ,  $V = 1001(3) \text{ \AA}^3$ ,  $d_{\text{calcd}} = 1.40 \text{ g cm}^{-3}$ ,  $Z = 2$ . For **22**:  $\text{C}_{24}\text{H}_{25}\text{N}$ , monoclinic, space group  $P2_1/n$ ,  $a = 11.119(3) \text{ \AA}$ ,  $b = 10.682(2) \text{ \AA}$ ,  $c = 15.428(3) \text{ \AA}$ ,  $\beta = 102.23(2)^\circ$ ,  $V = 1791(7) \text{ \AA}^3$ ,  $d_{\text{calcd}} = 1.21 \text{ g cm}^{-3}$ ,  $Z = 4$ . Besides these pyrroles, the expected bridgehead lactams **17a-d** were isolated from **13a-d** together with the lactone complex **18** in the case of **13b**. Crystal data for **18**:  $\text{C}_{19}\text{H}_{12}\text{O}_5\text{Cr}$ , orthorhombic, space group  $Pc2_1/b$ ,  $a = 10.356(1) \text{ \AA}$ ,  $b = 12.366(5) \text{ \AA}$ ,  $c = 12.529(2) \text{ \AA}$ ,  $V = 1604.4(8) \text{ \AA}^3$ ,  $d_{\text{calcd}} = 1.54 \text{ g cm}^{-3}$ ,  $Z = 4$ . However, **24b** gave as the major insertion product the aminofuran **26**, and pyrroline-derived carbene complexes **30a,b** gave lactams **32a,b** and trace amounts of pyrroles **31a,b**. Only trace amounts of pyrroles were detected starting from carbene complexes derived from azetidines (**33a-e**) and **36**, which gave mainly the lactams **35a,d** and **37**. Mechanisms for these new transformations of aminocarbene complexes of chromium based on the behavior of the Stevens-type acyl-stabilized *N*-ylides will be suggested.

## Introduction

The isolation of *N*-ylide complexes during the interaction of alkynes with aminocarbene complexes of chromium and their thermal transformation into lactams upon migration of alkyl groups from nitrogen to carbon atoms brought to light large analogies between these zwitterionic species and those discovered by Stevens, especially regarding the manner by which they rearrange thermally. In previous papers,<sup>1,2</sup> we described mainly products arising from the migration of the substituents from nitrogen to the  $\alpha$  and  $\gamma$  carbons of the intermediate *N*-ylide complexes. The present pub-

lication deals with the formation of pyrroles due to the migration of alkyl groups from nitrogen to the central carbon atom of the ketene function and the formation of aminofurans due to the cleavage of a carbon-nitrogen bond followed by the formation of a carbon-oxygen bond.

## Results

**Synthesis of the Aminocarbene Complexes.** Complexes **1**, **13a,c,d**, **24a,b**, **30a,b**, **33b-d**, and **36** were obtained by aminolysis of the corresponding ethoxy carbene complexes with the proper cycloamine,<sup>3,4</sup> complexes **4**, **8**, **13b**, **21**, **33a**, and **33e** were prepared from the formyl derivatives of the corresponding cycloamines

<sup>®</sup> Abstract published in *Advance ACS Abstracts*, May 1, 1995.

(1) Chelain, E.; Goumont, R.; Hamon, L.; Parlier, A.; Rudler, M.; Rudler, H.; Daran, J. C.; Vaissermann, J. *J. Am. Chem. Soc.* **1992**, *114*, 8088.

(2) Chelain, E.; Parlier, A.; Audouin, M.; Rudler, H.; Daran, J. C.; Vaissermann, J. *J. Am. Chem. Soc.* **1993**, *115*, 10568.

(3) Moser, E.; Fischer, E. O. *J. Organomet. Chem.* **1968**, *15*, 147.

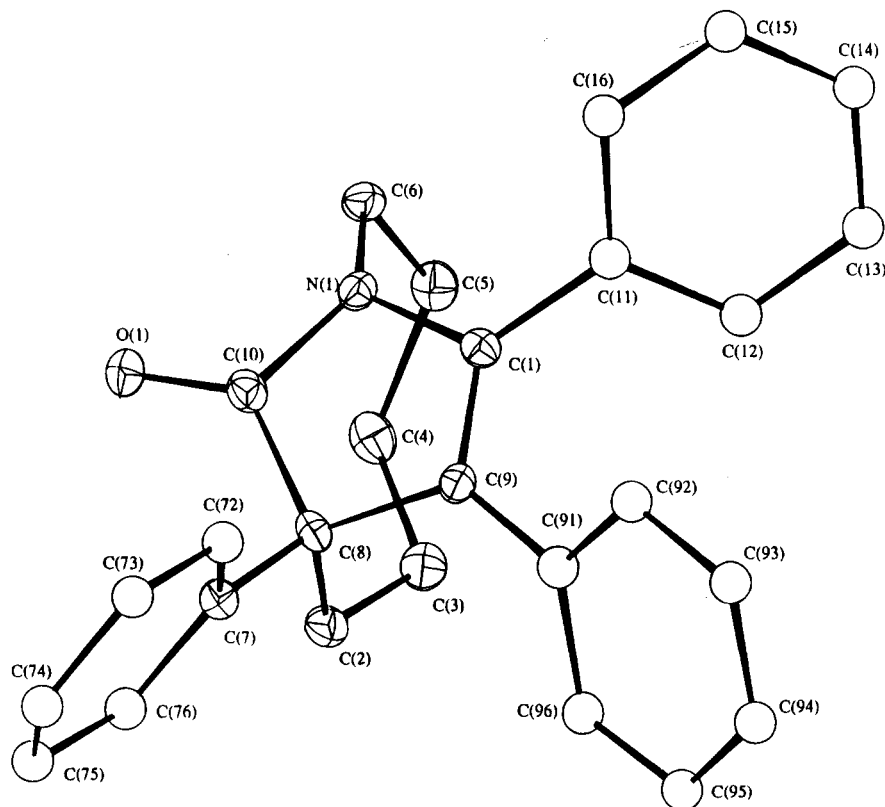
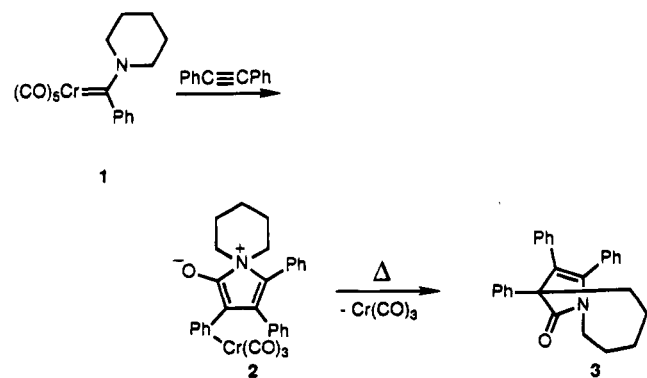


**Figure 1.** ORTEP drawing of compound **3** showing the atom-labeling scheme. The thermal ellipsoids are drawn at the 30% probability level.

and  $(\text{CO})_5\text{CrNa}_2$ .<sup>5</sup> Details for these syntheses are given in the Experimental Section.

In the case of **24a**, the two expected *E* and *Z* isomers, differing by the position of the sulfur atom with respect to the metal, were formed in 65% yield and were separated by silica gel chromatography.

**Reaction with Alkynes. Aminocarbene Complexes Derived from Six-, Seven-, and Eight-Membered Cycloamines: Formation of Bridgehead Lactams. Solid State Structure of Lactam 3.** When complex **1** was refluxed in cyclohexane in the presence of diphenylacetylene, the *N*-ylide complex **2** was obtained as yellow crystals in 65% yield. Heating this complex either in boiling toluene or pyridine led to formation of the metal-free bridgehead lactam **3** in 40% yield. Migration of the alkyl chain from nitrogen to the

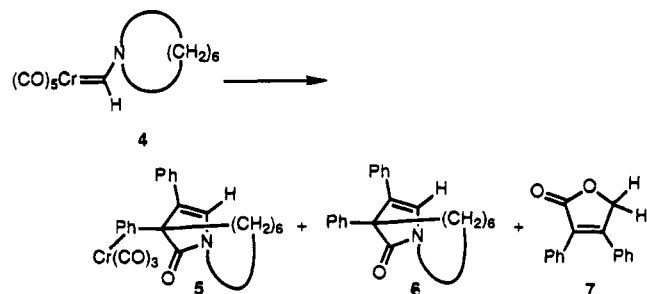


$\gamma$  carbon could be confirmed by an X-ray analysis carried out on crystals of **3**. The ORTEP projection of this lactam appears in Figure 1, the most important bond distances (Å) and bond angles (deg) being gathered in Table 1. Increasing the size of the cycle did not change the course of the reaction: the expected lactams could

**Table 1.** Selected Bond Distances (Å) and Bond Angles (deg) for Compound **3**

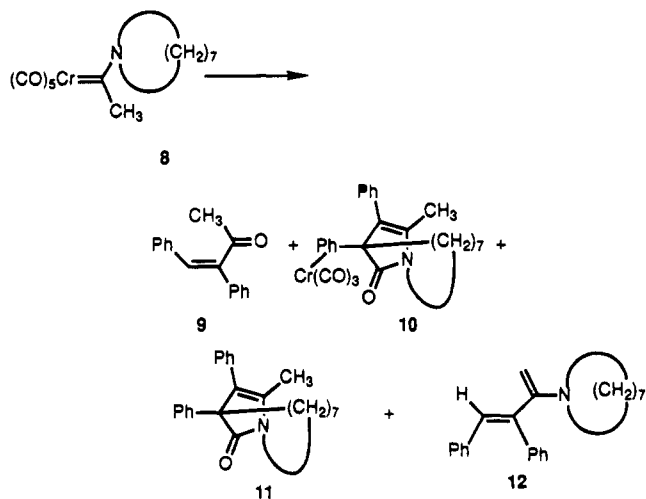
O(1)–C(10)	1.216(7)	N(1)–C(1)	1.420(7)
N(1)–C(6)	1.468(7)	N(1)–C(10)	1.388(7)
C(1)–C(9)	1.340(8)	C(1)–C(11)	1.475(8)
C(2)–C(3)	1.527(9)	C(2)–C(8)	1.561(9)
C(3)–C(4)	1.553(9)	C(4)–C(5)	1.541(9)
C(5)–C(6)	1.534(9)	C(7)–C(8)	1.519(8)
C(8)–C(9)	1.517(8)	C(8)–C(10)	1.528(9)
C(9)–C(91)	1.473(8)		
C(6)–N(1)–C(1)	122.8(5)	C(10)–N(1)–C(1)	109.3(5)
C(10)–N(1)–C(6)	117.5(5)	C(9)–C(1)–N(1)	111.4(5)
C(11)–C(1)–N(1)	118.9(5)	C(11)–C(1)–C(9)	129.7(6)
C(8)–C(2)–C(3)	116.7(5)	C(4)–C(3)–C(2)	119.8(6)
C(5)–C(4)–C(3)	118.4(6)	C(6)–C(5)–C(4)	115.8(5)
C(5)–C(6)–N(1)	110.3(5)	C(7)–C(8)–C(2)	114.2(5)
C(9)–C(8)–C(2)	111.0(5)	C(9)–C(8)–C(7)	114.9(5)
C(10)–C(8)–C(2)	102.1(5)	C(10)–C(8)–C(7)	111.1(5)
C(10)–C(8)–C(9)	102.1(5)	C(8)–C(9)–C(1)	108.5(5)
C(91)–C(9)–C(1)	125.7(6)	C(91)–C(9)–C(8)	125.8(5)
N(1)–C(10)–O(1)	125.7(6)	C(8)–C(10)–O(1)	127.0(6)
C(8)–C(10)–N(1)	107.0(5)		

be characterized either free or as their  $\text{Cr}(\text{CO})_3$  complexes. Minor products were isolated in these two cases: the lactone **7** in the case of complex **4** (vide infra)

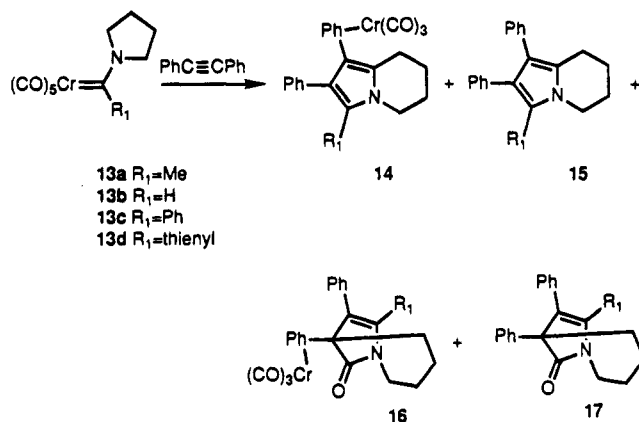


and the enamine **12** and its hydrolysis product, the already described ketone **9<sup>6</sup>** in the case of complex **8**.





**Pyrrolidine and Derivative-Substituted Carbene Complexes: Formation of Pyrroles.** When complex **13a** was heated in refluxing benzene in the presence of a slight excess of diphenylacetylene for 12 h, a mixture of new complexes and organic products was obtained. They could be separated as such (see the Experimental Section), but for the sake of simplicity the residue of the reaction was treated with pyridine in order to remove the metal. Silica gel chromatography led finally to two organic products. The less polar compound obtained in 25% yield was given the structure **15a**: its mass spectrum and elemental analysis confirmed that it was not a classical product arising either from the sole alkyne insertion (one more carbon observed) or from the alkyne and CO insertions (no oxygen present). The  $^1\text{H}$  and  $^{13}\text{C}$  NMR spectra were quite



simple: the first spectrum displayed signals for the aromatic protons and for the methylene groups of the pyrrolidine ring system. Moreover, a signal for a deshielded methyl group was present at  $\delta$  2.27 ppm. In the second spectrum, the  $\text{CH}_2$  groups gave signals at  $\delta$  43.13, 23.75, 23.40, and 21.12 ppm, confirming that ring-opening with rearrangement probably took place. The structure of the corresponding arene chromium complex **14a** was finally assessed by X-ray diffraction study. The ORTEP projection appears in Figure 2, the most important bond distances ( $\text{\AA}$ ) and bond angles (deg) being collected in Table 2. The figure indeed shows that, in addition to the insertion of the alkyne and of one carbon atom, a major rearrangement took place with migration of the alkyl chain from nitrogen to the inserted carbon atom C(9).

The second product (31% yield) was the expected bridgehead lactam **17a** resulting from the insertion of

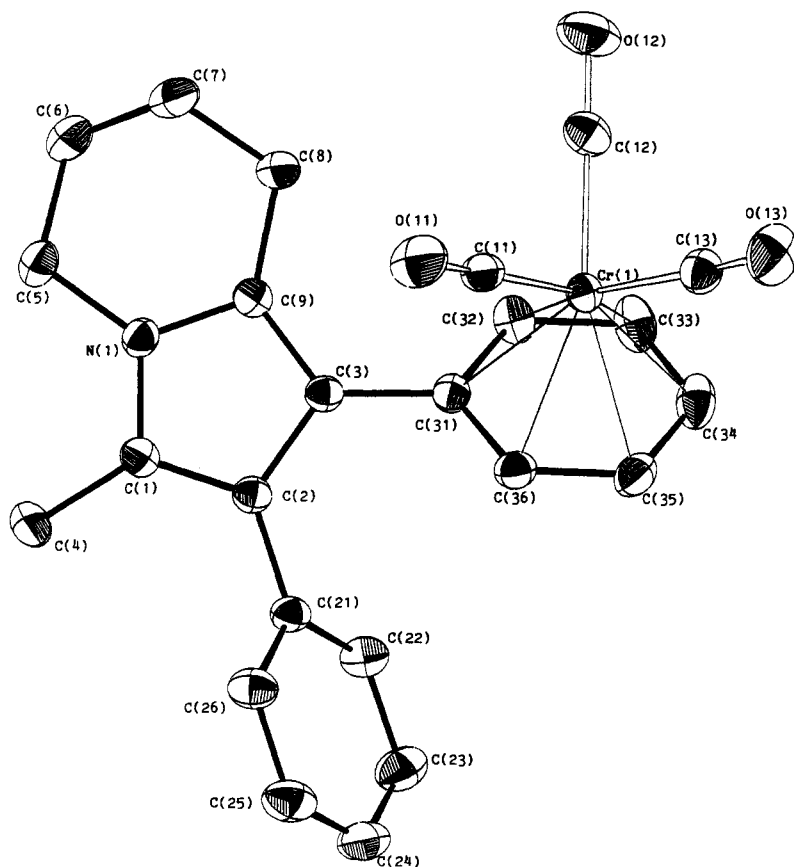


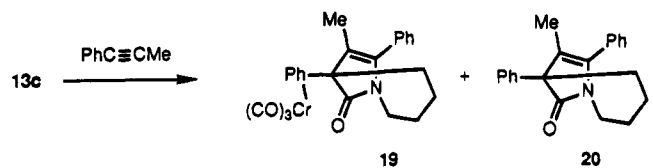
**Figure 2.** ORTEP drawing of compound **14a** showing the atom-labeling scheme. The thermal ellipsoids are drawn at the 30% probability level.

**Table 2. Selected Bond Distances (Å) and Bond Angles (deg) for Compound 14a**

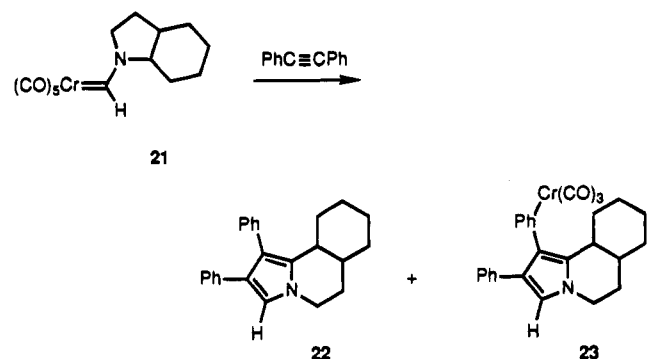
Cr(1)–C(11)	1.834(3)	C(11)–O(11)	1.146(3)
Cr(1)–C(12)	1.834(3)	C(12)–O(12)	1.150(3)
Cr(1)–C(13)	1.833(3)	C(13)–O(13)	1.146(3)
Cr(1)–C(31)	2.266(2)	Cr(1)–C(32)	2.213(3)
Cr(1)–C(33)	2.207(2)	Cr(1)–C(34)	2.216(3)
Cr(1)–C(35)	2.205(3)	Cr(1)–C(36)	2.210(2)
N(1)–C(1)	1.379(3)	N(1)–C(5)	1.462(3)
N(1)–C(9)	1.376(3)	C(1)–C(2)	1.370(3)
C(1)–C(4)	1.486(3)	C(2)–C(3)	1.431(3)
C(2)–C(21)	1.472(3)	C(3)–C(9)	1.379(3)
C(3)–C(31)	1.469(3)	C(5)–C(6)	1.502(4)
C(6)–C(7)	1.503(4)	C(7)–C(8)	1.507(4)
C(8)–C(9)	1.483(3)		
C(12)–Cr(1)–C(11)	90.0(1)	O(11)–C(11)–Cr(1)	179.1(2)
C(13)–Cr(1)–C(11)	87.8(1)	O(12)–C(12)–Cr(1)	179.4(3)
C(13)–Cr(1)–C(12)	87.1(1)	O(13)–C(13)–Cr(1)	178.0(2)
C(5)–N(1)–C(1)	125.3(2)	C(9)–N(1)–C(1)	109.8(2)
C(9)–N(1)–C(5)	124.9(2)	C(2)–C(1)–N(1)	107.9(2)
C(4)–C(1)–N(1)	121.7(2)	C(4)–C(1)–C(2)	130.3(2)
C(3)–C(2)–C(1)	107.3(2)	C(9)–C(3)–C(2)	107.5(2)
C(6)–C(5)–N(1)	111.8(2)	C(7)–C(6)–C(5)	111.7(2)
C(8)–C(7)–C(6)	110.6(2)	C(9)–C(8)–C(7)	111.9(2)
C(3)–C(9)–N(1)	107.4(2)	C(8)–C(9)–N(1)	120.7(2)
C(8)–C(9)–C(3)	131.8(2)		

both the alkyne and CO and from the migration of the alkyl chain from nitrogen to the  $\gamma$  position.

Complexes **13b–d** behaved similarly with diphenylacetylene and gave mixtures of pyrrole complexes **14** and pyrroles **15** and of lactam complexes **16** and lactams **17**. However, the insertion of 1-phenyl-1-propyne into carbene complex **13c** only gave a mixture of the complexed and metal-free bridgehead lactams **19** and **20**. In the case of complex **21**, derived from perhydroindole, the pyrrole **22** and its complex **23** were the major



products of the reaction (31% yield). The structure of



**22** could again be ascertained by an X-ray analysis. The ORTEP view appears in Figure 4, the most important bond distances (Å) and bond angles (deg) being displayed in Table 4. Notice here that in the case of complex **13b** the same lactone **7** as from complex **4** could be isolated and fully characterized as its  $\text{Cr}(\text{CO})_3$  complex **18**, the hydrolysis product of the aminofuran

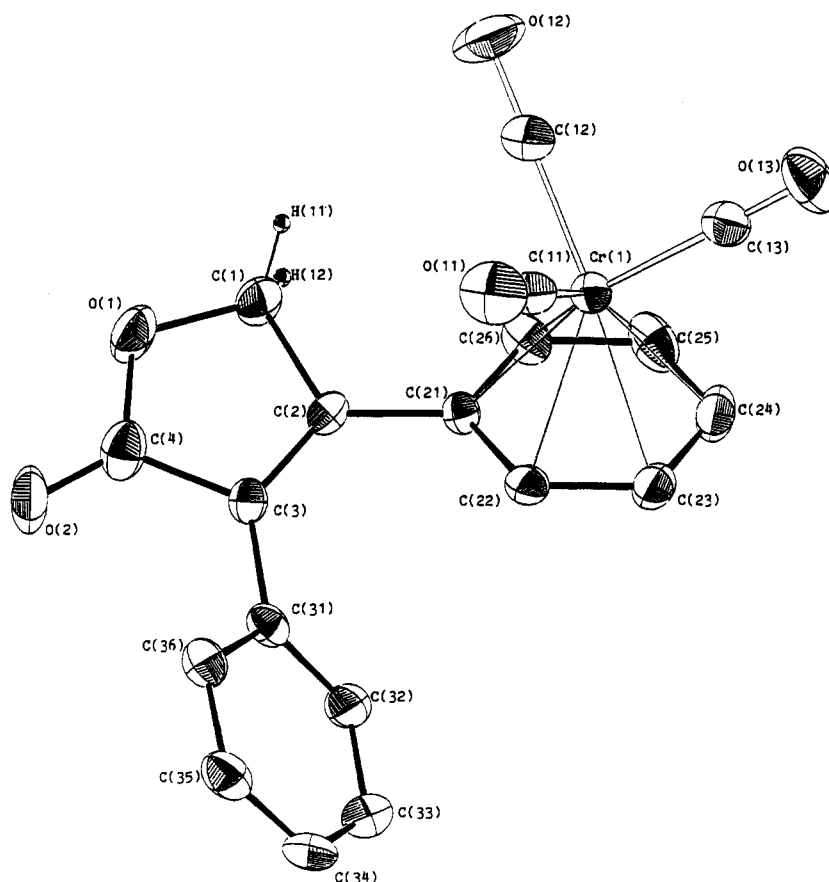


**Figure 3.** ORTEP drawing of compound **18** showing the atom-labeling scheme. The thermal ellipsoids are drawn at the 30% probability level.

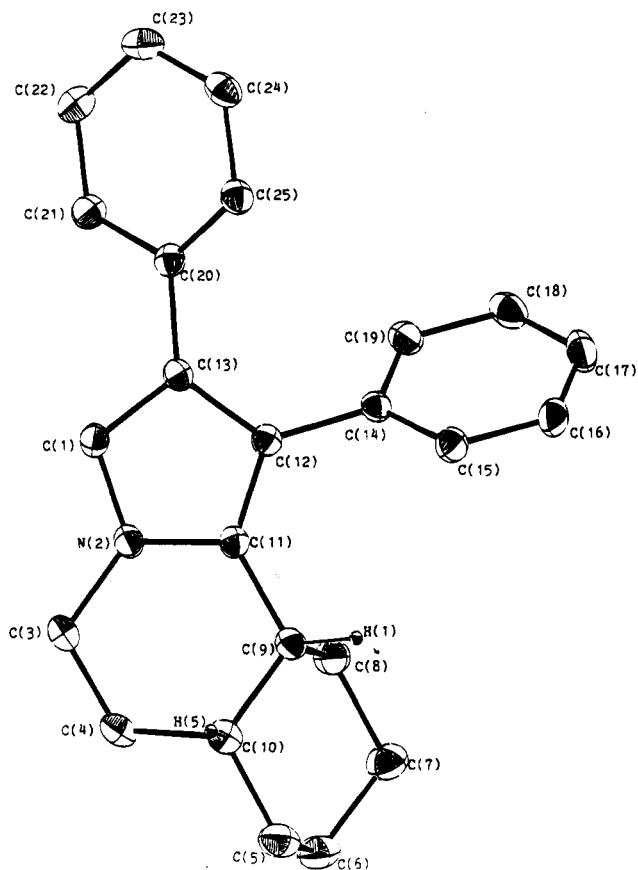
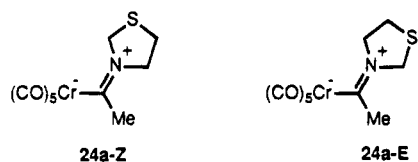


**Figure 4.** ORTEP drawing of compound **22** showing the atom-labeling scheme. The thermal ellipsoids are drawn at the 30% probability level.

complex **18a**. Its ORTEP projection appears in Figure 3, the most important bond distances (Å) and bond angles (deg) being gathered in Table 3.

**Thiazolidine-Derived Carbene Complexes 24a and 24b.** Since, in the case of the two rotamers **24a-Z** and **24a-E**, products arising from the cleavage of two



different carbon–nitrogen bonds, N–C(3) or N–C(4), could be expected, their structures were accurately determined by X-ray crystallography and the alkyne insertion reaction was carried out on the two complexes separately. Crystals of the less polar complex could be grown: as shown on the ORTEP projection provided in Figure 5 it corresponds to the *E* isomer. In agreement with the structures already established for other aminocarbene complexes of chromium, the bond distances are typical for such a complex with a short nitrogen–carbon bond (N(1)–C(1) = 1.300(4) Å) and a long metal–carbon bond (Cr–C(1) = 2.123(3) Å). The bond distances (Å) and bond angles (deg) are displayed in Table 5.

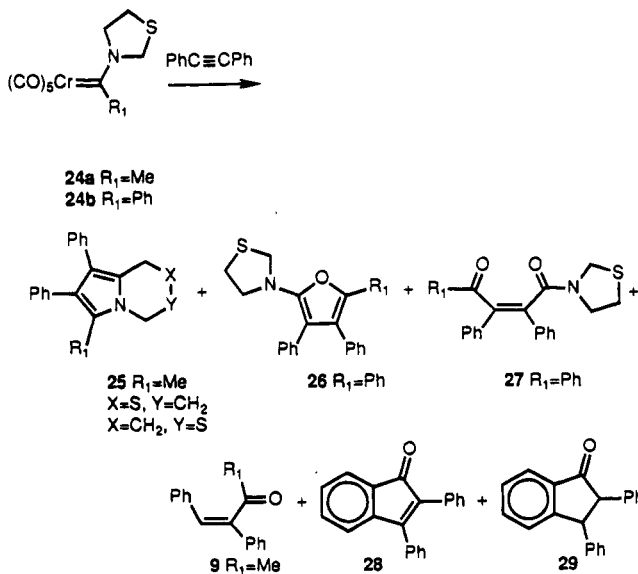
However, no variation in the product distribution was observed: both isomers reacted with diphenylacetylene and led to the same mixture of pyrrole **25a** and of its Cr(CO)<sub>3</sub> complex. According to the <sup>1</sup>H NMR spectrum, **25a** consisted of a mixture of isomers, one of them being largely predominant: for one isomer the isolated CH<sub>2</sub>

**Table 3.** Selected Bond Distances (Å) and Bond Angles (deg) for Compound **18**

Cr(1)–C(11)	1.815(6)	C(11)–O(11)	1.163(7)
Cr(1)–C(12)	1.823(6)	C(12)–O(12)	1.162(7)
Cr(1)–C(13)	1.825(6)	C(13)–O(13)	1.144(7)
Cr(1)–C(21)	2.242(5)	Cr(1)–C(22)	2.200(5)
Cr(1)–C(23)	2.215(6)	Cr(1)–C(24)	2.196(5)
Cr(1)–C(25)	2.213(6)	Cr(1)–C(26)	2.198(6)
O(1)–C(1)	1.430(7)	O(1)–C(4)	1.344(7)
C(1)–C(2)	1.495(7)	C(2)–C(3)	1.334(7)
C(2)–C(21)	1.460(7)	C(3)–C(4)	1.491(7)
C(3)–C(31)	1.471(6)	C(4)–O(2)	1.179(7)
C(12)–Cr(1)–C(11)	87.9(3)	O(11)–C(11)–Cr(1)	179.1(6)
C(13)–Cr(1)–C(11)	85.5(3)	O(12)–C(12)–Cr(1)	179.5(6)
C(13)–Cr(1)–C(12)	88.7(3)	O(13)–C(13)–Cr(1)	178.0(6)
C(4)–O(1)–C(1)	110.1(4)	C(2)–C(1)–O(1)	104.9(4)
C(3)–C(2)–C(1)	108.9(4)	C(21)–C(2)–C(1)	120.3(5)
C(21)–C(2)–C(3)	130.8(5)	C(4)–C(3)–C(2)	107.8(5)
C(31)–C(3)–C(2)	130.8(5)	C(31)–C(3)–C(4)	121.4(5)
C(3)–C(4)–O(1)	108.3(5)	O(2)–C(4)–O(1)	123.3(6)
O(2)–C(4)–C(3)	128.4(6)		

**Table 4.** Selected Bond Distances (Å) and Bond Angles (deg) for Compound **22**

C(1)–N(2)	1.364(4)	C(1)–C(13)	1.368(4)
N(2)–C(3)	1.460(4)	N(2)–C(11)	1.380(3)
C(3)–C(4)	1.509(4)	C(4)–C(10)	1.528(4)
C(5)–C(6)	1.510(5)	C(5)–C(10)	1.525(4)
C(6)–C(7)	1.511(5)	C(7)–C(8)	1.528(5)
C(8)–C(9)	1.524(4)	C(9)–C(10)	1.537(4)
C(9)–C(11)	1.497(4)	C(11)–C(12)	1.373(4)
C(12)–C(13)	1.430(4)		
C(13)–C(1)–N(2)	108.9(2)	C(3)–N(2)–C(1)	125.2(2)
C(11)–N(2)–C(1)	109.3(2)	C(11)–N(2)–C(3)	124.8(2)
C(4)–C(3)–N(2)	110.4(2)	C(10)–C(4)–C(3)	109.8(3)
C(10)–C(5)–C(6)	113.6(3)	C(7)–C(6)–C(5)	111.0(3)
C(8)–C(7)–C(6)	111.0(3)	C(9)–C(8)–C(7)	112.1(3)
C(11)–C(9)–C(8)	112.3(2)	C(11)–C(9)–C(10)	111.0(3)
C(11)–C(9)–C(10)	111.8(2)	C(5)–C(10)–C(4)	113.8(3)
C(9)–C(10)–C(4)	110.1(3)	C(9)–C(10)–C(5)	111.4(3)
C(9)–C(11)–N(2)	119.7(3)	C(12)–C(11)–N(2)	107.4(2)
C(12)–C(11)–C(9)	132.2(3)	C(13)–C(12)–C(11)	107.8(2)
C(12)–C(13)–C(1)	106.5(3)		



group gave a signal at  $\delta$  3.93 ppm, and for the other isomer it appeared at  $\delta$  3.90 ppm. In contrast to pyrroles **15**, pyrroles **25a** appeared to be very unstable, degradation of the product being observed both in chlorinated solvents and on silica gel. Thus the best yield (25%) was observed upon direct silica gel flash chromatography of the reaction residue. That both isomers gave the same result was probably linked to

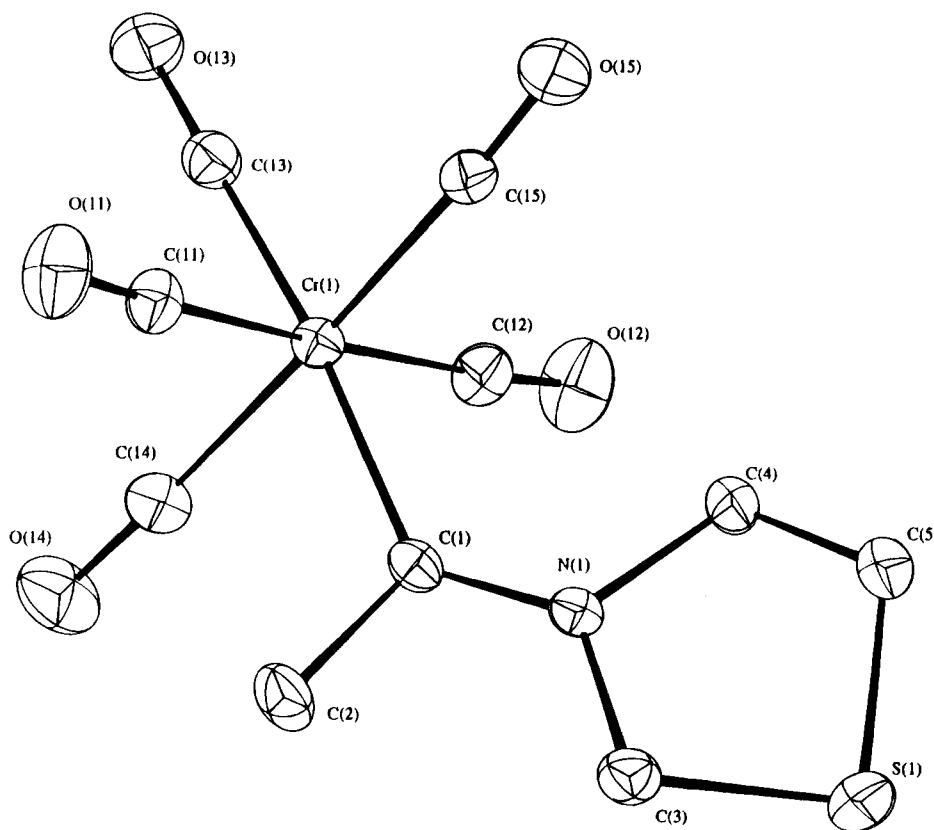


**Figure 5.** ORTEP drawing of compound **24a** showing the atom-labeling scheme. The thermal ellipsoids are drawn at the 30% probability level.

**Table 5. Bond Distances (Å) and Bond Angles (deg) for Compound 24a**

Cr(1)–C(1)	2.123(3)	Cr(1)–C(11)	1.888(3)
Cr(1)–C(12)	1.895(3)	Cr(1)–C(13)	1.864(3)
Cr(1)–C(14)	1.892(3)	Cr(1)–C(15)	1.893(3)
S(1)–C(3)	1.786(4)	S(1)–C(5)	1.785(4)
O(11)–C(11)	1.139(4)	O(12)–C(12)	1.130(4)
O(13)–C(13)	1.146(4)	O(14)–C(14)	1.134(4)
O(15)–C(15)	1.138(4)	N(1)–C(1)	1.300(4)
N(1)–C(3)	1.488(4)	N(1)–C(4)	1.482(4)
C(1)–C(2)	1.510(4)	C(4)–C(5)	1.487(5)
C(11)–Cr(1)–C(1)	89.0(1)	C(12)–Cr(1)–C(1)	92.5(1)
C(13)–Cr(1)–C(1)	174.6(1)	C(14)–Cr(1)–C(1)	86.4(1)
C(15)–Cr(1)–C(1)	94.9(1)	C(12)–Cr(1)–C(11)	177.9(1)
C(13)–Cr(1)–C(11)	89.2(1)	C(13)–Cr(1)–C(12)	89.5(1)
C(14)–Cr(1)–C(11)	90.4(1)	C(14)–Cr(1)–C(12)	91.2(1)
C(14)–Cr(1)–C(13)	88.5(1)	C(15)–Cr(1)–C(11)	87.6(1)
C(15)–Cr(1)–C(12)	90.8(1)	C(15)–Cr(1)–C(13)	90.1(1)
C(15)–Cr(1)–C(14)	177.6(2)		
O(11)–C(11)–Cr(1)	178.1(3)	O(12)–C(12)–Cr(1)	176.3(3)
O(13)–C(13)–Cr(1)	179.4(3)	O(14)–C(14)–Cr(1)	177.6(3)
O(15)–C(15)–Cr(1)	177.3(3)		
C(5)–S(1)–C(3)	90.1(2)	C(3)–N(1)–C(1)	124.6(2)
C(4)–N(1)–C(1)	124.4(2)	C(4)–N(1)–C(3)	111.1(2)
N(1)–C(1)–Cr(1)	129.5(2)	C(2)–C(1)–Cr(1)	117.6(2)
C(2)–C(1)–N(1)	112.8(3)	N(1)–C(3)–S(1)	107.9(2)
C(5)–C(4)–N(1)	108.5(3)	C(4)–C(5)–S(1)	105.2(2)

the interconversion of the isomers during the insertion reaction: indeed, heating **24a-E** or **24a-Z** in benzene for 12 h led to a 50/50 mixture of the two isomers.<sup>7</sup>

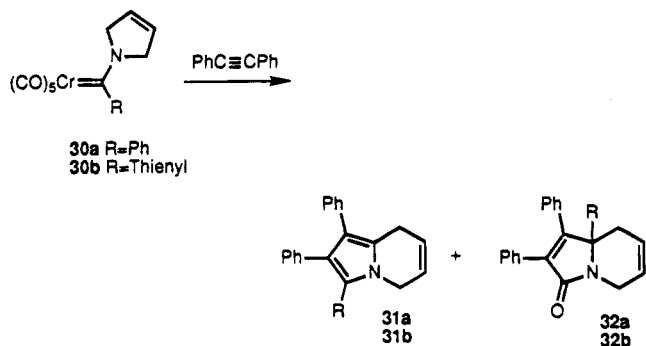
Complex **24b** ( $R_1 = \text{Ph}$ ), obtained as a 40/60 mixture of *E/Z* isomers behaved differently: no pyrrole could be detected. Instead, the major products of the reaction appeared to be the aminofuran **26b** and its  $\text{Cr}(\text{CO})_3$  complex. Treatment of the crude reaction product in

boiling pyridine, after silica gel chromatography, gave **26b** in 41% yield together with small and variable amounts of its oxidation product, the ketoamide **27**. The  $^1\text{H}$  NMR spectrum of **26b** confirmed the presence of the thiazolidine ring system, with signals at  $\delta$  4.35 ( $\text{NCH}_2\text{S}$ ), 3.62, and 3.10 ppm ( $2\text{CH}_2$ ). The  $^{13}\text{C}$  NMR spectrum was again typical for such a structure with a signal at  $\delta$  151.3 ppm for the NCO carbon and a signal at  $\delta$  109 ppm for the second carbon of the furan linked to oxygen. The spectroscopic data of **27** agreed with those of other ketoamides already isolated from aminofurans: the  $^{13}\text{C}$  NMR spectrum disclosed signals for the two carbonyl carbons at  $\delta$  197.04 and 168.06 ppm. Finally, small amounts of the benzannulation products **28** (11%) and **29** (7%) were also isolated.<sup>8</sup> In order to get a better insight into the mechanism of this reaction, attempts were made to isolate the presumable *N*-ylide which might be formed prior to the rearrangement reaction. However, heating the alkyne and the starting complex **24b** in refluxing cyclohexane led directly to the formation of **26b**, the complexed aminofuran.

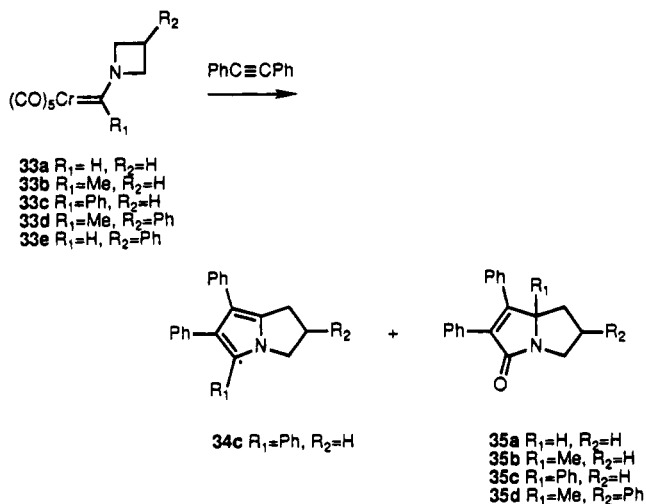
**Pyrroline and Azetidone-Substituted Carbene Complexes 30a,b, 33a–e, and 36.** Under the same conditions as for the pyrrolidine-substituted carbene complexes, no bridgehead lactams were isolated starting from the pyrrolidine-substituted carbene complexes. Thus, complexes **30a,b** led to the lactams **32a** and **32b** in respectively 61% and 43% yields. However, in the case of **30a**, a less polar compound could be detected. Both its mass spectrum ( $m/z = 347$ ) and its proton NMR spectrum, with signals at  $\delta$  3.95 and 3.31 ppm for the two  $\text{CH}_2$  groups, were consistent with a structure such as **31a**. A similar result was observed in the case of **30b** which led to trace amounts of **31b**. Likewise,

(4) Rudler, H.; Parlier, A.; Yefsah, R.; Denise, B.; Daran, J. C.; Vaissermann, J.; Knobler, C. *J. Organomet. Chem.* **1988**, *358*, 245.

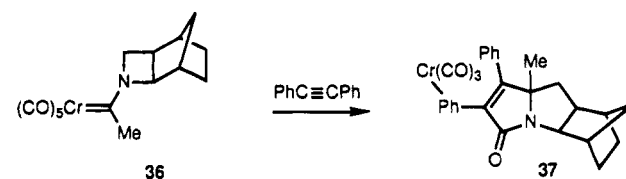
(5) Imwinkelried, R.; Hegedus, L. S. *Organometallics* **1988**, *7*, 702.



starting from azetidene-substituted carbene complexes **33a–d**, no bridgehead lactams were isolated. Thus,



when **33b** was heated in benzene in the presence of diphenylacetylene, the metal-free substituted pyrrolizidine **35b** was obtained in 40% yield as a white solid. The IR spectrum ( $\nu_{\text{CO}}, 1675 \text{ cm}^{-1}$ ) as well as the  $^{13}\text{C}$  NMR spectrum ( $\delta 173.7 \text{ ppm}$  (CO)) were in agreement with the presence of an unsaturated lactam. The  $^{13}\text{C}$  NMR spectrum disclosed signals for a quaternary N–C carbon at  $\delta 72.22 \text{ ppm}$ , for an NCH<sub>2</sub> group at  $\delta 41.34 \text{ ppm}$ , for two methylene groups at  $\delta 35.15$  and  $28.40 \text{ ppm}$ , and finally for the angular methyl group at  $\delta 22.24 \text{ ppm}$ . Similar results were observed for complexes **38a,c,d** and **36**, which gave the corresponding lactams **35a,c,d** and **37**. A slight difference in behavior was, however, observed for complex **33c** since small amounts (1.8%) of the corresponding pyrrole **34c** could be detected and isolated upon careful silica gel chromatog-



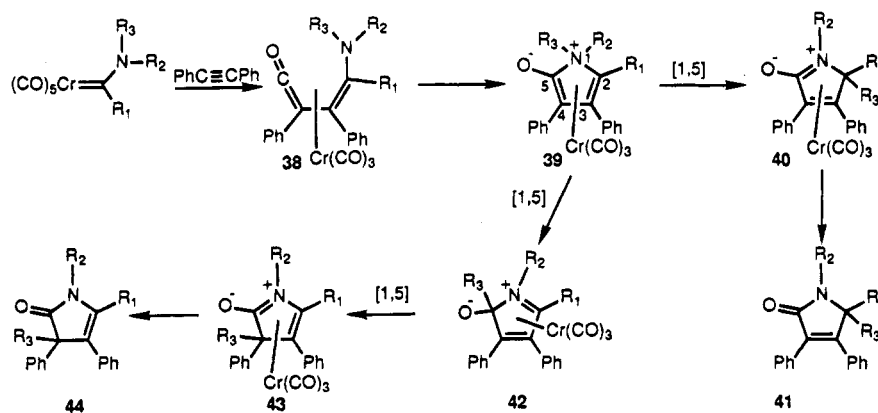
raphy. The spectroscopic data of **34c** were in accordance with those of the pyrroles so far isolated: the mass spectrum agreed with the absence of oxygen, whereas the  $^1\text{H}$  NMR spectrum depicted signals for three distinct CH<sub>2</sub> groups, at  $\delta 4.08$  (NCH<sub>2</sub>), 3.11, and 2.56 ppm. Surprisingly, whereas the phenyl-substituted azetidene carbene complex **33d** gave the insertion product **35d** as a mixture of two isomers, no reaction except for decomposition of the starting complex was observed in the case of complex **33e**.

## Discussion

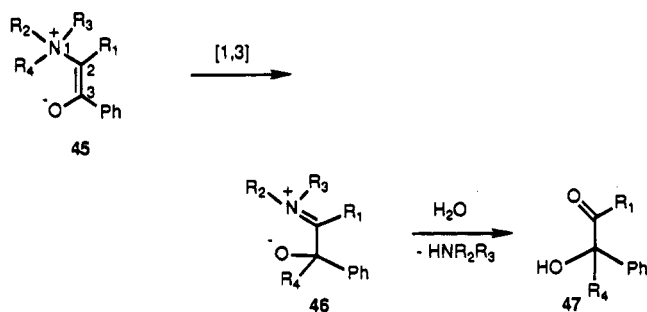
Up to now, most of the products obtained upon insertion of the alkynes into aminocarbene complexes of chromium could be derived from the  $\text{Cr}(\text{CO})_3$ -stabilized betaine **39** (Scheme 1), one of the limiting forms of the isolated intermediate, which can also be considered as the vinylog of the Stevens betaine **45** (Scheme 2).<sup>9</sup> Indeed and without taking into account the presence of the metal, successive (1,5) migrations of the alkyl group R<sub>3</sub> led either to **41** via **40** or to **44** via **42** and **43** (Scheme 1). However, products derived from **42** and resulting thus from the migration of the alkyl group on the central atom of the ketene function were still missing, although in the case of organic betaines **45**, products arising from the migration of an alkyl group from nitrogen to the carbon atom C(3) were observed (Scheme 2). Thus **45** ( $\text{R}_1 = \text{R}_2 = \text{R}_3 = \text{Me}$ ,  $\text{R}_2 = \text{CH}_2\text{Ph}$ ) led, in addition to the expected (1,2) migration product, to the hydroxy ketone **47** via **46**.<sup>10</sup> This gap has now been filled since pyrroles of the general structure **49** could be isolated during the insertion of alkynes into pyrrolidine-substituted carbene complexes of chromium. The structures of **14a** and **22** clearly indicate that ring opening took place together with the migration of the alkyl chain on carbon C(5) (**39**  $\rightarrow$  **42**).

However, in contrast to the iminium derivative **46**, which gave **47** upon hydrolysis, **42** rearranges according to another pathway to give the pyrrole **49**: loss of oxygen is indeed observed. Although the exact mechanism of this transformation is not known, one can tentatively assume that the metal is involved in this

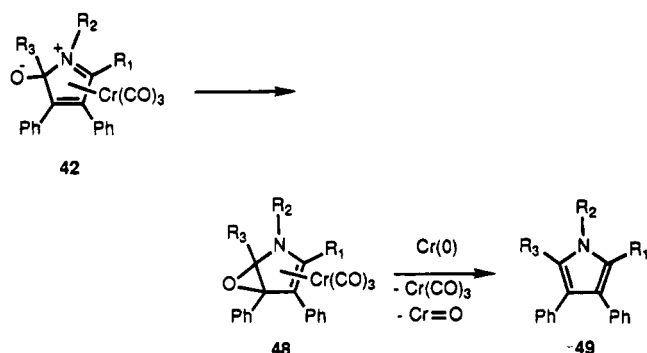
Scheme 1



Scheme 2



Scheme 3



last reaction: low-valent metal deoxygenation reactions are indeed known, and moreover, Cr(0)-mediated carbon–oxygen bond cleavages have been observed.<sup>11</sup> A possible mechanism for this transformation could thus involve the formation of **48** via an intramolecular nucleophilic addition followed by a Cr(0)-mediated deoxygenation reaction (Scheme 3).

That pyrroles are preferentially observed in the case of pyrrolidine-substituted carbene complexes might be due to the formation of a stable six-membered ring system upon the first (1,5) migration of the alkyl chain from nitrogen to the carbonyl carbon atom (**39** → **42**, Scheme 2, R<sub>2</sub>R<sub>3</sub> = (CH<sub>2</sub>)<sub>4</sub>) followed by the irreversible deoxygenation reaction (**42** → **49**).

**Comments on the Mechanism of Formation of Furans.** A last intriguing point concerns the formation of aminofurans during these alkyne insertion reactions.

Aminofurans have been observed in several instances during the reaction of aminocarbene complexes of chromium with alkynes: this was, for example, the case for complexes derived from *N*-methylaniline.<sup>8</sup> In the present report, complex **24b** gave as the main product the aminofuran **26** and its derivative **27** whereas complexes **13b** and **4** gave the lactone **18**, the hydrolysis product of the aminofuran **18a**. These types of products had also been obtained by Semmelhack from amino-

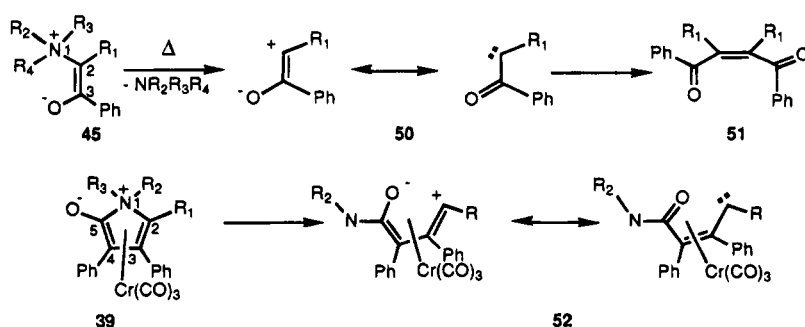
carbene complexes of iron.<sup>12</sup> More interestingly, the formation of furans is not limited to the case of aminocarbene complexes: indeed, Wulff and his co-workers observed the formation of alkoxyfurans from alkoxy-carbene complexes of chromium and molybdenum.<sup>13</sup> Labeling experiments clearly showed that migration of the alkoxy group from C(2) to C(5) took place. (Scheme 5, X = O). However, a mechanism via ylide complexes such as **39** (X = O) had been excluded. Let us again consider the Stevens rearrangement: a third reaction<sup>14</sup> which had been observed in the case of alkyl groups of low propensity for migration, was indeed the C(2)–N(1) bond rupture with formation of a tertiary amine together with products **51** formally derived from the carbenes **50**. (Scheme 4).

Applied to betaine **39** such a bond rupture would lead to the alkenone carbene complexes **52** (Scheme 4) or **54** (Scheme 5). Yet it is known that such intermediates which can be generated either photochemically from acetylcyclopropenes<sup>15</sup> or via carbene complexes from alkynyl diazo esters<sup>16</sup> rearrange to furans.

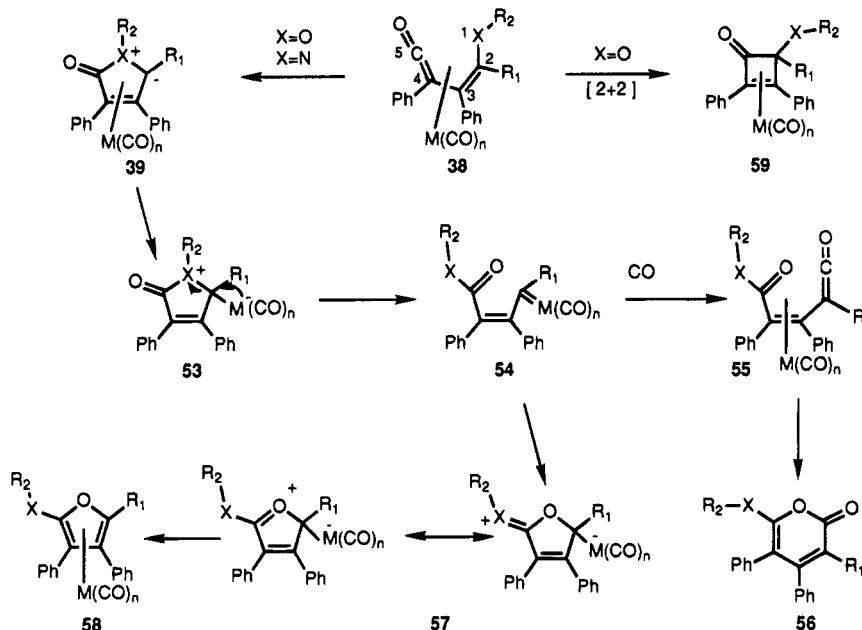
Thus, a mechanism which could account for the formation of both alkoxy and aminofurans might involve free- or metal-stabilized alkenone carbenes is outlined in the general Scheme 5: interaction of the heteroatom with the central carbon atom of the ketene function of **38** might lead to a metal-stabilized ylide **53**: for R<sub>2</sub> groups of low propensity for the migration, a metal-induced C(2)–X bond rupture could take place leading to a new carbene complex **54**. This complex might then undergo either of the two following transformations: (1) If the reaction is carried out under CO (as for the aminocarbene complexes of iron), CO insertion giving the ketene complex **55** followed by an electrocyclic reaction would lead to the pyrone **56**. Such products have indeed been observed in the case of aminocarbene complexes of iron.<sup>12</sup> (2) Interaction of the carbonyl group with the carbene function in **54** followed by a haptotropic shift of the metal would then lead to the furan complexes **58** via **57**.

That the interaction between X and the ketene function is less favored for X = O than for X = NR appears clearly since cyclobutenones **59** are present in almost all of the reaction mixtures obtained during the insertion of alkynes into alkoxy-carbene complexes of chromium as the result of a favored cycloaddition reaction of the two carbon–carbon double bonds in **38**.<sup>17</sup> The formation of aminocyclobutenones from aminocarbene complexes has, to the best of our knowledge, not been observed.

Scheme 4



Scheme 5



### Conclusion

Although several points concerning the interaction of aminocarbene complexes of chromium with alkynes have to be examined further, it is now clear that this reaction has many points in common with the Stevens rearrangement of acyl-stabilized nitrogen ylides. Most of the products which were expected from such a rearrangement have now been isolated or detected, in some cases in low yield.

### Experimental Section

**General Methods.**  $^1\text{H}$  NMR and  $^{13}\text{C}$  NMR spectra were recorded on a JEOL GX 400 or on a Bruker WM 200 spectrometer. IR spectra were recorded on a Perkin-Elmer 1420 spectrophotometer. Mass spectra were recorded on a ZAB HSQ (Fisons) instrument. Column chromatography was performed with Merck silica gel (70–230 mesh) using various ratios of ethyl acetate/light petroleum ether or dichloromethane/light petroleum ether as eluent. All reagents were obtained from commercial suppliers and used as received. Reactions were performed under an argon atmosphere in carefully dried glassware. Benzene, tetrahydrofuran (THF), and diethyl ether were distilled from sodium/benzophenone ketyl under a nitrogen atmosphere. Dichloromethane ( $\text{CH}_2\text{Cl}_2$ ) was distilled from calcium hydride under a nitrogen atmosphere.

Aminocarbene complexes **13a** were prepared according to a previous report.<sup>4</sup>

$(\text{CO})_5\text{Cr}=\text{C}(\text{Ph})\text{N}(\text{CH}_2)_5$  (**1**) was obtained from  $(\text{CO})_5\text{Cr}=\text{C}(\text{Ph})\text{OEt}$  and piperidine in diethyl ether upon evaporation of the volatiles under vacuum; yield 66%; yellow crystals: mp 81 °C; IR ( $\text{CHCl}_3$ ) 2020, 1970, 1920  $\text{cm}^{-1}$ ;  $^1\text{H}$  NMR (200 MHz,  $\text{CDCl}_3$ )  $\delta$  7.35–6.60 (m, 5H, ArH), 4.45 (t, 2H,  $\text{NCH}_2$ ), 3.37 (t, 2H,  $\text{CH}_2$ );  $^{13}\text{C}$  NMR (50 MHz,  $\text{CDCl}_3$ )  $\delta$  271.01 ( $\text{Cr}=\text{C}$ ), 224.05, 217.23 (CO), 128.46–118.99 (Ar), 61.47, 55.66 ( $\text{NCH}_2$ ), 27.99,

23.96 (3  $\text{CH}_2$ ). Anal. Calcd for  $\text{C}_{17}\text{H}_{15}\text{NO}_5\text{Cr}$ : C, 55.89; H, 4.11; N, 3.83. Found: C, 55.88; H, 4.06; N, 3.70.

**N-Ylide Complex  $\text{C}_{30}\text{H}_{25}\text{NO}_4\text{Cr}$  (**2**)** was obtained upon refluxing a solution of complex **1** (6.5 g, 17.6 mmol) and diphenylacetylene (4.7 g, 26.4 mmol) in cyclohexane (175 mL) for 24 h. Filtration of the precipitate gave complex **2** (5.8 g, 64.8%) as a yellow powder: mp 212 °C; IR ( $\text{CHCl}_3$ ) 1950, 1870, 1700  $\text{cm}^{-1}$ ;  $^1\text{H}$  NMR (200 MHz,  $\text{CDCl}_3$ )  $\delta$  7.28–7.11 (m, 10H, ArH), 5.40–4.85 (m, 5H, ArCr), 3.65 (m, 2H,  $\text{NCH}_2$ ), 3.30 (m, 2H,  $\text{NCH}_2$ ), 1.61 (m, 4H, 2  $\text{CH}_2$ );  $^{13}\text{C}$  NMR (100 MHz,  $\text{CDCl}_3$ )  $\delta$  234.01 (CO), 170.05 (CO), 134.13, 130.69–127.47, 114.05 ( $\text{C}=\text{C}$ , Ar), 95.71, 88.50, 86.86 (ArCr), (NC(Ph)), 55.99 ( $\text{NCH}_2$ ), 20.98, 20.23 ( $\text{CH}_2$ ). HRMS for  $\text{C}_{30}\text{H}_{25}\text{NO}_4\text{Cr}(\text{M}^+)$ . Calcd 515.1188. Found: 515.1188.

**Lactam **3** and lactam complex **3a**** were obtained upon refluxing complex **2** (0.5 g, 0.97 mmol) in anhydrous toluene for 18 h. Workup as usual gave lactam **3** (0.49 g, 28%), a white solid which was recrystallized from  $\text{CH}_2\text{Cl}_2$ /hexane: mp 195–196 °C; IR ( $\text{CHCl}_3$ ) 1700, 1590  $\text{cm}^{-1}$ ;  $^1\text{H}$  NMR (200 MHz,  $\text{CDCl}_3$ )  $\delta$  7.42–6.86 (m, 15H, Ar), 4.18 (m, 1H, NCH), 3.23 (m, 1H, NCH), 2.98 (m, 1H, COCCH), 2.70 (m, 1H, COCCH), 2.17 (m, 1H), 1.78 (m, 2H), 1.45 (m, 3H);  $^{13}\text{C}$  NMR (50 MHz,  $\text{CDCl}_3$ )  $\delta$  188.68 (CO), 141.98–123.44 ( $\text{C}=\text{C}$ , Ar), 62.52 (COC(Ph)), 45.98 ( $\text{NCH}_2$ ), 43.17, 35.43, 25.81, 25.57 ( $\text{CH}_2$ ). Anal. Calcd for  $\text{C}_{27}\text{H}_{25}\text{NO}$ : C, 85.49; H, 6.60; N, 3.69. Found: C, 85.06; H, 6.57; N, 3.59. Lactam complex **3b** was also obtained (0.28 g, 12%); yellow crystals: mp 223 °C;  $^1\text{H}$  NMR (200 MHz,  $\text{CDCl}_3$ )  $\delta$  7.35–7.05 (m, 10H, ArH), 5.45 (m, 2H, ArCr), 5.25 (m, 1H, ArCr), 5.02 (m, 2H, ArCr), 4.19 (m, 1H, NCH), 3.26 (m, 1H, NCH), 2.85 (m, 1H), 2.55 (m, 1H), 1.84–1.24 (m, 4H);

(1) Tumer, S. U.; Herndon, J. W.; Mac Mullen, L. A. *J. Am. Chem. Soc.* **1992**, *114*, 8394.

(2) Semmelhack, M. F.; Park, J. *Organometallics* **1986**, *5*, 2550.

(3) McCallum, J. S.; Kung, F. A.; Gilbertson, S. R.; Wulff, W. D. *Organometallics* **1988**, *7*, 2346.

(4) Jemison, R. W.; Mageswaran, S.; Ollis, W. D.; Sutherland, I. O.; Thebtaranonth, Y. *J. Chem. Soc., Perkin Trans. 1*, **1981**, 1154.

(5) Padwa, A.; Akiba, M.; Chou, C. S.; Cohen, L. *J. Org. Chem.* **1982**, *47*, 183.

(6) Padwa, A.; Kinder, F. R. *J. Org. Chem.* **1993**, *58*, 21.

(7) Wulff, W. D.; Bax, B. M.; Brandvold, T. A.; Chan, K. S.; Gilbert, A. M.; Hsung, R. P.; Mitchell, J.; Clardy, J. *Organometallics* **1994**, *13*, 102 and references cited therein.

(8) Watkins, D. J.; Carruthers, J. R.; Betteridge, P. W. *Crystals User Guide*; Chemical Crystallography Laboratory, University of Oxford: Oxford, England, 1985.

(9) *International Tables for X-ray Crystallography*; Kynoch Press: Birmingham, U.K., 1974; Vol. 4.

(10) Sheldrick, G. M. *SHELXS 86, Program for Crystal Structure Solution*; University of Göttingen: Göttingen, Germany, 1986.

(6) Denise, B.; Dubost, P.; Parlier, A.; Rudler, M.; Rudler, H.; Daran, J. C.; Vaissermann, J.; Delgado, F.; Arevalo, A. R.; Toscano, R. A.; Alvarez, C. *J. Organomet. Chem.* **1991**, *418*, 377.

(7) Casey, C. P.; Shusterman, A. J.; Vollendorf, N. W.; Haller, K. J. *J. Am. Chem. Soc.* **1982**, *104*, 2417.

(8) Bouancheau, C.; Parlier, A.; Rudler, M.; Rudler, H.; Vaissermann, J.; Daran, J. C. *Organometallics* **1994**, *13*, 4708.

(9) Stevens, T. S.; Creighton, E. M.; Gordon, A. B.; Mac Nicol, M. J. *Chem. Soc.* **1928**, 3193.

(10) Chantropomma, K.; Ollis, W. D.; Sutherland, I. O. *J. Chem. Soc., Perkin Trans. 1* **1983**, 1049 and references cited therein.

**Table 6. Fractional Parameters for Compound 3**

atom	<i>x/a</i>	<i>y/b</i>	<i>z/c</i>	<i>U</i> (eq)	<i>U</i> (iso)
O(1)	0.6436(4)	0.2279(4)	0.2445(2)	0.0472	
N(1)	0.4227(5)	0.2910(4)	0.2351(3)	0.0335	
C(1)	0.3058(6)	0.2977(5)	0.1751(3)	0.0348	
C(2)	0.4553(6)	0.0644(6)	0.1445(4)	0.0446	
C(3)	0.3629(7)	0.0303(6)	0.1977(4)	0.0495	
C(4)	0.4099(7)	0.0504(6)	0.2846(4)	0.0494	
C(5)	0.3488(7)	0.1517(6)	0.3204(4)	0.0471	
C(6)	0.4151(6)	0.2681(6)	0.3142(4)	0.0402	
C(7)	0.5574(6)	0.2227(6)	0.0739(4)	0.0398	
C(8)	0.4674(6)	0.1946(5)	0.1290(4)	0.0341	
C(9)	0.3286(6)	0.2507(6)	0.1112(3)	0.0344	
C(10)	0.5281(6)	0.2407(6)	0.2084(4)	0.0378	
C(11)	0.1812(6)	0.3503(6)	0.1900(3)		0.038(2)
C(12)	0.0577(6)	0.2928(6)	0.1715(4)		0.045(2)
C(13)	-0.0585(7)	0.3414(7)	0.1885(4)		0.060(2)
C(14)	-0.0510(8)	0.4457(7)	0.2224(4)		0.063(2)
C(15)	0.0686(8)	0.5042(7)	0.2399(4)		0.057(2)
C(16)	0.1862(6)	0.4582(6)	0.2236(4)		0.046(2)
C(17)	0.5532(7)	0.3313(6)	0.0438(4)		0.056(2)
C(18)	0.6390(8)	0.3622(8)	-0.0047(5)		0.075(2)
C(19)	0.7274(8)	0.2839(8)	-0.0229(5)		0.073(2)
C(20)	0.7364(8)	0.1786(8)	0.0064(5)		0.077(3)
C(21)	0.6480(8)	0.1466(7)	0.0546(4)		0.067(2)
C(22)	0.2346(6)	0.2534(6)	0.0363(4)		0.041(2)
C(23)	0.1641(7)	0.3527(6)	0.0102(4)		0.048(2)
C(24)	0.0703(7)	0.3531(7)	-0.0601(4)		0.059(2)
C(25)	0.0486(8)	0.2590(8)	-0.1030(4)		0.067(2)
C(26)	0.1172(9)	0.1614(8)	-0.0810(5)		0.080(3)
C(27)	0.2131(8)	0.1579(7)	-0.0106(4)		0.065(2)

**Table 7. Fractional Parameters for Compound 14a**

atom	<i>x/a</i>	<i>y/b</i>	<i>z/c</i>	<i>U</i> (eq)
CR(1)	0.42595(6)	0.17187(4)	0.23322(3)	0.0325
C(11)	0.1824(4)	0.1086(3)	0.2435(2)	0.0410
O(11)	0.0294(3)	0.0706(3)	0.2491(2)	0.0619
C(12)	0.4885(4)	0.0328(3)	0.3387(2)	0.0458
O(12)	0.5266(4)	-0.0552(2)	0.4046(2)	0.0705
C(13)	0.5084(4)	0.0467(3)	0.1693(2)	0.0440
O(13)	0.5574(4)	-0.0345(2)	0.1314(2)	0.0672
N(1)	-0.1221(3)	0.4275(2)	0.4046(1)	0.0349
C(1)	-0.1609(3)	0.5375(2)	0.3268(2)	0.0351
C(2)	-0.0138(3)	0.5350(2)	0.2607(2)	0.0322
C(3)	0.1198(3)	0.4187(2)	0.2998(1)	0.0312
C(4)	-0.3326(4)	0.6385(3)	0.3251(2)	0.0481
C(5)	-0.2451(4)	0.3920(3)	0.4905(2)	0.0431
C(6)	-0.1467(4)	0.2808(3)	0.5663(2)	0.0503
C(7)	-0.0423(5)	0.1670(3)	0.5313(2)	0.0562
C(8)	0.1174(4)	0.2249(3)	0.4595(2)	0.0429
C(9)	0.0484(3)	0.3539(2)	0.3886(2)	0.0331
C(21)	0.0086(3)	0.6390(2)	0.1691(2)	0.0345
C(22)	0.1763(4)	0.7110(3)	0.1427(2)	0.0456
C(23)	0.1987(5)	0.8089(3)	0.0569(2)	0.0530
C(24)	0.0539(5)	0.8378(3)	-0.0040(2)	0.0513
C(25)	-0.1135(5)	0.7689(3)	0.0213(2)	0.0533
C(26)	-0.1366(4)	0.6699(3)	0.1067(2)	0.0461
C(31)	0.3007(3)	0.3777(2)	0.2534(2)	0.0332
C(32)	0.4714(4)	0.3324(3)	0.3004(2)	0.0401
C(33)	0.6478(4)	0.3009(3)	0.2551(2)	0.0460
C(34)	0.6560(4)	0.3127(3)	0.1616(2)	0.0484
C(35)	0.4863(4)	0.3545(3)	0.1130(2)	0.0442
C(36)	0.3107(4)	0.3846(2)	0.1581(2)	0.0383

<sup>13</sup>C NMR (50 MHz, CDCl<sub>3</sub>) δ 232.86 (CO), 186.01 (CO), 142.79, 134.25, 129.53–127.34, 121.27 (C=C, Ar), 108.93, 94.20, 93.91, 93.49, 89.99 (ArCr), 59.22, 46.50, 46.32, 35.32, 26.18, 24.39 (5 CH<sub>2</sub>). Lactam **3** (0.14 g, 40%) could also be obtained upon refluxing complex **2** (0.5 g, 0.97 mmol) in pyridine (30 mL) for 12 h followed by workup as usual.

(CO)<sub>5</sub>Cr=C(H)N(CH<sub>2</sub>)<sub>6</sub> (**4**) was obtained from formylheptamethylenimine and (CO)<sub>5</sub>CrNa<sub>2</sub> according to the method of Hegedus<sup>26</sup> in 70% yield as yellow crystals: mp 36–37 °C; IR (CHCl<sub>3</sub>) 2050, 1990, 1930 cm<sup>-1</sup>; <sup>1</sup>H NMR (200 MHz, CDCl<sub>3</sub>) δ 10.49 (s, 1H, Cr=CH), 4.14 (t, *J* = 6 Hz, 2H, NCH<sub>2</sub>), 3.27 (t, *J* = 6 Hz, 2H, NCH<sub>2</sub>), 2.0–1.67 (m, 8H, 4CH<sub>2</sub>); <sup>13</sup>C NMR (50 MHz, CDCl<sub>3</sub>) δ 262.63 (Cr=O), 224.23, 217.76 (CO), 65.72, 58.06 (NCH<sub>2</sub>), 29.37, 28.10, 27.20, 26.14 (CH<sub>2</sub>). Anal. Calcd

**Table 8. Fractional Parameters for Compound 18**

atom	<i>x/a</i>	<i>y/b</i>	<i>z/c</i>	<i>U</i> (eq)
CR(1)	0.06361(7)	0.0009(1)	0.46411(6)	0.0361
C(11)	0.0089(6)	-0.0978(5)	0.3669(5)	0.0475
O(11)	-0.0272(5)	-0.1616(4)	0.3056(4)	0.0708
C(12)	-0.0508(6)	0.0961(5)	0.4058(5)	0.0572
O(12)	-0.1244(5)	0.1562(4)	0.3687(5)	0.0788
C(13)	-0.0664(5)	-0.0508(5)	0.5481(5)	0.0479
O(13)	-0.1492(4)	-0.0849(5)	0.5983(4)	0.0735
O(1)	0.2817(5)	0.1864(3)	0.1335(3)	0.0557
C(1)	0.2247(6)	0.1803(4)	0.2373(5)	0.0464
C(2)	0.2895(5)	0.0863(4)	0.2900(4)	0.0303
C(3)	0.3751(5)	0.0438(4)	0.2225(4)	0.0352
C(4)	0.3698(7)	0.1075(5)	0.1215(5)	0.0514
O(2)	0.4315(5)	0.0959(4)	0.0433(3)	0.0611
C(21)	0.2544(5)	0.0553(4)	0.3987(4)	0.0317
C(22)	0.2619(5)	-0.0540(5)	0.4319(4)	0.0397
C(23)	0.2304(5)	-0.0838(5)	0.5367(5)	0.0469
C(24)	0.1865(5)	-0.0062(7)	0.6068(4)	0.0542
C(25)	0.1774(6)	0.1007(6)	0.5766(5)	0.0525
C(26)	0.2081(5)	0.1309(5)	0.4714(5)	0.0438
C(31)	0.4611(5)	-0.0502(4)	0.2338(4)	0.0365
C(32)	0.5402(6)	-0.0645(5)	0.3224(4)	0.0467
C(33)	0.6144(6)	-0.1529(6)	0.3316(5)	0.0583
C(34)	0.6131(5)	-0.2346(6)	0.2544(8)	0.0572
C(35)	0.5396(6)	-0.2202(5)	0.1653(5)	0.0509
C(36)	0.4645(5)	-0.1288(4)	0.1533(4)	0.0430

**Table 9. Fractional Parameters for Compound 22**

atom	<i>x/a</i>	<i>y/b</i>	<i>z/c</i>	<i>U</i> (eq)
C(1)	0.1839(3)	-0.0559(3)	-0.0148(2)	0.0442
N(2)	0.2203(2)	0.0535(2)	0.0283(2)	0.0427
C(3)	0.1588(3)	0.1741(3)	0.0085(2)	0.0495
C(4)	0.1963(3)	0.2626(3)	0.0857(2)	0.0525
C(5)	0.3839(3)	0.3707(3)	0.1807(2)	0.0585
C(6)	0.3665(3)	0.3414(3)	0.2730(2)	0.0641
C(7)	0.4243(4)	0.2171(3)	0.3049(2)	0.0648
C(8)	0.3726(3)	0.1120(3)	0.2405(2)	0.0531
C(9)	0.3879(3)	0.1393(3)	0.1465(2)	0.0424
C(10)	0.3365(3)	0.2682(3)	0.1133(2)	0.0478
C(11)	0.3337(2)	0.0367(3)	0.0843(2)	0.0398
C(12)	0.3666(2)	-0.0862(3)	0.0773(2)	0.0384
C(13)	0.2709(2)	-0.1457(3)	0.0143(2)	0.0384
C(14)	0.4780(3)	-0.1460(3)	0.1319(2)	0.0401
C(15)	0.5945(3)	-0.0932(3)	0.1389(2)	0.0485
C(16)	0.6952(3)	-0.1460(4)	0.1949(2)	0.0553
C(17)	0.6842(3)	-0.2518(4)	0.2416(2)	0.0592
C(18)	0.5704(3)	-0.3071(3)	0.2337(2)	0.0577
C(19)	0.4679(3)	-0.2547(3)	0.1795(2)	0.0493
C(20)	0.2615(3)	-0.2757(3)	-0.0185(2)	0.0406
C(21)	0.1474(3)	-0.3341(3)	-0.0404(2)	0.0489
C(22)	0.1354(3)	-0.4533(3)	-0.0760(2)	0.0564
C(23)	0.2364(3)	-0.5164(3)	-0.0911(2)	0.0558
C(24)	0.3495(3)	-0.4606(3)	-0.0687(2)	0.0531
C(25)	0.3633(3)	-0.3416(3)	-0.0329(2)	0.0474

for C<sub>12</sub>H<sub>13</sub>NO<sub>5</sub>Cr: C, 47.52; H, 4.29; N, 4.62. Found: C, 47.72; H, 4.23; N, 4.50.

Lactam complex **5**, lactam **6**, and lactone **7** were obtained upon refluxing a solution of complex **4** (2.5 g, 9 mmol) and diphenylacetylene (2 g, 11 mmol) in benzene (100 mL) for 12 h. Workup as usual followed by silica gel chromatography first gave complex **5** (1.5 g, 40%) as yellow crystals: mp 177–178 °C; IR (CHCl<sub>3</sub>) 1970, 1890, 1710 cm<sup>-1</sup>; <sup>1</sup>H NMR (200 MHz, CDCl<sub>3</sub>) δ 7.30 (m, 5H, ArH), 6.88 (s, 1H, Cr=CH), 5.60 (q, 2H, ArCr), 5.31 (q, 1H, ArCr), 5.07 (m, 1H, ArCr), 4.00 (m, 1H, NCH), 3.29 (m, 1H, NCH), 2.59 (m, 1H), 2.20 (m, 1H), 1.78 (m, 4H), 1.26 (m, 4H); <sup>13</sup>C NMR (50 MHz, CDCl<sub>3</sub>) δ 232.81 (CO), 179.02 (CO), 133.67–122.44 (C=C, Ar), 95.44–89.98 (ArCr), 58.50 (PhCCH), 43.80 (NCH<sub>2</sub>), 39.54, 26.32, 25.78, 21.83 (CH<sub>2</sub>). Anal. Calcd for C<sub>25</sub>H<sub>23</sub>NO<sub>4</sub>Cr: C, 66.22; H, 5.07; N, 3.09. Found: C, 65.54; H, 4.98; N, 2.94. Heating complex **5** in pyridine gave the lactam **6** as a white solid: mp 180–181 °C; IR (CHCl<sub>3</sub>) 1720 cm<sup>-1</sup>; <sup>1</sup>H NMR (200 MHz, CDCl<sub>3</sub>) δ 7.14 (m, 10H, ArH), 6.62 (s, 1H, =CH), 3.80 (m, 1H, NCH), 2.74 (m, 1H, NCH), 2.24 (m, 2H, PhCCH<sub>2</sub>), 1.64 (m, 8H, 4 CH<sub>2</sub>); <sup>13</sup>C NMR (50 MHz, C<sub>6</sub>D<sub>6</sub>) δ 180.65 (CO), 139.63–123.47 (C=C, Ar), 60.07 (PhC), 42.82 (NCH<sub>2</sub>), 35.11, 26.20, 25.86, 21.06



**Table 10. Fractional Parameters for Compound 24a**

atom	<i>x/a</i>	<i>y/b</i>	<i>z/c</i>	<i>U</i> (eq)	<i>U</i> (iso)
Cr(1)	0.25249(6)	0.15617(4)	0.41079(4)	0.0392	
S(1)	-0.2547(1)	0.4591(1)	0.48181(8)	0.0696	
O(11)	0.2059(3)	-0.0631(2)	0.5198(2)	0.0767	
O(12)	0.3035(4)	0.3658(2)	0.2887(2)	0.0776	
O(13)	0.5058(3)	0.0441(3)	0.2971(2)	0.0710	
O(14)	0.5197(3)	0.2191(3)	0.5748(2)	0.0800	
O(15)	-0.0054(4)	0.0760(2)	0.2470(2)	0.0771	
N(1)	-0.0304(3)	0.3016(2)	0.4775(2)	0.0385	
C(1)	0.0903(3)	0.2348(2)	0.5038(2)	0.0397	
C(2)	0.1184(4)	0.2170(4)	0.6183(2)	0.0584	
C(3)	-0.1304(4)	0.3569(3)	0.5510(2)	0.0526	
C(4)	-0.0872(4)	0.3319(3)	0.3702(2)	0.0542	
C(5)	-0.2543(5)	0.3773(3)	0.3678(3)	0.0646	
C(11)	0.2225(4)	0.0204(3)	0.4802(3)	0.0521	
C(12)	0.2814(4)	0.2895(3)	0.3365(3)	0.0509	
C(13)	0.4088(4)	0.0863(3)	0.3402(2)	0.0519	
C(14)	0.4190(4)	0.1979(3)	0.5129(2)	0.0517	
C(15)	0.0888(4)	0.1080(3)	0.30993(3)	0.0530	
H(21)	0.194(4)	0.162(3)	0.638(3)	0.084(4)	
H(22)	0.027(4)	0.207(3)	0.646(3)	0.084(4)	
H(23)	0.167(4)	0.287(3)	0.651(3)	0.084(4)	
H(31)	-0.193(4)	0.298(3)	0.575(3)	0.084(4)	
H(32)	-0.064(4)	0.397(3)	0.603(3)	0.084(4)	
H(41)	-0.086(4)	0.267(3)	0.325(3)	0.084(4)	
H(42)	-0.013(4)	0.385(3)	0.344(3)	0.084(4)	
H(51)	-0.283(4)	0.428(3)	0.310(3)	0.084(4)	
H(52)	-0.328(4)	0.316(3)	0.370(3)	0.084(4)	

(CH<sub>2</sub>). MS for C<sub>22</sub>H<sub>23</sub>NO. Calcd 317 (*m/z*). Found 317. Lactone **7** (0.21 g, 10%), a white solid, was also obtained: mp 137 °C; IR (CHCl<sub>3</sub>) 1750 cm<sup>-1</sup>; <sup>1</sup>H NMR (200 MHz, CDCl<sub>3</sub>) δ 7.49–7.34 (m, 10H, ArH), 4.34 (s, 2H, OCH<sub>2</sub>); <sup>13</sup>C NMR (50 MHz, CDCl<sub>3</sub>) δ 173.2 (CO), 155.34, 133.0–123.1 (C=C, Ar), 69.70 (OCH<sub>2</sub>). MS for C<sub>16</sub>H<sub>12</sub>O<sub>2</sub>. Calcd 236. Found 236.

(CO)<sub>5</sub>Cr=C(Me)N(CH<sub>2</sub>)<sub>7</sub> (**8**) was obtained from acetylheptamethylenimine according to the method of Hegedus<sup>5</sup> in 36% yield as a yellow solid: mp 82 °C; IR (CHCl<sub>3</sub>) 2040, 1965, 1920 cm<sup>-1</sup>; <sup>1</sup>H NMR (200 MHz, CDCl<sub>3</sub>) δ 4.29 (m, 2H, NCH<sub>2</sub>), 3.83 (m, 2H, NCH<sub>2</sub>), 2.79 (s, 3H, CH<sub>3</sub>), 2.01 (m, 2H, CH<sub>2</sub>), 1.77 (m, 4H, CH<sub>2</sub>), 1.30 (m, 4H, CH<sub>2</sub>); <sup>13</sup>C NMR (50 MHz, CDCl<sub>3</sub>) δ 272.59 (Cr=C), 223.78, 218.15 (CO), 66.66, 52.43 (NCH<sub>2</sub>), 40.11 (CH<sub>3</sub>), 27.50, 27.06, 26.17, 25.60, 23.08 (CH<sub>2</sub>). Anal. Calcd for C<sub>14</sub>H<sub>17</sub>NO<sub>5</sub>Cr: C, 50.75; H, 5.13; N, 4.23. Found: C, 50.90; H, 5.15; N, 4.22.

**Lactam complex 10, lactam 11, and enamine 12** were obtained upon heating complex **8** (2 g, 6 mmol) and diphenylacetylene (1.2 g, 7.0 mmol) in refluxing benzene (100 mL) for 12 h. After evaporation of the solvent under vacuum, the residue was chromatographed on silica gel with ethyl acetate/petroleum ether (5/95) as eluent which gave first ketone **9** (0.16 g, 12%) as an oil and then complex **10** (0.67 g, 25%) as an orange solid: mp 143 °C; <sup>1</sup>H NMR (200 MHz, CDCl<sub>3</sub>) δ 7.39 (m, 5H, ArH), 5.62 (d, 1H, ArCr), 5.21 (t, 2H, ArCr), 5.04 (t, 2H, ArCr), 4.00 (m, 1H, NCH), 3.27 (m, 1H, NCH), 2.39 (m, 1H), 2.07 (m, 1H), 1.62 (m, 5H), 1.24 (m, 5H); <sup>13</sup>C NMR (50 MHz, CDCl<sub>3</sub>) δ 232.85 (CO), 178.2 (CO), 130.11–127.40 (C=C, Ar), 93.51–90.51 (ArCr), 58.52, 40.76, 37.92, 27.69, 23.01, 22.70, 20.72, 20.18 (CH<sub>2</sub>). MS for C<sub>27</sub>H<sub>27</sub>NO<sub>4</sub>Cr. Calcd 481 (*m/z*). Found 481. Heating complex **10** in pyridine gave lactam **11** as a white solid: mp 126 °C; IR (CHCl<sub>3</sub>) 1690 cm<sup>-1</sup>; <sup>1</sup>H NMR (200 MHz, CDCl<sub>3</sub>) δ 7.24 (m, 8H, ArH), 6.82 (m, 2H, ArH), 4.03 (m, 1H, NCH), 3.34 (m, 1H, NCH), 2.13 (m, 5H), 1.45 (m, 10H); <sup>13</sup>C NMR (50 MHz, CDCl<sub>3</sub>) δ 181.33 (CO), 140.22, 137.72, 133.89, 129.24–126.51 (C=C, Ar), 60.49, 40.56, 32.09, 22.59, 20.20, 19.71 (CH<sub>2</sub>), 12.24 (CH<sub>3</sub>). Anal. Calcd for C<sub>24</sub>H<sub>27</sub>NO: C, 83.47; H, 7.82; N, 4.06. Found: C, 83.32; H, 7.85; N, 3.90. Enamine **12** was obtained last (1 g, 52%) as an oil: <sup>1</sup>H NMR (200 MHz, CDCl<sub>3</sub>) δ 7.68–7.23 (m, 10H, ArH), 6.84 (s, 1H, =CH), 3.86 (s, 1H), 3.66 (s, 1H, C=CHH), 3.24 (m, 4H, NCH<sub>2</sub>), 1.35 (m, 10H, CH<sub>2</sub>); <sup>13</sup>C NMR (50 MHz, CDCl<sub>3</sub>) δ 150.63 (N=C), 130.90, 129.44–126.82 (C=C, Ar), 80.52 (=CH<sub>2</sub>), 50.44 (NCH<sub>2</sub>), 27.51, 27.33, 26.04 (CH<sub>2</sub>). MS for C<sub>23</sub>H<sub>27</sub>N. Calcd 317 (*m/z*). Found 317.

(CO)<sub>5</sub>Cr=C(H)N-CH<sub>2</sub>CH<sub>2</sub>CH<sub>2</sub>CH<sub>2</sub> (**13b**) was obtained from the corresponding formylamide and (CO)<sub>5</sub>CrNa<sub>2</sub>; yield 70%, yellow crystals: mp 51 °C; IR (CHCl<sub>3</sub>) 2040, 1970, 1920 cm<sup>-1</sup>; <sup>1</sup>H NMR (200 MHz, CDCl<sub>3</sub>) δ 10.92 (s, 1H, Cr=C(H)), 4.01 (m, 2H, NCH<sub>2</sub>), 3.74 (m, 2H, NCH<sub>2</sub>), 2.15 (m, 4H, 2CH<sub>2</sub>); <sup>13</sup>C NMR (50 MHz, CDCl<sub>3</sub>) δ 257.45 (Cr=C), 227.26, 217.85 (CO), 62.00, 55.58 (NCH<sub>2</sub>), 25.84, 25.44 (CH<sub>2</sub>). Anal. Calcd for C<sub>10</sub>H<sub>9</sub>NO<sub>5</sub>Cr: C, 43.63; H, 3.27; N, 5.10. Found: C, 43.60; H, 3.32; N, 5.08.

(CO)<sub>5</sub>Cr=C(Ph)NCH<sub>2</sub>CH<sub>2</sub>CH<sub>2</sub>CH<sub>2</sub> (**13c**) was obtained from (CO)<sub>5</sub>Cr=(OEt)Ph and pyrrolidine; yield 80%, yellow crystals: mp 97 °C; IR (CHCl<sub>3</sub>) 2040, 1940, 1900 cm<sup>-1</sup>; <sup>1</sup>H NMR (200 MHz, CDCl<sub>3</sub>) δ 7.2–6.6 (m, 5H, Ar), 4.20 (m, 2H, NCH<sub>2</sub>), 3.15 (m, 2H, NCH<sub>2</sub>), 2.12 (m, 2H, CH<sub>2</sub>), 1.91 (m, 2H, CH<sub>2</sub>); <sup>13</sup>C NMR (100 MHz, CDCl<sub>3</sub>) δ 269.57 (Cr=C), 223.77, 217.50 (CO), 153.87, 128.70, 125.72, 118.39 (Ar), 59.39, 55.81 (NCH<sub>2</sub>), 25.37, 25.28 (CH<sub>2</sub>). Anal. Calcd for C<sub>16</sub>H<sub>13</sub>NO<sub>5</sub>Cr: C, 54.70; H, 3.70; N, 3.99. Found: C, 54.62; H, 3.62; N, 4.04.

(CO)<sub>5</sub>Cr=C(SC<sub>4</sub>H<sub>9</sub>)(NCH<sub>2</sub>CH<sub>2</sub>CH<sub>2</sub>CH<sub>2</sub>) (**13d**) was obtained from (CO)<sub>5</sub>Cr=C(SC<sub>4</sub>H<sub>9</sub>)OEt and pyrrolidine in 80% yield as a yellow solid: mp 114 °C; <sup>1</sup>H NMR (200 MHz, CDCl<sub>3</sub>) δ 7.25 (m, 1 H, HC=C), 6.98 (m, 1H, HC=C), 6.51 (m, 1H, CH=C), 4.27 (m, 2H, NCH<sub>2</sub>), 3.50 (m, 2H, NCH<sub>2</sub>), 2.20 (m, 2H, CH<sub>2</sub>), 2.00 (m, 2H, CH<sub>2</sub>); <sup>13</sup>C NMR (50 MHz, CDCl<sub>3</sub>) δ 265.0 (Cr=C), 223.87, 217.35 (CO), 153.91, 127.13, 123.73, 117.73 (C=C), 59.95 (NCH), 56.53 (NCH), 25.56 (2 CH<sub>2</sub>). Anal. Calcd for C<sub>14</sub>H<sub>11</sub>NO<sub>5</sub>SCr: C, 47.05; H, 3.08; N, 3.92. Found: C, 47.23; H, 3.08; N, 3.81.

**Pyrrole complex 14a, pyrrole 15a, lactam complex 16a, and lactam 17a** were obtained upon refluxing complex **13a** (R<sub>1</sub> = Me) (2.89 g, 10 mmol) in benzene (100 mL) for 12 h in the presence of diphenylacetylene (1.8 g, 10 mmol). Evaporation of the solvent under vacuum, followed by silica gel chromatography with petroleum ether/methylene chloride (95/5) first gave pyrrole **15a** (0.48 g, 17% as a white solid: mp 145 °C; IR (CHCl<sub>3</sub>) 1600 cm<sup>-1</sup>; <sup>1</sup>H NMR (200 MHz, CDCl<sub>3</sub>) δ 7.28–7.07 (m, 10H, Ar), 3.90 (m, 2H, NCH<sub>2</sub>), 2.88 (m, 2H, CH<sub>2</sub>), 2.27 (s, 3H, CH<sub>3</sub>), 2.03 (m, 2H, CH<sub>2</sub>), 1.82 (m, 2H, CH<sub>2</sub>); <sup>13</sup>C NMR (50 MHz, CDCl<sub>3</sub>) δ 155.36, 137.24–118.47 (Ar), 43.13 (NCH<sub>2</sub>), 23.75, 23.40, 21.12 (3CH<sub>2</sub>), 10.75 (CH<sub>3</sub>). MS for C<sub>21</sub>H<sub>21</sub>N<sup>+</sup>. Calcd 423. Found 423. Complex **14a** followed (0.22 g, 5%) as yellow crystals: mp 145 °C; IR (CHCl<sub>3</sub>) 1960, 1880 cm<sup>-1</sup>; <sup>1</sup>H NMR (200 MHz, CDCl<sub>3</sub>) δ 7.30–7.00 (m, 5H, Ar), 5.34–5.15 (m, 5H, ArCr), 3.85 (m, 2H, NCH<sub>2</sub>), 2.96 (m, 2H, CH<sub>2</sub>), 2.14 (s, 3H, CH<sub>3</sub>), 2.01 (m, 2H, CH<sub>2</sub>), 1.88 (m, 2H, CH<sub>2</sub>); <sup>13</sup>C NMR (50 MHz, CDCl<sub>3</sub>) δ 233.99 (CO), 135.86–125.96 (Ar), 100.0, 95.0, 93.21, 90.16 (ArCr), 43.31 (NCH<sub>2</sub>), 23.97, 23.38, 21.02 (3 CH<sub>2</sub>). Anal. Calcd for C<sub>24</sub>H<sub>21</sub>NO<sub>3</sub>Cr: C, 68.08; H, 4.96; N, 3.30. Found: C, 67.28; H, 4.93; N, 3.10. Lactam **17a** was then obtained (0.17 g, 5.5%) as white crystals: mp 146 °C; IR (CHCl<sub>3</sub>) 1730 cm<sup>-1</sup>; <sup>1</sup>H NMR (200 MHz, CDCl<sub>3</sub>) δ 7.27–6.84 (m, 10H, Ar), 3.64 (m, 1H, NCH), 3.05 (m, 1H, NCH), 2.50 (m, 1H, CH), 2.12 (s, 3H, CH<sub>3</sub>), 2.04 (m, 1H, CH), 1.88–1.63 (m, 4H, CH<sub>2</sub>); <sup>13</sup>C NMR (50 MHz, CDCl<sub>3</sub>) δ 189.93 (CO), 141.86, 137.81, 134.19, 128.70–126.43, 122.21 (Ar, C=C), 64.67 (CPh), 42.77 (NCH<sub>2</sub>), 36.97, 26.02, 22.64 (3 CH<sub>2</sub>), 11.78 (CH<sub>3</sub>). HRMS for C<sub>21</sub>H<sub>21</sub>NO<sup>+</sup>. Calcd 303.1623. Found 303.1623. Finally complex **16a** was obtained (1.145 g, 26%) as yellow crystals: mp 120 °C; IR (CHCl<sub>3</sub>) 1980, 1890, 1740 cm<sup>-1</sup>; <sup>1</sup>H NMR (200 MHz, C<sub>6</sub>D<sub>6</sub>) δ 7.18–6.77 (m, 5H, Ar), 5.17 (d, 1H, ArCr), 4.76 (d, 1H, ArCr), 4.49 (m, 1H, ArCr), 4.36 (m, 1H, ArCr), 4.19 (m, 1H, ArCr), 3.40 (m, 1H, NCH), 2.54 (m, 1H, NCH), 2.10–1.82 (m, 2H, CH<sub>2</sub>), 1.54 (s, 3H, CH<sub>3</sub>), 1.42–1.16 (m, 4H, CH<sub>2</sub>). MS for C<sub>24</sub>H<sub>21</sub>NO<sub>4</sub>Cr<sup>+</sup>. Calcd 439. Found 439. Treatment of complex **13a** under the same conditions with diphenylacetylene, followed by evaporation of the solvent and treatment of the residue with pyridine at reflux for 6 h, gave upon silica gel chromatography pyrrole **14a** in 25% yield and lactam **17a** in 19% yield.

**Pyrrole complex 14b, pyrrole 15b, lactam complex 16b, and lactam 17b** were obtained under the same conditions as above. Silica gel chromatography of the residue of the reaction with petroleum ether/methylene chloride as

eluents gave, by collecting appropriate fractions (from 5/95 to 20/80), successively pyrrole **15b** (0.30 g, 15%) as a white solid: mp 184 °C;  $^1\text{H NMR}$  (200 MHz,  $\text{CDCl}_3$ )  $\delta$  7.30–7.03 (m, 10H, Ar), 6.72 (s, 1H, C=CH), 4.02 (m, 2H,  $\text{NCH}_2$ ), 2.81 (m, 2H,  $\text{CH}_2$ ), 2.02 (m, 2H,  $\text{CH}_2$ ), 1.82 (m, 2H,  $\text{CH}_2$ );  $^{13}\text{C NMR}$  (50 MHz,  $\text{CDCl}_3$ )  $\delta$  130.24–117.68 (Ar), 45.62 ( $\text{NCH}_2$ ), 23.73, 22.99, 21.34 (3  $\text{CH}_2$ ). MS for  $\text{C}_{20}\text{H}_{19}\text{N}^+$ . Calcd 273. Found 273. Complex **14b** was then obtained (0.6 g, 19%) as yellow crystals: mp 175 °C; IR ( $\text{CHCl}_3$ ) 1960, 1890, 1735  $\text{cm}^{-1}$ ;  $^1\text{H NMR}$  (200 MHz,  $\text{C}_6\text{D}_6$ )  $\delta$  7.28–7.08 (5H, m, Ar), 6.21 (s, 1H, C=CH), 4.93 (d,  $J = 6.4$  Hz, 2H), 4.51 (t,  $J = 6.4$  Hz, 2H), 4.33 (t,  $J = 6.2$  Hz, 2H) (ArCr), 3.13 (t,  $J = 6.2$  Hz, 2H,  $\text{NCH}_2$ ), 2.78 (t,  $J = 6.2$  Hz, 2H, C=C– $\text{CH}_2$ ), 1.48 (m, 2H,  $\text{CH}_2$ ), 1.12 (m, 2H,  $\text{CH}_2$ );  $^{13}\text{C NMR}$  (50 MHz,  $\text{CDCl}_3$ )  $\delta$  234.21 (CO), 138.0–109.1 (Ar, C=C), 95.14, 92.92, 90.13 (ArCr), 45.30 ( $\text{NCH}_2$ ), 23.81, 23.13, 21.12 (3 $\text{CH}_2$ ). Anal. Calcd for  $\text{C}_{23}\text{H}_{19}\text{NO}_3\text{Cr}$ : C, 67.48; H, 4.64; N, 3.42. Found: C, 67.34; H, 4.52; N, 3.32. Lactam **17b** was obtained next (0.60 g, 20%) as a white solid: mp 148 °C; IR ( $\text{CHCl}_3$ ) 1735  $\text{cm}^{-1}$ ;  $^1\text{H NMR}$  (200 MHz,  $\text{C}_6\text{D}_6$ )  $\delta$  7.28–6.83 (m, 10H, Ar), 6.48 (s, 1H, C=CH), 3.47 (m, 1H, NCH), 2.26 (m, 1H), 2.11–1.97 (m, 3H) (ArCr), 1.36–1.24 (m, 3H);  $^{13}\text{C NMR}$  (50 MHz,  $\text{CDCl}_3$ )  $\delta$  188.02 (CO), 138.241, 135.89, 133.44, 128.49–124.73 (Ar, C=C), 63.53 (CPh), 45.58 ( $\text{NCH}_2$ ), 35.87, 26.79, 22.60 (3  $\text{CH}_2$ ). Anal. Calcd for  $\text{C}_{20}\text{H}_{19}\text{NO}$ : C, 83.04; H, 6.57; N, 4.84. Found: C, 83.09; H, 6.65; N, 4.80. Lactam complex **16b** was obtained last (0.60 g, 20%) as an oil; IR ( $\text{CHCl}_3$ ) 1970, 1900, 1735  $\text{cm}^{-1}$ ;  $^1\text{H NMR}$  (200 MHz,  $\text{C}_6\text{D}_6$ )  $\delta$  7.35–6.90 (m, 5H, Ar), 6.1 (s, 1H, CH=C), 5.25 (d, 1H, ArCr), 4.90 (d, 1H, ArCr), 4.35 (t, 1H, ArCr), t 1H, ArCr), 4.05 (t, 1H, ArCr), 3.55 (m, 1H, NCH), 2.35–1.65 (m, 4H), (m, 1H, NCH), 1.6–1.18 (m, 6H, 3 $\text{CH}_2$ ). MS for  $\text{C}_{23}\text{H}_{19}\text{NO}_4\text{Cr}^+$ . Calcd 425. Found 425.

**Pyrrole 15c, lactam 17c, and lactam complex 16c** were obtained from complex **1c** (3 g, 8.54 mmol) and diphenylacetylene (1.5 g, 8.6 mmol) as above. Appropriate fractions were collected to give first with petroleum ether/methylene chloride (70/30) a mixture of pyrrole complex **14c** and pyrrole **15c**, which was refluxed in pyridine to give after filtration through silica gel pyrrole **15c** as a white solid (0.40 g, 14%): mp 194 °C; IR ( $\text{CHCl}_3$ ) 1600  $\text{cm}^{-1}$ ;  $^1\text{H NMR}$  (200 MHz,  $\text{CDCl}_3$ )  $\delta$  7.28–6.88 (m, 15H Ar), 3.88 (m, 2H,  $\text{NCH}_2$ ), 2.94 (m, 2H,  $\text{CH}_2$ ), 1.91 (m, 4H, 2  $\text{CH}_2$ );  $^{13}\text{C NMR}$  (50 MHz,  $\text{CDCl}_3$ )  $\delta$  136.04–119.21 (C=C, Ar), 44.75 ( $\text{NCH}_2$ ), 23.93, 23.49, 21.21 (3  $\text{CH}_2$ ). Anal. Calcd for  $\text{C}_{26}\text{H}_{23}\text{N}$ : C, 89.36; H, 6.63; N, 4.00. Found: C, 89.27; H, 6.67; N, 3.89. Elution with the same mixture of solvents then gave complex **16c** (2.25 g, 42%) as yellow crystals: mp 177 °C; IR ( $\text{CHCl}_3$ ) 1980, 1895, 1740  $\text{cm}^{-1}$ ;  $^1\text{H NMR}$  (200 MHz,  $\text{CDCl}_3$ )  $\delta$  7.32–6.93 (m, 10H, Ar), 5.46 (d, 1H, ArCr), 5.28 (d, 2H, ArCr), 5.06 (t, 1H, ArCr), 4.93 (t, 1H, ArCr), 3.60 (m, 1H, NCH), 2.85–2.65 (m, 1H, NCH), 2.25–1.65 (m, 6H, 3  $\text{CH}_2$ );  $^{13}\text{C NMR}$  (50 MHz,  $\text{CDCl}_3$ )  $\delta$  232.86 (CrCO), 186.43 (CO), 146.04, 134.20–121.20 (Ar, C=C), 107.20, 94.67, 94.31, 89.17 (ArCr), 62.34 (CPh), 44.81 (NC), 43.06, 39.32, 25.94, 22.83 (4  $\text{CH}_2$ ). Anal. Calcd for  $\text{C}_{29}\text{H}_{23}\text{NO}_4\text{Cr}$ : C, 69.46; H, 4.59; N, 2.79. Found: C, 69.30; H, 4.45; N, 2.71. Lactam **17c** was then obtained (0.45 g, 16%) as a white solid: mp 185 °C; IR ( $\text{CHCl}_3$ ) 1740  $\text{cm}^{-1}$ ;  $^1\text{H NMR}$  (200 MHz,  $\text{CDCl}_3$ )  $\delta$  7.44–6.93 (m, 15H, Ar), 3.64–3.54 (m, 1H, NCH), 2.64–2.76 (m, 1H, NCH), 2.33–1.75 (m, 6H, 3  $\text{CH}_2$ );  $^{13}\text{C NMR}$  (50 MHz,  $\text{CDCl}_3$ )  $\delta$  189.75 (CO), 145.99, 137.33–122.49 (Ar, C=C), 65.93 (CPh), 44.11 ( $\text{NCH}_2$ ), 37.94, 26.21, 22.58 (3  $\text{CH}_2$ ). HRMS for  $\text{C}_{26}\text{H}_{23}\text{NO}^+$ . Calcd 365.1779. Found 365.1781.

**Pyrrole 15d and Lactam 17d.** A solution of complex **1d** (1.815 g, 5.08 mmol) in benzene (50 mL) was refluxed for 12 h in the presence of diphenylacetylene (1 g, 5.6 mmol). Evaporation of the solvent followed by silica gel chromatography with petroleum ether/methylene chloride (80/20) first gave a yellow oil, which was not further purified. Treatment in boiling pyridine for 6 h gave, after evaporation of the solvent and filtration through silica gel, pyrrole **15d** as a white solid (0.8 g, 44%): mp 172 °C;  $^1\text{H NMR}$  (200 MHz,  $\text{CDCl}_3$ )  $\delta$  7.29–6.91 (m, 13H, Ar), 3.93 (m, 2H,  $\text{NCH}_2$ ), 2.91 (m, 2H,  $\text{CH}_2$ ), 1.98 (m, 2H,  $\text{CH}_2$ ), 1.86 (m, 2H,  $\text{CH}_2$ );  $^{13}\text{C NMR}$  (50 MHz,  $\text{CDCl}_3$ )  $\delta$

135.77–119.61 (15 peaks, Ar), 44.54 ( $\text{NCH}_2$ ), 23.81, 23.52; 21.06 (3  $\text{CH}_2$ ). Anal. Calcd for  $\text{C}_{24}\text{H}_{21}\text{NS}$ : C, 81.12; H, 5.91; N, 3.94. Found: C, 81.18; H, 5.98; N, 3.79. Then petroleum ether/methylene chloride (50/50) eluted a second fraction, which was also treated with pyridine to give, after filtration through silica gel, lactam **17d** (0.86 g, 45.6%) as a white solid: mp 242 °C;  $^1\text{H NMR}$  (200 MHz,  $\text{CDCl}_3$ )  $\delta$  7.28–6.90 (m, 13H, Ar), 3.71–3.61 (m, 1H, NCH), 3.18–3.10 (m, 1H, NCH), 2.72–2.64 (m, 1H, CH), 2.26–2.13 (m, 2H,  $\text{CH}_2$ ), 1.96–1.83 (m, 3H,  $\text{CH}_2$ );  $^{13}\text{C NMR}$  (100 MHz,  $\text{CDCl}_3$ )  $\delta$  189.81 (CO), 139.74, 136.91, 133.41, 128.86–126.87 (Ar), 65.73 (CPh), 45.03 ( $\text{NCH}_2$ ), 37.22, 25.97, 22.41 (3  $\text{CH}_2$ ). Anal. Calcd for  $\text{C}_{24}\text{H}_{21}\text{NOS}$ : C, 77.62; H, 5.66; N, 3.77. Found: C, 77.02; H, 5.57; N, 3.60.

**Lactam complex 19 and lactam 20** were obtained upon heating of complex **13c** (1.5 g, 4.27 mmol) in refluxing benzene in the presence of 1-phenyl-1-propyne (1 mL, 8 mmol) as above. Silica gel chromatography of the residue with petroleum ether/ethyl acetate (80/20) first gave complex **19c** (0.7 g, 38%) as orange crystals: mp 164 °C; IR ( $\text{CHCl}_3$ ) 1980, 1890, 1740  $\text{cm}^{-1}$ ;  $^1\text{H NMR}$  (200 MHz,  $\text{CDCl}_3$ )  $\delta$  7.54–7.28 (m, 5H, Ar), 5.51–5.22 (m, 5H, ArCr), 3.49 (m, 1H, NCH), 2.71 (m, 1H, NCH), 2.23 (m, 1H), 2.01 (m, 2H), 1.86 (s, 3H,  $\text{CH}_3$ );  $^{13}\text{C NMR}$  (50 MHz,  $\text{CDCl}_3$ )  $\delta$  190.91 (CO), 145.17, 137.71, 131.78, 128.83–127.19, 119.41 (C=C, Ar), 65.03 (CPh), 39.25 ( $\text{NCH}_2$ ), 25.61, 22.87 ( $\text{CH}_2$ ), 10.35 ( $\text{CH}_3$ ). Anal. Calcd for  $\text{C}_{24}\text{H}_{21}\text{NO}_4\text{Cr}$ : C, 65.60; H, 4.55; N, 3.19. Found: C, 65.68; H, 4.65; N, 3.24. Heating complex **19c** in pyridine for 6 h gave after silica gel chromatography lactam **20** (0.3 g, 61%) as a white solid: mp 113 °C; IR ( $\text{CHCl}_3$ ) 1740  $\text{cm}^{-1}$ ;  $^1\text{H NMR}$  (50 MHz,  $\text{CDCl}_3$ )  $\delta$  7.58–7.27 (m, 10H, Ar), 3.55 (m, 1H, NCH), 2.75 (m, 1H, NCH), 2.38 (m, 1H, CH), 2.02 (m, 1H), 1.72 (m, 3H), 1.58 (s, 3H,  $\text{CH}_3$ ). Anal. Calcd for  $\text{C}_{21}\text{H}_{21}\text{NO}$ : C, 83.16; H, 6.93; N, 4.62. Found: C, 82.85; H, 6.99; N, 4.52.

$(\text{CO})_5\text{Cr}=\text{C}(\text{H})\text{N}(\text{C}_6\text{H}_{14})$  (**21**) was obtained from formylperhydroindole and  $(\text{CO})_5\text{CrNa}_2$  as a yellow solid: mp 40 °C; IR ( $\text{CHCl}_3$ ) 2020, 1970, 1925  $\text{cm}^{-1}$ ;  $^1\text{H NMR}$  (200 MHz,  $\text{CDCl}_3$ )  $\delta$  10.93, 10.80, 10.71, 10.70 (s, 1H, Cr=C(H) for the four isomers), 4.23 (m, 1H, NCH), 3.96 (m, 1H, NCH), 3.55 (m, 1H, NCH), 2.45 (m, 1H, CH), 2.10–1.0 (m, 10H,  $\text{CH}_2$ );  $^{13}\text{C NMR}$  (50 MHz,  $\text{CDCl}_3$ )  $\delta$  253.9 (Cr=C), 224.0, 218.1 (CO), 66.52, 59.02 ( $\text{NCH}_2$ , NCH), 37.21 (CH), 26.76, 25.49, 23.55, 19.90 ( $\text{CH}_2$ ). Anal. Calcd for  $\text{C}_{14}\text{H}_{15}\text{NO}_5\text{Cr}$ : C, 51.06; H, 4.56; N, 4.25. Found: C, 51.42; H, 4.61; N, 4.11.

**Pyrrole 22 and pyrrole complex 23** were obtained as above from complex **21** (3.5 g, 8.5 mmol) and diphenylacetylene (2 g, 11 mmol). Chromatography of the residue with petroleum ether/ethyl acetate (95/5) first gave compound **22** (0.9 g, 20%) as a white solid: mp 148 °C;  $^1\text{H NMR}$  (200 MHz,  $\text{CDCl}_3$ )  $\delta$  7.32–6.72 (m, 10H, Ar), 6.69 (s, 1H, C=CH), 4.16–3.90 (m, 2H,  $\text{NCH}_2$ ), 3.10 (m, 1H, =CCH), 2.34 (m, 1H), 2.17 (m, 1H), 1.71–1.04 (m, 9H);  $^{13}\text{C NMR}$  (50 MHz,  $\text{CDCl}_3$ )  $\delta$  130.45–116.95 (C=C, Ar), 45.72 ( $\text{NCH}_2$ ), 34.0 (CH), 32.45 (CH), 31.53, 28.64, 25.89, 24.41, 21.07 (5  $\text{CH}_2$ ). HRMS for  $\text{C}_{24}\text{H}_{25}\text{N M}^+$ . Calcd 327.1986. Found 327.1990. Elution with the same solvents gave complex **23** (0.4 g, 11%) as a yellow solid: mp 170.1 °C; IR ( $\text{CHCl}_3$ ) 1965, 1885  $\text{cm}^{-1}$ ;  $^1\text{H NMR}$  (200 MHz,  $\text{CDCl}_3$ )  $\delta$  7.33–7.21 (m, 5H, Ar), 6.83 (s, 1H, CH=C), 5.36–5.08 (m, 5H, ArCr), 4.07–3.93 (m, 2H,  $\text{NCH}_2$ ), 2.94 (m, 1H, C=CCH), 2.34–1.20 (m, 11H). MS for  $\text{C}_{27}\text{H}_{25}\text{NO}_3\text{Cr}$  ( $\text{M}^+$ ). Calcd 463. Found 463.

$(\text{CO})_5\text{Cr}=\text{C}(\text{Me})\text{NCH}_2\text{CH}_2\text{SCH}_2$  (**24a**) was obtained from  $(\text{CO})_5\text{Cr}=\text{C}(\text{Me})\text{OEt}$  and thiazolidine in 65% yield as a yellow solid. Silica gel chromatography with petroleum ether/methylene chloride (98/2) first gave **24a-E** as yellow crystals (36%): mp 101 °C;  $^1\text{H NMR}$  (200 MHz,  $\text{CDCl}_3$ )  $\delta$  4.60 (s, 2H,  $\text{NCH}_2\text{S}$ ), 4.56 (m, 2H,  $\text{NCH}_2$ ), 3.18 (m, 2H,  $\text{SCH}_2$ ), 2.77 (s, 3H,  $\text{CH}_3$ );  $^{13}\text{C NMR}$  (100 MHz,  $\text{CDCl}_3$ )  $\delta$  274.63 (Cr=C), 223.03, 217.52 (CO), 63.32 ( $\text{NCH}_2\text{S}$ ), 52.82 ( $\text{CH}_2\text{N}$ ), 41.43 ( $\text{CH}_2\text{S}$ ), 29.06 ( $\text{CH}_3$ ). Compound **24a-Z** was then obtained as yellow crystals: mp 103 °C;  $^1\text{H NMR}$  (200 MHz,  $\text{CDCl}_3$ )  $\delta$  5.19 (s, 2H,  $\text{NCH}_2\text{S}$ ), 3.86 (m, 2H,  $\text{NCH}_2$ ), 3.25 (m, 2H,  $\text{SCH}_2$ ), 2.76 (s, 3H,  $\text{CH}_3$ );  $^{13}\text{C NMR}$  (100 MHz,  $\text{CDCl}_3$ )  $\delta$  274.15 (Cr=C), 223.11,

217.55 (CO), 61.86 (NCH<sub>2</sub>S), 54.24 (CH<sub>2</sub>N), 41.96 (CH<sub>2</sub>S), 30.83 (CH<sub>3</sub>). Anal. Calcd for C<sub>10</sub>H<sub>9</sub>NO<sub>5</sub>Cr: C, 39.08; H, 2.93; N, 4.56. Found: C, 39.02; H, 2.92; N, 4.56.

(CO)<sub>5</sub>Cr=C(Ph)NCH<sub>2</sub>SCH<sub>2</sub>CH<sub>2</sub> (**24b**) was obtained from (CO)<sub>5</sub>Cr=C(Ph)OEt and thiazolidine in 66% yield as a yellow solid (60/40 *E/Z* mixture): mp 115 °C; <sup>1</sup>H NMR (200 MHz, CDCl<sub>3</sub>) δ (11*b-Z*) 7.43–6.72 (m, 5H, Ar), 5.32 (s, 2H, NCH<sub>2</sub>S), 3.56 (m, 2H, NCH<sub>2</sub>), 3.06 (m, 2H, CH<sub>2</sub>); (11*b-E*) 7.43–6.72 (m, 5H, Ar), 4.64 (m, 2H, NCH<sub>2</sub>), 4.24 (m, 2H, NCH<sub>2</sub>S), 3.29 (m, 2H, CH<sub>2</sub>); <sup>13</sup>C NMR (100 MHz, CDCl<sub>3</sub>) δ 275.72 (Cr=C), 223.07, 216.95 (CO), 153.20, 128.91, 126.37, 118.25 (Ar), 61.48, 61.30, 56.10, 56.02, 42.25, 29.68 (CH<sub>2</sub>). HRMS for C<sub>15</sub>H<sub>11</sub>NO<sub>5</sub>Scr (M<sup>+</sup> - CO). Calcd 340.9813. Found 340.9814.

**Pyrrrole 25a** was obtained upon heating a mixture of complex **24a** (3.5 g, 11.4 mmol) and diphenylacetylene (2.5 g, 14 mmol) as above. Silica gel chromatography first gave with petroleum ether/ethyl acetate (97/3) pyrrrole **25** (0.76 g, 22%) and then a fraction of complexed and uncomplexed products (1.6 g), which was treated with pyridine. The residue of this reaction was then chromatographed on silica gel. Elution with petroleum ether/ethyl acetate (95/5) first gave pyrrrole **25** (0.125 g), total yield 25.5%, as a white solid, unstable in solution: mp 74 °C; IR (CHCl<sub>3</sub>) 1600 cm<sup>-1</sup>; <sup>1</sup>H NMR (200 MHz, CDCl<sub>3</sub>) δ 7.27–7.01 (m, 10H, Ar), 4.12 (m, 2H, NCH<sub>2</sub>), 3.90 (s, 2H, NCH<sub>2</sub>S), 3.11 (m, 2H, CH<sub>2</sub>), 2.25 (s, 3H, CH<sub>3</sub>); <sup>13</sup>C NMR (50 MHz, CDCl<sub>3</sub>) δ 135.88–119.69 (Ar), 44.28 (NCH<sub>2</sub>), 27.50 (CH<sub>2</sub>), 24.61 (CH<sub>2</sub>), 10.31 (CH<sub>3</sub>). HRMS C<sub>20</sub>H<sub>19</sub>NS (M<sup>+</sup>). Calcd 305.1238. Found 305.1239. After elution with with petroleum ether/ethyl acetate (90/10) ketone **9** was obtained as an oil (0.22 g, 8.5%), in all respects identical with an authentic sample.

**Furan 26 and amido ketone 27** were obtained upon heating a mixture of complex **24b** (2.5 g, 6.77 mmol) and diphenylacetylene (2.35 g, 13.2 mmol) in benzene as above. Silica gel chromatography of the residue of the reaction with petroleum ether/ethyl acetate (95/5) as eluent gave the Cr-(CO)<sub>3</sub> complex of **26** followed by indenone **28** (0.13 g, 7%) and indanone **29** (0.20 g, 11%), the spectroscopic data of which were identical in all respects with those of previously synthesized samples. Treatment of the complex of the aminofuran in boiling pyridine for 6 h followed by evaporation of the solvent and chromatography of the residue first gave with petroleum ether/ethyl acetate (95/5) the aminofuran **26** (1.1 g, 42%) as a white solid: mp 108 °C; <sup>1</sup>H NMR (200 MHz, CDCl<sub>3</sub>) δ 7.28–7.16 (m, 15H, Ar), 4.35 (s, 2H, NCH<sub>2</sub>S), 3.62 (m, 2H, NCH<sub>2</sub>), 3.13 (m, 2H, CH<sub>2</sub>); <sup>13</sup>C NMR (50 MHz, CDCl<sub>3</sub>) δ 151.34 (NCO), 141.52 (C–O), 133.84–109.56 (Ar, C=C), 56.16, 54.40, 32.0 (CH<sub>2</sub>). HRMS C<sub>25</sub>H<sub>21</sub>NOS (M<sup>+</sup>). Calcd 383.1343. Found 383.1342. Amido ketone **27** (0.2 g, 7%) was then obtained as a 50/50 mixture of two isomers; white solid: mp 195 °C; IR (CHCl<sub>3</sub>) 1630, 1658 cm<sup>-1</sup>; <sup>1</sup>H NMR (200 MHz, CDCl<sub>3</sub>) δ 7.89–7.12 (m, 15H, Ar), 4.46 (s, 2H, NCH<sub>2</sub>S), 3.70 (m, 2H, NCH<sub>2</sub>), 2.92 (m, 2H, SCH<sub>2</sub>); <sup>13</sup>C NMR (100 MHz, CDCl<sub>3</sub>) δ 197.04 (CO), 168.07 (CO), 140.08–128.42 (Ar, C=C), 50.25 and 49.28, 48.22 and 47.63, 30.71 and 29.83 (CH<sub>2</sub>). HRMS for C<sub>25</sub>H<sub>21</sub>NO<sub>2</sub>S (M<sup>+</sup>). Calcd 399.1329. Found 399.133.

(CO)<sub>5</sub>Cr=C(Ph)N(CH<sub>2</sub>CH=CHCH<sub>2</sub>) (**30a**) was obtained from (CO)<sub>5</sub>Cr=C(Ph)OEt and pyrrolone as a yellow solid in 97% yield: mp 110 °C; <sup>1</sup>H NMR (200 MHz, CDCl<sub>3</sub>) δ 7.40 (m, 2H, Ar), 7.17 (m, 1H, Ar), 6.75 (m, 2H, Ar), 6.07 (m, 1H, CH=C), 5.79 (m, 1H, CH=C), 5.02 (m, 2H, NCH<sub>2</sub>), 3.97 (m, 2H, NCH<sub>2</sub>); <sup>13</sup>C NMR (50 MHz, CDCl<sub>3</sub>) δ 273.94 (Cr=C), 223.70, 217.51 (CO), 154.02, 129.05, 126.09, 125.12, 118.31 (Ar, C=C), 64.88 (NC), 61.05 (NC). Anal. Calcd for C<sub>16</sub>H<sub>11</sub>NO<sub>5</sub>Cr: C, 55.00; H, 3.15; N, 4.01. Found: C, 55.05; H, 3.12; N, 3.87.

(CO)<sub>5</sub>Cr=C(C<sub>4</sub>H<sub>9</sub>S)N(CH<sub>2</sub>CH=CHCH<sub>2</sub>) (**30b**) was obtained from (CO)<sub>5</sub>Cr=C(C<sub>4</sub>H<sub>9</sub>S)OEt and pyrrolone as a yellow solid in 88% yield: mp 62 °C; <sup>1</sup>H NMR (200 MHz, CDCl<sub>3</sub>) δ 7.28 (m, 1H, thienyl), 6.99 (m, 1H, thienyl), 6.50 (m, 1H, thienyl), 6.07 (m, 1H, CH=C), 5.83 (m, 1H, CH=C), 5.03 (m, 2H, NCH<sub>2</sub>), 4.23 (m, 2H, NCH<sub>2</sub>); <sup>13</sup>C NMR (50 MHz, CDCl<sub>3</sub>) δ 269.91 (Cr=C), 223.59, 217.16 (CO), 153.60, 127.19, 125.94, 125.06, 123.81, 117.38 (thienyl, C=C), 65.25 (NCH<sub>2</sub>), 61.04

(NCH<sub>2</sub>). Anal. Calcd for C<sub>14</sub>H<sub>9</sub>NO<sub>5</sub>Cr: C, 47.32; H, 2.53; N, 3.94. Found: C, 47.12; H, 2.61; N, 4.03.

**Lactam 32a and pyrrole 31a** were obtained upon heating a mixture of complex **30a** (2.5 g, 7.16 mmol) and diphenylacetylene (2.55 g, 14.0 mmol) in benzene as above. Silica gel chromatography of the residue of the reaction with petroleum ether/methylene chloride (90/10) as the eluent first gave pyrrole **31a** (0.045 g, 1.8%) as a white solid: mp 174 °C (decomp); <sup>1</sup>H NMR (200 MHz, CDCl<sub>3</sub>) δ 7.39–6.81 (m, 15H, Ar), 5.63 (m, 1H, CH=C), 5.38 (m, 1H, CH=C), 3.95 (m, 2H, NCH<sub>2</sub>), 3.32 (m, 2H, CH<sub>2</sub>). HRMS for C<sub>26</sub>H<sub>21</sub>N<sup>+</sup>. Calcd 347.1673. Found 347.1673. Elution with petroleum ether/ethyl acetate (80/20) gave lactam **32a** (1.6 g, 61.5%) as a white solid: mp 89–90 °C; <sup>1</sup>H NMR (200 MHz, CDCl<sub>3</sub>) δ 7.47–6.66 (m, 15H, Ar), 5.87 (m, 1H, CH=C), 5.69 (m, 1H, CH=C), 4.65 (m, 1H, NCH), 3.30 (m, 1H, NCH), 3.06 (m, 1H, HCH), 2.46 (m, 1H, HCH); <sup>13</sup>C NMR (50 MHz, CDCl<sub>3</sub>) δ 168.15 (CO), 158.52, 138.14, 132.87, 131.17, 129.44–126.67, 124.85, 122.06 (Ar, C=C), 66.08 (NC), 38.16 (NCH<sub>2</sub>), 31.12 (CH<sub>2</sub>). Anal. Calcd for C<sub>26</sub>H<sub>21</sub>NO: C, 85.95; H, 3.85; N, 5.78. Found: C, 85.40; H, 3.77; N, 6.03.

**Lactam 32b and pyrrole 31b** were obtained from complex **30b** (1.77 g, 4.9 mmol) and diphenylacetylene (1 g, 5.6 mmol) as above. Treatment of the residue of the reaction with pyridine for 6 h followed by silica gel chromatography with petroleum ether/methylene chloride (90/10) first gave pyrrole **31b** (0.025 g); <sup>1</sup>H NMR (200 MHz, CDCl<sub>3</sub>) δ 7.33–6.91 (m, 13H, Ar), 6.31 (m, 2H, CH=CH), 3.98 (m, 2H, CH<sub>2</sub>), 2.92 (m, 2H, CH<sub>2</sub>). Elution with petroleum ether/ethyl acetate (90/10) gave lactam **32b** (0.8 g, 43.5%) as a white solid: mp 137 °C; <sup>1</sup>H NMR (200 MHz, CDCl<sub>3</sub>) δ 7.45–6.79 (m, 15H, Ar), 5.81 (m, 2H, CH=CH), 4.66 (m, 1H, NCH), 3.54 (m, 1H, NCH), 2.95 (m, 1H, HCH), 2.55 (m, 1H, HCH); <sup>13</sup>C NMR (100 MHz, CDCl<sub>3</sub>) δ 167.74 (CO), 158.14, 142.23, 132.70–121.78 (Ar, CH=CH), 64.49 (NC), 38.26 (NCH<sub>2</sub>), 33.60 (CH<sub>2</sub>). Anal. Calcd for C<sub>24</sub>H<sub>19</sub>NOS: C, 78.04; H, 5.15; N, 3.79. Found: C, 77.67; H, 5.14; N, 3.85.

(CO)<sub>5</sub>Cr=C(H)N(CH<sub>2</sub>)<sub>3</sub> (**33a**) was obtained from formylazetidine and (CO)<sub>5</sub>CrNa<sub>2</sub> as a yellow solid in 93% yield: mp 61 °C; IR (CHCl<sub>3</sub>) 2040, 1970, 1920 cm<sup>-1</sup>; <sup>1</sup>H NMR (400 MHz, CDCl<sub>3</sub>) δ 10.36 (s, 1H, Cr=C(H)), 4.60 (t, *J* = 7.5 Hz, 2H, NCH<sub>2</sub>), 4.28 (t, *J* = 7.5 Hz, 2H, NCH<sub>2</sub>), 2.41 (m, 2H, CH<sub>2</sub>); <sup>13</sup>C NMR (100 MHz, CDCl<sub>3</sub>) δ 255.30 (Cr=O), 223.65, 217.58 (CO), 61.43, 58.43 (NCH<sub>2</sub>), 13.59 (CH<sub>2</sub>). Anal. Calcd for C<sub>9</sub>H<sub>7</sub>NO<sub>5</sub>Cr: C, 41.14; H, 2.68; N, 5.36. Found: C, 41.19; H, 2.74; N, 5.33.

(CO)<sub>5</sub>Cr=C(Me)NCH<sub>2</sub>CH<sub>2</sub>CH<sub>2</sub> (**33b**) was obtained from (CO)<sub>5</sub>Cr=C(Me)OEt and azetidine in 91% yield as a yellow solid: mp 31 °C; IR (CHCl<sub>3</sub>) 2040, 1970, 1920 cm<sup>-1</sup>; <sup>1</sup>H NMR (200 MHz, C<sub>6</sub>D<sub>6</sub>) δ 3.88 (m, 2H, NCH<sub>2</sub>), 2.66 (m, 2H, NCH<sub>2</sub>), 1.75 (s, 3H, CH<sub>3</sub>), 1.06 (m, 2H, CH<sub>2</sub>); <sup>13</sup>C NMR (50 MHz, CDCl<sub>3</sub>) δ 264.23 (Cr=C), 223.01, 218.23 (CO), 59.56 (NCH<sub>2</sub>), 55.82 (NCH<sub>2</sub>), 35.53 (CH<sub>2</sub>), 13.44 (CH<sub>3</sub>). Anal. Calcd for C<sub>10</sub>H<sub>9</sub>NO<sub>5</sub>Cr: C, 43.63; H, 3.27; N, 5.09. Found: C, 43.69; H, 3.32; N, 4.82.

(CO)<sub>5</sub>Cr=C(Ph)NCH<sub>2</sub>CH<sub>2</sub>CH<sub>2</sub> (**33c**) was obtained from (CO)<sub>5</sub>Cr=C(Ph)OEt and azetidine in 91% yield as yellow crystals: mp 124–126 °C; IR (CHCl<sub>3</sub>) 2040, 1940 cm<sup>-1</sup>; <sup>1</sup>H NMR (200 MHz, CDCl<sub>3</sub>) δ 7.37, 7.23, 6.78 (m, 5H, Ar), 4.84 (m, 2H, NCH<sub>2</sub>), 3.91 (m, 2H, NCH<sub>2</sub>), 2.36 (m, 2H, CH<sub>2</sub>); <sup>13</sup>C NMR (50 MHz, CDCl<sub>3</sub>) δ 266.76 (Cr=C), 223.50, 217.56 (CO), 149.87, 128.71, 126.64, 119.60 (Ar), 59.89 (NCH<sub>2</sub>), 57.38 (NCH<sub>2</sub>), 13.79 (CH<sub>2</sub>). Anal. Calcd for C<sub>15</sub>H<sub>11</sub>NO<sub>5</sub>Cr: C, 53.41; H, 3.26; N, 4.15. Found: C, 52.89; H, 3.24; N, 3.86. MS for C<sub>15</sub>H<sub>11</sub>NO<sub>5</sub>Cr<sup>+</sup>. Calcd 337. Found 337.

(CO)<sub>5</sub>Cr=C(Me)NCH<sub>2</sub>CH(Ph)CH<sub>2</sub> (**33d**) was obtained from (CO)<sub>5</sub>Cr=C(Me)OEt and 3-phenylazetidine in 94% yield as a yellow solid: mp 59–61 °C; IR (CHCl<sub>3</sub>) 2040, 1920 cm<sup>-1</sup>; <sup>1</sup>H NMR (200 MHz, CDCl<sub>3</sub>) δ 7.41–7.25 (m, 5H, Ar), 5.07 (m, 1H, NCH), 4.72 (m, 2H, NCH<sub>2</sub>), 4.33 (m, 1H, NCH), 4.01 (m, 1H, CHPh), 2.50 (s, 3H, CH<sub>3</sub>); <sup>13</sup>C NMR (50 MHz, CDCl<sub>3</sub>) δ 266.74 (Cr=C), 222.98, 218.25 (CO), 140.37, 129.28, 127.84, 126.65 (Ar), 66.50 (NCH<sub>2</sub>), 62.91 (NCH<sub>2</sub>), 36.02 (CH), 31.59

Table 11. Crystal Data for Compounds 3, 14a, 18, 22, and 24a

compd	C <sub>27</sub> H <sub>25</sub> ON (3)	C <sub>24</sub> H <sub>21</sub> O <sub>3</sub> NCr (14a)	C <sub>19</sub> H <sub>12</sub> O <sub>5</sub> Cr (18)	C <sub>24</sub> H <sub>25</sub> N (22)	C <sub>10</sub> H <sub>9</sub> O <sub>5</sub> NSCr (24a)
cryst params					
fw	379.5	423.43	372.3	327.47	275.18
cryst syst	monoclinic	triclinic	orthorhombic	monoclinic	monoclinic
space group	<i>P</i> 2 <sub>1</sub> / <i>n</i>	<i>P</i> -1	<i>Pc</i> 2 <sub>1</sub> / <i>b</i>	<i>P</i> 2 <sub>1</sub> / <i>n</i>	<i>P</i> 2 <sub>1</sub> / <i>n</i>
<i>a</i> , Å	10.080(4)	6.918(1)	10.356(1)	11.119(3)	8.3011(9)
<i>b</i> , Å	11.727(3)	10.057(1)	12.366(5)	10.682(2)	11.949(1)
<i>c</i> , Å	18.014(6)	15.193(2)	12.529(2)	15.428(3)	13.101(2)
$\alpha$ , deg		72.410(9)		102.23(2)	95.74(1)
$\beta$ , deg	102.40(3)	84.99(1)			
$\gamma$ , deg		84.66(3)			
<i>V</i> , Å <sup>3</sup>	2080(14)	1001(3)	1604.4(8)	1791(7)	1293(1)
<i>Z</i>	4	2	4	4	4
$\rho$ , g cm <sup>-3</sup>	1.21	1.40	1.54	1.21	1.41
$\mu$ (Mo K $\alpha$ ), cm <sup>-1</sup>	0.68	5.80	7.20	0.65	8.69
data collection					
diffractometer	CAD4	CAD4	CAD4	CAD4	CAD4
monochromator	graphite	graphite	graphite	graphite	graphite
radiation	Mo K $\alpha$	Mo K $\alpha$	Mo K $\alpha$	Mo K $\alpha$	Mo K $\alpha$
scan type	$\omega/2\theta$	$\omega/2\theta$	$\omega/2\theta$	$\omega/2\theta$	$\omega/2\theta$
scan range $q$ , deg	0.8 + 0.34 tan $\theta$	1.2 + 0.34 tan $\theta$	0.8 + 0.34 tan $\theta$	1.2 + 0.34 tan $\theta$	1.2 + 0.34 tan $\theta$
2 $\theta$ range, deg	3–50	3–60	2–50	2–50	3–56
no. of reflns collected	3648	5820	1486	3159	3103
no. of reflns used ( <i>I</i> > 3 $\sigma$ (1))	1327	3647	1089	1488	2137
refinement				0.036	0.036
<i>R</i>	0.065	0.037	0.029	0.034	0.035
<i>R</i> <sub>w</sub> *	0.063	0.037	0.029	DIFABS	DIFABS
abs. corr.**	DIFABS	DIFABS	DIFABS	0.87/1.13	0.89/1.12
min/max abs	0.90/1.10	0.83/1.16	0.81/1.12	no	93 × 10 <sup>-6</sup>
second extinct param	0.70 × 10 <sup>-4</sup>	no	no	unit wt	unit wt
weighting scheme	unit wt	unit wt	unit wt	303	193
ls params	180	238	264		

(CH<sub>3</sub>). Anal. Calcd for C<sub>16</sub>H<sub>13</sub>NO<sub>5</sub>Cr: C, 54.70; H, 3.70; N, 3.98. Found: C, 54.98; H, 3.74; N, 3.85.

(CO)<sub>5</sub>Cr=C(H)N-CH<sub>2</sub>CH(Ph)CH<sub>2</sub> (**33e**) was obtained from 1-formyl-3-phenylazetidine and (CO)<sub>5</sub>CrNa<sub>2</sub> as a yellow solid in 50% yield: mp 50 °C; IR (CHCl<sub>3</sub>) 2050, 1975, 1915 cm<sup>-1</sup>; <sup>1</sup>H NMR (200 MHz, CDCl<sub>3</sub>)  $\delta$  10.61 (s, 1H, Cr=C(H)), 7.40 (m, 5H, Ar), 5.05 (m, 1H, NCH), 4.68 (m, 2H, NCH<sub>2</sub>), 4.44 (m, 1H, NCH), 4.02 (m, 1H, CHPh); <sup>13</sup>C NMR (50 MHz, CDCl<sub>3</sub>)  $\delta$  257.63 (Cr=C), 223.6, 217.56, (CO), 139.98, 129.19, 127.61, 126.55 (Ar), 68.26, 65.20 (NCH<sub>2</sub>), 31.83 (CHPh). Anal. Calcd for C<sub>15</sub>H<sub>11</sub>NO<sub>5</sub>Cr: C, 53.41; H, 3.26; N, 4.15. Found: C, 53.41; H, 3.26; N, 4.13.

**Lactam 35a** was obtained upon heating complex **33a** (2.0 g, 7.6 mmol) in benzene in the presence of diphenylacetylene (1.5 g, 8.4 mmol) followed by silica gel chromatography. Elution with petroleum ether/ethyl acetate (80/20) gave lactam **35a** (0.63 g, 30%) as a white solid: mp 141 °C; IR (CHCl<sub>3</sub>) 1655, 1600 cm<sup>-1</sup>; <sup>1</sup>H NMR (200 MHz, CDCl<sub>3</sub>)  $\delta$  7.39 (m, 10H, Ar), 4.67 (m, 1H, NCH), 3.64 (m, 1H, NCH), 3.40 (m, 1H, NCH), 2.36 (m, 3H), 1.41 (m, 1H); <sup>13</sup>C NMR (100 MHz, CDCl<sub>3</sub>)  $\delta$  174.69 (CO), 153.86, 133.26, 131.88–129.49 (C=C, Ar), 66.77 (NC), 42.49 (NCH<sub>2</sub>), 29.98, 28.94 (2 CH<sub>2</sub>). HRMS for C<sub>19</sub>H<sub>17</sub>ON<sup>+</sup>. Calcd 275.1310. Found 275.1310.

**Lactam 35b** was obtained in 40% yield from complex **33b** as a white solid: mp 137 °C; IR (CHCl<sub>3</sub>) 1675 cm<sup>-1</sup>; <sup>1</sup>H NMR (200 MHz, CDCl<sub>3</sub>)  $\delta$  7.37 (m, 10H, Ar), 3.77 (m, 1H, NCH), 3.37 (m, 1H, NCH), 2.46 (m, 2H), 2.20 (m, 1H), 1.88 (m, 1H), 1.20 (s, 3H, CH<sub>3</sub>); <sup>13</sup>C NMR (50 MHz, CDCl<sub>3</sub>)  $\delta$  173.70 (CO), 159.21–127.83 (C=C, Ar), 72.22 (C–N), 41.34 (NCH<sub>2</sub>), 35.15, 28.40, 22.24 (CH<sub>2</sub>, CH<sub>3</sub>). Anal. Calcd for C<sub>20</sub>H<sub>19</sub>NO: C, 83.04; H, 6.57; N, 4.84. Found: C, 82.53; H, 6.48; N, 4.54. MS for C<sub>20</sub>H<sub>19</sub>NO<sup>+</sup>. Calcd 289. Found 289.

**Pyrrole 34c** and **lactam 35c** were obtained from complex **33c** (2.6 g, 7.71 mmol) and diphenylacetylene (2.85 g, 16 mmol) in benzene as above. Treatment of the residue of the reaction with pyridine under reflux for 6 h gave first, after silica gel chromatography with petroleum ether/methylene chloride (90/10), pyrrole **34c** (0.047 g, 1.8%) as a white solid: mp 218 °C; <sup>1</sup>H NMR (200 MHz, CDCl<sub>3</sub>)  $\delta$  7.25–7.00 (m, 15H, Ar), 4.08

(m, 2H, NCH<sub>2</sub>), 3.11 (m, 2H, CH<sub>2</sub>), 2.56 (m, 2H, CH<sub>2</sub>); <sup>13</sup>C NMR (50 MHz, CDCl<sub>3</sub>)  $\delta$  136.17–124.90 (Ar), 46.49 (NCH<sub>2</sub>), 27.23 (CH<sub>2</sub>), 24.99 (CH<sub>2</sub>). HRMS for C<sub>25</sub>H<sub>21</sub>N<sup>+</sup>. Calcd 335.1674. Found 335.1674. Eluting with petroleum ether/ethyl acetate (80/20), lactam **35c** was then obtained (0.65 g, 24%) as a white solid: mp 119 °C; IR (CHCl<sub>3</sub>) 1680 cm<sup>-1</sup>; <sup>1</sup>H NMR (200 MHz, CDCl<sub>3</sub>)  $\delta$  7.38–6.90 (m, 15H, Ar), 3.82 (m, 1H, NCH), 3.33 (m, 1H, NCH), 2.80 (m, 1H), 2.37 (m, 1H), 2.04 (m, 2H); <sup>13</sup>C NMR (50 MHz, CDCl<sub>3</sub>)  $\delta$  174.13 (CO), 159.62, 139.12, 133.87, 131.21–126.22 (C=C, Ar), 78.19 (NC), 41.46 (NCH<sub>2</sub>), 34.75 (CH<sub>2</sub>), 28.49 (CH<sub>2</sub>). Anal. Calcd for C<sub>25</sub>H<sub>21</sub>NO: C, 85.47; H, 5.98; N, 3.98. Found: C, 85.65; H, 5.93; N, 3.71.

**Lactam 35d** was obtained from complex **33d** (2 g, 5.6 mmol) and diphenylacetylene (1.5 g, 8.4 mmol) as above in 43% yield as a mixture of two isomers, which were separated by silica gel chromatography with petroleum ether/ethyl acetate (80/20) as eluent. First isomer (41%), white solid: mp 219 °C; IR (CHCl<sub>3</sub>) 1670 cm<sup>-1</sup>; <sup>1</sup>H NMR (200 MHz, CDCl<sub>3</sub>)  $\delta$  7.28 (m, 15H, Ar), 4.45 (m, 1H, CHPh), 3.58 (m, 1H, NCH), 3.28 (m, 1H, NCH), 2.94 (m, 1H, CCH), 2.14 (m, 1H, CCH), 1.48 (s, 3H, CH<sub>3</sub>); <sup>13</sup>C NMR (50 MHz, CDCl<sub>3</sub>)  $\delta$  174.70 (CO), 159.64, 141.45, 133.62, 131.55–127.03 (C=C, Ar), 71.75 (C–N), 49.44 (NCH<sub>2</sub>), 47.94 (CPh), 42.73 (CH<sub>2</sub>), 28.56 (CH<sub>3</sub>). Anal. Calcd for C<sub>26</sub>H<sub>23</sub>NO: C, 85.47; H, 6.30; N, 3.83. Found: C, 85.74; H, 6.21; N, 3.68. Second isomer (in trace amounts): mp 64 °C; <sup>1</sup>H NMR (200 MHz, CDCl<sub>3</sub>)  $\delta$  7.27 (m, 15H, Ar), 4.08 (m, 1H, CHPh), 3.82 (m, 2H, NCH<sub>2</sub>), 2.60 (m, 1H), 2.02 (m, 1H), 1.37 (s, 3H, CH<sub>3</sub>); <sup>13</sup>C NMR (50 MHz, CDCl<sub>3</sub>)  $\delta$  173.81 (CO), 159.33, 141.84, 133.76–127.17 (C=C, Ar), 72.89 (NC), 49.21 (NCH<sub>2</sub>), 48.67 (CPh), 44.90 (CH<sub>2</sub>), 22.62 (CH<sub>3</sub>). MS for C<sub>26</sub>H<sub>23</sub>NO<sup>+</sup>. Calcd 365. Found 365.

(CO)<sub>5</sub>Cr=C(Me)N(C<sub>8</sub>H<sub>12</sub>) (**36**) was obtained from the corresponding substituted azetidine and (CO)<sub>5</sub>Cr=C(Me)OEt in 73% yield as yellow crystals: mp 93–95 °C; IR (CHCl<sub>3</sub>) 2040, 1920 cm<sup>-1</sup>; <sup>1</sup>H NMR (200 MHz, CDCl<sub>3</sub>)  $\delta$  4.56 (m, 1H, NCH), 4.42 (m, 1H, NCH), 4.14 (m, 1H, NCH), 2.54 (m, 1H), 2.49 (s, 3H, CH<sub>3</sub>), 2.41 (m, 2H), 1.78 (m, 1H), 1.53 (m, 3H), 1.15 (m, 2H); <sup>13</sup>C NMR (50 MHz, CDCl<sub>3</sub>)  $\delta$  265.10 (Cr=C), 223.1, 218.48 (CO), 75.35 (NCH), 62.71 (NCH<sub>2</sub>), 39.95, 38.11, 33.98, 31.27,

27.20, 23.67. Anal. Calcd for  $C_{15}H_{15}NO_5Cr$ : C, 52.78; H, 4.35; N, 3.98. Found: C, 52.61; H, 4.35; N, 3.98. MS for  $C_{15}H_{15}NO_5Cr^+$ . Calcd 341. Found 341.

**Lactam complex 37** was obtained from complex **36** (1 g, 2.91 mmol) and diphenylacetylene (0.8 g, 4.49 mmol) as above after silica chromatography with petroleum ether/methylene chloride as eluent (65/35) as a yellow solid (0.65 g, 45%): mp 87 °C; IR ( $CHCl_3$ ) 1970, 1900, 1670  $cm^{-1}$ ;  $^1H$  NMR (200 MHz,  $CDCl_3$ )  $\delta$  7.35–7.24 (m, 5H, Ar), 6.01, 5.46, 5.25, 4.90 (m, 5H, ArCr), 4.08 (m, 1H, NCH), 3.61 (m, 1H), 2.77–2.28 (m, 4H), 1.85 (s, 3H,  $CH_3$ ), 1.63–1.08 (m, 6H);  $^{13}C$  NMR (50 MHz,  $CDCl_3$ )  $\delta$  232.22 (CO), 167.48 (CO), 130.00, 129.64, 128.82, 128.30 (Ar), 97.75, 95.68, 94.52, 89.50, 88.63 (ArCr), 71.50 (N–C), 55.76, 44.84, 43.41, 40.82, 40.04, 35.80, 29.75, 28.51, 22.50 (4 CH, 4  $CH_2$ ,  $CH_3$ ). HRMS for  $C_{28}H_{25}NO_4Cr$  ( $M^+ - 2 CO$ ). Calcd 435.1290. Found 435.1291.

**X-ray Studies.** Intensity data were collected at room temperature on a Nonius CAD4 diffractometer using graphite-monochromated Mo  $K\alpha$  radiation. Crystal data and data collection parameters are listed in Table 11. For each compound, the accurate cell dimensions and orientation matrix were obtained from least-squares refinements of the setting angles of 25 well-defined reflections. No decay in the intensities of two standard reflections was observed during the course of data collections. The usual corrections for Lorentz and polarization effects were applied.

Computations were performed by using CRYSTAL adapted on a Microvax-II computer.<sup>18</sup> Scattering factors and correc-

tions for anomalous dispersion were from ref 19. The structures were solved by using direct method (SHELXS)<sup>20</sup> for compounds **3**, **22**, and **24a** and by standard Patterson–Fourier techniques for compounds **14a** and **18**. Absorption corrections were applied (DIFABS). For **3**, non-hydrogen atoms were refined anisotropically except for the C atoms of the phenyl rings, which were left isotropic. For all other compounds all non-hydrogen atoms were refined anisotropically, hydrogen atoms were located on difference-Fourier maps, and their coordinates were refined with an overall refinable isotropic thermal parameter.

In Tables 1–5 are listed main bond lengths and angles for the five compounds.

**Acknowledgment** is made to Centre National de la Recherche Scientifique and to Commission of the European Communities (DGSRD, International Scientific Cooperation) for financial support.

**Supplementary Material Available:** Complete tables of atomic coordinates, anisotropic thermal parameters, bond lengths and angles (Tables S1–S15) (18 pages). This material is contained in many libraries on microfiche, immediately follows this article in the microfilm version of the journal, and can be ordered from the ACS; see any current masthead page for ordering information.

OM940582R

# 1,2-H Shift on Tetranuclear Ethynyl Complexes $(\mu_4\text{-C}_2\text{H})(\eta^5\text{-C}_5\text{R}_5)\text{FeMCo}_2(\text{CO})_n$ ( $\text{M} = \text{Fe, Ru}; n = 10, 11;$ $\text{R} = \text{H, Me})^1$

Munetaka Akita,\* Hideki Hirakawa, Kohsuke Sakaki, and Yoshihiko Moro-oka\*

Research Laboratory of Resources Utilization, Tokyo Institute of Technology, 4259 Nagatsuta, Midori-ku, Yokohama 226, Japan

Received January 26, 1995<sup>®</sup>

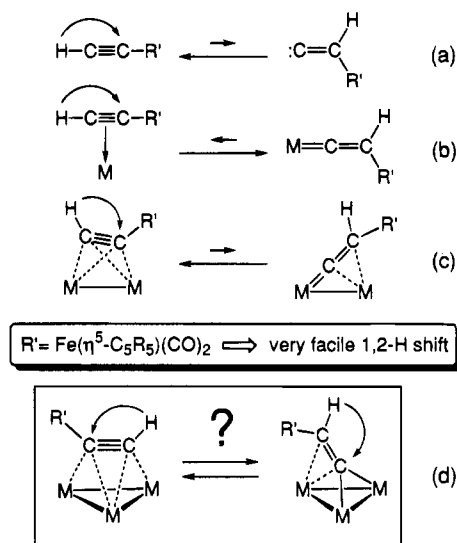
The interaction of the trinuclear ethynyl complexes  $\text{Co}_2(\text{CO})_6[\mu\text{-}(\eta^5\text{-C}_5\text{R}_5)\text{Fe}(\text{CO})_2\text{C}\equiv\text{CH}]$  (**3**: **a**,  $\text{R} = \text{H}$ ; **b**,  $\text{R} = \text{Me}$ ) with  $\text{Fe}_2(\text{CO})_9$  and the addition reaction of  $(\eta^5\text{-C}_5\text{R}_5)\text{Fe}(\text{CO})_2\text{C}\equiv\text{CH}$  (**1a,b**) to the trimetallic species  $\text{RuCo}_2(\text{CO})_{11}$  afford the tetranuclear vinylidene intermediates  $\text{Co}_2\text{M}(\text{CO})_9[\mu_3\text{-C}=\text{C}(\text{H})\text{Fe}(\eta^5\text{-C}_5\text{R}_5)(\text{CO})_2]$  (**4**,  $\text{M} = \text{Fe}$ ; **6**,  $\text{M} = \text{Ru}$ ), respectively, which are thermally decarbonylated to produce the tetranuclear acetylide clusters  $(\mu_4\text{-C}_2\text{H})(\eta^5\text{-C}_5\text{R}_5)\text{Fe}[\text{MCo}_2(\text{CO})_{10}]$  (**5**,  $\text{M} = \text{Fe}$ ; **7**,  $\text{M} = \text{Ru}$ ) with the spiked triangular metal array. The skeletal rearrangement  $[\text{HC}\equiv\text{CFe} (\mathbf{1}, \mathbf{3}) \rightarrow \text{C}=\text{C}(\text{H})\text{Fe} (\mathbf{4}, \mathbf{6}) \rightarrow \text{HC}\equiv\text{CFe} (\mathbf{5}, \mathbf{7})]$  can be explained in terms of a 1,2-H shift on the  $\text{C}_2$  bridge of the plausible alkyne-cluster type intermediates  $[\mu_3\text{-}(\eta^5\text{-C}_5\text{R}_5)\text{Fe}(\text{CO})_2\text{C}\equiv\text{CH}]\text{MCo}_2(\text{CO})_9$  [ $\text{M} = \text{Fe}$  (**9**),  $\text{Ru}$  (**10**)].

## Introduction

The 1,2-hydrogen shift of terminal alkynes within a coordination sphere of a transition metal (Scheme 1) has been recognized as an elementary step of organometallic chemistry.<sup>2</sup> Although the uncatalyzed process a has proved to be highly unfavorable owing to the thermodynamic instability of the vinylidene species, coordination to one or more transition metal centers results in inversion of the energetics to make the process feasible (processes b and c).<sup>3</sup> In particular, the process b on mononuclear complexes serves as a versatile preparative method for vinylidene complexes<sup>2</sup> and is involved as a key step of an increasing number of catalytic transformations.<sup>4</sup>

We have been studying the synthesis, structure, and chemical properties of polymetallic  $\text{C}_2\text{H}$  complexes derived from the ethynyliron complexes  $(\eta^5\text{-C}_5\text{R}_5)\text{Fe}(\text{CO})_2\text{C}\equiv\text{CH}$  [ $\text{R} = \text{H}$  (**1a**),  $\text{Me}$  (**1b**)].<sup>5</sup> As a result, it has been revealed that the introduction of the iron groups as the 1-alkyne substituents [ $\text{R}' = (\eta^5\text{-C}_5\text{R}_5)\text{Fe}(\text{CO})_2$  in Scheme 1] induces remarkable labilization of the H atom on the  $\text{C}_2$  moiety. For example, the cationic *diiron* complex  $[\text{Fp}^*_2(\mu\text{-C}\equiv\text{CH})]\text{BF}_4^{5a}$  (process b where  $\text{R}' = \text{M} = \text{Fp}^*$ ) and the *trinuclear* complexes  $\text{Cp}^2\text{Mo}_2(\text{CO})_4[\mu\text{-}\eta^2\text{:}\eta^2\text{-}(\eta^5\text{-C}_5\text{R}_5)\text{Fe}(\text{CO})_2\text{C}\equiv\text{CH}]^{5g}$  [process c where  $\text{R}' = (\eta^5\text{-C}_5\text{R}_5)\text{Fe}(\text{CO})_2$  and  $\text{M} = \text{MoCp}(\text{CO})_2$ ] exhibit dynamic behavior by way of the fast reversible 1,2-H shift on the  $\text{C}_2$  bridge as confirmed by  $^{13}\text{C}$ -NMR analyses. As an extension, we have examined the chemical properties

## Scheme 1



of mixed metal *tetranuclear*  $\text{C}_2\text{H}$  complexes [process d where  $\text{R}' = (\eta^5\text{-C}_5\text{R}_5)\text{Fe}(\text{CO})_2$ ]. The corresponding tautomerization of 1-alkyne on trinuclear cluster systems (process d where  $\text{R}' = \text{organic group}$ ) was already reported, and trinuclear vinylidene clusters have been prepared via this process.<sup>6</sup>

In a previous paper,<sup>5e</sup> we reported formation of a *tetranuclear*  $\text{C}_2\text{H}$  complex  $(\text{CpFe})(\text{CpNi})_2\text{Ni}(\text{CO})_2(\mu_4\text{-}$

<sup>®</sup> Abstract published in *Advance ACS Abstracts*, May 1, 1995.

(1) Abbreviations: Cp =  $\eta^5\text{-C}_5\text{H}_5$ ; Cp\* =  $\eta^5\text{-C}_5\text{Me}_5$ ; Fp = CpFe(CO)<sub>2</sub>; Fp\* = Cp\*Fe(CO)<sub>2</sub>. Throughout this paper the carbon atoms of the  $\text{C}_2\text{H}$  linkage are designated as Fe-C<sub>α</sub>-C<sub>β</sub> or Fe-C1-C2 irrespective of the structure.

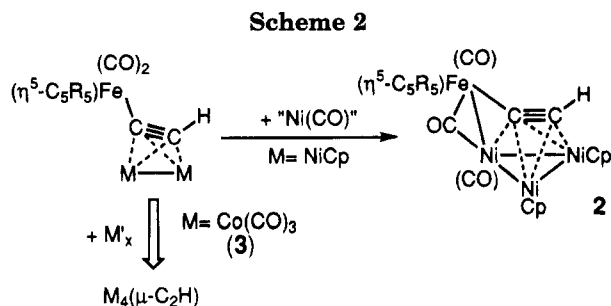
(2) (a) Bruce, M. I. *Chem. Rev.* **1991**, *91*, 197. (b) Bruce, M. I.; Swincer, A. G. *Adv. Organomet. Chem.* **1983**, *22*, 60.

(3) (a) Silvestre, J.; Hoffmann, R. *Helv. Chem. Acta* **1985**, *68*, 1461. (b) Wakatsuki, Y.; Koga, N.; Yamazaki, H.; Morokuma, K. *J. Am. Chem. Soc.* **1994**, *116*, 8105.

(4) (a) Wakatsuki, Y.; Yamazaki, H.; Kumegawa, N.; Satoh, T.; Satoh, J. Y. *J. Am. Chem. Soc.* **1991**, *113*, 9604. (b) Trost, B. M.; Kulawiec, R. J. *J. Am. Chem. Soc.* **1992**, *114*, 5579. (c) References cited in ref 2a.

(5) (a) Akita, M.; Terada, M.; Oyama, S.; Moro-oka, Y. *Organometallics* **1990**, *9*, 816. (b) Akita, M.; Terada, M.; Oyama, S.; Sugimoto, S.; Moro-oka, Y. *Organometallics* **1991**, *10*, 1561. (c) Akita, M.; Terada, M.; Moro-oka, Y. *Organometallics* **1991**, *10*, 2962. (d) Akita, M.; Terada, M.; Moro-oka, Y. *Organometallics* **1992**, *11*, 1825. (e) Akita, M.; Terada, M.; Moro-oka, Y. *Organometallics* **1992**, *11*, 3468. (f) Akita, M.; Sugimoto, S.; Tanaka, M.; Moro-oka, Y. *J. Am. Chem. Soc.* **1992**, *114*, 7581. (g) Akita, M.; Sugimoto, S.; Takabuchi, A.; Tanaka, M.; Moro-oka, Y. *Organometallics* **1993**, *12*, 2925. (h) Akita, M.; Ishii, N.; Takabuchi, A.; Tanaka, M.; Moro-oka, Y. *Organometallics* **1994**, *13*, 258. (i) Akita, M.; Takabuchi, A.; Terada, M.; Ishii, N.; Tanaka, M.; Moro-oka, Y. *Organometallics* **1994**, *13*, 2516–2520. (j) Akita, M.; Terada, M.; Ishii, N.; Hirakawa, H.; Moro-oka, Y. *J. Organomet. Chem.* **1994**, *473*, 175. (k) Akita, M.; Moro-oka, Y. *Bull. Chem. Soc. Jpn.* **1995**, *68*, 420.

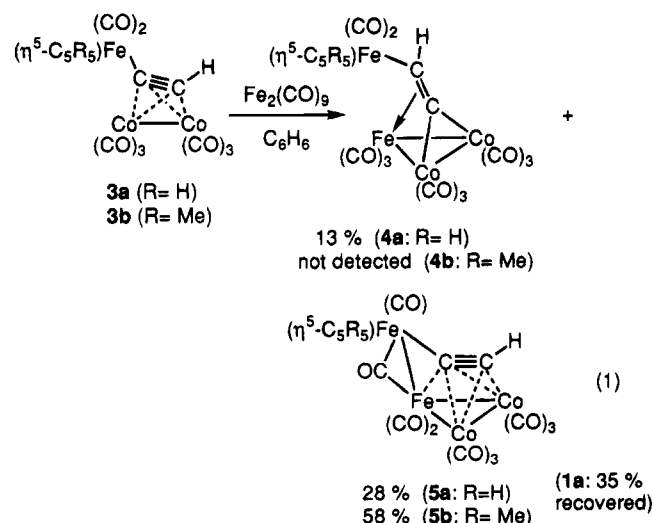




$\text{C}_2\text{H}$ ) (**2**) by addition reaction of  $\text{Ni}(\text{CO})_4$  to  $(\text{CpNi})_2(\mu\text{-}\eta^2\text{-}\eta^2\text{-FpC}\equiv\text{CH})$  (Scheme 2). This result prompted us to examine structure expansion of its Co analogues  $\text{Co}_2(\text{CO})_6[\mu\text{-}\eta^2\text{-}\eta^2\text{-}(\eta^5\text{-C}_5\text{R}_5)\text{Fe}(\text{CO})_2\text{C}\equiv\text{CH}]$  (**3**) [**3a** (R = H), **3b** (R = Me)].<sup>5c</sup> Of many attempts to expand the structure, we found that tetranuclear  $\text{Fe}_2\text{Co}_2$  complexes were obtained by interaction with  $\text{Fe}_2(\text{CO})_9$ . In addition, the isoelectronic  $\text{FeRuCo}_2$  complexes were also prepared by the reaction of **1** with the reactive heterotrinnuclear species  $\text{RuCo}_2(\text{CO})_{11}$ .<sup>7,8</sup> Herein we disclose the details of the reaction and structural aspects of the resulting tetranuclear  $(\mu_4\text{-C}_2\text{H})\text{FeMCo}_2$  (M = Fe, Ru) complexes relevant to the 1,2-H shift. The corresponding organic counterparts derived from 1-alkyne, i.e., trinnuclear  $(\mu_3\text{-R}'\text{C}_2\text{H})\text{MCo}_2$  clusters (M = Fe,<sup>9</sup> Ru<sup>8</sup>), were studied by Vahrenkamp et al.

## Results and Discussion

**Interaction of  $\text{Co}_2(\text{CO})_6[\mu\text{-}\eta^2\text{-}\eta^2\text{-}(\eta^5\text{-C}_5\text{R}_5)\text{Fe}(\text{CO})_2\text{C}\equiv\text{CH}]$  (**3a,b**) with  $\text{Fe}_2(\text{CO})_9$ .** When the trinuclear ethynyl complex  $\text{Co}_2(\text{CO})_6(\mu\text{-}\eta^2\text{-}\eta^2\text{-FpC}\equiv\text{CH})$  (**3a**)<sup>5c</sup> [the adduct of **1a** to  $\text{Co}_2(\text{CO})_8$ ] was treated with  $\text{Fe}_2(\text{CO})_9$  at room temperature, two products **4a** and **5a** were isolated as black crystals in 13% and 28% yields, respectively, after preparative TLC separation (eq 1). The thermally



unstable, minor product **4a** contains only terminal CO ligands as indicated by IR, whereas the major product **5a** contains the  $\nu(\mu\text{-CO})$  absorption at  $1838\text{ cm}^{-1}$ . In the case of the reaction of the  $\text{Fp}^*$  derivative **3b**, the adduct **5b** with the  $\nu(\mu\text{-CO})$  absorption was obtained exclusively without formation of any detectable amount of **4b**.

The deshielded  $\text{C}_2\text{H}$  signals ( $^1\text{H-NMR}$ ) of the tetranuclear complexes **4** and **5** [ $\delta_{\text{H}}$  7.18 (**4a**), 8.65 (**5a**), 8.68

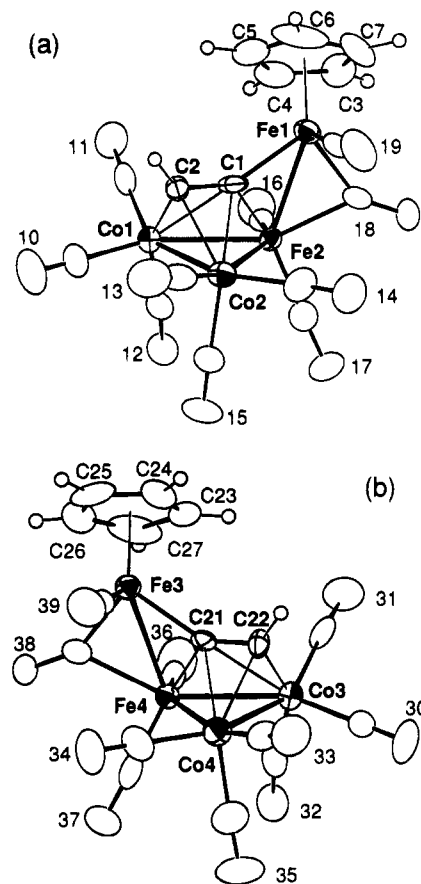


**Figure 1.** Molecular structure of the two independent molecules of **5a**: (a) molecule 1; (b) molecule 2. The numbers without the atom names are for the CO ligands.

(**5b**)] suggest that the  $\text{C}_2\text{H}$  ligands are incorporated in a cluster environment. The major products **5a,b** are readily assigned to acetylide cluster compounds on the basis of the large  $^1J_{\text{C-H}}$  values of the  $\text{C}_\beta$  signals<sup>1</sup> of the  $\text{C}_2\text{H}$  bridge [**5a**,  $\delta_{\text{C}}$  193.0 (s,  $\text{C}_\alpha$ ), 118.5 (d,  $^1J_{\text{C-H}} = 203\text{ Hz}$ ,  $\text{C}_\beta$ ); **5b**,  $\delta_{\text{C}}$  193.1 (s,  $\text{C}_\alpha$ ), 115.7 (d,  $^1J_{\text{C-H}} = 208\text{ Hz}$ ,  $\text{C}_\beta$ )]. The rather sharp singlets around 193 ppm, the chemical shift and shape of which do not change significantly in the temperature range of room temperature to  $-80\text{ }^\circ\text{C}$ ,<sup>10</sup> have been assigned to  $\text{C}_\alpha$ . Then the molecular structure of **5a** was determined by X-ray crystallography. ORTEP views of the two independent molecules with essentially the same geometry are reproduced in Figure 1a,b, and the crystallographic data and the selected structural parameters are listed in Tables 1 and 2. The four metal atoms are arranged in a spiked triangular array, with which the  $\text{C}_2\text{H}$  ligand interacts as a  $\mu\text{-}\eta^1(\text{Fe}1,3):\eta^1(\text{Fe}2,4)$ - as well as  $\mu\text{-}\eta^2\text{-}(\text{Co}1,3):\eta^2(\text{Co}2,4)$ -bridging ligand. As can be seen from

(6) (a) Sappa, E.; Tiripicchio, A.; Braunstein, P. *Chem. Rev.* **1983**, *83*, 203. (b) Silvestre, J.; Hoffmann, R. *Langmuir* **1985**, *1*, 621. (c) Raithby, P. R.; Rosales, M. J. *Adv. Inorg. Chem. Radiochem.* **1985**, *29*, 169. (d) Nast, R. *Coord. Chem. Rev.* **1982**, *47*, 89. (e) Carty, A. J. *Pure Appl. Chem.* **1982**, *54*, 113.

(7) (a) Roland, E.; Vahrenkamp, H. *Chem. Ber.* **1985**, *118*, 1133. (b) Vahrenkamp, H. *Inorg. Synth.* **1989**, *26*, 354.

(8) (a) Roland, E.; Vahrenkamp, H. *J. Mol. Catal.* **1983**, *21*, 233. (b) Bernhardt, W.; Vahrenkamp, H. *Angew. Chem., Int. Ed. Engl.* **1984**, *23*, 141. (c) Roland, E.; Bernhardt, W.; Vahrenkamp, H. *Chem. Ber.* **1985**, *118*, 2858.

(9) Albiez, T.; Bernhardt, W.; von Schnering, C.; Roland, E.; Bantel, H.; Vahrenkamp, H. *Chem. Ber.* **1990**, *123*, 141.

(10) The shape of the CO signals appearing in the region of 190–250 ppm depends on the temperature measured owing to the fluxionality of the CO ligands.

Table 1. Crystallographic Data for 5a, 6a, and 7b

comps	5a	6a	7b
formula	C <sub>17</sub> H <sub>6</sub> O <sub>10</sub> Fe <sub>2</sub> Co <sub>2</sub>	C <sub>18</sub> H <sub>6</sub> O <sub>11</sub> FeRuCo <sub>2</sub>	C <sub>22</sub> H <sub>16</sub> O <sub>10</sub> FeRuCo <sub>2</sub>
fw	599.79	673.02	715.15
space group	P2 <sub>1</sub> /n	Pca2 <sub>1</sub>	P $\bar{1}$
a/Å	9.213(3)	12.892(2)	9.390(4)
b/Å	19.731(6)	13.024(4)	15.882(4)
c/Å	22.486(6)	13.164(9)	9.243(6)
$\alpha$ /deg			97.43(4)
$\beta$ /deg	90.96(2)		108.93(4)
$\gamma$ /deg			99.07(3)
V/Å <sup>3</sup>	4087(2)	2210(2)	1263(1)
Z	8	4	2
$d_{\text{calcd}}/\text{g cm}^{-3}$	1.949	2.022	1.880
$\mu/\text{cm}^{-1}$	30.38	28.45	24.78
2 $\theta$ /deg	5–50	5–60	5–60
no. of data colld	7904	3590	4824
no. of unique data with $I > 3\sigma(I)$	4326	2347	3241
no. of variables	559	297	325
R <sup>a</sup>	0.063	0.036	0.032
R <sub>w</sub> <sup>b</sup>	0.044	0.026	0.028

<sup>a</sup>  $R = \sum(|F_o| - |F_c|)/\sum|F_o|$ , <sup>b</sup>  $R_w = \{\sum w(|F_o| - |F_c|)^2/\sum w|F_o|^2\}^{1/2}$ , where  $w = \{\sigma^2(F_o)\}^{-1}$ .

Table 2. Selected Structural Parameters for 5a<sup>a</sup>

Bond Lengths			
C1–C2	1.34(1)	C21–C22	1.34(1)
C1–Co1	2.30(1)	C21–Co3	2.30(1)
C1–Co2	2.12(1)	C21–Co4	2.14(1)
C1–Fe1	1.96(1)	C21–Fe3	1.96(1)
C1–Fe2	1.93(1)	C21–Fe4	1.90(1)
C2–Co1	1.94(1)	C22–Co3	1.99(1)
C2–Co2	2.07(1)	C22–Co4	2.05(1)
Co1–Co2	2.471(2)	Co3–Co4	2.467(2)
Co1–Fe2	2.617(2)	Co3–Fe4	2.608(2)
Co2–Fe2	2.573(2)	Co4–Fe4	2.584(2)
Fe1–Fe2	2.557(2)	Fe3–Fe4	2.589(2)
Bond Angles			
Co1–C1–CO2	67.8(3)	Co3–C21–Co4	67.4(3)
Co1–C1–C2	57.3(6)	Co3–C21–C22	59.5(6)
Co2–C1–Fe2	78.7(3)	Co4–C21–Fe4	79.3(4)
Co2–C1–C2	69.1(6)	Co4–C21–C22	67.6(6)
Fe1–C1–Fe2	82.2(5)	Fe3–C21–Fe4	84.1(5)
Fe1–C1–C2	147.2(9)	Fe3–C21–C22	144.0(9)
Fe2–C1–C2	130.1(9)	Fe4–C21–C22	131.8(8)
Co1–C2–CO2	76.1(3)	Co3–C22–Co4	75.4(4)
Co1–C2–C1	87.1(8)	Co3–C22–C21	84.9(7)
Co2–C2–C1	73.5(6)	Co4–C22–C21	75.1(6)
Co2–Co1–Fe2	60.67(6)	Co4–Co3–Fe4	61.15(6)
Co1–Co2–Fe2	62.47(6)	Co3–Co4–Fe4	62.11(6)
Co1–Fe2–Fe1	104.01(7)	Co3–Fe4–Fe3	104.27(8)
Co2–Fe2–Fe1	93.70(7)	Co4–Fe4–Fe3	93.35(7)
Co1–Fe2–Co2	56.87(6)	Co3–Fe4–Co4	56.75(6)

<sup>a</sup> Bond lengths in angstroms and bond angles in degrees.

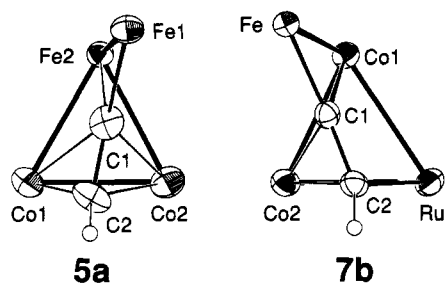


Figure 2. Top views of the core structures of 5a and 7b.

the top view of the core structure (Figure 2a), the C1–C2 (C21–C22) part lies almost perpendicular to the Co1–Co2 (Co3–Co4) vector. Although the chiral environment caused by the Fe<sub>1,3</sub> part slightly distorts the structure from a symmetrical one, the C1 (C21) and C2 (C22) atoms are located nearly equidistant from the  $\pi$ -coordinated Co<sub>1,3</sub> and Co<sub>2,4</sub> atoms. Although the tetra-

nuclear structure of 5 appears to be formed by a capping reaction of the FeCo<sub>2</sub> triangular face in 3 by an “Fe(CO)<sub>2</sub>” fragment, the formation of 5 follows a couple of processes as described below.

The other product 4a, which could not be fully characterized owing to its thermal instability, was assigned to the vinylidene cluster Co<sub>2</sub>Fe(CO)<sub>9</sub>[ $\mu_3$ -C=C(H)Fp] by comparison of the spectroscopic features with those of the structurally characterized Ru analogue 6a (see below), in particular (1) the olefinic nature of the CH moiety of the C<sub>2</sub>H part as suggested by the NMR data [ $\delta_{\text{H}}$  7.18;  $\delta_{\text{C}}$  123.7 (d,  $^1J_{\text{C-H}} = 151$  Hz, =C(H)Fp)] and (2) the absence of  $\nu(\mu\text{-CO})$  absorption. Unfortunately, the characteristic, highly deshielded C=C(H)-Fp signal could not be located despite several attempts. In accord with the composition, the molecular weight ( $m/z = 628$ ) determined by FDMS is larger than that of 5a ( $m/z = 600$ ) by 28 (CO), and upon being heated in refluxing benzene, the vinylidene cluster 4a was converted to the acetylide cluster 5a in a quantitative yield ( $^1\text{H-NMR}$ ) through a combination of thermal decarbonylation and H-migration. On the other hand, the Cp\* complex 4b could not be detected at all even by a  $^1\text{H-NMR}$  experiment, and the more stable acetylide cluster 5b was formed directly as mentioned above.

Thus the reaction of 3 with Fe<sub>2</sub>(CO)<sub>9</sub> gives the vinylidene cluster 4 via addition of an “Fe(CO)<sub>2</sub>” fragment followed by 1,2-H shift. Upon thermal decarbonylation of 4, backward H-shift coupled with the Fe–Co bond formation produces the acetylide cluster 5. These results indicate that the C<sub>2</sub>H atom migrates between the two carbon atoms.

**Interaction of ( $\eta^5\text{-C}_5\text{R}_5$ )Fe(CO)<sub>2</sub>C≡CH (1) with RuCo<sub>2</sub>(CO)<sub>11</sub>.** In order to examine the generality of the 1,2-H shift on tetranuclear C<sub>2</sub>H complexes, preparation of Ru analogues of 4 and 5 was attempted. When the core composition of the tetranuclear clusters 4 and 5 is compared with that of the starting mononuclear ethynyl complex 1, formal addition of “Fe(CO)<sub>2</sub>(CO)<sub>x</sub>” fragments ( $x = 8, 9$ ) to 1 leads to the composition of 4 and 5. Then we examined the addition reaction of 1 to the reactive trinuclear cluster RuCo<sub>2</sub>(CO)<sub>11</sub> reported by Vahrenkamp et al.<sup>7,8</sup>



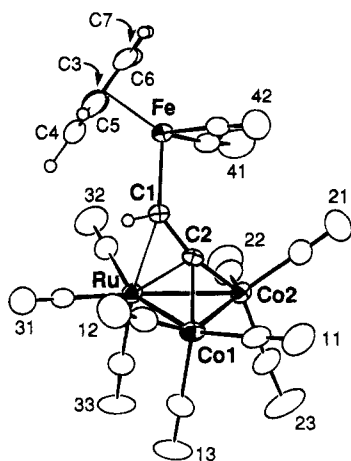
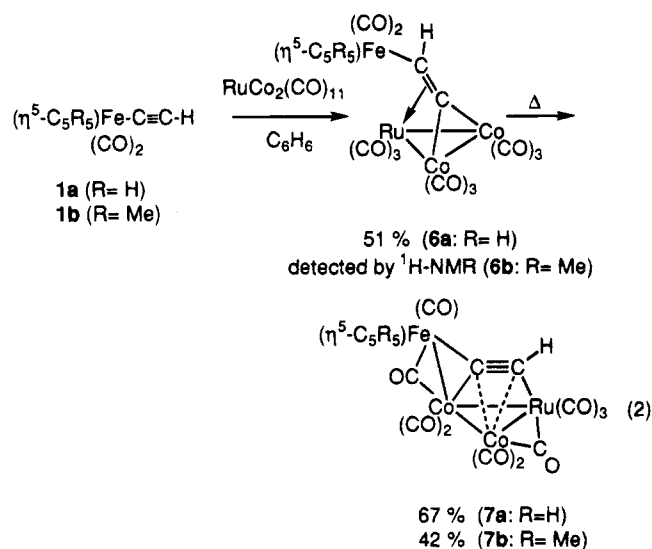


**Figure 3.** Molecular structure of **6a** drawn at the 30% probability level. The numbers without the atom names are for the CO ligands.

Treatment of **1a** with  $\text{RuCo}_2(\text{CO})_{11}$  in benzene at room temperature readily gave the dark red adduct **6a** (eq 2). The  $^{13}\text{C}$ -NMR parameters for the  $\text{C}_2\text{H}$  part, in



particular, the quaternary carbon signal observed in low field [ $\delta_{\text{C}}$  277.5 (s, C2), 107.1 (d,  $^1J_{\text{C-H}} = 151$  Hz, C1)], clearly indicate that **6a** contains a vinylidene-type  $\text{C}=\text{C}(\text{H})$  moiety, and the vinylidene structure has been confirmed by X-ray crystallography. The molecular structure is shown in Figure 3, and the selected structural parameters are summarized in Table 3. The  $\text{C}=\text{C}(\text{H})\text{Fp}$  moiety interacts with the  $\text{RuCo}_2$  cluster part as a vinylidene ligand. The C2 atom bridges the two Co atoms, and the C1-C2 part is  $\pi$ -bonded to the Ru center. The C1-C2 length [1.34(1) Å] falls in the typical range of the C=C lengths of trinuclear vinylidene cluster compounds.<sup>2</sup> The Fp part has no interaction with the  $\text{RuCo}_2$  cluster part and acts merely as a vinylidene substituent. In accord with this description, the geometry of the cluster part is close to that of the organic counterparts,  $\text{RuCo}_2(\text{CO})_9[\mu_3\text{-C}=\text{C}(\text{H})\text{R}]$  (R = *t*-Bu, Ph),<sup>9</sup> as compared with the typical *t*-Bu derivative (Table 2). On the basis of the similar spectroscopic features of **4a** and **6a** [(1)  $\text{C}_2\text{H}$  chemical shifts; (2) absence of  $\nu(\mu\text{-CO})$  absorption; (3) thermal transformation to the acetylide clusters **5a** and **7a**], **4a** has been assigned to the Fe analogue of **6a** as discussed above.

**Table 3.** Selected Structural Parameters for  $\text{RuCo}_2(\text{CO})_9[\mu_3\text{-C}=\text{C}(\text{H})\text{R}]$  [R = Fp (**6a**) and *t*-Bu]<sup>a</sup>

	R	
	Fp ( <b>6a</b> )	<i>t</i> -Bu <sup>b</sup>
Bond Lengths		
C1-C2	1.350(9)	1.37(1)
C1-Fe	2.014(7)	1.53(1) <sup>c</sup>
C1-Ru	2.445(7)	2.405(8)
C2-Co1	1.925(7)	1.901(7)
C2-Co2	1.895(7)	1.983(7)
C2-Ru	2.106(7)	2.099(8)
Ru-Co1	2.629(1)	2.618(1)
Ru-Co2	2.629(1)	2.628(1)
Co1-Co2	2.489(2)	2.489(1)
Bond Angles		
Ru-C1-Fe	126.3(3)	<i>d</i>
Ru-C1-C2	59.3(4)	<i>d</i>
Fe-C1-C2	133.8(5)	131(1) <sup>e</sup>
Ru-C2-Co1	81.3(2)	<i>d</i>
Ru-C2-Co2	82.0(3)	<i>d</i>
Ru-C2-C1	87.2(4)	<i>d</i>
Co1-C2-Co2	81.3(3)	<i>d</i>
Co1-C2-C1	132.8(5)	<i>d</i>
Co2-C2-C1	142.1(5)	<i>d</i>
Co1-Ru-Co2	56.53(3)	56.7(1)
Co1-Ru-C2	46.4(2)	<i>d</i>
Co2-Ru-C2	45.5(2)	<i>d</i>
Ru-Co1-Co2	61.74(4)	61.9(1)
Ru-Co1-C2	52.3(2)	<i>d</i>
Co2-Co1-C2	48.8(2)	<i>d</i>
Ru-Co2-Co1	61.73(4)	61.5(1)
Ru-Co2-C2	52.5(2)	<i>d</i>
Co1-Co2-C2	49.9(2)	<i>d</i>

<sup>a</sup> Bond lengths in angstroms and bond angles in degrees. <sup>b</sup> Reference 9. <sup>c</sup> The =C-C(quaternary carbon of the *t*-Bu group) length. <sup>d</sup> Not reported. <sup>e</sup> The C=C-C(quaternary carbon of the *t*-Bu group) angle.

The reaction of the Cp\* derivative **1b** with  $\text{RuCo}_2(\text{CO})_{11}$  followed a similar process to give the orange adduct **6b**. Although an analytically pure sample was not obtained owing to facile thermal decarbonylation (see below), **6b** was assigned to the vinylidene structure on the basis of the  $\text{C}_2\text{H}$  resonance ( $^1\text{H-NMR}$ ).

Thermolysis of the vinylidene clusters **6a,b** in refluxing benzene resulted in the formation of the deep green complexes **7a,b**, respectively, which showed spectroscopic features quite similar to those of **5a,b**. For example, **7** contains a  $\nu(\mu\text{-CO})$  absorption and the  $\text{C}_2\text{H}$  moiety may behave as an acetylide ligand as suggested by the large  $^1J_{\text{C-H}}$  values [**7a**,  $\delta_{\text{H}}$  8.07 (s),  $\delta_{\text{C}}$  198.6 (s,  $\text{C}_\alpha$ ), 106.2 (d,  $^1J_{\text{C-H}} = 196$  Hz,  $\text{C}_\beta$ ); **7b**,  $\delta_{\text{H}}$  7.98 (s),  $\delta_{\text{C}}$  198.9 (s,  $\text{C}_\alpha$ ), 106.7 (d,  $^1J_{\text{C-H}} = 193$  Hz,  $\text{C}_\beta$ )]. However, the structure of the Ru-containing tetranuclear cluster **7b** has proved to be considerably different from that of the above-mentioned Fe derivative **5a** as revealed by X-ray crystallography (Figure 4 and Table 4). While the four metal atoms are arranged in a spiked triangular array in a manner similar to those in **4a**, the spiked  $(\eta^5\text{-C}_5\text{R}_5)\text{Fe}$  part is not bonded to the group 8 metal (Ru) as in the case of **5a** but to Co1. Namely, the Ru atom does not occupy the hinge position of the basal  $\text{RuCo}_2$  triangle. Furthermore **7b** contains one more bridging CO(17) in addition of CO(11) and the C1-C2 part is coordinated to the Ru and Co1 atoms in an unsymmetrical manner. The  $\text{C}_2\text{H}$  ligand is formally  $\sigma$ -bonded to Fe, Ru, and Co1 and  $\pi$ -bonded to Co2, whereas that in **5a** is  $\pi$ -bonded to Co1 and Co2. As a result, the C1-C2 bond lies almost parallel to the Co1-Ru vector. Therefore the core part in **7b**, which is essentially the same as that of the Ph analogue of **7b**, (CpFe)-

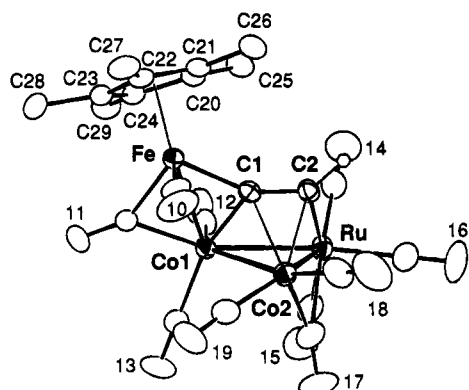


**Figure 4.** Molecular structure of **7b** drawn at the 30% probability level. The numbers without the atom names are for the CO ligands.

**Table 4. Selected Structural Parameters for 7b<sup>a</sup>**

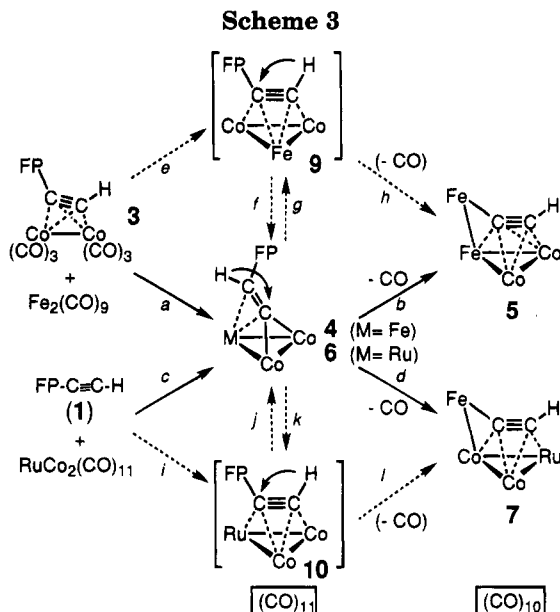
Bond Lengths			
C1–C2	1.340(6)	C2–Co1	2.849(5)
C1–Ru	2.701(5)	C2–Co2	2.066(5)
C1–Co1	1.923(5)	Ru–Co1	2.731(1)
C1–Co2	2.120(5)	Ru–Co2	2.587(1)
C1–Fe	1.917(5)	Co1–Co2	2.532(1)
C2–Ru	2.139(5)	Co1–Fe	2.565(1)
Bond Angles			
Co1–C1–Co2	77.4(2)	RuCo1–Co2	58.73(4)
Co1–C1–Fe	83.8(2)	RuCo1–Fe	114.23(4)
Co1–C1–C2	120.6(4)	RuCo1–C1	68.4(2)
Co2–C1–Fe	128.7(2)	Co2–Co1–Fe	91.16(4)
Co2–C1–C2	69.1(3)	Co2–Co1–C1	54.8(1)
Fe–C1–C2	154.4(4)	Fe–Co1–C1	48.0(2)
Ru–C2–Co2	75.9(2)	C1–Co2–C2	37.3(2)
Ru–C2–C1	99.3(3)	Ru–Co2–Co1	64.48(3)
Co2–C2–C1	73.6(3)	Ru–Co2–C1	69.2(1)
Co1–Ru–Co2	56.78(2)	Ru–Co2–C2	53.3(1)
Co1–Ru–C2	70.4(1)	Co1–Co2–C1	47.8(1)
Co2–Ru–C2	50.8(1)	Co1–Co2–C2	75.8(1)
Co1–Fe–C1	48.2(1)		

<sup>a</sup> Bond lengths in angstroms and bond angles in degrees.

$\text{RuCo}_2(\text{CO})_{10}(\mu_4\text{-C}_2\text{Ph})$  (**8**),<sup>11a</sup> can be viewed as a trimetalated ethylene  $\pi$ -coordinated to the fourth metal center (Figure 2b).

The structure of the tetranuclear  $\mu_4$ -acetylide cluster compounds (the  $\perp$ -structure like **4a** vs the  $\parallel$ -structure like **7b**) has been a subject of discussion.<sup>5c,12</sup> Several factors of the metal centers such as atomic radii, electron-donating ability, and electronic configuration have been assumed to be causes of the different structure. However, a definite conclusion has not been obtained so far, and a theoretical study is needed for the clear-cut description of the structure. Furthermore, as to the reason that the Fe and Ru atoms in the isoelectronic complexes **5** and **7** occupy different sites of the spiked-triangular metal array, we have no explanation at present.

Thus the interaction of the ethynyl complex **1a,b** with  $\text{RuCo}_2(\text{CO})_{11}$  follows a reaction pathway similar to eq 1 to give the vinylidene cluster **6** at first, and then thermal decarbonylation leads to the formation of the acetylide cluster **7** with a structure considerably different from that of the Fe derivative **4**.



**1,2-H Shift on Tetranuclear  $\text{C}_2\text{H}$  Cluster Compounds.** The results described above show that the reactions 1 and 2 produce the vinylidene clusters  $\text{MCo}_2(\text{CO})_9[\mu_3\text{-C}=\text{C}(\text{H})\text{Fe}(\eta^5\text{-C}_5\text{R}_5)(\text{CO})_2]$  **4** ( $\text{M} = \text{Fe}$ ) and **6** ( $\text{M} = \text{Ru}$ ) (paths *a* and *c*), which, upon thermal decarbonylation, are transformed to the acetylide clusters  $(\eta^5\text{-C}_5\text{R}_5)\text{FeMCo}_2(\text{CO})_{10}(\mu_4\text{-C}_2\text{H})$  **5** ( $\text{M} = \text{Fe}$ ) and **7** ( $\text{M} = \text{Ru}$ ) (paths *b* and *d*), respectively, as summarized in Scheme 3.

The transformations can be explained in terms of 1,2-H shift on the  $\eta^2$ -alkyne cluster intermediates  $\text{MCo}_2(\text{CO})_9[\mu_3\text{-}\eta^1\text{-}\eta^1\text{-}\eta^2\text{-}(\eta^5\text{-C}_5\text{R}_5)\text{Fe}(\text{CO})_2\text{C}\equiv\text{CH}]$  **9** ( $\text{M} = \text{Fe}$ ) and **10** ( $\text{M} = \text{Ru}$ ). Addition of an “ $\text{Fe}(\text{CO})_2$ ” fragment to the Co–Co bond in **3** (path *e*) and the displacement of CO ligands in  $\text{RuCo}_2(\text{CO})_{11}$  by  $(\eta^5\text{-C}_5\text{R}_5)\text{Fe}(\text{CO})_2\text{C}\equiv\text{CH}$  (path *i*) should form the intermediates **9** and **10**, detection of which has been unsuccessful despite several attempts. However, the corresponding 1-alkyne clusters containing an organic group in place of the  $(\eta^5\text{-C}_5\text{R}_5)\text{Fe}(\text{CO})_2$  moiety in **9** and **10** were isolated and structurally characterized.<sup>2,8,9</sup> The subsequent, very fast 1,2-H shift may give rise to the vinylidene clusters **4** (path *f*) and **6** (path *j*).

The intermediates **9** and **10** are also viable ones for the formation of the acetylide clusters **5** and **7** (paths *b* and *d*). The backward 1,2-H shift (paths *g* and *k*) may regenerate the intermediates **9** and **10**, which, upon thermal decarbonylation, should be transformed irreversibly to the acetylide clusters **5** and **7** via metal–metal bond formation. These results show that the 1,2-H shift on the tetranuclear  $\text{C}_2\text{H}$  complexes **4–7** (paths *f–g* and *j–k*) proceeds as fast as that on the di- and trinuclear derivatives (Scheme 1). Although the forward 1,2-H shift giving the vinylidene structure on cluster compounds has been reported already,<sup>2</sup> the backward process is confirmed by the present study for the first time.

## Experimental Section

All manipulations were carried out under an argon atmosphere by using standard Schlenk tube techniques. Ether, THF, hexanes, and benzene (Na–K alloy) and  $\text{CH}_2\text{Cl}_2$  ( $\text{P}_2\text{O}_5$ ) were treated with appropriate drying agents, distilled, and

(11) (a) Bernhardt, W.; Vahrenkamp, H. *J. Organomet. Chem.* **1988**, *355*, 427. (b) Roland, E.; Bernhardt, W.; Vahrenkamp, H. *Chem. Ber.* **1986**, *119*, 2566.

(12) (a) Ewing, P.; Farrugia, L. *J. Organometallics* **1989**, *8*, 1246. (b) Deeming, A. J.; Senior, A. M. *J. Organomet. Chem.* **1992**, *439*, 177.

stored under Ar. Organometallic compounds **1a**,<sup>13</sup> **1b**,<sup>5a</sup> **3a**,<sup>5c</sup> **3b**,<sup>5c</sup>  $\text{Fe}_2(\text{CO})_9$ ,<sup>14</sup> and  $\text{RuCo}_2(\text{CO})_{11}$ <sup>7</sup> were prepared according to the literature procedures. Column chromatography and preparative TLC were performed on alumina [column, activity II–IV (Merck Art. 1097)]; PTLC, aluminum oxide 60 PF<sub>254</sub> (Typ E) (Merck Art. 1103)]. <sup>1</sup>H- and <sup>13</sup>C-NMR spectra were recorded on JEOL EX-90 (<sup>1</sup>H, 90 MHz) and JEOL GX-270 spectrometers (<sup>1</sup>H, 270 MHz; <sup>13</sup>C, 67.9 MHz). Solvents for NMR measurements containing 1% TMS were dried over molecular sieves and distilled under reduced pressure. IR and FDMS spectra were obtained on a JASCO FT/IR 5300 spectrometer and a Hitachi M-80 mass spectrometer, respectively.

**Reaction of 3a with Fe<sub>2</sub>(CO)<sub>9</sub>.** A mixture of **3a** (400 mg, 0.820 mmol) and  $\text{Fe}_2(\text{CO})_9$  (401 mg, 1.10 mmol) dissolved in benzene (20 mL) was stirred for 30 h at room temperature. After removal of the volatiles, the residue was subjected to PTLC separation ( $\text{CH}_2\text{Cl}_2/\text{hexanes} = 1:6$ ). The tetranuclear adducts **4a** (69 mg, 0.109 mmol, 13% yield) and **5a** (138 mg, 0.230 mmol, 28% yield) were obtained from the brown ( $R_f = 0.8$ ) and dark brown bands ( $R_f = 0.6$ ), and **3a** (139 mg, 0.285 mmol, 35% recovered) was recovered from the greenish yellow band ( $R_f = 0.9$ ). **5a**: <sup>1</sup>H-NMR ( $\text{CDCl}_3$ )  $\delta$  5.06 (5 H, s, Cp), 8.60 (1H, s, C<sub>2</sub>H); <sup>13</sup>C-NMR ( $\text{CDCl}_3$ )  $\delta$  87.2 (d, <sup>1</sup> $J_{\text{CH}} = 181$  Hz, Cp), 118.5 (d, <sup>1</sup> $J_{\text{CH}} = 203$  Hz, C≡CH), 193.0 (s, C≡CH), 200–204 (br, Co–CO), 211.0, 214.0 (s × 2, Fe–CO), 245.9 ( $\mu$ -CO); IR ( $\text{CH}_2\text{Cl}_2$ )  $\nu(\text{C}=\text{O})$  2078, 2036, 2027, 2010, 1973, 1838  $\text{cm}^{-1}$ ; FDMS  $m/z$  600 ( $M^+$ ). Anal. Calcd for  $\text{C}_{17}\text{H}_6\text{O}_{10}\text{Fe}_2\text{Co}_2$ : C, 34.38; H, 0.93. Found: C, 34.04; H, 1.01. **4a**: <sup>1</sup>H-NMR ( $\text{CDCl}_3$ )  $\delta$  4.98 (5 H, s, Cp), 7.18 (1H, s, C<sub>2</sub>H); <sup>13</sup>C-NMR ( $\text{CDCl}_3$ )  $\delta$  86.9 (d, <sup>1</sup> $J_{\text{CH}} = 181$  Hz, Cp), 123.7 (d, <sup>1</sup> $J_{\text{CH}} = 151$  Hz, C≡CH), 205.5, 209.6 (s × 2,  $\text{Fe}_2\text{Co}-\text{CO}$ ), 213.4 (s, Fp–CO); IR ( $\text{CH}_2\text{Cl}_2$ )  $\nu(\text{C}=\text{O})$  2087, 2041, 2033  $\text{cm}^{-1}$ ; FDMS  $m/z$  628 ( $M^+$ ). An analytically pure sample was not obtained due to partial thermal decomposition.

**Reaction of 3b with Fe<sub>2</sub>(CO)<sub>9</sub>.** A mixture of **3b** (156 mg, 0.279 mmol) and  $\text{Fe}_2(\text{CO})_9$  (407 mg, 1.12 mmol) dissolved in benzene (10 mL) was stirred for 7.5 h at room temperature. After removal of the volatiles, the residue was extracted with ether and filtered through an alumina pad. Recrystallization from ether–hexanes gave **5b** (108 mg, 0.161 mmol, 58% yield) as black crystals. **5b**: <sup>1</sup>H-NMR ( $\text{CDCl}_3$ )  $\delta$  1.83 (15 H, s, Cp\*), 8.68 (1H, s, C<sub>2</sub>H). <sup>13</sup>C-NMR ( $\text{CDCl}_3$ )  $\delta$  9.5 (q, <sup>1</sup> $J_{\text{CH}} = 122$  Hz,  $\text{C}_5\text{Me}_5$ ), 97.8 (s,  $\text{C}_5\text{Me}_5$ ), 115.7 (d, <sup>1</sup> $J_{\text{CH}} = 208$  Hz, C≡CH), 206 (br, CO), 209–212 (br, Co–CO), 217.5 (s, Fe–CO), 247.3 ( $\mu$ -CO); IR ( $\text{CH}_2\text{Cl}_2$ )  $\nu(\text{C}=\text{O})$  2072, 2027, 2020, 2004, 1988, 1963, 1827  $\text{cm}^{-1}$ ; FDMS  $m/z$  670 ( $M^+$ ). Anal. Calcd for  $\text{C}_{22}\text{H}_{16}\text{O}_{10}\text{Fe}_2\text{Co}_2$ : C, 39.44; H, 2.41. Found: C, 39.53; H, 2.36.

**Reaction of 1a with RuCo<sub>2</sub>(CO)<sub>11</sub>.** A benzene solution (15 mL) of **1a** (118 mg, 0.586 mmol) and  $\text{RuCo}_2(\text{CO})_{11}$  (309 mg, 587 mmol) was stirred for 2 h at room temperature. After removal of the volatiles, the residue was extracted with ether and filtered through an alumina pad. Recrystallization from ether–hexanes gave **6a** (198 mg, 0.294 mmol, 50% yield) as red brown crystals. **6a**: <sup>1</sup>H-NMR ( $\text{CDCl}_3$ )  $\delta$  4.98 (5 H, s, Cp), 6.66 (1H, s, C<sub>2</sub>H); <sup>13</sup>C-NMR ( $\text{CDCl}_3$ )  $\delta$  86.8 (d, <sup>1</sup> $J_{\text{CH}} = 180$  Hz, Cp), 107.1 (d, <sup>1</sup> $J_{\text{CH}} = 151$  Hz, C≡CH), 199.5 (s,  $\text{RuCo}_2-\text{CO}$ ), 214.0 (s, Fp–CO), 277.5 (s, C≡CH); IR ( $\text{CH}_2\text{Cl}_2$ )  $\nu(\text{C}=\text{O})$  2087, 2046, 2037, 2015  $\text{cm}^{-1}$ . Anal. Calcd for  $\text{C}_{18}\text{H}_6\text{O}_{11}\text{FeRuCo}_2$ : C, 32.12; H, 0.90. Found: C, 32.33; H, 0.97.

**Thermal Decarbonylation of 6a Leading to 7a.** A benzene solution (20 mL) of **6a** (198 mg, 0.294 mmol) was refluxed for 2 h. After removal of the volatiles, the residue was extracted with ether and filtered through an alumina pad. Recrystallization from ether–hexanes gave **7a** (128 mg, 0.197 mmol, 67% yield) as deep green crystals. **7a**: <sup>1</sup>H-NMR ( $\text{CDCl}_3$ )  $\delta$  4.98 (5 H, s, Cp), 8.07 (1H, s, C<sub>2</sub>H); <sup>13</sup>C-NMR ( $\text{CDCl}_3$ )  $\delta$  86.8 (d, <sup>1</sup> $J_{\text{CH}} = 179$  Hz, Cp), 106.2 (d, <sup>1</sup> $J_{\text{CH}} = 196$  Hz, C≡CH), 190–194 (br, CO), 198.6 (s, C≡CH), 201–208 (br, CO). IR ( $\text{CH}_2-$

$\text{Cl}_2$ )  $\nu(\text{C}=\text{O})$  2086, 2045, 2025, 1997, 1833  $\text{cm}^{-1}$ . Anal. Calcd for  $\text{C}_{17}\text{H}_6\text{O}_{10}\text{FeRuCo}_2$ : C, 31.66; H, 0.94. Found: C, 31.67; H, 0.86.

**Reaction of 1b with RuCo<sub>2</sub>(CO)<sub>11</sub>.** A benzene solution (15 mL) of **1b** (298 mg, 1.09 mmol) and  $\text{RuCo}_2(\text{CO})_{11}$  (574 mg, 1.09 mmol) was stirred for 1 h at room temperature. The formation of **6b** was detected as a red orange spot by TLC. Then the mixture was heated for 17 h at 50 °C. After removal of the volatiles, the residue was extracted with  $\text{CH}_2\text{Cl}_2$  and filtered through an alumina pad. Recrystallization from  $\text{CH}_2\text{Cl}_2$ –hexanes gave **7b** (408 mg, 0.549 mmol, 55% yield) as red brown crystals. **6b**: <sup>1</sup>H-NMR ( $\text{CDCl}_3$ )  $\delta$  1.83 (15 H, s, Cp\*), 6.59 (1H, s, C<sub>2</sub>H). **7b**: <sup>1</sup>H-NMR ( $\text{CDCl}_3$ )  $\delta$  1.83 (15 H, s, Cp\*), 7.98 (1H, s, C<sub>2</sub>H); <sup>13</sup>C-NMR ( $\text{CDCl}_3$ )  $\delta$  9.3 (q, <sup>1</sup> $J_{\text{CH}} = 122$  Hz,  $\text{C}_5\text{Me}_5$ ), 98.2 (s,  $\text{C}_5\text{Me}_5$ ), 106.7 (d, <sup>1</sup> $J_{\text{CH}} = 193$  Hz, C≡CH), 198.9 (s, C≡CH), 205–208 (br, Co–CO), 237, (s, Fe–CO), 254 ( $\mu$ -CO); IR (KBr)  $\nu(\text{C}=\text{O})$  2088, 2032, 2004, 1988, 1971, 1956, 1933, 1890, 1815  $\text{cm}^{-1}$ . Anal. Calcd for  $\text{C}_{22}\text{H}_{16}\text{O}_{10}\text{FeRuCo}_2$ : C, 36.95; H, 2.26. Found: C, 36.70; H, 2.13.

**X-ray Crystallography of 5a, 6a, and 7b.** The tetranuclear cluster compounds **5a** and **6a** were recrystallized from ether–hexanes, and **7b** was recrystallized from  $\text{CH}_2\text{Cl}_2$ –hexanes. Suitable crystals were mounted on glass fibers. Diffraction measurements were made on a Rigaku AFC-5R automated four-circle diffractometer by using graphite-monochromated Mo K $\alpha$  radiation ( $\lambda = 0.71068$  Å). The unit cell was determined and refined by a least-squares method using 20–24 independent reflections. Data were collected with an  $\omega$ – $2\theta$  scan technique. If  $\sigma(F)/F$  was more than 0.1, a scan was repeated up to three times and the results were added to the first scan. Three standard reflections were monitored at every 150 measurements. The data processing was performed on a micro vax II computer (data collection) and an IRIS Indigo computer (structure analysis) by using the teXsan structure solving program system obtained from the Rigaku Corp., Tokyo, Japan. Neutral scattering factors were obtained from the standard source.<sup>15</sup> In the reduction of data, Lorentz, polarization, and empirical absorption corrections ( $\Psi$  scans) were made.

The structures were solved by a combination of the direct methods and Fourier syntheses (SAPI91 and DIRDIF). The unit cell of **5a** contained two independent molecules. All the non-hydrogen atoms were refined anisotropically. The C<sub>2</sub>H atoms were located by examination of the Fourier maps and were not refined. The hydrogen atoms of the Cp and Cp\* ligands were fixed at the calculated positions (C–H = 0.95 Å) and were not refined. The crystallographic data and selected structural parameters are summarized in Tables 1–4.

**Acknowledgment.** The financial support from the Ministry of Education, Science, and Culture of the Japanese Government is gratefully acknowledged (Grants-in-Aid for Scientific Research on Priority Area Nos. 04241105 and 05236103).

**Supplementary Material Available:** Tables of positional and thermal parameters and bond lengths and angles for **5a**, **6a**, and **7b** (16 pages). Ordering information is given on any current masthead page.

OM950071K

(13) Kim, P.; Masai, H.; Sonogashira, K.; Hagihara, N. *J. Inorg. Nucl. Chem. Lett.* **1970**, *6*, 181.

(14) King, R. B. *Organometallic Synthesis*; Academic Press: New York, 1965; Vol. 1, p 93.

(15) *International Tables for X-Ray Crystallography*; Kynoch Press: Birmingham, U.K., 1975; Vol. 4.

# Steric Effects in the Chemistry of Platinum Cluster Complexes

Leijun Hao, Ian R. Jobe, Jagadese J. Vittal, and Richard J. Puddephatt\*

Department of Chemistry, University of Western Ontario, London, Canada N6A 5B7

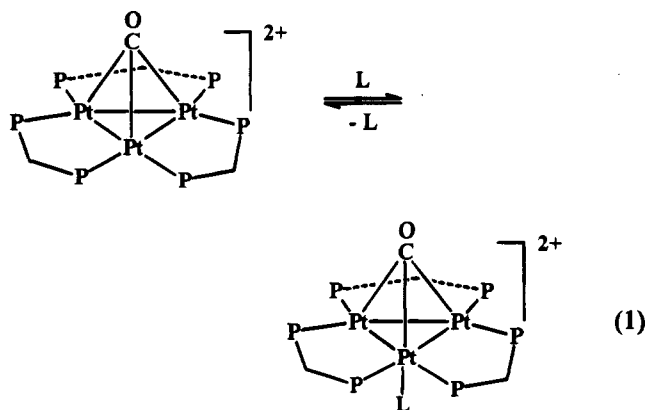
Received January 18, 1995<sup>®</sup>

A study of steric effects of the ligands  $R_2PCH_2PR_2$ ,  $R = \text{aryl}$ , on the formation and chemistry of the clusters  $[Pt_3(\mu_3\text{-CO})(\mu\text{-}R_2PCH_2PR_2)_3(O_2CCF_3)]^+$ , **4**, and  $[Pt_3(\mu_3\text{-CO})(\mu\text{-}R_2PCH_2PR_2)_3]^{2+}$ , **8**, is reported. When  $R = 2\text{-MeC}_6\text{H}_4$ , reduction of  $[Pt(O_2CCF_3)_2(R_2PCH_2PR_2)]$  by  $CO/H_2O$  gave only the binuclear complex  $[Pt_2H(CO)(\mu\text{-}R_2PCH_2PR_2)_2]^+$ , but with smaller groups  $R$ , further reduction to **4** ( $R = 4\text{-MeC}_6\text{H}_4$ ,  $3\text{-MeC}_6\text{H}_4$ ,  $3,5\text{-Me}_2\text{C}_6\text{H}_3$ ,  $3,5\text{-F}_2\text{C}_6\text{H}_3$ ,  $3,5\text{-Cl}_2\text{C}_6\text{H}_3$ ) or to  $[Pt_4(\mu\text{-CO})_2(\mu\text{-H})(\mu\text{-}R_2PCH_2PR_2)_3(R_2PCH_2PR_2)]^+$  ( $R = 4\text{-MeC}_6\text{H}_4$ ,  $3,5\text{-F}_2\text{C}_6\text{H}_3$ ) occurred. The complexes were characterized spectroscopically and for **4** ( $CF_3CO_2^-$ ),  $R = 3,5\text{-Cl}_2\text{C}_6\text{H}_3$ , crystallographically [ $C_{80}H_{42}Cl_{24}F_6O_5P_6Pt_3 \cdot 0.5CH_2Cl_2 \cdot 1.5H_2O$ , monoclinic,  $P2_1/n$ ,  $a = 23.365(4)$  Å,  $b = 24.599(4)$  Å,  $c = 19.141(7)$  Å,  $\beta = 102.44(2)^\circ$ ,  $Z = 4$ ,  $R = 0.0727$ ]. The complexes **8** can all form adducts with  $I^-$ ,  $SCN^-$ , and  $CF_3CO_2^-$  though evidence is presented that coordination of  $CF_3CO_2^-$  is reversible in solution when  $R = 3,5\text{-Cl}_2\text{C}_6\text{H}_3$ . Reactions of **8** with the ligands  $L = PPh_3$ ,  $PMePh_2$ ,  $P(OPh)_3$ , and  $P(OMe)_3$  to form the adducts  $[Pt_3(\mu_3\text{-CO})(\mu\text{-}R_2PCH_2PR_2)_3L]^{2+}$  are reversible, and the position of equilibrium depends on the steric effects of  $R$ , indicating the steric sequence  $R = 4\text{-MeC}_6\text{H}_4 < 3\text{-MeC}_6\text{H}_4 < 3,5\text{-Me}_2\text{C}_6\text{H}_3 < 3,5\text{-F}_2\text{C}_6\text{H}_3 < 3,5\text{-Cl}_2\text{C}_6\text{H}_3$ .

## Introduction

Steric effects of organophosphorus ligands can play an important role in the design of transition metal cluster complexes and in affecting their reactivity.<sup>1,2</sup> For example, the nuclearity and stoichiometry of platinum carbonyl phosphine clusters formed by reduction of platinum salts in the presence of CO and  $PR_3$  depend critically on the steric bulk of the phosphine ligand  $PR_3$ .<sup>3</sup> More specifically, the reactions of the clusters  $[Pt_3(\mu\text{-CO})_3(PR_3)_3]$  with  $PR_3$  to give  $[Pt_3(\mu\text{-CO})_3(PR_3)_4]$  are less favorable with bulkier phosphines such as  $PCy_3$  ( $Cy = \text{cyclohexyl}$ ) than with smaller phosphines such as  $PPh_3$ .<sup>3</sup> Similarly, the addition of phosphine and phosphite ligands to  $[Pt_3(\mu_3\text{-CO})(\mu\text{-dppm})_3]^{2+}$  (eq 1,  $dppm = Ph_2PCH_2PPh_2$ ) is possible with ligands  $L$  with steric bulk

the flexibility of  $dppm$ .<sup>4,5</sup> However, increasing the cavity size on one side of the  $Pt_3$  triangle of  $Pt_3(\mu\text{-dppm})_3$  clusters, by moving phenyl substituents away, necessarily reduces the cavity size on the other side.<sup>5</sup> This paper describes attempts to determine how greatly these cavities could be tailored by modifying the supporting diphosphine ligands,  $R_2PCH_2PR_2$ . Most previous work in this area has concentrated on the ligand  $dppm$ ,  $R = Ph$ , with some studies using  $dmpm$  ( $R = Me$ ).<sup>4-6</sup> In the present work, the substituents used are substituted phenyl groups, chosen so that differences in electronic effects of the ligands should be relatively small while allowing major differences in steric bulk. The aim is to investigate in a systematic way how variation of the steric properties of the ligand  $R_2PCH_2PR_2$  affects the formation and coordination chemistry of the clusters  $[Pt_3(\mu_3\text{-CO})(\mu\text{-}R_2PCH_2PR_2)_3]^{2+}$ . These clusters are co-



no greater than that of  $PPh_3$ .<sup>4</sup> In the above cluster, steric effects are between the incoming ligand and the phenyl substituents of the  $\mu\text{-dppm}$  ligands, which define a cavity whose size is to some extent adjustable due to

(1) (a) Darensbourg, D. J. In *The Chemistry of Metal Cluster Complexes*; Shriver, D. F., Kaesz, H. D., Adams, R. D., Eds.; VCH: New York, 1990. (b) Pignolet, L. H., Ed. *Homogeneous Catalysis with Metal Phosphine Complexes*; Plenum: New York, 1983. (c) McAuliffe, C. A., Ed. *Transition Metal Complexes of Phosphorus, Arsenic and Antimony Ligands*; Halsted: New York, 1973.

(2) (a) White, D.; Coville, N. J. *Adv. Organomet. Chem.* **1994**, *36*, 95. (b) Tolman, C. A. *Chem. Rev.* **1977**, *77*, 313. (c) Tolman, C. A. *J. Am. Chem. Soc.* **1970**, *92*, 2953. (d) Atwood, J. D.; Wovkulich, M. J.; Sonnenberger, D. C. *Acc. Chem. Res.* **1983**, *16*, 350. (e) Puddephatt, R. J. *Chem. Soc. Rev.* **1983**, *12*, 99.

(3) (a) Dahmen, K. H.; Moor, A.; Naegeli, R.; Venanzi, L. M. *Inorg. Chem.* **1991**, *30*, 4285. (b) Evans, D. G.; Hallam, M. F.; Mingos, D. M. P.; Wardle, R. W. M. *J. Chem. Soc., Dalton Trans.* **1987**, 1889. (c) Mingos, D. M. P.; Wardle, R. W. M. *Transition Met. Chem.* **1985**, *10*, 441. (d) Browning, C. S.; Farrar, D. H.; Gukathasan, R. R.; Morris, S. A. *Organometallics* **1985**, *4*, 1750. (e) Chatt, J.; Chini, P. *J. Chem. Soc. A* **1970**, 1538. (f) Imhof, D.; Venanzi, L. M. *Chem. Soc. Rev.* **1994**, 185.

(4) (a) Bradford, A. M.; Douglas, G.; Manojlovic-Muir, Lj.; Muir, K. W.; Puddephatt, R. J. *Organometallics* **1990**, *9*, 409. (b) Harvey, P. D.; Hubig, S. M.; Ziegler, T. *Inorg. Chem.* **1994**, *33*, 3700. (c) Provencher, R.; Aye, K.-T.; Drouin, M.; Gagnon, J.; Boudreault, N.; Harvey, P. D. *Inorg. Chem.* **1994**, *33*, 3689.

(5) Puddephatt, R. J.; Manojlovic-Muir, Lj.; Muir, K. W. *Polyhedron* **1990**, *9*, 2767.

(6) Ling, S. S. M.; Hadj-Bagheri, N.; Manojlovic-Muir, Lj.; Muir, K. W.; Puddephatt, R. J. *Inorg. Chem.* **1987**, *26*, 231.

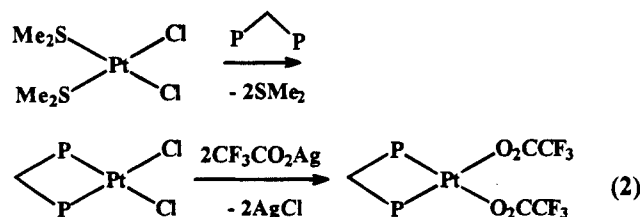
<sup>®</sup> Abstract published in *Advance ACS Abstracts*, May 1, 1995.

ordinatively unsaturated and can mimic some aspects of the reactivity of a platinum surface.<sup>4</sup>

## Results

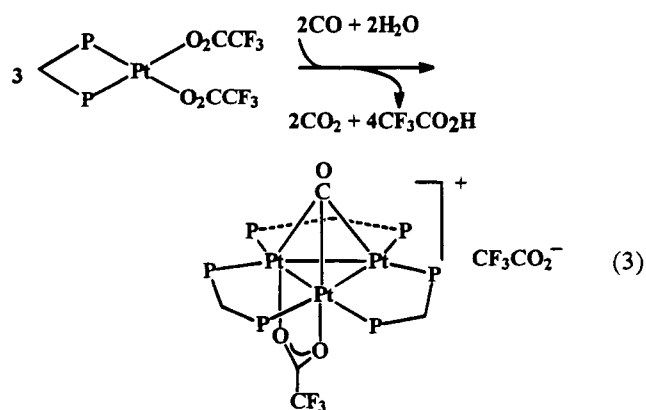
**Synthesis and Characterization of Ligands and Simple Platinum Complexes.** Several new diphosphine ligands  $R_2PCH_2PR_2$ , **1**, were prepared by reaction of  $Cl_2PCH_2PCL_2$  with the corresponding Grignard reagent. The ligands were easily characterized by their NMR spectra. For example, each gave a singlet in the  $^{31}P$  NMR with chemical shifts ranging from  $\delta = -17.3$  to 46.6. These ligands and their NMR parameters are listed in Table 1.

The above ligands were then used to prepare the mononuclear platinum complexes  $[PtCl_2(R_2PCH_2PR_2)]$ , **2**, and  $[Pt(O_2CCF_3)_2(R_2PCH_2PR_2)]$ , **3**, according to eq 2.



Most of the complexes **2** were very sparingly soluble; they were therefore easily isolated since they precipitated from the reaction mixtures in high yield, but most could not be characterized by NMR. However, complexes **3** were more soluble and NMR data were obtained. Each gave a singlet in the  $^{31}P$  NMR with the ranges of  $\delta(^{31}P) = -56.8$  to  $-92.2$  and  $^1J(PtP) = 3270$ – $3450$  Hz. The chemical shifts are typical for chelating ligands of the type  $R_2PCH_2PR_2$ .<sup>7</sup> It is noted that the most sterically hindered complex **3g** gives the most negative value of  $\delta(^{31}P)$  and the smallest value of  $^1J(PtP)$  and that the compounds with electronegative substituents on the aryl groups **3e,f** give the least negative values of  $\delta(^{31}P)$  and the largest values of  $^1J(PtP)$ . Full details of the NMR spectra are given in the Experimental Section, and selected parameters are in Table 1.

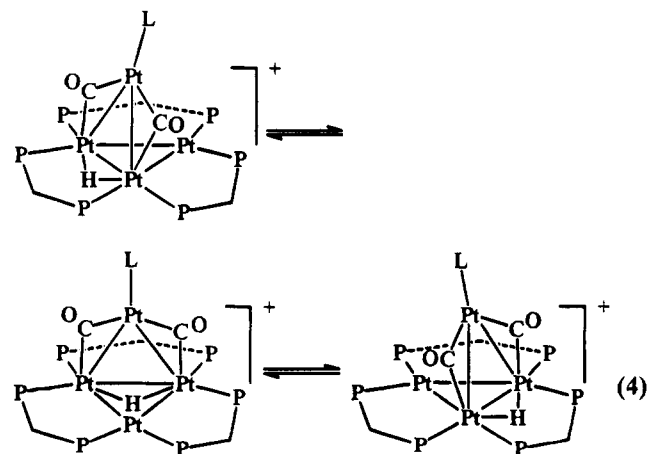
**Reduction of the Platinum(II) Complexes.** The reduction of the complexes  $[Pt(O_2CCF_3)_2(R_2PCH_2PR_2)]$  under water gas shift (WGS) conditions to give  $[Pt_3(\mu_3-CO)(\mu-R_2PCH_2PR_2)_3(O_2CCF_3)]^+$ , **4**, as the trifluoroacetate salt, was carried out as reported for the case with  $R = Ph$ .<sup>8</sup> The reaction occurred with the stoichiometry shown in eq 3.



The reaction was successful in the cases with para or meta, but not with ortho, substituted phenyl derivatives

**R.** When  $R = 2-MeC_6H_4$ , the product was the binuclear complex  $[Pt_2H(CO)(\mu-R_2PCH_2PR_2)_2][CF_3CO_2]$ , **5**, only, and this complex was stable to reduction to a triplatinum cluster. Unlike the corresponding dppe complex, it also failed to form an adduct with CO or to react with hydrogen to give the cation  $[Pt_2H_2(\mu-H)(\mu-R_2PCH_2PR_2)_2]^+$ , **6**.<sup>9,10</sup> However,  $[Pt_2H_2(\mu-H)(\mu-R_2PCH_2PR_2)_2]^+$ ,  $R = 2-MeC_6H_4$ , prepared by reduction of **3c** with  $NaBH_4$ , did react with CO to form  $[Pt_2H(CO)(\mu-R_2PCH_2PR_2)_2]^+$ . It seems evident that the hydrido(carbonyl)diplatinum(I) complex is stabilized by the presence of the 2-methyl substituent, presumably by steric effects. In other cases, the binuclear diplatinum(I) complexes are intermediates in the formation of the clusters  $[Pt_3(\mu_3-CO)(\mu-R_2PCH_2PR_2)_3(O_2CCF_3)](O_2CCF_3)$  and the hydride  $[Pt_2H_2(\mu-H)(\mu-R_2PCH_2PR_2)_2]^+$  is more stable than  $[Pt_2H(CO)(\mu-R_2PCH_2PR_2)_2]^+$ .<sup>9,10</sup> For example, when  $R = 3,5-Me_2C_6H_3$ , an equilibrium mixture of  $[Pt_2H(CO)(\mu-R_2PCH_2PR_2)_2]^+$  and  $[Pt_2H_2(\mu-H)(\mu-R_2PCH_2PR_2)_2]^+$  was detected at intermediate stages of reduction and, in the absence of CO,  $[Pt_2H(CO)(\mu-R_2PCH_2PR_2)_2]^+$  was unstable, reacting with water to give  $[Pt_2H_2(\mu-H)(\mu-R_2PCH_2PR_2)_2]^+$ .

In some cases, the reduction of the complexes **3** under WGS conditions led to tetranuclear products  $[Pt_4(\mu_2-CO)_2(\mu_2-H)(\mu-R_2PCH_2PR_2)_3(R_2PCH_2PR_2)]^+$ , **7**, isolated as the hexafluorophosphate salts.<sup>11</sup> These products reflect a degree of reduction beyond the clusters **4**. Their formation, although not completely predictable, was more likely under conditions where a buildup in the concentration of  $H_2$  was allowed as a result of WGS catalysis, for smaller substituents  $R$  and for longer reduction times. The complexes with  $R = 4-MeC_6H_4$  and  $R = 3,5-F_2C_6H_3$  have been studied in depth. Both undergo the same form of fluxionality established previously for  $R = Ph$  (eq 4).<sup>11</sup> Details of the NMR spectra are given in the Experimental Section.



**Spectra and Structure of Clusters **4**.** The clusters **4** reacted with  $NH_4[PF_6]$  to give the hexafluorophosphate salts  $[Pt_3(\mu_3-CO)(\mu-R_2PCH_2PR_2)_3(O_2CCF_3)][PF_6]$

(7) Grossel, M. C.; Batson, J. R.; Moulding, R. P.; Seddon, K. R. *J. Organomet. Chem.* **1986**, *304*, 391.

(8) Ferguson, G.; Lloyd, B. R.; Puddephatt, R. J. *Organometallics* **1986**, *5*, 344.

(9) Puddephatt, R. J. *Chem. Soc. Rev.* **1983**, 99.

(10) (a) Fisher, J. R.; Mills, A. J.; Sumner, S.; Brown, M. P.; Thomson, M. A.; Puddephatt, R. J.; Frew, A. A.; Manojlovic-Muir, Lj.; Muir, K. W. *Organometallics* **1982**, *1*, 1421. (b) McLeenan, A. J.; Puddephatt, R. J. *Organometallics* **1986**, *5*, 811.

(11) Douglas, G.; Manojlovic-Muir, Lj.; Muir, K. W.; Jennings, M. C.; Lloyd, B. R.; Rashidi, M.; Schoettel, G.; Puddephatt, R. J. *Organometallics* **1991**, *10*, 3927.

**Table 1. Selected NMR Data for the Ligands, 1, and Complexes, 3<sup>a</sup>**

R	compound				
	1		3		
	$\delta(\text{CH}_2)$ , $J(\text{PH})$	$\delta(\text{P})$	$\delta(\text{CH}_2)$ , $J(\text{PH}), J(\text{PtH})$	$\delta(\text{P})$ , $J(\text{PtP})$	
4-MeC <sub>6</sub> H <sub>4</sub> , <b>a</b>	2.71, 3	-26.9	4.84, 11, 85	-70.2, 3319	
3-MeC <sub>6</sub> H <sub>4</sub> , <b>b</b>	2.78, 1	-24.3	4.94, 12, 87	-68.3, 3324	
2-MeC <sub>6</sub> H <sub>4</sub> , <b>c</b>	2.68, 3	-46.6	5.31, 11, 80	-71.4, 3304	
3,5-Me <sub>2</sub> C <sub>6</sub> H <sub>3</sub> , <b>d</b>	2.78, 0	-23.6	4.85, 11, 88	-68.6, 3319	
3,5-F <sub>2</sub> C <sub>6</sub> H <sub>3</sub> , <b>e</b>	2.80, 0	-17.3	5.36, 12, 91	-56.8, 3450	
3,5-Cl <sub>2</sub> C <sub>6</sub> H <sub>3</sub> , <b>f</b>	2.70, 0	-17.4	5.48, 12, 92	-57.2, 3450	
2,4,6-Me <sub>3</sub> C <sub>6</sub> H <sub>2</sub> , <b>g</b>	2.74, 0	-32.2	5.26, 11, 60	-92.2, 3270	

<sup>a</sup>  $\delta$  in ppm;  $J$  in Hz.**Table 2. Selected NMR and IR Data for Clusters 4 and 8<sup>a</sup>**

R, compd	$\delta(\text{CH}^a\text{H}^b)$ , $J(\text{H}^a\text{H}^b)$	$\delta(\text{P})$ , $^1J(\text{PtP})$ , $^3J(\text{PP})$	$\nu(\text{CO})$
4-MeC <sub>6</sub> H <sub>4</sub> , <b>4a</b>	5.6, 5.8; 14	-11.1, 3753, 155	1740
<b>8a</b>	5.5, 6.0; 16	-7.4, 3706, 138	1754
3-MeC <sub>6</sub> H <sub>4</sub> , <b>4b</b>	5.6, 5.7; 13	-11.2, 3741, 157	1734
<b>8b</b>	5.3, 5.4; 15	-6.8, 3701, 144	1734
3,5-Me <sub>2</sub> C <sub>6</sub> H <sub>3</sub> , <b>4c</b>	5.3, 5.5; 12	-11.6, 3690, 160	1742
<b>8c</b>	5.2, 5.8; 14	-5.2, 3697, 139	1743
3,5-F <sub>2</sub> C <sub>6</sub> H <sub>3</sub> , <b>4d</b>	5.7, 6.7; 13.3	-7.1, 3706, 161	1783
<b>8d</b>	5.9, 6.4; 14	0.4, 3759, 110	1784
3,5-Cl <sub>2</sub> C <sub>6</sub> H <sub>3</sub> , <b>4e</b>	5.7, 6.6; 16	-8.4, 3673, 169	1771
<b>8e</b>	5.6, 6.5; 16	-8.4, 3672, 174	1771

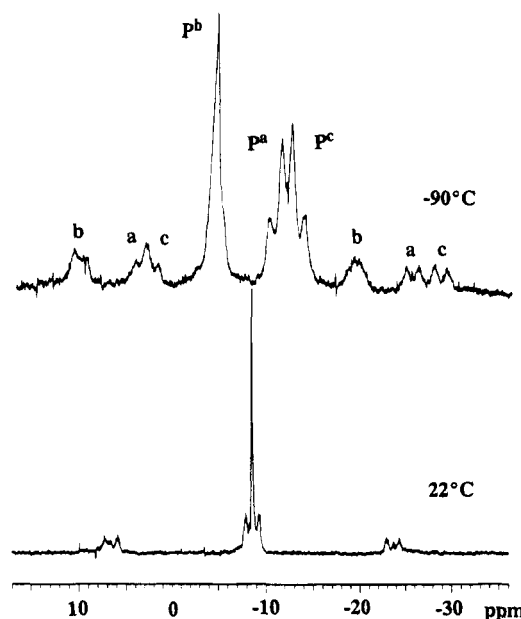
<sup>a</sup>  $\delta$  in ppm,  $J$  in Hz,  $\nu$  in cm<sup>-1</sup> (Nujol mull).

and, with excess [PF<sub>6</sub>]<sup>-</sup>, [Pt<sub>3</sub>( $\mu_3$ -CO)( $\mu$ -R<sub>2</sub>PCH<sub>2</sub>PR<sub>2</sub>)<sub>3</sub>]-[PF<sub>6</sub>]<sub>2</sub>, **8**. Selected NMR and IR data for the clusters **4** and **8** are given in Table 2.

The values of  $\nu(\text{CO})$  for the triply bridging carbonyl ligand fall in the range 1734–1784 cm<sup>-1</sup> and are similar for clusters **4** and **8**. The highest values of  $\nu(\text{CO})$  are observed for R = 3,5-F<sub>2</sub>C<sub>6</sub>H<sub>3</sub> and 3,5-Cl<sub>2</sub>C<sub>6</sub>H<sub>3</sub>, the aryl groups with electron-withdrawing substituents. This suggests that  $\nu(\text{CO})$  is mostly influenced by electronic effects of the ligands, as would be expected.

The <sup>1</sup>H NMR spectra of complexes **4** and **8** are similar, but there were differences in the <sup>31</sup>P NMR spectra. In general, the <sup>31</sup>P chemical shifts of clusters **4** were 3–7 ppm more negative than for the corresponding clusters **8**.<sup>8,12</sup> The only exception was for R = 3,5-Cl<sub>2</sub>C<sub>6</sub>H<sub>3</sub> for which the <sup>31</sup>P chemical shifts of **4e** and **8e** were identical. This is interpreted in terms of dissociation of trifluoroacetate from **4e** in solution to give the cluster **8e**, promoted by the bulky substituents.

In the idealized structure of **8**, the cluster has 3-fold symmetry and so should give a single resonance for the R<sub>2</sub>PCH<sub>2</sub>PR<sub>2</sub> ligands.<sup>5</sup> The symmetry of **4** is lower, but since the ligated trifluoroacetate is weakly held, fluxionality is easy and leads to effective 3-fold symmetry. In agreement with this picture the clusters **4a–d** and **8a–d** all give a single resonance in the <sup>31</sup>P NMR spectra in the diphosphine ligand region at either room temperature or at -80 °C. However, while the room temperature spectra of **4e** and **8e** give a single <sup>31</sup>P resonance, at low temperature the resonance splits into three equal intensity resonances (Figure 1). The low-temperature spectra of **4e** and **8e** and the coalescence temperature are the same within experimental error, suggesting that the ion in solution is the same, namely the dication **8e**, in both cases. Clearly, the cluster with

**Figure 1.** <sup>31</sup>P NMR spectra (121.47 MHz) of [Pt<sub>3</sub>( $\mu_3$ -CO)( $\mu$ -R<sub>2</sub>PCH<sub>2</sub>PR<sub>2</sub>)<sub>3</sub>]<sup>2+</sup>, R = 3,5-Cl<sub>2</sub>C<sub>6</sub>H<sub>3</sub>, **4e**, at -90 °C and at 22 °C.

R = 3,5-Cl<sub>2</sub>C<sub>6</sub>H<sub>3</sub> is the most sterically hindered of those studied and it seems that steric effects lead to easy dissociation of the trifluoroacetate ligand from **4e**. In addition, the ground state structure of **8e** must have lower symmetry than C<sub>3v</sub> and the bulky substituents give rise to a higher activation energy for flexing of the R<sub>2</sub>PCH<sub>2</sub>PR<sub>2</sub> ligands than in the other cases. Hence the variable-temperature NMR spectra can be understood.

In order to understand these effects, an X-ray structure determination of **4e** as the trifluoroacetate salt was carried out. Selected bond distances and angles are given in Table 3, and atomic coordinates are in Table 4. A view of the structure is given in Figure 2, and the steric effects are illustrated by the space-filling models in Figure 3.

The structure of **4e** is based on an approximately equilateral triangular Pt<sub>3</sub> metal core, with Pt–Pt distances 2.603(1), 2.610(1), and 2.624(1) Å and Pt–Pt–Pt angles 59.76(4), 59.89(4), and 60.46(3)°. The mean Pt–Pt distance (2.61(1) Å) is slightly shorter than that (2.63(2) Å) found in the [Pt<sub>3</sub>( $\mu_3$ -CO)( $\mu$ -dppm)<sub>3</sub>]<sup>2+</sup> and indicates the presence of Pt–Pt single bonds.<sup>8</sup> Each edge of the Pt<sub>3</sub> triangle is bridged by a diphosphine ligand, and the Pt–P distances have a mean value of 2.29(2) Å, slightly longer than that of 2.28(1) Å in [Pt<sub>3</sub>( $\mu_3$ -CO)( $\mu$ -dppm)<sub>3</sub>]<sup>2+</sup>.<sup>8</sup> One face of the Pt<sub>3</sub> triangle is bridged by a  $\mu_3$ -CO ligand, and the other, by a weakly bound  $\mu_2$ -trifluoroacetate ligand. All three R<sub>2</sub>PCH<sub>2</sub>PR<sub>2</sub> methylene carbon atoms C(10), C(20), and C(30) are folded away from the triply bridging carbonyl, being displaced from the Pt<sub>3</sub> plane by 0.80, 0.78, and 1.10 Å, respectively. In this conformation, all dichlorophenyl substituents on the carbonyl and CF<sub>3</sub>CO<sub>2</sub> sides of the Pt<sub>3</sub> plane are axial and equatorial, respectively. This arrangement leads to a larger cavity on the trifluoroacetate side of the cluster, as is necessary to accommodate the larger group (Figure 3). It also gives rise to a structure in which all the phenyl rings are paired, with each pair lying essentially parallel. Thus, there are three pairs of parallel dichlorophenyl rings on each side of the Pt<sub>3</sub> triangle. The distances between the parallel phenyl rings range from 3.2(1) to 3.6(1) Å,

(12) Lloyd, B. R.; Manojlovic-Muir, Lj.; Muir, K. W.; Puddephatt, R. J. *Organometallics* 1993, 12, 1231.

**Table 3. Selected Bond Distances (Å) and Angles (deg) for 4e**

Pt(1)–Pt(2)	2.610(1)	Pt(1)–Pt(3)	2.603(1)
Pt(1)–P(1)	2.301(6)	Pt(1)–P(6)	2.286(6)
Pt(1)–C(1)	2.04(2)	Pt(1)–O(2)	2.52(2)
Pt(2)–Pt(3)	2.624(1)	Pt(2)–P(2)	2.324(6)
Pt(2)–P(3)	2.286(6)	Pt(2)–C(1)	2.06(2)
Pt(2)–O(3)	2.52(2)	Pt(3)–P(4)	2.276(6)
Pt(3)–P(5)	2.282(6)	Pt(3)–C(1)	2.24(2)
P(1)–C(10)	1.73(2)	P(2)–C(10)	1.88(2)
P(3)–C(2)	1.80(2)	P(4)–C(20)	1.81(2)
P(5)–C(30)	1.80(2)	P(6)–C(30)	1.81(2)
C(1)–O(1)	1.20(2)	O(2)–C(2)	1.20(3)
O(3)–C(2)	1.21(3)	C(2)–C(3)	1.54(3)
C(3)–F(1)	1.23(4)	C(3)–F(2)	1.24(4)
C(3)–F(3)	1.24(5)		
Pt(2)–Pt(1)–Pt(3)	60.46(3)	Pt(2)–Pt(1)–P(1)	95.4(2)
Pt(2)–Pt(1)–P(6)	155.0(2)	Pt(2)–Pt(1)–C(1)	50.9(6)
Pt(2)–Pt(1)–O(2)	85.2(4)	Pt(3)–Pt(1)–P(1)	155.9(2)
Pt(3)–Pt(1)–P(6)	94.6(2)	Pt(3)–Pt(1)–C(1)	56.1(6)
Pt(3)–Pt(1)–O(2)	87.6(5)	P(1)–Pt(1)–P(6)	109.6(2)
P(1)–Pt(1)–C(1)	110.0(7)	P(1)–Pt(1)–O(2)	90.5(5)
P(6)–Pt(1)–C(1)	118.4(7)	P(6)–Pt(1)–O(2)	92.4(4)
C(1)–Pt(1)–O(2)	131.7(7)	Pt(1)–Pt(2)–Pt(3)	59.76(4)
Pt(1)–Pt(2)–P(2)	95.2(2)	Pt(1)–Pt(2)–P(3)	154.7(2)
Pt(1)–Pt(2)–C(1)	50.1(7)	Pt(1)–Pt(2)–O(3)	84.7(4)
Pt(3)–Pt(2)–P(2)	154.3(2)	Pt(3)–Pt(2)–P(3)	95.0(2)
Pt(3)–Pt(2)–C(1)	55.5(6)	Pt(3)–Pt(2)–O(3)	84.6(4)
P(2)–Pt(2)–P(3)	109.9(2)	P(2)–Pt(2)–C(1)	113.9(7)
P(2)–Pt(2)–O(3)	88.0(5)	P(3)–Pt(2)–C(1)	118.2(7)
P(3)–Pt(2)–O(3)	92.4(4)	C(1)–Pt(2)–O(3)	129.5(7)
Pt(1)–Pt(3)–Pt(2)	59.89(4)	Pt(1)–Pt(3)–P(4)	155.2(2)
Pt(1)–Pt(3)–P(5)	94.9(2)	Pt(1)–Pt(3)–C(1)	49.1(6)
Pt(2)–Pt(3)–P(4)	95.5(2)	Pt(2)–Pt(3)–P(5)	151.9(2)
Pt(2)–Pt(3)–C(1)	49.4(6)	P(4)–Pt(3)–P(5)	108.3(2)
P(4)–Pt(3)–C(1)	118.4(6)	P(5)–Pt(3)–C(1)	124.5(6)

**Table 4. Selected Atomic Coordinates and Thermal Parameters (Å<sup>2</sup>) for 4e**

atom	x	y	z	B <sub>iso</sub>
Pt(1)	0.24440(4)	0.80939(4)	0.10114(5)	2.76(4)
Pt(2)	0.24205(4)	0.70500(4)	0.07642(5)	2.76(4)
Pt(3)	0.27328(4)	0.77299(4)	-0.01426(5)	2.98(4)
P(1)	0.2142(3)	0.8029(2)	0.2076(3)	3.0(3)
P(2)	0.2019(3)	0.6821(3)	0.1735(3)	3.1(3)
P(3)	0.2514(2)	0.6289(2)	0.0112(3)	3.0(3)
P(4)	0.2841(2)	0.7085(3)	-0.0956(3)	3.0(3)
P(5)	0.2701(3)	0.8561(3)	-0.0680(3)	3.2(3)
P(6)	0.2559(3)	0.8988(2)	0.0748(3)	2.9(3)
C(10)	0.1704(10)	0.7458(9)	0.2044(13)	3.9(5)
C(20)	0.2425(9)	0.6488(9)	-0.0813(11)	3.3(5)
C(30)	0.2326(9)	0.9034(9)	-0.0217(10)	3.0(4)
C(1)	0.3124(10)	0.7574(9)	0.1014(12)	3.8(5)
O(1)	0.3627(6)	0.7511(6)	0.1303(8)	3.6(3)
O(2)	0.1393(8)	0.8083(8)	1.0327(10)	7.1(5)
O(3)	0.1396(8)	0.7226(7)	1.0064(10)	6.2(4)
C(2)	0.1172(8)	0.7670(8)	1.0060(13)	5.6(6)
C(3)	0.0518(8)	0.7699(11)	0.9692(15)	11.3(13)
F(1)	0.0253(10)	0.7294(14)	0.9835(21)	20.2(30)
F(2)	0.0446(10)	0.7713(16)	0.9031(13)	18.8(29)
F(3)	0.0290(12)	0.8125(16)	0.9844(22)	33.9(45)

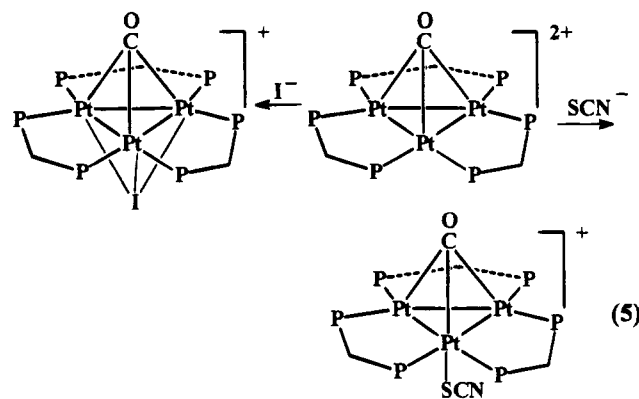
indicating weak  $\pi$ -stacking of the paired aryl rings. As a consequence, the structure has approximate  $C_s$  symmetry, the mirror plane passing through Pt(3), C(1), and the midpoint of the Pt(1)–Pt(2) bond. The phosphorus atoms P(1), P(2), P(3), P(4), P(5), and P(6) are displaced from the Pt<sub>3</sub> plane away from the  $\mu_3$ -CO ligand by 0.001, 0.226, 0.041, 0.123, 0.516, and 0.076 Å, respectively. The largest distortion involves the phosphorus atoms P(4) and P(5) which coordinate to Pt(3). The carbonyl ligand adopts a slightly distorted, triply bridging geometry, binding more strongly to Pt(1) and Pt(2) than to Pt(3) with the Pt–C distances 2.04(2), 2.06(2), and 2.24(2) Å, respectively. The shorter bonds are to the two platinum atoms bridged by the trifluoroacetate ligand. The

trifluoroacetate is weakly bonded as indicated by the long Pt–O distances, both 2.52(2) Å; most Pt–O single bonds fall in the range 2.0–2.2 Å. For example, in cluster complexes, Pt–O distances ranging 2.01–2.14 Å are seen in [Pt<sub>4</sub>( $\mu$ -CCl<sub>3</sub>COO)<sub>4</sub>( $\mu$ -CH<sub>3</sub>COO)<sub>4</sub>],<sup>13</sup> and distance ranging 1.97–2.19 Å, in [Pt<sub>4</sub>(CH<sub>3</sub>COO)<sub>8</sub>].<sup>14</sup> The calculated Pauling covalent Pt–O bond length is 2.03 Å. The observation of weak Pt···O bonds in 4e is clearly consistent with the hypothesis, outlined earlier, that the trifluoroacetate ligand dissociates in solution to give 8e.

By reference to the structure of 4e, the phosphorus atoms could be assigned to the pairs P(1), P(2); P(3), P(6); and P(4), P(5). If a similar conformation is present in 8e, this would be consistent with the low-temperature <sup>31</sup>P NMR spectrum which contains three resonances. However, it must be recognized that dissociation of the CF<sub>3</sub>CO<sub>2</sub> ligand is likely to lead to a change in conformation.

**Coordination Chemistry of the Triplatinum Clusters [Pt<sub>3</sub>( $\mu_3$ -CO)( $\mu$ -R<sub>2</sub>PCH<sub>2</sub>PR<sub>2</sub>)<sub>3</sub>]<sup>2+</sup>.** The cluster [Pt<sub>3</sub>( $\mu_3$ -CO)( $\mu$ -R<sub>2</sub>PCH<sub>2</sub>PR<sub>2</sub>)<sub>3</sub>]<sup>2+</sup> has a 42-electron count with each platinum having a 16-electron configuration. Hence each platinum atom is coordinatively unsaturated and the cluster is expected to form coordination complexes, although steric effects of the ligands R<sub>2</sub>PCH<sub>2</sub>PR<sub>2</sub> may limit the ability of the cluster to bind bulky donor ligands.

Clusters 8, as the [PF<sub>6</sub>]<sup>-</sup> salts, all react readily with MeI or NaI to form the clusters [Pt<sub>3</sub>( $\mu_3$ -CO)( $\mu_3$ -I)( $\mu$ -R<sub>2</sub>PCH<sub>2</sub>PR<sub>2</sub>)<sub>3</sub>]<sup>+</sup>, 9, according to eq 5. Similarly, all reacted with thiocyanate to form the adducts [Pt<sub>3</sub>( $\mu_3$ -CO)(SCN)( $\mu$ -R<sub>2</sub>PCH<sub>2</sub>PR<sub>2</sub>)<sub>3</sub>]<sup>+</sup>, 10. The corresponding reactions with R = Ph have been established earlier.<sup>5,15</sup>



Steric discrimination was most clearly observed with phosphite and phosphine ligands. It is known that reaction of [Pt<sub>3</sub>( $\mu_3$ -CO)( $\mu$ -dppm)<sub>3</sub>]<sup>2+</sup> with P(OR)<sub>3</sub> (R = Me or Ph) gives a thermally stable adduct [Pt<sub>3</sub>( $\mu_3$ -CO)(P(OR)<sub>3</sub>)( $\mu$ -dppm)<sub>3</sub>]<sup>2+</sup> but that, with the bulkier ligand PPh<sub>3</sub>, adduct formation is reversible and the product cannot be isolated.<sup>4</sup> Reaction of [Pt<sub>3</sub>( $\mu_3$ -CO)( $\mu$ -R<sub>2</sub>PCH<sub>2</sub>PR<sub>2</sub>)<sub>3</sub>]<sup>2+</sup>, 8, with P(OPh)<sub>3</sub> at low temperature gave the adducts [Pt<sub>3</sub>( $\mu_3$ -CO){P(OPh)<sub>3</sub>}( $\mu$ -R<sub>2</sub>PCH<sub>2</sub>PR<sub>2</sub>)<sub>3</sub>]<sup>2+</sup> (9) (eq 1, L = P(OPh)<sub>3</sub>) when R = 4-MeC<sub>6</sub>H<sub>4</sub>, 3-MeC<sub>6</sub>H<sub>4</sub>, 3,5-Me<sub>2</sub>C<sub>6</sub>H<sub>3</sub>, and 3,5-F<sub>2</sub>C<sub>6</sub>H<sub>3</sub>, as monitored by <sup>31</sup>P NMR spectroscopy, but no reaction occurred in the case of R

(13) Yamaguchi, T.; Sasaki, Y.; Nagasawa, A.; Ito, T.; Koga, N.; Morokuma, K. *Inorg. Chem.* **1989**, *28*, 4321.

(14) De Carrondo, C. T.; Skapski, A. C. *J. Chem. Soc., Chem. Commun.* **1976**, 410.

(15) Ferguson, G.; Lloyd, B. R.; Manojlovic-Muir, Lj.; Muir, K. W.; Puddephatt, R. *J. Inorg. Chem.* **1986**, *25*, 4190.



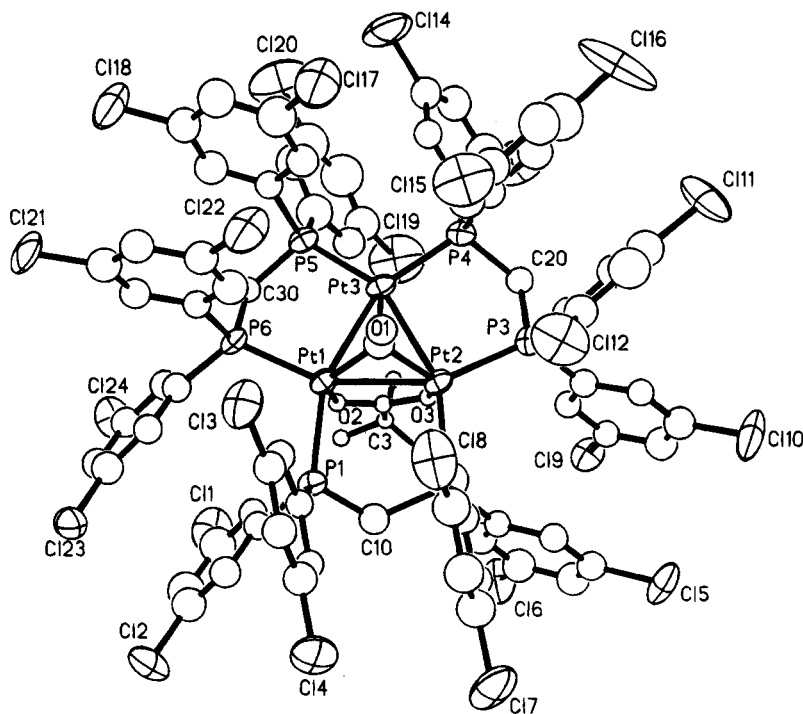


**Figure 2.** View of the structure of the cation  $[\text{Pt}_3(\mu_3\text{-CO})(\mu\text{-R}_2\text{PCH}_2\text{PR}_2)_3(\text{O}_2\text{CCF}_3)]^+$ ,  $\text{R} = 3,5\text{-Cl}_2\text{C}_6\text{H}_3$ , **4e**, showing 50% probability ellipsoids and the atom-labeling scheme. Atoms of the  $\text{CF}_3\text{CO}_2$  group are shown as spheres of arbitrary radius, and hydrogen atoms are omitted for clarity.

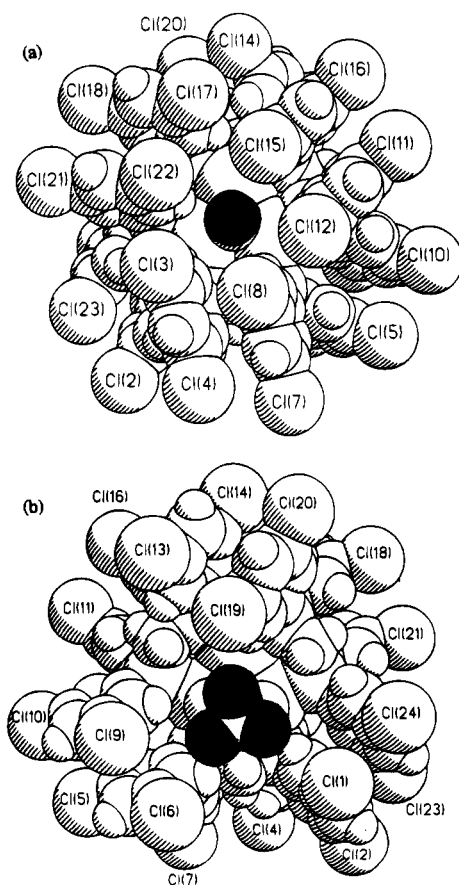


**Figure 3.** Space filling models of  $[\text{Pt}_3(\mu_3\text{-CO})(\mu\text{-R}_2\text{PCH}_2\text{PR}_2)_3(\text{O}_2\text{CCF}_3)]^+$ ,  $\text{R} = 3,5\text{-Cl}_2\text{C}_6\text{H}_3$ , **4e**, (a) on the carbonyl side (the carbonyl O atom is shaded) and (b) on the trifluoroacetate side (the F atoms are shaded) of the  $\text{Pt}_3$  triangle.

$= 3,5\text{-Cl}_2\text{C}_6\text{H}_3$ . These reactions are reversible, and the position of the equilibrium depends on the bulk of R. In the case of  $\text{R} = 3,5\text{-Me}_2\text{C}_6\text{H}_3$  and  $3,5\text{-F}_2\text{C}_6\text{H}_3$ , the

adducts **9** existed only at low temperature and fully dissociated to the corresponding starting material **8** and  $\text{P}(\text{O}^i\text{Ph})_3$  at room temperature. In the case of  $4\text{-MeC}_6\text{H}_4$  and  $3\text{-MeC}_6\text{H}_4$ , the adducts dissociated partially at room temperature. The reactions of **8**, with  $\text{R} = 3,5\text{-F}_2\text{C}_6\text{H}_3$  and  $3,5\text{-Cl}_2\text{C}_6\text{H}_3$ , with the less bulky ligand  $\text{P}(\text{OMe})_3$  were also studied. Both gave adducts at low temperature, but at room temperature, the adduct dissociated completely to the starting materials when  $\text{R} = 3,5\text{-Cl}_2\text{C}_6\text{H}_3$  but only partially when  $\text{R} = 3,5\text{-F}_2\text{C}_6\text{H}_3$  as determined by  $^{31}\text{P}$  NMR.<sup>4</sup> When L is the larger phosphine  $\text{PMePh}_2$ , reversible coordination is detected when  $\text{R} = 3,5\text{-Me}_2\text{C}_6\text{H}_3$  but not when  $\text{R} = 3,5\text{-F}_2\text{C}_6\text{H}_3$  or  $3,5\text{-Cl}_2\text{C}_6\text{H}_3$ .

## Discussion

The role of steric effects of the diphosphine ligands on the formation and chemistry of clusters  $[\text{Pt}_3(\mu_3\text{-CO})(\mu\text{-R}_2\text{PCH}_2\text{PR}_2)_3]^{2+}$  has been established, using substituted phenyl substituents R. In the case of the ortho-substituted derivative,  $\text{R} = 2\text{-MeC}_6\text{H}_4$ , the steric effects of the ligand  $\text{R}_2\text{PCH}_2\text{PR}_2$  are so great that formation of the corresponding triplatinum cluster is not possible and only dinuclear complexes can be formed.<sup>9,10</sup> With *meta*- and *para*-substituted phenyl groups R, the triplatinum clusters are formed and, in several cases, can be further converted to tetraplatinum clusters.<sup>11</sup> The ease of the conversion to the  $\text{Pt}_4$  cluster is greater with less bulky  $\text{R}_2\text{PCH}_2\text{PR}_2$  ligands, following the sequence  $\text{R} = 4\text{-MeC}_6\text{H}_4 \sim 3\text{-MeC}_6\text{H}_4 > 3,5\text{-Me}_2\text{C}_6\text{H}_3 \sim 3,5\text{-F}_2\text{C}_6\text{H}_3 > 3,5\text{-Cl}_2\text{C}_6\text{H}_3$ . The greater steric effects with  $\text{R} = 3,5\text{-Cl}_2\text{C}_6\text{H}_3$ , are also responsible for the cluster  $[\text{Pt}_3(\mu_3\text{-CO})(\mu\text{-R}_2\text{PCH}_2\text{PR}_2)_3]^{2+}$  giving three resonances in the low-temperature  $^{31}\text{P}$  NMR spectrum, whereas only one such resonance is observed in all other cases. The coordination of the anions  $\text{I}^-$  and  $\text{SCN}^-$  to the triplatinum clusters **8** occurs in all cases, but with the ligands  $\text{PPh}_3$ ,  $\text{PMePh}_2$ ,  $\text{P}(\text{OR})_3$ , and  $\text{CF}_3\text{CO}_2^-$ , there



is evidence for steric effects, which are greatest when  $R = 3,5\text{-Cl}_2\text{C}_6\text{H}_3$ . In this case, the cavity size, defined by the  $\text{R}_2\text{PCH}_2\text{PR}_2$  ligands of the  $\text{Pt}_3(\mu\text{-R}_2\text{PCH}_2\text{PR}_2)_3$  triangle, is so small that the  $\text{P(OPh)}_3$  ligand does not bind but is still large enough to bind  $\text{P(OMe)}_3$  at low temperature. Thus from experiments of this kind using phosphines and phosphites with different cone angles, it was determined that the steric effects of the  $\text{R}_2\text{PCH}_2\text{-PR}_2$  ligand to the triplatinum clusters  $[\text{Pt}_3(\mu_3\text{-CO})(\mu\text{-R}_2\text{PCH}_2\text{PR}_2)_3]^{2+}$  are in the order  $2\text{-MeC}_6\text{H}_4 > 3,5\text{-Cl}_2\text{C}_6\text{H}_3 > 3,5\text{-F}_2\text{C}_6\text{H}_3 > 3,5\text{-Me}_2\text{C}_6\text{H}_3 > 3\text{-MeC}_6\text{H}_4, 4\text{-MeC}_6\text{H}_4, \text{C}_6\text{H}_5$ . This assumes that electronic effects can be neglected. Although the electron density at the  $\text{Pt}_3$  center is unlikely to change to a major extent, there is evidence from the value of  $\nu(\mu_3\text{-CO})$  that minor changes can occur. It is also possible that electronic effects between fluoro or chloro substituents when  $R = 3,5\text{-F}_2\text{C}_6\text{H}_3$  or  $3,5\text{-Cl}_2\text{C}_6\text{H}_3$  and the incoming ligands L might be significant in some cases. However, it is clear that the major effects on the ability to form the clusters, and on their ability to bind phosphine and phosphite ligands in particular, arise from steric effects of the substituents R. The cavity size can indeed be tailored and does lead to size selectivity in ligand binding.

### Experimental Section

All reactions were performed under  $\text{N}_2$  atmosphere using standard Schlenk techniques unless otherwise noted. All solvents were dried and distilled before use. The phosphine ligand  $\text{Cl}_2\text{PCH}_2\text{PCL}_2$  was prepared using established methods.<sup>16</sup> NMR spectra were recorded by using a Varian Gemini-300 instrument. The proton and carbon chemical shifts are positive downfield relative to external  $\text{Me}_4\text{Si}$ .  $^{31}\text{P}\{^1\text{H}\}$  NMR spectra are externally referenced to 85%  $\text{H}_3\text{PO}_4$ , with downfield chemical shifts reported as positive.

**$\text{R}_2\text{PCH}_2\text{PR}_2$ .** A solution of  $4\text{-MeC}_6\text{H}_4\text{MgBr}$  was prepared from  $4\text{-MeC}_6\text{H}_4\text{Br}$  (22.6 mL, 0.184 mol) with Mg (4.46 g, 0.184 mol) in dry ether (50 mL), initiating the reaction with  $\text{C}_2\text{H}_4\text{-Br}_2$  (1 mL). The above solution was cooled to  $-7^\circ\text{C}$ , and a solution of  $\text{Cl}_2\text{PCH}_2\text{PCL}_2$  (6.15 mL, 0.0459 mol) in ether (10 mL) was added dropwise. The mixture was allowed to warm to room temperature and stirred for 15 h and then cooled to  $-7^\circ\text{C}$  and hydrolyzed by addition of saturated aqueous  $\text{NH}_4\text{Cl}$  (40 mL). The mixture was added to a solution of KOH (100 g) in water (300 mL) in a liquid-liquid continuous extractor. Ether (200 mL) was added, and the product was extracted for 12 h. The ether extract was dried over  $\text{MgSO}_4$ , and the ether was evaporated to give  $\{(4\text{-MeC}_6\text{H}_4)_2\text{P}\}_2\text{CH}_2$  as a yellow oil in 70% yield. A part was recrystallized from  $\text{CH}_2\text{Cl}_2/\text{EtOH}$  as colorless crystals. NMR in  $\text{CDCl}_3$ :  $\delta(^1\text{H}) = 7.29$  [m, 8H,  $^3\text{J}(\text{HH}) = 8$  Hz,  $^4\text{J}(\text{HH}) = 3$  Hz, aryl], 7.08 [d, 8H,  $^3\text{J}(\text{HH}) = 8$  Hz, aryl], 2.71 [t, 2H,  $^2\text{J}(\text{PH}) = 3$  Hz,  $\text{CH}_2\text{P}_2$ ], 2.30 [t, 12H,  $^4\text{J}(\text{HH}) = 3$  Hz, Me];  $\delta(^{31}\text{P}) = -26.9$  [s, P].

Similarly were prepared the following compounds.  $R = 3\text{-MeC}_6\text{H}_4$ : yield 65%; NMR in  $\text{CDCl}_3$   $\delta(^1\text{H}) = 7.1\text{--}7.4$  [m, 16H, aryl], 2.78 [t, 2H,  $^2\text{J}(\text{PH}) = 1$  Hz,  $\text{CH}_2\text{P}_2$ ], 2.26 [s, 12H, Me],  $\delta(^{31}\text{P}) = -24.3$  [s, P].  $R = 2\text{-MeC}_6\text{H}_4$ : yield 45%; NMR in  $\text{CDCl}_3$   $\delta(^1\text{H}) = 7.1\text{--}7.3$  [m, 16H, aryl], 2.68 [t, 2H,  $^2\text{J}(\text{PH}) = 3$  Hz,  $\text{CH}_2\text{P}_2$ ], 2.28 [s, 12H, Me],  $\delta(^{31}\text{P}) = -46.6$  [s, P].  $R = 3,5\text{-Me}_2\text{C}_6\text{H}_3$ : yield 60%; NMR in  $\text{CDCl}_3$   $\delta(^1\text{H}) = 7.18$  [s, 4H, aryl], 6.88 [d, 8H,  $^3\text{J}(\text{PH}) = 24$  Hz, aryl], 2.78 [s, 2H,  $\text{CH}_2\text{P}_2$ ], 2.27 [s, 24H, Me],  $\delta(^{31}\text{P}) = -23.6$  [s, P].  $R = 2,4,6\text{-Me}_3\text{C}_6\text{H}_2$ : yield 70%; NMR in  $\text{CDCl}_3$   $\delta(^1\text{H}) = 6.76$  [s, 8H, aryl], 2.74 [s, 2H,  $\text{CH}_2\text{P}_2$ ], 2.24, 2.33 [br s, 36H, Me],  $\delta(^{31}\text{P}) = -32.2$  [s, P]. The following compounds were prepared similarly, except that the reaction mixtures were extracted with ether using standard Schlenk techniques.  $R = 3,5\text{-Cl}_2\text{C}_6\text{H}_3$ : yield 82%; NMR in

$\text{CDCl}_3$   $\delta(^1\text{H}) = 7.4\text{--}6.9$  [m, 12H,  $\text{C}_6\text{H}_3$ ], 2.70 [br s, 2H,  $\text{CH}_2\text{P}_2$ ],  $\delta(^{31}\text{P}) = -17.4$  [s].  $R = 3,5\text{-F}_2\text{C}_6\text{H}_3$ : yield 85%; NMR in  $\text{CDCl}_3$   $\delta(^1\text{H}) = 7.3\text{--}6.8$  [m, 12H,  $\text{C}_6\text{H}_3$ ], 2.80 [br s, 2H,  $\text{CH}_2\text{P}_2$ ],  $\delta(^{31}\text{P}) = -17.3$  [s].

**$[\text{PtCl}_2(\text{R}_2\text{PCH}_2\text{PR}_2)]$ .** To a stirred solution of a mixture of *cis*- and *trans*- $[\text{PtCl}_2(\text{SMe}_2)_2]$  (2.67 g, 6.84 mmol) in  $\text{CH}_2\text{Cl}_2$  (20 mL) was added dropwise a solution of  $\text{R}_2\text{PCH}_2\text{PR}_2$  ( $R = 3,5\text{-Cl}_2\text{C}_6\text{H}_3$ , 6.84 mmol) in  $\text{CH}_2\text{Cl}_2$  (10 mL). A white precipitate formed immediately. After 6 h, the product was collected by filtration and washed with diethyl ether (10 mL) and pentane (10 mL) and dried under vacuum. Yield: 93%. Anal. Calcd for  $\text{C}_{25}\text{H}_{14}\text{Cl}_{10}\text{P}_2\text{Pt}$ : C, 32.43; H, 1.51. Found: C, 32.33; H, 1.27. NMR: insufficient solubility.

Similarly were prepared the following compounds.  $R = 3,5\text{-F}_2\text{C}_6\text{H}_3$ : yield 95%. Anal. Calcd for  $\text{C}_{25}\text{H}_{14}\text{Cl}_2\text{F}_8\text{P}_2\text{Pt}$ : C, 37.80; H, 1.78. Found: C, 38.12; H, 1.90. NMR: insufficient solubility.  $R = 4\text{-MeC}_6\text{H}_4$ : yield 88%. Anal. Calcd for  $\text{C}_{29}\text{H}_{30}\text{Cl}_2\text{P}_2\text{Pt}$ : C, 49.3; H, 4.3. Found: C, 48.9; H, 4.1. NMR in  $\text{CDCl}_3$ :  $\delta(^1\text{H}) = 7.05, 7.83$  [m, 16H, aryl], 4.54 [t, 2H,  $^2\text{J}(\text{PH}) = 14$  Hz,  $^3\text{J}(\text{PtH}) = 70$  Hz,  $\text{CH}_2\text{P}_2$ ], 2.21 [s, 12H, Me];  $\delta(^{31}\text{P}) = -68.6$  [s,  $^1\text{J}(\text{PtP}) = 3078$ , P].  $R = 3,5\text{-Me}_2\text{C}_6\text{H}_3$ : yield 35%. Anal. Calcd for  $\text{C}_{33}\text{H}_{38}\text{Cl}_2\text{P}_2\text{Pt}$ : C, 52.0; H, 5.0. Found: C, 51.0; H, 5.3. NMR: insufficient solubility.  $R = 2\text{-MeC}_6\text{H}_4$ : yield 75%. Anal. Calcd for  $\text{C}_{29}\text{H}_{30}\text{Cl}_2\text{P}_2\text{Pt}$ : C, 49.3; H, 4.3. Found: C, 49.0; H, 4.6. NMR in  $\text{CDCl}_3$ :  $\delta(^1\text{H}) = 7.53\text{--}8.07$  [m, 16H, aryl], 5.15 [t, 2H,  $^2\text{J}(\text{PH}) = 11$  Hz,  $^3\text{J}(\text{PtH}) = 68$  Hz,  $\text{CH}_2\text{P}_2$ ], 2.31 [s, 12H, Me];  $\delta(^{31}\text{P}) = -64.6$  [s,  $^1\text{J}(\text{PtP}) = 3068$ , P].  $R = 2,4,6\text{-Me}_3\text{C}_6\text{H}_2$ : yield 25%. Anal. Calcd for  $\text{C}_{37}\text{H}_{46}\text{Cl}_2\text{P}_2\text{Pt}$ : C, 54.3; H, 5.7. Found: C, 54.2; H, 5.9. NMR in  $\text{CDCl}_3$ :  $\delta(^1\text{H}) = 6.78$  [s, 8H, aryl], 5.23 [t, 2H,  $^2\text{J}(\text{PH}) = 10$  Hz,  $^3\text{J}(\text{PtH}) = 51$  Hz,  $\text{CH}_2\text{P}_2$ ], 2.24 [s, 12H, Me], 2.39 [s, 24H, Me];  $\delta(^{31}\text{P}) = -83.8$  [s,  $^1\text{J}(\text{PtP}) = 3089$ , P].

**$[\text{Pt}(\text{O}_2\text{CCF}_3)_2(\text{R}_2\text{PCH}_2\text{PR}_2)]$ .** To a stirred suspension of  $[\text{PtCl}_2(\text{R}_2\text{PCH}_2\text{PR}_2)]$ ,  $R = 3,5\text{-Cl}_2\text{C}_6\text{H}_4$  (1.05 g, 1.13 mmol), in acetone (25 mL) and trifluoroacetic acid (2 mL) was added silver trifluoroacetate (0.55 g, 2.5 mmol). The mixture was stirred at room temperature in the dark for 1 h and then refluxed for 3 h. The mixture was cooled to room temperature and filtered to remove the  $\text{AgCl}$  precipitate, and the solvent was evaporated under vacuum to give a yellow oil, which was triturated with ether at  $0^\circ\text{C}$  to give the product as a white solid. Yield: 86%. Anal. Calcd for  $\text{C}_{29}\text{H}_{14}\text{Cl}_8\text{F}_6\text{O}_4\text{P}_2\text{Pt}$ : C, 32.22; H, 1.31. Found: C, 32.41; H, 1.42. NMR in  $(\text{CD}_3)_2\text{CO}$ :  $\delta(^1\text{H}) = 8.10\text{--}8.02$  [m, 8H, aryl], 7.8 [t, 4H,  $^4\text{J}(\text{HH}) = 2$  Hz, aryl], 5.48 [t, 2H,  $^2\text{J}(\text{PH}) = 12$  Hz,  $^3\text{J}(\text{PtH}) = 92.5$  Hz,  $\text{CH}_2\text{P}_2$ ];  $\delta(^{31}\text{P}) = -57.2$  [s,  $^1\text{J}(\text{PtP}) = 3450$ , P].

Similarly were prepared the following complexes.  $R = 3,5\text{-F}_2\text{C}_6\text{H}_3$ : yield 80%. Anal. Calcd for  $\text{C}_{29}\text{H}_{14}\text{F}_{14}\text{O}_4\text{P}_2\text{Pt}$ : C, 36.69; H, 1.49. Found: C, 36.83; H, 1.51. NMR in  $(\text{CD}_3)_2\text{CO}$ :  $\delta(^1\text{H}) = 7.84\text{--}7.70$  [m, 8H, aryl], 7.39 [tt, 4H,  $^4\text{J}(\text{HH}) = 2$  Hz,  $^3\text{J}(\text{FH}) = 9$  Hz, aryl], 5.36 [t, 2H,  $^2\text{J}(\text{PH}) = 12$  Hz,  $^3\text{J}(\text{PtH}) = 91$  Hz,  $\text{CH}_2\text{P}_2$ ];  $\delta(^{31}\text{P}) = -56.8$  [s,  $^1\text{J}(\text{PtP}) = 3450$ , P].  $R = 4\text{-MeC}_6\text{H}_4$ : yield 60%. Anal. Calcd for  $\text{C}_{33}\text{H}_{30}\text{F}_6\text{O}_4\text{P}_2\text{Pt}$ : C, 46.0; H, 3.5. Found: C, 45.75; H, 3.7. NMR in  $(\text{CD}_3)_2\text{CO}$ :  $\delta(^1\text{H}) = 7.41\text{--}7.78$  [m, 16H, aryl], 4.94 [t, 2H,  $^2\text{J}(\text{PH}) = 12$  Hz,  $^3\text{J}(\text{PtH}) = 87$  Hz,  $\text{CH}_2\text{P}_2$ ], 2.31 [s, 12H, Me];  $\delta(^{31}\text{P}) = -68.3$  [s,  $^1\text{J}(\text{PtP}) = 3324$  Hz, P].  $R = 2\text{-MeC}_6\text{H}_4$ : yield 86%. Anal. Calcd for  $\text{C}_{33}\text{H}_{30}\text{F}_6\text{O}_4\text{P}_2\text{Pt}$ : C, 46.0; H, 3.5. Found: C, 46.5; H, 3.5. NMR in  $(\text{CD}_3)_2\text{CO}$ :  $\delta(^1\text{H}) = 7.32\text{--}8.12$  [m, 16H, aryl], 5.31 [t, 2H,  $^2\text{J}(\text{PH}) = 11$  Hz,  $^3\text{J}(\text{PtH}) = 80$  Hz,  $\text{CH}_2\text{P}_2$ ], 2.28 [s, 12H, Me];  $\delta(^{31}\text{P}) = -71.4$  [s,  $^1\text{J}(\text{PtP}) = 3304$  Hz, P].  $R = 3,5\text{-Me}_2\text{C}_6\text{H}_3$ : yield 49%. Anal. Calcd for  $\text{C}_{37}\text{H}_{38}\text{F}_6\text{O}_4\text{P}_2\text{Pt}$ : C, 48.4; H, 4.2. Found: C, 48.7; H, 4.6. NMR in  $(\text{CD}_3)_2\text{CO}$ :  $\delta(^1\text{H}) = 7.23$  [s, 4H, aryl], 7.55 [m, 8H, aryl], 4.85 [t, 2H,  $^2\text{J}(\text{PH}) = 11$  Hz,  $^3\text{J}(\text{PtH}) = 88$  Hz,  $\text{CH}_2\text{P}_2$ ], 2.28 [s, 24H, Me];  $\delta(^{31}\text{P}) = -68.6$  [s,  $^1\text{J}(\text{PtP}) = 3319$  Hz, P].  $R = 2,4,6\text{-Me}_3\text{C}_6\text{H}_2$ : yield 80%. Anal. Calcd for  $\text{C}_{41}\text{H}_{46}\text{F}_6\text{O}_4\text{P}_2\text{Pt}$ : C, 50.6; H, 4.8. Found: C, 51.0; H, 4.8. NMR in  $(\text{CD}_3)_2\text{CO}$ :  $\delta(^1\text{H}) = 6.80$  [s, 8H, aryl], 5.26 [t, 2H,  $^2\text{J}(\text{PH}) =$

(16) Hietkamp, S.; Sommer, H.; Stelzer, O. *Inorg. Synth.* **1989**, *25*, 120.

11 Hz,  $^3J(\text{PtH}) = 60$  Hz,  $\text{CH}_2\text{P}_2$ , 2.24 [s, 12H, Me], 2.35 [s, 24H, Me];  $\delta(^{31}\text{P}) = -92.2$  [s,  $^1J(\text{PtP}) = 3270$  Hz, P].

**[Pt<sub>3</sub>( $\mu_3$ -CO)( $\mu$ -R<sub>2</sub>PCH<sub>2</sub>PR<sub>2</sub>)<sub>3</sub>(O<sub>2</sub>CCF<sub>3</sub>)](O<sub>2</sub>CCF<sub>3</sub>)**. A mixture of [Pt(O<sub>2</sub>CCF<sub>3</sub>)<sub>2</sub>(R<sub>2</sub>PCH<sub>2</sub>PR<sub>2</sub>)], R = 3,5-Cl<sub>2</sub>C<sub>6</sub>H<sub>3</sub> (1.00 g, 0.93 mmol), MeOH (40 mL), distilled H<sub>2</sub>O (4 mL), and CF<sub>3</sub>-CO<sub>2</sub>H (1 mL) in a Parr pressure reactor (300 mL) was heated at 70 °C for 3 days under CO (14 atm). At 12 h intervals for the first 24 h and then 24 h intervals for the remaining 48 h, the pressure reactor was cooled and a fresh CO atmosphere was introduced. After this period, the reactor was cooled to room temperature and opened. The solution was filtered, and the resulting red filtrate was evaporated under vacuum. The orange residue was recrystallized from CH<sub>2</sub>Cl<sub>2</sub>/diethyl ether to give the product as an orange solid. Yield: 85%. Anal. Calcd for C<sub>80</sub>H<sub>42</sub>F<sub>6</sub>O<sub>5</sub>P<sub>6</sub>Cl<sub>2</sub>Pt<sub>3</sub>: C, 34.08; H, 1.50. Found: C, 33.98; H, 1.66. IR (Nujol):  $\nu(\text{CO}) = 1771$  (s) cm<sup>-1</sup>. NMR in (CD<sub>3</sub>)<sub>2</sub>CO:  $\delta(^1\text{H}) = 7.1$ – $7.6$  [m, 36H, C<sub>6</sub>H<sub>3</sub>], 6.6 [d, 3H,  $^2J(\text{HH}) = 16$  Hz, CH<sup>a</sup>H<sup>b</sup>], 5.7 [d, 3H,  $^2J(\text{HH}) = 16$  Hz, CH<sup>a</sup>H<sup>b</sup>];  $\delta(^{31}\text{P}) = -8.4$  [s,  $^1J(\text{PtP}) = 3673$  Hz,  $^2J(\text{PP}) = -5$  Hz,  $^3J(\text{PP}) = 169$  Hz];  $\delta(^{31}\text{P})$  at  $-60$  °C =  $-10.3$  [br,  $^1J(\text{PtP}) = 3624$ ];  $\delta(^1\text{H})$  at  $-90$  °C =  $5.72$  [m, CH<sup>a</sup>H<sup>b</sup>],  $4.80$  [m, CH<sup>a</sup>H<sup>b</sup>];  $\delta(^{31}\text{P})$  at  $-90$  °C =  $-4.6$  [s, 2P<sup>b</sup>,  $^1J(\text{PtP}) = 3628$  Hz,  $^3J(\text{P}^b\text{P}^b) = 144$  Hz],  $-10.6$  [d, 2P<sup>a</sup>,  $^1J(\text{PtP}) = 3616$  Hz,  $^3J(\text{P}^a\text{P}^a) = 160$  Hz],  $-13.2$  [d, 2P<sup>c</sup>,  $^1J(\text{PtP}) = 3746$  Hz,  $^3J(\text{P}^a\text{P}^c) = 160$  Hz]. NMR of <sup>13</sup>CO exchanged **1a** at 20 °C in (CD<sub>3</sub>)<sub>2</sub>CO:  $\delta(^{31}\text{P}) = -8.5$  [d,  $^1J(\text{PtP}) = 3676$  Hz,  $^2J(\text{PtP}) = 2$  Hz,  $^3J(\text{PP}) = 164$  Hz,  $^2J(\text{CP}) = 20$  Hz];  $\delta(^{13}\text{C}) = 188.8$  [quintet,  $^1J(\text{PtC}) = 945$  Hz,  $^2J(\text{PC}) = 20$  Hz, PtCO], 52.1 [br, CH<sub>2</sub>P<sub>2</sub>].

Similarly were prepared the following complexes. R = 3,5-F<sub>2</sub>C<sub>6</sub>H<sub>3</sub>: yield 80%. Anal. Calcd for C<sub>80</sub>H<sub>42</sub>F<sub>30</sub>O<sub>5</sub>P<sub>6</sub>Pt<sub>3</sub>: C, 39.64; H, 1.75. Found: C, 39.52; H, 1.78. IR (Nujol):  $\nu(\text{CO}) = 1783$  (s) cm<sup>-1</sup>. NMR in (CD<sub>3</sub>)<sub>2</sub>CO:  $\delta(^1\text{H}) = 7.4$ – $6.9$  [m, C<sub>6</sub>H<sub>3</sub>], 6.7 [d,  $^2J(\text{HH}) = 13.3$  Hz, CH<sup>a</sup>H<sup>b</sup>], 5.7 [d,  $^2J(\text{HH}) = 13.3$  Hz, CH<sup>a</sup>H<sup>b</sup>];  $\delta(^{31}\text{P}) = -7.1$  [s,  $^1J(\text{PtP}) = 3706$  Hz,  $^2J(\text{PtP}) = 13$  Hz,  $^3J(\text{PP}) = 161$  Hz]. R = 4-MeC<sub>6</sub>H<sub>4</sub>: yield 83%. Anal. Calcd for C<sub>92</sub>H<sub>90</sub>F<sub>6</sub>O<sub>5</sub>P<sub>6</sub>Pt<sub>3</sub>: C, 51.1; H, 4.2. Found: C, 50.5; H, 4.5. IR (Nujol):  $\nu(\text{CO}) = 1740$  (s) cm<sup>-1</sup>. NMR in (CD<sub>3</sub>)<sub>2</sub>CO:  $\delta(^1\text{H}) = 7.2$ – $6.7$  [m, C<sub>6</sub>H<sub>4</sub>], 5.8 [d,  $^2J(\text{HH}) = 14$  Hz, CH<sup>a</sup>H<sup>b</sup>], 5.6 [d,  $^2J(\text{HH}) = 14$  Hz, CH<sup>a</sup>H<sup>b</sup>];  $\delta(^{31}\text{P}) = -11.1$  [s,  $^1J(\text{PtP}) = 3753$  Hz,  $^2J(\text{PtP}) = 1$  Hz,  $^3J(\text{PP}) = 155$  Hz]. R = 3-MeC<sub>6</sub>H<sub>4</sub>: yield 98%. Anal. Calcd for C<sub>92</sub>H<sub>90</sub>F<sub>6</sub>O<sub>5</sub>P<sub>6</sub>Pt<sub>3</sub>: C, 51.1; H, 4.2. Found: C, 51.3; H, 4.7. IR (Nujol):  $\nu(\text{CO}) = 1734$  (s) cm<sup>-1</sup>. NMR in (CD<sub>3</sub>)<sub>2</sub>CO:  $\delta(^1\text{H}) = 7.3$ – $6.9$  [m, C<sub>6</sub>H<sub>4</sub>], 5.63 [d,  $^2J(\text{HH}) = 13$  Hz, CH<sup>a</sup>H<sup>b</sup>], 5.71 [d,  $^2J(\text{HH}) = 13$  Hz, CH<sup>a</sup>H<sup>b</sup>];  $\delta(^{31}\text{P}) = -11.2$  [s,  $^1J(\text{PtP}) = 3741$  Hz,  $^2J(\text{PtP}) = -2$  Hz,  $^3J(\text{PP}) = 157$  Hz]. R = 3,5-Me<sub>2</sub>C<sub>6</sub>H<sub>3</sub>: yield 98%. Anal. Calcd for C<sub>104</sub>H<sub>114</sub>F<sub>6</sub>O<sub>5</sub>P<sub>6</sub>Pt<sub>3</sub>: C, 53.6; H, 4.9. Found: C, 53.3; H, 4.7. IR (Nujol):  $\nu(\text{CO}) = 1742$  (s) cm<sup>-1</sup>. NMR in (CD<sub>3</sub>)<sub>2</sub>CO:  $\delta(^1\text{H}) = 7.1$ – $6.9$  [m, C<sub>6</sub>H<sub>3</sub>], 5.53 [d,  $^2J(\text{HH}) = 12$  Hz, CH<sup>a</sup>H<sup>b</sup>], 5.27 [d,  $^2J(\text{HH}) = 12$  Hz, CH<sup>a</sup>H<sup>b</sup>];  $\delta(^{31}\text{P}) = -11.6$  [s,  $^1J(\text{PtP}) = 3690$  Hz,  $^2J(\text{PtP}) = -3$  Hz,  $^3J(\text{PP}) = 160$  Hz].

**[Pt<sub>3</sub>( $\mu_3$ -CO)( $\mu$ -R<sub>2</sub>PCH<sub>2</sub>PR<sub>2</sub>)<sub>3</sub>](PF<sub>6</sub>)<sub>2</sub>**. To a solution of [Pt<sub>3</sub>( $\mu_3$ -CO)( $\mu$ -R<sub>2</sub>PCH<sub>2</sub>PR<sub>2</sub>)<sub>3</sub>(O<sub>2</sub>CCF<sub>3</sub>)](O<sub>2</sub>CCF<sub>3</sub>), R = 3,5-Cl<sub>2</sub>C<sub>6</sub>H<sub>3</sub> (0.240 g, 0.085 mmol), in MeOH (5 mL) was added dropwise a filtered solution of NH<sub>4</sub>PF<sub>6</sub> (0.222 g, 1.36 mmol) in MeOH (5 mL). An orange precipitate formed immediately. After 4 h, the product was collected by filtration and washed with MeOH (0.5 mL). Recrystallization from CH<sub>2</sub>Cl<sub>2</sub>/ether followed by vacuum drying afforded the orange-red crystalline product in 85% yield. Anal. Calcd for C<sub>76</sub>H<sub>42</sub>Cl<sub>2</sub>F<sub>12</sub>OP<sub>8</sub>Pt<sub>3</sub>: C, 31.66; H, 1.47. Found: C, 31.78; H, 1.65. IR (Nujol):  $\nu(\text{CO}) = 1771$  (s) cm<sup>-1</sup>. NMR in (CD<sub>3</sub>)<sub>2</sub>CO:  $\delta(^1\text{H}) = 7.6$ – $7.1$  [m, C<sub>6</sub>H<sub>3</sub>], 6.5 [d,  $^2J(\text{HH}) = 16$  Hz, CH<sup>a</sup>H<sup>b</sup>], 5.6 [d,  $^2J(\text{HH}) = 16$  Hz, CH<sup>a</sup>H<sup>b</sup>];  $\delta(^{31}\text{P}) = 8.4$  [s,  $^1J(\text{PtP}) = 3672$  Hz,  $^2J(\text{PtP}) = -3$  Hz,  $^3J(\text{PP}) = 174$  Hz];  $\delta(^1\text{H})$  at 90 °C =  $5.72$  [m, CH<sup>a</sup>H<sup>b</sup>],  $4.82$  [m, CH<sup>a</sup>H<sup>b</sup>];  $\delta(^{31}\text{P})$  at  $-90$  °C =  $-4.6$  [s, 2P<sup>b</sup>,  $^1J(\text{PtP}) = 3622$  Hz,  $^3J(\text{P}^b\text{P}^b) = 143$  Hz],  $-10.6$  [d, 2P<sup>a</sup>,  $^1J(\text{PtP}) = 3606$  Hz,  $^3J(\text{P}^a\text{P}^a) = 160$  Hz],  $-13.2$  [d, 2P<sup>c</sup>,  $^1J(\text{PtP}) = 3746$  Hz,  $^3J(\text{P}^a\text{P}^c) = 160$  Hz].

Similarly were prepared the following complexes. R = 3,5-F<sub>2</sub>C<sub>6</sub>H<sub>3</sub>: yield 84%. Anal. Calcd for C<sub>76</sub>H<sub>42</sub>F<sub>36</sub>OP<sub>8</sub>Pt<sub>3</sub>: C, 36.69; H, 1.70. Found: C, 36.99; H, 1.86. IR (Nujol):  $\nu(\text{CO}) = 1784$  (s) cm<sup>-1</sup>. NMR in (CD<sub>3</sub>)<sub>2</sub>CO:  $\delta(^1\text{H}) = 7.4$ – $6.7$  [m, C<sub>6</sub>H<sub>3</sub>], 6.4 [d,  $^2J(\text{HH}) = 14$  Hz, CH<sup>a</sup>H<sup>b</sup>], 5.9 [d,  $^2J(\text{HH}) = 14$

Hz, CH<sup>a</sup>H<sup>b</sup>];  $\delta(^{31}\text{P}) = 0.4$  [s,  $^1J(\text{PtP}) = 3759$  Hz,  $^2J(\text{PtP}) = 32$  Hz,  $^3J(\text{PP}) = 110$  Hz]. R = 4-MeC<sub>6</sub>H<sub>4</sub>: yield 94%. Anal. Calcd for C<sub>88</sub>H<sub>90</sub>F<sub>12</sub>OP<sub>8</sub>Pt<sub>3</sub>: C, 47.51; H, 4.08. Found: C, 47.74; H, 4.52. IR (Nujol):  $\nu(\text{CO}) = 1754$  (s) cm<sup>-1</sup>,  $\nu(^{13}\text{CO}) = 1711$  cm<sup>-1</sup>. NMR in (CD<sub>3</sub>)<sub>2</sub>CO:  $\delta(^1\text{H}) = 7.2$ – $6.9$  [m, C<sub>6</sub>H<sub>4</sub>], 6.0 [d,  $^2J(\text{HH}) = 16$  Hz, CH<sup>a</sup>H<sup>b</sup>], 5.55 [d,  $^2J(\text{HH}) = 16$  Hz, CH<sup>a</sup>H<sup>b</sup>], 2.26, 2.25 [s, MeC];  $\delta(^{31}\text{P}) = -7.39$  [s,  $^1J(\text{PtP}) = 3706$  Hz,  $^2J(\text{PtP}) = -3$  Hz,  $^3J(\text{PP}) = 138$  Hz];  $\delta(^{13}\text{C}) = 211.1$  [br s,  $^1J(\text{PtC}) = 750$  Hz]. R = 3-MeC<sub>6</sub>H<sub>4</sub>: yield 99%. Anal. Calcd for C<sub>88</sub>H<sub>90</sub>F<sub>12</sub>OP<sub>8</sub>Pt<sub>3</sub>: C, 47.51; H, 4.08. Found: C, 47.24; H, 4.50. IR (Nujol):  $\nu(\text{CO}) = 1734$  (s) cm<sup>-1</sup>,  $\nu(^{13}\text{CO}) = 1696$  cm<sup>-1</sup>. NMR in CD<sub>2</sub>Cl<sub>2</sub>:  $\delta(^1\text{H}) = 7.0$ – $6.8$  [m, C<sub>6</sub>H<sub>4</sub>], 5.4 [d,  $^2J(\text{HH}) = 15$  Hz, CH<sup>a</sup>H<sup>b</sup>], 5.3 [d,  $^2J(\text{HH}) = 15$  Hz, CH<sup>a</sup>H<sup>b</sup>], 2.12, 2.00 [s, Me];  $\delta(^{31}\text{P}) = -6.81$  [s,  $^1J(\text{PtP}) = 3701$  Hz,  $^3J(\text{PP}) = 144$  Hz];  $\delta(^{13}\text{C}) = 209.6$  [m,  $^1J(\text{PtC}) = 806$  Hz,  $^2J(\text{PC}) = 25$  Hz]. R = 3,5-Me<sub>2</sub>C<sub>6</sub>H<sub>3</sub>: yield 98%. Anal. Calcd for C<sub>106</sub>H<sub>114</sub>F<sub>12</sub>OP<sub>8</sub>Pt<sub>3</sub>: C, 50.19; H, 4.80. Found: C, 50.00; H, 5.08. IR (Nujol):  $\nu(\text{CO}) = 1743$  (s) cm<sup>-1</sup>,  $\nu(^{13}\text{CO}) = 1703$  cm<sup>-1</sup>. NMR in (CD<sub>3</sub>)<sub>2</sub>CO:  $\delta(^1\text{H}) = 7.2$ – $6.8$  [m, C<sub>6</sub>H<sub>3</sub>], 5.8 [d,  $^2J(\text{HH}) = 14$  Hz, CH<sup>a</sup>H<sup>b</sup>], 5.2 [d,  $^2J(\text{HH}) = 14$  Hz, CH<sup>a</sup>H<sup>b</sup>], 2.14, 1.99 [s, Me];  $\delta(^{31}\text{P}) = -5.2$  [s,  $^1J(\text{PtP}) = 3697$  Hz,  $^3J(\text{PP}) = 139$  Hz];  $\delta(^{13}\text{C}) = 213.4$  [m,  $^1J(\text{PtC}) = 670$  Hz]. NMR at  $-90$  °C:  $\delta(^{31}\text{P}) = -7.8$  [br s,  $^1J(\text{PtP}) = 3640$  Hz];  $\delta(^{13}\text{C}) = 210.4$  [m,  $^1J(\text{PtC}) = 800$  Hz,  $^2J(\text{PC}) = 18$  Hz].

**[Pt<sub>2</sub>H(CO)( $\mu$ -R<sub>2</sub>PCH<sub>2</sub>PR<sub>2</sub>)](CF<sub>3</sub>CO<sub>2</sub>), R = 2-MeC<sub>6</sub>H<sub>4</sub>**. A mixture of [Pt(O<sub>2</sub>CCF<sub>3</sub>)<sub>2</sub>(R<sub>2</sub>PCH<sub>2</sub>PR<sub>2</sub>)], (0.66 g), MeOH (35 mL), and H<sub>2</sub>O (3 mL) was heated in a 300 mL pressure reactor with CO (60 psi) for 3 days. Workup in the usual way gave the product as a yellow solid. Yield: 85%. Anal. Calcd for C<sub>61</sub>H<sub>61</sub>F<sub>3</sub>O<sub>3</sub>P<sub>4</sub>Pt<sub>2</sub>: C, 51.84; H, 4.35. Found: C, 51.47; H, 4.35. IR (Nujol):  $\nu(\text{CO}) = 2043$  (s) cm<sup>-1</sup>,  $\nu(^{13}\text{CO}) = 1993$  cm<sup>-1</sup>;  $\nu(\text{PtH}) = 2074$  cm<sup>-1</sup>. NMR in (CD<sub>3</sub>)<sub>2</sub>CO:  $\delta(^1\text{H}) = 8.6$ – $6.0$  [m, C<sub>6</sub>H<sub>4</sub>], 4.3 [m, CH<sub>2</sub>P<sub>2</sub>], 2.00, 1.99 [s, Me],  $-6.77$  [m,  $^1J(\text{PtH}) = 990$  Hz,  $^2J(\text{PtH}) = 120$  Hz,  $^2J(\text{PH}) = 20$  Hz, PtH];  $\delta(^{31}\text{P}) = 2.61$  [m,  $^1J(\text{PtP}) = 2720$  Hz, PtP<sup>a</sup>], 7.66 [m,  $^1J(\text{PtP}) = 3385$  Hz, PtP<sup>b</sup>];  $\delta(^{13}\text{C}) = 189.1$  [m,  $^1J(\text{PtC}) = 1138$  Hz,  $^2J(\text{PtC}) = 195$  Hz,  $^2J(\text{PC}) = 7$  Hz, CO]. NMR at  $-90$  °C:  $\delta(^{31}\text{P}) = -7.8$  [br s,  $^1J(\text{PtP}) = 3640$  Hz];  $\delta(^{13}\text{C}) = 210.4$  [m,  $^1J(\text{PtC}) = 800$  Hz,  $^2J(\text{PC}) = 18$  Hz].

**[Pt<sub>2</sub>H<sub>2</sub>( $\mu$ -H)( $\mu$ -R<sub>2</sub>PCH<sub>2</sub>PR<sub>2</sub>)<sub>2</sub>](PF<sub>6</sub>)<sub>2</sub>, R = 2-MeC<sub>6</sub>H<sub>4</sub>**. To a stirred suspension of [PtCl<sub>2</sub>(R<sub>2</sub>PCH<sub>2</sub>PR<sub>2</sub>)], (0.5 g) in MeOH (50 mL) was added a solution of Na[BH<sub>4</sub>] (0.35 g) in EtOH (30 mL). After 4 h, the mixture was filtered, NH<sub>4</sub>[PF<sub>6</sub>] (0.84 g) was added to the filtrate, and the solvent was evaporated. The residue was extracted with CH<sub>2</sub>Cl<sub>2</sub> (10 mL), and the product was obtained by precipitation with pentane (20 mL). Yield: 76%. Anal. Calcd for C<sub>58</sub>H<sub>63</sub>F<sub>6</sub>P<sub>5</sub>Pt<sub>2</sub>: C, 49.09; H, 4.47. Found: C, 49.12; H, 4.53. IR (Nujol):  $\nu(\text{PtH}) = 2130$  cm<sup>-1</sup>. NMR in (CD<sub>3</sub>)<sub>2</sub>CO:  $\delta(^1\text{H}) = -7.42$  [t,  $^1J(\text{PtH}) = 1170$  Hz,  $^2J(\text{PtH}) = 105$  Hz,  $^2J(\text{PH}) = 7$  Hz, PtH<sup>a</sup>],  $-6.06$  [m,  $^1J(\text{PtH}) = 570$  Hz, PtH<sup>b</sup>], 2.06 [s, Me], 5.05 [m,  $^3J(\text{PtH}) = 37$  Hz,  $^4J(\text{PH}) = 4$  Hz, CH<sub>2</sub>P<sub>2</sub>];  $\delta(^{31}\text{P}) = 9.04$  [s,  $^1J(\text{PtP}) = 2692$  Hz, dppm]. Similarly was prepared the corresponding trideuteride derivative by using NaBD<sub>4</sub>;  $\nu(\text{PtD}) = 1530$  cm<sup>-1</sup>. Similarly was prepared the complex with R = 3,5-Me<sub>2</sub>C<sub>6</sub>H<sub>3</sub>. Yield: 58%. Anal. Calcd for C<sub>66</sub>H<sub>79</sub>F<sub>6</sub>P<sub>5</sub>Pt<sub>2</sub>: C, 51.76; H, 5.20. Found: C, 51.05; H, 5.06. IR (Nujol):  $\nu(\text{PtH}) = 2105$  cm<sup>-1</sup>. NMR in (CD<sub>3</sub>)<sub>2</sub>CO:  $\delta(^1\text{H}) = -6.81$  [dt,  $^1J(\text{PtH}) = 1132$  Hz,  $^2J(\text{PtH}) = 106$  Hz,  $^2J(\text{PH}) = 6$  Hz,  $^2J(\text{H}^b\text{H}^a) = 15$  Hz, PtH<sup>a</sup>],  $-6.10$  [m,  $^1J(\text{PtH}) = 544$  Hz, PtH<sup>b</sup>], 2.24 [s, Me], 4.51 [m,  $^3J(\text{PtH}) = 34$  Hz, CH<sub>2</sub>P<sub>2</sub>];  $\delta(^{31}\text{P}) = 19.63$  [s,  $^1J(\text{PtP}) = 2758$  Hz,  $^3J(\text{PtP}) = 10$  Hz,  $^2J(\text{PP}) = -29, 76$  Hz, dppm].

**[Pt<sub>4</sub>( $\mu_2$ -CO)<sub>2</sub>( $\mu_2$ -H)(R<sub>2</sub>PCH<sub>2</sub>PR<sub>2</sub>)<sub>4</sub>](PF<sub>6</sub>)<sub>2</sub>, R = 3,5-F<sub>2</sub>C<sub>6</sub>H<sub>3</sub>**. A mixture of [Pt(R<sub>2</sub>PCH<sub>2</sub>PR<sub>2</sub>)(O<sub>2</sub>CCF<sub>3</sub>)<sub>2</sub>], R = 3,5-F<sub>2</sub>C<sub>6</sub>H<sub>3</sub> (1.00 g, 1.05 mmol), MeOH (40 mL), and triple distilled H<sub>2</sub>O (4 mL) in a Parr pressure reactor (300 mL) was heated at 65 °C for 4 d under CO (20 atm). At 12 h intervals for the first 24 h and then at 24 h intervals for the remaining 72 h, a fresh CO atmosphere was introduced. The reactor was cooled to room temperature and opened. The reddish solution was filtered, and the filtrate was evaporated to dryness under vacuum. The red residue was dissolved in MeOH (5 mL), and to this solution was added dropwise a prefiltered solution of NH<sub>4</sub>PF<sub>6</sub> (1.40 g, 8.59 mmol) in MeOH (5 mL). After 4 h, the solution was

filtered and the filtrate was evaporated to dryness. The residue was then extracted with  $\text{CH}_2\text{Cl}_2$ , and the product was isolated by evaporation of the solvent as a red crystalline product. Yield: 82%. Anal. Calcd for  $\text{C}_{102}\text{H}_{55}\text{F}_{38}\text{O}_2\text{P}_9\text{Pt}_4$ : C, 39.57; H, 1.86. Found: C, 39.85; H, 1.92%. IR (Nujol):  $\nu(\text{CO}) = 1824$  (s),  $1784$  (s)  $\text{cm}^{-1}$ . NMR in  $(\text{CD}_3)_2\text{CO}$ :  $\delta(^1\text{H}) = 4.26$  [d, 3H,  $^2J(\text{HH}) = 13$  Hz,  $^3J(\text{PtH}) = 25$  Hz,  $\text{CH}^a\text{H}^b$  of  $\mu\text{-PP}$ ],  $4.24$  [d, 3H,  $^2J(\text{HH}) = 13$  Hz,  $^3J(\text{PtH}) = 25$  Hz,  $\text{CH}^a\text{H}^b$  of  $\mu\text{-PP}$ ],  $3.66$  [d, 2H,  $^2J(\text{PH}) = 11$  Hz,  $^3J(\text{PtH}) = 62$  Hz,  $\text{CH}_2$  of  $\eta^1\text{-PP}$ ],  $-7.2$  [quin, 1H,  $^1J(\text{PtH}) = 532$  Hz,  $^2J(\text{PtH}) = 32$  Hz,  $\text{HPt}_2$ ];  $\delta(^{31}\text{P}) = -22.6$  [s, 1P,  $^1J(\text{PtP}) = 4520$  Hz,  $^2J(\text{PtP}) = 166$  Hz],  $-12.5$  [s, 6P,  $^1J(\text{PtP}) = 3271$  Hz,  $^2J(\text{PtP}) = 206$  Hz,  $^3J(\text{PP}) = 200$  Hz],  $-21.9$  [d, 1P,  $^3J(\text{PtP}) = 80$  Hz].

Similarly were prepared the following complexes.  $\text{R} = 4\text{-MeC}_6\text{H}_4$ : yield 45%. Anal. Calcd for  $\text{C}_{118}\text{H}_{121}\text{F}_6\text{O}_2\text{P}_9\text{Pt}_4$ : C, 51.64; H, 4.44. Found: C, 51.77; H, 5.06. IR (Nujol):  $\nu(\text{CO}) = 1800$  (s),  $1757$  (s)  $\text{cm}^{-1}$ ,  $\nu(^{13}\text{CO}) = 1760$  (s),  $1725$  (s)  $\text{cm}^{-1}$ . NMR in  $(\text{CD}_3)_2\text{CO}$  at  $-40$  °C:  $\delta(^1\text{H}) = 4.82$ ,  $4.78$ ,  $3.93$ ,  $3.87$  [m,  $\text{CH}^a\text{H}^b$  of  $\mu\text{-PP}$ ],  $3.45$  [d, 2H,  $^2J(\text{PH}) = 10$  Hz,  $^3J(\text{PtH}) = 50$  Hz,  $\text{CH}_2$  of  $\mu\text{-PP}$ ],  $-7.9$  [m, 1H,  $^1J(\text{PtH}) = 672$  Hz,  $^2J(\text{PtH}) = 175$  Hz,  $\text{HPt}_2$ ];  $\delta(^{13}\text{C}) = 247.8$  [m,  $^1J(\text{PtC}) = 821$  Hz,  $403$  Hz,  $^2J(\text{PC}) = 19$ ,  $^{13}\text{CO}$ ];  $\delta(^{31}\text{P}) = -24.9$  [m, 1P,  $^1J(\text{PtP}) = 4520$  Hz,  $^2J(\text{PtP}) = 166$  Hz],  $-12.5$  [s, 6P,  $^1J(\text{PtP}) = 3271$  Hz,  $^2J(\text{PtP}) = 206$  Hz,  $^3J(\text{PP}) = 200$  Hz],  $-21.9$  [d, 1P,  $^3J(\text{PtP}) = 80$  Hz].

$\text{Pt}_3(\mu_3\text{-CO})(\mu_3\text{-I})(\mu\text{-R}_2\text{PCH}_2\text{PR}_2)_3[\text{PF}_6]_2$ ,  $\text{R} = 3,5\text{-Cl}_2\text{C}_6\text{H}_3$ . To a solution of  $[\text{Pt}_3(\mu_3\text{-CO})(\mu\text{-R}_2\text{PCH}_2\text{PR}_2)_3](\text{PF}_6)_2$  (40 mg, 0.014 mmol) in acetone (10 mL) was added MeI (0.20 mL, 3.21 mmol) via microsyringe. The orange solution darkened immediately. After 4 h,  $\text{NH}_4\text{PF}_6$  (10 mg) was added, the solution was stirred for another 10 min, and the solvent was removed under vacuum. The residue was extracted with  $\text{CH}_2\text{Cl}_2$  (10 mL), and the solvent was removed under vacuum to give the product as an orange solid, which was recrystallized from acetone/*n*-pentane. Yield: 94%. Anal. Calcd for  $\text{C}_{76}\text{H}_{42}\text{Cl}_{24}\text{F}_6\text{IOP}_7\text{Pt}_3$ : C, 31.86; H, 1.48. Found: C, 31.74; H, 1.63. IR (Nujol):  $\nu(\text{CO}) = 1785$  (s)  $\text{cm}^{-1}$ . NMR in  $(\text{CD}_3)_2\text{CO}$ :  $\delta(^1\text{H}) = 7.6\text{--}7.3$  [m,  $\text{C}_6\text{H}_3$ ],  $6.6$  [d,  $^2J(\text{HH}) = 14$  Hz,  $\text{CH}^a\text{H}^b$ ],  $5.6$  [d,  $^2J(\text{HH}) = 14$  Hz,  $\text{CH}^a\text{H}^b$ ];  $\delta(^{31}\text{P}) = -10.1$  [s,  $^1J(\text{PtP}) = 3989$  Hz,  $^2J(\text{PtP}) = 55$  Hz,  $^3J(\text{PP}) = 131$  Hz].

Similarly were prepared the following complexes.  $\text{R} = 3,5\text{-F}_2\text{C}_6\text{H}_3$ : yield 89%. Anal. Calcd for  $\text{C}_{76}\text{H}_{42}\text{F}_{30}\text{IOP}_7\text{Pt}_3$ : C, 36.96; H, 1.71. Found: C, 36.99; H, 1.80. IR (Nujol):  $\nu(\text{CO}) = 1788$  (s)  $\text{cm}^{-1}$ . NMR in  $(\text{CD}_3)_2\text{CO}$ :  $\delta(^1\text{H}) = 7.2\text{--}7.1$  [m,  $\text{C}_6\text{H}_3$ ],  $6.6$  [d,  $^2J(\text{HH}) = 13.8$  Hz,  $\text{CH}^a\text{H}^b$ ],  $5.9$  [d,  $^2J(\text{HH}) = 13.8$  Hz,  $\text{CH}^a\text{H}^b$ ];  $\delta(^{31}\text{P}) = -8.5$  [s,  $^1J(\text{PtP}) = 3961$  Hz,  $^2J(\text{PtP}) = 28$  Hz,  $^3J(\text{PP}) = 168$  Hz, dppm].  $\text{R} = 4\text{-MeC}_6\text{H}_4$ : yield 93%. Anal. Calcd for  $\text{C}_{88}\text{H}_{90}\text{F}_6\text{IOP}_7\text{Pt}_3\cdot 2\text{Me}_2\text{CO}$ : C, 48.61; H, 4.43. Found: C, 48.89; H, 4.91. IR (Nujol):  $\nu(\text{CO}) = 1757$  (s)  $\text{cm}^{-1}$ . NMR in  $(\text{CD}_3)_2\text{CO}$ :  $\delta(^1\text{H}) = 7.2\text{--}6.9$  [m,  $\text{C}_6\text{H}_4$ ],  $5.77$  [d,  $^2J(\text{HH}) = 13$  Hz,  $\text{CH}^a\text{H}^b$ ],  $5.23$  [d,  $^2J(\text{HH}) = 13$  Hz,  $\text{CH}^a\text{H}^b$ ],  $2.20$ ,  $2.23$  [s, Me];  $\delta(^{31}\text{P}) = -16.1$  [s,  $^1J(\text{PtP}) = 3902$  Hz,  $^2J(\text{PtP}) = -28$  Hz,  $^3J(\text{PP}) = 160$  Hz, dppm].  $\text{R} = 3\text{-MeC}_6\text{H}_4$ : yield 75%. Anal. Calcd for  $\text{C}_{88}\text{H}_{90}\text{F}_6\text{IOP}_7\text{Pt}_3\cdot 2\text{Me}_2\text{CO}$ : C, 48.61; H, 4.43. Found: C, 48.20; H, 4.23. IR (Nujol):  $\nu(\text{CO}) = 1757$  (s)  $\text{cm}^{-1}$ . NMR in  $(\text{CD}_3)_2\text{CO}$ :  $\delta(^1\text{H}) = 7.2\text{--}6.95$  [m,  $\text{C}_6\text{H}_4$ ],  $5.81$  [d,  $^2J(\text{HH}) = 14$  Hz,  $\text{CH}^a\text{H}^b$ ],  $5.36$  [d,  $^2J(\text{HH}) = 14$  Hz,  $\text{CH}^a\text{H}^b$ ],  $2.09$ ,  $2.03$  [s, Me];  $\delta(^{31}\text{P}) = -15.4$  [s,  $^1J(\text{PtP}) = 3889$  Hz,  $^2J(\text{PtP}) = -30$  Hz,  $^3J(\text{PP}) = 162$  Hz, dppm].  $\text{R} = 3,5\text{-Me}_2\text{C}_6\text{H}_3$ : yield 99% from  $\text{CH}_2\text{Cl}_2$ . Anal. Calcd for  $\text{C}_{100}\text{H}_{114}\text{F}_6\text{IOP}_7\text{Pt}_3$ : C, 49.32; H, 4.75. Found: C, 49.03; H, 5.19. IR (Nujol):  $\nu(\text{CO}) = 1757$  (s)  $\text{cm}^{-1}$ . NMR in  $(\text{CD}_3)_2\text{CO}$ :  $\delta(^1\text{H}) = 7.6\text{--}6.8$  [m,  $\text{C}_6\text{H}_3$ ],  $5.66$  [d,  $^2J(\text{HH}) = 14$  Hz,  $\text{CH}^a\text{H}^b$ ],  $5.20$  [d,  $^2J(\text{HH}) = 14$  Hz,  $\text{CH}^a\text{H}^b$ ],  $2.03$ ,  $1.98$  [s, Me];  $\delta(^{31}\text{P}) = -16.0$  [s,  $^1J(\text{PtP}) = 3893$  Hz,  $^2J(\text{PtP}) = -27$  Hz,  $^3J(\text{PP}) = 162$  Hz, dppm].

$[\text{Pt}_3(\mu_3\text{-CO})(\text{SCN})(\mu\text{-R}_2\text{PCH}_2\text{PR}_2)_3][\text{PF}_6]_2$ ,  $\text{R} = 3,5\text{-Cl}_2\text{C}_6\text{H}_3$ . To a solution of  $[\text{Pt}_3(\mu_3\text{-CO})(\mu\text{-R}_2\text{PCH}_2\text{PR}_2)_3](\text{PF}_6)_2$  (50 mg, 0.017 mmol) in acetone (10 mL) was added  $\text{KSCN}$  (8.4 mg, 0.087 mmol). An immediate color change to orange-red occurred. The mixture was stirred for 4 h and then  $\text{NH}_4\text{PF}_6$  (10 mg) was added and stirred for another 10 min. The solvent was evaporated under vacuum, the residue was extracted with  $\text{CH}_2\text{Cl}_2$  (15 mL), and the  $\text{CH}_2\text{Cl}_2$  was evaporated to give the product as a red solid which was recrystallized from acetone/*n*-

*n*-pentane. Yield: 92%. Anal. Calcd for  $\text{C}_{77}\text{H}_{42}\text{Cl}_{24}\text{F}_6\text{NOP}_7\text{Pt}_3\text{S}$ : C, 33.08; H, 1.51. Found: C, 33.48; H, 1.72. IR (Nujol):  $\nu(\text{CN}) = 2089$  (s),  $2065$  (sh),  $\nu(\text{CO}) = 1786$  (s)  $\text{cm}^{-1}$ . NMR in  $(\text{CD}_3)_2\text{CO}$ :  $\delta(^1\text{H}) = 7.6\text{--}7.3$  [m,  $\text{C}_6\text{H}_3$ ],  $6.6$  [d,  $^2J(\text{HH}) = 12.5$  Hz,  $\text{CH}^a\text{H}^b$ ],  $5.9$  [d,  $^2J(\text{HH}) = 12.5$  Hz,  $\text{CH}^a\text{H}^b$ ];  $\delta(^{31}\text{P}) = -10.4$  [s,  $^1J(\text{PtP}) = 3670$  Hz,  $^2J(\text{PtP}) = 9$  Hz,  $^3J(\text{PP}) = 164$  Hz, dppm].

Similarly were prepared the following complexes.  $\text{R} = 3,5\text{-F}_2\text{C}_6\text{H}_3$ : yield 90%. Anal. Calcd for  $\text{C}_{77}\text{H}_{42}\text{F}_{30}\text{NOP}_7\text{Pt}_3\text{S}$ : C, 38.51; H, 1.76. Found: C, 38.97; H, 1.85. IR (Nujol):  $\nu(\text{CN}) = 2083$  (sh),  $2053$  (s),  $\nu(\text{CO}) = 1782$  (s)  $\text{cm}^{-1}$ . NMR in  $(\text{CD}_3)_2\text{CO}$ :  $\delta(^1\text{H}) = 7.3\text{--}7.0$  [m,  $\text{C}_6\text{H}_3$ ],  $6.5$  [d,  $^2J(\text{HH}) = 13.9$  Hz,  $\text{CH}^a\text{H}^b$ ],  $5.9$  [d,  $^2J(\text{HH}) = 13.9$  Hz,  $\text{CH}^a\text{H}^b$ ];  $\delta(^{31}\text{P}) = -10.5$  [s,  $^1J(\text{PtP}) = 3691$  Hz,  $^2J(\text{PtP}) = 4$  Hz,  $^3J(\text{PP}) = 168$  Hz, dppm].  $\text{R} = 3,5\text{-Me}_2\text{C}_6\text{H}_3$ : yield 93%. Anal. Calcd for  $\text{C}_{102}\text{H}_{114}\text{F}_6\text{NOP}_7\text{Pt}_3\text{S}$ : C, 52.60; H, 4.98. Found: C, 52.11; H, 5.15. IR (Nujol):  $\nu(\text{CN}) = 2080$  (sh),  $2053$  (s),  $\nu(\text{CO}) = 1752$  (s)  $\text{cm}^{-1}$ . NMR in  $(\text{CD}_3)_2\text{CO}$ :  $\delta(^1\text{H}) = 7.6\text{--}6.8$  [m,  $\text{C}_6\text{H}_3$ ],  $5.49$  [d,  $^2J(\text{HH}) = 12$  Hz,  $\text{CH}^a\text{H}^b$ ],  $5.35$  [d,  $^2J(\text{HH}) = 12$  Hz,  $\text{CH}^a\text{H}^b$ ],  $2.02$ ,  $1.98$  [s, Me];  $\delta(^{31}\text{P}) = -16.0$  [s,  $^1J(\text{PtP}) = 3656$  Hz,  $^2J(\text{PtP}) = -1$  Hz,  $^3J(\text{PP}) = 166$  Hz, dppm].

$\text{Pt}_3(\mu_3\text{-CO})(\text{P}(\text{O}Ph)_3)(\mu\text{-R}_2\text{PCH}_2\text{PR}_2)_3[\text{PF}_6]_2$ ,  $\text{R} = 3,5\text{-F}_2\text{C}_6\text{H}_3$ . To a solution of  $[\text{Pt}_3(\mu_3\text{-CO})(\mu\text{-R}_2\text{PCH}_2\text{PR}_2)_3][\text{PF}_6]_2$ ,  $\text{R} = 3,5\text{-F}_2\text{C}_6\text{H}_3$  (38 mg, 0.015 mmol), in  $(\text{CD}_3)_2\text{CO}$  (0.5 mL) in an NMR tube was added  $\text{P}(\text{O}Ph)_3$  (0.8  $\mu\text{L}$ , 0.030 mmol) via microsyringe at  $-78$  °C. Upon mixing, the solution changed from orange to orange red. The product was characterized spectroscopically at temperatures below  $-40$  °C. At temperatures from 0 to 25 °C, only starting materials were observed in solution by NMR. NMR spectra in  $(\text{CD}_3)_2\text{CO}$  at  $-90$  °C:  $\delta(^1\text{H}) = 5.80$  [m,  $\text{CH}^a\text{H}^b$ ],  $5.20$  [m,  $\text{CH}^a\text{H}^b$ ];  $\delta(^{31}\text{P}) = 88.8$  [t,  $1\text{P}^x$ ,  $^1J(\text{PtP}) = 5362$  Hz,  $^2J(\text{PtP}) = 525$  Hz],  $\delta = -0.03$  [s,  $2\text{P}^b$ ,  $^1J(\text{PtP}) = 3142$  Hz,  $^3J(\text{P}^b\text{P}^b) = 154$  Hz],  $-2.8$  [d,  $2\text{P}^a$ ,  $^1J(\text{PtP}) = 3896$  Hz,  $^3J(\text{P}^a\text{P}^a) = 177$  Hz],  $-28.4$  [d,  $2\text{P}^c$ ,  $^1J(\text{PtP}) = 2520$  Hz,  $^3J(\text{P}^a\text{P}^c) = 177$  Hz]. NMR at  $-60$  °C:  $\delta(^1\text{H}) = 5.84$  [m,  $\text{CH}^a\text{H}^b$ ],  $5.20$  [m,  $\text{CH}^a\text{H}^b$ ];  $\delta(^{31}\text{P}) = 88.8$  [t,  $1\text{P}^x$ ,  $^1J(\text{PtP}) = 5362$  Hz,  $^2J(\text{PtP}) = 525$  Hz],  $-0.15$  [s,  $2\text{P}^b$ ,  $^1J(\text{PtP}) = 3126$  Hz,  $^3J(\text{P}^b\text{P}^b) = 145$  Hz],  $-2.9$  [d,  $2\text{P}^a$ ,  $^1J(\text{PtP}) = 3894$  Hz,  $^3J(\text{P}^a\text{P}^c) = 177$  Hz],  $-28.8$  [d,  $2\text{P}^c$ ,  $^1J(\text{PtP}) = 2520$  Hz,  $^3J(\text{P}^a\text{P}^c) = 177$  Hz].

**Reaction of  $[\text{Pt}_3(\mu_3\text{-CO})(\mu\text{-R}_2\text{PCH}_2\text{PR}_2)_3](\text{PF}_6)_2$ ,  $\text{R} = 3,5\text{-Cl}_2\text{C}_6\text{H}_3$ , with  $\text{P}(\text{O}Ph)_3$ .** The same procedure as above was applied to the reaction of  $[\text{Pt}_3(\mu_3\text{-CO})(\mu\text{-R}_2\text{PCH}_2\text{PR}_2)_3](\text{PF}_6)_2$ ,  $\text{R} = 3,5\text{-Cl}_2\text{C}_6\text{H}_3$ , with  $\text{P}(\text{O}Ph)_3$ .  $^{31}\text{P}\{^1\text{H}\}$  NMR results showed only the existence of starting materials at temperatures between  $-90$  to 20 °C.

**Reactions with  $\text{P}(\text{Ph})_3$ .** Reaction of  $[\text{Pt}_3(\mu_3\text{-CO})(\mu\text{-R}_2\text{PCH}_2\text{PR}_2)_3](\text{PF}_6)_2$ ,  $\text{R} = 3,5\text{-F}_2\text{C}_6\text{H}_3$  or  $3,5\text{-Cl}_2\text{C}_6\text{H}_3$ , with  $\text{PPh}_3$  was studied as above. No reaction was detected at temperatures between  $-90$  and 20 °C according to NMR measurements.

$[\text{Pt}_3(\mu_3\text{-CO})(\text{P}(\text{OMe})_3)(\mu\text{-R}_2\text{PCH}_2\text{PR}_2)_3][\text{O}_2\text{CCF}_3]_2$ ,  $\text{R} = 3,5\text{-Cl}_2\text{C}_6\text{H}_3$ . To a solution of  $[\text{Pt}_3(\mu_3\text{-CO})(\mu\text{-R}_2\text{PCH}_2\text{PR}_2)_3](\text{O}_2\text{CCF}_3)_2$ ,  $\text{R} = 3,5\text{-Cl}_2\text{C}_6\text{H}_3$  (22 mg, 0.008 mmol), in  $(\text{CD}_3)_2\text{CO}$  (0.5 mL) in an NMR tube was added  $\text{P}(\text{OMe})_3$  (0.95  $\mu\text{L}$ , 0.008 mmol) via microsyringe at  $-78$  °C. Upon mixing, the solution changed from orange yellow to orange red. The product was characterized spectroscopically at temperatures below 60 °C. NMR spectra in  $(\text{CD}_3)_2\text{CO}$  at  $-90$  °C:  $\delta(^1\text{H}) = 5.62$  [br,  $\text{CH}^a\text{H}^b$ ],  $5.00$  [br,  $\text{CH}^a\text{H}^b$ ],  $3.95$  [m,  $\text{P}(\text{OCH}_2)_3$ ];  $\delta(^{31}\text{P}) = 100.9$  [t,  $1\text{P}^x$ ,  $^1J(\text{PtP}) = 4900$  Hz,  $^2J(\text{PtP}) = 460$  Hz],  $-1.1$  [s,  $2\text{P}^b$ ,  $^1J(\text{PtP}) = 3106$  Hz,  $^3J(\text{P}^b\text{P}^b) = 135$  Hz],  $-3.8$  [d,  $2\text{P}^a$ ,  $^1J(\text{PtP}) = 3929$  Hz,  $^3J(\text{P}^a\text{P}^c) = 172$  Hz],  $-28.5$  [d,  $2\text{P}^c$ ,  $^1J(\text{PtP}) = 2503$  Hz,  $^3J(\text{P}^a\text{P}^c) = 172$  Hz]. NMR at  $-60$  °C:  $\delta(^1\text{H}) = 5.58$  [br,  $\text{CH}^a\text{H}^b$ ],  $5.04$  [br,  $\text{CH}^a\text{H}^b$ ],  $4.00$  [m,  $\text{P}(\text{OCH}_2)_3$ ];  $\delta(^{31}\text{P}) = 100.7$  [t,  $1\text{P}^x$ ,  $^1J(\text{PtP}) = 4938$  Hz,  $^2J(\text{PtP}) = 452$  Hz],  $-1.6$  [s,  $2\text{P}^b$ ,  $^1J(\text{PtP}) = 3070$  Hz,  $^3J(\text{P}^b\text{P}^b) = 129$  Hz],  $-3.6$  [d,  $2\text{P}^a$ ,  $^1J(\text{PtP}) = 3946$  Hz,  $^3J(\text{P}^a\text{P}^c) = 174$  Hz],  $-28.7$  [d,  $2\text{P}^c$ ,  $^1J(\text{PtP}) = 2482$  Hz,  $^3J(\text{P}^a\text{P}^c) = 174$  Hz].

Similarly,  $[\text{Pt}_3(\mu_3\text{-CO})(\text{P}(\text{OMe})_3)(\mu\text{-R}_2\text{PCH}_2\text{PR}_2)_3][\text{PF}_6]_2$ ,  $\text{R} = 3,5\text{-F}_2\text{C}_6\text{H}_3$ , was prepared in solution by reaction of  $[\text{Pt}_3(\mu_3\text{-CO})(\mu\text{-R}_2\text{PCH}_2\text{PR}_2)_3][\text{PF}_6]_2$ ,  $\text{R} = 3,5\text{-F}_2\text{C}_6\text{H}_3$  (20 mg, 0.008 mmol), with  $\text{P}(\text{OMe})_3$  (0.95  $\mu\text{L}$ , 0.008 mmol) at  $-78$  °C. Compound **6b** was characterized spectroscopically at temper-

**Table 5. Crystal Data and Experimental Details for the Compound**

**[Pt<sub>3</sub>(R<sub>2</sub>PCH<sub>2</sub>PR<sub>2</sub>)<sub>3</sub>(μ<sub>3</sub>-CO)(O<sub>2</sub>CCF<sub>3</sub>)<sub>3</sub>-(CF<sub>3</sub>CO<sub>2</sub>)-0.5CH<sub>2</sub>Cl<sub>2</sub>·1.5H<sub>2</sub>O, R = 3,5-Cl<sub>2</sub>C<sub>6</sub>H<sub>3</sub>, 4e**

formula	C <sub>80</sub> H <sub>42</sub> Cl <sub>24</sub> F <sub>6</sub> O <sub>5</sub> P <sub>6</sub> Pt <sub>3</sub> ·0.5CH <sub>2</sub> Cl <sub>2</sub> ·1.5H <sub>2</sub> O
fw	2888.64
cryst system,	monoclinic, <i>P</i> 2 <sub>1</sub> / <i>n</i>
space group	
cell dimens	<i>a</i> = 23.365(4) Å <i>b</i> = 24.599(4) Å <i>c</i> = 19.141(7) Å <i>β</i> = 102.44(2)°
cell vol (Å <sup>3</sup> ), <i>Z</i>	10743(5), 4
density (gcm <sup>-3</sup> ):	1.76(5), 1.786
obsd, calcd	
radiation,	Mo Kα, 0.710 73
wavelength (Å)	
abs coeff (cm <sup>-1</sup> )	44.5
<i>R</i> <sup>a</sup>	0.0727

$$^a R = \sum (|F_o| - |F_c|) / \sum |F_o|.$$

atures below 40 °C. NMR in (CD<sub>3</sub>)<sub>2</sub>CO at -90 °C: δ(<sup>1</sup>H) = 6.28 [br, CH<sup>a</sup>H<sup>b</sup>], 5.02 [br, CH<sup>a</sup>H<sup>b</sup>], 3.90 [m, P(OCH<sub>2</sub>)<sub>3</sub>]; δ(<sup>31</sup>P) = 101.7 [t, 1P<sup>x</sup>, <sup>1</sup>*J*(PtP) = 4951 Hz, <sup>2</sup>*J*(PtP) = 414 Hz], -1.2 [s, 2P<sup>b</sup>, <sup>1</sup>*J*(PtP) = 3174 Hz, <sup>3</sup>*J*(P<sup>b</sup>P<sup>b</sup>) = 161], -3.1 [d, 2P<sup>a</sup>, <sup>1</sup>*J*(PtP) = 4032 Hz, <sup>3</sup>*J*(P<sup>a</sup>P<sup>c</sup>) = 168 Hz], -26.8 [d, 2P<sup>c</sup>, <sup>1</sup>*J*(PtP) = 2639 Hz, <sup>3</sup>*J*(P<sup>a</sup>P<sup>c</sup>) = 168 Hz]. NMR at -60 °C: δ(<sup>1</sup>H) = 6.27 [br, CH<sup>a</sup>H<sup>b</sup>], 5.01 [m, CH<sup>a</sup>H<sup>b</sup>], 3.93 [m, P(OCH<sub>2</sub>)<sub>3</sub>]; δ(<sup>31</sup>P) = 101.3 [t, 1P<sup>x</sup>, <sup>1</sup>*J*(PtP) = 4923 Hz, <sup>2</sup>*J*(PtP) = 424 Hz], -1.0 [s, 2P<sup>b</sup>, <sup>1</sup>*J*(PtP) = 3142 Hz, <sup>3</sup>*J*(P<sup>b</sup>P<sup>b</sup>) = 149 Hz], -2.9 [d, 2P<sup>a</sup>, <sup>1</sup>*J*(PtP) = 4050 Hz, <sup>3</sup>*J*(P<sup>a</sup>P<sup>c</sup>) = 169 Hz], -27.0 [d, 2P<sup>c</sup>, <sup>1</sup>*J*(PtP) = 2638 Hz, <sup>3</sup>*J*(P<sup>a</sup>P<sup>c</sup>) = 169 Hz]. <sup>31</sup>P NMR measurement at ambient temperature showed two broad peaks at -3 and -28 ppm. The product could not be isolated as a pure solid due to its thermal instability.

Similarly addition of PMePh<sub>2</sub> gave the following adducts. R = 3,5-Me<sub>2</sub>C<sub>6</sub>H<sub>3</sub>: NMR in CD<sub>2</sub>Cl<sub>2</sub> at -80 °C δ(<sup>31</sup>P) = -12.4 [t, 1P<sup>x</sup>, <sup>1</sup>*J*(PtP) = 2880 Hz], -15.9 [s, 2P<sup>b</sup>, <sup>1</sup>*J*(PtP) = 3300 Hz, <sup>3</sup>*J*(P<sup>b</sup>P<sup>b</sup>) = 140], -45.4 [d, 2P<sup>a</sup>, <sup>1</sup>*J*(PtP) = 2620 Hz, <sup>3</sup>*J*(P<sup>a</sup>P<sup>c</sup>) = 180 Hz], -15.5 [d, 2P<sup>c</sup>, <sup>1</sup>*J*(PtP) = 3720 Hz, <sup>3</sup>*J*(P<sup>a</sup>P<sup>c</sup>) = 180 Hz]. R = 3-MeC<sub>6</sub>H<sub>4</sub>: NMR in CD<sub>2</sub>Cl<sub>2</sub> at -80 °C δ(<sup>31</sup>P) = -9.1 [t, 1P, <sup>1</sup>*J*(PtP) = 2700 Hz, PMePh<sub>2</sub>], -15.0 [s, 2P<sup>b</sup>, <sup>1</sup>*J*(PtP) = 3300 Hz, <sup>3</sup>*J*(P<sup>b</sup>P<sup>b</sup>) = 140], -43.0 [d, 2P<sup>a</sup>, <sup>1</sup>*J*(PtP) = 2670 Hz, <sup>3</sup>*J*(P<sup>a</sup>P<sup>c</sup>) = 180 Hz], -15.1 [d, 2P<sup>c</sup>, <sup>1</sup>*J*(PtP) = 3760 Hz, <sup>3</sup>*J*(P<sup>a</sup>P<sup>c</sup>) = 180 Hz]. R = 4-MeC<sub>6</sub>H<sub>4</sub>: NMR in CD<sub>2</sub>Cl<sub>2</sub> at -80 °C δ(<sup>31</sup>P) = -21.9 [t, 1P, <sup>1</sup>*J*(PtP) = 2720 Hz, PMePh<sub>2</sub>], -13.6 [s, 2P<sup>b</sup>, <sup>1</sup>*J*(PtP) = 3200 Hz, <sup>3</sup>*J*(P<sup>b</sup>P<sup>b</sup>) = 150 Hz], -40.1 [d, 2P<sup>a</sup>, <sup>1</sup>*J*(PtP) = 2600 Hz, <sup>3</sup>*J*(P<sup>a</sup>P<sup>c</sup>) = 185 Hz], -14.2 [d, 2P<sup>c</sup>, <sup>1</sup>*J*(PtP) = 3800 Hz, <sup>3</sup>*J*(P<sup>a</sup>P<sup>c</sup>) = 185 Hz].

**X-ray Crystallography.** Orange-yellow, rodlike crystals of **4e**(CF<sub>3</sub>CO<sub>2</sub>) were grown with difficulty from CH<sub>2</sub>Cl<sub>2</sub>/Et<sub>2</sub>O. Data were collected at -50 °C, since solvent loss and crystal decay occurred at room temperature, by using an Enraf-Nonius CAD4F diffractometer<sup>17</sup> with graphite-monochromated Mo Kα radiation. Photo and automatic indexing routines, followed by least-squares fits of 21 automatically centered reflections (24.5 ≤ 2θ ≤ 31.3°), gave cell constants and an orientation matrix. The Niggli matrix suggested the monoclinic system with symmetry 2/*m*, and this was confirmed from an inspection of equivalent reflections. Intensity data were recorded in ω-2θ mode, at variable scan speeds (2.06-4.12 degmin<sup>-1</sup>) and a scan width of 1.0 + 0.35 tan θ, with a maximum time per datum of 45 s. Background measurements were made by extending the scan by 25% on each side. Three standard reflections were monitored every 120 min of X-ray exposure time, and orientation checks were done for every 250 reflections measured. There were 15 859 reflections in the 2θ range 0-45° (-25 ≤ *h*

≤ 25, -26 ≤ *k* ≤ 1, -20 ≤ *l* ≤ 1), and 90 repetitions of the standards were recorded. Corrections were made for Lorentz, monochromator and crystal polarization, background radiation effects, and decay using the NRCVAX crystal structure programs<sup>18</sup> running on a SUN 3/80 workstation. The data crystal had six faces which were indexed, and the distances between them were measured for absorption (μ = 44.5 cm<sup>-1</sup>). A Gaussian absorption correction was applied using the program "ABSO"; the maximum and minimum transmission values were 0.5266 and 0.4256. There were 14 042 independent reflections of which 6792 were considered observed (for *I* ≥ 2.5σ(*I*)). The systematic absences<sup>19</sup> indicated that the space group was *P*2<sub>1</sub>/*n*, and the correctness of the choice of the space group was confirmed by successful solution and refinement of the structure. The positions of the heavy atoms were determined by using the program SHELXS-86,<sup>20</sup> and the remaining atoms were located by subsequent difference Fourier techniques. Initial least-squares refinements were performed using SHELX-76,<sup>21</sup> and final full-matrix least-squares refinements on *F*<sup>2</sup> using SHELXL-93.<sup>22</sup> Anisotropic thermal parameters were assigned and refined for all the Pt, P, Cl, and the F atoms in the cation. The phenyl ring carbon atoms were treated as regular hexagons with *d*(C-C) = 1.390 Å, and their individual isotropic thermal parameters were refined in the least-squares cycles. The hydrogen atoms were placed in ideal calculated positions (*d*(C-H) = 0.97 and 0.93 Å for methylene and phenyl groups, respectively). Of the two trifluoroacetate groups one was found to be a part of the cation. Two fragments of the other trifluoroacetate anion were successfully located, and their occupancy factors were refined to 0.55 and 0.45. The trifluoroacetate groups were constrained to have equivalent C-F, C-C, and C-O bonds of equal length. A common isotropic thermal parameter was refined for the F atoms and for the CCO<sub>2</sub> group. A half-molecule of disordered dichloromethane was located, and the occupancy factors were assigned by comparing with the electron densities of other peaks in the difference Fourier. Three peaks found in the electron density maps were assigned as oxygen atoms of water molecules. No hydrogen atoms were included for these solvent molecules. The model converged to *R* = 0.0727 for 6958 data with *F*<sub>o</sub> > 4σ(*F*<sub>o</sub>). The maximum shift = 0.037 Å for C(11) and the maximum *dU* = 0.012 for F(3). Tables of crystal data, positional and thermal parameters, anisotropic thermal parameters, hydrogen atom positional parameters, selected weighted least-squares planes, and dihedral angles have been included in the depository materials.

**Acknowledgment.** We thank the NSERC (Canada) for financial support and Dr. N. C. Payne for access to X-ray facilities.

**Supplementary Material Available:** Tables of crystallographic experimental details, fractional coordinates and *B*<sub>iso</sub> values, bond distances and angles, anisotropic thermal parameters, hydrogen coordinates, and least-squares planes and dihedral angles (15 pages). Ordering information is given on any current masthead page.

OM950042+

(18) Gabe, E. J.; Le Page, Y.; Charland, J.-P.; Lee, F. C. *J. Appl. Crystallogr.* **1989**, *22*, 384.

(19) *International Tables for X-ray Crystallography*; D. Reidel Publishing Co.: Boston, MA, 1983; Vol. A.

(20) Sheldrick, G. M. SHELX-86. *Acta Crystallogr.* **1990**, *A46*, 467.

(21) Sheldrick, G. M. SHELX-76. University of Cambridge, England, 1976.

(22) Sheldrick, G. M. SHELXL-93. Inst. Anorg. Chem., Göttingen, Germany, 1993.

(17) *CAD4 Diffractometer Manual*; Enraf-Nonius: Delft, The Netherlands, 1988.

# Synthesis and Photochemistry of the Supramolecular $(\text{Cp}^{\text{A}})_2\text{Mo}_2(\text{CO})_6$ Complex ( $\text{Cp}^{\text{A}} = \eta^5\text{-C}_5\text{H}_4\text{CH}_2\text{CH}_2\text{NHC(O)-C}_{14}\text{H}_7\text{O}_2$ ; $\text{C}_{14}\text{H}_7\text{O}_2 = 2\text{-Anthraquinonyl}$ ). Reactivity of 19-Electron Complexes Covalently Bound to an Electron Acceptor

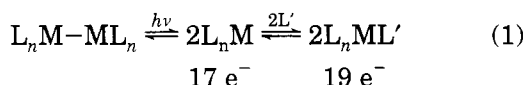
Alfred Avey, Gregory F. Nieckarz, Keith Keana, and David R. Tyler\*

Department of Chemistry, University of Oregon, Eugene, Oregon 97403

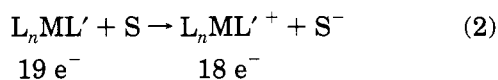
Received January 9, 1995<sup>®</sup>

The synthesis and photochemistry of the anthraquinone-derivatized  $(\text{Cp}^{\text{A}})_2\text{Mo}_2(\text{CO})_6$  molecule are described ( $\text{Cp}^{\text{A}} = \eta^5\text{-C}_5\text{H}_4\text{CH}_2\text{CH}_2\text{NHC(O)-C}_{14}\text{H}_7\text{O}_2$ ;  $\text{C}_{14}\text{H}_7\text{O}_2 = 2\text{-anthraquinonyl}$ ). The purpose of the attached anthraquinone is to act as an internal electron acceptor for 19-electron adducts generated from  $\text{Cp}_2\text{Mo}_2(\text{CO})_6$ . Such species may be useful in schemes for recycling the 19-electron adducts. Irradiation of the complex with low-energy light ( $\lambda > 525 \text{ nm}$ ) results in homolysis of the Mo-Mo bond. The resulting radicals can be trapped with  $\text{CCl}_4$  or TMIO (TMIO is the nitroxide radical trap 1,1,3,3-tetramethylisindoline-2-oxyl) or they can react with phosphine ligands to give net disproportionation reactions. The occurrence of disproportionation strongly suggests that the radicals react with phosphines to form 19-electron adducts. Although exogenous anthraquinone will inhibit disproportionation of the unsubstituted  $\text{Cp}_2\text{Mo}_2(\text{CO})_6$  dimer, disproportionation of  $(\text{Cp}^{\text{A}})_2\text{Mo}_2(\text{CO})_6$  occurs because  $(\text{Cp}^{\text{A}})^-(\text{Cp}^{\text{A}})\text{Mo}_2(\text{CO})_6$ , a key intermediate in the reaction, is photochemically fragmented to form  $(\text{Cp}^{\text{A}})\text{Mo}(\text{CO})_3^-$  and  $\text{Cp}^{\text{A}}\text{Mo}(\text{CO})_3$ . This reaction was demonstrated by independently generating  $(\text{Cp}^{\text{A}})^-(\text{Cp}^{\text{A}})\text{Mo}_2(\text{CO})_6$  and showing that it quickly fragmented when irradiated with visible light ( $\lambda > 525 \text{ nm}$ ). A scheme is proposed and tested for recycling 19-electron complexes generated photochemically from  $(\text{Cp}^{\text{A}})_2\text{Mo}_2(\text{CO})_6$ ; however, the scheme did not work. The net reaction in the proposed recycling scheme is thermodynamically uphill; a facile photochemical back-reaction pathway is one likely reason no net reaction is observed.

Nineteen-electron organometallic adducts, formed in the reactions of 17-electron radicals with 2-electron donors (eq 1), are important intermediates in many



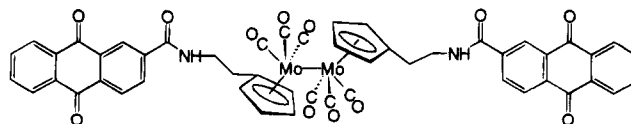
reactions.<sup>1</sup> The 19-electron adducts are powerful reductants, and their primary reactivity is electron transfer to reducible substrates:<sup>1</sup>



S = a reducible substrate

If reactions could be found that regenerated the 19-electron complexes, these electron transfer reactions

might be useful in catalytic redox reactions. However, viable methods for regenerating the 19-electron complexes are not readily apparent. One possible recycling scheme is presented in this paper. As explained in more detail below, the key to the proposed recycling scheme is to increase the lifetimes of the 19-electron adducts by shuttling the unpaired electron onto a ligand. For that reason we decided to synthesize the  $(\text{Cp}^{\text{A}})_2\text{Mo}_2(\text{CO})_6$  molecule ( $\text{Cp}^{\text{A}} = \eta^5\text{-C}_5\text{H}_4\text{CH}_2\text{CH}_2\text{NHC(O)-C}_{14}\text{H}_7\text{O}_2$ ;  $\text{C}_{14}\text{H}_7\text{O}_2 = 2\text{-anthraquinonyl}$ ), in which the anthraquinone is the attached electron acceptor.



The strategy of using rapid inner-sphere electron transfer to stabilize 19-electron adducts is a modification of the strategy used to synthesize  $18 + \delta$  complexes.<sup>2,3</sup> These latter complexes are 19-electron adducts in which the unpaired electron also occupies a ligand orbital. (These molecules are also called "radical anion ligand complexes".<sup>2</sup>) An example is the  $\text{Co}(\text{CO})_3\text{L}_2$  complex,

(2) Kaim, W. *Coord. Chem. Rev.* **1987**, *76*, 187.

(3) (a) Mao, F.; Tyler, D. R.; Bruce, M. R. M.; Bruce, A. E.; Rieger, A. L.; Rieger, P. H. *J. Am. Chem. Soc.* **1992**, *114*, 6418. (b) Mao, F.; Tyler, D. R.; Keszler, D. *J. Am. Chem. Soc.* **1989**, *111*, 130-134. (c) Fenske, D. *Chem. Ber.* **1979**, *112*, 363-375.

<sup>®</sup> Abstract published in *Advance ACS Abstracts*, May 1, 1995.

(1) (a) Tyler, D. R.; *Acc. Chem. Res.* **1991**, *24*, 325. (b) The adducts that form in the reactions of 17-electron species with ligands are known in the literature as "19-electron adducts" (or "19-electron complexes") simply because the sum of 17 valence electrons from the metal radical and the 2 electrons from the ligand is 19. No implication about the electronic or geometric structures of these complexes is necessarily implied by this name. "Slipped" Cp rings, bent CO ligands, (i.e., CO acting as a 1-electron donor), and phosphoranyl radical-type structures are all possible and would result in an 18- or 17-electron configuration at the metal center. Further details are found in ref 1a.

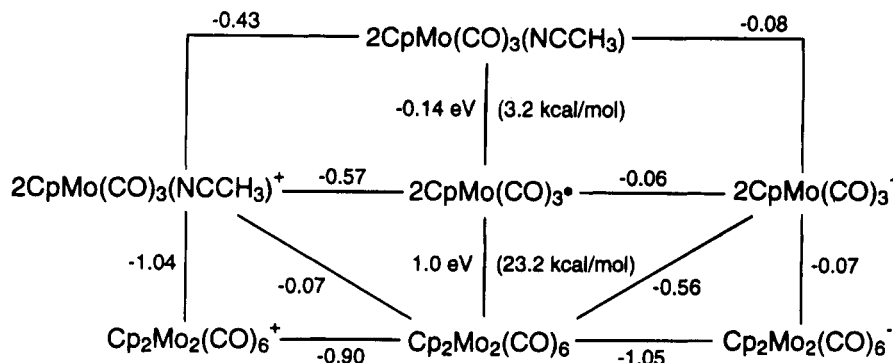
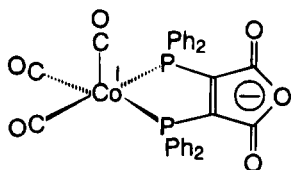


**Figure 1.** Latimer diagram for  $\text{Cp}_2\text{Mo}_2(\text{CO})_6$  including the 19-electron complex  $\text{CpMo}(\text{CO})_3(\text{NCCH}_3)$ . This diagram is based on the Latimer diagram in ref 4.

where  $\text{L}_2$  is the chelating 2,3-bis(diphenylphosphino)-maleic anhydride ligand; although this is nominally a  $\text{Co}(0)$  complex, EPR studies showed that the unpaired electron is localized on the  $\text{L}_2$  ligand.<sup>3</sup> The complex is thus more appropriately written as  $\text{Co}^{\text{I}}(\text{CO})_3(\text{L}_2^-)$ .



A noteworthy difference between the  $18 + \delta$  complexes and the 19-electron complexes derived from  $(\text{Cp}^{\text{A}})_2\text{Mo}_2(\text{CO})_6$  is that in an  $18 + \delta$  complex the reduced ligand is coordinated directly to the metal center. In  $(\text{Cp}^{\text{A}})_2\text{Mo}_2(\text{CO})_6$ , the acceptor is not directly coordinated to the metal but is merely attached by a covalent chain to the metal. The difference is nontrivial:  $18 + \delta$  complexes are generally so stabilized that their small reduction potentials make them useless as reductants.<sup>1-3</sup> On the other hand, because the acceptor is not directly coordinated to the metal in 19-electron adducts derived from  $(\text{Cp}^{\text{A}})_2\text{Mo}_2(\text{CO})_6$ , these molecules can retain much of the reducing ability of the reduced acceptor.

In this paper, we report the synthesis and photochemistry of the  $(\text{Cp}^{\text{A}})_2\text{Mo}_2(\text{CO})_6$  complex. Also described is an attempt to recycle 19-electron adducts using this molecule.

## Results and Discussion

**Choice of Electron Acceptor.** Anthraquinone was chosen as the electron acceptor for several reasons: First, it is easily derivatized and therefore easily attached to the metal-metal-bonded dimer precursors of the 19-electron adducts. Second, its reduction potential ( $E^\circ = -0.83$  V) is between the reduction potential of the metal-metal-bonded dimers and the oxidation potential of the metal anions which form in the disproportionation reactions of the  $\text{Cp}_2\text{Mo}_2(\text{CO})_6$  molecule. (See reactions 6 and 7 in a following section.) A reduction potential more positive than that of the metal anions would lead to spontaneous reduction by the metal anions, while a potential more negative than that of the dimers would lead to reduction of the dimers and no useful chemistry. Third, the molecule has an infrared spectroscopic handle (the  $\nu(\text{C}=\text{O})$  band) for easily monitoring its "oxidation state".

**Thermodynamics.** For the discussions which follow, it will be necessary to refer to several bond energies, reduction potentials, and other thermodynamic quantities. Meyer and Pugh reported much of this information in a recent paper.<sup>4</sup> Their data and some added information of our own involving 19-electron adducts are summarized in the Latimer diagram in Figure 1. Discussion of the chart and data is provided as supplementary material.

**Synthesis of  $(\text{Cp}^{\text{A}})_2\text{Mo}_2(\text{CO})_6$ .** The  $(\text{Cp}^{\text{A}})_2\text{Mo}_2(\text{CO})_6$  molecule was synthesized by the route in Scheme 1. The molecule was characterized by noting that its infrared spectrum is essentially identical to the infrared spectra of the analogous  $\text{Cp}_2\text{Mo}_2(\text{CO})_6$  and  $(\text{MeCp})_2\text{Mo}_2(\text{CO})_6$  dimers (Table 1). Likewise, the electronic spectrum of  $(\text{Cp}^{\text{A}})_2\text{Mo}_2(\text{CO})_6$  is identical to those of the other dimers (Table 2). The product was further characterized by <sup>1</sup>H NMR, by elemental analysis, and by FAB mass spectrometry. (Details are found in the Experimental Section.) Repeated attempts to grow crystals suitable for X-ray diffraction analysis were not successful.

**Electronic Spectrum of  $(\text{Cp}^{\text{A}})_2\text{Mo}_2(\text{CO})_6$ .** The electronic absorption spectrum of  $(\text{Cp}^{\text{A}})_2\text{Mo}_2(\text{CO})_6$  exhibits two bands in the visible/near-UV region (Table 2). There is a weak band at 503 nm ( $2100 \text{ M}^{-1} \text{ cm}^{-1}$ ) and an intense band at 388 nm ( $18\,000 \text{ M}^{-1} \text{ cm}^{-1}$ ). This spectrum is essentially identical to the spectra of  $\text{Cp}_2\text{Mo}_2(\text{CO})_6$  and  $(\text{MeCp})_2\text{Mo}_2(\text{CO})_6$  (Table 2), and similar band assignments are therefore proposed:<sup>5-7</sup> The band at 388 nm is assigned to the  $\sigma \rightarrow \sigma^*$  transition and the band at 503 nm to a  $d\pi \rightarrow \sigma^*$  transition. All of the photochemical reactions in this study were carried out by irradiation into the low-energy tail of the  $d\pi \rightarrow \sigma^*$  transition ( $\lambda > 525$  nm). Irradiation at these wavelengths results in metal-metal bond homolysis in  $\text{Cp}_2\text{Mo}_2(\text{CO})_6$  and  $(\text{MeCp})_2\text{Mo}_2(\text{CO})_6$ ; as established in the next section, similar photochemistry occurs with the  $(\text{Cp}^{\text{A}})_2\text{Mo}_2(\text{CO})_6$  molecule.

**Photolysis of the Mo-Mo Bond.** In order to use  $(\text{Cp}^{\text{A}})_2\text{Mo}_2(\text{CO})_6$  as a source of 17-electron radicals for the generation of 19-electron complexes, it was first necessary to establish that irradiation of the complex resulted in cleavage of the Mo-Mo bond and that anthraquinone was neither inhibiting this reactivity nor binding to the metal radicals subsequent to homolysis.

(4) Pugh, J. R.; Meyer, T. J. *J. Am. Chem. Soc.* **1992**, *114*, 3784.

(5) Goldman, A. S.; Tyler, D. R. *Organometallics* **1984**, *3*, 449.

(6) Wrighton, M. S.; Ginley, D. S. *J. Am. Chem. Soc.* **1975**, *97*, 4246.

(7) Geoffroy, G. L.; Wrighton, M. S. *Organometallic Photochemistry*; Academic: New York, 1979.



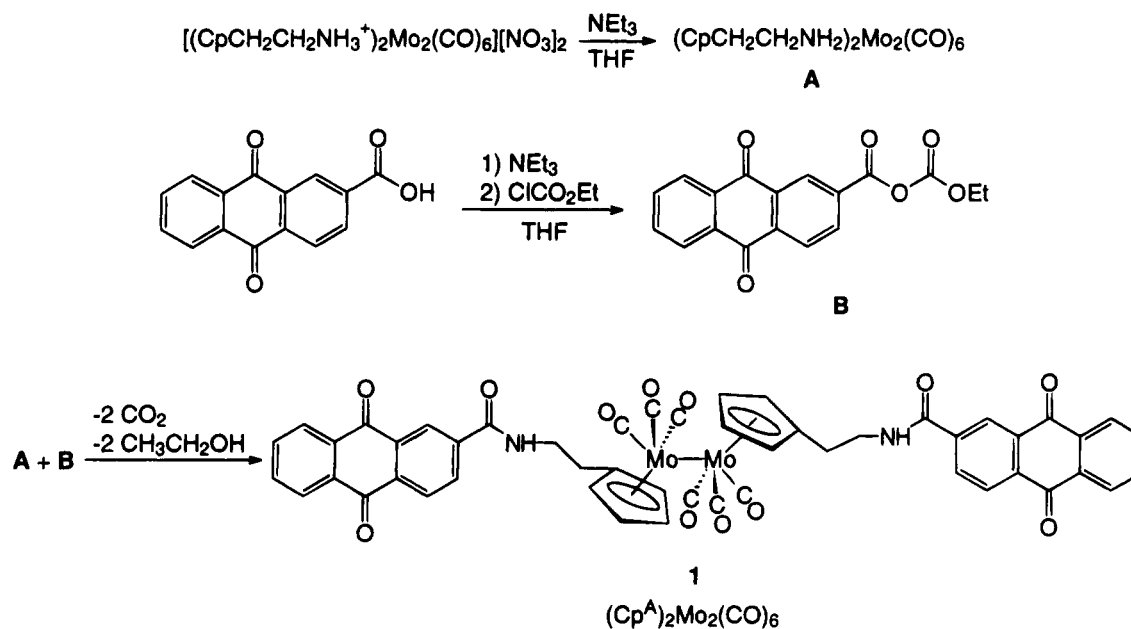
Scheme 1. Synthesis of the  $(\text{Cp}^{\text{A}})_2\text{Mo}_2(\text{CO})_6$  Complex

Table 1. Selected Infrared Data

complex <sup>a</sup>	$\nu(\text{CO}), \text{cm}^{-1}$	ref
$\text{Cp}_2\text{Mo}_2(\text{CO})_6^b$	2012 (w), 1956 (s), 1911 (s)	11
$(\text{MeCp})_2\text{Mo}_2(\text{CO})_6^b$	2009 (m), 1956 (s), 1912 (s)	5
$(\text{Cp}^{\text{A}})_2\text{Mo}_2(\text{CO})_6^c$	2009 (m), 1958 (s), 1908 (s)	this work
$[(\text{CpCH}_2\text{CH}_2\text{NH}_3^+)_2\text{Mo}_2(\text{CO})_6][\text{PF}_6^-]_2^c$	2010 (m), 1953 (8000), <sup>d</sup> 1913 (s)	24
$\text{CpMo}(\text{CO})_3\text{Me}^c$	2020 (vs), 1937 (vs)	this work
$\text{Cp}^{\text{A}}\text{Mo}(\text{CO})_3\text{Me}^c$	2016 (vs), 1927 (vs)	this work
$(\text{MeCp})\text{Mo}(\text{CO})_3\text{Cl}^c$	2051, 1981 (3300), <sup>d</sup> 1957	5, this work
$\text{Cp}^{\text{A}}\text{Mo}(\text{CO})_3\text{Cl}^c$	2050 (m), 1971 (s), 1956 (sh)	this work
$\text{CpMo}(\text{CO})_3\text{I}^c$	2040 (vs), 1968 (vs), 1955 (sh)	33
$\text{Cp}^{\text{A}}\text{Mo}(\text{CO})_3\text{I}^c$	2037 (vs), 1960 (vs), 1954 (sh)	this work
$(\text{MeCp})\text{Mo}(\text{CO})_2\text{TMIO}^c$	1944 (4700), <sup>d</sup> 1836 (5300) <sup>d</sup>	34
$\text{Cp}^{\text{A}}\text{Mo}(\text{CO})_2\text{TMIO}^c$	1944 (s), 1836 (s)	this work
$[\text{CpMo}(\text{CO})_3\text{PPh}_3^+][\text{BF}_4^-]^e$	2062 (s), 2001 (m), 1975 (s)	34
$[\text{Cp}^{\text{A}}\text{Mo}(\text{CO})_3(\text{PPh}_3)]^+{}^c$	2059 (s), 1987 (m), 1956 (s)	this work
$[\text{CpMo}(\text{CO})_2(\text{PPh}_3)_2^+][\text{BF}_4^-]^e$	1978 (s), 1901 (s)	34
$[\text{Cp}^{\text{A}}\text{Mo}(\text{CO})_2(\text{PPh}_3)_2]^+{}^c$	1965 (s), 1900 (s)	this work
$[\text{CpMo}^{\text{II}}(\text{CO})_2\text{dppe}^+][\text{BF}_4^-]^e$	1979, 1910	35
$[\text{Cp}^{\text{A}}\text{Mo}(\text{CO})_2\text{dppe}]^+{}^c$	1979 (s), 1900 (s)	this work
$\text{K}^+[\text{CpMo}(\text{CO})_3]^-{}^c$	1898 (s), 1790 (s), 1750 (s)	36
$[\text{Cp}^{\text{A}}\text{Mo}^0(\text{CO})_3]^-{}^c$	1895 (s), 1784 (3500), <sup>d</sup> 1766 (s)	this work
$\text{Cp}_2\text{Mo}_2(\text{CO})_5\text{PPh}_3^b$	1968 (s), 1900 (s), 1827 (m)	37
anthraquinone <sup>c</sup>	1678	this work

<sup>a</sup> Cp = ( $\eta^5$ -C<sub>5</sub>H<sub>5</sub>); MeCp = ( $\eta^5$ -C<sub>5</sub>H<sub>4</sub>CH<sub>3</sub>); Cp<sup>A</sup> = ( $\eta^5$ -C<sub>5</sub>H<sub>4</sub>CH<sub>2</sub>CH<sub>2</sub>NHC(O)-C<sub>14</sub>H<sub>7</sub>O<sub>2</sub>). <sup>b</sup> CCl<sub>4</sub>. <sup>c</sup> THF. <sup>d</sup>  $\epsilon$ , M<sup>-1</sup> cm<sup>-1</sup>. <sup>e</sup> CH<sub>2</sub>Cl<sub>2</sub>.

Table 2. Electronic Spectroscopic Data

complex <sup>a</sup>	$\lambda_{\text{max}}, \text{nm} (\epsilon, \text{M}^{-1} \text{cm}^{-1})$	ref
$(\text{Cp}^{\text{A}})_2\text{Mo}_2(\text{CO})_6^b$	503 (2100), 388 (18 000)	this work
$(\text{MeCp})_2\text{Mo}_2(\text{CO})_6^c$	506 (2400), 390 (20 000)	5
$\text{Cp}_2\text{Mo}_2(\text{CO})_6^d$	505 (1610), 385 (17 400)	6

<sup>a</sup> Cp = ( $\eta^5$ -C<sub>5</sub>H<sub>5</sub>); MeCp = ( $\eta^5$ -C<sub>5</sub>H<sub>4</sub>CH<sub>3</sub>); Cp<sup>A</sup> = ( $\eta^5$ -C<sub>5</sub>H<sub>4</sub>CH<sub>2</sub>CH<sub>2</sub>NHC(O)-C<sub>14</sub>H<sub>7</sub>O<sub>2</sub>). <sup>b</sup> THF. <sup>c</sup> CH<sub>2</sub>Cl<sub>2</sub>. <sup>d</sup> MeOH.

These points were demonstrated by doing standard metal-radical-trapping experiments.<sup>8</sup> Thus, irradiation of  $(\text{Cp}^{\text{A}})_2\text{Mo}_2(\text{CO})_6$  in 1 M CCl<sub>4</sub>, 1 M CH<sub>3</sub>I, or a 100-fold molar excess of TMIO<sup>9,10</sup> in THF led to the quantitative formation of  $\text{Cp}^{\text{A}}\text{Mo}(\text{CO})_3\text{Cl}$  (eq 3),  $\text{Cp}^{\text{A}}\text{Mo}(\text{CO})_3\text{I}$  (eq 4),

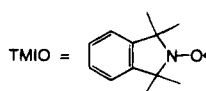
or  $\text{Cp}^{\text{A}}\text{Mo}(\text{CO})_2\text{TMIO}$  (eq 5), respectively. The reactions were monitored by infrared spectroscopy, which showed the disappearance of the  $(\text{Cp}^{\text{A}})_2\text{Mo}_2(\text{CO})_6$  bands at 2009, 1956, and 1912 cm<sup>-1</sup> and the formation of bands assigned to the products. The infrared spectra are summarized in Table 1. The products were identified by comparison to the spectra of analogous complexes containing Cp or MeCp rings. As Table 1 shows, the spectra of the Cp<sup>A</sup>- and Cp-containing molecules are virtually identical. The extinction coefficients used to

(10) In previous work,<sup>11</sup> we showed that  $\text{CpMo}(\text{CO})_3$  radicals can be trapped with the nitroxide TMIO. TMIO reacts with  $\text{CpMo}(\text{CO})_3$  radicals 77 times faster than CCl<sub>4</sub> in competition experiments. The most important feature of this new trap, however, is that it does not participate in any chemistry other than radical reactions. This feature is important because typical radical traps such as CCl<sub>4</sub> and CH<sub>3</sub>I often react with metal anions in an S<sub>N</sub>2 displacement reaction. The fact that TMIO reacts only with radicals makes it possible to easily separate the even-electron pathways from the radical pathways in this study.

(11) Tenhaeff, S. C.; Covert, K. J.; Castellani, M. P.; Grunkemeier, J.; Kunz, C.; Weakley, T. J. R.; Koenig, T.; Tyler, D. R. *Organometallics* **1993**, *12*, 5000.

(8) Meyer, T. J.; Caspar, J. V. *Chem. Rev.* **1985**, *85*, 187.

(9) See: Beckwith, A. L. J.; Bowry, V. W.; Moad, G. J. *Org. Chem.* **1988**, *53*, 1632.

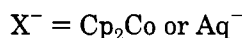
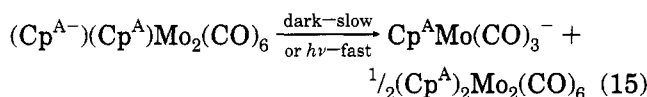
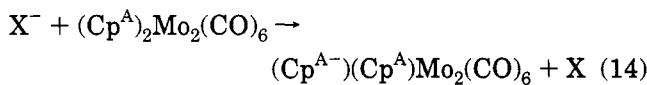






becomes clear after the results in the following section are presented.

**Thermal Fragmentation of  $(\text{Cp}^{\text{A}-})(\text{Cp}^{\text{A}})\text{Mo}_2(\text{CO})_6$ .** Several straightforward experiments showed that one-electron reduction of  $(\text{Cp}^{\text{A}})_2\text{Mo}_2(\text{CO})_6$  gives  $(\text{Cp}^{\text{A}-})(\text{Cp}^{\text{A}})\text{Mo}_2(\text{CO})_6$  and that this reduced species thermally fragments into  $(\text{Cp}^{\text{A}})\text{Mo}(\text{CO})_3^-$  and  $\text{Cp}^{\text{A}}\text{Mo}(\text{CO})_3$  (eqs 14 and 15;  $\tau_{1/2} \approx 10$  min). (The  $\text{Cp}^{\text{A}-}$  nomenclature indicates the anthraquinone appendage is reduced.)



(1) Infrared spectroscopic monitoring of the reaction between  $(\text{Cp}^{\text{A}})_2\text{Mo}_2(\text{CO})_6$  and 0.1 molar equiv of  $\text{Cp}_2\text{Co}$  in THF showed the immediate disappearance of 10% of the anthraquinone  $\nu(\text{C}=\text{O})$  peak at  $1678 \text{ cm}^{-1}$  but no shift in frequency or loss in intensity of any of the  $\nu(\text{C}=\text{O})$  bands ( $2009$ ,  $1958$ , and  $1908 \text{ cm}^{-1}$ ).<sup>16</sup> These spectroscopic results suggest that  $(\text{Cp}^{\text{A}-})(\text{Cp}^{\text{A}})\text{Mo}_2(\text{CO})_6$  forms when  $(\text{Cp}^{\text{A}})_2\text{Mo}_2(\text{CO})_6$  is reduced (eq 14) but that fragmentation (eq 15) does not occur immediately.<sup>17</sup> (The anthraquinone pendant is preferably reduced because its 1-electron reduction potential is more positive than that of the metal-metal unit:  $-0.86 \text{ V}$  vs  $-1.05 \text{ V}$ ; see Figure 1. The  $\nu(\text{C}=\text{O})$  band for reduced anthraquinone at  $1496 \text{ cm}^{-1}$ <sup>18</sup> could not be observed in these experiments because of strong absorptions by THF.) Over a period of about 30 min in the dark, the  $\nu(\text{C}=\text{O})$  peaks decreased in intensity by about 5% and new bands ( $1895$ ,  $1784$ , and  $1766 \text{ cm}^{-1}$ ) assigned to  $\text{Cp}^{\text{A}}\text{Mo}(\text{CO})_3^-$  appeared (Table 2). Equations 14 and 15 account for this observation.<sup>19</sup>

The formation and subsequent disappearance of the putative  $(\text{Cp}^{\text{A}-})(\text{Cp}^{\text{A}})\text{Mo}_2(\text{CO})_6$  intermediate were observed directly by EPR spectroscopy. Reaction between  $(\text{Cp}^{\text{A}})_2\text{Mo}_2(\text{CO})_6$  and 0.19 molar equiv of  $\text{Cp}_2\text{Co}$  in THF produced a product with a singlet signal at  $g = 2.004$ . On standing, the signal weakened in intensity, and after about 2 h, it was no longer detectable. For comparison, note that reduced anthraquinone has  $g = 2.003$ . (No other signals were observed in this experiment.<sup>20</sup>)

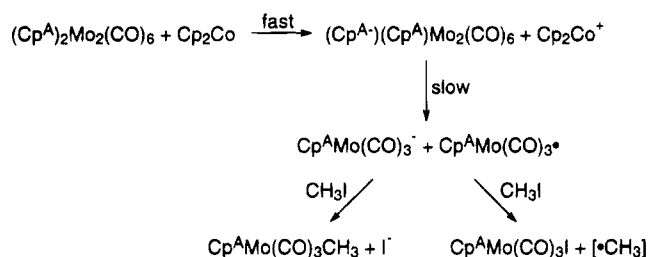
(16) The reduction of  $(\text{Cp}^{\text{A}-})(\text{Cp}^{\text{A}})\text{Mo}_2(\text{CO})_6$  to  $2(\text{Cp}^{\text{A}})\text{Mo}(\text{CO})_3^-$  is 270 mV downhill (Figure 1). Therefore, in order to rule out any 2-electron processes in the reactions of  $(\text{Cp}^{\text{A}})_2\text{Mo}_2(\text{CO})_6$  with  $\text{Cp}_2\text{Co}$ , only 0.1 molar equiv of the reductant was used.

(17) We rationalize the fact that  $(\text{Cp}^{\text{A}-})(\text{Cp}^{\text{A}})\text{Mo}_2(\text{CO})_6$  does not immediately fragment as follows. The anthraquinone and metal-metal units are separated by a saturated chain. Consequently, there will be little, if any, electronic communication between the two. The metal-metal bond should therefore not be strongly affected by reduction of the anthraquinone, and the reduced dimer does not fragment immediately.

(18) Clark, B. R.; Evans, D. H. *J. Electroanal. Chem. Interfacial Electrochem.* **1976**, *69*, 181.

(19) Attempts to obtain the electronic spectrum of the  $(\text{Cp}^{\text{A}-})(\text{Cp}^{\text{A}})\text{Mo}_2(\text{CO})_6$  species were unsuccessful. As explained, the molar ratio of  $\text{Cp}_2\text{Co}$  to  $(\text{Cp}^{\text{A}})_2\text{Mo}_2(\text{CO})_6$  was kept low so as to avoid the 2-electron reduction of the dimer. Thus, solutions containing  $(\text{Cp}^{\text{A}-})(\text{Cp}^{\text{A}})\text{Mo}_2(\text{CO})_6$  always contained large amounts of  $(\text{Cp}^{\text{A}})_2\text{Mo}_2(\text{CO})_6$ . The electronic spectra of such solutions showed no bands other than those attributable to  $(\text{Cp}^{\text{A}})_2\text{Mo}_2(\text{CO})_6$ .

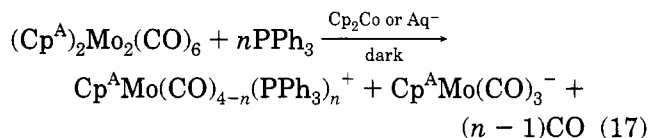
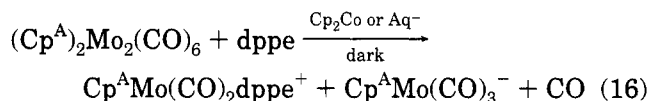
### Scheme 3



An important observation is that irradiation of a THF solution containing  $(\text{Cp}^{\text{A}-})(\text{Cp}^{\text{A}})\text{Mo}_2(\text{CO})_6$  (prepared as above) caused a rapid decrease in intensity of peaks assigned to the dimer ( $\nu(\text{C}=\text{O}) = 2009$ ,  $1958$ , and  $1908 \text{ cm}^{-1}$ ) and the formation of  $\text{Cp}^{\text{A}}\text{Mo}(\text{CO})_3^-$ , as indicated by the appearance of bands at  $1895$ ,  $1784$ , and  $1766 \text{ cm}^{-1}$  (eq 15).<sup>21</sup> Equations 14 and 15 also account for this reactivity.

(2) The dark reaction of  $(\text{Cp}^{\text{A}-})(\text{Cp}^{\text{A}})\text{Mo}_2(\text{CO})_6$  (prepared as above) with  $\text{CH}_3\text{I}$  resulted in the formation of  $\text{Cp}^{\text{A}}\text{Mo}(\text{CO})_3\text{I}$  and  $\text{Cp}^{\text{A}}\text{Mo}(\text{CO})_3\text{Me}$  as detected by infrared spectroscopy ( $\nu(\text{C}=\text{O}) = 2037$ ,  $1960$ , and  $1954 \text{ cm}^{-1}$  and  $2016$  and  $1927 \text{ cm}^{-1}$ , respectively; Table 1). The former is the radical-trapped product, and the latter is the anion-trapped product. The suggested reaction pathway is outlined Scheme 3.

(3) The dark reaction of  $(\text{Cp}^{\text{A}})_2\text{Mo}_2(\text{CO})_6$  with 0.1 molar equiv of cobaltocene or  $\text{Aq}^-$  in the presence of either dppe or  $\text{PPh}_3$  resulted in the complete disproportionation of the dimer over a period of about 30–40 min (eqs 16 and 17), as indicated by the disappearance of the dimer bands at  $2009$ ,  $1958$ , and  $1908 \text{ cm}^{-1}$  and the appearance of new bands assigned to the products in eqs 16 and 17. The products were identified by infrared



$$n = 1 \text{ or } 2$$

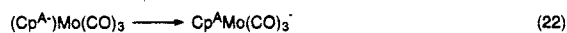
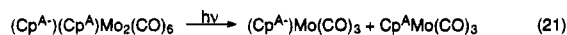
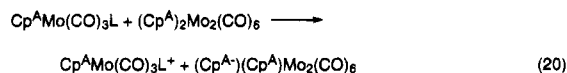
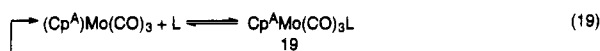
comparison to analogous Cp or MeCp species (Table 1). In prior work,<sup>22</sup> analogous reactivity was observed with the  $\text{Cp}_2\text{Mo}_2(\text{CO})_6$  dimer and was attributed to initiation of the disproportionation chain mechanism (Scheme 2) by reduction of the dimer and its subsequent fragmentation (eq 12). The same explanation undoubtedly applies to the  $(\text{Cp}^{\text{A}})_2\text{Mo}_2(\text{CO})_6$  complex. The fact that *all* of the  $(\text{Cp}^{\text{A}})_2\text{Mo}_2(\text{CO})_6$  disproportionated (as indicated by the complete disappearance of the bands at  $2009$ ,  $1956$ , and  $1912 \text{ cm}^{-1}$ ) when only 0.1 molar equiv

(20) Thermal fragmentation of the  $(\text{Cp}^{\text{A}-})(\text{Cp}^{\text{A}})\text{Mo}_2(\text{CO})_6$  species is expected because some homolysis occurs in most metal-metal dimers in solution at room temperature. In the case of  $(\text{Cp}^{\text{A}-})(\text{Cp}^{\text{A}})\text{Mo}_2(\text{CO})_6$ , fragmentation would yield  $(\text{Cp}^{\text{A}-})\text{Mo}(\text{CO})_3$  and  $(\text{Cp}^{\text{A}})\text{Mo}(\text{CO})_3$ . Fast intramolecular transfer in the former species yields  $(\text{Cp}^{\text{A}})\text{Mo}(\text{CO})_3^-$  (see eq 22), and the homolysis would be irreversible. For a further discussion of these homolysis reactions and equilibria, see ref 11.

(21) There was also a slight increase in intensity of the  $(\text{Cp}^{\text{A}})_2\text{Mo}_2(\text{CO})_6$  bands.

(22) Stieglman, A. E.; Stieglitz, M.; Tyler, D. R. *J. Am. Chem. Soc.* **1983**, *105*, 6032.

## Scheme 4



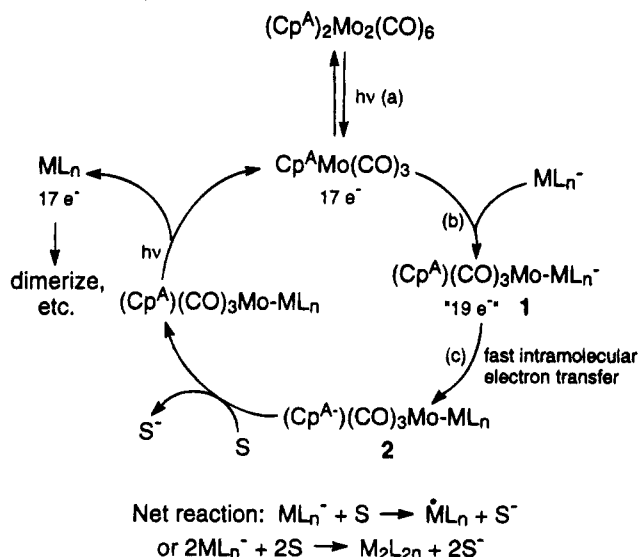
of reducing agent was added is evidence that the reaction follows a chain mechanism, likely analogous to Scheme II.

In summary, these experiments strongly suggest that 1-electron reduction of  $(Cp^A)_2Mo_2(CO)_6$  gives an intact dimer molecule in which a  $Cp^A$  ligand has been reduced:  $(Cp^{A-})(Cp^A)Mo_2(CO)_6$ .<sup>21</sup> This reduced dimer reacts quickly photochemically or more slowly thermally to give products derived by fragmentation into  $Cp^AMo(CO)_3^-$  and  $Cp^AMo(CO)_3$ .

**Why Does Photochemical Disproportionation of  $(Cp^A)_2Mo_2(CO)_6$  Occur?** In light of the results in the preceding section, the proposed chain mechanism in Scheme 4 accounts for why there is no suppression of the  $(Cp^A)_2Mo_2(CO)_6$  disproportionation reaction. Reactions 18–20 are similar to their counterparts in Scheme 2. However, in contrast to its  $Cp_2Mo_2(CO)_6^-$  analog in Scheme II, the  $(Cp^{A-})(Cp^A)Mo_2(CO)_6$  species in eq 20 does not immediately fragment.<sup>17</sup> Because the Mo–Mo bond is still intact, the bond will photolyze (eq 21) (see also eq 15); with the resulting formation of  $(Cp^{A-})Mo(CO)_3$ . This molecule in turn undergoes an intramolecular electron transfer reaction to form  $Cp^AMo(CO)_3^-$  (eq 22). (The electron transfer reaction is thermodynamically favorable, as shown in Figure 1.) The net result is disproportionation of the  $(Cp^A)_2Mo_2(CO)_6$  complex. The key to the mechanism in Scheme 4 is the fast electron transfer reaction in eq 22; the rate is fast because the reaction is intramolecular. Analogous reactivity does not occur with  $Cp_2Mo_2(CO)_6$ /anthraquinone solutions (eq 13) because the electron transfer from  $Aq^-$  to  $CpMo(CO)_3$  is bimolecular; the rate is apparently slow enough that no disproportionation will occur via a Scheme 4 type pathway.

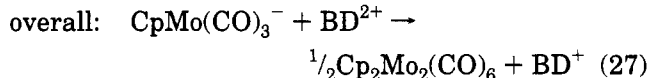
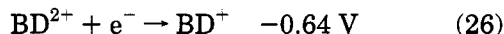
**Recycling 19-Electron Complexes.** A long-range goal in our laboratory is to exploit the reducing ability of 19-electron organometallic adducts in catalytic cycles (e.g. in photochemical water-splitting schemes for solar conversion).<sup>23,24</sup> A possible scheme for recycling 19-electron species using the  $(Cp^A)_2Mo_2(CO)_6$  molecule is shown in Scheme 5.<sup>25</sup> Unfortunately, all attempts to react  $(Cp^A)_2Mo_2(CO)_6$  according to Scheme 5 failed. In a typical experiment, butyl diquat ( $C_{18}H_{26}N_2^{2+}$ ;  $E^\circ =$

## Scheme 5. A Possible Scheme Involving Fast Intramolecular Electron Transfer for Recycling 19-Electron Complexes

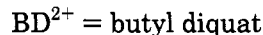


$-0.64 \text{ V}^{26}$ ) was used as the reducible substrate and  $CpMo(CO)_3^-$  as the “ligand” that bonds to the radical to form the 19-electron adduct (1). No reaction was observed even after several minutes of irradiation in an IR cell. Attempts at achieving Scheme 5 using the  $Cp_2Mo_2(CO)_6$ ,  $Cp_2W_2(CO)_6$ , or  $Cp_2Fe_2(CO)_4$  dimers and  $CpMo(CO)_3^-$  or  $CpW(CO)_3^-$  as the ligands also failed to give any net reactivity.

It is interesting to speculate on the reasons for the observed lack of reactivity. One obvious reason may simply be that the metal carbonyl anions are such poor ligands that adduct 1 (step b, Scheme 5) never forms, or if it does form, it is too short-lived for the intramolecular electron transfer to the anthraquinone to occur (step c).<sup>27</sup> The failure to react according to Scheme 5 might also be attributable to unfavorable reaction thermodynamics coupled with a facile back-reaction. Thus, the overall reaction with butyl diquat (eq 27) is endergonic (eqs 24–27). This fact by itself will not



$$\Delta G^\circ = 1.8 \text{ kcal/mol}$$



prohibit the reaction,<sup>30</sup> but coupled with the facile photochemical back-reaction pathway in eqs 28–30, it

(26) Tsukahara, K.; Wilkins, R. G. *J. Am. Chem. Soc.* **1988**, *110*, 2632.

(27) For example, the lifetime of  $[Mn_2(CO)_{10}]^-$  was found to be  $<10^{-7}$  s.<sup>28</sup> However, intramolecular electron transfer reactions are often in the range  $10^8$ – $10^{10}$  s<sup>-1</sup>.<sup>29</sup>

(28) Waltz, W. L.; Hackelberg, O.; Dorfman, L. M.; Wojcicki, A. *J. Am. Chem. Soc.* **1978**, *100*, 7259.

(29) See, for example: (a) Closs, G. L.; Miller, J. R. *Science* **1988**, *240*, 440. (b) Bowler, B. E.; Raphael, A. L.; Gray, H. B. *Prog. Inorg. Chem.* **1990**, *38*, 259.

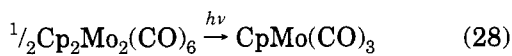
(30) In fact, this makes the reaction useful because it stores photonic energy.

(23) Avey, A.; Tenhaeff, S. C.; Weakley, T. J. R.; Tyler, D. R. *Organometallics* **1991**, *10*, 3607.

(24) Avey, A.; Tyler, D. R. *Organometallics* **1992**, *11*, 3856.

(25) Because the cycle in Scheme 5 did not work, a complete description of the logic that went into its design is not provided in the text. A thorough discussion is provided in the supplementary material. The key point to the scheme, however, is that the oxidized form of the “19-electron adduct” (i.e.,  $(Cp^A)(CO)_3Mo-ML_n$ ) reacts photochemically to form 17-electron radicals, which then continue in the cycle.

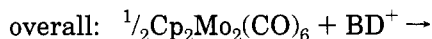
might prevent a *net* forward reaction from occurring.



$$\Delta G^\circ = 11.6 \text{ kcal/mol}$$



$$\Delta G^\circ = -13.4 \text{ kcal/mol}$$



$$\Delta G^\circ = -1.8 \text{ kcal/mol}$$

(The thermodynamic data are from ref 11 for eq 25, from Figure 1 for eq 24, and from ref 26 for eq 26.) In summary of this section,  $(\text{Cp}^A)_2\text{Mo}_2(\text{CO})_6$ , butyl diquat, and  $\text{CpMo}(\text{CO})_3^-$  cannot be used to recycle 19-electron complexes according to Scheme 5.

**Conclusions.** Standard radical-trapping and disproportionation experiments suggest that 19-electron adducts form when  $(\text{Cp}^A)_2\text{Mo}_2(\text{CO})_6$  is irradiated in the presence of ligands. The purpose of the attached anthraquinone is to act as an electron acceptor so as to prolong the lifetime of the 19-electron adduct for use in recycling schemes such as Scheme 5. However, recycling reactivity according to Scheme 5 was not realized. When the ligand is a metal carbonyl anion, the net reaction in Scheme 5 is thermodynamically uphill; a facile photochemical back-reaction pathway is likely why no net reaction was observed.

## Experimental Section

All manipulations of air-sensitive materials were carried out under a nitrogen atmosphere by using standard Schlenk line techniques or by handling the materials and solutions in a Vacuum Atmospheres Co. glovebox.

**Materials.**  $[(\text{CpCH}_2\text{CH}_2\text{NH}_3^+)_2\text{Mo}_2(\text{CO})_6][\text{NO}_3^-]_2$ ,<sup>24</sup>  $(\text{MeCp})_2\text{Mo}_2(\text{CO})_6$ ,<sup>18</sup> and TMIO<sup>9</sup> were synthesized using literature procedures.  $\text{PPh}_3$  (Aldrich) was recrystallized from hexanes. THF (Baker) was freshly distilled as needed from sodium benzophenone ketyl under nitrogen. Carbon tetrachloride (Baker) was distilled from  $\text{P}_2\text{O}_5$  under nitrogen and passed through a silica gel column before use. Triethylamine was dried over calcium sulfate. Cobaltocene, anthraquinone, and anthraquinone-2-carboxylic acid were obtained from Aldrich and used as received. Dppe (Aldrich) was recrystallized three times from ethanol. [Butyl diquat][ $\text{PF}_6^-$ ]<sub>2</sub> was prepared according to the literature.<sup>31</sup>

**Instrumentation.** Photochemical reactions were carried out with an Oriel Co. 200 W high-pressure mercury arc lamp. A Corning CS 3-68 cutoff filter ( $\lambda > 525 \text{ nm}$ ) was used for all of the irradiations. Infrared spectra were obtained with a Nicolet 5DXB FT-IR and a 0.10 mm path length calcium fluoride sealed cell. Electronic spectra were obtained with a Perkin-Elmer Lambda 6 UV/vis spectrophotometer. Proton NMR data were collected on a General Electric QE-300 spectrometer. EPR spectra were obtained with a Bruker ESP-300 spectrometer equipped with a Bruker ER035M NMR gaussmeter and a Hewlett Packard 5342A microwave frequency counter. All *g* values were calculated from recorded fields and frequencies. EPR control experiments were run on all solutions prior to reaction.

**Synthesis of  $(\text{Cp}^A)_2\text{Mo}_2(\text{CO})_6$ .** Anthraquinone-2-carboxylic acid (144 mg; 0.57 mmol) was dissolved in 30 mL of THF, and the solution was cooled in an ice bath. Triethylamine (2

mL; 14 mmol) was then added with a syringe. Ethyl chloroformate (0.055 mL; 0.570 mmol) was added slowly to the magnetically stirred solution. The solution was stirred for 1 h in an ice bath. In another flask, triethylamine (0.5 mL; 3.5 mmol) was added to a 10 mL THF solution containing 200 mg (0.285 mmol) of insoluble  $[(\text{CpCH}_2\text{CH}_2\text{NH}_3^+)_2\text{Mo}_2(\text{CO})_6][\text{NO}_3^-]_2$ , and the contents were mixed well with magnetic stirring. The dark red homogeneous solution was then cannulated into the flask containing the mixed anhydride anthraquinone. The red solution was stirred in an ice bath for 30 min. Deoxygenated  $\text{H}_2\text{O}$  was added via cannula to the red reaction solution, and a red precipitate formed almost immediately. The solution was vacuum-filtered in air, yielding a fine red precipitate. The precipitate was recrystallized from THF/hexanes. Yield: 0.212 g; 70%. IR (KBr):  $\nu(\text{CO})$  2007 (w), 1948 (vs), 1905 (s),  $\nu(\text{CO}$ , anthraquinone) 1675 (m), 1656 (amide I), 1543  $\text{cm}^{-1}$  (amide II). UV/vis (THF): 507, 388 nm.  $^1\text{H}$  NMR (THF-*d*<sub>5</sub>):  $\delta$  10.85 (s (br), 2H,  $\text{CpCH}_2\text{CH}_2\text{NHCOC}_{14}\text{H}_7\text{O}_2$ ), 8.33 (m, 14H,  $\text{CpCH}_2\text{CH}_2\text{NHCOC}_{14}\text{H}_7\text{O}_2$ ), 5.47 (s, 8H,  $\text{CpCH}_2\text{CH}_2\text{NHCOC}_{14}\text{H}_7\text{O}_2$ ), 2.77 (t, 4H,  $\text{CpCH}_2\text{CH}_2\text{NHCOC}_{14}\text{H}_7\text{O}_2$ ), 1.50 (m, 4H,  $\text{CpCH}_2\text{CH}_2\text{NHCOC}_{14}\text{H}_7\text{O}_2$ ). FAB mass spectrum (matrix = 3-nitrobenzyl alcohol), *m/e*: 1046 (50; molecular ion), 1018 (20; molecular ion - CO), 990 (15; molecular ion - 2CO), 962 (30; molecular ion - 3CO), 878 (100; molecular ion - 6CO). Elemental analyses showed the presence of variable amounts of water, as is typical for an amide.<sup>32</sup> Anal. Calcd for  $\text{C}_{50}\text{H}_{32}\text{N}_2\text{O}_{12}\text{Mo}_2 \cdot 1.5\text{H}_2\text{O}$ : C, 56.04; H, 3.29. Found: C, 55.91; H, 3.78.

**Photochemical Reaction of  $(\text{Cp}^A)_2\text{Mo}_2(\text{CO})_6$  with  $\text{CCl}_4$  in THF.** A THF solution of  $(\text{Cp}^A)_2\text{Mo}_2(\text{CO})_6$  (1 mM) and  $\text{CCl}_4$  (60 mM) was prepared and transferred to a sealed IR cell with a syringe. An initial spectrum and a spectrum taken after 5 min in the dark were compared, and no change was observed. The cell was irradiated for 1 min, after which time no  $(\text{Cp}^A)_2\text{Mo}_2(\text{CO})_6$  peaks were present but bands at 2050 and 1971  $\text{cm}^{-1}$  bands, corresponding to  $(\text{Cp}^A)\text{Mo}(\text{CO})_3\text{Cl}$  (Table 2), had grown in. The product formed in quantitative yield (100 ± 10%), as calculated by using the known extinction coefficients for  $[(\text{CpCH}_2\text{CH}_2\text{NH}_3^+)_2\text{Mo}_2(\text{CO})_6]$  and  $(\text{MeCp})\text{Mo}(\text{CO})_3\text{Cl}$  (see Table 2).

**Photochemical Reaction of  $(\text{Cp}^A)_2\text{Mo}_2(\text{CO})_6$  with TMIO.** A THF solution of  $(\text{Cp}^A)_2\text{Mo}_2(\text{CO})_6$  (1 mM) and TMIO (28 mM) was prepared and transferred to a sealed IR cell with a syringe. The initial spectrum and one taken after 5 min in the dark were identical. The solution was then irradiated and monitored every 15 s. After 1 min of irradiation, the reaction was complete, as indicated by the complete disappearance of the  $(\text{Cp}^A)_2\text{Mo}_2(\text{CO})_6$  bands at 2009, 1956, and 1912  $\text{cm}^{-1}$ . The product,  $(\text{Cp}^A)\text{Mo}(\text{CO})_2\text{TMIO}$ , was identified by the 1944 and 1836  $\text{cm}^{-1}$  bands in the IR spectrum by comparison to the spectrum of the known  $(\text{MeCp})\text{Mo}(\text{CO})_2\text{TMIO}$  complex.<sup>11</sup> The product was formed in quantitative yield, as calculated by using the known extinction coefficients for  $[(\text{CpCH}_2\text{CH}_2\text{NH}_3^+)_2\text{Mo}_2(\text{CO})_6]$  and  $(\text{MeCp})\text{Mo}(\text{CO})_2\text{TMIO}$  (see Table 2). No change in intensity of the anthraquinone  $\nu(\text{CO})$  peak was observed.

**Photochemical Reaction of  $(\text{Cp}^A)_2\text{Mo}_2(\text{CO})_6$  with  $\text{CH}_3\text{I}$ .** A THF solution of  $(\text{Cp}^A)_2\text{Mo}_2(\text{CO})_6$  (1 mM) and  $\text{CH}_3\text{I}$  (100 mM) was prepared, and the solution was transferred with a syringe to a sealed IR cell. The initial spectrum and one taken after 5 min in the dark were identical. The solution was then irradiated and the reaction monitored every 15 s. The reaction was complete after 1 min of irradiation, as indicated by the complete disappearance of the  $(\text{Cp}^A)_2\text{Mo}_2(\text{CO})_6$  bands at 2009,

(32) Bilmeyer, F. W., Jr. *Textbook of Polymer Science*, 3rd ed.; Wiley-Interscience: New York, 1984; p 14. For a specific example of this phenomenon, see the elemental analyses for the polyamides in: Ueda, M.; Kameyama, A.; Hashimoto, K. *Macromolecules* **1988**, *21*, 19-24.

(33) Piper, T. S.; Wilkinson, G. *J. Inorg. Nucl. Chem.* **1956**, *3*, 113.

(34) Sunkel, K.; Ernst, H.; Beck, W. *Z. Naturforsch.* **1981**, *36B*, 474.

(35) Beck, W.; Schloter, K. *Z. Naturforsch.* **1978**, *33B*, 1214.

(36) Ellis, J. E.; Flom, E. A. *J. Organomet. Chem.* **1975**, *99*, 263.

(37) Haines, R. J.; Nyholm, R. S.; Stiddard, M. H. *G. J. Chem. Soc. A* **1968**, 43.

(31) Homer, R. F.; Tomlinson, T. E. *J. Am. Chem. Soc.* **1960**, 2498.

1956, and 1912  $cm^{-1}$  and the appearance of bands at 2037, 1960, and 1954 (sh)  $cm^{-1}$ . The product,  $(Cp^A)Mo(CO)_3I$ , was identified by IR comparison to  $CpMo(CO)_3I$  (Table 2). No change in the intensity of the anthraquinone  $\nu(CO)$  peak was observed.

**Photochemical Disproportionation of  $(Cp^A)_2Mo_2(CO)_6$  with  $PPh_3$ .** A solution of  $(Cp^A)_2Mo_2(CO)_6$  (1 mM) and triphenylphosphine (115 mM) in THF was prepared and transferred to an IR cell with a syringe. No dark reaction was detected over a period of 5 min. The solution was irradiated in the IR cell and the reaction monitored every 15 s. The reaction was complete after 75 s of irradiation, as indicated by the loss of the dimer absorption bands at 2010, 1954, and 1912  $cm^{-1}$ . The products were  $[(Cp^A)Mo^{II}(CO)_3(PPh_3)]^{2+}$  (2059, 1987, and 1956  $cm^{-1}$ ),  $[Cp^AMo^{II}(CO)_2(PPh_3)_2]^{2+}$  (1978 and 1901  $cm^{-1}$ ), and  $Cp^AMo^0(CO)_3^-$  (1895, 1784, and 1766  $cm^{-1}$ ), identified by comparison of their IR spectra to those of analogous unsubstituted Cp complexes (see Table 2). No change in intensity of the anthraquinone  $\nu(CO)$  peak was observed.

**Photochemical Disproportionation of  $(Cp^A)_2Mo_2(CO)_6$  with Dppe.** A solution of dppe (28 mM) and  $(Cp^A)_2Mo_2(CO)_6$  (1 mM) in THF was prepared and transferred to an IR cell using a syringe. An initial spectrum and a spectrum taken after 5 min in the dark were identical. The solution was then irradiated for 1 min, after which time the reaction had gone to completion as indicated by the disappearance of the  $(Cp^A)_2Mo_2(CO)_6$  bands at 2009, 1956, and 1912  $cm^{-1}$ . New bands at 1979, 1900, 1895, 1784, and 1766 were assigned to  $[Cp^AMo^{II}(CO)_2dppe]^+$  and  $Cp^AMo(CO)_3^-$  (Table 2). Product identification was by comparison to unsubstituted Cp analogs, also shown in Table 2. The anthraquinone  $\nu(CO)$  peak did not change in intensity during the reaction.

**Reduction of  $(Cp^A)_2Mo_2(CO)_6$  with Cobaltocene.** A standard solution of cobaltocene (0.1 mM) in THF was prepared for use in this and the following experiments that were monitored by infrared spectroscopy.  $(Cp^A)_2Mo_2(CO)_6$  was added in the dark to the standard cobaltocene solution and the resulting mixture transferred to a sealed IR cell via syringe ( $[(Cp^A)_2Mo_2(CO)_6] = 1$  mM). The reaction was monitored by IR spectroscopy, and after 30 min the dimer absorbances had decreased by 5%. Peaks at 1895, 1784, and 1766  $cm^{-1}$ , corresponding to  $Cp^AMo(CO)_3^-$ , grew in (Table 2). A 10% increase in the intensity of the anthraquinone  $\nu(CO)$  peak at 1678  $cm^{-1}$  was also observed. (This result is indicative of a rapid initial reaction of  $Cp_2Co$  with  $(Cp^A)_2Mo_2(CO)_6$  to form  $(Cp^A)(Cp^A)Mo_2(CO)_6$ , which occurs before the first infrared spectrum (after mixing) can be taken.)

The EPR detection of  $(Cp^A)(Cp^A)Mo_2(CO)_6$  was done as follows. In the drybox, in the dark, a stock solution of 0.0159 mM  $(Cp^A)_2Mo_2(CO)_6$  was made by adding  $(Cp^A)_2Mo_2(CO)_6$  (34.3 mg, 0.0319 mmol) to a 2 mL volumetric flask and diluting with THF. Similarly, a stock solution of  $Cp_2Co$  (0.0030 mM) was prepared by placing  $Cp_2Co$  (2.8 mg, 0.015 mmol) in a 5 mL volumetric flask and diluting with THF. In the drybox, in the dark, two EPR tubes were charged with approximately 100  $\mu L$  each of the two solutions, each capped with a septum and wrapped in aluminum foil, and then removed from the drybox. The septa were secured with Parafilm, and control spectra of the reactants were obtained prior to mixing. The  $Cp_2Co$  solution was then syringed into the tube containing  $(Cp^A)_2Mo_2(CO)_6$  using an  $N_2$ -purged syringe. The resulting solution was thoroughly mixed and the EPR spectrum recorded. The spectrum consisted of a single line with a  $g$  value of 2.004. The signal disappeared after 2 h.

**Reaction of  $(Cp^A)_2Mo_2(CO)_6$  with Cobaltocene in the Presence of Dppe.**  $(Cp^A)_2Mo_2(CO)_6$  and dppe were added *in the dark* to an aliquot of the standard cobaltocene solution, and the mixture was then transferred to a sealed IR cell with a syringe ( $[(Cp^A)_2Mo_2(CO)_6] = 1$  mM and  $[dppe] = 28$  mM). The reaction was monitored by IR spectroscopy, and after 30 min the dimer absorbances (2009, 1956, and 1912  $cm^{-1}$ ) had disappeared. Peaks grew in at 1979, 1900, 1895, 1784,

and 1766  $cm^{-1}$ , corresponding to  $[(Cp^A)Mo(CO)_2dppe]^+$  and  $[(Cp^A)Mo(CO)_3]^-$  (Table 2). No change in intensity of the anthraquinone  $\nu(CO)$  peak at 1678  $cm^{-1}$  was observed, again indicative of the rapid initial reaction of  $Cp_2Co$  with  $(Cp^A)_2Mo_2(CO)_6$  to form  $(Cp^A)(Cp^A)Mo_2(CO)_6$  and  $Cp_2Co^+$ , which occurs before the first spectrum can be taken.

**Reaction of  $(Cp^A)_2Mo_2(CO)_6$  with Cobaltocene in the Presence of  $PPh_3$ .** A solution of  $(Cp^A)_2Mo_2(CO)_6$  (1 mM) and  $PPh_3$  (50 mM) was prepared in the dark with the standard cobaltocene solution and transferred to a sealed IR cell with a syringe. The reaction was monitored by IR spectroscopy; after 30 min the absorbances assigned to the dimer had disappeared and those for  $[Cp^AMo(CO)_2PPh_3]^+$  and  $(Cp^A)Mo(CO)_3^-$  had grown in.

**Photochemical Reaction of  $(Cp^A)_2Mo_2(CO)_6$  in the Presence of Cobaltocene.**  $(Cp^A)_2Mo_2(CO)_6$  was added in the dark to an aliquot of the standard cobaltocene solution ( $[(Cp^A)_2Mo_2(CO)_6] = 1$  mM). The solution was then transferred to a sealed IR cell with a syringe. The IR cell was irradiated, and the reaction was monitored by IR spectroscopy every 10 s. The reaction stopped after 5% of the dimer had disappeared ( $\sim 1$  min of irradiation), as indicated by the disappearance of the bands at 2009, 1956, and 1912  $cm^{-1}$ . The only product of the reaction was  $Cp^AMo(CO)_3^-$ , as detected by IR spectroscopy (1895, 1784, and 1766  $cm^{-1}$ ; Table 2). A 10% increase in the intensity of the anthraquinone  $\nu(CO)$  peak at 1678  $cm^{-1}$  was observed during the course of the reaction.

**Reaction of  $(Cp^A)_2Mo_2(CO)_6$  with Cobaltocene in the Presence of  $CH_3I$ .** A THF solution of  $(Cp^A)_2Mo_2(CO)_6$  (1 mM) and  $CH_3I$  (100 mM) was prepared in the dark using the standard cobaltocene solution (0.1 mM) and transferred to a sealed IR cell with a syringe. The reaction was monitored by IR spectroscopy; after 30 min the dimer absorbances at 2009, 1956, and 1912  $cm^{-1}$  had decreased by about 10% and new peaks at 2037, 2016, 1960, 1927  $cm^{-1}$  had appeared. These latter peaks are assigned to  $Cp^AMo(CO)_3Me$  and  $Cp^A(Mo(CO)_3)I$  (Table 2). A 10% increase in the intensity of the anthraquinone  $\nu(CO)$  peak at 1678  $cm^{-1}$  was observed (as compared to the initial spectrum).

**Reduction of  $(Cp^A)_2Mo_2(CO)_6$  with  $Aq^-$ .** A standard solution of 0.1 mM  $Aq^-$  in 0.1 M TBAP/THF was prepared by bulk electrolysis ( $Aq^- = 1$ -electron-reduced anthraquinone).  $(Cp^A)_2Mo_2(CO)_6$  was added in the dark to the standard  $Aq^-$  solution and transferred to a sealed IR cell via syringe ( $[(Cp^A)_2Mo_2(CO)_6] = 1$  mM). The reaction was monitored by IR spectroscopy. After 30 min, the dimer bands at 2009, 1956, and 1912  $cm^{-1}$  had decreased by 5% and peaks at 1895, 1784, and 1766  $cm^{-1}$ , corresponding to  $Cp^AMo(CO)_3^-$ , had appeared (Table 2). In comparison to the initial spectrum, no increase in the intensity of the anthraquinone  $\nu(CO)$  peak at 1678  $cm^{-1}$  was observed.

**Reduction of  $(Cp^A)_2Mo_2(CO)_6$  with  $Aq^-$  in the Presence of TMIO.** A solution containing  $(Cp^A)_2Mo_2(CO)_6$  (1 mM) and TMIO (28 mM) was prepared in the dark with the  $Aq^-$  standard solution and then transferred to a sealed IR cell with a syringe. The reaction was monitored by IR spectroscopy. After 20 min, the dimer bands at 2009, 1956, and 1912  $cm^{-1}$  had decreased by 10% and new peaks at 1944 and 1836  $cm^{-1}$  corresponding to  $Cp^AMo(CO)_2TMIO$  had appeared (Table 2).

**Reduction of  $(Cp^A)_2Mo_2(CO)_6$  with  $Aq^-$  in the Presence of  $CH_3I$ .** A THF solution containing  $(Cp^A)_2Mo_2(CO)_6$  (1 mM) and  $CH_3I$  (28 mM) was prepared in the dark using the  $Aq^-$  standard solution and then transferred to a sealed IR cell with a syringe. The reaction was monitored by IR spectroscopy. After 20 min, the dimer bands at 2009, 1956, and 1912  $cm^{-1}$  had decreased by  $\sim 10\%$  and new bands at 2037, 2016, 1960, and 1927 had appeared. These peaks were assigned to  $Cp^AMo(CO)_3CH_3$  and  $Cp^AMo(CO)_3I$  (Table 2).

**Photochemical Reduction of Anthraquinone with  $Cp_2Mo_2(CO)_6$  and  $PPh_3$ .** This reaction was analyzed by infrared spectroscopy as follows. A THF solution of  $Cp_2Mo_2(CO)_6$  (10 mM),  $PPh_3$  (100 mM), and anthraquinone (100 mM)

was prepared and transferred to an IR cell with a syringe. No reaction was observed after 5 min in the dark. The solution was irradiated, and the reaction was monitored by IR spectroscopy every 2 min for a total of 30 min. Over this period, the dimer bands at 2009, 1956, and 1912  $\text{cm}^{-1}$  disappeared and new bands appeared at 2059, 1978, 1968, 1956, 1901, 1900, and 1827  $\text{cm}^{-1}$ . These products were assigned to  $\text{Cp}^*\text{Mo}(\text{CO})_2(\text{PPh}_3)_2^+$ ,  $\text{Cp}^*\text{Mo}(\text{CO})_3\text{PPh}_3^+$ , and  $\text{Cp}'_2\text{Mo}_2(\text{CO})_5\text{PPh}_3$  (Table 2). In addition, the anthraquinone  $\nu(\text{CO})$  peak at 1678  $\text{cm}^{-1}$  decreased in intensity by 20%.

In this same reaction, reduced anthraquinone was detected by EPR as follows. A stock solution (0.192 mM) of  $\text{PPh}_3$  (50.4 mg, 0.192 mmol) in THF was prepared in a 1 mL volumetric flask. In addition, a stock solution (0.0206 mM) of  $(\text{MeCp})_2\text{Mo}_2(\text{CO})_6$  was prepared by adding 53.5 mg (0.103 mmol) of the dimer to a 5 mL volumetric flask and diluting with THF. In the drybox, in the dark, three EPR tubes were charged separately with approximately 100  $\mu\text{L}$  of the  $\text{PPh}_3$ ,  $\text{Cp}'_2\text{Mo}_2(\text{CO})_6$ , and anthraquinone (see next section) stock solutions, capped with septums, wrapped in aluminum foil, and removed from the drybox. The septums were secured using Parafilm, and control spectra of each reagent were recorded prior to mixing them. The solutions of  $\text{PPh}_3$  and anthraquinone were then transferred by syringe to the tube containing  $\text{Cp}'_2\text{Mo}_2(\text{CO})_6$ . The EPR spectrum of the mixed sample kept in the dark showed no signal. Irradiation of the sample for 10 min produced a single-line spectrum with a  $g$  value of 2.003. This experiment was repeated with a solution that contained no anthraquinone but that was otherwise identical. No EPR signals were observed either before or after irradiation. As a final control, the experiment was again repeated, but this time in the absence of  $\text{PPh}_3$ . Again, no signals were detected.

**Reduction of Anthraquinone Using  $\text{Cp}_2\text{Co}$ .** A stock solution (0.201 mM) of anthraquinone (83.7 mg, 0.402 mmol)

in THF (2 mL) was prepared. In the drybox, in the dark, an EPR tube was charged with approximately 100  $\mu\text{L}$  of this stock solution and another tube with 100  $\mu\text{L}$  of the previously prepared  $\text{Cp}_2\text{Co}$  stock solution. The tubes were capped with septums and removed from the drybox wrapped in aluminum foil. The septums were then secured using Parafilm, and control spectra of the solutions were obtained. The  $\text{Cp}_2\text{Co}$  solution was then syringed into the anthraquinone solution. The resulting solution was thoroughly mixed and the EPR spectrum recorded, with the exclusion of light. The spectrum consisted of a single line with a  $g$  factor of 2.003.

**Attempted Photochemical Reduction of Substrates with  $(\text{Cp}^A)_2\text{Mo}_2(\text{CO})_6$  and  $[\text{CpMo}(\text{CO})_3^-][\text{NBu}_4^+]$ .** A THF solution of  $(\text{Cp}^A)_2\text{Mo}_2(\text{CO})_6$  (1 mM),  $[\text{CpMo}(\text{CO})_3^-][\text{NBu}_4^+]$  (50 mM) and butyl diquat (50 mM) was prepared and transferred to a sealed IR cell with a syringe. The solution was irradiated and the reaction monitored by IR spectroscopy. No changes were observed in the infrared spectrum of the solution, even after 30 min of irradiation. In addition, no change in the intensity of the anthraquinone  $\nu(\text{CO})$  peak was observed.

**Acknowledgment** is made to the NSF for the support of this research. A.A. and G.F.N. were partially supported by U.S. Department of Education Areas of National Needs fellowships. Professor Phil Rieger (Brown University) is acknowledged for helpful discussions.

**Supplementary Material Available:** A discussion of Figure 1 and a more in-depth discussion of the 19-electron adduct recycling pathway shown in Scheme 5 (3 pages). Ordering information is given on any current masthead page.

OM9500127

# Mono(pentamethylcyclopentadienyl)thorium Chemistry. Formation and Structural Characterization of a Novel Triflate-Bridged Dimeric Thorium Complex

Raymond J. Butcher,<sup>1a</sup> David L. Clark,<sup>\*1b</sup> Steven K. Grumbine,<sup>1c</sup> and John G. Watkin<sup>\*1c</sup>

Chemical Science and Technology Division (CST), Los Alamos National Laboratory, Los Alamos, New Mexico 87545

Received January 26, 1995<sup>®</sup>

Reaction of  $[(\text{Me}_3\text{Si})_2\text{N}]_2\text{Th}[\text{N}(\text{SiMe}_3)(\text{SiMe}_2\text{CH}_2)]$  (**1**) with 1 equiv of trifluoromethanesulfonic acid (HOTf) produces the mono(triflate) species  $\text{Th}[\text{N}(\text{SiMe}_3)_2](\text{OTf})$  (**2**), whereas the reaction of **1** with 2 equiv of HOTf yields both **2** and the tris(triflate) complex  $\text{Th}[\text{N}(\text{SiMe}_3)_2](\text{OTf})_3$  (**3**) in approximately equal amounts. Heating a toluene solution of **2** with 1 equiv of  $\text{Cp}^*\text{H}$  ( $\text{Cp}^* = \text{C}_5\text{Me}_5$ ) leads to formation of the dimeric triflate-bridged complex  $\text{Cp}^*[(\text{Me}_3\text{Si})_2\text{N}]\text{Th}(\mu_2\text{-OSO}_2\text{CF}_3)_3\text{Th}[\text{N}(\text{SiMe}_3)(\text{SiMe}_2\text{CH}_2)]\text{Cp}^*$  (**4**). Reaction of **4** with 1 equiv of  $\text{KN}(\text{SiMe}_3)_2$  produces the dimeric species  $\{\text{Cp}^*(\text{TfO})\text{Th}[\text{N}(\text{SiMe}_3)(\text{SiMe}_2\text{CH}_2)]\}_2$  (**5**). Compounds **2–5** have been characterized by <sup>1</sup>H NMR and IR spectroscopy, elemental analysis, and, in the case of **4**, by a single-crystal X-ray diffraction study. Compound **4** consists of two mono(pentamethylcyclopentadienyl)thorium moieties ( $\text{Th}-\text{Cp}^*_{\text{centroid}} = 2.54$  and  $2.51 \text{ \AA}$ ) joined by means of three bridging triflate ligands. One thorium metal center bears a bis(trimethylsilyl)amide ligand ( $\text{Th}-\text{N} = 2.24(3) \text{ \AA}$ ) while the other features a cyclometalated amide ligand ( $\text{Th}-\text{N} = 2.26(4) \text{ \AA}$ ,  $\text{Th}-\text{C} = 2.43(5) \text{ \AA}$ ). A tentative mechanism is proposed for the formation of **4**. Crystal data for **4** at  $-70 \text{ }^\circ\text{C}$ : monoclinic space group  $P2_1/n$ ,  $a = 14.073(3) \text{ \AA}$ ,  $b = 23.242(5) \text{ \AA}$ ,  $c = 18.101(4) \text{ \AA}$ ,  $\beta = 105.70(3)^\circ$ ,  $V = 5699.5 \text{ \AA}^3$ ,  $d_{\text{calcd}} = 1.806 \text{ g cm}^{-3}$ ,  $Z = 4$ .

## Introduction

The organometallic chemistry of the early actinide elements has been dominated by complexes containing  $\text{Cp}^*_2\text{An}$  or  $\text{Cp}_3\text{An}$  frameworks ( $\text{Cp}^* = \eta\text{-C}_5\text{Me}_5$ ,  $\text{Cp} = \eta\text{-C}_5\text{H}_5$ ,  $\text{An} = \text{Th}, \text{U}$ ).<sup>2</sup> Reports of actinide compounds containing monocyclopentadienyl<sup>3</sup> or mono(pentamethylcyclopentadienyl)<sup>4</sup> ancillary ligand sets are considerably less common, with many of these complexes being

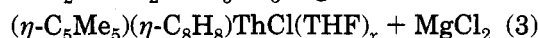
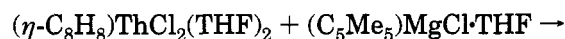
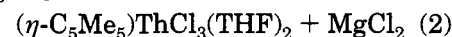
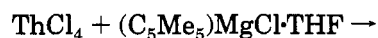
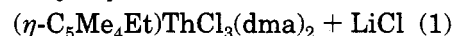
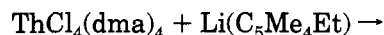
Lewis-base adducts of the  $\text{CpAnX}_3$  moiety ( $\text{X} = \text{halide}$ ). The steric and electronic unsaturation of the monocyclopentadienyl actinide framework, relative to the  $\text{Cp}^*_2\text{-An}$  or  $\text{Cp}_3\text{An}$  systems, makes it an attractive synthetic goal. Halide metathesis routes such as those shown in eqs 1–3 have been used to introduce a single  $\eta\text{-C}_5\text{Me}_5$  or the related  $\eta\text{-C}_5\text{Me}_4\text{Et}$  ligand into the coordination sphere of an early actinide element.<sup>4a–c</sup> We report here an alternative synthetic route to this most interesting class of compounds.

<sup>®</sup> Abstract published in *Advance ACS Abstracts*, May 1, 1995.

(1) (a) Current address: Department of Chemistry, Howard University, Washington, DC 20059. (b) LANL, Mail Stop G739. (c) LANL, Mail Stop C346.

(2) (a) Marks, T. J. In *Comprehensive Organometallic Chemistry*; Wilkinson, G., Stone, F. G. A., Abel, E. W., Eds.; Pergamon Press: Oxford, England, 1982; Vol. 3, p 211–223. (b) Ephritikhine, M. *New J. Chem.* **1992**, 16, 451.

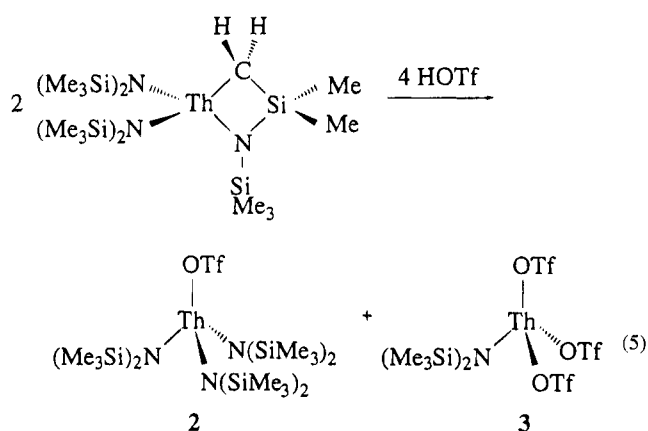
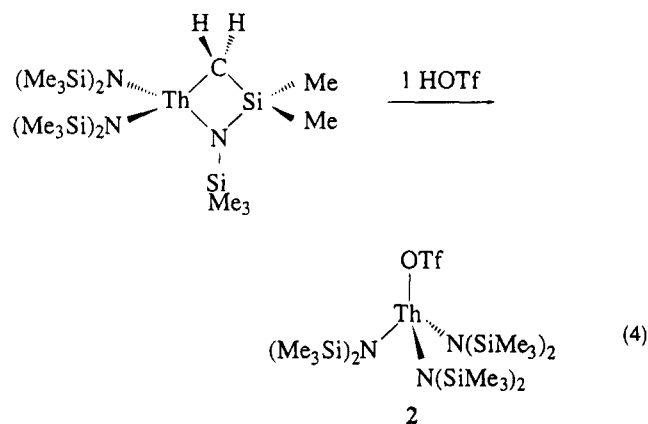
(3) See for example: (a) Cramer, R. E.; Bruck, M. A.; Gilje, J. W. *Organometallics* **1988**, 7, 1465. (b) Eigenbrot, C. W.; Raymond, K. N. *Inorg. Chem.* **1982**, 21, 2653. (c) Ernst, R. D.; Kenelly, W. J.; Day, C. S.; Day, V. W.; Marks, T. J. *J. Am. Chem. Soc.* **1979**, 101, 2656. (d) Bagnall, K. W.; Benetollo, F.; Bombieri, G.; de Paoli, G. *J. Chem. Soc., Dalton Trans.* **1984**, 67. (e) Bagnall, K. W.; Beheshti, A.; Heatley, F. *J. Less-Common Met.* **1978**, 61, 63. (f) Delavaux-Nicot, B.; Ephritikhine, M. *J. Organomet. Chem.* **1990**, 399, 77. (g) Baudry, D.; Dorion, P.; Ephritikhine, M. *J. Organomet. Chem.* **1988**, 356, 165. (h) Baudry, D.; Ephritikhine, M. *J. Organomet. Chem.* **1988**, 349, 123. (i) Domingos, A.; Marques, N.; Pires de Matos, A. *Polyhedron* **1990**, 9, 69. (j) Bagnall, K. W.; Edwards, J.; Tempest, A. C. *J. Chem. Soc., Dalton Trans.* **1978**, 295. (k) Bagnall, K. W.; Beheshti, A.; Edwards, J.; Heatley, F.; Tempest, A. C. *J. Chem. Soc., Dalton Trans.* **1979**, 1241. (l) Baudin, C.; Ephritikhine, M. *J. Organomet. Chem.* **1989**, 364, C1. (m) Edelman, M. A.; Lappert, M. F.; Atwood, J. L.; Zhang, H. *Inorg. Chim. Acta* **1987**, 139, 185. (n) Bombieri, G.; de Paoli, G.; Del Pra, A.; Bagnall, K. W. *Inorg. Nucl. Chem. Lett.* **1978**, 14, 359. (o) Cramer, R. E.; Mori, A. L.; Maynard, R. B.; Gilje, J. W.; Tatsumi, K.; Nakamura, A. *J. Am. Chem. Soc.* **1984**, 106, 5920. (p) Brianese, N.; Casellato, U.; Ossola, F.; Porchia, M.; Rossetto, G.; Zanella, P.; Graziani, R. *J. Organomet. Chem.* **1989**, 365, 223. (q) Rebizant, J.; Spirlet, M. R.; Apostolidis, A.; Kanellakopoulos, B. *Acta Cryst.* **1992**, 48C, 452.



(4) (a) Mintz, E. A.; Moloy, K. G.; Marks, T. J. *J. Am. Chem. Soc.* **1982**, 104, 4692. (b) Gilbert, T. M.; Ryan, R. R.; Sattelberger, A. P. *Organometallics* **1989**, 8, 857. (c) Bagnall, K. W.; Beheshti, A.; Heatley, F.; Tempest, A. C. *J. Less-Common Met.* **1979**, 64, 267. (d) Schake, A. R.; Avens, L. R.; Burns, C. J.; Clark, D. L.; Sattelberger, A. P.; Smith, W. H. *Organometallics* **1993**, 12, 1497. (e) Berthet, J. C.; Le Marechal, J. F.; Ephritikhine, M. *J. Organomet. Chem.* **1990**, 393, C47. (f) Cymbaluk, T. H.; Ernst, R. D.; Day, V. W. *Organometallics* **1983**, 2, 963. (g) Ryan, R. R.; Salazar, K. V.; Sauer, N. N.; Ritchey, J. M. *Inorg. Chim. Acta* **1989**, 162, 221.

## Results and Discussion

**Synthesis and Reactivity.** Treatment of a hexane solution of the thorium metallacycle  $[(\text{Me}_3\text{Si})_2\text{N}]_2\text{Th}[\text{N}(\text{SiMe}_3)(\text{SiMe}_2\text{CH}_2)]_5$  (**1**) with 1 equiv of a diethyl ether solution of trifluoromethanesulfonic acid (HOTf) at  $-40^\circ\text{C}$  resulted in the formation of the mono-triflate species  $\text{Th}[\text{N}(\text{SiMe}_3)_2]_3(\text{OTf})$  (**2**), which was isolated as a white crystalline solid in 55% yield as indicated in eq 4. Microanalytical data are consistent with the pro-



posed stoichiometry of **2**. Use of 2 equiv of HOTf in an analogous reaction produces a mixture of the mono-triflate complex (**2**) and the bis-triflate complex  $\text{Th}[\text{N}(\text{SiMe}_3)_2](\text{OTf})_2$  (**3**). The relative insolubility of **3** in common solvents results in straightforward separation of the two complexes, which may be isolated in 42% and 36% yields for **2** and **3**, respectively (eq 5). Although some spectroscopic evidence exists for the transient formation of the expected bis-triflate product  $\text{Th}[\text{N}(\text{SiMe}_3)_2]_2(\text{OTf})_2$ , it appears that this species undergoes rapid ligand redistribution to form the isolated reaction products **2** and **3**.

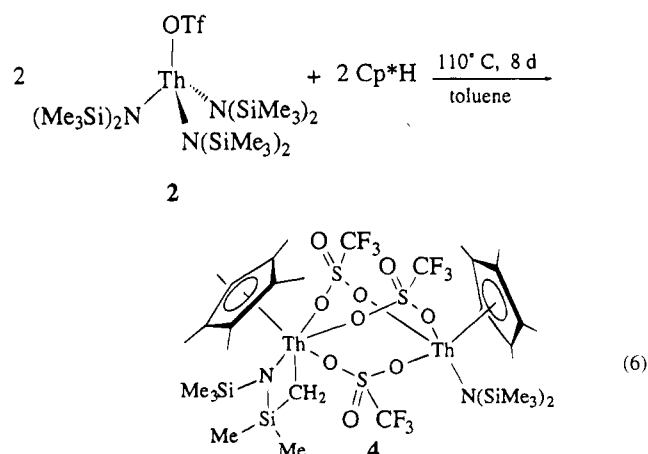
Initial attempts to form mono(pentamethylcyclopentadienyl)thorium complexes through metathesis of **2** or **3** with  $\text{KCp}^*$  were unsuccessful. Additionally, the reaction of metallacycle **1** with 1 equiv of  $\text{Cp}^*\text{H}$  was also unsuccessful, showing no reaction after heating at  $110^\circ\text{C}$  in toluene for 3 days. However, reaction of  $\text{Th}[\text{N}(\text{SiMe}_3)_2]_3(\text{OTf})$  (**2**) with  $\text{Cp}^*\text{H}$  in a refluxing toluene solution for 8 days allows the isolation of a dinuclear

**Table 1. Summary of Crystallographic Data for  $\text{Cp}^*[(\text{Me}_3\text{Si})_2\text{N}]\text{Th}(\mu_2\text{-OSO}_2\text{CF}_3)_3\text{-Th}[\text{N}(\text{SiMe}_3)(\text{SiMe}_2\text{CH}_2)]\text{Cp}^* \cdot \text{C}_7\text{H}_8$  (**4**)**

<b>Th</b> $[\text{N}(\text{SiMe}_3)(\text{SiMe}_2\text{CH}_2)]\text{Cp}^* \cdot \text{C}_7\text{H}_8$ ( <b>4</b> )	
empirical formula	$\text{C}_{39}\text{H}_{65}\text{F}_9\text{N}_2\text{O}_9\text{S}_3\text{Si}_4\text{Th}_2$
color, habit	colorless needle
cryst dimens, mm <sup>3</sup>	$0.30 \times 0.10 \times 0.08$
space group	$P2_1/n$
cell dimens	
<i>a</i> , Å	14.073(3)
<i>b</i> , Å	23.242(5)
<i>c</i> , Å	18.101(4)
$\beta$ , deg	105.70(3)
vol, Å <sup>3</sup>	5699.5
<i>Z</i> (molecules/cell)	4
fw	1549.6
<i>D</i> <sub>calcd</sub> , g cm <sup>-3</sup>	1.806
abs coeff, cm <sup>-1</sup>	54.83
$\lambda(\text{Mo K}\alpha)$	0.710 73
temp, °C	-70
$2\theta$ range, deg	2.0–50.0
measd reflns	10 737
unique intensities	10 027
obsd reflns	4902 ( $F > 3.0\sigma(F)$ )
<i>R</i> ( <i>F</i> ) <sup>a</sup>	0.0500
<i>R</i> <sub>w</sub> ( <i>F</i> ) <sup>b</sup>	0.0651
goodness-of-fit	1.95

<sup>a</sup>  $R(F) = \sum ||F_o| - F_c| / \sum |F_o|$ . <sup>b</sup>  $R_w(F) = [\sum w(|F_o| - |F_c|)^2 / \sum w|F_o|^2]^{1/2}$ ;  $w = 1/\sigma^2(|F_o|)$ .

thorium complex  $\text{Cp}^*[(\text{Me}_3\text{Si})_2\text{N}]\text{Th}(\mu_2\text{-OSO}_2\text{CF}_3)_3\text{Th}[\text{N}(\text{SiMe}_3)(\text{SiMe}_2\text{CH}_2)]\text{Cp}^*$  (**4**) as a white crystalline solid in 42% yield (eq 6). The <sup>1</sup>H NMR spectrum of **4** shows two  $\text{Cp}^*$  resonances and a number of resonances between 0.12–1.39 ppm in a 9:3:3:1:1 ratio consistent with cyclometalation of one bis(trimethylsilyl)amide ligand. The infrared spectrum shows vibrational features at 1332, 1237, and 1219 cm<sup>-1</sup>, consistent with the presence of bridging OTf ligands.<sup>6</sup> A single-crystal X-ray diffraction study (*vide infra*) confirmed that one silylamide ligand had been activated to form a four-membered metallacyclic ring, as shown schematically in eq 6.



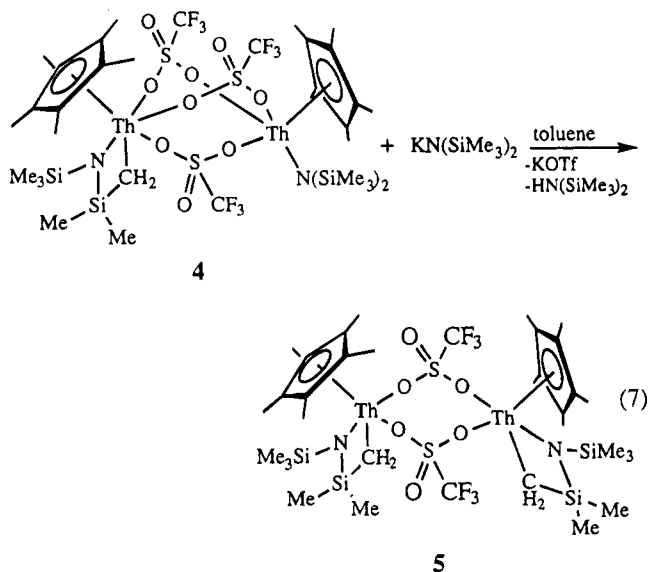
Compound **4** reacts with 1 equiv of  $\text{KN}(\text{SiMe}_3)_2$  in a toluene/THF solution to produce  $\{\text{Cp}^*(\text{TfO})\text{Th}[\text{N}(\text{SiMe}_3)(\text{SiMe}_2\text{CH}_2)]_2\}$  (**5**) in 50% yield (eq 7). The <sup>1</sup>H NMR spectrum of **5** shows a single  $\text{Cp}^*$  resonance, together with the distinctive pattern of resonances in a 9:3:3:2 ratio consistent with the presence of cyclometalated bis(trimethylsilyl)amide ligands (we believe that the two

(5) (a) Simpson, S. J.; Turner, H. W.; Andersen, R. A. *J. Am. Chem. Soc.* **1979**, *101*, 7728. (b) Simpson, S. J.; Turner, H. W.; Andersen, R. A. *Inorg. Chem.* **1981**, *20*, 2991. (c) Dormond, A.; El Bouadili, A. A.; Aaliti, A.; Moise C. *J. Organomet. Chem.* **1985**, *288*, C1.

(6) Lawrance, G. A. *Chem. Rev.* **1986**, *86*, 17.



diastereotopic Si-CH<sub>2</sub>-Th methylene protons within the metallacycle are coincidentally overlapping). Infrared absorption bands at 1324, 1306, 1258, and 1240 cm<sup>-1</sup> in the solid-state IR spectrum of **5** suggest the presence of a bidentate triflate ligand.<sup>6</sup> The dimeric structure shown in eq 7 is proposed on the basis of IR data, the comparable solubilities of **4** and **5**, the expected steric unsaturation of a monomeric species, and the results of a solution molecular weight determination which found the degree of oligomerization in solution to be 2.3 (found 1555; calcd 676, for monomeric Cp\*(TfO)Th[N(SiMe<sub>3</sub>)(SiMe<sub>2</sub>CH<sub>2</sub>)]). The two Cp\* ligands in **5** are shown in a *cis*-orientation by analogy with that observed in the solid-state structure of **4** (*vide infra*).



**Solid-State and Molecular Structure.** Crystals of **4** suitable for an X-ray diffraction study were grown by cooling a concentrated toluene solution to -40 °C, and the structure was determined from diffraction data collected at -70 °C. A summary of data collection and crystallographic parameters is given in Table 1. Selected fractional coordinates are given in Table 2, and selected bond lengths and angles are given in Table 3. A ball-and-stick drawing giving the atom-numbering scheme used in the tables is shown in Figure 1. The overall molecular structure of **4** consists of two mono(pentamethylcyclopentadienyl)thorium units joined by means of three bridging triflate ligands. One thorium metal center bears a bis(trimethylsilyl)amide ligand while the other features a cyclometalated amide ligand. The Th-centroid distances compare favorably to those observed in other examples of mono(pentamethylcyclopentadienyl)thorium complexes. For example, the Th-Cp\*<sub>centroid</sub> distances of 2.54 and 2.51 Å are very similar to those of 2.54 Å seen in both Cp\*Th(η-C<sub>8</sub>H<sub>8</sub>)Cl<sub>2</sub>Mg(t-Bu)(THF)<sup>4b</sup> and Cp\*Th(η-C<sub>8</sub>H<sub>8</sub>)[CH(SiMe<sub>3</sub>)<sub>2</sub>],<sup>4b</sup> while the average Th-C distances of 2.80 and 2.77 Å are consistent with that of 2.79 Å seen in Cp\*Th(CH<sub>2</sub>C<sub>6</sub>H<sub>5</sub>)<sub>3</sub>.<sup>4a</sup> To the best of our knowledge, the three structures referenced here represent the only previously reported examples of structurally characterized mono(pentamethylcyclopentadienyl)thorium complexes.

The bonding of the triflate ligands to thorium is somewhat asymmetric, with average Th-O bond lengths of 2.57(3) and 2.45(3) Å to Th(1) and Th(2), respectively.

**Table 2. Selected Atomic Coordinates and Equivalent Isotropic Displacement Coefficients for Cp\*[Me<sub>3</sub>Si]<sub>2</sub>N]Th(μ<sub>2</sub>-OSO<sub>2</sub>CF<sub>3</sub>)<sub>3</sub>-**

Th[N(SiMe <sub>3</sub> )(SiMe <sub>2</sub> CH <sub>2</sub> )]Cp* · C <sub>7</sub> H <sub>8</sub> (4)				
	10 <sup>4</sup> x	10 <sup>4</sup> y	10 <sup>4</sup> z	10 <sup>4</sup> U(eq), Å <sup>2</sup>
Th(1)	1920.6(1)	786.8(6)	3103(8)	481(5)
Th(2)	-1140.2(1)	2395.7(6)	3483.3(8)	430(4)
S(1)	-882(7)	809(4)	3005(5)	480(33)
S(2)	344(7)	2097(4)	2017(6)	488(34)
S(3)	1348(7)	1828(4)	4666(5)	464(33)
Si(1)	1925(10)	-535(5)	3235(8)	656(51)
Si(2)	995(9)	-219(5)	1517(8)	612(46)
Si(3)	-3511(8)	2108(5)	2602(7)	525(41)
Si(4)	-2869(9)	2013(5)	4383(6)	560(43)
O(1)	134(22)	682(11)	3213(14)	604(111)
O(2)	-1087(20)	1325(12)	3341(17)	658(119)
O(3)	-1404(21)	744(13)	2251(17)	706(120)
O(4)	832(21)	15455(11)	22438(15)	604(109)
O(5)	-337(17)	2249(10)	2474(15)	494(91)
O(6)	936(21)	2545(12)	1900(16)	645(112)
O(7)	1591(19)	1494(11)	4093(15)	576(101)
O(8)	349(19)	2063(11)	4397(13)	524(98)
O(9)	2058(21)	2226(12)	5084(15)	625(113)
N(1)	1631(24)	-55(15)	2476(19)	600(135)
N(2)	-2694(27)	2187(12)	3518(19)	605(136)
C(4)	2223(34)	10(21)	4032(26)	776(200)
C(10)	-2717(30)	2296(21)	1956(21)	692(172)
C(16)	3810(28)	1202(15)	3808(21)	478(87)
C(17)	4000(33)	708(19)	345(25)	645(111)
C(18)	3674(29)	819(17)	2670(22)	537(91)
C(19)	3305(35)	1369(20)	2526(26)	704(121)
C(20)	3395(32)	1623(18)	3259(24)	615(106)
C(26)	-325(32)	3357(17)	4318(24)	597(104)
C(27)	-1334(31)	3486(17)	4053(23)	58(10)
C(28)	-1614(26)	3551(15)	3284(20)	439(82)
C(29)	-784(27)	3491(15)	3013(20)	439(82)
C(30)	3(29)	3384(16)	3661(22)	519(92)

**Table 3. Selected Bond Distances (Å) and Angles (deg) for Cp\*[Me<sub>3</sub>Si]<sub>2</sub>N]Th(μ<sub>2</sub>-OSO<sub>2</sub>CF<sub>3</sub>)<sub>3</sub>-**

Th[N(SiMe <sub>3</sub> )(SiMe <sub>2</sub> CH <sub>2</sub> )]Cp* · C <sub>7</sub> H <sub>8</sub> (4)			
Th(1)-O(1)	2.59(3)	Th(2)-O(2)	2.50(3)
Th(1)-O(4)	2.57(3)	Th(2)-O(5)	2.42(3)
Th(1)-O(7)	2.57(3)	Th(2)-O(8)	2.42(2)
Th(1)-N(1)	2.24(3)	Th(2)-N(2)	2.26(4)
Th(1)-Cp* (cent)	2.54(4)	Th(2)-Cp* (cent)	2.51(4)
Th(1)-Cp* (av)	2.80(4)	Th(2)-Cp* (av)	2.77(4)
Th(1)-C(4)	2.43(5)	Th(2)-C(10)	3.05(3)
N(1)-Th(1)-C(4)	71.1(14)	N(2)-Th(2)-C(10)	62.4(12)
Th(1)-C(4)-Si(1)	90.5(18)	Th(2)-C(10)-Si(3)	82.1(12)
Th(1)-N(1)-Si(1)	100.9(15)	Th(2)-N(2)-Si(3)	112.9(20)
N(1)-Si(1)-C(4)	97.6(19)	N(2)-Si(3)-C(10)	102.5(18)

This may be due to the fact that Th(1) is more sterically encumbered (formally six-coordinate) than Th(2) (formally five-coordinate). A number of structurally characterized complexes have been found to contain bridging triflate ligands, although these have been predominantly in late transition metal complexes containing Cu,<sup>7</sup> Hg,<sup>8</sup> and Ag.<sup>9</sup> Structurally characterized examples of metal centers bridged by two triflate ligands appear to be limited to the complexes {[Cp\*Re(NO)(PPh<sub>3</sub>)](μ-C<sub>3</sub>H<sub>2</sub>O<sub>2</sub>)[Re(CO)<sub>4</sub>(PMe<sub>3</sub>)]<sub>2</sub>[μ-Li<sub>2</sub>(O<sub>3</sub>SCF<sub>3</sub>)<sub>2</sub>]<sup>10</sup> and [(η-C<sub>5</sub>H<sub>5</sub>)<sub>2</sub>Yb(μ-O<sub>3</sub>SCF<sub>3</sub>)<sub>2</sub>].<sup>11</sup> The structure of **4** in which

(7) See for example (a) Dedert, P. L.; Sorrell, T.; Marks, T. J.; Ibers, J. A. *Inorg. Chem.* **1982**, *21*, 3506. (b) Ferrara, J. D.; Tessier-Youngs, C.; Youngs, W. J. *Inorg. Chem.* **1988**, *27*, 2201.

(8) Balch, A. L.; Olmstead, M. M.; Rowley, S. P. *Inorg. Chem.* **1988**, *27*, 2275.

(9) (a) Arif, A. M.; Richmond, T. G. *J. Chem. Soc., Chem. Commun.* **1990**, 871. (b) Gleiter, R.; Karcher, M.; Kratz, D.; Zeigler, M. L.; Nuber, B. *Chem. Ber.* **1990**, *123*, 1461.



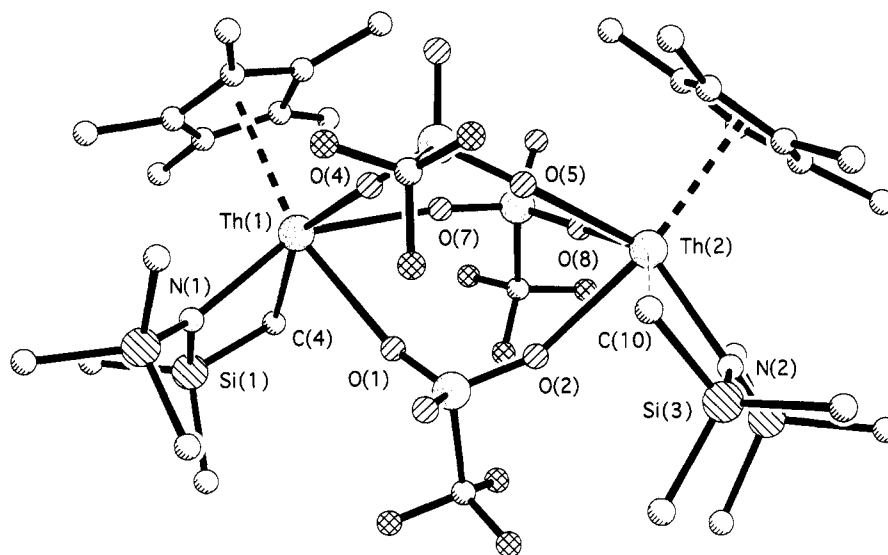


**Figure 1.** A ball and stick drawing of the solid-state structure of  $\text{Cp}^*[(\text{Me}_3\text{Si})_2\text{N}]\text{Th}(\mu_2\text{-OSO}_2\text{CF}_3)_3\text{Th}[\text{N}(\text{SiMe}_3)\text{-}(\text{SiMe}_2\text{CH}_2)]\text{Cp}^*$  (**4**) giving the atom-numbering scheme used in the tables.

three triflate groups bridge two metal centers is only the second documented example of this structural motif.<sup>12</sup> Furthermore, **4** appears to be the first crystallographically characterized example of an actinide triflate complex, with no other structures of these types being located in the Cambridge Structural Database.

The Th–N distances of 2.24(3) and 2.26(4) Å can be compared with the average Th–N distances of 2.34(1) Å in  $(\eta\text{-C}_5\text{H}_5)\text{Th}[\text{N}(\text{SiMe}_3)_2]_2$ ,<sup>13a</sup> 2.32(2) Å in  $(\eta^3\text{-BH}_4)\text{-Th}[\text{N}(\text{SiMe}_3)_2]_3$ ,<sup>13b</sup> and 2.31(1) Å in  $\text{Th}[\text{N}(\text{SiMe}_3)_2]_2\text{-}(\text{NMePh})_2$ .<sup>13c</sup> The Th–C distance of 2.43(5) has a relatively large error associated with it but can be compared with the average Th–C distances of 2.58(1) Å in  $\text{Cp}^*\text{Th}(\text{CH}_2\text{C}_6\text{H}_5)_3$ ,<sup>4a</sup> 2.55(2) Å in  $\text{Th}(\text{CH}_2\text{C}_6\text{H}_5)_4(\text{Me}_2\text{-PCH}_2\text{CH}_2\text{PMe}_2)$ ,<sup>14a</sup> 2.51(2) Å in  $[\text{Me}_2\text{Si}(\text{Me}_4\text{C}_5)]\text{Th}(\text{CH}_2\text{-SiMe}_3)_2$ ,<sup>14b</sup> and 2.49(1) Å in  $[\text{Cp}^*\text{Th}(\text{Me})(\text{THF})_2]^+$ .<sup>14c</sup> The close contact of Th(2) to the methyl carbon of the trimethylsilyl group (Th(2)–C(10) = 3.05(3) Å) is a further example of the  $\gamma$ -agostic or  $\beta$ -methyl interaction which is frequently observed in actinide and lanthanide structures containing bis(trimethylsilyl)amide or bis(trimethylsilyl)methyl ligands.<sup>4b,13a,15</sup>

## Discussion

We were intrigued by the process in which the dinuclear species **4** is formed during the reaction between  $\text{Th}[\text{N}(\text{SiMe}_3)_2]_3(\text{OTf})$  (**2**) and  $\text{Cp}^*\text{H}$ , and therefore performed some additional experiments to probe the possible mechanistic pathway depicted in Scheme 1. The first step in the proposed mechanism is the cyclometalation of a bis(trimethylsilyl)amide ligand in the mono(triflate) **2** to produce the metallacyclic complex

$[(\text{Me}_3\text{Si})_2\text{N}](\text{TfO})\text{Th}[\text{N}(\text{SiMe}_3)(\text{SiMe}_2\text{CH}_2)]$ . Precedence for this type of reaction has been observed during the thermolysis of the closely related actinide mono(aryloxide) complexes  $\text{An}[\text{N}(\text{SiMe}_3)_2]_3(\text{OAr})$  (Ar = 2,6-*t*-Bu<sub>2</sub>C<sub>6</sub>H<sub>3</sub>, An = Th, U) which lead to silylamide ligand activation and subsequent formation of a new metallacycle of formula  $(\text{ArO})[(\text{Me}_3\text{Si})_2\text{N}]\text{An}[\text{N}(\text{SiMe}_3)(\text{SiMe}_2\text{CH}_2)]$ .<sup>16</sup> In an attempt to verify this initial step in the reaction scheme, complex **2** was heated in toluene for 7 days (100 °C), but only the starting complex and a small amount of an unidentified product were observed. This may indicate either that the first step in our preliminary mechanism is reversible or that it involves direct protonation of the Th–N bond by  $\text{Cp}^*\text{H}$  to give the product of steps 1 and 2 directly. Although an example of direct protonation of the metal–nitrogen bond in  $\text{Zr}(\text{NEt}_2)_4$  and  $\text{Hf}(\text{NMe}_2)_4$  by a substituted cyclopentadiene has been reported very recently,<sup>17</sup> we feel that the significantly higher  $\text{pK}_a$  of  $\text{Cp}^*\text{H}$  compared with mono-substituted  $\text{C}_5\text{H}_5\text{SiMe}_2\text{X}$  (X = NPh, C<sub>5</sub>H<sub>5</sub>) makes a two-step pathway (metallacycle formation followed by Th–C protonation) more likely in the present case.

The protonation reaction of the metallacyclic species

$[(\text{Me}_3\text{Si})_2\text{N}](\text{TfO})\text{Th}[\text{N}(\text{SiMe}_3)(\text{SiMe}_2\text{CH}_2)]$  with  $\text{Cp}^*\text{H}$  to produce  $\text{Cp}^*\text{Th}[\text{N}(\text{SiMe}_3)_2]_2(\text{OTf})$  in the second step is favored based upon relative  $\text{pK}_a$  values, although a pathway involving a  $\sigma$ -bond metathesis process is

(10) O'Connor, J. M.; Uhrhammer, R.; Rheingold, A. L.; Staley, D. L. *J. Am. Chem. Soc.* **1989**, *111*, 7633.

(11) Stehr, J.; Fischer, R. D. *J. Organomet. Chem.* **1992**, *430*, C1.

(12) Frankland, A. D.; Hitchcock, P. B.; Lappert, M. F.; Lawless, G. A. *J. Chem. Soc., Chem. Commun.* **1994**, 2435.

(13) (a) Gilbert, T. M.; Ryan, R. R.; Sattelberger, A. P. *Organometallics* **1988**, *7*, 2514. (b) Turner, H. W.; Andersen, R. A.; Zalkin, A.; Templeton, D. H. *Inorg. Chem.* **1979**, *18*, 1221. (c) Barnhart, D. M.; Clark, D. L.; Grumbine, S. K.; Watkin, J. G. *Inorg. Chem.* **1995**, *34*, 1695.

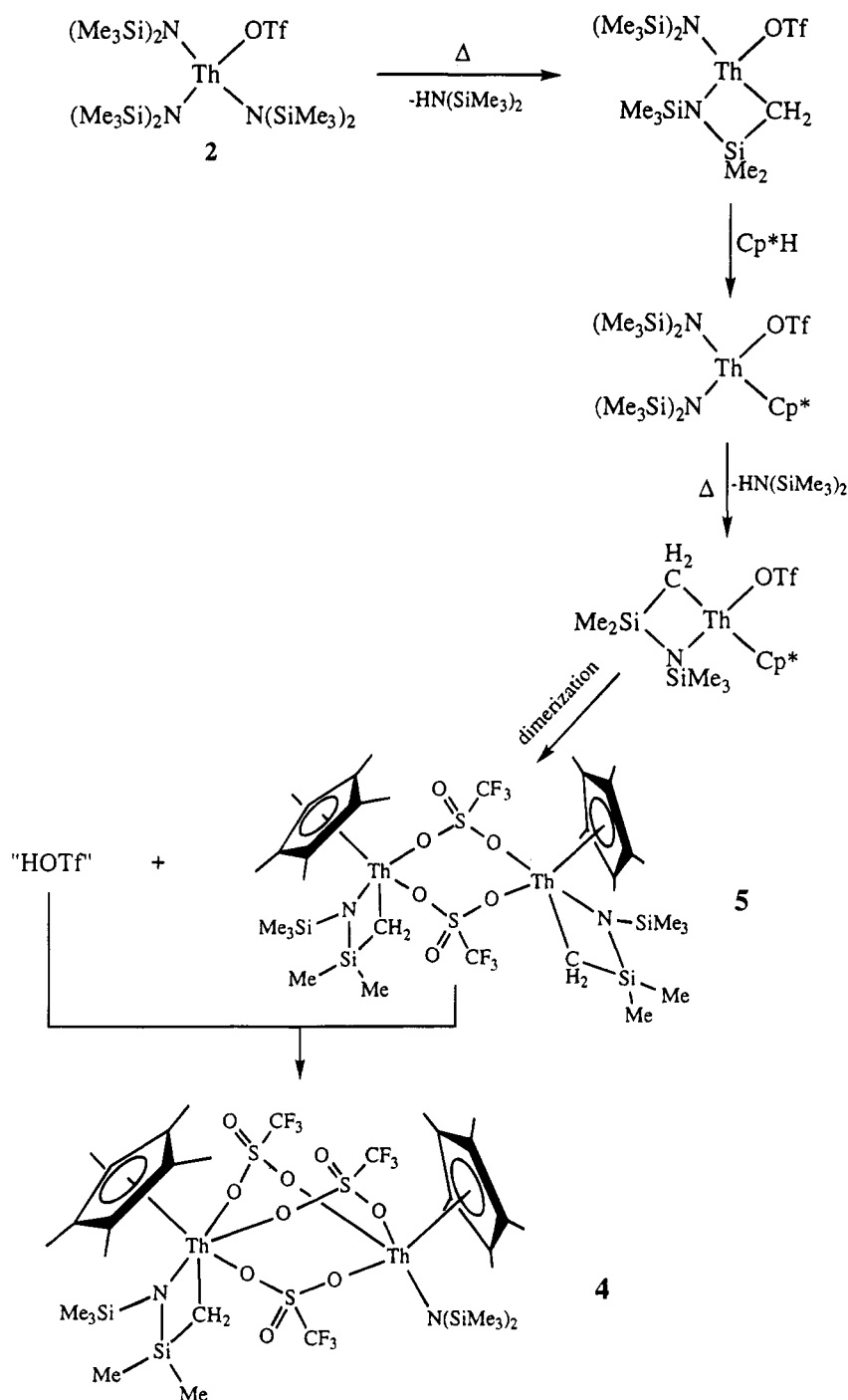
(14) (a) Edwards, P. G.; Andersen, R. A.; Zalkin, A. *Organometallics* **1984**, *3*, 293. (b) Fendrick, C. M.; Mintz, E. A.; Schertz, L. D.; Marks, T. J. *Organometallics* **1984**, *3*, 819. (c) Lin, Z.; Marechal, J.-L. L.; Sabat, M.; Marks, T. J. *J. Am. Chem. Soc.* **1987**, *109*, 4127.

(15) (a) Tilley, T. D.; Andersen, R. A.; Zalkin, A. *Inorg. Chem.* **1984**, *23*, 2271. (b) den Haan, K. H.; de Boer, J. L.; Teuben, J. H.; Spek, A. L.; Kojic-Prodic, B.; Hays, G. R.; Hues, R. *Organometallics* **1986**, *5*, 1726. (c) Schaverien, C. J.; Nesbitt, G. J. *J. Chem. Soc., Dalton Trans.* **1992**, 157. (d) Heeres, H. J.; Meetsma, A.; Teuben, J. H. *J. Chem. Soc., Chem. Commun.* **1988**, 962. (e) Tilley, T. D.; Andersen, R. A.; Zalkin, A. *J. Am. Chem. Soc.* **1982**, *104*, 3725. (f) Jeske, G.; Lauke, H.; Mauermann, H.; Swebston, P. N.; Schumann, H.; Marks, T. J. *J. Am. Chem. Soc.* **1985**, *107*, 8091. (g) Clark, D. L.; Miller, M. M.; Watkin, J. G. *Inorg. Chem.* **1993**, *32*, 772. (h) Barnhart, D. M.; Clark, D. L.; Gordon, J. C.; Huffman, J. C.; Watkin, J. G.; Zwick, B. D. *J. Am. Chem. Soc.* **1993**, *115*, 8461. (i) Van Der Sluys, W. G.; Burns, C. J.; Sattelberger, A. P. *Organometallics* **1989**, *8*, 855.

(16) Berg, J. M.; Clark, D. L.; Huffman, J. C.; Morris, D. E.; Sattelberger, A. P.; Streib, W. E.; Van der Sluys, W. G.; Watkin, J. G. *J. Am. Chem. Soc.* **1992**, *114*, 10811.

(17) Herrmann, W. A.; Morawietz, M. J. A.; Priermeier, T. *Angew. Chem., Int. Ed. Engl.* **1994**, *33*, 1946.

Scheme 1



perhaps more likely. Despite the fact that  $[(\text{Me}_3\text{Si})_2\text{N}]_2\text{Th}[\text{N}(\text{SiMe}_3)(\text{SiMe}_2\text{CH}_2)]$  (1) has been shown to be unreactive toward  $\text{Cp}^*\text{H}$  after 3 days at  $110^\circ\text{C}$  (*vide supra*), the reduced steric bulk of  $[(\text{Me}_3\text{Si})_2\text{N}](\text{TfO})\text{Th}[\text{N}(\text{SiMe}_3)(\text{SiMe}_2\text{CH}_2)]$  compared with metallacycle 1 may allow the reaction to proceed more readily in this case.

As mentioned above, the metallacycle formation proposed in step 3 has precedence in the literature,<sup>16</sup> and subsequent dimerization to form the independently synthesized complex  $\{\text{Cp}^*(\text{TfO})\text{Th}[\text{N}(\text{SiMe}_3)(\text{SiMe}_2\text{CH}_2)]\}_2$  (5) seems logical based upon steric requirements. The last step in our proposed mechanism requires the formal

incorporation of  $1/2$  equiv of triflic acid into 5 in order to facilitate the protonation of one metallacycle to an amide ligand and the concomitant introduction of the third bridging triflate ligand. We do indeed find that when 5 is allowed to react with  $1/2$  equiv of triflic acid at  $-40^\circ\text{C}$  in toluene, the major product isolated is complex 4. The actual source of the triflic acid in the formation of 4 from  $\text{Th}[\text{N}(\text{SiMe}_3)_2]_3(\text{OTf})$  (2) and  $\text{Cp}^*\text{H}$  is uncertain, but it could be a result of a small equilibrium concentration of triflic acid arising from the reverse of the reaction shown in eq 4. This postulate was investigated by heating (NMR tube,  $85^\circ\text{C}$ , 18 h) complexes 2 and 5 together in benzene- $d_6$  and observing in the  $^1\text{H}$  NMR spectrum the formation of complexes 1 and 4.

### Concluding Remarks

We have shown that the reaction of an actinide amide complex, such as  $\text{Th}[\text{N}(\text{SiMe}_3)_2]_3(\text{OTf})$  (**2**), with  $\text{Cp}^*\text{H}$  can provide an alternative to the traditional halide metathesis routes to mono(pentamethylcyclopentadienyl)actinide species. As reported recently for the Group IV metals,<sup>17</sup> this synthetic method can offer distinct advantages over halide metathesis procedures, most notably by eliminating the problem of salt retention by the actinide product.<sup>4b</sup>

The X-ray crystal structure of the dinuclear actinide complex  $\text{Cp}^*[(\text{Me}_3\text{Si})_2\text{N}]\text{Th}(\mu_2\text{-OSO}_2\text{CF}_3)_3\text{Th}[\text{N}(\text{SiMe}_3)(\text{SiMe}_2\text{CH}_2)]\text{Cp}^*$  (**4**), formed from reaction of **2** with  $\text{Cp}^*\text{H}$ , has been determined and reveals an unusual molecular geometry in which three  $\eta^2$ -triflate ligands bridge the two thorium metal centers. We have proposed a mechanism to explain the formation of **4** and have shown that several of the proposed mechanistic steps may be verified in independent reactions. Further studies of the reactivity and catalytic properties of mono- $\text{Cp}^*$  thorium complexes with alkoxide and alkyl supporting ligands are currently underway.

### Experimental Section

**General Procedures and Techniques.** All manipulations were carried out under an inert atmosphere of oxygen-free UHP grade argon using standard Schlenk techniques or under oxygen-free helium in a Vacuum Atmospheres glovebox. The metallacyclic complex  $[(\text{Me}_3\text{Si})_2\text{N}]_2\text{Th}[\text{N}(\text{SiMe}_3)(\text{SiMe}_2\text{CH}_2)]$  (**1**) was prepared as described previously.<sup>5,16</sup> Trifluoromethanesulfonic acid and pentamethylcyclopentadiene were obtained from Aldrich and degassed prior to use. Solvents were degassed and distilled from Na or Na/benzophenone ketyl under nitrogen. Benzene-*d*<sub>6</sub> was dried with Na/benzophenone ketyl and then trap-to-trap distilled before use. Solvents were taken into the glovebox, and small amounts were tested with a solution of sodium benzophenone in THF. Solvents that failed to maintain a purple coloration from this test were not used.

NMR spectra were recorded at 22 °C on a Bruker WM 300 spectrometer in benzene-*d*<sub>6</sub> solution. All <sup>1</sup>H NMR chemical shifts are reported in ppm relative to the <sup>1</sup>H impurity in benzene-*d*<sub>6</sub> set at  $\delta$  7.15. Infrared spectra were recorded as Nujol mulls or hexane solutions (KBr) on a Perkin-Elmer 1500 spectrophotometer interfaced with a 1502 central processor. Elemental analyses were performed on a Perkin-Elmer 2400 CHN analyzer. Elemental analysis samples were prepared and sealed in tin capsules in the glovebox prior to combustion.

**$\text{Th}[\text{N}(\text{SiMe}_3)_2]_3(\text{OTf})$  (**2**).** A 50 mL hexane solution of  $[(\text{Me}_3\text{Si})_2\text{N}]_2\text{Th}[\text{N}(\text{SiMe}_3)(\text{SiMe}_2\text{CH}_2)]$  (4.00 g, 5.62 mmol) was cooled to -40 °C in the drybox. To this solution was added with stirring a cold (-40 °C) trifluoromethanesulfonic acid (0.76 g, 5.1 mmol) and diethyl ether (10 mL) solution over a 5 min period, resulting in a small amount of precipitation. The mixture was stirred for 14 h, and the solvent was removed in vacuo. The resulting white solid was extracted into hexane (60 mL), filtered through Celite, and cooled to -40 °C. After 18 h, a crop of colorless crystals had formed, which were isolated by vacuum filtration inside the glovebox. Yield: 2.66 g (55%). <sup>1</sup>H NMR (300 MHz, C<sub>6</sub>D<sub>6</sub>, 22 °C):  $\delta$  0.36 (s, 54 H, SiMe<sub>3</sub>). IR (hexane, cm<sup>-1</sup>): 1367 (m), 1256 (s), 1238 (m), 1200 (s), 1162 (m), 972 (m), 917 (s), 896 (m sh), 852 (s), 772 (m), 656 (w), 633 (m), 613 (m). Anal. Calcd for C<sub>19</sub>H<sub>54</sub>F<sub>3</sub>N<sub>3</sub>O<sub>3</sub>SSi<sub>6</sub>Th: C, 26.47; H, 6.31; N, 4.87. Found: C, 26.53; H, 6.01; N, 4.82.

**$\text{Th}[\text{N}(\text{SiMe}_3)_2](\text{OTf})_3$  (**3**).** A 50 mL hexane solution of the metallacycle  $[(\text{Me}_3\text{Si})_2\text{N}]_2\text{Th}[\text{N}(\text{SiMe}_3)(\text{SiMe}_2\text{CH}_2)]$  (**1**) (3.00 g, 4.21 mmol) was cooled to -40 °C in the drybox. To this solution was added with stirring a cold (-40 °C) trifluoromethanesulfonic acid (1.29 g, 8.61 mmol) and diethyl ether (5 mL) solution over a 1 min period, resulting in a large amount of precipitation. The mixture was allowed to stir for 1 h, and the resulting white precipitate was isolated by vacuum filtration, washed with toluene (5 mL), and dried in vacuo to yield 1.30 g of **3** (36%). The precipitate is insoluble in toluene, diethyl ether, and methylene chloride. After concentrating and cooling the filtrate to -40 °C, 1.47 g (42%) of **2** was also isolated. IR (Nujol, cm<sup>-1</sup>): 1339 (m br), 1208 (s br), 1036 (s), 846 (w), 641 (m). Anal. Calcd for C<sub>9</sub>H<sub>18</sub>F<sub>9</sub>N<sub>3</sub>O<sub>3</sub>Si<sub>2</sub>Th: C, 12.87; H, 2.16; N, 1.67. Found: C, 12.66; H, 2.16; N, 1.17.

**$\text{Cp}^*[(\text{Me}_3\text{Si})_2\text{N}]\text{Th}(\mu_2\text{-OSO}_2\text{CF}_3)_3\text{Th}[\text{N}(\text{SiMe}_3)(\text{SiMe}_2\text{CH}_2)]\text{Cp}^*$  (**4**).** In a Schlenk reaction vessel, toluene (40 mL), pentamethylcyclopentadiene (0.46 g, 3.2 mmol), and **2** (2.40 g, 2.78 mmol) were combined and refluxed under argon for 8 days. All volatiles were removed in vacuo and the residue was extracted with hexane (3 × 10 mL), leaving a white microcrystalline powder (0.73 g). Upon cooling the solution to -40 °C more microcrystalline powder formed. Total yield: 0.94 g (43%). <sup>1</sup>H NMR (300 MHz, C<sub>6</sub>D<sub>6</sub>, 22 °C):  $\delta$  0.12 (s, 9 H, SiMe<sub>3</sub>), 0.16 (s, 9 H, SiMe<sub>3</sub>), 0.36 (s, 9 H, SiMe<sub>3</sub>), 0.53 (s, 3 H, SiMe), 0.54 (s, 3 H, SiMe), 1.34 (s, 1 H, ThCH<sub>2</sub>), 1.39 (s, 1 H, ThCH<sub>2</sub>), 2.08 (s, 15 H, C<sub>5</sub>Me<sub>5</sub>), 2.35 (s, 15 H, C<sub>5</sub>Me<sub>5</sub>). IR (Nujol, cm<sup>-1</sup>): 1332 (m), 1237 (s), 1219 (s), 1196 (m), 1183 (m), 1142 (w), 1030 (s), 1014 (s), 964 (m), 857 (m), 831 (m), 802 (w), 772 (w), 759 (w), 727 (w), 693 (w), 640 (m), 629 (s), 601 (w), 506 (w). Anal. Calcd for C<sub>35</sub>H<sub>65</sub>F<sub>9</sub>N<sub>2</sub>O<sub>9</sub>Si<sub>4</sub>Th<sub>2</sub> · 0.5C<sub>7</sub>H<sub>8</sub>: C, 29.88; H, 4.49; N, 1.81. Found: C, 29.74; H, 4.29; N, 1.45.

**$\{\text{Cp}^*(\text{TfO})\text{Th}[\text{N}(\text{SiMe}_3)(\text{SiMe}_2\text{CH}_2)]_2$  (**5**).** A toluene solution (5 mL) of  $\text{KN}(\text{SiMe}_3)_2$  (0.079 g, 0.40 mmol) was added to a toluene(20 mL)/THF(5 mL) solution of **4** (0.63 g, 0.40 mmol), and the solution was stirred for 4 h. All volatiles were removed under vacuum, and the solid was extracted with toluene (2 × 10 mL) and filtered through Celite. Upon cooling to -40 °C, a white powder was deposited (65 mg). The filtrate was pumped dry and washed with hexane, leaving a second crop of the white powder. Total yield: 0.28 g (50%). <sup>1</sup>H NMR (300 MHz, C<sub>6</sub>D<sub>6</sub>, 22 °C)  $\delta$  0.29 (s, 3 H, SiMe), 0.34 (s, 9 H, SiMe<sub>3</sub>), 0.40 (s, 3 H, SiMe), 0.58 (s, 2 H, ThCH<sub>2</sub>), 2.32 (s, 15 H, C<sub>5</sub>Me<sub>5</sub>). IR (Nujol, cm<sup>-1</sup>): 1324 (w), 1306 (s), 1258 (s), 1240 (s), 1201 (m), 964 (w), 857 (m), 828 (m), 804 (w), 770 (w), 634 (s), 625 (s), 602 (s), 548 (w), 515 (w). Anal. Calcd for C<sub>17</sub>H<sub>32</sub>F<sub>3</sub>N<sub>3</sub>O<sub>3</sub>Si<sub>2</sub>Th: C, 30.22; H, 4.77; N, 2.07. Found: C, 30.59; H, 4.42; N, 1.42.

**Crystallographic Studies.**  **$\text{Cp}^*[(\text{Me}_3\text{Si})_2\text{N}]\text{Th}(\mu_2\text{-OSO}_2\text{CF}_3)_3\text{Th}[\text{N}(\text{SiMe}_3)(\text{SiMe}_2\text{CH}_2)]\text{Cp}^* \cdot \text{C}_7\text{H}_8$  (**4**).** The clear, well-formed crystals were examined in mineral oil under an argon stream. A suitable crystal measuring 0.30 × 0.10 × 0.083 mm<sup>3</sup> was affixed to the end of a glass fiber using Apiezon grease. The crystal was then transferred to the goniostat of an Enraf-Nonius CAD4 diffractometer and cooled to -70 °C for characterization and data collection. Unit cell parameters were determined from the least-squares refinement of  $(\sin \theta/\lambda)^2$  values for 25 accurately centered reflections with a  $2\theta$  range between 16° and 32°. Three reflections were chosen as intensity standards and were measured every 3600 s of X-ray exposure time.

The data were reduced using the Structure Determination Package provided by Enraf-Nonius, and corrected for absorption empirically using the high- $\chi$   $\psi$ -scans. All data were corrected for Lorentz and polarization effects, and equivalent data were averaged to a unique set of intensities and associated  $\sigma$ 's in the usual manner. The structure was solved by Patterson and Fourier techniques and refined by full matrix

least squares. All non-hydrogen atoms were treated anisotropically except for the ring carbons of the pentamethylcyclopentadienyl ligands and the toluene of crystallization (C36–C39). All hydrogen atoms were placed in fixed, idealized positions in the final cycle of refinement. A final difference Fourier contained some residual electron density around the thorium, the largest peak being  $2.58 \text{ e}/\text{\AA}^3$ . All data solution calculations were performed using the Siemens SHELXTL PLUS computing package (Siemens Analytical X-ray Instruments, Inc, Madison, WI, 1990).

**Acknowledgment.** This work was performed under the auspices of the Laboratory Directed Research and Development Program. Los Alamos National Labora-

tory is operated by the University of California for the U.S. Department of Energy under Contract W-7405-ENG-36.

**Supplementary Material Available:** Tables of fractional atomic coordinates, bond lengths and angles, anisotropic thermal parameters, hydrogen atom coordinates, and an ORTEP drawing for  $\text{Cp}^*[(\text{Me}_3\text{Si})_2\text{N}]\text{Th}(\mu_2\text{-OSO}_2\text{CF}_3)_3\text{Th}[\text{N}(\text{SiMe}_3)(\text{SiMe}_2\text{CH}_2)]\text{Cp}^* \cdot \text{C}_7\text{H}_8$  (4) (11 pages). Ordering information is given on any current masthead page. Structure factor tables are available from the authors upon request.

OM950072C

# Aqueous Organometallic Chemistry: Structure and Dynamics in the Formation of ( $\eta^5$ -Pentamethylcyclopentadienyl)rhodium Aqua Complexes as a Function of pH

Moris S. Eisen,<sup>\*,†</sup> Ariel Haskel,<sup>†</sup> Hong Chen,<sup>‡</sup> Marilyn M. Olmstead,<sup>§</sup>  
David P. Smith,<sup>‡</sup> Marcos F. Maestre,<sup>‡</sup> and Richard H. Fish<sup>\*,‡</sup>

Lawrence Berkeley Laboratory, University of California, Berkeley, California 94720,  
Department of Chemistry, Technion—Israel Institute of Technology, Haifa, 32000, Israel, and  
Department of Chemistry, University of California, Davis, California 95616

Received February 22, 1995<sup>⊗</sup>

The structures of the ( $\eta^5$ -pentamethylcyclopentadienyl)rhodium aqua complexes, as a function of pH, were studied by  $^1\text{H}$ ,  $^{13}\text{C}$ ,  $^{17}\text{O}$ , and 2D NOESY NMR spectroscopic techniques as well as by FAB mass spectrometry and potentiometric titration. The starting complex for our NMR experiments,  $[\text{Cp}^*\text{Rh}(\text{H}_2\text{O})_3](\text{OTf})_2$ , **1**, was structurally characterized by single-crystal X-ray crystallography [130 K, Mo K $\alpha$  radiation,  $\lambda = 0.71073 \text{ \AA}$ ,  $a = 23.979(9) \text{ \AA}$ ,  $b = 9.726(4) \text{ \AA}$ ,  $c = 18.257(6) \text{ \AA}$ ,  $Z = 8$ , orthorhombic, space group  $Pna2_1$ , 3879 independent reflections,  $R = 0.0482$ ,  $R_w = 0.1062$ ]. Both  $^1\text{H}$  and  $^{13}\text{C}$  NMR titration experiments of the starting complex, **1**, were performed by dissolving **1** in  $\text{H}_2\text{O}$  ( $\text{D}_2\text{O}$ ) and obtaining spectra from pH 2–14. From pH 2–5 only one  $\text{Cp}^*$  signal ( $^1\text{H}$  NMR, 1.57 ppm;  $^{13}\text{C}$  NMR, 5.78 ppm) was observed, which was attributed to **1**. As the pH of the solution with **1** was increased from 5 to 7, a dynamic and rapid equilibrium was observed to provide putative  $[\text{Cp}^*\text{Rh}(\mu\text{-OH})(\text{H}_2\text{O})_2](\text{OTf})_2$ , **2**, and  $[(\text{Cp}^*\text{Rh})_2(\mu\text{-OH})_3](\text{OTf}/\text{OH})$ , **3**; unfortunately, only one  $^1\text{H}$  or  $^{13}\text{C}$  NMR signal for  $\text{Cp}^*\text{Rh}$  at 1.50 ( $\text{Cp}^*$ ) or 5.41 ppm ( $\text{C}-\text{CH}_3$ ), respectively, was found for the latter two species, with broadening of the signals at pH 5.5–6, indicating that conversion from putative **2** to **3** was very fast on the NMR time scale. As the pH was further increased from 7 to 10, only the  $^1\text{H}$  or  $^{13}\text{C}$  NMR signal for **3** was observed at 1.50 or 5.41 ppm, respectively. In addition, starting the equilibrium from **3** (**3**  $\rightleftharpoons$  **1** via putative **2**) within the pH range 14–2 provided similar results. The 2D NOESY NMR exchange phasing experiments at pH 5.8 and 11 showed correlations between the  $\text{Cp}^*$   $\text{CH}_3$  groups and the  $\text{H}_2\text{O}$  or  $\mu\text{-OH}$  groups attached to Rh and between both  $\text{Cp}^*$   $\text{CH}_3$  groups of the  $\text{Cp}^*\text{Rh}$  aqua complexes, although separate signals for bulk  $\text{H}_2\text{O}$  and  $\mu\text{-OH}$  or  $\text{H}_2\text{O}$  ligands bonded to Rh were not observed due to a rapid exchange process. A potentiometric titration study gave further evidence that the conversion of **1**  $\rightarrow$  **3** via putative **2** occurs rapidly with only one  $\text{p}K_a$  of 5.3 being observed, reaffirming the fact that the conversion of **1**  $\rightarrow$  **3** via putative **2** was extremely fast. The pseudo-first-order rate of conversion of **1**  $\rightarrow$  **3** at pH 5.8 was measured by an NMR spin population transfer technique to be  $k_1 = 7.18 \text{ s}^{-1}$  (**1**, 0.034 M;  $T_1 = 1.6 \text{ s}$ ), while  $k_{-1}$ , **3**  $\rightarrow$  **1**, was found to be  $2.93 \text{ s}^{-1}$  ( $T_1 = 1.5 \text{ s}$ ). The equilibrium constant,  $K_{\text{eq}}$ , at pH 5.8 for **1**  $\rightleftharpoons$  **3** was found to be 353.  $^{17}\text{O}$  NMR studies again showed that  $\text{H}_2\text{O}$  molecules bonded to  $\text{Cp}^*\text{Rh}$  and those in the bulk solution are in very fast exchange ( $k > 8150 \text{ s}^{-1}$ ).

Aqueous organometallic chemistry is a relatively new and exciting area that has primarily focused on catalysis studies<sup>1</sup> and, to a lesser extent, on the reactions of DNA/RNA nucleobases, nucleosides, nucleotides, and oligonucleotides,<sup>2</sup> as well as amino acids (MeOH solvent),<sup>3</sup> aniline and phenol derivatives,<sup>4</sup> and other biological systems.<sup>5</sup> Our entry into this new area of organometallic chemistry was instigated by our recent studies of the reactions of a ( $\eta^5$ -pentamethylcyclopentadienyl)rhodium aqua complex(es) with DNA/RNA nucleobases, nucleosides, and nucleotides in aqueous solution.<sup>2a–d</sup>

Moreover, from those results with DNA/RNA biological ligands, we felt it necessary to understand the structure and dynamics of the ( $\eta^5$ -pentamethylcyclo-

(2) (a) Smith, D. P.; Baralt, E.; Morales, B.; Olmstead, M. M.; Maestre, M. F.; Fish, R. H. *J. Am. Chem. Soc.* **1992**, *114*, 10647. (b) Smith, D. P.; Olmstead, M. M.; Noll, B. C.; Maestre, M. F.; Fish, R. H. *Organometallics* **1993**, *12*, 593. (c) Smith, D. P.; Kohen, E.; Maestre, M. F.; Fish, R. H. *Inorg. Chem.* **1993**, *32*, 4119. (d) Smith, D. P.; Griffin, M. T.; Olmstead, M. M.; Maestre, M. F.; Fish, R. H. *Inorg. Chem.* **1993**, *32*, 4677. (e) Kuo, L. Y.; Kanatzdis, M. G.; Sabat, M.; Tipton, A. L.; Marks, T. J. *J. Am. Chem. Soc.* **1991**, *113*, 9027 and references therein. (f) Presented at an Advanced NATO Workshop on Aqueous Organometallic Chemistry and Catalysis, Horváth, I., Joo, F., Co-Chairmen, Debrecen, Hungary, August 29–September 1, 1994.

(3) Kramer, R.; Polborn, K.; Robl, C.; Beck, W. *Inorg. Chim. Acta* **1992**, *198–200*, 415 and references therein.

(4) (a) Nutton, A.; Maitlis, P. M. *J. Chem. Soc., Dalton Trans.* **1981**, 2335. (b) Nutton, A.; Maitlis, P. M. *J. Chem. Soc., Dalton Trans.* **1981**, 2339. (c) Espinet, P.; Bailey, P. M.; Maitlis, P. M. *J. Chem. Soc., Dalton Trans.* **1979**, 1542.

(5) (a) Ryabov, A. D. *Angew. Chem., Int. Ed. Engl.* **1991**, *30*, 931. (b) Jaouen, G.; Vessieres, A.; Butler, I. S. *Acc. Chem. Res.* **1993**, *26*, 361.

\* To whom correspondence should be addressed.

<sup>†</sup> Technion.

<sup>‡</sup> Lawrence Berkeley Laboratory.

<sup>§</sup> University of California, Davis.

<sup>⊗</sup> Abstract published in *Advance ACS Abstracts*, May 1, 1995.

(1) (a) Barton, M.; Atwood, J. D. *J. Coord. Chem.* **1991**, *24*, 43. (b) Hermann, W. A.; Kohlpaintner, C. W. *Angew. Chem., Int. Ed. Engl.* **1993**, *32*, 1524.

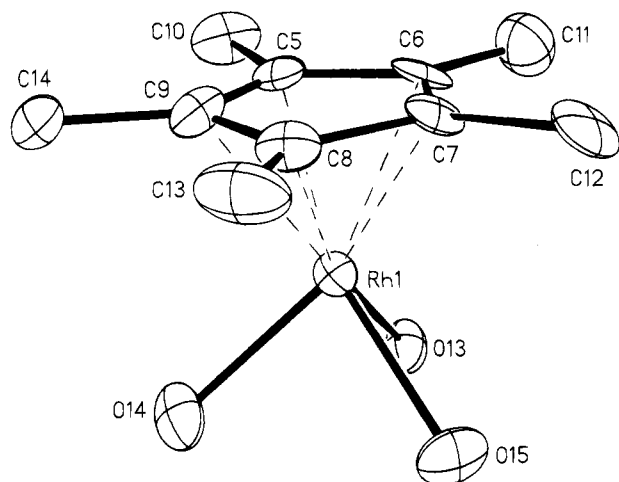


**Figure 1.** ORTEP drawing of the cationic portion of complex **1** (see Table 3 for selected bond distances and angles).

pentadienyl)rhodium aqua complex(es) as a function of pH.<sup>2f</sup> In our perusal of the literature, we found that several studies on these Cp\*Rh aqua complexes had been reported, the most notable being the pioneering studies of Maitlis and co-workers. They isolated and characterized by X-ray crystallography a product from the hydrolysis of [Cp\*RhCl<sub>2</sub>]<sub>2</sub> at pH 14, [(Cp\*Rh)<sub>2</sub>(μ-OH)<sub>3</sub>(OH)], **3**, and also obtained, in another reaction, a complex with an empirical formula of [Cp\*Rh(SO<sub>4</sub>)(H<sub>2</sub>O)<sub>2</sub>]<sub>k</sub>. This was thought to be the tris aqua complex [Cp\*Rh(H<sub>2</sub>O)<sub>3</sub>]<sup>2+</sup>, **1**; however, attempts to fully characterize this material were not successful.<sup>6</sup> Kölle and co-workers also speculated on this same complex as a low-pH structure, **1**, and reported a pK<sub>1</sub> value of 3.6.<sup>7a</sup>

Neither of those reported studies<sup>6,7a</sup> focused on the structure and dynamics of the Cp\*Rh aqua complexes as a function of pH, and, to reiterate, the relationship between the putative low-pH structure, **1**, and the high-pH structure, **3**, defined by X-ray crystallography, has never been unequivocally established; it may be important to state at this time that generally very little is known about the structure and dynamics of organometallic aqua complexes<sup>2e,7b,c</sup> in comparison to what has been reported for several inorganic aqua complexes.<sup>8</sup> Therefore, in lieu of the previously reported fragmentary results concerning the Cp\*Rh aqua complexes, we have performed an in-depth <sup>1</sup>H, <sup>13</sup>C, <sup>17</sup>O, and 2D NOESY NMR study of the structure and dynamics of the equilibrium of conversion of **1** → **3** via the plausible intermediacy of putative **2**, [Cp\*Rh(μ-OH)(H<sub>2</sub>O)<sub>2</sub>]<sup>2+</sup>, further studied the structure of **1** by single-crystal X-ray crystallography and fast atom bombardment mass spectrometry (FAB/MS), and also established the relationship between **1** and **3** by utilizing potentiometric titration techniques.

(6) Nutton, A.; Baily, P. M.; Maitlis, P. M. *J. Chem. Soc., Dalton Trans.* **1981**, 1997 and references therein.

(7) (a) Kölle, U.; Kläui, W. *Z. Naturforsch.* **1991**, *46B*, 75 and references therein. (b) Kölle, U.; Flunkert, G.; Görissen, R.; Schmidt, M.; Englert, U. *Angew. Chem., Int. Ed. Engl.* **1992**, *31*, 440 and references therein. (c) Dadci, L.; Elias, H.; Frey, U.; Hornig, A.; Kölle, U.; Merbach, A. E.; Paulus, H.; Schneider, J. S. *Inorg. Chem.* **1995**, *35*, 306.

(8) (a) Cervini, R.; Fallon, G. D.; Spiccia, L. *Inorg. Chem.* **1991**, *30*, 831. (b) Read, M. C.; Glaser, J.; Sandström, M.; Toth, I. *Inorg. Chem.* **1992**, *31*, 4155. (c) Wieghardt, K.; Schmidt, W.; Nuber, B.; Prikner, B.; Weiss, J. *Chem. Ber.* **1980**, *113*, 36.

**Table 1. Crystallographic Data for 1**

compound	[Cp*Rh(H <sub>2</sub> O) <sub>3</sub> ](OTf) <sub>2</sub>
formula	C <sub>12</sub> H <sub>21</sub> F <sub>6</sub> O <sub>9</sub> RhS <sub>2</sub>
fw	590.31
a, Å	23.979(9)
b, Å	9.726(4)
c, Å	18.257(6)
V, Å <sup>3</sup>	4258(3)
Z	8
cryst syst	orthorhombic
space group	Pna2 <sub>1</sub>
T, K	130 (2)
λ, Å	0.710 73
d(calcd), g/cm <sup>3</sup>	1.377
μ(Mo Kα), cm <sup>-1</sup>	9.4
range of transmissn factors	0.95–0.98
R	0.0482
R <sub>w</sub>	0.1062

**Table 2. Selected Atomic Coordinates (×10<sup>4</sup>) and Isotropic Thermal Parameters (Å<sup>2</sup> × 10<sup>3</sup>) for 1**

	x	y	z	U
Rh(1)	317 (1)	1441(1)	0(1)	20(1)
O(13)	223(3)	691(8)	1138(5)	28(2)
O(14)	1176(3)	1037(9)	223(5)	36(2)
O(15)	270(4)	-723(8)	-173(4)	35(2)
C(5)	108(5)	3556(11)	81(9)	31(3)
C(6)	-397(5)	2747(10)	-43(9)	26(3)
C(7)	-328(5)	2068(12)	-700(6)	22(2)
C(8)	213(6)	2378(11)	-1014(7)	26(3)
C(9)	464(5)	3340(12)	-526(8)	32(3)
C(10)	235(6)	4505(14)	708(7)	36(3)
C(11)	-866(6)	2684(15)	489(10)	44(4)
C(12)	-758(5)	1133(13)	-1037(8)	39(3)
C(13)	425(7)	1922(15)	-1727(8)	45(4)
C(14)	1023(6)	3998(13)	-639(9)	46(4)
Rh(2)	-2857(1)	-1145(1)	7276(1)	21(1)
O(16)	-3717(3)	-801(8)	7021(5)	31(2)
O(17)	-2751(4)	-204(9)	6213(5)	30(2)
O(18)	-2876(4)	981(9)	7597(5)	51(3)

**Table 3. Selected Bond Distances (Å) and Angles (deg) for 1**

Rh(1)–O(13)	2.213(8)	Rh(1)–O(14)	2.137(8)
Rh(1)–O(15)	2.131(8)	Rh(1)–C(5)	2.122(11)
Rh(1)–C(6)	2.134(10)	Rh(1)–C(7)	2.096(10)
Rh(1)–C(8)	2.079(12)	Rh(1)–C(9)	2.112(12)
Rh(2)–O(16)	2.140(8)	Rh(2)–O(17)	2.162(8)
Rh(2)–O(18)	2.150(9)	Rh(2)–C(15)	2.114(10)
O(14)–Rh(1)–O(13)	81.9(3)	O(15)–Rh(1)–O(13)	78.9(3)
O(15)–Rh(1)–O(14)	84.1(3)	C(5)–Rh(1)–O(13)	103.3(5)

## Results

### X-ray Crystal Structure of [Cp\*Rh(H<sub>2</sub>O)<sub>3</sub>](OTf)<sub>2</sub>,

**1.** Clearly, it would be informative to have the unequivocal structure of complex **1**, [Cp\*Rh(H<sub>2</sub>O)<sub>3</sub>](OTf)<sub>2</sub>, to be better able to define the equilibrium between **1** ↔ **3**. Initial attempts to accomplish this involved reaction of [Cp\*Rh(OTf)<sub>2</sub>]<sub>k</sub>, prepared from [Cp\*RhCl<sub>2</sub>]<sub>2</sub> with AgOTf in CH<sub>2</sub>Cl<sub>2</sub>, with H<sub>2</sub>O. This provided a complex that was always H<sub>2</sub>O deficient and gave a formula of [Cp\*Rh(H<sub>2</sub>O)<sub>2</sub>(OTf)<sub>2</sub>]<sub>k</sub>. We recently found, however, that this was a consequence of our recrystallization (CH<sub>2</sub>Cl<sub>2</sub>) and drying procedures, whereby the H<sub>2</sub>O ligand was partially lost during these processes. Moreover, we found that, by layering the CH<sub>2</sub>Cl<sub>2</sub> solution with 3 equiv of H<sub>2</sub>O/Cp\*Rh, X-ray-quality crystals were obtained for **1**.

The X-ray structure of complex **1** is shown in Figure 1, while Table 1 shows the crystallographic data, Table 2 provides selected atomic coordinates and isotropic thermal parameters, and Table 3 shows selected bond distances and angles. The structure consists of two

molecules of **1**, which are slightly different crystallographically (supplementary material). The cationic portions of both molecules have the typical piano stool geometry, with the sums of the O–Rh(1)–O and O–Rh(2)–O angles equal to 244.9° and 245.9°, respectively. These values are larger than those found in the structure of **3** (227.6° and 227.1°),<sup>6</sup> indicating less strain in the oxygen coordinations of **1**. Moreover, the mean Rh–O and Rh–C distances of 2.156 and 2.118 Å for **1** are comparable to those found in **3** (2.114 and 2.128 Å, respectively).

When complex **1** was dissolved in H<sub>2</sub>O, the pH was found to be 3.5. Therefore, the *in situ* preparation of **1** by reaction of [Cp\*RhCl<sub>2</sub>]<sub>2</sub> with AgOTf in H<sub>2</sub>O (measured pH = 3.5) provides a facile method for its formation in aqueous solution. Further attempts on understanding the monomeric nature of complex **1** in solution was provided by running the <sup>1</sup>H NMR spectrum of the pH 3.5 Cp\*Rh aqua complex, **1**, in DMSO-*d*<sub>6</sub>. Thus, the Cp\* signal at 1.53 ppm and the broad H<sub>2</sub>O signal at 3.38 ppm were found in the ratio Cp\*/H<sub>2</sub>O = 2.5, while a ratio of 2.5 is expected for the aqua complex **1**. Thus, we believe that the structure of **1** in water at a pH 3.5 is as shown in the solid state in Figure 1.

**<sup>1</sup>H and <sup>13</sup>C NMR Spectroscopic Titration Studies of Complexes **1** and **3**.** An <sup>1</sup>H and <sup>13</sup>C NMR pH titration study was initiated with [Cp\*Rh(H<sub>2</sub>O)<sub>3</sub>](OTf)<sub>2</sub>, **1**.<sup>2a</sup> Complex **1** was dissolved in D<sub>2</sub>O, and the pH was adjusted with either 0.01 M CF<sub>3</sub>SO<sub>3</sub>D (DOTf) or NaOD. Figure 2 shows the <sup>1</sup>H NMR titration results from pH 2–10 (in D<sub>2</sub>O, pD = pH + 0.4). From pH 2–5 only one sharp Cp\*Rh resonance for **1** is evident at 1.57 ppm, while the signal at 4.73 is that of H<sub>2</sub>O. As the pH is increased from 5 to 7, a second signal is observed at 1.50 ppm. Both signals, 1.57 and 1.50 ppm, are clearly broadened in this pH range (5–7) and reflect the possibility of several Cp\*Rh aqua complexes being in rapid equilibrium. Further increases in the pH to 10 (Figure 2) and then to 14 (not shown) provide only a sharp signal at 1.50 ppm.

A similar <sup>13</sup>C NMR pH titration experiment at pH 2.0 (supplementary material) provided the Cp\* ring carbons at 88.73 (doublet, *J*<sub>Rh–C</sub> = 6.1 Hz), while the Cp\* CH<sub>3</sub> groups appeared at 5.78 ppm. When the pH is raised to 5.5, two sets of signals are evident for both Cp\* ring and CH<sub>3</sub> carbon atoms. Thus, the Cp\* ring carbons appear as doublets at 92.02 (*J*<sub>Rh–C</sub> = 6.1 Hz) and 88.73 (*J*<sub>Rh–C</sub> = 6.1 Hz) ppm, while the Cp\* CH<sub>3</sub> resonances appear at 5.78 and 5.41 ppm (supplementary material). As the pH is raised to 10, only the signal for the Cp\* ring carbons is evident at 92.02 ppm, while the Cp\* CH<sub>3</sub> carbons show only the 5.41 ppm signal.

We also studied the Cp\*Rh aqua equilibrium starting from complex **3** at pH 14 and then proceeding to pH 5.2. Figure 3 shows a similar <sup>1</sup>H NMR pH titration experiment as in Figure 2. Although there is a very slight shift of complex **3** at pH 14, [(Cp\*Rh)<sub>2</sub>(μ-OH)<sub>3</sub>]<sup>+</sup>, the pH range from 12.5 to 5.2 provides the same two signals at 1.50 and 1.57 ppm and is further evidence for the equilibrium between the low-, intermediate-, and high-pH Cp\*Rh aqua species.

**Additional Structural Determinations of the Cp\*Rh Aqua Complexes **1** and **3** by 2D NOESY Exchange Phasing and FAB/MS Techniques.** The present study defined the structure of the low-pH

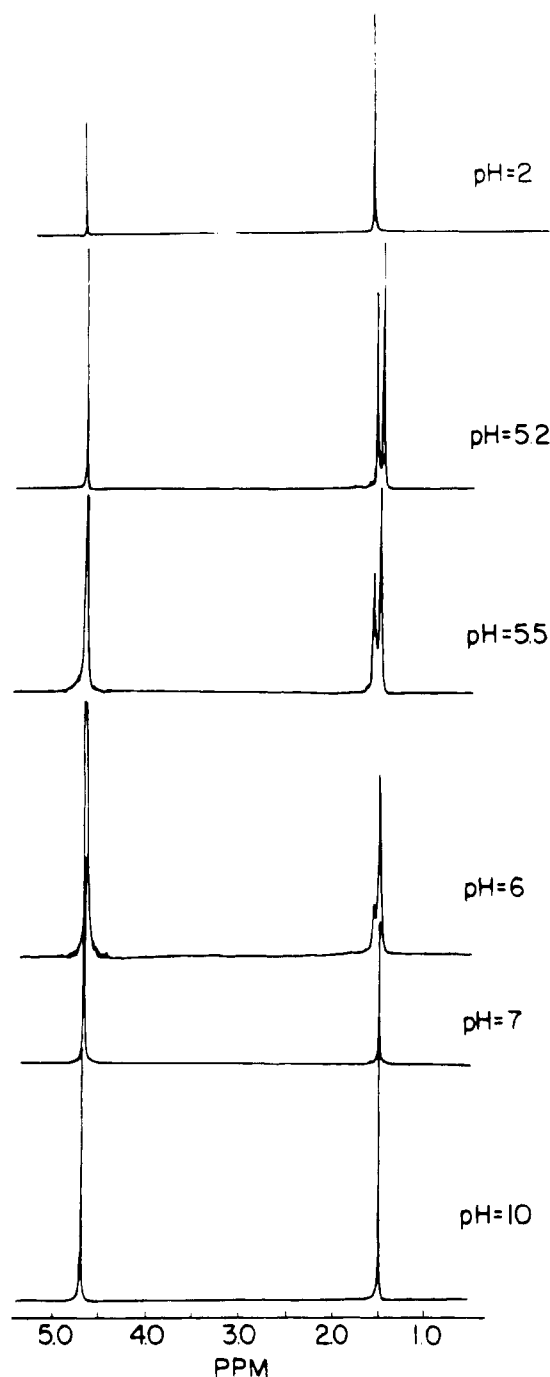


**Figure 2.** <sup>1</sup>H NMR spectral titration experiments of complex **1**, pH 2–10.

Cp\*Rh aqua complex as that of [Cp\*Rh(H<sub>2</sub>O)<sub>3</sub>]<sup>2+</sup>, **1**. In order to further clarify structure **1** as the pH 2–5 Cp\*Rh aqua complex (Figure 1), we used a 2D NOESY exchange phasing procedure, the basic premise being that the three H<sub>2</sub>O molecules complexed to the Rh metal center are in rapid exchange with the bulk H<sub>2</sub>O molecules (no separate signal for Cp\*Rh-complexed H<sub>2</sub>O was observed even at a lower temperature). Therefore, if structure **1**, [Cp\*Rh(H<sub>2</sub>O)<sub>3</sub>]<sup>2+</sup>, is correct in aqueous acidic solution, then there should be a NOESY cross-polarization effect between the three H<sub>2</sub>O molecules complexed to the Rh metal center and the CH<sub>3</sub> groups of Cp\*. The 2D NOESY experiment at pH 5.8 (Figure 4A) clearly verifies a strong correlation between complexed H<sub>2</sub>O and the Cp\* CH<sub>3</sub> groups as well as between both Cp\* and CH<sub>3</sub> in the equilibrium. As well, a similar

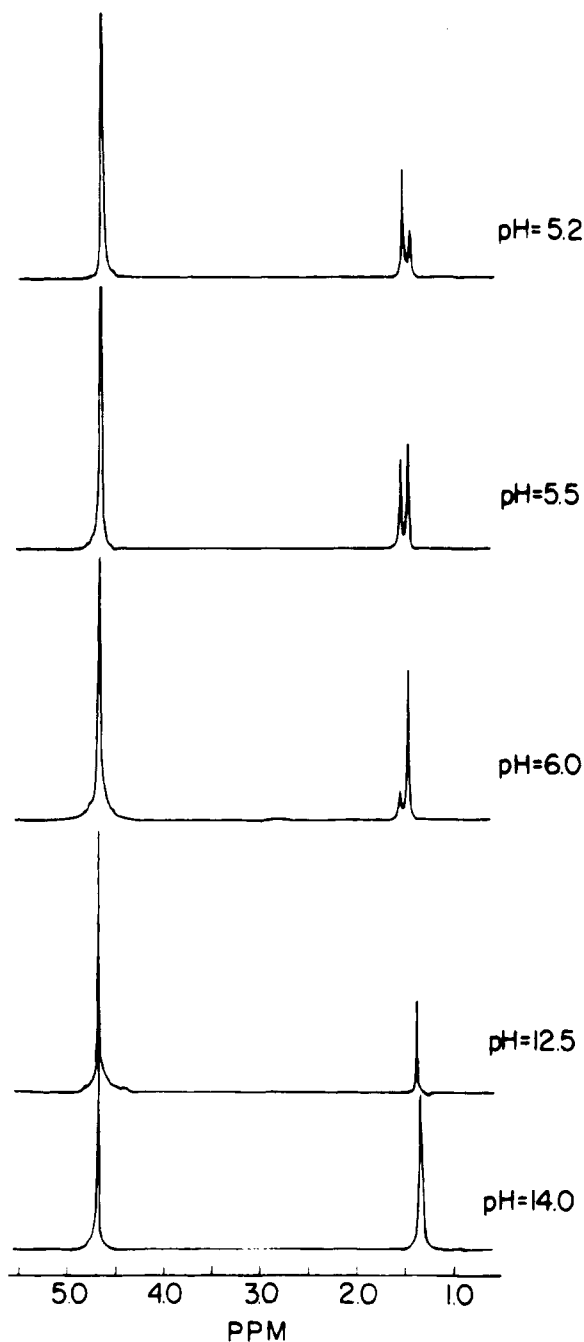


**Figure 3.**  $^1\text{H}$  NMR spectral titration experiments of complex **3**, pH 14–5.2.

NOESY correlation (Figure 4B) for  $\mu\text{-OH}$  groups bonded to  $\text{Cp}^*\text{Rh}$  and the  $\text{Cp}^*\text{CH}_3$  groups was also observed at pH 11, which corroborates that complex **3** is in equilibrium with the low-pH (<5) aqua complex **1** via putative **2**.

In addition, attempts to verify the structure of **1** by FAB/MS experiments (*p*-nitrobenzyl alcohol matrix) on acidic solutions (pH < 5) provided data that showed, under the FAB/MS conditions, that complex **1** forms a presumed  $\mu\text{-H}_2\text{O}$ -bridged dimeric species,  $[(\text{Cp}^*\text{Rh}(\text{H}_2\text{O})_2)_2(\mu\text{-H}_2\text{O})(\text{CF}_3\text{SO}_3)_2]^+$ ,  $m/e = 1013$  (15%), and a  $[(\text{Cp}^*\text{Rh})_2(\text{CF}_3\text{SO}_3)_2]^+$  ion, at  $m/e = 923$  (100%). This is consistent with our finding that under vacuum complex **1** may lose a water molecule, and this is reflected in the FAB/MS with formation of  $\mu\text{-H}_2\text{O}$ -bridged dimeric species. Interestingly, complex **3** at pH 14 shows a FAB/MS (*p*-nitrobenzyl alcohol matrix) peak

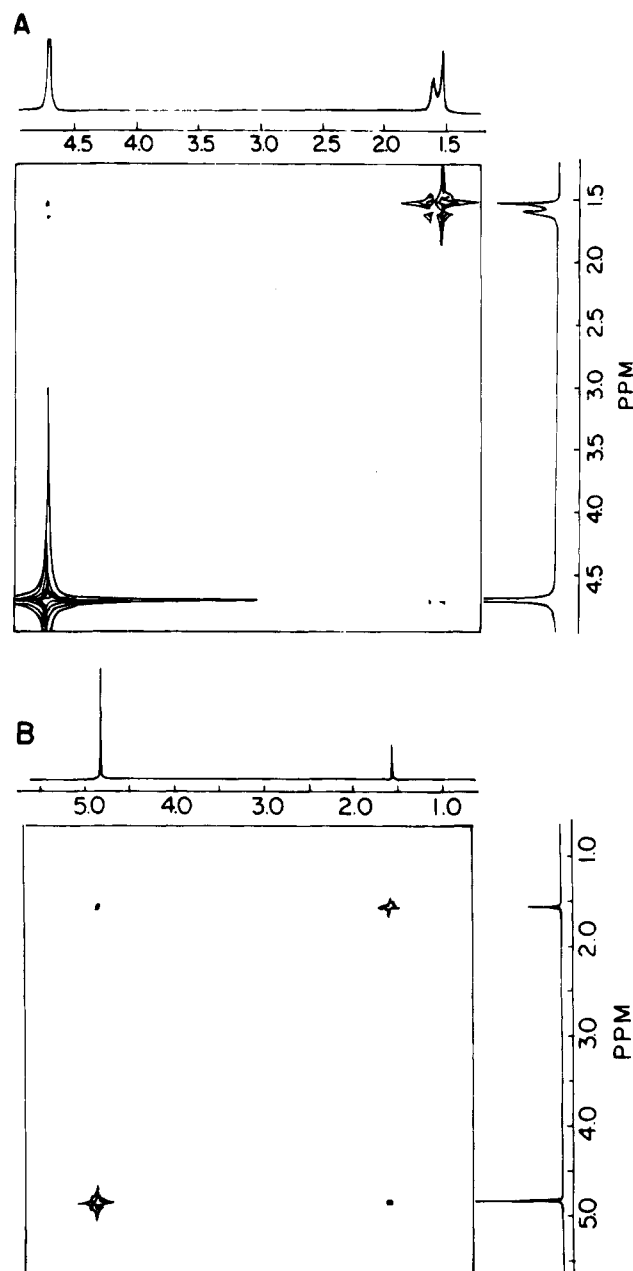


**Figure 4.** 2D NOESY for complex **1** at pH 5.8 (A) and pH 11 (B).

that provides the replacement of all three  $\mu\text{-OH}$  groups by three *p*-nitrobenzyl alcohol (PNA) groups to give the  $[(\text{Cp}^*\text{Rh})_2(\text{PNA})_3]^+$  ion, at  $m/e = 932$ .

**Potentiometric Titration Experiments.** A detailed potentiometric titration study of the  $\text{Cp}^*\text{Rh}$  aqua complexes would shed light on the equilibrium by determining the  $\text{p}K_a$  values. Complex **1** was dissolved in 0.02 M HOTf and titrated with 0.1 N NaOH. Figure 5A shows the results of this potentiometric titration, and it is clearly the classical titration of a mixture of a strong acid (HOTf) and a weak acid (**1**). The amount of NaOH from the first equivalence point for HOTf ( $\text{p}K_a = 2.5$ ) to the second equivalence point of the  $\text{Cp}^*\text{Rh}$  aqua complexes is 1.5 times the amount of starting aqua complex **1**; i.e., the ratio of  $\text{Cp}^*\text{Rh}$  aqua complex/NaOH is 1:1.5. Surprisingly, there is only one  $\text{p}K_a$  of 5.3 that was observed in this titration for the  $\text{Cp}^*\text{Rh}$  aqua species equilibrium. Alternatively, we studied the potentiometric titration of complex **3** from pH 14 to 2 and again



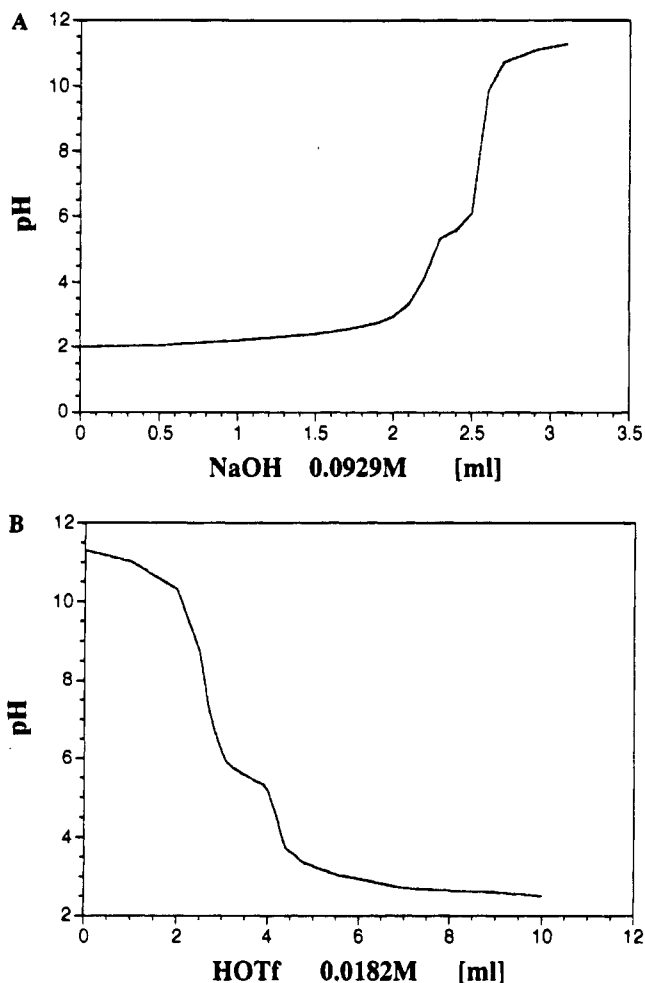
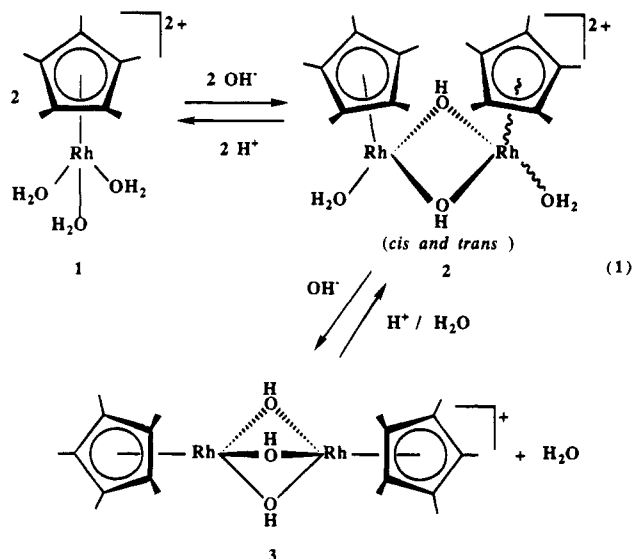


**Figure 5.** Potentiometric titration of complex **1** at pH 2–14 (A) and complex **3** at pH 14–2 (B).

found only one  $pK_a$  of 5.3 (Figure 5B). From the 1:1.5 ratio of complex **1** to NaOH and the fact that we see *only one* and *not two*  $pK_a$  values as we might have expected, we can now formulate the following equilibrium scheme, including the above-mentioned data generated by NMR, single-crystal X-ray, and FAB/MS experiments (eq 1).



**Kinetic and Equilibrium Constants for  $1 \rightleftharpoons 3$ .** The NMR pH titration experiments (Figures 2 and 3)

established the equilibrium between  $Cp^*Rh$  aqua complexes **1** and **3** via the plausible intermediate **2** (eq 1). Therefore, we decided to measure the equilibrium pseudo-first-order rate constants ( $k_1$  and  $k_{-1}$ ) at pH 5.8 by an NMR spin population transfer technique, followed by the use of the Bloch equation  $k = 1/T_{1A} [M_{0A}/M_{ZA\infty} - 1]$ , where  $T_{1A}$  is the longitudinal relaxation time of nucleus **A**,  $M_{0A}$  is the equilibrium magnetization of the nuclei at site **A** before perturbation by rf energy, and  $M_{ZA\infty}$  is the magnetization of nuclei **A** after equilibrium magnetization has been reached.

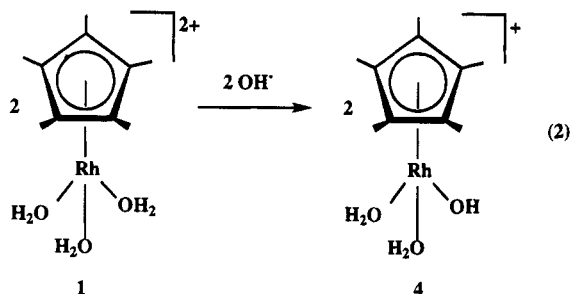
This analysis provided the following pseudo-first-order rate constant for conversion of **1**  $\rightarrow$  **3** at pH 5.8,  $k_1 = 7.18 \text{ s}^{-1}$ , with a  $T_1$  for **1** (0.034 M) of 1.6 s, while the rate constant,  $k_{-1}$ , for the reverse reaction, **3**  $\rightarrow$  **1**, is  $2.93 \text{ s}^{-1}$  with a  $T_1$  for **3** of 1.55 s. From these calculations, we can determine the equilibrium ratio for **1**  $\rightleftharpoons$  **3** to be 2.45 at pH 5.8, while from the integration ratio the equilibrium constant,  $K_{eq}$ , was found to be 353.

We also performed  $^{17}O$  NMR experiments over the pH range from 2 to 14 to elucidate exchange rates of bulk  $H_2O$  with  $H_2O$  or  $\mu-OH$  ligands bonded to the  $Cp^*Rh$  metal center. The spectra showed that the bulk  $H_2O$  with  $H_2O$  and  $\mu-OH$  ligands bonded to the  $Cp^*Rh$  metal center were in the very fast exchange regime, providing only one  $^{17}O$  signal; therefore, a rate of exchange can be estimated as  $k_{exchange} > 8150 \text{ s}^{-1}$ , by simply multiplying the chemical shift of the  $\mu-OH$  groups ( $\sim 150$  ppm, referenced to bulk  $H_2O$  at 0 ppm) by the Hz/ppm (54.2, frequency of  $^{17}O$ ) at 400 MHz.<sup>8b</sup> This  $k_{exchange}$  rate of  $> 8150 \text{ s}^{-1}$  can be compared to the number recently reported for *in situ*-generated **1**, via variable pressure  $^{17}O$  NMR studies, of  $1.6 \times 10^5 \text{ s}^{-1}$ , therefore, our reported value appears to be at the lower limits of this fast exchange process.<sup>7c</sup> It is also noteworthy to mention that in the latter variable pressure  $^{17}O$  NMR studies<sup>7c</sup> that only one signal was found for *in situ*-generated **1**, which implies that in solution at pH 2–5 this aqua complex is monomeric.

## Discussion

The most surprising aspect of our overall results on elucidating the structure and dynamics of the equilibrium between  $Cp^*Rh$  aqua complexes from pH 2–14 (eq 1) was that only two species were observed when the equilibrium was started from either **1** or **3**, the caveat being that only one broadened NMR signal was observed in the pH range 5–7 for both the putative intermediate **2** and for **3**, the tris- $\mu-OH$  complex. In addition, only one  $pK_a$  was found for both of these complexes, confirming the rapid equilibria between them. In our scheme for this equilibrium (eq 1), we designate the  $Cp^*Rh$  aqua complex **2** as the most logical intermediate between the conversion of **1** to **3**. This can be rationalized by the data generated in the potentiometric titration, by other similar  $[Cp^*Rh(\mu-OH)(L)_2]^{2+}$  dimer structures reported in the literature, as well as by precedent from inorganic models of the  $Cp^*Rh$  aqua equilibrium.

We believe that a mononuclear  $[Cp^*Rh(H_2O)_2(OH)]^+$  cationic complex, **4**, (eq 2) is formed first from reaction of 2 mol of **1** with 2 mol of NaOH. Complex **4**, a monocation, is the logical precursor to the putative dimer complex, **2**, a  $\mu-OH$  structure with terminal  $H_2O$  ligands (eq 1), via a rapid dimerization reaction.



The analogous structure depicted for **2** in eq 1 has been found for several nitrogen ligand complexes with the general formula  $[\text{Cp}^*\text{Rh}(\mu\text{-OH})(\text{L})_2]^{2+}$ , determined by single-crystal X-ray analysis, where L, a terminal ligand, was pyridine,<sup>9</sup> quinoline,<sup>10</sup> or 1-methylcytosine.<sup>2b</sup> In addition, a previous study by Wiegardt and co-workers<sup>8b</sup> on an inorganic model for the rapid equilibrium between **2** and **3** in eq 1 was reported for a (1,4,7-triazacyclononane)rhodium(III) cationic system. In this latter study, a *trans*-diaquabis( $\mu$ -hydroxo)bis[1,4,7-triazacyclononane]rhodium(III) cationic complex was isolated and characterized by single-crystal X-ray analysis. In solution, this analogue of complex **2** was converted to the tris( $\mu$ -hydroxo)bis[1,4,7-triazacyclononane]rhodium(III) cationic complex by a change in pH, a structure analogous to complex **3** that was elucidated by Maitlis and co-workers.<sup>6</sup>

The surprisingly rapid conversion from putative intermediate **2** to tris- $\mu$ -OH dimer **3** consumes 1 mol of NaOH and thereby explains the overall molar ratio of 1:1.5 of starting  $\text{Cp}^*\text{Rh}$  aqua complex, **1**, to the amount of NaOH added in the potentiometric titration from pH 2–12. More importantly, we have unequivocally ascertained the monomeric structure of **1** by X-ray crystallographic and <sup>1</sup>H NMR techniques and have clearly established the dynamic equilibria between  $\text{Cp}^*\text{Rh}$  aqua complexes **1** and **3** via the plausible intermediate **2**, including pseudo-first-order rate constants, an equilibrium constant, as well as the one  $\text{p}K_a$  value.

Finally, these results help further explain the structural studies we have reported and are still pursuing with the  $\text{Cp}^*\text{Rh}$  aqua complexes and nucleobases, nucleosides, nucleotides, and oligonucleotides as a function of pH.<sup>2a-d</sup> As the new field of aqueous organometallic chemistry continues to progress, with emphasis on elucidation of structure and dynamics and catalysis studies, we are hopeful that our present approach to the structure and dynamics of the  $\text{Cp}^*\text{Rh}$  aqua complexes will be a model for other studies on organometallic aqua complexes.

## Experimental Section

**Instrumentation and Materials.** Three Bruker NMR spectrometers, two WM 200 MHz instruments, and a WM 400 MHz instrument were used for all <sup>1</sup>H, <sup>13</sup>C, and 2D NMR experiments. The cross-polarization experiments utilized all three spectrometers with different probes and signal-to-noise ratios; similar results were obtained with each instrument. The <sup>1</sup>H NMR chemical shifts were referenced to an external D<sub>2</sub>O solution of 3-(trimethylsilyl)propionic acid-2,2,3,3-*d*<sub>4</sub> so-

dium salt. The <sup>13</sup>C NMR chemical shifts were referenced to the triflate anion at 120.532 ppm. A Bruker AM 400 spectrometer was used for the <sup>17</sup>O NMR measurements and the <sup>17</sup>O NMR spectra were recorded at 54.2 MHz for samples in 5 mm sealed J. Young NMR tubes. The 90° pulse width for <sup>17</sup>O NMR spectra was found to be 15.8  $\mu\text{s}$ . Pulses were used with a short pulse repetition time of 0.1 s. Chemical shifts were referenced to external H<sub>2</sub>O (distilled) at 298 K ( $\delta = 0$  ppm,  $T_1 = 5.2$  s). The NOESY experiments were performed using the commercial Bruker NOESYPH subroutine with a mixing time of 1.2 s.

The FAB/MS data were obtained with an MS-50 instrument. The potentiometric titration experiments were performed on a Corning model 340 pH meter with an Aldrich ultrathin long-stem pH electrode; solutions prepared in an oxygen-free environment and those prepared in the presence of air gave similar pH measurements. The potentiometer data was acquired and analyzed on an IBM computer. The acids and bases utilized were standardized with HCl and NaOH samples of known concentration.

**Preparation of  $[\text{Cp}^*\text{Rh}(\text{H}_2\text{O})_3](\text{OTf})_2$ , **1**.** A solution of  $[\text{Cp}^*\text{RhCl}_2]_2$  (0.050 g, 0.08 mmol) and AgOTf (0.083 g, 0.32 mmol) in anhydrous  $\text{CH}_2\text{Cl}_2$  (4 mL) was stirred at ambient temperature for 3 h, and then it was filtered. The filtrate was carefully layered with H<sub>2</sub>O (8.7  $\mu\text{L}$ , 0.48 mmol). The layered filtrate was allowed to stand at ambient temperature for 12 h to give an amber crystalline product in quantitative yield. The NMR sample was prepared in a Vacuum Atmospheres glovebox by dissolving an appropriate amount of  $[\text{Cp}^*\text{Rh}(\text{H}_2\text{O})_3](\text{OTf})_2$  in a 5 mm NMR tube in 0.6 mL of DMSO-*d*<sub>6</sub>, which was dried over activated molecular sieves. The <sup>1</sup>H NMR spectra were obtained on a Bruker AM 400 spectrometer with the reference peak set at 2.49 ppm for the solvent DMSO-*d*<sub>6</sub>. The proton integration of H<sub>2</sub>O was calculated by subtracting the spectrum of a sample of the 0.6 mL of blank DMSO-*d*<sub>6</sub> solvent containing trace amounts of H<sub>2</sub>O. The <sup>1</sup>H chemical shift of these trace amounts of H<sub>2</sub>O in the blank DMSO-*d*<sub>6</sub> solvent is at 3.32 ppm. It is noteworthy to mention that the <sup>1</sup>H resonance of H<sub>2</sub>O in the sample of **1** was downfield-shifted by 0.06 ppm, indicating that the H<sub>2</sub>O molecules were in an equilibrium process of occupying the coordination sites of  $\text{Cp}^*\text{Rh}$  even in the presence of DMSO. The <sup>1</sup>H NMR (400 MHz, DMSO-*d*<sub>6</sub>, 25 °C)  $\delta$  3.38 (s, 6H, 3H<sub>2</sub>O), 1.53 (s, 15H, Cp\*). FAB/MS (glycerol/H<sub>2</sub>O), *m/e* (relative intensity): 688.9 (43)  $[[\text{Cp}^*\text{Rh}(\text{OH})_2]_2(\text{OTf}) - 4\text{H}]$ ; 540.9 (100)  $[[\text{Cp}^*\text{Rh}(\text{OH})_2]_2 - 3\text{H}]$ . Elemental analysis for C<sub>12</sub>H<sub>21</sub>F<sub>6</sub>O<sub>9</sub>RhS<sub>2</sub>. Calcd C, 24.4; H, 3.56. Found: C, 24.1; H, 3.52. Alternatively, **1** can be generated *in situ* by reacting  $[\text{Cp}^*\text{RhCl}_2]_2$  and 4 equiv of AgOTf in H<sub>2</sub>O for 3 h and then filtering through Celite, measured pH = 3.5.

**X-ray Data Collection, Solution, and Refinement of **1**.** The X-ray data for **1** were collected by using a Siemens R3m/v diffractometer equipped with an Enraf-Nonius low-temperature apparatus. Only a random fluctuation of <0.5% in the intensities of two standard reflections was observed during data collection. All calculations were carried out on a MicroVAX 3200 computer using the SHELXTL Plus and SHELXL-93 program systems.<sup>11</sup> Crystals of **1** were transferred to a Petri dish and immediately covered with a layer of hydrocarbon oil. A single crystal was selected, mounted on a glass fiber, and immediately placed in a low-temperature N<sub>2</sub> stream.

Some details of the data collection and refinement are given in Table 1. Further details are provided in the supplementary material. The structure was solved in the space group *Pna*2<sub>1</sub> using direct and difference Fourier methods. Solution could not be obtained in the alternative space group, *Pnma*, because no mirror plane is present in the structure.

(9) Lahoz, F. G.; Carmona, D.; Oro, L. A.; Lamata, M. P.; Puebla, M. P.; Foces-Foces, C.; Cano, F. H. *J. Organomet. Chem.* **1986**, *316*, 221.

(10) Fish, R. H.; Kim, H.-S.; Babin, J. E.; Adams, R. D. *Organometallics* **1988**, *7*, 2250.

(11) Tables of neutral atom scattering factors,  $f'$  and  $f''$ , and absorption coefficients are from: *International Tables for Crystallography*; Wilson, A. J. C., Ed.; Kluwer Academic Publishers: Dordrecht, The Netherlands, 1992; Vol. C, Tables 6.1.1.3 (pp 500–502), 4.2.6.8 (pp 219–222), and 4.2.4.2 (pp 193–199), respectively.

Disorder in one of the triflate anions was modeled with two sites of relative weight 0.75/0.25 for the three oxygen atoms. Hydrogen atoms were added geometrically and refined with a riding model. An absorption correction (XABS2)<sup>12</sup> was applied. In the final cycles of refinement, all non-hydrogen atoms except those of the above disorder were refined with anisotropic thermal parameters. The largest feature in the final difference map had a peak value of 0.66 e Å<sup>-3</sup>, 1.3 Å from a triflate fluorine atom. Some atom coordinates and isotropic thermal parameters are given in Table 2. Selected bond distances and angles are listed in Table 3.

**NMR Titration Sample Preparations.** Complex **1** was dissolved in an argon-degassed solution of CF<sub>3</sub>SO<sub>3</sub>D in D<sub>2</sub>O. The pH adjustments were carried out by adding the necessary amounts of 0.01 M NaOD or 0.01 M CF<sub>3</sub>SO<sub>3</sub>D. The solutions were placed in J. Young NMR tubes and sealed with the total exclusion of air. The <sup>17</sup>O enrichment was performed by exchanging the D<sub>2</sub>O with enriched H<sub>2</sub><sup>17</sup>O purchased from ISO-YEDA Co. Ltd., Israel, (10.2% H<sub>2</sub><sup>17</sup>O) at pH 2.0, while further pH adjustments were made with a 0.01 M NaOH solution. The 2D NOESY NMR solutions were prepared at different pH values by utilizing a 50% mixture of H<sub>2</sub>O and D<sub>2</sub>O to increase cross-polarization.

**Potentiometric Titration of 1.** Complex **1** (10.7 mg, 0.0196 mmol) was dissolved in 0.018 M triflic acid (HOTf) and titrated with a standard solution of 0.093 M NaOH. The first equivalence point, belonging to the neutralization of the strong acid, HOTf, was achieved after addition of 2.2 mL of 0.093 M NaOH, at which point the pH was 4.3. The second equivalence point associated with **1** (i.e., **1** to [**2**] and **3**) was obtained after an additional 0.3 mL (0.028 mmol) of NaOH was added, the pH was 8.1. The two pK<sub>a</sub>'s corresponding to the two equivalence points were calculated to be 2.2 ± 0.1 (triflic acid) and 5.4 ± 0.1 (**1**), respectively. The reverse titration was also performed by dissolving **1** in a 0.093 M NaOH solution and titrating with a 0.0182 M HOTf solution. The first equivalence point is acquired after the addition of 2.59 mL (pH = 8.5) and

the second equivalence point was acquired after a total addition of 4.19 mL of HOTf. (Δ mL = 1.60, 0.029 mmol at pH 4.4).

**Potentiometric Titration of 3.** Complex **3**, [(Cp\*Rh)<sub>2</sub>(μ-OH)<sub>3</sub>]OTf, 39.2 mg (0.056 mmol) was dissolved in 10 mL of 0.093 M NaOH and titrated with a standard solution of HOTf (0.019 M). The first equivalence point occurred after the addition of 8.68 mL of HOTf (pH = 8.3). The pK<sub>a</sub> was calculated to be 5.5 ± 0.1. After an additional 1.80 mL (0.164 mmol) of HOTf had been added, the second equivalence point was obtained at pH = 3.53. The reverse titration was also done by dissolving **3** in a 0.019 M HOTf solution and titrating with a 0.093 M solution of NaOH. The first equivalence point was at pH = 3.83 after the addition of 2.69 mL of NaOH, and the second point was at pH = 7.98 after an additional 1.70 mL of NaOH had been added. The pK was 5.4 ± 0.1.

**Acknowledgment.** The studies at LBL were generously supported by NIH Grant A I 08427 (M.F.M.), Laboratory Directed Research and Development Funds (M.F.M. and R.H.F.), and the Department of Energy under Contract No. DE-ACO3-76SF00098, while those at the Technion were supported by Institute Funds to M.S.E. We also thank the reviewers for constructive comments concerning this manuscript.

**Supplementary Material Available:** The crystal data, data collection, and solution and refinement of **1**; tables of atomic coordinates and equivalent isotropic displacement parameters, bond distances and angles, anisotropic displacement parameters, hydrogen coordinates, and isotropic displacement parameters of **1**; figures of two crystallographically different molecules and the unit cell structure of **1**; <sup>13</sup>C NMR spectra of **1** in acidic solution, pH < 5 (Figure A) (the quartet at 118 ppm is due to the triflate anion, CF<sub>3</sub>SO<sub>3</sub><sup>-</sup> and CH<sub>3</sub> signal of Cp\* at pH 5.8 (Figure B) (16 pages). See any current masthead page for ordering information.

OM950140V

(12) Program XABS2 calculates 24 coefficients from a least-squares fit of (1/A vs sin<sup>2</sup>(θ)) to a cubic equation in sin<sup>2</sup>(θ) by minimization of F<sub>o</sub><sup>2</sup> and F<sub>c</sub><sup>2</sup> differences. Parkin, S. Department of Chemistry, University of California, Davis, CA, 1993.

# Thiapentadienyl–Iridium–Phosphine Chemistry<sup>1</sup>

John R. Bleeker,\* Michael F. Ortwerth, and Alicia M. Rohde

Department of Chemistry, Washington University, St. Louis, Missouri 63130-4899

Received January 30, 1995<sup>®</sup>

Potassium thiapentadienide ( $K^+C_4H_5S^-$ ) reacts cleanly with  $ClIr(PMe_3)_3$  in tetrahydrofuran at room temperature to generate ((1,2,5- $\eta$ )-5-thiapentadienyl)Ir( $PMe_3$ )<sub>3</sub> (**1**). Treatment of **1** with  $H^+BF_4^- \cdot OEt_2$  leads to protonation at C1 and production of [((2,3,4,5- $\eta$ )-5-thiapentadiene)-Ir( $PMe_3$ )<sub>3</sub>]<sup>+</sup>BF<sub>4</sub><sup>-</sup> (**2**), while treatment with  $CH_3O_3SCF_3$  results in methylation at sulfur and production of [((1,2,5- $\eta$ )-5-methyl-5-thiapentadienyl)Ir( $PMe_3$ )<sub>3</sub>]<sup>+</sup>O<sub>3</sub>SCF<sub>3</sub><sup>-</sup> (**3**). Compound **3** isomerizes to [((1,2,3,4- $\eta$ )-5-methyl-5-thiapentadiene)Ir( $PMe_3$ )<sub>3</sub>]<sup>+</sup>O<sub>3</sub>SCF<sub>3</sub><sup>-</sup> (**4**) at room temperature. Upon heating in toluene at reflux, compound **1** slowly converts to the iridathia-cyclopentene complex  $mer\text{-}CH_2=C-CH=CH-S-Ir(PMe_3)_3(H)$  (**5**), via intramolecular activation of the C–H<sub>2</sub> bond. Like compound **1**, **5** undergoes protonation at C1 when treated with  $H^+BF_4^- \cdot OEt_2$ , producing the “iridathiophene” complex,  $[mer\text{-}CH_3-C^{\bullet}H-CH^{\bullet}S^{\bullet}-Ir(PMe_3)_3(H)]^+BF_4^-$  (**6**), but undergoes methylation at sulfur when treated with  $CH_3O_3SCF_3$ , generating  $[mer\text{-}CH_2=C-CH=CH-S(CH_3)-Ir(PMe_3)_3(H)]^+O_3SCF_3^-$  (**7**). ((1,2,5- $\eta$ )-5-Thiapentadienyl)Ir( $PEt_3$ )<sub>3</sub> (**8**), the tris( $PEt_3$ ) analogue of **1**, is produced upon reacting potassium thiapentadienide with  $ClIr(PEt_3)_3$ . Unlike **1**, it undergoes intramolecular C–H bond activation upon stirring in tetrahydrofuran at room temperature. Initially, a mixture of the C–H<sub>1</sub> bond activation product,  $mer\text{-}CH=CH-CH=CH-S-Ir(PEt_3)_3(H)$  (**9**), and the C–H<sub>2</sub> bond activation product,  $mer\text{-}CH_2=C-CH=CH-S-Ir(PEt_3)_3(H)$  (**10**), are produced. However, the six-membered ring compound (**9**) gradually converts to the thermodynamically-preferred five-membered ring compound (**10**). Like its tris( $PMe_3$ ) analogue (**5**), compound **10** reacts with  $H^+BF_4^- \cdot OEt_2$  to produce the “iridathiophene” complex,  $mer\text{-}CH_3-C^{\bullet}H-CH^{\bullet}S^{\bullet}-Ir(PEt_3)_3(H)]^+BF_4^-$  (**11**), and with  $CH_3O_3SCF_3$  to generate the S-methylated compound,  $[mer\text{-}CH_2=C-CH=CH-S(CH_3)-Ir(PEt_3)_3(H)]^+O_3SCF_3^-$  (**12**). Excess  $Cl_2$  and  $I_2$  react with compound **11** exclusively at the metal center to produce the neutral dihalide compounds,  $trans\text{-}CH_3-C^{\bullet}H-CH^{\bullet}S^{\bullet}-Ir(PEt_3)_2(X)_2$  (**13**, X = Cl; **14**, X = I). In contrast, excess  $Br_2$  reacts with **11** at both the Ir center and C3 of the ring to form the electrophilic aromatic substitution product,  $trans\text{-}CH_3-C^{\bullet}C(Br)-CH^{\bullet}S^{\bullet}-Ir(PEt_3)_2(Br)_2$  (**15**). Molecular structures of  $mer\text{-}CH_2=C-CH=CH-S-Ir(PMe_3)_3(H)$  (**5**) and  $trans\text{-}CH_3-C^{\bullet}C(Br)-CH^{\bullet}S^{\bullet}-Ir(PEt_3)_2(Br)_2$  (**15**) have been determined by single-crystal X-ray diffraction studies. Crystal structure data for these compounds are as follows: **5**, orthorhombic,  $Pnma$ ,  $a = 11.935(3)$  Å,  $b = 14.251(3)$  Å,  $c = 11.908(3)$  Å,  $V = 2025.3(7)$  Å<sup>3</sup>,  $Z = 4$ ,  $R = 0.0206$  for 1127 reflections with  $I > 3\sigma(I)$ ; **15**, orthorhombic,  $Pca2_1$ ,  $a = 14.825(4)$  Å,  $b = 10.110(2)$  Å,  $c = 15.757(4)$  Å,  $V = 2361.7(10)$  Å<sup>3</sup>,  $Z = 4$ ,  $R = 0.0388$  for 3762 reflections with  $I > 3\sigma(I)$ .

## Introduction

During the past 15 years, pentadienyl–metal complexes have been extensively investigated.<sup>2</sup> The pentadienyl ligands in these complexes adopt a wide variety of bonding modes, and facile interconversion between those modes leads to interesting dynamic behavior and

reactivity. In contrast, relatively little effort has been directed toward synthesizing and studying the reactivity of heteropentadienyl–metal complexes, i.e., species in which one carbon of the pentadienyl chain has been replaced by a heteroatom.

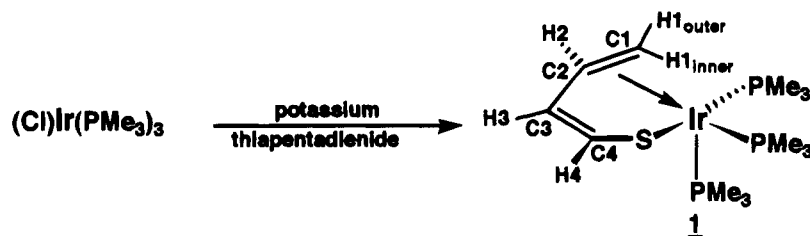
In order to learn more about the bonding preferences and reactivity features of heteropentadienyl ligands, we have begun to investigate a new family of heteropentadienyl–metal–phosphine complexes. These compounds are, in general, synthesized by treating halo–metal–phosphine precursors with anionic heteropentadienide reagents. Our initial studies have focussed

<sup>®</sup> Abstract published in *Advance ACS Abstracts*, May 1, 1995.

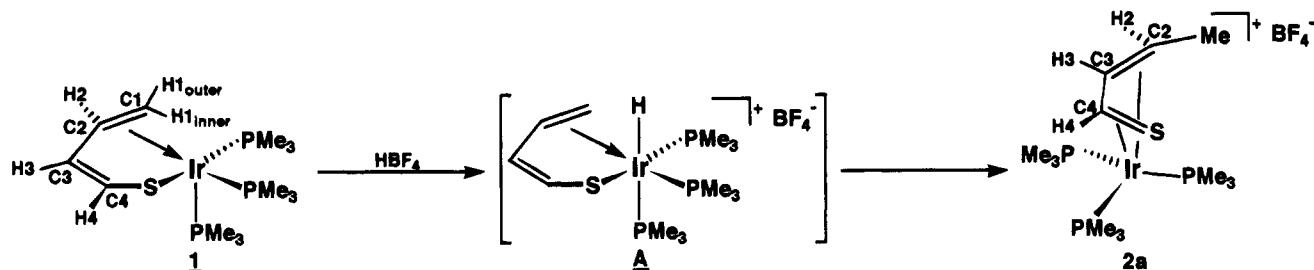
(1) Pentadienyl–Metal–Phosphine Chemistry. 30. Part 29: Bleeker, J. R.; Rohde, A. M.; Robinson, K. D. *Organometallics* 1995, 14, 1674.

(2) For recent reviews, see: (a) Ernst, R. D. *Chem. Rev.* 1988, 88, 1251. (b) Yasuda, H.; Nakamura, A. *J. Organomet. Chem.* 1985, 285, 15. (c) Powell, P. *Adv. Organomet. Chem.* 1986, 26, 125.

Scheme 1



Scheme 2



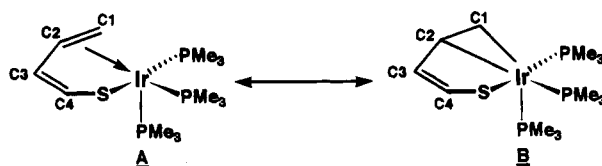
on electron-rich heteropentadienyl-iridium(I)-phosphine complexes because these species have a propensity to undergo C–H bond activation, generating novel metallacyclic products.<sup>3</sup> Previously, we reported our findings in the oxapentadienyl,<sup>3</sup> azapentadienyl,<sup>4</sup> and phosphapentadienyl<sup>5</sup> ligand systems. We now describe the results of a parallel study on iridium–phosphine complexes containing the sulfur-based ligand, thiapentadienyl.<sup>6</sup>

## Results and Discussion

**A. Reaction of ClIr(PMe<sub>3</sub>)<sub>3</sub> with Potassium Thiapentadienide.** Potassium thiapentadienide, prepared by the method of Kloosterziel,<sup>7</sup> reacts cleanly with ClIr(PMe<sub>3</sub>)<sub>3</sub> to produce ((1,2,5- $\eta$ )-5-thiapentadienyl)Ir(PMe<sub>3</sub>)<sub>3</sub> (**1**) (see Scheme 1).<sup>8</sup> The <sup>13</sup>C{<sup>1</sup>H} NMR spectrum of **1** shows two downfield peaks at  $\delta$  134.0 and 126.4 for the two uncomplexed olefinic carbons (C3 and C4, respectively) and two upfield peaks at  $\delta$  41.0 and 18.4 for the two  $\pi$ -complexed olefinic carbons (C2 and C1, respectively). The upfield signals are doublets ( $J = 28.3$  and 33.1 Hz) due to phosphorus coupling. Similarly, the <sup>1</sup>H NMR spectrum includes two downfield signals at  $\delta$  5.72 and 5.17 (H3 and H4) and three upfield signals at  $\delta$  2.67,

1.37, and 1.10 (H2 and H1's). The <sup>31</sup>P{<sup>1</sup>H} NMR spectrum is an AXY pattern; each of the three PMe<sub>3</sub> phosphorus nuclei gives rise to a doublet-of-doublets signal due to P–P coupling.

The X-ray crystal structure of **1**, which we reported earlier,<sup>6a</sup> shows the coordination geometry around iridium to be a distorted octahedron, with C1, C2, and S lying approximately *trans* to the three phosphorus atoms. Of course, the geometry is distorted because of the rigidity of the thiapentadienyl ligand. Carbon atoms C3 and C4 lie substantially out of the C1/C2/S plane (1.06 and 1.22 Å, respectively) and are directed away from the iridium center. The C3–C4 bond distance is 1.316(18) Å, normal for a carbon–carbon double bond. In contrast, the C1–C2 bond distance lengthens to 1.441(15) Å, as a result of strong  $\pi$ -backbonding from the electron-rich Ir center to the coordinated olefin. Hence, the metallacyclopropane resonance structure (**B** below) appears to be an important contributor to the bonding in **1**.



**B. Treatment of Compound 1 with Electrophiles.** As shown in Scheme 2, treatment of compound **1** with tetrafluoroboric acid (H<sup>+</sup>BF<sub>4</sub><sup>-</sup>·OEt<sub>2</sub>) produces [(2,3,4,5- $\eta$ )-5-thiapentadiene]Ir(PMe<sub>3</sub>)<sub>3</sub><sup>+</sup>BF<sub>4</sub><sup>-</sup> (**2a**).<sup>9</sup> This reaction probably involves initial protonation at iridium (intermediate **A**, Scheme 2), followed by “hydride” migration to carbon C1.<sup>10</sup> In the <sup>13</sup>C{<sup>1</sup>H} NMR spectrum of **2a**, internal carbons C3 and C4 resonate at  $\delta$

(3) See, for example: (a) Bleeke, J. R.; Haile, T.; Chiang, M. Y. *Organometallics* **1991**, *10*, 19. (b) Bleeke, J. R.; Haile, T.; New, P. R.; Chiang, M. Y. *Organometallics* **1993**, *12*, 517.

(4) Bleeke, J. R.; Luaders, S. T.; Robinson, K. D. *Organometallics* **1994**, *13*, 1592.

(5) Bleeke, J. R.; Rohde, A. M.; Robinson, K. *Organometallics* **1994**, *13*, 401.

(6) Two communications on this subject have already appeared: (a) Bleeke, J. R.; Ortwerth, M. F.; Chiang, M. Y. *Organometallics* **1992**, *11*, 2740. (b) Bleeke, J. R.; Ortwerth, M. F.; Chiang, M. Y. *Organometallics* **1993**, *12*, 985.

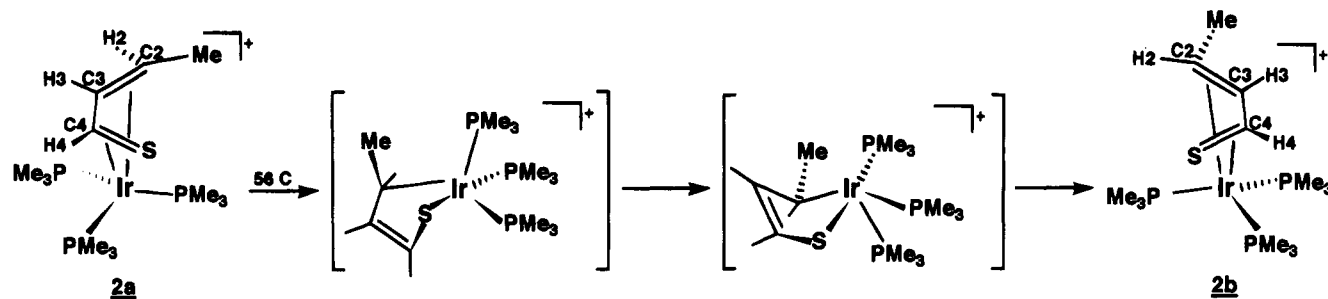
(7) Kloosterziel, H.; Van Drunen, J. A. A.; Galama, P. *J. Chem. Soc., Chem. Commun.* **1969**, 885.

(8) Several thiapentadienyl (or “butadienethiolate”) metal complexes have recently been obtained from (thiophene)metal precursors: (a) Spies, G. H.; Angelici, R. J. *Organometallics* **1987**, *6*, 1897. (b) Hachgenei, J. W.; Angelici, R. J. *Angew. Chem., Int. Ed. Engl.* **1987**, *26*, 909. (c) Hachgenei, J. W.; Angelici, R. J. *J. Organomet. Chem.* **1988**, *355*, 359. (d) Skaugset, A. E.; Rauchfuss, T. B.; Wilson, S. R. *Organometallics* **1990**, *9*, 2875. (e) Bianchini, C.; Meli, A.; Peruzzini, M.; Vizza, F.; Frediani, P.; Herrera, V.; Sanchez-Delgado, R. A. *J. Am. Chem. Soc.* **1993**, *115*, 2731.

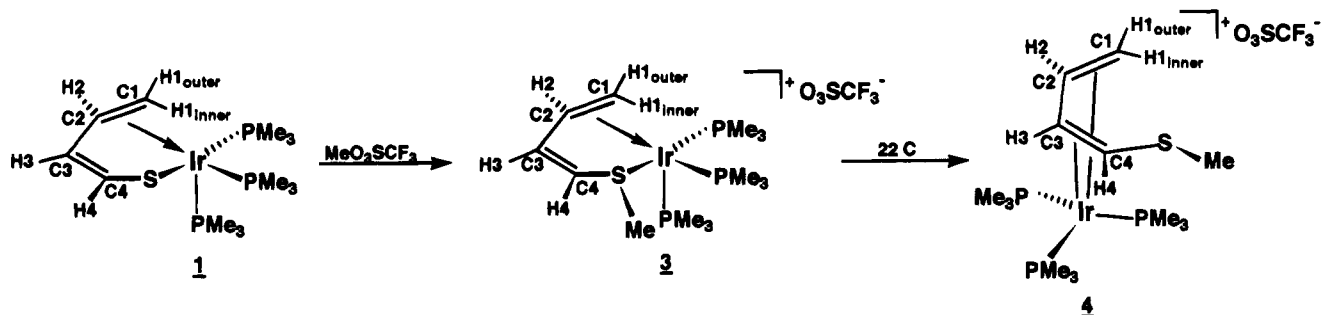
(9) Several other examples of  $\eta^4$ -bound  $\alpha,\beta$ -unsaturated thioaldehyde or thioketone ligands have been reported. (a) Harlow, R. L.; Pfluger, C. E. *Acta Crystallogr., Sect. B* **1973**, *B29*, 2633. (b) Dittmer, D. C.; Takahashi, K.; Iwanami, M.; Tsai, A. I.; Chang, P. L.; Blidner, B. C.; Stamos, I. K. *J. Am. Chem. Soc.* **1976**, *98*, 2795. (c) Skaugset, A. E.; Rauchfuss, T. B.; Wilson, S. R. *J. Am. Chem. Soc.* **1992**, *114*, 8521.

(10) However, the proposed metal–hydride intermediate is not observed by <sup>1</sup>H NMR, even when monitoring the protonation reaction at  $-80$  °C.

Scheme 3



Scheme 4

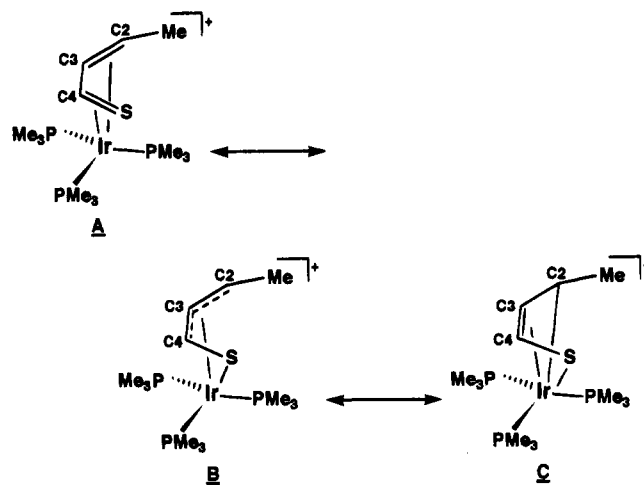


97.1 and 95.1, respectively, while carbon C2 resonates at  $\delta$  42.3 and appears as a  $^{31}\text{P}$ -coupled doublet ( $J = 41.3$  Hz). Methyl carbon C1 shifts upfield to  $\delta$  9.8. A similar pattern of chemical shifts is observed in the  $^1\text{H}$  NMR spectrum: H4 and H3 resonate downfield at  $\delta$  6.12 and 5.84, respectively, while H2 appears at  $\delta$  2.76 and the methyl protons (H1's) resonate at  $\delta$  1.59. The  $^{31}\text{P}\{^1\text{H}\}$  NMR spectrum is an AMX pattern consisting of three doublets-of-doublets for the three inequivalent  $\text{PMe}_3$  ligands. The *syn* orientation of the methyl substituent in **2a** has been verified by NOE difference spectroscopy.<sup>11</sup> Particularly diagnostic is the observation that irradiation of H2 causes significant enhancement of the H3 signal and *vice versa*.

When **2a** is heated in refluxing acetone, it gradually (over the course of 4 h) converts to the less-hindered *anti* isomer, **2b**. The  $^1\text{H}$  NMR spectrum of **2b** closely resembles that of **2a**. However, the coupling between H2 and H3 (measured while broadband decoupling the  $^{31}\text{P}$  nuclei) increases to 9.15 Hz (from 7.33 Hz in **2a**), reflecting the *trans* relationship of these two protons. Again, NOE difference spectroscopy confirms the *anti* geometry. In this case, irradiation of H2 gives no enhancement of the H3 signal.

One possible mechanism for this isomerization, outlined in Scheme 3, involves dissociation of C3–C4 from the metal center, followed by ring-flipping via a planar iridathiacyclopentene intermediate.<sup>12</sup> Reoordination of C3–C4 would then restore the  $\eta^4$ -thiapentadiene struc-

ture but with the methyl group in the *anti* position. The likelihood of this mechanism is enhanced if resonance structures such as **B** and **C** below contribute significantly to the bonding in **2**.



As shown in Scheme 4, treatment of compound **1** with methyl triflate ( $\text{CH}_3\text{O}_3\text{SCF}_3$ ) leads to  $\text{Me}^+$  attack at sulfur and production of  $[(\eta^4\text{-}5\text{-methyl-5-thiapentadienyl})\text{Ir}(\text{PMe}_3)_3]^+\text{O}_3\text{SCF}_3^-$  (**3**).<sup>13</sup> Hence, the site of  $\text{Me}^+$  attack differs from that of  $\text{H}^+$  attack (*vide supra*), reflecting the strongly nucleophilic character of sulfur.<sup>14</sup>

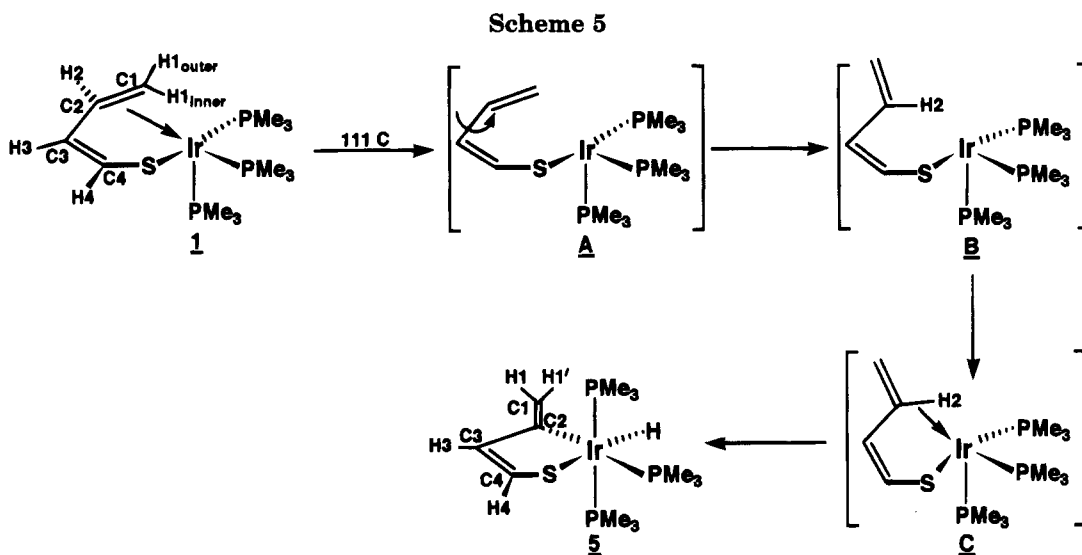
The bonding mode of the thiapentadienyl ligand in **3** is evident from the  $^{13}\text{C}\{^1\text{H}\}$  NMR spectrum. As in parent compound **1**, **3** exhibits two downfield signals at  $\delta$  157.8 and 114.7 for the uncomplexed carbons (C3 and

(11) Derome, A. E. *Modern NMR Techniques for Chemistry Research*; Pergamon Press: Oxford, 1987; p 113.

(12) This type of mechanism has been proposed for interconversion of *syn* and *anti* substituents on  $\eta^4$ -butadiene ligands. (a) Faller, J. W.; Rosan, A. M. *J. Am. Chem. Soc.* **1977**, *99*, 4858. (b) Benn, R.; Schroth, G. *J. Organomet. Chem.* **1982**, *228*, 71. (c) Erker, G.; Krüger, C.; Müller, G. *Adv. Organomet. Chem.* **1985**, *24*, 1. See also: Hersh, W. H.; Hollander, F. J.; Bergman, R. G. *J. Am. Chem. Soc.* **1983**, *105*, 5834.

(13) Several other S-methylated thiapentadienyl-metal complexes have been reported: see refs 8c and 8e.

(14) Gutsche, C. D.; Pasto, D. J. *Fundamentals of Organic Chemistry*; Prentice-Hall: Englewood Cliffs, NJ, 1975; pp 446–448.



C4, respectively), as well as two upfield signals at  $\delta$  38.7 and 25.0 for the  $\pi$ -complexed olefinic carbons (C2 and C1, respectively). The upfield signals exhibit strong phosphorus coupling ( $J = 33.8$  and  $34.0$  Hz, respectively). The S–Me peak is found at  $\delta$  23.8. In the  $^1\text{H}$  NMR spectrum, downfield peaks are observed for H3 and H4 ( $\delta$  7.13 and 5.50, respectively), while upfield peaks are found for H2 ( $\delta$  2.44) and the two H1's ( $\delta$  1.83 and 1.19). The S–Me signal appears at  $\delta$  2.40. The  $^{31}\text{P}\{^1\text{H}\}$  NMR spectrum of **3** is an AMX pattern, consisting of three doublets-of-doublets for the three inequivalent  $\text{PMe}_3$  ligands.

Upon stirring overnight in tetrahydrofuran at room temperature, compound **3** isomerizes to [(1,2,3,4- $\eta$ )-5-methyl-5-thiapentadiene] $\text{Ir}(\text{PMe}_3)_3]^+\text{O}_3\text{SCF}_3^-$  (**4**) (see Scheme 4). In the  $^{13}\text{C}\{^1\text{H}\}$  NMR spectrum of **4**, internal carbons C2 and C3 resonate at  $\delta$  95.8 and 82.1, respectively, while terminal carbons C4 and C1 resonate at  $\delta$  38.7 and 32.7, respectively, and exhibit strong phosphorus coupling ( $J = 50.8$  and  $32.2$  Hz, respectively). The S–Me signal appears at  $\delta$  21.3. In the  $^1\text{H}$  NMR spectrum of **4**, the H2 and H3 signals appear downfield at  $\delta$  5.50 and 5.33, respectively, while H4 and the two H1's resonate at  $\delta$  3.46, 2.50, and 2.24, respectively. The S–Me signal is observed at  $\delta$  2.08. The  $^{31}\text{P}\{^1\text{H}\}$  NMR spectrum is an AMX pattern, but since two of the P–P coupling constants are approximately 0, the signals consist of a singlet and two doublets.

NOE difference spectroscopy has confirmed that the S–Me group in **4** resides in the *syn* orientation as shown in Scheme 4. Irradiation of H4 causes significant enhancement of the signal due to H3 but *no* enhancement of the H1<sub>inner</sub> signal. Enhancement of the H1<sub>inner</sub> peak would be expected if the S–Me group were *anti* and H4 were, therefore, “inner”. In contrast to compound **2a**, compound **4** does not isomerize from the *syn* geometry to the *anti* geometry, even upon refluxing in acetone for 18 h.

**C. Thermal Conversion of Compound 1 to an Iridathiacyclopentene Complex.** Compound **1** is stable indefinitely in solution at room temperature. However, upon heating in toluene at reflux (111  $^\circ\text{C}$ ), it slowly (over the course of 4 h) converts to the iridathia-

cyclopentene complex, *mer*- $\text{CH}_2=\text{C}=\text{CH}=\text{CH}-\text{S}-\text{Ir}(\text{PMe}_3)_3(\text{H})$  (**5**) (see Scheme 5).<sup>15</sup> This reaction, which involves oxidative addition across the C–H2 bond, undoubtedly proceeds through the intermediacy of the 16e  $\eta^1$ -thiapentadienyl complexes, **A** and **B**, and perhaps through the 18e agostic species, **C**. High reaction temperatures are apparently required to release the coordinated olefin (C1=C2) from the metal center in **1**, thereby allowing the C–H bond activation to proceed.

In the  $^{13}\text{C}\{^1\text{H}\}$  NMR spectrum of **5**, the three ring carbons resonate at  $\delta$  163.0 (C2), 144.3 (C3), and 141.4 (C4), while exocyclic methylene carbon C1 resonates at  $\delta$  119.3. Carbon C2 appears as a doublet ( $J = 78.5$  Hz) of triplets ( $J = 14.5$  Hz) due to strong coupling to the *trans* phosphine and weaker coupling to the two equivalent *cis* phosphines. Similarly, the  $^1\text{H}$  NMR spectrum shows downfield peaks for H4, H3, and the two H1's at  $\delta$  6.17, 5.88, 5.83, and 5.05, respectively. The hydride resonates at  $\delta$  –15.4 and is split into a pseudoquartet as a result of phosphorus coupling ( $J = 16.1$  Hz). The  $^{31}\text{P}\{^1\text{H}\}$  NMR spectrum is an  $\text{A}_2\text{X}$  (doublet/triplet) pattern, as expected for a planar metallacycle with a *mer* arrangement of phosphine ligands.

Yellow prisms of compound **5** were obtained from an ether/pentane solution at –30  $^\circ\text{C}$ , and an X-ray crystal structure determination was performed. An ORTEP drawing of the solid state structure is shown in Figure 1. Atomic coordinates for the non-hydrogen atoms are listed in Table 1, while important bond distances and angles are reported in Table 2.<sup>16</sup> As expected, the phosphines adopt a meridional geometry, while the

(15) When the reaction is monitored by  $^{31}\text{P}\{^1\text{H}\}$  NMR, peaks consistent with the six-membered iridathiacycle (C–H1 activation product) are observed. However, these peaks are always small compared to those of **1** and **5** and ultimately vanish as the reaction proceeds to completion.

(16) Compound **5** is structurally related to a family of metallathiacyclopentene complexes which contain an oxygen atom in place of the exocyclic methylene carbon. (a) Davidson, J. L.; Shiralian, M.; Manojlovic-Muir, L.; Muir, K. W. *J. Chem. Soc., Chem. Commun.* **1979**, 30. (b) Manojlovic-Muir, L.; Muir, K. W. *J. Organomet. Chem.* **1979**, 168, 403. (c) Guerchais, J. E.; LeFloch-Perennou, F.; Petillon, F. Y.; Keith, A. N.; Manojlovic-Muir, L.; Muir, K. W.; Sharp, D. W. A. *J. Chem. Soc., Chem. Commun.* **1979**, 410. (d) Petillon, F. Y.; LeFloch-Perennou, F.; Guerchais, J. E.; Sharp, D. W. A. *J. Organomet. Chem.* **1979**, 173, 89. (e) Ashby, M. T.; Enemark, J. H. *Organometallics* **1987**, 6, 1318.

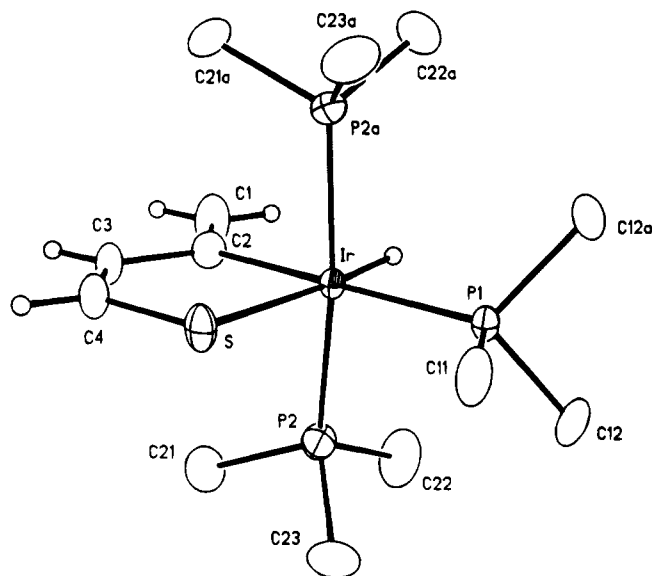


**Figure 1.** ORTEP drawing of  $mer\text{-CH}_2=\text{C}-\text{CH}=\text{CH}-\text{S}-\text{Ir}(\text{PMe}_3)_3(\text{H})$  (**5**).

**Table 1. Atomic Coordinates ( $\times 10^4$ ) and Equivalent Isotropic Displacement Coefficients ( $\text{\AA}^2 \times 10^3$ ) with Estimated Standard Deviations for Non-Hydrogen Atoms in**

$mer\text{-CH}_2=\text{C}-\text{CH}=\text{CH}-\text{S}-\text{Ir}(\text{PMe}_3)_3(\text{H})$ ( <b>5</b> )				
atom	x	y	z	U(eq)
Ir	2287(1)	2500	419(1)	31(1)
P1	3516(2)	2500	-1098(2)	40(1)
P2	2233(2)	4110(1)	573(2)	57(1)
S	545(2)	2500	-657(2)	56(1)
C1	1506(10)	2500	2879(8)	87(5)
C2	1210(8)	2500	1813(7)	52(4)
C3	7(8)	2500	1534(9)	59(4)
C4	-349(8)	2500	490(8)	58(4)
C11	2869(8)	2500	-2481(8)	70(4)
C12	4541(6)	3456(5)	-1220(7)	78(3)
C21	1095(7)	4611(5)	1395(8)	93(4)
C22	3460(7)	4625(6)	1254(9)	113(4)
C23	2050(9)	4789(6)	-716(8)	103(4)

**Table 2. Selected Bond Distances ( $\text{\AA}$ ) and Bond Angles (deg) with Estimated Standard Deviations**

for $mer\text{-CH}_2=\text{C}-\text{CH}=\text{CH}-\text{S}-\text{Ir}(\text{PMe}_3)_3(\text{H})$ ( <b>5</b> )			
Bond Distances			
Ir-P1	2.327(2)	S-C4	1.733(10)
Ir-P2	2.303(2)	C1-C2	1.318(13)
Ir-S	2.441(2)	C2-C3	1.474(14)
Ir-C2	2.099(9)	C3-C4	1.314(14)
Ir-H	1.504(90)		
Bond Angles			
P1-Ir-P2	94.6(1)	C2-Ir-H	88.0(37)
P1-Ir-S	97.4(1)	P2-Ir-P2A	170.3(1)
P2-Ir-S	91.1(1)	Ir-S-C4	96.4(3)
P1-Ir-C2	178.6(3)	Ir-C2-C1	126.8(8)
P2-Ir-C2	85.4(1)	Ir-C2-C3	114.7(6)
S-Ir-C2	83.9(3)	C1-C2-C3	118.5(9)
P1-Ir-H	90.6(37)	C2-C3-C4	121.9(9)
P2-Ir-H	88.3(3)	S-C4-C3	123.1(8)
S-Ir-H	171.9(37)		

hydride (which was located and refined) resides in the ring plane *cis* to C2 and *trans* to S. The molecule resides on a crystallographically-imposed mirror plane. Hence, the sum of the five internal angles of the metallacycle is required to equal  $540^\circ$ . The individual angles range

from  $83.9^\circ$  for C2-Ir-S to  $123.1^\circ$  for S-C4-C3. The carbon-carbon bonds in the metallacycle exhibit normal bond lengths, but the C4-S bond [1.733(10)  $\text{\AA}$ ] is somewhat shorter than a typical C-S single bond (1.82  $\text{\AA}$ ),<sup>17</sup> perhaps reflecting some participation by a sulfur lone pair in the ring  $\pi$ -bonding. The Ir-C2 and Ir-S distances of 2.099(9) and 2.441(2)  $\text{\AA}$  are normal single-bond lengths.

**D. Treatment of Compound 5 with Electrophiles.** As shown in Scheme 6, treatment of compound **5** with tetrafluoroboric acid ( $\text{H}^+\text{BF}_4^-\cdot\text{OEt}_2$ ) leads to proton attack at the exocyclic carbon center (C1), generating the "iridathiophene" complex, [ $mer\text{-CH}_3-\text{C}=\text{CH}=\text{CH}-\text{S}-\text{Ir}(\text{PMe}_3)_3(\text{H})$ ] $^+\text{BF}_4^-$  (**6**).

Although the crystal structure of **6** has not been obtained, its tris-(PEt<sub>3</sub>) analogue has been fully characterized by X-ray diffraction (*vide infra*) and exhibits the delocalized bonding of an aromatic ring system. Aromatic character is also suggested by the <sup>1</sup>H NMR spectrum of **6**. H4 and H3 are shifted dramatically downfield to  $\delta$  10.60 and 7.77, respectively (vs  $\delta$  6.17 and 5.88 in precursor **5**), while the ring methyl group resonates at  $\delta$  3.22. The hydride appears as a pseudoquartet ( $J_{\text{H-P}} = 15.9$  Hz) at  $\delta$  -14.31. The <sup>13</sup>C{<sup>1</sup>H} NMR spectrum of **6** shows similar downfield shifts for the ring carbons with C2, C3, and C4 resonating at  $\delta$  251.1, 154.6, and 213.6, respectively, and C1 (the ring methyl) resonating at  $\delta$  43.5. Carbon atom C2 is strongly coupled to the *trans* PMe<sub>3</sub> ligand ( $J = 77.6$  Hz). The <sup>31</sup>P{<sup>1</sup>H} NMR spectrum of **6** is the A<sub>2</sub>X (doublet/triplet) pattern characteristic of planar metallacycles with a *mer* arrangement of phosphine ligands.

In contrast to protonation, methylation of compound **5** occurs cleanly at the sulfur center. Hence, as shown in Scheme 6, treatment of **5** with methyl triflate ( $\text{CH}_3\text{O}_3\text{SCF}_3$ ) leads to the production of [ $mer\text{-CH}_2=\text{C}-\text{CH}=\text{CH}-\text{S}(\text{CH}_3)-\text{Ir}(\text{PMe}_3)_3(\text{H})$ ] $^+\text{O}_3\text{SCF}_3^-$  (**7**).

The X-ray crystal structure of the tris(PEt<sub>3</sub>) analogue of **7** has been determined (*vide infra*) and shows *localized* bonding around the metallacycle and a *pyramidal* sulfur center.

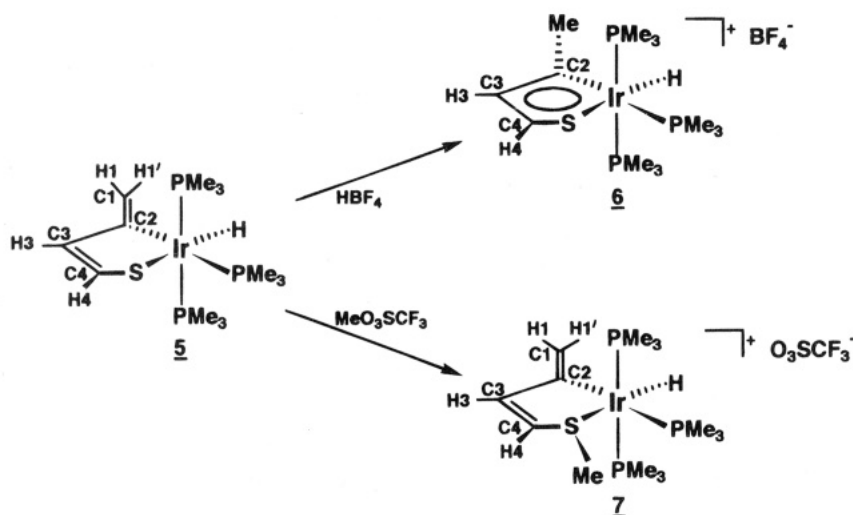
The localized, nonaromatic character of **7** is also reflected in its <sup>1</sup>H NMR spectrum, which bears a close resemblance to that of precursor **5**. Ring protons H4 and H3 resonate at  $\delta$  6.19 and 6.50, respectively, significantly upfield from their positions in aromatic compound **6**. Additional <sup>1</sup>H NMR peaks are observed at  $\delta$  6.41 and 5.52 (H1's), 2.69 (S-Me), and -16.44 (Ir-H). In the <sup>13</sup>C{<sup>1</sup>H} NMR, ring carbons C2, C3, and C4 resonate at  $\delta$  156.6, 155.6, and 125.7, respectively, while exocyclic carbon C1 resonates at  $\delta$  132.4 and the S-Me carbon appears at  $\delta$  24.0.

The pyramidal geometry about sulfur causes the *trans*-diaxial PMe<sub>3</sub> ligands to be inequivalent. Hence, these phosphines give rise to separate signals in the <sup>31</sup>P{<sup>1</sup>H} NMR spectrum at -80  $^\circ\text{C}$ . Because the P-P coupling constant is large with respect to the chemical shift difference ( $J_{\text{P-P}} = 323$  Hz,  $\Delta\delta = 85$  Hz), a second-order pattern is observed. As the temperature of the sample is raised, the environments of the *trans*-diaxial PMe<sub>3</sub> ligands become equivalent, causing the <sup>31</sup>P NMR peaks to broaden and ultimately coalesce at about -5

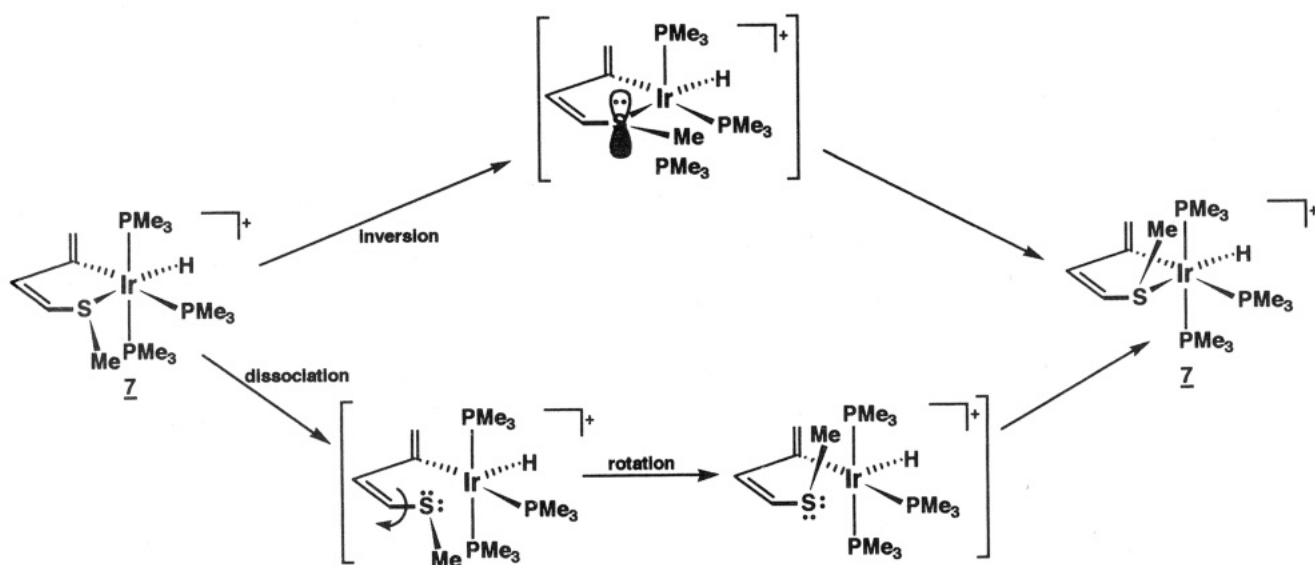
(17) Huheey, J. E. *Inorganic Chemistry*, 3rd ed.; Harper and Row: New York, 1983; Appendix E and references therein.



Scheme 6



Scheme 7



°C. The free energy of activation ( $\Delta G^\ddagger$ ) for the exchange process that is responsible for this behavior is calculated to be about 53.7 kJ/mol (12.8 kcal/mol) at the coalescence temperature.

As illustrated in Scheme 7, two reasonable mechanisms for this exchange process can be envisaged: (a) inversion at the pyramidal sulfur or (b) dissociation of sulfur, followed by C4-S bond rotation and reattachment to iridium. While the activation energy for this process appears to be unusually low for inversion about sulfonium sulfur,<sup>18</sup> the planar intermediate would be stabilized by overlap of the filled sulfur  $p\pi$  orbital with the ring's  $\pi$ -system. Furthermore, the presence of the metal and its ligands may promote inversion because bulky substituents generally lower the barrier to sulfonium inversion.<sup>18</sup>

**E. Reaction of  $\text{ClIr}(\text{PEt}_3)_3$  with Potassium Thiapentadienide.** Treatment of  $\text{ClIr}(\text{PEt}_3)_3$  with potassium thiapentadienide produces ((1,2,5- $\eta$ )-5-thiapentadienyl) $\text{Ir}(\text{PEt}_3)_3$  (**8**), the tris( $\text{PEt}_3$ ) analogue of **1**. Compound **8** can be isolated and crystallized in pure

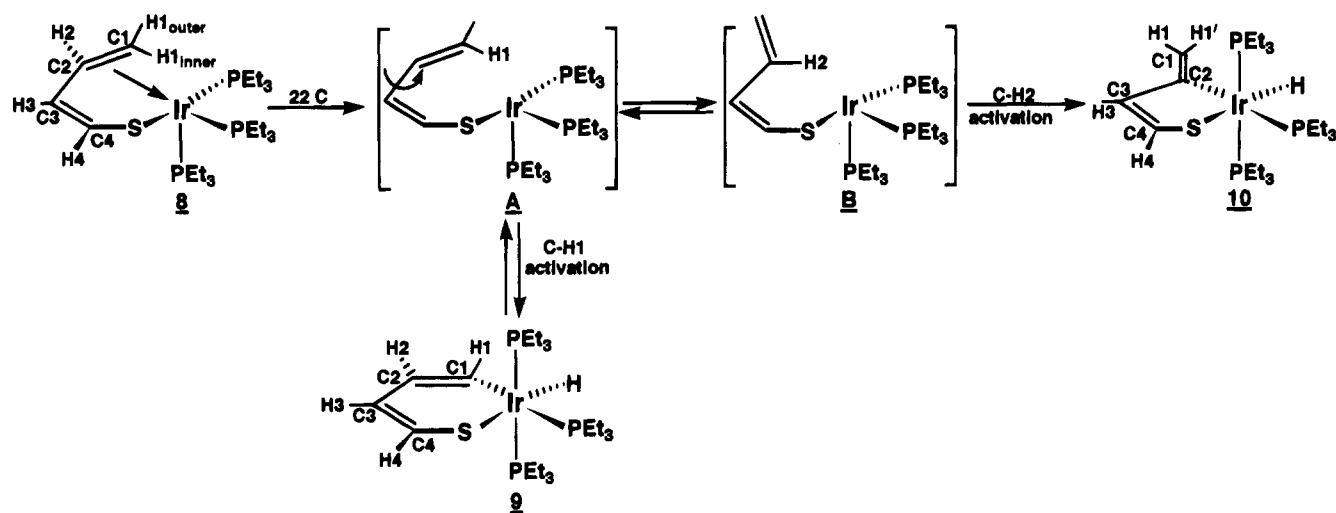
form, but unlike **1** it undergoes intramolecular C-H bond activation upon stirring in tetrahydrofuran at room temperature.<sup>19</sup> As shown in Scheme 8, compound **8** first converts to a mixture of the C-H1 bond activation product, *mer*-CH=CH-CH=CH-S-Ir(PEt<sub>3</sub>)<sub>3</sub>(H) (**9**), and the C-H2 bond activation product, *mer*-CH<sub>2</sub>=C-CH=CH-S-Ir(PEt<sub>3</sub>)<sub>3</sub>(H) (**10**), and then slowly to pure **10**. This conversion involves 16e thiapentadienyl species (**A** and **B** in Scheme 8) and perhaps 18e agostic species, in which  $\sigma$ -bonds C-H1 or C-H2 are weakly coordinated to Ir.

The system's thermodynamic preference for the five-membered ring product (**10**) over the six-membered ring product (**9**) can be understood by considering the ring strain in each metallacycle. In a planar five-membered ring, the sum of the internal angles must equal 540°, and in metallacycle **10** this requirement can be satisfied without introducing any serious strain. On the other

(18) Anderson, K. K. In *The Chemistry of the Sulphonium Group*; Stirling, C. J. M., Ed.; Wiley: Chichester, England, 1981; Part 1, pp 229-266.

(19) The enhanced reactivity of compound **8** vs its tris( $\text{PMe}_3$ ) analogue **1** probably results from steric destabilization of the  $\pi$ -component of the (1,2,5- $\eta$ )-5-thiapentadienyl bonding mode.  $\pi$ -Bond dissociation produces the key 16 e ( $\eta^1$ -thiapentadienyl) $\text{Ir}(\text{PR}_3)_3$  intermediate through which metallacycle formation proceeds.

Scheme 8



hand, in a planar six-membered ring,<sup>20</sup> the sum of the internal angles must equal 720°, and in octahedral complexes such as **9** where the C1–Ir–S angle is constrained to be approximately 90°, the other ring internal angles are forced to expand beyond 120°. This, in turn, introduces substantial ring strain.

Although pure **9** has not been obtained, its identity has been established through a series of NMR experiments conducted on mixtures of **9** and **10**. Particularly diagnostic for the iridathiacyclohexadiene ring structure<sup>20</sup> is the <sup>13</sup>C{<sup>1</sup>H} NMR spectrum, which shows four CH-type carbons in the downfield region ( $\delta$  122.8–121.1). These carbon peaks correlate with four downfield proton peaks ( $\delta$  7.18–5.70) in the 2D <sup>13</sup>C–<sup>1</sup>H HMQC spectrum. The <sup>31</sup>P{<sup>1</sup>H} NMR spectrum is an A<sub>2</sub>X (doublet/triplet) pattern, indicating that the three phosphines adopt a *mer* arrangement. This geometry is confirmed by the metal–hydride signal, which appears at  $\delta$  –16.74 and is split into a pseudoquartet by phosphorus coupling. Finally, C1 is strongly coupled to phosphorus ( $J = 72$  Hz), requiring that it reside *trans* to PEt<sub>3</sub> and, therefore, *cis* to the hydride.

Pure compound **10** can be obtained by stirring the mixture of **9** and **10** in tetrahydrofuran at room temperature for several days or by refluxing the mixture in tetrahydrofuran for 3 h. The solution-phase NMR spectra of **10** closely resemble those of its tris(PMe<sub>3</sub>) analogue, compound **5**. Its solid-state structure was

reported in an earlier communication;<sup>22</sup> key structural parameters are summarized in Table 3.

**F. Treatment of Compound 10 with Electrophiles.** Compound **10**, like its tris(PMe<sub>3</sub>) analogue (**5**), reacts cleanly with tetrafluoroboric acid (H<sup>+</sup>BF<sub>4</sub><sup>–</sup>·OEt<sub>2</sub>) to produce the “iridathiophene” complex, [*mer*-CH<sub>3</sub>–  
.....  
C<sup>••</sup>–CH<sup>••</sup>–CH<sup>••</sup>–S<sup>••</sup>–Ir(PEt<sub>3</sub>)<sub>3</sub>H]<sup>+</sup>BF<sub>4</sub><sup>–</sup> (**11**). Aromatic character is indicated by the <sup>1</sup>H NMR spectrum of **11**. Ring protons H4 and H3 are shifted downfield to  $\delta$  10.07 and 7.51, respectively (vs  $\delta$  6.14 and 5.84 in precursor **10**), while the ring methyl group resonates at  $\delta$  3.10. The <sup>13</sup>C NMR spectrum shows similar downfield shifts for the ring carbons with C2, C3, and C4 appearing at  $\delta$  245.8, 155.6, and 212.7, respectively. The solid-state structure of **11**, which we reported earlier,<sup>6b</sup> provides additional evidence for the presence of an aromatic ring system. Unlike precursor **10**, in which the bonding around the metallacycle is fully localized, compound **11** exhibits delocalized  $\pi$ -bonding. As summarized in Table 3, ring bonds Ir–C2 (2.042(10) Å), Ir–S (2.383(3) Å), and C4–S (1.647(11) Å) have all shortened significantly (with respect to their distances in **10**)<sup>22</sup> to values intermediate between normal single and double bonds. Similarly, the C–C distances within the ring have moved toward equalization, with C2–C3 shortening to 1.362(15) Å and C3–C4 lengthening to 1.399(16) Å. Overall, the circumference of the five-membered ring in **11** has shrunk by 0.233 Å from its value in **10**<sup>22</sup> (8.833 Å in **11** vs 9.066 Å in **10**).

The spectroscopic and structural data described above suggest that several resonance structures contribute to the overall bonding picture in **11**. Structure **A** is supported by the short Ir–C2 distance and the downfield “carbene-like” chemical shift position of C2. Resonance form **B**, on the other hand, accounts for the short C4–S bond distance. The aromatic character of **11** can be explained qualitatively by noting that both resonance structures **A** and **B** possess a closed loop of six  $\pi$ -electrons. In **A**, a lone pair on sulfur contributes two

(20) The ring in **9** is expected to be essentially planar, based on the structures of close carbon and oxygen analogues. See: Bleeke, J. R.; Peng, W.-J. *Organometallics* **1987**, *6*, 1576, and ref 3a.

(21) Other related metallathiacyclohexadienes have been synthesized via metal-centered cleavage of C–S bonds in thiophenes: (a) Ogilvy, A. E.; Draganjac, M.; Rauchfuss, T. B.; Wilson, S. R. *Organometallics* **1988**, *7*, 1171. (b) Chen, J.; Daniels, L. M.; Angelici, R. J. *J. Am. Chem. Soc.* **1990**, *112*, 199. (c) Chen, J.; Daniels, L. M.; Angelici, R. J. *Polyhedron* **1990**, *9*, 1883. (d) Jones, W. D.; Dong, L. *J. Am. Chem. Soc.* **1991**, *113*, 559. (e) Dong, L.; Duckett, S. B.; Ohman, K. F.; Jones, W. D. *J. Am. Chem. Soc.* **1992**, *114*, 151. (f) Jones, W. D.; Chin, R. M. *Organometallics* **1992**, *11*, 2698. (g) Luo, S.; Skaugset, A. E.; Rauchfuss, T. B.; Wilson, S. R. *J. Am. Chem. Soc.* **1992**, *114*, 1732. (h) Selna, H. E.; Merola, J. S. *Organometallics* **1993**, *12*, 1583. (i) Bianchini, C.; Meli, A.; Peruzzini, M.; Vizza, F.; Frediani, P.; Herrera, V.; Sanchez-Delgado, R. A. *J. Am. Chem. Soc.* **1993**, *115*, 2731. (j) Garcia, J. J.; Maitlis, P. M. *J. Am. Chem. Soc.* **1993**, *115*, 12200. (k) Buys, I. E.; Field, L. D.; Hambley, T. W.; McQueen, A. E. D. *J. Chem. Soc., Chem. Commun.* **1994**, 557. (l) Bianchini, C.; Meli, A.; Peruzzini, M.; Vizza, F.; Moneti, S.; Herrera, V.; Sanchez-Delgado, R. A. *J. Am. Chem. Soc.* **1994**, *116*, 4370. (m) Jones, W. D.; Chin, R. M.; Crane, T. W.; Baruch, D. M. *Organometallics* **1994**, *13*, 4448.

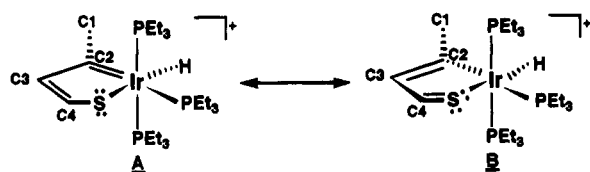
(22) The preliminary structure is reported in ref 6a. Bond distances from a subsequent, higher-quality structure determination are included in ref 6b. Because compound **10** crystallized with two independent molecules in the unit cell, average bond distances and angles are given.

**Table 3. Comparison of Key Bond Distances (Å) and Bond Angles (deg) with Estimated Standard Deviations for *mer*-CH<sub>2</sub>=C-CH=CH-S-Ir(PEt<sub>3</sub>)<sub>3</sub>H (10), [*mer*-CH<sub>3</sub>-C-CH=CH-S-Ir(PEt<sub>3</sub>)<sub>3</sub>(H)]<sup>+</sup>BF<sub>4</sub><sup>-</sup> (11), [*mer*-CH<sub>2</sub>=C-CH=CH-S(CH<sub>3</sub>)-Ir(PEt<sub>3</sub>)<sub>3</sub>H]<sup>-</sup>O<sub>3</sub>SCF<sub>3</sub><sup>-</sup> (12), and *trans*-CH<sub>3</sub>-C-C(Br)-CH-S-Ir(PEt<sub>3</sub>)<sub>2</sub>(Br)<sub>2</sub> (15)**

	compd 10 <sup>a</sup>	compd 11 <sup>b</sup>	compd 12 <sup>b</sup>	compd 15 <sup>c</sup>
Bond Distances				
Ir-C2	2.104(11)	2.042(10)	2.091(6)	1.958(13)
C2-C3	1.477(17)	1.362(15)	1.478(9)	1.362(19)
C3-C4	1.328(18)	1.399(16)	1.324(9)	1.370(22)
C4-S	1.713(13)	1.647(11)	1.747(6)	1.666(16)
S-Ir	2.444(3)	2.383(3)	2.419(2)	2.294(4)
C1-C2	1.309(15)	1.500(15)	1.330(9)	1.499(22)
Bond Angles				
S-Ir-C2	84.0(3)	82.3(3)	82.8(2)	84.3(4)
Ir-C2-C3	113.9(7)	118.0(8)	115.6(4)	117.3(11)
C2-C3-C4	122.4(11)	121.2(10)	123.4(6)	122.2(14)
C3-C4-S	122.8(10)	119.2(8)	118.6(5)	116.5(11)
C4-S-Ir	96.8(5)	99.2(4)	99.5(2)	99.4(6)
Ir-C2-C1	127.6(9)	124.3(8)	129.1(5)	125.2(10)
C1-C2-C3	118.6(11)	117.7(10)	115.2(6)	117.5(13)

<sup>a</sup> Reference 22. <sup>b</sup> Reference 6b. <sup>c</sup> This work.

$\pi$ -electrons, while in **B**, a pair of metal-based d-electrons completes the Hückel sextet.<sup>23</sup>



Compound **10** reacts with methyl triflate to produce the S-methylated ring compound, [*mer*-

CH<sub>2</sub>=C-CH=CH-S(CH<sub>3</sub>)-Ir(PEt<sub>3</sub>)<sub>3</sub>(H)]<sup>+</sup>O<sub>3</sub>SCF<sub>3</sub><sup>-</sup> (**12**). The <sup>1</sup>H NMR spectrum of this compound closely resembles that of its tris(PMe<sub>3</sub>) analogue (**7**) and is consistent with its formulation as a localized, nonaromatic system. Ring protons H4 and H3 resonate at  $\delta$  6.00 and 6.45, respectively, while the two H1 protons appear at  $\delta$  6.46 and 5.49 and the S-Me protons resonate at  $\delta$  2.61. The metal-hydride appears as a pseudoquartet ( $J_{\text{H-P}} = 14.8$  Hz) at  $\delta$  -16.37. The X-ray crystal structure of **12**, which we reported earlier,<sup>6b</sup> confirms the presence of localized bonding within the metallacycle. As summarized in Table 3, ring carbon-carbon distances of 1.478(9) and 1.324(9) Å are observed for C2-C3 and C3-C4, respectively. The remaining ring bond lengths [Ir-C2 = 2.091(6) Å, Ir-S = 2.419(2) Å, and C4-S = 1.747(6) Å] closely resemble the distances observed in precursor **10** and are typical single-bond lengths. The circumference of the five-membered ring in **12** is almost identical with that in **10** (9.059 Å in **12** vs 9.066 Å in **10**).<sup>22</sup> As anticipated, the sulfur center in **12** is *pyramidal*. The S-Me carbon atom (C5) lies 1.521 Å out of the ring plane, and the C4-S-C5 angle is 98.9(3)°.

(23) Fenske-Hall molecular orbital calculations have been performed on a related *manganafuran* system. See: DeShong, P.; Slough, G. A.; Sidler, D. R.; Rybczynski, P. J.; von Philipsborn, W.; Kunz, R. W.; Bursten, B. E.; Clayton, T. W., Jr. *Organometallics* **1989**, *8*, 1381.

As in the case of compound **7**, the pyramidal geometry about the sulfur atom causes the *trans*-diaxial phosphine ligands to be inequivalent. Hence in the low-temperature (-80 °C) <sup>31</sup>P{<sup>1</sup>H} NMR spectrum of **12**, separate peaks are observed for these phosphines. However, as the temperature is raised the peaks broaden and ultimately coalesce at  $\sim$ -25 °C. As discussed above (Scheme 7), the exchange process responsible for this variable-temperature NMR behavior could involve inversion at sulfur or dissociation of sulfur, followed by rotation and reattachment. The free energy of activation ( $\Delta G^\ddagger$ ) for this process at the coalescence temperature is calculated to be 47.3 kJ/mol (11.3 kcal/mol).

### G. Reactions of Compound **11** with Halogens.

Ring halogenation is one of the characteristic reactions of aromatic compounds. Therefore, we have explored the reactivity of "iridathiophene" **11** with Cl<sub>2</sub>, Br<sub>2</sub>, and I<sub>2</sub>. As shown in Scheme 9, excess Cl<sub>2</sub> and I<sub>2</sub> react with **11** exclusively at the metal center to produce the neutral

dihalide compounds, *trans*-CH<sub>3</sub>-C-CH=CH-S-Ir(PEt<sub>3</sub>)<sub>2</sub>(X)<sub>2</sub> (**13**, X = Cl; **14**, X = I). These reactions involve formal loss of H<sup>+</sup> and PEt<sub>3</sub> from the Ir center, but their detailed mechanisms have not been explored.

The <sup>1</sup>H NMR spectra of **13** and **14** show the presence of two downfield <sup>1</sup>H NMR signals (at  $\delta$  9.64 and 7.44 for **13** and at  $\delta$  9.66 and 7.19 for **14**), indicating that ring protons H4 and H3 have not been replaced by halogen and that the aromatic rings remain intact. The ring methyl group resonates at  $\delta$  3.11 in **13** and at  $\delta$  3.17 in **14**. No signals are observed in the upfield "hydride" region of the <sup>1</sup>H NMR spectrum. The <sup>31</sup>P{<sup>1</sup>H} NMR spectra of **13** and **14** each consist of a singlet, consistent with the presence of equivalent *trans*-diaxial phosphines. The <sup>13</sup>C{<sup>1</sup>H} NMR spectra of **13** and **14**, like those of parent **11**, include three downfield signals for ring carbons C2, C4, and C3, together with an upfield signal for the ring methyl carbon. The C2 signals for **13** and **14** exhibit no strong C-P coupling because they reside *trans* to a halide ligand, X.

Like Cl<sub>2</sub> and I<sub>2</sub>, excess Br<sub>2</sub> adds to **11** at the metal center, but unlike the other halogens it also reacts at C3 of the ring to form the electrophilic aromatic

substitution product, *trans*-CH<sub>3</sub>-C-C(Br)-CH-S-Ir(PEt<sub>3</sub>)<sub>2</sub>(Br)<sub>2</sub> (**15**) (see Scheme 9).<sup>24</sup> The substitution at C3 is apparent from the <sup>1</sup>H NMR spectrum of **15**.<sup>25</sup> The downfield region of the spectrum shows only one peak, a singlet at  $\delta$  10.14 due to H4; the H3 signal is absent as a result of the bromination. All other features of the <sup>1</sup>H, <sup>13</sup>C, and <sup>31</sup>P spectra of **15** closely resemble those of **13** and **14**.

The structure of **15** has been confirmed by single-crystal X-ray diffraction (see ORTEP drawing in Figure 2). Positional parameters are given in Table 4, while important bond distances and angles are reported in Table 5. A comparison of structural parameters in **15**

(24) Analogous bromination of a related *manganafuran* system has been reported. See: DeShong, P.; Sidler, D. R.; Rybczynski, P. J.; Slough, G. A.; Rheingold, A. L. *J. Am. Chem. Soc.* **1988**, *110*, 2575.

(25) The regiochemistry of this electrophilic substitution reflects the fact that ring carbon C3 in compound **11** is a more negative center than C4, due in part to resonance effects involving the sulfur lone pairs. This distribution of charge is also apparent from the <sup>13</sup>C NMR of **11**, wherein C3 resonates substantially upfield from C4 ( $\delta$  155.6 vs  $\delta$  212.7).

Scheme 9

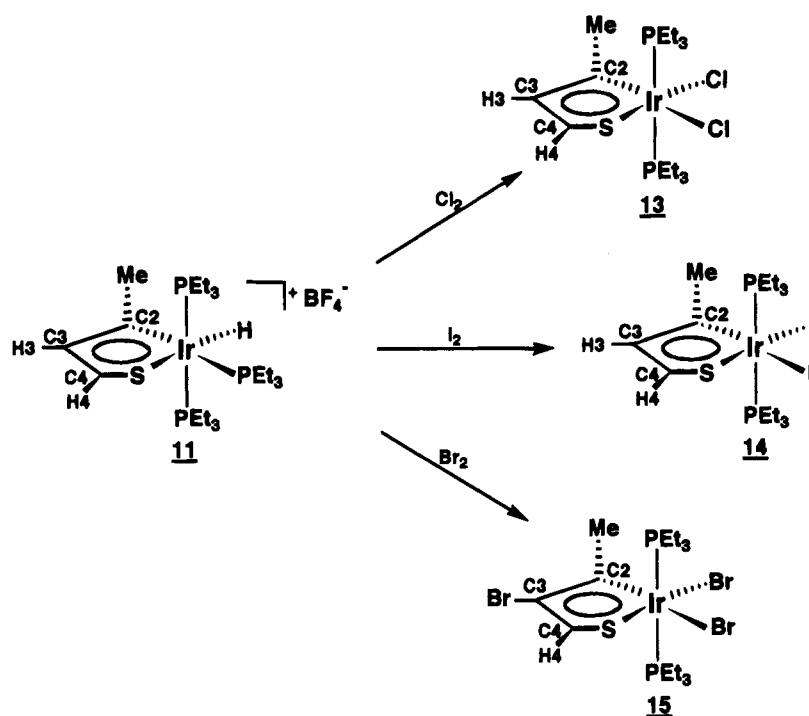


**Table 4. Atomic Coordinates ( $\times 10^4$ ) and Equivalent Isotropic Displacement Coefficients ( $\text{\AA}^2 \times 10^3$ ) with Estimated Standard Deviations for Non-Hydrogen Atoms in**

*trans*-CH<sub>3</sub>-C≡C(Br)-CH-S-Ir(PEt<sub>3</sub>)<sub>2</sub>(Br)<sub>2</sub> (15)

atom	x	y	z	U(eq)
Ir	1215(1)	1622(1)	2782	24(1)
Br1	2091(1)	-167(1)	3636(1)	44(1)
Br2	2615(1)	2360(2)	1968(1)	42(1)
Br3	-1370(1)	4129(2)	2048(2)	73(1)
S	-61(2)	904(3)	3464(3)	41(1)
P1	1623(3)	3126(3)	3882(2)	33(1)
P2	1014(2)	44(3)	1690(2)	32(1)
C1	678(11)	3952(16)	1633(11)	51(6)
C2	403(8)	2916(13)	2261(9)	33(4)
C3	-479(9)	2885(15)	2503(10)	44(5)
C4	-812(10)	1933(16)	3036(11)	48(5)
C11	2686(11)	2820(19)	4480(10)	52(5)
C12	3535(14)	2920(26)	3971(12)	74(8)
C13	854(14)	3199(18)	4816(10)	60(6)
C14	-4(14)	4034(25)	4666(13)	83(9)
C15	1704(10)	4841(14)	3540(11)	46(5)
C16	2020(17)	5856(16)	4183(13)	81(9)
C21	678(12)	821(19)	662(9)	51(5)
C22	-335(12)	1058(20)	547(12)	59(6)
C23	174(12)	-1234(17)	1843(12)	57(6)
C24	409(15)	-2280(22)	2536(14)	81(9)
C25	2077(10)	-856(17)	1452(12)	51(5)
C26	1993(15)	-1870(18)	711(11)	63(7)

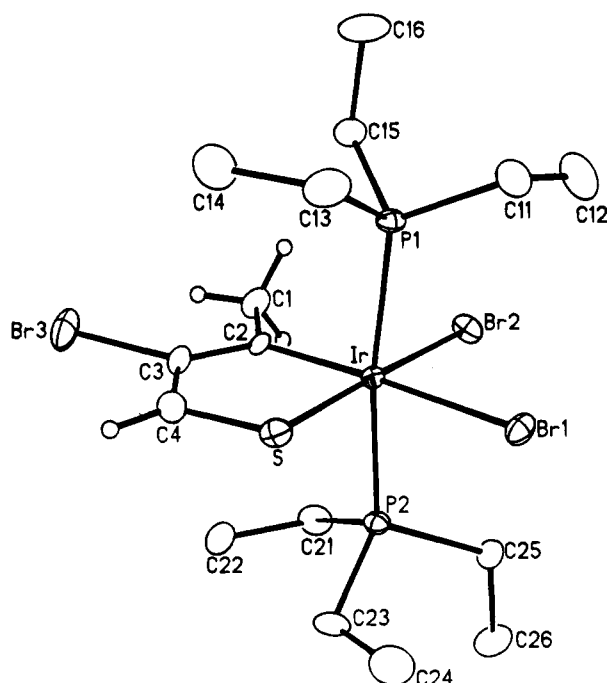


**Figure 2.** ORTEP drawing of *trans*-CH<sub>3</sub>-C≡C(Br)-CH-S-Ir(PEt<sub>3</sub>)<sub>2</sub>(Br)<sub>2</sub> (15).

with those of **10**, **11**, and **12** is provided in Table 3. As expected, the molecule adopts an octahedral coordination geometry with the bromine ligands lying *trans* to ring atoms C2 and S, and the PEt<sub>3</sub> ligands residing *trans* to one another. The metallacyclic ring is planar to within 0.035 Å. The five internal angles within the ring range from 84.3(4)° (for C2-Ir-S) to 122.2(14)° (for C2-C3-C4), but their sum of 539.7° falls very close to the theoretical value of 540° for planar five-membered rings. The bond distances within the ring exhibit the delocalization that is characteristic of aromatic systems.

The two ring carbon-carbon bond distances are essentially equal [1.362(19) and 1.370(22) Å] and intermediate in length between C-C single and double bonds. Similarly, the ring carbon-sulfur bond length of 1.666(16) Å lies between normal C-S single-bond (1.82 Å) and double-bond (1.60 Å) distances.<sup>17</sup> The iridium-ring atom bond distances of 1.958(13) Å for Ir-C2 and 2.294(4) Å for Ir-S are quite short, indicating substantial participation by the metal-ligand moiety in ring π-bonding. As a result of these strong π-interactions, the circumference of the metallacycle in **15** is reduced to 8.650 Å (vs 8.833 Å in **11**).

**Table 5. Selected Bond Distances (Å) and Angles (deg) with Estimated Standard Deviations for**

<i>trans</i> -CH <sub>3</sub> -C≡C(Br)-CH-S-Ir(PEt <sub>3</sub> ) <sub>2</sub> (Br) <sub>2</sub> (15)			
Bond Distances			
Ir-Br1	2.602(2)	S-C4	1.666(16)
Ir-Br2	2.550(2)	C1-C2	1.499(22)
Ir-P1	2.384(3)	C2-C3	1.362(19)
Ir-P2	2.366(4)	C3-C4	1.370(22)
Ir-S	2.294(4)	C3-Br3	1.959(15)
Ir-C2	1.958(13)		
Bond Angles			
Br-Ir-Br2	93.3(1)	P1-Ir-C2	92.0(4)
Br1-Ir-P1	86.6(1)	P2-Ir-C2	93.9(4)
Br2-Ir-P1	88.4(1)	S-Ir-C2	84.3(4)
Br1-Ir-P2	88.3(1)	Ir-S-C4	99.4(6)
Br2-Ir-P2	86.2(1)	Ir-C2-C1	125.2(10)
P1-Ir-P2	172.4(1)	Ir-C2-C3	117.3(11)
Br1-Ir-S	87.1(1)	C1-C2-C3	117.5(13)
Br2-Ir-S	177.5(1)	Br3-C3-C2	122.0(11)
P1-Ir-S	94.1(1)	Br3-C3-C4	115.6(11)
P2-Ir-S	91.3(1)	C2-C3-C4	122.2(14)
Br1-Ir-C2	171.1(4)	S-C4-C3	116.5(11)
Br2-Ir-C2	95.4(4)		

### Summary

A new approach to the synthesis of thiapentadienyl-metal complexes has been demonstrated. This approach, which utilizes *anionic* thiapentadienide reagents, is illustrated by the reaction of ClIr(PMe<sub>3</sub>)<sub>3</sub> with potassium thiapentadienide, which produces ((1,2,5- $\eta$ )-5-thiapentadienyl)Ir(PMe<sub>3</sub>)<sub>3</sub> (1) in high yield. Treatment of compound 1 with the electrophilic reagents H<sup>+</sup>BF<sub>4</sub><sup>-</sup>·OEt<sub>2</sub> and CH<sub>3</sub>O<sub>3</sub>SCF<sub>3</sub> results in electrophilic addition at *different* sites on the thiapentadienyl ligand. Protonation occurs at terminal carbon C1 (probably through the intermediacy of a metal-hydride) to produce [(2,3,4,5- $\eta$ )-5-thiapentadiene]Ir(PMe<sub>3</sub>)<sub>3</sub><sup>+</sup>BF<sub>4</sub><sup>-</sup> (2), while methylation occurs at the sulfur center to produce [((1,2,5- $\eta$ )-5-methyl-5-thiapentadienyl)Ir(PMe<sub>3</sub>)<sub>3</sub>]<sup>+</sup>O<sub>3</sub>SCF<sub>3</sub><sup>-</sup> (3). Compound 3 then rearranges to [((1,2,3,4- $\eta$ )-5-methyl-5-thiapentadiene)Ir(PMe<sub>3</sub>)<sub>3</sub>]<sup>+</sup>O<sub>3</sub>SCF<sub>3</sub><sup>-</sup> (4), a species which is stabilized by the metal center's strong interaction with a  $\pi$ -system of four contiguous carbon atoms. Upon heating in toluene at reflux, 1 undergoes intramolecular C-H bond activation at C-H<sub>2</sub>, generating the five-membered iridathiacycle, *mer*-CH<sub>2</sub>=C-CH=

CH-S-Ir(PMe<sub>3</sub>)<sub>3</sub>(H) (5). This species exhibits the same clean regiochemistry as 1 in its reactions with electrophiles. Protonation with H<sup>+</sup>BF<sub>4</sub><sup>-</sup>·OEt<sub>2</sub> occurs exclusively at carbon C1 (the exocyclic methylene carbon) to produce the "iridathiophene", [*mer*-CH<sub>3</sub>-C≡C-CH=CH-S-Ir(PMe<sub>3</sub>)<sub>3</sub>(H)]<sup>+</sup>BF<sub>4</sub><sup>-</sup> (6), while methylation with CH<sub>3</sub>O<sub>3</sub>SCF<sub>3</sub> proceeds exclusively at sulfur to generate [*mer*-CH<sub>2</sub>=C-CH=CH-S(CH<sub>3</sub>)-Ir(PMe<sub>3</sub>)<sub>3</sub>(H)]<sup>+</sup>O<sub>3</sub>SCF<sub>3</sub><sup>-</sup> (7).

ClIr(PEt<sub>3</sub>)<sub>3</sub> also reacts cleanly with potassium thiapentadienide to produce the tris(PEt<sub>3</sub>) analogue of 1, ((1,2,5- $\eta$ )-5-thiapentadienyl)Ir(PEt<sub>3</sub>)<sub>3</sub> (8). Compound 8 is less robust thermally than 1, undergoing intramolecular C-H bond activation at room temperature. Both the C-H1 bond activation product, *mer*-CH=CH-CH=CH-S-Ir(PEt<sub>3</sub>)<sub>3</sub>(H) (9), and the C-H2 bond activation product, *mer*-CH<sub>2</sub>=C-CH=CH-S-Ir-

(PEt<sub>3</sub>)<sub>3</sub>(H) (10), are formed initially, but 9 gradually converts to 10. The thermodynamic preference for 10 over 9 derives from the fact that ring strain is lower in five-membered planar iridacycles than in six-membered planar iridacycles. Compound 10, like its tris(PMe<sub>3</sub>) analogue (5), reacts with H<sup>+</sup>BF<sub>4</sub><sup>-</sup>·OEt<sub>2</sub> and CH<sub>3</sub>O<sub>3</sub>SCF<sub>3</sub> to form the "iridathiophene" [*mer*-

CH<sub>3</sub>-C≡C-CH=CH-S-Ir(PEt<sub>3</sub>)<sub>3</sub>(H)]<sup>+</sup>BF<sub>4</sub><sup>-</sup> (11) and the S-methylated metallacycle, [*mer*-CH<sub>2</sub>=C-CH=CH-S-(CH<sub>3</sub>)-Ir(PEt<sub>3</sub>)<sub>3</sub>(H)]<sup>+</sup>O<sub>3</sub>SCF<sub>3</sub><sup>-</sup> (12), respectively. The aromatic character of "iridathiophene" 11 is supported by (a) its spectroscopy (downfield <sup>1</sup>H NMR chemical shifts for ring protons H3 and H4), (b) its structure (delocalized  $\pi$ -bonding around the ring), and (c) its reactivity (electrophilic substitution at ring carbon C3 when treated with excess Br<sub>2</sub>).

### Experimental Section

**General Comments.** Experimental procedures were carried out under an inert nitrogen atmosphere, using either glovebox or double-manifold Schlenk techniques. Solvents were stored under nitrogen after being distilled from appropriate drying agents. Toluene, tetrahydrofuran, and diethyl ether were dried over sodium/benzophenone, pentane was dried over calcium hydride, and acetone, methanol, and ethanol were dried over magnesium sulfate. Deuterated NMR solvents were obtained from MSD Isotopes or Cambridge Isotope Laboratories in 1 g sealed ampules and used as received.

The following reagents were obtained from the supplier indicated and used without further purification: *cis*-1,4-dichloro-2-butene (Aldrich), sulfur powder (Fisher), sodium metal (Aldrich), sodium sulfide (Johnson-Matthey), dimethyl sulfoxide (Aldrich), anhydrous ammonia (Matheson), potassium metal (Aldrich), IrCl<sub>3</sub>·3H<sub>2</sub>O (Johnson-Matthey), cyclooctene (Aldrich), trimethylphosphine (Strem), triethylphosphine (Strem), tetrafluoroboric acid diethyl etherate (Aldrich), methyl triflate (Aldrich), Cl<sub>2</sub> (Matheson), Br<sub>2</sub> (Fisher), and I<sub>2</sub> (Fisher). Potassium thiapentadienide<sup>7</sup> and [(cyclooctene)<sub>2</sub>-IrCl]<sub>2</sub><sup>26</sup> were prepared using literature procedures.

Nuclear magnetic resonance experiments were carried out on Varian 300 (XL-series) and 500 (VXR-series) MHz spectrometers. <sup>1</sup>H and <sup>13</sup>C spectra were referenced to tetramethylsilane ( $\delta = 0$ ), while <sup>31</sup>P spectra were referenced to H<sub>3</sub>PO<sub>4</sub> ( $\delta = 0$ ). Generally, <sup>1</sup>H and <sup>13</sup>C peak assignments were established using data from COSY (homonuclear shift-correlated spectroscopy), ATP (attached proton test), HETCOR (heteronuclear shift-correlated spectroscopy), and HMQC (<sup>1</sup>H-detected multiple quantum coherence) experiments. In some instances, additional information was obtained through nuclear Overhauser effect (NOE) difference experiments. *Note: In all NMR spectra, carbon atoms and associated hydrogens are numbered by starting at the end of the chain opposite sulfur.*

Elemental microanalyses were performed by Galbraith Laboratories, Inc., Knoxville, TN.

**Synthesis of ((1,2,5- $\eta$ )-5-Thiapentadienyl)Ir(PMe<sub>3</sub>)<sub>3</sub> (1).** Under a nitrogen atmosphere, trimethylphosphine (0.38 g, 5.0 mmol) was added dropwise to a cold (-78 °C) stirred solution of [(cyclooctene)<sub>2</sub>Ir(Cl)]<sub>2</sub> (0.75 g, 0.84 mmol) in 100 mL of tetrahydrofuran (THF). Potassium thiapentadienide (0.21 g, 1.7 mmol) in 30 mL of THF was then added dropwise. After the solution was warmed to room temperature, the volatiles were removed under vacuum. Compound 1 was then extracted from the resulting residue with pentane and crystallized at -30 °C from a concentrated diethyl ether solution containing

(26) Herde, J. L.; Lambert, J. C.; Senoff, C. V. In *Inorganic Syntheses*; Parrshall, G. W., Ed.; McGraw-Hill: New York, 1974; Vol. 15, pp 18-20.

several drops of pentane: yield (yellow crystals) 0.51 g, 60%. Anal. Calcd for  $C_{13}H_{33}IrP_3S$ : C, 30.88; H, 6.39. Found: C, 30.56; H, 6.34.  $^1H$  NMR ( $(CD_3)_2CO$ , 22 °C, 300 MHz):  $\delta$  5.72 (m, 1, H3), 5.17 (m, 1, H4), 2.67 (m, 1, H2), 1.59 (d,  $J_{H-P}$  = 8.3 Hz, 9,  $PMe_3$ ), 1.51 (d,  $J_{H-P}$  = 7.1 Hz, 9,  $PMe_3$ ), 1.47 (d,  $J_{H-P}$  = 8.7 Hz, 9,  $PMe_3$ ), 1.37 (m, 1, H1), 1.10 (m, 1, H1).  $^{13}C\{^1H\}$  NMR ( $(CD_3)_2CO$ , 22 °C, 75 MHz):  $\delta$  134.0 (s, C3), 126.4 (d,  $J_{C-P}$  = 17.6 Hz, C4), 41.0 (d,  $J_{C-P}$  = 28.3 Hz, C2), 23.1 (d,  $J_{C-P}$  = 22.4 Hz,  $PMe_3$ ), 20.2 (d,  $J_{C-P}$  = 23.5 Hz,  $PMe_3$ ), 19.4 (d,  $J_{C-P}$  = 34.7 Hz,  $PMe_3$ ), 18.4 (d,  $J_{C-P}$  = 33.1 Hz, C1).  $^{31}P\{^1H\}$  NMR ( $(CD_3)_2CO$ , 22 °C, 121 MHz):  $\delta$  -37.0 (dd,  $J_{P-P}$  = 17.6, 16.0 Hz,  $PMe_3$ ), -51.6 (dd,  $J_{P-P}$  = 42.3, 17.6 Hz,  $PMe_3$ ), -52.1 (dd,  $J_{P-P}$  = 42.3, 16.0 Hz,  $PMe_3$ ).

**Synthesis of [(2,3,4,5- $\eta$ )-5-Thiapentadiene]Ir( $PMe_3$ ) $_3$ ] $^+$ BF $_4^-$  (*anti* Isomer, **2a**). Under a nitrogen atmosphere, tetrafluoroboric acid diethyl etherate was added in excess to a cold (-30 °C) solution of compound **1** (50 mg, 0.10 mmol) in 15 mL of tetrahydrofuran (THF). After the mixture was filtered through Celite and the volatiles were removed under vacuum, compound **2a** was extracted from the residue with THF. Removal of the solvent afforded pure **2a** as an oily solid: yield 43 mg, 72%. Anal. Calcd for  $C_{13}H_{33}BF_4IrP_3S$ : C, 26.31; H, 5.62. Found: C, 25.91; H, 5.42.  $^1H$  NMR ( $(CD_3)_2CO$ , 22 °C, 300 MHz):  $\delta$  6.12 (m, 1, H4), 5.84 (m, 1, H3), 2.76 (m, 1, H2), 1.95 (d,  $J_{H-P}$  = 10.5 Hz, 9,  $PMe_3$ ), 1.71 (d,  $J_{H-P}$  = 10.2 Hz, 9,  $PMe_3$ ), 1.68 (d,  $J_{H-P}$  = 9.6 Hz, 9,  $PMe_3$ ), 1.59 (m, 3, H1's).  $^{13}C\{^1H\}$  NMR ( $(CD_3)_2CO$ , 22 °C, 75 MHz):  $\delta$  97.1 (s, C3), 95.1 (d,  $J_{C-P}$  = 9.4 Hz, C4), 42.3 (d,  $J_{C-P}$  = 41.3 Hz, C2), 21.7 (d,  $J_{C-P}$  = 36.7 Hz,  $PMe_3$ ), 19.0 (d,  $J_{C-P}$  = 35.2 Hz,  $PMe_3$ ), 18.7 (d,  $J_{C-P}$  = 38.2 Hz,  $PMe_3$ ), 9.8 (s, C1).  $^{31}P\{^1H\}$  NMR ( $(CD_3)_2CO$ , 22 °C, 121 MHz):  $\delta$  -33.6 (dd,  $J_{P-P}$  = 16.6, 10.8 Hz,  $PMe_3$ ), -36.9 (dd,  $J_{P-P}$  = 10.8, 10.8 Hz,  $PMe_3$ ), -51.6 (dd,  $J_{P-P}$  = 16.6, 10.8 Hz,  $PMe_3$ ).**

**Synthesis of [(2,3,4,5- $\eta$ )-5-Thiapentadiene]Ir( $PMe_3$ ) $_3$ ] $^+$ BF $_4^-$  (*syn* Isomer, **2b**). Under nitrogen, compound **2a** was refluxed for 5 h in acetone. After the solution was cooled to room temperature and filtered through Celite, the volatiles were removed under vacuum, affording pure **2b** in essentially quantitative yield.  $^1H$  NMR ( $(CD_3)_2CO$ , 22 °C, 500 MHz):  $\delta$  6.04 (m, 1, H3), 5.68 (m, 1, H4), 2.43 (m, 1, H2), 1.88 (d,  $J_{H-P}$  = 9.9 Hz, 9,  $PMe_3$ ), 1.75 (d,  $J_{H-P}$  = 10.0 Hz, 9,  $PMe_3$ ), 1.71 (d,  $J_{H-P}$  = 9.9 Hz, 9,  $PMe_3$ ), 1.54 (m, 3, H1's).  $^{13}C\{^1H\}$  NMR ( $(CD_3)_2CO$ , 22 °C, 75 MHz):  $\delta$  103.1 (s, C3), 80.7 (d,  $J_{C-P}$  = 10.1 Hz, C4), 58.0 (d,  $J_{C-P}$  = 35.7 Hz, C2), 21.1 (d,  $J_{C-P}$  = 37.5 Hz,  $PMe_3$ ), 20.9 (d,  $J_{C-P}$  = 36.2 Hz,  $PMe_3$ ), 19.4 (d,  $J_{C-P}$  = 38.0 Hz,  $PMe_3$ ), 16.9 (s, C1).  $^{31}P\{^1H\}$  NMR ( $(CD_3)_2CO$ , 22 °C, 121 MHz):  $\delta$  -35.7 (dd,  $J_{P-P}$  = 18.4, 9.2 Hz,  $PMe_3$ ), -43.4 (dd,  $J_{P-P}$  = 9.2, 9.2 Hz,  $PMe_3$ ), -50.7 (dd,  $J_{P-P}$  = 18.4, 9.2 Hz,  $PMe_3$ ).**

**Synthesis of [(1,2,5- $\eta$ )-5-Methyl-5-thiapentadienyl]Ir( $PMe_3$ ) $_3$ ] $^+$ O $_3$ SCF $_3^-$  (**3**). Under nitrogen, cold (-30 °C) methyl triflate (33 mg, 0.20 mmol) was added to a cold (-30 °C) solution of compound **1** (100 mg, 0.20 mmol) in 15 mL of diethyl ether. The solution was stirred vigorously for a few seconds and then quickly returned to a -30 °C refrigerator, where **3** crystallized overnight: yield (yellow crystals) 122 mg, 91%. Anal. Calcd for  $C_{15}H_{35}F_3IrO_3P_3S_2$ : C, 26.90; H, 5.28. Found: C, 26.76; H, 5.23.  $^1H$  NMR ( $(CD_3)_2CO$ , -80 °C, 300 MHz):  $\delta$  7.13 (m, 1, H3), 5.50 (m, 1, H4), 2.44 (m, 1, H2), 2.40 (m, 3, SMe), 1.83 (m, 1, H1), 1.73 (d,  $J_{H-P}$  = 7.9 Hz, 9,  $PMe_3$ ), 1.59 (d,  $J_{H-P}$  = 9.7 Hz, 9,  $PMe_3$ ), 1.53 (d,  $J_{H-P}$  = 8.3 Hz, 9,  $PMe_3$ ), 1.19 (m, 1, H1).  $^{13}C\{^1H\}$  NMR ( $(CD_3)_2CO$ , -80 °C, 75 MHz):  $\delta$  157.8 (s, C3), 114.7 (d,  $J_{C-P}$  = 17.0 Hz, C4), 38.7 (d,  $J_{C-P}$  = 33.8, C2), 25.0 (d,  $J_{C-P}$  = 34.0 Hz, C1), 23.8 (d,  $J_{C-P}$  = 8.0 Hz, SMe), 20.1 (d,  $J_{C-P}$  = 29.3,  $PMe_3$ ), 19.0 (d,  $J_{C-P}$  = 28.4 Hz,  $PMe_3$ ), 16.1 (d,  $J_{C-P}$  = 39.7 Hz,  $PMe_3$ ).  $^{31}P\{^1H\}$  NMR ( $(CD_3)_2CO$ , -80 °C, 121 MHz):  $\delta$  -32.2 (dd,  $J_{P-P}$  = 25.0, 18.1 Hz,  $PMe_3$ ), -52.3 (dd,  $J_{P-P}$  = 25.0, 18.1 Hz,  $PMe_3$ ), -54.7 (dd,  $J_{P-P}$  = 25.0, 25.0 Hz,  $PMe_3$ ).**

**Synthesis of [(1,2,3,4- $\eta$ )-5-Methyl-5-thiapentadiene]Ir( $PMe_3$ ) $_3$ ] $^+$ O $_3$ SCF $_3^-$  (**4**). At room temperature, compound **3** in THF was stirred overnight under a nitrogen atmosphere.**

After the mixture was filtered through Celite, the volatiles were removed under vacuum, affording pure **4** in essentially quantitative yield.  $^1H$  NMR ( $(CD_3)_2CO$ , 22 °C, 300 MHz):  $\delta$  5.50 (m, 1, H2), 5.33 (m, 1, H3), 3.46 (m, 1, H4), 2.50 (m, 1, H1), 2.24 (m, 1, H1), 2.08 (m, 3, SMe), 1.88 (d,  $J_{H-P}$  = 11.0 Hz, 9,  $PMe_3$ ), 1.66 (d,  $J_{H-P}$  = 9.0 Hz, 9,  $PMe_3$ ), 1.59 (d,  $J_{H-P}$  = 8.5 Hz, 9,  $PMe_3$ ).  $^{13}C\{^1H\}$  NMR ( $(CD_3)_2CO$ , 22 °C, 75 MHz):  $\delta$  95.8 (s, C2), 82.1 (d,  $J_{C-P}$  = 6.9 Hz, C3), 38.7 (d,  $J_{C-P}$  = 50.8 Hz, C4), 32.7 (d,  $J_{C-P}$  = 32.2 Hz, C1), 22.2 (d,  $J_{C-P}$  = 35.8 Hz,  $PMe_3$ ), 21.3 (d,  $J_{C-P}$  = 7.2 Hz, SMe), 19.4 (d,  $J_{C-P}$  = 31.5 Hz,  $PMe_3$ 's).  $^{31}P\{^1H\}$  NMR ( $(CD_3)_2CO$ , 22 °C, 121 MHz):  $\delta$  -40.3 (s,  $PMe_3$ ), -48.8 (d,  $J_{P-P}$  = 20.5 Hz,  $PMe_3$ ), -51.0 (d,  $J_{P-P}$  = 20.5 Hz,  $PMe_3$ ).

**Synthesis of  $mer$ -CH $_2$ -C-CH=CH-S-Ir( $PMe_3$ ) $_3$ (H) (**5**).** Under nitrogen, compound **1** (0.35 g, 0.59 mmol) was refluxed for 4 h in 50 mL of toluene. The solution was then cooled to room temperature, and the volatiles were removed under vacuum. Compound **5** was extracted from the resulting residue with pentane and crystallized at -30 °C from a concentrated diethyl ether solution containing several drops of pentane: yield (yellow prisms) 0.30 g, 85%. Anal. Calcd for  $C_{13}H_{33}IrP_3S$ : C, 30.88; H, 6.37. Found: C, 31.43; H, 6.62.  $^1H$  NMR ( $(CD_3)_2CO$ , 22 °C, 300 MHz):  $\delta$  6.17 (m, 1, H4), 5.88 (m, 1, H3), 5.83 (m, 1, H1), 5.05 (m, 1, H1), 1.61 (d,  $J_{H-P}$  = 7.1 Hz, 9, equatorial  $PMe_3$ ), 1.44 (d,  $J_{H-P}$  = 6.8 Hz, 18, axial  $PMe_3$ 's), -15.42 (pseudo q,  $J_{H-P}$  = 16.1 Hz, Ir-H).  $^{13}C\{^1H\}$  NMR ( $(CD_3)_2CO$ , 22 °C, 75 MHz):  $\delta$  163.0 (d of t,  $J_{C-P}$  = 78.5, 14.5 Hz, C2), 144.3 (s, C3), 141.4 (d,  $J_{C-P}$  = 11.9 Hz, C4), 119.3 (m, C1), 22.7 (d,  $J_{C-P}$  = 25.8 Hz, equatorial  $PMe_3$ ), 17.8 (virtual t,  $J_{C-P}$  = 37.5 Hz, axial  $PMe_3$ 's).  $^{31}P\{^1H\}$  NMR ( $(CD_3)_2CO$ , 22 °C, 121 MHz):  $\delta$  -42.4 (d,  $J_{P-P}$  = 21.1 Hz, axial  $PMe_3$ 's), -53.4 (t,  $J_{P-P}$  = 21.1 Hz, equatorial  $PMe_3$ ).

**Synthesis of [ $mer$ -CH $_3$ -C-CH=CH-S-Ir( $PMe_3$ ) $_3$ (H)] $^+$ BF $_4^-$  (**6**).** Under nitrogen, cold (-30 °C) tetrafluoroboric acid diethyl etherate (74 mg, 0.45 mmol) was added to a cold (-30 °C) solution of compound **5** (230 mg, 0.45 mmol) in 15 mL of diethyl ether. After it was swirled briefly, the solution was stored overnight at -30 °C, causing **6** to precipitate as a light brown powder. The powder was collected by filtration and recrystallized from a 1:1 mixture of ethanol/diethyl ether: yield (red-brown prisms) 220 mg, 82%. Anal. Calcd for  $C_{13}H_{33}BF_4IrP_3S$ : C, 26.31; H, 5.62. Found: C, 25.91; H, 5.42.  $^1H$  NMR ( $(CD_3)_2CO$ , 22 °C, 300 MHz):  $\delta$  10.60 (m, 1, H4), 7.77 (m, 1, H3), 3.22 (m, 3, H1's), 1.86 (d,  $J_{H-P}$  = 8.7 Hz, 9, equatorial  $PMe_3$ ), 1.48 (m, 18, axial  $PMe_3$ 's), -14.31 (pseudo q,  $J_{H-P}$  = 15.9 Hz, 1, Ir-H).  $^{13}C\{^1H\}$  NMR ( $(CD_3)_2CO$ , 22 °C, 75 MHz):  $\delta$  251.1 (d of t,  $J_{C-P}$  = 77.6, 7.5 Hz, C2), 213.6 (m, C4), 154.6 (s, C3), 43.5 (m, C1), 20.0 (d,  $J_{C-P}$  = 31.9 Hz, equatorial  $PMe_3$ ), 19.0 (virtual t,  $J_{C-P}$  = 40.2 Hz, axial  $PMe_3$ 's).  $^{31}P\{^1H\}$  NMR ( $(CD_3)_2CO$ , 22 °C, 121 MHz):  $\delta$  -40.3 (d,  $J_{P-P}$  = 28.3 Hz, axial  $PMe_3$ 's), -55.2 (t,  $J_{P-P}$  = 28.3 Hz, equatorial  $PMe_3$ ).

**Synthesis of [ $mer$ -CH $_2$ -C-CH=CH-S(CH $_3$ )-Ir( $PMe_3$ ) $_3$ (H)] $^+$ O $_3$ SCF $_3^-$  (**7**).** Under nitrogen, cold (-30 °C) methyl triflate (52 mg, 0.32 mmol) was added to a cold (-30 °C) solution of compound **5** (160 mg, 0.32 mmol) in 15 mL of diethyl ether. The solution was stirred vigorously for a few seconds and then returned to a -30 °C refrigerator overnight, causing **7** to precipitate from solution. The precipitate was collected, redissolved in a 1:1 mixture of ethanol/diethyl ether, and crystallized at -30 °C: yield (yellow crystals) 200 mg, 92%. Anal. Calcd for  $C_{15}H_{35}F_3IrO_3P_3S_2$ : C, 26.90; H, 5.28. Found: C, 26.76; H, 5.23.  $^1H$  NMR ( $(CD_3)_2CO$ , 22 °C, 300 MHz):  $\delta$  6.50 (m, 1, H3), 6.41 (m, 1, H1), 6.19 (s, 1, H4), 5.52 (s, 1, H1), 2.69 (s, 3, SMe), 1.79 (m, 9, equatorial  $PMe_3$ ), 1.52 (m, 18, axial  $PMe_3$ 's), -16.44 (pseudo q,  $J_{H-P}$  = 16.7 Hz, Ir-H).  $^{13}C\{^1H\}$  NMR ( $(CD_3)_2CO$ , 22 °C, 75 MHz):  $\delta$  156.6 (d of t,  $J_{C-P}$  = 75.0, 14.1 Hz, C2), 155.6 (s, C3), 132.4 (s, C1), 125.7 (d,  $J_{C-P}$  = 10.0 Hz, C4), 24.0 (m, SMe), 22.7 (d,  $J_{C-P}$  = 31.6 Hz, equatorial  $PMe_3$ ), 18.5 (virtual t,  $J_{C-P}$  = 39.4 Hz, axial



PMe<sub>3</sub>'s). <sup>31</sup>P{<sup>1</sup>H} NMR ((CD<sub>3</sub>)<sub>2</sub>CO, -80 °C, 121 MHz, stopped exchange): δ -41.5 (dd, J<sub>P-P</sub> = 323.1, 20.1 Hz, axial PMe<sub>3</sub>), -42.2 (dd, J<sub>P-P</sub> = 323.1, 20.1 Hz, axial PMe<sub>3</sub>), -51.1 (dd, J<sub>P-P</sub> = 20.1, 20.1 Hz, equatorial PMe<sub>3</sub>).

**Synthesis of ((1,2,5-η)-5-Thiapentadienyl)Ir(PET<sub>3</sub>)<sub>3</sub> (8).** Under a nitrogen atmosphere, triethylphosphine (0.59 g, 5.0 mmol) was added dropwise to a room temperature stirred solution of [(cyclooctene)<sub>2</sub>Ir(Cl)]<sub>2</sub> (0.75 g, 0.84 mmol) in 100 mL of tetrahydrofuran (THF). After removal of the volatiles under vacuum, the reaction mixture was redissolved in 100 mL of THF and cooled to 0 °C. Potassium thiapentadienide (0.21 g, 1.7 mmol) in 30 mL of THF was then added dropwise. After this mixture was stirred for 4 h at 0 °C and warmed to room temperature, the volatiles were removed under vacuum. Compound **8** was extracted from the resulting residue with pentane and crystallized at -30 °C from a concentrated diethyl ether solution containing several drops of pentane: yield (orange-yellow crystals) 0.91 g, 86%. Anal. Calcd for C<sub>22</sub>H<sub>50</sub>IrP<sub>3</sub>S: C, 41.81; H, 7.99. Found: C, 41.60; H, 8.07. <sup>1</sup>H NMR ((CD<sub>3</sub>)<sub>2</sub>CO, 22 °C, 500 MHz): δ 5.73 (m, 1, H3), 5.07 (m, 1, H4), 2.88 (m, 1, H2), 2.10–1.71 (m's, 18, PEt<sub>3</sub> CH<sub>2</sub>'s) 1.51 (m, 1, H1), 1.24 (m, 1, H1), 1.12–1.03 (m, 27, PEt<sub>3</sub> CH<sub>3</sub>'s). <sup>13</sup>C{<sup>1</sup>H} NMR ((CD<sub>3</sub>)<sub>2</sub>CO, 22 °C, 75 MHz): δ 134.0 (s, C3), 126.0 (d, J<sub>C-P</sub> = 17.2 Hz, C4), 39.1 (d, J<sub>C-P</sub> = 33.5 Hz, C2), 23.2 (d, J<sub>C-P</sub> = 21.1 Hz, PEt<sub>3</sub> CH<sub>2</sub>'s), 20.0 (d, J<sub>C-P</sub> = 21.1 Hz, PEt<sub>3</sub> CH<sub>2</sub>'s), 19.9 (d, J<sub>C-P</sub> = 29.2 Hz, PEt<sub>3</sub> CH<sub>2</sub>'s), 15.8 (d, J<sub>C-P</sub> = 36.2 Hz, C1), 10.0 (s, PEt<sub>3</sub> CH<sub>3</sub>'s), 8.9 (s, PEt<sub>3</sub> CH<sub>3</sub>'s). <sup>31</sup>P{<sup>1</sup>H} NMR ((CD<sub>3</sub>)<sub>2</sub>CO, 22 °C, 121 MHz): δ -16.9 (dd, J<sub>P-P</sub> = 17.5, 12.5 Hz, PEt<sub>3</sub>), -25.0 (dd, J<sub>P-P</sub> = 36.8, 17.5 Hz, PEt<sub>3</sub>), -27.2 (dd, J<sub>P-P</sub> = 36.8, 12.5 Hz, PEt<sub>3</sub>).

**NMR Characterization of mer-CH=CH-CH=CH-S-Ir(PET<sub>3</sub>)<sub>3</sub>(H) (9).** In an NMR tube, compound **8** in acetone-*d*<sub>6</sub> was placed in the probe of a Varian XL-300 spectrometer at 35 °C and monitored by <sup>31</sup>P{<sup>1</sup>H} NMR. After several hours, **8** had fully converted to two metallacyclic isomers, the six-membered ring **9** and the five-membered ring compound mer-CH<sub>2</sub>=C-CH=CH-S-Ir(PET<sub>3</sub>)<sub>3</sub>(H) (**10**), in a 3:2 ratio. NMR signals for **9** were obtained from this mixture of products. Note: Longer reaction times resulted in gradual conversion of **9** to **10**. <sup>1</sup>H NMR ((CD<sub>3</sub>)<sub>2</sub>CO, 22 °C, 500 MHz): δ 7.18 (m, 1, H1), 6.43 (m, 1, H2), 5.79 (m, 1, H4), 5.70 (m, 1, H3), 2.09–1.69 (m's, 18, PEt<sub>3</sub> CH<sub>2</sub>'s), 1.13–1.02 (m, 27, PEt<sub>3</sub> CH<sub>3</sub>'s), -16.74 (m, 1, Ir-H). <sup>13</sup>C{<sup>1</sup>H} NMR ((CD<sub>3</sub>)<sub>2</sub>CO, 22 °C, 125 MHz): δ 122.8 (s, C3), 122.7 (d, J<sub>C-P</sub> = 17 Hz, C4), 122.6 (s, C2), 121.1 (d of t, J<sub>C-P</sub> = 72, 16 Hz, C1), 21.1 (d, J<sub>C-P</sub> = 24.0 Hz, equatorial PEt<sub>3</sub> CH<sub>2</sub>'s), 17.5 (virtual t, J<sub>C-P</sub> = 32.0 Hz, axial PEt<sub>3</sub> CH<sub>2</sub>'s), 8.6 (s, axial PEt<sub>3</sub> CH<sub>3</sub>'s), 8.4 (s, equatorial PEt<sub>3</sub> CH<sub>3</sub>'s). <sup>31</sup>P{<sup>1</sup>H} NMR ((CD<sub>3</sub>)<sub>2</sub>CO, 22 °C, 121 MHz): δ -13.3 (d, J<sub>P-P</sub> = 16.7 Hz, axial PEt<sub>3</sub>'s), -23.4 (t, J<sub>P-P</sub> = 16.7 Hz, equatorial PEt<sub>3</sub>).

**Synthesis of mer-CH<sub>2</sub>=C-CH=CH-S-Ir(PET<sub>3</sub>)<sub>3</sub>(H) (10).** Under nitrogen, compound **8** (0.91 g, 1.44 mmol) was refluxed for 3 h in 50 mL of tetrahydrofuran. The solution was then cooled to room temperature, and the volatiles were removed under vacuum. Compound **10** was extracted from the resulting residue with pentane and crystallized at -30 °C from a concentrated diethyl ether solution containing several drops of pentane: yield (orange-yellow crystals) 0.83 g, 91%. Anal. Calcd for C<sub>22</sub>H<sub>50</sub>IrP<sub>3</sub>S: C, 41.81; H, 7.99. Found: C, 41.00; H, 8.19. <sup>1</sup>H NMR ((CD<sub>3</sub>)<sub>2</sub>CO, 22 °C, 300 MHz): δ 6.14 (m, 1, H4), 5.90 (m, 1, H1), 5.84 (m, 1, H3), 4.96 (m, 1, H1), 2.12–1.61 (m's, 18, PEt<sub>3</sub> CH<sub>2</sub>'s), 1.13–1.01 (m, 27, PEt<sub>3</sub> CH<sub>3</sub>'s), -15.63 (pseudo q, J<sub>H-P</sub> = 16.0 Hz, 1, Ir-H). <sup>13</sup>C{<sup>1</sup>H} NMR ((CD<sub>3</sub>)<sub>2</sub>CO, 22 °C, 75 MHz): δ 161.9 (d of t, J<sub>C-P</sub> = 76.7, 14.2 Hz, C2), 144.4 (s, C3), 142.7 (m, C4), 120.6 (d, J<sub>C-P</sub> = 10.3 Hz, C1), 21.2 (d, J<sub>C-P</sub> = 23.9 Hz, equatorial PEt<sub>3</sub> CH<sub>2</sub>'s), 18.1 (virtual t, J<sub>C-P</sub> = 32.8 Hz, axial PEt<sub>3</sub> CH<sub>2</sub>'s), 8.7 (s, axial PEt<sub>3</sub> CH<sub>3</sub>'s), 8.5 (s, equatorial PEt<sub>3</sub> CH<sub>3</sub>'s). <sup>31</sup>P{<sup>1</sup>H} NMR ((CD<sub>3</sub>)<sub>2</sub>CO, 22 °C, 121 MHz): δ -19.9 (t, J<sub>P-P</sub> = 18.7 Hz, equatorial PEt<sub>3</sub>), -22.9 (d, J<sub>P-P</sub> = 18.7 Hz, axial PEt<sub>3</sub>'s).

**Synthesis of [mer-CH<sub>3</sub>-C-CH=CH-S-Ir(PET<sub>3</sub>)<sub>3</sub>(H)]<sup>+</sup>BF<sub>4</sub><sup>-</sup> (11).** Under nitrogen, cold (-30 °C) tetrafluoroboric acid diethyl etherate (41 mg, 0.25 mmol) was added to a cold (-30 °C) solution of compound **10** (160 mg, 0.25 mmol) in 15 mL of diethyl ether. After it was swirled briefly, the solution was stored overnight at -30 °C, causing **11** to precipitate as a light brown powder. The powder was collected by filtration and recrystallized from a 1:1 mixture of ethanol/diethyl ether: yield (red-brown prisms) 160 mg, 89%. Anal. Calcd for C<sub>22</sub>H<sub>51</sub>BF<sub>4</sub>IrP<sub>3</sub>S: C, 36.71; H, 7.16. Found: C, 36.27; H, 6.57. <sup>1</sup>H NMR ((CD<sub>3</sub>)<sub>2</sub>CO, 22 °C, 300 MHz): δ 10.07 (m, 1, H4), 7.51 (m, 1, H3), 3.10 (m, 3, H1's), 1.90–1.50 (m's, 18, PEt<sub>3</sub> CH<sub>2</sub>'s), 0.94 (m, 9, PEt<sub>3</sub> CH<sub>3</sub>'s), 0.82 (m, 18, PEt<sub>3</sub> CH<sub>3</sub>'s), -14.28 (pseudo q, J<sub>H-P</sub> = 14.8 Hz, 1, Ir-H). <sup>13</sup>C{<sup>1</sup>H} NMR ((CD<sub>3</sub>)<sub>2</sub>CO, 22 °C, 75 MHz): δ 245.8 (d of t, J<sub>C-P</sub> = 75.7, 13.9 Hz, C2), 212.7 (m, C4), 155.6 (s, C3), 43.7 (d, J<sub>C-P</sub> = 5.4 Hz, C1), 19.5 (m, PEt<sub>3</sub> CH<sub>2</sub>'s), 8.6 (s, axial PEt<sub>3</sub> CH<sub>3</sub>'s), 8.3 (s, equatorial PEt<sub>3</sub> CH<sub>3</sub>'s). <sup>31</sup>P{<sup>1</sup>H} NMR ((CD<sub>3</sub>)<sub>2</sub>CO, 22 °C, 121 MHz): δ -13.8 (d, J<sub>P-P</sub> = 24.9 Hz, axial PEt<sub>3</sub>'s), -25.5 (t, J<sub>P-P</sub> = 24.9 Hz, equatorial PEt<sub>3</sub>).

**Synthesis of [mer-CH<sub>2</sub>=C-CH=CH-S(CH<sub>3</sub>)<sub>3</sub>-Ir(PET<sub>3</sub>)<sub>3</sub>(H)]<sup>+</sup>O<sub>3</sub>SCF<sub>3</sub><sup>-</sup> (12).** Under nitrogen, cold (-30 °C) methyl triflate (39 mg, 0.24 mmol) was added to a cold (-30 °C) solution of compound **10** (150 mg, 0.24 mmol) in 15 mL of diethyl ether. The solution was stirred vigorously for a few seconds and then stored in a -30 °C refrigerator overnight, causing **12** to precipitate. The precipitate was collected by filtration, redissolved in a 1:1 mixture of ethanol/diethyl ether, and crystallized at -30 °C: yield (yellow crystals) 160 mg, 84%. Anal. Calcd for C<sub>24</sub>H<sub>53</sub>F<sub>3</sub>IrO<sub>3</sub>P<sub>3</sub>S<sub>2</sub>: C, 36.21; H, 6.72. Found: C, 36.60; H, 6.24. <sup>1</sup>H NMR (CD<sub>2</sub>Cl<sub>2</sub>, 22 °C, 300 MHz): δ 6.46 (m, 1, H1), 6.45 (s, 1, H3), 6.00 (d, J<sub>H-H</sub> = 4 Hz, 1, H4), 5.49 (m, 1, H1), 2.61 (m, 3, SCH<sub>3</sub>), 2.00–1.60 (m's, 18, PEt<sub>3</sub> CH<sub>2</sub>'s), 1.10–0.95 (m, 27, PEt<sub>3</sub> CH<sub>3</sub>'s), -16.37 (pseudo q, J<sub>H-P</sub> = 14.8 Hz, 1, Ir-H). <sup>13</sup>C{<sup>1</sup>H} NMR (CD<sub>2</sub>Cl<sub>2</sub>, 22 °C, 75 MHz): δ 156.0 (s, C3), 154.8 (d of t, J<sub>C-P</sub> = 83.2, 17.1 Hz, C2), 134.1 (d, J<sub>C-P</sub> = 8.1 Hz, C1), 124.9 (d, J<sub>C-P</sub> = 7.2 Hz, C4), 26.5 (s, SMe), 20.7 (d, J<sub>C-P</sub> = 23.9 Hz, equatorial PEt<sub>3</sub> CH<sub>2</sub>'s), 18.4 (virtual t, J<sub>C-P</sub> = 30.3 Hz, axial PEt<sub>3</sub> CH<sub>2</sub>'s), 8.41 (s, axial PEt<sub>3</sub> CH<sub>3</sub>'s), 8.34 (s, equatorial PEt<sub>3</sub> CH<sub>3</sub>'s). <sup>31</sup>P{<sup>1</sup>H} NMR ((CD<sub>3</sub>)<sub>2</sub>CO, -80 °C, 121 MHz, stopped exchange): δ -20.1 (dd, J<sub>P-P</sub> = 18.4, 18.4 Hz, equatorial PEt<sub>3</sub>), -20.9 (dd, J<sub>P-P</sub> = 300.4, 18.4 Hz, axial PEt<sub>3</sub>), -22.9 (dd, J<sub>P-P</sub> = 300.4, 18.4 Hz, axial PEt<sub>3</sub>).

**Synthesis of trans-CH<sub>3</sub>-C-CH=CH-S-Ir(PET<sub>3</sub>)<sub>2</sub>(Cl)<sub>2</sub> (13).** Under nitrogen, Cl<sub>2</sub> gas was bubbled through a cold (0 °C) THF solution of compound **11** (500 mg, 0.69 mmol) for a period of about 30 s to establish a static Cl<sub>2</sub> atmosphere. The solution was stirred under the Cl<sub>2</sub> atmosphere for 1 h at 0 °C before warming to room temperature. The volatiles were then removed under vacuum, and the resulting residue was washed with diethyl ether. Compound **13** was extracted from the remaining solid residue with pentane. Removal of the pentane afforded **13** as a pink powder: yield 320 mg, 79%. <sup>1</sup>H NMR ((CD<sub>3</sub>)<sub>2</sub>CO, 22 °C, 300 MHz): δ 9.64 (s, 1, H4), 7.44 (m, 1, H3), 3.11 (s, 3, H1's), 2.05–1.75 (m's, 12, PEt<sub>3</sub> CH<sub>2</sub>'s), 1.10–0.95 (m, 18, PEt<sub>3</sub> CH<sub>3</sub>'s). <sup>13</sup>C{<sup>1</sup>H} NMR ((CD<sub>3</sub>)<sub>2</sub>CO, 22 °C, 75 MHz): δ 239.0 (s, C2), 201.0 (s, C4), 152.5 (s, C3), 36.1 (s, C1), 13.5 (virtual t, J<sub>C-P</sub> = 33.7 Hz, PEt<sub>3</sub> CH<sub>2</sub>'s), 8.1 (s, PEt<sub>3</sub> CH<sub>3</sub>'s). <sup>31</sup>P{<sup>1</sup>H} NMR ((CD<sub>3</sub>)<sub>2</sub>CO, 22 °C, 121 MHz): δ -12.1 (s, PEt<sub>3</sub>'s).

**Synthesis of trans-CH<sub>3</sub>-C-CH=CH-S-Ir(PET<sub>3</sub>)<sub>2</sub>(I)<sub>2</sub> (14).** Under a nitrogen atmosphere, I<sub>2</sub> (260 mg, 1.0 mmol) was added to compound **11** (250 mg, 0.35 mmol) in THF, and the solution was refluxed for a period of 48 h. After the mixture was cooled to room temperature, the volatiles were removed under vacuum and the resulting residue was washed with diethyl ether. Compound **14** was then extracted from the remaining solid with pentane. Removal of the pentane afforded **14** as a red-brown powder: yield 220 mg, 83%. <sup>1</sup>H NMR

Table 6. X-ray Diffraction Structure Summary

compd	5	15
Crystal Parameters and Data Collection Summary		
formula	C <sub>13</sub> H <sub>32</sub> IrP <sub>3</sub> S	C <sub>16</sub> H <sub>34</sub> Br <sub>3</sub> IrP <sub>2</sub> S
fw	505.6	752.4
cryst syst	orthorhombic	orthorhombic
space group	<i>Pnma</i>	<i>Pca2<sub>1</sub></i>
<i>a</i> , Å	11.935(3)	14.825(4)
<i>b</i> , Å	14.251(3)	10.110(2)
<i>c</i> , Å	11.908(3)	15.757(4)
$\alpha$ , deg	90	90
$\beta$ , deg	90	90
$\gamma$ , deg	90	90
<i>V</i> , Å <sup>3</sup>	2025.3(7)	2361.7(10)
<i>Z</i>	4	4
cryst dims, mm <sup>3</sup>	0.31 × 0.16 × 0.28	0.62 × 0.24 × 0.60
cryst color and habit	yellow prism	deep red block
density <sub>calcd</sub> , g/cm <sup>3</sup>	1.658	2.116
radiation, Å	Mo K $\alpha$ ( $\lambda$ = 0.710 73 Å)	Mo K $\alpha$ ( $\lambda$ = 0.710 73 Å)
scan type	$\theta$ - $2\theta$	$\theta$ - $2\theta$
scan rate, deg/min in $\omega$	variable; 3.50-14.65	variable; 3.50-14.65
scan range ( $\omega$ ), deg	1.20 plus K $\alpha$ separation	1.20 plus K $\alpha$ separation
$2\theta$ range, deg	3.0-45.0	3.0-55.0
data collected	<i>h</i> , 0 → 12; <i>k</i> , -15 → 15; <i>l</i> , 0 → 12	<i>h</i> , -19 → 19; <i>k</i> , -13 → 13; <i>l</i> , -20 → 20
total decay	none detected	none detected
temp, K	295	296
Treatment of Intensity Data and Refinement Summary		
no. of data collected	2957	6125
no. of unique data	1391	5391
no. of data with $I > 3\sigma(I)$	1127	3762
Mo K $\alpha$ linear abs coeff, cm <sup>-1</sup>	69.19	109.51
abs corr applied	semiempirical	semiempirical
data to parameter ratio	11.5:1	17.9:1
<i>R</i> <sup>a</sup>	0.0206	0.0388
<i>R</i> <sub>w</sub> <sup>a</sup>	0.0268 <sup>b</sup>	0.0562 <sup>c</sup>
GOF <sup>d</sup>	0.75	0.61

<sup>a</sup>  $R = \sum ||F_o| - |F_c|| / \sum |F_o|$ .  $R_w = [\sum w(|F_o| - |F_c|)^2 / \sum w|F_o|^2]^{1/2}$ . <sup>b</sup>  $w = [\sigma^2(F_o) + 0.0008(F_o)^2]^{-1}$ . <sup>c</sup>  $w = [\sigma^2(F_o) + 0.0067(F_o)^2]^{-1}$ . <sup>d</sup> GOF =  $[\sum w(|F_o| - |F_c|)^2 / (N_{\text{observations}} - N_{\text{variables}})]^{1/2}$ .

((CD<sub>3</sub>)<sub>2</sub>CO, 22 °C, 500 MHz):  $\delta$  9.66 (m, 1, H4), 7.19 (m, 1, H3), 3.17 (s, 3, H1's), 2.30-2.00 (m's 12, PEt<sub>3</sub> CH<sub>2</sub>'s), 1.06-0.98 (m, 18, PEt<sub>3</sub> CH<sub>3</sub>'s). <sup>13</sup>C{<sup>1</sup>H} NMR ((CD<sub>3</sub>)<sub>2</sub>CO, 22 °C, 125 MHz):  $\delta$  235.3 (s, C2), 205.1 (s, C4), 150.3 (s, C3), 41.3 (s, C1), 17.9 (virtual t,  $J_{C-P} = 35.5$  Hz, PEt<sub>3</sub> CH<sub>2</sub>'s), 9.4 (s, PEt<sub>3</sub> CH<sub>3</sub>'s). <sup>31</sup>P{<sup>1</sup>H} NMR ((CD<sub>3</sub>)<sub>2</sub>CO, 22 °C, 121 MHz):  $\delta$  -33.4 (s, PEt<sub>3</sub>'s).

**Synthesis of *trans*-CH<sub>3</sub>-C<sup>.....</sup>-C(Br)-CH-Ir(PEt<sub>3</sub>)<sub>2</sub>(Br)<sub>2</sub> (15).** Under a nitrogen atmosphere, excess Br<sub>2</sub> was added dropwise to a room temperature THF solution of compound 11 (250 mg, 0.35 mmol). The solution was then stirred vigorously for 15 min, before removing the volatiles under vacuum. Compound 15 was extracted from the resulting residue with acetone and crystallized from acetone at -30 °C: yield (deep red crystals) 180 mg, 69%. Anal. Calcd for C<sub>16</sub>H<sub>34</sub>Br<sub>3</sub>IrP<sub>2</sub>S: C, 25.54; H, 4.56. Found: C, 25.62; H, 4.67. <sup>1</sup>H NMR ((CD<sub>3</sub>)<sub>2</sub>CO, 22 °C, 500 MHz):  $\delta$  10.14 (s, 1, H4), 2.97 (s, 3, H1's), 2.08-1.78 (m's, 12, PEt<sub>3</sub> CH<sub>2</sub>'s), 0.99-0.91 (m, 18, PEt<sub>3</sub> CH<sub>3</sub>'s). <sup>13</sup>C{<sup>1</sup>H} ((CD<sub>3</sub>)<sub>2</sub>CO, 22 °C, 125 MHz):  $\delta$  222.4 (s, C2), 201.5 (s, C4), 129.2 (s, C3), 37.2 (s, C1), 15.0 (virtual t,  $J_{C-P} = 34.2$  Hz, PEt<sub>3</sub> CH<sub>2</sub>'s), 8.2 (s, PEt<sub>3</sub> CH<sub>3</sub>'s). <sup>31</sup>P{<sup>1</sup>H} NMR ((CD<sub>3</sub>)<sub>2</sub>CO, 22 °C, 121 MHz):  $\delta$  -18.8 (s, PEt<sub>3</sub>'s).

**X-ray Diffraction Studies of *mer*-CH<sub>2</sub>=C-CH=CH-S-Ir(PMe<sub>3</sub>)<sub>3</sub>(H) (5) and *trans*-CH<sub>3</sub>-C<sup>.....</sup>-C(Br)-CH-S-Ir(PEt<sub>3</sub>)<sub>2</sub>(Br)<sub>2</sub> (15).** Single crystals of 5 and 15 were sealed in glass capillaries under an inert atmosphere. Data were collected at room temperature, using graphite-monochromated Mo K $\alpha$  radiation. Three standard reflections were measured every 100 events as check reflections for crystal deterioration and/or misalignment. All data reduction and refinement were done using the Siemens SHELXTL PLUS package on a Vax

3100 workstation.<sup>27</sup> Crystal data and details of data collection and structure analysis are listed in Table 6.

The iridium atom positions in 5 and 15 were determined by direct methods. In each case, remaining non-hydrogen atoms were found by successive full-matrix least-squares refinement and difference Fourier map calculations. All non-hydrogen atoms were refined anisotropically, while the metal-bound hydrogen atom in 5 was refined isotropically. All other hydrogens in 5 and 15 were placed at idealized positions and assumed the riding model. In each case, a common isotropic *U* value for all hydrogens was refined.

**Dynamic NMR Studies of [*mer*-CH<sub>2</sub>=C-CH=CH-S-(CH<sub>3</sub>)-Ir(PMe<sub>3</sub>)<sub>3</sub>(H)]<sup>+</sup>O<sub>3</sub>SCF<sub>3</sub><sup>-</sup> (7) and [*mer*-CH<sub>2</sub>=C-CH=CH-S(CH<sub>3</sub>)-Ir(PEt<sub>3</sub>)<sub>3</sub>(H)]<sup>+</sup>O<sub>3</sub>SCF<sub>3</sub><sup>-</sup> (12).** Determination of  $\Delta G^\ddagger$ . Variable temperature (-80 °C - 55 °C) <sup>31</sup>P{<sup>1</sup>H} NMR spectra of compounds 7 and 12 in acetone-*d*<sub>6</sub> were obtained on the Varian XL-300 NMR spectrometer. Exchange rate constants, *k*<sub>e</sub>, at the coalescence temperature, *T*<sub>c</sub>, were calculated by using the formula

$$k_e = \pi(\Delta\nu)/2^{1/2}$$

where  $\Delta\nu$  is the difference in frequency between the two exchanging sites in the stopped exchange limit<sup>28</sup> (i.e., the frequency difference between the <sup>31</sup>P NMR signals for the *trans*-di-axial phosphines at -80 °C).<sup>29</sup> These exchange rate

(27) Atomic scattering factors were obtained from the following: *International Tables for X-Ray Crystallography*; Kynoch Press: Birmingham, England, 1974; Vol. 4.

(28) Pople, J. A.; Schneider, W. G.; Bernstein, H. J. *High-Resolution Nuclear Magnetic Resonance*; McGraw-Hill: New York, 1959; p 223.



constants were then used to determine the free energies of activation,  $\Delta G^\ddagger$ , at the coalescence temperature,  $T_c$ , from the Eyring equation

$$k_c = \frac{k'}{h} T_c \Delta e^{-\Delta G^\ddagger/RT_c}$$

where  $k'$  = Boltzmann's constant,  $h$  = Planck's constant, and  $R$  = ideal gas constant.<sup>30</sup>

**Acknowledgment.** We thank the National Science Foundation (Grants CHE-9003159 and CHE-9303516) and the donors of the Petroleum Research Fund, ad-

---

(29) In both **7** and **12**, the *trans*-diaxial phosphines had very similar <sup>31</sup>P chemical shifts and large P-P couplings, giving rise to second-order AB patterns in the low-temperature (stopped-exchange) spectra. In order to obtain the actual chemical shift positions of these signals, the Varian spin simulation program was employed.

(30) Lowry, T. H.; Richardson, K. S. *Mechanism and Theory in Organic Chemistry*; Harper and Row: New York, 1976; p 194.

ministered by the American Chemical Society, for support of this research. A loan of IrCl<sub>3</sub>·3H<sub>2</sub>O from Johnson-Matthey Alfa/Aesar is gratefully acknowledged. Washington University's X-ray Crystallography Facility was funded by the National Science Foundation's Chemical Instrumentation Program (Grant CHE-8811456). The High Resolution NMR Service Facility was funded in part by National Institutes of Health Biomedical Support Instrument Grant 1 S10 RR02004 and by a gift from Monsanto Company.

**Supplementary Material Available:** Tables of structure determination summaries, final atomic coordinates, thermal parameters, bond lengths, and bond angles for compounds **5** and **15** (16 pages). Ordering information is given on any current masthead page.

OM950075P

# Unusual Hexacoordination in a Triorganotin Fluoride Supported by Intermolecular Hydrogen Bonds. Crystal and Molecular Structures of 1-Aza-5-stanna-5-halogenotricyclo[3.3.3.0<sup>1,5</sup>]undecanes N(CH<sub>2</sub>CH<sub>2</sub>CH<sub>2</sub>)<sub>3</sub>SnF·H<sub>2</sub>O and N(CH<sub>2</sub>CH<sub>2</sub>CH<sub>2</sub>)<sub>3</sub>SnX (X = Cl, Br, I)<sup>†</sup>

Ute Kolb,<sup>‡</sup> Martin Dräger,<sup>\*,‡,§</sup> Manfred Dargatz,<sup>||,⊥</sup> and Klaus Jurkschat<sup>\*,||,∇</sup>

Institut für Anorganische Chemie und Analytische Chemie der Johannes Gutenberg-Universität, Johann Joachim Becher-Weg 24, D-55099 Mainz, Germany, and Lehrstuhl für Anorganische Chemie II der Universität Dortmund, D-44221 Dortmund, Germany

Received December 19, 1994<sup>⊗</sup>

Synthesis of N(CH<sub>2</sub>CH<sub>2</sub>CH<sub>2</sub>)<sub>3</sub>SnF·H<sub>2</sub>O (**1a**) and MeN(CH<sub>2</sub>CH<sub>2</sub>CH<sub>2</sub>)<sub>2</sub>SnFMe·H<sub>2</sub>O (**5a**) and molecular structures of **1a** and N(CH<sub>2</sub>CH<sub>2</sub>CH<sub>2</sub>)<sub>3</sub>SnX (**2**, X = Cl; **3**, X = Br; **4**, X = I) are reported. Compound **1a** is a tetramer held together by intermolecular Sn···F interactions (2.797(6) Å) and F···H and O···H hydrogen bridges. It is the first example of an intermolecular hexacoordinated triorganotin halide. Compounds **2–4** exhibit the expected propellane (metallatrane) structure with pentacoordinate tin, with the shortest intramolecular Sn···N interaction of 2.28(2) Å found for **3**. The Sn···N distances in the other stannatranes are 2.393(5) and 2.426(6) Å (**1a**), 2.38(2) Å (**2**, hexagonal), 2.38(4) Å (**2**, monoclinic), and 2.375(6) Å (**4**).

## Introduction

Hypervalency is one of the most exciting concepts in modern main group element chemistry. It explains very well the stereochemical nonrigidity and unusual reactivity of a great variety of compounds.<sup>1</sup> Prominent representatives of hypervalent compounds are the so-called metallatranes,<sup>2</sup> among which the silatranes<sup>3</sup> and stannatranes<sup>4</sup> of type N(CH<sub>2</sub>CH<sub>2</sub>X)<sub>3</sub>ER (X = O, S, NR,

CH<sub>2</sub>; E = Si, Sn) are most extensively studied. These compounds are characterized by their unusual cage structures, intramolecular N–E interactions, and chirality of their molecular frameworks. Some derivatives exhibit remarkable biological activity.<sup>5</sup>

Recently, it has been shown that 1-aza-5-stannabicyclo[3.3.3]undecanes (tricarbastannatranes) of type A exhibit enhanced reactivity of the apical Sn–R bond, making these compounds interesting also from the viewpoint of synthetic application<sup>6</sup> (see Chart 1).

The enhanced reactivity of the Sn–C bond in the presence of an intramolecular donor is a common feature in organotin chemistry and has recently been reviewed.<sup>6c</sup> A better understanding of the strength and nature of such coordinative bonds is therefore of some interest. Solution NMR studies on tricarbastannatranes of type A did not give conclusive evidence for the influence of R on the Sn–N bond strength.<sup>4d</sup> We therefore decided to perform systematic X-ray studies on N(CH<sub>2</sub>CH<sub>2</sub>CH<sub>2</sub>)<sub>3</sub>SnR and present here the molecular structures of **1** (X = F, as its water adduct **1a**), **2** (X = Cl), **3** (X = Br), and **4** (X = I).

(4) (a) Tzschach, A.; Jurkschat, K. *Comments Inorg. Chem.* **1983**, *3*, 35. (b) Jurkschat, K.; Tzschach, A. *J. Organomet. Chem.* **1984**, *272*, C13. (c) Jurkschat, K.; Tzschach, A.; Meunier-Piret, J.; Van Meersche, M. *J. Organomet. Chem.* **1985**, *290*, 285. (d) Mügge, C.; Pepermans, H.; Gielen, M.; Willem, R.; Tzschach, A.; Jurkschat, K. *Z. Anorg. Allg. Chem.* **1988**, *567*, 122. (e) Jurkschat, K.; Tzschach, A.; Meunier-Piret, J. *J. Organomet. Chem.* **1986**, *315*, 45. (f) Plass, W.; Verkade, J. G. *Inorg. Chem.* **1993**, *32*, 5153.

(5) Tandura, S.; Voronkov, M. G.; Alekseev, N. Y. *Curr. Top. Chem.* **1986**, *131*, 99.

(6) (a) Vedejs, E.; Haight, A. R.; Moss, W. O. *J. Am. Chem. Soc.* **1992**, *114*, 6556. (b) Under the influence of ultrasound, even methanol cleaves the Sn–CH<sub>3</sub> bond of N(CH<sub>2</sub>CH<sub>2</sub>CH<sub>2</sub>)<sub>3</sub>SnCH<sub>3</sub>. Jurkschat, K. Unpublished results. (c) Jastrzebski, J. T. B. H.; Van Koten, G. *Adv. Organomet. Chem.* **1993**, *35*, 241.

<sup>†</sup> Dedicated to Professor Herbert Schumann on the occasion of his 60th birthday.

<sup>‡</sup> Gutenberg Universität Mainz.

<sup>§</sup> Tel.: +49-6131-395757. Fax: +49-6131-395380.

<sup>||</sup> Universität Dortmund.

<sup>⊥</sup> Present address: Department of Chemistry, Deakin University, Geelong, Vic. 3217, Australia.

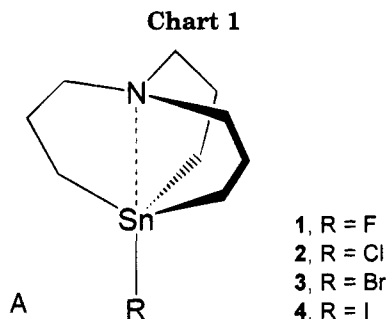
<sup>∇</sup> Tel.: +49-231-7553800. Fax: +49-231-5553771.

<sup>⊗</sup> Abstract published in *Advance ACS Abstracts*, May 1, 1995.

(1) (a) Musher, J. I. *Angew. Chem., Int. Ed. Engl.* **1969**, *8*, 54. (b) Kutzelnigg, W. *Angew. Chem., Int. Ed. Engl.* **1984**, *23*, 272. (c) Alcock, N. W. *Adv. Inorg. Chem. Radiochem.* **1972**, *15*, 1. (d) Holmes, R. R. *Chem. Rev.* **1990**, *90*, 17 and references cited therein. (e) Corriu, R. J. P.; Chuit, C.; Reye, C.; Young, J. C. *Chem. Rev.* **1993**, *93*, 1371 and references cited therein.

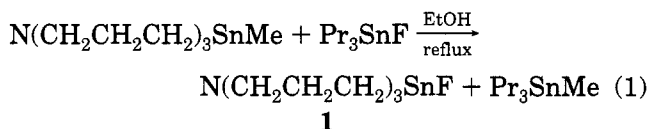
(2) (a) Voronkov, M. G.; Baryshok, V. B. *J. Organomet. Chem.* **1982**, *239*, 199 and references cited therein. (b) Verkade, J. G.; Menge, W. M. P. B. *Inorg. Chem.* **1991**, *30*, 4628 and references cited therein. (c) Plass, W.; Verkade, J. G. *J. Am. Chem. Soc.* **1992**, *114*, 2275. (d) Cummins, C. C.; Schrock, R. R.; Davis, W. M. *Organometallics* **1992**, *11*, 1452.

(3) (a) Voronkov, M. G.; Dyakov, V. M.; Kirpichenko, S. V. *J. Organomet. Chem.* **1982**, *233*, 1. (b) Hencsei, P.; Parkanyi, L. *Rev. Silicon, Germanium, Tin Lead Compds.* **1985**, *8*, 191 and references cited therein. (c) Jurkschat, K.; Mügge, C.; Schmidt, J.; Tzschach, A. *J. Organomet. Chem.* **1985**, *287*, C1. (d) Jurkschat, K.; Tzschach, A.; Meunier-Piret, J.; van Meersche, M. *J. Organomet. Chem.* **1986**, *317*, 145. (e) Jurkschat, K.; Tzschach, A.; Dargatz, M.; Pepermans, H.; Gielen, M.; Willem, R. *Recl. Trav. Chim. Pays-Bas* **1988**, *107*, 170. (f) Gudat, D.; Verkade, J. G. *Organometallics* **1989**, *8*, 2772. (g) Gordon, M. S.; Marshall, T. C.; Jensen, J. H. *Organometallics* **1991**, *10*, 2657. (h) Garant, R. J.; Daniels, L. M.; Das, S. K.; Janakiraman, M. N.; Jacobson, R. A.; Verkade, J. G. *J. Am. Chem. Soc.* **1991**, *113*, 5728. (i) Oh, A.-S.; Chung, Y. K.; Kim, S. *Organometallics* **1992**, *11*, 1394.

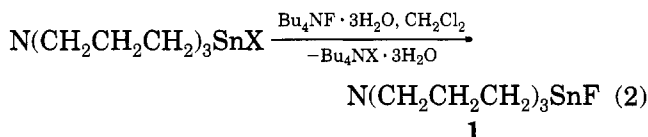


## Results and Discussion

**Synthetic Aspects.** Compound **1** was prepared almost quantitatively by reaction of  $N(\text{CH}_2\text{CH}_2\text{CH}_2)_3\text{SnMe}$  and  $\text{Pr}_3\text{SnF}$  in ethanol (eq 1).



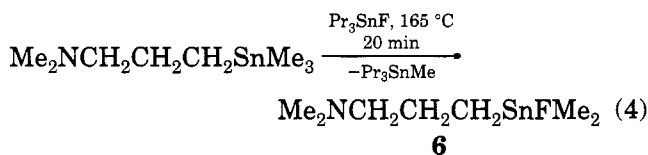
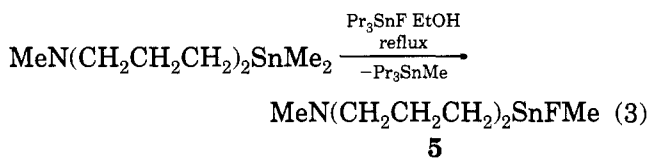
Compound **1** also forms quantitatively by reaction of  $N(\text{CH}_2\text{CH}_2\text{CH}_2)_3\text{SnX}$  ( $X = \text{Cl}, \text{Br}, \text{I}$ ) with  $\text{Bu}_4\text{NF} \cdot 3\text{H}_2\text{O}$  (eq 2), but not attempt was made to isolate it from this reaction mixture.



$^{119}\text{Sn}$  NMR reveals this reaction to be quantitative.

Because of the presence of water (from  $\text{Bu}_4\text{NX} \cdot 3\text{H}_2\text{O}$ ) **1** is very likely in a fast equilibrium with **1a** (see below).

For the sake of comparison,  $\text{MeN}(\text{CH}_2\text{CH}_2\text{CH}_2)_2\text{SnMeF}$  (**5**) and  $\text{Me}_2\text{NCH}_2\text{CH}_2\text{CH}_2\text{SnFMe}_2$  (**6**) were prepared by similar reactions (eqs 3 and 4). Crystalline



**1** and **5** were obtained only as their water adducts  $N(\text{CH}_2\text{CH}_2\text{CH}_2)_3\text{SnF} \cdot \text{H}_2\text{O}$ , hereafter referred to as **1a**, and  $\text{MeN}(\text{CH}_2\text{CH}_2\text{CH}_2)_2\text{SnMeF} \cdot \text{H}_2\text{O}$ , hereafter referred to as **5a**, from both toluene and ether/hexane, respectively. The origin of water is air moisture. Attempts to obtain crystals of **1** and **5**, respectively, were not successful under strictly inert conditions. Compound **6** is an oil which was not separated from  $\text{Pr}_3\text{SnMe}$  and which was identified by  $^{119}\text{Sn}$  and  $^{13}\text{C}$  NMR only.

**Molecular Structure of 1a.** The molecular structure of **1a** is shown in Figure 1, and selected bond lengths and bond angles are summarized in Table 1. Compound **1a** consists of two independent molecules which are held together by intermolecular  $\text{Sn}(1) \cdots \text{F}(2)$  interaction. This interaction is supported by the

**Table 1. Selected Bond Distances (Å) and Bond Angles (deg) in  $N(\text{CH}_2\text{CH}_2\text{CH}_2)_3\text{SnF} \cdot \text{H}_2\text{O}$  (**1a**) with Standard Deviations in Parentheses**

Bond Distances			
Sn(1)–N(1)	2.426(6)	Sn(2)–N(2)	2.393(5)
Sn(1)–C(11)	2.146(7)	Sn(2)–C(21)	2.145(8)
Sn(1)–C(14)	2.132(9)	Sn(2)–C(24)	2.135(8)
Sn(1)–C(17)	2.145(9)	Sn(2)–C(27)	2.126(7)
Sn(1)–F(1)	2.121(5)	Sn(2)–F(2)	2.115(6)
Sn(1) $\cdots$ F(2)	2.797(6)		
F(1)–O(1)	2.238(7)	F(2)–O(1)	2.214(8)
Sn(2) $\cdots$ O(1)	3.180(8)		
O(1) $\cdots$ O(2)	2.88(1)		
O(1) $\cdots$ O(2')	2.92(1)		
Bond Angles			
N(1)–Sn(1)–F(1)	172.7(2)	N(2)–Sn(2)–F(2)	174.0(2)
F(1)–Sn(1)–C(11)	102.3(2)	F(2)–Sn(2)–C(21)	102.4(3)
F(1)–Sn(1)–C(14)	94.1(3)	F(2)–Sn(2)–C(24)	93.6(3)
F(1)–Sn(1)–C(17)	106.9(3)	F(2)–Sn(2)–C(27)	104.4(3)
C(11)–Sn(1)–C(14)	119.5(3)	C(21)–Sn(2)–C(24)	117.6(3)
C(14)–Sn(1)–C(17)	112.8(4)	C(24)–Sn(2)–C(27)	115.0(3)
C(11)–Sn(1)–C(17)	116.8(3)	C(21)–Sn(2)–C(27)	118.1(3)
Sn(1) $\cdots$ F(2)–Sn(2)	151.4(2)		
N(1)–Sn(1) $\cdots$ F(2)	136.8(2)		
C(11)–Sn(1) $\cdots$ F(2)	76.7(2)		
C(14)–Sn(1) $\cdots$ F(2)	143.9(3)		
C(17)–Sn(1) $\cdots$ F(2)	81.4(3)		
N(2)–Sn(2) $\cdots$ O(1)	141.3(2)		
C(21)–Sn(2) $\cdots$ O(1)	75.9(3)		
C(24)–Sn(2) $\cdots$ O(1)	137.4(2)		
C(27)–Sn(2) $\cdots$ O(1)	86.7(2)		

water molecule O(1) which links the two stannatrane molecules by strong  $\text{F}(1) \cdots \text{H} \cdots \text{O}(1) \cdots \text{H} \cdots \text{F}(2)$  hydrogen bridges. This dimer is connected by an additional water molecule O(2) to a second dimer to form a centrosymmetric tetramer. The system of hydrogen bonds in **1a** is supported by IR absorptions  $\nu(\text{OH})$  at 3497 m, 3455 m, and 3300  $\text{sh cm}^{-1}$  (sample mullied in Nujol). The presence of water in the coordination sphere of organotin compounds is not an uncommon feature.<sup>7</sup> Further, FD mass spectrometry from a toluene solution shows a signal at  $m/e$  573. This signal can tentatively be assigned to  $\{[\text{N}(\text{CH}_2\text{CH}_2\text{CH}_2)_3\text{Sn}]_2\text{F} \cdot 2\text{H}_2\text{O}\}^+$  (strongest peak from computer simulation, 573) or  $\{[\text{N}(\text{CH}_2\text{CH}_2\text{CH}_2)_3\text{SnF}]_2 \cdot \text{H}_2\text{O}\}^+$  (strongest peak from computer simulation, 574). The fluorine-bridged dimer  $\{[\text{N}(\text{CH}_2\text{CH}_2\text{CH}_2)_3\text{Sn}]_2\text{F}\}^+$  ( $m/e$  539; computer simulation, 537) appears as a fragment of high intensity.

The coordination geometry at Sn(1) and Sn(2) can be best described as monocapped trigonal bipyramid, i.e., **1a** can be regarded as a model substance for the nucleophilic substitution at pentacoordinate triorganotin species. It also supports the idea that stereoisomerizations at chiral triorganotin halides and nucleophilic substitutions at pentacoordinate triorganotin compounds could proceed via hexacoordinate intermediates.<sup>8a,c</sup> The intermolecular  $\text{Sn}(1) \cdots \text{F}(2)$  interac-

(7) (a) Huber, F.; Preut, H.; Hoffmann, E.; Gielen, M. *Acta Crystallogr.* **1989**, C45, 51. (b) Gielen, M.; Acheddad, M.; Tiekink, E. R. T. *Main Group Met. Chem.* **1993**, 16, 367. (c) Johnson, S. E.; Polborn, K.; Nöth, H. *Inorg. Chem.* **1991**, 30, 1410.

(8) (a) Weichmann, H.; Mügge, C.; Grand, A.; Robert, J. B. J. *Organomet. Chem.* **1982**, 238, 343. (b) Kolb, U.; Dräger, M.; Jousseau, B. *Organometallics* **1991**, 10, 2737. (c) van Koten, G.; Jastrzebski, J. T. B. H.; Noltes, J. G.; Pontenagel, W. M. G. F.; Kroon, J.; Spek, A. L. *J. Am. Chem. Soc.* **1978**, 100, 5021. (d) Kolb, U.; Beuter, M.; Dräger, M. *Inorg. Chem.* **1994**, 33, 4522.

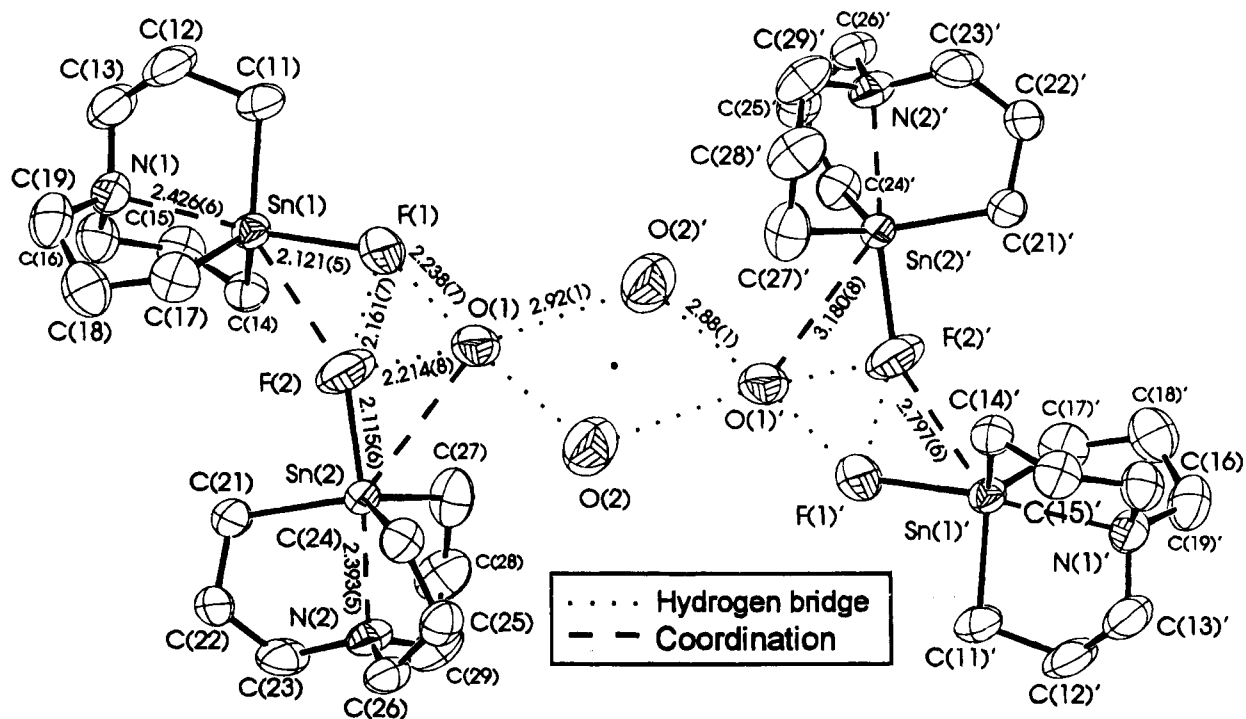


**Figure 1.** Molecular structure of  $N(\text{CH}_2\text{CH}_2\text{CH}_2)_3\text{SnF} \cdot \text{H}_2\text{O}$  (**1a**). Labels of atoms as given in Table 1. ORTEP drawing (thermal ellipsoids at the 50% probability level) without hydrogen atoms for better clarity. The network of the coordinations the hydrogen bonds and the main distances (Å) are shown.

tion amounts to 2.797(6) Å (Pauling-type bond order,<sup>8d</sup> 0.18) and is much stronger than that observed for the border line case between penta- and hexacoordination in  $\text{Me}_2\text{FSn-1,4-CHD-COOMe}$ .<sup>8b</sup> The intermolecular  $\text{Sn}(2) \cdots \text{O}(1)$  interaction is much weaker and amounts to 3.180(8) Å (Pauling-type bond order, 0.09). Both intermolecular attacks are face attacks and proceed on the planes defined by  $\text{F}(1), \text{C}(14), \text{C}(17)$  and  $\text{F}(2), \text{C}(24), \text{C}(27)$ , respectively. An intramolecular  $\text{Sn} \cdots \text{N}$  edge attack has recently been described for bis[8-(dimethylamino)-1-naphthyl]methyltin iodide.<sup>9</sup>

Both the surprisingly strong  $\text{Sn}(1) \cdots \text{F}(2)$  and the weaker  $\text{Sn}(2) \cdots \text{O}(1)$  contacts cause only slight distortions of the ideal atrane framework. Thus the  $\text{N}(1)-\text{Sn}(1)-\text{F}(1)$  and  $\text{N}(2)-\text{Sn}(2)-\text{F}(2)$  angles deviate by 7.3° and 6°, respectively, from the ideal value of 180° observed for **2-4**. However, the equatorial  $\text{C}-\text{Sn}-\text{C}$  angles are only slightly affected.

The lengthening of the  $\text{Sn}(1)-\text{F}(1)$  and  $\text{Sn}(2)-\text{F}(2)$  bonds by 0.161 and 0.155 Å, respectively, compared to a  $\text{Sn}-\text{F}$  single bond of 1.96 Å,<sup>8b,10,11</sup> is a result of intramolecular  $\text{Sn}-\text{N}$  coordination as well as of the intermolecular coordination accompanied with hydrogen bridging. The two long  $\text{Sn}-\text{F}$  distances are supported by vibrational data (IR ( $\text{cm}^{-1}$ ) 463 s and 444 s, broad; Raman ( $\text{cm}^{-1}$ ) 454 m and 445 m). The tetrahedral molecules  $\text{Me}_3\text{SnF}$  (gas phase) and  $\text{Me}_3\text{SnF}$  (solid state) show strong IR transitions at 588 and 554  $\text{cm}^{-1}$ , respectively.<sup>11,12a</sup>

The importance of the hydrogen bridging for the  $\text{Sn}-\text{F}$  lengthening becomes evident when comparing with other intramolecularly coordinated organotin fluo-

rides that do not contain water, such as  $\text{Me}_2\text{FSnCH}_2\text{-CH}_2\text{P}(\text{O})\text{Ph}_2$  ( $\text{Sn}-\text{F}$ , 2.035(2) Å)<sup>12b</sup> and  $\text{Me}_2\text{FSn-1,4-CHD-COOMe}$  ( $\text{Sn}-\text{F}$ , 1.974(8) Å, IR 486  $\text{s cm}^{-1}$ ).<sup>8b</sup> In fact, the presence of water associated with the possibility of forming hydrogen bridges seems to be essential in bringing the two stannatrane moieties close enough together to allow substantial intermolecular  $\text{Sn} \cdots \text{F}$  interaction. In other words, the  $\text{F} \cdots \text{H} \cdots \text{O}$  bond prevents the "movable charge" (lone pair) at fluorine  $\text{F}(1)$  from being shifted into the  $3\sigma^*$  LUMO at  $\text{Sn}(1)$  of the tetrahedron-trigonal bipyramid path<sup>8d</sup> and thus allows the fluorine  $\text{F}(2)$  of the neighboring stannatrane to use this orbital for intermolecular coordination. The  $\text{Sn}(1) \cdots \text{F}(2)$  coordination has the same effect on  $3\sigma^*$  at  $\text{Sn}(2)$ , making possible the weak  $\text{Sn}(2) \cdots \text{O}(1)$  interaction.

**Molecular Structures of 2, 3, and 4.** The structures of **2-4** are almost identical and are shown in Figure 2 by the representative structure of **3**. Selected bond lengths and bond angles are given in Table 2.

The molecular structure of the hexagonal modification of  $N(\text{CH}_2\text{CH}_2\text{CH}_2)_3\text{SnCl}$  (**2a**) has previously been reported.<sup>4c</sup> Its very long  $\text{Sn}-\text{Cl}$  distance of 2.613(7) Å made us suspicious that the actual crystal used in this investigation might have contained some percentage of bromine.<sup>4d</sup> In both modifications of  $N(\text{CH}_2\text{CH}_2\text{CH}_2)_3\text{-SnCl}$  (**2a** and **2b**) reported here the  $\text{Sn}-\text{Cl}$  distances turned out to be shorter.

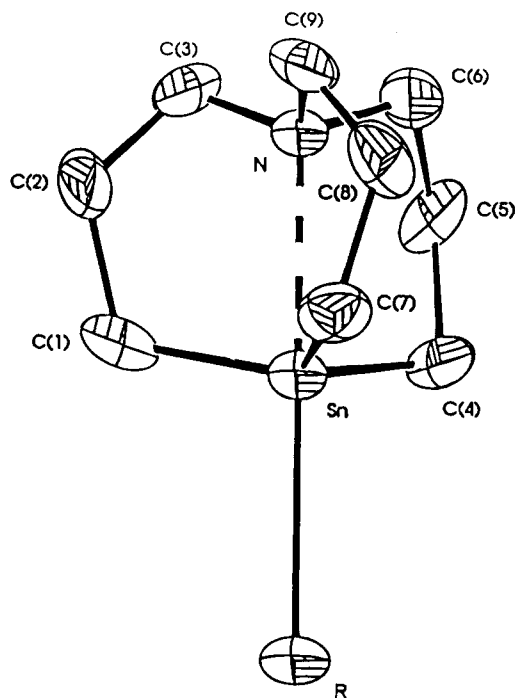
The tin atoms in **2-4** show a distorted trigonal bipyramidal configuration with nitrogen and halogen in axial positions and three methylene carbons in equatorial positions. The most interesting feature is that the minimum  $\text{Sn} \cdots \text{N}$  distance and hence the strongest

(9) Jastrzebski, J. T. B. H.; van der Schaaf, P. A.; Boersma, J.; van Koten, G.; de Ridder, D. J. A.; Heijdenrijk, D. *Organometallics* **1992**, *11*, 1521.

(10) Al-Juaid, S.; Dhaher, S. M.; Eaborn, C.; Hitchcock, P. B.; Smith, J. D. J. *Organomet. Chem.* **1987**, *325*, 117.

(11) Reuter, H.; Puff, H. *J. Organomet. Chem.* **1989**, *379*, 223.

(12) (a) Licht, K.; Geissler, H.; Koehler, P.; Hottmann, K.; Schnorr, H.; Kriegsmann, H. *Z. Anorg. Allg. Chem.* **1971**, *385*, 271. (b) Preut, H.; Godry, B.; Mitchell, T. *Acta Crystallogr.* **1992**, *C48*, 1894. (c) Mitchell, T. N. Private communication.



R		d (Sn...N) (Å)
Cl (hex)	(2a)	2.37 (3)
Cl (mon)	(2b)	2.384 (4)
Br	(3)	2.28 (2)
I	(4)	2.375 (6)
Me		2.624 (8)

**Figure 2.** Intramolecular coordination in  $N(\text{CH}_2\text{CH}_2\text{CH}_2)_3\text{SnR}$ , R = Cl (**2**), Br (**3**), I (**4**). Labels of atoms as given in Table 2. ORTEP drawing of **3** (thermal ellipsoids are at the 50% probability level). Hydrogen atoms are omitted for better clarity. The intramolecular Sn...N distances (Å) of **2a**, **2b**, **3**, **4**, and for comparison of  $N(\text{CH}_2\text{CH}_2\text{CH}_2)_3\text{SnMe}^{4e}$  are given.

**Table 2. Bond Lengths and Bond Angles at the Tin Atom in  $N(\text{CH}_2\text{CH}_2\text{CH}_2)_3\text{Sn-R}$  (R = Cl, Br, I) with Esd's in Parentheses**

	<b>2a</b> (R = Cl) hexagonal <sup>a</sup>	<b>2b</b> (R = Cl) monoclinic <sup>b</sup>	<b>3</b> (R = Br) hexagonal <sup>a</sup>	<b>4</b> (R = I) monoclinic <sup>b</sup>
Bond Lengths (Å)				
Sn...N	2.37(2)	2.384(4)	2.28(2)	2.375(6)
Sn-R	2.52(1)	2.554(1)	2.693(2)	2.896(1)
Sn-C	2.14(1)	2.157(5)	2.20(1)	2.152(8)
Bond Angles (deg)				
N-Sn-R	180	179.7(1)	180	179.6(1)
N-Sn-C	80.3(3)	79.7(2)	81.2(3)	80.5(3)
R-Sn-C	99.7(2)	100.3(1)	98.8(3)	99.5(2)
C-Sn-C	117.5(3)	116.9(2)	117.7(6)	117.3(3)
Shortest Intermolecular Distances (Å)				
Sn...R	5.27(1)	5.276(2)	5.469(2)	4.961(2)

<sup>a</sup> Sn, N, and R on a 3-fold axis. <sup>b</sup> Near to  $C_3$  symmetry. The values given are average values.

donor interaction is found for **3**, i.e., for bromine substitution at tin. For **2a**, **2b** (R = Cl), and **4** (R = I), the Sn...N distances are alike. The factors "electronegativity" and "lone pair interaction" of the halogen substituents are counteractive and in this series of compounds cancel each other at bromine.

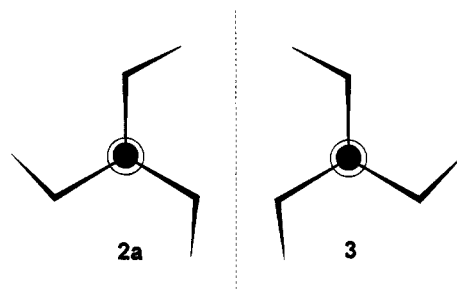


**Figure 3.** View of the two enantiomeric structures  $N(\text{CH}_2\text{CH}_2\text{CH}_2)_3\text{SnCl}$  (**2a**) and  $N(\text{CH}_2\text{CH}_2\text{CH}_2)_3\text{SnBr}$  (**3**) along the axis R-Sn...N.

The long axial tin-halogen distances are confirmed by their Raman emissions of 229 s and 240 s for **2** (single crystals of **2a** and **2b**), 156 s for **3**, and 121 s  $\text{cm}^{-1}$  for **4**. The tetrahedral molecules  $\text{Me}_3\text{Sn}-\text{Cl}/\text{Br}/\text{I}$  (distances 2.37/2.49/2.72 Å from gas phase electron diffraction<sup>13</sup>) have IR absorptions at 331/234/189  $\text{cm}^{-1}$  in cyclohexane solution.<sup>14</sup> With regard to the vibration  $\nu(\text{Sn}\cdots\text{N})$ , all four stannatranes **1-4** show IR and Raman transitions of medium intensity close to 375 and 390  $\text{cm}^{-1}$ . ( $\text{Sn}(\text{NMe}_2)_4$ :  $d(\text{Sn}-\text{N}) = 2.045$  Å,<sup>15</sup>  $\nu(\text{Sn}-\text{N})$  535 and 516  $\text{cm}^{-1}$ .<sup>16</sup>  $\text{Me}_3\text{SnNMe}_2$ :  $\nu(\text{Sn}-\text{N})$  618  $\text{cm}^{-1}$ .<sup>17</sup> A previous report of the vibrational data of the stannatranes **2-4** assigns the transition at 375  $\text{cm}^{-1}$  to  $\nu(\text{Sn}\cdots\text{N})$ .<sup>18</sup> If this assignment is correct, the transition at 390  $\text{cm}^{-1}$  would be the *gauche* deformation  $\delta(\text{CCC})_g$  of the cage (see supplementary material for a full assignment of the vibrational spectra). Neither the stretching  $\nu(\text{Sn}\cdots\text{N})$  nor the *gauche* bending at the central carbon is independent. The potential energy of both vibrations is spread over the whole range of 15  $\text{cm}^{-1}$ , and no direct connection to the distances  $d(\text{Sn}\cdots\text{N})$  exists.

Compounds **2-4** exhibit almost ideal  $C_3$  symmetry as a result of the uniform *envelope* conformations of the three five-membered rings. This conformation makes the molecules chiral, as can easily be seen by looking along the halogen-tin-nitrogen axis (Figure 3). The crystals of **2a** (monoclinic) and **4** contain both enantiomers, whereas **2b** (hexagonal) and **3** crystallize as pure enantiomers with *clockwise* and *anticlockwise* orientation of the propellers (Figure 3), respectively.

**Structure of 1a in Solution.** Osmometric molecular weight determination in  $\text{CHCl}_3$  shows **1a** to be essentially monomeric. The  $^{119}\text{Sn}$  NMR spectrum of **1a** in  $\text{CH}_2\text{Cl}_2$  displays a doublet at 23.0 ppm with a  $^1J(^{119}\text{Sn}-^{19}\text{F})$  of 2500 Hz. The  $^{19}\text{F}$  NMR spectrum of the same solution displays a singlet at -166.3 ppm with  $^{119}\text{Sn}$  satellites of 2512 Hz. Both  $^{19}\text{F}$  and  $^{119}\text{Sn}$  spectra are temperature (+40 to -95 °C) and concentration independent. The  $^{119}\text{Sn}$  NMR spectrum in  $\text{C}_6\text{D}_6$  of water-free **1**, generated in an NMR tube by heating  $N(\text{CH}_2\text{CH}_2\text{CH}_2)_3\text{SnMe}$  and  $\text{Pr}_3\text{SnF}$  for 10 min to 150 °C followed by addition of dry  $\text{C}_6\text{D}_6$ , displays a doublet at 13.6 ppm with a  $^1J(^{119}\text{Sn}-^{19}\text{F})$  coupling of 2583 Hz. A

(13) Skinner, H. A.; Sutton, L. E. *Trans. Faraday Soc.* **1944**, *40*, 164.

(14) Clark, R. J. H.; Davies, A. G.; Puddephatt, R. J. *J. Chem. Soc.* **1968**, 1828.

(15) Vilkov, L. V.; Tarasenko, N. A.; Prokofe, A. K. *J. Struct. Chem. (Engl. Transl.)* **1970**, *11*, 114.

(16) Bürger, H.; Sawodny, W. *Spectrochim. Acta* **1967**, *23A*, 2841.

(17) Marchand, A.; Forel, M.-T.; Riviere-Baudet, M. *J. Organomet. Chem.* **1978**, *156*, 341.

(18) Schenzel, K.; Kolbe, A.; Reich, P. *Monatsh. Chem.* **1990**, *121*, 615.

Chart 2

	2	7, R = Ph	8, R = Me	9, R = Ph	10, R = Me
Sn-N (Å)	2.38	2.435 <sup>25</sup>		2.578 <sup>26</sup>	2.487 <sup>24</sup>
$\Delta\Sigma(\vartheta)$ (°)	50	70		76	77
$\delta^{119}\text{Sn}$ (ppm)	19.4	-54.8 <sup>27</sup>	4.4	-138	-2.5
$^1J(^{119}\text{Sn}-^{13}\text{CH}_2)$ (Hz)	477	535	509	572	546
	1	5		11, R = Ph	6, R = Me
$\delta^{119}\text{Sn}$ (ppm)	13.6	3.1		-143.4	0.7
$^1J(^{119}\text{Sn}-^{19}\text{F})$ (Hz)	2583	2249		2078	1900
$^1J(^{119}\text{Sn}-^{13}\text{CH}_2)$ (Hz)	502	523		599	545

—————> goodness of the trigonal bipyramid

singlet appears at  $-8.2$  ppm, which is assigned to  $\text{Pr}_3\text{SnMe}$ . Addition of one droplet water causes only slight high-frequency shift to  $18.2$  ppm and a minor decrease of the  $^1J(^{119}\text{Sn}-^{19}\text{F})$  coupling to  $2543$  Hz. Addition of about  $0.2$  mL of methanol causes an additional high-frequency shift to  $36.7$  ppm and additional lowering of the  $^1J(^{119}\text{Sn}-^{19}\text{F})$  coupling to  $2400$  Hz.

The results indicate that there is an equilibrium between **1** plus free water and **1a**. The lowering of the  $^1J(^{119}\text{Sn}-^{19}\text{F})$  upon addition of water and/or methanol is likely to be a result of fluorine-hydrogen bridges rather than attack of these donors at tin, as suggested by the high  $^{119}\text{Sn}$  frequency shift. A similar effect has been observed for  $\text{Me}_3\text{SnF}_2^-$ .<sup>19</sup> Keeping the molecular weight determination in mind, this also means that in solution of **1a** the tin is not hexacoordinate.

Hypervalent triorganotin compounds having the substituent pattern  $\text{C}_3\text{XSnY}$  are excellent model substances for nucleophilic substitution at organotin compounds and map the tetrahedron-trigonal bipyramid path.<sup>20</sup> Along this path a donor Y approaches the tin atom, causing simultaneously a lengthening of Sn-X and a change of the CSnC angles from  $109.5^\circ$  (tetrahedron) to  $120^\circ$  (trigonal bipyramid). An elegant measure of the "goodness" of the trigonal bipyramid is the difference  $\Delta\Sigma(\vartheta)^\circ$  of equatorial and axial angles, which is  $90^\circ$  ( $3 \times 120 - 3 \times 90$ ) for the ideal trigonal bipyramid and  $0^\circ$  for the ideal tetrahedron. For the solid state this path has been well documented by a great number of X-ray structures.<sup>8d,20,21</sup> However, the existence of this path

can also be documented by NMR spectroscopy. Increasing the coordination number at tin from 4 to 5 in general causes (i) a low-frequency shift,<sup>22</sup> (ii) an increase of the  $^1J(^{119}\text{Sn})$  couplings to the atoms becoming equatorial,<sup>4b</sup> and (iii) a decrease of the  $^1J(^{119}\text{Sn})$  couplings to the atoms becoming axial,<sup>4b</sup> all with respect to the tetrahedral compound with the substituent pattern  $\text{C}_3\text{XSn}$ . Some of the first systematic studies<sup>8d</sup> showed that the chemical shift for a given system is mainly controlled electronically by the population of the LUMO of the three-center bond whereas steric factors (orientation of the HOMO) among others influence the  $^1J(^{119}\text{Sn})$  couplings.

In order to apply this concept to compounds **1**, **5**, and **6** (Chart 2), we first need a true tetrahedral triorganotin fluoride of substituent pattern  $(\text{sp}^3\text{-C})_3\text{SnF}$ . Such compounds are very rare because they usually polymerize via fluorine bridges. For tetracoordinate  $(\text{Me}_3\text{Si})_3\text{CSnMe}_2\text{F}$ , in which the bulky  $(\text{Me}_3\text{Si})_3\text{C}$  substituents prevent autoassociation, the  $^1J(^{119}\text{Sn}-^{19}\text{F})$  amounts to  $2376$  Hz.<sup>10</sup> Increasing the coordination should place the fluorine in the apical position of a trigonal bipyramid and consequently decrease the  $^1J(^{119}\text{Sn}-^{19}\text{F})$ . This is indeed the case for the intramolecularly coordinated  $\text{Ph}_2(\text{O})\text{PCH}_2\text{CH}_2\text{SnMe}_2\text{F}$  ( $^1J(^{119}\text{Sn}-^{19}\text{F}) = 1965$  Hz),<sup>12c</sup> *cis*-3-BzO-C<sub>6</sub>H<sub>10</sub>SnMe<sub>2</sub>F ( $^1J(^{119}\text{Sn}-^{19}\text{F}) = 2095$  Hz),<sup>23</sup> and  $\text{MeOOC-CHD-1,4-SnMe}_2\text{F}$  ( $^1J(^{119}\text{Sn}-^{19}\text{F}) = 2225$  Hz),<sup>8b</sup> and even more so for anionic species such as  $\text{Me}_3\text{SnF}_2^-$  ( $^1J(^{119}\text{Sn}-^{19}\text{F}) = 1500$  Hz) and  $\text{Me}_3\text{SnClF}^-$  ( $^1J(^{119}\text{Sn}-^{19}\text{F}) = 1514$  Hz).<sup>19</sup>

Regardless of the solvent the  $^1J(^{119}\text{Sn}-^{19}\text{F})$  of  $2400$ – $2583$  Hz found for **1/1a** are far too big to indicate

(19) Dakternieks, D.; Zhu, H. *Inorg. Chim. Acta* **1992**, *196*, 19.

(20) Bürgi, H.-B.; Dunitz, J. D. *Structure Correlation*; VCH Weinheim: New York, 1994; Chapter 7. Britton, D.; Dunitz, J. D. *J. Am. Chem. Soc.* **1981**, *103*, 2970.

(21) Kolb, U.; Beuter, M.; Gerner, M.; Dräger, M. *Organometallics* **1994**, *13*, 4413.

(22) Harrison, P. G. In *Chemistry of Tin*; Harrison, P. G., Ed.; Blackie: Glasgow, 1989, and references cited therein.

(23) Ochiai, M.; Iwaki, S.; Ukita, T.; Matsuura, Y.; Shiro, M.; Nagao, Y. *J. Am. Chem. Soc.* **1988**, *110*, 4606.

**Table 3. Crystallographic Data and Structure Determination Details for N(CH<sub>2</sub>CH<sub>2</sub>CH<sub>2</sub>)<sub>3</sub>SnF · H<sub>2</sub>O (1a), N(CH<sub>2</sub>CH<sub>2</sub>CH<sub>2</sub>)<sub>3</sub>SnCl (2a), (2b), N(CH<sub>2</sub>CH<sub>2</sub>CH<sub>2</sub>)<sub>3</sub>SnBr (3), and N(CH<sub>2</sub>CH<sub>2</sub>CH<sub>2</sub>)<sub>3</sub>SnI (4)**

	1a	2a	2b	3	4
		Crystal Data (Mo Kα <sub>1</sub> , λ = 0.709 26 Å)			
formula, M <sub>r</sub>	C <sub>18</sub> H <sub>40</sub> F <sub>2</sub> N <sub>2</sub> O <sub>2</sub> Sn <sub>2</sub> , 591.945	C <sub>9</sub> H <sub>18</sub> ClNSn, 292.396	C <sub>9</sub> H <sub>18</sub> ClNSn, 292.396	C <sub>9</sub> H <sub>18</sub> BrNSn, 338.863	C <sub>9</sub> H <sub>18</sub> INSn, 385.863
cryst habit, color	irregular square block	long hexagonal needle	square plate	long hexagonal needle	long square needle
face indices (distance from a common origin inside the crystal (mm))	010, 0, -1, 0 (0.47); -3, 1, 0, -3, -1, 0 (0.03); 210 (0.62); 2, -2, 0 (0.90)	100, -1, 0, 0 (0.08); 010, 0, -1, 0 (0.08); 001, 0, 0, -1 (0.70); -1, 1, 0, 1, -1, 0 (0.08)	100, -1, 0, 0 (0.26); 010, 0, -1, 0 (0.23); 001, 0, 0, -1 (0.05)	100, -1, 0, 0 (0.07); 010, 0, -1, 0 (0.07); 001, 0, 0, -1 (0.80); -1, 1, 0, 1, -1, 0 (0.07)	100, -1, 0, 0 (0.26); 010, 0, -1, 0 (0.23); 001, 0, 0, -1 (0.05)
cryst sys	monoclinic	hexagonal	monoclinic	hexagonal	monoclinic
space group	P2 <sub>1</sub> /n (No. 14)	P6 <sub>3</sub> (No. 173)	P2 <sub>1</sub> /c (No. 14)	P6 <sub>3</sub> (No. 173)	P2 <sub>1</sub> /c (No. 14)
unit cell dimens: α, b, c (Å); β (deg)	12.311(2), 13.527(1), 14.406(1); 104.55(1)	8.415(1), 8.415(1), 9.168(1)	7.602(1), 9.207(1), 16.03(3); 96.88(1)	8.472(5), 8.472(5), 9.299(1)	7.619(1), 9.653(1), 16.258(2); 93.55(1)
least-squares fit: no. of reflns, θ range (deg)	122, 28–30	100, 25–29	48, 26–29	75, 25–27	72, 26–29
packing: V (Å <sup>3</sup> ), Z, F(000)	2322(1), 4, 1172	562(1), 2, 292	1114(1), 4, 584	578(1), 2, 328	1193(1), 4, 728
D <sub>calcd</sub> /D <sub>exptl</sub> (g/Å <sup>3</sup> )	1.693/1.705	1.739/1.730	1.755/1.800	1.947/1.952	2.147/2.112
	Intensity Data Collection (Mo Kα, λ = 0.710 69 Å, graphite monochromator)				
temp (°C), θ range (deg)	23, 1.5–30	23, 1.5–35	23, 1.5–32	23, 1.5–30	23, 1.5–29
(sin θ) <sub>max</sub> /λ (Å <sup>-1</sup> )	0.7035	0.8071	0.7456	0.7035	0.6822
range of hkl	+17, +19, ±20	+13, +13, ±14	+11, +13, ±23	+12, +12, ±14	+10, +13, ±22
no. of ref reflns	3, 4000 s	3, 4000 s	3, 4000 s	3, 4000 s	3, 3000 s
loss of intensity (time)	10% (6 days)	2% (1 day)	8% (4 days)	2% (1 day)	5% (3 days)
corr	linear	linear	direct	direct	direct
no. of reflns measd, indep (int R)	7710, 6743 (0.075)	1071, 827	4328, 3852 (0.098)	1417, 595 (0.044)	3813, 3136 (0.036)
no. of reflns used, limit μ (cm <sup>-1</sup> ), abs corr	5842, 3σ(I) 20.03	727, 3σ(I) 22.77	3002, 3σ(I) 22.98	483, 3σ(I) 49.44	2483, 3σ(I) 43.52
range of transmissn		0.7283–0.6824	0.8149–0.3630		0.4204–0.3138
	Refinement				
choice of thermal params	Sn, F, C, N, O anisotropic, H isotropic fixed	Sn, Cl, C, N, O anisotropic, H isotropic fixed	Sn, Cl, C, N, O anisotropic, H isotropic fixed	Sn, Br, C, N, O anisotropic, H isotropic fixed	Sn, I, C, N, O anisotropic, H isotropic fixed
vars, ratio of reflns/var last shifts	238, 25 <0.001σ	42, 17 <0.001σ	112, 27 <0.001σ	38, 13 <0.001σ	112, 22 <0.001σ
final R, R <sub>w</sub>	0.0688, 0.1112	0.0575, 0.0710	0.0389, 0.0638	0.0471, 0.0649	0.0602, 0.0723
enantiomorphism (signif)		1.0070 (>99%)		1.0570 (>99.5%)	
weighting scheme w <sup>-1</sup>	σ <sup>2</sup> (F) + 0.000604F <sup>2</sup>	σ <sup>2</sup> (F) + 0.026723F <sup>2</sup>	σ <sup>2</sup> (F) + 0.001744F <sup>2</sup>	σ <sup>2</sup> (F) + 0.08950F <sup>2</sup>	σ <sup>2</sup> (F) + 0.000224F <sup>2</sup>
final difference Fourier maxima (e <sup>-</sup> /Å <sup>3</sup> )	0.5 near Sn	0.4 near Sn	2.27 near Cl, 1.38 near N	0.5 near Sn	1.5 near Sn

pentacoordination. At first sight this is even more surprising as the chemical shift of 1/1a (13.6 to 36.7 ppm, see above) is clearly low-frequency and in agreement with pentacoordination when compared with that of 124.5 ppm for (Me<sub>3</sub>Si)<sub>3</sub>CSnMe<sub>2</sub>F.<sup>10</sup> This obvious contradiction has its origin in the ring strain of the stannatranes framework which prevents a linear correlation between Sn···N interaction and goodness of the trigonal bipyramid. In other words, the particular cage frame of the tricarbostannatranes 1–4 allows or even forces substantial Sn···N contacts (associated with the <sup>119</sup>Sn low-frequency shift) but prevents the methylene carbons from becoming completely equatorial and the substituent R from becoming completely axial (associated with incomplete increase or decrease of coupling constants, respectively). Chart 2 illustrates this situation by comparing X-ray and selected NMR data of a series of related compounds.

The intramolecular Sn···N interaction decreases in the sequence N(CH<sub>2</sub>CH<sub>2</sub>CH<sub>2</sub>)<sub>3</sub>SnCl (2) > MeN(CH<sub>2</sub>CH<sub>2</sub>CH<sub>2</sub>)<sub>2</sub>SnMeCl (8) > Me<sub>2</sub>NCH<sub>2</sub>CH<sub>2</sub>CH<sub>2</sub>SnMe<sub>2</sub>Cl (10), whereas the difference of the sums of equatorial and axial angles increases. This increasing goodness of the trigonal bipyramid is associated with an increase of <sup>1</sup>J(<sup>119</sup>Sn–<sup>13</sup>CH<sub>2</sub>) as expected for methylene carbons becoming equatorial. A similar trend is observed for the corresponding fluorine derivatives N(CH<sub>2</sub>CH<sub>2</sub>CH<sub>2</sub>)<sub>3</sub>SnF (1), MeN(CH<sub>2</sub>CH<sub>2</sub>CH<sub>2</sub>)<sub>2</sub>SnMeF (5), and Me<sub>2</sub>NCH<sub>2</sub>CH<sub>2</sub>CH<sub>2</sub>SnMe<sub>2</sub>F (6). Here, in addition to the increasing <sup>1</sup>J(<sup>119</sup>Sn–<sup>13</sup>CH<sub>2</sub>), the decreasing <sup>1</sup>J(<sup>119</sup>Sn–<sup>19</sup>F) reflects very well the tetrahedron → trigonal bipyramid path.

The <sup>1</sup>J(<sup>119</sup>Sn–<sup>19</sup>F) of Me<sub>2</sub>NCH<sub>2</sub>CH<sub>2</sub>CH<sub>2</sub>SnMe<sub>2</sub>F (1900 Hz) is very close to that of Ph<sub>2</sub>(O)PCH<sub>2</sub>CH<sub>2</sub>SnMe<sub>2</sub>F (1965 Hz),<sup>12c</sup> and therefore both compounds should have a very similar structure. The molecular structure of the latter (ΔΣ(θ) = 72.6°)<sup>12b</sup> resembles the structure of Me<sub>2</sub>NCH<sub>2</sub>CH<sub>2</sub>CH<sub>2</sub>SnMe<sub>2</sub>Cl (ΔΣ(θ) = 77°).<sup>24</sup> The phenyl-substituted derivatives 7, 9, and 11 are given as additional information. They fit well into the general trend.

## Experimental Section

**General Considerations.** All solvents were dried by standard procedures. The <sup>1</sup>H (200.13, 499.843 MHz), <sup>13</sup>C (50.39, 125.697 MHz), <sup>19</sup>F (470.24 MHz), and <sup>119</sup>Sn (74.64, 186.409 MHz) NMR spectra were recorded on Bruker WP200 and Varian Unity 500 spectrometers using TMS, CFC<sub>3</sub>, and tetramethyltin as external references.

The FT-IR spectra were recorded on a Galaxy 2030 (Mattson) spectrometer with samples pressed into disks with polyethylene (700–200 cm<sup>-1</sup>) and as samples mullied in Nujol (4000–2500 cm<sup>-1</sup>). The Raman spectra were obtained on a Spex 1403 spectrometer; excitation by He/Ne laser (633 nm) or Kr laser (647 nm); 1500–50 cm<sup>-1</sup>, microcrystalline samples in capillaries and single crystals of 2a and 2b.

The mass spectra were recorded on a Finnigan MAT 8230 spectrometer. FD method: dipping the emission wire into a solution of some single crystals of 1a in toluene; field desorption potential, 6 kV; acceleration potential, 3 kV. EI activation: evaporation of one single crystal (fraction used for X-ray

(24) Cl–Sn···N 171.9°. Jurkschat, K.; Schollmeyer, D. Unpublished results.

**Table 4. Fractional Atomic Coordinates and Equivalent Isotropic Thermal Parameters for N(CH<sub>2</sub>CH<sub>2</sub>CH<sub>2</sub>)<sub>3</sub>SnF · H<sub>2</sub>O (1a) (Esd's in Parentheses)**

	atom	<i>x/a</i>	<i>y/b</i>	<i>z/c</i>	<i>U</i> <sub>eq</sub> <sup>a</sup> (Å <sup>2</sup> )	
H <sub>2</sub> O	O(1)	0.1063(7)	0.4829(8)	0.5939(5)	0.106(4)	
	O(2)	0.0707(5)	0.3704(6)	0.4193(6)	0.059(3)	
molecule 1	Sn(1)	0.16954(4)	0.23007(3)	0.20121(3)	0.0384(2)	
	F(1)	0.1016(4)	0.3400(3)	0.2754(3)	0.058(2)	
	N(1)	0.2287(5)	0.1101(4)	0.0985(4)	0.048(2)	
	C(11)	0.0931(6)	0.0975(5)	0.2369(5)	0.045(2)	
	C(12)	0.0795(7)	0.0247(5)	0.1534(6)	0.058(3)	
	C(13)	0.1873(8)	0.0116(5)	0.1222(6)	0.059(3)	
	C(14)	0.106(1)	0.2966(7)	0.0641(6)	0.067(3)	
	C(15)	0.164(1)	0.2536(8)	-0.0075(7)	0.078(4)	
	C(16)	0.172(1)	0.1378(7)	-0.0006(6)	0.077(4)	
	C(17)	0.3484(7)	0.2404(7)	0.2506(7)	0.069(3)	
	C(18)	0.3977(7)	0.1410(8)	0.2270(8)	0.077(4)	
	C(19)	0.3538(8)	0.1120(8)	0.1241(8)	0.076(4)	
	molecule 2	Sn(2)	0.20709(3)	0.19231(3)	0.53665(3)	0.0363(2)
		F(2)	0.1856(5)	0.2518(4)	0.3973(4)	0.067(2)
		N(2)	0.2363(5)	0.1089(4)	0.6875(4)	0.044(2)
		C(21)	0.0377(6)	0.1664(7)	0.5437(7)	0.063(3)
		C(22)	0.0357(8)	0.0842(9)	0.6134(7)	0.079(4)
C(23)		0.1240(8)	0.0956(8)	0.7066(6)	0.073(4)	
C(24)		0.3015(7)	0.0684(6)	0.5085(5)	0.055(2)	
C(25)		0.3664(8)	0.0252(6)	0.6029(5)	0.059(3)	
C(26)		0.2911(8)	0.0106(5)	0.6719(5)	0.057(3)	
C(27)		0.3015(7)	0.3013(5)	0.6291(5)	0.053(3)	
C(28)		0.2921(7)	0.2785(6)	0.7321(6)	0.054(3)	
C(29)	0.3146(8)	0.1710(5)	0.7567(5)	0.057(3)		

$$^a U_{\text{eq}} = \frac{1}{3} \sum_i \sum_j U_{ij} a_i^* a_j^* (a_i a_j).$$

crystallography) at 100 °C from a crucible; ionization potential, 70 eV.

N(CH<sub>2</sub>CH<sub>2</sub>CH<sub>2</sub>)<sub>3</sub>SnMe,<sup>4b</sup> MeN(CH<sub>2</sub>CH<sub>2</sub>CH<sub>2</sub>)<sub>2</sub>SnMe<sub>2</sub>,<sup>4b</sup> Me<sub>2</sub>NCH<sub>2</sub>CH<sub>2</sub>CH<sub>2</sub>SnMe<sub>3</sub>,<sup>28</sup> and 2-4<sup>4b,c</sup> were prepared according to literature procedures.

**Synthesis of the 5-Fluoro-1-aza-5-stannatricyclo[3.3.3.0<sup>1,5</sup>]undecane Water Adduct N(CH<sub>2</sub>CH<sub>2</sub>CH<sub>2</sub>)<sub>3</sub>SnF · H<sub>2</sub>O (1a).** N(CH<sub>2</sub>CH<sub>2</sub>CH<sub>2</sub>)<sub>3</sub>SnMe (0.666 g, 2.43 mmol) was added to a suspension of Pr<sub>3</sub>SnF (0.648 g, 2.43 mmol) in 25 mL of ethanol. The reaction mixture was refluxed with magnetic stirring for 2 h. The solvent was distilled off, and 15 mL of diethyl ether was added to the residue. The mixture was stirred for 10 min followed by filtration in order to remove traces of unreacted Pr<sub>3</sub>SnF. Hexane was added to the filtrate, and the mixture was kept at -20 °C for several days to yield 0.61 g (91% yield) of 1a as colorless needles. The crystals partially sublime at 120–130 °C and melt at 185–190 °C. <sup>1</sup>H NMR (CDCl<sub>3</sub>): SnCH<sub>2</sub>, 1.10 ppm (d of t, <sup>2</sup>J(<sup>119</sup>Sn–H) = 71 Hz, <sup>3</sup>J(<sup>1</sup>H–<sup>1</sup>H) = 6.7 Hz, <sup>3</sup>J(<sup>19</sup>F–<sup>1</sup>H) = 2.5 Hz, 6H); CH<sub>2</sub>, 1.82 ppm (m, <sup>3</sup>J(<sup>119</sup>Sn–<sup>1</sup>H) = 101 Hz, 6H); NCH<sub>2</sub>, 2.43 ppm (t, <sup>3</sup>J(<sup>1</sup>H–<sup>1</sup>H) = 5.5 Hz, 6H). <sup>13</sup>C NMR (CDCl<sub>3</sub>): SnCH<sub>2</sub>, 9.8 ppm (d, <sup>1</sup>J(<sup>119</sup>Sn–<sup>13</sup>C) = 511 Hz, <sup>2</sup>J(<sup>19</sup>F–<sup>13</sup>C) = 15.6 Hz); CH<sub>2</sub>, 23.1 ppm (<sup>2</sup>J(<sup>119</sup>Sn–<sup>13</sup>C) = 26.1 Hz); NCH<sub>2</sub>, 54.6 ppm (<sup>3</sup>J(<sup>119</sup>Sn–<sup>13</sup>C) = 39.9 Hz). <sup>19</sup>F NMR (CD<sub>2</sub>Cl<sub>2</sub>) -166.3 ppm (<sup>1</sup>J(<sup>119</sup>Sn–<sup>19</sup>F) = 2512 Hz); <sup>119</sup>Sn NMR (CH<sub>2</sub>Cl<sub>2</sub>) 23.0 ppm (d, <sup>1</sup>J(<sup>119</sup>Sn–<sup>19</sup>F) = 2500 Hz). Molecular weight determination (osmometrically, 175.8 mg in 25.1302 g of CHCl<sub>3</sub>): found, 283 g/mol. Anal. Found: C, 36.55; H, 6.83; N, 4.93. C<sub>9</sub>H<sub>20</sub>FNOSn (295.972). Calcd: C, 36.52; H, 6.81; N, 4.73%.

**Synthesis of the 1,5-Dimethyl-5-fluoro-1-aza-5-stannabicyclo[3.3.0<sup>1,5</sup>]cyclooctane Water Adduct MeN(CH<sub>2</sub>CH<sub>2</sub>CH<sub>2</sub>)<sub>2</sub>SnFMe · H<sub>2</sub>O (5a).** MeN(CH<sub>2</sub>CH<sub>2</sub>CH<sub>2</sub>)<sub>2</sub>SnMe<sub>2</sub> (0.618 g, 2.36 mmol) and Pr<sub>3</sub>SnF (0.7 g, 2.65 mmol) were refluxed for 3

**Table 5. Fractional Atomic Coordinates and Equivalent Isotropic Thermal Parameters for N(CH<sub>2</sub>CH<sub>2</sub>CH<sub>2</sub>)<sub>3</sub>SnCl (2a,b), N(CH<sub>2</sub>CH<sub>2</sub>CH<sub>2</sub>)<sub>3</sub>SnBr (3), and N(CH<sub>2</sub>CH<sub>2</sub>CH<sub>2</sub>)<sub>3</sub>SnI (4) (Esd's in Parentheses)**

atom	<i>x/a</i>	<i>y/b</i>	<i>z/c</i>	<i>U</i> <sub>eq</sub> <sup>a</sup> (Å <sup>2</sup> )
Compound 2a				
Sn(1)	-0.33330(0)	-0.66660(0)	-0.10730(0)	0.0376(2)
Cl(1)	-0.33330(0)	-0.66660(0)	0.1676(10)	0.058(2)
N(1)	-0.33330(0)	-0.66660(0)	-0.366(3)	0.034(4)
C(1)	-0.2373(10)	-0.3814(8)	-0.1468(9)	0.048(2)
C(2)	-0.1663(9)	-0.3355(7)	-0.304(1)	0.050(3)
C(3)	-0.2989(8)	-0.4840(9)	-0.4105(8)	0.042(2)
Compound 2b				
Sn(1)	0.68841(3)	0.60145(3)	0.38559(2)	0.03152(10)
Cl(1)	0.6737(2)	0.3243(1)	0.38404(7)	0.0436(3)
N(1)	0.7028(4)	0.8602(4)	0.38664(2)	0.0346(10)
C(1)	0.4147(6)	0.6535(5)	0.3469(3)	0.043(1)
C(2)	0.3812(6)	0.8081(5)	0.3739(3)	0.044(1)
C(3)	0.5245(6)	0.9108(4)	0.3491(3)	0.037(1)
C(4)	0.7887(7)	0.6395(6)	0.5151(3)	0.047(1)
C(5)	0.8685(7)	0.7898(6)	0.5204(3)	0.050(1)
C(6)	0.7468(8)	0.9023(5)	0.4750(3)	0.045(1)
C(7)	0.8674(7)	0.6364(5)	0.2922(3)	0.047(1)
C(8)	0.8445(7)	0.7909(5)	0.2597(3)	0.047(1)
C(9)	0.8429(6)	0.9010(4)	0.3341(3)	0.040(1)
Compound 3				
Sn(1)	0.33330(0)	0.66660(0)	0.10730(0)	0.0382(3)
Br(2)	0.33330(0)	0.66660(0)	-0.1823(2)	0.0512(8)
N(1)	0.33330(0)	0.66660(0)	0.353(2)	0.036(4)
C(1)	0.241(2)	0.388(2)	0.144(1)	0.060(6)
C(2)	0.169(1)	0.339(1)	0.299(2)	0.053(5)
C(3)	0.301(1)	0.483(1)	0.402(1)	0.051(4)
Compound 4				
Sn(1)	0.69280(5)	0.62052(4)	0.38290(3)	0.0307(2)
I(1)	0.69154(7)	0.32047(5)	0.38422(3)	0.0439(2)
N(1)	0.6942(7)	0.8666(6)	0.3809(3)	0.033(2)
C(1)	0.4187(8)	0.6574(8)	0.3524(5)	0.042(2)
C(2)	0.3784(8)	0.8073(7)	0.3742(5)	0.041(2)
C(3)	0.5182(9)	0.9078(8)	0.3471(4)	0.038(2)
C(4)	0.7934(10)	0.6598(9)	0.5075(4)	0.046(2)
C(5)	0.857(1)	0.8092(8)	0.5117(5)	0.049(3)
C(6)	0.730(1)	0.9073(7)	0.4675(5)	0.044(2)
C(7)	0.868(1)	0.6548(8)	0.2856(5)	0.050(3)
C(8)	0.842(1)	0.8013(8)	0.2557(5)	0.052(3)
C(9)	0.8324(10)	0.9047(8)	0.3265(5)	0.044(2)

$$^a U_{\text{eq}} = \frac{1}{3} \sum_i \sum_j U_{ij} a_i^* a_j^* (a_i a_j).$$

h in 20 mL of ethanol. The solvent was distilled off, and the residue was dissolved in diethyl ether and filtered in order to remove traces of unreacted Pr<sub>3</sub>SnF. Hexane was added to the filtrate, and the mixture was kept at -20 °C for several days to yield 0.63 g (85%) of 5a as colorless needles, mp 120–140 °C. <sup>1</sup>H NMR (C<sub>6</sub>D<sub>6</sub>): SnCH<sub>3</sub>, 0.34 ppm (s, <sup>2</sup>J(<sup>119</sup>Sn–<sup>1</sup>H) 61.8 Hz, 3H); SnCH<sub>2</sub>, 1.04 ppm (m, 4H); CH<sub>2</sub>, 1.26 ppm (m, 2H); 1.38 ppm (m, 2H); NCH<sub>2</sub>, 1.52 ppm (m, 2H), 1.69 ppm (m, 2H); NCH<sub>3</sub>, 1.52 ppm (s, 3H); H<sub>2</sub>O 0.73 ppm (s, 2H). <sup>13</sup>C NMR (C<sub>6</sub>D<sub>6</sub>): SnCH<sub>3</sub>, -4.7 ppm (d, <sup>2</sup>J(<sup>19</sup>F–<sup>13</sup>C) = 15 Hz); SnCH<sub>2</sub>, 12.1 ppm (d, <sup>2</sup>J(<sup>19</sup>F–<sup>13</sup>C) = 16 Hz, <sup>1</sup>J(<sup>119</sup>Sn–<sup>13</sup>C) = 523 Hz); CH<sub>2</sub>, 22.8 ppm (s, <sup>2</sup>J(<sup>119</sup>Sn–<sup>13</sup>C) = 26 Hz); NCH<sub>3</sub>, 43.5 ppm; NCH<sub>2</sub>, 57.9 ppm (s, <sup>1</sup>J(<sup>119</sup>Sn–<sup>13</sup>C) = 43 Hz). <sup>19</sup>F NMR (CDCl<sub>3</sub>): -162.5 ppm, (<sup>1</sup>J(<sup>119</sup>Sn–<sup>19</sup>F) = 2108 Hz). <sup>119</sup>Sn NMR (C<sub>6</sub>D<sub>6</sub>): 3.1 ppm (d, <sup>1</sup>J(<sup>119</sup>Sn–<sup>19</sup>F) 2249 Hz); (CDCl<sub>3</sub>) 14.2 ppm (d, <sup>1</sup>J(<sup>119</sup>Sn–<sup>19</sup>F) 2097 Hz); (C<sub>6</sub>D<sub>6</sub>, CH<sub>3</sub>OH, H<sub>2</sub>O) 23.4 ppm (d, <sup>1</sup>J(<sup>119</sup>Sn–<sup>19</sup>F) = 1988 Hz). IR (Nujol): ν(OH) 3430 cm<sup>-1</sup>; ν(Sn–F) IR 480 s, Raman 474 m cm<sup>-1</sup>. Molecular weight determination (osmometrically, 200.3 mg in 28.8709 g of CHCl<sub>3</sub>) found, 320 g/mol. Anal. Found: C, 33.42; H, 7.18; N, 5.09. C<sub>8</sub>H<sub>20</sub>FNOSn (265.944). Calcd: C, 33.84; H, 7.10; N, 4.93%.

**In Situ Generation of Water-Free 1 for NMR Experiment.** N(CH<sub>2</sub>CH<sub>2</sub>CH<sub>2</sub>)<sub>3</sub>SnMe (77 mg, 0.281 mmol) and Pr<sub>3</sub>SnF (75 mg, 0.281 mmol), both checked by IR for absence of H<sub>2</sub>O, were placed in a dry 5 mm NMR tube and heated to 150 °C for 10 min. C<sub>6</sub>D<sub>6</sub> was directly condensed into the NMR tube from a reservoir containing C<sub>6</sub>D<sub>6</sub>/LiAlH<sub>4</sub>.

(25) Kolb, U. Doctoral Dissertation, Johannes Gutenberg University, Mainz, Germany, 1994.

(26) Dakternieks, D.; Dräger, M.; Jurkschat, K.; Kolb, U.; Tozer, R. To be published.

(27) Beuter, M. Doctoral Dissertation, Johannes Gutenberg University, Mainz, Germany, 1995.

(28) Jurkschat, K. Doctoral Dissertation, Martin Luther University, Halle-Wittenberg, Germany, 1987.



**In Situ Generation of 6.**  $\text{Me}_2\text{NCH}_2\text{CH}_2\text{CH}_2\text{SnMe}_3$  (2.5 g, 10 mmol) and  $\text{Pr}_3\text{SnF}$  (2.67 g, 10 mmol) were placed in a 25 mL round bottom flask and kept at 165 °C for 20 min. After cooling to room temperature, ether was added and the mixture stirred for 5 min followed by filtration in order to remove traces of unreacted  $\text{Pr}_3\text{SnF}$ . The ether was removed *in vacuo*, and part of the resulting oil was dissolved in  $\text{C}_6\text{D}_6$  for NMR studies. The  $^{119}\text{Sn}$  spectrum displayed a doublet at 0.7 ppm ( $^1J(^{119}\text{Sn}-^{19}\text{F}) = 1900$  Hz) assigned to **6** and a singlet at -11.3 ppm assigned to  $\text{Pr}_3\text{SnMe}$ . In addition, a signal of low intensity is observed at -4.2 ppm belonging to a trace amount of unreacted  $\text{Me}_2\text{NCH}_2\text{CH}_2\text{CH}_2\text{SnMe}_3$ .

**Crystal Structure Determination.** Single crystals were obtained from toluene (**1a** and **2b**),  $\text{CH}_2\text{Cl}_2$ /diethyl ether (**3**) and  $\text{CH}_2\text{Cl}_2$ /hexane (**4**). Single crystals of **2a** were obtained from halide exchange of **1a** with  $\text{CDCl}_3$ . Crystal data as well as details of intensity data collections and refinements are given in Table 3.

Densities were obtained from neutral buoyancy in polytungstate solution. The crystals were fixed by gravity and sealed in small glass capillaries. The quality and symmetry of the crystals were examined by Weissenberg exposures. Integrated intensities were measured by means of  $\bar{\omega}/2\theta$  scans on a CAD4 diffractometer (Enraf-Nonius). The structures were solved by Patterson syntheses (Sn) and completed by Fourier syntheses (halogen, C, N, O). The refinements resulted in good convergences and in even distributions of the variances. Hydrogen atoms were calculated and refined as riding on their carbon atoms ( $U = 0.08 \text{ \AA}^2$ ). Fractional atomic coordinates and equivalent isotropic thermal parameters are given in Tables 4 and 5.

$\text{ClSn}(\text{CH}_2\text{CH}_2\text{CH}_2)_3\text{N}$  (**2a**) and  $\text{BrSn}(\text{CH}_2\text{CH}_2\text{CH}_2)_3\text{N}$  (**3**) both crystallize in the noncentrosymmetric space group  $P6_3$ , with Sn, Cl or Br, and N situated on the 3-fold axes. To check the significance of the chosen enantiomers, all coordinates were inverted. The ratios of the weighted  $R$ 's are 1.0070 (**2a**) and 1.0570 (**3**), which correspond to a significance level higher

than 90%. In comparison to the thermal parameters found for the halide atoms in **2a** and **3**, the value found for the earlier investigated structure<sup>4c</sup> ( $U_{\text{eq}}(\text{Cl}) = 0.036 \text{ \AA}^2$ ) is very low. Also, considering that the volume of the unit cell ( $V = 470 \text{ \AA}^3$ ) is situated between the volumes of **2a** and **3** may be explained by co-crystallization of chlorine and bromine in the earlier structure.

$\text{ClSn}(\text{CH}_2\text{CH}_2\text{CH}_2)_3\text{N}$  was obtained as well in a centrosymmetric modification (**2b**) exhibiting the space group  $P2_1/c$ . The refinement led to six higher final difference Fourier maxima that form two triangles. These triangles are situated around chlorine (triangle plane perpendicular to  $\text{Cl}-\text{Sn}\cdots\text{N}$ ) and nitrogen (triangle plane parallel to  $\text{Cl}-\text{Sn}\cdots\text{N}$ ). This effect may be connected to the high variance of the cell axis  $c$ .

$\text{ISn}(\text{CH}_2\text{CH}_2\text{CH}_2)_3\text{N}$  (**4**) also crystallizes in the centrosymmetric space group  $P2_1/c$ , which is isostructural to **2b** and to the earlier published structure of  $\text{MeSn}(\text{CH}_2\text{CH}_2\text{CH}_2)_3\text{N}$ .<sup>4e</sup>

$\text{FSn}(\text{CH}_2\text{CH}_2\text{CH}_2)_3\text{N} \cdot \text{H}_2\text{O}$  (**1a**) exhibits the monoclinic space group  $P2_1/n$  with two symmetrical independent molecules. In addition, two oxygen atoms could be located and refined anisotropically. The existence of two water molecules goes along with a higher density crystal, even though the hydrogen atoms could not be located.

In addition to several locally written routines, local versions of SHELX-76, and SHELX-86 were used for the calculations and ORTEP for drawing. Calculations were performed on an IBM RISC/6000.

**Supplementary Material Available:** Lists of all coordinates, anisotropic thermal displacement parameters, and all geometric data and a list of assigned IR absorptions and Raman emissions below  $600 \text{ cm}^{-1}$  for compounds **1a**, **2a**, **2b**, **3**, and **4** (13 pages). Ordering information is given on any current masthead page.

OM940966H

# Reductions of Cyclopentadienyltitanium Diolate and Dithiolate Species with Boron and Tin Hydrides

Yujin Huang and Douglas W. Stephan\*

Department of Chemistry and Biochemistry, University of Windsor,  
Windsor, Ontario, Canada N9B 3P4

Received January 23, 1995<sup>®</sup>

Reactions of various CpTi diolate and thiolate complexes with boron and tin hydrides are examined. Reaction of the species  $(\text{CpTiCl}_2)_2(\text{OCH}_2\text{CMe}_2\text{CH}_2\text{O})$  (**6**), generated *in situ*, with  $\text{LiBH}_4$  yields black crystals of  $[\text{CpTi}(\text{BH}_4)(\text{OCH}_2\text{CMe}_2\text{CH}_2\text{O})]_2\text{TiCp}$  (**7**). This trimetallic product is paramagnetic and has been characterized crystallographically. The reaction of  $\text{CpTiCl}(\text{SCH}_2\text{CH}_2\text{CH}_2\text{S})$  (**1**) with  $\text{LiBH}_4$  performed in THF at room temperature affords black crystals of the diamagnetic species **8**. NMR and crystallographic data confirmed the formulation of **8** as the dimeric species  $[\text{CpTi}(\text{SCH}_2\text{CH}_2\text{CH}_2\text{S})(\text{BH}_4)]_2$ . The similar reaction of **1** with  $\text{NaBEt}_3\text{H}$  also yielded black crystals whose characterization via spectroscopic methods was precluded by insolubility. Nonetheless, X-ray crystallographic study confirmed the formulation of **9** as the dimeric compound  $[\text{CpTi}(\text{SCH}_2\text{CH}_2\text{CH}_2\text{S})]_2$ . The reaction of **1** with  $\text{Bu}_3\text{SnH}$  proceeds to yield black, insoluble crystals of **10**. Repeated attempts to characterize **10** by X-ray crystallographic methods were made. Preliminary crystallographic data establish the connectivity and thus the formulation of **10** as  $\text{Cp}_3\text{Ti}_3\text{S}_2(\text{SCH}_2\text{CH}_2\text{CH}_2\text{S})_2$ . The reaction of  $[\text{CpTiCl}(\text{SCH}_2\text{CH}_2\text{S})]_2$  (**2**) with  $\text{Bu}_3\text{SnH}$  led to uncharacterized paramagnetic and diamagnetic products, although a small amount of the known species  $\text{Cp}_5\text{Ti}_5\text{S}_6$  (**12**) was isolated. The reaction of  $\text{CpTiCl}(\text{SCH}_2\text{CH}_2\text{SCH}_2\text{CH}_2\text{S})$  (**3**) with  $\text{Bu}_3\text{SnH}$  affords the dark, crystalline, sparingly soluble, product  $[\text{CpTi}(\text{SCH}_2\text{CH}_2\text{SCH}_2\text{CH}_2\text{S})]_2$  (**11**), which was formulated on the basis of X-ray crystallographic data. The structures of these products are described, and the implications of this chemistry are considered. X-ray data for the compounds presented herein are summarized below. Compound **7**:  $P2_1/a$ ,  $a = 16.117(8) \text{ \AA}$ ,  $b = 9.889(5) \text{ \AA}$ ,  $c = 19.533(7) \text{ \AA}$ ,  $\beta = 109.95(3)^\circ$ ,  $Z = 4$ ,  $V = 2926(2) \text{ \AA}^3$ . Compound **8**:  $P2_1/n$ ,  $a = 15.863(9) \text{ \AA}$ ,  $b = 16.025(7) \text{ \AA}$ ,  $c = 8.411(3) \text{ \AA}$ ,  $\beta = 90.082(4)^\circ$ ,  $Z = 4$ ,  $V = 2138(2) \text{ \AA}^3$ . Compound **9**:  $P2_1/n$ ,  $a = 8.750(2) \text{ \AA}$ ,  $b = 9.526(1) \text{ \AA}$ ,  $c = 11.732(2) \text{ \AA}$ ,  $\beta = 110.33(1)^\circ$ ,  $Z = 4$ ,  $V = 917.0(3) \text{ \AA}^3$ . Compound **10**:  $Cc$ ,  $a = 15.080(9) \text{ \AA}$ ,  $b = 15.747(9) \text{ \AA}$ ,  $c = 10.776(4) \text{ \AA}$ ,  $\beta = 91.26(7)^\circ$ ,  $Z = 4$ ,  $V = 2559(2) \text{ \AA}^3$ . Compound **11**:  $Aba2$ ,  $a = 19.684(10) \text{ \AA}$ ,  $b = 7.869(10) \text{ \AA}$ ,  $c = 14.408(6) \text{ \AA}$ ,  $Z = 4$ ,  $V = 2232(4) \text{ \AA}^3$ .

## Introduction

Interest in group 4 and 5 transition metal chalcogenide derivatives is motivated by a number of reasons. For example, these are relevant to bioinorganic systems, may act as models for metal chalcogenide supports, and may be utilized as synthons for heterobimetallics.<sup>1</sup> More recently applications of such species in metal mediated organic syntheses have been reported.<sup>2–7</sup> In

much of this previous work, the chemistry has focused on early metallocene oxides, sulfides, polysulfides, and alkoxide and thiolate derivatives.

In contrast, studies of monocyclopentadienyl early metal systems have received much less attention. Although an impressive variety of group 4 and 5 oxide and sulfide clusters have been reported by Bottomley et al.<sup>8</sup> and others,<sup>9,10</sup> studies of the related monocyclopentadienyl early metal thiolates and alkoxides are few.<sup>1,11</sup> Complexes of the form  $\text{CpMX}_{3-x}(\text{ER})_x$  have been known as early as 1968,<sup>12</sup> but only recently have species such as the “four-legged piano stool” type complexes  $\text{Cp}^*\text{Ta}(\text{SCH}=\text{CHS})_2$  and  $\text{Cp}^*\text{Ta}(\text{SPh})_4$  been character-

\* Corresponding author. E-mail: Stephan@UWindsor.ca

<sup>®</sup> Abstract published in *Advance ACS Abstracts*, April 15, 1995.

(1) Stephan, D. W.; Nadasdi, T. T. *Coord. Chem. Rev.*, in press.

(2) Huang, Y.; Nadasdi, T. T.; Stephan, D. W. *J. Am. Chem. Soc.* **1994**, *116*, 5483.

(3) Walsh, P. J.; Hollander, F. J.; Bergman, R. G. *J. Am. Chem. Soc.* **1988**, *110*, 8729. (b) Walsh, P. J.; Carney, M. J.; Bergman, R. G. *J. Am. Chem. Soc.* **1991**, *113*, 6343. (c) Walsh, P. J.; Hollander, F. J.; Bergman, R. G. *J. Organomet. Chem.* **1992**, *428*, 13. (d) Parkin, G.; Bercaw, J. E. *J. Am. Chem. Soc.* **1989**, *111*, 391. (e) Carney, M. J.; Walsh, P. J.; Hollander, F. J.; Bergman, R. G. *J. Am. Chem. Soc.* **1989**, *111*, 8751. (f) Whinnery, L. L.; Hening, L. M.; Bercaw, J. E. *J. Am. Chem. Soc.* **1991**, *113*, 7575. (g) Carney, M. J.; Walsh, P. J.; Bergman, R. G. *J. Am. Chem. Soc.* **1990**, *112*, 6426. (h) Proulx, G.; Bergman, R. G. *J. Am. Chem. Soc.* **1994**, *116*, 7953.

(4) Buchwald, S. L.; Nielsen, R. B.; Dewan, J. C. *J. Am. Chem. Soc.* **1987**, *109*, 1590. (b) Buchwald, S. L.; Nielsen, R. B. *J. Am. Chem. Soc.* **1988**, *110*, 3171. (c) Buchwald, S. L.; Fisher, R. A.; Davis, W. M. *Organometallics* **1989**, *8*, 2082. (d) Fisher, R. A.; Nielsen, R. B.; Davis, W. M.; Buchwald, S. L. *J. Am. Chem. Soc.* **1991**, *113*, 165.

(5) Park, J. W.; Henling, L. M.; Schaefer, W. P.; Grubbs, R. H. *Organometallics* **1990**, *9*, 1650.

(6) Bolinger, C. M.; Rauchfuss, T. B. *Inorg. Chem.* **1982**, *21*, 3947.

(b) Giolando, D. M.; Rauchfuss, T. B. *Organometallics* **1984**, *3*, 487.

(7) Steudel, R.; Holz, B.; Pickardt, J. *Angew. Chem., Int. Ed. Engl.* **1989**, *28*, 1269.

(8) Bottomley, F. *Polyhedron* **1992**, *11*, 1707. (b) Bottomley, F.; Drummond, D. F.; Egharevba, G. O.; White, P. S. *Organometallics* **1986**, *5*, 1620. (c) Bottomley, F.; Egharevba, G. O.; White, P. S. *J. Am. Chem. Soc.* **1985**, *107*, 4353. (d) Bottomley, F.; Drummond, D. F.; Paez, D. E.; White, P. S. *J. Am. Chem. Soc.* **1982**, *104*, 5651. (e) Bottomley, F.; Magill, C. P.; Zhao, B. *Organometallics* **1990**, *9*, 1700. (f) Bottomley, F.; Magill, C. P.; Zhao, B. *Organometallics* **1991**, *10*, 1946. (g) Bottomley, F.; Keizer, P. N.; White, P. S.; Preston, K. F. *Organometallics* **1990**, *9*, 1917. (h) Bottomley, F.; Karslioglu, S. *Organometallics* **1991**, *11*, 326. (i) Bottomley, F.; Boyle, P. D.; Karslioglu, S. *Organometallics* **1993**, *12*, 4090. (j) Bottomley, F.; Day, R. W. *Organometallics* **1991**, *10*, 2560.



Table 1. Crystallographic Data

	7	8	9	10	11
formula	C <sub>25</sub> H <sub>43</sub> B <sub>2</sub> O <sub>4</sub> Ti <sub>3</sub>	C <sub>16</sub> H <sub>30</sub> B <sub>2</sub> S <sub>4</sub> Ti <sub>2</sub>	C <sub>16</sub> H <sub>22</sub> S <sub>4</sub> Ti <sub>2</sub>	C <sub>18</sub> H <sub>26</sub> S <sub>6</sub> Ti <sub>2</sub>	C <sub>18</sub> H <sub>26</sub> S <sub>6</sub> Ti <sub>2</sub>
formula weight	572.93	468.17	438.38	615.50	530.56
cryst System	monoclinic	monoclinic	monoclinic	monoclinic	orthorhombic
cryst descrip	black blocks	purple blocks	purple-black blocks	black rhombs	purple-black blocks
crystal size	0.30 × 0.25 × 0.27	0.30 × 0.25 × 0.25	0.25 × 0.35 × 0.22	0.15 × 0.40 × 0.12	0.20 × 0.40 × 0.24
space group	P2 <sub>1</sub> /a	P2 <sub>1</sub> /n	P2 <sub>1</sub> /n	Cc	Aba2
a (Å)	16.117(8)	15.863(9)	8.750(2)	15.080(9)	19.684(10)
b (Å)	9.889(5)	16.025(7)	9.526(1)	15.747(9)	7.869(10)
c (Å)	19.533(7)	8.411(3)	11.732(2)	10.776(4)	14.408(6)
β (deg)	109.95(3)	90.082(4)	110.33(1)	91.26(7)	
V (Å <sup>3</sup> )	2926(2)	2138(2)	917.0(3)	2559(2)	2232(4)
Z	4.00	4.00	4.00	4	8
μ (cm <sup>-1</sup> )	8.26	11.13	12.94	14.12	12.79
d (calc) g/cm <sup>3</sup>	1.30	1.45	1.59	1.60	1.58
λ (Mo Kα)	0.710 69	0.710 69	0.710 69	0.710 69	0.710 69
temp (°C)	24	24	24	24	24
scan speed (deg/min)	8.0	8.0	8.0	8.0	8.0
scan range (deg)	1.0 above Kα <sub>1</sub> , 1.0 below Kα <sub>2</sub>	1.0 above Kα <sub>1</sub> , 1.0 below Kα <sub>2</sub>	1.0 above Kα <sub>1</sub> , 1.0 below Kα <sub>2</sub>	1.0 above Kα <sub>1</sub> , 1.0 below Kα <sub>2</sub>	1.0 above Kα <sub>1</sub> , 1.0 below Kα <sub>2</sub>
bkgd/scan time ratio	0.5	0.5	0.5	0.5	0.5
2θ index range	4.5–50.0, ±hkl	4.5–50.0, ±hkl	4.5–50.0, ±hkl	4.5–50.0, ±hkl	4.5–50.0, ±hkl
data collectd	4373	3923	1852	7932 (full sphere)	1145
data F <sub>o</sub> <sup>2</sup> > 3s(F <sub>o</sub> <sup>2</sup> )	905	1309	1089	905	681
variables	145.00	167	100.00	117.00	92
transmission factors	0.925–1.000	0.639–1.000	0.916–1.000	0.526–1.000	0.615–1.000
R (%) <sup>a</sup>	9.12	4.90	3.68	8.95	5.01
R <sub>w</sub> (%) <sup>a</sup>	7.77	7.92	4.17	9.10	6.53
goodness of fit	2.71	2.08	1.62	2.36	2.75

$$^a R = \sum |F_o| - |F_c| / \sum |F_o|, R_w = [\sum (|F_o| - |F_c|)^2 / \sum |F_o|^2]^{0.5}.$$

**Synthesis of [CpTi(SCH<sub>2</sub>CH<sub>2</sub>CH<sub>2</sub>S)]<sub>2</sub> (9).** (i) To a THF (10 mL) solution of **1** (130 mg, 0.5 mmol) was added Super-Hydride (0.6 mL, 1.0 M in THF). Gas evolution was observed, and the solution became black in color. After the solution was stirred for 3 h, about 3 mL of hexane was added, and the solution was allowed to stand for several days. Black, insoluble crystals of the product **9** precipitated from solution. Separation was achieved by decantation of the mother liquid, and the solid was washed with hexane (yield 86%). (ii) The compound **8** (46 mg, 0.10 mmol) was stirred for 48 h at 30 °C in 5 mL of THF. The solution was allowed to stand for 3 days, and insoluble, black crystals of **9** were formed in 20% yield, while 66% of compound **9** was ultimately recovered. (iii) A mixture of **1** (30 mg, 0.1 mmol), LiH (20 mg, 2.5 mmol) in 2 mL of THF was stirred for 1 h, during which the solution became dark. The mixture was stirred for 15 days. After workup, **9** was obtained in 65% yield. Anal. Calcd for C<sub>16</sub>H<sub>22</sub>S<sub>4</sub>Ti<sub>2</sub>: C, 43.84; H, 5.06. Found: C, 43.50; H, 5.00.

**Synthesis of [Cp<sub>2</sub>Ti<sub>3</sub>S<sub>2</sub>(SCH<sub>2</sub>CH<sub>2</sub>CH<sub>2</sub>S)<sub>2</sub>]** (**10**). (i) To a THF (3 mL) solution of **1** (130 mg, 0.5 mmol) was added Bu<sub>3</sub>SnH (2.0 mmol, 580 mg). The solution gradually became dark and was allowed to stand over the period of 2 days, after which time black crystals of **10** were formed. Separation was achieved by decantation of the mother liquid. The insoluble solid **10** was washed with hexane. Yield 39%. (ii) Compound **10** was also isolated as a by-product in very low yield (1%) from preparation (i) for **8** described above. Anal. Calcd for C<sub>18</sub>H<sub>26</sub>S<sub>6</sub>Ti<sub>2</sub>: C, 40.98; H, 4.42. Found: C, 40.12; H, 4.07.

**Synthesis of [CpTi(SCH<sub>2</sub>CH<sub>2</sub>SCH<sub>2</sub>CH<sub>2</sub>S)]<sub>2</sub> (**11**).** To a THF (3 mL) solution of **1** (90 mg, 0.3 mmol) was added Bu<sub>3</sub>SnH (318 mg, 1.2 mmol). As the solution was stirred for 0.5 h, the evolution of gas was observed. The solution became dark and was allowed to stand for 1 day. About 1 mL of hexane was added, and the solution was allowed to stand for 2 days. Black crystals of **11** were obtained. Separation was achieved by decantation

of mother liquid, and the solid was washed with 2 × 1 mL of hexane (yield 73%). Anal. Calcd for C<sub>18</sub>H<sub>26</sub>S<sub>6</sub>Ti<sub>2</sub>: C, 40.25; H, 4.94. Found: C, 39.98; H, 4.63.

**Reaction of 2 with Bu<sub>3</sub>SnH.** To a solution of **2** in 3 mL of THF was added an excess of Bu<sub>3</sub>SnH. As the solution was stirred for 0.5 h, the evolution of gas was observed. The solution became dark and was allowed to stand for 1 day. About 1 mL of hexane was added, and the solution was allowed to stand for 2 days. A few crystals of Cp<sub>5</sub>Ti<sub>5</sub>S<sub>6</sub> were formed in low yield (2%) and isolated via decantation of the mother liquor.

**Reaction of 11 with CDCl<sub>3</sub>.** In a NMR tube, **11** (14 mg 0.05 mmol) was dissolved with 0.8 mL of CDCl<sub>3</sub>. Upon standing for 1 h, <sup>1</sup>H NMR showed that 10% of **11** was converted to **3**. After another 2 days, the conversion was 100%.

**X-ray Data Collection and Reduction.** X-ray quality crystals of **7–11** were obtained directly from the preparation as described above. The crystals were manipulated and mounted in capillaries in a glovebox, thus maintaining a dry, O<sub>2</sub>-free environment for each crystal. Diffraction experiments were performed on a Rigaku AFC6 diffractometer equipped with graphite-monochromatized Mo Kα radiation. The initial orientation matrix was obtained from 20 machine-centered reflections selected by an automated peak search routine. These data were used to determine the crystal systems. Automated Laue system check routines around each axis were consistent with the crystal system. Ultimately, 25 reflections (20° < 2θ < 25°) were used to obtain the final lattice parameters and the orientation matrices. Crystal data are summarized in Table 1. The observed extinctions were consistent with the space groups. The data sets were collected in three shells (4.5° < 2θ < 50.0°), and three standard reflections were recorded every 197 reflections. Fixed scan rates were employed. Up to four repetitive scans of each reflection at the respective scan rates were averaged to ensure meaningful statistics. The number of scans of each reflections was determined by the intensity. The in-

tensities of the standards showed no statistically significant change over the duration of the data collections. The data were processed using the TEXSAN crystal solution package operating on a SGI Challenger mainframe with remote X-terminals. The reflections with  $F_o^2 > 3\sigma F_o^2$  were used in the refinements.

**Structure Solution and Refinement.** Non-hydrogen atomic scattering factors were taken from the literature tabulations.<sup>20,21</sup> The Ti atom positions were determined using direct methods employing either the SHELX-86 or Mithril direct methods routines. The remaining non-hydrogen atoms were located from successive difference Fourier map calculations. The refinements were carried out by using full-matrix least-squares techniques on  $F$ , minimizing the function  $\omega(|F_o| - |F_c|)^2$ , where the weight  $\omega$  is defined as  $4F_o^2/2\sigma(F_o^2)$  and  $F_o$  and  $F_c$  are the observed and calculated structure factor amplitudes. In the final cycles of each refinement, all the Ti, O, and S atoms were assigned anisotropic temperature factors with the exception of **10**, where only the Ti and sulfide S atoms were assigned anisotropic temperature factors. Some of the carbon atoms were assigned anisotropic thermal parameters, while others were treated isotropically so as to maintain a reasonable data:variable ratio. In the cases of **7** and **10**, the cyclopentadienyl groups were constrained to be rigid pentagons. Empirical absorption corrections were applied to the data sets based either on  $\Psi$ -scan data or a DIFABS calculation and employing the software resident in the TEXSAN package. Hydrogen atom positions were calculated and allowed to ride on the carbon to which they are bonded, assuming a C–H bond length of 0.95 Å. In the case of **8**, the hydride and hydrogen atoms on B were located via difference map calculations. Hydrogen atom temperature factors were fixed at 1.10 times the isotropic temperature factor of the carbon atom to which the hydrogen atoms are bonded. The hydrogen atom contributions were calculated but not refined. In the refinement of **10**, disorder of the alkyl chains of the dithiolate moieties was evidenced by the carbon thermal parameters. Numerous and repeated attempts to model this disorder were made. The most acceptable model is presented, although residual evidence of the disorder resides in the large thermal parameters on the carbons of one of the alkyl chains and in the C–C and S–C bond distances. Attempts to obtain improved crystallographic data for **10** were made.<sup>22</sup> Although crystals of **10** could be obtained from the same reaction in benzene, the crystallographic data were also plagued by disorder problems. The final values of  $R$ ,  $R_w$ , and the maximum D/s on any of the parameters in the final cycles of the refinements are given in Table 1. The locations of the largest peaks in the final difference Fourier map calculation as well as the magnitudes of the residual electron densities in each case were of no chemical significance. The following data are tabulated: selected positional parameters

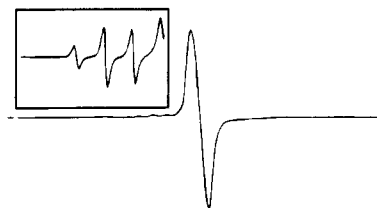


**Figure 1.** EPR spectrum of **7**. Expansion shows the Ti hyperfine coupling.

(Table 2) and selected bond distances and angles (Table 3). Positional parameters, hydrogen atom parameters, thermal parameters, and bond distances and angles have been deposited as supplementary material.

## Results and Discussion

**Synthesis. Diolate Species.** We have previously described the synthesis of **6** via the straightforward reaction of alcohol, base, and  $\text{CpTiCl}_3$ .<sup>18</sup> This species was generated *in situ* and then allowed to react with  $\text{LiBH}_4$ . The reaction mixture became black, and black crystals of **7** were deposited. This product is paramagnetic, exhibiting a singlet EPR spectrum ( $g = 1.978$ ) with hyperfine coupling to Ti of 15G (Figure 1), indicative of a Ti(III) species. The nature of this compound was determined unequivocally by X-ray methods. This confirmed the formulation of **7** as the trimeric species,  $[\text{CpTi}(\text{BH}_4)(\text{OCH}_2\text{CMe}_2\text{CH}_2\text{O})]_2\text{TiCp}$  (*vide infra*, Figure 2).

**Thiolate Species.** The reaction of **1** with  $\text{LiBH}_4$  was performed in THF at room temperature. A black, benzene-soluble product **8** was isolated from this reaction and recrystallized from benzene/hexane.  $^1\text{H}$  and  $^{13}\text{C}\{^1\text{H}\}$  NMR data for **8** showed resonances attributable to protons of the cyclopentadienyl ring and the methylene groups of the dithiolate moiety. In addition, a broad  $^1\text{H}$  NMR resonance was observed around  $-0.7$  ppm at room temperature. This latter resonance was attributed to a  $\text{BH}_4$  group coordinated to Ti. On cooling **8** to  $-70$  °C, this signal sharpened but was not resolved into its constituent resonances. Consequently, the nature of the binding mode of the  $\text{BH}_4^-$  moiety to Ti in solution was not discernable. Nonetheless, the NMR data, integration, and combustion analyses were all consistent with the empirical formulation of **8** as  $\text{CpTi}(\text{SCH}_2\text{CH}_2\text{CH}_2\text{S})(\text{BH}_4)$  (Scheme 1). Two NMR resonances attributable to inequivalent methylene groups  $\alpha$  to S are consistent with a dimeric structure in which two sulfur atoms bridge two titanium centers. This geometry was subsequently confirmed by X-ray crystallographic data (*vide infra*, Figure 3).

A similar reaction of **1** with  $\text{NaBEt}_3\text{H}$  was performed in THF. The evolution of gas, presumably  $\text{H}_2$ , was evident immediately. The solution became black, and following addition of hexane to the solution and several days of standing, black crystals of the species **9** were obtained in 86% yield. Once **9** was isolated, its insolubility precluded spectroscopic characterization. Subsequent X-ray crystallographic study confirmed the formulation of **9** as  $[\text{CpTi}(\text{SCH}_2\text{CH}_2\text{CH}_2\text{S})]_2$  (*vide infra*, Figure 4). An alternative, albeit low-yield (20%) route to crystals of compound **9** was found by simply allowing compound **8** to stand in THF for 72 h.

The reaction of **1** with  $\text{Bu}_3\text{SnH}$  in THF or benzene proceeds to give a dark solution along with the evolution of gas. After the solution was allowed to stand for 48

(20) Cromer, D. T.; Mann, J. B. *Acta Crystallogr., Sect. A: Cryst. Phys., Theor. Gen. Crystallogr.* **1968**, *24*, 324; (b) **1968**, *A24*, 390.

(21) Cromer, D. T.; Waber, J. T. *International Tables for X-ray Crystallography*; Knoch Press: Birmingham England, **1974**.

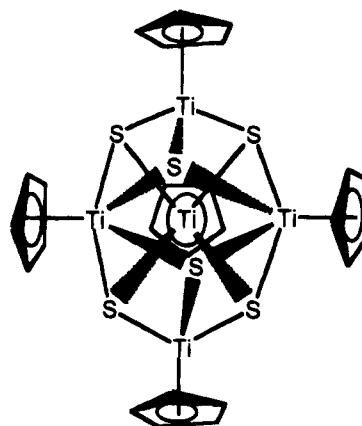
(22) Crystals of **9** were also obtained from the reaction described above employing benzene as the solvent. In this case, the crystals obtained were monoclinic, space group  $P2_1/c$ , with  $a = 11.836(6)$  Å,  $b = 14.359(4)$  Å,  $c = 18.263(8)$  Å,  $\beta = 105.43^\circ$ ,  $V = 2992(2)$  Å<sup>3</sup>. The preliminary solution appeared to be  $\text{C}_6\text{H}_6$ , although a complete refinement was not possible. Disorder of the alkyl chains of the two dithiolate ligands as well as the benzene molecule was evident; however, repeated attempts to model the disorder were unsuccessful.

Table 2. Positional Parameters

atom	x	y	z	atom	x	y	z
[CpTi(BH <sub>4</sub> (OCH <sub>2</sub> CMe <sub>2</sub> CH <sub>2</sub> O)) <sub>2</sub> TiCp (7)							
Ti(1)	0.5757(3)	0.0292(5)	0.7428(3)	C(11)	0.661(1)	0.374(2)	0.976(1)
Ti(2)	0.3837(4)	-0.0514(6)	0.6350(3)	C(12)	0.693(1)	0.242(2)	0.9931(9)
Ti(3)	0.5947(3)	0.2348(5)	0.8729(3)	C(13)	0.742(1)	0.209(2)	0.949(1)
O(1)	0.582(1)	0.044(2)	0.8481(8)	C(14)	0.741(1)	0.321(2)	0.9041(9)
O(2)	0.473(1)	-0.103(2)	0.7308(9)	C(15)	0.691(1)	0.423(1)	0.921(1)
O(3)	0.583(1)	0.229(2)	0.770(1)	C(16)	0.575(2)	-0.070(3)	0.887(2)
O(4)	0.477(1)	0.091(2)	0.651(1)	C(17)	0.492(2)	-0.157(3)	0.856(2)
C(1)	0.653(1)	-0.160(2)	0.714(1)	C(18)	0.474(2)	-0.204(3)	0.779(2)
C(2)	0.642(1)	-0.066(3)	0.659(1)	C(19)	0.410(2)	-0.069(3)	0.858(2)
C(3)	0.690(1)	0.050(2)	0.689(1)	C(20)	0.496(2)	-0.279(3)	0.907(2)
C(4)	0.731(1)	0.028(2)	0.764(1)	C(21)	0.576(2)	0.332(3)	0.718(2)
C(5)	0.708(1)	-0.102(2)	0.780(1)	C(22)	0.495(2)	0.336(3)	0.653(2)
C(6)	0.266(2)	0.082(3)	0.601(2)	C(23)	0.483(2)	0.203(4)	0.609(2)
C(7)	0.258(2)	-0.032(5)	0.557(2)	C(24)	0.418(2)	0.370(3)	0.673(2)
C(8)	0.264(2)	-0.147(3)	0.600(3)	C(25)	0.506(2)	0.451(3)	0.602(2)
C(9)	0.277(2)	-0.104(3)	0.671(2)	B(1)	0.398(3)	-0.206(5)	0.554(3)
C(10)	0.278(2)	0.037(4)	0.672(2)	B(2)	0.457(2)	0.312(4)	0.872(2)
[CpTi(SCH <sub>2</sub> CH <sub>2</sub> CH <sub>2</sub> S)BH <sub>4</sub> ] <sub>2</sub> (8)							
Ti(1)	0.6806(2)	0.0654(2)	0.1129(3)	C(7)	0.682(1)	-0.009(1)	0.350(2)
Ti(2)	0.8227(2)	0.0453(2)	-0.1618(3)	C(8)	0.714(1)	-0.061(1)	0.235(2)
S(1)	0.5605(3)	0.1637(3)	0.1002(5)	C(9)	0.648(1)	-0.078(1)	0.129(2)
S(2)	0.6696(3)	0.0509(3)	-0.1689(5)	C(10)	0.579(1)	-0.037(1)	0.180(2)
S(3)	0.8318(3)	0.0854(3)	0.1107(5)	C(11)	0.600(1)	0.010(1)	0.319(2)
S(4)	0.9317(3)	0.1534(3)	-0.2181(6)	C(12)	0.824(1)	-0.098(1)	-0.115(2)
C(1)	0.553(1)	0.228(1)	-0.075(2)	C(13)	0.803(1)	-0.088(1)	-0.273(2)
C(2)	0.616(1)	0.217(1)	-0.200(3)	C(14)	0.869(1)	-0.053(1)	-0.355(2)
C(3)	0.622(1)	0.136(1)	-0.280(2)	C(15)	0.933(2)	-0.041(1)	-0.238(3)
C(4)	0.868(1)	0.192(1)	0.152(2)	C(16)	0.905(1)	-0.071(1)	-0.102(2)
C(5)	0.861(2)	0.252(1)	0.023(2)	B(1)	0.643(1)	0.214(1)	0.242(2)
C(6)	0.920(1)	0.250(1)	-0.105(3)	B(2)	0.845(2)	0.155(2)	-0.392(3)
[CpTi(SCH <sub>2</sub> CH <sub>2</sub> CH <sub>2</sub> S) <sub>2</sub> (9)							
Ti(1)	0.5511(1)	0.4410(1)	0.91793(8)	C(4)	0.7595(7)	0.4141(9)	0.8348(7)
S(1)	0.2608(1)	0.4250(2)	0.9093(1)	C(5)	0.623(1)	0.4612(7)	0.7420(6)
S(2)	0.4151(2)	0.6726(1)	0.8831(1)	C(6)	0.1948(7)	0.2585(6)	0.9528(5)
C(1)	0.5096(8)	0.360(1)	0.7190(6)	C(7)	0.6824(8)	0.8521(7)	1.0015(6)
C(2)	0.567(1)	0.2493(7)	0.7924(8)	C(8)	0.5456(7)	0.8221(6)	0.8848(5)
C(3)	0.722(1)	0.2796(9)	0.8662(6)				
[CpTi(SCH <sub>2</sub> CH <sub>2</sub> SCH <sub>2</sub> CH <sub>2</sub> S) <sub>2</sub> (11)							
Ti(1)	0.5784(1)	0.1039(3)	0.0104	C(4)	0.6666(9)	0.258(2)	0.081(1)
S(1)	0.5761(3)	0.2367(7)	-0.1389(4)	C(5)	0.6629(9)	0.095(2)	0.126(1)
S(2)	0.6819(2)	-0.0521(6)	-0.0732(4)	C(6)	0.6599(8)	0.200(2)	-0.197(1)
S(3)	0.5431(2)	-0.1933(5)	0.0144(5)	C(7)	0.679(1)	0.020(3)	-0.194(1)
C(1)	0.6034(9)	0.083(3)	0.173(1)	C(8)	0.6580(8)	-0.274(2)	-0.089(1)
C(2)	0.569(1)	0.234(3)	0.156(2)	C(9)	0.5811(8)	-0.294(2)	-0.093(1)
C(3)	0.6076(9)	0.344(2)	0.101(1)				

h, black, insoluble crystals of **10** were deposited in moderate yield (39%). Repeated attempts to characterize **10** by X-ray crystallographic methods were made. Crystallographic data were obtained on crystals isolated from reactions performed in either THF or benzene. In either case, the crystals were of poor quality. Nonetheless, diffraction data were obtained, and the solutions permitted the establishment of the connectivity and thus the formulation of **10** as Cp<sub>3</sub>Ti<sub>3</sub>S<sub>2</sub>(SCH<sub>2</sub>CH<sub>2</sub>CH<sub>2</sub>S)<sub>2</sub> (*vide infra*, Figure 5). This species **10** was also obtained as a very minor byproduct (1%) from the reaction yielding **8**.

The reaction of **2** with Bu<sub>3</sub>SnH was performed under conditions similar to those employed to obtain **10**. The reaction appears to proceed in a manner analogous to that affording **8**, with gas evolution and the generation of a black solution. However, attempts to characterize the products in this reaction mixture were inconclusive. Unknown diamagnetic and paramagnetic species were observed according to NMR and EPR data. Following addition of hexane to the mixture, a small number of black crystals of **12** were isolated in 1% yield. The isolated product **12** exhibited a singlet EPR signal. This, together with the crystallographic cell parameters, confirmed the identity of this minor product as the



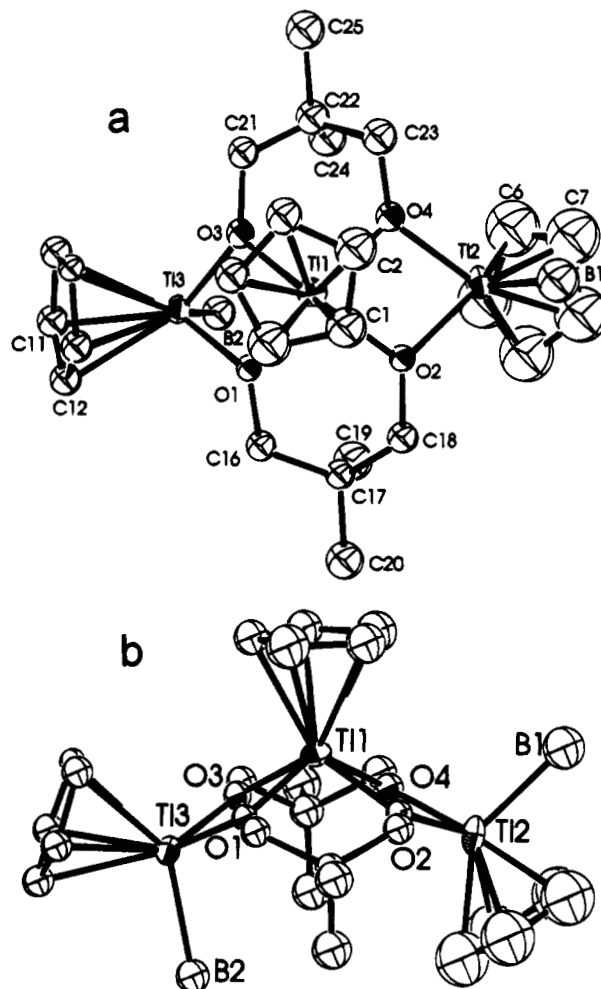
12

species Cp<sub>5</sub>Ti<sub>5</sub>S<sub>6</sub> (**7**), a compound previously prepared and characterized by Bottomley et al.<sup>8</sup>

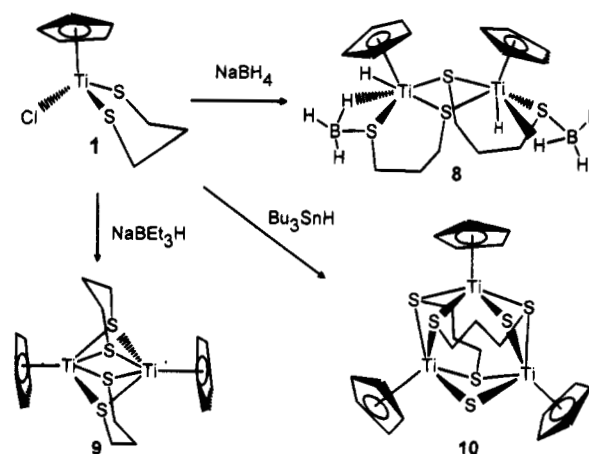
The reaction of **3** with Bu<sub>3</sub>SnH was performed in a manner similar to that described above. In this case, the dark, crystalline, sparingly soluble product **11** was isolated. Reaction of **11** with CHCl<sub>3</sub> led to the formation of the known species **3**, suggesting the formulation of **11** as a Ti(III) species. A subsequent crystallographic

**Table 3. Selected Bond Distances and Angles**

[CpTi(BH <sub>4</sub> )(OCH <sub>2</sub> CMe <sub>2</sub> CH <sub>2</sub> O)] <sub>2</sub> TiCp (7)			
Ti(1)–O(1)	2.03(2)	Ti(1)–O(2)	2.06(2)
Ti(1)–O(3)	2.03(2)	Ti(1)–O(4)	2.04(2)
Ti(2)–O(2)	2.01(2)	Ti(2)–O(4)	2.02(2)
Ti(3)–O(1)	1.95(2)	Ti(3)–O(3)	1.95(2)
Ti(1)–C(1)	2.43(2)	Ti(1)–C(2)	2.43(2)
Ti(1)–C(3)	2.41(3)	Ti(1)–C(4)	2.39(2)
Ti(1)–C(5)	2.40(2)	Ti(2)–B(1)	2.27(5)
Ti(2)–C(6)	2.23(3)	Ti(2)–C(7)	2.14(3)
Ti(2)–C(8)	2.08(3)	Ti(2)–C(9)	2.14(4)
Ti(2)–C(10)	2.23(4)	Ti(3)–B(2)	2.34(4)
Ti(3)–C(11)	2.38(2)	Ti(3)–C(12)	2.35(2)
Ti(3)–C(13)	2.35(2)	Ti(3)–C(14)	2.38(2)
Ti(3)–C(15)	2.40(2)	O(1)–C(16)	1.38(4)
O(2)–C(18)	1.39(4)	O(3)–C(21)	1.43(4)
O(4)–C(23)	1.42(4)		
O(1)–Ti(1)–O(2)	85.0(7)	O(1)–Ti(1)–O(3)	71.7(8)
O(1)–Ti(1)–O(4)	128.4(7)	O(1)–Ti(1)–C(1)	115.8(8)
O(1)–Ti(1)–C(2)	146.2(7)	O(1)–Ti(1)–C(3)	130.8(6)
O(2)–Ti(1)–O(3)	127.6(7)	O(2)–Ti(1)–O(4)	75.1(7)
O(2)–Ti(2)–O(4)	76.7(7)	O(2)–Ti(2)–B(1)	105(1)
O(3)–Ti(1)–O(4)	83.7(7)	O(4)–Ti(2)–B(1)	109(1)
O(1)–Ti(3)–O(3)	75.3(7)	O(1)–Ti(3)–B(2)	107(1)
Ti(1)–O(1)–Ti(3)	106.5(8)	Ti(1)–O(2)–Ti(2)	103.8(8)
O(3)–Ti(3)–B(2)	104(1)	Ti(1)–O(3)–Ti(3)	106.4(9)
Ti(1)–O(4)–Ti(2)	103.7(8)		
[CpTi(SCH <sub>2</sub> CH <sub>2</sub> CH <sub>2</sub> S)BH <sub>4</sub> ] <sub>2</sub> (8)			
Ti(1)–S(1)	2.474(5)	Ti(1)–S(2)	2.388(5)
Ti(1)–S(3)	2.421(5)	Ti(2)–S(2)	2.431(6)
Ti(2)–S(3)	2.385(5)	Ti(2)–S(4)	2.495(6)
Ti(1)–C(1)	2.32(2)	Ti(2)–C(9)	2.33(2)
Ti(1)–C(2)	2.33(2)	Ti(2)–C(10)	2.35(2)
Ti(1)–C(3)	2.36(2)	Ti(2)–C(11)	2.38(2)
Ti(1)–C(4)	2.36(2)	Ti(2)–C(12)	2.32(2)
Ti(1)–C(5)	2.33(2)	Ti(2)–C(13)	2.33(2)
S(1)–C(6)	1.80(2)	S(2)–C(8)	1.83(2)
S(3)–C(14)	1.84(2)	S(4)–C(16)	1.83(2)
S(1)–B(1)	1.95(2)	S(4)–B(2)	2.00(2)
S(1)–Ti(1)–S(2)	87.9(2)	S(1)–Ti(1)–S(3)	132.7(2)
S(2)–Ti(1)–S(3)	94.4(2)	S(2)–Ti(2)–S(3)	94.2(2)
S(2)–Ti(2)–S(4)	131.5(2)	S(3)–Ti(2)–S(4)	87.3(2)
Ti(1)–S(1)–C(6)	116.7(7)	Ti(1)–S(1)–B(1)	73.6(6)
C(6)–S(1)–B(1)	108(1)	Ti(1)–S(2)–Ti(2)	84.7(2)
Ti(1)–S(2)–C(8)	117.7(7)	Ti(2)–S(2)–C(8)	116.7(8)
Ti(1)–S(3)–Ti(2)	85.0(2)	Ti(1)–S(3)–C(14)	115.4(6)
Ti(2)–S(3)–C(14)	117.0(6)	Ti(2)–S(4)–C(16)	115.0(8)
Ti(2)–S(4)–B(2)	70.8(7)	C(16)–S(4)–B(2)	108(1)
[CpTiSCH <sub>2</sub> CH <sub>2</sub> CH <sub>2</sub> S] <sub>2</sub> (9)			
Ti(1)–Ti(1)	2.640(2)	Ti(1)–S(1)	2.512(2)
Ti(1)–S(1)	2.475(2)	Ti(1)–S(2)	2.473(2)
Ti(1)–S(2)	2.496(2)	Ti(1)–C(1)	2.363(6)
Ti(1)–C(2)	2.380(6)	Ti(1)–C(3)	2.364(6)
Ti(1)–C(4)	2.362(5)	Ti(1)–C(5)	2.367(5)
S(1)–C(6)	1.821(6)	S(2)–C(8)	1.821(6)
S(1)–Ti(1)–S(1)	116.09(4)	S(1)–Ti(1)–S(2)	68.00(5)
S(1)–Ti(1)–S(2)	78.52(5)	S(1)–Ti(1)–S(2)	79.65(5)
S(1)–Ti(1)–S(2)	68.20(5)	S(2)–Ti(1)–S(2)	115.82(4)
Ti(1)–S(1)–Ti(1)	63.91(4)	Ti(1)–S(1)–C(6)	117.1(2)
Ti(1)–S(1)–C(6)	113.9(2)	Ti(1)–S(2)–Ti(1)	64.18(4)
Ti(1)–S(2)–C(8)	115.6(2)	Ti(1)–S(2)–C(8)	117.3(2)
[CpTiSCH <sub>2</sub> CH <sub>2</sub> SCH <sub>2</sub> CH <sub>2</sub> S] <sub>2</sub> (11)			
Ti(1)–S(1)	2.392(5)	Ti(1)–S(2)	2.666(6)
Ti(1)–S(3)	2.441(5)	Ti(1)–S(3)	2.493(5)
Ti(1)–C(1)	2.40(2)	Ti(1)–C(2)	2.34(2)
Ti(1)–C(3)	2.37(2)	Ti(1)–C(4)	2.35(2)
Ti(1)–C(5)	2.36(2)	S(1)–C(6)	1.87(2)
S(2)–C(7)	1.83(2)	S(2)–C(8)	1.83(2)
S(3)–C(9)	1.90(2)		
S(1)–Ti(1)–S(2)	79.0(2)	S(1)–Ti(1)–S(3)	115.8(2)
S(1)–Ti(1)–S(3)	83.1(2)	S(2)–Ti(1)–S(3)	77.7(2)
S(2)–Ti(1)–S(3)	150.8(2)	S(3)–Ti(1)–S(3)	89.8(1)
Ti(1)–S(1)–C(6)	108.4(6)	Ti(1)–S(2)–C(7)	105.1(6)
Ti(1)–S(2)–C(8)	107.4(6)	C(7)–S(2)–C(8)	99.9(9)
Ti(1)–S(3)–Ti(1)	90.1(1)	Ti(1)–S(3)–C(9)	105.7(6)
Ti(1)–S(3)–C(9)	118.6(6)		



**Figure 2.** ORTEP drawing of **7**, showing 30% thermal ellipsoids. Hydrogen atoms are omitted for clarity. The two views **a** and **b** are approximately orthogonal to each other.

**Scheme 1**

study of **11** identified it as [CpTi(SCH<sub>2</sub>CH<sub>2</sub>SCH<sub>2</sub>CH<sub>2</sub>S)<sub>2</sub>]*(vide infra*, Scheme 2, Figure 6).

**Structural Studies.** The structure of **7** determined by X-ray methods is depicted in Figure 2. The molecule contains three CpTi fragments. Two are linked by two dialkoxide ligands forming a 12-membered macrocyclic ring. The four oxygen atoms of this macrocycle complete the coordination sphere of the central CpTi unit. The O–Ti1–O' angles are typical of a "four-legged piano stool" geometry, with the slight perturbation introduced by the presence of the four-membered Ti<sub>2</sub>O<sub>2</sub> rings.



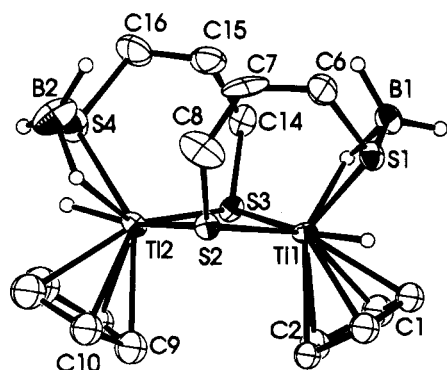


**Figure 3.** ORTEP drawing of **8**, showing 30% thermal ellipsoids. Some of the hydrogen atoms are omitted for clarity.

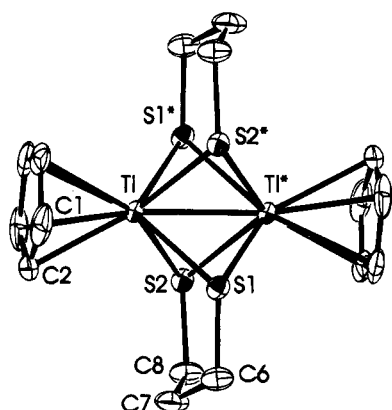


**Figure 4.** ORTEP drawing of **9**, showing 30% thermal ellipsoids. Hydrogen atoms are omitted for clarity.

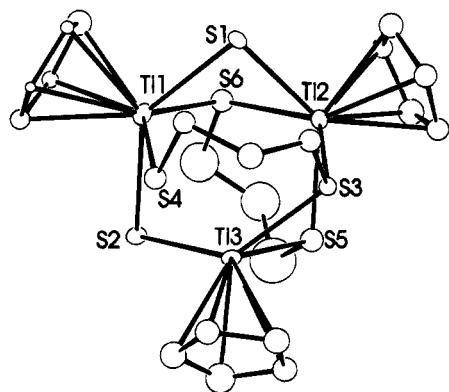
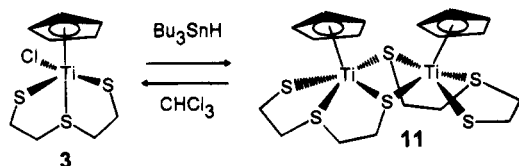


**Figure 5.** ORTEP drawing of **10**, showing 30% thermal ellipsoids. Hydrogen atoms are omitted for clarity.

#### Scheme 2



Thus, O1-Ti1-O3 and O2-Ti1-O4 are 71.7(8) and 75.1(7)°, which is significantly smaller than the O1-Ti1-O2 and O3-Ti1-O4 angles of 85.0(7) and 83.7(7)°, respectively. The coordination spheres of the outer Ti atoms are completed by the BH<sub>4</sub><sup>-</sup>. The nature of the bonding mode of these moieties was not determined since the hydrogen atoms could not be located. The Ti2-B1 and Ti3-B2 distances are 2.27(5) and 2.34(2) Å. The B-Ti-O angles about the "outer" Ti centers range from 104(1) to 109(1)° while the O-Ti-O angles

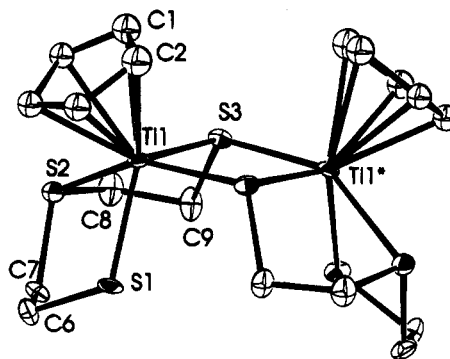


**Figure 6.** ORTEP drawing of **11**, showing 30% thermal ellipsoids. Hydrogen atoms are omitted for clarity.

at Ti2 and Ti3 are 76.7(7) and 75.2(7)°, respectively. These data are consistent with the description of the coordination sphere geometry at Ti2 and Ti3 as that of a distorted "three-legged piano stool" which is constrained by the presence of the four-membered Ti<sub>2</sub>O<sub>2</sub> ring. Viewing the macrocycle side-on (Figure 2b) reveals that the cyclopentadienyl and borohydride ligands of the outer Ti atoms adopt *transoid* dispositions with respect to the plane through the four oxygen atoms. The bridging Ti-O distances in **7** average 2.01(4) Å. This is typical of bridging Ti-O distances and is significantly longer than the terminal Ti-alkoxide bond lengths of 1.733(6) and 1.750(4) Å seen in (CpTiCl<sub>2</sub>)<sub>2</sub>(OCH<sub>2</sub>CMe-CH<sub>2</sub>O) and (CpTiCl<sub>2</sub>)<sub>2</sub>(OCHMeCH<sub>2</sub>CHMeO), respectively.<sup>18</sup> The Ti-O-Ti angles indicate a slight dissymmetry in the molecule. These angles at O1 and O3 are 106.5(8) and 106.4(9)°, while, at O2 and O4, the angles are 103.8(8) and 103.7(8)°, respectively. This small dissymmetry is also reflected in the Ti-Ti distances, (Ti1-Ti2, 3.194(7) Å, Ti1-Ti3, 3.186(8) Å) and may be attributed to a steric interaction of the Cp ligand on Ti2 with the *gem*-dimethyl groups on the diolate ligands.

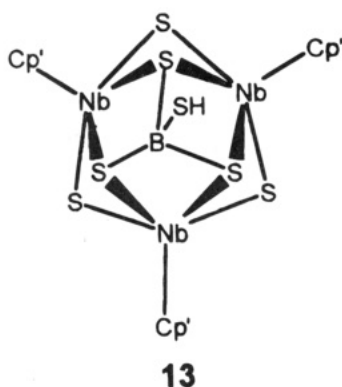
The structure of **8** determined by crystallography is shown in Figure 3. Each of the two titanium atoms is coordinated to a cyclopentadienyl ring and three sulfur atoms. Two of the sulfur atoms bridge the two Ti atoms. The bridging Ti-S bonds alternate in length about the Ti<sub>2</sub>S<sub>2</sub> core. The shorter Ti1-S2 and Ti2-S3 bonds are 2.388(5) and 2.395(5) Å, respectively, while the longer Ti1-S3 and Ti2-Ti2 bond lengths are 2.421(4) and 2.431(4) Å, respectively. The Ti-Ti separation is 3.246(4) Å. The other Ti-S bond distances, which average 2.484(7) Å, are significantly longer than either the bridging Ti-S distances or typical terminal Ti-S bond lengths.<sup>16</sup> This lengthening is consistent with the interaction of these sulfur centers with the Lewis acidic B atoms, giving average S-B distances of 1.97(2) Å. One of the three hydrogen atoms of each BH<sub>3</sub> moiety also bridges to the adjacent Ti center. The Ti-H distances in these cases are 1.90 Å. Terminal hydride atoms are also found bonded to each metal center, with Ti-H distances of 1.45 Å. The two cyclopentadienyl rings adopt a *cisoid* disposition with respect to the slightly puckered Ti<sub>2</sub>S<sub>2</sub> core; the angle between the two TiS<sub>2</sub> planes is 14.75°.

X-ray structural data for **9** confirmed it to be a centrosymmetric dimer in which the four thiolate sulfur atoms of two propane dithiolate ligands symmetrically bridge two titanium centers, each of which is also coordinated to a cyclopentadienyl ligand (Figure 4). The Ti-S distances average 2.490(4) Å, while the Ti-S-Ti angles average 65.05(4)°. The Ti-Ti separation in **9** is



2.640(2) Å, significantly shorter than in **8** or **7**, which is consistent with the presence of four bridging atoms. This metal–metal distance compares with those of 2.425(1) and 2.448(3) Å seen in  $[\text{CpV}(\text{SCH}_2\text{CH}_2\text{S})_2]_2^{23}$  and  $[\text{CpV}(\text{S}_2\text{C}_6\text{H}_4)_2]_2^{24}$  respectively.

The X-ray crystallographic data for compound **10** confirmed that the complex is a trimeric Ti species in which three CpTi units form a triangular arrangement in which two sulfur atoms bridge each edge of the triangle (Figure 5). Two pairs of the sulfur atoms are part of two propanedithiolate fragments while the others are simple sulfide bridges. Thus, compound **7** is formulated as  $[(\text{CpTi})_3(\mu\text{-S})_2(\mu\text{-SCH}_2\text{CH}_2\text{CH}_2\text{S})_2]$ . While the crystallographic data confirm the connectivity of **10**, the poor crystal quality and ligand disorder preclude a detailed discussion of the metric parameters. It is, however, pertinent to point out the structural similarity of the CpTi–S core of **10** to that recently reported for  $[(\text{C}_5\text{Me}_4\text{Et})\text{NbS}_2]_3\text{BSH}$  (**13**).<sup>9a</sup>



The structural characterization of **11** by X-ray crystallography (Figure 6) revealed the dimeric nature of the complex. Each titanium center is coordinated to a cyclopentadienyl ligand as well as a diethanethiolate sulfide ligand. One of the thiolate sulfur atoms from each  $\text{S}_3$  ligand bridges the two titanium centers. Thus, a cyclopentadienyl ligand, a terminal thiolate sulfur, two bridging thiolate sulfurs and the thioether sulfur atoms constitute the pseudo-four-legged piano stool coordination sphere about each of the titanium center. The terminal, bridging, and thioether Ti–S distances of 2.392(5), 2.441(5), and 2.666(6) Å follow the expected order. The two cyclopentadienyl ligands in **11** adopt a cisoid disposition with respect to the planar  $\text{Ti}_2\text{S}_2$  core.

The above structural data are consistent with a greater degree of  $\pi$ -bonding between Ti and O than between Ti and S. This is evident in the trimeric species **7** and **10**. The geometry about the bridging oxygen atoms in **7** is planar, as the Ti–O–Ti and Ti–O–C angles sum to  $360^\circ$ . Interaction of the O p-orbitals orthogonal to the Ti–O–C planes with metal-based d-orbitals accounts for this  $\pi$ -interaction (Figure 7). In contrast, the angles about the sulfur atoms in **10** are approximately tetrahedral. As has been previously concluded, the longer M–S  $\sigma$ -bond precludes a more significant  $\pi$ -interaction.<sup>25</sup>

**Mechanistic Considerations.** Little is known about the mechanism by which early metal chalcogenide

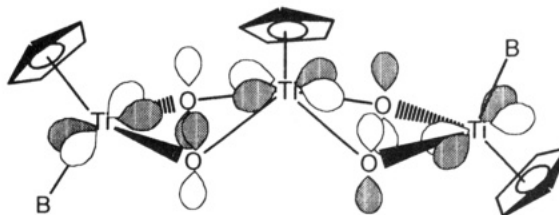
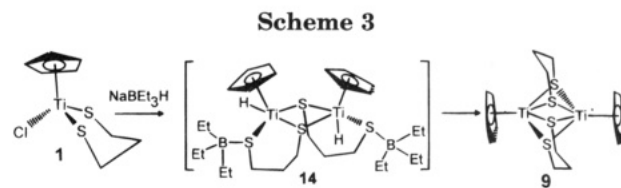


**Figure 7.** Schematic depiction of the extended Ti–O  $\pi$ -interaction in **7**. The alkyl chains of the diolate ligands have been omitted for clarity.



clusters are reduced. Some implications of mechanistic information may be derived from the present results. The formation of **7** is clearly a complex reaction. Monitoring the reaction mixture via NMR suggests the intermediacy of a macrocyclic dimer  $[\text{CpTiCl}(\text{OCH}_2\text{-CMe}_2\text{CH}_2\text{O})_2]$  analogous to **5**, although attempts to intercept or prepare this species directly led to loss of the cyclopentadienyl ligand.<sup>18</sup>

The isolation of **8** suggests an analogous intermediate **14** in the reaction of Super-Hydride with **1**. The steric bulk of the  $\text{BEt}_3$  moiety, as well as the absence of a chelating interaction with Ti which stabilizes the association of  $\text{BH}_3$  between Ti and S in **8**, may account for the subsequent reaction affording **9** (Scheme 3).

## Summary

In this paper we have characterized the first examples of CpTi(III) diolate and thiolate complexes. The structures of these species are dependent not only on the nature of the ligands but also on the method of reduction of the metal. The observation of C–S bond cleavage in some of these reductions as evidenced by formation of **10** and **12** further suggests that intermediates similar to **15** or **16** may offer a route to monocyclopentadienyl early metal sulfides. While recent studies<sup>26</sup> have yielded early metal chalcogenides from the corresponding chalcogenolates via C–S bond cleavage, mononuclear monocyclopentadienyl early metal sulfides are unknown and yet are expected to be highly reactive. The reactivity and trapping of such molecules containing the  $\text{CpM}=\text{S}$  fragment is the focus of an ongoing study.

**Acknowledgment.** Support from the PRF, administered by the American Chemical Society, is gratefully acknowledged. Additional support from the NSERC of Canada is also acknowledged.

**Supplementary Material Available:** Tables of crystallographic parameters, hydrogen atom parameters and thermal parameters (25 pages). Ordering information is given on any current masthead page.

OM950052A

(23) Rajan, O. A.; Noordik, J.; Haltiwanger, R. C.; Rakowski Du Bois, M. *Organometallics* **1984**, *3*, 831.

(24) Stephan, D. W. *Inorg. Chem.* **1992**, *31*, 4218.

(25) Stephan, D. W. *J. Chem. Soc., Chem. Commun.* **1991**, 129. (b) Stephan, D. W. *Organometallics* **1991**, *10*, 2037. (c) Stephan, D. W. *Organometallics* **1990**, *9*, 2718.

(26) Piers, W. E.; Koch, L.; Ridge, D. S.; MacGillivray, L. R.; Zaworotko, M. J. *Organometallics* **1992**, *11*, 3147 and references therein.

# Insertion of Isocyanides into Tantalum–Carbon Bonds of Azatantalacyclopropane Complexes. Crystal Structures of $\text{TaCp}^*\text{Cl}_3(\eta^2\text{-NRCMe}_2\text{CNHR})$ , $\text{TaCp}^*\text{Me}(\text{NR})(\text{NRCMe}=\text{CMe}_2)$ , and $\text{TaCp}^*\text{Me}(\text{NR})(\eta^2\text{-NR}=\text{CCMe}_2\text{CMe}=\text{NR})$ ( $\text{R} = 2,6\text{-Me}_2\text{C}_6\text{H}_3$ )

Mikhail V. Galakhov, Manuel Gómez, Gerardo Jiménez, and Pascual Royo\*

*Departamento de Química Inorgánica, Universidad de Alcalá de Henares, Campus Universitario, E-28871 Alcalá de Henares, Spain*

Maria Angela Pellinghelli and Antonio Tiripicchio

*Dipartimento di Chimica Generale ed Inorganica, Chimica Analitica, Chimica Fisica, Università di Parma, Centro di Studio per la Strutturistica Diffattometrica del CNR, Viale delle Scienze 78, I-43100 Parma, Italy*

Received January 6, 1995\*

Reaction of  $\text{TaCp}^*\text{Cl}_2\text{Me}_2$  with 2 equiv of isocyanides or addition of 1 equiv of isocyanides to azatantalacyclopropane complexes  $\text{TaCp}^*\text{Cl}_2(\eta^2\text{-NRCMe}_2)$  ( $\text{R} = 2,6\text{-Me}_2\text{C}_6\text{H}_3$ , **1a**,  $2,4,6\text{-Me}_3\text{C}_6\text{H}_2$ , **1b**) at room temperature afforded new imido derivatives  $\text{TaCp}^*\text{Cl}_2(\text{NR})$  ( $\text{R} = 2,6\text{-Me}_2\text{C}_6\text{H}_3$ , **2a**,  $2,4,6\text{-Me}_3\text{C}_6\text{H}_2$ , **2b**) in almost quantitative yields, with simultaneous elimination of the imino ketene,  $\text{RN}=\text{C}=\text{CMe}_2$ . When the same reactions were carried out in the presence of traces of water, small amounts of cyclic  $\eta^2$ -amido–carbene species  $\text{TaCp}^*\text{Cl}_3(\eta^2\text{-NRCMe}_2\text{CNHR}')$  ( $\text{R} = \text{R}' = 2,6\text{-Me}_2\text{C}_6\text{H}_3$ , **3a**,  $\text{R} = 2,6\text{-Me}_2\text{C}_6\text{H}_3$ ,  $\text{R}' = 2,4,6\text{-Me}_3\text{C}_6\text{H}_2$ , **3b**) were simultaneously obtained. Complexes **3** can also be prepared by heating the corresponding trichloro-isopropylamido complexes  $\text{TaCp}^*\text{Cl}_3(\text{NR}'\text{Pr})$ , **4**, at 90 °C in the presence of isocyanide and decompose by further heating at 120 °C to give the imido compounds **2**. A similar reaction of  $\text{TaCp}^*\text{Cl}_n\text{Me}_{4-n}$  ( $n = 0, 1$ ) with 1 equiv of  $\text{CN}(2,6\text{-Me}_2\text{C}_6\text{H}_3)$  afforded mono- and dimethylated azatantalacyclopropane derivatives  $\text{TaCp}^*\text{Cl}_n\text{Me}_{2-n}[\eta^2\text{-N}(2,6\text{-Me}_2\text{C}_6\text{H}_3)\text{CMe}_2]$  ( $n = 1$ , **5a**;  $n = 0$ , **5b**), which react with one additional equivalent of isocyanide to give imido alkenylamido species  $\text{TaCp}^*\text{X}[\text{N}(2,6\text{-Me}_2\text{C}_6\text{H}_3)](\text{NR}'\text{CMe}=\text{CMe}_2)$  ( $\text{X} = \text{Cl}$ ,  $\text{R}' = 2,6\text{-Me}_2\text{C}_6\text{H}_3$ , **6a**, and  $2,4,6\text{-Me}_3\text{C}_6\text{H}_2$ , **6b**;  $\text{X} = \text{Me}$ ,  $\text{R}' = 2,6\text{-Me}_2\text{C}_6\text{H}_3$ , **6c**, and  $2,4,6\text{-Me}_3\text{C}_6\text{H}_2$ , **6d**). Reaction of complexes **6a,c** with a third 1 equiv of isocyanide afforded new  $\eta^2$ -imino acyl compounds  $\text{TaCp}^*\text{X}[\text{N}(2,6\text{-Me}_2\text{C}_6\text{H}_3)](\eta^2\text{-NR}''=\text{CCMe}_2\text{CMe}=\text{NR}')$  ( $\text{X} = \text{Cl}$ ,  $\text{R}' = \text{R}'' = 2,6\text{-Me}_2\text{C}_6\text{H}_3$ , **7a**;  $\text{X} = \text{Me}$ ,  $\text{R}' = \text{R}'' = 2,6\text{-Me}_2\text{C}_6\text{H}_3$ , **7b**,  $\text{R}' = 2,6\text{-Me}_2\text{C}_6\text{H}_3$ ,  $\text{R}'' = 2,4,6\text{-Me}_3\text{C}_6\text{H}_2$ , **7c**, and  $\text{R}' = 2,6\text{-Me}_2\text{C}_6\text{H}_3$ ,  $\text{R}'' = \text{tBu}$ , **7d**). All compounds were characterized by IR and  $^1\text{H}$  and  $^{13}\text{C}$  NMR measurements, and the activation barrier to rotation around the  $\text{C}=\text{C}$  double bond of the alkenyl group of **6a,c** was determined in solution. Molecular structures of **3a**, **6c**, and **7b** were studied by X-ray diffraction methods. Crystals of **3a** are monoclinic, space group  $P2_1/n$ , with  $Z = 4$  in a unit cell of dimensions  $a = 8.774(4)$  Å,  $b = 18.338(8)$  Å,  $c = 18.470(7)$  Å, and  $\beta = 91.62(2)^\circ$ . Crystals of **6c** are monoclinic, space group  $P2_1/c$ , with  $Z = 4$  in a unit cell of dimensions  $a = 8.635(4)$  Å,  $b = 34.156(9)$  Å,  $c = 10.090(4)$  Å, and  $\beta = 105.94(2)^\circ$ . Crystals of **7b** are orthorhombic, space group  $P2_12_12_1$ , with  $Z = 4$  in a unit cell of dimensions  $a = 11.622(3)$  Å,  $b = 14.141(5)$  Å, and  $c = 22.755(9)$  Å. All three structures were solved from diffractometer data by Patterson and Fourier methods and refined by full-matrix least-squares on the basis of 6620 (**3a**), 3442 (**6c**), and 3667 (**7b**) observed reflections to  $R$  and  $R_w$  values of 0.0271 and 0.0394 (**3a**), 0.0272 and 0.0336 (**6c**), and 0.0450 and 0.0419 (**7b**), respectively.

## Introduction

We have reported<sup>1</sup> recently the isolation of azatantalacyclopropane complexes by insertion of isocyanides into tantalum–methyl bonds of  $\text{TaCp}^*\text{Cl}_2\text{Me}_2$  ( $\text{Cp}^* = \eta^5\text{-C}_5\text{Me}_5$ ) with migration of two methyl groups. Similar compounds have also been reported for other transition

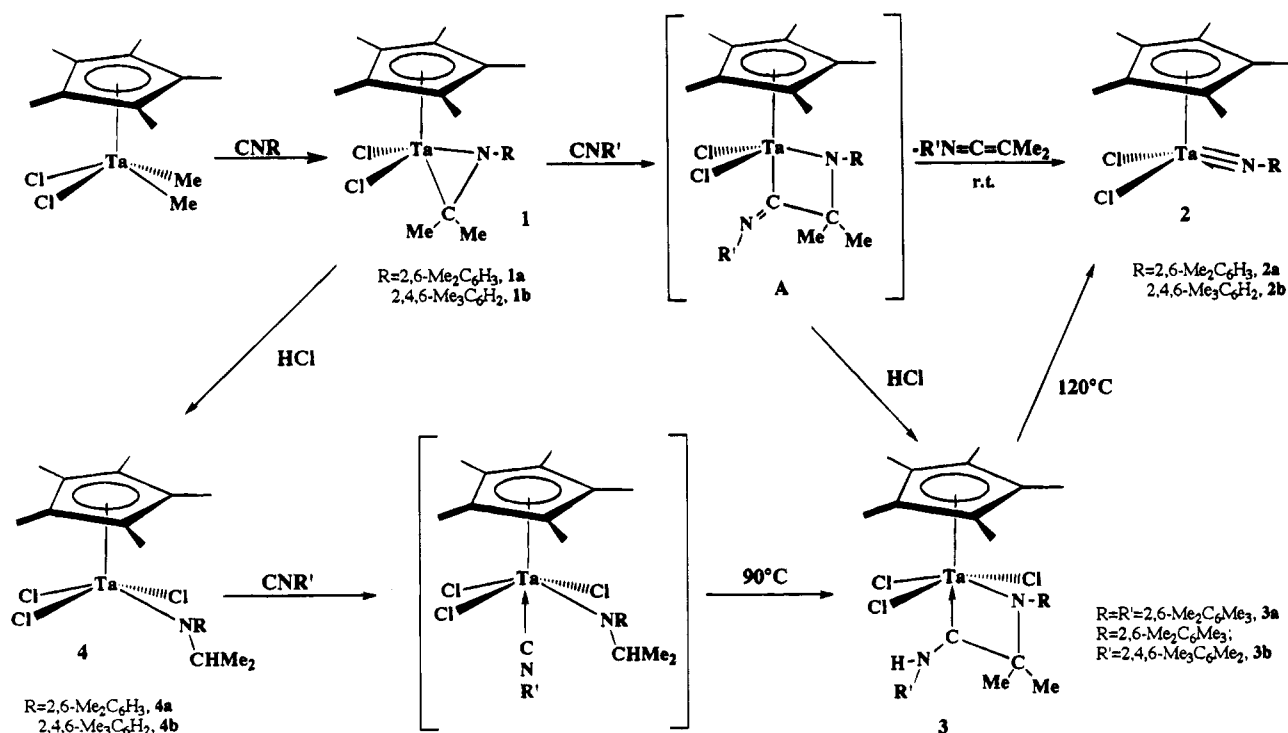
metals.<sup>2</sup> Further insertion of isocyanide is known<sup>3</sup> to occur when more than two alkyl groups are bound to the metal, leading to imido alkenylamido complexes

(2) (a) Takahashi, Y.; Onoyama, N.; Ishikawa, Y.; Motojima, S.; Sugiyama, K. *Chem. Lett.* **1978**, 525. (b) Wolczanski, P. T.; Bercaw, J. E. *J. Am. Chem. Soc.* **1979**, *101*, 6450. (c) Mayer, J. M.; Curtis, C. J.; Bercaw, J. E. *J. Am. Chem. Soc.* **1983**, *105*, 2651. (d) Nugent, W. A.; Overall, D. W.; Holmes, S. J. *Organometallics* **1983**, *2*, 161. (e) Sielisch, T.; Behrens, U. *J. Organomet. Chem.* **1986**, *310*, 179. (f) Brunner, H.; Wachter, J.; Schmidbauer, J. *Organometallics* **1986**, *5*, 2212. (g) Durfee, L. D.; Fanwick, P. E.; Rothwell, I. P. *J. Am. Chem. Soc.* **1987**, *109*, 4720. (h) Durfee, L. D.; Hill, J. E.; Fanwick, P. E.; Rothwell, I. P. *Organometallics* **1990**, *9*, 75.

\* Abstract published in *Advance ACS Abstracts*, May 1, 1995.

(1) Galakhov, M. V.; Gómez, M.; Jiménez, G.; Pellinghelli, M. A.; Royo, P.; Tiripicchio, A. *Organometallics* **1995**, *14*, 1901.

Scheme 1



which are analogous to the oxido enolate derivatives isolated<sup>4</sup> when the same reaction is carried out by using CO. The interest of this type of compounds in relation with many synthetic applications moved us to extend the study to other (pentamethylcyclopentadienyl)-tantalum chloro methyl complexes and to investigate the reactivity of the azatantalacyclopropane derivatives.

Here we describe the results found when 1 equiv of isocyanide is inserted in tri- and tetramethyltantalum complexes  $\text{TaCp}^*\text{Cl}_n\text{Me}_{4-n}$  ( $n = 0, 1$ ) and the behavior of the resulting azatantalacyclopropane complexes in further insertions of isocyanides. The X-ray structures of the three most significant complexes and the dynamical behavior of the alkenylamido derivatives in solution are also described.

## Results and Discussion

### Reactions of $\text{TaCp}^*\text{Cl}_2\text{Me}_2$ with Isocyanides.

Reaction of  $\text{TaCp}^*\text{Cl}_2\text{Me}_2$  with 1 equiv of isocyanide allowed us<sup>1</sup> to isolate dichloroazatantalacyclopropane complexes **1**. When the same reaction is repeated at room temperature by using 2 equiv of isocyanides under a rigorously dry inert atmosphere or in a sealed NMR tube, a different sequence of reactions takes place leading finally to the dichloro imido derivatives **2** as the unique reaction products in an almost quantitative yield.

As shown in Scheme 1, exactly the same imido compounds are obtained when 1 equiv of the corresponding isocyanide is added at room temperature to toluene solutions of the azatantalacyclopropane com-

plexes **1**. However, when the same reaction is carried out in the presence of traces of water, the same imido complexes **2** are formed as the main products, but a small amount of air-stable  $\eta^2$ -amido-carbene complexes **3** are simultaneously obtained.

This behavior can be explained assuming that the azatantalacyclopropane complexes coordinate the isocyanide, which is inserted into the Ta-C bond by migration of the alkyl group of the metallacycle, to give the intermediate azatantalacyclobutane species **A**. Spontaneous thermal decomposition of this species at room temperature is so fast that **A** cannot be either isolated or observed by NMR spectroscopy. The decomposition takes place with elimination of the arylimine ketene. The imine ketene formed from **1a** in a sealed NMR tube was identified by its <sup>13</sup>C spectrum, which shows the characteristic resonances of this species<sup>5</sup> at  $\delta$  52.9 and 193.3, and its IR spectrum,<sup>6</sup> which shows  $\nu(\text{CN})$  at  $2015\text{ cm}^{-1}$ .

In the presence of traces of water, hydrolysis of **A** or its precursor complex **1** takes place with evolution of HCl, which further reacts at room temperature to give complexes **3**. Formation of complex **A** is required for **2** to be formed at room temperature, because complexes **3** only decompose by heating at  $120^\circ\text{C}$  in a sealed tube, being transformed into the same imido derivatives **2**, with elimination of an unidentified organic residue.

Complexes **3** can alternatively be obtained in an almost quantitative yield when a mixture of equimolar amounts of the already reported<sup>1</sup> amido complexes **4**, with the corresponding isocyanide, is heated at  $90^\circ\text{C}$ . This reaction probably takes place by migration of the isopropyl hydrogen to the coordinated isocyanide, with simultaneous carbon-carbon bond formation.

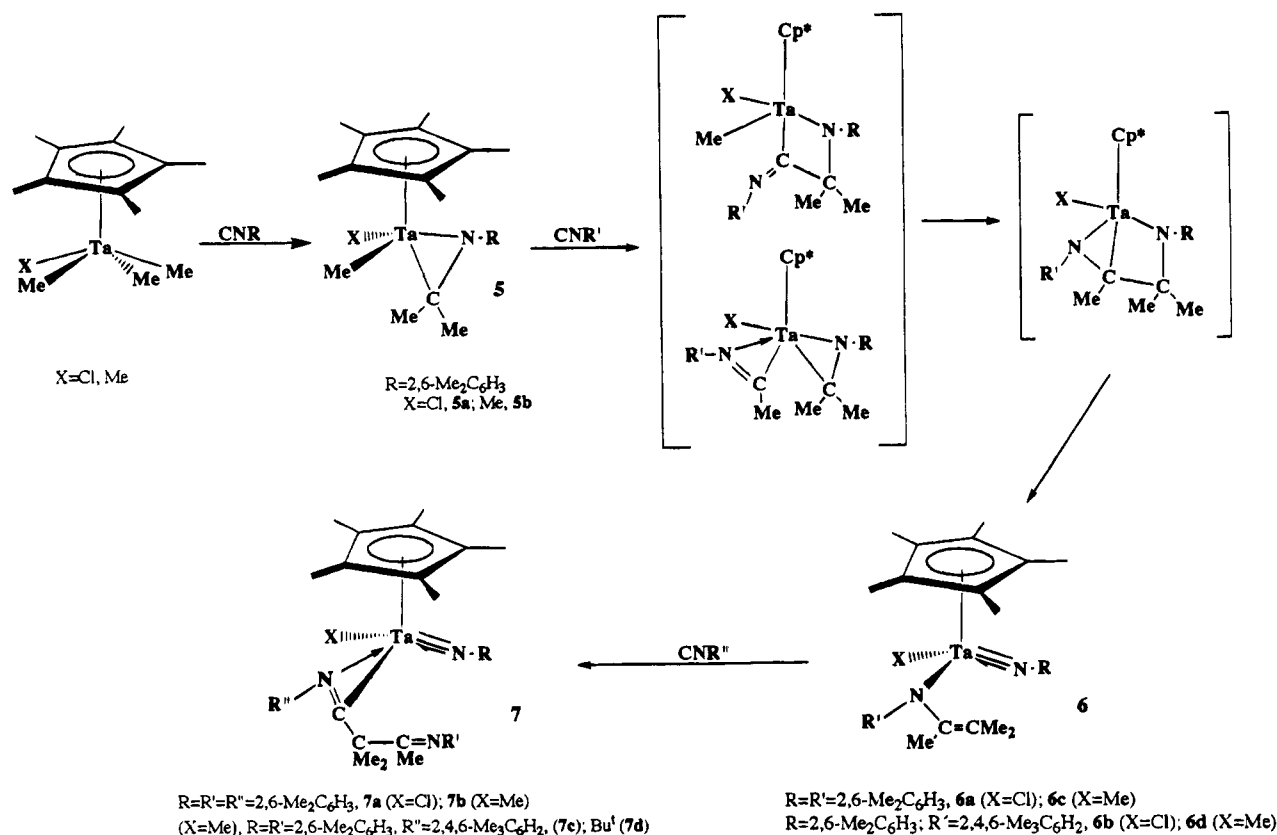
(3) (a) Chiu, K. W.; Jones, R. A.; Wilkinson, G.; Galas, A. M. R.; Hursthouse, M. B. *J. Am. Chem. Soc.* **1980**, *102*, 7978. (b) Chiu, K. W.; Jones, R. A.; Wilkinson, G.; Galas, A. M. R.; Hursthouse, M. B. *J. Chem. Soc., Dalton Trans.* **1981**, 2088. (c) Chamberlain, L. R.; Rothwell, I. P.; Huffman, J. C. *J. Chem. Soc., Chem. Commun.* **1986**, 1203. (d) Chamberlain, L. R.; Steffy, B. D.; Rothwell, I. P.; Huffman, J. D. *Polyhedron* **1989**, *8*, 341.

(4) Wood, C. D.; Schrock, R. R. *J. Am. Chem. Soc.* **1979**, *101*, 5421.

(5) Collier, C.; Webb, G. A. *Org. Magn. Reson.* **1979**, *12*, 659.

(6) Bestmann, H. J.; Lienert, J.; Mott, L. *Liebigs Ann. Chem.* **1968**, *718*, 24.

Scheme 2



The IR spectra of complexes **3** show the  $\nu(\text{N-H})$  and  $\nu(\text{C=N})$  absorptions at 3112 and 1628  $\text{cm}^{-1}$ , respectively. Their formulation is based on the observed NMR behavior. The  $^{13}\text{C}\{^1\text{H}\}$  NMR spectra of **3** show one singlet due to the carbene carbon at  $\delta$  261.2. The  $^1\text{H}$  NMR spectra of **3** exhibit one broad signal at  $\delta$  12.2 due to the aminocarbene proton, one singlet at  $\delta$  1.17 (**3a**),  $\delta$  1.23 (**3b**) for the two equivalent methyl-methylene protons, and two singlets at  $\delta$  2.23 (**3a,b**) and  $\delta$  2.43 (**3a**),  $\delta$  2.44 (**3b**) due to also equivalent *ortho*-methylphenyl protons of the amido and amino phenyl groups, respectively. The structure of complex **3a** was fully elucidated by X-ray diffraction analysis. It shows the amido nitrogen directly bonded to the tantalum atom occupying one equatorial position together with the three chlorine atoms, whereas the carbene end of the ligand occupies the axial position.

**Reactions of  $\text{TaCp}^*\text{ClMe}_3$  and  $\text{TaCp}^*\text{Me}_4$  with Isocyanides.** When 1 equiv of the isocyanide is added to a toluene solution of the chlorotrimethyltantalum complex, a red solution is obtained, which after manipulation affords the monomethylated azatantalacyclopropane complex **5a**, as shown in Scheme 2.

The addition of a second 1 equiv of isocyanide to solutions of this azatantalacyclopropane complex **5a** produces a new insertion leading finally to the imido alkenylamido derivatives **6a,b**.

When 1 equiv of  $\text{CN}(2,6\text{-Me}_2\text{C}_6\text{H}_3)$  is added to the tetramethyltantalum complex in a sealed NMR tube, an intense red solution is obtained, which according to its  $^1\text{H}$  NMR spectrum consists of a mixture of three different components. The main product is complex **6c**, together with a small amount of the expected dimethylazatantalacyclopropane derivative **5b**, recently<sup>1</sup> isolated by methylation of **1a**, and an amount of unreacted

starting material. This behavior means that the insertion of  $\text{CNR}$  is much more favorable for complex **5b** than for the starting tetramethyl derivative. However, when 2 equiv of  $\text{CN}(2,6\text{-Me}_2\text{C}_6\text{H}_3)$  is added to the tetramethyltantalum complex in toluene, a yellow-green product characterized as complex **6c** is obtained in almost quantitative yield. The still remaining methyl substituent does not migrate, probably because it would lead to a much less favorable unsaturated electron deficient compound.<sup>3b</sup> Neither does such a migration take place for  $\text{TaCp}^*\text{Me}(\eta^2\text{-ArC}\equiv\text{CAr})(\eta^2\text{-Bu}^t\text{N}=\text{CMe})$ <sup>9</sup> in spite of containing a *cis*-methyl group.

The first step in both reactions with the trimethyl- and tetramethyltantalum complexes consists in the insertion of the first coordinated isocyanide molecule, with migration of two methyl groups to give **5a,b**, containing the same azatantalacyclopropane system already studied<sup>1</sup> for compounds **1** and analogous to other reported<sup>4,7,8</sup> " $\eta^2$ -ketone" complexes. Coordination of a second isocyanide to the vacant position is followed by a double migration of one methyl group and the met-

(7) (a) Masai, H.; Sonogashira, K.; Hagihara, N. *Bull. Chem. Soc. Jpn.* **1968**, *41*, 750. (b) Fachinetti, G.; Floriani, C. *J. Chem. Soc., Chem. Commun.* **1979**, 654. (c) Girolami, G. S.; Mainz, V. V.; Andersen, R. A.; Völlmer, S. H.; Day, V. W. *J. Am. Chem. Soc.* **1991**, *113*, 3953. (d) Hessen, B.; Teuben, J.; Lemmen, T. H.; Huffman, J. C.; Caulton, K. G. *Organometallics* **1985**, *4*, 946. (e) Negishi, E.; Takahashi, T. *Synthesis* **1988**, 1.

(8) (a) Rosenfeldt, F.; Erker, G. *Tetrahedron Lett.* **1980**, *21*, 1637. (b) Waymouth, R. M.; Clauser, K. R.; Grubbs, R. H. *J. Am. Chem. Soc.* **1986**, *108*, 638. (c) Stella, S.; Floriani, C. *J. Chem. Soc., Chem. Commun.* **1986**, 1053. (d) Erker, G.; Dorf, V.; Czisch, P.; Petersen, J. L. *Organometallics* **1986**, *5*, 668.

(9) (a) Curtis, M. D.; Real, J. *J. Am. Chem. Soc.* **1986**, *108*, 4668. (b) Curtis, M. D.; Real, J.; Hirpo, W.; Butler, W. M. *Organometallics* **1990**, *9*, 66. (c) Hirpo, W.; Curtis, M. D. *Organometallics* **1994**, *13*, 2706.

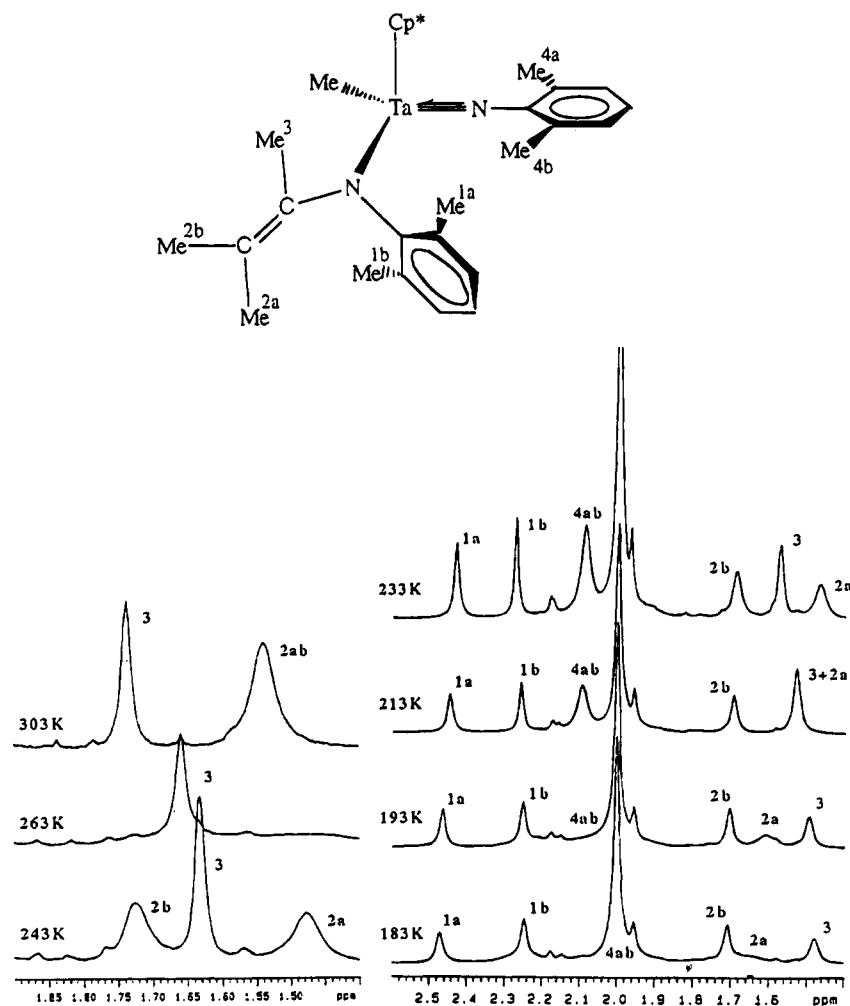


Figure 1.  $^1\text{H}$  NMR spectra at variable temperature for complex **6c** in  $\text{CD}_2\text{Cl}_2$ .

allacycle alkyl group to the electrophilic isocyanide carbon atom.

As shown in Scheme 2, two different pathways may be proposed depending on which is the order of migration of both groups, leading in any case to the same unidentified intermediate species that spontaneously rearranges, breaking the Ta–C and C–N(amido) bonds with simultaneous C=C bond formation, to give the resultant products **6**.

This behavior is similar to that observed in the formation of complexes **2**, for which the C–N bond breaking also takes place, but the coordinating capacity of the resulting imino ketene is low, resulting in its dissociation. However, when a third methyl group is present, its migration transforms the imino into an amido group, which remains occupying its coordination position. Complexes **6a–c** are reasonably stable compounds that can be easily crystallized and characterized by NMR spectroscopy.

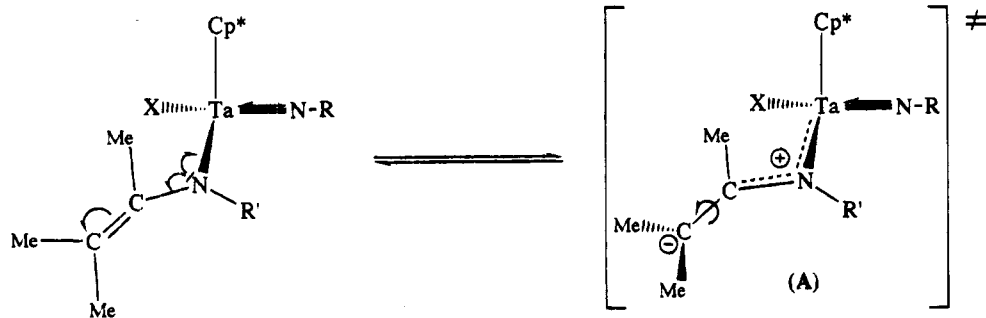
In order to favor the migration of the methyl group by addition of bases, we studied the reaction of complexes **6a** and **6c** with an additional 1 equiv of the isocyanides. Addition of 1 equiv of CNR to a toluene solution of the previously isolated **6a,c** produces a very slow reaction to give after 7 days at room temperature (2–3 days at 50–60 °C) pale yellow-green solutions, which after evaporation render complexes **7a–d**. Therefore, the still remaining methyl group does not migrate to the electrophilic carbon atom of the new isocyanide

ligand, which instead attacks the terminal olefinic carbon atom of the amido ligand, leading to the new  $\eta^2$ -acylimido complexes **7a–d**. The structures of the complexes **6c** and **7b** were determined by X-ray diffraction methods. Formulation of the complexes **6** and **7** is also in agreement with the NMR structural behavior described (see Experimental Section).

**Structural and Dynamic NMR Studies.** The structural characterization of complexes **1**, **2**, **4**, and **5b** has already been reported.<sup>1</sup> The NMR behavior of complexes **3** has been discussed above, and the structure of **3a** was determined by X-ray diffraction methods (see below). Complex **5a** shows the NMR behavior expected for a molecule which does not contain the plane of symmetry observed for **5b**; therefore, the  $^1\text{H}$  and  $^{13}\text{C}$  NMR spectra of **5a** show two singlets for the pair of nonequivalent methyl groups bound to the carbon atom of the azatantalacyclopropane ring, along with the singlet due to the *ortho*-methylphenyl groups made equivalent by rotation and that due to the methyl group bound to the metal. The NMR spectra of complexes **6** show that one of the two phenyl rings is freely rotating whereas the other does not rotate in the NMR scale time. A comparison between the two  $^1\text{H}$  NMR spectra of complexes **6a,b** or **6c,d** (Figure 1) shows that the phenyl ring of the imido substituent possesses  $C_{2v}$  symmetry.

Broad  $^1\text{H}$  and  $^{13}\text{C}$  signals are always observed for the  $=\text{CMe}_2$  methyl groups ( $\text{Me}^{2a}$ ,  $\text{Me}^{2b}$ ) in all complexes

Scheme 3



Scheme 4

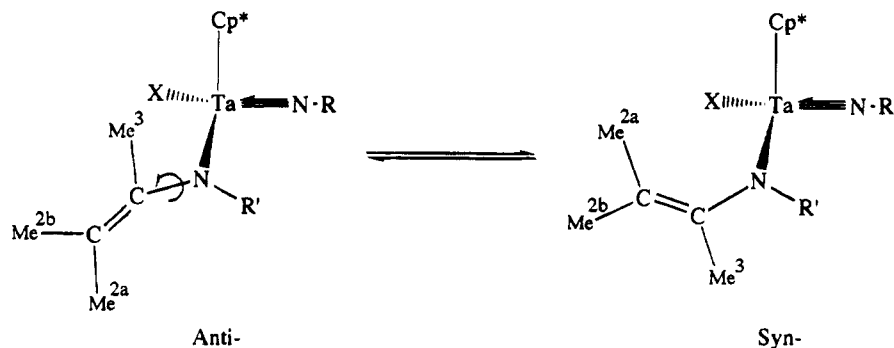


Table 1. Kinetic Parameters of Rotation around the C=C Double Bond of Complexes 6a,c

	$E_a$ , kcal/mol	$\log A$	$\Delta H^\ddagger$ , kcal/mol	$\Delta S^\ddagger$ , eu	$\Delta G^\ddagger$ 298K, kcal/mol
6a	$10.0 \pm 0.4$	$11.5 \pm 1.8$	$9.5 \pm 0.4$	$-15.8 \pm 1.7$	14.2
	$r = 0.998$		$r = 0.998$		
6c	$8.0 \pm 0.1$	$11.1 \pm 0.9$	$7.5 \pm 0.1$	$-16.3 \pm 0.4$	12.2
	$r = 0.999$		$r = 0.999$		

**6** at 303 K and also for the  $^1\text{H}$  resonance due to the  $\text{Me}^3$  group that can be resolved as a septuplet by coupling with the protons of the two  $\text{Me}^{2a}$  and  $\text{Me}^{2b}$  groups, which seem to be equivalent at higher temperatures. When a  $\text{CDCl}_3$  solution of **6c** is cooled from 303 K down to 243 K, the  $\text{Me}^2$  signal broadens with a coalescence point at 263 K ( $\Delta G^\ddagger = 12.2 \text{ kcal mol}^{-1}$ ), being split into two signals observed at  $\delta$  1.47 and  $\delta$  1.73 at 243 K. A similar behavior is observed for complex **6a** with the coalescence point at 313 K ( $\Delta G^\ddagger = 14.2 \text{ kcal mol}^{-1}$ ).

Kinetic parameters calculated on the basis of  $^1\text{H}$  DNMR data by NMR line shape analysis<sup>11</sup> (see Table 1) show that this transformation is an intramolecular process [ $\log A = 11.5$  (**6a**), 11.1 (**6c**)] taking place with negative  $\Delta S^\ddagger$  values, due to solvation effects with a highly polar transition state.

The values found for these parameters are consistent with a transition state **A** (Scheme 3) resulting from the heterolytic dissociation of the C=C  $\pi$  bond, similar to that reported<sup>12</sup> for enamines, in this case, with electron delocalization of the nitrogen lone pair over the C-N-Ta system. This delocalization is affected by the X substituent, as found from a comparison between the kinetic parameters for both complexes **6a** and **6c** that allows to conclude that  $E_a$ ,  $\Delta H^\ddagger$ , and  $\Delta G^\ddagger$  values are

lower for the less electronegative substituent X bound to the metal.

Rotation around the C-C axis in species **A** renders the terminal methyl groups ( $\text{Me}^{2a}$ ,  $\text{Me}^{2b}$ ) equivalent on the NMR time scale at higher temperatures. A transition  $\pi$ -azaallylic species, whose rapid  $\sigma$ - $\pi$ - $\sigma$  conversion would allow the exchange between the *syn*- and *anti*-methyl groups at the Ta-C  $\sigma$ -stage, cannot be considered because the presence of a chiral metal center would make both methyl groups diastereotopic and therefore not equivalent. When the solution of **6c** in  $\text{CD}_2\text{Cl}_2$  is cooled at decreasing temperatures to the coalescence point, the width and chemical shift of one of the two  $\text{Me}^2$  signals is unaffected, whereas the other broadens and shifts to lower field and simultaneously the resonances due to  $\text{Me}^3$  and one of the two  $\text{Me}^1$  groups are slightly broadened and shifted. It is well-known<sup>11</sup> that spin-relaxation times depend on the number of adjacent protons and their distances. Spin-lattice relaxation times ( $T_1$ ) have been measured for **6c** at different temperatures. The  $T_1$  values at 193 K combined with X-ray data can be used to assign the resonances at  $\delta$  1.6 and 1.7 to  $\text{Me}^{2a}$  ( $T_1 = 0.428 \pm 0.001 \text{ s}$ ) and  $\text{Me}^{2b}$  ( $T_1 = 0.200 \pm 0.001 \text{ s}$ ) protons, respectively.

The behavior of  $\text{Me}^{2a}$  and  $\text{Me}^3$  signals between 233 and 183 K can be explained by exchange of these signals with upfield and downfield lines, respectively, of the signals of the other isomer present in ca. 10% amount. Several signals of the minor isomer of **6c** can be detected in the  $^{13}\text{C}\{^1\text{H}\}$  NMR spectrum at 173 K. We propose that the second process is an exchange between the *anti* (major) and *syn* (minor) isomers (Scheme 4) due to rotation around the C-N bond as reported<sup>12</sup> for organic enamines. Finally at 193 K is possible to detect the coalescence of the 2,6- $\text{Me}_2\text{C}_6\text{H}_3$  methyl proton resonances ( $\Delta G^\ddagger = 8.7 \text{ kcal mol}^{-1}$ ) corresponding to the rotation around the  $\text{C}_{\text{ipso}}\text{-N}$  bond.

(10) Weber, W. P.; Gokel, G. W.; Ugi, I. K. *Angew. Chem., Int. Ed. Engl.* **1972**, *11*, 530.

(11) (a) Abragam, S. *The principles of nuclear magnetism*; Clarendon Press: Oxford, U.K., 1961. (b) Jackman, K. M.; Cotton, F. A. *DNMR Spectroscopy*; Academic Press: New York, 1975.

(12) Bakmutov, V. I.; Fedin, E. I. *Bull. Magn. Reson.* **1984**, *6*, 142.

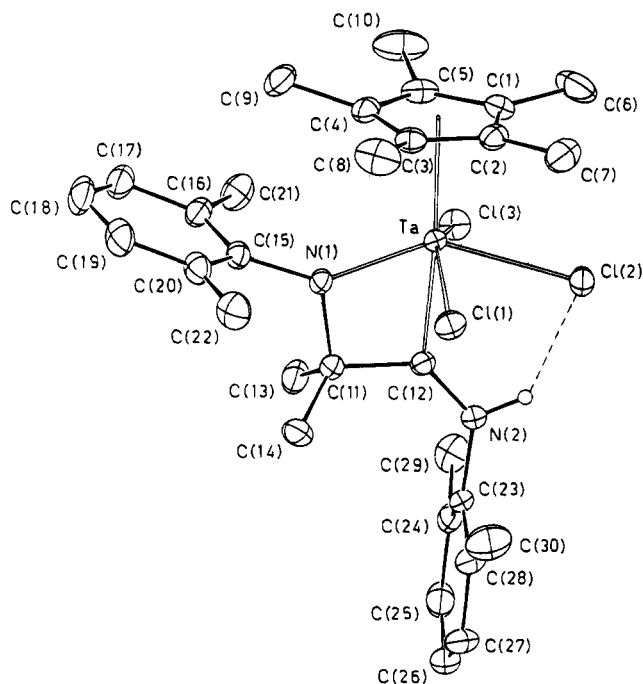


**Figure 2.** ORTEP view of the molecular structure of  $\text{TaCp}^*\text{Cl}_3(\eta^2\text{-NRCMe}_2\text{CNHR})$  ( $\text{R} = 2,6\text{-Me}_2\text{C}_6\text{H}_3$ ) (**3a**) with the atom-numbering scheme. The thermal ellipsoids are drawn at the 30% probability level.

**Table 2.** Selected Bond Distances (Å) and Angles (deg) with Esd's in Parentheses for Compound **3a**

Ta-CE(1) <sup>a</sup>	2.199(4)	N(1)-C(11)	1.527(4)
Ta-Cl(1)	2.452(1)	N(1)-C(15)	1.439(4)
Ta-Cl(2)	2.526(1)	C(11)-C(12)	1.505(5)
Ta-Cl(3)	2.450(1)	N(2)-C(12)	1.289(4)
Ta-N(1)	2.029(3)	N(2)-C(23)	1.454(4)
Ta-C(12)	2.195(3)		
CE(1)-Ta-Cl(1)	103.9(1)	Cl(3)-Ta-N(1)	92.2(1)
CE(1)-Ta-Cl(2)	104.6(1)	Cl(3)-Ta-C(12)	76.1(1)
CE(1)-Ta-Cl(3)	104.5(1)	N(1)-Ta-C(12)	63.5(1)
CE(1)-Ta-N(1)	112.4(1)	Ta-N(1)-C(11)	104.2(2)
CE(1)-Ta-C(12)	175.9(1)	Ta-N(1)-C(15)	139.6(2)
Cl(1)-Ta-Cl(2)	78.7(1)	C(11)-N(1)-C(15)	116.3(3)
Cl(1)-Ta-Cl(3)	148.1(1)	C(12)-N(2)-C(23)	129.9(3)
Cl(1)-Ta-N(1)	90.4(1)	N(1)-C(11)-C(12)	94.6(3)
Cl(1)-Ta-C(12)	76.7(1)	Ta-C(12)-N(2)	132.8(3)
Cl(2)-Ta-Cl(3)	80.2(1)	Ta-C(12)-C(11)	97.7(2)
Cl(2)-Ta-N(1)	142.9(1)	N(2)-C(12)-C(11)	129.5(3)
Cl(2)-Ta-C(12)	79.5(1)		

<sup>a</sup> CE(1) is the centroid of the C(1)··C(5) cyclopentadienyl ring.

**X-ray Crystal Structures of 3a, 6c, and 7b.** A view of the complex  $\text{TaCp}^*\text{Cl}_3(\eta^2\text{-NRCMe}_2\text{CNHR})$  ( $\text{R} = 2,6\text{-Me}_2\text{C}_6\text{H}_3$ ) (**3a**) is shown in Figure 2 together with the atom-numbering scheme. Selected bond distances and angles are given in Table 2. The pentamethylcyclopentadienyl ring is bound to the Ta atom in a nearly symmetric  $\eta^5$ -fashion (the Ta-C distances range from 2.472(4) to 2.562(4) Å, with the distance between the metal and the centroid of the ring being 2.199(4) Å. The Ta atom is bound to the N(1) and C(12) atoms of the chelating amido carbene ligand. The Ta atom is bound also to three Cl atoms with Ta-Cl bond lengths of 2.450(1), 2.452(1), and 2.526(1) Å, the longest one involving the Cl atom trans to the amido N(1) atom. The complex can be described as pseudooctahedral if the centroid of the Cp\* ring is considered as occupying one coordination site. The Ta atom is displaced by 0.621(1) Å from the equatorial plane, containing the three Cl atoms and the

N(1) atom, toward the Cp\* ring, and the carbene C(12) atom is positioned trans to the Cp\* ring. The Ta-N(1) and Ta-C(12) bond distances involving the chelating atoms are 2.029(3) and 2.195(3) Å, respectively. The Ta-N(1) distance shows a double bond character similar to that found in the complex  $\text{TaCp}^*\text{Me}_2(\eta^2\text{-Me}_2\text{CNR})$ , where the value of this distance has been found much shorter, 1.930(4) Å.<sup>1</sup> Also the value of the Ta-C(12) bond distance is much shorter than that found, 2.321(12) Å, with the carbene carbon atom in the complex  $\text{TaCp}^*\text{Cl}_4[\text{C}(\text{Me})\text{NHR}]$ .<sup>1</sup> This remarkable shortening could be due to the steric effect of the narrow bite of the chelating ligand, as shown by the very different angles at the carbene C(12) atom [the C(11)-C(12)-Ta angle is 97.7(2)° against 125.9(9)°, the N(2)-C(12)-Ta one is 132.8(3)° against 123.0(8)°, and the N(2)-C(12)-C(11) one is 129.5(3)° against 111.1(10)°]. The four-membered ring containing the Ta, N(1), C(11), and C(12) atoms is planar with the C(11)-C(12) and N(1)-C(11) bond distances being consistent with single bonds. This plane forms a dihedral angle of 89.5(2)° with the mean plane passing through the cyclopentadienyl ring. The N(2)-C(12) bond length of the aminocarbene moiety is 1.289(4) Å, corresponding to a localized double bond. Also the C(11)C(12)N(2)C(23) moiety is perfectly planar with the Ta and N(1) atoms deviating by 0.132(1) and 0.056(1) Å from this plane. The N(2)-bound hydrogen is involved in an intramolecular hydrogen bond with the coordinated Cl(2) atom. The N(2)··Cl(2) and H··Cl(2) distances of 3.029(3) and 2.34(6) Å, respectively, as well as the N(2)-H··Cl(2) angle of 132(5)° are in agreement with this bonding. It is noteworthy the very large Ta-N(1)-C(15) angle, 139.6(2)°, is probably due to steric hindrance of the C(9) atom from the methyl group with the C(15) and C(16) atoms. The C(9)··C(15) and C(9)··C(16) contacts are of 3.112(7) and 3.210(7) Å, respectively, and the C(9) atom is displaced from the mean plane of the cyclopentadienyl ring plane by 0.401(5) Å, much more than the other methyl carbon atoms deviate (in the range 0.132(5)-0.210(6) Å).

A view of the complex  $\text{TaCp}^*\text{Me}(\text{NR})(\text{NRCMe}=\text{CMe}_2)$  ( $\text{R} = 2,6\text{-Me}_2\text{C}_6\text{H}_3$ ) (**6c**) is shown in Figure 3 together with the atom-numbering scheme. Selected bond distances and angles are given in Table 3. The pentamethylcyclopentadienyl ring is bound to the Ta atom in a slightly asymmetric  $\eta^5$ -fashion (the Ta-C distances range from 2.392(8) to 2.564(6) Å), with the distance between the metal and the centroid of the ring being 2.179(7) Å. The Ta atom is also bound to the C(32) atom of a methyl group and to the two N(1) and N(2) atoms of the phenylimido and alkenylamido ligands. The complex, which can be described as pseudotetrahedral if the centroid of the Cp\* ring is considered as occupying one coordination site, is chiral, and both enantiomers are present in the crystal. The Ta-C(32) bond distance [Ta-C(32) = 2.181(7) Å] is quite normal and can be compared with those found, 2.178(7) and 2.179(7) Å, in  $\text{TaCp}^*\text{Me}_2(\eta^2\text{-Me}_2\text{CNR})$ .<sup>1</sup> The values of the Ta-N(1) bond length, 1.784(4) Å, consistent with a triple bond character, and the nearly linear Ta-N(1)-C(11) angle of 168.0(4)° are expected for an imido ligand and are strictly comparable with those found for the same ligand in complex **7b** (see below). The Ta-N(2) bond length, 2.050(5) Å, involving the alkenylamido ligand, is consistent with a double bond character and is comparable



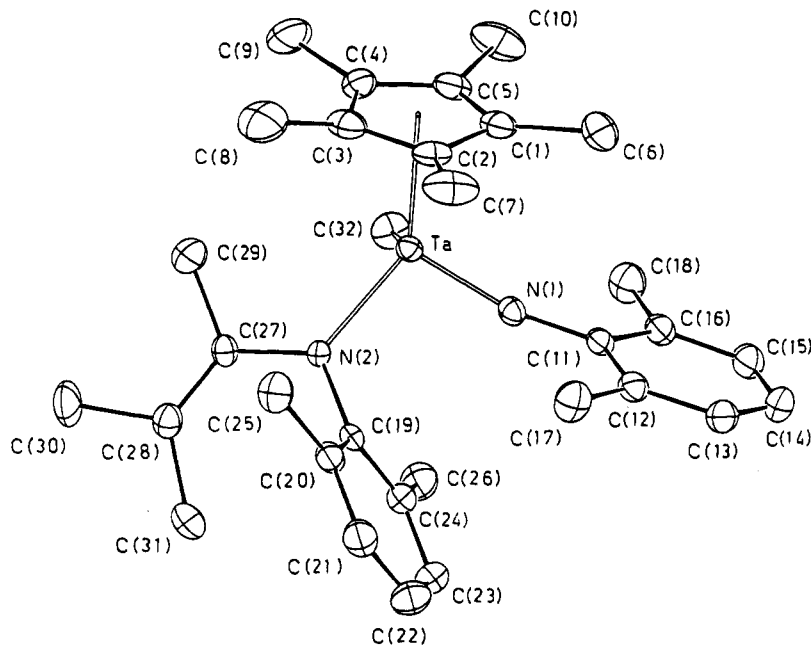


**Figure 3.** ORTEP view of the molecular structure of  $\text{TaCp}^*\text{Me}(\text{NR})(\text{NRCMe}=\text{CMe}_2)$  (**6c**) with the atom-numbering scheme. The thermal ellipsoids are drawn at the 30% probability level.

**Table 3.** Selected Bond Distances (Å) and Angles (deg) with Esd's in Parentheses for Compound **6c**

Ta-CE(1) <sup>a</sup>	2.179(7)	N(2)-C(27)	1.431(7)
Ta-N(1)	1.784(4)	C(27)-C(28)	1.354(10)
Ta-N(2)	2.050(5)	C(27)-C(29)	1.507(8)
Ta-C(32)	2.181(7)	C(28)-C(30)	1.504(9)
N(1)-C(11)	1.382(7)	C(28)-C(31)	1.512(9)
N(2)-C(19)	1.453(6)		
CE(1)-Ta-N(1)	114.7(2)	Ta-N(2)-C(27)	125.9(4)
CE(1)-Ta-N(2)	133.2(2)	C(19)-N(2)-C(27)	116.1(4)
CE(1)-Ta-C(32)	106.3(3)	N(2)-C(27)-C(29)	112.6(5)
N(1)-Ta-N(2)	99.4(2)	N(2)-C(27)-C(28)	128.3(5)
N(1)-Ta-C(32)	100.9(2)	C(28)-C(27)-C(29)	119.2(6)
N(2)-Ta-C(32)	96.9(2)	C(27)-C(28)-C(31)	128.9(6)
Ta-N(1)-C(11)	168.0(4)	C(27)-C(28)-C(30)	120.2(6)
Ta-N(2)-C(19)	117.9(3)	C(30)-C(28)-C(31)	110.9(6)

<sup>a</sup> CE(1) is the centroid of the C(1)··C(5) cyclopentadienyl ring.

to that found for the Ta-N(1) bond length involving the nitrogen atom of the amido group in **3a**. In the alkenylamido ligand the C(27)-C(28) bond distance, 1.354(10) Å, agrees with a double bond character. The alkenylamido and phenyl groups are almost perpendicular one to another, the dihedral angle between them being 85.0(1)°. Also in **6c** the Ta-N(2)-C(27) angle, 125.9(4)°, is large probably due to steric hindrance of the C(8) atom from the methyl group with the C(29) atom [the C(8)··C(29) contact is of 3.349(14) Å and moreover the C(8) atom is that which deviates more remarkably from the cyclopentadienyl ring plane].

A view of the structure of  $\text{TaCp}^*\text{Me}(\text{NR})(\eta^2\text{-NR}=\text{CCMe}_2\text{CMe}=\text{NR})$  (**7b**) is shown in Figure 4 together with the atom-numbering scheme.

Selected bond distances and angles are given in Table 4. The pentamethylcyclopentadienyl ring is bound to the Ta atom in a nearly symmetric  $\eta^5$ -fashion (the Ta-C distances range from 2.432(11) to 2.508(11) Å), with the distance between the metal and the centroid of the ring being 2.155(11) Å. The Ta atom is also bound to the C(11) atom of a methyl group, to the N(1) atom from the phenylimido ligand, and to N(2) and C(28) from the  $\eta^2$ -coordinated  $\text{NR}=\text{CCMe}_2\text{CMe}=\text{NR}$  ligand. The coordination geometry is a distorted square pyramid if the

$\text{Cp}^*$  is considered as occupying the apical coordination site with the Ta atom deviating 0.984(1) Å from the mean plane passing through atoms C(11), N(1), N(2), and C(28) toward the Cp\* ring. The complex is chiral, and in the crystals only one of the two enantiomers is present. The values of the Ta-N(1) bond length, 1.812(8) Å, and of the Ta-N(1)-C(12) angle, 171.1(8)°, are comparable with those found for the same phenylimido ligand in complex **6c**. The value of the Ta-C(11) bond distance [Ta-C(11) = 2.203(11) Å] is very similar to that found in **6c**. The imino acyl  $\text{NR}=\text{CCMe}_2\text{CMe}=\text{NR}$  ligand is dihapto coordinated to the Ta atom through the N(2) and C(28) atoms. The Ta-C(28) bond distance, 2.188(9) Å, is comparable to that involving the methyl group and also to that found, 2.209(6) Å, for the azatantalacyclopropane ligand in  $\text{TaCp}^*\text{Me}_2(\eta^2\text{-Me}_2\text{-CNR})$ .<sup>1</sup> The value of the Ta-N(2) bond length, 2.148(7) Å, is much longer than that found, 1.930(4) Å, for the azatantalacyclopropane ligand in  $\text{TaCp}^*\text{Me}_2(\eta^2\text{-Me}_2\text{-CNR})$ ,<sup>1</sup> denoting a single bond character instead of the double bond character evidenced in the azatantalacyclopropane ligand. Both imino acyl and isopropylideneamine ligands show a clearly different behavior as illustrated by the following observations. The values of the N(2)-C(28) and N(3)-C(30) bond lengths, 1.294(13) and 1.271(13) Å, are consistent with a double bond character. The TaN(2)C(28) plane forms dihedral angles of 131.8(4)° with the cyclopentadienyl ring, of 104.6(4)° with the TaC(11)N(1) plane, and of 83.1(4)° with the aryl group, whereas in  $\text{TaCp}^*\text{Me}_2(\eta^2\text{-Me}_2\text{-CNR})$  the azatantalacyclopropane ring was almost perpendicular to the cyclopentadienyl ring.<sup>1</sup> Moreover, in this last complex the centroid of the cyclopentadienyl ring was coplanar with the triatomic ring, whereas in **7b** the centroid is out of the plane of the triatomic ring by 1.49(1) Å.

## Conclusions

With this and a previously reported work<sup>1</sup> we have completed a systematic study of the isocyanide insertion reactions into tantalum-methyl bonds of different ha-



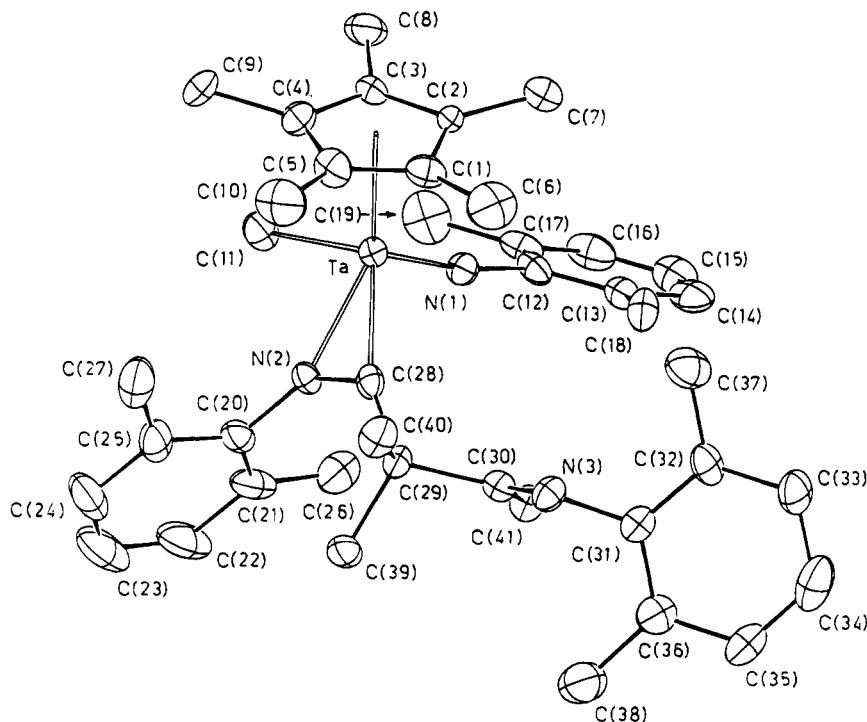


**Figure 4.** ORTEP view of the molecular structure of  $\text{TaCp}^*\text{Me}(\text{NR})(\eta^2\text{-NR}=\text{CCMe}_2\text{CMe}=\text{NR})$  (**7b**) with the atom-numbering scheme. The thermal ellipsoids are drawn at the 30% probability level.

**Table 4.** Selected Bond Distances (Å) and Angles (deg) with Esd's in Parentheses for Compound **7b**

Ta-CE(1) <sup>a</sup>	2.155(11)	N(2)-C(20)	1.435(14)
Ta-N(1)	1.812(8)	N(2)-C(28)	1.294(13)
Ta-N(2)	2.148(7)	N(3)-C(30)	1.271(13)
Ta-C(11)	2.203(11)	N(3)-C(31)	1.419(13)
Ta-C(28)	2.188(9)	C(28)-C(29)	1.548(14)
Ta-CE(2)	2.069(8)	C(29)-C(30)	1.564(14)
N(1)-C(12)	1.380(14)		
CE(1)-Ta-N(1)	118.6(4)	CE(2)-Ta-C(11)	96.1(4)
CE(1)-Ta-N(2)	134.5(4)	Ta-N(1)-C(12)	171.1(8)
CE(1)-Ta-C(11)	104.3(4)	Ta-N(2)-C(28)	74.3(5)
CE(1)-Ta-C(28)	118.5(4)	Ta-N(2)-C(20)	148.4(7)
N(1)-Ta-N(2)	105.2(3)	C(20)-N(2)-C(28)	137.2(9)
N(1)-Ta-C(11)	99.7(4)	C(30)-N(3)-C(31)	120.9(8)
N(1)-Ta-C(28)	101.3(4)	Ta-C(28)-N(2)	71.0(5)
N(2)-Ta-N(1)	78.6(4)	Ta-C(28)-C(29)	161.2(7)
N(2)-Ta-C(28)	34.7(3)	N(2)-C(28)-C(29)	127.6(9)
C(11)-Ta-C(28)	113.2(4)	N(3)-C(30)-C(29)	117.3(8)
CE(1)-Ta-CE(2)	128.0(4)	N(3)-C(30)-C(41)	126.2(9)
CE(2)-Ta-N(1)	103.9(3)	C(29)-C(30)-C(41)	116.5(8)

<sup>a</sup> CE(1) is the centroid of the C(1)-C(5) cyclopentadienyl ring, and CE(2) the midpoint of the N(2)-C(28) bond.

lomethyl(pentamethylcyclopentadienyl)tantalum complexes  $\text{TaCp}^*\text{Cl}_{4-n}\text{Me}_n$ . Whereas the monomethyl complex ( $n = 1$ ) leads to the formation of the  $\eta^2$ -coordinated imino acyl compound, the dimethyl derivative ( $n = 2$ ) gives the dichloroazatantalacyclopropane complex by double migration of two methyl groups. Similar chloromethyl- and dimethylazatantalacyclopropane complexes are also obtained by insertion into tri- and tetramethyl ( $n = 3, 4$ ) complexes, respectively, but these compounds take part in a simultaneous further insertion of isocyanide leading to the chloro- and methylimido alkenylamido complexes, which are almost quantitatively obtained when an additional 1 equiv of isocyanide is used. Attack of the isocyanide to the terminal olefinic carbon of the alkenyl moiety in these complexes converts the amido into an imino acyl ligand containing a terminal ketimine function. Activation barriers for the

intramolecular isomerization of the azatantalacyclopropane complexes ( $\Delta G^\ddagger = 11.5\text{--}11.6\text{ kcal mol}^{-1}$ ) and for the rotation around the C=C double bond of the alkenyl group in imido alkenyl complexes ( $\Delta G^\ddagger = 12.2\text{--}14.2\text{ kcal mol}^{-1}$ ) were determined by dynamic NMR measurements. Carbene, amido, and imido derivatives can be easily obtained by protonation, rearrangement, or thermal transformation of these imino acyl and azatantalacyclopropane compounds.

## Experimental Section

**General Procedures.** All manipulations were carried out under an atmosphere of argon using conventional Schlenk-tube and glovebox techniques. Solvents were purified by distillation from an appropriate drying agent: *n*-hexane (Na/K alloy) and toluene (sodium).  $\text{NC}^t\text{Bu}$  was purchased from Fluka and used without further purification. Isocyanides<sup>10</sup>  $\text{CNR}$  ( $R = 2,6\text{-Me}_2\text{C}_6\text{H}_3, 2,4,6\text{-Me}_3\text{C}_6\text{H}_2$ ) and starting materials  $\text{TaCp}^*\text{Cl}_n\text{Me}_{4-n}$  ( $n = 0, 4, 13, 14, 215$ ) and  $\text{TaCp}^*\text{Cl}_2(\eta^2\text{-RN-CMe}_2)$ <sup>1</sup> were synthesized according to literature procedures.

Infrared spectra were recorded on a Perkin-Elmer 583 spectrophotometer ( $4000\text{--}200\text{ cm}^{-1}$ ) as Nujol mulls between CsI pellets or polyethylene films.  $^1\text{H}$  and  $^{13}\text{C}$  NMR spectra were recorded on a Varian Unity-300 MHz spectrometer, and DNMR studies were carried out on a Varian Unity-500 MHz spectrometer. Chemical shifts are reported in  $\delta$  units,  $\text{CDCl}_3$  or  $\text{C}_6\text{D}_6$  being used as the reference signal. C, H, and N analyses were carried out with a Perkin-Elmer 240C microanalyzer.

**Reaction of  $\text{TaCp}^*\text{Cl}_2\text{Me}_2$  with CNR.** CNR (1.06 mmol) was added under rigorously anhydrous conditions to a solution of  $\text{TaCp}^*\text{Cl}_2\text{Me}_2$  (0.22 g, 0.53 mmol) in toluene (20 mL), and the reaction mixture was stirred for 24 h. The red solution obtained was evaporated to dryness and the residue washed

(13) Sanner, R. D.; Carter, S. T.; Bruton, W., Jr. *J. Organomet. Chem.* **1982**, *240*, 157.

(14) McLain, S. L.; Wood, C. D.; Schrock, R. R. *J. Am. Chem. Soc.* **1979**, *101*, 4558.

(15) Gómez, M.; Jiménez, G.; Royo, P.; Selas, J. M.; Raithby, P. R. *J. Organomet. Chem.* **1992**, *439*, 147.

twice with *n*-hexane (2 × 5 mL) to give microcrystalline red solids identified as **2a** (R = 2,6-Me<sub>2</sub>C<sub>6</sub>H<sub>3</sub>; yield 0.21 g, 78%) or **2b** (R = 2,4,6-Me<sub>3</sub>C<sub>6</sub>H<sub>2</sub>; yield 0.19 g, 70%). Analytical and structural data for **2a,b** are coincidental with those previously reported.<sup>1</sup>

**Reaction of TaCp\*Cl<sub>2</sub>(η<sup>2</sup>-RNCMe<sub>2</sub>) (1a,b) with CNR'.** Toluene solutions (50 mL) of **1a** or **1b** (1.20 mmol) were treated with CNR' (1.20 mmol) under rigorously anhydrous conditions (drybox) and stirred for 24 h. Solutions were concentrated to dryness and the residues extracted with *n*-hexane (3 × 20 mL). Solutions were concentrated to ca. 20 mL and cooled to -40 °C to yield red microcrystalline solids identified<sup>1</sup> as **2a** (yield: 0.44 g, 80%) or **2b** (yield: 0.44 g, 76%).

**Preparation of TaCp\*Cl<sub>3</sub>(η<sup>2</sup>-NR-CMe<sub>2</sub>-CNHR') (R = R' = 2,6-Me<sub>2</sub>C<sub>6</sub>H<sub>3</sub>, **3a**; R = 2,6-Me<sub>2</sub>C<sub>6</sub>H<sub>3</sub>, R' = 2,4,6-Me<sub>3</sub>C<sub>6</sub>H<sub>2</sub>, **3b**). Method A.** In a standard vacuum line, CN(2,6-Me<sub>2</sub>C<sub>6</sub>H<sub>3</sub>) (0.18 g, 1.44 mmol) was added to a toluene (30 mL) solution of TaCp\*Cl<sub>2</sub>Me<sub>2</sub> (0.30 g, 0.72 mmol) under not rigorously dry argon and the reaction mixture stirred for 12 h. The resulting red solution was filtered, the solvent evaporated to dryness, and the residue extracted with *n*-hexane (2 × 25 mL). The solution was cooled to -40 °C to give **3a** as yellow crystals, which were filtered out and dried under vacuum. Yield: 0.05 g (10%). The residual solution containing a mixture of red **2a** as the main product and still a small amount of **3a** was not further worked.

**Method B.** A mixture of equimolar amounts of the amido complex **4a** and isocyanide CNR' in benzene was heated at 90 °C for 1 week in a sealed tube. After the tube was opened, the solution was evaporated to dryness and the residue recrystallized from toluene/hexane to give yellow crystals of **3a** or **3b**. Yield: 90%. The data for **3a** follow. IR (Nujol mull, ν, cm<sup>-1</sup>): 3112 (w), 1628 (m), 1252 (w), 1230 (w), 1198 (w), 1138 (m), 1022 (w), 910 (w), 834 (w), 790 (m), 350 (m), 290 (m). <sup>1</sup>H NMR (δ ppm, in C<sub>6</sub>D<sub>6</sub>): 12.20 (br, 1H, TaCNHR), 6.85 m, 6.51 d (<sup>3</sup>J<sub>H-H</sub> = 7.5 Hz, m-H<sub>3</sub>C<sub>6</sub>Me<sub>2</sub>), 6.85 m, 6.71 t (<sup>3</sup>J<sub>H-H</sub> = 7.5 Hz, p-H<sub>3</sub>C<sub>6</sub>Me<sub>2</sub>), 2.43 s, 2.23 s (2,6-Me<sub>2</sub>C<sub>6</sub>H<sub>3</sub>), 2.00 (s, 15H, C<sub>5</sub>Me<sub>5</sub>), 1.17 (s, 6H, CMe<sub>2</sub>). <sup>13</sup>C NMR (δ ppm, in C<sub>6</sub>D<sub>6</sub>): 261.2 (m, TaCNHR), 145.0 m, 138.4 m (i-C<sub>6</sub>H<sub>3</sub>Me<sub>2</sub>), 140.2 m, 135.5 m (o-C<sub>6</sub>H<sub>3</sub>Me<sub>2</sub>), 129.3 d, 129.2 d (<sup>1</sup>J<sub>C-H</sub> = 158.2 Hz, <sup>1</sup>J<sub>C-H</sub> = 157.9 Hz, m-C<sub>6</sub>H<sub>3</sub>Me<sub>2</sub>), 128.0, 126.2 d (<sup>1</sup>J<sub>C-H</sub> = 159.2 Hz, p-C<sub>6</sub>H<sub>3</sub>Me<sub>2</sub>), 125.7 (m, C<sub>5</sub>Me<sub>5</sub>), 87.4 (spt, <sup>1</sup>J<sub>C-H</sub> = 75 Hz, CMe<sub>2</sub>), 22.1 (qd, <sup>1</sup>J<sub>C-H</sub> = 127.1 Hz, <sup>3</sup>J<sub>C-H</sub> = 4.9 Hz, 2,6-Me<sub>2</sub>C<sub>6</sub>H<sub>3</sub>), 21.9 (qd, <sup>1</sup>J<sub>C-H</sub> = 126.3 Hz, <sup>3</sup>J<sub>C-H</sub> = 5.1 Hz, 2,6-Me<sub>2</sub>C<sub>6</sub>H<sub>3</sub>), 18.7 (qq, <sup>1</sup>J<sub>C-H</sub> = 128.1 Hz, <sup>3</sup>J<sub>C-H</sub> = 4.6 Hz, CMe<sub>2</sub>), 11.7 (q, <sup>1</sup>J<sub>C-H</sub> = 128.2 Hz, C<sub>5</sub>Me<sub>5</sub>). Anal. Calcd for TaCl<sub>3</sub>C<sub>30</sub>H<sub>40</sub>N<sub>2</sub>: C, 50.33; H, 5.63; N, 3.90. Found: C, 50.23; H, 5.68; N, 3.86. The data for **3b** follow. <sup>1</sup>H (δ ppm, in C<sub>6</sub>D<sub>6</sub>): 12.20 (br, 1H, TaCNHR), 6.85 (m, 3H, H<sub>3</sub>C<sub>6</sub>Me<sub>2</sub>), 6.33 (s, 2H, H<sub>2</sub>C<sub>6</sub>Me<sub>3</sub>), 2.44 (s, 6H, 2,4,6-Me<sub>3</sub>C<sub>6</sub>H<sub>2</sub>), 2.23 (s, 6H, 2,6-Me<sub>2</sub>C<sub>6</sub>H<sub>3</sub>), 2.01 (s, 15H, C<sub>5</sub>Me<sub>5</sub>), 1.86 (s, 3H, 2,4,6-Me<sub>3</sub>C<sub>6</sub>H<sub>2</sub>), 1.23 (s, 6H, CMe<sub>2</sub>). <sup>13</sup>C{<sup>1</sup>H} NMR (δ ppm, in C<sub>6</sub>D<sub>6</sub>): 261.2 (s, TaCNHR), 144.7 s, 139.8 s, 129.3 s, 135.6 s (C<sub>i</sub>, C<sub>o</sub>, C<sub>m</sub>, C<sub>p</sub>, C<sub>6</sub>H<sub>3</sub>Me<sub>2</sub>), 138.7 s, 134.8 s, 128.0 s, 125.8 s (C<sub>i</sub>, C<sub>o</sub>, C<sub>m</sub>, C<sub>p</sub>, C<sub>6</sub>H<sub>2</sub>Me<sub>3</sub>), 125.7 (s, C<sub>5</sub>Me<sub>5</sub>), 87.1 (s, CMe<sub>2</sub>), 21.8 (s, 2,6-Me<sub>2</sub>C<sub>6</sub>H<sub>3</sub>), 21.6 (s, 2,4,6-Me<sub>3</sub>C<sub>6</sub>H<sub>2</sub>), 20.7 (s, 2,4,6-Me<sub>3</sub>C<sub>6</sub>H<sub>2</sub>), 18.3 (s, CMe<sub>2</sub>), 11.8 (s, C<sub>5</sub>Me<sub>5</sub>).

**Preparation of TaCp\*ClMe(η<sup>2</sup>-NRCMe<sub>2</sub>) (R = 2,6-Me<sub>2</sub>C<sub>6</sub>H<sub>3</sub>, **5a**).** To a green solution of TaCp\*ClMe<sub>3</sub> (1.06 g, 2.67 mmol) in toluene (50 mL) was added CNR (0.35 g, 2.67 mmol) at room temperature. The color quickly changed to dark red, and after 20 min the solution was evaporated to dryness and the residue extracted with *n*-hexane (3 × 15 mL). The suspension was filtered and the solution concentrated to ca. 20 mL and cooled to -40 °C to give a red microcrystalline solid identified as **5a**. Yield: 0.85 g (60%). The data for **5a** follow. IR (Nujol mull, ν, cm<sup>-1</sup>): 1259 (m), 1229 (m), 1105 (w), 1025 (w), 782 (w), 764 (m), 485 (m), 341 (m). <sup>1</sup>H NMR (δ ppm, in C<sub>6</sub>D<sub>6</sub>): 7.06 (d, 2H, <sup>3</sup>J<sub>H-H</sub> = 7.2 Hz, m-H<sub>3</sub>C<sub>6</sub>Me<sub>2</sub>), 6.94 (t, 1H, <sup>3</sup>J<sub>H-H</sub> = 7.2 Hz, p-H<sub>3</sub>C<sub>6</sub>Me<sub>2</sub>), 2.28 (s, 3H, Me<sub>2</sub>CNR), 2.22 (s, 3H, Me<sub>2</sub>CNR), 2.11 (s, 6H, 2,6-Me<sub>2</sub>C<sub>6</sub>H<sub>3</sub>), 1.66 (s, 15H, C<sub>5</sub>Me<sub>5</sub>), 0.60 (s, 3H, Ta-Me). <sup>13</sup>C NMR (δ ppm, in C<sub>6</sub>D<sub>6</sub>): 151.7 (m, i-C<sub>6</sub>H<sub>3</sub>Me<sub>2</sub>), 133.7 (m, o-C<sub>6</sub>H<sub>3</sub>Me<sub>2</sub>), 128.9 (dm, <sup>1</sup>J<sub>C-H</sub>

= 157.5 Hz, m-C<sub>6</sub>H<sub>3</sub>Me<sub>2</sub>), 124.7 (d, <sup>1</sup>J<sub>C-H</sub> = 159.3 Hz, p-C<sub>6</sub>H<sub>3</sub>Me<sub>2</sub>), 118.6 (m, C<sub>5</sub>Me<sub>5</sub>), 89.3 (m, Me<sub>2</sub>CNR), 52.5 (q, <sup>1</sup>J<sub>C-H</sub> = 120.8 Hz, Ta-Me), 29.8 qq, 27.9 qq (<sup>1</sup>J<sub>C-H</sub> = 124.5 Hz, <sup>3</sup>J<sub>C-H</sub> = 3.7 Hz, Me<sub>2</sub>CNR), 20.7 (qm, <sup>1</sup>J<sub>C-H</sub> = 129.1 Hz, 2,6-Me<sub>2</sub>C<sub>6</sub>H<sub>3</sub>), 10.5 (q, <sup>1</sup>J<sub>C-H</sub> = 128.2 Hz, C<sub>5</sub>Me<sub>5</sub>). Anal. Calcd for TaClC<sub>22</sub>H<sub>33</sub>N: C, 50.05; H, 6.30; N, 2.65. Found: C, 50.15; H, 6.28; N, 2.69.

**Reaction between TaCp\*Me<sub>4</sub> and CNR in Molar Ratio 1:1.** A C<sub>6</sub>D<sub>6</sub> solution of TaCp\*Me<sub>4</sub> (0.10 g, 0.27 mmol) was placed into a NMR tube, and under rigorously anhydrous conditions, CNR (0.035 g, 0.27 mmol) was added and the tube sealed under vacuum. The reaction was monitored by <sup>1</sup>H NMR spectroscopy until no further change was observed. The spectrum showed the presence of a mixture of the three following components: a new complex **6c** as the major product, **5b**, and a small amount of unreacted starting material TaCp\*Me<sub>4</sub>.

**Preparation of TaCp\*X(NR)(NR'CMe=CMe<sub>2</sub>) (X = Cl, R = R' = 2,6-Me<sub>2</sub>C<sub>6</sub>H<sub>3</sub>, **6a**; X = Cl, R = 2,6-Me<sub>2</sub>C<sub>6</sub>H<sub>3</sub>, R' = 2,4,6-Me<sub>3</sub>C<sub>6</sub>H<sub>2</sub>, **6b**; X = Me, R = R' = 2,6-Me<sub>2</sub>C<sub>6</sub>H<sub>3</sub>, **6c**; X = Me, R = 2,6-Me<sub>2</sub>C<sub>6</sub>H<sub>3</sub>, R' = 2,4,6-Me<sub>3</sub>C<sub>6</sub>H<sub>2</sub>, **6d**).** **6a.** To a toluene (60 mL) solution of TaCp\*ClMe<sub>3</sub> (1.07 g, 2.71 mmol) was added CNR (0.71 g, 5.42 mmol). After being stirred at room temperature for 12 h, the resulting solution was evaporated to dryness in vacuo, the resulting yellow residue was extracted with *n*-hexane (2 × 25 mL), and the solution was cooled to -30 °C to afford **6a** (Yield: 0.99 g, 56%). The same compound can also be prepared by addition of 1 equiv of isocyanide to **5a**. The data for **6a** follow. IR (Nujol mull, ν, cm<sup>-1</sup>): 1625 (w), 1575 (w), 1315 (s), 1252 (m), 1189 (m), 1155 (m), 1095 (m), 1022 (m), 937 (m), 875 (m), 805 (m), 765 (m), 350 (m), 335 (m). <sup>1</sup>H NMR (δ ppm, in C<sub>6</sub>D<sub>6</sub>): 6.92 (d, 2H, <sup>3</sup>J<sub>H-H</sub> = 7.5 Hz, m-H<sub>3</sub>C<sub>6</sub>Me<sub>2</sub>, R), 6.7 (m, 3H, H<sub>2</sub>C<sub>6</sub>Me<sub>2</sub>, R'), 6.55 (t, 1H, <sup>3</sup>J<sub>H-H</sub> = 7.5 Hz, p-H<sub>3</sub>C<sub>6</sub>Me<sub>2</sub>, R), 2.61 (s, 3H, 2,6-Me<sub>2</sub>C<sub>6</sub>H<sub>3</sub>, R), 2.27 (s, 6H, 2,6-Me<sub>2</sub>C<sub>6</sub>H<sub>3</sub>, R'), 2.25 (s, 3H, 2,6-Me<sub>2</sub>C<sub>6</sub>H<sub>3</sub>, R), 1.89 (s, 15H, C<sub>5</sub>Me<sub>5</sub>), 1.86 [spt, 3H, <sup>3</sup>J<sub>H-H</sub> = 0.93 Hz, C(Me)=CMe<sub>2</sub>], 1.6 br, 1.3 br [Me<sub>2</sub>C=C(Me)]. <sup>13</sup>C NMR (δ ppm, in C<sub>6</sub>D<sub>6</sub>): 154.5 (m, i-C<sub>6</sub>H<sub>3</sub>Me<sub>2</sub>, R'), 151.3 (m, i-C<sub>6</sub>H<sub>3</sub>Me<sub>2</sub>, R), 135.2 (m, o-C<sub>6</sub>H<sub>3</sub>Me<sub>2</sub>, R), 135.1 m, 132.9 m (o-C<sub>6</sub>H<sub>3</sub>Me<sub>2</sub>, R'), 128.6 d, 127.6 d (<sup>1</sup>J<sub>C-H</sub> = 157.0 Hz, m-C<sub>6</sub>H<sub>3</sub>Me<sub>2</sub>, R'), 126.5 (dm, <sup>1</sup>J<sub>C-H</sub> = 157.5 Hz, m-C<sub>6</sub>H<sub>3</sub>Me<sub>2</sub>, R), 124.2 (d, <sup>1</sup>J<sub>C-H</sub> = 161.2 Hz, p-C<sub>6</sub>H<sub>3</sub>Me<sub>2</sub>, R'), 122.1 (d, <sup>1</sup>J<sub>C-H</sub> = 161.2 Hz, p-C<sub>6</sub>H<sub>3</sub>Me<sub>2</sub>, R), 135.1 [m, C(Me)=CMe<sub>2</sub>], 119.3 (m, C<sub>5</sub>Me<sub>5</sub>), 112.4 [m, C(Me)=CMe<sub>2</sub>], 23.1 [q, <sup>1</sup>J<sub>C-H</sub> = 125.5 Hz, C(Me)=CMe<sub>2</sub>], 22.0 [v br, C(Me)=CMe<sub>2</sub>], 20.3 (qd, <sup>1</sup>J<sub>C-H</sub> = 126.8 Hz, <sup>3</sup>J<sub>C-H</sub> = 4.5 Hz, 2,6-Me<sub>2</sub>C<sub>6</sub>H<sub>3</sub>, R), 20.1 (qd, <sup>1</sup>J<sub>C-H</sub> = 125.9 Hz, <sup>3</sup>J<sub>C-H</sub> = 5.1 Hz, 2,6-Me<sub>2</sub>C<sub>6</sub>H<sub>3</sub>, R'), 19.4 (qd, <sup>1</sup>J<sub>C-H</sub> = 126.4 Hz, <sup>3</sup>J<sub>C-H</sub> = 5.5 Hz, 2,6-Me<sub>2</sub>C<sub>6</sub>H<sub>3</sub>, R), 11.6 (q, <sup>1</sup>J<sub>C-H</sub> = 127.4 Hz, C<sub>5</sub>Me<sub>5</sub>). Anal. Calcd for TaClC<sub>31</sub>H<sub>42</sub>N<sub>2</sub>: C, 56.49; H, 6.42; N, 4.25. Found: C, 56.37; H, 6.40; N, 4.23.

**6b.** C<sub>6</sub>D<sub>6</sub> (0.6 mL) was added to a mixture of complex **5a** (0.13 g, 0.25 mmol) and CN(2,4,6-Me<sub>3</sub>C<sub>6</sub>H<sub>2</sub>) (0.036 g, 0.25 mmol) in a NMR tube. The reaction was monitored by <sup>1</sup>H NMR until complete reaction. Formation of **6b** was confirmed by its <sup>1</sup>H and <sup>13</sup>C NMR spectra and the data follow. <sup>1</sup>H NMR (δ ppm, in CDCl<sub>3</sub>): 6.76 (d, 2H, <sup>3</sup>J<sub>H-H</sub> = 7.5 Hz, m-H<sub>3</sub>C<sub>6</sub>Me<sub>2</sub>, R), 6.61 d, 6.58 d (<sup>4</sup>J<sub>H-H</sub> = 1.9 Hz, m-H<sub>2</sub>C<sub>6</sub>Me<sub>3</sub>, R'), 6.50 (t, 1H, <sup>3</sup>J<sub>H-H</sub> = 7.5 Hz, p-H<sub>3</sub>C<sub>6</sub>Me<sub>2</sub>, R), 2.31 s, 2.25 s (2,4,6-Me<sub>3</sub>C<sub>6</sub>H<sub>2</sub>, R'), 2.12 (s, 3H, 2,4,6-Me<sub>3</sub>C<sub>6</sub>H<sub>2</sub>), 2.09 (s, 15H, C<sub>5</sub>Me<sub>5</sub>), 2.05 (s, 6H, 2,6-Me<sub>2</sub>C<sub>6</sub>H<sub>3</sub>, R), 1.86 [spt, 3H, <sup>3</sup>J<sub>H-H</sub> = 0.87 Hz, C(Me)=CMe<sub>2</sub>], 1.7 vbr, 1.3 vbr [C(Me)=CMe<sub>2</sub>]. <sup>13</sup>C NMR (δ ppm, in CDCl<sub>3</sub>): 151.8 (m, i-C<sub>6</sub>H<sub>2</sub>Me<sub>3</sub>, R'), 151.4 (m, i-C<sub>6</sub>H<sub>3</sub>Me<sub>2</sub>, R), 135.3 [m, C(Me)=CMe<sub>2</sub>], 135.1 (m, o-C<sub>6</sub>H<sub>3</sub>Me<sub>2</sub>, R), 134.6 (t, <sup>2</sup>J<sub>C-H</sub> = 5.5 Hz, p-C<sub>6</sub>H<sub>2</sub>Me<sub>3</sub>, R'), 133.4 m, 132.5 m (o-C<sub>6</sub>H<sub>2</sub>Me<sub>3</sub>, R'), 129.2 (dm, <sup>1</sup>J<sub>C-H</sub> = 153.9 Hz, m-C<sub>6</sub>H<sub>2</sub>Me<sub>3</sub>, R'), 128.1 (dm, <sup>1</sup>J<sub>C-H</sub> = 154.4 Hz, m-C<sub>6</sub>H<sub>2</sub>Me<sub>3</sub>, R'), 126.4 (dm, <sup>1</sup>J<sub>C-H</sub> = 157.2 Hz, m-C<sub>6</sub>H<sub>3</sub>Me<sub>2</sub>, R), 122.0 (d, <sup>1</sup>J<sub>C-H</sub> = 160.3 Hz, p-C<sub>6</sub>H<sub>3</sub>Me<sub>2</sub>, R), 119.1 (m, C<sub>5</sub>Me<sub>5</sub>), 112.6 [m, C(Me)=CMe<sub>2</sub>], 22.8 [q, <sup>1</sup>J<sub>C-H</sub> = 125.5 Hz, C(Me)=CMe<sub>2</sub>], 22.0 [vbr, C(Me)=CMe<sub>2</sub>], 20.5 (qt, <sup>1</sup>J<sub>C-H</sub> = 125.9 Hz, <sup>3</sup>J<sub>C-H</sub> = 4.6 Hz, 2,4,6-Me<sub>3</sub>C<sub>6</sub>H<sub>2</sub>, R'), 20.2 (qd, <sup>1</sup>J<sub>C-H</sub> = 126.9 Hz, <sup>3</sup>J<sub>C-H</sub> = 5.5 Hz, 2,4,6-Me<sub>3</sub>C<sub>6</sub>H<sub>2</sub>, R'), 20.0 (qd, <sup>1</sup>J<sub>C-H</sub> = 125.9 Hz, <sup>3</sup>J<sub>C-H</sub> = 5.05 Hz, 2,4,6-

$\text{Me}_3\text{C}_6\text{H}_2$ , R'), 19.5 (qd,  $^1J_{\text{C-H}} = 126.8$  Hz,  $^3J_{\text{C-H}} = 5.5$  Hz, 2,6- $\text{Me}_2\text{C}_6\text{H}_3$ , R), 11.6 (q,  $^1J_{\text{C-H}} = 127.7$  Hz,  $\text{C}_5\text{Me}_5$ ).

**6c.** A sample of  $\text{TaCp}^*\text{Me}_4$  (1.769 g, 4.70 mmol) was dissolved in 30 mL of toluene in a Schlenk tube in the glovebox. After the addition of a toluene (10 mL) solution of CNR (1.23 g, 9.40 mmol), the color of the solution changed quickly from green to red. The reaction mixture was stirred for 1 h at room temperature and then evaporated to dryness. The oily residue was extracted with *n*-hexane ( $2 \times 10$  mL) and cooled to  $-40$  °C to give **6c** as yellow crystals. Yield: 2.75 g (92%). The same compound can also be prepared by addition of 1 equiv of isocyanide to **5b**. The data for **6c** follow. IR (Nujol mull,  $\nu$ ,  $\text{cm}^{-1}$ ): 1612 (w), 1585 (w), 1320 (s), 1254 (m), 1192 (m), 1154 (m), 1095 (m), 1025 (m), 939 (m), 879 (m), 800 (m), 763 (m), 383 (m), 338 (m).  $^1\text{H}$  NMR ( $\delta$  ppm, in  $\text{C}_6\text{D}_6$ ): 6.9 (d, 2H,  $^3J_{\text{H-H}} = 7.5$  Hz, **m-H** $_3\text{C}_6\text{Me}_2$ , R), 6.7 (m, **H** $_3\text{C}_6\text{Me}_2$ , R'), 6.6 (t, 1H,  $^3J_{\text{H-H}} = 7.5$  Hz, **p-H** $_3\text{C}_6\text{Me}_2$ , R), 2.48 s, 2.35 s (2,6- $\text{Me}_2\text{C}_6\text{H}_3$ , R'), 2.24 (s, 2,6- $\text{Me}_2\text{C}_6\text{H}_3$ , R), 1.77 (s, 15H,  $\text{C}_5\text{Me}_5$ ), 1.64 [spt, 3H,  $^5J_{\text{H-H}} = 0.95$  Hz, **C(Me)=CMe** $_2$ ], 1.5 [br, 6H, **C(Me)=CMe** $_2$ ], 0.87 (s, 3H, **Ta-Me**).  $^{13}\text{C}$  NMR ( $\delta$  ppm, in  $\text{C}_6\text{D}_6$ ): 153.4 (m, **i-C** $_6\text{H}_3\text{Me}_2$ , R'), 152.7 (m, **i-C** $_6\text{H}_3\text{Me}_2$ , R), 135.7 [m, **C(Me)=CMe** $_2$ ], 133.7 (qd,  $^2J_{\text{C-H}} = ^3J_{\text{C-H}} = 6.5$  Hz, **o-C** $_6\text{H}_3\text{Me}_2$ , R'), 134.6 (qd,  $^2J_{\text{C-H}} = ^3J_{\text{C-H}} = 5.9$  Hz, **o-C** $_6\text{H}_3\text{Me}_2$ , R'), 134.2 (qd,  $^2J_{\text{C-H}} = ^3J_{\text{C-H}} = 5.8$  Hz, **o-C** $_6\text{H}_3\text{Me}_2$ , R), 128.4 (dm,  $^1J_{\text{C-H}} = 157.4$  Hz, **m-C** $_6\text{H}_3\text{Me}_2$ , R'), 127.6 (dm,  $^1J_{\text{C-H}} = 156.6$  Hz, **m-C** $_6\text{H}_3\text{Me}_2$ , R'), 126.4 (dm,  $^1J_{\text{C-H}} = 155.7$  Hz, **m-C** $_6\text{H}_3\text{Me}_2$ , R), 123.3 (d,  $^1J_{\text{C-H}} = 159.3$  Hz, **p-C** $_6\text{H}_3\text{Me}_2$ , R'), 120.6 (d,  $^1J_{\text{C-H}} = 160.3$  Hz, **p-C** $_6\text{H}_3\text{Me}_2$ , R), 116.2 (m,  $\text{C}_5\text{Me}_5$ ), 111.3 [m, **C(Me)=CMe** $_2$ ], 33.4 (q,  $^1J_{\text{C-H}} = 102.9$  Hz, **Ta-Me**), 21.6 [br, **C(Me)=CMe** $_2$ ], 21.4 [q,  $^1J_{\text{C-H}} = 125.2$  Hz, **C(Me)=CMe** $_2$ ], 20.8 (qd,  $^1J_{\text{C-H}} = 125.8$  Hz,  $^3J_{\text{C-H}} = 5.9$  Hz, 2,6- $\text{Me}_2\text{C}_6\text{H}_3$ , R'), 20.4 (qd,  $^1J_{\text{C-H}} = 128.1$  Hz,  $^3J_{\text{C-H}} = 5.2$  Hz, 2,6- $\text{Me}_2\text{C}_6\text{H}_3$ , R'), 19.4 (qd,  $^1J_{\text{C-H}} = 125.6$  Hz,  $^3J_{\text{C-H}} = 5.25$  Hz, 2,6- $\text{Me}_2\text{C}_6\text{H}_3$ , R), 11.3 (q,  $^1J_{\text{C-H}} = 127.5$  Hz,  $\text{C}_5\text{Me}_5$ ). Anal. Calcd for  $\text{TaC}_{32}\text{H}_{45}\text{N}_2$ : C, 60.18; H, 7.10; N, 4.39. Found: C, 60.38; H, 7.00; N, 4.35.

**6d.** Complex **5b** (0.12 g, 0.236 mmol), CNR' (0.034 g, 0.236 mmol), and  $\text{C}_6\text{D}_6$  (0.6 mL) were placed in a NMR tube. The reaction was instantaneous and checked by NMR confirmed the formation of **6d** in quantitative yield. The data for **6d** follow.  $^1\text{H}$  NMR ( $\delta$  ppm, in  $\text{C}_6\text{D}_6$ ): 6.91 (d, 2H,  $^3J_{\text{H-H}} = 7.5$  Hz, **m-H** $_3\text{C}_6\text{Me}_2$ , R), 6.68 d, 6.57 d ( $^4J_{\text{H-H}} = 2$  Hz, **m-H** $_2\text{C}_6\text{Me}_3$ , R'), 6.21 (t, 1H,  $^3J_{\text{H-H}} = 7.5$  Hz, **p-H** $_3\text{C}_6\text{Me}_2$ , R), 2.46 s, 2.33 s (2,4,6- $\text{Me}_3\text{C}_6\text{H}_2$ , R'), 2.25 (s, 6H, 2,6- $\text{Me}_2\text{C}_6\text{H}_3$ , R), 2.06 (s, 3H, 2,4,6- $\text{Me}_3\text{C}_6\text{H}_2$ , R'), 1.78 (s, 15H,  $\text{C}_5\text{Me}_5$ ), 1.66 [spt, 3H,  $^5J_{\text{H-H}} = 1.2$  Hz, **C(Me)=CMe** $_2$ ], 1.5 [vbr, 6H, **C(Me)=CMe** $_2$ ], 0.86 (s, 3H, **Ta-Me**).  $^{13}\text{C}\{^1\text{H}\}$  NMR ( $\delta$  ppm, in  $\text{C}_6\text{D}_6$ ): 152.7 (s, **i-C** $_6\text{H}_2\text{Me}_3$ , R'), 150.8 (s, **i-C** $_6\text{H}_3\text{Me}_2$ , R), 135.5 [s, **C(Me)=CMe** $_2$ ], 133.7 (s, **o-C** $_6\text{H}_3\text{Me}_2$ , R), 134.2 s, 132.9 s (**o-C** $_6\text{H}_2\text{Me}_3$ , R'), 132.8 (s, **p-C** $_6\text{H}_2\text{Me}_3$ , R'), 129.3 s, 128.1 s (**m-C** $_6\text{H}_2\text{Me}_3$ , R'), 127.6 (s, **m-C** $_6\text{H}_3\text{Me}_2$ , R), 121.0 (s, **p-C** $_6\text{H}_3\text{Me}_2$ , R), 115.5 (s,  $\text{C}_5\text{Me}_5$ ), 109.6 [s, **C(Me)=CMe** $_2$ ], 32.2 (s, **Ta-Me**), 21.43 [s, **C(Me)=CMe** $_2$ ], 21.0 [br, **C(Me)=CMe** $_2$ ], 20.1 s, 20.0 s (2,4,6- $\text{Me}_3\text{C}_6\text{H}_2$ , R'), 19.8 (s, 2,4,6- $\text{Me}_3\text{C}_6\text{H}_2$ , R'), 19.3 (s, 2,6- $\text{Me}_2\text{C}_6\text{H}_3$ , R), 11.2 (s,  $\text{C}_5\text{Me}_5$ ).

**Preparation of  $\text{TaCp}^*\text{X}(\text{NR})\{\eta^2\text{-N}(\text{R}')\text{=CCMe}_2\text{-CMe=NR}'\}$  (**X = Cl, R = R' = 2,6-Me<sub>2</sub>C<sub>6</sub>H<sub>3</sub>, 7a**; **X = Me, R = R' = 2,6-Me<sub>2</sub>C<sub>6</sub>H<sub>3</sub>, 7b**; **X = Me, R = R' = 2,6-Me<sub>2</sub>C<sub>6</sub>H<sub>3</sub>, R'' = 2,4,6-Me<sub>3</sub>C<sub>6</sub>H<sub>2</sub>, 7c**; **X = Me, R = R' = 2,6-Me<sub>2</sub>C<sub>6</sub>H<sub>3</sub>, R'' = Bu<sup>t</sup>, 7d**). **7a.** CNR'' (0.09 g, 0.69 mmol) was added to a solution of **6a** (0.45 g, 0.69 mmol) in toluene (30 mL) and the reaction mixture heated for 3 days at 60 °C. The resulting yellow-green solution was evaporated to dryness. The residue was extracted with *n*-hexane ( $3 \times 15$  mL) and the solution filtered, concentrated to ca. 15 mL, and cooled to  $-40$  °C to give **7a** as yellow crystals. Yield: 0.46 g (85%). The data for **7a** follow. IR (Nujol mull,  $\nu$ ,  $\text{cm}^{-1}$ ): 1655 (s), 1600 (s), 1326 (s), 1209 (m), 1165 (m), 1122 (m), 1080 (m), 1020 (m), 978 (m), 746 (m), 343 (m), 339 (m).  $^1\text{H}$  NMR ( $\delta$  ppm, in  $\text{C}_6\text{D}_6$ ): 6.8 (m, 9H, **H** $_3\text{C}_6\text{Me}_2$ , R, R'), 2.68 s, 2.44 s, 2.02 s, 2.00 s, 1.59 s, 1.45 s (2,6- $\text{Me}_2\text{C}_6\text{H}_3$ , R, R'), 1.99 (s, 15H,  $\text{C}_5\text{Me}_5$ ), 1.79 (s, 3H, **NCCMe<sub>2</sub>CMeN**), 1.68 (s, 3H, **NCCMe<sub>2</sub>CMeN**), 1.35 (s, 3H, **NCCMe<sub>2</sub>CMeN**).  $^{13}\text{C}\{^1\text{H}\}$  NMR ( $\delta$  ppm, in  $\text{C}_6\text{D}_6$ ): 240.0**

**Table 5. Experimental Data for the X-ray Diffraction Studies**

	<b>3a</b>	<b>6c</b>	<b>7b</b>
mol formula	$\text{C}_{30}\text{H}_{40}\text{Cl}_3\text{N}_2\text{Ta}$	$\text{C}_{32}\text{N}_{45}\text{N}_2\text{Ta}$	$\text{C}_{41}\text{H}_{54}\text{N}_3\text{Ta}$
mol wt	715.97	638.67	769.85
cryst system	monoclinic	monoclinic	orthorhombic
space group	$P2_1/n$	$P2_1/c$	$P2_12_12_1$
radiatn (Mo K $\alpha$ )	graphite-monochromated ( $\lambda = 0.71073$ Å)		
<i>a</i> , Å	8.774(4)	8.635(4)	11.622(3)
<i>b</i> , Å	18.338(8)	34.156(9)	14.141(5)
<i>c</i> , Å	18.470(7)	10.090(4)	22.755(9)
$\beta$ , deg	91.62(2)	105.94(2)	
<i>V</i> , Å <sup>3</sup>	2971(2)	2861(2)	3740(2)
<i>Z</i>	4	4	4
<i>D</i> <sub>calcd</sub> , g cm <sup>-3</sup>	1.601	1.482	1.367
<i>F</i> (000)	1432	1296	1576
cryst dimens, mm	0.25 × 0.30 × 0.35	0.27 × 0.32 × 0.40	0.23 × 0.27 × 0.30
$\mu$ (Mo K $\alpha$ ), cm <sup>-1</sup>	39.92	38.63	29.70
diffractometer	Siemens AED	Phillips PW 1100	Siemens AED
$2\theta$ range, deg	6–60	6–54	6–60
reflens measd	$\pm h, k, l$	$\pm h, k, l$	$\pm h, k, l$
no. of unique tot. data	8712	6223	5994
no. of unique obsd data	6620	3442	3667
	[ <i>I</i> > 2 $\sigma$ ( <i>I</i> )]	[ <i>I</i> > 2 $\sigma$ ( <i>I</i> )]	[ <i>I</i> > 2 $\sigma$ ( <i>I</i> )]
<i>R</i>	0.0271	0.0272	0.0450
<i>R</i> <sub>w</sub>	0.0394	0.0336	0.0419
goodness of fit	0.96	1.06	1.02

(s, **NCCMe<sub>2</sub>CMeN**), 171.0 (s, **NCCMe<sub>2</sub>CMeN**), 150.8 s, 149.8 s, 141.7 s (**i-C** $_6\text{H}_3\text{Me}_2$ , R, R'), 136.1 s, 130.5 s, 128.9 s, 128.3 s, 128.2 s, 125.7 s (**o-C** $_6\text{H}_3\text{Me}_2$ , R, R'), 128.0 s, 127.9 s, 127.5 s, 127.2 s, 126.7 s, 126.4 s (**m-C** $_6\text{H}_3\text{Me}_2$ , R, R'), 126.2 s, 122.9 s, 120.6 s (**p-C** $_6\text{H}_3\text{Me}_2$ , R, R'), 116.8 (s,  $\text{C}_5\text{Me}_5$ ), 55.5 (s, **NCCMe<sub>2</sub>CMeN**), 26.2 s, 26.0 s (**NCCMe<sub>2</sub>CMeN**), 20.7 (s, **NCCMe<sub>2</sub>CMeN**), 20.1 s, 19.4 s, 19.3 s, 19.0 s, 18.1 s, 17.6 s (2,6- $\text{Me}_2\text{C}_6\text{H}_3$ , R, R'), 11.9 (s,  $\text{C}_5\text{Me}_5$ ). Anal. Calcd for  $\text{TaClC}_{40}\text{H}_{51}\text{N}_3$ : C, 60.78; H, 6.51; N, 5.31. Found: C, 60.92; H, 6.25; N, 5.25.

**7b.** CNR'' (0.11 g, 0.83 mmol) was added to a solution of **6c** (0.53 g, 0.83 mmol) in toluene (30 mL). The reaction mixture was heated for 2 days at 50–60 °C. The resulting yellow-green solution was evaporated to dryness. Recrystallization from *n*-hexane at  $-40$  °C afforded **7b** as yellow crystals in 92% yield (0.59 g). The data for **7b** follow. IR (Nujol mull,  $\nu$ ,  $\text{cm}^{-1}$ ): 1652 (s), 1599 (s), 1325 (s), 1210 (m), 1153 (m), 1123 (m), 1090 (m), 1019 (m), 976 (m), 759 (m), 515 (w), 487 (m), 343 (m).  $^1\text{H}$  NMR ( $\delta$  ppm, in  $\text{C}_6\text{D}_6$ ): 6.9 (m, **H** $_3\text{C}_6\text{Me}_2$ , R, R'), 2.52 s, 2.44 s, 2.08 s, 1.93 s, 1.72 s, 1.68 s (2,6- $\text{Me}_2\text{C}_6\text{H}_3$ , R, R'), 1.89 (s, 15H,  $\text{C}_5\text{Me}_5$ ), 1.66 (s, 3H, **NCCMe<sub>2</sub>CMeN**), 1.52 (s, 3H, **NCCMe<sub>2</sub>CMeN**), 1.31 (s, 3H, **NCCMe<sub>2</sub>CMeN**), 0.43 (s, 3H, **Ta-Me**).  $^{13}\text{C}$  NMR ( $\delta$  ppm, in  $\text{C}_6\text{D}_6$ ): 241.2 (s, **NCCMe<sub>2</sub>CMeN**), 171.9 (q,  $^2J_{\text{C-H}} = 2.8$  Hz, **NCCMe<sub>2</sub>CMeN**), 154.3 m, 147.1 m, 142.0 m (**i-C** $_6\text{H}_3\text{Me}_2$ , R, R'), 134.2 qd, 130.0 qd, 130.0 qd, 129.0 qd, 127.8 qd, 126.3 qd ( $^2J_{\text{C-H}} = ^3J_{\text{C-H}} = 7.0$  Hz, **o-C** $_6\text{H}_3\text{Me}_2$ , R, R'), 128.6 dd, 128.0 dd, 127.9 dd, 127.6 dd, 126.8 dd, 126.4 dd ( $^1J_{\text{C-H}} = 158.2$  Hz,  $^3J_{\text{C-H}} = 5$  Hz, **m-C** $_6\text{H}_3\text{Me}_2$ , R, R'), 125.6 d, 122.7 d, 118.9 d ( $^1J_{\text{C-H}} = 157.8$  Hz, **p-C** $_6\text{H}_3\text{Me}_2$ , R, R'), 113.4 (m,  $\text{C}_5\text{Me}_5$ ), 57.4 (spt,  $^2J_{\text{C-H}} = 3.4$  Hz, **NCCMe<sub>2</sub>CMeN**), 25.8 qq, 25.5 qq ( $^1J_{\text{C-H}} = 128.3$  Hz,  $^2J_{\text{C-H}} = 4.6$  Hz, **NCCMe<sub>2</sub>CMeN**), 21.6 (q,  $^1J_{\text{C-H}} = 118.1$  Hz, **Ta-Me**), 20.3 (q,  $^1J_{\text{C-H}} = 127.4$  Hz, **NCCMe<sub>2</sub>CMeN**), 20.1 qd, 19.5 qd, 19.0 qd, 18.8 qd, 18.1 qd, 17.7 qd ( $^1J_{\text{C-H}} = 126.4$  Hz,  $^3J_{\text{C-H}} = 4.5$  Hz, 2,6- $\text{Me}_2\text{C}_6\text{H}_3$ , R, R'), 11.5 (q,  $^1J_{\text{C-H}} = 125.9$  Hz,  $\text{C}_5\text{Me}_5$ ). Anal. Calcd for  $\text{TaC}_{41}\text{H}_{54}\text{N}_3$ : C, 63.97; H, 7.07; N, 5.46. Found: C, 63.66; H, 6.99; N, 5.43.

**7c.** To a solution of **6c** (0.13 g, 0.20 mmol) in  $\text{C}_6\text{D}_6$  (0.6 mL) was added CNR'' (0.03 g, 0.20 mmol) at room temperature in a NMR tube. The reaction mixture was heated to 50 °C during 3 days and then was checked by  $^1\text{H}$  NMR showing **7c** as the unique product. The data for **7c** follow.  $^1\text{H}$  NMR ( $\delta$  ppm, in  $\text{C}_6\text{D}_6$ ): 6.8 (m, **H** $_3\text{C}_6\text{Me}_2$ , R, R'; **H** $_2\text{C}_6\text{Me}_3$ , R''), 2.54 s, 2.45 s,

**Table 6. Atomic Coordinates ( $\times 10^4$ ) and Isotropic Thermal Parameters ( $\text{\AA}^2 \times 10^4$ ) with Esd's in Parentheses for the Non-Hydrogen Atoms of Compound 3a**

atom	<i>x/a</i>	<i>y/b</i>	<i>z/c</i>	<i>U<sup>a</sup></i>
Ta	1997(1)	2871(1)	5251(1)	250(1)
Cl(1)	-222(1)	2233(1)	5721(1)	422(3)
Cl(2)	2207(1)	3194(1)	6579(1)	423(3)
Cl(3)	4734(1)	3129(1)	5362(1)	416(3)
N(1)	2330(3)	2050(2)	4536(2)	297(7)
N(2)	3410(3)	1668(2)	6341(2)	325(8)
C(1)	1700(5)	4210(2)	5176(2)	404(11)
C(2)	233(4)	3923(2)	5248(2)	383(10)
C(3)	-158(4)	3524(2)	4604(2)	378(10)
C(4)	1081(4)	3588(2)	4130(2)	398(10)
C(5)	2230(4)	3995(2)	4481(2)	446(12)
C(6)	2524(8)	4720(3)	5689(4)	759(20)
C(7)	-851(6)	4061(3)	5855(3)	626(17)
C(8)	-1710(5)	3220(3)	4407(4)	706(20)
C(9)	989(7)	3449(3)	3334(2)	690(19)
C(10)	3638(6)	4290(3)	4141(4)	832(23)
C(11)	3002(4)	1433(2)	5000(2)	341(9)
C(12)	2977(4)	1859(2)	5696(2)	299(8)
C(13)	4605(5)	1220(3)	4772(2)	488(12)
C(14)	2003(6)	749(2)	5010(3)	534(14)
C(15)	2113(4)	1898(2)	3776(2)	352(9)
C(16)	3284(5)	2088(2)	3290(2)	422(11)
C(17)	3028(7)	1981(3)	2543(2)	558(15)
C(18)	1674(7)	1678(3)	2285(2)	682(19)
C(19)	570(6)	1496(3)	2760(3)	596(16)
C(20)	750(5)	1596(2)	3503(2)	460(12)
C(21)	4771(5)	2437(3)	3521(2)	542(14)
C(22)	-579(5)	1396(3)	3964(3)	587(15)
C(23)	3946(4)	965(2)	6611(2)	354(10)
C(24)	5499(5)	805(2)	6602(2)	417(11)
C(25)	5948(6)	127(3)	6883(2)	582(15)
C(26)	4901(7)	-339(3)	7176(3)	642(18)
C(27)	3389(7)	-144(2)	7208(3)	578(16)
C(28)	2880(5)	515(2)	6928(2)	455(12)
C(29)	6680(5)	1339(3)	6352(3)	593(16)
C(30)	1212(6)	713(3)	6979(3)	730(20)

<sup>a</sup> Equivalent isotropic *U* defined as one-third of the trace of the orthogonalized  $U_{ij}$  tensor.

2.10 s, 2.06 s, 1.92 s, 1.75 s, 1.69 s (2,6- $\text{Me}_2\text{C}_6\text{H}_3$ , R, R'); 2,4,6- $\text{Me}_3\text{C}_6\text{H}_2$ , R'), 1.92 (s, 15H,  $\text{C}_5\text{Me}_5$ ), 1.67 (s, 3H,  $\text{NCCMe}_2\text{CMeN}$ ), 1.52 (s, 3H,  $\text{NCCMe}_2\text{CMeN}$ ), 1.37 (s, 3H,  $\text{NC-CMe}_2\text{CMeN}$ ), 0.46 (s, Ta-Me). <sup>13</sup>C NMR ( $\delta$  ppm, in  $\text{C}_6\text{D}_6$ ): 242.1 (s,  $\text{NCCMe}_2\text{CMeN}$ ), 172.0 (q,  $^2J_{\text{C-H}} = 2.8$  Hz,  $\text{NC-CMe}_2\text{CMeN}$ ), 154.4 m, 147.2 m, 139.2 m (i- $\text{C}_6\text{H}_3\text{Me}_2$ , R, R'; i- $\text{C}_6\text{H}_2\text{Me}_3$ , R'), 135.1 m, 134.2 m, 129.8 m, 126.8 m, 126.3 m, 125.6 m (o- $\text{C}_6\text{H}_3\text{Me}_2$ , R, R'; o- $\text{C}_6\text{H}_2\text{Me}_3$ , R'), 129.4 dm, 128.4 dm, 128.0 dm, 127.9 dm, 127.6 dm, 126.4 dm ( $^1J_{\text{C-H}} = 158.2$  Hz, m- $\text{C}_6\text{H}_3\text{Me}_2$ , R, R'; m- $\text{C}_6\text{H}_2\text{Me}_3$ , R'), 122.7 d, 118.9 d, 116.2 m ( $^1J_{\text{C-H}} = 158.9$  Hz, p- $\text{C}_6\text{H}_3\text{Me}_2$ , R, R'; p- $\text{C}_6\text{H}_2\text{Me}_3$ , R'), 113.4 (m,  $\text{C}_5\text{Me}_5$ ), 54.6 (m,  $\text{NCCMe}_2\text{CMeN}$ ), 25.8 qq, 25.6 qq ( $^1J_{\text{C-H}} = 129.1$  Hz,  $^3J_{\text{C-H}} = 4.6$  Hz,  $\text{NCCMe}_2\text{CMeN}$ ), 21.7 (q,  $^1J_{\text{C-H}} = 119.5$  Hz, Ta-Me), 20.2 (q,  $^1J_{\text{C-H}} = 127.1$  Hz,  $\text{NCCMe}_2\text{CMeN}$ ), 20.7 qt, 19.4 qd, 18.9 qd, 18.8 qd, 18.7 qd, 18.1 qd, 17.6 qd ( $^1J_{\text{C-H}} = 127.3$  Hz,  $^3J_{\text{C-H}} = 4.8$  Hz, 2,6- $\text{Me}_2\text{C}_6\text{H}_3$ , R, R'; 2,4,6- $\text{Me}_3\text{C}_6\text{H}_2$ , R'), 11.5 (q,  $^1J_{\text{C-H}} = 127.3$  Hz,  $\text{C}_5\text{Me}_5$ ).

**7d.** A sample of **6c** (0.56 g, 0.87 mmol) was added at room temperature to a solution of  $\text{CN}^t\text{Bu}$  (0.1 mL, 0.88 mmol) in toluene (50 mL). The reaction mixture was heated at 60 °C for 2 days, the resulting solution was concentrated to dryness, and the residue was extracted with *n*-hexane (3  $\times$  10 mL). The solution was filtered, concentrated to ca. 15 mL, and cooled to -40 °C to give **7d** as a yellow microcrystalline solid. Yield: 0.51 g (81%). The data for **7d** follow. IR (Nujol mull,  $\nu$ ,  $\text{cm}^{-1}$ ): 1639 (s), 1606 (m), 1591 (m), 1326 (s), 1208 (m), 1190 (m), 1113 (m), 1096 (m), 1023 (m), 954 (m), 765 (s), 503 (w), 473 (m), 341 (m). <sup>1</sup>H NMR ( $\delta$  ppm, in  $\text{C}_6\text{D}_6$ ): 7.0 (d,  $^3J_{\text{H-H}} = 7.5$  Hz, 2H, m- $\text{H}_3\text{C}_6\text{Me}_2$ , R), 6.93 (m, 2H, m- $\text{H}_3\text{C}_6\text{Me}_2$ , R'), 6.93 (m, 1H, p- $\text{H}_3\text{C}_6\text{Me}_2$ , R), 6.68 (t,  $^3J_{\text{H-H}} = 7.5$  Hz, 1H, p- $\text{H}_3\text{C}_6\text{Me}_2$ , R), 2.54 s, 2.03 s, 1.95 s (2,6- $\text{Me}_2\text{C}_6\text{H}_3$ , R, R'), 1.88 (s, 15H,

**Table 7. Atomic Coordinates ( $\times 10^4$ ) and Isotropic Thermal Parameters ( $\text{\AA}^2 \times 10^4$ ) with Esd's in Parentheses for the Non-Hydrogen Atoms of Compound 6c**

atom	<i>x/a</i>	<i>y/b</i>	<i>z/c</i>	<i>U<sup>a</sup></i>
Ta	2163(1)	1118(1)	1022(1)	266(1)
N(1)	3721(6)	855(1)	2219(5)	310(17)
N(2)	1769(5)	1551(1)	2295(4)	259(16)
C(1)	3440(8)	885(2)	-743(6)	470(27)
C(2)	3550(8)	1299(2)	-638(6)	422(25)
C(3)	1991(10)	1456(2)	-1225(7)	459(27)
C(4)	907(7)	1144(2)	-1593(6)	444(23)
C(5)	1805(8)	792(2)	-1261(7)	469(27)
C(6)	4845(9)	607(3)	-402(8)	755(38)
C(7)	5092(9)	1533(3)	-290(7)	708(37)
C(8)	1666(13)	1876(3)	-1620(8)	844(43)
C(9)	-850(9)	1163(3)	-2347(8)	780(37)
C(10)	1172(11)	382(2)	-1616(9)	790(39)
C(11)	4995(7)	620(2)	2902(6)	328(21)
C(12)	6553(7)	772(2)	3485(6)	374(22)
C(13)	7769(8)	525(2)	4162(6)	465(25)
C(14)	7518(9)	131(3)	4299(7)	593(32)
C(15)	5999(9)	-21(2)	3754(7)	522(29)
C(16)	4743(8)	215(2)	3057(6)	403(24)
C(17)	6884(8)	1200(2)	3348(8)	547(30)
C(18)	3089(8)	39(2)	2468(8)	535(29)
C(19)	3041(7)	1635(2)	3542(5)	292(19)
C(20)	3985(7)	1974(2)	3572(6)	381(23)
C(21)	5175(8)	2058(2)	4765(7)	510(27)
C(22)	5457(9)	1821(2)	5887(8)	613(31)
C(23)	4536(9)	1491(2)	5858(7)	549(29)
C(24)	3294(8)	1395(2)	4700(6)	395(24)
C(25)	3712(8)	2240(2)	2331(7)	509(28)
C(26)	2195(9)	1049(2)	4727(7)	534(29)
C(27)	363(7)	1793(2)	2049(6)	316(21)
C(28)	-152(7)	2010(2)	2967(7)	398(23)
C(29)	-618(8)	1787(2)	562(7)	581(30)
C(30)	-1651(8)	2255(2)	2493(8)	628(32)
C(31)	547(9)	2039(2)	4512(7)	618(32)
C(32)	68(8)	762(2)	1028(7)	485(27)

<sup>a</sup> Equivalent isotropic *U* defined as one-third of the trace of the orthogonalized  $U_{ij}$  tensor.

$\text{C}_5\text{Me}_5$ ), 1.75 (s, 3H,  $\text{NCCMe}_2\text{CMeN}$ ), 1.69 (s, 3H,  $\text{NCCMe}_2\text{CMeN}$ ), 1.25 (s, 9H,  $\text{Me}_3\text{C}$ , R'), 1.21 (s, 3H,  $\text{NCCMe}_2\text{CMeN}$ ), 0.88 (s, 3H, Ta-Me). <sup>13</sup>C NMR ( $\delta$  ppm, in  $\text{C}_6\text{D}_6$ ): 248.5 (s,  $\text{NCCMe}_2\text{CMeN}$ ), 174.7 (q,  $^2J_{\text{C-H}} = 2.6$  Hz,  $\text{NCCMe}_2\text{CMeN}$ ), 155.4 m, 147.5 m (i- $\text{C}_6\text{H}_3\text{Me}_2$ , R, R'), 132.2 m, 132.2 m, 126.2 m, 125.7 m (o- $\text{C}_6\text{H}_3\text{Me}_2$ , R, R'), 128.3 dm, 128.3 dm, 126.9 dm, 126.9 dm ( $^1J_{\text{C-H}} = 155.5$  Hz, m- $\text{C}_6\text{H}_3\text{Me}_2$ , R, R'), 122.8 d, 118.9 d ( $^1J_{\text{C-H}} = 159.2$  Hz, p- $\text{C}_6\text{H}_3\text{Me}_2$ , R, R'), 113.8 (m,  $\text{C}_5\text{Me}_5$ ), 63.3 (m,  $^2J_{\text{C-H}} = 3.7$  Hz,  $\text{CMe}_3$ , R'), 52.7 (m,  $\text{NCCMe}_2\text{CMeN}$ ), 33.7 qq, 24.8 qq ( $^1J_{\text{C-H}} = 128.7$  Hz,  $^2J_{\text{C-H}} = 5.05$  Hz,  $\text{NCCMe}_2\text{CMeN}$ ), 30.9 (qspt,  $^1J_{\text{C-H}} = 126.9$  Hz,  $^3J_{\text{C-H}} = 4.1$  Hz,  $\text{Me}_3\text{C}$ , R'), 19.6 (q,  $^1J_{\text{C-H}} = 127.8$  Hz,  $\text{NCCMe}_2\text{CMeN}$ ), 19.5 (q,  $^1J_{\text{C-H}} = 119.5$  Hz, Ta-Me), 20.2 qd, 20.2 qd, 19.6 qd, 18.5 qd ( $^1J_{\text{C-H}} = 126.2$  Hz,  $^3J_{\text{C-H}} = 5$  Hz, 2,6- $\text{Me}_2\text{C}_6\text{H}_3$ , R, R'), 11.8 (q,  $^1J_{\text{C-H}} = 126.4$  Hz,  $\text{C}_5\text{Me}_5$ ). Anal. Calcd for  $\text{TaC}_37\text{H}_{54}\text{N}_3$ : C, 61.57; H, 7.54; N, 5.82. Found: C, 61.59; H, 7.53; N, 5.80.

**X-ray Data Collection, Structure Determination, and Refinement for Compounds 3a, 6c, and 7b.** The crystallographic data for the three compounds are summarized in Table 5. Data were collected at room temperature (22 °C) on a Siemens AED diffractometer (**3a** and **7b**) and on a Phillips PW 1100 (**6c**), using graphite-monochromated Mo K $\alpha$  radiation and the  $\theta/2\theta$  scan type.

The reflections for both compounds were collected with a variable scan speed of 3–12° min<sup>-1</sup> and a scan width (deg) of 1.20 + 0.346 tan  $\theta$ . One standard reflection was monitored every 50 measurements; no significant decay was noticed over the time of data collection. The individual profiles have been analyzed following Lehmann and Larsen.<sup>16</sup> Intensities were

(16) Lehmann, M. S.; Larsen, F. K. *Acta Crystallogr., Sect. A* **1974**, *30*, 580.

**Table 8. Atomic Coordinates ( $\times 10^4$ ) and Isotropic Thermal Parameters ( $\text{\AA}^2 \times 10^4$ ) with Esd's in Parentheses for the Non-Hydrogen Atoms of Compound 7b**

atom	<i>x/a</i>	<i>y/b</i>	<i>z/c</i>	<i>U<sup>a</sup></i>
Ta	631(1)	337(1)	4441(2)	345(1)
N(1)	927(7)	-471(7)	5040(3)	411(29)
N(2)	2213(6)	428(6)	3956(3)	360(25)
N(3)	1507(8)	-2608(6)	3152(4)	445(30)
C(1)	-1210(10)	-5(8)	3975(5)	507(41)
C(2)	-1437(8)	95(6)	4590(5)	399(35)
C(3)	-1192(9)	1022(7)	4747(4)	417(33)
C(4)	-903(10)	1536(8)	4228(5)	532(40)
C(5)	-918(10)	893(9)	3760(5)	530(43)
C(6)	-1493(12)	-867(10)	3615(7)	839(60)
C(7)	-1895(11)	-632(9)	5007(6)	697(52)
C(8)	-1362(11)	1458(9)	5348(5)	646(46)
C(9)	-769(13)	2610(7)	4186(7)	811(54)
C(10)	-799(14)	1134(11)	3113(5)	875(61)
C(11)	1387(11)	1640(8)	4806(5)	533(40)
C(12)	976(7)	-1066(7)	5521(5)	438(31)
C(13)	730(10)	-2050(7)	5463(4)	467(34)
C(14)	851(10)	-2640(10)	5954(6)	620(49)
C(15)	1208(11)	-2272(11)	6487(6)	691(53)
C(16)	1439(11)	-1325(11)	6541(5)	650(52)
C(17)	1317(10)	-725(10)	6074(5)	488(41)
C(18)	273(11)	-2456(8)	4903(5)	590(45)
C(19)	1554(12)	336(11)	6140(5)	795(54)
C(20)	3302(10)	885(8)	3870(5)	471(38)
C(21)	4214(10)	650(9)	4251(6)	642(46)
C(22)	5264(12)	1105(13)	4162(8)	914(68)
C(23)	5410(16)	1722(14)	3716(9)	1121(89)
C(24)	4471(18)	2024(11)	3377(8)	983(70)
C(25)	3427(13)	1580(8)	3456(6)	643(49)
C(26)	4060(11)	-50(8)	4757(6)	680(49)
C(27)	2404(14)	1896(8)	3082(6)	797(61)
C(28)	1661(8)	-283(8)	3735(4)	379(28)
C(29)	2072(10)	-964(7)	3245(5)	422(33)
C(30)	2020(9)	-2006(7)	3473(4)	376(31)
C(31)	1521(10)	-3585(7)	3295(5)	408(35)
C(32)	511(11)	-4010(8)	3473(4)	516(38)
C(33)	457(13)	-4970(8)	3574(5)	625(45)
C(34)	1447(17)	-5525(10)	3483(7)	890(70)
C(35)	2442(14)	-5110(9)	3270(6)	669(52)
C(36)	2486(11)	-4131(9)	3179(6)	574(46)
C(37)	-576(12)	-3446(9)	3541(6)	745(50)
C(38)	3559(12)	-3700(10)	2935(7)	921(67)
C(39)	3353(9)	-813(7)	3048(5)	518(39)
C(40)	1306(11)	-810(8)	2698(5)	576(44)
C(41)	2640(10)	-2210(7)	4038(4)	428(35)

<sup>a</sup> Equivalent isotropic *U* defined as one-third of the trace of the orthogonalized  $U_{ij}$  tensor.

corrected for Lorentz and polarization effects. A correction for absorption was applied (maximum and minimum values for and transmission factors were 1.092 and 0.939 (**3a**), 1.098 and 0.905 (**6c**), and 1.109 and 0.836 (**7b**)).<sup>17</sup> Only the observed reflections were used in the structure solutions and refinements.

(17) Walker, N.; Stuart, D. *Acta Crystallogr., Sect. A* **1983**, *39*, 158. Ugozzoli, F. *Comput. Chem.* **1987**, *11*, 109.

The structures were solved by Patterson and Fourier methods and refined by full-matrix least-squares first with isotropic thermal parameters and then with anisotropic thermal parameters for the non-hydrogen atoms. In order to test the chirality of the complex **7b**, a refinement of the non-hydrogen atoms with anisotropic thermal parameters was carried out using the coordinates  $-x, -y, -z$ ; a remarkable increase of the *R* and *R<sub>w</sub>* values was obtained [ $R(x, y, z) = 0.0508$ ,  $R_w(x, y, z) = 0.0541$ ;  $R(-x, -y, -z) = 0.0600$ ,  $R_w(-x, -y, -z) = 0.0710$ ]. The former model was selected, and the reported data refer to this model. All hydrogen atoms, excepting for HN(2) of **3a**, clearly localized in the final  $\Delta F$  map and refined isotropically, were placed at their geometrically calculated positions (C-H = 0.96 Å) and refined "riding" on the corresponding carbon atoms (with isotropic thermal parameters). The final cycles of refinement were carried out on the basis of 338 (**3a**), 325 (**6c**), and 412 (**7b**) variables; after the last cycles, no parameters shifted by more than 0.81 (**3a**), 0.92 (**6c**), and 0.31 (**7b**) esd. The highest remaining peak in the final difference map was equivalent to about 0.70 (**3a**), 0.69 (**6c**), and 0.66 (**7b**) e/Å<sup>3</sup>. In the final cycles of refinement a weighting scheme  $w = K[\sigma^2(F_o) + gF_o^2]^{-1}$  was used; at convergence the *K* and *g* values were 0.570 and 0.0047 (**3a**), 0.722 and 0.0044 (**6c**), and 1.025 and 0.0002 (**7b**), respectively. The analytical scattering factors, corrected for the real and imaginary parts of anomalous dispersion, were taken from ref 18. All calculations were carried out on the Gould Powernode 6040 and Encore 91 computers of the "Centro di Studio per la Strutturistica Diffraattometrica" del CNR, Parma, Italy, using the SHELX-76 and SHELXS-86 systems of crystallographic computer programs.<sup>19</sup> The final atomic coordinates for the non-hydrogen atoms are given in Table 6 (**3a**), Table 7 (**6c**), and Table 8 (**7b**).

**Acknowledgment.** We are grateful to the DGICYT (Grant PB92-0178-C) and the Consiglio Nazionale delle Ricerche, Rome, for financial support.

**Supplementary Material Available:** Atomic coordinates of the hydrogen atoms (Tables SI (**3a**) SII (**6c**), and SIII (**7b**), thermal parameters (Tables SIV (**3a**), SV (**6c**), and SVI (**7b**), complete bond distances and angles (Tables SVII (**3a**), SVIII (**6c**), and SIX (**7b**), chemical shifts for **6a** and **6c** at variable temperature in solution (**6a**-CDCl<sub>3</sub>, **6c**-CD<sub>2</sub>Cl<sub>2</sub>) and in the solid (Table SX), spin-lattice relaxation times for **6c** in CD<sub>2</sub>-Cl<sub>2</sub> solution (Table SXI), <sup>1</sup>H NMR spectra at variable temperature for complex **6c** in CD<sub>2</sub>Cl<sub>2</sub> solution (Figure SI), and a <sup>13</sup>C{<sup>1</sup>H} NMR spectrum (**6c**) in CD<sub>2</sub>Cl<sub>2</sub> solution (Figure SII) (18 pages). Ordering information is given on any current masthead page.

OM950009N

(18) *International Tables for X-Ray Crystallography*; Kynoch Press: Birmingham, England, 1974; Vol. IV.

(19) Sheldrick G. M. SHELX-76 Program for crystal structure determination, University of Cambridge, England, 1976; SHELXS-86 Program for the solution of crystal structures, University of Göttingen, 1986.



## ((Trityloxy)methyl)boronic Esters

Oliver C. Ho, Raman Soundararajan, Jianhui Lu, Donald S. Matteson,\*  
Zhenming Wang, Xin Chen, Mingyi Wei, and Roger D. Willett\*

Department of Chemistry, Washington State University, Pullman, Washington 99164-4630

Received February 7, 1995<sup>®</sup>

Sodium trityl oxide with 2-(bromomethyl)-4,4,5,5-tetramethyl-1,3,2-dioxaborolane [pinacol (bromomethyl)boronate (**1**)] in dimethyl sulfoxide efficiently yields 4,4,5,5-tetramethyl-2-[(triphenylmethoxy)methyl]-1,3,2-dioxaborolane (**3**), which can be transesterified with chiral diols to form other [(triphenylmethoxy)methyl]-1,3,2-dioxaborolanes. These can undergo chain extension with (dichloromethyl)lithium in the normal manner and are potentially useful synthetic intermediates. The majority of known boronic esters are liquids, but the trityl group confers crystallinity on several examples. Six structures have been determined: 4,4,5,5-tetramethyl-2-[(triphenylmethoxy)methyl]-1,3,2-dioxaborolane (**3**), [*R*-(4 $\alpha$ ,5 $\beta$ )]-4,5-dicyclohexyl-2-[(triphenylmethoxy)methyl]-1,3,2-dioxaborolane (**4**), [*S*-(4 $\alpha$ ,5 $\beta$ )]-4,5-bis(1-methylethyl)-2-[(triphenylmethoxy)methyl]-1,3,2-dioxaborolane (**5**), (*R*)-pinanediol ((trityloxy)methyl)boronate (*ent*-**6**), (*S*)-pinanediol (*S*)-(1-chloro-2-(trityloxy)ethyl)boronate (**7a**), and (*S*)-pinanediol (*S*)-(1-bromo-2-(trityloxy)ethyl)boronate (**7b**). The 1,3,2-dioxaborolane ring is very nearly planar, consistent with strong oxygen–boron  $\pi$ -bonding.

### Introduction

The boronic ester function is known to facilitate nucleophilic displacement of halide at the adjacent carbon.<sup>1</sup> The nucleophile generally attacks the boron atom first to form a borate complex and then displaces the  $\alpha$ -halide in an internal rearrangement, permitting the use of unusual nucleophiles such as Grignard reagents<sup>2</sup> or lithio(hexamethyldisilazane).<sup>3</sup>

Reported nucleophilic displacements by trityl oxide ion at carbon are confined to the reaction of its potassium salt with methyl iodide<sup>4</sup> or sulfate<sup>5</sup> to form trityl methyl ether or with benzyl bromide to form trityl benzyl ether.<sup>5</sup> With ethyl iodide, elimination to ethylene resulted.<sup>4</sup> There is also a report that (trityloxy)(ethyl)zinc reacts with ethylene oxide at both the Zn–O and the Zn–C bonds.<sup>6</sup>

Though originally chosen for potential synthetic utility, several trityloxy-substituted boronic esters have provided crystals suitable for X-ray crystallography. Most known boronic esters are liquids. Crystal structures of simple boronic acids or esters appear to be confined to phenylboronic acid,<sup>7</sup> its mannitol ester,<sup>8</sup> and some of its six-membered cyclic esters.<sup>9</sup> Alkylboron-dioxy compounds are represented by a hybrid boroxin/borazine (CH<sub>3</sub>B)<sub>3</sub>O<sub>2</sub>NAr<sup>10</sup> and a bis(ethylboryl) 2,3-dihydroxyfumarate.<sup>11</sup> In other structures, the boron

atom is tetracoordinate, though the fourth bond may be relatively weak, as in the ethylene glycol ester of (*1R*)-1-acetamido-3-(methylthio)propylboronic acid.<sup>12</sup>

### Results

In exploratory experiments, lithium trityl oxide was prepared in THF from butyllithium and trityl alcohol and treated with pinacol (chloromethyl)boronate,<sup>13</sup> (bromomethyl)boronate (**1**),<sup>14</sup> or (iodomethyl)boronate. Yields of pinacol ((trityloxy)methyl)boronate (**3**) varied, usually between 30% and 60% but occasionally 0% or 90%, with no perceptible relationship to any controlled experimental variables, including the presence or absence of DMSO (1 equiv), the radical initiator azobis(isobutyronitrile), the photosensitizer benzophenone, the use of DME in place of THF, or reaction temperatures between 0 °C and reflux.

Consistent high yields of pinacol ((trityloxy)methyl)boronate (**3**) were obtained when sodium trityl oxide in DMSO, easily prepared from trityl alcohol and sodium hydride, was treated with pinacol (bromomethyl)boronate (**1**). The reaction is complete at room temperature overnight. Conventional aqueous workup yielded solid **3** with ~10% of unchanged trityl alcohol as the major

(9) (a) Shimanouchi, H.; Saito, N.; Sasada, Y. *Bull. Chem. Soc. Jpn.* **1969**, *42*, 1239–1247. (b) Cox, P. J.; Cradwick, C. D.; Sim, G. A. *J. Chem. Soc., Perkin Trans. 2* **1976**, 110–113. (c) Kliegel, W.; Preu, L.; Rettig, S. J.; Trotter, J. *Can. J. Chem.* **1985**, *63*, 509–515. (d) Kliegel, W.; Preu, L.; Rettig, S. J.; Trotter, J. *Can. J. Chem.* **1986**, *64*, 1855–1858.

(10) Wang, A. H.-J.; Paul, I. C. *J. Am. Chem. Soc.* **1976**, *98*, 4612–4619.

(11) Meller, A.; Habben, C.; Noltemeyer, M.; Sheldrick, G. M. *Z. Naturforsch., Teil B* **1982**, *37*, 1504–1506.

(12) Matteson, D. S.; Michnick, T. J.; Willett, R. D.; Patterson, C. *D. Organometallics* **1989**, *8*, 726–729.

(13) Sadhu, K. M.; Matteson, D. S. *Organometallics* **1985**, *4*, 1687–1689.

(14) (a) Michnick, T. J.; Matteson, D. S. *Synlett* **1991**, 631–632. (b) *Chemical Abstracts* name: 2-(bromomethyl)-4,4,5,5-tetramethyl-1,3,2-dioxaborolane.

<sup>®</sup> Abstract published in *Advance ACS Abstracts*, May 15, 1995.

(1) Matteson, D. S. *Chem. Rev.* **1989**, *89*, 1535–1551.

(2) Matteson, D. S.; Mah, R. W. H. *J. Am. Chem. Soc.* **1963**, *85*, 2599–2603.

(3) (a) Matteson, D. S.; Sadhu, K. M. *Organometallics*, **1984**, *3*, 614–618. (b) Brown, H. C.; De Lue, N. R.; Yamamoto, Y.; Maruyama, K.; Kasahara, T.; Murahashi, S.; Sonoda, A. *J. Org. Chem.* **1977**, *42*, 4088–4092.

(4) Blicke, F. F. *J. Am. Chem. Soc.* **1923**, *45*, 1965–1969.

(5) Bowden, S. T.; John, T. *J. Chem. Soc.* **1939**, 314–317.

(6) Dodonov, V. A.; Krasnov, Yu. N. *Zh. Obshch. Khim.* **1980**, *50*, 352–357; *Chem. Abstr.* **1980**, *93*, 71891x.

(7) Rettig, S. J.; Trotter, J. *Can. J. Chem.* **1977**, *55*, 3071–3075.

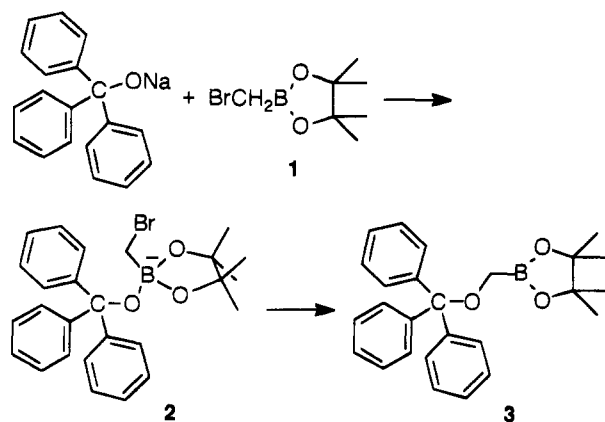
(8) Gupta, A.; Kirfel, A.; Will, G.; Wulff, G. *Acta Crystallogr., Sect. B* **1977**, *33*, 637–641.

Table 1. Bond Distances in 1,3,2-Dioxaborolane Rings

compd	bond	distance (Å)	bond	distance (Å)	bond	distance (Å)
<b>3</b>	B(1)–C(1)	1.560(4)	B(1)–O(2)	1.316(4)	B(1)–O(3)	1.314(4)
	C(3)–O(2)	1.438(4)	C(2)–O(3)	1.426(4)	C(2)–C(3)	1.543(4)
<b>3<sup>a</sup></b>	B(2)–C(33)	1.555(4)	B(2)–O(4)	1.318(4)	B(2)–O(5)	1.333(3)
	C(28)–O(4)	1.448(3)	C(27)–O(5)	1.441(4)	C(27)–C(28)	1.545(4)
<b>4</b>	B(1)–C(6)	1.552(9)	B(1)–O(2)	1.339(7)	B(1)–O(5)	1.383(6)
	C(3)–O(2)	1.478(7)	C(4)–O(5)	1.441(7)	C(3)–C(4)	1.539(7)
<b>4<sup>a</sup></b>	B(51)–C(56)	1.581(10)	B(51)–O(52)	1.331(8)	B(51)–O(55)	1.353(9)
	C(53)–O(52)	1.429(7)	C(54)–O(55)	1.435(7)	C(53)–C(54)	1.553(8)
<b>5</b>	B(1)–C(6)	1.554(13)	B(1)–O(2)	1.356(11)	B(1)–O(5)	1.347(14)
	C(3)–O(2)	1.456(11)	C(4)–O(5)	1.433(9)	C(3)–C(4)	1.560(14)
<i>ent</i> - <b>6</b>	B(1)–C(6)	1.605(16)	B(1)–O(2)	1.346(14)	B(1)–O(5)	1.336(15)
	C(3)–O(2)	1.473(12)	C(4)–O(5)	1.444(12)	C(3)–C(4)	1.553(15)
<b>7a</b>	B(1)–C(6)	1.580(8)	B(1)–O(2)	1.362(7)	B(1)–O(5)	1.343(8)
	C(3)–O(2)	1.440(7)	C(4)–O(5)	1.478(6)	C(3)–C(4)	1.531(8)
<b>7b</b>	B(1)–C(6)	1.566(17)	B(1)–O(2)	1.372(15)	B(1)–O(5)	1.361(16)
	C(3)–O(2)	1.444(14)	C(4)–O(5)	1.454(13)	C(3)–C(4)	1.539(16)

<sup>a</sup> At second site in unit cell.

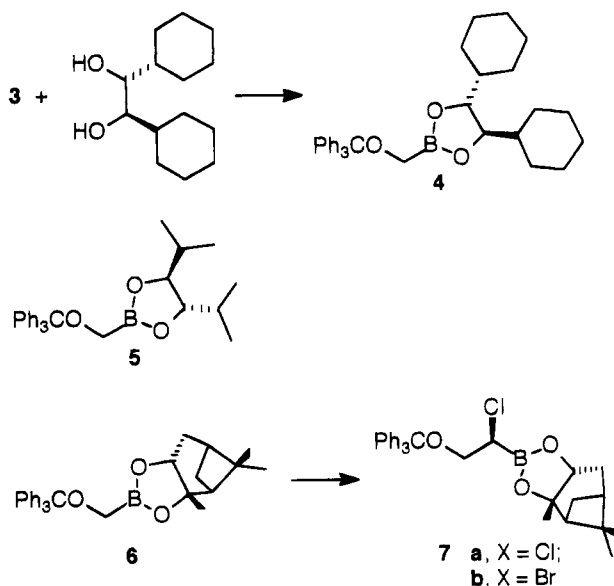
impurity, and the relative solubilities of the two species were not promising for purification by recrystallization.



Separation of the product **3** from unchanged trityl alcohol could be accomplished by chromatography, but for preparative purposes a more efficient process was required. Basic hydrolysis of **3** was carried out in a two-phase (ether/water) system with the aid of pentaerythritol, which assists in solubilizing the sodium salt of the boronic acid in water<sup>15</sup> and leaves the trityl alcohol and pinacol in the ether. Regeneration of **3** was accomplished by acidification and treatment with pinacol in pentane, from which excess pinacol can be extracted with water.

Transesterification of **3** with the chiral diols (*R,R*)-1,2-dicyclohexylethanol<sup>16</sup> or (*S,S*)-2,5-dimethyl-3,4-hexanediol<sup>17</sup> to form the boronic ester **4** or **5**, respectively, occurred readily in pentane at room temperature. The pinanediol ester<sup>18</sup> **6** was similarly prepared from **3** and (*S*)-pinanediol, or its enantiomer *ent*-**6** from (*R*)-

pinanediol, and **6** was converted to the (1-chloro-2-(trityloxy)ethyl)boronic ester **7a** or the bromo analogue **7b** by treatment with (chloromethyl)lithium or (bromomethyl)lithium followed by zinc chloride according to previously reported methods.<sup>19,20</sup> The boronic esters **3**, **4**, **5**, **6** (or its enantiomer *ent*-**6**), **7a**, and **7b** all crystallized from pentane and yielded crystals suitable for X-ray analysis.



(15) Matteson, D. S.; Man, H.-W. To be published.

(16) (a) Ditrich, K.; Bube, T.; Stürmer, R.; Hoffmann, R. W. *Angew. Chem.* **1986**, *98*, 1016–1018. (b) Matteson, D. S.; Man, H.-W. *J. Org. Chem.* **1993**, *58*, 6545–6547.

(17) Matteson, D. S.; Beedle, E. C.; Kandil, A. A. *J. Org. Chem.* **1987**, *52*, 5034–5036.

(18) *Chemical Abstracts* name: {3*aS*-[3*αα*,4*β*,6*β*,7*αα*]}-2-[(trityloxy)methoxy)methyl]hexahydro-3*α*,5,5-trimethyl-4,6-methano-1,3,2-dioxaborole. The structures drawn for **6** and **7** are plane projections of computer molecular models viewed from a suitable angle. The substituents on the dioxaborolane ring which are believed to direct the chiral synthesis are marked as pointing toward or away from the viewer to emphasize the analogy between **6** or **7** and **4** or **5**.

Boron–carbon and boron–oxygen bond distances in 1,3,2-dioxaborolane rings are summarized in Table 1. The average of the sixteen B–O bond distances found in the six crystal structures is 1.344 (±0.020) Å, and the average of the eight exocyclic B–C distances is 1.569 (±0.018) Å. The other C–O and C–C distances within the five-membered ring are also tabulated.

The 1,3,2-dioxaborolane rings of all six compounds **3**–**7a** are close to planar, and *syn* pairs of substituents are in an eclipsed conformation. Dihedral angles observed for the C–C–C linkages involving *trans* and *cis* 4,5-substituents are summarized in Table 2, which also includes recalculated data for the only previously studied *C*<sub>2</sub>-symmetric 1,3,2-dioxaborolane in mannitol

(19) Matteson, D. S.; Sadhu, K. M.; Peterson, M. L. *J. Am. Chem. Soc.* **1986**, *108*, 812–819.

(20) Matteson, D. S.; Peterson, M. L. *J. Org. Chem.* **1987**, *52*, 5116–5121.

Table 2. Dihedral Angles at Positions 4 and 5 of 1,3,2-Dioxaborolane Rings

compd	diol moiety	atom set ( $\sim 120^\circ$ )	angle (deg)	atom set ( $\sim 0^\circ$ )	angle (deg)
3	pinacol	C(7)–C(3)–C(2)–C(4)	138.6	C(6)–C(3)–C(2)–C(4)	11.7
		C(6)–C(3)–C(2)–C(5)	116.5	C(7)–C(3)–C(2)–C(5)	10.4
3	pinacol	C(32)–C(27)–C(28)–C(29)	120.0	O(2)–C(3)–C(2)–O(3)	10.2
		C(30)–C(28)–C(27)–C(31)	134.5	C(29)–C(28)–C(27)–C(31)	6.8
				C(30)–C(28)–C(27)–C(32)	7.7
				O(4)–C(28)–C(27)–O(5)	6.9
4	DICHEd <sup>a</sup>	C(11)–C(3)–C(4)–C(11')	112.6	O(5)–C(4)–C(3)–O(2)	2.7
4	DICHEd <sup>a</sup>	C(61')–C(54)–C(53)–C(61)	120.1	O(55)–C(54)–C(53)–O(52)	6.5
5	DIPED <sup>b</sup>	C(12)–C(4)–C(3)–C(9)	131.3	O(5)–C(4)–C(3)–O(2)	7.9
ent-6	pinanediol	C(10)–C(4)–C(3)–C(9)	131.3	C(10)–C(4)–C(3)–C(11)	0.9
				O(5)–C(4)–C(3)–O(2)	4.3
7a	pinanediol	C(11)–C(3)–C(4)–C(18)	127.9	C(14)–C(4)–C(3)–C(11)	4.9
7b	pinanediol	C(11)–C(3)–C(4)–C(18)	127.9	O(2)–C(3)–C(4)–O(5)	2.0
				C(14)–C(4)–C(3)–C(11)	2.8
PhB <sup>c</sup>	mannitol	C(2)–C(3)–C(4)–C(5)	136.3	O(2)–C(3)–C(4)–O(5)	4.0
				O(5)–C(3)–C(4)–O(6)	8.3

<sup>a</sup> 1,2-Dicyclohexyl-1,2-ethanediol. <sup>b</sup> 1,2-Diisopropyl-1,2-ethanediol (= 2,5-dimethyl-3,4-hexanediol). <sup>c</sup> Calculated for the central 1,3,2-dioxaborolane ring ( $C_2$ -symmetric) of mannitol tris(phenylboronate) from data in ref 8.

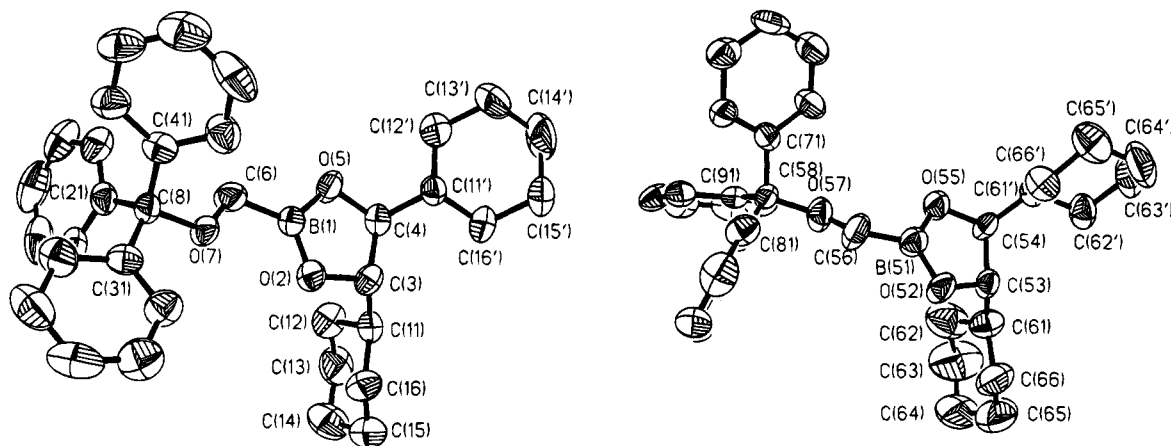


Figure 1. ORTEP drawings of the two crystallographically independent molecules in  $[R-(4\alpha,5\beta)]$ -4,5-dicyclohexyl-2-[(triphenylmethoxy)methyl]-1,3,2-dioxaborolane (**4**) (H atoms omitted).

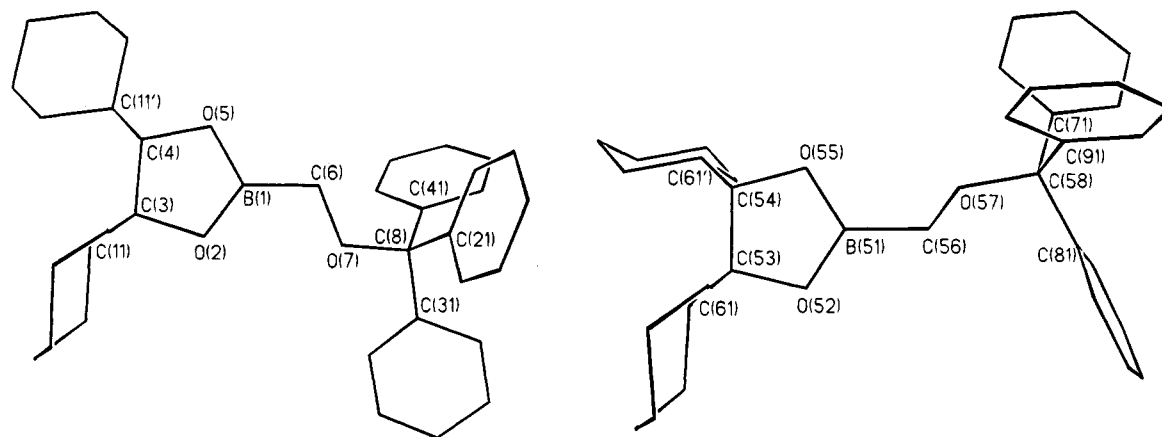


Figure 2. Line drawings of the two crystallographically independent molecules in  $[R-(4\alpha,5\beta)]$ -4,5-dicyclohexyl-2-[(triphenylmethoxy)methyl]-1,3,2-dioxaborolane (**4**) (H atoms omitted).

tris(phenylboronate).<sup>8</sup> ORTEP drawings of **4** at the two different crystal lattice sites are shown in Figure 1, line drawings in Figure 2. The planarity of the rings is shown by the dihedral angles of the C–C–O–B and O–B–O–C linkages within the rings in Table 3.

The sums of the bond angles around the boron atoms of the 1,3,2-dioxaborolane rings are all very close to  $360^\circ$ , indicating that the boron atoms are strictly planar. Mannitol tris(phenylboronate) also has planar boron atoms.<sup>8</sup> Bond angles involving the dioxaborolane rings are summarized in Table 4.

## Discussion

The trityl oxide anion is extremely sterically hindered and would not ordinarily be useful as a nucleophile in  $S_N2$  reactions, as the scanty literature indicates.<sup>4–6</sup> Neighboring group assistance by the boronic ester function is presumably a major factor in the displacement of bromide from **1** by trityl oxide, and the formation of intermediates analogous to the postulated borate **2** has been supported strongly by previous evidence.<sup>1,2</sup> The critical step is rearrangement of **2** with loss of



**Table 3. Dihedral Angles (B–O–C–C and O–B–O–C) in 1,3,2-Dioxaborolanes**

compd	diol moiety	atom set	angle (deg)	atom set	angle (deg)
<b>3</b>	pinacol	C(2)–C(3)–O(2)–B(1)	7.8	O(2)–B(1)–O(3)–C(2)	5.5
		B(1)–O(3)–C(2)–C(3)	9.9	O(3)–B(1)–O(2)–C(3)	2.0
<b>3</b>	pinacol	C(27)–C(28)–O(4)–B(2)	7.0	O(5)–B(2)–O(4)–C(28)	4.3
		B(2)–O(5)–C(27)–C(28)	4.9	C(27)–O(5)–B(2)–O(4)	0.6
<b>4</b>	DICHED <sup>a</sup>	B(1)–O(2)–C(3)–C(4)	1.5	O(5)–B(1)–O(2)–C(3)	0.2
		C(3)–C(4)–O(5)–B(1)	2.9	O(2)–B(1)–O(5)–C(4)	2.1
<b>4</b>	DICHED <sup>a</sup>	B(51)–O(52)–C(53)–C(54)	4.7	C(53)–O(52)–B(51)–O(55)	1.1
		C(53)–C(54)–O(55)–B(51)	6.0	O(52)–B(51)–O(55)–C(54)	3.4
<b>5</b>	DIPED <sup>a</sup>	C(4)–C(3)–O(2)–B(1)	7.1	O(5)–B(1)–O(2)–C(3)	3.6
		B(1)–O(5)–C(4)–C(3)	6.3	C(4)–O(5)–B(1)–O(2)	2.0
<b>ent-6</b>	pinanediol	C(3)–C(4)–O(5)–B(1)	4.9	O(5)–B(1)–O(2)–C(3)	0.9
		B(1)–O(2)–C(3)–C(4)	2.2	O(2)–B(1)–O(5)–C(4)	3.9
<b>7a</b>	pinanediol	C(3)–C(4)–O(5)–B(1)	0.6	O(5)–B(1)–O(2)–C(3)	4.6
		C(4)–C(3)–O(2)–B(1)	3.8	O(2)–B(1)–O(5)–C(4)	3.3
<b>7b</b>	pinanediol	B(1)–O(5)–C(4)–C(3)	0.2	O(5)–B(1)–O(2)–C(3)	6.9
		C(4)–C(3)–O(2)–B(1)	6.4	O(2)–B(1)–O(5)–C(4)	4.1
Mannitol tris(BPh) <sup>b</sup>		B(3)–O(6)–C(4)–C(3)	4.7	O(6)–B(3)–O(5)–C(3)	6.5
		C(4)–C(3)–O(5)–B(3)	8.9	O(5)–B(3)–O(6)–C(4)	0.8

<sup>a</sup> Defined in Table 2. <sup>b</sup> Calculated for central 1,3,2-dioxaborolane ring (*C*<sub>2</sub>-symmetric) from data in ref 8.

**Table 4. Bond Angles in 1,3,2-Dioxaborolane Rings**

compd	atom set	angle (deg)	atom set	angle (deg)	atom set	angle (deg)
<b>3</b>	O(3)–B(1)–O(2)	111.9(3)	O(4)–B(2)–O(5)	113.0(2)	O(3)–C(2)–C(3)	103.5(2)
	O(3)–B(1)–C(1)	127.7(2)	O(4)–B(2)–C(33)	126.5(2)	C(2)–C(3)–O(2)	101.6(2)
	C(1)–B(1)–O(2)	120.4(3)	C(33)–B(2)–O(5)	120.5(3)	O(4)–C(28)–C(27)	103.5(2)
	B(1)–O(3)–C(2)	110.5(2)	B(2)–O(4)–C(28)	109.8(2)	C(28)–C(27)–O(5)	102.9(2)
	B(1)–O(2)–C(3)	111.3(3)	B(2)–O(5)–C(27)	110.2(2)		
<b>4</b>	O(5)–B(1)–O(2)	113.4(5)	O(52)–B(51)–O(55)	114.5(6)	O(2)–C(3)–C(4)	103.6(4)
	O(5)–B(1)–C(6)	119.7(5)	O(52)–B(51)–C(56)	123.4(6)	O(5)–C(4)–C(3)	105.6(4)
	O(2)–B(1)–C(6)	126.8(5)	O(55)–B(51)–C(56)	122.1(5)	O(52)–C(53)–C(54)	103.4(4)
	B(1)–O(2)–C(3)	109.0(4)	B(51)–O(52)–C(53)	109.4(5)	O(55)–C(54)–C(53)	104.8(5)
	B(1)–O(5)–C(4)	108.3(4)	B(51)–O(55)–C(54)	107.5(4)		
<b>5</b>	O(2)–B(1)–O(5)	113.1(8)	O(2)–B(1)–C(6)	123.1(10)	O(5)–B(1)–C(6)	123.8(8)
	B(1)–O(2)–C(3)	108.8(8)	B(1)–O(5)–C(4)	110.0(7)		
	O(2)–C(3)–C(4)	103.6(6)	O(5)–C(4)–C(3)	103.9(7)		
	O(2)–B(1)–O(5)	116.6(10)	O(2)–B(1)–C(6)	119.2(10)	O(5)–B(1)–C(6)	124.2(9)
<b>ent-6</b>	B(1)–O(2)–C(3)	106.8(8)	B(1)–O(5)–C(4)	107.6(8)		
	O(2)–C(3)–C(4)	103.7(8)	C(3)–C(4)–O(5)	105.1(8)		
	O(2)–B(1)–O(5)	114.5(5)	O(2)–B(1)–C(6)	122.0(6)	O(5)–B(1)–C(6)	123.5(5)
<b>7a</b>	B(1)–O(2)–C(3)	107.7(4)	B(1)–O(5)–C(4)	108.1(4)		
	O(5)–C(4)–C(3)	103.5(4)	O(2)–C(3)–C(4)	106.0(4)		
	O(2)–B(1)–O(5)	113.4(10)	O(2)–B(1)–C(6)	122.2(11)	O(5)–B(1)–C(6)	124.4(10)
<b>7b</b>	B(1)–O(2)–C(3)	108.4(9)	B(1)–O(5)–C(4)	107.9(8)		
	O(2)–C(3)–C(4)	104.5(8)	O(5)–C(4)–C(3)	105.2(8)		

bromide ion. Dipolar aprotic solvents in general<sup>21</sup> and DMSO in particular<sup>22</sup> often accelerate S<sub>N</sub>2 reactions, though the effects depend strongly on relative polarities and solvations of starting materials and transition states and are not necessarily predictable in systems that lack clear precedents.

In the light of subsequent findings, it is conceivable that the irreproducible reactions observed during the exploratory phase of the work actually occurred during aqueous workup, which was always done before NMR spectra were taken.

Although previous literature has provided B–C and B–O bond distances for a scattered group of boronic esters and related compounds,<sup>7–12</sup> the present results are the first to correlate a series of simple boronic esters of the 1,3,2-dioxaborolane type. Compounds of this class have proved particularly useful in asymmetric synthesis,<sup>1,13,16,23</sup> and insight into their steric properties is therefore useful.

The near planarity of the 1,3,2-dioxaborolane ring places considerable eclipsing strain on the carbon atoms in the ring. MMX calculations with the PC Model program<sup>24</sup> using parameters that neglect oxygen–boron  $\pi$ -bonding suggest that the 4,5-carbon atoms would twist to a semistaggered conformation, and thus are an unsatisfactory model. Parameters that make the O–B–O group as rigid as an allyl anion yield approximately the right degree of flatness in the ring. All of the transition states of interest for asymmetric synthesis involve some degree of coordination of a Lewis base with the boron atom. When the boron atom is made tetracoordinate, even though the fourth ligand is weakly bound, the groups around the 4,5-carbon–carbon bond in the five-membered ring become semistaggered in a known structure,<sup>12</sup> and the modeling program is in reasonable agreement. Both the modeling program and organic chemist's experience agree in predicting that large *trans* substituents on the ring will adopt the pseudoequatorial conformation, but structure data to test this prediction are not yet available.

(21) Parker, A. *J. Chem. Rev.* **1969**, *69*, 1–32.

(22) Buncl, E.; Wilson, H. *Adv. Phys. Org. Chem.* **1977**, *14*, 133–202.

(23) (a) Roush, W. R.; Ratz, A. M.; Jablonski, J. A. *J. Org. Chem.* **1992**, *57*, 2047. (b) Roush, W. R.; Hoong, L. K.; Palmer, M. A. J.; Park, J. C. *J. Org. Chem.* **1990**, *55*, 4109. Roush, W. R.; Hoong, L. K.; Palmer, M. A. J.; Straub, J. A.; Palkowitz, A. D. *J. Org. Chem.* **1990**, *55*, 4117.

(24) Available from Serena Software, Bloomington, IN. We thank Professor Mark Midland, University of California, Riverside, CA, for assistance in translating our X-ray data into suitable parameters for boron for this program.

Table 5. Crystal Structure Data

compd	3	4	5	6	7a	7b
empirical formula	C <sub>26</sub> H <sub>29</sub> BO <sub>3</sub>	C <sub>34</sub> H <sub>41</sub> BO <sub>3</sub>	C <sub>28</sub> H <sub>33</sub> BO <sub>3</sub>	C <sub>30</sub> H <sub>33</sub> BO <sub>3</sub>	C <sub>31</sub> H <sub>34</sub> BClO <sub>3</sub>	C <sub>31</sub> H <sub>34</sub> BBro <sub>3</sub>
mol wt	400.3	509.0	428.4	452.4	500.8	543.3
cryst class	triclinic	monoclinic	trigonal	orthorhombic	orthorhombic	orthorhombic
space group	<i>P</i> $\bar{1}$	<i>P</i> 2 <sub>1</sub>	<i>P</i> 3 <sub>2</sub>	<i>P</i> 2 <sub>1</sub> 2 <sub>1</sub> 2 <sub>1</sub>	<i>P</i> 2 <sub>1</sub> 2 <sub>1</sub> 2 <sub>1</sub>	<i>P</i> 2 <sub>1</sub> 2 <sub>1</sub> 2 <sub>1</sub>
<i>a</i> (Å)	10.173(2)	14.827(3)	9.450(2)	12.592(3)	10.074(2)	10.096(2)
<i>b</i> (Å)	10.518(2)	9.225(2)		13.912(3)	15.457(3)	15.473(3)
<i>c</i> (Å)	21.905(4)	22.465(4)	24.719(5)	14.843(3)	17.825(4)	17.961(4)
$\alpha$ (deg)	96.40(3)					
$\beta$ (deg)	95.47(3)	107.74(3)				
$\gamma$ (deg)	97.61(3)					
<i>V</i> (Å <sup>3</sup> )	2294.2(8)	2926.6(10)	1911.7(7)	2600.2(10)	2775.6(10)	2805.8 (7)
<i>Z</i>	4	4	3	4	4	4
<i>R</i> <sup>a</sup>	0.062	0.060	0.066	0.075	0.050	0.071
<i>wR</i> <sup>b</sup>	0.127	0.080	0.070	0.047	0.056	0.085

$$^a R = \sum ||F_o| - |F_c|| / \sum |F_o|, \quad ^b wR = \sum w(|F_o| - |F_c|)^2 / \sum w|F_o|^2.$$

### Experimental Section

**X-ray Data Analysis.** X-ray data were collected on a Syntex P2<sub>1</sub> diffractometer upgraded to Siemens P4 specifications (6) or a Nicolet P3 diffractometer upgraded to Siemens P4 specifications (3–5, 7a, b). Each diffractometer was equipped with a graphite monochromator for Mo K $\alpha$  radiation (6) or Cu K $\alpha$  radiation (3–5, 7a, b). Data collections were based on the Siemens XSCANS software.<sup>25</sup> Structure solutions were obtained via the subroutine SOLV in the SHELXTL PLUS program package,<sup>26</sup> and all subsequent calculations were carried out with the routines in this package. Pertinent crystallographic data are given in Table 5, and full listings of collection and refinement parameters, as well as bond distances and angles, are available as supplementary material. Solution and refinement generally was straightforward. Absolute configurations were determined only for 7a and 7b. For the other chiral structures (4–6), the unit cells were chosen so as to give the chemically correct chirality.

In the case of 3 (space group *P* $\bar{1}$ ) and 4 (space group *P*2<sub>1</sub>), the structures contained two crystallographically independent molecules. In 3, the conformations of the two independent molecules are essentially identical. The only difference is a slight rotation of the triphenylmethoxy moiety. In 4, on the other hand, the two independent molecules have distinctly different conformations, as seen in Figure 1. The cyclohexyl groups all assume a chair conformation, but the orientations of the cyclohexane rings with respect to the dioxaborolane rings are different. Similarly, the orientations of the three phenyl groups are nearly the same in each triphenylmethoxy group, but their orientation relative to the dioxaborolane rings are different. In fact, the orientations of the three phenyl groups are nearly identical in all of the compounds. For compounds 3–6, the conformation of the triphenylmethoxy groups relative to the dioxaborolane rings are also essentially identical, except for the molecule containing B(51) in 4.

**4,4,5,5-Tetramethyl-2-[(triphenylmethoxy)methyl]-1,3,2-dioxaborolane (3).** A solution of 0.40 mol of sodium trityl oxide was prepared by addition of sodium hydride (17.6 g, 0.44 mol) (60% dispersion in mineral oil) to trityl alcohol (*Chemical Abstracts* name:  $\alpha, \alpha$ -diphenylbenzenemethanol) (104.1 g, 0.40 mol) in dimethyl sulfoxide (800 mL) at room temperature overnight. To this mixture was added pinacol (bromomethyl)boronate (1) (88.4 g, 0.40 mol) at 0 °C via cannula. The solution warmed to room temperature and was stirred for 18 h. The mixture was worked up by addition of saturated aqueous ammonium chloride (800 mL) and extracted with diethyl ether (2  $\times$  500 mL). The ether layer was concentrated in a rotary evaporator until only a small amount of ether remained. Pentane was added (100 mL), and on evaporation

of the pentane the mixture solidified. The solid was washed several times with distilled water to remove DMSO residue. The crude mixture contained ~10% unchanged trityl alcohol together with the major product, 4,4,5,5-tetramethyl-2-[(triphenylmethoxy)methyl]-1,3,2-dioxaborolane (155 g), which was redissolved in diethyl ether (1 L). The ether solution was treated with aqueous sodium hydroxide (1 M, 1.2 L) and pentaerythritol (136 g, 1 mol). After stirring at room temperature for 18 h, the organic layer was separated from the solution, and the aqueous phase was neutralized by hydrochloric acid (pH ~6) in an ice bath. After 10 min, the cloudy mixture was filtered and the solid was collected. A solution of the solid and pinacol (47.2 g, 400 mmol) in pentane (1 L) was stirred at room temperature for 2 h. The pentane solution was washed with water (3  $\times$  1 L) and dried over magnesium sulfate. Concentration in a rotary evaporator gave pure 4,4,5,5-tetramethyl-2-[(triphenylmethoxy)methyl]-1,3,2-dioxaborolane (3) (136 g, 85%): mp 107–109 °C, 300-MHz <sup>1</sup>H-NMR (CDCl<sub>3</sub>)  $\delta$  0.88–1.26 (s, 12H, CH<sub>3</sub>), 2.86 (s, 2H, CH<sub>2</sub>B), 7.18–7.48 (m, 15H, C<sub>6</sub>H<sub>5</sub>); 75-MHz <sup>13</sup>C-NMR (CDCl<sub>3</sub>)  $\delta$  24.80, 83.61, 87.68, 126.71, 127.65, 128.85, 144.13; HRMS calcd for C<sub>26</sub>H<sub>29</sub>BO<sub>3</sub> (M<sup>+</sup>) 400.2210, found 400.2207.

**[*R*-(4 $\alpha$ ,5 $\beta$ )]-4,5-Dicyclohexyl-2-[(triphenylmethoxy)methyl]-1,3,2-dioxaborolane (4).** To a solution of pinacol [(triphenylmethoxy)methyl]boronate (3) (100 g, 250 mmol) in pentane (500 mL) was added (*R,R*)-1,2-dicyclohexyl-1,2-ethanediol (56.5 g, 250 mmol), and the mixture was stirred for 4 h at room temperature. The solution was washed with water (3  $\times$  500 mL) to remove pinacol. Concentration in a rotary evaporator gave [*R*-(4 $\alpha$ ,5 $\beta$ )]-4,5-dicyclohexyl-2-[(triphenylmethoxy)methyl]-1,3,2-dioxaborolane (4) (121 g, 98%): mp 95–98 °C, 300-MHz <sup>1</sup>H-NMR (CDCl<sub>3</sub>)  $\delta$  0.88–1.39 and 1.60–1.83 (m, 22, C<sub>6</sub>H<sub>11</sub>), 2.84 (AB, *J* = 15.7 Hz, 1, CH<sub>2</sub>B), 2.94 (AB, *J* = 15.7 Hz, 1, CH<sub>2</sub>B), 3.91–3.95 (m, 2, BOCH), 7.20–7.49 (m, 15, C<sub>6</sub>H<sub>5</sub>); 75-MHz <sup>13</sup>C-NMR (CDCl<sub>3</sub>)  $\delta$  25.87, 26.01, 27.37, 28.37, 42.93, 83.75, 87.67, 126.74, 127.68, 128.85, 144.18; HRMS calcd for C<sub>34</sub>H<sub>41</sub>O<sub>3</sub>B (M<sup>+</sup>) 508.3149, found 508.3158. Anal. Calcd for C<sub>34</sub>H<sub>41</sub>BO<sub>3</sub>: C, 80.31; H, 8.13; B, 2.13. Found: C, 80.48; H, 8.27; B, 2.09.

**[*S*-(4 $\alpha$ ,5 $\beta$ )]-4,5-Bis(1-methylethyl)-2-[(triphenylmethoxy)methyl]-1,3,2-dioxaborolane (5).** To a solution of 4,4,5,5-tetramethyl-2-[(triphenylmethoxy)methyl]-1,3,2-dioxaborolane (3) (40 g, 100 mmol) in pentanes (300 mL) was added (*S,S*)-2,5-dimethyl-3,4-hexanediol (14.6 g, 0.10 mol), and the mixture was stirred for 1 h (until the solid dissolved) at room temperature. The solution was washed with water (3  $\times$  300 mL) to remove pinacol. Concentration in a rotary evaporator gave 5 (41.5 g, 97%): mp 48–50 °C, 200-MHz <sup>1</sup>H-NMR (CDCl<sub>3</sub>)  $\delta$  0.95 (d, 12, CH<sub>3</sub>), 1.7 (m, 1, CH<sub>2</sub>B), 2.91 (AB, 2, CH<sub>2</sub>B), 3.92 (m, 2, BOCH), 7.20–7.51 (m, 15, C<sub>6</sub>H<sub>5</sub>); HRMS calcd for C<sub>28</sub>H<sub>33</sub>O<sub>3</sub>B (M<sup>+</sup>) 428.2523, found 428.2481. Anal. Calcd for C<sub>28</sub>H<sub>33</sub>O<sub>3</sub>B: C, 78.46; H, 7.77; B, 2.57. Found: C, 78.09; H, 7.62; B, 2.18.

(25) Nicolet Crystallographic Systems Users Guide, Release 81.3; Nicolet X-ray Instruments: Madison, WI, 1985.

(26) SHELXTL PLUS, Release 4.0; Siemens Analytical Instruments, Inc.: Madison, WI, 1990.

**(S)-Pinanediol ((Tritylloxymethyl)boronate (6)).**<sup>27</sup> A mixture of 4,4,5,5-tetramethyl-2-[(triphenylmethoxy)methyl]-1,3,2-dioxaborolane (**3**) (5.14 g, 12.85 mmol) and (*S*)-pinanediol (2.18 g, 12.85 mmol) in pentane (120 mL) was stirred at room temperature overnight. The solution was washed with water (3 × 100 mL) to remove pinacol. Concentration in a rotary evaporator gave **6** (5.37 g, 92.5%): mp 85–87 °C, 300-MHz <sup>1</sup>H-NMR (CDCl<sub>3</sub>) δ 0.853 (s, 3, CH<sub>3</sub>), 1.168 (d, 1, *J* = 10.8 Hz, pinyl CH), 1.294 (s, 3, CH<sub>3</sub>), 1.399 (s, 3, CH<sub>3</sub>), 1.50–2.45 (m, 5, pinyl CH), 2.9124 (s, 2, OCH<sub>2</sub>B), 4.355 (dd, 1, *J* = 1.86 and 8.7 Hz, CHOB), 7.15–7.55 (m, 15 C<sub>6</sub>H<sub>5</sub>); 75-MHz <sup>13</sup>C-NMR (CDCl<sub>3</sub>) δ 23.993, 26.438, 27.052, 28.541, 35.391, 38.107, 39.477, 51.218, 78.076, 86.111, 87.719, 126.75, 127.69, 128.86, 144.12. Anal. Calcd for C<sub>30</sub>H<sub>33</sub>BO<sub>3</sub>: C, 79.65; H, 7.35; B, 2.39. Found: C, 79.24, 79.35; H, 7.17, 7.26; B, 2.30.

The enantiomer *ent*-**6** was similarly prepared from (*R*)-pinanediol and was used for the X-ray crystal structure determination.

**(S)-Pinanediol (S)-(1-Chloro-2-(trityloxy)ethyl)boronate (7a).**<sup>27</sup> To a solution of dichloromethane (2.28 mL, 35.37 mmol) in THF (15 mL) was added 1-butyllithium (10.57 mL, 1.45 M, 15.33 mmol) at –100 °C via cannula. The butyllithium solution was allowed to run down the cold wall of the reaction flask to be chilled before contacting the dichloromethane solution. After 5 min, a solution of (*S*)-pinanediol ((trityloxy)methyl)boronate (**6**) (5.33 g, 11.7 mmol) was added to the solution via cannula. After 10 min, zinc chloride (2.89 g, 21.2 mmol), which was fused before use, was added to the solution. The solution warmed to room temperature and was kept for 18 h, and then it was worked up by treatment with aqueous ammonium chloride and pentane. The pentane solution was filtered through a column of anhydrous magnesium sulfate (10–15 g) and then concentrated to yield solid **7a** containing 0.9% unchanged **6**, recrystallized from 3:1 pentane/diethyl ether, 4.81 g (81%): mp 165–167 °C, 300-MHz <sup>1</sup>H-NMR (CDCl<sub>3</sub>) δ 0.824 (s, 3, CH<sub>3</sub>), 1.211 (d, 1, *J* = 10.8 Hz, pinyl CH), 1.270 (s, 1, CH<sub>3</sub>), 1.382 (s, 3, CH<sub>3</sub>), 1.8–2.4 (m, 5, pinyl CH), 3.470 (m, 2, OCH<sub>2</sub>CHCl), 3.5823 (dd, 1, *J* = 4.92 and 6.39 Hz, OCH<sub>2</sub>CHCl), 4.3599 (dd, 1, *J* = 1.95 and 8.79 Hz, CHOB),

7.15–7.55 (m, 15, C<sub>6</sub>H<sub>5</sub>); 75-MHz <sup>13</sup>C-NMR (CDCl<sub>3</sub>) δ 23.942, 26.341, 26.989, 28.431, 35.104, 38.151, 39.275, 51.051, 65.559, 78.683, 86.584, 87.025, 126.97, 127.73, 128.73, 143.79. Anal. Calcd for C<sub>31</sub>H<sub>34</sub>O<sub>3</sub>BCl: C, 74.34; H, 6.84. Found: C, 74.49; H, 6.73.

**(S)-Pinanediol (S)-(1-Bromo-2-(trityloxy)ethyl)boronate (7b).** A solution of (*S*)-pinanediol ((trityloxy)methyl)boronate (**6**) (4.16 g, 9.20 mmol) and 1.94 mL (27.6 mmol) of dibromomethane in 25 mL of THF was stirred at –78 °C during the dropwise addition of LDA (6.0 mL, 2 M, 12.0 mmol). After 10 min, zinc chloride (3.88 g, 28.5 mmol), which was fused before use, was added to the solution. The solution warmed to room temperature and was kept for 18 h, then was worked up by treatment with saturated aqueous ammonium chloride and pentane. The pentane solution was filtered through a column of anhydrous magnesium sulfate (10–15 g), then concentrated to yield solid (*S*)-pinanediol (S)-(1-chloro-2-(trityloxy)ethyl)boronate (**7b**) containing 3% unchanged **6**, recrystallized from 3:1 pentane/diethyl ether, 3.51 g (70%): mp 176–177 °C, 300-MHz <sup>1</sup>H-NMR (CDCl<sub>3</sub>) δ 0.829 (s, 3, CH<sub>3</sub>), 1.25–1.28 (m, 4), 1.39 (s, 3, CH<sub>3</sub>), 1.8–2.4 (m, 5, pinyl CH), 3.40 (dd, 1, OCH<sub>2</sub>CHBr), 3.47–3.52 (m, 2, OCH<sub>2</sub>CHBr), 4.35 (dd, 1, *J* = 1.95 and 8.79 Hz, CHOB), 7.2–7.5 (m, 15, C<sub>6</sub>H<sub>5</sub>); 75-MHz <sup>13</sup>C-NMR (CDCl<sub>3</sub>) δ 23.95, 26.26, 26.99, 28.38, 35.15, 38.23, 39.27, 51.16, 64.96, 78.55, 86.73, 126.99, 127.75, 128.73, 143.83; HRMS calcd for C<sub>31</sub>H<sub>34</sub>O<sub>3</sub>BBr (M<sup>+</sup>) 544.1784, found 544.1771.

**Acknowledgment.** We thank the National Institutes of Health (Grants GM39063 and GM50298) and the National Science Foundation (Grant CHE-9303074, to D.S.M.) for support.

**Supplementary Material Available:** Tables of data collection parameters, atomic coordinates and equivalent isotropic displacement coefficients, bond lengths, bond angles, anisotropic thermal parameters, and illustrations for compounds **3–6** and **7a,b** (85 pages). Ordering information is given on any current masthead page.

OM950100R

(27) Systematic names: **6** is {3*aS*-[3*αα*,4*β*,6*β*,7*αα*]}-2-[(triphenylmethoxy)methyl]hexahydro-3*α*,5,5-trimethyl-4,6-methano-1,3,2-benzodioxaborole; **7a** is {3*aS*-[2(*R*<sup>\*</sup>),3*αα*,4*β*,6*β*,7*αα*]}-2-[1-chloro-2-(triphenylmethoxy)ethyl]hexahydro-3*α*,5,5-trimethyl-4,6-methano-1,3,2-benzodioxaborole.

# The Aldol Reaction for 2,3- $\eta^2$ -Furan Complexes of Osmium(II): Cyclization across C(2) and C(4) To Form a New Heterocycle

Ronggang Liu, Huiyuan Chen, and W. Dean Harman\*,†

Department of Chemistry, University of Virginia, Charlottesville, Virginia 22901

Received March 20, 1995<sup>⊗</sup>

The pentaammineosmium(II) complex of 5-methylfuran (**2**) undergoes stereoselective aldol reactions with various aldehydes in the presence of a Lewis acid ( $\text{Sn}(\text{OTf})_2$  or  $\text{BF}_3\cdot\text{OEt}_2$ ) to give 4-acetylated-4,5-dihydrofuran complexes where the aldehyde carbonyl group has been incorporated into the dihydrofuran nucleus. A detailed analysis of the substitution pattern and stereochemistry of these products reveals a reaction sequence involving an aldol reaction at C(4) of the  $\eta^2$ -furan followed by nucleophilic displacement at C(2) of the furan oxygen by the aldol-derived alkoxide. When the parent furan complex is subjected to otherwise identical reaction conditions, this rearrangement does not occur. Instead, two diastereomers of a novel bicyclic diacetal are formed.

## Introduction

Furans show a pronounced tendency to undergo electrophilic addition preferentially at an  $\alpha$  carbon.<sup>1a</sup> In the presence of a Lewis acid, furan typically reacts with aldehydes and ketones, to give oligomers or resins.<sup>1b</sup> However, through the use of the Paternó–Büchi [2 + 2] photocycloaddition,<sup>2</sup> the stereoselective attachment of an aldehyde carbon to the  $\beta$  carbon of the furan may be accomplished, and this approach has led to a methodology for the synthesis of several carbohydrate-based natural products.<sup>3</sup>

Dihapto complexation of the furan has been shown to markedly enhance the nucleophilic character of the unbound  $\beta$  carbon. For example, treatment of the complex  $[\text{Os}(\text{NH}_3)_5(2,3\text{-}\eta^2\text{-furan})]^{2+}$  with carbon-based electrophiles results in 4*H*-furanium intermediates that are subject to deprotonation at C(4) or nucleophilic addition, at either C(5) or C(2) (Figure 1).<sup>4</sup> Our hope was that a dihapto-coordinated furan complex might also react with aldehydes selectively at the  $\beta$  carbon and, in the presence of a nucleophile, give the functional equivalent of an aldol condensation (Figure 2). Instead, we find that the alkoxide generated from the aldol reaction at C(4) undergoes an intramolecular addition to C(2) to form a new heterocyclic ring.

## Results

Furan complexes such as  $[\text{Os}(\text{NH}_3)_5(2,3\text{-}\eta^2\text{-furan})]^{2+}$ , **1**, are prepared from the reduction of  $\text{Os}(\text{NH}_3)_5(\text{OTf})_3$  in the presence of an excess of the furan ligand as previously described.<sup>4</sup> When **1** is combined with an

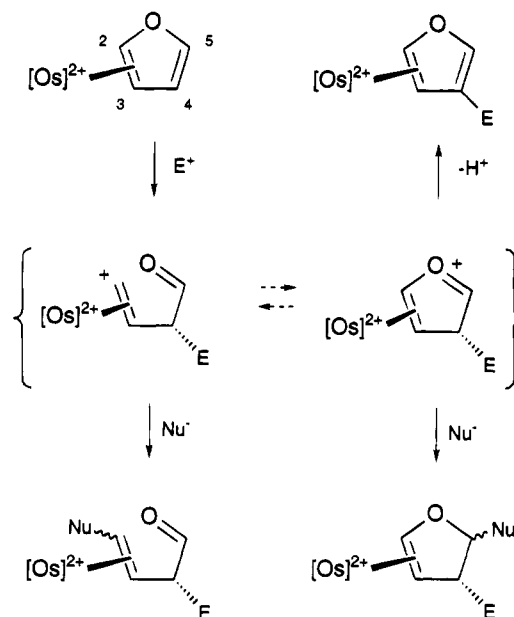


Figure 1. Sequential electrophile–nucleophile addition process for an 2,3- $\eta^2$ -furan complex.

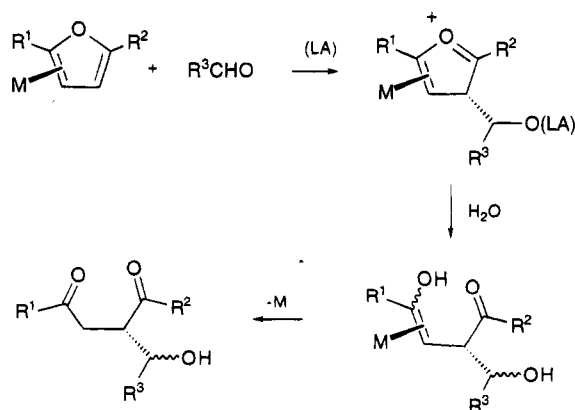


Figure 2. Functional equivalent of an aldol condensation for an  $\eta^2$ -furan and aldehyde.

excess of benzaldehyde dimethyl acetal in the presence of a Lewis acid ( $\text{BF}_3\cdot\text{OEt}_2$ ; 0.5–1.0 equiv; 20 °C;  $\text{CH}_3$ -

\* Alfred P. Sloan Research Fellow (1994–96); NSF Young Investigator (1993–98); Camille and Henry Dreyfus Teacher-Scholar (1992–95).

<sup>⊗</sup> Abstract published in *Advance ACS Abstracts*, May 15, 1995.

(1) (a) Sargent, M. V.; Dean, F. W. In *Comprehensive Heterocycle Chemistry*; Karritzky, E. R., Rees, C. W., Eds.; Pergamon Press: New York, 1984; Part 3, Vol. 4, p 607. (b) Pennanen, S.; Nyman, G. *Acta Chem. Scand.* **1972**, 216, 1018.

(2) Büchi, G.; Inman, C. G.; Lipinsky, E. S. *J. Am. Chem. Soc.* **1954**, 76, 4327.

(3) For example, see: Schreiber, S. L. *Science* **1985**, 227, 857.

(4) Chen, H.; Hodges, L. M.; Liu, R.; Stevens, W. C.; Sabat, M.; Harman, W. D. *J. Am. Chem. Soc.* **1994**, 116, 5499.

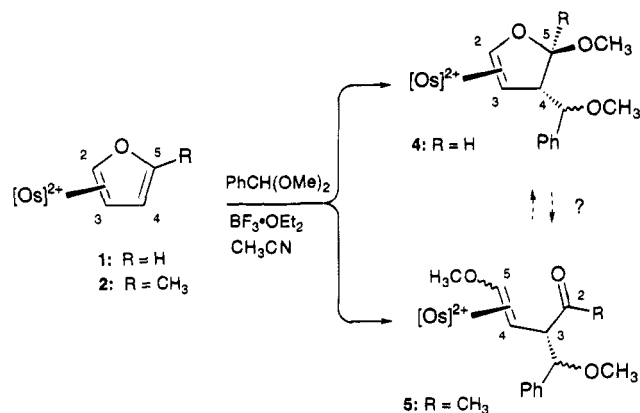


**Figure 3.** Contrasting reactions of furan and 5-methylfuran complexes with benzaldehyde dimethyl acetal.

CN), electrophilic addition occurs at C(4). The resulting 4*H*-furanium species is subsequently attacked by the methoxide nucleophile at C(5) to generate the acetal **4** (Figure 3).<sup>5</sup> Repeating this reaction for the 5-methylfuran analog (**2**) gives an entirely different outcome under otherwise identical reaction conditions. When a sample of **2** is combined with benzaldehyde dimethyl acetal in acetonitrile solution and treated with BF<sub>3</sub>·OEt<sub>2</sub>, (0.5–1.0 equiv; 20 °C; CH<sub>3</sub>CN), a new product (**5**) is generated whose <sup>1</sup>H NMR spectrum strongly resembles the cyclic acetal formed from the parent furan complex (**4**) (Figure 3). However, <sup>13</sup>C data include a carbonyl signal at 208.5 ppm suggesting that the furan ring has been severed. A complete spectroscopic analysis reveals that compound **5** is a constitutional isomer of the expected cyclic acetal where methoxide has displaced the furan oxygen at C(2) of the product (Figure 3). Compound **5** is isolated as a single diastereomer, where the stereochemistry of C(3) is assigned according to precedent with the electrophilic addition occurring on the ring-face opposite to that of metal coordination (Figure 3).<sup>6</sup>

When the 5-methylfuran complex **2** is combined with benzaldehyde and a Lewis acid (e.g. 0.1–0.5 equiv of Sn(OTf)<sub>2</sub>), the solution is allowed to stand 17 h at –40 °C. After pyridine is added to neutralize the Lewis acid, addition of a mixture of CH<sub>2</sub>Cl<sub>2</sub> and Et<sub>2</sub>O precipitates a new dihydrofuran complex, **6a**, in 78% yield. <sup>1</sup>H and <sup>13</sup>C NMR spectra and electrochemical data<sup>7</sup> for **6a** are consistent with the formation of a 4,5-disubstituted η<sup>2</sup>-dihydrofuran complex bearing a phenyl group. Coupling and DEPT data indicate that, like **5**, complex **6a** has four contiguous methines, one methyl group, and an unconjugated carbonyl (214.7 ppm). Taken together, these observations indicate the formation of a pentaammineosmium(II) complex of 4-acetyl-5-phenyl-4,5-dihydrofuran (Figure 4). Irradiation of the *cis* amines causes a 24% NOE enhancement of H(5) indicating that the metal is *anti* to the phenyl group, and a 9% NOE

(5) Similar results have been observed for simple vinyl ethers and acetals. See for example: Inokuchi, T.; Takagishi, S.; Ogawa, K.; Kurokawa, Y.; Torii, S. *Chem. Lett.* **1988**, 1347.

(6) The stereochemical assignment is made in consideration of the large number of examples of electrophilic addition at the β-carbon of η<sup>2</sup>-furans, pyrroles, and arenes that occur from the uncoordinated ring-face. See ref 15.

(7) The complex [Os(NH<sub>3</sub>)<sub>5</sub>(2,3-dihydrofuran)]<sup>2+</sup> has been prepared for comparison (*E*<sub>1/2</sub> = 0.63 V). In contrast to furan complexes, the dihydrofuran analogs show chemically reversible behavior at moderate scan rates (50–500 mV/s).

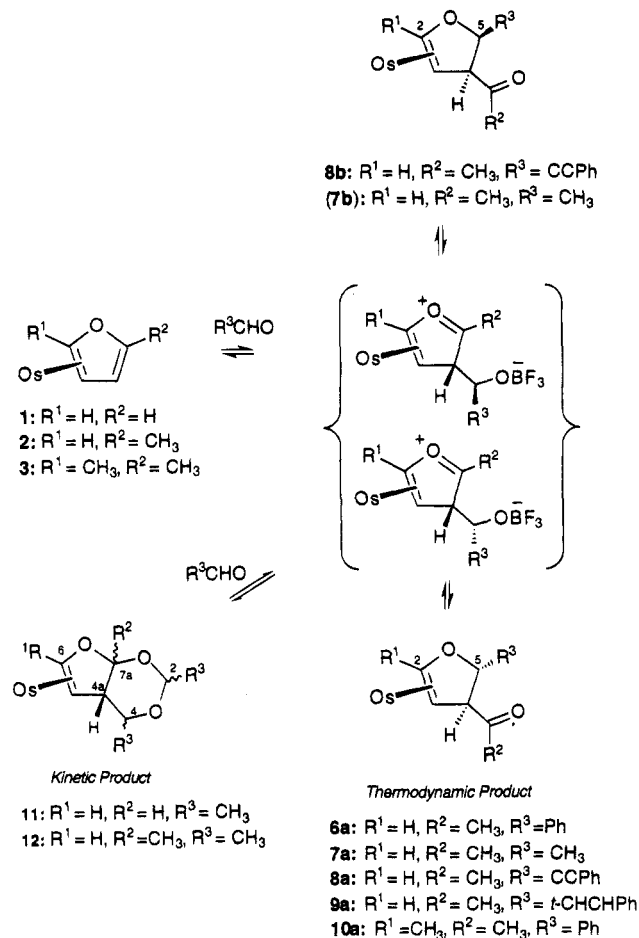


**Figure 4.** Aldol reactions of the osmium(II)–2,3-η<sup>2</sup>-furan complexes and their rearrangements to 4-acetyl-4,5-dihydrofuran species. Os = [Os(NH<sub>3</sub>)<sub>5</sub>]<sup>2+</sup> (triflate salts).

enhancement is observed between H(4) and the phenyl ring. Consistent with these data, the relative stereochemistry of **6a** is assigned as shown in Figure 4.

Using reaction and workup conditions similar to those used in the synthesis of **6a**, acetaldehyde is combined with the methylfuran complex (**2**) to form compound **7a**, the pentaammineosmium(II) complex of *trans*-4-acetyl-5-methyl-4,5-dihydrofuran (80% yield). <sup>1</sup>H NMR data are virtually identical to that of **6a** with the exception that the phenyl signals have been replaced with a doublet in the proton spectrum at 1.22 ppm. As in the case of the phenyl derivative (**6a**), NOE and coupling data indicate that the dihydrofuran complex **7a** is generated as a single diastereomer with the acetyl group oriented *syn* to the osmium while the methyl group of C(5) is *anti* to the metal (Figure 4).

Given that complex **1**, [Os(NH<sub>3</sub>)<sub>5</sub>(2,3-η<sup>2</sup>-furan)]<sup>2+</sup>, undergoes a Michael addition with methyl vinyl ketone,<sup>4</sup> the 5-methylfuran analog (**2**) was also combined with acrolein, crotonaldehyde, cinnamaldehyde, and phenylpropargyl aldehyde and Lewis acid. While the reaction of **2** with acrolein or crotonaldehyde resulted in a complex mixture of products,<sup>8</sup> the reaction with cinnamaldehyde or phenylpropargyl aldehyde delivers the

(8) Reaction conditions: –40 °C, 17 h, 1.0 equiv of Sn(OTf)<sub>2</sub>; pyridine quench. The mixture of products include a 4-acetyl-4,5-dihydrofuran complex as well as two or more isomers of what is thought to be the benzofuran nucleus resulting from Michael–Michael–ring-closure reaction.

desired *trans*-4-acetyl-5-phenylethynyl-4,5-dihydrofuran (**8a**) and *trans*-4-acetyl-5-phenylethenyl-4,5-dihydrofuran (**9a**) complexes, respectively, each as a single diastereomer. Similar to that observed with compounds **6a** and **7a**, coupling and NOE data support the assignment of the osmium *syn* to the acetyl group and *trans* to the C(5) substituent ( $R^3$ ) (Figure 4).

When the reaction of **2** with phenylpropargyl aldehyde is quenched with pyridine after a considerably shorter reaction time (e.g. 15 min instead of 17 h), a new species **8b** is isolated along with **8a** in a 3:2 ratio.  $^{13}\text{C}$  and  $^1\text{H}$  NMR, DEPT, and NOE data confirm that **8b** is the C(5) epimer of **8a** with the phenylethynyl group now oriented *syn* to the osmium (Figure 4).<sup>9</sup> When this product mixture of **8a,b** was redissolved in solution along with Lewis acid for an extended reaction period (~24 h) and then quenched with base, isomer **8a** was the only compound isolated.

The aldol/displacement sequence illustrated in Figure 4 also occurs for the 2,5-dimethylfuran complex. For example, treatment of the complex  $[\text{Os}(\text{NH}_3)_5(\eta^2\text{-2,5-dimethylfuran})](\text{OTf})_2$  (**3**) with benzaldehyde and a Lewis acid generates the pentaammineosmium(II) complex of 4-acetyl-2-methyl-5-phenyl-4,5-dihydrofuran (**10a**) as a single diastereomer. Judging from the strong correlation of coupling constants for the three methine ring protons of **10a** and those of the methylfuran analogs (**6–9a**), the stereochemistry of the 2,5-dimethylfuran analog is identical to the latter compounds with the phenyl and acetyl groups *anti* and *syn* to the metal, respectively.

For the parent complex  $[\text{Os}(\text{NH}_3)_5(2,3\text{-}\eta^2\text{-furan})]^{2+}$  (**1**), the reaction takes a different course. The initial aldol product undergoes a subsequent cyclization with acetaldehyde to generate the bicyclic diacetal, **11**, as a mixture of two diastereomers (Figure 4).<sup>10</sup> Key spectroscopic features for **11** include two methyl groups, four methine groups with proton signals from 3.8 to 6 ppm, and no  $^{13}\text{C}$  carbonyl resonances. Interestingly, when the methylfuran complex (**2**) is combined with an excess of acetaldehyde under reaction conditions used to generate the acetyldihydrofuran complex **7a** ( $\text{CH}_3\text{CN}/\text{CH}_3\text{-CH}_2\text{CN}/-40^\circ\text{C}/\text{Sn}(\text{OTf})_2$ ), except that the reaction is quenched with pyridine after a much shorter reaction time (3 h instead of 17 h), a complex product mixture results, but several of the major components appear by  $^1\text{H}$  NMR to be isomers of a bicyclic acetal similar to **11**. When **2**, an excess of acetaldehyde, and  $\text{BF}_3\cdot\text{OEt}_2$  are combined at room temperature in *methanol*, the major product, **12**, isolated as a single diastereomer, has  $^{13}\text{C}$  and  $^1\text{H}$  NMR data virtually identical to **11** with the exception of an additional methyl group at C(5) (Figure 4). Finally, when the bicyclic ketal **12** is returned to  $\text{CH}_3\text{CN}$  with 0.5 equiv of  $\text{BF}_3\cdot\text{OEt}_2$  and allowed to stand 8 h at  $-40^\circ\text{C}$ , the acetyldihydrofuran **7a** is recovered as the sole product.

Whereas the reaction of the methylfuran complex **2** with aldehydes appears to be general, when **2** is combined with acetone or acetophenone, a  $^1\text{H}$  NMR of the isolated reaction mixture indicates no incorporation of the ketone. Rather, the major product of the reaction

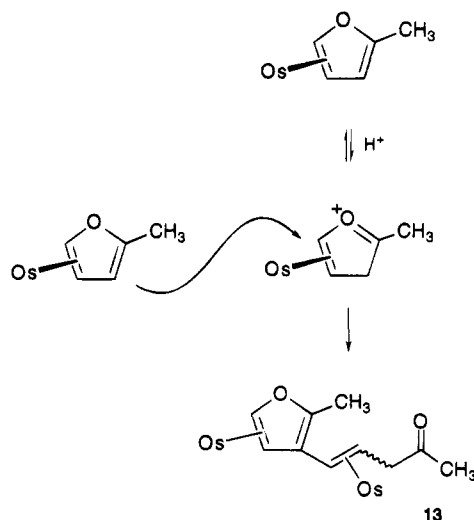


**Figure 5.** Formation of the dimerization product (**13**) for the methylfuran complex **2**.

(**13**) is a dimer of **2** with  $^1\text{H}$  NMR data now showing two sets of *cis*- and *trans*-ammine resonances of equal intensity. The dimer (**13**) is also obtained from a control reaction where a solution of methylfuran complex **2** is treated with Lewis acid alone and allowed to stand at  $-40^\circ\text{C}$  for ~48 h (Figure 5). The synthesis and characterization of the dimer (**13**) is described in detail in a separate study.<sup>11</sup>

Dihydrofuran is readily displaced from the complex  $[\text{Os}(\text{NH}_3)_5(2,3\text{-}\eta^2\text{-4,5-dihydrofuran})]^{2+}$  by  $1e^-$  oxidants,<sup>12</sup> and treatment of the bicyclic species **11** and **12** with DDQ also liberates the organic ligands.<sup>13</sup> Unfortunately, for compounds **6–8a**, one-electron oxidants catalyze an intramolecular condensation of the acetyl group with a *cis*-ammine ligand (Figure 6, **14–16**).<sup>14</sup> This process, originally observed for the condensation of acetone with hexammineosmium(II), is initiated by oxidation of the metal to osmium(III). Once in this form, an acidic ammine ligand readily loses a proton and undergoes condensation with the acetyl group of the organic ligand. The resulting imine complex is rendered somewhat more oxidizing than its pentaammineosmium(III) precursor and consequently is reduced by uncondensed starting material back to osmium(II) (Figure 6). Thus, no organic products are generated by the usual route. Efforts to remove these acetylated dihydrofuran ligands through the use of stoichiometric amounts of harsher oxidants (e.g.  $\text{Ce}(\text{IV})$  or  $\text{NO}^+$ ) also have failed. Chemical modification of the acetyl group or the ammine ligand may be required in order to generate useful amounts of the organic products.

(11) Chen, H.; Liu, R.; Harman, W. D. Manuscript in preparation.

(12) Typical reaction conditions: 1.0 equiv of DDQ; DMF;  $-40^\circ\text{C}$ .

(13) NMR characterization of the bicyclic ligand recovered from **12**:  $^1\text{H}$  NMR (benzene- $d_6$ , 300 MHz)  $\delta$  6.20 (t,  $J = 2.7$  Hz, 1H, H-C6), 4.78 (t,  $J = 2.1$  Hz, 1H, H-C5), 4.53 (q, 1H,  $J = 5.1$  Hz, H-C2), 3.35 (qd,  $J = 6.3, 3.6$  Hz, 1H, H-C4), 2.10 (m, 1H, H-C4a), 1.43 (s, 3H,  $\text{CH}_3$ ), 1.33 (d,  $J = 5.1$  Hz, 3H,  $\text{CH}_3$ ), 1.25 (d,  $J = 6.3$  Hz, 3H,  $\text{CH}_3$ );  $^{13}\text{C}$  NMR ( $\text{CD}_3\text{CN}$ , 75 MHz)  $\delta$  145.8 (C6), 99.9 (C5), 95.0 (C2), 69.7 (C4), 49.9 (C4a), 22.9 ( $\text{CH}_3$ ), 21.9 ( $\text{CH}_3$ ), 19.2 ( $\text{CH}_3$ ), C7a overlaps with solvent peak.

(14) For an example of a redox-catalyzed condensation of acetone and an osmium(II)-ammine ligand, see: Harman, W. D.; Taube, H. *Inorg. Chem.* **1988**, *27*, 3261.

(15) (a) Myers, W. H.; Koontz, J. I.; Harman, W. D. *J. Am. Chem. Soc.* **1992**, *114*, 5684. (b) Hodges, L. M.; Gonzalez, J.; Koontz, J. I.; Myers, W. H.; Harman, W. D. *J. Org. Chem.* **1993**, *58*, 4788. (c) Hodges, L. M.; Gonzalez, J.; Koontz, J. I.; Myers, W. H.; Harman, W. D. *J. Org. Chem.* **1995**, *60*, 2125.

(9) Complex **8b** shows a 12% NOE between H(4) and H(5), and no detectable NOE is observed for either of these protons with the *cis*-ammines.

(10) A similar reaction occurs for benzaldehyde.



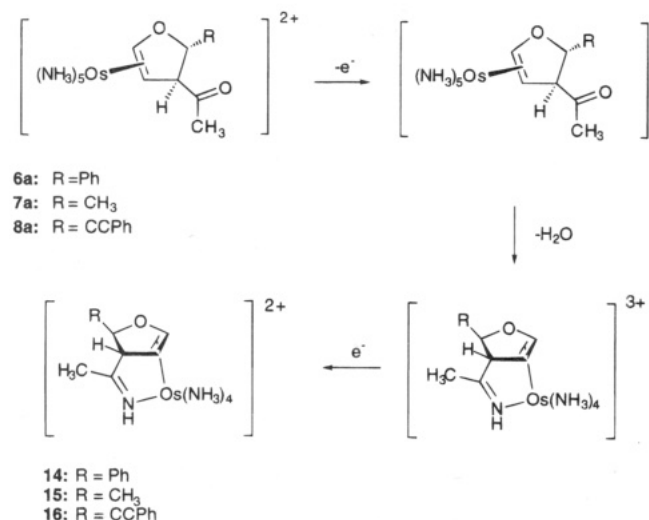


**Figure 6.** Redox-catalyzed condensation of 4-acetyl-4,5-dihydrofuran and ammine ligands.

### Discussion

The contrast between the reaction of  $[\text{Os}(\text{NH}_3)_5(\eta^2\text{-furan})]^{2+}$  (**1**) and its 5-methylated analog (**2**) with benzaldehyde dimethyl acetal (Figure 3) highlights a fundamental difference in the chemistry of these ( $\eta^2$ -furan)osmium complexes compared to their pyrrole analogs. Whereas the latter react with carbon electrophiles at the unbound  $\beta$  carbon (C(4)) to generate *stable* 4*H*-pyrrolium complexes,<sup>15</sup> the more electron-deficient 4*H*-furanium species show a distinct tendency to sever the bond between the heteroatom and C(2) (e.g. compound **5**). It is not clear if the difference in reaction pathways illustrated in Figure 3 is a consequence of thermodynamics or kinetics. Arguably, with R = CH<sub>3</sub>, the carbonyl group in **5** is stabilized relative to its aldehyde counterpart (R = H), and this factor alone could be responsible for the contrast in reactivities of **1** and **2** with the benzaldehyde acetal. Alternatively, if **4** and **5** were formed under kinetic control, the observed differences in reactivity could be rationalized by invoking that the methyl group sufficiently hinders nucleophilic attack at C(5) of the 4*H*-furanium species so that C(2) addition becomes competitive. Although our observations do not lead to any firm conclusions in this regard, it is clear that *the addition of a methyl group to C(5) enhances the chances for nucleophilic addition at C(2)*.

The methylfuran complex (**2**) and its furan analog undergo an aldol reaction at C(4) stereospecifically with the electrophile coming from the ring face *anti* to metal coordination. Thus, the *syn* stereochemistry at C(4), common to complexes **6–10a**, is at first glance surprising. However, the observed substitution pattern for the products requires a rearrangement involving cleavage and formation of a new furan ring. The acid-catalyzed aldol reaction is expected to occur at C(4) of the furan complex *anti* to the osmium. In the absence of nucleophilic addition at C(5), the hypothesized 4*H*-furanium intermediate undergoes a nucleophilic displacement at C(2) to form the final dihydrofuran product. Although it has not been determined whether this displacement is stepwise or concerted, connecting the *anti*-oriented alkoxide substituent to C(2) requires a rotation of the C(3)–C(4) bond, and consequently, the newly formed

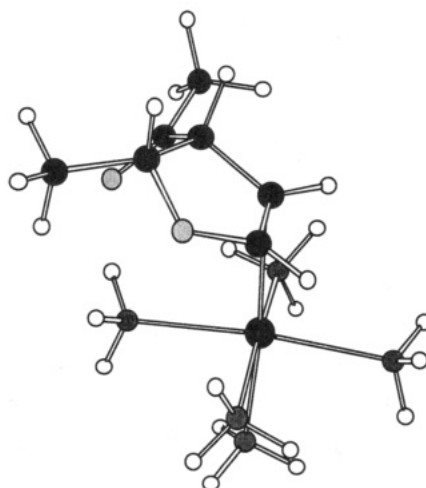


**Figure 7.** Molecular model of the hypothetical diastereomer of **7a**,  $[\text{Os}(\text{NH}_3)_5(2\alpha,3\alpha\text{-}\eta^2\text{-4a-acetyl-5}\alpha\text{-methyl-4,5-dihydrofuran})]^{2+}$  (**7b**; not observed) showing steric interaction between pentaammineosmium and methyl groups.

acetyl group is required to have a *syn* stereochemistry with respect to the metal. The chirality of C(5) also originates from the aldol reaction, but in contrast to C(4), the stereochemistry of C(5) is governed by thermodynamics. The epimerization of **8b** to its more stable isomer (**8a**) probably occurs through a reversible reaction sequence where the methylfuran complex and aldehyde are temporarily re-formed. Supporting this hypothesis is the observation that when a reaction mixture containing only **8a,b** is subjected to an excess of acetaldehyde in the presence of the Lewis acid, a significant amount ( $\sim 20\%$ ) of compound **7a** is isolated. For every case examined, the thermodynamically favored isomer has the C(5) substituent *anti* to the pentaammineosmium moiety, and we interpret this preference as a consequence of minimizing the steric interactions between these groups. In Figure 7, this point is illustrated by consideration of a molecular model of the unobserved isomer **7b** that has the C(5) methyl group *syn* to the osmium.

The primary reaction competing with the C(2) displacement is the formation of a furodioxin (**11**, **12**). Similar products have been observed for the reaction of simple vinyl ethers with saturated aldehydes.<sup>16</sup> For the case of acetaldehyde and the 5-methylfuran complex **2**, quenching the reaction after 3 h ( $-40^\circ\text{C}$ ) results in significant amounts of **12** (Figure 4). Under identical conditions, running the reaction for longer periods (e.g. 17 h) yields the acetyldihydrofuran complex **7a** as the sole product. Finally, a sample of **12** prepared from methanol solution readily converts to **7a** when treated with Lewis acid in acetonitrile. Together, these observations confirm that the bicyclic ketals such as **12** are kinetically favored products that under acidic conditions readily eliminate 1 equiv of aldehyde to form the acetyldihydrofuran products. By analogy, the furodioxin complexes formed from the furan analog (e.g. **11**) may also be unstable with respect to such a transformation. Indeed, treatment of **11** with  $\text{BF}_3\cdot\text{OEt}_2$  in acetonitrile over 24 h does result in a decomposition product ( $\sim 40\%$ ) whose  $^1\text{H}$  NMR features match those expected for a

(16) Satsumabayashi, S.; Nakajo, K.; Soneda, R.; Mototi, S. *Bull. Chem. Soc. Jpn.* **1970**, *43*, 1586.



4-formyl-4,5-dihydrofuran complex, but attempts to produce this material in high yield have failed.

In contrast to typical (thermal) reactions of furans with aldehydes, complexation with osmium(II) serves to alter the regiochemistry of electrophilic addition, inhibit possible deprotonation of the resulting 4*H*-furanium species, activate C(2) toward nucleophilic addition, and control the stereochemistry for these transformations. In related studies, the pentaammine-osmium(II) moiety has proven to be an effective promoter of both electrophilic and nucleophilic additions for arenes and aromatic heterocycles, but such transformations heretofore were observed only for *uncoordinated* ring-carbons. Of significance, this study demonstrates a complementary chemistry for pentaammine-osmium(II) where nucleophilic addition occurs at a bound carbon of a heterocycle,<sup>4</sup> in this case to generate a functionalized dihydrofuran with a high degree of stereocontrol.

### Experimental Section

**General Methods.** Routine <sup>1</sup>H and <sup>13</sup>C NMR spectra were recorded on a General Electric QE-300 or GN-300 spectrometer at 23 °C (room temperature) unless otherwise noted. Unless otherwise noted, <sup>1</sup>H and <sup>13</sup>C spectra were obtained at 300 and 75 MHz, respectively. Chemical shifts are reported in ppm and are referenced to residual protonated solvent ( $\delta(\text{acetone-}d_6) = 2.04$ ;  $\delta(\text{acetonitrile-}d_2) = 1.93$ ;  $\delta(\text{methanol-}d_3) = 3.30$ ). Two-dimensional NMR spectra (e.g., DEPT, COSY, NOESY, HETCOR) were recorded on a General Electric GN-300 spectrometer. Electrochemical experiments were performed under nitrogen using a PAR Model 362 potentiostat driven by a PAR Model 175 universal programmer. Cyclic voltammograms were recorded (Kipp & Zonen BD90 XY recorder) in a standard three-electrode cell<sup>17</sup> from +1.8 to -1.8 V with a glassy carbon electrode. All potentials are reported vs NHE and, unless otherwise noted, were determined in acetonitrile (~0.5 M TBAH) using ferrocene ( $E_{1/2} = +0.55$  V) or cobaltocenium hexafluorophosphate ( $E_{1/2} = -0.78$  V) *in situ* as a calibration standard. The peak-to-peak separation ( $E_{p,a} - E_{p,c}$ ) was between 80 and 100 mV for all reversible couples unless otherwise noted. This work was carried out under a nitrogen atmosphere in a Vacuum Atmospheres Co. glovebox, separate boxes being used for aqueous and nonaqueous reactions. When necessary, furan complexes were purified by ion-exchange chromatography using Sephadex SP C-25 resin with aqueous NaCl as the mobile phase. The purified salts were precipitated as the tetraphenylborate salt by adding an excess of aqueous NaBPh<sub>4</sub>. Elemental analyses were obtained on a Perkin-Elmer PE-2400 Series II CHN analyzer.

**Solvents.** All solvents were deoxygenated by purging with nitrogen for at least 15 min; deuterated solvents were deoxygenated either by repeated freeze-pump-thaw cycles or vacuum distillation. All distillations were performed under nitrogen. Methylene chloride was refluxed over either CaH<sub>2</sub> or P<sub>2</sub>O<sub>5</sub> for at least 8 h and distilled. Diethyl ether was refluxed for at least 8 h over sodium/benzophenone and distilled. Methanol was refluxed over Mg(OMe)<sub>2</sub> prepared *in situ* from magnesium activated by I<sub>2</sub> and distilled. Acetonitrile and propionitrile were refluxed over CaH<sub>2</sub> and distilled. Aldrich anhydrous grade DMAc and DME were used without further purification, except that they were deoxygenated prior to use.

**Reagents.** [Os(NH<sub>3</sub>)<sub>5</sub>OTf](OTf)<sub>2</sub> was synthesized as described by Lay et al.<sup>18</sup> Magnesium powder (Aldrich, 50 mesh) was activated by treating with iodine in DME under nitrogen, stirring for 1 h, filtering, and washing with DMAc, acetone, and diethyl ether. All liquid reagents were used as received except that they were deoxygenated prior to use.

**Complexes.** The synthesis and characterization of the furan complex [Os(NH<sub>3</sub>)<sub>5</sub>( $\eta^2$ -furan)]OTf<sub>2</sub> (1) and compound 4 have been previously reported,<sup>4</sup> and the 2,5-dimethyl analog (3) was prepared in a similar fashion to that of 1.

[Os(NH<sub>3</sub>)<sub>5</sub>(2,3- $\eta^2$ -5-methylfuran)](OTf)<sub>2</sub> (2). To a solution of [Os(NH<sub>3</sub>)<sub>5</sub>(OTf)](OTf)<sub>2</sub> (2.55 g, 3.53 mmol) in methanol (14.5 g) is added 2-methylfuran (10.9 g, 132 mmol), followed by Zn/Hg (9.97 g). After being stirred for 5 min, the slurry was filtered through a fine frit into a flask containing Et<sub>2</sub>O (800 mL), producing a light yellow precipitate, that was collected, washed with CH<sub>2</sub>Cl<sub>2</sub> and Et<sub>2</sub>O, and dried *in vacuo*. Yield of light yellow powder: 2.10 g, 91%. The title compound can also be synthesized by reducing [Os(NH<sub>3</sub>)<sub>5</sub>(OTf)](OTf)<sub>2</sub> with Mg<sup>0</sup> in DMAc. <sup>1</sup>H NMR (300 MHz, acetone-*d*<sub>6</sub>):  $\delta$  7.38 (d, *J* = 3.6 Hz, 1H, H-C2), 5.81 (d, *J* = 1.5 Hz, 1H, H-C4), 5.00 (dd, *J* = 3.6, 1.5 Hz, 1H, H-C3), 4.63 (br s, 3H, *trans*-NH<sub>3</sub>), 3.46 (br s, 12H, *cis*-NH<sub>3</sub>), 1.97 (s, 3H, CH<sub>3</sub>). <sup>13</sup>C NMR (75 MHz, acetone-*d*<sub>6</sub>):  $\delta$  153.1 (C5), 107.2 (C4), 97.8 (C2), 50.4 (C3), 13.1 (CH<sub>3</sub>). Anal. Calcd for C<sub>7</sub>H<sub>21</sub>O<sub>7</sub>N<sub>5</sub>S<sub>2</sub>OsF<sub>6</sub>: C, 12.83; H, 3.23; N, 10.68. Found: C, 12.51; H, 3.19; N, 10.57. CV (CH<sub>3</sub>CN, TBAH, 100 mV/s):  $E_{p,a} = 0.60$  V (NHE).

[Os(NH<sub>3</sub>)<sub>5</sub>(4,5- $\eta^2$ -3-(methoxyphenylmethyl)-5-methoxy-pent-4-ene-2-one)](OTf)<sub>2</sub> (5). Benzaldehyde dimethyl acetal (522 mg, 3.43 mmol) and 2 (76.5 mg, 0.117 mmol) were dissolved in acetonitrile (1.86 g), and the solution was cooled to -40 °C. BF<sub>3</sub>·OEt<sub>2</sub> (16.7 mg, 0.118 mmol) was added to the reaction solution. The solution was stirred at -40 °C for 1 h and then quenched with pyridine (32.3 mg, 0.408 mmol). After 10 min, the product was precipitated with ether (150 mL), and the light yellow solid was collected (61.6 mg, 66%). From <sup>1</sup>H-NMR, the product appeared to be a single diastereomer. <sup>1</sup>H NMR (CD<sub>3</sub>CN, 300 MHz):  $\delta$  7.20-7.50 (m, 5H, Ph), 5.78 (d, *J* = 6.0 Hz, 1H, H-C5), 4.61 (d, *J* = 10.5 Hz, 1H, H-CPh), 4.13 (br s, 3H, *trans*-NH<sub>3</sub>), 3.82 (dd, *J* = 6.0, 4.2 Hz, 1H, H-C4), 3.55 (s, 3H, OCH<sub>3</sub>), 3.22 (br s, 12H, *cis*-NH<sub>3</sub>), 3.19 (s, 3H, OCH<sub>3</sub>), 2.39 (dd, *J* = 10.5, 4.2 Hz, 1H, H-C3), 1.99 (s, 3H, CH<sub>3</sub>). <sup>13</sup>C NMR (CD<sub>3</sub>CN, 75 MHz):  $\delta$  208.5 (C=O), 139.4 (Ph), 129.8 (Ph), 129.6 (Ph), 129.4 (Ph), 95.1 (C2), 84.7 (CPh), 64.0 (C3), 62.7 (OCH<sub>3</sub>), 56.6 (OCH<sub>3</sub>), 40.0 (C4), 28.8 (CH<sub>3</sub>). Anal. Calcd for C<sub>16</sub>H<sub>33</sub>N<sub>5</sub>O<sub>9</sub>S<sub>2</sub>OsF<sub>6</sub>: C, 23.79; H, 4.12; N, 8.67. Found: C, 24.02; H, 4.17; N, 8.92. CV (CH<sub>3</sub>CN, TBAH, 100 mV/s):  $E_{p,a} = 0.97$  V (NHE). When this reaction was carried out at room temperature, the same complex was obtained but in lower yield.

[Os(NH<sub>3</sub>)<sub>5</sub>(2 $\alpha$ ,3 $\alpha$ - $\eta^2$ -4 $\alpha$ -acetyl-5 $\beta$ -phenyl-4,5-dihydro-furan)](OTf)<sub>2</sub> (6a). Benzaldehyde (145.3 mg, 1.37 mmol) and 2 (60.6 mg, 0.092 mmol) were dissolved in a mixture of acetonitrile (1 g) and propionitrile (0.5 g), and the solution was cooled to -40 °C. Sn(OTf)<sub>2</sub> (38.2 mg, 0.092 mmol) dissolved in 500 mg of acetonitrile was added. After stirring for 17 h (-40 °C), the solution was quenched with pyridine (200 mg), and the product was precipitated with a mixture of ether (100 mL) and CH<sub>2</sub>Cl<sub>2</sub> (75 mL) and collected (71%, 50.2 mg). <sup>1</sup>H NMR (300 MHz, CD<sub>3</sub>CN):  $\delta$  7.30-7.40 (m, 5H, Ph), 6.39 (d, *J* = 4.2 Hz, 1H, H-C2), 4.31 (dd, *J* = 10.5, 4.2 Hz, 1H, H-C4), 4.17 (d, *J* = 10.5 Hz, 1H, H-C5), 4.05 (br s, 3H, *trans*-NH<sub>3</sub>), 3.79 (t, *J* = 4.2 Hz, 1H, H-C3), 3.21 (br s, 12H, *cis*-NH<sub>3</sub>), 2.10 (s, 3H, CH<sub>3</sub>). <sup>13</sup>C NMR (75 MHz, CD<sub>3</sub>CN):  $\delta$  214.7 (C=O), 142.5 (Ph), 129.4 (Ph), 129.0 (Ph), 127.4 (Ph), 96.68 (C2), 82.3 (C5), 69.6 (C4), 37.4 (C3), 32.5 (CH<sub>3</sub>). This compound was purified by ion-exchange chromatography and isolated as its tetraphenylborate salt monohydrate. Anal. Calcd for C<sub>60</sub>H<sub>67</sub>-

(17) Bard, A. J.; Faulkner, L. R. *Electrochemical Methods*; John Wiley & Sons: New York, 1980.

(18) (a) Lay, P. A.; Magnuson, R. H.; Taube, H. *Inorg. Chem.* **1989**, *28*, 3001. (b) Lay, P. A.; Magnuson, R. H.; Taube, H. *Inorg. Synth.* **1986**, *24*, 269.

$\text{N}_5\text{O}_2\text{B}_2\text{O}_8\cdot\text{H}_2\text{O}$ : C, 64.34; H, 6.21; N, 6.25. Found: C, 64.73; H, 6.32; N, 6.01. CV ( $\text{CH}_3\text{CN}$ , TBAH, 100 mV/s):  $E_{p,a} = 0.76$  V (NHE).

**[Os(NH<sub>3</sub>)<sub>5</sub>(2 $\alpha$ ,3 $\alpha$ - $\eta^2$ -4 $\alpha$ -acetyl-5 $\beta$ -methyl-4,5-dihydrofuran)](OTf)<sub>2</sub> (7a).** Acetaldehyde (6.0 mg, 0.136 mmol) and **2** (54.3 mg, 0.083 mmol) were dissolved in a mixture of acetonitrile (1 g) and propionitrile (0.5 g), and the solution was cooled to  $-40^\circ\text{C}$ . Sn(OTf)<sub>2</sub> (33.6 mg, 0.081 mmol) dissolved in 500 mg of acetonitrile was added. After being stirred for 17 h at  $-40^\circ\text{C}$ , the solution was quenched with pyridine (200 mg), and the product was precipitated with a mixture of ether (60 mL) and  $\text{CH}_2\text{Cl}_2$  (40 mL) and collected (78%, 45.2 mg). <sup>1</sup>H NMR ( $\text{CD}_3\text{CN}$ , 300 MHz):  $\delta$  6.18 (d,  $J = 4.2$  Hz, 1H, H-C2), 3.98 (br s, 3H, *trans*-NH<sub>3</sub>), 3.96 (dd,  $J = 10.5$ , 4.2 Hz, 1H, H-C4), 3.66 (t,  $J = 4.2$  Hz, 1H, H-C3), 3.20–3.40 (m, 1H, H-C5), 3.12 (br s, 12H, *cis*-NH<sub>3</sub>), 2.31 (s, 3H, COCH<sub>3</sub>), 1.22 (d,  $J = 5.7$  Hz, 3H, CH<sub>3</sub>-C5). <sup>13</sup>C NMR ( $\text{CD}_3\text{CN}$ , 75 MHz):  $\delta$  215.37 (C=O), 96.58 (C2), 77.22 (C5), 67.11 (C4), 37.87 (C3), 32.49 (CH<sub>3</sub>), 22.22 (CH<sub>3</sub>-C5). This compound was purified by ion-exchange chromatography and isolated as its tetraphenylborate monohydrate salt. Anal. Calcd for  $\text{C}_{55}\text{H}_{65}\text{O}_2\text{N}_5\text{B}_2\text{O}_8\cdot\text{H}_2\text{O}$ : C, 62.44; H, 6.38; N, 6.62. Found: C, 62.63; H, 6.33; N, 6.66. CV ( $\text{CH}_3\text{CN}$ , TBAH, 100 mV/s):  $E_{p,a} = 0.72$  V (NHE).

**[Os(NH<sub>3</sub>)<sub>5</sub>(2 $\alpha$ ,3 $\alpha$ - $\eta^2$ -4 $\alpha$ -acetyl-5 $\beta$ -phenylethynyl-4,5-dihydrofuran)](OTf)<sub>2</sub> (8a).** Phenylpropargylaldehyde (40.2 mg, 0.31 mmol) and **2** (142 mg, 0.22 mmol) were dissolved in a mixture of acetonitrile (3 g) and propionitrile (3 g), and the solution was cooled to  $-40^\circ\text{C}$ . Sn(OTf)<sub>2</sub> (90.3 mg, 0.22 mmol) dissolved in 1500 mg of acetonitrile was added. After being stirred for 17 h, the solution was quenched with pyridine (200 mg), and the product was precipitated with a mixture of ether (350 mL) and  $\text{CH}_2\text{Cl}_2$  (200 mL) and collected (80%, 136 mg). <sup>1</sup>H NMR ( $\text{CD}_3\text{CN}$ , 300 MHz) (**8a**):  $\delta$  7.30–7.52 (m, 5H, Ph), 6.31 (d,  $J = 4.2$  Hz, 1H, H-C2), 4.50 (dd,  $J = 10.5$ , 4.2 Hz, 1H, H-C4), 4.06 (d,  $J = 10.5$  Hz, 1H, H-C5), 4.05 (br s, 3H, *trans*-NH<sub>3</sub>), 3.73 (t,  $J = 4.2$  Hz, 1H, H-C3), 3.16 (br s, 12H, *cis*-NH<sub>3</sub>), 2.41 (s, 3 H, CH<sub>3</sub>). <sup>13</sup>C NMR ( $\text{CD}_3\text{CN}$ , 75 MHz):  $\delta$  213.57 (C=O), 132.34 (Ph), 129.92 (Ph), 129.51 (Ph), 123.83 (Ph), 96.53 (C2), 87.78 (C=C), 87.51 (C=C), 70.20 (C5), 66.72 (C4), 36.30 (C3), 32.30 (CH<sub>3</sub>). This compound was purified by ion-exchange chromatography and isolated as its tetraphenylborate monohydrate salt. Anal. Calcd for  $\text{C}_{62}\text{H}_{67}\text{O}_2\text{N}_5\text{B}_2\text{O}_8\cdot\text{H}_2\text{O}$ : C, 65.09; H, 6.08; N, 6.12. Found: C, 65.05; H, 6.16; N, 6.42. CV ( $\text{CH}_3\text{CN}$ , TBAH, 100 mV/s):  $E_{p,a} = 0.82$  V (NHE).

**8b (Minor Isomer).** <sup>1</sup>H NMR ( $\text{CD}_3\text{CN}$ , 300 MHz):  $\delta$  7.30–7.52 (m, 5H, Ph), 6.40 (d,  $J = 4.2$  Hz, 1H, H-C2), 5.82 (d,  $J = 12.0$  Hz, 1H, H-C5), 4.93 (dd,  $J = 12.0$ , 4.2 Hz, 1H, H-C4), 4.05 (br s, 3H, *trans*-NH<sub>3</sub>), 3.73 (t,  $J = 4.2$  Hz, 1H, H-C3), 3.19 (br s, 12H, *cis*-NH<sub>3</sub>), 2.29 (s, 3H, COCH<sub>3</sub>). <sup>13</sup>C NMR ( $\text{CD}_3\text{CN}$ , 75 MHz):  $\delta$  212.70 (C=O), 132.34 (Ph), 130.37 (Ph), 129.57 (Ph), 122.77 (Ph), 98.33 (C2), 87.78 (C=C), 87.13 (C=C), 71.11 (C5), 60.71 (C4), 37.29 (C3), 32.41 (CH<sub>3</sub>).

**[Os(NH<sub>3</sub>)<sub>5</sub>(2 $\alpha$ ,3 $\alpha$ - $\eta^2$ -4 $\alpha$ -acetyl-5 $\beta$ -*t*-phenylethenyl-4,5-dihydrofuran)](OTf)<sub>2</sub> (9a).** *trans*-Cinnamaldehyde (113.7 mg, 0.86 mmol) and **2** (55.1 mg, 0.084 mmol) were dissolved in a mixture of acetonitrile (1 g) and propionitrile (1 g), and the solution was cooled to  $-40^\circ\text{C}$ . Sn(OTf)<sub>2</sub> (38.9 mg, 0.093 mmol) dissolved in 500 mg of acetonitrile was added. After being stirred for 17 h at  $-40^\circ\text{C}$ , the solution was quenched with pyridine (200 mg), and the product was precipitated with a mixture of ether (75 mL) and  $\text{CH}_2\text{Cl}_2$  (30 mL) and collected (90%, 60.2 mg). <sup>1</sup>H-NMR (300 MHz,  $\text{CD}_3\text{CN}$ ):  $\delta$  7.55 (m, 5H, C<sub>6</sub>H<sub>5</sub>), 6.55 (d,  $J = 15.9$  Hz, 1H, PhCH), 6.28 (dd,  $J = 6.9$ , 15.9 Hz, 1H, H-C5), 6.26 (d,  $J = 4.2$  Hz, 1H, H-C2), 4.25 (dd,  $J = 4.5$ , 10.5 Hz, 1H, H-C4), 4.02 (br s, 3H, NH<sub>3</sub>), 3.80 (dd,  $J = 6.9$ , 10.5 Hz, 1H, H-C5), 3.71 (dd,  $J = 4.2$ , 4.5 Hz, 1H, H-C3), 3.16 (br s, 12H, NH<sub>3</sub>), 2.26 (s, 3H, COCH<sub>3</sub>). <sup>13</sup>C NMR (75 MHz,  $\text{CD}_3\text{CN}$ ):  $\delta$  194.07 (CO), 145.79 (C), 132.52 (CH), 129.78 (CH), 129.54 (CH), 123.86 (C), 119.64 (C), 93.00 (CH), 79.51 (CH), 61.71 (CH), 51.09 (CH), 24.00 (CH<sub>3</sub>).

**Os(NH<sub>3</sub>)<sub>5</sub>(2 $\alpha$ ,3 $\alpha$ - $\eta^2$ -4 $\alpha$ -acetyl-2-methyl-5 $\beta$ -phenyl-4,5-dihydrofuran)](OTf)<sub>2</sub> (10a).** Benzaldehyde (38.5 mg, 0.36 mmol) and [Os(NH<sub>3</sub>)<sub>5</sub>( $\eta^2$ -2,5-dimethylfuran)](OTf)<sub>2</sub> (**3**) (48.5 mg, 0.072 mmol) were dissolved in a mixture of acetonitrile (1 g) and propionitrile (1 g), and the solution was cooled to  $-40^\circ\text{C}$ . Sn(OTf)<sub>2</sub> (26.7 mg, 0.064 mmol) dissolved in 500 mg of acetonitrile was added. After being stirred for 17 h at  $-40^\circ\text{C}$ , the solution was quenched with pyridine (200 mg), and the product was precipitated with a mixture of ether (50 mL) and  $\text{CH}_2\text{Cl}_2$  (50 mL) and collected (80%, 45 mg). <sup>1</sup>H-NMR (300 MHz,  $\text{CD}_3\text{CN}$ ):  $\delta$  7.28–7.40 (m, 5H, C<sub>6</sub>H<sub>5</sub>), 4.50 (dd,  $J = 4.8$ , 9.6 Hz, 1H, H-C4), 4.31 (d,  $J = 9.6$  Hz, 1H, H-C5), 4.05 (br s, 3H, *trans*-NH<sub>3</sub>), 3.81 (d,  $J = 4.8$  Hz, 1H, H-C3), 3.23 (br s, 12H, *cis*-NH<sub>3</sub>), 2.14 (s, 3H, COCH<sub>3</sub>), 1.77 (t, 3H, CH<sub>3</sub>-C2). <sup>13</sup>C-NMR (75 MHz,  $\text{CD}_3\text{CN}$ ):  $\delta$  215.22 (CO), 144.15 (C), 129.47 (CH), 128.80 (CH), 127.02 (CH), 97.65 (C), 83.47 (CH), 69.16 (CH), 39.90 (CH), 32.80 (CH<sub>3</sub>), 19.26 (CH<sub>3</sub>).

**[Os(NH<sub>3</sub>)<sub>5</sub>(5,6- $\eta^2$ -2,4-dimethyl-4a,7a-dihydro-4H-furo[2,3-*d*]-1,3-dioxin)](OTf)<sub>2</sub> (11).** Acetaldehyde (50.5 mg, 1.15 mmol) and **1** (63.3 mg, 0.0987 mmol) were dissolved in a mixture of  $\text{CH}_3\text{CN}$  (2.78 g) and  $\text{CH}_2\text{Cl}_2$  (1.09 g), and the solution was cooled to  $-40^\circ\text{C}$ . BF<sub>3</sub>·OEt<sub>2</sub> (17.1 mg, 0.121 mmol) was added, and the solution was stirred at  $-40^\circ\text{C}$  for 12 h. The reaction was quenched with pyridine (64.5 mg, 0.815 mmol), and the product was precipitated with a mixture of ether (50 mL) and  $\text{CH}_2\text{Cl}_2$  (50 mL) and collected (83%, 59.7 mg). From the <sup>1</sup>H NMR, the product appeared to be a mixture of two isomers with a 1:2 ratio. Anal. Calcd for  $\text{C}_{10}\text{H}_{27}\text{N}_5\text{O}_9\text{S}_2\text{OsF}_6$ : C, 16.46; H, 3.73; N, 9.60. Found: C, 16.04; H, 3.85; N, 10.00. CV ( $\text{CH}_3\text{CN}$ , TBAH, 100 mV/s):  $E_{1/2} = 0.77$  V (NHE).

**Major Isomer.** <sup>1</sup>H NMR ( $\text{CD}_3\text{CN}$ , 300 MHz):  $\delta$  5.97 (d,  $J = 4.2$  Hz, 1H, H-C6), 5.05 (q,  $J = 5.1$  Hz, 1H, H-C2), 4.19 (d,  $J = 5.4$  Hz, 1H, H-C7a), 3.80 (m, 1H, H-C4), 3.97 (br s, 3H, *trans*-NH<sub>3</sub>), 3.05 (br s, 12 H, *cis*-NH<sub>3</sub>), 2.92 (d,  $J = 4.2$  Hz, 1H, H-C5), 1.79 (dd,  $J = 9.9$ , 5.7 Hz, 1H, H-C4a), 1.35 (d,  $J = 6.0$  Hz, 3H, CH<sub>3</sub>), 1.26 (d,  $J = 5.1$  Hz, 3H, CH<sub>3</sub>). <sup>13</sup>C NMR ( $\text{CD}_3\text{CN}$ , 75 MHz):  $\delta$  100.0 (C7a), 93.8 (C2), 90.1 (C6), 77.9 (C4), 44.6 (C4a), 35.6 (C5), 21.1 (CH<sub>3</sub>), 20.5 (CH<sub>3</sub>).

**Minor Isomer.** <sup>1</sup>H NMR ( $\text{CD}_3\text{CN}$ , 300 MHz):  $\delta$  6.72 (d,  $J = 4.2$  Hz, 1H, H-C6), 5.40 (d,  $J = 3.6$  Hz, 1H, H-C7a), 4.70 (q,  $J = 5.1$  Hz, H-C2), 4.05 (m, 1H, H-C4), 4.05 (br s, 3H, *trans*-NH<sub>3</sub>), 3.80 (m, 1H, H-C5), 3.01 (br s, 12H, *cis*-NH<sub>3</sub>), 1.83 (m, 1H, H-C4), 1.30 (d,  $J = 6.6$  Hz, 3H, CH<sub>3</sub>), 1.26 (d,  $J = 5.1$  Hz, 3H, CH<sub>3</sub>). <sup>13</sup>C NMR ( $\text{CD}_3\text{CN}$ , 75 MHz):  $\delta$  107.6 (C7a), 98.2 (C6), 95.6 (C2), 71.8 (C4), 46.7 (C4a), 38.1 (C5), 21.5 (CH<sub>3</sub>), 20.1 (CH<sub>3</sub>).

**[Os(NH<sub>3</sub>)<sub>5</sub>(5,6- $\eta^2$ -2,4,7a-trimethyl-4a,7a-dihydro-4H-furo[2,3-*d*]-1,3-dioxin)](OTf)<sub>2</sub> (12).** Acetaldehyde (1.28 g, 29.0 mmol) and **2** (116 mg, 0.180 mmol) were dissolved in  $\text{CH}_3\text{OH}$  (635 mg). BF<sub>3</sub>·OEt<sub>2</sub> (11.5 mg, 0.0810 mmol) was added, and the solution was stirred at ambient temperature for 45 min. The reaction was quenched with pyridine (60.4 mg, 0.764 mmol), and the product was precipitated with a mixture of Et<sub>2</sub>O (120 mL) and  $\text{CH}_2\text{Cl}_2$  (30 mL) and collected (74%, 98.5 mg). From the <sup>1</sup>H NMR, the product appeared to be a mixture of a single diastereomer of **12** and **7a** (<10%). <sup>1</sup>H NMR ( $\text{CD}_3\text{CN}$ , 300 MHz):  $\delta$  6.56 (d,  $J = 3.9$  Hz, 1H, H-C6), 4.71 (q,  $J = 5.1$  Hz, 1H, H-C2), 3.86 (1H, overlap with H-C3, H-C4), 3.86 (1H, overlap with H-C4, H-C3), 4.12 (br s, 3H, *trans*-NH<sub>3</sub>), 3.08 (br s, 12H, *cis*-NH<sub>3</sub>), 1.66 (s, 1H, H-C4a), 1.28 (s, 3H, CH<sub>3</sub>), 1.27 (d,  $J = 6.6$  Hz, 3H, CH<sub>3</sub>), 1.25 (d,  $J = 5.1$  Hz, 3H, CH<sub>3</sub>). <sup>13</sup>C NMR ( $\text{CD}_3\text{CN}$ , 75 MHz):  $\delta$  114.2 (C7a), 96.3 (C6), 95.3 (C2), 71.2 (C4), 50.2 (C4a), 40.7 (C5), 21.6 (CH<sub>3</sub>), 20.2 (CH<sub>3</sub>), 19.2 (CH<sub>3</sub>). CV ( $\text{CH}_3\text{CN}$ , TBAH, 100 mV/s):  $E_{1/2} = 0.77$  V (NHE).

**Compound 14 (NMR Characterization).** <sup>1</sup>H-NMR (300 MHz,  $\text{CD}_3\text{OD}$ ):  $\delta$  7.20–7.50 (m, 5 H, C<sub>6</sub>H<sub>5</sub>), 6.97 (d, 1 H,  $J = 3.3$  Hz, H-C2), 4.69 (d, 1 H,  $J = 2.1$  Hz, H-C5), 4.53 (br s, 3H, NH<sub>3</sub>), 4.21 (dd, 1 H,  $J = 3.3$ , 5.0 Hz, 5.0 Hz, H-C3), 4.01 (dd, 1 H,  $J = 2.1$ , 5.0 Hz, H-C4), 3.70 (br s, 6H, NH<sub>3</sub>), 3.27 (br s, 3H, NH<sub>3</sub>), 2.35 (s, 3 H, CH<sub>3</sub>). <sup>13</sup>C-NMR (75 MHz,  $\text{CD}_3\text{O}$

OD):  $\delta$  195.29 (C=NH), 144.89 (C), 129.73 (CH), 128.67 (CH), 125.68 (CH), 94.62 (CH), 90.29 (CH), 63.75 (CH), 49.83 (CH), 23.96 (CH<sub>3</sub>).

**Compound 15.** Pyridine (21.9 mg, 0.277 mmol) and [7a](OTf)<sub>2</sub> (53.8 mg, 0.0769 mmol) were dissolved in CH<sub>3</sub>OH (700 mg), and the solution was cooled to -40 °C. DDQ (5.1 mg, 0.022 mmol, dissolved in 100 mg of CH<sub>3</sub>OH), was added into the reaction mixture. After 7 min, the product was precipitated with a mixture of Et<sub>2</sub>O (25 mL) and CH<sub>2</sub>Cl<sub>2</sub> (25 mL). A yellow-green solid was collected, washed with Et<sub>2</sub>O and CH<sub>2</sub>Cl<sub>2</sub>, and dried in *vacuo* (58%, 30.3 mg). Anal. Calcd for C<sub>9</sub>H<sub>23</sub>N<sub>5</sub>O<sub>9</sub>S<sub>2</sub>OsF<sub>6</sub>: C, 15.86; H, 3.40; N, 10.28. Found: C, 16.29; H, 3.52; N, 10.19. CV (CH<sub>3</sub>CN, TBAH, 100 mV/s):  $E_{1/2}$  = 0.71 V (NHE).

<sup>1</sup>H NMR (300 MHz, CD<sub>3</sub>CN):  $\delta$  9.94 (br s, 1H, NH), 6.60 (d, 1 H,  $J$  = 3.3 Hz, H-C2), 4.24 (dd, 1 H,  $J$  = 3.3, 5.1 Hz, H-C3), 4.08 (br s, 3H, NH<sub>3</sub>), 3.76 (dq, 1 H,  $J$  = 1.8, 6.3 Hz, H-C5), 3.70 (dd, 1 H,  $J$  = 1.8, 5.1 Hz, H-C4), 3.23 (br s, 3H, NH<sub>3</sub>), 3.20 (br s, 3H, NH<sub>3</sub>), 2.81 (br s, 3H, NH<sub>3</sub>), 2.17 (s, 3 H, CH<sub>3</sub>), 1.21 (d, 3 H,  $J$  = 6.3 Hz, CH<sub>3</sub>-C5). <sup>13</sup>C-NMR (75 MHz, CD<sub>3</sub>CN):  $\delta$  195.0 (C=NH), 91.7 (CH), 84.0 (CH), 59.7 (CH), 49.6 (CH), 23.0 (CH<sub>3</sub>), 22.4 (CH<sub>3</sub>).

<sup>1</sup>H NMR (300 MHz, CD<sub>3</sub>OD):  $\delta$  6.61 (d, 1 H,  $J$  = 3.3 Hz, H-C2), 4.45 (br s, 3H, NH<sub>3</sub>), 4.26 (dd, 1 H,  $J$  = 3.3, 5.1 Hz, H-C3), 3.83 (dq, 1 H,  $J$  = 1.8, 6.3 Hz, H-C5), 3.73 (dd, 1 H,  $J$  = 1.8, 5.1 Hz, H-C4), 3.70 (br s, 6H, NH<sub>3</sub>), 3.17 (br s, 3H, NH<sub>3</sub>), 2.22 (s, 3 H, CH<sub>3</sub>), 1.25 (d, 3 H,  $J$  = 6.3 Hz, CH<sub>3</sub>-C5). <sup>13</sup>C-NMR (75 MHz, CD<sub>3</sub>OD):  $\delta$  195.53 (C=NH), 92.59 (CH), 85.79 (CH), 61.27 (CH), 50.49 (CH), 23.79 (CH<sub>3</sub>), 23.59 (CH<sub>3</sub>).

**Compound 16.** <sup>1</sup>H-NMR (300 MHz, CD<sub>3</sub>OD):  $\delta$  7.08–7.60 (m, 5 H, Ph), 6.78 (d, 1 H,  $J$  = 3.6 Hz, H-C2), 4.77 (d, 1 H,  $J$  = 2.1 Hz, H-C5), 4.55 (br s, 3H, NH<sub>3</sub>), 4.43–4.50 (m, 1 H, H-C3), 4.27–4.31 (m, 1 H, H-C4), 3.75 (br s, 6H, NH<sub>3</sub>), 3.22 (br s, 3H, NH<sub>3</sub>), 2.31 (s, 3 H, CH<sub>3</sub>). <sup>13</sup>C-NMR (75 MHz, CD<sub>3</sub>OD):  $\delta$  194.07 (C=NH), 145.79 (C), 132.52 (CH), 129.78 (CH), 129.54 (CH), 123.86 (C), 119.64 (C), 93.00 (CH), 79.51 (CH), 61.71 (CH), 51.09 (CH), 24.00 (CH<sub>3</sub>).

**Acknowledgment** is made to the Camille and Henry Dreyfus Foundation, the National Science Foundation (NSF Young Investigator program), the Alfred P. Sloan Foundation, and Colonial Metals Inc. (Elkton, MD) for their generous support of this work.

OM950203+

# Unusual Rate Enhancement in the RhCl(PPh<sub>3</sub>)<sub>3</sub>-Catalyzed Hydrosilylation by Organosilanes Having Two Si–H Groups at Appropriate Distances: Mechanistic Aspects

Hideo Nagashima, Kazuo Tatebe, Toshinori Ishibashi, Akihito Nakaoka, Jun Sakakibara, and Kenji Itoh\*

Department of Materials Science, Toyohashi University of Technology, Toyohashi, Aichi 440, Japan

Received October 13, 1994<sup>®</sup>

Unusual rate enhancement observed in the RhCl(PPh<sub>3</sub>)<sub>3</sub>-catalyzed hydrosilylation of carbonyl compounds with certain  $\alpha,\omega$ -bifunctional organosilanes was studied in two series of experiments. First, the reactions with Me<sub>2</sub>HSi(CH<sub>2</sub>)<sub>n</sub>SiHMe<sub>2</sub> [**1** ( $n = 1$ ), **2** ( $n = 2$ ), **3** ( $n = 3$ ), and **4** ( $n = 4$ )], R<sub>2</sub>HSi(CH<sub>2</sub>)<sub>2</sub>SiHPh<sub>2</sub> [**8** (R = Me) and **9** (R = Ph)], and 1,2-[Me<sub>2</sub>HSi(CH<sub>2</sub>)<sub>n</sub>][Me<sub>2</sub>HSi(CH<sub>2</sub>)<sub>n'</sub>]C<sub>6</sub>H<sub>4</sub> [**5** ( $n = n' = 0$ ), **6** ( $n = 0, n' = 1$ ), and **7** ( $n = n' = 1$ )] were investigated in order to understand the rate acceleration by these two closely spaced Si–H groups. The reactions of five of these bifunctional organosilanes, **2**, **3**, and **5–7**, with acetone were unusually rapid and resulted in selective conversion of only one of their Si–H bonds to a Si–OiPr group within several hours at room temperature. The reaction of their remaining Si–H bonds was as slow as the hydrosilylation with monofunctional organosilanes such as EtMe<sub>2</sub>SiH and PhMe<sub>2</sub>SiH; the conversion was below 25% after 1 day at room temperature. The rate of the reaction of acetone with **1** or **4** was similar to that of EtMe<sub>2</sub>SiH or PhMe<sub>2</sub>SiH. These results suggest that the large enhancement in rate occurred in those bifunctional organosilanes in which two closely spaced Si–H groups were connected by 2–4 carbon units. Similar rate enhancement, compared with monofunctional organosilanes, was observed at 50 °C in the hydrosilylation of **8** or **9** and led to the selective conversion of one Si–H group to a Si–OiPr moiety. Analysis of the products revealed involvement of redistribution of methyl groups in the reaction with **5**. Hydrosilylation of unsymmetrical bifunctional organosilanes, **6** or **8**, gave a 1:1 mixture of two isomers. In the second approach, the stoichiometric reaction of **8** or **9** with RhCl(PPh<sub>3</sub>)<sub>3</sub> was studied by <sup>1</sup>H and <sup>31</sup>P NMR spectroscopy. The product obtained was dependent on the solvent used; in CDCl<sub>3</sub>, Rh(III)-oxidative adducts, R<sup>1</sup><sub>2</sub>HSi(CH<sub>2</sub>CH<sub>2</sub>)R<sup>2</sup><sub>2</sub>Si–RhHCl(PPh<sub>3</sub>)<sub>2</sub> (R<sup>1</sup>, R<sup>2</sup> = Me or Ph), having a trigonal bipyramidal structure with two PPh<sub>3</sub> ligands at the apical positions were obtained, whereas the spectra of such reaction mixtures obtained in toluene-*d*<sub>8</sub> suggested the formation of Rh(V)-double oxidative adducts, R<sup>1</sup><sub>2</sub>Si(CH<sub>2</sub>CH<sub>2</sub>)R<sup>2</sup><sub>2</sub>Si–RhH<sub>3</sub>(PPh<sub>3</sub>)<sub>2</sub>. Since the catalytic hydrosilylation of acetone with **2** or **8** proceeded in toluene-*d*<sub>8</sub>, but did not in CDCl<sub>3</sub>, it is likely that the Rh(V)-double oxidative adducts play an important role in the rapid hydrosilylation of ketones with one end of the bifunctional organosilanes. These experimental results allow us to discuss two probable mechanisms involving disilametallacyclic intermediates for the rate enhancement by the two closely spaced Si–H groups.

## Introduction

The hydrosilylation of unsaturated organic molecules in which a Si–H bond adds across a carbon–carbon, carbon–oxygen, or carbon–nitrogen multiple bond with the aid of a transition metal catalyst is an important industrial and laboratory process for the synthesis of organosilicon compounds.<sup>1</sup> Numerous studies have been carried out using a variety of hydrosilanes, catalysts, and unsaturated substrates from various facets of the

reaction since its discovery in the late 1940s, and the hydrosilylation reaction continues to receive much attention.

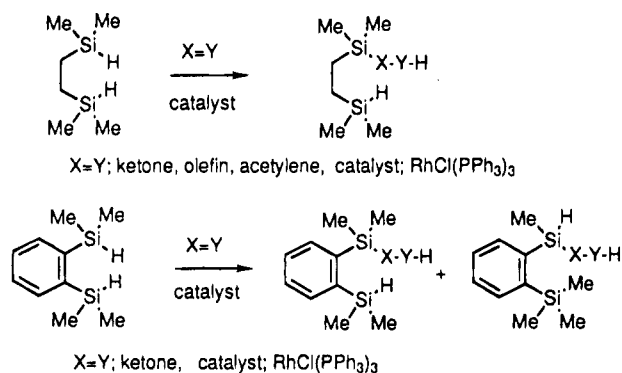
In 1989, we reported an unusual selectivity observed in the RhCl(PPh<sub>3</sub>)<sub>3</sub>-catalyzed hydrosilylation of unsaturated molecules with Me<sub>2</sub>HSiCH<sub>2</sub>CH<sub>2</sub>SiHMe<sub>2</sub>, in which only one of the Si–H group in the molecule reacts with the unsaturated substrate (X = Y) while the other one remains intact (Scheme 1).<sup>2a</sup> This selectivity was caused by the fact that the first step of the reaction, i.e., from Me<sub>2</sub>HSiCH<sub>2</sub>CH<sub>2</sub>SiHMe<sub>2</sub> (**2**) to Me<sub>2</sub>HSiCH<sub>2</sub>CH<sub>2</sub>Si(XYH)Me<sub>2</sub>, was several to several 10 times faster than the second step, i.e., from Me<sub>2</sub>HSiCH<sub>2</sub>CH<sub>2</sub>Si(XYH)Me<sub>2</sub>

<sup>®</sup> Abstract published in *Advance ACS Abstracts*, May 1, 1995.

(1) (a) Speier, J. L. *Adv. Organomet. Chem.* **1979**, *17*, 407. (b) Ojima, I. In *The Chemistry of Organic Silicon Compounds*; Patai, S., Rappport, Z., Eds.; Wiley: New York, 1989. (c) Marciniec, B.; Gulinski, J. J. *Organomet. Chem.* **1993**, *446*, 15. (d) *Comprehensive Handbook on Hydrosilylation*; Marciniec, B., Ed.; Pergamon: Oxford, U.K., 1992.

(2) (a) Nagashima, H.; Tatebe, K.; Ishibashi, I.; Sakakibara, J.; Itoh, K. *Organometallics* **1989**, *8*, 2495. (b) Nagashima, H.; Tatebe, K.; Itoh, K. *J. Chem. Soc. Perkin Trans. 1* **1989**, 1707.

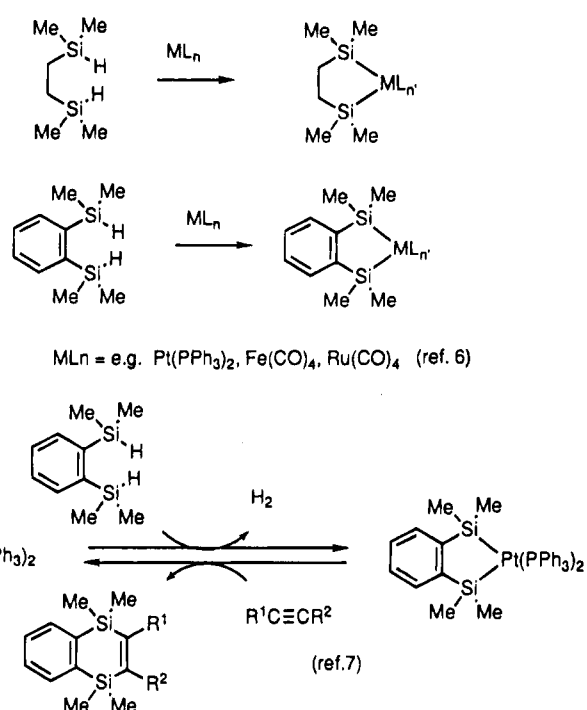
Scheme 1



to Me<sub>2</sub>(HYX)SiCH<sub>2</sub>CH<sub>2</sub>Si(XYH)Me<sub>2</sub>. Since the hydrosilylation of unsaturated molecules with monofunctional organosilanes such as EtMe<sub>2</sub>SiH and PhMe<sub>2</sub>SiH was as slow as the second reaction, the first reaction apparently was accelerated for some unrecognized reason. Similar rapid reaction and selective conversion of only one Si-H group were also observed in the hydrosilylation of ketones with 1,2-bis(dimethylsilyl)benzene (**5**), which was accompanied by a curious redistribution of methyl groups on the silicon atoms to give a mixture of two products as shown in Scheme 1.<sup>2b</sup> Despite the numerous studies reported in the literature on the catalytic hydrosilylation reaction little is known concerning such reactions of bifunctional organosilanes **2** and **5**.<sup>1</sup> The only example of the catalytic hydrosilylation with bifunctional organosilanes to our knowledge is that of the RhCl(PPh<sub>3</sub>)<sub>3</sub>-catalyzed reactions of nitriles reported by Corriu, which afforded N,N-disilylated amines and enamines by the concomitant reaction of both of the Si-H groups with nitriles.<sup>3</sup> Since nitriles are not hydrosilylated with monofunctional organosilanes under the same conditions, this reaction may suggest a higher reactivity of bifunctional silanes, similar to our observation in the hydrosilylation of ketones, olefins, and acetylenes. However, no detailed study of the mechanism of the reaction has been undertaken.

How does the rate enhancement occur? It is well-known that inductive and steric factors of the substituents on the silicon atom affect the rate of the hydrosilylation, and these are sometimes accompanied by significant differences in selectivities of the reaction.<sup>1d</sup> As a typical example, the RhCl(PPh<sub>3</sub>)<sub>3</sub>-catalyzed hydrosilylation of ketones with dialkyldihydrosilanes proceeded more rapidly than that with trialkylmonohydrosilanes.<sup>4,5</sup> The reaction of α,β-unsaturated ketones with Ph<sub>2</sub>SiH<sub>2</sub> resulted in the addition of an Si-H bond to the carbonyl group to give the corresponding silyl ether of allylic alcohols, whereas the reaction with Et<sub>3</sub>SiH proceeded in a 1,4-addition mode to form the corresponding silyl enol ethers.<sup>4</sup> Stereoselectivity for the hydrosilylation of 4-*tert*-butylcyclohexanone was significantly different between Ph<sub>2</sub>SiH<sub>2</sub> and Et<sub>3</sub>SiH.<sup>5</sup> These features depend on steric and inductive influence around Si-H bonds between dihydrosilanes and monohydrosilanes. In contrast, the hydrosilylation of mesityl oxide or 4-*tert*-butylcyclohexanone with bifunctional

Scheme 2



organosilanes, **2** or **5**, is much faster than that with EtMe<sub>2</sub>SiH or PhMe<sub>2</sub>SiH, but the selectivities are similar. Since there is little difference on the substituents of the silicon atom between **2** or **5** and EtMe<sub>2</sub>SiH or PhMe<sub>2</sub>SiH, inductive or steric effects may not be a major reason for the rate enhancement in the reaction with **2** or **5**.

A probable factor which may result in the special reactivity of **2** or **5** is their bifunctional structure, two Si-H bonds of which can concomitantly interact with the catalyst. Fink and Graham reported that a stoichiometric reaction of **2** or **5** with certain transition metal complexes results in release of molecular hydrogen to form stable disilametallacyclic compounds (Scheme 2).<sup>6</sup> Double oxidative addition of two Si-H groups in **2** or **5** to the metal center followed by reductive elimination of H<sub>2</sub> is the probable mechanism for the formation of these disilametallacyclic compounds. Tanaka and co-workers reported a platinum-catalyzed dehydrogenative double silylation of unsaturated molecules with **5** and proposed a platinadisilacyclopentane intermediate formed by double oxidative addition of two of the Si-H bonds in **5** followed by release of H<sub>2</sub>.<sup>7</sup> The disilametallacyclic intermediate undergoes insertion of unsaturated molecules between Pt-Si bonds to accomplish the dehydrogenative disilylation as shown in Scheme 2. An important requirement for these reactions is the proximity of the two Si-H bonds in the bifunctional structure of **2** or **5**, which is crucial in facilitating the double oxidative addition to the metal center. In fact, the above

(6) Fink, W. *Helv. Chim. Acta.* **1974**, *57*, 1010; **1976**, *59*, 606. Corriu, R. J. P.; Moreau, J.; Pataud-Sat, M. *Organometallics* **1985**, *4*, 623. Vancea, L.; Graham, W. A. G. *Inorg. Chem.* **1974**, *13*, 511. Recent advances for disilarhodacycles: Osakada, K.; Hataya, K.; Tanaka, M.; Nakamura, Y.; Yamamoto, T. *J. Chem. Soc., Chem. Commun.* **1993**, 576.

(7) (a) Uchimaru, Y.; Lautenschlager, H. J.; Wynd, A. J.; Tanaka, M.; Goto, M. *Organometallics* **1992**, *11*, 2639. (b) Tanaka, M.; Uchimaru, Y.; Lautenschlager, H. J. *J. Organomet. Chem.* **1992**, *428*, 1. (c) Reddy, N. P.; Uchimaru, Y.; Lautenschlager, H. J.; Tanaka, M. *Chem. Lett.* **1992**, 45. (d) Tanaka, M.; Uchimaru, Y.; Lautenschlager, H. J. *Organometallics* **1991**, *10*, 16.

(3) Corriu, R. J. P.; Moreau, J. J. E.; Pataud-Sat, M. *J. Organomet. Chem.* **1982**, *228*, 301.

(4) Ojima, I.; Nihonyanagi, M.; Kogure, T.; Kumagai, M.; Horiuchi, S.; Nakatsugawa, K. *J. Organomet. Chem.* **1975**, *94*, 449. Ojima, I.; Kogure, T. *Organometallics* **1982**, *1*, 1390.

(5) Semmelhack, M. F.; Misra, R. N. *J. Org. Chem.* **1982**, *47*, 2469.

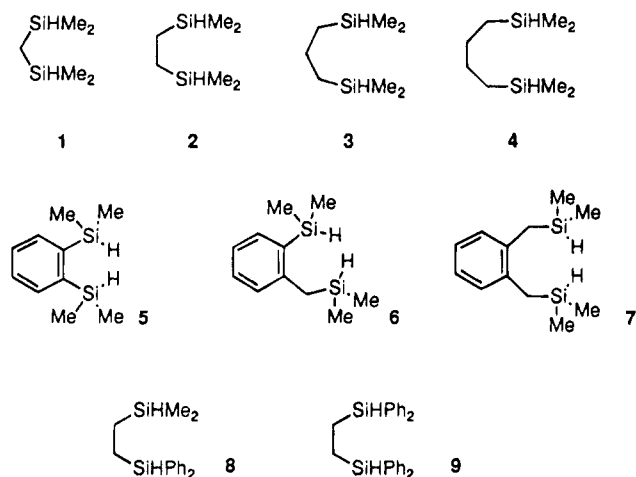


**Figure 1.** Bifunctional organosilanes.

stoichiometric and catalytic reactions were not accessible with the monofunctional organosilanes. These results are consistent with the fact that the rapid  $\text{RhCl}(\text{PPh}_3)_3$ -catalyzed hydrosilylation was only accomplished by the bifunctional organosilanes, **2** or **5**, but not by  $\text{EtMe}_2\text{SiH}$  or  $\text{PhMe}_2\text{SiH}$ , which strongly suggests that concomitant interaction of the two Si-H groups in **2** or **5** with the rhodium center is a clue to understanding the mechanism.

In this paper, we wish to report two experiments performed to understand this unusual rate enhancement of bifunctional organosilanes in the  $\text{RhCl}(\text{PPh}_3)_3$ -catalyzed hydrosilylation reaction. First, nine bifunctional organosilanes, shown in Figure 1, which had either a different number of carbon units between the two Si-H groups or different substituents on the silicon atoms, were used in the catalytic hydrosilylation of acetone. The results revealed that the structure of the bifunctional organosilanes appropriate for the concomitant interaction of both of the Si-H groups to the Rh center generally showed a rate enhancement. Second, direct detection of the interaction of two Si-H groups in the bifunctional organosilanes, **2**, **8**, and **9**, with  $\text{RhCl}(\text{PPh}_3)_3$  was examined by  $^1\text{H}$  and  $^{31}\text{P}$  NMR spectroscopy, and provided evidence for double oxidative addition, i.e., formation of a  $\text{Rh}(\text{V})$ -disilametalacyclic intermediate,

$\text{H}_3\text{Rh}(\text{R}_2\text{SiCH}_2\text{CH}_2\text{SiR}_2)(\text{PPh}_3)_2$ . These results indicate the key role of  $\text{Rh}(\text{V})$ -disilametalacyclic intermediates in the catalytic hydrosilylation with bifunctional organosilanes.

In contrast to the great success of the hydrosilylation in organic and organometallic synthesis, the reaction mechanism still remains uncertain.<sup>1</sup> The Chalk-Harrod cycle proposed for the platinum-catalyzed hydrosilylation of olefins offered the first reasonable mechanism, which involves the oxidative addition of a Si-H bond to a platinum-alkene complex, followed by alkene insertion into the Pt-H bond and reductive elimination of the alkyl and silyl groups to form a new silane.<sup>8</sup> The Chalk-Harrod cycle and its variants have been extensively used to explain various transition metal-catalyzed hydrosilylations including those mediated by  $\text{RhCl}(\text{PPh}_3)_3$ .<sup>4</sup> However, recent publications claimed the

involvement of higher oxidation states such as  $\text{Rh}(\text{V})$ ,<sup>9,10</sup>  $\text{Ir}(\text{V})$ ,<sup>11</sup> and  $\text{Pt}(\text{IV})$ <sup>12</sup> and metal colloidal catalysis.<sup>13</sup> Two reaction pathways involving silylmetalation and hydro-metalation of unsaturated molecules also were a subject of controversy.<sup>14-17</sup> The present report offers a mechanistic discussion on the catalytic hydrosilylation from a fresh perspective.

## Results and Discussion

**I. Catalytic Hydrosilylation of Acetone with Bifunctional Organosilanes 1-9.** Organosilanes of general formula  $\text{HMe}_2\text{Si}(\text{CH}_2)_n\text{SiMe}_2\text{H}$  (**1-4** ( $n = 1-4$ )) were synthesized and used for the catalytic hydrosilylation of acetone (an equimolar amount with respect to the silane) in the presence of  $\text{RhCl}(\text{PPh}_3)_3$  (1 mol %) in  $\text{C}_6\text{D}_6$  at 30 °C under a nitrogen atmosphere. Reaction profiles following the disappearance of acetone as determined by  $^1\text{H}$  NMR spectroscopy are shown in Figure 2. The rate apparently was dependent on the number of carbon units ( $n$ ) between the two  $\text{Me}_2\text{SiH}$  groups; the reactions with silanes **2** and **3** were complete within 1 h, whereas the conversion of acetone in the reactions of **1** and **4** was less than a few percent after 1 h. Similar reactions of  $\text{EtMe}_2\text{SiH}$  and  $\text{PhMe}_2\text{SiH}$  were as slow as those of **1** and **4**. It was estimated from the initial rate analysis that the reactions of **2** and **3** were approximately 50 and 120 times faster, respectively, than those of **1**, **4**,  $\text{EtMe}_2\text{SiH}$ , and  $\text{PhMe}_2\text{SiH}$ .<sup>18</sup> That no rate acceleration occurred in the hydrosilylation with **1** and **4** indicates that the distance between the two Si-H groups in the bifunctional organosilane is particularly important; that in **1** is too short, whereas that in **4** is too long.

(9) (a) Millan, A.; Fernandez, M. J.; Bentz, P.; Maitlis, P. M. *J. Mol. Catal.* **1984**, *26*, 89. (b) Ruiz, J.; Bentz, P. O.; Mann, B. E.; Spencer, C. M.; Taylor, B. F.; Maitlis, P. M. *J. Chem. Soc., Dalton Trans.* **1987**, 2709.

(10) (a) Duckett, S. B.; Perutz, R. N. *Organometallics* **1992**, *11*, 90. (b) Duckett, S. B.; Haddleton, D. M.; Jackson, S. A.; Perutz, R. N.; Poliakov, M.; Upmacis, R. K. *Organometallics* **1988**, *7*, 1526.

(11) Tanke, R. S.; Crabtree, R. H. *J. Chem. Soc., Chem. Commun.* **1990**, 1056; *J. Am. Chem. Soc.* **1990**, *112*, 7984; *Organometallics* **1991**, *10*, 415.

(12) Chu, H. K.; Frye, C. L. *J. Organomet. Chem.* **1993**, *446*, 183. (13) Lewis, L. N. *J. Am. Chem. Soc.* **1990**, *112*, 5998. Lewis, L. N.; Lewis, N. *J. Am. Chem. Soc.* **1986**, *108*, 7228.

(14) Ojima, I.; Clos, N.; Donovan, R. J.; Ingallina, P. *Organometallics* **1990**, *9*, 3127. Ojima, I.; Donovan, R. J.; Clos, N. *Organometallics* **1991**, *10*, 2606.

(15) Brookhart, M.; Grant, B. E. *J. Am. Chem. Soc.* **1993**, *115*, 2151.

(16) (a) Tamao, K.; Nakagawa, Y.; Ito, Y. *Organometallics* **1993**, *12*, 2297. (b) Bergens, S. H.; Noheda, P.; Whelan, J.; Bosnich, B. *J. Am. Chem. Soc.* **1992**, *114*, 2121, 2128.

(17) Seitz, F.; Wrighton, M. S. *Angew. Chem., Int. Ed. Engl.* **1988**, *27*, 289. Mitchener, J. C.; Wrighton, M. S. *J. Am. Chem. Soc.* **1981**, *103*, 975. Schroeder, M. A.; Wrighton, M. S. *J. Organomet. Chem.* **1977**, *128*, 345.

(18) One may consider that a further kinetic study could contribute to a better understanding of the reaction profiles. However, the large experimental errors observed in each run made us hesitate to do kinetic experiments in detail. Three kinetic runs with **2** under the same conditions as above (under a nitrogen atmosphere) gave a rate constant with  $\pm 20\%$  experimental error, whereas four experiments conducted in an NMR tube sealed in vacuum gave a smaller rate constant with  $\pm 50\%$  experimental error. The origin of the large experimental errors was attributed to oxygen contamination of the reaction mixture, because it is known that a trace amount of oxygen accelerates the  $\text{RhCl}(\text{PPh}_3)_3$ -catalyzed hydrosilylation of olefins.<sup>19</sup> As long as the reaction was carried out under a nitrogen atmosphere, at least three repeated runs with each hydrosilane (**1-9**) proved reproducibility of the initial rate constant with maximum uncertainty  $\pm 30\%$ , which is enough for qualitative comparison of the reaction rate as described in the text. However, we consider that attempted quantitative analysis using these data would be unproductive.

(19) Dickers, H. M.; Haszeldine, R. N.; Malkin, L. S.; Mather, A. P.; Parish, R. V. *J. Chem. Soc., Dalton Trans.* **1980**, 308. Faltynek, R. A. *Inorg. Chem.* **1981**, *20*, 1357.

(8) Chalk, A. J.; Harrod, J. F. *J. Am. Chem. Soc.* **1965**, *87*, 16. Harrod, J. F.; Chalk, A. J. In *Organic Synthesis via Metal Carbonyls*; Wender, I.; Pino, P., Eds.; Wiley: New York, 1977; Vol. 2.



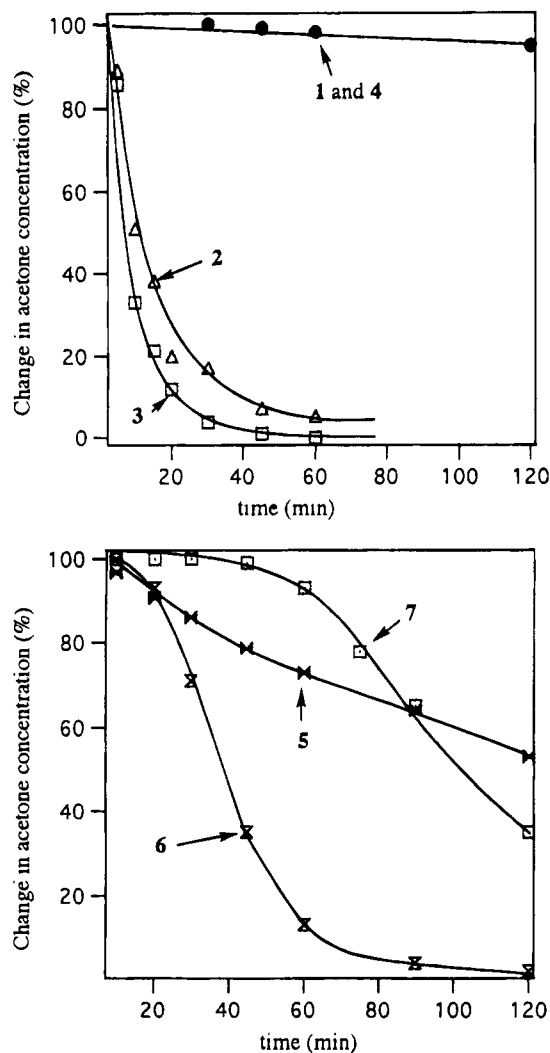


**Figure 2.** Reaction profiles for the catalytic hydrosilylation of bifunctional organosilanes 1–7. All reactions were carried out in C<sub>6</sub>D<sub>6</sub> at 30 °C in the presence of 1 mol % of RhCl(PPh<sub>3</sub>)<sub>3</sub> as the catalyst. The reaction was monitored by following the decrease of acetone against toluene as the internal standard.

In Figure 2 are also illustrated reaction profiles of the hydrosilylation with the silanes 1,2-[Me<sub>2</sub>HSi(CH<sub>2</sub>)<sub>n</sub>][Me<sub>2</sub>HSi(CH<sub>2</sub>)<sub>n'</sub>]C<sub>6</sub>H<sub>4</sub> [**5** ( $n = n' = 0$ ), **6** ( $n = 0, n' = 1$ ), and **7** ( $n = n' = 1$ )], under the same conditions as above. The reactions of these silanes were slower than those of **2** or **3** but were significantly faster than those of **1**, **4**, EtMe<sub>2</sub>SiH, and PhMe<sub>2</sub>SiH. The relative rate of **5** to PhMe<sub>2</sub>SiH was 20:1. A significant induction period was observed in the reactions of **6** and **7**, but after the induction period, rapid hydrosilylation occurred (260 and 70 times faster than PhMe<sub>2</sub>SiH for **6** and **7**, respectively). The additional two experiments apparently showed that the rate of the reaction is sensitive to the structure of the bifunctional organosilanes; an isomer of **5**, 1,4-(HMe<sub>2</sub>Si)<sub>2</sub>C<sub>6</sub>H<sub>4</sub>, reacted with acetone as slowly as PhMe<sub>2</sub>SiH, whereas 1,8-bis(dimethylsilyl)naphthalene did not react at all. Similar to **2** and **3**, silanes **5** and **6**, in which two of the Si–H groups are connected by two or three carbon units, showed higher reactivity than **1** and **4**. Although there are four carbon units between them, the rate enhancement occurred in the reaction with **7** (unlike **4**). This can be attributed to the presence of the benzene ring in **7**, which restricts

the distance between the two Si–H moieties. Thus, an adequate distance between the two Si–H groups is important for the rate acceleration. The distance between the two silicon groups is too long in 1,4-(HMe<sub>2</sub>Si)C<sub>6</sub>H<sub>4</sub> but is too short in 1,8-bis(dimethylsilyl)naphthalene.

Diphenylsilyl derivatives also were the subjects of a similar study. The hydrosilylation of acetone with diphenylsubstituted organosilanes, **8** and **9**, was substantially slower than that of their methyl analogue **2**. In reactions at 50 °C, the relative rates between **8** and EtMe<sub>2</sub>SiH were estimated to be 8:1. Although **9** reacted with acetone slowly (the rate was approximately 0.2 times that of EtMe<sub>2</sub>SiH), EtPh<sub>2</sub>SiH did not react with acetone at all under the same conditions. The order of the reaction rate, **8** > EtMe<sub>2</sub>SiH and **9** >> EtPh<sub>2</sub>SiH, clearly demonstrates that the bifunctional structure of **8** and **9** enhances the reactivity of both the Me<sub>2</sub>SiH and the Ph<sub>2</sub>SiH moieties.

In Table 1 are summarized the products and the yields of the enhanced hydrosilylation of bifunctional organosilanes. All of the reactions were carried out in benzene in the presence of RhCl(PPh<sub>3</sub>)<sub>3</sub> (1 mol %) at room temperature under a nitrogen atmosphere. In all cases, only one Si–H group of the silane was converted to a Si–OiPr moiety. The results provided two interesting problems with respect to the products. One is that redistribution of the substituents on the silicon atoms was only observed for **5**. The fact that no methyl group migration was observed in the reactions of **6** or **7** as was seen in those of **5** suggests that both of the dimethylsilyl groups must be bonded directly to an aromatic ring for the redistribution of the methyl groups to occur.<sup>20</sup> Since methyl group migration is not a general reaction of the bifunctional organosilanes, we will not discuss this further.<sup>21</sup> The second problem was raised in the reactions of the unsymmetrical organosilanes **6** and **8**, which gave a 1:1 mixture of isomers. The result obtained with **8** is especially curious, because the experiments with EtMe<sub>2</sub>SiH or EtPh<sub>2</sub>SiH described above showed that the Me<sub>2</sub>SiH group is much more reactive than the Ph<sub>2</sub>SiH moiety. If the two Si–H groups in **8** were independently activated by the catalyst, this large difference in reactivity would result in selective conversion of the Me<sub>2</sub>SiH bond in **8** to Me<sub>2</sub>SiOiPr group with the Ph<sub>2</sub>SiH moiety remaining intact. Thus, the lack of chemoselectivity implicates the activation pathways of both of Me<sub>2</sub>SiH and Ph<sub>2</sub>SiH moieties in **8** during the reaction.

In summary, the above experiments revealed that bifunctional organosilanes with two Si–H groups connected by two or three carbon units generally showed accelerated hydrosilylation of acetone. It should be pointed out that all of the bifunctional organosilanes showing the rate enhancement also have a structure conducive to the concomitant activation of both Si–H

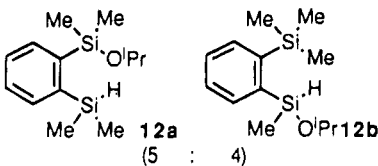
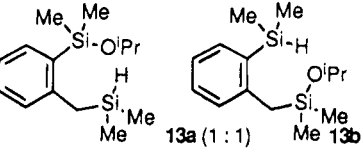
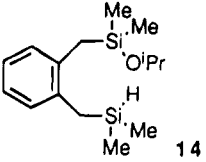
(20) The methyl group migration also occurred in the hydrosilylation of acetone with 3,4-bis(dimethylsilyl)toluene. A mixture of four isomers, two regioisomers of rearranged and unrearranged compounds, was obtained.

(21) Redistribution of alkyl groups of organosilanes was extensively observed in the transition metal-catalyzed reactions of hydrosilanes.<sup>22</sup> It was pointed out that oxidative addition of low-valent metal species between Si–alkyl bonds might induce the redistribution.<sup>22</sup> A possible mechanism for the 1,4-methyl group migration in the hydrosilylation with **5** is shown in Scheme 8.

(22) Curtis, M. D.; Epstein, P. S. *Adv. Organomet. Chem.* **1981**, *19*, 220. For a recent publication for the alkyl group redistribution in the platinum-catalyzed process with **5**, see ref 7b.



**Table 1. Isolation of Monohydrosilylation Products of Bidentate Organosilanes with Acetone<sup>a</sup>**

Entry	Substrate	Temp (°C)	Time(h)	Products	Yield(%)
1	2	r.t.	3	Me <sub>2</sub> HSiCH <sub>2</sub> CH <sub>2</sub> Si(O <sup>i</sup> Pr)Me <sub>2</sub> (10)	75
2	3	r.t.	3	Me <sub>2</sub> HSiCH <sub>2</sub> CH <sub>2</sub> CH <sub>2</sub> Si(O <sup>i</sup> Pr)Me <sub>2</sub> (11)	71
3	5	r.t.	19	 12a (5) : 12b (4)	74
5	6	r.t.	3	 13a (1 : 1) : 13b	88
6	7	r.t.	48	 14	73
7	8	50	5	Ph <sub>2</sub> HSiCH <sub>2</sub> CH <sub>2</sub> Si(O <sup>i</sup> Pr)Me <sub>2</sub> (15a) Ph <sub>2</sub> ( <sup>i</sup> PrO)SiCH <sub>2</sub> CH <sub>2</sub> SiHMe <sub>2</sub> (15b) (1 : 1)	64
8	9	50	10	Ph <sub>2</sub> HSiCH <sub>2</sub> CH <sub>2</sub> Si(O <sup>i</sup> Pr)Ph <sub>2</sub> (16)	20 <sup>b</sup>

<sup>a</sup> All reactions were carried out with 1 mol % of RhCl(PPh<sub>3</sub>)<sub>3</sub> in benzene. <sup>b</sup> It was difficult to isolate 16. Conversion determined by NMR is reported.

groups as in the double oxidative addition to form disilametallacyclic intermediates. As noted above, the lack of chemoselectivity in the hydrosilylation with unsymmetrical bifunctional organosilanes, **6** and **8**, supports the concomitant activation of both of the Si-H groups in **6** and **8**. To examine the interaction of bifunctional organosilanes with the catalyst, we carried out stoichiometric reaction of RhCl(PPh<sub>3</sub>)<sub>3</sub> with some bifunctional organosilanes as described below.

**II. Double Oxidative Addition of 2, 8, and 9 to RhCl(PPh<sub>3</sub>)<sub>3</sub>: An NMR Study.** The RhCl(PPh<sub>3</sub>)<sub>3</sub>-catalyzed hydrosilylation of unsaturated molecules usually is explained by variants of the Chalk-Harrod cycle, in which the oxidative addition of R<sub>3</sub>SiH to RhCl(PPh<sub>3</sub>)<sub>3</sub> to form (R<sub>3</sub>Si)RhCl(H)(PPh<sub>3</sub>)<sub>2</sub> is the probable initial step of the catalytic cycle.<sup>4,8</sup> Studies of the reaction of monohydrosilanes R<sub>3-n</sub>Cl<sub>n</sub>SiH (*n* = 0–3) with RhCl(PPh<sub>3</sub>)<sub>3</sub> were actively carried out in the 1960s by Wilkinson<sup>23</sup> and Haszeldine,<sup>24</sup> and several oxidative adducts, generally formulated as (R<sub>3-n</sub>Cl<sub>n</sub>Si)RhHCl(PPh<sub>3</sub>)<sub>2</sub>, were isolated and characterized. The structure of a stable oxidative adduct (Cl<sub>3</sub>Si)RhHCl(PPh<sub>3</sub>)<sub>3</sub> was determined by X-ray analysis to be that of a trigonal bipyramid with trans-phosphines at the apices and H,

Cl, and SiCl<sub>3</sub> in the trigonal plane.<sup>25</sup> The NMR spectra of the oxidative adducts suggested that the structure in solution would be analogous to that formed in the crystal structure; the five-coordinate complexes (R<sub>3-n</sub>Cl<sub>n</sub>Si)RhHCl(PPh<sub>3</sub>)<sub>2</sub> generally showed a Rh-H peak split into a doublet of triplets due to the coupling with <sup>103</sup>Rh (*J*<sub>H-Rh</sub> = 21–27 Hz) and two equivalent PPh<sub>3</sub> ligands (*J*<sub>H-Rh-P</sub> = 13–15 Hz).<sup>23,24</sup> We confirmed that the reaction mixture of RhCl(PPh<sub>3</sub>)<sub>3</sub> and HSiMe<sub>2</sub>Ph in CDCl<sub>3</sub> gave a characteristic Rh-H peak split into a doublet of triplets at -15.33 ppm (*J*<sub>H-Rh</sub> = 22.7 Hz and *J*<sub>H-Rh-P</sub> = 15.4 Hz) in the <sup>1</sup>H NMR spectrum, whereas a doublet was observed at 35.7 ppm (*J*<sub>Rh-P</sub> = 124.5 Hz) in <sup>31</sup>P{<sup>1</sup>H} NMR.<sup>26</sup> Similar NMR spectra were obtained in toluene-*d*<sub>8</sub>; a Rh-H peak appeared at -14.60 ppm as a doublet of triplets in the <sup>1</sup>H NMR spectrum, and a Rh-P signal at 36.0 ppm as a doublet. These spectral features are consistent with HRhCl(SiMe<sub>2</sub>Ph)(PPh<sub>3</sub>)<sub>2</sub> (**17**) having the structure shown in Figure 3. The reaction was reversible, and the equilibrium favored the reactant. Appropriate spectra, in which only small peaks derived from the starting materials appeared, were obtained in the reaction of 2 molar equiv of PhMe<sub>2</sub>SiH with 1 equiv of RhCl(PPh<sub>3</sub>)<sub>3</sub>. Two ill-resolved Rh-H signals also appeared at -10.2 ppm as a broad doublet and at -17.5 ppm as a broad singlet in the <sup>1</sup>H

(23) de Charentenay, F.; Osborn, J. A.; Wilkinson, G. *J. Chem. Soc. A* **1968**, 787.

(24) Haszeldine, R. N.; Parish, R. V.; Parry, D. J. *J. Chem. Soc. (A)* **1969**, 683. Haszeldine, R. N.; Parish, R. V.; Taylor, R. J. *J. Chem. Soc. A* **1974**, 2311.

(25) Muir, K. W.; Ibers, J. A. *Inorg. Chem.* **1970**, *9*, 440.

(26) <sup>31</sup>P NMR of several rhodium-phosphine complexes: Brown, T. H.; Green, P. J. *J. Am. Chem. Soc.* **1970**, *92*, 2359.

Table 2. NMR Data for the Oxidative Adducts<sup>a-d</sup>

	$\delta_{\text{Rh-H}}$	$\delta_{\text{Rh-P}}$
<b>17</b>	-15.33 <sup>a</sup> (dt, $J = 15.4, 22.7$ Hz), -14.60 <sup>b</sup> (dt, $J = 15.4, 22.0$ Hz)	35.7 <sup>a</sup> (d, $J = 124.5$ Hz), 36.0 <sup>b</sup> (d, $J = 124.5$ Hz)
<b>19<sup>a</sup></b>	-15.54 (dt, $J = 15.4, 23.5$ Hz)	37.4 (d, $J = 128.5$ Hz)
<b>20<sup>a</sup></b>	-15.18 (dt, $J = 15.4, 22.0$ Hz)	31.6 (d, $J = 128.5$ Hz)
<b>21<sup>b</sup></b>	-10.8 (brd, $J = 125$ Hz, 1H), -7.3 (brs, 1H), -6.7 (brs, 1H)	27.7 (dd, $J = 16.1, 84.4$ , 1P), 36.6 (dd, $J = 16.1, 104.4$ Hz, 1P)
<b>22<sup>b</sup></b>	-10.9 (brd, $J = 130$ Hz, 1H), -6.3 (brs, 2H)	32.1 (dd, $J = 16.1, 86.3$ Hz, 1P)

<sup>a</sup> In CDCl<sub>3</sub>. <sup>b</sup> In toluene-*d*<sub>8</sub> at -60.0 °C. <sup>c</sup> <sup>1</sup>H NMR spectral data for other parts are as follows. **17**: (CDCl<sub>3</sub>)  $\delta$  0.01 (s, Rh-SiMe), 6.8-7.7 (m, Ph); (toluene-*d*<sub>8</sub>)  $\delta$  0.4 (rRh-SiMe), 6.7-7.9 (m, Ph). **19**:  $\delta$  -0.25 (s, RhSiMe), 0.4-0.55 and 1.0-1.15 (m, SiCH<sub>2</sub>), 4.44 (br-s, Ph<sub>2</sub>SiH), 6.8-7.8 (m, Ph). **20**:  $\delta$  1.15 (s, SiCH<sub>2</sub>), 4.32 (brs, Ph<sub>2</sub>SiH), 6.8-8.7 (m, Ph). **21**:  $\delta$  -0.1 to 1.3 (m, MeSiCH<sub>2</sub>), 6.5-8.1 (m, Ph). **22**:  $\delta$  1.1-1.5 (m, SiCH<sub>2</sub>), 6.5-8.0 (m, Ph). Spectra in CDCl<sub>3</sub> were measured in the presence of cyclohexane as the internal standard. <sup>d</sup> RhCl(PPh<sub>3</sub>)<sub>3</sub>:  $\delta_{\text{Rh-P}}$  29.6 (dd,  $J = 38, 145$  Hz, 2P), 46.8 (dt,  $J = 38, 190$  Hz, 1P) in CDCl<sub>3</sub>; 28.7 (dd,  $J = 38, 145$  Hz, 2P), 46.0 (dt,  $J = 38, 190$  Hz, 1P) in toluene-*d*<sub>8</sub>. RhH<sub>2</sub>Cl(PPh<sub>3</sub>)<sub>2</sub> (**18**):  $\delta_{\text{Rh-H}}$  -17.5 (brs, 1H), -10.2 (brd,  $J = 125$  Hz, 1H) in CDCl<sub>3</sub> and -16.6 (brs, 1H), -9.3 (brd,  $J = 125$  Hz, 1H) in toluene-*d*<sub>8</sub>;  $\delta_{\text{Rh-P}}$  35.2 (d,  $J = 116.4$ ) in CDCl<sub>3</sub> and 32.8 (d,  $J = 116.4$  Hz) in toluene-*d*<sub>8</sub>.

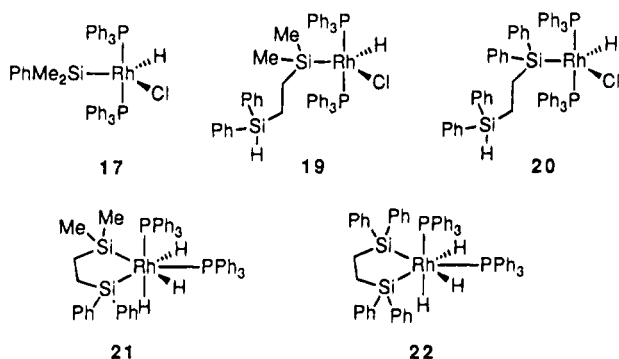


Figure 3. Oxidative adducts formed by the reactions of RhCl(PPh<sub>3</sub>)<sub>3</sub> with PhMe<sub>2</sub>SiH, **8**, or **9**.

NMR spectrum. These could be assigned as Rh-H signals derived from RhH<sub>2</sub>Cl(PPh<sub>3</sub>)<sub>2</sub> (**18**).<sup>27</sup> A Si-Me signal assignable to (PhMe<sub>2</sub>Si)<sub>2</sub>O indicates that the oxidative addition product to RhCl(PPh<sub>3</sub>)<sub>3</sub> reacted with adventitious moisture to give (PhMe<sub>2</sub>Si)<sub>2</sub>O and **18**. The <sup>31</sup>P NMR spectrum of **18** showed a doublet at 35.2 ppm. It was difficult to suppress the reaction of the oxidative adduct with moisture even by careful removal of water from the solvent and the NMR tube.

The NMR studies of the reaction of RhCl(PPh<sub>3</sub>)<sub>3</sub> with **2** were hampered by the high moisture sensitivity of the oxidative adduct. Three sets of Rh-H signals as doublets of triplets at -15.41, -15.45, and -15.65 ppm were observed in the <sup>1</sup>H NMR spectrum at the initial stage of the reaction, all of which diminished after several hours. The <sup>31</sup>P{<sup>1</sup>H} NMR spectrum of the same sample showed a doublet at 37.71 ppm corresponding to the species affording the Rh-H signal at -15.41 ppm, accompanied by small two doublets at 37.51 and 38.00 ppm. These results seemed to suggest the formation of a complex similar to **17** and its structural isomers. However, the reaction mixture was very sensitive to moisture, and the rapid decrease of the peak intensity of the oxidative adducts accompanied by the formation of **18** prevented detailed studies.

Since the reaction of **8** and **9** with moisture was slower than that of **2** in the presence of RhCl(PPh<sub>3</sub>)<sub>3</sub>, NMR spectra without serious contamination of **18** were obtained in CDCl<sub>3</sub> at -20 °C from a 1:2 reaction mixture of **8** and **9** with RhCl(PPh<sub>3</sub>)<sub>3</sub>. The oxidative adduct of **8** provided a doublet of triplets at -15.54 ppm (Rh-H) in the <sup>1</sup>H NMR spectrum. In the <sup>31</sup>P{<sup>1</sup>H} NMR spectrum, a doublet appeared at 37.4 ppm. In contrast, the reaction mixture of **9** and RhCl(PPh<sub>3</sub>)<sub>3</sub> gave a <sup>1</sup>H NMR

spectrum that showed a doublet of triplets at -15.18 ppm (Rh-H) and a <sup>31</sup>P{<sup>1</sup>H} NMR spectrum showing a doublet at 31.6 ppm (Table 2). These NMR data are consistent with the oxidative adducts **19** and **20** shown in Figure 3, in which one of the Si-H bond of **8** and **9** reacted with the Rh center with the other Si-H group remaining intact. In the <sup>31</sup>P{<sup>1</sup>H} NMR spectrum of **20**, large peaks derived from RhCl(PPh<sub>3</sub>)<sub>3</sub> were observed. This is attributed to the fact that the oxidative addition is reversible and that the equilibrium to give **20** is less favorable for the product than for **19**. In other words, activation of Ph<sub>2</sub>SiH moieties by RhCl(PPh<sub>3</sub>)<sub>3</sub> is more difficult than activation of Me<sub>2</sub>SiH groups, which results in the observation of complete chemoselectivity in the oxidative addition of unsymmetrical organosilane **8** to RhCl(PPh<sub>3</sub>)<sub>3</sub>, in which only Me<sub>2</sub>SiH moiety reacted with the Rh center.

To our surprise, similar experiments with **8** and **9** using toluene-*d*<sub>8</sub> as the solvent gave completely different spectra from those in CDCl<sub>3</sub>. An NMR sample of a mixture of **8**, RhCl(PPh<sub>3</sub>)<sub>3</sub>, and toluene-*d*<sub>8</sub> was prepared at -78 °C, warmed to room temperature, kept for 10 min, and quickly cooled again to -60 °C. Three ill-resolved Rh-H peaks were observed at -6.7, -7.3, and -10.8 ppm (singlet, singlet, and doublet, respectively) in an integral ratio of 1:1:1. <sup>31</sup>P{<sup>1</sup>H} NMR measurement of this novel species revealed two sets of doublets of doublets at 27.7 and 36.6 ppm. The reaction of **9** with RhCl(PPh<sub>3</sub>)<sub>3</sub> in toluene-*d*<sub>8</sub> also gave NMR spectra different from those obtained in CDCl<sub>3</sub>. The <sup>1</sup>H NMR spectrum showed two ill-resolved Rh-H signals at -6.3 and -10.9 ppm, in an integral ratio of 2:1. The former appeared as a singlet, whereas the latter split into a doublet. <sup>31</sup>P{<sup>1</sup>H} NMR afforded two sets of doublets of doublets at 26.7 and 32.1 ppm. All of the NMR data are summarized in Table 2, and <sup>1</sup>H NMR spectra of **21** and **22** including that of **17** in CDCl<sub>3</sub> for comparison are shown in Figure 4.

These new species can be reasonably assigned as the Rh(V)-disilyl-trihydride complexes **21** and **22** shown in Figure 3 for the following reasons.<sup>28</sup> First, <sup>31</sup>P{<sup>1</sup>H} NMR peaks split into two sets of a doublet of doublets

(28) Complexes having  $\eta^2\text{-H}_2$  or  $\eta^2\text{-Si-H}$  ligands have recently received considerable attention.<sup>29</sup> A reviewer suggested that two of the hydrides of the trisilyl dihydride complexes, **21** and **22**, might be a coordinated hydrogen molecule. Alternatively, these complexes may involve  $\eta^2\text{-Si-H}$  ligands as proposed in silane alkoxylation catalyzed by a cationic iridium complex by Crabtree.<sup>30</sup> These nonclassical intermediates should not be completely ruled out, though it is difficult to replace the disilyl trihydride intermediates shown in Scheme 6 and Scheme 7 by  $\eta^2\text{-H}_2$  or  $\eta^2\text{-Si-H}$  intermediates.

(29) Reviews of  $\eta^2\text{-H}_2$  complexes: Kubas, G. J. *Acc. Chem. Res.* **1988**, *21*, 120. Crabtree, R. H. *Adv. Organomet. Chem.* **1988**, *28*, 299.  $\eta^2\text{-Si-H}$  complexes: Shubert, U. *Adv. Organomet. Chem.* **1990**, *30*, 151.

(30) Luo, X. L.; Crabtree, R. H. *J. Am. Chem. Soc.* **1989**, *111*, 2527.

(27) Osborn, J. A.; Jardine, F. H.; Young, J. F.; Wilkinson, G. J. *Chem. Soc. A* **1966**, 1711.

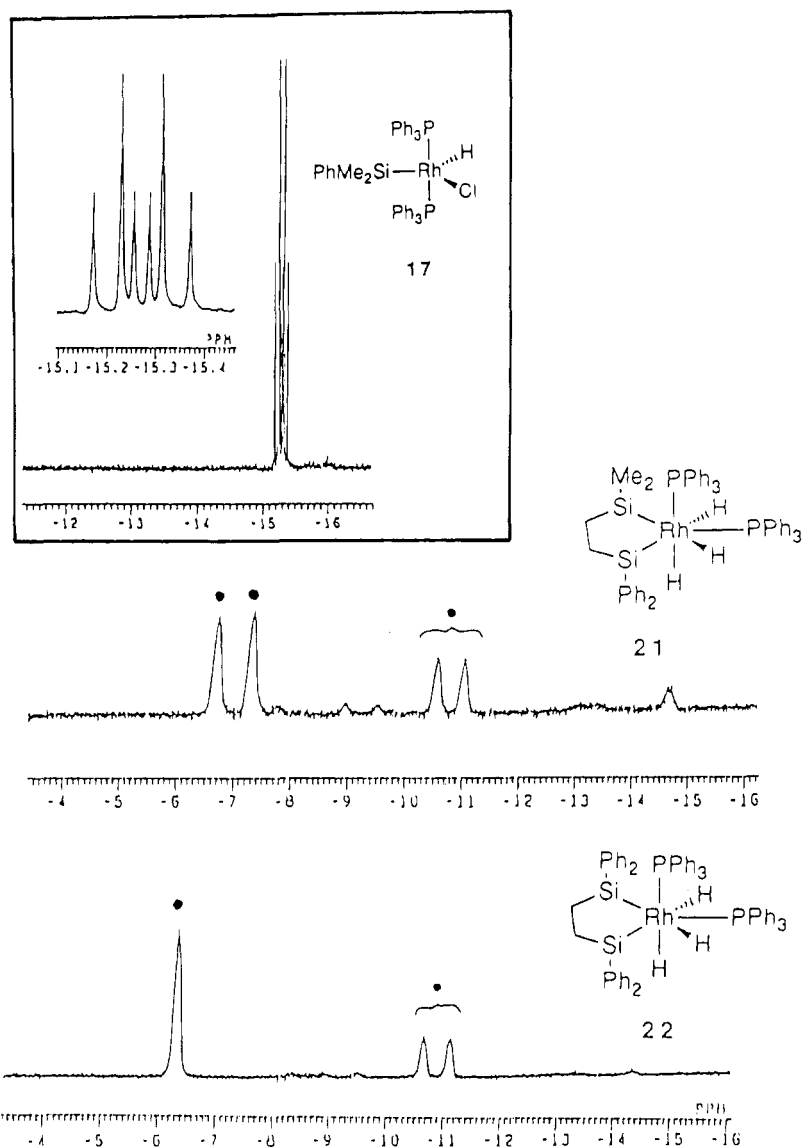


**Figure 4.**  $^1\text{H}$  NMR spectra of Rh–H peaks in **21** and **22** at  $-60^\circ\text{C}$ . Two broad singlets and one broad doublet are seen in **21**, whereas one broad singlet and one broad doublet in an integral ratio of 2:1 are visible in **22**. The Rh–H resonance of **17** in  $\text{CDCl}_3$  is shown in the inset above as a typical example of a Rh–H signal for the Rh(III)-monoxidative adducts, **17**, **19**, and **20**. The peak splits into a doublet of triplets.

with coupling constants of 16 Hz ( $J_{\text{P-P}}$ ) and 84–105 Hz ( $J_{\text{Rh-P}}$ ), which indicates that the molecule includes two  $\text{PPh}_3$  ligands cis to each other as shown in **21** and **22**. Second, the presence of three Rh–H peaks observed in the  $^1\text{H}$  NMR spectrum of **21** indicates the existence of three Rh–H moieties in the molecule. The fact that two of the three Rh–H peaks have the same chemical shift in the spectrum of **22**, which showed two Rh–H signals in a ratio of 2:1, suggests that **22** has a symmetry plane in the molecule. The difference between **21** and **22** can be explained in terms of the additional symmetry of **22** derived from the two identical organosilyl groups in the molecule compared with **21**. The complex **21** has an unsymmetrical  $\text{Me}_2\text{Si}(\text{CH}_2)_2\text{SiPh}_2$  group, whereas **22** contains a symmetrical  $\text{Ph}_2\text{Si}(\text{CH}_2)_2\text{SiPh}_2$  moiety. Third, two of the Rh–H signals are singlets, whereas the remaining one splits into a doublet with the coupling constant,  $J = 125\text{--}130$  Hz, due to coupling with a phosphine ligand at the trans position. Thus, only one of the Rh–H species is located trans to one of the phosphine ligands, whereas the other two do not have any trans-phosphines. These results are most readily

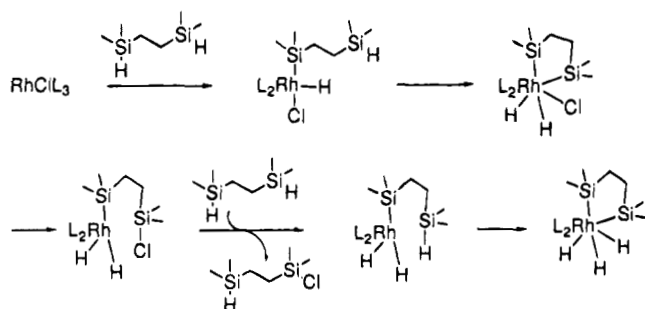
interpreted in terms of the seven-coordinated structures shown in Figure 3.

The compounds **21** and **22** showed a characteristic fluxional behavior in their NMR spectra due to stereochemical nonrigidity of seven-coordinated complexes.<sup>31</sup> Compound **21** showed two singlets and one doublet below  $-40^\circ\text{C}$ . At  $-20^\circ\text{C}$ , the singlet at  $-6.7$  ppm and the doublet began to broaden and then disappeared at  $0^\circ\text{C}$ . From 20 to  $60^\circ\text{C}$ , all of the peaks coalesced to a broad peak, and above  $60^\circ\text{C}$  the complex decomposed. Similarly, two Rh–P signals appearing as a sharp doublet of doublets at  $-60^\circ\text{C}$  turned into two broad doublets at  $-40^\circ\text{C}$ . Above  $-20^\circ\text{C}$ , the peaks coalesced to extensively broadened signals. Similar results were obtained in variable-temperature NMR studies of **22**. The results are provided in the supplementary material.

How do these seven-coordinate species form? When the NMR samples of a mixture of **21**,  $\text{RhCl}(\text{PPh}_3)_3$ , and toluene- $d_6$  were prepared at  $-78^\circ\text{C}$ , warmed to room

(31) Hoffmann, R.; Beier, B. F.; Muetterties, E. L.; Rossi, A. R. *Inorg. Chem.* **1977**, *16*, 511. See also: Luo, X.-L.; Schulte, G. K.; Demou, P.; Crabtree, R. H. *Inorg. Chem.* **1990**, *29*, 4268.

Scheme 3

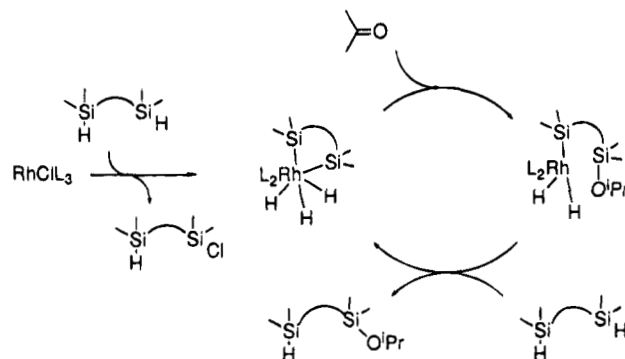


temperature for 1 min, and cooled again to  $-40\text{ }^{\circ}\text{C}$ , the Rh-H signal was observed as a well-resolved doublet of triplets [ $\delta -14.7$  (dt,  $J = 15.4, 23.5$  Hz)], whereas the Rh-P peaks appeared at 38.5 ppm (d,  $J = 128.5$  Hz). These NMR data are consistent with the Rh(III)-monooxidative adduct **19**. After this sample was warmed to room temperature again, kept for 10 min, and then cooled to  $-60\text{ }^{\circ}\text{C}$ , its  $^1\text{H}$  NMR spectrum was completely changed to that of **21**. Thus, the reaction of **8** with RhCl(PPh<sub>3</sub>)<sub>3</sub> initially resulted in the formation of the five-coordinate Rh(III) oxidative adduct **19**; however, it was quickly converted to **21** by warming, during which intramolecular oxidative addition of the second Si-H group was followed by reductive elimination of HSiR<sub>2</sub>(CH<sub>2</sub>)<sub>2</sub>R<sub>2</sub>SiCl and double oxidative addition of another molecule of **8** as shown in Scheme 3. Appearance of a singlet around 0.4 ppm in the  $^1\text{H}$  NMR spectrum of **21**, which is typical for the Me<sub>2</sub>ClSi group, could support this mechanism. Replacement of a chlorine atom on the metal by a hydride was reported in the reaction of RuCl<sub>2</sub>(PPh<sub>3</sub>)<sub>3</sub> or IrCl(CO)(PPh<sub>3</sub>)<sub>2</sub> with several organosilanes.<sup>32,33</sup>

**Role of the Oxidative Adducts in the Catalytic Reaction.** As noted above, the RhCl(PPh<sub>3</sub>)<sub>3</sub>-catalyzed hydrosilylations were explained by the Chalk-Harrod cycle and its variants.<sup>1d,4</sup> Although a Rh(III)-oxidative adduct such as **17** was proposed as an intermediate,<sup>4</sup> it was claimed that **17** might not be a net catalytic species.<sup>1d</sup> Lewis and co-workers claimed that metal colloids formed from interaction of the metal complex with oxygen and the silane may operate as the actual catalyst.<sup>13</sup> This can be eliminated in our case by the fact that the reaction proceeds with high selectivity to give monofunctionalization of the bifunctional organosilanes. It is unlikely that metal colloids would activate selectively only one of the Si-H groups in the bifunctional organosilanes.

We confirmed that two types of oxidative adducts could be observed, depending on the solvent, in the stoichiometric reaction of RhCl(PPh<sub>3</sub>)<sub>3</sub> and two bifunctional organosilanes. To determine which is involved in the catalytic reactions, acetone was hydrosilylated with **2** in the presence of a catalytic amount of RhCl(PPh<sub>3</sub>)<sub>3</sub> in either CDCl<sub>3</sub> or toluene-*d*<sub>8</sub>. In toluene-*d*<sub>8</sub> at room temperature, the reaction proceeded smoothly to form **10**, while, in sharp contrast, the hydrosilylation did not occur at all in CDCl<sub>3</sub>. On heating at 50  $^{\circ}\text{C}$  for 30 min in CDCl<sub>3</sub>, a part of the acetone (ca. 20%) was hydrosilylated, but a large peak at 0.41 ppm, which could be assigned to ClMe<sub>2</sub>Si(CH<sub>2</sub>CH<sub>2</sub>)SiMe<sub>2</sub>Cl, was

Scheme 4



observed in the  $^1\text{H}$  NMR spectrum of the reaction mixture, indicating that radical chlorination of the Si-H group<sup>34</sup> is a major reaction pathway in CDCl<sub>3</sub>. We also carried out experiments with **8** at 50  $^{\circ}\text{C}$  in CDCl<sub>3</sub> and toluene-*d*<sub>8</sub>, which afforded similar results to those observed with **2**. In the reaction in toluene-*d*<sub>8</sub>, the Rh(V) disilametallacyclic species **21** actually was detected by NMR spectroscopy. These results clearly suggest that the Rh(V)-double oxidative adducts **21** and **22** are more reasonable active species in the catalytic cycle than the generally accepted Rh(III) adducts, **17**, **19**, and **20**.

The double oxidative addition involves replacement of a chlorine atom of RhCl(PPh<sub>3</sub>)<sub>3</sub> by a hydride. Thus, one might claim that the bifunctional organosilanes merely act to produce a Rh-H species generally active for the catalytic hydrosilylations. This possibility is excluded, however, by the fact that catalytic hydrosilylation of acetone with a 1:10 mixture of **2** and EtMe<sub>2</sub>SiH in toluene-*d*<sub>8</sub> at room temperature was terminated with EtMe<sub>2</sub>SiH remaining unreacted, after all of **2** was consumed. The reaction of RhCl(PPh<sub>3</sub>)<sub>3</sub> with **2** produces a Rh-H species which is not an active catalyst for the hydrosilylation with a monofunctional organosilane EtMe<sub>2</sub>SiH. Thus, the bifunctional structure is crucially important for the rapid hydrosilylation described above.

Replacement of the chlorine ligand in the rhodium catalyst may play an important role in the induction period observed in the hydrosilylation with **6** and **7** as described above. These bifunctional organosilanes produce larger-membered disilametallacycles than **2** or **5**, which may cause a substantially slower reaction for the oxidative addition of the second Si-H group followed by reductive elimination to form a Si-Cl bond. An induction period is required for generation of Rh-H species, and thereafter the reaction of **6** or **7** proceeds rapidly.

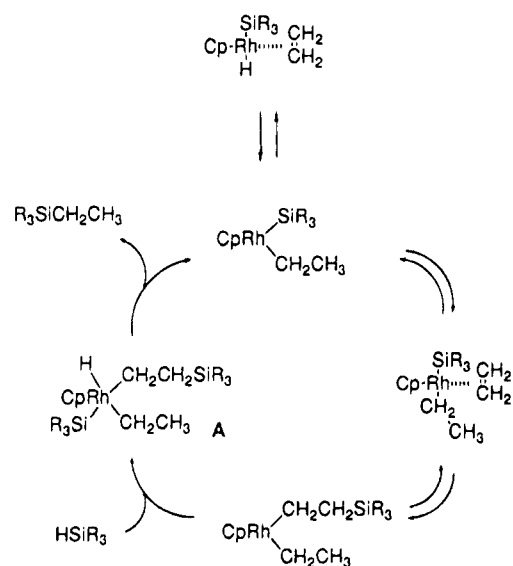
**Mechanistic Consideration.** A reaction scheme illustrating the initial and final step of the catalytic cycle is shown in Scheme 4. The catalyst, RhCl(PPh<sub>3</sub>)<sub>3</sub>, undergoes the double oxidative addition by bifunctional organosilanes to form the Rh(V) species, which readily reacts with acetone to form the Rh(III)-monooxidative adduct containing an isopropoxysilyl group. The reductive elimination of the monoisopropoxymonohydrosilane and oxidative addition of another molecule of the bifunctional organosilane regenerate the Rh(V)-double oxidative adduct. As noted above, the RhCl(PPh<sub>3</sub>)<sub>3</sub>-catalyzed hydrosilylations had heretofore been ex-

(32) Kono, H.; Wakao, N.; Ito, K.; Nagai, Y. *J. Organomet. Chem.* **1977**, *132*, 53.

(33) Chalk, A. J.; Harrod, J. F. *J. Am. Chem. Soc.* **1967**, *89*, 1640.

(34) Nagai, Y.; Matsumoto, H.; Hayashi, M.; Tajima, E.; Ohtsuki, M.; Sekikawa, N. *J. Organomet. Chem.* **1971**, *29*, 209.

Scheme 5



plained in terms of the Chalk–Harrod cycle,<sup>8</sup> in which the Rh(III)-oxidative adduct  $\text{ClRhH}(\text{SiR}_3)(\text{PPh}_3)_2$  was a reasonable intermediate in the catalytic cycle in the conventional mechanism.<sup>4</sup> In sharp contrast, our results clearly exclude this type of oxidative adduct in the catalytic reaction, suggesting that mechanisms involving Rh(V) intermediates, which were reported in certain rhodium complexes,<sup>9,10</sup> are rather important.

Dehydrogenative silylation of olefins catalyzed by several rhodium complexes containing cyclopentadienyl ligands were reported by Maitlis<sup>9</sup> and Perutz.<sup>10</sup> An important suggestion in their reports is that double oxidative addition of trialkylsilanes to the rhodium complexes actually gives Rh(V) complexes, Cp- or Cp\*Rh-(H)<sub>2</sub>(SiR<sub>3</sub>)<sub>2</sub>. These double oxidative adducts themselves did not undergo olefin insertion into their Rh–H or Rh–Si bonds and were essentially inert in catalysis. The net catalyst species proposed was Cp- or Cp\*Rh(H)-(SiR<sub>3</sub>)(olefin), whose formation is followed by insertion and reductive elimination to complete the catalytic cycle. The mechanism proposed by Perutz is shown in Scheme 5.<sup>10</sup> Reductive elimination of one H–SiR<sub>3</sub> molecule from Cp\*Rh(H)<sub>2</sub>(SiR<sub>3</sub>)<sub>2</sub> followed by coordination of olefin can generate Cp\*Rh(H)(SiR<sub>3</sub>)(olefin) according to Maitlis et al.<sup>9</sup> This reaction can initiate the catalytic reaction but is considered to be a minor reaction pathway in the catalytic dehydrogenative silylation because of great stability of the double oxidative adducts. Perutz suggested that the other Rh(V) species (A in Scheme 5) might be involved in the catalytic cycle, in which insertion of olefin into a Rh–Si bond of CpRh(Et)(SiR<sub>3</sub>)-(olefin) forms a dialkyl Rh(III) intermediate, to which oxidative addition of another molecule of R<sub>3</sub>SiH facilitates the reductive elimination via A.<sup>10</sup>

Analysis by Maitlis and Perutz gives a clue which provides an answer to the question of how the rate enhancement is achieved in our RhCl(PPh<sub>3</sub>)<sub>3</sub>-catalyzed hydrosilylation with bifunctional organosilanes. A plausible candidate is shown in Scheme 6. The double oxidative addition of bifunctional organosilanes to RhCl-(PPh<sub>3</sub>)<sub>3</sub> results in formation of a Rh(V)–disilametallacyclic intermediate B, which reversibly produces a catalytically active Rh(III) species C by reductive elimination of one of the Si–H groups and coordination of

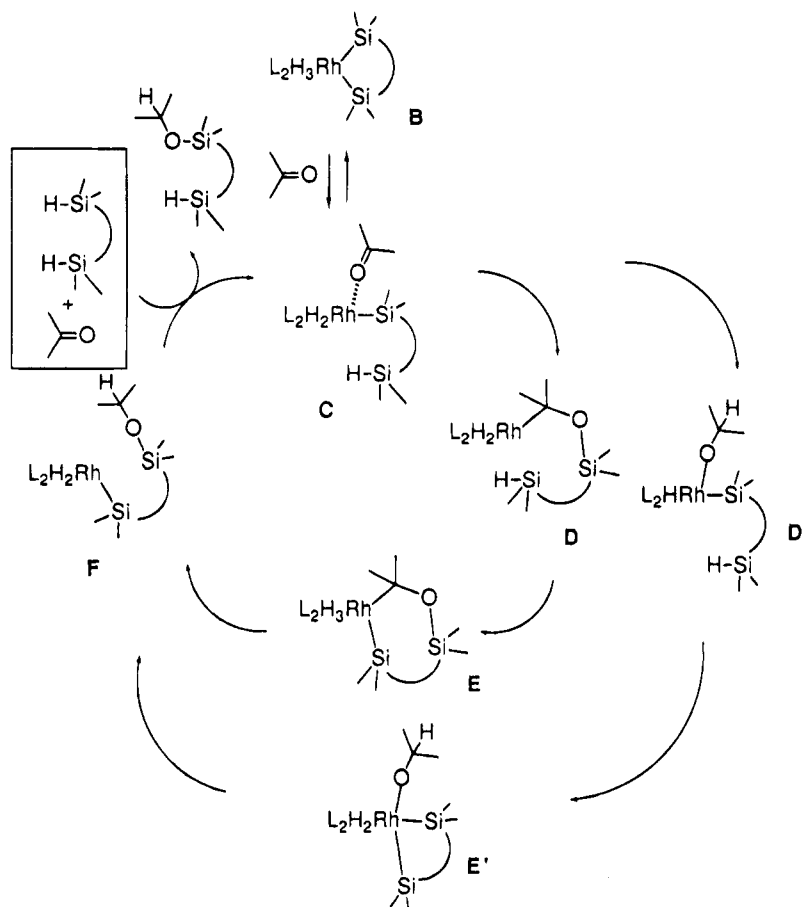
ketones. Migratory insertion of ketones between either a Rh–Si or Rh–H bond in C<sup>35</sup> provides D or D', from which reductive elimination of a Si–OiPr group is induced by intramolecular oxidative addition of the uncoordinated Si–H bond. A key point of this scheme is the reductive elimination of the product facilitated by the oxidative addition of the Si–H bond, i.e., D (D') to F via E (E'). Since this second oxidative addition step is an intramolecular process in the hydrosilylation of bifunctional organosilanes, reductive elimination is much more facile compared with that of monofunctional organosilanes, in which the reductive elimination has to occur via the intermolecular oxidative addition of another molecule of organosilane.

This mechanism also can explain the selective monofunctionalization of the bifunctional organosilanes. As described above, the second oxidative addition facilitates the formation of the intermediate F. Although coordination of acetone and subsequent insertion may occur from F, the hydrosilylation of acetone by the second Si–H group is no longer assisted by the intramolecular oxidative addition process. Thus, reductive elimination of the product having two Si–OiPr groups is inhibited. As a consequence, reductive elimination of the monoisopropoxy monohydrosilane from F becomes the only way to produce the product. The lack of the chemoselectivity in the hydrosilylation with unsymmetrical organosilanes 8 is presumably attributable to the small energy difference between the Me<sub>2</sub>SiH moiety and the Ph<sub>2</sub>SiH group in the total oxidative addition step.

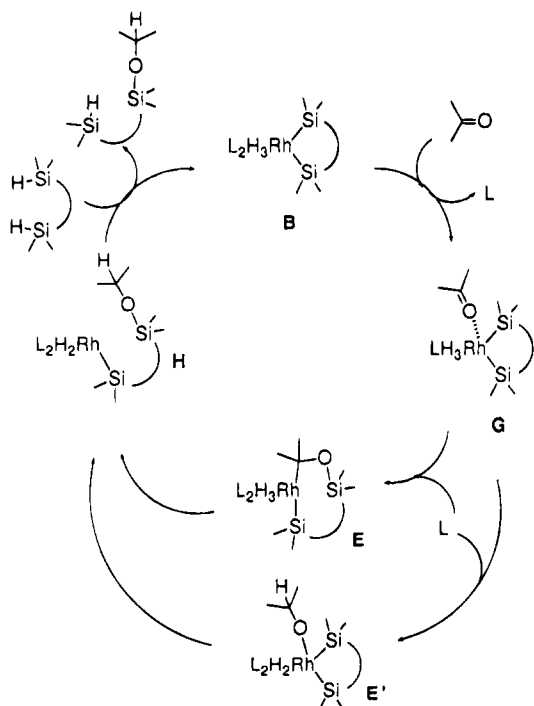
We consider this mechanism adaptable to explain all of the experimental results described above. However, it should be pointed out that there is another possibility of an alternative catalytic cycle involving the Rh(V)-double oxidative adducts inside the catalytic cycle as shown in Scheme 7. Since the double oxidative adducts, Cp- or Cp\*Rh(H)<sub>2</sub>(SiR<sub>3</sub>)<sub>2</sub>, used for dehydrogenative silylation of olefins by Maitlis and Perutz are coordinatively saturated, reductive elimination of H–SiR<sub>3</sub> is the only process to open a coordination site for olefins (except for the less common  $\eta^5 \rightarrow \eta^3$  slippage of the Cp ring<sup>9,10</sup>). In the double oxidative adducts 21 and 22, there is another possible pathway to produce coordinatively unsaturated species which then can react with ketones, dissociation of PPh<sub>3</sub>. If the replacement of PPh<sub>3</sub> by ketones occurs, the coordinated ketones could subsequently insert into either a Rh–Si or a Rh–H bond,<sup>35</sup> followed by coordination of PPh<sub>3</sub>, to form E or E', which are the same intermediates discussed in the mechanism shown in Scheme 6. The rate enhancement is derived from the high reactivity of the Rh(V)–trihydride–disilyl species toward insertion of the carbon–oxygen double bond of ketones. If we assume that this high reactivity was only observed in the Rh(V)–trihydride–disilyl species (G) and not in the product (H) obtained by the insertion, the selective monofunctionalization can also be explained. It is also easy to explain the nonselective functionalization of unsymmetrical

(35) Insertion of unsaturated molecules into the oxidative adduct, H–M–SiR<sub>3</sub>, has recently been a subject of controversy. Two possibilities were discussed: one is that the insertion takes place into a H–M bond, and the other that it does so into a Si–M bond. Our results cannot provide unequivocal evidence to this problem. However, it should be noted that a pathway involving hydrogen migration more easily explains the catalytic cycle, because the Si migration pathway results in formation of unfavorable disilametallacycle intermediates having larger ring size E.

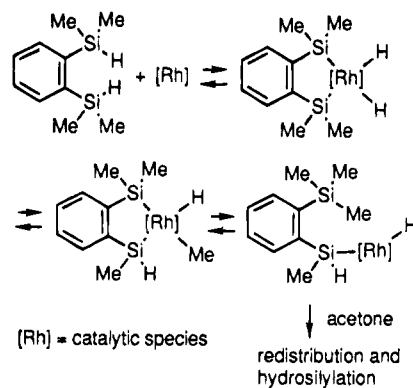
Scheme 6



Scheme 7



Scheme 8



tionalization. In contrast, that shown in Scheme 7 involves the double oxidative adducts as a highly reactive intermediate for insertion of ketones. To obtain experimental evidence to differentiate between these two mechanisms, we attempted to carry out the reaction of the double oxidative adducts, **21** or **22**, with ketones. Unfortunately, however, the high moisture and temperature sensitivity of these adducts did not give NMR spectra clear enough to provide information on this problem.

### Conclusion

We have described here our studies on the unusual rate enhancement observed in the RhCl(PPh<sub>3</sub>)<sub>3</sub>-catalyzed hydrosilylation of ketones with bifunctional organosilanes. Experiments in which the structure of the

organosilanes if we assume there is little difference in energy among the possible insertion steps from **G**.

In the mechanism shown in Scheme 6, the bifunctional structure of organosilanes effects the reductive elimination to eliminate the product from the catalyst, giving the rate enhancement and selective monofunc-

silanes was changed and others to detect the double oxidative adducts which might be involved in the catalytic cycle were carried out. In the former study, two characteristic features, the significant rate acceleration compared with monofunctional organosilanes and the selective functionalization of one of the Si–H bonds, were observed only when we used the bifunctional organosilanes having two Si–H bonds at an appropriate distance apart. The structure of “reactive” organosilanes, namely **2**, **3**, and **5–9**, suggests that those which allow formation of disilametallacyclic intermediates by double oxidative addition of both of the Si–H bonds to  $\text{RhCl}(\text{PPh}_3)_3$  can result in such reactivity. Spectral evidence for the double oxidative adducts was obtained in the latter study, in which  $\text{Rh}(\text{V})$ -disilyltrihydride species, **21** and **22**, actually were detected in toluene- $d_8$ . It also was confirmed that the solution containing this species is catalytically active for the hydrosilylation reactions of bifunctional organosilanes. Conventional  $\text{Rh}(\text{III})$ -oxidative adducts **17**, **19**, and **20** also were detected in  $\text{CDCl}_3$ . However, these species were inactive to the catalytic reaction.

An important point of these results is that neither the conventional Chalk–Harrod cycle or its variants, nor a mechanism involving metal colloids, can explain both the rate enhancement and selective monofunctionalization. Mechanisms involving  $\text{Rh}(\text{V})$  intermediates such as the ones proposed by Maitlis<sup>9</sup> and Perutz<sup>10</sup> are reasonable possibilities to explain all of the results, which prompted us to propose the two possible mechanisms shown in Schemes 6 and 7. It is important that both mechanisms involve intramolecular oxidative addition of the second Si–H bond of the bifunctional organosilanes to the  $\text{Rh}(\text{III})$  species to form  $\text{Rh}(\text{V})$  adducts. This is essential for the rate enhancement and selective functionalization in either the reductive elimination step (Scheme 6) or the double oxidative addition step (Scheme 7). In either mechanism, the role of the  $\text{Rh}(\text{V})$  intermediates is crucial.

We suspect that the involvement of  $\text{Rh}(\text{V})$  intermediates may commonly play an important role in the  $\text{RhCl}(\text{PPh}_3)_3$ -catalyzed hydrosilylation with other organosilanes. For example, Ojima and Kogure reported that the rate and selectivities of hydrosilylation of ketones with  $\text{Ph}_2\text{SiH}_2$  were high when no solvent was used for the reaction.<sup>4</sup> They suggested from the fact that dilution with benzene reduced both the rate and selectivities that a bimolecular process could be involved in the reaction. If this bimolecular process corresponds to the reductive elimination step facilitated by the oxidative addition of another molecule of  $\text{Ph}_2\text{SiH}_2$ , this suggestion would be consistent with our proposed mechanism shown in Scheme 6, in which the intramolecular oxidative addition of the second Si–H facilitates the reductive elimination of the product. Alternatively, the bimolecular process suggested by Ojima may be related to the double oxidative addition of two molecules of  $\text{Ph}_2\text{SiH}_2$  to  $\text{RhCl}(\text{PPh}_3)_3$ , similar to the mechanism shown in Scheme 7. The Wilkinson complex is a synthetically well-known but mechanistically little understood hydrosilylation catalyst. The present report will stimulate mechanistic controversy on the  $\text{RhCl}(\text{PPh}_3)_3$ -catalyzed hydrosilylations.<sup>35,36</sup>

## Experimental Section

**General Methods.** All manipulations were carried out using standard Schlenk technique under an argon or nitrogen atmosphere. NMR spectra ( $^1\text{H}$ , 270 MHz;  $^{13}\text{C}$ , 67.8 MHz;  $^{31}\text{P}$ , 109.25 MHz), which were measured in  $\text{CDCl}_3$  unless otherwise noted, are recorded by  $\delta$ -values (ppm) and coupling constants ( $J$ ; Hz). Many of the organosilicon compounds listed below are volatile oils, and it was very difficult to remove small amounts of organic impurities such as siloxanes and solvents. Some of the compounds are sensitive to moisture. Thus, determination of the products was mainly carried out by  $^1\text{H}$  and  $^{13}\text{C}$  NMR as well as high-resolution mass spectra. All of the solvents were distilled from drying reagents (acetone,  $\text{B}_2\text{O}_3$ ; benzene, toluene, ether, THF,  $\text{Na}/\text{Ph}_2\text{CO}$ ) just before use.

**Preparation of 1-(Dimethylsilyl)-2-(dimethylsilylmethyl)benzene (6) and 1,2-Bis(dimethylsilylmethyl)benzene (7).** Preparation of **6** was carried out by the reaction of  $\text{Me}_2\text{SiHCl}$ , Mg, and 1-bromo-2-(bromomethyl)benzene. In a typical example, 1-bromo-2-(bromomethyl)benzene (2 g, 8 mmol) in THF (8 mL) was added dropwise to a mixture of  $\text{Me}_2\text{SiHCl}$  (1.86 mL, 16.8 mmol) and Mg (0.41 g, 16.8 mmol) in THF (2 mL). The mixture was heated under reflux for 1 h. After removal of the solvent, distillation of the residue gave **6** in 49% yield (0.81 g). With a similar procedure, **7** was prepared from 1,2-bis(bromomethyl)benzene in 75% yield.

**6:** colorless liquid (bp 62 °C/1.2 mmHg);  $^1\text{H}$  NMR ( $\text{C}_6\text{D}_6$ )  $\delta$  0.18 (d,  $J = 3.7$ , 6H,  $\text{CH}_2\text{SiMe}_2$ ), 0.44 (d, 6H,  $J = 3.9$ ,  $\text{ArSiMe}_2$ ), 2.47 (d, 2H,  $J = 3.41$ ,  $\text{CH}_2$ ), 4.35 (sep, 1H,  $J = 3.7$ ,  $\text{CH}_2\text{SiH}$ ), 4.74 (sep, 1H,  $J = 3.7$ ,  $\text{ArSiH}$ ), 7.15–7.59 (m, 4H, aryl);  $^{13}\text{C}$  NMR ( $\text{CDCl}_3$ )  $\delta$  -5.72 (Me), -4.48 (Me), 22.8 ( $\text{CH}_2$ ), 122.5, 126.8, 127.9, 133.2, 133.3, and 144.4 (aromatic); IR (neat) 2140  $\text{cm}^{-1}$  HRMS ( $m/e$ ): calcd for  $\text{C}_{11}\text{H}_{20}\text{Si}_2$ , 208.1104; found, 208.1101.

**7:** colorless liquid (bp 56–58 °C/1.2 mmHg);  $^1\text{H}$  NMR ( $\text{C}_6\text{D}_6$ )  $\delta$  0.01 (d,  $J = 3.4$ , 12H,  $\text{SiMe}_2$ ), 2.09 (d,  $J = 3.4$ , 4H,  $\text{CH}_2$ ), 4.20 (sep,  $J = 3.4$ , 2H, Si–H), 6.98 (m, 4H, aryl).  $^{13}\text{C}$  NMR ( $\text{CDCl}_3$ )  $\delta$  -4.20 (Me), 21.7 ( $\text{CH}_2$ ), 125.0, 129.6, and 130.7 (aromatic). IR (neat): 2140  $\text{cm}^{-1}$ . Anal. Calcd for  $\text{C}_{12}\text{H}_{22}\text{Si}_2$ : C, 64.79; H, 9.97. Found: C, 64.45; H, 9.97.

**Preparation of Phenyl-Substituted Organosilanes 8 and 9.** To a mixture of  $\text{ClPh}_2\text{Si}(\text{CH}=\text{CH}_2)$  (8 mL, 36 mmol) and 0.1 M  $\text{H}_2\text{PtCl}_6$  in  $^i\text{PrOH}$  (5 drops) was added  $\text{Me}_2\text{SiHCl}$  (4.5 mL, 40 mmol). The mixture was heated under reflux for 3 h. Distillation of the crude product at 142–154 °C/2 mmHg gave  $\text{ClPh}_2\text{SiCH}_2\text{CH}_2\text{SiMe}_2\text{Cl}$  in 88% yield (10.8 g) [ $^1\text{H}$  NMR ( $\text{C}_6\text{D}_6$ )  $\delta$  0.41 (s,  $\text{SiMe}_2$ ), 0.7–1.0 and 1.1–1.5 (m,  $\text{SiCH}_2$ ), 7.3–7.5 (m, Ph)]. This chlorosilane (10.7 g, 31.5 mmol) was reduced with  $\text{LiAlH}_4$  (1.2 g, 31.5 mmol) in ether (35 mL) at 40 °C for 6 h.  $\text{NaF}$  (5.3 g, 126 mmol) dissolved in water (2.3 g, 128 mmol) was added, and the mixture was filtered. The filtrate was dried over  $\text{MgSO}_4$ . After removal of the solvents, the residue was distilled to give **8** in 34% yield (3.29 g). A similar two-step procedure from  $\text{ClPh}_2\text{Si}(\text{CH}=\text{CH}_2)$  and  $\text{ClSiHPh}_2$  afforded **9** in overall 15% yield.

**8:** colorless oil (bp 110–124 °C/2 mmHg);  $^1\text{H}$  NMR  $\delta$  0.05 (d, 6H,  $J = 3.9$ , Si–Me), 0.59–0.67 and 1.04–1.13 (m, 2H each,

(36) In our preliminary communications,<sup>2</sup> we reported that the rapid and selective monofunctionalization of **2** or **5** was also achieved with olefins and acetylenes. There were some points that differ from the reactions with ketones. First, the magnitude of rate enhancement giving rise to the selective monofunctionalization was large in ketones and acetylenes but not in olefins in the hydrosilylation with **2**. Second, in the hydrosilylation with **5**, selective monofunctionalization was also achieved by olefins; however, no 1,4-methyl group migration such as that observed in the reaction of ketones was observed. Third, hydrosilylation of acetylenes with **5** did not occur under the conditions used. It is well-known that features of hydrosilylation differ among ketones, olefins, and acetylenes, which has made mechanistic studies on catalytic hydrosilylation extremely complicated.<sup>1</sup> The analysis presented in this paper can be adaptable to the reaction with ketones and can stimulate the mechanistic studies of the reaction with olefins or acetylenes; further detailed investigation, however, will be required for full clarification.



Si-CH<sub>2</sub>), 3.83 (septet, 1H, *J* = 3.9, Me<sub>2</sub>SiH), 4.82 (t, 1H, *J* = 3.9, Ph<sub>2</sub>SiH), 7.31–7.56 (m, 10H, Ph); <sup>13</sup>C NMR δ -4.77 (Me), 5.28 and 7.44 (CH<sub>2</sub>), 128.0, 129.5, 134.5, and 135.2 (Ph); IR (neat) 2100 cm<sup>-1</sup>. Anal. Calcd for C<sub>16</sub>H<sub>22</sub>Si<sub>2</sub>: C, 71.04; H, 8.20. Found: C, 71.43; H, 8.25.

**9**: white solid (mp 84.5–85 °C; bp 220 °C/2 mmHg (Kugelrohr)); <sup>1</sup>H NMR δ 1.19 (s, 4H, CH<sub>2</sub>), 4.85 (s, 2H, SiH), 7.30–7.53 (m, 20H, Ph); <sup>13</sup>C NMR δ 5.45 (CH<sub>2</sub>), 128.0, 129.6, 134.2, and 135.2 (Ph); IR (CH<sub>2</sub>Cl<sub>2</sub>) 2110 cm<sup>-1</sup>. Anal. Calcd for C<sub>26</sub>H<sub>22</sub>Si<sub>2</sub>: C, 79.13; H, 6.64. Found: C, 78.86; H, 6.56.

**General Procedure for the Monohydrosilylation of Bidentate Organosilanes 1–7 with Acetone.** A mixture of silane (2 mmol), anhydrous acetone (2 mmol), and RhCl(PPh<sub>3</sub>)<sub>3</sub> (0.02 mmol) dissolved in dry benzene (6 mL) was stirred at room temperature for a few hours. After removal of the solvent in vacuo, bulb-to-bulb distillation of the residue gave the corresponding monoisopropoxymonohydrosilane. Because of the facile hydrolysis of either Si-H or Si-OR bonds in the presence of metallic residues, careful work-up to avoid contact with air or moisture is necessary.

**10**: colorless liquid (bp 88–90 °C/34 mmHg); <sup>1</sup>H NMR (C<sub>6</sub>D<sub>6</sub>) δ 0.04 (d, 6H, *J* = 3.4, SiHMe<sub>2</sub>), 0.11 (s, 6H, SiMe<sub>2</sub>OiPr), 0.56 (s, 4H, SiCH<sub>2</sub>), 1.10 (d, 6H, *J* = 5.8, OCHMe<sub>2</sub>), 3.85 (sep, 1H, *J* = 5.8, OCHMe<sub>2</sub>), 4.12 (br-s, 1H, Si-H); <sup>13</sup>C NMR (C<sub>6</sub>D<sub>6</sub>) δ -4.72 and -1.88 (SiMe), 6.19 and 9.99 (SiCH<sub>2</sub>), 26.1 (Me or iPr), 64.9 (CH of iPr); IR (neat) 2160 cm<sup>-1</sup>. HRMS (*m/e*): calcd for C<sub>9</sub>H<sub>24</sub>O<sub>2</sub>Si<sub>2</sub>; 204.1366; found, 204.1365.

**11**: colorless liquid (bp 50–52 °C/2 mmHg); <sup>1</sup>H NMR δ 0.03 (d, 6H, *J* = 3.4, SiHMe<sub>2</sub>), 0.06 (s, 6H, SiMe<sub>2</sub>OiPr), 0.61–0.67 (m, 4H, SiCH<sub>2</sub>), 1.12 (d, 6H, *J* = 5.8, Me of iPr), 1.41 (m, 2H, CH<sub>2</sub>), 3.82 (sep, 1H, *J* = 3.4, SiH), 3.95 (sep, 1H, *J* = 5.8, CH of iPr). IR (neat) 2110 cm<sup>-1</sup>. Anal. Calcd for C<sub>10</sub>H<sub>26</sub>Si<sub>2</sub>O; C, 54.98; H, 11.99. Found: C, 54.08; H, 11.96.

**12a and 12b**: These were obtained as a mixture of isomers (**12a:12b** = 5:4) (colorless liquid; bp 60–65 °C/0.8 mmHg). IR (neat): 2150 cm<sup>-1</sup>. Anal. Calcd for C<sub>13</sub>H<sub>24</sub>Si<sub>2</sub>O; C, 61.72; H, 9.59. Found: C, 61.84; H, 9.58. NMR samples were separated by preparative GC. <sup>1</sup>H NMR (C<sub>6</sub>D<sub>6</sub>): **12a**, δ 0.33 (d, 6H, *J* = 3.9, SiHMe<sub>2</sub>), 0.43 (s, 6H, Si(OiPr)Me<sub>2</sub>), 1.14 (d, 6H, *J* = 5.9, Me of iPr), 3.95 (sep, 1H, *J* = 5.9, CH of iPr), 4.99 (sep, 1H, *J* = 3.9, SiH), 7.22–7.65 (m, 4H, aromatic). **12b**, δ 0.30 (s, 9H, SiMe<sub>3</sub>), 0.40 (d, 3H, *J* = 2.4, SiH(OiPr)Me), 1.09 and 1.11 (two d, 3H each, *J* = 6.8, Me of iPr), 3.93 (sep, 1H, *J* = 6.8, CH of iPr), 5.55 (q, 1H, *J* = 2.4, SiH), 7.22–7.84 (m, 4H, aromatic). <sup>13</sup>C NMR (C<sub>6</sub>D<sub>6</sub>): **12a**, δ -2.03 (SiHMe<sub>2</sub>), 1.16 (Si(OiPr)Me<sub>2</sub>), 25.94 (Me of iPr), 65.60 (CH of iPr), 128.8 (2C), 134.6, 134.8, 144.3 and 144.5 (aromatic); **12b**, δ -0.60 (SiMe<sub>3</sub>), 1.40 (SiH(OiPr)Me), 25.4 and 25.5 (Me of iPr), 66.9 (CH of iPr), 129.1 (2C), 134.7, 135.1, 144.4 and 146.4 (aromatic).

**13**: This was obtained as a 1:1 mixture of two isomers (colorless liquid; bp 90–95 °C/2 mmHg). <sup>1</sup>H NMR (C<sub>6</sub>D<sub>6</sub>): δ 0.07 (d, 6H, *J* = 3.9, CH<sub>2</sub>SiHMe<sub>2</sub>), 0.11 (s, 6H, CH<sub>2</sub>Si(OiPr)Me<sub>2</sub>), 0.30 (d, 6H, *J* = 3.9, ArSiHMe<sub>2</sub>), 0.40 (s, 6H, ArSi(OiPr)Me<sub>2</sub>), 1.08 and 1.10 (two d, 6H each, *J* = 6.3, OCHMe<sub>2</sub>), 2.46 (s, 2H, ArCH<sub>2</sub>Si(OiPr)Me<sub>2</sub>), 2.52 (d, 2H, *J* = 3.4, ArCH<sub>2</sub>-SiHMe<sub>2</sub>), 3.78–3.94 (m, 2H total, two CH of iPr), 4.25 (sep, 1H, *J* = 3.9, CH<sub>2</sub>SiH), 4.85 (sep, *J* = 3.9, 1H, ArSiH), 7.0–7.2 (m, 4H total, aromatic), 7.43 (d, 2H total, *J* = 7.1, aromatic), 7.57 (d, 2H total, *J* = 7.4, aromatic). IR (neat): 2110 cm<sup>-1</sup>. HRMS (*m/e*): calcd for C<sub>14</sub>H<sub>26</sub>Si<sub>2</sub>O; 266.1523; found, 266.1520.

**14**: colorless liquid (bp 90–100 °C/1.2 mmHg); <sup>1</sup>H NMR (C<sub>6</sub>D<sub>6</sub>) δ 0.00 (d, *J* = 3.4, 6H, SiHMe), 0.09 (s, 6H, SiMeOiPr), 1.07 (d, *J* = 5.9, 6H, OCHMe<sub>2</sub>), 2.18 (d, *J* = 3.4, 2H, CH<sub>2</sub>SiH),

2.23 (s, 2H, CH<sub>2</sub>SiOiPr), 3.82 (sep, *J* = 5.9, 1H, CHMe<sub>2</sub>), 4.21 (sep, *J* = 3.4, 1H, Si-H), 6.9–7.1 (m, 4H, aromatic); <sup>13</sup>C NMR -4.31 (SiMe), -1.32 (SiMe), 21.8 (CH<sub>2</sub>), 24.3 (CH<sub>2</sub>), 25.8 (OCHMe), 65.2 (OCH), 124.2, 124.7, 129.0, 129.3, 136.0, and 136.8 (aromatic); IR (neat) 2130 cm<sup>-1</sup>. Anal. Calcd for C<sub>15</sub>H<sub>28</sub>O<sub>2</sub>Si<sub>2</sub>: C, 64.22; H, 10.06. Found: C, 63.62; H, 10.03. HRMS (*m/e*): calcd, 280.1679; found, 280.1676.

**Monohydrosilylation of 8 and 9 with Acetone.** The reactions were carried out at 50 °C; other procedures were the same as above. The reaction of **9** gave **16** containing some amounts of **9**, which could not be separated.

**15a and 15b**: These were obtained as a 1:1 mixture of isomers (colorless oil; bp 140–150 °C/2 mmHg). <sup>1</sup>H NMR (C<sub>6</sub>D<sub>6</sub>): δ -0.01 (d, 6H, *J* = 4.4 Hz, SiHMe<sub>2</sub>), 0.07 (s, 6H, Si(OiPr)Me<sub>2</sub>), 0.70–0.76 (m, 4H total, CH<sub>2</sub>SiHMe<sub>2</sub> and CH<sub>2</sub>Si(OiPr)Me<sub>2</sub>), 1.07 (d, 6H, *J* = 5.9, Si(OCHMe<sub>2</sub>)Me<sub>2</sub>), 1.11 (d, 6H, *J* = 6.4, Si(OCHMe<sub>2</sub>)Ph<sub>2</sub>), 1.14–1.22 (m, 4H total, CH<sub>2</sub>SiHPh<sub>2</sub> and CH<sub>2</sub>Si(OiPr)Ph<sub>2</sub>), 3.80 (m, 1H, Si(OCHMe<sub>2</sub>)Me<sub>2</sub>), 4.04 (m, 1H, Si(OCHMe<sub>2</sub>)Ph<sub>2</sub>), 4.10 (quintet, 1H, *J* = 3.1, SiHMe<sub>2</sub>), 5.12 (t, 1H, *J* = 4.1, SiHPh<sub>2</sub>), 7.02–7.72 (m, 20H total, Ph). IR (neat): 2110 cm<sup>-1</sup>. Anal. Calcd for C<sub>19</sub>H<sub>28</sub>Si<sub>2</sub>O; C, 69.45; H, 8.59. Found: C, 69.69; H, 8.57.

**16**: a mixture with **9** (colorless oil); <sup>1</sup>H NMR δ 1.08 (d, 6H, *J* = 6.3, Me of iPr), 1.25 (s, 4H, SiCH<sub>2</sub>), 3.98 (m, 1H, CH of iPr), 5.12 (t, 1H, *J* = 3.0, SiH), 7.08–7.40 (m, 20H, Ph); IR (neat) 2110 cm<sup>-1</sup>. MS (*m/e*): 452 (M), 453 (M + 1) [100:86].

**NMR Studies for the Detection of Double Oxidative Adducts.** All of the oxidative adducts reported in this paper were highly moisture sensitive, and careful removal of water from the NMR solvents and from the NMR sample tube was critically important to obtain appropriate NMR charts. Most of the manipulations were carried out using the vacuum line (10<sup>-4</sup> to 10<sup>-3</sup> Torr) technique. The NMR solvents were repeatedly distilled in the presence of drying reagents (CDCl<sub>3</sub>, P<sub>2</sub>O<sub>5</sub>; toluene-*d*<sub>8</sub>, Na/Ph<sub>2</sub>CO) in vacuum and stored in a vacuum line. Organosilanes were distilled just before use. RhCl(PPh<sub>3</sub>)<sub>3</sub> was dried in vacuo overnight. The NMR sample tube (5 mm diameter) was flame-dried in vacuum just before use. Into the NMR tube were placed RhCl(PPh<sub>3</sub>)<sub>3</sub> (36 mg, 0.04 mmol) and the organosilane (0.08–0.16 mmol) under argon atmosphere. In the case using toluene-*d*<sub>8</sub>, half amounts of the rhodium complex and the organosilane were used because of the low solubility of the oxidative adducts. The tube was quickly connected to the vacuum line and evacuated at -78 °C. After the solvent was distilled under vacuum the tube was sealed. The NMR sample prepared was kept at -78 °C until the NMR measurement. The NMR sample was quickly warmed, kept at room temperature for several minutes, and then subjected to the NMR measurement. Most of the measurements were carried out at -20 °C in CDCl<sub>3</sub> and at -40 °C in toluene-*d*<sub>8</sub>, unless otherwise noted in the text.

**Acknowledgment.** This work was supported by Grants from the Ministry of Education, Culture, and Science of Japan (02247210, 03233212, 042172212, and 06805080).

**Supplementary Material Available:** Details on the NMR studies for the oxidative addition of PhMe<sub>2</sub>SiH, **8**, and **9** including text and figures (25 pages). Ordering information is given on any current masthead page.

OM940791B

# Use of Tetradentate (N<sub>2</sub>O<sub>2</sub>) Ligands To Form Monomeric, Trimetallic Gallium Complexes

David A. Atwood\* and Drew Rutherford

Department of Chemistry, North Dakota State University, Fargo, North Dakota 58105

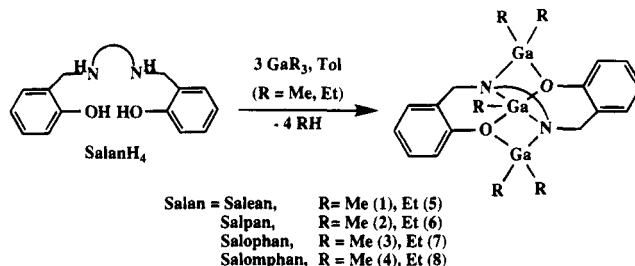
Received February 27, 1995<sup>®</sup>

Members of the SalanH<sub>4</sub> class of tetradentate (N<sub>2</sub>O<sub>2</sub>) ligand, *N,N'*-bis(*o*-hydroxybenzyl)-1,2-diaminoethane (SaleanH<sub>4</sub>), *N,N'*-bis(*o*-hydroxybenzyl)-1,3-diaminopropane (SalpanH<sub>4</sub>), *N,N'*-bis(*o*-hydroxybenzyl)-1,2-diaminobenzene (SalophanH<sub>4</sub>), and *N,N'*-bis(*o*-hydroxybenzyl)-1,2-diamino-4,5-dimethylbenzene (SalomphanH<sub>4</sub>), react with 3 equiv of GaMe<sub>3</sub> to form the trimetallic complexes SaleanGaMe(GaMe<sub>2</sub>)<sub>2</sub> (**1**), SalpanGaMe(GaMe<sub>2</sub>)<sub>2</sub> (**2**), SalophanGaMe(GaMe<sub>2</sub>)<sub>2</sub> (**3**), and SalomphanGaMe(GaMe<sub>2</sub>)<sub>2</sub> (**4**). Similar reactions of the SalanH<sub>4</sub> ligands with GaEt<sub>3</sub> form SaleanGaEt(GaEt<sub>2</sub>)<sub>2</sub> (**5**), SalpanGaEt(GaEt<sub>2</sub>)<sub>2</sub> (**6**), SalophanGaEt(GaEt<sub>2</sub>)<sub>2</sub> (**7**), and SalomphanGaEt(GaEt<sub>2</sub>)<sub>2</sub> (**8**). For these compounds, the <sup>1</sup>H NMR data indicate the presence of rigid solution state geometries. A crystallographic study of **1**, **2**, and **5** demonstrates that the molecules contain a central GaR group (R = Me, Et) which is coordinated in a planar array to the nitrogens and oxygens of the ligand. The remaining GaR<sub>2</sub> groups each bridge an oxygen and nitrogen atom. Compound **1** contains one molecule of toluene as solvent of crystallization. Crystal data are as follows. **1**: C<sub>28</sub>H<sub>39</sub>Ga<sub>3</sub>N<sub>2</sub>O<sub>2</sub>, space group P2<sub>1</sub>/c (no. 14), with *a* = 10.694(2) Å, *b* = 14.101(2) Å, *c* = 19.184(2) Å, β = 94.040(10)°, *V* = 2885.5(7) Å<sup>3</sup>, and *Z* = 4. With 316 parameters refined on 2615 reflections having *F* > 4.0σ(*F*), the final *R* values were *R* = 0.0498 and *R*<sub>w</sub> = 0.0545. **2**: C<sub>22</sub>H<sub>33</sub>Ga<sub>3</sub>N<sub>2</sub>O<sub>2</sub>, space Group P2<sub>1</sub>/c (no. 14), with *a* = 16.247(12) Å, *b* = 9.588(9) Å, *c* = 17.131(8) Å, β = 116.21(4)°, *V* = 2395(3) Å<sup>3</sup> and *Z* = 4. With 262 parameters refined on 1777 reflections having *F* > 6.0σ(*F*), the final *R* values were *R* = 0.0690 and *R*<sub>w</sub> = 0.0763. **5**: C<sub>26</sub>H<sub>41</sub>Ga<sub>3</sub>N<sub>2</sub>O<sub>2</sub>, space group monoclinic P2<sub>1</sub>/n (no. 14), with *a* = 8.433(1) Å, *b* = 22.010(2) Å, *c* = 15.241(1) Å, β = 98.81(1)°, *V* = 2795.4(5) Å<sup>3</sup>, and *Z* = 4. With 298 parameters refined on 2111 reflections having *F* > 4.0σ(*F*), the final *R* values were *R* = 0.0458 and *R*<sub>w</sub> = 0.0492.

## Introduction

The SalanH<sub>4</sub> molecules (*N,N'*-bis(*o*-hydroxybenzyl)-1,2-diaminoalkane or -arene) (Figure 1a) are unique and useful ligands with which to explore fundamental aspects of structure and bonding in the main group elements, specifically for the group 12–14 elements. For instance, the OH and NH groups in these molecules may be used to form σ or donor bonding, or a combination of the two, depending on the oxophilicity and the oxidation state of the metal being bound. Additional properties such as chelate size, solubility, and chirality may be manipulated by varying the groups at R<sup>1</sup>, R<sup>2</sup>, and R<sup>3</sup>. It is evident that these molecules should be ideal ligands for both the transition and main group metal elements. In fact, these ligands have been used previously in the synthesis of transition metal complexes<sup>1</sup> and various main group examples, including complexes of general formula SalanH<sub>2</sub>M (where M = Zn<sup>2+</sup> and Sn<sup>3+</sup>), [(SalanAl)-Li(THF)<sub>2</sub>]<sub>2</sub>,<sup>4</sup> SalanH<sub>2</sub>AlMe,<sup>5</sup> and [SalanAl(AlMe<sub>2</sub>)<sub>2</sub>]<sub>2</sub>.<sup>5</sup>

## Scheme 1. General Syntheses of Compounds 1–8



In the present study we wish to expand the range of trimetallic derivatives of formula SalanMR(MR<sub>2</sub>)<sub>2</sub> to include those with M = Ga and R = Me and Et. Specifically, we will examine the gallium complexes of formula SalanGaR(GaR<sub>2</sub>)<sub>2</sub>, where Salan = Salean [R = Me (**1**), Et (**5**)], Salpan [R = Me (**2**), Et (**6**)], Salophan [R = Me (**3**), Et (**7**)], and Salomphan [R = Me (**4**), Et (**8**)]. The structures of compounds **1**, **2**, and **5** have been determined by single-crystal X-ray analysis.

## Results and Discussion

**Synthesis and Characterization.** Compounds **1–8** were prepared by the exothermic reaction of the respective SalanH<sub>4</sub> ligand with trialkylgallium in a 1:3 stoi-

(6) Shannon, R. D. *Acta Crystallogr.* **1976**, A32, 751.

<sup>®</sup> Abstract published in *Advance ACS Abstracts*, May 15, 1995.

(1) (a) Gheller, S. F.; Hambley, T. W.; Snow, M. R.; Murray, K. S.; Wedd, A. G. *Aust. J. Chem.* **1984**, 7, 911. (b) Bottcher, A.; Elias, H.; Jager, E.-G.; Langfelderova, H.; Mazur, M.; Muller, L.; Paulus, H.; Pelikan, P.; Rudolph, M.; Valko, M. *Inorg. Chem.* **1993**, 32, 4131.

(2) Atwood, D. A.; Benson, J.; Jegier, J. A.; Lindholm, N. F.; Martin, K. J.; Rutherford, D. *Main Group Chem.* **1995**, in press.

(3) Atwood, D. A.; Jegier, J. A.; Martin, K. J.; Rutherford, D. *J. Organomet. Chem.* **1995**, in press.

(4) Atwood, D. A.; Rutherford, D. *Inorg. Chem.* **1995**, in press.

(5) Atwood, D. A.; Jegier, J. A.; Martin, K. J.; Rutherford, D. *Organometallics*, **1995**, 14, 1453.

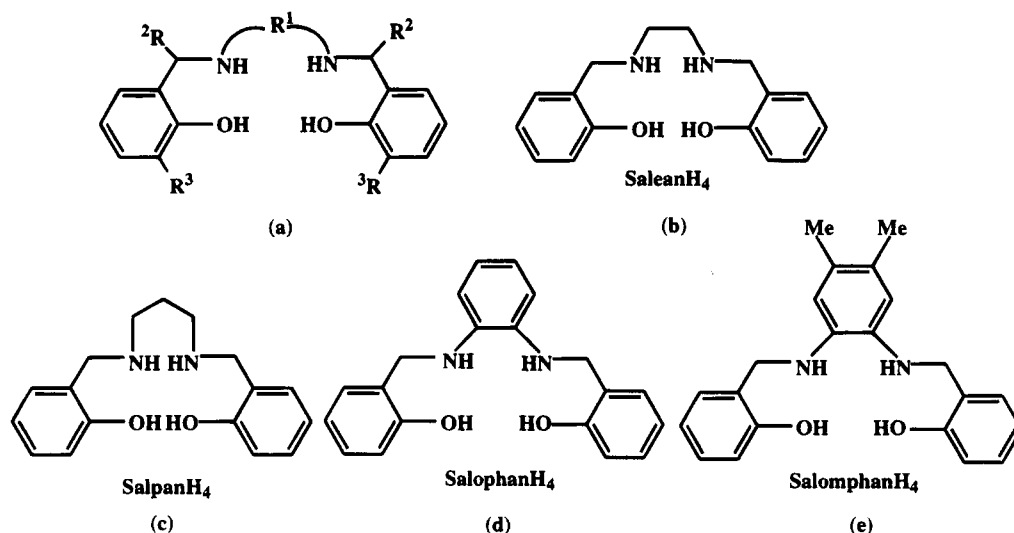


**Figure 1.** General depiction of the SalanH<sub>4</sub> class of ligands (a) and the ligands used in this study: SaleanH<sub>4</sub> (b), SalpanH<sub>4</sub> (c), SalophanH<sub>4</sub> (d), and SalomphanH<sub>4</sub> (e).

**Table 1.** Selected NMR Data for Compounds 1–8

compd	$\delta(^1\text{H})$			
	GaR	NCH <sub>2</sub> CH <sub>2</sub>	NCH <sub>2</sub>	PhCH <sub>2</sub>
SaleanGaMe(GaMe <sub>2</sub> ) <sub>2</sub> (1)	-0.25, 0.03, 0.20		2.40, 2.92	3.33, 4.46
SalpanGaMe(GaMe <sub>2</sub> ) <sub>2</sub> (2)	-0.10, 0.07, 0.29	1.18	2.53, 2.72	3.12, 4.40
SalophanGaMe(GaMe <sub>2</sub> ) <sub>2</sub> (3)	-0.72, 0.13, 0.53			3.94, 4.62
SalomphanGaMe(GaMe <sub>2</sub> ) <sub>2</sub> (4)	-0.62, 0.16, 0.56			3.96, 4.64
SaleanGaEt(GaEt <sub>2</sub> ) <sub>2</sub> (5)	-0.22–0.99, 1.16–1.23		2.47, 2.96	3.51, 4.58
SalpanGaEt(GaEt <sub>2</sub> ) <sub>2</sub> (6)	-0.47–0.88, 1.20–1.48	0.95–1.07	2.61, 2.78	3.31, 4.53
SalophanGaEt(GaEt <sub>2</sub> ) <sub>2</sub> (7)	-0.19–0.10, 0.40–1.50			4.13, 4.74
SalomphanGaEt(GaEt <sub>2</sub> ) <sub>2</sub> (8)	-0.16–0.02, 0.43–1.52			4.18, 4.76

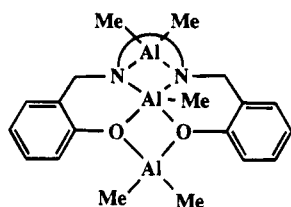


**Figure 2.** General depiction of the SalanAlMe(AlMe<sub>2</sub>)<sub>2</sub> molecule showing the cis disposition of the nitrogens and oxygens.

chemistry (Scheme 1). The products were isolated in yields of  $\geq 92\%$ . In each case the disposition of the alkyl amine backbone was determined to be trans by the <sup>1</sup>H NMR data (see Table 1). In this configuration the gallium–alkyl groups were manifested as a series of three singlets (for Ga–Me) and three pairs of multiplets (for Ga–Et) in the region  $\delta$  0.6 to  $-0.4$  ppm. By comparison, when the alkylamine backbone is oriented such that the oxygens and nitrogens are cis to one another, in for example, SalpanAlMe(AlMe<sub>2</sub>)<sub>2</sub>,<sup>5</sup> there are five Al–Me resonances (Figure 2). Another unique feature of 1–8 is the maintenance of a rigid solution state geometry. This is manifested as AB-type coupling within each Ph–CH<sub>2</sub> group, leading to a doublet-of-doublets in the NMR spectrum. The alkylamine backbones also demonstrate this type of coupling. In Figure 3 is shown the <sup>1</sup>H NMR spectrum for 2 which illustrates this point. Resonances 1 and 2 can be attributed to the Ph–CH<sub>2</sub> groups. The backbone propylamine protons are designated by 3–5. Irradiation experiments were used to confirm the assignments given for 1–8.

We were interested to see if the SalanMR(MR<sub>2</sub>)<sub>2</sub> (M = Al, Ga; R = Me, Et) molecules would undergo

exchange of either the metal–alkyl units or the individual alkyl groups in solution. In order to test this, three types of reactions were examined. In the first, equimolar amounts of SalpanGaMe(GaMe<sub>2</sub>)<sub>2</sub> (2) and SalpanAlMe(AlMe<sub>2</sub>)<sub>2</sub> (9)<sup>5</sup> were mixed together in toluene and then stirred at 25 °C for 8 h. Analysis by <sup>1</sup>H NMR of the solid remaining after solvent removal indicated that 2 and 9 were unchanged from the mixing. The second and third reactions were directed at the possibility of exchange of the alkyl groups between Ga atoms and were conducted in situ in 5 mm NMR tubes. Thus, the trimetallic derivatives SalpanGaMe(GaMe<sub>2</sub>)<sub>2</sub> (2) and SalpanGaEt(GaEt<sub>2</sub>)<sub>2</sub> (6) were mixed in C<sub>6</sub>D<sub>6</sub> at 25 °C and stirred for 2 h. Similarly, 2 was mixed with a 50-fold excess of GaEt<sub>3</sub> and stirred for 2 h. The NMR spectra of these mixtures were comprised of well-defined resonances which could be attributed to unchanged mixtures of 2/6 and 2/GaEt<sub>3</sub>. These experiments served to indicate that compounds of this type are nonfluxional and nondissociative at 25 °C in aryl solvents.

**Structural Characterization.** An X-ray crystallographic study of 1, 2, and 5 was undertaken in order to determine whether the proposed solution structures were the same as that found in the solid state. A summary of crystallographic data for these molecules is given in Table 2. Selected bond distances and angles are given in Table 3, and positional parameters are given in Tables 4–6. Molecular structures and atom-numbering schemes are shown in Figures 4–6. In each structure the ligand adopts a trans orientation with respect to the location of the nitrogen and oxygen atoms. In this conformation each of the GaR<sub>2</sub> units bridge both a nitrogen and oxygen atom. This is in contrast to the

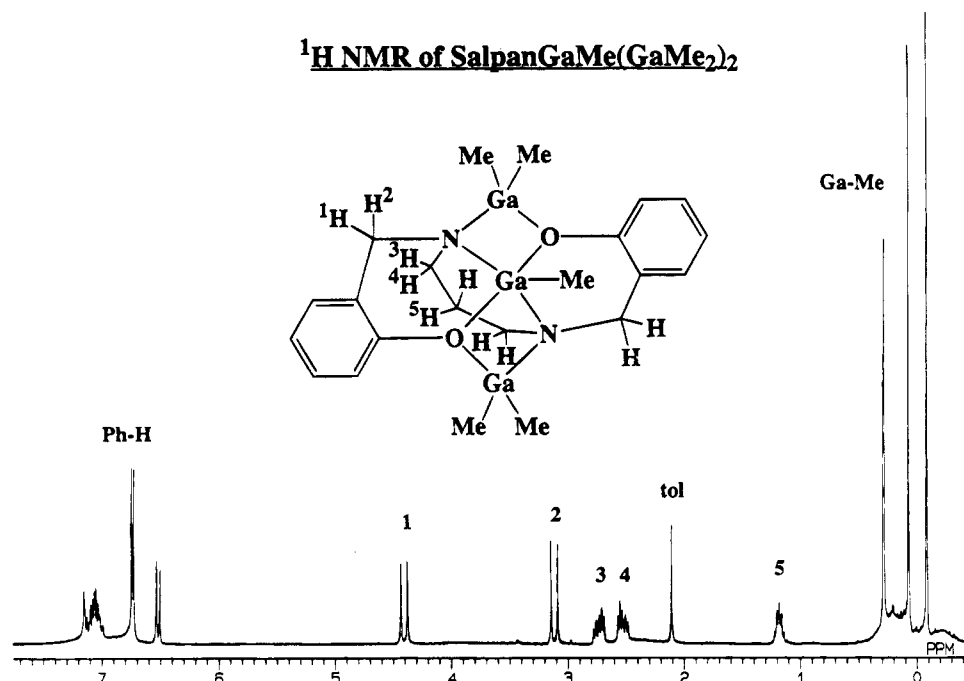


**Figure 3.** <sup>1</sup>H NMR spectrum of **2** with chemical shift assignments.

**Table 2. Crystal Data for SaleanGaMe(GaMe<sub>2</sub>)<sub>2</sub> (1), SalpanGaMe(GaMe<sub>2</sub>)<sub>2</sub> (2), and SaleanGaEt(GaEt<sub>2</sub>)<sub>2</sub> (5)**

compd	<b>1</b>	<b>2</b>	<b>5</b>
formula	C <sub>28</sub> H <sub>39</sub> Ga <sub>3</sub> N <sub>2</sub> O <sub>2</sub>	C <sub>22</sub> H <sub>33</sub> Ga <sub>3</sub> N <sub>2</sub> O <sub>2</sub>	C <sub>26</sub> H <sub>41</sub> Ga <sub>3</sub> N <sub>2</sub> O <sub>2</sub>
fw	644.8	566.7	622.8
cryst system	monoclinic	monoclinic	monoclinic
space group	P2 <sub>1</sub> /c	P2 <sub>1</sub> /c	P2 <sub>1</sub> /n
a (Å)	10.694(2)	16.247(12)	8.433(1)
b (Å)	14.101(2)	9.588(9)	22.010(2)
c (Å)	19.184(2)	17.131(8)	15.241(1)
β (deg)	94.040(10)	116.21(4)	98.81(1)
V (Å <sup>3</sup> )	2885.5(7)	2395(3)	2795.4(5)
Z	4	4	4
D <sub>calc</sub> (g/cm <sup>3</sup> )	1.484	1.572	1.480
cryst size (mm)	0.5 × 0.5 × 0.5	1.6 × 0.2 × 0.1	1.0 × 0.5 × 0.4
temp (K)	223	223	298
2θ range (deg)	3.5–45	3.5–45	2.0–45
scan type	2θ-θ	2θ-θ	2θ-θ
scan speed (deg/min)	6–60	8–60	6–60
scan range (deg)	0.39	0.53	0.40
reflcs collcd	4881	3979	3679
indp reflcs	3740	3107	3393
obsd reflcs	2615 (F > 4.0σ(F))	1777 (F > 6.0σ(F))	2111 (F > 4.0σ(F))
no. of params	316	262	298
R	0.0498	0.0690	0.0458
R <sub>w</sub>	0.0545	0.0763	0.0492
GOF	3.37	5.09	3.07
largest diff peak (e/Å <sup>3</sup> )	0.66	1.49	0.50

structures that were determined for SalpanAlMe(AlMe<sub>2</sub>)<sub>2</sub> (**9**) and SalophanAlMe(AlMe<sub>2</sub>)<sub>2</sub> (**10**), in which the N and O atoms were cis, but correspond to that seen for SaleanAlMe(AlMe<sub>2</sub>)<sub>2</sub> (**11**).<sup>5</sup> For these aluminum complexes the presence of a trans orientation for **11** was attributed to both the bond strain and the presence of eclipsing hydrogens in the cis-directed ethylamine backbone. The resulting N–N separation for this compound was 2.863 Å. For compounds **1** and **5** a similar argument may be used to explain the trans disposition. The N–N distances in these complexes are 2.823 and 2.835 Å, respectively. However, a different argument must be used when considering the trans disposition of the propylamine backbone in **2**. Although five-coordinate Ga(III) and Al(III) have very similar ionic radii (0.62 and 0.69 Å, respectively), the difference of 0.07 Å can have a sizable effect. In the present case this is apparently responsible for the difference in

geometries found between **9** and **2**. In **9** the N and O atoms form a square plane (maximum deviation = 0.031 Å for O(1)) above which the aluminum is located at a distance of 0.6109 Å. The geometry is then distorted square pyramidal. In contrast, the geometry for the central gallium in **2** is best described as a distorted trigonal bipyramid with O(1) and O(2) occupying the axial positions and N(1), N(2), and C(3) occupying the equatorial sites. For the central Ga atom, this leads to average Ga–N bonds (1.93 Å) that are shorter than the Ga–O bonds (2.08 Å). By comparison, the central Al atom of **9** contains average Al–N and Al–O bond distances that are 2.004 and 1.934 Å, respectively.

### Conclusion

In summary, we have demonstrated that there is an interesting range of complexes that are accessible in

**Table 3. Bond Lengths (Å) and Angles (deg) for Compounds 1, 2, and 5**

	1	2	5
Distances			
Ga(1)–N(1)	2.044(7)	2.044(16)	2.018(7)
Ga(1)–O(1)	1.981(6)	2.000(12)	1.988(7)
Ga(2)–O(1)	2.156(6)	2.064(14)	2.116(6)
Ga(2)–O(2)	2.155(6)	2.103(15)	2.135(6)
Ga(2)–N(1)	1.953(7)	1.941(15)	1.959(9)
Ga(2)–N(2)	1.958(7)	1.910(12)	1.966(8)
Ga(3)–O(2)	1.970(6)	1.957(11)	1.955(7)
Ga(3)–N(2)	2.030(7)	2.053(17)	2.029(7)
Angles			
O(1)–Ga(1)–N(1)	84.1(3)	80.5(6)	82.1(3)
O(1)–Ga(2)–O(2)	162.2(2)	164.5(4)	162.2(3)
O(1)–Ga(2)–N(1)	81.8(3)	81.4(6)	80.3(3)
O(1)–Ga(2)–N(2)	86.5(3)	89.3(6)	86.7(3)
O(2)–Ga(2)–N(1)	86.0(2)	90.9(6)	87.5(3)
O(2)–Ga(2)–N(2)	81.1(3)	80.6(6)	80.9(3)
N(1)–Ga(2)–N(2)	92.4(3)	109.9(6)	92.5(3)
Ga(2)–O(2)–Ga(3)	92.2(2)	94.1(6)	93.3(3)
Ga(1)–N(1)–Ga(2)	96.5(3)	96.1(7)	97.9(4)
O(2)–Ga(3)–N(2)	84.1(3)	80.8(6)	83.9(3)
Ga(1)–O(1)–Ga(2)	92.2(2)	93.6(6)	93.9(3)
Ga(2)–N(2)–Ga(3)	96.5(3)	97.1(7)	96.3(3)

**Table 4. Atomic Coordinates ( $\times 10^5$ ) and Equivalent Isotropic Displacement Coefficients ( $\text{Å}^2 \times 10^4$ ) for  $\text{SalanGaMe}(\text{GaMe}_2)_2$  (1)**

atom	x	y	z	U(eq)
Ga(1)	50594(9)	3551(7)	17412(5)	344(3)
Ga(2)	74170(9)	14923(6)	18538(5)	299(3)
Ga(3)	98583(9)	12753(7)	26835(5)	341(3)
O(1)	55543(53)	15601(42)	22147(28)	349(20)
O(2)	93025(51)	10413(38)	16973(32)	329(20)
N(1)	69474(62)	1663(48)	16993(37)	310(24)
N(2)	79969(64)	12543(50)	28291(36)	314(24)
C(1)	52509(85)	18163(61)	28626(49)	364(33)
C(2)	39928(87)	18991(63)	29916(51)	396(33)
C(3)	36309(91)	21498(70)	36332(51)	430(35)
C(4)	45190(102)	23709(74)	41748(59)	553(42)
C(5)	57884(99)	22925(65)	40510(52)	456(37)
C(6)	61707(84)	20130(60)	34039(45)	327(30)
C(7)	75899(84)	19688(68)	33350(51)	422(34)
C(8)	75126(81)	2807(59)	29686(48)	352(30)
C(9)	75039(76)	-3389(58)	23229(41)	285(28)
C(10)	73476(79)	-2079(64)	10306(46)	364(31)
C(11)	87419(76)	-3223(64)	9834(43)	314(29)
C(12)	91558(87)	-10572(64)	5723(48)	390(33)
C(13)	104272(93)	-12116(73)	4947(51)	465(37)
C(14)	112878(96)	-6318(69)	8517(52)	453(36)
C(15)	109077(82)	1065(64)	12413(52)	396(33)
C(16)	96331(82)	2927(62)	13136(45)	337(30)
C(17)	43709(87)	7035(75)	8110(47)	450(35)
C(18)	42815(89)	-4995(70)	23870(58)	516(39)
C(19)	73388(94)	25937(71)	12572(55)	508(38)
C(20)	107650(90)	1770(76)	30858(59)	550(40)
C(21)	103783(92)	26014(66)	27064(55)	481(37)
C(22)	31105(204)	50648(134)	-1723(96)	1550(111)
C(23)	26182(154)	42974(95)	2438(69)	766(57)
C(24)	34590(187)	38086(123)	7114(73)	1091(77)
C(25)	30731(302)	31451(159)	10852(96)	1672(157)
C(26)	17515(472)	28104(199)	10138(185)	2156(249)
C(27)	10327(339)	32921(182)	5930(166)	2502(244)
C(28)	13988(160)	40088(134)	1858(92)	1098(79)

combinations of the  $\text{SalanH}_4$  ligands with 3 equiv of  $\text{GaR}_3$  (where  $\text{R} = \text{Me}$  and  $\text{Et}$ ). For instance, the trimetallic derivatives of general formula  $\text{SalanGaR}(\text{GaR}_2)_2$  offer evidence for solution state rigidity. Additionally, no exchange occurs upon mixing  $\text{SalanAlMe}(\text{AlMe}_2)_2$  with  $\text{SalpanGaMe}(\text{GaMe}_2)_2$  (2),  $\text{SalpanGaMe}(\text{GaMe}_2)_2$  (2) with  $\text{SalpanGaEt}(\text{GaEt}_2)_2$  (6), and  $\text{SalpanGaMe}(\text{GaMe}_2)_2$  (2) with  $\text{GaEt}_3$ . The solution state geometry of these molecules was shown by X-ray crystallography to be the same as that of the solid state.

**Table 5. Atomic Coordinates ( $\times 10^5$ ) and Equivalent Isotropic Displacement Coefficients ( $\text{Å}^2 \times 10^4$ ) for  $\text{SalpanGaMe}(\text{GaMe}_2)_2$  (2)**

atom	x	y	z	U(eq)
Ga(1)	59235(12)	-19000(22)	70098(13)	387(8)
Ga(2)	71044(12)	5923(21)	73100(13)	344(8)
Ga(3)	89386(12)	19432(23)	80202(13)	394(9)
O(1)	64013(69)	-3902(123)	79052(77)	413(54)
O(2)	80890(72)	11852(117)	68886(82)	429(57)
N(1)	70177(81)	-12543(147)	68150(89)	344(60)
N(2)	81591(90)	7008(149)	84102(96)	404(69)
C(1)	65251(102)	-2597(175)	87277(113)	330(75)
C(2)	59105(107)	-8159(187)	89836(112)	374(80)
C(3)	59826(124)	-6169(203)	98060(135)	485(100)
C(4)	67166(137)	1267(232)	104033(133)	601(105)
C(5)	73306(111)	7084(190)	101378(119)	422(84)
C(6)	72697(101)	5306(169)	93291(107)	293(71)
C(7)	79635(111)	13287(208)	91315(118)	481(88)
C(8)	86155(111)	-6692(220)	87223(119)	510(88)
C(9)	86970(101)	-15187(193)	80252(119)	433(82)
C(10)	78362(102)	-22523(167)	73476(122)	416(87)
C(11)	68917(106)	-11708(196)	59025(119)	430(83)
C(12)	77027(104)	-6074(183)	57852(111)	335(74)
C(13)	78867(122)	-11947(209)	51433(124)	500(90)
C(14)	85763(131)	-6629(232)	49406(130)	572(103)
C(15)	90870(112)	4458(202)	53915(123)	465(87)
C(16)	89427(110)	10790(204)	60592(112)	445(87)
C(17)	82318(99)	4983(180)	62415(109)	337(73)
C(18)	47732(107)	-12495(243)	60209(130)	687(101)
C(19)	60490(130)	-37295(222)	75305(142)	695(106)
C(20)	62263(115)	20846(206)	67493(151)	635(106)
C(21)	85906(126)	39449(177)	79917(143)	544(105)
C(22)	102106(105)	12993(204)	84007(150)	626(102)

**Table 6. Atomic Coordinates ( $\times 10^5$ ) and Equivalent Isotropic Displacement Coefficients ( $\text{Å}^2 \times 10^4$ ) for  $\text{SalanGaEt}(\text{GaEt}_2)_2$  (5)**

atom	x	y	z	U(eq)
Ga(1)	-10263(14)	80245(5)	6629(7)	442(4)
Ga(2)	19409(13)	84637(5)	18316(7)	369(4)
Ga(3)	29426(15)	96582(5)	26517(8)	489(5)
O(1)	11836(82)	82472(27)	4796(38)	418(24)
O(2)	21659(81)	88983(29)	30973(40)	434(25)
N(1)	-3886(101)	84932(35)	18003(49)	422(30)
N(2)	20262(94)	93139(34)	14455(48)	370(28)
C(1)	16769(127)	85262(43)	-2258(63)	419(37)
C(2)	13300(146)	82458(51)	-10617(68)	565(44)
C(3)	18157(165)	85106(64)	-17964(75)	731(56)
C(4)	26254(177)	90434(63)	-17276(78)	777(59)
C(5)	29388(142)	93341(51)	-9017(73)	566(45)
C(6)	24869(126)	90784(45)	-1358(63)	426(37)
C(7)	29797(135)	94219(44)	7265(63)	488(40)
C(8)	2946(124)	94745(44)	11555(65)	458(39)
C(9)	-7742(120)	91528(43)	17358(64)	423(36)
C(10)	-9246(132)	82168(47)	26110(62)	484(40)
C(11)	-3277(120)	85285(43)	35012(62)	402(36)
C(12)	-13090(137)	84769(49)	41517(67)	521(42)
C(13)	-8829(161)	87500(52)	49744(78)	630(51)
C(14)	5083(149)	90600(56)	51494(71)	599(48)
C(15)	15408(145)	91160(47)	45253(71)	552(44)
C(16)	11087(127)	88492(43)	36874(63)	413(38)
C(17)	-9266(156)	71485(47)	8922(73)	633(48)
C(18)	-905(176)	67972(57)	2476(89)	848(62)
C(19)	-26269(139)	84294(56)	-2075(73)	634(46)
C(20)	-35568(149)	80149(60)	-8641(81)	784(55)
C(21)	36400(146)	78656(51)	20976(72)	604(47)
C(22)	46194(172)	77464(68)	13950(82)	952(68)
C(23)	52470(146)	95840(54)	28292(77)	673(50)
C(24)	60827(174)	98290(64)	36918(88)	937(65)
C(25)	18215(161)	103656(51)	30179(76)	679(51)
C(26)	23680(219)	109462(58)	26687(89)	1053(78)

Future studies will be directed at the use of bulky group 13 reagents and chiral  $\text{SalanH}_4$  ligands.

### Experimental Section

**General Methods.** All manipulations were conducted using Schlenk techniques in conjunction with an inert atmo-

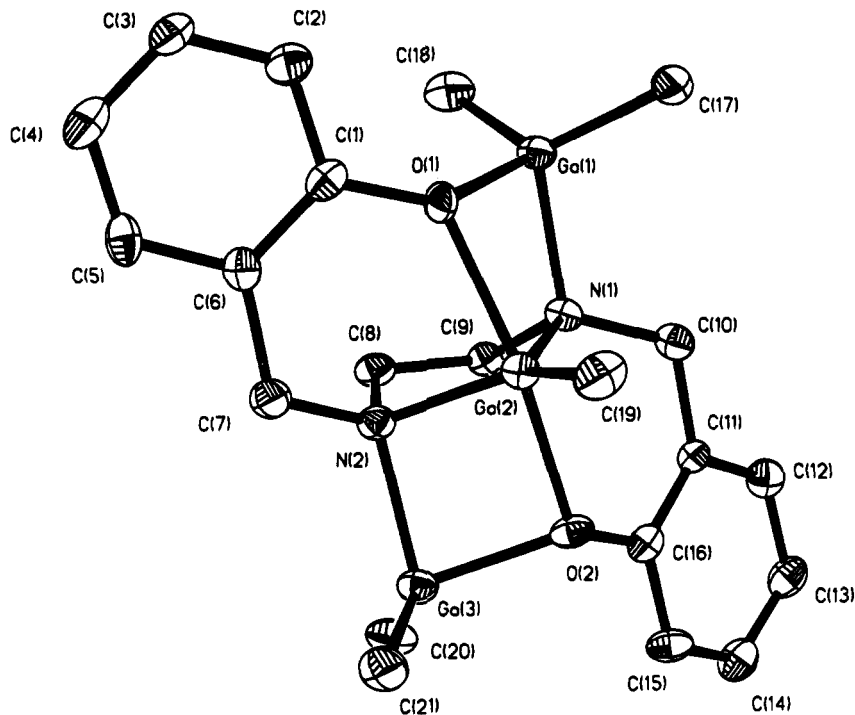


**Figure 4.** Molecular structure and atom-numbering scheme for **1**.

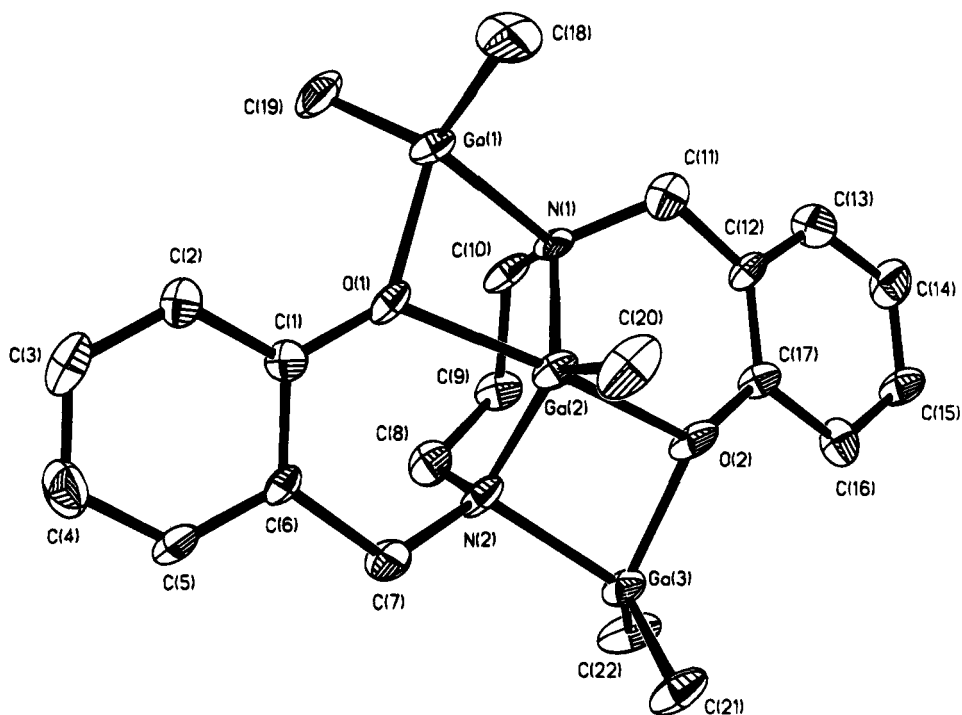


**Figure 5.** Molecular structure and atom-numbering scheme for **2**.

sphere glovebox. All solvents were rigorously dried prior to use. The ligands SaleanH<sub>4</sub>, SalpanH<sub>4</sub>, SalophanH<sub>4</sub>, and SalomphanH<sub>4</sub> were synthesized as previously described.<sup>2</sup> NMR data were obtained on JEOL-GSX-400 and -270 instruments at 270.17 (<sup>1</sup>H) and 62.5 (<sup>13</sup>C) MHz. Chemical shifts are reported relative to SiMe<sub>4</sub> and are in ppm. Elemental analyses were obtained on a Perkin-Elmer 2400 analyzer. Mass spectral data were obtained on a Hewlett-Packard 5988 spectrometer using electron impact ionization (70 eV) with a direct ionization probe (DIP). Infrared data were recorded as KBr pellets on a Matheson Instruments 2020 Galaxy Series spectrometer and are reported in cm<sup>-1</sup>. For **1**, **2**, and **5**, crystals suitable for X-ray analysis were grown by dissolution in toluene and cooling to -30 °C.

**SaleanGaMe(GaMe<sub>2</sub>)<sub>2</sub> (1).** Trimethylgallium (0.646 g, 5.62 mmol) was added neat to a rapidly stirring solution of SaleanH<sub>4</sub> (0.501 g, 1.84 mmol) in 50 mL of toluene at 25 °C. The exothermic reaction was stirred at 25 °C until the evolution of gas ceased (15 min) and then heated at reflux for 8 h. The toluene was removed in vacuo leaving the title compound as a white solid (0.946 g, 93%): mp 85–87 °C; <sup>1</sup>H NMR (270 MHz, C<sub>6</sub>D<sub>6</sub>) δ -0.25 (s, 6H, GaCH<sub>3</sub>), 0.03 (s, 6, GaCH<sub>3</sub>), 0.20 (s, 3H, GaCH<sub>3</sub>), 2.40 (d, *J* = 8 Hz, 2H, NCH<sub>2</sub>), 2.92 (d, *J* = 8 Hz, 2H, NCH<sub>2</sub>), 3.33 (d, *J* = 16 Hz, 2H, PhCH<sub>2</sub>), 4.46 (d, *J* = 16 Hz, 2H, PhCH<sub>2</sub>), 6.52–7.19 (m, 8H, Ph H); <sup>13</sup>C NMR (62.5 MHz, C<sub>6</sub>D<sub>6</sub>) δ -11.3 (GaCH<sub>3</sub>), -6.8 (GaCH<sub>3</sub>), 1.4 (GaCH<sub>3</sub>), 48.1 (NCH<sub>2</sub>), 53.9 (PhCH<sub>2</sub>), 120.0 (Ph), 121.7 (Ph), 128.6 (Ph), 129.3 (Ph), 130.3 (Ph), 156.9 (Ph); IR (KBr) 2981

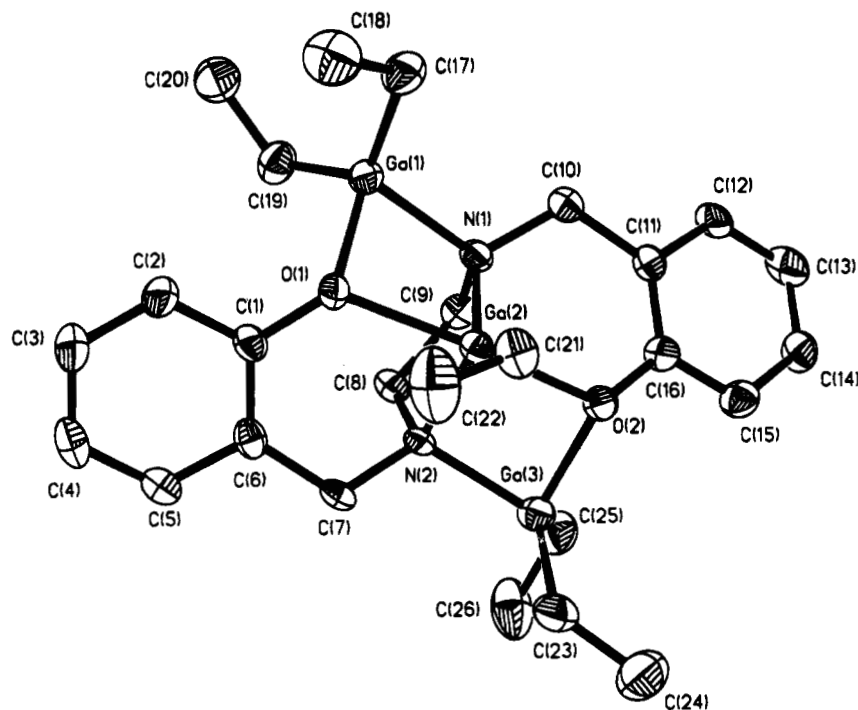


**Figure 6.** Molecular structure and atom-numbering scheme for **5**.

m, 2870 s, 1603 vs, 1487 vs, 1235 vs, 1055 s, 885 vs, 758 vs, 729 vs, 584 vs  $\text{cm}^{-1}$ ; MS (DIP/MS)  $m/e$  552 ( $\text{M}^+$ ), 537 ( $\text{M}^+ - \text{Me}$ ), 453 ( $\text{M}^+ - \text{GaMe}_2$ ), 437 ( $\text{M}^+ - \text{Me} - \text{GaMe}_2$ ), 422 ( $\text{M}^+ - 2\text{Me} - \text{GaMe}_2$ ), 407 ( $\text{M}^+ - 3\text{Me} - \text{GaMe}_2$ ), 337 ( $\text{M}^+ - \text{Me} - 2\text{GaMe}_2$ ), 245 ( $\text{PhOCH}_2\text{N}(\text{CH}_2)_3\text{NGa}^+$ ), 99 ( $\text{GaMe}_2^+$ ), 69 ( $\text{Ga}^+$ ). Anal. Calcd: C, 45.64; H, 5.65. Found: C, 45.58; H, 5.70.

**SalpanGaMe(GaMe<sub>2</sub>)<sub>2</sub> (2).** The procedure was as described for **1**, with trimethylgallium (0.623 g, 5.42 mmol) and SalpanH<sub>4</sub> (0.500 g, 1.75 mmol) yielding **2** as a white solid (0.951 g, 96%): mp 172–174 °C; <sup>1</sup>H NMR (270 MHz, C<sub>6</sub>D<sub>6</sub>)  $\delta$  -0.10 (s, 6H, GaCH<sub>3</sub>), 0.07 (s, 6H, GaCH<sub>3</sub>), 0.29 (s, 3H, GaCH<sub>3</sub>), 1.18 (m, 2H, CH<sub>2</sub>CH<sub>2</sub>), 2.53 (m, 2H, NCH<sub>2</sub>), 2.72 (m, 2H, NCH<sub>2</sub>), 3.12 (d,  $J = 16$  Hz, 2H, PhCH<sub>2</sub>), 4.40 (d,  $J = 16$  Hz, 2H, PhCH<sub>2</sub>), 6.52 (d,  $J = 6$  Hz, 2H, Ph H), 6.75 (d,  $J = 6$  Hz, 2H, Ph H), 6.98–7.13 (m, 4H, Ph H); <sup>13</sup>C NMR (62.5 MHz, C<sub>6</sub>D<sub>6</sub>)  $\delta$  -8.0 (GaCH<sub>3</sub>), -6.4 (GaCH<sub>3</sub>), -5.1 (GaCH<sub>3</sub>), 28.0 (CH<sub>2</sub>CH<sub>2</sub>), 51.8 (NCH<sub>2</sub>), 56.0 (PhCH<sub>2</sub>), 118.9 (Ph), 119.6 (Ph), 125.6 (Ph), 129.1 (Ph), 131.2 (Ph), 158.3 (Ph); IR (KBr) 2963 m, 1598 m, 1485 s, 1449 s, 1259 s, 1078 s, 1025 s, 801 s, 754 vs, 580 s, 536 s  $\text{cm}^{-1}$ ; MS (DIP/MS)  $m/e$  566 ( $\text{M}^+$ ), 551 ( $\text{M}^+ - \text{Me}$ ), 467 ( $\text{M}^+ - \text{GaMe}_2$ ), 451 ( $\text{M}^+ - \text{Me} - \text{GaMe}_2$ ), 436 ( $\text{M}^+ - 2\text{Me} - \text{GaMe}_2$ ), 421 ( $\text{M}^+ - 3\text{Me} - \text{GaMe}_2$ ), 351 ( $\text{M}^+ - \text{Me} - 2\text{GaMe}_2$ ), 245 ( $\text{PhOCH}_2\text{N}(\text{CH}_2)_3\text{NGa}^+$ ), 99 ( $\text{GaMe}_2^+$ ), 69 ( $\text{Ga}^+$ ). Anal. Calcd: C, 46.63; H, 5.87. Found: C, 46.66; H, 5.82.

**SalophanGaMe(GaMe<sub>2</sub>)<sub>2</sub> (3).** The procedure was as described for **1**, with trimethylgallium (0.548 g, 4.77 mmol) and SalophanH<sub>4</sub> (0.500 g, 1.56 mmol) yielding **3** as a yellow solid (0.889 g, 95%): mp 172 °C (dec); <sup>1</sup>H NMR (270 MHz, C<sub>6</sub>D<sub>6</sub>)  $\delta$  -0.72 (s, 6H, GaCH<sub>3</sub>), 0.13 (s, 6H, GaCH<sub>3</sub>), 0.53 (s, 3H, GaCH<sub>3</sub>), 3.94 (d,  $J = 16$  Hz, 2H, PhCH<sub>2</sub>), 4.62 (d,  $J = 16$  Hz, 2H, PhCH<sub>2</sub>), 6.32 (d,  $J = 8$  Hz, 2H, Ph H), 6.48–7.12 (m, 10H, Ph H); <sup>13</sup>C NMR (62.5 MHz, C<sub>6</sub>D<sub>6</sub>)  $\delta$  -8.6 (GaCH<sub>3</sub>), -8.5 (GaCH<sub>3</sub>), -6.4 (GaCH<sub>3</sub>), -5.9 (GaCH<sub>3</sub>), 52.0 (PhCH<sub>2</sub>), 52.1 (PhCH<sub>2</sub>), 119.3 (Ph), 121.5 (Ph), 123.7 (Ph), 123.9 (Ph), 124.2 (Ph), 125.6 (Ph), 128.5 (Ph), 129.2 (Ph), 130.4 (Ph), 142.7 (Ph), 159.5 (Ph); IR (KBr) 3077 m, 3028 m, 1599 s, 1487 vs, 1451 vs, 1280 vs, 1018 s, 880 s, 752 vs, 592 s  $\text{cm}^{-1}$ ; MS (DIP/EI)  $m/e$  600 ( $\text{M}^+$ ), 501 ( $\text{M}^+ - \text{GaMe}_2$ ), 486 ( $\text{M}^+ - \text{Me} - \text{GaMe}_2$ ), 471 ( $\text{M}^+ - 2\text{Me} - \text{GaMe}_2$ ), 385 ( $\text{M}^+ - \text{Me} - 2\text{GaMe}_2$ ), 383 ( $\text{M}^+ - \text{Me} - 2\text{GaMe}_2 - 2\text{H}$ ), 279 ( $\text{PhOCH}_2\text{NPhNGa}^+$ ), 203 ( $\text{PhOCH}_2\text{NNGa}^+$ ), 189 ( $\text{PhOCH}_2\text{NGa}^+$ ), 99 ( $\text{GaMe}_2^+$ ), 69 ( $\text{Ga}^+$ ). Anal. Calcd: C, 49.99; H, 5.20. Found: C, 49.95; H, 5.18.

**SalomphanGaMe(GaMe<sub>2</sub>)<sub>2</sub> (4).** The procedure was as described for **1**, with trimethylgallium (0.507 g, 4.41 mmol)

and SalomphanH<sub>4</sub> (0.500 g, 1.44 mmol) yielding **4** as a gray solid (0.877 g, 97%): mp 238 °C (dec); <sup>1</sup>H NMR (270 MHz, C<sub>6</sub>D<sub>6</sub>)  $\delta$  -0.62 (s, 6H, GaCH<sub>3</sub>), 0.16 (s, 6H, GaCH<sub>3</sub>), 0.56 (s, 3H, GaCH<sub>3</sub>), 1.61 (s, 6H, Ph-CH<sub>3</sub>), 3.96 (d,  $J = 16$  Hz, 2H, PhCH<sub>2</sub>), 4.64 (d,  $J = 16$  Hz, 2H, PhCH<sub>2</sub>), 6.35 (d,  $J = 7$  Hz, 2H, Ph H), 6.53 (s, 2H, Ph H), 6.61–7.13 (m, 6H, Ph H); <sup>13</sup>C NMR (62.5 MHz, C<sub>6</sub>D<sub>6</sub>)  $\delta$  -8.5 (GaCH<sub>3</sub>), -6.4 (GaCH<sub>3</sub>), -5.9 (GaCH<sub>3</sub>), 19.1 (Ph-CH<sub>3</sub>), 52.3 (PhCH<sub>2</sub>), 119.2 (Ph), 121.6 (Ph), 123.9 (Ph), 124.9 (Ph), 127.9 (Ph), 128.1 (Ph), 129.2 (Ph), 130.4 (Ph), 132.6 (Ph), 137.2 (Ph), 140.2 (Ph), 159.6 (Ph); IR (KBr) 2966 m, 2363 vs, 2342 vs, 1599 m, 1487 vs, 1263 vs, 1086 m, 752 s, 588 m  $\text{cm}^{-1}$ ; MS (DIP/MS)  $m/e$  530 ( $\text{M}^+ - \text{GaMe}_2$ ), 514 ( $\text{M}^+ - \text{Me} - \text{GaMe}_2$ ), 499 ( $\text{M}^+ - 2\text{Me} - \text{GaMe}_2$ ), 413 ( $\text{M}^+ - \text{Me} - 2\text{GaMe}_2$ ), 411 ( $\text{M}^+ - \text{Me} - 2\text{GaMe}_2 - 2\text{H}$ ), 307 ( $\text{PhOCH}_2\text{NPhNGa}^+$ ), 99 ( $\text{GaMe}_2^+$ ), 69 ( $\text{Ga}^+$ ). Anal. Calcd: C, 51.58; H, 5.61. Found: C, 51.62; H, 5.57.

**SaleanGaEt(GaEt<sub>2</sub>)<sub>2</sub> (5).** The procedure was as described for **1**, with triethylgallium (0.871 g, 5.55 mmol) and SaleanH<sub>4</sub> (0.500 g, 1.84 mmol) yielding colorless crystals of **5** (1.140 g, 93%): mp 125–127 °C; <sup>1</sup>H NMR (270 MHz, C<sub>6</sub>D<sub>6</sub>)  $\delta$  -0.22–0.99 (m, 10H, CH<sub>2</sub>CH<sub>3</sub>), 1.16–1.23 (m, 12H, CH<sub>2</sub>CH<sub>3</sub>), 1.46 (app. t, 3H, CH<sub>2</sub>CH<sub>3</sub>), 2.47 (d,  $J = 8$  Hz, 2H, NCH<sub>2</sub>), 2.96 (d,  $J = 8$  Hz, 2H, NCH<sub>2</sub>), 3.51 (d,  $J = 16$  Hz, 2H, PhCH<sub>2</sub>), 4.58 (d,  $J = 16$  Hz, 2H, PhCH<sub>2</sub>), 6.64–7.12 (m, 8H, Ph H); <sup>13</sup>C NMR (62.5 MHz, C<sub>6</sub>D<sub>6</sub>)  $\delta$  0.5 (CH<sub>2</sub>CH<sub>3</sub>), 3.0 (CH<sub>2</sub>CH<sub>3</sub>), 5.7 (CH<sub>2</sub>CH<sub>3</sub>), 9.5 (CH<sub>2</sub>CH<sub>3</sub>), 9.6 (CH<sub>2</sub>CH<sub>3</sub>), 10.2 (CH<sub>2</sub>CH<sub>3</sub>), 10.3 (CH<sub>2</sub>CH<sub>3</sub>), 48.8 (NCH<sub>2</sub>), 54.5 (PhCH<sub>2</sub>), 120.0 (Ph), 121.6 (Ph), 125.6 (Ph), 128.5 (Ph), 128.7 (Ph), 129.3 (Ph), 130.2 (Ph), 157.4 (Ph); IR (KBr) 2949 s, 2866 vs, 1597 s, 1485 vs, 1447 vs, 1285 vs, 1035 s, 756 vs, 585 vs  $\text{cm}^{-1}$ ; MS (DIP/EI)  $m/e$  593 ( $\text{M}^+ - \text{Et}$ ), 465 ( $\text{M}^+ - \text{Et} - \text{GaEt}_2$ ), 335 ( $\text{M}^+ - \text{Et} - 2\text{GaEt}_2$ ), 232 ( $\text{PhOCH}_2\text{N}(\text{CH}_2)_2\text{NGa}^+$ ), 204 ( $\text{PhOCH}_2\text{NCH}_2\text{Ga}^+$ ), 127 ( $\text{GaEt}_2^+$ ), 69 ( $\text{Ga}^+$ ). Anal. Calcd: C, 50.14; H, 6.64. Found: C, 50.10; H, 6.63.

**SalpanGaEt(GaEt<sub>2</sub>)<sub>2</sub> (6).** The procedure was as described for **1**, with triethylgallium (0.832 g, 5.30 mmol) and SalpanH<sub>4</sub> (0.500 g, 1.75 mmol) yielding **6** as a white solid (1.04 g, 93%): mp 178–182 °C; <sup>1</sup>H NMR (270 MHz, C<sub>6</sub>D<sub>6</sub>)  $\delta$  -0.47–0.88 (m, 10H, CH<sub>2</sub>CH<sub>3</sub>), 0.95–1.07 (m, 2H, CH<sub>2</sub>CH<sub>2</sub>), 1.20–1.48 (m, 15H, CH<sub>2</sub>CH<sub>3</sub>), 2.58–2.65 (m, 2H, NCH<sub>2</sub>), 2.75–2.82 (m, 2H, NCH<sub>2</sub>), 3.31 (d,  $J = 16$  Hz, 2H, PhCH<sub>2</sub>), 4.53 (d,  $J = 16$  Hz, 2H, PhCH<sub>2</sub>), 6.60 (d,  $J = 8$  Hz, 2H, Ph H), 6.72 (d,  $J = 5$  Hz, 4H, Ph H), 7.06–7.12 (m, 2H, Ph H); <sup>13</sup>C NMR (62.5 MHz, C<sub>6</sub>D<sub>6</sub>)  $\delta$  1.3 (CH<sub>2</sub>CH<sub>3</sub>), 2.7 (CH<sub>2</sub>CH<sub>3</sub>), 3.5 (CH<sub>2</sub>CH<sub>3</sub>), 6.4 (CH<sub>2</sub>CH<sub>3</sub>), 10.1 (CH<sub>2</sub>CH<sub>3</sub>), 10.3 (CH<sub>2</sub>CH<sub>3</sub>), 28.3 (CH<sub>2</sub>CH<sub>2</sub>), 52.2



(NCH<sub>2</sub>), 56.7 (PhCH<sub>2</sub>), 119.0 (Ph), 119.4 (Ph), 124.0 (Ph), 129.1 (Ph), 131.1 (Ph), 158.7 (Ph); IR (KBr) 2944 s, 2866 s, 1599 m, 1485 s, 1271 vs, 1076 m, 1026 m, 881 m, 754 s, 578 m, 557 m cm<sup>-1</sup>; MS (DIP/EI) *m/e* 607 (M<sup>+</sup> - Et), 479 (M<sup>+</sup> - Et - GaEt<sub>2</sub>), 450 (M<sup>+</sup> - 2Et - GaEt<sub>2</sub>), 421 (M<sup>+</sup> - 3Et - GaEt<sub>2</sub>), 349 (M<sup>+</sup> - Et - 2GaEt<sub>2</sub>), 273 (PhOCH<sub>2</sub>N(CH<sub>2</sub>)<sub>3</sub>NGaEt<sup>+</sup>), 244 (PhOCH<sub>2</sub>N(CH<sub>2</sub>)<sub>3</sub>NGa<sup>+</sup>), 127 (GaEt<sub>2</sub><sup>+</sup>), 69 (Ga<sup>+</sup>). Anal. Calcd: C, 50.92; H, 6.81. Found: C, 50.91; H, 6.78.

**SalophanGaEt(GaEt<sub>2</sub>)<sub>2</sub> (7).** The procedure was as described for **1**, with triethylgallium (0.738 g, 4.70 mmol) and SalophanH<sub>4</sub> (0.500 g, 1.56 mmol) yielding **7** as a pale solid (0.962 g, 92%): <sup>1</sup>H NMR (270 MHz, C<sub>6</sub>D<sub>6</sub>) δ -0.19–0.10 (5, m, CH<sub>2</sub>CH<sub>3</sub>), 0.40–1.50 (m, 20H, CH<sub>2</sub>CH<sub>3</sub>), 4.13 (d, *J* = 16 Hz, 2H, PhCH<sub>2</sub>), 4.74 (d, *J* = 16 Hz, 2H, PhCH<sub>2</sub>), 6.47–6.93 (m, 12H, Ph *H*); <sup>13</sup>C NMR (62.5 MHz, C<sub>6</sub>D<sub>6</sub>) δ 2.3 (CH<sub>2</sub>CH<sub>3</sub>), 4.1 (CH<sub>2</sub>CH<sub>3</sub>), 6.1 (CH<sub>2</sub>CH<sub>3</sub>), 9.6 (CH<sub>2</sub>CH<sub>3</sub>), 9.7 (CH<sub>2</sub>CH<sub>3</sub>), 10.1 (CH<sub>2</sub>CH<sub>3</sub>), 52.2 (PhCH<sub>2</sub>), 119.4 (Ph), 121.3 (Ph), 123.1 (Ph), 123.7 (Ph), 124.2 (Ph), 128.5 (Ph), 130.3 (Ph), 142.8 (Ph), 159.9 (Ph); IR (KBr) 2887 m, 1597 m, 1485 s, 1265 s, 1116 s, 1018 s, 877, 754 vs, 642 vs, 576 vs cm<sup>-1</sup>.

**SalomphanGaEt(GaEt<sub>2</sub>)<sub>2</sub> (8).** The synthetic procedure was as described for **1**, with triethylgallium (0.681 g, 4.34 mmol) and SalomphanH<sub>4</sub> (0.500 g, 1.44 mmol) yielding **8** as a gray solid (0.950 g, 95%): mp 146–148 °C (dec); <sup>1</sup>H NMR (270 MHz, C<sub>6</sub>D<sub>6</sub>) δ -0.16–0.02 (m, 5H, CH<sub>2</sub>CH<sub>3</sub>), 0.43–1.52 (m, 20H, CH<sub>2</sub>CH<sub>3</sub>), 1.67 (s, 6H, PhCH<sub>3</sub>), 4.18 (d, *J* = 16 Hz, 2H, PhCH<sub>2</sub>), 4.76 (d, *J* = 16 Hz, 2H, PhCH<sub>2</sub>), 6.47–6.91 (m, 10H, Ph *H*); <sup>13</sup>C NMR (62.5 MHz, C<sub>6</sub>D<sub>6</sub>) δ 2.4 (CH<sub>2</sub>CH<sub>3</sub>), 4.1 (CH<sub>2</sub>CH<sub>3</sub>), 6.2 (CH<sub>2</sub>CH<sub>3</sub>), 9.6 (CH<sub>2</sub>CH<sub>3</sub>), 9.8 (CH<sub>2</sub>CH<sub>3</sub>), 10.2 (CH<sub>2</sub>CH<sub>3</sub>), 19.2 (PhCH<sub>3</sub>), 52.5 (PhCH<sub>2</sub>), 119.4 (Ph), 121.4 (Ph), 124.2 (Ph), 128.5 (Ph), 130.3 (Ph), 132.5 (Ph), 132.5 (Ph), 140.2 (Ph), 160.0 (Ph); IR (KBr) 2945 s, 2864 s, 1599 m, 1485 vs, 1448 vs, 1265 vs, 1091 m, 1004 m, 879 m, 754 s, 648 m, 589 m, 490 m cm<sup>-1</sup>;

MS (DIP/EI) *m/e* 698 (M<sup>+</sup>), 671 (M<sup>+</sup> - Et), 572 (M<sup>+</sup> - GaEt<sub>2</sub>), 542 (M<sup>+</sup> - Et - GaEt<sub>2</sub>), 513 (M<sup>+</sup> - 2Et - GaEt<sub>2</sub>), 484 (M<sup>+</sup> - 3Et - GaEt<sub>2</sub>), 411 (M<sup>+</sup> - Et - 2GaEt<sub>2</sub> - 2H), 127 (GaEt<sub>2</sub><sup>+</sup>), 69 (Ga<sup>+</sup>). Anal. Calcd: C, 54.99; H, 6.49. Found: C, 54.95; H, 6.46.

**X-ray Experimental Methods.** Details of the crystal data and a summary of data collection parameters for **1**, **2**, and **5** are given in Table 2. Data were collected on a Siemens P4 diffractometer using graphite monochromated Mo Kα (0.710 73 Å) radiation. The check reflections, measured every 100 reflections, indicated a less than 5% decrease in intensity over the course of data collection, and hence, no correction was applied. All calculations were performed on a personal computer using the Siemens software package, SHELXTL-Plus. The structures were solved by direct methods and successive interpretation of difference Fourier maps, followed by least-squares refinement. All non-hydrogen atoms were refined anisotropically. The hydrogen atoms were included in the refinement in calculated positions using fixed isotropic parameters.

**Acknowledgment.** Gratitude is expressed to the National Science Foundation NSF-EPSCoR program (Grant RII-861075) and the NDSU Grant-in-Aid program for generous financial support.

**Supplementary Material Available:** Tables of bond lengths and angles, hydrogen positional and thermal parameters, anisotropic thermal parameters, and unit cell views (28 pages). Ordering information is given on any current mast-head page.

OM950152G

# Alkyne Insertions into Metal–Metal Bonds. Synthesis of Heteronuclear Dimetalated Olefins by Insertion of $\text{MeO}_2\text{CC}\equiv\text{CCO}_2\text{Me}$ into an Re–Fe Single Bond

Richard D. Adams\* and Mingsheng Huang

Department of Chemistry and Biochemistry, University of South Carolina,  
Columbia, South Carolina 29208

Received January 3, 1995<sup>⊙</sup>

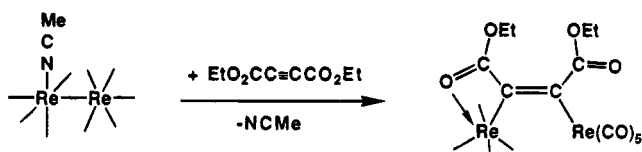
Activation of the complex  $\text{CpFe}(\text{CO})_2\text{Re}(\text{CO})_5$ , **1**, by  $\text{Me}_3\text{NO}$  followed by treatment with  $\text{MeO}_2\text{CC}\equiv\text{CCO}_2\text{Me}$  yielded the *Z*-dimetalated olefin complex  $\text{CpFe}(\text{CO})_2[\mu-(Z)-(\text{MeO}_2\text{C})\text{C}=\text{C}(\text{CO}_2\text{Me})]\text{Re}(\text{CO})_4$ , **2**, in 78% yield. Compound **2** was isomerized to *E*-isomer  $\text{CpFe}(\text{CO})_2[\mu-(E)-(\text{MeO}_2\text{C})\text{C}=\text{C}(\text{CO}_2\text{Me})]\text{Re}(\text{CO})_4$ , **3**, 18% yield, by heating solutions in heptane solvent to reflux for 70 min. When compound **2** was treated with  $\text{MeO}_2\text{CC}\equiv\text{CCO}_2\text{Me}$  in heptane solvent at reflux, the metallacyclic complex  $\text{CpFeRe}(\text{CO})_4[\mu-\text{C}(\text{CO}_2\text{Me})\text{C}(\text{CO}_2\text{Me})\text{C}(\text{CO}_2\text{Me})\text{C}(\text{CO}_2\text{Me})]$ , **4**, was formed in 59% yield. Compounds **2**, **3**, and **4** were characterized by single crystal x-ray diffraction analyses. Compound **2** is a *Z*-dimetalated olefin complex in which the carbonyl oxygen atom of one of the carboxylate groups is coordinated to the rhenium atom to form a four-membered ring. Compound **3** is an *E*-isomer of **2** in which the carbonyl oxygen atom of the other carboxylate group is coordinated to the rhenium atom to form a five-membered ring. In compound **4** the two alkynes are coupled to each other and to the rhenium atom to form a metallacycle that is  $\pi$ -bonded to the iron atom. Crystal data for **2**: space group =  $P2_1/n$ ,  $a = 14.010(2)$  Å,  $b = 10.259(3)$  Å,  $c = 14.116(3)$  Å,  $\beta = 105.96(1)^\circ$ ,  $Z = 4$ , 2274 reflections,  $R = 0.023$ . For **3**: space group =  $P\bar{1}$ ,  $a = 8.967(1)$  Å,  $b = 16.106(2)$  Å,  $c = 7.143(1)$  Å,  $\alpha = 101.69(1)^\circ$ ,  $\beta = 99.10(1)^\circ$ ,  $\gamma = 98.30(1)^\circ$ ,  $Z = 2$ , 2581 reflections,  $R = 0.024$ . For **4**: space group =  $P2_1/c$ ,  $a = 16.335(3)$  Å,  $b = 7.622(2)$  Å,  $c = 19.382(4)$  Å,  $\beta = 96.39(2)^\circ$ ,  $Z = 4$ , 2342 reflections,  $R = 0.032$ .

## Introduction

In recent studies we have characterized some of the first examples of the intramolecular insertion of carboxylated substituted alkynes into unsupported metal–metal bonds of reactive dimanganese and dirhenium carbonyl complexes.<sup>1</sup> The products are dimetalated olefins that are frequently stabilized by coordination of one of the oxygen atoms of the carboxylate groups to one of the metal atoms (e.g., eq 1).<sup>2,3</sup> Products with *Z*

olefins can be functionalized by a variety of insertion reactions at the metal–carbon bonds.<sup>3,5–7</sup> CO insertions are easily accomplished. Some of these products have led to new organic molecules.<sup>3</sup>

In this study we report the first example of the insertion of  $\text{MeO}_2\text{CC}\equiv\text{CCO}_2\text{Me}$  into the iron–rhenium bond in an activated derivative of the complex  $\text{CpFe}(\text{CO})_2\text{Re}(\text{CO})_5$ , **1**, to yield the *Z*-dimetalated olefin complex  $\text{CpFe}(\text{CO})_2[\mu-(Z)-(\text{MeO}_2\text{C})\text{C}=\text{C}(\text{CO}_2\text{Me})]\text{Re}(\text{CO})_4$ , **2**. Complex **2** can be thermally isomerized to the *E*-dimetalated olefin complex  $\text{CpFe}(\text{CO})_2[\mu-(E)-(\text{MeO}_2\text{C})\text{C}=\text{C}(\text{CO}_2\text{Me})]\text{Re}(\text{CO})_4$ , **3**, and in the presence of an additional quantity of  $\text{MeO}_2\text{CC}\equiv\text{CCO}_2\text{Me}$  it reacts to yield the metallacyclic complex  $\text{CpFeRe}(\text{CO})_4[\mu-\text{C}(\text{CO}_2\text{Me})\text{C}(\text{CO}_2\text{Me})\text{C}(\text{CO}_2\text{Me})\text{C}(\text{CO}_2\text{Me})]$ , **4**, by a coupling of a second equivalent of alkyne to the first with formation of a metallacycle by incorporating the rhenium atom.



- and *E*-stereochemistry can be obtained, but it appears that all the reactions proceed initially via species having *Z*-stereochemistry.

The activation of alkynes by metal atoms is well known to provide routes to new organic compounds.<sup>4</sup> We have shown that the alkyne grouping in the dimetalated

## Experimental Section

Unless specified otherwise, all reactions were carried out under an atmosphere of nitrogen. Hexane, heptane, and toluene solvents were freshly distilled from sodium/benzophenone solutions prior to use. MeCN was dried over CaH<sub>2</sub> and distilled before use. Re<sub>2</sub>(CO)<sub>10</sub> was purchased from Strem Chemical Co. [CpFe(CO)<sub>2</sub>]<sub>2</sub> was purchased from Pressure

<sup>⊙</sup> Abstract published in *Advance ACS Abstracts*, May 15, 1995.

(1) Adams, R. D. *Chem. Soc. Rev.* **1994**, 335.

(2) (a) Adams, R. D.; Chen, L. *Organometallics* **1994**, *13*, 1264. (b) Adams, R. D.; Chen, L.; Wu, W. *Organometallics* **1993**, *12*, 1257.

(3) (a) Adams, R. D.; Chen, L.; Huang, M. *Organometallics* **1994**, *13*, 2696. (b) Adams, R. D.; Chen, L. *J. Am. Chem. Soc.* **1994**, *116*, 4467.

(4) (a) Shore, N. E. *Chem. Rev.* **1988**, *88*, 1081. (b) Colquhoun, H. M.; Thompson, D. J.; Twigg, M. V. *Carbonylation. Direct Synthesis of Carbonyl Compounds*; Plenum Press: New York, 1991. (c) Pino, P.; Braca, G. In *Organic Synthesis via Metal Carbonyls*; Wender, I., Pino, P., Eds.; Wiley: New York, 1977; Vol. 2, pp 420–516.

(5) (a) Adams, R. D.; Chen, L.; Wu, W. *Organometallics* **1994**, *13*, 1257. (b) Adams, R. D.; Chen, L.; Wu, W. *Organometallics* **1993**, *12*, 4962.

(6) (a) Adams, R. D.; Chen, L.; Wu, W. *Organometallics* **1993**, *12*, 4112. (b) Lemke, F. R.; Szalda, D. J.; Bullock, R. M. *J. Am. Chem. Soc.* **1991**, *113*, 8466.

(7) Adams, R. D.; Huang, M. *Organometallics* **1995**, *14*, 506.

Chemical Co., and  $\text{MeO}_2\text{CC}\equiv\text{CCO}_2\text{Me}$  (99%) was purchased from Aldrich. These reagents were used without further purification.  $\text{Me}_3\text{NO}\cdot 2\text{H}_2\text{O}$  was purchased from Aldrich and was dehydrated by using a Dean–Stark apparatus with benzene solvent before use.<sup>8</sup> UV irradiations were performed on solutions in Pyrex glassware by using an externally positioned 125-WPI high-pressure mercury lamp (purchased from American Ultraviolet Co., Santa Anna, CA) operating at 500 W of power. TLC separations were performed in air by using silica gel (60 Å,  $F_{254}$ ) on plates (Whatman, 0.25 mm). IR spectra were recorded on a Nicolet 5DXB FT-IR spectrophotometer. <sup>1</sup>H NMR spectra were taken at 400 MHz on a Bruker AM-400 spectrometer. Elemental analyses were performed by Oneida Research Services Inc., Whitesboro, NY.

**Preparation of  $\text{CpFe}(\text{CO})_2\text{Re}(\text{CO})_5$ , 1.** A 200.0-mg amount (0.310 mmol) of  $\text{Re}_2(\text{CO})_{10}$  and a 217.0-mg amount (0.610 mmol) of  $[\text{CpFe}(\text{CO})_2]_2$  were dissolved in 300 mL of toluene. (The  $[\text{CpFe}(\text{CO})_2]_2$  was used in excess simply to maximize the consumption of the expensive reagent,  $\text{Re}_2(\text{CO})_{10}$ . The excess  $[\text{CpFe}(\text{CO})_2]_2$  can be recovered and reused if desired.) The solution was purged with CO for 1 h and was then exposed to UV irradiation for 1 h in the presence of a slow CO purge. After this period the solvent was removed in vacuo, and the residue was separated by column chromatography (silica gel) under an atmosphere of nitrogen. Elution with hexane yielded the following: 129.5 mg of  $[\text{CpFe}(\text{CO})_2]_2$ , 242.0 mg of orange  $\text{CpFe}(\text{CO})_2\text{Re}(\text{CO})_5$ , **1** (79% yield), and 13.1 mg of  $\text{Re}_2(\text{CO})_{10}$ . The product **1** is spectroscopically identical to the compound with the same formula reportedly obtained from the reaction of  $\text{Na}[\text{Re}(\text{CO})_5]$  with  $[\text{CpFe}(\text{CO})_2\text{I}]$ .<sup>9</sup> Without providing details, Johnston et al. also noted a similar photo-synthesis of **1**, but claimed the yield was only 20%.<sup>9</sup> Photo reactions can be strongly influenced and directed by the intensity of the radiation source which could explain our higher yield using a 0.5-kW UV source.

**Preparation of  $\text{CpFe}(\text{CO})_2[\mu\text{-(Z)-(MeO}_2\text{C)C=C(CO}_2\text{Me)}]\text{-Re}(\text{CO})_4$ , 2.** In a 250-mL three-neck flask wrapped with aluminum foil, a 150.0-mg amount (0.30 mmol) of **1** and a 27.0-mg amount (0.36 mmol) of  $\text{Me}_3\text{NO}$  in 100 mL of MeCN were stirred at 25 °C for 30 min. The solvent was then removed under vacuum, and 200 mL of hexane was introduced into the flask via cannula. A 44.4- $\mu\text{L}$  amount (0.36 mmol) of  $\text{MeO}_2\text{CC}\equiv\text{CCO}_2\text{Me}$  was then added via syringe, and the mixture was stirred at 25 °C for 15 h. The solvent was removed under vacuum, and the residue was pumped for 12 h to remove any excess  $\text{MeO}_2\text{CC}\equiv\text{CCO}_2\text{Me}$ . The residue was then extracted with 5 × 100-mL of hexane. Concentration of the hexane solution yielded 142.8 mg of pale yellow  $\text{CpFe}(\text{CO})_2[\mu\text{-(Z)-(MeO}_2\text{C)C=C(CO}_2\text{Me)}]\text{Re}(\text{CO})_4$ , **2**, in 78% yield upon cooling. Note: Infrared spectra of the reaction solution at the end of the 15 h reaction period showed at most only a trace of  $[\text{CpFe}(\text{CO})_2]_2$  coproduct and no evidence for  $\text{Re}_2(\text{CO})_{10}$  formation. Spectral data for **2**: IR ( $\nu_{\text{CO}}$  in hexane,  $\text{cm}^{-1}$ ): 2096 (w), 2032 (s), 1996 (s), 1984 (s), 1979 (s), 1930 (s), 1705 (w, br), 1527 (w, br). <sup>1</sup>H NMR ( $\delta$  in  $\text{C}_6\text{D}_6$ , ppm): 4.44 (s, 5H,  $\text{C}_5\text{H}_5$ ), 3.59 (s, 3H, OMe), 2.96 (s, 3H, OMe). Anal. Calcd (found): C, 33.08 (33.42); H, 1.80 (1.78).

**Preparation of  $\text{CpFe}(\text{CO})_2[\mu\text{-(E)-(MeO}_2\text{C)C=C(CO}_2\text{Me)}]\text{-Re}(\text{CO})_4$ , 3.** A 15.0-mg amount (0.024 mmol) of **2** was dissolved in 25 mL of heptane. The solution was heated to reflux for 70 min. After cooling to room temperature, the solvent was evaporated under vacuum, and the residue was separated by TLC using a hexane/ $\text{CH}_2\text{Cl}_2$  (1/1) solvent mixture. This yielded 2.7 mg of pale yellow  $\text{CpFe}(\text{CO})_2[\mu\text{-(E)-(MeO}_2\text{C)C=C(CO}_2\text{Me)}]\text{Re}(\text{CO})_4$ , **3**, 18% yield. Spectral data for **3**: IR ( $\nu_{\text{CO}}$  in hexane,  $\text{cm}^{-1}$ ): 2097 (w), 2026 (s), 1995 (s), 1984 (s), 1978 (s), 1954 (w), 1943 (s), 1705 (w, br), 1537 (w, br). <sup>1</sup>H NMR

( $\delta$  in  $\text{C}_6\text{D}_6$ , ppm): 4.25 (s, 5H,  $\text{C}_5\text{H}_5$ ), 3.77 (s, 3H, OMe), 3.21 (s, 3H, OMe). Anal. Calcd (found): C, 33.08 (33.11); H, 1.80 (1.80).

**Preparation of  $\text{CpFeRe}(\text{CO})_4[\mu\text{-C(CO}_2\text{Me)C(CO}_2\text{Me)C(CO}_2\text{Me)C(CO}_2\text{Me)}]$ , 4.** A 15.0-mg amount (0.024 mmol) of **2** and a 4.5- $\mu\text{L}$  amount (0.036 mmol) of  $\text{MeO}_2\text{CC}\equiv\text{CCO}_2\text{Me}$  were dissolved in 30 mL of heptane, and the solution was heated to reflux for 70 min. After cooling to room temperature, the solvent was removed in vacuo, and the residue was separated by TLC using a hexane/ $\text{CH}_2\text{Cl}_2$  1/2 solvent mixture to give 0.8 mg of **3** (5%) and 10.0 mg of green  $\text{CpFeRe}(\text{CO})_4[\mu\text{-C(CO}_2\text{Me)C(CO}_2\text{Me)C(CO}_2\text{Me)C(CO}_2\text{Me)}]$ , **4**, in 59% yield. Spectral data for **4**: IR ( $\nu_{\text{CO}}$  in hexane,  $\text{cm}^{-1}$ ): 2095 (s), 2024 (s), 1975 (s), 1741 (w, br), 1712 (w, br). <sup>1</sup>H NMR ( $\delta$  in  $\text{C}_6\text{D}_6$ , ppm): 4.80 (s, 5H,  $\text{C}_5\text{H}_5$ ), 3.86 (s, 6H, OMe), 3.81 (s, 6H, OMe). Anal. Calcd (found): C, 35.86 (35.92); H, 2.44 (2.27).

**Crystallographic Analysis.** Crystals of **2** suitable for X-ray diffraction analysis were obtained by recrystallization from solution in a hexane/ethylacetate 2/1 solvent mixture by cooling to  $-4$  °C. Crystals of **3** were obtained from a solution in a hexane/ $\text{CH}_2\text{Cl}_2$  2/1 solvent mixture by cooling to  $-4$  °C. Crystals of **4** were obtained by slow evaporation of solvent from a solution in a hexane/ $\text{CH}_2\text{Cl}_2$  2/1 solvent mixture at 25 °C. All crystals that were used in diffraction intensity measurements were mounted in thin-walled glass capillaries. Diffraction measurements were made on a Rigaku AFC6S fully automated four-circle diffractometer by using graphite-monochromated Mo K $\alpha$  radiation. The unit cells were determined and refined from 15 randomly selected reflections obtained by using the AFC6 automatic search, center, index, and least-squares routines. All data processing was performed on a Digital Equipment Corp. VAXstation 3520 computer by using the TEXSAN motif structure-solving program library obtained from Molecular Structure Corp., The Woodlands, TX. Neutral atom scattering factors were calculated by the standard procedures.<sup>10a</sup> Anomalous dispersion corrections were applied to all non-hydrogen atoms.<sup>10b</sup> Lorentz/polarization (Lp) and absorption corrections were applied to the data for each analysis. Full-matrix least-squares refinements minimized the function  $\sum_{hkl} w(|F_o| - |F_c|)^2$ , where  $w = 1/\sigma(F_o)^2$ ,  $\sigma(F_o) = \sigma(F_o^2)/2F_o$ , and  $\sigma(F_o^2) = [\sigma(I_{\text{raw}})^2 + (0.02I_{\text{net}})^2]^{1/2}/Lp$ . All structures were solved by a combination of direct methods (MITHRIL) and difference Fourier syntheses. Crystal data and results of the analyses are listed in Table 1.

Compounds **2** and **4** crystallized in the monoclinic crystal system. The space groups  $P2_1/n$  and  $P2_1/c$ , respectively, were identified uniquely from the patterns of systematic absences observed in the data. For both structures least-squares refinements were completed using anisotropic thermal parameters for all non-hydrogen atoms. The positions of all hydrogen atoms were calculated by assuming idealized geometries and C–H distances of 0.95 Å. The scattering contributions of the hydrogen atoms were added to the structure factor calculations, but their positions were not refined.

Compound **3** crystallized in the triclinic crystal system. The space group  $P\bar{1}$  was assumed and confirmed by the successful solution and refinement of the structure. All non-hydrogen atoms were refined using anisotropic thermal parameters. The positions of all hydrogen atoms were calculated by assuming idealized geometries and C–H distances of 0.95 Å. The scattering contributions of the hydrogen atoms were added to the structure factor calculations, but their positions were not refined.

## Results

When  $\text{CpFe}(\text{CO})_2\text{Re}(\text{CO})_5$ , **1**, was treated with a sequence of  $\text{Me}_3\text{NO}$  in the presence of NCMe followed

(8) Smith, C.; Boekelheide, J. In *Organic Synthesis*; Wiley: New York, 1973; Collective Vol. 5, p 872.

(9) Johnston, P.; Hutchings, G. J.; Denner, L.; Boeyene, J. C. A.; Coville, N. J. *Organometallics* **1987**, *6*, 1292.

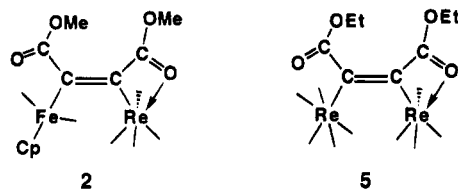
(10) (a) *International Tables for X-ray Crystallography*; Kynoch Press: Birmingham, England, 1975; Vol. 4, Table 2.2B, pp 99–101. (b) *Ibid.*, Table 2.3.1, pp 149–150.

Table 1. Crystal Data for Compounds 2–4

compd	2	3	4
formula	ReFeO <sub>10</sub> C <sub>17</sub> H <sub>11</sub>	ReFeO <sub>10</sub> C <sub>17</sub> H <sub>11</sub>	ReFeO <sub>12</sub> C <sub>21</sub> H <sub>17</sub>
fw	617.32	617.32	703.41
cryst syst	monoclinic	triclinic	monoclinic
lattice params			
<i>a</i> (Å)	14.010(2)	8.967(1)	16.335(3)
<i>b</i> (Å)	10.259(3)	16.106(2)	7.622(2)
<i>c</i> (Å)	14.116(3)	7.143(1)	19.382(4)
$\alpha$ (deg)	90.0	101.69(1)	90.0
$\beta$ (deg)	105.96(1)	99.10(1)	96.39(2)
$\gamma$ (deg)	90.0	98.30(1)	90.0
<i>V</i> (Å <sup>3</sup> )	1950.7(7)	980.8(2)	2398.1(9)
space group	<i>P</i> 2 <sub>1</sub> / <i>n</i> (No.14)	<i>P</i> 1̄ (No. 2)	<i>P</i> 2 <sub>1</sub> / <i>c</i> (No.14)
<i>Z</i>	4	2	4
$\rho_{\text{calcd}}$ (g/cm <sup>3</sup> )	2.10	2.09	1.95
$\mu$ (Mo K $\alpha$ ) (cm <sup>-1</sup> )	69.98	69.59	57.12
temp	20	20	20
2 $\theta_{\text{max}}$ (deg)	45.0	46.0	43.0
no. of obsd rflns ( <i>I</i> > 3 $\sigma$ )	2274	2581	2342
goodness of fit	1.80	2.35	2.55
residuals: <sup>a</sup> <i>R</i> ; <i>R</i> <sub>w</sub>	0.023; 0.026	0.024; 0.030	0.032; 0.037
abs corr	empirical	empirical	empirical
largest peak in final diff	1.00	0.90	0.87
map (e/Å <sup>3</sup> )			

<sup>a</sup>  $R = \sum_{hkl} (|F_o| - |F_c|) / \sum_{hkl} |F_o|$ ;  $R_w = [\sum_{hkl} w(|F_o| - |F_c|)^2 / \sum_{hkl} |F_o|^2]^{1/2}$ ,  $w = 1/\sigma^2(F_o)$ ; GOF =  $[\sum_{hkl} (|F_o| - |F_c|/\sigma(F_o))^2 / (n_{\text{data}} - n_{\text{vars}})]^{1/2}$ .

by MeO<sub>2</sub>CC≡CCO<sub>2</sub>Me, the new compound CpFe(CO)<sub>2</sub>[ $\mu$ -(*Z*)-(MeO<sub>2</sub>C)C=C(CO<sub>2</sub>Me)]Re(CO)<sub>4</sub>, **2**, was obtained in 72% yield. It is notable that there was no evidence for the formation of Re<sub>2</sub>(CO)<sub>10</sub> and at most only a trace of [CpFe(CO)<sub>2</sub>]<sub>2</sub> coproduct was formed in this reaction. Compound **2** was characterized by IR, <sup>1</sup>H NMR, and



single-crystal X-ray diffraction analyses. The <sup>1</sup>H NMR spectrum shows only three singlets at  $\delta$  4.44 (Cp), 3.59 (OCH<sub>3</sub>), and 2.96 (OCH<sub>3</sub>) ppm. An ORTEP diagram of **2** is shown in Figure 1. Final atomic positional parameters are listed in Table 2. The compound is a *Z*-dimetalated olefin complex. The C–C double bond is short, C(1)–C(2) = 1.332(8) Å, as expected. This distance is very similar to that found in the related  $\mu$ -(*Z*)-dirhenium dimetalated olefin complex Re(CO)<sub>5</sub>[ $\mu$ -(*Z*)-(MeO<sub>2</sub>C)C=C(CO<sub>2</sub>Me)]Re(CO)<sub>4</sub>, **5**, 1.34(1) Å.<sup>2a</sup> A CpFe(CO)<sub>2</sub> grouping is bonded to C(2), Fe–C(2) = 2.007(5) Å, and a Re(CO)<sub>4</sub> grouping is bonded to C(1), Re–C(1) = 2.211(6) Å. The oxygen atom of the carbonyl group bonded to C(1) is coordinated to the rhenium atom, Re–O(1) = 2.218(4) Å, to form a four-membered ring, Re–C(1)–C(3)–O(1). A similar arrangement was also found in **5** which contained very similar Re–C and Re–O distances, 2.193(8) and 2.214(6) Å, respectively. Evidence for strain in the system is indicated by the very large bond angle, Re–C(1)–C(2) = 146.3(4)°. The corresponding angle in **5** is virtually the same, 146.8(7)°. This is probably a result of steric interactions between the iron and rhenium groups which may also affect the planarity of the olefinic grouping. For example, the dihedral angle between the planes Re–C(1)–C(3) and Fe–C(2)–C(4) is 7.8°. It is notable that the C–O distance of the coordinated carbonyl group, C(3)–O(1)

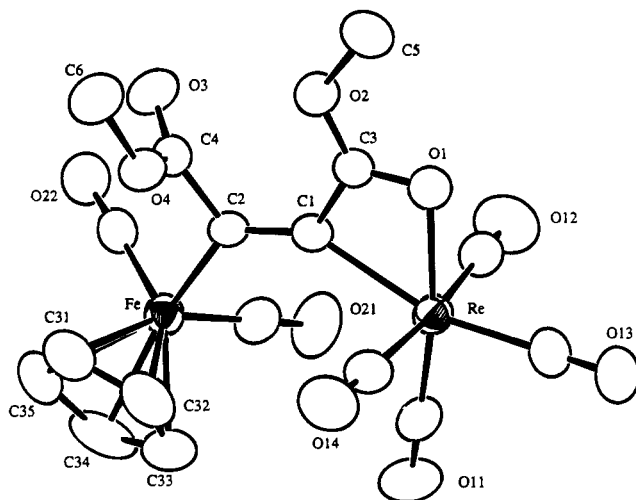
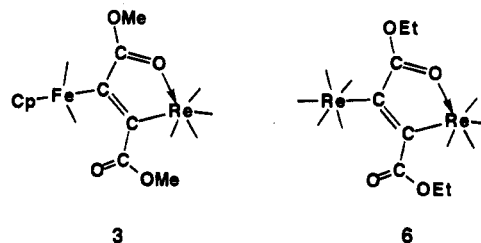


Figure 1. An ORTEP diagram of CpFe(CO)<sub>2</sub>[ $\mu$ -(*Z*)-(MeO<sub>2</sub>C)C=C(CO<sub>2</sub>Me)]Re(CO)<sub>4</sub>, **2**, showing 50% probability thermal ellipsoids. Selected bond distances (Å) and angles (deg) are as follows: Re–O(1) = 2.218(4), Fe–C(2) = 2.007(5), Re–C(1) = 2.211(6), C(1)–C(2) = 1.332(8), C(1)–C(3) = 1.457(7), C(2)–C(4) = 1.485(8), C(3)–O(1) = 1.264(6), and C(4)–O(3) = 1.200(7) Å; Re–C(1)–C(2) = 146.3(4), Fe–C(2)–C(1) = 127.8(4)°, Re–C(1)–C(3) = 88.9(3)°, Fe–C(2)–C(4) = 113.5(4)°, C(2)–C(1)–C(3) = 124.1(5)°, and C(1)–C(2)–C(4) = 118.7(5)°.

= 1.264(6) Å, is significantly longer than that of the uncoordinated carbonyl group C(4)–O(3) = 1.200(7) Å. This is reflected in their stretching frequencies observed in the infrared spectrum, 1527 vs 1705 cm<sup>-1</sup>.

When solutions of **2** were heated to reflux in heptane solvent, the new compound CpFe(CO)<sub>2</sub>[ $\mu$ -(*E*)-(MeO<sub>2</sub>C)C=C(CO<sub>2</sub>Me)]Re(CO)<sub>4</sub>, **3**, was obtained in 18% yield. Compound **3** was characterized by IR, <sup>1</sup>H NMR, and



single-crystal X-ray diffraction analyses. Its <sup>1</sup>H NMR spectrum is similar to that of **2**, exhibiting three singlets at  $\delta$  4.25 (Cp), 3.77 (OCH<sub>3</sub>), and 3.21 (OCH<sub>3</sub>) ppm. An ORTEP diagram of **3** is shown in Figure 2. Final atomic positional parameters are listed in Table 3. This compound is an *E*-dimetalated olefin complex, i.e., the metal atoms lie on opposite sides of the C–C double bond. The C–C double bond distance C(1)–C(2) = 1.344(8) Å is not significantly different from those in **2** and **5**.<sup>2a</sup> The CpFe(CO)<sub>2</sub> grouping remains bonded to C(2) via a Fe–C single bond at a distance identical to that in **2**, Fe–C(2) = 2.007(6) Å. The Re(CO)<sub>4</sub> grouping is still bonded to C(1), but the Re–C distance is now shorter than that in **2** and **5**, Re–C(1) = 2.168(8) Å. A carbonyl oxygen atom of one of the carboxylate groups is bonded to the rhenium atom, but this is now the carboxylate group that is bonded to the other carbon atom of the C–C double bond. The ring that is formed is five membered, Re–C(1)–C(2)–C(3)–O(1) and the Re–O distance is also shorter than that in **2**, Re–O(3)

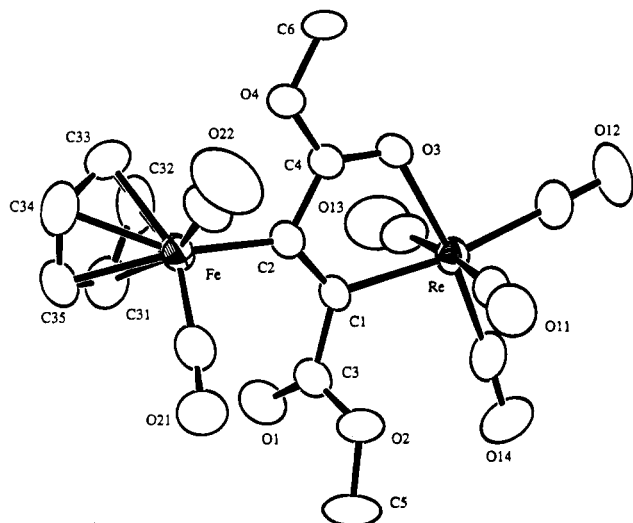


**Figure 2.** An ORTEP diagram of  $\text{CpFe}(\text{CO})_2\text{-}\mu\text{-(E)-(MeO}_2\text{C)C=C(CO}_2\text{Me)Re(CO)}_4$ , **3**, showing 50% probability thermal ellipsoids. Selected bond distances ( $\text{\AA}$ ) and angles (deg) are as follows:  $\text{Re-O}(3) = 2.170(4)$ ,  $\text{Fe-C}(2) = 2.007(6)$ ,  $\text{Re-C}(1) = 2.175(5)$ ,  $\text{C}(1)\text{-C}(2) = 1.344(8)$ ,  $\text{C}(1)\text{-C}(3) = 1.482(8)$ ,  $\text{C}(2)\text{-C}(4) = 1.471(8)$ ,  $\text{C}(3)\text{-O}(1) = 1.202(7)$ , and  $\text{C}(4)\text{-O}(3) = 1.252(7)$   $\text{\AA}$ ;  $\text{Re-C}(1)\text{-C}(2) = 119.0(4)^\circ$ ,  $\text{Fe-C}(2)\text{-C}(1) = 129.8(4)^\circ$ ,  $\text{Re-C}(1)\text{-C}(3) = 117.0(4)^\circ$ ,  $\text{Fe-C}(2)\text{-C}(4) = 120.9(4)^\circ$ ,  $\text{C}(2)\text{-C}(1)\text{-C}(3) = 124.0(5)^\circ$ , and  $\text{C}(1)\text{-C}(2)\text{-C}(4) = 109.1(5)^\circ$ .

**Table 2. Positional Parameters and  $B(\text{eq})$  for **2****

atom	x	y	z	$B(\text{eq})$
Re	0.69623(2)	0.02132(2)	0.02443(2)	2.73(1)
Fe	0.82235(6)	-0.37673(7)	0.05615(6)	2.80(3)
O(1)	0.7774(3)	0.1095(4)	-0.0741(3)	3.4(2)
O(2)	0.8963(3)	0.0078(4)	-0.1230(3)	3.7(2)
O(3)	1.0014(3)	-0.2501(4)	-0.0551(3)	3.8(2)
O(4)	0.8597(3)	-0.2617(4)	-0.1762(3)	3.5(2)
O(11)	0.6061(3)	-0.1352(4)	0.1625(4)	5.2(2)
O(12)	0.8602(4)	0.1058(5)	0.2130(4)	6.3(3)
O(13)	0.5588(4)	0.2578(4)	0.0246(4)	5.4(2)
O(14)	0.5506(4)	-0.1103(5)	-0.1570(4)	5.3(2)
O(21)	0.8419(4)	-0.2206(5)	0.2309(3)	5.2(2)
O(22)	1.0303(4)	-0.4465(4)	0.1200(3)	4.5(2)
C(1)	0.8081(4)	-0.1002(5)	-0.0178(4)	2.5(2)
C(2)	0.8456(4)	-0.2192(5)	-0.0187(4)	2.6(2)
C(3)	0.8297(4)	0.0092(5)	-0.0742(4)	2.7(2)
C(4)	0.9126(4)	-0.2439(5)	-0.0819(4)	2.7(2)
C(5)	0.9120(7)	0.1254(7)	-0.1721(6)	4.5(4)
C(6)	0.9155(6)	-0.2706(8)	-0.2475(6)	4.7(4)
C(11)	0.6385(4)	-0.0762(6)	0.1099(5)	3.5(3)
C(12)	0.8019(5)	0.0787(6)	0.1427(5)	3.7(3)
C(13)	0.6108(5)	0.1700(6)	0.0272(5)	3.8(3)
C(14)	0.6016(5)	-0.0596(6)	-0.0917(5)	3.4(3)
C(21)	0.8338(4)	-0.2803(6)	0.1615(5)	3.5(3)
C(22)	0.9483(5)	-0.4168(5)	0.0926(4)	3.1(3)
C(31)	0.7543(6)	-0.4918(7)	-0.0656(6)	4.9(4)
C(32)	0.6857(6)	-0.4058(7)	-0.0479(6)	5.0(4)
C(33)	0.6738(5)	-0.4297(8)	0.0449(6)	5.1(4)
C(34)	0.7381(7)	-0.5313(8)	0.0861(6)	5.5(4)
C(35)	0.7857(6)	-0.5716(7)	0.0155(7)	5.1(4)

$= 2.170(4)$   $\text{\AA}$ . The shortening of the  $\text{Re-C}$  and  $\text{Re-O}$  bonds in the five-membered ring may be a result of a decrease in ring strain in going from **2** to **3** and the ability to achieve bond angles more favorable to the coordination of the carbon and oxygen atoms. A similar shortening of the  $\text{Re-C}$  and  $\text{Re-O}$  distances was found in **5** when was transformed to its *E*-isomer  $\text{Re}(\text{CO})_5[\mu\text{-(E)-(MeO}_2\text{C)C=C(CO}_2\text{Me)Re(CO)}_4$ , **6**,<sup>2a</sup>

When **2** was allowed to react with an additional quantity of  $\text{MeO}_2\text{CC}\equiv\text{CCO}_2\text{Me}$  in a heptane solution at reflux, the new compound  $\text{CpFeRe}(\text{CO})_4[\mu\text{-C(CO}_2\text{Me)C-}$

**Table 3. Positional Parameters and  $B(\text{eq})$  for **3****

atom	x	y	z	$B(\text{eq})$
Re	0.16237(2)	0.38553(1)	0.88503(3)	2.50(1)
Fe	-0.27911(9)	0.15009(5)	0.5094(1)	2.96(3)
O(1)	0.1241(5)	0.1304(3)	0.6903(7)	4.7(2)
O(2)	0.0928(5)	0.1848(3)	0.9955(6)	4.0(2)
O(3)	-0.0418(4)	0.4074(2)	0.7078(5)	2.8(1)
O(4)	-0.2655(4)	0.3476(2)	0.5117(6)	3.3(1)
O(11)	0.0005(6)	0.3779(3)	1.2389(7)	4.9(2)
O(12)	0.3138(6)	0.5787(3)	1.0383(8)	5.9(2)
O(13)	0.3253(7)	0.3654(4)	0.5282(8)	6.5(3)
O(14)	0.4252(5)	0.3222(3)	1.1119(7)	5.0(2)
O(21)	-0.2242(7)	0.0533(3)	0.8053(8)	6.0(2)
O(22)	-0.5167(7)	0.2252(4)	0.680(1)	8.6(3)
C(1)	0.0196(6)	0.2592(3)	0.7582(8)	2.5(2)
C(2)	-0.1189(6)	0.2541(3)	0.6475(8)	2.7(2)
C(3)	0.0817(6)	0.1837(4)	0.804(1)	3.1(2)
C(4)	-0.1389(6)	0.3408(4)	0.6252(8)	2.7(2)
C(5)	0.167(1)	0.1203(5)	0.1065(1)	5.7(3)
C(6)	-0.2824(7)	0.4327(4)	0.486(1)	3.8(2)
C(11)	0.0566(7)	0.3839(4)	1.110(1)	3.2(2)
C(12)	0.2592(7)	0.5075(4)	0.9187(9)	3.5(2)
C(13)	0.2645(8)	0.3729(4)	0.656(1)	3.8(2)
C(14)	0.3289(7)	0.3488(4)	1.0266(9)	3.5(2)
C(21)	-0.2442(7)	0.0947(4)	0.693(1)	4.0(2)
C(22)	-0.4220(8)	0.1969(4)	0.613(1)	4.7(3)
C(31)	-0.1687(9)	0.0820(5)	0.309(1)	5.0(3)
C(32)	-0.188(1)	0.1608(5)	0.260(1)	5.3(3)
C(33)	-0.343(1)	0.1632(5)	0.224(1)	5.6(3)
C(34)	-0.4222(9)	0.0843(5)	0.245(1)	5.7(3)
C(35)	-0.315(1)	0.0355(4)	0.296(1)	5.0(3)

$(\text{CO}_2\text{Me)C(CO}_2\text{Me)C(CO}_2\text{Me)}$ , **4**, was obtained in 59% yield by the loss of 2 equiv of  $\text{CO}$  and the addition of 1 equiv of  $\text{MeO}_2\text{CC}\equiv\text{CCO}_2\text{Me}$ . Compound **4** was characterized by IR,  $^1\text{H}$  NMR, and single-crystal X-ray diffraction analyses. The  $^1\text{H}$  NMR spectrum shows only three singlets,  $\delta$  4.80 (Cp), 3.86 (2 OMe), and 3.81 (2 OMe) ppm, indicating that the  $\text{CO}_2\text{Me}$  groups have formed two equivalent pairs. An ORTEP diagram of **4** is shown in Figure 3. Final atomic positional parameters are listed in Table 4. This complex contains  $\text{CpFe}$  and  $\text{Re}(\text{CO})_4$  groups that are joined by a  $\text{Fe-Re}$  single bond, 2.717(1)  $\text{\AA}$ . The two alkynes have been coupled to each other and to the rhenium atom to form a rheniacyclopentadienyl group that is  $\pi$ -bonded to the iron atom. The  $\text{C-C}$  bonds in the ring are all similar, 1.43(1), 1.46(1), and 1.41(1)  $\text{\AA}$ , indicating that there is considerable delocalization of the  $\pi$ -bonding. The coupling of alkynes at diiron centers is well-known to produce such metallacycles,<sup>11</sup> but there have been only a few recent reports a similar alkyne coupling at dirhenium centers,<sup>12</sup> and **4** is the first example of such a coupling in a mixed iron-rhenium system. Both metal atoms possess 18-electron configurations.

## Discussion

In our previous studies we have demonstrated that carboxylate-substituted alkynes can add to activated dirhenium and dimanganese carbonyl complexes by insertion of the alkyne into the metal-metal bond to produce dimetalated olefin complexes.<sup>1-3</sup> Results in those studies indicated that the insertions occur by

(11) (a) Fehlhammer, W. P.; Stolzenberg, H. In *Comprehensive Organometallic Chemistry*; Wilkinson, G., Stone, F. G. A., Abel, E., Eds.; Pergamon: Oxford, U.K., 1982; Chapter 31.4. (b) Adams, R. D.; Daran, J.-C.; Jeannin, Y. *J. Cluster Sci.* **1992**, *3*, 1.

(12) (a) Adams, R. D.; Chen, G.; Yin, J. *Organometallics* **1991**, *10*, 1278. (b) Pourreau, D. B.; Whittle, R. R.; Geoffroy, G. L. *J. Organomet. Chem.* **1984**, *273*, 333.

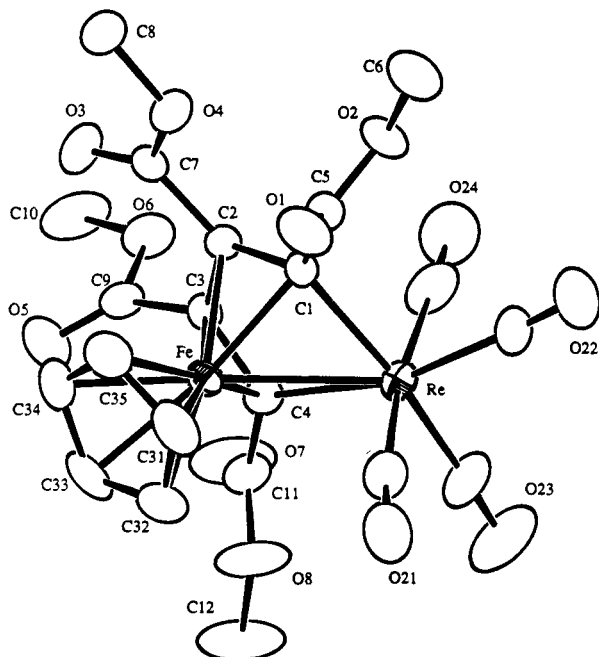


**Figure 3.** An ORTEP diagram of  $\text{CpFeRe}(\text{CO})_4[\mu\text{-C}(\text{CO}_2\text{Me})\text{C}(\text{CO}_2\text{Me})\text{C}(\text{CO}_2\text{Me})\text{C}(\text{CO}_2\text{Me})]$ , **4**, showing 50% probability thermal ellipsoids. Selected bond distances (Å) and angles (deg) are as follows:  $\text{Re-Fe} = 2.717(1)$ ,  $\text{Re-C}(1) = 2.168(8)$ ,  $\text{Re-C}(4) = 2.185(8)$ ,  $\text{Fe-C}(1) = 2.000(7)$ ,  $\text{Fe-C}(2) = 2.038(7)$ ,  $\text{Fe-C}(3) = 2.035(7)$ ,  $\text{Fe-C}(4) = 1.963(8)$ ,  $\text{C}(1)\text{-C}(2) = 1.43(1)$ ,  $\text{C}(2)\text{-C}(3) = 1.46(1)$ , and  $\text{C}(3)\text{-C}(4) = 1.41(1)$  Å;  $\text{C}(1)\text{-Re-C}(4) = 74.6(3)^\circ$ ,  $\text{Re-C}(1)\text{-C}(2) = 115.4(5)^\circ$ ,  $\text{Re-C}(4)\text{-C}(3) = 114.4(5)^\circ$ ,  $\text{Fe-C}(1)\text{-Re} = 81.3(3)^\circ$ ,  $\text{Fe-C}(4)\text{-Re} = 81.7(3)^\circ$ ,  $\text{C}(1)\text{-C}(2)\text{-C}(3) = 113.7(7)^\circ$ , and  $\text{C}(2)\text{-C}(3)\text{-C}(4) = 115.2(6)^\circ$ .

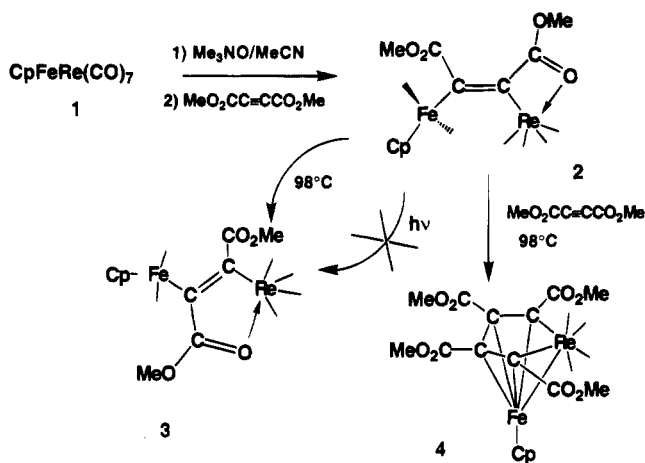
intramolecular mechanisms. The current investigation shows that a suitably activated form of **1** will also react with  $\text{MeO}_2\text{CC}\equiv\text{CCO}_2\text{Me}$  by insertion into the Fe–Re bond to yield the dimetalated olefin complex **2**. A summary of the results of this study are shown in Scheme 1. The treatment of **1** with  $\text{Me}_3\text{NO}$  in MeCN produces a decarbonylation which probably occurs at the CO-rich  $\text{Re}(\text{CO})_5$  grouping. A molecule of MeCN probably occupies temporarily the site of CO elimination. The MeCN ligand is subsequently displaced by the alkyne, and the alkyne is inserted into the metal–metal bond. This is followed by the coordination of the oxygen atom of the proximate carbonyl group to the rhenium atom. The absence of formation of any significant amounts of  $[\text{CpFe}(\text{CO})_2]_2$  or  $\text{Re}_2(\text{CO})_{10}$  is consistent with a nondissociative process. Compound **2** can be isomerized to the *E*-isomer **3** under relatively mild thermal conditions, but the yield is low. The thermal isomerization of **5** to **6** also gives a low yield. The transformation of **5** to **6** was improved by photoassistance. Unfortunately, irradiations of **2** produced no **3** at all. Hoffman et al. have calculated that such isomerizations should have activation barriers in excess of 60 kcal/mol.<sup>13</sup> We have rationalized the facile isomerization of **5** to **6** by employing a  $\mu\text{-}\eta^2\text{-alkenyl}$  intermediate.<sup>2</sup> A similar intermediate could be invoked to explain the isomerization of **2** to **3**.

When treated with  $\text{MeO}_2\text{CC}\equiv\text{CCO}_2\text{Me}$ , **2** loses two CO ligands and adds 1 equiv of  $\text{MeO}_2\text{CC}\equiv\text{CCO}_2\text{Me}$  to form **4** by the formation of a C–C bond between the two

**Table 4.** Positional Parameters and  $B(\text{eq})$  for **4**

atom	<i>x</i>	<i>y</i>	<i>z</i>	<i>B</i> (eq)
Re	0.13054(2)	0.47888(4)	0.86650(2)	3.28(2)
Fe	0.27726(7)	0.5973(1)	0.92919(6)	2.86(5)
O(1)	0.1859(4)	0.4313(8)	1.0677(3)	5.2(3)
O(2)	0.1572(4)	0.1722(7)	1.0181(3)	4.2(3)
O(3)	0.4310(4)	0.2247(9)	0.9647(4)	5.3(4)
O(4)	0.3393(3)	0.2087(8)	1.0409(3)	4.4(3)
O(5)	0.4493(4)	0.4808(9)	0.8419(4)	6.2(4)
O(6)	0.3988(4)	0.2155(8)	0.8152(3)	5.0(3)
O(7)	0.2980(6)	0.528(1)	0.7210(4)	8.9(5)
O(8)	0.2421(5)	0.7604(9)	0.7626(3)	6.9(4)
O(21)	0.0825(4)	0.841(1)	0.9239(5)	8.3(5)
O(22)	-0.0208(5)	0.338(1)	0.9327(5)	7.7(5)
O(23)	0.0453(6)	0.607(2)	0.7252(5)	10.9(6)
O(24)	0.1464(5)	0.109(1)	0.7997(5)	8.3(5)
C(1)	0.2157(4)	0.382(1)	0.9517(4)	2.6(3)
C(2)	0.2955(5)	0.333(1)	0.9339(4)	2.6(4)
C(3)	0.3142(5)	0.403(1)	0.8675(4)	2.7(3)
C(4)	0.2530(5)	0.514(1)	0.8333(4)	3.0(3)
C(5)	0.1887(5)	0.336(1)	1.0195(5)	3.3(4)
C(6)	0.1271(7)	0.113(1)	1.0819(6)	6.2(6)
C(7)	0.3637(6)	0.250(1)	0.9801(5)	3.2(4)
C(8)	0.4014(6)	0.132(1)	1.0908(5)	5.5(5)
C(9)	0.3964(6)	0.376(1)	0.8416(5)	3.7(4)
C(10)	0.4745(7)	0.169(2)	0.7883(6)	7.6(7)
C(11)	0.2681(6)	0.598(1)	0.7665(5)	4.1(5)
C(12)	0.251(1)	0.855(2)	0.6999(6)	9.3(8)
C(21)	0.1049(6)	0.710(1)	0.9060(7)	6.3(6)
C(22)	0.0332(6)	0.391(1)	0.9066(5)	4.5(5)
C(23)	0.0747(6)	0.559(2)	0.7785(7)	6.4(6)
C(24)	0.1402(7)	0.243(1)	0.8222(6)	6.1(6)
C(31)	0.2653(7)	0.784(1)	1.0045(6)	5.3(6)
C(32)	0.2775(7)	0.867(1)	0.9411(6)	5.6(6)
C(33)	0.3530(7)	0.814(1)	0.9212(6)	5.4(6)
C(34)	0.3884(6)	0.698(1)	0.9717(6)	5.2(5)
C(35)	0.3357(8)	0.681(1)	1.0230(6)	5.3(5)

**Scheme 1**



alkynes. Such coupling processes are not uncommon, but this appears to be the first example in a mixed Re–Fe system. Further studies of the reactivity of **2** and **3** are in progress.

**Acknowledgment.** This research was supported by the Office of Basic Energy Sciences of U.S. Department of Energy.

**Supplementary Material Available:** Tables of hydrogen atom positional parameters, anisotropic thermal parameters, and bond distances and angles for all three structural analyses (19 pages). Ordering information is given on any current masthead page.

# Synthesis and Reactivity of Platinum Complexes of Cyclic Alkynes and Tropyne

Jerzy Klosin, Khalil A. Abboud, and W. M. Jones\*

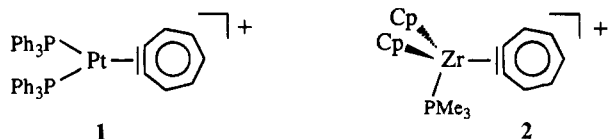
Department of Chemistry, University of Florida, Gainesville, Florida 32611

Received January 10, 1995\*

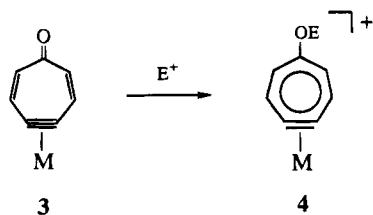
Platinum complexes of dibenzannelated didehydrotropone **5**, didehydrooxepin **6**, and didehydrocycloheptatriene **7** have been synthesized in good yields by base-induced dehydrobromination from the corresponding bromoalkenes in the presence of Pt(PPh<sub>3</sub>)<sub>3</sub>. Complex **5** crystallizes in triclinic space group  $P\bar{1}$ :  $a = 11.221(2)$  Å,  $b = 11.318(2)$  Å,  $c = 16.621(4)$  Å,  $\alpha = 74.22(2)^\circ$ ,  $\beta = 78.86(2)^\circ$ ,  $\gamma = 73.56(2)^\circ$ ,  $V = 2445.0(9)$  Å<sup>3</sup>,  $Z = 2$ ,  $R = 5.79\%$ . Reaction of **5** with *tert*-butyl isocyanide gives a single phosphine displacement product **11**, and reaction with HBF<sub>4</sub> and HBr gives oxidative addition products **8** and **12**, respectively. Bis-(dicyclohexylphosphino)ethane displaces triphenylphosphine from **5** and **6** to give **9** and **10**. Complex **5** reacts with tetracyanoethylene to give the highly distorted substituted benzene **14** which was characterized by X-ray diffraction. Crystal data for **14**: Space group  $P\bar{1}$ ,  $a = 11.274(2)$  Å,  $b = 11.826(1)$  Å,  $c = 13.474(2)$  Å,  $\alpha = 111.79(1)^\circ$ ,  $\beta = 106.34(1)^\circ$ ,  $\gamma = 98.54(1)^\circ$ ,  $V = 1534.9(4)$  Å<sup>3</sup>,  $Z = 2$ ,  $R = 6.17\%$ . Complex **6** reacts with TCNE to give the platinumacyclopent-2-ene **15** (55%). Complex **15** crystallizes in monoclinic space group *Ia*:  $a = 17.175(3)$  Å,  $b = 15.411(2)$  Å,  $c = 18.661(2)$  Å,  $\beta = 91.86(1)^\circ$ ,  $V = 4915(2)$  Å<sup>3</sup>,  $R = 4.74\%$ . Reaction of **7** with triphenylcarbenium tetrafluoroborate gives the dibenzannelated tropyne complex **16** which can be converted back to **7** with KBET<sub>3</sub>H. Reaction of **16** with bis(dicyclohexylphosphino)ethane gives **17** (60%), and reaction with HBr gives the oxidative addition product **18** which slowly isomerizes to **19**.

## Introduction

We recently reported the synthesis and characterization of platinum<sup>1</sup> (**1**) and zirconium<sup>2</sup> (**2**) complexes of



tropyne by hydride abstraction from the corresponding complexes of cycloheptadienyne. By analogy with well-established chemistry of tropones, it occurred to us that, in principle, it should be possible to prepare alkoxy- and hydroxy-substituted tropyne complexes by alkylation or protonation of didehydrotropone complexes.<sup>3</sup>



To test this hypothesis, preparation of a metal complex of didehydrotropone was considered. However, synthesis of appropriate starting materials was formidable. We therefore decided to focus initially on the much more

readily available dibenzannelated analogue **5** (Scheme 1). At this time we report the successful synthesis of **5** which, although it could be neither alkylated nor protonated on the carbonyl oxygen, underwent reaction with TCNE to give the highly cluttered and distorted benzene derivative **14** (Scheme 3). This surprising result induced us to prepare platinum complexes of two other dibenzannelated cycloheptadienyne (**6** and **7**), and although neither underwent trimerization when treated with TCNE, one (**6**) underwent a rare coupling to form **15** (Scheme 3) and the other (**7**), upon hydride abstraction, gave the new tropyne complex **16** (Scheme 4).

## Results and Discussion

### Preparation of Platinum Alkyne Complexes.

Dibenzannelated didehydrotropone **5**, didehydrooxepin **6**, and didehydrocycloheptatriene **7** have been synthesized from the corresponding bromoalkenes as shown in Scheme 1. After workup yellow (**5**, **6**) and off-white (**7**) crystalline solids were obtained in 60–75% yield. All new complexes were characterized by <sup>1</sup>H, <sup>13</sup>C, <sup>31</sup>P, and <sup>195</sup>Pt NMR (Table 2), HRMS, and elemental analysis. The proton NMR spectrum of these complexes is somewhat surprising in that the chemical shifts of the protons nearest the triple bond (H1) are in the range 5.8–6.5 ppm which is uncommonly high field for aromatic compounds. This upfield shift was shown in two ways to be due to diamagnetic shielding by triphenylphosphine coordinated to the platinum. First, in an NOE study of **6**, irradiation of the ortho protons of triphenylphosphine led to an 11.9% enhancement of H1. Second, analogues of **5** and **6** that are incapable of significant shielding (**9**, **10**) were prepared by ligand

\* Abstract published in *Advance ACS Abstracts*, April 15, 1995.

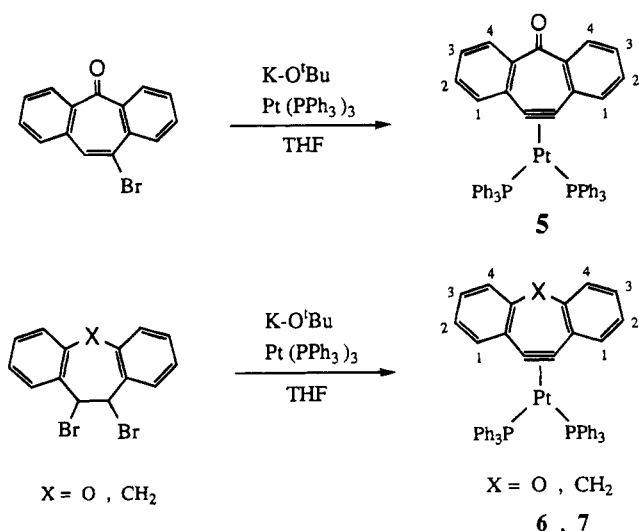
(1) Lu, Z.; Abboud, K. A.; Jones, W. M. *J. Am. Chem. Soc.* **1992**, *114*, 10991.

(2) Lu, Z.; Jones, W. M. *Organometallics* **1994**, *13*, 1539.

(3) Douglas, L. *Non-Benzenoid Conjugated Carbocyclic Compounds*; Elsevier Science Publishers: Amsterdam, 1984.



Scheme 1



exchange and their spectra compared with **5** and **6**. All aromatic resonances appear below 7 ppm.<sup>4</sup> The infrared spectra of the alkyne complexes **5**, **6**, and **7** showed the expected alkyne absorptions at 1708, 1691, and 1689  $\text{cm}^{-1}$ , respectively. These are in the range normally expected for platinum alkyne complexes (1630–1780  $\text{cm}^{-1}$ ) and are at a lower frequency than those of the corresponding complexes of cycloheptyne (1771  $\text{cm}^{-1}$ ) and cyclohexyne<sup>5</sup> (1721  $\text{cm}^{-1}$ ) as would be expected from conjugation with the aryl rings.

**X-ray Crystal Structure of 5.** Crystals of **5** were obtained from a mixture of toluene and hexane as yellow plates. Complex **5** crystallizes in the  $P\bar{1}$  space group together with one molecule of toluene which is disordered in two different positions. A thermal ellipsoid drawing of the structure is given in Figure 1, while crystal data are listed in Table 5. Selected bond lengths and angles and final fractional atomic coordinates are provided in Tables 1 and 6, respectively. The alkyne bond length in **5** is 1.283(15) Å and is equal, within experimental error, to that in platinum complexes of cyclohexyne and cycloheptyne.<sup>6</sup> The alkyne ligand is bent, with a dihedral angle between the phenyls of 146.8(5)°. This value is almost the same as in dibenzotropone<sup>7</sup> [142.8(6)°]; coordination of platinum has virtually no effect on the geometry of the ligand. Complexes of this type have an essentially square planar geometry with the donor phosphine groups occupying *cis* coordination sites. The coordinated alkyne is slightly rotated from the P1–Pt–P2 planes. In complex **5** the dihedral angle between planes defined by Pt, P1, P2 and Pt, C10, C11 is 12.3(7)° and is one of the largest among all known platinum alkyne complexes.<sup>6</sup>

**Reactions of Alkyne Complexes.** Some reactions of the alkyne complexes **5**–**7** are summarized in Scheme 2. Overall, the reactivity of these complexes is quite moderate. They show no reaction with weak acids such as ethanol and acetonitrile even when warmed to 80 °C for 2 days. They also show no reaction with methyl iodide, dimethyl acetylenedicarboxylate or phenylacety-

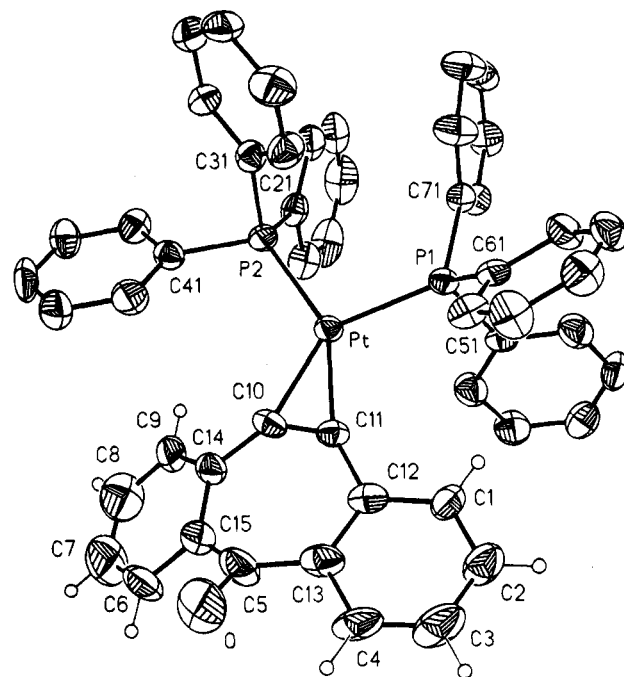


Figure 1. Structure and labeling scheme for **5** with 40% probability of thermal ellipsoids.

Table 1. Selected Bond Lengths (Å) and Angles (deg) for Complex **5**

Bond Lengths (Å)			
Pt–P1	2.290(3)	P2–C21	1.840(11)
Pt–P2	2.277(3)	P2–C31	1.836(12)
Pt–C10	2.056(13)	P2–C41	1.826(11)
Pt–C11	2.031(13)	C5–O	1.27(2)
P1–C51	1.839(11)	C11–C10	1.283(15)
P1–C61	1.826(10)	C14–C10	1.42(2)
P1–C71	1.844(13)	C12–C11	1.43(2)
Bond Angles (deg)			
P1–Pt–P2	102.04(12)	C13–C5–O	115.7(13)
P1–Pt–C10	144.4(3)	C15–C5–O	116.3(13)
P2–Pt–C10	113.0(3)	C11–C10–C14	135.8(14)
P2–Pt–C11	148.9(3)	C14–C10–Pt	152.3(10)
C10–Pt–C11	36.6(4)	C12–C11–Pt	154.1(8)
C11–Pt–P1	109.0(3)	Pt–C11–C10	72.8(8)

lene. Attempts to protonate **5** on the carbonyl oxygen to give the hydroxytropone complex also failed; as Bennett observed for an analogous complex of cyclohexyne,<sup>5</sup> the electrophile apparently attacks the metal which leads to the  $\sigma$  complexes **8** and **12** from  $\text{HBF}_4$  and  $\text{HBr}$ , respectively. As mentioned above, complexes **5** and **6** react readily with bis(dicyclohexylphosphino)ethane to give **9** and **10**.<sup>5,8</sup> The carbon–carbon triple bond in **9** shows a red shift of 18  $\text{cm}^{-1}$  as compared with **6** which could be expected from the increased basicity of the phosphine ligand. However, the frequency of the same bond in **10** is almost identical to that of **5**. Complex **5** also reacted rapidly with *tert*-butyl isocyanide to give **11** in good yield; further ligand exchange or other reactions could not be induced, even at elevated temperature. The IR of **11** shows bands at 1710.9 and 2155.5  $\text{cm}^{-1}$  due to the coordinated triple bond and the isocyanide ligand, respectively. The  $^{195}\text{Pt}\{^1\text{H}\}$  spectrum shows a signal at –4694 ppm as a broad doublet which is a result of coupling to one phosphine and  $^{14}\text{N}$ .

Bennett has found that TCNE reacts with bis(triphenylphosphine)platinum complexes of cyclohexyne and cycloheptyne to give the bis(triphenylphosphine)-plat-

(4) For a recent similar effect in organometallic complexes see: Seino, H.; Ishii, Y.; Hidai, M. *J. Am. Chem. Soc.* **1994**, *116*, 7433.

(5) Bennett, M. A.; Yoshida, T. *J. Am. Chem. Soc.* **1978**, *100*, 1750.

(6) Robertson, G. B.; Whimp, P. O. *J. Am. Chem. Soc.* **1975**, *97*, 1051.

(7) Odden, P. Y.; Darbon, N.; Reboul, J. P.; Cristau, B.; Soyfer, J. C.; Pepe, G. *Acta Crystallogr.* **1984**, *C40*, 524

(8) Bennett, M. A.; Rokieki, A. *Aust. J. Chem.* **1985**, *38*, 1307.

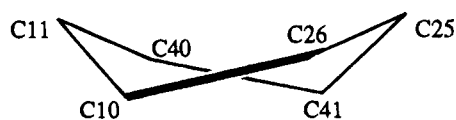
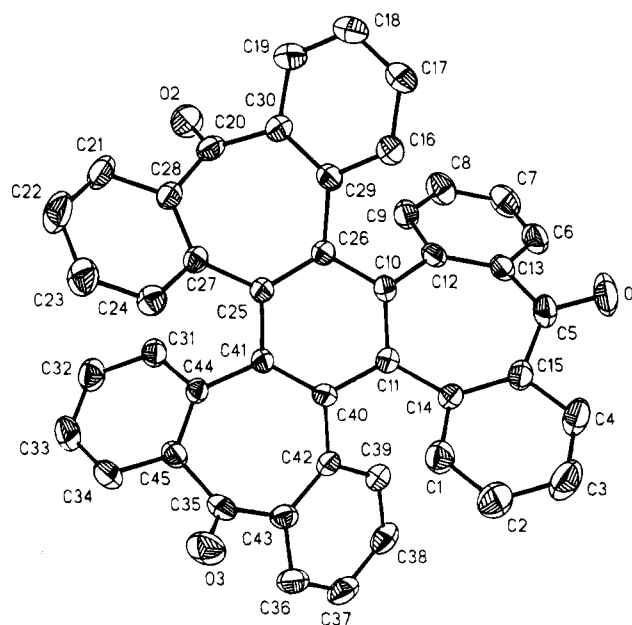
**Table 2.**  $^{195}\text{Pt}\{^1\text{H}\}$  NMR and  $^{31}\text{P}\{^1\text{H}\}$  NMR Spectroscopic Data for Platinum Complexes<sup>a</sup>

complex no.	$^{195}\text{Pt}\{^1\text{H}\}$ (ppm)	$^{31}\text{P}\{^1\text{H}\}$ (ppm)
5	-4745.2 (t, $^1J_{\text{Pt-P}} = 3391.4$ Hz)	23.73 (s)
6	-4749.6 (t, $^1J_{\text{Pt-P}} = 3418.3$ Hz)	23.75 (s)
7	-4732.4 (t, $^1J_{\text{Pt-P}} = 3385.7$ Hz)	24.42 (s)
8	-4071.8 (t, $^1J_{\text{Pt-P}} = 3137.6$ Hz)	24 (s)
9	-5101.5 (t, $^1J_{\text{Pt-P}} = 3056$ Hz)	69.29 (s)
10	-5047.9 (t, $^1J_{\text{Pt-P}} = 3010.4$ Hz)	68.03 (s)
11	-4694 (d, br, $^1J_{\text{Pt-P}} = 3196.4$ Hz)	25.99 (s)
12	-4554.3 (dd, $^1J_{\text{Pt-P1}} = 1686.2$ Hz, $^1J_{\text{Pt-P2}} = 4432.2$ Hz)	15.2 (d, $^2J_{\text{P-P}} = 15.4$ , P2), 16.77 (d, $^2J_{\text{P-P}} = 15.4$ , P1)
13	-4868 (t, $^1J_{\text{Pt-P}} = 3743$ Hz)	16.03 (s)
13a	-5257.3 (t, $^1J_{\text{Pt-P}} = 3310$ Hz)	67.2 (s)
15	-4347.3 (dd, $^1J_{\text{Pt-P1}} = 3259.4$ Hz, $^1J_{\text{Pt-P2}} = 1918.2$ Hz)	13.68 (d, $^2J_{\text{P-P}} = 20.5$ Hz), 14.57 (d, $^2J_{\text{P-P}} = 20.5$ )
16	-4060.2 (t, $^1J_{\text{Pt-P}} = 3189.2$ Hz)	19.96 (s)
20	-5257.3 (t, $^1J_{\text{Pt-P}} = 3310$ Hz)	67.2 (s)
17	-4733.4 (t, $^1J_{\text{Pt-P}} = 3366.6$ Hz)	21.95 (s, $\text{PPh}_3$ ), 34.93 (s, $\text{PCy}_2$ )
18	-4434.8 (dd, $^1J_{\text{Pt-P}} = 849$ Hz, $^1J_{\text{Pt-P2}} = 4121$ Hz)	13.96 (d, $^2J_{\text{P-P}} = 18$ Hz, P1), 15.03 (d, $^2J_{\text{P-P}} = 18$ Hz, P2)
19	-4221.5 (t, $^1J_{\text{Pt-P}} = 2863$ Hz)	19.84 (s)

<sup>a</sup> All spectra were recorded in  $\text{CD}_2\text{Cl}_2$  except for spectra of complexes 9, 11, and 13 which were measured in  $\text{C}_6\text{D}_6$ .

inum complex of TCNE and presumably, although not identified, free cycloheptyne and cyclohexyne.<sup>5</sup> It occurred to us that it might be possible to release dibenzotropynone from **5** in the same way. Indeed, treatment of a  $\text{C}_6\text{D}_6$  solution of **5** with 1 equiv of TCNE led to a rapid change in color from yellow to dark red-brown. The  $^1\text{H}$  NMR spectrum of the crude reaction mixture showed complete loss of **5**. Workup gave the TCNE adduct of bis(triphenylphosphine)platinum (essentially quantitatively) and a 45% yield of a hydrocarbon that showed spectra consistent with a very interesting substituted benzene **14**, a formal trimer of dibenzotropynone (Scheme 3). This structure was confirmed by an X-ray crystal structure analysis.

**Crystal Structure of Trimer 14.** Crystals of **14** were grown by slow evaporation of a methylene chloride/hexane solution at room temperature. The structure of **14** was solved in a triclinic space group  $P\bar{1}$  using direct methods. Thermal ellipsoid and stereographic drawings of **14** are presented in Figures 3 and 4, respectively, while crystal data are listed in Table 5. Selected bond lengths and angles and final fractional atomic coordinates are provided in Tables 3 and 7, respectively. The structure shows three dibenzotropone fragments fused to the benzene ring located in the center of the molecule. To minimize nonbonding interactions between the large dibenzotropone fragments, two of them bend in opposite directions forming dihedral angles between phenyl rings in the two fragments of 112.3 and 115.9°, respectively. The third fragment with a dihedral angle between phenyl rings of 158.2° is positioned in a unique way with one phenyl ring above and the other below the middle benzene ring. The consequence of such a spatial arrangement of these three fragments is a substantial twisted boat deformation (Figure 2) of the benzene ring in the center of the molecule. This distortion is quite severe and is comparable to other previously reported distorted benzenes. For example, the dihedral angle between planes C10–C11–C40 and C26–C25–C41, 38.4(4)°, is equal, within experimental error, to the corresponding dihedral angle in 8,9-dicarbomethoxy-[6]-*para*-cyclophane<sup>9</sup> (38.9°) but is less than the most highly distorted ring reported to date, perchlorotriphenylene,<sup>10</sup> which has a dihedral angle of 54.1°. Other more severely distorted benzenes

**Figure 2.****Figure 3.** Structure and labeling scheme for **14** with 40% probability of thermal ellipsoids.

include tetramethyl-[6](9,10)anthracenophane<sup>11</sup> (49.3° dihedral) and [6](1,4)anthracenophane<sup>12</sup> (42° dihedral). Theoretical work on deformed benzenes has also recently appeared.<sup>13</sup> There is a slight bond alternation (0.03 Å) in the middle benzene ring of **14**, presumably as a result of a distortion. In perchlorotriphenylene this value is larger (0.06 Å), which is consistent with more severe distortion in this molecule.<sup>14</sup>

The trimer **14** exhibits approximately  $\text{C}_2$  geometry in the solid state. If this structure is maintained in solution, however, it must undergo a rapid conformational equilibrium because the  $^1\text{H}$  NMR clearly shows only 4 different kinds of aromatic hydrogens (if **14** were not equilibrating it should show 12) and the  $^{13}\text{C}$  NMR

(11) Tobe, Y.; Ishii, H.; Saiki, S.; Kakiuchi, K.; Naemura, K. *J. Am. Chem. Soc.* **1993**, *115*, 11604.

(12) Bickelhaupt, F. *Pure Appl. Chem.* **1990**, *62*, 373.

(13) Tsuzuki, S.; Tanabe, K. *J. Chem. Soc., Perkin Trans. 2*, **1990**, 1687.

(9) Krieger, C.; Liebe, J.; Tochtermann, W. T. *Tetrahedron Lett.* **1983**, *24*, 707.

(10) Shibata, K.; Kulkarni, A. A.; Ho, D. M.; Pascal, R. A., Jr. *J. Am. Chem. Soc.* **1994**, *116*, 5983.

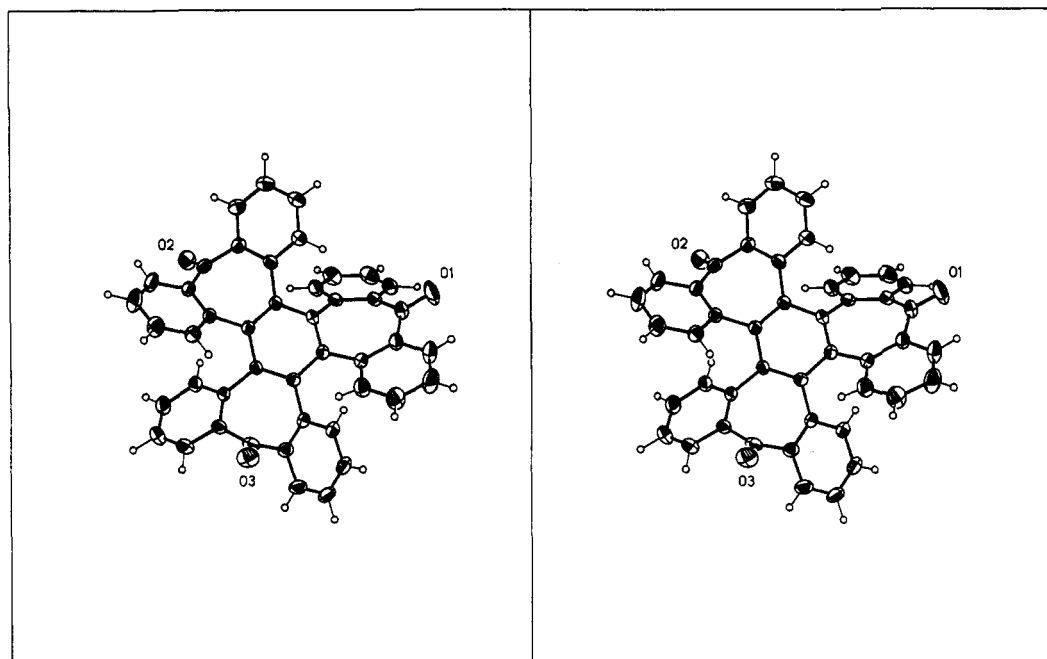
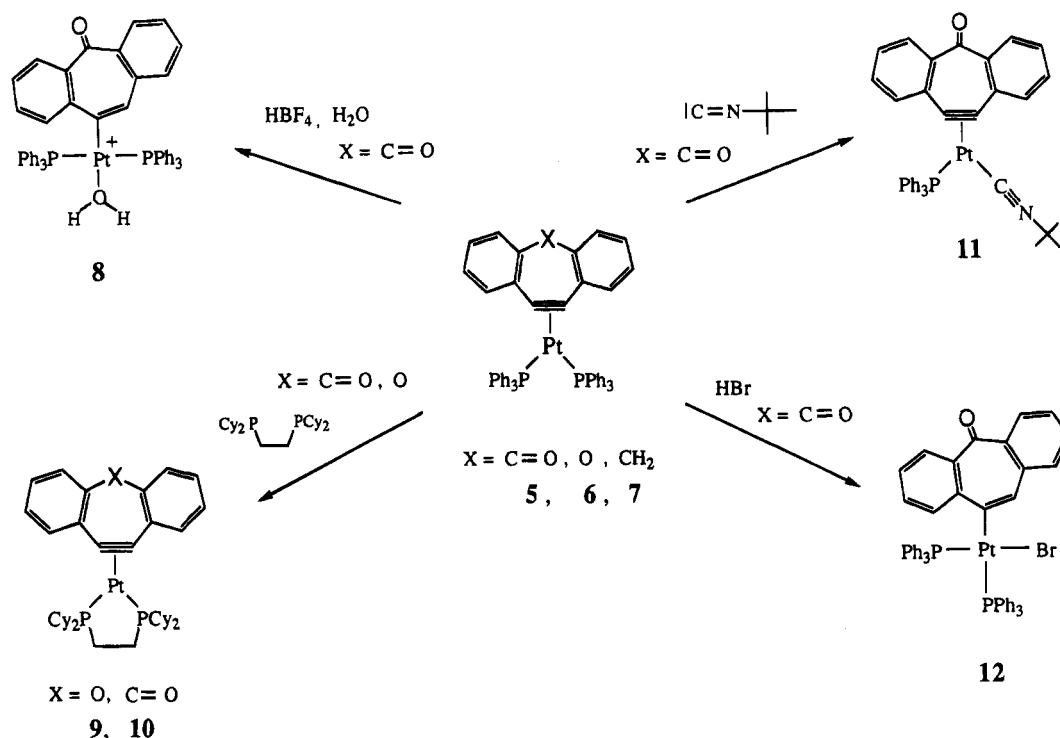


Figure 4. Stereoview of compound 14.

## Scheme 2



spectrum shows only 8 kinds of carbon while nonequilibrating 14 should show 23. Furthermore, if it has  $C_2$  symmetry in solution, the inversion barrier must be quite low since the  $^1\text{H}$  NMR spectrum at  $-80^\circ\text{C}$  ( $\text{C}_6\text{D}_5\text{-CD}_3$ ) showed no significant broadening.

**Synthesis and Structure of Complex 15.** To test the generality of the trimerization reaction other alkyne complexes were subjected to reaction with TCNE. Complex 11, when treated with TCNE in  $\text{C}_6\text{D}_6$ , gave trimer 14 in yields comparable to those of complex 5 together with two unidentified platinum products which were detected in the  $^{31}\text{P}\{^1\text{H}\}$  NMR. When the same reaction was carried out with complex 10, a mixture of organic products containing only about 5–10% (by  $^1\text{H}$  NMR) 14 was formed.  $[(\text{Cy}_2\text{PCH}_2)_2\text{Pt}(\text{TCNE})]$  (13a) was

formed quantitatively in this reaction. The reason for this difference in behavior is not clear.

Treatment of 6 with TCNE (Scheme 3) led to an interesting product. In addition to 10% of the TCNE complex of bis(triphenylphosphine)platinum ( $^{31}\text{P}\{^1\text{H}\}$  NMR), 6 gave the coupling product 15 (55% yield isolated); this type of reaction is quite unusual for platinum alkyne complexes.<sup>15</sup> The initial structural assignment to 15 was based on elemental analysis and multinuclear NMR. The  $^1\text{H}$  NMR of this material

(14) For other examples of benzene rings with significant bond alternation see: Boese, R.; Blaser, D.; Billups, E. W.; Haley, M. M.; Maulitz, A. H.; Mohler, D. L.; Vollhardt, K. P. C. *Angew. Chem., Int. Ed. Engl.* 1994, 33, 313, and references therein.

(15) Moseley, K.; Maitlis, M. P. *J. Chem. Soc., Dalton Trans.* 1974, 169.

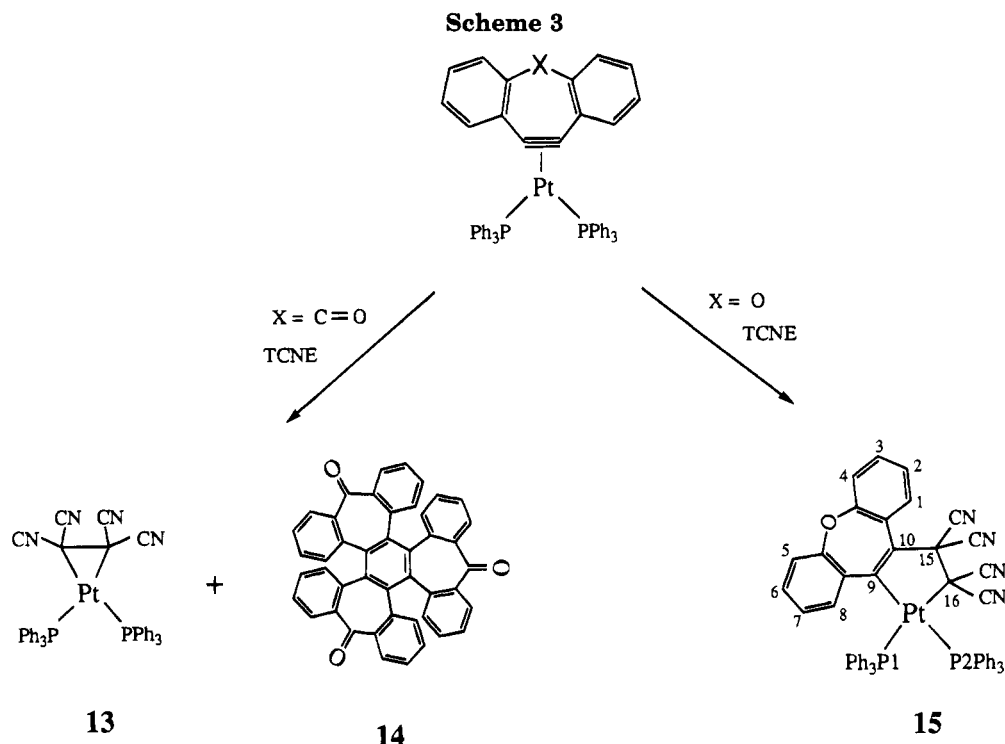


**Table 3. Selected Bond Lengths (Å) and Angles (deg) for Compound 14**

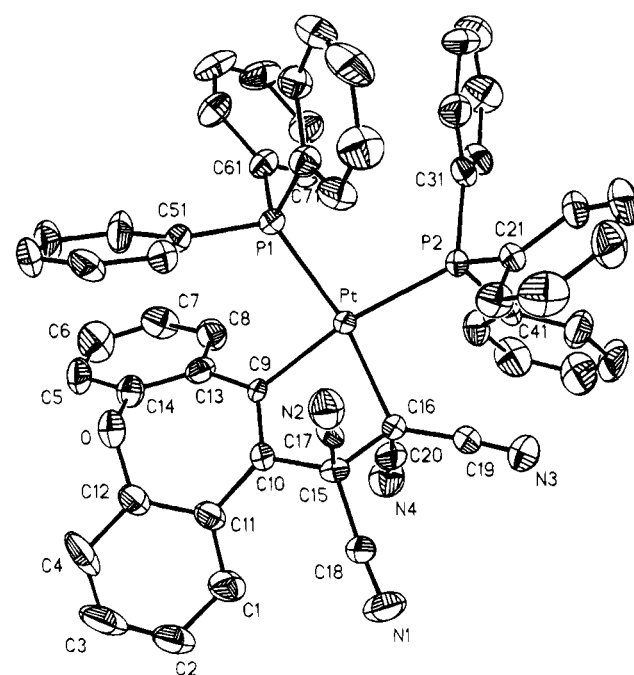
Bond Lengths (Å)			
C11–C10	1.404(5)	C30–C20	1.491(5)
C26–C10	1.433(4)	C27–C25	1.487(3)
C26–C25	1.398(4)	C29–C26	1.489(5)
C41–C25	1.424(5)	C43–C35	1.488(3)
C41–C40	1.394(4)	C42–C40	1.490(5)
C40–C11	1.430(5)	C44–C41	1.494(5)
C14–C11	1.490(5)	C12–C13	1.405(4)
C12–C10	1.488(4)	C14–C15	1.418(5)
C5–O1	1.224(5)	C27–C28	1.397(5)
C20–O2	1.210(5)	C29–C30	1.404(5)
C35–O3	1.214(4)	C42–C43	1.402(5)
C13–C5	1.482(6)	C44–C45	1.403(5)
C28–C20	1.492(5)		

Bond Angles (deg)			
C25–C41–C40	119.0(3)	C28–C20–C30	114.3(3)
C26–C10–C11	117.6(3)	C30–C20–O2	122.7(3)
C41–C40–C11	119.5(3)	C27–C25–C41	118.5(3)
C41–C25–C26	118.4(2)	C29–C26–C10	117.2(3)
C10–C26–C25	119.1(3)	C43–C35–C45	113.8(3)
C40–C11–C10	116.3(3)	C42–C40–C11	118.1(3)
C14–C11–C40	120.6(3)	C44–C41–C40	123.4(3)
C12–C10–C26	119.9(3)	C43–C35–O3	122.3(3)
C13–C5–C15	124.5(3)	C45–C35–O3	123.2(3)
C13–C5–O1	116.9(4)	C28–C20–O2	122.1(3)
C15–C5–O1	118.6(4)	C41–C40–C42	121.7(3)
C29–C26–C25	123.4(2)	C26–C25–C27	123.1(3)
C28–C20–C30	114.3(3)	C11–C10–C12	121.2(2)

showed eight different protons belonging to the ligand. In the  $^{31}\text{P}\{^1\text{H}\}$  NMR, two phosphorus nuclei (P1 and P2) were observed as nonequivalent doublets at 13.7 and 14.6 ppm, respectively ( $^2J_{\text{P1-P2}} = 20.5$  Hz). The  $^{195}\text{Pt}\{^1\text{H}\}$  NMR exhibited a doublet of doublets centered at  $-4347.3$  ppm with two different coupling constants to P1 ( $^1J_{\text{Pt-P1}} = 3259.4$  Hz) and P2 ( $^1J_{\text{Pt-P2}} = 1918.2$  Hz). This difference in coupling constants is presumably due to a stronger trans influence on P2 than on P1.

Crystals of complex **15** were obtained by slow evaporation of a methylene chloride/hexane solution. Complex **15** crystallizes in monoclinic space group  $Ia$  together with one molecule of methylene chloride solvent. The thermal ellipsoid drawing of the structure is shown in Figure 5, while crystal data are listed in Table 5.



**Figure 5.** Structure and labeling scheme for **15** with 40% probability of thermal ellipsoids.

Selected bond lengths and angles and final fractional atomic coordinates are provided in Tables 4 and 8, respectively. Complex **15** can be viewed as a platinumacyclopent-2-ene with platinum bonded to two phosphorus and two carbon atoms. The Pt–P1 bond [2.305(3) Å] is shorter than Pt–P2 [2.370(3) Å] as expected from two different  $^{195}\text{Pt}$ – $^{31}\text{P}$  coupling constants. Correlation between bond distances of Pt–P and  $^{195}\text{Pt}$ – $^{31}\text{P}$  coupling constants is well established.<sup>16</sup> The Pt–C9 bond [2.090(9) Å] is shorter than Pt–C16 [2.161(9) Å], a difference which is attributed to the different hybridization of the two carbons bonded to the platinum atom. From this data it is clear that C9 ( $\text{sp}^2$ ) exerts a stronger trans influence than does C16 ( $\text{sp}^3$ ). The Pt–C9 and Pt–C16 bond lengths are equal within experimental error to the

**Table 4. Selected Bond Lengths (Å) and Angles (deg) for Complex 15**

Bond Lengths (Å)			
Pt-P1	2.305(3)	C18-N1	1.10(2)
Pt-P2	2.370(3)	C17-N2	1.11(2)
Pt-C9	2.090(9)	C19-N3	1.14(2)
Pt-C16	2.161(9)	C20-N4	1.14(2)
P1-C51	1.825(11)	C10-C9	1.327(14)
P1-C61	1.833(12)	C13-C9	1.474(15)
P1-C71	1.833(11)	C11-C10	1.475(14)
P2-C21	1.796(11)	C16-C15	1.609(14)
P2-C31	1.831(11)	C17-C15	1.51(2)
P2-C41	1.828(11)	C18-C15	1.51(2)
C12-O	1.375(14)	C19-C16	1.465(14)
C14-O	1.42(2)	C20-C16	1.46(2)
Bond Angles (deg)			
P1-Pt-P2	97.50(11)	C16-C15-C18	108.7(8)
P2-Pt-C16	93.2(3)	C16-C15-C10	104.7(8)
P2-Pt-C9	168.2(2)	C12-O-C14	108.5(9)
P1-Pt-C16	165.0(3)	C17-C15-C18	106.6(9)
C9-Pt-C16	77.0(3)	C17-C15-C10	109.2(8)
Pt-C16-C15	98.7(6)	C18-C15-C10	118.6(8)
C10-C9-Pt	117.0(7)	C19-C16-C20	108.2(9)
C10-C9-C13	121.1(9)	C19-C16-Pt	121.7(7)
C13-C9-Pt	121.4(7)	N2-C17-C15	177.4(12)
C11-C10-C15	120.7(9)	N1-C18-C15	174.4(13)
C11-C10-C9	127.4(9)	N3-C19-C16	175.3(13)
C16-C15-C17	108.7(8)	N4-C20-C16	178.0(14)

corresponding bond distances observed in Pt(cyclohexenyl)(CH<sub>2</sub>COC<sub>6</sub>H<sub>5</sub>)(diphos) [Pt-C(sp<sup>2</sup>) = 2.068(10) Å, Pt-C(sp<sup>3</sup>) = 2.175(10) Å].<sup>17</sup> Complex 15 has a distorted square planar geometry around the Pt atom with the dihedral angle between the planes defined by Pt, P1, P2 and Pt, C9, C16 equal to 12.5(3)°. The dihedral angle between the phenyl ring planes of the dibenzoxepin ligand [109.6(4)°] is much smaller than that of free dibenzoxepin<sup>18</sup> [134(2)°]. The most pronounced feature of the structure of 15 is the presence of a platinacyclopent-2-ene ring which has a geometry of a half-chair. The atoms Pt, C9, C10, and C15 are coplanar (maximum deviation from the least squares plane is 0.016 Å for C10) while C16 lies 0.97 Å below the plane. The dihedral angle between the Pt-C9-C10-C15 and the Pt-C16-C15 plane is 54.7(6)°. Such distortions from planarity are a common feature of metallacyclopent-2-enes.<sup>19</sup> This distortion, however, is significantly larger in 15 than in any other metallacyclopent-2-enes known for which crystal structure data are available.<sup>20</sup> It is not clear why 5 and 6 react differently with TCNE.

**Preparation of Dibenzotropyne 16.** The platinum complex of tropyne (1) was prepared by hydride abstraction from the corresponding cycloheptadienyne complex. The dibenzannelated analogue (7) behaved similarly. Treatment of 7 with triphenylcarbenium tetrafluoroborate in methylene chloride at -78 °C, followed by warming to room temperature, gave a deep blue solution. Addition of diethyl ether gave 16 as deep blue-

black needles (Scheme 4). Complex 16 was characterized by <sup>1</sup>H, <sup>13</sup>C, <sup>19</sup>F, <sup>31</sup>P, and <sup>195</sup>Pt NMR, HRMS, and elemental analysis. In the <sup>1</sup>H NMR all protons belonging to the ligand are deshielded relative to 7. The electronic structure of 16 is somewhat different from that of 1 in that the positive charge in 16 resides to a greater extent on the ligand. This is best shown by the <sup>1</sup>H and <sup>195</sup>Pt{<sup>1</sup>H} NMR. The chemical shift of H5 in 16 is the same (10.45 ppm) as that of the corresponding proton in the dibenzotropylium ion.<sup>21</sup> However, the same proton in complex 1 (8.64 ppm) shows a significant upfield shift when compared to the tropylium ion (9.55 ppm).<sup>1</sup> Similarly, the chemical shift in the <sup>195</sup>Pt{<sup>1</sup>H} NMR of 16 is 280 ppm upfield relative to 1. Both of these differences are expected if the platinum atom more effectively delocalizes the positive charge in 1 than in 16.

**Reactivity of Platinum Tropyne Complex 16.** Tropyne complexes of platinum have two reaction sites, one on the ring which is susceptible to nucleophilic attack and the other on the metal center where electrophilic attack would be expected. Examples of these two reaction types for 16 are shown in Scheme 4. Reaction with KBET<sub>3</sub>H is rapid and gives 7 in 70% yield (<sup>1</sup>H and <sup>31</sup>P{<sup>1</sup>H} NMR). Three minor phosphorus-containing platinum products were formed in this reaction as shown by <sup>31</sup>P{<sup>1</sup>H} NMR, but they were not characterized. The bidentate phosphine bis(dicyclohexylphosphino)ethane also reacts rapidly (within seconds) with 16 to form the bis(alkyne) complex 17. The <sup>31</sup>P{<sup>1</sup>H} NMR of this material exhibits two peaks, one centered at 21.95 ppm (PPh<sub>3</sub>, <sup>195</sup>Pt satellites) and the other at 34.93 ppm (PCy<sub>2</sub>). The ratio of cyclohexyl to phenyl protons in the <sup>1</sup>H NMR is consistent with the stoichiometry of complex 17. This reaction parallels the reaction of metal η<sup>7</sup>-tropylium complexes with diphosphines.<sup>22</sup> Addition of HBr in acetic acid to a THF solution of 16 led to a rapid color change from deep blue to purple. Addition of ether gave 18 as a purple precipitate. The <sup>31</sup>P{<sup>1</sup>H} NMR of 18 showed only two doublets with <sup>195</sup>Pt satellites corresponding to the *cis*-isomer. Upon standing, this slowly isomerized to the *trans*-isomer (ca. 70% conversion within 4 weeks at room temperature in CD<sub>2</sub>Cl<sub>2</sub>). The same type of products was obtained from reaction of 1 with HBr and HCl.<sup>1</sup>

## Experimental Section

**General Considerations.** All experiments involving organometallic compounds were carried out under an atmosphere of purified N<sub>2</sub> using Schlenk, vacuum line, and drybox techniques. Solvents were distilled under nitrogen prior to use: toluene, THF, and Et<sub>2</sub>O from sodium benzophenone ketyl; hexane from sodium benzophenone ketyl/tetraglyme mixture; methylene chloride from CaH<sub>2</sub>. NMR spectra were measured on a Varian XL-300 (FT 300 MHz, <sup>1</sup>H; 75 MHz, <sup>13</sup>C; 282 MHz, <sup>19</sup>F; 121 MHz, <sup>31</sup>P; 64 MHz, <sup>195</sup>Pt). <sup>1</sup>H NMR and <sup>13</sup>C{<sup>1</sup>H} NMR spectra were referenced to residual solvent peaks and are reported in ppm relative to tetramethylsilane. <sup>19</sup>F NMR spectra were referenced to external CFCl<sub>3</sub>. <sup>31</sup>P{<sup>1</sup>H} NMR spectra were referenced to external 85% H<sub>3</sub>PO<sub>4</sub> in D<sub>2</sub>O. <sup>195</sup>Pt{<sup>1</sup>H} NMR spectra were referenced to an external saturated solution of Na<sub>2</sub>PtCl<sub>6</sub> in D<sub>2</sub>O. Infrared spectra were measured in KBr pellets on a Perkin-Elmer 1600 FTIR spectrometer.

(21) Cecon, A.; Gambaro, A. R.; Venzo, A. *Angew. Chem., Int. Ed. Engl.* **1983**, *22*, 559.

(22) Brown, D. A.; Burns, J.; Glass, W. K.; Cunningham, D.; Higgins, T.; McArdle, P.; Salama, M. *Organometallics* **1994**, *13*, 2662.

(16) (a) Pregosin, P. S.; Kunz, R. W. *<sup>31</sup>P and <sup>31</sup>C NMR of Transition Metal Phosphine Complexes*; Springer-Verlag: Berlin, 1979; p 25. (b) Yamamoto, A. *Oganotransition Metal Chemistry, Fundamental Concepts and Applications*; Wiley-Interscience: New York, 1986; p 180.

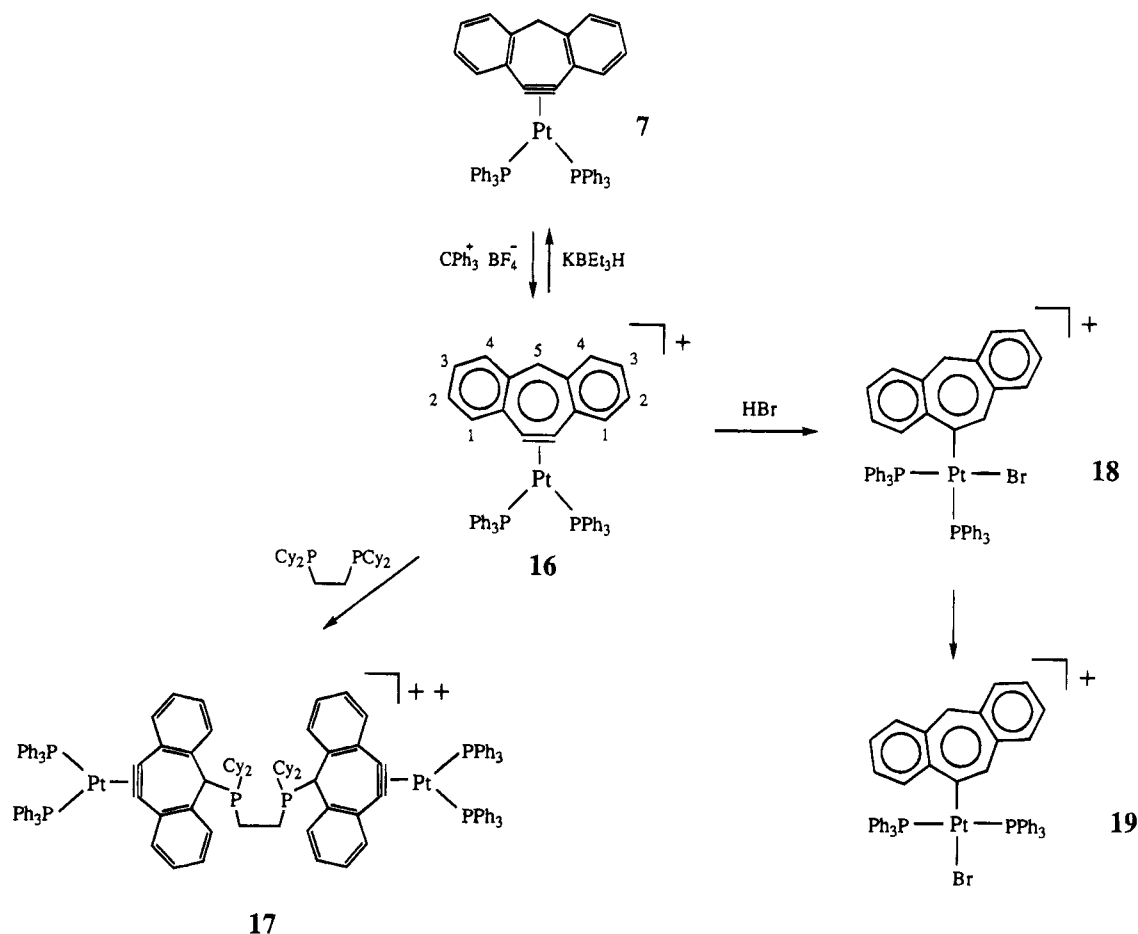
(17) Bennett, M. A.; Robertson, B. G.; Whimp, O. P.; Yoshida, T. *J. Am. Chem. Soc.* **1973**, *95*, 3028.

(18) Drake, J. A. G.; Jones, D. W. *Acta Crystallogr.* **1982**, *B38*, 200.

(19) (a) Wakatsuki, Y.; Aoki, K.; Yamazaki, H. *J. Am. Chem. Soc.* **1979**, *101*, 1123. (b) Bhide, V. V.; Faron, F. M.; Djebli, W. J.; Youngs, W. J. *Organometallics* **1990**, *9*, 1766. (c) Erker, G.; Korek, U.; Petrenz, R.; Rheingold, A. L. *J. Organomet. Chem.* **1991**, *421*, 215. (d) Bennett, M. A.; Hambley, T. W.; Roberts, N. K.; Robertson, G. B. *Organometallics* **1985**, *4*, 1992. (e) Erker, G.; Dorf, U.; Rheingold, A. L. *Organometallics* **1988**, *7*, 138.

(20) Cambridge Data Base.

Scheme 4



Mass spectra (positive FAB) were obtained on a Finnigan Mat 95Q. Elemental analyses were performed in the microanalysis lab in the Chemistry Department at the University of Florida. Melting points were measured in open capillaries and are not corrected. Potassium *tert*-butoxide, tetrafluoroboric acid, hydrogen bromide (30 wt % solution in acetic acid), potassium triethylborohydride (1.0 M solution in THF), tetracyanoethylene, *tert*-butyl isocyanide, and triphenylcarbenium tetrafluoroborate were purchased from Aldrich Chemical Co., and 1,2-bis(dicyclohexylphosphino)ethane was purchased from Strem Chemicals. All compounds were used as received. The following compounds were prepared as described in the literature without any modification:  $\text{Pt}(\text{PPh}_3)_3$ ,<sup>23</sup> 10-bromodibenzosuberone,<sup>24</sup> 10,11-dibromodibenzooxepin,<sup>25</sup> 10,11-dibromodibenzocycloheptene.<sup>26</sup>

**(10,11-Didehydrodibenzotropone)bis(triphenylphosphine)platinum- $\text{C}_6\text{H}_5\text{CH}_3$  (5).**  $\text{Pt}(\text{PPh}_3)_3$  (0.3 g, 0.306 mmol) and  $\text{K-O}^t\text{Bu}$  (0.068 g, 0.612 mmol) were dissolved in 10 mL of THF. To this solution was added very slowly 10-bromodibenzosuberone (0.142 g, 0.5 mmol) in 2 mL of THF at room temperature. After stirring of the mixture for 1 h, the solvent was evaporated and the residue was extracted with 5–10 mL of toluene. To this mixture was added 3 mL of hexane, and the yellow solution was filtered. To the filtrate was added 30 mL of hexane, and the Schlenk tube was put aside in the refrigerator for 4 days to give 200 mg yellow crystals (65%). The compound crystallizes as a toluene solvate. Mp: 225 °C dec. IR (KBr): 1708, 1622, 1585.8, 1479, 1434.6, 1303.9, 1092.6, 754.4, 695.7  $\text{cm}^{-1}$ .  $^1\text{H}$  NMR ( $\text{CD}_2\text{Cl}_2$ ):  $\delta$  8.22 (d, 2H,  $^3J_{\text{H}_4-\text{H}_3} = 7.9$  Hz, H4), 7.62 (m, 12H, *PPh*<sub>3</sub>, ortho), 7.26

(m, 25H), 7.02 (td, 2H,  $^3J_{\text{H}_2-\text{H}_{1,3}} = 7.9$  Hz,  $^4J_{\text{H}_2-\text{H}_4} = 1.44$  Hz, H2), 6.43 (d, 2H,  $^3J_{\text{H}_1-\text{H}_2} = 7.9$  Hz, H1).  $^{13}\text{C}\{^1\text{H}\}$  NMR ( $\text{CD}_2\text{Cl}_2$ ):  $\delta$  195.66, 140.33 (t,  $J_{\text{C}-\text{P}} = 3.56$  Hz,  $J_{\text{C}-\text{Pt}} = 44.01$  Hz), 136.39 (vd,  $^1J_{\text{C}-\text{P}} = 49.34$  Hz, *PPh*<sub>3</sub>, ipso), 134.56 (m, *PPh*<sub>3</sub>, ortho), 132.43 (dd,  $^2J_{\text{C}-\text{P}_{\text{cis}}} = 8.23$  Hz,  $^2J_{\text{C}-\text{P}_{\text{trans}}} = 84.56$  Hz), 131.55, 130.86, 130.69 (t, 20.7 Hz), 130.41, 129.92 (s, *PPh*<sub>3</sub>, para), 128.44 (t,  $^3J_{\text{C}-\text{P}} = 4.62$  Hz, *PPh*<sub>3</sub>, meta), 127.01. HRMS (FAB) (*m/e*): calcd for (*M* + 1)<sup>+</sup>, 924.2124, found, 924.2114. Anal. Calcd for  $\text{C}_{58}\text{H}_{46}\text{OP}_2\text{Pt}$ : C, 68.54; H, 4.56. Found: C, 68.54; H, 4.65.

**(10,11-Didehydrodibenzooxepin)bis(triphenylphosphine)platinum (6).**  $\text{Pt}(\text{PPh}_3)_3$  (0.5 g, 0.51 mmol) and  $\text{K-O}^t\text{Bu}$  (0.252 g, 0.225 mmol) were dissolved in 15 mL of THF. To this solution was added very slowly 10,11-dibromodibenzooxepin (0.318 g, 0.9 mmol) in 3 mL of THF at room temperature. After stirring of the mixture for 4 h, the solvent was evaporated and the residue was extracted with 20 mL of toluene and 30 mL of hexane was added causing quick precipitation of **17** containing 15% of starting material. This solid was recrystallized from a mixture of toluene and hexane to give 286 mg of analytically pure yellow crystals (61.6%). Mp: 223–225 °C dec. IR (KBr): 3052.2 w, 1691.5, 1586.6 w, 1478.4, 1434.9, 1195.1, 1094, 777, 742.8, 693.6, 536.8, 519.3  $\text{cm}^{-1}$ .  $^1\text{H}$  NMR ( $\text{CD}_2\text{Cl}_2$ ):  $\delta$  7.48 (m, 12H, *PPh*<sub>3</sub>, ortho), 7.2 (m, 18H, *PPh*<sub>3</sub>), 7.05 (td, 2H,  $^3J_{\text{H}_3-\text{H}_{4,2}} = 7.6$  Hz,  $^4J_{\text{H}_3-\text{H}_1} = 1.6$  Hz, H3), 6.54 (td, 2H,  $^3J_{\text{H}_2-\text{H}_{3,1}} = 7.4$  Hz,  $^4J_{\text{H}_2-\text{H}_4} = 1.5$  Hz, H2), 6.43 (dd, 2H,  $^3J_{\text{H}_1-\text{H}_2} = 7.6$  Hz,  $^4J_{\text{H}_1-\text{H}_3} = 1.4$  Hz, H1).  $^{13}\text{C}\{^1\text{H}\}$  NMR ( $\text{CD}_2\text{Cl}_2$ ):  $\delta$  155.2 (t,  $J_{\text{C}-\text{P}} = 2.7$  Hz,  $J_{\text{C}-\text{Pt}} = 37.94$  Hz), 136.64 (vd,  $^1J_{\text{C}-\text{P}} = 46.79$  Hz, *PPh*<sub>3</sub>, ipso), 134.43 ( $^2J_{\text{C}-\text{P}} = 6.5$  Hz, *PPh*<sub>3</sub>, ortho), 133.39 (dd,  $^2J_{\text{C}-\text{P}_{\text{cis}}} = 8.01$  Hz,  $^2J_{\text{C}-\text{P}_{\text{trans}}} = 86.9$  Hz), 129.78 (s, *PPh*<sub>3</sub>, para), 128.59, 128.44, 128.27 (t,  $^3J_{\text{P}-\text{C}} = 4.6$  Hz, *PPh*<sub>3</sub>, meta), 127.44 (t, 10.35 Hz), 124.8, 121.16. HRMS (FAB) (*m/e*): calcd for (*M* + 1)<sup>+</sup>, 912.2124; found, 912.2103. Anal. Calcd for  $\text{C}_{50}\text{H}_{38}\text{OP}_2\text{Pt}$ : C, 65.86; H, 4.2. Found: C, 66.05; H, 4.21.

**(10,11-Didehydrodibenzocycloheptene)bis(triphenyl-**

(23) Ugo, R.; Cariati, F.; La Monica, G. *Inorg. Chem.* **1968**, *7*, 105.(24) Treibs, W. *Chem. Ber.* **1951**, *84*, 671.(25) Tochtermann, W.; Oppenlander, K.; Nguyen-Duong Hoang, M. *Liebigs. Ann. Chem.* **1967**, *701*, 117.(26) Bellucci, G.; Bianchini, R.; Chiappe, C.; Marioni, F. *Tetrahedron* **1988**, *44*, 4863.

Table 5. Crystallographic Data

	5	14	15
A. Crystal Data (298 K)			
<i>a</i> , Å	11.221(2)	11.274(2)	17.175(3)
<i>b</i> , Å	14.318(2)	11.826(1)	15.411(2)
<i>c</i> , Å	16.621(4)	13.474(2)	18.661(2)
$\alpha$ , deg	74.22(2)	111.79(1)	90
$\beta$ , deg	78.86(2)	106.34(1)	91.86(1)
$\gamma$ , deg	73.56(2)	98.54(1)	90
<i>V</i> , Å <sup>3</sup>	2445.0(9)	1534.9(4)	4937(1)
<i>d</i> <sub>calc</sub> , g cm <sup>-3</sup> (298 K)	1.380	1.326	1.520
empirical formula	C <sub>51</sub> H <sub>38</sub> OP <sub>2</sub> Pt·C <sub>7</sub> H <sub>8</sub>	C <sub>45</sub> H <sub>24</sub> O <sub>3</sub>	C <sub>56</sub> H <sub>38</sub> N <sub>4</sub> OP <sub>2</sub> Pt·CH <sub>2</sub> Cl <sub>2</sub>
fw	1015.98	612.64	1124.86
cryst system	triclinic	triclinic	monoclinic
space group	<i>P</i> $\bar{1}$	<i>P</i> $\bar{1}$	<i>Ia</i>
<i>Z</i>	2	2	4
<i>F</i> (000), electrons	1020	636	2240
cryst size, mm <sup>3</sup>	0.63 × 0.30 × 0.06	0.42 × 0.38 × 0.34	0.61 × 0.19 × 0.11
B. Data Collection (298 K)			
radiation ( $\lambda$ , Å)		Mo K $\alpha$ (0.710 73)	
mode		$\omega$ -scan	
scan range		symmetrically over 1.2° about K $\alpha_{1,2}$ maximum	
background		offset 1.0 and -1.0 in $\omega$ from K $\alpha_{1,2}$ maximum	
scan rate, deg min <sup>-1</sup>	4-8	3-6	3-6
2 $\theta$ range, deg	3-55	3-50	3-58
range of <i>hkl</i>	0 ≤ <i>h</i> ≤ 13 -16 ≤ <i>k</i> ≤ 16 -19 ≤ <i>l</i> ≤ 19	0 ≤ <i>h</i> ≤ 14 -15 ≤ <i>k</i> ≤ 15 -17 ≤ <i>l</i> ≤ 17	0 ≤ <i>h</i> ≤ 24 0 ≤ <i>k</i> ≤ 22 -26 ≤ <i>l</i> ≤ 26
tot. reflns measd	9103	5695	6853
unique reflns	8619	5394	6625
abs coeff $\mu$ (Mo K $\alpha$ ), mm <sup>-1</sup>	2.97	0.08	3.07
C. Structure Refinement			
<i>S</i> , goodness-of-fit	1.8940	1.6522	1.4121
reflens used	6230, <i>I</i> > 3 $\sigma$ ( <i>I</i> )	3722, <i>I</i> > 2 $\sigma$ ( <i>I</i> )	5569, <i>I</i> > 2 $\sigma$ ( <i>I</i> )
no. of variables	554	529	587
<i>R</i> , w <i>R</i> , <sup>a</sup> (%)	5.79, 6.75	6.17, 6.13	4.74, 4.76
<i>R</i> <sub>int</sub> , %	0.000	0.0352	0.000
max shift/esd	0.009	0.001	0.002
min peak in diff Fourier map, e Å <sup>-3</sup>	-1.9	-0.2	-1.6
max peak in diff Fourier map, e Å <sup>-3</sup>	1.2	0.3	1.8

<sup>a</sup> Relevant expressions are as follows, where in the footnote *F*<sub>o</sub> and *F*<sub>c</sub> represent, respectively, the observed and calculated structure-factor amplitudes. Function minimized was  $w(|F_o| - |F_c|)^2$ , where  $w = (\sigma(F))^2$ .  $R = \sum(|F_o| - |F_c|)/\sum|F_o|$ ;  $wR = [\sum w(|F_o| - |F_c|)^2/\sum|F_o|^2]^{1/2}$ ;  $S = [\sum w(|F_o| - |F_c|)^2/(m - n)]^{1/2}$ .

**ylphosphine)platinum (7).** To a solution of Pt(PPh<sub>3</sub>)<sub>3</sub> (0.45 g, 0.458 mmol) and K-O<sup>t</sup>Bu (228 mg, 2 mmol) in 15 mL of THF was added very slowly (1 h) 10,11-dibromodibenzocycloheptene (285 mg, 0.81 mmol) in 3 mL of THF at room temperature. After stirring of the mixture for 2 h, the solvent was removed and the residue was extracted with 5–10 mL of toluene. To this filtrate was added hexane, and the Schlenk tube was cooled to -26 °C to give 280 mg (67%) of **7** as an off-white solid. An analytically pure sample was obtained by recrystallization from a mixture of toluene and hexane. Mp: 219–222 °C dec. IR (KBr): 3051.2 w, 1688.7, 1586.7 w, 1477.8, 1434.3, 1092.8, 751.5, 693.2, 540.1, 519, 496.8 cm<sup>-1</sup>. <sup>1</sup>H NMR (CD<sub>2</sub>Cl<sub>2</sub>):  $\delta$  7.5 (m, 12H, PPh<sub>3</sub>), 7.31 (d, 2H, <sup>3</sup>J<sub>H4-H3</sub> = 7.3 Hz, H4), 7.23 (m, 18H, PPh<sub>3</sub>), 7.08 (td, 2H, <sup>3</sup>J<sub>H3-H4,2</sub> = 7.4 Hz, <sup>4</sup>J<sub>H3-H1</sub> = 1.3 Hz, H3), 6.65 (td, 2H, <sup>3</sup>J<sub>H2-H3,1</sub> = 7.5 Hz, <sup>4</sup>J<sub>H2-H4</sub> = 1.2 Hz, H2), 6.43 (dd, 2H, <sup>3</sup>J<sub>H1-H2</sub> = 7.6 Hz, <sup>4</sup>J<sub>H1-H3</sub> = 1.2 Hz, H1), 3.85 (s, 2H, CH<sub>2</sub>). <sup>13</sup>C{<sup>1</sup>H} NMR (CD<sub>2</sub>Cl<sub>2</sub>):  $\delta$  134.4 (m), 134.65 (m, PPh<sub>3</sub>), 132.62 (t, J<sub>C-P</sub> = 9.5 Hz), 129.78 (s, PPh<sub>3</sub>), 128.53, 128.31 (m, PPh<sub>3</sub>), 127.52 (s, J<sub>C-Pt</sub> = 25.35 Hz), 126.92, 126.27, 44.08. HRMS (FAB) (*m/e*): calcd for (M + 1)<sup>+</sup>, 910.2332; found, 910.2323. Anal. Calcd for C<sub>51</sub>H<sub>40</sub>P<sub>2</sub>Pt: C, 67.32; H, 4.43. Found: C, 67.36; H, 4.55.

**Preparation of Complex 8.** To a Schlenk tube containing 120 mg of **5** (0.12 mmol) in 10 mL of CH<sub>2</sub>Cl<sub>2</sub>, 22.5 mg of HBF<sub>4</sub> (0.118 mmol) in 2 mL of CH<sub>2</sub>Cl<sub>2</sub> was added slowly at -78 °C. After slow warming of the solution to room temperature, hexane was added and the Schlenk tube was placed in a refrigerator for a few days. Solvent removal gave 105 mg of **8** (86%). IR (KBr): 3050 w, 1637, 1596, 1572, 1482, 1437, 1313, 1098, 745, 693, 523 cm<sup>-1</sup>. <sup>1</sup>H NMR (CD<sub>2</sub>Cl<sub>2</sub>):  $\delta$  9.0 (dd, 1H, <sup>3</sup>J<sub>H-H</sub> = 7.8 Hz, <sup>4</sup>J<sub>H-H</sub> = 1 Hz), 7.77 (dd, 1H, <sup>3</sup>J<sub>H-H</sub> = 7.1 Hz, <sup>4</sup>J<sub>H-H</sub> = 2.1 Hz), 7.56 (dd, 1H, <sup>3</sup>J<sub>H-H</sub> = 7.8 Hz, <sup>4</sup>J<sub>H-H</sub> = 1.5 Hz),

7.2–7.5 (m, 33H, PPh<sub>3</sub>) 7.15 (td, 1H, <sup>3</sup>J<sub>H-H</sub> = 7.3 Hz, <sup>4</sup>J<sub>H-H</sub> = 1.2 Hz), 7.03 (s, 1H, <sup>3</sup>J<sub>H-Pt</sub> = 99.7 Hz), 6.43 (dd, 1H, <sup>3</sup>J<sub>H-H</sub> = 7.1 Hz, <sup>4</sup>J<sub>H-H</sub> = 1.9 Hz), 3.73 (s, br). <sup>13</sup>C{<sup>1</sup>H} NMR (CD<sub>2</sub>Cl<sub>2</sub>):  $\delta$  193.08, 139.3, 138.19 (s, br), 137.49, 136.52, 135.7, 135.55, 134.37 (t, <sup>2</sup>J<sub>C-P</sub> = 6.2 Hz, PPh<sub>3</sub>, ortho), 131.98 (s, PPh<sub>3</sub>, para), 131.42, 130.65, 129.7, 129.39 (t, <sup>3</sup>J<sub>C-P</sub> = 5.45 Hz, PPh<sub>3</sub>, meta), 128.91, 127.94, 127.42, 127.09, 127.05, 126.67. <sup>19</sup>F NMR (CD<sub>2</sub>Cl<sub>2</sub>):  $\delta$  -150.58. HRMS (FAB) (*m/e*): calcd for (M - H<sub>2</sub>O)<sup>+</sup>, 925.2203; found, 925.2283. Anal. Calcd for C<sub>52</sub>H<sub>44</sub>Cl<sub>2</sub>BF<sub>4</sub>O<sub>2</sub>P<sub>2</sub>Pt: C, 56.00; H, 3.97. Found: C, 55.82; H, 3.96.

**(10,11-Didehydrodibenzooxepin)[bis(dicyclohexylphosphino)ethane]platinum (9).** A 100 mg (0.108 mmol) amount of **6** and 50 mg (0.118 mmol) of bis(dicyclohexylphosphino)ethane were dissolved in 0.5 mL of C<sub>6</sub>D<sub>6</sub> in an NMR tube. After 4 days at room temperature the <sup>31</sup>P{<sup>1</sup>H} NMR showed formation of complex **9** in about 95% yield. The solution from the NMR tube was transferred to a Schlenk tube, and 4 mL of hexane was added. After 1 week at 6 °C yellow crystals had formed: 45 mg (yield 50.6%); mp 248–250 °C dec. IR (KBr): 2926, 2848, 1674, 1469, 1438, 1193, 742 cm<sup>-1</sup>. <sup>1</sup>H NMR (C<sub>6</sub>D<sub>6</sub>):  $\delta$  7.68 (dd, 2H, <sup>3</sup>J<sub>H-H</sub> = 7.4 Hz, <sup>4</sup>J<sub>H-H</sub> = 1.7 Hz), 7.29 (d, 2H, <sup>3</sup>J<sub>H-H</sub> = 7.9 Hz), 7.15 (td, 2H, <sup>3</sup>J<sub>H-H</sub> = 7.4 Hz, <sup>4</sup>J<sub>H-H</sub> = 1.4 Hz), 7.06 (td, 2H, <sup>3</sup>J<sub>H-H</sub> = 7.8, <sup>4</sup>J<sub>H-H</sub> = 1.7 Hz), 2.19 (d, 4H, *J* = 11.8 Hz), 0.95–2 (m, 44H, PCy<sub>3</sub>). <sup>13</sup>C{<sup>1</sup>H} NMR (C<sub>6</sub>D<sub>6</sub>):  $\delta$  156.2 (t, J<sub>C-P</sub> = 2.7 Hz), 144.23 (dd, <sup>2</sup>J<sub>C-P<sub>trans</sub></sub> = 13.46 Hz, <sup>2</sup>J<sub>C-P<sub>trans</sub></sub> = 99.6 Hz), 131.51 (t, J<sub>C-P</sub> = 11.3 Hz), 129.07, 128.12, 124.93, 121.89, 36.35 (m), 30.33, 29.22, 27.25 (m), 26.38, 24.8 (m). HRMS (FAB) (*m/e*): calcd for (M + 1)<sup>+</sup>, 810.3533; found, 810.3428. Anal. Calcd for C<sub>40</sub>H<sub>56</sub>OP<sub>2</sub>Pt: C, 59.30; H, 6.97. Found: C, 59.15; H, 7.01.

**(10,11-Didehydrodibenzotropone)[bis(dicyclohexylphosphino)ethane]platinum (10).** A 130 mg (0.13



**Table 6. Fractional Coordinates and Equivalent Isotropic<sup>a</sup> Thermal Parameters (Å<sup>2</sup>) for the Non-H Atoms of Complex 5**

atom	x	y	z	U
Pt	0.96571(4)	0.15781(3)	0.77442(3)	0.0350(2)
P1	1.1114(3)	0.0522(2)	0.7019(2)	0.0368(11)
P2	0.7913(3)	0.1002(2)	0.7891(2)	0.0369(11)
O	0.9708(11)	0.5478(7)	0.8214(9)	0.115(7)
C1	1.2663(11)	0.2716(10)	0.7399(8)	0.059(6)
C2	1.3582(13)	0.3241(10)	0.7190(10)	0.074(7)
C3	1.327(2)	0.4162(13)	0.7383(11)	0.096(9)
C4	1.2092(14)	0.4579(10)	0.7770(10)	0.074(7)
C5	0.9989(15)	0.4528(10)	0.8409(10)	0.073(7)
C6	0.852(2)	0.4509(12)	0.9753(12)	0.095(9)
C7	0.771(2)	0.408(2)	1.0386(11)	0.113(12)
C8	0.746(2)	0.324(2)	1.0346(11)	0.098(10)
C9	0.7991(11)	0.2806(11)	0.9704(8)	0.062(6)
C10	0.9408(11)	0.2663(8)	0.8399(7)	0.044(5)
C11	1.0467(10)	0.2592(8)	0.7930(6)	0.038(4)
C12	1.1435(11)	0.3111(9)	0.7782(7)	0.051(5)
C13	1.1184(13)	0.4039(9)	0.7986(9)	0.060(6)
C14	0.8795(11)	0.3157(8)	0.9057(7)	0.048(5)
C15	0.9119(13)	0.4059(11)	0.9050(9)	0.068(7)
C21	0.8101(10)	-0.0325(8)	0.8436(7)	0.044(5)
C22	0.7826(11)	-0.1028(9)	0.8115(8)	0.055(5)
C23	0.8091(12)	-0.2025(9)	0.8593(10)	0.063(6)
C24	0.8530(15)	-0.2285(12)	0.9294(12)	0.083(8)
C25	0.8786(13)	-0.1596(13)	0.9624(9)	0.081(7)
C26	0.8591(11)	-0.0585(9)	0.9185(8)	0.057(5)
C31	0.7221(10)	0.1206(8)	0.6924(7)	0.042(5)
C32	0.6083(10)	0.1030(9)	0.6928(8)	0.051(5)
C33	0.5538(12)	0.1251(10)	0.6189(8)	0.058(6)
C34	0.6106(13)	0.1683(10)	0.5451(9)	0.064(7)
C35	0.7277(15)	0.1882(11)	0.5411(8)	0.073(7)
C36	0.7832(11)	0.1637(10)	0.6149(7)	0.057(6)
C41	0.6513(10)	0.1629(8)	0.8486(7)	0.044(5)
C42	0.5629(11)	0.1139(11)	0.8984(7)	0.057(6)
C43	0.4552(12)	0.1679(11)	0.9376(8)	0.063(6)
C44	0.4355(12)	0.2671(12)	0.9317(9)	0.071(7)
C45	0.5217(13)	0.3165(11)	0.8818(9)	0.069(7)
C46	0.6296(12)	0.2641(10)	0.8408(8)	0.060(6)
C51	1.2474(10)	-0.0063(8)	0.7604(7)	0.040(5)
C52	1.2372(12)	-0.0010(9)	0.8436(7)	0.055(5)
C53	1.3351(12)	-0.0505(10)	0.8909(8)	0.063(6)
C54	1.4476(12)	-0.1024(9)	0.8543(8)	0.060(6)
C55	1.4591(11)	-0.1099(10)	0.7717(8)	0.061(6)
C56	1.3580(12)	-0.0608(10)	0.7252(8)	0.060(6)
C61	1.1794(10)	0.1096(8)	0.5976(7)	0.040(5)
C62	1.2556(11)	0.0520(9)	0.5395(7)	0.055(5)
C63	1.3134(12)	0.0995(10)	0.4646(7)	0.060(6)
C64	1.2979(12)	0.2022(11)	0.4454(8)	0.063(6)
C65	1.2257(13)	0.2567(10)	0.4999(8)	0.065(6)
C66	1.1656(11)	0.2072(9)	0.5772(7)	0.054(6)
C71	1.0786(10)	-0.0615(7)	0.6885(6)	0.036(4)
C72	1.1043(10)	-0.1497(9)	0.7479(7)	0.048(5)
C73	1.0752(12)	-0.2333(9)	0.7379(9)	0.060(6)
C74	1.0188(13)	-0.2288(11)	0.6715(9)	0.070(7)
C75	0.9888(13)	-0.1404(11)	0.6109(8)	0.068(7)
C76	1.0217(13)	-0.0577(10)	0.6196(7)	0.060(6)

<sup>a</sup> For anisotropic atoms, the  $U$  value is  $U_{eq}$ , calculated as  $U_{eq} = \frac{1}{3} \sum_i \sum_j U_{ij} a_i^* a_j^* A_{ij}$ , where  $A_{ij}$  is the dot product of the  $i$ th and  $j$ th direct space unit cell vectors.

mmol) amount of **5** and 60 mg (0.14 mmol) of bis(dicyclohexylphosphino)ethane were dissolved in 3 mL of  $C_6H_6$  in a Schlenk tube, and the mixture was stirred for 20 h at room temperature. A 10 mL volume of hexane was added, and the solution was filtered through a canula. The filtrate was cooled for 1 week at  $-20$  °C to give 80 mg of crystalline pure **10** (74%), mp 265 °C dec. IR (KBr): 2928, 2850, 1707, 1615, 1578, 1447, 1302, 751  $cm^{-1}$ . <sup>1</sup>H NMR ( $CD_2Cl_2$ ):  $\delta$  8.25 (dd, 2H, <sup>3</sup> $J_{H_4-H_3} = 8.07$  Hz, <sup>4</sup> $J_{H_4-H_2} = 1.4$  Hz, H4), 7.81 (dd, 2H, <sup>3</sup> $J_{H_1-H_2} = 7.8$  Hz, <sup>4</sup> $J_{H_1-H_3} = 1.2$  Hz, H1), 7.68 (td, 2H, <sup>3</sup> $J_{H_3-H_2,4} = 7.14$  Hz, <sup>4</sup> $J_{H_3-H_1} = 1.5$  Hz, H3), 7.06 (td, 2H, <sup>3</sup> $J_{H_2-H_1,3} = 7.55$ , <sup>4</sup> $J_{H_2-H_4} = 1.4$  Hz, H2), 1–2.2 (m, 44H,  $PCy_3$ ). <sup>13</sup>C{<sup>1</sup>H} NMR ( $CD_2Cl_2$ ):  $\delta$  195.8, 144.2 (dd, <sup>2</sup> $J_{C-P_{cis}} = 14.3$  Hz, <sup>2</sup> $J_{C-P_{trans}} = 97.3$  Hz), 140.7 (t,  $J_{C-P} = 3.8$  Hz), 133.27 (t,  $J_{C-P} = 10.6$  Hz), 132.18 (m), 131.14, 128.76, 126.9, 36.8 (m), 30.8 (s,  $J_{C-Pt} = 23.5$  Hz), 29.5 (s,  $J_{C-Pt} = 21$  Hz), 27.54 (m) 26.7, 25 (t,  $J_{C-P} = 20.5$  Hz). HRMS (FAB)

**Table 7. Fractional Coordinates and Equivalent Isotropic<sup>a</sup> Thermal Parameters (Å<sup>2</sup>) for the Non-H Atoms of Compound 14**

atom	x	y	z	U
O1	0.2157(3)	1.0224(2)	0.9121(3)	0.081(2)
O2	0.4222(2)	0.4639(2)	0.3601(2)	0.0566(13)
O3	0.0782(2)	0.1800(2)	0.7596(2)	0.0608(13)
C1	0.0944(3)	0.6117(4)	0.8857(3)	0.049(2)
C2	0.0243(4)	0.6545(4)	0.9527(4)	0.062(2)
C3	0.0350(4)	0.7828(4)	1.0024(4)	0.069(2)
C4	0.1080(4)	0.8625(4)	0.9770(3)	0.058(2)
C5	0.2442(3)	0.9222(3)	0.8849(3)	0.047(2)
C6	0.4407(4)	1.0271(3)	0.8750(3)	0.051(2)
C7	0.5397(4)	1.0346(3)	0.8370(3)	0.056(2)
C8	0.5477(4)	0.9259(3)	0.7552(3)	0.054(2)
C9	0.4565(3)	0.8129(3)	0.7144(3)	0.044(2)
C10	0.2733(3)	0.6695(3)	0.7099(3)	0.0329(14)
C11	0.2420(3)	0.6256(3)	0.7854(2)	0.0324(13)
C12	0.3528(3)	0.8019(3)	0.7520(3)	0.0355(14)
C13	0.3466(3)	0.9131(3)	0.8357(3)	0.039(2)
C14	0.1790(3)	0.6916(3)	0.8644(2)	0.0356(14)
C15	0.1782(3)	0.8205(3)	0.9063(3)	0.042(2)
C16	0.1636(3)	0.7111(3)	0.5071(3)	0.043(2)
C17	0.1440(4)	0.7583(3)	0.4266(3)	0.053(2)
C18	0.1919(4)	0.7172(3)	0.3400(3)	0.057(2)
C19	0.2574(4)	0.6271(3)	0.3341(3)	0.051(2)
C20	0.3287(3)	0.4647(3)	0.3874(3)	0.039(2)
C21	0.2094(4)	0.2387(3)	0.2727(3)	0.052(2)
C22	0.1237(4)	0.1294(4)	0.2518(3)	0.067(2)
C23	0.0729(4)	0.1258(3)	0.3317(3)	0.054(2)
C24	0.1090(3)	0.2310(3)	0.4345(3)	0.039(2)
C25	0.2389(3)	0.4501(3)	0.5768(2)	0.0304(13)
C26	0.2511(3)	0.5768(3)	0.5967(2)	0.0317(14)
C27	0.1958(3)	0.3441(3)	0.4599(2)	0.0318(13)
C28	0.2445(3)	0.3472(3)	0.3761(3)	0.0358(14)
C29	0.2297(3)	0.6197(3)	0.5039(3)	0.0343(14)
C30	0.2747(3)	0.5754(3)	0.4133(3)	0.0382(15)
C31	0.3857(3)	0.2678(3)	0.6002(3)	0.039(2)
C32	0.4104(4)	0.1505(3)	0.5729(3)	0.053(2)
C33	0.3494(4)	0.0635(3)	0.6005(3)	0.060(2)
C34	0.2689(4)	0.0951(3)	0.6599(3)	0.053(2)
C35	0.1780(3)	0.2493(3)	0.7729(3)	0.040(2)
C36	0.2834(3)	0.3550(4)	0.9834(3)	0.047(2)
C37	0.3600(4)	0.4564(4)	1.0860(3)	0.052(2)
C38	0.4052(3)	0.5728(4)	1.0873(3)	0.048(2)
C39	0.3733(3)	0.5861(3)	0.9865(3)	0.040(2)
C40	0.2619(3)	0.5058(3)	0.7752(2)	0.0321(14)
C41	0.2673(3)	0.4212(3)	0.6730(2)	0.0296(13)
C42	0.2960(3)	0.4840(3)	0.8804(2)	0.0334(14)
C43	0.2516(3)	0.3670(3)	0.8807(3)	0.0366(15)
C44	0.3031(3)	0.3010(3)	0.6589(2)	0.0328(13)
C45	0.2480(3)	0.2142(3)	0.6928(3)	0.0376(14)

<sup>a</sup> For anisotropic atoms, the  $U$  value is  $U_{eq}$ , calculated as  $U_{eq} = \frac{1}{3} \sum_i \sum_j U_{ij} a_i^* a_j^* A_{ij}$ , where  $A_{ij}$  is the dot product of the  $i$ th and  $j$ th direct space unit cell vectors.

( $m/e$ ): calcd for  $(M + 1)^+$ , 822.3533; found, 822.3559. Anal. Calcd for  $C_{41}H_{56}OP_2Pt$ : C, 59.91; H, 6.94. Found: C, 60.34; H, 6.93.

**(10,11-Didehydrodibenzotropone)(triphenylphosphine)(*tert*-butyl isocyanide)platinum (11).** To a Schlenk tube containing 100 mg of **5** (0.1 mmol) in 2 mL of  $C_6H_6$ , was added 22 mg of *tert*-butyl isocyanide (0.26 mmol) in 30 mL of  $C_6H_6$ . After the solution was stirred for 20 min at room temperature, the solvent was evaporated and the residue was dissolved in 1 mL of  $C_6H_6$  followed by addition of 6 mL of hexane. After 2 days at 6 °C yellow-orange needles had formed: 63 mg (84%); mp 210 °C dec. IR (KBr): 3054 w, 2982 w, 2156, 1711, 1618, 1583 1436, 1304, 1206, 1096, 754, 696, 531, 518  $cm^{-1}$ . <sup>1</sup>H NMR ( $CD_2Cl_2$ ):  $\delta$  8.35 (d, 1H, <sup>3</sup> $J_{H-H} = 7.8$  Hz), 8.28 (d, 1H, <sup>3</sup> $J_{H-H} = 7.7$  Hz), 7.87 (d, 1H, <sup>3</sup> $J_{H-H} = 7.1$  Hz), 7.74 (m, 7H,  $PPH_3$ ), 7.53 (t, 1H, <sup>3</sup> $J_{H-H} = 7$  Hz), 7.43 (m, 9H,  $PPH_3$ ), 7.35 (t, 1H, <sup>3</sup> $J_{H-H} = 8.1$  Hz), 7.15 (t, 1H, <sup>3</sup> $J_{H-H} = 7.5$  Hz), 6.81 (d, 1H, <sup>3</sup> $J_{H-H} = 7.8$  Hz), 1.39 (s, 9H). <sup>13</sup>C{<sup>1</sup>H} NMR ( $CD_2Cl_2$ ):  $\delta$  194.73, 140.99 (s,  $J_{P-C} = 44.6$  Hz), 139.97 (s,  $J_{P-C} = 8$  Hz), 138.03, 136.53, 136.17 (d,  $J_{C-P} = 44.8$  Hz,  $J_{P-C} = 24.6$  Hz ( $PPH_3$ , ipso), 134.6 (m,  $PPH_3$ , ortho), 132.59, 132.01, 131.95 (d,  $J_{C-P} = 4.7$  Hz), 131.5 (m), 131.32 (m), 131.02, 130.48

(s,  $PPh_3$ , para), 128.78 (d,  $J_{C-P} = 9.8$ ,  $PPh_3$ , meta), 128.43 (t,  $J_{C-P} = 5.1$  Hz) 127.79, 127.39, 78.28, 57.51, 30.58. HRMS (FAB) ( $m/e$ ): calcd for  $(M + 1)^+$ , 745.1948; found, 745.1980. Anal. Calcd for  $C_{38}H_{32}NOPt$ : C, 61.29; H, 4.33; N, 1.88. Found: C, 61.43; H, 4.32; N, 1.84.

**Preparation of Complex 12.** To a Schlenk tube containing **5** (50 mg, 0.05 mmol) in 4 mL of THF was added HBr (16.2 mg, 12  $\mu$ L of 30 wt % solution in acetic acid dissolved in 1 mL of THF) at room temperature. The color changed immediately from yellow to pale yellow. The mixture was stirred for 15 min at room temperature. Solvent was evaporated in vacuo, and the residue was dissolved in 3 mL of  $CH_2Cl_2$  followed by addition of 10 mL of hexane. After 1 day off-white needles had formed: 35 mg (64%), mp 278–279 °C. IR (KBr): 3044 w, 2992 w, 1624, 1584, 1578, 1479, 1437, 1312, 750, 692, 524  $cm^{-1}$ .  $^1H$  NMR ( $CD_2Cl_2$ ):  $\delta$  9.15 (dd, 1H,  $^3J_{H-H} = 7.9$  Hz,  $^4J_{H-H} = 1$  Hz), 7.82 (d, 1H,  $^3J_{H-H} = 7.6$  Hz), 7.7 (d, 1H,  $^3J_{H-H} = 8.2$  Hz), 7.63 (t, 1H,  $^3J_{H-H} = 7.6$  Hz), 6.9–7.55 (m, 34H,  $PPh_3$ ).  $^{13}C\{^1H\}$  NMR ( $CD_2Cl_2$ ):  $\delta$  193.3, 137.46, 137.32, 137.14, 136.32, 135.39 (m,  $PPh_3$ ), 134.32 (m,  $PPh_3$ ), 132.5, 131.9, 131.34, 130.98, 130.23, 129.99, 129.7, 129.27, 129, 128.2, 128.05 (d), 126.67, 126.29. HRMS (FAB) ( $m/e$ ): calcd for  $(M + 1)^+$ , 1004.1386; found, 1004.1402. Anal. Calcd for  $C_{51}H_{39}OP_2BrPt \cdot 1.5CH_2Cl_2$ : C, 55.69; H, 3.74. Found: C, 55.87; H, 3.81.

**Preparation of Trimer 14.** A Schlenk tube was charged with **5** (100 mg, 0.1 mmol), and 2 mL of  $C_6H_6$  was added. To this solution was added tetracyanoethylene (30 mg, 0.234 mmol). The color changed immediately from yellow to brown. To this solution was added 5 mL of hexane. The solution was filtered through a short silica gel column using methylene chloride/hexane (7/3, v/v) as the eluent. Methylene chloride was evaporated in vacuum leaving yellow trimer **14** (9 mg, 45%). IR (KBr): 3058.7 w, 2957.6 w, 1696, 1590, 1289.2, 1261.5, 1246.2, 931.9, 800.1, 751, 733, 641.7  $cm^{-1}$ .  $^1H$  NMR ( $C_6D_6$ ):  $\delta$  7.43 (dd, 6H,  $^3J_{H4-H3} = 7.5$  Hz,  $^4J_{H4-H2} = 1$  Hz, H4), 6.83 (d, 6H,  $^3J_{H1-H2} = 7.9$  Hz, H1), 6.7 (td, 6H,  $^3J_{H2-H1,3} = 7.5$  Hz,  $^4J_{H2-H4} = 1$  Hz, H2), 6.49 (td, 2H,  $^3J_{H3-H4,2} = 7.7$  Hz,  $^4J_{H3-H1} = 1.4$  Hz, H3).  $^{13}C\{^1H\}$  NMR ( $C_6D_6$ ):  $\delta$  197.42, 146.71, 138.18, 134.78, 133.15, 129.09, 127.93, 125.05. HRMS (FAB) ( $m/e$ ): calcd for  $(M + 1)^+$ , 613.1804; found, 613.1835.

**Preparation of Complex 15.** To a solution of **6** (130 mg, 0.13 mmol) in 2 mL of benzene was added 22 mg (0.17 mmol) of TCNE at room temperature. After stirring of the mixture for 0.5 h, the solvent was evaporated in vacuo. The residue was dissolved in 5–10 mL of  $CH_2Cl_2$ , and 15 mL of hexane was added. The solution was kept at  $-20$  °C for 2 days to give 82 mg (55%) of yellow-brown crystals. An analytically pure sample (off-white crystals) was obtained by recrystallization from  $CH_2Cl_2$ /hexane solution. Mp: 208 °C. IR (KBr): 3060 w, 2216 w, 1481, 1439, 1203, 1096, 744, 697  $cm^{-1}$ .  $^1H$  NMR ( $CD_2Cl_2$ ):  $\delta$  7.88 (dd, 1H,  $^3J_{H4-H3} = 8.1$  Hz,  $^4J_{H4-H2} = 1.4$  Hz, H4), 7.6 (dd, 1H,  $^3J_{H5-H6} = 7.6$  Hz,  $^4J_{H5-H7} = 1.5$  Hz, H5), 7.24 (td, 1H,  $^3J_{H2-H1,3} = 8$  Hz,  $^4J_{H2-H4} = 1.5$  Hz, H2), 7.09 (td, 1H,  $^3J_{H3-H4,2} = 8$  Hz,  $^4J_{H3-H1} = 1.4$  Hz, H3), 7 (dd, 1H,  $^3J_{H1-H2} = 8$  Hz,  $^4J_{H1-H3} = 1$  Hz, H1), 6.79 (td, 1H,  $^3J_{H7-H6,8} = 7.7$  Hz,  $^4J_{H7-H5} = 1.3$  Hz, H7), 6.37 (d, 1H,  $^3J_{H8-H7} = 8.3$  Hz, H8), 6.32 (td, 1H,  $^3J_{H6-H5,7} = 7.5$  Hz,  $^4J_{H6-H8} = 1.2$  Hz, H6), 7.1–7.56 (m, 30H,  $PPh_3$ ).  $^{13}C\{^1H\}$  NMR ( $CD_2Cl_2$ ):  $\delta$  165.71 (d,  $J_{C-P} = 3.8$  Hz), 164.37 (d,  $J_{C-P} = 4.6$  Hz), 161.05, 157.78 (d,  $J_{C-P} = 3.9$  Hz), 135.93 (d,  $J_{C-P} = 10.6$  Hz,  $PPh_3$ ), 134.44 (br), 131.43 (s,  $PPh_3$ ), 130.93, 130.40, 130.22, 129.45, 128.81, 128.41 (d,  $J_{C-P} = 9.9$  Hz,  $PPh_3$ ), 128.09, 126.81 (d,  $J_{C-P} = 6.1$  Hz), 124.58, 123.8, 120.78, 120.17, 117.89 (d,  $J_{C-P} = 4.6$  Hz). HRMS (FAB) ( $m/e$ ): calcd for  $(M + 1)^+$ , 1040.2247; found, 1040.2203. Anal. Calcd for  $C_{56}H_{38}N_4OP_2Pt \cdot CH_2Cl_2$ : C, 60.86; H, 3.58; N, 4.98. Found: C, 60.55; H, 3.54; N, 4.92.

**(Dibenzotropyne)bis(triphenylphosphine)platinum (16).** To a solution of **7** (160 mg, 0.175 mmol) in 3 mL of  $CH_2Cl_2$  was added dropwise at  $-78$  °C triphenylcarbenium tetrafluoroborate (61 mg, 0.184 mmol) in 2 mL of  $CH_2Cl_2$ . The resulting solution was stirred for 5 h at  $-78$  °C and subsequently warmed slowly to room temperature. The resulting

**Table 8. Fractional Coordinates and Equivalent Isotropic<sup>a</sup> Thermal Parameters ( $\text{\AA}^2$ ) for Non-H Atoms of Complex 15**

atom	x	y	z	U
Pt	0.27993	0.01260(2)	0.08525	0.02981(8)
P1	0.2791(2)	0.0807(2)	-0.02475(14)	0.0344(8)
P2	0.3059(2)	0.1369(2)	0.15691(14)	0.0344(8)
O	0.2019(5)	-0.2173(6)	-0.0703(4)	0.051(3)
N1	0.1269(8)	-0.2217(8)	0.2398(6)	0.072(5)
N2	0.0695(6)	-0.0251(7)	0.0982(6)	0.053(3)
N3	0.2013(8)	-0.0033(7)	0.2943(6)	0.064(4)
N4	0.3705(8)	-0.1693(8)	0.2061(7)	0.066(5)
C1	0.2029(8)	-0.3253(7)	0.1027(7)	0.057(5)
C2	0.1873(8)	-0.4114(8)	0.0800(9)	0.064(5)
C3	0.1730(11)	-0.4249(9)	0.0088(10)	0.085(7)
C4	0.1779(9)	-0.3646(10)	-0.0398(9)	0.080(6)
C5	0.3249(9)	-0.2244(8)	-0.1288(6)	0.059(5)
C6	0.4009(9)	-0.2013(10)	-0.1332(8)	0.072(6)
C7	0.4346(8)	-0.1485(9)	-0.0824(8)	0.060(5)
C8	0.3910(8)	-0.1160(8)	-0.0271(7)	0.050(4)
C9	0.2669(6)	-0.1109(6)	0.0402(4)	0.031(3)
C10	0.2224(7)	-0.1668(6)	0.0742(5)	0.036(3)
C11	0.2064(7)	-0.2580(7)	0.0549(6)	0.043(4)
C12	0.1943(7)	-0.2802(7)	-0.0188(6)	0.046(4)
C13	0.3141(8)	-0.1389(7)	-0.0203(6)	0.043(4)
C14	0.2818(7)	-0.1942(7)	-0.0731(6)	0.047(4)
C15	0.1855(7)	-0.1255(6)	0.1400(5)	0.039(3)
C16	0.2538(6)	-0.0674(6)	0.1765(5)	0.034(3)
C17	0.1199(7)	-0.0665(7)	0.1154(6)	0.039(3)
C18	0.1530(8)	-0.1844(7)	0.1963(6)	0.047(4)
C19	0.2269(7)	-0.0297(7)	0.2494(6)	0.045(4)
C20	0.3199(9)	-0.1236(9)	0.1938(7)	0.052(5)
C21	0.2246(7)	0.1919(6)	0.1946(5)	0.036(3)
C22	0.2319(7)	0.2741(7)	0.2254(6)	0.047(4)
C23	0.1702(9)	0.3181(9)	0.2540(7)	0.067(5)
C24	0.0984(9)	0.2807(9)	0.2518(8)	0.068(5)
C25	0.0866(9)	0.2009(12)	0.2213(9)	0.075(7)
C26	0.1504(8)	0.1548(9)	0.1921(8)	0.050(5)
C31	0.3611(6)	0.2288(6)	0.1228(6)	0.037(3)
C32	0.3236(8)	0.2946(7)	0.0840(7)	0.054(4)
C33	0.3652(10)	0.3649(8)	0.0589(7)	0.068(6)
C34	0.4442(11)	0.3708(10)	0.0688(9)	0.082(7)
C35	0.4823(8)	0.3059(10)	0.1084(9)	0.070(5)
C36	0.4425(10)	0.2371(10)	0.1347(8)	0.055(5)
C41	0.3669(7)	0.0999(6)	0.2330(5)	0.040(3)
C42	0.4297(7)	0.0458(8)	0.2182(6)	0.048(4)
C43	0.4808(10)	0.0218(9)	0.2731(9)	0.071(6)
C44	0.4682(11)	0.0468(12)	0.3417(9)	0.083(7)
C45	0.4066(11)	0.0975(11)	0.3568(7)	0.080(6)
C46	0.3554(9)	0.1243(9)	0.3019(6)	0.062(5)
C51	0.2301(7)	0.0219(7)	-0.0981(5)	0.042(3)
C52	0.1498(9)	0.0174(8)	-0.1004(7)	0.057(5)
C53	0.1103(10)	-0.0214(9)	-0.1579(8)	0.067(5)
C54	0.1490(12)	-0.0577(9)	-0.2121(7)	0.076(6)
C55	0.2266(11)	-0.0563(9)	-0.2102(7)	0.071(6)
C56	0.2687(9)	-0.0166(8)	-0.1540(6)	0.060(4)
C61	0.3718(7)	0.1175(7)	-0.0602(6)	0.039(3)
C62	0.4371(8)	0.1194(9)	-0.0177(7)	0.047(5)
C63	0.5062(8)	0.1563(9)	-0.0403(7)	0.058(5)
C64	0.5083(9)	0.1872(8)	-0.1093(7)	0.066(5)
C65	0.4438(8)	0.1826(9)	-0.1534(7)	0.061(5)
C66	0.3757(7)	0.1472(8)	-0.1301(6)	0.050(4)
C71	0.2178(7)	0.1779(7)	-0.0234(6)	0.040(4)
C72	0.2318(8)	0.2501(7)	-0.0659(6)	0.048(4)
C73	0.1791(9)	0.3200(8)	-0.0684(8)	0.065(5)
C74	0.1141(9)	0.3160(8)	-0.0275(9)	0.076(6)
C75	0.0994(11)	0.2448(12)	0.0151(9)	0.070(6)
C76	0.1524(7)	0.1764(8)	0.0164(7)	0.051(4)

<sup>a</sup> For anisotropic atoms, the  $U$  value is  $U_{eq}$ , calculated as  $U_{eq} = 1/3 \sum_i \sum_j U_{ij} a_i^* a_j^* A_{ij}$ , where  $A_{ij}$  is the dot product of the  $i$ th and  $j$ th direct space unit cell vectors.

very deep blue solution was filtered, and to the filtrate was added 15 mL of ether. After 2 h deep blue needles had formed. The solvent was removed by decantation, and the crystals (100 mg, 57%) were dried under vacuum. Mp: 197 °C dec. IR (KBr): 3057 w, 1654 w, 1648 w, 1436, 1084, 745, 694, 523  $cm^{-1}$ .  $^1H$  NMR ( $CD_2Cl_2$ ):  $\delta$  10.43 (s, 1H, H5), 8.78 (d, 2H,  $^3J_{H4-H3} = 8.3$  Hz, H4), 7.94 (td, 2H,  $^3J_{H3-H4,2} = 8.3$  Hz,  $^4J_{H3-H1} = 1.2$  Hz, H3), 7.75 (td, 2H,  $^3J_{H2-H1,3} = 8.3$  Hz,  $^4J_{H2-H4} = 1.2$  Hz, H2),

7.55 (m, 12H, *PPh*<sub>3</sub>, ortho), 7.4 (m, 6H, *PPh*<sub>3</sub>, para), 7.25 (m, 12H, *PPh*<sub>3</sub>, meta), 7.02 (d, 2H, <sup>3</sup>*J*<sub>H1-H2</sub> = 8.3 Hz, H1). <sup>13</sup>C{<sup>1</sup>H} NMR (CD<sub>2</sub>Cl<sub>2</sub>): δ 160.15 (dd, <sup>2</sup>*J*<sub>C-Pcis</sub> = 4.04 Hz, <sup>2</sup>*J*<sub>C-Ptrans</sub> = 84.03 Hz), 155.86, 140.2 (t, *J*<sub>C-P</sub> = 4.5 Hz), 139.5, 137.22, 135.39 (t, *J*<sub>C-P</sub> = 8.85 Hz), 134.74, 134.52 (p, <sup>2</sup>*J*<sub>C-P</sub> = 6.4 Hz, *PPh*<sub>3</sub>, ortho), 133.94 (d, <sup>1</sup>*J*<sub>C-P</sub> = 49.72 Hz, *PPh*<sub>3</sub>, ipso), 132.88, 131.08 (s, *PPh*<sub>3</sub>, para), 129.04 (t, <sup>3</sup>*J*<sub>C-P</sub> = 5.1 Hz, *PPh*<sub>3</sub>, meta). <sup>19</sup>F NMR (CD<sub>2</sub>Cl<sub>2</sub>): δ -152.82. HRMS (FAB) (*m/e*): calcd for (M - BF<sub>4</sub>)<sup>+</sup>, 908.2175; found, 908.220. Anal. Calcd for C<sub>51</sub>H<sub>38</sub>BF<sub>4</sub>P<sub>2</sub>Pt<sup>1/2</sup>CH<sub>2</sub>Cl<sub>2</sub>: C, 59.58; H, 3.88. Found: C, 59.31; H, 4.02.

**Reaction of 16 with KBet<sub>3</sub>H.** To a solution of **16** (30 mg, 0.03 mmol) in 3 mL of THF was added quickly KBet<sub>3</sub>H (35 μL, 0.035 mmol of 1 M solution in THF) at room temperature. The color changed at once from deep blue to light yellow. After 5 min THF was removed in vacuum and the residue dissolved in CD<sub>2</sub>Cl<sub>2</sub>. <sup>1</sup>H and <sup>31</sup>P{<sup>1</sup>H} NMR showed formation of **7** in about 70% together with three minor platinum products which were not characterized.

**Preparation of Complex 17.** To a solution of **16** (100 mg, 0.1 mmol) in 3 mL of CH<sub>2</sub>Cl<sub>2</sub> at room temperature was added 30 mg (0.7 mmol) of bis(dicyclohexylphosphino)ethane. The color changed immediately from deep blue to light yellow. After 15 min of stirring, 15 mL hexane was added causing precipitation of an off-white solid. This solid was dissolved in 2 mL of CH<sub>2</sub>Cl<sub>2</sub>, and 10 mL of Et<sub>2</sub>O was added causing precipitation of **17** (80 mg, 66%). An analytically pure sample was obtained by recrystallization from CH<sub>2</sub>Cl<sub>2</sub>/hexane. Mp: 206–208 °C dec. IR (KBr): 3052, 2933, 2854, 1689, 1476, 1437, 1085 (br), 753, 694 cm<sup>-1</sup>. <sup>1</sup>H NMR (CD<sub>2</sub>Cl<sub>2</sub>): δ 7.71 (d, 4H, <sup>3</sup>*J*<sub>H-H</sub> = 7.5 Hz), 7.43 (m, 24H, *PPh*<sub>3</sub>, ortho), 7.28 (m, 12H, *PPh*<sub>3</sub>, para), 7.18 (m, 24H, *PPh*<sub>3</sub>, meta), 6.74 (t, 4H, <sup>2</sup>*J*<sub>H-H</sub> = 7.6 Hz), 5.97 (d, 4H, <sup>2</sup>*J*<sub>H-H</sub> = 6.2 Hz), 5.64 (d, 2H, <sup>2</sup>*J*<sub>P-H</sub> = 19.8 Hz), 2.95 (m, 4H), 2.5 (m, 2H), 0.8–2 (m, 42H, PCy<sub>2</sub>). <sup>13</sup>C{<sup>1</sup>H} NMR (CD<sub>2</sub>Cl<sub>2</sub>): δ 136.48, 135.85, 134.46 (m, *PPh*<sub>3</sub>), 133.45 (t, *J*<sub>P-C</sub> = 9.4 Hz), 132.45, 130.11 (s, *PPh*<sub>3</sub>), 129.66, 129.45, 128.66, 128.32 (m, *PPh*<sub>3</sub>), 127.26 (m), 66.02, 51.71 (t, *J*<sub>P-C</sub> = 17.5 Hz), 31.71 (br) 26.4–27.5 (m, PCy<sub>2</sub>), 25.62. <sup>19</sup>F NMR (CD<sub>2</sub>Cl<sub>2</sub>): δ -148.3. Anal. Calcd for C<sub>128</sub>H<sub>126</sub>B<sub>2</sub>F<sub>8</sub>P<sub>6</sub>Pt<sub>2</sub>: C, 63.69; H, 5.26. Found: C, 63.39; H, 5.61.

**Preparation of Complexes 18 and 19.** To a solution of **16** (110 mg, 0.11 mmol) in 5 mL of CH<sub>2</sub>Cl<sub>2</sub> was added HBr (27 μL of 30% HBr in acetic acid dissolved in 1 mL of CH<sub>2</sub>Cl<sub>2</sub>) within 20 s. The color changed at once from deep blue to deep purple. The mixture was stirred for 5 min, and then the solvent was removed in vacuo. The residue was dissolved in 5 mL of CH<sub>2</sub>Cl<sub>2</sub>, and then 15 mL of hexane was added causing precipitation of **18**. After 2 h at -16 °C the supernatant was discarded leaving 102 mg of product (85% yield). Mp: 268–269 °C dec. IR (KBr): 3053 w, 1602, 1514, 1480, 1435, 1384, 1095 br, 1055 br, 750, 695, 542, 525.5, 496 cm<sup>-1</sup>. <sup>1</sup>H NMR (CD<sub>2</sub>Cl<sub>2</sub>): δ 10.28 (d, 1H, *J*<sub>H-H</sub> = 8.4 Hz), 9.97 (d, 1H, <sup>4</sup>*J*<sub>H-P</sub> = 9 Hz, <sup>3</sup>*J*<sub>H-Pt</sub> = 41.1 Hz), 9.62 (s, 1H), 8.5 (m, 3H), 8.36 (s, 1H), 8.35 (s, 1H), 8.1 (t, 1H, <sup>3</sup>*J*<sub>H-H</sub> = 7.2 Hz), 8.04 (m, 1H), 6.8–7.6 (m, 30H, *PPh*<sub>3</sub>). <sup>13</sup>C{<sup>1</sup>H} NMR (CD<sub>2</sub>Cl<sub>2</sub>): δ 177.15, 164.98, 153.78, 152.37, 140.79, 140.24, 139.58, 137.75, 137.31, 136.34, 135.35 (d, *J*<sub>C-P</sub> = 10 Hz), 134.51, 133.83 (d, *J*<sub>C-P</sub> = 11 Hz), 132.43, 131.74, 131.55, 131.02, 130.34, 128.61 (d, *J*<sub>C-P</sub> = 10 Hz), 127.68. <sup>19</sup>F NMR (CD<sub>2</sub>Cl<sub>2</sub>): δ -152.5. HRMS (FAB) (*m/e*): calcd for (M + 1)<sup>+</sup>, 988.1437; found, 988.1390. Anal. Calcd for C<sub>51</sub>H<sub>40</sub>BF<sub>4</sub>BrP<sub>2</sub>Pt: C, 57.00; H, 3.74. Found: C, 56.67; H, 3.82.

The sample was kept in CD<sub>2</sub>Cl<sub>2</sub> for 1 month at room temperature. After that time the <sup>1</sup>H and <sup>31</sup>P{<sup>1</sup>H} showed

formation of **19** in about 75% with unreacted **18** and some decomposition products. <sup>1</sup>H NMR (CD<sub>2</sub>Cl<sub>2</sub>) spectroscopic data for **19**: δ 10.3 (d, 1H, *J*<sub>H-H</sub> = 8.2 Hz), 9.64 (s, 1H), 9.45 (s, 1H), <sup>3</sup>*J*<sub>H-Pt</sub> = 70.2 Hz), 8.25 (t of mult. 2H, *J*<sub>H-H</sub> = 7.6 Hz), 7.77 (d, 1H, <sup>3</sup>*J*<sub>H-H</sub> = 8.1 Hz), 8.5 (m, 2H), 8.1 (m, 2H), 6.8–7.6 (m, 30H, *PPh*<sub>3</sub>).

**Crystallographic Analysis.** Crystal data and numerical details of the structures are given in Table 2. Data were collected at room temperature on a Siemens P3m/V diffractometer equipped with a graphite monochromator utilizing Mo Kα radiation (λ = 0.710 73 Å). A total of 32 reflections with 20.0° ≤ 2θ ≤ 22.0° were used to refine the cell parameters of each crystal. Four reflections were measured every 96 reflections to monitor instrument and crystal stability for each data set (maximum corrections on *I* were 4, 1, and 4% for **5**, **14**, and **15**, respectively). Absorption corrections were applied based on measured crystal faces using *SHELXTL plus*.<sup>27</sup> All of the three structures were refined in *SHELXTL plus* using full-matrix least squares. The structures of **5** and **15** were solved by the heavy-atom method in *SHELXTL plus* from which the locations of the Pt atoms were obtained. The rest of the non-hydrogen atoms were obtained from subsequent difference Fourier maps. All non-H atoms were refined with anisotropic thermal parameters, while positions of all of the H atoms were calculated in ideal positions and their isotropic thermal parameters were fixed. Methylene chloride was found along with the Pt complex in **15**, and its non-H atoms were fully refined. In **5** disordered two partial toluene molecules were found and refined with isotropic thermal parameters. One of the toluene molecules (65% occupancy) is disordered in a general position, and the other (35% occupancy) is disordered around a center of inversion. The first toluene molecule was disordered in the methyl group only. While all of the ring C atoms were not disordered, two methyl groups of 32.5% occupancy were refined in *para* positions. The structure of **14** was solved by direct methods. The non-H atoms were refined with anisotropic thermal parameters, and the H atoms were located from a subsequent difference Fourier map and refined without any constraints. The linear absorption coefficients were calculated from values from the ref 28. Scattering factors for non-hydrogen atoms were taken from Cromer and Mann<sup>29</sup> with anomalous-dispersion corrections from Cromer and Liberman,<sup>30</sup> while those of hydrogen atoms were from Stewart, Davidson and Simpson.<sup>31</sup>

**Acknowledgment.** Support of this research by the National Science Foundation and the Chevron Research and Technology Co. is gratefully acknowledged.

**Supplementary Material Available:** Tables of atomic positions and *U* values, anisotropic thermal parameters for non-hydrogen atoms, and comprehensive bond lengths and angles (22 pages). Ordering information is given on any current masthead page.

OM9500174

(27) Sheldrick, G. M. *SHELXTL plus*, version 4.21/V; Siemens XRD, Madison, WI, 1990.

(28) *International Tables for X-ray Crystallography*; Kynoch Press: Birmingham, (present distributor; D. Reidel, Dordrecht, The Netherlands).

(29) Cromer, D. T.; Mann, J. B. *Acta Cryst.* **1968**, *A24*, 321–324.

(30) Cromer, D. T.; Liberman, D. *J. Chem. Phys.* **1970**, *53*, 1891–1898.

(31) Stewart, R. F.; Davidson, E. R.; Simpson, W. T. *J. Chem. Phys.* **1965**, *42*, 3175–3187.

# Organoaluminum and -gallium Thiolates. 1. Synthetic and X-ray Structural Studies

Majid Taghiof, Mary Jane Heeg, Marcia Bailey, David G. Dick, Rajesh Kumar, D. Greg Hendershot, Hamid Rahbarnoochi, and John P. Oliver\*

Department of Chemistry, Wayne State University, Detroit, Michigan 48202

Received February 27, 1995\*

Organoaluminum and -gallium thiolates are prepared in high yield by the reaction of triorganoaluminum and -gallium derivatives with thiols. In this way,  $[\text{Mes}_2\text{Al}(\mu\text{-SBz})]_2$  ( $\text{Mes} = 2,4,6\text{-Me}_3\text{C}_6\text{H}_2$ ;  $\text{Bz} = \text{CH}_2\text{C}_6\text{H}_5$ ) (**1**),  $[\text{Me}_2\text{Al}(\mu\text{-SSiPh}_3)]_2$  (**2**),  $[\text{Mes}_2\text{Al}(\mu\text{-SPh})]_2$  (**3**),  $\{\text{Me}_2\text{Al}[\mu\text{-S}(2\text{-}t\text{-BuC}_6\text{H}_4)]\}_3$  (**4**),  $\{\text{Me}_2\text{Al}[\mu\text{-S}(2\text{-Me}_3\text{SiC}_6\text{H}_4)]\}_3$  (**5**),  $\{\text{Me}_2\text{Al}[\mu\text{-S}(2\text{-}i\text{-PrC}_6\text{H}_4)]\}_3$  (**6**),  $\{i\text{-Bu}_2\text{Al}[\mu\text{-S}(2,4,6\text{-}i\text{-Pr}_3\text{C}_6\text{H}_2)]\}_3$  (**7**),  $\{\text{Me}_2\text{Al}[\mu\text{-S}(2,6\text{-Me}_2\text{C}_6\text{H}_3)]\}_4$  (**8**), and  $\{\text{Me}_2\text{Ga}[\mu\text{-S}(2,6\text{-Me}_2\text{C}_6\text{H}_3)]\}_4$  (**9**) were prepared and crystallographically characterized. The dimethyl- and dimesitylaluminum thiolates **1–3** were determined to be dimeric with four-membered  $(\text{AlS})_2$  rings. The structure of **1** was determined in space group  $P2_1/n$  (No. 14):  $a = 10.660(4)$  Å,  $b = 12.268(2)$  Å,  $c = 17.793(3)$  Å,  $\beta = 106.94(2)^\circ$ ,  $Z = 4$ ,  $R = 6.7\%$ , and  $R_w = 6.1\%$ . The structures of **2** and **3** were determined in space group  $P\bar{1}$  (No. 2):  $a = 9.077(2)$  Å,  $b = 13.847(3)$  Å,  $c = 16.724(4)$  Å,  $\alpha = 101.08(2)^\circ$ ,  $\beta = 95.34(2)^\circ$ ,  $\gamma = 103.38(2)^\circ$ ,  $Z = 2$  (dimers),  $R = 5.2\%$ , and  $R_w = 5.1\%$  for **2**, and  $a = 11.068(5)$  Å,  $b = 12.470(3)$  Å,  $c = 17.654(5)$  Å,  $\alpha = 90.97(2)^\circ$ ,  $\beta = 107.77(3)^\circ$ ,  $\gamma = 112.23(3)^\circ$ ,  $Z = 4$ ,  $R = 5.9\%$ , and  $R_w = 4.8\%$  for **3**. The dialkylaluminum thiolates, **4–7**, were found to be trimeric in the solid state. The structure of **4** was determined in space group  $P2_1/c$  (No. 14),  $a = 9.324(7)$  Å,  $b = 18.632(5)$  Å,  $c = 23.959(9)$  Å,  $\beta = 98.31(5)^\circ$ ,  $Z = 4$  (trimers),  $R = 7.6\%$ , and  $R_w = 5.2\%$ ; **5** in space group  $P\bar{1}$  (No. 2),  $a = 10.149(4)$  Å,  $b = 14.427(5)$  Å,  $c = 15.159(4)$  Å,  $\alpha = 88.19(3)^\circ$ ,  $\beta = 89.39(3)^\circ$ ,  $\gamma = 88.57(3)^\circ$ ,  $Z = 2$  (trimers),  $R = 5.0\%$ , and  $R_w = 5.0\%$ ; **6** in space group  $P\bar{1}$  (No. 2),  $a = 12.538(5)$  Å,  $b = 13.180(2)$  Å,  $c = 13.873(2)$  Å,  $\alpha = 74.38(1)^\circ$ ,  $\beta = 64.18(2)^\circ$ ,  $\gamma = 69.44(2)^\circ$ ,  $Z = 2$  (trimers),  $R = 5.2\%$  and  $R_w = 4.4\%$ ; and **7** in space group  $P2_1/c$  (No. 14),  $a = 13.935(2)$  Å,  $b = 22.563(4)$  Å,  $c = 25.044(4)$  Å,  $\beta = 101.44(1)^\circ$ ,  $Z = 4$  (trimers),  $R = 12.5\%$ , and  $R_w = 14.2\%$ . The sulfur atoms in **7** are in a planar environment. Compounds **8** and **9** are tetrameric with eight-membered  $(\text{MS})_4$  ( $\text{M} = \text{Al}, \text{Ga}$ ) ring systems. They are isomorphous, and their structures were determined in space group  $P\bar{1}$  (No. 2). For **8**  $a = 8.555(1)$  Å,  $b = 11.869(1)$  Å,  $c = 12.688(1)$  Å,  $\alpha = 96.546(8)^\circ$ ,  $\beta = 106.34(1)^\circ$ ,  $\gamma = 109.06(1)^\circ$ ,  $Z = 2$ ,  $R = 5.0\%$ , and  $R_w = 5.2\%$ , and for **9**  $a = 8.525(2)$  Å,  $b = 11.805(3)$  Å,  $c = 12.714(4)$  Å,  $\alpha = 96.36(2)^\circ$ ,  $\beta = 106.46(2)^\circ$ ,  $\gamma = 108.90(2)^\circ$ ,  $Z = 2$ ,  $R = 6.1\%$ , and  $R_w = 6.6\%$ .

## Introduction

The structural features of group 13 organometallic compounds have been of fundamental interest because of the three-center, two-electron bonds that are commonly observed in these systems.<sup>1</sup> When diorgano-group 13 pnictinides or chalcogenides are prepared, these electron-deficient bonds are replaced by normal two-electron bonds, giving rise to a new series of compounds with similar structures but differing electronic properties because of the electron-rich bridging atoms.

Earlier work has been reviewed by Matteson,<sup>2</sup> Coates,<sup>3</sup> Eisch,<sup>4</sup> and Mole.<sup>5</sup> Extensive reviews of these topics in "Coordination Chemistry of Aluminum"<sup>6</sup> provide de-

tailed information on the structures, bonding, and reactivity of Group 13–15 and Group 13–16 compounds. We have recently reviewed the work on the thiolates, selenolates, and tellurolates of group 13 derivatives.<sup>7,8</sup>

These compounds exhibit a variety of structural types depending on the metal, the chalcogen, and the substituents on each. The derivatives with very bulky substituents are monomeric with the substituents surrounding the metal atom preventing dimerization. These include the oxygen derivatives,  $\text{MeAl}[2,6\text{-}(t\text{-Bu})_2\text{-4-MeC}_6\text{H}_2\text{O}]_2$ <sup>9</sup> and  $(t\text{-Bu})_2\text{GaOCPh}_3$ ,<sup>10</sup> the sulfur derivatives,  $\text{Al}(\text{SMes}^*)_3$  and  $\text{Ga}(\text{SMes}^*)_3$  ( $\text{Mes}^* = 2,4,6\text{-}t\text{-Bu}_3\text{-C}_6\text{H}_2$ ),<sup>11</sup> the selenium derivative,  $\text{Ga}(\text{SeMes}^*)_3$ ,<sup>12</sup> and the tellurium compound,  $[(\text{Me}_3\text{Si})_2\text{CH}]_2\text{GaTeSi}(\text{SiMe}_3)_3$ .<sup>13</sup>

\* Abstract published in *Advance ACS Abstracts*, May 15, 1995.

(1) Oliver, J. P. In *The Chemistry of the Metal-Carbon Bond*; Hartley, F. R., Patai, S., Eds.; John Wiley and Sons: New York, 1985; Vol. 2, pp 789–826.

(2) Matteson, D. S. *Organometallic Reaction Mechanisms*; Academic Press: New York, 1974.

(3) Coates, G. E.; Wade, K. *The Main Group Elements* 3rd ed.; Methuen: London, 1967; Vol. 1.

(4) Eisch, J. J. In *Comprehensive Organometallic Chemistry*; Wilkinson, G., Stone, F. G. A., Abel, E. W., Eds.; Pergamon: Oxford, 1982; Vol. 1, pp 555–683.

(5) Mole, T.; Jeffrey, E. A. *Organoaluminum Compounds*; Elsevier: Amsterdam, 1972.

(6) Robinson, G. H. *Coordination Chemistry of Aluminum*; VCH: New York, 1993.

(7) Oliver, J. P.; Kumar, R. *Polyhedron* **1990**, *9*, 409.

(8) Oliver, J. P.; Kumar, R.; Taghiof, M. In *Coordination Chemistry of Aluminum*; Robinson, G. H., Ed.; VCH: New York, 1993; pp 167–195.

(9) Robinson, G. H.; Sangokoya, S. A. *J. Am. Chem. Soc.* **1987**, *109*, 6862.

(10) Cleaver, W. M.; Barron, A. R. *Organometallics* **1993**, *12*, 1001.

The dimeric derivatives,  $[\text{R}_2\text{M}(\mu\text{-ER}')_2]$  (R and R' = alkyl, aryl; M = Al, Ga, In; E = O, S, Se, Te) constitute a second class of structures. In addition to the alkoxides which have been studied extensively, these include  $[\text{Me}_2\text{Al}(\mu\text{-SC}_6\text{F}_5)_2]_2$ ,<sup>14</sup>  $[(t\text{-Bu})_2\text{Al}(\mu\text{-Te-}t\text{-Bu})_2]_2$ ,<sup>15</sup>  $[\text{Ph}_2\text{Ga}(\mu\text{-S-Et})_2]_2$ ,<sup>16</sup>  $[t\text{-Bu}_2\text{Ga}(\mu\text{-SH})_2]_2$ ,<sup>17</sup>  $[\text{Ph}_2\text{Ga}(\mu\text{-SSn}(\text{C}_6\text{H}_{11})_3)_2]_2$ ,<sup>18</sup>  $[\text{Ph}_2\text{Ga}(\mu\text{-SeMe})_2]_2$ ,<sup>19</sup> and  $[\text{Np}_2\text{Ga}(\mu\text{-TePh})_2]_2$ .<sup>20</sup> These examples all have planar or nearly planar  $(\text{ME})_2$  rings with the substituent on the chalcogen in the *trans* configuration.

The third class of compounds are those which involve six-membered  $(\text{ME})_3$  rings, but there are very few examples with chalcogens. The reported structures include  $[\text{Me}_2\text{Al}(\mu\text{-OMe})_3]_3$ <sup>21</sup> and  $[\text{Me}_2\text{In}(\mu\text{-SSiPh}_3)_3]_3$ .<sup>22</sup> There also is an unusual sulfide derivative,  $[(t\text{-Bu})(\text{Py})\text{-Ga}(\mu\text{-S})_3]_3$ .<sup>23</sup> For Group 13–15 derivatives, there are a number of examples of  $[\text{R}_2\text{M}(\mu\text{-ER}'_2)]_3$  (E = N, P, As; R = H, Me, Ph).<sup>24–28</sup> No trimeric derivatives of aluminum or gallium with thiolate, selenolate, or telluroate bridges have been reported. The only two eight-membered ring systems that have been reported for group 13 derivatives are  $[\text{Me}_2\text{Al}(\mu\text{-F})_4]_4$ <sup>29</sup> with bridging fluorine atoms between the  $\text{Me}_2\text{Al}$  units and  $[\text{Me}_2\text{Ga}(\mu\text{-OH})_4]_4$ <sup>30</sup> with bridging hydroxyl groups.

Other studies have provided isolated examples of chains such as  $[\text{Me}_2\text{Al}(\mu\text{-SMe})_\infty]_n$ ,<sup>31</sup>  $[\text{MeIn}(\text{SePh})(\mu\text{-SePh})_\infty]_n$ ,<sup>32</sup> and  $[\text{In}(\text{SePh})_3]_\infty$ .<sup>33</sup> Small heteronuclear cluster compounds, including  $[t\text{-BuGa}(\mu_3\text{-S})_4]_4$ ,<sup>15,34</sup> and  $[t\text{-BuGa}(\mu_3\text{-S})_6]_6$ ,<sup>23</sup> have been reported with sulfide bridging groups.

The studies reported do not provide adequate data to develop an understanding of those factors which deter-

mine the aggregate size or structure for the group 13–16 organometallic derivatives of the type  $[\text{R}_2\text{M}(\mu\text{-ER}')_n]_n$ . To address this problem, we have started a systematic study of the syntheses and structures of these derivatives and in this paper present our findings on a series of dialkylaluminum thiolates with four-membered  $(\text{AlS})_2$ , six-membered  $(\text{AlS})_3$ , and eight-membered  $(\text{AlS})_4$  rings and an example of a gallium thiolate with an eight-membered  $(\text{GaS})_4$  ring. A detailed study of the equilibria and the dynamic behavior of these systems in solution as followed by NMR spectroscopy will be discussed in a subsequent paper.<sup>35</sup>

## Experimental Section

**General Data.** The compounds synthesized are both air and moisture sensitive, so they were prepared and manipulated under an argon atmosphere using standard Schlenk line and glovebox techniques. Argon was purified by passing it through a series of columns containing Deox catalyst (Alfa), calcium sulfate, and phosphorus pentoxide. All solvents used were dried using standard techniques,<sup>36</sup> and all glassware was oven- or flame-dried. Trimethylaluminum (2.0 M in toluene), *i*-Bu<sub>3</sub>Al (1.0 M in toluene), decalin, 2-bromomesitylene, 2-isopropylthiophenol, benzylthiol, benzenethiol, 2,6-dimethylthiophenol, and 2,4,6-triisopropylbenzenesulfonyl chloride were purchased from Aldrich and used without further purification. Me<sub>3</sub>Ga was obtained from Strem, and 2-*t*-butylthiophenol was obtained from Lancaster. 2-(Me<sub>3</sub>Si)C<sub>6</sub>H<sub>4</sub>SH,<sup>37</sup> Ph<sub>3</sub>SiSH,<sup>38</sup> and Mes<sub>3</sub>Al (Mes = 2,4,6-Me<sub>3</sub>C<sub>6</sub>H<sub>2</sub>)<sup>39</sup> were prepared according to published procedures. <sup>1</sup>H and <sup>13</sup>C NMR spectra were recorded on a General Electric QE300 or GN300 NMR spectrometer at ambient temperature. The proton chemical shifts were referenced to C<sub>6</sub>D<sub>5</sub>H ( $\delta$  = 7.15 ppm), the carbon resonances to C<sub>6</sub>D<sub>6</sub> ( $\delta$  = 128.0 ppm), and the <sup>29</sup>Si NMR spectra (59.60 MHz) to Si(CH<sub>3</sub>)<sub>4</sub> ( $\delta$  = 0 ppm) in benzene. Analyses were performed at Galbraith Laboratories, Knoxville, TN. Melting points were measured on a Haake-Buchler melting point apparatus and are uncorrected. Mass spectrometry data were obtained on a Kratos MS80 RFA mass spectrometer using electron ionization (70 eV).

**Synthesis of 2,4,6-*i*-Pr<sub>3</sub>C<sub>6</sub>H<sub>2</sub>SH.** The thiol, 2,4,6-*i*-Pr<sub>3</sub>C<sub>6</sub>H<sub>2</sub>SH, was prepared as described previously and purified by distillation under reduced pressure.<sup>40</sup> <sup>1</sup>H NMR (C<sub>6</sub>D<sub>6</sub>): 1.196 (d,  $J_{\text{H-H}}$  = 6.9 Hz, 12H, 2,6-CH(CH<sub>3</sub>)<sub>2</sub>), 1.199 (d,  $J_{\text{H-H}}$  = 6.6 Hz, 6H, 4-CH(CH<sub>3</sub>)<sub>2</sub>), 2.79 (sept, 1H, 4-CH(CH<sub>3</sub>)<sub>2</sub>), 2.90 (s, 1H, SH), 3.52 (sept, 2H, 2,6-CH(CH<sub>3</sub>)<sub>2</sub>), 7.05 (s, 2H, aryl H). <sup>13</sup>C-<sup>1</sup>H NMR (C<sub>6</sub>D<sub>6</sub>): 23.4, 24.3 (CH(CH<sub>3</sub>)<sub>2</sub>), 32.2, 34.6 (CH(CH<sub>3</sub>)<sub>2</sub>), 121.5, 124.8, 147.3, 148.5 (aryl).

**Synthesis of [Mes<sub>2</sub>Al(μ-SBz)]<sub>2</sub> (1).** Benzylthiol (Bz = CH<sub>2</sub>C<sub>6</sub>H<sub>5</sub>) (0.3 mL, 2.55 mmol) was added dropwise to a solution of Mes<sub>3</sub>Al (Mes = 2,4,6-Me<sub>3</sub>C<sub>6</sub>H<sub>2</sub>) (1.0 g, 2.6 mmol) in 50 mL of toluene. The product precipitated from the reaction mixture and was recrystallized from warm toluene. Yield: ~60%. MP: 279–280 °C. <sup>1</sup>H NMR (C<sub>6</sub>D<sub>6</sub>,  $\delta$ , ppm): 2.13 (s, 6H, 4-CH<sub>3</sub> of Mes), 2.66 (s, 12H, 2,6-CH<sub>3</sub> of Mes), 3.56 (s, 2H, SCH<sub>2</sub>Ph), 6.72 (s, 2H, H of Mes), 6.78 (m, 3H, SCH<sub>2</sub>Ph), 6.90 (m, 2H, SCH<sub>2</sub>Ph). <sup>13</sup>C NMR (C<sub>6</sub>D<sub>6</sub>,  $\delta$ , ppm): 21.2 (4-CH<sub>3</sub> of Mes), 26.0 (2,6-CH<sub>3</sub> of Mes), 36.1 (SCH<sub>2</sub>Ph), 127.3, 128.9, 138.4, 138.7, 145.7 (aryl). Anal. for C<sub>25</sub>H<sub>29</sub>AlS. Calcd (found): C, 77.28 (75.62); H, 7.52 (7.48).

(35) Kumar, R.; Bailey, M.; Barber, M.; Hendershot, D. G.; Taghiof, M.; Rahbarnoohi, H.; Dick, D. G.; Oliver, J. P. To be submitted for publication.

(36) Shriver, D. F.; Drezdson, M. A. *The Manipulation of Air-Sensitive Compounds*; John Wiley & Sons: New York, 1986.

(37) Block, E.; Eswarakrishnan, V.; Gernon, M.; Ofori-Okai, G.; Saha, C.; Tang, K.; Zubieta, J. *J. Am. Chem. Soc.* **1989**, *111*, 658.

(38) Calas, R.; Duffaut, N.; Martel, B.; Paris, C. *Bull. Soc. Chim. Fr.* **1961**, 886.

(39) Seidel, W. Z. *Anorg. Allg. Chem.* **1985**, *524*, 101. Jerius, J. T.; Hahn, J. M.; Rahman, A. F. M. M.; Mols, O.; Iisley, W. H.; Oliver, J. P. *Organometallics* **1986**, *5*, 1812.

(40) Pearson, D. E.; Caine, D.; Field, L. *J. Org. Chem.* **1960**, *25*, 867.

(11) Ruhlandt-Senge, K.; Power, P. P. *Inorg. Chem.* **1991**, *30*, 2633.

(12) Ruhlandt-Senge, K.; Power, P. P. *Inorg. Chem.* **1991**, *30*, 3683.

(13) Uhl, W.; Layh, M.; Becker, G.; Klinkhammer, K. W.; Hildenbrand, T. *Chem. Ber.* **1992**, *125*, 1547.

(14) de Mel, V. S. J.; Kumar, R.; Oliver, J. P. *Organometallics* **1990**, *9*, 1303.

(15) Cowley, A. H.; Jones, R. A.; Harris, P. R.; Atwood, D. A.; Contreras, L.; Burek, C. J. *Angew. Chem., Int. Ed. Engl.* **1991**, *30*, 1143.

(16) Hoffmann, G. G.; Burschka, C. *J. Organomet. Chem.* **1984**, *267*, 229.

(17) Power, M. B.; Barron, A. R. *J. Chem. Soc., Chem. Commun.* **1991**, 1315.

(18) Ghazi, S. U.; Heeg, M. J.; Oliver, J. P. *Inorg. Chem.* **1994**, *33*, 4517.

(19) Kumar, R.; Dick, D. G.; Ghazi, S. U.; Taghiof, M.; Heeg, M. J.; Oliver, J. P. *Organometallics* **1995**, *14*, 1601.

(20) Banks, M. A.; Beachley, O. T., Jr.; Gysling, H. J.; Luss, H. R. *Organometallics* **1990**, *9*, 1979.

(21) Drew, D. A.; Haaland, A.; Weidlein, J. Z. *Anorg. Allg. Chem.* **1973**, *398*, 241.

(22) Rahbarnoohi, H.; Taghiof, M.; Heeg, M. J.; Dick, D. G.; Oliver, J. P. *Inorg. Chem.* **1994**, *33*, 6307.

(23) Power, M. B.; Ziller, J. W.; Barron, A. R. *Organometallics* **1992**, *11*, 2783.

(24) Beachley, O. T., Jr.; Royster, T. L., Jr.; Arhar, J. R.; Rheingold, A. L. *Organometallics* **1993**, *12*, 1976.

(25) McLaughlin, G. M.; Sim, G. A.; Smith, J. D. *J. Chem. Soc., Dalton Trans.* **1972**, 2197.

(26) Semenenko, K. N.; Lobkovskii, E. B.; Dorosinskii, A. L. *J. Struct. Chem. (Engl. Transl.)* **1972**, *13*, 743.

(27) Harrison, W.; Storr, A.; Trotter, J. *J. Am. Chem. Soc., Dalton Trans.* **1972**, 1554.

(28) Cowley, A. H.; Jones, R. A.; Kidd, K. B.; Nunn, C. M.; Westmoreland, D. L. *J. Organomet. Chem.* **1988**, *341*, C1.

(29) Gunderson, G.; Haugen, T.; Haaland, A. *J. Organomet. Chem.* **1973**, *54*, 77.

(30) Smith, G. S.; Hoard, J. L. *J. Am. Chem. Soc.* **1959**, *81*, 3907.

(31) Brauer, D. J.; Stucky, G. D. *J. Am. Chem. Soc.* **1969**, *91*, 5462.

(32) Rahbarnoohi, H.; Kumar, R.; Heeg, M. J.; Oliver, J. P. *Organometallics*, in press.

(33) Annan, T.; Kumar, R.; Mabrouk, H. E.; Tuck, D. G.; Chadha, R. K. *Polyhedron* **1989**, *8*, 865.

(34) Power, M. B.; Ziller, J. W.; Tyler, A. N.; Barron, A. R. *Organometallics* **1992**, *11*, 1055.

**Synthesis of [Me<sub>2</sub>Al(μ-SSiPh<sub>3</sub>)<sub>2</sub>] (2).** Me<sub>3</sub>Al (2.0 mL, 4.00 mmol) was added at room temperature to Ph<sub>3</sub>SiSH (1.00 g, 3.42 mmol) in pentane. Gas evolution was noted during the course of the reaction. The product precipitated and subsequently was recrystallized from a pentane/toluene mixture at room temperature resulting in X-ray quality crystals. Yield: ~70%. MP: 195 °C. <sup>1</sup>H NMR (C<sub>6</sub>D<sub>6</sub>, δ, ppm): -0.56 (s, trimer), -0.45 (s, Al(CH<sub>3</sub>)<sub>2</sub>, dimer). (An equilibrium for the process 2 trimer ⇌ 3 dimer is established with *K*<sub>eq</sub> = 31 mol/L. Details are discussed elsewhere.<sup>35</sup>) 7.04 (m, 9H, Ph), 7.74 (m, 6H, Ph). <sup>13</sup>C NMR (C<sub>6</sub>D<sub>6</sub>, δ, ppm): -4.36, -3.12 (Al(CH<sub>3</sub>)<sub>2</sub>), 128.3, 128.5, 130.7, 130.8, 133.5, 133.7, 136.1, 136.6 (aryl). <sup>29</sup>Si NMR (C<sub>6</sub>D<sub>6</sub>, δ, ppm): -2.2, -1.7 (SiPh<sub>3</sub>). Anal. for C<sub>20</sub>H<sub>21</sub>-AlSiS. Calcd (found): C, 68.94 (69.23%); H, 6.01% (5.65%).

**Synthesis of [Mes<sub>2</sub>Al(μ-SPh)]<sub>2</sub> (3).** Compound 3 was prepared by reaction of PhSH (8.4 mL, 0.195 M, 1.63 mmol) with Mes<sub>3</sub>Al (0.630 g, 1.64 mmol) in hexane as described for 2. This material was recrystallized from hot hexane/toluene (50:50 solution), resulting in X-ray quality crystals. Yield: 24%. MP: 233 °C. <sup>1</sup>H NMR (C<sub>6</sub>D<sub>6</sub>, δ, ppm): 2.03 (s, 6H, 4-CH<sub>3</sub> of Mes), 2.74 (s, 12H, 2,6-CH<sub>3</sub> of Mes), 6.51 (m, 3H, Ph), 6.56 (s, 4H, aryl of Mes), 6.98 (m, 2H, Ph). <sup>13</sup>C{<sup>1</sup>H} NMR (C<sub>6</sub>D<sub>6</sub>, δ, ppm): 21.1 (4-CH<sub>3</sub> of Mes), 25.6 (2,6-CH<sub>3</sub> of Mes), 127.9, 129.1, 133.9, 134.3, 138.0, 145.29. MS (EI, *m/e*): 483 (Mes<sub>2</sub>Al(SPh)<sub>2</sub>, 0.1), 438 (Mes<sub>2</sub>Al(SPh)<sub>2</sub> - 3Me, 1.0).

**Synthesis of {Me<sub>2</sub>Al[μ-S(2-*t*-BuC<sub>6</sub>H<sub>4</sub>)]<sub>3</sub> (4).** Compound 4 was prepared by reaction of Me<sub>3</sub>Al (2.5 mL, 2.0 M soln) with 2-*tert*-butylthiophenol as described for 2. The solid was recrystallized from pentane at -10 °C. Yield: ~60%. MP: 171 °C. <sup>1</sup>H NMR (C<sub>6</sub>D<sub>6</sub>, δ, ppm): -0.43 (s, 3H, Al(CH<sub>3</sub>)<sub>2</sub>), -0.23 (s, 6H, Al(CH<sub>3</sub>)<sub>2</sub>), -0.11 (s, 6H, Al(CH<sub>3</sub>)<sub>2</sub>), 0.19 (s, 3H, Al(CH<sub>3</sub>)<sub>2</sub>), 1.55 (s, 9H, *t*-Bu), 1.53 (s, 18H, *t*-Bu), 6.98 (m, 6H, Ar), 7.94 (m, 2H, Ar), 7.26 (m, 3H, Ar), 8.13 (m, 1H, Ar). <sup>13</sup>C-{<sup>1</sup>H} NMR (C<sub>6</sub>D<sub>6</sub>, δ, ppm): -8.1 (Al(CH<sub>3</sub>)<sub>2</sub>), -7.2 (Al(CH<sub>3</sub>)<sub>2</sub>), -5.5, (Al(CH<sub>3</sub>)<sub>2</sub>), 30.7 (C(CH<sub>3</sub>)), 30.7 (C(CH<sub>3</sub>)), 36.5 (C(CH<sub>3</sub>)), 125.4, 126.6, 128.2, 128.7, 138.0, 138.6, 139.1, 152.3, 152.4 (aryl). Anal. for C<sub>12</sub>H<sub>19</sub>AlS. Calcd (found): C, 64.83 (61.87); H, 8.61 (7.98).

**Synthesis of {Me<sub>2</sub>Al[μ-S(2-Me<sub>3</sub>Si)C<sub>6</sub>H<sub>4</sub>]}<sub>3</sub> (5).** Compound 5 was prepared by reaction of the thiol, HS(2-Me<sub>3</sub>Si)C<sub>6</sub>H<sub>4</sub> (0.60 mL, 3.4 mmol), with Me<sub>3</sub>Al (1.7 mL, 2.0 M solution, 3.4 mmol) following the procedure used for 2. The white solid was recrystallized from pentane, yielding colorless crystals. Yield: ~60%. MP: 169 °C. <sup>1</sup>H NMR (C<sub>6</sub>D<sub>6</sub>, δ, ppm): -0.42 (s, 3H, Al(CH<sub>3</sub>)<sub>2</sub>-trimer), -0.34 (s, 6H, Al(CH<sub>3</sub>)<sub>2</sub>-trimer), -0.15 (s, 12H, Al(CH<sub>3</sub>)<sub>2</sub>-dimer), -0.05 (s, 6H, Al(CH<sub>3</sub>)<sub>2</sub>-trimer), 0.13 (s, 3H, Al(CH<sub>3</sub>)<sub>2</sub>-trimer), 0.42 (s, 18H, SiMe<sub>3</sub>-dimer), 0.43 (s, 9H, SiMe<sub>3</sub>-trimer), 0.44 (s, 18H, Si(CH<sub>3</sub>)<sub>3</sub>-trimer) (An equilibrium for the process 2 trimer ⇌ 3 dimer is established with *K*<sub>eq</sub> = 0.4 mol/L. Details are discussed elsewhere.<sup>35</sup>) 7.01 (m, 5H, aryl), 7.21 (d of t, *J*<sub>H-H</sub> = 7.2 and 1.5 Hz, 1H, aryl), 7.39 (d of d, 3H, *J*<sub>H-H</sub> = 1.2 and 7.2 Hz, aryl), 7.87 (d, *J*<sub>H-H</sub> = 6.9 Hz, 2H, aryl), 8.06 (d, *J*<sub>H-H</sub> = 7.8 Hz, 1H, aryl). <sup>13</sup>C NMR (C<sub>6</sub>D<sub>6</sub>, δ, ppm): -7.9, -7.3, -6.8, -5.4, (Al(CH<sub>3</sub>)<sub>2</sub>), 0.7, 0.3 (Si(CH<sub>3</sub>)<sub>3</sub>-trimer), 0.01 (Si(CH<sub>3</sub>)<sub>3</sub>-dimer), 127.1, 127.4, 129.3, 130.1, 130.3, 133.1, 133.3, 135.0, 136.0, 136.2, 136.5, 136.9, 145.3, 145.5 (aryl of dimer and trimer). Anal. for C<sub>11</sub>H<sub>19</sub>AlSiS. Calcd (found): C, 55.42 (51.97), H, 8.03 (7.76).

**Synthesis of {Me<sub>2</sub>Al[μ-S(2-*i*-PrC<sub>6</sub>H<sub>4</sub>)]<sub>3</sub> (6).** Trimethylaluminum (3.5 mL, 2.0 M soln, 7.0 mmol) was added to 1.0 mL (6.89 mmol) of 2-isopropylthiophenol in approximately 50 mL of pentane. Colorless crystals were obtained from the solution by cooling to -10 °C. Yield: ~50%. MP 125 °C. <sup>1</sup>H NMR (C<sub>6</sub>D<sub>6</sub>, δ, ppm): -0.17 (s, 6H, Al(CH<sub>3</sub>)<sub>2</sub>), 1.13 (d, *J*<sub>H-H</sub> = 7 Hz, 6H, -CH(CH<sub>3</sub>)<sub>2</sub>), 3.80 (sept, *J*<sub>H-H</sub> = 7 Hz, 1H, CH(CH<sub>3</sub>)<sub>2</sub>), 7.00 (m, 3H, Ar), 7.91 (m, 1H, Ar). <sup>13</sup>C NMR (C<sub>6</sub>D<sub>6</sub>, δ, ppm): -7.6 (Al(CH<sub>3</sub>)<sub>2</sub>), 23.0 (-CH(CH<sub>3</sub>)<sub>2</sub>), 31.3 (-CH(CH<sub>3</sub>)<sub>2</sub>), 124.9, 126.5, 126.8, 129.1, 135.6, 151.8 (aryl). Anal. for C<sub>11</sub>H<sub>17</sub>AlS. Calcd (found): C, 63.43 (61.56); H, 8.23 (7.76).

**Synthesis of {*i*-Bu<sub>2</sub>Al[μ-S(2,4,6-*i*-Pr<sub>3</sub>C<sub>6</sub>H<sub>2</sub>)]<sub>3</sub> (7).** Compound 7 was prepared by reaction of triisobutylaluminum (5.0 mL, 1.0 M soln, 5.0 mmol) with 2,4,6-triisopropylthiophenol

(1.0 mL, 4.45 mmol) by the procedure used for 2. Cooling the pentane solution to -10 °C produced crystals. Yield: ~30%. MP: 107 °C. <sup>1</sup>H NMR (C<sub>6</sub>D<sub>6</sub>, δ, ppm): 0.73 (d, *J*<sub>H-H</sub> = 6.9 Hz, 4H, Al-CH<sub>2</sub>CH(CH<sub>3</sub>)<sub>2</sub>), 0.89 (d, *J*<sub>H-H</sub> = 6.3 Hz, 12H, Al-CH<sub>2</sub>-CH(CH<sub>3</sub>)<sub>2</sub>), 1.13 (d, *J*<sub>H-H</sub> = 6.6 Hz, 6H, 2,6-CH(CH<sub>3</sub>)<sub>2</sub>), 1.51 (d, *J*<sub>H-H</sub> = 6.3 Hz, 12H, 4-CH(CH<sub>3</sub>)<sub>2</sub>), 1.93 (sept, *J*<sub>H-H</sub> = 6.8 Hz, 2H, Al-CH<sub>2</sub>CH(CH<sub>3</sub>)<sub>2</sub>), 2.70 (sept, *J*<sub>H-H</sub> = 6.9 Hz, 1H, 4-CH(CH<sub>3</sub>)<sub>2</sub>), 4.30 (sept, *J*<sub>H-H</sub> = 6.8 Hz, 2H, 2,6-CH(CH<sub>3</sub>)<sub>2</sub>), 7.13 (s, 2H, aryl). <sup>13</sup>C NMR (C<sub>6</sub>D<sub>6</sub>, δ, ppm): 23.9, 24.8, 25.7, 25.9, 28.2, 32.5, 34.3, 122.5, 123.1, 149.8, 153.1. Anal. for C<sub>23</sub>H<sub>41</sub>AlS. Calcd (found): C, 73.35 (68.61); H, 10.97 (10.08).

**Synthesis of {Me<sub>2</sub>Al[μ-S(2,6-Me<sub>2</sub>C<sub>6</sub>H<sub>3</sub>)]<sub>4</sub> (8).** Compound 8 was prepared by the procedure used for 2 by addition of 2,6-dimethylthiophenol (1.0 mL, 7.51 mmol) to Me<sub>3</sub>Al (3.75 mL, 2.0 M solution, 7.5 mmol). The reaction mixture stood at -20 °C for 24 h during which time crystalline 8 deposited. Yield: 90%. MP: 140–143 °C. <sup>1</sup>H NMR (C<sub>6</sub>D<sub>6</sub>, δ, ppm): -0.30 (s, 6H, Al(CH<sub>3</sub>)<sub>2</sub>-trimer), -0.23 (s, 6H, Al(CH<sub>3</sub>)<sub>2</sub>-dimer), 2.60 (s, 6H, 2,6-(CH<sub>3</sub>)<sub>2</sub>C<sub>6</sub>H<sub>3</sub>-trimer), 2.60 (s, 6H, 2,6-(CH<sub>3</sub>)<sub>2</sub>C<sub>6</sub>H<sub>3</sub>-dimer), 6.85 (s, 3H, 2,6-(CH<sub>3</sub>)<sub>2</sub>C<sub>6</sub>H<sub>3</sub>-trimer), 6.87 (s, 3H, 2,6-(CH<sub>3</sub>)<sub>2</sub>C<sub>6</sub>H<sub>3</sub>-dimer). (An equilibrium for the process 2 trimer ⇌ 3 dimer is established with *K*<sub>eq</sub> = 0.6 mol/L. Details are discussed elsewhere.<sup>35</sup>) <sup>13</sup>C NMR (C<sub>6</sub>D<sub>6</sub>, δ, ppm): -6.7 (Al(CH<sub>3</sub>)<sub>2</sub>), -6.2 (Al(CH<sub>3</sub>)<sub>2</sub>), 24.0 (2,6-(CH<sub>3</sub>)<sub>2</sub>C<sub>6</sub>H<sub>3</sub>), 24.3 (2,6-(CH<sub>3</sub>)<sub>2</sub>C<sub>6</sub>H<sub>3</sub>), 128.2, 128.3, 128.8, 128.9, 142.5, 142.7, (aryl). MW (cryoscopically in benzene): 0.1976 g of 8 in 5.244 g of benzene, Δ*T* = 0.340 °C, MW = 567, *n* = 2.92; 0.468 g of 8, in 5.681 g of benzene, Δ*T* = 0.763 °C, MW = 574, *n* = 2.96; calcd for trimer, 583.2. Anal. for C<sub>10</sub>H<sub>15</sub>AlS. Calcd (found): C, 61.83 (60.83); H, 7.78 (7.78).

**Synthesis of {Me<sub>2</sub>Ga[μ-S(2,6-Me<sub>2</sub>C<sub>6</sub>H<sub>3</sub>)]<sub>4</sub> (9).** Trimethylgallium (0.36 mL, 3.62 mmol) was added to 0.500 g (0.48 mL, 3.62 mmol) of 2,6-dimethylthiophenol in 20 mL of toluene at 0 °C, and the solution was stirred overnight. The volatiles were removed under vacuum, leaving a white solid which was recrystallized from a mixture of toluene and pentane at -20 °C. Yield: 88%. <sup>1</sup>H NMR (C<sub>6</sub>D<sub>6</sub>, δ, ppm): 0.08, 0.10, 0.12, 0.20 (s, 6H, Ga(CH<sub>3</sub>)<sub>2</sub>), 2.55, 2.58, 2.61 (s, 6H, 2,6-(CH<sub>3</sub>)<sub>2</sub>C<sub>6</sub>H<sub>3</sub>), 6.88 (s, 3H, 2,6-(CH<sub>3</sub>)<sub>2</sub>C<sub>6</sub>H<sub>3</sub>). <sup>13</sup>C NMR (C<sub>6</sub>D<sub>6</sub>, δ, ppm): -1.9, -1.7, -0.7 (Ga(CH<sub>3</sub>)<sub>2</sub>), 24.2 (br, 2,6-(CH<sub>3</sub>)<sub>2</sub>C<sub>6</sub>H<sub>3</sub>), 127.4, 127.5, 128.4, 128.6, 128.7, 142.5 (aryl).

**X-ray Data Collection and Structure Refinement.** Suitable crystals of compounds 1–9 were prepared using the procedures described in the Experimental Section. Crystals of each compound were inserted into thin-walled glass capillaries under an argon atmosphere in a drybox, which were plugged with grease, removed from the drybox, flame-sealed, and mounted on a goniometer head. Diffraction data were collected on a Syntex/Siemens P2<sub>1</sub> or R3 diffractometer using nickel-filtered Cu radiation (λ = 1.581 84 Å) or graphite-monochromatized MoKα radiation (λ = 0.710 73 Å). The initial orientation matrices were obtained from 15 to 25 machine-centered reflections chosen from rotation photographs. Axial photographs were consistent with the crystal systems selected for all compounds. Ultimately, 25 high-angle reflections were used to determine the final cell constants and orientation matrices. The symmetries of the cells for 2, 3, 5, 6, 8, and 9 were consistent with the space groups *P*1 and *P*1̄. Successful refinement of the structures confirmed the space groups as *P*1̄ for these six structures. Compounds 1, 4, and 7 were consistent with the monoclinic system and were assigned to the space groups *P*2<sub>1</sub>/*c* for 4 and 7 and *P*2<sub>1</sub>/*n* for 1. In the cases of 1, 2, and 8, absorption corrections were applied (ψ scans). Selected crystal and data collection parameters for all compounds are listed in Table 1.

For compounds 1, 2, and 4–9, data reduction was carried out using the SHELXTL programs,<sup>41</sup> and data refinement was performed with SHELX-76.<sup>42</sup> For compound 3, data reduction and solution were carried out using SHELXTL PC.<sup>43</sup> Scat-

(41) Sheldrick, G. M. *SHELXTL*; University of Göttingen: Göttingen, Federal Republic of Germany, 1978.



**Table 1. Selected Experimental Parameters for the X-ray Diffraction Studies of [Mes<sub>2</sub>Al(μ-SBz)]<sub>2</sub> (1), [Me<sub>2</sub>Al(μ-SSiPh<sub>3</sub>)]<sub>2</sub> (2), [Mes<sub>2</sub>Al(μ-SPh)]<sub>2</sub> (3), {Me<sub>2</sub>Al[μ-S(2-*t*-BuC<sub>6</sub>H<sub>4</sub>)]<sub>3</sub> (4), {Me<sub>2</sub>Al[μ-S(2-Me<sub>3</sub>Si)C<sub>6</sub>H<sub>4</sub>]}<sub>3</sub> (5), {Me<sub>2</sub>Al[μ-S(2-*i*-PrC<sub>6</sub>H<sub>4</sub>)]<sub>3</sub> (6), {*i*-Bu<sub>2</sub>Al[μ-S(2,4,6-*i*-Pr<sub>3</sub>C<sub>6</sub>H<sub>2</sub>)]<sub>3</sub> (7), {Me<sub>2</sub>Al[μ-S(2,6-Me<sub>2</sub>C<sub>6</sub>H<sub>3</sub>)]<sub>4</sub> (8), and {Me<sub>2</sub>Ga[μ-S(2,6-Me<sub>2</sub>C<sub>6</sub>H<sub>3</sub>)]<sub>4</sub> (9)**

cmpd	1	2	3	4	5	6	7	8	9
formula	C <sub>25</sub> H <sub>29</sub> AlS	C <sub>40</sub> H <sub>42</sub> Al <sub>2</sub> -S <sub>2</sub> Si <sub>2</sub>	C <sub>24</sub> H <sub>27</sub> AlS	C <sub>36</sub> H <sub>57</sub> Al <sub>3</sub> S <sub>3</sub>	C <sub>35</sub> H <sub>57</sub> Al <sub>3</sub> -Si <sub>3</sub> S <sub>3</sub>	C <sub>33</sub> H <sub>51</sub> Al <sub>3</sub> S <sub>3</sub>	C <sub>69</sub> H <sub>123</sub> Al <sub>3</sub> S <sub>3</sub>	C <sub>20</sub> H <sub>30</sub> Al <sub>2</sub> S <sub>2</sub>	C <sub>20</sub> H <sub>30</sub> Ga <sub>2</sub> S <sub>2</sub>
fw (amu)	388.55	697.03	374.52	666.98	715.20	624.90	1129.87	388.55	474.02
space group	P2 <sub>1</sub> /n (No. 14)	P1̄ (No. 2)	P1̄ (No. 2)	P2 <sub>1</sub> /c (No. 14)	P1̄ (No. 2)	P1̄ (No. 2)	P2 <sub>1</sub> /c (No. 14)	P1̄ (No. 2)	P1̄ (No. 2)
α(Å)	10.660(4)	9.077(2)	11.068(5)	9.324(7)	10.149(4)	12.538(5)	13.935(2)	8.555(1)	8.525(2)
b(Å)	12.268(2)	13.847(3)	12.470(3)	18.632(5)	14.427(5)	13.180(2)	22.563(4)	11.869(1)	11.805(3)
c(Å)	17.793(3)	16.724(4)	17.654(5)	23.959(9)	15.159(4)	13.873(2)	25.044(4)	12.688(1)	12.714(4)
α (deg)		101.08(2)	90.97(2)		88.19(3)	74.38(1)		96.546(8)	96.36(2)
β (deg)	106.94(2)	95.34(2)	107.77(3)	98.31(5)	89.39(3)	64.18(2)	101.44(1)	106.34(1)	106.46(2)
γ (deg)		103.38(2)	112.23(3)		88.57(3)	69.44(2)		109.06(1)	108.90(2)
Z	4	2 (dimers)	4	4 (trimers)	2 (trimers)	2 (trimers)	4 (trimers)	2	2
volume (Å <sup>3</sup> )	2226.0(9)	1986.0(7)	2143(2)	4119(4)	2218(1)	1913.7(9)	7718(2)	1137.9(3)	1131.6(6)
D <sub>calcd</sub> (g/cm <sup>3</sup> )	1.16	1.17	1.16	1.08	1.07	1.08	1.03	1.13	1.39
radiation type	Mo Kα <sup>a</sup>	Mo Kα <sup>a</sup>	Mo Kα <sup>a</sup>	Mo Kα <sup>a</sup>	Mo Kα <sup>a</sup>	Mo Kα <sup>a</sup>	Mo Kα <sup>a</sup>	Cu Kα <sup>b</sup>	Cu Kα <sup>b</sup>
temp (°C)	22	22	20	22	22	22	22	20	20
μ (cm <sup>-1</sup> )	1.82	2.25	1.97	2.33	3.17	2.49	1.35	27.5	47.67
R <sup>c</sup>	0.067	0.0520	0.0593	0.0755	0.050	0.520	0.125	0.0495	0.0608
R <sub>w</sub> <sup>d</sup>	0.061	0.0514	0.0480	0.0517	0.050	0.0441	0.142	0.0522	0.0660

<sup>a</sup> Graphite monochromator, λ = 0.710 73 Å. <sup>b</sup> Nickel filter, λ = 1.541 78 Å. <sup>c</sup> R = Σ(|F<sub>o</sub>| - |F<sub>c</sub>|)/Σ|F<sub>o</sub>|. <sup>d</sup> R<sub>w</sub> = [Σw(|F<sub>o</sub>| - |F<sub>c</sub>|)<sup>2</sup>/Σw|F<sub>o</sub>|<sup>2</sup>]<sup>1/2</sup>.

tering factors<sup>44</sup> for neutral non-hydrogen atoms were used, and the data were corrected for Lorentz and polarization effects. Direct methods were used to obtain an initial solution for all of the structures and the positions for heavy atoms. The positions of the non-hydrogen atoms not found by the direct methods were located from successive difference Fourier map calculations. Full-matrix, least-squares refinement of positional and thermal parameters for non-hydrogen atoms was carried out by minimizing the function Σ(w|F<sub>o</sub>| - |F<sub>c</sub>|)<sup>2</sup> for all compounds except **3** and **4** which were refined using two- and three-blocked matrices, respectively. The hydrogen atoms were placed in calculated positions with a C-H bond distance of 0.96 Å, and their isotropic thermal parameters were fixed at 0.08 (**2**, **4**, **6**, **8**, and **9**), 0.10 (**1**), and 0.15 (**5**). All hydrogen atom positional parameters were allowed to ride with their parent carbon atoms during subsequent refinement.

In the final cycles of refinement all non-hydrogen atoms of **1**–**6**, **8**, and **9** were refined anisotropically. For compound **7**, only the Al and S atoms were refined anisotropically. The carbon atoms were refined isotropically, and the hydrogen atoms were not modeled because of the limited number of data. The structural solution of **7** was further complicated by disorder of one of the *i*-Pr and two of the *i*-Bu groups. The phenyl rings of **5** were refined as regular hexagons with C-C distances of 1.395 Å. The asymmetric unit for **1** is a Mes<sub>2</sub>-AlSBz moiety, the asymmetric unit for **2** is a complete dimeric molecule, and the asymmetric unit for **3** consists of two independent Mes<sub>2</sub>AlSPh moieties. The asymmetric units of **4**–**7** are complete trimeric molecules, and the asymmetric units of **8** and **9** contain one-half of a tetrameric molecule. One and 14 reflections were omitted in the refinement of **5** and **7**, respectively, because of secondary extinction.

The residual electron densities are of no chemical significance (<0.5 electrons). Atomic coordinates and isotropic thermal parameters for the non-hydrogen atoms are presented in Tables 2–10. Selected bond distances and angles are listed in Tables 11 (**1**–**3**), 12 (**4**–**7**), and 13 (**8**, **9**). A complete listing of crystal and X-ray data collection parameters, bond distances and angles, anisotropic thermal parameters for the non-hydrogen atoms, and atomic coordinates and isotropic thermal

**Table 2. Atomic Coordinates and Isotropic Thermal Parameters for the Non-Hydrogen Atoms of [Mes<sub>2</sub>Al(μ-SBz)]<sub>2</sub> (1)**

atom	x	y	z	U <sub>eq</sub> (Å <sup>2</sup> ) <sup>a</sup>
Al1	0.0124(2)	0.1050(2)	0.9404(1)	0.0421(8)
S1	-0.1307(2)	-0.0491(1)	0.9317(1)	0.0428(7)
C1	-0.2928(6)	-0.0032(5)	0.9398(4)	0.045(3)
C2	-0.3865(6)	-0.0987(5)	0.9252(4)	0.042(3)
C3	-0.4170(7)	-0.1569(6)	0.8555(4)	0.057(3)
C4	-0.5086(8)	-0.2400(6)	0.8432(5)	0.073(4)
C5	-0.5677(8)	-0.2683(6)	0.9001(7)	0.078(4)
C6	-0.5357(8)	-0.2104(7)	0.9699(5)	0.071(4)
C7	-0.4449(6)	-0.1253(6)	0.9828(4)	0.052(3)
C8	0.1358(6)	0.0962(6)	0.8758(3)	0.040(3)
C9	0.1999(6)	0.1928(5)	0.8640(4)	0.047(3)
C10	0.1811(8)	0.3010(6)	0.8995(5)	0.077(4)
C11	0.2899(7)	0.1904(6)	0.8193(4)	0.055(3)
C12	0.3172(6)	0.0954(7)	0.7860(4)	0.053(3)
C13	0.4132(7)	0.0941(6)	0.7383(4)	0.074(4)
C14	0.2572(6)	0.0001(6)	0.7995(4)	0.052(3)
C15	0.1690(6)	-0.0002(6)	0.8429(4)	0.044(3)
C16	0.1120(7)	-0.1091(5)	0.8563(4)	0.060(3)
C17	-0.1049(6)	0.2314(5)	0.9293(4)	0.044(3)
C18	-0.2060(8)	0.2389(6)	0.8576(5)	0.060(4)
C19	-0.2118(7)	0.1611(6)	0.7895(4)	0.070(4)
C20	-0.2993(8)	0.3206(7)	0.8448(6)	0.083(5)
C21	-0.2968(9)	0.3963(8)	0.9008(8)	0.101(6)
C22	-0.403(1)	0.4842(8)	0.8896(7)	0.146(7)
C23	-0.196(1)	0.3946(6)	0.9699(6)	0.080(5)
C24	-0.0974(7)	0.3148(6)	0.9854(5)	0.056(4)
C25	0.0140(9)	0.3266(5)	1.0578(5)	0.067(4)

<sup>a</sup> U<sub>eq</sub> (Å<sup>2</sup>) = 1/3Σ<sub>i</sub>Σ<sub>j</sub>U<sub>ij</sub>a<sub>i</sub>\*a<sub>j</sub>\*a<sub>i</sub>a<sub>j</sub>.

parameters for the hydrogen atoms are deposited as supplementary material.

## Results and Discussion

The aluminum and gallium thiolates prepared are colorless crystalline materials, sensitive to moisture and oxygen. All nine compounds have been characterized by single-crystal X-ray diffraction and form three separate classes of structures in the solid state: dimeric molecular units with four-membered (AlS)<sub>2</sub> rings, trimeric units with six-membered (AlS)<sub>3</sub> rings, and tetrameric units with eight-membered (AlS)<sub>4</sub> and (GaS)<sub>4</sub> rings.

Compounds **1**–**3** are dimeric in the solid state with planar or nearly planar four-membered (AlS)<sub>2</sub> rings.

(42) Sheldrick, G. M. *SHELX-76*; University Chemical Laboratory: Cambridge, England, 1976.

(43) *SHELXTL PC*; Siemens Analytical X-Ray Instruments, Inc.: Madison, WI, 1990.

(44) *International Tables for X-ray Crystallography*; Kynoch: Birmingham, England, 1974; Vol. 4 (present distributor, D. Reidel, Dordrecht, The Netherlands).



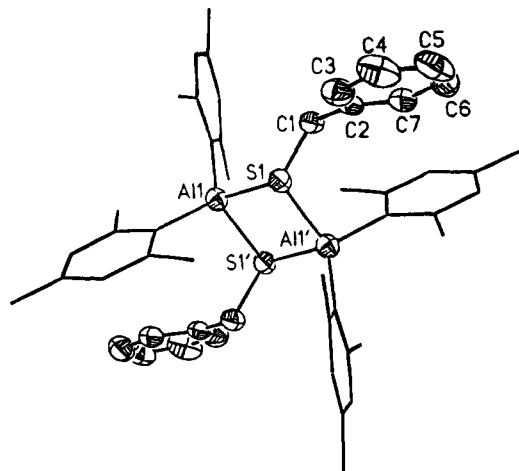


**Figure 1.** Diagram (50% thermal ellipsoids) of  $[\text{Me}_2\text{Al}(\mu\text{-SBz})]_2$  (**1**) showing the atom-labeling scheme. The mesityl rings have been shown as wire frames, and the hydrogen atoms have been omitted for clarity.

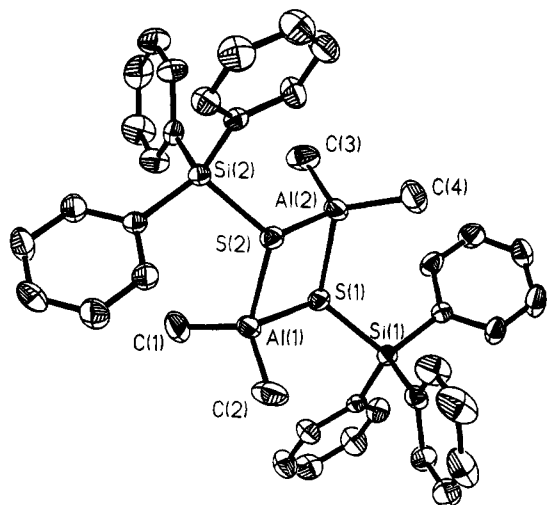


**Figure 2.** Diagram (20% thermal ellipsoids) of  $[\text{Me}_2\text{Al}(\mu\text{-SSiPh}_3)]_2$  (**2**) showing the atom-labeling scheme. Hydrogen atoms have been omitted for clarity.

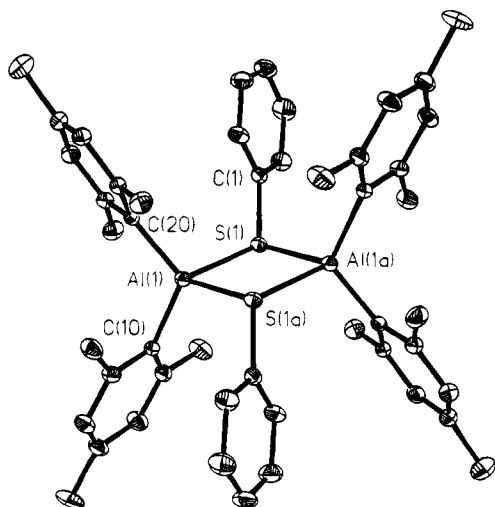


**Figure 3.** Diagram (20% thermal ellipsoids) of  $[\text{Me}_2\text{Al}(\mu\text{-SPh})]_2$  (**3**) showing the atom-labeling scheme. Hydrogen atoms have been omitted for clarity.

ORTEP or thermal ellipsoid diagrams are given in Figures 1, 2, and 3. The average Al–C bond lengths are 1.977, 1.928, and 1.968 Å. Compounds **1** and **3**, with

**Table 3.** Atomic Coordinates and Isotropic Thermal Parameters for the Non-Hydrogen Atoms of  $[\text{Me}_2\text{Al}(\mu\text{-SSiPh}_3)]_2$  (**2**)

atom	x	y	z	$U_{\text{eq}}$ (Å <sup>2</sup> ) <sup>a</sup>
S1	0.3175(2)	0.6140(1)	0.21865(8)	0.0472(5)
S2	0.1773(2)	0.3970(1)	0.26775(8)	0.0462(5)
Al1	0.3975(2)	0.4615(1)	0.2108(1)	0.0569(7)
Al2	0.0859(2)	0.5422(1)	0.2641(1)	0.0594(7)
Si1	0.4682(2)	0.7532(1)	0.29042(8)	0.0382(5)
Si2	0.0272(2)	0.2496(1)	0.20981(8)	0.0381(5)
C3	-0.0693(7)	0.5257(4)	0.1726(4)	0.092(3)
C4	0.0624(8)	0.6018(5)	0.3753(4)	0.114(4)
C1	0.3935(8)	0.4068(5)	0.0953(4)	0.102(3)
C2	0.5705(6)	0.4686(5)	0.2901(4)	0.091(3)
C11	0.3470(5)	0.8428(3)	0.3190(3)	0.040(2)
C12	0.2064(6)	0.8356(4)	0.2756(3)	0.063(2)
C13	0.1204(7)	0.9033(5)	0.2994(4)	0.076(3)
C14	0.1719(8)	0.9792(5)	0.3657(4)	0.072(3)
C15	0.3123(8)	0.9918(5)	0.4098(3)	0.082(3)
C16	0.3979(7)	0.9227(4)	0.3857(3)	0.064(3)
C17	0.5998(5)	0.7959(4)	0.2177(3)	0.040(2)
C18	0.6210(6)	0.8895(4)	0.1994(3)	0.057(2)
C19	0.7125(8)	0.9170(4)	0.1415(4)	0.075(3)
C20	0.7853(7)	0.8500(5)	0.1021(4)	0.073(3)
C21	0.7707(7)	0.7581(5)	0.1198(4)	0.071(3)
C22	0.6775(6)	0.7308(4)	0.1769(3)	0.057(2)
C23	0.5818(6)	0.7373(4)	0.3840(3)	0.050(2)
C24	0.5118(7)	0.6858(5)	0.4393(4)	0.087(3)
C25	0.600(1)	0.6754(7)	0.5082(4)	0.116(5)
C26	0.752(1)	0.7154(7)	0.5205(4)	0.107(5)
C27	0.8218(8)	0.7672(6)	0.4697(4)	0.093(4)
C28	0.7394(7)	0.7786(4)	0.4003(3)	0.066(3)
C29	-0.1027(6)	0.2508(4)	0.1170(3)	0.043(2)
C30	-0.2579(6)	0.2153(4)	0.1116(3)	0.061(2)
C31	-0.3556(6)	0.2162(5)	0.0423(4)	0.077(3)
C32	-0.2999(8)	0.2530(5)	-0.0196(4)	0.080(3)
C33	-0.1470(8)	0.2872(5)	-0.0168(4)	0.086(3)
C34	-0.0464(6)	0.2856(4)	0.0510(3)	0.065(2)
C35	-0.0892(5)	0.2161(4)	0.2915(3)	0.041(2)
C36	-0.1571(7)	0.2848(4)	0.3334(4)	0.064(3)
C37	-0.2452(8)	0.2605(5)	0.3946(4)	0.078(3)
C38	-0.2613(8)	0.1701(6)	0.4144(4)	0.082(3)
C39	-0.1961(8)	0.0998(5)	0.3738(4)	0.079(3)
C40	-0.1084(6)	0.1221(4)	0.3122(3)	0.056(2)
C41	0.1539(5)	0.1636(4)	0.1832(3)	0.041(2)
C42	0.2900(6)	0.1721(4)	0.2329(3)	0.056(2)
C43	0.3814(7)	0.1071(5)	0.2127(4)	0.070(3)
C44	0.3401(7)	0.0323(5)	0.1420(4)	0.071(3)
C45	0.2097(7)	0.0223(5)	0.0925(3)	0.073(3)
C46	0.1162(6)	0.0874(4)	0.1130(3)	0.060(2)

$$^a U_{\text{eq}} (\text{Å}^2) = \frac{1}{3} \sum_i \sum_j U_{ij} a_i^* a_j^* \mathbf{a}_i \cdot \mathbf{a}_j$$

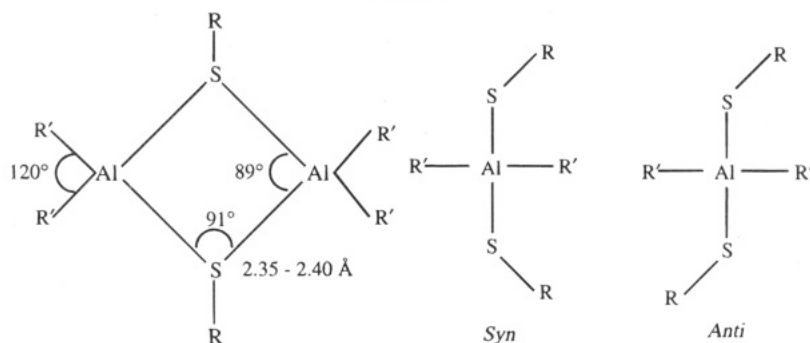
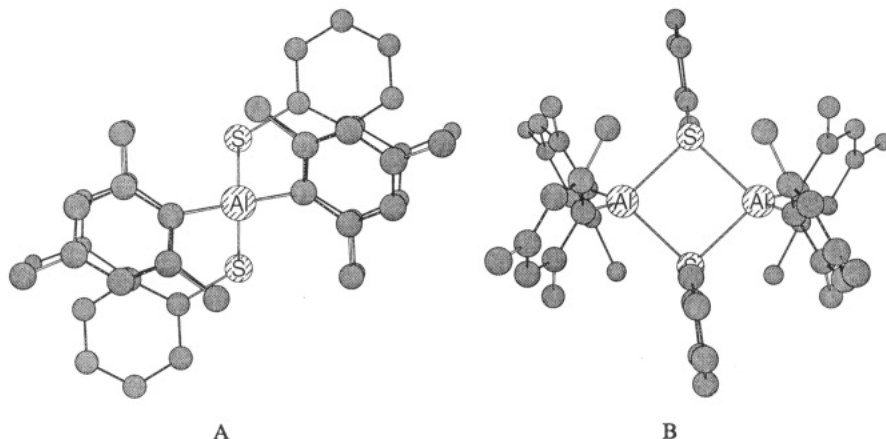
the longer bond lengths, are mesityl derivatives while **2** has methyl groups attached to the aluminum. The C–Al–C angles in **1–3** are in a narrow range between 118.7°–121.7°. Selected bond distances and angles are summarized in Table 11.

The bridging groups in these three compounds are found in the *anti* conformation in the solid state. The sulfur atoms are pyramidal with the average value for the sum of the bond angles at the sulfur atom of **1**, **2**, and **3** being 306°, 330°, and 316°, respectively. The sum of these angles in  $[\text{Me}_2\text{Al}(\mu\text{-SMe})]_2$  is 306.7° in the gas phase<sup>45</sup> and 310.3° in the solid state.<sup>31</sup> In  $[\text{Me}_2\text{Al}(\mu\text{-SC}_6\text{F}_5)]_2$ ,<sup>14</sup> this sum is 304.5°, and in the isostructural  $[\text{Me}_2\text{Ga}(\mu\text{-SC}_6\text{F}_5)]_2$ ,<sup>46</sup> the sum of the angles around sulfur is 304.1°. In **1** and **3** the central (AlS)<sub>2</sub> ring is planar as required by symmetry, but in **2** the central ring deviates slightly from planarity with an angle of 7.2(2)° calculated between the Al(3)–S(1)–Al(4) and Al-

(45) Haaland, A.; Stokkeland, O.; Weidlein, J. J. *Organomet. Chem.* **1975**, *94*, 353.

(46) Hendershot, D. G.; Kumar, R.; Barber, M.; Oliver, J. P. *Organometallics* **1991**, *10*, 1917.

Chart 1

Chart 2. Views of **3** (A) along the Al-Al Vector and (B) Perpendicular to the  $(\text{AlS})_2$  Plane

(3)-S(2)-Al(4) planes. The butterfly conformation of **2** compares with that observed in  $[\text{Me}_2\text{Al}(\mu\text{-SC}_6\text{F}_5)]_2$  ( $17.7^\circ$ ),<sup>14</sup> in  $[\text{I}_2\text{Ga}(\mu\text{-S-}i\text{-Pr})]_2$  ( $36.7(2)^\circ$ ),<sup>47</sup> and in  $[\text{Me}_2\text{Ga}(\mu\text{-SC}_6\text{F}_5)]_2$  ( $27.7^\circ$ ).<sup>46</sup> The structures of the cores of  $[\text{Ph}_2\text{Ga}(\mu\text{-SEt})]_2$ <sup>16</sup> and  $[\text{Me}_2\text{Al}(\mu\text{-SMe})]_2$  in the gas phase<sup>45</sup> are planar. All of the compounds so far studied are found to have the groups attached to the sulfur atom in the *anti* conformation, but evidence gained from solution studies shows the energy difference between the *syn* and *anti* conformations is small.<sup>19,35</sup> Typical values for the structural parameters for the four-membered  $(\text{AlS})_2$  ring system along with projections showing the *syn* and *anti* conformations are shown in Chart 1.

Examination of the nonbonding distances in **1** and **3** shows that the shortest interaction in the mesitylaluminum derivatives is between the *ortho* methyl groups and the aluminum with ranges of  $3.107\text{--}3.345$  and  $3.039\text{--}3.466 \text{ \AA}$  and average values of  $3.272$  and  $3.260 \text{ \AA}$ , respectively. These short distances have minimal impact on the aggregation state but have often been involved in discussions on C-H bond activation.<sup>48</sup> The interactions of most importance to our arguments on aggregate formation and conformation stability are those occurring between the *ortho* methyl groups and those between these groups and the sulfur atom. Other interactions that may destabilize the aggregate or influence its conformation include those between the substituent on the sulfur and the aluminum, the interannular interactions, and those between the substituents on the aluminum atom. Many of these distances

are within the range  $3.4\text{--}4.0 \text{ \AA}$  and may contribute to the stability of the aggregate. Detailed calculations taking all of these interactions into account have not been made because of the large number of parameters and the unavailability of the force constants in these molecules. Chart 2, A and B, shows views of **3** along the Al-Al vector and perpendicular to the  $(\text{AlS})_2$  ring. The mesityl groups bound to aluminum and the phenyl groups bound to sulfur are oriented so that there are minimal steric interactions between them.

The conclusions that can be reached from these observations are that the central four-membered ring deviates little from planarity and that the orientation of the SR groups is normally found in the *anti* conformation in the solid state. The energy difference between the *anti* and the *syn* conformations is small, with both present in solution.<sup>35</sup> In the solid state, only the *anti* conformation has been reported and may be accounted for by small intermolecular interactions or crystal-packing forces.

Compounds **4**–**7** are the first trimeric organoaluminum thiolates that have been reported. The central  $(\text{AlS})_3$  rings in compounds **4**–**6** are in the chair conformation (Figures 4–6) with two of the substituents on the sulfur atoms oriented in an equatorial position and the other in an axial position. Compound **7** is in the skew-boat or twist conformation (Figure 7). Selected bond distances and bond angles for **4**–**7** are given in Table 12. The average Al-C bond distances in **4**–**7** are  $1.94$ ,  $1.945$ ,  $1.934$ , and  $1.96 \text{ \AA}$ . The first three of these are for methyl derivatives and are very close to the value observed for **2**. In **7**, the substituent is an isobutyl group. Examination of the axial and equatorial Al-C bond lengths (see Table 13) for **4**–**6** shows that the axial

(47) Hoffmann, G. G.; Burschka, C. *Angew. Chem., Int. Ed. Engl.* **1985**, *24*, 970.

(48) Waggoner, K. M.; Power, P. P. *J. Am. Chem. Soc.* **1991**, *113*, 3385.

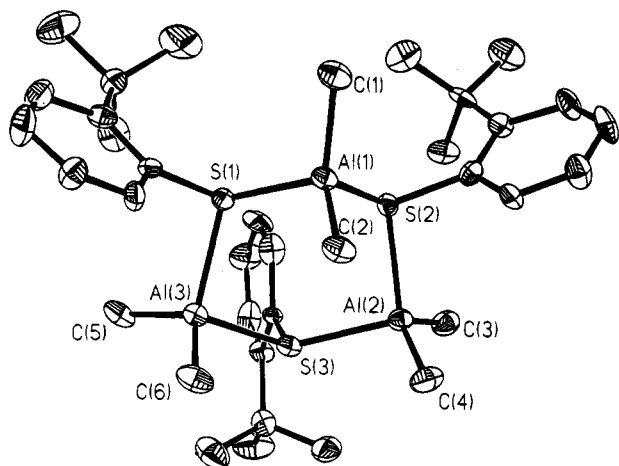


**Figure 4.** Diagram (20% thermal ellipsoids) of  $\{\text{Me}_2\text{Al}[\mu\text{-S}(2\text{-}t\text{-BuC}_6\text{H}_4)]_3\}$  (4) showing the atom-labeling scheme. Hydrogen atoms have been omitted for clarity.

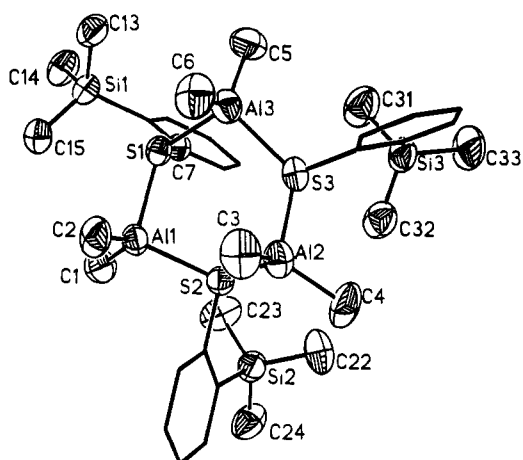


**Figure 5.** Diagram (50% thermal ellipsoids) of  $\{\text{Me}_2\text{Al}[\mu\text{-S}(2\text{-Me}_3\text{Si})\text{C}_6\text{H}_4]\}_3$  (5) showing the atom-labeling scheme. The aromatic rings have been shown as wire frames, and the hydrogen atoms have been omitted for clarity.

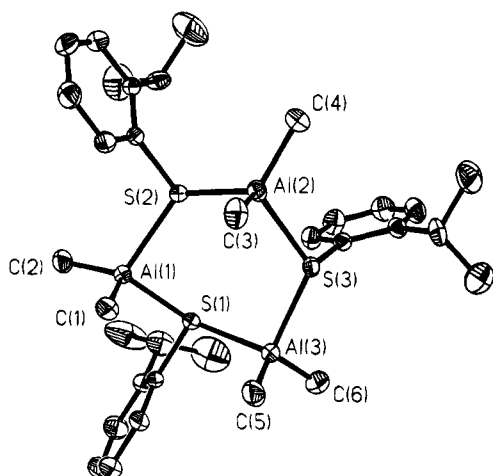


**Figure 6.** Diagram (20% thermal ellipsoids) of  $\{\text{Me}_2\text{Al}[\mu\text{-S}(2\text{-}i\text{-PrC}_6\text{H}_4)]_3\}$  (6) showing the atom-labeling scheme. Hydrogen atoms have been omitted for clarity.

Al–C bond distances are all longer by approximately 0.02 Å than the equatorial Al–C distances, which suggests some differences in bond length as a function of orientation.

In 4–6, the C–Al–C angles are between 118.3° and 123.2°, comparable to those observed in dimers, 1–3.

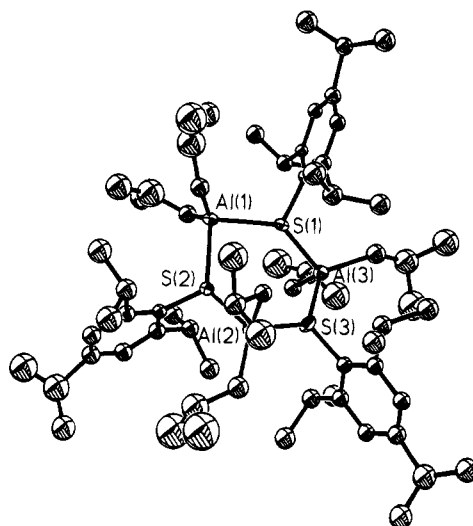


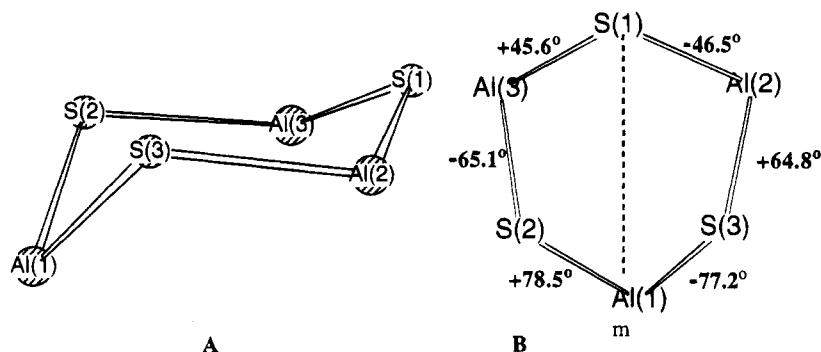
**Figure 7.** Diagram (5% thermal ellipsoids) of  $\{i\text{-Bu}_2\text{Al}[\mu\text{-S}(2,4,6\text{-}i\text{-Pr}_3\text{C}_6\text{H}_2)]_3\}$  (7) showing the atom-labeling scheme. Hydrogen atoms have been omitted for clarity.

In 7, these angles increase to 129°–130°, most probably as a result of the change of substituent on the metal from a methyl to an isobutyl group which also influences the ring conformation.

In 4–7, there are fewer nonbonding distances shorter than 4.0 Å between groups on adjacent atoms in the ring than are observed in the dimers, suggesting that, with less steric crowding, trimers are favored. Increasing the bulk of the substituents on the metal by replacing the methyl groups with isobutyl groups and by adding isopropyl groups to the 2,6-positions on the aromatic rings attached to sulfur increases the number of nonbonding distances less than 4.0 Å, leading to added steric interactions and a change in the conformation of the ring. A comparison of the torsion angles in the two conformations and views of the ring structures are shown in Chart 3, A and B, and Chart 4, A and B.

This difference in ring conformation is seen in other ways. The sums of the angles around sulfur for compounds 4–6 are in the range 320°–338.5°. In compound 7, the sum of the angles around sulfur is in the range 357°–360°; thus, the sulfur atoms in 7 are essentially planar. The sum of the angles around sulfur in the trimeric units is generally larger than in the dimers (304°–330°), showing that the sulfur atoms are approaching planarity. The changes in geometry appear to be associated with steric interactions and with angle strain in the ring system. In the trimeric oxygen-bridged compounds, the oxygen atom is planar or nearly planar in all cases, but additional O → Al π-interactions have been proposed that may account for this observation in these derivatives.<sup>49</sup> The implications of these differing geometries on reorganizational barriers will be discussed elsewhere.<sup>35</sup> A comparison of the endocyclic angles in 4–6 shows that the S–Al–S and Al–S–Al angles differ by about 10°, but the large angle around sulfur occurs at the apex while the corresponding angle around aluminum is the smallest in the ring, as shown in Chart 5. The greatest difference between 7 and 4–6 is observed at the sulfur atom where the angles around sulfur range from 127° to 132° in 7 and from 114° to

(49) Barron, A. R.; Dobbs, K. D.; Francl, M. M. *J. Am. Chem. Soc.* 1991, 113, 39.

Chart 3. Chair Conformation of  $\{\text{Me}_2\text{Al}[\mu\text{-S}(2\text{-}t\text{-BuC}_6\text{H}_4)]\}_3$  (4)<sup>a</sup>

<sup>a</sup> The six torsion angles are given adjacent to the central bond associated with the angle in B.

Table 4. Atomic Coordinates ( $\times 10^4$ ) and Isotropic Thermal Parameters ( $\times 10^3$ ) for the Non-Hydrogen Atoms of  $[\text{Me}_2\text{Al}(\mu\text{-SPh})]_2$  (3)

atom	x	y	z	$U_{\text{eq}} (\text{\AA}^2)^a$
Al1	428(1)	-1208(1)	4927(1)	37(1)
S1	1589(1)	817(1)	5554(1)	39(1)
C1	2861(4)	1768(4)	5176(3)	38(2)
C2	3939(5)	2713(4)	5710(3)	56(3)
C3	4930(6)	3502(5)	5443(4)	79(3)
C4	4849(6)	3348(5)	4655(4)	76(4)
C5	3798(6)	2404(5)	4134(3)	66(3)
C6	2794(5)	1614(4)	4386(3)	53(3)
C10	89(5)	-2391(4)	5659(3)	37(2)
C11	621(5)	-2233(4)	6506(3)	48(3)
C12	273(6)	-3187(5)	6917(3)	62(3)
C13	-558(5)	-4311(4)	6527(3)	56(3)
C14	-1069(5)	-4471(4)	5698(3)	55(3)
C15	-767(5)	-3542(4)	5269(3)	44(2)
C16	1597(6)	-1044(4)	6996(3)	72(3)
C17	-932(6)	-5347(5)	6989(3)	90(4)
C18	-1371(5)	-3823(4)	4358(3)	61(3)
C20	1279(5)	-1401(3)	4140(3)	36(2)
C21	2632(5)	-1322(4)	4474(3)	45(3)
C22	3412(5)	-1350(4)	3998(4)	59(3)
C23	2892(7)	-1461(4)	3181(4)	61(3)
C24	1548(7)	-1579(4)	2829(3)	56(3)
C25	738(5)	-1564(4)	3287(3)	43(3)
C26	3293(5)	-1220(4)	5375(3)	63(3)
C27	3747(7)	-1460(5)	2654(4)	101(4)
C28	-733(6)	-1761(4)	2840(3)	62(3)
Al2	3762(2)	5181(1)	10337(1)	40(1)
S2	3941(1)	4734(1)	9061(1)	41(1)
C30	4026(5)	5901(4)	8476(3)	40(2)
C31	4871(5)	7064(4)	8797(3)	51(3)
C32	4952(6)	7918(4)	8301(3)	68(3)
C33	4204(7)	7623(5)	7502(3)	78(4)
C34	3344(7)	6490(5)	7191(3)	89(4)
C35	3243(6)	5613(4)	7670(3)	63(3)
C40	2641(5)	3857(4)	10760(3)	38(2)
C41	1776(5)	2707(4)	10364(3)	44(2)
C42	1259(5)	1821(4)	10792(3)	54(3)
C43	1536(5)	2023(4)	11612(3)	56(3)
C44	2307(5)	3161(5)	11996(3)	57(3)
C45	2874(5)	4064(4)	11590(3)	44(2)
C46	1333(6)	2374(4)	9469(3)	69(3)
C47	1011(7)	1049(5)	12064(3)	100(4)
C48	3780(6)	5271(4)	12086(3)	64(3)
C50	3523(5)	6664(4)	10316(3)	41(2)
C51	4459(5)	7795(4)	10740(3)	44(3)
C52	4143(5)	8760(4)	10593(3)	51(3)
C53	2899(6)	8658(4)	10052(3)	55(3)
C54	1949(5)	7564(5)	9655(3)	59(3)
C55	2238(5)	6587(4)	9775(3)	45(3)
C56	5826(5)	7983(4)	11363(3)	61(3)
C57	2577(6)	9730(5)	9898(4)	87(4)
C58	1146(5)	5413(5)	9300(3)	66(3)

<sup>a</sup>  $U_{\text{eq}} (\text{\AA}^2) = 1/3 \sum_i \sum_j U_{ij} a_i^* a_j^* \mathbf{a}_i \cdot \mathbf{a}_j$ .

Table 5. Atomic Coordinates and Isotropic Thermal Parameters for the Non-Hydrogen Atoms of  $\{\text{Me}_2\text{Al}[\mu\text{-S}(2\text{-}t\text{-BuC}_6\text{H}_4)]\}_3$  (4)

atom	x	y	z	$U_{\text{eq}} (\text{\AA}^2)^a$
S1	0.1892(3)	0.1650(2)	0.2308(1)	0.046(1)
S2	0.2333(3)	0.2545(2)	0.3505(1)	0.048(1)
S3	0.1343(3)	0.0689(2)	0.3572(1)	0.047(1)
Al1	0.1009(4)	0.2743(2)	0.2601(2)	0.052(2)
Al2	0.1206(4)	0.1757(2)	0.4083(2)	0.051(2)
Al3	0.0716(4)	0.0618(2)	0.2593(2)	0.052(2)
C1	0.194(1)	0.3524(6)	0.2267(5)	0.074(6)
C2	-0.111(1)	0.2725(6)	0.2589(5)	0.066(6)
C3	0.245(1)	0.1673(7)	0.4792(5)	0.079(6)
C4	-0.087(1)	0.1936(6)	0.4046(5)	0.086(7)
C5	0.167(1)	-0.0204(6)	0.2321(5)	0.085(6)
C6	-0.138(1)	0.0668(6)	0.2463(5)	0.078(6)
C7	0.145(1)	0.1641(7)	0.1580(5)	0.049(5)
C8	0.242(1)	0.1575(7)	0.1185(6)	0.057(6)
C9	0.188(2)	0.1550(8)	0.0598(7)	0.082(8)
C10	0.039(2)	0.161(1)	0.0403(6)	0.098(8)
C11	-0.046(1)	0.1707(9)	0.0779(6)	0.067(6)
C12	-0.004(2)	0.1709(8)	0.1338(5)	0.063(6)
C13	0.407(2)	0.1533(9)	0.1370(6)	0.076(8)
C14	0.495(2)	0.146(1)	0.0868(7)	0.135(9)
C15	0.449(1)	0.0878(9)	0.1744(6)	0.093(7)
C16	0.464(1)	0.2211(9)	0.1678(8)	0.14(1)
C17	0.236(2)	0.3401(7)	0.3835(4)	0.052(6)
C18	0.369(1)	0.3773(8)	0.4052(6)	0.055(6)
C19	0.352(2)	0.4450(8)	0.4301(6)	0.072(7)
C20	0.221(2)	0.4748(7)	0.4309(6)	0.090(8)
C21	0.097(2)	0.4400(9)	0.4096(6)	0.077(7)
C22	0.104(2)	0.3737(8)	0.3875(5)	0.057(6)
C23	0.523(2)	0.3463(7)	0.4013(6)	0.060(6)
C24	0.642(1)	0.3953(8)	0.4319(6)	0.108(8)
C25	0.543(1)	0.2741(7)	0.4320(5)	0.076(7)
C26	0.545(1)	0.3395(8)	0.3392(6)	0.096(7)
C27	0.317(1)	0.0324(7)	0.3733(5)	0.044(6)
C28	0.353(2)	-0.0296(7)	0.4018(5)	0.058(6)
C29	0.502(2)	-0.0479(8)	0.4070(6)	0.083(8)
C30	0.599(2)	-0.005(1)	0.3819(8)	0.10(1)
C31	0.562(2)	0.0560(9)	0.3564(6)	0.085(8)
C32	0.416(2)	0.0767(8)	0.3509(5)	0.072(7)
C33	0.246(2)	-0.0774(8)	0.4273(6)	0.065(7)
C34	0.168(2)	-0.0355(7)	0.4696(6)	0.099(8)
C35	0.129(2)	-0.1064(7)	0.3805(7)	0.118(8)
C36	0.319(2)	-0.1412(8)	0.4594(7)	0.124(8)

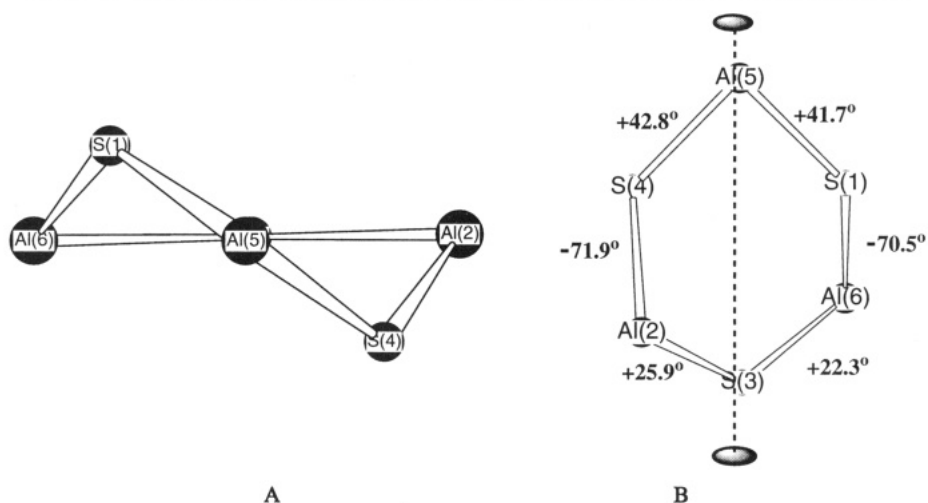
<sup>a</sup>  $U_{\text{eq}} (\text{\AA}^2) = 1/3 \sum_i \sum_j U_{ij} a_i^* a_j^* \mathbf{a}_i \cdot \mathbf{a}_j$ .

The trimeric structure is established with  $[\text{Me}_2\text{Al}(\mu\text{-OMe})]_3$  (gas phase),<sup>21</sup>  $[\text{Me}_2\text{Al}(\mu\text{-N}(\text{H})\text{Me})]_3$ ,<sup>25</sup>  $[\text{H}_2\text{Al}(\mu\text{-NMe}_2)]_3$ ,<sup>26</sup> and  $[t\text{-Bu}_2\text{Al}(\mu\text{-NH}_2)]_3$ <sup>50</sup> ring systems. Other Group 13 metals form six-membered rings such as  $[\text{Me}_2\text{-In}(\mu\text{-AsMe}_2)]_3$ ,<sup>28</sup>  $[t\text{-Bu}_2\text{Ga}(\mu\text{-OH})]_3$ ,<sup>51</sup>  $[t\text{-Bu}_2\text{Ga}(\mu\text{-NH}_2)]_3$ ,<sup>51</sup>

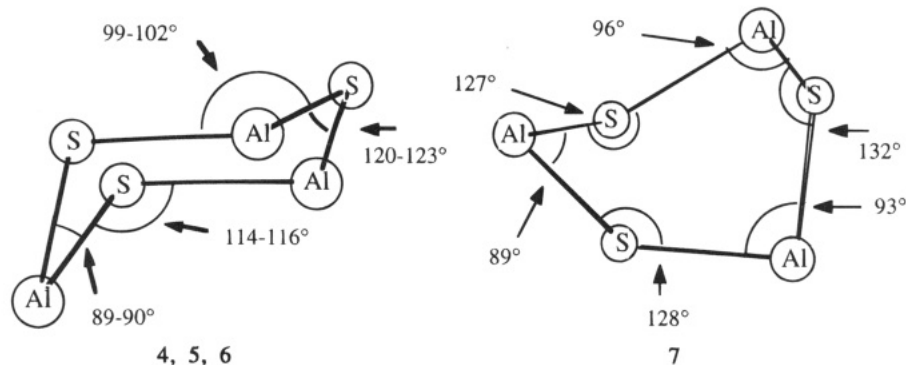
(50) Interrante, L. V.; Sigel, G. A.; Garbaskas, M.; Hejna, C.; Slack, G. A. *Inorg. Chem.* **1989**, *28*, 252.

(51) Atwood, D. A.; Cowley, A. H.; Harris, P. R.; Jones, R. A.; Koschmieder, S. U.; Nunn, C. M.; Atwood, J. L.; Bott, S. G. *Organometallics* **1993**, *12*, 24.

123° in 4–6. Again this shows the distorted configuration of 7.

**Chart 4. Twist-Boat Conformation of  $\{i\text{-Bu}_2\text{Al}[\mu\text{-S}(2,4,6\text{-}i\text{-Pr}_3\text{C}_6\text{H}_2)]\}_3$  (7)<sup>a</sup>**


<sup>a</sup> The six torsion angles are given adjacent to the central bond associated with the angle in B.

**Chart 5**


$[(\text{CH}_2)_2\text{NGaH}_2]_3$ ,<sup>27</sup> and  $\{\text{Me}_2\text{Ga}[\mu\text{-P}(\text{Me})(\text{Ph})]\}_3$ .<sup>24</sup> Chair and skew-boat conformations have been observed for these derivatives with the primary difference in the structures related to the bridging chalcogen which is three-coordinate and the pnictinides which are four-coordinate.

Compounds **8** and **9** represent the first structurally-characterized cyclic tetrameric organoaluminum and -gallium thiolates. They are isomorphous and crystallize in an extended-chair conformation with alternating (2,6-dimethylphenyl)thiolato ligands bridging  $\text{Me}_2\text{M}$  moieties to form an eight-membered  $(\text{MS})_4$  ring with the Al or Ga atoms occupying the apical positions (Figures 8 and 9). Selected bond distances and angles are summarized in Table 13. The C–M–C bond angles show differences between the two independent metal atoms. In **8** these values are  $126.0^\circ$  and  $120.3^\circ$  while in **9** they are  $129.5^\circ$  and  $124.2^\circ$ . These values are in the range observed for  $[\text{Ph}_2\text{Ga}(\mu\text{-SEt})]_2$  ( $121.2^\circ$ )<sup>16</sup> and for the aluminum derivative cited earlier. The average Al–C bond length in **8** is  $1.943 \text{ \AA}$ , with equatorial bond lengths approximately  $0.015 \text{ \AA}$  longer than the axial bond lengths. All of the Al–C bonds are in the range observed for organoaluminum compounds and compare favorably with the Al–C distances in other aluminum sulfur derivatives such as  $[\text{Me}_2\text{Al}(\mu\text{-SMe})]_2$  in the gas phase ( $1.945 \text{ \AA}$ ),<sup>45</sup>  $[\text{Me}_2\text{Al}(\mu\text{-SMe})]_\infty$  in the solid state ( $1.945 \text{ \AA}$ ),<sup>31</sup> and  $[\text{Me}_2\text{Al}(\mu\text{-SC}_6\text{F}_5)]_2$  ( $1.942 \text{ \AA}$  average).<sup>14</sup> The Ga–C bond lengths in **9** (average  $1.936 \text{ \AA}$ ) are also comparable to those observed in other organogallium

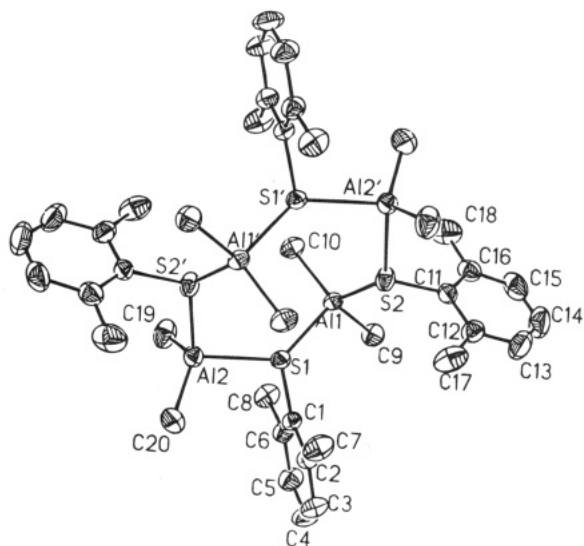


**Figure 8.** Diagram (50% thermal ellipsoids) of  $\{\text{Me}_2\text{Al}[\mu\text{-S}(2,6\text{-Me}_2\text{C}_6\text{H}_3)]\}_4$  (**8**) showing the atom-labeling scheme. Hydrogen atoms have been omitted for clarity.

derivatives such as  $[\text{Me}_2\text{Ga}(\mu\text{-SC}_6\text{F}_5)]_2$  ( $1.94 \text{ \AA}$ ),<sup>46</sup>  $[\text{Ph}_2\text{Ga}(\mu\text{-SEt})]$  ( $1.964 \text{ \AA}$ ),<sup>16</sup> and  $[\text{Me}_2\text{Ga}(\mu\text{-C}\equiv\text{CPh})]_2$  ( $1.952 \text{ \AA}$ ).<sup>52</sup>

In both the aluminum and the gallium derivatives, the geometry around the sulfur atom is pyramidal with the sum of the angles around sulfur being  $342.8^\circ$  and

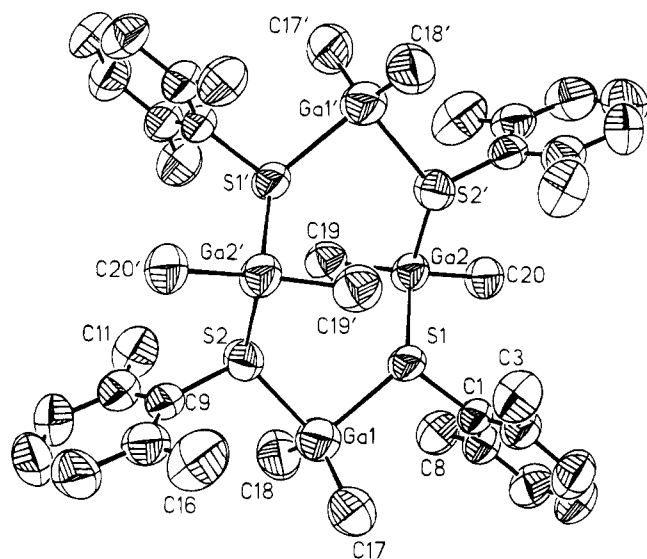


**Figure 9.** Diagram (50% thermal ellipsoids) of  $\{\text{Me}_2\text{Ga}[\mu\text{-S}(2,6\text{-Me}_2\text{C}_6\text{H}_3)]_4\}$  (**9**) showing the atom-labeling scheme. Hydrogen atoms have been omitted for clarity.

**Table 6. Atomic Coordinates and Isotropic Thermal Parameters for the Non-Hydrogen Atoms of  $\{\text{Me}_2\text{Al}[\mu\text{-S}(2\text{-SiMe}_3\text{C}_6\text{H}_4)]_3\}$  (**5**)**

atom	x	y	z	$U_{\text{eq}} (\text{\AA}^2)^a$
S1	0.3266(1)	0.70685(9)	0.37788(9)	0.0498(5)
S2	0.2388(1)	0.73399(9)	0.14653(9)	0.0520(5)
S3	0.2915(1)	0.92511(9)	0.2570(1)	0.0586(6)
Al1	0.3389(2)	0.6250(1)	0.2462(1)	0.0563(7)
Al2	0.3644(2)	0.8680(1)	0.1196(1)	0.0647(7)
Al3	0.4034(2)	0.8603(1)	0.3814(1)	0.0627(7)
Si1	0.2394(2)	0.5814(1)	0.5605(1)	0.0588(6)
Si2	-0.0446(2)	0.6907(1)	0.0376(1)	0.0680(7)
Si3	0.0439(2)	1.0858(1)	0.2732(1)	0.0831(8)
C1	0.2239(6)	0.5196(4)	0.2525(4)	0.084(3)
C2	0.5295(5)	0.6060(4)	0.2315(4)	0.083(3)
C3	0.5542(5)	0.8433(4)	0.1120(4)	0.094(3)
C4	0.2817(6)	0.9421(4)	0.0258(4)	0.098(3)
C5	0.3313(6)	0.9152(4)	0.4866(4)	0.090(3)
C6	0.5937(5)	0.8482(4)	0.3647(4)	0.090(3)
C7	0.1601(3)	0.7090(2)	0.4144(2)	0.048(2)
C8	0.0680(3)	0.7637(2)	0.3675(2)	0.061(2)
C9	-0.0624(3)	0.7699(2)	0.3971(2)	0.074(3)
C10	-0.1008(3)	0.7212(2)	0.4738(2)	0.076(3)
C11	-0.0087(3)	0.6664(2)	0.5207(2)	0.065(2)
C12	0.1217(3)	0.6603(2)	0.4911(2)	0.050(2)
C13	0.3663(6)	0.6522(4)	0.6132(4)	0.080(3)
C14	0.1384(6)	0.5217(4)	0.6489(4)	0.084(3)
C15	0.3165(5)	0.4891(4)	0.4932(4)	0.071(2)
C16	0.2460(4)	0.6755(2)	0.0454(2)	0.054(2)
C17	0.3690(4)	0.6497(2)	0.0107(2)	0.070(3)
C18	0.3773(4)	0.6046(2)	-0.0693(2)	0.088(3)
C19	0.2628(4)	0.5852(2)	-0.1146(2)	0.093(3)
C20	0.1399(4)	0.6109(2)	-0.0799(2)	0.079(3)
C21	0.1315(4)	0.6560(2)	0.0001(2)	0.058(2)
C22	-0.0660(6)	0.8186(4)	0.0222(5)	0.100(3)
C23	-0.0817(6)	0.6518(5)	0.1530(4)	0.094(3)
C24	-0.1648(6)	0.6337(4)	-0.0348(4)	0.097(3)
C25	0.3268(5)	1.0452(2)	0.2483(3)	0.070(3)
C26	0.4570(5)	1.0714(2)	0.2348(3)	0.099(3)
C27	0.4868(5)	1.1651(2)	0.2263(3)	0.131(4)
C28	0.3864(5)	1.2327(2)	0.2313(3)	0.145(5)
C29	0.2562(5)	1.2064(2)	0.2448(3)	0.115(4)
C30	0.2264(5)	1.1127(2)	0.2533(3)	0.077(3)
C31	0.0227(7)	1.0380(5)	0.3874(4)	0.110(3)
C32	-0.0219(6)	1.0043(4)	0.1935(4)	0.092(3)
C33	-0.0560(8)	1.1959(5)	0.2612(5)	0.126(4)

$$^a U_{\text{eq}} (\text{\AA}^2) = \frac{1}{3} \sum_i \sum_j U_{ij} a_i^* a_j^* a_i a_j$$

**Chart 6. Comparison of Structural Parameters for  $\{\text{Me}_2\text{Al}[\mu\text{-S}(2,6\text{-Me}_2\text{C}_6\text{H}_3)]_4\}$  (**8**),  $\{\text{Me}_2\text{Ga}[\mu\text{-S}(2,6\text{-Me}_2\text{C}_6\text{H}_3)]_4\}$  (**9**), and  $[\text{Me}_2\text{Ga}(\mu\text{-OH})]_4$**

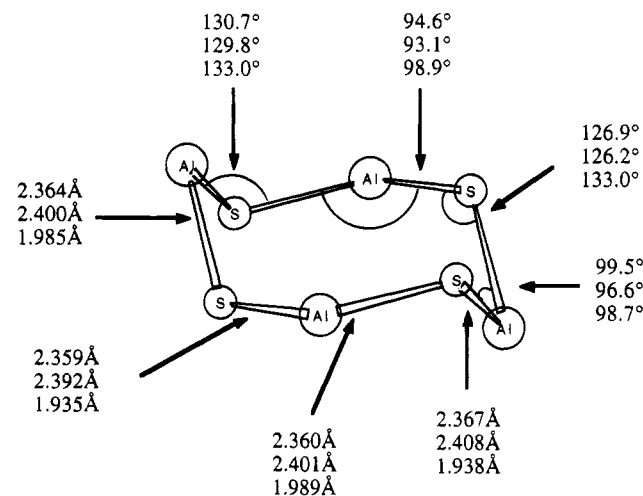
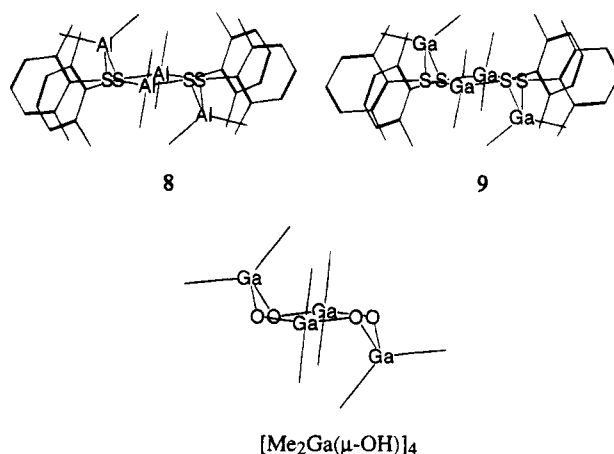


**Chart 7**



and pyramidal geometries, suggesting that the chalcogen centers are slightly flattened. The endocyclic angles for **8** and **9** are listed in Table 13 and summarized in Chart 6, which shows the relationships between **8**, **9**, and the cyclic tetramer,  $[\text{Me}_2\text{Ga}(\mu\text{-OH})]_4$ .<sup>30</sup> The similarities of the three tetrameric derivatives are illustrated in Chart 7, which shows the three molecules viewed along the plane containing the four chalcogen atoms. These angles are substantially larger than the Al-S-Al angles of **1** ( $90.89^\circ$ ), **2** ( $92.2^\circ$  average), **3** ( $93.6^\circ$  average),  $[\text{Me}_2\text{Al}(\mu\text{-SMe})]_2$  in the gas phase ( $94.5^\circ$ ),<sup>45</sup>  $[\text{Me}_2\text{Al}(\mu\text{-SC}_6\text{F}_5)]_2$  ( $87.10^\circ$ ),<sup>14</sup> and the Ga-S-Ga angle of  $[\text{I}_2\text{Ga}(\mu\text{-S-}i\text{-Pr})]_2$  ( $84.7^\circ$ )<sup>47</sup> and  $[\text{Ph}_2\text{Ga}(\mu\text{-SEt})]_2$  ( $86.42^\circ$ ).<sup>16</sup> They are also larger than those in **4-6** (summarized in Chart 5) but comparable to those in **7**.

In **8**, the C-Al-C angles are  $120.3^\circ$  and  $126.0^\circ$ . The corresponding angles in **9** are  $124.2^\circ$  and  $129.5^\circ$ . All other C-Al-C angles fall into the  $115^\circ$ - $125^\circ$  range typically observed for organoaluminum derivatives.<sup>7,8</sup> The C-M-C angles in **8** and **9** are at the top of this range, and this slight increase may be attributed to the high degree of flexibility of the eight-membered ring.

The Al-S and Ga-S bond lengths for all nine compounds are comparable to those observed in a number of aluminum and gallium thiolate bridged compounds as shown in Table 14. The Al-S bonds in thiolate bridges are longer than the distances observed

$348.3^\circ$  (**8**) and  $340.7^\circ$  and  $346.0^\circ$  (**9**). These values are intermediate with respect to the ideal values for planar

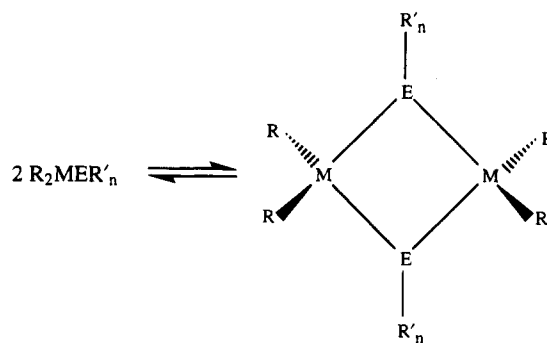
**Table 7. Atomic Coordinates and Isotropic Thermal Parameters for the Non-Hydrogen Atoms of  $\{Me_2Al[\mu-S(2-i-PrC_6H_4)]_3\}_3$  (**6**)**

atom	x	y	z	$U_{eq} (\text{\AA}^2)^a$
S1	0.01457(9)	0.17500(8)	0.18960(8)	0.0524(5)
S2	0.17019(9)	0.31140(7)	0.22777(7)	0.0473(5)
S3	0.31928(9)	0.17467(8)	-0.01352(7)	0.0504(5)
Al1	0.0613(1)	0.17969(9)	0.33527(9)	0.0507(6)
Al2	0.3683(1)	0.2384(1)	0.10083(9)	0.0551(6)
Al3	0.1753(1)	0.0709(1)	0.0532(1)	0.0643(7)
C1	0.1588(4)	0.0389(3)	0.3788(3)	0.072(2)
C2	-0.0870(4)	0.2548(4)	0.4428(3)	0.078(2)
C3	0.4607(4)	0.1076(4)	0.1648(3)	0.080(3)
C4	0.4338(4)	0.3617(4)	0.0204(4)	0.087(3)
C5	0.2583(5)	-0.0705(4)	0.1115(4)	0.102(3)
C6	0.1172(5)	0.0898(5)	-0.0594(4)	0.107(4)
C7	-0.1050(4)	0.1047(3)	0.2557(3)	0.053(2)
C8	-0.2239(4)	0.1609(4)	0.2663(4)	0.068(3)
C9	-0.3134(4)	0.1015(5)	0.3204(4)	0.094(3)
C10	-0.2818(6)	-0.0054(6)	0.3601(4)	0.100(4)
C11	-0.1663(6)	-0.0597(4)	0.3488(4)	0.088(3)
C12	-0.0753(4)	-0.0048(4)	0.2966(3)	0.070(3)
C13	-0.2592(5)	0.2785(5)	0.2208(6)	0.104(4)
C14	-0.2461(8)	0.2904(6)	0.1068(9)	0.198(8)
C15	-0.3828(7)	0.3445(6)	0.2817(9)	0.217(7)
C16	0.2128(3)	0.3529(3)	0.3167(3)	0.048(2)
C17	0.1919(3)	0.4640(3)	0.3180(3)	0.054(2)
C18	0.2321(4)	0.4884(4)	0.3870(4)	0.073(3)
C19	0.2859(5)	0.4093(5)	0.4505(4)	0.087(3)
C20	0.3021(4)	0.3035(4)	0.4503(4)	0.079(3)
C21	0.2672(4)	0.2731(4)	0.3828(3)	0.065(2)
C22	0.1286(4)	0.5537(3)	0.2531(4)	0.073(3)
C23	0.0037(6)	0.6102(6)	0.3231(6)	0.147(5)
C24	0.1981(7)	0.6373(6)	0.1891(6)	0.165(5)
C25	0.2701(4)	0.2916(3)	-0.1020(3)	0.049(2)
C26	0.3496(4)	0.3122(3)	-0.2079(3)	0.056(2)
C27	0.3024(5)	0.4048(4)	-0.2705(4)	0.082(3)
C28	0.1837(5)	0.4699(4)	-0.2312(4)	0.086(3)
C29	0.1102(4)	0.4471(4)	-0.1296(4)	0.082(3)
C30	0.1509(4)	0.3594(3)	-0.0625(3)	0.069(2)
C31	0.4777(4)	0.2409(4)	-0.2565(3)	0.073(2)
C32	0.4879(5)	0.1789(5)	-0.3375(5)	0.115(4)
C33	0.5737(5)	0.3041(6)	-0.3064(5)	0.133(4)

$$^a U_{eq} (\text{\AA}^2) = 1/3 \sum_i \sum_j U_{ij} a_i^* a_j^* a_i \cdot a_j$$

for single Al-S bonds in the monomeric derivative, Al-[S(2,4,6-*t*-Bu<sub>3</sub>C<sub>6</sub>H<sub>2</sub>)<sub>3</sub>]<sub>3</sub>, (2.185 Å)<sup>11</sup> and in the bridging sulfido ligands of I<sub>4</sub>Al<sub>4</sub>(μ<sub>3</sub>-S)<sub>2</sub>(μ<sub>3</sub>-SR)<sub>2</sub> (2.1 Å).<sup>53</sup> The Al-S distances involving the thiolate ligands of I<sub>4</sub>Al<sub>4</sub>(μ<sub>3</sub>-S)<sub>2</sub>(μ<sub>3</sub>-SR)<sub>2</sub> (2.30 Å)<sup>53</sup> are only slightly shorter than those of **2**, **5**, and **8**. Other dimeric and trimeric aluminum thiolates display Al-S separations which are in good agreement with those reported here. For example, distances of 2.406, 2.338, 2.348, and 2.370 Å are found for [Me<sub>2</sub>Al(μ-SC<sub>6</sub>F<sub>5</sub>)<sub>2</sub>]<sub>2</sub>,<sup>14</sup> [Me<sub>2</sub>Al(2-SPy)]<sub>2</sub>,<sup>54</sup> [Me<sub>2</sub>Al(μ-SMe)]<sub>∞</sub> (solid state),<sup>31</sup> and [Me<sub>2</sub>Al(μ-SMe)]<sub>2</sub> (gas phase),<sup>45</sup> respectively. The average Ga-S distance in **9** is 2.400 Å which is slightly longer than the analogous distances in [I<sub>2</sub>Ga(μ-S-*i*-Pr)]<sub>2</sub> (2.329 Å)<sup>47</sup> and [Ph<sub>2</sub>Ga(μ-SEt)]<sub>2</sub> (2.379 Å)<sup>16</sup> and significantly longer than the Ga-S distances in [*t*-BuGa(μ-S)Py]<sub>3</sub> (2.242 Å)<sup>23</sup> and [*t*-BuGa(μ-S)]<sub>4</sub> (2.359 Å).<sup>34</sup> Simple addition compounds, (R<sub>3</sub>Al · SR<sub>2</sub>), all have longer Al-S bonds which fall in the range 2.5–2.7 Å.<sup>8</sup>

A comparison of the endocyclic angles at the metal atom in the four-, six-, and eight-membered rings shows some increase around the metal center from 89° to 100°. These angles are similar to the S-M-S angles in four-

**Chart 8**


membered ring systems such as [I<sub>2</sub>Ga(μ-S-*i*-Pr)]<sub>2</sub> (89.1°),<sup>47</sup> [Me<sub>2</sub>Al(μ-SMe)]<sub>2</sub> (gas phase) (85.5°),<sup>45</sup> [Me<sub>2</sub>Al(μ-SC<sub>6</sub>F<sub>5</sub>)<sub>2</sub>]<sub>2</sub> (89.51°),<sup>14</sup> [Ph<sub>2</sub>Ga(μ-SEt)]<sub>2</sub> (93.58°),<sup>16</sup> and the six-membered ring of **5** (89.35–100.84°). In the linear polymer, [Me<sub>2</sub>Al(μ-SMe)]<sub>∞</sub> (solid state),<sup>31</sup> an angle of 100.1° is found, suggesting that there is little strain at the metal atoms in the four-, six-, and eight-membered rings. The only other cyclic tetramers of this type reported are the [Me<sub>2</sub>Al(μ-F)]<sub>4</sub> molecule, which has bridging fluorine atoms,<sup>29</sup> and [Me<sub>2</sub>Ga(μ-OH)]<sub>4</sub>.<sup>30</sup> The differences between the present systems and the [Me<sub>2</sub>Al(μ-F)]<sub>4</sub> derivative are in the description of the ring with the thiolate forming an “extended chair” and the fluoride a puckered ring. The center of inversion in the [Me<sub>2</sub>Ga(μ-OH)]<sub>4</sub> derivative gives similar features to the present systems. A comparison of the three chalcogen-bridged molecules is shown in Chart 7, all viewed parallel to the plane described by the four chalcogen atoms. The gross structural features are the same, but some differences occur as a result of the size of the bridging atoms and the changes in steric interactions. The internal angles in the rings differ substantially, and it appears that this results from the tendency of the oxygen to become planar when serving as a bridge between aluminum or gallium atoms.

The observation that diorganoaluminum thiolates form monomers, dimers, trimers, tetramers, and chains raises a number of questions concerning the factors which influence the aggregation states of these molecules in the solid state and in solution. In the present study, we can make some qualitative observations concerning these factors, but a more detailed discussion and the ability to predict aggregation states is still beyond our grasp. Coates<sup>3</sup> provided a brief comment on factors which may govern aggregation states nearly 30 years ago. The factors which he suggested are the “balance between entropy factors (favoring the formation of the maximum number of molecules, hence monomers or dimers) and steric factors.” While this statement gives the broad overview of the problem, the difficulties are in assessing each of the interactions. The first distinction to be made is between monomers and dimers where the differences are the greatest since the monomer contains a single M-chalcogen (or pnictinide) bond while the dimer replaces this with a bridge of the form shown in Chart 8.

From the studies published, it is apparent that monomers result only when very bulky groups such as 2,4,6-*t*-Bu<sub>3</sub>C<sub>6</sub>H<sub>2</sub>S are present on the metal center. This shows that the energy released in going from two single M-E bonds to two M-E-M bonds containing four M-E interactions in the bridge is sufficient to overcome the

(53) Boardman, A.; Small, R. W. H.; Worrall, I. J. *Inorg. Chim. Acta* **1986**, *120*, L23.

(54) Kumar, R.; de Mel, V. S. J.; Oliver, J. P. *Organometallics* **1989**, *8*, 2488.



**Table 8. Atomic Coordinates and Isotropic Thermal Parameters for the Non-Hydrogen Atoms of  $\{i\text{-Bu}_2\text{Al}[\mu\text{-S}(2,4,6\text{-}i\text{-Pr}_3\text{C}_6\text{H}_2)]_3\}$  (7)**

atom	x	y	z	$U_{\text{eq}} (\text{\AA}^2)^a$	atom	x	y	z	$U_{\text{eq}} (\text{\AA}^2)^a$
S1	0.7562(4)	0.3076(3)	0.2018(3)	0.058(3)	C38	0.706(2)	0.287(2)	0.365(1)	0.12(1)
S2	0.5338(5)	0.2896(3)	0.1263(3)	0.061(3)	C39	1.003(2)	0.444(1)	0.396(1)	0.077(9)
S3	0.6906(6)	0.1664(3)	0.1557(3)	0.075(3)	C40	0.925(2)	0.490(1)	0.410(1)	0.11(1)
Al1	0.6213(6)	0.3712(4)	0.1709(3)	0.062(3)	C41	1.041(2)	0.403(1)	0.446(1)	0.11(1)
Al2	0.5278(5)	0.1929(4)	0.1613(3)	0.059(3)	C42	0.909(2)	0.407(1)	0.193(1)	0.075(9)
Al3	0.8263(5)	0.2307(4)	0.1575(3)	0.058(3)	C43	1.013(2)	0.387(1)	0.182(1)	0.09(1)
C1	0.820(2)	0.255(1)	0.083(1)	0.084(9)	C44	0.903(2)	0.476(1)	0.183(1)	0.09(1)
C2	0.920(3)	0.276(2)	0.065(2)	0.16(2)	C50	0.436(1)	0.3078(7)	0.0704(6)	0.051(7)
C3	0.969(4)	0.226(3)	0.050(2)	0.24(2)	C51	0.343(1)	0.3205(7)	0.0792(6)	0.072(8)
C4	0.900(4)	0.325(3)	0.029(3)	0.27(3)	C52	0.265(1)	0.3278(7)	0.0349(6)	0.086(9)
C5	0.941(2)	0.204(1)	0.212(1)	0.10(1)	C53	0.282(1)	0.3223(7)	-0.0181(6)	0.088(9)
C6	1.031(3)	0.177(2)	0.198(2)	0.17(2)	C54	0.375(1)	0.3096(7)	-0.0268(6)	0.085(9)
C7	1.106(3)	0.161(2)	0.250(2)	0.19(2)	C55	0.453(1)	0.3023(7)	0.0174(6)	0.077(9)
C8	0.993(4)	0.118(3)	0.171(2)	0.24(2)	C56	0.557(2)	0.290(1)	0.004(1)	0.085(9)
C9	0.646(2)	0.422(1)	0.111(1)	0.086(9)	C57	0.583(2)	0.338(1)	-0.037(1)	0.11(1)
C10	0.602(4)	0.482(3)	0.099(2)	0.22(2)	C58	0.558(2)	0.227(1)	-0.019(1)	0.11(1)
C11	0.634(3)	0.508(2)	0.047(2)	0.16(2)	C59	0.149(4)	0.370(2)	-0.078(2)	0.21(2)
C12	0.516(3)	0.503(2)	0.111(2)	0.18(2)	C60	0.196(3)	0.320(3)	-0.078(2)	0.19(2)
C13	0.569(2)	0.392(1)	0.237(1)	0.084(9)	C61	0.152(3)	0.260(2)	-0.080(2)	0.15(1)
C14	0.599(4)	0.450(2)	0.262(2)	0.20(2)	C62	0.320(2)	0.329(1)	0.139(1)	0.10(1)
C15	0.688(3)	0.481(2)	0.270(1)	0.14(1)	C63	0.227(3)	0.295(2)	0.144(2)	0.16(1)
C16	0.562(4)	0.451(2)	0.322(2)	0.22(2)	C64	0.313(3)	0.395(2)	0.148(1)	0.14(1)
C17	0.526(2)	0.204(1)	0.240(1)	0.069(8)	C70	0.711(1)	0.0876(5)	0.1520(8)	0.061(8)
C18	0.421(2)	0.200(1)	0.254(1)	0.10(1)	C71	0.726(1)	0.0530(5)	0.1991(8)	0.069(8)
C19	0.429(3)	0.240(2)	0.310(2)	0.18(2)	C72	0.733(1)	-0.0084(5)	0.1954(8)	0.072(8)
C20	0.405(3)	0.139(2)	0.274(2)	0.19(2)	C73	0.726(1)	-0.0353(5)	0.1446(8)	0.085(9)
C21	0.455(2)	0.140(1)	0.109(1)	0.11(1)	C74	0.711(1)	-0.0008(5)	0.0975(8)	0.072(8)
C22	0.338(4)	0.147(2)	0.091(2)	0.18(2)	C75	0.703(1)	0.0607(5)	0.1012(8)	0.074(8)
C23	0.307(5)	0.149(3)	0.031(3)	0.29(3)	C76	0.693(2)	0.095(1)	0.048(1)	0.090(9)
C24	0.292(5)	0.106(3)	0.112(3)	0.31(4)	C77	0.601(2)	0.072(1)	0.006(1)	0.11(1)
C30	0.839(1)	0.3409(6)	0.2590(6)	0.049(7)	C78	0.789(2)	0.090(2)	0.024(1)	0.12(1)
C31	0.898(1)	0.3881(6)	0.2501(6)	0.042(6)	C79	0.731(3)	-0.104(2)	0.137(2)	0.14(1)
C32	0.952(1)	0.4189(6)	0.2943(6)	0.056(7)	C80	0.632(3)	-0.130(2)	0.110(1)	0.13(1)
C33	0.947(1)	0.4025(6)	0.3473(6)	0.066(8)	C81	0.785(2)	-0.135(2)	0.186(1)	0.13(1)
C34	0.887(1)	0.3553(6)	0.3562(6)	0.063(8)	C82	0.738(2)	0.083(1)	0.259(1)	0.09(1)
C35	0.833(1)	0.3245(6)	0.3120(6)	0.066(8)	C83	0.837(2)	0.065(1)	0.294(1)	0.11(1)
C36	0.773(2)	0.267(1)	0.325(1)	0.10(1)	C84	0.651(2)	0.060(2)	0.283(1)	0.12(1)
C37	0.845(2)	0.217(1)	0.347(1)	0.10(1)					

$$^a U_{\text{eq}} (\text{\AA}^2) = 1/3 \sum_i \sum_j U_{ij} a_i^* a_j^* \mathbf{a}_i \cdot \mathbf{a}_j.$$

**Table 9. Atomic Coordinates and Isotropic Thermal Parameters for the Non-Hydrogen Atoms of  $\{\text{Me}_2\text{Al}[\mu\text{-S}(2,6\text{-Me}_2\text{C}_6\text{H}_3)]_4\}$  (8)**

atom	x	y	z	$U_{\text{eq}} (\text{\AA}^2)^a$
S1	0.0230(1)	0.41374(9)	0.66207(8)	0.0475(4)
S2	0.0992(2)	0.7206(1)	0.62097(8)	0.0577(5)
Al1	0.2595(1)	0.5988(1)	0.68751(9)	0.0441(5)
Al2	-0.0351(2)	0.2207(1)	0.5528(1)	0.0543(6)
C1	0.0027(5)	0.3807(3)	0.7932(3)	0.047(2)
C2	-0.1510(5)	0.3765(4)	0.8146(3)	0.056(2)
C3	-0.1714(7)	0.3456(5)	0.9125(4)	0.080(3)
C4	-0.0443(8)	0.3207(5)	0.9886(4)	0.085(3)
C5	0.1052(7)	0.3253(4)	0.9672(4)	0.073(3)
C6	0.1333(5)	0.3547(4)	0.8700(3)	0.056(2)
C7	-0.2941(6)	0.4033(5)	0.7331(4)	0.082(3)
C8	0.3003(6)	0.3561(5)	0.8506(4)	0.072(2)
C9	0.3807(6)	0.6696(4)	0.8490(3)	0.066(2)
C10	0.3671(5)	0.5621(4)	0.5789(4)	0.065(2)
C11	0.1548(5)	0.8510(4)	0.7297(3)	0.051(2)
C12	0.0207(6)	0.8582(4)	0.7709(4)	0.065(2)
C13	0.064(1)	0.9550(6)	0.8596(5)	0.093(3)
C14	0.229(1)	1.0400(6)	0.9056(5)	0.105(4)
C15	0.3581(8)	1.0352(5)	0.8654(5)	0.090(3)
C16	0.3243(6)	0.9401(4)	0.7749(4)	0.067(2)
C17	-0.1629(7)	0.7665(6)	0.7245(5)	0.101(3)
C18	0.4674(7)	0.9374(6)	0.7305(5)	0.104(3)
C19	0.1673(7)	0.1765(5)	0.5625(4)	0.087(3)
C20	-0.2347(7)	0.1131(4)	0.5816(5)	0.095(3)

$$^a U_{\text{eq}} (\text{\AA}^2) = 1/3 \sum_i \sum_j U_{ij} a_i^* a_j^* \mathbf{a}_i \cdot \mathbf{a}_j.$$

steric and entropy factors in all but the most hindered molecules. The differences between the dimers and higher aggregates are not so readily assessed since the

number of bonds remains constant. This is represented in Chart 9.

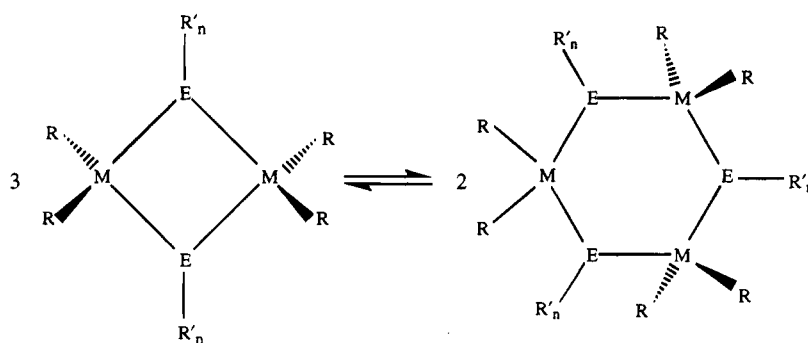
In these systems the balance is between entropy and the variety of steric interactions possible. It is not likely that any significant contribution from changes in bond energy occurs since the number and type of bonds remain constant. The steric interactions include the repulsion between groups on the same atom, the repulsion between those on adjacent atoms, cross-ring or chain interactions such as 1-3 diaxial interactions, and the various kinds of ring strain that may occur. As pointed out by many authors, the interaction between groups on adjacent atoms should increase as the ring size expands; at the same time, cross-ring interactions should diminish and the flexibility of the ring may decrease any ring strain present. To account for all of this stretching and bending, force constants are needed for all bonds. Barron has studied a number of  $[\text{R}_2\text{Al}(\mu\text{-OR})]_n$  derivatives which contain four- and six-membered rings by NMR spectroscopy and has carried out a few calculations designed to provide information about the stability of these rings and their conformations.<sup>55</sup> He has shown that increasing chain length of the R' group favors dimers but has noted that it is

(55) Rogers, J. H.; Apblett, A. W.; Cleaver, W. M.; Tyler, A. N.; Barron, A. R. *J. Chem. Soc., Dalton Trans.* **1992**, 3179.

(56) Fernholt, L.; Haaland, A.; Hargittai, M.; Seip, R.; Weidlein, J. *Acta Chem. Scand.* **1981**, A35, 529.

(57) Boardman, A.; Jeffis, S. E.; Small, R. W. H.; Worrall, I. *J. Inorg. Chim. Acta* **1985**, 99, L39.

Chart 9


**Table 10. Atomic Coordinates and Isotropic Thermal Parameters for the Non-Hydrogen Atoms of  $\{Me_2Ga[\mu-S(2,6-Me_2C_6H_3)]\}_4$  (9)**

atom	x	y	z	$U_{eq}$ ( $\text{\AA}^2$ ) <sup>a</sup>
Ga1	-0.0356(2)	0.2161(1)	0.5541(1)	0.0936(7)
Ga2	0.2655(2)	0.5994(1)	0.68897(8)	0.0724(5)
S1	0.0201(3)	0.4133(2)	0.6614(2)	0.068(1)
S2	-0.0949(3)	0.2799(2)	0.3789(2)	0.078(1)
C1	0.001(1)	0.3797(7)	0.7935(6)	0.063(4)
C2	-0.149(1)	0.3774(8)	0.8151(7)	0.075(4)
C3	-0.297(1)	0.405(1)	0.7347(9)	0.098(6)
C4	-0.169(1)	0.346(1)	0.9158(9)	0.093(6)
C5	-0.042(2)	0.321(1)	0.9886(8)	0.099(6)
C6	0.104(2)	0.324(1)	0.9661(8)	0.090(6)
C7	0.133(1)	0.3544(8)	0.8693(7)	0.074(4)
C8	0.297(1)	0.356(1)	0.8498(8)	0.090(5)
C9	-0.153(1)	0.1506(8)	0.2706(7)	0.069(4)
C10	-0.021(2)	0.1419(9)	0.2286(8)	0.087(5)
C11	0.165(2)	0.231(1)	0.275(1)	0.117(7)
C12	-0.064(2)	0.044(1)	0.138(1)	0.106(7)
C13	-0.229(3)	-0.040(1)	0.092(1)	0.125(9)
C14	-0.362(2)	-0.035(1)	0.133(1)	0.111(6)
C15	-0.322(1)	0.0621(9)	0.2242(8)	0.085(5)
C16	-0.465(2)	0.068(1)	0.268(1)	0.128(7)
C17	-0.239(2)	0.114(1)	0.5815(9)	0.120(6)
C18	0.168(2)	0.175(1)	0.5638(9)	0.107(6)
C19	0.368(1)	0.5632(9)	0.5767(8)	0.080(5)
C20	0.381(1)	0.6714(9)	0.8513(7)	0.086(5)

$${}^a U_{eq} (\text{\AA}^2) = 1/3 \sum_i \sum_j U_{ij} a_i^* a_j^* \mathbf{a}_i \cdot \mathbf{a}_j.$$

difficult to make quantitative predictions for these systems. Alternatively, *ab initio* calculations describing the system could be carried out. At the present time, a

number of the necessary force constants are unavailable, and an *ab initio* calculation is beyond the scope of this work.

We have, however, looked at several of these parameters in which the major differences arise from substituent interactions and compared these with compounds reported in the literature to obtain a qualitative understanding of the critical factors governing these equilibria. The only monomer reported for an aluminum thiolate is  $Al(SMes^*)_3$ .<sup>11</sup> The shortest nonbonding interactions, in the range of 2.5–2.8  $\text{\AA}$ , are between hydrogen atoms on the *tert*-butyl groups and the metal atom. The separations between *tert*-butyl groups on adjacent rings are in the range 3.73–3.83  $\text{\AA}$ . The *tert*-butyl groups effectively form a cage around the aluminum center, preventing dimerization.

In the typical dimeric compounds the closest nonbonding interactions that are likely to influence the state of aggregation substantially are those between the groups bound to aluminum and the groups on sulfur and interactions which occur across the ring. The groups bound to sulfur are normally separated by large distances because of their orientation in the *trans* configuration in the dimers or in equatorial positions on the larger rings. In the trimeric molecules, the rings become more flexible, in many cases undergoing inversion with relatively low energy barriers.<sup>35</sup> In the solid state, the rings are found in chair and skew-boat conformation, and the closest nonbonding interactions

**Table 11. Selected Bond Distances ( $\text{\AA}$ ) and Angles (deg) for  $[Mes_2Al(\mu-SBz)]_2$  (1),  $[Me_2Al(\mu-SSiPh_3)]_2$  (2), and  $[Mes_2Al(\mu-SPh)]_2$  (3)**

$[Mes_2Al(\mu-SBz)]_2$ (1)		$[Me_2Al(\mu-SSiPh_3)]_2$ (2)		$[Mes_2Al(\mu-SPh)]_2$ (3)	
Bond Distances					
Al1-S1	2.405(3)	Al1-S1	2.372(2)	Al1-S1	2.416(2)
Al1'-S1	2.358(2)	Al2-S1	2.368(2)	Al1'-S1	2.371(2)
		Al1-S2	2.358(2)	Al2-S2	2.395(2)
		Al2-S2	2.355(2)	Al2'-S2	2.398(2)
Al1-C17	1.966(7)	Al2-C4	1.936(5)	Al1-C20	1.958(6)
Al1-C8	1.987(5)	Al2-C3	1.921(6)	Al1-C10	1.982(5)
		Al1-C2	1.930(6)	Al2-C40	1.969(5)
		Al1-C1	1.927(5)	Al2-C50	1.964(6)
S1-C1	1.863(6)	S1-Si1	2.147(2)	S1-C1	1.781(5)
		S2-Si2	2.160(2)	S2-C30	1.789(5)
Bond Angles					
S1-Al1-S1'	89.11(8)	S1-Al1-S2	87.51(6)	S1-Al1-S1'	85.6(1)
Al1-S1-Al1'	90.89(8)	S1-Al2-S2	87.68(6)	S2-Al2-S2'	87.2(1)
		Al1-S1-Al2	91.85(6)	Al1-S1-Al1'	94.4(1)
		Al1-S2-Al2	92.54(6)	Al2-S2-Al2'	92.8(1)
C8-Al1-C17	119.6(3)	C3-Al2-C4	121.4(3)	C10-Al1-C20	118.7(2)
		C1-Al1-C2	120.7(3)	C40-Al2-C50	121.7(3)
Al1-S1-C1	110.0(2)	Al1-S1-Si1	118.35(7)	Al1-S1-C1	116.8(2)
Al1'-S1-C1	105.1(2)	Al2-S1-Si1	91.85(6)	Al1'-S1-C1	108.3(2)
		Al2-S2-Si2	118.21(7)	Al2-S2-C30	112.2(2)
		Al1-S2-Si2	119.97(6)	Al2'-S2-C30	108.5(2)

**Table 12. Selected Bond Distances (Å) and Angles (deg) for {Me<sub>2</sub>Al[μ-S(2-*t*-BuC<sub>6</sub>H<sub>4</sub>)]<sub>3</sub>} (4), {Me<sub>2</sub>Al[μ-S(2-SiMe<sub>3</sub>)C<sub>6</sub>H<sub>4</sub>]}<sub>3</sub> (5), {Me<sub>2</sub>Al[μ-S(2-*i*-PrC<sub>6</sub>H<sub>4</sub>)]<sub>3</sub>} (6), and {*i*-Bu<sub>2</sub>Al[μ-S(2,4,6-*i*-Pr<sub>3</sub>C<sub>6</sub>H<sub>2</sub>)]<sub>3</sub>} (7)**

4		5		6		7	
Bond Distances							
Al1-S1	2.340(5)	Al1-S1	2.351(2)	Al1-S1	2.357(3)	Al1-S1	2.37(1)
Al3-S1	2.363(5)	Al3-S1	2.368(2)	Al3-S1	2.380(2)	Al3-S1	2.37(1)
Al1-S2	2.363(4)	Al1-S2	2.365(2)	Al1-S2	2.366(2)	Al1-S2	2.36(1)
Al2-S2	2.367(5)	Al2-S2	2.365(2)	Al2-S2	2.371(2)	Al2-S2	2.36(1)
Al2-S3	2.349(5)	Al2-S3	2.369(2)	Al2-S3	2.352(3)	Al2-S3	2.38(1)
Al3-S3	2.336(4)	Al3-S3	2.366(2)	Al3-S3	2.358(2)	Al3-S3	2.38(1)
Al3-C6 (a)	1.93(1)	Al3-C6 (a)	1.949(6)	Al3-C6 (e)	1.92(1)	Al3-C1	1.94(3)
Al3-C5 (e)	1.93(1)	Al3-C5 (e)	1.932(7)	Al3-C5 (a)	1.939(7)	Al3-C5	1.98(3)
Al2-C4 (a)	1.95(1)	Al2-C4 (e)	1.937(7)	Al2-C4 (e)	1.930(6)	Al2-C17	1.99(2)
Al2-C3 (e)	1.92(1)	Al2-C3 (a)	1.953(6)	Al2-C3 (a)	1.942(6)	Al2-C21	1.91(3)
Al1-C2 (a)	1.97(1)	Al1-C2 (a)	1.958(6)	Al1-C2 (e)	1.936(6)	Al1-C13	1.99(2)
Al-C1 (e)	1.92(1)	Al1-C1 (e)	1.940(6)	Al1-C1 (a)	1.936(6)	Al1-C9	1.95(3)
Bond Angles							
S1-Al1-S2	88.8(2)	S1-Al1-S2	100.84(8)	S1-Al1-S2	90.22(8)	S1-Al1-S2	89.1(3)
S1-Al3-S3	100.6(2)	S1-Al3-S3	99.20(8)	S1-Al3-S3	99.89(8)	S1-Al3-S3	93.2(3)
S2-Al2-S3	99.1(2)	S2-Al2-S3	89.35(8)	S2-Al2-S3	101.52(7)	S2-Al2-S3	96.1(3)
Al1-S1-Al3	115.0(2)	Al1-S1-Al3	120.13(8)	Al1-S1-Al3	115.83(7)	Al1-S1-Al3	131.5(3)
Al1-S1-C7	105.5(5)	Al1-S1-C7	108.0(1)	Al1-S1-C7	101.9(2)	Al1-S1-C30	110.2(6)
Al3-S1-C7	103.3(5)	Al3-S1-C7	107.6(1)	Al3-S1-C7	106.9(2)	Al3-S1-C30	114.6(6)
Al1-S2-Al2	114.6(2)	Al1-S2-Al2	113.53(8)	Al1-S2-Al2	114.24(7)	Al1-S2-Al2	126.8(3)
Al1-S2-C17	103.9(4)	Al1-S2-C16	102.7(1)	Al2-S2-C16	99.8(1)	Al2-S2-C50	115.2(6)
Al2-S2-C17	106.1(4)	Al2-S2-C16	104.4(1)	Al1-S2-C16	105.9(2)	Al1-S2-C50	115.4(6)
Al2-S3-Al3	123.2(2)	Al2-S3-Al3	114.85(8)	Al2-S3-Al3	122.5(1)	Al2-S3-Al3	127.6(4)
Al2-S3-C27	108.9(4)	Al2-S3-C25	103.5(2)	Al2-S3-C25	107.3(2)	Al2-S3-C70	114.3(6)
Al3-S3-C27	106.4(4)	Al3-S3-C25	108.1(2)	Al3-S3-C25	107.3(2)	Al3-S3-C70	118.1(6)
C1-Al1-C2	121.1(5)	C1-Al1-C2	120.2(3)	C1-Al1-C2	119.6(3)	C9-Al1-C13	130(1)
C3-Al2-C4	121.5(5)	C3-Al2-C4	118.3(3)	C3-Al2-C4	122.6(2)	C17-Al2-C21	130(1)
C5-Al3-C6	119.3(5)	C5-Al3-C6	120.2(3)	C5-Al3-C6	123.2(3)	C1-Al3-C5	129(1)

**Table 13. Selected Bond Distances (Å) and Angles (deg) for {Me<sub>2</sub>Al[μ-S(2,6-Me<sub>2</sub>C<sub>6</sub>H<sub>3</sub>)]<sub>4</sub>} (8) and {Me<sub>2</sub>Ga[μ-S(2,6-Me<sub>2</sub>C<sub>6</sub>H<sub>3</sub>)]<sub>4</sub>} (9)**

8		9	
Bond Distances			
Al1-S1	2.364(1)	Ga1-S1	2.392(2)
Al2-S1	2.359(1)	Ga1-S2	2.401(1)
Al1-S2	2.367(1)	Ga2-S1	2.400(2)
Al2'-S2	2.360(1)	Ga2-S2'	2.408(2)
Al1-C9	1.955(3) (e)	Ga1-C17 (e)	1.91(1)
Al1-C10	1.944(3) (a)	Ga1-C18 (a)	1.92(1)
Al2-C19	1.944(5) (e)	Ga2-C20 (e)	1.967(6)
Al2-C20	1.927(5) (a)	Ga2-C19 (a)	1.946(6)
S1-C1	1.794(2)	S1-C1	1.768(5)
S2-C11	1.785(3)	S2-C9	1.807(4)
Bond Angles			
Al1-S1-Al2	126.92(5)	Ga1-S1-Ga2	126.21(8)
Al1-S2-Al2'	130.68(4)	Ga2'-S2-Ga1	129.77(7)
S1-Al1-S2	99.46(5)	S1-Ga1-S2	93.07(5)
S1-Al2-S2'	94.60(4)	S1-Ga2-S2'	96.6(5)
C9-Al1-C10	126.0(2)	C19-Ga2-C20	129.5(4)
C19-Al2-C20	120.3(2)	C17-Ga1-C18	124.2(3)

between the groups on aluminum and sulfur are on the order of 3.4 Å. The average C-Al-C angles for 1-6 are in a very narrow range between 119.6° and 121.8°. In 7 this angle opens up to 129.7°. In the dimers, 1-3, the endocyclic angles are all near 90°. In the trimers, 4-6, these angles range from 115° to 122° for Al-S-Al and from 89° to 100° for S-Al-S. In the seat of the chair, the angles at aluminum are 100° and those at sulfur are slightly larger at 115°. The angles at the other positions differ substantially with those around the aluminum at 89° and around sulfur at 122°. In 7 there are substantial changes with all S-Al-S angles near 90° and those around sulfur averaging 128.6°. In the tetrameric structures, the rings have even more flexibility, and the shortest nonbonded interactions are typically 3.5 Å or greater for carbon on adjacent aluminum and sulfur atoms. The endocyclic angles

around the ring are 93° to 100° at the metal and 126° to 130° at the sulfur.

It is apparent from these observations that large groups which give rise to significant interactions between groups on adjacent atoms in the ring favor dimers. This, along with the entropy which favors dimers over higher aggregates, takes precedence. When the steric requirements are reduced, the larger aggregates may form. These may be enhanced by reduction of transannular interactions such as axial-axial interactions. The substantial number of these interactions and the lack of information on force constants for deformation of the molecular units make quantitative prediction of the aggregation states difficult. This is further complicated in the solid state by the inclusion of lattice energies which may favor a single conformation or aggregation state. In a paper to follow we will provide a detailed discussion of the behavior of these compounds in solution in which we show that the difference in energy between dimers and trimers is often very small and also describe the flexibility of the rings in solution.

It is interesting to consider the groups that give rise to dimers, trimers, and tetramers. In the dimeric systems, the bridging chalcogen atoms are bound to a variety of groups, i.e., Et, Bu, Ph, and SiPh<sub>3</sub>. In the observed trimeric aluminum derivatives, the substituents on the bridging atoms are all phenyl groups with substituents on the 2- or 2- and 6-positions. The substituents on the metal are methyl groups in all but one compound where isobutyl groups are present. In the tetramers, very small groups, OH, or large 2,6-Me<sub>2</sub>C<sub>6</sub>H<sub>3</sub> groups are bound to the chalcogen, and methyl groups are bound to the metal. From these observations, one may conclude that the substituent on the chalcogen may have some influence on the aggregate formed, but the most important contributions appear

Table 14. Selected Structural Data on Aluminum and Gallium Thiolates and Related Compounds

	M-S distance (Å) (av)	S-M-S (deg)	M-S-M (deg)	sum of angles around S
Aluminum Derivatives				
[Mes <sub>2</sub> Al( $\mu$ -SBz)] <sub>2</sub> (1) <sup>a</sup>	2.381	89.1	90.9	305.99
[Me <sub>2</sub> Al( $\mu$ -SSiPh <sub>3</sub> )] <sub>2</sub> (2) <sup>a</sup>	2.363	87.5, 87.7	91.9	330.2
			92.5	330.7
[Mes <sub>2</sub> Al( $\mu$ -SPh)] <sub>2</sub> (3) <sup>a</sup>	2.395	86.4	92	319.5
				313.5
{Me <sub>2</sub> Al[ $\mu$ -S(2- <i>t</i> -BuC <sub>6</sub> H <sub>4</sub> )] <sub>3</sub> } (4) <sup>a</sup>	2.35	100.6	115.1	323.9
		88.8	123.2	338.5
		99.1	114.6	324.6
{Me <sub>2</sub> Al[ $\mu$ -S(2-Me <sub>3</sub> Si)C <sub>6</sub> H <sub>4</sub> ]} <sub>3</sub> (5) <sup>a</sup>	2.36	100.84	120.13	335.73
		89.35	113.53	320.63
		99.20	114.85	326.45
{Me <sub>2</sub> Al[ $\mu$ -S(2- <i>i</i> -PrC <sub>6</sub> H <sub>4</sub> )] <sub>3</sub> } (6) <sup>a</sup>	2.36	101.5	115.8	324.5
		99.9	114.2	337.1
		90.2	122.5	320.0
<i>i</i> -Bu <sub>2</sub> Al[ $\mu$ -S(2,4,6- <i>i</i> -Pr <sub>3</sub> C <sub>6</sub> H <sub>2</sub> )] <sub>3</sub> (7) <sup>a</sup>	2.37	89.1	127.6	360.0
		93.2	126.8	357.4
		96.1	131.5	356.3
{Me <sub>2</sub> Al[ $\mu$ -S(2,6-Me <sub>2</sub> C <sub>6</sub> H <sub>3</sub> )] <sub>4</sub> } (8) <sup>a</sup>	2.363	99.5	126.9	342.8
		94.6	130.7	348.3
[Me <sub>2</sub> Al( $\mu$ -SMe)] <sub>∞</sub> (solid state) <sup>b</sup>	2.348	100.1	103.0	310.3
[Me <sub>2</sub> Al( $\mu$ -SMe)] <sub>2</sub> (gas phase) <sup>c</sup>	2.370	85.5	94.5	
[Me <sub>2</sub> Al( $\mu$ -SC <sub>6</sub> F <sub>5</sub> )] <sub>2</sub> <sup>d</sup>	2.402	89.4	86.9	301.0
		89.6	87.3	308.0
Me <sub>3</sub> Al·SMe <sub>2</sub> (gas phase) <sup>e</sup>	2.55			
[Me <sub>2</sub> Al( $\mu$ -PyS)] <sub>2</sub> <sup>f</sup>	2.338	97.34		
Al[S(2,4,6- <i>t</i> -Bu <sub>3</sub> C <sub>6</sub> H <sub>2</sub> )] <sub>3</sub> <sup>g</sup>	2.185	119.8		
Gallium Derivatives				
[Ph <sub>2</sub> Ga( $\mu$ -SEt)] <sub>2</sub> <sup>h</sup>	2.373	93.58	86.42	294.92
[ <i>t</i> -Bu <sub>2</sub> Ga( $\mu$ -SH)] <sub>2</sub> <sup>i</sup>	2.433	90.5	89.5	282.5
[Me <sub>2</sub> Ga( $\mu$ -SC <sub>6</sub> F <sub>5</sub> )] <sub>2</sub> <sup>j</sup>	2.449	89.45	87.75	302.55
		88.59	87.99	304.99
[I <sub>2</sub> Ga( $\mu$ -SMe)] <sub>2</sub> <sup>k</sup>	2.379	94.5	85.5	
[I <sub>2</sub> Ga( $\mu$ -S- <i>i</i> -Pr)] <sub>2</sub> <sup>l</sup>	2.329	89.1	84.7	
[ <i>t</i> -BuGa( $\mu$ -S)] <sub>4</sub> <sup>m</sup>	2.359	97.3	82.1	
Ga[S(2,4,6- <i>t</i> -Bu <sub>3</sub> C <sub>6</sub> H <sub>2</sub> )] <sub>3</sub> <sup>n</sup>	2.205	119.8		
{Me <sub>2</sub> Ga[ $\mu$ -S(2,6-Me <sub>2</sub> C <sub>6</sub> H <sub>3</sub> )] <sub>4</sub> } (9) <sup>a</sup>	2.397	93.07	126.21	340.71
		96.6	129.8	346.0

<sup>a</sup> This work. <sup>b</sup> Reference 31. <sup>c</sup> Reference 45. <sup>d</sup> Reference 14. <sup>e</sup> Reference 56. <sup>f</sup> Reference 54. <sup>g</sup> Reference 11. <sup>h</sup> Reference 16. <sup>i</sup> Reference 17. <sup>j</sup> Reference 46. <sup>k</sup> Reference 57. <sup>l</sup> Reference 47. <sup>m</sup> References 15 and 17. <sup>n</sup> Reference 11.

to come from the substituents on the metal with methyl groups favoring formation of larger aggregates. Work is now in progress to determine if it is possible to predict the degree of aggregation by consideration of the substituents on the metal and chalcogen atoms in these cyclic derivatives.

**Acknowledgment.** Acknowledgment is made to the donors of the Petroleum Research Fund administered

by the American Chemical Society for the support of this research.

**Supplementary Material Available:** Complete listings of crystal and X-ray data collection parameters, bond distances and angles, anisotropic thermal parameters for the non-hydrogen atoms, and atomic coordinates and isotropic thermal parameters for the hydrogen atoms (41 pages). Ordering information is given on any current masthead page.

OM950150W

# Synthesis, Structure, and Reactivity of the Anionic Trinuclear Methanide $\text{NBu}_4[\{\text{Au}(\text{C}_6\text{F}_5)_3(\text{PPh}_2\text{CHPPh}_2)\}_2\text{Au}]$

Eduardo J. Fernández,<sup>†</sup> M. Concepción Gimeno,<sup>‡</sup> Peter G. Jones,<sup>§</sup> Antonio Laguna,<sup>\*,‡</sup> Mariano Laguna,<sup>‡</sup> and José M. López-de-Luzuriaga<sup>†</sup>

Departamento de Química, Universidad de La Rioja, E-26001 Logroño, Spain, Departamento de Química Inorgánica, Instituto de Ciencia de Materiales de Aragón, Universidad de Zaragoza, CSIC, E-50009 Zaragoza, Spain, and Institut für Anorganische und Analytische Chemie der Technische Universität, Postfach 3329, D-38023 Braunschweig, Germany

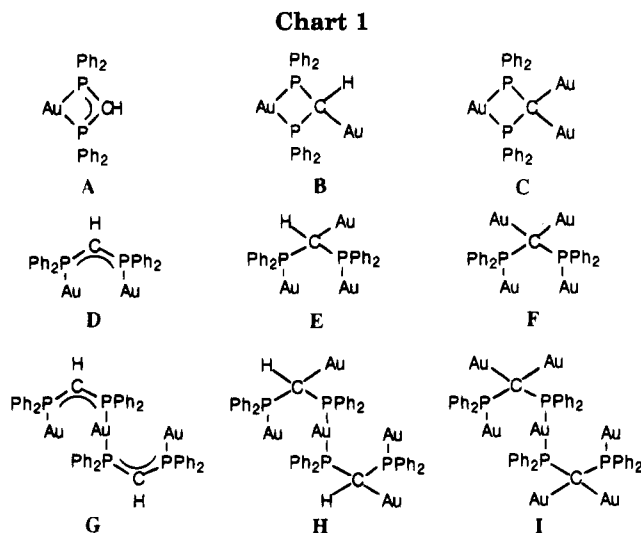
Received January 10, 1995<sup>®</sup>

The reaction of  $[\text{Au}(\text{tht})_2]\text{ClO}_4$  or  $\text{NBu}_4[\text{Au}(\text{acac})_2]$  with 2 equiv of  $[\text{Au}(\text{C}_6\text{F}_5)_3\text{PPh}_2\text{CH}_2\text{PPh}_2]$  affords the cationic  $[\{\text{Au}(\text{C}_6\text{F}_5)_3\text{PPh}_2\text{CH}_2\text{PPh}_2\}_2\text{Au}]\text{ClO}_4$  (**1**) or anionic complex  $\text{NBu}_4[\{\text{Au}(\text{C}_6\text{F}_5)_3\text{PPh}_2\text{CHPPh}_2\}_2\text{Au}]$  (**2**), respectively, in high yield. The methanide complex **2** can displace tetrahydrothiophene from  $[\text{AuX}(\text{tht})]$  to give the pentanuclear  $\text{NBu}_4[\{\text{Au}(\text{C}_6\text{F}_5)_3\text{PPh}_2\text{CH}(\text{AuX})\text{PPh}_2\}_2\text{Au}]$  ( $\text{X} = \text{Cl}, \text{C}_6\text{F}_5$ ). The heptanuclear  $[\{\text{Au}(\text{C}_6\text{F}_5)_3\text{PPh}_2\text{C}(\text{AuPPh}_3)_2\text{PPh}_2\}_2\text{Au}]\text{ClO}_4$  is obtained by reaction of **1** with  $[\text{Au}(\text{acac})\text{PPh}_3]$  (molar ratio 1:4). The structure of **2** has been determined by a single-crystal X-ray diffraction study. It crystallizes in the space group  $P\bar{1}$  with  $a = 14.213(4)$  Å,  $b = 16.067(4)$  Å,  $c = 23.840(6)$  Å,  $\alpha = 88.60(2)^\circ$ ,  $\beta = 89.27(2)^\circ$ ,  $\gamma = 71.23(2)^\circ$ ,  $Z = 2$ , and  $T = -100$  °C. It does not display gold–gold interactions.

## Introduction

We have reported the synthesis of methanide or methanediide complexes of gold starting from (bis(diphenylphosphino)methane)gold complexes, such as  $[\text{Au}(\text{C}_6\text{F}_5)_2\{\text{PPh}_2\}_2\text{CH}_2]\text{ClO}_4$  or  $[\text{CH}_2\{\text{PPh}_2\text{AuPPh}_2\}_2\text{CH}_2](\text{ClO}_4)_2$ , and by reaction with sodium hydride,<sup>1</sup> (acetylacetonato)gold derivatives,<sup>2,3</sup> and other deprotonating agents.<sup>1</sup> However, in these complexes, the diphosphine acts as a chelating or bridging ligand, respectively, and after deprotonation the only possibility for further coordination is through the methanide carbon atom. The reaction of  $[\text{Au}(\text{acac})\text{PPh}_3]$  with  $(\text{PPh}_2)_2\text{CH}_2$  (dppm) leads to the deprotonation of the  $\text{CH}_2$  group and formation of a dinuclear eight-membered-ring complex in which the donor atoms at gold are the phosphorus atoms of the phosphine.<sup>4</sup> The different coordination forms reported<sup>1–4</sup> for these ligands are in Chart 1 (A–F). There is no example of a derivative with three gold centers bonded by two methanide or methanediide ligands (forms G–I). Most of the gold methanide complexes described so far are neutral or cationic; there are very few examples of anionic complexes.

In this paper we describe the preparation of the trinuclear  $\text{NBu}_4[\{\text{Au}(\text{C}_6\text{F}_5)_3\text{PPh}_2\text{CHPPh}_2\}_2\text{Au}]$  by reaction of  $[\text{Au}(\text{C}_6\text{F}_5)_3\text{PPh}_2\text{CH}_2\text{PPh}_2]$  with  $\text{NBu}_4[\text{Au}(\text{acac})_2]$ . Its molecular structure has been established by X-ray studies and shows the presence of two  $\text{PPh}_2\text{CHPPh}_2$



groups bridging the gold(I) and gold(III) centers. The excess electron density on the C-methanide can be used to coordinate to new gold centers.

## Results and Discussion

The diphosphine in  $[\text{Au}(\text{C}_6\text{F}_5)_3\text{PPh}_2\text{CH}_2\text{PPh}_2]$  acts as a monodentate ligand,<sup>5</sup> and the free phosphorus atom can be used to coordinate other gold centers. Thus, the reaction with  $[\text{Au}(\text{tht})_2]\text{ClO}_4$  (molar ratio 2:1) leads to the trinuclear complex  $[\{\text{Au}(\text{C}_6\text{F}_5)_3\text{PPh}_2\text{CH}_2\text{PPh}_2\}_2\text{Au}]\text{ClO}_4$  (**1**) (Scheme 1).

The use of acetylacetonato (acac) complexes, such as  $[\text{Au}(\text{acac})_2]^-$  or  $[\text{Au}(\text{acac})\text{PPh}_3]$ , as deprotonating agents which allow one to form Au–C bonds very easily has been previously reported.<sup>2,3,6,7</sup> The reaction of  $\text{NBu}_4$ –

<sup>†</sup> Universidad de La Rioja.

<sup>‡</sup> Universidad de Zaragoza.

<sup>§</sup> Technischen Universität.

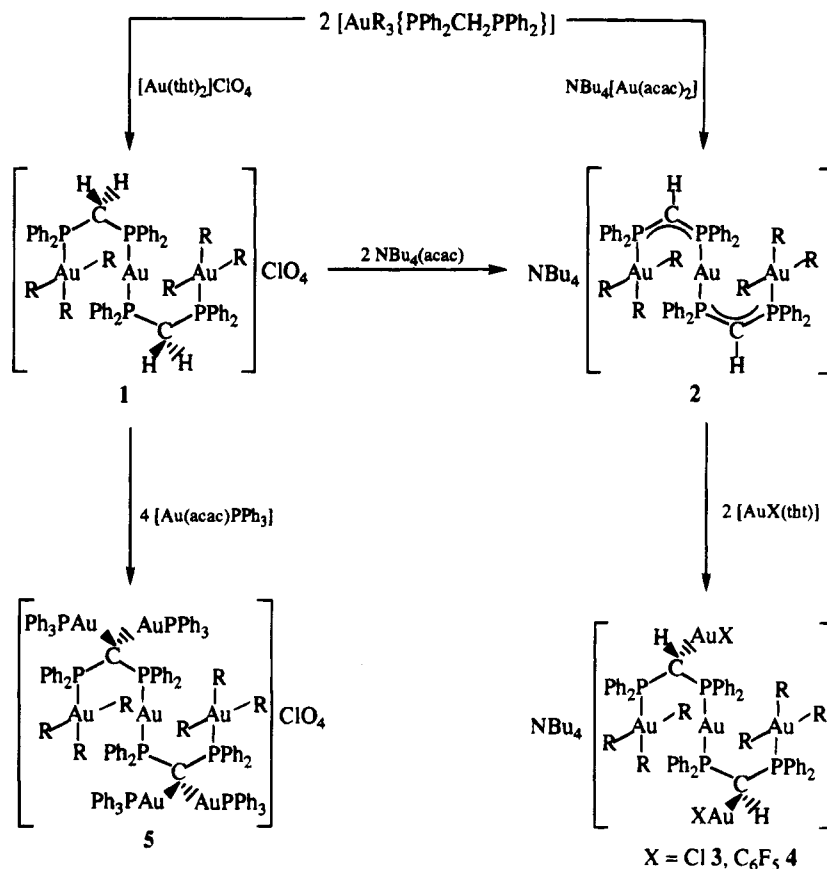
<sup>®</sup> Abstract published in *Advance ACS Abstracts*, May 1, 1995.

(1) Laguna, A.; Laguna, M. *J. Organomet. Chem.* **1990**, *394*, 743.  
(2) Fernández, E. J.; Gimeno, M. C.; Jones, P. G.; Laguna, A.; Laguna, M.; Lopez-de-Luzuriaga, J. M. *J. Chem. Soc., Dalton Trans.* **1992**, 3365.

(3) Fernández, E. J.; Gimeno, M. C.; Jones, P. G.; Laguna, A.; Laguna, M.; Lopez-de-Luzuriaga, J. M. *Angew. Chem., Int. Ed. Engl.* **1994**, *33*, 87.

(4) Gimeno, M. C.; Laguna, A.; Laguna, M.; Sanmartín, F.; Jones, P. G. *Organometallics* **1993**, *12*, 3984; *Organometallics* **1994**, *13*, 1538.

(5) Usón, R.; Laguna, A.; Laguna, M.; Fernández, E. J.; Jones, P. G.; Sheldrick, G. M. *J. Chem. Soc., Dalton Trans.* **1982**, 1971.

Scheme 1<sup>a</sup><sup>a</sup> R = C<sub>6</sub>F<sub>5</sub>.

[Au(acac)<sub>2</sub>] with [Au(C<sub>6</sub>F<sub>5</sub>)<sub>3</sub>PPh<sub>2</sub>CH<sub>2</sub>PPh<sub>2</sub>] (molar ratio 1:2) leads to the deprotonation of the CH<sub>2</sub> group and formation of the trinuclear complex **2** (Scheme 1). The gold(I) center is coordinated to the free phosphorus atom instead of the C-methanide, as we have observed in other complexes.<sup>4,8</sup> Complex **2** can also be obtained by reaction of **1** with NBu<sub>4</sub>(acac), in molar ratio 1:2, but in this case a mixture of **2** and NBu<sub>4</sub>ClO<sub>4</sub> is obtained, and separation of these two products is difficult because of their similar solubilities in common organic solvents.

The presence of excess electron density on the methanide carbons causes them to act as C-donor nucleophiles, and they are able to displace tetrahydrothiophene (tht) from [AuX(tht)] (X = Cl or C<sub>6</sub>F<sub>5</sub>) to give the pentanuclear complexes **3** or **4** (Scheme 1).

The reaction of the trinuclear complex **1** with 4 equiv of [Au(acac)PPh<sub>3</sub>] affords the heptanuclear [Au(C<sub>6</sub>F<sub>5</sub>)<sub>3</sub>-PPh<sub>2</sub>C(AuPPh<sub>3</sub>)<sub>2</sub>PPh<sub>2</sub>]<sub>2</sub>Au]ClO<sub>4</sub> (**5**) in which the bis(diphenylphosphino)methanediide acts as an eight-electron donor ligand bonded to four gold atoms. Only two examples are known<sup>3,9</sup> in which this ligand bridges four metal centers. [Au(acac)PR<sub>3</sub>] was previously used in the preparation of complexes with two =C{Au(PR<sub>3</sub>)<sub>2</sub>}<sub>2</sub> groups, as in the synthesis of [Au(PPh<sub>3</sub>)<sub>2</sub>]<sub>2</sub>C(PPh<sub>2</sub>-AuPPh<sub>2</sub>)<sub>2</sub>C{Au(PPh<sub>3</sub>)<sub>2</sub>}(ClO<sub>4</sub>)<sub>2</sub><sup>3</sup> or [Au(PMe<sub>2</sub>Ph)]<sub>4</sub>{μ-C(PPh<sub>3</sub>)<sub>2</sub>CO}(ClO<sub>4</sub>)<sub>2</sub>.<sup>6</sup>

Complexes **1**–**5** are air- and moisture-stable white (**1**, **5**), pale yellow (**3**, **4**), or yellow (**2**) solids. They behave as 1:1 electrolytes in acetone solution [118 (**1**), 110 (**2**), 119 (**3**), 140 (**4**), or 80 (**5**) Ω<sup>-1</sup> cm<sup>2</sup> mol<sup>-1</sup> for 5 × 10<sup>-4</sup> M solutions]. Their IR spectra show bands at ca. 1505 (vs), 967 (vs), and 800 (s) cm<sup>-1</sup> arising from C<sub>6</sub>F<sub>5</sub> groups bonded to gold(III) centers.<sup>5</sup> Furthermore, complex **2** shows a band at 1174 (m) cm<sup>-1</sup> assigned to the methanide (P–CH–P) system.<sup>1</sup> For complexes **3** the ν(Au–Cl) vibration appears at 320 (m) cm<sup>-1</sup>.

The <sup>19</sup>F NMR spectra of complexes **1**, **2**, and **5** are characteristic of tris(pentafluorophenyl) compounds, showing three groups of signals associated with the two different types of C<sub>6</sub>F<sub>5</sub>. However, for complex **3** several signals appear in the region of the *ortho*-fluorine at δ –118.1 (m) and –122.3 (m) (relative intensities 2:1, for the two mutually *trans* C<sub>6</sub>F<sub>5</sub> and one *cis* C<sub>6</sub>F<sub>5</sub> groups, respectively) and at –119.1 (m) and –120.8 (m) (relative intensities 2:1) indicating the presence of two diastereomers with relative abundance 1:0.58. Since complex **3** has two chiral centers, four isomers or two diastereomers are possible. The spectrum of complex **4** also shows the presence of two diastereomers; six resonances due to the *ortho*-fluorine atoms at –115.1 (m), –118.6 (m), –120.6 (m) (relative intensities 1:1:2) and –116.0 (m), –118.3 (m), –122.1 (m) (relative intensities 1:1:2) appear (relative abundance between isomers 0.7:1). In both complexes the signals corresponding to *para*- and *meta*-fluorine atoms are overlapped for the two isomers and appear as multiplets at δ –157.5 (m) and –157.8 (m) (*para*-F) and –161.3 (m) and –162.3 (m) (*meta*-F) (**3**) and at –157.8 (m), –158.3 (m), and –159.4 (m)

(6) Vicente, J.; Chicote, M. T.; Saura-Llamas, I.; Jones, P. G.; Meyer-Bäse, K.; Erdbrügger, C. F. *Organometallics* **1988**, *7*, 997.

(7) Vicente, J.; Chicote, M. T.; Saura-Llamas, I.; Lagunas, M. C. *J. Chem. Soc., Chem. Commun.* **1992**, 915.

(8) Fernández, E. J.; Gimeno, M. C.; Jones, P. G.; Laguna, A.; Laguna, M.; López-de-Luzuriaga, J. M. *J. Chem. Soc., Dalton Trans.* **1993**, 3401.

(9) Luser, M.; Peringer, P. *Organometallics* **1984**, *3*, 1916.

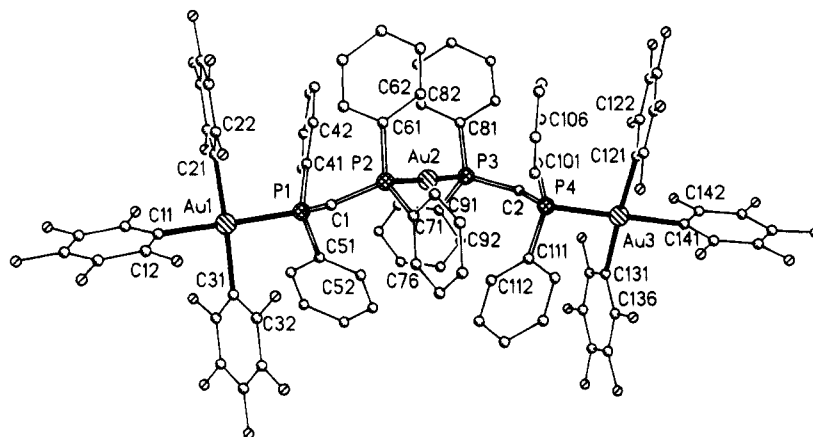


**Figure 1.** Anion of complex **2** in the crystal. Hydrogen atoms are omitted for clarity.

(*para*-F) and  $-161.8$  (m),  $-162.7$  (m), and  $-163.5$  (m) (*meta*-F) (**4**).

The presence of two diastereomers in complex **4** can also be observed in the  $^1\text{H}$  NMR spectrum. Thus, the resonances of the methine protons appear as two doublets of doublets (dd), one for each isomer, at 3.27 ppm [ $J(\text{H}-\text{P}) = 11.3$  and 6.0 Hz] and 2.93 ppm [ $J(\text{H}-\text{P}) = 14.0$  and 6.0 Hz]. In complex **3** only one resonance is observed at 3.4 ppm (dd) [ $J(\text{H}-\text{P}) = 11.9$  and 5.9 Hz] probably caused by the overlapping of the other signal with one of the resonances due to the tetrabutylammonium cation [3.2(m) ppm]. For complexes **1** or **2** the resonance of the methine groups appear at 4.7 (m) or 3.55 ("t") [ $J(\text{H}-\text{P}) = 11$  Hz], respectively.

The  $^{31}\text{P}\{^1\text{H}\}$  NMR spectra of **1**–**5** show two broad signals corresponding to a poorly resolved AA'XX' system, even at low temperature. In complex **5** the signal due to  $\text{PPh}_3$  appears as a singlet (see Experimental Section).

The structure of complex **2** was confirmed by an X-ray structure determination (Figure 1). Atomic coordinates are collected in Table 1, and selected bond lengths and angles, in Table 2. The gold(III) centers Au(1) and Au(3) display the expected planar coordination; the gold atoms lie 0.04 and 0.01 Å, respectively, out of their ligand planes. The Au–C bond lengths lie in the range 2.057(8)–2.080(8) Å, similar to those in other tris(pentafluorophenyl)gold(III) derivatives.<sup>10</sup> The Au(III)–P distances are both 2.367(2) Å, longer than in  $[\text{AuCl}_3(\text{PPh}_3)]^{11}$  (2.335(4) Å),  $[\text{AuMe}_3(\text{PPh}_3)]^{12}$  [2.350(6) and 2.347(6) Å, two independent molecules], or  $[\text{Au}(\text{C}_6\text{F}_5)(\text{S}_2\text{C}_6\text{H}_4)(\text{PPh}_3)]^{13}$  (2.340(1) Å), reflecting the higher *trans* influence of the pentafluorophenyl groups. The central gold(I) atom Au(2) is linearly coordinated [Au–P = 2.311(2) and 2.314(2) Å and P–Au–P = 177.95(7)°]. There are no short gold–gold interactions; the intramolecular contacts Au(1)···Au(2) = 6.28 Å and Au(2)···Au(3) = 6.10 Å are the shortest. The P–C<sub>methanide</sub> bond distances lie in the range 1.701(8)–1.722(7) Å, shorter than in the bis(diphenylphosphino)methane ligand; e.g., the P–C distance in  $[\text{Au}(\text{C}_6\text{F}_5)_2\{(\text{PPh}_2)_2-$

$\text{CH}_2\}\text{ClO}_4^{14}$  is 1.845(9) Å. This difference arises from a degree of multiple P–C bonding in the methanide ligand. The angles around the methanide carbons are P(4)–C(2)–P(3) = 123.9(5) and P(1)–C(1)–P(2) = 129.0(5)°, close to the ideal value of 120° for  $\text{sp}^2$  hybridization.

The molecular backbone consists of two extended peripheral sections, with torsion angles C(11)···P(1)–C(1)–P(2) =  $-163^\circ$ , P(1)–C(1)–P(2)···P(3) =  $-19^\circ$ , P(2)···P(3)–C(2)–P(4) =  $-1^\circ$ , and P(3)–C(2)–P(4)···C141 =  $-174^\circ$ ; the conformation about the central gold is *gauche*, with C(1)–P(2)···P(3)–C(2) =  $-137^\circ$ .

## Experimental Section

**Materials and Instrumentation.** All compounds described in this report are air-stable, but reactions were performed under nitrogen atmosphere and at room temperature. Solvents were purified by standard methods and distilled under nitrogen prior to use. Infrared spectra were recorded in the range 4000–200  $\text{cm}^{-1}$  on a Perkin-Elmer 883 spectrophotometer using Nujol mulls between polyethylene sheets. Conductivities were measured with a Jenway 4010 digital conductimeter. C, H, and N analyses were carried out with a Perkin-Elmer 240C microanalyzer. NMR spectra were recorded on Bruker ARX-300 spectrometer. Chemical shifts are cited relative to  $\text{SiMe}_4$  (external,  $^1\text{H}$ ), 85%  $\text{H}_3\text{PO}_4$  (external,  $^{31}\text{P}$ ), and  $\text{CFCl}_3$  (external,  $^{19}\text{F}$ ).

**Safety Note!** Perchlorate salts of metal complexes with organic ligands are potentially explosive. Only small amounts of material should be prepared, and these should be handled with great caution.

**Synthesis.**  $[\text{NBu}_4][\text{Au}(\text{acac})\text{Cl}]$ . To a solution of  $[\text{AuCl}(\text{tht})]^{15}$  (0.32 g, 1 mmol) in dichloromethane (30 mL) was added  $[\text{NBu}_4][\text{acac}]$  (0.34 g, 1 mmol). After 30 min the solution was filtered over Celite and the solvent was concentrated to ca. 5 mL. Addition of diethyl ether (15 mL) gave  $[\text{NBu}_4][\text{Au}(\text{acac})\text{Cl}]$  as a white solid. Yield: 68%. Decomposes at 42 °C. Anal. Calcd for  $\text{C}_{21}\text{H}_{43}\text{AuNO}_2\text{Cl}$ : C, 44.0; H, 7.55; N, 2.45. Found: C, 44.0; H, 8.0; N, 2.45.  $\Lambda_M$ : 119  $\Omega^{-1}\text{cm}^2\text{mol}^{-1}$ . IR: 1654 (vs) and 1639 (vs) [ $\nu(\text{CO})$ ], 318 (m) [ $\nu(\text{AuCl})$ ].  $^1\text{H}$  NMR ( $\text{CDCl}_3$ ): 4.31 (s, CH), 3.15 (m,  $\text{CH}_2$ ), 2.17 [s,  $\text{CH}_3$  (acac)], 1.59 (m,  $\text{CH}_2$ ), 1.37 (m,  $\text{CH}_2$ ) and 0.91 [t,  $\text{CH}_3$  (Bu),  $J(\text{HH}) = 7.3$  Hz].

$[\text{NBu}_4][\text{Au}(\text{acac})_2]$ . To a solution of  $[\text{NBu}_4][\text{Au}(\text{acac})\text{Cl}]$  (0.574 g, 1 mmol) in dichloromethane (30 mL) was added  $\text{Ti}(\text{acac})_3$  (0.30 g, 1 mmol). After the mixture was stirred for 4 h, the precipitated  $\text{TiCl}_3$  was filtered off. The solution was evaporated to ca. 5 mL, and addition of diethyl ether (15 mL)

(10) Usón, R.; Laguna, A.; Laguna, M.; Castilla, M. L.; Jones, P. G.; Fittschen, C. *J. Chem. Soc., Dalton Trans.* **1987**, 3017.

(11) Bandoli, G.; Clemente, D. A.; Marangoni, G.; Cattalini, L. *J. Chem. Soc., Dalton Trans.* **1973**, 886.

(12) Stein, J.; Fackler, J. P., Jr.; Paparizos, C.; Chen, H. W. *J. Am. Chem. Soc.* **1981**, *103*, 2192.

(13) Cerrada, E.; Fernández, E. J.; Gimeno, M. C.; Laguna, A.; Laguna, M.; Terroba, R.; Villacampa, M. D. *J. Organomet. Chem.*, in press.

(14) Usón, R.; Laguna, A.; Laguna, M.; Fernández, E.; Villacampa, M. D.; Jones, P. G.; Sheldrick, G. M. *J. Chem. Soc., Dalton Trans.* **1983**, 1679.

(15) Usón, R.; Laguna, A. *Organomet. Synth.* **1986**, *3*, 322.



Table 1. Atomic Coordinates ( $\times 10^4$ ) and Equivalent Isotropic Displacement Parameters ( $\text{\AA}^2 \times 10^3$ ).

	<i>x</i>	<i>y</i>	<i>z</i>	<i>U</i> (eq) <sup>a</sup>		<i>x</i>	<i>y</i>	<i>z</i>	<i>U</i> (eq) <sup>a</sup>
Au(1)	-906.8(2)	7470.9(2)	3735.50(12)	25.50(15)	C(93)	3126(4)	1935(4)	3529(2)	49(2)
Au(2)	1675.8(2)	4723.1(2)	2033.62(12)	24.29(15)	C(94)	2293(5)	2258(4)	3870(2)	55(3)
Au(3)	5450.7(2)	2287.4(2)	969.55(12)	24.60(15)	C(95)	1422(4)	2841(4)	3649(2)	58(3)
P(1)	80.7(14)	6262.9(13)	3213.7(8)	24.5(10)	C(96)	1384(3)	3101(4)	3087(2)	44(2)
P(2)	1104.5(14)	6241.0(12)	2052.6(8)	23.0(9)	C(101)	3276(3)	4108(3)	906(2)	25(2)
P(3)	2190.1(14)	3203.0(12)	2018.1(8)	23.2(9)	C(102)	3403(4)	4923(3)	811(2)	32(2)
P(4)	4041.8(14)	3272.3(13)	1409.2(8)	24.1(9)	C(103)	2911(4)	5464(3)	371(2)	37(2)
C(1)	566(5)	6715(5)	2674(3)	27(2)	C(104)	2292(4)	5192(3)	25(2)	40(2)
C(2)	3327(5)	2709(5)	1707(3)	26(2)	C(105)	2165(4)	4378(3)	119(2)	36(2)
C(11)	-1768(5)	8544(5)	4173(3)	35(2)	C(106)	2657(4)	3836(3)	560(2)	30(2)
C(12)	-1611(6)	9350(5)	4148(3)	42(2)	C(111)	4553(4)	3889(3)	1886(2)	27(2)
C(13)	-2154(6)	10060(5)	4451(3)	52(2)	C(112)	4260(4)	3991(4)	2446(2)	40(2)
C(14)	-2899(6)	9981(6)	4801(4)	58(3)	C(113)	4678(4)	4450(4)	2800(2)	51(2)
C(15)	-3091(6)	9196(5)	4839(3)	45(2)	C(114)	5389(4)	4806(4)	2595(2)	48(2)
C(16)	-2525(5)	8502(5)	4531(3)	35(2)	C(115)	5681(4)	4703(4)	2035(2)	39(2)
F(12)	-881(4)	9454(3)	3814(2)	51(3)	C(116)	5264(4)	4245(4)	1681(2)	35(2)
F(13)	-1970(5)	10832(3)	4424(3)	77(5)	C(121)	4817(4)	2656(3)	190(3)	27(2)
F(14)	-3435(5)	10674(4)	5109(3)	85(5)	C(122)	4313(5)	2176(5)	-75(3)	33(2)
F(15)	-3827(4)	9125(4)	5180(2)	64(3)	C(123)	3871(5)	2419(5)	-588(3)	37(2)
F(16)	-2737(4)	7739(3)	4585(2)	48(3)	C(124)	3913(6)	3184(4)	-849(4)	44(2)
C(21)	-2084(5)	7618(3)	3207(3)	31(2)	C(125)	4416(6)	3679(5)	-597(3)	43(2)
C(22)	-2269(5)	8229(3)	2775(3)	39(2)	C(126)	4857(5)	3407(4)	-86(3)	30(2)
C(23)	-3048(6)	8359(5)	2399(3)	47(2)	F(122)	4231(4)	1439(3)	178(2)	44(3)
C(24)	-3667(7)	7866(4)	2454(4)	52(2)	F(123)	3385(4)	1936(4)	-831(2)	58(3)
C(25)	-3514(6)	7257(5)	2880(3)	47(2)	F(124)	3473(4)	3442(4)	-1346(2)	65(4)
C(26)	-2727(5)	7138(5)	3249(3)	40(2)	F(125)	4457(4)	4421(3)	-848(2)	59(4)
F(22)	-1684(4)	8743(3)	2701(2)	44(3)	F(126)	5338(3)	3914(3)	149(2)	42(3)
F(23)	-3193(4)	8977(4)	1984(2)	67(4)	C(131)	6132(5)	1851(4)	1733(3)	35(2)
F(24)	-4439(4)	8002(4)	2107(3)	81(4)	C(132)	5897(6)	1237(5)	2076(3)	42(2)
F(25)	-4121(4)	6759(4)	2941(3)	72(3)	C(133)	6363(7)	937(6)	2580(4)	60(3)
F(26)	-2615(4)	6526(3)	3664(2)	50(3)	C(134)	7115(7)	1239(6)	2745(5)	74(3)
C(31)	246(5)	7431(4)	4264(3)	29(2)	C(135)	7384(7)	1844(6)	2418(4)	64(3)
C(32)	1047(5)	7706(5)	4106(3)	36(2)	C(136)	6888(6)	2143(5)	1923(3)	40(2)
C(33)	1806(6)	7678(5)	4464(3)	48(2)	F(132)	5180(4)	911(3)	1927(2)	49(3)
C(34)	1802(7)	7350(5)	4997(3)	54(2)	F(133)	6101(5)	342(4)	2901(2)	83(6)
C(35)	1036(6)	7070(5)	5178(3)	48(2)	F(134)	7594(6)	946(5)	3239(3)	120(8)
C(36)	276(5)	7124(5)	4817(3)	38(2)	F(135)	8124(5)	2138(5)	2585(3)	101(5)
F(32)	1082(4)	8028(3)	3578(2)	45(3)	F(136)	7196(4)	2711(4)	1610(2)	52(3)
F(33)	2553(4)	7961(4)	4280(3)	75(4)	C(141)	6694(5)	1475(4)	558(3)	29(2)
F(34)	2548(5)	7310(4)	5350(3)	86(5)	C(142)	6838(5)	598(4)	474(3)	33(2)
F(35)	1017(5)	6755(4)	5705(2)	74(5)	C(143)	7614(5)	72(5)	162(3)	36(2)
F(36)	-487(4)	6862(3)	5013(2)	49(3)	C(144)	8306(6)	419(4)	-66(3)	40(2)
C(41)	-653(4)	5584(3)	2961(2)	27(2)	C(145)	8197(5)	1291(5)	16(3)	39(2)
C(42)	-1120(4)	5800(3)	2444(2)	32(2)	C(146)	7402(5)	1798(4)	323(3)	31(2)
C(43)	-1722(4)	5335(4)	2255(2)	40(2)	F(142)	6191(3)	219(3)	697(2)	46(3)
C(44)	-1857(4)	4654(3)	2582(2)	39(2)	F(143)	7722(4)	-781(3)	82(2)	53(3)
C(45)	-1390(4)	4438(3)	3099(2)	39(2)	F(144)	9079(4)	-87(3)	-371(2)	59(3)
C(46)	-788(4)	4903(3)	3289(2)	35(2)	F(145)	8868(4)	1633(4)	-211(2)	59(3)
C(51)	987(3)	5494(3)	3687(2)	28(2)	F(146)	7320(3)	2657(3)	379(2)	44(3)
C(52)	1960(4)	5082(4)	3514(2)	35(2)	N	2007(5)	9871(5)	2620(3)	38(2)
C(53)	2630(3)	4500(4)	3875(2)	49(2)	C(151)	1346(6)	9414(6)	2361(4)	38(2)
C(54)	2327(4)	4330(4)	4410(2)	50(2)	C(152)	534(8)	9975(7)	1975(5)	54(3)
C(55)	1353(4)	4742(4)	4583(2)	42(2)	C(153)	-159(9)	9475(8)	1822(5)	64(3)
C(56)	684(3)	5324(3)	4222(2)	32(2)	C(154)	-1007(10)	9992(9)	1449(6)	78(4)
C(61)	262(3)	6642(3)	1456(2)	27(2)	C(155)	2471(6)	10300(6)	2170(4)	38(2)
C(62)	438(3)	6175(3)	961(2)	31(2)	C(156)	3164(7)	9660(6)	1763(4)	42(2)
C(63)	-178(4)	6485(3)	501(2)	45(2)	C(157)	3460(7)	10120(6)	1265(4)	40(2)
C(64)	-971(4)	7262(4)	537(2)	49(2)	C(158)	4230(7)	9496(6)	907(4)	44(2)
C(65)	-1147(3)	7729(3)	1032(2)	42(2)	C(159)	2802(7)	9178(6)	2949(4)	42(2)
C(66)	-531(4)	7419(3)	1491(2)	33(2)	C(160)	3590(7)	9477(6)	3225(4)	46(2)
C(71)	2111(3)	6704(4)	1898(2)	28(2)	C(161)	4293(7)	8745(6)	3563(4)	48(2)
C(72)	2198(3)	7097(4)	1382(2)	36(2)	C(162)	5131(8)	8989(7)	3819(5)	57(3)
C(73)	3006(4)	7386(4)	1275(2)	45(2)	C(1')	1395(7)	10614(6)	2999(4)	44(2)
C(74)	3728(3)	7283(4)	1682(2)	38(2)	C(2')	1099(12)	10239(9)	3561(5)	42(4)
C(75)	3641(4)	6890(4)	2198(2)	48(2)	C(3')	277(9)	11026(8)	3843(5)	74(3)
C(76)	2833(4)	6601(4)	2306(2)	42(2)	C(4')	249(22)	10734(17)	4471(7)	92(8)
C(81)	1216(4)	2871(4)	1676(2)	29(2)	C(2'')	574(12)	10373(11)	3347(6)	51(5)
C(82)	228(4)	3261(4)	1831(3)	67(3)	C(4'')	1059(17)	10691(16)	4308(9)	83(8)
C(83)	-517(3)	3041(5)	1560(3)	78(4)	C(3)	5632(23)	1901(20)	4238(7)	233(14)
C(84)	-274(4)	2432(4)	1134(3)	57(3)	C1(1)	5406(7)	2689(6)	3678(4)	223(4)
C(85)	714(4)	2041(4)	979(2)	41(2)	C1(2)	4790(8)	2573(7)	4750(4)	244(4)
C(86)	1459(3)	2261(3)	1250(2)	34(2)	C(4)	5466(16)	6004(21)	4372(18)	310(21)
C(91)	2217(4)	2777(4)	2746(2)	31(2)	C1(3)	4348(10)	5949(8)	4055(6)	306(6)
C(92)	3088(3)	2195(4)	2967(2)	38(2)	C1(4)	6226(13)	4899(11)	4220(7)	379(8)

<sup>a</sup> *U*(eq) is defined as one-third of the trace of the orthogonalized  $U_{ij}$  tensor.

**Table 2. Selected Bond Lengths (Å) and Angles (deg)**

Au(1)–C(21)	2.057(8)	Au(1)–C(11)	2.063(8)
Au(1)–C(31)	2.063(8)	Au(1)–P(1)	2.367(2)
Au(2)–P(2)	2.311(2)	Au(2)–P(3)	2.314(2)
Au(3)–C(121)	2.064(8)	Au(3)–C(131)	2.069(9)
Au(3)–C(141)	2.080(8)	Au(3)–P(4)	2.367(2)
P(1)–C(1)	1.706(8)	P(1)–C(51)	1.845(4)
P(1)–C(41)	1.849(4)	P(2)–C(1)	1.736(8)
P(2)–C(61)	1.838(4)	P(2)–C(71)	1.843(4)
P(3)–C(2)	1.722(7)	P(3)–C(81)	1.842(5)
P(3)–C(91)	1.845(4)	P(4)–C(1)	1.701(8)
P(4)–C(111)	1.828(4)	P(4)–C(101)	1.856(4)
C(21)–Au(1)–C(11)	89.1(2)	C(21)–Au(1)–C(31)	175.4(2)
C(11)–Au(1)–C(31)	87.5(2)	C(21)–Au(1)–P(1)	90.4(2)
C(11)–Au(1)–P(1)	178.56(15)	C(31)–Au(1)–P(1)	93.0(2)
P(2)–Au(2)–P(3)	177.95(7)	C(121)–Au(3)–C(131)	176.8(2)
C(121)–Au(3)–C(141)	87.5(2)	C(131)–Au(3)–C(141)	89.7(2)
C(121)–Au(3)–P(4)	90.8(2)	C(131)–Au(3)–P(4)	92.1(2)
C(141)–Au(3)–P(4)	177.08(13)	C(1)–P(1)–C(51)	116.1(3)
C(1)–P(1)–C(41)	112.1(3)	C(51)–P(1)–C(41)	102.7(2)
C(1)–P(1)–Au(1)	105.2(3)	C(51)–P(1)–Au(1)	109.0(2)
C(41)–P(1)–Au(1)	111.8(2)	C(1)–P(2)–C(61)	111.4(3)
C(1)–P(2)–C(71)	105.5(3)	C(61)–P(2)–C(71)	102.8(2)
C(1)–P(2)–Au(2)	117.0(3)	C(61)–P(2)–Au(2)	107.9(2)
C(71)–P(2)–Au(2)	111.3(2)	C(2)–P(3)–C(81)	110.5(3)
C(2)–P(3)–C(91)	109.0(3)	C(81)–P(3)–C(91)	104.4(3)
C(2)–P(3)–Au(2)	115.7(3)	C(81)–P(3)–Au(2)	108.1(2)
C(91)–P(3)–Au(2)	108.5(2)	C(2)–P(4)–C(111)	116.3(3)
C(2)–P(4)–C(101)	109.0(3)	C(111)–P(4)–C(101)	105.0(2)
C(2)–P(4)–Au(3)	110.1(3)	C(111)–P(4)–Au(3)	104.5(2)
C(101)–P(4)–Au(3)	111.8(2)	P(1)–C(1)–P(2)	129.0(5)
P(4)–C(2)–P(3)	123.9(5)	C(16)–C(11)–C(12)	114.8(8)
C(22)–C(21)–C(26)	115.5(8)	C(32)–C(31)–C(36)	114.4(7)
C(126)–C(121)–C(122)	116.5(7)	C(132)–C(131)–C(136)	115.7(8)
C(142)–C(141)–C(146)	115.7(7)		

led to  $[\text{NBu}_4][\text{Au}(\text{acac})_2]$  as a white solid. Yield: 85%. Decomposes at 59 °C. Anal. Calcd for  $\text{C}_{26}\text{H}_{50}\text{AuNO}_4$ : C, 48.95; H, 7.9; N, 2.2. Found: C, 48.95; H, 8.5; N, 2.25.  $\Lambda_M$ : 98  $\Omega^{-1} \text{cm}^2 \text{mol}^{-1}$ . IR: 1642 (vs) and 1633 (vs) [ $\nu(\text{CO})$ ].  $^1\text{H}$  NMR ( $\text{CDCl}_3$ ): 4.35 (s, CH), 3.28 (m,  $\text{CH}_2$ ), 2.34 [s,  $\text{CH}_3$  (acac)], 1.61 (m,  $\text{CH}_2$ ), 1.41 (m,  $\text{CH}_2$ ) and 0.98 [t,  $\text{CH}_3$  (Bu)] ( $J(\text{HH}) = 7.3 \text{ Hz}$ ).

**$[\text{Au}(\text{C}_6\text{F}_5)_3\text{PPh}_2\text{CH}_2\text{PPh}_2]_2\text{Au}(\text{I})\text{ClO}_4$  (1).** To a solution of  $[\text{Au}(\text{C}_6\text{F}_5)_3\text{PPh}_2\text{CH}_2\text{PPh}_2]^{5+}$  (0.216 g, 0.2 mmol) in dichloromethane (20 mL) was added  $[\text{Au}(\text{tht})_2]\text{ClO}_4^{16}$  (0.047 g, 0.1 mmol). A white precipitate of **1** was formed, and the mixture was stirred for 30 min. The solvent was concentrated to ca. 5 mL. Addition of 20 mL of hexane completed the precipitation of complex **1**. Yield: 85%. Mp: 205 °C dec. Anal. Calcd for  $\text{C}_{86}\text{H}_{44}\text{Au}_3\text{ClF}_{30}\text{O}_4\text{P}_4$ : C, 41.95; H, 1.8. Found: C, 41.45; H, 1.6.  $^{31}\text{P}\{^1\text{H}\}$  NMR [ $(\text{CD}_3)_2\text{CO}$ ]:  $\delta$  15.6 [m, P–Au(III)], 37.5 [m, P–Au(I)].

**$\text{NBu}_4[\text{Au}(\text{C}_6\text{F}_5)_3\text{PPh}_2\text{CHPPH}_2]_2\text{Au}$  (2).** To a diethyl ether solution (20 mL) of  $[\text{Au}(\text{C}_6\text{F}_5)_3\text{PPh}_2\text{CH}_2\text{PPh}_2]^{5+}$  (0.216 g, 0.2 mmol) was added  $\text{NBu}_4[\text{Au}(\text{acac})_2]$  (0.063 g, 0.1 mmol), and the mixture was stirred for 2 h. Concentration of the solution to ca. 5 mL and addition of 20 mL of hexane led to precipitation of complex **2**. Yield: 90%. Mp: 80 °C dec. Anal. Calcd for  $\text{C}_{102}\text{H}_{80}\text{Au}_3\text{F}_{30}\text{NP}_4$ : C, 47.1; H, 3.0; N, 0.55. Found: C, 47.15; H, 2.95; N, 0.55.  $^{31}\text{P}\{^1\text{H}\}$  NMR ( $\text{CDCl}_3$ ):  $\delta$  15.4 [m, P–Au(III)], 33.8 [m, P–Au(I)].

**$\text{NBu}_4[\text{Au}(\text{C}_6\text{F}_5)_3\text{PPh}_2\text{CH}(\text{AuX})\text{PPh}_2]_2\text{Au}$  (X = Cl (3),  $\text{C}_6\text{F}_5$  (4)).** To a yellow solution of complex **2** (0.260 g, 0.1 mmol) in 20 mL of dichloromethane was added  $[\text{AuX}(\text{tht})]^{15}$  (0.2 mmol; X = Cl, 0.064 g; X =  $\text{C}_6\text{F}_5$ , 0.090 g), and the mixture

**Table 3. Details of Data Collection and Structure Refinement for Complex 2·2CH<sub>2</sub>Cl<sub>2</sub>**

chem formula	$\text{C}_{104}\text{H}_{82}\text{Au}_3\text{Cl}_4\text{F}_{30}\text{NP}_4$	$2\theta_{\text{max}}/\text{deg}$	50
cryst habit	yellow prism	$\mu(\text{Mo K}\alpha)/\text{mm}^{-1}$	4.53
cryst size/mm	$0.55 \times 0.25 \times 0.20$	transm	0.65–0.85
space group	P1	no. of reflns measd	20894
a/Å	14.213(4)	no. of unique reflns	18166
b/Å	16.067(4)	no. of reflns used	18150
c/Å	23.840(6)	$R_{\text{int}}$	0.058
$\alpha/\text{deg}$	88.60(2)	$R^a(I, I > 2\sigma(I))$	0.043
$\beta/\text{deg}$	89.27(2)	$wR^b(F^2, \text{all reflns})$	0.118
$\gamma/\text{deg}$	71.23(2)	no. of params	684
$V/\text{Å}^3$	5153(2)	no. of restraints	364
Z	2	$S^c$	1.065
$D_c/\text{Mg m}^{-3}$	1.787	max $\Delta\rho/e \text{ Å}^{-3}$	2.18
M	2772.29	max $\Delta\sigma$	0.012
F(000)	2696		
$T/^\circ\text{C}$	–100		

$^a R(F) = \sum |F_o| - |F_c| / \sum |F_o|$ .  $^b wR(F)^2 = [\sum \{w(F_o^2 - F_c^2)^2 / \sum \{w(F_o^2)^2\}]^{0.5}$ ;  $w^{-1} = \sigma^2(F_o^2) + (aP)^2 + bP$ , where  $P = [F_o^2 + F_c^2]/3$  and  $a$  and  $b$  are constants adjusted by the program.  $^c S = [\sum \{w(F_o^2 - F_c^2)^2\} / (n - p)]^{0.5}$ , where  $n$  is the number of data and  $p$  the number of parameters.

was stirred for 1 h. The resulting colorless solution was evaporated to ca. 5 mL. Addition of 20 mL of hexane gave complexes **3** or **4**. **3**. Yield: 57%. Mp: 70 °C dec. Anal. Calcd for  $\text{C}_{102}\text{H}_{80}\text{Au}_3\text{Cl}_2\text{F}_{30}\text{NP}_4$ : C, 39.4; H, 2.55; N, 0.45. Found: C, 39.3; H, 2.55; N, 0.55.  $^{31}\text{P}\{^1\text{H}\}$  NMR ( $\text{CDCl}_3$ ):  $\delta$  19.5 [m, P–Au(III)] and 27.6 [m, P–Au(I)]. **4**. Yield: 60%. Mp: 78 °C dec. Anal. Calcd for  $\text{C}_{114}\text{H}_{80}\text{Au}_3\text{F}_{40}\text{NP}_4$ : C, 41.1; H, 2.35; N, 0.4. Found: C, 41.45; H, 2.4; N, 0.65.  $^{31}\text{P}\{^1\text{H}\}$  NMR ( $\text{CDCl}_3$ ):  $\delta$  21.2 [m, P–Au(III)] and 38.0 [m, P–Au(I)].

**$[\text{Au}(\text{C}_6\text{F}_5)_3\text{PPh}_2\text{C}(\text{AuPPh}_3)_2\text{PPh}_2]_2\text{Au}(\text{I})\text{ClO}_4$  (5).** To a suspension of complex **1** (0.246 g, 0.1 mmol) in dichloromethane (20 mL) was added  $[\text{Au}(\text{acac})\text{PPh}_3]^{17}$  (0.223 g, 0.4 mmol). After being stirred for 48 h, the turbid solution was filtered through a 1 cm pad of Celite. Concentration of the solvent to ca. 4 mL and addition of hexane led to complex **5**. Yield: 80%. Mp: 99 °C dec. Anal. Calcd for  $\text{C}_{158}\text{H}_{106}\text{Au}_7\text{ClF}_{30}\text{O}_4\text{P}_8$ : C, 46.3; H, 2.45. Found: C, 46.5; H, 2.55.  $^{31}\text{P}\{^1\text{H}\}$  NMR ( $\text{CDCl}_3$ ):  $\delta$  22.1 [m, 2P–Au(III)], 35.2 [m, 2P–Au(I)], and 39.0 [s, 4P (PPh<sub>3</sub>)].

**Crystal Structure Determination of Compound 2·2CH<sub>2</sub>Cl<sub>2</sub>.** The crystal was mounted in inert oil on a glass fiber. Data were collected using monochromated Mo K $\alpha$  radiation ( $\lambda = 0.71073 \text{ Å}$ ) on a Siemens R3 diffractometer with an LT-2 low-temperature attachment. The scan type was  $\omega$ . Cell constants were refined from setting angles of 50 reflections in the range  $2\theta = 20\text{--}21^\circ$ . Absorption corrections were applied on the basis of  $\psi$ -scans.

The structure was solved by the heavy-atom method and refined anisotropically (except for the C atoms and solvent) on  $F^2$  using the program SHELXL-93.<sup>18</sup> One butyl group of the cation is disordered over two sites, and the solvent is not well resolved. Hydrogen atoms were included using a riding model. Other data are collected in Table 3.

**Acknowledgment.** We thank the Dirección General de Investigación Científica y Técnica (Grant No. PB91-0122), the Instituto de Estudios Riojanos, and the Fonds der Chemischen Industrie for financial support.

**Supplementary Material Available:** Tables of crystal data, data collection, and solution and refinement parameters, hydrogen atomic coordinates and thermal parameters, bond distances and angles, and anisotropic thermal parameters (8 pages). Ordering information is given on any current masthead page.

OM950018W

(16) Usón, R.; Laguna, A.; Laguna, M.; Jiménez, J.; Gómez, M. P.; Sáinz, A.; Jones, P. G. *J. Chem. Soc., Dalton Trans.* **1990**, 3457.

(17) Gibson, D.; Johnson, B. F. G.; Lewis, J.; *J. Chem. Soc. A* **1970**, 367.

(18) Sheldrick, G. M. SHELXL-93. A program for Crystal Structure Refinement. University of Göttingen, Göttingen, 1993.

# Aminolysis of Dicationic Ruthenium Thiophene Complexes

Qian Feng, Thomas B. Rauchfuss,\* and Scott R. Wilson

School of Chemical Sciences, University of Illinois, Urbana, Illinois 61801

Received February 8, 1995<sup>®</sup>

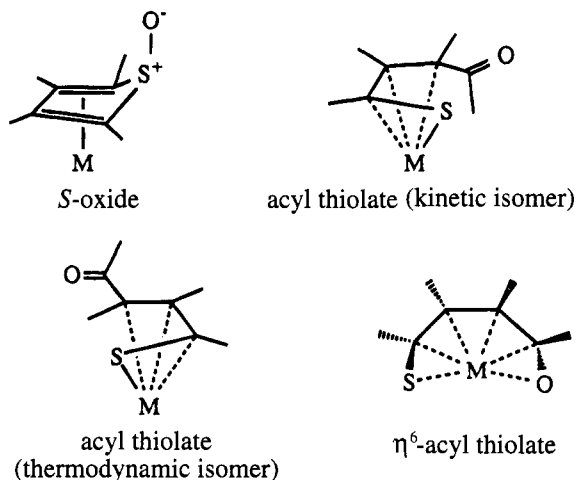
Dicationic sandwich complexes containing thiophene, 2-methylthiophene, 2,5-dimethylthiophene, and tetramethylthiophene react with ammonia to give salts of the formula [(ring)-Ru(SC<sub>4</sub>R<sub>4</sub>NH<sub>2</sub>)]X where ring = C<sub>6</sub>Me<sub>6</sub> or cymene. The thiophene, 2-methylthiophene, and 2,5-dimethylthiophene complexes undergo C–S cleavage to give iminium–thiolato derivatives. In the case of the 2,5-dimethylthiophene complex, a kinetic isomer was isolated which slowly isomerized to a thermodynamic isomer. The ammonia adducts of the tetramethylthiophene complexes [(cymene)Ru(C<sub>4</sub>Me<sub>4</sub>S)]<sup>2+</sup> and [(C<sub>5</sub>Me<sub>5</sub>)Rh(C<sub>4</sub>Me<sub>4</sub>S)]<sup>2+</sup> do not undergo C–S cleavage. These 2-NH<sub>2</sub>C<sub>4</sub>Me<sub>4</sub>S complexes react with protic acids to regenerate the starting dication [(ring)M(C<sub>4</sub>Me<sub>4</sub>S)]<sup>2+</sup>. The aniline adducts of thiophene, 2-methylthiophene, and 2,5-dimethylthiophene are similar to the ammonia derivatives. The structures of the kinetic isomer of [(C<sub>6</sub>Me<sub>6</sub>)Ru(SC<sub>3</sub>H<sub>2</sub>MeCHNHP)]PF<sub>6</sub> and the thermodynamic isomer of [(cymene)Ru(SC<sub>3</sub>H<sub>2</sub>MeCMeNHP)]OTf were established by single-crystal X-ray diffraction. The crystallographic study proves that the isomerization in this family of compounds arises from the relative configuration at the terminal carbon of the alkenyl thiolate ligand. Bond distance data indicate an interaction between the iminium carbon center and the Ru atom in the kinetic isomer.

## Introduction

In previous papers we have described the reactions of dicationic thiophene complexes with hydroxide.<sup>1–3</sup> The work was motivated by the prospect of developing nonconventional methods for the desulfurization of thiophenes.<sup>4</sup> The chemistry proved to be particularly rich, leading to the isolation of four isomeric forms of oxygenated thiophene ligands C<sub>4</sub>Me<sub>4</sub>SO (Chart 1). This work provided the first evidence for nucleophilic addition to the sulfur center of thiophene. In addition, the hydrolyzed thiophene complexes display extensive ligand-based reactions.<sup>2</sup> Variants of the base hydrolysis reaction of coordinated thiophenes are of interest in that they illustrate new pathways for breaking C–S bonds.

Nucleophilic addition to metal arene complexes has been recognized for many years.<sup>5,6</sup> The first extension of this pattern to thiophene complexes was provided by studies on nucleophilic addition to thiophene complexes of Mn(CO)<sub>3</sub><sup>+</sup> and (C<sub>5</sub>H<sub>5</sub>)Ru<sup>+</sup>.<sup>7,8</sup> For the Ru complexes, these reactions result in C–S bond cleavage and show some potential for the synthesis of organo–sulfur

Chart 1



compounds. Our recent studies<sup>2,3</sup> on base hydrolysis focused on dicationic arene–thiophene complexes (ring)-Ru(C<sub>4</sub>R<sub>4</sub>S)<sup>2+</sup> (ring = C<sub>4</sub>Me<sub>4</sub>S, cymene, and hexamethylbenzene) and (C<sub>5</sub>Me<sub>5</sub>)Rh(C<sub>4</sub>Me<sub>4</sub>S)<sup>2+</sup>. The (arene)Ru<sup>2+</sup> moiety is of particular interest since it forms stable adducts of most thiophenes<sup>9,10</sup> and the resulting dicationic sandwich complexes are highly electrophilic. The present work deals with their reactions with ammonia and aniline. These results provide new methods of C–S cleavage with common reagents. The associated structural studies clarify the mechanistic and stereochemical facets of nucleophilic addition to η<sup>5</sup>-thiophene ligands.

(9) Ganja, E. A.; Rauchfuss, T. B.; Stern, C. L. *Organometallics* **1991**, *10*, 270.

(10) Luo, S.; Rauchfuss, T. B.; Wilson, S. R. *J. Am. Chem. Soc.* **1992**, *114*, 8515.

(11) Dalmay, L.-V.; Colthup, N. B.; Fateley, W. G.; Grasselli, J. G. *The Handbook of Infrared and Raman Characteristic Frequencies of Organic Molecules*; Academic Press: New York, 1991; p 200.

<sup>®</sup> Abstract published in *Advance ACS Abstracts*, May 15, 1995.

(1) Skaugset, A. E.; Rauchfuss, T. B.; Wilson, S. R. *J. Am. Chem. Soc.* **1992**, *114*, 8521.

(2) Krautscheid, H.; Feng, Q.; Rauchfuss, T. B. *Organometallics* **1993**, *12*, 3273.

(3) Feng, Q.; Krautscheid, H.; Rauchfuss, T. B.; Skaugset, A. E.; Venturelli, A. *Organometallics* **1995**, *14*, 297.

(4) (a) Ogilvy, A. E.; Draganjac, M. E.; Rauchfuss, T. B.; Wilson, S. R. *Organometallics* **1988**, *7*, 1171. (b) Riaz, U.; Curnow, O.; Curtis, D. M. *J. Am. Chem. Soc.* **1991**, *113*, 1416. (c) Garcia, J. J.; Mann, B. E.; Adams, H.; Bailey, N. A.; Maitlis, P. M. *J. Am. Chem. Soc.* **1995**, *117*, 2179.

(5) Hegedus, L. S. *Transition Metals in the Synthesis of Complex Organic Molecules*; University Science Books: Mill Valley, CA, 1994.

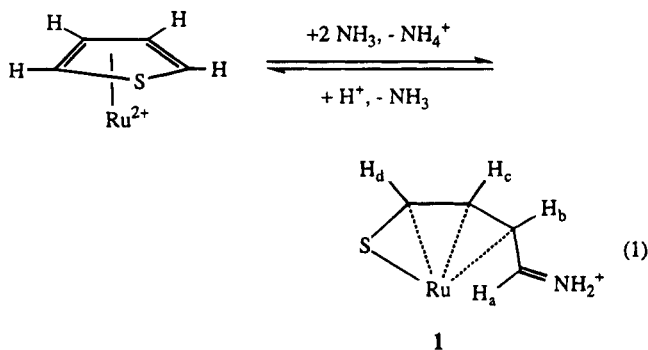
(6) Kane-Maguire, L. A. P.; Honig, E. D.; Sweigart, D. A. *Chem. Rev.* **1984**, *84*, 525.

(7) Lesch, D. A.; Richardson, J. W.; Jacobson, R. A.; Angelici, R. J. *J. Am. Chem. Soc.* **1984**, *106*, 2901.

(8) Hachgenei, J. W.; Angelici, R. J. *J. Organomet. Chem.* **1988**, *355*, 359. Spies, G. H.; Angelici, R. J. *Organometallics* **1987**, *6*, 1897.

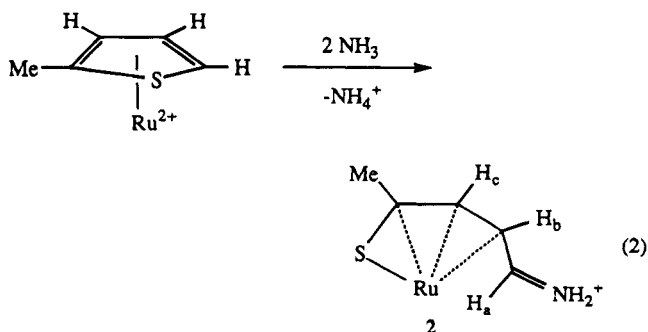
## Results

**Ammonolysis of  $C_4H_4S$  and 2-Me $C_4H_3S$  Complexes.** We started with the addition of the simplest amine, ammonia, to a complex of the simplest thiophene,  $[(C_6Me_6)Ru(C_4H_4S)](OTf)_2$ . Treatment of the solid ruthenium complex with gaseous ammonia resulted in a rapid color change from yellow to red. The product was purified by simple extraction into  $CH_2Cl_2$  and filtration from the  $NH_4OTf$ . This new compound analyzed as  $[(C_6Me_6)Ru(SC_3H_3CHNH_2)]OTf$  (**1**, eq 1; in this and subse-



quent equations, the spectator  $\eta^6$ -arene ligand is not shown). The IR spectrum of **1** shows a moderately strong band at  $1620\text{ cm}^{-1}$  assigned to  $\nu_{C=N}$  and strong bands at  $3336$  and  $3208\text{ cm}^{-1}$  assigned to  $\nu_{NH}$ . The  $^1H$  NMR spectrum was analyzed by decoupling and difference nOe experiments that probed the relative positions of the  $SC_4H_4NH_2$  protons. Three of the thiophene-derived signals showed strong nOe's, indicating that they are cis and coplanar. For instance, irradiation of  $H_b$  increases the intensity  $H_c$ , which is cis, by 15%, and at the same time only a much smaller (3%) nOe is observed for the trans  $H_a$ . This solution structure is consistent with the results of a single-crystal structural analysis of an analogous complex (*vide infra*). Solutions of **1** revert to the starting complex  $[(C_6Me_6)Ru(C_4H_4S)]^{2+}$  upon treatment with triflic acid.

Ammonolysis of the 2-methylthiophene complex afforded a related product,  $[(cymene)Ru(SC_3H_2MeCHNH_2)]OTf$  (**2**) (eq 2). The addition and C–S cleavage processes

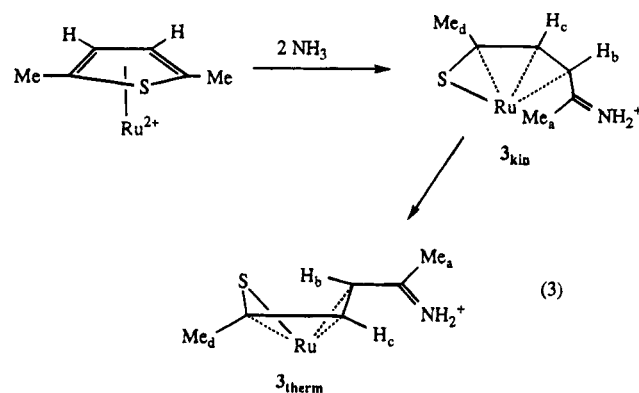


occur regioselectively at the CH–S linkage, not at C(Me)–S. The presence of only one isomer was established by  $^1H$  NMR spectroscopy, which, for instance, showed only one set of cymene resonances. The  $CH=NH_2^+$  signal was found in a position similar to that for the aforementioned thiophene product. Angelici had previously observed that nucleophiles ( $OR^-$ ,  $H^-$ ,  $CR_3^-$ ) selectively add to the unsubstituted carbon in  $(C_5H_5)Ru(2-MeC_4H_3S)^+$ .<sup>8</sup>

## Ammonolysis of $[(cymene)Ru(2,5-Me_2C_4H_2S)]^{2+}$ .

Additional stereochemical insights into the ammonolysis reaction were provided by studies on the dimethylthiophene complex  $[(cymene)Ru(2,5-Me_2C_4H_2S)]^{2+}$ . Acetonitrile solutions of this salt reacted readily with ammonia. When the reaction was allowed to proceed for a brief interval, we obtained pure samples of a single isomer of  $[(cymene)Ru(SC_3H_2MeCMeNH_2)]^+$  (**3<sub>kin</sub>**). The spectroscopic evidence supports a structure analogous to those of the aforementioned products derived from thiophene and 2-methylthiophene complexes. The  $^1H$  and  $^{13}C$  NMR data point to a chiral complex, and the IR spectrum shows bands attributable to both  $\nu_{NH}$  ( $3346$  and  $3153\text{ cm}^{-1}$ ) and  $\nu_{C=N}$  ( $1648\text{ cm}^{-1}$ ).<sup>11</sup> Care must be taken in this synthesis because the product tends to isomerize (see below). The degree of isomerization can be minimized by conducting the ammonolysis on solid samples of  $[(cymene)Ru(2,5-Me_2C_4H_2S)](OTf)_2$ .

In solution, **3** isomerizes via a first-order process with  $t_{1/2} = 54\text{ min}$  ( $35\text{ }^\circ\text{C}$ ). Notice that, according to this mechanism, isomerization does not result in racemization. We refer to these isomers as kinetic and thermodynamic, **3<sub>kin</sub>** and **3<sub>therm</sub>**, respectively (eq 3). It was

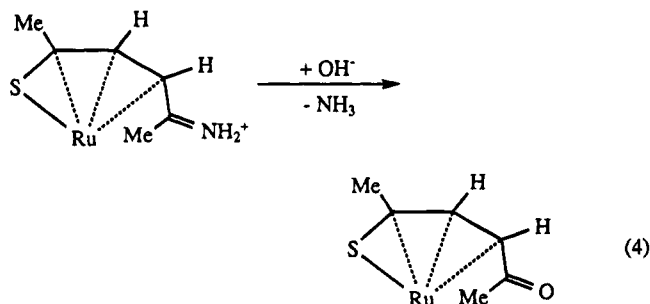


found that solid samples of **3<sub>kin</sub>** rearranged upon standing at  $30\text{ }^\circ\text{C}$ .

The spectroscopic characteristics of the **3<sub>kin</sub>** and **3<sub>therm</sub>** isomers are similar. The UV–vis spectra differ only slightly even though the isomers have noticeably different colors, the kinetic isomer being more red while the other isomer is more purple. The  $C_4H_2Me_2$  signals on the thiophene are most sensitive to the identity of the isomer. The  $^1H$  NMR shift for  $H_b$  occurs at  $3.88\text{ ppm}$  for **3<sub>kin</sub>** and  $1.80\text{ ppm}$  for **3<sub>therm</sub>**. Attempts to isomerize **1** and **2** led only to unidentified decomposition products.

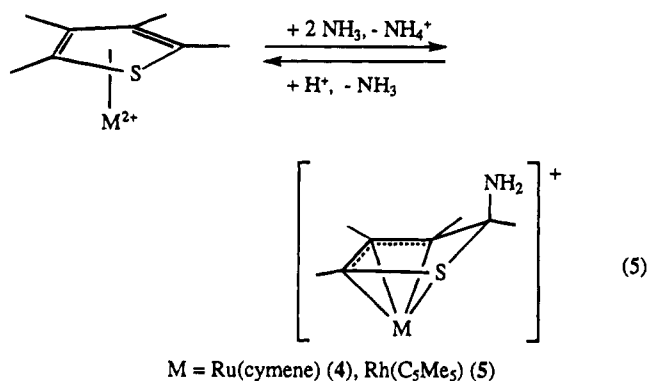
Solutions of **3<sub>kin</sub>** were shown to react with aqueous KOH to give the kinetic isomer of the corresponding acyl thiolate<sup>2</sup> (eq 4).

**Ammonolysis of  $C_4Me_4S$  Complexes.** To our initial surprise, the ammonolysis of tetramethylthiophene complexes proceeds rather differently from the cases for less substituted thiophenes. Solutions of the tetramethylthiophene complexes  $[(cymene)Ru(C_4Me_4S)]^{2+}$  and  $[(C_5Me_5)Rh(C_4Me_4S)]^{2+}$  react with ammonia to give orange-yellow microcrystalline adducts  $[(ring)M(C_4Me_4S-2-NH_2)]^+$  ( $M = Ru$ , ring = cymene (**4**);  $M = Rh$ , ring =  $C_5Me_5$  (**5**)). The  $^1H$  NMR data for **4** indicate that it is

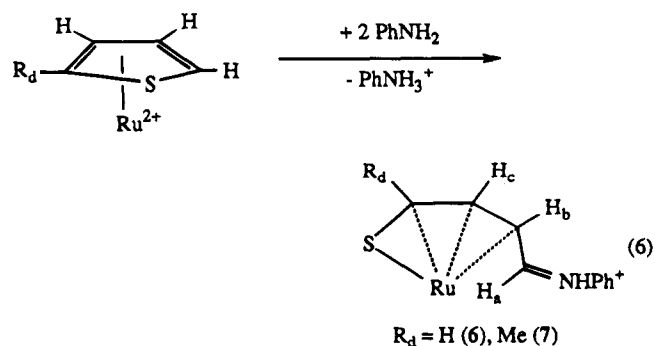


chiral as we observe four  $\text{MeC}_6\text{H}_4\text{CHMe}_2$  multiplets. Its IR spectrum is dominated by a strong band at  $3300\text{ cm}^{-1}$  corresponding to  $\nu_{\text{NH}}$ . We do not observe strong bands in the range for  $\nu_{\text{C=N}}$ , as seen in the amine derivatives of other thiophenes. Solutions of **4** react with HOTf to recover the starting  $[(\text{cymene})\text{Ru}(\text{C}_4\text{Me}_4\text{S})]^{2+}$ .

The  $^1\text{H}$  NMR data for **5** proved comparable to those for **4**, with the exception of a signal for one methyl group which is split due to  $^{103}\text{Rh}$  coupling. This long-range splitting had been previously observed for  $[(\text{C}_5\text{Me}_5)\text{Rh}(\text{C}_4\text{Me}_4\text{S}-2\text{-OH})]^+$ , which was shown by crystallography to feature an  $\eta^4\text{-C}_4\text{Me}_4\text{S}-2\text{-OH}$  ligand.<sup>1</sup> Solutions of **5** react with HOTs to regenerate the starting  $[(\text{C}_5\text{Me}_5)\text{Rh}(\text{C}_4\text{Me}_4\text{S})]^{2+}$  (eq 5).



**Reactions with Aniline.** The corresponding reactions of the dicationic thiophene complexes with aniline were also examined in an attempt to probe the generality of the amination. These experiments also afforded X-ray-quality crystals of both kinetic and thermodynamic isomers. The complexes of thiophene and 2-methylthiophene  $[(\text{C}_6\text{Me}_6)\text{Ru}(\text{C}_4\text{H}_4\text{-}x\text{Me}_x\text{S})]^{2+}$  ( $x = 0, 1$ ) reacted readily with aniline to give deep red crystalline products  $[(\text{C}_6\text{Me}_6)\text{Ru}(\text{SC}_3\text{H}_3\text{CHNHPH})]\text{OTf}$  (**6**) and  $[(\text{C}_6\text{Me}_6)\text{Ru}(\text{SC}_3\text{H}_2\text{MeCHNHPH})]\text{PF}_6$  (**7**), respectively (eq 6).



In both cases, the  $^1\text{H}$  NMR spectra indicated single isomers whose spectroscopic properties were consistent

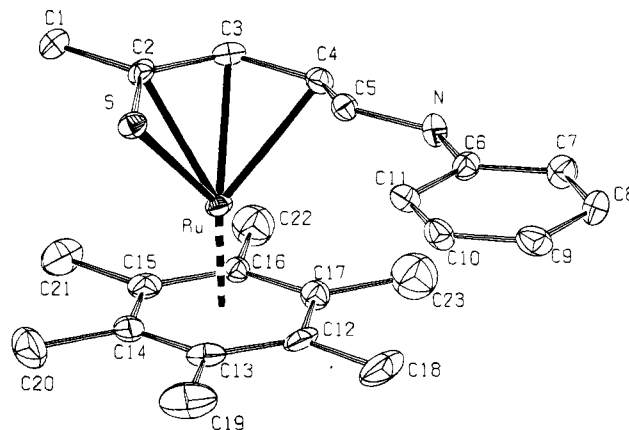
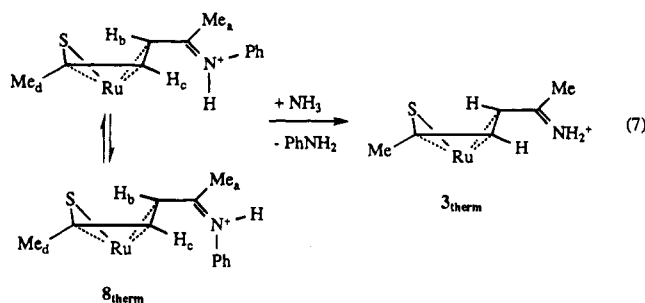


**Figure 1.** ORTEP plot of one of two enantiomeric cations in the salt  $[(\text{C}_6\text{Me}_6)\text{Ru}(\eta^4\text{-SC}_3\text{H}_2\text{MeCHNHPH})]\text{PF}_6$  (**7**).

with the aforementioned kinetic isomers. The critical data were the chemical shift and coupling patterns for the protons on the thiolate ligand.

The addition of aniline to  $[(\text{cymene})\text{Ru}(\text{2,5-Me}_2\text{C}_4\text{H}_2\text{S})]^{2+}$  was also rapid; however, in this case we only obtained the thermodynamic isomer of  $[(\text{cymene})\text{Ru}(\text{SC}_3\text{H}_2\text{MeCMENHPH})]\text{OTf}$  (**8<sub>therm</sub>**). Actually, the  $^1\text{H}$  NMR data revealed what appear to be two thermodynamic isomers in a ratio of 4:1. Since the chemical shift and coupling patterns for the two are quite similar, we suggest that these species differ according to the relative orientation of the phenyl substituent on the iminium nitrogen center. The rapid formation of the thermodynamic isomer(s) suggests that the presence of the phenyl group destabilizes **8<sub>kin</sub>**. The elusive **8<sub>kin</sub>** was observed when the reaction was monitored by  $^1\text{H}$  NMR spectroscopy at  $-10^\circ\text{C}$ .

Using **8<sub>therm</sub>**, we demonstrated amine exchange, in that treatment of a solution of this salt with an excess of ammonia gave free aniline and the aforementioned **3<sub>therm</sub>**, as demonstrated by  $^1\text{H}$  NMR studies (eq 7).



**Crystallographic Studies on  $[(\text{C}_6\text{Me}_6)\text{Ru}(\text{SC}_3\text{H}_2\text{MeCHNHPH})]\text{PF}_6$  (**7**) and  $[(\text{cymene})\text{Ru}(\text{SC}_3\text{H}_2\text{MeCMENHPH})]\text{OTf}$  (**8<sub>therm</sub>**).** The spectroscopic evidence that **8<sub>therm</sub>** is stable only as the thermodynamic isomer was confirmed by the crystallographic analysis. The connectivity and metrical details are unexceptional. The assignment of this species as an iminium derivative is supported by the bond distances and angles at C5; the C=N distance of  $1.34(2)\text{ \AA}$  is appropriate for a double bond and far shorter than the bond between nitrogen and phenyl ( $1.47(2)\text{ \AA}$ ) (Figure 2).

The structure of **7** in the solid state reveals a sandwich structure wherein the thiophene ligand is cleaved (Figure 1). The bond distances and angles in the  $\text{C}_3\text{S}$  portion of the ligand are similar to those found

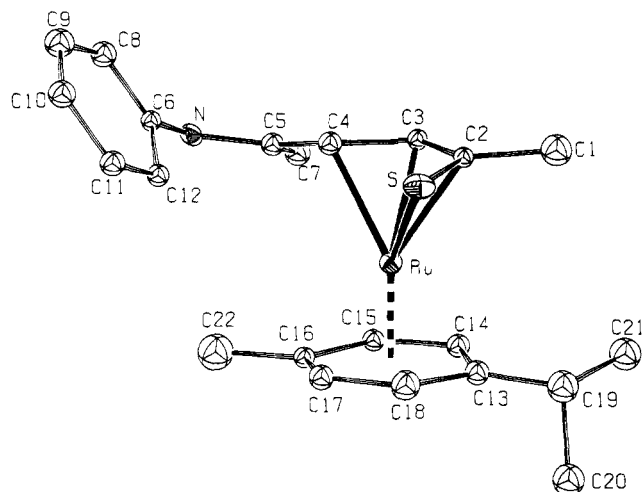


**Figure 2.** ORTEP plot of one of two enantiomeric cations in the salt [(cymene)Ru( $\eta^4$ -SC<sub>3</sub>H<sub>2</sub>MeCMeNHP)]OTf (**8<sub>therm</sub>**).

in **8<sub>therm</sub>**. It is seen that the nucleophile has added to the less substituted carbon  $\alpha$  to sulfur. Furthermore, the stereochemistry of the carbon  $\gamma$  to sulfur is consistent with the kinetic isomer, as assigned in previous papers dealing with acyl analogues.<sup>2</sup> This compound is not a direct analogue of an acyl, since it is an iminium derivative, not an imine. Related to this difference is some ambiguity in classifying the iminium thiolate as an  $\eta^4$  ligand. The iminium carbon C5 is situated 2.627 Å from Ru, vs 2.192(5), 2.222(10), and 2.288(6) Å for Ru–C2, –C3, and –C4, respectively. For comparison, the iminium C–Ru distance is 3.08 Å in **8<sub>therm</sub>**.

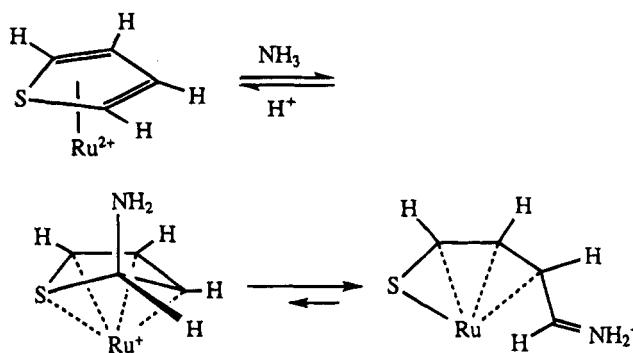
### Discussion

Dicationic  $\pi$ -thiophene complexes readily add ammonia and amines.<sup>12</sup> The transformations are efficient, and the scope of the reaction appears to be broad. The structural chemistry is consistent with, but more complete than, other cases of nucleophilic additions to dicationic thiophene complexes. The results are especially relevant to our studies on the base hydrolysis of thiophene complexes.<sup>2</sup> Meriting further discussion are mechanistic relationships and structural trends in these compounds.

The structural chemistry of these compounds is controlled by a number of subtle but systematic factors even though all of the ammonia derivatives have the same basic formula (arene)Ru(C<sub>4</sub>R<sub>4</sub>SNH<sub>2</sub>)<sup>+</sup>. The amination of tetramethylthiophene complexes afforded ring-closed structures, analogous to that of (C<sub>5</sub>Me<sub>5</sub>)Rh(C<sub>4</sub>Me<sub>4</sub>S-2-OH)<sup>+</sup>.<sup>1</sup> The related dimethylthiophene complex on the other hand gives ring-opened isomers. We previously observed that ring opening depends on the degree of ring methylation for the species (C<sub>6</sub>Me<sub>6</sub>)Ru(C<sub>4</sub>R<sub>4</sub>HS)<sup>+</sup>.<sup>13</sup>

For the first time, we have crystallographically confirmed the stereochemistry of a kinetic isomer of a ring-opened thiophene complex. One interesting detail of this structure is the Ru–iminium carbon distance of 2.627 Å, which is only 0.3 Å longer than other Ru–C distances in this complex. We also observe the isomer-

**Scheme 1**



ization of (cymene)Ru(SC<sub>3</sub>H<sub>2</sub>MeCMeNH<sub>2</sub>)<sup>+</sup> whereby the kinetically formed endo isomer converts to the thermodynamically favored exo isomer, i.e., **3<sub>kin</sub>** to **3<sub>therm</sub>**. The facility of the isomerization depends on the steric bulk of the added nucleophile as well as the substituents on thiophene.

The products of the C–S cleavage reaction feature iminium centers. This assignment is supported by a number of factors including the details of the <sup>1</sup>H NMR spectra. The presence of two thermodynamic isomers for the PhNH<sub>2</sub> addition compound with 2,5-dimethylthiophene is also consistent with slow cis–trans isomerization at the iminium center. The crystallographic studies indicate that these iminium centers are conjugated via a  $\pi$ -bonding network with the rest of the allyl thiolate. The iminium carbon is demonstrably electrophilic, since it is susceptible to attack by OH<sup>–</sup> (base hydrolysis) and NH<sub>3</sub> (transamination). This same reactivity pattern provides a plausible pathway for reclosure of the thiophene ring via nucleophilic attack of the thiolate on the imine carbon (Scheme 1). Recyclization of the thiophene ligand proceeds rapidly when the kinetic isomers are treated with protic sources. It was also found that the aminated ring-closed compounds derived from tetramethylthiophene revert to the dicationic sandwich structures upon treatment with acids.

The transformations reported in this paper are so well behaved that it is tempting to consider further extensions of these results. One possibility would be to attempt the reductive cleavage of the aminated thiophenes as a route to amino thiols.

### Experimental Section

**Materials and Methods.** Hydrated ruthenium trichloride was obtained from PGM Ltd. (Gerrinston, Republic of South Africa), 2,5-dimethylthiophene from Penta, and AgOTf from Aldrich. Tetramethylthiophene and [(*p*-cymene)RuCl<sub>2</sub>]<sub>2</sub> were prepared according to published procedures.<sup>14</sup> Syntheses and workups were performed under an inert atmosphere using purified nitrogen. The thiophene complexes have been described in previous publications.<sup>1–3</sup> The reagent grade solvents were distilled from Na/benzophenone (ether, THF, toluene, hexanes) or CaH<sub>2</sub> (acetonitrile, methylene chloride).

IR spectra were acquired on KBr pellets using a Mattson Galaxy Series FTIR 3000 spectrometer. NMR spectra were collected on a U-400 Varian spectrometer. Coupling patterns are described with the following abbreviations: s, singlet; d, doublet; t, triplet; dd, doublet of doublets; ps, pseudo, br, broad. Coupling constants in hertz are indicated parenthetically. Field desorption mass spectra were measured on a VG 70-VSE

(12) In separate work we have demonstrated that alkylamines work well also: Kocazja, K. M.; Rauchfuss, T. B. Unpublished results.

(13) Luo, S.; Rauchfuss, T. B.; Gan, Z. *J. Am. Chem. Soc.* **1993**, *115*, 4943.

(14) Bennett, M. A.; Huang, T.-N.; Matheson, T. W.; Smith, A. K. *Inorg. Syntheses* **1982**, *21*, 74.

or a Finnigan MAT-731; fast atom bombardment spectra, on a VG ZAB-SE. Mass spectral data are reported in units of  $m/z$ . Elemental analyses were performed by the University of Illinois Microanalytical Laboratory.

**[(C<sub>6</sub>Me<sub>6</sub>)Ru( $\eta^4$ -SC<sub>3</sub>H<sub>3</sub>CHNH<sub>2</sub>)]OTf (1).** Anhydrous NH<sub>3</sub> was passed through a powdered sample of 300 mg (0.465 mmol) of [(C<sub>6</sub>Me<sub>6</sub>)Ru(C<sub>4</sub>H<sub>4</sub>S)](OTf)<sub>2</sub> with stirring for 30 s. The resulting red solid was extracted into 10 mL of CH<sub>2</sub>Cl<sub>2</sub>. The extract was concentrated and diluted with 20 mL of hexanes giving a red powder. Yield: 203 mg (85%). <sup>1</sup>H NMR (CD<sub>3</sub>CN) (see eq 1 for labeling scheme): 7.02 (virtual q,  $J_{\text{NH-H}} = 11.0$ ,  $J_{4,3} = 11.5$ , 1H, H<sub>a</sub> of SC<sub>3</sub>H<sub>3</sub>CHNH<sub>2</sub>), 6.08 (dd,  $J_{1,2} = 4.88$ , 1H, H<sub>a</sub> of SC<sub>3</sub>H<sub>3</sub>CHNH<sub>2</sub>), 6.02 (br s, 2H, NH<sub>2</sub>), 5.58 (dd,  $J_{2,3} = 6.6$ , 1H, H<sub>c</sub> of SC<sub>3</sub>H<sub>3</sub>CHNH<sub>2</sub>), 3.99 (ddd, 1H, H<sub>b</sub> of SC<sub>3</sub>H<sub>3</sub>CHNH<sub>2</sub>), 2.17 (s, 15H, C<sub>6</sub>Me<sub>6</sub>). <sup>13</sup>C{<sup>1</sup>H} NMR (CD<sub>3</sub>CN): 142.1 (C<sub>a</sub> of SC<sub>3</sub>H<sub>3</sub>CHNH<sub>2</sub>), 121.0 (q, CF<sub>3</sub>), 100.8 (C<sub>d</sub> of SC<sub>3</sub>H<sub>3</sub>CHNH<sub>2</sub>), 99.8 (C<sub>6</sub>Me<sub>6</sub>), 89.6 (C<sub>c</sub> of SC<sub>3</sub>H<sub>3</sub>CHNH<sub>2</sub>), 68.4 (C<sub>b</sub> of SC<sub>3</sub>H<sub>3</sub>CHNH<sub>2</sub>), 16.2 (C<sub>6</sub>Me<sub>6</sub>). IR (KBr):  $\nu_{\text{NH}} = 3336$  and  $3208$ ,  $\nu_{\text{C-N}} = 1649$  cm<sup>-1</sup>. UV-vis: 500, 340 nm. FAB-MS: 364 (M<sup>+</sup>). Anal. Calcd for C<sub>17</sub>H<sub>24</sub>NF<sub>3</sub>O<sub>3</sub>RuS<sub>2</sub>: C, 39.83; H, 4.72; N, 2.73; Ru, 19.68; S, 12.51. Found: C, 39.97; H, 4.79; N, 2.80; Ru, 19.60; S, 12.36.

**[(cymene)Ru( $\eta^4$ -SC<sub>3</sub>H<sub>2</sub>MeCHNH<sub>2</sub>)]OTf (2).** Anhydrous NH<sub>3</sub> was passed over 200 mg (0.32 mmol) of solid [(cymene)Ru(2-MeC<sub>4</sub>H<sub>3</sub>S)](OTf)<sub>2</sub> for 30 s. The red oily product was extracted into 10 mL of CH<sub>2</sub>Cl<sub>2</sub>, and this extract was evaporated, leaving a red oil. Yield: 127 mg (80%). <sup>1</sup>H NMR (acetone-*d*<sub>6</sub>) (see eq 2 for labeling scheme): 7.96 (br s, 2H, NH<sub>2</sub>), 7.61 (br d,  $J_{1,2} = 11.2$ , 1H, H<sub>a</sub> of SC<sub>3</sub>H<sub>2</sub>MeCHNH<sub>2</sub>), 6.06 (d, 1H, <sup>1</sup>PrC<sub>6</sub>H<sub>4</sub>Me), 5.94 (m, 2H, <sup>1</sup>PrC<sub>6</sub>H<sub>4</sub>Me and 1H, H<sub>c</sub> of SC<sub>3</sub>H<sub>2</sub>MeCHNH<sub>2</sub>), 5.60 (d, 1H, <sup>1</sup>PrC<sub>6</sub>H<sub>4</sub>Me), 4.52 (dd,  $J_{2,1} = 11.2$ ,  $J_{2,3} = 6.4$ , 1H, H<sub>b</sub> of SC<sub>3</sub>H<sub>2</sub>MeCHNH<sub>2</sub>), 2.76 (sept, 1H, CH(Me)<sub>2</sub>C<sub>6</sub>H<sub>4</sub>Me), 2.38 (s, 3H), 2.20 (s, 3H), 1.30 (dd, 6H, CH(Me)<sub>2</sub>C<sub>6</sub>H<sub>4</sub>Me). <sup>13</sup>C{<sup>1</sup>H} NMR (CD<sub>3</sub>CN): 158.5 (C<sub>a</sub> of SC<sub>3</sub>H<sub>2</sub>MeCHNH<sub>2</sub>), 121.0 (q, CF<sub>3</sub>), 113.7, 111.3 (C<sub>d</sub> of SC<sub>3</sub>H<sub>2</sub>MeCHNH<sub>2</sub>), 100.2, 86.4, 85.9 (C<sub>c</sub> of SC<sub>3</sub>H<sub>2</sub>MeCHNH<sub>2</sub>), 85.8, 85.5, 84.3, 58.9 (C<sub>b</sub> of SC<sub>3</sub>H<sub>2</sub>MeCHNH<sub>2</sub>), 30.5, 28.3, 22.5, 21.8, 16.2. IR:  $\nu_{\text{NH}} = 3328$  and  $3219$ ,  $\nu_{\text{C-N}} = 1651$  cm<sup>-1</sup>. UV-vis: 512 nm. FAB-MS: 350 (M<sup>+</sup>). Anal. Calcd for C<sub>16</sub>H<sub>22</sub>NF<sub>3</sub>O<sub>3</sub>RuS<sub>2</sub>·0.25CH<sub>2</sub>Cl<sub>2</sub>: C, 37.56; H, 4.36; N, 2.69. Found: C, 37.87; H, 4.33; N, 2.51.

**[(cymene)Ru( $\eta^4$ -SC<sub>3</sub>H<sub>2</sub>MeCMeNH<sub>2</sub>)]OTf (3<sub>kin</sub>). Method a.** Gaseous NH<sub>3</sub> was bubbled through a solution of 400 mg (0.62 mmol) of [(cymene)Ru(2,5-Me<sub>2</sub>C<sub>4</sub>H<sub>3</sub>S)](OTf)<sub>2</sub> in 20 mL of CH<sub>3</sub>CN for 30 s. After a few minutes of stirring, the solvent was removed under vacuum. The red residue was extracted into 15 mL of CH<sub>2</sub>Cl<sub>2</sub>, leaving a white residue. The solution was filtered, and the filtrate was concentrated to 2 mL, followed by dilution with 20 mL of hexanes to give a red precipitate. Yield: 280 mg (89%).

**Method b.** Gaseous NH<sub>3</sub> was bubbled through 200 mg (0.31 mmol) of solid [(cymene)Ru(C<sub>4</sub>H<sub>2</sub>Me<sub>2</sub>S)](OTf)<sub>2</sub> for 30 s. The red product was extracted into 10 mL of CH<sub>2</sub>Cl<sub>2</sub>. This extract was concentrated and diluted with 20 mL of hexanes resulting in a red precipitate. Yield: 142 mg (90%). <sup>1</sup>H NMR (CD<sub>3</sub>CN) (see eq 3 for labeling scheme) 7.18 (br s, 2H, NH<sub>2</sub>), 5.95 (ps d, 1H, <sup>1</sup>PrC<sub>6</sub>H<sub>4</sub>Me), 5.68 (m, 2H, <sup>1</sup>PrC<sub>6</sub>H<sub>4</sub>Me), 5.58 (ps d, 1H, <sup>1</sup>PrC<sub>6</sub>H<sub>4</sub>Me), 5.40 (d,  $J = 5.4$ , 1H, H<sub>c</sub> of SC<sub>3</sub>H<sub>2</sub>MeCMeNH<sub>2</sub>), 3.88 (d,  $J = 5.6$ , 1H, H<sub>b</sub> of SC<sub>3</sub>H<sub>2</sub>MeCMeNH<sub>2</sub>), 2.69 (sept, 1H, CH(Me)<sub>2</sub>C<sub>6</sub>H<sub>4</sub>Me), 2.28 (s, 3H), 2.17 (s, 3H), 2.11 (s, 3H), 1.24 (dd, 6H, CH(Me)<sub>2</sub>C<sub>6</sub>H<sub>4</sub>Me). <sup>13</sup>C{<sup>1</sup>H} NMR (acetone-*d*<sub>6</sub>): 175.2 (C<sub>a</sub> of SC<sub>3</sub>H<sub>2</sub>MeCMeNH<sub>2</sub>), 121.0 (q, CF<sub>3</sub>), 111.3, 109.1 (C<sub>d</sub> of SC<sub>3</sub>H<sub>2</sub>MeCMeNH<sub>2</sub>), 98.3, 85.4, 84.7, 83.9, 83.8, 83.0 (C<sub>c</sub> of SC<sub>3</sub>H<sub>2</sub>MeCMeNH<sub>2</sub>), 49.5 (C<sub>b</sub> of SC<sub>3</sub>H<sub>2</sub>MeCMeNH<sub>2</sub>), 31.6 (CH(Me)<sub>2</sub>C<sub>6</sub>H<sub>4</sub>Me), 25.9, 22.8, 22.2, 22.1, 18.35. IR:  $\nu_{\text{NH}} = 3381$  and  $3151$ ,  $\nu_{\text{C-N}} = 1648$  cm<sup>-1</sup>. UV-vis: 516, 388 nm. FAB-MS: 364 (M<sup>+</sup>). Anal. Calcd for C<sub>17</sub>H<sub>24</sub>NF<sub>3</sub>O<sub>3</sub>RuS<sub>2</sub>: C, 39.83; H, 4.70; N, 2.73; Ru, 19.68; S, 12.50. Found: C, 39.60; H, 4.76; N, 2.73; Ru, 19.55; S, 12.46.

**[(cymene)Ru( $\eta^4$ -SC<sub>3</sub>H<sub>2</sub>MeCMeNH<sub>2</sub>)]OTf (3<sub>therm</sub>).** A solid sample of the kinetic isomer was maintained at 45 °C. Over the course of 24 h, the red powder assumed a dark purple-red

coloration. On the basis of <sup>1</sup>H NMR analysis, the transformation was quantitative. A solution of the kinetic isomer in CH<sub>3</sub>CN gave the thermodynamic isomer of [(cymene)Ru( $\eta^4$ -SC<sub>3</sub>H<sub>2</sub>MeCMeNH<sub>2</sub>)]OTf after 12 h (~25 °C), which was isolated as a dark red oil. The kinetics of the isomerization were examined on 10 mg sample dissolved in 0.6 mL of CD<sub>3</sub>CN, the solution of which was sealed in a 5 mm NMR tube. The progress of the reaction was monitored at 35 °C, and integrated spectra were recorded after 6 min, followed by 20 min intervals. Eight data points were collected. Plots of ln[**3**<sub>kin</sub>] vs time were linear with a slope of  $k = 2.13 \times 10^{-4}$  s<sup>-1</sup>. <sup>1</sup>H NMR (acetone-*d*<sub>6</sub>) (see eq 3 for labeling scheme): 9.93 (br s, 1H, NH<sub>2</sub>), 9.68 (br s, 1H, NH<sub>2</sub>), 6.17 (br d, 1H, H<sub>c</sub> of SC<sub>3</sub>H<sub>2</sub>MeCMeNH<sub>2</sub>), 6.07 (ps d, 1H, <sup>1</sup>PrC<sub>6</sub>H<sub>4</sub>Me), 5.74 (ps d, 1H, <sup>1</sup>PrC<sub>6</sub>H<sub>4</sub>Me), 5.59 (ps d, 1H, <sup>1</sup>PrC<sub>6</sub>H<sub>4</sub>Me), 5.06 (ps d, 1H, <sup>1</sup>PrC<sub>6</sub>H<sub>4</sub>Me), 2.72 (sept, 1H, CH(Me)<sub>2</sub>C<sub>6</sub>H<sub>4</sub>Me), 2.40 (s, 3H, Me<sub>a</sub> of SC<sub>3</sub>H<sub>2</sub>MeCMeNH<sub>2</sub>), 2.38 (s, 3H, Me<sub>d</sub> of SC<sub>3</sub>H<sub>2</sub>MeCMeNH<sub>2</sub>), 2.16 (s, 3H, CH(Me)<sub>2</sub>C<sub>6</sub>H<sub>4</sub>Me), 1.86 (br s, 1H, H<sub>b</sub> of SC<sub>3</sub>H<sub>2</sub>MeCMeNH<sub>2</sub>), 1.32 (dd, 6H, CH(Me)<sub>2</sub>C<sub>6</sub>H<sub>4</sub>Me). <sup>13</sup>C{<sup>1</sup>H} NMR (acetone-*d*<sub>6</sub>): 191.7 (C<sub>a</sub> of SC<sub>3</sub>H<sub>2</sub>MeCMeNH<sub>2</sub>), 122.0 (q, CF<sub>3</sub>), 110.5, 108.4 (C<sub>d</sub> of SC<sub>3</sub>H<sub>2</sub>MeCMeNH<sub>2</sub>), 99.3, 86.7, 84.7, 84.6, 84.1 82.0 (C<sub>c</sub> of SC<sub>3</sub>H<sub>2</sub>MeCMeNH<sub>2</sub>), 54.2 (C<sub>b</sub> of SC<sub>3</sub>H<sub>2</sub>MeCMeNH<sub>2</sub>), 31.7, 26.93, 26.90, 23.7, 23.4, 18.0. IR:  $\nu_{\text{NH}} = 3328$  and  $3153$ ,  $\nu_{\text{C-N}} = 1668$  cm<sup>-1</sup>. UV-vis: 536, 418 nm. FAB-MS: 364 (M<sup>+</sup>). Anal. Calcd for C<sub>17</sub>H<sub>24</sub>NF<sub>3</sub>O<sub>3</sub>RuS<sub>2</sub>: C, 39.83; H, 4.70; N, 2.73; Ru, 19.68; S, 12.50. Found: C, 39.63; H, 4.66; N, 2.63; Ru, 19.38; S, 12.35.

**Reaction of 3<sub>kin</sub> with KOH.** A solution of 30 mg (58.5  $\mu$ mol) of [(cymene)Ru( $\eta^4$ -SC<sub>3</sub>H<sub>2</sub>MeCMeNH<sub>2</sub>)]OTf in 2 mL of H<sub>2</sub>O was treated with 3.9 mL of 0.03 M KOH. The color of the solution changed from red to orange. After 1 min, the product was extracted into 5 mL of CH<sub>2</sub>Cl<sub>2</sub>. The extract was concentrated to dryness to give an orange oil whose <sup>1</sup>H NMR spectrum matched that of the known [(cymene)Ru( $\eta^4$ -SC<sub>3</sub>H<sub>2</sub>MeCOMe)] (kinetic isomer).<sup>2</sup>

**[(cymene)Ru( $\eta^4$ -C<sub>4</sub>Me<sub>4</sub>S-2-NH<sub>2</sub>)]BF<sub>4</sub> (4).** Anhydrous NH<sub>3</sub> was bubbled through a solution of 200 mg (0.36 mmol) of [(cymene)Ru(C<sub>4</sub>Me<sub>4</sub>S)](BF<sub>4</sub>)<sub>2</sub> in 15 mL of CH<sub>3</sub>CN for 1 min. The color of the reaction solution changed to bright yellow. After the solvent was removed, the residue was extracted into 15 mL of CH<sub>2</sub>Cl<sub>2</sub>. The filtrate was filtered away from the NH<sub>4</sub>OTf and diluted with hexanes to give yellow crystals. Yield: 150 mg (86%). <sup>1</sup>H NMR (acetone-*d*<sub>6</sub>): 6.09 (m, 1H), 6.0 (m, 1H), 5.82 (m, 1H), 5.64 (m, 1H), 3.62 (br s, 2H, NH<sub>2</sub>), 2.80 (sept, 1H), 2.44 (s, 3H), 2.23 (s, 3H), 2.12 (s, 3H), 1.74 (s, 3H), 1.68 (s, 3H), 1.29 (dd, 6H). <sup>13</sup>C{<sup>1</sup>H} NMR (acetone-*d*<sub>6</sub>): 114.6 (<sup>1</sup>PrC<sub>6</sub>H<sub>4</sub>Me), 108.5 (SC<sub>4</sub>Me<sub>4</sub>NH<sub>2</sub>), 102.5 (<sup>1</sup>PrC<sub>6</sub>H<sub>4</sub>Me), 95.8 (SC<sub>4</sub>Me<sub>4</sub>NH<sub>2</sub>), 88.9 (<sup>1</sup>PrC<sub>6</sub>H<sub>4</sub>Me), 87.6 (<sup>1</sup>PrC<sub>6</sub>H<sub>4</sub>Me), 86.1 (<sup>1</sup>PrC<sub>6</sub>H<sub>4</sub>Me), 85.4 (<sup>1</sup>PrC<sub>6</sub>H<sub>4</sub>Me), 85.3 (SC<sub>4</sub>Me<sub>4</sub>NH<sub>2</sub>), 77.2 (SC<sub>4</sub>Me<sub>4</sub>NH<sub>2</sub>), 32.2 (CH(Me)<sub>2</sub>C<sub>6</sub>H<sub>4</sub>Me), 24.0, 23.4, 23.2, 18.6, 17.2, 13.8, 13.2. IR:  $\nu_{\text{NH}} = 3431$  and  $3352$  cm<sup>-1</sup>. FAB-MS: 392 (M<sup>+</sup>). Anal. Calcd for C<sub>18</sub>H<sub>28</sub>NBF<sub>4</sub>RuS: C, 45.20; H, 5.90; N, 2.90; Ru, 21.10; S, 6.70. Found: C, 45.19; H, 5.93; N, 2.91; Ru, 21.27; S, 6.64.

**Reaction of 4 with HOTf.** Addition of 9.0  $\mu$ L (0.115 mmol) of HOTf to a solution of 50 mg (0.105 mmol) of [(cymene)Ru( $\eta^4$ -C<sub>4</sub>Me<sub>4</sub>S-2-NH<sub>2</sub>)]BF<sub>4</sub> in 8 mL of CH<sub>2</sub>Cl<sub>2</sub> precipitated a yellow solid, which was collected and recrystallized from acetone/Et<sub>2</sub>O. <sup>1</sup>H NMR spectroscopy showed that the product was [(cymene)Ru(C<sub>4</sub>Me<sub>4</sub>S)]<sup>2+</sup>.<sup>9</sup>

**[(C<sub>5</sub>Me<sub>5</sub>)Rh( $\eta^4$ -C<sub>4</sub>Me<sub>4</sub>S-2-NH<sub>2</sub>)]OTf (5).** A pale yellow solution of 200 mg (0.295 mmol) of [(C<sub>5</sub>Me<sub>5</sub>)Rh(C<sub>4</sub>Me<sub>4</sub>S)](OTf)<sub>2</sub> in 15 mL of CH<sub>3</sub>CN was purged with gaseous NH<sub>3</sub> for ~1 min, resulting in a yellow-orange solution. The solvent was removed, and the residue was extracted into 15 mL of CH<sub>2</sub>Cl<sub>2</sub>, leaving a white residue of NH<sub>4</sub>OTf. The solution was concentrated to 2 mL and diluted with 15 mL of hexanes, affording light orange microcrystals. Yield: 140 mg (87%). <sup>1</sup>H NMR (CD<sub>3</sub>CN): 3.10 (br s, 2H, NH<sub>2</sub>), 2.28 (s, 3H), 1.92 (d,  $J_{\text{H-Rh}} = 1.0$ , 3H), 1.83 (s, 15H, C<sub>5</sub>Me<sub>5</sub>), 1.69 (s, 3H), 1.48 (s, 3H), <sup>13</sup>C{<sup>1</sup>H} NMR (acetone-*d*<sub>6</sub>): 122.1 (q, CF<sub>3</sub>), 108.8 (d,  $J = 2.28$ ), 99.9 (d,  $J = 6.87$ , C<sub>5</sub>Me<sub>5</sub>), 99.1 (d,  $J = 6.87$ ), 91.5 (d,  $J = 9.15$ ),



**Table 1. Selected Bond Distances (Å) and Angles (deg) of [(C<sub>6</sub>Me<sub>6</sub>)Ru(η<sup>4</sup>-SC<sub>3</sub>H<sub>2</sub>MeCHNHPPh)]PF<sub>6</sub> (7) and [(cymene)Ru(η<sup>4</sup>-SC<sub>3</sub>H<sub>2</sub>MeCMeNHPPh)]OTf (8<sub>therm</sub>)**

	7	8 <sub>therm</sub>
Ru-S	2.335(3)	2.392(6)
Ru-C2	2.192(5)	2.160(2)
Ru-C3	2.222(10)	2.14(2)
Ru-C4	2.288(6)	2.22(2)
Ru-C5	2.627(6)	3.08(2)
S-C2	1.74(3)	1.73(2)
C2-C3	1.39(3)	1.36(2)
C3-C4	1.435(11)	1.44(2)
C4-C5	1.389(10)	1.46(2)
C5-N	1.348(8)	1.34(2)
N-C6	1.433(9)	1.47(2)
Ru-C <sub>6R6</sub>	2.218(3)-2.222(3)	2.17-2.29(2)
S-C2-C3	120.7(5)	121(1)
C2-C3-C4	127.8(10)	115(2)
C3-C4-C5	129.0(7)	122(2)
C4-C5-N	120.4(6)	123(2)
C5-N-C6	124.8(6)	124(1)
C2-C3-C4	127.8(10)	115(2)
C3-C4-C5	129.0(7)	122(2)
C4-C5-N	120.4(6)	123(2)
C5-N-C6	124.8(6)	124(1)

81.9 (d,  $J = 10.68$ ), 24.4, 15.0, 11.1, 10.7, 9.3 (C<sub>6</sub>Me<sub>6</sub>). IR:  $\nu_{\text{NH}} = 3407$  and  $3330 \text{ cm}^{-1}$ . FAB-MS: 394 (M<sup>+</sup>). Anal. Calcd for C<sub>19</sub>H<sub>29</sub>NF<sub>3</sub>O<sub>3</sub>RhS<sub>2</sub>: C, 41.99; H, 5.38; N, 2.58; Rh, 18.94; S, 11.8. Found: C, 41.87; H, 5.37; N, 2.52; Rh, 18.58; S, 12.0.

**Reaction of [(C<sub>5</sub>Me<sub>5</sub>)Rh(η<sup>4</sup>-C<sub>4</sub>Me<sub>4</sub>S-2-NH<sub>2</sub>)]OTf with HOTs.** Addition of 30 mg (0.178 mmol) of HOSO<sub>2</sub>C<sub>6</sub>H<sub>4</sub>Me<sub>2</sub>O to a solution of 70 mg (0.13 mmol) of [(C<sub>5</sub>Me<sub>5</sub>)Rh(η<sup>4</sup>-C<sub>4</sub>Me<sub>4</sub>S-2-NH<sub>2</sub>)]OTf in 10 mL of CH<sub>2</sub>Cl<sub>2</sub> precipitated a yellow solid, which was collected and recrystallized from acetone/Et<sub>2</sub>O. The product was identified as [(C<sub>5</sub>Me<sub>5</sub>)Rh(C<sub>4</sub>Me<sub>4</sub>S)]<sup>2+</sup> by its <sup>1</sup>H NMR spectrum.<sup>1</sup>

**[(C<sub>6</sub>Me<sub>6</sub>)Ru(η<sup>4</sup>-SC<sub>3</sub>H<sub>3</sub>CHNHPPh)]OTf (6).** A solution of 200 mg of [(C<sub>6</sub>Me<sub>6</sub>)Ru(C<sub>4</sub>H<sub>4</sub>S)](OTf)<sub>2</sub> (0.31 mmol) in 20 mL of CH<sub>3</sub>CN was treated with 56 μL (0.62 mmol) of PhNH<sub>2</sub>, resulting in a color change from pale yellow to orange-red. After 3 h, the solvent was removed under vacuum and the residue was extracted into 20 mL of CH<sub>2</sub>Cl<sub>2</sub>, leaving a gray powder of PhNH<sub>3</sub>(OTf). The filtrate was concentrated to 2 mL and diluted with 15 mL of hexanes giving red crystals. Yield: 156 mg (85%). <sup>1</sup>H NMR (CD<sub>3</sub>CN) (see eq 6 for labeling scheme): 8.02 (br d,  $J_{\text{NH-H}} = 12.7$ , 1H, NHPPh), 7.39 (m, 2H, C<sub>6</sub>H<sub>5</sub>NH), 7.10 (m, 1H, C<sub>6</sub>H<sub>5</sub>NH), 6.92 (m, 2H, C<sub>6</sub>H<sub>5</sub>NH), 6.77 (dd,  $J_{1,2} = 11.1$ , 1H, H<sub>a</sub> of SC<sub>3</sub>H<sub>3</sub>CHNHPPh), 6.25 (d,  $J_{4,3} = 5.4$ , 1H, H<sub>a</sub> of SC<sub>3</sub>H<sub>3</sub>CHNHPPh), 5.82 (dd,  $J_{3,2} = 6.4$ , 1H, H<sub>c</sub> of SC<sub>3</sub>H<sub>3</sub>CHNHPPh), 4.69 (dd, 1H, H<sub>b</sub> of SC<sub>3</sub>H<sub>3</sub>CHNHPPh), 2.16 (s, 18H, C<sub>6</sub>Me<sub>6</sub>). <sup>13</sup>C{<sup>1</sup>H} NMR (CD<sub>3</sub>NO<sub>2</sub>): 141.9 (C<sub>a</sub> of SC<sub>3</sub>H<sub>3</sub>CHNHPPh), 131.3 (C<sub>6</sub>H<sub>5</sub>NH), 126.8 (C<sub>6</sub>H<sub>5</sub>NH), 124.3 (C<sub>6</sub>H<sub>5</sub>NH), 120.4 (q, CF<sub>3</sub>), 116.7 (C<sub>6</sub>H<sub>5</sub>NH), 104.1 (C<sub>d</sub> of SC<sub>3</sub>H<sub>3</sub>CHNHPPh), 103.0 (C<sub>6</sub>-Me<sub>6</sub>), 90.8 (C<sub>c</sub> of SC<sub>3</sub>H<sub>3</sub>CHNHPPh), 75.2 (C<sub>d</sub> of SC<sub>3</sub>H<sub>3</sub>CHNHPPh), 16.9 (C<sub>6</sub>Me<sub>6</sub>). IR:  $\nu_{\text{NH}} = 3252 \text{ cm}^{-1}$ . FAB-MS: 440 (M<sup>+</sup>) Anal. Calcd for C<sub>23</sub>H<sub>28</sub>NF<sub>3</sub>O<sub>3</sub>RuS<sub>2</sub>: C, 46.92; H, 4.79; N, 2.38; Ru, 17.17; S, 10.89. Found: C, 46.93; H, 4.79; N, 2.40; Ru, 17.30; S, 10.72.

**[(C<sub>6</sub>Me<sub>6</sub>)Ru(η<sup>4</sup>-SC<sub>3</sub>H<sub>2</sub>MeCHNHPPh)]PF<sub>6</sub> (7).** A solution of 200 mg (0.307 mmol) of [(C<sub>6</sub>Me<sub>6</sub>)Ru(2-MeC<sub>4</sub>H<sub>2</sub>S)](PF<sub>6</sub>)<sub>2</sub> in 10 mL of CH<sub>3</sub>CN was treated with 56 μL (0.614 mmol) of PhNH<sub>2</sub>, resulting in a color change from pale yellow to purple-red. After 10 min, the solvent was removed under vacuum and the residue was extracted into 8 mL of CH<sub>2</sub>Cl<sub>2</sub>, leaving a gray powder of PhNH<sub>3</sub>(PF<sub>6</sub>). The filtrate was concentrated to 2 mL and diluted with 15 mL of hexanes, giving a red powder. A CH<sub>2</sub>Cl<sub>2</sub> solution of this product was further purified by chromatography on silica gel. Yield: 137 mg (75%). <sup>1</sup>H NMR (CD<sub>3</sub>CN) (see eq 6 for labeling scheme): 9.02 (br d,  $J_{\text{NH-H}} = 12.7$ , 1H, NHPPh), 7.42 (m, 2H, C<sub>6</sub>H<sub>5</sub>NH), 7.11 (m, 1H, C<sub>6</sub>H<sub>5</sub>-NH), 6.99 (m, 2H, C<sub>6</sub>H<sub>5</sub>NH), 6.97 (dd, 1H, H<sub>a</sub> of SC<sub>3</sub>H<sub>2</sub>MeCHNHPPh), 5.87 (d,  $J_{3,2} = 6.6$ , 1H, H<sub>c</sub> of SC<sub>3</sub>H<sub>2</sub>MeCHNHPPh),

**Table 2. Atomic Coordinates and Equivalent Isotropic Thermal Parameters for 7**

	x	y	z	U(eq), Å <sup>2</sup>
Ru	-361(1)	2500	1441(1)	23(1)
S	1508(3)	3903(2)	870(1)	26(1)
N	3440(7)	1350(5)	2721(3)	31(1)
C1	-46(8)	2687(14)	-501(3)	32(3)
C2	858(7)	2569(34)	328(3)	26(2)
C3	1186(14)	1380(10)	648(6)	29(2)
C4	1900(8)	1067(6)	1438(4)	28(1)
C5	2877(8)	1816(7)	2002(4)	28(1)
C6	4302(16)	2067(8)	3363(5)	29(2)
C7	5059(17)	1428(8)	4024(5)	36(2)
C8	5870(16)	2084(7)	4666(5)	33(3)
C9	5862(17)	3379(8)	4657(5)	39(2)
C10	5108(18)	4001(8)	3996(6)	35(2)
C11	4302(17)	3352(8)	3354(6)	35(2)
C12	-1475(6)	2500	2610(3)	38(1)
C13	-1911(4)	3652(3)	2213(2)	36(1)
C14	-2828(4)	3645(3)	1437(2)	35(1)
C15	-3269(6)	2500	1052(3)	34(1)
C18	-548(3)	2500	3432(3)	67(2)
C19	-1431(7)	4892(4)	2615(3)	70(1)
C20	-3341(6)	4868(4)	1023(3)	63(1)
C21	-4214(7)	2500	222(3)	61(2)
P1	3343(3)	7536(16)	2560(1)	45(1)
F1	3048(13)	8747(7)	2028(5)	98(3)
F2	3659(16)	6379(8)	3100(5)	118(3)
F3	1335(7)	7234(11)	2348(3)	102(3)
F4	5328(8)	7914(8)	2738(5)	134(4)
F5	3709(12)	6758(8)	1818(5)	101(3)
F6	2816(13)	8347(9)	3289(5)	99(3)
Cl	1169(3)	3848(2)	5365(1)	101(1)
C24	1376(21)	2500	5917(5)	136(5)

4.82 (dd,  $J_{2,1} = 10.9$ , 1H, H<sub>b</sub> of SC<sub>3</sub>H<sub>2</sub>MeCHNHPPh), 2.30 (s, 3H, Me<sub>d</sub> of SC<sub>3</sub>H<sub>2</sub>MeCHNHPPh), 2.21 (s, 18H, C<sub>6</sub>Me<sub>6</sub>). <sup>13</sup>C{<sup>1</sup>H} NMR (acetone-*d*<sub>6</sub>): 141.3, 141.2, 130.6, 123.6, 115.9, 115.8, 101.3, 87.5 (C<sub>c</sub> of SC<sub>3</sub>H<sub>2</sub>MeCHNHPPh), 73.0 (C<sub>b</sub> of SC<sub>3</sub>H<sub>2</sub>MeCHNHPPh), 28.65 (Me<sub>d</sub> of SC<sub>3</sub>H<sub>2</sub>MeCHNHPPh), 16.15 (C<sub>6</sub>Me<sub>6</sub>). IR:  $\nu_{\text{NH}} = 3364 \text{ cm}^{-1}$ . FAB-MS: 454 (M<sup>+</sup>). Anal. Calcd for C<sub>23</sub>H<sub>30</sub>NF<sub>6</sub>O<sub>3</sub>PRuS-0.3CH<sub>2</sub>Cl<sub>2</sub>: C, 44.84; H, 4.94; N, 2.24. Found: C, 44.96; H, 4.95; N, 2.35.

**[(cymene)Ru(η<sup>4</sup>-SC<sub>3</sub>H<sub>2</sub>MeCMeNHPPh)]OTf (8).** A solution of 200 mg (0.31 mmol) of [(cymene)Ru(2,5-Me<sub>2</sub>C<sub>4</sub>H<sub>2</sub>S)](OTf)<sub>2</sub> in 10 mL of CH<sub>3</sub>CN was treated with 60 μL (0.62 mmol) of PhNH<sub>2</sub>, resulting in a color change from pale yellow to purple-red. After 10 min, the solvent was removed under vacuum and the residue was extracted into 8 mL of CH<sub>2</sub>Cl<sub>2</sub> to give a red solution and gray powder of PhNH<sub>3</sub>(OTf). The CH<sub>2</sub>Cl<sub>2</sub> extract was filtered, concentrated to 2 mL, and diluted with 15 mL of hexanes, giving 160 mg (88%) of purple-red needle crystals. The <sup>1</sup>H NMR spectrum showed two thermodynamic isomers formed in a ratio of 4:1. <sup>1</sup>H NMR (CD<sub>3</sub>CN, major isomer of 8<sub>therm</sub>) (see eq 7 for labeling scheme): 10.51 (br s, 1H, NH), 7.51 (m, 2H), 7.39 (m, 3H), 5.96 (d,  $J = 6.8$ , 1H, H<sub>c</sub> of SC<sub>3</sub>H<sub>2</sub>MeCMeNHPPh), 5.76 (m, 1H), 5.68 (ps d, 1H), 5.63 (ps d, 1H), 5.11 (ps d, 1H), 2.39 (s, 3H), 2.37 (s, 3H), 2.18 (s, 3H), 1.93 (sept, 1H), 1.86 (d,  $J = 7.0$ , 1H, H<sub>b</sub> of SC<sub>3</sub>H<sub>2</sub>MeCMeNHPPh), 1.26 (dd, 6H). <sup>13</sup>C{<sup>1</sup>H} NMR (acetone-*d*<sub>6</sub>, major isomer): 185.0 (C<sub>a</sub> of SC<sub>3</sub>H<sub>2</sub>MeCMeNHPPh), 137.1, 130.2, 129.0, 125.0, 122.1 (q, CF<sub>3</sub>), 111.3, 109.8, 100.1, 86.6, 85.3, 85.1, 84.9, 84.2, 83.7, 55.7 (C<sub>b</sub> of SC<sub>3</sub>H<sub>2</sub>MeCMeNHPPh), 32.3, 26.8, 23.8, 23.6, 21.2, 18.6. IR:  $\nu_{\text{NH}} = 3223 \text{ cm}^{-1}$ . FAB-MS: 440 (M<sup>+</sup>). Anal. Calcd for C<sub>23</sub>H<sub>28</sub>NF<sub>3</sub>O<sub>3</sub>RuS<sub>2</sub>: C, 46.92; H, 4.79; N, 2.38; Ru, 17.17; S, 10.89. Found: C, 46.88; H, 4.84; N, 2.38; Ru, 17.08; S, 10.93. In an NMR tube, a solution of 30 mg (0.047 mmol) of [(cymene)Ru(2,5-Me<sub>2</sub>C<sub>4</sub>H<sub>2</sub>S)](OTf)<sub>2</sub> in 0.65 mL of CD<sub>3</sub>CN was cooled to -10 °C and treated with 10 μL (0.10 mmol) of PhNH<sub>2</sub>, resulting in a color change from pale yellow to purple-red. The reaction was monitored by <sup>1</sup>H NMR spectroscopy at -10 °C, which showed that only one kinetic isomer formed, isomerizing to two thermodynamic isomers upon warming to ambient temperatures. <sup>1</sup>H NMR (CD<sub>3</sub>CN, -10 °C, 8<sub>kin</sub>): 8.02 (br s, 1H, NH), 7.35 (m, 3H), 7.10 (m, 2H), 6.01 (ps d, 1H), 5.76 (ps d,

Table 3. Atomic Coordinates for **8**<sub>therm</sub>

	<i>x/a</i>	<i>y/b</i>	<i>z/c</i>
Ru	0.1486(1)	0.09637(5)	0.0
S	0.1211(5)	0.0704(2)	0.3042(8)
N	0.074(1)	0.2358(5)	0.061(2)
C1	0.351(1)	0.0576(6)	0.269(2)
C2	0.252(1)	0.0904(6)	0.238(2)
C3	0.266(1)	0.1343(6)	0.164(2)
C4	0.166(1)	0.1627(6)	0.159(2)
C5	0.159(2)	0.2048(6)	0.052(2)
C6	-0.022(1)	0.2309(6)	0.186(2)
C7	0.247(2)	0.2193(6)	-0.076(2)
C8	-0.044(2)	0.2663(6)	0.299(2)
C9	-0.136(2)	0.2648(7)	0.404(2)
C10	-0.211(2)	0.2276(7)	0.411(2)
C11	-0.185(2)	0.1913(6)	0.288(2)
C12	-0.091(1)	0.1915(6)	0.184(2)
C13	0.181(1)	0.0299(7)	-0.168(3)
C14	0.239(2)	0.0707(6)	-0.240(2)
C15	0.178(1)	0.1139(6)	-0.288(2)
C16	0.059(1)	0.1184(6)	-0.260(2)
C17	0.003(2)	0.0808(6)	-0.177(2)
C18	0.065(2)	0.0385(7)	-0.138(3)
C19	0.239(2)	-0.0153(7)	-0.130(2)
C20	0.192(3)	-0.048(1)	-0.278(4)
C21	0.366(2)	-0.011(1)	-0.148(5)
C22	-0.005(2)	0.1624(7)	-0.310(3)
S2A	0.4544(6)	-0.1554(3)	-0.7896(10)
O1A	0.5693(7)	-0.1418(5)	-0.774(2)
O2A	0.430(1)	-0.2026(3)	-0.729(2)
O3A	0.4020(10)	-0.1423(4)	-0.956(1)
C23A	0.3826(9)	-0.1173(4)	-0.620(1)
F1A	0.401(2)	-0.0740(3)	-0.664(2)
F2A	0.2778(8)	-0.1272(7)	-0.626(2)
F3A	0.425(1)	-0.1273(5)	-0.465(1)
S2B	0.462(1)	-0.1602(5)	-0.735(2)
O1B	0.409(2)	-0.2019(6)	-0.806(3)
O2B	0.548(1)	-0.141(1)	-0.848(3)
O3B	0.489(2)	-0.1625(8)	-0.547(2)
C23B	0.349(2)	-0.1147(7)	-0.744(2)
F1B	0.314(2)	-0.1128(10)	-0.908(3)
F2B	0.392(3)	-0.0751(6)	-0.694(4)
F3B	0.271(2)	-0.128(1)	-0.636(4)

1H), 5.73 (ps d, 1H), 5.61 (ps d, 1H), 5.43 (d, *J* = 5.1, 1H, H<sub>c</sub> of SC<sub>3</sub>H<sub>2</sub>MeCMeNHPPh), 4.10 (d, *J* = 5.1, 1H, H<sub>b</sub> of SC<sub>3</sub>H<sub>2</sub>MeCMeNHPPh), 2.69 (sept, 1H), 2.28 (s, 3H), 2.18 (s, 3H), 2.05 (s, 3H), 1.24 (dd, 6H).

**Reaction of **8**<sub>therm</sub> with NH<sub>3</sub>.** Gaseous NH<sub>3</sub> was passed over a solution of 50 mg (0.085 mmol) of **8** in 10 mL of CH<sub>3</sub>CN for 30 s. The color of the solution changed to purple-red. The solution was evaporated to dryness. The residue was dissolved in acetone-*d*<sub>6</sub> and examined by <sup>1</sup>H NMR spectroscopy which established that the mixture consisted of PhNH<sub>2</sub> and the thermodynamic isomer of [(cymene)Ru(η<sup>4</sup>-SC<sub>3</sub>H<sub>2</sub>MeCMeNH<sub>2</sub>)]<sup>+</sup>.

**Crystallographic Characterization of **7**.** Red, prismatic crystals of [(C<sub>8</sub>Me<sub>6</sub>)Ru(η<sup>4</sup>-SC<sub>3</sub>H<sub>2</sub>MeCHNHPPh)]PF<sub>6</sub>·CH<sub>2</sub>Cl<sub>2</sub> were obtained by layering a CH<sub>2</sub>Cl<sub>2</sub> solution with diethyl ether. The crystal of dimensions 0.40 × 0.32 × 0.22 mm was mounted in oil (Paratone-N, Exxon) to a thin glass fiber with the (212) scattering planes roughly normal to the spindle axis. The salt crystallized in the monoclinic space group *P*2<sub>1</sub>/*m*, with *a* = 7.528(2) Å, *b* = 10.665(2) Å, *c* = 17.029(4) Å, α = γ = 90°, β = 96°, *Z* = 2, and *d*<sub>calcd</sub> = 1.669 g/cm<sup>3</sup>. The data crystal was bound by the (001), (00 $\bar{1}$ ), (011), (0 $\bar{1}\bar{1}$ ), (10 $\bar{1}$ ), and ( $\bar{1}$ 01) faces. Distances from the crystal center to these facial boundaries were 0.11, 0.11, 0.16, 0.16, 0.20, and 0.20 mm, respectively. Data were measured at 198 K on an Enraf-Nonius diffractometer. Systematic conditions suggested the ambiguous space group *P*2<sub>1</sub>; however, refinement supported the presence of a symmetry center. Periodically monitored standard intensities showed no decay. Step-scanned intensity data were reduced by profile analysis<sup>15</sup> and corrected for Lorentz-

(15) Coppens, P.; Blessing, R. H.; Becker, P. *J. Appl. Crystallogr.* **1972**, *7*, 488.

Table 4. Crystal Data and Structure Refinement for **7**

empirical formula	C <sub>24</sub> H <sub>32</sub> Cl <sub>2</sub> F <sub>6</sub> NPRuS
formula weight	683.51
temperature	198(2) K
wavelength	0.710 73 Å
crystal system	monoclinic
space group	<i>P</i> 2 <sub>1</sub> / <i>m</i>
unit cell dimensions	<i>a</i> = 7.528(2) Å, <i>b</i> = 10.665(2) Å, <i>c</i> = 17.029(4) Å, α = γ = 90°, β = 96.00(2)°
volume	1359.75(5) Å <sup>3</sup>
<i>Z</i>	2
density (calculated)	1.669 Mg/m <sup>3</sup>
absorption coefficient	0.956 mm <sup>-1</sup>
<i>F</i> (000)	692
crystal size	0.40 × 0.32 × 0.22 mm
θ range for data collection	2.26 to 24.95°
index ranges	0 ≤ <i>h</i> ≤ 8, 0 ≤ <i>k</i> ≤ 12, -20 ≤ <i>l</i> ≤ 20
reflections collected	2723
no. of independent reflections	2519 [ <i>R</i> (i) = 0.0217]
absorption correction	integration
max and min transmission	0.8411 and 0.7135
refinement method	full-matrix least-squares on <i>F</i> <sup>2</sup>
data/restraints/parameters	2519/145/280
goodness-of-fit on <i>F</i> <sup>2</sup>	1.135
final <i>R</i> indices [ <i>I</i> > 2σ( <i>I</i> )]	<i>R</i> <sub>1</sub> = 0.0357, <i>R</i> <sub>w2</sub> = 0.0894
<i>R</i> indices (all data)	<i>R</i> <sub>1</sub> = 0.0400, <i>R</i> <sub>w2</sub> = 0.0918
extinction coefficient	0.0022(6)
largest diff peak and hole	0.546 and -0.755 e/Å <sup>3</sup>

polarization effects and for absorption.<sup>16</sup> Scattering factors and anomalous dispersion terms were taken from standard tables.<sup>17</sup>

The structure was solved in the acentric space group *P*2<sub>1</sub> by Patterson methods (Sheldrick, 1990); positions Ru and P1 were deduced from a vector map. Partial structure expansion revealed positions for the remaining non-H atoms including disordered positions with pseudomirror symmetry for both the anion and the asymmetric ligand of the cation. Subsequent calculations imposed mirror symmetry on the cation, anion, and solvate molecules in the centric space group *P*2<sub>1</sub>/*m*. Methyl H atom positions C-CH<sub>3</sub>, were optimized by rotation about C-C bonds while maintaining idealized C-H, C-H, and H-H distances were maintained. Positions for atoms H3-H6 were independently refined. Remaining H atoms were included as fixed idealized contributors. H atom U's were assigned as 1.2 *U*<sub>eq</sub> of adjacent non-H atoms. Geometric restraints were imposed on both disordered moieties. Octahedral geometry with an effective standard deviation of 0.03 Å was imposed on the anion; the mean P-F bond length converged at 1.562(6) Å. Phenyl carbon atoms C6-C11 were restrained to have equivalent 1,2- and 1,3-distances (esd = 0.02 Å). No restraints were imposed on atomic positions S, C2-C5, N6, or H3-H5. Rigid bond restraints were imposed on the anisotropic displacement parameters refined for all non-H atoms. Successful convergence of the full-matrix least-squares refinements on *F*<sup>2</sup> was indicated by the maximum shift/error for the last cycle.<sup>18</sup> The highest peak in the final difference Fourier map was in the vicinity of solvate molecule; the final map had no other significant features. A final analysis of variance between observed and calculated structure factors showed no dependence on amplitude or resolution. Selected bond distances and angles are presented in Table 1, refined atomic coordinates are presented in Table 2, and crystal data and structure refinement parameters are presented in Table 4.

(16) Sheldrick, G. M. *SHELX-76: Program for Crystal Structure Determination*; University of Cambridge: Cambridge, England.

(17) Wilson, A. J. C., Ed. *International Tables for X-ray Crystallography*; Kluwer Academic Publishers: Dordrecht, The Netherlands, Vol. C.

(18) Sheldrick, G. M. *SHELX-93: A Program for Structure Refinement*; University of Göttingen: Göttingen, Germany, 1994.

**Table 5. Crystal Data and Structure Refinement for  $\mathbf{8}_{\text{therm}}$** 

empirical formula	$\text{C}_{23}\text{H}_{28}\text{F}_3\text{NO}_3\text{PRuS}_2$
formula weight	588.67
crystal system	orthorhombic
wavelength	0.710 73 Å
temperature	-75 °C
space group	$Pna2_1$
unit cell dimensions	$a = 11.935(3)$ Å, $b = 28.162(11)$ Å, $c = 7.407(2)$ Å $\alpha = \beta = \gamma = 90^\circ$
volume	$2490$ Å <sup>3</sup>
Z	4
density (calculated)	$1.570$ g/cm <sup>3</sup>
absorption coefficient	$\mu = 8.24$ cm <sup>-1</sup>
$F(000)$	1200
crystal size	$0.07 \times 0.08 \times 0.05$ mm
radiation	Mo $K\alpha$
scan mode	$\omega-2\theta$
scan limits	$2^\circ < 2\theta < 51^\circ$
scan rate	$2-8^\circ/\text{min}$
no. of data collected	3029
no. of data observed	1286
no. of variables	182
$R^a$	0.062
$R_w^b$	0.049
maximum shift/error	0.05
weighting scheme	1.40
highest peak in final diff map	$+0.75 > e/\text{Å} > -0.78$
refinement method	SHELXS-86

$$^a R = \sum(|F_o| - |F_c|)/\sum|F_o|. \quad ^b R_w = [(\sum w(|F_o| - |F_c|)^2)/\sum w|F_o|^2]^{1/2}.$$

**Crystallographic Characterization of  $\mathbf{8}_{\text{therm}}$ .** The purple-red, translucent, and columnar crystals of [(cymene)Ru( $\eta^4$ -SC<sub>3</sub>H<sub>2</sub>MeCMeNHPPh)]OTf were obtained by layering a CH<sub>2</sub>Cl<sub>2</sub> solution with hexanes. The crystal of dimensions  $0.07 \times 0.08 \times 0.50$  mm was mounted in oil (Paratone-N) to a thin glass fiber and then cooled to -75 °C with the (118) scattering planes roughly normal to the spindle axis. The salt crystallized in the orthorhombic space group  $Pna2_1$  with  $a = 11.935(3)$  Å,  $b = 28.162(11)$  Å,  $c = 7.407(22)$  Å,  $\alpha = \beta = \gamma = 90^\circ$ ,  $Z = 4$  and  $d_{\text{calcd}} = 1.570$  g/cm<sup>3</sup>. The structure was solved by Patterson

methods;<sup>19</sup> the correct Ru atom position was deduced from a vector map, and partial structure expansion revealed positions for the S atom. Subsequent least-squares refinement and difference Fourier syntheses gave positions for the remaining non-H atoms, including disordered positions for all anion atoms in addition to cation C20 and C21. Equivalent 3-fold symmetry was imposed on the disordered anion positions and a common C-C bond length was imposed on the disordered methyl atoms C20 and C21. No N-bound H atom position ever surfaced. Disordered H atoms positions were not included in structure factor calculations; however, the remaining H atoms were included as fixed contributors in "ideal" positions. Common isotropic thermal parameters were refined for the H atoms, the disordered methyl C atoms of the cation, and the S, F, O, and C atoms of the anion. Anisotropic thermal coefficients were refined for the Ru, N, and cation S atoms, and independent isotropic thermal coefficients were refined for the ordered C atoms. Successful convergence was indicated by the maximum shift/error for the last cycle. The highest peak in the final difference Fourier map was in the vicinity of the anion. A final analysis of variance between observed and calculated structure factors showed dependence on  $\sin \theta$  and amplitude. Selected bond distances and angles are presented in Table 1, refined atomic coordinates are presented in Table 3, and crystal data and structure refinement parameters are presented in Table 5.<sup>20</sup>

**Acknowledgment.** This research was supported by the U.S. Department of Energy. We thank H. Krautscheid, A. K. Verma, and T. Prussak for assistance.

**Supplementary Material Available:** Labeled ORTEP diagrams and tables of bond distances, bond angles, and thermal parameters (11 pages). Ordering information is given on any current masthead page.

OM950104W

(19) Sheldrick, G. M. *Acta Crystallogr.* **1990**, *A46*, 467.

(20) Plots in Figures 1 and 2 employed A. L. Spek's PLATON-92 software (Vakgroep Kristalene Structuurchemie, University of Utrecht, Padualaan 8, 3584 CH Utrecht, The Netherlands, 1992).

# Structural Characterization of Intermediates in the Rhodium-Catalyzed Reductive Carbonylation of Methanol: $\text{Rh}(\text{COCH}_3)(\text{I})_2(\text{dppp})$ and $[\text{Rh}(\text{H})(\text{I})(\mu\text{-I})(\text{dppp})]_2$

Kenneth G. Moloy\*

Union Carbide Corporation, P.O. Box 8361, South Charleston, West Virginia 25303-0361

Jeffrey L. Petersen

Department of Chemistry, West Virginia University, Morgantown, West Virginia 26505-6045

Received February 21, 1995<sup>®</sup>

X-ray structural analyses of  $\text{Rh}(\text{COCH}_3)(\text{I})_2(\text{dppp})$  (**1**) and  $[\text{Rh}(\text{H})(\text{I})(\mu\text{-I})(\text{dppp})]_2$  (**2**) are reported. Complex **1** is converted to hydride **2** with  $\text{H}_2$ , and this reaction is believed to be the critical step in the conversion of methanol to acetaldehyde, catalyzed by **1**. Unsaturated complex **1** possesses a distorted five-coordinate geometry that is intermediate between sbp and tbp structures. Complex **2** achieves coordinative saturation *via* formation of iodo bridges.  $\text{H}_2$  activation by **1** is discussed in view of these structural results. Complex **1** further is found to heterolytically activate  $\text{H}_2$  in the presence of base.

## Introduction

In a previous report<sup>1</sup> we described a rhodium catalyst for the reductive carbonylation of methanol to acetaldehyde. This catalyst is unique in that it gives good rates and selectivities (80%) under much milder temperatures and pressures (140 °C, 1000 psig) than previously reported catalysts (typically cobalt-based, > 200 °C, 3000–5000 psig). The rhodium acetyl complex  $\text{Rh}(\text{COCH}_3)(\text{I})_2(\text{dppp})$  (**1**, dppp = 1,3-bis(diphenylphosphino)propane) is isolable in essentially quantitative yield from spent catalyst solutions. This observation, the demonstration that **1** can be reused for catalysis and again be recovered, and also kinetic and mechanistic studies led us to postulate that **1** is a key intermediate in the catalytic reaction.

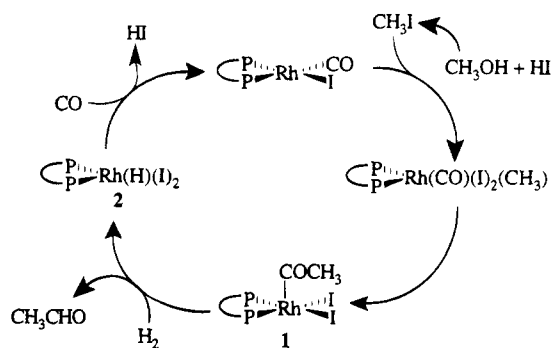
The catalytic cycle proposed for this transformation is shown in Scheme 1. In what appears to be the rate-determining step, **1** reacts with  $\text{H}_2$  to produce acetaldehyde and hydride **2**. In a separate catalytic cycle (not shown) **1** is believed to add a CO ligand; the resulting carbonyl complex then reductively eliminates  $\text{CH}_3\text{COI}$ , forming  $\text{Rh}(\text{I})(\text{CO})(\text{dppp})$ . Liberated  $\text{CH}_3\text{COI}$  is rapidly converted to  $\text{HOAc/MeOAc}$ , resulting in the major inefficiency (*ca.* 20%) with this catalyst. If these hypotheses are correct, **1** is seen to play a pivotal role in this catalysis, governing both the rate- and selectivity-determining steps.

Due to the importance of the conversion of **1** to **2** in the catalytic cycle, we became interested in understanding the mechanism of this step. The hydrogenolysis of Rh–C bonds is a well-studied transformation owing to its importance in rhodium-catalyzed olefin hydroformy-

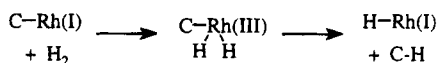
\* Author to whom correspondence should be addressed. Current address: E. I. du Pont de Nemours and Company, Central Research and Development, Experimental Station E328/215A, P.O. Box 80328, Wilmington, DE 19880-0328. E-mail: moloykg@esvax.dnet.dupont.com.

<sup>®</sup> Abstract published in *Advance ACS Abstracts*, May 1, 1995.  
(1) (a) Moloy, K. G.; Wegman, R. W. *Organometallics* 1989, 8, 2883.  
(b) Moloy, K. G.; Wegman, R. W. In *Homogeneous Transition Metal Catalyzed Reactions*; Moser, W. R., Slocum, D. W., Eds.; Advances in Chemistry Series 230; American Chemical Society: Washington, D.C., 1992; p 323.

## Scheme 1

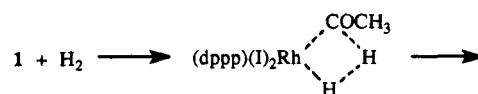


## Scheme 2



lation and hydrogenation.<sup>2</sup> The Rh–C intermediates in these latter transformations involve Rh(I), and the hydrogenolysis is believed to involve oxidative addition of  $\text{H}_2$ , followed by reductive elimination of C–H from the resulting Rh(III) dihydride (Scheme 2).

Complex **1**, however, presents a possible dilemma in that it contains Rh(III). In our previous report<sup>1</sup> we demonstrated the reaction of **1** with  $\text{H}_2$  to liberate  $\text{CH}_3\text{CHO}$  and **2**. The lack of reactivity of **1** toward hydride or proton donors, as well as kinetic evidence, suggested that the catalytic reaction may involve direct reaction of **1** with  $\text{H}_2$ . While many potential mechanisms for this transformation can be envisioned, an intriguing possibility is the  $\sigma$ -bond metathesis shown in eq 1. Rhod-



**2** +  $\text{CH}_3\text{CHO}$  (1)  
ium in **1** is  $d^6$ , 16 e, and therefore unsaturated. It is

(2) Collman, J. P.; Hegedus, L. S.; Norton, J. R.; Finke, R. G. *Principles and Applications of Organotransition Metal Chemistry*; University Science Books: Mill Valley, CA, 1987; p 524, 625.

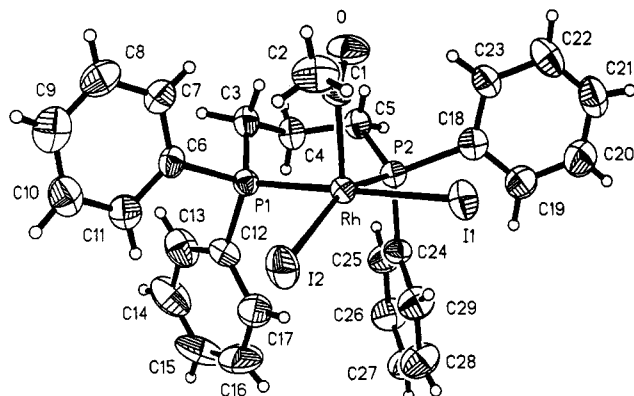


**Figure 1.** Perspective (ORTEP) drawing of complex **1** showing the atom-labeling scheme.

possible that the empty coordination site may be available to activate  $H_2$  in such a manner, possibly *via* a Rh- $(\eta^2-H_2)$  intermediate.<sup>3</sup> A concern with this proposal is that, by analogy with related structurally characterized complexes  $RhP_2X_2Y$ ,<sup>4,5</sup> **1** is presumed to possess the sbp geometry shown in Scheme 1. This places the empty orbital available for  $H_2$  activation in a position *trans* to the acetyl ligand. Although five-coordinate molecules are characteristically fluxional, we sought to determine if **1** indeed possesses a sbp geometry. The solid state structure of hydride **2** is also described, which shows that this complex is actually a dimer. This result corrects our previous structural assignment<sup>1a</sup> for **2** and also serves to underscore the unsaturated nature of **1**. Finally, we report a preliminary observation on the heterolytic activation of  $H_2$  by **1**.

### Results and Discussion

The solid state structure of complex **1** was determined by X-ray crystallography, and an ORTEP drawing of the molecule is shown in Figure 1; important bond lengths and angles are provided in Table 1. As expected, the complex contains a five-coordinate Rh(III) ion. The dppp bite angle of  $90.5^\circ$  is within the range found for other complexes of this ligand. The conformation of the chelate ring is that of a "flattened boat" as generally found for this particular ligand.<sup>6</sup>

The bonding parameters involving the acetyl group are not unusual. The Rh-C bond length, 1.981(6) Å, is within the range observed for similar acyl complexes of the type  $Rh(COR)X_2P_2$  (X = halide).<sup>4</sup> While previous reports of related acyl complexes have suggested that these Rh-C bond lengths (1.95–2.0 Å) are unusually short and indicative of substantial metal to ligand back-bonding, we disagree with this conclusion. The Rh-C bond length in **1** is slightly shorter than that recently

(3) (a) Kubas, G. J. *Acc. Chem. Res.* **1988**, *21*, 120. (b) Jessop, P. G.; Morris, R. H. *Coord. Chem. Rev.* **1992**, *121*, 155.

(4) (a) Shie, J.-Y.; Lin, Y.-C.; Wang, Y. *J. Organomet. Chem.* **1989**, *371*, 383. (b) McGuigan, M. F.; Doughty, D. H.; Pignolet, L. H. *J. Organomet. Chem.* **1980**, *185*, 241. (c) Slack, D. A.; Egglestone, D. L.; Baird, M. C. *J. Organomet. Chem.* **1978**, *146*, 71. (d) Egglestone, D. L.; Baird, M. C.; Lock, C. J. L.; Turner, G. J. *J. Chem. Soc. Dalton* **1977**, 1576. (e) Cheng, C.-H.; Eisenberg, R. *Inorg. Chem.* **1979**, *18*, 1418. (f) Cheng, C.-H.; Spivack, B. D.; Eisenberg, R. *J. Am. Chem. Soc.* **1977**, *99*, 3003.

(5) (a) Fawcett, J.; Holloway, J. H.; Saunders, G. C. *Inorg. Chim. Acta* **1992**, *202*, 111. (b) The structure of  $Rh(CH_3)(I)_2(PPh_3)_2$  has also been reported (Rh-CH<sub>3</sub> = 2.081 Å): Troughton, P. G. H.; Skapski, A. C. *J. Chem. Soc., Chem. Commun.* **1968**, 575.

(6) Andrews, M. A.; Voss, E. J.; Gould, G. L.; Klooster, W. T.; Koetzle, T. F. *J. Am. Chem. Soc.* **1994**, *116*, 5730.

**Table 1.** Selected Interatomic Distances (Å) and Bond Angles (deg) in  $Rh[Ph_2P(CH_2)_3PPh_2](COCH_3)I_2$  (**1**)<sup>a</sup>

Interatomic Distances			
Rh-I1	2.6768(5)	Rh-I2	2.7263(5)
Rh-P1	2.299(1)	Rh-P2	2.276(1)
P1-C3	1.817(6)	P2-C5	1.829(6)
P1-C6	1.821(5)	P2-C18	1.830(5)
P1-C12	1.806(5)	P2-C24	1.834(5)
Rh-C1	1.981(6)	O-C1	1.182(7)
C1-C2	1.513(9)	C3-C4	1.527(8)
C4-C5	1.526(8)		

Range of C-C distances in phenyl rings: 1.350(11)–1.399(9)

Bond Angles			
I1-Rh-I2	89.15(2)	P1-Rh-P2	90.49(5)
I1-Rh-P1	179.36(4)	I2-Rh-P2	156.79(4)
I1-Rh-P2	90.15(3)	I2-Rh-P1	90.23(4)
C1-Rh-I1	90.4(2)	C1-Rh-I2	108.6(2)
C1-Rh-P1	89.7(2)	C1-Rh-P2	94.6(2)
Rh-P1-C3	113.6(2)	Rh-P2-C5	118.4(2)
Rh-P1-C6	115.6(2)	Rh-P2-C18	119.8(2)
Rh-P1-C12	115.7(2)	Rh-P2-C24	105.3(2)
C3-P1-C6	102.4(3)	C5-P2-C18	100.1(2)
C3-P1-C12	103.3(2)	C5-P2-C24	107.0(2)
C6-P1-C12	104.6(2)	C18-P2-C24	105.1(2)
P1-C3-C4	114.5(4)	P2-C5-C4	117.3(4)
C3-C4-C5	115.0(4)	Rh-C1-O1	125.7(5)
Rh-C1-C2	113.1(4)	C2-C1-O	121.1(6)

range of C-C-C bond angles: 117.8(5)–121.2(7)

range of P-C-C bond angles: 117.9(4)–122.7(4)

<sup>a</sup> The esd's for the interatomic distances and bond angles were calculated from the standard errors of the fractional coordinates of the corresponding atomic parameters.

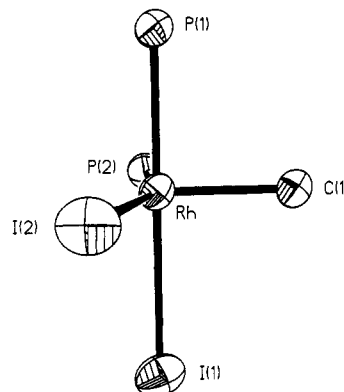
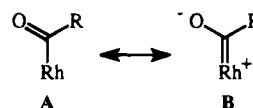


**Figure 2.** ORTEP view of **1** showing the coordination environment about rhodium.

reported for *trans*- $Rh(Ph)(Cl)_2(PPh_3)_2$  (2.016(3) Å).<sup>5a</sup> In addition, the carbonyl stretching frequency for **1** ( $1698\text{ cm}^{-1}$ ) is found at the high end of the range for  $\eta^1$ -acyl complexes, which more commonly are found to absorb at or below *ca.*  $1650\text{ cm}^{-1}$ .<sup>7</sup> Also, we reported previously that **1** is unreactive toward even very potent acids. For example, the IR spectrum of **1** is unchanged upon the addition of HOTf. Together, these results lead us to disfavor a significant resonance contribution involving metal to ligand back-bonding such as that shown by **B**.



While the gross structural features are within expectations, close inspection reveals a significant distortion

(7) (a) Reference 2, p 107. (b) Hitam, R. B.; Narayanaswamy, R.; Rest, A. J. *J. Chem. Soc., Dalton Trans.* **1983**, 615.

of the molecular structure of **1** from an ideal sbp geometry. Most notable is the linear ( $179.4^\circ$ ) P(1)–Rh–I(1) arrangement, which may be compared with the P(2)–Rh–I(2) angle of  $156.8^\circ$ . As a result of this disparity the four basal donor atoms of the ideal square base pyramid (P(1), P(2), I(1), and I(2)) no longer lie in a plane. Figure 2 depicts clearly this distortion of the rhodium coordination sphere. This structural feature should be compared and contrasted with the related complexes Rh(COPh)Cl<sub>2</sub>(dppp) (P–Rh–Cl =  $163.5^\circ$ ,  $169.8^\circ$ )<sup>4b</sup> and *cis*-Rh(COCH<sub>2</sub>CH<sub>3</sub>)Cl<sub>2</sub>(PPh<sub>3</sub>)<sub>2</sub> (P–Rh–Cl =  $166.7^\circ$ ,  $161.2^\circ$ )<sup>4a</sup> in which each pair of corresponding angles are much more similar and the four basal donor atoms nearly form a plane. Related structurally-characterized complexes of the type *trans*-Rh(R)(X)<sub>2</sub>(PPh<sub>3</sub>)<sub>2</sub> also exhibit nearly ideal sbp geometries.<sup>5</sup> The structure of **1** appears to be approaching that of a trigonal bipyramid. This distortion does not lie on the Berry coordinate, however.<sup>8</sup> Such interconversions involve a concerted movement of ligands, and this is not observed in **1**. The deviation from the "tbp" geometry is reflected by the varied bond angles in the equatorial plane passing through C(1), P(2), and I(2). Although the sum of these angles is  $360^\circ$ , the individual values vary widely from  $94.6^\circ$  (C(1)–Rh–P(2)) to  $108.6^\circ$  (C(1)–Rh–I(2)) to  $156.8^\circ$  (P(2)–Rh–I(2)). Similar distortions have been reported<sup>9</sup> for five-coordinate, d<sup>6</sup> complexes with bulky, mutually *trans* monodentate phosphine ligands. It is not yet clear how or if the electronic explanations for the distortions in the *trans* structures apply to **1**, where the phosphines are *cis*.

Although rhodium in complex **1** is 16 e we find no evidence for an additional donor interaction to alleviate this unsaturation. Inspection of the crystal-packing diagram shows that there are no intermolecular distances within bonding range. It has been reported<sup>5a</sup> that the sbp complex *trans*-Rh(Ph)Cl<sub>2</sub>(PPh<sub>3</sub>)<sub>2</sub> possesses agostic interactions with *ortho* hydrogens on two of the phosphine phenyl groups (Rh–H = 2.87, 2.84 Å). Although two of the dppp phenyl rings flank the empty coordination site *trans* to the acetyl ligand, the shortest Rh–H contact involving the dppp ligand in **1** is 2.99 Å. We do not attribute this to a bonding interaction. The shortest intramolecular contact of this type in **1** involves the acetyl methyl group with a Rh–H distance of 2.85 Å. Agostic interactions with acetyl ligands have been observed previously.<sup>10</sup> However, they are accompanied by significant angular distortions about the carbonyl carbon. The acetyl ligand in **1** is tilted slightly so as to move the methyl group closer to rhodium, but this distortion is significantly smaller than that previously found for agostic acyls. The absence of a significant decrease in the Rh–C–O angle of **1** further demon-

strates the lack of an  $\eta^2$ -acetyl interaction.<sup>11</sup> This result is perhaps surprising considering that the related complexes Ru(COR)(Cl)(CO)(PPh<sub>3</sub>)<sub>2</sub> achieve saturation *via* formation of an  $\eta^2$  acyl linkage (in fact, these are the first  $\eta^2$ -acyl complexes to have been reported).<sup>12</sup> It is possible that rhodium, being less oxophilic than ruthenium, prefers  $\pi$ -donation from the iodide ligands<sup>13</sup> to alleviate this unsaturation as an alternative to  $\eta^2$ -acetyl formation.

The unsaturated nature of the rhodium center in complex **1** is nicely demonstrated by the structure of hydride **2**. An ORTEP drawing of the molecule is shown in Figure 3, and selected bond distances and angles are provided in Table 2. X-ray crystallography shows that **2** is actually a centrosymmetric dimer, correcting our previous structural assignment. This dimeric structure resembles that assigned by Osborn to related iridium complexes.<sup>14</sup> Thus, simply replacing the acetyl ligand with a sterically less demanding hydride ligand is sufficient to allow the formation of iodo bridges and a more stable 18 e configuration at rhodium.<sup>15</sup> Bond distances and angles for **2** are all within the expected ranges.

The structural data presented here demonstrate the unsaturated nature of **1**. Moreover, the distorted nature of this complex suggests the potential for an open coordination site *cis* to the acetyl ligand as the limiting *tbp* geometry places this vacant coordination site in the equatorial plane defined by C(1), P(2), and I(2). Extensive NMR studies have to date failed to detect any interaction between **1** and H<sub>2</sub> (e.g., Rh–( $\eta^2$ -H<sub>2</sub>)). It is known, however, that such species are very acidic and that they may often be intercepted with base.<sup>3, 9a, 16</sup> To test this possibility we examined the reactivity of **1** with H<sub>2</sub> in the presence of amine bases such as Et<sub>3</sub>N and DMAP.

Complex **1** reacts with H<sub>2</sub> only under forcing conditions (120 °C, 120 psi) to generate **2** and CH<sub>3</sub>CHO. These conditions approach those employed in the catalytic reaction, consistent with the conclusion that hydrogenolysis of **1** to **2** is the catalytic rate-determining step. In the presence of base (DMAP, Et<sub>3</sub>N), however, **1** activates H<sub>2</sub> at significantly reduced temperature. NMR and IR spectral monitoring show the formation of Et<sub>3</sub>NH<sup>+</sup> and a new rhodium complex. This new complex exhibits an acetyl band in the IR at 1708 cm<sup>-1</sup>, which is shifted to a slightly higher frequency than **1**.

(11) Durfee, L. D.; Rothwell, I. P. *Chem. Rev.* **1988**, *88*, 1059.

(12) (a) Roper, W. R.; Taylor, G. E.; Waters, J. M.; Wright, L. J. *J. Organomet. Chem.* **1979**, *182*, C46. (b) Hitch, R. R.; Gondal, S. K.; Sears, C. T. *J. Chem. Soc., Chem. Commun.* **1971**, 777.

(13) (a) Poulton, J. T.; Sigalas, M. P.; Eisenstein, O.; Caulton, K. G. *Inorg. Chem.* **1993**, *32*, 5490. (b) Poulton, J. T.; Foltling, K.; Streib, W. E.; Caulton, K. G. *Inorg. Chem.* **1992**, *31*, 3190.

(14) (a) Ng Cheong Chan, Y.; Osborn, J. A. *J. Am. Chem. Soc.* **1990**, *112*, 9400. (b) RhHCl<sub>2</sub>(dppp) has been formulated as both a dimer and a monomer: Faraone, F.; Bruno, G.; Schiavo, S. L.; Tresoldi, G.; Bombieri, G. *J. Chem. Soc., Dalton Trans.* **1983**, 433.

(15) The unsaturated nature of **1** is also demonstrated by the reports that the Rh(III) acyl complexes Rh(COR)X<sub>2</sub>(CO)(PR<sub>3</sub>)<sub>1.5a</sub> and [Me<sub>3</sub>PhN]<sub>2</sub>[Rh<sub>2</sub>(COCH<sub>3</sub>)<sub>2</sub>(CO)<sub>2</sub>]<sub>1.5b</sub> are dimeric, achieving saturation through the formation of halide bridges. (a) Doyle, M. J.; Mayanza, A.; Bonnet, J.-J.; Kalck, P.; Poilblanc, R. *J. Organomet. Chem.* **1978**, *146*, 293. (b) Adamson, G. W.; Daly, J. J.; Forster, D. *J. Organomet. Chem.* **1974**, *71*, C17.

(16) (a) Cappellani, E. P.; Drouin, S. D.; Jia, G.; Maltby, P. A.; Morris, R. H.; Schweitzer, C. T. *J. Am. Chem. Soc.* **1994**, *116*, 3375. (b) Chinn, M. S.; Heinekey, D. M. *J. Am. Chem. Soc.* **1987**, *109*, 5865. (c) Kristjansdottir, S. S.; Norton, J. R. In *Transition Metal Hydrides: Recent Advances in Theory and Experiment*; Dedieu, A., Ed.; VCH: New York, 1991; Chapter 10.

(8) Holmes, R. R. *Progress in Inorganic Chemistry*; Lippard, S. J., Ed.; John Wiley & Sons: New York, 1984; Vol. 32, p 119.

(9) (a) Albinati, A.; Bakmutov, V. I.; Caulton, K. G.; Clot, E.; Eckert, J.; Eisenstein, O.; Gusev, D. G.; Grushin, V. V.; Hauger, B. E.; Klooster, W. T.; Koetzle, T. F.; McMullan, R. K.; O'Loughlin, T. J.; Pélissier, M.; Ricci, J. S.; Sigalas, M. P.; Vymenits, A. B. *J. Am. Chem. Soc.* **1993**, *115*, 7300. (b) Riehl, J.-F.; Jean, Y.; Eisenstein, O.; Pélissier, M. *Organometallics* **1992**, *11*, 729. (c) Rachidi, I. E.-I.; Jean, Y.; Eisenstein, O. *New J. Chem.* **1990**, *14*, 671. (d) Harlow, R. L.; Thorn, D. L.; Baker, R. T.; Jones, N. L. *Inorg. Chem.* **1992**, *31*, 993.

(10) (a) Contreras, L.; Monge, A.; Pizzano, A.; Ruiz, C.; Sánchez, L.; Carmona, E. *Organometallics* **1992**, *11*, 3971. (b) Carmona, E.; Contreras, L.; Poveda, M. L.; Sánchez, L. *J. Am. Chem. Soc.* **1991**, *113*, 4322.

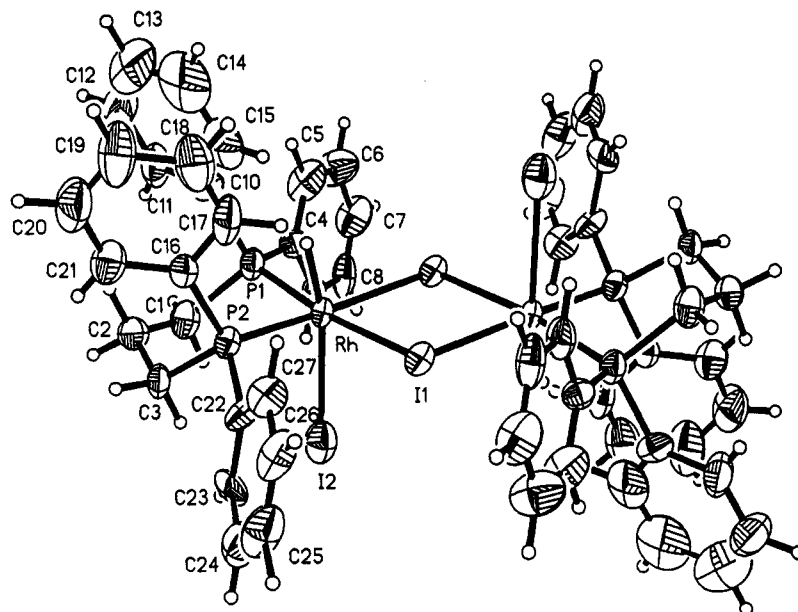


**Figure 3.** ORTEP drawing of hydride **2** (molecule **1**).

**Table 2. Selected Interatomic Distances (Å) and Bond Angles (deg) in  $\{\text{Rh}[\text{Ph}_2\text{P}(\text{CH}_2)_3\text{PPh}_2](\text{H})\text{I}(\mu\text{-I})_2\}_2$**

	Molecule A	Molecule B
Interatomic Distances		
Rh...Rh*	4.085(2)	4.085(2)
Rh-I1	2.709(1)	2.710(1)
Rh-I1*	2.712(1)	2.711(2)
Rh-I2	2.861(2)	2.859(1)
Rh-P1	2.261(4)	2.264(3)
Rh-P2	2.259(3)	2.261(4)
I1...I1*	3.564(2)	3.563(2)
P1...P2	3.185(4)	3.194(6)
P1-C1	1.82(2)	1.84(1)
P1-C4	1.83(1)	1.82(2)
P1-C10	1.82(1)	1.83(1)
P2-C3	1.82(2)	1.81(1)
P2-C16	1.81(1)	1.83(1)
P2-C22	1.83(1)	1.84(2)
C1-C2	1.53(2)	1.54(3)
C2-C3	1.57(2)	1.56(2)
Bond Angles		
I1-Rh-I1*	82.20(4)	82.19(4)
I1-Rh-I2	91.19(4)	91.25(4)
I1-Rh-P1	172.8(1)	172.6(1)
I1-Rh-P2	94.4(1)	94.4(1)
I2-Rh-I1*	93.78(4)	93.88(4)
I2-Rh-P1	94.8(1)	94.7(1)
I2-Rh-P2	91.1(1)	91.1(1)
P1-Rh-I1*	93.3(1)	93.1(1)
P1-Rh-P2	89.6(1)	89.8(1)
P2-Rh-I1*	174.1(1)	174.0(1)
Rh-I1-Rh*	97.80(4)	97.81(4)
C1-P1-C4	105.2(7)	105.2(7)
C1-P1-C10	102.6(7)	102.6(7)
C4-P1-C10	103.4(5)	103.6(7)
C3-P2-C16	105.7(7)	105.8(6)
C3-P2-C22	102.1(7)	102.4(6)
C16-P2-C22	102.1(6)	102.3(7)
C2-C1-P1	112(1)	112.6(9)
C1-C2-C3	115(1)	113(1)
C2-C3-P2	115(9)	116.4(9)

This new complex has been identified as the dichloride  $\text{Rh}(\text{COCH}_3)\text{Cl}_2(\text{dppp})$  (**3**). Confirmation of this assignment was obtained through an alternate synthesis of **3** (reaction of **1** with  $\text{Cl}^-$ ). Reaction of **1** with  $\text{D}_2$  in the presence of  $\text{Et}_3\text{N}$  cleanly produces  $\text{Et}_3\text{ND}^+$  and **3**. Presumably, a rhodium hydride is generated which abstracts chloride from the  $\text{CH}_2\text{Cl}_2$  solvent, generating

$\text{Rh}-\text{Cl}$  bonds and  $\text{CH}_3\text{Cl}$ ; formation of the latter has not yet been confirmed.<sup>17</sup>

These preliminary results reveal that **1** is indeed able to participate in the heterolytic activation of  $\text{H}_2$ . Although cleavage of  $\text{Rh}-\text{I}$  bonds, rather than  $\text{Rh}-\text{COCH}_3$ , occurs under the conditions reported here, these observations suggest that the vacant coordination site on **1** may be an important consideration in the catalytic conversion of methanol to acetaldehyde. Further studies of the activation of  $\text{H}_2$  by **1**, as well as careful consideration of other potential mechanisms for the conversion of **1** to **2**, are required to more fully understand the chemistry of this pivotal intermediate.

## Experimental Section

**General Considerations.** The syntheses and spectroscopic properties of **1** and **2** have been reported previously. Crystals suitable for X-ray diffraction were grown by slowly cooling saturated methanol (**1**) or toluene (**2**) solutions of the complex. All manipulations were routinely conducted under an inert atmosphere ( $\text{N}_2$ ) using Schlenk or glovebox techniques. Solvents were Aldrich anhydrous grade material and used as received. DMAP (4-(dimethylamino)pyridine) and  $\text{Et}_3\text{N}$  were obtained from commercial sources.

Proton and phosphorus NMR data were collected in the Union Carbide Corp. NMR Skill Center using General Electric GN-300NB and QE-300 spectrometers (each are 300 MHz  $^1\text{H}$ ).  $^1\text{H}$  NMR spectra were referenced to TMS *via* solvent peaks, and the  $^{31}\text{P}$  spectra were referenced externally to 85% phosphoric acid. Infrared spectra were recorded on a Nicolet 205 FTIR spectrometer as solutions in  $\text{CaF}_2$  cells.

**X-ray Structural Analyses of  $\text{Rh}[\text{Ph}_2\text{P}(\text{CH}_2)_3\text{PPh}_2](\text{COCH}_3)\text{I}_2$  and  $\{\text{Rh}[\text{Ph}_2\text{P}(\text{CH}_2)_3\text{PPh}_2](\text{H})\text{I}(\mu\text{-I})_2\}_2$ .** The same general procedures were utilized to perform the X-ray structural analyses of  $\text{Rh}[\text{Ph}_2\text{P}(\text{CH}_2)_3\text{PPh}_2](\text{COCH}_3)\text{I}_2$  and  $\{\text{Rh}[\text{Ph}_2\text{P}(\text{CH}_2)_3\text{PPh}_2](\text{H})\text{I}(\mu\text{-I})_2\}_2$ . Crystalline samples of these two

(17) In related chemistry the complexes  $\text{L}_2\text{Rh}(\text{H})\text{Cl}_2$  ( $\text{L} = \text{P}^i\text{Pr}_3, \text{PCy}_3$ ) have been reported to catalyze the hydrogenolysis of chloroarenes to arenes. It has been suggested that these reactions may proceed through  $\text{Rh}-(\eta^2\text{-H}_2)$  intermediates. See: (a) Grushin, V. V.; Alper, H. *Chem. Rev.* **94**, 1047. (b) Grushin, V. V.; Alper, H. *Organometallics* **1991**, *10*, 1620. (c) Grushin, V. V. *Acc. Chem. Res.* **1993**, *26*, 279.



**Table 3. Crystallographic Data for the X-ray Diffraction Analysis of Rh[Ph<sub>2</sub>P(CH<sub>2</sub>)<sub>3</sub>PPh<sub>2</sub>](COCH<sub>3</sub>)I<sub>2</sub> and {Rh[Ph<sub>2</sub>P(CH<sub>2</sub>)<sub>3</sub>PPh<sub>2</sub>](H)(I)(μ-I)}<sub>2</sub>**

Crystal Data		
empirical formula	C <sub>26</sub> H <sub>26</sub> RhI <sub>2</sub> OP <sub>2</sub>	C <sub>54</sub> H <sub>54</sub> Rh <sub>2</sub> I <sub>4</sub> P <sub>4</sub>
color	red-orange	red
cryst dimens, mm <sup>3</sup>	0.125 × 0.325 × 0.55	0.140 × 0.210 × 0.275
temp, K	295(2)	295(2)
cryst syst	monoclinic	triclinic
space group	P2 <sub>1</sub> /n (C <sub>2h</sub> <sup>5</sup> , No. 14)	P $\bar{1}$ (C <sub>i</sub> <sup>1</sup> , No. 2)
a, Å	10.339(2)	10.037(3)
b, Å	10.238(2)	15.108(4)
c, Å	27.269(6)	20.131(5)
α, deg		78.87(2)
β, deg	95.17(2)	75.59(2)
γ, deg		70.60(2)
V, Å <sup>3</sup>	2874.6(11)	2768.3(9)
Z	4	2
fw, amu	812.21	1540.34
calcd density, g/cm <sup>3</sup>	1.876	1.848
μ, cm <sup>-1</sup>	29.215	30.13
F(000)	1088	784
Data Collection and Structural Analyses		
scan type	θ-2θ, fixed	θ-2θ, fixed
scan rate, deg/min	2.00	4.00
scan width	1.1 + 0.9 tan θ	1.1 + 0.8 tan θ
2θ range, deg	5.0-50.0	5.0-45.0
index ranges	-12 ≤ h ≤ 12; 0 ≤ k ≤ 12; 0 ≤ l ≤ 32	-12 ≤ h ≤ 12; -17 ≤ k ≤ 17; 0 ≤ l ≤ 32
no. of reflns collected	5218	8460
agreement between equiv data, R <sub>av</sub> (F <sub>o</sub> )	0.035	0.019
total no. of unique data	5103	
obsd data criteria	F <sub>o</sub> > σ(F <sub>o</sub> )	F <sub>o</sub> > σ(F <sub>o</sub> )
no. of obsd data	4508	5466
abs corr	face-indexed	face-indexed
range of transmissn coeff	0.534-0.785	0.57-0.70
p	0.03	0.03
refinement method	full matrix on F <sup>2</sup>	full matrix on F <sup>2</sup>
discrepancy indices		
R(F <sub>o</sub> )	0.044	0.056
R(F <sub>o</sub> <sup>2</sup> )	0.050	0.072
R <sub>w</sub> (F <sub>o</sub> <sup>2</sup> )	0.080	0.116
σ <sub>1</sub> , GOF	1.67	2.23
no. of variables	408	577
data to param ratio	12.5:1	9.5:1

compounds were sealed in glass capillary tubes under a nitrogen atmosphere and then optically aligned on a Picker full-circle goniostat under computer control by a Krisel Control diffractometer automation system. After the indexing<sup>18</sup> of a series of low-angle reflections and the calculation of a preliminary set of lattice parameters, the orientation angles of 20 higher order reflections were optimized by an automatic peak-centering routine<sup>19</sup> and then least-squares fitted to provide the corresponding refined lattice parameters and the orientation matrix.

Intensity data were measured with Zr-filtered Mo Kα radiation with a take-off angle of 2°. Peak scans employed a fixed scan rate and a variable scan width. The integrated intensity, *I*, and its standard deviation, σ(*I*), for each measured reflection were calculated from the expressions  $I = \omega(S/t_s - B/t_b)$  and  $\sigma(I) = \omega(S/t_s^2 + B/t_b^2)^{1/2}$ , where *S* is the total scan count measured in time *t<sub>s</sub>* and *B* is the combined background count in time *t<sub>b</sub>*. The standard deviation of the square of each structure factor,  $F_o^2 = AI/Lp$ , was calculated from  $\sigma(F_o^2) = [\sigma_c(F_o^2)^2 + (pF_o^2)^2]^{1/2}$ . The observed data were corrected for sample decay, absorption,<sup>20</sup> and Lorentz-polarization effects. Duplicate reflections were averaged. Additional crystallographic information is provided in Table 1.

The initial coordinates for the Rh and I atoms of Rh[Ph<sub>2</sub>P(CH<sub>2</sub>)<sub>3</sub>PPh<sub>2</sub>](COCH<sub>3</sub>)I<sub>2</sub> and {Rh[Ph<sub>2</sub>P(CH<sub>2</sub>)<sub>3</sub>PPh<sub>2</sub>](H)(I)(μ-I)}<sub>2</sub>

I<sub>2</sub> were interpolated from an E-map calculated on the basis of the initial phases determined by MULTAN78.<sup>21</sup> Approximate coordinates for the remaining non-hydrogen atoms were obtained by Fourier methods and then refined with anisotropic thermal parameters. The hydrogen atoms were initially located using difference Fourier calculations based on only low-angle data with (sin θ/λ) < 0.40 Å<sup>-1</sup> and then later adjusted with the aid of MIRAGE.<sup>22</sup>

During the refinement of Rh[Ph<sub>2</sub>P(CH<sub>2</sub>)<sub>3</sub>PPh<sub>2</sub>](COCH<sub>3</sub>)I<sub>2</sub>, it became apparent that the sample contained a detectable amount of Rh[Ph<sub>2</sub>P(CH<sub>2</sub>)<sub>3</sub>PPh<sub>2</sub>]<sub>3</sub>. A small residual peak in the difference Fourier map is located at ca. 2.7 Å from the central Rh atom and occupies the same general coordination site as the acyl ligand. A correction for the residual iodide was introduced by reducing the occupancy factors of O, C1, C2, H1, H2, and H3 from 1.000 to 0.977 and introducing a third iodine atom with an occupancy of 0.023. The position and occupancy factor of the residual iodine atom were refined with an isotropic thermal model. Full-matrix refinement<sup>23</sup> of the positional and anisotropic thermal parameters for the 35 non-hydrogen atoms, the coordinated and isotropic temperature factors for the residual iodide, and the positional para-

(20) The absorption correction was performed with the use of the general polyhedral shape routine of DTALIB. The distance from the crystal center to each face and the orientation angles (φ and χ) used to place each face in diffracting position are required to define the crystal's shape, size, and orientation with respect to the diffractometer's coordinate system.

(21) Declercq, J. P.; Germain, D.; Main, P.; Woolfson, M. M. *Acta Crystallogr. Sect. A* **1973**, *A29*, 231.

(22) Calabrese, J. C. Ph.D. Dissertation, University of Wisconsin, Madison, WI, 1971; Appendix II.

(18) This automatic reflection-indexing algorithm is based upon Jacobson's procedure: Jacobson, R. A. *J. Appl. Crystallogr.* **1976**, *9*, 115.

(19) This peak-centering algorithm is similar to that described by Busing; Busing, W. R. *Crystallographic Computing*; Ahmed, F. R., Ed.; Munksgaard: Copenhagen, Denmark, 1970; p 319. The ω, χ, and 2θ angles were optimized with respect to the Kα<sub>1</sub> peak (λ = 0.709 26 Å).

meters with fixed isotropic contributions for the 29 hydrogen atoms converged with final discrepancy indices of  $R(F_o) = 0.044$ ,  $R(F_o^2) = 0.050$ , and  $R_w(F_o^2) = 0.080$  with  $\sigma_1 = 1.67$  for the 4508 reflections with  $F_o^2 > \sigma(F_o^2)$ . The final difference map contained no additional regions of significant electron density. Selected interatomic distances and bond angles and their esd's for the non-hydrogen atoms are given in Table 2.

In the crystallographic setting used to collect the X-ray data for  $\{\text{Rh}[\text{Ph}_2\text{P}(\text{CH}_2)_3\text{PPh}_2](\text{H})\text{I}(\mu\text{-I})\}_2$ , the two molecular dimers lie on different crystallographic centers of inversion. Therefore, the asymmetric unit consists of two independent  $\text{Rh}[\text{Ph}_2\text{P}(\text{CH}_2)_3\text{PPh}_2](\text{H})\text{I}_2$  molecular fragments. The terminal hydride ligand, H27, was located but not varied. Full-matrix refinement<sup>23</sup> (based on  $F_o^2$ ) of the positional and anisotropic thermal parameters for the 64 non-hydrogen atoms with fixed isotropic contributions for the 54 hydrogen atoms converged with final discrepancy indices of  $R(F_o) = 0.056$ ,  $R(F_o^2) = 0.072$ , and  $R_w(F_o^2) = 0.116$  with  $\sigma_1 = 2.23$  for the 5466 reflections with  $F_o^2 > \sigma(F_o^2)$ . The final difference map contained a residual peak at *ca.* 1.0 Å from the terminal iodine atom, I2, and was lying nearly along the Rh–I2 vector. Interatomic distances and bond angles and their esd's for the non-hydrogen atoms are given in Table 3.

**Preparation of  $\text{Rh}(\text{dppp})(\text{COCH}_3)(\text{Cl})_2$  (**3**) from **1**,  $\text{H}_2$ , and Base.** A glass pressure reactor (Fischer–Porter bottle) was charged with 1.03 g (1.27 mmol) of **1**, 0.200 g (1.63 mmol) of DMAP, 55 mL of  $\text{CH}_2\text{Cl}_2$ , and a magnetic stir bar. The bottle was connected to a high-pressure gas manifold. After purging, the vessel was charged with 80 psi of  $\text{H}_2$  and then immersed in a 70 °C oil bath. After *ca.* 15 h the solution turned from yellow–orange to yellow. A small amount of precipitate was removed by filtration, and the solvent was removed under vacuum. The residue was washed with MeOH, and the solid product was dried. Recrystallization from  $\text{CH}_2\text{Cl}_2$

$\text{Cl}_2$  provided yellow crystals of **3** contaminated with small amounts of  $\text{Rh}(\text{COCH}_3)(\text{Cl})(\text{I})(\text{dppp})$  (see below). Yield: 0.40 g, 50%. <sup>31</sup>P NMR ( $\text{CD}_2\text{Cl}_2$ ):  $\delta$  24.3, d,  $J_{\text{Rh-P}} = 136$  Hz. <sup>1</sup>H NMR ( $\text{CD}_2\text{Cl}_2$ ):  $\delta$  7.8–7.2 (m, 20H), 2.93 (s, 3H), 2.44 (m, 4H), 1.64 (m, 2H). These data are consistent with those previously reported<sup>4c</sup> for **3**. Analysis (IR, NMR) of the MeOH extracts showed the presence of  $[\text{DMAPH}][\text{I}]$  and unreacted DMAP.

Similar results are obtained with  $\text{Et}_3\text{N}$ . A control experiment, omitting base, resulted in recovery of intact **1** after the above treatment.

**Preparation of **3** From **1** and  $\text{Et}_4\text{NCl}$ .** Solutions of **1** (0.095 g, 0.12 mmol, in 6 mL) and  $\text{Et}_4\text{NCl}$  (0.055 g, 0.33 mmol, in 2 mL) were prepared in  $\text{CH}_2\text{Cl}_2$ . The  $\text{Et}_4\text{NCl}$  solution was added to the solution of **1** in 0.5 mL aliquots, and the reaction was monitored by IR. The solution turned from yellow–orange to yellow during the titration, and the carbonyl absorption attributable to the acetyl ligand shifted from 1698 to 1708  $\text{cm}^{-1}$ . The solvent was then removed in vacuo, and the resulting product was washed well with MeOH. <sup>31</sup>P NMR ( $\text{CD}_2\text{Cl}_2$ ) showed the product to be complex **3**.

In a separate experiment, **1** was treated with 1 equiv of  $\text{Et}_4\text{NCl}$ , and the product was isolated as described above. <sup>31</sup>P NMR showed, in addition to resonances attributable to **1** and **3**, an ABX spectrum assignable to the mixed halide  $\text{Rh}(\text{COCH}_3)(\text{Cl})(\text{I})(\text{dppp})$ :  $P_a$   $\delta$  21.3, dd,  $J_{\text{Rh-P}_a} \approx 169$  Hz;  $P_b$   $\delta$  20.2, dd,  $J_{\text{Rh-P}_b} \approx 162$  Hz;  $J_{P_a-P_b} \approx 22$  Hz.<sup>25</sup>

**Acknowledgment.** Helpful discussions with Professor K. G. Caulton are gratefully acknowledged. T. L. Fortin is thanked for laboratory assistance. This work was partially funded by the U.S. Department of Energy under Contracts DE-AC22-84PC70022 and DE-AC22-86PC90013. We thank Union Carbide Corporation for permission to publish these results.

**Supplementary Material Available:** Tables of positional parameters, thermal parameters, and bond distances and angles, for complexes **1** and **2** (14 pages). Ordering information is given on any current page.

OM950139W

(23) The least-squares refinements<sup>24</sup> of the X-ray diffraction data were based upon the minimization of  $\sum w_i |F_o^2 - S^2 F_c^2|^2$ , where  $w_i$  is the individual weighting factor and  $S$  is the scale factor. The discrepancy indices were calculated from the expressions  $R(F_o) = \sum |F_o| - |F_c| / \sum |F_o|$ ,  $R(F_o^2) = \sum |F_o^2 - F_c^2| / \sum F_o^2$ , and  $R_w(F_o^2) = [\sum (w_i |F_o^2 - F_c^2|^2) / \sum (w_i F_o^4)]^{1/2}$ . The standard deviation of an observation of unit weight (GOF) was computed from  $[\sum (w_i |F_o^2 - F_c^2|^2) / (n - p)]^{1/2}$ , where  $n$  is the number of reflections and  $p$  is the number of parameters varied during the last refinement cycle.

(24) The scattering factors employed in all of the structure factor calculations were those of Cromer and Mann<sup>24a</sup> for the non-hydrogen atoms and those of Stewart *et al.*<sup>24b</sup> for the hydrogen atoms with corrections included for anomalous dispersion.<sup>24c</sup> (a) Cromer, D. T.; Mann, J. B. *Acta Crystallogr., Sect. A* **1968**, *A24*, 321. (b) Stewart, R. F.; Davidson, E. R.; Simpson, W. T. *J. Chem. Phys.* **1965**, *42*, 3175. (c) Cromer, D. T.; Liberman, D. J. *J. Chem. Phys.* **1970**, *53*, 1891.

(25) The observation of inequivalent phosphorus resonances in the <sup>31</sup>P NMR of **3**, while **1** shows equivalent phosphorus resonances, indicates that in solution this class of compounds adopt rigid (on the NMR time scale) sbp geometries or that any fluxional processes that are occurring involve pairwise motion of transoid phosphorus and halogen ligands. We have not conducted variable temperature <sup>31</sup>P NMR measurements on either complex to investigate this in more detail.

# Reactions of 2-Butyne with Group 6–Group 10 Heterobimetallics. New Mixed-Metal Metallacycle Chemistry

Michael J. Chetcuti,<sup>\*,†</sup> Brian E. Grant,<sup>†</sup> and Philip E. Fanwick<sup>‡</sup>

Department of Chemistry and Biochemistry, University of Notre Dame, Notre Dame, Indiana 46556, and Department of Chemistry, Purdue University, West Lafayette, Indiana 47907

Received January 23, 1995<sup>®</sup>

The reactions of disubstituted alkynes with the mixed-metal complexes  $\text{NiCp}^*\text{M}(\text{CO})_3\text{Cp}$  (**1**,  $\text{M} = \text{Mo}, \text{W}$ ) are presented, and the chemistry of the resultant products is developed. Complexes **1** react with nonterminal alkynes to afford nickelacyclic products of the type  $\text{NiCp}^*\{\mu\text{-}\eta^2(1,3\text{-Ni}), \eta^2(1,2\text{-M})\text{-C}(\text{R})\text{C}(\text{R}')\text{C}(\text{O})\}\text{M}(\text{CO})_2\text{Cp}''$  (**3**) [ $\text{M} = \text{Mo}, \text{W}$ ;  $\text{R} = \text{R}' = \text{Me}$ ;  $\text{R} = \text{Me}, \text{R}' = \text{Ph}$ .  $\text{Cp}'' = \text{Cp}, \text{Cp}'$ ; not all combinations made]. Complexes **3** may be thermally decarbonylated to the  $\mu$ -alkyne (dimetallatetrahedrane) complexes  $\text{NiCp}^*\{\mu\text{-}\eta^2, \eta^2\text{-RC}_2\text{R}'\}\text{M}(\text{CO})_2\text{Cp}''$  (**2**). Complex **3a** ( $\text{R} = \text{R}' = \text{Me}$ ;  $\text{M} = \text{Mo}$ ;  $\text{Cp}'' = \text{Cp}$ ) may be protonated or alkylated at the metallacyclic acyl-like carbonyl ligand with  $\text{HBF}_4\cdot\text{Et}_2\text{O}$  or  $\text{R}_3\text{O}^+\text{BF}_4^-$  ( $\text{R} = \text{Me}, \text{Et}$ ), respectively, to afford the cationic species  $[\text{NiCp}^*\{\mu\text{-}\eta^2(1,3\text{-Mo}), \eta^2(1,2\text{-Ni})\text{-C}(\text{Me})\text{C}(\text{Me})\text{C}(\text{OH})\}\text{Mo}(\text{CO})_2\text{Cp}]^+\text{BF}_4^-$  (**4**, Ni–Mo) and  $[\text{NiCp}^*\{\mu\text{-}\eta^2(1,3\text{-Mo}), \eta^2(1,2\text{-Ni})\text{-C}(\text{Me})\text{C}(\text{Me})\text{C}(\text{OR})\}\text{Mo}(\text{CO})_2\text{Cp}]^+\text{BF}_4^-$  (Ni–Mo; **5a**,  $\text{R} = \text{Me}$ ; **5b**,  $\text{R} = \text{Et}$ ), respectively. On the basis of an analysis of the  $^{13}\text{C}$  NMR spectrum of **5c'**, a Ni–W analog of **5a**, complexes **4** and **5** are believed to contain molybdenacycle, not nickelacycle, rings—i.e. a “ring flip” takes place during the protonation or the alkylation reaction. The attempted substitution of a carbonyl ligand in **5a** with  $t\text{BuNC}$  in the presence of the oxidant  $\text{Me}_3\text{NO}$  led to oxidation at the molybdenum center, loss of all carbonyl ligands, rupture of the Ni–Mo bond, and insertion of an isocyanide ligand into one of the Mo–C  $\sigma$ -bonds. The structure of the resulting cationic molybdenum oxo species **7**,  $\text{NiCp}^*\{\mu\text{-}\eta^3(1,2,3\text{-Ni})\text{-C}(\text{OMe})\text{C}(\text{Me})\text{C}(\text{Me})\text{C}(\text{N}^t\text{Bu})\}\text{Mo}(\text{O})\text{Cp}^+\text{BF}_4^-$  was established by an X-ray diffraction study. Crystal data for **7**,  $\text{NiMoC}_{26}\text{H}_{38}\text{BF}_4\text{NO}_2$ : monoclinic,  $P2_1/c$  (No. 14),  $a = 12.288(3)$  Å,  $b = 13.130(2)$  Å,  $c = 17.013(4)$  Å,  $\beta = 93.47(1)^\circ$ ,  $Z = 4$ ,  $R(F) = 0.042$ , and  $R_w(F) = 0.051$ . Complex **5a** reacts with  $\text{KHBET}_3$  affording what is believed to be the hydrido-acyl species  $\text{NiCp}^*\{\mu\text{-}\eta^3(1,2,3\text{-Ni}), \eta^2(1,4\text{-Mo})\text{-C}(\text{OMe})\text{C}(\text{Me})\text{C}(\text{Me})\text{C}(\text{O})\}\text{MoH}(\text{CO})\text{Cp}$  (**8**, Ni–Mo). A carbonyl ligand in **5a** may be substituted with an iodide ion to afford the neutral molybdenum iodo species  $\text{NiCp}^*\{\mu\text{-}\eta^3\text{-Ni}, \eta^2(1,3\text{-Mo})\text{-C}(\text{Me})\text{C}(\text{Me})\text{C}(\text{OMe})\}\text{MoI}(\text{CO})\text{Cp}$  (**9**, Ni–Mo). Alkylation of **9** with  $\text{MeLi}$  afforded the very air-sensitive Mo–Me complex  $\text{NiCp}^*\{\mu\text{-}\eta^3\text{-Ni}, \eta^2(1,3\text{-Mo})\text{-C}(\text{Me})\text{C}(\text{Me})\text{C}(\text{OMe})\}\text{MoMe}(\text{CO})\text{Cp}$  (**10**, Ni–Mo).

## Introduction

Alkynes are virtually unparalleled in the diverse reactivity patterns and the variety of bonding modes they exhibit toward organometallic and inorganic complexes. Alkynes bind terminally to metal complexes and are known to bridge two, three, or four metal centers, where they exhibit a plurality of bonding modes. When alkynes react with metal carbonyl species, the linkage of one or more alkyne groups with carbonyl ligand(s) is often observed. Quinone or cyclopentadienone species resulting from such reactions have long been recognized, and other simple or more complex linkages between these two ligands have since been reported. These results and others are discussed and summarized in

reviews of transition metal alkyne chemistry and references cited therein.<sup>1–4</sup>

Our group has been interested in the chemistry of early–late mixed-metal systems. We have focused on the chemistry of Ni–Mo/W and Co–Mo/W compounds in recent years. Alkyne reactions with mixed-metal species remain an important component of our current work.<sup>5–12</sup> Preliminary alkyne research concentrated on the reactions of the coordinatively saturated complexes  $\text{Ni}(\text{CO})\text{Cp}\text{-M}(\text{CO})_3\text{Cp}'$ <sup>6,13</sup> with alkynes. The synthesis

(1) Bruce, M. I. *Pure Appl. Chem.* **1990**, *62*, 1021–1026.

(2) Puddephatt, R. J.; Manojlovic-Muir, L.; Muir, K. *Polyhedron* **1990**, *9*, 2767–2802.

(3) Colborn, R. E.; Vollhardt, K. P. C. *J. Am. Chem. Soc.* **1986**, *108*, 5470–5477.

(4) Winter, M. J. In *The Chemistry of the Metal–Carbon Bond*; Hartley, F. R., Patai, S., Eds.; John Wiley & Sons: Chichester, New York, Brisbane, Toronto, Singapore, 1985; Vol. 3; pp 259–294.

(5) Chetcuti, M. J.; Eigenbrot, C.; Green, K. A. *Organometallics* **1987**, *6*, 2298–2306.

(6) Chetcuti, M. J.; Green, K. A. *Organometallics* **1988**, *7*, 2450–2457.

\* To whom correspondence should be addressed. E-mail address: chetcuti.1@nd.edu.

<sup>†</sup> University of Notre Dame.

<sup>‡</sup> Purdue University.

<sup>®</sup> Abstract published in *Advance ACS Abstracts*, May 15, 1995.

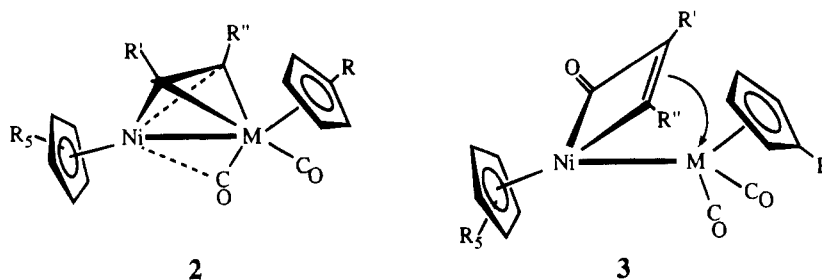


**Figure 1.** Structures of complexes **2** and **3** (M = Mo, W; R = H or Me; R', R'' = Me, Et, Ph).

of the electronically and coordinatively unsaturated permethylated cyclopentadienyl nickel–molybdenum and nickel–tungsten complexes  $\text{Ni}(\text{CO})\text{Cp}^*\text{M}(\text{CO})_3\text{Cp}$  (Ni–M, M = Mo, W)<sup>14</sup> has triggered an investigation into their chemistry. The large, electron-rich Cp\* ligand dramatically affects the chemistry of these heterobimetallic complexes as compared to their cyclopentadienyl analogs. It enabled the isolation of the coordinatively unsaturated complexes  $\text{NiCp}^*\text{M}(\text{CO})_3\text{Cp}$  (Ni–M, M = Mo, W), whose nickel–cyclopentadienyl derivatives are unknown. The steric protection afforded by the large Cp\* ligands imparts a substantial stabilizing effect to these complexes but does not preclude a rich chemistry that stems from their electronic unsaturation.

Some preliminary reactions of these complexes with butyne have already been reported.<sup>14</sup> In this manuscript, we attempt to bring together data we have assembled these past few years concerning the reactions of the complexes  $\text{Ni}(\text{CO})\text{Cp}^*\text{M}(\text{CO})_3\text{Cp}$  (Ni–M, M = Mo, W) with disubstituted alkynes (principally 2-butyne). The reactions of these complexes with ethyne and phenylacetylene are discussed in a separate manuscript as there are some major differences in the reaction chemistry of these alkynes with Ni–M (M = Mo, W) species. Initially we present a brief summary of previously reported reactions of the complexes  $\text{Ni}(\text{CO})\text{CpM}(\text{CO})_3\text{Cp}'$  (Ni–M, M = Mo, W). We then describe the reactions of the pentamethylcyclopentadienyl nickel–molybdenum and –tungsten complexes with 2-butyne and 1-phenylpropyne and develop the chemistry of some of the products derived from the reaction of the nickel–molybdenum complexes with 2-butyne.

## Results and Discussion

**(a) Reactions of the NiCp Complexes  $\text{Ni}(\text{CO})\text{CpM}(\text{CO})_3\text{Cp}'$  (M = Mo, W) with Alkynes.** Various combinations of either the NiMo or the NiW complex

have been reacted with alkynes to afford bridging  $\eta^2, \eta^2$ -alkyne complexes of generic formula  $\text{NiCp}(\mu\text{-}\eta^2, \eta^2\text{-RC}_2\text{R}')\text{M}(\text{CO})_2\text{Cp}'$  (**2**) (M = Mo, W;  $\text{RC}_2\text{R}' = \text{HC}_2\text{H}$ ,  $\text{MeC}_2\text{Me}$ ,  $\text{MeC}_2\text{Et}$ ,  $\text{PhC}_2\text{H}$ ,  $\text{PhC}_2\text{Ph}$ ,  $\text{MeCO}_2\text{C}_2\text{CO}_2\text{-Me}$ ).<sup>5,15</sup> These products have dimetallatetrahedrane type geometries. Compounds in this class have also been accessed by other synthetic routes, either from mononuclear alkyne complexes<sup>16</sup> or, with different metals, from propargyl species.<sup>17</sup>

Nickelacyclobutenone complexes of general formula  $\text{NiCp}\{\mu\text{-}\eta^2(1,2\text{-Mo}), \eta^2(1,3\text{-Ni})\text{-C(R)C(R')C(O)}\}\text{Mo}(\text{CO})_2\text{-Cp}'$  (Ni–Mo, **3**) are also obtained when  $\text{Ni}(\text{CO})\text{CpMo}(\text{CO})_3\text{Cp}'$  (Ni–Mo) is treated with alkynes, but in general these species are not observed in reactions of the corresponding nickel–tungsten complex.<sup>5</sup> The four-membered metallacycles result from alkyne–carbonyl coupling reactions, and they contain a nickel–acyl linkage. The formal alkyne-derived C=C double bond is  $\pi$ -coordinated to the molybdenum atom. Unsymmetrical alkynes afford isomers in which either alkyne-derived C(R) or C(R') groups are linked to the metallacyclic carbonyl ligand. Such complexes are generally obtained from the nickel–molybdenum species: nickel–tungsten metallacycles of this type were not generally accessible. The structures of complexes **2** and **3** are shown in Figure 1.

Complexes encompassing a metallacyclobutenone complex  $\pi$ -ligated to another metal are uncommon. Among the few reported examples are  $\text{W}(\text{CO})_2\text{Cp}\{\mu\text{-}\eta^2, \eta^2\text{-C(R)C(R')C(O)}\}\text{W}(\text{CO})_2\text{Cp}$  (W–W),<sup>18</sup>  $\text{PtCp}\{\mu\text{-}\eta^2, \eta^2\text{-C(R)C(R')C(O)}\}\text{PtCp}$  (Pt–Pt),<sup>19</sup> and  $\text{M}(\text{CO})\text{Cp}^*\{\mu\text{-}\eta^2, \eta^2\text{-C(R)C(R')C(O)}\}\text{M}(\text{CO})\text{Cp}^*$  (M–M, M = Co,<sup>20</sup> Rh<sup>21</sup>). Mixed-metal examples are rare; the complex  $\text{W}(\text{CO})_2\text{Cp}\{\mu\text{-C(Tol)C(O)C(Tol)}\}\text{Co}(\text{CO})_3$  (W–Co), which contains an isomeric C(R)C(O)C(R')M linkage, has been prepared and crystallographically characterized.<sup>22</sup> Other homodinuclear complexes which contain C(R)C(O)C(R) linkages are known.<sup>23–25</sup>

The metallacycle complexes **3** exhibit poor thermal

(7) Molecules of types **2** and **3**, and other species, which contain W–C  $\pi$ -bonds typically exhibit a relatively small <sup>183</sup>W–<sup>13</sup>C coupling of  $\leq 30$  Hz, which is not always observed. See ref 5 and: Chetcuti, M. J.; Gordon, J. C.; Green, K. A.; Fanwick, P. E.; Morgenstern, D. *Organometallics* **1989**, *8*, 1790–1799.

(8) Chetcuti, M. J.; Grant, B. E.; Fanwick, P. E. *J. Am. Chem. Soc.* **1989**, *111*, 2743–2744.

(9) Chetcuti, M. J.; Fanwick, P. E.; Gordon, J. C. *Inorg. Chem.* **1990**, *29*, 3781–3787.

(10) Chetcuti, M. J.; DeLiberato, L.; Fanwick, P. E.; Grant, B. E. *Inorg. Chem.* **1990**, *29*, 1295–1298.

(11) Chetcuti, M. J.; Grant, B. E.; Fanwick, P. E. *Organometallics* **1991**, *10*, 3003–3004.

(12) Chetcuti, M. J.; Fanwick, P. E.; Gordon, J. C. *Inorg. Chem.* **1991**, *30*, 4710–4717.

(13) Throughout this manuscript, Cp =  $\eta^5\text{-C}_5\text{H}_5$ , Cp' =  $\eta^5\text{-C}_5\text{H}_4\text{Me}$ , and Cp\* =  $\eta^5\text{-C}_5\text{Me}_5$ .

(14) Chetcuti, M. J.; Grant, B. E.; Fanwick, P. E. *Organometallics* **1990**, *9*, 1345–1347.

(15) Azar, M. C.; Chetcuti, M. J.; Eigenbrot, C.; Green, K. A. *J. Am. Chem. Soc.* **1985**, *107*, 7209–7210.

(16) Jaouen, G.; Marinetti, A.; Saillard, J.-Y.; Sayer, B. G.; McGlinchey, M. J. *Organometallics* **1982**, *1*, 225–227.

(17) Wido, T. M.; Young, G. H.; Wojcicki, A.; Calligaris, M.; Nardin, G. *Organometallics* **1988**, *7*, 452–458.

(18) Finnimore, S. R.; Knox, S. A. R.; Taylor, G. E. *J. Chem. Soc., Dalton Trans.* **1982**, 1783–1788.

(19) Boag, N. M.; Goodfellow, R. J.; Green, M.; Hessner, B.; Howard, J. A. K.; Stone, F. G. A. *J. Chem. Soc., Dalton Trans.* **1983**, 2585–2591.

(20) Dickson, R. S.; Evans, G. S.; Fallon, G. D. *Aust. J. Chem.* **1985**, *38*, 273–291.

(21) Herrmann, W. A.; Bauer, C.; Weichmann, J. *J. Organomet. Chem.* **1983**, *243*, C21–C26.

(22) Hart, I. J.; Jardin, A. E.; Jeffery, J. C.; Stone, F. G. A. *J. Organomet. Chem.* **1988**, *341*, 391–406.

(23) Green, M.; Howard, J. A. K.; Porter, S. J.; Stone, F. G. A.; Tyler, D. C. *J. Chem. Soc., Dalton Trans.* **1984**, 2553–2559.

Chart 1<sup>a</sup>

- 1a** NiCp\*Mo(CO)<sub>3</sub>Cp (Ni-Mo)  
**1b** NiCp\*W(CO)<sub>3</sub>Cp (Ni-W)  
**1b'** NiCp\*W(CO)<sub>3</sub>Cp' (Ni-W)  
**2a** NiCp\*(μ-η<sup>2</sup>,η<sup>2</sup>-MeC<sub>2</sub>Me)Mo(CO)<sub>2</sub>Cp (Ni-Mo)  
**2b'** NiCp\*(μ-η<sup>2</sup>,η<sup>2</sup>-MeC<sub>2</sub>Me)W(CO)<sub>2</sub>Cp' (Ni-W)  
**2c** NiCp\*(μ-η<sup>2</sup>,η<sup>2</sup>-MeC<sub>2</sub>Ph)W(CO)<sub>2</sub>Cp (Ni-W)  
**2c'** NiCp\*(μ-η<sup>2</sup>,η<sup>2</sup>-MeC<sub>2</sub>Ph)W(CO)<sub>2</sub>Cp' (Ni-W)  
**3a** NiCp\*{μ-η<sup>2</sup>(1,3-Ni),η<sup>2</sup>(1,2-Mo)-C(Me)C(Me)C(O)}Mo(CO)<sub>2</sub>Cp (Ni-Mo)  
**3b'** NiCp\*{μ-η<sup>2</sup>(1,3-Ni),η<sup>2</sup>(1,2-W)-C(Me)C(Me)C(O)}W(CO)<sub>2</sub>Cp' (Ni-W)  
**3c** NiCp\*{μ-η<sup>2</sup>(1,3-Ni),η<sup>2</sup>(1,2-W)-C(Ph)C(Me)C(O)}W(CO)<sub>2</sub>Cp (Ni-W)  
**3d** NiCp\*{μ-η<sup>2</sup>(1,3-Ni),η<sup>2</sup>(1,2-Mo)-C(Me)C(Et)C(O)}Mo(CO)<sub>2</sub>Cp (Ni-Mo)  
**3e** NiCp\*{μ-η<sup>2</sup>(1,3-Ni),η<sup>2</sup>(1,2-Mo)-C(Et)C(Me)C(O)}Mo(CO)<sub>2</sub>Cp (Ni-Mo)  
**4** [NiCp\*{μ-η<sup>2</sup>(1,3-Mo),η<sup>2</sup>(1,2-Ni)-C(Me)C(Me)C(OH)}Mo(CO)<sub>2</sub>Cp]<sup>+</sup> BF<sub>4</sub><sup>-</sup> (Ni-Mo)  
**5a** [NiCp\*{μ-η<sup>2</sup>(1,3-Mo),η<sup>2</sup>(1,2-Ni)-C(Me)C(Me)C(OMe)}Mo(CO)<sub>2</sub>Cp]<sup>+</sup> BF<sub>4</sub><sup>-</sup> (Ni-Mo)  
**5b** [NiCp\*{μ-η<sup>2</sup>(1,3-Mo),η<sup>2</sup>(1,2-Ni)-C(Me)C(Me)C(OEt)}Mo(CO)<sub>2</sub>Cp]<sup>+</sup> BF<sub>4</sub><sup>-</sup> (Ni-Mo)  
**5c'** [NiCp\*{μ-η<sup>2</sup>(1,3-W),η<sup>2</sup>(1,2-Ni)-C(Me)C(Me)C(OMe)}W(CO)<sub>2</sub>Cp']<sup>+</sup> BF<sub>4</sub><sup>-</sup> (Ni-W)  
**6** [NiCp\*{μ-η<sup>2</sup>(1,3-Mo),η<sup>2</sup>(1,2-Ni)-C(Me)C(Me)C(OMe)}Mo(BuNC)(CO)Cp]<sup>+</sup> BF<sub>4</sub><sup>-</sup> (Ni-Mo)  
**7** [NiCp\*{μ-C(OMe)C(Me)C(Me)C(N<sup>+</sup>Bu)}Mo(O)Cp]<sup>+</sup> BF<sub>4</sub><sup>-</sup>  
**8** NiCp\*{μ-η<sup>2</sup>(1,4-Mo)η<sup>3</sup>(1,2,3-Ni)-C(OMe)C(Me)C(Me)C(O)}MoH(CO)Cp (Ni-Mo)  
**9** NiCp\*{μ-η<sup>3</sup>(Ni)η<sup>2</sup>(1,3-Mo)C(Me)C(Me)C(OMe)}MoI(CO)Cp (Ni-Mo)  
**10** NiCp\*{μ-η<sup>3</sup>(Ni)η<sup>2</sup>(1,3-Mo)C(Me)C(Me)C(OMe)}MoMe(CO)Cp (Ni-Mo)  
**11a, b** NiMo(CO)<sub>2</sub>C(Me)C(Me)C(OMe)CpMe(C<sub>5</sub>Me<sub>5</sub>)

<sup>a</sup> Compounds of a similar class are differentiated by letters: e.g. all μ-η<sup>2</sup>,η<sup>2</sup>-alkyne complexes are numbered **2** and are distinguished by letters (**2a**, **2b'**, etc.). Unprimed compounds (e.g. **2a**) contain MoCp or WCp groups; primed compounds contain MoCp' or WCp' groups.

stability and lose CO slowly at room temperature over a period of months in the solid state (and in a few days in solution) to afford the corresponding μ-η<sup>2</sup>,η<sup>2</sup>-alkyne species. The decarbonylation takes place quantitatively when solutions of the metallacycle are heated. The structures of representative complexes from both sets of compounds—NiCp(μ-η<sup>2</sup>,η<sup>2</sup>-MeC<sub>2</sub>Me)W(CO)<sub>2</sub>Cp (Ni-W) and NiCp{μ-η<sup>2</sup>(1,2-Mo),η<sup>2</sup>(1,3-Ni)-C(Me)C(Me)C(O)}-Mo(CO)<sub>2</sub>Cp' (Ni-Mo)—have been fully determined by X-ray diffraction studies.<sup>5,15</sup>

**(b) Reactions of the NiCp\* Species NiCp\*M-(CO)<sub>3</sub>Cp (Ni-M; 1a, M = Mo; 1b, M = W) with Disubstituted Alkynes.** (i) **General Comments.** The NiCp\* complexes **1** (Chart 1) react with alkynes in a somewhat similar fashion to their NiCp analogs, as shown in Scheme 1. However the metallacycle derivatives that are produced in these reactions appear to be significantly more thermally stable than their NiCp analogs. They are also obtained in higher yields, or occasionally exclusively, depending on the alkyne in question. The major products obtained for disubstituted alkynes are metallacyclic species of type **3** (Figure 1).

Occasionally μ-η<sup>2</sup>,η<sup>2</sup>-alkyne complexes are obtained (complex **2**, Figure 1) in yields that depend on the alkyne in question and also on the reaction conditions. (Pronounced differences are observed in the reactions of these species with the terminal alkynes HC<sub>2</sub>H and PhC<sub>2</sub>H. These reactions will be discussed elsewhere.<sup>26</sup>)

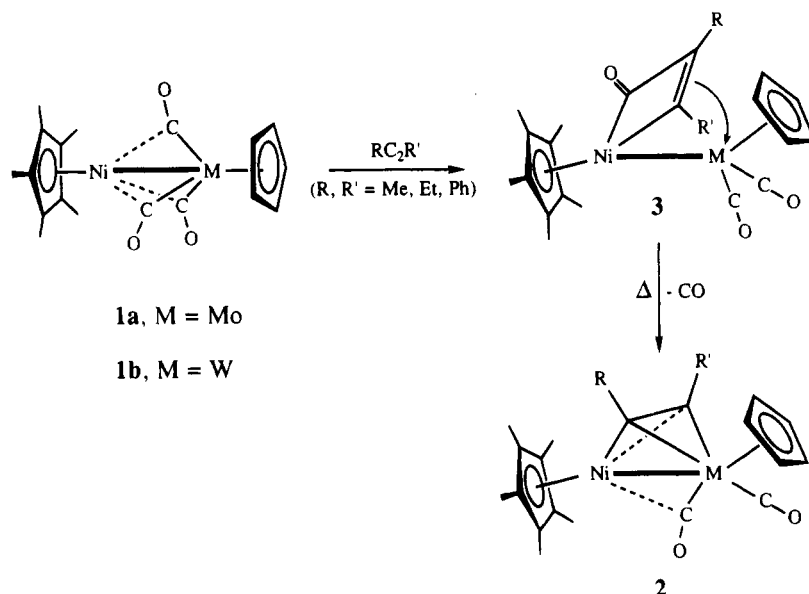
**(ii) Reactions of Complexes 1 with 2-Butyne.** Complexes **1a** and **1b'** (Chart 1) react with 2-butyne at low temperature to afford the orange brown products **3a** and **3b'**, respectively. NMR and IR data of both the Ni-Mo and of the Ni-W species (Tables 1–3, respectively) closely parallel those of fully characterized heterobimetallic nickelacyclobutenone Cp complexes.<sup>5</sup> The resonances of the metallacyclic CO and the alkyne derived carbon atoms of **3b'** exhibit slightly broadened peaks in their <sup>13</sup>C NMR spectra, and no <sup>183</sup>W–<sup>13</sup>C coupling could definitively be observed. However, the more upfield peak assigned to one of the two alkyne methyl groups exhibited a <sup>183</sup>W–<sup>1</sup>H coupling of ≈4 Hz. On the basis of trends seen from other compounds in our labs, we assign this resonance to the methyl substituent α-to the CO group. We conclude that these products are the species NiCp{μ-η<sup>2</sup>(1,2-M),η<sup>2</sup>(1,3-Ni)-C(Me)C(Me)C(O)}M(CO)<sub>2</sub>Cp'' (**3a**, M = Mo, Cp'' = Cp;

(24) Sheridan, J. B.; Geoffroy, G. L.; Rheingold, A. R. *Organometallics* **1986**, *5*, 1514–1515.

(25) Carroll, W. E.; Green, M.; Howard, J. A. K.; Pfeffer, M.; Stone, F. G. A. *J. Chem. Soc., Dalton Trans.* **1978**, 1472–1478.

(26) Chetcuti, M. J.; Grant, B. E.; Fanwick, P. E. Manuscript in preparation.

**Scheme 1. General Scheme of the Reaction of Nonterminal Alkynes with NiCp\*M(CO)<sub>3</sub>Cp (Ni-M; M = Mo, W)<sup>a</sup>**



<sup>a</sup> The structures of NiCp analogs of **2** and **3** were established by X-ray diffraction (Chetcuti, M. J.; Eigenbrot, C.; Green, K. A. *Organometallics* **1987**, *6*, 2298–2306).

**Table 1. <sup>1</sup>H NMR Data for New Complexes<sup>a</sup>**

complex	Cp*	Cp or Cp'	OMe	R	R'
<b>2a<sup>b</sup></b> (R, R' = Me)	1.70	5.22		2.31	2.31
<b>2c</b> (R, R' = Me, Ph)	1.47	5.24		7.18–7.38	2.68
<b>2c'</b> (R, R' = Me, Ph)	1.49	4.82–5.12, 1.98		7.16–7.33	2.66
<b>3a<sup>b</sup></b> (R, R' = Me)	1.75	5.16		2.38	1.19
<b>3b'</b> (R, R' = Me)	1.68	5.09, 5.20, 5.28, 5.37, 2.09		2.56	1.11 ( <i>J</i> <sub>WH</sub> = 3.0 Hz)
<b>3c</b> (R, R' = Me, Ph)	1.45	5.41		7.40, 7.38, 7.20	1.33 ( <i>J</i> <sub>WH</sub> = 3.9 Hz)
<b>4<sup>b</sup></b> (R, R' = Me)	1.84	5.25	9.69 <sup>d</sup>	1.96	1.39
<b>5a<sup>b</sup></b> (R, R' = Me)	1.86	5.36	3.65	2.05	1.46
<b>5b</b> (R, R' = Me)	1.85	5.28	4.85 (d), <sup>c</sup> 1.64 (q)	1.96	1.40
<b>5c'</b> (R, R' = Me)	1.85	5.28–5.41, 2.11	3.57	1.98	1.52
<b>7<sup>c</sup></b> (R, R' = Me)	1.64	6.10	3.97	1.97	1.92
<b>8<sup>f</sup></b> (R, R' = Me)	1.76	4.96	3.86	2.04	1.59
<b>9</b> (R, R' = Me)	1.87	4.84	3.52	2.32	1.44
<b>10<sup>g</sup></b> (R, R' = Me)	1.78	4.98	3.70	1.84	1.18

<sup>a</sup> Spectra recorded in acetone-*d*<sub>6</sub> and chemical shifts are in ppm relative to CHD<sub>2</sub>C(O)CD<sub>3</sub> set at 2.04 ppm. For Cp' resonances (all ABCD-type multiplets) the center of each multiplet or the aromatic proton range is given, followed by the Me resonance. <sup>b</sup> Spectrum recorded in chloroform-*d*<sub>1</sub> with CHCl<sub>3</sub> set at 7.24 ppm. <sup>c</sup> OCH<sub>2</sub>Me, OCH<sub>2</sub>Me. *J*<sub>HH</sub> = 15.2 Hz. <sup>d</sup> OH chemical shift. <sup>e</sup> <sup>t</sup>Bu (s, 9H), 1.59 ppm. <sup>f</sup> Mo–H (s, br, H), –6.90 ppm. <sup>g</sup> Mo–CH<sub>3</sub> (s, 3H), –0.82 ppm.

**Table 2. <sup>13</sup>C NMR Data for the New Complexes<sup>a</sup>**

complex	CO	C(O)R and/or C(OMe)	C <sub>5</sub> Me <sub>5</sub> , C <sub>5</sub> Me <sub>5</sub>	Cp or Cp'(Me)	CR, CR'	R	R'		
<b>2a<sup>b</sup></b>	236.4		100.5, 8.8	92.0	92.9, 92.9	16.9	16.9		
<b>2c</b>	225.3	219.3	99.8	8.8	90.7	81.2	75.9		
<b>2c'</b>	226.4, 218.8		99.6, 8.5	107.3, 90.2, 89.8, 89.2, 88.2, 13.6	80.9, 74.8	142.9, 131.0, 128.9, 126.9	18.3		
<b>3a<sup>b</sup></b>	231.7, 229.5	184.1	100.5, 9.0	92.2	147.0, 67.3	22.1	14.7		
<b>3b'<sup>b</sup></b>	220.0, <sup>c</sup> 218.6 <sup>d</sup>	179.5	100.5, 8.4	106.4, 92.5, 88.1, 87.7, 85.7, 13.2	130.7, 89.1	23.6	10.2		
<b>3c<sup>b</sup></b>	217.8	217.6	185.8	100.8, 8.5	89.9	***, 57.0	145.7, 129.5, 128.4, 125.9	16.3	
<b>4</b>	225.8	225.5	173.6,	105.2	8.4	92.1	139.5, 123.5	24.5	7.4
<b>5a</b>	227.2, 224.3	178.0, 63.2	105.8	8.8	92.4	138.1	125.0	24.4	7.4
<b>5a<sup>b</sup></b>	225.5, 222.7	177.1, 62.6	104.7	8.6	91.1	137.5	124.1	24.2	7.1
<b>5b<sup>b</sup></b>	227.7, 222.7	179.0, <sup>e</sup> 53.5, 14.9	103.7, 8.2	90.4	138.4	119.5	24.6	12.4	
<b>5c'<sup>b</sup></b>	214.8, <sup>f</sup> 212.6 <sup>g</sup>	161.6, <sup>h</sup> 62.7	104.1, 8.5	109.1, 90.3, 89.8, 87.0, 86.4, 13.7	157.1, 128.0	23.5	8.8		
<b>8</b>	215.3	176.5, ***, 63.0	102.2	9.4	88.4	***, ***	15.2	14.5	
<b>9<sup>b</sup></b>	244.8	178.7, 59.9	101.2, 9.1	90.3	148.8, 119.1	25.3	7.1		
<b>10<sup>i</sup></b>	***	***, 61.0	99.4, 9.8	92.0	***, ***	18.1	8.8		

<sup>a</sup> In acetone-*d*<sub>6</sub>;  $\delta$  (ppm) referenced to the acetone-*d*<sub>6</sub> methyl resonance, set at 29.8. Cp', Cp\*, and Ph signals given in the following order: *ipso* carbon, other aromatic carbon atoms, Me. Unobserved resonances denoted \*\*\*. <sup>b</sup> In chloroform-*d*<sub>1</sub> (set at 77.0 ppm). *J*<sub>WC</sub> (Hz) = 150.2,<sup>c</sup> 152.9.<sup>d</sup> <sup>e</sup> OCH<sub>2</sub>Me, OCH<sub>2</sub>Me. *J*<sub>WC</sub> (Hz) = 140.1,<sup>f</sup> 135.9,<sup>g</sup> 67.4.<sup>h</sup> <sup>i</sup> Quaternary carbons not observed. Mo–CH<sub>3</sub>, –10.8 ppm.

**3b'**, M = W, Cp'' = Cp'), with structures shown in Figure 1 (structure **3**).

In contrast to what is observed for the NiCp species, "dimetallatetrahedrane type"  $\mu$ -alkyne complexes are

not obtained from reactions of **1a** and **1b'** with 2-butyne at ambient temperatures. Furthermore, **3a** and **3b'** are stable when stored under an inert atmosphere, and their CDCl<sub>3</sub> solutions show little decomposition after over-

Table 3. IR  $\nu(\text{CO})$  Data ( $\text{cm}^{-1}$ ) for New Complexes<sup>a</sup>

complex	$\nu(\text{CO})$	complex	$\nu(\text{CO})$
<b>2a</b> <sup>b</sup>	1918 (s), 1810 (s)	<b>5c'</b>	2002 (s), 1946 (s)
<b>2c'</b> <sup>b</sup>	1956 (m), 1937 (s), 1871 (m), 1815 (w)	<b>6</b>	2141 (s), <sup>f</sup> 1936 (s)
<b>3a</b> <sup>c</sup>	1972 (s), 1915 (s), 1662 (s)	<b>7</b>	1664 (m, br.)
<b>3b'</b> <sup>d</sup>	1965 (s), 1899 (s), 1648 (s)	<b>8<sup>d</sup></b>	2011 (w), <sup>g</sup> 1901 (s)
<b>3c</b> <sup>b</sup>	1975 (s), 1920 (s), 1660 (m)	<b>9<sup>d</sup></b>	1901 (s)
<b>4<sup>d,e</sup></b>	2002 (s), 1962 (s)	<b>10<sup>b</sup></b>	1869 (s)
<b>5a</b>	2011 (s), 1961 (s)	<b>11a,b</b> <sup>b</sup>	1932 (s), 1861 (s), 1846 (m)
<b>5b</b>	2007 (s), 1955 (s)		

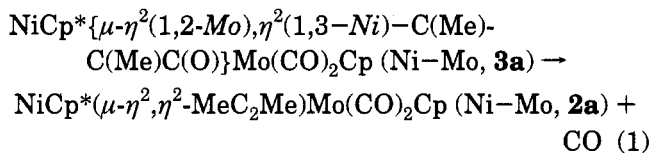
<sup>a</sup> In  $\text{CH}_2\text{Cl}_2$ . <sup>b</sup> In hexanes. <sup>c</sup> Nujol mull. <sup>d</sup> In thf. <sup>e</sup>  $\nu(\text{OH}) = 3291 \text{ cm}^{-1}$ . <sup>f</sup>  $\nu(\text{NC})$ . <sup>g</sup>  $\nu(\text{MoH})$ .

Table 4. Mass Spectral Data (EI) ( $m/e$ )

complex	$\text{M}^+$	$(\text{M} - \text{CO})^+$	other
<b>2a</b>	466	438	410, $(\text{M} - 2\text{CO})^+$ ; 356, $(\text{NiCp}^*\text{MoCp})^+$
<b>3a</b>	494	466	438, $(\text{M} - 2\text{CO})^+$ ; 410, $(\text{M} - 3\text{CO})^+$ ; 356, $(\text{NiCp}^*\text{MoCp})^+$
<b>5a</b>	509		491, $(\text{M} - \text{H}_2\text{O})^+$ ?; 466, $(\text{M} - \text{CO} - \text{Me})^+$ ; 356, $(\text{NiCp}^*\text{MoCp})^+$ ; 296
<b>7</b>	552		571, $(\text{M} + \text{F})^+$ ; 488, $(\text{M} + \text{F} - \text{tBuNC})^+$ ; 469, $(\text{M} - \text{tBuNC})^+$
<b>8<sup>a,b</sup></b>	510	482	466, $(\text{M} - \text{Me} - \text{CO} - \text{H})^+$
<b>9<sup>a</sup></b>	608	580	481, $(\text{M} - \text{I})^+$
<b>10<sup>a,b</sup></b>	496	468	480, $(\text{M} - \text{Me} - \text{H})^+$
<b>11a,b<sup>a</sup></b>	524	496	

<sup>a</sup> CI, using isobutane. <sup>b</sup>  $\text{M}^+$  and  $(\text{M} + \text{H})^+$  both observed.

night storage. However, refluxing thf solutions of **3a** can be decarbonylated to form the corresponding  $\mu$ -alkyne species **2a**, as indicated in eq 1. Scheme 1 shows this reaction and the generic structures of **2** and **3**.



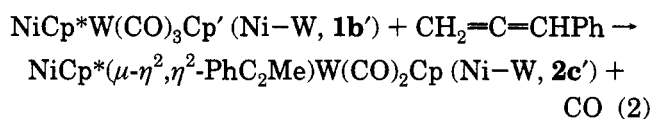
Complex **2a** is believed to have a structure similar to that of its NiCp analog shown in Figure 1 on the basis of the similarity of the two compound's spectroscopic data (Tables 1–3 and ref 5). Both complexes have a semibridging and a terminal carbonyl ligand and both exhibit a single signal for the 2-butyne Me resonances in their  $^1\text{H}$  NMR spectra. A (semi)bridging CO-terminal CO exchange process, operative in both molecules, generates an effective mirror plane of symmetry on the NMR time scale that makes the alkyne Me resonances equivalent in each molecule.<sup>5</sup>

(iii) **Reactions of 1-Phenylpropyne, 2-Pentyne, and 1-Phenylallene with Complexes 1.** The reaction of **1b** with 1-phenylpropyne ( $\text{MeC}_2\text{Ph}$ ) at  $-20^\circ\text{C}$  afforded three products. In contrast to the reaction with 2-butyne, the major product, obtained in 60–70% yield, was the  $\mu$ -alkyne complex  $\text{NiCp}^*(\mu\text{-}\eta^2,\eta^2\text{-MeC}_2\text{Ph})\text{W(CO)}_2\text{Cp (Ni-W, } \mathbf{2c})$ . Minor yields of one of the possible isomers (**3c**) of a metallacyclic complex were also isolated. On the basis of a careful comparison of the spectroscopic data of this species with those of **3b'**, complex **3c** is tentatively believed to a nickelalacycle species. It was assigned the structure  $\text{NiCp}\{\mu\text{-}\eta^2(1,3\text{-Ni}),\eta^2(1,2\text{-W})\text{-C(Me)C(Ph)C(O)}\}\text{W(CO)}_2\text{Cp (Ni-W, } \mathbf{3c})$  on the basis of its NMR data (Tables 1 and 2). The third reaction product, obtained in tiny quantities, was not characterized.

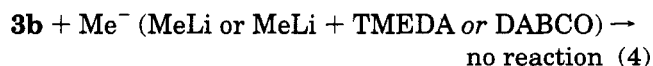
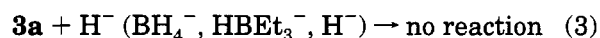
The reaction of **1a** with 2-pentyne ( $\text{MeC}_2\text{Et}$ ) was attempted by reacting **1a** with excess  $\text{MeC}_2\text{Et}$  over a 24 h period. The principal products of this reaction were a mixture of the metallacycles  $\text{NiCp}\{\mu\text{-}\eta^2(1,3\text{-Ni}),\eta^2(1,2\text{-Mo})\text{-C(R)C(R')C(O)}\}\text{Mo(CO)}_2\text{Cp (Ni-Mo; } \mathbf{3d}, \text{R} = \text{Et, R}' = \text{Me; } \mathbf{3e}, \text{R} = \text{Me, R}' = \text{Et})$ . Complexes **3d,e** were

obtained in an  $\approx 2:1$  ratio, respectively, as shown by  $^1\text{H}$  NMR spectroscopy. Further purification was not attempted.

The reaction of 1-phenylallene,  $\text{CH}_2=\text{C}=\text{CHPh}$ , with **1b'** did not afford a  $\mu$ -allene species. This contrasts with the reactions of allenes with other metal-metal-bonded species, which usually afforded  $\mu\text{-}\eta^2,\eta^2$ -allene species.<sup>27–30</sup> Furthermore,  $\mu$ -metalloallyl species, such as  $\text{NiCp}\{\mu\text{-}\eta^1(\text{Ni}),\eta^3(\text{M})\text{-CH}_2\text{CCMe}_2\}\text{M(CO)}_2\text{Cp}' (\text{Ni-M, } \mathbf{31})$  were not obtained. Instead, an effective 1,3-hydrogen migration ensued and the product obtained was the  $\mu$ -alkyne species  $\text{NiCp}^*(\mu\text{-}\eta^2,\eta^2\text{-MeC}_2\text{Ph})\text{W(CO)}_2\text{Cp (Ni-W, } \mathbf{2c'})$ , the Cp' analog of complex **2c**. Spectroscopic data for **2c** and **2c'** are, as expected, very similar. The reaction is summarized in eq 2.



(c) **Reactions of the Metallacyclic Complexes 3.**  
(i) **Reaction of 3 with Nucleophiles.** Complexes **3**, especially those in which a  $\text{NiCp}^*$  group are present, are electron-rich species which are not susceptible to nucleophilic attack. Complex **3a** for example is inert to sources of  $\text{H}^-$  ( $\text{NaBH}_4$ ,  $\text{LiHBEt}_3$ ,  $\text{NaH}$ ) as shown in eq 3. Solutions of **3b** remain inert to methyllithium, even when the latter species is activated with TMEDA or DABCO (eq 4).



(27) Wu, I.-Y.; Tseng, T.-W.; Chen, C.-T.; Cheng, M.-C.; Lin, Y.-C.; Wang, Y. *Inorg. Chem.* **1993**, *32*, 1539–1540.

(28) Chisholm, M. H.; Rankel, L. A.; Bailey, W. I. J.; Cotton, F. A.; Murillo, C. A. *J. Am. Chem. Soc.* **1977**, *99*, 1261–1262.

(29) Bailey, W. I. J.; Chisholm, M. H.; Cotton, F. A.; Murillo, C. A.; Rankel, L. A. *J. Am. Chem. Soc.* **1978**, *100*, 802–807.

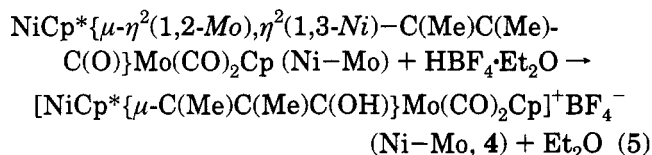
(30) Meyer, A.; McCabe, D. J.; Curtis, M. D. *Organometallics* **1987**, *6*, 1491–1498.

(31) Chetcuti, M. J.; Fanwick, P. E.; McDonald, S. R.; Rath, N. P. *Organometallics* **1991**, *10*, 1551–1560.



(ii) **Reactions of NiCp\* $\{\mu\text{-}\eta^2(1,2\text{-Mo}),\eta^2(1,3\text{-Ni})\text{-C(Me)C(Me)C(O)}\}\text{Mo(CO)}_2\text{Cp}$  (Ni–Mo) (**3b**) with H<sup>+</sup>.** In contrast to their reactions with nucleophiles, complexes **3** undergo ready attack by electrophiles. Etheral solutions of **3a** react instantaneously with HBF<sub>4</sub>·Et<sub>2</sub>O, and a yellow powder (**4**) precipitates quantitatively. The solubility properties of **4** suggest that the compound is ionic—the compound is insoluble in ether, hexane, or toluene but soluble in dichloromethane. Spectroscopic data indicate that protonation of the metallacyclic carbonyl oxygen atom of **3a** has occurred to afford a cationic hydroxy species. IR data of the yellow solid indicate that the acyl-like  $\nu(\text{CO})$  stretch has vanished. Two  $\nu(\text{CO})$  stretches are still present, but these are shifted to higher frequencies as expected for a cation. A broad new  $\nu(\text{OH})$  absorbance appears, centered around 3300 cm<sup>-1</sup>.

The NMR and other data for **4** support its formulation as a hydroxy cation. In addition to similar resonances to those in **3a** the <sup>1</sup>H NMR spectrum shows a new signal assigned to the single OH proton at  $\delta = 9.69$  ppm. Furthermore, there is no new resonance in the 0 to -20 ppm range typical of metal hydride species, indicating that neither the metals nor the metal–metal bond was protonated. When solutions of **4** in CH<sub>2</sub>Cl<sub>2</sub> are stirred over a suspension of Na<sub>2</sub>CO<sub>3</sub>, complex **3a** is re-formed. The OH <sup>1</sup>H NMR resonance present in **3a** vanishes when **4** was exposed to D<sub>2</sub>O. Presumably, H/D exchange takes place. Complex **4** was therefore formulated as the salt [NiCp\* $\{\mu\text{-C(Me)C(Me)C(OH)}\}\text{Mo(CO)}_2\text{Cp}\}^+\text{BF}_4^-$ . Its formation is described by eq 5.



The structure of this species, specifically the likely bonding mode of the C(Me)C(Me)C(OH) moiety to the dimetal center in **4**, will be discussed shortly. However, it is noteworthy that while there is a relatively small change in most of the <sup>13</sup>C NMR chemical shifts of **4** as compared to **3a**, there is a significant chemical shift difference between the metallacyclic ring carbon atom <sup>13</sup>C NMR chemical shifts found in the two species. The CMe signals for the C(Me)C(Me) resonances are assigned shifts of 147.3 and 67.3 in **3a** and 139.5 and 123.5 ppm, respectively, in **4**.

The protonation of carbonyl groups that form part of a metallacyclic ligand has been reported, and structural changes occasionally follow the protonation reaction. The mixed-metal species W(CO)<sub>4</sub> $\{\mu\text{-}\eta^2(\text{Co}),\eta^3(\text{W})\text{-C(Tol)C(Me)C(Me)C(O)}\}\text{Co(CO)}_2(\text{PPh}_3)$  (W–Co), which was prepared from a cobalt–tungsten  $\mu$ -alkylidyne complex, was protonated to form the cationic hydroxy complex [W(CO)<sub>4</sub> $\{\mu\text{-}\eta^2(\text{Co})\eta^3(\text{W})\text{-C(Tol)C(Me)C(Me)C(OH)}\}\text{Co(CO)}_2(\text{PPh}_3)\}^+$ . Both species were characterized crystallographically.<sup>32</sup> Data for these Co–W complexes indicate that there was a significant structural change on protonation: the C(OH) carbon in the cationic complex is  $\sigma$ -bonded to the tungsten atom; this is not the case for the neutral species. Protonation of the structurally

characterized complex W(CO)<sub>2</sub>Cp\* $\{\mu\text{-C(Tol)C(O)C(Me)C(Me)C(O)}\}\text{Fe(CO)}_3$  (W–Fe) to [W(CO)<sub>2</sub>Cp\* $\{\mu\text{-C(Tol)C(OH)C(Me)C(Me)C(O)}\}\text{Fe(CO)}_3\}^+$  (W–Fe) is also believed to occur with the formation of a C(OH)–Fe bond, but the protonated species was not structurally characterized.<sup>33</sup>

In contrast, when the complex W<sub>2</sub> $\{\mu\text{-C(Tol)C(O)C(Tol)}\}\text{(CO)}_4\text{Cp}_2$  (W–W)<sup>23,24,34</sup> was protonated (at the metallacyclic carbonyl oxygen), the same geometry was maintained. Indeed, neglecting distances involving the protonated CO group, bond length and bond angle differences between the structurally characterized neutral species<sup>24,34</sup> and the protonated complex [W<sub>2</sub> $\{\mu\text{-C(Tol)C(OH)C(Tol)}\}\text{(CO)}_4\text{Cp}_2\}^+\text{BF}_4^-$  (W–W)<sup>35</sup> were minimal. The chemical shift of the carbon atom of the carbonyl ligand that is protonated also shows an upfield chemical shift on protonation, in the <sup>13</sup>C NMR spectrum, as is observed in the work reported here [ $\delta(\text{C(O)})$  in W<sub>2</sub> $\{\mu\text{-C(Tol)C(O)C(Tol)}\}\text{(CO)}_4\text{Cp}_2$  (W–W) = 177.3 ppm;<sup>34</sup>  $\delta(\text{C(OH)})$  in [W<sub>2</sub> $\{\mu\text{-C(Tol)C(OH)C(Tol)}\}\text{(CO)}_4\text{Cp}_2\}^+\text{BF}_4^-$  (W–W) = 160.9 ppm].<sup>35</sup>

(iii) **Reactions of NiCp\* $\{\mu\text{-}\eta^2(1,2\text{-Mo}),\eta^2(1,3\text{-Ni})\text{-C(Me)C(Me)C(O)}\}\text{Mo(CO)}_2\text{Cp}$  (Ni–Mo, **3a**) with Me<sup>+</sup> and Et<sup>+</sup>.** The alkylation of **3a** also proceeded in a straightforward fashion. Treatment of **3a** with a 1 molar ratio of Me<sub>3</sub>O<sup>+</sup>BF<sub>4</sub><sup>-</sup> led to the formation of a new complex (**5a**). Spectroscopic properties of **5a** were consistent with electrophilic attack taking place on the acyl oxygen atom of **3a**. The IR spectrum of **5a** exhibited two terminal  $\nu(\text{CO})$  stretches in the carbonyl region, shifted to higher energies when compared to those of their neutral precursor. A new Me signal at 3.66 ppm in the <sup>1</sup>H NMR spectrum of **5a** was assigned to MeO group resulting from electrophilic attack at the acyl oxygen atom of **3a** by Me<sup>+</sup>. The collective spectroscopic properties (Tables 1–3) are consistent with **5a** being a methylated acyl species.

The alkylation reaction on **3a** was also performed with Et<sub>3</sub>O<sup>+</sup>BF<sub>4</sub><sup>-</sup> to afford **5b**. The results and spectroscopic data **5b** parallel those of the methylation reaction. Both alkylation products are believed to be isostructural to the hydroxy complex **4**. They may be formulated as [NiCp\* $\{\mu\text{-C(Me)C(Me)C(OR)}\}\text{Mo(CO)}_2\text{Cp}\}^+\text{BF}_4^-$  (Ni–Mo, **5a**, R = Me; **5b**, R = Et).

(iv) **Structures of the Protonated or Alkylated Metallacycles **4**, **5a**, and **5b**.** The chemical shifts of corresponding proton and carbon atoms in the <sup>1</sup>H and <sup>13</sup>C NMR spectra of all species are very similar (Tables 1 and 2), as are their  $\nu(\text{CO})$  stretches (Table 3). All three of these cationic species likely have similar structures. The protonation or alkylation reactions leading to the formation of **4**, **5a**, and **5b** and four alternative structures for the products are shown in Scheme 2. Whether the structures of these species are delocalized or not, and whether the cationic species are nickelacycles or molybdenacycles, will now be discussed.

On the basis of the chemical shifts of the metallacyclic carbon atoms, the carbon spine of the metallacycle is probably best considered to bind as a  $\mu\text{-}\eta^2,\eta^3$ -allyl species, as shown in Scheme 2, structure B or D. Carbonium ion representations (structure A or C) or

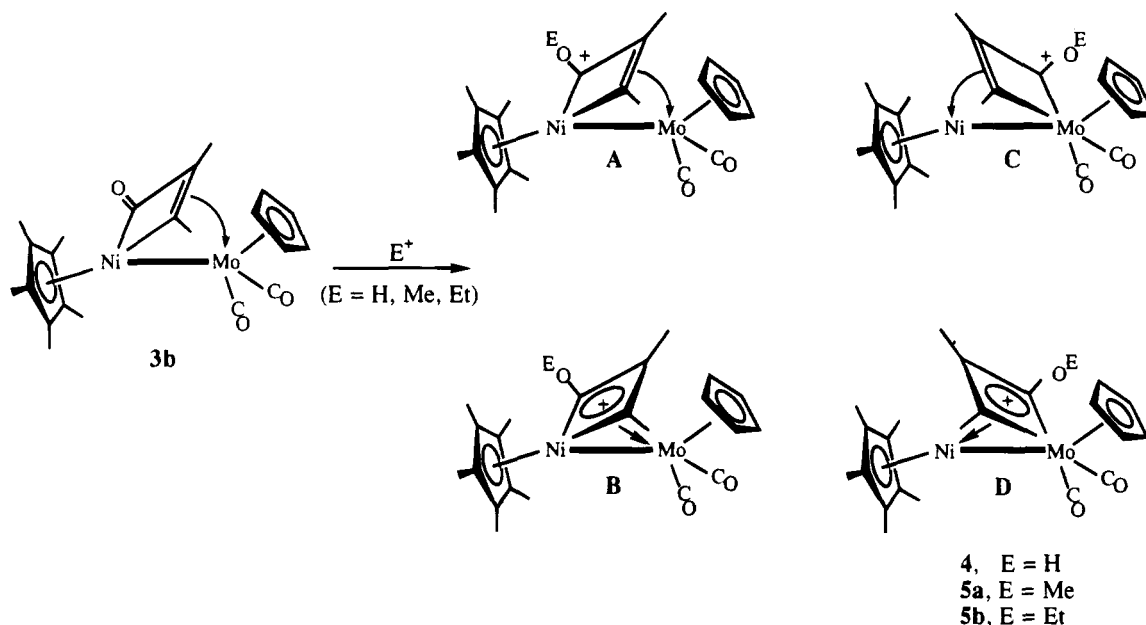
(32) Hein, J.; Jeffery, J. C.; Sherwood, P.; Stone, F. G. A. *J. Chem. Soc., Dalton Trans.* **1987**, 2211–2218.

(34) Sheridan, J. B.; Pourreau, D. B.; Geoffroy, G. L.; Rheingold, A. L. *Organometallics* **1988**, *7*, 289–294.

(35) Sheridan, J. B.; Garrett, K.; Geoffroy, G. L.; Rheingold, A. L. *Inorg. Chem.* **1988**, *27*, 3248–3250.

(32) Hart, I. J.; Jeffery, J. C.; Grosse-Ophoff, M. J.; Stone, F. G. A. *J. Chem. Soc., Dalton Trans.* **1988**, 1867–1877.

**Scheme 2. Alkylation or Protonation of Metallacycle 3a and Some Possible Structures (A–D) of the Products 4 and 5**



carbene-type representations (not shown) with metal-acyl-carbon double bonds, are unlikely to be strongly contributing as the C(OH) or C(OR) (R = Me, Et) carbon atom for all three complexes resonates at relatively high field in the  $^{13}\text{C}$  NMR spectrum (Table 2).

The question then arises as to whether the metallacycle remains a nickelacycle  $\pi$ -coordinated to the group 6 metal atom on protonation or alkylation (corresponding to Scheme 2, structure B). This geometry, which can be described as a 1,3-nickelallyl species  $\pi$ -complexed to the group 6 metal, might be expected. However, a "ring flip", which would result in a molybdenacycle,  $\pi$ -coordinated to the nickel atom (as shown in Scheme 2, structure D), would also be consistent with the NMR data and cannot be ruled out.

(v) **Alkylation of [NiCp\* $\{\mu\text{-C}(\text{Me})\text{C}(\text{Me})\text{C}(\text{O})\text{-W}(\text{CO})_2\text{Cp}'\}$  (Ni–W, 3b') and the Structures of the Cationic Metallacycles 4 and 5.** Other data suggest that 3a in fact does have a metallacycle geometry different from that of the protonated or alkylated complexes. The structure of 5a was established by carrying out the analogous methylation reaction on the WCp' analog of 3a (complex 3b'). This WCp' derivative was chosen as it was significantly more soluble in organic solvents than its WCp analog. The methylated cationic product, [NiCp\* $\{\mu\text{-C}(\text{Me})\text{C}(\text{Me})\text{C}(\text{OMe})\text{-W}(\text{CO})_2\text{Cp}'\}^+\text{BF}_4^-$  (5c') readily is formed from the methylation of 3b', in similar fashion to the methylation of 3a to give 5b. Observable  $^{183}\text{W}$ – $^{13}\text{C}$  coupling in the  $^{13}\text{C}$  NMR spectra of 5c' led to informative structural conclusions.

Chemical shifts of all the pertinent resonances of 5c' were very similar to respective signals found in 5a,b, strongly suggesting that the two species are isostructural. (We are aware of no example in the literature where a Cp' derivative has a structure substantially different from its Cp congener in di- or polynuclear compounds.) Furthermore, the methoxy carbon atom of 5c' exhibited a  $^{183}\text{W}$ – $^{13}\text{C}$  coupling of 67 Hz, whose magnitude suggested a direct W–C  $\sigma$ -bond.<sup>7</sup> In compounds in which there are direct W–C  $\sigma$ -bonds, such

as are found in W  $\sigma$ -bound alkenyl species or in other metallacycles, larger and more readily observable  $^{183}\text{W}$ – $^{13}\text{C}$  coupling is exhibited. Some examples of  $^{183}\text{W}$ – $^{13}\text{C}$  couplings for the carbon atom  $\sigma$ -bonded to the tungsten atom are listed as illustrative examples: NiCp $\{\mu\text{-}\eta^1\text{-}(\text{W}),\eta^2(\text{Ni})\text{-CH=CH}_2\}\text{W}(\text{CO})_2(\text{CO}_2\text{CF}_3)\text{Cp}'$  (Ni–W) [78 Hz];<sup>7</sup> W $_2\{\mu\text{-C}(\text{Tol})\text{C}(\text{O})\text{C}(\text{Tol})\}(\text{CO})_4\text{Cp}_2$  (W–W) [40 Hz];<sup>34</sup> W(CO) $_2\text{Cp}'^*\{\mu\text{-C}(\text{Tol})\text{C}(\text{O})\text{C}(\text{Me})\text{C}(\text{Me})\}\text{Fe}(\text{CO})_3$  (W–Fe) [64 and 73 Hz].<sup>33</sup>

These NMR data strongly suggest that a "ring flip" has taken place in the alkylation (and by analogy, the protonation) reactions. The structures of 5c' (and, by extension, 5a,b) are thus believed to contain tungstenacycle or molybdenacycle rings. The complexes can be formulated as [NiCp\* $\{\mu\text{-}\eta^2(1,3\text{-M}),\eta^3(\text{Ni})\text{-C}(\text{Me})\text{C}(\text{Me})\text{-C}(\text{OR})\}\text{M}(\text{CO})_2\text{Cp}''\}^+\text{BF}_4^-$  (Ni–M) (M = Mo, Cp'' = Cp; 5a, R = Me; 5b, R = Et. M = W, Cp'' = Cp'; 5c', R = Me). This "ring-flip" and the structures of 5 are shown in Scheme 3. On the basis of its similar spectroscopic data, 4, [NiCp\* $\{\mu\text{-}\eta^2(1,3\text{-Mo}),\eta^3(\text{Ni})\text{-C}(\text{Me})\text{C}(\text{Me})\text{-C}(\text{OH})\}\text{Mo}(\text{CO})_2\text{Cp}'\}^+\text{BF}_4^-$ , is believed to have a similar structure and a similar allylic  $\eta^2(1,3\text{-Mo}),\eta^3(\text{Ni})$  ligation mode for the three-carbon chain.

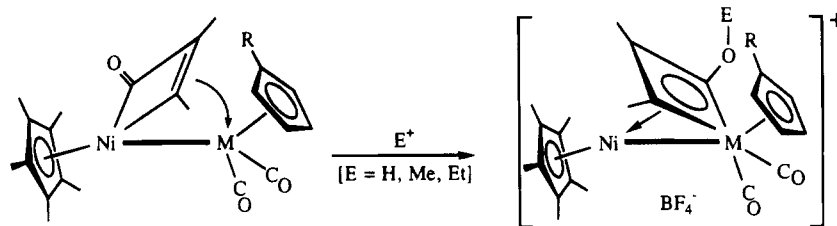
Both homo- and heterobimetallic complexes that contain a  $\mu\text{-}\eta^2,\eta^3$ -allylic group are known. Many of these species result from reactions of  $\mu$ -carbyne complexes with alkynes. Mathieu and co-workers have reported examples of alkoxy-substituted  $\mu\text{-}\eta^2,\eta^3$ -allyl complexes that were prepared through the reactions of a diiron  $\mu$ -methoxycarbyne complex with alkynes.<sup>36</sup> Stone and his group have reported many mixed-metal examples of  $\mu\text{-}\eta^2,\eta^3$ -allyl species, of which Mo(CO) $_2\text{Cp}\{\eta^2(1,3\text{-Mo}),\eta^3(\text{Fe})\text{-C}(\text{Tol})\text{C}(\text{OMe})\text{C}(\text{H})\}\text{Fe}(\text{CO})_3$  (Mo–Fe) and W(CO) $_2\text{Cp}\{\mu\text{-}\eta^2(1,3\text{-W}),\eta^3(\text{Fe})\text{-C}(\text{Tol})\text{C}(\text{Me})\text{C}(\text{Me})\}\text{Fe}(\text{CO})_3$  (W–Fe) are typical.<sup>23,33,37,38</sup> The previously

(36) Ros, J.; Commenges, G.; Mathieu, R.; Solans, X.; Font-Altaba, M. *J. Chem. Soc., Dalton Trans.* **1985**, 1087.

(37) Dare, H. F.; Howard, J. A. K.; Spaniol, T. P.; Stone, F. G. A.; Szameitat, J. *J. Chem. Soc., Dalton Trans.* **1990**, 495–504.

(38) Garcia, M. E.; Tran-Huy, N. H.; Jeffery, J. C.; Sherwood, P.; Stone, F. G. A. *J. Chem. Soc., Dalton Trans.* **1987**, 2201–2209.

**Scheme 3. Electrophilic Attack of Metallacycles 3a and 3b', Showing the Ring Flip That Occurs on Formation of the Protonated or Alkylated Products 4, 5a, 5b, and 5c'**



3a, M = Mo, R = H

3b', M = W, R = Me

4, M = Mo, R = H, E = H

5a, M = Mo, R = H, E = Me

5b, M = Mo, R = H, E = Et

5c', M = W, R = Me, E = Me

referred to protonated complex  $[W_2\{\mu-\eta^2, \eta^2-C(\text{Tol})-C(\text{OH})C(\text{Tol})\}(\text{CO})_4\text{Cp}_2]^+\text{BF}_4^-$  (W-W) is also considered to contain an allylic organic bridge.<sup>34</sup>

The structural rearrangement observed in going from 3a to 4 or 5a is not unprecedented. In the  $W_2$  complexes of general formula  $W(\text{CO})_2\text{Cp}\{\mu-C(\text{R})C(\text{R})C(\text{O})\}W(\text{CO})_2\text{Cp}$ , the bridging organic  $C(\text{R})C(\text{R})C(\text{O})$  fragments bind to the  $W_2$  framework in the same  $\mu-\eta^2(1,3), \eta^2(1,2)$ -bonding mode as is found in complexes 3.<sup>18</sup> When these species are protonated, cationic  $[W(\text{CO})_2\text{Cp}\{\mu-C(\text{R})C(\text{R})C(\text{OH})\}W(\text{CO})_2\text{Cp}]^+$  complexes form that are designated as hydroxy carbene species. The dynamic behavior of these cations has been explained by invoking a rapid series of "ring flips" of the kind that occur in going from a group 6 metallacycle in complexes 3 to a nickelaallyl complex found in 5c'. Neutral precursors to the cationic  $W_2$  species also exhibit this dynamic behavior. Furthermore, as has been remarked earlier, new W-C bonds form when the cationic hydroxy complexes  $[W(\text{CO})_4\{\mu-\eta^2(\text{CO}), \eta^4(W)-C(\text{Tol})C(\text{Me})C(\text{Me})C(\text{OH})\}-\text{Co}(\text{CO})_2(\text{PPh}_3)]^+$  (W-Co) and  $[W(\text{CO})_2\text{Cp}^*\{\mu-\eta^2(W), \eta^4(\text{Fe})-C(\text{Tol})C(\text{OH})C(\text{Me})C(\text{Me})\}Fe(\text{CO})_3]^+$  (W-Fe) are generated from their respective neutral precursors.<sup>32,33</sup>

**(d) Reaction of the Cationic Complex  $[\text{NiCp}^*\{\mu-\eta^2(1,3-\text{Mo}), \eta^3(\text{Ni})-C(\text{Me})C(\text{Me})C(\text{OMe})\}Mo(\text{CO})_2\text{Cp}]^+\text{BF}_4^-$  (Ni-Mo, 5a) with Nucleophiles. (i) Reaction with <sup>t</sup>BuNC.** Some preliminary chemistry of the cationic  $\mu-\eta^2, \eta^3$ -allyl species  $[\text{NiCp}^*\{\mu-C(\text{Me})C(\text{Me})C(\text{OMe})\}Mo(\text{CO})_2\text{Cp}]^+\text{BF}_4^-$  (5a) was investigated. A high-energy IR  $\nu(\text{CO})$  stretch [ $\nu(\text{CO}) = 2011\text{ cm}^{-1}$ ] in 5a suggested that carbonyl ligand substitution would be facile. Treatment of 5a with <sup>t</sup>BuNC and  $\text{Me}_3\text{NO}$  (trimethylamine *N*-oxide, TMNO)<sup>39,40</sup> in refluxing dichloromethane led to a reaction. Two new absorbances in the  $\nu(\text{CO})$  region of the IR spectrum were assigned to a terminal  $\nu(\text{NC})$  stretch at  $2141\text{ cm}^{-1}$  and a  $\nu(\text{CO})$  stretch at  $1935\text{ cm}^{-1}$ . These data suggested that <sup>t</sup>BuNC for CO substitution of a CO group had occurred.

Nevertheless, despite repeated attempts, we were unable to isolate the major product, believed to be the isocyanide-substituted complex  $[\text{NiCp}^*\{\mu-\eta^2(1,3-\text{Mo}), \eta^3(\text{Ni})-C(\text{Me})C(\text{Me})C(\text{OMe})\}Mo(\text{<sup>t</sup>BuNC})(\text{CO})\text{Cp}]^+\text{BF}_4^-$ , 6, present in this dark red solution. However, while we attempted to isolate 6, small quantities of bright green

crystals (7) were collected. NMR data of 7 showed that one <sup>t</sup>Bu group was present and indicated that a <sup>t</sup>BuNC moiety was incorporated. Complex 7 exhibited no  $\nu(\text{NC})$  or  $\nu(\text{CO})$  stretches in its IR spectrum. MS analysis suggested that a single Ni and a single Mo atom were present. The mass of the  $M^+$  ion suggested that 7 differed from the expected cationic substitution product  $[\text{NiCp}^*\{\mu-C(\text{Me})C(\text{Me})C(\text{OMe})\}Mo(\text{<sup>t</sup>BuNC})(\text{CO})\text{Cp}]^+\text{BF}_4^-$  (6) by carbonyl ligand loss and the incorporation of an oxygen atom. This premise was supported by the absence of a  $\nu(\text{CO})$  stretch in the IR spectrum. Solubility properties of 7 (insoluble in nonpolar organic solvents; soluble in  $\text{CH}_2\text{Cl}_2$ , thf) corroborated its ionic nature.

**(ii) Molecular Structure of Complex 7. X-ray Diffraction Study of  $[\text{NiCp}^*\{C(\text{OMe})C(\text{Me})C(\text{Me})C(\text{N}^t\text{Bu})\}Mo(\text{O})\text{Cp}]^+\text{BF}_4^-$ .** An X-ray diffraction study was carried out on a single crystal of 7. An ORTEP diagram and a sketch of the structure are shown in Figure 2. Tables 5-8, respectively, list key crystal and data collection parameters, positional parameters of all atoms, bond lengths, and bond angles of important atoms of 7.

The X-ray diffraction study showed that 7 could be formulated as  $\text{NiCp}^*\{-C(\text{OMe})C(\text{Me})C(\text{Me})C(\text{N}^t\text{Bu})\}Mo(\text{O})\text{Cp}^+\text{BF}_4^-$ . The molecule consists of  $\text{Cp}^*\text{Ni}$  and  $\text{Cp}-Mo(\text{O})$  fragments spanned by an unusual organic framework. This group consists of an almost planar  $C(\text{OMe})C(\text{Me})C(\text{Me})C(\text{N}^t\text{Bu})$  chain formed by the formal insertion of the <sup>t</sup>BuNC group into one of the Mo-C  $\sigma$ -bonds present in 5a. The  $C_{\text{MeO}}-\text{Mo}$   $\sigma$ -bond originally present in 5a remains, and the isocyanide-derived N and C atoms in the inserted <sup>t</sup>BuNC group also ligate to the molybdenum atom. All four carbon atoms in the  $C_4\text{N}$  chain bind to the nickel atom. An internuclear distance of  $3.0625(9)\text{ \AA}$  between the two metal atoms rules out significant metal-metal bonding but does not entirely preclude some bonding interactions. (Typical Ni-Mo single bonds lie in the  $2.55-2.65\text{ \AA}$  range.<sup>5,31,41-44</sup>) While the length of Mo=O double bonds, including those

(41) Chetcuti, M. J.; McDonald, S. R.; Huffman, J. C. *Inorg. Chem.* **1989**, *28*, 238-242.

(42) Curtis, M. D.; Ping, L. *J. Am. Chem. Soc.* **1989**, *111*, 8279-8280.

(43) Mlekuz, M.; Bougeard, P.; Sayer, B. G.; Peng, S.; McGlinchey, M. J.; Marinetti, A.; Saillard, J.-Y.; Naceur, J. B.; Mentzen, B.; Jaouen, G. *Organometallics* **1985**, *4*, 1123-1130.

(44) Beurich, H.; Blumhofer, R.; Vahrenkamp, H. *Chem. Ber.* **1982**, *115*, 2409-2422.

(39) Abers, M. O.; Coville, N. J. *Coord. Chem. Rev.* **1984**, *53*, 227.

(40) Luh, T.-Y. *Coord. Chem. Rev.* **1984**, *60*, 255.

**Table 5. Crystal Data and Data Collection Parameters for [NiCp\* $\{\mu\text{-}\eta^3(1,2,3\text{-Ni})\text{-C(OMe)C(Me)C(Me)CN}(\text{tBu})\text{Mo(O)Cp}\}^+\text{BF}_4^-$  (7)**

param	value	param	value
formula	C <sub>26</sub> H <sub>38</sub> BF <sub>4</sub> MoNNiO <sub>2</sub>	fw	638.05
space group	P2 <sub>1</sub> /c (No. 14)	a, Å	12.288(3)
b, Å	13.130(2)	c, Å	17.013(4)
$\beta$ , deg	93.47(1)	V, Å <sup>3</sup>	2739(2)
Z	4	$d_{\text{calc}}$ , g cm <sup>-3</sup>	1.547
cryst Dimens, mm	0.52 × 0.41 × 0.25	temp, °C	20
radiation, $\lambda$ (Å)	Mo K $\alpha$ , 0.710 69	monochromator	graphite
abs coeff $\mu$ , cm <sup>-1</sup>	11.87	abs corr applied	empirical
transm factors	0.75 (min), 1.00 (max)	diffractometer	Enraf-Nonius CAD4
scan method	$\omega$ -2 $\theta$	2 $\theta$ range, deg	4.00–45.00
<i>h, k, l</i> limits	-13 to 13, 0 to 14, 0 to 18	scan width, deg	0.70 + 0.35 tan $\theta$
		programs used	Enraf-Nonius SDP
take-off angle, deg	2.95	weighing <i>p</i> -factor	0.040
$F_{000}$	1312.0	unique data	3755
data colled	3755	no. of variables	325
data with $I > 3.0\sigma(I)$	2497	R <sup>a</sup>	0.042
		R <sub>w</sub> <sup>b</sup>	0.051
max shift/esd in final cycle	0.01	goodness of fit	1.45

$$^a R = \sum |F_o - F_c| / \sum F_o. \quad ^b R_w = [\sum w(|F_o - F_c|)^2 / \sum w F_o^2]^{1/2}.$$

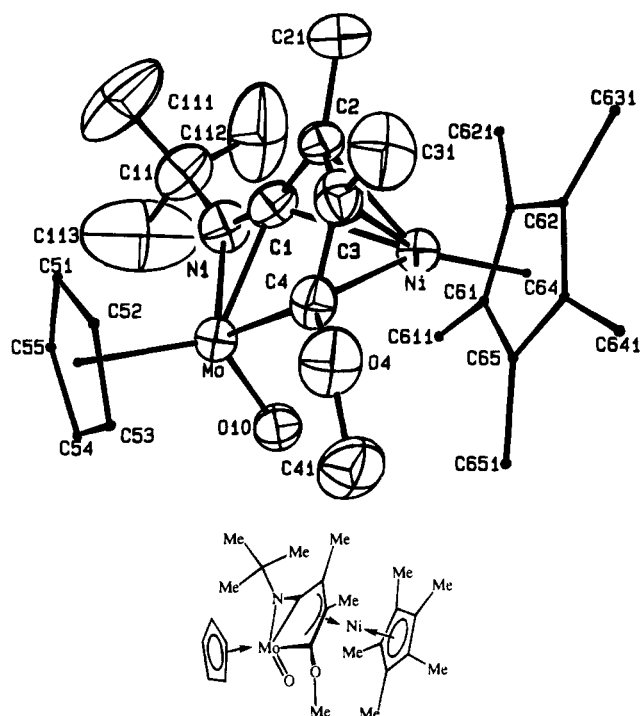


**Figure 2.** ORTEP diagram of [NiCp\* $\{\text{C(OMe)C(Me)C(Me)CN}(\text{tBu})\text{Mo(O)Cp}\}^+$ , the cationic part of **7**. The plot shows the thermal ellipsoids at the 50% probability level. Hydrogen atoms are not shown and Cp and Cp\* atoms are shown as arbitrarily small spheres, for clarity. A sketch of the structure is also shown.

bonds where there could be significant triple bond character (from O  $\pi$ -donation), "appears to vary little with oxidation state",<sup>45</sup> the value of 1.702(1) Å observed here for what is formally a Mo(IV) species is typical for such species.<sup>45–47</sup> Other compounds with similar Mo=O bond lengths (Å) include the complexes MoOCl<sub>2</sub>Cp [Mo=O = 1.740(6)],<sup>48</sup> its Cp\* analog MoOCl<sub>2</sub>Cp\* [Mo=O

**Table 6. Positional and Isotropic Thermal Parameters of the Non-Hydrogen Atoms in [NiCp\* $\{\mu\text{-}\eta^3(1,2,3\text{-Ni})\text{-C(OMe)C(Me)C(Me)CN}(\text{tBu})\text{Mo(O)Cp}\}^+\text{BF}_4^-$  (7) with Estimated Standard Deviations in Parentheses<sup>a</sup>**

atom	x	y	z	B (Å <sup>2</sup> )
Mo	0.09146(5)	0.09720(5)	0.20547(4)	3.01(1)
Ni	0.33294(7)	0.13749(6)	0.18245(5)	2.76(2)
O(4)	0.1758(4)	0.1285(4)	0.0346(3)	5.0(1)
O(10)	0.0894(4)	0.2237(4)	0.2271(3)	4.0(1)
N(1)	0.1759(5)	0.0268(5)	0.2979(3)	3.8(1)
C(1)	0.2340(6)	0.0222(5)	0.2385(4)	3.2(2)
C(2)	0.3143(5)	-0.0149(5)	0.1911(4)	3.3(2)
C(3)	0.2877(6)	0.0207(5)	0.1120(4)	3.6(2)
C(4)	0.2008(5)	0.0935(5)	0.1089(4)	3.3(1)
C(11)	0.1771(7)	-0.0308(6)	0.3754(4)	4.8(2)
C(21)	0.4004(7)	-0.0904(6)	0.2145(6)	5.4(2)
C(31)	0.3439(7)	-0.0126(7)	0.0401(5)	5.7(2)
C(41)	0.1284(8)	0.2259(7)	0.0257(5)	6.1(2)
C(51)	-0.0126(7)	-0.0596(6)	0.1872(6)	6.2(2)
C(52)	-0.0048(7)	-0.0173(7)	0.1147(5)	6.2(2)
C(53)	-0.0566(7)	0.0784(7)	0.1145(6)	6.3(2)
C(54)	-0.0990(7)	0.0904(8)	0.1880(6)	6.9(3)
C(55)	-0.0675(7)	0.0079(8)	0.2321(6)	7.1(2)
C(61)	0.3736(6)	0.2537(5)	0.2620(4)	3.3(2)
C(62)	0.4613(6)	0.1839(6)	0.2604(4)	3.7(2)
C(63)	0.4998(6)	0.1854(6)	0.1844(4)	3.8(2)
C(64)	0.4338(6)	0.2524(5)	0.1369(4)	3.7(2)
C(65)	0.3556(5)	0.2958(5)	0.1880(4)	3.3(2)
C(111)	0.165(1)	-0.1404(8)	0.3592(7)	10.2(4)
C(112)	0.281(1)	-0.007(1)	0.4228(7)	11.4(4)
C(113)	0.088(1)	0.011(1)	0.4231(7)	14.5(5)
C(611)	0.3137(7)	0.2841(7)	0.3328(5)	5.4(2)
C(621)	0.5119(7)	0.1276(7)	0.3284(6)	6.3(2)
C(631)	0.5975(7)	0.1272(7)	0.1594(6)	6.7(3)
C(641)	0.4470(8)	0.2786(8)	0.0511(5)	6.4(2)
C(651)	0.2784(7)	0.3794(6)	0.1673(6)	6.0(2)
F(1001)	0.2016(6)	0.7472(6)	0.6718(4)	11.0(2)
F(1002)	0.1794(8)	0.8811(5)	0.5971(5)	14.4(3)
F(1003)	0.2808(6)	0.7685(7)	0.5578(5)	12.7(3)
F(1004)	0.1176(7)	0.7357(8)	0.5544(5)	19.7(3)
B(1000)	0.1861(9)	0.7807(9)	0.5970(7)	6.9(3)

<sup>a</sup> B values for anisotropically refined atoms are given in the form of the isotropic equivalent thermal parameter defined as  $(4/3)[a^2\beta(1,1) + b^2\beta(2,2) + c^2\beta(3,3) + ab(\cos \gamma)\beta(1,2) + ac(\cos \beta)\beta(1,3) + bc(\cos \alpha)\beta(2,3)]$ .

= 1.683(2)],<sup>49</sup> and the bent sandwich species MoOCp'<sub>2</sub> [Mo=O = 1.721(2)],<sup>50</sup> among others.<sup>46</sup>

The short and near identical Mo–C and Mo–N bond distances [2.058(6) and 2.052(5) Å, respectively] indicate that the isocyanide ligand is bound in  $\pi$  fashion to the

(45) Pope, M. T. In *Progress in Inorganic Chemistry*; Lippard, S. J., Ed.; John Wiley and Sons: New York, 1991; Vol. 39, pp 181–257.

(46) Bottomley, F.; Sutin, L. *Adv. Organomet. Chem.* **1988**, *28*, 338–396.

(47) Tytko, K.-H.; Trobisch, U. In *Gmelin Handbook of Inorganic Chemistry*, 8th ed.; Springer Verlag: Berlin, 1987; Vol. 7, pp 67–358.

(48) Bottomley, F.; Ferris, E. C.; White, P. S. *Organometallics* **1990**, *9*, 1166–1171.

**Table 7. Key Bond Lengths (Å) for [NiCp\* $\{\mu\text{-}\eta^3(1,2,3\text{-Ni})\text{-C(OMe)C(Me)C(Me)CN}(\text{tBu})\text{Mo(O)Cp}\}^+\text{BF}_4^-$  (7) with Estimated Standard Deviations in Parentheses**

Mo-Ni	3.0625(9)	O(4)-C(4)	1.363(7)
Mo-O(10)	1.701(4)	O(4)-C(41)	1.410(9)
Mo-N(1)	2.052(5)	N(1)-C(1)	1.273(7)
Mo-C(1)	2.058(6)	N(1)-C(11)	1.518(8)
Mo-C(4)	2.185(6)	C(1)-C(2)	1.399(8)
C(2)-C(3)	1.443(8)	C(2)-C(21)	1.486(9)
C(3)-C(4)	1.432(8)	C(3)-C(31)	1.506(9)
Ni-C(1)	2.195(6)	Ni-C(2)	2.020(6)
Ni-C(3)	2.004(6)	Ni-C(4)	2.071(6)

**Table 8. Key Bond Angles (deg) for the Complex [NiCp\* $\{\mu\text{-}\eta^3(1,2,3\text{-Ni})\text{-C(OMe)C(Me)C(Me)CN}(\text{tBu})\text{Mo(O)Cp}\}^+\text{BF}_4^-$  (7) with Estimated Standard Deviations in Parentheses**

Ni-Mo-O(10)	83.5(1)	Ni-Mo-N(1)	74.1(1)
Ni-Mo-C(1)	45.8(2)	Ni-Mo-C(4)	42.5(1)
C(1)-Mo-C(4)	69.1(2)	O(10)-Mo-N(1)	106.7(2)
O(10)-Mo-C(1)	115.5(2)	O(10)-Mo-C(4)	101.7(2)
C(2)-Ni-C(3)	42.0(2)	C(2)-Ni-C(4)	71.3(2)
Mo-Ni-C(1)	42.2(2)	Mo-Ni-C(2)	72.8(2)
Mo-Ni-C(3)	73.1(2)	Mo-Ni-C(4)	45.5(2)
C(3)-Ni-C(4)	41.1(2)	C(1)-Ni-C(2)	38.5(2)
C(1)-Ni-C(3)	65.9(2)	C(1)-Ni-C(4)	68.6(2)
Mo-C(1)-N(1)	71.7(4)	Mo-C(1)-C(2)	128.8(4)
Ni-C(1)-N(1)	131.6(5)	Ni-C(1)-C(2)	63.9(3)
N(1)-C(1)-C(2)	157.3(6)	Ni-C(2)-C(1)	77.6(3)
Ni-C(2)-C(3)	68.4(3)	Ni-C(2)-C(21)	126.7(5)
C(1)-C(2)-C(3)	107.3(5)	C(1)-C(2)-C(21)	126.4(6)
C(3)-C(2)-C(21)	125.6(6)	Ni-C(3)-C(2)	69.6(3)
Ni-C(3)-C(4)	71.9(3)	Ni-C(3)-C(31)	125.7(5)
C(4)-O(4)-C(41)	118.3(6)	C(2)-C(3)-C(4)	112.1(5)
Mo-N(1)-C(1)	72.2(3)	C(2)-C(3)-C(31)	125.1(6)
Mo-N(1)-C(11)	150.2(4)	C(4)-C(3)-C(31)	122.8(6)
C(1)-N(1)-C(11)	133.5(6)	Mo-C(4)-Ni	92.0(2)
Mo-C(1)-Ni	92.1(2)	Mo-C(4)-O(4)	125.1(4)
Mo-C(4)-C(3)	118.6(4)	Ni-C(4)-O(4)	126.2(4)
Ni-C(4)-C(3)	67.0(3)	O(4)-C(4)-C(3)	112.6(5)

molybdenum atom, with the C $\equiv$ N triple bond acting as a four-electron donor to the group 6 metal. Multiple C-N bond character still exists: the <sup>t</sup>BuN-C distance is only 1.273(7) Å. The two dienyl groups are in a transoid geometry (Cp<sub>centroid</sub>-Mo-Ni-Cp<sub>centroid</sub> = 157.2°). Both the relatively large thermal anisotropies observed for the pendant Me carbon atoms of the <sup>t</sup>Bu group and the disorder observed for the BF<sub>4</sub><sup>-</sup> anion are not unusual for these moieties.

It is unclear how **7** is formed. Its structure and the reaction conditions from which it was isolated suggest that the substitution product of **6** (which was observed spectroscopically but was not isolated) could be a precursor to **7**. The observation that excess Me<sub>3</sub>NO and longer reaction times lead to greater yields of **7** is consistent with this. A possible mechanism could be the insertion of <sup>t</sup>BuNC into the metallacycle ring of **6**. This would open a coordination site at the molybdenum center, allowing attack by Me<sub>3</sub>NO to take place: formation of **7** would follow carbonyl loss. The failure to isolate the simple substitution product **6**, despite repeated attempts, has prevented a more thorough investigation into the sequence of steps that lead to the formation of complex **7**. Scheme 4 shows the formation of **6** and **7**.

(iii) Reaction of [NiCp\* $\{\mu\text{-}\eta^2(1,3\text{-Mo}),\eta^3(\text{Ni})\text{-C(Me)C(Me)C(OMe)}\}\text{Mo(CO)}_2\text{Cp}\}^+\text{BF}_4^-$  (Ni-Mo, **5a**) with KHBET<sub>3</sub>. Formation of NiCp\* $\{\mu\text{-}\eta^2(1,4\text{-Mo}),\eta^3(1,2,3\text{-Ni})\text{-C(OMe)C(Me)C(Me)C(O)}\}\text{MoH(CO)Cp}$  (Ni-Mo, **8**). Complex **5a** reacts with KHBET<sub>3</sub> to afford a single product (**8**) after workup. The IR spectrum of **8** exhibited two  $\nu(\text{CO})$  stretches at 1925 and 1605 cm<sup>-1</sup>, respectively, which suggests that both a terminal carbonyl ligand and an acyl group are present in **8**. This was corroborated by <sup>13</sup>C NMR data (Table 3). A broad singlet at -7.0 ppm in the <sup>1</sup>H NMR spectrum of **5a** is indicative of a metal hydride species. The molybdenum-bound Cp ligand resonances appeared as a doublet ( $J_{\text{H-H}} = 0.5$  Hz), which places the hydride ligand on the molybdenum atom.

The presence an acyl group in **8** implies that a carbonyl insertion reaction has occurred to possibly yield a metallacyclopentenone species. The connectivity of the newly formed ring could not be deduced unambiguously by spectroscopy, but on the basis of the formation and structure of complex **7**, in which formal isocyanide insertion into the Mo-C(Me) bond has taken place, the proposed structure of **8** features a Mo-C(O)-C(Me) linkage (shown in Scheme 5). The formulation of complex **8** as NiCp\* $\{\mu\text{-}\eta^3(1,2,3\text{-Ni})\eta^2(1,4\text{-Mo})\text{-C(OMe)C(Me)C(Me)C(O)}\}\text{MoH(CO)Cp}$  (Ni-Mo) is in accord with the observed data. Such a structure would be consistent with the formation of **8** resulting from nucleophilic attack at the molybdenum atom. Carbonyl insertion into the Mo-C(Me) bond would leave an open coordination site on the molybdenum, which could be satisfied by re-formation of a (dative) metal-metal bond. Nucleophilic induction of "CO insertion" reactions is well recognized in many monometallic systems.

(iv) Reaction of [NiCp\* $\{\mu\text{-}\eta^2(1,3\text{-Mo}),\eta^3(\text{Ni})\text{-C(Me)C(Me)C(OMe)}\}\text{Mo(CO)}_2\text{Cp}\}^+\text{BF}_4^-$  (Ni-Mo, **5a**) with I<sup>-</sup>. Formation of NiCp\* $\{\mu\text{-}\eta^2(1,3\text{-Mo}),\eta^3(\text{Ni})\text{-C(Me)C(Me)C(OMe)}\}\text{MoI(CO)Cp}$  (Ni-Mo, **9**). As complex **5a** is a cationic species, effecting a iodide-for-carbonyl ligand substitution in this species would lead to a neutral iodide complex. When **5a** was treated with 1 equiv of [<sup>n</sup>NBu<sub>4</sub>]<sup>+</sup>I<sup>-</sup>, IR spectroscopy showed that no reaction had taken place (**3a** was not regenerated either). Upon addition of Me<sub>3</sub>NO, the solution rapidly changed color (brown to red) and a new product **9** formed.

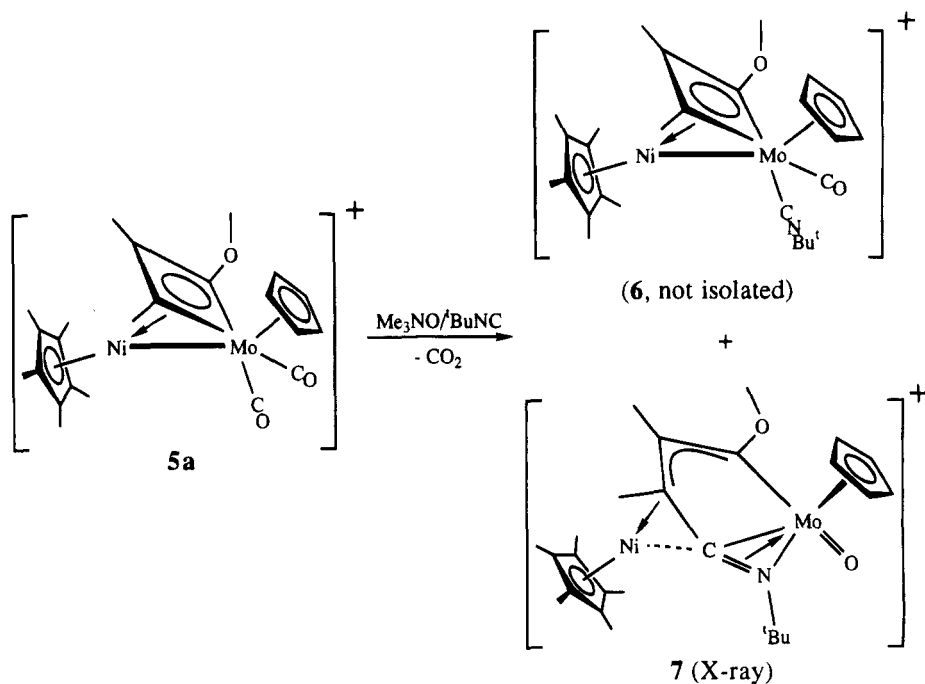
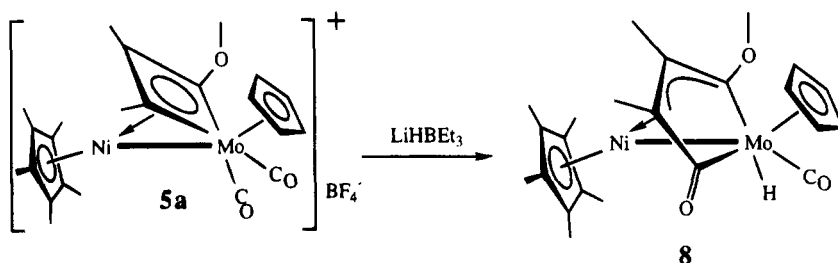
The IR spectrum of **9** showed only one  $\nu(\text{CO})$  stretch at 1900 cm<sup>-1</sup>, and a downfield <sup>13</sup>C NMR chemical shift signal was assigned to a terminal carbonyl ligand. These and other data are consistent with **9** being the neutral iodide complex NiCp\* $\{\mu\text{-}\eta^2(1,3\text{-Mo}),\eta^3(\text{Ni})\text{-C(Me)C(Me)C(OMe)}\}\text{MoI(CO)Cp}$  (Ni-Mo). The presumed structure of **9** and the reaction leading to its formation is shown in the top part of Scheme 6.

Two features of **9** are worthy of comment. In order to maintain an 18 electron count at each metal center a dative Ni-Mo bond must be invoked. Unambiguous examples of dative metal-metal bonds, with no bridging ligands, are now firmly established. These include both anionic species such as [Cr(CO)<sub>5</sub>Fe(CO)<sub>4</sub>]<sup>2-</sup> (Cr-Fe)<sup>51</sup> and neutral complexes such as W(CO)<sub>5</sub>Ir(CO)<sub>2</sub>Cp\* (W-Ir)<sup>52</sup> and [Mo(CO)<sub>5</sub>Os(CO)<sub>4</sub>{P(OMe)<sub>3</sub>}] (Mo-Os),<sup>53</sup> to name but a few. In **9**, relief from excess density on the

(49) Bottomley, F.; Boyle, P. D.; Chen, J. *Organometallics* **1994**, *13*, 370-373.

(50) Silavwe, N. D.; Chiang, M. Y.; Tyler, D. R. *Inorg. Chem.* **1990**, *24*, 4219-4221.

(51) Arndt, L. W.; Darensbourg, M. Y.; DeLord, T.; Trzcinska Bancroft, B. *J. Am. Chem. Soc.* **1986**, *108*, 2617-2627.

Scheme 4. Reaction of 5a with Me<sub>3</sub>NO/<sup>t</sup>BuNC Leading to 6 and 7Scheme 5. Reaction of 5a with LiHBET<sub>3</sub> To Afford 8

Mo atom seemingly comes not from a semibridging interaction but from enhanced  $d\pi-p\pi$  back-bonding to the terminal carbonyl ligand bound to it. The relatively low IR  $\nu(\text{CO})$  stretching frequency observed and the low-field chemical shift of the carbonyl carbon resonance in the  $^{13}\text{C}$  NMR spectrum of **9** corroborate this.

The other noteworthy feature of this reaction was that *only one* of two possible isomeric products was formed. If the group 6 metal is considered to adopt a four-legged "piano stool" geometry (ignoring the metal-metal bond), two carbonyl substitution isomers are possible in principle, depending on whether the CO ligand trans to the C(Me) or to the C(OMe) group is replaced. Steric factors could lead to differing accessibilities of the two carbonyls toward attack by Me<sub>3</sub>NO. The different *trans* effects of the asymmetric metallacycle on opposite carbonyl ligands may also account for the observed selectivity.

Which carbonyl ligand is removed is not definitively known. An X-ray diffraction study of the related nickel-tungsten PhC<sub>2</sub>H derived metallacyclic complex NiCp\* $\{\mu-\eta^2(1,3-W),\eta^3(Ni)-C(H)C(Ph)C(OMe)\}WI(CO)Cp'$  (Ni-W) indicated that the CO ligand trans to the C(OMe) group of the metallacycle was labilized and

replaced by an iodide ligand. This isomer is also assumed to be obtained here and is shown in Scheme 6.

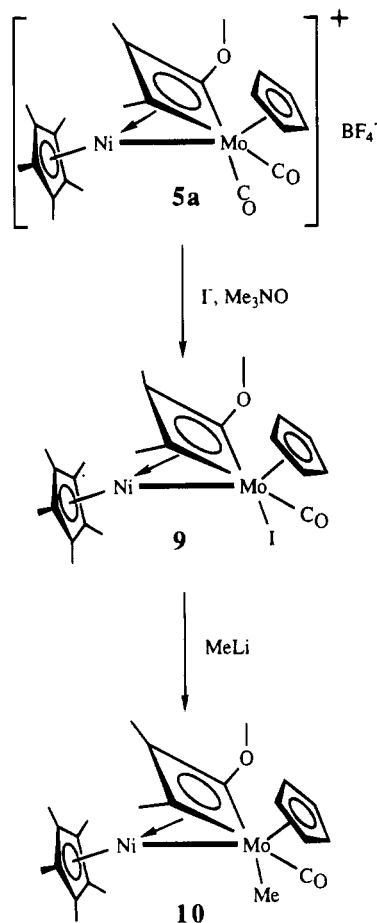
(v) **Nucleophilic Attack of NiCp\* $\{\mu-\eta^2(1,3-Mo),\eta^3(Ni)-C(Me)C(Me)C(OMe)\}MoI(CO)Cp$  (Ni-Mo, **9**) with MeLi.** Methylation of the iodo complex **9** should be possible and does indeed proceed smoothly. Treatment of **9** with 1 molar equiv of MeLi led to a new product (**10**). Complex **10** proved to be extremely air sensitive and was unstable toward chromatography. Direct crystallization as a means of purification was therefore mandatory. IR analysis of the crude reaction mixture only showed one new  $\nu(\text{CO})$  stretch.

NMR spectra of **10** are consistent with its formulation as the molybdenum methyl species NiCp\* $\{\mu-\eta^2(1,3-Mo),\eta^3(Ni)-C(Me)C(Me)C(OMe)\}MoMe(CO)Cp$  (Ni-Mo). A singlet resonance for the Mo-Me hydrogen atoms was observed at -0.82 ppm in the  $^1\text{H}$  NMR spectrum of **10**; this methyl carbon signal was similarly shifted upfield in its  $^{13}\text{C}$  NMR spectrum, appearing at -10.7 ppm. The reaction leading to the formation of **10** and the proposed structure of this compound are shown in the bottom portion of Scheme 6. As seen for **9**, only one isomer is obtained for **10**.

(vi) **Nucleophilic Attack of [NiCp\* $\{\mu-\eta^2(1,3-Mo),\eta^3(Ni)-C(Me)C(Me)-C(OMe)\}Mo(CO)_2Cp\}^+BF_4^-$  (Ni-Mo, **5a**) with MeLi.** The reaction of **5a** with MeLi was less clear. Stirring an ethereal slurry of **5a** with 1 equiv

(52) Einstein, F. W. B.; Pomeroy, R. K.; Rushman, P.; Willios, A. C. *Organometallics* **1985**, *4*, 250-255.

(53) Batchelor, R. J.; Davis, H. B.; Einstein, F. W. B.; Johnston, V. J.; Jones, R. H.; Pomeroy, R. K.; Ramos, A. F. *Organometallics* **1992**, *11*, 3555-3565.

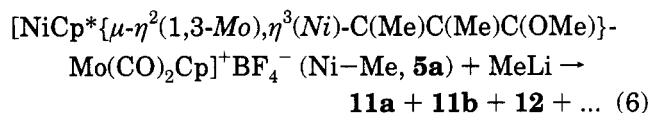
**Scheme 6. Syntheses of Complexes 9 and 10 from 5a**

of MeLi, followed by filtration and removal of solvent, led to the isolation of a mixture of products. At least three products were observed in the  $^1\text{H}$  NMR spectrum of the crude mixture. These included complexes **11a**, **11b**, and **12**. Resonances corresponding to compound **10** were not observed.

Chromatography led to the isolation of the compounds (**11a,b**) as an inseparable mixture; other products including **12** decomposed during chromatography were not further characterized. IR spectra of the mixture only show terminal  $\nu(\text{CO})$  bands (Table 3). The mass of the  $\text{M}^+$  ions and their isotopomer patterns are consistent with **11a,b** being isomers. MS data suggest that  $\text{Me}^-$  attack on **5a** takes place without further loss of ligands. Further structural elucidation of **11a,b** is clearly warranted, but X-ray-quality crystals have not yet been obtained.

The  $^1\text{H}$  NMR spectrum of the **11a/11b** mixture presents a complicated set of signals that can be interpreted by using the  $\approx 2:1$  ratio of isomers. All protons originally present in **5a** appear in both isomers, and there is an extra *Me* resonance present in the spectrum of each compound (presumably resulting from  $\text{Me}^-$  addition to **5a**). Each complex exhibits five separate methyl resonances arising from each  $\text{Cp}^*$  ligand. The integrated intensities and number of the methyl signals are consistent with two isomeric products resulting from  $\text{Me}^-$  attack on **5a** and a rearrangement involving the  $\text{Cp}^*$  such that, in each case, the five  $\text{Cp}^*$  methyl resonances are no longer equivalent. The  $^{13}\text{C}$  NMR, is not fully assignable, but corroborates this

interpretation. Structures of **11a,b** remain speculative. The reaction is summarized in eq 6.



### Conclusions

The heterobimetallic unsaturated complexes  $\text{NiCp}^*\text{M}(\text{CO})_3\text{Cp}$  ( $\text{Ni-M}$ ;  $\text{M} = \text{Mo}, \text{W}$ ) and their  $\text{WCp}'$  congeners react with alkynes to afford nickelacyclic species as the major product in which a carbonyl ligand has linked up with an alkyne. The  $\text{NiC}_3$  ring in these  $\text{NiCp}\{\mu\text{-}\eta^2(1,2\text{-M},\eta^2(1,3\text{-Ni})\text{-C}(\text{Me})\text{C}(\text{Me})\text{C}(\text{O})\}\text{M}(\text{CO})_2\text{Cp}$  ( $\text{Ni-M}$ ) species are immune to nucleophilic attack but may be protonated or alkylated with  $\text{H}^+$  or  $\text{R}^+$  sources. This electrophilic attack leads to a "ring-flip" reaction in which molybdenacycle or tungstenacycle rings are formed. The  $\text{C}(\text{Me})\text{C}(\text{Me})\text{C}(\text{OR})$  ( $\text{R} = \text{H}, \text{Me}, \text{Et}$ ) fragment in these species is best considered to be  $\eta^3$ -coordinated, in a  $\pi$ -allyl fashion, to the nickel atom.

An attempt was made to effect  $^t\text{BuNC}$  for CO substitution in the cationic  $\text{Ni-Mo}$  species  $[\text{NiCp}^*\{\mu\text{-}\eta^2(1,3\text{-Mo}),\eta^3(\text{Ni})\text{-C}(\text{Me})\text{C}(\text{Me})\text{C}(\text{OR})\}\text{Mo}(\text{CO})_2\text{Cp}]^+\text{BF}_4^-$  ( $\text{Ni-Mo}$ , **5a**):  $\text{Me}_3\text{NO}$  was added to facilitate CO removal. The only isolated product was not the expected  $^t\text{BuNC}$  substituted species (which was observed spectroscopically) but compound **8**, which results from a  $^t\text{BuNC-C}(\text{Me})\text{C}(\text{Me})\text{C}(\text{OMe})$  coupling reaction, oxidation at the molybdenum center affording a  $\text{Mo}=\text{O}$  bond and  $\text{Ni-Mo}$  bond rupture. Complex **8** was crystallographically characterized. A carbonyl ligand in the complex  $[\text{NiCp}^*\{\mu\text{-}\eta^2(1,3\text{-Mo}),\eta^3(\text{Ni})\text{-C}(\text{Me})\text{C}(\text{Me})\text{C}(\text{OR})\}\text{Mo}(\text{CO})_2\text{Cp}]^+\text{BF}_4^-$  ( $\text{Ni-Mo}$ , **5a**) may be substituted with  $\text{I}^-$ , to afford the neutral metallacyclic compound  $\text{NiCp}^*\{\mu\text{-}\eta^2(1,3\text{-Mo}),\eta^3(\text{Ni})\text{-C}(\text{Me})\text{C}(\text{Me})\text{-C}(\text{OMe})\}\text{MoI}(\text{CO})\text{Cp}$  ( $\text{Ni-Mo}$ , **9**). A straightforward Me-for-I substitution results when  $\text{NiCp}^*\{\mu\text{-}\eta^2(1,3\text{-Mo}),\eta^3(\text{Ni})\text{-C}(\text{Me})\text{C}(\text{Me})\text{C}(\text{OMe})\}\text{MoI}(\text{CO})\text{Cp}$  ( $\text{Ni-Mo}$ ) was treated with MeLi to afford the  $\text{Mo-Me}$  species  $\text{NiCp}^*\{\mu\text{-}\eta^2(1,3\text{-Mo}),\eta^3(\text{Ni})\text{-C}(\text{Me})\text{C}(\text{Me})\text{C}(\text{OMe})\}\text{MoMe}(\text{CO})\text{Cp}$  ( $\text{Ni-Mo}$ , **10**).

The methylated cationic complex  $[\text{NiCp}^*\{\mu\text{-}\eta^2(1,3\text{-Mo}),\eta^3(\text{Ni})\text{-C}(\text{Me})\text{C}(\text{Me})\text{C}(\text{OR})\}\text{Mo}(\text{CO})_2\text{Cp}]^+\text{BF}_4^-$  ( $\text{Ni-Mo}$ , **5a**) was also reacted with an  $\text{H}^-$  source ( $\text{LiHBEt}_3$ ) and with  $\text{Me}^-$  ( $\text{MeLi}$ ). The first reaction afforded the complex  $\text{NiCp}^*\{\mu\text{-}\eta^2(1,4\text{-Mo}),\eta^3(1,2,3\text{-Ni})\text{-C}(\text{OMe})\text{C}(\text{Me})\text{C}(\text{Me})\text{C}(\text{O})\}\text{MoH}(\text{CO})\text{Cp}$  ( $\text{Ni-Mo}$ ), which was spectroscopically characterized. The second reaction afforded a mixture of products, which included two isomeric species; their structures remain speculative.

Why the  $\text{NiC}_3$  rings present in **3** become  $\text{MC}_3$  ( $\text{M} = \text{Mo}, \text{W}$ ) rings when complexes **3** are protonated or alkylated and why complex **6** cannot be isolated is not obvious. These results demonstrate the rich and frequently unpredictable chemistry that results when simple reactions are attempted on an organic framework that spans two dissimilar metal centers. Further work to elucidate the identity of isomers **11a,b** and to examine other related reactions is planned.

### Experimental Section

(a) **General Techniques.** All manipulations were carried out under a  $\text{N}_2$  atmosphere using standard Schlenk tube techniques and flame-dried glassware. Reagent grade chemi-



cals were used. Solvents were purified as follows: toluene, hexanes, tetrahydrofuran (THF), and diethyl ether were distilled from blue or purple Na-benzophenone ketyl solutions under an atmosphere of prepurified nitrogen. Methylene chloride was distilled over CaH<sub>2</sub> under a N<sub>2</sub> atmosphere; reagent grade acetone was stored over 4 Å molecular sieves and deoxygenated by bubbling N<sub>2</sub> through it immediately prior to use. Deuterated NMR solvents were stored over molecular sieves under N<sub>2</sub> and were subjected to three freeze-thaw-degas cycles prior to use.

The heterodinuclear species NiCp\**M*(CO)<sub>3</sub>(C<sub>5</sub>H<sub>4</sub>R) (Ni-M, **1**) were prepared according to published procedures.<sup>14</sup> The alkynes 2-butyne and 1-phenylpropyne and phenylallene were purchased from Aldrich and used as received. Trimethyl- and triethyloxonium tetrafluoroborate (Aldrich) were stored in an oven-dried Schlenk tube under an atmosphere of nitrogen and were rinsed with several portions of dry CH<sub>2</sub>Cl<sub>2</sub> immediately prior to use. <sup>t</sup>BuNC (Aldrich) was stored under an atmosphere of nitrogen in a freezer.

**(b) Spectroscopic Measurements.** IR spectra were obtained on an IBM IR-32 FT spectrometer: the solvent-subtract function was utilized for solution spectra. Mass spectra were obtained on JEOL JMS-AX505 HA or Finnegan-Matt mass spectrometers. Low-resolution spectra were obtained using chemical ionization (CI), with isobutane as the ionization source; high-resolution spectra employed electron impact (EI) ionization and PFK as a standard. All low-resolution spectra were compared with calculated isotopomer patterns. The <sup>1</sup>H and <sup>13</sup>C NMR spectra were recorded on a GE GN-300 instrument at 300 and 75 MHz, respectively; Cr(acac)<sub>3</sub> (≈0.01 M) was added to the <sup>13</sup>C NMR samples as a shiftless relaxation agent.

**(c) Compound Syntheses.** **(i) Synthesis of NiCp\*{μ-η<sup>2</sup>(1,2-Mo),η<sup>2</sup>(1,3-Ni)-C(Me)C(Me)C(O)}Mo(CO)<sub>2</sub>Cp (Ni-Mo, **3a**).** A crude sample of **1a**, prepared on a 2.0 mmol scale, was dissolved in 30 mL of toluene and cooled to -78 °C. (As impure samples of **1a** contaminated with the homonuclear dimers [Ni(CO)Cp\*]<sub>2</sub> (Ni-Ni) and [Mo(CO)<sub>3</sub>Cp]<sub>2</sub> (Mo-Mo) do not interfere with the formation of **3a**, the prior purification of freshly prepared **1a** is unnecessary and was frequently omitted in this synthesis.) 2-Butyne (0.2 mL, 3.0 mmol) was added via syringe, and the reaction mixture was allowed to warm slowly to 0 °C. The solution was then concentrated, and applied to an alumina column. Elution with toluene gave a red band which was collected. When the eluent was changed from toluene to ether, a brown band developed, which, after collection and solvent removal, gave microcrystals of **3a** (540 mg, 55%—based on the original quantity of [Ni(CO)Cp\*]<sub>2</sub> (Ni-Ni) used to prepare **1a** and then **3a** in this one-pot procedure). Further chromatography of the red band with hexane-ether (5:1) showed that it only contained [Ni(CO)Cp\*]<sub>2</sub> (Ni-Ni) and [Mo(CO)<sub>3</sub>Cp]<sub>2</sub> (Mo-Mo) by IR spectroscopy.

**(ii) Synthesis of NiCp\*{μ-η<sup>2</sup>,η<sup>2</sup>-C(Me)C(Me)C(O)}W(CO)<sub>2</sub>Cp' (Ni-W, **3b'**).** **1b'** (≈150 mg, 0.30 mmol) was dissolved in CH<sub>2</sub>Cl<sub>2</sub> (15 mL) and cooled to -78 °C. 2-Butyne (0.05 mL, 0.6 mmol) was added, and the mixture was allowed to slowly warm to 0 °C. Filtration, followed by solvent removal, afforded **3b'** as a brown powder. Yield: >90% (by NMR).

**(iii) Synthesis of NiCp\*{μ-η<sup>2</sup>,η<sup>2</sup>-MeC<sub>2</sub>Me}Mo(CO)<sub>2</sub>Cp (Ni-Mo, **2a**).** **3a** (150 mg, 0.30 mmol) was placed in a Schlenk tube fitted with a reflux condenser, and THF (20 mL) was added. The solution was refluxed for 5 h, after which time the solvent was removed under reduced pressure, and the product was subjected to chromatography. A single orange band developed on elution with a hexane-ether mixture (5:1). Crystallization (hexane solution at -20 °C) afforded **2a** as orange needles (94 mg, 68%). HRMS (*m/e*, M<sup>+</sup>): 466.0322, calc; 466.0333, expt.

**(iv) Synthesis of NiCp\*{μ-η<sup>2</sup>,η<sup>2</sup>-C(Me)C(Ph)C(O)}W(CO)<sub>2</sub>Cp (Ni-W, **3c**) and NiCp\*{μ-η<sup>2</sup>,η<sup>2</sup>-MeC<sub>2</sub>Ph}W(CO)<sub>2</sub>Cp (Ni-W, **2c**).** **1b** (≈250 mg, 0.50 mmol) was dissolved in

toluene (20 mL), and 1-phenylpropyne (0.1 mL) was added. The mixture was stirred overnight. Chromatography and elution with a hexane-ether (29:1) mixture yielded, in order of elution, [Ni(CO)Cp\*]<sub>2</sub> (Ni-Ni), [W(CO)<sub>3</sub>Cp]<sub>2</sub> (W-W), and **2c**, isolated as an oily orange solid (140 mg, ≈46%). Adding thf to the eluent mixture afforded **3c** as a slow moving band; traces of an unidentified compound followed. **3c** was isolated as a brown crystalline solid (90 mg, ≈30%).

**(v) Protonation of Complex **3a**. Synthesis of [NiCp\*{μ-η<sup>2</sup>(1,3-Mo),η<sup>3</sup>(Ni)-C(R)C(R')C(OH)}Mo(CO)<sub>2</sub>Cp']<sup>+</sup>BF<sub>4</sub><sup>-</sup> (Ni-Mo, **4**).** **3a** (120 mg) was dissolved in ether (30 mL), and the solution was cooled to 0 °C. Excess HBF<sub>4</sub>·Et<sub>2</sub>O (≈3-4 equiv) was added, prompting immediate and complete precipitation. After the precipitation was allowed to settle, the (colorless) solvent was removed via syringe and the residue was subjected to sequential rinsings of ether (3 × 5 mL). Residual ether was evaporated under reduced pressure, leaving a reddish-black powder. <sup>1</sup>H NMR analysis of the product formed showed exclusive (>95%) formation of **4**.

**(vi) Alkylation of Metallacycles **3a** and **3b'**. Synthesis of [NiCp\*{μ-η<sup>2</sup>(1,3-Mo),η<sup>3</sup>(Ni)-C(OR'')C(R)C(R')}M(CO)<sub>2</sub>Cp']<sup>+</sup>BF<sub>4</sub><sup>-</sup> (Ni-M: M = Mo, **5a** (Cp'' = Cp, R'' = Me), **5b** (Cp'' = Cp, R'' = Et); M = W, **5c'** (R'' = Me, Cp'' = Cp')).** Alkylation of these metallacycles followed similar methods; the preparation of **5a** is typical. **3a** (691 mg, 1.16 mmol) was dissolved in CH<sub>2</sub>Cl<sub>2</sub> (20 mL), and Me<sub>3</sub>O<sup>+</sup>BF<sub>4</sub><sup>-</sup> (172 mg, 1.16 mmol) was added. The reaction mixture was stirred for 5 h. Solvent removal with a syringe led to the isolation of **5a** as a dark brown powder in quantitative yield (>95% by <sup>1</sup>H NMR). Methylation of **3b'** to afford **5c'** and ethylation of **3a** to **5b** proceeded with similar high yields. The use of 2-3 equiv of alkylating agent reduces the reaction time to 2-3 h but necessitates the filtration of unreacted R<sub>3</sub>O<sup>+</sup>BF<sub>4</sub><sup>-</sup>.

**(vii) Synthesis of [NiCp\*{μ-C(OMe)C(Me)C(Me)C(N<sup>t</sup>Bu)}Mo(O)Cp]<sup>+</sup>BF<sub>4</sub><sup>-</sup> (**7**) and the IR Detection of **6**.** A Schlenk tube was charged with **5a** (204 mg, 0.37 mmol), Me<sub>3</sub>NO (29 mg, 0.39 mmol), and CH<sub>2</sub>Cl<sub>2</sub> (30 mL). <sup>t</sup>BuNC (0.04 mL, 0.65 mmol) was added to this solution, and the mixture was refluxed for 1 h. IR bands in the resultant mixture could tentatively be assigned to **6**, but despite repeated attempts it could not be isolated. After solvent evaporation, extraction with acetone, and filtration, the brown filtrate was concentrated. Cooling to -20 °C deposited bright green crystals of **7** (including the one selected for the X-ray study).

**(viii) Nucleophilic Attack of **5a** with KBET<sub>3</sub>H. Synthesis of NiCp\*{μ-η<sup>2</sup>(1,4-Mo),η<sup>3</sup>(1,2,3-Ni)-C(OMe)C(Me)C(Me)C(O)}MoH(CO)Cp (Ni-Mo, **8**).** **5a** (150 mg, 0.25 mmol) was dissolved in CH<sub>2</sub>Cl<sub>2</sub> (15 mL) and the solution was cooled to -78 °C. KBET<sub>3</sub>H (0.25 mmol; 0.25 mL of a 1.0 M THF solution) was added. The mixture was warmed slowly to room temperature. Volatiles were removed under reduced pressure, and the product was extracted with ether. Filtration and evaporation led to the isolation of **8** as a tan powder (71 mg, 56%).

**(ix) Synthesis of NiCp\*{μ-η<sup>2</sup>(1,3-Mo),η<sup>3</sup>(Ni)-C(OMe)C(Me)C(Me)}MoI(CO)Cp (Ni-Mo, **9**).** A Schlenk tube was charged with **5a** (105 mg, 0.18 mmol), <sup>n</sup>Bu<sub>4</sub>N<sup>+</sup>I<sup>-</sup> (67 mg, 0.18 mmol), and Me<sub>3</sub>NO (17 mg, 0.22 mmol). CH<sub>2</sub>Cl<sub>2</sub> (30 mL) was added and the brown solution was refluxed for 30 min, during which time the color changed to red. Upon concentration of the solution, the mixture was filtered and subjected to chromatography. Elution with hexane-dichloromethane (2:1) gave a single, slow-moving red band. This red solution was concentrated and cooled to -20 °C. Reddish-black crystals of **9** deposited (90 mg, 82%).

**(x) Synthesis of NiCp\*{μ-η<sup>2</sup>(1,3-Mo),η<sup>3</sup>(Ni)-C(OMe)C(Me)C(Me)}MoMe(CO)Cp (Ni-Mo, **10**).** MeLi (0.22 mL of a 1.4 M solution; 0.30 mmol) was added to a solution of **9** (99 mg, 0.16 mmol) in diethyl ether (30 mL). The mixture was stirred overnight at room temperature. Excess MeLi was then quenched by adding 3 drops of water. After the solution was dried over MgSO<sub>4</sub> and filtered, solvent was removed under

reduced pressure. Hexane (10 mL) was used to redissolve the residue, and **10** was isolated as an oily brown solid ( $\approx 30$  mg, 37%) by recrystallization from hexane at  $-78$  °C. IR analysis showed that more of **10** was present in the mother liquor, but a second crop of crystals could not be grown.

**(xi) Nucleophilic Attack of 5a with MeLi. Synthesis of 11a,b.** **5a** (200 mg, 0.34 mmol) was suspended in ether (20 mL) at 0 °C. MeLi (0.25 mL of a 1.4 M ethereal solution; 0.35 mmol) was added, and the mixture was allowed to stir for 2 h. The mixture was then filtered, and the ether was removed under reduced pressure.  $^1\text{H}$  NMR analysis of the crude mixture showed three major products in a ratio of **11a**:**11b**:**12** = 62:20:18 (**12** is an unidentified product with an  $\eta^5$ -Cp\* ligand). The crude reaction mixture was subjected to chromatography on silica gel; **12** decomposed on the column. **11a,b** eluted with a hexane-dichloromethane mixture (2:1) as a single yellow band which yielded a small crop of yellow microcrystals (50 mg, 27%).  $^1\text{H}$  NMR spectral data (of the **11a,b** mixture, acetone- $d_6$ ,  $\delta$ , ppm) are as follows: **11a**, 5.13 (Cp), 3.36 (OMe), 1.92, 1.84, 1.442, 1.435, 1.414, 1.382, 1.306, 0.712 (Me signals); **11b**, 5.08 (Cp), 3.34 (OMe), 2.17, 2.12, 1.79, 1.60, 1.34, 1.25, 1.11, 0.66 (Me signals).  $^{13}\text{C}$  NMR spectral data (of **11a,b** mixture, acetone- $d_6$ ,  $\delta$ , ppm) **11a**, 248.9 (CO), 246.3 (CO), 141.5, 132.7, 106.1, 104.6, 102.7, 101.8, 99.8, 91.5 (Cp), 60.2, 57.0, 32.3 (Me), 23.8 (Me), 23.4 (Me), 11.6 (Me), 10.8 (Me), 10.5 (Me), 8.0 (Me), 7.7 (Me); **11b**, 251.9 (CO), 246.8 (CO), 150.4, 133.4, 110.6, 104.7, 103.1, 101.2, 91.5 (Cp), 57.2, 55.0, 23.3 (Me), 22.2 (Me), 11.1 (Me), 11.0 (Me), 9.4 (Me), 8.5 (Me).

**(d) X-ray Diffraction Study of  $[\text{NiCp}^*\{\mu\text{-C}(\text{OMe})\text{C}(\text{Me})\text{C}(\text{Me})\text{C}(\text{N}^t\text{Bu})\}\text{Mo}(\text{O})\text{Cp}]^+\text{BF}_4^-$  (**7**).** A small chunk of a crystal of **7**, obtained as indicated earlier, was mounted in a random orientation in a glass capillary tube, on a Enraf-Nonius CAD4 computer-controlled  $\kappa$  axis diffractometer. Cell constants and an orientation matrix for data collection were obtained from least squares refinement, using the setting angles of 25 reflections in the range  $16 < \theta < 21^\circ$ . Systematic absences of  $h0l$ ,  $l = 2n$ , and  $0k0$ ,  $k = 2n$ , and the subsequent successful refinement indicated that the space group was  $P2_1/c$  (No. 14). Lorentz-polarization corrections and an empirical absorption correction<sup>54</sup> were applied to the data.

A Patterson map located the position of the molybdenum atom: remaining atoms were located using DIRDIF and in succeeding difference Fourier syntheses. Hydrogen atoms were located and added to the structure factor calculations but their positions were not refined. The structure was refined in full-matrix least-squares where the function minimized was  $\sum w(|F_o| - |F_c|)^2$  and the weight  $w$  is defined as per the Killean and Lawrence method, with terms of 0.020 and 1.0.<sup>55</sup>

Scattering factors were from Cromer and Waber.<sup>56</sup> Anomalous dispersion effects were included in  $F_c$ ;<sup>57</sup> values for  $\partial f'$  and  $\partial f''$  were those of Cromer.<sup>58</sup> The highest peak in the final difference Fourier had a height of 0.75 e/Å<sup>3</sup>, with an estimated error based on  $\partial F'$  of 0.08.<sup>59</sup> All calculations were performed on a VAX computer using SDP/VAX software.<sup>60</sup>

**Acknowledgment.** We thank the American Chemical Society administered Petroleum Research Fund and the University of Notre Dame for support of this research.

**Supplementary Material Available:** Tables of structural data for **7**, including positional and thermal parameters for hydrogen atoms, anisotropic thermal parameters for non-hydrogen atoms, and bond lengths and bond angles for all atoms (11 pages). Ordering information is given on any current masthead page.

OM950050Q

(54) Walker, N.; Stuart, D. *Acta Crystallogr.* **1983**, *39A*, 158.

(55) Killean, R. C. G.; Lawrence, J. L. *Acta Crystallogr.* **1969**, *25B*, 1750.

(56) Cromer, D. T.; Waber, J. T. In *International Tables for X-ray Crystallography*; The Kynoch Press: Birmingham, England, 1974; Vol. IV, Table 2.2B.

(57) Ibers, J. A.; Hamilton, W. C. *Acta Crystallogr.* **1964**, *17*, 781.

(58) Cromer, D. T. In *International Tables for X-ray Crystallography*; The Kynoch Press: Birmingham, England, 1974; Vol. IV, Table 2.3.1.

(59) Cruickshank, D. W. J. *Acta Crystallogr.* **1949**, *2*, 154.

(60) Frenz, B. A. In *Computing in Crystallography*; Schenk, H., R. Olthof-Hazelkamp, R., van Koningsveld, H., Bassi, G. C., Eds.; Delft University Press: Delft, Holland, 1978; pp 64–71.

# Photochemical Metal-to-Oxo Migrations of Aryl and Alkyl Ligands

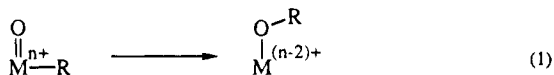
Seth N. Brown<sup>1</sup> and James M. Mayer<sup>\*,2</sup>

Department of Chemistry, P.O. Box 351700, University of Washington,  
Seattle, Washington 98195-1700

Received February 10, 1995<sup>®</sup>

Photolysis of the oxo-phenyl complex (HBpz<sub>3</sub>)ReO(Ph)Cl (HBpz<sub>3</sub> = hydrotris(1-pyrazolyl)borate) in the presence of pyridine or other donor ligands (MeCN, OPMe<sub>3</sub>) slowly gives paramagnetic rhenium(III) phenoxide complexes (HBpz<sub>3</sub>)Re(OPh)(Cl)(L). Phenyl-to-oxo migration is predominantly intramolecular, as indicated by a crossover experiment involving photolysis of (HBpz<sub>3</sub>)Re(<sup>18</sup>O)(C<sub>6</sub>H<sub>5</sub>)(Cl) and (HBpz<sub>3</sub>)Re(<sup>16</sup>O)(C<sub>6</sub>D<sub>5</sub>)(Cl). The radical traps, MeCN and PhSH, have little influence on the reaction, further ruling out the involvement of free phenyl radicals. Migration of substituted aryl ligands in (HBpz<sub>3</sub>)ReO(Cl)(Ar) (Ar = *p*-anisyl, *p*-phenoxyphenyl, 2,4-dimethylphenyl, 2,5-dimethylphenyl) occurs exclusively with carbon-oxygen bond formation to the *ipso* carbon of the aryl ligand. The reactions are therefore simple [1,2]-migrations; they are proposed to take place via nucleophilic attack of the oxo ligand on the aryl group in the excited state. Photochemical ethyl-to-oxo migration also occurs in (HBpz<sub>3</sub>)ReO(C<sub>2</sub>H<sub>5</sub>)Cl to give (HBpz<sub>3</sub>)Re(OC<sub>2</sub>H<sub>5</sub>)Cl(py). But net ethyl migration occurs by a process involving free ethyl radicals, as indicated by facile trapping by PhSH. Thus two different mechanisms are involved in these processes, the first clear examples of [1,2]-migration of hydrocarbon ligands from a metal to an oxo group.

Migration of an alkyl or aryl ligand to a coordinated oxo group (eq 1) has been proposed as a way of transferring oxidizing equivalents from a metal complex to an organic fragment.<sup>3</sup> This reaction has never been observed directly,<sup>4</sup> though the reverse reaction, involving alkyl or hydride migration to metal centers, has been documented in a handful of cases.<sup>5</sup>

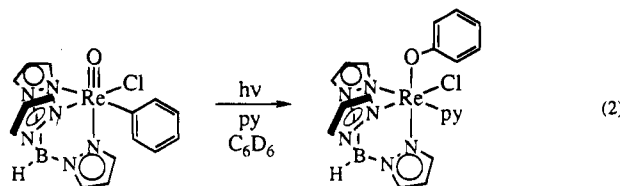


The selective oxidation of organic groups is of importance in a variety of areas of chemistry, and the involvement of organometallic complexes, as in eq 1, is an area of great promise. For instance, the transformation of eq 1, coupled with formation of metal-carbon bonds from hydrocarbons, could be a method of hydrocarbon oxidation with novel selectivity. We have previously reported the photochemical formation of rhenium(V) oxo-aryl complexes from rhenium(V) iodide com-

plexes and arenes.<sup>6</sup> In this paper, the subsequent photochemical aryl-to-oxo migration of these compounds to give aryloxo complexes is described. The preparation and analogous migration reaction of an oxo-ethyl complex is also discussed. Surprisingly, aryl and saturated alkyl ligands undergo the same formal migration by quite different mechanisms. A portion of this work has been previously reported.<sup>6a</sup>

## Results

**Synthesis and Structure of (HBpz<sub>3</sub>)Re(OPh)(Cl)(py).** When the oxo-phenyl complex (HBpz<sub>3</sub>)ReO(Ph)Cl (HBpz<sub>3</sub> = hydrotris(1-pyrazolyl)borate) is photolyzed in benzene in the presence of a few equivalents of pyridine, NMR signals for the oxo complex slowly decrease in intensity. They are replaced by signals due to a red paramagnetic complex, (HBpz<sub>3</sub>)Re(OPh)(Cl)(py) (eq 2), which can be separated from unreacted starting



material by column chromatography on silica gel. The phenoxide complex is stable to air for a few weeks in solution and indefinitely in the solid state. The photo-reaction takes place in good yield (85% based on converted rhenium) but goes rather slowly (~80% conversion in 10 days) and slows down dramatically as the reaction proceeds, presumably because of light

(6) (a) Brown, S. N.; Mayer, J. M. *J. Am. Chem. Soc.* **1994**, *116*, 2219–2220. (b) Brown, S. N. Ph.D. Thesis, University of Washington, Seattle, WA, 1994; Chapter 2.

<sup>®</sup> Abstract published in *Advance ACS Abstracts*, May 15, 1995.  
(1) Current address: Department of Chemistry 164-30, California Institute of Technology, Pasadena, CA 91125. Electronic mail: snbrown@cco.caltech.edu.

(2) Electronic mail: mayer@macmail.chem.washington.edu.  
(3) (a) Sharpless, K. B.; Teranishi, A. Y.; Bäckvall, J.-E. *J. Am. Chem. Soc.* **1977**, *99*, 3120–3128. (b) Hentges, S. G.; Sharpless, K. B. *J. Am. Chem. Soc.* **1980**, *102*, 4263–4265. (c) Göbel, T.; Sharpless, K. B. *Angew. Chem., Int. Ed. Engl.* **1993**, *32*, 1329–1331. (d) Gable, K. P.; Phan, T. N. *J. Am. Chem. Soc.* **1994**, *116*, 833–839. (e) Jørgensen, K. A.; Schiøtt, B. *Chem. Rev.* **1990**, *90*, 1483–1506.

(4) This or similar migrations have been proposed on the basis of indirect evidence, e.g.: (a) Reichle, W. T.; Carrick, W. L. *J. Organomet. Chem.* **1970**, *24*, 419–426. (b) Nugent, W. A.; Harlow, R. L. *J. Am. Chem. Soc.* **1980**, *102*, 1759–1760. (c) Vivanco, M.; Ruiz, J.; Floriani, C.; Chiesi-Villa, A.; Rizzoli, C. *Organometallics* **1993**, *12*, 1802–1810.

(5) (a) van Asselt, A.; Burger, B. J.; Gibson, V. C.; Bercaw, J. E. *J. Am. Chem. Soc.* **1986**, *108*, 5347–5349. (b) Parkin, G.; Bunel, E.; Burger, B. J.; Trimmer, M. S.; van Asselt, A.; Bercaw, J. E. *J. Mol. Catal.* **1987**, *41*, 21–41. (c) Nelson, J. E.; Parkin, G.; Bercaw, J. E. *Organometallics* **1992**, *11*, 2181–2189. (d) Tahmassebi, S. K.; Conry, R. R.; Mayer, J. M. *J. Am. Chem. Soc.* **1993**, *115*, 7553–7554.

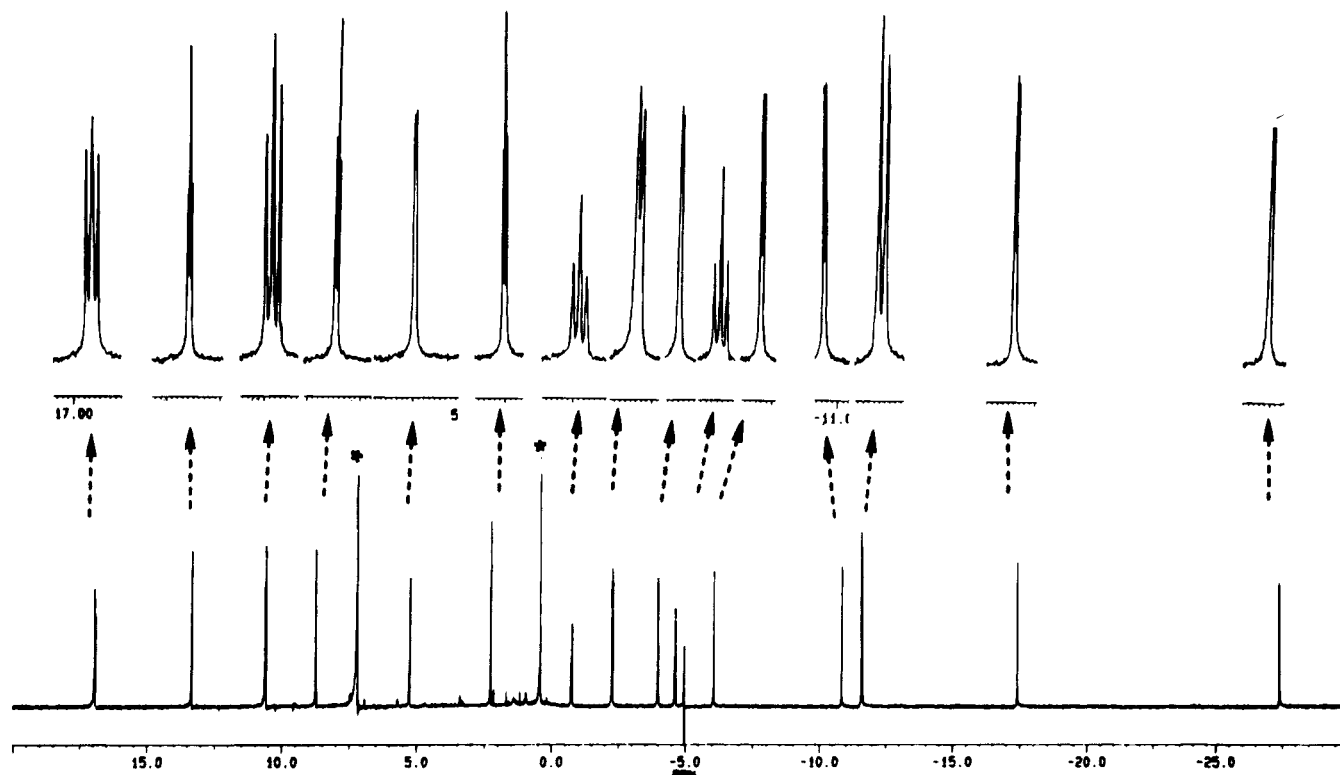


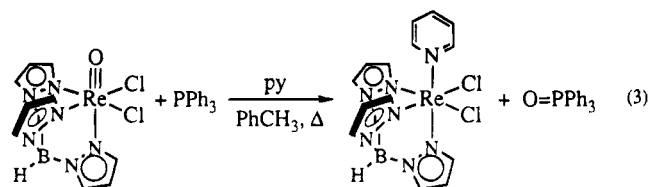
**Figure 1.**  $^1\text{H}$  NMR spectrum of  $(\text{HBpz}_3)\text{Re}(\text{OPh})(\text{Cl})(\text{py})$  in  $\text{C}_6\text{D}_6$ . An expanded plot of each peak is displayed on the upper part of the figure. Peaks due to  $\text{C}_6\text{D}_5\text{H}$  ( $\delta$  7.15) and  $\text{H}_2\text{O}$  ( $\delta$  0.40) are marked with asterisks.

absorption by the product. Since  $(\text{HBpz}_3)\text{ReO}(\text{Ph})\text{Cl}$  is formed in high yield on photolysis of  $(\text{HBpz}_3)\text{ReO}(\text{Cl})\text{I}$  in benzene in the presence of pyridine,<sup>6</sup>  $(\text{HBpz}_3)\text{Re}(\text{OPh})(\text{Cl})(\text{py})$  can be prepared in one pot simply by prolonged photolysis of  $(\text{HBpz}_3)\text{ReO}(\text{Cl})\text{I}$  under these conditions. This represents a net oxidation of benzene to phenoxide.

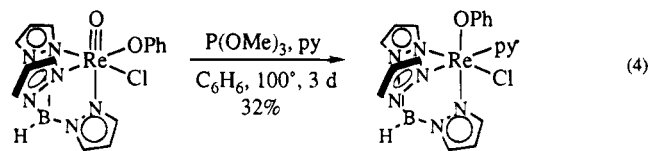
The product is identified as the phenoxide complex  $(\text{HBpz}_3)\text{Re}(\text{OPh})(\text{Cl})(\text{py})$  on the basis of spectroscopic, chemical, and structural data. Its mass spectrum shows a parent ion at  $m/z = 607$ , and the IR spectrum lacks a metal-oxo stretch but has a strong C–O stretch at  $1258\text{ cm}^{-1}$  absent in the starting material. The  $^1\text{H}$  NMR spectrum (Figure 1) is paramagnetically shifted but extremely sharp (the 2 Hz couplings of the pyrazole protons are easily seen), as expected for an octahedral rhenium(III) complex.<sup>7</sup> There are resonances due to three inequivalent pyrazole groups (three triplets and six doublets), indicating the absence of any symmetry in the molecule. There is also one pyridine ligand ( $\delta$   $-2.32$ ,  $+16.92$ , and  $-0.79$  ppm in  $\text{C}_6\text{D}_6$ ) and one phenyl group ( $\delta$   $-11.71$ ,  $+10.56$ , and  $-4.73$  ppm) whose resonances are absent if the compound is made from  $(\text{HBpz}_3)\text{ReO}(\text{C}_6\text{D}_5)\text{Cl}$ .

$(\text{HBpz}_3)\text{Re}(\text{OPh})(\text{Cl})(\text{py})$  can be synthesized independently by reduction of the rhenium(V) phenoxide complex  $(\text{HBpz}_3)\text{ReO}(\text{OPh})\text{Cl}$ , formed by treatment of  $(\text{HBpz}_3)\text{ReOCl}_2$  with  $\text{TiOPh}$ . Deoxygenation of rhenium(V) precursors in the presence of an appropriate ligand is a general route to rhenium(III) complexes,<sup>8</sup> as illustrated by the synthesis of  $(\text{HBpz}_3)\text{ReCl}_2(\text{py})$  (eq 3);

the diamagnetic 3-hexyne complex  $(\text{HBpz}_3)\text{ReCl}_2(\text{EtC}\equiv\text{CEt})$  may be prepared analogously.



Deoxygenation of  $(\text{HBpz}_3)\text{ReO}(\text{OPh})\text{Cl}$  is accomplished by treatment with trimethyl phosphite under forcing conditions. In the presence of pyridine, this forms  $(\text{HBpz}_3)\text{Re}(\text{OPh})(\text{Cl})(\text{py})$ , which is spectroscopically identical to that formed by photoinduced migration of the phenyl group in  $(\text{HBpz}_3)\text{ReO}(\text{Ph})\text{Cl}$  (eq 4).



Reduction of the rhenium(V) phenoxide complex is preferred over the photochemical reaction as a synthetic method for the rhenium(III) phenoxide despite its lower yield since the internal filtering effects in the latter procedure drastically limit the conversion possible in large-scale preparations. Attempts to synthesize the phenoxide complex by metathesis of a chloride ligand

(7) (a) Shaw, D.; Randall, E. W. *J. Chem. Soc., Chem. Commun.* **1965**, 82–83. (b) Chatt, J.; Leigh, G. J.; Mingos, D. M. P. *J. Chem. Soc. A* **1969**, 1674–1680. (c) Randall, E. W.; Shaw, D. *J. Chem. Soc. A* **1969**, 2867–2872.

(8) (a) Rouschias, G. *Chem. Rev.* **1974**, *74*, 531–566. (b) Abrams, M. J.; Davison, A.; Jones, A. G. *Inorg. Chim. Acta* **1984**, *82*, 125–128. (c) Conry, R. R.; Mayer, J. M. *Inorg. Chem.* **1990**, *29*, 4862–4867. (d) Paulo, A.; Domingos, A.; Pires de Matos, A.; Santos, I.; Carvalho, M. F. N. N.; Pombeiro, A. J. L. *Inorg. Chem.* **1994**, *33*, 4729–4737. (e) Brown, S. N.; Masui, C. S.; Mayer, J. M.; Schneemeyer, L. F.; Waszczak, J. V. Manuscript in preparation.

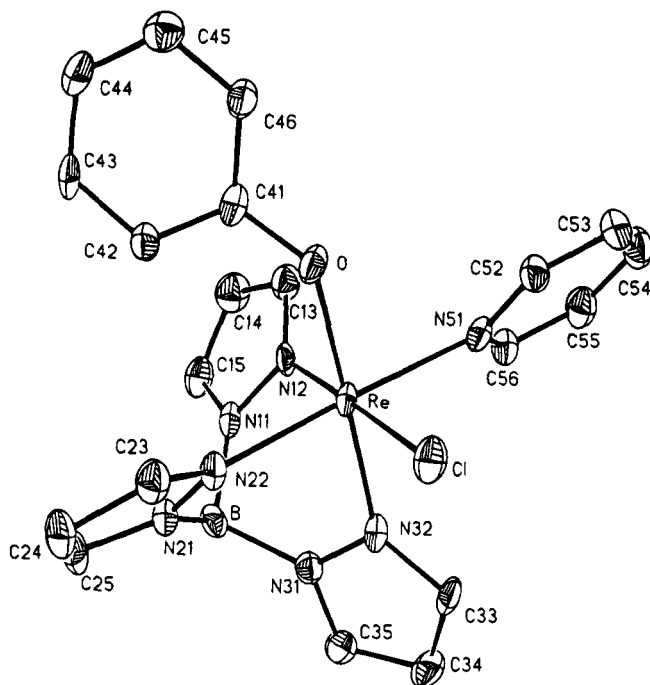
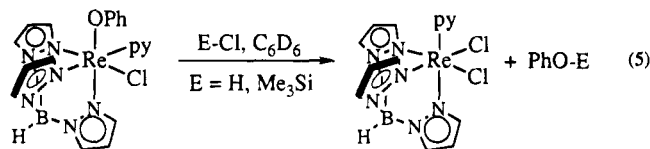


Figure 2. ORTEP diagram of  $(\text{HBpz}_3)\text{Re}(\text{OPh})(\text{Cl})(\text{py})$ .

in the rhenium(III) complex  $(\text{HBpz}_3)\text{ReCl}_2(\text{py})$  with lithium phenoxide or thallium alkoxides have been unsuccessful.

The phenoxide group in  $(\text{HBpz}_3)\text{Re}(\text{OPh})(\text{Cl})(\text{py})$  may be removed from the rhenium by electrophilic reagents. Concentrated aqueous HCl immediately releases phenol and forms  $(\text{HBpz}_3)\text{ReCl}_2(\text{py})$  from a benzene solution of the rhenium(III) phenoxide complex. Trimethylsilyl chloride reacts analogously, but more slowly (32 days, 85 °C), to give the same rhenium product and  $\text{PhOSiMe}_3$  (eq 5).



The structure of  $(\text{HBpz}_3)\text{Re}(\text{OPh})(\text{Cl})(\text{py})$  was determined by single-crystal X-ray diffraction. An ORTEP diagram is shown in Figure 2, crystallographic details are listed in Table 1, and bond distances and angles are in Table 2. The molecular structure is essentially superimposable with that of  $(\text{HBpz}_3)\text{ReCl}_2(\text{py})$ ,<sup>9</sup> with the phenoxide group substituted for one chloride. The coordination geometry in each case is a regular octahedron with a symmetrically bonded  $\text{HBpz}_3$  ligand (deviations from octahedral angles  $\leq 5^\circ$ ), in contrast to the [tris(pyrazolyl)borato]rhenium oxo complexes which invariably show substantial distortions due to the large *trans* influence of the oxo ligand.<sup>10</sup> The pyridine is bound 0.057(8) Å farther away from the rhenium than are the pyrazole nitrogens, on average. The pyridine ring and the phenyl ring of the phenoxide are oriented to bisect clefts between *cis* pyrazoles. This is also true of the phenyl groups in  $(\text{HBpz}_3)\text{ReO}(\text{Ph})_2$ <sup>6b</sup> and is presumably for steric reasons.

Table 1. Crystal Data for  $(\text{HBpz}_3)\text{Re}(\text{OPh})(\text{Cl})(\text{py}) \cdot \text{C}_6\text{D}_6$

formula	$\text{C}_{28}\text{H}_{20}\text{D}_6\text{BClN}_7\text{ORe}$
fw	691.05
cryst size, mm <sup>3</sup>	0.1 × 0.15 × 0.25
space group	$P\bar{1}$
$\lambda$ , Å	0.710 73
$T$ , °C	−90
$a$ , Å	8.874(2)
$b$ , Å	11.917(2)
$c$ , Å	13.070(3)
$\alpha$ , deg	92.58(2)
$\beta$ , deg	98.29(1)
$\gamma$ , deg	105.16(1)
$Z$	2
$V$ , Å <sup>3</sup>	1315.2(4)
$\rho_{\text{calcd}}$ , g cm <sup>−3</sup>	1.745
$\mu$ , cm <sup>−1</sup>	47.55
no. of reflns measd	6228
no. of unique reflns	4613
no. of obsd reflns	4010 ( $F > 4\sigma F$ )
no. of refined params	335
$R_{\text{av}}$	0.0195
$R$	0.0384
$R_w$	0.0412
goodness of fit	1.09

Table 2. Selected Bond Distances (Å) and Bond Angles (deg) in  $(\text{HBpz}_3)\text{Re}(\text{OPh})(\text{Cl})(\text{py}) \cdot \text{C}_6\text{D}_6$

Re—O	2.004(4)	Re—Cl	2.391(2)
Re—N(32)	2.091(5)	Re—N(51)	2.146(4)
Re—N(12)	2.084(5)	O—C(41)	1.351(6)
Re—N(22)	2.093(4)		
O—Re—Cl	91.7(1)	Cl—Re—N(51)	89.9(1)
O—Re—N(51)	86.9(2)	Cl—Re—N(12)	177.3(1)
O—Re—N(12)	91.1(2)	Cl—Re—N(22)	91.5(1)
O—Re—N(22)	95.3(2)	Cl—Re—N(32)	91.1(1)
O—Re—N(32)	177.1(2)	N(12)—Re—N(22)	88.5(2)
N(51)—Re—N(12)	90.0(2)	N(12)—Re—N(32)	86.2(2)
N(51)—Re—N(22)	177.4(2)	N(22)—Re—N(32)	83.6(2)
N(51)—Re—N(32)	94.1(2)	Re—O—C(41)	130.8(4)

The phenoxide group in  $(\text{HBpz}_3)\text{Re}(\text{OPh})(\text{Cl})(\text{py})$  is strongly bent ( $\angle \text{Re—O—C}(41) = 130.8(4)^\circ$ ). The rhenium—oxygen distance of 2.004(4) Å is slightly longer than that in the rhenium(III) oxo phenoxide complex  $(\text{MeC}\equiv\text{CMe})_2\text{Re}(\text{O})(\text{OPh})$  (1.966(14) Å),<sup>11</sup> in which some Re—O  $\pi$  bonding was proposed to be present, but significantly shorter than the distance in the  $d^5$ -cresolate complex *fac*-(CO)<sub>3</sub>(PPh<sub>3</sub>)<sub>2</sub>Re(OC<sub>6</sub>H<sub>4</sub>Me) (2.143(4) Å),<sup>12</sup> where only  $\pi$ -antibonding interactions are possible. Both of these structures also have small Re—O—C angles (124.5(11)° and 131.5(11)°). The rhenium—phenoxide bond appears to be normal, with neither significant  $\pi$ -bonding nor  $\pi$ -antibonding interactions, consistent with the complex's chemistry, which shows that the aryloxo linkage is not especially reactive.

**Mechanism and Scope of Aryl-to-Oxo Migration Reactions.** The oxo—phenyl complex  $(\text{HBpz}_3)\text{ReO}(\text{Ph})\text{Cl}$  is blue due to a d—d band ( $\lambda_{\text{max}} = 661 \text{ nm}$ ,  $\epsilon = 120 \text{ M}^{-1} \text{ cm}^{-1}$ ). However, intense visible light (filtered through a  $\lambda > 455 \text{ nm}$  filter) does not lead to rearrangement. Instead, the photochemically active band appears to be a charge-transfer band in the near UV (321 nm,  $\epsilon = 3000 \text{ M}^{-1} \text{ cm}^{-1}$ ). Though the complex has absorption bands at higher energy, these do not appear to contribute significantly to the reaction, since photolysis of acetonitrile solutions of  $(\text{HBpz}_3)\text{ReO}(\text{Ph})\text{Cl}$  in thin-

(9) (a) Brown, S. N. Ph.D. Thesis, University of Washington, Seattle, WA, 1994; Chapter 3. (b) Reference 8e.

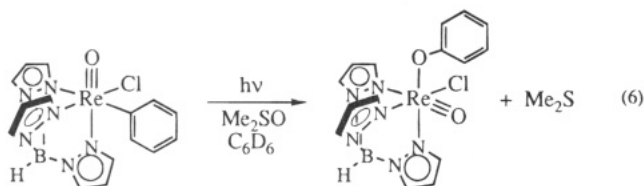
(10) (a) Brown, S. N.; Mayer, J. M. *Inorg. Chem.* **1992**, *31*, 4091–4100. (b) Reference 8d and references therein.

(11) Erikson, T. K. G.; Bryan, J. C.; Mayer, J. M. *Organometallics* **1988**, *7*, 1930–1938.

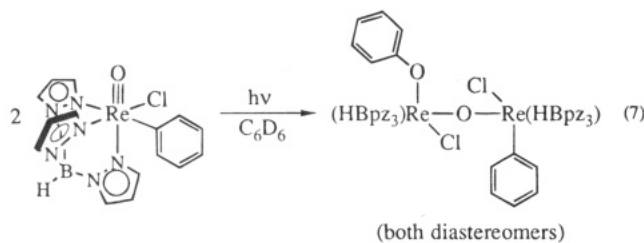
(12) Simpson, R. D.; Bergman, R. G. *Organometallics* **1993**, *12*, 781–796.

walled NMR tubes produces migration products at equal rates in the presence or absence of a thick-walled Pyrex beaker ( $\lambda > 300$  nm). The charge-transfer band at 321 nm is higher in energy than any associated with the chloride ligand, as the lowest-energy charge-transfer band in  $(\text{HBpz}_3)\text{ReOCl}_2$  is at 259 nm.<sup>8b</sup> Since the charge-transfer band shifts to lower energy in the anisyl complex  $(\text{HBpz}_3)\text{ReO}(p\text{-C}_6\text{H}_4\text{OMe})\text{Cl}$  ( $\lambda_{\text{max}} = 356$  nm),<sup>6</sup> it may be assigned as phenyl  $\pi$  to metal d (rhenium-oxo  $\pi^*$ ).

Photochemical phenyl-to-oxo migration does not depend on the presence of pyridine. Photolysis in neat  $\text{CH}_3\text{CN}$  or in benzene solutions containing  $\text{Me}_3\text{PO}$  produce paramagnetic adducts  $(\text{HBpz}_3)\text{Re}(\text{OPh})(\text{Cl})(\text{L})$  ( $\text{L} = \text{CH}_3\text{CN}, \text{Me}_3\text{PO}$ ) analogous to the pyridine complex described above. The  $\text{C}\equiv\text{N}$  stretching frequency drops slightly on coordination to the  $(\text{HBpz}_3)\text{Re}(\text{OPh})(\text{Cl})$  fragment ( $2244\text{ cm}^{-1}$  vs  $2255\text{ cm}^{-1}$  in free  $\text{CH}_3\text{CN}$ <sup>13</sup>), possibly indicating some degree of back-bonding by the rhenium(III) center.<sup>14</sup> Dimethyl sulfoxide presumably also binds, but the observed product is the diamagnetic oxo-phenoxide  $(\text{HBpz}_3)\text{ReO}(\text{OPh})(\text{Cl})$  due to net oxygen atom transfer from  $\text{Me}_2\text{SO}$  (eq 6). The apparent rate of disappearance of  $(\text{HBpz}_3)\text{ReO}(\text{Ph})\text{Cl}$  is in all cases unaffected by the nature of the added trap.



In the absence of added ligands, photolysis of  $(\text{HBpz}_3)\text{ReO}(\text{Ph})\text{Cl}$  causes the solution to darken and two new paramagnetic compounds to appear, tentatively assigned as the two diastereomers of an unsymmetric  $\mu$ -oxo rhenium(IV) dimer,  $(\text{HBpz}_3)\text{Re}(\text{OPh})(\text{Cl})(\mu\text{-O})(\text{Ph})(\text{Cl})\text{Re}(\text{HBpz}_3)$  (eq 7).



The dimers have been identified on the basis of FAB mass spectra ( $m/z = 1054$  with the expected isotope envelope) and their complex, paramagnetically shifted  $^1\text{H}$  NMR spectra (each isomer is expected to have 24 resonances). Two compounds are clearly present, as one precipitates selectively as the reaction proceeds. These dimers may be viewed as "adducts" of the photochemically generated rhenium(III) fragment  $[(\text{HBpz}_3)\text{Re}(\text{OPh})(\text{Cl})]$  with the unreacted oxo complex. Indeed,  $(\text{HBpz}_3)\text{ReO}(\text{Ph})\text{Cl}$  disappears twice as quickly in the absence of ligands as in their presence, consistent with each photochemical event consuming two molecules of the starting material.

(13) Butt, G.; Cilmi, J.; Hoobin, P. M.; Topsom, R. D. *Spectrochim. Acta* **1980**, *36A*, 521–524.

(14) Storhoff, B. N.; Lewis, H. C., Jr. *Coord. Chem. Revs.* **1977**, *23*, 1–29.

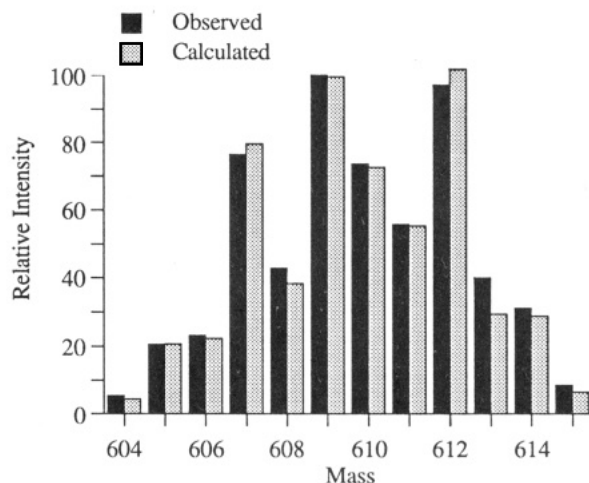
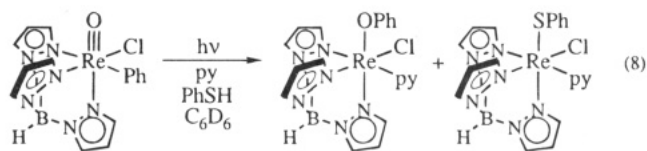


**Figure 3.** Observed and calculated isotope patterns for  $(\text{HBpz}_3)\text{Re}(\text{OPh})(\text{Cl})(\text{py})$  formed by photolysis of 44.8%  $(\text{HBpz}_3)\text{Re}^{16}\text{O}(\text{C}_6\text{D}_5)(\text{Cl})$  and 55.2%  $(\text{HBpz}_3)\text{Re}^{16}\text{O}(\text{C}_6\text{H}_5)(\text{Cl})$  ( $^{16}\text{O} = 64.4\%$   $^{18}\text{O}$ ). The calculated isotope pattern assumes an entirely intramolecular reaction.

Phenyl-to-oxo migration is predominantly intramolecular, as little crossover is observed by FABMS in the products of photolysis of a mixture of  $(\text{HBpz}_3)\text{Re}^{18}\text{O}(\text{C}_6\text{H}_5)(\text{Cl})$  and  $(\text{HBpz}_3)\text{Re}^{16}\text{O}(\text{C}_6\text{D}_5)(\text{Cl})$  in the presence of pyridine (Figure 3). The observed mass spectrum of  $(\text{HBpz}_3)\text{Re}(\text{OPh})(\text{Cl})(\text{py})$  is consistent with an entirely intramolecular migration, though small amounts of crossover ( $<15\%$ ) would not be detectable by this technique. In particular, this result indicates that free phenyl radicals do not participate in the migration. Phenyl radicals are further excluded by the observation that photolysis in neat  $\text{CD}_3\text{CN}$  smoothly produces  $(\text{HBpz}_3)\text{Re}(\text{OPh})(\text{Cl})(\text{NCCD}_3)$  with no sign of  $\text{C}_6\text{H}_5\text{D}$ .  $\text{Ph}^\cdot$  abstracts hydrogen atoms from  $\text{CH}_3\text{CN}$  at a rate of  $10^5\text{ M}^{-1}\text{ s}^{-1}$ ,<sup>15</sup> so neat acetonitrile (26 M) is a good radical trap (typical rhenium starting material concentrations are 0.02 M). The more reactive radical trap thiophenol ( $k = 10^9\text{ M}^{-1}\text{ s}^{-1}$  for  $\text{Ph}^\cdot + \text{PhSH}$ )<sup>15</sup> also does not interfere with rearrangement, though in this case some rhenium(III) thiophenoxide complex  $(\text{HBpz}_3)\text{Re}(\text{SPh})(\text{Cl})(\text{py})$  is formed in addition to the usual migration product (eq 8). Interaction of the  $\text{PhSH}$  with the rhenium presumably occurs after migration since reduction to rhenium(III) has already taken place.

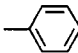
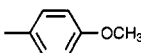
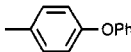
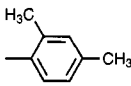
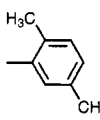


Photochemical aryl-to-oxo migration occurs in a variety of substituted phenyl complexes of the general formula  $(\text{HBpz}_3)\text{ReO}(\text{Cl})(\text{Ar})$  ( $\text{Ar} = p\text{-anisyl}, p\text{-phenoxyphenyl}, 2,4\text{-dimethylphenyl}, 2,5\text{-dimethylphenyl}$ ). In each case, migration occurs exclusively to the *ipso* carbon of the aromatic ligand (e.g., eq 9).

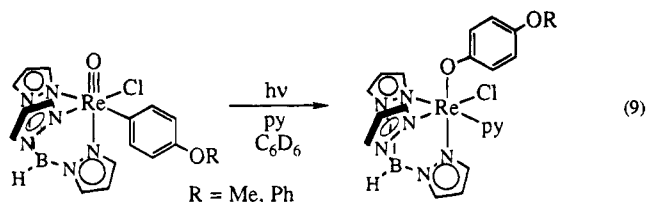
The NMR spectra of the various rhenium(III) aryloxide pyridine complexes are compiled in Table 3. In all

(15) Asmus, K.-D.; Bonifacic, M. In *Radical Reaction Rates in Liquids*; Fischer, H., Ed.; Landolt-Börnstein New Series; Springer-Verlag: Berlin, 1984; Vol. 13, Subvol. b, Carbon-centered Radicals II, pp 25–26, 182, 193.

Table 3.  $^1\text{H}$  NMR Spectra of  $(\text{HBpz}_3)\text{Re}(\text{OR})(\text{Cl})(\text{py})$  (in  $\text{C}_6\text{D}_6$ )

R	pyrazole 4-H <sup>a</sup>	pyrazole 3-H, 5-H <sup>b</sup>	py	R (aromatic)	R (other)
	2.22 8.74 13.30	-27.40 -17.48 -10.89 -6.12 -4.07 +5.22	-2.32 d, 4 Hz (2,6-H) 16.92 dd, 8, 6 Hz (3,5-H) -0.79 t, 8 Hz (4-H)	-11.71 d, 8 Hz (2,6-H) 10.56 t, 8 Hz (3,5-H) -4.73 t, 8 Hz (4-H)	
	2.23 8.95 13.44	-27.73 -17.01 -10.28 -5.53 -3.69 +5.37	-1.77 d, 5 Hz (2,6-H) 16.92 t, 7 Hz (3,5-H) -0.46 t, 8 Hz (4-H)	-12.10 d, 9 Hz (2,6-H) 10.00 d, 9 Hz (3,5-H)	3.30 (s, 3H; -OCH <sub>3</sub> )
	2.27 8.52 13.34	-27.05 -17.28 -10.85 -5.98 -4.13 +5.29	-2.23 d, 5 Hz (2,6-H) 16.98 t, 7 Hz (3,5-H) -0.71 t, 8 Hz (4-H)	-11.30 d, 9 Hz (2,6-H) 10.20 d, 9 Hz (3,5-H)	6.30 (d, 8 Hz, 2H; <i>o</i> -Ph) 6.98 (t, 8 Hz, 2H; <i>m</i> -Ph) 6.62 (t, 7 Hz, 1H; <i>p</i> -Ph)
	2.26 8.93 13.53	-27.52 -17.06 -9.94 -5.07 -4.04 +4.79	-1.67 d, 5 Hz (2,6-H) 17.10 t, 7 Hz (3,5-H) -0.47 tt, 8,1 Hz (4-H)	-12.09 d, 8 Hz (6-H) 8.74 d, 2 Hz (3-H) 13.35 d, 8 Hz (5-H)	3.16 (s, 3H; 2-CH <sub>3</sub> ) 11.07 (s, 3H; 4-CH <sub>3</sub> )
	2.29 8.95 13.59	-27.50 -17.27 -10.05 -5.21 -4.14 +4.78	-1.87 d, 5 Hz (2,6-H) 17.11 dd, 8,6 Hz (3,5-H) -0.59 tt, 8,1 Hz (4-H)	-12.06 s (6-H) 8.63 d, 8 Hz (3-H) -5.13 d, 8 Hz (4-H)	3.17 (s, 3H, 2-CH <sub>3</sub> ) -1.51 (s, 3H, 5-CH <sub>3</sub> )
-CH <sub>2</sub> CH <sub>3</sub>	2.39 10.22 13.44	-28.88 -14.89 -7.10 -3.50 -1.82 +5.71	-0.01 d, 5 Hz (2,6-H) 16.35 t, 7 Hz (3,5-H) 0.82 t, 8 Hz (4-H)		-10.00 (t, 7 Hz, 3H; CH <sub>2</sub> ) 76.94 (m <sup>c</sup> , 2H; CHHMe)

<sup>a</sup> All peaks t, 2 Hz, 1 H. <sup>b</sup> All peaks d, 2 Hz, 1 H. <sup>c</sup> Irradiating the methyl triplet at  $\delta -10.0$  ppm collapses the methylene multiplet to an AB pattern with  $J_{\text{AB}} = 12$  Hz and  $\Delta\delta = 0.03$  ppm.



cases the 2-, 4-, and 6-protons of both the pyridine and aryloxy ligands are shifted upfield from their normal positions in diamagnetic compounds, while the 3- and 5-protons are shifted downfield. The pyrazole protons show a similar general pattern, though there are exceptions. This alternation of the direction of shift of aromatic protons is characteristic of a Fermi contact interaction between the ligand and the metal-centered paramagnet; this is further borne out by the observation that methyl groups attached to the aromatic ring shift in the opposite sense of the protons they replace.<sup>16</sup> The nature of this paramagnetic shifting will be discussed in more detail in another report.<sup>8e</sup>

The phenyl, *p*-anisyl, and *p*-phenoxyphenyl complexes all undergo photochemical migration at comparable rates under comparable irradiation conditions. The two complexes with *ortho* methyl groups, however, have quantum yields for migration that are roughly 10 times

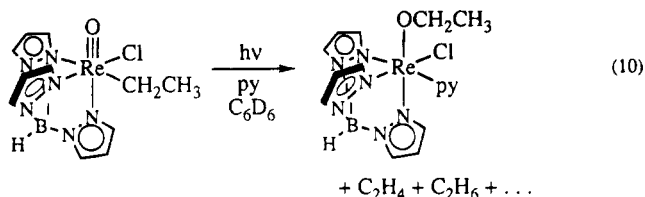
smaller under the same conditions. This is presumably a steric effect, since the alkoxy- or aryloxy-substituted aryl ligands would be expected to be at least as electron-rich as the dimethylaryl groups. Consistent with this trend, the oxo-mesityl complex  $(\text{HBpz}_3)\text{ReO}(2,4,6\text{-Me}_3\text{-C}_6\text{H}_2)\text{Cl}$  with its two *ortho* substituents is observed to be photochemically inert.

**Metal-to-Oxo Migration of a Rhenium Ethyl Complex.** The oxo-ethyl complex  $(\text{HBpz}_3)\text{ReO}(\text{C}_2\text{H}_5)\text{Cl}$  is prepared by treatment of the oxo dichloride complex  $(\text{HBpz}_3)\text{ReOCl}_2$  with  $1/2$  mol of diethylzinc. The crude reaction mixture contains large amounts of paramagnetic material, suggesting that reduction at rhenium accompanies ethylation. The ethyl complex  $(\text{HBpz}_3)\text{ReO}(\text{C}_2\text{H}_5)\text{Cl}$  may be separated from the paramagnetic byproducts by chromatography on silica gel and isolated as violet, diamagnetic, air-stable crystals. The diastereotopic methylene protons resonate at unusually low field and are well separated from each other ( $\delta$  6.06 and 7.81 in  $\text{C}_6\text{D}_6$ ).

Upon UV photolysis in benzene in the presence of a few equivalents of pyridine,  $(\text{HBpz}_3)\text{ReO}(\text{C}_2\text{H}_5)\text{Cl}$  is transformed into the red rhenium(III) ethoxide complex  $(\text{HBpz}_3)\text{Re}(\text{OC}_2\text{H}_5)(\text{Cl})(\text{py})$  (eq 10). The  $^1\text{H}$  NMR of this complex is similar to the aryloxy complexes (Table 3), except for the methyl triplet at  $\delta -10.00$  and the methylene multiplet at  $\delta +76.94$  ppm. Remarkably, despite the fact that the methylene protons are shifted some 70 ppm from their diamagnetic positions, the

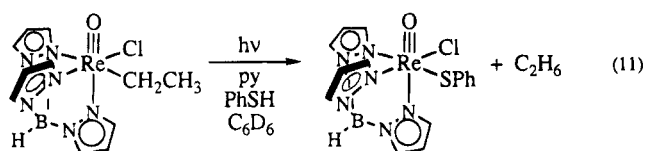
(16) La Mar, G. N., Horrocks, W. deW., Jr., Holm, R. H., Eds. *NMR of Paramagnetic Molecules: Principles and Applications*; Academic Press: New York, 1973; Chapter 4.





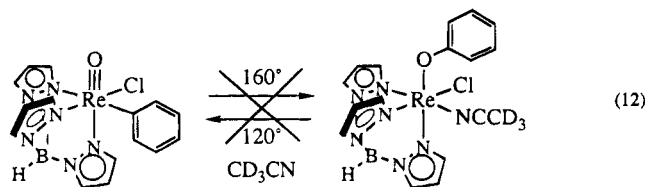
separation between the two diastereotopic resonances is only 0.03 ppm.

Photolysis of the ethyl complex is much faster than that of the phenyl complex, going to completion in about a day, but the yield of alkoxide product is lower (45% by NMR). The concurrent formation of ethane and small amounts of ethylene suggests that ethyl radicals are produced on irradiation of  $(\text{HBpz}_3)\text{ReO}(\text{C}_2\text{H}_5)\text{Cl}$ . These radicals are intimately involved in the migration, as addition of a few equivalents of thiophenol<sup>15</sup> suppresses rearrangement and instead produces ethane and  $(\text{HBpz}_3)\text{ReO}(\text{SPh})\text{Cl}$ <sup>17</sup> (eq 11; 77% yield by NMR). Addition of thiophenol does not affect the observed rate of disappearance of  $(\text{HBpz}_3)\text{ReO}(\text{C}_2\text{H}_5)\text{Cl}$ .



Other radical traps also inhibit rearrangement. In the presence of dioxygen, no rhenium(III) products are observed;  $(\text{HBpz}_3)\text{ReOCl}_2$ ,  $(\text{HBpz}_3)\text{ReO}_3$ , acetaldehyde, and unidentified organic and inorganic species are produced. Photolysis of  $(\text{HBpz}_3)\text{ReO}(\text{C}_2\text{H}_5)\text{Cl}$  in  $\text{CD}_2\text{Cl}_2$  with added pyridine gives predominantly  $(\text{HBpz}_3)\text{ReOCl}_2$  (80%) together with some reduction to  $(\text{HBpz}_3)\text{ReCl}_2(\text{py})$  (11%).

**Thermal Metal-to-Oxo Migrations.** The photochemical migrations described above do not go in reverse; for example, both  $(\text{HBpz}_3)\text{Re}(\text{O}(\text{Ph}))\text{Cl}(\text{py})$  and  $(\text{HBpz}_3)\text{Re}(\text{OEt})\text{Cl}(\text{py})$  are photochemically inert. Thermal rearrangements are not observed in either the metal-to-oxo or in the oxygen-to-metal directions. For example, the oxo-phenyl complex  $(\text{HBpz}_3)\text{ReO}(\text{Ph})\text{Cl}$  is very thermally robust. It may be heated at 160 °C in  $\text{CD}_3\text{CN}$  solution (sealed tube) for a month with only slight decomposition (<10%). Its rearrangement product,  $(\text{HBpz}_3)\text{Re}(\text{O}(\text{Ph}))\text{Cl}(\text{NCCD}_3)$ , decomposes over several days at 120 °C to give unidentified diamagnetic products but no  $(\text{HBpz}_3)\text{ReO}(\text{Ph})\text{Cl}$  (eq 12).



There is thus a substantial barrier to thermal rearrangement in this system:  $\Delta G^\ddagger > 40$  kcal/mol for  $\text{Re}(\text{O})\text{Ph} \rightarrow \text{Re}(\text{O}(\text{Ph}))$ ,  $\Delta G^\ddagger > 32$  kcal/mol for  $\text{Re}(\text{O}(\text{Ph})) \rightarrow \text{Re}(\text{O})\text{Ph}$ . The ethyl and ethoxide complexes show similar behavior, though with slightly less thermal

stability; both  $(\text{HBpz}_3)\text{ReO}(\text{C}_2\text{H}_5)\text{Cl}$  and  $(\text{HBpz}_3)\text{Re}(\text{OC}_2\text{H}_5)(\text{Cl})(\text{py})$  decompose over the course of several days at 110 °C without evidence of rearrangement ( $\Delta G^\ddagger > 32$  kcal/mol for rearrangement).

## Discussion

**Mechanism of Metal-to-Oxo Migrations.** The rhenium oxo-phenyl complex  $(\text{HBpz}_3)\text{ReO}(\text{Ph})\text{Cl}$  reacts slowly on UV irradiation to give products containing phenoxide ligands. The rearrangement proceeds in the presence of simple donor ligands (pyridine,  $\text{CH}_3\text{CN}$ , or  $\text{Me}_3\text{PO}$ ) to give octahedral paramagnetic rhenium(III) adducts, in the presence of the oxygen atom donor dimethyl sulfoxide to give  $(\text{HBpz}_3)\text{ReO}(\text{OPh})\text{Cl}$ , and in the absence of added ligand to give a product of conproportionation of a rhenium(III) phenoxide with the rhenium(V) oxo-phenyl complex (Scheme 1).

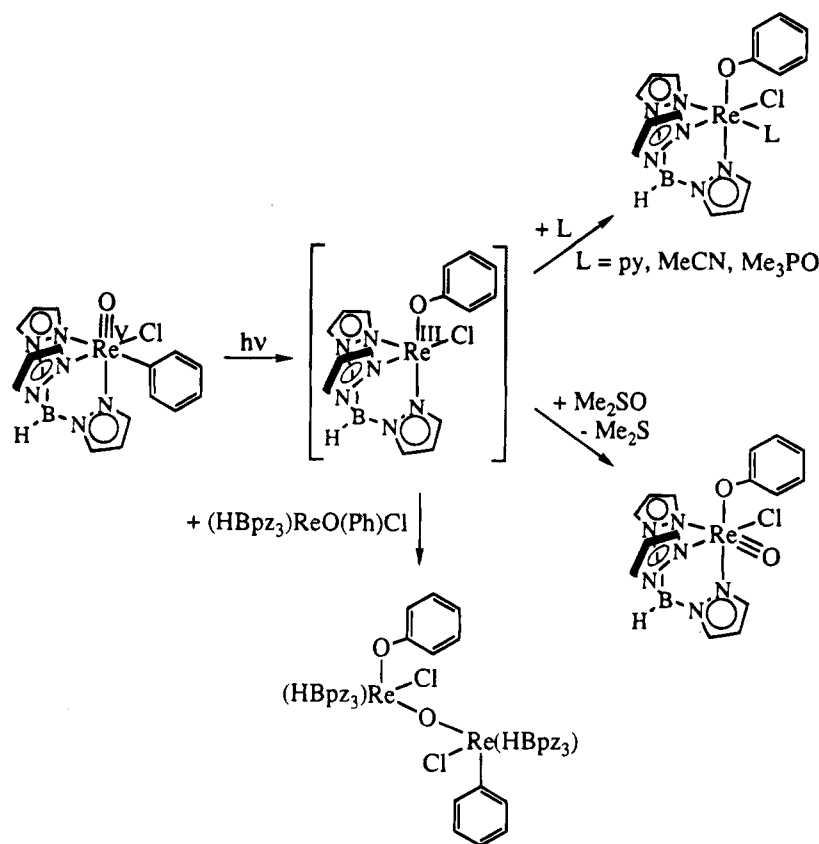
The apparent rate of disappearance of oxo-phenyl complex is independent of the nature or concentration of added trap, except in the absence of a trap where the apparent rate doubles since each rearrangement results in the consumption of two molecules of  $(\text{HBpz}_3)\text{ReO}(\text{Ph})\text{Cl}$ . The insensitivity of the apparent rate to added ligands and the intramolecularity of the rearrangement indicate that rearrangement takes place directly to give the five-coordinate rhenium(III) species  $[(\text{HBpz}_3)\text{Re}(\text{O}(\text{Ph}))\text{Cl}]$ , which then reacts with the available traps to give the observed products.

In all cases where substituted phenyl complexes undergo photochemical migration, the substitution pattern of the original aryl group is retained in the phenoxide product. In other words, the carbon originally attached to rhenium becomes attached to oxygen. This rules out any processes involving remote attack of the oxo group on the aromatic ring (for example, *ortho* attack of the oxo group on the ring followed by hydride migration to displace rhenium). The observed lack of crossover eliminates the possibility of dissociation of the phenyl group from the rhenium center, as by homolysis. Free phenyl radicals are clearly not involved because the rearrangement tolerates the radical traps acetonitrile and thiophenol. In sum, migration occurs via an intramolecular [1,2]-shift.

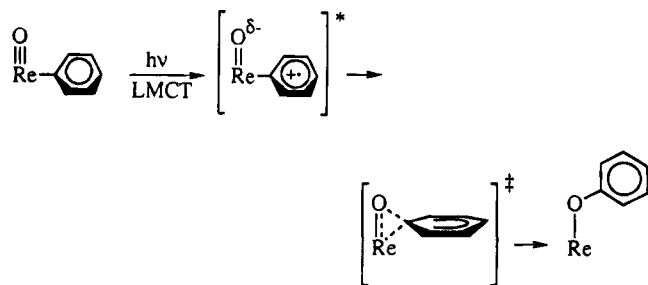
While none of the above data can eliminate the possible intermediacy of caged radical pairs, the observed steric effects on the migration rate are not consistent with this possibility. There is a marked inhibition of the reaction rate by *ortho* substitution of the aryl group, with 2,4- and 2,5-dimethylphenyl complexes reacting much more slowly than the sterically unencumbered aryls (phenyl, *p*-anisyl, or *p*-phenoxyphenyl), and the mesityl complex not rearranging at all. Dissociation to aryl radicals, even if they remain tightly held in a solvent cage, would be expected to lessen steric crowding at the metal and thus be accelerated by *ortho* substitution. Indeed, the apparent increase in congestion in the transition state for migration is noteworthy since the net reaction certainly involves motion of the phenyl group away from rhenium.

The proposed migration pathway is sketched in Scheme 2. The relevant excitation is assigned as aryl-to-rhenium charge transfer on the basis of its extinction coefficient and the fact that it shifts to the red as the aryl group becomes more electron-rich. The transition likely originates in the aryl  $\pi$  system, both because that

(17) Degnan, I. A.; Behm, J.; Cook, M. R.; Herrmann, W. A. *Inorg. Chem.* **1991**, *30*, 2165–2170.

Scheme 1. Products from Photochemical Phenyl-to-Oxo Rearrangements of (HBpz<sub>3</sub>)ReO(Ph)Cl

## Scheme 2. Proposed Mechanism of Photochemical Aryl-to-Oxo Migration



is expected to be the highest occupied ligand orbital and because the transition is observed at lower energy than in the ethyl complex. (The phenyl  $\sigma$  orbital should be lower in energy than the alkyl  $\sigma$  orbital, so a transition arising from it would be higher in energy than the corresponding one in the alkyl complex.) Absorption of a photon thus results in transfer of an electron from the aryl  $\pi$  system to the metal. The LUMO of the complex is metal-oxygen  $\pi$  antibonding in character; populating it would be expected to weaken the metal-oxo bond. Such an effect has been demonstrated by studies of the electronic spectra of metal-oxo complexes and from other data.<sup>18</sup> In addition to weakening the metal-oxo bond, population of the antibonding orbital is likely to increase the negative charge density at oxygen, as illustrated by the efficient quenching of metal-oxo  $d\pi^*$  excited states by proton donors.<sup>19</sup> De-

velopment of positive charge on the arene and negative charge on the oxygen would prime the molecule for C-O coupling and formation of the phenoxide ligand. Using the organic nomenclature for rearrangements,<sup>20</sup> one would regard this as an electrophilic migration, with the aryl group acting as an electrophile toward the oxo ligand.

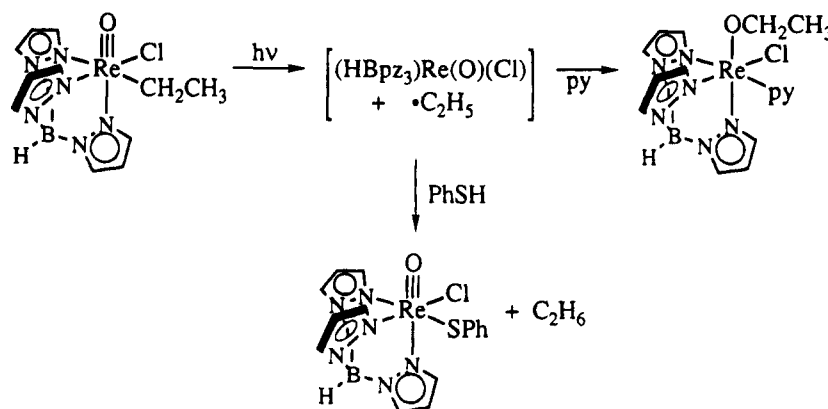
Optimal bond formation in this nucleophilic attack of the oxygen requires the plane of the phenyl group to be perpendicular to the metal-oxygen bond. In the ground state, however, the aryl group is most likely lined up in the wedge between the two *cis* pyrazoles (in (HBpz<sub>3</sub>)ReO(Ph)<sub>2</sub>,<sup>6b</sup> for example, the phenyl rings form angles of 30–45° with the Re-O bond). Thus some rotation of the phenyl group occurs during the migration (or, possibly, only those ground state molecules with perpendicular orientations are photoreactive). Such an alignment requirement is consistent with the low quantum yield and plausibly explains the observed steric inhibition, that aryl migration is less facile in complexes with larger barriers to phenyl rotation. Phenyl rotation in complexes with one *ortho* methyl group is somewhat hindered (the *o*-H and *o*-CH<sub>3</sub> resonances are broad at room temperature<sup>6b</sup>) and migration is 10 times slower than for *para*-substituted complexes. The mesityl complex, which is locked on the NMR time scale,<sup>6b</sup> is photochemically inert.

Migration of the saturated alkyl ligand in (HBpz<sub>3</sub>)ReO(C<sub>2</sub>H<sub>5</sub>)Cl occurs by an entirely different mechanism. UV irradiation of the ethyl complex induces homolysis of the rhenium-carbon bond, and rearrangement prod-

(18) (a) Winkler, J. R.; Gray, H. B. *Comments Inorg. Chem.* **1981**, 257–263. (b) Winkler, J. R.; Gray, H. B. *Inorg. Chem.* **1985**, *24*, 346–355. (c) Nugent, W. A.; Mayer, J. M. *Metal-Ligand Multiple Bonds*; Wiley-Interscience: New York, 1988. (d) Mayer, J. M. *Inorg. Chem.* **1988**, *27*, 3899–3903.

(19) Liu, W.; Welch, T. W.; Thorp, H. H. *Inorg. Chem.* **1992**, *31*, 4044–4045 and refs therein.

(20) Harwood, L. M. *Polar Rearrangements*; Oxford University Press: New York, 1992; p 2.

**Scheme 3. Pathway for Photochemical Alkyl-to-Oxo Rearrangement in (HBpz<sub>3</sub>)ReO(C<sub>2</sub>H<sub>5</sub>)Cl**

ucts are formed by subsequent recombination at oxygen (Scheme 3). The intervention of ethyl radical is demonstrated by the suppression of rearrangement by thiophenol. Alkyl radicals react with  $d^0$  complexes such as permanganate or chromate at rates near the diffusion limit, probably by alkylation at oxygen.<sup>21</sup> In the case of the low-valent oxo radical  $[(RC\equiv CR)_2Re(O)]$ , radical addition takes place at the metal to give oxo-alkyls.<sup>22</sup> In the system studied here, recombination of ethyl radical at the metal cannot be a significant process, at least in the presence of pyridine, because the addition of thiophenol does not change the rate at which  $(HBpz_3)ReO(C_2H_5)Cl$  disappears on irradiation. Pyridine may well bind to the transient rhenium(IV) oxo complex  $[(HBpz_3)Re(O)(Cl)]$  resulting from loss of the ethyl group; carbon-oxygen bond formation in such a pyridine adduct would directly form the observed  $(HBpz_3)Re(O(C_2H_5)(Cl)(py))$ . Et• addition to the five-coordinate oxo complex followed by binding of pyridine is also consistent with the observed product.

The difference in the mechanism of migration between the aryl and alkyl ligands is most likely due to the different excited states formed on irradiation of the two types of complexes. As discussed above, the relevant band in the aryl complexes involves removal of an electron from the  $\pi$  system of the aryl ligand. This should not significantly weaken the metal-carbon bond, so homolysis is not expected. Instead, charge transfer from the aryl ligand to the metal (and oxo) should enhance both the nucleophilicity of the oxo ligand and the electrophilicity of the aryl ring, accelerating migration. In contrast, the lowest-energy charge-transfer excitation in the ethyl complex most likely involves promotion of an electron from the rhenium-carbon  $\sigma$ -bonding orbital. Such an excitation would be expected to drastically weaken the rhenium-ethyl bond and lead efficiently to homolysis,<sup>23</sup> as is observed.

This study demonstrates that both homolysis-recombination and electrophilic migration are viable pathways for the photochemical transfer of  $\sigma$ -bonded organometallic groups from metal to oxygen. That such reactions are thermally inaccessible in this system is not surpris-

ing in light of these mechanisms. Rhenium-carbon bond homolysis would certainly have an impracticably large energetic barrier, given the strength of third-row transition metal bonds to carbon.<sup>24</sup> Nucleophilic attack by the oxo ligand on the phenyl group would also be expected to be difficult, since neither group in ground state  $(HBpz_3)ReO(Ph)Cl$  displays marked electrophilic or nucleophilic reactivity. A future report will describe the first example of *thermal* metal-to-oxo migrations, involving rhenium(VII) oxo complexes and a different mechanism.<sup>25</sup>

### Experimental Section

Unless otherwise noted, reactions were set up using standard vacuum line or inert atmosphere glovebox techniques, but purification was done on the benchtop since all compounds are air- and water-stable, the rhenium(V) complexes indefinitely so and the rhenium(III) compounds at least for brief periods. Photolyses were performed by placing the reaction vessel, in a Pyrex beaker of water, in the focused beam of a 200 W Hg/Xe lamp (Oriol), roughly 6 in. from the lamp. Aromatic solvents were dried over sodium, pyridine was dried over  $CaH_2$ , and acetonitrile and dichloromethane were dried over 4 Å molecular sieves followed by  $CaH_2$ . When dry solvents were needed, they were vacuum transferred from their drying agents before use and were stored in the drybox if not used immediately. Oxo-aryl complexes  $(HBpz_3)ReO(Ar)Cl$  were prepared by photolysis of  $(HBpz_3)ReO(I)Cl$  in neat arene in the presence of pyridine.<sup>6</sup>  $(HBpz_3)ReOCl_2$ <sup>10a</sup> and thallium phenoxide<sup>11</sup> were prepared according to literature procedures. Other reagents were commercially available and were used without further purification.

<sup>1</sup>H and <sup>13</sup>C{<sup>1</sup>H} NMR spectra were recorded on a Bruker AF-300 spectrometer at 300 and 75.4 MHz, respectively. The peaks due to the pyrazole protons in the <sup>1</sup>H NMR spectra are listed only as their chemical shifts and multiplicities; their coupling constants are always 2 Hz. IR spectra were obtained on a Perkin-Elmer 1604 FT-IR spectrometer; peaks are reported in wavenumbers, and the relatively invariant bands associated with the HBpz<sub>3</sub> ligand (see ref 10a) are not listed for the individual compounds. Fast atom bombardment mass spectra (FABMS) were acquired as previously described.<sup>10a</sup> Electron impact mass spectra were acquired on a Kratos Analytical mass spectrometer in the positive ion mode, with samples introduced as solids in the direct inlet probe. Elemental analyses were performed by Canadian Microanalytical Services, Ltd., Vancouver, BC.

(21) (a) Steenken, S.; Neta, P. *J. Am. Chem. Soc.* **1982**, *104*, 1244-1248. (b) Al-Sheikhly, M.; McLaughlin, W. L. *Radiat. Phys. Chem.* **1991**, *38*, 203-211. (c) Cook, G. K.; Mayer, J. M. *J. Am. Chem. Soc.* **1994**, *116*, 1855-1868.

(22) Conry, R. R.; Mayer, J. M. *Organometallics* **1991**, *10*, 3160-3166.

(23) (a) Luong, J. C.; Faltynek, R. A.; Wrighton, M. S. *J. Am. Chem. Soc.* **1980**, *102*, 7892-7900. (b) Pourreau, D. B.; Geoffroy, G. L. *Adv. Organomet. Chem.* **1985**, *24*, 249-352.

(24) Connor, J. A. *Top. Curr. Chem.* **1977**, *71*, 71-110.

(25) (a) Brown, S. N.; Mayer, J. M. Manuscript in preparation. (b) Brown, S. N. Ph.D. Thesis, University of Washington, Seattle, WA, 1994; Chapter 4.

**(HBpz<sub>3</sub>)ReO(OPh)Cl.** In the drybox to a flask containing 299 mg of solid (HBpz<sub>3</sub>)ReOCl<sub>2</sub> (0.614 mmol) was added 202 mg of TIOPh (0.681 mmol, 1.1 equiv). The flask was evacuated, 20 mL of CH<sub>2</sub>Cl<sub>2</sub> was vacuum transferred onto the solids, and the mixture was stirred at room temperature under vacuum for 3 days. The flask was then opened to the air, and the green solution was decanted away from the white solids and filtered through a plug of silica gel, eluting with dichloromethane. The CH<sub>2</sub>Cl<sub>2</sub> was removed from the eluate on a rotary evaporator, and the green oil dissolved into a minimum of toluene. This solution was loaded onto a long column of silica gel and eluted with toluene, which separates the green monophenoxide complex (HBpz<sub>3</sub>)ReO(OPh)Cl from the faster-moving blue starting material and from the slower-moving green bis(phenoxide) complex (HBpz<sub>3</sub>)ReO(OPh)<sub>2</sub>. The compound was crystallized from toluene/hexane to give 109 mg of green crystalline (HBpz<sub>3</sub>)ReO(OPh)Cl (33%). <sup>1</sup>H NMR (C<sub>6</sub>D<sub>6</sub>): δ 5.35, 5.65, 5.70 (t, 1 H); 6.72, 7.06, 7.11, 7.59, 7.67, 7.90 (d, 1 H); 6.90 (tt, 7, 1 Hz, 1 H; OPh *para*); 7.29 (d, 7 Hz, 2 H; OPh *ortho*); 7.45 (t, 7 Hz, 2 H; OPh *meta*). <sup>13</sup>C{<sup>1</sup>H} NMR (C<sub>6</sub>D<sub>6</sub>): δ 105.9, 108.0, 108.4, 133.7, 137.9, 138.7, 144.3, 146.5, 148.0 (pz), 121.2 (*ortho*), 121.9 (*para*), 128.7 (*meta*), 177.0 (*ipso*). IR (evaporated film): 2519 (m, ν<sub>BH</sub>), 1588, 1484 (s, ν<sub>C-C</sub>), 1391 (m), 1232 (s, ν<sub>C-O</sub>), 1162 (w), 973 (s, ν<sub>Re-O</sub>), 921 (w), 892 (w), 854 (m), 814 (w), 791 (w), 694 (w). MS: 544 (M<sup>+</sup>). Anal. Calcd for C<sub>15</sub>H<sub>15</sub>BClN<sub>6</sub>O<sub>2</sub>Re: C, 33.13; H, 2.78; N, 15.45. Found: C, 33.36; H, 2.81; N, 15.58.

**(HBpz<sub>3</sub>)Re(OPh)(Cl)(py).** In the drybox 66 mg of (HBpz<sub>3</sub>)ReO(OPh)(Cl) (0.12 mmol) was dissolved in a mixture of 4.5 mL of dry benzene and 0.30 mL of pyridine. The green solution was placed in a glass reaction vessel with a Teflon needle valve and freeze-pump-thaw degassed on the vacuum line. Onto the solution frozen at -196 °C was vacuum transferred the contents of a 280 mL bulb filled with 17 Torr of trimethyl phosphite vapor (0.26 mmol, 2.1 equiv). The valve on the reaction vessel was sealed, and the solution was thawed and then heated in a 100 °C oil bath. After 3 days, the solution had turned dark red and a small amount of dark solids had deposited on the walls of the flask. Heating was stopped, and the vessel opened to the air. The solution was poured out of the flask, combined with a toluene washing of the solids, and stripped down on a rotary evaporator. The residue was taken up in a minimum of toluene and chromatographed on a Pasteur pipet filled with silica gel, eluting first with dichloromethane to remove unreacted starting material, then with 3:1 CH<sub>2</sub>Cl<sub>2</sub>/EtOAc. (HBpz<sub>3</sub>)Re(OPh)(Cl)(py) elutes slowly in this solvent as an orange band; impure fractions containing it were rechromatographed as necessary to produce TLC-pure material. The fractions were combined and recrystallized by dissolving in toluene (4 mL) and layering with hexane (9 mL) and allowing to stand at room temperature overnight. The orange needles were filtered, washed with hexane, and air-dried to yield 23 mg of (HBpz<sub>3</sub>)Re(OPh)(Cl)(py) (32%). The compound is stable indefinitely in the air as a solid, but decomposes slowly in solutions exposed to air. <sup>1</sup>H NMR (C<sub>6</sub>D<sub>6</sub>): see Table 3. IR (evaporated film): 2508 (m, ν<sub>BH</sub>), 1584, 1479 (s, ν<sub>C-C</sub>), 1389 (m), 1258 (s, ν<sub>C-O</sub>), 1160 (m), 853 (m), 757 (s), 692 (m), 667 (w). MS: 607 (M<sup>+</sup>). Anal. Calcd for C<sub>20</sub>H<sub>20</sub>BClN<sub>7</sub>ORe: C, 39.58; H, 3.32; N, 16.16. Found: C, 39.87; H, 3.30; N, 16.00.

**Crossover Experiment: (HBpz<sub>3</sub>)Re<sup>18</sup>O(Ph)Cl.** A glass reaction vessel was charged with 26.5 mg of (HBpz<sub>3</sub>)ReO(Ph)Cl, 20 μL of H<sub>2</sub><sup>18</sup>O (Cambridge Isotope), and 2 mL of CH<sub>3</sub>CN. The Teflon stopcock was closed, and the solution was stirred at 85 °C for 6 days. Chromatography on silica with toluene, recrystallization from hot heptane, and washing with hexane yielded 9.6 mg (35%) of (HBpz<sub>3</sub>)Re<sup>18</sup>O(Ph)Cl. Mass spectra indicated 64.4 (4)% <sup>18</sup>O enrichment. **(HBpz<sub>3</sub>)ReO(C<sub>6</sub>D<sub>5</sub>)Cl** was prepared by photolysis of (HBpz<sub>3</sub>)ReO(I)Cl in C<sub>6</sub>D<sub>6</sub>, following the procedure for (HBpz<sub>3</sub>)ReO(C<sub>6</sub>H<sub>5</sub>)Cl.<sup>6</sup> **Crossover Experiment.** A sealable NMR tube was charged with 1.9 mg of (HBpz<sub>3</sub>)ReO(C<sub>6</sub>D<sub>5</sub>)Cl, 2.1 mg of (HBpz<sub>3</sub>)Re<sup>18</sup>O(C<sub>6</sub>H<sub>5</sub>)Cl, 6.2

μL of pyridine, 0.4 mL of C<sub>6</sub>D<sub>6</sub>, and Me<sub>4</sub>Si. The tube was sealed with a torch and photolyzed for 11 days. <sup>1</sup>H NMR indicated 38% starting material and 46% (HBpz<sub>3</sub>)Re(OPh)Cl(py) (75% yield based on converted Re). The tube was cut open and analyzed by FABMS. The intensities of parent ion peaks from 604–615 *m/z* were well fitted by a mixture of (HBpz<sub>3</sub>)Re(<sup>16</sup>OC<sub>6</sub>D<sub>5</sub>)Cl(py), (HBpz<sub>3</sub>)Re(<sup>16</sup>OC<sub>6</sub>H<sub>5</sub>)Cl(py), and (HBpz<sub>3</sub>)Re(<sup>18</sup>OC<sub>6</sub>H<sub>5</sub>)Cl(py), with the ratio of the last two equaling the enrichment in the (HBpz<sub>3</sub>)Re<sup>18</sup>O(C<sub>6</sub>H<sub>5</sub>)Cl starting material. Small amounts of crossover (<15%) would not be detectable by this analysis.

**(HBpz<sub>3</sub>)ReCl<sub>2</sub>(py)** was prepared by refluxing in the air, with stirring, a mixture of 154 mg of (HBpz<sub>3</sub>)ReOCl<sub>2</sub> (0.317 mmol), 106 mg of PPh<sub>3</sub> (0.404 mmol, 1.3 eq), 20 mL of toluene, and 1 mL of pyridine. After 18 h the solution was allowed to cool to room temperature, and the brick-red powder that precipitated was filtered and washed with hexane to furnish 149 mg of analytically pure (HBpz<sub>3</sub>)ReCl<sub>2</sub>(py) (85%). <sup>1</sup>H NMR (CD<sub>2</sub>Cl<sub>2</sub>): δ 11.25 (t, 1 H); 4.80 (t, 2 H); -9.59, 3.60 (d, 1 H); -15.92, -11.86 (d, 2 H); -7.94 (d, 5 Hz, 2 H; py 2,6-H); 17.07 (ddd, 8, 5, 1 Hz, 2 H; py 3,5-H); -4.32 (tt, 8, 1 Hz, 1 H; py 4-H). IR (Nujol): 2512 (m, ν<sub>BH</sub>), 1602 (w), 794, 760, 720, 692, 655 (m). MS: 549 (M<sup>+</sup>). Anal. Calcd for C<sub>14</sub>H<sub>15</sub>BCl<sub>2</sub>N<sub>7</sub>Re: C, 30.62; H, 2.75; N, 17.85. Found: C, 30.50; H, 2.76; N, 17.77.

**(HBpz<sub>3</sub>)ReCl<sub>2</sub>(EtC≡CEt).** Into a 50 mL round-bottom flask attached to a reflux condenser and containing 159 mg of (HBpz<sub>3</sub>)ReOCl<sub>2</sub> (0.33 mmol) and 90 mg of triphenylphosphine (0.34 mmol) were added 3 mL of 3-hexyne and 25 mL toluene by vacuum transfer. The solution was heated at reflux under a nitrogen atmosphere for 18 h. The flask was then opened to the atmosphere, and the toluene and excess hexyne were removed on the rotary evaporator. The orange residue was crystallized from hot toluene/hexane, and the orange needles so obtained were collected on a glass frit, washed thoroughly with hexane, and air-dried. Yield: 130 mg (72%). The alkyne adduct is air-stable in the solid state, but decomposes over the course of several days in solutions exposed to air. <sup>1</sup>H NMR (CD<sub>2</sub>Cl<sub>2</sub>): δ 1.06 (t, 7 Hz, 6H; CH<sub>2</sub>CH<sub>3</sub>); 6.21 (t, 1 H); 6.43 (t, 2 H); 6.61 (q, 7 Hz, 4 H; CH<sub>2</sub>CH<sub>3</sub>); 6.86, 7.20 (d, 2 H each); 7.06, 7.86 (d, 1 H each). <sup>13</sup>C{<sup>1</sup>H} NMR (CD<sub>2</sub>Cl<sub>2</sub>): δ 17.8 (CH<sub>2</sub>CH<sub>3</sub>); 22.0 (CH<sub>2</sub>CH<sub>3</sub>); 104.7, 136.6, 150.0 (pz *trans* to alkyne); 106.6, 138.2, 156.2 (pz *trans* to Cl); 212.9 (EtCCEt). IR (Nujol): 2528 (m, ν<sub>BH</sub>), 760 (m). FABMS: 552 (M<sup>+</sup>), 517 (M<sup>+</sup> - Cl), 470 (M<sup>+</sup> - EtCCEt). Anal. Calcd for C<sub>15</sub>H<sub>20</sub>BCl<sub>2</sub>N<sub>6</sub>Re: C, 32.62; H, 3.65; N, 15.22. Found: C, 32.31; H, 3.66; N, 14.98.

**(HBpz<sub>3</sub>)Re(SPh)(Cl)(py)** was generated on a small scale by heating a sealed tube containing 3.0 mg of (HBpz<sub>3</sub>)ReO(SPh)(Cl)<sup>17</sup> (5.4 μmol), 1.7 mg of PPh<sub>3</sub> (1.2 equiv), 4.2 μL of pyridine, and 0.4 mL of C<sub>6</sub>D<sub>6</sub> at 90 °C for 9 days. <sup>1</sup>H NMR (C<sub>6</sub>D<sub>6</sub>): δ 5.10, 5.39, 10.04 (t, 1 H); -20.73, -12.16, -11.25, -10.24, -9.87, +4.61 (d, 1 H); -6.83 (d, 8 Hz, 2 H; *o*-Ph), -3.55 (t, 8 Hz, 1 H; *p*-Ph), +11.18 (t, 8 Hz, 2 H; *m*-Ph); -7.22 (d, 4 Hz, 2 H; 2,6-H, py), -4.85 (t, 8 Hz, 1 H; 4-H, py), +14.65 (t, 4 Hz, 2 H; 3,5-H, py). FABMS: 623 (M<sup>+</sup>).

**(HBpz<sub>3</sub>)Re(OPh)(Cl)(NCCH<sub>3</sub>).** A sealed flask containing 114 mg of (HBpz<sub>3</sub>)ReO(Ph)(Cl) dissolved in 10 mL of dry, degassed CH<sub>3</sub>CN was placed in a Pyrex beaker filled with water. While being stirred magnetically, the solution was exposed to the output of a 200 W Hg/Xe arc lamp for 3 weeks. The volume of the solution, which had turned from blue to green, was reduced to ~3 mL, and this solution was stored at -10 °C in the drybox for 5 months. At this time, 8 mg of red crystalline (HBpz<sub>3</sub>)Re(OPh)(Cl)(NCCH<sub>3</sub>) was isolated by filtration. The filtrate was taken out into the air and chromatographed on silica gel. Elution with toluene led to the recovery of 83 mg of (HBpz<sub>3</sub>)ReO(Ph)(Cl) (28% conversion), and elution with 3:1 CH<sub>2</sub>Cl<sub>2</sub>/EtOAc provided another 2 mg of (HBpz<sub>3</sub>)Re(OPh)(Cl)(NCCH<sub>3</sub>) (10 mg total yield, 29% based on converted rhenium). <sup>1</sup>H NMR (C<sub>6</sub>D<sub>6</sub>): δ 2.58, 6.92, 12.04 (t, 1 H); -18.47, -15.60, -11.06, -7.33, -0.72, 6.23 (d, 1 H); -12.75 (d, 8 Hz, 2 H; OPh *ortho*); -5.63 (t, 7 Hz, 1 H; *para*); 9.44 (t, 8 Hz, 2 H;

*meta*); 59.32 (s, 3 H; CH<sub>3</sub>CN). IR (evaporated film): 2509 (m,  $\nu_{\text{BH}}$ ), 2244 (m,  $\nu_{\text{C}\equiv\text{N}}$ ), 1584 (m,  $\nu_{\text{C}-\text{C}}$ ), 1480 (s,  $\nu_{\text{C}-\text{C}}$ ), 1251 (s,  $\nu_{\text{C}-\text{O}}$ ), 1163 (m), 943 (w), 888 (w), 848 (m), 787 (m). FABMS: 569 (M<sup>+</sup>). Anal. Calcd for C<sub>17</sub>H<sub>18</sub>BClN<sub>7</sub>ORe: C, 35.89; H, 3.19; N, 17.24. Found: C, 35.57; H, 3.22; N, 16.78.

**(HBpz<sub>3</sub>)Re(OPh)(Cl)(OPMe<sub>3</sub>)** was prepared on a small scale by UV irradiation of a sealed NMR tube containing (HBpz<sub>3</sub>)ReO(Ph)(Cl) (5.3 mg) and a 6-fold excess of trimethylphosphine oxide (5.5 mg, Alfa) dissolved in 0.4 mL of C<sub>6</sub>D<sub>6</sub>. The product is sparingly soluble in benzene, and the orange crystals formed were separated from unreacted starting material and excess phosphine oxide by filtration. <sup>1</sup>H NMR (C<sub>6</sub>D<sub>6</sub>):  $\delta$  3.64, 9.29, 9.52 (t, 1 H); -20.33, -19.97, -18.43, -14.52, -9.75, +0.05 (d, 1 H); -8.12 (d, 8 Hz, 2 H; OPh *ortho*); -3.17 (t, 8 Hz, 1 H; OPh *para*); 10.51 (t, 8 Hz, 2 H; OPh *meta*); 1.46 (d,  $J_{\text{PH}} = 13$  Hz, 9 H; OPMe<sub>3</sub>). IR (evaporated film): 2507 (m,  $\nu_{\text{BH}}$ ), 1584, 1480 (s,  $\nu_{\text{C}-\text{C}}$ ), 1264 (s,  $\nu_{\text{C}-\text{O}}$ ), 1161 (m), 1100 (s,  $\nu_{\text{PO}}$ ), 949 (m), 855 (m). FABMS: 620 (M<sup>+</sup>).

**(HBpz<sub>3</sub>)Re(OPh)(Cl)( $\mu$ -O)(Ph)(Cl)Re(HBpz<sub>3</sub>)**. The two isomers of this compound were generated on a small scale by UV irradiation of a sealed tube containing (HBpz<sub>3</sub>)ReO(Ph)Cl dissolved in C<sub>6</sub>D<sub>6</sub>. As the photolysis proceeds, one isomer precipitates selectively from solution. <sup>1</sup>H NMR (C<sub>6</sub>D<sub>6</sub>) of the less soluble diastereomer:  $\delta$  -7.83, +1.72 (d, 8 Hz, 2 H ea.; *ortho*, *ortho'*); 9.55, 12.97 (t, 8 Hz, 2 H ea.; *meta*, *meta'*); -4.24, +2.67 (t, 7 Hz, 1 H ea.; *para*, *para'*); 4.30, 4.65, 6.77, 7.35, 7.41, 7.90 (t, 1 H); 2.25, 2.67, 2.85, 3.28, 3.59, 3.61, 3.74, 3.96, 4.08, 4.47, 5.29, 5.42 (d, 1 H). <sup>1</sup>H NMR of the more soluble diastereomer:  $\delta$  -9.14 (d, 7 Hz), -0.24 (d, 8 Hz) (2 H ea.; *ortho*, *ortho'*); 9.87 (t, 8 Hz), 13.74 (br) (2 H ea.; *meta*, *meta'*); -4.24, +2.67 (t, 7 Hz, 1 H ea.; *para*, *para'*); 4.14, 4.39, 6.94, 7.22, 7.96, 8.21 (t, 1 H); 0.94, 2.18, 2.29, 2.84, 3.10, 3.50, 4.09, 4.27, 4.33, 5.16 (d, 1 H); 6.24 (br,  $\Delta\nu_{1/2} = 20$  Hz, 1 H; pz 3- or 5-H); one pz 3- or 5-H not observed. FABMS (mixture of diastereomers): 1054 (M<sup>+</sup>).

**(HBpz<sub>3</sub>)Re(OAr)(Cl)(py)** were synthesized on a small scale by photolyzing a sealed NMR tube containing the desired aryl complex (HBpz<sub>3</sub>)ReO(Ar)Cl and 10 equiv of pyridine dissolved in C<sub>6</sub>D<sub>6</sub>. The product was separated from unreacted oxo-aryl complex by chromatography on silica gel, eluting first with methylene chloride to remove the starting material, then with ethyl acetate to elute the red product. <sup>1</sup>H NMR spectral data are given in Table 3. Other characterizations: **(HBpz<sub>3</sub>)Re( $\mu$ -OC<sub>6</sub>H<sub>4</sub>OMe)(Cl)(py)**. IR (evaporated film): 2508 (m,  $\nu_{\text{BH}}$ ), 1445 (m), 1389 (m), 1251 (m,  $\nu_{\text{C}-\text{O}}$ ), 1227 (s,  $\nu_{\text{C}-\text{O}}$ ), 864 (w), 829 (w), 690 (m), 656 (m). FABMS: 637 (M<sup>+</sup>). **(HBpz<sub>3</sub>)Re( $\mu$ -OC<sub>6</sub>H<sub>4</sub>OPh)(Cl)(py)**. IR (evaporated film): 2923 (w,  $\nu_{\text{CH}}$ ), 2507 (m,  $\nu_{\text{BH}}$ ), 1600 (m), 1587 (m), 1484 (s), 1445 (m), 1388 (w), 1272 (m), 1222 (s,  $\nu_{\text{C}-\text{O}}$ ), 851 (m), 839 (m), 691 (m). FABMS: 699 (M<sup>+</sup>). **(HBpz<sub>3</sub>)Re(O-2,4-Me<sub>2</sub>C<sub>6</sub>H<sub>3</sub>)(Cl)(py)**. IR (evaporated film): 2922 (s), 2855 (m) ( $\nu_{\text{CH}}$ ); 2506 (m,  $\nu_{\text{BH}}$ ), 1605 (w), 1486 (s), 1445 (m), 1389 (m), 1258 (s,  $\nu_{\text{C}-\text{O}}$ ), 931 (w), 822 (m), 812 (m), 691 (m). FABMS: 635 (M<sup>+</sup>). **(HBpz<sub>3</sub>)Re(O-2,5-Me<sub>2</sub>C<sub>6</sub>H<sub>3</sub>)(Cl)(py)**. FABMS: 635 (M<sup>+</sup>).

**(HBpz<sub>3</sub>)ReO(C<sub>2</sub>H<sub>5</sub>)Cl**. In the drybox, 350  $\mu$ L of a 1 M solution of diethylzinc in hexanes (Aldrich; 0.35 mmol) was added to a flask containing 340 mg of (HBpz<sub>3</sub>)ReOCl<sub>2</sub> (0.70 mmol) dissolved in 150 mL dry benzene. The resulting solution was stirred at room temperature with the exclusion of air for 3 h, as the solution turned from sky blue to bright green and finally to a slightly cloudy olive. The flask was then opened to the air, and the volatiles were stripped off on the rotary evaporator. The residue was extracted with small portions of toluene until no more product was present (as judged by TLC), and the portions were chromatographed on short columns of silica gel. Toluene elutes the monoethyl complex first as a blue-violet band, ahead of the lighter blue band due to unreacted starting material. The product can be isolated as a violet solid after removal of the eluant, slurring

the residue in hexane, and filtering; yield: 85 mg (25%). <sup>1</sup>H NMR (C<sub>6</sub>D<sub>6</sub>):  $\delta$  2.45 (t, 7.5 Hz, 3H; Re-CH<sub>2</sub>CH<sub>3</sub>); 6.06, 7.81 (d of q,  $^2J = 13$  Hz,  $^3J = 7.5$  Hz, 1 H ea.; Re-CHHCH<sub>3</sub>); 5.30, 5.69, 5.77 (t, 1 H each); 6.70, 7.08, 7.10, 7.23, 7.55, 8.35 (d, 1 H each). <sup>13</sup>C{<sup>1</sup>H} NMR (C<sub>6</sub>D<sub>6</sub>):  $\delta$  27.6, 31.5 (Re-CH<sub>2</sub>CH<sub>3</sub>), 105.8, 107.8, 108.3, 133.7, 137.3, 138.5, 144.2, 146.8, 147.0 (pyrazoles). IR (Nujol): 2518 (m,  $\nu_{\text{BH}}$ ), 980 (s,  $\nu_{\text{ReO}}$ ), 918 (w), 891 (w), 864 (w), 816 (w), 777 (m). UV-vis (CH<sub>3</sub>CN):  $\lambda_{\text{max}} = 690$  nm ( $\epsilon = 80$  M<sup>-1</sup> cm<sup>-1</sup>), 290 sh (2900), 236 (9500). FABMS: 480 (M<sup>+</sup>). Anal. Calcd for C<sub>11</sub>H<sub>15</sub>BClN<sub>6</sub>ORe: C, 27.54; H, 3.15; N, 17.52. Found: C, 27.61; H, 3.14; N, 17.50.

**(HBpz<sub>3</sub>)Re(OC<sub>2</sub>H<sub>5</sub>)(Cl)(py)**. In the drybox, 32 mg of (HBpz<sub>3</sub>)ReO(C<sub>2</sub>H<sub>5</sub>)Cl (0.066 mmol) was dissolved in 5 mL of benzene containing 60  $\mu$ L of pyridine (0.74 mmol, 11 equiv). The violet solution was poured into a small glass reaction vessel with a Teflon needle valve. After freeze-pump-thaw degassing on the vacuum line, the solution was thawed and photolyzed, while stirring, for 3.5 days. The volatiles were evaporated on the vacuum line, and the residue was exposed to the air. The residue was taken up in methylene chloride and chromatographed several times on short silica gel columns, eluting with 3:1 CH<sub>2</sub>Cl<sub>2</sub>/EtOAc, to afford 14 mg TLC-pure (HBpz<sub>3</sub>)Re(OC<sub>2</sub>H<sub>5</sub>)(Cl)(py) (38%). The analytical sample was recrystallized in the drybox by layering a toluene solution of the ethoxide complex with pentane and storing at -10 °C. Both the NMR spectrum and the analytical data of this sample indicated that about 5 mol % toluene remained included with the compound even after washing with pentane and drying *in vacuo*. <sup>1</sup>H NMR (C<sub>6</sub>D<sub>6</sub>): see Table 3. IR: 2956 (m), 2923 (s), 2853 (m,  $\nu_{\text{CH}}$ ); 2506 (m,  $\nu_{\text{BH}}$ ), 1480, 1445, 1390 (m); 1275, 1262 (m,  $\nu_{\text{C}-\text{O}}$ ); 920 (w), 894 (m), 811 (w), 689 (m), 636 (m). FABMS: 559 (M<sup>+</sup>). Anal. Calcd for (HBpz<sub>3</sub>)Re(OEt)(Cl)(py) · 0.05 C<sub>7</sub>H<sub>8</sub> (C<sub>16.35</sub>H<sub>20.4</sub>BN<sub>7</sub>ClORe): C, 34.85; H, 3.65; N, 17.40. Found: C, 35.08; H, 3.66; N, 17.04.

**X-ray Crystallography of (HBpz<sub>3</sub>)Re(OPh)(Cl)(py) · C<sub>6</sub>D<sub>6</sub>**. Crystals of (HBpz<sub>3</sub>)Re(OPh)(Cl)(py) · C<sub>6</sub>D<sub>6</sub> were obtained by allowing a sealed tube containing a slightly supersaturated solution of the rhenium(III) phenoxide complex in *d*<sub>6</sub>-benzene to stand for several weeks. Over this time the small crystals initially present gradually increased in size until they were suitable for study by single-crystal X-ray diffraction. A red-orange crystal 0.1 × 0.15 × 0.25 mm<sup>3</sup> was mounted on a glass fiber with viscous hydrocarbon oil and promptly frozen in the cold stream at -90 °C. The crystal was studied using an Enraf-Nonius CAD4 diffractometer using crystal-monochromated Mo K $\alpha$  radiation ( $\lambda = 0.71073$  Å). Decay was assessed by monitoring two standard reflections approximately every 2 h of exposure and was found to be negligible. An empirical absorption correction was applied. Data reduction was carried out using MOLLEN, and refinement was done using a PC version of Siemens SHELX. For other details of the crystal structures and data collection, see Table 1; selected bond distances and angles are presented in Table 2.

**Acknowledgment.** We are grateful to Dr. David Barnhart for assistance with the X-ray crystallography and to the National Science Foundation for financial support. S.N.B. would like to acknowledge a National Science Foundation Predoctoral Fellowship, a Shell Graduate Fellowship, and a Howard J. Ringold Fellowship of the University of Washington Department of Chemistry.

**Supplementary Material Available:** Tables of atomic positional and thermal parameters and bond distances and angles (5 pages). Ordering information is given on any current masthead page.

OM950110S

# Heterobimetallic $\sigma,\pi$ -Acetylide-Bridged Complexes from Disubstituted 1,3-Butadiynes

Uwe Rosenthal,\* Siegmund Pulst, Perdita Arndt, Andreas Ohff, Annegret Tillack, Wolfgang Baumann, Rhett Kempe, and Vladimir V. Burlakov†

Max-Planck-Gesellschaft, Arbeitsgruppe "Komplekxkatalyse" an der Universität Rostock, Buchbinderstrasse 5-6, D-18055 Rostock, Germany

Received December 12, 1994<sup>©</sup>

It has been shown that a nickel(0) complex of bis(trimethylsilyl)butadiyne,  $(\text{Ph}_3\text{P})_2\text{Ni}(\eta^2\text{-Me}_3\text{SiC}\equiv\text{CC}\equiv\text{CSiMe}_3)$ , readily reacts with the titanocene  $\text{Cp}_2\text{Ti}(\text{Me}_3\text{SiC}\equiv\text{CSiMe}_3)$  and zirconocene  $\text{Cp}_2\text{Zr}(\text{THF})(\text{Me}_3\text{SiC}\equiv\text{CSiMe}_3)$  complexes to form the heterobimetallic, doubly acetylide bridged complexes  $\text{Cp}_2\text{M}(\mu\text{-}\eta^1\text{:}\eta^2\text{-C}\equiv\text{CSiMe}_3)\text{Ni}(\text{PPh}_3)(\mu\text{-}\eta^1\text{:}\eta^2\text{-C}\equiv\text{CSiMe}_3)$  ( $\text{M} = \text{Ti}$  (1),  $\text{M} = \text{Zr}$  (2)). The structures of these complexes have been established by X-ray crystal structure analysis. Two  $\sigma,\pi$ -bridging acetylide units are  $\sigma$ -bonded to different metals and  $\pi$ -bonded to the second metal. Compound 1 in solution at 303 K is highly fluxional. An NMR study showed that at 190 K an equilibrium exists between one isomer with two nonequivalent and another isomer with two equivalent acetylide units. The cleavage of the central C–C single bond of the butadiyne was not observed in the reaction of the unsymmetrically substituted butadiyne  $\text{PhC}\equiv\text{CC}\equiv\text{CSiMe}_3$  with titanocene "Cp<sub>2</sub>Ti" generator  $\text{Cp}_2\text{Ti}(\text{Me}_3\text{SiC}\equiv\text{CSiMe}_3)$ . The product is a bridging tetrahydro-(1–3- $\eta$ ):-(2–4- $\eta$ )-*trans,trans*-butadiene unit (zigzag butadiyne) between two titanium centers in  $\text{Cp}_2\text{Ti}\{\mu\text{-}(1\text{-}3\text{-}\eta)\text{:}(2\text{-}4\text{-}\eta)\text{-trans,trans-PhC}\equiv\text{CC}\equiv\text{CSiMe}_3\}\text{TiCp}_2$  (5). If the phenyl(trimethylsilyl)butadiyne is complexed by nickel(0), the reaction with the titanocene generated from  $\text{Cp}_2\text{Ti}(\text{Me}_3\text{SiC}\equiv\text{CSiMe}_3)$  yields the heterobimetallic complex  $\text{Cp}_2\text{Ti}(\mu\text{-}\eta^1\text{:}\eta^2\text{-C}\equiv\text{CSiMe}_3)(\mu\text{-}\eta^1\text{:}\eta^2\text{-C}\equiv\text{CPh})\text{Ni}(\text{PPh}_3)$  (6). Both acetylide units are  $\sigma$ -bonded to the titanium atom and  $\pi$ -bonded to the nickel atom, giving a "tweezerlike" structure.

## Introduction

Recently we have reported the reaction of the titanocene complex  $\text{Cp}_2\text{Ti}(\text{Me}_3\text{SiC}\equiv\text{CSiMe}_3)$  with the disubstituted butadiyne  $\text{Me}_3\text{SiC}\equiv\text{CC}\equiv\text{CSiMe}_3$ , in which the starting butadiyne is cleaved by the generated "titanocene" to yield the dinuclear complex  $[\text{Cp}_2\text{Ti}(\mu\text{-}\eta^1\text{:}\eta^2\text{-C}\equiv\text{CSiMe}_3)]_2$  (3).<sup>1</sup> Later we could show that the reaction products of disubstituted butadiynes  $\text{R}^1\text{C}\equiv\text{CC}\equiv\text{CR}^2$  and titanocene "Cp<sub>2</sub>Ti" strongly depend on the nature of the substituents  $\text{R}^1$  and  $\text{R}^2$ . For  $\text{R}^1 = \text{R}^2 = \text{Ph}$ ,  $t\text{-Bu}$  and  $\text{R}^1 = \text{SiMe}_3$ ,  $\text{R}^2 = \text{Ph}$ ,  $t\text{-Bu}$  binuclear complexes with intact 1,4-disubstituted tetrahydro- $\mu\text{-}(1\text{-}3\text{-}\eta)\text{:}(2\text{-}4\text{-}\eta)\text{-trans,trans}$ -butadiene units between two titanium centers are formed.<sup>2</sup> The reason for the different reactions is the decrease of electron density in the central C–C bond caused by two  $\text{SiMe}_3$  substituents.<sup>2</sup>

On the other hand, with  $\text{Cp}_2\text{Zr}(\text{THF})(\text{Me}_3\text{SiC}\equiv\text{CSiMe}_3)$  the cleavage reaction is favored in all cases, yielding the symmetrically and unsymmetrically substituted  $\sigma,\pi$ -acetylide-bridged complexes  $\text{Cp}_2\text{Zr}(\mu\text{-}\eta^1\text{:}\eta^2\text{-C}\equiv\text{CR}^1)(\mu\text{-}\eta^1\text{:}\eta^2\text{-C}\equiv\text{CR}^2)\text{ZrCp}_2$ .<sup>3</sup> This result is explained by the larger size of Zr and longer Zr–C bond lengths which for Zr make the type of structure without a central C–C bond more stable compared to Ti.<sup>6d</sup>

Interestingly, in the reaction of  $\text{Cp}_2\text{Zr}(\text{py})(\text{Me}_3\text{SiC}\equiv\text{CSiMe}_3)$  and  $t\text{-BuC}\equiv\text{CC}\equiv\text{C}t\text{-Bu}$  cleavage was not observed but 1:1 complexation gave the smallest known cyclocumulene complex.<sup>4</sup> Also, the reactions of  $\text{L}_2\text{Ni}$  fragments with 1,4-disubstituted 1,3-butadiynes gave no cleavage product but 1:1 or 2:1  $\pi$ -complexes.<sup>5</sup>

In the series of binuclear complexes  $\text{L}_n\text{M}^1(\mu\text{-C}\equiv\text{CR}^1)\text{-}(\mu\text{-C}\equiv\text{CR}^2)\text{M}^2\text{L}_m$  the bonding of the  $\mu\text{-C}\equiv\text{CR}$  ligand can be widely varied, depending on different metals, ligands, and substituents.<sup>6</sup>

In the literature, complexes with  $\text{R}^1 = \text{R}^2$  usually were synthesized by reacting two alkali-metal acetylides with one  $\text{L}_n\text{M}^1\text{Cl}_2$  compound and subsequently adding the second metal fragment  $\text{L}_m\text{M}^2$ .<sup>6</sup> More re-

(4) Rosenthal, U.; Ohff, A.; Baumann, W.; Kempe, R.; Tillack, A.; Burlakov, V. V. *Angew. Chem.* **1994**, *106*, 1678.

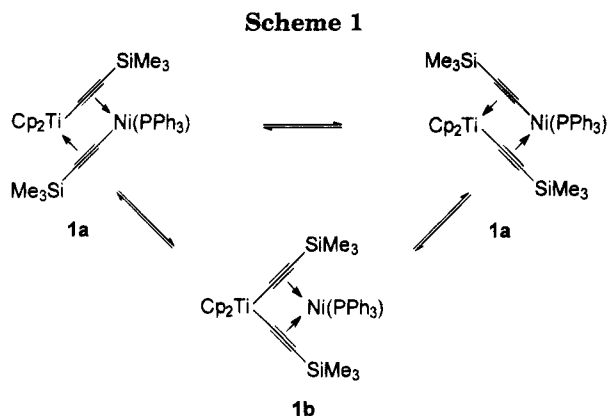
(5) (a) Rosenthal, U.; Pulst, S.; Arndt, P.; Baumann, W.; Tillack, A.; Kempe, R. *Z. Naturforsch.* **1995**, *50b*, 368. (b) Rosenthal, U.; Pulst, S.; Arndt, P.; Baumann, W.; Tillack, A.; Kempe, R. *Z. Naturforsch.* **1995**, *50b*, 377.

(6) (a) Erker, G.; Frömberg, W.; Mynott, R.; Gabor, B.; Krüger, C. *Angew. Chem.* **1986**, *98*, 456. (b) Erker, G.; Frömberg, W.; Bann, R.; Mynott, R.; Angermund, K.; Krüger, C. *Organometallics* **1989**, *8*, 911. (c) Erker, G.; Albrecht, M.; Krüger, C.; Nolte, M.; Werner, S. *Organometallics* **1993**, *12*, 4979. (d) Kumar, P. N. V. P.; Jemmis, E. D. *J. Am. Chem. Soc.* **1988**, *110*, 125. (e) Yasufuku, K.; Yamazaki, H. *Bull. Chem. Soc. Jpn.* **1972**, *45*, 2664. (f) Lang, H.; Zsolnai, L. *J. Organomet. Chem.* **1991**, *406*, C5. (g) Lang, H.; Herres, M.; Zsolnai, L.; Imhof, W. *J. Organomet. Chem.* **1991**, *409*, C7. (h) Lang, H.; Imhof, W. *Chem. Ber.* **1992**, *125*, 1307. (i) Lang, H.; Herres, M.; Zsolnai, L. *Bull. Chem. Soc. Jpn.* **1993**, *66*, 429. (j) Ciriano, M.; Howard, J. A. K.; Spencer, J. L.; Stone, F. G. A.; Wade, H. J. *Chem. Soc., Dalton Trans.* **1979**, 1749. (k) Fornies, J.; Gómez-Saso, M. A.; Lalinde, E.; Martínez, F.; Moreno, M. T. *Organometallics* **1992**, *11*, 2873. (l) Berenguer, J. R.; Falvello, L. R.; Fornies, J.; Lalinde, E.; Tomás, M. *Organometallics* **1993**, *12*, 6. (m) Berenguer, J. R.; Fornies, J.; Lalinde, E.; Martín, A. *Angew. Chem.* **1994**, *106*, 2196. (n) Lotz, S.; Van Rooyen, P. H.; Meyer, R. *Adv. Organomet. Chem.* **1995**, *37*, 219 and references therein.

\* Permanent address: Institute of Organoelement Compounds of the Russian Academy of Sciences, Moscow, Russia.

<sup>©</sup> Abstract published in *Advance ACS Abstracts*, May 15, 1995.

(1) Rosenthal, U.; Görls, H. *J. Organomet. Chem.* **1992**, *439*, C36.  
 (2) (a) Rosenthal, U.; Ohff, A.; Tillack, A.; Baumann, W.; Görls, H. *J. Organomet. Chem.* **1994**, *468*, C4. (b) Sekutowski, D. G.; Stucky, G. D. *J. Am. Chem. Soc.* **1976**, *98*, 1376.  
 (3) Rosenthal, U.; Ohff, A.; Baumann, W.; Kempe, R.; Tillack, A.; Burlakov, V. V. *Organometallics* **1994**, *13*, 2903.

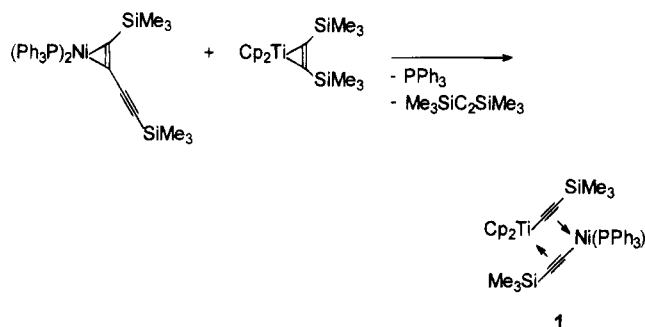


cently, the reaction of  $\text{Cp}_2\text{TiCl}_2$ , magnesium, and  $\text{Me}_3\text{SiC}\equiv\text{CC}\equiv\text{CSiMe}_3$  was reported to form a Ti–Mg bis(acetylide) complex in 40% yield.<sup>7</sup>

Here we describe further results of our method to cleave butadiynes by homo- or heterobimetallic systems and demonstrate the preparation of all possible combinations of such types of bis(acetylide)-bridged dinuclear complexes with (a)  $M^1 = M^2$  and  $R^1 = R^2$ ,<sup>1,3</sup> (b)  $M^1 = M^2$  and  $R^1 \neq R^2$ ,<sup>3</sup> (c)  $M^1 \neq M^2$  and  $R^1 = R^2$ , and (d)  $M^1 \neq M^2$  and  $R^1 \neq R^2$ .

## Results and Discussion

We found that a nickel(0) complex of bis(trimethylsilyl)butadiyne,  $(\text{Ph}_3\text{P})_2\text{Ni}(\eta^2\text{-Me}_3\text{SiC}\equiv\text{CC}\equiv\text{CSiMe}_3)$ ,<sup>5</sup> readily reacts in toluene at 50 °C with the titanocene generator  $\text{Cp}_2\text{Ti}(\text{Me}_3\text{SiC}\equiv\text{CSiMe}_3)$  to form the heterobimetallic, doubly acetylide bridged complex  $\text{Cp}_2\text{Ti}(\mu\text{-}\eta^1\text{:}\eta^2\text{-C}\equiv\text{CSiMe}_3)\text{Ni}(\text{PPh}_3)(\mu\text{-}\eta^1\text{:}\eta^2\text{-C}\equiv\text{CSiMe}_3)$  (**1**).



Complex **1** is a red-brown, crystalline solid (mp 127–133 °C under argon) which is soluble in THF and toluene and insoluble in *n*-hexane and was characterized by IR and NMR spectroscopy and X-ray crystallography.

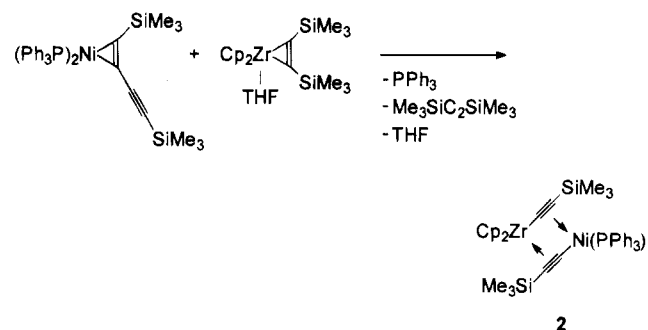
The infrared absorptions of the  $\text{C}\equiv\text{C}$  bond in **1** are in the region characteristic of  $\sigma,\pi$ -acetylide-bridged complexes. The assignment of the different metal  $\pi$ -complexed triple bonds was made in view of the fact that a more extended decrease in  $\nu_{\text{C}=\text{C}}$  is observed in titanocene alkyne complexes in comparison to nickel(0) complexes.<sup>8</sup> Therefore, the band at 1780  $\text{cm}^{-1}$  is assigned to the Ti- $\pi$ -complexed and the band at 1911  $\text{cm}^{-1}$  to the Ni- $\pi$ -complexed acetylide unit.

At 190 K the  $^{31}\text{P}$  NMR spectrum of **1** displays two signals, indicating that two isomers (Scheme 1) are

present. The  $^1\text{H}$  NMR spectrum shows two signals of the same intensity for the  $\text{SiMe}_3$  groups, in agreement with the unsymmetrical structure **1a**, together with one smaller signal, indicating a second isomer in solution have the symmetrical structure **1b**. Correspondingly, for the Cp rings two resonances of different intensity are observed as well. The ratio of the unsymmetrical isomer to the symmetrical one is about 5:1. The  $^{13}\text{C}$  NMR resonances of the acetylide carbon atoms could not be detected.

At 303 K the  $^{31}\text{P}$  NMR shows only one signal. The  $^1\text{H}$  NMR spectrum exhibits one signal for the  $\text{SiMe}_3$  groups and one signal for the Cp rings. The spectra at 303 K can be explained by a rapid exchange between a symmetrical and an unsymmetrical structure. A similar observation had been made in the case of the complex  $(\text{C}_5\text{H}_4\text{Bu})_2\text{Zr}(\mu\text{-C}\equiv\text{CR})\text{ZrCp}_2(\mu\text{-C}\equiv\text{CR})$  and was taken as evidence that the acetylide ligands rapidly change places between the two Zr centers.<sup>6b</sup>

The reaction of the nickel(0) complex  $(\text{Ph}_3\text{P})_2\text{Ni}(\eta^2\text{-Me}_3\text{SiC}\equiv\text{CC}\equiv\text{CSiMe}_3)$  with the zirconocene alkyne complex  $\text{Cp}_2\text{Zr}(\text{THF})(\text{Me}_3\text{SiC}\equiv\text{CSiMe}_3)$  in THF at 20 °C yields the heterobimetallic doubly acetylide bridged complex  $\text{Cp}_2\text{Zr}(\mu\text{-}\eta^1\text{:}\eta^2\text{-C}\equiv\text{CSiMe}_3)\text{Ni}(\text{PPh}_3)(\mu\text{-}\eta^1\text{:}\eta^2\text{-C}\equiv\text{CSiMe}_3)$  (**2**), the zirconocene analogue of **1**.



Complex **2** is a red-brown, crystalline solid (mp 145–150 °C under argon) which is soluble in THF and toluene and insoluble in *n*-hexane and was characterized by IR and NMR spectroscopy and X-ray crystallography.

The spectral data for the zirconocene complex **2** are very similar to those for the analogous titanocene complex **1**. On the basis of the same considerations, the absorption at 1876  $\text{cm}^{-1}$  in the IR spectrum of **2** is assigned to the nickel and that at 1771  $\text{cm}^{-1}$  to the zirconium  $\pi$ -complexed  $\text{C}\equiv\text{CSiMe}_3$  group.

In the  $^1\text{H}$  NMR spectrum of **2** at 303 K one signal due to the Cp rings and two signals due to the  $\text{SiMe}_3$  groups are observed. The  $^{13}\text{C}$  NMR spectrum displays one Cp-ring signal and four signals due to the acetylide carbon atoms. In contrast to compound **1**, the bridging acetylide units in **2** are nonequivalent at room temperature.

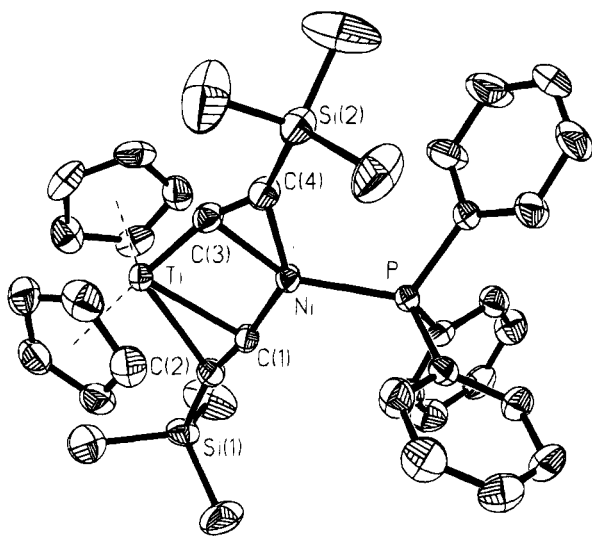
The structures of **1** (Figure 1) and **2** (Figure 2) have been established by X-ray diffraction. Table 1 lists crystallographic data. Positional parameters and selected bond lengths and angles of **1** are given in Tables 2 and 3 and those of **2** in Tables 4 and 5.

Table 6 lists selected structural data for **1** and **2** in comparison with those for the isostructural homobimetallic complexes  $[\text{Cp}_2\text{Ti}(\mu\text{-}\eta^1\text{:}\eta^2\text{-C}\equiv\text{CSiMe}_3)]_2$  (**3**)<sup>1,12</sup> and  $[\text{Cp}_2\text{Zr}(\mu\text{-}\eta^1\text{:}\eta^2\text{-C}\equiv\text{CSiMe}_3)]_2$  (**4**).<sup>3,13</sup>

(7) Troyanov, S. I.; Varga, V.; Mach, K. *Organometallics* **1993**, *12*, 2820.

(8) Rosenthal, U.; Oehme, G.; Burlakov, V. V.; Petrovskii, P. V.; Shur, V. B.; Vol'pin, M. E. *J. Organomet. Chem.* **1990**, *391*, 119.





**Figure 1.** Molecular structure of complex **1**, shown by an ORTEP plot at the 40% probability level.

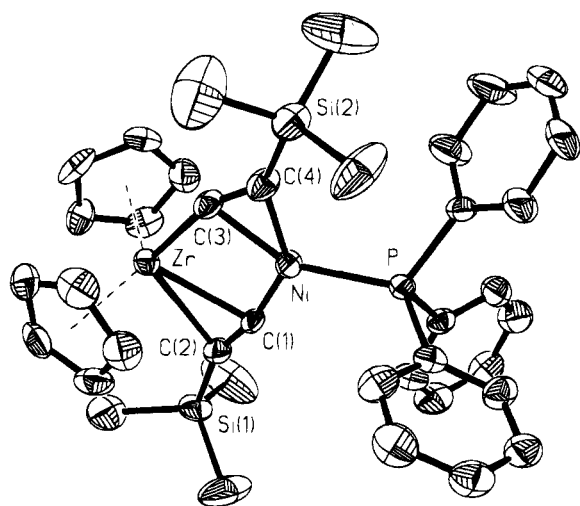


**Figure 2.** Molecular structure of complex **2**, shown by an ORTEP plot at the 40% probability level.

The most interesting feature of the structures of **1** and **2** is that they differ from the "tweezerlike" structure, e.g., in the titanium-nickel complex  $(\eta^5\text{-C}_5\text{H}_4\text{SiMe}_3)_2\text{Ti}(\mu\text{-}\eta^1\text{:}\eta^2\text{-C}\equiv\text{CR})_2\text{Ni}(\text{CO})$ .<sup>6h</sup> In this complex both acetylide groups are  $\sigma$ -bonded to the titanium atom and  $\pi$ -coordinated to the Ni(CO) fragment. The structures of **1** and **2** are unsymmetrical and display the two acetylide groups  $\sigma$ -bonded to different metals and  $\eta^2$ -bonded on  $\pi$ -coordination to the other metal, as in the recently published example  $\text{Cp}_2\text{Ti}(\mu\text{-}\eta^1\text{:}\eta^2\text{-C}\equiv\text{C}^t\text{Bu})\text{Pt}(\text{PPh}_3)(\mu\text{-}\eta^1\text{:}\eta^2\text{-C}\equiv\text{C}^t\text{Bu})$ .<sup>6m</sup>

In the complexes **1** and **2** the Ni- $\pi$ -complexed triple bond C(3) $\equiv$ C(4) (1.261(7) Å in **1** and 1.284(13) Å in **2**) is slightly longer than the Ti- or Zr- $\pi$ -complexed triple bond C(1) $\equiv$ C(2) (1.233(7) Å in **1** and 1.236(12) Å in **2**). The latter is almost identical with the distances in the homobimetallic complexes **3** (1.244(3) Å) and **4** (1.249(7) Å). Comparable monometallic alkyne complex C $\equiv$ C bond lengths are as follows:  $(\text{Ph}_3\text{P})_2\text{Ni}(\text{Me}_3\text{SiC}\equiv\text{CSiMe}_3)$  (1.256(2) Å);<sup>9a</sup>  $(\text{Ph}_3\text{P})_2\text{Ni}(\text{PhC}\equiv\text{CSiMe}_3)$  (1.273(8) Å);<sup>9b</sup>

$\text{Cp}_2\text{Ti}(\text{PhC}\equiv\text{CSiMe}_3)$  (1.289(4), 1.279(4) Å);<sup>11a</sup>  $\text{Cp}_2\text{Zr}(\text{THF})(\text{Me}_3\text{SiC}\equiv\text{CSiMe}_3)$  (1.302(9) Å).<sup>11b</sup>

In both complexes **1** and **2** the Ni-C(1)  $\sigma$ -bond (1.828(5) and 1.835(8) Å) is shorter than the Ti-C(3) (2.067(4) Å) and Zr-C(3)  $\sigma$ -bonds (2.178(9) Å). The latter are very similar to the  $\sigma$ -bonds in the corresponding complexes **3** (2.069(1) Å) and **4** (2.191(5) Å).

The angle C(3)-C(4)-Si(2) of the Ni(PPh<sub>3</sub>)-complexed triple bond in **1** (145.8(4)°) and **2** (141.7(7)°) is about 20° smaller than the angle C(1)-C(2)-Si(1) of the titanocene- or zirconocene-complexed triple bond in **1** (164.4(4)°) or **2** (159.2(7)°). The distances Ti-C(1) (2.331(4) Å) and Zr-C(1) (2.385(7) Å) are between 0.2 and 0.3 Å shorter than the Ti-C(2) (2.628 Å) and the Zr-C(2) (2.557 Å) distances. This might explain the large angles for the titanocene- or zirconocene-complexed triple bond in **1** and **2**. Comparable angles C-C-Si are found in the complexes **3** (141.5(2)°), **4** (142.5(4)°),  $\text{Cp}_2\text{Zr}(\text{THF})(\text{Me}_3\text{SiC}\equiv\text{CSiMe}_3)$  (143.5(6)°),<sup>11b</sup> 134.4(6)°,  $(\text{Ph}_3\text{P})_2\text{Ni}(\text{Me}_3\text{SiC}\equiv\text{CSiMe}_3)$  (143.3(1)°),<sup>9a</sup>  $\text{Cp}_2\text{Ti}(\text{PhC}\equiv\text{CSiMe}_3)$  (148.2(2)°, 151.9(2)°),<sup>11a</sup> and  $(\text{Ph}_3\text{P})_2\text{Ni}(\text{PhC}\equiv\text{CSiMe}_3)$  (138.7(5)°).<sup>9b</sup>

The distance M(1)-M(2) of 2.728(1) Å in **1** and 2.830(1) Å in **2** cannot be considered as a direct bonding interaction between the nickel atom and the metallocene center. Bonding interactions can be excluded for the bis(metallocene) species **3** (3.550(3) Å) and **4** (3.522(2) Å). Complex **1** is formally a Ti(III)/Ni(I) and complex **2** a Zr(III)/Ni(I) species and should therefore exhibit paramagnetism. However, both compounds are diamagnetic. The reason could be an antiferromagnetic coupling between the metal centers or an electronic coupling between the metals via the bridging alkynyl groups. Because of the long metal-metal distances in **1** and **2**, we favor an electronic coupling via the unsaturated bridging groups as in **3** and **4**.<sup>3,6b</sup>

The relatively short Ti-C(3) and Zr-C(3) bond lengths in **1** and **2** are good arguments for a considerable  $\pi$ -interaction between the metal centers and the organic  $\pi$ -system across the  $\sigma$ -bonds (Chart 1), as found for  $[\text{Cp}_2\text{Zr}(\mu\text{-}\eta^1\text{:}\eta^2\text{-C}\equiv\text{CR})_2\text{-type complexes}]$ .<sup>6b</sup>

In contrast, the Ni-C(1) distances (**1**, 1.828(5) Å; **2**, 1.835(8) Å) justify the description as single bonds which are slightly longer than those found in  $\text{NiBr}(\text{C}\equiv\text{CSiMe}_3)(\text{PMe}_3)_2$  (1.773(23) and 1.818(25)).<sup>10</sup>

Complexes **1** and **2** are stable at room temperature. Compound **1** reacts with an excess of CO to give a mixture of the "tweezerlike" titanium-nickel complex  $\text{Cp}_2\text{Ti}(\mu\text{-}\eta^1\text{:}\eta^2\text{-C}\equiv\text{CSiMe}_3)_2\text{Ni}(\text{CO})$ ,<sup>6h</sup>  $(\text{Ph}_3\text{P})\text{Ni}(\text{CO})_3$ , and  $\text{PPh}_3$ , as shown by comparison of IR and NMR spectra. Under analogous conditions for complex **2** mainly the unchanged starting material was obtained. Both complexes on reaction with an excess of  $\text{PhC}\equiv\text{CC}\equiv\text{CPh}$  and  $\text{Me}_3\text{SiC}\equiv\text{CC}\equiv\text{CSiMe}_3$  even at 90 °C in toluene gave only trimerization products of  $\text{PhC}\equiv\text{CC}\equiv\text{CPh}$  and not the unsymmetrically substituted diyne  $\text{PhC}\equiv\text{CC}\equiv\text{CSiMe}_3$  as a result of disproportionation in a "C-C  $\sigma$ -bond metathesis".

(10) Klein, H.-F.; Zwiener, M.; Petermann, A.; Jung, T.; Cordier, G.; Hammerschmitt, B.; Flörke, U.; Haupt, H.-J.; Dartiguenave, Y. *Chem. Ber.* **1994**, *127*, 1569.

(11) (a) Burlakov, V. V.; Polyakov, A. V.; Yanovsky, A. I.; Struchkov, Y. T.; Shur, V. B.; Vol'pin, M. E.; Rosenthal, U.; Görls, H. *J. Organomet. Chem.* **1994**, *476*, 197. (b) Rosenthal, U.; Ohff, A.; Michalik, M.; Görls, H.; Burlakov, V. V.; Shur, V. B. *Angew. Chem.* **1993**, *105*, 1228.

(12) Wood, G. L.; Knobler, C. B.; Hawthorne, M. F. *Inorg. Chem.* **1989**, *28*, 382.

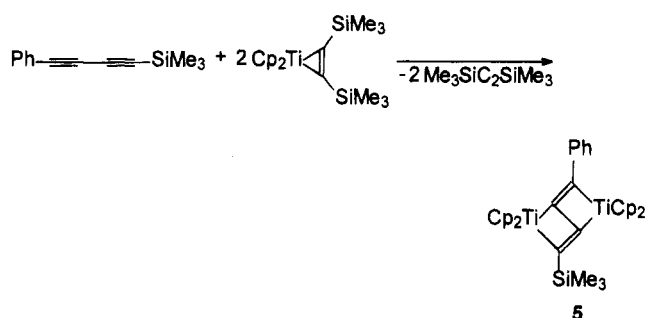
(13) Metzler, N.; Nöth, H. *J. Organomet. Chem.* **1993**, *454*, C5.

(9) (a) Rosenthal, U.; Schulz, W.; Görls, H. *Z. Anorg. Allg. Chem.* **1987**, *550*, 169. (b) Bartik, T.; Happ, B.; Iglewsky, M.; Bandmann, H.; Boese, R.; Heimbach, P.; Hoffmann, T.; Wenschuh, E. *Organometallics* **1992**, *11*, 1235.

Table 1. Crystallographic Data

compd	1·0.5THF	2·0.5THF	3	4
chem formula	C <sub>40.5</sub> H <sub>43</sub> NiPSi <sub>2</sub> Ti	C <sub>40</sub> H <sub>43</sub> NiO <sub>0.5</sub> PSiZr	C <sub>33</sub> H <sub>34</sub> SiTi <sub>2</sub>	C <sub>41</sub> H <sub>39</sub> NiPSiTi
lattice constants				
<i>a</i> (Å)	22.389(1)	22.537(2)	8.2232(6)	12.981(1)
<i>b</i> (Å)	9.4295(3)	9.4457(7)	32.86(1)	13.052(1)
<i>c</i> (Å)	36.182(3)	36.568(3)	10.479(1)	21.288(2)
$\beta$ (deg)	90.516(5)	90.390(8)	102.77(1)	95.008(7)
temp (K)	293	293	293	293
space group	<i>C2/c</i>	<i>C2/c</i>	<i>P2<sub>1</sub>/a</i>	<i>P2<sub>1</sub>/a</i>
cryst dimens (mm)	0.5 × 0.4 × 0.3	0.5 × 0.4 × 0.4	0.6 × 0.2 × 0.1	0.6 × 0.5 × 0.3
cryst color	red-brown	red-brown	green	red-brown
$\mu$ (mm <sup>-1</sup> )	0.833	0.881	0.642	0.851
abs cor	no	$\Psi$ -scan	$\Psi$ -scan	$\Psi$ -scan
$\theta$ range (deg)	2.13–24.10	2.40–24.99	2.61–24.97	2.36–24.98
no. of rflns (measd)	12 297	7684	5198	6618
no. of rflns (indep)	6049	6847	4843	6322
<i>R</i> (int)	0.049	0.088	0.045	0.038
no. of rflns (obsd), <i>I</i> > 2 $\sigma$ ( <i>I</i> )	4882	4937	3045	4642
<i>R</i> 1 ( <i>I</i> > 2 $\sigma$ ( <i>I</i> ))	0.078	0.057	0.066	0.040
w <i>R</i> 2 (all data)	0.210	0.232	0.245	0.123
non-H atoms refined	anisotropic (except solvent)	anisotropic (except solvent)	anisotropic	anisotropic
treatment of H atoms	geom riding	geom riding	geom riding	geom riding

As previously reported, "Cp<sub>2</sub>Ti" alone does not cleave disubstituted butadiynes R<sup>1</sup>C≡CC≡CR<sup>2</sup> with R<sup>1</sup> = R<sup>2</sup> = Ph, *t*-Bu and R<sup>1</sup> = SiMe<sub>3</sub>, R<sup>2</sup> = Ph, *t*-Bu. The reaction products are binuclear complexes with intact 1,4-disubstituted tetrahydro- $\mu$ -(1-3- $\eta$ ):(2-4- $\eta$ )-*trans,trans*-butadiene units between two titanium centers.<sup>2</sup> Preparation and some properties of **5** were reported in a preliminary communication.<sup>2</sup>



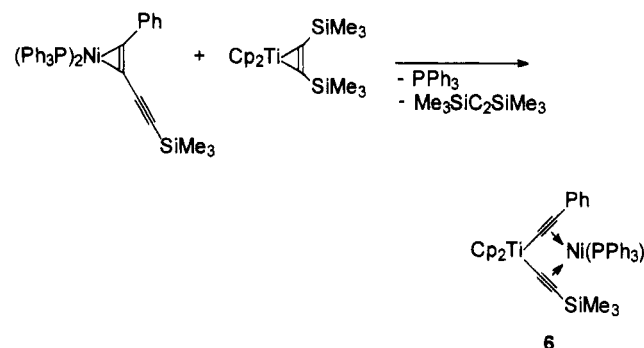
The structure of **5** has now been determined by X-ray diffraction (Figure 3). Table 1 lists crystallographic data. Positional parameters and selected bond distances and angles of **5** are given in Tables 7 and 8.

Structures with intact 1,4-disubstituted tetrahydro- $\mu$ -(1-3- $\eta$ ):(2-4- $\eta$ )-*trans,trans*-butadiene units between two titanocene centers are well-known.<sup>2</sup> They differ markedly from the type discussed above with  $\sigma,\pi$ -bridging acetylide units. The structure displays the intact C<sub>4</sub> chain ("zigzag butadiyne") between two titanium atoms. The titanium atoms and the diyne ligand are coplanar to within 0.017(5) Å with titanium-carbon  $\sigma$ -bond distances of 2.083(7) and 2.337(7) Å in the Ph-substituted part and 2.164(7) and 2.114(7) Å in the SiMe<sub>3</sub>-substituted part. The alternating C-C bond lengths of 1.327(9), 1.511(9), and 1.317(9) Å are close to those expected for a diolefin with the central C-C bond in the region typical of C-C single bonds. Also, the angles C(1)-C(2)-C(3) (126.6(6)°) and C(2)-C(3)-C(4) (128.4(6)°) approach those observed in butadienes.

Complex **5** is very stable and does not react with water, carbon dioxide, carbon monoxide, or triphenylphosphine. With an excess of PhC≡CC≡CSiMe<sub>3</sub> in

toluene at 90 °C only decomposition occurs and no symmetrically substituted diynes PhC≡CC≡CPh and Me<sub>3</sub>SiC≡CC≡CSiMe<sub>3</sub> were obtained as a result of a "C-C  $\sigma$ -bond metathesis".

Surprisingly, the cleavage reaction of PhC≡CC≡CSiMe<sub>3</sub>, which does not occur with "Cp<sub>2</sub>Ti" alone (see above), succeeded when a bimetallic Ni-Ti system was used. The reaction of nickel(0) complex (Ph<sub>3</sub>P)<sub>2</sub>Ni( $\eta^2$ -PhC≡CC≡CSiMe<sub>3</sub>)<sup>5b</sup> with the titanocene alkyne complex Cp<sub>2</sub>Ti(Me<sub>3</sub>SiC≡CSiMe<sub>3</sub>) in toluene at 80 °C yields the heterobimetallic, doubly acetylide bridged complex Cp<sub>2</sub>Ti( $\mu$ - $\eta^1$ : $\eta^2$ -C≡CPh)( $\mu$ - $\eta^1$ : $\eta^2$ -C≡CSiMe<sub>3</sub>)Ni(PPh<sub>3</sub>) (**6**), which has a structure different from those of **1** and **2**.



Complex **6** is a deep red, crystalline substance which is readily soluble in benzene and THF and melts at 184–185 °C under argon. The C≡C triple bond absorptions for **6** (1846, 1797 cm<sup>-1</sup>) are both in the region of  $\sigma,\pi$ -acetylide-bridged complexes. In order to assign the IR bands to the different acetylide groups, we note that a decrease in  $\nu_{C=C}$  is observed upon substitution with SiMe<sub>3</sub>.<sup>8</sup> Therefore, the absorption at 1797 cm<sup>-1</sup> should be assigned to the SiMe<sub>3</sub>-substituted and the other at 1846 cm<sup>-1</sup> to the Ph-substituted triple bond. At ambient temperature the SiMe<sub>3</sub> group and the Cp rings each exhibit a single resonance in the <sup>1</sup>H NMR spectrum. In the <sup>13</sup>C NMR spectrum four resonances for the acetylide carbon atoms were detected.

The structure of **6** has been determined by X-ray diffraction (Figure 4). Table 1 lists crystallographic data. Positional parameters and selected bond distances and angles of **6** are given in Tables 9 and 10.

**Table 2. Atomic Coordinates ( $\times 10^4$ ) and Equivalent Isotropic Displacement Parameters ( $\text{\AA}^2 \times 10^3$ ) for **1**<sup>a</sup>**

atom	x	y	z	$U_{eq}$
Ni	8304(1)	2630(1)	6239(1)	33(1)
Ti	7472(1)	2062(1)	6765(1)	31(1)
P	8864(1)	2689(1)	5754(1)	30(1)
Si(1)	6861(1)	-1203(2)	6115(1)	46(1)
Si(2)	9174(1)	5522(2)	6711(1)	50(1)
C(1)	7753(2)	1210(5)	6188(1)	35(1)
C(2)	7359(2)	300(5)	6206(1)	39(1)
C(3)	8157(2)	3511(5)	6705(1)	38(1)
C(4)	8609(2)	4183(6)	6595(1)	43(1)
C(5)	6463(3)	-1801(8)	6543(2)	76(2)
C(6)	7316(4)	-2700(7)	5952(3)	91(3)
C(7)	6299(4)	-719(9)	5758(3)	102(3)
C(8)	9920(3)	4998(11)	6564(3)	98(3)
C(9)	8988(6)	7274(9)	6496(4)	141(5)
C(10)	9188(4)	5714(13)	7223(2)	125(4)
C(20)	7548(3)	1458(7)	7404(1)	60(2)
C(21)	8120(3)	1683(7)	7281(2)	62(2)
C(22)	8252(3)	621(7)	7023(2)	57(2)
C(23)	7768(3)	-249(6)	6986(2)	53(1)
C(24)	7320(3)	261(6)	7217(2)	56(2)
C(30)	6871(2)	3683(6)	6423(2)	54(2)
C(31)	7003(3)	4336(6)	6760(2)	58(2)
C(32)	6733(3)	3568(8)	7032(2)	61(2)
C(33)	6425(2)	2443(7)	6871(2)	56(2)
C(34)	6508(3)	2516(6)	6495(2)	53(2)
C(40)	9548(2)	1634(5)	5785(1)	36(1)
C(41)	9883(2)	1296(6)	5473(1)	43(1)
C(42)	10395(3)	505(6)	5504(2)	55(1)
C(43)	10582(3)	13(7)	5848(2)	61(2)
C(44)	10250(3)	327(8)	6152(2)	68(2)
C(45)	9739(3)	1127(7)	6125(2)	54(1)
C(50)	9109(2)	4455(5)	5611(1)	37(1)
C(51)	8688(3)	5507(6)	5597(2)	77(2)
C(52)	8827(4)	6859(7)	5484(3)	95(3)
C(53)	9402(4)	7217(7)	5409(2)	75(2)
C(54)	9825(3)	6206(7)	5428(2)	72(2)
C(55)	9685(2)	4807(6)	5521(2)	57(2)
C(60)	8520(2)	2002(5)	5326(1)	34(1)
C(61)	8484(3)	2762(6)	4999(1)	46(1)
C(62)	8188(3)	2214(7)	4691(2)	56(2)
C(63)	7950(3)	895(7)	4706(2)	56(2)
C(64)	7990(3)	106(7)	5027(2)	62(2)
C(65)	8270(2)	660(5)	5338(1)	45(1)
O(100)	0	-1938(42)	2500	251(14)
C(100)	68(9)	352(22)	2295(4)	198(7)
C(101)	177(9)	-1102(25)	2203(6)	221(8)

<sup>a</sup>  $U_{eq}$  is defined as one-third of the trace of the orthogonalized  $U_{ij}$  tensor.

**Table 4. Atomic Coordinates ( $\times 10^4$ ) and Equivalent Isotropic Displacement Parameters ( $\text{\AA}^2 \times 10^3$ ) for **2**<sup>a</sup>**

atom	x	y	z	$U_{eq}$
Ni	8290(1)	2597(1)	6215(1)	37(1)
Zr	7436(1)	1914(1)	6751(1)	34(1)
P	8850(1)	2684(2)	5736(1)	33(1)
Si(1)	6867(1)	-1254(2)	6091(1)	51(1)
Si(2)	9165(1)	5426(3)	6687(1)	57(1)
C(1)	7746(3)	1166(7)	6158(2)	35(2)
C(2)	7353(3)	277(8)	6196(2)	41(2)
C(3)	8151(3)	3448(8)	6696(2)	40(2)
C(4)	8594(3)	4108(9)	6564(2)	47(2)
C(5)	6443(5)	-1813(12)	6498(4)	84(4)
C(6)	7336(6)	-2753(12)	5951(5)	122(6)
C(7)	6331(7)	-798(16)	5731(4)	131(7)
C(8)	9903(5)	4880(16)	6544(4)	107(5)
C(9)	8996(8)	7176(14)	6473(6)	144(7)
C(10)	9163(7)	5592(22)	7190(4)	146(8)
C(20)	7548(5)	1199(11)	7417(2)	63(3)
C(21)	8119(5)	1445(12)	7286(3)	68(3)
C(22)	8250(4)	425(11)	7019(3)	64(3)
C(23)	7754(4)	-489(10)	6992(3)	61(2)
C(24)	7319(5)	-10(10)	7230(2)	61(2)
C(30)	6762(4)	3652(10)	6434(3)	58(2)
C(31)	6904(4)	4259(9)	6769(3)	55(2)
C(32)	6656(4)	3414(11)	7039(2)	63(3)
C(33)	6348(4)	2301(11)	6875(2)	56(2)
C(34)	6410(4)	2429(10)	6508(3)	54(2)
C(40)	9529(3)	1615(8)	5760(2)	39(2)
C(41)	9871(3)	1304(9)	5463(2)	50(2)
C(42)	10383(4)	509(10)	5490(3)	58(2)
C(43)	10548(4)	-20(11)	5823(3)	64(2)
C(44)	10214(5)	253(12)	6139(3)	74(3)
C(45)	9705(4)	1093(11)	6098(3)	61(2)
C(50)	9105(3)	4444(8)	5601(2)	39(2)
C(51)	8685(4)	5487(10)	5573(4)	78(3)
C(52)	8832(6)	6841(10)	5470(4)	94(4)
C(53)	9404(5)	7192(10)	5409(3)	80(3)
C(54)	9825(5)	6195(11)	5434(3)	75(3)
C(55)	9677(4)	4813(10)	5518(3)	62(2)
C(60)	8518(3)	2020(8)	5309(2)	38(2)
C(61)	8486(4)	2805(9)	4988(2)	50(2)
C(62)	8196(5)	2250(11)	4688(3)	62(2)
C(63)	7955(4)	941(12)	4686(2)	62(2)
C(64)	7988(4)	149(10)	5007(3)	65(3)
C(65)	8270(4)	676(9)	5309(2)	53(2)
C(101)	29(16)	463(37)	2312(7)	244(14)
C(100)	107(14)	-977(38)	2169(9)	228(12)
O(100)	263(18)	-1913(46)	2500	258(20)

<sup>a</sup>  $U_{eq}$  is defined as one-third of the trace of the orthogonalized  $U_{ij}$  tensor.

**Table 3. Selected Bond Distances ( $\text{\AA}$ ) and Angles (deg) for **1****

C(1)-C(2)	1.233(7)	Ni-C(4)	2.061(5)
C(3)-C(4)	1.261(7)	Ti-C(3)	2.067(4)
C(2)-Si(1)	1.832(5)	Ti-C(1)	2.331(4)
C(4)-Si(2)	1.835(5)	Ti-C(2)	2.628
Ni-C(1)	1.828(5)	Ni-P	2.1674(13)
Ni-C(3)	1.909(5)	Ni-Ti	2.7277(10)
C(1)-C(2)-Si(1)	164.4(4)	Ni-C(1)-C(2)	170.4(4)
C(3)-C(4)-Si(2)	145.8(4)	Ti-C(3)-C(4)	164.5(4)

Heterobimetallic, tweezerlike complexes are well-known,<sup>6</sup> but compound **6** represents the first example of such a compound with different substituents at the acetylide groups. The structure shows that both of the acetylide groups in **6** are coordinatively  $\eta^2$ -side-on-bonded to the Ni( $\text{PPh}_3$ ) unit. There is no or only little influence of the different substituents at the C-C triple bond on the complexed C-C bond distances and on the Ni-C bond lengths to the carbon atoms, which are also  $\sigma$ -bonded to Ti. The other Ni-C bond distances to the carbon atoms not bonded to Ti are, as expected,<sup>9b</sup> shorter

**Table 5. Selected Bond Distances ( $\text{\AA}$ ) and Angles (deg) for **2****

C(1)-C(2)	1.236(12)	Ni-C(4)	2.035(9)
C(3)-C(4)	1.284(13)	Zr-C(3)	2.178(9)
C(2)-Si(1)	1.847(9)	Zr-C(1)	2.385(7)
C(4)-Si(2)	1.835(9)	Zr-C(2)	2.557
Ni-C(1)	1.835(8)	Ni-P	2.168(2)
Ni-C(3)	1.961(8)	Ni-Zr	2.8295(13)
C(1)-C(2)-Si(1)	159.2(7)	Ni-C(1)-C(2)	166.4(7)
C(3)-C(4)-Si(2)	141.7(7)	Zr-C(3)-C(4)	160.4(7)

for the Ph-substituted case (Ni-C(4) - 2.038(3)  $\text{\AA}$ ) than for the Si-substituted part of the structure (Ni-C(2) - 2.065(3)  $\text{\AA}$ ). The unexpected<sup>9b</sup> larger bending-back angle C(1)-C(2)-Si of 134.1(3) $^\circ$  in comparison with C(1)-C(2)-C(5) of 148.4(4) $^\circ$  is explained by steric effects and the possibility for the phenyl ring of the acetylide of finding a nearly parallel arrangement to a phenyl ring of the phosphine. The Ti-C distances are somewhat shorter compared to those in complexes **1** and **3**, indicating also the  $\pi$ -interaction discussed above (cf.

**Table 6. Selected Bond Distances and Angles for 1-4**

$$\begin{array}{c} L_n M(1) \cdot C(1) \equiv C(2) - Si(1) Me_3 \\ \uparrow \qquad \qquad \qquad \downarrow \\ Me_3 Si(2) - C(4) \equiv C(3) - M(2) Cp_2 \end{array}$$

	1	2	3	4 <sup>13</sup>
M(1)	Ni	Ni	Ti	Zr
M(2)	Ti	Zr	Ti	Zr
L <sub>n</sub>	PPh <sub>3</sub>	PPh <sub>3</sub>	Cp <sub>2</sub>	Cp <sub>2</sub>
	Distances (Å)			
C(1)-C(2)	1.233(7)	1.236(12)	1.244(3)	1.249(7)
C(3)-C(4)	1.261(7)	1.284(13)	1.244(3)	1.260(7)
M(1)-C(1)	1.828(5)	1.835(8)		
M(1)-C(3)	1.909(5)	1.961(8)		
M(1)-C(4)	2.061(5)	2.035(9)		
M(2)-C(3)	2.067(4)	2.178(9)	2.069(1)	2.191(5)
M(2)-C(1)	2.331(4)	2.385(7)	2.393(1)	2.426(5)
M(2)-C(2)	2.628	2.557	2.318(2)	2.407(5)
M(1)-M(2)	2.7277(10)	2.8295(13)	3.550(3) [12]	3.522(2)
	Angles (deg)			
C(1)-C(2)-Si(1)	164.4(4)	159.2(7)	141.5(2)	142.5(4)
C(3)-C(4)-Si(2)	145.8(4)	141.7(7)		
M(1)-C(1)-C(2)	170.4(4)	166.4(7)		
M(2)-C(3)-C(4)	164.5(4)	160.4(7)	176.4(1)	172.7(4)

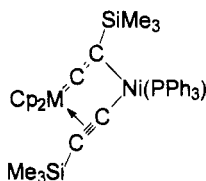
**Chart 1**

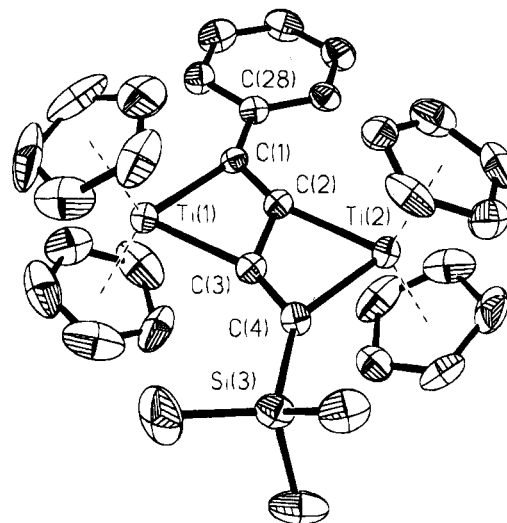
Chart 1). The long Ti-Ni distance suggests that there is little, if any, metal-metal interaction.

The different reaction pathways of PhC≡CC≡CSiMe<sub>3</sub> with "Cp<sub>2</sub>Ti" to **5** on the one hand and of (Ph<sub>3</sub>P)<sub>2</sub>Ni(η<sup>2</sup>-PhC≡CC≡CSiMe<sub>3</sub>) with "Cp<sub>2</sub>Ti" to **6** on the other hand can be explained in general by Scheme 2.

The first step is in all cases the formation of the cyclocumulene complex **A**, which is stable and was structurally characterized for R = R' = *t*-Bu<sup>14</sup> and also the zirconocene analogue.<sup>4</sup> The question is open as to whether such complexes **A** react (i) intramolecularly through bis(acetylide) complexes **B** or (ii) directly and intermolecularly with "Cp<sub>2</sub>Ti" to give **5** or with "(Ph<sub>3</sub>P)<sub>2</sub>-Ni" to give **6**. Possibly, the nickel fragment is acting mainly as a trapping agent for an intermediate of the cleavage reaction.

### Conclusion

Reactions of early-late transition-metal systems with 1,4-disubstituted 1,3-butadiynes proceed smoothly to give heterobimetallic complexes with σ,π-bridging acetylide units. In solution, an equilibrium of different structures obtains. In the solid state, a well-defined energy minimum of the structure, influenced by small effects of the substituents, the metal, and the ligands, is reached. Phenyl substituents at the acetylide unit and small ligands at the Ni center favor tweezerlike structures. In contrast, bulky *t*-Bu and SiMe<sub>3</sub> groups in combination with larger ligands on the Ni atom

**Figure 3.** Molecular structure of complex **5**, shown by an ORTEP plot at the 40% probability level.**Table 7. Atomic Coordinates (×10<sup>4</sup>) and Equivalent Isotropic Displacement Parameters (Å<sup>2</sup> × 10<sup>3</sup>) for 5<sup>a</sup>**

atom	x	y	z	U <sub>eq</sub>
Ti(1)	11625(2)	3983(1)	3549(1)	30(1)
Ti(2)	11148(2)	3431(1)	7062(1)	31(1)
Si(3)	13996(3)	4337(1)	7793(2)	42(1)
C(1)	10142(8)	3485(2)	3768(6)	30(2)
C(2)	10798(8)	3539(2)	5031(6)	29(2)
C(3)	11992(8)	3873(2)	5630(7)	31(2)
C(4)	12640(8)	3942(2)	6876(7)	31(2)
C(5)	14434(14)	4065(4)	3396(18)	96(5)
C(6)	13532(20)	4025(6)	2148(17)	109(6)
C(7)	12902(14)	3646(6)	2026(12)	93(5)
C(8)	13453(15)	3453(4)	3148(15)	81(4)
C(9)	14369(12)	3703(4)	4014(10)	73(3)
C(10)	8885(11)	4267(3)	2907(15)	79(4)
C(11)	9755(15)	4383(3)	1984(10)	73(3)
C(12)	10950(15)	4616(4)	2487(15)	84(4)
C(13)	11016(16)	4679(3)	3729(15)	89(4)
C(14)	9751(20)	4479(4)	4075(11)	90(5)
C(15)	11763(14)	2734(3)	6685(11)	66(3)
C(16)	13093(13)	2952(3)	6529(9)	58(3)
C(17)	13847(10)	3123(2)	7677(11)	58(3)
C(18)	12936(13)	3009(3)	8617(8)	62(3)
C(19)	11662(12)	2755(3)	7949(11)	62(3)
C(20)	9878(12)	3793(3)	8567(9)	62(3)
C(21)	9269(11)	3969(3)	7389(10)	53(2)
C(22)	8339(11)	3680(4)	6581(10)	71(3)
C(23)	8373(12)	3320(3)	7303(13)	76(3)
C(24)	9321(14)	3385(4)	8536(10)	73(3)
C(25)	15629(11)	4103(3)	9108(9)	58(2)
C(26)	12742(13)	4698(3)	8569(11)	74(3)
C(27)	15068(15)	4632(4)	6712(11)	91(4)
C(28)	8849(8)	3205(2)	3104(7)	32(2)
C(29)	8125(9)	2925(2)	3781(8)	40(2)
C(30)	6872(11)	2669(3)	3117(9)	53(2)
C(31)	6331(11)	2693(3)	1769(9)	55(2)
C(32)	7067(11)	2962(3)	1104(8)	56(2)
C(33)	8300(10)	3224(2)	1744(7)	44(2)

<sup>a</sup> U<sub>eq</sub> is defined as one-third of the trace of the orthogonalized U<sub>ij</sub> tensor.

prevent this structure and **1** and **2** are formed. For example, the acetylide phenyl group in **6** is almost parallel to one phenyl group of the triphenylphosphane. By this, the triphenylphosphane is put into a staggered position towards the trimethylsilyl group and a tweezer like structure results. For two trimethylsilyl groups as acetylide substituents this orientation would be more sterically hindered. This might explain the different

(14) Burlakov, V. V.; Ohff, A.; Lefebvre, C.; Tillack, A.; Baumann, W.; Kempe, R.; Rosenthal, U. *Chem. Ber.*, submitted for publication.

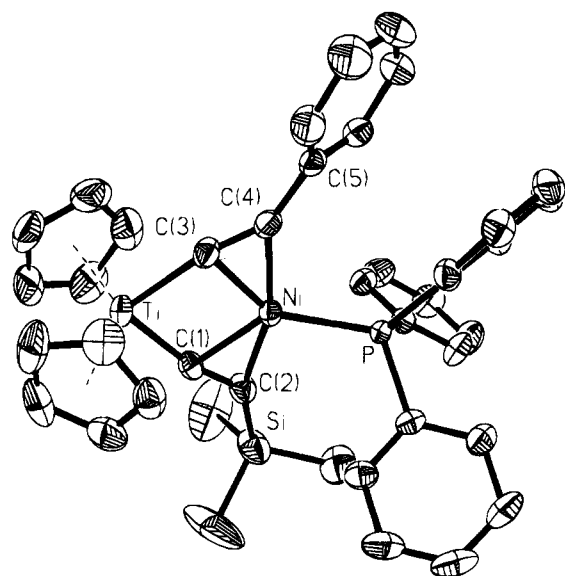


**Figure 4.** Molecular structure of complex **6**, shown by an ORTEP plot at the 40% probability level.

**Table 9.** Atomic Coordinates ( $\times 10^4$ ) and Equivalent Isotropic Displacement Parameters ( $\text{\AA}^2 \times 10^3$ ) for **6**<sup>a</sup>

atom	x	y	z	$U_{eq}$
Ti	6853(1)	1854(1)	567(1)	37(1)
Ni	8070(1)	3291(1)	1308(1)	32(1)
P	8813(1)	4574(1)	1809(1)	27(1)
Si	5900(1)	3804(1)	2384(1)	65(1)
C(1)	6635(3)	2770(3)	1321(2)	36(1)
C(2)	6737(3)	3395(3)	1766(2)	43(1)
C(3)	8346(3)	2370(3)	588(2)	41(1)
C(4)	9201(3)	2745(3)	792(2)	39(1)
C(5)	10315(3)	2749(3)	784(2)	40(1)
C(6)	10969(3)	2722(3)	1334(2)	48(1)
C(7)	12028(3)	2653(4)	1317(3)	68(1)
C(8)	12449(4)	2629(5)	755(4)	95(2)
C(9)	11819(4)	2664(5)	198(3)	89(2)
C(10)	10758(3)	2728(4)	210(2)	62(1)
C(11)	5663(7)	2627(6)	2851(3)	137(3)
C(12)	4672(4)	4260(8)	1964(3)	163(4)
C(13)	6400(4)	4842(4)	2927(2)	79(2)
C(20)	6076(4)	269(3)	781(3)	79(2)
C(21)	6502(4)	632(4)	1352(3)	74(2)
C(22)	7570(4)	655(4)	1318(3)	76(2)
C(23)	7796(4)	288(4)	739(3)	77(2)
C(24)	6863(5)	52(3)	411(3)	74(1)
C(30)	6788(4)	2579(4)	-460(2)	66(1)
C(31)	6460(4)	3345(3)	-67(2)	59(1)
C(32)	5530(3)	3024(4)	158(2)	62(1)
C(33)	5296(4)	2072(4)	-89(2)	70(1)
C(34)	6053(5)	1795(4)	-477(2)	77(2)
C(40)	10119(3)	4967(2)	1630(2)	33(1)
C(41)	10269(3)	5183(3)	1012(2)	43(1)
C(42)	11246(3)	5419(3)	835(2)	50(1)
C(43)	12076(3)	5436(3)	1286(2)	52(1)
C(44)	11930(3)	5247(3)	1905(2)	54(1)
C(45)	10958(3)	5010(3)	2076(2)	42(1)
C(50)	8125(3)	5799(3)	1673(2)	38(1)
C(51)	8587(3)	6726(3)	1823(2)	50(1)
C(52)	8061(4)	7641(3)	1715(2)	63(1)
C(53)	7074(4)	7629(4)	1434(2)	69(1)
C(54)	6612(4)	6724(4)	1265(2)	63(1)
C(55)	7129(3)	5810(3)	1383(2)	46(1)
C(60)	8956(3)	4381(3)	2667(2)	36(1)
C(61)	9076(3)	5168(3)	3107(2)	49(1)
C(62)	9181(4)	4966(3)	3747(2)	59(1)
C(63)	9170(4)	3973(4)	3953(2)	59(1)
C(64)	9068(4)	3182(3)	3525(2)	57(1)
C(65)	8951(3)	3385(3)	2887(2)	44(1)

<sup>a</sup>  $U_{eq}$  is defined as one-third of the trace of the orthogonalized  $U_{ij}$  tensor.

**Table 10.** Selected Bond Distances ( $\text{\AA}$ ) and Angles (deg) for **6**

C(1)–C(2)	1.250(5)	Ni–C(1)	1.986(3)
C(3)–C(4)	1.256(5)	Ni–C(3)	2.005(3)
C(2)–Si	1.855(4)	Ni–C(2)	2.065(3)
C(4)–C(5)	1.447(5)	Ni–C(4)	2.038(3)
Ti–C(1)	2.040(4)	Ni–P	2.1659(9)
Ti–C(3)	2.048(4)	Ti–Ni	2.840
C(1)–Ti–C(3)	89.25(13)	C(1)–C(2)–Si	134.1(3)
Ti–C(1)–C(2)	165.2(3)	C(3)–C(4)–C(5)	148.4(4)
Ti–C(3)–C(4)	160.4(3)		

H, SiMe<sub>3</sub>), 5.63 (s, 10 H, Cp); 190 K, symmetrical form,  $\delta$  -0.43 (s, 18 H, SiMe<sub>3</sub>), 5.47 (s, 10 H, Cp) (ratio unsymmetrical to symmetrical form ~5:1). <sup>13</sup>C NMR (THF-*d*<sub>6</sub>): 303 K,  $\delta$  1.1 (s, SiMe<sub>3</sub>), 105.9 (s, Cp), 128.9 (d, <sup>3</sup>J(C,P) = 9 Hz, Ph (meta)), 129.4 (s, Ph (para)), 135.2 (d, <sup>2</sup>J(C,P) = 13 Hz, Ph (ortho)), 137.0 (d, <sup>1</sup>J(C,P) = 35 Hz, Ph (ipso)). Anal. Calcd for C<sub>38</sub>H<sub>43</sub>NiP<sub>2</sub>Si<sub>2</sub>Ti·0.5C<sub>4</sub>H<sub>8</sub>O (*M*<sub>r</sub>, 729.5); <sup>15</sup>C, 65.85; H, 6.51; Ni, 8.05; Ti, 6.56. Found: C, 65.91; H, 6.73; Ni, 8.24; Ti, 6.61.

**Cp<sub>2</sub>Zr( $\mu$ - $\eta^1$ : $\eta^2$ -C≡CSiMe<sub>3</sub>)Ni(PPh<sub>3</sub>)( $\mu$ - $\eta^1$ : $\eta^2$ -C≡CSiMe<sub>3</sub>) (2).** A solution of 1.40 g (1.80 mmol) of (Ph<sub>3</sub>P)<sub>2</sub>Ni( $\eta^2$ -Me<sub>3</sub>SiC≡CC≡CSiMe<sub>3</sub>) in 10 mL of THF was added to 0.89 g (1.92 mmol) of Cp<sub>2</sub>Zr(THF)(Me<sub>3</sub>SiC≡CSiMe<sub>3</sub>) in 10 mL

**Table 8.** Selected Bond Distances ( $\text{\AA}$ ) and Angles (deg) for **5**

C(1)–C(2)	1.327(9)	Ti(1)–C(2)	2.337(7)
C(2)–C(3)	1.511(9)	Ti(1)–C(3)	2.164(7)
C(3)–C(4)	1.317(9)	Ti(2)–C(2)	2.114(7)
C(4)–Si(3)	1.838(7)	Ti(2)–C(3)	2.302(7)
Ti(1)–C(1)	2.083(7)	Ti(2)–C(4)	2.115(7)
C(1)–C(2)–C(3)	126.6(6)	C(4)–C(3)–Ti(1)	154.9(6)
C(2)–C(3)–C(4)	128.4(6)	C(2)–C(1)–C(28)	130.8(7)
C(1)–C(2)–Ti(2)	156.4(6)	C(3)–C(4)–Si(3)	135.0(6)

structures of complex **1** and **2**, where one acetylide group is  $\sigma$ -bonded to the nickel.

## Experimental Section

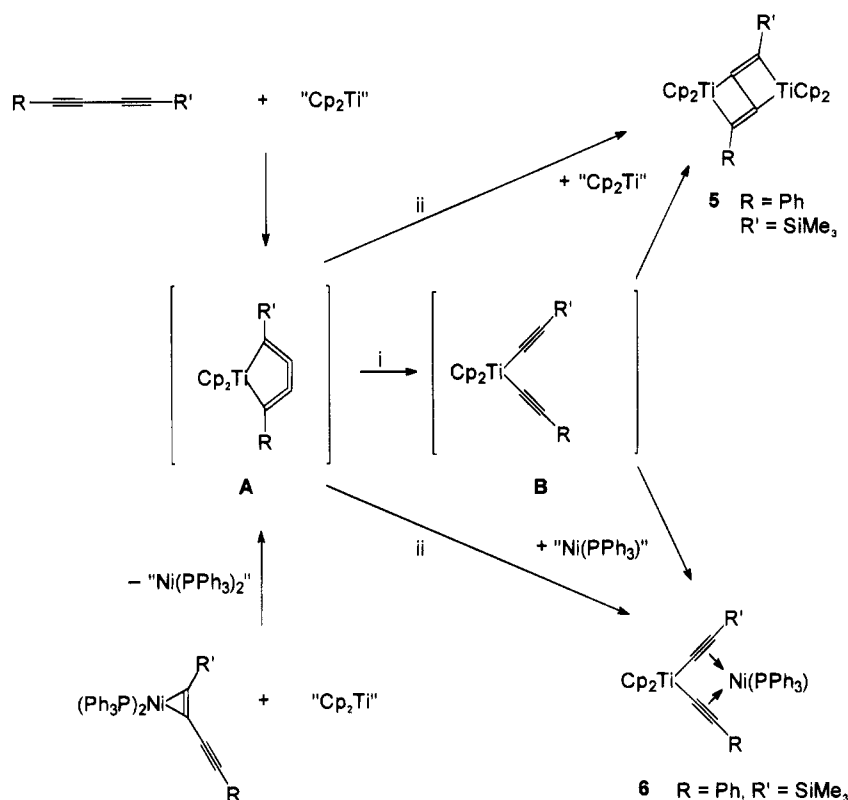
**General Considerations.** All operations were carried out under an inert atmosphere (argon) with standard Schlenk techniques. Solvents were freshly distilled from sodium tetraethylaluminate under argon prior to use. Deuterated solvents were treated with sodium or sodium tetraethylaluminate, distilled, and stored under argon. The following spectrometers were used: NMR, Bruker ARX 400; IR, Nicolet Magna 550 (Nujol mulls using KBr plates); MS, AMD 402. Melting points were measured in sealed capillaries on a Büchi 535 apparatus.

Diffraction data were collected on a CAD4 diffractometer using Mo K $\alpha$  radiation. The structure was solved by direct methods<sup>16a</sup> and refined by full-matrix least-squares techniques against  $F^2$ .<sup>16b</sup> Structural representation was obtained by using ORTEP.

**Cp<sub>2</sub>Ti( $\mu$ - $\eta^1$ : $\eta^2$ -C≡CSiMe<sub>3</sub>)Ni(PPh<sub>3</sub>)( $\mu$ - $\eta^1$ : $\eta^2$ -C≡CSiMe<sub>3</sub>) (1).** To a solution of 2.10 g (2.70 mmol) of (Ph<sub>3</sub>P)<sub>2</sub>Ni( $\eta^2$ -Me<sub>3</sub>SiC≡CC≡CSiMe<sub>3</sub>) in 20 mL of toluene was added 0.98 g (2.81 mmol) of Cp<sub>2</sub>Ti(Me<sub>3</sub>SiC≡CSiMe<sub>3</sub>) in 15 mL of toluene. As the yellowish brown reaction mixture was stirred for 4 h at 50 °C, the color changed to red-brown. The solvent was evaporated in vacuo, and the residue crystallized by diffusion of *n*-hexane into a THF solution. After 2 days, filtration left dark red-brown crystals, which were washed twice with *n*-hexane and dried in vacuo.

Yield: 1.39 g (70%) of **1**. Mp: 127–133 °C. MS: *m/z* 692 (M<sup>+</sup>). IR (Nujol mull): 1780, 1911 cm<sup>-1</sup> ( $\nu_{C=C}$ ). <sup>31</sup>P NMR (THF-*d*<sub>6</sub>): 303 K,  $\delta$  43.1; 190 K,  $\delta$  41.4, 42.7 (ratio ~5:1). <sup>1</sup>H NMR (THF-*d*<sub>6</sub>): 303 K,  $\delta$  -0.11 (s, 18 H, SiMe<sub>3</sub>), 5.53 (s, 10 H, C<sub>5</sub>H<sub>5</sub>), 7.31–7.36 (m, 10 H, Ph), 7.56–7.60 (m, 5 H, Ph); 190 K, unsymmetrical form,  $\delta$  -0.35 (s, 9 H, SiMe<sub>3</sub>), 0.25 (s, 9

Scheme 2



of THF, and the mixture was stirred at room temperature for 1 day. The color changed from yellow-brown to deep red-brown. The solvent was removed in vacuo and the residue crystallized from THF/*n*-hexane. After 4 days the solution afforded dark, red-brown crystals, which were washed with *n*-hexane and dried in vacuo.

Yield: 0.77 g (58%) of **2**. Mp: 145–150 °C. MS:  $m/z$  736 ( $M^+$ ). IR (Nujol mull): 1771, 1876  $cm^{-1}$  ( $\nu_{C=C}$ ).  $^{31}P$  NMR (THF- $d_6$ ):  $\delta$  40.0.  $^1H$  NMR (THF- $d_6$ ):  $\delta$  -0.19 (s, 9 H,  $SiMe_3$ ), 0.22 (s, 9 H,  $SiMe_3$ ), 5.72 (s, 10 H,  $C_5H_5$ ), 7.30–7.33 (m, 10 H, Ph), 7.50–7.60 (m, 10 H, Ph).  $^{13}C$  NMR (THF- $d_6$ ):  $\delta$  1.4 (s,  $SiMe_3$ ), 1.6 (s,  $SiMe_3$ ), 106.0 (s, Cp), 109.8 (d,  $^2J(C,P) = 6$  Hz,  $\beta-C\equiv$ ), 112.1 (d,  $^2J(C,P) = 1.5$  Hz,  $\beta-C\equiv$ ), 128.6 (d,  $^3J(C,P) = 9$  Hz, Ph (meta)), 129.8 (d,  $^4J(C,P) = 2$  Hz, Ph (para)), 135.0 (d,  $^2J(C,P) = 14$  Hz, Ph (ortho)), 138.1 (d,  $^1J(C,P) = 33$  Hz, Ph (ipso)), 214.6 (d,  $^2J(C,P) = 2$  Hz,  $\alpha-C\equiv$ ), 233.9 (d,  $^2J(C,P) = 3$  Hz,  $\alpha-C\equiv$ ). Anal. Calcd for  $C_{38}H_{43}NiPSi_2Zr \cdot 0.5C_4H_8O$  ( $M_r$  772.9):  $^{15}C$ , 62.16; H, 6.08; Ni, 7.59. Found: C, 62.18; H, 6.01; Ni, 8.04.

**$Cp_2Ti(\mu-(1-3\eta):(2-4\eta)-trans,trans-PhC\equiv CC\equiv CSiMe_3)-TiCp_2$  (**5**).<sup>2</sup>** A 0.31 mL (1.58 mmol) amount of 1-(trimethylsilyl)-4-phenyl-1,3-butadiyne was added to a solution of 1.10 g (3.16 mmol) of  $Cp_2Ti(Me_3SiC\equiv CSiMe_3)$  in 10 mL of THF and heated to 60 °C. After addition of 5 mL of *n*-hexane and cooling to room temperature, a green product crystallized, which was separated from the mother liquid, washed with cold *n*-hexane, and dried in vacuo.

Yield: 0.29 g (33%) of **5**. Mp: 280 °C. MS:  $m/z$  554 ( $M^+$ ).  $^1H$  NMR (THF- $d_6$ ):  $\delta$  0.36 (s, 9 H,  $SiMe_3$ ), 5.44 (s, 20 H,  $C_5H_5$ ) 7.23–7.53 (m, 5 H, C–Ph).  $^{13}C$  NMR (THF- $d_6$ ):  $\delta$  1.4 (s,  $SiMe_3$ ), 106.9, 107.2 (s, Cp), 128.1, 129.0, 132.3, 142.7 (Ph),

135.4 (C=CPh), 146.4 (C=CSiMe<sub>3</sub>), 221.9 (C=CPh), 227.4 (C=CSiMe<sub>3</sub>). Anal. Calcd for  $C_{33}H_{34}SiTi_2$  ( $M_r$  554.48): C, 71.48; H, 6.18; Si, 5.07; Ti, 17.27. Found: C, 71.98; H, 6.10; Si, 4.95; Ti, 16.95.

**$Cp_2Ti(\mu-\eta^1:\eta^2-C\equiv CPh)(\mu-\eta^1:\eta^2-C\equiv CSiMe_3)Ni(PPh_3)$  (**6**).** A 0.38 g (1.10 mmol) amount of  $Cp_2Ti(Me_3SiC\equiv CSiMe_3)$  in 5 mL of toluene was added to a reddish brown solution of 0.89 g (1.10 mmol) of  $(Ph_3P)_2Ni(\eta^2-PhC\equiv CC\equiv CSiMe_3)$  in 15 mL of toluene. Heating to 80 °C led to a brown color. After the mixture was stirred for 4 h, the solvent was removed in vacuo and the residual brown oil dissolved in THF. The solution was covered by *n*-hexane. After 2 days at room temperature well-formed, six-cornered, deep red crystals were formed. They were washed with *n*-hexane and dried in vacuo.

Yield: 0.52 g (62%) of **6**. Mp: 184–185 °C. MS:  $m/z$  696 ( $M^+$ ). IR (Nujol): 1797, 1846  $cm^{-1}$  ( $\nu_{C=C}$ ).  $^{31}P$  NMR (THF- $d_6$ ):  $\delta$  45.73.  $^1H$  NMR (THF- $d_6$ ):  $\delta$  -0.18 (s, 9 H,  $SiMe_3$ ), 5.55 (s, 10 H,  $C_5H_5$ ), 6.75–6.77 (m, 5 H, C–Ph), 7.19–7.24 (m, 9 H, P–Ph), 7.44–7.53 (m, 6 H, P–Ph).  $^{13}C$  NMR (THF- $d_6$ ):  $\delta$  1.6 (s,  $SiMe_3$ ), 104.8 (s, Cp), 115 (broad signal,  $\beta-C\equiv$ ), 119 (broad signal,  $\beta-C\equiv$ ), 125.0 ( $\equiv C-Ph$  (para)), 128.0 ( $\equiv C-Ph$  (meta)), 128.5 (d,  $^3J(C,P) = 9$  Hz, P–Ph (meta)), 129.8 (d,  $^4J(C,P) = 2$  Hz, P–Ph (para)), 130.3 ( $\equiv C-Ph$  (ortho)), 132.4 (d,  $^4J(C,P) = 5$  Hz,  $\equiv C-Ph$  (ipso)), 135.2 (d,  $^1J(C,P) = 13$  Hz, P–Ph (ortho)), 137.4 (d,  $^1J(C,P) = 36$  Hz, P–Ph (ipso)), 202.9 (broad signal,  $\alpha-C\equiv$ ), 222.9 (broad signal,  $\alpha-C\equiv$ ). Anal. Calcd for  $C_{41}H_{39}NiPSiTi$  ( $M_r$  697.4): C, 70.61; H, 5.64; Ni, 8.42; Ti, 6.87. Found: C, 70.41; H, 5.84; Ni, 7.79; Ti, 6.56.

**Supplementary Material Available:** For **1**, **2**, **5**, and **6**, figures giving ORTEP views of the structures and tables of crystal data and structure refinement details, all bond distances and angles, anisotropic thermal parameters, and H atom positional parameters (38 pages). Ordering information is given on any current masthead page.

OM940945N

(15) The compound crystallizes with 0.5 mol of THF. This was also detected by X-ray diffraction (see Tables 2 and 4) and NMR spectroscopy.

(16) (a) Sheldrick, G. Shelx-86. *Acta Crystallogr., Sect. A* **1990**, *46*, 467. (b) Sheldrick, G. Shelxl-93; University of Göttingen, Göttingen, Germany, 1993.

# Reactivity of Bimetallic Compounds Containing Planar Tetracoordinate Carbon toward Unsaturated Organic Substrates

Paul Binger,\* Frank Sandmeyer, and Carl Krüger

Max Planck Institut für Kohlenforschung, Kaiser Wilhelm Platz 1,  
45466 Mülheim an der Ruhr, Germany

Received February 6, 1995<sup>®</sup>

Anti van't Hoff/le Bel compound **1** consisting of titanocene tolan and diethylborane units reacts with ethene, acetylenes, phosphaacetylenes, and acetone to give metallacycles **2**, **3**, **6**, and **7**, and in most cases the corresponding diethylorganylboranes are formed by hydroboration of the carbon–carbon or carbon–heteroatom multiple bond in the substrate. With nitriles the new bimetallic systems **9a–c** (X-ray structure available for **9a**) with titanium and boron centers and **12** containing zirconium and aluminium centers are generated by the formal insertion of the nitrile into the B–C<sub>planar</sub> bond of **1** or the Al–C<sub>planar</sub> bond of **11**.

## Introduction

The synthetic and structural aspects of bimetallic complexes containing a planar tetracoordinate carbon atom bridging between a group 4 transition metal and a main group element are of current interest and have been treated extensively in recent publications.<sup>1</sup> For example we have successfully synthesized and characterized such anti van't Hoff/le Bel compounds that contain a zirconium or titanium atom with a boron atom.<sup>2</sup> Besides their structural characterization, the reactivity of these systems has been of great interest to use. Here we wish to report our results obtained by allowing two complexes of the type, **1** and **11**, to react with selected unsaturated organic substrates.

The X-ray crystallographic studies of **1** and **11** have revealed that the bonding situation can be approximated by the two mesomeric structures **A** (Figure 1). Since the reactivity characteristics of these complexes cannot satisfactorily be given by **A** alone, two alternative descriptions, **B** and **C**, are shown in Figure 1 which help explain how these compounds could react with suitable substrates.

Form **B** emphasizes the fact that the transition metal–carbon interaction, M–C2, is weaker than a conventional metal–carbon  $\sigma$ -bond by suggesting the bonding to be an agostic interaction. This formalism is reasonable in light of the results obtained by electron deformation density measurements made on Zr/Al

bimetallic systems.<sup>3</sup> A B–C2 bond activation might result. Cleavage of this bonding interaction is equivalent to the loss of the transition metal  $\sigma$ -acceptor effect which has been found to be essential for the stability of these molecules.<sup>4</sup> Form **C** is a much better description for the electronic situation than **A**; this form emphasizes that the anti van't Hoff/le Bel compounds contain two three-center, two-electron bonds between the transition metal M, the square planar carbon C2, the boron atom, and the hydridic hydrogen. Boranes which are connected by means of this bonding type show their typical reactions, e.g. hydroboration, after cleavage of the two-electron, three-center bond, which results in the fragmentation of the diborane structure. The analogous chemical behavior could occur when allowing the anti van't Hoff/le Bel compounds to react with appropriate substrates.

## Results and Discussion

When ethene is added to a suspension of complex **1** in pentane at ambient temperatures, a spontaneous reaction occurs to produce the titanacyclopentene **2** and triethylborane, as already reported in a preliminary communication.<sup>2a,5</sup> We have now extended our studies of the reactivity of **1** to various acetylenes, to acetone as a representative of the ketone family, and to various nitriles. Complex **1** does not react with bis(trimethylsilyl)acetylene possibly due to steric factors which would exist in the expected titanacyclopentadiene. With less bulky substituted acetylenes such as tolan, phenylacetylene, and 2-butyne, metallacyclopentadienyl complexes **3a,b,d** are formed in high yields at ambient temperatures.<sup>6</sup> The asymmetric phenylacetylene gives only one regioisomer **3d** with the aromatic group located

<sup>®</sup> Abstract published in *Advance ACS Abstracts*, May 15, 1995.  
(1) (a) Erker, G. *Comments Inorg. Chem.* **1992**, *13*, 111. (b) Erker, G. *Nachr. Chem. Tech. Lab.* **1992**, *40*, 1099. (c) Albrecht, M.; Erker, G.; Krüger, C. *Synlett* **1993**, 441. (d) Erker, G.; Albrecht, M.; Krüger, C.; Nolte, M.; Werner, S. *Organometallics* **1993**, *12*, 4979. (e) Erker, G.; Albrecht, M.; Krüger, C.; Werner, S. *J. Am. Chem. Soc.* **1992**, *114*, 8531. (f) Erker, G.; Albrecht, M.; Krüger, C.; Werner, S.; Binger, P.; Langhauser, F. *Organometallics* **1992**, *11*, 3517. (g) Erker, G.; Albrecht, M.; Werner, S.; Nolte, M.; Krüger, C. *Chem. Ber.* **1992**, *125*, 1953. (h) Erker, G.; Zwitter, R.; Krüger, C.; Noe, R.; Werner, S. *J. Am. Chem. Soc.* **1990**, *112*, 9620.  
(2) (a) Binger, P.; Sandmeyer, F.; Krüger, C.; Kuhnigk, J.; Goddard, R.; Erker, G. *Angew. Chem.* **1994**, *106*, 213; *Angew. Chem., Int. Ed. Engl.* **1994**, *33*, 197. (b) Binger, P.; Sandmeyer, F.; Krüger, C.; Erker, G. *Tetrahedron* **1995**, *51*, 4277.

(3) (a) Werner, S. Dissertation, Universität Münster, **1992**. (b) Krüger, C.; Werner, S. In *Transition Metal Carbyne Complexes*; Kreissl, F. R., Ed.; NATO ASI Series C; Plenum: New York, 1993; Vol. 392, p 131.  
(4) Gleiter, R.; Kryspin, I. H.; Niu, S.; Erker, G. *Angew. Chem.* **1993**, *105*, 753; *Angew. Chem., Int. Ed. Engl.* **1993**, *32*, 754.  
(5) Alt, H. G.; Herrmann, G. S. *J. Organomet. Chem.* **1990**, *390*, 159.  
(6) Shur, V. B.; Burlakov, V. V.; Vol'pin, M. E. *Bul. Acad. Sci. USSR* **1983**, *32*, 1753.



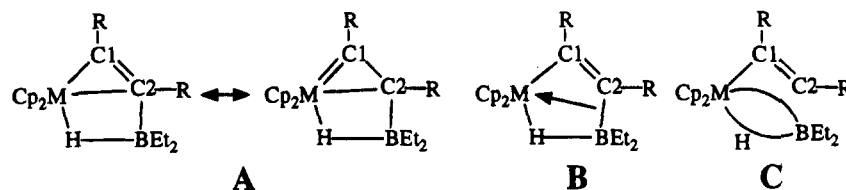
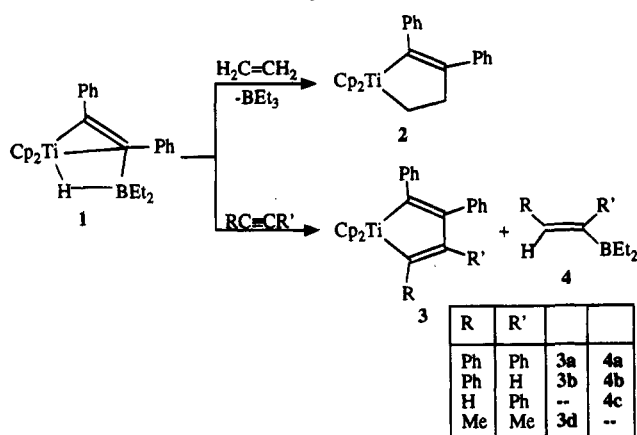


Figure 1.

### Scheme 1. Reactions of 1 with Ethene and Acetylenes

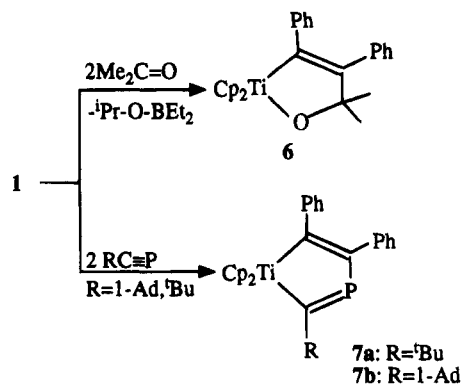


on the  $\alpha$ -carbon to the metal. With tolan and phenylacetylene the corresponding hydroborated acetylenes are obtained. Phenylacetylene produced both the Markovnikov and the anti-Markovnikov vinylboranes in a ratio of 2:3, estimated by  $^1\text{H}$  NMR spectroscopy. 2-Butyne formed one product which has not yet been isolated or identified. From  $^{11}\text{B}$  NMR spectroscopy, however, it can be concluded that this boron organic product is not the expected vinylborane (Scheme 1). A  $\delta(^{11}\text{B})$  value of 75.7 ppm should be observed for the latter. The new boron organic compound exhibits a resonance at  $\delta = -10.6$  ppm, which is in the region for borates or for carboranes.

The zirconocene complex  $\text{Cp}_2\text{Zr}(\text{PhCCPh})(\mu\text{-H})(\text{BEt}_2)$  (**5**), which is structurally analogous to **1**, does not react with acetylenes at ambient temperatures. When heated to 80 °C, the reactants undergo some as yet unknown transformation. No identifiable products could be observed.

The titanocene complex **1** reacts with acetone within a few minutes at ambient temperatures to give the red titanadihydrofuran **6**, which has been previously described by Vol'pin.<sup>7</sup> The only organoboron product formed in this reaction is diethylisopropoxyborane, which has been identified by the  $^{11}\text{B}$  resonance at  $\delta = 52.8$  ppm.<sup>8</sup> With phosphalkynes **1** reacts readily to give the dark red titanophospholes **7a**<sup>9</sup> and **7b**, bearing either a *tert*-butyl or an adamantyl substituent. Complex **7a** has been synthesized recently by the reaction of ( $\eta^2$ -*tert*-butylphosphaalkyne)(trimethylphosphine)titanocene with tolan in the presence of triethylborane at ambient temperatures.<sup>9</sup> The regioselectivity of this

### Scheme 2. Reaction of 1 with Acetone and Phosphaalkynes



cycloaddition as depicted in Scheme 2 is corroborated proved by the  $^{13}\text{C}$  NMR spectra of **7a** and **7b**. Both C atoms directly bonded to the transition metal exhibit resonances at considerably lower field than the  $\beta$ -C atoms (e.g. in **7a**:  $\delta = 303.8$  Ti-CtBu = P,  $^1J_{\text{P,C}} = 67.2$  Hz; 196.4 Ti-CPh = C, 118.9 Ti-C=CPh,  $^1J_{\text{P,C}} = 30.2$  Hz). No specific boron organic product can be identified, nor could any evidence for a hydroboration of the P-C triple bond be obtained.

The reactions described so far can be explained on the basis of the reactivity patterns implicit in structure **C** as discussed above. The starting complex can be considered to undergo fragmentation to give the two components, titanocene-tolan<sup>10</sup> and diethylborane, which then show their characteristic chemical behavior. In certain cases the diethylborane performs hydroboration reactions (where the reaction products could be identified), while the metallocene-tolan component oxidatively couples with the unsaturated organic substrate to give the corresponding five-membered ring system. Therefore diethylborane can be considered as a reversible protecting group for the titanocene-tolan complex.

A remarkably different and absolutely new reaction product is observed when acetonitrile, propionitrile, or benzonitrile is used as substrate for conversions with the titanocene anti van't Hoff/le Bel compound **1** (Scheme 3). In less than 1 h the reactions are completed in pentane at ambient temperatures. Instead of the hydroborated products and titanazoles only complexes **9** are detected containing the borane unit as well as the titanocene-tolan fragment. The same complex type (**9a**) is obtained by reaction of the titanazole **8**<sup>11</sup> with tetraethylidiborane at room temperature. Mass spec-

(10) Shur, V. B.; Burlakov, V. V.; Vol'pin, M. E. *J. Organomet. Chem.* **1988**, *347*, 77.

(11) Preparation as described for zirconium analogous: (a) Buchwald, S. L.; Watson, B. T.; Lum, R. T.; Nugent, W. A. *J. Am. Chem. Soc.* **1987**, *109*, 7137. (b) Buchwald, S. L.; Sayers, A.; Watson, B. T.; Dewan, J. C. *Tetrahedron Lett.* **1987**, *28*, 3245. (c) Buchwald, S. L.; Huffman, J. C.; Watson, B. T. *J. Am. Chem. Soc.* **1987**, *109*, 2544. (d) Takahashi, T.; Kageyama, M.; Denisov, V.; Hara, R.; Negishi, E. *Tetrahedron Lett.* **1993**, *34*, 687.

(7) Shur, V. B.; Burlakov, V. V.; Yanovsky, A. S. I.; Petrovsky, P. V.; Struchkov, Yu. T.; Vol'pin, M. E. *J. Organomet. Chem.* **1985**, *297*, 51.

(8) Wrackmeyer, B.; Köster, R. In *Houben Weyl, Methoden der organischen Chemie, Organbor-Verbindungen, Band XIII/3c*; Köster, R., Ed.; G. Thieme-Verlag: Stuttgart, New York, 1984; S 440 and references cited therein.

(9) Herrmann, A. T. Dissertation, University of Kaiserslautern, 1990.

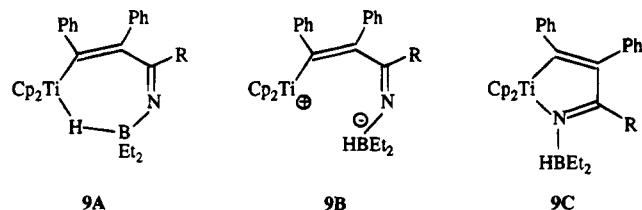
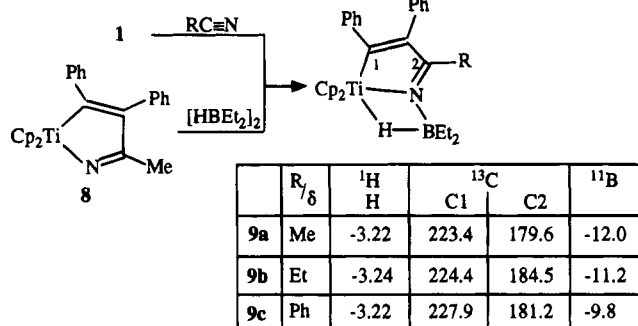


Figure 2.

### Scheme 3. Reaction of Nitriles with Anti-van't Hoff/le Bel Complexes



trometry and the elemental analysis prove that this new compound is a 1:1 adduct of the corresponding nitrile and 1. On the basis of the NMR-spectroscopic results it is not possible to distinguish between a monocyclic and a bicyclic structure. An X-ray investigation performed with a single crystal of compound **9a** proves these complexes to contain a bicyclo[3.2.0] skeleton as shown for **9a-c** (Scheme 3) thus ruling out the monocyclic alternative **9A** (Figure 2).

The presence of hydride bridges in **9a-c** can be corroborated by IR and NMR data. The proton resonances are located at high field ( $\delta \approx -3.2$  ppm) in the range expected for a hydrogen atom bridging the boron and the transition metal center.<sup>12</sup> A nonbridging B-H hydrogen atom features proton resonance signals at  $\delta = 3.76-4.40$  ppm.<sup>8</sup> The IR absorptions of the B-H-Ti units in **9-11** are located in the spectral range of 1675-1680  $\text{cm}^{-1}$ , a region typical for a bridging hydride.<sup>8</sup> Signals around 2340  $\text{cm}^{-1}$  usually belong to B-H bonds of amine adducts of dialkylboranes in which the hydrogen atoms are nonbridging.<sup>13</sup> Therefore structures of the type **9B,C** can be excluded (Figure 2). Further IR absorptions of analytical importance can be assigned to the C=N units. Their wavenumbers appear in the region from 1585 to 1595  $\text{cm}^{-1}$  due to the fact that the C-N double bond is part of a conjugated system.<sup>23</sup>

Splitting of the  $^1\text{H}$  NMR signals of the ethyl groups attached to boron into two signals with the methyl groups located at lower field as the methylene groups as well as the  $\delta(^{11}\text{B})$  values indicates that the boron atom is tetracoordinate.<sup>8</sup> The boron atoms give rise to  $^{11}\text{B}$  resonances in the region from -9.8 to -12.0 ppm, which amounts to an upfield shift of about 30 ppm compared to the absorptions of the starting complexes. The boron atoms of free imino boranes show absorptions

(12) (a) Kot, W. K.; Edelstein, N. M.; Zalkin, A. *Inorg. Chem.* **1987**, *26*, 1339. (b) Erker, G.; Hoffmann, U.; Zwettler, R.; Krüger, C. *J. Organomet. Chem.* **1989**, *367*, C15. (c) Erker, G.; Noe, R.; Wingbergmühle, D.; Petersen, J. L. *Angew. Chem.* **1993**, *105*, 1216; *Angew. Chem., Int. Ed. Engl.* **1993**, *32*, 1213.

(13) Köster, R.; Griasnow, G.; Larbig, W.; Binger, P. *Liebigs Ann. Chem.* **1964**, *672*, 1.

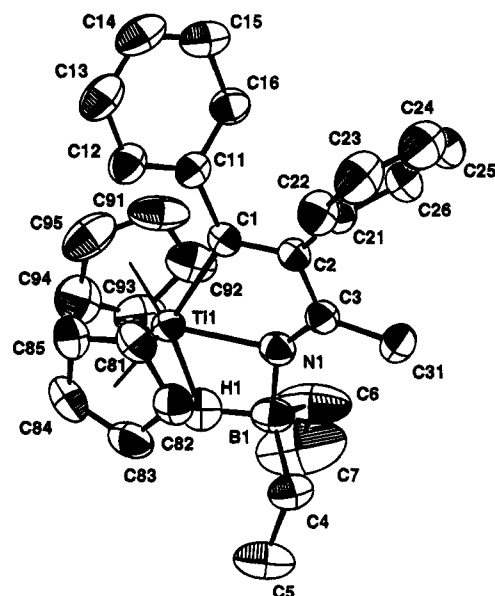
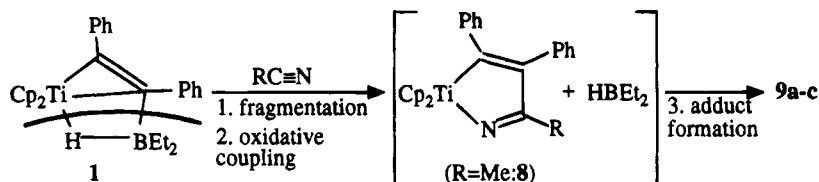


Figure 3. ORTEP plot of **9a** showing the atom-numbering scheme. The hydrogen atoms except the bridging hydride are omitted for clarity.

in the region of about  $\delta = 30$  ppm, while their dimers feature resonances in the region of -2.3 to 11.3 ppm.<sup>8</sup> As the two Cp signals give rise to only one signal in the  $^1\text{H}$  and the  $^{13}\text{C}$  spectra, the complex must be planar. As it is difficult to imagine that a monocycloheptadiene framework is perfectly planar, this observation strongly speaks in favor of the bicyclic structures of **9a-c**. Further valuable information is provided by  $^{13}\text{C}$  NMR spectroscopy. The carbon atoms C1 give rise to resonances above  $\delta = 220$  ppm which is in the typical region for  $\text{sp}^2$ -carbon atoms bonded to metals. Because of this feature a competing insertion of the nitrile into the metal-C1 bond can be excluded. The further question concerning the regioselectivity of the insertion remains to be answered. Of the two possibilities to be taken into consideration, Scheme 3 suggests an imino borane structure which is the result of B-N and C-C bond formation. The other possibility would be B-C and C-N bond formation to yield a vinyl borane. The  $\delta(^{13}\text{C})$  value of the nitrile carbon atom and the boron resonance provide the information necessary to solve this problem. The C=N carbon features a sharp singlet at  $\delta \approx 180$  ppm. If this carbon atom were bonded to the boron atom, the signal would have to show a striking line broadening as a result of the quadrupole coupling with the boron nucleus. From the spectroscopic data it can be unequivocally deduced that the insertion as shown in Scheme 3 is obtained. Another question however cannot be answered by NMR or IR spectroscopy: namely whether there is a bonding interaction between the transition metal and the nitrogen atom. Whether **9a-c** or **9A** is the correct structure can only be answered on the basis of the interatomic distances which were obtained for **9a** from the results of an X-ray investigation. Single crystals of **9a** were obtained by crystallization from a pentane-toluene solution (2:1; -20 °C). The ORTEP plot of **9a** is presented in Figure 3.

Complex **9a** exhibits a planar seven-membered framework consisting of the transition metal, the carbon atoms C1, C2, and C3, the nitrogen atom, and the B-H unit with the hydrogen atom bridging the transition and

## Scheme 4. Fragmentation Mechanism



the main group element. The skeleton is located in the plane bisecting the Cp(centroid)–Ti–Cp(centroid) angle. As the phenyl groups attached to C1 and C2 are twisted out of this plane, a stabilizing interaction of the aromatic ring systems with the C1–C2 double bond can be excluded. The boron atom is tetrahedrally coordinated with a bonding interaction to the nitrogen atom. Up to this point the routine spectroscopic results are fully confirmed. The vexing question as to whether there is a Ti–N interaction or not can now be answered by examining the most interesting datum, namely the distance between the Ti and the N atom. A separation of 2.075(2) Å is found for this pair of atoms. This value is within the range expected for a Ti–N bond with the nitrogen atom bonded to a  $sp^2$ -hybridized carbon atom<sup>14</sup> and indicates unequivocally the existence of a strong Ti–N interaction. This finding permits one to designate **9a–c** as the correct structures for these new complexes. Ti–N bonds in dialkylamides and bis(trimethylsilyl)amides are considerably shorter, e.g. 1.88 Å in  $CpTiCl_2[N(SiMe_3)_2]$ <sup>15</sup> and 1.89 Å in  $Fe[C_5H_4Ti(NEt_2)_3]$ .<sup>16</sup>

Pure Ti–N donor interactions are long by comparison, e.g. 2.293 Å in the pyridine complex  $Ti(OC_6H_3^tBuMe_2CH_2)(OC_6H_3^tBu_2)(CH_2SiMe_3)(py)$ <sup>14b</sup> or the pyridine-2,6-dicarboxylato compound  $Cp_2Ti[C_5H_3N-2,6-(CO_2)_2]$  (2.160 Å).<sup>17</sup> **9a** can very well be compared to the complex  $[Ti(salen)(BH_4)_2] \cdot 2thf$ <sup>18</sup> (**10**) (*salen* = *N,N'*-ethylenebis(salicylideneimine),  $C_{16}H_{16}N_2O_2$ ), which also exhibits a four-membered system consisting of Ti, B, N, and H. An averaged transition metal–nitrogen bond distance of 2.14 Å is found in this compound. Further bond distances and angles are listed in Table 1. The B–N distance of **9a** (1.515(4) Å) and those found in the Ti–salen complex (average 1.54 Å) are almost identical. Furthermore B–N distances in the range from 1.4 to 1.6 Å are rather common for organic boron compounds.<sup>19</sup> This result clearly support a strong boron nitrogen interaction in **9a**. The B–H bond length in **9a** (1.37(3) Å) is comparable to the corresponding value determined for **10** (averaged value:  $d_{av}(B-H) = 1.3(1)$  Å) whereas the Ti–H bond is remarkably longer in **9a** (2.01(3) Å) than in **10** ( $d_{av}(Ti-H) = 1.8(1)$  Å).

Formally the new compounds can be considered as insertion products of the corresponding nitrile into the boron–C<sub>planar</sub> bond, but this is quite unlikely, because

Table 1. Selected Bond Lengths (Å) and Angles (deg) for **9a**

Distances			
Ti–C1	2.289(2)	C1–C2	1.362(3)
Ti–N	2.075(2)	C2–C3	1.475(4)
Ti–H	2.01(3)	N–C3	1.276(3)
Ti–B	2.688(3)	B–H	1.37(3)
B–N	1.515(4)		
Angles			
H–Ti–C1	135.8(8)	B–N–Ti	95.7(2)
H–Ti–N	63.7(8)	C3–C2–C1	114.6(2)
C1–Ti–N	72.3(1)	C1–C2–Ti	43.0(1)
B–H–Ti	103(2)	C2–C1–Ti	113.0(2)
C3–N–B	139.4(2)	H–B–N	96.7(1)

in numerous insertion reactions of nitriles into Ti- or Zr-cyclic systems reported usually the nitriles insert into the bond of the group 4 transition metal to the carbon atom but not into a metal–heteroatom bond.<sup>20</sup>

As the titanazole **8** can be converted with tetraethylborane to give **9a** as well, we assume as an more likely alternative a fragmentation mechanism which could satisfactorily explain the formation of **9a–c**. As outlined in Scheme 4, this mechanistic concept designates three reaction steps starting with the fragmentation of **1** to give titanocene–tolan and diethylborane fragments. The subsequent oxidative coupling of the nitrile with the tolan in the coordination sphere of the transition metal leads to the titanazole intermediate. Up to this point the reaction would be identical to what has been observed when allowing **1** to react with carbon–carbon multiple bonds or with acetone. The deviation from the pattern shown in these reactions is to be seen in the third reaction step, namely the adduct formation leading to **9a–c** instead of leading to the hydroboration of the nitrile.

This reaction type resulting from the interaction between a titanacycle and a boron hydride is yet unknown in literature. Erker and co-workers observed an insertion of 9-bis(borabicyclononane) (9-BBN) and diisobutylaluminum hydride<sup>21</sup> into the zirconium–carbon bond of the dimeric zirconocene  $\eta^2$ -formaldehyde complex. In the course of these reactions the original ring system is enlarged by incorporation of the B–H or the Al–H unit.

On the basis of the above mentioned analytical data, the bonding properties of the complexes **9a–c** can be described as follows: The four-membered ring consisting of Ti, N, B, and H represents an electron-deficient unit with only six electrons available to form four bonds.

(14) (a) Bochmann, M.; Wilson, M. L. *Organometallics* **1987**, *6*, 2556.

(b) Chamberlain, L. R.; Durfee, L. D.; Fanwick, P. E.; Kobriger, L.; Latesky, S. L.; McMullen, A. K.; Rothwell, I. P.; Foltling, K.; Huffman, J. C.; Streib, W. E.; Wang, R. *J. Am. Chem. Soc.* **1987**, *109*, 390.

(15) Bochmann, M.; Wilson, M. L. *Organometallics* **1987**, *6*, 2556 and literature cited therein.

(16) Thewalt, U.; Schomburg, D. *Z. Naturforsch.* **1975**, *30B*, 636.

(17) Leik, R.; Zsolnai, L.; Huttner, G.; Neuse, E. W.; Brintzinger, H. H. *J. Organomet. Chem.* **1986**, *312*, 177.

(18) Dell'Amico, G.; Marchetti, F.; Floriani, C. *J. Chem. Soc., Dalton Trans.* **1982**, 2197.

(19) Allen, F. H.; Kennard, O.; Watson, G. D.; Brammer, L.; Orpen, A. G.; Taylor, R. *J. Chem. Soc., Perkin Trans. 2* **1987**, 1.

(20) (a) Reviews: Doxsee, K. M.; Mouser, J. K. M.; Farahi, J. B. *Synlett* **1992**, 13. Buchwald, S. L.; Nielsen, R. B. *Chem. Rev.* **1988**, *88*, 1047. (b) Doxsee, K. M.; Mouser, J. K. M. *Organometallics* **1990**, *9*, 3012. (c) Meinhard, J. D.; Grubbs, R. H. *Bull. Chem. Soc. Jpn.* **1988**, *61*, 171. (d) Erker, G.; Humphrey, M. G. *J. Organomet. Chem.* **1989**, *378*, 163. (e) Fisher, R. A.; Buchwald, S. L. *Organometallics* **1990**, *9*, 871.

(21) (a) Bendix, M.; Grehl, M.; Fröhlich, R.; Erker, G. *Organometallics* **1994**, *13*, 3366. (b) Erker, G.; Sosna, F.; Hoffmann, U. *J. Organomet. Chem.* **1989**, *372*, 41. (c) Erker, G.; Hoffmann, U.; Zwieter, R.; Krüger, C. *J. Organomet. Chem.* **1989**, *367*, C15.

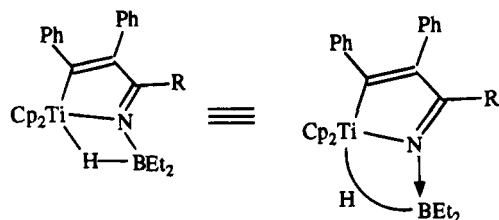
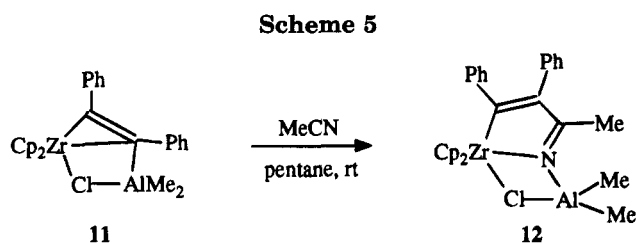


Figure 4.



We suggest that the bond between Ti, H, and B be considered as a three-center, two-electron bond. The bonding interaction between the nitrogen atom and the titanium should be a normal  $\sigma$ -bond as in the titanazole **8**, on the basis of crystallographic data. The nitrogen lone pair should provide the electrons for the bond between N and B, thus forming a donor-acceptor bond. The latter conclusion is drawn by analogy with the bonding situation found in the dimeric zirconaazole complex  $\text{Cp}_2\text{Zr}(\text{C}_6\text{H}_4)(\text{RCN})$ ,<sup>22</sup> derived from the reaction of an in situ-generated zirconocene-benzynes complex and a nitrile. This complex is dimeric due to the interactions of the nitrogen lone pairs with the zirconium atoms. Furthermore, the high-field position of the boron resonance can be explained by assuming that the nitrogen lone pair compensates for the electron deficiency of the boron atom.

The results obtained by allowing **1** to react with nitriles were not reflected in the reactions of the analogous zirconium-boron compounds. These complexes decompose slowly in the presence of the nitrile. In contrast to this, the zirconium aluminum compound  $\text{Cp}_2\text{Zr}(\text{PhCCPh})(\mu\text{-Cl})(\text{AlMe}_2)$  (**11**) reacts readily with acetonitrile to give the expected bicyclic ring system **12** (Scheme 5).

The reaction takes 2 days at ambient temperature for completion. The product was found to be analogous to the boron-containing complexes **9a-c** by comparison of the appropriate spectroscopic data.

The framework carbon atoms C1, C2, and C3 give rise to <sup>13</sup>C resonances at 222.5, 148.4, and 190.2 ppm which are located in the expected spectral regions. The methyl carbon atoms of the dimethylaluminum unit show a  $\delta$ -(<sup>13</sup>C) value at -6.8 ppm and the anticipated high-field resonance at  $\delta = -0.65$  ppm in the corresponding proton spectrum. The stretching frequency of the conjugated C=N unit is identified at 1585  $\text{cm}^{-1}$  in the IR spectrum. Compared with the values found for isolated C=N double bonds, this amounts to a shift of about 100  $\text{cm}^{-1}$  to lower wavenumbers.

By means of X-ray crystallographic studies, the Zr-N bond length has been determined to be 2.228 Å which is the usual range for a zirconium-nitrogen bond. For comparison Zr-N distances of 2.229 and 2.236 Å have been found for the 1-zirconabicyclo[3.2.0<sup>1,5</sup>]hepta-3,6-

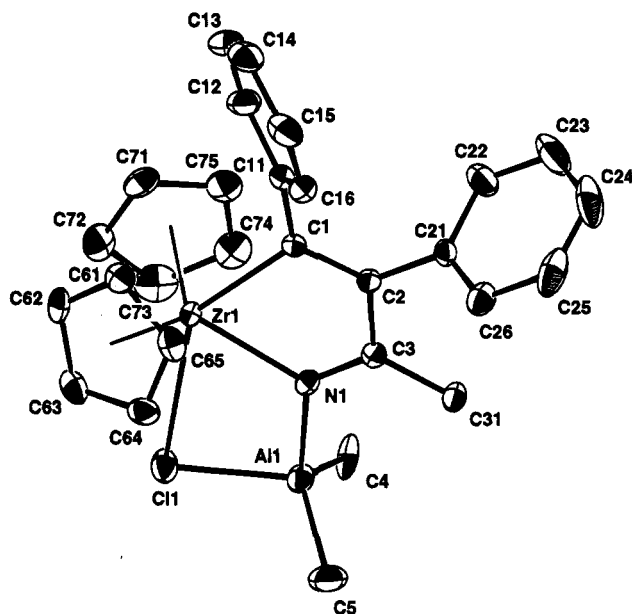


Figure 5. ORTEP plot of **12** showing the atom-numbering scheme. The hydrogen atoms are omitted for clarity.

diene system  $\text{Cp}_2\text{Zr}(\text{tBu})\text{CPNNC}(\text{tBu})\text{P}(\text{Me}_2)$ <sup>23</sup> and the 1-zirconabicyclo[4.2.0<sup>1,6</sup>]heteroocta-4,7-diene  $\text{Cp}_2\text{Zr}(\text{tBu})\text{CPNNC}(\text{H})\text{C}(\text{OMe})\text{O}$ <sup>23</sup> for which the Zr-N bonds are considered to be  $\sigma$ -bonds. A slightly shorter Zr-N bond length of 2.142 Å has been found in the ketenimine complex  $\text{Cp}_2\text{Zr}(\eta^2\text{-Ph}_2\text{CCNPh})(\text{PMe}_3)$ .<sup>24</sup> On the basis of interatom separations, the transition metal-nitrogen interaction is found to be rather strong. For the atom pair Al and N a bond distance of 1.888(2) Å is found which corresponds very nicely to the corresponding value already discussed for the analogous titanium-nitrogen bond in compound **9a** when taking the larger atomic radius of aluminum into account.

**12** can also be prepared by reacting the zirconaazole  $\text{Cp}_2\text{Zr}(\text{PhCCPh})(\text{MeCN})$  (**13**)<sup>11</sup> with dimethylaluminum chloride. When equimolar amounts of these two reagents are heated in toluene to 60 °C for 2 days, the complex **12** is obtained in 44% yield. Besides **12** the new compound **14** (ratio **12**:**14** = 10:3 as judged by the <sup>1</sup>H NMR intensities) is formed in the course of this reaction. **14** is analogous to **12** containing a methylaluminum dichloride fragment instead of dimethylaluminum chloride. The formation of **14** may be the result of the disproportionation of the aluminum organic reagent to give trimethylaluminum and methylaluminum dichloride during the reaction.

## Experimental Section

**General Considerations.** The preparations and handling of organometallic compounds were carried out in an inert argon atmosphere using Schlenk-type glassware. Solvents (pentane, toluene) were dried with sodium/potassium and distilled prior to use. Product characterization was performed by use of routine spectroscopic and physical methods. TMS serves as the standard for carbon and proton spectroscopy and

(23) Binger, P.; Herrmann, A. T. Unpublished results. Herrmann, A. T. Dissertation, University Kaiserslautern, 1990.

(24) Binger, P.; Langhauser, F. Unpublished results. Langhauser, F. Dissertation, University Kaiserslautern, 1991.

(22) Buchwald, S. L.; Sayers, A.; Watson, B. T.; Dewan, J. C. *Tetrahedron Lett.* **1987**, *28*, 3245.

Scheme 6

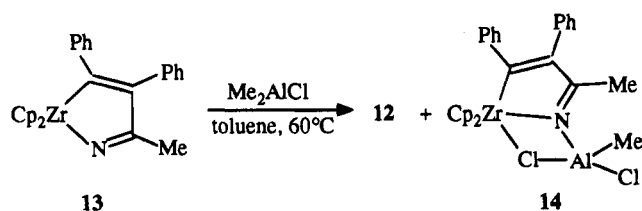


Table 2. Selected Bond Lengths (Å) and Angles (deg) for 12

Distances			
Zr-C1	2.363(3)	Al-N	1.888(2)
Zr-N	2.228(2)	C1-C2	1.359(4)
Zr-Cl	2.928(1)	C2-C3	1.479(4)
Al-Cl	2.247(1)	N-C3	1.285(3)
Angles			
Al-Cl-Zr	83.8(1)	Cl-Zr-N	72.0(1)
N-Al-Cl	91.3(1)	N-Zr-Cl	68.7(1)
C3-N-Zr	119.5(2)	C3-N-Al	124.7(2)
C2-C1-Zr	113.6(2)	Al-N-Zr	115.8(1)
C2-C3-N	118.9(2)	C3-C2-C1	116.1(2)

Table 3. Details of the Data Collection and Structure Solution of 9a and 12

	9a <sup>a</sup>	12
mol formula	C <sub>30</sub> H <sub>34</sub> TiBN	C <sub>28</sub> H <sub>29</sub> AlClN <sub>2</sub> Zr
mol wt	467.3	533.2
cryst color	yellow	light yellow
cryst syst	monoclinic	monoclinic
space group [no.]	P2 <sub>1</sub> /c [14]	P2 <sub>1</sub> /n [14]
a, Å	16.493(3)	15.568(2)
b, Å	8.100(1)	11.066(1)
c, Å	19.086(2)	15.840(3)
β, deg	101.78(1)	113.42(1)
V, Å <sup>3</sup>	2496.0	2504.1
Z	4	4
D <sub>calcd</sub> , g cm <sup>-3</sup>	1.24	1.41
μ, cm <sup>-1</sup>	3.55	5.89
λ(Kα radiation), Å	0.710 69	0.710 69
F(000), e	992	1096
diffractometer	Enraf-Nonius CAD4	
scan mode	ω-2θ	ω-2θ
[(sin θ)/λ] <sub>max</sub> , Å <sup>-1</sup>	0.65	0.65
T, °C	20	-173
no. of meas rflns	6276 (±h, ±k, ±l)	6240 (±h, ±k, ±l)
no. of indep rflns	5687	5722
no. of obsd rflns (I > 2σ(I))	4240	5285
no. of refined params	302	289
R	0.055	0.035
R <sub>w</sub> (w = 1/σ <sup>2</sup> (F <sub>o</sub> ))	0.064	0.063
resid electron dens, e Å <sup>-3</sup>	0.97	1.02
structure solution	heavy-atom method	

<sup>a</sup> The H1 atom position has been found and included in the final refinement stages. The other H atom positions were calculated and kept fixed in the final refinement stages.

H<sub>3</sub>PO<sub>4</sub> for <sup>31</sup>P NMR spectroscopy. The starting complexes **1** and **11** were prepared according to literature procedures.<sup>2</sup> Details of the X-ray crystallographic analysis (data collection and the structure solution) of **9a** and **12** are given in Table 3.

**Reaction of 1 with Ethylene.** Ethylene is passed through a solution of 0.5 g (1.2 mmol) of **1** in 15 mL of toluene at ambient temperatures for 5 min. The color changes almost immediately from orange to dark red. The solvent is removed in vacuo, the residue is suspended in 10 mL of pentane, and the red precipitate of **2** is filtered off. Yield: 0.44 g (95%). Triethylborane is obtained as the only organoboron product. When the reaction is performed in an NMR tube, no products other than the titanacycle and triethylborane can be detected. Anal. Calcd for C<sub>26</sub>H<sub>24</sub>Ti (384.4): C, 81.25; H, 6.25. Found: C, 81.66; H, 6.30. <sup>1</sup>H NMR ([D<sub>8</sub>]-THF, 29 °C, 300.1 MHz) (δ): 1.57, 2.81 (t, 4H, CH<sub>2</sub>, <sup>3</sup>J<sub>HH</sub> = 6.7 Hz), 6.27 (s, 10H, Cp), 6.92–6.42 (m, 10H, Ph). <sup>13</sup>C NMR ([D<sub>8</sub>]-THF, 29 °C, 75.5 MHz) (δ):

Table 4. Atomic Coordinates and Equivalent Isotropic Thermal Parameters (Å<sup>2</sup>) with Standard Deviations in Parentheses of Complex 9a<sup>a</sup>

atom	x	y	z	U <sub>eq</sub>
Ti1	0.8313(1)	0.0206(1)	0.3036(1)	0.041(1)
N1	0.7626(1)	-0.1327(3)	0.3563(1)	0.044(1)
B1	0.8202(2)	-0.1199(4)	0.4288(2)	0.053(2)
C1	0.7166(1)	-0.0617(3)	0.2223(1)	0.038(1)
C2	0.6728(1)	-0.1820(3)	0.2479(1)	0.039(1)
C3	0.7010(2)	-0.2183(3)	0.3247(1)	0.042(1)
C4	0.8688(2)	-0.2867(4)	0.4583(2)	0.063(2)
C5	0.9459(2)	-0.2692(5)	0.5168(2)	0.098(3)
C6	0.7768(3)	-0.0271(6)	0.4885(2)	0.111(3)
C7	0.8211(4)	0.0354(8)	0.5516(3)	0.169(6)
C11	0.6850(2)	0.0044(3)	0.1486(1)	0.042(1)
C12	0.7329(2)	0.0288(4)	0.0977(1)	0.054(2)
C13	0.6994(2)	0.0905(4)	0.0300(2)	0.067(2)
C14	0.6175(2)	0.1323(4)	0.0126(2)	0.070(2)
C15	0.5689(2)	0.1145(4)	0.0627(2)	0.065(2)
C16	0.6025(2)	0.0517(3)	0.1300(1)	0.051(2)
C21	0.6051(2)	-0.2815(3)	0.2037(1)	0.045(2)
C22	0.6211(2)	-0.3696(4)	0.1462(2)	0.061(2)
C23	0.5603(3)	-0.4633(4)	0.1035(2)	0.083(3)
C24	0.4832(3)	-0.4716(5)	0.1172(2)	0.089(3)
C25	0.4656(2)	-0.3874(5)	0.1739(2)	0.080(3)
C26	0.5257(2)	-0.2902(4)	0.2170(2)	0.062(2)
C31	0.6621(2)	-0.3476(4)	0.3627(2)	0.060(2)
C81	0.8725(2)	-0.1635(4)	0.2185(2)	0.054(2)
C82	0.8938(2)	-0.2391(4)	0.2856(2)	0.056(2)
C83	0.9562(2)	-0.1434(4)	0.3281(2)	0.064(2)
C84	0.9718(2)	-0.0072(4)	0.2886(2)	0.068(2)
C85	0.9197(2)	-0.0184(4)	0.2202(2)	0.062(2)
C91	0.7452(2)	0.2576(4)	0.2706(2)	0.076(2)
C92	0.7588(2)	0.2421(4)	0.3449(2)	0.064(2)
C93	0.8431(2)	0.2700(4)	0.3714(2)	0.067(2)
C94	0.8806(2)	0.2989(4)	0.3155(2)	0.078(3)
C95	0.8200(3)	0.2904(4)	0.2520(2)	0.082(3)
H1	0.873(2)	-0.006(3)	0.410(1)	0.065(9)

<sup>a</sup> U<sub>eq</sub> = 1/3 ijUijā<sub>i</sub>ā<sub>j</sub>.

[<sup>1</sup>J<sub>C,H</sub>]: 194.9 (s, Ti-C(Ph)=), 150.5 (s, =C(Ph)), 60.7 (t, Ti-CH<sub>2</sub> [124 Hz]), 40.8 (t, CH<sub>2</sub> [125 Hz]), 115.5 (d, Cp [173 Hz]), Ph 144.5 (s), 139.9 (s), 127.4 (d), 127.6 (d), 128.1 (d), 129.3 (d), 123.2 (d), 125.3 (d). MS (70 eV, 130 °C) (m/z (intensity [%])): 178 (Cp<sub>2</sub>Ti, PhCCPh [100]), 356 (M - C<sub>2</sub>H<sub>4</sub> [2]), 305 (M - 2H - C<sub>6</sub>H<sub>5</sub> [1]).

**Reaction of 1 with Diphenylacetylene.** To a suspension of 1.0 g (2.3 mmol) of **1** in 30 mL of pentane is added a solution of 1.0 g (5.6 mmol) of diphenylacetylene in 10 mL of diethyl ether at room temperature. The suspension slowly changes its color from yellowish green to dark green. The reaction mixture is stirred for 21 h. The green product **3a** is filtered off. To complete the isolation the mother liquor is cooled to -78 °C and a further crop of **3a** is obtained: yield 0.8 (65%); dec 134 °C; identification by comparison with the data of an authentic sample.<sup>25</sup> The residue is dried in vacuo. A green viscous oil is obtained which contains as the organoboron product the hydroborated tolan **4a**. Furthermore, stilbene, tolan, and small amounts of the titanacycle **3a** could be identified (<sup>1</sup>H NMR).

**Reaction of 1 with 2-Butyne.** To a solution of 1.2 g (2.8 mmol) of **1** in 35 mL of toluene is added by syringe 0.4 g (0.6 mL, 7.4 mmol) of 2-butyne. After 5 min of stirring at room temperature, the color of the reaction mixture has changed from orange to dark green. Suspended particles are filtered off, the solvent is removed in vacuo, and the residue is suspended in pentane. The green precipitate of **3d** is filtered off. Upon cooling of the mother liquor to -78 °C, another crop of the product **3d** is obtained: yield 1.1 g (93%); dec 126 °C. No organoboron product can be isolated in the pure state or be identified unequivocally (<sup>1</sup>H NMR ([D<sub>8</sub>]-THF, 27 °C, 200.1 MHz) (δ): 5.37 (q, J<sub>HH</sub> = 6.0 Hz), 1.15 (s), 1.10 (s), 0.77 (t, J<sub>HH</sub> = 7.8 Hz), 0.50 (t, 7.5 Hz), 1.59 (d, J<sub>HH</sub> = 6.4 Hz), 1.54 (s). <sup>11</sup>B

NMR ( $[D_8]$ -THF, 27 °C, 64.2 MHz) ( $\delta$ ): 10.6 ( $H_{1/2} = 115$  Hz). Anal. Calcd for  $C_{28}H_{26}Ti$  (410.4): C, 81.95; H, 6.34. Found: C, 81.78; H, 6.46.  $^1H$  NMR ( $[D_8]$ -THF, 29 °C, 300.1 MHz) ( $\delta$ ): 1.25, 1.42 (s, 6H, Me), 6.21 (s, 10H, Cp), 6.98–6.56 (m, 10H, Ph).  $^{13}C$  NMR ( $[D_8]$ -THF, 29 °C, 75.5 MHz) ( $\delta$  [ $^1J_{C,H}$ ]): 198.4 (s, Ti–C(Ph)=), 137.5 (s, =C(Ph)), 197.2 (s, Ti–C(Me)=), 127.1 (s, =C(Me)), 16.4, 20.9 (q, Me [125, 124 Hz]), Ph 148.8 (s), 143.2 (s), 130.8 (d), 127.6 (d), 125.1 (d), 123.1 (d), 127.7 (d), 127.3 (d). MS (70 eV): the sample decomposes in the temperature range 50–350 °C without giving identifiable fragments.

**Reaction of 1 with Phenylacetylene.** To a suspension of 1.2 g (2.8 mmol) of **1** in 45 mL of pentane is added by syringe 0.6 g (5.9 mmol) of phenylacetylene. After 30 min of stirring at ambient temperatures, the suspension has become dark green. The product **3b** is filtered off. Another crop of **3b** is obtained upon reducing the filtrate to two-thirds of its volume and cooling to –78 °C: yield 1.2 g (93%); dec 132 °C. The solvent is removed in vacuo. A green viscous residue is obtained which contains the Markovnikov and the anti-Markovnikov hydroboration products of phenylacetylene ( $^1H$ ,  $^{11}B$  NMR).  $^1H$  NMR ( $[D_8]$ -THF, 29 °C, 300.1 MHz) ( $\delta$ ): 6.25 (s, 10H, Cp), 6.35 (s, 1H, =CH), 7.19–6.41 (m, 15H, Ph)  $^{13}C$ -NMR ( $[D_8]$ -THF, 29 °C, 75.5 MHz) ( $\delta$  [ $^1J_{C,H}$ ]): 200.3 (s, Ti–C(Ph)=), 130.8 (s, =C(Ph)), 199.4 (s, Ti–C(Ph)=C(H)), 133.5 (d, =C(H) [158 Hz]), Ph 143.7 (s), 145.5 (s), 149.8 (s), 127.8 (d), 127.9 (d), 129.8 (d), 125.5 (d), 125.7 (d), 124.1 (d), 128.3 (d), 128.5(d), 128.1 (d).

**Reaction of 1 with Acetone.** To 1.1 g (2.6 mmol) of **1** in 30 mL of pentane is added by syringe 0.6 mL (0.4 g, 6.7 mmol) of acetone. After 2 h of stirring at ambient temperatures, the suspension has changed its color from orange to red. The red precipitate of **6** is filtered off. Further product is obtained upon cooling the mother liquor to –78 °C: yield 1.0 g (93%); dec 122 °C. Anal. Calcd for  $C_{27}H_{26}TiO$  (414.4): C, 78.26; H, 6.28. Found: C, 77.98; H, 6.20.  $^1H$  NMR ( $[D_8]$ -THF, 29 °C, 300.1 MHz) ( $\delta$ ): 1.27 (s, 6H, Me), 6.27 (s, 10H, Cp), 7.04–6.68 (m, 10H, Ph).  $^{13}C$ -NMR ( $[D_8]$ -THF, 29 °C, 75.5 MHz) ( $\delta$  [ $^1J_{C,H}$ ]): 192.4 (s, Ti–C(Ph)=), 159.4 (s, =C(Ph)), 91.3 (s, O–C), 27.9 (q,  $CH_3$  [126 Hz]), 116.5 (d, Cp, [173 Hz]), Ph 150.8 (s), 143.9 (s), 130.3 (d), 127.7 (d), 127.3 (d), 123.7 (d), 125.9 (d), 127.4 (d). MS (70 eV, 125 °C) ( $m/z$  (intensity [%])): 178 ( $Cp_2Ti$  [100]), 236 (M – PhCCPh [12]), 113 ( $CpTi$  [10]), 414 (M [4]). IR (KBr):  $\bar{\nu} = 1150, 965\text{ cm}^{-1}$  (C–O). From the mother liquor of **6** the solvent is removed in vacuo. A viscous red oil is obtained which contains the hydroborated acetone as the only boron organic compound (identified by its proton and  $^{11}B$  NMR properties)<sup>8</sup> besides small amounts of **6** and minor amounts of impurities.

**Reaction of 1 with *tert*-Butylphosphaalkyne.** To a suspension of 1.0 g (2.3 mmol) of **1** in 30 mL of pentane is added by syringe 0.5 g (5.0 mmol) of  $t\text{-BuCP}$ .<sup>26</sup> After 2 h the reaction is complete. The suspended red product **7a** is filtered off: yield 1.0 g (95%); dec 112 °C. Anal. Calcd for  $C_{29}H_{29}TiP$  (456.4): C, 76.31; H, 6.40. Found: C, 75.40; H, 6.26.  $^1H$  NMR ( $[D_8]$ -THF, –30 °C, 200.1 MHz) ( $\delta$ ): 1.46 (d, 9H,  $t\text{-Bu}$ ;  $^4J_{P,H} = 0.7$  Hz), 6.01 (s, 10H, Cp), 7.18–6.87 (m, 10H, Ph).  $^{13}C$  NMR ( $[D_8]$ -THF, –30 °C, 50.3 MHz) ( $\delta$  [ $^1J_{C,H}$ ]): 196.4 (s, Ti–C(Ph)),  $^2J_{P,C} = 63.5$  Hz), 118.9 (s, =C(Ph)),  $^1J_{P,C} = 30.2$  Hz), 303.8 (s, C=P,  $^1J_{P,C} = 67.2$  Hz), 49.9 (s,  $Me_3C$ ,  $^2J_{P,C} = 17.6$  Hz), 37.0 (q,  $CH_3$  [125 Hz]), 112.3 (d, Cp [175 Hz]), Ph 147.5 (s), 151.2 (s), 128.5 (d), 127.9 (d), 125.4 (d), 124.8 (d), 130.1 (d).  $^{31}P$  NMR ( $[D_8]$ -THF, –30 °C, 121.0 MHz) ( $\delta$ ): 121.1 ppm (s). MS (70 eV, 75–250 °C): decomposition of the sample.

**Reaction of 1 with 1-Adamantylphosphaalkyne.** To a suspension of 1.2 g (2.8 mmol) of **1** in 40 mL of pentane is added 0.75 g (4.2 mmol) of 1-AdCP. After 2 h **7b** is filtered off as a red precipitate: yield 1.4 g (93%); dec 136 °C. Anal. Calcd for  $C_{35}H_{35}TiP$  (534.5): C, 78.65; H, 6.54; P, 5.81. Found: C, 77.82; H, 6.68; P, 5.74.  $^1H$  NMR ( $[D_8]$ -THF, 27 °C,

200.1 MHz) ( $\delta$ ): Ad, 2.19, 2.07, 1.90, 1.82, 1.70 (15H), 6.00 (s, 10H, Cp), 7.20–6.79 (m, 10H, Ph).  $^{13}C$  NMR ( $[D_8]$ -THF, 27 °C, 50.3 MHz) ( $\delta$  [ $^1J_{C,H}$ ]): 195.0 (s, Ti–C(Ph=),  $^2J_{P,C} = 63.8$  Hz), 115.2 (s, =C(Ph),  $^1J_{P,C} = 31.2$  Hz), 338.9 (s, C=P,  $^1J_{P,C} = 67.7$  Hz), Ad 50.1 (s), 49.8 (t [126 Hz]), 31.2 (d [129 Hz]), 37.9 (t [126 Hz]), 112.1 (d, Cp [173 Hz]), Ph 148.3 (s), 148.1 (s), 130.9 (d), 128.8 (d), 127.9 (d), 127.4 (d), 125.4 (d), 124.7 (d).  $^{31}P$  NMR ( $[D_8]$ -THF, 27 °C, 81.0 MHz) ( $\delta$ ): 113.8 ppm (s). MS (70 eV, 100–300 °C) ( $m/z$  (intensity [%])): 178 ( $Cp_2Ti$ , PhCCPh, AdCP [100]).

Upon removal of the solvent, a red oil is obtained in which no product could be identified.

**Reaction of 1 with Acetonitrile.** To 1.3 g (3.1 mmol) of **1** in 45 mL of toluene is added by syringe 0.4 mL (0.3 g, 7.3 mmol) of acetonitrile. After 5 min the suspension becomes clear and the color changes from orange to red. Suspended particles are filtered off, the toluene is removed in vacuo, and the residue is suspended in pentane. The yellow precipitate of **9a** is filtered off and the mother liquor cooled to –20 °C to crystallize further product: yield 1.2 g (83%); dec 142 °C. The filtrate is evaporated to dryness. No further product was identified. Anal. Calcd for  $C_{30}H_{34}TiBN$  (467.3): C, 77.09; H, 7.28; N, 3.00; B, 2.36. Found: C, 76.89; H, 7.01; N, 2.95; B, 2.39.  $^1H$  NMR ( $[D_8]$ -THF, 29 °C, 300.1 MHz) ( $\delta$ ): –3.22 (s,  $H_{1/2} = 75$  Hz, 1H,  $\mu$ -H), 1.94 (s, 3H, NC– $CH_3$ ), 1.06 (t, 6H,  $CH_3$ ,  $^3J_{H,H} = 7.7$  Hz), 0.66, 0.38 (ddq, 4H, B– $CH_2$ ,  $^2J_{H,H} = 14.1$  Hz,  $^3J_{H,H} = 7.7$  Hz,  $^3J_{H,\mu-H} = 1.6$  Hz), 6.80–7.15 (m, 10H, Ph); 5.66 (s, 10H, Cp).  $^{13}C$  NMR ( $[D_8]$ -THF, 29 °C, 75.5 MHz) ( $\delta$  [ $^1J_{C,H}$ ]): 223.4 (s, Ti–C(Ph)=), 147.5 (s, =C(Ph)), 179.6 (s, C=N), 23.8 (q, NC– $CH_3$  [127 Hz]), 15.0 (t, B– $CH_2$ ), 12.8 (q, B– $CH_2$ – $CH_3$  [124 Hz]), 107.0 (d, Cp [175 Hz]), Ph 153.1 (s), 142.3 (s), 131.4 (d), 127.4 (d), 128.0 (d), 128.1 (d), 126.1 (d), 124.7 (d).  $^{11}B$  NMR ( $[D_8]$ -THF, 27 °C, 64.2 MHz) ( $\delta$ ): –12.0 ppm ( $H_{1/2} = 167$  Hz). MS (70 eV, 135 °C) ( $m/z$  (intensity [%])): 178 ( $Cp_2Ti$ , PhCCPh [100]), 219 ( $Cp_2Ti$ (MeCN) [14]), 41 (MeCN [12]), 438 (M–Et [7]), 401 (M–Ph [7]), 398 (M–BEt<sub>2</sub> [3]), 467 (M, [2]). IR (KBr):  $\bar{\nu} = 1675\text{ cm}^{-1}$  (B–H–Ti); 1590  $\text{cm}^{-1}$  (C=N).

**Reaction of 8 with Tetraethyldiborane.** A mixture of 1.3 g (3.3 mmol) of the titanaazole **8** in 45 mL of toluene and 0.4 mL (0.3 g, 2.3 mmol) of tetraethyldiborane is stirred for 4 days at room temperature. The color changes from brown to green. Suspended particles are filtered off, the toluene is removed in vacuo, and the residue is suspended in pentane. The yellow precipitate of **9a** is filtered off. The isolation is completed upon cooling of the mother liquor to –20 °C. Yield: 1.0 g (65%).

**Reaction of 1 with Propionitrile.** To a solution of 1.4 g (3.3 mmol) of **1** in 35 mL of toluene is added by syringe 0.4 g (0.5 mL, 7.3 mmol) of propionitrile. After 15 min the suspension has become clear and dark red. Suspended particles are filtered off, the solvent is removed in vacuo, and the residue is suspended in pentane. The yellow precipitate of **9b** is filtered off, half of the pentane is removed in vacuo, and the mother liquor is cooled to –78 °C for further product crystallization: yield 1.4 g (97%); dec 204 °C. Anal. Calcd for  $C_{31}H_{36}TiBN$  (481.4): C, 77.33; H, 7.48; N, 2.91; B, 2.29. Found: C, 75.24; H, 7.65; N, 2.96; B, 2.45.  $^1H$ -NMR ( $[D_8]$ -THF, 27 °C, 200.1 MHz) ( $\delta$ ): –3.24 (s,  $H_{1/2} = 24$  Hz, 1H,  $\mu$ -H), 2.41 (q, 2H, NC– $CH_2$ ,  $^3J_{H,H} = 7.4$  Hz), 0.67 (t, 3H, NC– $CH_2$ – $CH_3$ ,  $^3J_{H,H} = 7.4$  Hz), 0.44, 1.08 (m, 4H, B– $CH_2$ ), 1.12 (t, 6H, B– $CH_2$ – $CH_3$ ,  $^3J_{H,H} = 7.5$  Hz), 7.12–6.80 (m, 10H, Ph), 5.62 (s, 10H, Cp).  $^{13}C$  NMR ( $[D_8]$ -THF, 27 °C, 50.3 MHz) ( $\delta$  [ $^1J_{C,H}$ ]): 224.4 (s, Ti–C(Ph)=), 146.6 (s, =C(Ph)), 184.5 (s, C=N), 107.0 (d, Cp [175 Hz]), Ph 153.0 (s), 142.1 (s), 131.4 (d), 128.1 (d), 127.3 (d), 126.2 (d), 124.8 (d), 30.6 (t, NC– $CH_2$  [129 Hz]), 15.7 (t, B– $CH_2$ ,  $^1J_{C,H}$  superposed), 11.9 (q, NC– $CH_2$ – $CH_3$  [123 Hz]), 13.0 (q, B– $CH_2$ – $CH_3$  [127 Hz]).  $^{11}B$  NMR ( $[D_8]$ -THF, 27 °C, 64.2 MHz) ( $\delta$ ): 11.2 ppm ( $H_{1/2} = 542$  Hz). MS (70 eV, 210 °C) ( $m/z$  (intensity [%])): 178 ( $Cp_2Ti$ , PhCCPh [100]), 233 ( $Cp_2Ti$ (EtCN) [12]), 113 ( $CpTi$  [11]), 452 (M – Et [11]), 481 (M [3]). IR (KBr):  $\bar{\nu} = 1680\text{ cm}^{-1}$  (B–H–Ti); 1595  $\text{cm}^{-1}$  (C=N).

(26) Rösch, W.; Vogelbacher, U.; Allspach, T.; Regitz, M. *J. Organomet. Chem.* **1986**, *306*, 39.

**Reaction of 1 with Benzonitrile.** A 1.0 g (2.3 mmol) amount of the titanocene complex **1** and 0.5 g (0.5 mL, 4.9 mmol) of benzonitrile are mixed in 35 mL of toluene. After 45 min the color has changed from orange to red and a solution was formed. Suspended particles are filtered off, the solvent is removed in vacuo, and the residue is suspended in pentane. Filtration yields the first crop of **9c** as a yellow precipitate. Further product can be crystallized upon cooling the mother liquor to  $-20\text{ }^{\circ}\text{C}$ : yield 1.1 g (90%); dec  $224\text{ }^{\circ}\text{C}$ . Anal. Calcd for  $\text{C}_{35}\text{H}_{36}\text{TiBN}$  (529.5): C, 79.40; H, 6.81; N, 2.65; B, 2.08. Found: C, 79.63; H, 6.76; N, 2.50; B, 2.00.  $^1\text{H}$  NMR ( $[\text{D}_8]$ -THF,  $27\text{ }^{\circ}\text{C}$ , 200.1 MHz) ( $\delta$ ):  $-3.22$  (s,  $H_{1/2} = 22\text{ Hz}$ , 1H,  $\mu\text{-H}$ ),  $7.04\text{--}6.73$  (m, 15H, Ph),  $5.69$  (s, 10H, Cp),  $0.38$  (m, 4H, B-CH<sub>2</sub>),  $0.77$  (t, 6H, B-CH<sub>2</sub>-CH<sub>3</sub>,  $^3J_{\text{H,H}} = 6.9\text{ Hz}$ ).  $^{13}\text{C}$  NMR ( $[\text{D}_8]$ -THF,  $27\text{ }^{\circ}\text{C}$ , 50.3 MHz) ( $\delta$  [ $^1J_{\text{C,H}}$ ]):  $227.9$  (s, Ti-C(Ph)=),  $153.2$  (s, =C(Ph)),  $181.2$  (s, C=N),  $107.0$  (d, Cp [175 Hz]), Ph  $146.8$  (s),  $141.5$  (s),  $141.5$  (s),  $131.8$  (d),  $128.5$  (d),  $128.3$  (d),  $128.1$  (d),  $127.9$  (d),  $127.4$  (d),  $125.4$  (d),  $124.8$  (d),  $17.6$  (t, B-CH<sub>2</sub> [114 Hz]),  $12.7$  (q, CH<sub>3</sub> [123 Hz]).  $^{11}\text{B}$  NMR ( $[\text{D}_8]$ -THF,  $27\text{ }^{\circ}\text{C}$ , 64.2 MHz) ( $\delta$ ):  $9.8\text{ ppm}$  ( $H_{1/2} = 542\text{ Hz}$ ). MS (70 eV,  $130\text{ }^{\circ}\text{C}$ ) ( $m/z$  (intensity [%])):  $178$  (Cp<sub>2</sub>Ti, PhCCPh [100]),  $500$  (M - Et [53]),  $529$  (M [2]). IR (KBr):  $\bar{\nu} = 1685\text{ cm}^{-1}$  (B-H-Ti);  $1595\text{ cm}^{-1}$  (C=N).

**Reaction of 11 with Acetonitrile.** To a suspension of 1.2 g (2.4 mmol) of **11** in 35 mL of toluene is added by syringe 0.3 mL (0.2 g, 5.6 mmol) of acetonitrile. The reaction mixture is stirred for 27 h. Suspended particles are filtered off, the

solvent is removed in vacuo, and the residue is suspended in pentane. A 1.1 g (2.1 mmol) amount of the pale yellow product **12** can be isolated from this mixture by filtration. Upon crystallization at  $-20\text{ }^{\circ}\text{C}$  further product can be obtained: yield 1.2 g (96%); dec  $198\text{ }^{\circ}\text{C}$ . Anal. Calcd for  $\text{C}_{28}\text{H}_{29}\text{ZrAlClN}$  (533.2): C, 63.01; H, 5.48; N, 2.63. Found: C, 63.13; H, 5.41; N, 2.34.  $^1\text{H}$  NMR ( $[\text{D}_8]$ -THF,  $29\text{ }^{\circ}\text{C}$ , 300.1 MHz) ( $\delta$ ):  $-0.65$  (s, 6H, Al-CH<sub>3</sub>),  $1.91$  (s, 3H, CH<sub>3</sub>),  $7.10\text{--}6.78$  (m, 10H, Ph),  $6.18$  (s, 10H, Cp).  $^{13}\text{C}$  NMR ( $[\text{D}_8]$ -THF,  $29\text{ }^{\circ}\text{C}$ , 75.5 MHz) ( $\delta$  [ $^1J_{\text{C,H}}$ ]):  $222.5$  (s, Zr-C(Ph)=),  $148.4$  (s, =C(Ph)),  $190.2$  (s, C=N),  $112.6$  (d, Cp [174 Hz]), Ph  $152.0$  (s),  $142.4$  (s),  $130.7$  (d),  $126.4$  (d),  $125.7$  (d),  $124.4$  (d),  $128.1$  (d),  $128.0$  (d),  $28.3$  (q, CH<sub>3</sub> [127 Hz]),  $-6.8$  (q, Al-CH<sub>3</sub> [126 Hz]). MS (70 eV,  $130\text{ }^{\circ}\text{C}$ ) ( $m/z$  (intensity [%])):  $516$  (M - Me [100]),  $220$  (Cp<sub>2</sub>Zr [79]);  $261$  (Cp<sub>2</sub>Zr(MeCN) [20]),  $338$  (M - PhCCPh [20]),  $178$  (PhCCPh [17]).

**Acknowledgment.** F.S. thanks the "Fonds des Verbandes der Chemischen Industrie" for a stipendium.

**Supplementary Material Available:** Tables giving details of the X-ray structure analyses of **9a** and **12**, complete listings of bond lengths and angles and positional and thermal parameters, and an ORTEP diagram (14 pages). Ordering information is given on any current masthead page.

OM950094Z



# Regioselectivity of the Insertion of Dienes into Pd–R Bonds. Diastereoselection in the Isomerization of an ( $\eta^1$ - $\eta^2$ -Enyl)palladium Complex to an ( $\eta^3$ -Allyl)palladium Complex

Ana C. Albéniz, Pablo Espinet,<sup>\*,†</sup> and Yong-Shou Lin

Departamento de Química Inorgánica, Facultad de Ciencias, Universidad de Valladolid, 47005-Valladolid, Spain

Received May 4, 1994<sup>®</sup>

The regioselectivity of the olefin insertion reaction into Pd–pentafluorophenyl bonds has been examined by studying the reactions of  $[\text{Pd}(\text{C}_6\text{F}_5)\text{Br}(\text{NCMe})_2]$  and dienes with two nonequivalent double bonds, namely, isoprene, vinylcyclohexene, *R*-(+)-limonene,  $\alpha$ -terpinene, and  $\gamma$ -terpinene. Analysis of the structure of the final ( $\eta^3$ -allyl)palladium derivatives formed shows that in each case attack occurs selectively on the least substituted carbon of the least substituted double bond. The selectivity is very high except in the case of isoprene which leads to two products as a result of insertion of the least and the most substituted double bond in a 3:1 ratio, respectively. Total regioselective attack on the least substituted carbon of each double bond is still maintained for this diene. Vinylcyclohexene and *R*-(+)-limonene give at low temperature  $\eta^1$ - $\eta^2$ -enyl derivatives as a 1:1 mixture of two diastereoisomers in each case. These  $\eta^1$ - $\eta^2$ -enyl derivatives are intermediates in the allyl formation and isomerize to the corresponding  $\eta^3$ -allyl derivatives via Pd migration. Isomerization occurs simultaneously for the two diastereomeric  $\eta^1$ - $\eta^2$ -enyl complexes derived from vinylcyclohexene, but the  $\eta^1$ - $\eta^2$ -enyl derivatives from *R*-(+)-limonene form the corresponding  $\eta^3$ -allyl complexes with different activation energies. This selective isomerization is attributed to the difference in stability of the two diastereomeric  $\eta^1$ - $\eta^2$ -enyl complexes formed from *R*-(+)-limonene.

## Introduction

The Heck reaction (palladium-catalyzed arylation of olefins) and related processes are examples of cis addition of Pd–R to olefins, and they are widely used in organic synthesis.<sup>1</sup> Cis addition of Pd–R (also referred to as endo attack of the R group) is believed to proceed via the “in situ” formation of “PdRX” intermediates from the palladium salt and the arylating agent; coordination of the olefin cis to the R group will then allow insertion of the former into the Pd–R bond via a four center intermediate. The mechanism has been studied theoretically by Hoffmann et al.<sup>2</sup> When dienes are used as the substrates in this reaction ( $\eta^3$ -allyl)-palladium complexes<sup>3–7</sup> or ( $\eta^1$ - $\eta^2$ -enyl)palladium complexes<sup>8,9</sup> are obtained. Further reaction of these complexes with nucleophiles gives access to a wide variety of organic derivatives.<sup>10</sup>

A stable species corresponding to the stoichiometry of the intermediates proposed in the Heck reaction, namely  $[\text{Pd}(\text{C}_6\text{F}_5)\text{Br}]_n$ , was prepared in modest yield by Klabunde using the metal atom technique.<sup>11</sup> More recently we described a purely chemical method which made possible the preparation of “Pd( $\text{C}_6\text{F}_5$ )Br” solutions<sup>12</sup> and  $[\text{Pd}(\text{C}_6\text{F}_5)\text{Br}(\text{NCMe})_2]$ <sup>13</sup> in high yield. We could show that in fact any of these “Pd( $\text{C}_6\text{F}_5$ )Br” synthons react with dienes to give  $[\text{Pd}(\mu\text{-Br})_2(1\text{-}3\text{-}\eta^3\text{-C}_6\text{F}_5\text{-allyl})_2]$  complexes.<sup>9b,13</sup> The diolefins we used were linear or cyclic with two equivalent double bonds, and the Pd– $\text{C}_6\text{F}_5$  addition proved to be fully stereoselective cis and fully regioselective: The  $\text{C}_6\text{F}_5$  group always added to an external carbon of the diene system, and the allyl moiety was always formed at the position of the unattacked double bond. Using this model reaction, in this paper we look at the regio- and stereoselectivity of the insertion and subsequent Pd migration on dienes that offer two nonequivalent double bonds, hence four different carbon atoms susceptible to undergo  $\text{C}_6\text{F}_5$  endo attack.

When nonconjugated dienes undergo insertion of one double bond into a Pd–R bond, an ( $\eta^1$ - $\eta^2$ -enyl)palladium complex can be formed. These derivatives are intermediates in the formation of the thermodynamically

<sup>†</sup> E-mail: espinet@cpd.uva.es.

<sup>®</sup> Abstract published in *Advance ACS Abstracts*, April 15, 1995.

(1) (a) Trost, B. M.; Verhoever, T. R. In *Comprehensive Organometallic Chemistry*; Wilkinson, G., Stone, F. G., Abel, E. W., Eds.; Pergamon Press: London, 1982; Vol. 8, p 854 and references therein. (b) Heck, R. F. *Palladium Reagents in Organic Syntheses*; Academic Press: New York, 1985. (c) Hegedus, L. S. In *Organometallics in Synthesis*; Schlosser, M., Ed.; Wiley: New York, 1994; Chapter 5. (2) Thorn, D. L.; Hoffman, R. *J. Am. Chem. Soc.* **1978**, *100*, 2029. (3) Mabbot, D. J.; Maitlis, P. M. *J. Chem. Soc., Dalton Trans.* **1976**, 2156.

(4) Heck, R. F. *J. Am. Chem. Soc.* **1968**, *90*, 5542. (5) Stakem, F. G.; Heck, R. F. *J. Org. Chem.* **1980**, *45*, 3584. (6) Larock, R. C.; Takagi, K. *Tetrahedron Lett.* **1983**, *24* (33), 3457. (7) Larock, R. C.; Takagi, K. *J. Org. Chem.* **1984**, *49*, 2701. (8) Segnitz, A.; Bailey, P. M.; Maitlis, P. M. *J. Chem. Soc., Chem. Commun.* **1973**, 698. (9) (a) Albéniz, A. C.; Espinet, P.; Jeannin, Y.; Philoche-Levisalles, M.; Mann, B. E. *J. Am. Chem. Soc.* **1990**, *112*, 6594. (b) Albéniz, A. C.; Espinet, P. *Organometallics* **1991**, *10*, 2987.

(10) Bäckvall, J.-E. *Adv. Met. Org. Chem.* **1989**, *1*, 135.

(11) (a) Klabunde, K. J.; Low, J. Y. F. *J. Organomet. Chem.* **1973**, *51*, C33. (b) Klabunde, K. J.; Low, J. Y. F. *J. Am. Chem. Soc.* **1974**, *96*, 7674. (c) Klabunde, K. J.; Anderson, B. B.; Neuenchwander, K. *Inorg. Chem.* **1980**, *19*, 3719.

(12) Usón, R.; Fornies, J.; Nalda, J. A.; Lozano, M. J.; Espinet, P.; Albéniz, A. C. *Inorg. Chim. Acta* **1989**, *156*, 251.

(13) Albéniz, A. C.; Espinet, P.; Foces-Foces, C.; Cano, F. H. *Organometallics* **1990**, *9*, 1079.

Table 1. Summary of Reactivity<sup>a,b</sup>

diene	allyl moiety	compd	ratio
1		1a-syn, 1b	19
		1a-anti	5
1		1c-syn	7
		1c-anti	1
2		2a, 2b	7.8
		2c	1
3		3a, 3b	12.9
		3c	1
4		4a, 4b	
5		5a, 5b	18.6
		5c	1

a) = position of attack; = central allylic carbon in the complex; Pf = C<sub>6</sub>F<sub>5</sub>.

b) The conformations of the cyclohexenyl rings are tentative except 4a,b

more stable  $\eta^3$ -allyl derivatives through the Pd-migration mechanism (Pd-H elimination-readdition). This isomerization process has been observed in just a few cases,<sup>9b,14-16</sup> since it is common to observe only one species, either the allyl when the  $\eta^1$ - $\eta^2$ -enyl is unstable<sup>13</sup> or the  $\eta^1$ - $\eta^2$ -enyl when its stability is high.<sup>9a</sup> The reactions of [Pd(C<sub>6</sub>F<sub>5</sub>)Br(NCMe)<sub>2</sub>] with two dienes used in this work, vinylcyclohexene and *R*-(+)-limonene, allow the observation of the above-mentioned isomerization. The process for *R*-(+)-limonene offers a nice example of diastereoselection in the Pd-migration process.

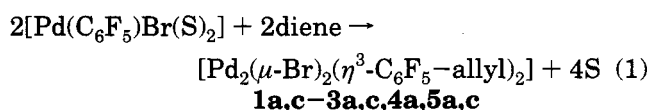
(14) (a) Albelo, G.; Wiger, G.; Rettig, M. F. *J. Am. Chem. Soc.* **1975**, *97*, 4510. (b) Parra-Hake, M.; Rettig, M. F.; Wing, R. M. *Organometallics* **1983**, *2*, 1013. (c) Parra-Hake, M.; Rettig, M. F.; Williams, J. L.; Wing, R. M. *Organometallics* **1986**, *5*, 1032.

(15) Peuckert, M.; Keim, W. *Organometallics* **1983**, *2*, 594.

(16) Goddard, R.; Green, M.; Hughes, R. P.; Woodward, P. *J. Chem. Soc., Dalton Trans.* **1976**, 1890.

## Results

The reactions of [Pd(C<sub>6</sub>F<sub>5</sub>)Br(NCMe)<sub>2</sub>]<sup>13</sup> or "Pd(C<sub>6</sub>F<sub>5</sub>)Br" solutions<sup>12</sup> with isoprene (**1**), vinylcyclohexene (**2**), (*R*)-(+)-limonene (**3**),  $\alpha$ -terpinene (**4**), and  $\gamma$ -terpinene (**5**) proceed easily at room temperature (eq 1) to give dimeric ( $\eta^3$ -C<sub>6</sub>F<sub>5</sub>-allyl)palladium compounds having the structures shown in Table 1. Both syn and anti isomers are observed for **1a** and **1c** (see below).



S = solvent or NCMe

All products, except the isomers **c** and **1a-anti**, were obtained as crystalline solids (analyses and yields are collected in the Experimental Section). The use of [Pd-(C<sub>6</sub>F<sub>5</sub>)Br(NCMe)<sub>2</sub>] makes it possible to follow up the

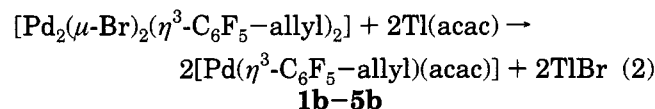
**Table 2.**  $^{19}\text{F}$  Data for the  $\text{C}_6\text{F}_5\text{-}\eta^3\text{-Allyl}$  Complexes at Different Temperatures<sup>a,b</sup>

compd	T (°C)	F <sub>para</sub> <sup>c</sup>	F <sub>meta</sub>	F <sub>ortho</sub>
<b>1a-syn</b>	20 <sup>d</sup>	-156.5 t	-162.2 m	-142.5 m
<b>1b-syn</b>	20 <sup>d</sup>	-157.7 t	-163.1 m	-142.7 m
<b>1a-anti</b>	20 <sup>d</sup>	-157.0 t	-162.5 m	-143.5 m
<b>1c-syn</b>	20 <sup>d</sup>	-155.7 t	-162.0 m	-141.7 m
<b>1c-anti</b>	20 <sup>d</sup>	-156.0 t	-162.2 m	-140.8 m
<b>2a</b>	20	-158.0 t	-162.9 m	-144.8 m
		-157.31 t		
	-60	-157.37 t		
		-157.40 t		
<b>2b</b>	20 <sup>d</sup>	-158.3 t	-163.1 m	-144.7 m
<b>2c</b>	20	-158.3 t	-163.1 m	-145.1 m
	-60	-157.7 t		
		-157.8 t		
<b>3a</b>	20 <sup>e</sup>	-157.8 t	-163.1 m	-143.4 m
		-157.9 t		
		-157.13 t		
	-50	-157.20 t		
		-157.22 t		
<b>3b</b>	20 <sup>d</sup>	-158.0 t	-163.1 m	-143.2 m
		-158.1 t		
<b>3c</b>	20	-158.0 m	-163.1 <sup>f</sup>	-145.1 <sup>f</sup>
<b>4a</b>	60	-157.09 t	-163.0 b	-142.0 b <sup>g</sup>
		-157.14 t		
		-156.75 t		
	20	-156.80 b		
		-156.83 t		
		-156.18 t		
	-50	-156.06 b		
		-156.02 t		
<b>4b</b>	20 <sup>d</sup>	-157.3 t	-163.2 m	-141.2 <sup>g</sup>
<b>5a</b>	20	-156.5 t	-162.4 b <sup>g</sup>	-140.5 b <sup>g</sup>
		-155.72 t		
	-50	-155.81 t		
		-155.86 t		
<b>5b</b>	20 <sup>d</sup>	-157.0 t	-162.6 m	-141.1 b <sup>g</sup>
<b>5c</b>	20	-156.2 b	-162.5 <sup>f</sup>	-140.5 <sup>f</sup>

<sup>a</sup>  $\delta$  multiplet. Measured on a Bruker AC-300 spectrometer using  $\text{CDCl}_3$  as solvent and  $\text{CFCl}_3$  as reference. <sup>b</sup>  $F_{\text{meta}}$  and  $F_{\text{ortho}}$  are given only when coalescence or maximum simplification is reached. <sup>c</sup>  $^3J_{\text{F-F}} = 20\text{--}21$  Hz. <sup>d</sup> The same  $F_{\text{para}}$  pattern is found in the range 60 to  $-50$  °C. <sup>e</sup> The product ratio is ca. 1:1. <sup>f</sup> Signal included in the resonance of the major isomer **3a**. <sup>g</sup> Broad resonance due to hindered rotation of the  $\text{C}_6\text{F}_5$  group.

reactions by  $^{19}\text{F}$  and  $^1\text{H}$  NMR in  $\text{CDCl}_3$  as a solvent and detect all the compounds formed.

In order to help structural assignment, monomeric derivatives were synthesized by treating the dimers with  $\text{Tl}(\text{acac})$  ( $\text{acac} = \text{acetylacetonate}$ ) (eq 2).<sup>13</sup> Although these reactions are virtually quantitative, the small scale used and the high solubility of the products prevented their isolation as solids in several cases.



The structures of the products were assigned on the basis of the  $^{19}\text{F}$  and  $^1\text{H}$  NMR data collected in Tables 2 and 3, using the approach discussed in detail in a previous paper.<sup>13</sup> Thus, the number of  $F_{\text{para}}$  resonances reveals the number of diastereoisomers of any kind formed in a given reaction; the spectra of the monomeric complexes allow one to discount stereoisomers due to the different arrangements of two allyl moieties in a dimer. Finally, the analysis of the  $^1\text{H}$  NMR spectra, using double resonance techniques, 2D homonuclear correlations, and previous literature data for related complexes,<sup>3-7,17-23</sup> leads to the structural assignments

contained in Table 3. The reactions with the different diolefins are discussed below.

**Reaction with Isoprene.** The reaction of " $\text{Pd}(\text{C}_6\text{F}_5)\text{-Br}$ ", or  $[\text{Pd}(\text{C}_6\text{F}_5)\text{Br}(\text{NCMe})_2]$ , with isoprene produces a mixture of Pd-allyl isomers, **1a** and **1c**, as a result of pentafluorophenyl attack to the least and the most substituted double bond, respectively. The preference for the least substituted one is clear as shown by the ratio **1a:1c** = 3:1. No significant change in the product ratio is observed when the reaction of isoprene with  $[\text{Pd}(\text{C}_6\text{F}_5)\text{Br}(\text{NCMe})_2]$  is carried out at  $-10$  °C (below this temperature the reaction is very slow) and monitored by  $^{19}\text{F}$  NMR. The attack is regiospecific in that the  $\text{C}_6\text{F}_5$  group adds, in each case, to the least substituted carbon of the coordinated double bond.

Both **1a** and **1c** appear as a mixture of their anti and syn isomers (Table 1), the syn derivatives being more abundant as corresponds to a less hindered arrangement in the allyl compound. The four isomers are formed in a ratio **1a-syn:1a-anti:1c-syn:1c-anti** = 19:5:7:1.

The major derivative, **1a-syn**, can be isolated by careful crystallization in 40% yield.

**Reactions with Vinylcyclohexene and (R)-(+)-Limonene.** Only in the case of these dienes was it possible to observe intermediates in the formation of the final allyls by  $^{19}\text{F}$  and  $^1\text{H}$  NMR monitoring of the reaction of vinylcyclohexene or (R)-(+)-limonene and  $[\text{Pd}(\text{C}_6\text{F}_5)\text{Br}(\text{NCMe})_2]$  at different temperatures. The insertion of vinylcyclohexene or limonene occurs slowly at  $-30$  °C to give initially two  $\eta^1\text{-}\eta^2\text{-enyl}$  derivatives **2d**<sub>1</sub> and **2d**<sub>2</sub> or **3d**<sub>1</sub> and **3d**<sub>2</sub> (Scheme 1). The chemical shifts for the  $F_{\text{ortho}}$  signals of **2d**<sub>1</sub> ( $\delta = -141.9$ ), **2d**<sub>2</sub> ( $\delta = -142.7$ ), **3d**<sub>1</sub> ( $\delta = -138.5$ ), and **3d**<sub>2</sub> ( $\delta = -139.5$ ) reveal a pentafluorophenyl group attached to carbon ( $\text{C}_6\text{F}_5\text{-C}$ ),<sup>13</sup> proving that insertion has occurred. In spite of some signals partially hidden by starting materials still unreacted and by free acetonitrile, the  $^1\text{H}$  NMR spectra show clearly a coordinated endocyclic double bond ( $\delta = 6.04, 5.76$  for **2d**<sub>1</sub> and **2d**<sub>2</sub>;  $\delta = 5.51$  for **3d**<sub>1</sub>;  $\delta = 5.53$  for **3d**<sub>2</sub>) and a  $\text{CH}_2\text{C}_6\text{F}_5$  group ( $\delta = 3.55, 3.40$  for **2d**<sub>1</sub>;  $\delta = 3.55, 3.00$  for **2d**<sub>2</sub>;  $\delta = 3.30, 2.60$  for **3d**<sub>1</sub>;  $\delta = 3.75, 3.42$  for **3d**<sub>2</sub>) revealing that the  $\text{C}_6\text{F}_5$  group has added to the external carbon of the exocyclic double bond. Homonuclear  $^1\text{H}$  correlation experiments were used to assign the proton resonances to the complexes (see Experimental Section). **2d**<sub>1</sub>, **2d**<sub>2</sub> and **3d**<sub>1</sub>, **3d**<sub>2</sub> are pairs of diastereoisomers arising from the new exocyclic chiral carbon formed (both configurations present, due to indiscriminate coordination of both faces of the exocyclic double bond before insertion) and the chiral cycle coordinated in a trans Pd-H<sup>4</sup> fashion; molecular models indicate that a cis Pd-H<sup>4</sup> coordination of the double bond is not possible.

Both ratios **2d**<sub>1</sub>:**2d**<sub>2</sub> and **3d**<sub>1</sub>:**3d**<sub>2</sub> at  $-30$  °C are ca. 1:1. As the temperature increases isomerization of the  $\eta^1\text{-}\eta^2\text{-enyl}$  derivatives to the corresponding  $\eta^3\text{-allyl}$ s is observed. Isomerization of **2d**<sub>1</sub> and **2d**<sub>2</sub> occurs at

(17) Van Leeuwen, P. W. N. M.; Lukas, J.; Praat, A. P.; Appelman, M. *J. Organomet. Chem.* **1972**, *38*, 199.

(18) Tibbetts, D. L.; Brown, T. L. *J. Am. Chem. Soc.* **1969**, *91*, 1108.

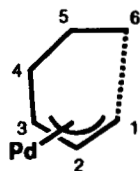
(19) Robinson, S. D.; Shaw, B. L. *J. Chem. Soc. A* **1963**, 4806.

(20) Rowe, J. M.; White, D. A. *J. Chem. Soc. A* **1967**, 1451.

(21) Hughes, R. P.; Powell, J. *J. Am. Chem. Soc.* **1972**, *94*, 7723.

(22) Hall, S. S.; Akermark, B. *Organometallics* **1984**, *3*, 1745.

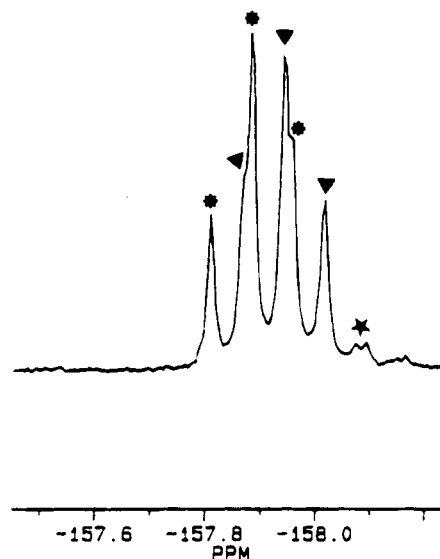
(23) Imaizumi, S.; Matsuhisa, T.; Senda, Y. *J. Organomet. Chem.* **1985**, *280*, 441.

Table 3.  $^1\text{H}$  NMR Data for the  $\text{C}_6\text{F}_5\text{-}\eta^3\text{-Allyl}$  Complexes<sup>a</sup>**1a, 1b:**  $\text{R}_1 = \text{R}'_1 = \text{H}$ ;  $\text{R}_2 = \text{Me}$ ;  $\text{R}_3 = \text{H}$ ;  $\text{R}_4 = \text{R}'_4 =$ **1c:**  $\text{R}_1 = \text{R}'_1 = \text{R}_2 = \text{H}$ ;  $\text{R}_3 = \text{Me}$ ;  $\text{R}_4 = \text{R}'_4 = \text{H}$ **2a, 2b:**  $\text{R}_1 = \text{R}_2 = \text{R}_3 = \text{H}$ ;  $\text{R}_4 = \text{CH}_2\text{CH}_2\text{C}_6\text{F}_5$ ;  $\text{R}'_4 = \text{H}$ ;  $\text{R}_5 = \text{R}'_5 = \text{R}_6 = \text{R}'_6 = \text{H}$ **2c:**  $\text{R}_1 = \text{R}_2 = \text{R}_3 = \text{R}_4 = \text{R}'_4 = \text{R}_5 = \text{H}$ ;  $\text{R}'_5 = \text{CH}_2\text{CH}_2\text{C}_6\text{F}_5$ ;  $\text{R}_6 = \text{R}'_6 = \text{H}$ **3a, 3b:**  $\text{R}'_1 = \text{Me}$ ;  $\text{R}_2 = \text{R}_3 = \text{H}$ ;  $\text{R}_4 = \text{CH}(\text{Me})\text{CH}_2\text{C}_6\text{F}_5$ ;  $\text{R}'_4 = \text{H}$ ;  $\text{R}_5 = \text{R}'_5 = \text{R}_6 = \text{R}'_6 = \text{H}$ **3c:**  $\text{R}'_1 = \text{H}$ ;  $\text{R}_2 = \text{Me}$ ;  $\text{R}_3 = \text{R}_4 = \text{R}'_4 = \text{R}_5 = \text{H}$ ;  $\text{R}'_5 = \text{CH}(\text{Me})\text{CH}_2\text{C}_6\text{F}_5$ ;  $\text{R}_6 = \text{R}'_6 = \text{H}$ **4a, 4b:**  $\text{R}'_1 = \text{H}$ ;  $\text{R}_2 = \text{CHMe}_2$ ;  $\text{R}_3 = \text{R}_4 = \text{H}$ ;  $\text{R}'_4 = \text{C}_6\text{F}_5$ ;  $\text{R}_5 = \text{H}$ ;  $\text{R}'_5 = \text{Me}$ ;  $\text{R}_6 = \text{R}'_6 = \text{H}$ **5a, 5b:**  $\text{R}'_1 = \text{CHMe}_2$ ;  $\text{R}_2 = \text{R}_3 = \text{H}$ ;  $\text{R}_4 = \text{Me}$ ;  $\text{R}'_4 = \text{H}$ ;  $\text{R}_5 = \text{C}_6\text{F}_5$ ;  $\text{R}'_5 = \text{H}$ ;  $\text{R}_6 = \text{R}'_6 = \text{H}$ **5c:**  $\text{R}'_1 = \text{Me}$ ;  $\text{R}_2 = \text{R}_3 = \text{R}_4 = \text{H}$ ;  $\text{R}'_4 = \text{CHMe}_2$ ;  $\text{R}_5 = \text{C}_6\text{F}_5$ ;  $\text{R}'_5 = \text{H}$ ;  $\text{R}_6 = \text{R}'_6 = \text{H}$ 

compd	$\text{R}_1$ (anti)	$\text{R}'_1$ (syn)	$\text{R}_2$	$\text{R}_3$	$\text{R}_4$	$\text{R}'_4$	$\text{R}_5$	$\text{R}'_5$	$\text{R}_6$	$\text{R}'_6$	other
<b>1a-syn</b>	2.67 s	3.86 s	2.10 s	3.77 m <sup>b</sup> (10.1; 4.7)	3.27 m <sup>b</sup> (14.9; 4.7)	3.15 m <sup>b</sup> (14.9; 10.1)					
<b>1b-syn</b>	2.63 s	3.62 s	2.24 s	3.39 m <sup>b</sup> (7.2; 5.4)	3.19 m <sup>b</sup> (15; 5.4)	2.97 m <sup>b</sup> (15; 7.2)					5.43 s (1H), 1.98 s (3H); 1.90 s (3H)
<b>1a-anti</b>	3.51 s	4.10 s	2.23 s	4.59 m	2.89 dd (14.8; 7)	2.59 dd (14.8; 7.7)					
<b>1c-syn</b>	3.23 d (12.6)	4.05 d (7.7)	5.37 dd (12.7; 7.5)	1.21 s							
<b>1c-anti</b>	3.45 d (12.7)	4.11 d (7.5)	5.11 dd (12.7; 7.5)	1.50 s							
<b>2a</b>		5.35 m	5.46 t (6.3)	5.08 d (6.3)	1.57 m ( $-\text{CH}_2-$ ) (14.4; 6.7), 1.68 m ( $-\text{CH}_2-$ ) (14.4; 6.7), 2.76 m ( $-\text{CH}_2\text{P}_f$ ) (13.5; 6.7), 2.80 m ( $-\text{CH}_2\text{P}_f$ ) (13.5; 6.7)	2.1 m	1.83 m	0.75 m	1.9 m	1.9 m	
<b>2b</b>		4.98 t (6.1)	5.58 t (6.1)	4.73 d (6.1)	1.58 m ( $-\text{CH}_2-$ ) (13.1; 7.9), 1.77 m (2H, $-\text{CH}_2-$ ), 2.78 t ( $-\text{CH}_2\text{P}_f$ ) (7.9)	1.9 m (3H)	1.77 m (2H)	0.67 m	1.9 m (3H)	1.9 m (3H)	
<b>2c</b>		5.10 <sup>c</sup>	5.45 <sup>c</sup>	5.10 <sup>c</sup>	0.96 m	2.22 dt (2H) (15.5; 5.5)	2.95 m	1.43 m ( $-\text{CH}_2-$ ), 2.61 m ( $-\text{CH}_2\text{P}_f$ ) (9; 7.5)	0.96 m	2.22 dt (2H) (15.5; 5.5)	
<b>3a</b>		1.63 s	5.35 d (6.4)	4.90 m <sup>d</sup> (6.4)	0.83 d (Me) (6.8), 1.8 m (2H, H), 2.5 m (1H $-\text{CH}_2\text{P}_f$ ), 2.8 m (1H, $-\text{CH}_2\text{P}_f$ )	2.1 m (2H)	0.9 m	1.7 m	1.8 m (2H)	2.1 m (2H)	
<b>3b</b>		1.48 s	5.36 d (6.3)	4.62 d (6.3), 4.25 d <sup>c</sup> (6.6)	0.82 d (Me), <sup>c,c</sup> 0.87 d (Me) (6.8), 1.8–2.0 m (H), 2.5 m (1H, $-\text{CH}_2\text{P}_f$ ), 2.8 m (1H, $-\text{CH}_2\text{P}_f$ )	2.0–1.8 m (4H)	0.8 m	1.6 m	2.0–1.8 m (4H)		5.27 s (1H), 1.96 s (3H), 1.92 s (3H)
<b>3c</b>		4.90 <sup>c</sup>	1.98 s	4.90 <sup>c</sup>	1.06 m	2.20 m	2.80 <sup>c</sup>	0.72 d (Me) (7.0), 1.51 (H), 2.36 t ( $-\text{CH}_2\text{P}_f$ ) (11.7), 2.76 m ( $-\text{CH}_2\text{P}_f$ )	1.06 m	2.20 m	

<b>4a<sup>f</sup></b>	4.86 m <sup>g</sup>	2.4 m (2H; H), 1.19 (Me + Me') (6.8)	4.46 s	2.65 m	3.75 b, <sup>h</sup> 3.52 b	0.85 d (5.8)	2.4 m (2H)	1.00 m
<b>4b</b>	4.55 m (4; 1.6; 1.6 <sup>f</sup> )	2.48 m (H), 1.23 d (Me (6.8), 1.20 d (Me') (6.8)	4.16 t (1.6)	2.57 dd (10.5; 1.6)	3.31 m	0.76 d (6.3)	2.3 m (15; 5.5; 4)	0.85 m 5.32 s (1H), 1.99 s (3H), 1.91 s (3H)
<b>5a</b>	2.2 m (3H; H), 1.23 d (Me) (6.8), 1.22 d (Me') (6.6)	5.39 d (6.8)	4.87 d (6.8)	0.98 d (6.8)	2.6 m (2H)	2.6 m (2H)	2.2 m (3H)	2.2 m (3H)
<b>5b</b>	1.24 d (Me) (6.8), 1.20 d (Me') (6.8)	5.43 d (6.3)	4.58 d (6.3)	0.99 d (6.4)	2.45	2.55 m	2.50 m	2.06 m
<b>5c<sup>i</sup></b>	1.62 s	5.45 d (6.5)	4.91 d (6.5)	1.38 m (H), 1.01 d (Me) (6.5), 0.54 d (6.5)	2.45	2.55 m	2.50 m	2.06 m

<sup>a</sup>  $\delta$  mult,  $J$  values (Hz) are given in parentheses.  $R_n$  = axial;  $R'_n$  = equatorial.  $CDCl_3$  used as solvent. <sup>b</sup> ABX pattern. <sup>c</sup> Partially overlapped signal. <sup>d</sup> Multiplet due to the presence of a 1:1 diastereoisomeric mixture. <sup>e</sup> Signal corresponding to the second diastereoisomer; only several signals of this species are distinctly observed. <sup>f</sup> Recorded at 60 °C. <sup>g</sup> Broad resonance due to the unresolved overlapping of signals. <sup>h</sup> Two resonances are observed for  $R_5$  showing that coalescence of the signals of the diastereoisomers derived from the dimer has not been reached yet. <sup>i</sup>  $J_{1-3}$ .  $J_{CD_3CN:CDCl_3} = 1:1$  mixture used as a solvent.



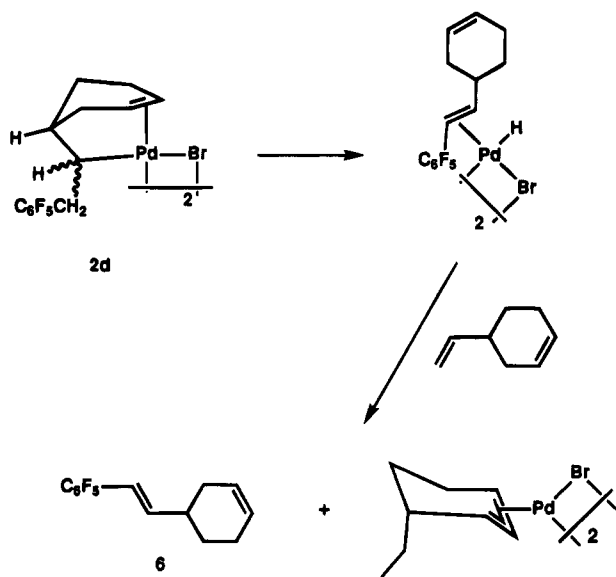
**Figure 1.**  $F_{para}$  signals (triplets) of **3a<sub>1</sub>** and **3a<sub>2</sub>** (\* +  $\blacktriangledown$ ) and the central peaks of the two minor isomers **3c** ( $\star$ ).

comparable rates and slowly at 25 °C (**2d<sub>1</sub>**:  $k_{obs}(298\text{ K}) = (3.12 \pm 0.02) \times 10^{-5} \text{ s}^{-1}$ ;  $\Delta G^\ddagger(298\text{ K}) = 98.7 \pm 0.3 \text{ kJ mol}^{-1}$ . **2d<sub>2</sub>**:  $k_{obs}(298\text{ K}) = (2.93 \pm 0.02) \times 10^{-5} \text{ s}^{-1}$ ;  $\Delta G^\ddagger(298\text{ K}) = 98.8 \pm 0.3 \text{ kJ mol}^{-1}$ ) to give the  $\eta^3$ -allyl derivatives **2a** and **2c** in 78% and 10% final yield, respectively, as estimated by integration of the  $^{19}\text{F}$  NMR resonances in the reaction mixture (Scheme 1). The isomerization  $\eta^1$ - $\eta^2$ -enyl  $\rightarrow$   $\eta^3$ -allyl occurs via a Pd migration process (cis hydride elimination–readdition mechanism)<sup>7,14a,b,24</sup> and necessarily creates the  $\eta^3$ -cyclohexenyl moiety stereospecifically with the Pd atom and the H<sup>4</sup> atom in a cis arrangement. Thus only one diastereoisomer is formed for the regioisomer **2a** from the  $\eta^1$ - $\eta^2$ -enyls **2d<sub>1</sub>** and **2d<sub>2</sub>**. This is also the case of the minor regioisomer **2c**. The major compound, **2a**, is formed by Pd–H elimination of the allylic H<sup>3</sup> atom. This is preferred to Pd–H<sup>5</sup> elimination which gives rise to the minor compound **2c**.

The isomerization of **3d<sub>1</sub>** and **3d<sub>2</sub>** occurs at different rates, **3d<sub>1</sub>** disappearing first to give **3a<sub>1</sub>** (Scheme 1). This process is first order in Pd complex, and the rate of isomerization was measured at 0 °C using  $^{19}\text{F}$  NMR:  $k_{obs}(273\text{ K}) = (5.9 \pm 0.3) \times 10^{-4} \text{ s}^{-1}$ ;  $\Delta G^\ddagger(273\text{ K}) = 83.5 \pm 0.3 \text{ kJ mol}^{-1}$ . At 25 °C the second  $\eta^1$ - $\eta^2$ -enyl complex, **3d<sub>2</sub>**, isomerizes to the second  $\eta^3$ -allyl diastereoisomer, **3a<sub>2</sub>**:  $k_{obs}(298\text{ K}) = (5.5 \pm 0.2) \times 10^{-4} \text{ s}^{-1}$ ;  $\Delta G^\ddagger(298\text{ K}) = 91.6 \pm 0.3 \text{ kJ mol}^{-1}$ . Note that, since we could not determine unequivocally the configuration of the  $\eta^1$ - $\eta^2$ -enyl diastereoisomer which isomerizes first, the assignments of **3d<sub>1</sub>** and **3d<sub>2</sub>** could be reversed. The two observed  $\eta^3$ -allyl diastereoisomers **3a** (ca. 1:1 ratio, Figure 1) correspond to a fixed configuration of the cyclohexenyl ring and the two configurations of the exocyclic chiral carbon produced in the reaction. **3a** can be isolated as a crystalline solid (albeit in low yield due to its high solubility), and the diastereomeric mixture is also present in the corresponding monomeric acac derivative **3b**, showing that both isomers are due to the allyl system itself and independent of the monomeric or dimeric nature of the compounds.



Scheme 2



along with two pentafluorophenyl–dienes which amount to 3% altogether: 1-Isopropyl-3-(pentafluorophenyl)-4-methyl-1,4-cyclohexadiene (**8**) and 3-isopropyl-5-(pentafluorophenyl)-6-methyl-1,3-cyclohexadiene (**9**) in a *ca.* 1:1 ratio (Chart 1). Several other minor <sup>19</sup>F resonances were detected (<2% each of them) which could not be identified. Excess  $\alpha$ -terpinene facilitates the formation of both C<sub>6</sub>F<sub>5</sub>-substituted dienes **8** and **9**; they increased to 7% for a ratio Pd:diene = 1:5 or to 19% for Pd:diene = 1:50, a behavior analogous to that observed for vinylcyclohexene.

The number of F<sub>para</sub> resonances for compound **4a** is temperature-dependent. **4a** shows two triplets and a broad signal at 20 °C, three clear triplets at –50 °C, but only two at 60 °C; its monomeric acac derivative **4b** shows only one F<sub>para</sub> signal (Table 2). Consequently only one allyl moiety is present, although isomers are produced in the dimer.<sup>13</sup> From the <sup>1</sup>H NMR data of Table 3, **4a,b** can be assigned the structures shown in Table 1. It can be seen that the C<sub>6</sub>F<sub>5</sub> group is attached to the least substituted carbon of the least substituted double bond and the Pd atom migration along the cyclohexenyl ring to form an allyl has occurred without isomerization of the unattacked double bond (Scheme 3). Stereochemical analysis of product **4b** based on <sup>1</sup>H NMR data reveals a chair conformation for the cyclohexenyl ring and a *cis* arrangement of Pd and the C<sub>6</sub>F<sub>5</sub> group, as expected from *cis* addition of these two moieties to the diene and subsequent Pd migration (see Experimental Section).

The insertion of the least substituted double bond of  $\gamma$ -terpinene into the Pd–C<sub>6</sub>F<sub>5</sub> bond gives product **5a** as the major regioisomer (93%); a minor compound **5c** (5%) is detected and identified as the result of insertion of the isopropyl substituted double bond into the Pd–C<sub>6</sub>F<sub>5</sub> bond. Attack at the least substituted carbon of each double bond takes place in both cases, and no isomerization of the unattacked double bond is observed. Less than 1% of organic C<sub>6</sub>F<sub>5</sub>-containing products are detected, and this percentage does not change noticeably with the amount of reactant diene added. The number of F<sub>para</sub> signals observed for **5a,c** show a temperature-dependent behavior similar to that observed for **4a**,

although coalescence is reached at 20 °C for both **5a** and **5c**, as collected in Table 2.

Hindered rotation of the C<sub>6</sub>F<sub>5</sub> group is also observed for derivatives **4a,b** and **5a,b**, as shown clearly by the broad F<sub>ortho</sub> resonances that split into two signals at low temperature.<sup>9a</sup>

The reaction of [Pd(C<sub>6</sub>F<sub>5</sub>)Br(NCMe)<sub>2</sub>] with  $\gamma$ -terpinene is significantly slower than the reaction with  $\alpha$ -terpinene. This fact and the small amount of pentafluorophenyl–dienes formed in the  $\gamma$ -terpinene case (independent on the quantities of starting diene used) seems to reflect a lower coordination ability of  $\gamma$ -terpinene, which competes with MeCN and C<sub>6</sub>F<sub>5</sub>-dienes less efficiently than  $\alpha$ -terpinene.

Complexes **4a** and **5a** are capable of forming what seem to be mixed dimers with unreacted starting material, i.e. [( $\eta^3$ -allyl)Pd( $\mu$ -Br)<sub>2</sub>Pd(C<sub>6</sub>F<sub>5</sub>)S] (S = NCMe). These species can be detected by <sup>19</sup>F NMR as the reaction with the diene proceeds or when [Pd(C<sub>6</sub>F<sub>5</sub>)Br(NCMe)<sub>2</sub>] is added to a CDCl<sub>3</sub> solution of pure **4a** or **5a**. The new F<sub>para</sub> signals which appear are as follows:  $\delta$  –155.9 (b) and –156.4 (b) for **4a**;  $\delta$  –156.1 (b) for **5a**. We had proposed the formation of similar species (undetected in that occasion) to explain the autocatalytic isomerization of [Pd(C<sub>6</sub>F<sub>5</sub>)Cl(COD)] (COD = 1,5-cyclooctadiene) to its insertion products.<sup>9a</sup>

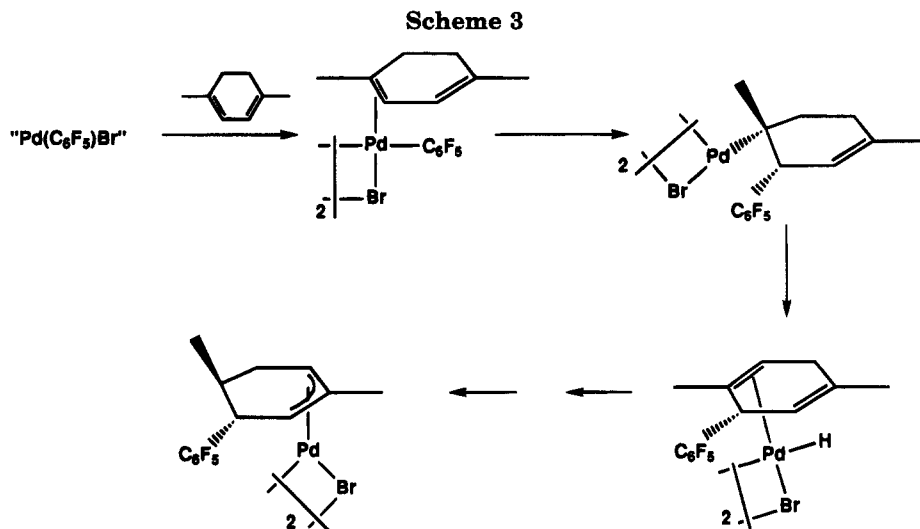
## Discussion

In previous papers<sup>9a,13</sup> we showed that the insertion of diolefins into Pd–C<sub>6</sub>F<sub>5</sub> bonds is fully stereoselective *cis* and this is also confirmed by the stereochemical analysis of product **4b**, so this point will not be further discussed here. The results in those papers and in this work illustrate some other regio- and stereochemical aspects of the *endo* attack of nucleophiles to diolefins.

It has been shown previously that when two inequivalent double bonds are susceptible to undergo *endo* attack, addition to the least substituted one (which coordinates more easily to the palladium center) is preferred.<sup>3–7,25,26</sup> This is also observed here, and insertion of only the least substituted double bond is found except in two cases: isoprene, for which insertion of both double bonds in a 3:1 ratio is observed, and  $\gamma$ -terpinene with a 18.6:1 ratio. The least substituted unsaturation is still favored in both cases. Other previous examples in the literature of *endo* attack using isoprene as substrate report either the insertion of only the least substituted unsaturation into the Pd–C or Pd–H bond<sup>3–5,25</sup> or insertion of both unsaturations, the least substituted one reacting preferentially.<sup>26</sup> Since the reported yields for the final allyl derivatives in the first case are sometimes noticeably less than 100%, unnoticed insertion of the second double bond cannot be ruled out. Thus, the ability of palladium to discriminate double bonds with close substitution patterns, as it is the case of isoprene, is moderate, although there are examples of insertion of isoprene with very good selection of the least substituted unsaturation.<sup>25</sup> Higher selectivity is observed for  $\gamma$ -terpinene, and although both unsaturations are 1,1,2-trisubstituted, coordination of the double bond bearing the less bulky methyl group is clearly preferred.

(25) Larock, R. C.; Colleen, A. F. *J. Am. Chem. Soc.* **1990**, *112*, 5882.  
(26) May, C. J.; Powell, J. J. *J. Organomet. Chem.* **1980**, *184*, 385.





In all the reactions studied in this and previous papers we have consistently observed attack of the C<sub>6</sub>F<sub>5</sub> group on the least substituted carbon atom of the double bond undergoing insertion; since this is often the terminal carbon of a conjugated diene system as well, one might think of electronic factors related to the conjugation influencing such selectivity. In this respect the case of  $\alpha$ -terpinene is interesting since the C<sub>6</sub>F<sub>5</sub> group adds to an *internal* carbon of the conjugated system in spite of the fact that if the addition had occurred on the external carbon an allyl would have been formed immediately, avoiding the need for palladium migration (Scheme 3). This shows that the addition occurs to the least substituted carbon of the coordinated double bond regardless of its position relative to the other double bond. Also, it is clear that, at least in this case, the unattacked double bond must remain uncoordinated during the endo attack and subsequent Pd migration<sup>13</sup> since coordination of the second double bond is sterically inconceivable in the four-center intermediate leading to addition of C<sub>6</sub>F<sub>5</sub> to the internal carbon. It is worth noting the reaction reported by Imaizumi et al. which is believed to involve insertion of  $\alpha$ -terpinene into a Pd-H bond to give [Pd<sub>2</sub>( $\mu$ -Cl)<sub>2</sub>(1-isopropyl-4-methyl-1-3- $\eta^3$ -cyclohexenyl)<sub>2</sub>].<sup>23</sup> In this case the hydrogen atom is incorporated onto the terminal carbon of the diene system. The reversibility of the Pd-H addition to double bonds does not give definite information about the kinetically preferred site of attack, although the smaller size of H versus C<sub>6</sub>F<sub>5</sub> could be important in making feasible the attack to the terminal carbon.

As we have discussed previously,<sup>9</sup> after insertion of one unsaturated group into the Pd-C<sub>6</sub>F<sub>5</sub> bond, coordination of the unattacked double bond can occur to give an  $\eta^1$ - $\eta^2$ -enyl complex. This is observed whenever the separation between double bonds allows for the formation of a stable metalacycle as it is the case for vinylcyclohexene and (*R*)-(+)-limonene, and the  $\eta^1$ - $\eta^2$ -enyl derivatives **2d** and **3d** (each as a mixture of two diastereoisomers) are observed. Their isomerization to the  $\eta^3$ -allyl through the palladium migration mechanism requires the placement of Pd and H<sup>4</sup> in a *cis* arrangement so Pd-H elimination can occur.<sup>7,9,14a,b,24</sup> For this, decoordination of the endocyclic double bond is needed, which will be easier and faster for the more hindered, and consequently less stable,  $\eta^1$ - $\eta^2$ -enyl. The rate of

isomerization observed for the  $\eta^1$ - $\eta^2$ -enyls, i.e. **3d**<sub>1</sub> > **3d**<sub>2</sub> > **2d**<sub>1</sub>  $\approx$  **2d**<sub>2</sub>, seems to correlate well with steric hindrance.  $\Delta G^\ddagger$  measured in each case gives in turn the value of the activation free energy for the decoordination step. Interestingly, although the insertion step is not stereoselective (as shown by the diastereomeric 1:1 mixture formed in both cases), diastereoselectivity is observed in the subsequent isomerization **3d**  $\rightarrow$  **3a** (Scheme 1).

Pd migration occurs to some extent through every possible way in the hydrocarbon chain to reach the uninserted double bond and form an  $\eta^3$ -allyl derivative, provided a *cis* Pd-H arrangement can be reached. This is the case in the **2d**  $\rightarrow$  allyl or **3d**  $\rightarrow$  allyl isomerizations; after the first elimination-readdition Pd migration from C<sup>4</sup> can proceed through Pd-H<sup>3</sup> or Pd-H<sup>5</sup> elimination. Elimination of the more activated allylic H<sup>3</sup> is clearly preferred, and this short way gives **2a** and **3a** as major regioisomers. It is worth noting how the requirement of a *cis* Pd-H<sup>4</sup> arrangement for the migration leads necessarily to a *cis* Pd-H<sup>4</sup> arrangement also in the final  $\eta^3$ -allyl derivatives **2a,c** and **3a,c**. Thus, the formation of endocyclic Pd-allyls via Pd migration from an exocyclic carbon through a chiral tertiary carbon must be fully stereoselective and can be of use for the stereospecific creation of a second endocyclic functionalized chiral carbon.

Small amounts of pentafluorophenyl-substituted organic derivatives are observed whenever the Pd-migration process is operating to form the final allyl compounds. The amount of these derivatives increases when a competing ligand is present in solution (i.e. excess of some diolefins) and promotes substitution of the C<sub>6</sub>F<sub>5</sub>-dienes. Fairly hindered double bonds are generated in some cases (a tetrasubstituted one in the formation of **3a**, for example) but the high yield in allyl formation indicates that readdition of Pd-H to the double bond is fast.

## Experimental Section

**General Comments.** Carbon, hydrogen, and nitrogen analyses were carried out on a Perkin-Elmer 240 microanalyzer. <sup>19</sup>F and <sup>1</sup>H NMR spectra were recorded on Bruker ARX-300 and AC-300 and AC-400 instruments. Chemical shifts (in  $\delta$  units, ppm) are reported downfield from Me<sub>4</sub>Si for <sup>1</sup>H and from CFC<sub>3</sub> for <sup>19</sup>F. Mixtures of organic products were

analyzed using an HP-5890 gas chromatograph connected to an HP-5988 mass spectrometer at an ionizing voltage of 70 eV and a quadrupole analyzer; chemical ionization using methane at 230 eV was also used.

[Pd(C<sub>6</sub>F<sub>5</sub>)Br(NCMe)<sub>2</sub>]<sup>13</sup> and "Pd(C<sub>6</sub>F<sub>5</sub>)Br" solutions<sup>12</sup> were prepared as described elsewhere. Diolefins were purchased from Lancaster, Aldrich, and Janssen and were used without further purification.

**Safety Note.** Although we have not had any problems using perchlorate salts, it is well-known that they are potentially explosive. Thus, *great caution* should be exercised when handling these materials.

**Preparation of the Complexes.** General syntheses are described. The yields reported refer to isolated crystalline products.

**Synthesis of [Pd<sub>2</sub>(μ-Br)<sub>2</sub>(1-3-η<sup>3</sup>-C<sub>6</sub>F<sub>5</sub>-allyl)<sub>2</sub>] Derivatives (1a, 2a-5a, 1c-3c, 5c). Method A. Synthesis of Bis(μ-bromo)bis(2-methyl-4-(pentafluorophenyl)-1-3-η<sup>3</sup>-butenyl)dipalladium(II) (1a-syn). To a suspension of AgClO<sub>4</sub> (0.0585 g, 0.282 mmol) in CH<sub>2</sub>Cl<sub>2</sub> (30 mL) were added isoprene (0.028 mL, 0.282 mmol) and (NBu<sub>4</sub>)<sub>2</sub>[Pd<sub>2</sub>(μ-Br)<sub>2</sub>(C<sub>6</sub>F<sub>5</sub>)<sub>2</sub>Br<sub>2</sub>] (0.191 g, 0.141 mmol). After 8 h of stirring the precipitate (AgBr) was filtered out, and the resulting solution was evaporated to dryness. The residue was extracted with 100 mL of Et<sub>2</sub>O, and the insoluble (NBu<sub>4</sub>)ClO<sub>4</sub> was removed. Evaporation of the Et<sub>2</sub>O solution to ca. 5 mL and cooling afforded a yellow product (1a-syn), which was filtered out and air dried (0.0478 g, 40.2% yield). The mother liquors were evaporated to dryness, and the residue was dissolved in CDCl<sub>3</sub> and checked by <sup>19</sup>F and <sup>1</sup>H NMR; it was found to be a mixture of 1c, 1a and traces of (NBu<sub>4</sub>)ClO<sub>4</sub>. Anal. Calcd for C<sub>22</sub>H<sub>16</sub>Br<sub>2</sub>F<sub>20</sub>Pd<sub>2</sub> (1a-syn): C, 31.34; H, 1.91. Found: C, 31.27; H, 1.93.**

The same procedure was applied for the rest of the dimers, with the following variations in the procedure of crystallization:

**2a.** Reaction time: 48 h. Procedure variation: Evaporation of the Et<sub>2</sub>O solution to dryness and trituration of the residue in *n*-hexane (5 mL); 30% yield. Anal. Calcd for C<sub>28</sub>H<sub>24</sub>Br<sub>2</sub>F<sub>10</sub>Pd<sub>2</sub>: C, 36.43; H, 2.62. Found: C, 36.17; H, 2.62.

**3a.** Procedure variation: Evaporation of the Et<sub>2</sub>O solution to dryness and trituration of the residue in *n*-hexane (5 mL); 10% yield. Anal. Calcd for C<sub>32</sub>H<sub>32</sub>Br<sub>2</sub>F<sub>10</sub>Pd<sub>2</sub>: C, 39.25; H, 3.29. Found: C, 39.43; H, 3.32.

**4a.** Procedure variation: Evaporation of the Et<sub>2</sub>O solution to dryness and trituration of the residue in cold 2-propanol (5 mL); 50% yield. Anal. Calcd for C<sub>32</sub>H<sub>32</sub>Br<sub>2</sub>F<sub>10</sub>Pd<sub>2</sub>: C, 39.25; H, 3.29. Found: C, 39.38; H, 3.24.

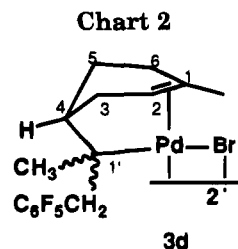
**5a.** Procedure variation: The solution obtained after filtration of the AgBr was evaporated to dryness, and the residue was trituated with ethanol (15 mL), where (NBu<sub>4</sub>)ClO<sub>4</sub> is soluble; the yellow solid (5a) was filtered out, washed with cold ethanol, and dried; 77% yield. Anal. Calcd for C<sub>32</sub>H<sub>32</sub>Br<sub>2</sub>F<sub>10</sub>Pd<sub>2</sub>: C, 39.25; H, 3.29. Found: C, 39.27; H, 3.28.

In each case, the mother liquors were evaporated to dryness, and the <sup>19</sup>F and <sup>1</sup>H NMR spectra of the residues were studied.

**Method B. Synthesis of Bis(μ-bromo)bis(1-methyl-4-(1-(pentafluorophenyl)-2-propyl)-1-3-η<sup>3</sup>-cyclohexenyl)dipalladium(II) (3a).** To a solution of [Pd(C<sub>6</sub>F<sub>5</sub>)Br(NCMe)<sub>2</sub>] (0.1410 g, 0.324 mmol) in CH<sub>2</sub>Cl<sub>2</sub> (10 mL) was added *R*-(+)-limonene (0.0525 mL, 0.324 mmol). The mixture was stirred for 4 h. The solvent was evaporated to dryness, and the residue was trituated with *n*-hexane (5 mL) and cooled. 3a was obtained as a yellow solid in 20% yield (0.0317 g).

1a and 4a can be obtained in a similar way using the solvents indicated above for crystallization. The synthesis of 2a or 5a requires a longer reaction time: The mixture was stirred for 2 days in the case of 2a and 12 h for 5a, and the products crystallized as indicated in method A.

**Synthesis of the acac Derivatives (1b-4b). (acetylacetonato)(1-isopropyl-4-methyl-5-(pentafluorophenyl)-1-3-η<sup>3</sup>-cyclohexenyl)palladium(II) (5b).** To a solution of 5a



(0.0727 g, 0.074 mmol) in CH<sub>2</sub>Cl<sub>2</sub> (10 mL) was added Tl(acac) (0.0451 g, 0.148 mmol) whereupon a TlBr precipitate appeared and the solution turned from yellow to pale yellow. The suspension was stirred for 15 min, and the precipitate was filtered off; the solution was evaporated to dryness, and the residue was trituated with *n*-hexane (2 mL) and cooled in the freezer. The white-yellowish solid was filtered out and identified as 5b (0.0376 g, 50% yield). The mother liquors were evaporated to dryness and studied by <sup>19</sup>F and <sup>1</sup>H NMR. Anal. Calcd for C<sub>21</sub>H<sub>23</sub>F<sub>5</sub>O<sub>2</sub>Pd (5b) C, 49.57; H, 4.56. Found: C, 49.70; H, 4.58.

The same procedure afforded solids 1b-syn (45% yield) and 4b (10% yield); their mother liquors were also studied by NMR. For 2b and 3b the residue was fully soluble in the *n*-hexane used for trituration; then, the *n*-hexane solution was evaporated to dryness to give an oily residue which was studied by <sup>1</sup>H and <sup>19</sup>F NMR to characterize 2b and 3b. 4b and 5b decompose slowly at room temperature and were stored at -20 °C.

**1b.** Anal. Calcd for C<sub>16</sub>H<sub>15</sub>F<sub>5</sub>O<sub>2</sub>Pd: C, 43.61; H, 3.43. Found: C, 43.51; H, 3.44.

**4b.** Anal. Calcd for C<sub>21</sub>H<sub>23</sub>F<sub>5</sub>O<sub>2</sub>Pd: C, 49.57; H, 4.56. Found: C, 49.42; H, 4.59.

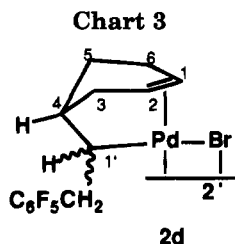
**Characterization of Bis(μ-bromo)bis(η¹-η²-(1-methylcyclohex-1-en-4-yl)methyl((pentafluorophenyl)methyl)methyl)dipalladium(II) (3d) and Rate Measurements.** A 5 mm NMR tube was charged with a solution of [Pd(C<sub>6</sub>F<sub>5</sub>)Br(NCMe)<sub>2</sub>] (0.0305 g, 0.070 mmol) in CDCl<sub>3</sub> (0.6 mL) and cooled to -30 °C. *R*-(+)-Limonene (0.0113 mL, 0.070 mmol) was added to this solution, and the reaction was monitored by <sup>19</sup>F and <sup>1</sup>H NMR. Compounds 3d<sub>1</sub> and 3d<sub>2</sub> were slowly formed (Chart 2).

**3d<sub>1</sub>.** <sup>19</sup>F NMR (CDCl<sub>3</sub>, δ, 243 K, 282 MHz): -162.4 (m, F<sub>meta</sub>), -155.3 (t, F<sub>para</sub>), -138.5 (m, F<sub>ortho</sub>). <sup>1</sup>H NMR (CDCl<sub>3</sub>, δ, 243 K, 300 MHz): 5.51 (H<sup>2</sup>), 3.30, 2.60 (CH<sub>2</sub>C<sub>6</sub>F<sub>5</sub>), 2.50 (H<sup>3</sup>), 1.75 (H<sup>4</sup>), 1.5-2.0 (H<sup>5</sup>, H<sup>5'</sup>, H<sup>6</sup>, H<sup>6'</sup>), 1.30 (Me<sup>1</sup>), 0.41 (H<sup>4</sup>).

**3d<sub>2</sub>.** <sup>19</sup>F NMR (CDCl<sub>3</sub>, δ, 243 K, 282 MHz): -162.5 (m, F<sub>meta</sub>), -155.2 (t, F<sub>para</sub>), -139.5 (m, F<sub>ortho</sub>). <sup>1</sup>H NMR (CDCl<sub>3</sub>, δ, 243 K, 300 MHz): 5.53 (H<sup>2</sup>), 3.75, 3.42 (CH<sub>2</sub>C<sub>6</sub>F<sub>5</sub>), 2.75 (H<sup>3</sup>), 1.80 (H<sup>3'</sup>), 1.5-2.0 (H<sup>5</sup>, H<sup>5'</sup>, H<sup>6</sup>, H<sup>6'</sup>), 0.89 (Me<sup>1</sup>), 0.22 (H<sup>4</sup>).

Rate constants were measured by recording <sup>19</sup>F NMR spectra every 10 min at 273 K for 3d<sub>1</sub> and 298 K for 3d<sub>2</sub> (relaxation delays of at least 5T<sub>1</sub>'s were used). A plot of ln[signal integral] versus time gave the first-order rate constants. The reported uncertainty in the isomerization rate constants corresponds to one standard deviation in the slope of the best fit line. Free energies of activation were calculated using the Eyring equation in the form ΔG<sup>‡</sup> = -2.3RT log(k<sub>B</sub>T/hk<sub>obs</sub>). Errors were calculated using the above-mentioned uncertainties in k<sub>obs</sub> and a temperature variation of ±1 °C.<sup>27</sup>

**Characterization of Bis(μ-bromo)bis(η¹-η²-(cyclohex-1-en-4-yl))((pentafluorophenyl)methyl)methyl)dipalladium(II) (2d).** A 5 mm NMR tube was charged with a solution of [Pd(C<sub>6</sub>F<sub>5</sub>)Br(NCMe)<sub>2</sub>] (0.0300 g, 0.069 mmol) in CDCl<sub>3</sub> (0.6 mL) and cooled to -30 °C. Vinylcyclohexene (0.009 mL, 0.069 mmol) was added to the solution, and the mixture was kept at -30 °C for 6 h. After this time <sup>19</sup>F NMR revealed the presence of compounds 2d<sub>1</sub> and 2d<sub>2</sub> (Chart 3) and about 8% of 2a.



**2d<sub>1</sub>.** <sup>19</sup>F NMR (CDCl<sub>3</sub>, δ, 243 K, 282 MHz): -162.7 (m, F<sub>meta</sub>), -157.4 (t, F<sub>para</sub>), -141.8 (m, F<sub>ortho</sub>). <sup>1</sup>H NMR (CDCl<sub>3</sub>, δ, 243 K, 300 MHz): 6.04 (b, H<sup>1</sup>), 5.76 (b, H<sup>2</sup>), 3.55 (d, *J* = 12.2 Hz, CH<sub>2</sub>C<sub>6</sub>F<sub>5</sub>), 3.40 (d, *J* = 12.2 Hz, CH<sub>2</sub>C<sub>6</sub>F<sub>5</sub>), 2.8–2.6 (H<sup>3</sup>, H<sup>6</sup>), 2.20 (H<sup>6</sup>), 1.8–1.5 (H<sup>5</sup>, H<sup>5</sup>, H<sup>3</sup>), 0.70 (H<sup>4</sup>).

**2d<sub>2</sub>.** <sup>19</sup>F NMR (CDCl<sub>3</sub>, δ, 243 K, 282 MHz): -162.8 (m, F<sub>meta</sub>), -157.6 (t, F<sub>para</sub>), -142.8 (m, F<sub>ortho</sub>). <sup>1</sup>H NMR (CDCl<sub>3</sub>, δ, 243 K, 300 MHz): 6.04 (b, H<sup>2</sup>), 5.76 (b, H<sup>1</sup>), 3.55 (d, *J* = 12.2 Hz, CH<sub>2</sub>C<sub>6</sub>F<sub>5</sub>), 3.00 (t, *J* = 12.2 Hz, CH<sub>2</sub>C<sub>6</sub>F<sub>5</sub>), 2.8–2.6 (H<sup>1</sup>, H<sup>6</sup>), 2.3–2.1 (H<sup>6</sup>, H<sup>3</sup>), 1.8–1.5 (H<sup>5</sup>, H<sup>5</sup>, H<sup>3</sup>), 0.82 (H<sup>4</sup>).

The rate of isomerization **2d** → **2a**, **2c** was measured by <sup>19</sup>F NMR at 298 K as reported above.

**Identification of the Pentafluorophenyl-Substituted Organic Byproducts.** To a solution of [Pd(C<sub>6</sub>F<sub>5</sub>)Br(NCMe)<sub>2</sub>] (0.1000 g, 0.230 mmol) in CH<sub>2</sub>Cl<sub>2</sub> (1.5 mL) was added α-terpinene (0.0562 mL, 0.345 mmol). The reaction was monitored by <sup>19</sup>F NMR, and when it was complete, the solvent was evaporated and the residue was chromatographed on a silica column (neutral, 230–400 mesh) and eluted with *n*-hexane. This operation separated the C<sub>6</sub>F<sub>5</sub>-organic derivatives. Elution with Et<sub>2</sub>O yielded the Pd-allyl compound **4a**. The first fraction was analyzed by <sup>19</sup>F, <sup>1</sup>H NMR, and then GC-MS. Two main compounds were found as follows:

**1-Isopropyl-3-(pentafluorophenyl)-4-methyl-1,4-cyclohexadiene (8).** <sup>19</sup>F NMR (CDCl<sub>3</sub>, δ, 282 MHz): -163.5 (m, F<sub>meta</sub>), -158.1 (t, F<sub>para</sub>), -144.5 (m, F<sub>ortho</sub>). <sup>1</sup>H NMR (CDCl<sub>3</sub>, δ, 300 MHz): 5.64 (m, 1H, H<sup>5</sup>), 5.29 (1H, H<sup>2</sup>), 4.29 (m, 1H, H<sup>3</sup>), 2.70 (m, H<sup>6</sup> + H<sup>6</sup>), 2.3 (m, CHMe<sub>2</sub>), 1.54 (s, Me<sup>4</sup>), 1.02 (dd, *J* = 6.6 Hz, 6H, CHMe<sub>2</sub>). MS (EI) [*m/z* (relative intensity)]: 302 (M<sup>+</sup>, 40), 259 (100), 181 (47), 91 (84), 43 (82), 41 (56).

**3-Isopropyl-5-(pentafluorophenyl)-6-methyl-1,3-cyclohexadiene (9).** <sup>19</sup>F NMR (CDCl<sub>3</sub>, δ, 282 MHz): -163.1 (m, F<sub>meta</sub>), -157.7 (t, F<sub>para</sub>), -139.1 (m, F<sub>ortho</sub>). <sup>1</sup>H NMR (CDCl<sub>3</sub>, δ, 300 MHz): 5.96, 5.71 (AB system, *J* = 9.6 Hz, H<sup>1</sup> + H<sup>2</sup>), 5.29 (m, H<sup>4</sup>), 3.70 (d, *J* = 16 Hz, H<sup>5</sup>), 2.66 (m, H<sup>6</sup>), 2.30 (m, CHMe<sub>2</sub>), 1.05 (d, *J* = 6.6 Hz, CH(Me)Me), 1.04 (d, *J* = 6.6 Hz, CH(Me)Me), 0.96 (d, *J* = 6.7 Hz, Me<sup>6</sup>). MS (EI) [*m/z* (relative intensity)]: 302 (M<sup>+</sup>, 36), 259 (96), 181 (31), 91 (100), 43 (70), 41 (56).

The rest of the reaction mixtures were analyzed in a similar way, and the following products were identified:

**Reaction of [Pd(C<sub>6</sub>F<sub>5</sub>)Br(NCMe)<sub>2</sub>] with Vinylcyclohexene. 4-(1-Pentafluorophenylethen-2-yl)-1-cyclohexene (6).** <sup>19</sup>F NMR (CDCl<sub>3</sub>, δ, 282 MHz): -163.9 (m, F<sub>meta</sub>), -158.3 (t, F<sub>para</sub>), -144.1 (m, F<sub>ortho</sub>). <sup>1</sup>H NMR (CDCl<sub>3</sub>, δ, 300 MHz):

6.56 (m, *J* = 16.5; 7.3 Hz, -CH=CHC<sub>6</sub>F<sub>5</sub>), 6.29 (m, *J* = 16.5; 1 Hz, -CH=CHC<sub>6</sub>F<sub>5</sub>), 5.70 (s, 2H, H<sup>1</sup>, H<sup>2</sup>), 2.45 (m, H<sup>4</sup>), 2.25–2.10 (m, H<sup>3</sup>, H<sup>5</sup>, H<sup>6</sup>), 2.0 (m, H<sup>3</sup>), 1.85 (m, H<sup>6</sup>), 1.52 (m, H<sup>5</sup>). MS (EI) [*m/z* (relative intensity)]: 274 (M<sup>+</sup>, 0.86), 181 (5), 151 (18), 80 (100), 41 (7).

**[Pd<sub>2</sub>(μ-Br)<sub>2</sub>(4-ethyl-1-3-η<sup>3</sup>-cyclohexenyl)<sub>2</sub>].** The product was obtained along with **2a** and **2c** using Et<sub>2</sub>O as eluent after separating the organic products as above. <sup>1</sup>H NMR (CDCl<sub>3</sub>, δ, 300 MHz): 5.45 (t, *J* = 6.4 Hz, H<sup>2</sup>), 5.32 (m, H<sup>1</sup>), 5.12 (m, H<sup>3</sup>), 1.95 (m, H<sup>4</sup>), 1.9–1.8 (H<sup>6</sup>, H<sup>6</sup>), 1.75 (m, H<sup>5</sup>), 1.5 (m, CHHMe), 1.33 (m, CHHMe), 0.96 (t, *J* = 7.4 Hz, CH<sub>2</sub>Me), 0.65 (m, H<sup>5</sup>).

**Reaction with *R*-(+)-Limonene. 4-(3-(Pentafluorophenyl)-1-propen-2-yl)-1-methylcyclohexene (7).** <sup>19</sup>F NMR (CDCl<sub>3</sub>, δ, 282 MHz): -163.2 (m, F<sub>meta</sub>), -157.7 (t, F<sub>para</sub>), -143.8 (m, F<sub>ortho</sub>). <sup>1</sup>H NMR (CDCl<sub>3</sub>, δ, 300 MHz): 5.40 (s, 1H, H<sub>2</sub>), 4.85 (s, 1H, -CH(CH<sub>2</sub>C<sub>6</sub>F<sub>5</sub>)=CHH), 4.50 (s, 1H, -CH(CH<sub>2</sub>C<sub>6</sub>F<sub>5</sub>)=CHH), 3.42 (s, 2H, -CH(CH<sub>2</sub>C<sub>6</sub>F<sub>5</sub>)=CH<sub>2</sub>), 2.15 (m, H<sup>3</sup>), 2.0 (m, H<sup>3</sup>), 2.10–1.80 (m, 4H, H<sup>4</sup>, H<sup>5</sup>, H<sup>6</sup>, H<sup>6</sup>), 1.66 (s, 3H, Me<sup>1</sup>), 1.55 (m, 1H, H<sup>5</sup>). MS (CI) [*m/z*]: 303 (MH<sup>+</sup>), 81 (base peak).

**Stereochemical Assignment of Product 4b.** Analysis of the coupling constant values in (1-3-η<sup>3</sup>-cyclohexenyl)-palladium derivatives can give information about the conformation of the ring and the arrangement of the substituents.<sup>22</sup> A pseudochair conformation is expected when <sup>3</sup>*J*<sub>1-6a</sub> (*a* = axial; *e* = equatorial) or <sup>3</sup>*J*<sub>3-4a</sub> are *ca.* 1.5–3.5 Hz and <sup>3</sup>*J*<sub>1-6e</sub> and <sup>3</sup>*J*<sub>3-4e</sub> are *ca.* 2.5–4 Hz. <sup>3</sup>*J*<sub>1-6a</sub> ≈ <sup>3</sup>*J*<sub>3-4a</sub> ≈ 6 Hz and <sup>3</sup>*J*<sub>1-6e</sub> ≈ <sup>3</sup>*J*<sub>3-4e</sub> ≈ 0 Hz are expected for a pseudoboat conformation. Thus, **4b** adopts a pseudochair conformation as can be seen by the <sup>3</sup>*J* values collected in Table 3 (<sup>3</sup>*J*<sub>1-6a</sub> = 1.6 Hz; <sup>3</sup>*J*<sub>1-6e</sub> = 4 Hz; <sup>3</sup>*J*<sub>3-4a</sub> = 1.6 Hz). This leaves the pentafluorophenyl group attached to C-4 in an equatorial position and so *cis* to Pd, which confirms the *cis* stereochemistry if Pd–C<sub>6</sub>F<sub>5</sub> adds to the diene.

The small <sup>3</sup>*J*<sub>3-4</sub> values detected for the rest of the complexes (<sup>3</sup>*J*<sub>3-4</sub> < 2 Hz) are inconsistent with either a pseudoboat (<sup>3</sup>*J*<sub>3-4a</sub> ≈ 6 Hz) or a pseudochair (<sup>3</sup>*J*<sub>3-4e</sub> ≈ 2.5–4 Hz) conformation of the rings. Unfortunately the complication of the <sup>1</sup>H NMR prevented the determination of other coupling constants that could help in the assignment of the ring conformation and the mutual arrangement of Pd and the C<sub>6</sub>F<sub>5</sub> group. We represent the cyclohexenyl derivatives **2a–c**, **3a–c**, and **5a,b** as pseudochair conformers which seem to provide a sterically comfortable arrangement in most cases.

**Acknowledgment.** Financial support by the Dirección General de Investigación Científica y Técnica (Project PB93-0222) and the Commission of the European Communities (Network “Selective Processes and Catalysis Involving Small Molecules”, CHR-X-CT93-0147) is gratefully acknowledged as well as the Ministerio de Educación y Ciencia for a fellowship to Y.-S.L.

OM940345O

# Steric and "Indenyl" Effects in the Chemistry of Alkylidyne Complexes of Tungsten and Molybdenum

Stephen Anderson, Anthony F. Hill,\* and Bashir A. Nasir

Department of Chemistry, Imperial College, London SW7 2AY, U.K.

Received January 24, 1995<sup>⊗</sup>

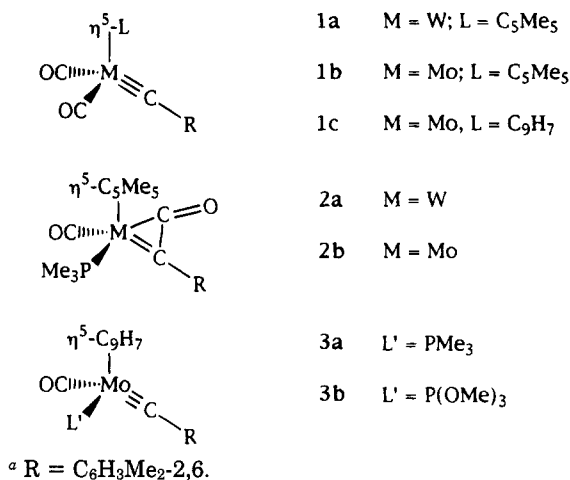
Reaction between  $\text{LiC}_5\text{Me}_5$  or  $\text{KC}_9\text{H}_7$  and  $[\text{M}(\equiv\text{C}_6\text{H}_3\text{Me}_2-2,6)(\text{CO})_2(\text{NC}_5\text{H}_4\text{Me-4})_2\text{Br}]$  affords the complexes  $[\text{M}(\equiv\text{CC}_6\text{H}_3\text{Me}_2-2,6)(\text{CO})_2\text{L}]$  ( $\text{L} = \eta\text{-C}_5\text{Me}_5$ ,  $\text{M} = \text{W}$  (**1a**);  $\text{Mo}$  (**1b**);  $\text{L} = \eta^5\text{-C}_9\text{H}_7$ ,  $\text{M} = \text{Mo}$  (**1c**)). The complexes **1a** and **1b** react with  $\text{PMe}_3$  to give  $\eta^2$ -ketenyl compounds  $[\text{M}\{\eta^2\text{-C}(\text{O})\text{CC}_6\text{H}_3\text{Me}_2-2,6\}(\text{CO})(\text{PMe}_3)(\eta\text{-C}_5\text{Me}_5)]$  ( $\text{M} = \text{W}$  (**2a**),  $\text{Mo}$  (**2b**)) while the reaction of **1c** with  $\text{PMe}_3$  or  $\text{P}(\text{OMe})_3$  gives  $[\text{Mo}(\equiv\text{CC}_6\text{H}_3\text{Me}_2-2,6)(\text{CO})\text{L}'(\eta^5\text{-C}_9\text{H}_7)]$  ( $\text{L}' = \text{PMe}_3$  (**3a**),  $\text{P}(\text{OMe})_3$  (**3b**)). Thermolysis of **2a** provides **1a** rather than the anticipated complex  $[\text{W}(\equiv\text{CC}_6\text{H}_3\text{Me}_2-2,6)(\text{CO})(\text{PMe}_3)(\eta\text{-C}_5\text{Me}_5)]$ . Compound **1b** has been employed to prepare the range of heterobimetallic compounds  $[\text{MoFe}(\mu\text{-CC}_6\text{H}_3\text{Me}_2-2,6)(\text{CO})_5(\eta\text{-C}_5\text{Me}_5)]$  (**4**),  $[\text{MoFe}(\mu\text{-CC}_6\text{H}_3\text{Me}_2-2,6)(\text{CO})_3(\mu\text{-dppm})(\eta\text{-C}_5\text{Me}_5)]$  (**5**),  $[\text{MoFe}(\mu\text{-}\eta^2\text{-SeCC}_6\text{H}_3\text{Me}_2-2,6)(\text{CO})_5(\eta\text{-C}_5\text{Me}_5)]$  (**6**), and  $[\text{MoCu}(\mu\text{-CC}_6\text{H}_3\text{Me}_2-2,6)(\text{CO})(\mu\text{-CO})(\eta\text{-C}_5\text{Me}_5)_2]$  (**8b**), with bonds between molybdenum and iron or copper supported by the xylylmethylidyne unit, to assess the effects of steric encumbrance on bridge-assisted cluster assembly.

## Introduction

The compounds  $[\text{M}(\equiv\text{CR})(\text{CO})_2\text{L}]$  ( $\text{M} = \text{Cr}, \text{Mo}, \text{W}, \text{Mn}^+, \text{Re}^+$ ;  $\text{R} = \text{alkyl, aryl, alkynyl}$ ;  $\text{L} = \eta\text{-C}_5\text{H}_5, \eta\text{-C}_5\text{Me}_5, \text{HB}(\text{pyrazol-1-yl})_3$ ) have proven to be useful precursors for the synthesis of metal cluster compounds in which alkylidyne groups bridge metal-metal bonds.<sup>1</sup> In these studies, however, it has become increasingly obvious that considerations of steric bulk are of primary importance in dictating the geometries and degree of coordinative saturation in the resulting polymetallic species.<sup>2</sup> In particular, the reactions of the (alkylidyne)-tungsten complex  $[\text{W}(\equiv\text{CC}_6\text{H}_4\text{Me-4})(\text{CO})_2(\eta\text{-C}_5\text{Me}_5)]$  were informative: with  $[\text{Fe}_2(\text{CO})_9]$  the major products are the bimetallic species  $[\text{WFe}(\mu\text{-CC}_6\text{H}_4\text{Me-4})(\text{CO})_n(\eta\text{-C}_5\text{Me}_5)]$  ( $n = 5, 6$ ),<sup>3</sup> while similar treatment of  $[\text{W}(\equiv\text{CC}_6\text{H}_4\text{Me-4})(\text{CO})_2(\eta\text{-C}_5\text{H}_5)]$  leads to the trinuclear derivatives  $[\text{WFe}_2(\mu_3\text{-CC}_6\text{H}_4\text{Me-4})(\mu\text{-CO})(\text{CO})_8(\eta\text{-C}_5\text{H}_5)]$  and  $[\text{WFe}_2(\mu_3\text{-C}_2(\text{C}_6\text{H}_4\text{Me-4})_2)(\text{CO})_6(\eta\text{-C}_5\text{H}_5)]$ .<sup>4</sup> Alternatively, the steric bulk may be increased by variation of the alkylidyne substituent, as shown by the reaction of  $[\text{W}(\equiv\text{CC}_6\text{H}_3\text{Me}_2-2,6)(\text{CO})_2(\eta\text{-C}_5\text{H}_5)]$  with  $[\text{Fe}_2(\text{CO})_9]$ , which produces exclusively the dinuclear 32-valence-electron complex  $[\text{WFe}(\mu\text{-CC}_6\text{H}_3\text{Me}_2-2,6)(\text{CO})_5(\eta\text{-C}_5\text{H}_5)]$ <sup>2a</sup> with no indication of the formation of complexes of higher nuclearity or coordinative saturation.

We describe herein the synthesis and reactions of complexes  $[\text{M}(\equiv\text{CC}_6\text{H}_3\text{Me}_2-2,6)(\text{CO})_2\text{L}]$  ( $\text{L} = \eta\text{-C}_5\text{Me}_5$ ,  $\text{M} = \text{W}$  (**1a**),  $\text{Mo}$  (**1b**);  $\text{L} = \eta^5\text{-C}_9\text{H}_7$ ,  $\text{M} = \text{Mo}$  (**1c**)) which combine steric congestion at the metal center and alkylidyne substituent. The effect of this steric encum-

Chart 1. Alkylidyne and Ketenyl Complexes of Tungsten and Molybdenum<sup>a</sup>



brance is then assessed in reactions expected to be sensitive to such pressures. In ligand addition reactions of **1c** there is strong evidence for "indenyl" effects.

## Results and Discussion

The  $\gamma$ -picoline-stabilized (alkylidyne)metal complexes  $[\text{M}(\equiv\text{CR})(\text{CO})_2(\text{NC}_5\text{H}_4\text{Me-4})_2\text{Br}]$  ( $\text{R} = \text{C}_6\text{H}_3\text{Me}_2-2,6$ ) offer increased thermal stability over the tetracarbonyl derivatives  $[\text{M}(\equiv\text{CR})(\text{CO})_4\text{X}]$ , and this feature greatly enhances the convenience and yields involved in the introduction of the ligands  $\eta\text{-C}_5\text{H}_5$ ,  $\eta\text{-C}_5\text{Me}_5$ , and  $\eta^5\text{-C}_9\text{H}_7$ . For our work we employed a modification of Mayr's method for the preparation of  $[\text{W}(\equiv\text{CPh})(\text{CO})_2(\text{py})_2(\text{O}_2\text{CCF}_3)]$ <sup>5</sup> via the reaction of  $[\text{W}(\text{CO})_6]$  with  $\text{PhLi}$ , followed by cation metathesis to provide  $[\text{NMe}_4][\text{W}\{\text{C}(\text{=O})\text{R}\}(\text{CO})_5]$ , which is then reacted with  $(\text{CF}_3\text{CO})_2\text{O}$  and pyridine. We find that if the cation metathesis step is omitted, then the process may be conveniently carried out in one pot to provide  $[\text{W}(\equiv\text{CC}_6\text{H}_3$

(5) Mayr, A.; McDermott, G. A.; Dorries, A. M. *Organometallics* 1985, 4, 608.

<sup>⊗</sup> Abstract published in *Advance ACS Abstracts*, May 1, 1995.

(1) Stone, F. G. A. *Pure Appl. Chem.* 1986, 58, 529; *ACS Symp. Ser.* 1983, No. 211, 383; *Angew. Chem., Int. Ed. Engl.* 1984, 23, 89.

(2) (a) Dossett, S. J.; Hill, A. F.; Jeffery, J. C.; Marken, F.; Sherwood, P.; Stone, F. G. A. *J. Chem. Soc., Dalton Trans.* 1988, 2453. (b) Dossett, S. J.; Hill, A. F.; Howard, J. A. K.; Nasir, B. A.; Spaniol, T. P.; Sherwood, P.; Stone, F. G. A. *J. Chem. Soc., Dalton Trans.* 1989, 1871. (c) Hart, I. J.; Hill, A. F.; Stone, F. G. A. *J. Chem. Soc., Dalton Trans.* 1989, 2261.

(3) Delgado, E.; Hein, J.; Jeffery, J. C.; Ratermann, A. L.; Stone, F. G. A.; Farrugia, L. J. *J. Chem. Soc., Dalton Trans.* 1987, 1191.

(4) Busetto, L.; Jeffery, J. C.; Mills, R. M.; Stone, F. G. A.; Went, M. J.; Woodward, P. *J. Chem. Soc., Dalton Trans.* 1983, 101.

Table 1. Analytical<sup>a</sup> and Physical Data for the Complexes

compd (R = C <sub>6</sub> H <sub>3</sub> Me <sub>2</sub> -2,6)	yield (%)	IR $\nu_{\max}(\text{CO})^b/\text{cm}^{-1}$	analyses (%)	
			C	H
[W(=CR)(CO) <sub>2</sub> ( $\eta$ -C <sub>5</sub> Me <sub>5</sub> )] ( <b>1a</b> , red)	67	1970 vs, 1892 vs	51.5 (51.2)	5.2 (4.9)
[Mo(=CR)(CO) <sub>2</sub> ( $\eta$ -C <sub>5</sub> Me <sub>5</sub> )] ( <b>1b</b> , red)	70	1979 vs, 1903 vs	62.4 (62.4)	6.4 (6.0)
[Mo(=CR)(CO) <sub>2</sub> ( $\eta^5$ -C <sub>9</sub> H <sub>7</sub> )] ( <b>1c</b> , red)	63	1998 vs, 1925 vs	62.4 (62.5)	4.3 (4.2)
[W( $\eta^2$ -OCCR)(CO)(PMe <sub>3</sub> )( $\eta$ -C <sub>5</sub> Me <sub>5</sub> )] ( <b>2a</b> , violet)	84	1898 vs, 1729 m (br)	49.2 (50.7)	5.9 (5.5)
[Mo( $\eta^2$ -OCCR)(CO)(PMe <sub>3</sub> )( $\eta$ -C <sub>5</sub> Me <sub>5</sub> )] ( <b>2b</b> , violet)	80	1888 vs, 1733 w (br)	60.2 (60.0)	7.2 (6.9)
[Mo(=CR)(CO)(PMe <sub>3</sub> )( $\eta^5$ -C <sub>9</sub> H <sub>7</sub> )] ( <b>3a</b> )	62	1887 vs	60.3 (61.1)	6.1 (5.8)
[Mo(=CR)(CO){P(OMe) <sub>3</sub> }( $\eta^5$ -C <sub>9</sub> H <sub>7</sub> )] ( <b>3b</b> , yellow)	66	1910 vs	55.4 (55.0)	4.4 (5.3)
[MoFe( $\mu$ -CR)(CO) <sub>5</sub> ( $\eta$ -C <sub>5</sub> Me <sub>5</sub> )] ( <b>4</b> , violet)	61	2038 vs, 1975, 1965 s, 1859 w (br)	52.8 (53.0)	4.5 (4.4)
[MoFe( $\mu$ -CR)(CO) <sub>3</sub> ( $\mu$ -dppm)( $\eta$ -C <sub>5</sub> Me <sub>5</sub> )] ( <b>5</b> , green)	89	1962 vs, 1907 s, 1748 w (br)	64.1 (64.7)	5.8 (5.3)
[MoFe( $\mu$ - $\eta^2$ -SeCR)(CO) <sub>5</sub> ( $\eta$ -C <sub>5</sub> Me <sub>5</sub> )] ( <b>6</b> , orange)	83	2038 vs, 1976 s, 1962 m (sh), 1945 w (sh) 1903 w (br)	46.0 (46.3)	4.2 (3.9)
[MoCu( $\mu$ -CR)(CO) <sub>2</sub> ( $\eta$ -C <sub>5</sub> Me <sub>5</sub> ) <sub>2</sub> ] ( <b>8b</b> , blue)	60	1950 vs, 1856 s	60.3 (61.7)	6.7 (6.5)
[Mo( $\kappa^2$ -S <sub>2</sub> CR)(CO) <sub>2</sub> ( $\eta$ -C <sub>5</sub> Me <sub>5</sub> )] ( <b>9</b> , pink)	71	1952 vs, 1876 s	53.1 (53.8)	5.4 (5.2)

<sup>a</sup> Calculated values given in parentheses. <sup>b</sup> Data for dichloromethane solutions.

Me<sub>2</sub>-2,6)(CO)<sub>2</sub>(NC<sub>5</sub>H<sub>4</sub>Me-4)<sub>2</sub>Br]. The presence of a bromide ligand in the final product was initially surprising; however, this originates from the 1 equiv of lithium bromide present as a consequence of the lithium reagent synthesis. The  $\gamma$ -picoline ligand was chosen purely for spectroscopic (<sup>1</sup>H NMR) purposes.

Heating a solution of [W(=CC<sub>6</sub>H<sub>3</sub>Me<sub>2</sub>-2,6)(CO)<sub>2</sub>(NC<sub>5</sub>H<sub>4</sub>Me-4)<sub>2</sub>Br] and LiC<sub>5</sub>Me<sub>5</sub> in tetrahydrofuran leads to clean formation of the pentamethylcyclopentadienyl complex [W(=CC<sub>6</sub>H<sub>3</sub>Me<sub>2</sub>-2,6)(CO)<sub>2</sub>( $\eta$ -C<sub>5</sub>Me<sub>5</sub>)] (**1a**) in high yield. The molybdenum alkylidyne [Mo(=CC<sub>6</sub>H<sub>3</sub>Me<sub>2</sub>-2,6)(CO)<sub>2</sub>(L)] (L =  $\eta$ -C<sub>5</sub>Me<sub>5</sub> (**1b**),  $\eta^5$ -C<sub>9</sub>H<sub>7</sub> (**1c**)) are obtained in a similar manner from [Mo(=CC<sub>6</sub>H<sub>3</sub>Me<sub>2</sub>-2,6)(CO)<sub>2</sub>(NC<sub>5</sub>H<sub>4</sub>Me-4)<sub>2</sub>Br] and LiC<sub>5</sub>Me<sub>5</sub> or KC<sub>9</sub>H<sub>7</sub>, respectively, with the exception that the reactions proceed readily at room temperature. Data for the complexes **1a–c** are given in Tables 1 and 2 and are unremarkable. Indenyl(alkylidyne)molybdenum complexes have been prepared previously by hydrogen-transfer reactions of suitable  $\sigma$ , $\pi$ -vinyl precursors, a reaction clearly not applicable to the synthesis of arylmethylidyne complexes.<sup>6</sup>

The reactions of the complexes **1a–c** with trimethylphosphine were investigated in order to compare the results with those obtained previously and in view of the current interest in the formation of ketenyl complexes *via* alkylidyne–carbonyl coupling.<sup>7,8</sup> Typically, reaction of the compounds [M(=CR)(CO)<sub>2</sub>( $\eta$ -C<sub>5</sub>H<sub>5</sub>)] with phosphines leads to either simple substitution of a carbonyl ligand or formation of ketenyl ligands. In some cases the ketenyl complexes formed may be decarbonylated to give the phosphine-substituted product;<sup>9</sup> however, this is not generally the case.

Reaction of the compounds **1a** and **1b** with PMe<sub>3</sub> in tetrahydrofuran both lead to the  $\eta^2$ -ketenyl complexes [M{ $\eta^2$ -C(O)CC<sub>6</sub>H<sub>3</sub>Me<sub>2</sub>-2,6}(CO)(PMe<sub>3</sub>)( $\eta$ -C<sub>5</sub>Me<sub>5</sub>)] (M = W (**2a**), Mo (**2b**)), in contrast with the corresponding reaction of [W(=CC<sub>6</sub>H<sub>3</sub>Me<sub>2</sub>-2,6)(CO)<sub>2</sub>( $\eta$ -C<sub>5</sub>H<sub>5</sub>)] (**1c**), in which a mixture of [W(=CC<sub>6</sub>H<sub>3</sub>Me<sub>2</sub>-2,6)(CO)(PMe<sub>3</sub>)( $\eta$ -C<sub>5</sub>H<sub>5</sub>)] (**3c**) and [W{ $\eta^2$ -C(O)CC<sub>6</sub>H<sub>3</sub>Me<sub>2</sub>-2,6}(CO)(PMe<sub>3</sub>)( $\eta$ -C<sub>5</sub>H<sub>5</sub>)] (**2c**) is obtained. Excess phosphine fails to induce formation of a monodentate ketenyl complex, as has been observed in the reaction of [W(=CC<sub>6</sub>H<sub>4</sub>Me-4)(CO)<sub>2</sub>( $\eta$ -C<sub>5</sub>H<sub>5</sub>)] with excess PMe<sub>3</sub> to provide [W{C(CO)-C<sub>6</sub>H<sub>4</sub>Me-4}(CO)(PMe<sub>3</sub>)<sub>2</sub>( $\eta$ -C<sub>5</sub>H<sub>5</sub>)].<sup>10</sup> Surprisingly, heating **2a** in tetrahydrofuran results in loss of PMe<sub>3</sub> rather than CO, as might have been expected with re-formation of the dicarbonyl precursor **1a**.

Substitution reactions at metal centers ligated by the  $\eta^5$ -indenyl ligand are often faster than for analogous  $\eta$ -C<sub>5</sub>H<sub>5</sub> and  $\eta$ -C<sub>5</sub>Me<sub>5</sub> derivatives, this being the so-called "indenyl effect" attributed to transient coordinatively unsaturated  $\eta^3$ -indenyl species.<sup>11</sup> The reaction of **1c** with PMe<sub>3</sub> was therefore of interest. Treating **1c** with PMe<sub>3</sub> leads to rapid formation of the phosphine-substituted alkylidyne complex [Mo(=CC<sub>6</sub>H<sub>3</sub>Me<sub>2</sub>-2,6)(CO)(PMe<sub>3</sub>)( $\eta^5$ -C<sub>9</sub>H<sub>7</sub>)] (**3a**), with no evidence for the formation of ketenyl intermediates. Similarly, reaction of **1c** with trimethyl phosphite leads to [Mo(=CC<sub>6</sub>H<sub>3</sub>Me<sub>2</sub>-2,6)(CO){P(OMe)<sub>3</sub>}( $\eta^5$ -C<sub>9</sub>H<sub>7</sub>)] (**3b**). The related complex [Mo(=CC<sub>6</sub>H<sub>4</sub>OMe-2)(CO){P(OMe)<sub>3</sub>}( $\eta$ -C<sub>5</sub>H<sub>5</sub>)] (**3c**) may be prepared either by photolysis (12 h, low-power visible light) of [Mo(=CC<sub>6</sub>H<sub>4</sub>OMe-2)(CO)<sub>2</sub>( $\eta$ -C<sub>5</sub>H<sub>5</sub>)] in the presence of trimethyl phosphite or by reaction of

(9) Geoffroy, G. L.; Bassner, S. L. *Adv. Organomet. Chem.* **1988**, *28*, 1.

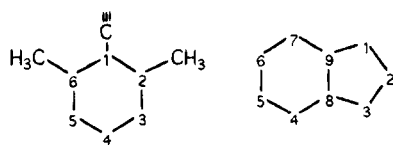
(10) Uedelhoven, W.; Eberl, K.; Kreissl, F. R. *Chem. Ber.* **1979**, *112*, 3376. Kreissl, F. R.; Friedrich, P.; Huttner, G. *Angew. Chem., Int. Ed. Engl.* **1977**, *16*, 102.

(11) O'Connor, J. M.; Casey, C. P. *Chem. Rev.* **1987**, *87*, 307.

(6) Allen, S. R.; Green, M.; Orpen, A. G.; Williams, I. D. *J. Chem. Soc., Chem. Commun.* **1982**, 826.

(7) Mayr, A.; Hofmeister, H. *Adv. Organomet. Chem.* **1992**, *32*, 227.

(8) Mayr, A.; Bastos, C. M. *Prog. Inorg. Chem.* **1992**, *40*, 1.

Table 2. Hydrogen-1 NMR Data<sup>a</sup> for the Complexes

compd	<sup>1</sup> H (δ)
<b>1a</b> (CDCl <sub>3</sub> )	2.19 [s, 15 H, C <sub>5</sub> Me <sub>5</sub> ], 2.46 [s, 6 H, C <sub>6</sub> H <sub>3</sub> Me <sub>2</sub> ], 6.87, 7.11 [m × 2, 3 H, C <sub>6</sub> H <sub>3</sub> Me <sub>2</sub> ]
<b>1b</b> (CD <sub>2</sub> Cl <sub>2</sub> )	2.06 [s, 15 H, C <sub>5</sub> Me <sub>5</sub> ], 2.53 [s, 6 H, C <sub>6</sub> H <sub>3</sub> Me <sub>2</sub> ], 6.85, 6.99 [m × 2, 3 H, C <sub>6</sub> H <sub>3</sub> Me <sub>2</sub> ]
<b>1c</b> (CDCl <sub>3</sub> )	2.48 [s, 6 H, C <sub>6</sub> H <sub>3</sub> Me <sub>2</sub> ], 5.89 [t, 1 H, H <sup>2</sup> (C <sub>9</sub> H <sub>7</sub> ), <i>J</i> (HH) 3.1 Hz], 6.15 [d, 2 H, H <sup>1,3</sup> (C <sub>9</sub> H <sub>7</sub> ), <i>J</i> (HH) 3.1 Hz], 6.86, 6.96, 7.42 [m × 3, 7 H, C <sub>6</sub> H <sub>4</sub> and C <sub>6</sub> H <sub>3</sub> ]
<b>2a</b> (CD <sub>2</sub> Cl <sub>2</sub> )	1.49 [d, 9 H, PMe <sub>3</sub> , <i>J</i> (PH) 9.2 Hz], 1.85 [s, 3 H, C <sub>6</sub> H <sub>3</sub> Me <sub>2</sub> ], 1.93 [s, 15 H, C <sub>5</sub> Me <sub>5</sub> ], 2.21 [s, 3 H, C <sub>6</sub> H <sub>3</sub> Me <sub>2</sub> ], 6.91, 7.02 [m × 2, 3 H, C <sub>6</sub> H <sub>3</sub> ]
<b>2b</b> (CD <sub>2</sub> Cl <sub>2</sub> )	1.38 [d, 9 H, PMe <sub>3</sub> , <i>J</i> (PH) 8.8 Hz], <i>ca</i> 1.78 [s(br), 3 H, C <sub>6</sub> H <sub>3</sub> Me <sub>2</sub> ], 1.82 [s, 15 H, C <sub>5</sub> Me <sub>5</sub> ], 2.17 [s(br), 3 H, C <sub>6</sub> H <sub>3</sub> Me <sub>2</sub> ], 6.96, 7.00 [m × 2, 3 H, C <sub>6</sub> H <sub>3</sub> ]
<b>3a</b> (CDCl <sub>3</sub> )	1.18 [d, 9 H, PMe <sub>3</sub> , <i>J</i> (PH) 8.4 Hz], 2.47 [s, 6 H, C <sub>6</sub> H <sub>3</sub> Me <sub>2</sub> ], 5.85 [d, 2 H, H <sup>1,3</sup> (C <sub>9</sub> H <sub>7</sub> ), <i>J</i> (HH) 2.8 Hz], 6.23 [t, 1 H, H <sup>2</sup> (C <sub>9</sub> H <sub>7</sub> ), <i>J</i> (HH) 3.11 Hz], 6.82, 6.8, 7.30 [m × 3, 7 H, C <sub>6</sub> H <sub>4</sub> and C <sub>6</sub> H <sub>3</sub> ]
<b>3b</b> (CDCl <sub>3</sub> )	2.51 [s, 6 H, C <sub>6</sub> H <sub>3</sub> Me <sub>2</sub> ], 3.22 [d, 9 H, POCH <sub>3</sub> , <i>J</i> (PH) 14 Hz], 5.84 [t, 1 H, H <sup>2</sup> (C <sub>9</sub> H <sub>7</sub> ), <i>J</i> (HH) 3.1 Hz], 5.98, 6.22 [m × 2, 2 H, 2 H, H <sup>1,3</sup> (C <sub>9</sub> H <sub>7</sub> )], 6.82, 6.84, 6.91, 7.3–7.4 [m × 4, 7 H, C <sub>6</sub> H <sub>4</sub> and C <sub>6</sub> H <sub>3</sub> ]
<b>4</b> (CDCl <sub>3</sub> )	1.55 [s, 6 H, C <sub>6</sub> H <sub>3</sub> Me <sub>2</sub> ], 1.71 [s, 15 H, C <sub>5</sub> Me <sub>5</sub> ], 7.04 [m, 3 H, C <sub>6</sub> H <sub>3</sub> ]
<b>5</b> (CDCl <sub>3</sub> )	1.46 [s, 15 H, C <sub>5</sub> Me <sub>5</sub> ], 1.83, 1.92 [s × 2, 6 H, C <sub>6</sub> H <sub>3</sub> Me <sub>2</sub> ], 4.48, 5.24 [m × 2, 2 H, P <sub>2</sub> CH <sub>2</sub> ], 6.44, 6.69, 6.74, 7.00, 7.11, 7.36, 7.78 [m × 6, 23 H, C <sub>6</sub> H <sub>5</sub> and C <sub>6</sub> H <sub>3</sub> ]
<b>6</b> (CDCl <sub>3</sub> )	1.88 [s, 15 H, C <sub>5</sub> Me <sub>5</sub> ], 2.47, 2.63 [s × 2, 6 H, C <sub>6</sub> H <sub>3</sub> Me <sub>2</sub> ], 7.13 [m, 3 H C <sub>6</sub> H <sub>3</sub> ]
<b>8b</b> (CDCl <sub>3</sub> )	1.67 [s, 30 H, MoC <sub>5</sub> Me <sub>5</sub> and CuC <sub>5</sub> Me <sub>5</sub> ], 1.99 [s, 6 H, C <sub>6</sub> H <sub>3</sub> Me <sub>2</sub> ], 7.00 [m, 3 H, C <sub>6</sub> H <sub>3</sub> ]
<b>9</b> (CD <sub>2</sub> Cl <sub>2</sub> )	1.95 [s, 15 H, C <sub>5</sub> Me <sub>5</sub> ], 2.00, 2.27 [s × 2, 6 H, C <sub>6</sub> H <sub>3</sub> Me <sub>2</sub> ], 7.02, 7.12 [m × 2, 3 H, C <sub>6</sub> H <sub>3</sub> ]

<sup>a</sup> Chemical shifts (δ) in ppm, coupling constants in Hz, measurements at room temperature.

[Mo(≡CC<sub>6</sub>H<sub>4</sub>OMe-2)Cl(CO){P(OMe)<sub>3</sub>}]<sub>3</sub> with sodium cyclopentadienide. The formation of the simple phosphite substitution complex **3c** by photolysis is itself somewhat unusual, since Geoffroy has shown that ketenyl complexes are usually the photoproducts in related systems.<sup>9</sup> These transformations are summarized in Scheme 1.

The reactions of complex **1b** with metal–ligand fragments were addressed next. As mentioned above, permethylation of the cyclopentadienyl ligand or the 2,6-positions of the arylmethylidyne ligand in the complex [W(≡C–aryl)(CO)<sub>2</sub>(η-C<sub>5</sub>H<sub>5</sub>)] introduces considerable steric congestion into the tungsten coordination sphere.<sup>2,3</sup> This is manifest in the reactions of [W(≡CC<sub>6</sub>H<sub>4</sub>Me-4)(CO)<sub>2</sub>(η-C<sub>5</sub>Me<sub>5</sub>)],<sup>3</sup> where treatment with coordinatively unsaturated metal–ligand fragment precursors lead in general to complexes of lower nuclearity than do those reactions involving the analogous cyclopentadienyl derivatives.

Reaction of **1b** with [Fe<sub>2</sub>(CO)<sub>9</sub>] leads to exclusive formation of the 32-valence-electron bimetallic complex [MoFe(μ-CC<sub>6</sub>H<sub>3</sub>Me<sub>2</sub>-2,6)(CO)<sub>5</sub>(η-C<sub>5</sub>Me<sub>5</sub>)] (**4a**). Most conspicuous among the spectroscopic data for such a complex<sup>2</sup> is the abnormally low field shift in the <sup>13</sup>C resonance due to the bridging carbyne carbon nucleus. This has been interpreted<sup>3</sup> by reference to similar downfield shifts observed in the <sup>13</sup>C NMR data for coordinatively unsaturated complexes of alkynes which have been extensively documented by Templeton and co-workers.<sup>12</sup> Such a low-field resonance is observed for **4a** at δ 404.2 ppm. The formal coordinative unsaturation of **4a** is reflected in its reactions with bis(diphenylphosphino)methane (dppm) and elemental selenium to provide respectively [Fe(μ-CC<sub>6</sub>H<sub>3</sub>Me<sub>2</sub>-2,6)(CO)<sub>3</sub>(μ-

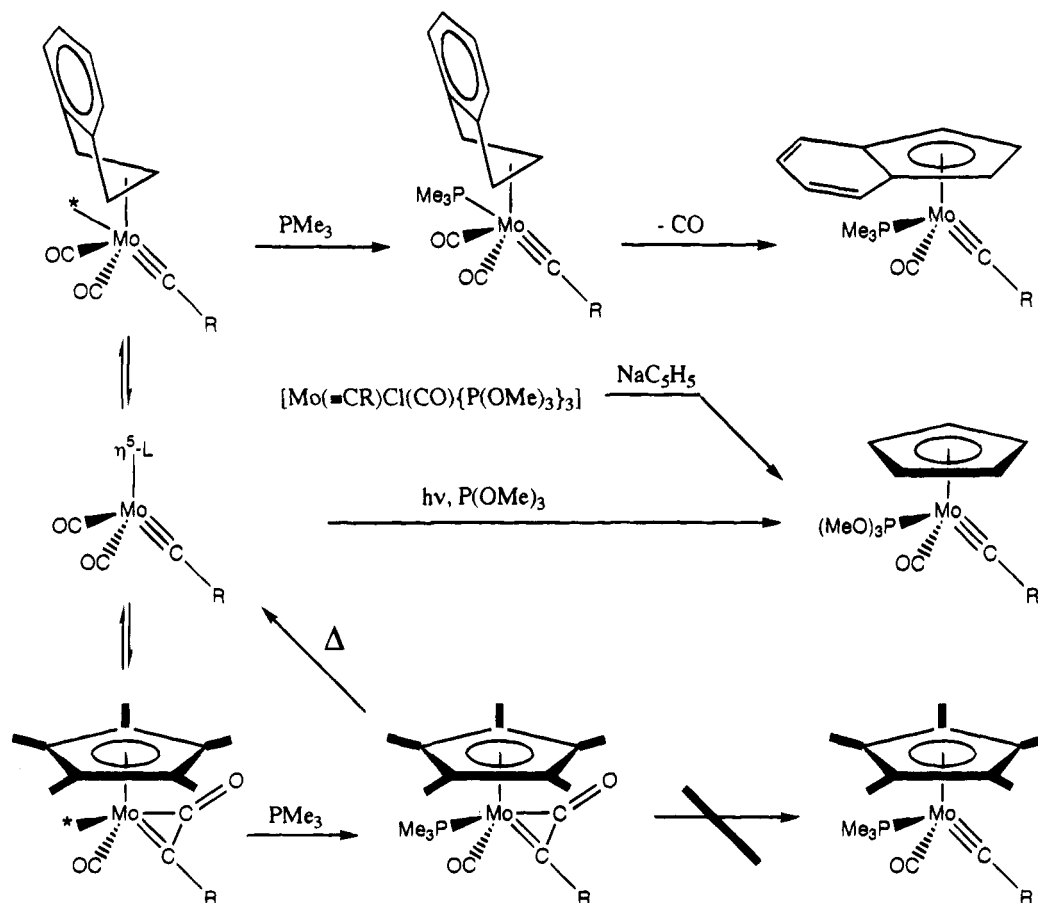
dppm)(η-C<sub>5</sub>Me<sub>5</sub>)] (**5**) and [Fe(μ-η<sup>2</sup>-SeCC<sub>6</sub>H<sub>3</sub>Me<sub>2</sub>-2,6)(CO)<sub>5</sub>(η-C<sub>5</sub>Me<sub>5</sub>)] (**6**), which are analogous to derivatives of the simple cyclopentadienyl-ligated compounds.<sup>2a,13,14</sup>

A departure in the reactivity of **1b** from that of [M(≡CC<sub>6</sub>H<sub>4</sub>Me-4)(CO)<sub>2</sub>(η-C<sub>5</sub>H<sub>5</sub>)], which is clearly steric in origin, is observed in its reaction with the “Cu(η-C<sub>5</sub>Me<sub>5</sub>)” transfer reagent obtained from CuCl and LiC<sub>5</sub>Me<sub>5</sub> in tetrahydrofuran.<sup>15</sup> This reagent (presumably [Cu(thf)(η-C<sub>5</sub>Me<sub>5</sub>)] reacts with [W(≡CC<sub>6</sub>H<sub>4</sub>Me-4)(CO)<sub>2</sub>(η-C<sub>5</sub>H<sub>5</sub>)] to provide the trimetallic complex [WCu<sub>2</sub>(μ<sub>3</sub>-CC<sub>6</sub>H<sub>4</sub>Me-4)(CO)<sub>2</sub>(η-C<sub>5</sub>H<sub>5</sub>)(η-C<sub>5</sub>Me<sub>5</sub>)<sub>2</sub>] (**7**), with no evidence being obtained for the presumed transient intermediate bimetallic complex [WCu(μ-CC<sub>6</sub>H<sub>4</sub>Me-4)(CO)<sub>2</sub>(η-C<sub>5</sub>H<sub>5</sub>)(η-C<sub>5</sub>Me<sub>5</sub>)] (**8a**). Such a complex is, however, isolated in the reaction of **1b** with the transfer reagent. The deep blue species [WCu(μ-CC<sub>6</sub>H<sub>3</sub>Me<sub>2</sub>-2,6)(CO)<sub>2</sub>(η-C<sub>5</sub>H<sub>5</sub>)(η-C<sub>5</sub>Me<sub>5</sub>)] (**8b**) is the only product isolated from this reaction even when the organocopper reagent is used in excess. The presence of a carbyne group bridging two metals is supported by the low-field shift of the carbyne carbon resonance (δ 319.2 ppm), which is considerably lower than that for **7** which is observed at δ 275.5 ppm. Infrared data for the carbonyl ligands (ν(CO) 1950, 1856 cm<sup>-1</sup>) suggest that one of these adopts a semibridging role, partially alleviating the excessive electron density at the electron-rich d<sup>10</sup> (formally) copper center. <sup>13</sup>C NMR data, however, indicate that the terminal and semibridging carbonyls interchange in solution (single resonance at δ 228.5 ppm).

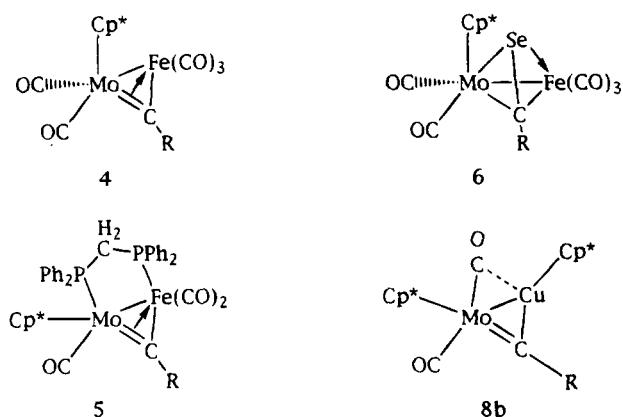
(13) Byrne, P.; Garcia, M. E.; Jeffery, J. C.; Sherwood, P.; Stone, F. G. A. *J. Chem. Soc., Dalton Trans.* **1987**, 1215.

(14) Hill, A. F.; Nasir, B. A.; Stone, F. G. A. *Polyhedron* **1989**, *8*, 179.

(15) Carriedo, G. A.; Howard, J. A. K.; Stone, F. G. A. *J. Chem. Soc., Dalton Trans.* **1984**, 1555; *J. Organomet. Chem.* **1983**, *250*, C28.

Scheme 1. Ligand Substitution via Ketenyl Formation or Indenyl Ring Slippage<sup>a</sup>

<sup>a</sup> L = C<sub>5</sub>H<sub>5</sub>, C<sub>5</sub>Me<sub>5</sub>, C<sub>9</sub>H<sub>7</sub>; \* = vacant coordination site.

Chart 2. Alkyldiene-Bridged Bimetallic Complexes<sup>a</sup>

<sup>a</sup> R = C<sub>6</sub>H<sub>3</sub>Me<sub>2</sub>-2,6; Cp\* = η<sup>5</sup>-C<sub>5</sub>Me<sub>5</sub>.

Two different types of ligands result from the reactions of terminal carbyne complexes with elemental sulfur. The electron-rich osmium carbyne [Os(≡CC<sub>6</sub>H<sub>4</sub>Me-4)Cl(CO)(PPh<sub>3</sub>)<sub>2</sub>] reacts to provide the thiobenzoyl complex [Os(η<sup>2</sup>-SCC<sub>6</sub>H<sub>4</sub>Me-4)Cl(CO)(PPh<sub>3</sub>)<sub>2</sub>],<sup>16</sup> which fails to react with further sulfur. In contrast, the half-sandwich carbyne complex [W(≡CC<sub>6</sub>H<sub>4</sub>Me-4)(CO)<sub>2</sub>(η-C<sub>5</sub>H<sub>5</sub>)] reacts with either sulfur or selenium to provide the dithio- or diselenobenzoyl complexes [W(κ<sup>2</sup>-A<sub>2</sub>-CC<sub>6</sub>H<sub>4</sub>Me-4)(CO)<sub>2</sub>(η-C<sub>5</sub>H<sub>5</sub>)] (A = S, Se).<sup>17</sup> Employing a deficiency of chalcogen fails to lead to any isolable

chalcogenoacyl complex of the form [W(η<sup>2</sup>-ACC<sub>6</sub>H<sub>4</sub>Me-4)(CO)<sub>2</sub>(η-C<sub>5</sub>H<sub>5</sub>)]. It seemed reasonable that steric pressures might partially explain this dichotomy of reactivity; however, this appears not to be the case. Reaction of **1b** with sulfur leads exclusively to the pink dithiobenzoyl complex [Mo(κ<sup>2</sup>-S<sub>2</sub>CC<sub>6</sub>H<sub>3</sub>Me<sub>2</sub>-2,6)(CO)<sub>2</sub>(η-C<sub>5</sub>Me<sub>5</sub>)] (**9**), spectroscopic data for which are completely analogous to those reported for [Mo(κ<sup>2</sup>-S<sub>2</sub>CC<sub>6</sub>H<sub>4</sub>Me-4)(CO)<sub>2</sub>(η-C<sub>5</sub>H<sub>5</sub>)].<sup>17</sup> It therefore appears likely that electronic, rather than steric, effects determine the outcome of this reaction.

## Experimental Section

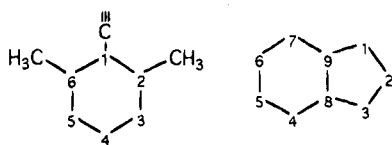
**General Procedures.** All manipulations were carried out under an atmosphere of prepurified dinitrogen using conventional Schlenk-tube techniques. Solvents were purified by distillation from an appropriate drying agent (ethers and paraffins from sodium/potassium alloy with benzophenone as indicator; halocarbons from CaH<sub>2</sub>). <sup>1</sup>H, <sup>13</sup>C{<sup>1</sup>H}, and <sup>31</sup>P{<sup>1</sup>H} NMR spectra were recorded on either a JEOL GX270 or FX90 NMR spectrometer and calibrated against internal Me<sub>4</sub>Si (<sup>1</sup>H), internal CDCl<sub>3</sub> (<sup>13</sup>C), or external H<sub>3</sub>PO<sub>4</sub> (<sup>31</sup>P). Infrared spectra were recorded using a Perkin-Elmer 1720-X FT-IR spectrometer. Light petroleum ether refers to that fraction with bp 40–60 °C. Data for the new complexes are given in Tables 1–5.

[W(≡CC<sub>6</sub>H<sub>3</sub>Me<sub>2</sub>-2,6)(CO)<sub>2</sub>(η-C<sub>5</sub>Me<sub>5</sub>)] (**1a**). A solution of [W(≡CC<sub>6</sub>H<sub>3</sub>Me<sub>2</sub>-2,6)(CO)<sub>2</sub>(NC<sub>5</sub>H<sub>4</sub>Me-4)<sub>2</sub>Br] (10.0 g, 15.2 mmol) in tetrahydrofuran (100 cm<sup>3</sup>) was treated with LiC<sub>5</sub>Me<sub>5</sub> (2.84 g, 20.0 mmol; from MeLi and C<sub>5</sub>Me<sub>5</sub>H) and heated under reflux

(16) Clark, G. R.; Marsden, K.; Roper, W. R.; Wright, L. *J. Am. Chem. Soc.* **1980**, *102*, 6570.

(17) Gill, D. S.; Green, M.; Marsden, K.; Moore, I.; Orpen, A. G.; Stone, F. G. A.; Williams, I. D.; Woodward, P. *J. Chem. Soc., Dalton Trans.* **1984**, 1343.



Table 3. Carbon-13 NMR Data<sup>a</sup> for the Complexes

compd	<sup>13</sup> C (δ)
<b>1a</b> (CDCl <sub>3</sub> )	299.9 [W≡C, <i>J</i> (WC) 212 Hz], 226.4 [WCO, <i>J</i> (WC) 195 Hz], 147.8 [C <sup>1</sup> (C <sub>6</sub> H <sub>3</sub> ), <i>J</i> (WC) 38 Hz], 139.1, 127.8, 127.1 [C <sup>2-6</sup> (C <sub>6</sub> H <sub>3</sub> )], 104.4 [C <sub>5</sub> Me <sub>5</sub> ], 20.6 [C <sub>6</sub> H <sub>3</sub> Me <sub>2</sub> ], 11.2 [C <sub>5</sub> Me <sub>5</sub> ]
<b>1b</b> (CD <sub>2</sub> Cl <sub>2</sub> )	312.4 [Mo≡C], 234.1 [MoCO], 144.5 [C <sup>1</sup> (C <sub>6</sub> H <sub>3</sub> )], 140.5, 128.8, 127.5 [C <sup>2-6</sup> (C <sub>6</sub> H <sub>3</sub> )], 106.0 [C <sub>5</sub> Me <sub>5</sub> ], 20.8 [C <sub>6</sub> H <sub>3</sub> Me <sub>2</sub> ], 11.4 [C <sub>5</sub> Me <sub>5</sub> ]
<b>1c</b> (CDCl <sub>3</sub> )	312.5 [Mo≡C], 228.6 [MoCO], 144.0 [C <sup>1</sup> (C <sub>6</sub> H <sub>3</sub> )], 140.0, 128.8, 127.3 [C <sup>2-6</sup> (C <sub>6</sub> H <sub>3</sub> )], 124.3, 122.6 [C <sup>4-7</sup> (C <sub>9</sub> H <sub>7</sub> )], 117.3 [C <sup>8,9</sup> (C <sub>9</sub> H <sub>7</sub> )], 98.3 [C <sup>2</sup> (C <sub>9</sub> H <sub>7</sub> )], 78.3 [C <sup>1,3</sup> (C <sub>9</sub> H <sub>7</sub> )], 21.0 [C <sub>6</sub> H <sub>3</sub> Me <sub>2</sub> ]
<b>2a</b> (CD <sub>2</sub> Cl <sub>2</sub> )	231.9 [WOC(C <sub>6</sub> H <sub>3</sub> Me <sub>2</sub> ), <i>J</i> (PC) 8.5, <i>J</i> (WC) 167 Hz], 201.6 [WCO, <i>J</i> (PC) not resolved], 195.4 [WOC(C <sub>6</sub> H <sub>3</sub> Me <sub>2</sub> ), <i>J</i> (PC) not resolved, <i>J</i> (WC) 68 Hz], 141.7 [C <sup>1</sup> (C <sub>6</sub> H <sub>3</sub> )], 131.0, 129.6 [C <sup>2,6</sup> (C <sub>6</sub> H <sub>3</sub> )], 126.2, 125.7 [C <sup>3,5</sup> (C <sub>6</sub> H <sub>3</sub> )], 124.4 [C <sup>4</sup> (C <sub>6</sub> H <sub>3</sub> )], 105.0 [C <sub>5</sub> Me <sub>5</sub> ], 20.7, 20.1 [C <sub>6</sub> H <sub>3</sub> Me <sub>2</sub> ], 18.3 [d, PMe <sub>3</sub> , <i>J</i> (PC) 34 Hz], 10.0 [C <sub>5</sub> Me <sub>5</sub> ]
<b>2b</b> (CD <sub>2</sub> Cl <sub>2</sub> )	238.8 [MoOCC(C <sub>6</sub> H <sub>3</sub> Me <sub>2</sub> ), <i>J</i> (PC) 17.0 Hz], 213.4 [MoCO, <i>J</i> (PC) 8.5 Hz], 205.0 [MoOCC(C <sub>6</sub> H <sub>3</sub> Me <sub>2</sub> )], 141.2 [C <sup>1</sup> (C <sub>6</sub> H <sub>3</sub> )], 131.0, 129.2 [C <sup>2,6</sup> (C <sub>6</sub> H <sub>3</sub> )], 125.9 [C <sup>3,5</sup> (C <sub>6</sub> H <sub>3</sub> )], 124.4 [C <sup>4</sup> (C <sub>6</sub> H <sub>3</sub> )], 106.1 [C <sub>5</sub> Me <sub>5</sub> ], 20.5, 20.0 [C <sub>6</sub> H <sub>3</sub> Me <sub>2</sub> ], 17.2 [d, PMe <sub>3</sub> , <i>J</i> (PC) 30 Hz], 9.7 [C <sub>5</sub> Me <sub>5</sub> ]
<b>3b</b> (CDCl <sub>3</sub> )	302.4 [d, Mo≡C, <i>J</i> (PC) 28 Hz], 242.1 [d, MoCO, <i>J</i> (PC) 17.0 Hz], 143.7 [C <sup>1</sup> (C <sub>6</sub> H <sub>3</sub> )], 137.8, 126.1, 125.9 [C <sup>2-6</sup> (C <sub>6</sub> H <sub>3</sub> )], 122.4, 121.9, 121.7 [C <sup>4-7</sup> (C <sub>9</sub> H <sub>7</sub> )], 117.3, 115.3 [C <sup>8,9</sup> (C <sub>9</sub> H <sub>7</sub> )], 95.9 [C <sup>2</sup> (C <sub>9</sub> H <sub>7</sub> )], 75.8 [C <sup>1,3</sup> (C <sub>9</sub> H <sub>7</sub> )], 50.0 [POMe], 20.0 [C <sub>6</sub> H <sub>3</sub> Me <sub>2</sub> ]
<b>4</b> (CDCl <sub>3</sub> )	404.2 [MeFe(μ-C)], 236.0 [MoCO], 212.7 [FeCO], 158.5 [C <sup>1</sup> (C <sub>6</sub> H <sub>3</sub> )], 126.3 [C <sup>3,5</sup> (C <sub>6</sub> H <sub>3</sub> )], 124.8 [C <sup>4</sup> (C <sub>6</sub> H <sub>3</sub> )], 123.4 [C <sup>2,6</sup> (C <sub>6</sub> H <sub>3</sub> )], 107.8 [C <sub>5</sub> Me <sub>5</sub> ], 20.3 [C <sub>6</sub> H <sub>3</sub> Me <sub>2</sub> ], 9.0 [C <sub>5</sub> Me <sub>5</sub> ]
<b>5</b> (CDCl <sub>3</sub> )	376.6 [d, MoFe(μ-C)], 253.1 [d, MoFe(μ-CO)], 220.7, 217.7 [MoFe(CO) <sub>2</sub> ], 162.2 [C <sup>1</sup> (C <sub>6</sub> H <sub>3</sub> )], 140–123 [C <sub>6</sub> H <sub>5</sub> and C <sub>6</sub> H <sub>3</sub> ], 105.1 [C <sub>5</sub> Me <sub>5</sub> ], 43.7 [dd, P <sub>A</sub> P <sub>B</sub> CH <sub>2</sub> , <i>J</i> (PC) 15, 32 Hz], 23.1, 22.3 [C <sub>6</sub> H <sub>3</sub> Me <sub>2</sub> ], 10.3 [C <sub>5</sub> Me <sub>5</sub> ]
<b>6</b> (CDCl <sub>3</sub> )	231.8, 230.8 [MoCO], 211.9 [FeCO], 144.9 [C <sup>1</sup> (C <sub>6</sub> H <sub>3</sub> )], 136.6, 133.2 [C <sup>2,6</sup> (C <sub>6</sub> H <sub>3</sub> )], 129.4 [C <sup>3,5</sup> (C <sub>6</sub> H <sub>3</sub> )], 124.4 [C <sup>4</sup> (C <sub>6</sub> H <sub>3</sub> )], 103.4 [C <sub>5</sub> Me <sub>5</sub> ], 27.4, 23.1 [C <sub>6</sub> H <sub>3</sub> Me <sub>2</sub> ], 10.5 [C <sub>5</sub> Me <sub>5</sub> ]
<b>8b</b> (CDCl <sub>3</sub> )	319.2 [MoCu(μ-C)], 228.5 [MoCO], 154.7 [C <sup>1</sup> (C <sub>6</sub> H <sub>3</sub> )], 132.3 [C <sup>3,5</sup> (C <sub>6</sub> H <sub>3</sub> )], 128.0 [C <sup>2,6</sup> (C <sub>6</sub> H <sub>3</sub> )], 127.0 [C <sup>4</sup> (C <sub>6</sub> H <sub>3</sub> )], 107.5 [MoC <sub>5</sub> Me <sub>5</sub> ], 93.3 [CuC <sub>5</sub> Me <sub>5</sub> ], 21.8 [C <sub>6</sub> H <sub>3</sub> Me <sub>2</sub> ], 9.5 [CuC <sub>5</sub> Me <sub>5</sub> and MoC <sub>5</sub> Me <sub>5</sub> ]
<b>9</b> (CD <sub>2</sub> Cl <sub>2</sub> )	255.1 [MoCO], 237.7 [MoS <sub>2</sub> C], 150.3 [C <sup>1</sup> (C <sub>6</sub> H <sub>3</sub> )], 134.5, 128.8, 127.8, 127.6, 127.0 [C <sup>2-6</sup> (C <sub>6</sub> H <sub>3</sub> )], 106.4 [C <sub>5</sub> Me <sub>5</sub> ], 20.3 [C <sub>6</sub> H <sub>3</sub> Me <sub>2</sub> ], 11.3 [C <sub>5</sub> Me <sub>5</sub> ]

<sup>a</sup> Chemical shifts (δ) in ppm, coupling constants in Hz, measurements at room temperature in CDCl<sub>3</sub>. Spectra are hydrogen-1 decoupled; chemical shifts are positive to high frequency of SiMe<sub>4</sub>.

Table 4. Mass Spectral Data for Selected Complexes

compd	<i>m/z</i> (%) [assignt]
<b>1a</b>	492 (57) [M] <sup>+</sup> , 436 (100) [M - 2CO] <sup>+</sup>
<b>1b</b>	406 [M] <sup>+</sup> , 378 [M - CO] <sup>+</sup> , 438 [M - 2CO] <sup>+</sup>
<b>2a</b>	524 (1.9) [W(HPC(C <sub>6</sub> H <sub>3</sub> Me <sub>2</sub> )(CO) <sub>2</sub> (C <sub>5</sub> Me <sub>5</sub> )) <sup>+</sup> ], 451 (5.7) [W(CO) <sub>2</sub> (PMe <sub>3</sub> )(C <sub>5</sub> Me <sub>5</sub> ) <sup>+</sup> ], 423 (3.3) [W(CO)(PMe <sub>3</sub> )(C <sub>5</sub> Me <sub>5</sub> ) <sup>+</sup> ]
<b>4</b>	406 (34) [M - 5CO] <sup>+</sup> , 406 (100) [M - Fe - 5CO] <sup>+</sup>
<b>5</b>	734 (3.2) [M - Fe - 3CO] <sup>+</sup>
<b>6</b>	624 (3.5) [M] <sup>+</sup> , 566 (2.8) [M - 2CO] <sup>+</sup> , 542 (11.2) [M - 3CO] <sup>+</sup> , 512 (7.6) [M - 4CO] <sup>+</sup>
<b>8b</b>	604 (3.0) [M] <sup>+</sup> , 546 (0.9) [M - 2CO] <sup>+</sup> , 469 (3.5) [M - C <sub>5</sub> Me <sub>5</sub> ] <sup>+</sup> , 438 (2.2) [M - C <sub>5</sub> Me <sub>5</sub> - CO] <sup>+</sup> , 413 (34.1) [M - C <sub>5</sub> Me <sub>5</sub> - 2CO] <sup>+</sup> , 348 [Mo(CC <sub>6</sub> H <sub>3</sub> Me <sub>2</sub> )(C <sub>5</sub> Me <sub>5</sub> ) <sup>+</sup> ]
<b>9</b>	470 (27.0) [M] <sup>+</sup> , 414 (100) [M - 2CO] <sup>+</sup> , 380 (14.9) [M - S - 2CO] <sup>+</sup> , 264 (54.4) [MoSC <sub>5</sub> Me <sub>5</sub> ] <sup>+</sup>

Table 5. Phosphorus-31 NMR Data<sup>a</sup> for the Complexes

compd	<sup>31</sup> P (δ)
<b>2a</b>	-16.6 [ <i>J</i> (WP) 397 Hz]
<b>2b</b>	9.6
<b>3a</b>	12.7
<b>3b</b>	198.4
<b>5</b>	41.0 [ <i>J</i> (AB) 76 Hz] 48.2

<sup>a</sup> Chemical shifts (δ) in ppm, coupling constants in Hz, measurements at room temperature in CDCl<sub>3</sub>. Spectra are hydrogen-1 decoupled; chemical shifts are positive to high frequency of H<sub>3</sub>PO<sub>4</sub>.

for 5 h. After the mixture was cooled to room temperature, the solvent was removed under reduced pressure and the residue extracted with a mixture of dichloromethane and light petroleum ether (1:2) and the combined extracts chromatographed on a cryostatally cooled (-40 °C) column loaded with

silica gel. Elution with dichloromethane developed a red band, which was freed of solvent in vacuo. The residue was then crystallized from light petroleum ether; yield 5.02 g (67%).

Similar procedures were used for the molybdenum complexes **1b** and **1c**, except that the reaction mixture was not heated but rather, stirred for 18 h. Reaction of [Mo(≡CC<sub>6</sub>H<sub>3</sub>-Me<sub>2</sub>-2,6)(CO)<sub>2</sub>(NC<sub>5</sub>H<sub>4</sub>Me-4)<sub>2</sub>Br] with LiC<sub>5</sub>Me<sub>5</sub> and KC<sub>9</sub>H<sub>7</sub> (from potassium and indene) provided the compounds **1b** (yield 4.98 g (70%)) and **1c** (yield 4.26 g (63%)).

[W(η<sup>2</sup>-OCC(C<sub>6</sub>H<sub>3</sub>Me<sub>2</sub>-2,6)(CO)(PMe<sub>3</sub>)(η<sup>-</sup>C<sub>5</sub>Me<sub>5</sub>)] (**2a**). A solution of **1a** (1.00 g, 2.03 mmol) in diethyl ether (20 cm<sup>3</sup>) was treated with PMe<sub>3</sub> (0.20 g, 2.63 mmol) and the mixture stirred for 12 h. The solvent was removed under reduced pressure and the residue crystallized from a mixture of dichloromethane and light petroleum ether (1:3) at -20 °C; yield 0.97 g (84%). Analogous treatment of **1b** provided **2b**; yield 0.95 g (80%).

[Mo(≡CC<sub>6</sub>H<sub>3</sub>Me<sub>2</sub>-2,6)(CO)(PMe<sub>3</sub>)(η<sup>5</sup>-C<sub>9</sub>H<sub>7</sub>)] (**3a**). A solu-

tion of **1c** (1.00 g, 2.06 mmol) in diethyl ether (20 cm<sup>3</sup>) was treated with PMe<sub>3</sub> (0.20 g, 2.63 mmol) and the mixture was stirred for 6 h. The solvent was removed in vacuo and the residue extracted with a mixture of dichloromethane and light petroleum ether (1:2), and the combined extracts were chromatographed on a cryostatically cooled (−40 °C) column loaded with silica gel. Elution with a mixture of dichloromethane and light petroleum ether (1:2) developed an orange band which was freed of solvent in vacuo. The residue was then crystallized from light petroleum ether; yield 0.74 g (62%). Similar treatment of **1c** with P(OMe)<sub>3</sub> provided **3b** (yield 0.87 g (66%)).

**[MoFe(μ-CC<sub>6</sub>H<sub>3</sub>Me<sub>2</sub>-2,6)(CO)<sub>5</sub>(η-C<sub>5</sub>Me<sub>5</sub>)] (4)**. A mixture of compound **1b** (2.00 g, 4.94 mmol) and [Fe<sub>2</sub>(CO)<sub>9</sub>] (3.64 g, 10 mmol) in THF (50 cm<sup>3</sup>) was stirred for 12 h and then freed of solvent and [Fe(CO)<sub>5</sub>] (*Caution!*) in vacuo. The black residue was dissolved in CH<sub>2</sub>Cl<sub>2</sub> (10 cm<sup>3</sup>), light petroleum ether (10 cm<sup>3</sup>) was added, and the solution was chromatographed on an alumina-loaded cryostatically cooled (−20 °C) column. Elution with the same solvent mixture removed a yellow zone ([Fe(CO)<sub>5</sub>] and a green zone ([Fe<sub>3</sub>(CO)<sub>12</sub>]), which were discarded. Further elution provided a violet fraction from which solvent was slowly removed in vacuo to provide deep violet microcrystals, yield 1.35 g (61%).

**[MoFe(μ-CC<sub>6</sub>H<sub>3</sub>Me<sub>2</sub>-2,6)(CO)<sub>3</sub>(μ-dppm)(η-C<sub>5</sub>Me<sub>5</sub>)] (5)**. A solution of **4** (1.00 g, 1.84 mmol) in diethyl ether (30 cm<sup>3</sup>) was treated with dppm (0.71 g, 1.84 mmol) and the mixture stirred for 10 h, by which time a deep green precipitate had formed. This was isolated by filtration, washed with light petroleum ether, and dried in vacuo; yield 1.43 g (89%).

**[MoFe(μ-η<sup>2</sup>-SeCC<sub>6</sub>H<sub>3</sub>Me<sub>2</sub>-2,6)(CO)<sub>5</sub>(η-C<sub>5</sub>Me<sub>5</sub>)] (6)**. A solution of **4** (0.50 g, 0.92 mmol) in diethyl ether (50 cm<sup>3</sup>) was

treated with elemental black selenium (0.3 g, excess) and the mixture stirred rapidly for 1 day. The solution was filtered through a plug of diatomaceous earth and then freed of solvent under reduced pressure. The residue was extracted twice with a mixture of CH<sub>2</sub>Cl<sub>2</sub> (6 cm<sup>3</sup>) and light petroleum ether (14 cm<sup>3</sup>). The combined extracts were chromatographed on a water-cooled column with the same solvent mixture as eluent. The major orange band was collected and reduced to ca. 4 cm<sup>3</sup> in vacuo and cooled to −78 °C to provide orange microcrystals of **6**, yield 0.48 g (83%).

**[MoCu(μ-CC<sub>6</sub>H<sub>3</sub>Me<sub>2</sub>-2,6)(CO)<sub>2</sub>(η-C<sub>5</sub>Me<sub>5</sub>)<sub>2</sub>] (8b)**. A solution of "Cu(η-C<sub>5</sub>Me<sub>5</sub>)" (0.50 mmol) in THF prepared according to the literature procedure at −80 °C<sup>15</sup> was treated with **1b** (1.00 g, 0.25 mmol) and the mixture stirred at −80 °C for 24 h and then warmed to room temperature. The solvent was removed in vacuo and the residue extracted with a mixture of dichloromethane and light petroleum ether (1:3). The combined extracts were chromatographed on a cryostatically cooled (−20 °C) column loaded with silica gel. The deep blue band was collected and freed of solvent under reduced pressure. The residue was then crystallized from light petroleum ether at −78 °C; yield 0.90 g (60%).

**Acknowledgment.** We are grateful to Professor F. G. A. Stone for guidance and the generous provision of research facilities at the University of Bristol. We thank the Royal Society and the SERC (U.K.) for support and for a research studentship (to S.A.)

OM950060R

# Early Metal Carborane Chemistry. Generation and Reactivity of $(C_5Me_5)(\eta^5-C_2B_9H_{11})TiMe$

Carsten Kreuder and Richard F. Jordan\*

Department of Chemistry, University of Iowa, Iowa City, Iowa 52242

Hongming Zhang

Department of Chemistry, Southern Methodist University, Dallas, Texas 75275

Received March 21, 1995<sup>®</sup>

The methane elimination reaction of  $Cp^*TiMe_3$  ( $Cp^* = C_5Me_5$ ) and  $C_2B_9H_{13}$  yields the thermally sensitive titanacarborane  $(Cp^*)(\eta^5-C_2B_9H_{11})TiMe$  (**4**), which has been characterized by  $^1H$ ,  $^{13}C$ , and  $^{11}B$  NMR spectroscopy. Complex **4** decomposes at 23 °C to the fulvene complex  $(\eta^6-C_5Me_4CH_2)(\eta^5-C_2B_9H_{11})Ti$  (**5**, 30% isolated) and forms labile adducts with  $PMe_3$  and THF. Complex **4** inserts  $CH_3CN$ , yielding  $(Cp^*)(\eta^5-C_2B_9H_{11})Ti(N=CMe_2)(MeCN)$  (**7**), which loses  $MeCN$  upon recrystallization from toluene to afford  $(Cp^*)(\eta^5-C_2B_9H_{11})(Ti(N=CMe_2))$  (**8**). X-ray diffraction analyses establish that **7** and **8** adopt monomeric bent metallocene structures with  $\eta^5-C_2B_9H_{11}$  ligands. Data for **7**: space group  $P\bar{1}$ ,  $a = 9.588(6)$  Å,  $b = 9.940(4)$  Å,  $c = 13.034(5)$  Å,  $\alpha = 96.69(3)^\circ$ ,  $\beta = 97.13(4)^\circ$ ,  $\gamma = 96.70(4)^\circ$ ,  $V = 1213(1)$  Å<sup>3</sup>,  $Z = 2$ ,  $R = 0.081$ ,  $R_w = 0.091$ . Data for **8**: space group  $C2/c$ ,  $a = 23.058(7)$  Å,  $b = 13.042(6)$  Å,  $c = 15.411(6)$  Å,  $\beta = 118.66(3)^\circ$ ,  $V = 4179(3)$  Å<sup>3</sup>,  $Z = 8$ ,  $R = 0.088$ ,  $R_w = 0.088$ . Complex **4** also inserts 2-butyne, yielding  $(Cp^*)(\eta^5-C_2B_9H_{11})Ti(CMe=CMe_2)$  (**9**). The reaction of **4** with ethylene yields propene and  $(Cp^*)(\eta^5-C_2B_9H_{11})TiEt$  (**10**), which adopts a  $\beta$ -agostic structure. The  $^{11}B$  NMR spectra of **4–10** are similar and indicate that all of these compounds have bent metallocene structures analogous to those established crystallographically for **7** and **8**. Complex **10** catalyzes the slow dimerization of ethylene to 1-butene; this contrasts with the ethylene polymerization catalysis observed for the analogous  $d^0$  metallocenes  $Cp^*_2ScR$  and  $Cp^*_2Ti(R)^+$ .

## Introduction

We recently described the synthesis and reactivity of a new class of zirconium and hafnium carborane complexes of stoichiometry  $[(Cp^*)(C_2B_9H_{11})M(Me)]_n$  (**1a**,  $M = Zr$ ; **1b**,  $M = Hf$ ;  $Cp^* = \eta^5-C_5Me_5$ ) which contain  $C_2B_9H_{11}^{2-}$  (dicarbollide) ligands.<sup>1</sup> These species insert 2-butyne, yielding  $(Cp^*)(\eta^5-C_2B_9H_{11})M(CMe=CMe_2)$  alkene complexes (**2a,b**), and undergo thermal elimination of methane, yielding bridged methylene complexes  $[(Cp^*)(\eta^5-C_2B_9H_{11})M]_2(\mu-CH_2)$  (**3a,b**). Zirconium complexes **2a** and **3a** have been shown by X-ray crystallography to adopt bent-metallocene structures in which the dicarbollide ligands bind in an  $\eta^5$ -manner. Thus, these compounds are isostructural and isolobal with  $(C_5R_5)_2M(R)$  ( $M = \text{group 3, lanthanide}$ )<sup>2</sup> and  $(C_5R_5)_2M(R)^+$  ( $M = \text{group 4, actinide}$ ) species<sup>3</sup> and provide an opportunity to probe the influence of metal charge on reactivity. The structures of **1a,b** have not yet been

fully elucidated.<sup>4</sup> Several other early metal and f-element carborane complexes with bent-metallocene structures have also been prepared.<sup>5,6</sup>

We are interested in extending our studies of the  $(Cp^*)(C_2B_9H_{11})M(X)$  system to titanium dicarbollide species  $(Cp^*)(\eta^5-C_2B_9H_{11})Ti(R)$ , because the smaller metal radius should favor monomeric structures which may simplify the chemistry. Additionally, it is of interest to compare the reactivity of  $(Cp^*)(C_2B_9H_{11})Ti(R)$  species to that of related  $d^0$  first-row metal complexes, i.e.,  $(C_5R_5)_2Sc(R)^{4b,7}$  and  $(C_5R_5)_2Ti(R)^+^{8,9}$ . Here we describe the generation and reactivity of the simplest

(3) (a) Jordan, R. F. *Adv. Organomet. Chem.* **1991**, *32*, 325. (b) Hlatky, G. G.; Turner, H. W.; Eckman, R. R. *J. Am. Chem. Soc.* **1989**, *111*, 2728. (c) Hlatky, G. G.; Eckman, R. R.; Turner, H. W. *Organometallics* **1992**, *11*, 1413. (d) Marks, T. J. *Acc. Chem. Res.* **1992**, *25*, 57.

(4) NMR data indicate that **1a,b** adopt unsymmetrical dimeric structures.

(5) Group 3: (a) Bazan, G. C.; Schaefer, W. P.; Bercaw, J. E. *Organometallics* **1993**, *12*, 2126. (b) Marsh, R. E.; Schaefer, W. P.; Bazan, G. C.; Bercaw, J. E. *Acta Crystallogr.* **1992**, *C48*, 1416. Group 5: (c) Uhrhammer, R.; Crowther, D. J.; Olson, J. D.; Swenson, D. C.; Jordan, R. F. *Organometallics* **1992**, *11*, 3098. (d) Uhrhammer, R.; Su, Y.; Swenson, D. C.; Jordan, R. F. *Inorg. Chem.* **1994**, *33*, 4398. (e) Fronczek, F. R.; Halstead, G. W.; Raymond, K. N. *J. Am. Chem. Soc.* **1977**, *99*, 1769. (f) Manning, M. J.; Knobler, C. B.; Khattar, R.; Hawthorne, M. F. *Inorg. Chem.* **1991**, *30*, 2009. See also: (g) Oki, A. R.; Zhang, H.; Hosmane, N. S. *Organometallics* **1991**, *10*, 3964. (h) Siriwardane, U.; Zhang, H.; Hosmane, N. S. *J. Am. Chem. Soc.* **1990**, *112*, 9637. (i) Zhang, H.; Jia, L.; Hosmane, N. S. *Acta Crystallogr.* **1993**, *C49*, 453. (j) Houseknecht, K. L.; Stockman, K. E.; Sabat, M.; Finn, M. G.; Grimes, R. N. *J. Am. Chem. Soc.* **1995**, *117*, 1163.

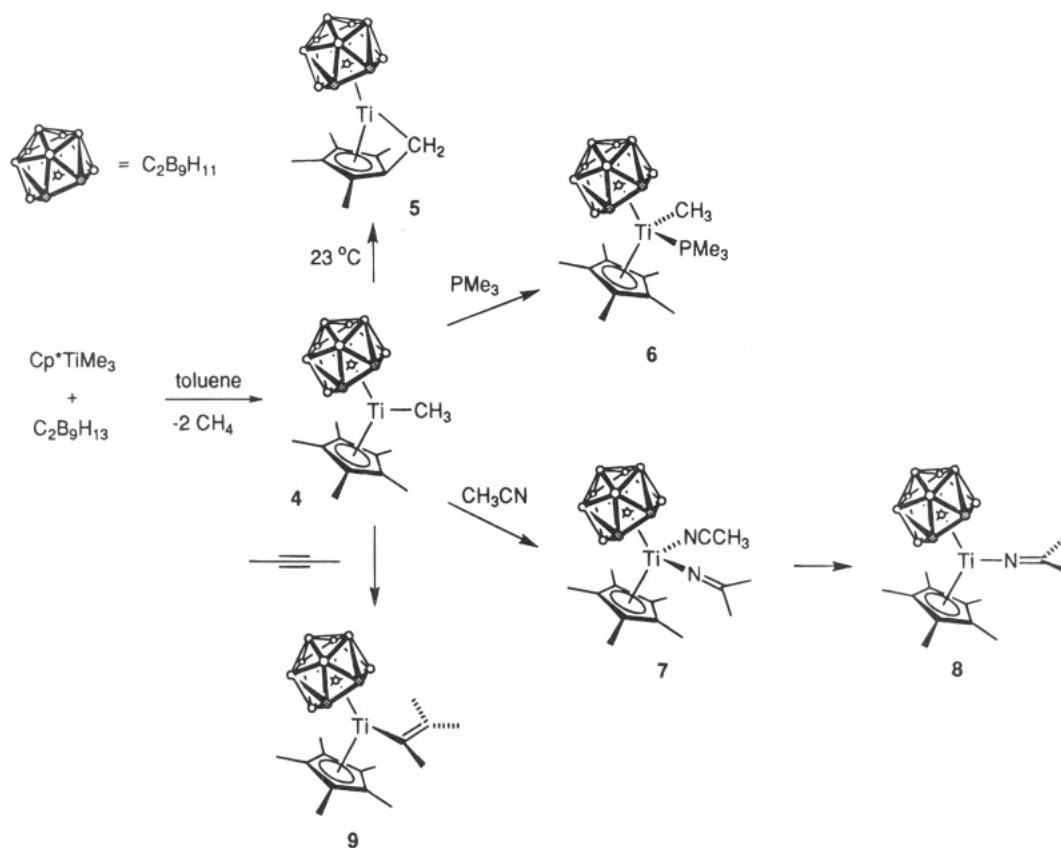
(6) For a recent review see: Saxena, A. K.; Hosmane, N. S. *Chem. Rev.* **1993**, *93*, 1081.

<sup>®</sup> Abstract published in *Advance ACS Abstracts*, June 1, 1995.

(1) (a) Crowther, D. J.; Baenziger, N. C.; Jordan, R. F. *J. Am. Chem. Soc.* **1991**, *113*, 1455. (b) Crowther, D. J.; Jordan, R. F. *Makromol. Chem., Macromol. Symp.* **1993**, *66*, 121. (c) Jordan, R. F. New Organometallic Models for Ziegler-Natta Catalysts. In *Proceedings of the World Metalocene Conference*; Catalyst Consultants Inc.: Spring House, PA, 1993; pp 89–96.

(2) Leading references: (a) Watson, P. L.; Parshall, G. W. *Acc. Chem. Res.* **1985**, *18*, 51. (b) Thompson, M. E.; Bercaw, J. E. *Pure Appl. Chem.* **1984**, *56*, 1. (c) Jeske, G.; Lauke, H.; Mauermann, H.; Sweptson, P. N.; Schumann, H.; Marks, T. J. *J. Am. Chem. Soc.* **1985**, *107*, 8091. (d) Booi, M.; Deelman, B. J.; Duchateau, R.; Postma, D. S.; Meetsma, A.; Teuben, J. H. *Organometallics* **1993**, *12*, 3531. (e) Schumann, H. *Angew. Chem., Int. Ed. Engl.* **1984**, *23*, 474. (f) Evans, W. J. *Adv. Organomet. Chem.* **1985**, *24*, 131. (g) Schaverien, C. J. *Adv. Organomet. Chem.* **1994**, *36*, 283.

Scheme 1



member of this series,  $(\text{Cp}^*)(\eta^5\text{-C}_2\text{B}_9\text{H}_{11})\text{Ti}(\text{Me})$ . Earlier, Hawthorne and co-workers described the synthesis of several classes of titanacarboranes which adopt sandwich structures, including  $\text{Ti}(\eta^6\text{-R}_2\text{C}_2\text{B}_{10}\text{H}_{10})_2^{2-}$  ( $\text{R} = \text{H}, \text{Me}$ ),  $\text{CpTi}(\eta^6\text{-R}_2\text{C}_2\text{B}_{10}\text{H}_{10})^-$  ( $\text{R} = \text{H}, \text{Me}$ ), and  $(\eta^8\text{-C}_8\text{H}_8)\text{-Ti}(\eta^5\text{-C}_2\text{B}_9\text{H}_{11})^{n-}$  ( $n = 0, 1$ ).<sup>10</sup> Grimes and co-workers prepared a related sandwich complex  $(\eta^8\text{-C}_8\text{H}_8)\text{Ti}(\eta^5\text{-Et}_2\text{C}_2\text{B}_4\text{H}_4)$  and several iodinated derivatives.<sup>11</sup> Recently Hosmane described the synthesis of several bent-titanocene species incorporating the  $\text{C}_2\text{B}_4(\text{SiMe}_3)_2\text{H}_4^{2-}$  ligand.<sup>12</sup> The reactivity of these systems has not been extensively investigated.

## Results

### Synthesis and Fate of $(\text{Cp}^*)(\eta^5\text{-C}_2\text{B}_9\text{H}_{11})\text{Ti}(\text{Me})$

(4). The reaction of equimolar amounts of  $\text{Cp}^*\text{TiMe}_3$  and  $\text{C}_2\text{B}_9\text{H}_{13}$  in benzene or toluene (23 °C, minutes) results in rapid methane elimination and the formation of  $(\text{Cp}^*)(\eta^5\text{-C}_2\text{B}_9\text{H}_{11})\text{Ti}(\text{Me})$  (4, Scheme 1).<sup>13</sup> Complex 4 could not be isolated due to thermal decomposition (*vide infra*); however, NMR monitoring experiments using an internal standard establish that 1 is formed in greater than 85% yield. The NMR properties of 4 are consistent with a  $C_s$ -symmetric bent-metalocene structure and are unchanged over the temperature range  $-80$  to  $+25$  °C. Singlets are observed for the dicarbollide CH units in both the <sup>1</sup>H and <sup>13</sup>C{<sup>1</sup>H} spectra, and a 1:2:2:1:2:1 pattern is observed in the <sup>11</sup>B{<sup>1</sup>H} spectrum. The <sup>11</sup>B chemical shifts are similar to those observed for other group 4 and 5 metal  $\eta^5$ -dicarbollide complexes and support the proposed  $\eta^5$ -coordination.<sup>1,5</sup> This issue is addressed in more detail below. The thermal sensitivity of 4 precluded accurate solution molecular weight measurements. However, as the dimeric structures adopted by early metal metallocenes with a similar degree of steric crowding are usually unsymmetrical (e.g.  $\text{Cp}^*_2\text{Lu}(\mu\text{-CH}_3)\text{Lu}(\text{Me})(\text{Cp}^*)$ ,  $\text{Cp}^*_2\text{Y}(\mu\text{-CH}_3)\text{Y}(\text{Me})(\text{Cp}^*)$ , and  $\text{Cp}^*_2\text{Lu}(\mu\text{-Cl})\text{Lu}(\text{Cl})(\text{Cp}^*)$ )<sup>14</sup> and as the NMR spectra of 4 are consistent with a symmetric structure even at low temperatures, it is likely that 4 is monomeric in solution.

Complex 4 decomposes at 23 °C ( $t_{1/2}$  ca. 2 h) to a mixture of fulvene ("tuck-in") complex 5 (40% NMR vs

(7) (a) Thompson, M. E.; Baxter, S. M.; Bulls, A. R.; Burger, B. J.; Nolan, M. C.; Santarsiero, B. D.; Schaefer, W. P.; Bercaw, J. E. *J. Am. Chem. Soc.* **1987**, *109*, 203. (b) Burger, B. J.; Thompson, M. E.; Cotter, W. D.; Bercaw, J. E. *J. Am. Chem. Soc.* **1990**, *112*, 1566.

(8) (a) Eisch, J. J.; Pombrik, S. I.; Zheng, G. *Organometallics* **1993**, *12*, 3856. (b) Eisch, J. J.; Caldwell, K. R.; Werner, S.; Krüger, C. *Organometallics* **1991**, *10*, 3417. (c) Eisch, J. J.; Piotrowski, A. M.; Brownstein, S. K.; Gabe, E. J.; Lee, F. L. *J. Am. Chem. Soc.* **1985**, *107*, 7219. (d) Taube, R.; Krukowka, L. *J. Organomet. Chem.* **1988**, *347*, C9. (e) Bochmann, M.; Jaggard, A. J. *J. Organomet. Chem.* **1992**, *424*, C5. (f) Bochmann, M.; Jaggard, A. J.; Wilson, L. M.; Hursthouse, M. B.; Motevalli, M. *Polyhedron* **1989**, *8*, 1838. (g) Bochmann, M.; Lancaster, S. J. *J. Organomet. Chem.* **1992**, *434*, C1. (h) Bochmann, M.; Wilson, L. M.; Hursthouse, M. B.; Motevalli, M. *Organometallics* **1988**, *7*, 1148. (i) Bochmann, M.; Wilson, L. M.; Hursthouse, M. B.; Short, R. L. *Organometallics* **1987**, *6*, 2556. (j) Amorose, D. M.; Lee, R. A.; Petersen, J. L. *Organometallics* **1991**, *10*, 2191. (k) Bochmann, M.; Jaggard, A. J.; Nicholls, J. C. *Angew. Chem., Int. Ed. Engl.* **1990**, *29*, 780. (l) Borkovsky, S. L.; Baenziger, N. C.; Jordan, R. F. *Organometallics* **1993**, *12*, 486. (m) Eshuis, J. J. W.; Tan, Y. Y.; Teuben, J. H. *J. Mol. Catal.* **1990**, *62*, 277.

(9) See also: (a) Tritto, I.; Sacchi, M. C.; Li, S. *Makromol. Chem., Rapid Commun.* **1994**, *15*, 217. (b) Tritto, I.; Li, S.; Sacchi, M. C.; Zannoni, G. *Macromolecules* **1993**, *26*, 7111. (c) Dyachkovskii, F. S. In *Catalyst Design for Tailor-Made Polyolefins*; Soga, K., Terano, M., Eds.; Elsevier: New York, 1994; p 201.

(10) (a) Salentine, C. G.; Hawthorne, M. F. *Inorg. Chem.* **1976**, *15*, 2872. (b) Lo, F. Y.; Strouse, C. E.; Callahan, K. P.; Knobler, C. B.; Hawthorne, M. F. *J. Am. Chem. Soc.* **1975**, *97*, 428.

(11) Swisher, R. G.; Sinn, E.; Grimes, R. N. *Organometallics* **1984**, *13*, 599.

(12) Hosmane, N. S.; Wang, Y.; Zhang, H.; Maguire, J. A.; Waldhoer, E.; Kaim, W.; Binder, H.; Kremer, R. K. *Organometallics* **1994**, *13*, 4156.

(13) Attempted preparation of titanium dicarbollide complexes by halide displacement (e.g.  $\text{Cp}^*\text{TiCl}_3 + \text{C}_2\text{B}_9\text{H}_{11}^{2-}$ ) was unsuccessful.

internal standard, 30% isolated, Scheme 1), unidentified insoluble organometallic product(s), methane, and ethane. NMR monitoring experiments suggest that paramagnetic species also are formed. The NMR parameters for the dicarbollide and  $C_5Me_4CH_2$  groups of **5** are consistent with a  $C_s$ -symmetric structure. The fulvene methylene  $^{13}C$  resonance appears at low field ( $\delta = 81$ ) and the  $J_{CH}$  value is large (155 Hz). These data are in the range observed for monomeric early metal fulvene complexes including, for example,  $(Cp^*)(\eta^6-C_5Me_4CH_2)-Ti(Me)$  ( $\delta = 73.9$ ,  $J_{CH} = 150$  Hz),<sup>15</sup>  $(C_5Me_4H)(\eta^6-C_5Me_3H(CH_2))/Ti(Me)$  ( $\delta = 74.4$ ,  $J_{CH} = 150$  Hz),<sup>16</sup> and  $(Cp^*)(\eta^7-C_5Me_3(CH_2)_2)/Ti$  ( $\delta = 67.4$ ,  $J_{CH} = 160$  Hz).<sup>17-19</sup> The large  $J_{CH}$  values for these complexes result from the small C-C-M angles and/or significant  $sp^2$  character at the fulvene carbon.<sup>20</sup> Several early metal complexes with bridging  $\eta^5, \eta^1-C_5Me_4CH_2$  ligands have been characterized by X-ray diffraction, including  $[(Cp^*)Sc(\mu-\eta^5, \eta^1-C_5Me_4CH_2)]_2$ <sup>21</sup> and  $[(Cp^*)Ti]_2(\mu-\eta^5, \eta^1-C_5Me_4CH_2)(\mu-O)_2$ .<sup>22</sup> In these cases, the fulvene carbons exhibit normal tetrahedral ( $sp^3$ ) geometries.<sup>23</sup> While  $^{13}C$  data have not been reported for these  $\mu-C_5Me_4CH_2$  species, lower  $\delta$  values and  $J_{CH}$  values ( $<125$  Hz) typical of early metal alkyls are expected. On the basis of these considerations, **5** is assigned the monomeric tuck-in structure shown in Scheme 1.

The solubility of **5** in aromatic solvents decreases considerably after recrystallization. This is a general property of group 4 metal carborane species, and its origin is still under investigation. It is possible that intermolecular B-H-M interactions between the hy-

drinic dicarbollide B-H bonds and the electrophilic metal centers are responsible.<sup>24</sup>

**Reactions of 4 with Lewis Bases.** The Lewis acid properties of **4** were probed by NMR monitoring of reactions with representative Lewis bases. Addition of  $PMe_3$  to **4** results in formation of  $(Cp^*)(\eta^5-C_2B_9H_{11})Ti(Me)(PMe_3)$  (**6**, Scheme 1). The low-temperature ( $-30$  °C)  $^{13}C$  and  $^1H$  spectra of **6** each contain two dicarbollide CH resonances, indicating that the sides of the dicarbollide ligand are inequivalent, and the low-temperature  $^{13}C\{^1H\}$  spectrum contains a doublet for the Ti-Me group ( $^2J_{CP} = 15$  Hz), indicating that a single  $PMe_3$  is coordinated. Above 0 °C,  $PMe_3$  exchange is rapid on the NMR time scale. Addition of excess  $PMe_3$  at 23 °C does not shift the resonances for **6**, indicating that coordination of a second  $PMe_3$  ligand does not occur in solution. Similarly, addition of THF to **4** causes extensive shifting of the NMR resonances. However, in this case, decomposition occurs at 23 °C ( $t_{1/2}$  ca. 1 h) and THF exchange is rapid down to  $-70$  °C, so discrete  $Cp^*(\eta^5-C_2B_9H_{11})Ti(Me)(THF)_x$  species could not be characterized.<sup>25</sup>

**Reaction of 4 with Acetonitrile.** The reactions of **4** with several unsaturated substrates were explored to prepare more stable derivatives. Complex **4** reacts with excess MeCN to yield the insertion product  $Cp^*(\eta^5-C_2B_9H_{11})Ti(N=CMe_2)(MeCN)$  (**7**), which is isolated as a sparingly soluble pale green solid (Scheme 1). The spectroscopic properties of **7** are similar to those for related Sc, Ti, and Zr azomethine species,<sup>8b,26</sup> in particular, a characteristic low-field  $^{13}C$  resonance is observed for the imine carbon ( $\delta = 169.0$ ) and strong  $\nu(C=N)$  ( $1678\text{ cm}^{-1}$ ) and  $\nu(C\equiv N)$  ( $2316, 2287\text{ cm}^{-1}$ )<sup>27</sup> bands are observed in the IR spectrum. In toluene- $d_8$  solvent, **7** undergoes MeCN dissociation ( $K_D = 0.01$  M at  $-40$  °C)<sup>28</sup> and rapid exchange (NMR time scale) of free and coordinated MeCN. The MeCN exchange results in effective  $C_s$  symmetry and is not frozen out at  $-70$  °C.<sup>29</sup> Recrystallization of **7** from toluene yields

(14) (a) Watson, P. J. *J. Am. Chem. Soc.* **1983**, *105*, 6491. (b) Evans, W. J.; Peterson, T. T.; Rausch, M. D.; Hunter, W. E.; Zhang, H.; Atwood, J. L. *Organometallics* **1985**, *4*, 554. (c) However less crowded analogues adopt symmetric dimeric structures, e.g.  $[Cp_2MMe]_2$  ( $M = Y, Yb$ ): Holton, J.; Lappert, M. F.; Ballard, D. G. H.; Pearce, R.; Atwood, J. L.; Hunter, W. E. *J. Chem. Soc., Dalton Trans.* **1979**, 54.

(15) (a) McDade, C.; Green, J. C.; Bercaw, J. E. *Organometallics* **1982**, *1*, 1629. (b) Bercaw, J. E.; Marvich, R. H.; Bell, L. G.; Brintzinger, H. H. *J. Am. Chem. Soc.* **1972**, *94*, 1219.

(16) (a) Mach, K.; Varga, V.; Hanus, V.; Sedmera, P. *J. Organomet. Chem.* **1991**, *415*, 87. (b) Vondrák, T.; Mach, K.; Varga, V.; Terpstra, A. *J. Organomet. Chem.* **1992**, *425*, 27.

(17) Pattiasina, J. W.; Hissink, C. E.; de Boer, J. L.; Meetsma, A.; Teuben, J. H. *J. Am. Chem. Soc.* **1985**, *107*, 7758.

(18) For other Ti fulvene species see: (a) Bercaw, J. E. *J. Am. Chem. Soc.* **1974**, *96*, 5087. (b) Bandy, J. A.; Mtetwa, V. S. B.; Prout, K.; Green, J. C.; Davies, C. E.; Green, M. L. H.; Hazel, N. J.; Izquierdo, A.; Martin-Polo, J. J. *J. Chem. Soc., Dalton Trans.* **1985**, 2037. (c) Luinstra, G. A.; Teuben, J. H. *Organometallics* **1992**, *11*, 1793. (d) Luinstra, G. A.; Teuben, J. H. *J. Am. Chem. Soc.* **1992**, *114*, 3361.

(19) For other group 4 metal fulvene complexes see: (a) Schock, L. E.; Brock, C. P.; Marks, T. J. *Organometallics* **1987**, *6*, 232. (b) Bulls, A. R.; Schaefer, W. P.; Serfas, M.; Bercaw, J. E. *Organometallics* **1987**, *6*, 1219. (c) Sinnema, P. J.; Meetsma, A.; Teuben, J. H. *Organometallics* **1993**, *12*, 184.

(20) The IR spectrum of **5** contains a weak band at  $3012\text{ cm}^{-1}$  which may be due to the fulvene  $\nu(C=CH_2)$  absorption. This band is absent from the IR spectra of  $Cp^*TiMe_3$  and other  $(Cp^*)(\eta^5-C_2B_9H_{11})Ti(X)$  species. For comparison, a band at  $3040\text{ cm}^{-1}$  for  $(Cp^*)(\eta^6-C_5Me_4CH_2)-Ti(Me)$  was assigned to  $\nu(C=CH_2)$ . However, dicarbollide  $\nu(CH)$  absorptions also may appear in this range (e.g.:  $Si(\eta^5-C_2B_9H_{11})_2$ ,  $3047\text{ cm}^{-1}$ ;  $[NMe_4][Ni(\eta^5-C_2B_9H_{11})_2]$ ,  $3037\text{ cm}^{-1}$ ) so this assignment is not definitive: (a) Schubert, D. M.; Rees, W. S., Jr.; Knobler, C. B.; Hawthorne, M. F. *Organometallics* **1990**, *9*, 2938. (b) Hawthorne, M. F.; Young, D. C.; Andrews, T. D.; Howe, D. V.; Pilling, R. L.; Pitts, A. D.; Reintjes, M.; Warren, L. F., Jr.; Wegner, P. A. *J. Am. Chem. Soc.* **1968**, *90*, 879.

(21) Hajela, S.; Schaefer, W. P.; Bercaw, J. E. *Acta Crystallogr.* **1992**, *C48*, 1771.

(22) Bottomley, F.; Egharevba, G. O.; Lin, I. J. B.; White, P. S. *Organometallics* **1985**, *4*, 550.

(23) However, more acute C-CH<sub>2</sub>-M angles are observed in early metal complexes with bridging  $C_5R_3(CH_2)_2$  ligands: (a) Booi, M.; Meetsma, A.; Teuben, J. H. *Organometallics* **1991**, *10*, 3246. (b) Troyanov, S. I.; Mach, K.; Varga, V. *Organometallics* **1993**, *12*, 3387.

(24) In the case of  $(\eta^6-C_5Me_4CH_2)(\eta^5-C_2B_9H_{11})Ti$ , it is also possible that dimeric or oligomeric structures containing bridging fulvene ligands are formed in the solid state.

(25) (a) The low-temperature  $^1H$  NMR ( $-70$  °C) and  $^{13}C$  NMR ( $-40$  °C) spectra of **4** in the presence of excess THF exhibit single dicarbollide CH resonances and a single set of THF resonances, indicating that THF exchange is rapid on the NMR time scale. Poor solubility precluded experiments at lower temperatures. (b) NMR data for  $(Cp^*)(\eta^5-C_2B_9H_{11})Ti(Me)(THF)_x$  generated by addition of excess THF to a toluene- $d_8$  solution of **4**:  $^1H$  NMR ( $-40$  °C)  $\delta$  3.39 (br s, 2H, dicarbollide CH), 1.81 (s, 15H,  $C_5Me_5$ ), 1.05 (s, 3H, TiMe);  $^{13}C\{^1H\}$  NMR ( $-40$  °C)  $\delta$  130.1 ( $C_5Me_5$ ), 71.5 (q,  $^1J_{CH} = 122$ , TiMe), 62.1 (br d,  $^1J_{CH} = 169$ ,  $C_2B_9H_{11}$ ), 13.7 (s,  $^1J_{CH} = 127$ ,  $C_5Me_5$ );  $^{11}B\{^1H\}$  NMR (25 °C)  $\delta$  14.1 (1B), 0.7 (2B), 0.0 (2B),  $-9.7$  (2B),  $-11.8$  (1B),  $-14.3$  (1B).

(26) (a) Alelyunas, Y. W.; Jordan, R. F.; Echols, S. F.; Borkowsky, S. L.; Bradley, P. K. *Organometallics* **1991**, *10*, 1406. (b) den Haan, K. H.; Luinstra, G. A.; Meetsma, A.; Teuben, J. H. *Organometallics* **1987**, *6*, 1509. (c) Evans, W. J.; Meadows, J. H.; Hunter, W. E.; Atwood, J. L. *J. Am. Chem. Soc.* **1984**, *106*, 1291. (d) Bercaw, J. E.; Davies, D. L.; Wolczanski, P. T. *Organometallics* **1986**, *5*, 443. (e) Erker, G.; Fromberg, W.; Atwood, J. L.; Hunter, W. E. *Angew. Chem., Int. Ed. Engl.* **1984**, *23*, 68.

(27) The  $\nu(C=N)$  bands are shifted from the bands for free MeCN ( $2293, 2257\text{ cm}^{-1}$ ). See: (a) Jordan, R. F.; Bajgur, C. S.; Dasher, W. E.; Rheingold, A. L. *Organometallics* **1987**, *6*, 1041. (b) Bruce, M. R. M.; Tyler, D. R. *Organometallics* **1985**, *4*, 528.

(28)  $K_D$  was estimated from the chemical shifts of **7** (under conditions of partial dissociation and fast MeCN exchange),  $Cp^*(\eta^5-C_2B_9H_{11})Ti(N=CMe_2)$  (**8**), and **7** in the presence of excess MeCN (where no **8** is present). At  $-40$  °C, **7** (ca. 0.01 M) undergoes ca. 20% MeCN dissociation. The extent of dissociation increases at higher temperatures.

(29) Solubility limitations precluded NMR analysis at lower temperatures.

**Table 1. Summary of Crystallographic Data for Cp\*( $\eta^5$ -C<sub>2</sub>B<sub>9</sub>H<sub>11</sub>)Ti(N=CMe<sub>2</sub>)(NCMe) (7) and Cp\*( $\eta^5$ -C<sub>2</sub>B<sub>9</sub>H<sub>11</sub>)Ti(N=CMe<sub>2</sub>) (8)<sup>a</sup>**

	7	8
formula	C <sub>17</sub> H <sub>35</sub> N <sub>2</sub> B <sub>9</sub> Ti	C <sub>15</sub> H <sub>32</sub> NB <sub>9</sub> Ti
fw	412.7	371.6
crystal system	triclinic	monoclinic
space group	P1	C2/c
a, Å	9.588(6)	23.058(7)
b, Å	9.940(4)	13.042(6)
c, Å	13.034(5)	15.411(6)
α, deg	96.69(3)	90
β, deg	97.13(4)	118.66(3)
γ, deg	96.70(4)	90
V, Å <sup>3</sup>	1213(1)	4179(3)
Z	2	8
D <sub>calcd</sub> , g cm <sup>-3</sup>	1.13	1.18
abs coeff, mm <sup>-1</sup>	0.359	0.409
crystal dmns, mm	0.25 × 0.15 × 0.05	0.05 × 0.20 × 0.10
scan type	ω/2θ	ω/2θ
scan sp in ω, deg:	5.0, 15.0	5.0, 15.0
min, max		
2θ range, deg	3.0–40.0	3.0–38.0
T, K	220	220
decay, %	0	0
no. of data collected	2406	1772
no. of obsd reflns,	1085	749 [F > 4.0σ(F)]
F > 6.0σ(F)		
no. of params refined	247	150
GOF	1.72	1.43
Δρ(max, min), e/Å <sup>3</sup>	0.54, -0.44	0.46, -0.56
R <sup>b</sup>	0.081	0.088
R <sub>w</sub> <sup>b</sup>	0.091	0.088

<sup>a</sup> Graphite-monochromatized Mo Kα radiation, λ = 0.710 73 Å.

<sup>b</sup> R = Σ||F<sub>o</sub> - |F<sub>c</sub>||/Σ|F<sub>o</sub>|; R<sub>w</sub> = [Σw(F<sub>o</sub> - F<sub>c</sub>)<sup>2</sup>/Σw(F<sub>o</sub>)<sup>2</sup>]<sup>1/2</sup>; w = 1/[σ<sup>2</sup>(F<sub>o</sub>) + 0.001(F<sub>o</sub>)<sup>2</sup>].

the base-free complex (Cp\*)( $\eta^5$ -C<sub>2</sub>B<sub>9</sub>H<sub>11</sub>)Ti(N=CMe<sub>2</sub>) (8). The spectroscopic properties of 8 are very similar to those of 7.

**Structures of Cp\*( $\eta^5$ -C<sub>2</sub>B<sub>9</sub>H<sub>11</sub>)Ti(N=CMe<sub>2</sub>)(Me-CN)<sub>n</sub> (7, n = 0; 8, n = 1).** The molecular structures of 7 and 8 have been determined by X-ray crystallography. Crystallographic data, atomic coordinates, and key bond distances and angles for 7 and 8 are listed in Tables 1–3, and ORTEP views are shown in Figures 1 and 2. Complex 7 adopts a monomeric bent-metallocene structure and contains an  $\eta^5$ -dicarbollide ligand. The azomethine and acetonitrile ligands lie in the equatorial plane between the  $\eta^5$  ligands as invariably observed in bent-metallocene compounds. The carborane cage is disordered between two orientations such that the atom position designated by Cb(2) is 60% occupied by B and 40% occupied by C and that designated by Cb(4) is 40% occupied by B and 60% occupied by C. The centroid–Ti–centroid angle (138.7°) is in the range observed for Cp\*<sub>2</sub>Ti<sup>IV</sup> bent metallocenes (137–141°) (e.g.: Cp\*<sub>2</sub>TiCl<sub>2</sub>, 137.4°;<sup>30</sup> Cp\*<sub>2</sub>Ti(CH<sub>3</sub>)(THF)<sup>+</sup>, 137.8°;<sup>3f</sup> Cp\*<sub>2</sub>Ti{ $\eta^2$ (O,C)(=NC<sub>6</sub>H<sub>11</sub>)C(=CH<sub>2</sub>)}, 140.8°),<sup>31</sup> as expected given the similar cone angles of  $\eta^5$ -C<sub>2</sub>B<sub>9</sub>H<sub>11</sub><sup>2-</sup> and Cp\*<sup>-</sup>.<sup>32</sup> The N(31)–Ti–N(35) angle (85.6°) is ca. 10° smaller than the X–M–X angles normally observed in d<sup>0</sup> Cp<sub>2</sub>MX<sub>2</sub> species (94–100°).<sup>33</sup> This is a manifestation of the high degree of steric crowding in this system; a similar reduction in X–M–X angle was observed for Cp\*<sub>2</sub>-Ti(Me)(THF)<sup>+</sup> (O–Ti–Me angle 88.9°)<sup>3f</sup> and ( $\eta^5$ -C<sub>2</sub>B<sub>9</sub>H<sub>11</sub>)<sub>2</sub>-

**Table 2. Atomic Coordinates (×10<sup>4</sup>) and Equivalent Isotropic Displacement Coefficients (Å<sup>2</sup> × 10<sup>3</sup>) for Cp\*( $\eta^5$ -C<sub>2</sub>B<sub>9</sub>H<sub>11</sub>)Ti(N=CMe<sub>2</sub>)(NCMe) (7) and Cp\*( $\eta^5$ -C<sub>2</sub>B<sub>9</sub>H<sub>11</sub>)Ti(N=CMe<sub>2</sub>) (8)**

	x	y	z	U(eq) <sup>a</sup>
	Compound 7			
Ti	2536(3)	5618(3)	2450(2)	30(1)
Cb(2)	4564(17)	4334(14)	2150(12)	28(7)
C(3)	3832(17)	4665(13)	1072(10)	28(6)
Cb(4)	2080(18)	4003(15)	805(12)	31(7)
B(5)	1797(25)	3104(16)	1883(13)	44(9)
B(6)	3367(19)	3449(17)	2731(15)	35(8)
B(7)	4989(21)	3487(17)	1008(13)	34(8)
B(8)	3422(22)	3231(16)	182(14)	38(8)
B(9)	2098(22)	2194(16)	676(14)	37(8)
B(10)	2958(24)	1841(16)	1893(14)	42(8)
B(11)	4721(25)	2615(16)	2132(14)	43(9)
B(12)	3900(22)	1907(15)	848(13)	35(8)
C(21)	1816(25)	7263(17)	3743(14)	59(9)
C(22)	2105(18)	6074(16)	4197(12)	36(7)
C(23)	1003(21)	5006(14)	3702(12)	38(7)
C(24)	109(22)	5502(16)	2869(14)	53(9)
C(25)	663(22)	6935(17)	2956(13)	47(8)
C(26)	2542(20)	8709(14)	4118(12)	62(8)
C(27)	3086(22)	6018(16)	5131(12)	73(10)
C(28)	694(18)	3642(14)	4133(12)	52(5)
C(29)	-1182(20)	4807(16)	2236(13)	59(8)
C(30)	-89(18)	7910(15)	2350(12)	54(5)
N(31)	4156(15)	6855(13)	2899(10)	40(6)
C(32)	5275(24)	7710(16)	3123(14)	47(8)
C(33)	5505(21)	8913(14)	2449(12)	72(9)
C(34)	6462(22)	7690(16)	4008(14)	67(9)
N(35)	2118(14)	6893(12)	1217(9)	32(5)
C(36)	2052(21)	7556(15)	575(13)	50(8)
C(37)	1901(18)	8406(15)	-262(12)	47(5)
	Compound 8			
Ti	3470(2)	1986(3)	8099(3)	34(2)
C(2)	2479(9)	2713(15)	7949(13)	33(6)
C(3)	2732(8)	1862(15)	8800(12)	27(5)
B(4)	2831(11)	781(19)	8434(18)	37(7)
B(5)	2556(11)	864(18)	7127(16)	30(7)
B(6)	2343(10)	2183(19)	6834(15)	31(7)
B(7)	1931(10)	2314(18)	8341(16)	30(7)
B(8)	2168(11)	1024(18)	8647(16)	32(7)
B(9)	2016(11)	410(18)	7547(17)	34(7)
B(10)	1718(12)	1235(19)	6594(18)	32(7)
B(11)	1666(12)	2413(17)	7046(19)	42(8)
B(12)	1473(11)	1322(18)	7519(17)	29(7)
C(21)	4395(10)	2660(16)	8024(14)	33(6)
C(22)	3867(9)	2604(16)	7019(14)	21(6)
C(23)	3705(9)	1669(16)	6736(14)	35(6)
C(24)	4119(10)	1035(18)	7595(15)	36(6)
C(25)	4547(9)	1688(15)	8345(15)	34(6)
C(26)	4757(9)	3609(14)	8533(14)	46(12)
C(27)	3568(9)	3492(14)	6325(14)	39(12)
C(28)	3255(9)	1280(17)	5719(13)	66(14)
C(29)	4134(10)	-81(19)	7622(16)	72(16)
C(30)	5107(10)	1365(18)	9331(15)	80(15)
N(31)	3952(8)	2600(14)	9352(12)	49(9)
C(32)	4223(9)	2935(18)	10193(15)	27(5)
C(33)	4572(9)	2273(16)	11083(13)	59(13)
C(34)	4270(9)	4024(16)	10401(14)	65(14)

<sup>a</sup> Equivalent isotropic U defined as one-third of the trace of the orthogonalized U<sub>ij</sub> tensor.

TaMe<sub>2</sub><sup>-</sup> (Me–Ta–Me angle 82.5°).<sup>5d</sup> The Ti–(dicarbollide centroid) distance (2.02 Å) in 7 is ca. 0.07 Å shorter than the Ti–(Cp\* centroid) distance (2.09 Å). Complex 8 also adopts a monomeric bent-metallocene structure; however the centroid–Ti–centroid angle is 5.9° larger

(30) McKenzie, T. C.; Sanner, R. D.; Bercaw, J. E. *J. Organomet. Chem.* **1975**, *102*, 457.

(31) Beckhaus, R.; Strauss, I.; Wagner, T.; Kiprof, P. *Angew. Chem., Int. Ed. Engl.* **1993**, *32*, 264.

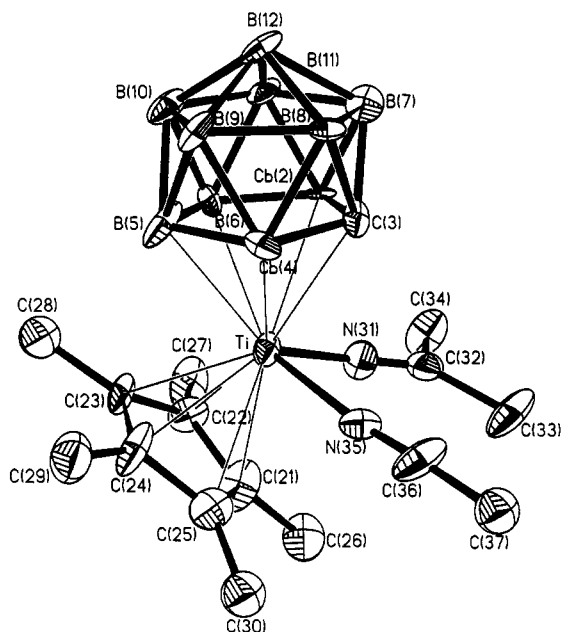
(32) Hanusa, T. P. *Polyhedron* **1982**, *1*, 661.

(33) (a) Prout, K.; Cameron, T. S.; Forder, R. A.; Crithley, S. R.; Denton, B.; Rees, G. V. *Acta Crystallogr.* **1974**, *B30*, 2290. (b) Lauher, J. W.; Hoffmann, R. *J. Am. Chem. Soc.* **1976**, *98*, 1729. (c) Cardin, D. J.; Lappert, M. F.; Raston, C. L. *Chemistry of Organo-Zirconium and Hafnium Compounds*; John Wiley and Sons: New York, 1986; Chapter 4.

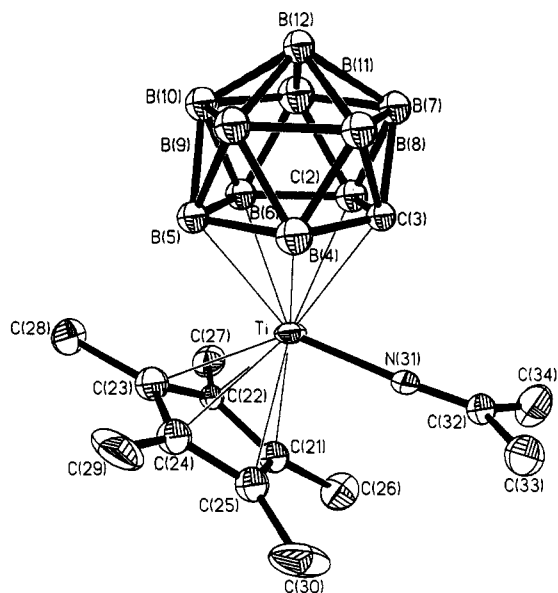
**Table 3. Selected Bond Distances (Å) and Angles (deg) for Cp\*( $\eta^5$ -C<sub>2</sub>B<sub>9</sub>H<sub>11</sub>)Ti(N=CMe<sub>2</sub>)(NCMe) (7) and Cp\*( $\eta^5$ -C<sub>2</sub>B<sub>9</sub>H<sub>11</sub>)Ti(N=CMe<sub>2</sub>) (8)<sup>a</sup>**

Compound 7			
Ti-Cnt(b1)	2.02	Ti-Cnt(c1)	2.09
Ti-Cb(2)	2.49(2)	Ti-C(3)	2.47(2)
Ti-Cb(4)	2.48(1)	Ti-B(5)	2.51(2)
Ti-B(6)	2.44(2)	Ti-C(21)	2.43(2)
Ti-C(22)	2.36(2)	Ti-C(23)	2.41(2)
Ti-C(24)	2.45(2)	Ti-C(25)	2.45(2)
Ti-N(31)	1.85(1)	Ti-N(35)	2.19(1)
N(35)-C(36)	1.12(2)	N(31)-C(32)	1.27(2)
C(32)-C(33)	1.58(2)	C(36)-C(37)	1.46(2)
av B-B	1.77	C(32)-C(34)	1.52(3)
Cnt(b1)-Ti-Cnt(c1)	138.7	Cnt(b1)-Ti-N(31)	107.8
Cnt(b1)-Ti-N(35)	105.0	Cnt(c1)-Ti-N(31)	103.9
Cnt(c1)-Ti-N(35)	103.2	N(31)-Ti-N(35)	85.6(5)
Ti-N(31)-C(32)	175(1)	N(31)-C(32)-C(33)	119(2)
N(31)-C(32)-C(34)	126(2)	Ti-N(35)-C(36)	172(1)
N(35)-C(36)-C(37)	177(2)	C(33)-C(32)-C(34)	115(2)
Compound 8			
Ti-Cnt(b2)	1.91	Ti-Cnt(c2)	2.07
Ti-C(2)	2.39(2)	Ti-C(3)	2.42(2)
Ti-B(4)	2.40(3)	Ti-B(5)	2.43(2)
Ti-B(6)	2.40(2)	Ti-C(21)	2.37(2)
Ti-C(22)	2.40(2)	Ti-C(23)	2.44(3)
Ti-C(24)	2.36(3)	Ti-C(25)	2.36(2)
Ti-N(31)	1.89(2)	av C-B	1.70
N(31)-C(32)	1.22(3)	av B-B	1.78
Cnt(b2)-Ti-N(31)	111.0	N(31)-C(32)-C(33)]	122(2)
Cnt(b2)-Ti-Cnt(c2)	114.6	Ti-N(31)-C(32)	173(2)
Cnt(c2)-Ti-N(31)	104.4	N(31)-C(32)-C(34)	122(2)
C(33)-C(32)-C(34)	116(2)		

<sup>a</sup> Cnt(b1) and Cnt(c1) are the centroids of the  $\eta^5$  faces of the C<sub>2</sub>B<sub>9</sub>H<sub>11</sub> and Cp\* ligands for compound 7, and Cnt(b2) and Cnt(c2) are the corresponding centroids for 8.

**Figure 1.** Molecular structure of Cp\*( $\eta^5$ -C<sub>2</sub>B<sub>9</sub>H<sub>11</sub>)Ti(N=CMe<sub>2</sub>)(MeCN) (7).

and the Ti-(dicarbollide centroid) distance 0.11 Å shorter than the corresponding values for 7, due to the lower coordination number. The azomethine ligand in 8 occupies the central coordination site (i.e. Ti, N(31), and the two centroids are coplanar to within 0.004 Å). The azomethine ligands in both 7 and 8 are oriented such that the methyl groups lie in the equatorial plane between the two  $\eta^5$  ligands. This orientation minimizes

**Figure 2.** Molecular structure of Cp\*( $\eta^5$ -C<sub>2</sub>B<sub>9</sub>H<sub>11</sub>)Ti(N=CMe<sub>2</sub>) (8).

steric interactions between the methyl groups and the Cp\* and dicarbollide ligands and maximizes Ti-N  $\pi$ -bonding. The metrical parameters for the azomethine ligands in 7 and 8 are similar to those for other d<sup>0</sup> metallocene azomethine complexes (e.g. (indenyl)<sub>2</sub>Ti(N=CMePh)(PhCN)<sup>+</sup> and Cp<sub>2</sub>Zr(N=CHPh)Cl).<sup>8h,26e</sup> The short Ti-N<sub>azomethine</sub> distances (7, 1.85 Å; 8, 1.89 Å) are consistent with strong Ti-N  $\pi$ -bonding.

**Reaction of 4 with 2-Butyne.** Complex 4 undergoes single insertion of 2-butyne, yielding the alkenyl complex Cp\*( $\eta^5$ -C<sub>2</sub>B<sub>9</sub>H<sub>11</sub>)Ti(CMe=CMe<sub>2</sub>) (9, Scheme 1), which is isolated as a red-brown solid. The <sup>1</sup>H and <sup>13</sup>C NMR spectra of 9 each contain two dicarbollide CH resonances, indicating that a symmetry plane is not present. Additionally, one of the alkenyl methyl <sup>1</sup>H resonances appears at unusually high field ( $\delta$  = 0.05). These observations imply that the alkenyl ligand lies in the equatorial plane between the Cp\* and dicarbollide ligands and that rotation about the Ti-alkenyl bond is slow on the NMR time scale, and suggest that the alkenyl  $\alpha$ -Me group is close to the metal center. X-ray diffraction studies established the presence of "in-plane"  $\beta$ -agostic M-CMe=CMe<sub>2</sub> ligands in Cp\*( $\eta^5$ -C<sub>2</sub>B<sub>9</sub>H<sub>11</sub>)-Zr(CMe=CMe<sub>2</sub>) (2a)<sup>1a</sup> and (C<sub>5</sub>H<sub>4</sub>Me)<sub>2</sub>Zr(C(Me)=CMe<sub>2</sub>)-(THF)<sup>+</sup>.<sup>34</sup> However, there is no definitive evidence for a  $\beta$ -agostic interaction in 9.<sup>35</sup> The <sup>1</sup>H NMR spectrum of 9 in THF-*d*<sub>8</sub> is significantly perturbed from that in toluene-*d*<sub>6</sub>; in particular, the high-field alkenyl methyl resonance shifts downfield to the normal range ( $\delta$  = 0.86). This suggests that 9 forms a THF adduct; however 9 is isolated in base-free form by recrystallization from THF/hexane.<sup>36</sup>

**Reaction of 4 with Ethylene.** Complex 4 reacts rapidly with ethylene (23 °C, minutes, 1–3 atm, Scheme 2) to yield propene and (Cp\*)( $\eta^5$ -C<sub>2</sub>B<sub>9</sub>H<sub>11</sub>)Ti(CH<sub>2</sub>CH<sub>3</sub>) (10), via ethylene insertion,  $\beta$ -H elimination, and rapid

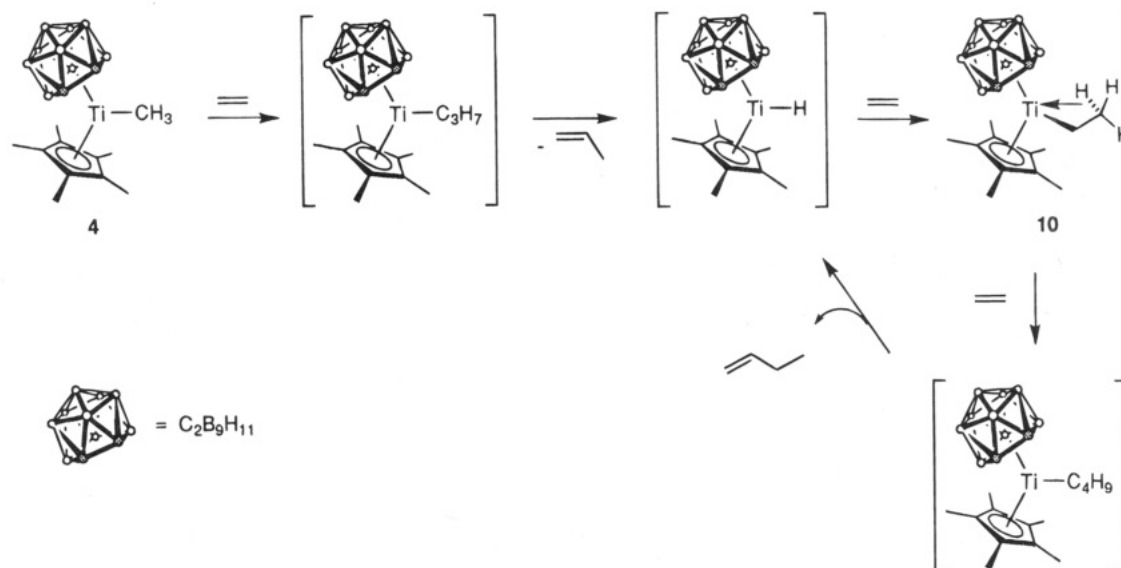
(34) Jordan, R. F.; LaPointe, R. E.; Bradley, P. K.; Baenziger, N. C. *Organometallics* 1989, 8, 2892.

(35) The *J*<sub>CH</sub> values for the alkenyl methyl groups are normal (125 Hz).

(36) <sup>1</sup>H NMR of 9 (THF-*d*<sub>8</sub>):  $\delta$  3.77 (br s, 1H, dicarbollide CH), 3.53 (br s, 1H, dicarbollide CH), 2.15 (s, 15H, C<sub>5</sub>Me<sub>5</sub>), 1.78 (s, 3H, C=CMe<sub>2</sub>), 1.22 (s, 3H, C=CMe<sub>2</sub>), 0.86 (s, 3H, TiC(Me)).



Scheme 2



ethylene insertion of the resulting hydride  $(\text{Cp}^*)(\eta^5\text{-C}_2\text{B}_9\text{H}_{11})\text{Ti}(\text{H})$  (not observed).<sup>37</sup> In a secondary process, ethylene is catalytically dimerized to 1-butene (ca. 4 t.o./h at 2–3 atm, 23 °C) via an insertion/ $\beta$ -H elimination process. The catalyst resting state is ethyl complex **10**.

NMR data establish that **10** adopts a  $\beta$ -H agostic structure similar to those of  $\text{Cp}^*_2\text{Sc}(\text{CH}_2\text{CH}_3)$  and  $(\text{C}_5\text{R}_5)_2\text{Zr}(\text{CH}_2\text{CH}_2\text{R})(\text{L})^+$  ( $\text{L} = \text{PR}_3, \text{RCN}$ ) complexes.<sup>7a,38</sup> Key NMR data for **10** include a high-field  $\beta\text{-CH}_3$   $^1\text{H}$  resonance ( $\delta = -0.8$ , characteristic of a  $\text{M-H}$  interaction), a large  $J_{\text{C}\alpha\text{-H}}$  value (144 Hz, characteristic of an acute  $\text{M-C-C}$  angle), and a reduced  $J_{\text{C}\alpha\text{-C}\beta}$  value (28.5 Hz, characteristic of acute  $\text{M-C-C}$  and  $\text{C}\alpha\text{-C}\beta\text{-H}_{\text{bridge}}$  angles).<sup>38</sup>

Exchange of the terminal and bridging  $\beta$ -hydrogens of **10** is rapid on the NMR time scale even at  $-90$  °C.<sup>39</sup> The  $^1\text{H}$  and  $^{13}\text{C}$  NMR spectra (singlets for the dicarbollide CH units) and the  $^{11}\text{B}$  spectrum (1,2,2,3,1 pattern) imply that **10** maintains effective  $C_s$  symmetry over the temperature range  $-90$  to  $+23$  °C. No exchange of the  $\alpha$ - and  $\beta$ -hydrogens is observed. As bridge/terminal  $\beta$ -H exchange via "in-place" methyl rotation would not render the sides of the dicarbollide ligand equivalent, these observations imply that **10** is in equilibrium with a nonagostic species.<sup>40</sup> The  $J_{\text{C}\beta\text{-H}}$  value (124 Hz) is consistent with the expected average of one small ( $\mu\text{-H}$ ) and two large (terminal H) values.<sup>38</sup>

Complex **10** undergoes thermal decomposition ( $t_{1/2} < 12$  h at 23 °C) to insoluble product(s) and thus could not be isolated.<sup>41</sup>

(37) Compound **4** does not react with propylene and higher  $\alpha$ -olefins (toluene, 1 atm, 23 °C).

(38) (a) Guo, Z.; Swenson, D. C.; Jordan, R. F. *Organometallics* **1994**, *13*, 1424. (b) Alelyunas, Y. W.; Guo, Z.; LaPointe, R. E.; Jordan, R. F. *Organometallics* **1993**, *12*, 544. (c) Jordan, R. F.; Bradley, P. K.; Baenziger, N. C.; LaPointe, R. E. *J. Am. Chem. Soc.* **1990**, *112*, 1289.

(39) Some broadening of the  $\text{Ti-CH}_2\text{CH}_3$  resonances of **10** is observed at  $-90$  °C. Solubility limitations precluded NMR analysis at lower temperatures.

(40) (a) Green, M. L. H.; Wong, L.-L. *J. Chem. Soc., Chem. Commun.* **1988**, 677. (b) Casey, C. P.; Yi, C. S. *Organometallics* **1991**, *10*, 33. (c) McNally, J. P.; Cooper, N. J. *Organometallics* **1988**, *7*, 1704. (d) Bercaw, J. E.; Burger, B. J.; Green, M. L. H.; Santarsiero, B. D.; Sella, A.; Trimmer, M. S.; Wong, L.-L. *J. Chem. Soc., Chem. Commun.* **1989**, 734.

**$^{11}\text{B}$  NMR Spectra and Structures of 4–10.** The  $^{11}\text{B}$  NMR spectra for **4–10** are schematically illustrated in Figure 3, in which compounds are grouped together by coordination number for clarity (i.e.: **4, 5, 8–10**, 3-coordinate, counting the  $\eta^5\text{-C}_2\text{B}_9\text{H}_{11}$  and  $\text{Cp}^*$  as unidentate ligands and excluding agostic interactions; **6, 7**, 4-coordinate). The spectra of 3-coordinate species **4, 5**, and **8–10** are similar. Each contains a low-field resonance in the range  $\delta$  10–20 (1B) and a high-field resonance in the range  $\delta$   $-14$  to  $-18$  (1B). These resonances may be assigned to the unique boron on the  $\text{C}_2\text{B}_3$  face and the capping boron trans to Ti, respectively, on the basis of comparison with data for  $(\eta^5\text{-C}_2\text{B}_9\text{H}_{11})_2\text{TaX}_2^-$  compounds, for which assignments were made from  $^{11}\text{B}\text{-}^{11}\text{B}$  COSY spectra.<sup>5d</sup> Additionally, each spectrum contains a set of resonances between  $\delta$   $+6$  and  $-13$  for the remaining borons. The similarity of these spectra indicate that **4, 5**, and **8–10** all adopt similar structures; i.e., these compounds all adopt bent-metalloocene structures similar to that established crystallographically for **8**.

The spectra of **6** and **7** are also quite similar. Each contains a low-field resonance assignable to the unique boron on the  $\text{C}_2\text{B}_3$  face and a collection of high-field resonances lying in a relatively narrow range of ca. 15 ppm. The spectrum of **7** is shifted upfield by ca. 7 ppm relative to the spectrum of **6**. The similarity of these spectra indicates that **6** and **7** adopt similar structures, i.e., that both adopt bent-metalloocene structures as established crystallographically for **7**. Additionally, the  $^{11}\text{B}$  NMR spectrum of **4** in the presence of THF is very similar to that of **6**. This suggests that **4** forms a mono-THF adduct; however as noted above, this could not be confirmed from the other NMR spectra.

## Discussion

**Structure, Bonding, and Reactivity.** The alkane elimination reaction of  $\text{C}_2\text{B}_9\text{H}_{13}$  and  $\text{Cp}^*\text{TiMe}_3$  provides a simple route to the bent-metalloocene complex  $(\text{Cp}^*)\text{-}$

(41) Attempts to isolate **10** yielded mixtures of **10** and unidentified organometallic product(s). The  $^1\text{H}$  NMR of these contained ethylene resonances, indicating that **10** undergoes  $\beta$ -H elimination.

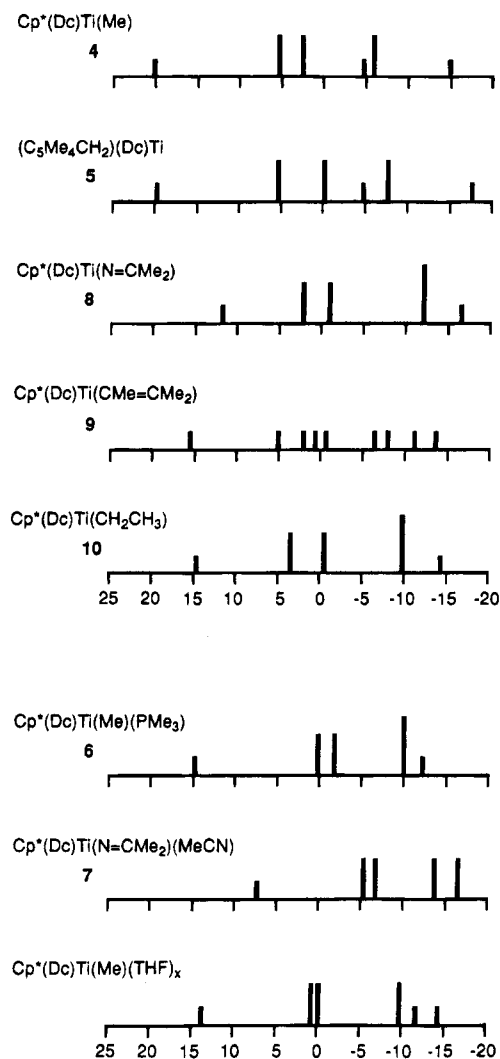


**Figure 3.** Schematic representation of  $^{11}\text{B}$  NMR data for 4–10. Three- and 4-coordinate compounds are grouped together for consistency with the discussion in the text. “Dc” denotes  $\eta^5\text{-C}_2\text{B}_9\text{H}_{11}$ .  $\text{Cp}^*(\text{Dc})\text{Ti}(\text{Me})(\text{THF})_x$  denotes the species formed upon reaction of 4 with THF.

$(\eta^5\text{-C}_2\text{B}_9\text{H}_{11})\text{Ti}(\text{Me})$  (4) in base-free form. Compound 4 is formally derived from the closo carborane  $\text{C}_2\text{B}_{10}\text{H}_{12}$  (*o*-carborane) by replacement of a “BH” vertex by a  $\text{d}^2$  “ $\text{Cp}^*\text{Ti}(\text{Me})$ ” fragment, which provides two electrons for cluster bonding. Compound 4 is also related to  $\text{Cp}^*_2\text{Ti}(\text{Me})^+$  by replacement of a  $\text{C}_5\text{Me}_5^-$  ligand by an  $(\eta^5\text{-C}_2\text{B}_9\text{H}_{11})^{2-}$  ligand. EMO calculations show that  $\text{d}^0$   $(\text{C}_5\text{R}_5)(\eta^5\text{-C}_2\text{B}_9\text{H}_{11})\text{M}(\text{H})$  species contain two low-lying metal-centered empty orbitals similar to those of  $\text{d}^0$   $(\text{C}_5\text{R}_5)_2\text{M}(\text{H})^{n+}$  species,<sup>1b</sup> and structural comparisons indicate that the steric properties of  $\text{Cp}^*$  and  $(\eta^5\text{-C}_2\text{B}_9\text{H}_{11})^{2-}$  ligands are similar.<sup>32</sup> Thus, 4 and other  $(\text{Cp}^*)(\eta^5\text{-C}_2\text{B}_9\text{H}_{11})\text{Ti}(\text{X})$  complexes are best considered as a 14-electron Ti(IV) species, analogous to  $\text{Cp}^*_2\text{Ti}(\text{Me})^+$  and  $\text{Cp}^*_2\text{Sc}(\text{Me})$ . Consistent with this picture,  $(\text{Cp}^*)(\eta^5\text{-C}_2\text{B}_9\text{H}_{11})\text{Ti}(\text{X})$  species display structural features and reactivity patterns characteristic of electrophilic metal complexes (Schemes 1, 2) including agostic interactions (10), ligand coordination (6, 7), insertion (6, 9, 10), and (intramolecular) C–H activation (5).  $(\text{Cp}^*)(\eta^5\text{-C}_2\text{B}_9\text{H}_{11})\text{Ti}(\text{X})$  complexes appear not to form 18-electron  $(\text{Cp}^*)(\eta^5\text{-C}_2\text{B}_9\text{H}_{11})\text{Ti}(\text{X})(\text{L})_2$  adducts, and 4 decomposes predominantly to mononuclear fulvene complex 5 rather than to binuclear  $\{(\text{Cp}^*)(\eta^5\text{-C}_2\text{B}_9\text{H}_{11})\text{Ti}\}(\mu\text{-CH}_2)$

species analogous to Zr and Hf complexes 3a,b. These results manifest the high degree of steric crowding in  $(\text{Cp}^*)(\eta^5\text{-C}_2\text{B}_9\text{H}_{11})\text{Ti}(\text{X})$  species.

**Ethylene Reactivity.**  $\text{Cp}^*_2\text{ScR}$  and analogous group 3 and lanthanide compounds polymerize ethylene to high molecular weight linear polyethylene with high activity.<sup>2,7,42</sup> Cationic  $(\text{C}_5\text{R}_5)_2\text{M}(\text{R})^+$  species ( $\text{M}$  = group 4, actinide) are also highly active ethylene polymerization catalysts; activities and polymer properties depend strongly on the steric and electronic properties of the  $(\text{C}_5\text{R}_5)_2\text{M}$  framework, the presence or absence of Lewis bases, and counterion/cocatalyst properties.<sup>43</sup> For example,  $(\text{C}_5\text{Me}_4\text{Pr})_2\text{TiCl}_2/\text{MAO}$ , in which the active species is almost certainly  $(\text{C}_5\text{Me}_4\text{Pr})_2\text{Ti}(\text{R})^+$ , catalyzes ethylene polymerization, though with much lower activity than less crowded Ti catalysts, e.g.  $\text{Cp}_2\text{TiX}_2/\text{MAO}$  ( $\text{X} = \text{Ph}, \text{Cl}$ ) or  $\text{Cp}(\text{C}_5\text{Me}_4\text{Pr})\text{TiCl}_2/\text{MAO}$ .<sup>44–46</sup> In contrast,  $(\text{Cp}^*)(\eta^5\text{-C}_2\text{B}_9\text{H}_{11})\text{TiR}$  catalyzes the slow dimerization of ethylene to butene (Scheme 2); evidently the unobserved intermediate  $(\text{Cp}^*)(\eta^5\text{-C}_2\text{B}_9\text{H}_{11})\text{Ti}(\text{nBu})$  undergoes  $\beta\text{-H}$  elimination much faster than ethylene insertion. This observation is reminiscent of the reactivity of the Zr and Hf dicarbollide complexes 1 and 3. These species polymerize ethylene with activity comparable to that of sterically similar  $(\text{C}_5\text{Me}_5)_2\text{M}(\text{R})^+$  species<sup>3b,42b,47</sup> but produce polymer of much lower molecular weight as a result of rapid  $\beta\text{-H}$  elimination.<sup>1b,c,48</sup>

The striking difference in the molecular weights of oligomers/polymers produced by group 4  $(\text{Cp}^*)(\text{C}_2\text{B}_9\text{H}_{11})\text{M}(\text{R})$  and  $\text{Cp}^*_2\text{M}(\text{R})^{n+}$  catalysts may be due in part to bond strength effects. Thermochemical studies clearly establish that  $\beta\text{-H}$  elimination processes are endothermic for early metal alkyl complexes.<sup>49</sup> Factors which increase the  $\text{M-R}$  bond strength relative to the  $\text{M-H}$  bond strength should tend to disfavor  $\beta\text{-H}$  elimination (other factors being equal). There is strong theoretical and experimental evidence that  $^+\text{M-R}$  bonds in cationic metal species are selectively strengthened relative to corresponding  $^+\text{M-H}$  bonds, due to the higher polarizability and  $\pi$ -donor ability of alkyl ligands vs the hydride ligand, which stabilizes the metal charge.<sup>50</sup> This effect may disfavor  $\beta\text{-H}$  elimination in cationic olefin polymerization catalysts, resulting in higher molecular weight product. In contrast, this effect is absent in the neutral dicarbollide systems and lower molecular weights are observed.<sup>51</sup>

(42) (a) Watson, P. L. *J. Am. Chem. Soc.* **1982**, *104*, 337. (b) Ballard, D. G. H.; Courtis, A.; Holton, J.; McMeeking, J.; Pearce, R. *J. Chem. Soc., Chem. Commun.* **1978**, 994. (c) Evans, W. J.; Chamberlain, L. R.; Ulibarri, T. A.; Ziller, J. W. *J. Am. Chem. Soc.* **1988**, *110*, 6423. (d) den Haan, K. H.; Wielstra, Y.; Eshuis, J. J. W.; Teuben, J. H. *J. Organomet. Chem.* **1987**, *323*, 181.

(43) For a recent review see: Möhring, P. C.; Coville, N. J. *J. Organomet. Chem.* **1994**, *479*, 1.

(44) Mallin, D. T.; Rausch, M. D.; Mintz, E. A.; Rheingold, A. L. *J. Organomet. Chem.* **1990**, *381*, 35.

(45) (a) Ewen, J. A. *J. Am. Chem. Soc.* **1984**, *106*, 6355. (b) Ewen, J. A. *Stud. Surf. Sci. Catal.* **1986**, *25*, 271. (c) Giannetti, E.; Nicoletti, G. M.; Mazzocchi, R. *J. Polym. Sci., Polym. Chem. Ed.* **1985**, *23*, 2117.

(46) However, the discrete cationic systems  $[(\text{C}_5\text{Me}_5)_2\text{Ti}(\text{Me})][\text{BPh}_4]$  and  $[(\text{C}_5\text{Me}_5)_2\text{Ti}(\text{Me})(\text{tetrahydrothiophene})][\text{BPh}_4]$  are reported to be inactive with ethylene.<sup>56a</sup>

(47) Kaminsky, W.; Külper, K.; Niedoba, S. *Makromol. Chem., Macromol. Symp.* **1986**, *3*, 377.

(48) (a) Jordan, R. F.; Crowther, D. J. U.S. Patent 5,214,173, 1993. (b) Karol, F. J.; Kao, S.; Brady, R. C. U.S. Patent 5,162,466, 1993.

(49) Schock, L. E.; Marks, T. J. *J. Am. Chem. Soc.* **1988**, *110*, 7701.

(50) (a) Ziegler, T.; Tschinke, V.; Becke, A. *J. Am. Chem. Soc.* **1987**, *109*, 1351. (b) Mandich, M. L.; Halle, L. F.; Beauchamp, J. L. *J. Am. Chem. Soc.* **1984**, *106*, 4403.

Ethylene insertion of  $\beta$ -agostic Ti–Et species **10** is much slower than for Ti–Me species **4**. Previously, Bercaw found that the  $\beta$ -agostic ethyl complex  $\text{Cp}^*\text{ScEt}$  inserts ethylene more slowly than do  $\text{Cp}^*\text{ScMe}$  or higher nonagostic  $\text{Cp}^*\text{ScCH}_2\text{CH}_2\text{R}$  species.<sup>7b</sup> The  $\beta$ -agostic interactions in **10** and  $\text{Cp}^*\text{ScEt}$  probably disfavors ethylene coordination by utilizing the coordination site required for ethylene binding and perhaps may need to be broken for insertion to occur.

**Unresolved Issue.** An unresolved issue in the chemistry of the  $(\text{Cp}^*)(\text{C}_2\text{B}_9\text{H}_{11})\text{TiX}$  series is the possible role of paramagnetic species in the thermolysis and other reactions of **4** and **10**. We previously observed that  $\text{Cp}_2\text{Ti}(\text{CH}_2\text{Ph})^+$  species decompose via Ti– $\text{CH}_2\text{Ph}$  homolysis to  $\text{Ti}^{\text{III}}$  products.<sup>81</sup> Similar processes may be important in the chemistry of **4** and **10**. Our studies of this problem will be reported in due course.

## Experimental Section

**General Procedures.** All manipulations were performed by using vacuum-line or Schlenk techniques or in a glovebox under a purified  $\text{N}_2$  atmosphere. Solvents were distilled from appropriate drying/deoxygenating agents and stored under  $\text{N}_2$  or vacuum prior to use: toluene, benzene, hexane, THF,  $\text{Et}_2\text{O}$  (Na/benzophenone); MeCN ( $\text{P}_2\text{O}_5$ , molecular sieves), 2-butyne (molecular sieves),  $\text{PMe}_3$  (Na, molecular sieves).  $\text{C}_2\text{B}_9\text{H}_{13}$  and  $\text{Cp}^*\text{TiMe}_3$  were synthesized using literature procedures.<sup>5c,52</sup> NMR spectra were recorded on a Bruker AMX-360 instrument in flame-sealed or Teflon-valved tubes at 25 °C, unless indicated otherwise.  $^1\text{H}$  and  $^{13}\text{C}$  chemical shifts are reported versus  $\text{Me}_4\text{Si}$  and were determined by reference to the residual solvent peaks.  $^{11}\text{B}\{^1\text{H}\}$  NMR spectra were referenced to external  $\text{BF}_3\cdot\text{Et}_2\text{O}$  and  $^{31}\text{P}\{^1\text{H}\}$  NMR spectra to external  $\text{H}_3\text{PO}_4$ . The  $^1\text{H}$  NMR spectra of **4**–**10** contain broad BH resonances which are not listed. Elemental analyses were performed by E&R Microanalytical Laboratory, Inc.

**(Cp\*)( $\eta^5$ - $\text{C}_2\text{B}_9\text{H}_{11}$ )Ti(Me) (4). NMR Scale.** An NMR tube was charged with  $\text{Cp}^*\text{TiMe}_3$  (12 mg, 0.052 mmol) and  $\text{C}_2\text{B}_9\text{H}_{13}$  (7.0 mg, 0.052 mmol), toluene- $d_8$  (0.4 mL) was added under vacuum at  $-196$  °C, and the tube was warmed to  $-78$  °C. The solids dissolved with  $\text{CH}_4$  evolution, and the solution turned intensely yellow. The tube was warmed to 0 °C, and  $\text{CH}_4$  evolution continued; within 5 min, the reaction mixture turned deep red-brown. The tube was warmed to 23 °C for 5 min, and NMR spectra were recorded. The  $^1\text{H}$  NMR spectrum of the deep red solution established the formation of **4** in >85% yield.  $^1\text{H}$  NMR (toluene- $d_8$ ):  $\delta$  3.74 (br s, 2H, dicarbollide CH), 2.17 (s, 3H, TiMe), 1.71 (s, 15H,  $\text{C}_5\text{Me}_5$ ).  $^{13}\text{C}$  NMR (toluene- $d_8$ ,  $-30$  °C):  $\delta$  133.8 (s,  $\text{C}_5\text{Me}_5$ ), 81.0 (q,  $^1J_{\text{CH}} = 122$ , TiMe), 69.2 (br d,  $^1J_{\text{CH}} = 170$ ,  $\text{C}_2\text{B}_9\text{H}_{11}$ ), 13.3 (q,  $^1J_{\text{CH}} = 128$ ,  $\text{C}_5\text{Me}_5$ ).  $^{11}\text{B}\{^1\text{H}\}$  NMR ( $\text{C}_6\text{D}_6$ ):  $\delta$  20.0 (1B), 5.4 (2B), 2.5 (2B),  $-4.4$  (1B),  $-6.0$  (2B),  $-14.7$  (1B).

**Preparative Scale.** A solution of  $\text{C}_2\text{B}_9\text{H}_{13}$  (202 mg, 1.50 mmol) in toluene (40 mL) was added to a solution of  $\text{Cp}^*\text{TiMe}_3$  (343 mg, 1.50 mmol) in toluene (50 mL) at  $-78$  °C. The reaction mixture was warmed to 0 °C (30 min) and then to 23 °C (10 min). Attempts to isolate pure solid **4** were thwarted by its thermal decomposition and yielded partially soluble mixtures of **4** and **5**; therefore, solutions of **4** prepared in this manner were used for further reaction chemistry.

**( $\eta^6$ - $\text{C}_5\text{Me}_4\text{CH}_2$ )( $\eta^5$ - $\text{C}_2\text{B}_9\text{H}_{11}$ )Ti (5).** A solution of  $\text{Cp}^*(\eta^5$ - $\text{C}_2\text{B}_9\text{H}_{11})\text{Ti}(\text{Me})$  **4** (484 mg, 1.46 mmol) in toluene (30 mL) was stirred for 18 h at 23 °C. The dark reaction mixture was

filtered and the residue washed with toluene. The filtrate and wash were combined, concentrated to 15 mL, and cooled to  $-30$  °C overnight. The solid was collected by filtration. The filtrate was concentrated to 7 mL and layered with hexane (5 mL) to obtain a second crop of product. Total yield: 140 mg (30%).  $^1\text{H}$  NMR ( $\text{C}_6\text{D}_6$ ):  $\delta$  2.86 (br s, 2H, dicarbollide CH), 2.43 (s, 2H,  $\text{C}_5\text{Me}_4\text{CH}_2$ ), 1.54 (s, 6H,  $\text{C}_5\text{Me}_4\text{CH}_2$ ), 0.33 (s, 6H,  $\text{C}_5\text{Me}_4\text{CH}_2$ ).  $^{13}\text{C}$  NMR (toluene- $d_8$ ):  $\delta$  138.2 (s,  $\text{C}_5\text{Me}_4\text{CH}_2$ ), 134.9 (s,  $\text{C}_5\text{Me}_4\text{CH}_2$ ), 125.6 (s,  $\text{C}_5\text{Me}_4\text{CH}_2$ ), 92.5 (t,  $^1J_{\text{CH}} = 154$ ,  $\text{C}_5\text{Me}_4\text{CH}_2$ ), 65.6 (br d,  $^1J_{\text{CH}} = 166$ ,  $\text{C}_2\text{B}_9\text{H}_{11}$ ), 11.2 (q,  $^1J_{\text{CH}} = 129$ ,  $\text{C}_5\text{Me}_4\text{CH}_2$ ), 11.1 (q,  $^1J_{\text{CH}} = 128$ ,  $\text{C}_5\text{Me}_4\text{CH}_2$ ).  $^{11}\text{B}\{^1\text{H}\}$  NMR ( $\text{C}_6\text{D}_6$ ):  $\delta$  19.2 (1B), 5.3 (2B),  $-0.2$  (2B),  $-4.9$  (1B),  $-7.8$  (2B),  $-17.7$  (1B). IR (KBr,  $\text{cm}^{-1}$ ): 3012 (w), 2959 (w), 2915 (w), 2870 (sh), 2583 (vs,  $\nu(\text{BH})$ ), 2535 (vs  $\nu(\text{BH})$ ), 1449 (w), 1381 (m), 1081 (w), 1022 (m), 971 (w), 776 (w), 729 (m), 639 (w). Anal. Calcd for  $\text{C}_{12}\text{H}_{25}\text{B}_9\text{Ti}$ : C, 45.83; H, 8.01. Found: C, 45.61; H, 8.04.

**(Cp\*)( $\eta^5$ - $\text{C}_2\text{B}_9\text{H}_{11}$ )Ti(Me)( $\text{PMe}_3$ ) (6).** A solution of **4** (16 mg, 0.05 mmol) in toluene- $d_8$  (0.4 mL) was prepared in an NMR tube,  $\text{PMe}_3$  (ca. 0.5 mmol) was added by vacuum transfer at  $-78$  °C, and the tube was warmed to 23 °C. The volatiles were removed under vacuum, and the residue was dried under vacuum for 1 h.  $^1\text{H}$  NMR (toluene- $d_8$ ,  $-30$  °C):  $\delta$  3.93 (br s, 1H, dicarbollide CH), 2.57 (br s, 1H, dicarbollide CH), 1.78 (s, 15H,  $\text{C}_5\text{Me}_5$ ), 0.48 (br s, 9H,  $\text{PMe}_3$ ),  $-0.13$  (s, 3H, TiMe).  $^{13}\text{C}\{^1\text{H}\}$  NMR (toluene- $d_8$ ,  $-30$  °C):  $\delta$  122.0 (s,  $\text{C}_5\text{Me}_5$ ), 70.2 (br d,  $^2J_{\text{CP}} = 15$ , TiMe), 61.8 (s,  $\text{C}_2\text{B}_9\text{H}_{11}$ ), 59.6 (s,  $\text{C}_2\text{B}_9\text{H}_{11}$ ), 14.5 (d,  $^1J_{\text{CP}} = 18$ ,  $\text{PMe}_3$ ), 13.9 (s,  $\text{C}_5\text{Me}_5$ ).  $^{11}\text{B}\{^1\text{H}\}$  NMR (toluene- $d_8$ ):  $\delta$  14.6 (1B), 0.4 (2B),  $-1.6$  (2B),  $-10.1$  (3B),  $-12.1$  (1B).  $^{31}\text{P}\{^1\text{H}\}$  NMR (toluene- $d_8$ ,  $-30$  °C):  $\delta$   $-7.8$  ( $\text{PMe}_3$ ).

**(Cp\*)( $\eta^5$ - $\text{C}_2\text{B}_9\text{H}_{11}$ )Ti(N=CMe<sub>2</sub>)(MeCN) (7).** A solution of acetonitrile (110 mg, 2.7 mmol) in toluene (30 mL) was added to a solution of **4** (0.500 g, 1.51 mmol) in toluene (90 mL) at  $-78$  °C, and the reaction mixture was warmed to 23 °C and stirred for 15 h. The green-yellow microcrystalline precipitate was collected by filtration (75 mg). The filtrate was cooled to  $-30$  °C for 48 h, and a second crop (180 mg) of the same material was isolated (combined yield 255 mg, 41%). Compound **7** is dichromic, appearing green to reflected light and orange to transmitted light. The following NMR spectra were recorded in the presence of excess acetonitrile (ca. 20 equiv), which was added to disfavor MeCN dissociation.  $^1\text{H}$  NMR (toluene- $d_8$ ):  $\delta$  3.05 (br s, 2H, dicarbollide CH), 1.88 (s, 15H,  $\text{C}_5\text{Me}_5$ ), 1.43 (s, 6H, = $\text{CMe}_2$ ), 0.7 (br s, excess MeCN).  $^{13}\text{C}$  NMR (toluene- $d_8$ ):  $\delta$  169.0 (s, = $\text{CMe}_2$ ), 123.5 (s,  $\text{C}_5\text{Me}_5$ ), 117 (br s, MeCN), 56.5 (br d,  $^1J_{\text{CH}} = 169$ ,  $\text{C}_2\text{B}_9\text{H}_{11}$ ), 24.1 (q,  $^1J_{\text{CH}} = 128$ , = $\text{CMe}_2$ ), 13.5 (q,  $^1J_{\text{CH}} = 127$ , Cp\*),  $-0.4$  (br s, MeCN).  $^{11}\text{B}\{^1\text{H}\}$  NMR (toluene- $d_8$ ):  $\delta$  7.3 (1B),  $-5.3$  (2B),  $-6.5$  (2B),  $-13.2$  (2B),  $-16.4$  (2B). IR (KBr,  $\text{cm}^{-1}$ ): 2316 ( $\nu(\text{C}\equiv\text{N})$ ), 2287 ( $\nu(\text{C}\equiv\text{N})$ ), 1678 ( $\nu(\text{C}=\text{N})$ ). Anal. Calcd for  $\text{C}_{17}\text{H}_{35}\text{B}_9\text{N}_2\text{Ti}$ : C, 49.48; H, 8.54. Found: C, 49.17; H, 8.67.

**(Cp\*)( $\eta^5$ - $\text{C}_2\text{B}_9\text{H}_{11}$ )Ti(N=CMe<sub>2</sub>) (8).** The filtrate obtained after isolation of the second crop of **7** above was concentrated to 20 mL under vacuum and cooled to  $-30$  °C for 14 h. Red-brown crystals (140 mg, 25% based on **4**) were collected by filtration.  $^1\text{H}$  NMR (toluene- $d_8$ ):  $\delta$  3.62 (br s, 2H, dicarbollide CH), 1.77 (s, 15H,  $\text{C}_5\text{Me}_5$ ), 1.23 (s, 6H, = $\text{CMe}_2$ ).  $^{11}\text{B}\{^1\text{H}\}$  NMR (toluene- $d_8$ ):  $\delta$  11.9 (1B), 2.3 (2B),  $-1.0$  (2B),  $-12.0$  (3B),  $-16.6$  (1B). IR (KBr,  $\text{cm}^{-1}$ ): 1678 ( $\nu(\text{C}=\text{N})$ ).

**(Cp\*)( $\eta^5$ - $\text{C}_2\text{B}_9\text{H}_{11}$ )Ti(CMe=CMe<sub>2</sub>) (9).** Excess 2-butyne (ca. 0.9 mmol) was added to a solution of  $(\text{Cp}^*)(\eta^5$ - $\text{C}_2\text{B}_9\text{H}_{11})\text{Ti}(\text{Me})$  (60 mg, 0.18 mmol) in  $\text{C}_6\text{D}_6$  (0.6 mL) in an NMR tube via vacuum transfer. The NMR tube was maintained at 23 °C and agitated for 5 min. The volatiles were removed under vacuum, and the residue was dissolved in THF (3 mL). The solution was layered with hexane (3 mL) and cooled to  $-30$  °C. A red-brown solid was isolated by filtration (55 mg, 79%).  $^1\text{H}$  NMR (toluene- $d_8$ ):  $\delta$  3.84 (br s, 1H, dicarbollide CH), 3.31 (br s, 1H, dicarbollide CH), 1.74 (s, 15H,  $\text{C}_5\text{Me}_5$ ), 1.44 (s, 3H, C=CMe<sub>2</sub>), 0.89 (s, 3H, C=CMe<sub>2</sub>), 0.14 (s, 3H, TiC(Me)=).  $^{13}\text{C}$  NMR (toluene- $d_8$ ):  $\delta$  131.3 (s,  $\text{C}_5\text{Me}_5$ ), 65.1 (br d,  $^1J_{\text{CH}} = 174$ ,  $\text{C}_2\text{B}_9\text{H}_{11}$ ), 64.6 (br d,  $^1J_{\text{CH}} = 168$ ,  $\text{C}_2\text{B}_9\text{H}_{11}$ ), 24.0 (q,  $^1J_{\text{CH}} = 126$ ,

(51) The higher effective metal charge (i.e. lower metal electronegativity) and lower degree of steric crowding in group 3/lanthanide ( $\text{C}_5\text{R}_5$ )<sub>2</sub>MR complexes (vs group 4 ( $\text{Cp}^*)(\text{C}_2\text{B}_9\text{H}_{11})\text{MR}$  complexes) may promote olefin insertion relative to  $\beta$ -H elimination.

(52) Mena, M.; Royo, P.; Serrano, R.; Pellinghelli, M. A.; Tiripicchio, A. *Organometallics* **1989**, *8*, 476.

C=CMeMe), 23.3 (q,  $^1J_{\text{CH}} = 125$ , C=CMeMe), 19.8 (q,  $^1J_{\text{CH}} = 125$ , TiC(Me)=), 13.5 (q,  $^1J_{\text{CH}} = 128$ , C<sub>5</sub>Me<sub>5</sub>), vinyl carbons not observed.  $^{13}\text{C}$  NMR (THF-*d*<sub>8</sub>):  $\delta$  213.7 (s, TiC(Me)=), 132.0 (s, C<sub>5</sub>Me<sub>5</sub>), 130.0 (s, =CMe<sub>2</sub>), 65.1 (br d, partially obscured by solvent resonance, C<sub>2</sub>B<sub>9</sub>H<sub>11</sub>), 64.3 (br d,  $^1J_{\text{CH}} = 165$ , C<sub>2</sub>B<sub>9</sub>H<sub>11</sub>), 24.2 (q,  $^1J_{\text{CH}} = 126$ , C=CMe<sub>2</sub>), 23.6 (q,  $^1J_{\text{CH}} = 125$ , C=CMe<sub>2</sub>), 19.8 (q,  $^1J_{\text{CH}} = 125$ , TiC(Me)=), 13.7 (q,  $^1J_{\text{CH}} = 128$ , C<sub>5</sub>Me<sub>5</sub>).  $^{11}\text{B}\{^1\text{H}\}$  NMR (C<sub>6</sub>D<sub>6</sub>):  $\delta$  15.3, 5.1, 1.9, 0.7, -0.6, -6.4, -7.9, -11.2, -14.3 (each 1B). Anal. Calcd for C<sub>17</sub>H<sub>35</sub>B<sub>9</sub>Ti: C, 53.08; H, 9.17. Found: C, 51.89; H, 8.89.

**(Cp\*)( $\eta^5$ -C<sub>2</sub>B<sub>9</sub>H<sub>11</sub>)Ti(CH<sub>2</sub>CH<sub>3</sub>) (10).** An NMR tube containing a solution of (Cp\*)( $\eta^5$ -C<sub>2</sub>B<sub>9</sub>H<sub>11</sub>)Ti(Me) (16 mg, 0.050 mmol) in toluene-*d*<sub>8</sub> (0.4 mL) was charged with 2–3 atm of ethylene or doubly labeled  $^{13}\text{C}_2\text{H}_4$  at -196 °C. The tube was warmed to 23 °C for 5 min and stored at -30 °C prior to NMR measurements.  $^1\text{H}$  NMR (toluene-*d*<sub>8</sub>):  $\delta$  3.18 (br s, 2H, dicarbollide CH), 2.93 (q,  $^3J_{\text{HH}} = 7.9$ , 2H, CH<sub>2</sub>CH<sub>3</sub>), 1.65 (s, 15H, C<sub>5</sub>Me<sub>5</sub>), -0.75 (t,  $^3J_{\text{HH}} = 7.8$ , 3H, CH<sub>2</sub>CH<sub>3</sub>).  $^{13}\text{C}$  NMR (doubly  $^{13}\text{C}$ -labeled compound, toluene-*d*<sub>8</sub>, -30 °C):  $\delta$  89.5 (td,  $^1J_{\text{CH}} = 144$ ,  $^1J_{\text{CC}} = 28.5$ ,  $^{13}\text{CH}_2^{13}\text{CH}_3$ ), 64.7 (br d,  $^1J_{\text{CH}} = 169$ , C<sub>2</sub>B<sub>9</sub>H<sub>11</sub>), 26.1 (qd,  $^1J_{\text{CH}} = 124$ ,  $^1J_{\text{CC}} = 28.5$ ,  $^{13}\text{CH}_2^{13}\text{CH}_3$ ), 13.0 (q,  $^1J_{\text{CH}} = 128$ , C<sub>5</sub>Me<sub>5</sub>), Cp\*(C<sub>ipso</sub>) not observed.  $^{11}\text{B}\{^1\text{H}\}$  NMR (toluene-*d*<sub>8</sub>):  $\delta$  14.3 (1B), 3.2 (2B), -0.6 (2B), -10.1 (3B), -14.3 (1B).

**X-ray Crystallographic Analysis of 7.** Crystals of 7 were grown from a cold toluene solution. An orange, plate-shaped crystal was mounted on a Siemens R3m/V diffractometer under a low-temperature nitrogen stream. Key crystallographic data are summarized in Table 1. Final unit cell parameters were obtained from 25 accurately centered reflections ( $12^\circ < 2\theta < 20^\circ$ ). Three standard reflections monitored after every 150 reflections did not show any significant change in intensity during the data collection. The data were corrected for Lorentz and polarization effects. The structure was solved by direct-methods and subsequent difference Fourier syntheses using the SHELXTL-Plus package.<sup>53,54</sup> Full-matrix refinement was performed. All non-H atoms were refined

anisotropically. The carborane cage is disordered between two orientations. In the major orientation (60%), Cb(2) is a C atom and Cb(4) is a B atom. In the minor orientation (40%), Cb(2) is a B atom and Cb(4) is a C atom. The carborane H atoms were located in difference Fourier maps, and the methyl H atoms were placed at idealized positions (C–H = 0.96 Å).

**X-ray Crystallographic Analysis of 8.** Crystals of 8 were grown from a cold toluene solution. A red, plate-shaped crystal was mounted on the diffractometer under a low-temperature nitrogen stream. Key crystallographic data are summarized in Table 1. Final unit cell parameters were obtained from 25 accurately centered reflections ( $10^\circ < 2\theta < 18^\circ$ ). Three standard reflections monitored after every 150 reflections did not show any significant change in intensity during the data collection. The data were corrected for Lorentz and polarization effects. The structure was solved by direct-methods and subsequent difference Fourier syntheses using the SHELXTL-Plus package.<sup>53,54</sup> Full-matrix refinement was performed. The Ti, N, and methyl C atoms were refined anisotropically; the remaining C and B atoms were refined isotropically. The carborane H atoms were located in difference Fourier maps, and the methyl H atoms were placed at idealized positions (C–H = 0.96 Å).

**Acknowledgment.** This work was supported by NSF Grant CHE-9413022. C.K. is grateful to the Deutsche Forschungsgemeinschaft for a fellowship.

**Supplementary Material Available:** For 7 and 8, tables of complete bond distances and angles, anisotropic displacement coefficients, and hydrogen atom coordinates and isotropic displacement coefficients (8 pages). Ordering information is given on any current masthead page.

OM950207E

(53) Sheldrick, G. M. SHELXTL-PLUS; Siemens Analytical X-ray Instruments, Inc., 1990.

(54) *International Tables for X-ray Crystallography*; Kynoch Press: Birmingham, England, 1994; Vol. IV.

# Synthesis and Characterization of a Series of Mononuclear Tantalum(V) Hydride Compounds Containing Aryloxy Ligation

Bernardeta C. Parkin, Janet R. Clark, Valerie M. Visciglio,  
Phillip E. Fanwick, and Ian P. Rothwell\*

Department of Chemistry, 1393 Brown Building, Purdue University,  
West Lafayette, Indiana 47907-1393

Received March 27, 1995<sup>®</sup>

A series of seven-coordinate, mononuclear tantalum–hydride compounds  $[\text{Ta}(\text{OC}_6\text{H}_3\text{Pr}^i\text{-2,6})_2(\text{Cl})_{3-n}(\text{H})_n]$  (**1**,  $n = 1$ ; **2**,  $n = 2$ ; **3**,  $n = 3$ ;  $\text{OC}_6\text{H}_3\text{Pr}^i\text{-2,6} = 2,6\text{-diisopropylphenoxide}$ ; L = tertiary phosphines) can be obtained either by hydrogenolysis of the corresponding tantalum alkyl substrate, producing **2** and **3**, or by reacting the trichloride  $[\text{Ta}(\text{OC}_6\text{H}_3\text{Pr}^i\text{-2,6})_2\text{Cl}_3]$  with one (for **1**) or two (for **2**) equiv of  $\text{Bu}^n\text{SnH}$  in the presence of ligand. The hydrogenolysis of the substrate  $[\text{Ta}(\text{OC}_6\text{H}_3\text{Pr}^i\text{-2,6})_2(\text{CH}_2\text{C}_6\text{H}_4\text{-4Me})_3]$  in the presence of  $\text{PMe}_2\text{Ph}$  or  $\text{PMePh}_2$  produces the complexes  $[\text{Ta}(\text{OC}_6\text{H}_3\text{Pr}^i\text{-2,6})_2(\text{H})_3(\text{L})_2]$  (**3a**, L =  $\text{PMe}_2\text{Ph}$ ; **3b**, L =  $\text{PMePh}_2$ ), while the compounds  $[\text{Ta}(\text{OC}_6\text{H}_3\text{Ph}_2\text{-2,6})_2(\text{R})_3]$  (R =  $\text{CH}_2\text{C}_6\text{H}_4\text{-4Me}$ ,  $\text{CH}_2\text{SiMe}_3$ ) produce  $[\text{Ta}(\text{OC}_6\text{H}_3\text{Cy}_2\text{-2,6})_2(\text{H})_3(\text{L})_2]$  (**3c**, L =  $\text{PMe}_2\text{Ph}$ ; **3d**, L =  $\text{PMePh}_2$ ) with the 2,6-dicyclohexylphenoxide ligand being generated by intramolecular hydrogenation of the *ortho* phenyl rings in the 2,6-diphenylphenoxide substrate. The hydrogenolysis of the bisalkyl  $[\text{Ta}(\text{OC}_6\text{H}_3\text{Pr}^i\text{-2,6})_3(\text{CH}_2\text{C}_6\text{H}_4\text{-4Me})_2]$  in the presence of  $\text{PMe}_2\text{Ph}$  produces the six-coordinate  $[\text{Ta}(\text{OC}_6\text{H}_3\text{Pr}^i\text{-2,6})_3(\text{PMe}_2\text{Ph})(\text{H})_2]$ , **4b**, which will exchange the phosphine ligand to produce a series of substituted derivatives. A related series of six-coordinate dihydride compounds  $[\text{Ta}(\text{OC}_6\text{H}_3\text{Bu}^t\text{-2,6})_2(\text{L})(\text{Cl})(\text{H})_2]$ , **5**, are produced by addition of  $\text{Bu}^n\text{SnH}$  (2 Sn per Ta) to  $[\text{Ta}(\text{OC}_6\text{H}_3\text{Bu}^t\text{-2,6})_2\text{Cl}_3]$  in the presence of added L. Single-crystal X-ray diffraction analyses of seven-coordinate **1**, **2b**, and **3c** (all cases L =  $\text{PMe}_2\text{Ph}$ ) show them to adopt pentagonal bipyramidal geometries with *trans* axial aryloxy ligands. In monohydride **1** the unique hydride ligand is *cis* to both phosphine ligand, while in dihydride **2b** the hydride ligands are mutually *cis* but *trans* to the chloride group within the pentagonal plane. A crystallographic 2-fold axis in trihydride **3c** passes through the unique Ta–H bond and bisects the remaining *cis* hydride ligands within the pentagonal plane. The solution <sup>1</sup>H NMR spectra of **1**, **2**, and **3** are consistent with the solid state structure being maintained in solution. Furthermore, analysis and simulation of the downfield hydride resonances in **2** and **3** show these seven-coordinate molecules to be stereochemically rigid on the NMR time scale. The coupling constants obtained from simulations conclusively rule out the formulation of **2** or **3** as containing  $\eta^2\text{-H}_2$  ligands. The solid state structures of six-coordinate  $[\text{Ta}(\text{OC}_6\text{H}_3\text{Pr}^i\text{-2,6})_3(\text{PMe}_2\text{Ph})(\text{H})_2]$ , **4b**, and  $[\text{Ta}(\text{OC}_6\text{H}_3\text{Bu}^t\text{-2,6})_2(\text{PMePh}_2)(\text{Cl})(\text{H})_2]$ , **5c**, show a geometry severely distorted from octahedral. In both compounds the mutually *trans* hydride ligands are bent toward the phosphine ligand with H–Ta–P angles of 66(2)° and 69(1)° for **4a** and 56(2)° and 62(2)° for **5b**. A steric origin to this distortion is ruled out by the structure of **5b** in which the hydride ligands are bent toward the bulky phosphine ligand and away from the Ta–Cl bond. Strong support for the distorted structures of **4** and **5** comes from solution and solid state infrared spectra where two sharp  $\bar{\nu}(\text{Ta}-\text{H})$  vibrations are observed. Analysis of the intensity ratio for the symmetric and asymmetric bands yields predicted H–Ta–H angles very close to those observed in the solid state structure. The summary of the crystal data is as follows for  $[\text{Ta}(\text{OC}_6\text{H}_3\text{Pr}^i\text{-2,6})_2(\text{PMe}_2\text{Ph})_2(\text{Cl})_2(\text{H})]$ , **1**, at 20 °C:  $a = 26.025(4)$  Å,  $b = 10.7954(5)$  Å,  $c = 18.509(3)$  Å,  $\beta = 128.31(1)^\circ$ ,  $Z = 4$ ,  $d_{\text{calcd}} = 1.438$  g cm<sup>-3</sup> in space group *C2/c*. For  $[\text{Ta}(\text{OC}_6\text{H}_3\text{Pr}^i\text{-2,6})_2(\text{PMe}_2\text{Ph})_2(\text{Cl})(\text{H})_2]$ , **2b**, at 20 °C:  $a = 9.735(1)$  Å,  $b = 24.310(3)$  Å,  $c = 17.735(2)$  Å,  $\beta = 90.76(1)^\circ$ ,  $Z = 4$ ,  $d_{\text{calcd}} = 1.344$  g cm<sup>-3</sup> in space group *P2<sub>1</sub>/n*. For  $[\text{Ta}(\text{OC}_6\text{H}_3\text{-Cy}_2\text{-2,6})_2(\text{PMe}_2\text{Ph})_2(\text{H})_3]$ , **3c**, at 20 °C:  $a = 24.065(3)$  Å,  $b = 13.530(2)$  Å,  $c = 20.263(3)$  Å,  $\beta = 131.633(9)^\circ$ ,  $Z = 4$ ,  $d_{\text{calcd}} = 1.313$  g cm<sup>-3</sup> in space group *C2/c*. For  $[\text{Ta}(\text{OC}_6\text{H}_3\text{Pr}^i\text{-2,6})_3(\text{PMe}_2\text{Ph})(\text{H})_2]$ , **4b**, at 20 °C:  $a = 10.637(1)$  Å,  $b = 12.820(2)$  Å,  $c = 31.799(4)$  Å,  $\beta = 98.76(1)^\circ$ ,  $Z = 4$ ,  $d_{\text{calcd}} = 1.322$  g cm<sup>-3</sup> in space group *P2<sub>1</sub>/n*. For  $[\text{Ta}(\text{OC}_6\text{H}_3\text{Bu}^t\text{-2,6})_2(\text{PMePh}_2)(\text{Cl})(\text{H})_2]$ , **5c**, at -100 °C,  $a = 10.851(5)$  Å,  $b = 18.110(7)$  Å,  $c = 20.09(1)$  Å,  $\beta = 96.67(5)^\circ$ ,  $Z = 4$ ,  $d_{\text{calcd}} = 1.404$  g cm<sup>-3</sup> in space group *P2<sub>1</sub>/n*.

## Introduction

The study of transition metal hydride compounds remains an extremely active area of chemical research.<sup>1</sup>

This interest stems not only from the important chemical reactivity demonstrated by these species but also by their structural and spectroscopic properties.<sup>2</sup> Another facet to this chemistry has been added with the discovery and characterization of  $\eta^2$ -dihydrogen complexes.<sup>3</sup> During our studies of the early d-block organometallic

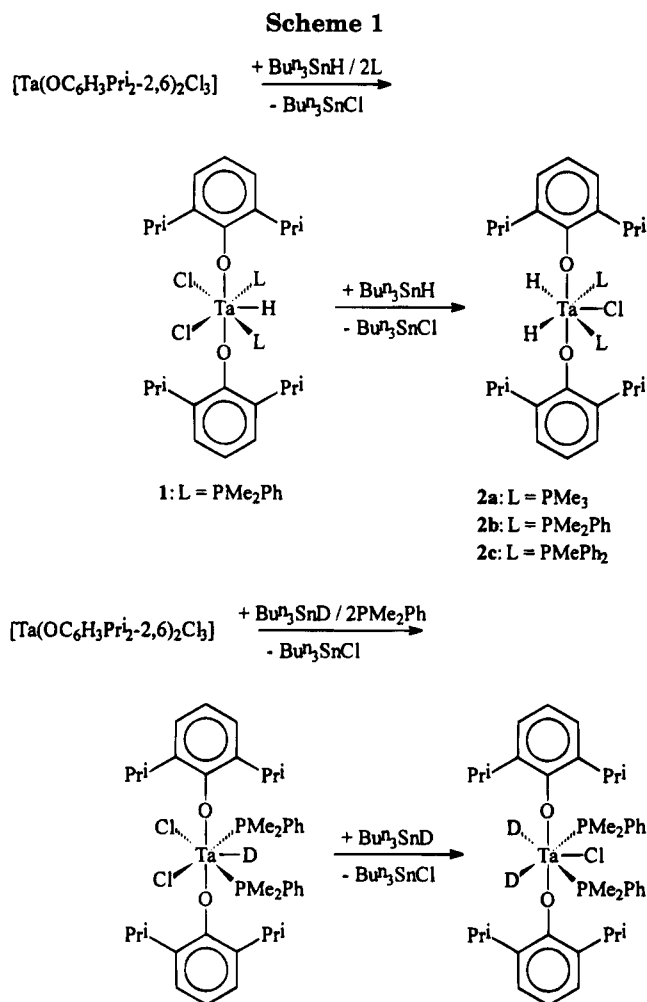
<sup>®</sup> Abstract published in *Advance ACS Abstracts*, May 15, 1995.

chemistry associated with bulky aryloxy ligation we have demonstrated the ability of mixed hydrido aryloxides of niobium and tantalum to carry out the catalytic hydrogenation of arene rings along with other unsaturated substrates.<sup>4</sup> In this paper we report on the synthesis, structure and spectroscopic properties of an extensive series of mononuclear hydride compounds of tantalum(V).<sup>5</sup>

## Results and Discussion

**Synthesis of Compounds.** There are numerous methods in the literature for the formation of transition metal hydride bonds.<sup>1</sup> Using as our basic starting materials the chloro aryloxides  $[\text{Ta}(\text{OC}_6\text{H}_3\text{R}_{2-2,6})_n\text{Cl}_{5-n}]$  ( $\text{R} = \text{Pr}^i$ ,  $n = 2, 3$ ;  $\text{R} = \text{Ph}$ ,  $n = 2, 3$ ; and  $\text{R} = \text{Bu}^t$ ,  $n = 2$ )<sup>6,7</sup> we have evaluated many of these methods for the generation of the corresponding hydride derivatives. We find that two synthetic procedures are superior for the formation of hydrido aryloxides in high yield. The first involves addition of  $\text{Bu}^n_3\text{SnH}$  to the corresponding chloride in the presence of phosphine ligands.<sup>8</sup> The second involves initial formation of the corresponding alkyl intermediate followed by hydrogenolysis, again in the presence of a suitable phosphine ligand.<sup>5k,9</sup>

The trichloride  $[\text{Ta}(\text{OC}_6\text{H}_3\text{Pr}^i_{2-2,6})_2\text{Cl}_3]$  forms a 1:1 adduct in hydrocarbon solution with phosphine ligands.<sup>10</sup> In the presence of an excess (>2 equiv) of  $\text{PMe}_2\text{Ph}$ , the addition of  $\text{Bu}^n_3\text{SnH}$  to these mixtures does not lead to any detectable evolution of hydrogen gas. Instead sequential formation of the seven-coordinate mono- and dihydrido derivatives **1** and **2b** occurs (Scheme 1). The



(1) (a) Crabtree, R. H. In *Comprehensive Coordination Chemistry*; Wilkinson, G.; Gillard, R. D.; McCleverty, J. A., Eds.; Pergamon Press: Oxford, 1987; Vol. 2, Chapter 19. (b) Hlatky, G. G.; Crabtree, R. H. *Coord. Chem. Rev.* **1985**, *65*, 2. (c) Moore, D. S.; Robinson, S. D. *Chem. Soc. Rev.* **1983**, 415. Some recent articles: (d) Bakhmutov, V.; Burgi, T.; Burger, P.; Ruppli, U.; Berke, H. *Organometallics* **1994**, *13*, 4203. (e) Lin, Z.; Hall, M. B. *J. Am. Chem. Soc.* **1994**, *116*, 4446. (f) Heinekey, D. M.; Oldham, W. J., Jr. *J. Am. Chem. Soc.* **1994**, *116*, 3137. (g) Hauger, B. E.; Gusev, D. G.; Caulton, K. G. *J. Am. Chem. Soc.* **1994**, *116*, 208. (h) Dmitry, G.; Gusev, D. G.; Kuhlman, R.; Sini, G.; Eisenstein, O.; Caulton, K. G. *J. Am. Chem. Soc.* **1994**, *116*, 2685. (i) Heinekey, D. M.; Oldham, W. J., Jr. *J. Am. Chem. Soc.* **1994**, *116*, 3375. (j) Heinekey, D. M.; Schomber, B. M.; Radzewich, C. E. *J. Am. Chem. Soc.* **1994**, *116*, 4515. (k) Budzichowski, T. A.; Chisholm, M. H.; Strieb, W. E. *J. Am. Chem. Soc.* **1994**, *116*, 389. (l) Moreno, B.; Sabo-Etienne, S.; Chaudret, B.; Rodriguez-Fernandez, A.; Trofimenko, F. J. S. *J. Am. Chem. Soc.* **1994**, *116*, 2635. (m) Burrell, A. K.; Bryan, J. C.; Kubas, G. J. *J. Am. Chem. Soc.* **1994**, *116*, 1575. (n) Fryzuk, M. D.; Lloyd, B. R.; Clentsmith, G. K. B.; Rettig, S. J. *J. Am. Chem. Soc.* **1994**, *116*, 3804. (o) Cappellani, E. P.; Drouin, S. D.; Jia, G.; Maltby, P. A.; Morris, R. H.; Schweitzer, C. T. *J. Am. Chem. Soc.* **1994**, *116*, 3375. (p) Shapiro, P. J.; Cotter, W. D.; Schefer, W. P.; Labinger, J. A.; Bercaw, J. E. *J. Am. Chem. Soc.* **1994**, *116*, 4623. (q) Paneque, M.; Poveda, M. L.; Taboada, S. *J. Am. Chem. Soc.* **1994**, *116*, 4519.

(2) (a) Teller, R. G.; Bau, R. *Struct. Bonding (Berlin)* **1981**, *44*, 1. (b) Zilm, K. W.; Millar, J. M. *Adv. Magn. Opt. Reson.* **1990**, *15*, 163.

(3) (a) Kubas, G. J.; Ryan, R. R.; Swanson, B. I.; Vergamini, P. J.; Wasserman, J. J. *J. Am. Chem. Soc.* **1984**, *106*, 451. (b) Kubas, G. J. *Acc. Chem. Res.* **1988**, *21*, 120. (c) Crabtree, R. H. *Chem. Rev.* **1985**, *85*, 245. (d) Crabtree, R. H. *Acc. Chem. Res.* **1990**, *23*, 95. (e) Jessop, P. G.; Morris, R. H. *Coord. Chem. Rev.* **1992**, *121*, 155. (f) Heinekey, D. M.; Oldham, W. J. *Chem. Rev.* **1993**, *93*, 913. (g) Kubas, G. J.; Burns, C. J.; Eckert, J.; Johnson, S. W.; Larson, A. C.; Vergamini, P. J.; Unkefer, C. J.; Khalsa, G. R. K.; Jackson, S. A.; Eisenstein, O. *J. Am. Chem. Soc.* **1993**, *115*, 569 and references therein. (h) Crabtree, R. H. *Angew. Chem., Int. Ed. Engl.* **1993**, *32*, 789.

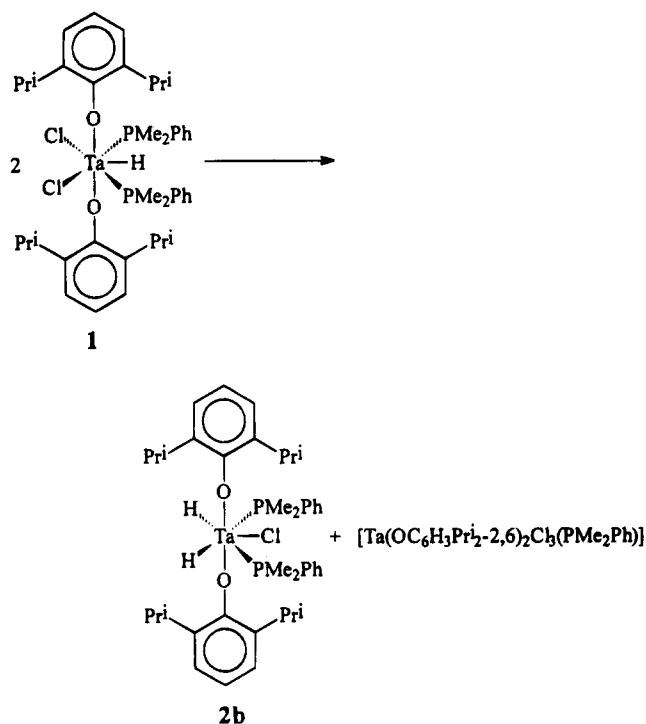
(4) (a) Steffey, B. D.; Chesnut, R. W.; Kerschner, J. L.; Pellechia, P. J.; Fanwick, P. E.; Rothwell, I. P. *J. Am. Chem. Soc.* **1989**, *111*, 378. (b) Ankaniec, B. C.; Fanwick, P. E.; Rothwell, I. P. *J. Am. Chem. Soc.* **1991**, *113*, 4710. (c) Visciglio, V. M.; Fanwick, P. E.; Rothwell, I. P. *J. Chem. Soc., Chem. Commun.* **1992**, 1505. (d) Yu, J. S.; Rothwell, I. P. *J. Chem. Soc., Chem. Commun.* **1992**, 632. (e) Clark, J. R.; Fanwick, P. E.; Rothwell, I. P. *J. Chem. Soc., Chem. Commun.* **1993**, 1233. (f) Yu, J. S.; Ankaniec, B. C.; Nguyen, M. T.; Rothwell, I. P. *J. Am. Chem. Soc.* **1992**, *114*, 1927.

slightly soluble monohydride **1** is obtained in >80% yield directly from an unstirred reaction mixture, while formation of **2b** requires the stirring of a suspension of

(5) (a) Toreki, R.; LaPointe, R. E.; Wolczanski, P. T. *J. Am. Chem. Soc.* **1987**, *109*, 7558. (b) LaPointe, R. E.; Wolczanski, P. T.; Mitchell, J. F. *J. Am. Chem. Soc.* **1986**, *108*, 6382. (c) LaPointe, R. E.; Wolczanski, P. T.; VanDuyne, G. D. *Organometallics* **1985**, *4*, 1810. (d) Belmonte, P. A.; Cloke, G. N.; Schrock, R. R. *J. Am. Chem. Soc.* **1983**, *105*, 2643. (e) Turner, H. W.; Schrock, R. R.; Fellmann, J. D.; Holmes, S. J. *J. Am. Chem. Soc.* **1983**, *105*, 4942. (f) Nelson, J. E.; Parkin, G.; Bercaw, J. E. *Organometallics* **1992**, *11*, 2181. (g) Quan, R. W.; Bercaw, J. E.; Schaefer, W. P. *Acta Crystallogr. C* **1991**, *47*, 2057. (h) Nelson, J. E.; Bercaw, J. E.; Marsh, R. E.; Henling, L. M. *Acta Crystallogr. C* **1992**, *48*, 1023. (i) Bell, R. A.; Cohen, S. A.; Doherty, N. M.; Threlkel, R. S.; Bercaw, J. E. *Organometallics* **1986**, *5*, 972. (j) Asselt, A. V.; Burger, B. J.; Gibson, V. C.; Bercaw, J. E. *J. Am. Chem. Soc.* **1986**, *108*, 5347. (k) Mayer, J. M.; Bercaw, J. E. *J. Am. Chem. Soc.* **1982**, *104*, 2157. (l) Parkin G.; Asselt, A. V.; Leahy, D. J.; Whinnery, L.; Hua, N. G.; Quan, R. W.; Henling, L. M.; Schaefer, W. P.; Santarsiero, B. D.; Bercaw, J. E. *Inorg. Chem.* **1992**, *31*, 82. (m) Mayer, J. M.; Wolczanski, P. T.; Santarsiero, B. D.; Olson, W. A.; Bercaw, J. E. *Inorg. Chem.* **1983**, *22*, 1149. (n) Sattelberger, A. P.; Wilson, R. B., Jr.; Huffman, J. C. *Inorg. Chem.* **1982**, *21*, 2392. (o) Sattelberger, A. P.; Wilson, R. B., Jr.; Huffman, J. C. *Inorg. Chem.* **1982**, *21*, 4179. (p) Luetkens, M. L., Jr.; Elcesser, W. L.; Huffman, J. C.; Sattelberger, A. P. *Inorg. Chem.* **1984**, *23*, 1718. (q) Luetkens, M. L., Jr.; Hopkins, M. D.; Schultz, A. J.; Williams, J. M.; Fair, C. K.; Ross, F. K.; Huffman, J. C.; Sattelberger, A. P. *Inorg. Chem.* **1987**, *26*, 2430. (r) Sattelberger, A. P.; Wilson, R. B., Jr.; Huffman, J. C. *J. Am. Chem. Soc.* **1980**, *102*, 7111. (s) Luetkens, M. L., Jr.; Huffman, J. C.; Sattelberger, A. P. *J. Am. Chem. Soc.* **1983**, *105*, 4474. (t) Luetkens, M. L., Jr.; Huffman, J. C.; Sattelberger, A. P. *J. Am. Chem. Soc.* **1985**, *107*, 3361. (u) Luetkens, M. L., Jr.; Elcesser, W. L.; Huffman, J. C.; Sattelberger, A. P. *J. Chem. Soc., Chem. Commun.* **1983**, 1072. (v) Luetkens, M. L., Jr.; Santure, D. J.; Huffman, J. C.; Sattelberger, A. P. *J. Chem. Soc., Chem. Commun.* **1985**, 552. (w) Scioly, A. J.; Luetkens, M. L., Jr.; Wilson, R. B., Jr.; Huffman, J. C.; Sattelberger, A. P. *Polyhedron* **1987**, *6*, 741. (x) Curtis, M. D.; Bell, L. G.; Butler, W. M. *Organometallics* **1985**, *4*, 701. (y) Profflet, R. D.; Fanwick, P. E.; Rothwell, I. P. *Polyhedron* **1992**, *11*, 1559.



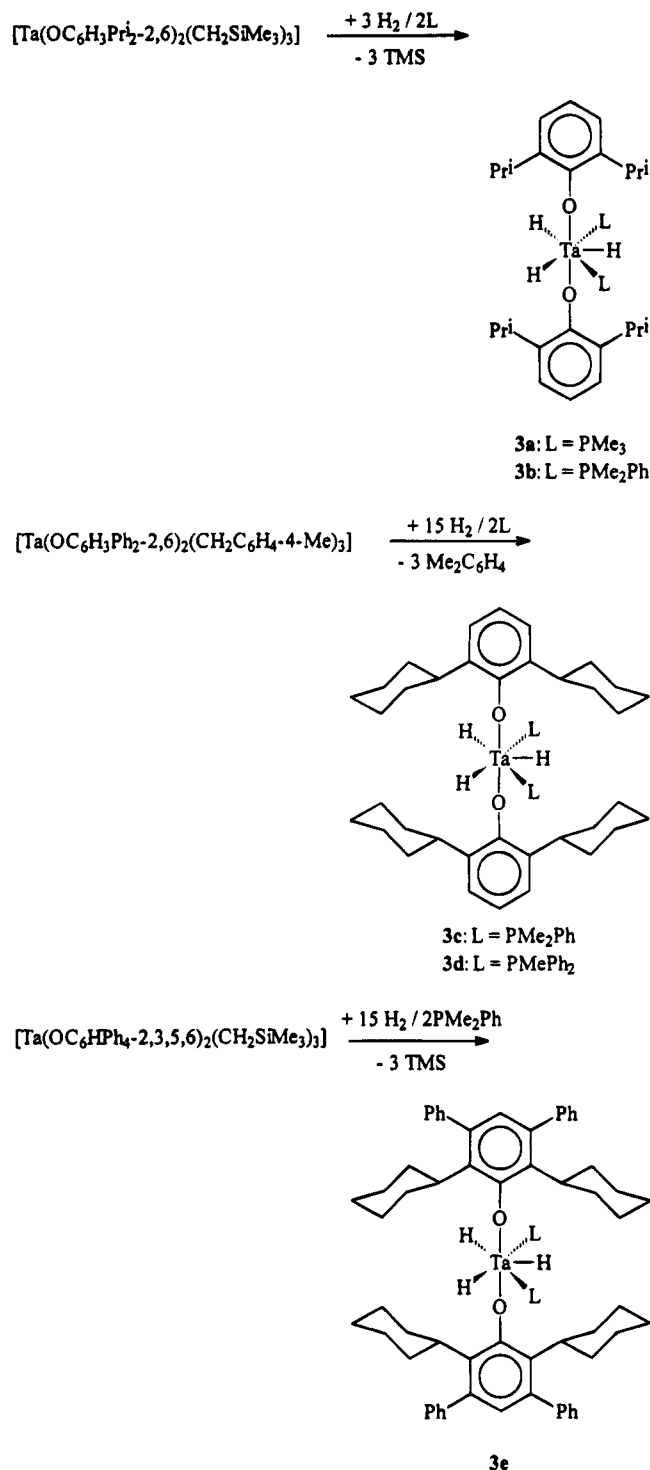
Scheme 2



**1** in the presence of an excess of Bu<sup>n</sup><sub>3</sub>SnH. The procedure can be used to obtain the corresponding deuterium-labeled compounds by using Bu<sup>n</sup><sub>3</sub>SnD as reagent (Scheme 1).

A suspension of sparingly soluble **1** in C<sub>6</sub>D<sub>6</sub> was found (<sup>1</sup>H and <sup>31</sup>P NMR) to produce **2** upon heating for several hours at 90 °C along with 1 equiv of the monophosphine adduct of the trichloride and free phosphine (Scheme 2). This ligand exchange reaction presumably proceeds via an intermediate containing two tantalum metal centers bridged by chloro and hydrido ligands. In the presence of an excess of Bu<sup>n</sup><sub>3</sub>SnH, the final chloride ligand in **2** is not replaced. The corresponding trihydride compounds **3** can, however, be obtained by the hydrogenolysis of the tris(4-methylbenzyl) complex [Ta(OC<sub>6</sub>H<sub>3</sub>Pr<sup>i</sup><sub>2</sub>-2,6)<sub>2</sub>(CH<sub>2</sub>C<sub>6</sub>H<sub>4</sub>-4Me)<sub>3</sub>]<sup>11</sup> in the presence of a suitable phosphine ligand (Scheme 3). The use of 2,6-diphenylphenoxide and 2,3,5,6-tetraphenylphenoxide alkyl substrates for reaction with H<sub>2</sub> leads to the formation of the corresponding 2,6-dicyclohexylphenoxide and 2,6-dicyclohexyl-3,5-diphenylphenoxide trihydride derivatives due to the intramolecular hydrogenation

Scheme 3



(6) (a) Chamberlain, L. R.; Keddington, J.; Rothwell, I. P. *Organometallics* **1982**, *1*, 1098. (b) Chamberlain, L. R.; Rothwell, I. P.; Huffman, J. C. *Inorg. Chem.* **1984**, *23*, 2575. (c) Chesnut, R. W.; Durfee, L. D.; Fanwick, P. E.; Rothwell, I. P. *Polyhedron* **1987**, *6*, 2019. (d) Steffey, B. D.; Chamberlain, L. R.; Chesnut, R. W.; Chebi, D. E.; Fanwick, P. E.; Rothwell, I. P. *Organometallics* **1989**, *8*, 1419. (e) Chesnut, R. W.; Yu, J. S.; Fanwick, P. E.; Rothwell, I. P. *Polyhedron* **1990**, *9*, 1051.

(7) Lockwood, M. A.; Potyen, M. C.; Steffey, B. D.; Fanwick, P. E.; Rothwell, I. P. *Polyhedron*, submitted for publication.

(8) (a) Roskamp, E. J.; Pedersen, S. F. *J. Am. Chem. Soc.* **1987**, *109*, 3152. (b) Roskamp, E. J.; Pedersen, S. F. *J. Am. Chem. Soc.* **1987**, *109*, 6551. (c) Cotton, F. A.; Maoyu Shang, J. L.; Wojtczak, W. A. *J. Am. Chem. Soc.* **1994**, *116*, 4364.

(9) (a) McAlister, D. R.; Erwin, D. K.; Bercaw, J. E. *J. Am. Chem. Soc.* **1978**, *100*, 5966. (b) Gell, K. I.; Schwartz, J. J. *J. Am. Chem. Soc.* **1978**, *100*, 3246.

(10) Potyen, M. C.; Clark, J. R.; Nguyen, M. T.; Fanwick, P. E.; Rothwell, I. P. *Polyhedron*, submitted for publication.

(11) Steffey, B. D.; Fanwick, P. E.; Rothwell, I. P. *Polyhedron* **1990**, *9*, 963.

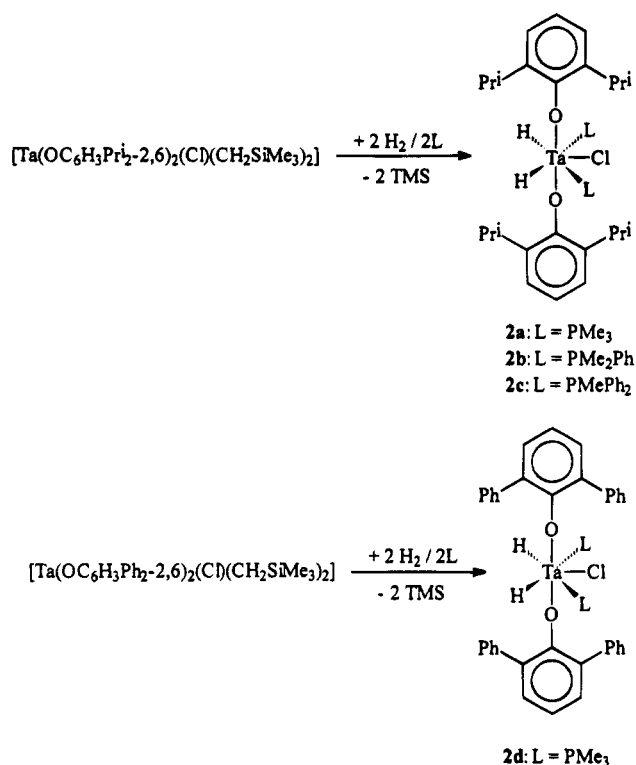
tion of the *ortho* phenyl rings (Scheme 3). The hydrogenolysis method can also be applied to the synthesis of the dihydride complexes **2** (Scheme 4). In the case of the monochloride precursor [Ta(OC<sub>6</sub>H<sub>3</sub>Ph<sub>2</sub>-2,6)<sub>2</sub>Cl(CH<sub>2</sub>SiMe<sub>3</sub>)<sub>2</sub>] the dihydride product obtained after 24 h contained unhydrogenated aryloxy ligands (Scheme 4).

Two sets of six-coordinate dihydride complexes were obtained either by the hydrogenolysis of the bisalkyl [Ta(OC<sub>6</sub>H<sub>3</sub>Pr<sup>i</sup><sub>2</sub>-2,6)<sub>3</sub>(CH<sub>2</sub>C<sub>6</sub>H<sub>4</sub>-4Me)<sub>2</sub>] or by treating the trichloride [Ta(OC<sub>6</sub>H<sub>3</sub>Bu<sup>t</sup><sub>2</sub>-2,6)<sub>2</sub>Cl<sub>3</sub>] with Bu<sup>n</sup><sub>3</sub>SnH/L in benzene solution (Scheme 5).

Some alternative methods have been evaluated for the synthesis of the tantalum-hydride compounds **1–5**. The



Scheme 4



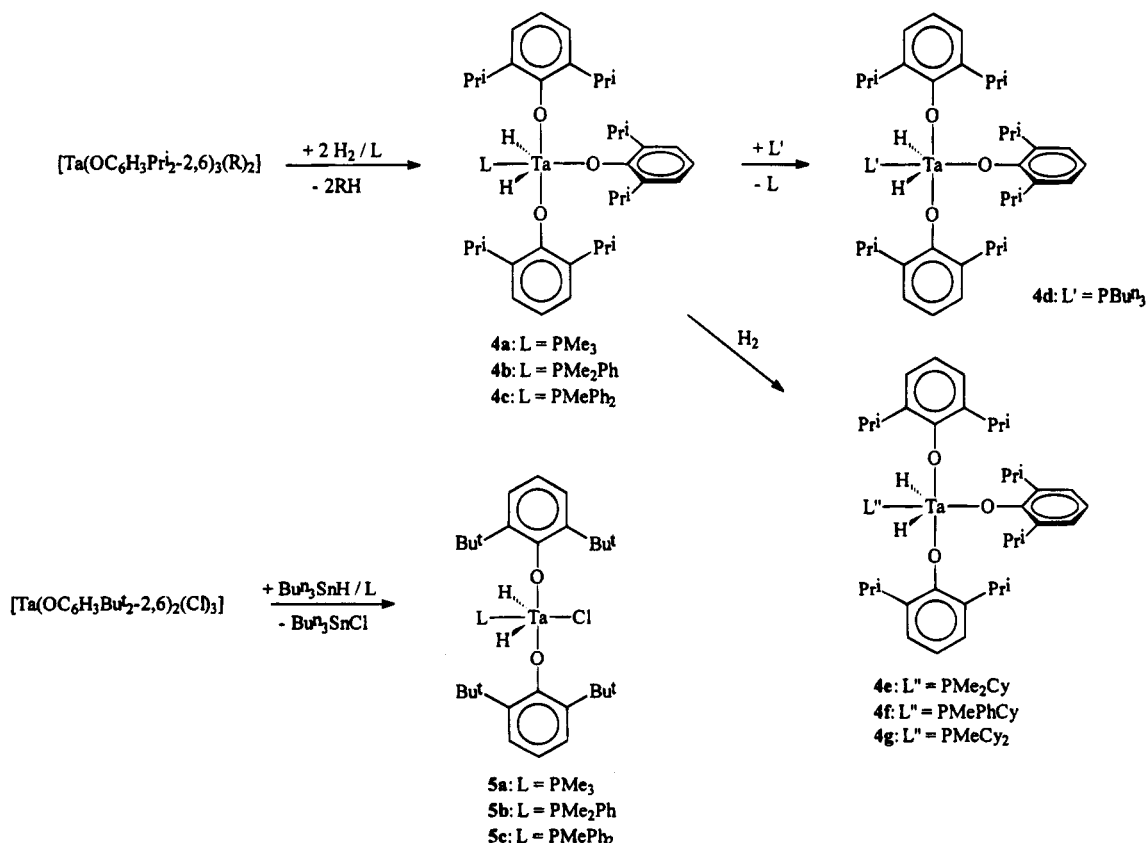
addition of hydride reagents such as LiBH<sub>4</sub> and LiAlH<sub>4</sub> to hydrocarbon solutions of phosphine ligands and halides such as [Ta(OC<sub>6</sub>H<sub>3</sub>Pr<sup>i</sup><sub>2-2,6</sub>)<sub>2</sub>Cl<sub>3</sub>] will generate detectable amounts of hydrido complexes such as **1** and **2** in solution (<sup>1</sup>H NMR), but isolation of the compounds from the reaction mixtures was not convenient. The

work of Wolczanski et al. has shown that siloxy hydrides of tantalum can be obtained by sodium amalgam reduction of the corresponding chloride precursor under an H<sub>2</sub> atmosphere.<sup>5a</sup> We find that hydride compounds such as **4** are generated by this procedure, although again yields of isolated material are lower than these obtained via hydrogenolysis of the alkyl precursor.

**Solid State Structures of the Tantalum Hydride Compounds.** Single-crystal X-ray diffraction analyses of representative examples of each class of compound **1–5** have been carried out. In each case the hydride ligands about the metal were located and refined. Furthermore the position of these hydride ligands was also supported by spectroscopic studies (*vide infra*). ORTEP views of the five molecules are shown in Figures 1–5, while selected interatomic distances and angles are collected in Tables 1–5.

The seven-coordinate compounds **1**, **2b**, and **3c** adopt a pentagonal bipyramidal arrangement of ligands about the tantalum metal centers. In all three molecules there are two mutually *trans* axial aryloxy ligands; O–Ta–O angles of 174.7(3)° in **1**, 178.6(2)° in **2b**, and 179.2(5)° in **3c**. The Ta–O distances are essentially identical for all three compounds at 1.90 Å (av). The Ta–O–Ar angles are all greater than 170°. Large angles at oxygen are typical of aryloxy derivatives of Ta(V).<sup>11</sup> The pentagonal planes of all three compounds contain the two phosphine ligands in nonadjacent positions. The angles within this plane reflect the steric requirements of the phosphine, chloride, and hydride ligands present. In **1** the H–Ta–P angles are compressed to 65.92(3)°, while the Cl–Ta–Cl angle is opened up to 86.66(7)°. In monochloride **2b**, the mutually *cis* hydride ligands are separated by 61(3)° while the Cl–Ta–P angles open up

Scheme 5



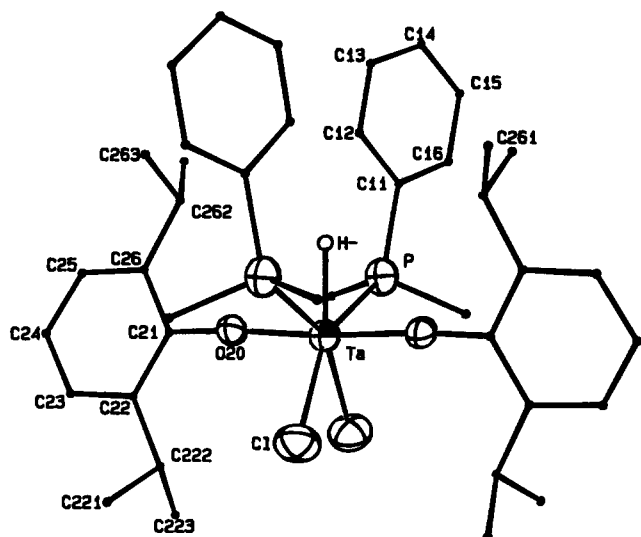


**Figure 1.** Molecular structure of  $[\text{Ta}(\text{OC}_6\text{H}_3\text{Pr}^i\text{-2,6})_2(\text{H})(\text{Cl})(\text{PMe}_2\text{Ph})_2]$ , **1**. Selected interatomic distances and angles are contained in Table 1. The molecule contains a crystallographically imposed 2-fold rotation axis.

to  $84.03(9)^\circ$  and  $84.88(8)^\circ$ . The trihydride **3c** is closest to adopting a true pentagonal bipyramidal structure with an  $\text{H}(1)\text{-Ta-H}(1)'$  angle of  $75(5)^\circ$  and *cis*  $\text{H-Ta-P}$  angles of  $65(3)^\circ$  and  $77.49(7)^\circ$ .

In compounds **2b** and **3c** the *cis*  $\text{H-Ta-H}$  angles of  $61(3)^\circ$  and  $75(5)^\circ$  are too large for there to be any significant interaction between the hydrogen ligands. This structural data combined with the spectroscopy of those colorless compounds strongly argues against their formulation as  $\eta^2$ -dihydrogen derivatives of  $\text{Ta}(\text{III})$ .<sup>2</sup>

The solid state structures of six-coordinate **4b** and **5c** are of particular interest. It can be seen (Figures 4 and 5) that both compounds adopt related structures. There are two mutually *trans* aryloxy ligands,  $\text{O-Ta-O}$  angles of  $173.3(1)^\circ$  and  $172.2(1)^\circ$ , and a phosphine ligand *trans* to either an aryloxy oxygen atom **4b**,  $\text{P-Ta-O}(30) = 174.5(1)^\circ$ , or a chloride group **5c**,  $\text{P-Ta-Cl} = 174.96(5)^\circ$ . This results in a square planar arrangement

**Table 1.** Selected Interatomic Distances (Å) and Angles (deg) for  $[\text{Ta}(\text{OC}_6\text{H}_3\text{Pr}^i\text{-2,6})_2(\text{H})(\text{Cl})(\text{PMe}_2\text{Ph})_2]$ , **1**

Ta-H <sup>-</sup>	1.70(7)	Ta-P	2.647(1)
Ta-Cl	2.478(1)	Ta-O(20)	1.902(3)
Cl-Ta-H <sup>-</sup>	139(3)	Cl-Ta-O(20)	87.82(9)
P-Ta-H <sup>-</sup>	65(3)	P-Ta-P	131.84(6)
O(20)-Ta-H <sup>-</sup>	87(5)	P-Ta-O(20)	92.19(9)
Cl-Ta-Cl	86.66(7)	P-Ta-O(20)	85.94(9)
Cl-Ta-P	153.84(5)	O(20)-Ta-O(20)	175.4(2)
Cl-Ta-P	73.73(4)	Ta-O(20)-C(21)	174.7(3)

for the  $[\text{TaO}_3\text{P}]$  and  $[\text{TaO}_2\text{PCl}]$  cores in **4b** and **5c** respectively. The two hydride ligands are positioned above and below this plane. The location and refinement of these hydrides show that they are distorted away from the positions predicted for an octahedral geometry. Instead in both cases the hydrides are bent toward the phosphine ligand with acute  $\text{H-Ta-P}$  angles of  $66(2)^\circ$  and  $69(1)^\circ$  in **4b** and  $56(2)^\circ$  and  $62(2)^\circ$  in **5c**. The positioning of these hydride ligands is supported by the infrared spectroscopy (*vide infra*) of **4** and **5** where analysis of the intensity of the two observed  $\bar{\nu}(\text{Ta-H})$  bands is consistent with the  $\text{H-Ta-H}$  angles of only  $135(3)^\circ$  in **4b** and  $118(2)^\circ$  in **5c** predicted by the X-ray diffraction studies.

The Ta-O(aryloxy) distances of 1.888(3) and 1.896(3) Å in **5c** are slightly shorter on average than the distances in **1**, **2b**, **3c**, and **4b**. In all five compounds the Ta-P distances span the very narrow range of 2.615(3) to 2.655(1) Å.

The pentagonal bipyramidal structures adopted by the seven-coordinate hydrides **1**, **2**, and **3** can be rationalized using steric and electronic arguments. The formation of a pentagonal bipyramid requires the use of seven atomic orbitals ( $s$ ,  $p_x$ ,  $p_y$ ,  $p_z$ ,  $d_{z^2}$ ,  $d_{xy}$ , and  $d_{x^2-y^2}$ ) on the metal center for  $\sigma$ -bonding. The *trans* axial arrangement of the bulky aryloxy groups not only minimizes steric crowding but also allows  $\pi$ -donation from the oxygen atoms into the vacant  $d_{xz}$  and  $d_{yz}$  pair of atomic orbitals on tantalum. The arrangement of

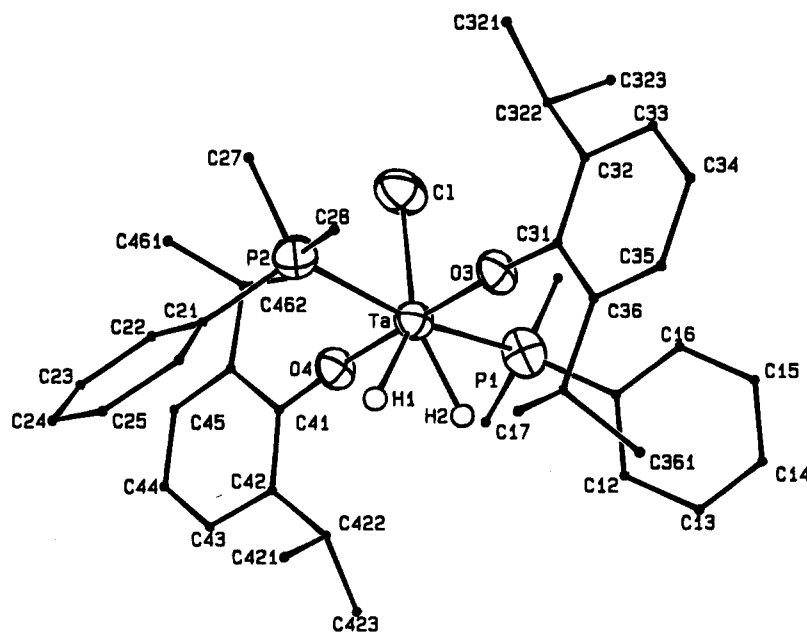


**Figure 2.** Molecular structure of  $[\text{Ta}(\text{OC}_6\text{H}_3\text{Pr}^i\text{-2,6})_2(\text{Cl})(\text{H})_2(\text{PMe}_2\text{Ph})_2]$ , **2b**. Selected interatomic distances and angles are contained in Table 2.

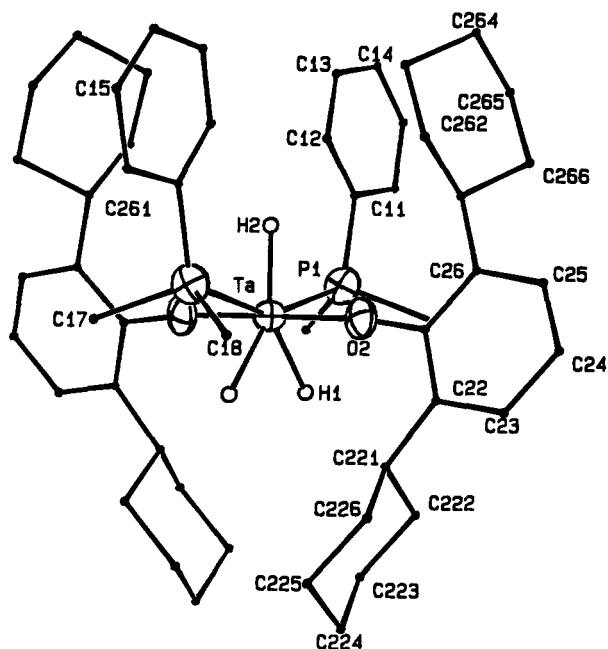


**Figure 3.** Molecular structure of  $[\text{Ta}(\text{OC}_6\text{H}_3\text{Cy}_{2-2,6})_2(\text{H})_3(\text{PMe}_2\text{Ph})_2]$ , **3c**. Selected interatomic distances and angles are contained in Table 3. The molecule contains a crystallographically imposed 2-fold rotation axis.

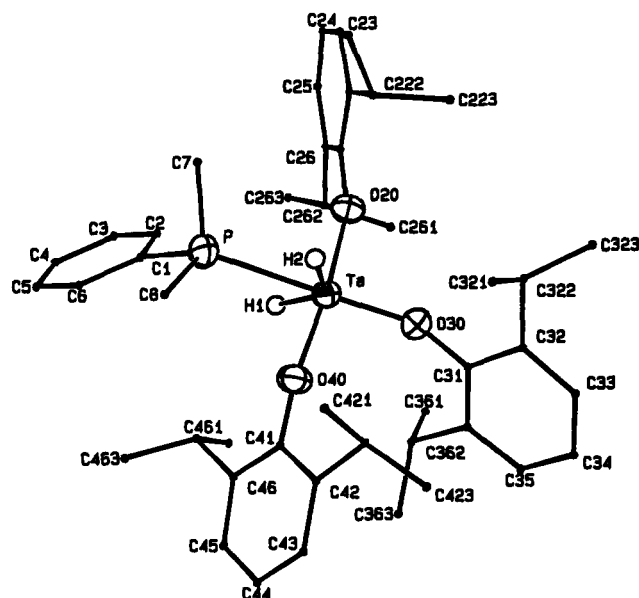


**Figure 4.** Molecular structure of  $[\text{Ta}(\text{OC}_6\text{H}_3\text{Pr}_{2-2,6})_3(\text{H})_2(\text{PMe}_2\text{Ph})]$ , **4a**. Selected interatomic distances and angles are contained in Table 4.

ligands within the pentagonal plane can be rationalized on steric grounds.

The structures adopted by six-coordinate **4b** and **5c** are intriguing. The bending of the hydride ligands toward the phosphine group cannot be rationalized on steric grounds; in **5c** a steric argument would predict a bending toward the chloride group. Despite the acute P-Ta-H angles in **4b** and **5c** the hydride ligands still lie 2.2–2.5 Å away from the phosphorus atom, which is too far (typical P-H bond distances are 1.4 Å) for any electronic interaction. A better description of the molecular structures of **4b** and **5c** involves a pentagonal bipyramidal arrangement of the "anionic" groups (hydride, chloride, aryloxy) with the phosphine ligand coordinated between the two equatorial hydride groups.

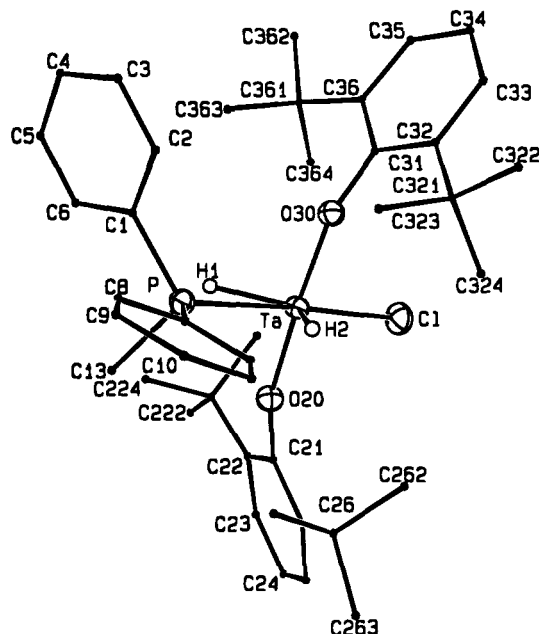


**Figure 5.** Molecular structure of  $[\text{Ta}(\text{OC}_6\text{H}_3\text{Bu}_{2-2,6})_2(\text{Cl})(\text{H})_2(\text{PMe}_2\text{Ph})]$ , **5c**. Selected interatomic distances and angles are contained in Table 5.

**Table 2. Selected Interatomic Distances (Å) and Angles (deg) for  $[\text{Ta}(\text{OC}_6\text{H}_3\text{Pr}_{2-2,6})_2\text{Cl}(\text{H})_2(\text{PMe}_2\text{Ph})_2]$ , **2b****

Ta-H(1)	1.90(9)	Ta-P(2)	2.617(3)
Ta-H(2)	1.76(7)	Ta-O(3)	1.899(5)
Ta-Cl	2.532(2)	Ta-O(4)	1.900(5)
Ta-P(1)	2.616(3)		
H(1)-Ta-H(2)	61(3)	Cl-Ta-P(2)	84.88(8)
Cl-Ta-H(1)	152(3)	Cl-Ta-O(3)	91.2(2)
Cl-Ta-H(2)	146(2)	Cl-Ta-O(4)	90.2(2)
P(1)-Ta-H(1)	123(3)	P(1)-Ta-P(2)	168.86(8)
P(1)-Ta-H(2)	62(2)	P(1)-Ta-O(3)	90.1(2)
P(2)-Ta-H(1)	68(3)	P(1)-Ta-O(4)	90.1(2)
P(2)-Ta-H(2)	129(2)	P(2)-Ta-O(3)	89.1(2)
O(3)-Ta-H(1)	95(3)	P(2)-Ta-O(4)	90.9(2)
O(3)-Ta-H(2)	92(2)	O(3)-Ta-O(4)	178.6(2)
O(4)-Ta-H(1)	84(3)	Ta-O(3)-C(31)	174.2(5)
O(4)-Ta-H(2)	87(2)	Ta-O(3)-C(41)	71.4(5)
Cl-Ta-P(1)	84.03(9)		

**Table 3. Selected Interatomic Distances (Å) and Angles (deg) for  $[\text{Ta}(\text{OC}_6\text{H}_3\text{Cy}_{2-2,6})_2(\text{H})_3(\text{PMe}_2\text{Ph})_2]$ , **3c****

Ta-H(1)	1.77(9)	Ta-P(1)	2.615(3)
Ta-H(2)	1.6(2)	Ta-O(2)	1.901(6)
H(1)-Ta-H(1)	75(5)	O(2)-Ta-H(2)	90.4(3)
H(1)-Ta-H(2)	143(3)	P(1)-Ta-P(1)	155.0(1)
P(1)-Ta-H(1)	65(3)	P(1)-Ta-O(2)	89.0(2)
P(1)-Ta-H(2)	140(3)	P(1)-Ta-O(2)	91.2(2)
P(1)-Ta-H(2)	77(3)	O(2)-Ta-O(2)	179.2(5)
O(2)-Ta-H(1)	84(3)	Ta-O(2)-C(21)	172.1(8)
O(2)-Ta-H(1)	95(3)		

The adoption of unexpected structures by some s- and p-block metal derivatives has been attributed to the presence of primary (typically covalent) and secondary (typically dative) bonds.<sup>12</sup> The secondary bonds are argued to be less stereochemically active than the primary bonds in determining the adopted structure. A similar argument can be applied to compounds **4b** and **5c** and a number of other transition metal compounds in the literature.<sup>13</sup>

(12) Goel, S. C.; Chiang, M. Y.; Buhro, W. E. *J. Am. Chem. Soc.* **1990**, *112*, 6724. (b) Haaland, A. *Angew. Chem., Int. Ed. Engl.* **1989**, *28*, 992. (c) Alcock, N. W. *Adv. Inorg. Chem. Radiochem.* **1972**, *15*, 1.

**Table 4. Selected Interatomic Distances (Å) and Angles (deg) for [Ta(OC<sub>6</sub>H<sub>3</sub>Pr<sup>i</sup>-2,6)<sub>3</sub>(H)<sub>2</sub>(PMe<sub>2</sub>Ph)], **4b****

Ta-H(1)	1.74(4)	Ta-O(20)	1.907(3)
Ta-H(2)	1.83(6)	Ta-O(30)	1.912(4)
Ta-P	2.650(1)	Ta-O(40)	1.897(3)
H(1)-Ta-H(2)	135(3)	P-Ta-O(20)	89.3(1)
P-Ta-H(1)	69(1)	P-Ta-O(30)	174.5(1)
P-Ta-H(2)	66(2)	P-Ta-O(40)	85.4(1)
O(20)-Ta-H(1)	89(1)	O(20)-Ta-O(30)	92.0(2)
O(20)-Ta-H(2)	91(2)	O(20)-Ta-O(40)	173.3(1)
O(30)-Ta-H(1)	116(1)	O(30)-Ta-O(40)	93.6(2)
O(30)-Ta-H(2)	109(2)	Ta-C(20)-C(21)	160.7(3)
O(40)-Ta-H(1)	86(1)	Ta-O(30)-C(31)	153.6(3)
O(40)-Ta-H(2)	91(2)	Ta-O(4)-C(41)	169.5(4)

**Table 5. Selected Interatomic Distances (Å) and Angles (deg) for [Ta(OC<sub>6</sub>H<sub>3</sub>Bu<sup>t</sup>-2,6)<sub>2</sub>Cl(H)<sub>2</sub>(PMePh<sub>2</sub>)], **5c****

Ta-H(1)	1.73(5)	Ta-P	2.655(1)
Ta-H(2)	1.54(5)	Ta-O(20)	1.896(3)
Ta-Cl	2.397(1)	Ta-O(30)	1.888(3)
H(1)-Ta-H(2)	118(2)	O(30)-Ta-H(1)	99(2)
Cl-Ta-H(1)	128(2)	O(30)-Ta-H(2)	88(2)
Cl-Ta-H(2)	113(2)	Cl-Ta-P	174.96(5)
P-Ta-H(1)	56(2)	Cl-Ta-O(20)	86.5(1)
P-Ta-H(2)	62(2)	Cl-Ta-O(30)	86.5(1)
O(20)-Ta-H(1)	83(2)	P-Ta-O(20)	92.7(1)
O(20)-Ta-H(2)	99(2)	P-Ta-O(30)	94.6(1)
O(20)-Ta-O(30)	172.2(1)		

**NMR Spectroscopic Properties.** The most important spectroscopic feature of these compounds is due to the tantalum hydride ligands in the <sup>1</sup>H NMR spectrum (Table 6). The resonances due to the other ligands in the <sup>1</sup>H, <sup>13</sup>C, and <sup>31</sup>P NMR spectra are unexceptional and are consistent with the observed solid state structures. The hydride ligands in compounds **1–5** resonate to low field in the δ 10–20 ppm region of the <sup>1</sup>H NMR spectrum. In sparingly soluble monohydride **1** the hydride ligand appears as a sharp triplet at δ 18.93 ppm due to coupling to the two equivalent <sup>31</sup>P nuclei, <sup>2</sup>J(<sup>31</sup>P–<sup>1</sup>H) = 88.0 Hz. In dihydrides **2** a multiplet is observed for the two equivalent hydride ligands (Figure 6). The position of the multiplet is highly sensitive to the nature of the phosphine ligand, moving to higher field as the basicity of the phosphine ligand increases. Analysis of these multiplets shows them to contain 10 resolvable lines with some of the lines being very weak. The peaks were successfully simulated as being half of an AA'XX' pattern (the X nucleus being phosphorus). This simulation (Figure 7) and the derived coupling constants (Table 7) have some important ramifications. The generation of an AA'XX' pattern necessitates a lack of exchange on the NMR time scale between the chemically identical, but magnetically nonequivalent, hydride ligands. The multiplet for the hydride ligands in **2b** was found to remain essentially unchanged at temperatures up to 80 °C. This indicates that molecules **2** exhibit stereochemical rigidity on the <sup>1</sup>H NMR time scale. Any facile processes involving formation of an η<sup>2</sup>-dihydrogen complex in **2** followed by rotation can be excluded. The values of the coupling constants derived from the simulation are also informative. The H–H coupling constants of 6–7 Hz are too low to indicate significant interaction between these ligands. The magnitudes of

the P–P coupling constants were confirmed by the <sup>31</sup>P NMR spectrum of a mixture of **2b** and added PMe<sub>3</sub>. A well-resolved AB pattern for the mixed (PMe<sub>2</sub>Ph)(PMe<sub>3</sub>) complex was observed with a <sup>2</sup>J coupling constant of 158 Hz, comparable in magnitude to these derived from the simulation studies.

In the trihydride **3**, two multiplets in the ratio of 2:1 are observed in the <sup>1</sup>H NMR spectrum for the two chemically distinct hydride ligands. The unique hydride appears as a triplet of triplets due to coupling to both phosphines and the other two hydride ligands. The {<sup>31</sup>P}<sup>1</sup>H NMR spectrum shows the small <sup>2</sup>J coupling between the chemically nonequivalent hydride ligands (Figure 8). The more complex pattern for the remaining two hydrides can again be ascribed to the stereochemical rigidity of these molecules.

In both seven-coordinate compounds **2** and **3**, restricted rotation about the Ta–O–Ar bond is evidenced by the presence of nonequivalent resonances for the *ortho* substituents on the aryloxy ligands (Figure 6).

**Vibrational Spectroscopy.** The existence of tantalum–hydride ligands in these compounds can be detected by the presence of bands in the 1550–1950 cm<sup>-1</sup> region of the infrared spectrum. The detection and assignment of ν̄(M–H) bands in the infrared spectra of metal–hydride compounds can be challenging.<sup>1a</sup> The monohydride **1** shows a single, sharp infrared band at 1850 cm<sup>-1</sup>. In dihydrides **2** and trihydrides **3** the tantalum–hydride bands are broader and weaker. The most interesting infrared spectra are those of six-coordinate dihydrides **4** and **5**. In both sets of compounds two well-resolved ν̄(Ta–H) vibrations are observed. In the case of highly soluble **4**, the spectra are due to *solutions* of the compound in Nujol. In the case of **5**, however, the spectra are due to *mulls* (Figure 9). The use of infrared spectroscopy as a structural tool for inorganic compounds has excellent precedence in metal–carbonyl chemistry. A common text book illustration involves the angular dependence of the intensities of the symmetric and asymmetric stretching vibrations for two carbonyl ligands.<sup>14</sup> An identical analysis should apply to metal–hydride compounds. In practice it is unusual to be able to obtain vibrational spectra of hydrides in which simple ν̄(M–H) stretching vibrations are not strongly coupled to other ligand vibrations or metal–hydride bends. In compounds **4** and **5** the presence of two tantalum–hydride stretches is consistent with a nonlinear arrangement of hydride ligands (Figure 9). If one assigns the higher frequency band to the symmetric stretch, then the intensity ratio of the two bands yields an estimate of the H–Ta–H angle (Figure 10). The angles estimated by this analysis (typically within 10°) are consistent with the values determined from the X-ray diffraction studies.

## Experimental Section

All operations were carried out under a dry nitrogen atmosphere or *in vacuo* either in a Vacuum Atmosphere Dri-Lab or by standard Schlenk techniques. Hydrocarbon solvents were dried by distillation from sodium/benzophenone and stored under dry nitrogen. Tributyltin hydride and tributyltin deuteride were purchased from Aldrich Chemical Co. Phosphines were all purchased from Strem Chemical Co. and were

(13) (a) Fryzuk, M. D.; Carter, A.; Rettig, S. J. *Organometallics* **1992**, *11*, 469. (b) Kobriger, L. M.; McMullen, A. K.; Fanwick, P. E.; Rothwell, I. P. *Polyhedron* **1989**, *8*, 77.

(14) Cotton, F. A.; Wilkinson, G. *Advanced Inorganic Chemistry*, 5th ed.; Wiley-Interscience: New York, 1988; p 1037.

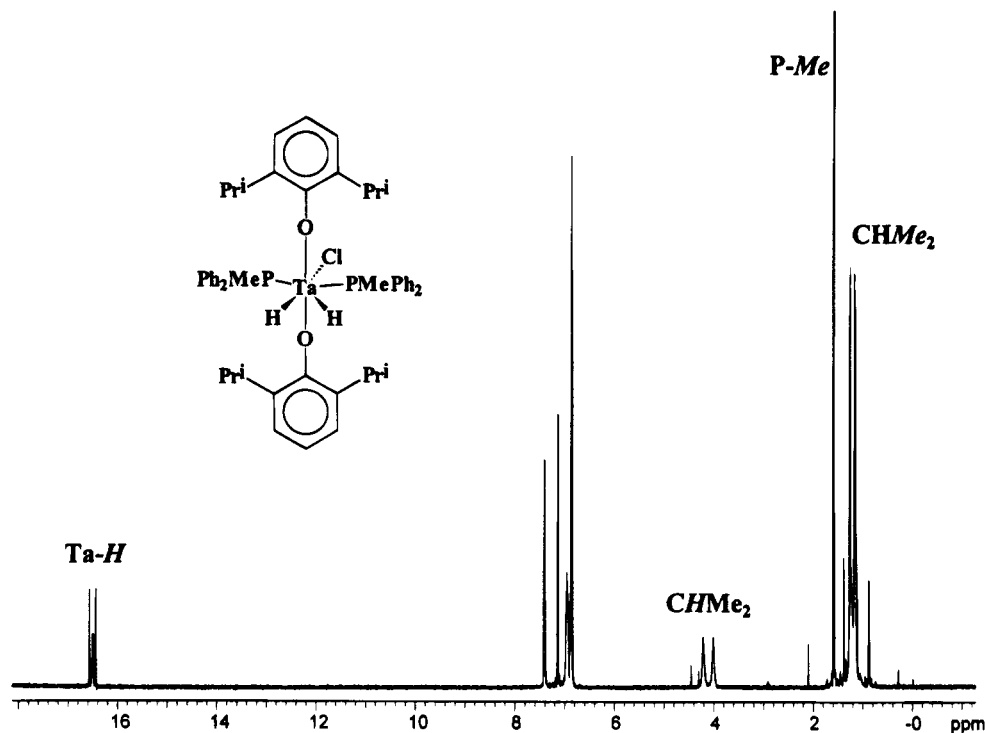


Figure 6.  $^1\text{H}$  NMR (500 MHz) spectrum of  $[\text{Ta}(\text{OC}_6\text{H}_3\text{Pr}^i\text{-}2,6)_2(\text{Cl})(\text{H})_2(\text{PMePh}_2)_2]$ , **2c**.

Table 6. Selected NMR Data for Tantalum-Hydride Compounds

	$\delta(\text{Ta-H})$	$^2J(^{31}\text{P}-^1\text{H})/\text{Hz}$	$\delta(\text{Ta-P})$
$[\text{Ta}(\text{OC}_6\text{H}_3\text{Pr}^i\text{-}2,6)_2\text{H}(\text{Cl})_2(\text{PMe}_2\text{Ph})_2]$ , <b>1</b>	18.93 (t)	88	7.8
$[\text{Ta}(\text{OC}_6\text{H}_3\text{Pr}^i\text{-}2,6)_2\text{Cl}(\text{H})_2(\text{PMe}_3)_2]$ , <b>2a</b>	15.89 (m)		-12.3
$[\text{Ta}(\text{OC}_6\text{H}_3\text{Pr}^i\text{-}2,6)_2\text{Cl}(\text{H})_2(\text{PMe}_2\text{Ph})_2]$ , <b>2b</b>	16.55 (m)		-3.7
$[\text{Ta}(\text{OC}_6\text{H}_3\text{Pr}^i\text{-}2,6)_2\text{Cl}(\text{H})_2(\text{PMePh}_2)_2]$ , <b>2c</b>	17.77 (m)		7.6
$[\text{Ta}(\text{OC}_6\text{H}_3\text{Ph}_2\text{-}2,6)_2\text{Cl}(\text{H})_2(\text{PMe}_3)_2]$ , <b>2d</b>	16.73 (m)		-12.4
$[\text{Ta}(\text{OC}_6\text{H}_3\text{Pr}^i\text{-}2,6)_2(\text{H})_3(\text{PMe}_3)_2]$ , <b>3a</b>	13.20 (m); 12.32 (tt)		-12.0
$[\text{Ta}(\text{OC}_6\text{H}_3\text{Pr}^i\text{-}2,6)_2(\text{H})_3\text{PMe}_2\text{Ph})_2]$ , <b>3b</b>	13.54 (m); 12.80 (tt)		3.2
$[\text{Ta}(\text{OC}_6\text{H}_3\text{Cy}_2\text{-}2,6)_2(\text{H})_3(\text{PMe}_2\text{Ph})_2]$ , <b>3c</b>	13.00 (m); 12.98 (tt)		2.3
$[\text{Ta}(\text{OC}_6\text{H}_3\text{Cy}_2\text{-}2,6)_2(\text{H})_3(\text{PMePh}_2)_2]$ , <b>3d</b>	13.52 (m); 13.34 (tt)		22.5
$[\text{Ta}(\text{OC}_6\text{HPh}_2\text{-}3,5\text{-Cy}_2\text{-}2,6)_2(\text{H})_3(\text{PMe}_2\text{Ph})_2]$ , <b>3e</b>	13.76 (m); 13.15 (tt)		-2.2
$[\text{Ta}(\text{OC}_6\text{H}_3\text{Pr}^i\text{-}2,6)_3(\text{H})_2(\text{PMe}_3)]$ , <b>4a</b>	14.46 (d)	63	-17.4
$[\text{Ta}(\text{OC}_6\text{H}_3\text{Pr}^i\text{-}2,6)_3(\text{H})_2(\text{PMe}_2\text{Ph})]$ , <b>4b</b>	14.89 (d)	60	-6.5
$[\text{Ta}(\text{OC}_6\text{H}_3\text{Pr}^i\text{-}2,6)_3(\text{H})_2(\text{PMePh}_2)]$ , <b>4c</b>	15.34 (d)	59	8.2
$[\text{Ta}(\text{OC}_6\text{H}_3\text{Pr}^i\text{-}2,6)_3(\text{H})_2(\text{PBu}^n_3)]$ , <b>4d</b>	14.67 (d)	59	10.7
$[\text{Ta}(\text{OC}_6\text{H}_3\text{Pr}^i\text{-}2,6)_3(\text{H})_2(\text{PMe}_2\text{Cy})]$ , <b>4e</b>	14.65 (d)	60	-3.6
$[\text{Ta}(\text{OC}_6\text{H}_3\text{Pr}^i\text{-}2,6)_3(\text{H})_2(\text{PMePhCy})]$ , <b>4f</b>	15.23 (d)	58	11.9
$[\text{Ta}(\text{OC}_6\text{H}_3\text{Pr}^i\text{-}2,6)_3(\text{H})_2(\text{PMeCy}_2)]$ , <b>4g</b>	14.82 (d)	57	18.2
$[\text{Ta}(\text{OC}_6\text{H}_3\text{Bu}^t\text{-}2,6)_2\text{Cl}(\text{H})_2(\text{PMe}_3)]$ , <b>5a</b>	17.12 (d)	77	-5.6
$[\text{Ta}(\text{OC}_6\text{H}_3\text{Bu}^t\text{-}2,6)_2\text{Cl}(\text{H})_2(\text{PMe}_2\text{Ph})]$ , <b>5b</b>	17.47 (d)	76	3.9
$[\text{Ta}(\text{OC}_6\text{H}_3\text{Bu}^t\text{-}2,6)_2\text{Cl}(\text{H})_2(\text{PMePh}_2)]$ , <b>5c</b>	17.69 (d)	74	24.1

dried over 3 Å molecular sieves prior to use.  $[\text{Ta}(\text{OC}_6\text{H}_3\text{Pr}^i\text{-}2,6)_2\text{Cl}_3]$ ,  $[\text{Ta}(\text{OC}_6\text{H}_3\text{Bu}^t\text{-}2,6)_2\text{Cl}_3]$ ,  $[\text{Ta}(\text{OC}_6\text{H}_3\text{Pr}^i\text{-}2,6)_3(\text{CH}_2\text{C}_6\text{H}_4\text{-p-CH}_3)_2]$ ,  $[\text{Ta}(\text{OC}_6\text{H}_3\text{Pr}^i\text{-}2,6)_2\text{Cl}(\text{CH}_2\text{SiMe}_3)_2]$ ,  $[\text{Ta}(\text{OC}_6\text{H}_3\text{Pr}^i\text{-}2,6)_2(\text{CH}_2\text{SiMe}_3)_3]$ ,  $[\text{Ta}(\text{OC}_6\text{H}_3\text{Ph}_2\text{-}2,6)_2\text{Cl}(\text{CH}_2\text{SiMe}_3)_2]$ ,  $[\text{Ta}(\text{OC}_6\text{H}_3\text{Ph}_2\text{-}2,6)_2(\text{R})_3]$ , ( $\text{R} = \text{CH}_2\text{SiMe}_3$ ,  $\text{CH}_2\text{C}_6\text{H}_4\text{-p-CH}_3$ ), and  $[\text{Ta}(\text{OC}_6\text{HPh}_4\text{-}2,3,5,6)_2(\text{CH}_2\text{SiMe}_3)_3]$  were prepared by reported procedures.<sup>6,7,15</sup> The  $^1\text{H}$  and  $^{31}\text{P}$  NMR spectra were recorded on Varian Associates Gemini 200 and General Electric QE-300 spectrometers and were referenced to 85%  $\text{H}_3\text{PO}_4$  using protio impurities of commercial benzene- $d_6$  as an internal standard. The infrared spectra were obtained using a Perkin-Elmer 1800 Fourier transform infrared spectrophotometer. High-pressure operations were performed with a Parr Instrument Co. model 4561 300 mL stainless steel high-pressure minireactor connected to a Parr 4841 temperature controller. Microanalyses were obtained in-house at Purdue. Considerable difficulties were encountered in obtaining accurate microanalytical data for some of these compounds. In particular,

the values for the percentage of carbon were consistently found to be low, a fact we ascribe to the possible formation of metal carbides on combustion. Due to the similarity of some of the synthetic procedures, only representative methods will be presented for each type of compound.

**$[\text{Ta}(\text{OC}_6\text{H}_3\text{Pr}^i\text{-}2,6)_2\text{H}(\text{Cl})_2(\text{PMe}_2\text{Ph})_2]$ , **1**.** To a suspension of  $[\text{Ta}(\text{OC}_6\text{H}_3\text{Pr}^i\text{-}2,6)_2\text{Cl}_3]$  (2.0 g, 3.12 mmol) in benzene (5 mL) was added (dimethylphenyl)phosphine (1.08 g, 7.79 mmol) followed by tri-*n*-butyltin hydride (1.36 g, 4.67 mmol). The resulting clear yellow mixture was allowed to stand for 15 h to yield the crystalline product. The colorless crystals were washed with hexane and dried *in vacuo*; yield: 2.14 g (88.6%). Anal. Calcd for  $\text{C}_{40}\text{H}_{57}\text{Cl}_2\text{P}_2\text{O}_2\text{Ta}$ : C, 54.37; H, 6.50; Cl, 8.03; P, 7.01. Found: C, 54.17; H, 6.51; Cl, 7.89.  $^1\text{H}$  NMR ( $\text{C}_6\text{D}_6$ , 30 °C): 7.63 (m, 4H, *P-Ph ortho*); 6.62–6.85 (m, 12H, aromatics); 3.61 (septet, 2H, *CHMe*); 2.78 (septet, 2H, *CHMe*); 1.94 (t, 12H, *P-Me*); 1.64 (d, 12H, *CHMe*); 1.52 (d, 12H, *CHMe*). IR (Nujol): 1850  $\text{cm}^{-1}$  (Ta-H).

**$[\text{Ta}(\text{OC}_6\text{H}_3\text{Pr}^i\text{-}2,6)_2\text{Cl}(\text{H})_2(\text{PMe}_3)_2]$ , **2a**.** This compound was obtained by the hydrogenolysis of  $[\text{Ta}(\text{OC}_6\text{H}_3\text{Pr}^i\text{-}2,6)_2(\text{CH}_2\text{-}$

(15) Parkin, B. C.; Clark, J. R.; Fanwick, P. E.; Rothwell, I. P. Results to be published.

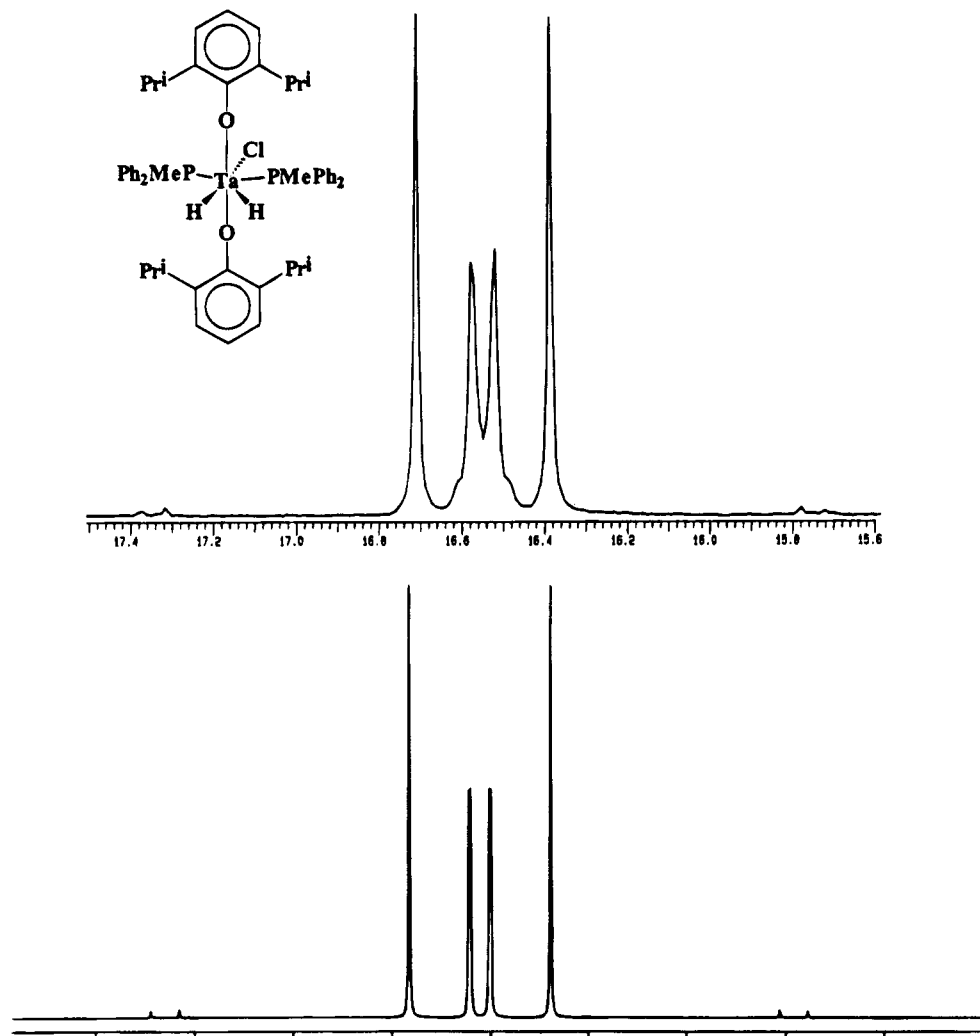


**Figure 7.** Observed and simulated spectra for the hydride ligands (AA'XX' pattern) in the  $^1\text{H}$  NMR spectrum of  $[\text{Ta}(\text{OC}_6\text{H}_3\text{Pr}^i\text{-2,6})_2\text{Cl}(\text{H})_2(\text{PMePh}_2)_2]$ , **2c**. The coupling constants used in the simulation are contained in Table 7.

**Table 7. Coupling Constants Obtained by Simulation for Dihydrides 2**

	$^2J(^{31}\text{P}'\text{-}^1\text{H})$	$^2J(^{31}\text{P}\text{-}^1\text{H})$	$^2J(^1\text{H}\text{-}^1\text{H})$	$^2J(^{31}\text{P}\text{-}^{31}\text{P})$
$[\text{Ta}(\text{OC}_6\text{H}_3\text{Pr}^i\text{-2,6})_2\text{Cl}(\text{H})_2(\text{PMe}_3)_2]$ , <b>2a</b>	65.8	7.0	-7.4	163.6
$[\text{Ta}(\text{OC}_6\text{H}_3\text{Pr}^i\text{-2,6})_2\text{Cl}(\text{H})_2(\text{PMe}_2\text{Ph})_2]$ , <b>2b</b>	64.4	7.2	-7.9	159.0
$[\text{Ta}(\text{OC}_6\text{H}_3\text{Pr}^i\text{-2,6})_2\text{Cl}(\text{H})_2(\text{PMePh}_2)_2]$ , <b>2c</b>	65.0	7.0	-6.2	156.7

$\text{SiMe}_3)_2\text{Cl}]$  in the presence of  $\text{PMe}_3$  using a procedure analogous to that used for compound **2b**. Anal. Calcd for  $\text{C}_{30}\text{H}_{54}\text{ClO}_2\text{P}_2\text{Ta}$ : C, 49.69; H, 7.51; Cl, 4.89; P, 8.54. Found: C, 49.32; H, 7.40; Cl, 4.44; P, 8.07.  $^1\text{H}$  NMR ( $\text{C}_6\text{D}_6$ , 30  $^\circ\text{C}$ ):  $\delta$  6.87–7.17 (m, 6H, aromatics);  $\delta$  4.24 (septet, 2H, CHMe);  $\delta$  4.20 (septet, 2H, CHMe);  $\delta$  1.33 (d, 24H, CHMe);  $\delta$  1.21 (t, 18H, P-Me),  $^2J(^{31}\text{P}\text{-}^1\text{H}) = 7.4$  Hz. IR (Nujol): 1764, 1730  $\text{cm}^{-1}$ , br (Ta-H).

**$[\text{Ta}(\text{OC}_6\text{H}_3\text{Pr}^i\text{-2,6})_2\text{Cl}(\text{H})_2(\text{PMe}_2\text{Ph})_2]$ , **2b**, by Hydrogenolysis.** To a solution of  $[\text{Ta}(\text{OC}_6\text{H}_3\text{Pr}^i\text{-2,6})(\text{CH}_2\text{SiMe}_3)_2\text{Cl}]$  (0.30 g, 0.40 mmol) in cyclohexane (3 mL) was added (dimethylphenyl)phosphine (0.24 g, 1.20 mmol). The solution was placed in a glass flask within the high-pressure reactor, pressurized to 1200 psi of  $\text{H}_2$ , and heated unstirred at 80  $^\circ\text{C}$  for 24 hrs. The pressure reactor was allowed to cool slowly to ambient temperatures before being depressurized and opened in the drybox. Decanting the brown supernatant gave pale yellow crystals of product, which were washed with hexane and dried *in vacuo*. In a number of runs the yield of **2b** varied from 35%–65%. Anal. Calcd for  $\text{C}_{40}\text{H}_{58}\text{ClO}_2\text{P}_2\text{Ta}$ : C, 56.57; H, 6.88; Cl, 4.17; P, 7.29. Found: C, 56.63; H, 7.23; Cl, 4.61; P, 7.14.  $^1\text{H}$  NMR ( $\text{C}_6\text{D}_6$ , 30  $^\circ\text{C}$ ):  $\delta$  7.42 (m, 4H, P-Ph ortho);  $\delta$  6.82–6.95 (m, 12H, aromatics);  $\delta$  4.21 (septet, 2H, CHMe);  $\delta$

4.02 (septet, 2H, CHMe);  $\delta$  1.60 (t, 12H, P-Me),  $^2J(^{31}\text{P}\text{-}^1\text{H}) = 4.1$  Hz;  $\delta$  1.23 (d, 12H, CHMe);  $\delta$  1.17 (d, 12H, CHMe). IR (Nujol): 1848, 1754  $\text{cm}^{-1}$ , br (Ta-H).

**$[\text{Ta}(\text{OC}_6\text{H}_3\text{Pr}^i\text{-2,6})_2\text{Cl}(\text{H})_2(\text{PMe}_2\text{Ph})_2]$ , **2b**, by Addition of  $\text{Bu}_3\text{SnH}$ .** To a suspension of  $[\text{Ta}(\text{OC}_6\text{H}_3\text{Pr}^i\text{-2,6})_2\text{Cl}_3]$  (2.0 g, 3.11 mmol) in benzene (5 mL) was added (dimethylphenyl)phosphine (1.08 g, 7.81 mmol) followed by tri-*n*-butyltin hydride (2.72 g, 9.35 mmol). The resulting clear yellow mixture was stirred for 20 h to generate a dark orange solution. Removal of benzene solvent led to the crude product as a white solid, which was washed with hexane and dried *in vacuo* to yield 1.1 g (42%).

**$[\text{Ta}(\text{OC}_6\text{H}_3\text{Pr}^i\text{-2,6})_2\text{Cl}(\text{H})_2(\text{PMePh}_2)_2]$ , **2c**.** This compound was obtained by the hydrogenolysis of  $[\text{Ta}(\text{OC}_6\text{H}_3\text{Pr}^i\text{-2,6})(\text{CH}_2\text{SiMe}_3)_2\text{Cl}]$  in the presence of  $\text{PMePh}_2$  using a procedure analogous to that used for compound **2b**. Anal. Calcd for  $\text{C}_{50}\text{H}_{82}\text{ClO}_2\text{P}_2\text{Ta}$ : C, 61.70; H, 6.42; Cl, 3.64; P, 6.36. Found: C, 61.30; H, 6.72; Cl, 3.65; P, 6.07.  $^1\text{H}$  NMR ( $\text{C}_6\text{D}_6$ , 30  $^\circ\text{C}$ ):  $\delta$  7.69 (m, 8H, P-Ph ortho);  $\delta$  6.77–7.21 (m, 18H, aromatics);  $\delta$  4.02 (septet, 4H, CHMe);  $\delta$  2.07 (t, 6H, P-Me),  $^2J(\text{P-H}) = 4.4$  Hz;  $\delta$  1.11 (d, 12H, CHMe);  $\delta$  1.02 (d, 12H, CHMe). IR (Nujol): 1852, 1796, 1758  $\text{cm}^{-1}$ , br (Ta-H).

**$[\text{Ta}(\text{OC}_6\text{H}_3\text{Pr}^i\text{-2,6})_2\text{Cl}(\text{H})_2(\text{PMe}_3)_2]$ , **2d**.** This compound

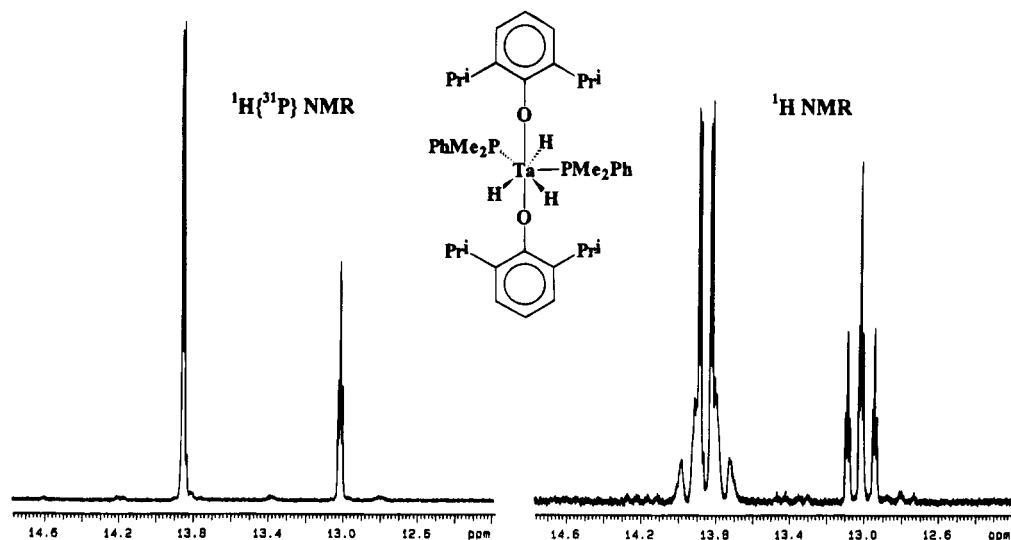


Figure 8.  $^1\text{H}\{^{31}\text{P}\}$  and  $^1\text{H}$  NMR (500 MHz) spectra of the hydride resonances in  $[\text{Ta}(\text{OC}_6\text{H}_3\text{Pr}^i\text{-2,6})_2(\text{H})_3(\text{PMe}_2\text{Ph})_2]$ , **3b**.

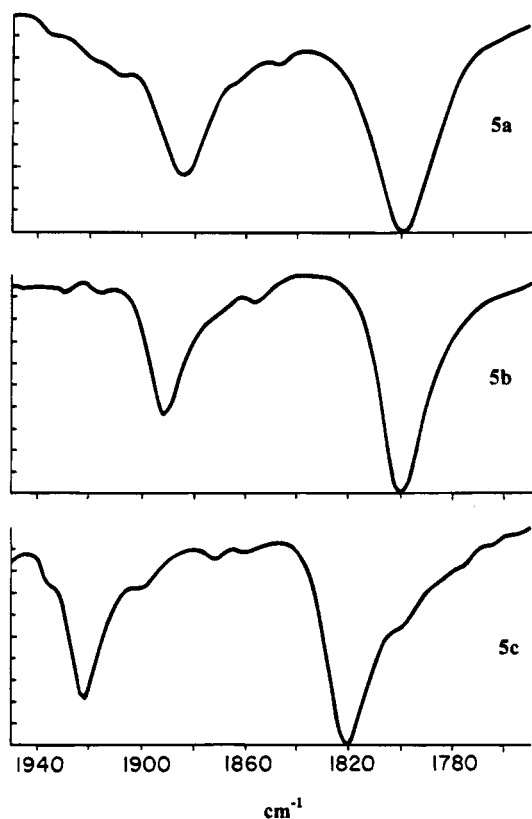


Figure 9. Infrared spectra (Nujol mulls) of dihydrides **5a–c** showing the symmetric and asymmetric  $\nu(\text{Ta-H})$  vibrations.

was obtained by the hydrogenolysis of  $[\text{Ta}(\text{OC}_6\text{H}_3\text{Ph}_2\text{-2,6})_2(\text{CH}_2\text{-SiMe}_3)_2\text{Cl}]$  in the presence of  $\text{PMe}_3$  using a procedure analogous to that used for compound **2b**.  $^1\text{H}$  NMR ( $\text{C}_6\text{D}_6$ , 30 °C):  $\delta$  6.49–7.75 (m, 26H, aromatics);  $\delta$  0.91 (d, 9H, P-Me),  $^2J(\text{P-H}) = 3.73$  Hz;  $\delta$  0.89 (d, 9H, P-Me),  $^2J(\text{P-H}) = 3.73$  Hz. IR (Nujol): 1730  $\text{cm}^{-1}$ , br (Ta-H).

$[\text{Ta}(\text{OC}_6\text{H}_3\text{Pr}^i\text{-2,6})_2(\text{H})_3(\text{PMe}_3)_2]$ , **3a**. This compound was obtained by the hydrogenolysis of  $[\text{Ta}(\text{OC}_6\text{H}_3\text{Pr}^i\text{-2,6})_2(\text{CH}_2\text{-SiMe}_3)_3]$  in the presence of  $\text{PMe}_3$  using a procedure analogous to that used for compound **3b**. Anal. Calcd for  $\text{C}_{30}\text{H}_{55}\text{O}_2\text{P}_2\text{Ta}$ : C, 52.17; H, 8.03; P, 8.97. Found: C, 53.80; H, 8.30.  $^1\text{H}$  NMR ( $\text{C}_6\text{D}_6$ , 30 °C):  $\delta$  6.86–7.00 (m, 6H, aromatics);  $\delta$  4.18 (septet, 2H, CHMe);  $\delta$  3.95 (septet, 2H, CHMe);  $\delta$  1.35 (d, 18 H, P-Me),  $^2J(^{31}\text{P}-^1\text{H}) = 7.4$  Hz;  $\delta$  1.31 (d, 12H, CHMe);  $\delta$  1.21 (d, 12H, CHMe).

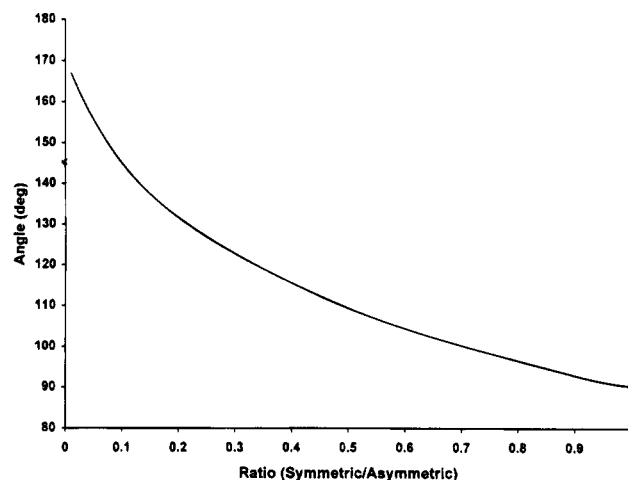


Figure 10. Plot showing the calculated relationship of the ratio of symmetric/asymmetric intensities with the angle between two vibrationally coupled ligands.

$[\text{Ta}(\text{OC}_6\text{H}_3\text{Pr}^i\text{-2,6})_2(\text{H})_3(\text{PMe}_2\text{Ph})_2]$ , **3b**. To a cyclohexane (3 mL) solution of  $[\text{Ta}(\text{OC}_6\text{H}_3\text{Pr}^i\text{-2,6})_2(\text{CH}_2\text{SiMe}_3)_3]$  (0.15 g, 0.19 mmol) was added (dimethylphenyl)phosphine (0.078 g, 0.56 mmol). The solution was placed in a glass flask within the high-pressure reactor, pressurized to 1200 psi of  $\text{H}_2$ , and heated unstirred at 80 °C for 24 h. The pressure reactor was allowed to cool slowly to ambient temperatures before being depressurized and opened in the drybox. Decanting the brown supernatant gave colorless crystals of product, which were washed with hexane and dried *in vacuo*. Typical yields: 35–65%. Anal. Calcd for  $\text{C}_{40}\text{H}_{59}\text{O}_2\text{P}_2\text{Ta}$ : C, 58.96; H, 7.30; P, 7.60. Found: C, 58.58; H, 7.50; P, 7.41.  $^1\text{H}$  NMR ( $\text{C}_6\text{D}_6$ , 30 °C):  $\delta$  7.99 (m, 4H, P-Ph ortho);  $\delta$  6.77–7.10 (m, 12H, aromatics);  $\delta$  4.10 (septet, 2H, CHMe);  $\delta$  3.77 (septet, 2H, CHMe);  $\delta$  1.67 (d, 12H, P-Me),  $^2J(^{31}\text{P}-^1\text{H}) = 6.3$  Hz;  $\delta$  1.26 (d, 12H, CHMe);  $\delta$  0.98 (d, 12H, CHMe). IR (Nujol): 1648  $\text{cm}^{-1}$ , br (Ta-H); 1196  $\text{cm}^{-1}$ , (Ta-D).

$[\text{Ta}(\text{OC}_6\text{H}_3\text{Cy}_2\text{-2,6})_2(\text{H})_3(\text{PMe}_2\text{Ph})_2]$ , **3c**. To a cyclohexane (3 mL) solution of  $[\text{Ta}(\text{OC}_6\text{H}_3\text{Ph}_2\text{-2,6})_2(\text{CH}_2\text{C}_6\text{H}_4\text{-p-CH}_3)_3]$  (0.50 g, 0.51 mmol) was added (dimethylphenyl)phosphine (0.21 g, 1.52 mmol). The solution was placed in a glass flask within the high-pressure reactor, pressurized to 1200 psi of  $\text{H}_2$ , and heated unstirred at 80 °C for 24 h. The pressure reactor was allowed to cool slowly to ambient temperatures before being depressurized and opened in the drybox. Decanting the dark-brown supernatant gave colorless crystals of product, which were washed with hexane and dried *in vacuo*. Anal. Calcd for  $\text{C}_{52}\text{H}_{75}\text{O}_2\text{P}_2\text{Ta}$ : C, 64.05; H, 7.75; P, 6.35. Found: C, 63.97;



Table 8. Crystal Data and Data Collection Parameters

formula	TaCl <sub>2</sub> P <sub>2</sub> O <sub>2</sub> C <sub>40</sub> H <sub>57</sub>	TaClP <sub>2</sub> O <sub>2</sub> C <sub>40</sub> H <sub>58</sub>	TaP <sub>2</sub> O <sub>2</sub> C <sub>52</sub> H <sub>75</sub>	TaPO <sub>3</sub> C <sub>44</sub> H <sub>64</sub>	TaClPO <sub>2</sub> C <sub>41</sub> H <sub>57</sub>
fw	883.70	849.26	975.07	852.92	829.29
space group	C2/c (No. 15)	P2 <sub>1</sub> /n (No. 14)	C2/c (No. 15)	P2 <sub>1</sub> /n (No. 14)	P2 <sub>1</sub> /n (No. 14)
a, Å	26.025(4)	9.735(1)	24.065(3)	10.637(1)	10.851(5)
b, Å	10.7954(5)	24.310(3)	13.530(2)	12.820(2)	18.110(7)
c, Å	18.509(3)	17.735(2)	20.263(3)	31.799(4)	20.09(1)
β, deg	128.31(1)	90.76(1)	131.633(9)	98.76(1)	96.67(5)
V, Å <sup>3</sup>	4080(2)	4196(1)	4931(3)	4285(2)	3921(6)
Z	4	4	4	4	4
d <sub>calcd</sub> , g cm <sup>-3</sup>	1.438	1.344	1.313	1.322	1.404
cryst dimens, mm <sup>3</sup>	0.47 × 0.47 × 0.30	0.47 × 0.28 × 0.06	0.44 × 0.20 × 0.05	0.50 × 0.46 × 0.29	0.50 × 0.25 × 0.19
temp, K	293	293	293	293	173
radiation (wavelength)	Mo Kα (0.710 73 Å)	Mo Kα (0.710 73 Å)	Mo Kα (0.710 73 Å)	Mo Kα (0.710 73 Å)	Mo Kα (0.710 73 Å)
monochromator	graphite	graphite	graphite	graphite	graphite
linear abs coeff, cm <sup>-1</sup>	29.02	27.56	23.01	26.05	29.09
abs corr appl	empirical	empirical	empirical	empirical	empirical
transmissn factors:	0.64, 1.00	0.78, 1.00	0.65, 1.00	0.76, 1.00	0.68, 1.00
min, max					
diffractometer	Enraf-Nonius CAD4	Enraf-Nonius CAD4	Enraf-Nonius CAD4	Enraf-Nonius CAD4	Enraf-Nonius CAD4
scan method	ω-2θ	ω-2θ	ω-2θ	ω-2θ	ω-2θ
h,k,l range	0-30; 0-12; -21 to 17	-10 to +10; 0-26; 0-19	0-25; 0-14; -21-16	-12 to +12; 0-15; 0-37	-11 to +11; -19 to 0; 0-21
2θ range, deg	4.00-50.00	4.00-45.00	4.00-45.00	4.00-50.00	5.04-45.00
scan width, deg	0.65 + 0.35 tan θ	0.57 + 0.35 tan θ	0.63 + 0.35 tan θ	0.42 + 0.35 tan θ	0.50 + 0.92 tan θ
Takeoff angle, deg	2.95	2.95	2.95	2.95	3.00
programs used	Enraf-Nonius Mo1EN	Enraf-Nonius SDP	Enraf-Nonius SDP	Enraf-Nonius Mo1EN	Enraf-Nonius Mo1EN
F <sub>000</sub>	1800.0	1736.0	2024.0	1760.0	1696.0
p-factor used in weighting	0.040	0.040	0.040	0.040	0.040
w no. of data collected	3784	5633	3377	7944	5504
no. of unique data	3784	5633	3377	7944	5332
no. of data with I > 3.0σ(I)	2631	3571	2213	5127	4111
no. of variables	215	423	264	450	423
largest shift/esd in final cycle	0.00	0.28	0.03	0.03	0.25
R	0.027	0.032	0.048	0.029	0.029
R <sub>w</sub>	0.033	0.306	0.053	0.036	0.037
goodness of fit	1.148	0.895	1.148	0.956	1.075

H, 7.99; P, 5.96. <sup>1</sup>H NMR (C<sub>6</sub>D<sub>6</sub>, 30 °C): δ 7.91 (m, 4H, *P-Ph ortho*); δ 6.81-7.18 (m, 12H, aromatics); δ 4.08 (m, 2H, *cy-CH*); δ 3.27 (m, 2H, *cy-CH*); δ 1.06-2.38 (m, 40H, cyclohexyl); δ 1.71 (d, 12H, *P-Me*), <sup>2</sup>J(<sup>31</sup>P-<sup>1</sup>H) = 9.0 Hz. IR (Nujol): 1654, 1588 cm<sup>-1</sup>, br (Ta-H); 1193 cm<sup>-1</sup>, (Ta-D).

[Ta(OC<sub>6</sub>H<sub>3</sub>Cy<sub>2</sub>-2,6)<sub>2</sub>(H)<sub>3</sub>(PMePh<sub>2</sub>)<sub>2</sub>], **3d**. This compound was obtained by the hydrogenolysis of [Ta(OC<sub>6</sub>H<sub>3</sub>Ph<sub>2</sub>-2,6)<sub>2</sub>(CH<sub>2</sub>C<sub>6</sub>H<sub>4</sub>-*p*-CH<sub>3</sub>)<sub>3</sub>] in the presence of PMePh<sub>2</sub> using a procedure analogous to that used for compound **3c**. Anal. Calcd for C<sub>62</sub>H<sub>76</sub>O<sub>2</sub>P<sub>2</sub>Ta: C, 67.75; H, 7.24; P, 5.64. Found: C, 67.41; H, 7.61; P, 5.79. <sup>1</sup>H NMR (C<sub>6</sub>D<sub>6</sub>, 30 °C): δ 7.96 (m, 8H, *P-Ph ortho*); δ 6.76-7.17 (m, 18H, aromatics); δ 3.80 (m, 2H, *cy-CH*); δ 3.31 (m, 2H, *cy-CH*); δ 1.05-2.12 (m, 40H, cyclohexyl); δ 1.94 (d, 6H, *P-Me*), <sup>2</sup>J(<sup>31</sup>P-<sup>1</sup>H) = 6.5 Hz. IR (Nujol): 1670, 1596 cm<sup>-1</sup>, br (Ta-H).

[Ta(OC<sub>6</sub>HPh<sub>2</sub>-3,5-Cy<sub>2</sub>-2,6)<sub>2</sub>(H)<sub>3</sub>(PMe<sub>2</sub>Ph)<sub>2</sub>], **3e**. This compound was obtained by the hydrogenolysis of [Ta(OC<sub>6</sub>HPh<sub>4</sub>-2,3,5,6)<sub>2</sub>(CH<sub>2</sub>SiMe<sub>3</sub>)<sub>3</sub>] in the presence of PMe<sub>2</sub>Ph using a procedure analogous to that used for compound **3c**. <sup>1</sup>H NMR (C<sub>6</sub>D<sub>6</sub>, 30 °C): δ 7.58 (m, 4H, *P-Ph ortho*); δ 7.01-7.39 (m, 38H, aromatics); δ 6.54 (s, 2H, OC<sub>6</sub>H); δ 4.23 (m, 2H, *cy-CH*); δ 3.88 (m, 2H, *cy-CH*); δ 1.05-2.39 (m, 40H, cyclohexyl); δ 1.92 (d, 12H, *P-Me*), <sup>2</sup>J(<sup>31</sup>P-<sup>1</sup>H) = 6.4 Hz. IR (Nujol): 1656, 1572 cm<sup>-1</sup>, br (Ta-H).

[Ta(OC<sub>6</sub>H<sub>3</sub>Pr<sup>i</sup>-2,6)<sub>3</sub>(H)<sub>2</sub>(PMe<sub>3</sub>)], **4a**. This compound was obtained by the hydrogenolysis of [Ta(OC<sub>6</sub>H<sub>3</sub>Pr<sup>i</sup>-2,6)<sub>3</sub>(CH<sub>2</sub>C<sub>6</sub>H<sub>4</sub>-*p*-CH<sub>3</sub>)<sub>2</sub>] in the presence of PMe<sub>3</sub> using a procedure identical to that used for compound **4b**. <sup>1</sup>H NMR (C<sub>6</sub>D<sub>6</sub>, 30 °C): δ 6.9-7.2 (m, 9H, aromatics); δ 3.80 (m, 6H, *CHMe*); δ 1.23 (d, 36H, *CHMe*); δ 1.06 (d, 9H, *P-Me*).

[Ta(OC<sub>6</sub>H<sub>3</sub>Pr<sup>i</sup>-2,6)<sub>3</sub>(H)<sub>2</sub>(PMe<sub>2</sub>Ph)], **4b**. To a cyclohexane solution (3 mL) of [Ta(OC<sub>6</sub>H<sub>3</sub>Pr<sup>i</sup>-2,6)<sub>3</sub>(CH<sub>2</sub>C<sub>6</sub>H<sub>4</sub>-*p*-CH<sub>3</sub>)<sub>2</sub>] (1.0 g, 1.08 mmol) was added (dimethylphenyl)phosphine (0.35 g, 2.5 mmol). The solution was placed in a glass flask within the high-pressure reactor, pressurized to 1200 psi of H<sub>2</sub>, and

heated unstirred at 90 °C for 24 h. The pressure reactor was allowed to cool slowly to ambient temperatures before being depressurized and opened in the drybox. Decanting the supernatant left colorless crystals of product, which were washed with hexane and dried *in vacuo* to yield 0.55 g (60%). Anal. Calcd for C<sub>44</sub>H<sub>64</sub>PO<sub>3</sub>Ta: C, 61.96; H, 7.56; P, 3.63. Found: C, 61.82; H, 7.57; P, 3.90. <sup>1</sup>H NMR (C<sub>6</sub>D<sub>6</sub>, 30 °C): δ 7.58 (m, 2H, *P-Ph ortho*); δ 6.8-7.2 (m, 12H, aromatics); δ 3.82 (septet, 4H, *CHMe*); δ 3.73 (septet, 2H, *CHMe*); δ 1.49 (d, 6H, *P-Me*); δ 1.29 (d, 24H, *CHMe*); δ 1.16 (d, 12H, *CHMe*). IR (Nujol): 1824, 1758 cm<sup>-1</sup>.

[Ta(OC<sub>6</sub>H<sub>3</sub>Pr<sup>i</sup>-2,6)<sub>3</sub>(H)<sub>2</sub>(PMePh<sub>2</sub>)], **4c**. This compound was obtained by the hydrogenolysis of [Ta(OC<sub>6</sub>H<sub>3</sub>Pr<sup>i</sup>-2,6)<sub>3</sub>(CH<sub>2</sub>C<sub>6</sub>H<sub>4</sub>-*p*-CH<sub>3</sub>)<sub>2</sub>] in the presence of PMePh<sub>2</sub> using a procedure identical to that used for compound **4b**. <sup>1</sup>H NMR (C<sub>6</sub>D<sub>6</sub>, 30 °C): δ 7.37 (m, 4H, *P-Ph ortho*); δ 6.8-7.2 (m, 15H, aromatics); δ 3.81 (septet, 4H, *CHMe*); δ 3.58 (septet, 2H, *CHMe*); δ 1.35 (d, 3H, *P-Me*); δ 1.17 (d, 24H, *CHMe*); δ 1.08 (d, 12H, *CHMe*). IR (Nujol): 1846, 1742 cm<sup>-1</sup>.

[Ta(OC<sub>6</sub>H<sub>3</sub>Pr<sup>i</sup>-2,6)<sub>3</sub>(H)<sub>2</sub>(PBu<sup>n</sup>)], **4d**. This compound was only spectroscopically characterized and was obtained by the addition of PBu<sup>n</sup> to C<sub>6</sub>D<sub>6</sub> solutions of **4b**. <sup>1</sup>H NMR (C<sub>6</sub>D<sub>6</sub>, 30 °C): δ 6.8-7.2 (m, 9H, aromatics); δ 3.77 (m, 6H, *CHMe*); δ 1.72 (pentet, 2H, PCH<sub>2</sub>CH<sub>2</sub>CH<sub>2</sub>CH<sub>3</sub>); δ 1.35 (d, 36H, *CHMe*); δ 1.20 (m, 2H, PCH<sub>2</sub>CH<sub>2</sub>CH<sub>2</sub>CH<sub>3</sub>); δ 0.82 (m, 2H, PCH<sub>2</sub>CH<sub>2</sub>CH<sub>2</sub>CH<sub>3</sub>); δ 0.68 (t, 3H, PCH<sub>2</sub>CH<sub>2</sub>CH<sub>2</sub>CH<sub>3</sub>). IR (Nujol): 1794, 1742 cm<sup>-1</sup>.

[Ta(OC<sub>6</sub>H<sub>3</sub>Pr<sup>i</sup>-2,6)<sub>3</sub>(H)<sub>2</sub>(L)] (L = PMe<sub>2</sub>Cy, **4e**; L = PMePhCy, **4f**; L = PMeCy<sub>2</sub>, **4g**). These compounds were obtained by exposing solutions of **4b** or **4c** to hydrogen (1200 psi, 90 °C) for extended periods of time. The compounds were not isolated but were characterized in reaction mixtures by <sup>1</sup>H and <sup>31</sup>P NMR (Table 6).

[Ta(OC<sub>6</sub>H<sub>3</sub>Bu<sup>i</sup>-2,6)<sub>2</sub>Cl(H)<sub>2</sub>(PMe<sub>3</sub>)], **5a**. This compound was obtained by a procedure analogous to that used for

compound **5c**.  $^1\text{H}$  NMR ( $\text{C}_6\text{D}_6$ , 30 °C):  $\delta$  6.84–7.36 (m, 6H, aromatics);  $\delta$  1.67 (s, 36H, *CMe*);  $\delta$  1.35 (d, 9H, *P-Me*),  $^2J(^{31}\text{P}-^1\text{H}) = 8.61$  Hz. IR (Nujol): 1884, 1800  $\text{cm}^{-1}$  (Ta–H).

**[Ta(OC<sub>6</sub>H<sub>3</sub>Bu<sup>t</sup>-2,6)<sub>2</sub>Cl(H)<sub>2</sub>(PMe<sub>2</sub>Ph)], 5b.** This compound was obtained by a procedure analogous to that used for compound **5c**.  $^1\text{H}$  NMR ( $\text{C}_6\text{D}_6$ , 30 °C):  $\delta$  7.45 (m, 2H, *P-Ph ortho*);  $\delta$  6.82–7.33 (m, 9H, aromatics);  $\delta$  1.77 (d, 9H, *P-Me*),  $^2J(^{31}\text{P}-^1\text{H}) = 8.06$  Hz;  $\delta$  1.62 (s, 36H, *CMe*). IR (Nujol): 1892, 1800  $\text{cm}^{-1}$  (Ta–H).

**[Ta(OC<sub>6</sub>H<sub>3</sub>Bu<sup>t</sup>-2,6)<sub>2</sub>Cl(H)<sub>2</sub>(PMePh<sub>2</sub>)], 5c.** To a suspension of [Ta(OC<sub>6</sub>H<sub>3</sub>Bu<sup>t</sup>-2,6)<sub>2</sub>Cl<sub>3</sub>] (1.0 g, 1.43 mmol) in benzene (5 mL) was added methyldiphenylphosphine (0.43 g 2.15 mmol) followed by tri-*n*-butyltin hydride (1.04 g, 3.58 mmol), and the resulting mixture was allowed to stand for 24 h. The product crystallized from the mixture, and, after decanting the supernatant, the yellow crystals were washed with hexane and dried *in vacuo* to yield 0.64 g (54%).  $^1\text{H}$  NMR ( $\text{C}_6\text{D}_6$ , 30 °C):  $\delta$  7.68 (m, 4H, *P-Ph ortho*);  $\delta$  6.76–7.42 (m, 12H, aromatics);  $\delta$  2.02

(d, 3H, *P-Me*),  $^2J(^{31}\text{P}-^1\text{H}) = 7.43$ ;  $\delta$  1.62 (s, 36H, *CMe*). IR (Nujol): 1922, 1820  $\text{cm}^{-1}$  (Ta–H); 1382, 1316  $\text{cm}^{-1}$  (Ta–D).

**Crystallographic Studies.** Crystal data and data collection parameters are contained in Table 8. Further details of the crystallographic study are contained in the supplementary material.

**Acknowledgment.** We thank the U.S. Department of Energy for financial support of this research.

**Supplementary Material Available:** Descriptions of experimental procedures and tables of thermal parameters, bond distances and angles, intensity data, torsional angles, and multiplicities for **1**, **2b**, **3c**, **4a**, and **5c** (99 pages). Ordering information is given on any current masthead page.

OM950221R

# C<sub>2</sub>B<sub>3</sub> and C<sub>2</sub>B<sub>4</sub> Carborane Ligands as Cyclopentadienyl Analogues: Early Transition Metal Complexes<sup>1</sup>

Kenneth E. Stockman, Karl L. Houseknecht, Eric A. Boring, Michal Sabat, M. G. Finn,\* and Russell N. Grimes\*

Department of Chemistry, University of Virginia, Charlottesville, Virginia 22901

Received February 27, 1995\*

This paper reports the directed synthesis, characterization, and reactivity of a series of tantalum, niobium, and zirconium sandwich complexes incorporating small carborane or cobaltacarborane ligands, centered on the development of suitable families of reagents for eventual application to organic synthesis. Complexes of the types (R<sup>1</sup><sub>2</sub>C<sub>2</sub>B<sub>4</sub>H<sub>4</sub>)MCl<sub>2</sub>Cp' and (Et<sub>2</sub>C<sub>2</sub>B<sub>4</sub>H<sub>4</sub>)ZrCl·THFCp' (R<sup>1</sup> = Et, SiMe<sub>3</sub>, or Me; Cp' = C<sub>5</sub>H<sub>5</sub> or C<sub>5</sub>Me<sub>5</sub>; M = Ta, Nb) were prepared from Cp'MCl<sub>n</sub> reagents (M = Ta, Nb, Zr) and the R<sup>1</sup><sub>2</sub>C<sub>2</sub>B<sub>4</sub>H<sub>5</sub><sup>-</sup> monoanion in THF. Similar treatment of the Cp\*Co(Et<sub>2</sub>C<sub>2</sub>B<sub>3</sub>H<sub>4</sub>)<sup>-</sup> cobaltacarborane anion (Cp\* = C<sub>5</sub>Me<sub>5</sub>) afforded the bent triple-decker sandwich complexes [Cp\*Co(Et<sub>2</sub>C<sub>2</sub>B<sub>3</sub>H<sub>3</sub>)]MCl<sub>2</sub>Cp' (M = Ta, Nb). Both families of compounds were obtained generally in high yield as air-stable crystalline solids that are readily soluble in organic solvents. In the Ta and Nb species, replacement of one or both chlorines with a variety of alkyl groups was effected via reactions with alkylating agents to generate (R<sup>1</sup><sub>2</sub>C<sub>2</sub>B<sub>4</sub>H<sub>4</sub>)Ta(L)ClCp' or (R<sup>1</sup><sub>2</sub>C<sub>2</sub>B<sub>4</sub>H<sub>4</sub>)ML<sub>2</sub>Cp' (M = Ta, Nb), and the corresponding alkylated triple-deckers [Cp\*Co(Et<sub>2</sub>C<sub>2</sub>B<sub>3</sub>H<sub>3</sub>)]Ta(L)ClCp' and [Cp\*Co(Et<sub>2</sub>C<sub>2</sub>B<sub>3</sub>H<sub>3</sub>)]-TaL<sub>2</sub>Cp' (L = Me, Et, Ph, CH<sub>2</sub>Ph, CH<sub>2</sub>CMe<sub>3</sub>, or OPh). Yields of the mono- and dialkyl derivatives ranged from moderate to quantitative. The new complexes were characterized via <sup>1</sup>H, <sup>13</sup>C, and <sup>11</sup>B NMR, mass spectrometry, and elemental analysis supplemented by FTIR and UV-visible spectroscopic data for many compounds, electrochemical studies on selected species, and crystal structure determinations on seven products. Exploratory studies of the reactivities of these complexes revealed significant differences from those of standard organometallic species such as Cp<sub>2</sub>TiCl<sub>2</sub> or Cp<sub>2</sub>ZrR<sub>2</sub>. Thus, tantalum and niobium C<sub>2</sub>B<sub>4</sub> dichloro complexes on treatment with Al<sub>2</sub>Me<sub>6</sub> gave dimethyl derivatives rather than methylenes. The reaction of (Et<sub>2</sub>C<sub>2</sub>B<sub>4</sub>H<sub>4</sub>)TaMe<sub>2</sub>Cp with excess HBF<sub>4</sub> in acetonitrile formed a single isolable product identified as a difluoro derivative, (Et<sub>2</sub>C<sub>2</sub>B<sub>4</sub>H<sub>4</sub>)TaF<sub>2</sub>-Cp. X-ray crystal structures were obtained for [(Me<sub>3</sub>Si)<sub>2</sub>C<sub>2</sub>B<sub>4</sub>H<sub>4</sub>]TaCl<sub>2</sub>Cp (**1b**), (Et<sub>2</sub>C<sub>2</sub>B<sub>4</sub>H<sub>4</sub>)TaCl<sub>2</sub>-Cp\* (**1c**), [Cp\*Co(Et<sub>2</sub>C<sub>2</sub>B<sub>3</sub>H<sub>3</sub>)]TaCl<sub>2</sub>Cp (**4a**), (Et<sub>2</sub>C<sub>2</sub>B<sub>4</sub>H<sub>4</sub>)TaPh<sub>2</sub>Cp (**6d**), Cp\*Co(Et<sub>2</sub>C<sub>2</sub>B<sub>3</sub>H<sub>3</sub>)TaMe<sub>2</sub>-Cp (**7b**), Cp\*Co(Et<sub>2</sub>C<sub>2</sub>B<sub>3</sub>H<sub>3</sub>)Ta(CH<sub>2</sub>Ph)ClCp (**7c**), and (Et<sub>2</sub>C<sub>2</sub>B<sub>4</sub>H<sub>4</sub>)NbMe<sub>2</sub>Cp (**8a**). Crystal data for **1b**: space group P2<sub>1</sub>/a; Z = 4; a = 14.292(4) Å, b = 9.008(2) Å, c = 17.899(7) Å, β = 112.61(2)°; R = 0.043 for 2854 independent reflections. For **1c**: space group P2<sub>1</sub>/c; Z = 4; a = 8.650(2) Å, b = 12.362(5) Å, c = 18.601(7) Å, β = 90.10(3)°; R = 0.038 for 1831 independent reflections. For **4a**: space group P2<sub>1</sub>/n; Z = 4; a = 8.874(2) Å, b = 14.303(4) Å, c = 18.585(6) Å, β = 91.53(2)°; R = 0.036 for 3033 independent reflections. For **6d**: space group P $\bar{1}$ ; Z = 2; a = 8.943(1) Å, b = 15.726(2) Å, c = 7.843(2) Å, α = 90.58(2)°; β = 102.78(2)°; γ = 103.53(1)°; R = 0.024 for 3376 independent reflections. For **7b**: space group P2<sub>1</sub>/n; Z = 4; a = 8.998(2) Å, b = 14.374(2) Å, c = 18.508(3) Å, β = 92.98(2)°; R = 0.027 for 3169 independent reflections. For **7c**: space group P2<sub>1</sub>/n; Z = 4; a = 12.780(2) Å, b = 16.084(2) Å, c = 13.442(2) Å, β = 104.16(1)°; R = 0.030 for 3684 independent reflections. For **8a**: space group P2<sub>1</sub>/c; Z = 4; a = 14.148(3) Å, b = 7.781(5) Å, c = 15.315(2) Å, β = 116.32(1)°; R = 0.031 for 2297 independent reflections.

The small carborane ligands *nido*-[RR'C<sub>2</sub>B<sub>4</sub>H<sub>4</sub>]<sup>2-</sup> and *arachno*-[RR'C<sub>2</sub>B<sub>3</sub>H<sub>5</sub>]<sup>2-</sup> (R, R' = H, alkyl, SiMe<sub>3</sub>) are six-electron donors that form stable η<sup>5</sup> complexes with a variety of metal and metalloid fragments.<sup>2</sup> These groups are isoelectronic with C<sub>5</sub>H<sub>5</sub><sup>-</sup>, as are other boron-containing ligands including *nido*-[RR'C<sub>2</sub>B<sub>9</sub>H<sub>9</sub>]<sup>2-</sup> (di-

carbollide), R<sub>4</sub>C<sub>4</sub>BR' (boroly), and R<sub>3</sub>C<sub>3</sub>B<sub>2</sub>R'<sub>2</sub> (diboroly). The latter two ligand types,<sup>3</sup> along with the bridge-deprotonated planar carborane unit [RR'C<sub>2</sub>B<sub>3</sub>H<sub>3</sub>]<sup>4-</sup>, have a special property that adds a further dimension to metal coordination chemistry: they readily bind in η<sup>5</sup> fashion to metals on opposite sides of the ring plane, generating extended families of stable multidecker sandwich complexes.<sup>1a,2a,3-5</sup> Carborane-bridged systems of this type include triple-decker,<sup>2a</sup> tetradecker,<sup>4a,b</sup> and

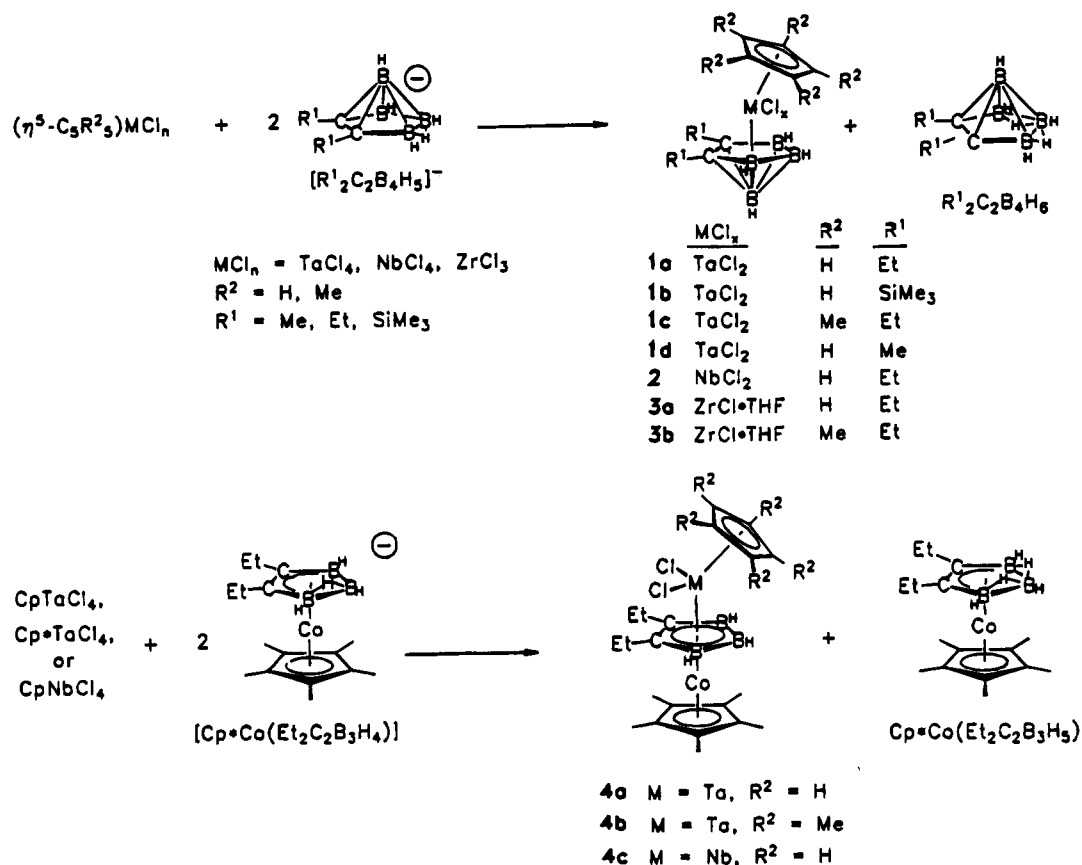
\* Abstract published in *Advance ACS Abstracts*, June 1, 1995.

(1) Organotransition-Metal Metallacarboranes. 38. (a) Part 37: Stephan, M.; Müller, P.; Zenneck, U.; Pritzkow, H.; Siebert, W.; Grimes, R. N. *Inorg. Chem.* **1995**, *34*, 2058. (b) Reported in part at the Fourth Boron U.S.A. Workshop, Syracuse, NY, July 1994; see Abstracts 9 and 68. Taken in part from: Stockman, K. E. Ph.D. Thesis, University of Virginia, 1995.

(2) Recent reviews: (a) Grimes, R. N. *Chem. Rev.* **1992**, *92*, 251. (b) Saxena, A. K.; Hosmane, N. S. *Chem. Rev.* **1993**, *93*, 1081.

(3) (a) Siebert, W. *Adv. Organomet. Chem.* **1993**, *35*, 187. (b) Herberich, G. E.; Carstensen, T.; Koeffler, D. P. J.; Klaff, N.; Boese, R.; Hyla-Krypsin, I.; Gleiter, R.; Stephan, M.; Meth, H.; Zenneck, U. *Organometallics* **1994**, *13*, 619 and references therein.

Scheme 1



(very recently) hexadecker<sup>4c</sup> complexes as well as linked-sandwich oligomers.<sup>5</sup> Moreover, the carborane ligands have a well-documented ability to stabilize many transition metal organometallic systems whose C<sub>5</sub>H<sub>5</sub> or C<sub>5</sub>-Me<sub>5</sub> counterparts are nonexistent or unstable, such as Fe(III)- and Ru(III)-arene complexes.<sup>6</sup> While there are exceptions, most metallacarboranes are resistant to air, heat, and moisture, and survive a far wider range of conditions (including multiple metal oxidation states) than do typical metal-hydrocarbon systems.

Extensive studies of the synthesis, structures, and reactivity of small carborane metal complexes in one of our laboratories have included the development of methods for placing a variety of organic and inorganic substituents at specific boron and carbon locations.<sup>2a,7</sup> This relatively facile tailorability enhances the utility of the carborane ligands as synthons, affording them a range of steric and electronic properties that is unmatched by cyclopentadienyl or any single family of cyclopentadienyl analogues. An aspect of small carborane chemistry that has been little explored is their complexation with early transition metals.<sup>2b</sup> Large

(12–13-vertex) metallacarborane complexes of these elements were first reported by Hawthorne,<sup>8</sup> but this area has been reignited by the recent work of Jordan,<sup>9</sup> Bercaw,<sup>10</sup> and extensive studies by Stone.<sup>11</sup> In the small metallacarborane area, ( $\eta^8-C_8H_8$ )M(Et<sub>2</sub>C<sub>2</sub>B<sub>4</sub>H<sub>4</sub>) (M = Ti, V) and ( $\eta^7-C_7H_7$ )Cr(Et<sub>2</sub>C<sub>2</sub>B<sub>4</sub>H<sub>4</sub>) were characterized in our laboratories a decade ago,<sup>12</sup> and Hosmane et al. have prepared a number of Ti, Cr, Y, Zr, and Hf complexes incorporating C<sub>2</sub>B<sub>4</sub> ligands.<sup>2b,13</sup> Motivated by the potential for development for new, stable catalytic systems involving the early transition elements, we have initiated a study of the synthesis and characterization of a family of Nb, Ta, and Zr complexes of C<sub>2</sub>B<sub>3</sub> and C<sub>2</sub>B<sub>4</sub>

(4) (a) Piepgrass, K. W.; Hölscher, M.; Meng, X.; Sabat, M.; Grimes, R. N. *Inorg. Chem.* **1992**, *31*, 5202. (b) Pipal, J. R.; Grimes, R. N. *Organometallics* **1993**, *12*, 4452 and 4459. (c) Wang, X.; Sabat, M.; Grimes, R. N. *J. Am. Chem. Soc.* **1994**, *116*, 2687.

(5) Meng, X.; Sabat, M.; Grimes, R. N. *J. Am. Chem. Soc.* **1993**, *115*, 6143.

(6) (a) Merkert, J. M.; Geiger, W. E.; Attwood, M. D.; Grimes, R. N. *Organometallics* **1991**, *10*, 3545. (b) Stephan, M.; Davis, J. H., Jr.; Meng, X.; Chase, K. P.; Hauss, J.; Zenneck, U.; Pritzkow, H.; Siebert, W.; Grimes, R. N. *J. Am. Chem. Soc.* **1992**, *114*, 5214.

(7) (a) Piepgrass, K. W.; Grimes, R. N. *Organometallics* **1992**, *11*, 2397. (b) Piepgrass, K. W.; Stockman, K. E.; Sabat, M.; Grimes, R. N. *Organometallics* **1992**, *11*, 2404. (c) Benvenuto, M. A.; Grimes, R. N. *Inorg. Chem.* **1992**, *31*, 3897. (d) Benvenuto, M. A.; Sabat, M.; Grimes, R. N. *Inorg. Chem.* **1992**, *31*, 3904.

(8) (a) Lo, F. Y.; Strouse, C. E.; Callahan, K. P.; Knobler, C. B.; Hawthorne, M. F. *J. Am. Chem. Soc.* **1975**, *97*, 428. (b) Salentine, C. G.; Hawthorne, M. F. *Inorg. Chem.* **1976**, *15*, 2872.

(9) (a) Crowther, D. J.; Baenziger, N. C.; Jordan, R. F. *J. Am. Chem. Soc.* **1991**, *113*, 1455. (b) Uhrhammer, R.; Crowther, D. J.; Olson, J. D.; Swenson, D. C.; Jordan, R. F. *Organometallics* **1992**, *11*, 3098. (c) Crowther, D. J.; Jordan, R. F. *Makromol. Chem., Macromol. Symp.* **1993**, *66*, 121. (d) Uhrhammer, R.; Su, Y.-X.; Swenson, D. C.; Jordan, R. F. *Inorg. Chem.* **1994**, *33*, 4398.

(10) (a) Bazan, G. C.; Schaefer, W. P.; Bercaw, J. E. *Organometallics* **1993**, *12*, 2126. (b) Marsh, R. E.; Schaefer, W. P.; Bazan, G. C.; Bercaw, J. E. *Acta Crystallogr.* **1992**, *C48*, 1416.

(11) (a) Stone, F. G. A. *Adv. Organometal. Chem.* **1990**, *31*, 53 and references therein. (b) Brew, S. A.; Stone, F. G. A. *Adv. Organomet. Chem.* **1993**, *35*, 135.

(12) Swisher, R. G.; Sinn, E.; Grimes, R. N. *Organometallics* **1984**, *3*, 599.

(13) (a) Siriwardane, U.; Zhang, H.; Hosmane, N. S. *J. Am. Chem. Soc.* **1990**, *112*, 9637. (b) Oki, A. R.; Zhang, H.; Hosmane, N. S. *Organometallics* **1991**, *10*, 3964. (c) Oki, A. R.; Zhang, H.; Maguire, J. A.; Hosmane, N. S.; Ro, H.; Hatfield, W. E. *Organometallics* **1991**, *10*, 2996. (d) Oki, A. R.; Zhang, H.; Maguire, J. A.; Hosmane, N. S.; Ro, H.; Hatfield, W. E.; Moscherosch, M.; Kaim, W. *Organometallics* **1992**, *11*, 4202. (e) Zhang, H.; Jia, L.; Hosmane, N. S. *Acta Crystallogr.* **1993**, *C49*, 453. (f) Hosmane, N. S.; Wang, Y.; Zhang, H.; Maguire, J. A.; Waldhoer, E.; Kaim, W.; Binder, H.; Kremer, R. K. *Organometallics* **1994**, *13*, 4156.

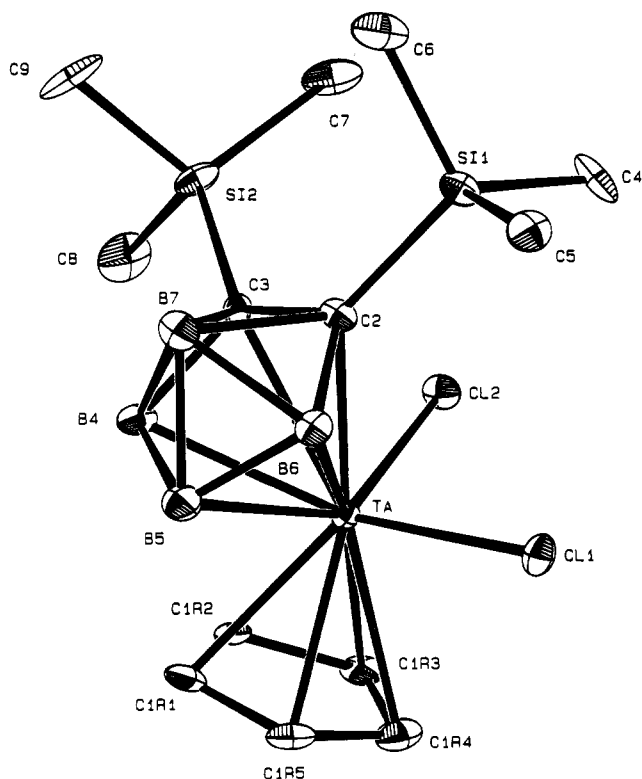


**Figure 1.** Molecular structure of  $[(\text{Me}_3\text{Si})_2\text{C}_2\text{B}_4\text{H}_4]\text{TaCl}_2\text{-Cp}$  (**1b**).

ligands that bear halide, alkyl, and/or hydride units on the metals.

## Results and Discussion

**Synthesis and Structure of (Ligand) $\text{M}(\text{C}_2\text{B}_4)$  and (Ligand) $\text{M}(\text{C}_2\text{B}_3)\text{CoCp}^*$  Complexes.** Carboranyl-cyclopentadienyl complexes of tantalum, niobium, and zirconium were prepared via disproportionation reactions between 2 equiv of  $[\text{R}^1_2\text{C}_2\text{B}_4\text{H}_5]^-$  *nido*-carborane monoanions and  $\text{CpTaCl}_4$ ,  $\text{Cp}^*\text{TaCl}_4$ ,  $\text{CpNbCl}_4$ , or  $\text{CpZrCl}_3$ , forming the species **1a-d**, **2**, and **3a,b** together with neutral  $\text{R}^1_2\text{C}_2\text{B}_4\text{H}_4$ , which was recovered (Scheme 1). Compounds **1a-d** and their derivatives (*vide infra*) are the only known tantalacarboranes other than the  $\text{TaC}_2\text{B}_9$  icosahedral clusters reported earlier by Jordan et al.<sup>9</sup> and a benzyne complex we reported recently (*vide infra*), while **2** is the first reported niobium carborane complex of any type. As shown in Scheme 1 (bottom), analogous reactions of the *nido*- $[\text{Cp}^*\text{Co}(\text{Et}_2\text{C}_2\text{B}_3\text{H}_4)]^-$  monoanion gave the bent triple-decker complexes **4a-c**. This method proved to be far more efficient than an earlier approach involving reactions of metal dihalides with the carborane dianions.<sup>14</sup>

All new complexes were characterized by  $^1\text{H}$ ,  $^{13}\text{C}$ , and  $^{11}\text{B}$  NMR, mass spectrometry, and elemental analysis, supported in many cases by FTIR and UV-visible spectroscopic data. X-ray crystal structures were obtained for **1b,c** and **4a**, the molecular geometries of which are depicted in Figures 1–3. Data collection parameters and crystal data are presented in Table 1, bond distances and bond angles are listed in Tables 2–4, and tables of positional parameters as well as mean

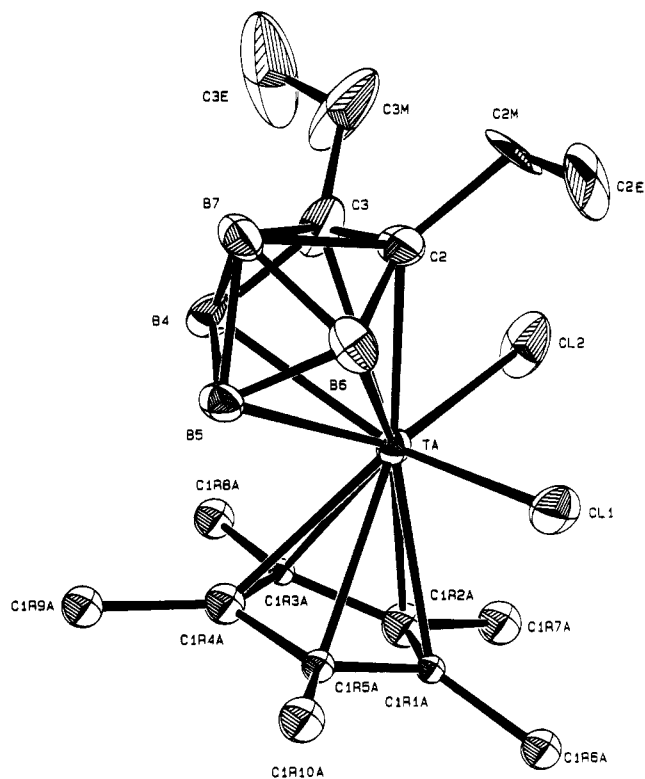


**Figure 2.** Molecular structure of  $(\text{Et}_2\text{C}_2\text{B}_4\text{H}_4)\text{TaCl}_2\text{Cp}^*$  (**1c**).

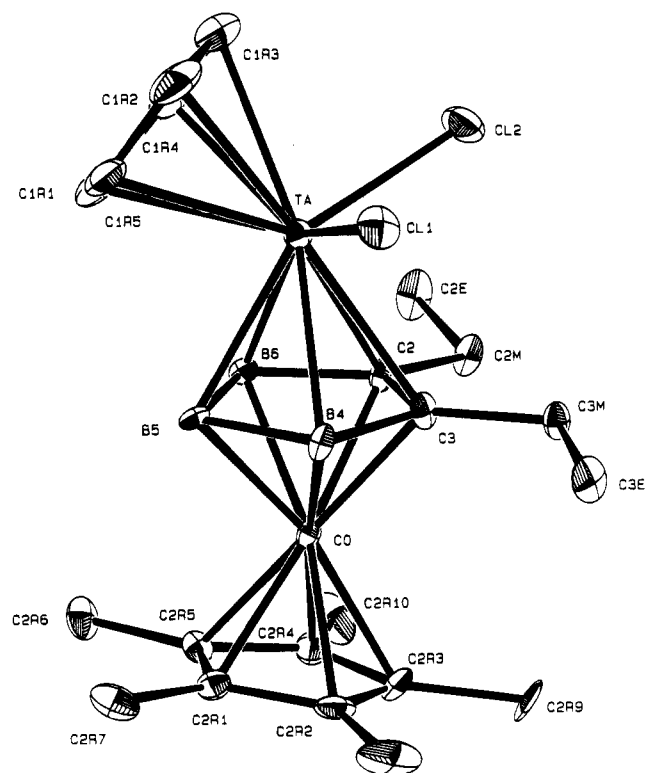


**Figure 3.** Molecular structure of  $[\text{Cp}^*\text{Co}(\text{Et}_2\text{C}_2\text{B}_3\text{H}_3)]\text{TaCl}_2\text{-Cp}$  (**4a**).

plane calculations are included in the supporting information.

The principal structural features in all three complexes, several of which are summarized in Table 5, are typical of metallocene dihalides and include normal metal-Cp, metal-carborane, and metal-Cl bond distances and Cp-M-Cl and Cl-M-Cl bond angles. In

(14) Davis, J. H., Jr.; Sinn, E.; Grimes, R. N. *J. Am. Chem. Soc.* **1989**, *111*, 4776.

Table 1. Experimental X-ray Diffraction Parameters and Crystal Data

compd	1b	1c	4a	6d	7b	7c	8a
empirical formula	TaCl <sub>2</sub> Si <sub>2</sub> Cl <sub>13</sub> B <sub>4</sub> H <sub>27</sub>	TaCl <sub>2</sub> C <sub>16</sub> B <sub>4</sub> H <sub>29</sub>	TaCoCl <sub>2</sub> C <sub>21</sub> B <sub>3</sub> H <sub>33</sub>	TaC <sub>23</sub> B <sub>4</sub> H <sub>29</sub>	TaCoC <sub>23</sub> B <sub>3</sub> H <sub>39</sub>	TaCoClC <sub>28</sub> B <sub>3</sub> H <sub>40</sub>	NbC <sub>13</sub> B <sub>4</sub> H <sub>25</sub>
fw	534.62	516.50	628.71	529.67	587.87	684.39	317.49
cryst color, habit	orange prism	yellow plate	black prism	yellow prism	dark prism	dark prism	yellow plate
cryst. dimens (mm <sup>3</sup> )	0.45 × 0.37 × 0.26	0.46 × 0.24 × 0.12	0.44 × 0.36 × 0.23	0.46 × 0.38 × 0.32	0.45 × 0.33 × 0.21	0.44 × 0.38 × 0.17	0.46 × 0.32 × 0.18
space group	P2 <sub>1</sub> /a	P2 <sub>1</sub> /c	P2 <sub>1</sub> /n	P1	P2 <sub>1</sub> /n	P2 <sub>1</sub> /n	P2 <sub>1</sub> /c
a, Å	14.292(4)	8.650(2)	8.874(2)	8.943(1)	8.998(2)	12.780(2)	14.148(3)
b, Å	9.008(2)	12.362(5)	14.303(4)	15.726(2)	14.374(2)	16.084(2)	7.781(5)
c, Å	17.899(7)	18.601(7)	18.565(6)	7.843(2)	18.508(3)	13.442(2)	15.315(2)
α, deg	112.61(2)	90.10(3)	91.53(2)	90.58(2)	92.98(2)	104.16(1)	116.32(1)
β, deg	2127	1989	2358	1044	2391	2679	1511
γ, deg	4	4	4	4	4	4	4
V, Å <sup>3</sup>	54.63	57.27	55.20	52.09	52.20	47.68	7.40
Z	0.62–1.00	0.46–1.00	0.72–1.00	0.58–1.00	0.48–1.00	0.61–1.00	0.93–1.00
μ, cm <sup>-1</sup> (Mo Kα)	1.669	1.725	1.771	1.685	1.633	1.697	1.395
transmissn factors	50.0	46.0	50.0	50.0	50.0	50.0	50.0
D(calcd), g cm <sup>-3</sup>	4191	3033	4609	3940	4684	5131	3002
2θ <sub>max</sub>	2854	1831	3033	3376	3169	3684	2297
reflms measd	0.043	0.038	0.036	0.024	0.027	0.030	0.031
reflms obsd <sup>c</sup>	0.055	0.058	0.051	0.039	0.037	0.041	0.057
R <sub>w</sub>	2.46	0.81	1.15	0.71	0.71	0.83	0.54
largest peak in final diss. map, e/Å <sup>3</sup>							

<sup>a</sup> I > 3.00σ(I).

Table 2. Bond Distances and Selected Bond Angles for [(Me<sub>3</sub>Si)<sub>2</sub>C<sub>2</sub>B<sub>4</sub>H<sub>4</sub>]TaCl<sub>2</sub>Cp (1b)

Bond Distances, Å			
Ta–Cl(1)	2.364(2)	Si(2)–C(8)	1.84(1)
Ta–Cl(2)	2.354(2)	Si(2)–C(9)	1.88(1)
Ta–C(2)	2.427(9)	C(2)–C(3)	1.51(1)
Ta–C(3)	2.427(9)	C(2)–B(6)	1.55(1)
Ta–C(1R1)	2.42(1)	C(2)–B(7)	1.74(1)
Ta–C(1R2)	2.41(1)	C(3)–B(4)	1.57(1)
Ta–C(1R3)	2.44(1)	C(3)–B(7)	1.73(1)
Ta–C(1R4)	2.44(1)	C(1R1)–C(1R2)	1.42(1)
Ta–C(1R5)	2.38(1)	C(1R1)–C(1R5)	1.41(1)
Ta–B(4)	2.41(1)	C(1R2)–C(1R3)	1.39(1)
Ta–B(5)	2.42(1)	C(1R3)–C(1R4)	1.40(1)
Ta–B(6)	2.42(1)	C(1R4)–C(1R5)	1.40(2)
Si(1)–C(2)	1.88(1)	B(4)–B(5)	1.71(2)
Si(1)–C(4)	1.85(1)	B(4)–B(7)	1.77(2)
Si(1)–C(5)	1.85(1)	B(5)–B(6)	1.66(2)
Si(1)–C(6)	1.86(1)	B(5)–B(7)	1.79(2)
Si(2)–C(3)	1.90(1)	B(6)–B(7)	1.79(2)
Si(2)–C(7)	1.86(1)	B(6)–B(7)	1.79(2)

Selected Bond Angles, deg			
Cl(1)–Ta–Cl(2)	95.50(9)	C(2)–C(3)–B(4)	110.9(8)
Cl(1)–Ta–C(2)	85.4(2)	C(2)–C(3)–B(7)	64.4(6)
Ta–C(2)–Si(1)	135.0(5)	B(4)–C(3)–B(7)	64.6(7)
Ta–C(2)–C(3)	71.9(5)	B(4)–B(5)–B(6)	104.1(9)
Ta–C(2)–B(6)	71.2(5)	C(3)–B(4)–B(5)	105.7(8)
Ta–C(2)–B(7)	95.8(6)	C(2)–B(6)–B(5)	107.2(9)
Si(1)–C(2)–C(3)	127.8(7)	C(2)–Si(1)–C(4)	113.2(4)
Si(1)–C(2)–B(6)	118.8(7)	C(2)–Si(1)–C(5)	108.5(5)
Si(1)–C(2)–B(7)	128.9(6)	C(2)–Si(1)–C(6)	110.3(5)
C(3)–C(2)–B(6)	112.1(8)	C(4)–Si(1)–C(5)	106.4(5)
C(3)–C(2)–B(7)	64.1(6)	C(4)–Si(1)–C(6)	112.2(6)
B(6)–C(2)–B(7)	65.5(7)	C(5)–Si(1)–C(6)	105.9(5)
Ta–C(3)–Si(2)	133.8(5)	C(3)–Si(2)–C(7)	117.0(5)
Ta–C(3)–C(2)	71.9(5)	C(3)–Si(2)–C(8)	107.9(5)
Ta–C(3)–B(4)	70.5(5)	C(3)–Si(2)–C(9)	105.8(5)
Ta–C(3)–B(7)	95.9(6)	C(7)–Si(2)–C(8)	107.4(5)
Si(2)–C(3)–C(2)	131.9(7)	C(7)–Si(2)–C(9)	110.4(6)
Si(2)–C(3)–B(4)	116.0(7)	C(8)–Si(2)–C(9)	107.9(6)
Si(2)–C(3)–B(7)	129.1(7)		

each case, the carborane ligand is oriented with the sterically more demanding R<sup>1</sup>–C–C–R<sup>1</sup> array on the "open" side of the complex. The dihedral (bending) angle subtended by the C<sub>5</sub> and C<sub>2</sub>B<sub>3</sub> ring planes is closely similar (50–54°) in the three structures, and is significantly larger than the corresponding angle (ca. 48°) in the bent-sandwich (SiMe<sub>3</sub>)<sub>2</sub>C<sub>2</sub>B<sub>4</sub>H<sub>4</sub>–titanium complexes reported by Hosmane et al.<sup>13f</sup> This small but significant difference can be accounted for by steric interaction between the Cp and carborane ligands in the titanium complex, which limits the degree of bending; in the tantalum species, this limitation is less severe owing to the larger metal center, allowing a slightly more bent geometry.

The Cp\* and C<sub>2</sub>B<sub>3</sub> planes in **4a**, on the other hand, are nearly parallel with a dihedral angle of only 8.4°, typical of Cp\*–metal–C<sub>2</sub>B<sub>3</sub> arrays (as discussed in earlier papers<sup>4</sup>). In the absence of other ligands on cobalt that could give rise to steric effects, this slight observed tilt is clearly of electronic origin and is related to the interaction between the bonding orbitals on cobalt and the available bonding MOs on the heterocyclic carborane ligand.<sup>4</sup>

Comparison of the structures of the C<sub>2</sub>B<sub>4</sub>Ta complexes **1b** and **1c** reveals close similarity in the bending angle, defined as above, and in other relevant parameters (Table 5). An exception, however, is seen in the carborane C–C bond distance which is significantly longer in **1b** than in **1c** (or in any of the other structures reported in this paper). This finding correlates with the

**Table 3. Bond Distances and Selected Bond Angles for (Et<sub>2</sub>C<sub>2</sub>B<sub>4</sub>H<sub>4</sub>)/TaCl<sub>2</sub>Cp\* (1c)**

Bond Distances, Å			
Ta-Cl(1)	2.343(4)	C(1R1A)-C(1R2A)	1.33(5)
Ta-Cl(2)	2.355(4)	C(1R1A)-C(1R5A)	1.46(4)
Ta-C(2)	2.42(2)	C(1R1A)-C(1R6A)	1.51(4)
Ta-C(3)	2.47(2)	C(1R1B)-C(1R2B)	1.41(5)
Ta-C(1R1A)	2.44(3)	C(1R1B)-C(1R5B)	1.41(4)
Ta-C(1R1B)	2.43(4)	C(1R1B)-C(1R6B)	1.57(5)
Ta-C(1R2A)	2.52(3)	C(1R2A)-C(1R3A)	1.42(4)
Ta-C(1R2B)	2.40(3)	C(1R2A)-C(1R7A)	1.63(5)
Ta-C(1R3A)	2.46(2)	C(1R2B)-C(1R3B)	1.40(4)
Ta-C(1R3B)	2.37(3)	C(1R2B)-C(1R7B)	1.62(5)
Ta-C(1R4B)	2.37(3)	C(1R3A)-C(1R4A)	1.37(4)
Ta-C(1R4A)	2.51(3)	C(1R3A)-C(1R8A)	1.50(4)
Ta-C(1R5B)	2.39(3)	C(1R3B)-C(1R4B)	1.32(5)
Ta-C(1R5A)	2.49(3)	C(1R3B)-C(1R8B)	1.41(4)
Ta-B(4)	2.39(2)	C(1R4B)-C(1R5B)	1.49(4)
Ta-B(5)	2.42(2)	C(1R4B)-C(1R9B)	1.64(4)
Ta-B(6)	2.42(2)	C(1R4A)-C(1R5A)	1.49(4)
C(2M)-C(2)	1.59(2)	C(1R4A)-C(1R9A)	1.57(4)
C(2M)-C(2E)	1.61(4)	C(1R5B)-C(1R10B)	1.54(4)
C(2)-C(3)	1.40(2)	C(1R5A)-C(1R10A)	1.52(4)
C(2)-B(6)	1.53(2)	B(4)-B(5)	1.77(2)
C(2)-B(7)	1.76(2)	B(4)-B(7)	1.78(2)
C(3)-C(3M)	1.51(3)	B(5)-B(6)	1.65(2)
C(3)-B(4)	1.50(3)	B(5)-B(7)	1.77(3)
C(3)-B(7)	1.73(2)	B(6)-B(7)	1.76(3)
C(3M)-C(3E)	1.23(4)		
Selected Bond Angles, deg			
Cl(1)-Ta-Cl(2)	95.0(2)	Ta-C(3)-B(4)	69(1)
Cl(1)-Ta-C(2)	86.8(5)	Ta-C(3)-B(7)	96(1)
Ta-C(2)-C(2M)	131(1)	C(2)-C(3)-C(3M)	116(2)
Ta-C(2)-C(3)	75(1)	C(2)-C(3)-B(4)	114(1)
Ta-C(2)-B(6)	71(1)	C(2)-C(3)-B(7)	68(1)
Ta-C(2)-B(7)	97.0(9)	C(3M)-C(3)-B(4)	129(2)
C(2M)-C(2)-C(3)	121(2)	C(3M)-C(3)-B(7)	127(2)
C(2M)-C(2)-B(6)	125(2)	B(4)-C(3)-B(7)	66(1)
C(2M)-C(2)-B(7)	132(1)	C(2)-C(2M)-C(2E)	113(2)
C(3)-C(2)-B(6)	113(2)	C(3)-C(3M)-C(3E)	123(3)
C(3)-C(2)-B(7)	65(1)	C(3)-B(4)-B(5)	105(1)
B(6)-C(2)-B(7)	64(1)	B(4)-B(5)-B(6)	100(1)
Ta-C(3)-C(2)	71(1)	C(2)-B(6)-B(5)	107(1)
Ta-C(3)-C(3M)	136(1)		

release of electron density by the SiMe<sub>3</sub> groups on **1b**, which would tend to mitigate the electron-deficiency in the region of the cage carbon atoms and hence reduce the multiple-bond character<sup>14</sup> of the C-C interaction in the C<sub>2</sub>B<sub>4</sub> ligand.

All of the isolated metal dihalide complexes are significantly more stable than their bis(cyclopentadienyl) counterparts. Thus, the tantalum compounds **1a-d** and **4a,b** are air-stable solids, and the niobium complexes **2** and **4c** are only mildly reactive with atmospheric moisture and can be handled on the benchtop. However, the zirconium species **3a** and **3b** form colorless precipitates (presumably oxygen-bridged polymers) on exposure to air in solution or in the solid state.

The zirconium cyclopentadienyl complex **3a** was isolated with 1 equiv of THF as solvent of crystallization. In this compound, the appearance of diastereotopic signals for the carboranyl ethyl groups indicates a comparatively slow process for ligand exchange. The permethylcyclopentadienyl complex **3b** was isolated with 2-3 equiv of THF; in contrast to **3a**, its carboranyl ethyl <sup>1</sup>H NMR signals were not split in a diastereotopic pattern, suggesting a more rapid ligand exchange process. This is consistent with the more hindered nature of the metal center, which is expected to enhance the rate of THF dissociation.

**Ligand Substitution Reactions: Synthesis of Alkyl, Aryl, and Phenoxide Complexes.** The re-

**Table 4. Bond Distances and Selected Bond Angles for [Cp\*Co(Et<sub>2</sub>C<sub>2</sub>B<sub>3</sub>H<sub>3</sub>)]TaCl<sub>2</sub>Cp (4a)**

Bond Distances, Å			
Ta-Cl(1)	2.376(2)	C(2M)-C(2E)	1.53(1)
Ta-Cl(2)	2.391(2)	C(2)-C(3)	1.48(1)
Ta-C(2)	2.469(8)	C(2)-B(6)	1.55(1)
Ta-C(3)	2.442(8)	C(3M)-C(3)	1.52(1)
Ta-C(1R1)	2.40(1)	C(3M)-C(3E)	1.53(1)
Ta-C(1R2)	2.38(1)	C(3)-B(4)	1.57(1)
Ta-C(1R3)	2.42(1)	C(1R1)-C(1R2)	1.39(1)
Ta-C(1R4)	2.45(1)	C(1R1)-C(1R5)	1.41(1)
Ta-C(1R5)	2.39(1)	C(1R2)-C(1R3)	1.40(2)
Ta-B(4)	2.44(1)	C(1R3)-C(1R4)	1.40(2)
Ta-B(5)	2.366(9)	C(1R4)-C(1R5)	1.36(1)
Ta-B(6)	2.39(1)	C(2R1)-C(2R2)	1.43(1)
Co-C(2)	2.030(8)	C(2R1)-C(2R5)	1.43(1)
Co-C(3)	2.046(8)	C(2R1)-C(2R6)	1.48(1)
Co-C(2R1)	2.043(8)	C(2R2)-C(2R3)	1.40(1)
Co-C(2R2)	2.037(8)	C(2R2)-C(2R7)	1.51(1)
Co-C(2R3)	2.067(8)	C(2R3)-C(2R4)	1.44(1)
Co-C(2R4)	2.067(9)	C(2R3)-C(2R8)	1.48(1)
Co-C(2R5)	2.068(8)	C(2R4)-C(2R5)	1.40(1)
Co-B(4)	2.09(1)	C(2R4)-C(2R9)	1.52(1)
Co-B(5)	2.06(1)	C(2R5)-C(2R10)	1.51(1)
Co-B(6)	2.055(9)	B(4)-B(5)	1.69(1)
C(2M)-C(2)	1.51(1)	B(5)-B(6)	1.73(1)
Selected Bond Angles, deg			
Cl(1)-Ta-Cl(2)	32.3(1)	C(2)-C(3)-C(3M)	118.6(7)
Cl(1)-Ta-C(2)	119.8(2)	C(2)-C(3)-B(4)	114.6(7)
Ta-C(2)-Co	103.0(3)	C(3M)-C(3)-B(4)	126.7(7)
Ta-C(2)-C(2M)	131.2(6)	Ta-C(3)-C(3M)	127.1(6)
Ta-C(2)-C(3)	71.4(5)	Ta-C(3)-B(4)	71.3(5)
Ta-C(2)-B(6)	68.6(4)	Co-C(3)-C(2)	68.1(4)
Co-C(2)-C(2M)	125.8(6)	Co-C(3)-C(3M)	129.3(6)
Co-C(2)-C(3)	69.3(4)	Co-C(3)-B(4)	69.1(5)
Co-C(2)-B(6)	68.5(4)	C(2)-C(2M)-C(2E)	114.6(7)
C(2M)-C(2)-C(3)	121.5(7)	C(3)-C(3M)-C(3E)	113.9(7)
C(2M)-C(2)-B(6)	127.0(7)	C(3)-B(4)-B(5)	104.4(7)
C(3)-C(2)-B(6)	111.4(7)	B(4)-B(5)-B(6)	104.0(7)
Ta-C(3)-Co	103.5(3)	C(2)-B(6)-B(5)	105.6(7)
Ta-C(3)-C(2)	73.5(5)		

placement of halide ligands by alkyl and aryl groups was found to be facile in most cases using standard alkylating reagents. Schemes 2 and 3 summarize the mono- and disubstitution reactions, respectively, for the dichlorotantalum carborane substrates. In general, the first chloride proved to be substantially more reactive than the second. Thus, monoalkyl complexes were selectively obtained when relatively mild alkylating agents were used in excess (Scheme 2): Al<sub>2</sub>Me<sub>6</sub> for short reaction times (**5a,b**), dialkylzinc reagents (**5a-c**, **5e-g**), and dialkylmagnesiums (**5h,i**). It is notable that, while dineopentylmagnesium generated complex **5h** from **1a** in 58% yield, dineopentylzinc was unreactive with **1a**.<sup>15</sup>

Disubstitution was achieved with more powerful nucleophiles (Scheme 3), as shown in the preparation of **6a-k** in good yield via treatment of the dichloro species with Grignard reagents.<sup>16,17</sup> The sterically hindered dineopentyl complexes **6h-j** were obtained in yields of 90, 68, and 68%, respectively, on treatment

(15) One exception has been noted: the monoethyl complex **5d** was obtained with EtMgCl.

(16) We have recently found that the reaction of **1a** with dimethylzinc in THF instead of toluene produces the dimethyl complex **6a** in good yield.

(17) The proton NMR spectra for both the dihalide and the dialkyl complexes exhibit dramatic solvent effects for the cyclopentadienyl resonances. For example, **1a** shows a shift of 0.83 ppm, from δ 5.60 in C<sub>6</sub>D<sub>6</sub> to δ 6.43 CDCl<sub>3</sub>. The dimethyl complex **6a** is similar, with signals at δ 5.37 in C<sub>6</sub>D<sub>6</sub> and δ 6.02 CDCl<sub>3</sub>. Interestingly, the Cp resonances for these species in CD<sub>3</sub>CN and CD<sub>2</sub>Cl<sub>2</sub> solvents are within 0.06 ppm of those recorded in CDCl<sub>3</sub>.

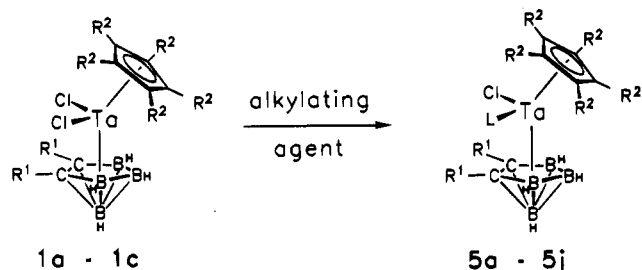


Table 5. Comparison of Structural Parameters

	1b	1c	4a	6d	7b	7c	8a
Cp(Cp*)-C <sub>2</sub> B <sub>3</sub> dihedral angle, deg	53.10	50.42	54.00, 8.38	51.10	51.98, 8.81	51.56, 8.56	48.92
Co-Ta distance, Å			3.531		3.559	3.560	
carborane C2-C3 distance, Å	1.51(1)	1.40(2)	1.48(1)	1.460(8)	1.483(8)	1.470(8)	1.463(5)
Ta-C <sub>2</sub> B <sub>3</sub> distance, Å <sup>a</sup>	2.001	2.018	1.995	2.019	2.011	2.019	2.024 <sup>e</sup>
Co-C <sub>2</sub> B <sub>3</sub> distance, Å <sup>a</sup>			1.536		1.548	1.541	
Ta-Cp(Cp*) distance, Å <sup>c</sup>	2.098	2.165	2.096	2.100	2.115	2.098	2.114 <sup>f</sup>
Co-Cp(Cp*) distance, Å <sup>c</sup>			1.664		1.666	1.672	
X-Ta-X (X = Cl, Me, Ph) angle, deg	95.50(9)	95.0	92.3	110.2 <sup>b</sup>	91.4(2) <sup>c</sup>	91.5(2) <sup>d</sup>	97.0(1) <sup>g</sup>

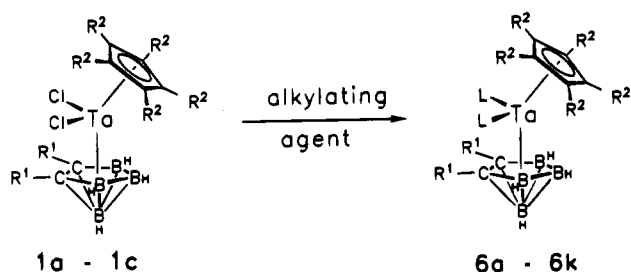
<sup>a</sup> Metal-ring plane distance. <sup>b</sup> C10-Ta-C4 (Ph-Ta-Ph) angle. <sup>c</sup> C11-Ta-C12 (Me-Ta-Me) angle. <sup>d</sup> C11-Ta-Cl (phenyl-Ta-Cl) angle. <sup>e</sup> Nb-C<sub>2</sub>B<sub>3</sub> distance. <sup>f</sup> Nb-Cp distance. <sup>g</sup> C4-Nb-C5 (Me-Nb-Me) angle.

Scheme 2



	R <sup>1</sup>	R <sup>2</sup>	L	alk. agent
5a	Et	H	Me	Al <sub>2</sub> Me <sub>6</sub> or Me <sub>2</sub> Zn
5b	SiMe <sub>3</sub>	H	Me	
5c	Et	Me	Me	EtMgCl
5d	Et	H	Et	
5e	Et	H	CH <sub>2</sub> Ph	Zn(CH <sub>2</sub> Ph) <sub>2</sub>
5f	SiMe <sub>3</sub>	H	CH <sub>2</sub> Ph	
5g	Et	Me	CH <sub>2</sub> Ph	
5h	Et	H	CH <sub>2</sub> tBu	Np <sub>2</sub> Mg·dioxane
5i	Et	Me	CH <sub>2</sub> tBu	

Scheme 3



	R <sup>1</sup>	R <sup>2</sup>	L	alk. agent
6a	Et	H	Me	CH <sub>3</sub> MgBr
6b	SiMe <sub>3</sub>	H	Me	
6c	Et	Me	Me	PhLi
6d	Et	H	Ph	
6e	Et	H	CH <sub>2</sub> Ph	PhCH <sub>2</sub> MgBr
6f	SiMe <sub>3</sub>	H	CH <sub>2</sub> Ph	
6g	Et	Me	CH <sub>2</sub> Ph	
6h	Et	H	CH <sub>2</sub> tBu	tBuCH <sub>2</sub> Li
6i	SiMe <sub>3</sub>	H	CH <sub>2</sub> tBu	
6j	Et	Me	CH <sub>2</sub> tBu	
6k	Et	H	OPh	PhONa

with 2.5–3 equiv of neopentyllithium. The displacement of both chloro ligands on **1a** by sodium phenoxide also proceeds smoothly to form **6k** in nearly quantitative yield.

Similar patterns were observed in the alkylation of the Cp\*Co analogue **4a**, depicted in Scheme 4 (top),

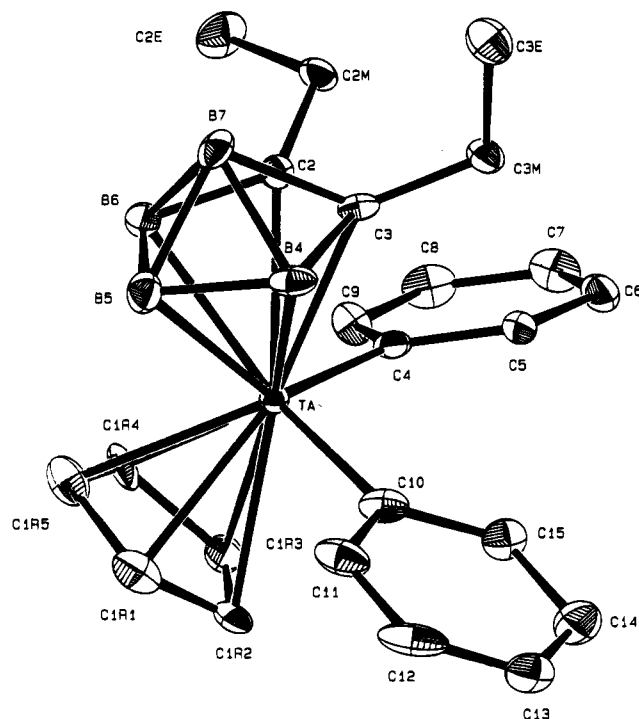


Figure 4. Molecular structure of (Et<sub>2</sub>C<sub>2</sub>B<sub>4</sub>H<sub>4</sub>)/TaPh<sub>2</sub>Cp (**6d**).

which afforded the mono- and dialkylated derivatives **7a–f**. The isolated yields of compounds **7a–d** were quantitative, while those of the neopentyl species **7e** and **7f** were 80% and 58%, respectively.

With two exceptions, all alkyl-, aryl-, and phenoxantantalum carborane complexes described here are air-stable in the solid state for weeks and for at least 1 day in solution. Decomposition under these conditions appears to consist mostly of slow hydrolysis to form oxo-bridged species (to be described in a subsequent paper).<sup>18</sup> In contrast, the Et<sub>2</sub>C<sub>2</sub>B<sub>4</sub>-bis(neopentyl) complexes **6h–j** are unstable, decomposing into uncharacterized products while standing in solution under N<sub>2</sub> for several hours. However, the reddish-purple Cp\*CoC<sub>2</sub>B<sub>3</sub> neopentyl analogues **7e** and **7f** are quite robust compounds.

Complexes **6d** and **7b,c** were characterized by X-ray crystallography, with the structures depicted in Figures 4–6 and the relevant information listed in Tables 1, 5, and 6–8. Comparison of the parameters in these molecules with the corresponding values in the dichloro species **1b,c** and **4a**, which are very similar (Table 5), suggests that replacement of Cl by organic moieties in

(18) When stored in CDCl<sub>3</sub>, the chloroalkyl complexes **5a** and **5d** decompose on standing to the parent dichloride **1a**. The process requires about 1 week for the methyl complex but only 2 days for the ethyl complex under similar conditions.

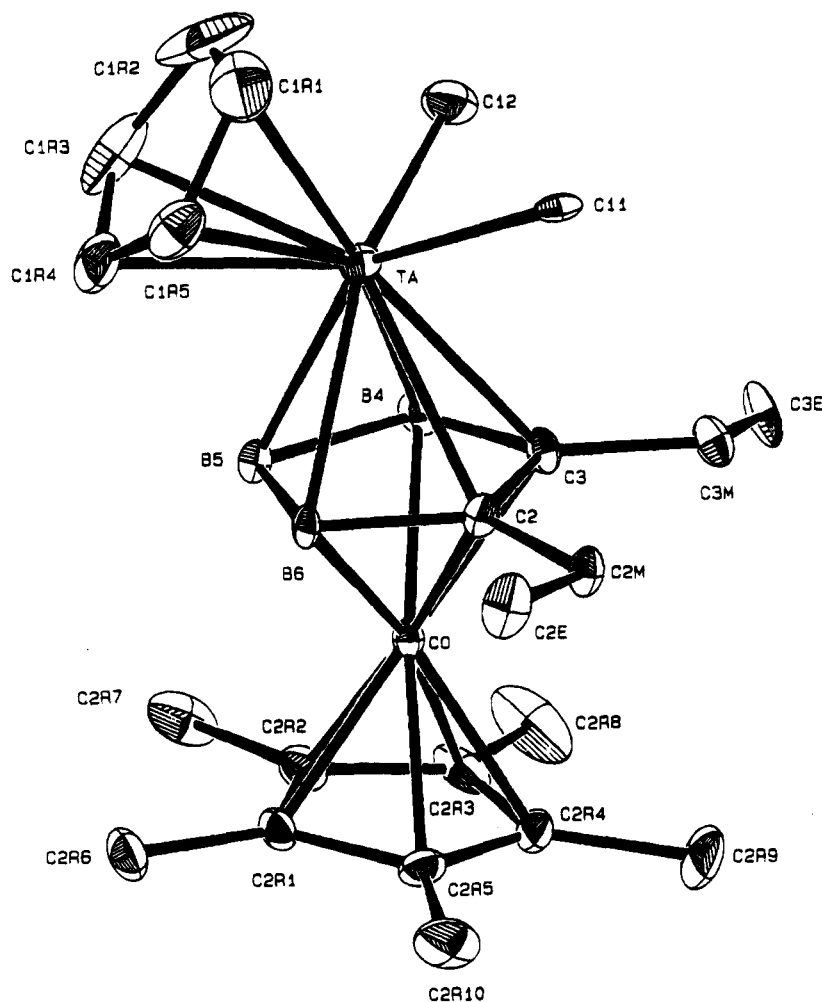
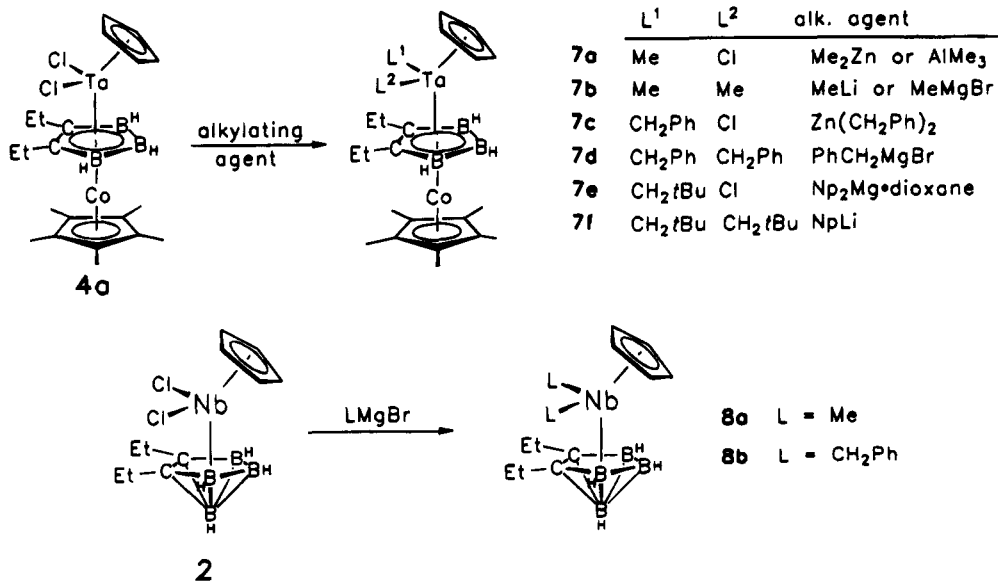


**Figure 5.** Molecular structure of  $\text{Cp}^*\text{Co}(\text{Et}_2\text{C}_2\text{B}_3\text{H}_3)\text{TaMe}_2\text{Cp}$  (**7b**).

**Scheme 4**



**6d**, and **7b,c** has little effect on the structures. Thus, the bend (dihedral) angle of the ring ligands on tantalum is  $51.1^\circ$ – $52.0^\circ$  for these structures, nearly identical with those observed in the analogous dichloro compounds. As is the case in the  $\text{CoTa}$  species **4a**, the  $\text{Cp}^*$  and  $\text{C}_2\text{B}_3$  ring planes in the bent triple-deckers **7b** and **7c** are only slightly tilted, with dihedral angles of  $8.8^\circ$  and  $8.6^\circ$ , respectively.

The dialkylation of the niobium dichloro complex **2** was accomplished in analogous fashion to the tantalum system, generating the dialkyls **8a** and **8b** on treatment with Grignard reagents (Scheme 4, bottom). An X-ray structure determination on **8a** (Table 9 and Figure 7) provided the first structural characterization of a niobium carborane complex and revealed general similarity with the corresponding  $\text{TaC}_2\text{B}_4$  species **1b,c** and **6d**

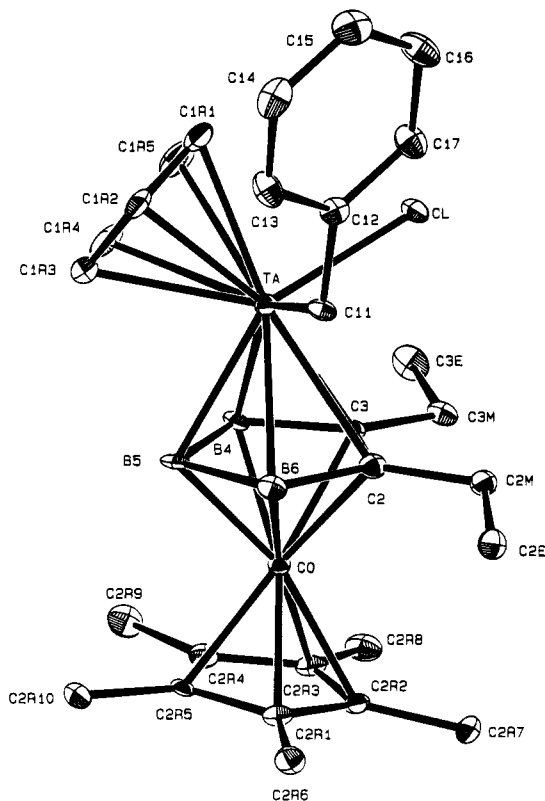


Figure 6. Molecular structure of  $\text{Cp}^*\text{Co}(\text{Et}_2\text{C}_2\text{B}_3\text{H}_3)\text{Ta}(\text{CH}_2\text{-Ph})\text{ClCp}$  (**7c**).

Table 6. Bond Distances and Selected Bond Angles for  $(\text{Et}_2\text{C}_2\text{B}_4\text{H}_4)\text{TaPh}_2\text{Cp}$  (**6d**)

Bond Distances, Å			
Ta-C(2)	2.466(5)	C(4)-C(9)	1.395(8)
Ta-C(3)	2.462(5)	C(5)-C(6)	1.397(7)
Ta-C(4)	2.237(5)	C(6)-C(7)	1.395(8)
Ta-C(10)	2.213(6)	C(7)-C(8)	1.397(8)
Ta-C(1R1)	2.429(5)	C(8)-C(9)	1.381(7)
Ta-C(1R2)	2.434(5)	C(10)-C(11)	1.395(7)
Ta-C(1R3)	2.403(5)	C(10)-C(15)	1.409(8)
Ta-C(1R4)	2.423(5)	C(1R1)-C(1R2)	1.380(9)
Ta-C(1R5)	2.414(5)	C(1R1)-C(1R5)	1.431(8)
Ta-B(4)	2.453(6)	C(11)-C(12)	1.38(1)
Ta-B(5)	2.395(6)	C(1R2)-C(1R3)	1.436(8)
Ta-B(6)	2.395(6)	C(12)-C(13)	1.383(9)
C(2)-C(2M)	1.516(7)	C(13)-C(14)	1.383(9)
C(2)-C(3)	1.460(8)	C(1R3)-C(1R4)	1.42(1)
C(2)-B(6)	1.558(7)	C(14)-C(15)	1.407(8)
C(2)-B(7)	1.731(7)	C(1R4)-C(1R5)	1.417(8)
C(2M)-C(2E)	1.501(8)	B(4)-B(5)	1.696(9)
C(3)-C(3M)	1.501(7)	B(4)-B(7)	1.793(9)
C(3)-B(4)	1.558(8)	B(5)-B(6)	1.693(9)
C(3)-B(7)	1.738(7)	B(5)-B(7)	1.757(8)
C(3M)-C(3E)	1.536(7)	B(6)-B(7)	1.778(8)
C(4)-C(5)	1.407(7)		
Selected Bond Angles, deg			
C(4)-Ta-C(10)	110.2(2)	C(2)-C(3)-C(3M)	122.8(5)
Ta-C(2)-C(2M)	137.4(3)	C(2)-C(3)-B(4)	114.0(5)
Ta-C(2)-C(3)	72.6(3)	C(2)-C(3)-B(7)	64.9(4)
Ta-C(2)-B(6)	68.8(3)	C(3M)-C(3)-B(4)	121.9(5)
Ta-C(2)-B(7)	95.3(3)	C(3M)-C(3)-B(7)	129.8(4)
C(2M)-C(2)-C(3)	120.0(4)	B(4)-C(3)-B(7)	65.6(4)
C(2M)-C(2)-B(6)	126.5(5)	Ta-C(3)-C(2)	72.9(3)
C(2M)-C(2)-B(7)	127.2(4)	Ta-C(3)-C(3M)	134.9(3)
C(3)-C(2)-B(6)	112.1(5)	C(2)-C(2M)-C(2E)	115.1(4)
C(3)-C(2)-B(7)	65.4(3)	C(3)-C(3M)-C(3E)	113.5(4)
B(6)-C(2)-B(7)	65.2(3)	C(3)-B(4)-B(5)	104.1(5)
Ta-C(3)-B(4)	71.2(3)	C(2)-B(6)-B(5)	105.3(5)
Ta-C(3)-B(7)	95.3(3)	B(4)-B(5)-B(6)	104.5(4)

(Table 5). A notable difference, however, is found in the reduced Cp-C<sub>2</sub>B<sub>3</sub> dihedral angle in **8a** (48.9°) which is

Table 7. Bond Distances and Selected Bond Angles for  $\text{Cp}^*\text{Co}(\text{Et}_2\text{C}_2\text{B}_3\text{H}_3)\text{TaMe}_2\text{Cp}$  (**7b**)

Bond Distances, Å			
Ta-C(2)	2.484(6)	C(2)-C(3)	1.483(8)
Ta-C(3)	2.499(6)	C(2)-B(6)	1.547(8)
Ta-C(1R1)	2.428(8)	C(2M)-C(2E)	1.523(8)
Ta-C(11)	2.321(6)	C(3)-C(3M)	1.515(8)
Ta-C(1R2)	2.419(8)	C(3)-B(4)	1.556(8)
Ta-C(12)	2.202(7)	C(3M)-C(3E)	1.526(8)
Ta-C(1R3)	2.397(8)	C(1R1)-C(1R2)	1.37(1)
Ta-C(1R4)	2.413(7)	C(1R1)-C(1R5)	1.39(1)
Ta-C(1R5)	2.417(7)	C(1R2)-C(1R3)	1.40(2)
Ta-B(4)	2.449(7)	C(1R3)-C(1R4)	1.35(1)
Ta-B(5)	2.354(7)	C(1R4)-C(1R5)	1.34(1)
Ta-B(6)	2.378(7)	C(2R1)-C(2R2)	1.426(9)
Co-C(2)	2.032(6)	C(2R1)-C(2R5)	1.431(8)
Co-C(3)	2.056(6)	C(2R1)-C(2R6)	1.501(9)
Co-C(2R1)	2.039(6)	C(2R2)-C(2R3)	1.42(1)
Co-C(2R2)	2.036(6)	C(2R2)-C(2R7)	1.509(9)
Co-C(2R3)	2.065(6)	C(2R3)-C(2R4)	1.42(1)
Co-C(2R4)	2.095(6)	C(2R3)-C(2R8)	1.49(1)
Co-C(2R5)	2.066(6)	C(2R4)-C(2R5)	1.42(1)
Co-B(4)	2.087(7)	C(2R4)-C(2R9)	1.51(1)
Co-B(5)	2.061(7)	C(2R5)-C(2R10)	1.50(1)
Co-B(6)	2.055(6)	B(4)-B(5)	1.673(9)
C(2)-C(2M)	1.523(7)	B(5)-B(6)	1.71(1)
Selected Bond Angles, deg			
C(11)-Ta-C(12)	91.4(2)	Ta-C(3)-C(3M)	130.4(4)
Ta-C(2)-Co	103.7(2)	Ta-C(3)-B(4)	69.9(3)
Ta-C(2)-C(2M)	129.7(4)	Co-C(3)-C(2)	67.9(3)
Ta-C(2)-C(3)	73.2(3)	Co-C(3)-C(3M)	126.9(4)
Ta-C(2)-B(6)	67.8(3)	Co-C(3)-B(4)	69.0(3)
Co-C(2)-C(2M)	126.5(4)	C(2)-C(3)-C(3M)	119.6(5)
Co-C(2)-C(3)	69.6(3)	C(2)-C(3)-B(4)	112.8(5)
Co-C(2)-B(6)	68.5(3)	C(3M)-C(3)-B(4)	127.4(5)
C(2M)-C(2)-C(3)	120.5(5)	C(2)-C(2M)-C(2E)	113.7(5)
C(2M)-C(2)-B(6)	127.5(5)	C(3)-C(3M)-C(3E)	114.2(5)
C(3)-C(2)-B(6)	111.9(5)	C(3)-B(4)-B(5)	105.8(5)
Ta-C(3)-Co	102.5(2)	B(4)-B(5)-B(6)	103.9(5)
Ta-C(3)-C(2)	72.1(3)	C(2)-B(6)-B(5)	105.7(5)

attributed to the slightly smaller covalent radius of Nb(V) relative to Ta(V), forcing closer Cp-carborane interaction in **8a** than in the tantalum species (an effect previously mentioned).

**Electrochemistry.** Transition metal-carborane complexes exhibit reversible multielectron redox chemistry, thereby defining the metallacarborane fragment as an "electron reservoir".<sup>4b,6b,19</sup> The C<sub>2</sub>B<sub>4</sub> tantalum complexes **1a-c** undergo quasireversible reduction at -1.40, -1.35, and -1.65 V vs Fc/Fc<sup>+</sup>, respectively, and no oxidation is observed. In contrast, the CoCp\*-capped tantalum complex **4a** exhibits quasireversible oxidation (+0.67 V vs Fc/Fc<sup>+</sup>) and reduction (-1.65 V) waves in the cyclic voltammogram at all scan rates (20-500 mV/sec). However, the Cp\*Co niobium compound **4c** exhibits no oxidation wave within the solvent window and quasireversible reduction at -1.11 V.

**Reactions.** Alkyl and aryl complexes bearing carborane ligands reported here proved to be less reactive than their isoelectronic Cp<sub>2</sub> analogues toward a variety of reagents and conditions, as follows.

(1) The treatment of complexes **1a** and **2** with Al<sub>2</sub>Me<sub>6</sub>, in an effort to prepare Tebbe-type reagents suitable as catalysts for ring-opening metathesis polymerization

(19) (a) Geiger, W. E., Jr. In *Metal Interactions with Boron Clusters*; Grimes, R. N., Ed.; Plenum Press: New York, 1982; Chapter 6, pp 239-268. (b) Merkert, J. M.; Geiger, W. E.; Davis, J. H., Jr.; Attwood, M. D.; Grimes, R. N. *Organometallics* **1989**, *8*, 1580. (c) Merkert, J. M.; Geiger, W. E.; Attwood, M. D.; Grimes, R. N. *Organometallics* **1991**, *10*, 3545. (d) Merkert, J.; Davis, J. H., Jr.; Geiger, W.; Grimes, R. N. *J. Am. Chem. Soc.* **1992**, *114*, 9846.

**Table 8. Bond Distances and Selected Bond Angles for Cp\*Co(Et<sub>2</sub>C<sub>2</sub>B<sub>3</sub>H<sub>3</sub>)/Ta(CH<sub>2</sub>Ph)ClCp (7c)**

Bond Distances, Å			
Ta-Cl	2.394(1)	C(3M)-C(3E)	1.520(9)
Ta-C(2)	2.508(6)	C(3)-B(4)	1.565(8)
Ta-C(3)	2.481(6)	C(11)-C(12)	1.509(8)
Ta-C(11)	2.277(6)	C(1R1)-C(1R2)	1.41(1)
Ta-C(1R1)	2.406(7)	C(1R1)-C(1R5)	1.41(1)
Ta-C(1R2)	2.429(6)	C(1R2)-C(1R3)	1.40(1)
Ta-C(1R3)	2.423(7)	C(12)-C(13)	1.398(9)
Ta-C(1R4)	2.428(6)	C(12)-C(17)	1.374(9)
Ta-C(1R5)	2.388(6)	C(1R3)-C(1R4)	1.398(9)
Ta-B(4)	2.381(6)	C(13)-C(14)	1.39(1)
Ta-B(5)	2.373(6)	C(1R4)-C(1R5)	1.41(1)
Ta-B(6)	2.463(7)	C(14)-C(15)	1.39(1)
Co-C(2)	2.043(6)	C(15)-C(16)	1.37(1)
Co-C(3)	2.039(6)	C(16)-C(17)	1.40(1)
Co-C(2R1)	2.049(6)	C(2R1)-C(2R2)	1.426(8)
Co-C(2R2)	2.100(6)	C(2R1)-C(2R5)	1.418(8)
Co-C(2R3)	2.099(6)	C(2R1)-C(2R6)	1.503(8)
Co-C(2R4)	2.046(6)	C(2R2)-C(2R3)	1.427(8)
Co-C(2R5)	2.031(5)	C(2R2)-C(2R7)	1.501(8)
Co-B(4)	2.056(7)	C(2R3)-C(2R4)	1.420(8)
Co-B(5)	2.055(7)	C(2R3)-C(2R8)	1.485(9)
Co-B(6)	2.087(7)	C(2R4)-C(2R5)	1.428(8)
C(2)-C(2M)	1.527(8)	C(2R4)-C(2R9)	1.516(8)
C(2)-C(3)	1.470(8)	C(2R5)-C(2R10)	1.511(8)
C(2)-B(6)	1.56(1)	B(4)-B(5)	1.717(9)
C(2M)-C(2E)	1.531(9)	B(5)-B(6)	1.68(1)
C(3M)-C(3)	1.520(8)		

Selected Bond Angles, deg			
Cl-Ta-C(11)	91.5(2)	Ta-C(3)-C(3M)	130.6(4)
Ta-C(11)-C(12)	120.1(4)	Ta-C(3)-B(4)	67.8(3)
Ta-C(2)-Co	102.6(2)	Co-C(3)-C(2)	69.0(3)
Ta-C(2)-C(2M)	128.7(4)	Co-C(3)-C(3M)	125.7(4)
Ta-C(2)-C(3)	71.9(3)	Co-C(3)-B(4)	68.1(3)
Ta-C(2)-B(6)	70.1(3)	C(2)-C(3)-C(3M)	120.8(5)
Co-C(2)-C(2M)	128.5(4)	C(2)-C(3)-B(4)	111.6(5)
Co-C(2)-C(3)	68.7(3)	C(3M)-C(3)-B(4)	127.3(5)
Co-C(2)-B(6)	69.3(3)	C(2)-C(2M)-C(2E)	114.1(5)
C(2M)-C(2)-C(3)	119.3(5)	C(3)-C(3M)-C(3E)	113.6(5)
C(2M)-C(2)-B(6)	127.0(5)	C(3)-B(4)-B(5)	105.4(5)
C(3)-C(2)-B(6)	113.6(5)	B(4)-B(5)-B(6)	103.9(5)
Ta-C(3)-Co	103.7(2)	C(2)-B(6)-B(5)	105.4(5)
Ta-C(3)-C(2)	73.9(3)		

(ROMP),<sup>20</sup> afforded only the dimethyl compounds **6a** and **8a**, respectively, in slow reactions, rather than Ta or Nb methylidene complexes. These observations thus stand in contrast to the preparation of Tebbe's reagent from Cp<sub>2</sub>TiCl<sub>2</sub>.<sup>21</sup> In addition, unlike the isoelectronic bis(Cp) complexes of group 4 metals, thermolysis of dialkyl (Et<sub>2</sub>C<sub>2</sub>B<sub>4</sub>H<sub>4</sub>)TaRR'Cp complexes in the presence or absence of PMe<sub>3</sub> leads to uncharacterized decomposition rather than to metal alkylidene compounds.

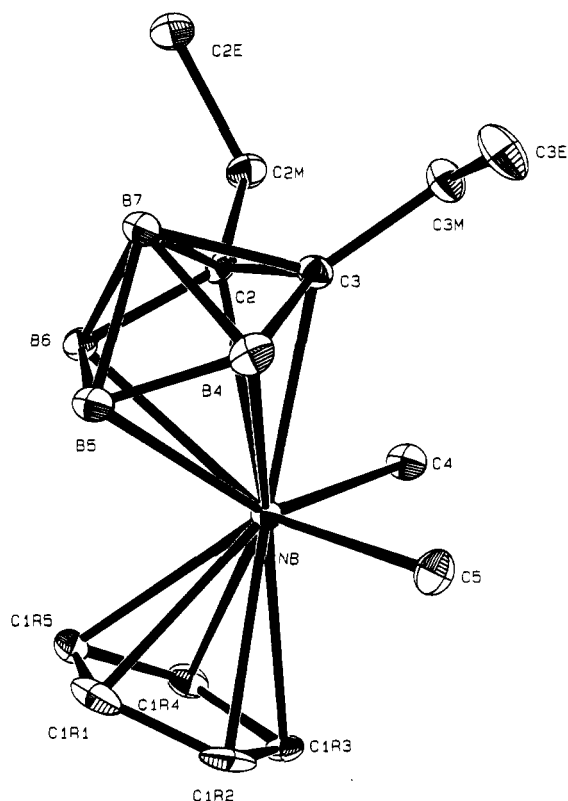
(2) While Cp<sub>2</sub>ZrR<sub>2</sub> (R = Me or benzyl) undergoes rapid reactions with Cp'FePh<sub>4</sub>B (Cp' = Cp or C<sub>5</sub>H<sub>4</sub>Me) to form cationic species,<sup>22</sup> treatment of the dimethyl complex **6a** or the dibenzyl species **6e** with these reagents did not lead to the formation of the desired Ta-R cation (R = Me or benzyl). Instead, the ferrocenium salt decomposed and the tantalum complex was recovered. Similarly, insertion and elimination processes that are facile for bis(cyclopentadienyl) complexes

**Table 9. Bond Distances and Selected Bond Angles for (Et<sub>2</sub>C<sub>2</sub>B<sub>4</sub>H<sub>4</sub>)NbMe<sub>2</sub>Cp (8a)**

Bond Distances, Å			
Nb-C(2)	2.433(3)	C(2)-B(7)	1.740(5)
Nb-C(3)	2.459(4)	C(3)-C(3M)	1.524(5)
Nb-C(4)	2.226(4)	C(3)-B(4)	1.568(6)
Nb-C(5)	2.222(4)	C(3)-B(7)	1.738(6)
Nb-C(1R1)	2.412(4)	C(3M)-C(3E)	1.502(6)
Nb-C(1R2)	2.427(4)	C(1R1)-C(1R2)	1.402(7)
Nb-C(1R3)	2.430(4)	C(1R1)-C(1R5)	1.405(6)
Nb-C(1R4)	2.449(4)	C(1R2)-C(1R3)	1.409(6)
Nb-C(1R5)	2.423(4)	C(1R3)-C(1R4)	1.392(5)
Nb-B(4)	2.456(4)	C(1R4)-C(1R5)	1.411(6)
Nb-B(5)	2.410(4)	B(4)-B(5)	1.669(7)
Nb-B(6)	2.414(4)	B(4)-B(7)	1.805(6)
C(2M)-C(2)	1.521(5)	B(5)-B(6)	1.688(6)
C(2M)-C(2E)	1.512(6)	B(5)-B(7)	1.760(6)
C(2)-C(3)	1.463(5)	B(6)-B(7)	1.772(6)
C(2)-B(6)	1.545(6)		

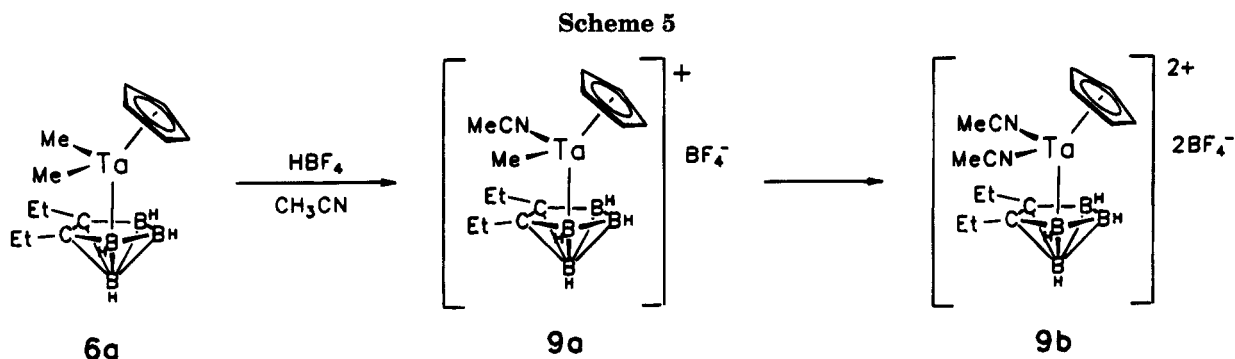
  

Selected Bond Angles, deg			
C(4)-Nb-C(5)	97.0(1)	Nb-C(3)-B(4)	71.3(2)
Nb-C(2)-C(2M)	133.9(2)	Nb-C(3)-B(7)	96.1(2)
Nb-C(2)-C(3)	73.6(2)	C(2)-C(3)-C(3M)	120.4(3)
Nb-C(2)-B(6)	70.7(2)	C(2)-C(3)-B(4)	113.1(3)
Nb-C(2)-B(7)	97.0(2)	C(2)-C(3)-B(7)	65.2(2)
C(2M)-C(2)-C(3)	122.3(3)	C(3M)-C(3)-B(4)	125.6(3)
C(2M)-C(2)-B(6)	124.0(3)	C(3M)-C(3)-B(7)	129.8(3)
C(2M)-C(2)-B(7)	129.1(3)	B(4)-C(3)-B(7)	65.9(3)
C(3)-C(2)-B(6)	112.5(3)	C(2)-C(2M)-C(2E)	112.9(3)
C(3)-C(2)-B(7)	65.1(2)	C(3)-C(3M)-C(3E)	114.9(3)
B(6)-C(2)-B(7)	65.0(2)	C(3)-B(4)-B(5)	104.1(3)
Nb-C(3)-C(2)	71.6(2)	B(4)-B(5)-B(6)	105.4(3)
Nb-C(3)-C(3M)	133.9(3)	C(2)-B(6)-B(5)	104.9(3)

**Figure 7. Molecular structure of (Et<sub>2</sub>C<sub>2</sub>B<sub>4</sub>H<sub>4</sub>)NbMe<sub>2</sub>Cp (8a).**

of group 4 metals<sup>22b,23</sup> appear to require irradiation in the isoelectronic CpTa(carborane) series. Thus, while all attempts at inducing thermal insertion reactions of alkynes and nitriles have failed with the carborane

(20) Gilliom, L. R.; Grubbs, R. H. *J. Am. Chem. Soc.* **1986**, *108*, 733.(21) (a) Tebbe, F. N.; Parshall, G. W.; Reddy, G. S. *J. Am. Chem. Soc.* **1978**, *100*, 3611. (b) Canizzo, L. F.; Grubbs, R. H. *J. Org. Chem.* **1985**, *50*, 2386.(22) (a) Jordan, R. F.; LaPointe, R. E.; Bradley, P. K.; Baenziger, N. *Organometallics* **1989**, *8*, 2892. (b) Alelyunas, Y. W.; Jordan, R. F.; Echols, S. F.; Borkowsky, S. L.; Bradley, P. K. *Organometallics* **1991**, *10*, 1406.(23) (a) Horton, A. D.; Orpen, A. G. *Organometallics* **1991**, *10*, 3910. (b) Ambrose, D. M.; Lee, R. A.; Petersen, J. L. *Organometallics* **1991**, *10*, 2191. (c) Guram, A. S.; Jordan, R. F. *J. Org. Chem.* **1993**, *58*, 5595.



dialkyl species reported here, these processes are stimulated by photolysis.<sup>24</sup> Another example is provided by the diphenyl complex **6d**, which decomposes on heating in toluene to form an intractable mixture but on irradiation produces biphenyl in quantitative yield.

(3) The dimethyl complex **6a** was found to react rapidly with 2 or more equiv of  $\text{HBF}_4$  in  $\text{CH}_3\text{CN}$  or  $\text{CD}_3\text{CN}$  to give a single carborane-containing product with properties consistent with the four-coordinate dicationic species **9b** (Scheme 5). The identity of **9b** is supported by its elemental analysis and its  $^1\text{H}$ ,  $^{11}\text{B}$ , and  $^{13}\text{C}$  NMR spectra, all of which are consistent with a symmetric structure indicating disubstitution. Significantly, the Ta–Me resonance of **6a** has been completely replaced by a coordinated acetonitrile singlet at  $\delta$  2.01 that integrates for two  $\text{CH}_3\text{CN}$  units. This signal appears both in spectra of the reaction mixture in  $\text{CH}_3\text{CN}$  solvent and in the spectrum of the product obtained (in  $\text{CDCl}_3$ ) after removal of the volatile reaction components followed by overnight drying in vacuo, suggesting that loss of the bound acetonitrile is slow. Consistent with this observation is the absence of insertion or polymerization reactivity when **6a** is protonated in the presence of a large excess of ethylene or propylene. Preliminary data suggest that monoprotonation of **6a** to give a methyl monocationic complex proceeds cleanly. When protonation was attempted with 3,5-[( $\text{CF}_3$ ) $_2\text{C}_6\text{H}_3$ ] $_2\text{B}[\text{H}(\text{OEt})_2]$ ,<sup>25</sup> gas evolution was accompanied by decomposition of the carborane complex.

Complex **9b** may be compared with the analogous five-coordinate bis(cyclopentadienyl)zirconium complex  $[\text{Cp}_2\text{Zr}(\text{CH}_3\text{CN})_3][\text{BPh}_4]_2$  reported by Jordan and Echols.<sup>26</sup> Consistent with the greater degree of electron donation, enhanced complex stabilization, and greater steric demand to be expected from carborane ligands relative to  $\eta^5\text{-C}_5\text{H}_5$ , complex **9b** has shown no propensity to bind a third  $\text{CH}_3\text{CN}$  donor, is stable to air for brief periods, and does not abstract fluoride from the  $\text{BF}_4^-$  counterion.

**Summary.** Early transition metal carborane sandwich complexes incorporating small carborane or cobaltacarborane ligands present a wide array of possibilities for exploitation in the design of reagents for organic synthesis, tailored via choice of metals and selective substitution on the cage or at the metal centers. In this paper we have described efficient routes to several classes of such compounds. However, the proper development of this area will require detailed exploration of their reactivity, and investigations of several aspects

of this chemistry are well under way in our laboratories. These include (i) preparation of metal hydride complexes via hydride transfer reactions, and their reactions with alkynes; (ii) introduction of chiral functional groups; (iii) photochemical reactions; (iv) alkyl/aryl eliminations and rearrangements; and (v) synthesis and reactions of cationic  $\text{Cp}(\text{carborane})\text{MR}^+$  and  $(\text{carborane})\text{MR}_2^+$  complexes.<sup>27</sup> As an example of (iv), we have recently reported<sup>28</sup> the conversion of the diphenyl complex **6d** to a strikingly robust benzyne complex,  $\text{Cp}(\text{PMe}_3)(\eta^2\text{-C}_6\text{H}_4)\text{Ta}(\text{Et}_2\text{C}_2\text{B}_4\text{H}_4)$ , via refluxing in toluene in the presence of excess  $\text{PMe}_3$ . In contrast to benzyne–metal complexes in general, this compound is stable in methanol solvent and can be purified by silica gel chromatography in air.<sup>28</sup> Subsequent papers will describe in detail our findings in these and related aspects of this chemistry.

## Experimental Section

**Instrumentation.**  $^1\text{H}$  (300 and 500 MHz),  $^{11}\text{B}$  (115.8 MHz), and  $^{13}\text{C}$  (75.5 and 125.3 MHz) NMR spectra were acquired on Nicolet NT-360, GE QE-300, or GE Omega-500 spectrometers. In the proton NMR spectra of new compounds, all ethyl  $\text{CH}_2$  signals were observed as doublets of quartets with coupling constants ( $J$  values) of 7.5 and 15 Hz, and ethyl  $\text{CH}_3$  resonances appeared as triplets with  $J = 7.5$  Hz, unless otherwise stated. Visible–ultraviolet spectra were recorded on a Hewlett-Packard 8452A diode array with a HP Vectra computer interface. Unit resolution mass spectra were obtained on a Finnegan MAT 4600 GC/MS spectrometer using perfluorotributylamine (FC43) as a calibration standard. In all cases, strong parent envelopes were observed, and the observed and calculated unit-resolution spectral patterns were in close agreement. Elemental analyses were obtained in this department on a Perkin-Elmer 2400 CHN Analyzer using 2,4-dinitrophenylhydrazine as a standard. Infrared spectra were recorded as thin films on a Mattson Cygnus FTIR spectrometer.

**Electrochemistry.** Cyclic voltammetry was conducted in a one-compartment cell with a Pt disk (3 mm diameter) working electrode, a saturated  $\text{Ag}/\text{AgCl}$  reference electrode, and a platinum wire as the auxiliary electrode, using a Bioanalytical Systems CV27 voltammograph. Scan rates from 20 mV/sec to 1 V/sec were employed; values reported were obtained at 200 mV/sec. The solvent was dimethoxyethane (DME), which was purified by twice distilling from  $\text{CaH}_2$ ; the

(27) Insertion reactions of the isoelectronic  $\text{Cp}_2\text{ZrR}^+$  family of complexes are the basis for extensive work in olefin polymerization processes. For examples, see ref 22 and (a) Jordan, R. F. *Adv. Organomet. Chem.* **1991**, *32*, 325. (b) Jordan, R. F.; Bajgur, C. S.; Willett, R.; Scott, B. *J. Am. Chem. Soc.* **1986**, *108*, 7410. (c) Bochmann, M.; Lancaster, S. J. *Organometallics* **1993**, *12*, 633. (d) Bierwagen, E. P.; Bercaw, J. E.; Goddard, W. A. *J. Am. Chem. Soc.* **1994**, *116*, 1481 and references cited therein.

(28) Houseknecht, K. L.; Stockman, K. E.; Sabat, M.; Finn, M. G.; Grimes, R. N. *J. Am. Chem. Soc.* **1995**, *117*, 1163.

(24) Curtis, M. A.; Houseknecht, K. E.; Finn, M. G.; Grimes, R. N. Studies in progress.

(25) Brookhart, M.; Grant, B.; Volpe, A. F., Jr. *Organometallics* **1992**, *11*, 3920.

(26) Jordan, R. F.; Echols, S. F. *Inorg. Chem.* **1987**, *26*, 383.

supporting electrolyte was 0.5 M Bu<sub>4</sub>NPF<sub>6</sub>, used as received and stored in the dry box. Potentials were measured against internal Cp<sub>2</sub>Fe/Cp<sub>2</sub>Fe<sup>+</sup> (+0.55 V vs NHE) and are reported vs NHE.

**Materials.** The starting compounds Me<sub>3</sub>CCH<sub>2</sub>Mg(dioxane)<sup>29</sup> (PhCH<sub>2</sub>)<sub>2</sub>Zn,<sup>30</sup> and Me<sub>3</sub>CCH<sub>2</sub>Li<sup>30</sup> were prepared by literature methods. Complexes CpTaCl<sub>4</sub>, CpZrCl<sub>3</sub>, and CpNbCl<sub>4</sub> were synthesized via reactions of C<sub>5</sub>H<sub>5</sub>SiMe<sub>3</sub> with the corresponding metal halides.<sup>31</sup> C<sub>5</sub>H<sub>5</sub>SiMe<sub>3</sub> was prepared via treatment of NaCp with SiMe<sub>3</sub>Cl in ether.<sup>29</sup> CpNa was obtained from the reaction of NaH with freshly cracked dicyclopentadiene. NaH (80% in mineral oil) was washed with petroleum ether and dried prior to use. Cp\*TaCl<sub>4</sub> (Strem), Cp\*ZrCl<sub>4</sub> (Strem), HBF<sub>4</sub>, MeMgBr, PhCH<sub>2</sub>MgBr, AlMe<sub>3</sub>, PhLi, BuLi, PhOH, and Me<sub>2</sub>Zn were purchased from commercial sources and used as received. The carborane Et<sub>2</sub>C<sub>2</sub>B<sub>4</sub>H<sub>6</sub> was synthesized on a multigram scale via the reaction of B<sub>5</sub>H<sub>9</sub> and diethylacetylene in diethyl ether solution, employing a recent major modification<sup>32</sup> of the literature method.<sup>33</sup> The disilyl carborane (Me<sub>3</sub>Si)<sub>2</sub>C<sub>2</sub>B<sub>4</sub>H<sub>6</sub><sup>34</sup> and the complex Cp\*Co(Et<sub>2</sub>C<sub>2</sub>B<sub>4</sub>H<sub>6</sub>)<sup>14</sup> were obtained as described elsewhere. Petroleum ether was used as received, and methylene chloride was distilled from CaH<sub>2</sub>. THF was distilled from Na/K alloy–benzophenone immediately prior to use. Column chromatography was performed on silica gel 60 (Merck). All reactions were conducted under an inert atmosphere unless otherwise indicated. Workup of products was generally carried out in air using benchtop procedures.

**Syntheses. (Et<sub>2</sub>C<sub>2</sub>B<sub>4</sub>H<sub>6</sub>)TaCl<sub>2</sub>Cp (1a).** A 250 mL flask was charged with NaH (1.00 g, 42.0 mmol) and 125 mL of THF. At room temperature, Et<sub>2</sub>C<sub>2</sub>B<sub>4</sub>H<sub>6</sub> (2.75 g, 20.6 mmol) was added dropwise via syringe over a 45 min period, carefully avoiding excessive H<sub>2</sub> evolution, after which the mixture was stirred for 1 h. The NaEt<sub>2</sub>C<sub>2</sub>B<sub>4</sub>H<sub>6</sub> solution was allowed to settle, and the supernatant was transferred by cannula into a 250 mL flask containing a suspension of CpTaCl<sub>4</sub> (4.00 g, 10.3 mmol) in 50 mL of THF. The yellow-brown solution was stirred for 4 h, after which the solvent was removed in vacuo to another flask to collect the neutral Et<sub>2</sub>C<sub>2</sub>B<sub>4</sub>H<sub>6</sub>, which was subsequently used in another reaction. The dark yellow residue left in the reaction flask was filtered twice through a pad of Celite with CH<sub>2</sub>Cl<sub>2</sub>. The resulting sticky yellow solid was washed with cold petroleum ether (3 × 5 mL) to give **1a** (3.97 g, 8.76 mmol, 85%) as a yellow powder. <sup>1</sup>H NMR (δ, CDCl<sub>3</sub>): 6.43 (C<sub>5</sub>H<sub>5</sub>, s, 5H), 3.14 (CH<sub>2</sub>, dq, 2H), 2.70 (CH<sub>2</sub>, dq, 2H), 1.23 (CH<sub>3</sub>, t, 6H). <sup>1</sup>H NMR (δ, C<sub>6</sub>D<sub>6</sub>): 5.60 (C<sub>5</sub>H<sub>5</sub>, s, 5H), 3.12 (CH<sub>2</sub>, dq, 2H), 2.48 (CH<sub>2</sub>, dq, 2H), 1.17 (CH<sub>3</sub>, t, 6H). <sup>13</sup>C NMR (δ, CDCl<sub>3</sub>): 126.7 (C<sub>2</sub>B<sub>4</sub>, br), 114.6 (C<sub>5</sub>H<sub>5</sub>), 23.1 (CH<sub>2</sub>), 14.6 (CH<sub>3</sub>). <sup>11</sup>B NMR (δ, CH<sub>2</sub>Cl<sub>2</sub>): 33.1 (1B, d, *J* = 137 Hz), 25.5 (2B, d, *J* = 162 Hz), 1.1 (1B, d, *J* = 157 Hz). FTIR (cm<sup>-1</sup>): 3215 m, 2970 m, 2934 m, 2914 m, 2876 w, 2571 s, 2361 w, 2341 w. UV–vis (nm, in CH<sub>2</sub>Cl<sub>2</sub>): 328 (45%), 248 (100%). MS *m/z* 447 (molecular ion envelope). Anal. Calcd for C<sub>11</sub>H<sub>19</sub>B<sub>4</sub>Cl<sub>2</sub>Ta: C, 29.60; H, 4.29. Found: C, 29.88; H, 4.40.

**[(Me<sub>3</sub>Si)<sub>2</sub>C<sub>2</sub>B<sub>4</sub>H<sub>6</sub>]TaCl<sub>2</sub>Cp (1b).** The same procedure was followed employing NaH (1.00 g, 42.0 mmol), (Me<sub>3</sub>Si)<sub>2</sub>C<sub>2</sub>B<sub>4</sub>H<sub>6</sub> (3.60 g, 16.4 mmol), and CpTaCl<sub>4</sub> (3.2 g, 8.2 mmol). Following the addition to CpTaCl<sub>4</sub>, the orange brown solution was stirred overnight. In this case, the solvent was removed by rotary evaporation and the orange-brown solid was filtered through Celite. Column chromatography (4:1 petroleum ether–CH<sub>2</sub>Cl<sub>2</sub>) yielded a single orange band, which upon evaporation gave

red orange crystals of **1b** (3.0 g, 5.6 mmol, 68%). The neutral carborane byproduct was lost on the silica gel. <sup>1</sup>H NMR (δ, CDCl<sub>3</sub>): 6.36 (C<sub>5</sub>H<sub>5</sub>, s, 5H), 0.42 (SiMe<sub>3</sub>, s, 18H). <sup>13</sup>C NMR (δ, CDCl<sub>3</sub>): 127.1 (C<sub>2</sub>B<sub>3</sub>, br), 114.6 (C<sub>5</sub>H<sub>5</sub>), 3.2 (SiMe<sub>3</sub>). <sup>11</sup>B NMR (δ, CH<sub>2</sub>Cl<sub>2</sub>): 34.3 (1B, d, *J* = 153 Hz), 30.9 (2B, d, *J* = 158 Hz), -2.6 (1B, d, *J* = 160 Hz). FTIR (cm<sup>-1</sup>): 3126 m, 2968 m, 2962 m, 2899 w, 2588 s, 2575 s, 2552 s, 2389 w, 2341 w. UV–vis (nm, in CH<sub>2</sub>Cl<sub>2</sub>): 334 (38%), 246 (100%). MS *m/z* 534 (molecular ion envelope), 519 (-Me), 499 (-Cl). Anal. Calcd for C<sub>13</sub>H<sub>27</sub>B<sub>4</sub>Cl<sub>2</sub>Si<sub>2</sub>Ta: C, 29.21; H, 4.99. Found: C, 29.15; H, 4.86.

**(Et<sub>2</sub>C<sub>2</sub>B<sub>4</sub>H<sub>6</sub>)TaCl<sub>2</sub>Cp\* (1c).** The same procedure was followed using NaH (0.50 g, 21 mmol), Et<sub>2</sub>C<sub>2</sub>B<sub>4</sub>H<sub>6</sub> (0.520 g, 3.93 mmol), and Cp\*TaCl<sub>4</sub> (0.900 g, 1.97 mmol). The reaction mixture was stirred overnight followed by workup as above. Washing twice with cold petroleum ether yielded yellow crystalline **1c** (0.687 g, 1.33 mmol, 68%). <sup>1</sup>H NMR (δ, CDCl<sub>3</sub>): 3.09 (CH<sub>2</sub>, dq, 2H), 2.57 (CH<sub>2</sub>, dq, 2H), 1.78 (C<sub>5</sub>Me<sub>5</sub>, s, 15H), 2.55 (CH<sub>3</sub>, t, 6H). <sup>13</sup>C NMR (δ, CDCl<sub>3</sub>): 94.6 (C\*<sub>5</sub>Me<sub>5</sub>), 17.2 (CH<sub>2</sub>), 13.2 (CH<sub>2</sub>), 9.6 (C<sub>5</sub>Me\*<sub>5</sub>). <sup>11</sup>B NMR (δ, CH<sub>2</sub>Cl<sub>2</sub>): 34.8 (1B, d, *J* = 116 Hz), 25.7 (2B, d, *J* = 152 Hz), -0.9 (1B, d, *J* = 185 Hz). UV–vis (nm, in CH<sub>2</sub>Cl<sub>2</sub>): 364 (33%), 246 (100%). MS *m/z* 516 (molecular ion envelope). Anal. Calcd for C<sub>16</sub>H<sub>29</sub>B<sub>4</sub>Cl<sub>2</sub>Ta: C, 37.21; H, 5.66. Found: C, 37.38; H, 5.98.

**(Me<sub>2</sub>C<sub>2</sub>B<sub>4</sub>H<sub>6</sub>)TaCl<sub>2</sub>Cp (1d).** The same procedure was followed employing NaH (0.50 g, 20.8 mmol), Me<sub>2</sub>C<sub>2</sub>B<sub>4</sub>H<sub>6</sub> (0.50 g, 4.8 mmol), and CpTaCl<sub>4</sub> (0.90 g, 2.4 mmol). The yellow-brown solution (total volume 225 mL) was stirred for 4 h and distilled in vacuo to another flask to collect the Et<sub>2</sub>C<sub>2</sub>B<sub>4</sub>H<sub>6</sub> product. The remaining dark yellow-brown residue was filtered twice through Celite in CH<sub>2</sub>Cl<sub>2</sub>, yielding **1d** as bright yellow crystals (230 mg, 0.55 mmol, 23%). <sup>1</sup>H NMR (δ, CDCl<sub>3</sub>): 6.44 (C<sub>5</sub>H<sub>5</sub>, s, 5H), 2.55 (CH<sub>3</sub>, s, 6H). <sup>13</sup>C NMR (δ, CDCl<sub>3</sub>): 123.1 (C<sub>2</sub>B<sub>4</sub>, br), 114.6 (C<sub>5</sub>H<sub>5</sub>), 17.2 (CH<sub>3</sub>). <sup>11</sup>B NMR (δ, CH<sub>2</sub>Cl<sub>2</sub>): 33.9 (1B, d, *J* = 144 Hz), 26.0 (2B, d, *J* = 153 Hz), 3.1 (1B, d, *J* = 164 Hz). FTIR (cm<sup>-1</sup>): 3225 m, 3120 m, 3110 m, 3084 w, 2962 m, 2929 w, 2871 w, 2568 s, 2561 s, 2532 m, 2340 w, 2327 w. UV–vis (nm, in CH<sub>2</sub>Cl<sub>2</sub>): 374 (20%), 248 (100%). MS *m/z* 418 (molecular ion envelope), 382 (-Cl). Anal. Calcd for C<sub>9</sub>H<sub>15</sub>B<sub>4</sub>Cl<sub>2</sub>Ta: C, 25.84; H, 3.61. Found: C, 26.04; H, 4.01.

**(Et<sub>2</sub>C<sub>2</sub>B<sub>4</sub>H<sub>6</sub>)NbCl<sub>2</sub>Cp (2).** The same procedure was followed with NaH (0.800 g, 33.3 mmol), Et<sub>2</sub>C<sub>2</sub>B<sub>4</sub>H<sub>6</sub> (0.885 g, 6.71 mmol), and CpNbCl<sub>4</sub> (1.00 g, 3.36 mmol). The red-brown solution (total volume 125 mL) was stirred for 4 h, followed by evaporation in vacuo to another flask to collect the neutral Et<sub>2</sub>C<sub>2</sub>B<sub>4</sub>H<sub>6</sub>. The dark red residue left in the reaction flask was filtered twice through Celite with CH<sub>2</sub>Cl<sub>2</sub> to yield **2** as a bright red crystalline solid (0.878 g, 2.45 mmol, 73%). <sup>1</sup>H NMR (δ, CDCl<sub>3</sub>): 6.51 (C<sub>5</sub>H<sub>5</sub>, s, 5H), 3.12 (CH<sub>2</sub>, dq, 2H), 2.59 (CH<sub>2</sub>, dq, 2H), 1.25 (CH<sub>3</sub>, t, 6H). <sup>13</sup>C NMR (δ, CDCl<sub>3</sub>): 130.9 (C<sub>2</sub>B<sub>4</sub>, br), 113.6 (C<sub>5</sub>H<sub>5</sub>), 23.6 (CH<sub>2</sub>), 14.2 (CH<sub>3</sub>). <sup>11</sup>B NMR (δ, CH<sub>2</sub>Cl<sub>2</sub>): 31.7 (1B, d, *J* = 146 Hz), 18.0 (2B, d, *J* = 158 Hz), -1.2 (1B, d, *J* = 165 Hz). FTIR (cm<sup>-1</sup>): 3215 m, 3124 m, 3115 m, 3088 w, 2968 m, 2935 w, 2877 w, 2575 s, 2561 s, 2538 m, 2361 w, 2343 w. UV–vis (nm, in CH<sub>2</sub>Cl<sub>2</sub>): 370 (20%), 250 (100%). MS *m/z* 358 (parent ion envelope), 322 (-Cl). Anal. Calcd for C<sub>11</sub>H<sub>19</sub>B<sub>4</sub>Cl<sub>2</sub>Nb: C, 36.87; H, 5.34. Found: C, 37.06; H, 5.61.

**(Et<sub>2</sub>C<sub>2</sub>B<sub>4</sub>H<sub>6</sub>)ZrCl<sub>2</sub>Cp-THF (3a).** A 250 mL flask was charged with NaH (0.500 g, 20.8 mmol) and 125 mL of THF. At room temperature Et<sub>2</sub>C<sub>2</sub>B<sub>4</sub>H<sub>6</sub> (1.22 g, 9.26 mmol) was added dropwise via syringe over a 15 min period, and the mixture was stirred for 1 h. The excess NaH was allowed to settle, and the supernatant was transferred by cannula to a 250 mL flask containing a suspension of CpZrCl<sub>3</sub> (1.45 g, 4.63 mmol) in 50 mL of THF. The yellow solution was stirred for 2 h, and then the solvent was removed in vacuo to another flask to collect the neutral Et<sub>2</sub>C<sub>2</sub>B<sub>4</sub>H<sub>6</sub>. The yellow residue was dissolved in CH<sub>2</sub>Cl<sub>2</sub> and filtered through Celite under a dry nitrogen atmosphere to yield **3a** as a moisture- and air-sensitive yellow solid (1.78 g, 3.84 mmol, 83%). <sup>1</sup>H NMR (δ, CDCl<sub>3</sub>): 6.37 (C<sub>5</sub>H<sub>5</sub>, s, 5H), 4.10 (THF, m, 2H), 3.93 (THF, m, 2H), 3.06 (CH<sub>2</sub>,

(29) Schrock, R. R.; Fellman, J. D. *J. Am. Chem. Soc.* **1978**, *100*, 3359.

(30) Schrock, R. R. *J. Organomet. Chem.* **1976**, *22*, 209.

(31) Cardoso, A. M.; Clark, R. J. H.; Moorhouse, S. *J. Chem. Soc., Dalton Trans.* **1980**, 1156.

(32) (a) Stockman, K. E., Ph.D. Dissertation, University of Virginia, 1995. (b) Stockman, K. E.; Müller, P. M.; Curtis, M. A.; Grimes, R. N. Manuscript in preparation.

(33) Maynard, R. B.; Borodinsky, L.; Grimes, R. *Inorg. Synth.* **1983**, *22*, 211.

(34) Hosmane, N. S.; Sirmokadam, N. N.; Mollenhauer, M. N. *J. Organomet. Chem.* **1985**, *279*, 359.

dq, 1H), 2.68 (CH<sub>2</sub>, m, 2H), 2.24 (CH<sub>2</sub>, dq, 1H), 2.09 (THF, m, 2H), 1.24 (CH<sub>3</sub>, t, 3H), 1.09 (CH<sub>3</sub>, t, 3H). <sup>13</sup>C NMR (δ, CDCl<sub>3</sub>): 129.5 (C<sub>2</sub>B<sub>4</sub>, br), 128.0 (C<sub>2</sub>B<sub>4</sub>, br), 113.7 (C<sub>5</sub>H<sub>5</sub>), 23.6 (CH<sub>2</sub>), 14.2 (CH<sub>3</sub>). <sup>11</sup>B NMR (δ, CH<sub>2</sub>Cl<sub>2</sub>): 33.9 (1B, d, *J* = 130 Hz), 25.2 (2B, d, *J* = 146 Hz), 2.1 (1B, d, *J* = 157 Hz).

**(Et<sub>2</sub>C<sub>2</sub>B<sub>4</sub>H<sub>4</sub>)ZrClCp\*·THF (3b).** The same procedure was followed using NaH (200 mg, 830 mmol), Et<sub>2</sub>C<sub>2</sub>B<sub>4</sub>H<sub>5</sub> (199 mg, 1.51 mmol), and Cp\*ZrCl<sub>3</sub> (250 mg, 0.75 mmol). The yellow solution was stirred for 4 h. The solvent and carborane were removed as before, and yellow residue was filtered through Celite with CH<sub>2</sub>Cl<sub>2</sub>, and the volatiles were removed to yield **3b** as an adduct containing approximately 3 equiv of THF (258 mg, 0.425 mmol, 58% based on 3 equiv of THF). <sup>1</sup>H NMR (δ, CDCl<sub>3</sub>): 3.83 (THF, m, 16H), 2.78 (CH<sub>2</sub>, dq, 2H), 2.39 (CH<sub>2</sub>, dq, 2H), 2.00 (C<sub>5</sub>Me<sub>5</sub>, s, 15H), 1.92 (THF, m, 16H), 1.14 (CH<sub>3</sub>, t, 3H). <sup>13</sup>C NMR (δ, CDCl<sub>3</sub>): 130.1 (C<sub>2</sub>B<sub>4</sub>, br), 128.5 (C<sub>2</sub>B<sub>4</sub>, br), 112.0 (C<sub>5</sub>H<sub>5</sub>), 23.6 (CH<sub>2</sub>), 14.2 (CH<sub>3</sub>). <sup>11</sup>B NMR (δ, CH<sub>2</sub>Cl<sub>2</sub>): 33.9 (1B, d, *J* = 130 Hz), 25.2 (2B, d, *J* = 146 Hz), 2.1 (1B, d, *J* = 157 Hz).

**[Cp\*Co(Et<sub>2</sub>C<sub>2</sub>B<sub>3</sub>H<sub>3</sub>)]TaCl<sub>2</sub>Cp (4a).** (Et<sub>2</sub>C<sub>2</sub>B<sub>3</sub>H<sub>5</sub>)CoCp\* (1.00 g, 3.15 mmol) was dissolved in 50 mL of THF, and to this solution was added an equimolar amount of *tert*-butyllithium (1.74 mL, 1.8 M in hexane, 3.15 mmol) at room temperature, resulting in a red-orange solution. After 30 min the solution was added to a flask containing CpTaCl<sub>4</sub> (0.61 g, 1.57 mmol) in 25 mL of THF, resulting in an immediate color change to deep green and then green-black. After the solution was stirred for 4 h, the solvent was removed by rotary evaporation and the residue was purified by column chromatography on silica in 4:1 petroleum ether-CH<sub>2</sub>Cl<sub>2</sub> to afford two bands. The first band was recovered (Et<sub>2</sub>C<sub>2</sub>B<sub>3</sub>H<sub>5</sub>)CoCp\* (0.20 g, 0.64 mmol), and the second was dark green **4a** (0.40 g, 0.64 mmol, 40% based on recovered starting material). <sup>1</sup>H NMR (δ, CDCl<sub>3</sub>): 6.10 (C<sub>5</sub>H<sub>5</sub>, s, 5H), 3.09 (CH<sub>2</sub>, dq, 2H), 2.69 (CH<sub>2</sub>, dq, 2H), 1.68 (C<sub>5</sub>Me<sub>5</sub>, s, 15H), 1.36 (CH<sub>3</sub>, t, 6H). <sup>13</sup>C NMR (δ, CDCl<sub>3</sub>): 112.5 (C<sub>5</sub>H<sub>5</sub>), 111.3 (C<sub>2</sub>B<sub>3</sub>, br), 91.9 (C\*<sub>5</sub>Me<sub>5</sub>), 23.1 (CH<sub>2</sub>), 14.7 (CH<sub>3</sub>), 10.2 (C<sub>5</sub>Me\*<sub>5</sub>). <sup>11</sup>B NMR (δ, CH<sub>2</sub>Cl<sub>2</sub>): 62.4 (1B, d, *J* = 108 Hz), 36.6 (2B, d, *J* = 123 Hz). FTIR (cm<sup>-1</sup>): 3215 w, 3113 w, 3099 w, 2967 m, 2918 m, 2501 s, 2362 m, 2342 m. UV-vis (nm, in CH<sub>2</sub>Cl<sub>2</sub>): 602 (10%), 308 (100%), 252 (52%). MS *m/z* 628 (parent ion envelope), 592 (-Cl). Anal. Calcd for C<sub>21</sub>H<sub>33</sub>B<sub>3</sub>Cl<sub>2</sub>TaCo: C, 40.12; H, 5.29. Found: C, 40.18; H, 5.52.

**[Cp\*Co(Et<sub>2</sub>C<sub>2</sub>B<sub>3</sub>H<sub>3</sub>)]TaCl<sub>2</sub>Cp\* (4b).** The same procedure was followed employing *tert*-butyllithium (0.87 mL, 1.8 M in hexane, 1.57 mmol), (Et<sub>2</sub>C<sub>2</sub>B<sub>3</sub>H<sub>5</sub>)CoCp\* (0.500 g, 1.57 mmol) and Cp\*TaCl<sub>4</sub> (0.61 g, 0.78 mmol). After stirring for 4 h, the solvent was removed by rotary evaporation and the residue was purified by column chromatographed in 4:1 petroleum ether-CH<sub>2</sub>Cl<sub>2</sub> to afford two bands. The first was recovered neutral (Et<sub>2</sub>C<sub>2</sub>B<sub>3</sub>H<sub>5</sub>)CoCp\* (102 mg, 0.64 mmol), and the second was dark green **4b** (187 mg, 0.64 mmol, 42% based on recovered starting material). <sup>1</sup>H NMR (δ, CDCl<sub>3</sub>): 3.05 (CH<sub>2</sub>, dq, 2H), 2.69 (CH<sub>2</sub>, dq, 2H), 2.08 (C<sub>5</sub>Me<sub>5</sub>, s, 15H), 1.70 (C<sub>5</sub>Me<sub>5</sub>, s, 15H), 1.33 (CH<sub>3</sub>, t, 6H). <sup>13</sup>C NMR (δ, CDCl<sub>3</sub>): 110.1 (C<sub>2</sub>B<sub>3</sub>, br), 122.6 (C<sub>5</sub>Me\*<sub>5</sub>-Ta), 91.3 (C\*<sub>5</sub>Me<sub>5</sub>-Co), 23.7 (CH<sub>2</sub>), 14.3 (CH<sub>3</sub>), 13.4 (C<sub>5</sub>Me\*<sub>5</sub>), 10.3 (C<sub>5</sub>Me\*<sub>5</sub>). <sup>11</sup>B NMR (δ, CH<sub>2</sub>Cl<sub>2</sub>): 63.4 (1B, d, *J* = 110 Hz), 33.1 (2B, d, *J* = 133 Hz). FTIR (cm<sup>-1</sup>): 3210 m, 3101 w, 2977 m, 2510 s, 2363 m, 2339 m. UV-vis (nm, in CH<sub>2</sub>Cl<sub>2</sub>): 615 (19%), 312 (100%), 245 (45%). MS *m/z* 698 (molecular ion), 622 (-Cl). Anal. Calcd for C<sub>26</sub>H<sub>43</sub>B<sub>3</sub>Cl<sub>2</sub>TaCo: C, 44.69; H, 6.20. Found: C, 44.31; H, 6.11.

**[Cp\*Co(Et<sub>2</sub>C<sub>2</sub>B<sub>3</sub>H<sub>3</sub>)]NbCl<sub>2</sub>Cp (4c).** The same procedure was followed using *tert*-butyllithium (0.87 mL, 1.8 M in hexane, 1.57 mmol), (Et<sub>2</sub>C<sub>2</sub>B<sub>3</sub>H<sub>5</sub>)CoCp\* (0.500 g, 1.57 mmol), and CpNbCl<sub>4</sub> (0.238 g, 0.785 mmol). After the solution was stirred for 4 h, the solvent was removed by rotary evaporation and the residue was purified by column chromatographed in 4:1 petroleum ether-CH<sub>2</sub>Cl<sub>2</sub> to afford two bands, the first of which was recovered neutral (Et<sub>2</sub>C<sub>2</sub>B<sub>3</sub>H<sub>5</sub>)CoCp\* (104 mg, 0.64 mmol). The second band was dark green **4c** (163 mg, 0.30 mmol, 38% based on recovered starting material). <sup>1</sup>H NMR

(δ CDCl<sub>3</sub>): 6.12 (C<sub>5</sub>H<sub>5</sub>, s, 5H), 2.98 (CH<sub>2</sub>, dq, 2H), 2.61 (CH<sub>2</sub>, dq, 2H), 1.71 (C<sub>5</sub>Me<sub>5</sub>, s, 15H), 1.32 (CH<sub>3</sub>, t, 6H). <sup>13</sup>C NMR (δ, CDCl<sub>3</sub>): 112.2 (C<sub>5</sub>H<sub>5</sub>), 110.5 (C<sub>2</sub>B<sub>3</sub>, br), 92.1 (C\*<sub>5</sub>Me<sub>5</sub>), 23.4 (CH<sub>2</sub>), 14.2 (CH<sub>3</sub>), 9.4 (C\*<sub>5</sub>Me<sub>5</sub>). <sup>11</sup>B NMR (δ, CH<sub>2</sub>Cl<sub>2</sub>): 63.0 (1B, d, *J* = 128 Hz), 31.7 (2B, d, *J* = 122 Hz). FTIR (cm<sup>-1</sup>): 3217 m, 3115 m, 3012 m, 2978 m, 2923 w, 2504 s, 2351 m, 2333 m. MS *m/z* 539 (parent ion envelope), 504 (-Cl). Anal. Calcd for C<sub>21</sub>H<sub>33</sub>B<sub>3</sub>Cl<sub>2</sub>NbCo: C, 46.65; H, 6.15. Found: C, 47.00; H, 6.23.

**(Et<sub>2</sub>C<sub>2</sub>B<sub>4</sub>H<sub>4</sub>)TaClMeCp (5a).** A 2.0 M solution of AlMe<sub>3</sub> (1.75 mL, 2.35 mmol, 2.1 equiv) in toluene was added dropwise via syringe to **1a** (0.500 g, 1.12 mmol) in 25 mL of THF. The mixture was stirred for 0.5 h, and the solvent was removed by rotary evaporation. The yellow solid was taken up in CH<sub>2</sub>Cl<sub>2</sub> and filtered through Celite to yield **5a** as lemon yellow crystals (405 mg, 0.95 mmol, 85%). Alternatively, 2.0 equiv of 1.0 M dimethylzinc can be used as a monomethylating agent to obtain **5a** (83%). <sup>1</sup>H NMR (δ, C<sub>6</sub>D<sub>6</sub>): 5.45 (C<sub>5</sub>H<sub>5</sub>, s, 5H), 3.08 (CH<sub>2</sub>, dq, 1H), 2.88 (CH<sub>2</sub>, dq, 1H), 2.72 (CH<sub>2</sub>, dq, 1H), 2.36 (CH<sub>2</sub>, dq, 1H), 1.36 (CH<sub>3</sub>, t, 3H), 1.10 (CH<sub>3</sub>, t, 3H), 0.76 (Ta-CH<sub>3</sub>, s, 3H). <sup>1</sup>H NMR (δ, CDCl<sub>3</sub>): 6.18 (C<sub>5</sub>H<sub>5</sub>, t, 2H), 3.12 (CH<sub>2</sub>, dq, 1H), 3.00-2.71 (CH<sub>2</sub>, m, 2H), 2.51 (CH<sub>2</sub>, dq, 1H), 1.42 (CH<sub>3</sub>, d, 3H), 1.13 (CH<sub>3</sub>, d, 3H), 1.13 (Ta-CH<sub>3</sub>, s, 3H). <sup>13</sup>C NMR (δ, CDCl<sub>3</sub>): 110.4 (C<sub>5</sub>H<sub>5</sub>), 41.8 (Ta-CH<sub>3</sub>), 23.2 (CH<sub>2</sub>), 23.1 (CH<sub>2</sub>), 15.0 (CH<sub>3</sub>), 14.5 (CH<sub>3</sub>). <sup>11</sup>B NMR (δ, CH<sub>2</sub>Cl<sub>2</sub>): 37.1 (1B, d, *J* = 140 Hz), 26.7 (1B, d, *J* = 148 Hz), 17.5 (1B, d, *J* = 149 Hz), 0.1 (1B, d, *J* = 162 Hz). FTIR (cm<sup>-1</sup>): 3211 m, 2970 m, 2934 w, 2874 w, 2575 s, 2544 s, 2361 w. MS *m/z* 425 (molecular ion), 410 (-CH<sub>3</sub>). Anal. Calcd for C<sub>12</sub>H<sub>22</sub>B<sub>4</sub>ClTa: C, 33.84; H, 5.21. Found: C, 33.96; H, 5.28.

**[(Me<sub>3</sub>Si)<sub>2</sub>C<sub>2</sub>B<sub>4</sub>H<sub>4</sub>]TaClMeCp (5b).** The above procedure was followed using AlMe<sub>3</sub> (0.983 mL of a 2.0 M solution, 1.87 mmol, 2.1 equiv) in toluene and **1b** (0.500 g, 0.936 mmol) in 25 mL of THF. The yellow solid was taken up in CH<sub>2</sub>Cl<sub>2</sub> and filtered through Celite to yield **5b** as lemon yellow crystals (433 mg, 0.84 mmol, 90%). <sup>1</sup>H NMR (δ, CDCl<sub>3</sub>): 6.14 (C<sub>5</sub>H<sub>5</sub>, s, 5H), 0.81 (Ta-CH<sub>3</sub>, s, 6H), 0.51 (SiMe<sub>3</sub>, s, 9H), 0.33 (SiMe<sub>3</sub>, s, 9H). <sup>13</sup>C NMR (δ, CDCl<sub>3</sub>): 111.2 (C<sub>5</sub>H<sub>5</sub>), 44.9 (Ta-CH<sub>3</sub>), 3.0 (SiMe<sub>3</sub>), 2.8 (SiMe<sub>3</sub>). <sup>11</sup>B NMR (δ, CH<sub>2</sub>Cl<sub>2</sub>): 40.3 (1B, d, *J* = 144 Hz), 32.1 (1B, d, *J* = 150 Hz), 27.5 (1B, d, *J* = 157 Hz), -2.3 (1B, d, *J* = 162 Hz). MS *m/z* 515 (molecular ion), 500 (-CH<sub>3</sub>). Anal. Calcd for C<sub>14</sub>H<sub>30</sub>B<sub>4</sub>Si<sub>2</sub>TaCl: C, 36.49; H, 6.94. Found: C, 36.79; H, 7.35.

**(Et<sub>2</sub>C<sub>2</sub>B<sub>4</sub>H<sub>4</sub>)TaClMeCp\* (5c).** The preceding procedure was followed employing AlMe<sub>3</sub> (0.20 mL, 2.0 M in toluene, 0.40 mmol, 2.1 equiv) and **1c** (100 mg, 0.19 mmol), affording **5c** as yellow crystals (86 mg, 0.17 mmol, 88%). Alternatively, use of diethylzinc gave **5c** in 83% yield. <sup>1</sup>H NMR (δ, CDCl<sub>3</sub>): 3.10 (CH<sub>2</sub>, dq, 1H), 2.91 (CH<sub>2</sub>, dq, 1H), 2.77 (CH<sub>2</sub>, dq, 1H), 2.55 (CH<sub>2</sub>, dq, 2H), 2.09 (C<sub>5</sub>Me<sub>5</sub>, s, 15H), 1.43 (CH<sub>3</sub>, t, 3H), 1.13 (CH<sub>3</sub>, t, 3H), 0.32 (Ta-CH<sub>3</sub>, s, 3H). <sup>13</sup>C NMR (δ, CDCl<sub>3</sub>): 120.2 (C\*<sub>5</sub>Me<sub>5</sub>), 46.7 (Ta-CH<sub>3</sub>), 23.1 (CH<sub>2</sub>), 23.0 (CH<sub>2</sub>), 15.2 (CH<sub>3</sub>), 14.7 (CH<sub>3</sub>), 12.9 (C<sub>5</sub>Me\*<sub>5</sub>). <sup>11</sup>B NMR (δ, CH<sub>2</sub>Cl<sub>2</sub>): 36.5 (1B, d, *J* = 142 Hz), 25.5 (1B, d, *J* = 142 Hz), 18.9 (1B, d, *J* = 147 Hz), 0.9 (1B, d, *J* = 160 Hz). FTIR (cm<sup>-1</sup>): 3113 m, 2969 s, 2890 w, 2571 s, 2545 s, 2266 w, 1986 m, 1575 m, 1567 m. MS *m/z* 498 (molecular ion), 483 (-CH<sub>3</sub>). Anal. Calcd for C<sub>17</sub>H<sub>32</sub>B<sub>4</sub>ClTa: C, 41.16; H, 6.50. Found: C, 40.95; H, 6.58.

**(Et<sub>2</sub>C<sub>2</sub>B<sub>4</sub>H<sub>4</sub>)TaClEtCp (5d).** A 2.0 M solution of ethylmagnesium chloride (1.75 mL, 2.35 mmol, 2.1 equiv) in toluene was added dropwise via syringe to **1a** (0.500 g, 1.12 mmol) in 25 mL of THF. The mixture was stirred for 0.5 h, and the solvent was removed by rotary evaporation. The yellow solid was taken up in CH<sub>2</sub>Cl<sub>2</sub> and filtered through Celite to yield **5d** as yellow crystals (192 mg, 0.44 mmol, 78%). <sup>1</sup>H NMR (δ, CDCl<sub>3</sub>): 6.17 (C<sub>5</sub>H<sub>5</sub>, s, 5H), 3.15 (CH<sub>2</sub>, dq, 1H), 2.85 (CH<sub>2</sub>, dq, 2H), 2.46 (Ta-CH<sub>2</sub>CH<sub>3</sub>, m, 2H), 2.36 (Ta-CH<sub>2</sub>CH<sub>3</sub>, t, 3H), 1.84 (CH<sub>3</sub>, t, 3H), 1.43 (CH<sub>3</sub>, t, 3H). <sup>13</sup>C NMR (δ, CDCl<sub>3</sub>): 111.0 (C<sub>5</sub>H<sub>5</sub>), 55.1 (Ta-C\*H<sub>2</sub>CH<sub>3</sub>), 23.2 (CH<sub>2</sub>), 23.0 (CH<sub>2</sub>), 20.4 (Ta-CH<sub>2</sub>C\*H<sub>3</sub>), 15.5 (CH<sub>3</sub>), 14.7 (CH<sub>3</sub>). <sup>11</sup>B NMR (δ, CH<sub>2</sub>Cl<sub>2</sub>): 35.1 (1B, d, *J* = 132 Hz), 24.5 (1B, d, *J* = 146 Hz), 13.9 (1B, d, *J* = 161 Hz), 0.1 (1B, d, *J* = 161 Hz). FTIR (cm<sup>-1</sup>): 2918 m, 2872



s, 2359 w, 2341 w, 1458 m, 1379 w. UV (nm): 368 (100), 332 (83.4), 298 (60.4). MS  $m/z$  439 (molecular ion), 410 ( $\text{CH}_2\text{CH}_3$ ).

**(Et<sub>2</sub>C<sub>2</sub>B<sub>4</sub>H<sub>4</sub>)Ta(CH<sub>2</sub>Ph)ClCp (5e).** A sample of **1a** (300 mg, 0.67 mmol) was dissolved in THF, and solid dibenzylzinc (180 mg, 0.84 mmol, 2.5 equiv of benzyl) was added under inert gas. The mixture was stirred for 2 h, following which the solvent was removed in vacuo. The residue was filtered through 3 cm of silica gel with  $\text{CH}_2\text{Cl}_2$ , and the solvent was removed to yield **5e** (335 mg, 0.67 mmol, quantitative) as a red-orange solid. <sup>1</sup>H NMR ( $\delta$ ,  $\text{CDCl}_3$ ): 7.23 (Ph, t, 2H), 6.91 (Ph, t, 1H), 6.81 (Ph d, 2H), 5.90 ( $\text{C}_5\text{H}_5$ , s, 5H), 3.29 ( $\text{CH}_2$ , dq, 1H), 3.20 ( $\text{CH}^*\text{Ph}$ , d, 1H), 3.04–2.90 ( $\text{CH}_2$ , m, 2H), 2.60 ( $\text{CH}_2$ , dq, 1H), 2.22 ( $\text{CH}^*\text{Ph}$ , d, 1H), 1.46 ( $\text{CH}_2$ , t, 3H), 1.14 ( $\text{CH}_2$ , t, 3H). <sup>13</sup>C NMR ( $\delta$ ,  $\text{CDCl}_3$ ): 149.0 (ipso  $\text{C}_6$ ), 129.5 (Ph), 128.1 (Ph), 123.3 (Ph), 114.8 ( $\text{C}_5\text{H}_5$ ), 72.1 ( $\text{CH}^*\text{Ph}$ ), 24.5 ( $\text{CH}_2$ ), 24.3 ( $\text{CH}_2$ ), 14.1 ( $\text{CH}_3$ ), 13.0 ( $\text{CH}_3$ ). <sup>11</sup>B NMR ( $\delta$ ,  $\text{CH}_2\text{Cl}_2$ ): 36.4 (1B, d,  $J$  = 140 Hz), 25.7 (1B, d,  $J$  = 145 Hz), 17.0 (1B, d,  $J$  = 141 Hz), -0.3 (1B, d,  $J$  = 160 Hz). FTIR ( $\text{cm}^{-1}$ ): 3200 m, 2996 m, 2918 s, 2895 m, 2568 s, 2549 s, 2367 m, 1980 m, 1568 m. MS  $m/z$  502 (molecular ion). Anal. Calcd for  $\text{C}_{15}\text{H}_{26}\text{B}_4\text{TaCl}$ : 43.06; H, 5.22. Found: C, 43.70; H, 5.56.

**[(Me<sub>3</sub>Si)<sub>2</sub>C<sub>2</sub>B<sub>4</sub>H<sub>4</sub>]Ta(CH<sub>2</sub>Ph)ClCp (5f).** A sample of **1b** (300 mg, 0.56 mmol) was dissolved in THF, and solid dibenzylzinc (180 mg, 0.70 mmol, 2.5 equiv of benzyl) was added under inert gas. The mixture was stirred for 2 h, following which the solvent was removed in vacuo. The residue was filtered through 3 cm of silica gel with  $\text{CH}_2\text{Cl}_2$ , and the solvent was removed to yield **5f** (320 mg, 0.54, 96%) as a red orange solid. <sup>1</sup>H NMR ( $\delta$ ,  $\text{CDCl}_3$ ): 7.26 (Ph, t,  $J$  = 7.8 Hz, 2H), 6.91 (Ph, t,  $J$  = 7.2 Hz, 1H), 6.76 (Ph, d,  $J$  = 7.5 Hz, 2H), 5.84 ( $\text{C}_5\text{H}_5$ , s, 5H), 3.58 ( $\text{CH}^*\text{Ph}$ , d,  $J$  = 13.8 Hz, 1H), 1.83 ( $\text{CH}^*\text{Ph}$ , d,  $J$  = 13.8 Hz, 1H), 0.57 ( $\text{SiMe}_3$ , s, 9H), 0.35 ( $\text{SiMe}_3$ , s, 9H). <sup>13</sup>C NMR ( $\delta$ ,  $\text{CDCl}_3$ ): 149.2 (ipso  $\text{C}_6$ ), 129.6 (Ph), 128.2 (Ph), 124.6 (Ph), 111.8 ( $\text{C}_5\text{H}_5$ ), 70.5 ( $\text{CH}_2\text{Ph}$ ), 3.4 ( $\text{SiMe}_3$ ), 3.0 ( $\text{SiMe}_3$ ). <sup>11</sup>B NMR ( $\delta$ ,  $\text{CH}_2\text{Cl}_2$ ): 41.1 (1B, d,  $J$  = 141 Hz), 31.1 (1B, d,  $J$  = 145 Hz), 27.1 (1B, d,  $J$  = 155 Hz), -2.9 (1B, d,  $J$  = 165 Hz). FTIR ( $\text{cm}^{-1}$ ): 3102 m, 2957 s, 2939 m, 2891 m, 2569 s, 2548 s, 2250 m, 1886 m. MS  $m/z$  590 (molecular ion). Anal. Calcd for  $\text{C}_{20}\text{H}_{34}\text{B}_4\text{Si}_2\text{TaCl}$ : 40.69; H, 5.81. Found: C, 41.01; H, 6.02.

**(Et<sub>2</sub>C<sub>2</sub>B<sub>4</sub>H<sub>4</sub>)Ta(CH<sub>2</sub>Ph)ClCp\* (5g).** The same procedure was followed employing **1c** (200 mg, 0.39 mmol) and dibenzylzinc (120 mg, 0.48 mmol, 2.5 equiv of benzyl). Removal of the solvent yielded **5g** as an orange solid (194 mg, 0.34 mmol, 87%). <sup>1</sup>H NMR ( $\delta$ ,  $\text{CDCl}_3$ ): 7.13 (Ph, t, 2H), 6.95 (Ph, t, 1H), 6.85 (Ph, d, 2H), 3.18 ( $\text{CH}_2$ , dq, 1H), 3.15 ( $\text{C}^*\text{H}_2\text{Ph}$ , d, 1H), 3.00–2.85 ( $\text{CH}_2$ , m, 1H), 2.60 ( $\text{CH}_2$ , dq, 1H), 2.28 ( $\text{CH}^*\text{Ph}$ , d, 1H), 1.67 ( $\text{C}_5\text{Me}_5$ , s, 15H), 1.48 ( $\text{CH}_2$ , t, 3H), 1.11 ( $\text{CH}_2$ , t, 3H). <sup>13</sup>C NMR ( $\delta$ ,  $\text{CDCl}_3$ ): 149.9 (ipso  $\text{C}_6$ ), 129.1 (Ph), 128.0 (Ph), 124.3 (Ph), 94.2 ( $\text{C}^*\text{Me}_5$ ), 71.3 ( $\text{C}^*\text{H}_2\text{Ph}$ ), 24.3 ( $\text{CH}_2$ ), 24.0 ( $\text{CH}_2$ ), 15.2 ( $\text{CH}_3$ ), 13.5 ( $\text{CH}_3$ ), 9.4 ( $\text{C}_5\text{Me}_5$ ). <sup>11</sup>B NMR ( $\delta$ ,  $\text{CH}_2\text{Cl}_2$ ): 38.0 (1B, d,  $J$  = 139 Hz), 28.3 (1B, d,  $J$  = 144 Hz), 18.3 (1B, d,  $J$  = 150 Hz), -1.9 (1B, d,  $J$  = 162 Hz). MS  $m/z$  572 (molecular ion). Anal. Calcd for  $\text{C}_{23}\text{H}_{32}\text{B}_4\text{ClTa}$ : C, 48.62; H, 5.68. Found: C, 48.31; H, 5.15.

**(Et<sub>2</sub>C<sub>2</sub>B<sub>4</sub>H<sub>4</sub>)Ta(CH<sub>2</sub>CMe<sub>3</sub>)ClCp (5h).** A sample of **1a** (100 mg, 0.22 mmol) was dissolved in 25 mL of THF, and solid dineopentylmagnesium dioxane (70 mg, 0.27 mmol, 2.5 equiv of neopentyl) was added to the solution, producing an instant color change from yellow to dark brown-black. The mixture was stirred for 2 h, after which the solvent was removed in vacuo and the residue was filtered through 3 cm of silica gel with  $\text{CH}_2\text{Cl}_2$ ; the solvent was then removed, and the residue was washed with 5 mL of cold petroleum ether to yield **5h** (90 mg, 0.19 mmol, 86%) as a yellow oil. <sup>1</sup>H NMR ( $\delta$ ,  $\text{CDCl}_3$ ): 6.33 ( $\text{C}_5\text{H}_5$ , s, 5H), 3.22 ( $\text{CH}_2$ , dq, 1H), 2.94–2.83 ( $\text{CH}_2/\text{C}^*\text{H}_2\text{tBu}$ , m, 3H), 2.40 ( $\text{CH}_2$ , dq, 1H), 1.48 ( $\text{CH}_3$ , t, 3H), 1.24 ( $\text{C}^*\text{H}_2\text{tBu}^*/\text{CH}_3$ , m, 13H). <sup>13</sup>C NMR ( $\delta$ ,  $\text{CDCl}_3$ ): 110.3 ( $\text{C}_5\text{H}_5$ ), 83.2 ( $\text{C}^*\text{H}_2\text{tBu}$ ), 37.5 ( $\text{C}^*\text{Me}_3$ ), 36.2 ( $\text{CMe}^*_3$ ), 23.3 ( $\text{CH}_2$ ), 23.1 ( $\text{CH}_2$ ), 15.0 ( $\text{CH}_3$ ), 14.7 ( $\text{CH}_3$ ). <sup>11</sup>B NMR ( $\delta$ ,  $\text{CH}_2\text{Cl}_2$ ): 40.9 (1B, d,  $J$  = 146

Hz), 33.2 (1B, d,  $J$  = 142 Hz), 28.0 (1B, d,  $J$  = 156 Hz), 0.3 (1B, d,  $J$  = 161 Hz). MS  $m/z$  480 (molecular ion), 411 ( $-\text{CH}_2\text{CMe}_3$ ).

**(Et<sub>2</sub>C<sub>2</sub>B<sub>4</sub>H<sub>4</sub>)Ta(CH<sub>2</sub>CMe<sub>3</sub>)ClCp\* (5i).** The same procedure described for the synthesis of **5h** was followed employing **1c** (100 mg, 0.19 mmol) and solid dineopentylmagnesium dioxane (61 mg, 0.24 mmol, 2.5 equiv of neopentyl). The mixture was stirred for 2h, with a gradual color change from yellow to dark yellow-brown, followed by workup as above to yield **5i** (90 mg, 0.16 mmol, 86%) as a yellow oil. <sup>1</sup>H NMR ( $\delta$ ,  $\text{CDCl}_3$ ): 3.34 ( $\text{CH}_2$ , dq, 1H), 2.83–2.70 ( $\text{CH}_2$ , m, 2H), 2.51 ( $\text{CH}_2$ , dq, 1H), 2.25 ( $\text{C}^*\text{H}_2\text{tBu}$ , d,  $J$  = 11.8 Hz, 1H), 2.12 ( $\text{C}_5\text{Me}_5$ , s, 15H), 1.50 ( $\text{CH}_3$ , t, 3H), 1.44 ( $\text{CH}_3$ , t, 3H), 1.25 ( $\text{tBu}$ , s, 9H), 0.65 ( $\text{C}^*\text{H}_2\text{tBu}$ , d,  $J$  = 11.8 Hz, 1H). <sup>13</sup>C NMR ( $\delta$ ,  $\text{CDCl}_3$ ): 96.6 ( $\text{C}_5\text{Me}_5$ ), 81.1 ( $\text{C}^*\text{H}_2\text{tBu}$ ), 36.1 ( $\text{C}^*\text{Me}_3$ ), 32.4 ( $\text{CMe}^*_3$ ), 24.5 ( $\text{CH}_2$ ), 24.4 ( $\text{CH}_2$ ), 15.3 ( $\text{CH}_3$ ), 14.9 ( $\text{CH}_3$ ), 10.2 ( $\text{C}_5\text{Me}_5$ ). <sup>11</sup>B NMR ( $\delta$ ,  $\text{CH}_2\text{Cl}_2$ ): 39.2 (1B, d,  $J$  = 140 Hz), 34.3 (1B, d,  $J$  = 147 Hz), 26.2 (1B, d,  $J$  = 150 Hz), 1.2 (1B, d,  $J$  = 159 Hz). MS  $m/z$  552 (molecular ion), 481 ( $-\text{CH}_2\text{CMe}_3$ ).

**(Et<sub>2</sub>C<sub>2</sub>B<sub>4</sub>H<sub>4</sub>)TaMe<sub>2</sub>Cp (6a).** A 1.4 M solution of methylmagnesium bromide (1.75 mL, 2.35 mmol, 2.1 equiv) in ether was added dropwise via syringe to **1a** (0.500 g, 1.12 mmol) in 25 mL of THF. The mixture was stirred for 0.5 h, and the solvent was removed by rotary evaporation. The yellow solid was taken up in  $\text{CH}_2\text{Cl}_2$  and filtered through Celite to yield **6a** as yellow fluffy crystals (413 mg, 1.02 mmol, 91%). Alternatively, 2.5 equiv of 1.4 MeLi in hexane can be used as a methylating agent to obtain approximately the same yield (87%). <sup>1</sup>H NMR ( $\delta$ ,  $\text{CDCl}_3$ ): 6.02 ( $\text{C}_5\text{H}_5$ , s, 5H), 2.92–2.65 ( $\text{CH}_2$ , m, 4H), 1.30 ( $\text{CH}_3$ , t, 6H), -0.10 (Ta- $\text{CH}_3$ , s, 6H). <sup>1</sup>H NMR ( $\delta$ ,  $\text{CD}_2\text{Cl}_2$ ): 6.06 ( $\text{C}_5\text{H}_5$ , s, 5H), 2.88–2.60 ( $\text{CH}_2$ , m, 4H), 1.31 (Me, t, 6H), -0.08 (Ta- $\text{CH}_3$ , s, 6H). <sup>1</sup>H NMR ( $\delta$ ,  $\text{C}_6\text{D}_6$ ): 5.37 ( $\text{C}_5\text{H}_5$ , s, 5H), 2.64 ( $\text{CH}_2$ , dq, 2H), 2.49 ( $\text{CH}_2$ , dq, 2H), 1.24 ( $\text{CH}_3$ , t, 6H), -0.25 (Ta- $\text{CH}_3$ , s, 6H). <sup>13</sup>C NMR ( $\delta$ ,  $\text{CDCl}_3$ ): 110.1 ( $\text{C}_5\text{H}_5$ ), 50.4 (Ta- $\text{CH}_3$ ), 23.0 ( $\text{CH}_2$ ), 15.3 ( $\text{CH}_3$ ). <sup>11</sup>B NMR ( $\delta$ ,  $\text{CH}_2\text{Cl}_2$ ): 29.8 (1B, d,  $J$  = 134 Hz), 22.1 (2B, d,  $J$  = 145 Hz), -0.7 (1B, d,  $J$  = 160 Hz). FTIR ( $\text{cm}^{-1}$ ): 3115 m, 3051 w, 2967 m, 2931 m, 2876 m, 2538 s. UV-vis (nm, in  $\text{CH}_2\text{Cl}_2$ ): 352 (100%), 316 (85%), 248 (85%). MS  $m/z$  405 (parent ion envelope), 390 ( $-\text{CH}_3$ ). Anal. Calcd for  $\text{C}_{13}\text{H}_{25}\text{B}_4\text{Ta}$ : C, 38.50; H, 6.21. Found: C, 38.14; H, 6.59.

**[(Me<sub>3</sub>Si)<sub>2</sub>C<sub>2</sub>B<sub>4</sub>H<sub>4</sub>]TaMe<sub>2</sub>Cp (6b).** A 1.4 M solution of methylmagnesium bromide (2.0 mL, 2.8 mmol, 3 equiv) in ether was added dropwise via syringe to **1b** (0.500 g, 0.94 mmol) in 25 mL THF at 0 °C. The mixture was stirred for 0.5 h at 0 °C and then at room temperature for 1 h. The solvent was removed by rotary evaporation, the yellow solid was taken up in  $\text{CH}_2\text{Cl}_2$ , filtered through Celite, and the solvent was removed to yield **6b** as yellow crystals (460 mg, 0.93 mmol, 99%). <sup>1</sup>H NMR ( $\delta$ ,  $\text{CDCl}_3$ ): 5.97 ( $\text{C}_5\text{H}_5$ , s, 5H), 0.41 ( $\text{SiMe}_3$ , s, 18H), 0.01 (Ta- $\text{CH}_3$ , s, 6H). <sup>13</sup>C NMR ( $\delta$ ,  $\text{CDCl}_3$ ): 109.2 ( $\text{C}_5\text{H}_5$ ), 51.9 (Ta- $\text{CH}_3$ ), 3.3 ( $\text{SiMe}_3$ ). <sup>11</sup>B NMR ( $\delta$ ,  $\text{CDCl}_3$ ): 30.1 (1B, d,  $J$  = 141 Hz), 24.7 (2B, d,  $J$  = 147 Hz), -0.9 (1B, d,  $J$  = 163 Hz). FTIR ( $\text{cm}^{-1}$ ): 3207 m, 3115 w, 2965 m, 2955 m, 2899 w, 2563 s, 2557 s, 2521 s, 2361 w, 2343 w. UV-vis (nm, in  $\text{CH}_2\text{Cl}_2$ ): 328 (38%), 246 (100%). MS  $m/z$  494 (molecular ion), 481 ( $-\text{CH}_3$ ). Anal. Calcd for  $\text{C}_{15}\text{H}_{33}\text{B}_4\text{Si}_2\text{Ta}$ : C, 36.49; H, 6.94. Found: C, 36.79; H, 7.35.

**(Et<sub>2</sub>C<sub>2</sub>B<sub>4</sub>H<sub>4</sub>)TaMe<sub>2</sub>Cp\* (6c).** A 1.4 M solution of methylmagnesium bromide (1.0 mL, 1.5 mmol, 3 equiv) in ether was added dropwise via syringe to **1c** (250 mg, 0.48 mmol) in 25 mL THF at 0 °C. Purification as in the preceding syntheses afforded **6c** as yellow fluffy crystals (225 mg, 0.46 mmol, 97%). <sup>1</sup>H NMR ( $\delta$ ,  $\text{CDCl}_3$ ): 2.82–2.61 ( $\text{CH}_2$ , m, 4H), 1.98 ( $\text{C}_5\text{Me}_5$ , s, 15H), 1.29 ( $\text{CH}_3$ , t, 6H), -0.53 (Ta- $\text{CH}_3$ , s, 6H). <sup>13</sup>C NMR ( $\delta$ ,  $\text{CDCl}_3$ ): 117.7 ( $\text{C}^*\text{Me}_5$ ), 53.4 (Ta- $\text{CH}_3$ ), 22.9 ( $\text{CH}_2$ ), 15.3 ( $\text{CH}_3$ ), 12.5 ( $\text{C}_5\text{Me}_5$ ). <sup>11</sup>B NMR ( $\delta$ ,  $\text{CH}_2\text{Cl}_2$ ): 31.7 (1B, d,  $J$  = 136 Hz), 23.9 (1B, d,  $J$  = 138 Hz), -2.5 (1B, d,  $J$  = 158 Hz). FTIR ( $\text{cm}^{-1}$ ): 3225 m, 2954 s, 2943 m, 2554 s, 1965 s, 1876 m. UV-vis (nm, in  $\text{CH}_2\text{Cl}_2$ ): 370, (66%), 248 (100%). MS  $m/z$  476 (parent ion envelope), 461 ( $-\text{CH}_3$ ). Anal. Calcd for  $\text{C}_{18}\text{H}_{35}\text{B}_4\text{TaC}$ : 45.45; H, 7.42. Found: C, 42.45; H, 7.70.

(**Et<sub>2</sub>C<sub>2</sub>B<sub>4</sub>H<sub>4</sub>)TaPh<sub>2</sub>Cp (6d)**. A 2 M solution of phenylmagnesium bromide in diethyl ether (11.2 mL, 33.6 mmol, 15 equiv) was added via syringe to a stirred solution of **1a** (1.00 g, 2.24 mmol) in 20 mL of toluene under argon. The mixture was stirred for 1 h, filtered in air, and the solvent was removed under vacuum. The yellow-brown residue was extracted with CH<sub>2</sub>Cl<sub>2</sub> and filtered through silica gel. The solvent was removed by rotary evaporation, and the solid residue was washed with pentane to afford **6d** as yellow crystals in quantitative yield (1.18 g, 2.24 mmol). <sup>1</sup>H NMR (δ, CDCl<sub>3</sub>): 7.29 (Ph, t, 4H), 7.19 (Ph, d, 4H), 7.06 (Ph, t, 2H), 6.01 (C<sub>5</sub>H<sub>5</sub>, s, 5H), 2.05 (CH<sub>2</sub>, dq, 2H), 1.97 (CH<sub>2</sub>, dq, 2H), 1.07 (CH<sub>3</sub>, dd, 6H). <sup>13</sup>C NMR (δ, CDCl<sub>3</sub>): 194.4 (ipso Ph), 137.0 (Ph), 129.0 (Ph), 128.1 (Ph), 125.7 (Ph), 123.6 (Ph), 121 (C<sub>2</sub>B<sub>3</sub>, br), 110.8 (C<sub>5</sub>H<sub>5</sub>), 24.4 (CH<sub>2</sub>), 14.6 (CH<sub>2</sub>). <sup>11</sup>B NMR (δ, CH<sub>2</sub>Cl<sub>2</sub>): 34.1 (1B, d, *J* = 122 Hz), 22.1 (2B, d, *J* = 109 Hz), 2.9 (1B, d, *J* = 136 Hz). MS *m/z* 529 (molecular ion).

(**Et<sub>2</sub>C<sub>2</sub>B<sub>4</sub>H<sub>4</sub>)Ta(CH<sub>2</sub>Ph)<sub>2</sub>Cp (6e)**. A 2 M solution of benzylmagnesium chloride (0.67 mL, 1.35 mmol, 3 equiv) in ether was added dropwise via syringe to **1a** (200 mg, 0.45 mmol) in 25 mL of THF. Over the course of the addition the color slowly changed from yellow to red-orange. The mixture was stirred for 0.5 h, and the solvent was removed in vacuo. The red residue was taken up in CH<sub>2</sub>Cl<sub>2</sub>, filtered through Celite, and chromatographed with 4:1 petroleum ether-CH<sub>2</sub>Cl<sub>2</sub>. One major orange band was eluted, which yielded **6e** as an orange oil (241 mg, 0.43 mmol, 96%). <sup>1</sup>H NMR (δ, CDCl<sub>3</sub>): 7.18 (Ph, t, *J* = 7.2 Hz, 2H), 6.96–6.89 (Ph, m, 3H), 5.57 (C<sub>5</sub>H<sub>5</sub>, s, 5H), 3.01 (CH<sub>2</sub>, dq, 2H), 2.89–2.75 (CH<sub>2</sub>/CH<sup>\*</sup><sub>2</sub>Ph, m, 3H), 1.42 (CH<sub>3</sub>, t, 6H), 0.73 (CH<sup>\*</sup><sub>2</sub>Ph, d, *J* = 11.4 Hz, 1H). <sup>13</sup>C NMR (δ, CDCl<sub>3</sub>): 150.4 (ipso C<sub>6</sub>), 128.9 (Ph), 128.4 (Ph), 124.5 (Ph), 119.7 (C<sub>5</sub>H<sub>5</sub>), 77.3 (CH<sup>\*</sup><sub>2</sub>Ph), 22.9 (CH<sub>2</sub>), 15.1 (CH<sub>3</sub>). <sup>11</sup>B NMR (δ, CH<sub>2</sub>Cl<sub>2</sub>): 31.6 (1B, d, *J* = 122 Hz), 22.8 (2B, d, *J* = 109 Hz), -0.2 (1B, d, *J* = 136 Hz). MS *m/z* 557 (parent ion envelope), 466 (-CH<sub>2</sub>Ph). Anal. Calcd for C<sub>25</sub>H<sub>33</sub>B<sub>4</sub>Ta: C, 53.84; H, 5.96. Found: C, 54.02; H, 6.10.

(**(Me<sub>3</sub>Si)<sub>2</sub>C<sub>2</sub>B<sub>4</sub>H<sub>4</sub>Ta(CH<sub>2</sub>Ph)<sub>2</sub>Cp (6f)**). The same procedure was followed employing benzylmagnesium chloride (0.67 mL, 1.35 mmol) and **1b** (200 mg, 0.37 mmol) in 15 mL of THF. Over the course of the addition the color slowly changed from yellow to brown-orange. Workup as before yielded **6f** (224 mg, 0.35 mmol, 96%) as an orange-red viscous oil. <sup>1</sup>H NMR (δ, CDCl<sub>3</sub>): 7.18 (Ph, t, 2H), 6.90–6.89 (Ph, t, 3H), 2.92 (CH<sup>\*</sup><sub>2</sub>Ph, d, 2H), 1.13 (CH<sup>\*</sup><sub>2</sub>Ph, d, 1H), 0.24 (SiMe<sub>3</sub>, s, 18H). <sup>13</sup>C NMR (δ, CDCl<sub>3</sub>): 148.2 (ipso C<sub>6</sub>), 130.9 (Ph), 127.7 (Ph), 124.5 (Ph), 119.7 (C<sub>5</sub>H<sub>5</sub>), 80.0 (CH<sub>2</sub>Ph), 22.6 (CH<sub>2</sub>), 15.6 (CH<sub>3</sub>). <sup>11</sup>B NMR (δ, CH<sub>2</sub>Cl<sub>2</sub>): 32.5 (1B, d, *J* = 129 Hz), 23.0 (2B, d, *J* = 115 Hz), -1.4 (1B, d, *J* = 146 Hz). MS *m/z* 645 (molecular ion), 554 (-CH<sub>2</sub>Ph).

(**Et<sub>2</sub>C<sub>2</sub>B<sub>4</sub>H<sub>4</sub>)Ta(CH<sub>2</sub>Ph)<sub>2</sub>Cp\* (6g)**. A 2.0 M solution of benzylmagnesium chloride (0.58 mL, 1.14 mmol, 3 equiv) in ether was added dropwise via syringe to **1c** (200 mg, 0.39 mmol) in 15 mL of THF. Over the course of the addition the color slowly changed from yellow to red-orange. The mixture was stirred for 0.5 h, and the solvent was removed in vacuo. The orange-red residue was taken up in CH<sub>2</sub>Cl<sub>2</sub>, filtered through Celite, and chromatographed with 4:1 petroleum ether-CH<sub>2</sub>Cl<sub>2</sub>. One major orange band was eluted, which yielded **6g** as an orange oil (228 mg, 0.36 mmol, 94%). <sup>1</sup>H NMR (δ, CDCl<sub>3</sub>): 7.23 (Ph, t, *J* = 7.2 Hz, 2H), 6.98–6.80 (Ph, m, 3H), 2.55–2.30 (CH<sub>2</sub>, m, 4H), 2.14 (CH<sup>\*</sup><sub>2</sub>Ph, d, *J* = 11.4 Hz, 1H), 1.97 (C<sub>5</sub>Me<sub>5</sub>, s, 15H), 1.14 (CH<sup>\*</sup><sub>2</sub>Ph, d, *J* = 11.4 Hz, 1H), 1.05 (CH<sub>3</sub>, t, 6H). <sup>13</sup>C NMR (δ, CDCl<sub>3</sub>): 149.5 (ipso C<sub>6</sub>), 130.4 (Ph), 127.2 (Ph), 125.2 (Ph), 95.7 (C<sup>\*</sup><sub>5</sub>Me<sub>5</sub>), 80.1 (C<sup>\*</sup>H<sub>2</sub>-Ph), 24.1 (CH<sub>2</sub>), 14.1 (CH<sub>3</sub>), 10.9 (C<sub>5</sub>Me<sub>5</sub>). <sup>11</sup>B NMR (δ, CH<sub>2</sub>Cl<sub>2</sub>): 32.0 (1B, d, *J* = 127 Hz), 22.4 (2B, d, *J* = 118 Hz), -1.2 (1B, d, *J* = 145 Hz). MS *m/z* 628 (parent ion envelope), 535 (-CH<sub>2</sub>Ph). Anal. Calcd for C<sub>30</sub>H<sub>43</sub>B<sub>4</sub>Ta: C, 57.84; H, 6.90. Found: C, 58.80; H, 7.12.

(**Et<sub>2</sub>C<sub>2</sub>B<sub>4</sub>H<sub>4</sub>)Ta(CH<sub>2</sub>CMe<sub>3</sub>)<sub>2</sub>Cp (6h)**. A sample of **1a** (100 mg, 0.22 mmol) was dissolved in 25 mL of THF, and solid neopentylolithium (44 mg, 0.56 mmol, 2.5 equiv) was added to

the solution, producing an instant color change from yellow to dark brown. The mixture was stirred for 0.5 h, following which the solvent was removed in vacuo. The residue was filtered through 3 cm of silica gel with CH<sub>2</sub>Cl<sub>2</sub>, and the solvent was removed, after which the residue was washed with 5 mL of cold petroleum ether to yield **6h** (102 mg, 0.20 mmol, 90%) as a yellow oil which decomposed overnight, under inert gas, generating an uncharacterizable brown residue. <sup>1</sup>H NMR (δ, CDCl<sub>3</sub>): 6.13 (C<sub>5</sub>H<sub>5</sub>, s, 5H), 2.73 (CH<sub>2</sub>, dq, 2H), 2.51 (CH<sub>2</sub>, dq, 2H), 1.29 (CH<sub>3</sub>, t, 6H), 1.24 (CH<sup>\*</sup><sub>2</sub>tBu, d, 2H), 1.00 (tBu, s, 18H), -0.34 (CH<sup>\*</sup><sub>2</sub>tBu, d, 2H). <sup>13</sup>C NMR (δ, CDCl<sub>3</sub>): 120 (C<sub>2</sub>B<sub>3</sub>), 106.6 (C<sub>5</sub>H<sub>5</sub>), 90.2 (C<sup>\*</sup>H<sub>2</sub>tBu), 38.4 (C<sup>\*</sup>Me<sub>3</sub>), 35.2 (CMe<sup>\*</sup><sub>3</sub>), 22.6 (CH<sub>2</sub>), 15.1 (CH<sub>3</sub>). <sup>11</sup>B NMR (δ, CH<sub>2</sub>Cl<sub>2</sub>): 31.5 (1B, d, *J* = 135 Hz), 24.5 (2B, d, *J* = 119 Hz), -2.6 (1B, d, *J* = 137 Hz). MS *m/z* 517 (molecular ion), 446 (-CH<sub>2</sub>CMe<sub>3</sub>).

(**(Me<sub>3</sub>Si)<sub>2</sub>C<sub>2</sub>B<sub>4</sub>H<sub>4</sub>Ta(CH<sub>2</sub>CMe<sub>3</sub>)<sub>2</sub>Cp (6i)**). The preceding procedure was followed employing neopentylolithium (37 mg, 0.48 mmol) and **1b** (100 mg, 0.19 mmol), which produced a red-orange solution on addition of the latter reagent. The solution was stirred for 30 min, after which solvent was removed, and the orange-brown solid was filtered through silica gel and chromatographed on silica to give a single yellow band that afforded **6i** (78 mg, 0.13 mmol, 68%) as a yellow oil. <sup>1</sup>H NMR (δ, CDCl<sub>3</sub>): 6.14 (C<sub>5</sub>H<sub>5</sub>, s, 5H), 1.14 (CH<sup>\*</sup><sub>2</sub>CMe<sub>3</sub>, d, 2H), 1.02 (CMe<sub>3</sub>, s, 18H), 0.43 (SiMe<sub>3</sub>, s, 18H), 0.81 (CH<sub>3</sub>-Ta, s, 3H), -0.37 (CH<sup>\*</sup><sub>2</sub>CMe<sub>3</sub>, d, 2H). <sup>13</sup>C NMR (δ, CDCl<sub>3</sub>): 105.8 (C<sub>5</sub>H<sub>5</sub>), 92.1 (C<sub>2</sub>B<sub>3</sub>), 35.2 (CMe<sup>\*</sup><sub>3</sub>), 31.6 (C<sup>\*</sup>Me<sub>3</sub>), 29.6 (CH<sub>2</sub>), 3.6 (SiMe<sub>3</sub>). <sup>11</sup>B NMR (δ, CH<sub>2</sub>Cl<sub>2</sub>): 40.0 (1B, d, *J* = 150 Hz), 25.2 (2B, d, *J* = 145 Hz), 0.9 (1B, d, *J* = 155 Hz). MS *m/z* 605 (molecular ion), 534 (-CH<sub>2</sub>CMe<sub>3</sub>).

(**Et<sub>2</sub>C<sub>2</sub>B<sub>4</sub>H<sub>4</sub>)Ta(CH<sub>2</sub>CMe<sub>3</sub>)<sub>2</sub>Cp\* (6j)**. The same procedure was followed employing neopentylolithium (30 mg, 36.0 mmol) and **1c** (50 mg, 0.09 mmol). Filtration through silica gel gave **6j** as a yellow solid (39 mg, 0.06 mmol, 75%). As with **6h**, this product decomposed overnight under inert gas. <sup>1</sup>H NMR (δ, CDCl<sub>3</sub>): 2.69 (CH<sup>\*</sup><sub>2</sub>, dq, 2H), 2.49 (CH<sup>\*</sup><sub>2</sub>, dq, 2H), 2.02 (C<sub>5</sub>-Me<sub>5</sub>, s, 15H), 1.19 (CH<sup>\*</sup><sub>2</sub>CMe<sub>3</sub>, d, 2H), 1.07 (CH<sub>3</sub>, t, 6H), 0.88 (CMe<sub>3</sub>, s, 18H), -0.30 (CH<sup>\*</sup><sub>2</sub>CMe<sub>3</sub>, d, 2H). <sup>13</sup>C NMR (δ, CDCl<sub>3</sub>): 122 (C<sub>2</sub>B<sub>3</sub>), 96.4 (C<sup>\*</sup><sub>5</sub>Me<sub>5</sub>), 91.0 (C<sup>\*</sup>H<sub>2</sub>CMe<sub>3</sub>), 39.1 (CMe<sup>\*</sup><sub>3</sub>), 35.4 (CMe<sup>\*</sup><sub>3</sub>), 22.5 (CH<sub>2</sub>), 15.0 (CH<sub>3</sub>), 9.6 (C<sub>5</sub>Me<sup>\*</sup><sub>5</sub>). MS *m/z* 587 (molecular ion), 516 (-CH<sub>2</sub>CMe<sub>3</sub>).

(**Et<sub>2</sub>C<sub>2</sub>B<sub>4</sub>H<sub>4</sub>)Ta(OPh)<sub>2</sub>Cp (6k)**. Phenol (126 mg, 1.3 mmol) was added dropwise to a suspension of NaH (100 mg, 4.1 mmol) in 15 mL of THF. The PhONa solution was allowed to settle and then was decanted to a solution of **1a** (200 mg, 0.45 mmol) in 10 mL of THF. The solution was stirred for 2 h, the solvent was removed, and the residue was taken up in CH<sub>2</sub>Cl<sub>2</sub> and filtered through 3 cm of silica gel to give **6k** (245 mg, 0.44 mmol, 97%) as an opaque yellow oil. <sup>1</sup>H NMR (δ, CDCl<sub>3</sub>): 7.35 (Ph, t, *J* = 7.8 Hz, 2H), 6.98 (Ph, t, *J* = 7.2 Hz, 1H), 6.73 (Ph, d, *J* = 8.1 Hz, 2H), 6.26 (C<sub>5</sub>H<sub>5</sub>, s, 5H), 2.92 (CH<sub>2</sub>, dq, 2H), 2.51 (CH<sub>2</sub>, dq, 2H), 1.25 (CH<sub>3</sub>, t, 6H). <sup>13</sup>C NMR (δ, CDCl<sub>3</sub>): 165.0 (ipso C<sub>6</sub>), 129.9 (Ph), 126.1 (C<sub>2</sub>B<sub>3</sub>, br), 121.6 (Ph), 118.3 (Ph), 112.2 (C<sub>5</sub>H<sub>5</sub>), 23.0 (CH<sub>2</sub>), 14.9 (CH<sub>3</sub>). <sup>11</sup>B NMR (δ, CH<sub>2</sub>Cl<sub>2</sub>): 20.7 (3B, unresolved coupling), -9.8 (1B, d, *J* = 150 Hz). FTIR (cm<sup>-1</sup>): 3132 w, 3063 w, 3030 w, 2967 m, 2931 m, 2874 w, 2561 s, 2343 w, 1587 s, 1481 s, 1248 s, 1161 m, 891 m, 869 m, 839 m. UV-vis (nm, in CH<sub>2</sub>Cl<sub>2</sub>): 344 (40%), 296 (100%), 260 (83%). Anal. Calcd for C<sub>23</sub>H<sub>29</sub>B<sub>4</sub>O<sub>2</sub>Ta: C, 49.18; H, 5.20. Found: C, 49.45; H, 5.24.

**Cp\*Co(Et<sub>2</sub>C<sub>2</sub>B<sub>3</sub>H<sub>3</sub>)TaMeClCp (7a)**. A 1.0 M solution of dimethylzinc (1.0 mL, 0.96 mmol, 1 equiv) in ether was added dropwise via syringe to **4a** (204 mg, 0.32 mmol) in 25 mL of THF at room temperature causing a color change from dark green to dark red. The mixture was stirred for 0.5 h, after which the solvent was removed by rotary evaporation. The red-black solid was chromatographed in 3:1 petroleum ether-CH<sub>2</sub>Cl<sub>2</sub> affording red-black **7a** (190 mg, 0.32 mmol, quantitative). <sup>1</sup>H NMR (δ, CDCl<sub>3</sub>): 5.78 (C<sub>5</sub>H<sub>5</sub>, s, 5H), 2.98 (CH<sub>2</sub>, dq, 1H), 2.79 (CH<sub>2</sub>, m, 2H), 2.61 (CH<sub>2</sub>, dq, 1H), 1.80 (CH<sub>3</sub>, t, 3H), 1.75 (C<sub>5</sub>Me<sub>5</sub>, s, 15H), 1.61 (CH<sub>3</sub>, t, 3H), 0.58 (Ta-CH<sub>3</sub>, s, 3H). <sup>13</sup>C NMR (δ, CDCl<sub>3</sub>): 109.1 (C<sub>5</sub>H<sub>5</sub>), 104.0 (C<sub>2</sub>B<sub>3</sub>, br), 102.5

(C<sub>2</sub>B<sub>3</sub>, br), 91.3 (C<sub>5</sub>Me<sub>5</sub>), 40.7 (Ta-CH<sub>3</sub>), 23.1 (CH<sub>2</sub>), 22.8 (CH<sub>2</sub>), 15.1 (CH<sub>3</sub>), 14.4 (CH<sub>3</sub>), 9.9 (C<sub>5</sub>Me<sub>5</sub>). <sup>11</sup>B NMR (δ, CH<sub>2</sub>Cl<sub>2</sub>): 65.7 (1B, d, *J* = 110 Hz), 30.8 (1B, d, *J* = 101 Hz), 22.4 (1B, d, *J* = 98 Hz). UV-vis (nm, in CH<sub>2</sub>Cl<sub>2</sub>): 322 (100%), 243 (51%). MS *m/z* 608 (molecular ion), 594 (- CH<sub>3</sub>). Anal. Calcd for C<sub>22</sub>H<sub>36</sub>B<sub>3</sub>CoTaCl: C, 43.44; H, 5.97. Found: C, 44.01; H, 5.51.

**Cp\*Co(Et<sub>2</sub>C<sub>2</sub>B<sub>3</sub>H<sub>3</sub>)TaMe<sub>2</sub>Cp (7b).** A 1.4 M solution of methylmagnesium bromide (0.86 mL, 1.2 mmol, 3 equiv) in ether was added dropwise via syringe to **4a** (251 mg, 0.40 mmol) in 25 mL of THF at room temperature causing a color change from dark green to dark red. The mixture was stirred for 0.5 h, after which solvent was removed by rotary evaporation. The red-black solid was chromatographed in 3:1 petroleum ether-CH<sub>2</sub>Cl<sub>2</sub> affording red-black **7b** (233 mg, 0.40 mmol, quantitative). <sup>1</sup>H NMR (δ, CDCl<sub>3</sub>): 5.73 (C<sub>5</sub>H<sub>5</sub>, s, 5H), 2.85-2.65 (CH<sub>2</sub>, m, 4H), 1.70 (C<sub>5</sub>Me<sub>5</sub>, s, 15H), 1.35 (CH<sub>3</sub>, t, 6H), -0.44 (Ta-CH<sub>3</sub>, s, 6H). <sup>13</sup>C NMR (δ, CDCl<sub>3</sub>): 108.5 (C<sub>5</sub>H<sub>5</sub>), 104.2 (C<sub>2</sub>B<sub>3</sub>, br), 90.4 (C<sub>5</sub>Me<sub>5</sub>), 52.1 (Ta-CH<sub>3</sub>), 23.0 (CH<sub>2</sub>), 15.3 (CH<sub>3</sub>), 10.4 (C<sub>5</sub>Me<sub>5</sub>). <sup>11</sup>B NMR (δ, CH<sub>2</sub>Cl<sub>2</sub>): 17.7 (1B, d, *J* = 103 Hz), 27.8 (2B, d, *J* = 102 Hz). FTIR (cm<sup>-1</sup>): 3214 m, 3112 w, 3095 w, 2977 m, 2928 m, 2505 s, 2352 m, 2341 m. UV-vis (nm, in CH<sub>2</sub>Cl<sub>2</sub>): 312 (100%), 246 (33%). MS *m/z* 586 (molecular ion), 571 (- CH<sub>3</sub>). Anal. Calcd for C<sub>23</sub>H<sub>39</sub>B<sub>3</sub>CoTa: C, 46.99; H, 6.69. Found: C, 49.39; H, 6.43.

**Cp\*Co(Et<sub>2</sub>C<sub>2</sub>B<sub>3</sub>H<sub>3</sub>)Ta(CH<sub>2</sub>Ph)ClCp (7c).** A sample of **4a** (180 mg, 0.29 mmol) was dissolved in 25 mL of THF and solid dibenzylzinc (214 mg, 0.87 mmol) was added to the solution causing a gradual color change from dark green to dark red over 1 h. The mixture was stirred for 2 h, following which the solvent was removed in vacuo. The residue was filtered through 3 cm of silica gel with CH<sub>2</sub>Cl<sub>2</sub>, and the solvent was removed, after which the residue was washed with 5 mL of cold petroleum ether to yield **7c** (191 mg, 0.28 mmol, quantitative) as a dark red solid. <sup>1</sup>H NMR (δ, CDCl<sub>3</sub>): 7.16 (Ph, t, *J* = 7.8 Hz, 2H), 6.85 (Ph, d, *J* = 7.8 Hz, 2H), 6.80 (Ph, d, *J* = 7.2 Hz, 1H), 5.60 (C<sub>5</sub>H<sub>5</sub>, s, 5H), 3.20 (CH<sub>2</sub>, dq, 1H), 3.01 (CH<sub>2</sub>, m, 2H), 2.68 (CH\*<sub>2</sub>Ph, d, *J* = 12.6 Hz, 1H), 2.53 (CH<sub>2</sub>, dq, 1H), 2.25 (CH\*<sub>2</sub>Ph, d, *J* = 12.6 Hz, 1H), 1.74 (CH<sub>3</sub>, t, 3H), 1.72 (C<sub>5</sub>Me<sub>5</sub>, s, 15H) 1.01 (CH<sub>3</sub>, t, 3H). <sup>13</sup>C NMR (δ, CDCl<sub>3</sub>): 151 (ipso C<sub>6</sub>), 129.5 (Ph), 127.8 (Ph), 123.4 (Ph), 110.4 (C<sub>5</sub>H<sub>5</sub>), 91.4 (C\*<sub>5</sub>Me<sub>5</sub>), 67.8 (C\*<sub>2</sub>H<sub>2</sub>Ph), 23.8 (CH<sub>2</sub>), 22.1 (CH<sub>2</sub>), 15.2 (CH<sub>3</sub>), 15.1 (CH<sub>3</sub>), 10.4 (C<sub>5</sub>Me\*<sub>5</sub>). <sup>11</sup>B NMR (δ, CH<sub>2</sub>Cl<sub>2</sub>): 65.9 (1B, d, *J* = 137 Hz), 31.3 (1B, d, *J* = 125 Hz), 24.2 (1B, d, *J* = 139 Hz). UV-vis (nm, in CH<sub>2</sub>Cl<sub>2</sub>): 250 (58%), 310 (100%), 548 (10%), MS *m/z* 685 (molecular ion). Anal. Calcd for C<sub>28</sub>H<sub>40</sub>B<sub>3</sub>CoTaCl: C, 49.14; H, 5.89. Found: C, 48.94; H, 5.60.

**Cp\*Co(Et<sub>2</sub>C<sub>2</sub>B<sub>3</sub>H<sub>3</sub>)Ta(CH<sub>2</sub>Ph)<sub>2</sub>Cp (7d).** A 2 M solution of benzylmagnesium chloride (0.60 mL, 1.20 mmol, 3 equiv) in ether was added dropwise via syringe to a sample of **4a** (250 mg, 0.16 mmol) in 25 mL of THF causing a gradual color change from dark green to dark red over 1 h. The mixture was stirred for 2 h, following which the solvent was removed in vacuo. The residue was filtered through 3 cm of silica gel with CH<sub>2</sub>Cl<sub>2</sub>, and the solvent was removed, after which the residue was washed with 5 mL of cold petroleum ether to yield **7d** (294 mg, 0.16 mmol, quantitative) as a reddish purple solid. <sup>1</sup>H NMR (δ, CDCl<sub>3</sub>): 7.14 (Ph, t, 2H), 6.80 (Ph, t, *J* = 7.2 Hz, 1H), 6.74 (Ph, d, 2H), 5.26 (C<sub>5</sub>H<sub>5</sub>, s, 5H), 3.00-2.80 (CH<sub>2</sub>, m, 4H), 2.35 (CH\*<sub>2</sub>Ph, d, *J* = 11.4 Hz, 2H), 1.75 (C<sub>5</sub>Me<sub>5</sub>, s, 15H), 1.48 (CH<sub>3</sub>, t, 6H), 0.84 (CH\*<sub>2</sub>Ph, d, *J* = 11.4 Hz, 2H). <sup>13</sup>C NMR (δ, CDCl<sub>3</sub>): 153.4 (ipso C<sub>6</sub>), 128.2 (Ph), 127.9 (Ph), 123.2 (Ph), 110.0 (C<sub>5</sub>H<sub>5</sub>), 105.5 (C<sub>2</sub>B<sub>3</sub>), 90.8 (C<sub>5</sub>Me<sub>5</sub>), 76.9 (C\*<sub>2</sub>H<sub>2</sub>Ph), 22.2 (CH<sub>2</sub>), 15.4 (CH<sub>3</sub>), 10.4 (C<sub>5</sub>Me<sub>5</sub>). <sup>11</sup>B NMR (δ, CH<sub>2</sub>Cl<sub>2</sub>): 63.0 (1B, d, *J* = 157 Hz), 28.2 (1B, d, *J* = 145 Hz). UV-vis (nm, in CH<sub>2</sub>Cl<sub>2</sub>): 250 (58%), 310 (100%), 548 (10%), MS *m/z* 741 (molecular ion). Anal. Calcd for C<sub>23</sub>H<sub>36</sub>B<sub>3</sub>CoTa: C, 56.80; H, 6.40. Found: C, 57.06; H, 6.61.

**Cp\*Co(Et<sub>2</sub>C<sub>2</sub>B<sub>3</sub>H<sub>3</sub>)Ta(CH<sub>2</sub>CMe<sub>3</sub>)ClCp (7e).** A sample of **7a** (100 mg, 0.16 mmol) was dissolved in 25 mL of THF, and solid dioneopentylmagnesium dioxane (50 mg, 0.20 mmol, 2.5 equiv of neopentyl) was added to the solution producing a color change from dark green to dark red over 1 h. The mixture

was stirred for 2 h, following which the solvent was removed in vacuo. The residue was filtered through 3 cm of silica gel with CH<sub>2</sub>Cl<sub>2</sub>, and the solvent was removed, after which the residue was washed with 5 mL of cold petroleum ether to yield **7e** (80 mg, 0.13 mmol, 80%) as a reddish solid. <sup>1</sup>H NMR (δ, CDCl<sub>3</sub>): 5.95 (C<sub>5</sub>H<sub>5</sub>, s, 5H), 3.03 (CH<sub>2</sub>, dq, 1H), 2.85 (CH<sub>2</sub>, dq, 2H), 2.38 (CH<sub>2</sub>, dq, 1H), 2.08 (CH<sub>2</sub>tBu, d, *J* = 12 Hz, 1H), 1.75 (CH<sub>3</sub>, t, 3H), 1.69 (C<sub>5</sub>Me<sub>5</sub>, s, 15H), 1.18 (CH<sub>2</sub>tBu, d, *J* = 12 Hz, 1H), 1.04 (CMe<sub>3</sub>, t, 9H), 1.01 (CH<sub>3</sub>, t, 3H). <sup>13</sup>C NMR (δ, CDCl<sub>3</sub>): 108.3 (C<sub>5</sub>H<sub>5</sub>), 84.5 (CH<sub>2</sub>tBu), 91.5 (C<sub>5</sub>Me<sub>5</sub>), 36.4 (CMe<sub>3</sub>), 35.1 (CMe<sub>3</sub>), 22.1 (CH<sub>2</sub>), 22.5 (CH<sub>2</sub>), 15.1 (CH<sub>3</sub>), 13.4 (CH<sub>3</sub>), 10.2 (C<sub>5</sub>Me\*<sub>5</sub>). MS *m/z* 665 (molecular ion). <sup>11</sup>B NMR (δ, CH<sub>2</sub>Cl<sub>2</sub>): 65.4 (1B, d, *J* = 140 Hz), 30.4 (1B, unresolved), 23.5 (1B, unresolved).

**Cp\*Co(Et<sub>2</sub>C<sub>2</sub>B<sub>3</sub>H<sub>3</sub>)Ta(CH<sub>2</sub>CMe<sub>3</sub>)<sub>2</sub>Cp (7f).** A sample of **4a** (100 mg, 0.16 mmol) was dissolved in 25 mL of THF, and solid neopentyllithium (31 mg, 0.40 mmol, 2.5 equiv of neopentyl) was added to the solution causing a color change from dark green to dark red over 1 h. The mixture was stirred for 2 h, following which the solvent was removed in vacuo. The residue was filtered through 3 cm of silica gel with CH<sub>2</sub>Cl<sub>2</sub>, and the solvent was removed, after which the residue was washed with 5 mL of cold petroleum ether to yield **7f** (65 mg, 0.09 mmol, 58%) as a reddish solid. <sup>1</sup>H NMR (δ, CDCl<sub>3</sub>): 5.84 (C<sub>5</sub>H<sub>5</sub>, s, 5H), 2.69 (CH<sub>2</sub>, dq, 2H), 2.54 (CH<sub>2</sub>, dq, 2H), 1.70 (C<sub>5</sub>Me<sub>5</sub>, s, 15H), 1.65 (CH<sub>2</sub>, d, 2H), 1.34 (CH<sub>3</sub>, t, 3H), 0.93 (CMe<sub>3</sub>, s, 18H), -0.26 (CH<sub>2</sub>, d, *J* = 12 Hz, 2H). <sup>13</sup>C NMR (δ, CDCl<sub>3</sub>): 106.3 (C<sub>5</sub>H<sub>5</sub>), 104.2 (C<sub>2</sub>B<sub>3</sub>, br), 90.9 (CH<sub>2</sub>), 90.1 (C\*<sub>5</sub>Me<sub>5</sub>), 37.4 (C\*Me<sub>3</sub>), 35.3 (CMe\*<sub>3</sub>), 22.1 (CH<sub>2</sub>), 15.0 (CH<sub>3</sub>), 10.4 (C<sub>5</sub>Me\*<sub>5</sub>). <sup>11</sup>B NMR (δ, CH<sub>2</sub>Cl<sub>2</sub>): 60.1 (1B, d, *J* = 145 Hz), 27.3 (2B, d, *J* = 131 Hz). MS *m/z* 700 (molecular ion), 628 (- CH<sub>2</sub>CMe<sub>3</sub>).

**(Et<sub>2</sub>C<sub>2</sub>B<sub>4</sub>H<sub>4</sub>)NbMe<sub>2</sub>Cp (8a).** A 1.4 M solution of methylmagnesium bromide (4.9 mL, 6.9 mmol, 10 equiv) in ether was added dropwise via syringe to (Et<sub>2</sub>C<sub>2</sub>B<sub>4</sub>H<sub>4</sub>)NbCl<sub>2</sub>Cp (250 mg, 0.69 mmol) in 25 mL of THF at 0 °C. The mixture was stirred for 0.5 h at 0 °C and then at room temperature for 1 h. The solvent was removed by rotary evaporation, the yellow solid was taken up in CH<sub>2</sub>Cl<sub>2</sub> and filtered through Celite, and the solvent was removed to yield **8a** as yellow crystals (206 mg, 0.65 mmol, 95%). <sup>1</sup>H NMR (δ, CDCl<sub>3</sub>): 6.01 (C<sub>5</sub>H<sub>5</sub>, s, 5H), 2.75 (CH<sub>2</sub>, m, 4H), 1.33 (CH<sub>3</sub>, t, 6H), 0.23 (Ta-CH<sub>3</sub>, s, 6H). <sup>13</sup>C NMR (δ, CDCl<sub>3</sub>): 108.8 (C<sub>5</sub>H<sub>5</sub>), 44.4 (Nb-CH<sub>3</sub>), 23.5 (CH<sub>2</sub>), 15.2 (CH<sub>3</sub>). <sup>11</sup>B NMR (δ, CH<sub>2</sub>Cl<sub>2</sub>): 34.1 (1B, d, *J* = 130 Hz), 23.6 (1B, d, *J* = 138 Hz), -3.1 (1B, d, *J* = 161 Hz). FTIR (cm<sup>-1</sup>): 2937 s, 2874 m, 2361 s, 1458 m, 1379 m. UV-vis (nm, in CH<sub>2</sub>Cl<sub>2</sub>): 372 (25%), 236 (100%). MS *m/z* 315 (parent ion envelope), 302 (- Me). Anal. Calcd for C<sub>13</sub>H<sub>25</sub>B<sub>4</sub>Nb: C, 49.18; H, 7.94. Found: C, 48.44; H, 7.58.

**(Et<sub>2</sub>C<sub>2</sub>B<sub>4</sub>H<sub>4</sub>)Nb(CH<sub>2</sub>Ph)<sub>2</sub>Cp (8b).** A 2.0 M solution of benzylmagnesium chloride (0.84 mL, 1.35 mmol) in ether was added dropwise via syringe to **2** (200 mg, 0.55 mmol) in 15 mL of THF. Over the course of the addition the color slowly changed from red-orange to brown-orange. The mixture was stirred for 0.5 h, and the solvent was removed in vacuo. The brown residue was taken up in CH<sub>2</sub>Cl<sub>2</sub>, filtered through Celite, and chromatographed with 4:1 petroleum ether-CH<sub>2</sub>Cl<sub>2</sub>. One major orange band was eluted, which yielded **8d** as a yellow solid (241 mg, 0.43 mmol, 96%). <sup>1</sup>H NMR (δ, CDCl<sub>3</sub>): 7.19 (Ph, t, 2H), 6.95 (Ph, t, 1H), 6.72 (Ph, d, *J* = 2H), 5.46 (C<sub>5</sub>H<sub>5</sub>, s, 5H), 3.53 (CH\*<sub>2</sub>Ph, d, 2H), 2.97 (CH<sub>2</sub>, dq, 2H), 2.79 (CH<sub>2</sub>, dq, 2H), 1.43 (CH<sub>3</sub>, t, 6H), 0.62 (CH\*<sub>2</sub>Ph, d, 1H). <sup>13</sup>C NMR (δ, CDCl<sub>3</sub>): 150.5 (ipso C<sub>6</sub>), 128.4 (Ph), 128.2 (Ph), 124.3 (Ph), 110.3 (C<sub>5</sub>H<sub>5</sub>), 121 (C<sub>2</sub>B<sub>4</sub>, br), 75.6 (C\*<sub>2</sub>H<sub>2</sub>Ph), 22.9 (CH<sub>2</sub>), 15.4 (CH<sub>3</sub>). <sup>11</sup>B NMR (δ, CH<sub>2</sub>Cl<sub>2</sub>): 32.5 (1B, d, *J* = 129 Hz), 23.8 (2B, d, *J* = 124 Hz), 2.0 (1B, d, *J* = 139 Hz). MS *m/z* 469 (parent ion envelope), 378 (- CH<sub>2</sub>Ph).

**Reaction of 6a with HBF<sub>4</sub> in Acetonitrile.** A 50 mg sample (0.12 mmol) of **6a** was dissolved in 5 mL of CH<sub>3</sub>CN in a scintillation vial, following which 912 mg of HBF<sub>4</sub>·OEt<sub>2</sub> in 9.5 g of CH<sub>3</sub>CN was added. Slight gas evolution was observed during the addition, but there was no color change. The solution was allowed to stand at room temperature for 4 h,

after which the solvent was removed in vacuo to yield  $(Et_2C_2B_4H_4)Ta(NCMe)_2Cp$  (**9b**) as a yellow solid which was insoluble in nonpolar solvents, slightly soluble in  $CH_2Cl_2$ , and readily soluble in polar solvents ( $CH_3CN$ , THF).  $^1H$  NMR ( $\delta$ ,  $CDCl_3$ ): 6.45 ( $C_5H_5$ , s, 5H), 2.82 ( $CH_2$ , dq, 2H), 2.52 ( $CH_2$ , dq, 2H), 2.01 ( $CH_3CN$ , s, 6H), 1.22 ( $CH_3$ , t, 6H).  $^1H$  NMR ( $\delta$ ,  $CD_3CN$ ): 6.57 ( $C_5H_5$ , s, 5H), 2.74 ( $CH_2$ , dq, 2H), 2.51 ( $CH_2$ , dq, 2H), 2.01 ( $CH_3CN$ , s, 6H), 1.16 ( $CH_3$ , t, 6H).  $^1H$  NMR ( $\delta$ ,  $(CD_3)_2C=O$ ): 6.59 ( $C_5H_5$ , s, 5H), 2.70 ( $CH_2$ , dq, 2H), 2.50 ( $CH_2$ , dq, 2H), 2.01 ( $CH_3CN$ , s, 6H), 1.18 ( $CH_3$ , t, 6H).  $^1H$  NMR ( $\delta$ ,  $CD_2Cl_2$ ): 6.46 ( $C_5H_5$ , s, 5H), 4.20 (q,  $Et_2O$ ), 2.89 ( $CH_2$ , dq, 2H), 2.49 ( $CH_2$ , dq, 2H), 2.03 ( $CH_3CN$ , s), 1.40 (t,  $Et_2O$ ), 1.22 ( $CH_3$ , t, 6H).  $^{11}B$  NMR ( $\delta$ ,  $CH_3CN$ ): 25.7 (1B, d,  $J = 162$  Hz), 23.3 (1B, d,  $J = 157$  Hz), -0.8 (1B, s), -9.6 (1B, d,  $J = 166$  Hz). MS  $m/z$  414 (molecular ion). Anal. Calcd for  $C_{15}H_{25}B_6N_2F_3$ -Ta: C, 28.54; H, 3.99; N, 4.44. Found: C, 29.51; H, 4.40; N, 4.27.

#### X-ray Data Collection and Structure Determination.

All measurements were conducted on a Rigaku AFC6S diffractometer either at  $-100$  °C (**1b**, **4a**, and **7b,c**) or at  $-120$  °C (**1c**, **6d**, and **8a**) using Mo  $K\alpha$  radiation ( $\lambda = 0.71069$  Å). Details of the measurement and structure analysis procedures are summarized in Table 1. For each crystal, the intensities of three standard reflections were monitored, showing no significant variation. Empirical absorption corrections were applied following  $\Psi$  scanning of several reflections with the  $\chi$  angle close to  $90^\circ$  (transmission factors are reported in Table 1). All calculations were performed on a VAX station 3520 computer employing the TEXSAN 5.0 crystallographic software package.<sup>35</sup> The structures of **1c**, **6d**, and **8a** were solved by heavy atom techniques applying Patterson and Fourier

maps, and those of the remaining compounds by direct methods using the SIR88 program.<sup>36</sup> The structures were refined using full-matrix least-squares calculations with anisotropic thermal displacement parameters for all non-hydrogen atoms except the carbon atoms of the Cp\* group in **1c**. In the latter case, the ring was found to be disordered between two orientations related by a ca.  $20^\circ$  rotation around an axis perpendicular to the plane of the ring. The carbon atoms belonging to the two orientations were refined with the population parameters of 0.5 and isotropic thermal parameters. The final difference Fourier maps were essentially featureless except that for **1b** which showed a peak ca.  $2.5$   $e/\text{\AA}^3$  high located in the vicinity of the Ta atom.

**Acknowledgment.** This work was supported in part by the National Science Foundation, Grant No. DHE-9322490 to R.N.G., and by the American Cancer Society (Junior Faculty Research Award No. C-66910) to M.G.F.

**Supplementary Material Available:** Tables of thermal parameters, atom coordinates, and calculated least-squares planes (24 pages). Ordering information is given on any current masthead page.

OM950160X

(35) TEXSAN 5.0: Single-Crystal Structure Analysis Software; Molecular Structure Corporation: The Woodlands, TX 77381, 1989.

(36) SIR88; Burla, M. C.; Camalli, M.; Cascarano, G.; Giacovazzo, C.; Polidori, G.; Spagna, R.; Viterbo, D. *J. Appl. Crystallogr.* **1989**, *22*, 389.

# Structural Characterization and Simple Synthesis of {Pd[P(*o*-Tol)<sub>3</sub>]<sub>2</sub>}, Dimeric Palladium(II) Complexes Obtained by Oxidative Addition of Aryl Bromides, and Corresponding Monometallic Amine Complexes

Frédéric Paul, Joe Patt, and John F. Hartwig\*

Department of Chemistry, Yale University, P.O. Box 208107,  
New Haven, Connecticut 06520-8107

Received December 13, 1994<sup>⊗</sup>

The palladium(0) complex {Pd[P(*o*-Tol)<sub>3</sub>]<sub>2</sub>} was prepared by addition of P(*o*-Tol)<sub>3</sub> to crude "[Pd(DBA)<sub>2</sub>]", which is an approximately equimolar mixture of Pd<sub>2</sub>(DBA)<sub>3</sub> and Pd(DBA)<sub>3</sub>, followed by crystallization from the reaction medium by addition of ether. The formation of {Pd[P(*o*-Tol)<sub>3</sub>]<sub>2</sub>} appeared to be driven by its insolubility in the benzene/ether solvent mixture. Benzene solutions of "[Pd(DBA)<sub>2</sub>]" and P(*o*-Tol)<sub>3</sub> did not contain amounts of the L<sub>2</sub>Pd compound that could be detected by <sup>31</sup>P NMR spectroscopy. {Pd[P(*o*-Tol)<sub>3</sub>]<sub>2</sub>} was characterized crystallographically and showed an exactly linear geometry. Similar Pd(0) compounds {Pd[P(2,4-dimethylphenyl)<sub>3</sub>]<sub>2</sub>}, {Pd[P(2-methyl-4-fluorophenyl)<sub>3</sub>]<sub>2</sub>}, and the low-coordinate trialkylphosphine complex {Pd[P(*t*-Bu)<sub>3</sub>]<sub>2</sub>} were also prepared by this method, but [Pd(PCy<sub>3</sub>)<sub>2</sub>(DBA)] was produced from reactions involving PCy<sub>3</sub> and "[Pd(DBA)<sub>2</sub>]", and [Pd(TMPP)(DBA)<sub>2</sub>] was isolated after addition of tris(1,3,5-trimethoxyphenyl)phosphine (TMPP) to "[Pd(DBA)<sub>2</sub>]". The oxidative addition of aryl halides to {Pd[P(*o*-Tol)<sub>3</sub>]<sub>2</sub>} at room temperature led to dimeric products {Pd[P(*o*-Tol)<sub>3</sub>](Ar)(Br)<sub>2</sub>}. An example of these compounds was characterized crystallographically as well as by solution molecular weight analysis. This aryl halide complex was shown to be dimeric in the solid state as well as in solution. The NMR spectra of the large triarylphosphine complexes showed temperature dependent behavior, presumably due to isomerizations and ligand rotations that occurred on the NMR time scale. The aryl halide compounds did not form four-coordinate monometallic species in the presence of excess P(*o*-Tol)<sub>3</sub>, but they did undergo cleavage to four-coordinate monometallic complexes upon addition of primary and secondary amines.

## Introduction

Tri-*o*-tolylphosphine complexes of palladium are widely used in catalysis. Examples of these catalytic reactions often involve aryl halide activation and include Heck reactions,<sup>1-5</sup> as well as cross-coupling chemistry that forms carbon-carbon bonds.<sup>6</sup> This large phosphine ligand is often preferred over the less expensive triphenylphosphine ligand because tri-*o*-tolylphosphine complexes can give rise to more active catalysts. This increased activity has been attributed to the resistance of the bulky ligand to undergo quaternization.<sup>7</sup> The increases in reaction rates have also been attributed to the lability of the tri-*o*-tolylphosphine ligand.<sup>6,7</sup> The proposed mechanistic scheme for homo-cross-coupling catalysis with this ligand involves a phosphine palladium(0) complex on the reaction pathway. Recently, we have been studying the use of tri-*o*-tolylphosphine

complexes of palladium in hetero-cross-coupling processes that form arylamines from aryl bromides and tin amides. We have proposed a mechanistic scheme for C-N bond forming chemistry that is similar to the accepted mechanism for C-C bond forming coupling reactions.<sup>8,9</sup>

A typical procedure for conducting catalysis with complexes of P(*o*-Tol)<sub>3</sub> involved *in situ* reduction of a Pd(II) starting complex or addition of the phosphine to a Pd(0) species such as the DBA complexes.<sup>6,10,11</sup> It was surprising to us that the only report of the simple Pd(0) complex {Pd[P(*o*-Tol)<sub>3</sub>]<sub>2</sub>} was included in a patent that used IR spectroscopy as the sole spectroscopic characterization.<sup>12</sup> Moreover, no report of the simple oxidative addition of aryl bromides to the Pd(0) species was known, and no aryl halide complexes containing this phosphine ligand had been isolated and characterized. One discussion of the Heck chemistry of these compounds formulated the aryl halide complex as a monomer, but no spectroscopic data was provided.<sup>7</sup>

The dramatic difference between the ability of [Pd(PPh<sub>3</sub>)<sub>4</sub>] and {Pd[P(*o*-Tol)<sub>3</sub>]<sub>2</sub>Cl<sub>2</sub>} to catalyze the forma-

<sup>⊗</sup> Abstract published in *Advance ACS Abstracts*, May 1, 1995.

(1) Mitsudo, T.-A.; Fischetti, W.; Heck, R. F. *J. Org. Chem.* **1984**, *49*, 1640-1646.

(2) Fischetti, W.; Mak, K. T.; Stakem, F. G.; Kim, J.-I.; Rheingold, A. L.; Heck, R. F. *J. Org. Chem.* **1983**, *48*, 948-955.

(3) Patel, B. A.; Dickerson, J. E.; Heck, R. F. *J. Org. Chem.* **1978**, *43*, 5018-5020.

(4) Patel, B. A.; Heck, R. F. *J. Org. Chem.* **1978**, *43*, 3898-3903.

(5) Patel, B. A.; Kao, L.-C. K.; Cortese, N. A.; Minkiewicz, J. V.; Heck, R. F. *J. Org. Chem.* **1979**, *44*, 918-921.

(6) Farina, V.; Krishnan, B. *J. Am. Chem. Soc.* **1991**, *113*, 9585-9595.

(7) Ziegler, C. B. J.; Heck, R. F. *J. Org. Chem.* **1978**, *43*, 2941-2946.

(8) Stille, J. K. *Pure Appl. Chem.* **1985**, *57*, 1771-1780.

(9) Stille, J. K. *Angew. Chem., Int. Ed. Engl.* **1986**, *25*, 508-524.

(10) Rubezhov, A. Z. *Russ. Chem. Rev.* **1988**, *57*, 2078-2101.

(11) Huser, M.; Youinou, M.-T.; Osborn, J. A. *Angew. Chem., Int. Ed. Engl.* **1988**, *28*, 1386-88.

(12) Enomoto, S.; Wada, H.; Nishita, S.; Mukaida, Y.; Yanaka, M.; Takita, H. U.S. Patent 904407, 1980.

tion of arylamines from aryl bromides and tin amides<sup>13-16</sup> prompted us to prepare potential intermediates on the catalytic pathways. It became clear that, unlike their  $PPh_3$  analogues, the aryl bromide complexes containing the  $P(o-Tol)_3$  ligand were not simple monomers and that addition of  $P(o-Tol)_3$  to DBA complexes of palladium did not give the simple compound  $\{Pd[P(o-Tol)_3]_2\}$  *in situ*.

We report here a method to produce crystalline samples of  $\{Pd[P(o-Tol)_3]_2\}$  and other  $L_2Pd$  complexes of large phosphine ligands directly from a reaction medium. Furthermore, we have conducted careful characterization of the aryl bromide complexes resulting from oxidative addition and have shown that they are clearly dimeric in the solid state and in solution. A brief account of some of this chemistry has appeared,<sup>16</sup> and herein we report more extensive synthetic studies and experimental details concerning these compounds that are intermediates in a number of important catalytic processes.

### Experimental Section

**Materials.** Unless otherwise specified, all reagents were purchased from commercial suppliers and used without further purification. *n*-Pentane (technical grade) was distilled under nitrogen from purple sodium/benzophenone ketyl made soluble by addition of tetraglyme to the still. Diethyl ether, THF, benzene, and toluene were distilled from sodium/benzophenone ketyl under nitrogen. Dichloromethane was vacuum transferred from  $CaH_2$ . Deuterated solvents for use in NMR experiments were dried as their protiated analogs, but were vacuum transferred from the drying agent.  $\{Pd[P(o-Tol)_3]_2Cl_2\}$ ,<sup>12</sup> tri-*o*-tolylphosphine,<sup>7</sup> tris(2,4-dimethylphenyl)phosphine,<sup>17</sup> DBA,<sup>18</sup> and 2-iodo-2'-aminobiphenyl<sup>19</sup> were synthesized following reported procedures. Tris(2-methyl-4-fluorophenyl)phosphine and trimesitylphosphine were prepared by procedures analogous to those for tri-*o*-tolylphosphine.

$\{Pd[P(o-Tol)_3]_2Br_2\}$ <sup>20</sup> was synthesized by reacting 2 equiv of  $P(o-Tol)_3$  with  $[Pd(MeCN)_2Br_2]$  obtained after refluxing  $PdBr_2$  in acetonitrile. The starting complex " $[Pd(DBA)_2]$ " was obtained following a synthesis reported for  $[Pd_2(DBA)_3]$  without recrystallizing the crude precipitate obtained at the end of the synthesis.<sup>21</sup> This material is an equimolar mixture of  $Pd_2(DBA)_3$  and  $Pd(DBA)_3$ .<sup>22,23</sup>

**Methods.** Unless otherwise noted, all manipulations were carried out in an inert atmosphere glovebox or by using standard Schlenk or vacuum line techniques. <sup>1</sup>H NMR spectra were obtained on a GE QE 300 MHz or an Omega 300 MHz Fourier transform spectrometer. <sup>19</sup>F and <sup>31</sup>P NMR spectra were obtained on the Omega 300 operating at 96.38 and 121.65 MHz, respectively. <sup>1</sup>H NMR spectra were recorded relative to residual protiated solvent. <sup>19</sup>F shifts were assigned relative to  $CFCl_3$ . <sup>31</sup>P{<sup>1</sup>H} chemical shifts are reported in units of parts

(13) Guram, A. S.; Buchwald, S. L. *J. Am. Chem. Soc.* **1994**, *116*, 7901-7902.

(14) Kosugi, M.; Kameyama, M.; Migita, T. *Chem. Lett.* **1983**, 927-928.

(15) Kosugi, M.; Kameyama, M.; Sano, H.; Migita, T. *Nippon Kagaku Kaishi* **1985**, 547-551.

(16) Paul, F.; Patt, J.; Hartwig, J. F. *J. Am. Chem. Soc.* **1994**, *116*, 5969-5970.

(17) Culcasi, M.; Bechardski, Y.; Gronchi, G.; Tordo, P. *J. Org. Chem.* **1991**, *56*, 3537-3542.

(18) Conrad, C. R.; Dolliver, M. A. In *Organic Syntheses*, 6th ed.; Blatt, A. H., Ed.; John Wiley & Sons, Inc.: New York, 1950; Collective Vol. 2, pp 167-169.

(19) Cade, J. A.; Pilbeam, A. *J. Chem. Soc.* **1964**, 114-121.

(20) Bennett, M. A.; Longstaff, P. A. *J. Am. Chem. Soc.* **1969**, *91*, 6266-6280.

(21) Ukai, T.; Kawazura, H.; Ishii, Y.; Bonnet, J. J.; Ibers, J. A. *J. Organomet. Chem.* **1974**, *65*, 253-266.

(22) Pierpont, C. G.; Mazza, M. C. *Inorg. Chem.* **1974**, *13*, 1891-1895.

(23) Mazza, M. C.; Pierpont, C. G. *Inorg. Chem.* **1973**, *12*, 2955-2959.

**Table 1. Crystal Data for 1a**

empirical formula	$C_{21}H_{21}PPd_{0.5}$
fw	357.57
cryst color/habit	pale yellow/prism
cryst dimens (mm <sup>3</sup> )	$0.10 \times 0.19 \times 0.32$
cryst syst	triclinic
no. of reffns used for unit cell determination ( $2\theta$ range)	25 ( $20.2^\circ$ - $30.5^\circ$ )
$\omega$ -scan peak width at half-height	0.22
lattice params	$a = 9.936(3) \text{ \AA}$ $b = 11.943(3) \text{ \AA}$ $c = 8.576(4) \text{ \AA}$ $\alpha = 106.84(3)^\circ$ $\beta = 111.84(3)^\circ$ $\gamma = 72.66(3)^\circ$ $V = 883.0(6) \text{ \AA}^3$
space group	$P\bar{1}$ (No. 2)
Z	2
$D_{\text{calcd}}$	1.345 g/cm <sup>3</sup>
$F(000)$	370
$\mu$ (Mo K $\alpha$ )	6.34 cm <sup>-1</sup>

**Table 2. Crystal Data for  $\{[(o-Tol)_3P](p-n-BuC_6H_4)Pd(Br)\}_2$  (2b)**

empirical formula	$C_{62}H_{68}P_2Br_2Pd_2$
fw	1247.77
cryst color/habit	very pale yellow/prism
cryst dimens (mm <sup>3</sup> )	$0.19 \times 0.19 \times 0.39$
cryst syst	monoclinic
no. of reflections used for unit cell determination ( $2\theta$ range)	25 ( $5.3^\circ$ - $13.4^\circ$ )
$\omega$ -scan peak width at half-height	0.26
lattice params	$a = 11.440(4) \text{ \AA}$ $b = 10.264(5) \text{ \AA}$ $c = 23.068(8) \text{ \AA}$ $\beta = 97.14(3)^\circ$ $V = 2688(3) \text{ \AA}^3$
space group	$P2_1/c$ (No. 14)
Z	2
$D_{\text{calcd}}$	1.542 g/cm <sup>3</sup>
$F(000)$	1264
$\mu$ (Mo K $\alpha$ )	22.29 cm <sup>-1</sup>

per million relative to 87%  $H_3PO_4$ . A positive value of the chemical shift denotes a resonance downfield from the reference. Unless noted, NMR spectra were obtained at ambient temperatures. Infrared spectra were recorded on a MIDAC Fourier transform spectrometer. Mass spectral studies were conducted at the University of Illinois. Samples for elemental analysis were submitted to Atlantic Microlab, Inc.

**X-ray Structural Determination.** Crystals for **1a** and **2b** were obtained directly from the reaction media. In both cases, the reactions were filtered, and ether was added. Crystalline samples of **1a** and **2b** were deposited after several days. The crystal data and details of measurements for **1a** and **2b** are reported in Tables 1 and 2.

Diffraction data were collected at  $-120 \pm 1^\circ \text{ C}$  for **1a** and  $-125 \pm 1^\circ \text{ C}$  for **2b** on a Rigaku AFC5S diffractometer with graphite-monochromated Mo K $\alpha$  radiation ( $\lambda = 0.71073 \text{ \AA}$ ). Cell constants and the orientation matrix for data collection were obtained from a least-squares refinement using the setting angles of 25 carefully centered reflections in the range  $20.24 < 2\theta < 30.55^\circ$  for **1a** corresponding to a triclinic cell and in the range  $5.35 < 2\theta < 13.36^\circ$  for **2b** corresponding to a triclinic cell. For **1a**, packing considerations, a statistical analysis of intensity distribution, and the successful solution and refinement of the structure showed the space group to be  $P\bar{1}$  (No. 2). In this space group, the metal center was situated on a crystallographic inversion center. For **2b**, the systematic absences of  $h0l$ ,  $l = 2n + 1$ , and  $0k0$ ,  $k = 2n + 1$ , and the successful solution and refinement of the structure showed the space group to be  $P2_1/c$  (No. 14).

The data were collected using the  $\omega$ - $2\theta$  scan to a maximum  $2\theta$  value of  $50.0^\circ$  for **1a** and  $45^\circ$  for **2b**. The  $\omega$ -scans of several intense reflections made prior to data collection had an average width at half-height of  $0.22^\circ$  for **1a** and  $0.26^\circ$  for **1b**, with a



take-off angle of  $6.0^\circ$  for both. Scans of  $(1.15 + 0.30 \tan \theta)^\circ$  for **1a** and  $(1.00 + 0.30 \tan \theta)^\circ$  for **2b** were made at speeds of  $8.0^\circ/\text{min}$  for **1a** and  $6.0^\circ/\text{min}$  for **2b** (in  $\omega$ ). The weak reflections ( $I < 10.0s(I)$ ) were rescanned (maximum 3 rescans), and the counts were accumulated to assure good counting statistics. Stationary background counts were recorded on each side of the reflection. The ratio of peak-counting time to background-counting time was 2:1. The diameter of the incident beam collimator was 0.5 mm, and the crystal to detector distance was 285.0 mm.

Of the 3307 reflections which were collected for **1a**, 3111 were unique ( $R_{\text{int}} = 0.025$ ). Of the 2440 reflections which were collected for **2b**, 2221 were unique ( $R_{\text{int}} = 0.065$ ). The intensities of the three representative reflections which were measured after every 150 reflections remained constant in both cases throughout data collection, indicating crystal and electronic stability (no decay correction was applied). The linear absorption coefficient for Mo K $\alpha$  was  $6.3 \text{ cm}^{-1}$  for **1a** and  $22.3 \text{ cm}^{-1}$  for **2b**. Azimuthal scans of several reflections indicated no need for an absorption correction in either case. The data were corrected for Lorentz and polarization effects.

The structure was solved by the Patterson method for **1a** and by a combination of the Patterson method and direct methods for **2b**. The Pd atom was located at 0, 0, 0 on an inversion center for **1a**. The non-hydrogen atoms were refined anisotropically. The hydrogen atoms were included in calculated positions. One hydrogen atom was located in the difference map of methyl groups to set the orientation of the other two hydrogen atoms. The final cycle of full-matrix least-squares refinement was based on 2399 observed reflections for **1a** and 1309 observed reflections for **2b** ( $I > 3.00s(I)$ ), 205 variable parameters for **1a**, 307 variable parameters for **2b** and converged (the largest parameter shift was 0.00 times its esd) with unweighted and weighted agreement factors of  $R = S||F_o| - |F_c||/S|F_o| = 0.034$  (**1a**) and 0.032 (**2b**) and  $R_w = [(Sw(|F_o| - |F_c|)^2/S|F_o|)]^{1/2} = 0.035$  (**1a**) and 0.031 (**2b**).

The standard deviation of an observation of unit weight was 1.41 for **1a** and 1.53 for **2b**. The weighting scheme was based on counting statistics and included a factor ( $p = 0.01$ ) to downweight the intense reflections. Plots of  $Sw(|F_o| - |F_c|)^2$  versus  $|F_o|$  reflection order in data collection,  $\sin \theta/l$ , and various classes of indices showed no unusual trends in either case. The maximum and minimum peaks on the final difference Fourier map corresponded to 0.41 and  $-0.39 \text{ e}/\text{\AA}^3$  for **1a** and 0.40 and  $-0.33 \text{ e}/\text{\AA}^3$  for **2b**. Neutral atom scattering factors were taken from Cromer and Waber.<sup>24</sup> Anomalous dispersion effects were included in  $F_c$ ; the values for  $\Delta f'$  and  $\Delta f''$  were also those of Cromer and Waber. All calculations were performed using the TEXSAN crystallographic software package of Molecular Structure Corporation.

**Synthesis of {Pd[P(o-Tol)<sub>3</sub>]<sub>2</sub>} (1a).** To 500 mg of "[Pd(DBA)<sub>2</sub>]" (0.87 mmol) suspended in 60 mL of benzene was added a solution of 2.10 g of tri-*o*-tolylphosphine (6.90 mmol) in 60 mL of benzene. The reaction mixture was stirred at room temperature for 20 h. The purple-brown solution was filtered and concentrated to dryness. The resulting orange-yellow precipitate was suspended in 150 mL of diethyl ether. This suspension was allowed to stand 24 h at  $-30^\circ\text{C}$  to complete precipitation of the yellow, powdery **1a** (70–80%). Recrystallization of this compound was achieved in the presence of excess phosphine from a benzene/ether solvent mixture. However, crystalline material was also obtained directly from a filtered reaction medium after addition of ether. This procedure was slower than the above method for obtaining **1a** as a powder. Quantitative crystallization of the **1a** from the reaction medium can require standing for 2 weeks. IR (KBr): 3055 (m), 3004 (m), 2964 (m), 2926 (m), 2855 (w) 1587 (m), 1563 (w), 1465 (s), 1447 (s), 1377 (m), 1274 (m), 1206 (m), 1158 (m), 1125 (m), 1068 (m), 1031 (m), 1027 (s), 800 (m), 751 (s), 711 (s), 675 (w), 665 (m), 556 (s), 518 (s), 461 (s), 406 (s)  $\text{cm}^{-1}$ .

<sup>1</sup>H NMR (C<sub>6</sub>D<sub>6</sub>):  $\delta$  6.98 (m, 18H), 6.77 (m, 6H), 2.92 (s, 18H). <sup>31</sup>P{<sup>1</sup>H} NMR (C<sub>6</sub>D<sub>6</sub>):  $\delta$  -6.72 (s). FAB MS (*m*-nitrobenzyl alcohol/trifluoroacetic acid)  $m/z$  714 ( $M^+$ ). Anal. Calcd for C<sub>42</sub>-H<sub>42</sub>P<sub>2</sub>Pd: C, 70.54; H, 5.92. Found: C, 70.57; H, 5.97.

**Synthesis of {Pd[P(2,4-(Me)<sub>2</sub>C<sub>6</sub>H<sub>3</sub>)]<sub>2</sub>} (1b).** To 200 mg of "[Pd(DBA)<sub>2</sub>]" (0.34 mmol) suspended in 60 mL of benzene was added a solution of 1.00 g of tris(2,4-dimethylphenyl)phosphine (2.89 mmol) in 60 mL of benzene. The reaction mixture was stirred at room temperature for 30 h. The orange solution was then filtered and concentrated to 10 mL. Diethyl ether (350 mL) was added to this solution, and the resulting mixture was allowed to stand overnight at  $-30^\circ\text{C}$  to complete precipitation of **1b**. The product was isolated by decanting the mother liquor, washing the solid with ether, and drying the solid *in vacuo* (175 mg, 65%). IR (KBr): 3055 (w), 3003 (m), 2960 (m), 2918 (m), 2860 (w) 1602 (s), 1557 (w), 1476 (s), 1442 (s), 1376 (w), 1281 (w), 1230 (s), 1170 (m), 1033 (m), 927 (s), 816 (s), 727 (m), 713 (w), 628 (m), 605 (m), 558 (m), 468 (s), 445 (m), 411 (m)  $\text{cm}^{-1}$ . <sup>1</sup>H NMR (C<sub>6</sub>D<sub>6</sub>):  $\delta$  7.00 (m, 6H), 6.85 (s, 6H), 6.68 (d,  $J = 8 \text{ Hz}$ , 6H), 3.05 (s, 18H), 1.98 (s, 18H). <sup>31</sup>P{<sup>1</sup>H} NMR (C<sub>6</sub>D<sub>6</sub>):  $\delta$  -8.50 (s). Anal. Calcd for C<sub>48</sub>H<sub>54</sub>P<sub>2</sub>-Pd: C, 72.13; H, 6.81. Found: C, 72.33; H, 6.73.

**Synthesis of {Pd[P(2-Me-4-FC<sub>6</sub>H<sub>3</sub>)]<sub>2</sub>} (1c).** To 80 mg of "[Pd(DBA)<sub>2</sub>]" (0.14 mmol) suspended in 10 mL of benzene was added a solution of 500 mg of tris(2-methyl-4-fluorophenyl)phosphine (1.40 mmol) in 60 mL of benzene. The reaction mixture was stirred at room temperature for 4 h. The orange solution was then filtered through Celite and evaporated to dryness, and 25 mL of degassed methanol was added to yield an orange solution and a yellow precipitate that was mainly free phosphine. This mixture was immediately filtered again through Celite. After standing at room temperature, yellow crystals of **1c** formed from the filtrate. The product was isolated by decanting the mother liquor, washing the solid with ether, and drying the solid *in vacuo* (55 mg, 48%). IR (KBr): 3054 (m), 2969 (s), 2922 (m), 2858 (w), 1600 (vs), 1578 (vs), 1475 (vs), 1439 (s), 1397 (m), 1279 (vs), 1226 (vs), 1158 (s), 1115 (w), 1058 (m), 1032 (w), 1001 (m), 947 (vs), 868 (vs), 816 (vs), 728 (s), 710 (w), 655 (vw), 636 (vw), 607 (m), 576 (s), 545 (s), 502 (m), 487 (vs), 458 (vs), 420 (vs)  $\text{cm}^{-1}$ . <sup>1</sup>H NMR (C<sub>6</sub>D<sub>6</sub>):  $\delta$  6.70 (m, 12H), 6.51 (m, 6H), 2.70 (s, 18H). <sup>31</sup>P{<sup>1</sup>H} NMR (C<sub>6</sub>D<sub>6</sub>):  $\delta$  -9.52 (s).

**Synthesis of {Pd[P(*t*-Bu)<sub>3</sub>]<sub>2</sub>} (1d).** To 200 mg of "[Pd(DBA)<sub>2</sub>]" (0.34 mmol) suspended in 10 mL of benzene was added a solution of 350 mg of tri-*tert*-butylphosphine (1.7 mmol) in 5 mL of benzene. The reaction mixture was stirred at room temperature for 15 h. The orange solution was then filtered, evaporated to dryness, dissolved in 5 mL of diethyl ether, and cooled at  $-30^\circ\text{C}$ . After 15 h, 160 mg (65%) of yellow {Pd[P(*t*-Bu)<sub>3</sub>]<sub>2</sub>} (**1d**) was obtained. The compound<sup>25,26</sup> was identified by <sup>1</sup>H and <sup>31</sup>P{<sup>1</sup>H} NMR spectroscopy and was found to be spectroscopically pure.

**Isolation of [Pd(TMPP)(DBA)<sub>2</sub>].** To 200 mg of "[Pd(DBA)<sub>2</sub>]" (0.34 mmol) suspended in 10 mL of benzene was added a solution of 2.10 g of tris(2,4,6-trimethoxyphenyl)phosphine (0.68 mmol) in 50 mL of benzene. The reaction mixture was stirred at room temperature for 20 h. The purple-red solution was then filtered through a plug of Celite and concentrated to 30 mL. Diethyl ether was added (100 mL). The solution was cooled at  $-30^\circ\text{C}$  and allowed to stand overnight. A first crop of the orange complex (TMPP)Pd(DBA)<sub>2</sub> (40%) was separated and washed three times with diethyl ether. A second crop was obtained by layering with additional ether. Crystalline material was also obtained by slow diffusion of *n*-pentane into a benzene solution of the complex at room temperature. IR (KBr): 3054 (w), 2998 (w), 2934 (m), 2834 (w) 1652 (m), 1593 (vs), 1452 (s), 1406 (s), 1331 (s), 1285 (w), 1225 (s), 1204 (s), 1158 (s), 1125 (s), 1088 (s), 1036 (m), 981 (w), 951 (m), 922 (w), 875 (vw), 808 (m), 762 (m), 698 (m), 634 (vw), 554 (w), 552 (w), 476 (m), 439 (w)  $\text{cm}^{-1}$ . <sup>1</sup>H NMR (THF-

(24) Cromer, D. T.; Waber, J. T. *International Tables for X-ray Crystallography*; The Kynoch Press: Birmingham England, 1974; Vol. 4.

(25) Yoshida, T.; Otsuka, S. *Inorg. Synth.* **1985**, *28*, 113–119.

(26) Yoshida, T.; Otsuka, S. *J. Am. Chem. Soc.* **1977**, *99*, 2134–2140.



$d_8$ ):  $\delta$  7.21 (broad s, 30H), 6.02 (broad s, 4H), 3.73 (broad s, 9H), 3.41 (broad s, 18H).  $^{31}P\{^1H\}$  NMR ( $C_6D_6$ ):  $\delta$  31.6 (s). Anal. Calcd for  $C_{61}H_{61}O_{11}PPd$ : C, 66.15; H, 5.55. Found: C, 66.13; H, 5.97.

**Isolation of  $[Pd(PCy_3)_2(DBA)]$ .** To 250 mg of "[Pd(DBA) $_2$ ]" (0.43 mmol) suspended in 60 mL of benzene was added 4.75 g (3.42 mmol) of tricyclohexylphosphine as a 20% solution in toluene. The reaction mixture was stirred at room temperature for 24 h. The resulting orange solution was then filtered through a plug of Celite and concentrated to 5 mL. Diethyl ether (15 mL) was added. Cooling of the solution at  $-30^\circ C$  precipitated 225 mg of an orange solid along with yellow crystals. The yellow crystals were separated from the orange solid and identified as free phosphine by NMR spectroscopy. The orange precipitate was identified as the known<sup>11</sup>  $[Pd(PCy_3)_2(DBA)]$  (68%).  $^{31}P\{^1H\}$  NMR ( $C_6D_6$ ,  $60^\circ C$ ):  $\delta$  31.

**General Procedure for the Synthesis of the Dimeric Compounds 2.** Compound **1a** (500 mg, 0.70 mmol) was suspended in a solution of 5 equiv of the corresponding aryl bromide in 20 mL of benzene. The reaction mixture was stirred at room temperature for 5 h. The resulting yellow solution was then filtered and concentrated to 2–5 mL, and 100 mL of diethyl ether was added. The solution was cooled at  $-30^\circ C$  for 1 h in order to complete precipitation of the yellow air-stable aryl halide complexes **2a–g**. Alternatively, the compounds were obtained as crystalline materials by slow diffusion of *n*-pentane or diethyl ether into the filtered reaction solution.

$\{Pd[P(o-Tol)_3](p-MeC_6H_4)(Br)\}_2$  (**2a**). IR (KBr): 3056 (w), 3010 (w), 2919 (w), 2861 (w), 1589 (m), 1563 (w), 1478 (vs), 1446 (vw), 1381 (m), 1277 (m), 1206 (m), 1134 (m), 1068 (m), 1056 (m), 1031 (m), 1018 (s), 797 (s), 750 (vs), 712 (s), 673 (m), 569 (s), 537 (s), 463 (w)  $cm^{-1}$ .  $^1H$  NMR ( $C_7D_8$ ,  $100^\circ C$ ):  $\delta$  7.95 (broad s, 6H), 7.00 (m, 10H), 6.84 (m, 12H), 6.39 (d, 8.4 Hz, 4H), 2.35 (s, 18H), 1.85 (s, 6H).  $^{31}P\{^1H\}$  NMR ( $C_7D_8$ ,  $25^\circ C$ ):  $\delta$  28.6 (broad s).  $^{31}P\{^1H\}$  NMR ( $C_7D_8$ ,  $-80^\circ C$ ):  $\delta$  30.3 (s), 27.7 (s), approximate ratio 5:6. FAB MS (*m*-nitrobenzyl alcohol)  $m/z$  501  $[M - Br]^+$ , 410  $[M - Tol - Br]^+$ . Anal. Calcd for  $C_{28}H_{28}PBrPd$ : C, 57.8; H, 4.85; Br, 13.73. Found: C, 57.95; H, 5.01; Br, 13.60. 87% yield.

$\{Pd[P(o-Tol)_3][p-(n-Bu)C_6H_4](Br)\}_2$  (**2b**). IR (KBr): 3056 (m), 2955 (vs), 2926 (vs), 2854 (m), 1588 (m), 1580 (m), 1564 (w), 1477 (vs), 1447 (vs), 1381 (m), 1280 (m), 1201 (m), 1130 (m), 1068 (m), 1052 (m), 1031 (m), 1008 (s), 803 (s), 752 (vs), 714 (s), 678 (s), 564 (s), 534 (s), 477 (vs)  $cm^{-1}$ .  $^1H$  NMR ( $C_6D_6$ ,  $80^\circ C$ ):  $\delta$  7.95 (broad s, 6H), 7.00 (m, 10H), 6.87 (m, 12H), 6.45 (d, 8.4 Hz, 4H), 2.45–2.05 (m, *o*-Me groups on phosphine and  $-CH_2CH_2CH_2CH_3$ , 22H), 1.22–1.06 (m,  $-CH_2CH_2CH_2CH_3$ , 8H), 0.9 (m,  $-CH_2CH_2CH_2CH_3$ , 6H).  $^{31}P\{^1H\}$  NMR ( $CD_2Cl_2$ ,  $25^\circ C$ ):  $\delta$  28.8 (broad s).  $^{31}P\{^1H\}$  NMR ( $CD_2Cl_2$ ,  $-80^\circ C$ ):  $\delta$  29.9 (s), 27.5 (s), approximate ratio 1:4. Anal. Calcd for  $C_{31}H_{34}PBrPd$ : C, 59.68; H, 5.49. Found: C, 60.13; H, 5.56. 89% yield.

$\{Pd[P(o-Tol)_3][p-(t-Bu)C_6H_4](Br)\}_2$  (**2c**). This compound was obtained in 42% yield by identical methods to those for other aryl bromide complexes. It was more soluble than the other derivatives, and concentration of the reaction medium to dryness, addition of the diethyl ether, and cooling at  $-30^\circ C$  gave 72% yield. IR (KBr): 3056 (m), 3007 (m), 2959 (vs), 2900 (sh), 2863 (m), 1590 (m), 1576 (m), 1565 (w), 1472, 1446 (vs), 1383 (m), 1360 (m), 1280 (m), 1200 (m), 1164 (w), 1130 (m), 1112 (s), 1068 (m), 1031 (m), 1006 (s), 808 (s), 751 (vs), 716 (s), 676 (w), 663 (w), 554 (s), 549 (s), 535 (s), 530 (w), 526 (w), 480 (vs), 466 (vs)  $cm^{-1}$ .  $^1H$  NMR ( $C_6D_6$ ,  $70^\circ C$ ):  $\delta$  7.90 (broad s, 6H), 6.94–7.15 (m, 14H), 6.79 (broad s, 6H), 6.55 (d, 9 Hz, 4H), 2.22 (broad s, 18H), 1.03 (s, 18H).  $^{31}P\{^1H\}$  NMR ( $C_7D_8$ ):  $\delta$  28.6 (broad s).  $^{31}P\{^1H\}$  NMR ( $C_7D_8$ ,  $-80^\circ C$ ):  $\delta$  30.2 (s), 28.2 (s), approximate ratio 5:3. Anal. Calcd for  $C_{31}H_{34}PBrPd$ : C, 59.68; H, 5.49. Found: C, 59.68; H, 5.66.

$\{Pd[P(o-Tol)_3](p-FC_6H_4)(Br)\}_2$  (**2d**). IR (KBr): 3056 (s), 3009 (m), 2966 (m), 2918 (m), 1590 (m), 1567 (m), 1475 (vs), 1447 (vs), 1382 (m), 1281 (m), 1216 (vs), 1156 (w), 1131 (m),

1068 (w), 1044 (m), 1007 (s), 950 (vw), 872 (vw), 809 (vs), 752 (vs), 716 (s), 678 (s), 661 (w), 565 (s), 534 (s), 510 (m), 466 (vs)  $cm^{-1}$ .  $^1H$  NMR ( $C_6D_6$ ,  $20^\circ C$ ):  $\delta$  6.2–8.0 (broad m, 32H), 1.75 (v broad s, 18H).  $^{31}P\{^1H\}$  NMR ( $C_6D_6$ ):  $\delta$  28.2 (broad s).  $^{19}F$  NMR ( $CD_2Cl_2$ ):  $\delta$  -126.15 (s). Anal. Calcd for  $C_{28}H_{27}BrFP-Pd^{1/3}C_6H_6$ : C, 57.58; H, 4.67. Found: C, 57.24; H, 4.67. 89% yield.

$\{Pd[(o-Tol)_3P][2,4,6-(CH_3)_3C_6H_2](Br)\}_2$  (**2e**). This compound was too insoluble in common organic solvents after isolation to allow NMR spectroscopic characterization, but it could be characterized by  $^{31}P\{^1H\}$  NMR when analyzed after generation in an NMR sample tube from **1a** and 2,4,6-( $CH_3$ ) $_3C_6H_2Br$ . IR (KBr): 3054, 3006 (m), 2955 (s), 2915 (s), 2861 (w), 1589 (m), 1563 (w), 1447 (vs), 1382 (m), 1281 (m), 1202 (m), 1166 (m), 1129 (m), 1068 (m), 1031 (m), 1013 (w), 945 (w), 846 (m), 804 (m), 751 (vs), 712 (m), 704 (m), 676 (m), 563 (m), 537 (s), 468 (vs)  $cm^{-1}$ .  $^{31}P\{^1H\}$  NMR ( $C_7D_8$ ):  $\delta$  26.2 (broad s).  $^{31}P\{^1H\}$  NMR ( $C_7D_8$ ,  $-80^\circ C$ ):  $\delta$  26.3 (s), 25.7 (s), approximate ratio 4:1. Anal. Calcd for  $C_{28}H_{28}PBrPd$ : C, 58.99; H, 5.45; Br, 13.08. Found: C, 59.22; H, 5.46; Br, 12.95. 70% yield.

$\{Pd[P(o-Tol)_3](p-MeC_6H_4)(I)\}_2$  (**2f**). IR (KBr): 3054 (m), 3008 (m), 2917 (m), 2862 (w), 1586 (m), 1564 (w), 1472 (vs), 1445 (vs), 1381 (m), 1276 (m), 1202 (m), 1163 (m), 1131 (m), 1068 (m), 1051 (m), 1032 (m), 1008 (s), 795 (sh), 788 (s), 753 (vs), 714 (s), 676, 564 (w), 562 (m), 535 (s), 519 (m), 480 (vs), 463 (vs)  $cm^{-1}$ .  $^1H$  NMR ( $CD_2Cl_2$ ,  $20^\circ C$ ):  $\delta$  7–7.4 (v broad m, 28 H), 6.38 (broad s, 4H), 2.5 (flat s, 18H), 2.02 (s, 6H).  $^{31}P\{^1H\}$  NMR ( $CD_2Cl_2$ ):  $\delta$  25.6 (broad s). Anal. Calcd for  $C_{28}H_{28}IPPd$ : C, 53.48; H, 4.49; I, 20.18. Found: C, 53.53; H, 4.71; I, 20.43. 77% yield.

$\{Pd[P(o-Tol)_3](p-NO_2C_6H_4)(I)\}_2$  (**2g**). Due to its very low solubility, this compound precipitated from the reaction medium before addition of ether. IR (KBr): 3057 (s), 3006 (m), 2954 (m), 2862 (m), 1711 (m), 1588 (m), 1553 (vs), 1503 (vs), 1465 (s), 1445 (s), 1380 (w), 1336 (vs), 1220 (m), 1202 (m), 1163 (m), 1131 (m), 1070 (m), 1050 (m), 1042 (s), 1008 (s), 848 (s), 833 (s), 803 (w), 753 (s), 740 (s), 714 (m), 678 (m), 563 (m), 534 (s), 515 (m), 466 (m)  $cm^{-1}$ . Anal. Calcd for  $C_{27}H_{25}INO_2PPd$ : C, 49.15; H, 3.82; N, 2.12. Found: C, 49.25; H, 3.87; N, 2.06. 87% yield.

$\{Pd[P(o-Tol)_3][p-(n-Bu)C_6H_4](Br)\}_2$  (**2h**). Compound **2h** was prepared following a preparation analogous to the one described above for **2b**, but employing Pd(0) complex **1b**. This pale yellow compound was more soluble than was **2b** in the reaction medium, and *n*-pentane was used instead of diethyl ether to precipitate **2h** at  $-30^\circ C$ . The yield of isolated compound was 47%. IR (KBr): 3056 (w), 3003 (m), 2954 (s), 2922 (vs), 2856 (9m), 1603 (s), 1582 (w), 1557 (m), 1478 (vs), 1445 (vs), 1380 (m), 1282 (m), 1229 (s), 1173 (m), 1100 (s), 1056 (s), 1011 (s), 985 (vs), 929 (m), 877 (w), 814 (s), 790 (sh), 770 (sh), 715 (w), 634 (s), 608 (s), 558 (s), 550 (w), 491 (s), 470 (s), 455 (s), 409 (w)  $cm^{-1}$ .  $^{31}P\{^1H\}$  NMR ( $C_7D_8$ ,  $25^\circ C$ ):  $\delta$  26.3 (broad s).  $^{31}P\{^1H\}$  NMR ( $C_7D_8$ ,  $-80^\circ C$ ):  $\delta$  28.4 (s), 26.0 (s), approximate ratio 4:3.

**Synthesis of 2a–c from  $\{Pd[P(o-Tol)_3]_2Cl_2\}$ .** In air, 1.80 g (2.29 mmol) of  $\{Pd[P(o-Tol)_3]_2Cl_2\}$  was suspended in 10 mL of a toluene solution of 800 mg (2.63 mmol) of  $P(o-Tol)_3$ . To this suspension was added 200 mg of NaOH in 10 mL of ethanol. The medium was heated with a reflux condenser at  $90^\circ C$  for 5.5 h under a blanket of nitrogen. After cooling to room temperature, the yellow precipitate was separated from the dark red mother liquor by filtration in air and washed several times with water, ethanol, and finally with ether before being dried under vacuum. Typically, 1.5–1.7 g of powder was obtained, consisting mainly of light yellow **1a** but also containing visible amounts of black palladium side product and presumably significant amounts of starting complex and/or NaCl, as shown by the elemental analysis of the crude product. Anal. Calcd for  $C_{48}H_{54}P_2Pd$ : C, 72.13; H, 6.81. Found: C, 62.61; H, 5.33; Cl, 6.76.

An 800 mg amount of this crude product was stirred with 1–1.3 g of desired aryl bromide (ca. 6 equiv) in 25 mL of

benzene for 5–10 h. The resulting dark suspension was filtered and concentrated to an oil. Addition of 25 mL of ether and cooling at  $-30\text{ }^{\circ}\text{C}$  precipitated **2a–c**. The yellow, air-stable compounds were then washed several times with ether and dried under vacuum. Typical yields were 530–550 mg (79–82%) of **2a**, or 550–600 mg (72–84%) of **2b**. Only 103 mg (18%) of **2c** was isolated from the mother liquor, but 391 mg was obtained by recrystallization of the dark precipitate from  $\text{CH}_2\text{Cl}_2$  layered with ether at  $-30\text{ }^{\circ}\text{C}$ . 67% overall yield based on  $\{\text{Pd}[\text{P}(\text{o-Tol})_3]_2\text{Cl}_2\}$ .

**General Procedure for the Synthesis of the Amine Adducts 3.** To a suspension of **2a–c** in benzene was added 5–10 equiv of amine. In minutes, the yellow aryl halide complex dissolved to give a colorless or very pale yellow solution, depending on the amine. After 20 min, the solution was filtered to separate any black precipitate. The solvent and amine were evaporated to give a white or light yellow solid or an oil. A minimum amount of toluene was then added to dissolve the solid or to double the volume of the oil. *n*-Pentane was then added (10–20 volume equiv), and the solution was cooled to  $-30\text{ }^{\circ}\text{C}$ . The amine adduct precipitated as an air-stable, cream or pale yellow solid, which was washed several times with pentane and dried under vacuum.

**$\{\text{Pd}[\text{P}(\text{o-Tol})_3]_2(\text{Br})(\text{HNET}_2)(\text{p-MeC}_6\text{H}_4)\}$  (3a).** IR (KBr): 3218 (m), 3054 (m), 3053 (m), 2070 (s), 2924 (m), 2860 (m), 1596 (s), 1564 (m), 1482 (s), 1471 (s), 1447 (vs), 1380 (s), 1270 (m), 1202 (m), 1131 (m), 1030 (m), 1013 (s), 850 (w), 826 (w), 793 (s), 757 (vs), 713 (s), 676 (m), 670 (w), 562 (s), 560–490 (w), 537 (s), 480 (s), 467 (s), 433 (w)  $\text{cm}^{-1}$ .  $^1\text{H}$  NMR ( $\text{C}_6\text{D}_6$ ,  $80\text{ }^{\circ}\text{C}$ ):  $\delta$  1.32 (broad s, 6H), 2.02 (s, 3H), 2.09 (broad s, 2H), 2.36 (broad s, 9H), 2.65 (broad s, 2H), 3.60 (broad s, 1H), 6.55 (d, 7.7 Hz, 2H), 6.92 (broad s, 9H), 6.97 (d, 7.7 Hz, 2H), 8.02 (v broad s, 3H).  $^{31}\text{P}\{^1\text{H}\}$  NMR ( $\text{C}_7\text{D}_8$ ,  $25\text{ }^{\circ}\text{C}$ ):  $\delta$  28.6 (broad s).  $^{31}\text{P}\{^1\text{H}\}$  NMR ( $\text{C}_7\text{D}_8$ ,  $-80\text{ }^{\circ}\text{C}$ ):  $\delta$  29.0 (s), 28.5 (s), 26.6 (s), approximate ratio 4:1:2. FAB MS (*m*-nitrobenzyl alcohol)  $m/z$  655  $[\text{M} + \text{H}]^+$ . 30% yield.

**$\{\text{Pd}[\text{P}(\text{o-Tol})_3]_2(\text{H}_2\text{N-}t\text{-Bu})(\text{Br})(\text{p-MeC}_6\text{H}_4)\}$  (3b).** IR (KBr): 3264 (m), 3203 (m), 3125 (w), 3054 (m), 3004 (m), 2965 (m), 2921 (m), 2862 (w), 1588 (m), 1577 (m), 1566 (m), 1480 (s), 1471 (s), 1446 (s), 1395 (m), 1362 (m), 1370 (m), 1279 (m), 1260 (m), 1206 (s), 1164 (w), 1131 (s), 1101 (w), 1068 (w), 1050 (w), 1032 (w), 1012 (m), 942 (w), 924 (w), 817 (m), 802 (s), 752 (vs), 717 (s), 677 (w), 665 (w), 560 (m), 536 (m), 480 (s), 465 (s), 432 (w)  $\text{cm}^{-1}$ .  $^{31}\text{P}\{^1\text{H}\}$  NMR ( $\text{C}_6\text{D}_6$ ):  $\delta$  29.0 (s).  $^{31}\text{P}\{^1\text{H}\}$  NMR ( $\text{C}_7\text{D}_8$ ,  $-80\text{ }^{\circ}\text{C}$ ):  $\delta$  28.9 (s), 27.8 (s), approximate ratio 1:1. Anal. Calcd for  $\text{C}_{32}\text{H}_{39}\text{BrNPPd}$ : C, 58.68; H, 6.00; N, 2.14. Found: C, 58.78; H, 6.10; N, 2.19. 33% yield.

**$\{\text{Pd}[\text{P}(\text{o-Tol})_3]_2(\text{H}_2\text{NPh})(\text{Br})(\text{p-MeC}_6\text{H}_4)\}$  (3c).** IR (KBr): 3224 (w), 3114 (vw), 3054 (m), 3007 (m), 2919 (m), 2862 (w), 1618 (m), 1601 (s), 1588 (m), 1564 (w), 1494 (s), 1479 (s), 1469 (s), 1447 (s), 1381 (m), 1280 (m), 1224 (w), 1204 (w), 1164 (w), 1131 (w), 1068 (m), 1051 (m), 1031 (m), 1010 (s), 999 (w), 873 (w), 791 (s), 752 (vs), 715 (s), 693 (s), 677 (w), 663 (w), 561 (m), 535 (m), 480 (s), 466 (s)  $\text{cm}^{-1}$ .  $^{31}\text{P}\{^1\text{H}\}$  NMR ( $\text{C}_6\text{D}_6$ ):  $\delta$  28.8 (s).  $^{31}\text{P}\{^1\text{H}\}$  NMR ( $\text{C}_7\text{D}_8$ ,  $-80\text{ }^{\circ}\text{C}$ ):  $\delta$  29.7 (s), 29.3 (s), 27.5 (s), approximate ratio 4:2:1. 35% yield.

**$\{\text{Pd}[\text{P}(\text{o-Tol})_3]_2(\text{HNET}_2)(\text{Br})[\text{p-}(n\text{-Bu})\text{C}_6\text{H}_4]\}$  (3d).** Suitable crystals of this compound were obtained, and an X-ray diffraction study was conducted.<sup>27</sup> Although the data set was of poor quality, and detailed conclusions on geometry are unwarranted, trans disposition of phosphine and amine were clearly determined. IR (KBr): 3290 (w), 3203 (m), 3124 (w), 3053 (s), 3004 (m), 2960 (vs), 2926 (vs), 2868 (s), 1584 (s), 1569 (m), 1469 (vs), 1448 (vs), 1378 (s), 1280 (m), 1262 (m), 1162 (w), 1149 (w), 1131 (m), 1103 (w), 1068 (m), 1052 (m), 1027 (s), 1010 (s), 865 (vw), 823 (m), 751 (vs), 736 (m), 717 (s), 696 (w), 677 (m), 664 (w), 563 (s), 550 (m), 520 (m), 479 (s), 465 (s), 433 (w)  $\text{cm}^{-1}$ .  $^{31}\text{P}\{^1\text{H}\}$  NMR ( $\text{C}_7\text{D}_8$ ):  $\delta$  29.4 (s).  $^{31}\text{P}\{^1\text{H}\}$  NMR ( $\text{C}_7\text{D}_8$ ,  $-80\text{ }^{\circ}\text{C}$ ):  $\delta$  30.2 (s), 29.4 (s), approximate ratio 1:20.  $^{31}\text{P}\{^1\text{H}\}$  NMR (THF,  $20\text{ }^{\circ}\text{C}$ ):  $\delta$  28.9 (s).  $^{31}\text{P}\{^1\text{H}\}$  NMR (THF,  $-70\text{ }^{\circ}\text{C}$ ):  $\delta$  28.6 (s). 55% yield.

**$\{\text{Pd}[\text{P}(\text{o-Tol})_3]_2(\text{H}_2\text{N-}t\text{-Bu})(\text{Br})[\text{p-}(n\text{-Bu})\text{C}_6\text{H}_4]\}$  (3e).** IR (KBr): 3307 (m), 3225 (m), 3142 (w), 3052 (s), 3006 (m), 2960 (vs), 2928 (vs), 2858 (s), 1590 (m), 1566 (s), 1470 (vs), 1446 (vs), 1395 (m), 1370 (m), 1281 (m), 1261 (m), 1202 (s), 1163 (w), 1131 (s), 1067 (w), 1055 (w), 1027 (w), 1010 (s), 925 (vw), 899 (w), 803 (s), 676 (w), 664 (w), 562 (m), 536 (s), 520 (m), 480 (s), 464 (s), 416 (w)  $\text{cm}^{-1}$ .  $^{31}\text{P}\{^1\text{H}\}$  NMR ( $\text{C}_7\text{D}_8$ ):  $\delta$  29.4 (s).  $^{31}\text{P}\{^1\text{H}\}$  NMR ( $\text{C}_7\text{D}_8$ ,  $-80\text{ }^{\circ}\text{C}$ ):  $\delta$  29.5 (s). Anal. Calcd for  $\text{C}_{35}\text{H}_{45}\text{BrNPPd}$ : C, 60.31; H, 6.51; N, 2.01. Found: C, 60.41; H, 6.49; N, 2.04. 50% yield.

**$\{\text{Pd}[\text{P}(\text{o-Tol})_3]_2(\text{H}_2\text{NPh})(\text{Br})[\text{p-}(n\text{-Bu})\text{C}_6\text{H}_4]\}$  (3f).** IR (KBr): 3307 (m), 3231 (m), 3142 (w), 3054 (m), 3006 (m), 2955 (s), 2923 (s), 2855 (m), 1618 (w), 1600 (vs), 1587 (s), 1565 (m), 1491 (s), 1468 (vs), 1448 (vs), 1380 (m), 1282 (m), 1224 (m), 1200 (m), 1164 (w), 1131 (m), 1108 (vw), 1068 (m), 1055 (m), 1031 (vs), 1010 (s), 997 (m), 872 (vw), 802 (s), 777 (m), 753 (vs), 715 (s), 649 (s), 678 (m), 664 (w), 642 (w), 619 (vw), 562 (m), 550 (m), 535 (s), 521 (m), 481 (s), 468 (vs), 432 (w)  $\text{cm}^{-1}$ .  $^{31}\text{P}\{^1\text{H}\}$  NMR ( $\text{C}_7\text{D}_8$ ):  $\delta$  29.8 (s).  $^{31}\text{P}\{^1\text{H}\}$  NMR ( $\text{C}_7\text{D}_8$ ,  $-80\text{ }^{\circ}\text{C}$ ):  $\delta$  29.8 (s), 27.9 (s), approximate ratio 5:1. Anal. Calcd for  $\text{C}_{37}\text{H}_{41}\text{BrNPPd}$ : C, 61.98; H, 5.76; N, 1.95. Found: C, 61.95; H, 5.83; N, 2.06. 30% yield.

**$\{\text{Pd}[\text{P}(\text{o-Tol})_3]_2(\text{HNET}_2)(\text{Br})[\text{p-}(t\text{-Bu})\text{C}_6\text{H}_4]\}$  (3g).** IR (KBr): 3261 (vw), 3207 (m), 3125 (vw), 3054 (s), 3006 (m), 2963 (vs), 2926 (sh), 2866 (s), 1590 (s), 1578 (m), 1569 (w), 1471 (vs), 1447 (vs), 1381 (s), 1360 (m), 1282 (m), 1269 (m), 1201 (m), 1163 (w), 1149 (w), 1131 (m), 1114 (m), 1103 (w), 1069 (m), 1017 (s), 1009 (vs), 865 (vw), 812 (s), 753 (vs), 736 (m), 716 (s), 678 (m), 664 (w), 562 (s), 536 (s), 520 (m), 485 (s), 479 (s), 468 (s), 433 (w)  $\text{cm}^{-1}$ .  $^{31}\text{P}\{^1\text{H}\}$  NMR ( $\text{C}_7\text{D}_8$ ):  $\delta$  27.8 (s).  $^{31}\text{P}\{^1\text{H}\}$  NMR ( $\text{C}_7\text{D}_8$ ,  $-80\text{ }^{\circ}\text{C}$ ):  $\delta$  29.1 (s), 28.4 (s), 26.4 (s), approximate ratio 4:1:5. Anal. Calcd for  $\text{C}_{35}\text{H}_{45}\text{BrNPPd}$ : C, 60.31; H, 6.51; N, 2.01. Found: C, 60.20; H, 6.57; N, 2.01. 69% yield.

**$\{\text{Pd}[\text{P}(\text{o-Tol})_3]_2(\text{H}_2\text{N-}t\text{-Bu})(\text{Br})[\text{p-}(t\text{-Bu})\text{C}_6\text{H}_4]\}$  (3h).** IR (KBr): 3310 (m), 3242 (w), 3127 (vw), 3056 (s), 3006 (sh), 2963 (vs), 2928 (sh), 2865 (s), 1590 (m), 1564 (s), 1471 (vs), 1446 (vs), 1396 (m), 1372 (s), 1283 (m), 1257 (m), 1203 (s), 1163 (w), 1131 (s), 1116 (s), 1101 (m), 1068 (w), 1033 (w), 1021 (w), 1007 (s), 925 (vw), 900 (w), 813 (s), 657 (vs), 649 (vs), 728 (w), 717 (m), 678 (m), 663 (vw), 562 (s), 536 (m), 519 (m), 511 (w), 482 (s), 478 (s), 464 (vs), 416 (vw)  $\text{cm}^{-1}$ .  $^{31}\text{P}\{^1\text{H}\}$  NMR ( $\text{C}_7\text{D}_8$ ):  $\delta$  29.3 (s).  $^{31}\text{P}\{^1\text{H}\}$  NMR ( $\text{C}_7\text{D}_8$ ,  $-80\text{ }^{\circ}\text{C}$ ):  $\delta$  29.8 (s), 29.3 (s), approximate ratio 1:4. Anal. Calcd for  $\text{C}_{35}\text{H}_{45}\text{BrNPPd}$ : C, 60.31; H, 6.51; N, 2.01. Found: C, 60.30; H, 6.54; N, 2.03. 35% yield.

**Synthesis of 4.** Reaction of **1a** with 2-Iodo-2'-amino-biphenyl. A 100 mg amount of **1a** (0.14 mmol) was suspended in a solution of 105 mg of 2-iodo-2'-aminobiphenyl (0.36 mmol) in 10 mL of benzene. The reaction mixture was stirred at room temperature for 12 h. The resulting yellow solution was then filtered and evaporated to dryness. Diethyl ether (5 mL) was added to dissolve the resulting solid, and this solution was layered with 20 mL of *n*-pentane. After cooling at  $-30\text{ }^{\circ}\text{C}$  for 2 days, a light-orange, air-stable crystalline product was isolated (80 mg, 81%). Crystalline material was also obtained by slow evaporation of a methylene chloride solution. IR (KBr): 3325 (m), 3252 (m), 3201 (w), 3052 (m), 2971 (m), 1609 (w), 1586 (s), 1565 (s), 1491 (s), 1443 (vs), 1423 (s), 1381 (m), 1243 (w), 1200 (w), 1162 (m), 1129 (m), 1098 (s), 1070 (m), 1032 (s), 1020 (s), 1002 (s), 931 (w), 870 (w), 840 (w), 821 (w), 803 (m), 751 (vs), 729 (s), 712 (s), 676 (w), 663 (w), 653 (w), 616 (w), 570 (m), 562 (m), 548 (m), 535 (m), 516 (m), 481 (s), 467 (s), 439 (w)  $\text{cm}^{-1}$ .  $^1\text{H}$  NMR (toluene- $d_6$ ):  $\delta$  9.34 (broad d, 12 Hz, 1H), 6.4–7.4 (m, 19H), 4.84 (broad s, 1H), 3.74 (broad s, 1H), 3.47 (broad s, 3H), 1.49 (broad s, 3H), 0.96 (broad s, 3H).  $^{31}\text{P}\{^1\text{H}\}$  NMR (toluene- $d_6$ ):  $\delta$  31.6 (broad s).  $^{31}\text{P}\{^1\text{H}\}$  NMR ( $\text{CD}_2\text{Cl}_2$ ,  $-80\text{ }^{\circ}\text{C}$ ):  $\delta$  34.0 (s), 31.6 (s), approximate ratio 1:6. Anal. Calcd for  $\text{C}_{33}\text{H}_{31}\text{NIPdC}_4\text{H}_{10}\text{O}$ : C, 56.97; H, 5.30; N, 1.80. Found: C, 57.05; H, 5.30; N, 1.73.

## Results and Discussion

**Synthesis of  $\{\text{Pd}[\text{P}(\text{o-Tol})_3]_2\}$  (1a).** Although a number of Pd(0) complexes containing phosphine ligands

(27)  $P_{21}/c$  (No. 14);  $a = 12.27(8)\text{ \AA}$ ,  $b = 10.9(1)\text{ \AA}$ ,  $c = 30.3(2)\text{ \AA}$ ,  $\beta = 94(1)^\circ$ ,  $V = 4.0(1) \times 10^3$ ,  $Z = 4$ ;  $R_{\text{int}} = 7.0$ .

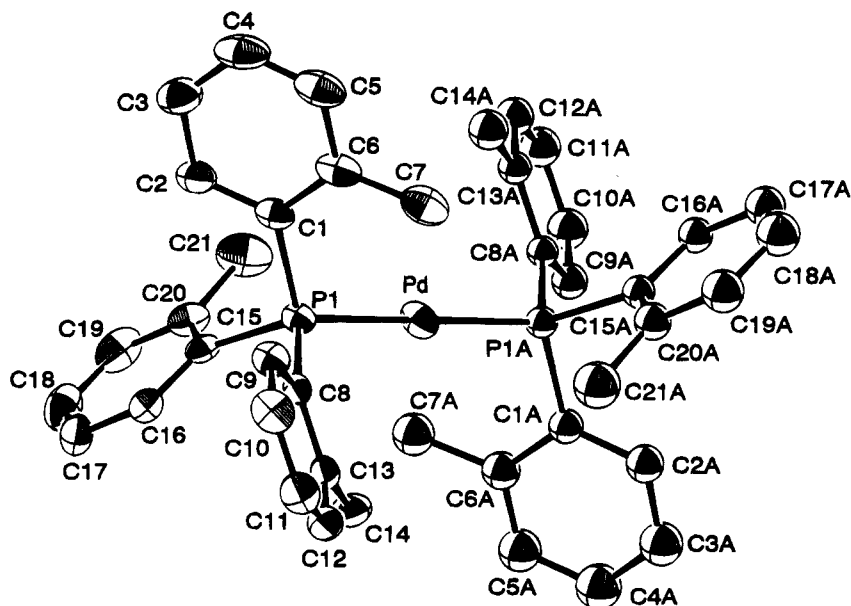
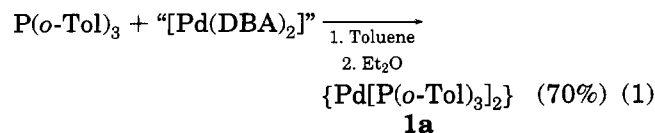


Figure 1. ORTEP diagram of  $[(o-Tol)_3P]_2Pd$  (**1a**).

are known, the only reported preparation of  $\{Pd[P(o-Tol)_3]_2\}$  (**1a**), an important intermediate in catalysis, was contained in a patent. The spectroscopic characterization was limited to IR spectroscopy. This synthetic procedure was reported on a 40 g scale and involved reduction of  $\{Pd[P(o-Tol)_3]_2Cl_2\}$  by alcohol in the presence of base. However, our initial attempts to reproduce this preparation on a smaller scale did not provide pure samples of **1a**. The major byproducts were a black insoluble material, typical of reduced palladium, and the starting dichloride.

We made a number of attempts to optimize the conditions of the reaction in order to obtain complete reaction of starting material without significant product decomposition. It proved difficult to achieve quantitative reduction of the very slightly soluble  $\{Pd[P(o-Tol)_3]_2Cl_2\}$  while limiting the decomposition of the thermally sensitive **1a**.  $PhNO_2$  rather than toluene solvent, MeOH or *i*-PrOH rather than EtOH, and  $\{Pd[P(o-Tol)_3]_2Br_2\}$  instead of  $\{Pd[P(o-Tol)_3]_2Cl_2\}$  were all less effective than was using a reaction temperature of 90 °C and a reaction time of 5.5 h. However, even under these optimized conditions, we were not able to isolate **1a** in pure form. Since the low solubility and thermal instability of **1a** precluded separation from  $\{Pd[P(o-Tol)_3]_2Cl_2\}$ , a different route to pure **1a** was required.

We investigated the possibility of isolating this complex from the labile palladium(0) compound  $[Pd_2(DBA)_3]$ , since it was known that bisphosphine palladium(0) complexes could be generated *in situ* from this precursor. From reaction of crude  $[Pd(DBA)_2]$ <sup>21</sup> with a 7-fold excess of tri-*o*-tolylphosphine, we were able to crystallize **1a** from the reaction medium (eq 1). After



reaction of phosphine with  $[Pd(DBA)_2]$  in benzene for 20 h, followed by filtration of any solid material remaining, ether was added, and upon standing at room temperature, crystalline **1a** was obtained after 3 to 4 days. Alternatively, evaporation of the solvent and

washing of the resulting solid several times with ether gave pure **1a** as a yellow powder. The stoichiometry of **1a** was assessed by an X-ray diffraction study (Figure 1) and elemental analysis.

Complex **1a** was not present in reaction solutions at high enough concentrations for it to be detected by  $^{31}P\{-^1H\}$  NMR spectroscopy. No sharp resonance for **1a** at  $\delta -6.72$  was observed. Rather, the reaction solution displayed a broad resonance near  $\delta 20$ , whose precise chemical shift depended on the relative amount of DBA and phosphine present in the medium. We assigned this resonance to Pd(0) compounds containing both DBA and phosphine. These complexes are likely to account for the deep orange-red color of the reaction mixture. Indeed, addition of DBA to a suspension of pure **1a** in benzene led to immediate formation of a homogeneous solution with both the same orange-red color and  $^{31}P\{-^1H\}$  NMR resonance near  $\delta 20$  as the reaction medium from which **1a** was isolated.  $^{31}P\{-^1H\}$  NMR spectra of solutions generated from **1a** and DBA also showed a sharp resonance for free  $P(o-Tol)_3$  of equal intensity to that at  $\delta 20$ , indicating that one ligand from **1a** had been displaced. Palladium complexes containing both DBA and tertiary phosphines are known,<sup>10</sup> but their stoichiometry is difficult to establish by spectroscopic means. The broad  $^{31}P\{-^1H\}$  resonance corresponding to the Pd(0) complex with both DBA and phosphine sharpened to a large number of singlets at low temperature and further attempts at spectroscopic characterization were not conclusive.

It appears that the preparation of **1a** from  $P(o-Tol)_3$  and  $[Pd(DBA)_2]$  is made possible by crystallization of the small amounts of **1a** created by the equilibria of eq 2. These equilibria would be constantly reestablished as **1a** crystallized or precipitated from solution. Thus, high yields of **1a** can be obtained, although the concentration of this compound in solution was below the detection limits of  $^{31}P$  NMR spectroscopy.

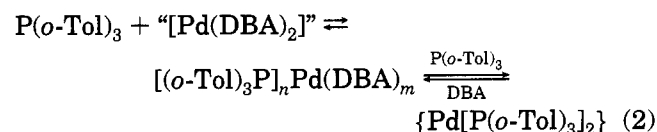


**Table 3. Bond Distances (Å) for Non-Hydrogen Atoms in [(*o*-Tol)<sub>3</sub>P]<sub>2</sub>Pd (1a)<sup>a</sup>**

Pd-P1	2.276(1)	C8-C13	1.402(5)
Pd-P1	2.276(1)	C9-C10	1.391(5)
P1-C1	1.840(4)	C10-C11	1.371(5)
P1-C8	1.842(3)	C11-C12	1.383(5)
P1-C15	1.845(4)	C12-C13	1.387(5)
C1-C2	1.392(5)	C13-C14	1.511(5)
C1-C6	1.410(5)	C15-C16	1.392(5)
C2-C3	1.397(5)	C15-C20	1.404(5)
C3-C4	1.381(6)	C16-C17	1.393(5)
C4-C5	1.371(6)	C17-C18	1.369(6)
C5-C6	1.398(5)	C18-C19	1.377(6)
C6-C7	1.503(6)	C19-C20	1.395(5)
C8-C9	1.398(4)	C20-C21	1.506(5)

<sup>a</sup> Distances are in angstroms. Estimated standard deviations in the least significant figure are given in parentheses.

**Table 4. Bond Angles (deg) for Non-Hydrogen Atoms in [(*o*-Tol)<sub>3</sub>P]<sub>2</sub>Pd (1a)<sup>a</sup>**

P1-Pd-P1	180.00	C9-C8-C13	119.1(3)
Pd-P1-C1	113.2(1)	C8-C9-C10	121.0(3)
Pd-P1-C8	115.3(1)	C9-C10-C11	119.6(3)
Pd-P1-C15	115.9(1)	C10-C11-C12	119.9(3)
C1-P1-C8	103.4(1)	C11-C12-C13	121.8(3)
C1-P1-C15	104.7(2)	C8-C13-C12	118.6(3)
C8-P1-C15	102.8(2)	C8-C13-C14	122.3(3)
P1-C1-C2	121.4(3)	C12-C13-C14	119.1(3)
P1-C1-C6	118.9(3)	P1-C15-C16	120.9(3)
C2-C1-C6	119.6(3)	P1-C15-C20	120.1(3)
C1-C2-C3	120.7(4)	C16-C15-C20	118.9(3)
C2-C3-C4	119.4(4)	C15-C16-C17	121.6(3)
C3-C4-C5	120.3(4)	C16-C17-C18	119.5(4)
C4-C5-C6	121.7(4)	C17-C18-C19	119.4(4)
C1-C6-C5	118.3(4)	C18-C19-C20	122.6(4)
C1-C6-C7	122.7(3)	C15-C20-C19	118.0(4)
C5-C6-C7	119.1(4)	C15-C20-C21	122.8(4)
P1-C8-C9	120.7(3)	C19-C20-C21	119.2(4)
P1-C8-C13	120.2(2)		

<sup>a</sup> Angles are in degrees. Estimated standard deviations in the least significant figure are given in parentheses.

**Spectroscopic and Structural Characterization of {Pd[P(*o*-Tol)<sub>3</sub>]<sub>2</sub>} (1a).** Yellow blocks of **1a** that were suitable for X-ray diffraction studies were obtained directly from the reaction. An ORTEP drawing is given in Figure 1; relevant bond lengths and angles are given in Tables 3 and 4. The palladium atom lay on an inversion center, creating a geometry about the palladium center that was exactly linear, with the metal center protected by the bulk of the two phosphines. Computed intramolecular distances between the nearest hydrogen atom on each phosphine methyl group in **1a** were 2.508(1), 2.502(1), and 2.699(1) Å. The first two distances listed are roughly 0.2 Å shorter than those attributed to a nonbonding interaction of *t*-Bu hydrogens with the palladium center in other L<sub>2</sub>Pd(0) complexes of P(*t*-Bu)<sub>3</sub> and P(Ph)(*t*-Bu)<sub>2</sub>.<sup>28</sup> However, the symmetry and distances in **1a** would require that a C-H bond on at least four and perhaps all six methyl groups be interacting with the metal. We feel that this number of C-H-M interactions is unreasonable, that these distances reflect simple geometric constraints of the tri-*o*-tolylphosphine ligand, and that it is not possible to support the presence of a C-H-M interaction from these structural and spectroscopic data.

Consistent with the absence of a strong C-H bond interaction with the palladium center, IR spectroscopy in the solid state showed no C-H vibrations at frequencies that are reduced from the typical values for P(*o*-

Tol)<sub>3</sub>. The IR spectrum for **1a** was essentially identical to that for {Pd[P(*o*-Tol)<sub>3</sub>]<sub>2</sub>Cl<sub>2</sub>}. Moreover, the <sup>1</sup>H NMR spectroscopic resonance of the ligand methyl group was located downfield rather than upfield of the free ligand.

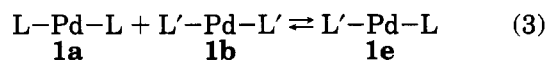
**Attempted Synthesis of Other Bisphosphine Complexes.** We attempted to isolate other bisphosphine complexes of large phosphines. Ligands possessing a larger cone angle than P(*o*-Tol)<sub>3</sub>, such as trimesitylphosphine gave no compound analogous to **1a**. In fact, only free phosphine was detected in the <sup>31</sup>P NMR spectrum of the reaction mixture, indicating that this ligand did not displace any of the coordinated DBA. L<sub>2</sub>-Pd compounds with ligands possessing a cone angle comparable to that of P(*o*-Tol)<sub>3</sub> were isolated in the case of tris(2,4-dimethylphenyl)phosphine and tris(2-methyl-4-fluorophenyl)phosphine. Reactions with tris(2,4,6-trimethoxyphenyl)phosphine (TMPP) gave an orange, crystalline product that contained coordinated DBA. This isolated material displayed integrations in the <sup>1</sup>H NMR spectra and elemental analysis that corresponded to the stoichiometry [Pd(TMPP)(DBA)<sub>2</sub>]. Tris(2-methoxyphenyl)phosphine failed to yield the corresponding bisphosphine complex due to inappropriate solubilities. The free phosphine ligand was only slightly soluble in benzene/ether mixtures, leading to its precipitation from the medium and displacement of the equilibria that are analogous to those in eq 2, but involving tris(2-methoxyphenyl)phosphine, in the undesired direction. The trialkylphosphine ligand P(*t*-Bu)<sub>3</sub>, which has a cone angle similar to or smaller than that of P(*o*-Tol)<sub>3</sub>, also gave an L<sub>2</sub>Pd compound. In this case, {Pd[P(*t*-Bu)<sub>3</sub>]<sub>2</sub>} was soluble in diethyl ether at room temperature, and the complex was obtained by crystallization from this solvent at -30 °C. Reactions with tricyclohexylphosphine gave only [Pd(Cy<sub>3</sub>P)<sub>2</sub>(DBA)].

This synthetic route is, therefore, not general to all large phosphines. It is strongly dependent on the electronic and steric factors of the phosphines, as well as the solubilities of the phosphines and L<sub>2</sub>Pd complexes. Nevertheless, the examples described constitute the simplest method to obtain these low-coordination number compounds in pure form. It is important to emphasize that the reaction solutions did not contain detectable amounts of the material that crystallized from solution and that the dominant Pd(0) complexes generated *in situ* are not the L<sub>2</sub>Pd species.

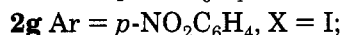
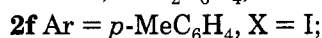
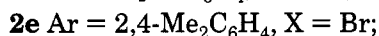
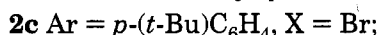
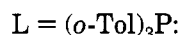
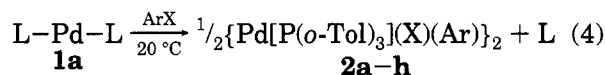
**Phosphine Exchanges with 1a.** When an excess of *p*-methyl-labeled tris(2,4-dimethylphenyl)phosphine was placed in a benzene solution with **1a**, the <sup>1</sup>H NMR spectrum of the reaction medium showed the formation of **1b** and liberation of free tri-*o*-tolylphosphine. Addition of excess of tri-*o*-tolylphosphine to **1b** formed **1a**. Importantly, the presence of excess phosphine did not lead to any detectable formation of an L<sub>3</sub>Pd complex. No new resonances or changes in chemical shifts were observed in the presence of added ligand. Mixing equimolar amounts of **1a** and **1b** led to the appearance of a new set of signals in the <sup>31</sup>P{<sup>1</sup>H} NMR spectrum whose AB pattern was consistent with the mixed phosphine complex **1e**. <sup>31</sup>P NMR spectroscopy of **1a** and **1b** showed no detectable quantities of free P(*o*-Tol)<sub>3</sub>. Thus, it seemed likely that the rapid equilibration between **1a** and **1b** involved phosphine dissociation from these compounds. Exchange of ligands after phosphine dissociation can occur by two processes: recombination with a different monoligated palladium complex also

(28) Otsuka, S.; Yoshida, T.; Matsumoto, M.; Nakatsu, K. *J. Am. Chem. Soc.* **1976**, *98*, 5850-5858.

generated by ligand dissociation or associative displacement of coordinated ligand from another bis(ligand)-metal complex by the free phosphine generated in small quantities by the initial dissociation (eq 3).



**Reaction of 1a and 1b with Aryl Bromides and Iodides.** A suspension of **1a** or **1b** in aromatic or THF solvents reacted quantitatively with various aryl bromides or aryl iodides at room temperature to give yellow solutions. The new air-stable aryl halide complexes were precipitated in 70–90% yields by addition of ether to the reaction solutions. <sup>31</sup>P{<sup>1</sup>H} NMR spectroscopic monitoring of the reaction indicated that 1 equiv of phosphine was released during the reaction. A sharp resonance at δ -29 for free ligand and a broad resonance between δ 25 and δ 29 for the palladium complex were observed in a 1:1 ratio of intensities. Once precipitated or crystallized, the dimeric complexes were slow to redissolve, even in the solvents used for their synthesis. However, the NMR spectra obtained after dissolution of isolated samples were identical to those obtained on the reaction mixtures, indicating that the isolated species had not undergone any irreversible transformation from the compound formed directly from the reaction. Gentle warming of suspensions of this material in aromatic solvents led to their dissolution (eq 4).



**NMR Spectroscopic Characterization of Aryl Bromide Complexes.** The aryl bromide complexes were all dimers in solution and in the solid state, in contrast to their previous formulation as monomers.<sup>7</sup> Solution molecular weight analysis of **2a** by the Signer method in benzene gave values that were within 10% of the molecular weight of the dimeric form, as expected from the observation of phosphine extrusion during synthesis. Moreover, the dimeric form in the solid state was revealed by X-ray diffraction.

The aryl bromide complexes displayed NMR spectra that were consistent with rotational barriers and isomerization processes that were occurring on the time scale of <sup>1</sup>H and <sup>31</sup>P{<sup>1</sup>H} NMR spectroscopy. At high temperatures, the <sup>1</sup>H and <sup>31</sup>P{<sup>1</sup>H} NMR spectra were straightforward. A single sharp resonance was observed in the <sup>31</sup>P{<sup>1</sup>H} NMR spectrum, and the <sup>1</sup>H NMR spectrum showed sharp lines. At 100 °C, the expected 1:1 ratio of palladium-bound aryl group to coordinated phosphine ligand was observed. Coupled with the solution molec-

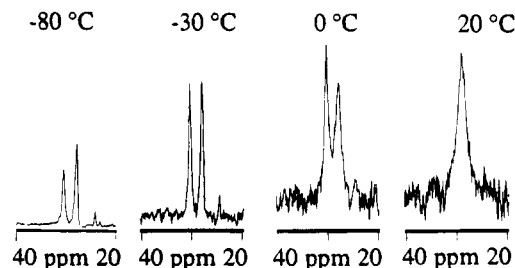


**Figure 2.** <sup>31</sup>P{<sup>1</sup>H} NMR spectra of analytically pure [(*o*-Tol)<sub>3</sub>P](*p*-MeC<sub>6</sub>H<sub>4</sub>)Pd(Br)<sub>2</sub> in toluene-*d*<sub>8</sub>.

ular weight data for **2a**, the compounds **2a-g** appear to be bimetallic aryl bromide complexes in solution as well as the solid state, although conformational and stereochemical differences may exist between the structures of the compounds in the two phases.

At low temperatures, the <sup>1</sup>H NMR spectrum was uninformative because only broad resonances were observed in the tolyl region. However, the broad <sup>31</sup>P NMR signal corresponding to coordinated phosphine in **2a** was resolved into two singlets at -20 °C in toluene-*d*<sub>8</sub> solvent. Moreover, the relative intensity of the two singlets varied as function of temperature (Figure 2). Dilution of the complexes in solution did not affect the ratio of the intensities of the two resonances, suggesting that the compounds corresponding to these signals possessed the same nuclearity. The position and ratio of the two singlets were not affected by the addition of free phosphine, and the resonance corresponding to the coordinated phosphine remained sharp at temperatures where the coordinated phosphine resonances were broad. Thus, added ligand had no effect on the processes involving **2a** that occurred on the NMR time scale. The presence of excess aryl bromide also had no effect on the <sup>31</sup>P{<sup>1</sup>H} NMR spectrum. Spectra obtained in more polar and potentially coordinating solvents such as THF and dichloromethane contained additional resonances. However, the ratio between the two main peaks showed a similar temperature dependence. We propose that the two main species observed in toluene-*d*<sub>8</sub> solvent are the *cis* and *trans* isomers of the dimeric aryl halide complex. Evidently, the *trans* form is less soluble, as it is the isomer contained in crystalline **2a**. Other minor species observed in THF and CD<sub>2</sub>Cl<sub>2</sub> may be attributed to different conformations of these isomers, since the chemical shifts of all those species are very close and all spectral changes were reversible.

**Crystal Structure of {Pd[P(*o*-Tol)<sub>3</sub>][*p*-(*n*-Bu)C<sub>6</sub>H<sub>4</sub>](Br)<sub>2</sub>}. Suitable crystals for an X-ray structure determination of **2b** were obtained directly from the toluene reaction solution by slow diffusion of ether. An ORTEP drawing is provided in Figure 3; relevant bond lengths and angles are given in Tables 5 and 6. The two palladium units display a square planar geometry with only minor distortions. The sum of the four angles about the palladium center is 359.75°, demonstrating the planarity at the metal. The Br-Pd-Ar angle is small (84.04(5)°) and the Br-Pd-P angle is large (98.91(9)°), while the other two angles are close to 90°. Thus, the large size of the phosphine leads to coordination of only one phosphine, but it does not lead to large distortions from a square planar geometry once the dimeric structure is adopted.**

**Attempts To Isolate the Dimeric Compounds 2 from Other Pd Precursors.** We attempted to isolate the aryl halide complexes starting directly from "[Pd-



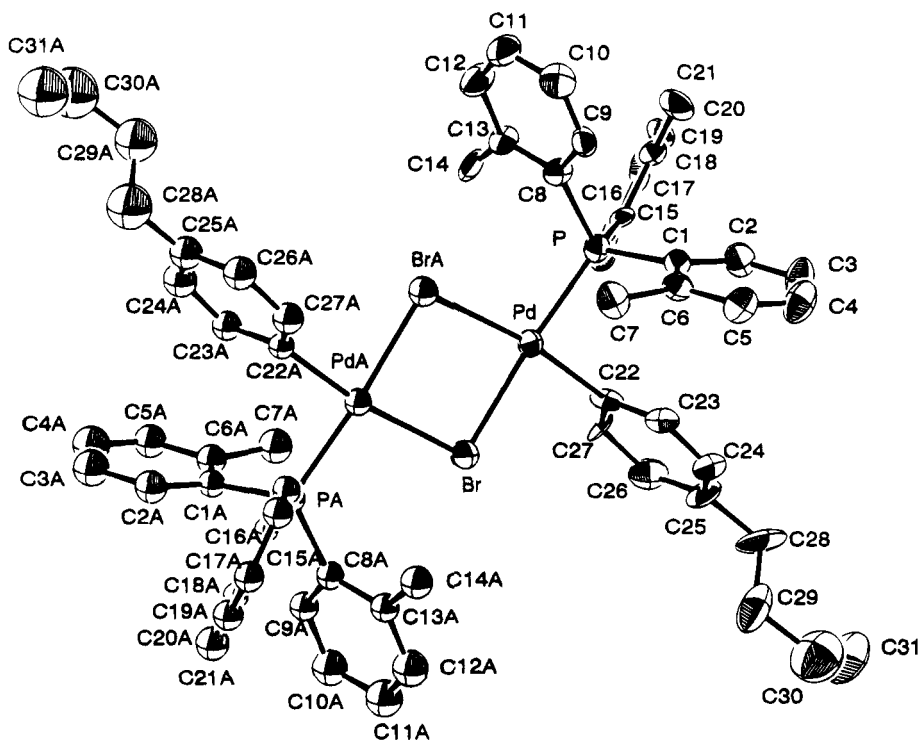


Figure 3. ORTEP diagram of  $[(o\text{-Tol})_3\text{P}]_2(p\text{-}n\text{-BuC}_6\text{H}_4)\text{Pd}(\text{Br})_2$ .

Table 5. Bond Distances for Non-Hydrogen Atoms (Å) in  $[(o\text{-Tol})_3\text{P}](p\text{-}n\text{-BuC}_6\text{H}_4)\text{Pd}(\text{Br})$  (**2b**)<sup>a</sup>

Pd-Br	2.527(2)	C12-C13	1.38(1)
Pd-Br	2.582(2)	C13-C14	1.50(1)
Pd-P	2.288(3)	C15-C16	1.36(1)
Pd-C22	2.02(1)	C15-C20	1.42(1)
P-C1	1.85(1)	C16-C17	1.38(2)
P-C8	1.83(1)	C17-C18	1.39(1)
P-C15	1.85(1)	C18-C19	1.35(1)
C1-C2	1.40(1)	C19-C20	1.38(2)
C1-C6	1.39(1)	C20-C21	1.50(1)
C2-C3	1.37(1)	C22-C23	1.40(1)
C3-C4	1.39(2)	C22-C27	1.35(1)
C4-C5	1.36(2)	C23-C24	1.37(1)
C5-C6	1.39(1)	C24-C25	1.40(2)
C6-C7	1.49(1)	C25-C26	1.36(2)
C8-C9	1.39(1)	C25-C28	1.55(2)
C8-C13	1.39(1)	C26-C27	1.39(1)
C9-C10	1.39(1)	C28-C29	1.43(2)
C10-C11	1.37(2)	C29-C30	1.56(2)
C11-C12	1.37(1)	C30-C31	1.42(2)

<sup>a</sup> Distances are in angstroms. Estimated standard deviations in the least significant figure are given in parentheses.

(DBA)<sub>2</sub>]<sup>+</sup>, aryl bromide, and tri-*o*-tolylphosphine. However, these reactions gave **2a-c** in lower yields than from **1a** and with accompanying impurities of {Pd[P(*o*-Tol)<sub>3</sub>Br<sub>2</sub>]} and black precipitates. In the presence of a poorly coordinating base such as NEt<sub>3</sub> in order to trap HBr that may be formed by DBA insertions and β-hydrogen eliminations, the aryl bromide complexes were obtained in pure form. However, the yields were not higher than the two-step synthesis involving **1a** (35%).

The synthesis of **2a-c** from crude **1a** that was obtained from the basic ethanol reduction of {Pd[P(*o*-Tol)<sub>3</sub>Cl<sub>2</sub>]} proved useful in some cases. The black palladium precipitate and {Pd[P(*o*-Tol)<sub>3</sub>Cl<sub>2</sub>]} were separated from **2a-c** by filtration after reaction with the aryl bromide. Thus, the soluble dimeric aryl bromide complexes could be easily prepared by this route on a large scale and obtained as spectroscopically pure material.

Table 6. Bond Angles (deg) for Non-Hydrogen Atoms in  $[(o\text{-Tol})_3\text{P}](p\text{-}n\text{-BuC}_6\text{H}_4)\text{Pd}(\text{Br})$  (**2b**)<sup>a</sup>

Br-Pd-Br	84.04(5)	C8-C9-C10	122(1)
Br-Pd-P	174.76(9)	C9-C10-C11	118(1)
Br-Pd-C22	87.1(3)	C10-C11-C12	120(1)
Br-Pd-P	98.81(9)	C11-C12-C13	122(1)
Br-Pd-C22	171.0(3)	C8-C13-C12	119(1)
P-Pd-C22	89.8(3)	C8-C13-C14	124(1)
Pd-Br-Pd	95.96(5)	C12-C13-C14	116(1)
Pd-P-C1	109.5(4)	P-C15-C16	116(1)
Pd-P-C8	114.4(4)	P-C15-C20	124(1)
Pd-P-C15	117.6(5)	C16-C15-C2	120(1)
C1-P-C8	106.6(6)	C15-C16-C17	121(1)
C1-P-C15	106.0(6)	C16-C17-C18	120(1)
C8-P-C15	101.7(5)	C17-C18-C19	118(1)
P-C1-C2	118(1)	C18-C19-C20	124(1)
P-C1-C6	122(1)	C15-C20-C19	117(1)
C2-C1-C6	120(1)	C15-C20-C21	125(1)
C1-C2-C3	121(1)	C19-C20-C21	118(1)
C2-C3-C4	120(1)	Pd-C22-C23	121(1)
C3-C4-C5	120(1)	Pd-C22-C27	120(1)
C4-C5-C6	122(1)	C23-C22-C27	118(1)
C1-C6-C5	118(1)	C22-C23-C24	120(1)
C1-C6-C7	122(1)	C23-C24-C25	122(1)
C5-C6-C7	119(1)	C24-C25-C26	118(1)
P-C8-C9	122(1)	C24-C25-C28	119(2)
P-C8-C13	120(1)	C26-C25-C28	123(2)
C9-C8-C13	118(1)	C25-C26-C27	121(1)
C22-C27-C26	122(1)	C25-C28-C29	110(1)
C28-C29-C30	115(1)	C29-C30-C31	117(2)

<sup>a</sup> Angles are in degrees. Estimated standard deviations in the least significant figure are given in parentheses.

**Exchange Processes Involving Aryl Bromide Complexes.** Addition of an excess of free phosphine to **2a** did not allow the observation of any new signals in the <sup>31</sup>P NMR spectrum at room temperature or below. However, free phosphine rapidly exchanged with coordinated phosphine. Excess tris(2,4-dimethylphenyl)phosphine was incorporated in **2b** to give **2h** within minutes. In order to determine if the dimeric complexes cleaved to monomers under mild conditions, we investigated the reaction between dimeric complexes containing different phosphines and between complexes containing different palladium-bound aryl groups. Unfortu-





# Cationic Vinylidene-Bridged Complexes and Their Reactions with Alkynes To Yield Either Alkyne- and Vinylidene-Bridged or Bis(vinylidene) Products. Facile Interconversion between Terminal and Bridging Vinylidene Bonding Modes

Li-Sheng Wang and Martin Cowie\*

Department of Chemistry, University of Alberta, Edmonton, Alberta, Canada T6G 2G2

Received December 23, 1994<sup>⊗</sup>

Reaction of the cationic A-frame complex  $[\text{Ir}_2(\text{CO})_2(\mu\text{-I})(\text{dppm})_2][\text{SO}_3\text{CF}_3]$  (**2**) (dppm =  $\text{Ph}_2\text{PCH}_2\text{PPh}_2$ ) with either acetylene or phenylacetylene at  $-78^\circ\text{C}$  yields the respective species  $[\text{Ir}_2(\text{CO})(\text{HCCR})(\mu\text{-I})(\mu\text{-CO})(\text{dppm})_2][\text{SO}_3\text{CF}_3]$  ( $\text{R} = \text{H}, \text{Ph}$ ), in which the alkyne is terminally bound to one metal. At ambient temperature these alkyne adducts slowly rearrange to the vinylidene-bridged species  $[\text{Ir}_2(\text{CO})_2(\mu\text{-I})(\mu\text{-CC}(\text{H})\text{R})(\text{dppm})_2][\text{SO}_3\text{CF}_3]$ . An analogous allene adduct is obtained in the reaction of **2** with allene. Reaction of the neutral, vinylidene-bridged complexes  $[\text{Ir}_2\text{I}_2(\text{CO})_2(\mu\text{-CC}(\text{H})\text{R})(\text{dppm})_2]$  ( $\text{R} = \text{H}, \text{Ph}$ ) with methyl triflate yields the same cationic vinylidene-bridged species through loss of  $\text{CH}_3\text{I}$ . Protonation of this neutral vinylidene-bridged species ( $\text{R} = \text{H}$ ) at  $-40^\circ\text{C}$  yields an ethynylidene-bridged product which rearranges to a vinylidene- and hydride-bridged product at ambient temperature. Reaction of  $[\text{Ir}_2(\text{CO})_2(\mu\text{-I})(\mu\text{-CC}(\text{H})\text{Ph})(\text{dppm})_2][\text{SO}_3\text{CF}_3]$  with either acetylene or phenylacetylene yields alkyne- and phenylvinylidene-bridged products  $[\text{Ir}_2\text{I}(\text{CO})_2(\mu\text{-CC}(\text{H})\text{Ph})(\mu\text{-HCCR})(\text{dppm})_2][\text{SO}_3\text{CF}_3]$  ( $\text{R} = \text{H}, \text{Ph}$ ), and the X-ray structure of a derivative,  $[\text{Ir}_2\text{I}_2(\text{CO})_2(\mu\text{-CC}(\text{H})\text{Ph})(\mu\text{-HCCH})(\text{dppm})_2]$  (**15**), has been carried out. The reaction of  $[\text{Ir}_2(\text{CO})_2(\mu\text{-I})(\mu\text{-CCH}_2)(\text{dppm})_2][\text{SO}_3\text{CF}_3]$  with phenylacetylene yields an unusual bis(vinylidene) product,  $[\text{Ir}_2\text{I}(\text{CO})_2(\text{CCH}_2)(\text{CC}(\text{H})\text{Ph})(\text{dppm})_2][\text{SO}_3\text{CF}_3]$  (**19**), in which each vinylidene is terminally bound to a different metal. Reaction of **19** with either  $\text{I}^-$  or  $\text{CO}$  converts the terminal vinylidenes to bridging groups yielding  $[\text{Ir}_2\text{I}(\text{L})(\text{CO})_2(\mu\text{-CCH}_2)(\mu\text{-CC}(\text{H})\text{Ph})(\text{dppm})_2]^{n+}$  ( $\text{L} = \text{I}, n = 0; \text{L} = \text{CO}, n = 1$ ). The structure of the diiodo species (**20b**) has been determined by X-ray techniques. Compound **15**, as the  $\text{CH}_2\text{Cl}_2$  solvate, crystallizes in the monoclinic space group  $P2_1/c$  with  $a = 15.799(3) \text{ \AA}$ ,  $b = 18.029(2) \text{ \AA}$ ,  $c = 21.126(5) \text{ \AA}$ ,  $\beta = 99.48(2)^\circ$ ,  $V = 5935(4) \text{ \AA}^3$  ( $T = -65^\circ\text{C}$ ), and  $Z = 4$ . On the basis of 7406 unique observations and 441 parameters varied, the structure refined to  $R = 0.034$  and  $R_w = 0.040$ . This complex has a bridging phenylvinylidene and a bridging acetylene group with the iodo ligands bound cis to the alkyne bridge. Compound **20b** crystallizes in the tetragonal space group  $I4_1/a$  with  $a = 30.407(5) \text{ \AA}$ ,  $c = 13.065(6) \text{ \AA}$ ,  $V = 12079(6) \text{ \AA}^3$ , and  $Z = 8$  ( $T = 22^\circ\text{C}$ ). On the basis of 3730 unique observations and 305 parameters varied, the structure refined to  $R = 0.045$  and  $R_w = 0.050$ . In this product both the vinylidene and the phenylvinylidene groups are bridging, with the iodo ligands having an anti arrangement on adjacent metals.

## Introduction

Vinylidene ( $:\text{C}=\text{CH}_2$ ) is an unstable isomer of acetylene, which can be stabilized by coordination to one or more metal centers.<sup>1,2</sup> Since the first vinylidene complex was established, only 28 years ago,<sup>3</sup> interest in this fascinating group has grown dramatically, and its close analogy to the ubiquitous carbonyl ligand<sup>2</sup> suggests that a rich chemistry will continue to develop for vinylidene and its derivatives. Parallels between the two groups show up clearly in their coordination chemistry, in which vinylidene can function as either a terminal or a bridging group;<sup>1,2</sup> in addition the bridged vinylidene can

be either symmetrically bridging or bound in a side-on manner ( $\mu\text{-}\sigma,\eta^2$ ),<sup>4</sup> much as is observed for carbonyls.<sup>5</sup> This ability to function as either a terminal or bridging group has led to a strategy in which vinylidene-bridged heterobinuclear complexes are prepared through the reaction of a terminal-vinylidene complex with an unsaturated metal fragment.<sup>6</sup>

Much of the recent interest in vinylidene ligands focuses on their involvement in C-C bond-forming reactions.<sup>1,7-18</sup> On the basis of evidence of vinylidene

(4) (a) Doherty, N. M.; Elschenbroich, C.; Kneuper, H.-J.; Knox, S. A. R. *J. Chem. Soc., Chem. Commun.* **1985**, 170. (b) Mercer, R. J.; Green, M.; Orpen, A. G. *J. Chem. Soc., Chem. Commun.* **1986**, 567.

(5) (a) Cotton, F. A. *Prog. Inorg. Chem.* **1976**, *21*, 1. (b) Commons, C. J.; Hoskins, B. F. *Aust. J. Chem.* **1975**, *28*, 1663.

(6) Werner, H.; Garcia Alonso, F. J.; Otto, H.; Peters, K.; von Schnering, H. G. *Chem. Ber.* **1988**, *121*, 1565.

(7) Hoel, E. L.; Answil, G. B.; Leta, S. *Organometallics* **1984**, *3*, 1633.

(8) Casey, C. P.; Miles, W. H.; Fagan, P. J.; Haller, K. J. *Organometallics* **1985**, *4*, 559.

(9) Casey, C. P.; Austin, E. A. *Organometallics* **1986**, *5*, 584.

<sup>⊗</sup> Abstract published in *Advance ACS Abstracts*, April 15, 1995.

(1) Bruce, M. I. *Chem. Rev.* **1991**, *91*, 197 and references therein.

(2) Werner, H. *Angew. Chem., Int. Ed. Engl.* **1990**, *29*, 1077 and references therein.

(3) (a) Mills, O. S.; Redhouse, A. D. *J. Chem. Soc., Chem. Commun.* **1966**, 444. (b) Mills, O. S.; Redhouse, A. D. *J. Chem. Soc. A* **1968**, 1282.

species on the surface of Fischer–Tropsch catalysts,<sup>19</sup> a mechanism for hydrocarbon chain lengthening, resulting from surface-bound vinylidene species, has been presented.<sup>20</sup> Vinylidene groups have also been attracting attention for applications in organic synthesis<sup>21,22</sup> and in alkyne polymerization, for which vinylidenes are suggested as polymerization initiators.<sup>10</sup>

The idea that binuclear complexes could function as effective models for processes occurring on metal surfaces, by allowing the substrate of interest to interact with more than one metal, led us to investigate binuclear vinylidene complexes. In a recent paper<sup>23</sup> we reported that the vinylidene-bridged species  $[\text{Ir}_2\text{I}_2(\text{CO})_2(\mu\text{-CCH}_2)(\text{dppm})_2]$  reacted with excess acetylene to yield products which were proposed to have a bridging vinylidene and a bridging acetylene group on opposite faces of the complex. Since the vinylidene-bridged precursor is coordinatively saturated, it appeared that removal of  $\text{I}^-$  should lead to unsaturation which might make preparation of these mixed alkyne–vinylidene species more facile. It also appeared that the preparation of bis(vinylidene) species should be possible starting from coordinatively unsaturated mono(vinylidene) precursors. In this paper we report the preparation of cationic vinylidene-bridged species starting from either  $[\text{Ir}_2(\text{CO})_2(\mu\text{-I})(\text{dppm})_2][\text{X}]$  or  $[\text{Ir}_2\text{I}_2(\text{CO})_2(\mu\text{-CC}(\text{H})\text{R})(\text{dppm})_2]$  and some subsequent reactions of these products.

## Experimental Section

**General Procedures.** Purified argon and carbon monoxide were obtained from Linde, and allene was from Matheson. The 99% carbon-13-enriched carbon monoxide was purchased from Isotec Inc., and the 99% carbon-13-enriched acetylene, from Cambridge Isotope Laboratories. All gases were used as received. Diethyl ether, THF, and hexane were dried over Na–benzophenone ketyl whereas  $\text{CH}_2\text{Cl}_2$  was dried by  $\text{P}_2\text{O}_5$  and MeOH by magnesium metal; all solvents were distilled under argon before use. The perdeuterated methylene chloride was dried over molecular sieves and deoxygenated by repeated freeze–pump–thaw cycles. The compounds phenylacetylene, silver tetrafluoroborate, methyl lithium, tetrafluoroboric acid–dimethyl etherate, triflic acid, methyl triflate, and *tert*-butyl isocyanide were used as received from Aldrich; potassium iodide was purchased from BDH Chemicals. Reactions were

(10) Alt, H. G.; Engelhardt, H. E.; Rausch, M. D.; Kool, L. B. *J. Organomet. Chem.* **1987**, 329, 61.

(11) Berry, D. H.; Eisenberg, R. *Organometallics* **1987**, 6, 1796.

(12) Gamble, A. S.; Birdwhistell, K. R.; Templeton, J. L. *Organometallics* **1988**, 7, 1046.

(13) Etienne, M.; Guerchais, J. E. *J. Chem. Soc., Dalton Trans.* **1989**, 2187.

(14) Gibson, V. C.; Parkin, G.; Bercaw, J. E. *Organometallics* **1991**, 10, 220.

(15) Selna, H. E.; Merola, J. S. *J. Am. Chem. Soc.* **1991**, 113, 4008.

(16) Etienne, M.; Talarmin, J.; Toupet, L. *Organometallics* **1992**, 11, 2058.

(17) Fryzuk, M. D.; Huang, L.; McManus, N. T.; Paglia, P.; Rettig, S. J.; White, G. S. *Organometallics* **1992**, 11, 2979.

(18) Wiedemann, R.; Steinert, P.; Schäfer, M.; Werner, H. *J. Am. Chem. Soc.* **1993**, 115, 9864.

(19) (a) Ibach, H.; Lehwald, S. *J. Vac. Sci. Technol.* **1978**, 15, 407.

(b) Demuth, J. E. *Surf. Sci.* **1979**, 80, 367. (c) Kesmodel, L. L.; Gates, J. A. *J. Electron. Spectrosc. Relat. Phenom.* **1983**, 29, 307. (d) Koestner, R. J.; Frost, J. C.; Stair, P. C.; Van Hove, M. A.; Somorjai, G. A. *Surf. Sci.* **1982**, 116, 85. (e) Hills, M. M.; Parmenter, J. E.; Weinberg, W. H. *J. Am. Chem. Soc.* **1987**, 109, 597.

(20) McCandlish, L. E. *J. Catal.* **1983**, 83, 362.

(21) Buchwald, S. L.; Grubbs, R. H. *J. Am. Chem. Soc.* **1983**, 105, 5490.

(22) Trost, B. M.; Dyker, G.; Kulawiec, R. *J. Am. Chem. Soc.* **1990**, 112, 7809.

(23) Xiao, J.; Cowie, M. *Organometallics* **1993**, 12, 463.

routinely conducted under Schlenk conditions. Ammonium hexachloroiridate(IV) was purchased from Victoria Precious Metals. Compounds  $[\text{Ir}_2\text{I}_2(\text{CO})(\mu\text{-CO})(\text{dppm})_2]$  ( $\text{dppm} = \text{Ph}_2\text{-PCH}_2\text{PPh}_2$ ) (**1**)<sup>24</sup> and  $[\text{Ir}_2\text{I}_2(\text{CO})_2(\mu\text{-CC}(\text{H})\text{R})(\text{dppm})_2]$  ( $\text{R} = \text{H}$  (**8**),  $\text{Ph}$  (**9**))<sup>23</sup> were prepared as previously reported.

All routine NMR experiments were conducted on a Bruker AM-400 spectrometer, whereas the  $^{13}\text{C}\{^{31}\text{P}\}$  NMR experiments were conducted on a Bruker AM-200 spectrometer (this capability is not available on the AM-400 instrument). For all NMR experiments  $\text{CD}_2\text{Cl}_2$  was used as solvent. IR spectra were recorded either on a Nicolet 7199 Fourier transform interferometer or a Perkin-Elmer 883 spectrophotometer as solids (Nujol mull or  $\text{CH}_2\text{Cl}_2$  cast) or  $\text{CH}_2\text{Cl}_2$  solutions. Elemental analyses were performed by the microanalytical service within the department. The spectral data for all compounds are given in Table 1.

**Preparation of Compounds.** (a)  $[\text{Ir}_2(\text{CO})_2(\mu\text{-I})(\text{dppm})_2][\text{SO}_3\text{CF}_3]$  (**2**). To a  $\text{CH}_2\text{Cl}_2$  solution of compound **1** (100 mg in 5 mL, 68  $\mu\text{mol}$ ) was added 7.8  $\mu\text{L}$  of methyl triflate (68  $\mu\text{mol}$ ) causing the color of the solution to change from orange to burgundy immediately. Removal of the solvent and recrystallization from  $\text{CH}_2\text{Cl}_2$ /hexane gave a burgundy solid (yield 86%). The compound was very air sensitive, and the elemental analysis was not attempted.

(b)  $[\text{Ir}_2(\eta^2\text{-HCCH})(\text{CO})(\mu\text{-I})(\mu\text{-CO})(\text{dppm})_2][\text{SO}_3\text{CF}_3]$  (**3**). To a  $\text{CH}_2\text{Cl}_2$  solution of compound **2** (100 mg in 5 mL, 67  $\mu\text{mol}$ ) was added 5 mL of acetylene (0.2 mmol) at  $-78^\circ\text{C}$  causing the color of the solution to change from burgundy to yellow immediately. The solution was partially evacuated to remove excess acetylene, and 30 mL of hexane was slowly added to the solution to precipitate the pale yellow solid (80%). The solid was found to be stable for short periods at room temperature; however, the  $\text{CH}_2\text{Cl}_2$  solution was not stable at ambient temperature and therefore the NMR sample was prepared at  $-78^\circ\text{C}$ . Characterization was by NMR and IR spectroscopies.

(c)  $[\text{Ir}_2(\text{CO})_2(\mu\text{-I})(\mu\text{-CCH}_2)(\text{dppm})_2][\text{SO}_3\text{CF}_3]$  (**4-SO}\_3\text{CF}\_3**). To a  $\text{CH}_2\text{Cl}_2$  solution of compound **8** (100 mg, 67  $\mu\text{mol}$  in 10 mL) was added 7.6  $\mu\text{L}$  of  $\text{CF}_3\text{SO}_3\text{CH}_3$  (67  $\mu\text{mol}$ ), and the solution was stirred for 1 h. Removal of the solvent and recrystallization from  $\text{CH}_2\text{Cl}_2$ /Et<sub>2</sub>O gave a yellow crystalline solid (yield 90%). Anal. Calcd for  $\text{Ir}_2\text{I}_2\text{F}_4\text{O}_5\text{C}_{55}\text{H}_{46}$ : C, 43.70; H, 3.05; I, 8.40. Found: C, 43.48; H, 2.91; I, 8.40.

(d)  $[\text{Ir}_2(\text{CO})_2(\mu\text{-I})(\mu\text{-CCH}_2)(\text{dppm})_2][\text{BF}_4]$  (**4-BF}\_4**). To a  $\text{CH}_2\text{Cl}_2$  solution of compound **8** (50 mg, 34  $\mu\text{mol}$  in 5 mL) was added 6.6  $\mu\text{L}$  of  $\text{AgBF}_4$  (34  $\mu\text{mol}$ ), and the solution was stirred for 15 min and filtered to remove AgI. Removal of the solvent from the yellow filtrate and recrystallization from  $\text{CH}_2\text{Cl}_2$ /Et<sub>2</sub>O gave a yellow crystalline solid (yield 84%). Anal. Calcd for  $\text{Ir}_2\text{IP}_4\text{F}_4\text{O}_2\text{BC}_{54}\text{H}_{46}$ : C, 44.75; H, 3.18. Found: C, 44.43; H, 3.12.

(e)  $[\text{Ir}_2(\eta^2\text{-HCCPh})(\text{CO})(\mu\text{-I})(\mu\text{-CO})(\text{dppm})_2][\text{SO}_3\text{CF}_3]$  (**5a,b**). To a  $\text{CD}_2\text{Cl}_2$  solution of compound **2** (10 mg in 0.5 mL in an NMR tube, 7  $\mu\text{mol}$ ) was added 3  $\mu\text{L}$  of phenylacetylene (27  $\mu\text{mol}$ ) at  $-78^\circ\text{C}$ . The solution turned to yellow from burgundy, and the variable-temperature NMR experiments were undertaken. These species were characterized by NMR and IR techniques, showing two isomers (**5a,b**).

(f)  $[\text{Ir}_2(\eta^2\text{-HCCPh})(\text{CO})(\mu\text{-I})(\mu\text{-CO})(\text{dppm})_2][\text{SO}_3\text{CF}_3]$  (**5b**). To a  $\text{CH}_2\text{Cl}_2$  solution of compound **2** (50 mg in 5 mL, 34  $\mu\text{mol}$ ) was added 6  $\mu\text{L}$  of phenylacetylene (54  $\mu\text{mol}$ ) at  $-78^\circ\text{C}$ . The solution turned to yellow from burgundy, and 30 mL of hexane was slowly added to the solution to precipitate the pale yellow solid (80%). The solid was found to be stable for short periods at room temperature; however the  $\text{CH}_2\text{Cl}_2$  solution was not stable at ambient temperature and therefore the NMR sample was prepared at  $-78^\circ\text{C}$ . Characterization was by NMR and IR spectroscopies, showing only **5b**.

(24) Vaartstra, B. A.; Xiao, J.; Jenkins, J. A.; Verhagen, R.; Cowie, M. *Organometallics* **1991**, 10, 2708.

Table 1. Spectroscopic Data for the Compounds<sup>a</sup>

compd	IR (cm <sup>-1</sup> )	NMR		
		$\delta(^{31}\text{P}\{^1\text{H}\})$	$\delta(^1\text{H})$	$\delta(^{13}\text{C}\{^1\text{H}\})$
$[\text{Ir}_2(\text{CO})_2(\mu\text{-I}(\text{dppm})_2)[\text{SO}_3\text{CF}_3] \text{ (2)}$	1971 (st) <sup>c</sup>	10.4 (t, $^2J_{\text{P}(\text{Ir})\text{C}} = 5 \text{ Hz}$ ) <sup>d</sup>	4.67 (m, 4H, $\text{PCH}_2\text{P}$ ) <sup>d</sup>	166.8 (qui, CO, $^2J_{\text{P}(\text{Ir})\text{C}} = 5 \text{ Hz}$ ) <sup>d</sup>
$[\text{Ir}_2(\eta^2\text{-C}_2\text{H}_2)(\text{CO})(\mu\text{-I})(\mu\text{-CO})(\text{dppm})_2][\text{SO}_3\text{CF}_3] \text{ (3)}$	1966 (vs), <sup>b</sup> 1824 (m), 1660 (w)	-4.4 (ddm, P <sup>1</sup> , $^2J_{\text{P}(\text{Ir})\text{C}^1} = 14 \text{ Hz}$ , $^2J_{\text{P}(\text{Ir})\text{C}^{\text{brn}}} = 4 \text{ Hz}$ ) <sup>e</sup> , -13.2 (dm, P <sup>2</sup> , $^2J_{\text{P}(\text{Ir})\text{C}^{\text{brn}}} = 4 \text{ Hz}$ )	4.98 (dd, 1H <sub>b</sub> , $^1J_{\text{CHb}} = 234 \text{ Hz}$ , $^2J_{\text{CCHb}} = 24 \text{ Hz}$ , H <sub>b</sub> CCH <sub>a</sub> ) <sup>g</sup> , 4.11 (m, 2H, $\text{PCH}_2\text{P}$ ), 3.90 (m, 2H, $\text{PCH}_2\text{P}$ ), 3.42 (dd, 1H <sub>a</sub> , $^1J_{\text{CHa}} = 237 \text{ Hz}$ , $^2J_{\text{CCHa}} = 26 \text{ Hz}$ , H <sub>a</sub> CCH <sub>a</sub> )	187.7 (ddm, C <sup>brn</sup> O, $^2J_{\text{C}^{\text{brn}}(\text{Ir})\text{C}^1} = 10 \text{ Hz}$ , $^2J_{\text{C}^{\text{brn}}(\text{Ir})\text{Ca}} = 7.5 \text{ Hz}$ ) <sup>g</sup> , 179.0 (dt, C <sup>1</sup> O, $^2J_{\text{C}^{\text{brn}}(\text{Ir})\text{C}^1} = 10 \text{ Hz}$ , $^2J_{\text{P}(\text{Ir})\text{C}^1} = 14 \text{ Hz}$ ), 75.2 (dd, C <sub>a</sub> , $^1J_{\text{CaCb}} = 102 \text{ Hz}$ , $^2J_{\text{C}^{\text{brn}}(\text{Ir})\text{Ca}} = 7.5 \text{ Hz}$ ), 62.0 (d, C <sub>b</sub> , $^1J_{\text{CaCb}} = 102 \text{ Hz}$ )
$[\text{Ir}_2(\text{CO})_2(\mu\text{-CCH}_2)(\mu\text{-I})(\text{dppm})_2][\text{SO}_3\text{CF}_3] \text{ (4-SO}_3\text{CF}_3)$	1949 (st), <sup>b</sup> 1588 (w); 1963 (st), <sup>c</sup> 1587 (w)	-7.9 (dt, $^2J_{\text{Ca}(\text{Ir})\text{P}} = 7 \text{ Hz}$ , $^2J_{\text{C}(\text{Ir})\text{P}} = 7 \text{ Hz}$ ) <sup>d</sup>	4.63 (m, 2H, $\text{PCH}_2\text{P}$ ) <sup>d</sup> , 3.92 (m, 2H, $\text{PCH}_2\text{P}$ ), 3.72 (d, $^1J_{\text{C}\beta\text{H}} = 161 \text{ Hz}$ , CCH <sub>2</sub> )	219.6 (dtm, $^1J_{\text{Ca}\beta} = 65 \text{ Hz}$ , $^2J_{\text{Ca}(\text{Ir})\text{C}} = 9 \text{ Hz}$ , CCH <sub>2</sub> ) <sup>d</sup> , 181.7 (dquin, $^2J_{\text{Ca}(\text{Ir})\text{C}} = 9 \text{ Hz}$ , $^2J_{\text{P}(\text{Ir})\text{C}} = 8 \text{ Hz}$ , CO), 129.9 (d, $^1J_{\text{Ca}\beta} =$ 65 Hz, CCH <sub>2</sub> )
$[\text{Ir}_2(\text{CO})_2(\mu\text{-CCH}_2)(\mu\text{-I})(\text{dppm})_2][\text{BF}_4] \text{ (4-BF}_4)$		-7.9 (d, $^2J_{\text{Ca}(\text{Ir})\text{P}} = 7 \text{ Hz}$ ) <sup>d</sup>	4.60 (m, 2H, $\text{PCH}_2\text{P}$ ) <sup>d</sup> , 3.92 (m, 2H), $\text{PCH}_2\text{P}$ ), 3.72 (d, $^1J_{\text{C}\beta\text{H}} = 161 \text{ Hz}$ , CCH <sub>2</sub> )	219.6 (dqui, $^1J_{\text{Ca}\beta} = 65 \text{ Hz}$ , $^2J_{\text{P}(\text{Ir})\text{Ca}} =$ 7 Hz, CCH <sub>2</sub> ) <sup>d</sup> , 129.9 (d, $^1J_{\text{Ca}\beta} = 65$ Hz, CCH <sub>2</sub> )
$[\text{Ir}_2(\eta^2\text{-PhCCH}(\text{CO})(\mu\text{-I})(\mu\text{-CO})(\text{dppm})_2)[\text{SO}_3\text{CF}_3] \text{ (5a)}$		-2.7 (ddm, P <sup>1</sup> , $^2J_{\text{P}(\text{Ir})\text{C}^1} = 14 \text{ Hz}$ , $^2J_{\text{P}(\text{Ir})\text{C}^{\text{brn}}} = 4 \text{ Hz}$ ) <sup>h</sup> , -10.8 (dm, P <sup>2</sup> , $^2J_{\text{P}(\text{Ir})\text{C}^{\text{brn}}} = 4 \text{ Hz}$ )	4.30 (s, 1H, PhCCH) <sup>h</sup> , 3.92 (m, 2H, $\text{PCH}_2\text{P}$ ), 3.81 (m, 2H, $\text{PCH}_2\text{P}$ )	190.2 (dquin, 1C <sup>brn</sup> O, $^2J_{\text{C}^{\text{brn}}(\text{Ir})\text{C}^1} = 8 \text{ Hz}$ , $^2J_{\text{P}(\text{Ir})\text{C}^{\text{brn}}} = 2J_{\text{P}(\text{Ir})\text{C}^{\text{brn}}} = 4 \text{ Hz}$ ) <sup>h</sup> , 179.2 (dt, 1C <sup>1</sup> O, $^2J_{\text{C}^{\text{brn}}(\text{Ir})\text{C}^1} = 8 \text{ Hz}$ , $^2J_{\text{P}(\text{Ir})\text{C}^1} =$ 14 Hz)
$[\text{Ir}_2(\eta^2\text{-PhCCH}(\text{CO})(\mu\text{-I})(\mu\text{-CO})(\text{dppm})_2)[\text{SO}_3\text{CF}_3] \text{ (5b)}$	1977 (w), <sup>b</sup> 1965 (vs), 1810 (st)	-4.7 (ddm, P <sup>1</sup> , $^2J_{\text{P}(\text{Ir})\text{C}^1} = 15 \text{ Hz}$ , $^2J_{\text{P}(\text{Ir})\text{C}^{\text{brn}}} = 4 \text{ Hz}$ ) <sup>d</sup> , -19.1 (dm, P <sup>2</sup> , $^2J_{\text{P}(\text{Ir})\text{C}^{\text{brn}}} = 4 \text{ Hz}$ )	5.39 (s, 1H, PhCCH) <sup>d</sup> , 4.20 (m, 2H, $\text{PCH}_2\text{P}$ ), 3.88 (m, 2H, $\text{PCH}_2\text{P}$ )	188.3 (dquin, 1C <sup>brn</sup> O, $^2J_{\text{C}^{\text{brn}}(\text{Ir})\text{C}^1} = 11 \text{ Hz}$ , $^2J_{\text{P}(\text{Ir})\text{C}^{\text{brn}}} = 2J_{\text{P}(\text{Ir})\text{C}^{\text{brn}}} = 4 \text{ Hz}$ ) <sup>d</sup> , 179.2 (dt, 1C <sup>1</sup> O, $^2J_{\text{C}^{\text{brn}}(\text{Ir})\text{C}^1} = 11 \text{ Hz}$ , $^2J_{\text{P}(\text{Ir})\text{C}^1} = 15 \text{ Hz}$ )
$[\text{Ir}_2(\text{CO})_2(\mu\text{-CC}(\text{H})\text{Ph})(\mu\text{-I})(\text{dppm})_2][\text{SO}_3\text{CF}_3] \text{ (6)}$	1972 (vs), <sup>b</sup> 1589 (w); 1968 (vs), <sup>c</sup> 1590 (w)	-5.2 (m), <sup>d</sup> -8.5 (m)	5.08 (s, 1H, CC(H)Ph) <sup>d</sup> , 4.54 (m, 2H, $\text{PCH}_2\text{P}$ ), 3.90 (m, 2H, $\text{PCH}_2\text{P}$ )	220.7 (m, CC(H)Ph) <sup>d</sup> , 182.5 (t, $^2J_{\text{P}(\text{Ir})\text{C}} =$ 15 Hz, CO), 181.5 (t, $^2J_{\text{P}(\text{Ir})\text{C}} = 15 \text{ Hz}$ , CO), 129.2 (s, CC(H)Ph)
$[\text{Ir}_2(\eta^2\text{-H}_2\text{CCCH}_2)(\text{CO})(\mu\text{-I})(\mu\text{-CO})(\text{dppm})_2][\text{SO}_3\text{CF}_3] \text{ (7a-SO}_3\text{CF}_3)$	1965 (st), <sup>b</sup> 1801 (st); 1978 (st), <sup>c</sup> 1815 (m)	-7.1 (m), <sup>d</sup> -10.5 (m)	5.95 (m, 1H) <sup>d</sup> , 5.34 (m, 1H), 4.30 (m, 2H), 4.01 (m, 2H), 1.33 (m, 2H)	189.9 (dquin, 1CO) <sup>d</sup> , 179.9 (dt, 1CO)
$[\text{Ir}_2(\eta^2\text{-H}_2\text{CCCH}_2)(\text{CO})(\mu\text{-I})(\mu\text{-CO})(\text{dppm})_2][\text{I}] \text{ (7a-I)}$	1963 (st), <sup>b</sup> 1801 (m); 1983 (st), <sup>c</sup> 1819 (m)	-6.9 (m, P <sup>1</sup> ) <sup>d</sup> , -10.4 (m, P <sup>2</sup> )	5.93 (dt, 1H <sub>a</sub> , $^2J_{\text{gem}} = 2.4 \text{ Hz}$ , $^4J_{\text{HaHc}} = 3.4 \text{ Hz}$ , (H <sub>c</sub> ) <sub>2</sub> CCC- H <sub>a</sub> H <sub>b</sub> ) <sup>d</sup> , 5.33 (dt, 1H <sub>b</sub> , $^2J_{\text{gem}} = 2.4 \text{ Hz}$ , $^4J_{\text{HbHc}} =$ 3.4 Hz, (H <sub>c</sub> ) <sub>2</sub> CCCH <sub>a</sub> H <sub>b</sub> ), 4.29 (m, 2H, $\text{PCH}_2\text{P}$ ), 4.08 (m, 2H, $\text{PCH}_2\text{P}$ ), 1.31 (ddt, 2H <sub>c</sub> , $^3J_{\text{P}(\text{Ir})\text{CHc}} = 7$ Hz, (H <sub>c</sub> ) <sub>2</sub> CCCH <sub>a</sub> H <sub>b</sub> )	189.9 (dquin, C <sup>brn</sup> O, $^2J_{\text{C}(\text{Ir})\text{C}^{\text{brn}}} = 8 \text{ Hz}$ ) <sup>d</sup> , $^2J_{\text{P}(\text{Ir})\text{C}^{\text{brn}}} = 6.5 \text{ Hz}$ ), 179.9 (dt, C <sup>1</sup> O, $^2J_{\text{C}(\text{Ir})\text{C}^{\text{brn}}} = 8 \text{ Hz}$ , $^2J_{\text{P}(\text{Ir})\text{C}^1} = 14 \text{ Hz}$ )
$[\text{Ir}_2(\eta^2\text{-H}_2\text{CCCH}_2)(\text{CO})(\mu\text{-I})(\mu\text{-CO})(\text{dppm})_2][\text{SO}_3\text{CF}_3] \text{ (7b-SO}_3\text{CF}_3)$	1921 (st), <sup>b</sup> 1760 (st)	-7.2 (m), <sup>d</sup> -8.2 (m)	5.26 (m, 1H, (H <sub>c</sub> ) <sub>2</sub> CCCH <sub>a</sub> H <sub>b</sub> ) <sup>d</sup> , 4.27 (m, 2H, $\text{PCH}_2\text{P}$ ), 4.05 (m, 2H, $\text{PCH}_2\text{P}$ ), 2.70 (m, 2H, (H <sub>c</sub> ) <sub>2</sub> CCCH <sub>a</sub> H <sub>b</sub> )	190.4 (dquin, C <sup>brn</sup> O, $^2J_{\text{C}(\text{Ir})\text{C}^{\text{brn}}} = 10 \text{ Hz}$ , $^2J_{\text{P}(\text{Ir})\text{C}^{\text{brn}}} = 6 \text{ Hz}$ ) <sup>d</sup> , 179.9 (dt, C <sup>1</sup> O, $^2J_{\text{C}(\text{Ir})\text{C}^{\text{brn}}} = 10 \text{ Hz}$ , $^2J_{\text{P}(\text{Ir})\text{C}^1} = 12 \text{ Hz}$ )
$[\text{Ir}_2(\eta^2\text{-H}_2\text{CCCH}_2)(\text{CO})(\mu\text{-I})(\mu\text{-CO})(\text{dppm})_2][\text{I}] \text{ (7b-I)}$		-7.1 (m), <sup>d</sup> -8.1 (m)	5.25 (m, 1H, (H <sub>c</sub> ) <sub>2</sub> CCCH <sub>a</sub> H <sub>b</sub> ) <sup>d</sup> , 4.28 (m, 2H, $\text{PCH}_2\text{P}$ ), 4.10 (m, 2H, $\text{PCH}_2\text{P}$ ), 2.67 (m, 2H, (H <sub>c</sub> ) <sub>2</sub> CCCH <sub>a</sub> H <sub>b</sub> )	
$[\text{Ir}_2\text{I}_2(\text{CO})_2(\mu\text{-CCH}_3)(\text{dppm})_2][\text{SO}_3\text{CF}_3] \text{ (10-SO}_3\text{CF}_3)$		-14.7 (m), <sup>g</sup> -20.3 (m)	4.78 (m, 2H), <sup>g</sup> 4.56 (m, 2H), 4.00 (d, 3H, $^1J_{\text{C}\beta\text{H}} = 128 \text{ Hz}$ )	
$[\text{Ir}_2\text{I}_2(\text{CO})_2(\mu\text{-CCH}_3)(\text{dppm})_2][\text{BF}_4] \text{ (10-BF}_4)$		-14.9 (m, P <sup>1</sup> ) <sup>g</sup> , -20.3 (m, P <sup>2</sup> )	4.73 (m, 2H, $\text{PCH}_2\text{P}$ ) <sup>g</sup> , 4.51 (m, 2H, $\text{PCH}_2\text{P}$ ), 3.99 (d, 3H, $^1J_{\text{C}\beta\text{H}} = 128 \text{ Hz}$ , CCH <sub>3</sub> )	409.1 (dd, $^1J_{\text{Ca}\beta} = 23 \text{ Hz}$ , $^2J_{\text{Ca}(\text{Ir})\text{C}} = 23$ Hz, C <sub>a</sub> C <sub>β</sub> H <sub>3</sub> ) <sup>g</sup> , 179.0 (dt, $^2J_{\text{Ca}(\text{Ir})\text{C}^2} = 23 \text{ Hz}$ , $^2J_{\text{P}(\text{Ir})\text{C}^2} = 15 \text{ Hz}$ , C <sub>2</sub> O), 166.5 (t, $^2J_{\text{P}(\text{Ir})\text{C}^1} =$ 10 Hz, C <sub>1</sub> O), 68.5 (d, $^1J_{\text{Ca}\beta} = 23 \text{ Hz}$ , C <sub>a</sub> C <sub>β</sub> H <sub>3</sub> )

$[\text{Ir}_2\text{I}_2(\text{CO})_2(\mu\text{-CCH}_2)(\mu\text{-H})(\text{dppm})_2][\text{SO}_3\text{CF}_3]$ ( <b>11-SO<sub>3</sub>CF<sub>3</sub></b> )	2066 (st), <sup>b</sup> 2020 (st), 1605 (w); 2081 (st), <sup>c</sup> 2028 (st), 1594 (w)	-21.2 (m), <sup>d</sup> -48.2 (m)	8.18 (d, 1H, <sup>2</sup> J <sub>gem</sub> = 7 Hz), <sup>d</sup> 5.02 (m, 2H), 4.13 (m, 2H), -12.47 (b, 1H)	187.5 (ddqui, C <sub>α</sub> <sup>1</sup> J <sub>CaCβ</sub> = 70 Hz, <sup>2</sup> J <sub>Ca(Ir)C</sub> = 26 Hz, <sup>2</sup> J <sub>P(Ir)C</sub> = 7 Hz, CCH <sub>2</sub> ), <sup>d</sup> 167.9 (t, <sup>2</sup> J <sub>P(Ir)C</sub> = 12 Hz, CO), 166.3 (dt, <sup>2</sup> J <sub>Ca(Ir)C</sub> = 26 Hz, <sup>2</sup> J <sub>P(Ir)C</sub> = 9 Hz, CO), 132.3 (d, <sup>1</sup> J <sub>CaCβ</sub> = 70 Hz, C <sub>β</sub> , CCH <sub>2</sub> )
$[\text{Ir}_2\text{I}_2(\text{CO})_2(\mu\text{-CCH}_2)(\mu\text{-H})(\text{dppm})_2][\text{BF}_4]$ ( <b>11-BF<sub>4</sub></b> )		-21.3 (m), <sup>d</sup> -48.2 (m)	8.17 (dd, 1H, <sup>1</sup> J <sub>CβH</sub> = 156 Hz, <sup>2</sup> J <sub>gem</sub> = 7 Hz, CCH <sub>2</sub> ), <sup>d</sup> 5.01 (m, 2H, PCH <sub>2</sub> P), 4.12 (m, 2H, PCH <sub>2</sub> P), -12.48 (b, 1H, hydrido)	188.3 (ddqui, C <sub>α</sub> <sup>1</sup> J <sub>CaCβ</sub> = 67 Hz, <sup>2</sup> J <sub>Ca(Ir)C</sub> = 3 Hz, <sup>2</sup> J <sub>P(Ir)Ca</sub> = 5 Hz, CCH <sub>2</sub> ), <sup>d</sup> 172.9 (ddt, C <sup>1</sup> O, <sup>3</sup> J <sub>C<sup>1</sup>C<sup>2</sup></sub> = 8 Hz, <sup>2</sup> J <sub>Ca(Ir)C</sub> = 3 Hz, <sup>2</sup> J <sub>P<sup>1</sup>(Ir)C</sub> = 8 Hz), 166.3 (dt, C <sup>2</sup> O, <sup>3</sup> J <sub>C<sup>1</sup>C<sup>2</sup></sub> = 8 Hz, <sup>2</sup> J <sub>P<sup>2</sup>(Ir)C</sub> = 8 Hz), 132.0 (d, <sup>1</sup> J <sub>CaCβ</sub> = 67 Hz, C <sub>β</sub> , CCH <sub>2</sub> )
$[\text{Ir}_2\text{I}(\text{CN-}t\text{-Bu})(\text{CO})_2(\mu\text{-CCH}_2)(\text{dppm})_2][\text{SO}_3\text{CF}_3]$ ( <b>12</b> )	2184 (st), <sup>c</sup> 1990 (sh), 1976 (vs), 1585 (w)	-20.4 (m, P <sup>1</sup> ), <sup>d</sup> -22.8 (m, P <sup>2</sup> )	6.75 (d, 2H, <sup>1</sup> J <sub>CβH</sub> = 157 Hz, CCH <sub>2</sub> ), <sup>d</sup> 6.05 (m, 2H, PCH <sub>2</sub> P), 4.49 (m, 2H, PCH <sub>2</sub> P), 0.89 (s, 9H, CN- <i>t</i> -Bu)	188.3 (ddm), C <sub>α</sub> <sup>1</sup> J <sub>CaCβ</sub> = 67 Hz, <sup>2</sup> J <sub>Ca(Ir)C</sub> = 15 Hz, <sup>2</sup> J <sub>P(Ir)Ca</sub> = 7 Hz, CCH <sub>2</sub> ), <sup>d</sup> 174.1 (dt(dd), CO, <sup>2</sup> J <sub>Ca(Ir)C</sub> = 15 Hz, <sup>2</sup> J <sub>P(Ir)C</sub> = 9 Hz), 170.0 (t(ddd), CO, <sup>2</sup> J <sub>P(Ir)C</sub> = 9 Hz), 162.4 (t(ddd), CO, <sup>2</sup> J <sub>P(Ir)C</sub> = 8 Hz), 131.4 (d, CCH <sub>2</sub> , <sup>1</sup> J <sub>CaCβ</sub> = 67 Hz)
$[\text{Ir}_2\text{I}(\text{CO})_3(\mu\text{-CCH}_2)(\text{dppm})_2][\text{SO}_3\text{CF}_3]$ ( <b>13</b> )	2060 (st), <sup>c</sup> 2015 (vs), 1985 (vs), 1586 (w)	-21.2 (m), <sup>d</sup> -23.5 (m)	6.88 (dd, 1H, <sup>1</sup> J <sub>CβH</sub> = 158 Hz, <sup>2</sup> J <sub>gem</sub> = 6 Hz, CCH <sub>2</sub> ), <sup>d</sup> 6.77 (dd, 1H, <sup>1</sup> J <sub>CβH</sub> = 158 Hz, <sup>2</sup> J <sub>gem</sub> = 6 Hz, CCH <sub>2</sub> ), 5.56 (m, 2H, PCH <sub>2</sub> P), 4.43 (m, 2H, PCH <sub>2</sub> P)	177.3 (t, <sup>2</sup> J <sub>P<sup>1</sup>(Ir)C</sub> = 6 Hz, C <sup>1</sup> O), <sup>d</sup> 169.2 (dt, <sup>2</sup> J <sub>Cb(Ir)C</sub> = 30 Hz, <sup>2</sup> J <sub>P<sup>2</sup>(Ir)C</sub> = 9 Hz, C <sup>2</sup> O), 133.8 (ddtt, <sup>1</sup> J <sub>CaCb</sub> = 60 Hz, <sup>2</sup> J <sub>Cb(Ir)C</sub> = 30 Hz, <sup>2</sup> J <sub>P<sup>2</sup>(Ir)Cb</sub> = 11 Hz, <sup>2</sup> J <sub>P<sup>1</sup>(Ir)Cb</sub> = 6.5 Hz, HC <sub>a</sub> C <sub>b</sub> H), 120.8 (dqui, <sup>1</sup> J <sub>CaCb</sub> = 60 Hz, <sup>2</sup> J <sub>P<sup>1</sup>(Ir)Ca</sub> = <sup>2</sup> J <sub>P<sup>2</sup>(Ir)Ca</sub> = 7.5 Hz, HC <sub>a</sub> C <sub>b</sub> H)
$[\text{Ir}_2\text{I}(\text{CO})_2(\mu\text{-HCCH})(\mu\text{-CC(H)Ph})(\text{dppm})_2][\text{SO}_3\text{CF}_3]$ ( <b>14-SO<sub>3</sub>CF<sub>3</sub></b> )	2054 (sh), <sup>b</sup> 2040 (st), 1592 (w); 2051 (sh), <sup>c</sup> 2034 (st), 1598 (w)	-9.4 (m, P <sup>1</sup> ), <sup>d</sup> -33.0 (m, P <sup>2</sup> )	8.60 (d, 1H, <sup>1</sup> J <sub>CbH</sub> = 146 Hz, HCCH), <sup>d</sup> 8.53 (s, 1H, CC(H)Ph), 4.46 (m, 2H, PCH <sub>2</sub> P), 2.87 (m, 2H, PCH <sub>2</sub> P)	173.0 (dt, <sup>2</sup> J <sub>Ca(Ir)C</sub> = 29 Hz, <sup>2</sup> J <sub>P<sup>1</sup>(Ir)C</sub> = 5 Hz, C <sup>1</sup> O), <sup>d</sup> 172.5 (dt, <sup>2</sup> J <sub>Cb(Ir)C</sub> = 28 Hz, <sup>2</sup> J <sub>P<sup>2</sup>(Ir)C</sub> = 5 Hz, C <sup>2</sup> O), 147.7 (ddtt, <sup>1</sup> J <sub>CaCb</sub> = 53 Hz, <sup>2</sup> J <sub>C<sup>2</sup>(Ir)Cb</sub> = 29 Hz, <sup>2</sup> J <sub>P<sup>2</sup>(Ir)Cb</sub> = 9 Hz, <sup>2</sup> J <sub>P<sup>1</sup>(Ir)Cb</sub> = 6.5 Hz, HC <sub>a</sub> C <sub>b</sub> H), 144.1 (ddtt, <sup>1</sup> J <sub>CaCb</sub> = 53 Hz, <sup>2</sup> J <sub>C<sup>1</sup>(Ir)Ca</sub> = 29 Hz, <sup>2</sup> J <sub>P<sup>1</sup>(Ir)Ca</sub> = 9 Hz, <sup>2</sup> J <sub>P<sup>2</sup>(Ir)Ca</sub> = 6 Hz, HC <sub>a</sub> C <sub>b</sub> H)
$[\text{Ir}_2\text{I}(\text{CO})_2(\mu\text{-HCCH})(\mu\text{-CC(H)Ph})(\text{dppm})_2][\text{BPh}_4]$ ( <b>14-BPh<sub>4</sub></b> )		-9.4 (m), <sup>d</sup> -33.0 (m)	8.61 (s), <sup>d</sup> 8.54 (s, 1H), 4.46 (m, 2H), 2.81 (m, 2H)	171.6 (t, <sup>2</sup> J <sub>P(Ir)C</sub> = 5 Hz, 1CO), <sup>d</sup> 164.6 (t, <sup>2</sup> J <sub>P(Ir)C</sub> = 6 Hz, 1CO), 162.8 (t, <sup>2</sup> J <sub>P(Ir)C</sub> = 5 Hz, 1CO)
$[\text{Ir}_2\text{I}_2(\text{CO})_2(\mu\text{-HCCH})(\mu\text{-CC(H)Ph})(\text{dppm})_2]$ ( <b>15</b> )	2027 (vs), <sup>b</sup> 1587 (w); 2023 (vs), <sup>c</sup> 1590 (w)	-29.9 (m, P <sup>1</sup> ), <sup>d</sup> -33.6 (m, P <sup>2</sup> )	9.55 (dm, 1H, <sup>1</sup> J <sub>CH</sub> = 146 Hz, HCCH), <sup>d</sup> 9.00 (dm, 1H, <sup>1</sup> J <sub>CH</sub> = 146 Hz, HCCH), 8.41 (s, 1H, CC(H)Ph), 4.83 (m, 2H, PCH <sub>2</sub> P), 2.87 (m, 2H, PCH <sub>2</sub> P)	164.6 (t, <sup>2</sup> J <sub>P(Ir)C</sub> = 5 Hz, 1CO), <sup>d</sup> 163.4 (t, <sup>2</sup> J <sub>P(Ir)C</sub> = 6 Hz, 1CO), 162.9 (t, <sup>2</sup> J <sub>P(Ir)C</sub> = 5 Hz, 1CO), 162.6 (t, <sup>2</sup> J <sub>P(Ir)C</sub> = 5 Hz, 1CO)
$[\text{Ir}_2\text{I}(\text{CO})_3(\mu\text{-HCCH})(\mu\text{-CC(H)Ph})(\text{dppm})_2]$ - [SO <sub>3</sub> CF <sub>3</sub> ] ( <b>16</b> )	2092 (st), <sup>c</sup> 2052 (st), 2046 (st)	-20.3 (m), <sup>d</sup> -30.0 (m)	9.91 (m, 1H, HCCH), <sup>d</sup> 8.57 (m, 1H, HCCH), 4.73 (m, 2H), PCH <sub>2</sub> P), 3.03 (m, 2H, PCH <sub>2</sub> P)	181.1 (t, <sup>2</sup> J <sub>P(Ir)C</sub> = 11 Hz, CO), <sup>d</sup> 162.9 (t, <sup>2</sup> J <sub>P(Ir)C</sub> = 8 Hz, CO)
$[\text{Ir}_2\text{I}(\text{CO})_4(\mu\text{-HCCH})(\mu\text{-CC(H)Ph})(\text{dppm})_2]$ - [SO <sub>3</sub> CF <sub>3</sub> ] <sub>2</sub> ( <b>17</b> )	2101 (st), <sup>c</sup> 2067 (st)	-19.8 (m), <sup>d</sup> -20.6 (m)	9.06 (m, 1H, HCCH), <sup>d</sup> 8.70 (b, 1H, CC(H)Ph), 8.31 (m, 1H, HCCH), 4.43 (m, 2H, PCH <sub>2</sub> P), 3.79 (m, 2H, PCH <sub>2</sub> P)	179.9 (t, <sup>2</sup> J <sub>P<sup>1</sup>(Ir)C</sub> = 10 Hz, C <sup>1</sup> O), <sup>d</sup> 174.6 (ddt, <sup>1</sup> J <sub>CaCβ</sub> = 64 Hz, <sup>2</sup> J <sub>Ca(Ir)C</sub> = 35 Hz, <sup>2</sup> J <sub>P<sup>2</sup>(Ir)Ca</sub> = 10 Hz, CCH <sub>2</sub> ), 174.3 (m, CC(H)Ph), 163.8 (dt, <sup>2</sup> J <sub>Ca(Ir)C</sub> = 35 Hz, <sup>2</sup> J <sub>P<sup>2</sup>(Ir)C</sub> = 9 Hz, C <sup>2</sup> O), 143.9 (s, CC(H)Ph), 133.6 (d, <sup>1</sup> J <sub>CaCβ</sub> = 64 Hz, CCH <sub>2</sub> )
$[\text{Ir}_2\text{I}(\text{CO})_2(\mu\text{-HCCPh})(\mu\text{-CC(H)Ph})(\text{dppm})_2]$ - [SO <sub>3</sub> CF <sub>3</sub> ] ( <b>18</b> )	2071 (m), <sup>c</sup> 1967 (st)	-7.9 (m), <sup>d</sup> -36.1 (m)	8.60 (s, 1H, CC(H)Ph), <sup>d</sup> 7.95 (s, 1H, HCCPh), 4.12 (m, 2H, PCH <sub>2</sub> P), 3.12 (m, 2H, PCH <sub>2</sub> P)	
$[\text{Ir}_2\text{I}(\text{CCH}_2)(\text{CC(H)Ph})(\text{CO})_2(\text{dppm})_2][\text{SO}_3\text{CF}_3]$ ( <b>19-SO<sub>3</sub>CF<sub>3</sub></b> )	2065 (m), <sup>b</sup> 1991 (st), 1580 (w); 2064 (m), <sup>c</sup> 1989 (st), 1577 (w)	-7.8 (dm, P <sup>1</sup> , <sup>2</sup> J <sub>P<sup>1</sup>(Ir)C</sub> = 10 Hz), <sup>g</sup> -34.8 (ddm, P <sup>2</sup> , <sup>2</sup> J <sub>P<sup>2</sup>(Ir)Ca</sub> = 9 Hz, <sup>2</sup> J <sub>P<sup>2</sup>(Ir)C</sub> = 9 Hz)	8.20 (d, 1H, <sup>4</sup> J <sub>C<sup>1</sup>(Ir)CCH</sub> = 4 Hz, CC(H)Ph), <sup>d</sup> 6.54 (ddt, 1H, <sup>1</sup> J <sub>CβH</sub> = 157 Hz, <sup>2</sup> J <sub>gem</sub> = 10 Hz, <sup>4</sup> J <sub>P(Ir)CCH</sub> = 2 Hz, CCH <sub>2</sub> ), 6.04 (ddt, 1H, <sup>1</sup> J <sub>CβH</sub> = 157 Hz, <sup>2</sup> J <sub>gem</sub> = 10 Hz, <sup>4</sup> J <sub>P(Ir)CCH</sub> = 2 Hz, CCH <sub>2</sub> ), 4.40 (m, 2H, PCH <sub>2</sub> P), 3.02 (m, 2H, PCH <sub>2</sub> P)	

Table 1 (Continued)

compd	IR (cm <sup>-1</sup> )	NMR		
		$\delta(^{31}\text{P}\{^1\text{H}\})$	$\delta(^1\text{H})$	$\delta(^{13}\text{C}\{^1\text{H}\})$
$[\text{Ir}_2\text{I}(\text{CCH}_2)(\text{CC}(\text{H})\text{Ph})(\text{CO})_2(\text{dppm})_2]\text{-}[\text{BF}_4]$ ( <b>19-BF<sub>4</sub></b> )		-8.0 (m, P <sup>1</sup> ), <sup>d</sup> -34.8 (dm, P <sup>2</sup> , <sup>2</sup> J <sub>P<sup>2</sup>(Ir)Ca</sub> = 10 Hz)	8.20 (s, 1H, CC(H)Ph), <sup>d</sup> 6.54 (ddt, 1H, CCH <sub>2</sub> ), 6.04 (ddt, 1H, CCH <sub>2</sub> ), 4.39 (m, 2H, PCH <sub>2</sub> P), 2.98 (m, 2H, PCH <sub>2</sub> P)	174.6 (dt, <sup>1</sup> J <sub>CaCβ</sub> = 64 Hz, <sup>2</sup> J <sub>P<sup>2</sup>(Ir)Ca</sub> = 10 Hz, CCH <sub>2</sub> ), <sup>d</sup> 133.7 (d, <sup>1</sup> J <sub>CaCβ</sub> = 64 Hz, CCH <sub>2</sub> )
$[\text{Ir}_2\text{I}_2(\text{CO})_2(\mu\text{-CCH}_2)(\mu\text{-CC}(\text{H})\text{Ph})(\text{dppm})_2]$ ( <b>20a</b> )	2027 (st), <sup>c</sup>	-32.3 (m), <sup>d</sup> -37.7 (m)	9.19 (d, 1H, <sup>1</sup> J <sub>CβH</sub> = 153 Hz, CCH <sub>2</sub> ), <sup>d</sup> 9.16 (d, 1H, <sup>1</sup> J <sub>CβH</sub> = 153 Hz, CCH <sub>2</sub> ), 4.65 (m, 2H, PCH <sub>2</sub> P), 2.45 (m, 2H, PCH <sub>2</sub> P)	171.9 (dt, <sup>2</sup> J <sub>Ca(Ir)C</sub> = 27 Hz, <sup>2</sup> J <sub>P(Ir)C</sub> = 7 Hz, CO), <sup>g</sup> 170.4 (dt, <sup>2</sup> J <sub>Ca(Ir)C</sub> = 27 Hz, <sup>2</sup> J <sub>P(Ir)C</sub> = 5 Hz, CO), 143.3 (d, <sup>1</sup> J <sub>CaCβ</sub> = 61 Hz, CCH <sub>2</sub> ), 102.2 (dtm, <sup>1</sup> J <sub>CaCβ</sub> = 61 Hz, <sup>2</sup> J <sub>Ca(Ir)C</sub> = 27 Hz, CCH <sub>2</sub> )
$[\text{Ir}_2\text{I}_2(\text{CO})_2(\mu\text{-CCH}_2)(\mu\text{-CC}(\text{H})(\text{Ph}))(\text{dppm})_2]$ ( <b>20b</b> )	2009 (st), <sup>b</sup>	-9.6 (m), <sup>i</sup> -10.3 (m), -31.3 (m), -36.5 (m)		174.7 (dt, <sup>2</sup> J <sub>Ca(Ir)C</sub> = 30 Hz, <sup>2</sup> J <sub>P(Ir)C</sub> = 8 Hz, CO), <sup>g</sup> 172.7 (t, <sup>2</sup> J <sub>P(Ir)C</sub> = 8 Hz, CO), 133.0 (d, <sup>1</sup> J <sub>CaCβ</sub> = 61 Hz, CCH <sub>2</sub> ), 102.2 (m, CCH <sub>2</sub> )
$[\text{Ir}_2\text{I}(\text{CO})_3(\mu\text{-CCH}_2)(\mu\text{-CC}(\text{H})\text{Ph})(\text{dppm})_2]\text{-}[\text{SO}_3\text{CF}_3]$ ( <b>21a</b> )	2094 (st), <sup>c</sup> 2050 (st), 2034 (sh)	-19.4 (m, P <sup>1</sup> ), <sup>c</sup> -33.3 (m, P <sup>2</sup> )	8.81 (d, 1H, <sup>1</sup> J <sub>CβH</sub> = 157 Hz, CCH <sub>2</sub> ), <sup>g</sup> 8.14 (d, 1H, <sup>1</sup> J <sub>CβH</sub> = 157 Hz, CCH <sub>2</sub> ), 4.01 (m, 2H, PCH <sub>2</sub> P), 3.26 (m, 2H, PCH <sub>2</sub> P)	171.4 (dt, <sup>2</sup> J <sub>Ca(Ir)C</sub> = 31 Hz, <sup>2</sup> J <sub>P<sup>2</sup>(Ir)C</sub> = 7 Hz, C <sup>2</sup> O), <sup>g</sup> 166.7 (t, <sup>2</sup> J <sub>P<sup>1</sup>(Ir)C</sub> = 6 Hz, C <sup>1</sup> O), 164.4 (dt, <sup>2</sup> J <sub>Ca(Ir)C</sub> = 21 Hz, <sup>2</sup> J <sub>P<sup>1</sup>(Ir)C</sub> = 5 Hz, C <sup>1</sup> O), 141.9 (d, <sup>1</sup> J <sub>CaCβ</sub> = 60 Hz, CCH <sub>2</sub> ), 101.0 (m, CCH <sub>2</sub> )
$[\text{Ir}_2\text{I}(\text{CO})_3(\mu\text{-CCH}_2)(\mu\text{-CC}(\text{H})\text{Ph})(\text{dppm})_2]\text{-}[\text{SO}_3\text{CF}_3]_2$ ( <b>21b</b> )		-20.7 (m, P <sup>1</sup> ), <sup>e</sup> -30.7 (m, P <sup>2</sup> )	8.72 (d, 1H, <sup>1</sup> J <sub>CβH</sub> = 152 Hz, CCH <sub>2</sub> ), <sup>g</sup> 8.18 (d, 1H, <sup>1</sup> J <sub>CβH</sub> = 152 Hz, CCH <sub>2</sub> ), 4.26 (m, 2H, PCH <sub>2</sub> P), 3.26 (m, 2H, PCH <sub>2</sub> P)	170.0 (dt, <sup>2</sup> J <sub>Ca(Ir)C</sub> = 32 Hz, <sup>2</sup> J <sub>P<sup>2</sup>(Ir)C</sub> = 7 Hz, C <sup>2</sup> O), <sup>g</sup> 166.2 (t, <sup>2</sup> J <sub>P(Ir)C</sub> = 9 Hz, C <sup>1</sup> O), 164.0 (dt, <sup>2</sup> J <sub>Ca(Ir)C</sub> = 22 Hz, <sup>2</sup> J <sub>P<sup>1</sup>(Ir)C</sub> = 5 Hz, C <sup>3</sup> O), 142.8 (d, <sup>1</sup> J <sub>CaCβ</sub> = 60 Hz, CCH <sub>2</sub> ), 99.8 (m, CCH <sub>2</sub> )
$[\text{Ir}_2(\text{CO})_4(\mu\text{-CCH}_2)(\mu\text{-CC}(\text{H})\text{Ph})(\text{dppm})_2]\text{-}[\text{SO}_3\text{CF}_3]$ ( <b>22</b> )	2102 (st), <sup>c</sup> 2066 (st)	-17.4 (m), <sup>d</sup> -19.1 (m)	8.19 (t, 1H, <sup>4</sup> J <sub>C(Ir)CCH</sub> = 5.5 Hz, CC(H)Ph), <sup>d</sup> 7.94 (dd, 1H, <sup>1</sup> J <sub>CH</sub> = 148 Hz, <sup>2</sup> J <sub>gem</sub> = 2.5 Hz, CCH <sub>2</sub> ), 7.82 (dd, 1H, <sup>1</sup> J <sub>CH</sub> = 148 Hz, <sup>2</sup> J <sub>gem</sub> = 2.5 Hz, CCH <sub>2</sub> ), 4.60 (m, 2H, PCH <sub>2</sub> P), 3.90 (m, 2H, PCH <sub>2</sub> P)	165.8 (dt, <sup>2</sup> J <sub>Ca(Ir)C</sub> = 26 Hz, <sup>2</sup> J <sub>P(Ir)C</sub> = 6 Hz, 1CO), <sup>d</sup> 165.7 (dt, <sup>2</sup> J <sub>Ca(Ir)C</sub> = 26 Hz, <sup>2</sup> J <sub>P(Ir)C</sub> = 6 Hz, 1CO), 164.7 (t, <sup>2</sup> J <sub>P(Ir)C</sub> = 6 Hz, CO), 164.1 (t, <sup>2</sup> J <sub>P(Ir)C</sub> = 7 Hz, CO), 142.6 (d, <sup>1</sup> J <sub>CaCβ</sub> = 61 Hz, CCH <sub>2</sub> ), 98.2 (dtqui, <sup>1</sup> J <sub>CaCβ</sub> = 61 Hz, <sup>2</sup> J <sub>Ca(Ir)C</sub> = 26 Hz, <sup>2</sup> J <sub>P(Ir)Ca</sub> = 8 Hz, CCH <sub>2</sub> )
$[\text{Ir}_2(\text{CH}_3)_2(\text{CO})_2(\mu\text{-CCH}_2)(\mu\text{-CC}(\text{H})\text{Ph})(\text{dppm})_2]$ ( <b>23</b> )		-10.7 (m, P <sup>1</sup> ), <sup>d</sup> -12.8 (m, P <sup>2</sup> )	-0.45 (t, 3H, <sup>3</sup> J <sub>P<sup>2</sup>(Ir)CH</sub> = 4.5 Hz, CH <sub>3</sub> ), <sup>d</sup> -0.92 (t, 3H, <sup>3</sup> J <sub>P<sup>1</sup>(Ir)CH</sub> = 4.5 Hz, CH <sub>3</sub> )	177.9 (dt, <sup>2</sup> J <sub>Ca(Ir)C</sub> = 26 Hz, <sup>2</sup> J <sub>P(Ir)C</sub> = 9 Hz, 1CO), <sup>d</sup> 177.5 (t, 1CO, <sup>2</sup> J <sub>P(Ir)C</sub> = 6 Hz), 133.4 (d, <sup>1</sup> J <sub>CaCβ</sub> = 59 Hz, CCH <sub>2</sub> ), 106.0 (m, CCH <sub>2</sub> )

<sup>a</sup> Abbreviations used are as follows. IR: w = weak; m = medium; st = strong; vs = very strong. NMR: s = singlet; d = doublet; t = triplet; q = quartet; qui = quintet; m = multiplet; b = broad; or any combination; bri = bridging. In all samples, except where noted in the text, the NMR data are for <sup>13</sup>CO, <sup>13</sup>C=<sup>13</sup>CH<sub>2</sub>, and H<sup>13</sup>C≡<sup>13</sup>CH groups; however, IR results are for the natural abundance samples. <sup>b</sup> Nujol mull. <sup>c</sup> CH<sub>2</sub>Cl<sub>2</sub> solution. <sup>d</sup> 22 °C. <sup>e</sup> 0 °C. <sup>f</sup> -20 °C. <sup>g</sup> -40 °C. <sup>h</sup> -60 °C. <sup>i</sup> -80 °C.

(g)  $[\text{Ir}_2(\text{CO})_2(\mu\text{-I})(\mu\text{-CC(H)Ph})(\text{dppm})_2][\text{SO}_3\text{CF}_3]$  (**6**). To a  $\text{CH}_2\text{Cl}_2$  solution of compound **9** (100 mg, 64  $\mu\text{mol}$  of 5 mL) was added 15  $\mu\text{L}$  of  $\text{CF}_3\text{SO}_3\text{CH}_3$  (128  $\mu\text{mol}$ ), and the solution was stirred for 0.5 h, resulting in a color change from yellow to orange. Removal of the solvent and recrystallization from  $\text{CH}_2\text{Cl}_2/\text{Et}_2\text{O}$  gave a yellow crystalline solid (yield 85%). Anal. Calcd for  $\text{Ir}_2\text{ISP}_4\text{F}_3\text{O}_5\text{C}_{61}\text{H}_{50}$ : C, 46.15; H, 3.15. Found: C, 45.76; H, 3.03.

(h)  $[\text{Ir}_2(\eta^2\text{-H}_2\text{CCCH}_2)(\text{CO})(\mu\text{-I})(\mu\text{-CO})(\text{dppm})_2][\text{SO}_3\text{CF}_3]$  (**7a-SO<sub>3</sub>CF<sub>3</sub>** and **7b-SO<sub>3</sub>CF<sub>3</sub>**). To a  $\text{CH}_2\text{Cl}_2$  solution of compound **2** (50 mg in 5 mL, 34  $\mu\text{mol}$ ) was added 5 mL of allene (0.2 mmol). The color of the solution changed from burgundy to light yellow immediately. Removal of the solvent and recrystallization from  $\text{CH}_2\text{Cl}_2/\text{Et}_2\text{O}$  gave a pale yellow solid (yield 90%). The  $^{31}\text{P}$  NMR showed a ratio of *ca* 2:1 of **7a-SO<sub>3</sub>CF<sub>3</sub>** and **7b-SO<sub>3</sub>CF<sub>3</sub>**, respectively. Elemental analyses were not carried out on this species but were done instead for the iodide salts which have essentially identical spectroscopic parameters.

(i)  $[\text{Ir}_2(\eta^2\text{-H}_2\text{CCCH}_2)(\text{CO})(\mu\text{-I})(\mu\text{-CO})(\text{dppm})_2][\text{I}]$  (**7a-I** and **7b-I**). To a  $\text{CH}_2\text{Cl}_2$  solution of compound **1** (50 mg in 5 mL, 34  $\mu\text{mol}$ ) was added 5 mL of allene (0.2 mmol). The solution was stirred for 1 h, during which time the yellow color of the solution lightened. Removal of the solvent and recrystallization from  $\text{THF}/\text{Et}_2\text{O}$  gave a pale yellow solid (yield 84%). The  $^{31}\text{P}$  NMR showed a ratio of *ca* 10:1 of **7a-I** and **7b-I**, respectively. Anal. Calcd for  $\text{Ir}_2\text{I}_2\text{P}_4\text{O}_2\text{C}_{55}\text{H}_{48}$ : C, 43.94; H, 3.20. Found: C, 44.58; H, 3.36.

(j)  $[\text{Ir}_2\text{I}_2(\text{CO})_2(\mu\text{-CCH}_3)(\text{dppm})_2][\text{SO}_3\text{CF}_3]$  (**10-SO<sub>3</sub>CF<sub>3</sub>**). To a  $\text{CD}_2\text{Cl}_2$  solution of compound **8** (10 mg in 0.5 mL in an NMR tube, 7  $\mu\text{mol}$ ) was added 1  $\mu\text{L}$  of  $\text{CF}_3\text{SO}_3\text{H}$  (11  $\mu\text{mol}$  at  $-78^\circ\text{C}$ ). The compound was characterized by NMR experiments at  $-40^\circ\text{C}$ .

(k)  $[\text{Ir}_2\text{I}_2(\text{CO})_2(\mu\text{-CCH}_3)(\text{dppm})_2][\text{BF}_4]$  (**10-BF<sub>4</sub>**). To a  $\text{CD}_2\text{Cl}_2$  solution of compound **1** (5 mg in 0.5 mL in an NMR tube, 3.4  $\mu\text{mol}$ ) was added 1  $\mu\text{L}$  of  $\text{HBF}_4\cdot\text{Me}_2\text{O}$  (8  $\mu\text{mol}$ ) at  $-78^\circ\text{C}$ . The NMR characterization was undertaken at  $-40^\circ\text{C}$ .

(l)  $[\text{Ir}_2\text{I}_2(\text{CO})_2(\mu\text{-CCH}_2)(\text{dppm})_2][\text{SO}_3\text{CF}_3]$  (**11-SO<sub>3</sub>CF<sub>3</sub>**). To a  $\text{CH}_2\text{Cl}_2$  solution of compound **8** (50 mg in 0.5 mL, 34  $\mu\text{mol}$ ) was added 3  $\mu\text{L}$  of  $\text{CF}_3\text{SO}_3\text{H}$  (34  $\mu\text{mol}$ ). Removal of the solvent and recrystallization from  $\text{THF}/\text{Et}_2\text{O}$  gave a yellow solid (yield 90%). Anal. Calcd for  $\text{Ir}_2\text{I}_2\text{P}_4\text{SF}_3\text{O}_5\text{C}_{55}\text{H}_{47}\text{C}_4\text{H}_5\text{O}$ : C, 41.40; H, 3.22. Found: C, 41.27; H, 2.95. The 1 equiv of THF was verified from the  $^1\text{H}$  NMR spectrum.

(m)  $[\text{Ir}_2\text{I}_2(\text{CO})_2(\mu\text{-H})(\mu\text{-CCH}_2)(\text{dppm})_2][\text{BF}_4]$  (**11-BF<sub>4</sub>**). To a  $\text{CH}_2\text{Cl}_2$  solution of compound **8** (50 mg in 0.5 mL, 34  $\mu\text{mol}$ ) was added 4.2  $\mu\text{L}$  of  $\text{HBF}_4\cdot\text{Me}_2\text{O}$  (34  $\mu\text{mol}$ ). Removal of the solvent and recrystallization from  $\text{CH}_2\text{Cl}_2/\text{Et}_2\text{O}$  gave a yellow solid (yield 82%).

(n)  $[\text{Ir}_2\text{I}(\text{t-BuNC})(\text{CO})_2(\mu\text{-CCH}_2)(\text{dppm})_2][\text{SO}_3\text{CF}_3]$  (**12**). To a  $\text{CH}_2\text{Cl}_2$  solution of compound **4a** (50 mg, 33  $\mu\text{mol}$  in 5 mL) was added 5  $\mu\text{L}$  of *tert*-butyl isocyanide (43  $\mu\text{mol}$ ), and the solution was stirred for 0.5 h, during which time the yellow color lightened. Removal of the solvent and recrystallization from  $\text{CH}_2\text{Cl}_2/\text{Et}_2\text{O}$  gave a pale yellow solid (yield 96%). Anal. Calcd for  $\text{Ir}_2\text{ISP}_4\text{F}_3\text{O}_5\text{NC}_{60}\text{H}_{55}$ : C, 45.20; H, 3.45. Found: C, 45.12; H, 3.26.

(o)  $[\text{Ir}_2\text{I}(\text{CO})_3(\mu\text{-CCH}_2)(\text{dppm})_2][\text{SO}_3\text{CF}_3]$  (**13**). A  $\text{CH}_2\text{Cl}_2$  solution of compound **4-SO<sub>3</sub>CF<sub>3</sub>** (50 mg, 33  $\mu\text{mol}$  in 5 mL) was put under CO (1 atm), and the solution was stirred for 0.5 h, during which time the yellow color lightened. Removal of the solvent under a stream of CO and recrystallization from  $\text{CH}_2\text{Cl}_2/\text{Et}_2\text{O}$  gave a pale yellow solid (yield 90%). An elemental analysis was not obtained for this compound owing to reversible CO loss regenerating **4-SO<sub>3</sub>CF<sub>3</sub>**.

(p)  $[\text{Ir}_2\text{I}(\text{CO})_2(\mu\text{-HCCH})(\mu\text{-CC(H)Ph})(\text{dppm})_2][\text{SO}_3\text{CF}_3]$  (**14-SO<sub>3</sub>CF<sub>3</sub>**). To a  $\text{CH}_2\text{Cl}_2$  solution of compound **6** (100 mg, 63  $\mu\text{mol}$  in 5 mL) was added 10 mL of  $\text{C}_2\text{H}_2$  (0.4 mmol). The solution was allowed to stir for 24 h causing a color change from orange to brown. Removal of the solvent and recrystallization from  $\text{CH}_2\text{Cl}_2/\text{Et}_2\text{O}$  gave a pale yellow solid (yield 82%).

Anal. Calcd for  $\text{Ir}_2\text{ISP}_4\text{F}_3\text{O}_5\text{C}_{63}\text{H}_{52}$ : C, 46.90; H, 3.23. Found: C, 46.88; H, 3.20.

(q)  $[\text{Ir}_2\text{I}(\text{CO})_2(\mu\text{-HCCH})(\mu\text{-CC(H)Ph})(\text{dppm})_2][\text{BPh}_4]$  (**14-BPh<sub>4</sub>**). To a  $\text{CH}_2\text{Cl}_2$  solution of compound **14-SO<sub>3</sub>CF<sub>3</sub>** (50 mg, 31  $\mu\text{mol}$  in 5 mL) was added 5 mL of an acetone solution of  $\text{NaBPh}_4$  (106 mg in 5 mL, 310  $\mu\text{mol}$ ), and the solution was stirred for 1 h. The solvent was removed, the residue was dissolved in 5 mL of  $\text{CH}_2\text{Cl}_2$ , and the solution was filtered. Removal of the solvent of the filtrate and recrystallization of the residue gave a yellow powder (yield 70%).

(r)  $[\text{Ir}_2\text{I}_2(\text{CO})_2(\mu\text{-HCCH})(\mu\text{-CC(H)Ph})(\text{dppm})_2]$  (**15**). To a  $\text{CH}_2\text{Cl}_2$  solution of compound **14-SO<sub>3</sub>CF<sub>3</sub>** (100 mg, 63  $\mu\text{mol}$  in 5 mL) was added a solution of KI (130 mg in a minimum volume of MeOH, 783  $\mu\text{mol}$ ) causing the color to change from light orange to light yellow immediately. The solution was stirred for 0.5 h, and then the solvent was removed. The residue was dissolved in 5 mL of  $\text{CH}_2\text{Cl}_2$ , and the solution was filtered. The filtrate was washed by  $3 \times 5$  mL of degassed water. Removal of the solvent and recrystallization from  $\text{CH}_2\text{Cl}_2/\text{Et}_2\text{O}$  gave a yellow solid (yield 76%). Anal. Calcd for  $\text{Ir}_2\text{I}_2\text{SP}_4\text{O}_2\text{C}_{62}\text{H}_{52}\text{CH}_2\text{Cl}_2$ : C, 45.13; H, 3.22. Found: C, 44.76; H, 3.03. One equivalent of  $\text{CH}_2\text{Cl}_2$  was verified from crystal structure determination.

(s)  $[\text{Ir}_2\text{I}(\text{CO})_3(\mu\text{-HCCH})(\mu\text{-CC(H)Ph})(\text{dppm})_2][\text{SO}_3\text{CF}_3]$  (**16**). A  $\text{CD}_2\text{Cl}_2$  solution of compound **14-SO<sub>3</sub>CF<sub>3</sub>** (15 mg in 0.5 mL in an NMR tube, 10  $\mu\text{mol}$ ) was put under CO (10 psi), and the NMR experiments were carried out. Removal of the CO atmosphere reversed the reaction.

(t)  $[\text{Ir}_2(\text{CO})_4(\mu\text{-HCCH})(\mu\text{-CC(H)Ph})(\text{dppm})_2][\text{SO}_3\text{CF}_3]$  (**17**). A  $\text{CD}_2\text{Cl}_2$  solution of compound **14-SO<sub>3</sub>CF<sub>3</sub>** (15 mg in 0.5 mL in an NMR tube, 10  $\mu\text{mol}$ ) was put under CO (10 psi), and 2  $\mu\text{L}$  of  $\text{CF}_3\text{SO}_3\text{CH}_3$  (18  $\mu\text{mol}$ ) was added and the NMR experiments were undertaken. The iodomethane was observed in the  $^1\text{H}$  NMR. Removal of CO caused the generation of unknown species at the cost of compound **17**.

(u)  $[\text{Ir}_2\text{I}(\text{CO})_2(\mu\text{-HCCPh})(\mu\text{-CC(H)Ph})(\text{dppm})_2][\text{SO}_3\text{CF}_3]$  (**18**). To a  $\text{CH}_2\text{Cl}_2$  solution of compound **6** (50 mg, 32  $\mu\text{mol}$  in 5 mL) was added 1 mL of phenyl acetylene (8.92 mmol). The solution was allowed to stir for 3 days causing a color change from orange to burgundy. Removal of the solvent and recrystallization from  $\text{CH}_2\text{Cl}_2/\text{Et}_2\text{O}$  gave a burgundy solid (yield 76%). The compound was not stable even in the solid owing to the slow loss of phenylacetylene.

(v)  $[\text{Ir}_2\text{I}(\text{CCH}_2)(\text{CC(H)Ph})(\text{CO})_2(\text{dppm})_2][\text{SO}_3\text{CF}_3]$  (**19-SO<sub>3</sub>CF<sub>3</sub>**). To a  $\text{CH}_2\text{Cl}_2$  solution of compound **4-SO<sub>3</sub>CF<sub>3</sub>** (100 mg, 66  $\mu\text{mol}$  in 10 mL) was added 500  $\mu\text{L}$  of phenylacetylene (4.46 mmol), and the solution was stirred for 2 days. The color changed gradually from yellow to deep burgundy. Removal of the solvent and recrystallization from  $\text{CH}_2\text{Cl}_2/\text{Et}_2\text{O}$  gave a burgundy solid (yield 92%). Anal. Calcd for  $\text{Ir}_2\text{ISP}_4\text{F}_3\text{O}_5\text{C}_{63}\text{H}_{52}$ : C, 46.90; H, 3.23. Found: C, 46.14; H, 3.12.

(w)  $[\text{Ir}_2\text{I}(\text{CCH}_2)(\text{CC(H)Ph})(\text{CO})_2(\text{dppm})_2][\text{BF}_4]$  (**19-BF<sub>4</sub>**). To a  $\text{CH}_2\text{Cl}_2$  solution of compound **4-BF<sub>4</sub>** (50 mg, 35  $\mu\text{mol}$  in 5 mL) was added 250  $\mu\text{L}$  of phenylacetylene (2.23 mmol), and the solution was stirred for 24 h. The color changed from yellow to deep burgundy. Removal of the solvent and recrystallization from  $\text{CH}_2\text{Cl}_2/\text{Et}_2\text{O}$  gave a burgundy solid (yield 86%).

(x)  $[\text{Ir}_2\text{I}_2(\text{CO})_2(\mu\text{-CCH}_2)(\mu\text{-CC(H)Ph})(\text{dppm})_2]$  (**20a,b**). To a  $\text{CH}_2\text{Cl}_2$  solution of compound **19-SO<sub>3</sub>CF<sub>3</sub>** (50 mg, 33  $\mu\text{mol}$  in 5 mL) was added a solution of KI (100 mg in a minimum volume of MeOH, 602  $\mu\text{mol}$ ) causing the color to change from burgundy to yellow. After the solution was stirred for 0.5 h, the solvent was removed, the residue was dissolved in 5 mL of  $\text{CH}_2\text{Cl}_2$ , and the solution was filtered. Removal of the solvent of the filtrate and recrystallization from  $\text{CH}_2\text{Cl}_2/\text{Et}_2\text{O}$  gave a yellow solid (yield 68%).

(y)  $[\text{Ir}_2\text{I}(\text{CO})_3(\mu\text{-CCH}_2)(\mu\text{-CC(H)Ph})(\text{dppm})_2][\text{SO}_3\text{CF}_3]$  (**21a,b**). A  $\text{CD}_2\text{Cl}_2$  solution of compound **19-SO<sub>3</sub>CF<sub>3</sub>** (15 mg in 0.5 mL in an NMR tube, 10  $\mu\text{mol}$ ) was put under CO (10

Table 2. Crystallographic Data

compd	15	20b
formula	C <sub>63</sub> H <sub>54</sub> Cl <sub>2</sub> I <sub>2</sub> Ir <sub>2</sub> O <sub>2</sub> P <sub>4</sub>	C <sub>62</sub> H <sub>52</sub> I <sub>2</sub> Ir <sub>2</sub> O <sub>2</sub> P <sub>4</sub>
fw	1676.14	1591.20
space group	P2 <sub>1</sub> /c (No. 14)	I4 <sub>1</sub> /a (No. 88)
unit cell parameters		
<i>a</i> (Å)	15.799(3)	30.407(5)
<i>b</i> (Å)	18.029(2)	
<i>c</i> (Å)	21.126(5)	13.065(6)
β (deg)	99.48(2)	
<i>V</i> (Å <sup>3</sup> )	5935(4)	12079(6)
<i>Z</i>	4	8
ρ (calcd) (g cm <sup>-3</sup> )	1.876	1.75
μ (cm <sup>-1</sup> )	57.3	55.8
diffractometer	Enraf-Nonius CAD4	Rigaku AFC7R
temperature (°C)	-65	22
radiation (λ (Å))	graphite-monochromated Mo Kα (0.710 69)	
take-off angle (deg)	3.0	6.0
detector aperture (mm)	(3.00 + tan θ) horiz × 4.00 vert	3.0 × 3.0
crystal-detector distance (mm)	173	235
scan type	ω-2θ	ω-2θ
scan rate (deg min <sup>-1</sup> )	6.71-1.73	4.00
scan width (deg)	0.80 + 0.344 tan θ	0.94 + 0.35 tan θ
max 2θ (deg)	50.0	55.0
tot. unique reflcns	10684 (± <i>h</i> , ± <i>k</i> , ± <i>l</i> )	7235 (+ <i>h</i> , + <i>k</i> , + <i>l</i> )
tot. obsvns (NO)	7406 ( <i>F</i> <sub>o</sub> <sup>2</sup> ≥ 3.0σ( <i>F</i> <sub>o</sub> <sup>2</sup> ))	3730
range of abs corr factors	0.85-1.21	0.83-1.20
final no. params varied (NV)	441	305
<i>R</i> <sup>a</sup>	0.034	0.045
<i>R</i> <sub>w</sub> <sup>b</sup>	0.040	0.050
error in obs of unit weight (GOF) <sup>c</sup>	1.274	1.80

$$^a R = \sum(|F_o| - |F_c|)/\sum|F_o|. \quad ^b R_w = [\sum w(|F_o| - |F_c|)^2/\sum w F_o^2]^{1/2}. \quad ^c GOF = [\sum w(|F_o| - |F_c|)^2/(NO - NV)]^{1/2}.$$

psi) for 1 h, and the NMR experiments were carried out. Removal of the CO atmosphere reversed the reaction.

(z) [Ir<sub>2</sub>(CO)<sub>4</sub>(μ-CCH<sub>2</sub>)(μ-CC(H)Ph)(dppm)<sub>2</sub>][SO<sub>3</sub>CF<sub>3</sub>]<sub>2</sub> (22).

A CD<sub>2</sub>Cl<sub>2</sub> solution of compound 19-SO<sub>3</sub>CF<sub>3</sub> (10 mg in 0.5 mL in an NMR tube, 7 μmol) was put under CO (10 psi), 4 μL of CF<sub>3</sub>SO<sub>3</sub>CH<sub>3</sub> (36 μmol) was added, and the NMR experiments were undertaken. Iodomethane was found in the <sup>1</sup>H NMR spectra. Removal of CO caused the transformation of compound 14 to unknown species.

(aa) [Ir<sub>2</sub>(Me)<sub>2</sub>(CO)<sub>2</sub>(μ-CCH<sub>2</sub>)(μ-CC(H)Ph)(dppm)<sub>2</sub>] (23).

To a CD<sub>2</sub>Cl<sub>2</sub> solution of compound 19-SO<sub>3</sub>CF<sub>3</sub> (25 mg in 0.5 mL in an NMR tube, 17 μmol) was added 50 μL of LiMe (1.4 M in Et<sub>2</sub>O, 70 μmol), and NMR experiments were carried out. The <sup>31</sup>P NMR showed that 1 equiv of compound 20 accompanies compound 23.

**X-ray Data Collection.** (a) [Ir<sub>2</sub>I<sub>2</sub>(CO)<sub>2</sub>(μ-CC(H)Ph)(μ-HCCH)(dppm)<sub>2</sub>] (15). Crystals were obtained, with 1 equiv of CH<sub>2</sub>Cl<sub>2</sub> of crystallization, from CH<sub>2</sub>Cl<sub>2</sub>/Et<sub>2</sub>O and mounted in capillaries. Unit cell parameters, at -65 °C, were obtained from a least-squares analysis of 25 reflections in the range 20.1° ≤ 2θ ≤ 23.9°, which were accurately centered on a CAD4 diffractometer. The systematic absences (*h*0*l*, *l* ≠ 2*n*; 0*k*0, *k* ≠ 2*n*) defined the space group as P2<sub>1</sub>/c (No. 14).

Intensity data were collected on the CAD4 diffractometer at -65 °C, employing the θ/2θ scan technique in the bisecting mode up to 2θ = 50°. Peaks were collected using variable scan speeds (between 1.73 and 6.71 deg min<sup>-1</sup>) with backgrounds scanned for 25% of the peak scan on either side of the peak. The intensities of three standard reflections were checked every 1 h of exposure time. No variation was observed so no correction was applied. A value of 0.04 was used for *p*,<sup>25</sup> and data were corrected for Lorentz and polarization effects and for absorption.<sup>26</sup> See Table 2 for additional information.

(b) [Ir<sub>2</sub>I<sub>2</sub>(CO)<sub>2</sub>(μ-CCH<sub>2</sub>)(μ-CC(H)Ph)(dppm)<sub>2</sub>] (20b). Yellow crystals suitable for an X-ray diffraction study were grown from CH<sub>2</sub>Cl<sub>2</sub>/Et<sub>2</sub>O, and one was wedged into a capillary which was flame sealed. Unit cell parameters were obtained from a least-squares analysis of the setting angles of 18 reflections

in the range 14.1° ≤ 2θ ≤ 15.8°, which were accurately centered on a Rigaku AFC7R diffractometer with graphite-monochromated MoKα radiation and 12 kW rotating anode generator. The systematic absences (*hkl*, *h* + *k* + *l* ≠ 2*n*; *hk*0, *h* (*k*), ≠ 2*n*; 00*l*, *l* ≠ 4*n*) and the 4/*m* Laue symmetry defined the space group as I4<sub>1</sub>/a (No. 88).

Intensity data were collected on the Rigaku diffractometer at 22 °C, employing the θ/2θ scan technique in the bisecting mode up to 2θ = 55°, at scan speeds of 4.0 deg min<sup>-1</sup>; weak reflections (*I* < 10σ(*I*)) were rescanned up to three times and the counts accumulated. Stationary backgrounds were collected on each side of the reflection for a total duration of half of the time of the peak scan. The intensities of three standard reflections were measured every 150 reflections to monitor crystal and electronic stability; no significant variation was observed so no correction was applied. The data were processed in the usual manner assuming a value of 0.013 used for *p* to downweight intense reflections. Corrections for Lorentz and polarization effects and for absorption were made. See Table 2 for pertinent crystal data and details of intensity collection.

**Structure Solution and Refinement.** Both compounds were solved by a combination of Patterson and direct methods techniques to locate the Ir and I atoms, and all other atoms were located in subsequent difference Fourier maps. For compound 15 all hydrogens were located but were input in the idealized positions except for the phenylvinylidene hydrogen which was allowed to refine. Although they were located, the hydrogens on the acetylene ligand did not refine well so were input at the idealized positions. In compound 20b the vinylidene groups were disordered about the inversion center at 1/2, 1/2, 0. Attempts to refine the two half-occupancy, inversion-related phenyl rings allowing the phenyl carbons to refine individually resulted in a slightly distorted geometry for this group. It was therefore refined as a rigid group with a single thermal parameter refined for all carbon atoms. All hydrogen atoms, except on the disordered phenylvinylidene, were located but were input in idealized coordinates and assigned thermal parameters of 1.2 times those of the attached carbon.

Refinements were carried out using full-matrix, least-squares techniques<sup>27,28</sup> minimizing the function  $\sum w(|F_o| -$

(25) Doedens, R. J.; Ibers, J. A. *Inorg. Chem.* **1967**, *6*, 204.

(26) Walker, N.; Stuart, D. *Acta Crystallogr., Sect. A: Found. Crystallogr.* **1983**, *A39*, 158.



**Table 3. Atomic Coordinates and Thermal Parameters for the Core Atoms of Compound 15<sup>a</sup>**

atom	x	y	z	B <sup>b</sup> (Å <sup>2</sup> )
Ir(1)	0.34732(2)	0.03235(1)	0.26634(1)	1.808(6)
Ir(2)	0.20380(2)	-0.10432(2)	0.31382(1)	1.994(6)
I(1)	0.47655(3)	0.13735(3)	0.30735(3)	3.04(1)
I(2)	0.13086(4)	-0.17685(3)	0.40899(3)	4.27(1)
P(1)	0.4502(1)	-0.0617(1)	0.27880(9)	2.04(4)
P(2)	0.3159(1)	-0.1880(1)	0.3153(1)	2.39(5)
P(3)	0.2332(1)	0.1152(1)	0.26892(9)	2.01(4)
P(4)	0.1065(1)	-0.0065(1)	0.30832(9)	2.19(4)
O(1)	0.3707(4)	0.0919(3)	0.1350(3)	4.0(2)
O(2)	0.0741(4)	-0.2040(3)	0.2282(3)	4.3(2)
C(1)	0.3597(5)	0.0647(4)	0.1807(4)	2.3(2)
C(2)	0.1240(5)	-0.1656(4)	0.2576(4)	2.8(2)
C(3)	0.3428(5)	0.0045(4)	0.3612(3)	2.3(2)
C(4)	0.2885(5)	-0.0437(4)	0.3786(4)	2.4(2)
C(5)	0.2558(4)	-0.0508(4)	0.2403(3)	2.0(2)
C(6)	0.2277(5)	-0.0733(4)	0.1804(4)	2.8(2)
C(7)	0.4044(4)	-0.1557(4)	0.2754(4)	2.5(2)
C(8)	0.1295(4)	0.0681(4)	0.2550(3)	2.2(2)

<sup>a</sup> Parameters for solvent molecule and phenyl rings are given as supplementary material. <sup>b</sup> All atoms given were refined anisotropically. Displacement parameters for the anisotropically refined atoms are given in the form of the equivalent isotropic Gaussian displacement parameter,  $B\{\text{eq}\}$ , defined as  $\frac{1}{3}[a^2\beta_{11} + b^2\beta_{22} + c^2\beta_{33} + ab(\cos \gamma)\beta_{12} + ac(\cos \beta)\beta_{13} + bc(\cos \alpha)\beta_{23}]$ .

**Table 4. Atomic Coordinates and Thermal Parameters for the Inner Core Atoms of Compound 20b<sup>a</sup>**

atom	x	y	z	B <sup>b</sup> (Å <sup>2</sup> )
Ir	0.46133(2)	0.51955(2)	0.07445(4)	2.38(1)
I	0.40802(4)	0.59642(3)	0.07318(9)	4.93(3)
P(1)	0.5175(1)	0.5542(1)	0.1700(3)	2.73(7)
P(2)	0.5904(1)	0.5164(1)	0.0306(3)	2.63(7)
O(1)	0.4115(3)	0.4966(4)	0.2661(8)	5.4(3)
C(1)	0.4283(4)	0.5047(5)	0.197(1)	4.4(4)
C(2)	0.5000(4)	0.4638(4)	0.0559(9)	2.3(3)
C(3)	0.4989(5)	0.4266(4)	0.103(1)	3.8(4)
C(4)	0.5671(4)	0.5649(4)	0.0955(10)	2.7(3)

<sup>a</sup> Phenyl carbons are given as supplementary material. <sup>b</sup> See Table 3 for definition of  $B$ .

$|F_c|^2$ , where  $w = 4F_o^2/\sigma^2(F_o^2)$ . The neutral atom scattering factors<sup>29,30</sup> and anomalous dispersion terms<sup>31</sup> used in structure solution were obtained from the usual sources. Both structures refined well as shown in Table 2. Positional parameters for the core atoms of compounds **15** and **20b** are given in Tables 3 and 4, respectively.

## Results and Discussion

**(a) Mono(vinylidene) Complexes.** In our previous study of alkyne-to-vinylidene transformations at an "Ir<sub>2</sub>" core<sup>23</sup> the majority of reactions carried out utilized the neutral diiodo species  $[\text{Ir}_2\text{I}_2(\text{CO})(\mu\text{-CO})(\text{dppm})_2]$  (**1**) as precursor; only preliminary studies were done with the closely related cationic A-frame  $[\text{Ir}_2(\text{CO})_2(\mu\text{-I})(\text{dppm})_2][\text{X}]$  (**2**). In the current paper we extend our investiga-

tions of cationic vinylidene complexes, reasoning that the removal of an anionic ligand should generate a coordination site for additional substrate molecules. Using this strategy the reaction with additional alkynes should be capable of generating bis(vinylidene) complexes or, alternatively, monovinylidene-alkyne complexes.

The cationic precursor used (**2**) had been previously prepared by the reaction of **1** with 1 equiv of the appropriate silver salt.<sup>24</sup> We now find that a more convenient preparation involves the reaction of **1** with methyl triflate, yielding **2** as the triflate salt, together with methyl iodide.

The reaction of **2** (as the triflate salt) with a 3-fold excess of acetylene at  $-80^\circ\text{C}$  yields the cationic acetylene adduct  $[\text{Ir}_2(\text{CO})(\text{HC}_2\text{H})(\mu\text{-I})(\mu\text{-CO})(\text{dppm})_2][\text{SO}_3\text{CF}_3]$  (**3**) as shown in Scheme 1 (note that in all schemes the dppm ligands above and below the plane of the drawing are omitted for clarity). This product can be isolated as a pale yellow solid at this temperature. The  $^{13}\text{C}\{^1\text{H}\}$  NMR spectrum of **3** (at  $-40^\circ\text{C}$ ) shows two carbonyl signals at  $\delta$  179.0 and 187.7, and selective and broad-band  $^{31}\text{P}$  decoupling experiments demonstrate a 10 Hz coupling between these carbonyls as well as coupling of the high-field carbonyl to the  $^{31}\text{P}$  nuclei on one metal and coupling of the low-field carbonyl to all four  $^{31}\text{P}$  nuclei, identifying the former as terminal and the latter as bridging. The acetylenic carbons resonate at  $\delta$  75.2 and 62.0 with a mutual coupling of 102 Hz. This coupling is intermediate between those for ethylene (67.6 Hz) and acetylene (171.5 Hz),<sup>32</sup> consistent with the expected rehybridization upon coordination to a metal center. In the  $^1\text{H}$  NMR spectrum the acetylenic protons resonate at  $\delta$  4.98 and 3.42 and, when  $^{13}\text{C}_2\text{H}_2$  is used, display coupling to the attached carbons of 234 and 237 Hz, respectively. These values are close to that observed in acetylene (249 Hz)<sup>32</sup> suggesting little rehybridization of this group (although it appears that this parameter may not be as sensitive to changes at carbon as  $^1J_{\text{C-C}}$ ). In the IR spectrum a stretch for the terminal carbonyl is observed at  $1966\text{ cm}^{-1}$  while the bridging CO appears at  $1824\text{ cm}^{-1}$ . A weak shoulder at  $1660\text{ cm}^{-1}$  is identified as the alkyne  $\text{C}\equiv\text{C}$  stretch, which is significantly lower than that in the free acetylene ( $1974\text{ cm}^{-1}$ ),<sup>33</sup> consistent with the significant change in C-C coupling constant noted above. This stretch is at higher frequency than values of ca.  $1590\text{ cm}^{-1}$  reported later for vinylidene ligands in which rehybridization to  $\text{sp}^2$  and bond-order reduction from three to two is complete. As expected for a low-valent, late transition metal, this alkyne, without electron-withdrawing substituents, is weakly bound,<sup>34</sup> as seen by the facile loss of acetylene from **3** under vacuum, even in the solid, which slowly develops a burgundy tinge, characteristic of **2**.

The structure proposed for compound **3** is analogous to that observed in the X-ray study of the hexafluorobutene adduct  $[\text{Ir}_2(\text{CO})(\text{CF}_3\text{C}_2\text{CF}_3)(\mu\text{-S})(\mu\text{-CO})(\text{dppm})_2]$ .<sup>35</sup>

(27) For compound **15**, programs used were those of the Enraf-Nonius Structure Determination Package by B. A. Frenz, in addition to local programs by R. G. Ball.

(28) For compound **20b**, the teXsan Crystal Structure Analysis Package, by Molecular Structure Corp. (1985 and 1992), was used.

(29) Cromer, D. T.; Waber, J. T. *International Tables for X-ray Crystallography*; The Kynoch Press: Birmingham, England, 1974; Vol. IV, Table 2.2A.

(30) Stewart, R. F.; Davidson, E. R.; Simpson, W. T. *J. Chem. Phys.* **1965**, *42*, 3175.

(31) (a) Cromer, D. T.; Liberman, D. *J. Chem. Phys.* **1970**, *53*, 1891.

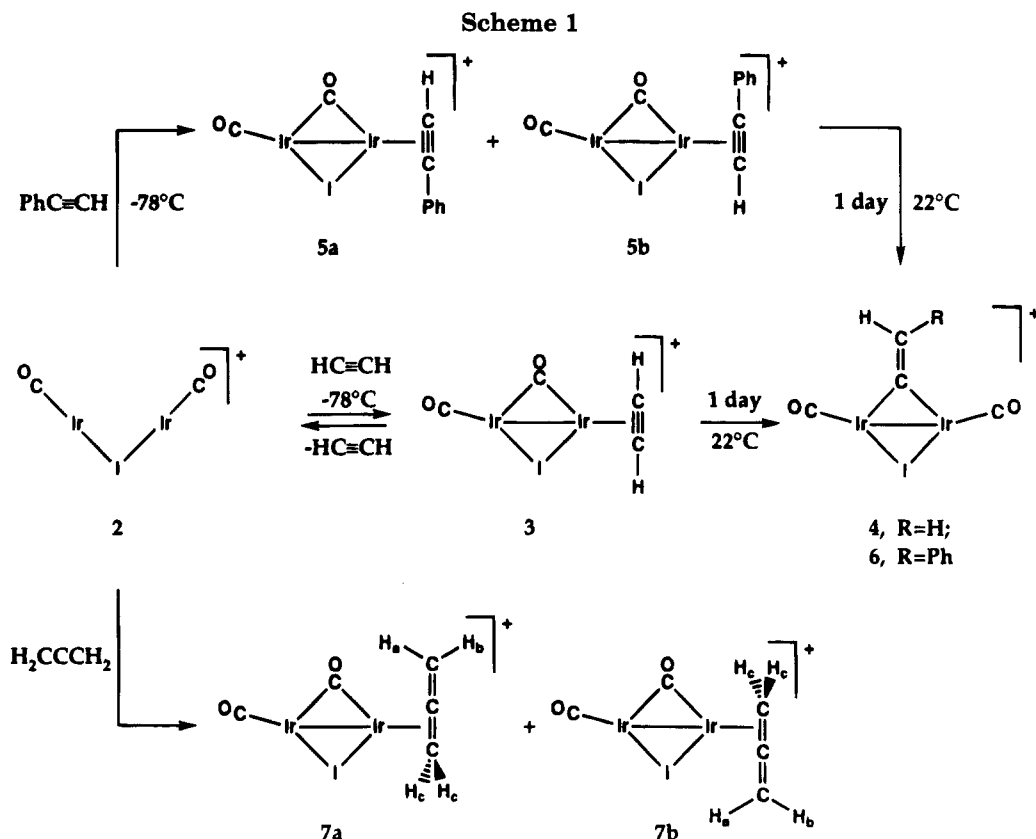
(b) Creagh, D. C.; McAuley, W. J. *International Tables for Crystallography*; Wilson, A. J. C., Ed.; Kluwer Academic Publishers: Boston, MA, 1992; Vol. C, Table 4.2.6.8, pp 219–222.

(32) Friebolin, H. *Basic One- and Two-Dimensional NMR Spectroscopy*; VCH Verlagsgesellschaft Publishers: Weinheim, Federal Republic of Germany, 1991; Chapter 3.

(33) Jones, R. N.; Sandorfy, C. *Technique of Organic Chemistry*; West, W., Ed.; Interscience Publishers: New York, 1956; Vol. IX, p 385.

(34) Collman, J. P.; Hegedus, L. S.; Norton, J. R.; Finke, R. G. *Principles and Applications of Organotransition Metal Chemistry*; University Science Books: Mill Valley, CA, 1987.

(35) Vaartstra, B. A.; Cowie, M. *Organometallics* **1989**, *8*, 2388.



This is the structure expected for alkyne attack at the less sterically encumbered coordination site on the outside of the A-frame, remote from the adjacent metal. However, it is surprising that **3** has not rearranged to an alkyne-bridged product, since such rearrangements are usually extremely facile in these complexes.<sup>36</sup> It may be that rearrangement is unfavorable because of the large bulk of the iodo ligand. Compound **3** is also isoelectronic with the series of tricarbonyl A-frames derived from CO addition to **2** and its analogues,<sup>24,37</sup> in which the terminal alkyne has been replaced by a carbonyl.

In the absence of excess acetylene, compound **3** rearranges to the vinylidene-bridged  $[\text{Ir}_2(\text{CO})_2(\mu\text{-I})(\mu\text{-CCH}_2)(\text{dppm})_2][\text{SO}_3\text{CF}_3]$  (**4**) after 24 h at ambient temperature. Although no intermediates were observed in this transformation, it appears that it is not a trivial process since the 1,2-hydrogen shift is accompanied by a reshuffling of the vinylidene and a carbonyl ligand to give the symmetric **4**. The  $^{13}\text{C}\{^1\text{H}\}$  NMR spectrum shows the vinylidene  $\text{C}_\alpha$  and  $\text{C}_\beta$  resonances at  $\delta$  219.6 and 129.9, and the coupling between these nuclei (65 Hz) is consistent with a  $\text{C}=\text{C}$  double bond between  $\text{sp}^2$ -hybridized carbons, comparing well to the value for ethylene (67.6 Hz).<sup>32</sup>  $\text{C}_\alpha$  also displays coupling to all

four phosphorus nuclei (7 Hz) and to both carbonyls (9 Hz,  $^{13}\text{C}$ -enriched), confirming its bridging nature. One resonance for both carbonyls is observed at  $\delta$  181.7, displaying coupling to  $\text{C}_\alpha$  ( $^{13}\text{C}$ -enriched vinylidene) in addition to being virtually coupled to all four phosphorus nuclei. The  $^1\text{H}$  NMR spectrum shows the vinylidene protons at  $\delta$  3.72, with coupling (in the  $^{13}\text{C}_2\text{H}_2$  sample) to the  $\beta$  carbon of 161 Hz, which is again close to that in ethylene (156.4 Hz)<sup>32</sup> but substantially different from that noted in the acetylene adduct **3**. In the IR spectrum only one carbonyl stretch is observed ( $1949 \text{ cm}^{-1}$ , Nujol) together with a weak band at  $1588 \text{ cm}^{-1}$  ( $1536 \text{ cm}^{-1}$  in the  $^{13}\text{C}=\text{C}$  sample) corresponding to the vinylidene  $\text{C}=\text{C}$  stretch. Compound **4** was obtained as the  $\text{SO}_3\text{CF}_3^-$  or the  $\text{BF}_4^-$  salt, starting from compound **2** having the appropriate anion, and both salts display identical spectroscopic parameters for the cations indicating that these anions behave as innocent, noncoordinating counterions.

Extending this chemistry to include unsymmetrical, terminal alkynes, such as phenylacetylene, gives similar chemistry with **2**, yielding two isomers of  $[\text{Ir}_2(\text{CO})(\text{HC}\equiv\text{CPh})(\mu\text{-I})(\mu\text{-CO})(\text{dppm})_2][\text{SO}_3\text{CF}_3]$  (**5a,b**) at  $-60^\circ\text{C}$ , as shown in Scheme 1. The existence of two isomers presumably results from the differing orientations of the unsymmetrical alkyne, in which the phenyl substituent faces the bridging iodo (**5a**) or carbonyl (**5b**) groups. All spectroscopic parameters for these isomers closely resemble those of **3**, supporting the structural assignments. At  $-60^\circ\text{C}$  **5a** is dominant (*ca.* 5:2 mole ratio); however, as the temperature is raised to ambient, this isomer disappears leaving only **5b**. It is assumed that this is the thermodynamically favored isomer on the basis of less repulsion of the phenyl substituent with the smaller carbonyl ligand, as opposed to the large iodo group. At ambient temperature compound **5b** slowly

(36) See for example: (a) Cowie, M.; Dickson, R. S. *Inorg. Chem.* **1981**, *20*, 2682. (b) Cowie, M.; Southern, T. G. *Inorg. Chem.* **1982**, *21*, 246. (c) Sutherland, B. R.; Cowie, M. *Organometallics* **1984**, *3*, 1869. (d) Vaartstra, B. A.; Xiao, J.; Jenkins, J. A.; Verhagen, R.; Cowie, M. *Organometallics* **1991**, *10*, 2708. (e) Jenkins, J. A.; Cowie, M. *Organometallics* **1992**, *11*, 2774. (f) Johnson, K. A.; Gladfelter, W. L. *Organometallics* **1989**, *8*, 2866. (g) Johnson, K. A.; Gladfelter, W. L. *Organometallics* **1992**, *11*, 2534. (h) Mague, J. T. *Organometallics* **1986**, *5*, 918. (i) Mague, J. T. *Polyhedron* **1990**, *9*, 2635.

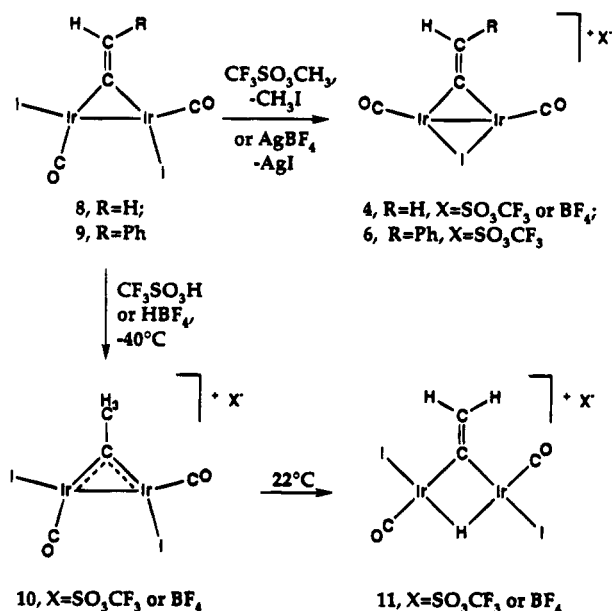
(37) (a) Kubiak, C. P.; Woodcock, C.; Eisenberg, R. *Inorg. Chem.* **1980**, *19*, 2733. (b) Kubiak, C. P.; Woodcock, C.; Eisenberg, R. *Inorg. Chem.* **1982**, *21*, 2119. (c) Cowie, M. *Inorg. Chem.* **1979**, *18*, 286. (d) Sutherland, B. R.; Cowie, M. *Inorg. Chem.* **1984**, *23*, 2324. (e) Sutherland, B. R.; Cowie, M. *Can. J. Chem.* **1986**, *64*, 464.

transforms into several (four or more) intermediates which in turn, after 24 h, transform into **6**, the phenylvinylidene-bridged analogue of **4**. Unfortunately, these intermediates were never present in large enough quantities and were always present as a complex mixture, so could not be identified. However, at least one of these intermediates displays a high-field resonance in the  $^1\text{H}$  NMR spectrum, suggesting the involvement of a hydride-acetylide species, as has been observed in other acetylene-to-vinylidene rearrangements.<sup>23,38-41</sup> The presence of several intermediates is consistent with our earlier hypothesis that this transformation from a terminally bound alkyne to a bridging vinylidene in **4** and **6** must require several steps.

An allene product,  $[\text{Ir}_2(\text{CO})(\text{C}_3\text{H}_4)(\mu\text{-I})(\mu\text{-CO})(\text{dppm})_2][\text{X}]$  (**7**), analogous to the alkyne species **3** and **5**, is obtained in the reaction of **2** with allene at ambient temperature. As was observed with phenylacetylene, two isomers, **7a,b**, are obtained in *ca.* 5:1 ratio. It is proposed that the major isomer (**7a**) has the  $\text{CH}_2$  moiety, which is not coordinated to the metal, aimed toward the smaller carbonyl rather than the iodo ligand, whereas this unit is closer to I in **7b**. For the major isomer ( $\text{I}^-$  salt) a terminal ( $\delta$  179.9) and a bridging ( $\delta$  189.9) carbonyl is identified in the  $^{13}\text{C}\{^1\text{H}\}$  NMR spectra, based on their coupling to the appropriate  $^{31}\text{P}$  nuclei, and this assignment is substantiated by the IR spectrum which shows a terminal and a bridging ( $1983, 1819\text{ cm}^{-1}$ ,  $\text{CH}_2\text{-Cl}_2$ ) carbonyl stretch. The  $^1\text{H}$  NMR spectrum shows the allene protons at  $\delta$  5.93, 5.33, and 1.31 in a 1:1:2 intensity ratio, respectively. The high-field signal corresponds to the protons on the coordinated  $\text{CH}_2$  group, which display coupling to two phosphorus nuclei ( $^3J_{\text{PH}} = 7\text{ Hz}$ ) and to each of the other allene protons ( $^4J_{\text{H}_a\text{H}_c} = ^4J_{\text{H}_b\text{H}_c} = 3.4\text{ Hz}$ ). In addition the inequivalent protons on the unbound end of the allene ( $\text{H}_a, \text{H}_b$ ) show geminal coupling of 2.4 Hz. For the less abundant isomer **7b** the spectroscopic data in Table 1 are very similar to those of **7a**. The subsequent chemistry of these allene products, with regards C-H activation or condensation reactions, has not yet been investigated.

In an attempt to probe the reactivity of the bridging vinylidene moiety in the previously reported complexes,  $[\text{Ir}_2\text{I}_2(\text{CO})_2(\mu\text{-CC}(\text{H})\text{R})(\text{dppm})_2]$  ( $\text{R} = \text{H}$  (**8**),  $\text{Ph}$  (**9**)),<sup>23</sup> methyl triflate was added on the assumption that electrophilic attack at the vinylidene  $\beta$ -carbon would occur.<sup>41</sup> Instead, as shown in Scheme 2, loss of  $\text{CH}_3\text{I}$  occurs (as detected in the  $^1\text{H}$  NMR by a resonance at  $\delta$  2.16) to generate the previously described cationic, vinylidene-bridged complexes **4** and **6**. No intermediates were detected, so whether initial  $\text{CH}_3^+$  attack occurs at a metal or directly at an iodo ligand is not known. The same species, having  $\text{BF}_4^-$  anions instead of  $\text{CF}_3\text{SO}_3^-$ , can be obtained by the addition of 1 equiv of  $\text{AgBF}_4$  to **8** or **9**. The vinylidene-bridged, cationic compounds **4** and **6** can therefore be prepared either by reaction of the appropriate alkyne with the cationic precursor **2** or by iodide removal from the preformed neutral vinylidene complexes **8** and **9**.

Scheme 2



Although, as noted above, electrophilic attack by  $\text{CH}_3^+$  apparently did not occur at the vinylidene  $\beta$ -carbon, protonation of **8** does yield the expected ethylidyne-bridged species **10** when protonation is carried out at  $-40^\circ\text{C}$ , as shown in Scheme 2. In the  $^{13}\text{C}\{^1\text{H}\}$  NMR spectrum of **10** ( $\text{BF}_4^-$  salt) two carbonyl resonances at  $\delta$  179.0 and 166.5 are observed and each shows coupling to a different pair of  $^{31}\text{P}$  nuclei, indicating that these carbonyls are terminally bound to different metals. When the ethylidyne ligand is  $^{13}\text{C}$ -enriched, the low-field  $^{13}\text{CO}$  resonance of **10** also shows 23 Hz coupling to the  $\alpha$ -carbon of the ethylidyne unit. The ethylidyne carbons resonate at  $\delta$  409.1 ( $\text{C}_\alpha$ ) and 68.5 ( $\text{C}_\beta$ ), comparing closely to the values reported ( $\delta$  405–453,  $\text{C}_\alpha$ ;  $\delta$  58,  $\text{C}_\beta$ ) in some ethylidyne-bridged heterobinuclear complexes,<sup>6,43</sup> and display a mutual coupling of 23 Hz. Although we were unable to find reports of C-C coupling in bridging ethylidyne groups, presumably because these groups were not  $^{13}\text{C}$  enriched, the value observed for **10** is comparable to the value reported for ethane (34.6 Hz) and is consistent with a C-C single bond. In the  $^1\text{H}$  NMR spectrum of ethylidyne methyl protons resonate as a singlet at  $\delta$  3.99 or as a doublet with 128 Hz coupling to  $\text{C}_\beta$  when the ethylidyne is  $^{13}\text{C}$  enriched; again this coupling is in good agreement with that reported for ethane (124.9 Hz) consistent with  $\text{sp}^3$  hybridization of the carbon.

Upon warming of **10** to ambient temperature an immediate and surprising rearrangement occurs in which an ethylidyne proton transfers to the metals to give the hydride- and vinylidene-bridged product  $[\text{Ir}_2\text{I}_2(\text{CO})_2(\mu\text{-H})(\mu\text{-CCH}_2)(\text{dppm})_2][\text{X}]$  (**11**). The  $^{13}\text{C}\{^1\text{H}\}$  NMR spectrum of the  $\text{BF}_4^-$  salt shows the carbonyl ligands at  $\delta$  167.9 and 166.3 with the latter displaying 26 Hz coupling to the vinylidene  $\text{C}_\alpha$  ( $^{13}\text{C}$  enriched). Resonances for the vinylidene group appear at  $\delta$  187.5 ( $\text{C}_\alpha$ ) and 132.3 ( $\text{C}_\beta$ ) with a mutual coupling of 70 Hz; in addition the  $\text{C}_\alpha$  resonance displays equal coupling to all four phosphorus nuclei, confirming the bridged arrange-

(38) Wolf, J.; Werner, H.; Sehadli, O.; Ziegler, M. L. *Angew. Chem., Int. Ed. Engl.* **1983**, *22*, 414.

(39) Garcia Alonso, F. J.; Höhn, A.; Wolf, J.; Otto, H.; Werner, H. *Angew. Chem., Int. Ed. Engl.* **1985**, *24*, 406.

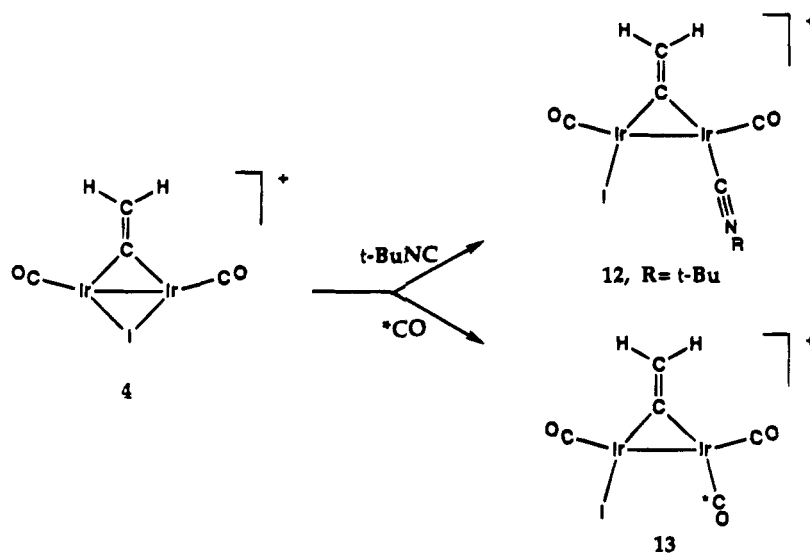
(40) Höhn, A.; Otto, H.; Dzialis, M.; Werner, H. *J. Chem. Soc., Chem. Commun.* **1987**, 852.

(41) Höhn, A.; Werner, H. *J. Organomet. Chem.* **1990**, *382*, 255.

(42) Kostic, N. M.; Fenske, R. F. *Organometallics* **1982**, *1*, 974.

(43) Awang, M. R.; Jeffery, J. C.; Stone, F. G. A. *J. Chem. Soc., Dalton Trans.* **1983**, 2091.

Scheme 3



ment, and to the carbonyl ligand. In the  $^1\text{H}$  NMR spectrum only one resonance for a vinylidene hydrogen is observed at  $\delta$  8.17 with the other presumably being obscured by the phenyl protons. This resonance displays 7 Hz geminal coupling to the other vinylidene proton and 156 Hz coupling to  $\text{C}_\beta$  ( $^{13}\text{C}$  enriched). The hydride resonance appears as a multiplet at  $\delta$  -12.48 and is shown to be bridging based on selective and broad-band  $^{31}\text{P}$  decoupling experiments. Protonation of **8** to give **11** has resulted in a net oxidation of the metals, and this is mirrored by the change in carbonyl stretches from 1960 and  $1985\text{ cm}^{-1}$  to 2020 and  $2066\text{ cm}^{-1}$ . The vinylidene stretch appears at  $1605\text{ cm}^{-1}$ .

This transformation is the opposite of what one intuitively expects, with protonation generally occurring first at the metals with subsequent transfer to the hydrocarbyl ligand, and certainly the opposite has been observed in related mononuclear vinylidene complexes in which protonation at Ir with subsequent transfer to the  $\beta$ -carbon occurred.<sup>41,44</sup> Apparently in **8** the most nucleophilic site is at the  $\beta$ -carbon yielding **10** as the kinetic product, but with the hydride- and vinylidene-bridged species being thermodynamically favored. In spite of the favorable C-H bond enthalpy in **10**, we assume that the delocalized Ir-C $_\alpha$ -Ir multiple bond is not sufficient to overcome the C=C bond and the Ir-H-Ir interaction that results in the final product **11**.

Although the cationic vinylidene-bridged complexes **4** and **6** are saturated, by virtue of the iodo ligand assuming a bridging position, they have incipient unsaturation, since movement of  $\text{I}^-$  to a terminal site on one metal can generate unsaturation at the other. Consistent with this proposal, compound **4** (as the triflate salt) reacts readily at ambient temperature with *t*-BuNC or CO, as shown in Scheme 3, to give the respective compounds  $[\text{Ir}_2\text{I}(\text{CO})_2(\textit{t}\text{-BuNC})(\mu\text{-CCH}_2)(\text{dppm})_2][\text{SO}_3\text{CF}_3]$  (**12**) and  $[\text{Ir}_2\text{I}(\text{CO})_3(\mu\text{-CCH}_2)(\text{dppm})_2][\text{SO}_3\text{CF}_3]$  (**13**). The  $^{13}\text{C}\{^1\text{H}\}$  NMR spectrum of **12** shows the terminal carbonyls at  $\delta$  172.9 and 166.3, and selective  $^{31}\text{P}$  decoupling shows that each CO is bound to a different metal. These carbonyls show 8 Hz mutual coupling which argues in favor of a structure in which

the carbonyls are close to the trans position with respect to the Ir-Ir bond; large 3-bond coupling through a metal-metal bond has been previously noted.<sup>45</sup> An arrangement of ligands like that proposed for **12** has been observed in the X-ray structures of **8** and **9**.<sup>23</sup> The vinylidene carbons ( $^{13}\text{C}$  enriched) are observed at  $\delta$  188.3 ( $\text{C}_\alpha$ ) and 132.0 ( $\text{C}_\beta$ ) and display the usual  $\text{C}_\alpha\text{-C}_\beta$  coupling of 67 Hz. As expected,  $\text{C}_\alpha$  displays additional coupling to all phosphorus nuclei, confirming its bridged arrangement, whereas  $\text{C}_\beta$  shows no additional coupling.  $\text{C}_\alpha$  also shows coupling to one of the carbonyls, but this is only 3 Hz, indicating that the vinylidene is cis to both carbonyls. In the  $^1\text{H}$  NMR the vinylidene protons appear as a singlet at  $\delta$  6.75 and the *t*-BuNC protons also appear as a singlet; however cooling the sample shows that the chemical shifts of the vinylidene protons are temperature dependent since the singlet resolves into an AB quartet. At ambient temperature the use of  $^{13}\text{C}$ -enriched vinylidene splits the vinylidene proton signal into a doublet ( $^1J_{\text{CH}} = 157\text{ Hz}$ ). The IR spectrum supports the structural assignment showing the terminal carbonyl bands at 1990 and  $1976\text{ cm}^{-1}$ , the C $\equiv$ N stretch of the isocyanide at  $2184\text{ cm}^{-1}$ , and the vinylidene C=C stretch at  $1585\text{ cm}^{-1}$ . The increase in the isocyanide stretch from *ca.*  $2125\text{ cm}^{-1}$  in the free molecule indicates that this ligand functions mainly as a  $\sigma$  donor.<sup>46</sup>

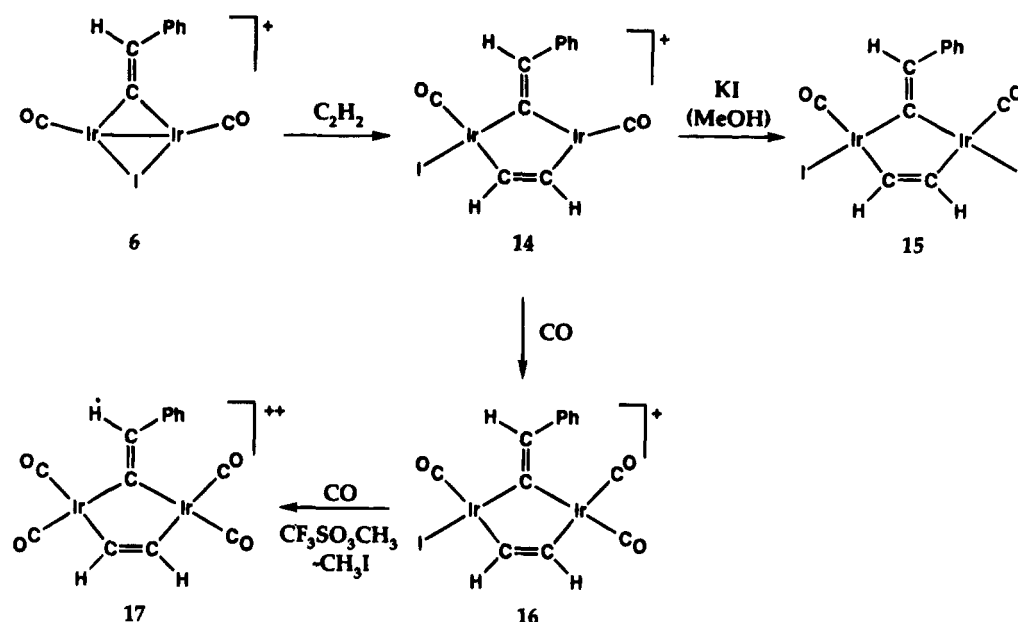
For the carbonyl adduct **13** the spectroscopic data are closely comparable. In the  $^{13}\text{C}\{^1\text{H}\}$  NMR three carbonyl resonances are now observed at  $\delta$  174.1, 170.0, and 162.4, and all are shown to correspond to terminally bound CO's, based on  $^{31}\text{P}$  decoupling experiments. All carbonyls display weak coupling (<3 Hz) with each other, but only the low-field resonance displays substantial coupling (15 Hz) to  $\text{C}_\alpha$  of the  $^{13}\text{C}$ -enriched vinylidene. This coupling suggests an arrangement of this carbonyl and the vinylidene group which is close to trans. If the  $^{13}\text{C}$ -enriched sample of **4** is reacted with  $^{12}\text{CO}$ , the  $^{13}\text{C}\{^1\text{H}\}$  NMR of the product shows that the low-field carbonyl signal is substantially weaker (*ca.* 50%) than the other two, supporting the structural

(44) Höhn, A.; Werner, H. *Angew. Chem., Int. Ed. Engl.* **1986**, *25*, 737.

(45) Brown, M. P.; Fisher, J. R.; Hill, R. H.; Puddephatt, R. J.; Seddon, K. R. *Inorg. Chem.* **1981**, *20*, 3516.

(46) Treichel, P. M. *Adv. Organomet. Chem.* **1973**, *11*, 21.

Scheme 4



assignment shown for **13** in which the attacking group binds at the site vacated by the bridging I<sup>-</sup> ligand. The partial occupancy of this site by <sup>13</sup>CO in the latter experiment indicates either scrambling of the carbonyls on the metals or some attack by CO adjacent to the vinylidene group.

**(b) Mixed Vinylidene–Acetylene-Bridged Complexes.** In our previous study<sup>23</sup> we had reported that the neutral vinylidene-bridged complex **8** reacted with acetylene to give two cationic species containing both a bridging vinylidene and a bridging acetylene group,<sup>47</sup> and that the same two species could be obtained in the reaction of [Ir<sub>2</sub>(CO)<sub>2</sub>(μ-I)(dppm)<sub>2</sub>][BF<sub>4</sub>] with excess acetylene. It appeared likely that a cationic monobridged vinylidene intermediate such as **4** was involved in this reaction. The previously described reactions of **4** with <sup>t</sup>BuNC and CO demonstrated ligand attack on the face of the complex opposite the vinylidene group. Similar reactivity of **4** with acetylene, followed by movement of acetylene to the bridging position, would give products analogous to those proposed in the earlier study. In agreement with these ideas the reaction of **4** with acetylene does give one of the two previously reported complexes, containing a bridged vinylidene and a bridged acetylene ligand (on the basis of a comparison of spectral parameters with those previously reported). However the present reaction is complex, yielding a large number of additional unidentified species. Owing to the complexity of this reaction we turned instead to the reaction of the analogous phenylvinylidene-bridged species **6** with acetylene. In this case the anticipated product, [Ir<sub>2</sub>I(CO)<sub>2</sub>(μ-CC(H)Ph)(μ-HC<sub>2</sub>H)(dppm)<sub>2</sub>][SO<sub>3</sub>CF<sub>3</sub>] (**14**), containing a bridging phenylvinylidene and bridging acetylene group was obtained cleanly, as outlined in Scheme 4.

Since the phenylvinylidene ligand was not <sup>13</sup>C enriched, we do not have <sup>13</sup>C NMR parameters for it; however it is assumed to remain bridging on the basis

of the subsequent structure determination of a derivative (**15**) (*vide infra*) and on the spectral data. The <sup>13</sup>C{<sup>1</sup>H} NMR spectrum of **14** (SO<sub>3</sub>CF<sub>3</sub><sup>-</sup> salt), in which the carbonyl and acetylene ligands are <sup>13</sup>C enriched, shows two resonances for the terminal carbonyls (δ 177.3, 169.2) and two acetylenic resonances at δ 133.8 and 120.8, with the latter two showing a mutual coupling of 60 Hz. Of the two CO resonances, only one displays strong coupling (30 Hz) to one of the acetylenic carbons indicating a *trans* arrangement at one metal—presumably at the saturated metal for which an octahedral geometry is proposed. Although the <sup>13</sup>C NMR parameters are not enough to differentiate between an acetylene and a vinylidene group, the <sup>31</sup>P coupling pattern strongly supports the acetylene-bridged formulation since *both* carbons show coupling to all <sup>31</sup>P nuclei; while one carbon shows 11 Hz coupling to one pair of <sup>31</sup>P nuclei and 6.5 Hz to the other, the adjacent carbon shows 7.5 Hz coupling to all <sup>31</sup>P nuclei. A similar coupling pattern is observed for the structurally characterized compound **15** (*vide infra*), and this coupling pattern is in contrast to that of bridging vinylidenes for which we find that only C<sub>α</sub> generally displays coupling to the <sup>31</sup>P nuclei. In the <sup>1</sup>H NMR spectrum of **14** one acetylenic proton is observed at δ 8.60, with coupling to an acetylenic carbon (<sup>1</sup>J<sub>CH</sub> = 146 Hz), and the phenylvinylidene hydrogen is observed at δ 8.53; the second acetylenic proton resonance is presumably obscured by phenyl resonances.

Reaction of **14** with KI yields the neutral diiodo product [Ir<sub>2</sub>I<sub>2</sub>(CO)<sub>2</sub>(μ-CC(H)Ph)(μ-HCCH)(dppm)<sub>2</sub>] (**15**). Although the local geometries at both Ir centers in **15** are identical, the orientation of the bridging phenylvinylidene ligand renders the metals inequivalent. As a result two closely spaced <sup>31</sup>P resonances are observed. Significantly, these resonances appear close to that observed for the saturated end of complex **14**, suggesting that this metal center in **14** has a similar environment to both metals in **15**, as shown in Scheme 4. Most other spectroscopic parameters for **15** compare well with those of **14** apart from the strong coupling of *both* carbonyls to an acetylenic carbon (<sup>13</sup>C enriched) in **15**, in line with

(47) It now appears that the compound previously reported in ref 23 as dicationic is in fact a neutral diiodo species analogous to **15** and should therefore be reformulated as [Ir<sub>2</sub>I(CO)<sub>2</sub>(μ-CCH<sub>2</sub>)(μ-HCCH)(dppm)<sub>2</sub>].

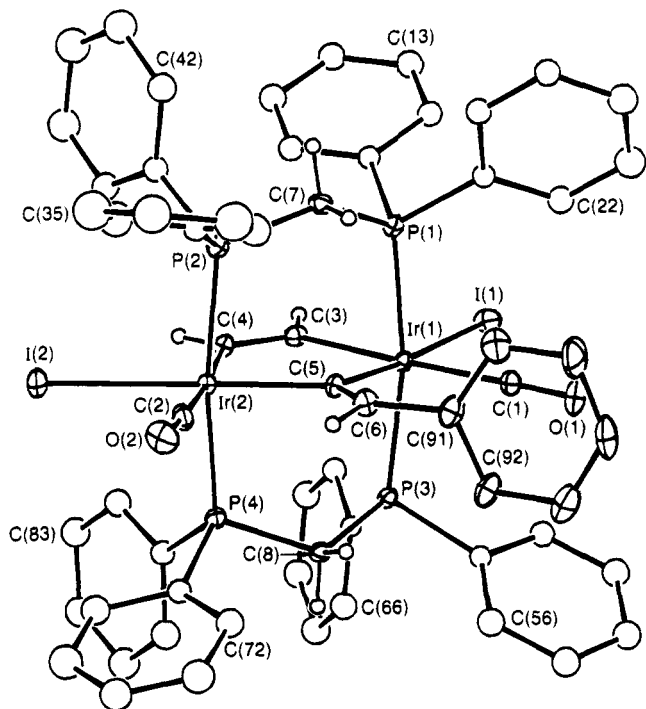


**Figure 1.** Perspective drawing of  $[\text{Ir}_2\text{I}_2(\text{CO})_2(\mu\text{-CC}(\text{H})\text{Ph})(\mu\text{-HCCH})(\text{dppm})_2]$  (**15**), showing the numbering scheme. Numbering on the phenyl carbons starts at the ipso position and proceeds sequentially around the ring. Thermal ellipsoids are shown at the 20% level except for methylene and vinylidene hydrogens which are shown arbitrarily small and phenyl hydrogens which are omitted.

the trans arrangement between these groups as shown. This geometry is consistent with  $\text{I}^-$  attack at **14** being directed away from the bulky phenyl substituent on the vinylidene group and is confirmed by the X-ray structure determination.

The geometry shown for compound **15** in Figure 1 has the expected octahedral coordinations at both metals. Selected bond lengths and angles are given in Table 5. Around each metal the angles are close to the idealized values, with the major distortions appearing to result from the very long Ir–Ir separation of 3.6011(6) Å, which has resulted from formal insertion of acetylene into the Ir–Ir bond of the precursor. By comparison the metal–metal-bonded, vinylidene-bridged species **8** and **9** have Ir–Ir separations of 2.828(1) and 2.783(1) Å, respectively.<sup>23</sup> All angles at the acetylene carbons and at the  $\alpha$ -carbon (C(5)) of the phenylvinylidene group are close to the idealized  $\text{sp}^2$  values. The slight distortion at C(6), resulting in a C(91)–C(6)–C(5) angle of 131.5(7)°, appears to be steric in origin, with the phenyl substituent being forced away from the adjacent carbonyl C(1)O(1). This also appears to cause a slight tilting of the vinylidene, resulting in the Ir(1)–C(5)–C(6) angle being slightly larger than Ir(2)–C(5)–C(6) (125.0(5)° vs 116.9(5)°). Both C=C bonds of the acetylene (1.316(9) Å) and the phenylvinylidene (1.335(9) Å) groups are close to the value expected for a double bond, in keeping with the 1,2-dimetallated olefin formulation for the acetylene group. All other parameters are essentially as expected.

Compound **14** also reacts with CO to give the cationic tricarbonyl species  $[\text{Ir}_2\text{I}(\text{CO})_3(\mu\text{-CC}(\text{H})\text{Ph})(\mu\text{-HCCH})(\text{dppm})_2][\text{SO}_3\text{CF}_3]$  (**16**), having a structure analogous to **15**. Again the  $^{31}\text{P}$  nuclei bound to the metal center

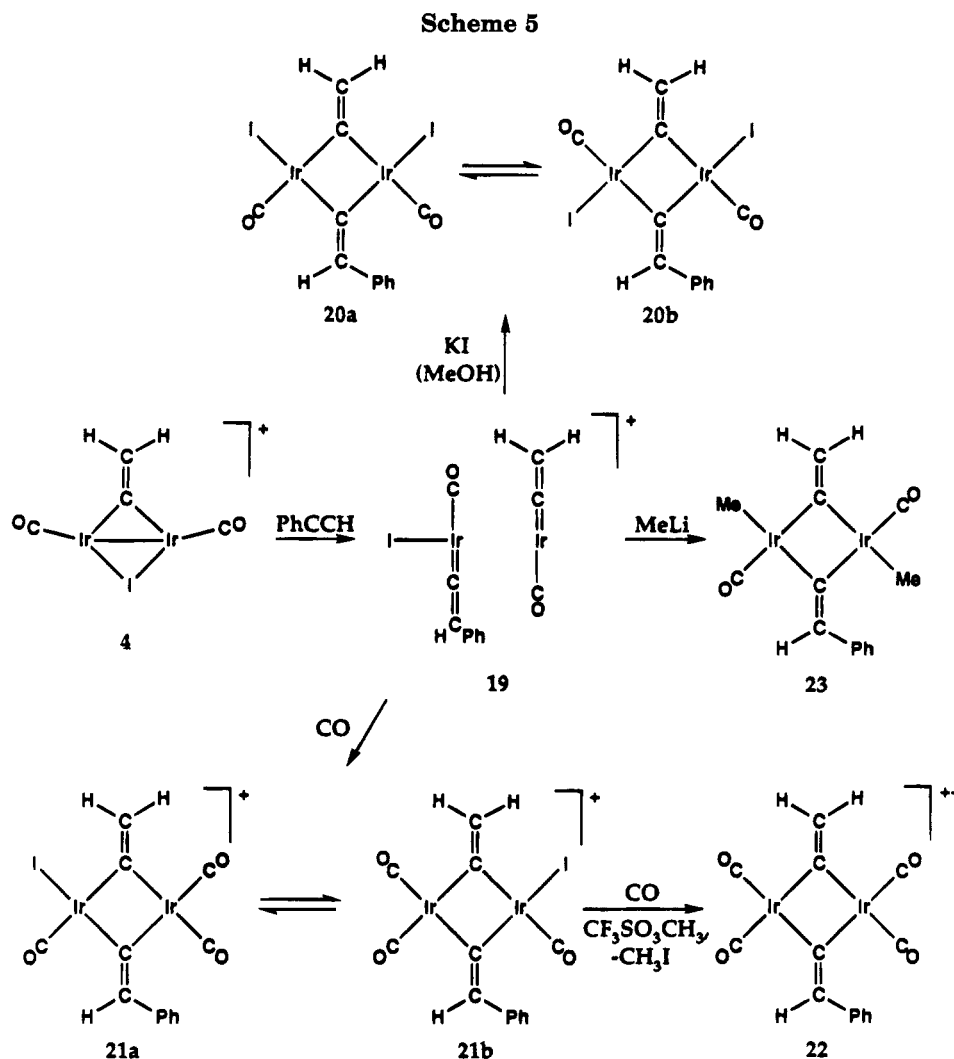
**Table 5.** Selected Bond Lengths (Å) and Angles (deg) for Compound **15**

Bond Lengths			
Ir(1)–I(1)	2.8144(7)	Ir(2)–C(2)	1.931(8)
Ir(1)–P(1)	2.333(2)	Ir(2)–C(4)	2.063(7)
Ir(1)–P(3)	2.349(2)	Ir(2)–C(5)	2.106(6)
Ir(1)–C(1)	1.942(7)	O(1)–C(1)	1.120(8)
Ir(1)–C(3)	2.078(7)	O(2)–C(2)	1.150(8)
Ir(1)–C(5)	2.092(6)	C(3)–C(4)	1.316(9)
Ir(2)–I(2)	2.8006(8)	C(5)–C(6)	1.335(9)
Ir(2)–P(2)	2.323(2)	C(6)–C(91)	1.48(1)
Ir(2)–P(4)	2.330(2)	C(6)–H(6)	1.08(8)
Bond Angles			
I(1)–Ir(1)–P(1)	89.87(5)	P(2)–Ir(2)–P(4)	171.00(6)
I(1)–Ir(1)–P(3)	94.93(4)	P(2)–Ir(2)–C(2)	93.2(2)
I(1)–Ir(1)–C(1)	84.6(2)	P(2)–Ir(2)–C(4)	85.7(2)
I(1)–Ir(1)–C(3)	90.2(2)	P(2)–Ir(2)–C(5)	85.3(2)
I(1)–Ir(1)–C(5)	176.1(2)	P(4)–Ir(2)–C(2)	92.5(2)
P(1)–Ir(1)–P(3)	169.26(6)	P(4)–Ir(2)–C(4)	89.0(2)
P(1)–Ir(1)–C(1)	98.5(2)	P(4)–Ir(2)–C(5)	87.2(2)
P(1)–Ir(1)–C(3)	81.3(2)	C(2)–Ir(2)–C(4)	176.2(3)
P(1)–Ir(1)–C(5)	87.0(2)	C(2)–Ir(2)–C(5)	95.9(3)
P(3)–Ir(1)–C(1)	91.5(2)	C(4)–Ir(2)–C(5)	87.5(2)
P(3)–Ir(1)–C(3)	89.0(2)	Ir(1)–C(1)–O(1)	170.9(6)
P(3)–Ir(1)–C(5)	87.8(2)	Ir(2)–C(2)–O(2)	174.8(6)
C(1)–Ir(1)–C(3)	174.8(3)	Ir(1)–C(3)–C(4)	123.8(5)
C(1)–Ir(1)–C(5)	98.2(3)	Ir(2)–C(4)–C(5)	123.1(5)
C(3)–Ir(1)–C(5)	87.0(3)	Ir(1)–C(5)–Ir(2)	118.1(3)
I(2)–Ir(2)–P(2)	95.18(5)	Ir(1)–C(5)–C(6)	125.0(5)
I(2)–Ir(2)–P(4)	92.46(5)	Ir(2)–C(5)–C(6)	116.9(5)
I(2)–Ir(2)–C(2)	82.5(2)	C(5)–C(6)–C(91)	131.5(7)
I(2)–Ir(2)–C(4)	94.0(2)	C(5)–C(6)–H(6)	128(5)
I(2)–Ir(2)–C(5)	178.4(2)	C(91)–C(6)–H(6)	100(5)

having the iodo and carbonyl ligand resonate in the same region as both similar centers in **15** and the similar center in **14** suggesting that they all have similar environments. In the  $^{13}\text{C}\{^1\text{H}\}$  NMR spectrum three resonances for the terminal carbonyls are observed. For both this product and **17** neither the acetylene nor the phenylvinylidene ligand were  $^{13}\text{C}$  enriched so  $^{13}\text{C}$  resonances for these groups were not observed. The  $^1\text{H}$  NMR spectrum shows the acetylenic protons as multiplets at typically low field ( $\delta$  9.91, 8.57); the phenylvinylidene proton was not observed. Consistent with the two  $\text{Ir}^{3+}$  centers and an overall positive charge on the complex, the carbonyl stretches are at high frequency.

Reaction of **16** with methyl triflate under carbon monoxide results in loss of  $\text{CH}_3\text{I}$  and formation of the dicationic species  $[\text{Ir}_2(\text{CO})_4(\mu\text{-CC}(\text{H})\text{Ph})(\mu\text{-HCCH})(\text{dppm})_2][\text{SO}_3\text{CF}_3]_2$  (**17**). Each metal center in **17** has an environment analogous to the dicarbonyl center in **16**, and again the  $^{31}\text{P}\{^1\text{H}\}$  resonances appear in the same region, consistent with the proposal that they have similar environments. Four resonances appear in the  $^{13}\text{C}\{^1\text{H}\}$  NMR spectrum for the four terminal carbonyls, and in the IR spectrum the carbonyl stretches are at even higher frequency than in **15**, consistent with the replacement of  $\text{I}^-$  by CO. In the  $^1\text{H}$  NMR spectrum both the acetylenic ( $\delta$  9.06, 8.70) and the phenylvinylidene protons ( $\delta$  8.31) appear.

Reaction of **6** with phenylacetylene also yields a mixed vinylidene–alkyne-bridged product  $[\text{Ir}_2\text{I}(\text{CO})_2(\mu\text{-CC}(\text{H})\text{Ph})(\mu\text{-HCCPh})(\text{dppm})_2][\text{SO}_3\text{CF}_3]$  (**18**), analogous to **14**. Although no  $^{13}\text{C}$  NMR parameters were obtained for the vinylidene and alkyne groups, since the phenylacetylene used was not enriched, the other spectroscopic parameters are closely comparable to those of **14**, so an analogous structure is assigned. Although we have no supporting data, we propose that the phenyl group on



the bridging phenyl acetylene ligand is directed toward the unsaturated Ir in order to avoid unfavorable contacts with the iodo ligand at the opposite end.

**(c) Bis(vinylidene) Complexes.** As noted earlier, the reaction of **4** with acetylene was complex yielding a number of unidentified species. However one product was identified as an acetylene–vinylidene-bridged species analogous to that observed in the reaction of **6** with acetylene, for which an acetylene–phenylvinylidene species,  $[\text{Ir}_2\text{I}(\text{CO})_2(\mu\text{-CC}(\text{H})\text{Ph})(\mu\text{-HCCH})(\text{dppm})_2][\text{SO}_3\text{CF}_3]$  (**14**), was obtained. It was assumed that the reaction of **4**, having a bridging  $\text{CCH}_2$  group, and phenylacetylene would yield an analogous species containing the opposite isomer combination, i.e., vinylidene and phenylacetylene. Surprisingly this is not the case, and instead a bis(vinylidene) complex,  $[\text{Ir}_2(\text{CO})_2(\text{CCH}_2)(\text{CC}(\text{H})\text{Ph})(\text{dppm})_2][\text{SO}_3\text{CF}_3]$  (**19**), results as outlined in Scheme 5. Compound **19** presents a rare example of a binuclear species in which the vinylidene ligands are not bridging but are terminal. Terminal vinylidene groups in binuclear complexes and clusters have been observed,<sup>48</sup> however in the previous cases the substituents on the  $\beta$ -carbon were bulky so the terminal coordination appeared to be sterically driven. In contrast, there appears to be no steric reason that demands terminal vinylidene coordination in **19**. The present

compound also appears to be the only bis(vinylidene) system reported on a binuclear framework. Higher clusters containing two vinylidene groups have been reported, however.<sup>49</sup> In a sample of **19** (triflate salt) that was  $^{13}\text{C}$  enriched at the vinylidene ( $^{13}\text{C}=\text{CH}_2$ ) and at the carbonyls, the  $^{13}\text{C}\{^1\text{H}\}$  NMR spectrum shows the  $\text{C}_\alpha$  resonance at  $\delta$  174.6 with coupling to  $\text{C}_\beta$  of 64 Hz, to one of the carbonyls of 35 Hz, and to two phosphorus nuclei on one metal of 10 Hz. The  $\text{C}_\beta$  resonance is observed at  $\delta$  133.6, with coupling only to  $\text{C}_\alpha$ . This  $\text{C}_\alpha$ – $\text{C}_\beta$  coupling is typical for vinylidenes, and coupling of  $\text{C}_\alpha$  to only two phosphorus nuclei identifies this group as terminal. The high coupling between  $\text{C}_\alpha$  and the adjacent carbonyl (35 Hz) indicates that the two groups are mutually trans. Overnight data acquisition on the sample containing natural-abundance phenylvinylidene allows the  $\text{C}_\alpha$  of this group to be identified as a broad multiplet at  $\delta$  174.3, close to that for the unsubstituted vinylidene, and  $\text{C}_\beta$  to be observed at  $\delta$  143.9. Appropriate decoupling experiments could not be carried out to simplify the  $\text{C}_\alpha$  resonance. The carbonyl resonances, at  $\delta$  179.9 and 163.8, each display coupling to two different sets of  $^{31}\text{P}$  nuclei establishing that they are terminally bound to different metals, and the high-field resonance also shows the aforementioned coupling to  $\text{C}_\alpha$ . In the

(48) (a) Umland, H.; Behrens, U. *J. Organomet. Chem.* **1984**, 273, C39. (b) Ewing, P.; Farrugia, L. J. *J. Organomet. Chem.* **1989**, 373, 259.

(49) (a) Kolobova, N. E.; Ivanov, L. L.; Zhvanko, O. S. *Izvest. Akad. Nauk. SSSR, Ser. Khim.* **1983**, 956. (b) Kolobova, N. E.; Ivanov, L. L.; Zhvanko, O. S.; Batsanov, A. S.; Struchkov, Yu. T. *J. Organomet. Chem.* **1985**, 279, 419.



$^1\text{H}$  NMR spectrum the phenylvinylidene proton resonates at  $\delta$  8.20 and displays weak coupling to the low-field carbonyl resonance, further supporting our proposal that these two groups are bound to one metal and in a trans orientation. The protons on the unsubstituted vinylidene group appear at  $\delta$  6.54 and 6.04, displaying a mutual coupling of 10 Hz and coupling to  $C_\beta$  of ca. 157 Hz ( $^{13}\text{C}$ -enriched vinylidene). These chemical shifts for the vinylidene and phenylvinylidene protons of **19** are not abnormal for such groups of binuclear complexes in which they are usually bridging but are far downfield of those reported for terminally bound groups as observed in mononuclear vinylidene complexes of iridium.<sup>17,41</sup> In particular the  $^1\text{H}$  resonances for the closely related complexes  $[\text{Ir}(\text{CC}(\text{H})\text{R})(\text{PPr}^i_3)_2]$  ( $\text{R} = \text{H}, \text{Ph}$ ) appear at  $\delta$  -5.25 and -3.58, respectively.<sup>41</sup> The geometry proposed, in which the iodo group is bound adjacent to the phenylvinylidene rather than the unsubstituted vinylidene group, is based on analogies with the chemistry described of **4** with CO and  $t\text{BuNC}$ , in which ligand attack occurred at one Ir center on the face opposite the bridging vinylidene. Assuming an analogous attack by phenylacetylene and subsequent rearrangement to a phenylvinylidene moiety, the most likely geometry which minimizes ligand rearrangements, would have the unsubstituted vinylidene moving to a terminal position on the opposite face of the metal vacated by the iodo ligand. The orientation of the phenyl substituent on the phenylvinylidene group is uncertain. Although we could not find a mononuclear analogue of the saturated  $\text{Ir}^+$  site having a carbonyl and a vinylidene unit together, a very analogous species  $[\text{Ir}(\text{CCH}_2)(\text{PPr}^i_3)_2]$  was reported to react with CO, but in this case transformation to an  $\text{Ir}^{3+}$  hydride-acetylide product resulted.<sup>41</sup>

Although the spectroscopic data for **19** do not unequivocally rule out the presence of a phenylacetylene instead of a phenylvinylidene group, two important observations strongly support the phenylvinylidene formulation. First, in the slow transformation of **4** to **19** a hydride intermediate is observed in the  $^1\text{H}$  NMR spectra. Such a species is consistent with the involvement of a hydride-acetylide intermediate, of the type previously shown to be involved in alkyne-to-vinylidene rearrangements in related binuclear systems.<sup>23</sup> Unfortunately this species is never present in high enough concentrations to obtain additional spectroscopic data, so could not be characterized. Furthermore, the transformation of **19** to **20**, which has been unambiguously characterized as a bis(vinylidene) species (*vide infra*), is essentially instantaneous—so is clearly inconsistent with an alkyne-to-vinylidene rearrangement occurring during this step. All such rearrangements previously noted in related systems have been slow (24–72 h).<sup>23</sup> If **19** had been a mixed alkyne-vinylidene species like **14**, the transformation of **19** to **20** should also have been slow.

The spectroscopic parameters for the triflate and tetrafluoroborate salts of **19** are virtually identical, in spite of the differing anions, suggesting that the anions are noncoordinating. In addition, the conductivity of the  $\text{BF}_4^-$  salt in  $\text{CH}_3\text{NO}_2$  indicates a 1:1 electrolyte (73  $\Omega$   $\text{cm}^2$   $\text{mol}^{-1}$ ), which also indicates that the iodo ligand remains coordinated. The IR spectrum of  $\text{19}\cdot\text{SO}_3\text{CF}_3$  shows a band at  $1580\text{ cm}^{-1}$ , separating into two bands,

at  $1575$  and  $1525\text{ cm}^{-1}$  when  $^{13}\text{C}$ -labeled vinylidene is used. It appears that in the latter spectrum the higher frequency band corresponds to phenylvinylidene whereas the lower frequency stretch is due to  $^{13}\text{C}=\text{CH}_2$ ; when natural abundance vinylidene is used both bands overlap.

The addition of either an anionic ( $\text{I}^-$ ) or a neutral (CO) ligand to **19** results in the unusual transformation of the terminal vinylidene ligands to bridging—a transformation that appears to be unprecedented, although it has previously been suggested.<sup>8,50</sup> In addition, the preparation of heterobimetallic, vinylidene complexes from the reaction of a mononuclear vinylidene complex with an unsaturated species is another example of terminal-to-bridging vinylidene rearrangement,<sup>6</sup> and the transfer of a vinylidene from one mononuclear complex to another also presumably occurs via a bridged intermediate.<sup>40</sup> Reaction of **19** with potassium iodide results in iodide coordination to give two isomers of  $[\text{Ir}_2\text{I}_2(\text{CO})_2(\mu\text{-CCH}_2)(\mu\text{-CC}(\text{H})\text{Ph})(\text{dppm})_2]$  (**20**), as shown in Scheme 5. Although other isomers, having an iodo ligand adjacent to the phenyl substituent of the phenylvinylidene group, are possible, they appear not to be favored owing to destabilizing steric repulsions involving these larger groups. At ambient temperature in  $\text{CH}_2\text{Cl}_2$  only isomer **20a** is observed. Its  $^{31}\text{P}\{^1\text{H}\}$  NMR spectrum shows two resonances indicating two phosphorus environments, and the  $^{13}\text{C}\{^1\text{H}\}$  NMR also shows two terminal-carbonyl resonances at  $\delta$  171.9 and 170.4. Each carbonyl shows coupling to two adjacent phosphorus nuclei, and in the  $^{13}\text{C}=\text{CH}_2$  sample each shows coupling (27 Hz) to  $C_\alpha$  of this vinylidene group, indicating that both are trans to it. The vinylidene carbon nuclei resonate at  $\delta$  102.2 ( $C_\alpha$ ) and 143.3 ( $C_\beta$ ) with a mutual coupling of 61 Hz. Coupling of  $C_\alpha$  to the  $^{31}\text{P}$  nuclei is not resolved. The chemical shift for  $C_\alpha$  is at exceptionally high field and can be compared with previous determinations for bridged vinylidenes which are usually downfield of  $\delta$  230;<sup>1</sup> the value observed for **20a** is at even higher field than those noted earlier in the paper, which are already unusual in their chemical shift (*vide supra*). In the  $^1\text{H}$  NMR spectrum the vinylidene protons appear at  $\delta$  9.19 and 9.16 with coupling (for  $^{13}\text{C}=\text{CH}_2$ ) of 153 Hz to  $C_\beta$ . No resonance for the phenylvinylidene proton is observed so it is presumed to lie under the phenyl resonances. The IR spectrum of **20a** shows a carbonyl stretch at  $2027\text{ cm}^{-1}$ .

At  $-80\text{ }^\circ\text{C}$  in  $\text{CH}_2\text{Cl}_2$  both isomers, **20a** and **20b**, appear in the approximate molar ratio of 2:1. The  $^{31}\text{P}\{^1\text{H}\}$  NMR spectrum of **20b** displays four different signals indicating a top-bottom as well as a left-right asymmetry in the complex. Although the iodo, carbonyl, and vinylidene ligands all form a plane perpendicular to the plane of the phosphorus atoms, the top-bottom asymmetry can be broken by a skewing of the phenylvinylidene about the  $\text{C}=\text{C}$  bond, as is shown in the X-ray structure (*vide infra*). In support of the structure shown only the carbonyl resonance at  $\delta$  174.7 displays trans coupling (30 Hz) with the  $^{13}\text{C}=\text{CH}_2$  group; the carbonyl at  $\delta$  172.7 is cis to the vinylidene ligand, displaying no coupling to it. The resonance for  $C_\alpha$  coincidentally occurs at exactly the chemical shift as for **20a**, whereas  $C_\beta$  resonates at  $\delta$  133.0. In the  $^1\text{H}$  NMR spectrum the

(50) Garcia Alonso, F. J.; Riera, V.; Ruiz, M. A.; Tiripicchio, A.; Tiripicchio Camellini, M. *Organometallics* **1992**, *11*, 370.

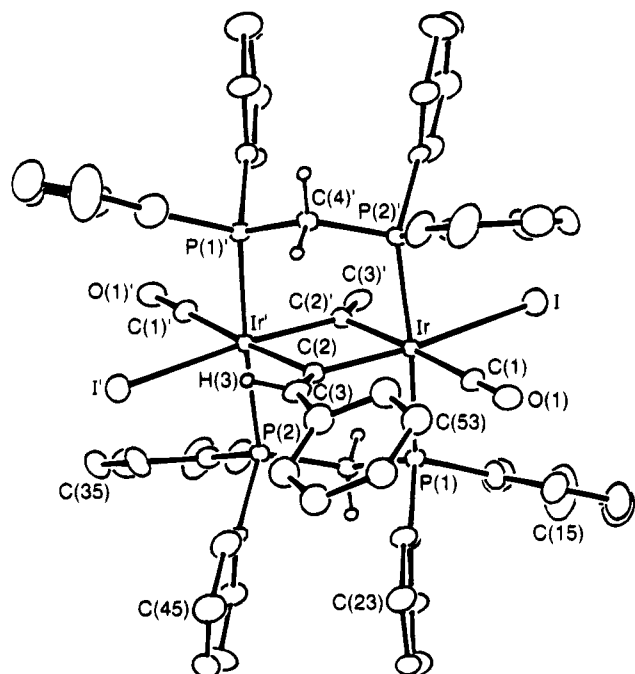


**Figure 2.** Perspective drawing of  $[\text{Ir}_2\text{I}_2(\text{CO})_2(\mu\text{-CCH}_2)(\mu\text{-CC(H)Ph})(\text{dppm})_2]$  (**20b**). Numbering and thermal ellipsoids are as described for Figure 1.

**Table 6. Selected Bond Lengths (Å) and Angles (deg) for Compound 20b**

Bond Lengths			
Ir–I	2.844(1)	Ir–P(1)	2.363(3)
Ir–P(2)	2.356(3)	Ir–C(1)	1.94(2)
Ir–C(2)	2.08(1)	Ir–C(2)	2.13(1)
O(1)–C(1)	1.07(2)	C(2)–C(3)	1.28(2)
C(3)–C(51)	1.58(2)		
Bond Angles			
I–Ir–P(1)	92.78(8)	I–Ir–P(2)	89.85(9)
I–Ir–C(1)	84.3(5)	I–Ir–C(2)	173.0(3)
I–Ir–C(2)	96.6(3)	P(1)–Ir–P(2)	175.5(1)
P(1)–Ir–C(1)	92.5(5)	P(1)–Ir–C(2)	90.9(3)
P(1)–Ir–C(2)	85.3(3)	P(2)–Ir–C(1)	91.6(5)
P(2)–Ir–C(2)	86.1(3)	P(2)–Ir–C(2)	90.8(3)
C(1)–Ir–C(2)	101.5(6)	C(1)–Ir–C(2)	177.5(5)
C(2)–Ir–C(2)	77.8(5)	Ir–C(1)–O(1)	177(1)
Ir–C(2)–Ir	102.2(5)	Ir–C(2)–C(3)	130.3(10)
Ir–C(2)–C(3)	127.2(10)	C(2)–C(3)–C(51)	149(1)

vinylidene protons appear at  $\delta$  8.81 and 8.14, and again the phenylvinylidene proton is not observed. Although **20a** is the only species observed in solution at ambient temperature, crystallization at this temperature yields only **20b** as a solid, as shown by IR spectroscopy and the X-ray structure. This isomer shows only one carbonyl stretch at  $2009\text{ cm}^{-1}$ . The facile interconversion of the two isomers presumably occurs by  $\text{I}^-$  loss and recoordination.

The structure of **20b** is shown in Figure 2, confirming the geometry assigned in Scheme 5 on the basis of the spectroscopic analysis. Important structural parameters are given in Table 6. Although the phenyl substituent on the phenylvinylidene group is inversion disordered, having half-occupancy on C(3) and half on C(3'), the rest of the molecule is well behaved and the disorder was satisfactorily resolved. In this disorder the two vinylidene carbons are directly superimposed on those of the phenylvinylidene, masking any subtle differences that there might be in their parameters. Nevertheless the structure unambiguously establishes both the bridging nature of the two vinylidene groups

and the mutually trans arrangement of the iodo ligands for this isomer. The metals in **20b** have slightly distorted octahedral geometries that are characteristic of  $\text{Ir}^{3+}$ , in which case the bridging vinylidene units are considered as dianionic ligands. Structurally this species is closely related to the monovinylidene species **8** and **9** via formal insertion of the second vinylidene ( $\text{CCH}_2$  or  $\text{CC(H)Ph}$ ) into the Ir–Ir bond of the respective monobridged species. The major structural differences in the two classes of species is therefore a much longer Ir–Ir separation in **20b** ( $3.275(1)\text{ \AA}$  compared to  $2.828(1)\text{ \AA}$  (**8**) and  $2.783(1)\text{ \AA}$  (**9**)) and a wider angle at the bridging vinylidene ( $102.2(5)^\circ$  vs  $84.6(7)^\circ$  (**8**) and  $86.0(9)^\circ$  (**9**)). Even so, in **20b**, the idealized  $120^\circ$  angle at C(2) is not attained, presumably because this would generate too acute an angle between the vinylidene at Ir, with the resulting poor Ir– $\text{C}_\alpha$  overlap; this angle is already quite acute ( $77.8(5)^\circ$ ). By comparison, the structure of **15**, having the acetylene tautomer instead of vinylidene, displays angles involving the bridging groups that are close to ideal. Since the acetylene ligand binds with one end to each metal, rather than to both metals through only one carbon atom, as for the vinylidene group, the metals are able to move apart by over  $0.3\text{ \AA}$ , compared to **20b**. In this geometry the undistorted angles at the acetylenic and vinylidene carbons and at the metals give rise to optimal metal–ligand overlap. All other parameters within **20b** compare well with those of **8** and **9**, and in particular, the vinylidene C(2)–C(3) separation  $1.28(2)\text{ \AA}$  is typical of a double bond.

Upon reaction of **19** with CO, transformation of the terminal vinylidene ligands to bridging again occurs yielding  $[\text{Ir}_2\text{I}(\text{CO})_3(\mu\text{-CCH}_2)(\mu\text{-CC(H)Ph})(\text{dppm})_2][\text{SO}_3\text{-CF}_3]$  (**21a,b**) and again two isomers are observed, corresponding to two orientations of the iodo ligand with respect to the phenylvinylidene group (isomers **21a,b** have been arbitrarily assigned since they differ only in the orientations of the substituents on the  $\beta$ -carbon of the phenylvinylidene, which could not be identified). In both of these isomers the iodo ligand remains on the same face of the  $\text{Ir}_2\text{P}_4$  plane opposite the  $\text{CC(H)Ph}$  moiety, presumably to minimize steric repulsions. Although it appears that the isomer having the iodo ligand adjacent to the hydrogen substituent on the phenylvinylidene ligand is equivalent to isomers **21a,b**, its absence suggests that the dominant repulsions involve the dppm phenyl groups, the orientations of which will be most affected by the large iodo ligand and the vinylidene phenyl group. Both possible isomers, in which the iodo group is adjacent to  $\text{CC(H)Ph}$ , can be ruled out by the  $^{13}\text{C}\{^1\text{H}\}$  NMR of a sample containing  $^{13}\text{CO}$  and  $^{13}\text{C}=\text{CH}_2$ , since both isomers observed display three carbonyl resonances of which two show strong coupling (between 21 and 32 Hz) to  $\text{C}_\alpha$  of the unsubstituted vinylidene, indicating that both of these CO's are opposite this group. At ambient temperature only isomer **21a** is observed, whereas at  $-60^\circ\text{C}$  the **21a**:**21b** ratio is ca. 1:0.75. Although the previously discussed interconversion between isomers **20a** and **20b** can occur via  $\text{I}^-$  loss and recoordination, since this occurs at the same metal center, the interconversion between **21a** and **21b** appears to be different, since the iodo ligand appears to migrate from metal to metal. If this occurs by  $\text{I}^-$  dissociation, there must also be an

accompanying loss of CO with its subsequent recoordination, since with the bridging vinylidene groups there is no simple way (such as a turnstile motion) that allows ligand exchange between the two metals. Iodide dissociation from **21** also appears less likely than in **20** owing to the positive charge of the former. Another possibility is that exchange between **21a** and **21b** can occur by rotation of the phenylvinylidene group about the C=C axis. Facile rotation of terminal vinylidenes has been previously noted,<sup>2</sup> and examples of rotation about the C=C bond in a bridged group are also known.<sup>51,52</sup> In both isomers of compound **21** the <sup>13</sup>C<sub>α</sub> resonance is again at unusually high field (δ 101.0 (**a**), 99.8 (**b**)), but all other parameters are as expected.

Under an atmosphere of CO compound **21** reacts with methyl triflate resulting in iodide abstraction (as CH<sub>3</sub>I) and yielding [Ir<sub>2</sub>(CO)<sub>4</sub>(μ-CCH<sub>2</sub>)(μ-CC(H)Ph)(dppm)<sub>2</sub>][SO<sub>3</sub>-CF<sub>3</sub>]<sub>2</sub> (**22**), which is not stable in the absence of CO. This product shows the expected four terminal carbonyl resonances, with two of them displaying strong coupling (26 Hz) to <sup>13</sup>C<sub>α</sub> of the enriched vinylidene, which is again observed at high field. The <sup>1</sup>H NMR spectrum of **22** shows the phenylvinylidene proton resonance at δ 8.19, which appears as an apparent triplet due to coupling to the two <sup>13</sup>CO's opposite the phenylvinylidene group, and this signal appears as a singlet when natural abundance CO is used. The protons of the unsubstituted vinylidene appear at δ 7.94 and 7.82 with the usual parameters observed when <sup>13</sup>C<sup>13</sup>CH<sub>2</sub> is used.

The dialkyl derivative, [Ir<sub>2</sub>(CH<sub>3</sub>)<sub>2</sub>(CO)<sub>2</sub>(μ-CCH<sub>2</sub>)(μ-CC(H)Ph)(dppm)<sub>2</sub>] (**23**), can be prepared from **19** by reaction with *ca.* 4-fold excess of MeLi. Also obtained in this reaction is compound **20**, resulting from I<sup>-</sup> attack on **19** by the LiI produced in the reaction. Compound **23** is unstable and transforms to unidentified products at ambient temperature, so was characterized only by NMR. Two carbonyl resonances, at δ 177.9 and 177.5, are observed in the <sup>13</sup>C{<sup>1</sup>H} NMR spectrum, and in the <sup>13</sup>C=CH<sub>2</sub>-containing sample the lower field carbonyl signal displays trans coupling (26 Hz) to <sup>13</sup>C<sub>α</sub>. The vinylidene carbons resonate at δ 106.0 (C<sub>α</sub>) and 133.4 (C<sub>β</sub>) and display the normal couplings. Although signals were observed in the <sup>1</sup>H NMR in the regions expected for vinylidene protons, we were unable to unambiguously assign them owing to many impurities in the sample. However the two methyl resonances are obvious at δ -0.45 and -0.92 and are shown, by selective <sup>31</sup>P decoupling, to be bound to different metals, by displaying coupling to only the <sup>31</sup>P nuclei bound to the respective metal. We had prepared **23** with the intention of studying migratory insertions involving the vinylidene ligands; however the instability of the species has precluded this study. It may be, however, that this instability is induced by migratory insertion which creates unsaturation in the complex. Further studies are underway, investigating other alkyl and aryl derivatives of **23**.

### Conclusions

The cationic, vinylidene-bridged complexes [Ir<sub>2</sub>(CO)<sub>2</sub>(μ-I)(μ-CC(H)R)(dppm)<sub>2</sub>][X] (R = H (**4**), Ph (**6**)) were studied with the idea that their incipient coordinative

unsaturation could result in the incorporation of alkynes, leading to unusual products, containing the vinylidene group together with a modified or unmodified alkyne. Verification that unsaturation in these species could result from movement of the bridging iodo ligand to a terminal site came from the products in the reactions of **4** with <sup>t</sup>BuNC and CO, which showed each of these ligands in the respective products occupying the site vacated by the iodo group. Reaction of **4** or **6** with alkynes appears to proceed in much the same manner yielding two unusual classes of complexes, in which the added alkyne either remains unmodified or undergoes tautomerism to a second vinylidene group.

With the phenylvinylidene-bridged precursor **6**, reaction with either acetylene or phenylacetylene yielded products [Ir<sub>2</sub>I(CO)<sub>2</sub>(μ-CC(H)Ph)(μ-HCCR)(dppm)<sub>2</sub>][X] (R = H (**14**), Ph (**18**)) bridged by a phenylvinylidene group and the alkyne molecule. In addition to the spectroscopic evidence supporting the presence of two alkyne tautomers in the same complex, an X-ray structure determination of the neutral diiodo species (**15**) confirmed the formulation.

Reaction of the vinylidene-bridged precursor **4** with acetylene gives an analogous vinylidene- and acetylene-bridged product (together with unidentified products); however the reaction of **4** with phenylacetylene yields the unusual bis(vinylidene) species [Ir<sub>2</sub>I(CO)<sub>2</sub>(CCH<sub>2</sub>)(CC(H)Ph)(dppm)<sub>2</sub>][X] (**19**), which appears to have each vinylidene group terminally bound to a different metal. Reaction of this species with I<sup>-</sup>, CH<sub>3</sub><sup>-</sup>, or CO yields the respective adducts in which the vinylidene groups move to the bridging sites. This formulation is confirmed by an X-ray determination of the diiodo species, which is isomeric with **15**, with the two differing in the tautomer of acetylene present. Compound **19** is an unusual example in which a vinylidene ligand is terminally bound in a binuclear system. The previous rare examples involving terminal, instead of bridging vinylidenes, have large vinylidene substituents suggesting that their terminal coordination is sterically driven. This appears not to be the case with **19**, since the addition of ligands leads to a bridged arrangement. The facile reversible interconversion between the terminal and bridging modes is also unusual.

The obvious question that arises from these results relates to the generation of a mixed vinylidene-acetylene complex by one route and a divinylidene complex by another. Why does the unsubstituted vinylidene-bridged compound **4** yield a bis(vinylidene) compound when reacted with phenylacetylene while the other reactions attempted yield the mixed vinylidene-alkyne products? It is noteworthy that only **4** yields the bis(vinylidene) species, and this occurs only with phenylacetylene. We assume that the tendency to yield the bis(vinylidene) species results from the tendency to undergo initial oxidative addition to yield the hydride-acetylide intermediate, which is presumed to precede vinylidene formation.<sup>23,38-41</sup> If our assumption is correct, formation of a bis(vinylidene) complex from the vinylidene-bridged **4**, but *not* from the phenylvinylidene-bridged **6**, can be rationalized on the basis that the stronger π-acidity of the phenylvinylidene group,<sup>53</sup> should leave the metals less electron rich and less prone to oxidative addition. Why this oxidative addition to **4** apparently occurs only with phenylacetylene and

(51) Afzoli, D.; Lukehart, C. M. *Organometallics* **1987**, *6*, 546.

(52) Wang, L.-S.; Cowie, M. *Organometallics* **1995**, *14*, 2374.

not with acetylene is somewhat more puzzling, since the relative tendencies of these alkynes to oxidatively add has to our knowledge not been reported. However, if these tendencies parallel their acidities,<sup>54</sup> we might expect the phenylacetylene to oxidatively add more readily. It must be noted, however, that the reactivity of **4** with acetylene was not studied in depth owing to the number of resulting products, so we cannot rule out that at least one of the unidentified products may have been a bis(vinylidene) species. These ideas remain to be tested through the use of different substituents on the vinylidene precursor and with different terminal alkynes.

---

(53) This can be seen from the IR spectra of **4** and **6** and of **8** and **9** (ref 23), which show that the carbonyl stretches for the vinylidene-bridged species are at lower frequency than those of the phenyl-vinylidene species.

(54) Streitwieser, A., Jr.; Hammons, J. H. *Prog. Phys. Org. Chem.* **1965**, *3*, 41.

**Acknowledgment.** We thank the Natural Sciences and Engineering Research Council (NSERC) of Canada and the University of Alberta for financial support. Dr. R. McDonald is thanked for assistance in preparing the tables of data for compound **15**, and Drs. H. Liu, P. N. Swepston, J. M. Troup, and B. R. Vincent at Molecular Structure Corp. are acknowledged for data collection and processing for compound **20b**.

**Supplementary Material Available:** Tables of positional and thermal parameters for the phenyl carbons, anisotropic thermal parameters, idealized hydrogen parameters, and bond distances and angles involving the phenyl rings for compounds **15** and **20b** (10 pages). Ordering information is given on any current masthead page.

OM940982E

# Observation of a Slow Dissociative Process in Palladium(II) Complexes

Juan A. Casares, Silverio Coco, Pablo Espinet,\* and Yong-Shou Lin

Departamento de Química Inorgánica, Facultad de Ciencias, Universidad de Valladolid,  
E-47005 Valladolid, Spain

Received March 13, 1995<sup>®</sup>

The dynamic behavior of complexes  $[\text{Pd}(\text{C}_6\text{F}_5)\text{X}(\text{SPPy}_n\text{Ph}_{3-n})]$  (Py = pyridin-2-yl; X = Br,  $n = 1$  (**1**), 3 (**3**);  $n = 2$ , X = Cl (**2a**), Br (**2b**), I (**2c**)) has been studied by NMR spectroscopy. Complex **1** has a S,N-chelating ligand and shows no isomers. Complexes **2** show two isomers, N,N- and N,S-bonded, the latter being dominant (>95%). Rotation of the  $\text{C}_6\text{F}_5$  group in the N,S-isomers in  $\text{CDCl}_3$  occurs slowly with  $\Delta H^\ddagger$  (kJ mol<sup>-1</sup>) = 60.0 (**2a**), 57.1 (**2b**), 50.2 (**2c**) and  $\Delta S^\ddagger$  (J K<sup>-1</sup> mol<sup>-1</sup>) = -35.8 (**2a**), -37.5 (**2b**), -51.1 (**2c**). Evidence strongly supports that this rotation is severely hindered in a square-planar complex and occurs in a contact ion pair  $[\text{Pd}(\text{C}_6\text{F}_5)(\text{SPPy}_2\text{Ph}-\text{N,S})] \cdot \text{X}$  formed by halide dissociation. Complex **3** shows also two isomers, and its N,N-isomer shows apparent  $\text{C}_6\text{F}_5$  rotation corresponding in reality to exchange of the Py group *trans* to the Pd-C bond and the uncoordinated Py group. The structure of  $[\text{Pd}(\text{C}_6\text{F}_5)\text{Br}(\text{SPPy}_2\text{Ph}-\text{N,S})]$  has been studied by X-ray diffraction:  $P2_1/c$ ,  $a = 8.273(2)$  Å,  $b = 14.240(2)$  Å,  $c = 19.547(4)$  Å,  $\beta = 95.10(2)^\circ$ ,  $V = 2293.6(7)$  Å<sup>3</sup>,  $Z = 4$ .

## Introduction

A dissociative process, usually of a neutral ligand, is often invoked as the initial step in many reactions involving Pd(II), Pt(II), and other square-planar d<sup>8</sup> organometallic complexes. This preliminary dissociation enables  $\beta$ -H elimination,<sup>1a-c</sup> isomerization,<sup>1d-j</sup> reductive elimination,<sup>1d-i</sup> or exchange reactions<sup>1k</sup> to occur. Surprisingly only limited thermodynamic data are available after much excellent work, and support for the dissociation step comes mostly from observation of rate-retarding effects by added ligands.

For Pt(II) clear-cut evidence for dissociative mechanisms in simple ligand-substitution processes, which are always associative in classical complexes, has been provided by the study of the reactions  $\text{cis}[\text{PtR}_2\text{L}_2] + 2^*\text{L} = \text{cis}[\text{PtR}_2^*\text{L}_2] + 2\text{L}$  (R = Ph or Me, L = Me<sub>2</sub>SO; R = Ph, L = SME<sub>2</sub>; \*L = labeled L) for which clearly positive  $\Delta V^\ddagger$  values were found.<sup>2</sup> These results show that the presence of Pt-C bond can produce a sharp changeover of reaction pathways from associative modes of activation in classical complexes to dissociative in organometallics. More recently, the displacement of thioether by pyridines has been demonstrated to be dissociative for  $[\text{PtPh}_2(\text{SEt}_2)_2]$  but associative for  $[\text{PtPh}_2(\text{SEt}_2)(\text{CO})]$ .<sup>2c</sup> The presence in the latter of a LUMO

perpendicular to the plane, prone to the nucleophilic attack, is the reason for the changeover of mechanism. Finally, the considerable acceleration in rate observed for the substitution of the aqua ligand *trans* to the Pt-C bond in the orthoplatinated complex  $[\text{Pt}\{\text{C}_6\text{H}_3\text{X}(\text{CH}_2\text{-NMe}_2)\}(\text{NC}_5\text{H}_4\text{SO}_3\text{-}3)(\text{H}_2\text{O})]$ , largely due to a strong decrease in  $\Delta H^\ddagger$ , is not associated with a changeover in mechanism, which is still associative.<sup>3</sup> Altogether the occurrence of dissociative substitutions in Pt(II) organometallic complexes seems to be "a combined result of ground-state destabilization and of a concurrent increase of electron density at the metal, preventing the approach of nucleophiles".<sup>2a</sup> On the other hand, studies by Romeo *et al.* on the uncatalyzed *cis* to *trans* isomerization of complexes of the type  $[\text{PtRXL}_2]$  in alcohol solvents and on some other processes have accumulated much consistent evidence for the operation of dissociative mechanisms usually involving halide dissociation<sup>4a</sup> but sometimes L dissociation.<sup>4b</sup>

The thermodynamic data in the literature for dissociative processes in Pd(II) are very scarce and recent and mostly refer to the dissociation of a neutral ligand: Sen *et al.* have determined the values of  $\Delta G^\circ$ ,  $\Delta H^\circ$ , and  $\Delta S^\circ$  for the reaction  $\text{Pd}(\text{COCOPh})\text{Cl}(\text{PPh}_3)_2 = \text{Pd}(\text{COCOPh})\text{Cl}(\text{PPh}_3) + \text{PPh}_3$ .<sup>5</sup>  $\Delta G^\ddagger$  values have been reported on the mechanism of apparent rotation in ( $\pi$ -allyl)-palladium complexes with bidentate nitrogen ligands, which seems to occur *via* cleavage of a Pd-N bond although some aspects remain obscure.<sup>6</sup>  $\Delta H^\ddagger$  and  $\Delta S^\ddagger$  values have been reported in another recent paper concerning the *cis*-*trans* isomerization of  $[\text{Pd}(\text{C}_6\text{F}_5)_2(\text{tht})_2]$  (tht = tetrahydrothiophene) which involves tht

<sup>®</sup> Abstract published in *Advance ACS Abstracts*, May 1, 1995.

(1) Some classic examples of the cited reactions: (a) McCarty, T. T.; Nuzzo, R. G.; Whitesides, G. M. *J. Am. Chem. Soc.* **1981**, *103*, 3396. (b) *Ibid.* **1981**, *103*, 3404. (c) Komiyama, S.; Morimoto, Y.; Yamamoto, T.; Yamamoto, A. *Organometallics* **1982**, *1*, 1528. (d) Komiyama, S.; Albright, T. A.; Hoffmann, R.; Kochi, J. K. *J. Am. Chem. Soc.* **1976**, *98*, 7255. (e) Gillie, A.; Stille, J. K. *J. Am. Chem. Soc.* **1980**, *102*, 4933. (f) Loar, M.; Stille, J. K. *J. Am. Chem. Soc.* **1981**, *103*, 4174. (g) Moravskiy, A.; Stille, J. K. *J. Am. Chem. Soc.* **1981**, *103*, 4182. (h) Ozawa, F.; Ito, T.; Nakamura, Y.; Yamamoto, A. *Bull. Chem. Soc. Jpn.* **1981**, *54*, 1868. (i) Paonessa, R. S.; Troglor, W. C. *J. Am. Chem. Soc.* **1982**, *104*, 3529. (j) Nakazawa, H.; Ozawa, F.; Yamamoto, A. *Organometallics* **1983**, *2*, 241. (k) Scott, J. D.; Puddephatt, R. J. *Organometallics* **1983**, *2*, 1643 and references therein.

(2) (a) Frey, U.; Helm, L.; Merbach, A. E.; Romeo, R. *J. Am. Chem. Soc.* **1989**, *111*, 8161 and references therein. (b) Lanza, S.; Minniti, D.; Moore, P.; Sachindis, J.; Romeo, R.; Tobe, M. *Inorg. Chem.* **1984**, *23*, 4428. (c) Romeo, R.; Grassi, A.; Monsù Scolaro, L. *Inorg. Chem.* **1992**, *31*, 4383.

(3) Schmülling, M.; Ryabov, A. D.; van Eldik, R. *J. Chem. Soc., Dalton Trans.* **1994**, 1257.

(4) (a) Romeo, R. *Comments Inorg. Chem.* **1990**, *11*, 21 and references therein. (b) Alibrandi, G.; Monsù Scolaro, L.; Romeo, R. *Inorg. Chem.* **1991**, *30*, 4007.

(5) Sen, A.; Chen, J.-T.; Vetter, W. M.; Whittle, R. R. *J. Am. Chem. Soc.* **1987**, *109*, 148, and literature cited in reference 10 in this paper.

(6) Gogoll, A.; Örnebro, J.; Grennberg, H.; Bäckvall, J.-E. *J. Am. Chem. Soc.* **1994**, *116*, 3631.

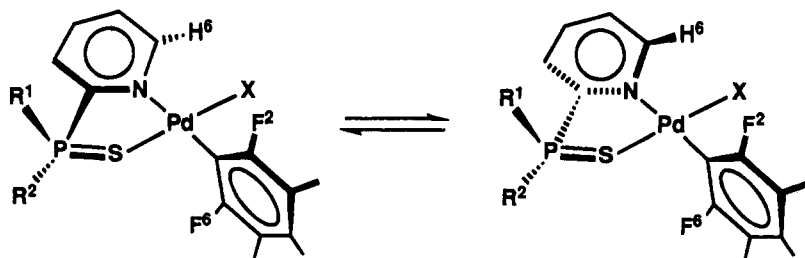


**Figure 1.** General schematic representation of the N,S-chelated species, showing the fast envelope shift making the five-membered ring appear as coplanar with the coordination plane on the NMR time scale.

dissociation.<sup>7</sup> Finally, as a result of the study of the thermolysis behavior of *trans*-[PdEt(OAc)(PMe<sub>3</sub>)<sub>2</sub>] the following values were obtained for the dissociation of OAc<sup>-</sup> in EtOH:  $\Delta H^\ddagger = 41.4 \text{ kJ mol}^{-1}$  and  $\Delta S^\ddagger = -171.4 \text{ J K}^{-1} \text{ mol}^{-1}$ .<sup>8</sup> The large negative  $\Delta S^\ddagger$  value was interpreted as the dissociation of the acetate being assisted by solvent coordination.

Whenever a dissociation process is followed by subsequent steps leading to products different from the starting materials (e.g., isomers, coupling products of a thermal decomposition, products of a ligand exchange, etc.), there is some uncertainty whether the thermodynamic parameters determined are related to the dissociative step (assumed to be the rate-determining step) or to a subsequent step in the whole process (if that assumption is not correct). The observation of a rate retardation by added ligand does not prove that the dissociation is the rate-determining step, since a mass-law effect will retard the reaction no matter what the rate-determining step is in the absence of added ligand (moreover, there is also the ambiguity of whether the rate retardation comes from blocking the formation of a three-coordinate species or from the formation of an unreactive five-coordinate species). In order to avoid these uncertainties it is necessary to carry out studies on systems offering the dissociation process as isolated as possible from further processes, preferably as the only process occurring.

Our studies on the dynamic behavior of some Pd and Pt organometallic compounds of the type [M(C<sub>6</sub>F<sub>5</sub>)X(EPPy<sub>n</sub>Ph<sub>3-n</sub>)] (M = Pd, Pt; X = C<sub>6</sub>F<sub>5</sub>, halide; E = O, S; n = 1, 2, 3; Py = pyridin-2-yl) have given us the opportunity to (i) observe dissociative processes involving either halide or a neutral ligand, as well as associative processes, not followed by further transformations; (ii) evaluate the corresponding activation parameters; and (iii) compare identical Pd and Pt systems in substitution reactions. This first paper deals with complexes of the type [Pd(C<sub>6</sub>F<sub>5</sub>)X(SPPy<sub>n</sub>Ph<sub>3-n</sub>)] (X = Br for n = 1, 2, 3; X = Cl, I for n = 2), and proves that rotation of the C<sub>6</sub>F<sub>5</sub> group is severely hindered in the square-planar complexes but occurs easily in a three-coordinate intermediate produced by halide dissociation.

## Results and Discussion

**A. Synthesis and Characterization of the Complexes in the Solid State.** The complexes [Pd(C<sub>6</sub>F<sub>5</sub>)Br(SPPy<sub>n</sub>Ph<sub>3-n</sub>)] (n = 1 (1), 2 (2b), and 3 (3)) were synthesized by reacting [Pd(C<sub>6</sub>F<sub>5</sub>)Br(NCMe)<sub>2</sub>] or (NBu<sub>4</sub>)<sub>2</sub>[Pd<sub>2</sub>(μ-Br)<sub>2</sub>(C<sub>6</sub>F<sub>5</sub>)<sub>2</sub>Br<sub>2</sub>] with a slight excess of the

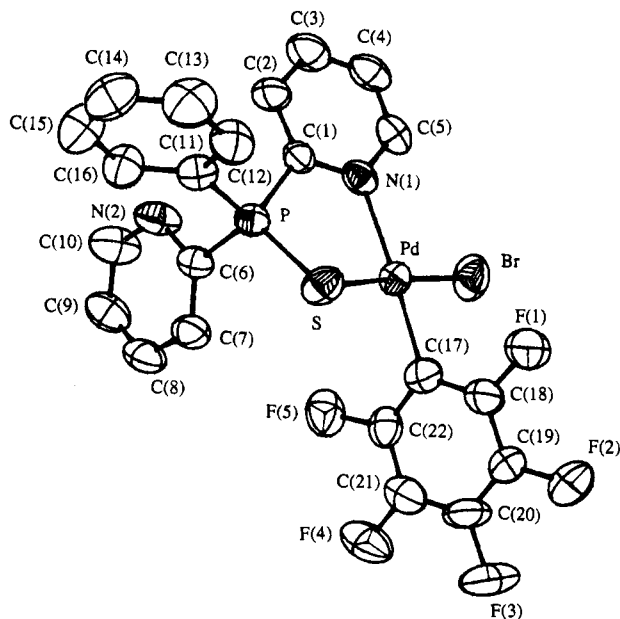
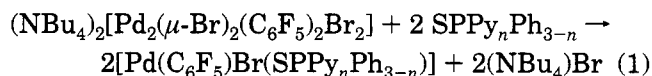


**Figure 2.** ORTEP drawing of the complex [Pd(C<sub>6</sub>F<sub>5</sub>)Br(SPPy<sub>2</sub>Ph)] (2b), with the labeling scheme indicated. Atoms are represented by their 50% probability ellipsoids.

corresponding SPPy<sub>n</sub>Ph<sub>3-n</sub> ligand (eq 1). The chloro (2a)



and iodo (2c) derivatives with SPPy<sub>2</sub>Ph were obtained by metathetical reactions in acetone from 2b and AgCl or KI, respectively.

The solid state IR spectra of all the complexes show the  $\nu(\text{P}=\text{S})$  absorption at 620–625 cm<sup>-1</sup>, i.e., shifted 25–35 cm<sup>-1</sup> downwards compared to the free ligand. This supports that, at least in the solid state, the ligands SPPy<sub>n</sub>Ph<sub>3-n</sub> are acting as S,N-chelates (Figure 1).

The molecular structure of 2b was studied by X-ray diffraction, and an ORTEP drawing of the molecule is shown in Figure 2 (note that the atom labeling in Figure 2 holds only for the X-ray data description and tables, whereas a chemical labeling will be used for the rest of the discussion, as defined at the beginning of section B). The bond distances and angles observed (Table 1) can be considered as normal. The palladium atom has an essentially square-planar geometry, and the neutral ligand is acting as S,N-chelate, as expected. The five-membered metallacycle is not planar: C1 and P are respectively 0.4814(55) and 0.9642(16) Å above the mean coordination plane containing Pd, Br, S, N1, and C17. The C<sub>6</sub>F<sub>5</sub> group is *cis* to the sulfur atom (in agreement with the expected antisymbiotic behavior of palladium)<sup>9</sup> and lies roughly perpendicular to the

(7) Minniti, D. *Inorg. Chem.* **1994**, *33*, 2631.

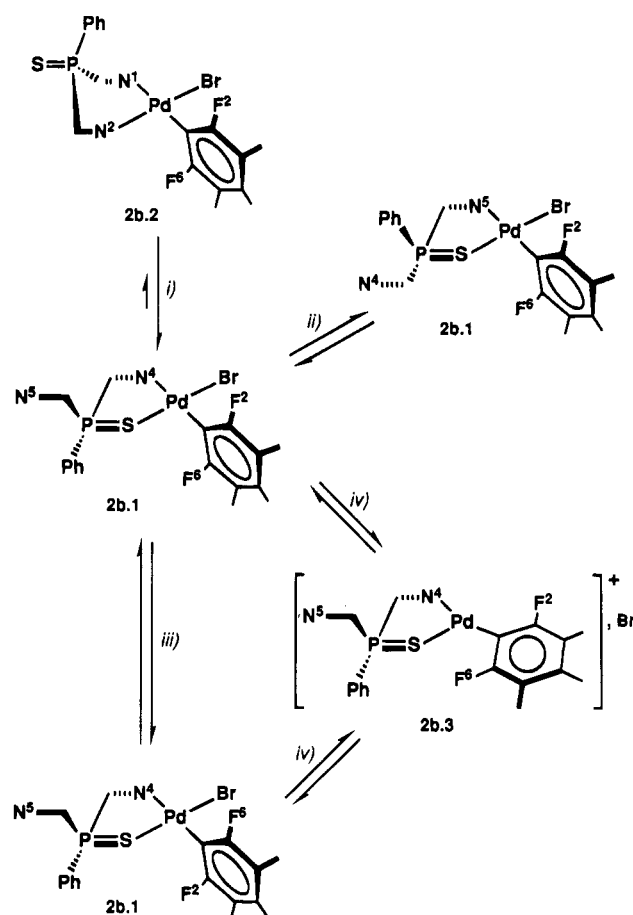
(8) Kawataka, S.; Kayaki, Y.; Shimizu, I.; Yamamoto, A. *Organometallics* **1994**, *13*, 3517.

**Table 1. Selected Bond Distances and Angles and Their Estimated Standard Deviations for [Pd(C<sub>6</sub>F<sub>5</sub>)Br(SPPy<sub>2</sub>Ph-N,S)] (2b)**

Distances, Å			
Pd-Br	2.425(1)	C(3)-C(4)	1.37(2)
Pd-S	2.307(2)	C(4)-C(5)	1.37(1)
Pd-N(1)	2.141(5)	C(6)-C(7)	1.364(9)
Pd-C(17)	1.978(7)	C(7)-C(8)	1.40(1)
S-P	1.991(2)	C(8)-C(9)	1.36(1)
P-C(1)	1.801(6)	C(9)-C(10)	1.36(1)
P-C(6)	1.811(6)	C(11)-C(12)	1.384(9)
P-C(11)	1.794(6)	C(11)-C(16)	1.382(9)
F(1)-C(18)	1.348(9)	C(12)-C(13)	1.37(2)
F(2)-C(19)	1.338(9)	C(13)-C(14)	1.39(1)
F(3)-C(20)	1.34(1)	C(14)-C(15)	1.35(1)
F(4)-C(21)	1.337(8)	C(15)-C(16)	1.38(2)
F(5)-C(22)	1.349(7)	C(17)-C(18)	1.36(1)
N(1)-C(1)	1.340(8)	C(17)-C(22)	1.363(9)
N(1)-C(5)	1.344(8)	C(18)-C(19)	1.37(1)
N(2)-C(6)	1.336(8)	C(19)-C(20)	1.35(1)
N(2)-C(10)	1.336(9)	C(20)-C(21)	1.36(2)
C(1)-C(2)	1.377(9)	C(21)-C(22)	1.374(9)
C(2)-C(3)	1.39(1)		
Angles, deg			
Br-Pd-S	175.23(5)	C(8)-C(9)-C(10)	119.8(7)
Br-Pd-N(1)	94.3(1)	N(2)-C(10)-C(9)	123.2(7)
Br-Pd-C(17)	86.4(2)	P-C(11)-C(12)	118.0(5)
S-Pd-N(1)	89.9(1)	P-C(11)-C(16)	122.0(5)
S-Pd-C(17)	89.7(2)	C(12)-C(11)-C(16)	120.0(6)
N(1)-Pd-C(17)	176.8(2)	C(11)-C(12)-C(13)	119.8(6)
Pd-S-P	94.23(8)	C(12)-C(13)-C(14)	119.9(7)
S-P-C(1)	107.6(2)	C(13)-C(14)-C(15)	119.9(7)
S-P-C(6)	113.7(3)	C(14)-C(15)-C(16)	121.4(7)
S-P-C(11)	112.3(3)	C(11)-C(16)-C(15)	119.0(6)
C(1)-P-C(6)	106.4(3)	Pd-C(17)-C(18)	124.7(5)
C(1)-P-C(11)	107.8(3)	Pd-C(17)-C(22)	121.4(5)
C(6)-P-C(11)	108.9(3)	C(18)-C(17)-C(22)	113.9(6)
Pd-N(1)-C(1)	118.6(4)	F(1)-C(18)-C(17)	119.3(7)
Pd-N(1)-C(5)	123.3(4)	F(1)-C(18)-C(19)	116.8(6)
N(1)-N(1)-C(5)	118.2(5)	C(17)-C(18)-C(19)	123.8(7)
C(6)-N(2)-C(10)	116.5(6)	F(2)-C(19)-C(18)	120.7(7)
P-C(1)-N(1)	115.9(4)	F(2)-C(19)-C(20)	120.0(7)
P-C(1)-C(2)	121.7(5)	C(18)-C(19)-C(20)	119.4(7)
N(1)-C(1)-C(2)	122.4(6)	F(3)-C(20)-C(19)	120.0(7)
C(1)-C(2)-C(3)	118.6(6)	F(3)-C(20)-C(21)	119.8(7)
C(2)-C(3)-C(4)	119.0(7)	C(19)-C(20)-C(21)	120.2(8)
C(3)-C(4)-C(5)	119.3(6)	F(4)-C(21)-C(20)	119.8(6)
N(1)-C(5)-C(4)	122.4(6)	F(4)-C(21)-C(22)	122.2(7)
P-C(6)-N(2)	113.3(4)	C(20)-C(21)-C(22)	118.1(7)
P-C(6)-C(7)	122.5(4)	F(5)-C(22)-C(17)	119.8(6)
N(2)-C(6)-C(7)	124.1(6)	F(5)-C(22)-C(21)	115.5(6)
C(6)-C(7)-C(8)	117.6(6)	C(17)-C(22)-C(21)	124.7(7)
C(7)-C(8)-C(9)	118.8(6)		

coordination plane (dihedral angle 98.64(18)°). The coordinated Py ring makes a dihedral angle of 20.84(36)° with the coordination plane. The N atom of the noncoordinated Py group is away from the metal.

**B. Solution Behavior of the Complexes.** The complexes have been studied in CDCl<sub>3</sub> and acetone-*d*<sub>6</sub> solution by <sup>1</sup>H, <sup>31</sup>P, and <sup>19</sup>F NMR spectroscopies (Table 2). The latter is particularly clear and informative: The number of F<sub>para</sub> (F<sup>4</sup>) signals reveals the number of isomers in solution, whereas the F<sub>ortho</sub> signals (F<sup>2</sup> and F<sup>6</sup>) report on the equivalence or inequivalence of the two halves of a given C<sub>6</sub>F<sub>5</sub> group (Figure 1).<sup>10,11</sup> In the <sup>1</sup>H NMR spectra the chemical shift of H<sup>6</sup> (the H atom on C<sup>6</sup> in the Py groups) is very sensitive to the coordinated or noncoordinated nature of the group and, when coordinated, to the *cis* ligand.<sup>12</sup>

**Scheme 1**

**B.1. Complex 1.** Complex 1 (Figure 1, R<sup>1</sup> = R<sup>2</sup> = Ph) shows only one isomer both in CDCl<sub>3</sub> and in acetone-*d*<sub>6</sub>. The chemical shift of H<sup>6</sup> ( $\delta$ (H<sup>6</sup>) = 9.78 ppm) is similar to that found for the coordinated Py in complex **2b.1** (see below and Scheme 1); hence, this group in **1** must be also *cis* to Br. In a rigid structure for **1**, identical to that found for complex **2b** in the solid, the two halves of the C<sub>6</sub>F<sub>5</sub> ring should be strictly inequivalent, but they appear as equivalent in the <sup>19</sup>F spectrum at all temperatures, both in CDCl<sub>3</sub> and in acetone-*d*<sub>6</sub>. This equivalence can be achieved by either of the two following processes: (a) Rotation of the C<sub>6</sub>F<sub>5</sub> ring, which can be discounted because it should be slow in CDCl<sub>3</sub> (see below, discussion for complexes **2**); and (b) a fast envelope-shift movement taking C<sup>2</sup> and P up and down the coordination plane, as represented in Figure 1, which must be the process operating. This allows us to continue the rest of the discussion as if the five-membered metallacycle defined by the N,S-chelating ligand was planar.

**B.2. Complexes 2a, 2b, and 2c.** Possible species and mechanisms operating for these complexes are depicted in Scheme 1. The <sup>19</sup>F, <sup>1</sup>H, and <sup>31</sup>P NMR spectra of complex **2b** in CDCl<sub>3</sub> at room temperature show the presence of two isomers. The <sup>1</sup>H spectrum of the major isomer (**2b.1**, >95%) displays the signals expected for two inequivalent Py groups: one noncoordinated ( $\delta$ (H<sup>6</sup>) = 8.82 ppm) and the other coordinated *cis* to Br ( $\delta$ (H<sup>6</sup>) = 9.81 ppm), as found in the X-ray structure determination. In the <sup>19</sup>F spectrum (Figure

(9) Pearson, R. G. *Inorg. Chem.* **1973**, *12*, 712.(10) Albéniz, A. C.; Espinet, P.; Foces-Foces, C.; Cano, F. H. *Organometallics* **1990**, *9*, 1079.(11) Albéniz, A. C.; Espinet, P.; Jeannin, Y.; Philoche-Levisalles, M.; Mann, B. E. *J. Am. Chem. Soc.* **1990**, *112*, 6594.(12) Byers, P. K.; Canty, A. J. *Organometallics* **1990**, *9*, 210.



Table 2. Relevant  $^{31}\text{P}$ ,  $^1\text{H}$ , and  $^{19}\text{F}$  NMR Data for the Complexes<sup>a</sup>

complex	P <sup>b</sup>	H <sup>6</sup> Py <sub>coord</sub> <sup>c</sup>	H <sup>6</sup> Py <sub>free</sub> <sup>c</sup>	F <sup>6</sup> and F <sup>2</sup> or F <sup>6</sup> + F <sup>2</sup> <sup>c</sup>	F <sup>5</sup> and F <sup>3</sup> or F <sup>5</sup> + F <sup>3</sup> <sup>c</sup>	F <sup>4</sup> <sup>d</sup>
1	52.6	9.74		-118.4	-164.6	-161.5
2a.1	46.9	9.62	8.82	-118.7, -119.5	-164.0	-160.8
2a.2		9.75		-118.2, -122.3	-162.8, -163.2	-160.2
2b.1	45.9	9.81	8.82	-118.1, -118.9	-164.1	-161.0
2b.2		9.73, 8.36		-117.7, -121.4	-162.9, -173.8	-160.1
2b.1 <sup>e</sup>		9.72	8.90	-113.2	-161.7	-158.6
2b.2 <sup>e</sup>		9.64, 8.47		-111.5, -116.0	-160.5, -161.4	-158.3
2c.1	43.5	10.02	8.81	-115.9, -116.5	-164.4	-161.0
2c.2		9.95		-114.6, -118.5	-163.2, -163.8	-160.1
3.1	42.3	9.09	8.90	-118.7	-163.1	-159.9
3.2	39.5	9.73, 8.40	8.94	-119.5, -122.0	-161.7, -162.4	-159.2

<sup>a</sup> All data at 294 K, except **3.2** at 213 K. In CDCl<sub>3</sub> unless otherwise stated. <sup>b</sup> Singlet. <sup>c</sup> Multiplet. <sup>d</sup> Triplet. <sup>e</sup> In acetone-*d*<sub>6</sub>.

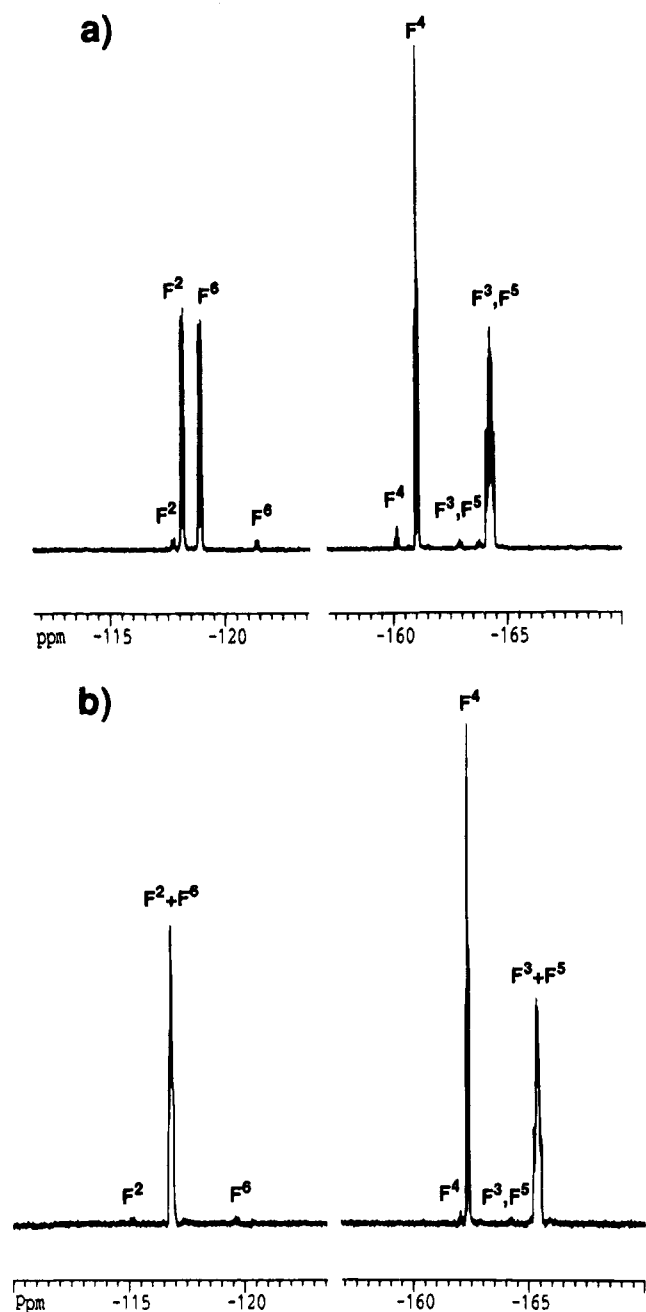


Figure 3.  $^{19}\text{F}$  NMR spectrum of  $[\text{Pd}(\text{C}_6\text{F}_5)\text{Br}(\text{SPPy}_2\text{Ph})]$  (**2b**) at 294 K in CDCl<sub>3</sub> (a) and in acetone-*d*<sub>6</sub> (b).

3a) the five fluorine atoms of this isomer give rise to five signals, i.e., the two halves of the C<sub>6</sub>F<sub>5</sub> ring appear as inequivalent. This result would indicate a rigid structure in which the C<sub>6</sub>F<sub>5</sub> group is not rotating around

the Pd-C bond; in fact a slow rotation is taking place, as discussed later. The minor isomer also shows inequivalence for the two halves of the C<sub>6</sub>F<sub>5</sub> ring, and the signals observed in the  $^1\text{H}$  and  $^{19}\text{F}$  spectra suggest for it structure **2b.2**, in which the neutral ligand is acting as a N,N-chelate. This is the kind of structure found for the corresponding complex with OPPy<sub>2</sub>Ph and is not considered in detail here as it will be discussed in a forthcoming paper on OPPy<sub>n</sub>Ph<sub>3-n</sub> complexes.

In acetone-*d*<sub>6</sub>, the NMR spectra of complex **2b** show again the presence of two isomers (Figure 3b), but now the  $^{19}\text{F}$  spectrum of the major isomer **2b.1** shows only three signals (2:1:2), i.e., the two halves of the C<sub>6</sub>F<sub>5</sub> ring appear as equivalent, even at 213 K. Meanwhile, its  $^1\text{H}$  spectrum shows the two Py groups to be still inequivalent, one noncoordinated and the other coordinated *cis* to Br. Hence, the mechanism producing equivalence of the two halves of the C<sub>6</sub>F<sub>5</sub> ring does not involve exchange of free and coordinated Py groups (i.e., equilibrium ii in Scheme 1 is very slow). In addition, the signals of the second and very minor isomer are still observed, thus excluding any process going *via* the N,N-chelated structure (i.e., equilibrium i in Scheme 1 is also very slow; its rate is measured later for the related complex **3**).

This led us to C<sub>6</sub>F<sub>5</sub> rotation as the mechanism producing equivalence, and we must address the question whether this rotation occurs (a) directly on the square-planar complex **2b.1** (path iii); (b) *via* an associative process on the pentacoordinate intermediate (not depicted in Scheme 1); or (c) *via* a dissociative process, on a three-coordinate intermediate (such as **2b.3** in Scheme 1, path iv).

The first possibility, rotation directly on **2b.1**, can be discounted because (1) the solvent should not have a marked effect on the rate of rotation, whereas the observed behavior is fast rotation in acetone-*d*<sub>6</sub> and slow rotation in CDCl<sub>3</sub> (see below, kinetic experiments); and (2) the rotation in the square-planar complex looks severely hindered sterically. In effect, by applying the data found in the X-ray determination of **2b** to a rotamer in which the C<sub>6</sub>F<sub>5</sub> ring becomes coplanar with the coordination plane (Figure 4), a very short distance (202 pm) is calculated between the *ortho* fluorines and the coordinated Br and S atoms. This distance means a contraction to about 62% of the sum of the van der Waals radii (330 and 320 pm, respectively),<sup>13</sup> which seems unacceptable. To avoid this the complex should undergo severe distortions at this stage of rotation,

(13) Emsley, J. *The Elements*, 2nd ed.; Clarendon Press: Oxford, England, 1991; pp 36, 70, and 182.

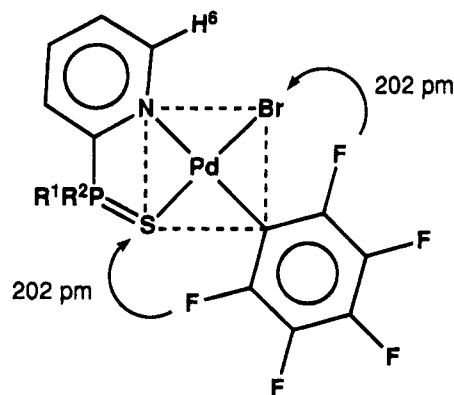


**Figure 4.** Chart of a hypothetical square-planar rotamer with the  $C_6F_5$  ring coplanar with the coordination plane.

implying a very high activation energy for the rotation.<sup>14</sup> As a matter of fact, our results discussed below mean that the most accessible distortion turns out to be the heterolytic cleavage of the Pd–Br bond.

The second possibility, an associative mechanism involving coordination of the solvent, would be consistent with the acceleration of rate observed in acetone, but it is not clear whether the  $C_6F_5$  rotation should be less hindered in a five-coordinate intermediate than in a square-planar complex. Moreover, it is difficult to understand why in the absence of a coordinating solvent ( $CDCl_3$ ) this mechanism should not be triggered by the pendant Py group.

The third possibility, a dissociative mechanism, might involve Pd–S or Pd–Br dissociation, both facilitating equally the  $C_6F_5$  rotation. The former can be discounted because it should not be so very sensitive to a change of solvent and, more importantly, because it should predictably trigger simultaneously equilibrium i, which is not observed. Dissociation of anionic  $Br^-$  might explain the acceleration observed in acetone, a more polar solvent with a higher dielectric constant than chloroform.

Overall, qualitative considerations seem to favor  $Br^-$  dissociation, but kinetic studies are needed to substantiate any decision between the associative and the dissociative path.

**Kinetic Studies.** The  $C_6F_5$  rotation for  $[Pd(C_6F_5)Br(SPPy_2Ph-N,S)]$  in acetone- $d_6$  is fast (see Figure 3b and ref 30). In  $CDCl_3$ , the  $^{19}F$  spectra show the molecule as apparently rigid (Figure 3a,  $F^2$  and  $F^6$  inequivalent) in the range of temperatures accessible, but magnetization transfer experiments on the  $F_{ortho}$  signals confirm that a slow rotation exchanging  $F^2$  and  $F^6$  is occurring and allow kinetic studies to be undertaken (Figure 5). In this way the rotation rate constants can be evaluated from the experimental magnetization transfer constants as  $k_{rot} = 2k_{MT}(F^2 \rightarrow F^6)$ .<sup>15</sup>

**(i) Influence of the Halide.** The temperature dependence of the rotation rate was determined for  $[Pd-$

**Table 3.** Temperature Dependence of  $C_6F_5$  Rotation Rate in Complexes **2a.1**, **2b.1**, and **2c.1** in  $CDCl_3$  ( $k_{rot}$  in  $s^{-1}$ )

$k_{rot}(2a.1)/$ $T$ (K)	$k_{rot}(2b.1)/$ $T$ (K)	$k_{rot}(2c.1)/$ $T$ (K)
1.41/291.6	3.54/291.6	2.13/269.8
2.23/296.6	6.33/296.6	4.49/276.3
3.74/302.5	9.81/302.6	6.93/283.5
7.59/311.5	16.68/311.5	12.09/289.9
12.52/317.5	29.32/317.0	22.47/299.6
17.01/323.2	41.72/323.2	38.89/306.6

**Table 4.** Activation Parameters for  $C_6F_5$  Rotation in  $[Pd(C_6F_5)X(SPPy_2Ph-N,S)]$  (**2b.1**) in  $CDCl_3$  (Standard Deviations in Parentheses)

X	Cl	Br	I
$\Delta H^\ddagger$ ( $kJ\ mol^{-1}$ )	60.0(1.2)	57.1(2.5)	50.2(0.6)
$\Delta S^\ddagger$ ( $J\ K^{-1}\ mol^{-1}$ )	-35.8(3.9)	-37.5(8.2)	-51.1(2.0)

**Table 5.** Thermodynamic Differences for Cl, Br, and I Involved in a Heterolytic Cleavage  $[Pd-X] \rightarrow [Pd]^+ + X^-$

X–X'	$\Delta_D(Pt)$	$\Delta_{EA}$	$\Delta_{free}$	$\Delta_{exp}$	$\Delta_{hydr}$	$\Delta_{solv}$
Cl–Br	33.5	-24.4	9.1	2.9	-31.35	-22.25
Br–I	48.5	-29.4	19.9	6.9	-40.96	-21.86
Cl–I	82.0	-53.8	28.2	9.8	-72.31	-44.11

<sup>a</sup> In  $kJ\ mol^{-1}$ ;  $\Delta$  taken as {(value for X) – (value for X')}.

( $C_6F_5$ )Br(SPPy<sub>2</sub>Ph–N,S)] (**2b**) and for their Cl (**2a**) and I (**2c**) derivatives, Table 3). The Eyring plots in Figure 6 yield the activation parameters in Table 4. A decrease in  $\Delta H^\ddagger$  is observed in the sequence Cl > Br > I. Again this trend discounts rotation directly in the four-coordinate species **2b.1**, where the bulkiest halogen atom should produce the biggest hindrance and the highest  $\Delta H^\ddagger$ . Furthermore, it supports the notion that rotation is preceded by halide dissociation, which we believe should be easiest for the heaviest halogen. The sequence of lability observed, Cl < Br < I is in contrast to that observed for the isomerization of *cis*-[Pt(YC<sub>6</sub>H<sub>4</sub>)X-(PEt<sub>3</sub>)<sub>2</sub>] in methanol, which occurs *via* dissociative loss of the X<sup>–</sup> ligand.<sup>16</sup> In that work the sequence of lability, Cl > Br > I, is said to reflect a variation of the bond strength of the halide ions to the “soft” metal center in the order Cl < Br < I, but there is much evidence against this affirmation. It is rather general that M–X dissociation energies for transition metals follow the order Cl > Br > I.<sup>17</sup> For a heterolytic cleavage a rough calculation of the differences for the three halides is given in Table 5, along with the parameters involved. The differences in bond dissociation energy ( $\Delta_D$ ) for Pt (as the element closest to Pd for which we have found data) are taken<sup>18</sup> and are corrected for the differences in electron affinity of the halogens ( $\Delta_{EA}$ ).<sup>19</sup> This provides the difference in energy ( $\Delta_{free}$ ) for the formation of well-separated unsolvated ion pairs (i.e., assuming equal electrostatic energy for the three anions), which is unfavorable for the dissociation of Cl<sup>–</sup> by about 9 kJ mol<sup>–1</sup> as compared to Br<sup>–</sup> and by 28 kJ mol<sup>–1</sup> as compared to I<sup>–</sup> (the experimental differences in activa-

(14) Examples of restriction to rotation in aryl derivatives are not uncommon. See, for instance: (a) Alcock, W.; Brown, J. M.; Pérez-Torrente, J. *Tetrahedron Lett.* **1992**, *33*, 389. (b) Alsters, P. L.; Boersma, J.; Smeets, W. J. J.; Spek, A. L.; van Koten, G. *Organometallics* **1993**, *12*, 1639. (c) Wada, M.; Sameshima, K. *J. Chem. Soc., Dalton Trans.* **1981**, 240. (d) Baumgärtner, R.; Brune, H. A. *J. Organomet. Chem.* **1988**, *350*, 115. (e) Anderson, G. K.; Cross, R. J.; Manojlovic-Muir, L.; Muri, K. W.; Rocamora, M. *Organometallics* **1988**, *7*, 1520.

(15) Green, M. L. H.; Wong, L.-L.; Sella, A. *Organometallics* **1992**, *11*, 2660.

(16) Romeo, R.; Minniti, D.; Lanza, S. *Inorg. Chem.* **1979**, *18*, 2362.

(17) Kerr, J. A. *Strengths of Chemical Bonds*. In *CRC Handbook of Chemistry and Physics*, 73rd ed; CRC Press Inc.: Boca Raton, FL, 1992; pp 9-129–137.

(18) Levy, C. J.; Puddephatt, R. J.; Vittal, J. J. *Organometallics* **1994**, *13*, 1559.

(19) Huheey, J. E.; Keiter, E. A.; Keiter, R. L. *Inorganic Chemistry. Principles of Structure and Reactivity*, 4th ed; Harper Collins College Publishers: New York, 1993; p 43.

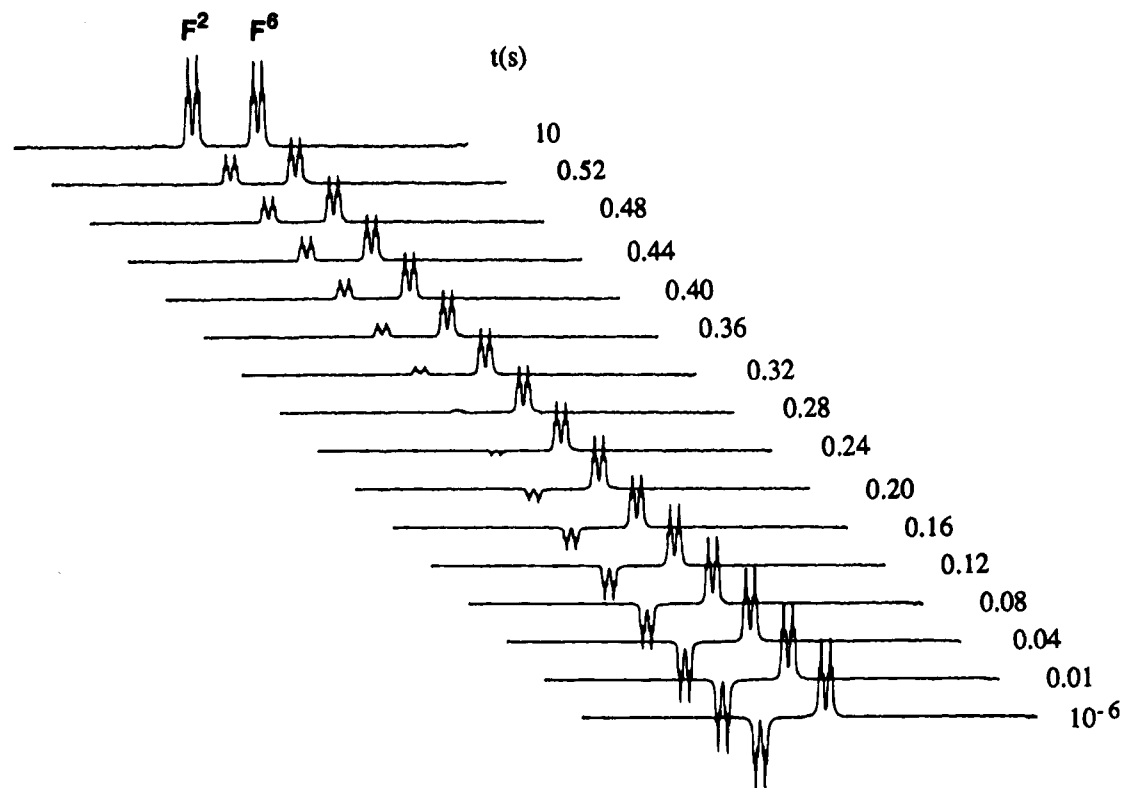


Figure 5. Plot of magnetization transfer,  $F^2 \rightarrow F^6$ .

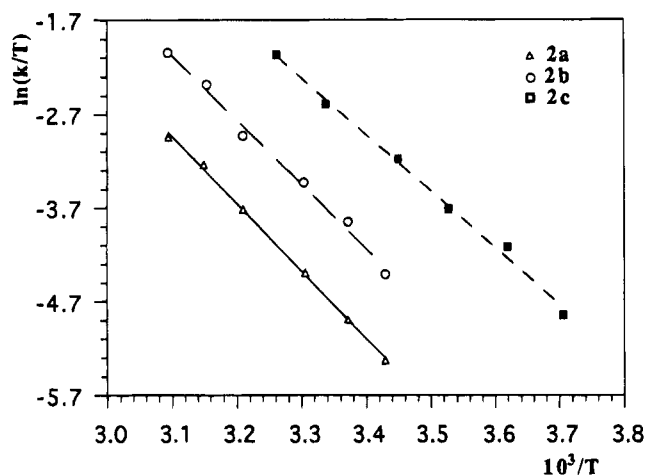


Figure 6. Eyring plots of  $k_{rot}$  of  $C_6F_5$  for the compounds  $[Pd(C_6F_5)X(SPPy_2Ph)]$  ( $X = Cl, 2a; Br, 2b; I, 2c$ ).

tion enthalpy,  $\Delta_{exp}$ , are 2.9 and 9.8, respectively). If the heterolytic cleavage occurs in the presence of a solvating solvent, then the differences in solvation energies for the three anions (for a common cation) have to be considered. These can be rather high and overcome the previous differences, as is the case with hydration energies ( $\Delta_{hydr}$ ).<sup>20,21</sup> The heterolytic cleavage of the hydrated ions (estimated as  $\Delta_{solv} = \Delta_{free} + \Delta_{hydr}$ ) is favorable for the dissociation of  $Cl^-$  by about  $22 \text{ kJ mol}^{-1}$  as compared to  $Br^-$ , and by  $44 \text{ kJ mol}^{-1}$  as compared to  $I^-$ . Still making the reasonable assumption that the order of stabilities in the rate-determining transition state is the same as for the dissociated systems one can be rather sure, even at this very crude level of ap-

proximation, that the order of lability toward heterolytic dissociation,  $Cl < Br < I$ , found in this paper in the nonsolvating  $CDCl_3$ , reflects the relative bond strength of the three "soft" halide ions to the "soft" Pd center; the inverse order found previously for  $cis-[Pt(YC_6H_4)X-(PEt_3)_2]$  was deduced from kinetic studies in MeOH and reflects the very important contribution of the solvation energies, not the bond strengths.

The negative values of  $\Delta S^\ddagger$  found in our system do not contradict a dissociative process in solution. For instance, the DMSO exchange in  $[PtPh_2(Me_2SO)_2]$ , which is undoubtedly dissociative ( $\Delta V^\ddagger = +4.9 \pm 0.5 \text{ cm}^3 \text{ mol}^{-1}$ ),<sup>2a</sup> shows a  $\Delta S^\ddagger = -16 \pm 2 \text{ cal K}^{-1} \text{ mol}^{-1}$ .<sup>2b</sup> The dissociation of the halo ligand in our system produces a tight ion pair in a cage of solvent (see next section); hence, the leaving group is not very much loosened in the transition state and a large positive  $\Delta S^\ddagger$  is not to be expected. In addition, some  $Pd \cdots F_{ortho}$  interaction in the transition state, assisting the dissociation, might reduce the rotational entropy. On the other hand, the ion pair must induce some solvent ordering in the transition state, leading to a negative contribution to  $\Delta S^\ddagger$ . Altogether, the positive contributions to  $\Delta S^\ddagger$  are expected to be small and can be compensated by the negative contributions.

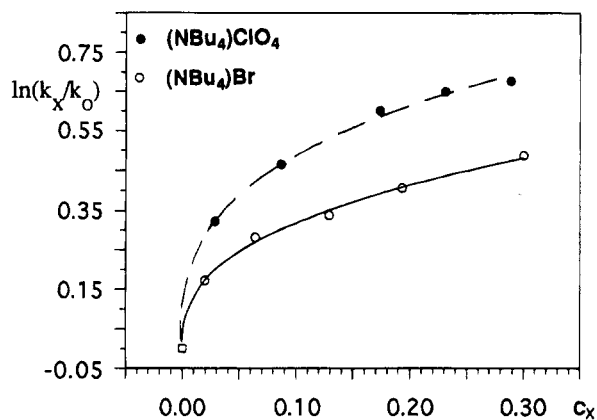
(ii) **Salt Effects.** The effect of adding  $(n-Bu_4N)Br$  or  $(n-Bu_4N)ClO_4$  on the rotation rate of  $[Pd(C_6F_5)-Br(SPPy_2Ph-N,S)]$  in  $CDCl_3$  (Table 6) is shown in Figure 7. Both salts produce a moderate acceleration effect which is more pronounced at the initial stage and somewhat stronger for  $(n-Bu_4N)ClO_4$ . The meaning of these results needs to be considered very cautiously: Compared to the many studies on the effect of added salts on reaction rates in polar and dissociating solvents,<sup>22-24</sup> salt effects in nonpolar solvents have been little studied. Kinetic studies in nonpolar solvents are complicated by the nonideal nature of solutions of ionic

(20) Morris, D. F. C. Ionic Radii and Enthalpies of Hydration of Ions. In *Structure and Bonding*; Springer Verlag: Berlin, Germany, 1968; Vol. 4, p 77.

(21) Duncan, A.; Pople, J. *Trans. Faraday Soc.* **1953**, *49*, 217.

**Table 6.** Salt Effects on the C<sub>6</sub>F<sub>5</sub> Rotation Rate in Complex **2b.1** in CDCl<sub>3</sub><sup>a</sup>

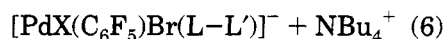
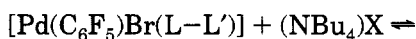
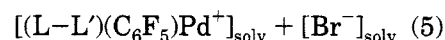
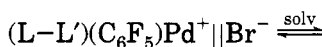
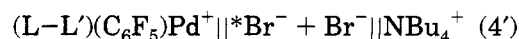
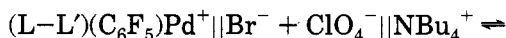
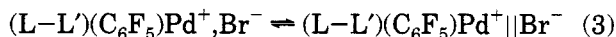
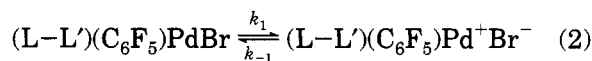
[(NBu <sub>4</sub> )ClO <sub>4</sub> ]/k <sub>rot</sub>	[(NBu <sub>4</sub> )ClO <sub>4</sub> ]/k <sub>rot</sub>
0.000/2.70	0.000/2.70
0.020/3.20	0.029/3.73
0.064/3.58	0.087/4.30
0.128/3.79	0.174/4.92
0.193/4.05	0.231/5.17
0.300/4.39	0.289/5.31

<sup>a</sup> Salt concentration in mol L<sup>-1</sup>; k<sub>rot</sub> in s<sup>-1</sup>.**Figure 7.** Plot of  $\ln(k_x/k_0)$  versus  $c$  ( $c$  = concentration of (NBu<sub>4</sub>)ClO<sub>4</sub> or (NBu<sub>4</sub>)Br).

species and the possible aggregation of reactants and products.<sup>25,26</sup> This must be particularly true for a very poorly dissociating solvent with a low dipole moment, such as CDCl<sub>3</sub> ( $\epsilon_r = 4.80$ ,  $\mu = 1.04$  for CHCl<sub>3</sub>)<sup>27</sup> and highly concentrated solutions (obliged by the use of NMR spectroscopy for the kinetic studies).

The possible steps to be considered in the dissociation of the Pd–Br bond are shown in eqs 2–5: heterolytic cleavage of the Pd–Br bond to give contact ion pairs in a cage of solvent (eq 2); formation of solvent-separated ion pairs (eq 3); exchange reaction between ion pairs (eq 4 for the perchlorate salt or eq 4' for the bromide salt); and complete ion dissociation (eq 5). In the event of an associative mechanism (unlikely with the information already discussed) we should also consider anion coordination with formation of a pentacoordinate species in which (supposedly) the C<sub>6</sub>F<sub>5</sub> rotation should occur more easily (eq 6).

For an associative mechanism (eq 6) an accelerating effect can be expected for the bromide but not for the perchlorate salt;<sup>28</sup> thus, the observation of a larger effect for perchlorate is evidence against the operation of an associative mechanism. On the other hand, the difference between the effects of the two salts is quantitatively small. This is the kind of behavior expected for nonpolar solvents in which the salts are present as ion pairs or higher aggregates (i.e., in which eqs 3, 4, and 5 are not operating).<sup>25,26,29</sup>

(22) Loupy, A.; Tchoubar, B. *Salt Effects in Organic and Organometallic Chemistry*; VCH: Weinheim, Germany, 1992; pp 11–53.(23) Fainberg, A. H.; Winstein, S. *J. Am. Chem. Soc.* **1956**, *78*, 2763.(24) Fainberg, A. H.; Winstein, S. *J. Am. Chem. Soc.* **1956**, *78*, 2767.(25) Smith, P. J.; Wilcox, C. S. *J. Org. Chem.* **1990**, *55*, 5675 and references therein.(26) Smith, P. J.; Kim, E.; Wilcox, C. S. *Angew. Chem., Int. Ed. Engl.* **1993**, *32*, 1648.(27) Chastrette, M.; Rajzmann, M.; Chanon, M.; Purcell, K. F. *J. Am. Chem. Soc.* **1985**, *107*, 1.(28) See, for example: Hansson, S.; Norrby, P.-O.; Sjögren, P. T.; Åkermark, B.; Cucciolito, M. E.; Giordano, F.; Vitagliano, A. *Organometallics* **1993**, *12*, 4940.

Consequently, the evidence points to rotation in a three-coordinate cation **2b.3** (Scheme 1) forming part of a contact ion pair in a cage of solvent (eq 2). This agrees with the simple model proposed by Perrin and Pressing for salt effects in less polar solvents. In this model the transition state (in a vanishingly small concentration) is a dipole rather than an ion, and the added salts are also present as ion pairs or higher aggregates. The effect of these dipolar interactions for a single added salt and low salt concentrations should obey eq 7, where  $b$  can be calculated ( $b_{\text{calcd}}$  for Bu<sub>4</sub>NClO<sub>4</sub> = 6.8;  $b_{\text{calcd}}$  for Bu<sub>4</sub>NBr = 4.3).<sup>29</sup>

$$\ln \frac{k}{k_0} = b[\text{salt}] \quad (7)$$

$$\frac{\ln[k(ClO_4^-)/k_0]}{\ln[k(Br^-)/k_0]} = \frac{b_{\text{calcd}}(\text{for } NBu_4ClO_4)}{b_{\text{calcd}}(\text{for } NBu_4Br)} = 1.58 \quad (8)$$

The ratio of salt effects for the two salts at the same concentration should be 1.58, according to eq 8. It is remarkable that, even though the concentrations used in this work are high, the ratio of the effects produced by the two salts is in the range 1.6–1.4, as can be seen in Figure 7.

Our results illustrate clearly the enormous changes in salt effects when nondissociating solvents are used. Thus the effect of addition of a common ion salt on a dissociative process is not a retardation of rate by the common ion mass effect, as in dissociating solvents. Rather to the contrary, an acceleration is produced as a consequence of the stabilization of the dipolar transition state in the increasingly polar atmosphere produced by the increasing concentration of dipoles or multipoles of the added salt in the nonpolar solvent.

Figure 8 shows a pictorial model of the concerted C<sub>6</sub>F<sub>5</sub> rotation in CDCl<sub>3</sub> according to the evidence discussed. In each half rotation the C<sub>6</sub>F<sub>5</sub> group will “push” the dissociated halide away from its coordination site, but not very far away since this is happening in a cage of solvent. It is a reasonable speculation that the halide

(29) Perrin, C. L.; Pressing, J. *J. Am. Chem. Soc.* **1971**, *93*, 5705.

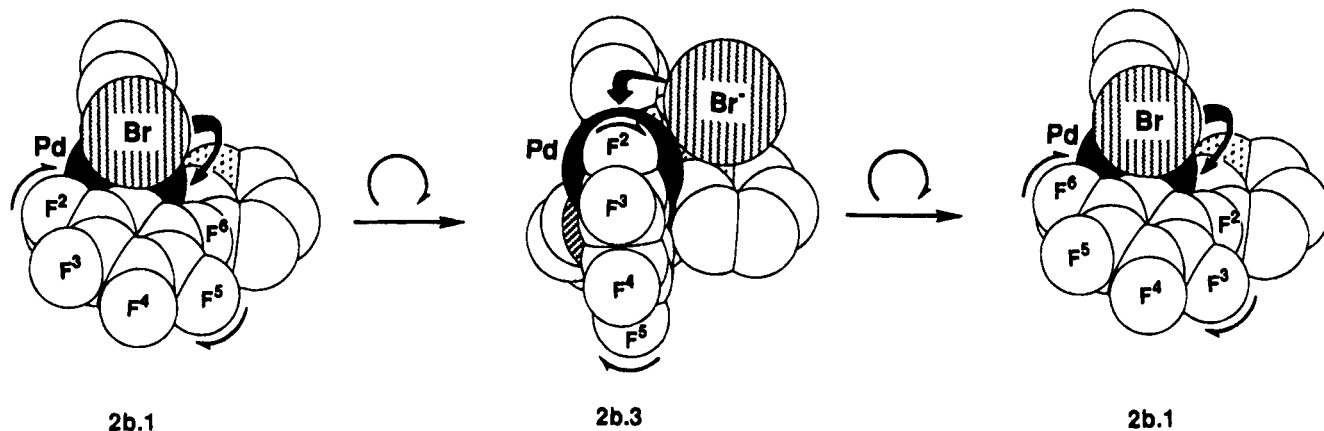
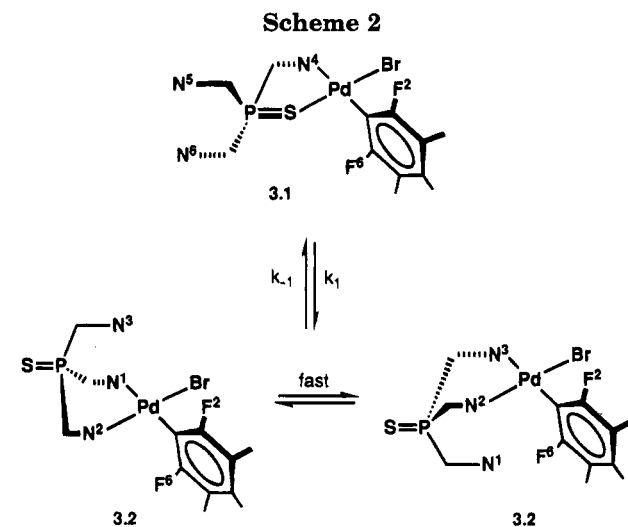


**Figure 8.** Space-filling model for the  $C_6F_5$  rotation in  $[Pd(C_6F_5)Br(SPPy_2Ph)]$  (**2b**) in  $CDCl_3$ ; the molecule is viewed along the bisectrix of the  $Br-Pd-C$  angle, and the labels refer to Scheme 1.

will move to some location over the coordination square plane where the anion-cation distance can be shorter and the electrostatic interactions can be higher and will fall back to its coordination site as soon as it is available. In dissociating solvents (e.g., acetone), separated solvated ions will be produced (eq 5). In other words, the halide is engaged or declutched from the rotor depending on the environment, the dissociating solvents letting out the clutch to allow faster rotation of the  $C_6F_5$  group.<sup>30,31</sup>

**B.3. Complex 3.** The species and mechanisms operating for complex **3** are shown in Scheme 2. The solubility of the compound in acetone is very low, and studies could be carried out only in  $CDCl_3$ . Two isomers are observed: the N,S-chelate **3.1** and the N,N-chelate **3.2** in an approximate 3:2 ratio at 298 K. The increase in proportion of the N,N-chelate isomer in **3** as compared to complex **2b** is very much higher than the factor of 2 expected from the higher effective concentration of the Py group in the former.<sup>32</sup> Two plausible explanations are a decrease in nucleophilicity of the sulfur atom in  $SPPy_3$  induced by the higher electron-attracting ability of the Py groups compared to the Ph groups or a weak bonding interaction of the third Py group to Pd (in a square-pyramidal geometry), since we observe three inequivalent Py groups at low temperature.<sup>33</sup>

The equilibrium  $3.1 \leftrightarrow 3.2$  is slow ( $k_1 = 0.33 \text{ s}^{-1}$ ;  $k_{-1} = 0.52 \text{ s}^{-1}$ , measured by magnetization transfer experi-



ments on the  $^{31}P$  signals at 298 K).  $F^2$  and  $F^6$  in **3.1** are inequivalent at room temperature; slow  $C_6F_5$  rotation in **3.1** via  $Br^-$  dissociation should be occurring, as in **2b.1**, but this was not studied. In isomer **3.2**,  $F^2$  and  $F^6$  are equivalent at room temperature but become inequivalent at low temperature (coalescence temperature = 243 K at 75 MHz;  $\Delta G^\ddagger = 44.25 \text{ kJ mol}^{-1}$ ). This apparent  $C_6F_5$  rotation is in reality a consequence of exchange of the uncoordinated Py group and the Py group *trans* to the  $Pd-C$  bond ( $N^1$  and  $N^3$  in Scheme 2). This can be clearly seen in the  $^1H$  spectra in Figure 9 that show exchange of  $H^6$  signals between only two Py groups. Detailed studies on related complexes with  $OPPy_3$ , to be presented in a forthcoming paper, support an associative mechanism for this process.

## Conclusion

The rotation of the  $C_6F_5$  group around the  $Pd-C$  bond in complexes  $[Pd(C_6F_5)X(SPPy_nPh_{3-n}-N,S)]$  in  $CDCl_3$  involves a simple halide dissociation not followed by any subsequent process except the rotation itself. The

(30) Coalescence in acetone- $d_6$  is observed at  $228 \pm 15 \text{ K}$  (a more precise value is difficult to assign due to the proximity of the signals) for the signals of  $F^3$  and  $F^5$ , for which the chemical shift difference below coalescence is  $\delta\nu = 83.9 \text{ Hz}$ . Then, applying the equation for the coalescence temperature  $k = 2\pi\delta\nu/\sqrt{2}$ , a value of  $k_{rot}$ (chloride in acetone) =  $186 \text{ s}^{-1}$  at  $T = 228 \text{ K}$  is obtained. This can be compared with the value calculated from the Eyring plots for the rotation in chloroform,  $k_{rot}$ (chloride in chloroform) =  $8.94 \times 10^{-3} \text{ s}^{-1}$  at  $T = 228 \text{ K}$ . Hence, the rotation is about 20 000 times faster in acetone than in chloroform. Possibly in acetone the dissociated species  $[Pd(C_6F_5)(SPPy_2Ph-N,S)(acetone)]^+X^-$  are formed, and the fast rotation indicates that decoordination of the hard ligand acetone from  $[Pd(C_6F_5)(SPPy_2Ph-N,S)(acetone)]^+$  is very easy.

(31) Molecular motors and brakes are fashionable nowadays (see, for instance: (a) Kelly, T. R.; Bowyer, M. C.; Bhaskar, K. V.; Bebbington, D.; Garcia, A.; Lang, F.; Kim, M. H.; Jette, M. P. *J. Am. Chem. Soc.* **1994**, *116*, 3657. (b) Fanizzi, F. P.; Lanfranchi, M.; Natile, G.; Tiripicchio, A. *Inorg. Chem.* **1994**, *33*, 3331). Ours offers the novelty that, in  $CDCl_3$ , the dissociated halide should show marked preference for one of the two faces of the coordination plane (either the Py side or the Ph side), thus producing a preferable "sense" for the ionization in each enantiomer (our compound is a racemic mixture). The rotation itself converts degenerate states and cannot have a preferred sense, according to the microscopic reversibility principle.

(32) Carter, M. J.; Beattie, J. K. *Inorg. Chem.* **1970**, *9*, 1233.

(33) We consider this latter possibility unlikely. In Pt, which shows a much greater tendency to pentacoordination than Pd, good N-donor ligands (ours is weak) and some  $\pi$ -acceptor ancillary ligand are necessary to promote five-coordination. Moreover, with trispyrazolylborates the resulting geometry is bipyramidal with two equatorial (hence equivalent) pyrazolyl groups. See, for instance: Albano, V. G.; Demartin, F.; De Renzi, A.; Morelli, G.; Saporito, A. *Inorg. Chem.* **1985**, *24*, 2032 and references therein.

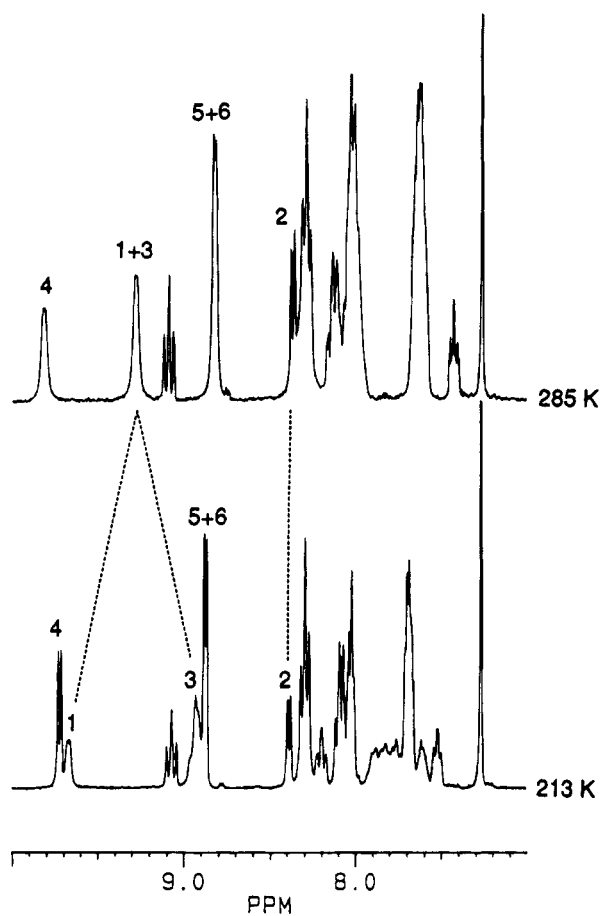


**Figure 9.**  $^1\text{H}$  NMR spectrum of  $[\text{Pd}(\text{C}_6\text{F}_5)\text{Br}(\text{SPPy}_3)]$  (**3**) at the temperatures indicated. Labels refer to the  $\text{H}^6$  atom of each Py ring in Scheme 2. For instance, 2 stands for  $\text{H}^6$  in the Py ring containing  $\text{N}^2$ .

rotation occurs in a contact ion pair in a cage of solvent,  $[\text{Pd}(\text{C}_6\text{F}_5)(\text{SPPy}_n\text{Ph}_{3-n})]^+\text{X}^-$ . The fact that the rotation is very fast in acetone shows that the rotation itself has a low activation energy. Hence the enthalpy values observed for the slow rotation in  $\text{CDCl}_3$  must correspond closely to the dissociation. The activation enthalpies decrease in the order  $\text{Cl} > \text{Br} > \text{I}$ , reflecting the decreasing affinity of the three "soft" halides for the "soft" palladium(II) in the absence of important solvation effects. The activation entropies for these dissociative processes in  $\text{CDCl}_3$  are negative.

### Experimental Section

**General Methods.** C, H, and N analyses were carried out on a Perkin-Elmer 240 microanalyzer. IR spectra were recorded (in the range  $4000\text{--}200\text{ cm}^{-1}$ ) on a Perkin-Elmer 883 spectrometer.  $[\text{Pd}(\text{C}_6\text{F}_5)_2(\text{NCMe})_2]^{10}$  and  $(\text{NBu}_4)_2[\text{Pd}_2(\mu\text{-Br})_2(\text{C}_6\text{F}_5)_2\text{Br}_2]$  were prepared as described elsewhere. The phosphines<sup>35</sup> and their sulfides<sup>36</sup> were made by methods in the literature.

**NMR Measurements.** NMR spectra were recorded on a Bruker AC300 spectrometer with a thermostated multinuclear QNP probehead operating in the FT mode at 300 MHz ( $^1\text{H}$ ),

(34) Usón, R.; Forniés, J.; Nalda, J. A.; Lozano, M. J.; Espinet, P.; Albéniz, A. C. *Inorg. Chim. Acta*, **1989**, *156*, 251.

(35) (a) Maisonnat, A.; Farr, J. P.; Olmstead, M. M.; Hunt, C. T.; Balch, A. L. *Inorg. Chem.* **1982**, *21*, 3961. (b) Xie, Y.; Lee, C.; Yang, Y.; Rettig, S. J.; James, B. R. *Can. J. Chem.* **1992**, *70*, 751. (c) Kurtev, K.; Ribola, D.; Jones, R. A.; Wilkinson, G.; Cole-Hamilton, D. J. *J. Chem. Soc., Dalton Trans.* **1980**, 55.

(36) Mann, F. G.; Watson, J. *J. Org. Chem.* **1948**, *13*, 502.

**Table 7. Selected Crystal and Refinement Data for  $[\text{Pd}(\text{C}_6\text{F}_5)\text{Br}(\text{SPPy}_2\text{Ph-N,S})]$  (**2b**)**

formula	$\text{C}_{22}\text{H}_{13}\text{BrF}_5\text{N}_2\text{PPdS}$
$M_r$	649.70
cryst syst	monoclinic
space group	$P2_1/c$
$a$ , Å	8.273(2)
$b$ , Å	14.240(2)
$c$ , Å	19.547(4)
$\beta$ , deg	95.10(2)
$V$ , Å <sup>3</sup>	2293.6(7)
$F(000)$	1264
$Z$	4
$D_{\text{calcd}}$ , g/cm <sup>3</sup>	1.88
$\mu$ , cm <sup>-1</sup>	27.3
no. of rflns collected	4745
no. of indepndt rflns	3134 ( $\geq 3\sigma(I)$ )
no. of refined params	298
largest peak/hole, e/Å <sup>3</sup>	+0.70/−0.65
$R^a$	0.042
$R_w^b$	0.047

$$^a R = \sum[|F_o| - |F_c|/\sum|F_o|]. \quad ^b R_w = \sum[w(|F_o| - |F_c|)^2/\sum w|F_o|^2]^{1/2}, \quad w = 1/[\sigma(F_o)^2 + (0.010F_o)^2 + 1.000].$$

282.38 MHz ( $^{19}\text{F}$ ), and 121.44 MHz ( $^{31}\text{P}$ ).  $^1\text{H}$ ,  $^{19}\text{F}$ , and  $^{31}\text{P}$  shifts are reported relative to TMS,  $\text{CFCl}_3$ , and 85%  $\text{H}_3\text{PO}_4$  as external standards, respectively. Temperature control of the NMR probe was achieved using a Bruker Cryo Controller. The actual temperature was measured before and after spectral accumulation by replacing the sample with Bruker standard samples of methanol-methanol- $d_4$  for low temperatures and ethylene glycol in  $\text{DMSO-}d_6$  (80/20) for high temperatures and using the equations provided by the manufacturer.

The magnetization transfer measurements were performed using the inversion-recovery technique. Selective inversion of one signal was achieved using the "1, −1" pulse train ( $90^\circ\text{--}D_1\text{--}90^\circ$ ); after a variable time  $t$  a nonselective  $90^\circ$  pulse allows observation of the signals. Data analysis was carried out as described in the literature.<sup>15</sup> The most popular "1, −3, 3, −1" pulse train ( $25.5^\circ\text{--}D_1\text{--}67.5^\circ\text{--}D_1\text{--}67.5^\circ\text{--}D_1\text{--}25.5^\circ$ ) gives worse results for our samples; it may be due to the loss of coherence of the components of each multiplet during three  $D_1$  delays. For the magnetization transfer experiments, 4000 data points were recorded over a sweep width of 1795 Hz (0.414 Hz/point) and required 8 scans with a delay between scans of at least  $5T_1$ . Special care was taken to accurately measure the pulse length for each sample.

The samples for the salt effect studies were prepared as follows: A stock 0.04 M solution of the palladium complex was prepared in deoxygenated  $\text{CDCl}_3$ . To one aliquot of this solution was added  $(\text{NBu}_4)\text{X}$  ( $\text{X} = \text{ClO}_4^-, \text{Br}^-$ ) to obtain a solution 0.4 M in the added salt; different salt concentrations were obtained by mixing measured volumes of this solution and of the stock solution.

**X-ray Structure Analysis of  $[\text{Pd}(\text{C}_6\text{F}_5)\text{Br}(\text{SPPy}_2\text{Ph-N,S})]$  (**2b**).** Recrystallization of  $[\text{Pd}(\text{C}_6\text{F}_5)\text{Br}(\text{SPPy}_2\text{Ph})]$  from  $\text{CHCl}_3$  gave a yellow-orange crystal suitable for X-ray diffraction. A total of 4745 independent reflections were measured by  $\omega\text{--}2\theta$  scan mode in the range  $\theta \leq 26^\circ$  (scan rate  $16^\circ\text{ min}^{-1}$ ).

The structure was solved by the heavy-atom method and Fourier techniques and refined by the full-matrix least-squares method to final  $R = 0.042$  and  $R_w = 0.047$ . The highest peak in the final difference Fourier map was of  $0.70\text{ e}\text{--}\text{Å}^{-3}$ . All H atoms were located theoretically and fixed during the structure refining.

All measurements were made on a Rigaku AFC5R diffractometer at room temperature using  $\text{Mo K}\alpha$  ( $\lambda = 0.71069\text{ Å}$ ) radiation with a graphite monochromator. All calculations were performed on a Micro Vax-II computer using the SDP program package. Details of crystal and refinement data for the structure are given in Table 7. Other pertinent X-ray data are given in the supplementary material.

**Preparation of the Complexes.** All reactions were carried out under nitrogen atmosphere in deoxygenated solvents.

Although the isolated products are stable in the air, the syntheses give some side products and lower yields when an inert atmosphere was not used.

**[Pd(C<sub>6</sub>F<sub>5</sub>)Br(SPPyPh<sub>2</sub>)] · 0.5OEt<sub>2</sub> (1).** To a solution of [Pd(C<sub>6</sub>F<sub>5</sub>)Br(NCMe)<sub>2</sub>] (0.200 g, 0.463 mmol) in diethyl ether (30 mL) was added SPPyPh<sub>2</sub> (0.1367 g, 0.464 mmol), and the solution was stirred for 15 min. Addition of *n*-hexane (10 mL) and evaporation of the solution to ca. 10 mL produced a yellow solid, which was filtered, washed with *n*-hexane, and air-dried. Yield: 0.239 g, 80%. Calcd: 43.78% C; 2.79% H; 2.04% N. Found: 43.42% C; 2.52% H; 2.02% N.

**[Pd(C<sub>6</sub>F<sub>5</sub>)Br(SPPy<sub>2</sub>Ph)] (2b).** To a solution of (NBu<sub>4</sub>)<sub>2</sub>[Pd<sub>2</sub>(μ-Br)<sub>2</sub>(C<sub>6</sub>F<sub>5</sub>)<sub>2</sub>Br<sub>2</sub>] (0.200 g, 0.131 mmol) in dichloromethane (30 mL) was added SPPy<sub>2</sub>Ph (0.086 g, 0.286 mmol). The solution was stirred for 30 min. Evaporation to a small volume (ca. 10 mL) and addition of ethanol (30 mL) afforded a yellow solid, which was filtered, washed with ethanol, and air-dried. Yield: 0.129 g, 76%. Calcd: 40.73% C; 2.02% H; 4.37% N. Found: 40.98% C; 2.09% H; 4.16% N.

**[Pd(C<sub>6</sub>F<sub>5</sub>)Br(SPPy<sub>3</sub>)] (3)** was prepared similarly starting from (NBu<sub>4</sub>)<sub>2</sub>[Pd<sub>2</sub>(μ-Br)<sub>2</sub>(C<sub>6</sub>F<sub>5</sub>)<sub>2</sub>Br<sub>2</sub>] (0.200 g, 0.131 mmol) and SPPy<sub>3</sub> (0.080 g, 0.27 mmol). Yield: 0.143 g, 84%. Calcd: 38.79% C; 1.86% H; 6.46% N. Found: 38.91% C; 2.06% H; 6.54% N.

**[Pd(C<sub>6</sub>F<sub>5</sub>)Cl(SPPy<sub>2</sub>Ph)] (2a).** To [Pd(C<sub>6</sub>F<sub>5</sub>)Br(SPPy<sub>2</sub>Ph)] (0.150 g, 0.220 mmol) in acetone (50 mL) was added an excess of AgCl, freshly prepared and wet. The mixture was stirred, shielded from light, for 24 h, and the insoluble silver salts were filtered off. Evaporation of the acetone solution and addition of ethanol (10 mL) afforded a pale yellow compound, which

was filtered, washed with ethanol, and air-dried. Yield: 0.120 g, 85%. Calcd: 43.66% C; 2.16% H; 4.63% N. Found: 43.44% C; 2.26% H; 4.56% N.

**[Pd(C<sub>6</sub>F<sub>5</sub>)I(SPPy<sub>2</sub>Ph)] (2c).** To [Pd(C<sub>6</sub>F<sub>5</sub>)Br(SPPy<sub>2</sub>Ph)] (0.150 g, 0.220 mmol) in acetone (50 mL) was added KI (0.0415 g, 0.25 mmol). The mixture was stirred for 1 h. The acetone solution was evaporated to dryness, and the residue was extracted with dichloromethane (2 × 15 mL). The potassium salts were insoluble. Addition of ethanol (15 mL) and evaporation of the solution to ca. 10 mL afforded an orange compound, which was filtered, washed with ethanol, and air-dried. Yield: 0.194 g, 84%. Calcd: 38.82% C; 1.92% H; 4.11% N. Found: 38.79% C; 1.85% H; 4.01% N.

**Acknowledgment.** We thank the Dirección General de Investigación Científica y Técnica (Projects PB90-0360 and PB93-0222) and the European Community (Contract CHRX-CT93-0147 (DG 12 DSCS)) for financial support. J.A.C. and Y.-S.L. very gratefully acknowledge studentships from the Ministerio de Educación y Ciencia, the Agencia Española de Cooperación Internacional/Instituto de Cooperación para el Desarrollo, and the Universidad de Valladolid.

**Supplementary Material Available:** Listing of atomic coordinates, full tables of bond distances and bond angles, and a listing of anisotropic displacement parameters (4 pages). Ordering information is given on any current masthead page.

OM950192K



## $\mu$ -Hydride Geometry and Dynamics in the Protic Acid Adducts of Triosmium Imidoyl Clusters

Roberto Gobetto,<sup>†</sup> Kenneth I. Hardcastle,<sup>\*,‡</sup> Shariff E. Kabir,<sup>§</sup> Luciano Milone,<sup>\*,†</sup> Nobuko Nishimura,<sup>‡</sup> M. Botta,<sup>†</sup> Edward Rosenberg,<sup>\*,§</sup> and Mingzhi Yin<sup>‡</sup>

Department of Chemistry, The University of Montana, Missoula, Montana 59812, Department of Chemistry, California State University at Northridge, Northridge, California 91330, and Dipartimento di Chimica Inorganica Chimica Fisica e Chimica dei Materiali, Università di Torino, Torino, Italy 10125

Received October 28, 1994<sup>®</sup>

The  $\mu_3$ -imidoyl cluster,  $(\mu\text{-H})\text{Os}_3(\text{CO})_9(\mu_3\text{-}\eta^2\text{-C}=\text{NCH}_2\text{CH}_2\text{CH}_2)$  (**1**) forms the neutral acid adducts  $(\mu\text{-H})_2\text{Os}_3(\text{CO})_9(\mu\text{-}\eta^2\text{-C}=\text{NCH}_2\text{CH}_2\text{CH}_2)\text{X}$  ( $\text{X} = \text{Cl}$  (**2**),  $\text{Br}$  (**3**),  $\text{CF}_3\text{CO}_2$  (**4**),  $\text{CF}_3\text{SO}_3$  (**6**)), upon addition of the corresponding acids  $\text{HX}$  to chloroform solutions of the  $\mu_3$ -imidoyl cluster at room temperature. Solid state structures of **3** and **4** reveal that  $\text{X}$  is in an axial position on the third Os atom and on the same face of the cluster as the  $\mu$ -imidoyl ligand which bridges two Os atoms. Thermolysis, at 40–80 °C under CO, of **3** isomerizes it to **8** where the bromide has migrated 180° to occupy an axial position in the opposite face of the cluster. In addition, loss of  $\text{HBr}$  to form **1** and competitive formation of  $(\mu\text{-H})(\mu\text{-Br})\text{Os}_3(\text{CO})_{10}$  (**7**) occurs. For  $\text{X} = \text{CF}_3\text{CO}_2$  and  $\text{CF}_3\text{SO}_3$  partial dissociation of the neutral adduct into  $(\mu\text{-H})_2\text{Os}_3(\text{CO})_9(\mu_3\text{-imidoyl})^+$  (**5**) and  $\text{X}^-$  is observed in solution, while for  $\text{X} = \text{Cl}$  and  $\text{Br}$  this cation is only observed when the acid adduct is treated with  $\text{AgSbF}_6$ . The same cation can be generated by treatment of **1** with the noncoordinating acid  $\text{HBF}_4$ . The location of the metal-bound hydrogens in the solid state structures of **3** and **8** reveals that the halogen atom is loosely associated with one of the metal-bound hydrogens while this is not the case for the trifluoroacetate derivative **4**. An investigation of the variable-temperature  $^1\text{H}$ - and  $^{13}\text{C}$ -NMR using one and two-dimensional methods reveals the presence of three isomers in solution for **2**, **3**, and **8** but only two for **4** and **6**. For **2** and **3**, exchange between two of the three isomers precedes direct exchange of the two hydride ligands, while for **8** direct exchange of the inequivalent hydrides is the lowest energy process. Mechanisms for these diverse exchange processes are presented in the light of their solid state structures and the two-dimensional NMR results. Compound **3** crystallizes in the orthorhombic space group  $Pna2_1$  with unit cell parameters  $a = 29.608(6)$  Å,  $b = 7.687(2)$  Å,  $c = 17.121(6)$  Å,  $V = 3.897(3)$  Å<sup>3</sup>, and  $Z = 4$ . Least squares refinement of 4051 observed reflections gave a final agreement factor of  $R = 0.044$  ( $R_w = 0.045$ ). Compound **4** crystallizes in the trigonal space group  $P3_1$  with unit cell parameters  $a = 8.976(3)$  Å,  $c = 23.27(1)$  Å,  $V = 1624(2)$  Å<sup>3</sup>, and  $Z = 3$ . Least squares refinement of 2973 observed reflections gave a final agreement factor of  $R = 0.030$  ( $R_w = 0.036$ ). Compound **8** crystallizes in the monoclinic space group  $P2_1/c$  with  $a = 18.253(8)$  Å,  $b = 14.129(5)$  Å,  $c = 17.728(6)$  Å,  $\beta = 116.32(3)^\circ$ ,  $V = 4098(6)$  Å<sup>3</sup>, and  $Z = 8$ . Least squares refinement of 2948 observed reflections gave a final agreement factor of  $R = 0.056$  ( $R_w = 0.050$ ).

### Introduction

The isolation of stable organometallic molecules whose structures are thought to resemble those of reactive intermediates at catalytically active metal centers has been an integral part of the progress that has been made in our understanding of both homogeneous and heterogeneous catalytic processes.<sup>1</sup> In the case of heterogeneous catalysis, the manipulation of small organic molecules on polynuclear complexes has expanded our view of how many simple chemical transformations take place on a metal surface.<sup>2</sup> Most of this work has

centered on hydrocarbon–metal interactions, but many heterogeneous catalytic processes utilize hydrohalic or oxyacids as cocatalysts or reagents. The reactions of polymeric clusters with protic acids have been extensively studied and exhibit a range of reactivity patterns. Most common are simple protonation to give a stable cationic hydride and cleavage of a metal–carbon<sup>3–5</sup> or a metal–metal bond.<sup>6</sup> In some cases, stable polymeric species where the acid's conjugate base has

(2) Shriver, D. F.; Kaesz, H. D.; Adams, R. D. *The Chemistry of Metal Cluster Complexes*; VCH: New York, 1990.

(3) Rosenberg, E.; Barner-Thorsen, C.; Saatjian, G.; Aime, S.; Milone, L.; Osella, D. *Inorg. Chem.* **1981**, *20*, 1592.

(4) Rosenberg, E.; Skinner, D. M.; Aime, S.; Gobetto, R.; Milone, L.; Osella, D. *Gaz. Chim. Ital.* **1991**, *121*, 313 and references therein.

(5) Frauenhoff, G. R.; Wilson, S. R.; Shapley, J. R. *Inorg. Chem.* **1991**, *30*, 78.

(6) Adams, R. D.; Golembeski, N. M.; Selegue, J. P. *Organometallics* **1982**, *1*, 240.

<sup>†</sup> Università di Torino.

<sup>‡</sup> CSU, Northridge.

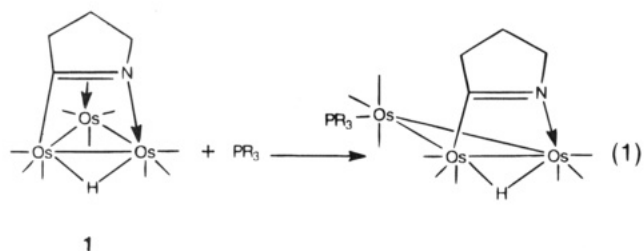
<sup>§</sup> The University of Montana.

<sup>®</sup> Abstract published in *Advance ACS Abstracts*, May 15, 1995.

(1) Gates, B. C. *Catalytic Chemistry*; J. Wiley & Sons: New York, 1992.

coordinated to the cluster in place of an organic ligand<sup>5</sup> or a metal–metal bond<sup>6</sup> can be isolated. Such acid adducts are also available from the reaction of lightly stabilized clusters such as  $\text{Os}_3(\text{CO})_{10}(\text{CH}_3\text{CN})_2$ , which give clusters of the general type  $(\mu\text{-H})(\mu\text{-X})\text{Os}_3(\text{CO})_{10}$  ( $\text{X} = \text{RCO}_2$ , halogen,  $\text{MeO}$ ).<sup>7,8</sup> Direct adduct formation not accompanied by ligand displacement or metal–metal bond cleavage has not been reported, and more importantly, there have been no detailed investigations of the thermal and dynamical properties of acid adducts of polynuclear species over a range of  $\text{HX}$  acid strengths except for one recent report.<sup>5a</sup>

We have been studying the chemistry of  $\mu_3$ -imidoyl clusters such as  $(\mu\text{-H})\text{Os}_3(\text{CO})_9(\mu_3\text{-}\eta^2\text{-C}=\text{NCH}_2\text{CH}_2\text{CH}_2)$  (**1**), which is obtained from the reaction of pyrrolidine with  $\text{Os}_3(\text{CO})_{10}(\text{CH}_3\text{CN})_2$  in good yields.<sup>9</sup> The hydrocarbyl analogs of **1** (e.g.,  $(\mu\text{-H})_2(\mu_3\text{-}\eta^2\text{-RC}_2\text{R})\text{Os}_3(\text{CO})_9$ ,  $(\mu\text{-CO})(\mu_3\text{-}\eta^2\text{-RC}_2\text{R})\text{Os}_3(\text{CO})_9$ ,  $(\mu\text{-H})(\mu_3\text{-}\eta^2\text{-C}_2\text{R})\text{Os}_3(\text{CO})_9$ , and  $(\mu\text{-H})(\mu_3\text{-}\eta^2\text{-RC}=\text{C}=\text{CR}_2)\text{Os}_3(\text{CO})_9$ ) react with two electron donor ligands to give carbonyl substitution products only at elevated temperatures.<sup>9b</sup> These formally saturated,  $48e^-$ ,  $\mu_3$ -imidoyl clusters show room-temperature addition chemistry giving adducts with two electron donors in which the carbon–nitrogen  $\pi$ -bond to one osmium atom has been displaced (eq 1).<sup>9,10</sup> Thus,



complexes such as **1** qualify as lightly stabilized clusters and we thought it would be interesting to study their reactions with a range of protic acids to see if simple protonation or acid adduct formation occurs depending on the nucleophilicity of the conjugate base of the acid used. We report here the results of our studies on the reactions of **1** with  $\text{HX}$  where we observe acid adduct formation ( $\text{X} = \text{Cl}$ ,  $\text{Br}$ ), monoprotection ( $\text{X} = \text{BF}_4$ ), or equilibrium mixtures of monoprotated cation and acid adduct ( $\text{X} = \text{CF}_3\text{CO}_2$ ,  $\text{CF}_3\text{SO}_3$ ). The subsequent one- and two-dimensional NMR studies of these species illustrate some important relationships between metal hydride geometries and their dynamic behavior.

## Results and Discussion

### A. Synthesis and Characterization of $(\mu\text{-H})_2\text{Os}_3(\text{CO})_9(\mu\text{-}\eta^2\text{-C}=\text{NCH}_2\text{CH}_2\text{CH}_2)\text{X}$ ( $\text{X} = \text{Cl}$ (**2**), $\text{Br}$ (**3**)).

The reaction of excess gaseous  $\text{HX}$  ( $\text{X} = \text{Cl}$ ,  $\text{Br}$ ) with **1** at room temperature in hexane gives essentially quantitative conversion to the compounds  $(\mu\text{-H})_2\text{Os}_3(\text{CO})_9(\mu\text{-}\eta^2\text{-C}=\text{NCH}_2\text{CH}_2\text{CH}_2)\text{X}$  ( $\text{X} = \text{Cl}$  (**2**),  $\text{Br}$  (**3**)).

(7) Ditzel, E. J.; Johnson, B. F. G.; Lewis, J. J. *Chem. Soc., Dalton Trans.* **1987**, 1293.

(8) Day, M.; Kabir, S. E.; Wolf, E.; Rosenberg, E.; Hardcastle, K. I. *J. Cluster Sci.* **1990**, *1*, 355 and references therein.

(9) (a) Day, M.; Espitia, D.; Hardcastle, K. I.; Kabir, S. E.; McPhillips, T.; Rosenberg, E.; Gobetto, R.; Milone, L.; Osella, D. *Organometallics* **1993**, *12*, 2309. (b) Rosenberg, E.; Freeman, W.; Carlos, Z.; Hardcastle, K. I.; Yoo, Y. J.; Milone, L.; Gobetto, R. *J. Cluster Sci.* **1992**, *3*, 439.

(10) Day, M.; Espitia, D.; Hardcastle, K. I.; Kabir, S. E.; Rosenberg, E.; Gobetto, R.; Milone, L.; Osella, D. *Organometallics* **1991**, *10*, 3550.

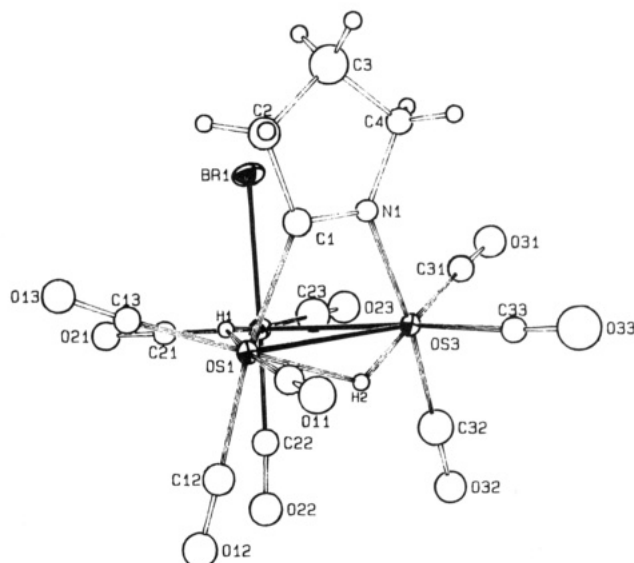


**Figure 1.** Solid state structure of  $(\mu\text{-H})_2\text{Os}_3(\text{CO})_9(\mu\text{-}\eta^2\text{-C}=\text{NCH}_2\text{CH}_2\text{CH}_2)\text{Br}$  (**3**).

$\text{C}=\text{NCH}_2\text{CH}_2\text{CH}_2\text{X}$  ( $\text{X} = \text{Cl}$  (**2**),  $\text{X} = \text{Br}$  (**3**)). The compounds can be isolated analytically pure by slow evaporation of the solvent or by preparative thin-layer chromatography. The compounds were characterized by  $^1\text{H}$  NMR, infrared spectroscopy, and elemental analysis. To our knowledge, **2** and **3** represent the first straightforward adducts of hydrogen halides with a trinuclear cluster although a closely related compound results from  $\text{Os}\text{-Os}$  bond cleavage in  $(\mu_3\text{-S})(\mu_3\text{-}\eta^2\text{-CH}_2\text{S})\text{Os}_3(\text{CO})_8(\text{PMe}_2\text{Ph})$ .<sup>6</sup> We therefore undertook a solid state structure determination of **3** to elucidate the actual mode of bonding of the  $\text{HX}$  molecule to the cluster.

The solid state structure of **3** is shown in Figure 1, crystal data are given in Table 1, important bond distances and angles are given in Table 2, and atomic coordinates are given in Table 3. The complex consists of an osmium triangle (molecule A) with two longer ( $\text{Os}(1)\text{-Os}(3) = 2.99(1)$  Å) and  $\text{Os}(1)\text{-Os}(2) = 3.08(1)$  Å) and one shorter metal–metal bond ( $\text{Os}(3)\text{-Os}(2) = 2.85(1)$  Å). The imidoyl ligand bridges the  $\text{Os}(1)\text{-Os}(3)$  edge with the bromine occupying the axial position on  $\text{Os}(2)$  on the same face of the triangle as the imidoyl ligand (i.e., the position formerly coordinated by carbon–nitrogen double bond). The osmium–bromine distance ( $\text{Os}(1)\text{-Br} = 2.59(1)$  Å) is significantly elongated compared to the osmium–halide distance in the higher oxidation state mononuclear osmium bromides ( $2.51(1)$  Å in  $\text{OsBr}_6^{2-}$ ).

The hydride ligands were located in **3** by Fourier synthesis of selected slices of the electron density map. Significantly,  $\text{H}(1)$ , which bridges the  $\text{Os}(1)\text{-Os}(2)$  edge, is tilted distinctly above the  $\text{Os}_3$  triangle toward the halogen atom. In related dihydride trinuclear clusters, the hydride ligands are generally located in the  $\text{Os}_3$  plane or tilted toward the opposite face of a bridging or face-capping organic ligand.<sup>11,12</sup> The resulting  $\text{H}(1)\text{-Br}$  distances are significantly shorter than the sum of the van der Waals radii of  $\text{H}$  and  $\text{Br}$  ( $2.96$  vs  $3.20$  Å). There is also significant asymmetry in the  $\text{H}(1)\text{-Os}(2)$  and  $\text{H}(1)\text{-Os}(3)$  bond distances with the bond vector to the halide-bound osmium atom being significantly

Table 1. Crystallographic Data

	compound		
	3	4	8
formula	C <sub>13</sub> H <sub>8</sub> BrOs <sub>3</sub> NO <sub>9</sub>	C <sub>15</sub> H <sub>8</sub> Os <sub>3</sub> F <sub>3</sub> NO <sub>11</sub>	C <sub>13</sub> H <sub>8</sub> BrOs <sub>3</sub> NO <sub>9</sub>
fw	972.72	1005.83	972.72
cryst dimen, mm <sup>3</sup>	0.13 × 0.22 × 0.52	0.20 × 0.33 × 0.53	0.05 × 0.15 × 0.31
radiation; wavelength, Å	Mo; 0.710 73	Mo; 0.710 73	Mo; 0.710 73
temp, °C	-100 ± 1	-98 ± 1	25 ± 1
cryst system	orthorhombic	trigonal	monoclinic
space group	<i>Pna</i> 2 <sub>1</sub>	<i>P</i> 3 <sub>1</sub>	<i>P</i> 2 <sub>1</sub> / <i>c</i>
<i>a</i> , Å	29.608(6)	8.976(3)	18.253(8)
<i>b</i> , Å	7.687(2)		14.129(5)
<i>c</i> , Å	17.121(6)	23.271(10)	17.728(6)
β, deg			116.32(3)
<i>V</i> , Å <sup>3</sup>	3897(3)	1624(2)	4098(6)
<i>Z</i>	4	3	8
density, g/cm <sup>3</sup>	3.32	3.09	3.15
abs coeff μ, cm <sup>-1</sup>	216.2	176.7	205.6
Re. transm coeff.	0.008–0.016	0.730–0.994	0.138–0.997
scan type	ω-2θ	ω-2θ	ω-2θ
scan rate, deg/min	8.23	8.23	8.23
scan width, deg	0.9 + 0.350 tan θ	0.9 + 0.350 tan θ	0.9 + 0.350 tan θ
<i>hkl</i> ranges	<i>h</i> : -39 to 39 <i>k</i> : 0 to 10 <i>l</i> : 0 to 22	<i>h</i> : -12 to 12: <i>k</i> : -12 to 12: <i>l</i> : 0 to 32	<i>h</i> : -17 to 17 <i>k</i> : 0 to 13 <i>l</i> : -17 to 17
2θ range, deg	48.0–56.0	48.0–60.0	2.0–40.0
structure solution	Patterson method	Patterson method	Patterson method
no. of unique data	5295	3310	4037
no. of data used in L.S. refinement with <i>F</i> <sub>o</sub> > 3.0 σ( <i>F</i> <sub>o</sub> )	4051	2973	2948
weighting scheme, <i>w</i>	4 <i>F</i> <sub>o</sub> <sup>2</sup> /[σ( <i>F</i> <sub>o</sub> ) <sup>2</sup> ] <sup>2</sup>	4 <i>F</i> <sub>o</sub> <sup>2</sup> /[σ( <i>F</i> <sub>o</sub> ) <sup>2</sup> ] <sup>2</sup>	4 <i>F</i> <sub>o</sub> <sup>2</sup> /[σ( <i>F</i> <sub>o</sub> ) <sup>2</sup> ] <sup>2</sup>
no. of params refined	256	297	293
<i>R</i> <sup>a</sup>	0.0442	0.0298	0.0558
<i>R</i> <sub>w</sub> <sup>b</sup>	0.0448	0.0356	0.0495
esd of obs of unit weight (GOF)	0.92	0.92	1.02
largest shift/esd	0.01	0.02	0.06
high peak in final diff map, e/Å <sup>3</sup>	2.10(46)	2.41(31)	2.08(39)

$$^a R = \sum[|F_o| - |F_c|]/\sum|F_o|, \quad ^b R_w = [\sum w(|F_o| - |F_c|)^2/\sum w|F_o|^2]^{1/2}.$$

shorter. Taken together, these facts seem to suggest some residual bonding interaction between H and Br in **3**. Although we have no conclusive evidence for persistence of this interaction in solution (vide infra), the fact that **3** can lose HBr on heating (40–80 °C) supports the idea of residual HX bonding in these complexes.

The structures of compounds **2** and **3** were reported in preliminary form. The difficulty in distinguishing between carbon and nitrogen in the symmetrical pyrrolidine ring led to some uncertainties in the relative disposition of the hydride ligands with respect to these atoms.<sup>11</sup> The structure of **3** which was determined from data obtained at -100 °C allowed a more distinct location of the electron density due to the hydrides relative to the residual electron density observed in the Fourier slices taken (see Experimental Section). The structure of **3** shown in Figure 1 is a more recent and careful refinement of the low-temperature data set and it is assumed on the basis of the solution NMR data that **2** is completely analogous. The asymmetric unit of the solid state structure of **3** consists of two molecules which differ from each other by small differences in the bond distances and angles.

**B. Synthesis and Solid State Structure of (μ-H)<sub>2</sub>Os<sub>3</sub>(CO)<sub>9</sub> (μ-η<sup>2</sup>-C=NCH<sub>2</sub>CH<sub>2</sub>CH<sub>2</sub>)(CF<sub>3</sub>CO<sub>2</sub>) (**4**).** Treatment of a chloroform solution of **1** with trifluoro-

acetic acid at 25 °C followed by cooling the solution to -20 °C leads to isolation of the product (μ-H)<sub>2</sub>Os<sub>3</sub>(CO)<sub>9</sub>(μ-η<sup>2</sup>-C=NCH<sub>2</sub>CH<sub>2</sub>CH<sub>2</sub>)(CF<sub>3</sub>CO<sub>2</sub>) (**4**). The solid state structure of **4** is shown in Figure 2, crystal data are listed in Table 1, and selected distances and bond angles are listed in Table 4 and atomic coordinates in Table 5. The overall structural features of **4** are very similar to **3** with the trifluoroacetate group η<sup>1</sup>-bound to Os(2) in an analogous position to the Br in **3**. The Os(2)–O(1) distance of 2.10(1) Å is slightly shorter than that reported for the related η<sup>1</sup>-trifluoroacetate derivative (μ-H)Os<sub>3</sub>(CO)<sub>10</sub>(CNPr)(η<sup>1</sup>-OCOCF<sub>3</sub>) (2.14(1) Å).<sup>5b</sup> However, there are some significant differences in the bonding characteristics of H(1) compared to **3**. First, H(1) is located distinctly in the plane of the metal triangle and the H(1)–O distance to the metal-bound oxygen is 2.83 Å, almost the same as the sum of the van der Waals radii (2.85 Å). Furthermore, H(1) is located symmetrically between Os(1) and Os(2) (1.84(1) and 1.83(1) Å, respectively). Interestingly, H(2) bridges Os(1)–Os(3) unsymmetrically in **3** and **4** with the Os(3)–H(2) distances being shorter than the Os(1)–H(2) distances by 0.13 and 0.79 Å, respectively in the series. That the hydride ligand is always found closer to the nitrogen-bound osmium leads one to propose that this atom is more electron rich than the carbon bound osmium in this series of complexes. In both the structures of **3** and **4** the error in hydride locations is estimated to be ±0.07 Å.

**C. Solution Structure and Dynamics of Complexes 2–4.** Complexes **2** and **3** both exhibit dynamic

(11) Hardcastle, K. I.; Irving, M. *J. Cluster. Sci.* **1993**, *4*, 77.

(12) Day, M.; Freeman, W.; Hardcastle, K. I.; Isomaki, M.; Kabir, S. E.; McPhillips, T.; Rosenberg, E.; Scott, L. G.; Wolf, E. *Organometallics* **1992**, *11*, 3376.

**Table 2. Selected Bond Distances (Å) and Angles (deg) for 3<sup>a</sup>**

Distances			
molecule A		molecule B	
Os(1)–Os(2)	3.077(1)	Os(1B)–Os(2B)	2.851(1)
Os(1)–Os(3)	2.988(1)	Os(1B)–Os(3B)	2.997(1)
Os(2)–Os(3)	2.854(1)	Os(2B)–Os(3B)	3.062(1)
Os(1)–H(1)	1.77(4)	Os(2B)–H(1B)	1.69(4)
Os(1)–H(2)	1.87(4)	Os(3B)–H(2B)	1.93(4)
Os(2)–H(1)	1.46(4)	Os(3B)–H(1B)	1.93(4)
Os(3)–H(2)	1.53(4)	Os(1B)–H(2B)	1.75(4)
Os–Br	2.587(2)	Os(2B)–BrB	2.587(2)
Os(1)–C(1)	2.08(2)	Os(3B)–C(1B)	2.10(2)
Os(3)–N(1)	2.12(2)	Os(1B)–N(1B)	2.10(2)
C(1)–N(1)	1.23(3)	C(1B)–N(1B)	1.26(3)
Os–C(CO)	1.92(2) <sup>b</sup>	OsB–C(CO)B	1.89(2) <sup>b</sup>
C–O	1.13(3) <sup>b</sup>	CB–OB	1.15(3) <sup>b</sup>

Angles			
molecule A		molecule B	
Os(1)–Os(2)–Os(3)	60.35(3)	Os(1B)–Os(2B)–Os(3B)	60.72(3)
Os(1)–Os(3)–Os(2)	63.53(3)	Os(1B)–Os(3B)–Os(2B)	56.26(3)
Os(2)–Os(1)–Os(3)	56.12(2)	Os(2B)–Os(1B)–Os(3B)	63.02(3)
Os(1)–Os(2)–Br	96.65(6)	Os(1B)–Os(2B)–BrB	93.19(6)
Os(3)–Os(2)–Br	92.58(6)	Os(3B)–Os(2B)–BrB	95.54(6)
Os(1)–Os(2)–H(1)	19.47(2)	Os(3B)–Os(2B)–H(1B)	34.72(2)
Os(2)–Os(1)–H(1)	16.05(2)	Os(2B)–Os(3B)–H(1B)	30.02(6)
Os(3)–Os(1)–H(2)	25.65(2)	Os(3B)–Os(1B)–H(2B)	37.43(2)
Os(1)–Os(3)–H(2)	31.99(3)	Os(1B)–Os(3B)–H(2B)	33.53(2)
Os(2)–Os(1)–C(1)	83.6(6)	Os(2B)–Os(3B)–C(1B)	86.41(5)
Os(2)–Os(3)–N(1)	88.4(5)	Os(2B)–Os(1B)–N(1B)	87.5(5)
C(1)–C(2)–C(3)	105(2)	C(1B)–C(2B)–C(3B)	105(2)
C(1)–N(1)–C(4)	116(2)	C(1B)–N(1B)–C(4B)	110(2)
Os–C–O <sup>b</sup>	177(2)	OsB–CB–OB	177(2)

<sup>a</sup> Numbers in parenthesis are estimated standard deviations.<sup>b</sup> Average values.

behavior on the NMR time scale in solution. The low-temperature limiting spectrum for both complexes is reached at  $-40\text{ }^{\circ}\text{C}$ , and the hydride regions show three pairs of singlet hydride signals (each pair in a ratio of 1:1) indicating the presence of three isomers in solution. In both **2** and **3** one isomer predominates with the two other isomers present in only minor amounts of 10 and 3% for **2** and 10 and 4% for **3**. The chemical shifts of the hydride resonances are in the range  $-13.5$  to  $-16.5$  ppm and do not provide compelling evidence for the persistence of even weak bonding interactions between H(1) and the halide in solution. As the temperature is raised above  $-40\text{ }^{\circ}\text{C}$  broadening of all three pairs of hydride resonances is observed until at  $+22\text{ }^{\circ}\text{C}$  a broadened single pair of hydride resonances is observed (Figure 3). Above this temperature, the two hydrides begin to coalesce but the onset of decomposition of **2** and **3** precluded achieving the high-temperature limit. Assuming that the major isomer found in solution is the same as that found in the solid state, the two minor isomers of **2** and **3** are likely to differ from it in the location of H(1) and/or H(2) (Scheme 1). Edge hopping of H(1) would interchange only two of the three observed isomers without interchanging H(1) and H(2), while H(1) and H(2) interchange would be expected to overlap with exchange of the third proposed isomer where the hydrides are located on the Os(1) and Os(2) and Os(2)–Os(3) edges (Scheme 1, numbering of Os atoms refers to Figure 1).

In order to further elucidate the nature of the isomers in **2** and **3** and the observed dynamical processes, we

**Table 3. Positional Parameters and B Values and Their Estimated Standard Deviations for 3**

atom	<i>x</i>	<i>y</i>	<i>z</i>	<i>B</i> <sup>a</sup> (Å <sup>2</sup> )
Os(1)	0.23704(3)	0.4257(1)	-0.097	1.14(1)
Os(2)	0.19400(3)	0.1892(1)	0.02789(5)	1.29(1)
Os(3)	0.26903(3)	0.4038(1)	0.06865(5)	1.23(1)
N(1)	0.3087(6)	0.260(2)	-0.011(1)	1.1(3)*
C(1)	0.2935(8)	0.270(3)	-0.078(1)	1.7(4)*
C(2)	0.3223(8)	0.164(3)	-0.133(1)	2.1(4)*
C(3)	0.3553(9)	0.068(4)	-0.079(2)	3.3(5)*
C(4)	0.3482(7)	0.151(3)	-0.001(1)	1.6(4)*
Br(1)	0.24501(8)	-0.0785(3)	0.0034(2)	2.2(5)
C(11)	0.2720(7)	0.611(3)	-0.137(1)	1.7(4)*
C(12)	0.1837(8)	0.583(3)	-0.095(2)	2.3(4)*
C(13)	0.2216(7)	0.328(3)	-0.194(1)	1.5(4)*
C(14)	0.1445(7)	0.054(3)	-0.007(1)	1.5(4)*
C(22)	0.1536(8)	0.376(3)	0.048(1)	1.9(4)*
C(23)	0.1878(9)	0.094(4)	0.131(2)	3.4(6)*
C(31)	0.2821(8)	0.257(3)	0.160(1)	1.9(4)*
C(32)	0.2283(9)	0.536(4)	0.132(2)	3.2(5)*
C(33)	0.3178(7)	0.568(3)	0.084(1)	1.4(3)*
O(11)	0.2939(6)	0.719(2)	-0.161(1)	2.5(3)*
O(12)	0.1548(6)	0.674(2)	-0.099(1)	2.6(3)*
O(13)	0.2158(5)	0.269(2)	-0.251(1)	2.3(3)*
O(21)	0.1147(5)	-0.023(2)	-0.0328(9)	2.3(3)*
O(22)	0.1285(6)	0.483(2)	0.058(1)	2.9(3)*
O(23)	0.1846(6)	0.036(2)	0.195(1)	3.1(4)*
O(31)	0.2896(6)	0.181(2)	0.213(1)	2.8(3)*
O(32)	0.2035(6)	0.617(2)	0.171(1)	2.6(3)*
O(33)	0.3478(7)	0.656(3)	0.092(1)	4.1(4)*
Os(3B)	0.02281(3)	-0.4247(1)	-0.11951(5)	1.15(1)
Os(2B)	0.06110(3)	-0.1999(1)	-0.25147(5)	1.24(1)
Os(1B)	-0.01676(3)	-0.4097(1)	-0.28046(5)	1.24(1)
N(1B)	-0.0496(7)	-0.267(3)	-0.193(1)	2.2(4)*
C(1B)	-0.0343(6)	-0.263(3)	-0.124(1)	1.1(3)*
C(2B)	-0.0595(8)	-0.147(3)	-0.068(1)	2.6(5)*
C(3B)	-0.0963(8)	-0.067(3)	-0.115(1)	2.6(4)*
C(4B)	-0.0917(8)	-0.143(3)	-0.199(1)	2.7(5)*
Br(1B)	0.01351(8)	0.0729(3)	-0.2189(2)	2.26(5)
C(32B)	0.0736(7)	-0.580(3)	-0.121(1)	1.6(3)*
C(33B)	0.0411(8)	-0.318(3)	-0.021(1)	2.2(4)*
C(21B)	0.0597(8)	-0.118(3)	-0.352(1)	1.8(4)*
C(22B)	0.0959(7)	-0.386(3)	-0.273(1)	1.6(4)*
C(11B)	-0.0677(7)	-0.568(3)	-0.278(1)	1.9(4)*
C(12B)	0.0208(7)	-0.545(3)	-0.349(1)	1.9(4)*
C(13B)	-0.0351(8)	-0.269(3)	-0.360(1)	2.2(4)*
O(31B)	-0.0346(6)	-0.695(2)	-0.034(1)	2.9(3)*
O(32B)	0.1032(6)	-0.672(2)	-0.121(1)	2.8(3)*
O(33B)	0.0506(6)	-0.260(2)	0.038(1)	3.0(4)*
O(21B)	0.0618(6)	-0.063(2)	-0.412(1)	3.5(4)*
O(22B)	0.1190(6)	-0.509(2)	-0.286(1)	2.7(3)*
O(23B)	0.1449(5)	0.013(2)	-0.205(1)	2.3(3)*
O(11B)	-0.0959(6)	-0.671(2)	-0.284(1)	2.6(3)*
O(12B)	0.0400(6)	-0.619(2)	-0.390(1)	2.9(3)*
O(13B)	-0.0476(6)	-0.171(2)	-0.411(1)	3.0(4)*
C(23B)	0.1130(8)	-0.072(3)	-0.218(1)	2.1(4)*
C(31B)	-0.0126(8)	-0.592(3)	-0.067(1)	2.3(4)*
H(21)	0.338	0.238	-0.168	4.0
H(22)	0.304	0.085	-0.162	4.0
H(31)	0.386	0.080	-0.096	4.0
H(32)	0.348	-0.052	-0.076	4.0
H(41)	0.344	0.067	0.039	4.0
H(42)	0.374	0.220	0.012	4.0
H(41B)	-0.118	-0.205	-0.215	4.0
H(42B)	-0.086	-0.052	-0.236	4.0
H(31B)	-0.094	0.056	-0.115	4.0
H(32B)	-0.125	-0.100	-0.094	4.0
H(21B)	-0.040	-0.059	-0.049	4.0
H(22B)	-0.071	-0.212	-0.025	4.0
H(1)	0.207	0.258	-0.049	6.0
H(2)	0.251	0.517	0.002	6.0
H(1B)	0.052	-0.214	-0.154	6.0
H(2B)	0.001	-0.555	-0.208	6.0

<sup>a</sup> Starred *B* values are for atoms that were refined isotropically. *B* values for anisotropically refined atoms are given in the form of the isotropic equivalent displacement parameter defined as  $\frac{1}{3}[a^2B(1,1) + b^2B(2,2) + c^2B(3,3) + ab(\cos \gamma)B(1,2) + ac(\cos \beta)B(1,3) + bc(\cos \alpha)B(2,3)]$ .

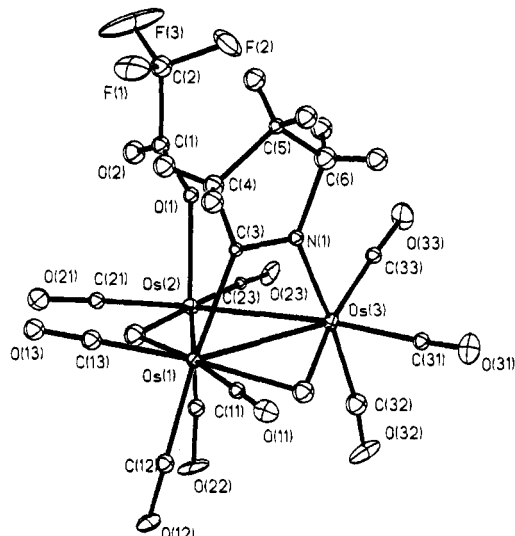


**Figure 2.** Solid state structure of  $(\mu\text{-H})_2\text{Os}_3(\text{CO})_9(\mu\text{-}\eta^2\text{-C=NCH}_2\text{CH}_2\text{CH}_2)(\eta^1\text{-CF}_3\text{CO}_2)$  (**4**).

**Table 4.** Selected Bond Distances (Å) and Angles (deg) for **4**<sup>a</sup>

Distances			
Os(1)–Os(2)	3.040(1)	Os(2)–O(1)	2.10(1)
Os(1)–Os(3)	2.999(1)	Os(1)–C(3)	2.12(2)
Os(3)–Os(2)	2.835(1)	Os(3)–N(1)	2.09(1)
Os(1)–H(1)	1.85(3)	C(3)–N(1)	1.29(2)
Os(1)–H(2)	2.10(4)	C(1)–O(1)	1.28(2)
Os(2)–H(1)	1.83(3)	C(1)–O(2)	1.24(2)
Os(3)–H(2)	1.65(4)	Os–C(CO) <sup>b</sup>	1.94(2)
		C–O(CO) <sup>b</sup>	1.13(2)
Angles			
Os(1)–Os(2)–Os(3)	61.25(2)	Os(3)–Os(1)–C(3)	67.3(4)
Os(1)–Os(3)–Os(2)	62.74(2)	Os(2)–Os(3)–N(1)	86.6(3)
Os(2)–Os(1)–Os(3)	56.00(2)	C(3)–C(4)–C(5)	103(1)
Os(3)–Os(2)–O(1)	87.7(3)	C(3)–N(1)–C(6)	108(1)
Os(1)–Os(2)–O(1)	94.1(3)	Os–(3)–O	176(2)
Os(1)–Os(2)–H(1)	34.32(2)		
Os(3)–Os(1)–H(1)	95.57(3)		
Os(3)–Os(1)–H(2)	31.83(2)		
Os(1)–Os(2)–H(2)	78.71(2)		

<sup>a</sup> Numbers in parentheses are estimated standard deviations.

<sup>b</sup> Average values.

undertook <sup>1</sup>H-2D-EXSY investigations of **2** and **3**, VT-<sup>13</sup>C-NMR of **3** and **4**, and <sup>13</sup>C-EXSY investigations of **4**. The <sup>1</sup>H-2D-EXSY spectrum of **3** at –40 °C shows relatively intense diagonal peaks between the major isomer and the more abundant of the two minor isomers (Figure 4a). There are also less intense off diagonal elements indicating exchange between the two lower field hydrides of the minor isomers with the major isomer (Figure 4a). At shorter mixing times, these less intense off diagonal elements are not observed (Figure 4b). There are thus two distinct dynamical processes occurring in **3** (and **2** which gives exactly the same <sup>1</sup>H-2D-EXSY spectra).

Using the method of Abel *et al.*,<sup>13</sup> we have treated these two processes independently as two 2 × 2 exchange matrices and obtained forward and reverse rate constants  $k_{ba} = 1.15 \text{ s}^{-1}$  and  $k_{ab} = 0.20 \text{ s}^{-1}$  for the more

**Table 5.** Positional Parameters and *B* Values and Their Estimated Standard Deviations for **4**

atom	<i>x</i>	<i>y</i>	<i>z</i>	<i>B</i> <sup>a</sup> (Å <sup>2</sup> )
Os(1)	0.44871(5)	0.53287(5)	0.000	0.996(7)
Os(3)	0.13687(5)	0.32249(5)	0.07298(2)	1.087(7)
Os(2)	0.18227(5)	0.63638(5)	0.2833(2)	0.986(7)
F(1)	–0.038(1)	0.424(2)	–0.1540(5)	4.5(3)
F(2)	–0.252(2)	0.266(2)	–0.1077(4)	4.9(3)
F(3)	–0.238(1)	0.488(2)	–0.1479(6)	8.0(3)
O(1)	0.030(1)	0.496(1)	–0.0406(4)	1.6(2)
O(2)	–0.097(1)	0.655(1)	–0.0528(5)	2.5(2)
O(11)	0.621(1)	0.314(1)	0.0068(6)	2.6(2)
O(12)	0.727(1)	0.814(1)	0.0809(5)	2.5(2)
O(13)	0.635(1)	0.735(1)	–0.1036(5)	2.2(2)
O(31)	0.151(1)	0.001(1)	0.1137(5)	2.7(2)
O(33)	–0.244(1)	0.176(1)	0.0923(6)	3.1(3)
O(32)	0.199(1)	0.475(1)	0.1983(5)	3.3(3)
O(21)	0.263(1)	0.984(1)	–0.0183(5)	2.7(2)
O(23)	–0.132(1)	0.581(1)	0.1001(5)	2.7(2)
O(22)	0.412(1)	0.829(1)	0.1309(5)	2.7(2)
N(1)	0.114(1)	0.242(1)	–0.0094(5)	1.7(2)
C(1)	–0.066(2)	0.541(2)	–0.0659(6)	1.6(3)
C(2)	–0.152(2)	0.428(2)	–0.1190(7)	2.5(3)
C(3)	0.246(1)	0.328(1)	–0.0409(6)	1.2(2)
C(4)	0.221(2)	0.264(2)	–0.1008(6)	1.8(3)
C(5)	0.043(2)	0.107(2)	–0.1007(6)	1.7(3)
C(6)	–0.027(2)	0.099(1)	–0.0403(6)	1.8(3)
C(11)	0.557(2)	0.395(2)	0.0046(6)	1.7(2)
C(12)	0.623(1)	0.712(1)	0.0537(6)	1.7(2)
C(13)	0.568(1)	0.660(1)	–0.0647(6)	1.5(2)
C(31)	0.141(1)	0.120(2)	0.0999(6)	1.7(2)
C(33)	–0.103(2)	0.233(2)	0.0857(6)	1.9(3)
C(32)	0.173(2)	0.417(2)	0.1525(6)	2.0(3)
C(21)	0.227(1)	0.848(1)	–0.0023(6)	1.6(2)
C(23)	–0.017(1)	0.601(1)	0.0744(6)	1.3(2)
C(22)	0.325(1)	0.753(2)	0.0952(7)	1.7(2)
H(41)	0.306	0.235	–0.111	3.0
H(42)	0.226	0.348	–0.127	3.0
H(52)	0.050	0.007	–0.108	3.0
H(51)	–0.028	0.118	–0.129	3.0
H(61)	–0.126	0.113	–0.042	3.0
H(62)	–0.057	–0.007	–0.022	3.0
H(2)	0.344	0.396	0.078	4.0
H(1)	0.382	0.695	–0.010	4.0

<sup>a</sup> *B* values for anisotropically refined atoms are given in the form of the isotropic equivalent displacement parameter defined as  $(4/3)[a^2B(1,1) + b^2B(2,2) + c^2B(3,3) + ab(\cos \gamma)B(1,2) + ac(\cos \beta)B(1,3) + bc(\cos \alpha)B(2,3)]$ .

rapid process involving the major isomer and the more abundant of the two minor isomers (**a** and **b** in Scheme 1). These values are averages of values obtained from two calculations involving the directly exchanging higher field and lower field sets of hydride resonances (Figure 4a). The errors for rate constants in the range of 5 to 0.1 are estimated to be <10%.<sup>13</sup> Note that no off diagonal elements are seen between the hydride resonances of a given isomer. This leads to the conclusion that the hydride bridge of H(2) opens more rapidly on one side and is consistent with the fact that one of the two Os–H bonds is significantly shorter than the other (i.e., the Os–H bonds with the osmium when bound to the nitrogen of the imidoyl ligand). This tentative conclusion represents an unusual example of a direct relation between metal hydride bond lengths and the mechanisms of hydride migrations in polymetallic clusters. The possibility that the minor isomers of **3** involve migration of the bromine atom to a radial or the other axial site on Os(2) can be excluded on the basis of our previous work which shows that axial–radial exchange at an Os(CO)<sub>3</sub>L group in these types of complexes is a much higher energy process<sup>9</sup> and by the thermolysis of **3** discussed below. Isomers **a–c** (Scheme 1) as well as H(1) and H(2) do eventually interchange as evidenced

(13) Abel, E. W.; Costen, T. P. J.; Orrell, K. G.; Sik, V.; Stephenson, D. *J. Magn. Reson.* **1986**, *70*, 34.

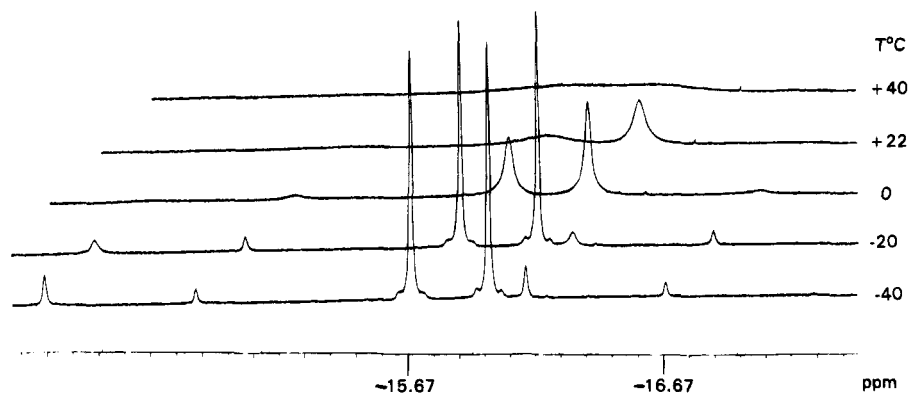
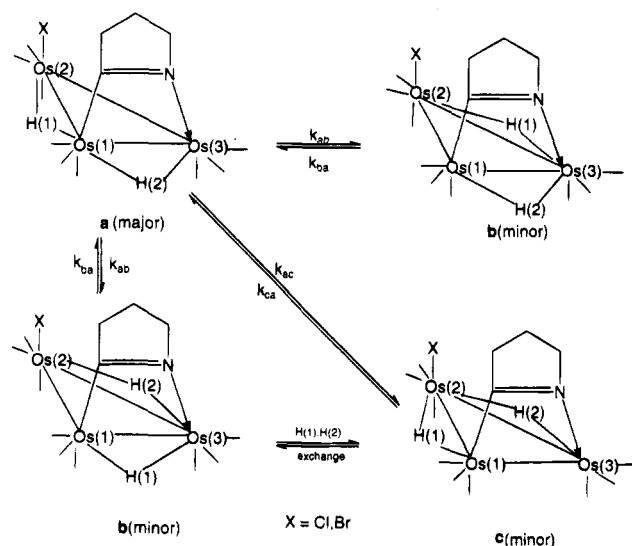


Figure 3. VT- $^1\text{H}$ -NMR of **3** at 360 MHz.

Scheme 1. Hydride Exchange Pathways for **2** and **3**



by the coalescence of the hydride signals at  $+50\text{ }^\circ\text{C}$ . Using this coalescence temperature, we estimate a barrier of  $76 \pm 2\text{ kJ/mol}$  for H(1) and H(2) exchange in the major isomer.

The VT- $^1\text{H}$ -NMR of **4** reveals the presence of only two isomers at the low-temperature limit in a ratio of 4.8 to 1. As the temperature is increased, we observe an averaging process consistent with interchange between isomers of type **a** and **b** (Scheme 1). In order to corroborate the nature of this single stage exchange process, we obtained VT- $^{13}\text{C}$ -NMR and a 2D- $^{13}\text{C}\{^1\text{H}\}$ -EXSY spectra of a  $^{13}\text{C}$ O-enriched ( $\sim 30\%$ ) sample of **4**.

The  $^{13}\text{C}$ -NMR of **4** remains unchanged from  $-40$  to  $-20\text{ }^\circ\text{C}$  and shows the expected nine resonances for the major isomer at 165.56, 166.18, 168.69, 173.07, 174.97, 175.22, 175.46, 175.57, and 176.31 ppm and nine companion resonances for the minor isomer at 163.17, 163.43, 166.66, 173.44, 175.29, 175.73, 176.16, 176.85, and 177.20 ppm with the ratio of major to minor resonances 4.5 to 1 in reasonable agreement with the proton data (Figure 5). The proton-coupled  $^{13}\text{C}$ -NMR of **4** allows at least a partial assignment of these resonances. The two-bond carbonyl-hydride couplings in these triosmium clusters fall into three distinct categories: *trans*-radial ( $^2J(^{13}\text{C}-^1\text{H}) = 10\text{--}12\text{ Hz}$ ), *cis*-radial ( $^2J(^{13}\text{C}-^1\text{H}) = 3\text{--}4\text{ Hz}$ ), and axial ( $^2J(^{13}\text{C}-^1\text{H}) < 1\text{ Hz}$ ).<sup>9</sup> On the basis of these established trends, we can interchangeably assign the resonances at 165.56 and

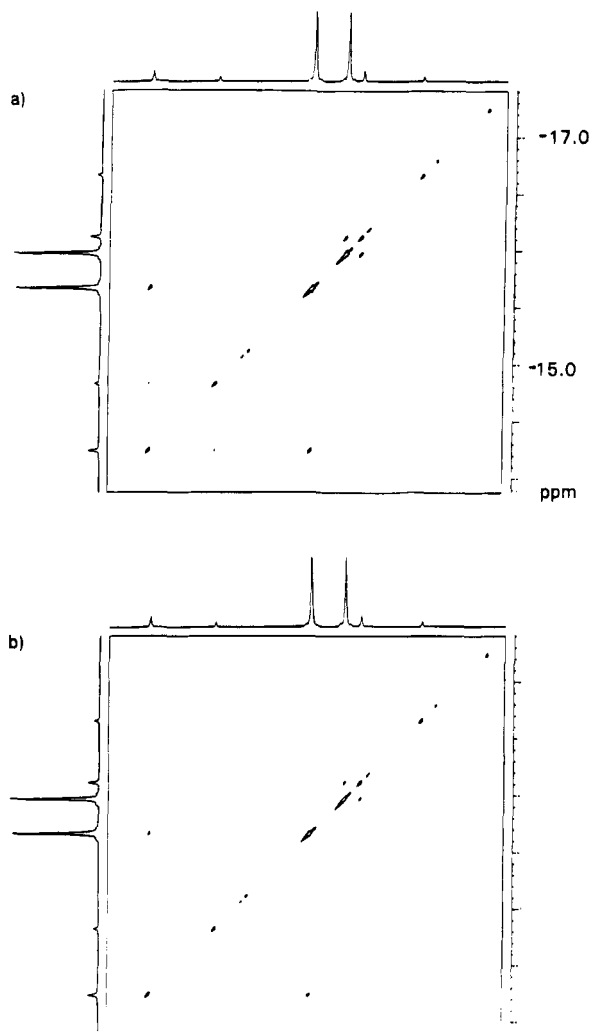
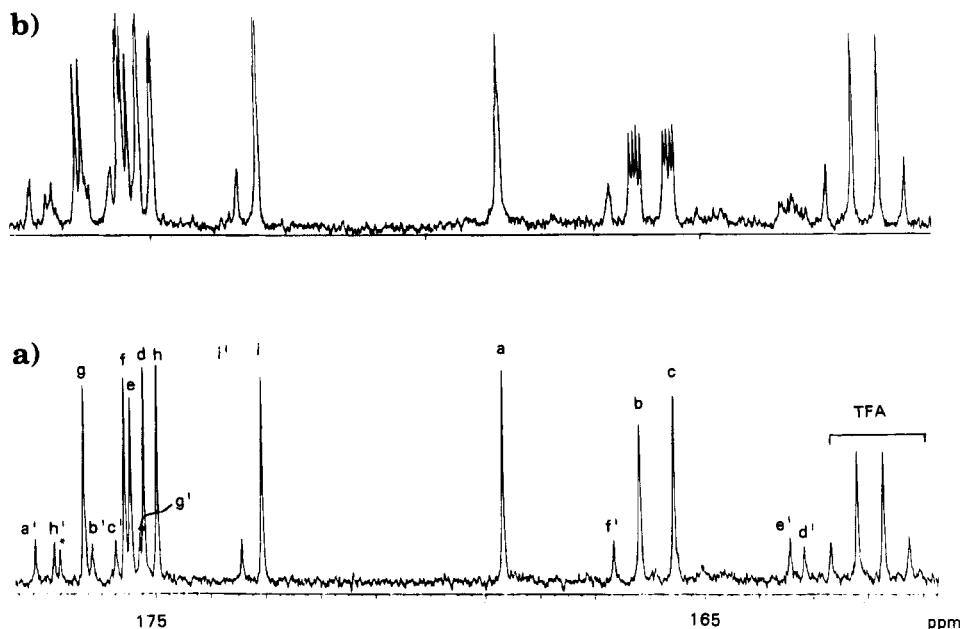


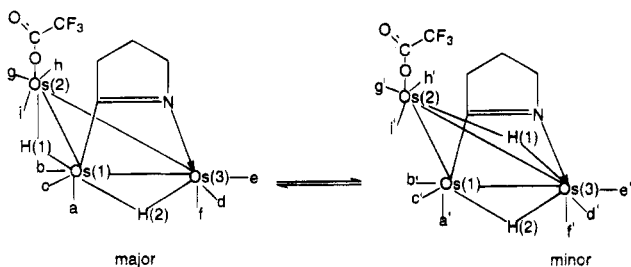
Figure 4.  $^1\text{H}$ -2D-EXSY spectra of **3** at  $-49\text{ }^\circ\text{C}$ : (a) mixing time = 500 ms; (b) mixing time = 200 ms (different scale than that of Figure 5a).

166.18 ppm each of which appears as a doublet of doublets to the radial carbonyls **b** and **c** on Os(1) (Scheme 2). The resonance at 168.69 ppm which appears as a triplet can be unambiguously assigned to the axial carbonyl on Os(1). Similarly, equivocal assignments of **g** and **e** to the resonances at 176.31 and 175.46 ppm can be made while the assignments of the remaining four resonances are more difficult owing to the similarity in coupling constants and partial overlap of resonances. The appearance of the nine companion resonances of the minor isomer in the coupled spectrum closely resembles those of the major isomer and gives



**Figure 5.**  $^{13}\text{C}$ -NMR of **4** in the carbonyl region at 90 MHz at  $-20^\circ\text{C}$ : (a) proton decoupled; (b) proton coupled; asterisk indicates minor impurity.

**Scheme 2. Carbonyl Assignments Based on the Exchange Process in 4**



evidence that the two isomers differ as illustrated in Scheme 2. We then obtained the  $^{13}\text{C}$ -2D-EXSY spectrum of **4** at  $-10^\circ\text{C}$  (Figure 6). Imposing the proposed hydride edge hopping (Scheme 2) on the off diagonal peaks observed (nine) gives a self-consistent picture of the exchange process between the major and minor isomers of **4** and allows an unambiguous assignment of all of the  $^{13}\text{CO}$  resonances. Thus, according to Scheme 2, edge hopping of H(1) would exchange resonance b, a doublet of doublets, with b', a doublet of the minor isomer with an 8–10 Hz coupling constant, as is observed (Figure 6). Resonance a, which is unambiguously assigned to the axial carbonyl on Os(1), would be expected to be correlated with a minor isomer resonance with a small ( $<1$  Hz) coupling constant as observed. This type of correlation follows through consistently for all nine resonances in the major and minor isomers and leads unequivocally to the assignments shown in Figure 5. The precise specification of the exchange process in **4** lends further credence to the structure of the isomers in **3** and their proposed exchange (Scheme 1).

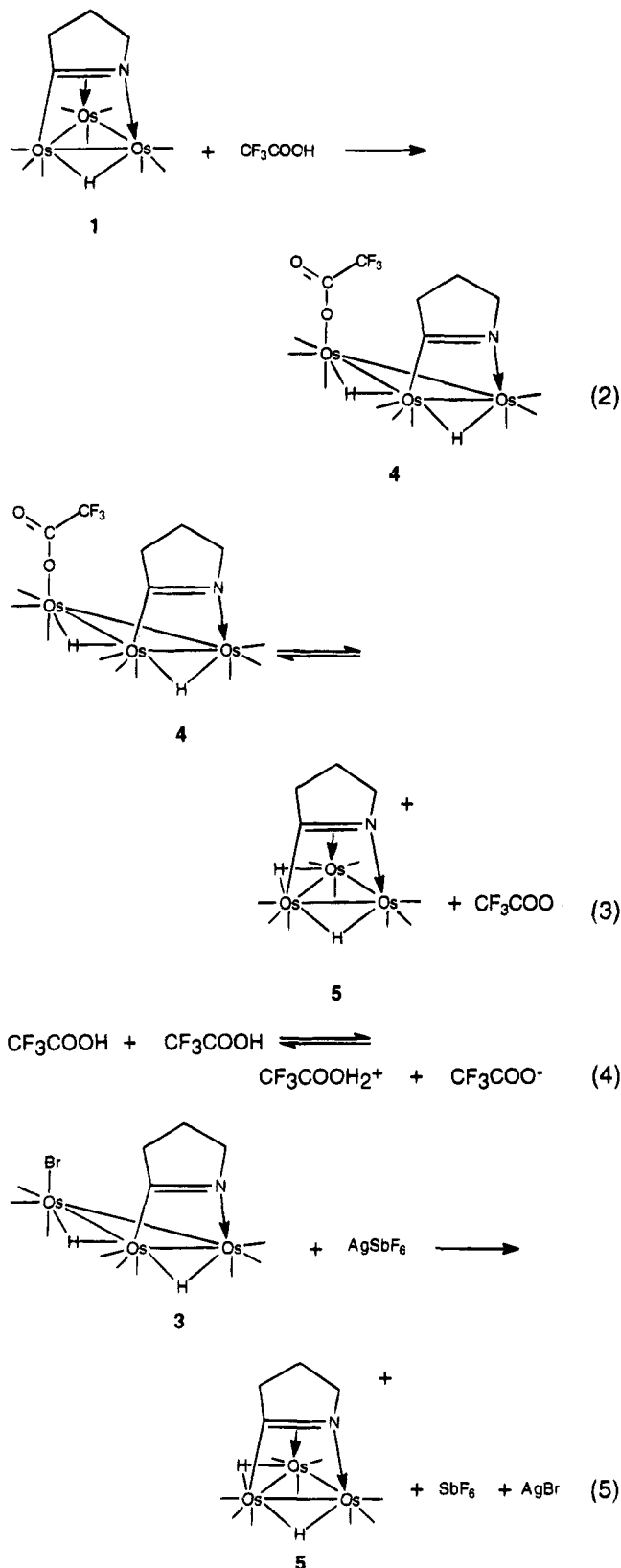
**D. Titrations of 1 with HX (X =  $\text{CF}_3\text{CO}_2$ ,  $\text{CF}_3\text{SO}_3$ ,  $\text{BF}_4$ ).** During the course of our studies on the synthesis of **4**, we followed the addition of trifluoroacetic acid to **1** by  $^1\text{H}$ -NMR (Figure 7). It was observed that at  $-40^\circ\text{C}$  in the presence of 1.5–8.0 equiv of trifluoroacetic acid there were detectable amounts of **1**, the two isomers of **4**, and two additional hydride signals at  $-17.01$  and  $-19.93$  ppm in a relative intensity of 1:1. On addition

of more trifluoroacetic acid, these resonances and the hydride resonance of **1** decreased in intensity while the resonances associated with the two isomers of **4** increased in relative intensity. A reasonable explanation for this phenomenon is the existence of three simultaneous equilibria; that between **1** and **4** (eq 2), between **4** and the monocation  $(\mu\text{-H})_2\text{Os}_3(\text{CO})_9(\mu_3\text{-}\eta^2\text{-C}=\text{NCH}_2\text{-CH}_2\text{CH}_2)^+$  (**5**)–trifluoroacetate (eq 3), and that between trifluoroacetic acid and self-protonated trifluoroacetic acid–trifluoroacetate anion (eq 4).

Supporting this hypothesis is the fact that the  $^{19}\text{F}$ -NMR of these solutions shows only two resonances at 2.17 and 2.14 ppm in the same relative intensity as the two isomers of **4** as measured by  $^1\text{H}$ -NMR. The  $\text{CF}_3\text{-COOH}$  resonance at 0.0 ppm shifts downfield as more  $\text{CF}_3\text{COOH}$  is added and is undoubtedly due to averaging of  $\text{CF}_3\text{COOH}$  with self-protonated  $\text{CF}_3\text{COOH}$  and trifluoroacetate anion (eq 4). As more  $\text{CF}_3\text{COOH}$  is added, more self-protonation takes place and shifts eq 3 to the left and eq 2 to the right. Using the relative intensity data from the  $^1\text{H}$ -NMR spectra, we can estimate the equilibrium constant for formation of the adduct (eq 2) to be  $2.50 \pm 0.3$  and the equilibrium constant for dissociation of the adduct (eq 3) to be  $(7.0 \pm 0.4) \times 10^{-3}$  in  $\text{CDCl}_3$  at  $-40^\circ\text{C}$ .

Additional proof that the new species observed is indeed **5** comes from an examination of the  $^1\text{H}$ -NMR spectrum of a sample of **3** after treatment with  $\text{AgSbF}_6$  in  $\text{CDCl}_3$  followed by filtration of the  $\text{AgBr}$  precipitate (eq 5). This solution showed the same two resonances at  $-19.93$  and  $-17.01$  ppm at  $-40^\circ\text{C}$ . Similarly, solutions of **1** treated with a 10-fold excess of  $\text{HBF}_4\cdot\text{Et}_2\text{O}$  show the same two hydride resonances at  $-40^\circ\text{C}$ . At room temperature these resonances appear broadened indicating the onset of hydride site exchange. The  $^{13}\text{C}$ -NMR of solutions of **5** at  $-40^\circ\text{C}$  show eight resonances, one of relative intensity two at 157.83 ppm which appears as a doublet of doublets in the proton-coupled spectrum. Two resonances at 170.56 and 168.54 ppm appear as doublets with  $^2J(^1\text{H}\text{-}^{13}\text{C}) = 8$  and 10 Hz,



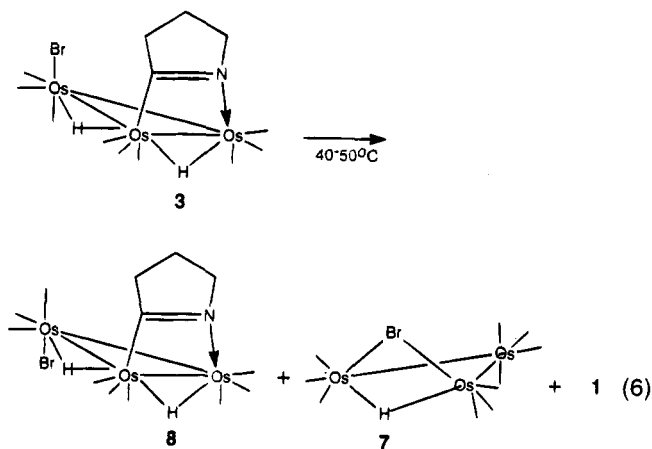


respectively, while the remaining resonances appear as slightly broadened singlets. These data and the relatively high-field chemical shifts observed for the hydrides of **5** are consistent with a  $\mu_3\text{-}\eta^2$ -imidoyl-nona-carbonyl cluster as indicated in eq 3.<sup>9</sup> Analytically pure samples of the tetrafluoroborate and hexafluoroantimonate salts of **5** could be isolated, but the crystals were not suitable for X-ray diffraction.

The simultaneous equilibria represented by eqs 2 and

3 can also be attained by treating solutions of **1** with CF<sub>3</sub>SO<sub>3</sub>H. In the case of this stronger acid, however, adduct formation is virtually quantitative. Since no free acid could be detected, no estimate of the equilibrium constant for adduct formation could be obtained. Interestingly though, in a slight deficiency of this acid, the major species detected in solution at -40 °C were the two isomers of the adduct  $(\mu\text{-H})_2\text{Os}_3(\text{CO})_9(\mu\text{-}\eta^2\text{-C=NCH}_2\text{CH}_2\text{CH}_2)(\eta^1\text{-CF}_3\text{SO}_3)$  (**6**) present in a 4:1 ratio and **1** along with a trace of the cation **5**. In the presence of ~1.0 equiv of CF<sub>3</sub>SO<sub>3</sub> no **1** was detected but the two hydride resonances associated with **6** appeared. From these data we can estimate that the equilibrium constant between the adduct **6** and the cation **5** is 0.15. We can infer from this experiment that initial reaction of trifluoroacetic or triflic acid with **1** gives the adducts **4** and **6** which then undergo partial dissociation to the cation, **5**. The stronger, triflic acid drives adduct formation further and not simple protonation, while the corresponding dissociation into the cation **5** and the acid's conjugate base occurs to a greater extent with **6** vs **4**. Further titration of **1** with CF<sub>3</sub>SO<sub>3</sub>H at -40 °C was precluded by the limited solubility of this acid in CDCl<sub>3</sub> or CD<sub>2</sub>Cl<sub>2</sub>. On warming, solutions of **6** showed the onset of isomer exchange as observed for **4**. The values of the equilibrium constants reported here do not take into account any ion pairing between **5** and its gegen ion.

**E. Thermolysis of 3.** The thermolysis of **3** was studied in the temperature range 40–50 °C in benzene under CO and N<sub>2</sub> atmospheres. Under a CO atmosphere, virtually complete conversion of **3** to three triosmium clusters was observed:  $(\mu\text{-H})(\mu\text{-Br})\text{Os}_3(\text{CO})_{10}$  (**7**, 14%), **1** (32%), and what proved to be an isomer of **3**,  $(\mu\text{-H})_2\text{Os}_3(\text{CO})_9(\mu\text{-}\eta^2\text{-C=NCH}_2\text{CH}_2\text{CH}_2)\text{Br}$  (**8**, 46%) (eq 6). Under an N<sub>2</sub> atmosphere, the same three triosmium



products are obtained but in much lower yields with associated nonspecific decomposition. An attempt was made to identify the organic product associated with the formation **7** by GC-mass spectroscopy of the reaction volatiles. A band with a retention time of 2.5 min (oven  $T = 85$  °C) at molecular mass = 108 amu was observed (which corresponds to C<sub>7</sub>H<sub>10</sub>N or C<sub>6</sub>H<sub>6</sub>NO) but in insufficient quantities to identify further. Further heating of isolated **8** (10–20 h at 40–50 °C) leads to **1** and **7**, but the formation of small amounts of  $(\mu\text{-H})_2\text{Os}_3(\text{CO})_{10}$  could also be detected by <sup>1</sup>H-NMR and thin-layer chromatography.

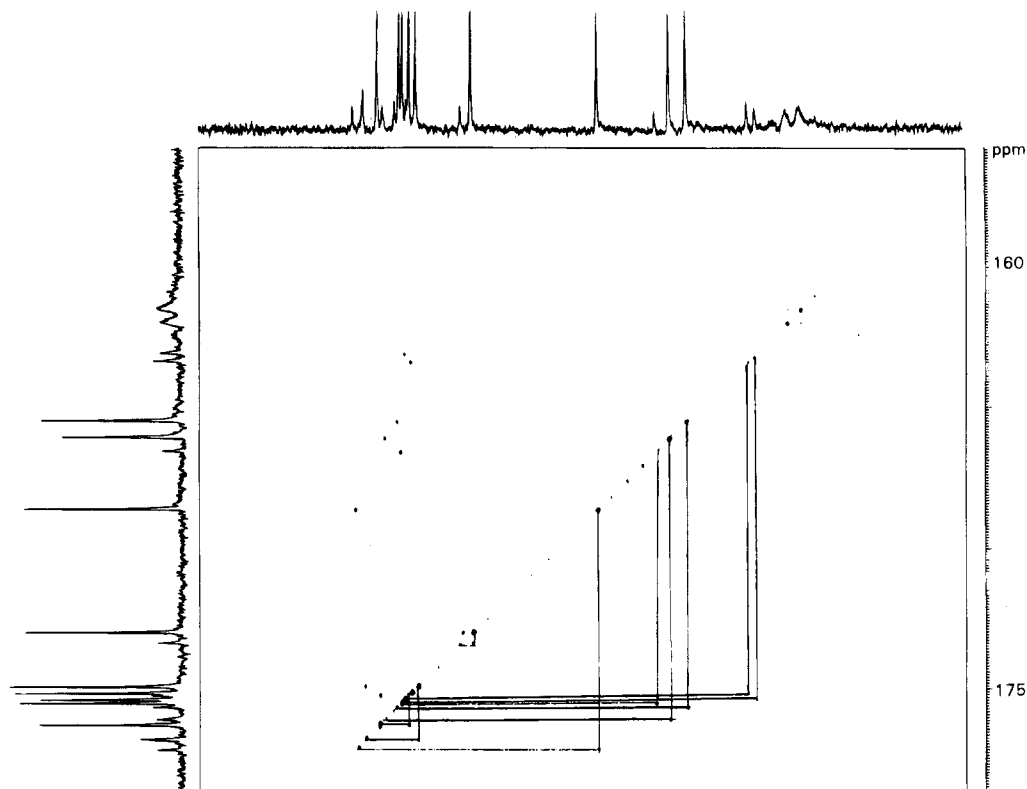


**Figure 6.** 2D- $^{13}\text{C}$ -EXSY spectrum of **4** at  $-20\text{ }^\circ\text{C}$  showing the off diagonal element correlations.

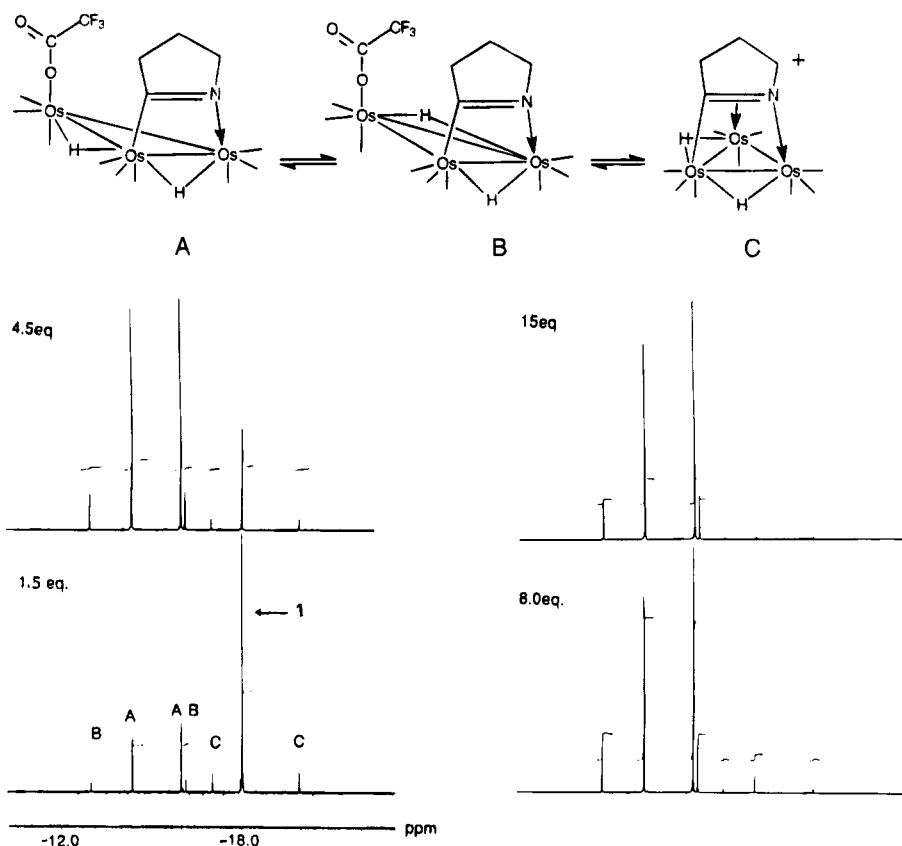


**Figure 7.** Titration of **1** with  $\text{CF}_3\text{COOH}$  followed by  $^1\text{H}$ -NMR at 360 MHz at  $-40\text{ }^\circ\text{C}$ .

The structure of **8** is shown in Figure 8, selected distances and bond angles are given in Table 6, atomic coordinates are given in Table 7, and crystal data and collection parameters are given in Table 1. The overall structure of **8** is the same as **3** except that the bromine atom is in an axial position on the opposite face of the

cluster as the imido ligand. Again, the average  $\text{Br}-\text{H}(1)$  distance of  $2.78(4)\text{ \AA}$  in the two molecules observed here as for **3** is less than the sum of the van der Waals radii. In **8**, however, the Br atom tilts toward H(1) as well, whereas in **3** the  $\text{Br}-\text{Os}(2)$  vector is essentially perpendicular to the  $\text{Os}_3$  plane. The type of isomeriza-

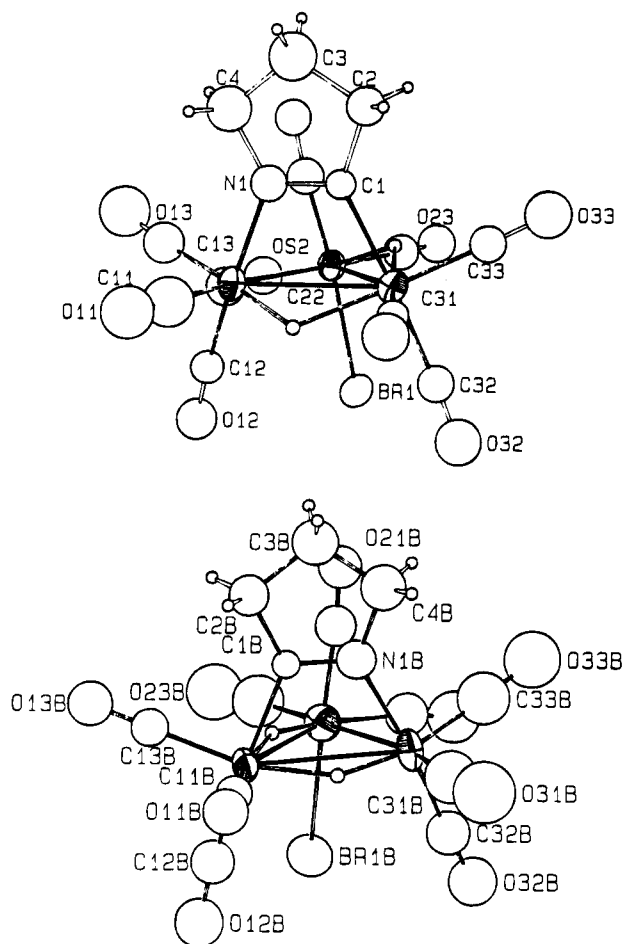


**Figure 8.** Solid state structure of  $(\mu\text{-H})_2\text{Os}_3(\text{CO})_9(\mu\text{-}\eta^2\text{-C=NCH}_2\text{CH}_2\text{CH}_2)\text{Br}$  (**8**).

tion exhibited by the conversion of **3** to **8** is, to our knowledge, unprecedented in cluster chemistry, where polytopal isomers normally interchange reversibly and indicates that **2**–**4** are the kinetic products of HX addition to **1**.

Perhaps the most interesting aspect of the structural difference between **3** and **8** is that exchange between H(1) and H(2) is much more rapid on the NMR time scale in **8**, (Figure 9). In **8**, coalescence is observed at +10 °C, and we can estimate a barrier of  $\Delta G^\ddagger = 54.5 \pm 2 \text{ kJ/mol}$  for this exchange process. As for **3**, we observe three isomers at the low-temperature limit which are probably analogous to isomers **a**–**c** in Scheme 1 except for the interchange of the Br atom and the axial carbonyl group on Os(2) in **3** and **8**. The 2D-<sup>1</sup>H-EXSY spectrum of **8** at –50 °C showed that the fastest process is the direct exchange of H(1) and H(2) in the major isomer, followed by exchange of H(1) and H(2) in one of the minor isomers and exchange between isomers of the type **a** and **b**. Exchange at –50 °C was too rapid to make use of the off diagonal element intensities for accurate evaluation of rate constants by the method of Abel *et al.*, and going to lower temperatures was precluded by the insolubility of **8** below –50 °C.<sup>13</sup> The substantial difference in the rate of H(2) and H(1) exchange rates between **3** and **8** (~20 kJ/mol) is difficult to rationalize on the basis of the differences in their hydride geometries. A careful inspection of the located hydride geometries in **3** and **8** fails to bring to light any significant differences in distances and angles. These

**Table 6.** Selected Bond Distances (Å) and Angles (deg) for **8**

	Distances	
	molecule A	molecule B
Os(1)–Os(2)	2.829(2)	Os(1B)–Os(2B) 3.085(2)
Os(1)–Os(3)	2.986(1)	Os(1B)–Os(3B) 3.993(2)
Os(2)–Os(3)	3.089(1)	Os(2B)–Os(3B) 2.839(2)
Os(1)–H(2)	1.63(4)	Os(1B)–H(1B) 1.86(4)
Os(2)–H(1)	1.75(4)	Os(1B)–H(2B) 1.67(4)
Os(3)–H(1)	1.80(4)	Os(2B)–H(1B) 1.33(4)
Os(3)–H(2)	1.90(4)	Os(3B)–H(2B) 1.42(4)
Os(2)–Br	2.591(3)	Os(2B)–BrB 2.585
Os(3)–C(1)	2.06(2)	Os(1B)–C(1B) 2.08(2)
Os(1)–N(1)	2.11(2)	Os(3B)–N(1B) 2.09(2)
C(1)–N(1)	1.30(2)	C(1B)–N(1B) 1.25(3)
Os–C(9)CO	1.86(3) <sup>b</sup>	OsB–CB(CO) 1.88(3) <sup>b</sup>
C–O	1.17(3) <sup>b</sup>	CB–OB 1.16(4)
Angles		
	molecule A	molecule B
Os(1)–Os(2)–Os(3)	60.42(3)	Os(1)–Os(2)–Os(3) 60.51(4)
Os(1)–Os(3)–Os(2)	55.47(3)	Os(1)–Os(3)–Os(2) 68.87(4)
Os(2)–Os(1)–Os(3)	64.10(4)	Os(2)–Os(1)–Os(3) 55.66(4)
Os(1)–Os(2)–Br	96.69(8)	Os(1B)–Os(2B)–BrB 86.9(1)
Os(3)–Os(2)–Br	87.34(7)	Os(3B)–Os(2B)–BrB 95.84(8)
Os(2)–Os(3)–H(1)	29.23(2)	Os(1B)–Os(2B)–H(1B) 17.25(3)
Os(3)–Os(2)–H(1)	30.18(3)	Os(2B)–Os(1B)–H(1B) 12.31(2)
Os(3)–Os(1)–H(2)	34.90(3)	Os(3B)–Os(1B)–H(2B) 13.08(3)
Os(1)–Os(3)–H(2)	29.43(2)	Os(1B)–Os(3B)–H(2B) 15.45(3)
Os(2)–Os(3)–C(1)	85.2(6)	Os(2B)–Os(1B)–C(1B) 83.3(7)
Os(2)–Os(1)–N(1)	88.0(6)	Os(2B)–Os(3B)–N(1B) 86.6(5)
C(1)–C(2)–C(3)	104.2(2)	C(1B)–C(2B)–C(3B) 101.(2)
C(1)–N(1)–C(4)	114.2(2)	C(1B)–N(1B)–C(4B) 111.(2)
Os–C–O	174.2(2) <sup>b</sup>	OsB–CB–OB 175.(3)

<sup>a</sup> Numbers in parenthesis are estimated standard deviations.  
<sup>b</sup> Average values.

results merely point to the fact that subtle differences in cluster structure can have profound effects on hydride dynamics.

## Conclusions

From the data presented, we conclude that the weak bonding interaction between hydrogen and bromine seen in the solid state for **3** and **8** has no distinct effect on the geometry assumed by the hydride H(1) but that the change in the position of the Br atom has a significant impact on hydride mobility. The observed asymmetric bonding in the H(2)–Os bond lengths accounts nicely for the restricted exchange matrix observed for **3** in the 2D-EXSY spectra. It is also tempting to propose that the lack of dissociation of the conjugate base in **2** and **3** vs **4** and **6** is due to the weak agostic hydrogen halide interaction observed in the solid state. However, it must be pointed out that the energy of solvation of the conjugate base and its ability to form hydrogen-bonded oligomers with the corresponding acid in the nonpolar solvents examined here are probably more important factors.

## Experimental Section

**Materials and General Methods.** Compound **1** was synthesized by published procedures.<sup>9</sup> Solvents were purified by distillation from CaH<sub>2</sub> (acetonitrile, CH<sub>2</sub>Cl<sub>2</sub>) or sodium benzophenone ketyl (benzene). Deuterated NMR solvents were stored over type 4 Å molecular sieves (Linde). Trifluoro-

**Table 7. Positional Parameters and B Values and Their Estimated Standard Deviations for 8**

atom	x	y	z	B <sup>a</sup> (Å <sup>2</sup> )
Os(1)	0.71236(6)	0.21773(7)	0.54231(6)	3.30(3)
Os(2)	0.60577(6)	0.33522(7)	0.57740(5)	3.01(3)
Os(3)	0.54758(6)	0.25039(7)	0.39951(5)	3.09(3)
Br(1)	0.5261(2)	0.2003(2)	0.6074(2)	4.31(7)
O(11)	0.802(1)	0.087(1)	0.476(1)	7.6(6)*
O(12)	0.699(1)	0.079(1)	0.667(1)	5.8(5)*
O(13)	0.859(1)	0.304(2)	0.677(1)	9.2(7)*
O(21)	0.706(1)	0.494(1)	0.5575(9)	4.8(4)*
O(22)	0.718(1)	0.320(1)	0.762(1)	6.7(5)*
O(23)	0.480(1)	0.466(1)	0.592(1)	6.1(5)*
O(31)	0.557(1)	0.115(1)	0.2699(9)	5.4(4)*
O(32)	0.421(1)	0.111(1)	0.407(1)	6.7(5)*
O(33)	0.416(1)	0.373(1)	0.270(1)	6.8(5)*
C(1)	0.637(1)	0.334(1)	0.393(1)	2.6(5)*
N(1)	0.709(1)	0.320(1)	0.454(1)	4.2(5)*
C(4)	0.775(2)	0.378(2)	0.448(1)	6.1(8)*
C(3)	0.729(2)	0.437(2)	0.373(2)	6.6(8)*
C(2)	0.641(1)	0.406(2)	0.332(1)	4.2(6)*
C(11)	0.769(2)	0.136(2)	0.503(2)	7.5(9)*
C(12)	0.707(2)	0.133(2)	0.619(1)	3.7(6)*
C(13)	0.801(2)	0.266(2)	0.627(2)	5.9(7)*
C(21)	0.670(2)	0.430(2)	0.567(1)	5.0(7)*
C(22)	0.677(2)	0.330(2)	0.691(2)	6.0(8)*
C(23)	0.525(2)	0.414(2)	0.582(1)	5.1(7)*
C(31)	0.549(1)	0.168(1)	0.318(1)	2.7(5)*
C(32)	0.465(2)	0.168(2)	0.410(1)	4.4(6)*
C(33)	0.466(2)	0.326(2)	0.322(1)	4.1(6)*
H(41)	0.8038	0.4152	0.4971	8.8
H(42)	0.8124	0.3386	0.4388	6.7
H(21)	0.6269	0.3778	0.2783	4.7
H(22)	0.6042	0.4571	0.3248	4.5
H(31)	0.7518	0.4272	0.3342	7.9
H(32)	0.7332	0.5024	0.3872	7.9
Os(3B)	0.90701(7)	-0.30091(8)	0.55413(6)	4.36(3)
Os(2B)	0.87152(7)	-0.16882(8)	0.42179(6)	4.19(3)
Os(1B)	0.74001(7)	-0.21460(7)	0.48104(6)	3.36(3)
Br(1B)	0.7975(2)	-0.2878(2)	0.3008(2)	7.1(1)
O(31B)	0.916(2)	-0.443(2)	0.686(1)	12.0(9)*
O(32B)	0.917(1)	-0.455(1)	0.440(1)	7.7(6)*
O(33B)	1.087(2)	-0.267(2)	0.621(1)	10.8(8)*
O(21B)	0.961(1)	-0.029(1)	0.556(1)	6.0(5)*
O(23B)	0.812(2)	-0.018(2)	0.286(1)	11.0(8)*
O(13B)	0.629(1)	-0.044(1)	0.435(1)	6.4(5)*
N(1B)	0.892(1)	-0.188(1)	0.623(1)	4.8(5)*
C(1B)	0.822(1)	-0.151(1)	0.592(1)	2.4(5)*
C(2B)	0.814(2)	-0.069(2)	0.643(1)	5.0(7)*
C(3B)	0.902(2)	-0.060(2)	0.710(2)	6.6(8)*
C(4B)	0.945(2)	-0.144(2)	0.702(2)	6.4(8)*
C(31B)	0.908(2)	-0.387(2)	0.633(2)	9(1)*
C(32B)	0.911(2)	-0.398(2)	0.485(2)	6.3(8)*
C(33B)	1.013(2)	-0.284(2)	0.593(2)	9(1)*
C(21B)	0.930(2)	-0.083(2)	0.507(1)	5.4(7)*
C(23B)	0.840(2)	-0.073(2)	0.338(2)	9(1)*
C(13B)	0.671(2)	-0.110(2)	0.452(1)	4.6(6)*
O(11B)	0.660(1)	-0.308(1)	0.582(1)	6.4(5)*
O(12B)	0.625(1)	-0.331(1)	0.322(1)	7.6(6)*
C(11B)	0.691(2)	-0.274(2)	0.545(1)	4.1(6)*
C(12B)	0.665(2)	-0.283(2)	0.381(2)	6.2(8)*
O(22B)	1.027(1)	-0.218(2)	0.411(1)	9.5(7)*
C(22B)	0.973(2)	-0.194(2)	0.417(2)	6.4(8)*
H(21B)	0.7963	-0.0137	0.6090	6.2
H(22B)	0.7779	-0.0840	0.6657	6.2
H(31B)	0.9243	-0.0036	0.7010	8.2
H(32B)	0.9021	-0.0583	0.7639	8.2
H(41B)	0.9566	-0.1850	0.7484	7.7
H(42B)	0.9940	-0.1236	0.7017	7.7
H(1)	0.550	0.346	0.468	6.0
H(2)	0.634	0.168	0.466	6.0
H(2B)	0.822	-0.286	0.518	6.0
H(1B)	0.805	-0.165	0.434	6.0

<sup>a</sup> Starred B values are for atoms that were refined isotropically. B values for anisotropically refined atoms are given in the form of the isotropic equivalent displacement parameter defined as  $(4/3)[a^2B(1,1) + b^2B(2,2) + c^2B(3,3) + ab(\cos \gamma)B(1,2) + ac(\cos \beta)B(1,3) + bc(\cos \alpha)B(2,3)]$ .

acetic acid, HBF<sub>4</sub>·(CH<sub>3</sub>CH<sub>2</sub>)<sub>2</sub>O, and triflic acid (Aldrich) were handled in an inert atmosphere and used as received. Hydrogen chloride and hydrogen bromide (Matheson) were used as received.

<sup>1</sup>H- and <sup>13</sup>C-NMR spectra were run on Bruker AMX-360 and AM-400 spectrometers. Two-dimensional EXSY spectra were obtained using the Bruker microprogram NOESY-TPPI in the phase sensitive mode (modified to allow composite pulse decoupling for <sup>13</sup>C) using 1024 and 512 data points, 8–32 transients, with a relaxation delay of 1–2 s. Infrared spectra were obtained on a Perkin-Elmer 1420 dispersive infrared spectrometer, and microanalyses were performed by Schwarzkopf Microanalytical Laboratory, New York.

**Synthesis of (μ-H)<sub>2</sub>Os<sub>3</sub>(CO)<sub>9</sub>(μ-η<sup>2</sup>-C=NCH<sub>2</sub>CH<sub>2</sub>CH<sub>2</sub>)X (X = Cl (2) Br (3)).** Into 100 mL of previously nitrogen-purged hexane was bubbled HX (X = Cl, Br) for ~3–5 min. A solution of **1** (100 mg, 0.112 mmol) in 20 mL of hexane was added and the solution stirred for 1 h. The orange-yellow solution was rotary evaporated to dryness, taken up in a minimum of methylene chloride/hexane (1:4), and recrystallized at -20 °C to yield 100–105 mg of **2** or **3** (95–100%).

**Spectral and Analytical Data for 2 and 3. Data for 2:** Anal. Calcd for C<sub>13</sub>H<sub>8</sub>ClNO<sub>9</sub>Os<sub>3</sub>: C, 16.82; H, 0.86; N, 1.51. Found: C, 16.89; H, 0.80; N, 1.54. IR (ν(CO) in hexane): 2121 w, 2113 m, 2086 s, 2058 s, 2044 s, 2028 s, 2020 m, 2004 s, 1987 m, 1968 cm<sup>-1</sup>. <sup>1</sup>H-NMR (CDCl<sub>3</sub>, -40 °C): major isomer, 3.42 (m, 2H), 2.43 (m, 2H), 1.76 (m, 2H), -15.12 (s, 1H), -15.93 (s, 1H) ppm; minor isomers, -13.76 (s, 1H), -16.06 (s, 1H) and -14.29 (s, 1H), -16.07 (s, 1H) ppm.

**Data for 3:** Anal. Calcd for C<sub>13</sub>H<sub>8</sub>BrNO<sub>9</sub>Os<sub>3</sub>: C, 16.05; H, 0.82; N, 1.44. Found: C, 16.20; H, 0.91; N, 1.44. IR (ν(CO) in hexane): 2019 m, 2113 m, 2085 s, 2058 vs, 2045 s, 2028 s, 2020 m, 2004 s, 1987 m, 1970 w cm<sup>-1</sup>. <sup>1</sup>H-NMR (CDCl<sub>3</sub> at -40 °C): major isomer, 3.43 (m, 2H), 2.45 (m, 2H), 1.78 (m, 2H), -15.67 (s, 1H), -15.98 (s, 1H) ppm; minor isomers, -14.25 (s, 1H), -16.12 (s, 1H) and -14.84 (s, 1H), -16.67 (s, 1H) ppm. The pyrrolidine ring protons overlap with major isomers for **2** and **3**. <sup>13</sup>C-NMR (CDCl<sub>3</sub>, at -40 °C, carbonyl region): 165.28 (dd, <sup>2</sup>J(<sup>1</sup>H-<sup>13</sup>C) = 5.2 and 11.1 Hz), 167.01 (dd, <sup>2</sup>J(<sup>1</sup>H-<sup>13</sup>C) = 6.1 and 11.9 Hz), 169.68 (t, <sup>2</sup>J(<sup>1</sup>H-<sup>13</sup>C) < 2 Hz), 172.08 (s), 173.47 (d, <sup>2</sup>J(<sup>1</sup>H-<sup>13</sup>C) = 3.1 Hz), 175.58 (d, <sup>2</sup>J(<sup>1</sup>H-<sup>13</sup>C) = 9.0 Hz), 175.79 (d, <sup>2</sup>J(<sup>1</sup>H-<sup>13</sup>C) < 2 Hz), 176.42 (d, <sup>2</sup>J(<sup>1</sup>H-<sup>13</sup>C) = 8.2 Hz), 176.81 (d, <sup>2</sup>J(<sup>1</sup>H-<sup>13</sup>C) = 2.9 Hz) ppm.

**Synthesis of (μ-H)<sub>2</sub>Os<sub>3</sub>(CO)<sub>9</sub>(μ-η<sup>2</sup>-C=NCH<sub>2</sub>CH<sub>2</sub>CH<sub>2</sub>)-(CF<sub>3</sub>CO<sub>2</sub>) (4).** To a methylene chloride (2.0 mL) solution of **1** (40 mg, 0.045 mmol) was added trifluoroacetic acid (20 μL, 0.26 mmol) by syringe under a nitrogen atmosphere. The solution was allowed to slowly evaporate at -20 °C to one-half of its original volume at which time large yellow prisms of **4** formed which were isolated and washed with hexane to yield 26 mg of **4** (57.5%). Anal. Calcd for C<sub>15</sub>H<sub>8</sub>F<sub>3</sub>NO<sub>11</sub>Os<sub>3</sub>: C, 17.9; H, 0.80; N, 1.39. Found: C, 17.72; H, 0.78; N, 1.42. IR (ν(CO) in CH<sub>2</sub>Cl<sub>2</sub>): 2056 s, 2039 m, br, 2021 m, 1996 m cm<sup>-1</sup>; (carboxyl) 1695 cm<sup>-1</sup>. <sup>1</sup>H-NMR (CDCl<sub>3</sub>, -20 °C): major isomer, 3.48 (m, 2H), 2.32 (m, 2H), 1.76 (m, 2H), -14.38 (s, 1H), -16.03 (s, 1H) ppm; minor isomer, -13.01 (s, 1H), -16.15 (s, 1H) ppm. <sup>19</sup>F-NMR (referenced to CF<sub>3</sub>CO<sub>2</sub>H, -20 °C): major isomer, 1.99 ppm; minor isomer, 2.02 ppm (ratio 4.8:1). <sup>13</sup>C-NMR: data in text.

**Preparation of (μ-H)<sub>2</sub>Os<sub>3</sub>(CO)<sub>9</sub>(μ-η<sup>2</sup>-C=NCH<sub>2</sub>CH<sub>2</sub>CH<sub>2</sub>)<sup>+</sup>X<sup>-</sup> (5) (X = BF<sub>4</sub><sup>-</sup>, SbF<sub>6</sub><sup>-</sup>).** Solutions of **1** (30 mg, 0.033 mmol) in 1.0 mL of CD<sub>2</sub>Cl<sub>2</sub> were treated with 85% HBF<sub>4</sub>·Et<sub>2</sub>O (40 μL, 0.27 mmol) or AgSbF<sub>6</sub> (12 mg, 0.035 mmol) in 0.5 mL of CD<sub>2</sub>Cl<sub>2</sub>. The solution treated with AgSbF<sub>6</sub> was filtered under an inert atmosphere into an NMR tube. The <sup>1</sup>H-NMR of the solution treated with HBF<sub>4</sub>·Et<sub>2</sub>O was determined, and both solutions gave identical <sup>1</sup>H-NMR spectra. Both solutions yielded powders on cooling at -20 °C which could be isolated as analytically pure materials. Anal. Calcd for C<sub>13</sub>H<sub>8</sub>F<sub>6</sub>NO<sub>9</sub>Os<sub>3</sub>Sb: C, 13.47; H, 0.69; N, 1.21. Found: C, 14.48; H,

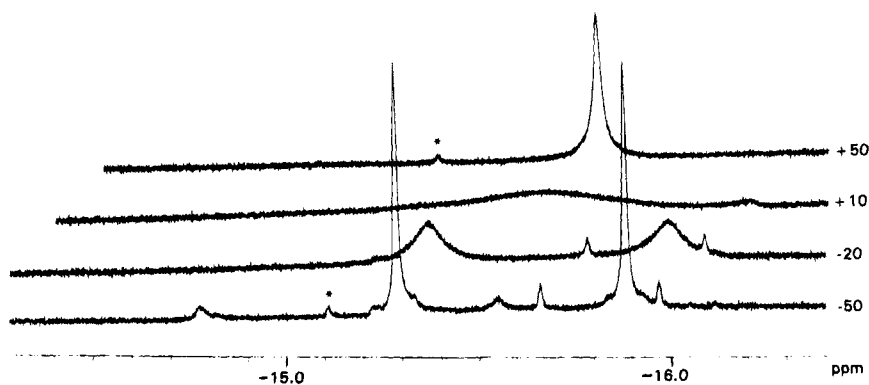


Figure 9. VT- $^1\text{H}$ -NMR of **8** in the hydride region at 360 MHz (asterisk denotes slight impurity).

0.74; N, 1.28. Anal. Calcd for  $\text{C}_{13}\text{H}_3\text{BF}_4\text{NO}_9\text{Os}_3$ : C, 15.94; H, 0.82; N, 1.43. Found: C, 16.19; H, 0.76; N, 1.38.  $^1\text{H}$ -NMR ( $\text{CD}_2\text{Cl}_2$ ,  $-20^\circ\text{C}$ ) of **5**: 3.45 (m, 2H), 2.34 (m, 2H), 1.78 (m, 2H),  $-17.01$  (s, 1H),  $-19.93$  (s, 1H) ppm.  $^{13}\text{C}$ -NMR ( $-20^\circ\text{C}$  in  $\text{CD}_2\text{Cl}_2$ , carbonyl region): 157.38 (dd, 2C,  $^2J(^1\text{H}-^{13}\text{C}) = 12.5$  Hz,  $< 2$  Hz), 160.85 (s, 1C), 164.09 (s, 1C), 168.54 (d, 1C,  $^2J(^1\text{H}-^{13}\text{C}) = 7.5$  Hz), 169.25 (s, 1C), 169.22 (s, 1C), 170.56 (d, 1C,  $^2J(^1\text{H}-^{13}\text{C}) = 8.0$  Hz), 174.74 (s, 1C) ppm.

**Treatment of 1 with  $\text{CF}_3\text{SO}_3\text{H}$ : Preparation of  $(\mu\text{-H})_2\text{Os}_3(\text{CO})_9(\mu\text{-}\eta^2\text{-C}=\text{NCH}_2\text{CH}_2\text{CH}_2)\text{CF}_3\text{SO}_3$  (**6**).** To 0.5 mL of a  $\text{CDCl}_3$  solution of **1** (30.0 mg, 0.033 mmol) was added by microsyringe 1.0  $\mu\text{L}$  of  $\text{CF}_3\text{SO}_3\text{H}$  (0.017 mmol) in a 5 mm NMR tube under an  $\text{N}_2$  atmosphere (septum capped). The  $^1\text{H}$ -NMR was monitored from  $-20$  to  $+22^\circ\text{C}$ , and then an additional 1.5  $\mu\text{L}$  was added and spectra were obtained again in the same temperature range. After the addition of 1 equiv of acid, only resonances associated with **6** and **5** could be detected.  $^1\text{H}$ -NMR data for **6** at  $-40^\circ\text{C}$  in  $\text{CDCl}_3$ : major isomer, 3.48 (m, 2H), 2.43 (m, 2H), 1.70 (m, 2H),  $-14.08$  (s, 1H),  $-16.02$  (s, 1H) ppm; minor isomer,  $-12.83$  (s, 1H),  $-16.13$  (s, 1H) ppm.  $^{19}\text{F}$ -NMR data for **6** (referenced to external  $\text{CF}_3\text{COOH}$ ) at  $-40^\circ\text{C}$  in  $\text{CDCl}_3$ : major isomer, 2.79 ppm; minor isomer 2.75 ppm (ratio 4.2:1).

**Thermolysis of 3.** A benzene (50 mL) solution of **4** (51.7 mg, 0.053 mmol) was heated for 24 h at  $40\text{--}50^\circ\text{C}$  in an oil bath under a CO atm. The reaction was monitored by analytical thin-layer chromatography (silica gel, 1:4,  $\text{CH}_2\text{Cl}_2$ /hexane), and almost all of **3** was consumed after this period. The solvent was rotary evaporated, the residue was taken up in  $\sim 1.0$  mL of  $\text{CH}_2\text{Cl}_2$ , and the solution was applied to preparative thin-layer chromatography (silica gel). After two elutions with 3:7  $\text{CH}_2\text{Cl}_2$ /hexane three major bands were resolved. The top band was shown to be  $(\mu\text{-H})(\mu\text{-Br})\text{Os}_3(\text{CO})_{10}$  (**7**, 7.5 mg, 14%) by IR and  $^1\text{H}$ -NMR,<sup>14</sup> the middle band proved to be **1** (15.5 mg, 32%), and the third band was **8** (24.1 mg, 46%). Similar products were obtained under a nitrogen atmosphere but in much lower yields and with small amounts of  $\text{H}_2\text{Os}_3(\text{CO})_{10}$  as a coproduct.

**Analytical Data for 8.** IR ( $\nu(\text{CO})$  in hexane): 2118 m, 2088 s, 2064 vs, 2054 s, 2022 vs, 2009 s, 1987 m, 1968  $\text{cm}^{-1}$ .  $^1\text{H}$ -NMR in  $\text{CDCl}_3$  at  $-50^\circ\text{C}$ : major isomer, 3.46 (m, 2H), 2.49 (m, 2H), 1.74 (m, 2H),  $-15.29$  (s, 1H),  $-15.89$  (s, 1H) ppm; minor isomers,  $-14.79$  (s, 1H),  $-15.56$  (s, 1H) and  $-15.67$  (s, 1H),  $-15.98$  (s, 1H) ppm.  $^{13}\text{C}$ -NMR in  $\text{CDCl}_3$  at  $-40^\circ\text{C}$  (carbonyl region, proton decoupled): major isomer, 165.51 (1C), 167.71 (1C), 169.62 (1C), 174.72 (2C), 175.03 (1C), 175.07 (1C), 175.61 (1C), 177.12 (1C) ppm.

**X-ray Structure Determination of 3, 4, and 8.** Crystals of **3**, **4**, and **8** for X-ray examination were obtained from saturated solutions of each in hexane/dichloromethane solvent systems at  $-20^\circ\text{C}$ . Suitable crystals of each were mounted on glass fibers, placed in a goniometer head on an Enraf-Nonium CAD4 diffractometer, and centered optically. Unit cell parameters and an orientation matrix for data collection were obtained by using the centering program in the CAD4 system. Details of the crystal data are given in Table 1. For each crystal, the actual scan range was calculated by scan width = scan range +  $0.35 \tan \theta$  and backgrounds were measured by using the crystal-moving counter technique at the beginning and end of each scan. Two or three representative reflections were monitored every 2 h as a check on instrument and crystal stability, and an additional two reflections were monitored for crystal orientation control. Lorentz, polarization, and decay corrections were applied as was an empirical absorption correction based on a series of  $\psi$  scans.

Each of the structures was solved by the Patterson method using SHELXS-86,<sup>20</sup> which revealed the positions of the metal atoms. All other non-hydrogen atoms were found by successive difference Fourier synthesis. Hydrogens on the pyrrolidine ring were placed in their calculated positions for compound **4** and bridging hydride ligand positions were obtained from different Fourier sections for all three compounds. The hydrides were located by taking 10–15 Fourier sections above and below the triosmium plane. In the low-temperature structure determinations (**3**, **4**, **8**), the electron density corresponding to the hydrides was distinct and separate from the other residual electron density in the Fourier map. The uncertainty in the position of the hydrides determined from this Fourier analysis technique is estimated to be about 0.07 Å, from the reproducibility of determinations. The hydride positions discovered in this manner differed by 0.1–0.5 Å from those calculated using HYDEX.<sup>11,16</sup> The positions of all hydrides thus determined were incorporated in the final least-squares refinements as fixed atoms. Hydrogen atom positions were included in the structure factor calculations but not refined, in the final least-squares cycles. Metal atoms were refined anisotropically as were some of the other non-hydrogen atoms depending upon the quality of the crystal and quality and quantity of data.

In compounds **3** and **8**, the crystals contained several isomers. The major isomers were those with hydride ligands bridging the Os–Os edges under the pyrrolidine ring and the edge containing the osmium atom bonded to the carbon of the pyrrolidine ring and their enantiomers. Other isomers included those in which the hydride ligand bridge was on the Os–Os edge to which the nitrogen was bonded. Attempts were made but it was not possible to model the pyrrolidine ring disorder adequately in order to determine percentage populations of isomers. Altering the populations of these isomers over

(14) Churchill, M. R.; Lashewycz, R. A. *Inorg. Chem.* **1979**, *18*, 3261.

(15) Bryan, E. G.; Jackson, W. G.; Johnson, B. F. G.; Kelland, J. W.; Lewis, J.; Schorpp, K. T. *J. Organometal. Chem.* **1976**, *108*, 385.

(16) Orpen, A. G. *J. Chem. Soc., Dalton Trans.* **1980**, 2509.

(17) Keister, J. B.; Shapley, J. R. *Inorg. Chem.* **1982**, *21*, 3304.

(18) Rosenberg, E. *Polyhedron* **1989**, *8*, 383.

(19) Keister, J. B.; Frey, V.; Zbinden, D.; Merbach, A. E. *Organometallics* **1991**, *10*, 1497.

(20) Sheldrick, G. M. *Acta Crystallogr.* **1990**, 467–473.

a significant range did not lead to a better refinement of the data. Final refinement parameters for each crystal are listed in Table 1.

Scattering factors were taken from Cromer and Waber.<sup>21</sup> Anomalous dispersion corrections were those of Cromer.<sup>22</sup> All calculations were carried out on a DEC MicroVAX II computer using the Molen system of programs for data reduction, decay and absorption corrections, and refinement except for compound **4**, which was refined and completed by using SHELXL-93.<sup>23</sup>

**Acknowledgment.** We gratefully acknowledge the National Science Foundation (E.R., Grants CHE-

9016495 and CHE-9319062) for support and for a Chemical Instrumentation Grant (CHE 9302468) for purchase of a 400 MHz NMR. We also thank the NATO Science Program for a travel grant (E.R. and L.M., 27505) and the CNR, Italy (L.M.).

**Supplementary Material Available:** Tables 8–10, listing anisotropic displacement factors, and Tables 11–13, listing complete bond distances and angles, for **3**, **4**, and **8** (19 pages). Ordering information is given on any current masthead page.

OM9408270

---

(21) Cromer, D. T.; Waber, J. T. *International Tables for X-Ray Crystallography*; The Kynoch Press: Birmingham, England, 1974; Vol. IV, Table 2.2B.

---

(22) Cromer, D. T. *International Tables for X-Ray Crystallography*; The Kynoch Press: Birmingham, England, 1974; Vol. IV, Table 2.3.1.

(23) Sheldrick, G. M. Program for Structure Refinement, University of Gottingen, Germany, 1993.

# New Diphosphine Ligands Based on Heterocyclic Aromatics Inducing Very High Regioselectivity in Rhodium-Catalyzed Hydroformylation: Effect of the Bite Angle

Mirko Kranenburg, Yuri E. M. van der Burgt, Paul C. J. Kamer, and Piet W. N. M. van Leeuwen\*

*J. H. van 't Hoff Research Institute, Department of Inorganic Chemistry, University of Amsterdam, Nieuwe Achtergracht 166, 1018 WV Amsterdam, The Netherlands*

Kees Goubitz and Jan Fraanje

*Amsterdam Institute for Molecular Studies, Department of Crystallography, University of Amsterdam, Nieuwe Achtergracht 166, 1018 WV Amsterdam, The Netherlands*

Received February 8, 1995<sup>⊗</sup>

The effect of the bite angle on regioselectivity in the rhodium-catalyzed hydroformylation reaction was studied with a series of bidentate diphosphines based on xanthene-like backbones as ligands. The bite angles of these ligands are fine-tuned by subtle alterations of the backbone of the ligands. When the bridge (X) in the 10-position of xanthene is varied, the bite angle as calculated from molecular mechanics increases stepwise from 102 to 131°, whereas the changes in steric bulk and electronic effects are virtually absent for the following ligands: bis(2-(diphenylphosphino)phenyl) ether (DPEphos, **1**), X = H; 4,6-bis(diphenylphosphino)-10,10-dimethylphenoxasilin (Sixantphos, **2**), X = Si(CH<sub>3</sub>)<sub>2</sub>; 2,8-dimethyl-4,6-bis(diphenylphosphino)phenoxathiin (Thixantphos, **3**), X = S; 9,9-dimethyl-4,6-bis(diphenylphosphino)xanthene (Xantphos, **4**), X = C(CH<sub>3</sub>)<sub>2</sub>; 4,6-bis(diphenylphosphino)dibenzofuran (DBFphos, **5**), X = bond. In the hydroformylation of 1-octene the regioselectivity increased regularly with increasing bite angle: at 40 °C up to 98.3% *n*-aldehyde was obtained with Xantphos, without isomerization or hydrogenation of 1-octene. DBFphos does not form chelates, and consequently no increased selectivity was observed. The selectivity of the catalyst was almost unaffected by raising of the temperature to 80 °C, resulting in a higher turnover frequency (tof) with a constant selectivity: 97.7% *n*-aldehyde, 0.5% isomerization, and a tof value of 800 mol (mol of Rh)<sup>-1</sup> h<sup>-1</sup>. Xantphos induces the highest selectivity for the formation of the linear aldehyde reported for diphosphines in the hydroformylation of 1-alkenes until now. The complexes (diphosphine)Rh(H)(CO)(PPh<sub>3</sub>) and (diphosphine)-Rh(H)(CO)<sub>2</sub> were prepared and identified with <sup>1</sup>H, <sup>31</sup>P, and <sup>13</sup>C NMR. The enhanced selectivity to the linear aldehyde was also observed for styrene (70% *n*-aldehyde with xantphos compared to 11% with triphenylphosphine). An X-ray crystal structure of the Xantphos ligand is presented (orthorhombic, space group *Pbnm*, with *a* = 8.7678(8) Å, *b* = 18.967(1) Å, *c* = 19.181(1) Å, *V* = 3189.8(4) Å<sup>3</sup>, and *Z* = 4).

## Introduction

Hydroformylation of alkenes is one of the most important homogeneously catalyzed reactions in industry.<sup>1–5</sup> Much effort has been made to enhance the regioselectivity of the reaction toward the formation of the more desirable normal aldehyde and to minimize the undesired side reaction of isomerization of the

substrate alkene. The rhodium phosphine catalysts, introduced by Wilkinson,<sup>6,7</sup> have been shown to be more selective, and they give higher rates under milder conditions than the older cobalt carbonyl catalysts. The generally accepted mechanism for the dissociative pathway as proposed by Wilkinson, a modification of the reaction mechanism as proposed by Heck and Breslow for the cobalt-catalyzed hydroformylation,<sup>8</sup> is shown in Scheme 1.

The steric and electronic properties of the ligands have a dramatic influence on the reactivity of organometallic complexes. The concept of the cone angle as a measure for the steric bulk of monodentate phosphine

<sup>⊗</sup> Abstract published in *Advance ACS Abstracts*, May 15, 1995.

(1) Parshall, G. W. *Homogeneous Catalysis: The Applications and Chemistry of Catalysis by Soluble Transition Metal Complexes*; Wiley: New York, 1980.

(2) Tkatchenko, I. In *Comprehensive Organometallic Chemistry*; Wilkinson, G., Stone, F. G. A., Abel, E. W., Eds.; Pergamon: Oxford, U.K., 1981; Vol. 8, pp 101–223.

(3) Tolman, C. A.; Faller, J. W. In *Homogeneous Catalysis with Metal Phosphine Complexes*; Pignolet, L. H., Ed.; Plenum: New York, 1983; pp 81–109.

(4) Masters, C. In *Homogeneous Transition-Metal Catalysis—A Gentle Art*; Chapman and Hall: London, 1981; pp 120–128.

(5) Mortreux, A.; Petit, F. In *Catalysis by Metal Complexes*; Ugo, R., James, B. R., Eds.; D. Reidel: Dordrecht, The Netherlands, 1988.

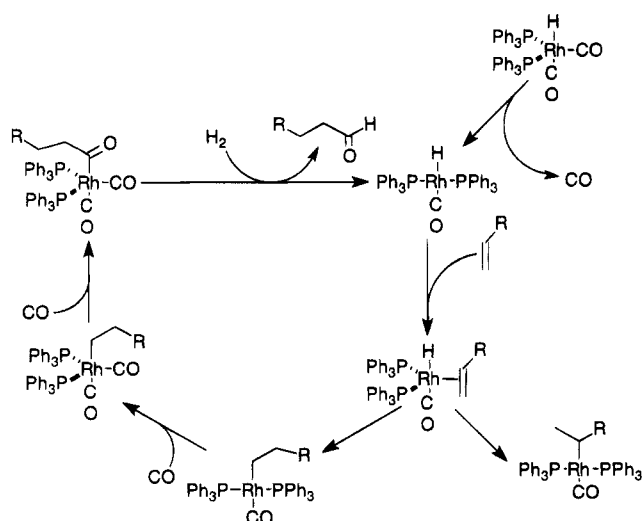
(6) Evans, D.; Yagupsky, G.; Wilkinson, G. *J. Chem. Soc. A* **1968**, 2660–2665.

(7) Brown, C. K.; Wilkinson, G. *J. Chem. Soc. A* **1970**, 2753–2764.

(8) Heck, R. F.; Breslow, D. S. *J. Am. Chem. Soc.* **1961**, *83*, 4023–4027.



Scheme 1



and phosphite ligands, introduced by Tolman,<sup>9</sup> has been widely accepted and applied in the development of new ligands.

Increasing the steric bulk of monodentate phosphines, i.e. increasing the cone angle, leads to higher regioselectivity in the hydroformylation.<sup>10</sup> Bulky phosphite and diphosphite ligands have been proven to be very successful for obtaining high normal to iso ratios,<sup>11,12</sup> although the monodentates also cause significant isomerization.<sup>11</sup> Work in our group has shown that bulky monophosphites can induce extremely high reaction rates,<sup>13,14</sup> whereas bulky diphosphites can give rise to good enantioselectivity.<sup>15-17</sup>

The effect of diphosphines on selectivity in rhodium-catalyzed hydroformylation has been studied by Hughes and Unruh.<sup>18</sup> They found that rhodium complexes formed from the reaction of  $(PPh_3)_3Rh(H)(CO)$  with various rigid chelating diphosphines led to increased linear to branched ratios when the ligand to rhodium ratio was 1.5 or higher. They proposed a mechanism in which three phosphines are coordinated to rhodium at the point where the aldehyde regiochemistry is determined. The complex proposed to account for this increase in linear to branched ratio is a dimeric rhodium complex, in which two ligands are chelating to one rhodium center, while one ligand is bridging between two rhodium centers (see Figure 1). This complex was later actually observed by <sup>31</sup>P NMR.<sup>19</sup>

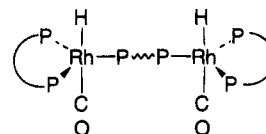
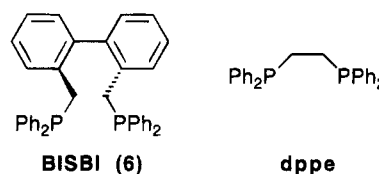


**Figure 1.** Bridged dimeric species as proposed by Hughes and Unruh.

An increase of rate due to possible intramolecular binuclear elimination, as observed by Stanley and co-workers,<sup>20,21</sup> was not found for these systems.

An important recent study by Casey and co-workers has indicated that the bite angle of bidentate diphosphines can have a dramatic influence on the regioselectivity of the rhodium-catalyzed hydroformylation of 1-alkenes. For the bis-equatorially coordinated 2,2'-bis((diphenylphosphino)methyl)-1,1'-biphenyl (BISBI; **6**), a linear to branched aldehyde ratio as high as 66:1 was reported, while the equatorially-axially coordinating (i.e.  $\angle P-Rh-P = 90^\circ$ ) 1,2-bis(diphenylphosphino)ethane (dpe) gave a linear to branched ratio of only 2.1.<sup>22,23</sup>



The observed selectivity is likely to be due to the bite angles of the ligands, but so far no detailed study has been done on the effect of subtle changes of the bite angle in a series of ligands with similar electronic properties and steric size, thus solely examining the influence of the bite angle.

Here we present a study of the effect of the bite angle alone in a series of new bidentate diphosphines, based on xanthene-like backbones, on the regioselectivity in the rhodium-catalyzed hydroformylation reaction. The bite angles of these ligands are fine-tuned by subtle alterations in the backbone of the ligands.

## Results and Discussion

**Molecular Mechanics.** We used molecular mechanics in our development of new bidentate diphosphines. The natural bite angle ( $\beta_n$ ) and flexibility range of new candidates were calculated using the Sybyl program<sup>24</sup> with an augmented TRIPOS force field, analogously to the method used by Casey and Whiteker.<sup>25</sup> The natural bite angle is defined as the preferred chelation angle determined only by ligand backbone constraints and not by metal valence angles. The flexibility range is defined as the accessible range of bite angles within less than 3 kcal mol<sup>-1</sup> excess strain energy from the calculated natural bite angle.

To examine the effect of the bite angle on the selectivity in rhodium-catalyzed hydroformylation, we

(9) Tolman, C. A. *Chem. Rev.* **1977**, *77*, 313-348.

(10) Pruet, R. L. In *Advances in Organometallic Chemistry*; Stone, F. G. A., West, R., Eds.; Academic Press: New York, 1979; Vol. 17, pp 1-60.

(11) Trzeciak, A. M.; Ziolkowski, J. J. *J. Mol. Catal.* **1988**, *48*, 319-324.

(12) Cuny, G. D.; Buchwald, S. L. *J. Am. Chem. Soc.* **1993**, *115*, 2066-2068.

(13) van Rooy, A.; Orij, E.; Kamer, P. C. J.; van Leeuwen, P. W. N. M. *Organometallics* **1995**, *14*, 34-43.

(14) van Rooy, A.; Orij, E. N.; Kamer, P. C. J.; van den Aardweg, F.; van Leeuwen, P. W. N. M. *J. Chem. Soc., Chem. Commun.* **1991**, 1096-1097.

(15) Babin, J. E.; Whiteker, G. T. PCT Int. Appl. WO 93/03839; U.S. Patent 911,518 (to Union Carbide), 1992.

(16) Buisman, G. J. H.; Kamer, P. C. J.; van Leeuwen, P. W. N. M. *Tetrahedron: Asymmetry* **1993**, *4*, 1625-1634.

(17) van Leeuwen, P. W. N. M.; Buisman, G. J. H.; van Rooy, A.; Kamer, P. C. J. *Recl. Trav. Chim. Pays-Bas* **1994**, *113*, 61-62.

(18) Hughes, O. R.; Unruh, J. D. *J. Mol. Catal.* **1981**, *12*, 71-83.

(19) Hughes, O. R.; Young, D. A. *J. Am. Chem. Soc.* **1981**, *103*, 6636-6642.

(20) Laneman, S. A.; Stanley, G. G. *Adv. Chem. Ser.* **1992**, No. 230, 349-366.

(21) Broussard, M. E.; Juma, B.; Train, S. G.; Peng, W.-J.; Laneman, S. A.; Stanley, G. G. *Science* **1993**, *260*, 1784-1788.

(22) Devon, T. J.; Philips, G. W.; Puckette, T. A.; Stavinocha, J. L.; Vanderbilt, J. J. U.S. Patent 4,694,109 (to Eastman Kodak), 1989.

(23) Casey, C. P.; Whiteker, G. T.; Melville, M. G.; Petrovich, L. M.; Gavney, J.; Powell, D. R. *J. Am. Chem. Soc.* **1992**, *114*, 5535-5543.

(24) Sybyl 6.03; Tripos Associates, 1699 S. Hanley Road, Suite 303, St. Louis, MO 63144.

(25) Casey, C. P.; Whiteker, G. T. *Isr. J. Chem.* **1990**, *30*, 299-304.

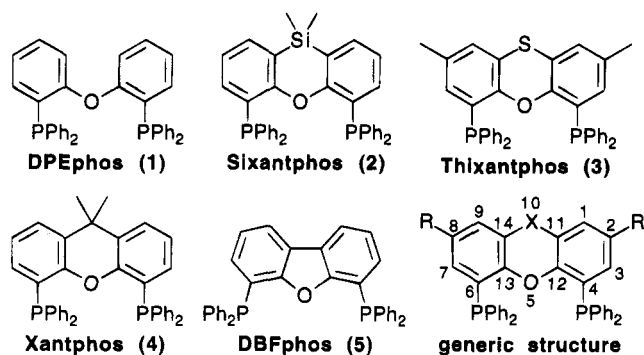


**Figure 2.** Ligands studied in this work and generic structure showing numbering scheme.

**Table 1. Calculated Natural Bite Angle and Flexibility Range for the Ligands 1–5**

ligand name	X	R	$\beta_n,^\circ$ deg	flexibility range, <sup>a</sup> deg
DPEphos (1)	H, H	H	102.2	86–120
Sixantphos (2)	Si(CH <sub>3</sub> ) <sub>2</sub>	H	108.7	93–132
Thixantphos (3)	S	CH <sub>3</sub>	109.4	94–130
Xantphos (4)	C(CH <sub>3</sub> ) <sub>2</sub>	H	111.7	97–135
DBFphos (5)	bond	H	131.1	117–147

<sup>a</sup> See text.

developed a series of new bidentate ligands based on rigid heterocyclic xanthene-like aromatics. By varying the bridge in the 10-position (Figure 2 and Table 1), we were able to induce small variations in the bite angle.

According to our molecular mechanics calculations, these ligands have natural bite angles ranging from 102 to 131° and a flexibility range of ca. 35°.

**Ligand Synthesis.** The ligands were easily obtained in good yields (typically 70–80%) by deprotonation of the backbones with 3 equiv of *sec*-butyllithium/TMEDA in ether. Due to the presence of the ether oxygen, selective dilithiation at the positions *ortho* to the ether bridge takes place.<sup>26,27</sup> The dilithiated species is then reacted with chlorodiphenylphosphine. Washing with water to remove lithium salts, followed by washing with hexanes to remove *sec*-butyldiphenylphosphine, yielded the pure product as a powder. No purification by column chromatography is necessary, but all ligands were recrystallized before utilization in catalysis. These reaction conditions lead to a considerably more efficient synthesis of DBFphos, for which Haenel and co-workers<sup>28</sup> reported a yield of 50% after repeated recrystallizations to remove the monophosphine. The ligands are very stable and insensitive toward oxidation by air, both in solution and in the solid phase.

The X-ray crystal structure of the free Xantphos ligand is shown in Figure 3. The symmetric unit contains a half-molecule, with four atoms (O, C1, C2, and C3) at special positions on a mirror plane. The structure clearly shows that only very little adjustment of the structure is necessary to form a chelate; the orientation of the diphenylphosphine moieties is nearly ideal. The observed P···P distance in the free ligand is 4.080 Å, while MM studies indicate that a decrease of the P···P distance to 3.84 Å is necessary for chelation

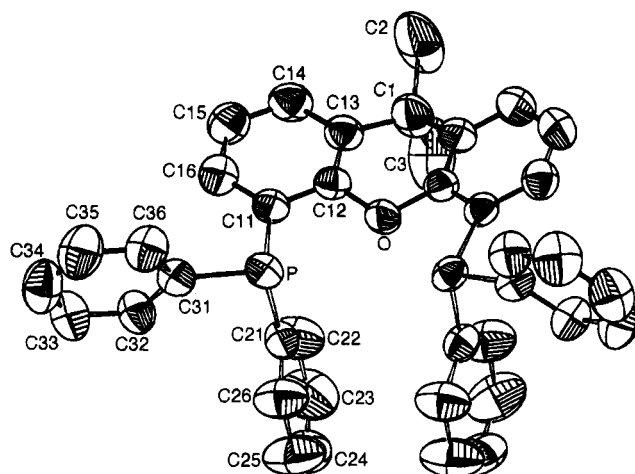


**Figure 3.** ORTEP representation of the Xantphos ligand. Thermal ellipsoids are drawn at the 50% probability level.

with a P–Rh–P angle of 111.7°, a decrease of only 0.24 Å. The P atoms are brought together by means of a slight decrease of the angle between the two phenyl planes in the backbone of the ligand from ca. 166 to 158°.

The <sup>13</sup>C NMR spectra of free Xantphos, Thixantphos, and Sixantphos all show a virtual triplet signal for *C-ipso* on the backbone. This resonance is the result of a through-space coupling of the two phosphorus atoms. The orientation of the lone pairs of the two phosphorus atoms is such that it causes degeneracy of the magnetic resonances of the P nuclei. In the <sup>13</sup>C NMR the degenerate magnetic resonance of the phosphorus causes the *ipso* carbon atom to couple with the two phosphorus atoms, with observed <sup>1</sup>J<sub>13C–P</sub> coupling constants of 40–60 Hz. This type of coupling has been reported for bulky diphosphites as an eight-bond coupling by Pastor and co-workers.<sup>29</sup> By simulation of the NMR spectra (using geNMR software<sup>30</sup>) it was possible to define a minimal P–P coupling for these ligands; a smaller coupling would lead to second-order signals above the noise level. The appearance of this P–P coupling is a strong indication that the structure in solution of the free ligands is similar to the crystal structure of Xantphos. This through-space coupling is not observed for DPEphos (due to the absence of such a rigid backbone) and DBFphos (in which the P···P distance is apparently too large: MM calculations gave P···P = 5.760 Å; PM3 calculations gave P···P = 5.956 Å).

Since electronic effects of the variations in the backbone are expected to be small<sup>9</sup> and the steric sizes of the substituents on phosphorus are identical in all ligands, the effect of solely the P–Rh–P chelation angle can be studied in detail.

**Hydroformylation of 1-Octene.** We tested the selectivity of our ligands in the rhodium-catalyzed hydroformylation of 1-octene. Work by Hughes and Unruh<sup>18</sup> on the effect of different ligand to rhodium ratios for bidentate diphosphines on the observed selectivity led us to investigate the optimal ligand to rhodium ratio for our ligands. Table 2 represents the data for Thixantphos as an example.

(26) Gschwend, H. W.; Rodriguez, H. R. *Org. React.* **1979**, *26*, 1–360.

(27) Schwarz, E. B.; Knobler, C. B.; Cram, D. J. *J. Am. Chem. Soc.* **1992**, *114*, 10775–10784.

(28) Haenel, M. W.; Jakubik, D.; Rothenberger, E.; Schroth, G. *Chem. Ber.* **1991**, *124*, 1705–1710.

(29) Pastor, S. D.; Shum, S. P.; Rodebaugh, R. K.; Debellis, A. D. *Helv. Chim. Acta* **1993**, *76*, 900–914.

(30) Budzelaar, P. H. M., geNMR 3.5M; IvorySoft, Amerbos 330, 1025 AV Amsterdam, the Netherlands.

**Table 2. Results of the Rhodium-Catalyzed Hydroformylation of 1-Octene with the Thixantphos Ligand at Different Ligand to Rhodium Ratios<sup>a</sup>**

L/Rh ratio	normal/ branched	% <i>n</i> -aldehyde
1.1	5.7	85.1
2.0	40.5	97.6
2.2	47.6	97.9
5.0	45.1	97.8
10.0	45.4	97.8

<sup>a</sup> Conditions:  $T = 40\text{ }^{\circ}\text{C}$ ,  $\text{CO}/\text{H}_2 = 1$ ,  $p(\text{CO}/\text{H}_2) = 10\text{ bar}$ , substrate/Rh = 674,  $[\text{Rh}] = 1.78\text{ mM}$ . In all cases the percent isomerization was <1 and the percent hydrogenation was zero.

L/Rh ratios from 1.1 to 10 were examined, and an optimum was found at 2.2. A higher ratio did not lead to improved regio- or chemoselectivity.

Molecular modeling studies, as well as CPK or Dreiding molecular models, show that due to the rigid structure of the ligands the presence of a binuclear species as proposed by Hughes and Unruh (see Figure 1) is very unlikely. Furthermore, a third phosphine ligand is readily replaced with carbon monoxide under an atmosphere of CO (see below). The observed optimal L/Rh ratio is probably the result of a dissociation equilibrium and is dependent on the absolute concentration.

We chose the following standard conditions to compare the selectivity and activity of the ligands:  $T = 40\text{ }^{\circ}\text{C}$ ,  $\text{CO}/\text{H}_2 = 1$ ;  $p(\text{CO}/\text{H}_2) = 10\text{ bar}$ , ligand/Rh = 2.2, substrate/Rh = 674,  $[\text{Rh}] = 1.78\text{ mM}$  (see Table 3).

DPEphos, with a calculated natural bite angle of  $102.2^{\circ}$ , induced an enhanced selectivity (compared to most diphosphines), but this selectivity was not very pronounced. The ligands with a one-atom bridge between C(11) and C(14) (Sixantphos, X = Si(CH<sub>3</sub>)<sub>2</sub>; Thixantphos, X = S; Xantphos, X = C(CH<sub>3</sub>)<sub>2</sub>) having a calculated natural bite angle near  $110^{\circ}$  showed a very high regioselectivity and a very low rate of isomerization to internal alkenes. DBFphos, with a calculated natural bite angle of  $131.1^{\circ}$ , proved not to be very selective.

Under these mild reaction conditions, the selectivities toward the linear aldehyde observed for Sixantphos, Thixantphos, and especially Xantphos are somewhat higher than that observed for BISBI. This is mainly due to the very low selectivity to isomerization of 1-octene. The normal to branched ratios of our ligands are very close to that of BISBI. Furthermore, no hydrogenation was observed.

Upon raising the temperature to  $80\text{ }^{\circ}\text{C}$ , we observed a large increase in the rate of the reaction (Table 4); the turnover frequency increases by a factor of 38 (for Sixantphos) to 80 (for Xantphos). The selectivity of the reaction, however, has hardly changed at this higher temperature. Hydrogenation is still not detected, the normal to branched ratios decrease slightly, and a slight increase of isomerization is observed. Especially for Xantphos, these effects are very small. The normal to branched ratio decreases from 57.1 to 53.5, with an increase of isomerization from 0% to 0.5%, resulting in a net decrease of selectivity for the formation of the linear aldehyde of only 0.5%.

At this temperature the difference between BISBI and our more rigid ligands becomes more pronounced. Even though the normal to branched ratio increases from 58.2 to 80.5 for BISBI, the selectivity toward the linear aldehyde decreases from 95.5% to 89.6%. This is a

result of the large increase of the selectivity to isomerization of 1-octene to 2-octene from 2.9% to 9.3%.

The increase of the linear to branched ratio in aldehyde with an increasing amount of isomerization is due to an increased tendency of the branched alkyl species to form the 2-alkene instead of the branched aldehyde (Scheme 2). In spite of the fact that the proportion of branched alkyl is higher at  $80\text{ }^{\circ}\text{C}$ , the net result is a higher normal to branched ratio. A similar effect was observed by Hughes and Unruh for other rigid ligands, based on cycloalkane backbones.<sup>18</sup>

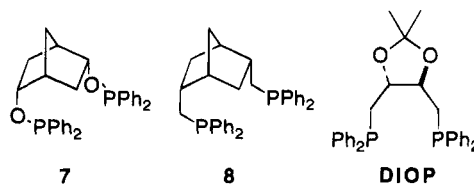
According to MM calculations, BISBI is very flexible; we calculated a natural bite angle of  $122.6^{\circ}$  and a flexibility range of  $101\text{--}148^{\circ}$  for a rhodium complex, while Casey and co-workers calculated a natural bite angle of  $113^{\circ}$  and a flexibility range of  $92\text{--}155^{\circ}$ .<sup>23</sup> These results are supported by studies of the fluxional behavior of BISBI in solution, in which a rapid exchange of the two phosphine moieties was observed.<sup>23</sup> Furthermore, X-ray structural analyses of transition-metal complexes of BISBI show a wide variety of P–M–P chelation angles:  $\angle\text{P–Mo–P} = 103.5^{\circ}$  in (BISBI)Mo(CO)<sub>4</sub>,<sup>31</sup>  $\angle\text{P–Ir–P} = 117.9^{\circ}$  in (BISBI)Ir(H)(CO)<sub>2</sub>,  $\angle\text{P–Rh–P} = 124.8^{\circ}$  in (BISBI)Rh(H)(CO)(PPh<sub>3</sub>),<sup>23</sup> and  $\angle\text{P–Fe–P} = 152.0^{\circ}$  in (BISBI)Fe(CO)<sub>3</sub>.<sup>32</sup>

The flexibility of BISBI allows the formation of a rhodium complex with a slightly less rigidly defined geometry, thus giving somewhat lower selectivity to *n*-alkyl intermediates. This effect of the flexibility on the observed selectivity becomes much more pronounced at higher temperatures.

**Hydroformylation of Styrene.** Hydroformylation of styrene with a (Xantphos)Rh catalyst resulted in relatively high selectivity for the linear aldehyde (a linear to branched ratio of up to 2.35 was obtained; see Table 5).

This is remarkable, since styrene is a substrate with a distinct preference for the formation of the branched aldehyde due to the stability of the 2-alkyl–rhodium species, induced by the formation of a  $\pi$ -allyl complex (ref 13 and references cited therein). Wilkinson<sup>7</sup> reported hydroformylation with (PPh<sub>3</sub>)<sub>3</sub>Rh(H)(CO) as a catalyst at  $25\text{ }^{\circ}\text{C}$  and 1 bar of CO/H<sub>2</sub>, yielding a linear to branched ratio of 0.13 (up to 0.27 using excess PPh<sub>3</sub>). Higher temperature and pressure (62 bar of CO/H<sub>2</sub> at  $70\text{ }^{\circ}\text{C}$ ) lead to higher selectivity for the branched aldehyde, yielding a linear to branched ratio of 0.08.<sup>33</sup>

The effect of ligands with a large bite angle on the rhodium-catalyzed hydroformylation of styrene was investigated by Yamamoto, who observed a very high selectivity for the branched aldehyde with **7**, a diphosphinite ligand with a calculated natural bite angle of  $118^{\circ}$ ,<sup>34</sup> and **8**, a diphosphine with a calculated natural bite angle of  $123^{\circ}$ .<sup>25,35</sup>



However, another ligand with a large natural bite angle, DIOP, showed much lower selectivity to the branched aldehyde and a resulting increased selectivity toward the linear aldehyde. For this ligand we (and

**Table 3. Results of the Hydroformylation of 1-Octene at 40 °C<sup>a</sup>**

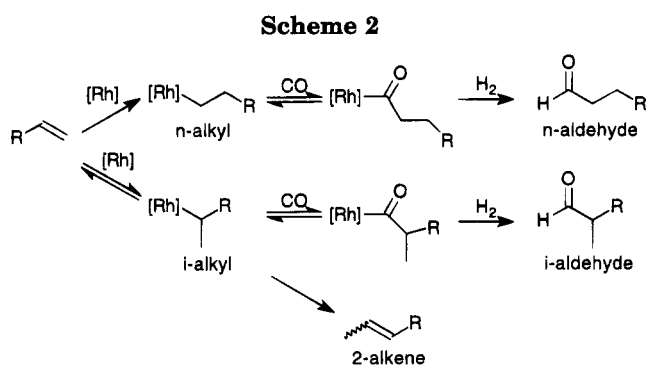
ligand	calcd bite angle, deg	flexibility range, deg	normal/branched	% n-aldehyde	% isomerization	tof <sup>b</sup>
DPEphos	102.2	86–120	10.5	91.3	0	5
Sixantphos	108.7	93–132	35.0	96.3	<1	4.4
Thixantphos	109.4	94–130	47.6	97.0	1	13.2
Xantphos	111.7	97–135	57.1	98.3	0	10
DBFphos	131.1	117–147	3.4	76.1	1.6	1.9
BISBI	122.6	101–148	58.2	95.5	2.9	30

<sup>a</sup> Conditions: CO/H<sub>2</sub> = 1, *p*(CO/H<sub>2</sub>) = 10 bar, substrate/Rh = 674, ligand/Rh = 2.2, [Rh] = 1.78 mM. In all cases the percent hydrogenation was zero. <sup>b</sup> Turnover frequency (mol of alkene (mol of Rh)<sup>-1</sup> h<sup>-1</sup>).

**Table 4. Results of the Hydroformylation of 1-Octene at 80 °C<sup>a</sup>**

ligand	calcd bite angle, deg	flexibility range, deg	normal/ branched	% n-aldehyde	% isomerization	tof
DPEphos	102.2	86–120	6.7	87.0	0	250
Sixantphos	108.7	93–132	34	94.2	3	168
Thixantphos	109.4	94–130	41	93.0	4.7	445
Xantphos	111.7	97–135	53.5	97.7	0.5	800
DBFphos	131.1	117–147	3	71	5.5	125
BISBI	122.6	101–148	80.5	89.6	9.3	850

<sup>a</sup> Conditions: CO/H<sub>2</sub> = 1, *p*(CO/H<sub>2</sub>) = 10 bar, substrate/Rh = 674, ligand/Rh = 2.2, [Rh] = 1.78 mM. In all cases the percent hydrogenation was zero.

**Table 5. Results of the Hydroformylation of Styrene<sup>a</sup>**

ligand	<i>T</i> , °C	<i>p</i> , bar	normal/ branched	% n-aldehyde	tof
Xantphos	60	10	0.77	43.5	128
	80		0.88	46.8	724
	120		2.35	70.1	4285
PPh <sub>3</sub> <sup>7</sup>	25	1	0.13	11.5	10
PPh <sub>3</sub> <sup>33</sup>	70	62	0.08	7.4	<i>b</i>
<b>7</b> <sup>34</sup>	30	40	0.03–0.05	3–5	9.7
<b>8</b> <sup>35</sup>	50	8	0.77	43.5	0.32
	50	40	0.12	11	(a)
DIOP <sup>36</sup>	20	25	0.04	4	2.1
	25	1	0.25–0.49 <sup>c</sup>	20–32.5 <sup>c</sup>	<i>b</i>

<sup>a</sup> Conditions: CO/H<sub>2</sub> = 1, substrate/Rh = 674, [Rh] = 1.78 mM.

<sup>b</sup> Not reported. <sup>c</sup> Depending on the rhodium precursor used.

Casey<sup>23</sup>) calculated a natural bite angle of 102.3°. A normal to branched ratio of 0.25–0.47 was obtained, depending on the rhodium precursor used.<sup>36</sup>

Casey and co-workers reported that they were unable to isolate any monomeric metal complexes of **8**. Furthermore, no enhanced selectivity for the linear aldehyde was found using the (**8**)Rh catalyst system in the

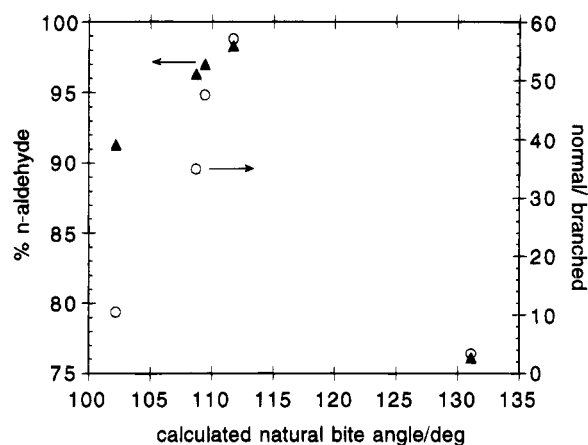


**Figure 4.** Selectivity versus calculated natural bite angle ( $\beta_n$ ) in the hydroformylation of 1-octene. Normal to branched ratio versus  $\beta_n$  is indicated by open circles and the percentage of linear aldehyde versus  $\beta_n$  with full triangles (data from Table 2).

hydroformylation of 1-hexene<sup>23</sup> or 1-octene.<sup>35</sup> Therefore, the effect of **8** on the selectivity (toward the branched aldehyde) in the hydroformylation of styrene remains unexplained.

In summary, the distinct effect of minor changes in the ligand backbone by alterations of the bridge between C11 and C14 on the observed selectivity shows that the effect of the bite angle is very subtle. For the chelating ligands in this series, we found a regular increase of both the normal/branched ratios and the percentage of linear aldehyde formed with increasing calculated natural bite angle in the hydroformylation of 1-octene (Figure 4). This correlation is observed at both 40 and 80 °C. For the ligand DBFphos no chelates were observed, and its selectivity is consequently out of the range. The very high selectivity of Xantphos (calculated natural bite angle 111.7°) and BISBI (our calculated natural bite angle 122.6° (lit.<sup>23</sup> 113°, X-ray (BISBI)Rh-(H)(CO)(PPh<sub>3</sub>) 124.8°)) indicates that the optimum is near 112–120°. Selectivity in the hydroformylation reaction increases when the bite angle of the ligand becomes larger. However, the rigidity of the ligand is also an important factor. This is strongly supported by the results obtained for the more flexible BISBI ligand, which shows a lower selectivity. The importance of this

(31) Herrmann, W. A.; Kohlpaintner, C. W.; Herdtweck, E.; Kiprof, P. *Inorg. Chem.* **1991**, *30*, 4271.

(32) Casey, C. P.; Whiteker, G. T.; Campana, C. F.; Powell, D. R. *Inorg. Chem.* **1990**, *29*, 3376–3381.

(33) Hayashi, T.; Tanaka, M.; Ogata, I. *J. Mol. Catal.* **1981**, *13*, 323–330.

(34) Yamamoto, K.; Momose, S.; Funahashi, M.; Ebata, S.; Ohmura, H.; Komatsu, H.; Miyazawa, M. *Chem. Lett.* **1994**, 189–192.

(35) Miyazawa, M.; Momose, S.; Yamamoto, K. *Synlett* **1990**, 711–712.

(36) Brown, J. M.; Cook, S. J.; Khan, R. *Tetrahedron* **1986**, *42*, 5105–5109.

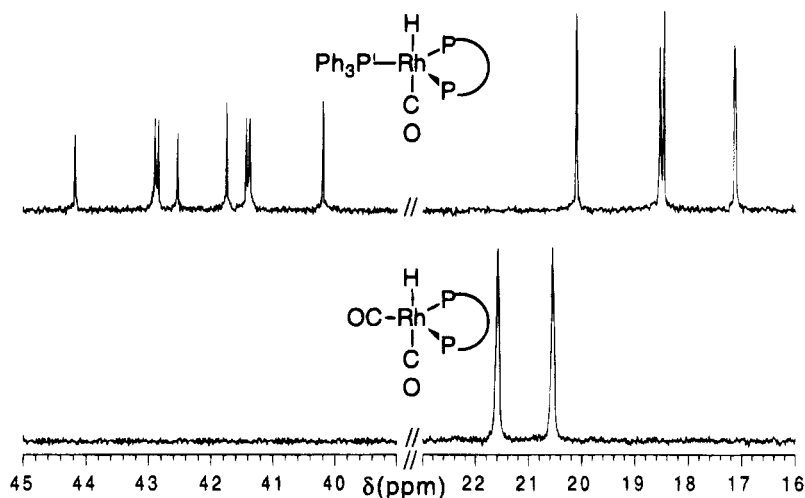


**Figure 5.**  $^{31}\text{P}$  NMR spectra for (Xantphos)Rh(H)(CO)(PPh<sub>3</sub>) (**9**; top) and (Xantphos)Rh(H)(CO)<sub>2</sub> (**10**; bottom) in C<sub>6</sub>D<sub>6</sub> at 25 °C.

ligand rigidity becomes even more pronounced at higher temperatures. Rigid ligands with a larger calculated bite angle are unable to form stable chelates, as was demonstrated with DBFphos and **8**.

**Rhodium Complexes.** In order to investigate the coordination behavior of our series of ligands, (diphosphine)Rh(H)(CO)(PPh<sub>3</sub>) complexes were synthesized for all ligands. Facile exchange of PPh<sub>3</sub> in (PPh<sub>3</sub>)<sub>3</sub>Rh(H)(CO) with the diphosphines gave quantitative yield (although some loss was observed during the workup procedure).

Detailed studies of the  $^{31}\text{P}\{^1\text{H}\}$  NMR spectra led to the conclusion that the two phosphine moieties of the diphosphine in the complex were equivalent for all ligands (except DBFphos). The coupling constants between the diphosphine P and PPh<sub>3</sub> ( $^2J = 114\text{--}129$  Hz) show that these ligands are indeed coordinated bis-equatorially. The attempts to synthesize (DBFphos)Rh(H)(CO)(PPh<sub>3</sub>) (DBFphos has a calculated natural bite angle of 131°) did not yield any characterizable complex.

Bubbling CO through a solution of (diphosphine)Rh(H)(CO)(PPh<sub>3</sub>) led to facile displacement of the remaining PPh<sub>3</sub>. The complex (diphosphine)Rh(H)(CO)<sub>2</sub> formed by this exchange (presumably the catalytically active species in the hydroformylation reaction) is stable under an atmosphere of CO. The  $^{31}\text{P}\{^1\text{H}\}$  NMR spectra of these compounds (see Figure 5 for the spectra of the Xantphos complexes) exhibit a clean doublet for the diphosphine, indicating that these ligands are also coordinated in a bis-equatorial fashion in these complexes.

The  $^1\text{H}$  NMR spectra of the (Xantphos)Rh(H)(CO)(PPh<sub>3</sub>) (**9**), (Xantphos)Rh(H)(CO)<sub>2</sub> (**10**), (Sixantphos)Rh(H)(CO)(PPh<sub>3</sub>) (**11**), and (Sixantphos)Rh(H)(CO)<sub>2</sub> (**12**) complexes show an inequivalence of the two methyl groups, indicating a rigid conformation of the ligand (formally, the absence of a mirror plane through the equatorial plane dictates the inequivalence of the methyl and phenyl groups). Furthermore, the *ortho* hydrogens of the phenyl groups on the diphenylphosphine moieties positioned in the equatorial plane and the axial plane are inequivalent in the (diphosphine)Rh(H)(CO)(PPh<sub>3</sub>) complexes. This is especially clear in the  $^1\text{H}$  NMR spectra of **9** and (Thixantphos)Rh(H)(CO)(PPh<sub>3</sub>) (**13**). This strongly indicates that in solution the two diphenylphosphine moieties are rigidly placed in space around the rhodium center.

Unfortunately, the crystals we have obtained for **9** are not suitable for a conclusive structure determination. The inequivalence of the phenyl groups at the phosphorus atoms of the ligands indicates, however, that the structure of the coordinated ligand (in solution) is probably very similar to the crystal structure of free Xantphos (Figure 3). The structure of the ligand determines therefore the geometry of the complex.

Therefore, we think that the enhanced selectivity for the linear aldehyde in the hydroformylation of styrene and the low isomerization of 1-octene (even at higher temperatures) is induced by a well-defined "docking area" on the rhodium center. The size of the bite angle dictates directly the shape of this docking area. The fact that isomerization is almost absent in these catalyst systems indicates that the strict geometry is inducing the formation of the 1-alkyl species (leading to the linear aldehyde) and actually inhibits the formation of 2-alkyls.

## Conclusion

A homologous series of diphosphines, based on rigid heterocyclic aromatics, allowed an investigation of the effect of slight alterations of the P–Rh–P bite angle only, without modifying other steric or electronic properties. The distinct effect of these alterations on the selectivity in the rhodium-catalyzed hydroformylation showed that the P–Rh–P bite angle has a pronounced effect on the selectivity. Comparison with BISBI shows that the rigidity of the ligand backbone is essential for obtaining high selectivity in the hydroformylation reaction. The rigidity of the ligands causes the chelated complexes to be stable, even at elevated temperatures. Therefore, selectivity was not lost at higher temperatures and the turnover frequency can be increased to a synthetically useful level. Comparison of the results obtained with these ligands revealed a regular increase of selectivity with an increasing bite angle, up to the point where the calculated bite angle has increased to such an extent that chelation is no longer possible. The Xantphos ligand has been shown to induce the highest selectivity reported so far for the formation of linear aldehydes with diphosphines in rhodium-catalyzed hydroformylation.

## Experimental Section

**Computational Details.** The molecular mechanics calculations were performed on a Silicon Graphics Indigo workstation using the program Sybyl, version 6.03,<sup>24</sup> with an augmented TRIPOS force field. We developed our own parameters for the phosphine-type phosphorus atom and the silane-type silicon atom, which are not defined in the standard TRIPOS force field. These parameters are included in the supplementary material.

Calculations were performed similarly to the method described by Casey and Whiteker,<sup>25</sup> using a Rh–P bond length of 2.315 Å.

Minimizations were performed using the standard Sybyl minimizer MAXIMIN2.

The structures were allowed to converge fully, with a termination criterion of a rms gradient of less than 0.001 kcal mol<sup>-1</sup> Å<sup>-1</sup>.

MOPAC-PM3 calculations<sup>37</sup> (CACHeMOPAC version 94.10, derived from MOPAC version 6.00<sup>38</sup>) were performed using the CACHe WorkSystem version 3.7,<sup>39</sup> on an Apple Power Macintosh 950, equipped with two CACHe CXP coprocessors. Geometry optimization was performed using eigenvector following (EF).

**Synthesis.** All preparations were carried out under an atmosphere of purified nitrogen using standard Schlenk techniques. Solvents were carefully dried and freshly distilled prior to use. Hexanes, THF, benzene, toluene, and ether were distilled from sodium, dichloromethane, and methanol from CaH<sub>2</sub>. Dibenzofuran, *sec*-butyllithium, and dimethyldichlorosilane were purchased from Janssen; dibenzofuran was recrystallized from ethanol before use. Chlorodiphenylphosphine and TMEDA were purchased from Aldrich and distilled prior to use. 9,9-Dimethylxanthene, diphenyl ether, and *n*-butyllithium were purchased from Aldrich and used as received. <sup>13</sup>C was purchased from Isotec Inc.

(PPh<sub>3</sub>)<sub>3</sub>Rh(H)(CO)<sup>40</sup> and dimethylphenoxathiin<sup>41</sup> were prepared according to literature procedures.

<sup>1</sup>H NMR (300 MHz) and <sup>31</sup>P NMR spectra (121.5 MHz, referenced to external 85% H<sub>3</sub>PO<sub>4</sub>) were recorded on a Bruker AMX-300 spectrometer; <sup>13</sup>C NMR spectra were recorded on a Bruker AC-200 (at 50 MHz), AMX-300 (at 75.5 MHz), or ARX-400 spectrometer (at 100 MHz). Assignments in complex NMR spectra were aided by simulation with geNMR 3.5M software.<sup>30</sup> P' represents the PPh<sub>3</sub> phosphorus atom in characterizations of couplings in NMR spectra. IR spectra were obtained on a Nicolet 510 FT-IR. Mass spectroscopy was measured on a JEOL JMS-SX/SX102A. Melting points were measured on a Gallenkamp MFB-595 melting point apparatus and are uncorrected.

Gas chromatography was performed on a Carlo Erba GC 6000 Vega series or an Interscience Mega 2 series apparatus (split/splitless injector, J&W Scientific, DB1 30 m column, film thickness 3.0 μm, carrier gas 70 kPa of He, FID detector).

**Bis(2-(diphenylphosphino)phenyl) Ether (DPEphos; 1).** At room temperature a solution of 4.00 g of diphenyl ether (23.5 mmol) in 15 mL of THF was added dropwise to a stirred mixture of 20.6 mL of *n*-butyllithium (2.5 M in hexane, 51.7 mmol) and 8.3 mL of TMEDA (51.7 mmol). The reaction mixture was stirred for 16 h. Then a solution of 9.3 mL of chlorodiphenylphosphine (51.7 mmol) in 15 mL of hexanes was added dropwise to the reaction mixture at room temperature. During the addition, the temperature was kept constant with a water bath. A white precipitate was formed. The mixture was stirred for another 16 h; then 30 mL of CH<sub>2</sub>Cl<sub>2</sub> and 30

mL of water were added and the mixture was stirred vigorously. The water layer was then removed, the organic phase was dried with MgSO<sub>4</sub>, and the solvent was removed *in vacuo*. The resulting sticky solid was washed with acetone and then dried *in vacuo*. Yield: 10.5 g of white powder (83%).

<sup>1</sup>H NMR (CDCl<sub>3</sub>): δ 7.40–7.18 (ar, 11 H), 6.98 (dt, *J* = 0.7, 7.3 Hz), 6.84 (ddd, *J* = 4.5, 7.5, 14 Hz), 6.71 (ddd, *J* = 0.7, 4.3, 7.5 Hz). <sup>31</sup>P{<sup>1</sup>H} NMR (CDCl<sub>3</sub>): δ -16.4. <sup>13</sup>C{<sup>1</sup>H} NMR (CDCl<sub>3</sub>): δ 159.8 (d, *J* = 22.65 Hz), 137.2 (d, *J* = 11.3 Hz), 14.6, 134.3, 130.7, 129.6 (d, *J* = 16.6 Hz), 129.0, 128.9, 128.7, 124.1, 118.6. IR (CHCl<sub>3</sub>, cm<sup>-1</sup>): 3073 (m), 3005 (m), 1585 (s), 1566 (s), 1479 (s), 1461 (s), 1434 (s), 1183 (s), 1070 (m), 877 (m), 697 (m). Exact mass (MS, FAB): 539.1656 (M + H) (calcd for C<sub>36</sub>H<sub>28</sub>OP<sub>2</sub> 538.1615), Mp: 175–176 °C.

**10,10-Dimethylphenoxasilin (14),<sup>42,43</sup>** At room temperature a solution of 8.00 g of diphenyl ether (47.0 mmol) in 35 mL of THF was added dropwise to a mixture of 41.4 mL of 2.5 M *n*-butyllithium in hexanes (103.4 mmol) and 16.7 mL of TMEDA (103.4 mmol). When all the phenyl ether was added, the reaction mixture was stirred for 16 h. The ethereal solution of bis(2-lithiophenyl) ether and a solution of 5.7 mL of dimethyldichlorosilane (47.0 mmol) in 75 mL of ether were added simultaneously to 40 mL of ether over 1 h. The reaction mixture was stirred for 16 h and then hydrolyzed by addition of 30 mL of water. The hydrolyzed mixture was stirred for 2 h. The organic layer was separated and the aqueous layer was extracted with 30 mL of ether. The combined organic layers were treated with Norit and dried with MgSO<sub>4</sub>. The solvent was removed *in vacuo*. Small crystals formed during the concentration. The semisolid oil was crystallized from methanol, resulting in white crystals with a grassy odor. Yield: 4.82 g (45%).

<sup>1</sup>H NMR (CDCl<sub>3</sub>): δ 7.56 (dd, 2H, *J* = 7.2, 1.7 Hz), 7.45 (dt, 2H, *J* = 7.7, 1.7 Hz), 7.22 (d, 2H, *J* = 8.4 Hz), 7.17 (dt, 2H, *J* = 7.2, 0.9 Hz), 0.51 (s, 6H, (CH<sub>3</sub>)<sub>2</sub>Si). <sup>13</sup>C{<sup>1</sup>H} NMR (CDCl<sub>3</sub>): δ 160.2, 134.5, 131.7, 123.1, 119.7 (C–Si), 118.5, 0.2 ((CH<sub>3</sub>)<sub>2</sub>Si). IR (CHCl<sub>3</sub>, cm<sup>-1</sup>): 3070, 3008, 2957, 2901, 1604, 1593, 1574, 1426, 1370, 1301, 1270, 885, 845, 807. Exact mass (MS): 226.0808 (calcd for C<sub>14</sub>H<sub>14</sub>O<sub>2</sub>Si 226.0814).

**4,6-Bis(diphenylphosphino)-10,10-dimethylphenoxasilin (Sixantphos; 2).** At room temperature 12.6 mL of *sec*-butyllithium (1.3 M in 98/2 cyclohexane/hexane, 13.3 mmol) was added dropwise to a stirred solution of 1.00 g of 14 (4.42 mmol) and 2.1 mL of TMEDA (13.3 mmol) in 50 mL of dry ether. When all *sec*-butyllithium was added, the reaction mixture was stirred for 16 h. Then a solution of 2.6 mL of chlorodiphenylphosphine (13.3 mmol) in 15 mL of hexanes was added dropwise, and the reaction mixture was stirred for another 16 h. The solvent was removed *in vacuo*. The resulting solid oil was dissolved in CH<sub>2</sub>Cl<sub>2</sub>; this solution was washed with water and dried with MgSO<sub>4</sub> and the solvent removed *in vacuo*. The resulting oil was washed with hexanes and crystallized from 1-propanol. The resulting white crystals are air-stable. Yield: 1.78 g white crystals (68%).

<sup>1</sup>H NMR (CDCl<sub>3</sub>): δ 7.50 (dd, 2H, *J* = 7.2, 1.7 Hz, CHCH<sub>3</sub>Si), 7.16–7.31 (ar, 20 H, P(C<sub>6</sub>H<sub>5</sub>)<sub>2</sub>), 7.00 (t, 2H, *J* = 7.3 Hz, PCCH<sub>3</sub>CH), 6.79 (dq, 2 H, *J* = 7.5, 1.7 Hz, OCPCCH), 0.50 (s, 6 H, (CH<sub>3</sub>)<sub>2</sub>Si). <sup>31</sup>P{<sup>1</sup>H} NMR (CDCl<sub>3</sub>): δ -17.6. <sup>13</sup>C{<sup>1</sup>H} NMR (CDCl<sub>3</sub>): δ 137.9 (t, *J* = 6.8 Hz), through-space P–P coupling ≥ 60 Hz, 136.4, 134.5, 133.9 (t, *J* = 10.6 Hz, P–C(Ph)), 127.9, 127.3 (t, *J* = 10.9 Hz, CO), 122.8, 118.5, -0.4 ((CH<sub>3</sub>)<sub>2</sub>Si). IR (CHCl<sub>3</sub>, cm<sup>-1</sup>): 3059, 3007, 2960, 1580, 1572, 1434, 1399, 1370, 1120, 885, 857. Exact mass (MS): 595.1741 (M + H) (calcd for C<sub>38</sub>H<sub>32</sub>OP<sub>2</sub>Si 594.1698). Mp: 245–245.5 °C. Anal. Calcd for C<sub>38</sub>H<sub>32</sub>OP<sub>2</sub>Si: C, 76.75; H, 5.43. Found: C, 76.04; H, 5.61.

**2,8-Dimethyl-4,6-bis(diphenylphosphino)phenoxathiin (Thixantphos; 3).** This compound was prepared

(37) Stewart, J. J. P. *J. Comput. Chem.* **1989**, *10*, 209–264 and references cited therein.

(38) Stewart, J. J. P. QCPE No. 455.

(39) CACHe WorkSystem 3.7; CACHe Scientific Inc., 18700 N. W. Walker Road, Building 92-01, Beaverton, OR 97006.

(40) Ahmad, N.; Levison, J. J.; Robinson, S. D.; Uttley, M. F. *Inorg. Synth.* **1974**, *15*, 59–60.

(41) Feigel, M. *Liebigs Ann. Chem.* **1989**, 459–468.

(42) Oita, K.; Gilman, H. *J. Am. Chem. Soc.* **1957**, *79*, 339–342.

(43) Gilman, H.; Trepka, W. *J. Org. Chem.* **1961**, *26*, 5202.

similarly to Sixantphos from 3.00 g of dimethylphenoxathiin (13.14 mmol). Yield: 5.56 g of white crystals (71%). Analytically pure material was obtained by crystallization from hot 1-propanol.

$^1\text{H}$  NMR ( $\text{CDCl}_3$ ):  $\delta$  7.16–7.35 (ar, 20 H,  $\text{P}(\text{C}_6\text{H}_5)_3$ ), 6.87 (“d”,  $J = 1.6$  Hz,  $\text{C}(\text{P}(\text{Ph})_2)\text{CHC}(\text{CH}_3)_2$ ), 6.23 (bs, 2H,  $\text{C}(\text{S})\text{CHC}(\text{CH}_3)_2$ ), 2.07 (s, 6H,  $\text{CH}_3$ ).  $^{31}\text{P}\{^1\text{H}\}$  NMR ( $\text{CDCl}_3$ ):  $\delta$  -17.3.  $^{13}\text{C}\{^1\text{H}\}$  NMR ( $\text{CDCl}_3$ ):  $\delta$  137.0 (t,  $J = 6.8$  Hz), through-space P–P coupling  $\geq 40$  Hz, 133.7 (t,  $J = 10.6$  Hz), 133.7, 132.5, 128.0–128.1 (ar), 127.1 (t,  $J = 12.1$  Hz), 119.3, 20.4 ( $\text{CH}_3$ ). IR ( $\text{CHCl}_3$ ,  $\text{cm}^{-1}$ ): 3004 (m), 2961 (m), 2926 (m), 1435 (s), 1407 (vs), 1244 (m), 695 (m). Exact mass (MS): 596.1483 (calcd for  $\text{C}_{38}\text{H}_{30}\text{OP}_3\text{S}$  596.1492). Mp: 179.5–180 °C. Anal. Calcd for  $\text{C}_{38}\text{H}_{30}\text{OP}_3\text{S}$ : C, 76.49; H, 5.07. Found: C, 75.64; H, 5.53.

**9,9-Dimethyl-4,6-bis(diphenylphosphino)xanthene (Xantphos; 4).** This compound was prepared similarly to Sixantphos from 1.00 g of 9,9-dimethylxanthene (4.76 mmol). Yield: 2.05 g of yellow-white powder (74.6%).  $^1\text{H}$  NMR ( $\text{CDCl}_3$ ):  $\delta$  7.40 (dd, 2H,  $J = 7.8$ , 1.0 Hz, CPCHCH), 7.15–7.26 (ar, 20 H,  $\text{P}(\text{C}_6\text{H}_5)_3$ ), 6.96 (t, 2H,  $J = 7.7$  Hz, CHCHCH), 6.54 (dd, 2H,  $J = 7.4$ , 1.4 Hz, CHCHCC), 1.65 (s, 6H,  $\text{CH}_3$ ).  $^{31}\text{P}\{^1\text{H}\}$  NMR ( $\text{CDCl}_3$ ):  $\delta$  -17.5.  $^{13}\text{C}\{^1\text{H}\}$  NMR ( $\text{CDCl}_3$ ):  $\delta$  137.2 (t,  $J = 5.3$  Hz), through-space P–P coupling  $\geq 60$  Hz, 133.7 (t,  $J = 10.1$  Hz), 131.9, 129.7, 128.0 (ar), 126.1, 125.7 (t,  $J = 9.8$  Hz), 123.1, 67.8 ( $\text{CMe}_2$ ), 31.6 ( $\text{CH}_3$ ). IR ( $\text{CHCl}_3$ ,  $\text{cm}^{-1}$ ): 3073 (w), 2974 (w), 1435 (s), 1405 (vs), 1243 (m), 695 (m). Exact mass (MS): 578.1916 (calcd for  $\text{C}_{39}\text{H}_{32}\text{OP}_2$  578.1928). Mp: 221–222 °C. Anal. Calcd for  $\text{C}_{39}\text{H}_{32}\text{OP}_2$ : C, 80.94; H, 5.58. Found: C, 80.69; H, 5.87.

**X-ray Crystal Structure Determination of Xantphos.** Crystals of Xantphos suitable for X-ray diffraction were grown from hot 1-propanol. Xantphos crystallizes in the orthorhombic space group  $Pbnm$ , with  $a = 8.7678(8)$  Å,  $b = 18.967(1)$  Å,  $c = 19.181(1)$  Å,  $V = 3189.8(4)$  Å<sup>3</sup> and  $Z = 4$ . The data collection was carried out at room temperature. The structure was solved by direct methods.<sup>44</sup> The hydrogen atoms were calculated. The structure was refined to  $R = 0.063$  and  $R_w = 0.085$ , for 1825 observed reflections. The symmetric unit contains a half-molecule with four atoms (O, C1, C2, and C3) at special positions on a mirror plane. Crystal data and collection parameters, atomic coordinates, bond lengths, bond angles, anisotropic thermal parameters, and H atom coordinates are included in the supplementary material.

**1,8-Bis(diphenylphosphino)dibenzofuran (DBFphos; 5).** At -65 °C 66.2 mL of *sec*-butyllithium (1.3 M in 98/2 cyclohexane/hexane, 84.0 mmol) was added dropwise to a stirred solution of 4.82 g of dibenzofuran (28.7 mmol) and 12.8 mL of TMEDA (84.0 mmol) in 280 mL of dry ether. After all the *sec*-butyllithium was added, the cooling bath was removed, and the reaction mixture was warmed to room temperature. After 16 h, the mixture was cooled to -65 °C, and a solution of 18.53 mL of chlorodiphenylphosphine (84.0 mmol) in 50 mL of hexanes was added dropwise. The cooling bath was removed, and the reaction mixture was stirred for another 16 h. The ether was removed *in vacuo*; the resulting solid oil was dissolved in 100 mL of  $\text{CH}_2\text{Cl}_2$  and the solution washed with 60 mL of deoxygenated water, dried with  $\text{MgSO}_4$ , and evaporated to dryness. The resulting oil was washed twice with 30 mL of hexanes and dried *in vacuo*. The resulting white crystals are air-stable. Yield: 12.2 g of white powder (81%).

$^1\text{H}$  NMR ( $\text{CDCl}_3$ ):  $\delta$  7.95 (dd, 2H,  $J = 7.7$ , 0.9 Hz, CHCHCC), 7.2–7.35 (ar, 22H,  $\text{P}(\text{C}_6\text{H}_5)_2 + \text{CHCHCH}$ ), 7.08 (dt, 2H,  $J = 6.9$ , 0.84 Hz, PCCHCHCH).  $^{31}\text{P}\{^1\text{H}\}$  NMR ( $\text{CDCl}_3$ ):  $\delta$  -16.5.  $^{13}\text{C}\{^1\text{H}\}$  NMR ( $\text{CDCl}_3$ ):  $\delta$  136.3 (d,  $J = 10.5$  Hz, *C-*ipso**), 134.5, 134.2, 132.6 (d,  $J = 9.8$  Hz, OCCPCH), 129.2, 128.9, 128.9, 124.1 (CO), 123.7, 122.2, 122.0, 121.9. IR ( $\text{CHCl}_3$ ,  $\text{cm}^{-1}$ ): 3059 (w), 3004 (w), 1435 (vs), 1411 (vs), 1390 (vs), 1180 (vs), 395 (m). Exact mass (MS): 536.1469 (calcd for  $\text{C}_{36}\text{H}_{26}\text{OP}_2$  536.1459). Mp: 211–214 °C (lit.<sup>28</sup> mp 212–216 °C).

**(Xantphos)Rh(H)(CO)(PPh<sub>3</sub>) (9).** A solution of  $(\text{PPh}_3)_3\text{-Rh(H)(CO)}$  (100 mg, 0.11 mmol) and Xantphos (63.6 mg, 0.11 mmol) in 10 mL of benzene was stirred for 4 h at 30 °C. The solvent was evaporated *in vacuo*. The resulting yellow solid was washed with 1 mL of methanol and dried *in vacuo*. The  $^{13}\text{C}$  resonances of the carbonyl were measured on a  $^{13}\text{C}$ -enriched complex.

$^1\text{H}$  NMR ( $\text{C}_6\text{D}_6$ ):  $\delta$  7.82 (apparent q, 4H,  $J = 4.8$  Hz, ar), 7.66 (m, 6H, ar), 7.53 (apparent q, 4H,  $J = 4.9$  Hz, ar), 7.11 (dd, 2H,  $J = 7.3$ , 1.3 Hz, CHCHCC), 7.0–6.9 (ar), 6.79 (“d”, 4H), 1.48 (s, 3H,  $\text{CCH}_3$ ), 1.38 (s, 3H,  $\text{CCH}_3$ ), -9.14 ( $J_{\text{H-P}} = 12.2$  Hz,  $J_{\text{H-Rh}} = 18.2$  Hz,  $J_{\text{H-Rh}} = 1.7$  Hz).  $^{31}\text{P}\{^1\text{H}\}$  NMR ( $\text{C}_6\text{D}_6$ ):  $\delta$  42.67 ( $J_{\text{P-Rh}} = 151.1$  Hz,  $J_{\text{P-P}} = 119.1$  Hz,  $\text{PPh}_3$ ), 25.65 ( $J_{\text{P-Rh}} = 127.9$  Hz,  $J_{\text{P-P}} = 119.1$  Hz, Xantphos-P).  $^{13}\text{C}\{^1\text{H}\}$  NMR (100 MHz,  $\text{C}_6\text{D}_6$ ):  $\delta$  156.9 (t,  $J = 5.6$  Hz), 141.9 (dt,  $J = 4.4$ , 31.1 Hz), 140.1 (t,  $J = 18.9$  Hz), 137.6 (t,  $J = 18$  Hz), 135.6 (s), 134.9 (ar), 134.8 (ar), 134.6 (ar), 134.6 (ar), 134.5 (ar), 134.4 (ar), 134.2 (ar), 36.9 (s,  $\text{C}(\text{CH}_3)_2$ ), 31.0, (s,  $\text{CH}_3$ ), 24.7 (s,  $\text{CH}_3$ ). IR ( $\nu_{\text{CO}}$ ,  $\text{CHCl}_3$ ,  $\text{cm}^{-1}$ ): 1996.9 (vs), 1909.66 (m). MS ( $m/z$ ): 961 (M - CO), 726 (M -  $\text{PPh}_3$  - 2H), 698 (M -  $\text{PPh}_3$  - CO - 2H). Anal. Calcd for  $\text{C}_{58}\text{H}_{48}\text{O}_2\text{P}_3\text{Rh}$ : C, 71.61; H, 4.98. Found: C, 71.02; H, 4.95.

**(Xantphos)Rh(H)( $^{13}\text{C}$ O)(PPh<sub>3</sub>) (9- $^{13}\text{C}$ O).** The  $^{13}\text{C}$  resonances of the carbonyl were measured on  $^{13}\text{C}$ -enriched **9**. The complex was synthesized as for **9**, but a gentle stream of  $^{13}\text{C}$ O was led through the reaction mixture for ca. 2 min, after which the workup procedure described for **9** was performed.

$^{13}\text{C}\{^1\text{H}\}$  NMR (100 MHz,  $\text{C}_6\text{D}_6$ ):  $\delta$  205.5 (“dq”,  $J_{\text{C-Rh}} = 53.8$  Hz,  $J_{\text{C-P}} = 10.3$  Hz, Rh-CO).

**(Xantphos)Rh(H)(CO)<sub>2</sub> (10) and (Xantphos)Rh(H)( $^{13}\text{C}$ O)<sub>2</sub> (10- $^{13}\text{C}$ O).** A gentle stream of CO was led through a  $\text{C}_6\text{D}_6$  solution of **9** in an NMR tube for 45 min. The tube was sealed under 1 atm of CO.

$^{10-13}\text{C}$ O was prepared similarly to **10**, using  $^{13}\text{C}$ O for ca. 10 min.

$^1\text{H}$  NMR ( $\text{C}_6\text{D}_6$ ):  $\delta$  7.1–7.02 (ar, 10H), 6.91–6.85 (ar, 12H), 6.70 (t,  $J = 7.7$  Hz, 2H), 6.60 (ar, 2H), 1.38 (s, 6H,  $\text{CH}_3$ ), -8.53 (m, 1H,  $J_{\text{Rh-H}} = 6.4$  Hz,  $J_{\text{P-H}} = 10.0$  Hz,  $J_{\text{C-H}} = 16.5$ , Rh-H).  $^{31}\text{P}\{^1\text{H}\}$  NMR ( $\text{C}_6\text{D}_6$ ):  $\delta$  21.08 (dt,  $J_{\text{P-Rh}} = 126.5$  Hz,  $J_{\text{P-C}} = 10.8$  Hz).  $^{13}\text{C}$  NMR ( $\text{C}_6\text{D}_6$ ):  $\delta$  201.1 (dt,  $J_{\text{C-Rh}} = 65.7$  Hz,  $J_{\text{C-P}} = 10.6$  Hz). IR ( $\nu_{\text{CO}}$ ,  $\text{C}_6\text{H}_6$ ,  $\text{cm}^{-1}$ ): 1989.9 (s), 1969.2 (vs), 1940.1 (vs).

**(Sixantphos)Rh(H)(CO)(PPh<sub>3</sub>) (11).** This compound was prepared similarly to **9**.

$^1\text{H}$  NMR ( $\text{C}_6\text{D}_6$ ):  $\delta$  7.64–7.58 (9H, ar), 7.46–7.35 (6H, ar), 7.23 (dd, 2H, CHCHCSi), 6.9–6.80 (ar, 22 H), 6.76 (t,  $J = 7.3$  Hz, 2H), 0.28 (s, 3H,  $\text{SiCH}_3$ ), 0.20 (s, 3H,  $\text{SiCH}_3$ ), -9.11 ( $J_{\text{H-P}} = 11.8$  Hz,  $J_{\text{H-P}} = 18.2$  Hz,  $J_{\text{H-Rh}} = 2.3$  Hz).  $^{31}\text{P}\{^1\text{H}\}$  NMR ( $\text{C}_6\text{D}_6$ ):  $\delta$  43.34 ( $J_{\text{P-Rh}} = 167.8$  Hz,  $J_{\text{P-P}} = 125.0$  Hz,  $\text{PPh}_3$ ), 27.82 ( $J_{\text{P-Rh}} = 146.5$  Hz,  $J_{\text{P-P}} = 125.0$  Hz, Sixantphos-P).  $^{13}\text{C}\{^1\text{H}\}$  NMR (50 MHz,  $\text{C}_6\text{D}_6$ ):  $\delta$  162.4 (t), 140.4 (dt), 139.1 (t), 136.3 (dd), 134.4–122 (ar), -1.0 ( $\text{CH}_3$ ), -3.0 ( $\text{CH}_3$ ). IR ( $\nu_{\text{CO}}$ ,  $\text{C}_6\text{H}_6$ ,  $\text{cm}^{-1}$ ): 1996.9 (vs), 1911.0 (w).

**(Sixantphos)Rh(H)(CO)<sub>2</sub> (12).** This compound was prepared similarly to **10**.

$^1\text{H}$  NMR ( $\text{C}_6\text{D}_6$ ):  $\delta$  7.51 (b, ar, ortho  $\text{PPh}_2$ ), 7.38 (m, ar, meta, para  $\text{PPh}_2$ ), 7.22 (dd,  $J = 7.0$ , 1.8 Hz, 2 H), 7.1–7.0 (m, ar,  $\text{PPh}_3$ ), 6.9–6.8 (m, ar), 6.77 (dd,  $J = 7.9$ , 2.0 Hz, 2 H), 6.71 (t,  $J = 10$  Hz, 2 H), 0.26 (s, 6H,  $\text{Si}(\text{CH}_3)_2$ ), -8.45 (dt, 1H,  $J_{\text{P-H}} = 22.7$  Hz,  $J_{\text{Rh-H}} = 7.7$  Hz).  $^{31}\text{P}\{^1\text{H}\}$  NMR ( $\text{C}_6\text{D}_6$ ):  $\delta$  22.26 (d,  $J_{\text{P-Rh}} = 123.9$ ). IR ( $\nu_{\text{CO}}$ ,  $\text{C}_6\text{H}_6$ ,  $\text{cm}^{-1}$ ): 1989.9 (m), 1966.4 (m), 1940.1 (vs).

**(Thixantphos)Rh(H)(CO)(PPh<sub>3</sub>) (13).** This compound was prepared similarly to **9**.

$^1\text{H}$  NMR ( $\text{C}_6\text{D}_6$ ):  $\delta$  7.71 (apparent q, 5 H, ar), 7.58 (m, 7H, ar), 7.41 (apparent q, 5 H, ar), 6.83–7.0 (ar, 28 H, ar), 6.75 (“d”,  $J = 1.6$  Hz,  $\text{C}(\text{P}(\text{Ph})_2)\text{CHC}(\text{CH}_3)_2$ ), 6.44 (bs, 2H,  $\text{C}(\text{S})\text{CHC}(\text{CH}_3)_2$ ), 1.69 (s, 6H,  $\text{CH}_3$ ), -9.19 (ddt,  $J_{\text{H-Rh}} = 0.6$  Hz,  $J_{\text{H-P}} = 11.1$  Hz,  $J_{\text{H-P}} = 18.6$  Hz).  $^{31}\text{P}$  NMR ( $\text{C}_6\text{D}_6$ ):  $\delta$  42.84 ( $J_{\text{P-Rh}} = 143.8$  Hz,  $J_{\text{P-P}} = 113.9$  Hz,  $\text{PPh}_3$ ), 28.3 ( $J_{\text{P-Rh}} = 127.2$  Hz,  $J_{\text{PP-P}} = 113.9$  Hz, Thixantphos-P). IR ( $\nu_{\text{CO}}$ ,  $\text{C}_6\text{H}_6$ ,  $\text{cm}^{-1}$ ): 2000 (vs),

(44) X-TAL3.2 Reference Manual; Hall, S. R., Flack, H. D., Stewart, J. M., Eds.; Universities of Western Australia, Geneva, and Maryland, 1992.



1918 (m). MS ( $m/z$ ): 961 (M - CO), 726 (M - PPh<sub>3</sub> - 2H), 698 (M - PPh<sub>3</sub> - CO - 2H).

**(Thixantphos)Rh(H)(CO)<sub>2</sub> (15).** This compound was prepared similarly to **10**.

<sup>1</sup>H NMR (C<sub>6</sub>D<sub>6</sub>): δ 7.51 (ar, 8 H), 7.03 (ar, 10 H), 7.38 (ar, 6 H), 6.90 (ar, 14 H), 6.73 ("d", 2 H, C(P(Ph)<sub>2</sub>)CHC(CH<sub>3</sub>)), 6.33 (m, 2H, C(S)CHC(CH<sub>3</sub>)), 1.69 (s, 6H, CH<sub>3</sub>), -8.55 (dt,  $J_{H-Rh} = 6.3$  Hz,  $J_{H-P} = 14.7$ ). <sup>31</sup>P{<sup>1</sup>H} NMR (C<sub>6</sub>D<sub>6</sub>): δ 23.39 (d,  $J_{P-Rh} = 127.9$  Hz). IR ( $\nu_{CO}$ , C<sub>6</sub>H<sub>6</sub>, cm<sup>-1</sup>): 1993 (s), 1975 (s), 1940 (s).

**(DPEphos)Rh(H)(CO)(PPh<sub>3</sub>) (16).** This compound was prepared similarly to **9**.

<sup>1</sup>H NMR (C<sub>6</sub>D<sub>6</sub>): δ 7.66-7.48 (ar), 7.0-6.8 (ar), 7.06-6.95 (m, ar, PPh<sub>3</sub>), 6.63 (apparent t, ar), 6.51 (apparent t, ar), -8.87 (apparent dq,  $J_{P-H} = J_{P'-H} = 26.9$  Hz,  $J_{Rh-H} = 3.6$  Hz, 1H, Rh-H). <sup>31</sup>P NMR (C<sub>6</sub>D<sub>6</sub>): δ 44.192 ( $J_{P'-Rh} = 168.0$  Hz,  $J_{P-P} = 129.0$  Hz, PPh<sub>3</sub>), 27.8 ( $J_{P-Rh} = 148.2$  Hz,  $J_{P-P} = 129.0$  Hz, DPEphos-P). <sup>13</sup>C{<sup>1</sup>H} NMR (C<sub>6</sub>D<sub>6</sub>): δ 158.2 (t,  $J = 5.7$  Hz), 135.4 (t,  $J = 8$  Hz), 133.9 (t,  $J = 8.0$  Hz), 133.1, 132.8, 132.5, 132.0, 129.3, 128.4-126.9 (ar), 122.7, 120.8. IR ( $\nu_{CO}$ , C<sub>6</sub>H<sub>6</sub>, cm<sup>-1</sup>): 2009.3 (vs), 1924.9 (m).

**(DPEphos)Rh(H)(CO)<sub>2</sub> (17).** This compound was prepared similarly to **10**.

<sup>1</sup>H NMR (C<sub>6</sub>D<sub>6</sub>): δ 7.66-7.48 (ar), 7.0-6.8 (ar), 7.06-6.95 (m, ar, PPh<sub>3</sub>), 6.66 (apparent t, ar), 6.41 (apparent t, ar), -8.59 (dt, 1H,  $J_{P-H} = 45.1$  Hz,  $J_{Rh-H} = 10.6$  Hz). <sup>31</sup>P{<sup>1</sup>H} NMR (C<sub>6</sub>D<sub>6</sub>): δ 25.54 (d,  $J_{P-Rh} = 123.9$ ). IR ( $\nu_{CO}$ , C<sub>6</sub>H<sub>6</sub>, cm<sup>-1</sup>): 1992.7 (s), 1978.9 (m), 1940.1 (vs).

**Hydroformylation Experiments.** Hydroformylation reactions were performed in a 180 mL stainless steel autoclave, equipped with a glass inner beaker, a substrate inlet vessel, a liquid sampling valve, and a magnetic stirring rod. The temperature was controlled by an electronic heating mantle.

The desired amount of diphosphine was placed in the autoclave and the system was flushed three times with 10 bar of CO/H<sub>2</sub> (1/1). Then, 3.0 mL of a 5 mM solution of Rh(acac)(CO)<sub>2</sub> in toluene was added, and the autoclave was pressurized to 6 bar. The autoclave was heated to the desired temperature and was stirred for 16 h. The desired amount of substrate and *n*-decane (internal standard) were placed in the substrate vessel and then pressed into the autoclave with 10 bar of CO/H<sub>2</sub>.

Samples were removed via the liquid sampling valve and quenched immediately with excess triphenyl phosphite to avoid isomerization. The samples were analyzed by temperature-controlled gas chromatography.

**Acknowledgment.** We thank Dr. A. M. Brouwer, Department of Organic Chemistry, University of Amsterdam, for his help and suggestions concerning the MM calculations and Prof. Dr. F. Bickelhaupt, Free University, Amsterdam, for valuable discussions.

**Supplementary Material Available:** Tables giving additional parameters for phosphine-type phosphorus and phenoxasilin-type silicon for the TRIPOS force field in Sybyl 6.03 and text giving additional details of the X-ray structure determination and tables of crystal data and collection parameters, atomic coordinates, bond lengths, bond angles, and thermal parameters (11 pages). Ordering information is given on any current masthead page.

OM950105O

## Notes

## Reactions of the Schiff Bases HN=CPh<sub>2</sub> and PhN=CHPh with Titanocene- and Zirconocene-Generating Complexes

C. Lefeber, P. Arndt, A. Tillack, W. Baumann, R. Kempe, V. V. Burlakov,<sup>†</sup> and U. Rosenthal\*

Max-Planck-Gesellschaft, Arbeitsgruppe "Komplekxkatalyse" an der Universität Rostock, Buchbinderstrasse 5-6, D-18055 Rostock, Germany

Received January 17, 1995<sup>®</sup>

**Summary:** The titanocene and zirconocene derivatives Cp<sub>2</sub>Ti(Me<sub>3</sub>SiC<sub>2</sub>SiMe<sub>3</sub>) and Cp<sub>2</sub>Zr(pyridine)(Me<sub>3</sub>SiC<sub>2</sub>SiMe<sub>3</sub>) generate under mild conditions unstable metallocenes "Cp<sub>2</sub>M", which react in situ with two molecules of the ketimine HN=CPh<sub>2</sub> to form metallocene amido alkylideneamido complexes Cp<sub>2</sub>M(NH-CHPh<sub>2</sub>)(N=CPh<sub>2</sub>) (M = Ti (1), Zr (2)) by hydrogen transfer of the ketimine moieties. By C-C coupling of two aldimine molecules PhN=CHPh, "zirconocene" affords the cyclic diamido complex Cp<sub>2</sub>Zr-N(Ph)-CHPh-CHPh-N(Ph) (3). The structures of the products have been established by X-ray structure analysis.

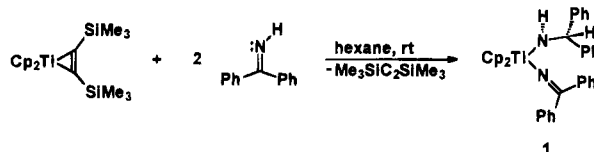
### Introduction

Zirconocene (IV) alkylideneamido complexes, for example aldimido complexes M-N=CHR or ketimido complexes M-N=CR<sub>2</sub> have attracted considerable attention.<sup>1</sup> In addition, group 4 metallocene amido (M-NR<sub>2</sub>) and metallocene imido complexes (M=NR)<sup>2</sup> have been described.<sup>3</sup> From zirconocene dichloride and LiN=CPh<sub>2</sub> the bis(alkylideneamido) complex Cp<sub>2</sub>Zr-(N=CPh<sub>2</sub>)<sub>2</sub> was prepared.<sup>4</sup> Alternatively, this complex became available by treatment of generated "Cp<sub>2</sub>Zr" with benzophenone azine (Ph<sub>2</sub>C=NN=CPh<sub>2</sub>).<sup>4</sup> Some η<sup>2</sup>-imine complexes, e.g. Cp<sub>2</sub>Zr(Me<sub>3</sub>SiN=CHPh)(THF), suggested the presence of a metallaziridine due to π-donation from Zr to the coordinated imine.<sup>5</sup> They react with unsaturated molecules, e.g. with alkynes or imines, to give metallacyclic products.<sup>5</sup> Other zirconocene imido complexes (Cp<sub>2</sub>Zr=NR) were generated as reactive intermediates by elimination of methane in Cp<sub>2</sub>Zr(CH<sub>3</sub>)-(NHR).<sup>2,6</sup>

Some of our recent results have shown that the complexes Cp<sub>2</sub>Ti(Me<sub>3</sub>SiC<sub>2</sub>SiMe<sub>3</sub>)<sup>7</sup> and Cp<sub>2</sub>Zr(L)(Me<sub>3</sub>SiC<sub>2</sub>SiMe<sub>3</sub>) (L = THF,<sup>8</sup> pyridine,<sup>9</sup> acetone<sup>10</sup>) are excellent metallocene generators under very mild conditions. They gave us the chance to investigate coupling reactions of unsaturated compounds without incorporation of alkynes. In a series of such studies we included selected aldimines and ketimines.

### Results and Discussion

We found that Cp<sub>2</sub>Ti(Me<sub>3</sub>SiC<sub>2</sub>SiMe<sub>3</sub>) reacts with 2 mol of the ketimine HN=CPh<sub>2</sub> in *n*-hexane at room temperature to give, after workup under argon, complex 1 in 91% yield.



Complex 1 is a dark red crystalline solid (mp 149–154 °C dec under argon), which is stable in air. In the IR spectrum of 1 the C=N double-bond stretching frequency at 1647 cm<sup>-1</sup> is in the expected region (cf. Cp<sub>2</sub>Zr-(N=CPh<sub>2</sub>)<sub>2</sub> 1630 cm<sup>-1</sup>).<sup>4</sup>

In the <sup>1</sup>H NMR spectrum the signals at δ 4.56 (d, *J* = 11.7 Hz) and 5.52 ppm (d, *J* = 11.7 Hz) are attributed to two different protons of the amido group.

The analogous Zr complex 2 is formed in 93% yield by the reaction of Cp<sub>2</sub>Zr(py)(Me<sub>3</sub>SiC<sub>2</sub>SiMe<sub>3</sub>)<sup>9</sup> with benzophenone imine in *n*-hexane. If the reaction was carried out in THF, only crude 2 was isolated. Recrystallization is not successful because complex 2 decomposes in solution. The acetone derivative "Cp<sub>2</sub>Zr-(acetone)(Me<sub>3</sub>SiC<sub>2</sub>SiMe<sub>3</sub>)", stabilized in the form of Cp<sub>2</sub>Zr-O-C(Me)<sub>2</sub>-C(SiMe<sub>3</sub>)-C(SiMe<sub>3</sub>),<sup>10</sup> is less reactive and does not react with benzophenone imine.

(7) Burlakov, V. V.; Rosenthal, U.; Beckhaus, R.; Polyakov, A. V.; Struchkov, Yu. T.; Oehme, G.; Shur, V. B.; Vol'pin, M. E. *Organomet. Chem. USSR* 1990, 3, 237.

(8) Rosenthal, U.; Ohff, A.; Michalik, M.; Görls, H.; Burlakov, V. V.; Shur, V. B. *Angew. Chem., Int. Ed. Engl.* 1993, 32, 1193.

(9) Rosenthal, U.; Ohff, A.; Baumann, W.; Tillack, A.; Görls, H.; Burlakov, V. V.; Shur, V. B. *Z. Anorg. Allg. Chem.* 1995, 621, 77.

(10) Rosenthal, U.; Ohff, A.; Baumann, W.; Tillack, A.; Görls, H.; Burlakov, V. V.; Shur, V. B. *J. Organomet. Chem.* 1994, 484, 203.

<sup>†</sup> On leave from the Institute of Organoelement Compounds of the Russian Academy of Sciences, Moscow, Russia.

<sup>®</sup> Abstract published in *Advance ACS Abstracts*, May 1, 1995.  
 (1) (a) Erker, G.; Frömberg, W.; Atwood, J. L.; Hunter, W. E. *Angew. Chem., Int. Ed. Engl.* 1984, 23, 68. (b) Bercaw, J. E.; Davies, D. L.; Wolczanski, P. T. *Organometallics* 1986, 5, 443. (c) Frömberg, W.; Erker, G. *J. Organomet. Chem.* 1985, 280, 343. (d) Boutonnet, F.; Dufour, N.; Straw, T.; Igau, A.; Majoral, J. P. *Organometallics* 1991, 10, 3939. (e) Erker, G.; Frömberg, W.; Krüger, C.; Raabe, E. *J. Am. Chem. Soc.* 1988, 110, 2400.

(2) Walsh, P. J.; Hollander, F. J.; Bergman, R. G. *J. Am. Chem. Soc.* 1988, 110, 8729.

(3) Hey-Hawkins, E. *Chem. Rev.* 1994, 94, 1661.

(4) Collier, M. R.; Lappert, M. F.; McMeeking, J. *Inorg. Nucl. Chem. Lett.* 1971, 7, 6898.

(5) Buchwald, S. L.; Watson, B. T.; Wannamaker, M. W.; Dewan, J. C. *J. Am. Chem. Soc.* 1989, 111, 4486.

(6) Negishi, E.; Cederbaum, F. E.; Takahashi, T. *Tetrahedron Lett.* 1986, 27, 2829.

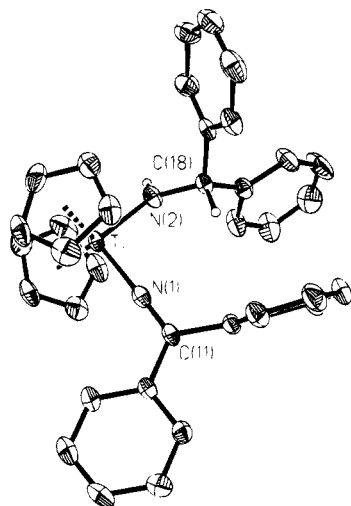


**Figure 1.** Molecular structure of complex **1**. Selected bond distances (Å) and angles (deg): Ti–N(1) = 1.891(3), Ti–N(2) = 1.980(3), N(1)–C(11) = 1.277(5), N(2)–C(18) = 1.447(5); Ti–N(1)–C(11) = 174.5(3), Ti–N(2)–C(18) = 129.6(2), N(1)–Ti–N(2) = 96.75(14).

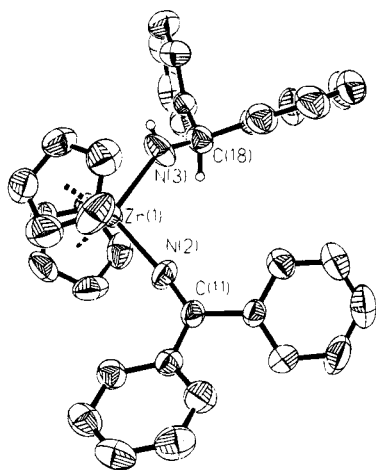


**Figure 2.** Molecular structure of complex **2**. Selected bond distances (Å) and angles (deg): Zr–N(2) = 2.043(3), Zr–N(3) = 2.089, N(2)–C(11) = 1.257(5), N(3)–C(18) = 1.372(6); Zr–N(2)–C(11) = 170.4(3), Zr–N(3)–C(18) = 138.5(3), N(2)–Zr–N(3) = 103.7(2).

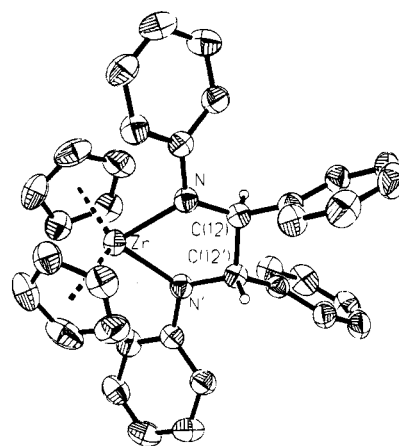
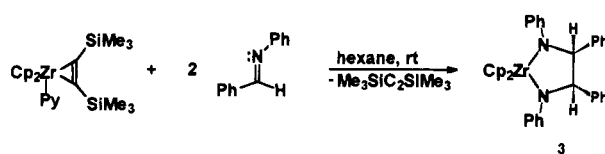
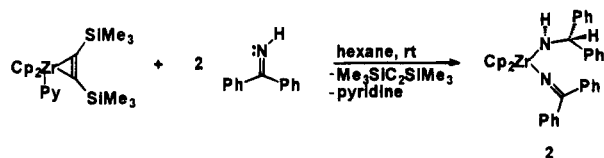


**Figure 3.** Molecular structure of complex **3**. Selected bond distances (Å) and angles (deg): Zr–N = 2.138(2), N–C(12) = 1.469(2), C(12)–C(12') = 1.545(4); Zr–N–C(12) = 116.1(8), N–C(12)–C(12') = 108.9(8), N–Zr–N' = 77.08(8).

1.372(6) Å) are distinguished, which are in the expected range for these C–N bond types.<sup>1a</sup> The angles at the shorter N atoms bonds (Ti(1)–N(1)–C(11) = 174.5(3)° and Zr(1)–N(2)–C(11) = 170.4(3)°) are not far from linear, confirming sp hybridization of the N atom. The angles at the other N atoms (Ti(1)–N(2)–C(18) = 129.6(2)° and Zr(1)–N(3)–C(18) = 138.5(2)°) are remarkably smaller.

The structure of **2** shows one alkylideneamido ligand (–N=CPh<sub>2</sub>) with typical structural parameters found in Cp<sub>2</sub>Zr(N=CPh<sub>2</sub>)<sub>2</sub><sup>1e</sup> (cf. Zr–N = 2.058(2) and 2.063(2) Å, C–N = 1.259(4) and 1.266(4) Å, Zr–N–C = 173.7(2) and 164.1(2)°), which is regarded to be the heteroallene Zr=N=CPh<sub>2</sub>. The second ligand –NH–CHPh<sub>2</sub> displays bonding parameters typical of saturated amido complexes.<sup>1e</sup>

The analogous reaction of Cp<sub>2</sub>Zr(py)(Me<sub>3</sub>SiC<sub>2</sub>SiMe<sub>3</sub>) with benzylideneaniline gives the coupling product **3** in 65% yield. A compound of the same type was described without experimental details for the reaction of the η<sup>2</sup>-imine complex Cp<sub>2</sub>Zr(Me<sub>3</sub>SiN=CHPh)(THF) with Me<sub>3</sub>SiN=CHPh.<sup>5</sup> The reaction of Cp<sub>2</sub>Ti(Me<sub>3</sub>SiC<sub>2</sub>SiMe<sub>3</sub>) with benzylideneaniline does not give the corresponding titanium complex.



Complex **2** is an orange-red crystalline substance. The spectral data are close to those of complex **1**. The IR spectrum of a Nujol suspension shows a C=N stretching frequency at 1625 cm<sup>-1</sup>, and the <sup>1</sup>H NMR exhibits two doublets at δ 3.76 and 5.76 ppm (*J* = 12.5 Hz) for the two different protons of the amido groups.

The structures of **1** (Figure 1) and **2** (Figure 2) were established by X-ray crystal structure analysis.

Compounds **1** and **2** are isostructural. They have a bent-metalloocene framework to which two different N atoms (**1** Ti(1)–N(1) = 1.891(3), Ti(1)–N(2) = 1.980(3) Å; **2**, Zr(1)–N(2) = 2.043(3), Zr(1)–N(3) = 2.089(3) Å) are coordinated. Correspondingly, two different C–N distances (**1**, N(1)–C(11) = 1.277(5), N(2)–C(18) = 1.447(5) Å; **2**, N(2)–C(11) = 1.257(5), N(3)–C(18) =

Complex **3** is a violet crystalline solid (mp 267–268 °C). The <sup>1</sup>H NMR spectrum exhibits, besides the signals of Cp and Ph groups, only two equivalent protons (δ 4.86 ppm) for the metallacycle, indicating that only one isomer is present in solution.

The structure of the racemate of **3** (Figure 3) was established by X-ray crystal structure analysis.

Crystals suitable for an X-ray structure analysis were obtained by recrystallization of **3** from THF and *n*-hexane at room temperature. In the crystal state **3** exhibits discrete molecular units, which are composed of a bent-metalloocene moiety (Cp<sub>2</sub>Zr) to which two equivalent nitrogen atoms are coordinated as a part of 1,3-diaza-2-zirconacyclopentane. The Zr–N bond distance (Zr(1)–N = 2.138(2) Å) is larger than in complexes

**1** and **2** and is typical for a zirconium–nitrogen single bond. The angle Zr–N–C12 is 116.1(11)° and indicates sp<sup>3</sup> hybridization of the nitrogen.

The symmetry of complex **3** is C<sub>2</sub> due to the trans configuration of the hydrogen atoms at the metallacycle. The cis isomer is not detected, either in the solid by X-ray crystal structure analysis or in solution by <sup>1</sup>H NMR spectra. The space group of **3** is centrosymmetrical. This indicates that both enantiomers of **3** (*R,R* and *S,S*) are present in the crystal.

The structure of **3** may be compared with that of the unsaturated zirconocene(IV) enediamido complex Cp<sub>2</sub>Zr–N(Ph)–CPh=CPh–N(Ph), which was prepared by oxidative addition of diazadienes to in situ generated zirconocene(II).<sup>11</sup> The Zr–N bonds in **3** are longer than those in the unsaturated complex (Zr(1)–N(1) = 2.100(4), Zr(1)–N(2) = 2.112(3) Å). The N–C distance of **3** (1.469(2) Å) is also longer in comparison with those of the unsaturated metallacycle (1.394(7) and 1.395(7) Å).

The most important difference in the two structures is the C<sub>β</sub>–C<sub>β'</sub> distance of 1.545(4) Å in the saturated complex **3** and that of 1.389(8) Å in the unsaturated complex, corresponding to N–C<sub>β</sub>–C<sub>β'</sub> angles of 108.9(11)° in **3** and 117.7(5) and 118.7(5)° in the unsaturated complex.

In contrast, the reactions of the sterically less demanding benzylidenemethylamine (MeN=CHPh) with metallocenes "Cp<sub>2</sub>Ti" and "Cp<sub>2</sub>Zr" gave products of another type. For example with, Cp<sub>2</sub>Ti(Me<sub>3</sub>SiC<sub>2</sub>SiMe<sub>3</sub>) no coupling products could be isolated. Treatment with Cp<sub>2</sub>Zr(py)(Me<sub>3</sub>SiC<sub>2</sub>SiMe<sub>3</sub>) provides a new type of zirconacycle, which is now under investigation.

## Conclusion

The reaction of the titanocene and zirconocene alkyne complexes Cp<sub>2</sub>Ti(Me<sub>3</sub>SiC<sub>2</sub>SiMe<sub>3</sub>) and Cp<sub>2</sub>Zr(L)(Me<sub>3</sub>SiC<sub>2</sub>SiMe<sub>3</sub>) (L = THF, pyridine) with Schiff bases such as aldimines and ketimines shows again the ability of such alkyne complexes to generate under mild conditions unstable "Cp<sub>2</sub>Ti" and "Cp<sub>2</sub>Zr" moieties, which react in situ with aldimines to yield amido-alkylideneamido complexes by hydrogen transfer.

Another reaction with ketimines giving cyclic diamido zirconacycles by a new C–C coupling reaction has a high synthetic potential for preparing diamines regioselectively and (by using chiral Cp ligands) stereoselectively. The reaction differs markedly from reversible alkyne–imine coupling reactions found earlier in the trapping of zirconocene η<sup>2</sup>-imine complexes by alkynes.<sup>12</sup>

Again the influence of alkyne substituents (SiMe<sub>3</sub>) is very important in destabilizing cocoupling and favoring homocoupling of substrates.

## Experimental Section

All operations were carried out under an inert atmosphere (argon) with standard Schlenk techniques. Prior to use, solvents were freshly distilled from sodium tetraethylaluminate under argon. Deuterated solvents were treated with

(11) Scholz, J.; Dlikan, M.; Stöhl, D.; Dietrich, A.; Schumann, H.; Thiele, K. H. *Chem. Ber.* **1990**, *123*, 2279.

(12) Coles, N.; Harris, M. C. J.; Whitby, R. J.; Blagg, J. *Organometallics* **1994**, *13*, 190.

sodium or sodium tetraethylaluminate, distilled, and stored under argon. The following spectrometers were used: NMR, Bruker ARX 400; IR, Nicolet Magna 550 (Nujol mulls using KBr plates); MS, AMD 402. Melting points were measured in sealed capillaries on a Büchi 535 apparatus.

**Preparation of Cp<sub>2</sub>Ti(NHCHPh<sub>2</sub>)(NCPPh<sub>2</sub>) (1).** A 0.38 g (1.10 mmol) amount of Cp<sub>2</sub>Ti(Me<sub>3</sub>SiC<sub>2</sub>SiMe<sub>3</sub>) was dissolved in 15 mL of THF, and 0.34 g (2.20 mmol) of benzophenone was added to the solution. The mixture was stirred for 1.5 h at room temperature, whereupon the color changed from brown to dark red. The solution was evaporated to dryness, and the oily residue was washed with diethyl ether. The resulting crystalline product was recrystallized from 10 mL of THF and 10 mL of *n*-hexane. When the solution stood at room temperature for 3 days, red crystals deposited. The crystals were washed twice with *n*-hexane and dried in vacuo to give 0.54 g (91%) of **1**, mp 149–154 °C. Anal. Calcd for C<sub>36</sub>H<sub>32</sub>N<sub>2</sub>Ti (540.54): C, 79.99; H, 5.97; N, 5.18. Found: C, 79.68; H, 5.76; N, 4.95. IR (Nujol mull): 3352 cm<sup>-1</sup> (ν<sub>N–H</sub>), 1647 cm<sup>-1</sup> (ν<sub>C=N</sub>); <sup>1</sup>H NMR (THF-*d*<sub>6</sub>): δ 4.56 (d, *J* = 11.7 Hz, 1H, N–H), 5.52 (d, *J* = 11.7 Hz, 1H, CHPh<sub>2</sub>), 5.84 (s, 10H, Cp), 7.06–7.38 (m, 20H, Ar H). <sup>13</sup>C{<sup>1</sup>H} NMR (THF-*d*<sub>6</sub>): δ 74.5 (CHPh<sub>2</sub>), 110.8 (Cp), 126.1, 127.8, 128.4, 128.5, 128.7, 128.9, 141.3, 151.0 (Ph), 167.5 (CPh<sub>2</sub>).

**Preparation of Cp<sub>2</sub>Zr(NHCHPh<sub>2</sub>)(NCPPh<sub>2</sub>) (2).** To a solution of 0.69 g (1.46 mmol) of Cp<sub>2</sub>Zr(py)(Me<sub>3</sub>SiC<sub>2</sub>SiMe<sub>3</sub>) in 20 mL of *n*-hexane was added 0.53 g (2.90 mmol) of benzophenone imine. The mixture was stirred for 10 min and was further kept at room temperature without stirring. After 5 h orange-red needles were formed and the liquid was decanted. The remaining crystals were washed with cold *n*-hexane and dried in vacuo to give 0.79 g (93%) of **2**: mp 127–130 °C. Anal. Calcd for C<sub>36</sub>H<sub>32</sub>N<sub>2</sub>Zr (583.88): C, 74.06; H, 5.52; N, 4.80. Found: C, 73.58; H, 5.80; N, 4.60. IR (Nujol mull): 3348 cm<sup>-1</sup> (ν<sub>N–H</sub>), 1625 cm<sup>-1</sup> (ν<sub>C=N</sub>). <sup>1</sup>H NMR (benzene-*d*<sub>6</sub>): δ 3.76 (d, *J* = 12.5 Hz, 1H, N–H), 5.76 (d, *J* = 12.5 Hz, 1H, CHPh<sub>2</sub>), 5.85 (s, 10 H, Cp), 7.16–7.79 (m, 20H, Ar H).

**Preparation of Cp<sub>2</sub>Zr–N(Ph)–CHPh–CHPh–N(Ph) (3).** A 0.77 g (1.63 mmol) amount of Cp<sub>2</sub>Zr(py)Me<sub>3</sub>SiC<sub>2</sub>SiMe<sub>3</sub> was dissolved in 20 mL of THF under argon, and 0.48 g (3.27 mmol) of benzylideneaniline was added. The solution was stirred at room temperature for 1 h, and the color slowly turned from black to red-violet. The solvent was removed in vacuo. The solid residue was dissolved in a mixture of 10 mL of THF and 10 mL of *n*-hexane. After 3 days violet crystals precipitated. The solvent was decanted and the obtained product was dried in vacuo to yield 0.62 g (65%) of **3**: mp 267–268 °C. Anal. Calcd for C<sub>36</sub>H<sub>32</sub>N<sub>2</sub>Zr (583.88): C, 74.06; H, 5.52; N, 4.80. Found: C, 74.11; H, 5.65; N, 4.74. <sup>1</sup>H NMR (benzene-*d*<sub>6</sub>): δ 4.86 (s, 2H, CHPh), 6.03 (s, 10H, Cp), 6.36 (d, 4H, Ar H), 6.96–7.05 (m, 16H, Ar H). <sup>13</sup>C{<sup>1</sup>H} NMR (benzene-*d*<sub>6</sub>): δ 74.0 (CHPh), 115.0 (Cp), 118.7, 118.9, 126.9, 127.8, 129.1, 129.5 (Ph), 143.9, 154.4 (Ph ipso).

**X-ray Crystallographic Study of Complexes 1–3.** Diffraction data were collected on a CAD4 Mach 3 diffractometer using Mo Kα radiation. The structure was solved by direct methods<sup>13</sup> and refined by full-matrix least-squares techniques against F<sup>2</sup>;<sup>14</sup> structural representations in the figures were obtained by using XP (Siemens). **1**: space group P1̄; *a* = 10.550(1) Å, *b* = 11.127(1) Å, *c* = 13.900(2) Å, α = 68.62(1)°, β = 82.64(1)°, γ = 66.14(1)°, *V* = 1389.2(3) Å<sup>3</sup>, crystal dimensions 0.4 × 0.3 × 0.2 mm, *Z* = 2, *D*<sub>c</sub> = 1.292 g/cm<sup>3</sup>, μ = 0.336 mm<sup>-1</sup>, θ range 2.35–24.98°; number of collected data at –80 °C 5156; number of unique data 4864; number of observed data with *I* > 2σ(*I*) 3734; non-hydrogen atoms were refined anisotropically; number of variables 359; *R*<sub>1</sub> = 0.070; *wR*<sub>2</sub> = 0.197. **2**: space group P2<sub>1</sub>/n; *a* = 14.155(1) Å, *b* = 10.708(1) Å, *c* = 19.669(1)

(13) Sheldrick, G. M. SHELXS-86. *Acta Crystallogr., Sect. A* **1990**, *46*, 467.

(14) Sheldrick, G. M. SHELXL-93; University of Göttingen, Göttingen, Germany, 1993.

$\text{\AA}$ ,  $\beta = 104.181(8)$ ,  $V = 2890.4(4) \text{\AA}^3$ , crystal dimensions  $0.4 \times 0.4 \times 0.2 \text{ mm}$ ,  $Z = 4$ ,  $D_c = 1.342 \text{ g/cm}^3$ ,  $\mu = 0.407 \text{ mm}^{-1}$ ,  $\theta$  range  $2.41\text{--}24.97^\circ$ ; number of collected data at  $20 \text{ }^\circ\text{C}$  5221; number of unique data 5064; number of observed data with  $I > 2\sigma(I)$  3441; non-hydrogen atoms were refined anisotropically; number of variables 357;  $R_1 = 0.043$ ;  $wR_2 = 0.093$ . **3**: space group  $C2/c$ ;  $a = 22.404(2) \text{\AA}$ ,  $b = 10.699(1) \text{\AA}$ ,  $c = 13.757(1) \text{\AA}$ ,  $\beta = 121.900(8)^\circ$ ,  $V = 2799.5(4) \text{\AA}^3$ , crystal dimensions  $0.5 \times 0.2 \times 0.2 \text{ mm}$ ,  $Z = 8$ ,  $D_c = 1.385 \text{ g/cm}^3$ ,  $\mu = 0.421 \text{ mm}^{-1}$ ,  $\theta$  range  $2.14\text{--}24.96^\circ$ ; number of collected data at  $20 \text{ }^\circ\text{C}$  2573; number of unique data 2460; number of observed data with  $I$

$> 2\sigma(I)$  2264; non-hydrogen atoms were refined anisotropically; number of variables 181;  $R_1 = 0.024$ ;  $wR_2 = 0.068$ .

**Supplementary Material Available:** Figures giving additional views of the structures and tables giving crystal data and structure refinement details, atomic coordinates, thermal parameters, and bond lengths and angles for **1-3** (31 pages). Ordering information is given on any current masthead page.

OM950029P

## H<sub>2</sub>- versus HSiMe<sub>3</sub>-Elimination in the Reactivity of HP(SiMe<sub>3</sub>)<sub>2</sub> with Me<sub>2</sub>AlH To Yield a Mixed Organoaluminum Phosphide Trimer

Larry K. Krannich,\* Charles L. Watkins,\* and Steven J. Schauer

Department of Chemistry, University of Alabama at Birmingham,  
Birmingham, Alabama 35294

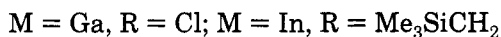
Received November 28, 1994<sup>⊗</sup>

**Summary:** The reaction of HP(SiMe<sub>3</sub>)<sub>2</sub> with Me<sub>2</sub>AlH was studied by variable temperature NMR. Spectral data indicate that HSiMe<sub>3</sub>-elimination is the preferred mode of reactivity for producing the Me<sub>2</sub>AlP(H)SiMe<sub>3</sub> moiety. However, this Al–P intermediate subsequently undergoes a transphosphination reaction with HP(SiMe<sub>3</sub>)<sub>2</sub> to produce several Me<sub>2</sub>AlP(SiMe<sub>3</sub>)<sub>2</sub>-containing species. The major product from the reaction is the mixed trimeric species [Me<sub>2</sub>AlP(H)SiMe<sub>3</sub>]<sub>2</sub>Me<sub>2</sub>AlP(SiMe<sub>3</sub>)<sub>2</sub> (**1**), which was isolated and characterized.

### Introduction

Phosphines containing P–H bonds react with organoalanes, R<sub>3</sub>Al, via a 1,2-elimination process followed by condensation to produce Al–P oligomeric species.<sup>1</sup> The utility of this reaction in organoaluminum phosphide synthesis is limited by the elevated temperatures that are required for alkane elimination.<sup>2</sup> However, more facile reactivity is observed when dialkylaluminum hydride species (R<sub>2</sub>AlH) are reacted with secondary phosphines, resulting in H<sub>2</sub>-elimination.<sup>3,4</sup>

Phosphines containing P–Si bonds react with Ga–Cl and In–Cl bond containing compounds via a dehalosilylation process to provide a route to Ga–P<sup>5</sup> and In–P<sup>6</sup> containing compounds (see eq 1). On the other



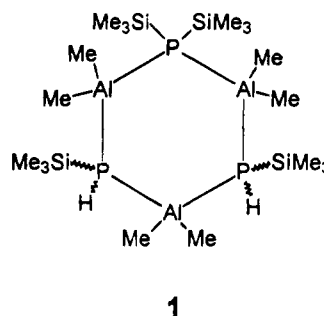
hand, P(SiMe<sub>3</sub>)<sub>3</sub> reacts with R<sub>2</sub>AlCl (R = Et, Bu<sup>i</sup>) and RAlCl<sub>2</sub> to yield adducts instead of dehalosilylation products.<sup>7</sup> More facile HSiMe<sub>3</sub>-elimination occurs when an Al–H bond containing organoaluminum species is used. For example, Cl<sub>2</sub>AlH and Me<sub>2</sub>AlH readily react with the P–Si bond in Et<sub>2</sub>PSiMe<sub>3</sub> to eliminate HSiMe<sub>3</sub> and form [Cl<sub>2</sub>AlPEt<sub>2</sub>]<sub>3</sub> and [Me<sub>2</sub>AlPEt<sub>2</sub>]<sub>2</sub>, respectively.<sup>8</sup> In addition, H<sub>2</sub>-elimination is the preferred mode of

reaction between Bu<sup>i</sup><sub>2</sub>AlH and the primary phosphine H<sub>2</sub>PSiPh<sub>3</sub>, producing [Bu<sup>i</sup><sub>2</sub>AlP(H)SiPh<sub>3</sub>]<sub>2</sub>.<sup>9</sup>

Thus, with silylphosphines that contain both P–H and P–Si bonds, both bonds can potentially be involved in elimination reactions. We have not found any reports on reactivity studies between the secondary silylphosphine HP(SiMe<sub>3</sub>)<sub>2</sub> and R<sub>3</sub>Al or R<sub>2</sub>AlH. In this paper, we report the first reactivity studies between HP(SiMe<sub>3</sub>)<sub>2</sub> and Me<sub>2</sub>AlH. These results establish that HSiMe<sub>3</sub>-elimination followed by transphosphination is the preferred mode of reaction to the isolated mixed organoaluminum phosphide.

### Results and Discussion

Me<sub>2</sub>AlH was allowed to react in a 1:1 stoichiometric mole ratio with HP(SiMe<sub>3</sub>)<sub>2</sub> at –115 °C in toluene-*d*<sub>8</sub> using our previously described reaction protocol.<sup>10</sup> <sup>1</sup>H, <sup>13</sup>C, and <sup>31</sup>P NMR spectra were recorded over the temperature range –90 °C to room temperature to monitor the progress of the reaction and elucidate the reaction pathway(s) to the thermodynamically stable products. <sup>31</sup>P NMR spectra of the reaction mixture at selected temperatures have been filed as supplementary material. The NMR spectra indicate that the mixed species [Me<sub>2</sub>AlP(H)SiMe<sub>3</sub>]<sub>2</sub>Me<sub>2</sub>AlP(SiMe<sub>3</sub>)<sub>2</sub> (**1**) was



**1**

formed as the major product in the 1:1 reaction system. Compound **1** was isolated as a pure white solid by vacuum sublimation of the solid reaction product mixture and was characterized using NMR, IR, and MS. The EI-MS fragmentation data (see Table 1) provide additional evidence to support a mixed trimeric Al–P compound.

From these results, one might conclude that the HSiMe<sub>3</sub>-elimination was favored over H<sub>2</sub>-elimination by a factor of 2 to 1. However, the NMR spectra indicate

<sup>⊗</sup> Abstract published in *Advance ACS Abstracts*, May 1, 1995.

(1) (a) Mole, T.; Jeffery, E. A. *Organoaluminum Compounds*; Elsevier: New York, 1972. (b) Davidson, N.; Brown, H. C. *J. Am. Chem. Soc.* **1942**, *64*, 316. (c) Coates, G. E.; Graham, J. J. *J. Chem. Soc.* **1963**, 233.

(2) For example, the reaction of Me<sub>3</sub>Al with HPMe<sub>2</sub> or HPEt<sub>2</sub> requires prolonged heating at 200 °C: Beachley, O. T.; Coates, G. E. *J. Chem. Soc.* **1965**, 3241.

(3) Beachley, O. T.; Victoriano, L. *Inorg. Chem.* **1966**, *25*, 1948.

(4) Beachley, O. T.; Tessier-Youngs, C. *Organometallics* **1983**, *2*, 796.

(5) Wells, R. L.; Self, M. F.; McPhail, A. T.; Aubuchon, S. A.; Woudenberg, R. C.; Jasinski, J. P. *Organometallics* **1993**, *12*, 2832.

(6) Wells, R. L.; McPhail, A. T.; Self, M. F. *Organometallics* **1992**, *11*, 221.

(7) Wells, R. L.; McPhail, A. T.; Self, M. F.; Laske, J. A. *Organometallics* **1993**, *12*, 3333.

(8) Fritz, G.; Emül, R. *Z. Anorg. Allg. Chem.* **1975**, *416*, 19.

(9) Cowley, A. H.; Jones, R. A.; Mardones, M. A.; Atwood, J. L.; Bott, S. G. *Angew. Chem., Int. Ed. Engl.* **1990**, *29*, 1409.

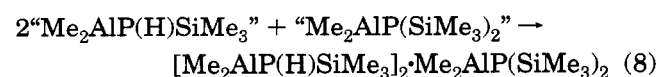
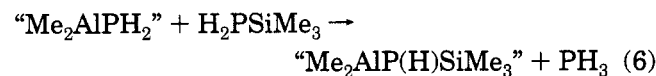
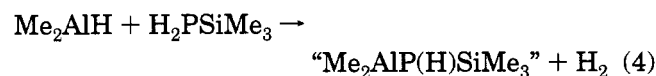
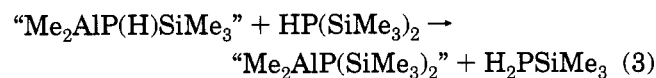
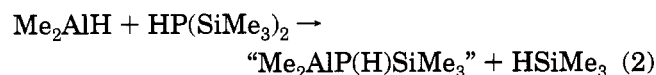
(10) Kannich, L. K.; Watkins, C. L.; Srivastava, D. K. *Polyhedron* **1990**, *9*, 289.

Table 1. EI-MS Data for  $[\text{Me}_2\text{AlP}(\text{H})\text{SiMe}_3]_2 \cdot \text{Me}_2\text{AlP}(\text{SiMe}_3)_2$ 

<i>m/z</i> (%)	fragment
543 (7.3)	$[\text{Me}_2\text{AlP}(\text{H})\text{SiMe}_3]_2 \cdot \text{Me}_2\text{AlP}(\text{SiMe}_3)_2 - \text{Me}^+$
527 (0.4)	$[\text{Me}_2\text{AlP}(\text{H})\text{SiMe}_3]_2 \cdot \text{Me}_2\text{AlP}(\text{SiMe}_3)_2 - 2\text{Me} - \text{H}^+$
471 (1.8)	$[\text{Me}_2\text{AlP}(\text{H})\text{SiMe}_3]_2 \cdot \text{Me}_2\text{AlP}(\text{SiMe}_3)_2 - \text{Me} - \text{SiMe}_3 + \text{H}^+$
453 (1.9)	$[\text{Me}_2\text{AlP}(\text{H})\text{SiMe}_3]_2 \cdot \text{Me}_2\text{AlP}(\text{SiMe}_3)_2 - \text{P}(\text{H})\text{SiMe}_3^+$
395 (0.7)	$\text{Me}_2\text{AlP}(\text{H})\text{SiMe}_3 \cdot \text{Me}_2\text{AlP}(\text{SiMe}_3)_2 - \text{H}^+$
381 (38.6)	$\text{Me}_2\text{AlP}(\text{H})\text{SiMe}_3 \cdot \text{Me}_2\text{AlP}(\text{SiMe}_3)_2 - \text{Me}^+$ or $[\text{Me}_2\text{AlP}(\text{H})\text{SiMe}_3]_2 \cdot \text{Me}_2\text{AlP}(\text{SiMe}_3)_2 - \text{P}(\text{SiMe}_3)_2^+$
365 (11.8)	$\text{Me}_2\text{AlP}(\text{H})\text{SiMe}_3 \cdot \text{Me}_2\text{AlP}(\text{SiMe}_3)_2 - 2\text{Me} - \text{H}^+$
309 (10.0)	$[\text{Me}_2\text{AlP}(\text{H})\text{SiMe}_3]_2 - \text{Me}^+$
293 (10.6)	$[\text{Me}_2\text{AlP}(\text{H})\text{SiMe}_3]_2 - 2\text{Me} - \text{H}^+$
291 (24.1)	$\text{Me}_2\text{AlP}(\text{H})\text{SiMe}_3 \cdot \text{Me}_2\text{AlP}(\text{SiMe}_3)_2 - \text{P}(\text{H})\text{SiMe}_3^+$
219 (33.9)	$[\text{Me}_2\text{AlP}(\text{H})\text{SiMe}_3]_2 - \text{P}(\text{H})\text{SiMe}_3^+$ or $\text{Me}_2\text{AlP}(\text{H})\text{SiMe}_3 \cdot \text{Me}_2\text{AlP}(\text{SiMe}_3)_2 - \text{P}(\text{SiMe}_3)_2^+$ or $\text{Me}_2\text{AlP}(\text{SiMe}_3)_2 - \text{Me}^+$
203 (10.5)	$\text{Me}_2\text{AlP}(\text{SiMe}_3)_2 - 2\text{Me} - \text{H}^+$
147 (30.5)	$\text{Me}_2\text{AlP}(\text{H})\text{SiMe}_3 - \text{Me}^+$
131 (24.1)	$\text{Me}_2\text{AlP}(\text{H})\text{SiMe}_3 - 2\text{Me} - \text{H}^+$
73 (100.0)	$\text{SiMe}_3^+$
57 (21.0)	$\text{AlMe}_2^+$

that a variety of mixed "Me<sub>2</sub>AlPH<sub>2</sub>", "Me<sub>2</sub>AlP(H)-SiMe<sub>3</sub>", and "Me<sub>2</sub>AlP(SiMe<sub>3</sub>)<sub>2</sub>"-containing<sup>11</sup> Al-P species are produced during the course of the reaction, including a trace of [Me<sub>2</sub>AlP(SiMe<sub>3</sub>)<sub>2</sub>]<sub>2</sub>.<sup>12</sup> In addition, the phosphines H<sub>2</sub>PSiMe<sub>3</sub> and PH<sub>3</sub> are observed as intermediates, indicating that the reaction pathways are not as straightforward as simply H<sub>2</sub>- versus HSiMe<sub>3</sub>-elimination. Our study establishes that trimethylsilane elimination is the preferred mode of reaction of HP-(SiMe<sub>3</sub>)<sub>2</sub> with Me<sub>2</sub>AlH; however, H<sub>2</sub>-elimination also occurs when Me<sub>2</sub>AlH reacts with H<sub>2</sub>PSiMe<sub>3</sub> and PH<sub>3</sub>, which are formed during the course of the overall reaction. Although intermediate and minor product species containing the Me<sub>2</sub>AlP(SiMe<sub>3</sub>)<sub>2</sub> moiety are observed in the spectra, this reactivity study suggests that these species do not arise *via* H<sub>2</sub>-elimination with HP(SiMe<sub>3</sub>)<sub>2</sub>, but through a transphosphination of "Me<sub>2</sub>AlP(H)SiMe<sub>3</sub>" and "Me<sub>2</sub>AlPH<sub>2</sub>" intermediates with HP(SiMe<sub>3</sub>)<sub>2</sub> and H<sub>2</sub>PSiMe<sub>3</sub>, respectively.

The variable temperature NMR data support the following reactions as being important in the Me<sub>2</sub>AlH/HP(SiMe<sub>3</sub>)<sub>3</sub> reaction system (eqs 2-8):

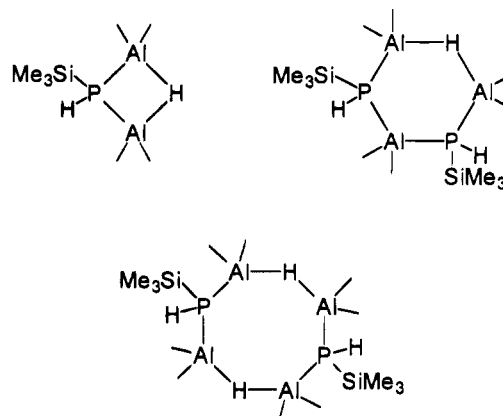


At low temperature (<-80 °C), the NMR spectra indicate no reaction between HP(SiMe<sub>3</sub>)<sub>2</sub> and Me<sub>2</sub>AlH.

(11) Due to the presence of mixed oligomeric Al-P species, specific monomers will be referred to as single species (i.e., "Me<sub>2</sub>AlP(H)SiMe<sub>3</sub>") without implying that they exist as true monomers in solution.

(12) Hey-Hawkins, E.; Lappert, M. F.; Atwood, J. L.; Bott, S. G. *J. Chem. Soc., Dalton Trans.* **1991**, 939.

Above -80 °C, reactivity is observed (eq 2) without any spectral evidence for adduct formation between the parent reactants. HSiMe<sub>3</sub> and eight-, six-, and four-membered oligomers containing the Me<sub>2</sub>AlP(H)SiMe<sub>3</sub> moiety, i.e., [Me<sub>2</sub>AlP(H)SiMe<sub>3</sub>]<sub>n</sub>[Me<sub>2</sub>AlH]<sub>m</sub> (*n* = 1, *m* = 1; *n* = 2, *m* = 1, 2), are observed in the spectra. Line drawings of these oligomers are as follows:



These oligomers arise from the interaction of "Me<sub>2</sub>AlP(H)SiMe<sub>3</sub>" with available Me<sub>2</sub>AlH in solution. In the absence of adduct formation, considerable amounts of HP(SiMe<sub>3</sub>)<sub>2</sub> and Me<sub>2</sub>AlH are available to react with initial products and produce intermediates whose compositions and/or amounts are dependent upon the concentration of the initial reactants. Conversion of the eight-membered ring, which has a 4:2 Al:P composition ratio with one molecule of Me<sub>2</sub>AlH per Me<sub>2</sub>AlP(H)SiMe<sub>3</sub> unit, to the six-membered ring, which has a 3:2 Al:P composition ratio, occurs with depletion of Me<sub>2</sub>AlH as the Me<sub>2</sub>AlH/HP(SiMe<sub>3</sub>)<sub>2</sub> reaction proceeds. With increasing temperature, the six-membered ring, [Me<sub>2</sub>AlP(H)SiMe<sub>3</sub>]<sub>2</sub>·Me<sub>2</sub>AlH, becomes one of the predominant species in solution. Also present in the reaction mixture are small amounts of the four-membered ring, Me<sub>2</sub>AlP(H)SiMe<sub>3</sub>·Me<sub>2</sub>AlH, which has a 2:1 Al:P composition ratio. Eventually the Me<sub>2</sub>AlH is consumed, allowing the final Al-P products to form. Analogous eight-, six-, and four-membered ring systems have been proposed, on the basis of NMR and solution molecular weight data, for Me<sub>2</sub>AlPR<sub>2</sub>-<sup>3</sup> and Me<sub>2</sub>AlNR<sub>2</sub>-containing<sup>13-16</sup> species in

(13) Glore, J. D.; Hall, R. E.; Schram, E. P. *Inorg. Chem.* **1972**, *11*, 550.

(14) Glore, J. D.; Schram, E. P. *Inorg. Chem.* **1972**, *11*, 1532.

(15) Bernstein, J. D. Ph.D. Thesis, SUNY-Buffalo, Buffalo, NY, 1975.



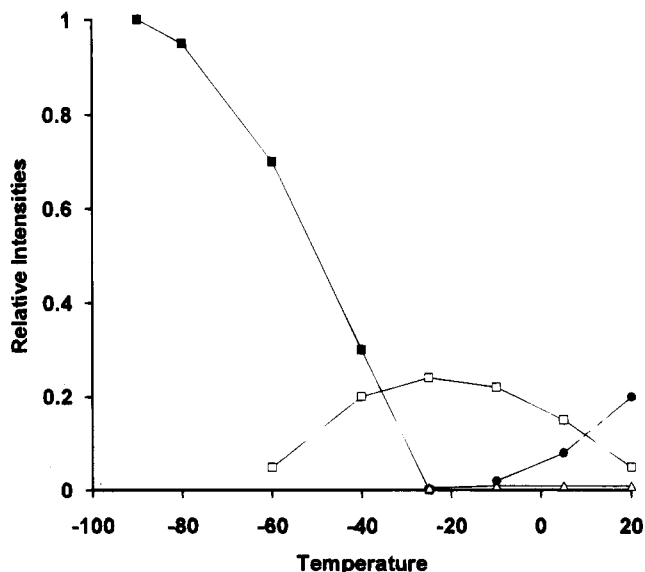


**Figure 1.** Relative amounts of selected P-containing species as a function of temperature (°C). HP(SiMe<sub>3</sub>)<sub>2</sub> (■), H<sub>2</sub>PSiMe<sub>3</sub> (□), PH<sub>3</sub> (△), compound 1 (●).

reactions involving Me<sub>2</sub>AlH. The eight-membered [Me<sub>2</sub>AlNMe<sub>2</sub>·Me<sub>2</sub>AlH]<sub>2</sub><sup>13</sup> and six-membered [Me<sub>2</sub>AlNMe<sub>2</sub>]<sub>2</sub>·Me<sub>2</sub>AlH<sup>14</sup> rings exist as isolable species.

The <sup>31</sup>P NMR spectra indicate the formation of H<sub>2</sub>PSiMe<sub>3</sub> above -60 °C and PH<sub>3</sub> above -10 °C. Coupled <sup>31</sup>P NMR data and comparisons with literature data confirm the formation of H<sub>2</sub>PSiMe<sub>3</sub><sup>17</sup> and PH<sub>3</sub>.<sup>18</sup> The assignments for various phosphorus-containing intermediates were made using information on the influence of H, Me, and Me<sub>3</sub>Si substituents in silylphosphines on <sup>1</sup>H and <sup>31</sup>P chemical shifts and coupling constants as previously reported.<sup>17</sup> Both coupled and <sup>1</sup>H-decoupled <sup>31</sup>P NMR spectra were recorded to indicate the number of hydrogen atoms directly bound to the phosphorus atom in each species. <sup>31</sup>P-decoupled <sup>1</sup>H NMR spectra were obtained to verify the <sup>1</sup>H NMR assignments.

After the formation of Me<sub>2</sub>AlP(H)SiMe<sub>3</sub>-containing oligomers, HP(SiMe<sub>3</sub>)<sub>2</sub> reacts with these oligomers to produce Me<sub>2</sub>AlP(SiMe<sub>3</sub>)<sub>2</sub>-containing species and H<sub>2</sub>PSiMe<sub>3</sub> (eq 3). The H<sub>2</sub>PSiMe<sub>3</sub> then reacts with available Me<sub>2</sub>AlH *via* H<sub>2</sub>-elimination to form the Me<sub>2</sub>AlP(H)SiMe<sub>3</sub>-containing oligomers (eq 4). Above -40 °C, H<sub>2</sub>PSiMe<sub>3</sub> also reacts with available Me<sub>2</sub>AlH *via* HSiMe<sub>3</sub>-elimination to produce Me<sub>2</sub>AlPH<sub>2</sub>-containing oligomers (eq 5). NMR spectral data suggest that these oligomers involve Me<sub>2</sub>AlPH<sub>2</sub> associated with the Me<sub>2</sub>AlP(H)SiMe<sub>3</sub> and Me<sub>2</sub>AlP(SiMe<sub>3</sub>)<sub>2</sub> moieties. Above -10 °C, H<sub>2</sub>PSiMe<sub>3</sub> reacts with the "Me<sub>2</sub>AlPH<sub>2</sub>" unit *via* transphosphination to yield PH<sub>3</sub> and "Me<sub>2</sub>AlP(H)SiMe<sub>3</sub>" (eq 6). PH<sub>3</sub> then reacts with Me<sub>2</sub>AlH *via* H<sub>2</sub>-elimination to form "Me<sub>2</sub>AlPH<sub>2</sub>"-containing oligomers (eq 7). The formation of 1 is first noted above -10 °C (eq 8). Figure 1 denotes the relative amounts of HP(SiMe<sub>3</sub>)<sub>2</sub>, H<sub>2</sub>PSiMe<sub>3</sub>, PH<sub>3</sub>, and 1 as obtained from <sup>31</sup>P NMR intensity data as a function of temperature.

NMR data indicate that the reaction produced 1, which is the first reported mixed trimeric organoalu-

minum phosphide, in yields greater than 90%. This implies that the overall yields of "Me<sub>2</sub>AlP(H)SiMe<sub>3</sub>" and "Me<sub>2</sub>AlP(SiMe<sub>3</sub>)<sub>2</sub>", regardless of how they were formed, must be in an approximate ratio of 2:1. The spectral data indicate that, while "Me<sub>2</sub>AlP(H)SiMe<sub>3</sub>" is formed primarily by HSiMe<sub>3</sub>-elimination from Me<sub>2</sub>AlH and HP(SiMe<sub>3</sub>)<sub>2</sub>, "Me<sub>2</sub>AlP(SiMe<sub>3</sub>)<sub>2</sub>" is formed *via* transphosphination of "Me<sub>2</sub>AlP(H)SiMe<sub>3</sub>" with HP(SiMe<sub>3</sub>)<sub>2</sub> rather than from a possible H<sub>2</sub>-elimination from the reaction of Me<sub>2</sub>AlH with HP(SiMe<sub>3</sub>)<sub>2</sub>. Thus unique combination of reaction pathways results in the formation of 1. The isolated product exists as a mixture of *cis* and *trans* isomers, in an approximate 5:1 ratio. Because 1 is presumed to exist in a chair conformation, the major isomer is assigned the *cis* form by analogy with 1,3-dimethylcyclohexane, whose *cis* isomer can adopt a conformation allowing the two methyl groups to occupy equatorial positions to minimize 1,3-diaxial interactions. The *trans* isomer, with both equatorial and axial methyl groups, should be less favored.

Additional evidence to support the proposed route to the formation of 1 was obtained by studying the reaction system at different stoichiometries.<sup>16</sup> In the 2:1 Me<sub>2</sub>AlH/HP(SiMe<sub>3</sub>)<sub>2</sub> reaction system reactivity proceeds *via* a pathway analogous to that observed in the 1:1 system, except the final reaction mixture consists of a mixture of the eight-, six-, and four-membered ring compounds without the formation of 1. Thus, the presence of the additional Me<sub>2</sub>AlH complexes the "Me<sub>2</sub>AlPH<sub>2</sub>", "Me<sub>2</sub>AlP(H)SiMe<sub>3</sub>", and "Me<sub>2</sub>AlP(SiMe<sub>3</sub>)<sub>2</sub>" moieties and thereby curtails further reactivity to 1.

In the 1:2 Me<sub>2</sub>AlH/HP(SiMe<sub>3</sub>)<sub>2</sub> reaction system, the NMR spectra of the final reaction mixture indicated the formation of 1 and HSiMe<sub>3</sub> as the major products. In addition to unreacted HP(SiMe<sub>3</sub>)<sub>2</sub>, the spectra also indicated the presence of H<sub>2</sub>PSiMe<sub>3</sub> and PH<sub>3</sub>. The latter are presumed to form *via* the pathways suggested in the 1:1 reaction system. Because of the additional quantity of HP(SiMe<sub>3</sub>)<sub>2</sub> present in the system, the eight-, six-, and four-membered ring oligomeric complexes and "Me<sub>2</sub>AlPH<sub>2</sub>"-containing species are not observed as reaction products.

## Experimental Section

**General Considerations.** HP(SiMe<sub>3</sub>)<sub>2</sub> was purchased from Quantum Design, Inc., Austin, TX, and used as obtained. Its purity was checked by <sup>1</sup>H, <sup>13</sup>C, and <sup>31</sup>P NMR. Me<sub>2</sub>AlH was obtained as a gift from Morton Advanced Materials, Danvers, MA. The variable temperature studies were carried out using a previously described procedure.<sup>10</sup> The reactions were monitored by <sup>1</sup>H, <sup>13</sup>C, and <sup>31</sup>P NMR spectroscopy on a GE (Nicolet) 300 MHz multinuclear FT-NMR operating at 300.1, 75.4, and 121.5 MHz, respectively. The 1:1, 2:1, and 1:2 Me<sub>2</sub>AlH/HP(SiMe<sub>3</sub>)<sub>2</sub> NMR tube reactions were prepared using 1:1, 2:1, and 0.5:1 mmol amounts, respectively, of the starting materials in a total of 3 mL of toluene-*d*<sub>8</sub> in 10 mm J. Young VNMR tubes. Low-resolution EI-MS data were recorded in DIP mode on a HP5986A GC/MS spectrometer operated at 70 eV with a 2400 V electron multiplier. Carbon and hydrogen analyses were obtained from E+R Microanalytical Laboratory, Inc., Corona, NY.

[Me<sub>2</sub>AlP(H)SiMe<sub>3</sub>]<sub>2</sub>·Me<sub>2</sub>AlP(SiMe<sub>3</sub>)<sub>2</sub> (1). A 1.5 mL solution of HP(SiMe<sub>3</sub>)<sub>2</sub> (0.178 g, 1 mmol) in toluene-*d*<sub>8</sub> was added to a 1.5 mL solution of Me<sub>2</sub>AlH (0.058 g, 1 mmol) in toluene-*d*<sub>8</sub>, which had been cooled to -115 °C with a liquid N<sub>2</sub>/ethanol

(16) Watkins, C. L.; Krannich, L. K.; Thomas, C. J.; Srivastava, D. *Polyhedron* **1994**, *13*, 3299.

(17) Fritz, G.; Schäfer, H. Z. *Anorg. Allg. Chem.* **1974**, *409*, 137.

(18) Crutchfield, M. M.; Dungan, C. H.; Letcher, J. H.; Mark, V.; Van Wazer, J. R. *Top. Phosphorus Chem.* **1967**, *5*, 238.

bath. The resultant mixture was slowly warmed to room temperature over an 8-h period and then remained at room temperature for 3 days to allow complete reaction. Removal of the solvent under vacuum yielded a white solid residue, which was then sublimed under vacuum at 80 °C. Compound **1** was isolated in 73% yield as a clear crystalline solid (mp 126–127 °C). NMR (toluene-*d*<sub>6</sub>): <sup>1</sup>H δ 1.40 (d, *PH*, <sup>1</sup>*J*<sub>PH</sub> = 263 Hz, *cis*), 1.15 (d, *PH*, <sup>1</sup>*J*<sub>PH</sub> = 250 Hz, *trans*), 0.37 (d, P(SiMe<sub>3</sub>)<sub>2</sub>, <sup>3</sup>*J*<sub>PH</sub> = 4.74 Hz, *cis*), 0.30 (vt, P(H)SiMe<sub>3</sub>, *J*<sub>sum</sub> = 5.31 Hz, *cis*), 0.32 (vt, P(H)SiMe<sub>3</sub>, *J*<sub>sum</sub> = 5.19 Hz, *trans*), 0.34 (d, P(SiMe<sub>3</sub>)<sub>2</sub>, *trans*), -0.15(-0.24) (m, MeAl, both isomers); <sup>13</sup>C δ 2.40 (vt, P(H)SiMe<sub>3</sub>, *J*<sub>sum</sub> = 8.85 Hz, *cis*), 3.46 (d, P(SiMe<sub>3</sub>)<sub>2</sub>, <sup>2</sup>*J*<sub>PC</sub> = 7.43 Hz, *cis*), 2.64 (vt, P(H)SiMe<sub>3</sub>, *J*<sub>sum</sub> = 8.39 Hz, *trans*), 3.87 (d, P(SiMe<sub>3</sub>)<sub>2</sub>, <sup>2</sup>*J*<sub>PC</sub> = 7.70 Hz, *trans*), -3.87 (br s, MeAl, both isomers); <sup>31</sup>P δ -221.49 (d, P(H)Si, <sup>2</sup>*J*<sub>PP</sub> = 41.3 Hz, *cis*), -222.08

(d, P(H)Si, <sup>2</sup>*J*<sub>PP</sub> = 43.7 Hz, *trans*), -253.00 (vt, P(Si)<sub>2</sub>, *J*<sub>sum</sub> = 85.0 Hz, *cis*), -252.46 (vt, P(Si)<sub>2</sub>, *J*<sub>sum</sub> = 91.1 Hz, *trans*). IR: (cm<sup>-1</sup>) 2929 (s), 2890 (s), 2819 (m), 1405 (m), 1306 (w), 1261 (w, sh), 1250 (m), 1206 (w), 1188 (w), 1090 (m, br), 1036 (w, sh), 843 (s), 806 (m, sh), 754 (w), 720 (w, sh), 690 (m), 680 (w, sh), 625 (m), 563 (w), 425 (m), 452 (w). EI-MS: *m/z* 543 (M - Me<sup>+</sup>, 7.3%). Anal. Calcd for C<sub>18</sub>H<sub>56</sub>Al<sub>3</sub>P<sub>3</sub>Si<sub>4</sub>: C, 10.10; H, 38.69. Found: C, 10.23; H, 38.14.

**Supplementary Material Available:** A figure showing NMR spectra (2 pages). Ordering information is given on any current masthead page.

OM940901E

# Boron Trihalide Mediated Cleavage of Diethyl Ether with [Tris(trimethylsilyl)methyl]lithium

Clifford L. Smith

Department of Natural Sciences, Albany State College, Albany, Georgia 31705

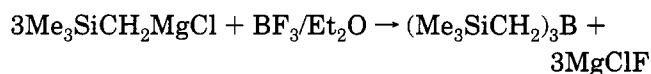
Received February 2, 1995<sup>®</sup>

**Summary:** Facile cleavage of Et<sub>2</sub>O occurs with [tris(trimethylsilyl)methyl]lithium in the presence of BX<sub>3</sub> (where X = F, Cl, or Br) yielding ethyl tris(trimethylsilyl)methyl ether instead of the expected [tris(trimethylsilyl)methyl]boron dihalide; an analogous Et<sub>2</sub>O cleavage also occurs with AlCl<sub>3</sub>. The sterically hindered ether formed was unreactive toward carbon-oxygen bond cleavage by HBr, BCl<sub>3</sub>, and Me<sub>3</sub>SiI.

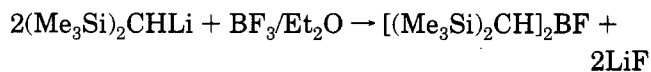
## Introduction

The very bulky tris(trimethylsilyl)methyl ligand (hereafter referred to as the "trisyl" moiety) imparts exceptional stability at metal and metalloid centers.<sup>1</sup> The alkyl halide trisyl bromide is also surprisingly unreactive toward nucleophilic substitution reactions<sup>2</sup> but is very reactive toward Li and Mg metals and organolithiums.<sup>3</sup> We now report on BX<sub>3</sub>- and AlCl<sub>3</sub>-mediated cleavage of Et<sub>2</sub>O by trisyllithium in hexane/Et<sub>2</sub>O affording ethyl trisyl ether.<sup>4</sup>

It is reported that 3 mol of [(trimethylsilyl)methyl]magnesium chloride react with BF<sub>3</sub> yielding tris[(trimethylsilyl)methyl]borane:<sup>5</sup>

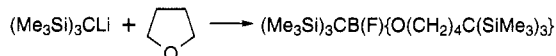


Only 2 mol of the bulkier [bis(trimethylsilyl)methyl]lithium reacted with BF<sub>3</sub>, even under forcing reaction conditions, yielding bis[bis(trimethylsilyl)methyl]boron fluoride:<sup>6</sup>



The formation of tris[bis(trimethylsilyl)methyl]borane is presumably prohibited by severe steric crowding that would be induced at the boron atom when bonded to three bulky bis(trimethylsilyl)methyl groups. Reaction of the bulkiest trisyllithium with BF<sub>3</sub> in THF/Et<sub>2</sub>O did not even afford the monoalkylated boron difluoride; (Me<sub>3</sub>Si)<sub>3</sub>CBF<sub>2</sub>, but instead yielded an unexpected prod-

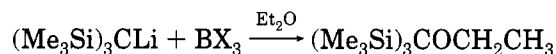
uct of ring-opening of THF:<sup>7</sup>



In contrast, the less reactive (PhMe<sub>2</sub>Si)<sub>3</sub>CLi reacts with BF<sub>3</sub> in the normal manner, yielding the monoalkylated boron difluoride product, (PhMe<sub>2</sub>Si)<sub>3</sub>CBF<sub>2</sub>.<sup>8</sup> The lower reactivity of (PhMe<sub>2</sub>Si)<sub>3</sub>CLi is reported to be associated with its molecular structure<sup>9a</sup> as opposed to the ionic nature of the more reactive trisyllithium.<sup>9b</sup>

## Results and Discussion

We recently discovered that cleavage of Et<sub>2</sub>O occurs in reactions of trisyllithium with BX<sub>3</sub> in hexane/Et<sub>2</sub>O affording the sublimable ethyl trisyl ether. When X = fluoro, a 40% yield of ethyl trisyl ether was obtained, the chloro gave 45%, and the bromo afforded 64%:



Contrary to BF<sub>3</sub>-induced ring-opening of THF, BX<sub>3</sub>-mediated cleavage of Et<sub>2</sub>O by trisyllithium is quite astonishing because the product, ethyl trisyl ether, does not contain a boron atom. Eaborn et al. reasoned that complexes of THF with either BF<sub>3</sub> or the monoalkylated product, (Me<sub>3</sub>Si)<sub>3</sub>CBF<sub>2</sub>, might be responsible for ring-opening of THF.<sup>7</sup> They also concluded that trisyllithium alone is unlikely to cause ring-opening in view of its exceptional stability in THF.<sup>10</sup> It is apparent from the structure of the products that cleavage reactions in THF/Et<sub>2</sub>O must involve different intermediate boron complexes than those occurring in hexane/Et<sub>2</sub>O.

The role of BX<sub>3</sub> in cleavage of Et<sub>2</sub>O by trisyllithium is perplexing, especially in view of the absence of boron in the product. Consistent with Eaborn's postulate, if complexes of Et<sub>2</sub>O with BX<sub>3</sub> or the intermediate (Me<sub>3</sub>Si)<sub>3</sub>CBX<sub>2</sub> are responsible for the cleavage of Et<sub>2</sub>O, then the expected products would be (Me<sub>3</sub>Si)<sub>3</sub>CB(X)OCH<sub>2</sub>CH<sub>3</sub> and CH<sub>3</sub>CH<sub>2</sub>X. For instance, facile cleavage of Et<sub>2</sub>O occurs in the presence of BCl<sub>3</sub> or BBr<sub>3</sub>, yielding the ethyl borate esters CH<sub>3</sub>CH<sub>2</sub>OBX<sub>2</sub> and the corresponding alkyl halides CH<sub>3</sub>CH<sub>2</sub>X.<sup>11a</sup> Reaction of trisyllithium with the borate esters is thereby expected to give (Me<sub>3</sub>Si)<sub>3</sub>CB-

<sup>®</sup> Abstract published in *Advance ACS Abstracts*, May 1, 1995.

(1) Eaborn, C. In *Organosilicon and Bioorganosilicon Chemistry*; Sakurai, H., Ed.; Ellis Horwood: Chichester, U.K., 1985; pp 123-130, and references cited therein.

(2) Cook, M. A.; Eaborn, C.; Walton, D. R. M. *J. Organomet. Chem.* **1971**, *29*, 389.

(3) (a) Smith, C. L.; James, L. M.; Sibley, K. L. *Organometallics* **1992**, *11*, 2938. (b) Seyferth, D.; Lefferts, J. L.; Lambert, R. L., Jr. *J. Organomet. Chem.* **1977**, *142*, 39.

(4) Smith, C. L. *Abstracts of Papers*, 209th National Meeting of the American Chemical Society, Anaheim, CA, April 2-6, 1995; American Chemical Society: Washington, DC, 1995; ORGN 228.

(5) Seyferth, D. *J. Am. Chem. Soc.* **1959**, *81*, 1844.

(6) Al-Hashimi, S.; Smith, J. D. *J. Organomet. Chem.* **1978**, *153*, 253.

(7) Eaborn, C.; Retta, N.; Smith, J. D.; Hitchcock, P. B. *J. Organomet. Chem.* **1982**, *235*, 265.

(8) Eaborn, C.; El-Kheli, M. N. A.; Hitchcock, P. B.; Smith, J. D. *J. Chem. Soc., Chem. Commun.* **1984**, 1673.

(9) (a) Eaborn, C.; Hitchcock, P. B.; Smith, J. D.; Sullivan, A. C. *J. Chem. Soc., Chem. Commun.* **1983**, 1390. (b) Eaborn, C.; Hitchcock, P. B.; Smith, J. D.; Sullivan, A. C. *J. Chem. Soc., Chem. Commun.* **1983**, 827.

(10) Cook, M. A.; Eaborn, C.; Jukes, A. E.; Walton, D. R. M. *J. Organomet. Chem.* **1979**, *24*, 529.

(11) (a) For a review on the cleavages of ethers see: Bhatt, M. V.; Kulkarni, S. U. *Synthesis* **1983**, 249. (b) Gerrard, W.; Lappert, M. F. *J. Chem. Soc.* **1952**, 1486. (c) Benton, F. L.; Dillon, T. L. *J. Am. Chem. Soc.* **1942**, *64*, 1128.

(X)OCH<sub>2</sub>CH<sub>3</sub> or products of its hydrolysis formed during workup, (Me<sub>3</sub>Si)<sub>3</sub>CB(OH)OCH<sub>2</sub>CH<sub>3</sub> and (Me<sub>3</sub>Si)<sub>3</sub>CB(OH)<sub>2</sub>. However, neither one of these compounds were isolated, the latter boronic acid having been synthesized by other methods.<sup>12,13</sup> On the other hand, reaction of trisyllithium with CH<sub>3</sub>CH<sub>2</sub>X (a reaction expected to be slower than attack at the boron center of CH<sub>3</sub>CH<sub>2</sub>O BX<sub>2</sub>) would yield (Me<sub>3</sub>Si)<sub>3</sub>CCH<sub>2</sub>CH<sub>3</sub>. This compound has been reported<sup>14</sup> by Seyferth et al. from reaction of trisyllithium with CH<sub>3</sub>CH<sub>2</sub>I; however, the elemental analysis for (Me<sub>3</sub>Si)<sub>3</sub>CCH<sub>2</sub>CH<sub>3</sub> and the reported mp 208–211 °C were not in agreement with the mp 248–251 °C of our product. If trisyllithium reacts with BX<sub>3</sub> to form (Me<sub>3</sub>Si)<sub>3</sub>CBX<sub>2</sub>, which subsequently cleaves Et<sub>2</sub>O, the product of the reaction also would be (Me<sub>3</sub>Si)<sub>3</sub>CB(X)OCH<sub>2</sub>CH<sub>3</sub>. The BF<sub>3</sub>-mediated cleavage of Et<sub>2</sub>O is even more remarkable because addition complexes of BF<sub>3</sub> with Et<sub>2</sub>O is perhaps its most readily accessible derivative<sup>15</sup> (being distilled at bp 124 °C/760 Torr without decomposition); thus the cleavage fragments CH<sub>3</sub>CH<sub>2</sub>OBF<sub>2</sub> and CH<sub>3</sub>CH<sub>2</sub>F should not be significant intermediates available for reaction with trisyllithium. In view of these findings that BF<sub>3</sub> is unreactive toward cleavage of Et<sub>2</sub>O, then it seems reasonable that an intermediate (Me<sub>3</sub>Si)<sub>3</sub>CBF<sub>2</sub> should also be even more unreactive toward cleavage of Et<sub>2</sub>O because nucleophilic attack upon boron would be sterically inhibited by the trisyl group.<sup>16</sup> It is therefore apparent that trisyllithium complexed with BF<sub>3</sub> is more reactive toward Et<sub>2</sub>O cleavage than complexes of Et<sub>2</sub>O with either BF<sub>3</sub> or (Me<sub>3</sub>Si)<sub>3</sub>CBF<sub>2</sub>.

The monoalkylated dichloride compound (Me<sub>3</sub>Si)<sub>3</sub>-AlCl<sub>2</sub> (15%) was obtained along with (Me<sub>3</sub>Si)<sub>3</sub>C(CH<sub>2</sub>)<sub>4</sub>-OH (20%) and some (Me<sub>3</sub>Si)<sub>3</sub>CH from reaction between trisyllithium and AlCl<sub>3</sub> in THF/Et<sub>2</sub>O.<sup>13</sup> In contrast, we obtained a 54% yield of ethyl trisyl ether from reaction of trisyllithium with AlCl<sub>3</sub> in hexane/Et<sub>2</sub>O.

In summary, the following results illustrate the diverse nature of reactions occurring between (RMe<sub>2</sub>-Si)<sub>3</sub>CLi and BX<sub>3</sub>: (a) trisyllithium cleaves Et<sub>2</sub>O in the presence of BF<sub>3</sub> in hexane/Et<sub>2</sub>O, affording a trisyl-bearing ether without incorporation of a boron atom; (b) trisyllithium reacts with BF<sub>3</sub> in THF/Et<sub>2</sub>O by ring-opening of THF, yielding a trisyl-bearing ether with incorporation of a boron atom;<sup>7</sup> (c) trisyllithium also reacts in THF/Et<sub>2</sub>O with B(OMe)<sub>3</sub>, giving the expected alkylated product, (Me<sub>3</sub>Si)<sub>3</sub>CB(OMe)<sub>2</sub>,<sup>12</sup> and (d) the related alkylithium, (PhMe<sub>2</sub>Si)<sub>3</sub>CLi, reacts with BF<sub>3</sub> in THF/Et<sub>2</sub>O, yielding the expected alkylated difluoride, (PhMe<sub>2</sub>Si)<sub>3</sub>CBF<sub>2</sub>.<sup>8</sup>

Ethyl trisyl ether is unreactive toward BCl<sub>3</sub> in methylene chloride, toward Me<sub>3</sub>SiI in acetonitrile, and

toward HBr in acetic acid, presumably because of the steric effect of the bulky trisyl group.<sup>1</sup>

## Experimental Section

**General Procedure.** All glassware was oven-dried and purged with nitrogen while hot before reactants were introduced. Unless specified, the standard apparatus consisted of a 500 mL three-necked round-bottomed flask with ground glass joints which was fitted with a Trubore stirrer, a Friedrich condenser, and an addition funnel.

Trisyllithium was synthesized from trisyl bromide and lithium metal in Et<sub>2</sub>O according to published directions<sup>3a</sup> and standardized by acid titration of hydrolyzed aliquots using phenolphthalein as the indicator. Diethyl ether was dried over sodium wire, and other solvents were dried over molecular sieves. All other reagents were used as obtained from commercial sources without further purification.

Ethyl trisyl ether was routinely characterized by comparison of its physical properties, IR and NMR spectral data, and GC retention times with those of authentic samples. Elemental analyses and the molecular weights were performed by Galbraith Laboratories, Inc., Knoxville, TN.

Melting points were determined with an electrothermal melting point apparatus in sealed capillary tubes and were uncorrected. IR spectra were obtained on a Perkin-Elmer Model 710B double-beam grating IR spectrophotometer. GC measurements were effected with a Perkin-Elmer Sigma 3B instrument using a 3% OV-101 on 80/100 mesh Chromosorb W packed column (4 ft × 1/8 in.). <sup>1</sup>H NMR spectra were recorded on a Varian EM 3630L spectrometer using carbon tetrachloride as the solvent. Chemical shifts are reported in δ units (ppm) from internal chloroform.

**Trisyllithium with BBr<sub>3</sub>.** Trisyllithium (0.2 mol) in 250 mL of Et<sub>2</sub>O was added dropwise over a 30 min period to stirred BBr<sub>3</sub> (50 g, 0.2 mol) in 250 mL of hexane which was cooled to ca. 5 °C with an external ice-water bath. Upon completed addition, the bath was removed and the mixture was refluxed for 2 h prior to hydrolysis with 250 mL of ice-cold water. The organic layer was separated, and the aqueous layer was extracted once with Et<sub>2</sub>O (100 mL). The combined organic layers were dried over molecular sieves and filtered, and the volatiles were removed from the filtrate via distillation leaving a solid. Recrystallization from ethyl acetate/95% ethanol prior to sublimation at 150 °C/0.1 mmHg afforded pure ethyl trisyl ether (35 g, 64% yield), mp 248–251 °C (sealed tube). Anal. Calcd for C<sub>12</sub>H<sub>32</sub>OSi<sub>3</sub>: C, 52.03; H, 11.65; Si, 30.42. Found: C, 52.21; H, 11.90; Si, 30.09. The molecular weight was determined by vapor pressure osmometry in benzene: found 272 (calcd 277). The <sup>1</sup>H NMR spectrum showed δ at 0.11 (s, 27H, SiMe<sub>3</sub>), 1.18 (t, 3H, Me), and 1.77 (q, 2H, CH<sub>2</sub>).

**Trisyllithium with BCl<sub>3</sub>.** To a stirred solution of trisyllithium (0.15 mol) in 315 mL of Et<sub>2</sub>O, cooled to ca. 5 °C with an external ice-water bath, was added dropwise BCl<sub>3</sub> (0.19 mol) in 180 mL of hexane over a 30 min period. The ice water bath was removed and the mixture was refluxed for 3 h prior to hydrolysis with 250 mL of ice-cold water. Workup in the usual manner followed by removal of the volatiles by distillation

(12) Trisyllithium reacts with the borate ester B(OMe)<sub>3</sub> in Et<sub>2</sub>O/THF to give (Me<sub>3</sub>Si)<sub>3</sub>CB(OMe)<sub>2</sub>, which was partially hydrolyzed during workup yielding a mixture of (Me<sub>3</sub>Si)<sub>3</sub>CB(OMe)<sub>2</sub>, (Me<sub>3</sub>Si)<sub>3</sub>CB(OH)OMe, and (Me<sub>3</sub>Si)<sub>3</sub>CB(OH)<sub>2</sub>; Lickiss, P. D. *J. Organomet. Chem.* **1986**, *308*, 261.

(13) Eaborn, C.; El-Kheli, M. N.; Retta, N.; Smith, J. D. *J. Organomet. Chem.* **1983**, *249*, 23.

(14) Seyferth, D.; Lefferts, J. L.; Lambert, R. L., Jr. *J. Organomet. Chem.* **1977**, *142*, 39.

(15) Brown, H. C.; Adams, R. M. *J. Am. Chem. Soc.* **1942**, *64*, 2557.

(16) The trichloride (Me<sub>3</sub>Si)<sub>3</sub>CSiCl<sub>3</sub> is stable to boiling MeOH and PhLi, illustrating the very large steric hindrance toward nucleophilic substitution at silicon caused by the trisyl group: Dua, S. S.; Eaborn, C.; Happer, D. A. R.; Hopper, S. P.; Safa, K. D.; Walton, D. R. M. *J. Organomet. Chem.* **1979**, *178*, 75.

yielded a viscous liquid which, upon further heating under reduced pressure ( $\sim 2$  mmHg), afforded 33 g of a solid. Recrystallization from ethyl acetate/methanol prior to sublimation at  $150$  °C/ $0.1$  mmHg afforded pure ethyl trisyl ether (18.5 g, 44.5%), mp  $246$ – $248$  °C (sealed tube).

**Trisyllithium with  $\text{BF}_3$ .** To stirred trisyllithium (0.15 mol) dissolved in 155 mL of  $\text{Et}_2\text{O}$  was added  $\text{BF}_3 \cdot \text{Et}_2\text{O}$  (45.4 g, 0.32 mol) dissolved in 150 mL of hexane over a 5 min period prior to continued stirring at room temperature for 24 h. The reaction mixture was thereafter refluxed for 8 h prior to hydrolysis with 250 mL of ice-cold water. Workup in the usual manner was followed by removal of the volatiles by distillation to a viscous liquid which, upon heating under reduced pressure ( $\sim 2$  mmHg), afforded a 34 g of a solid. Recrystallization of the solid from ethyl acetate/methanol prior to sublimation at  $150$  °C/ $0.1$  mmHg afforded pure ethyl trisyl ether (15.5 g, 40% yield), mp  $246$ – $248$  °C (sealed tube).

**Trisyllithium with  $\text{AlCl}_3$ .** Trisyllithium (0.06 mol) in 105 mL of  $\text{Et}_2\text{O}$  was added over a 10 min period to a stirred suspension of anhydrous  $\text{AlCl}_3$  (7.5 g, 0.06 mol) in 200 mL of hexane at room temperature. The exothermic (ca.  $48$  °C) reaction mixture was maintained at reflux for 1 h with external heating. Volatiles were removed by distillation under nitrogen until the temperature of the mixture reached  $70$ – $72$  °C, and thereafter the mixture was refluxed for an additional 2 h. After this time, about 100 mL of the solvent was removed by distillation under nitrogen and the mixture was allowed to cool to room temperature, depositing crystals of salts which were collected by filtration under reduced pressure. Volatiles were removed from the filtrate by distillation yielding a viscous liquid which, upon heating under reduced pressure (ca.  $140$  °C/ $0.5$  mmHg), afforded 15 g of a solid. Recrystallization from methanol prior to sublimation at  $150$  °C/ $0.1$  mmHg afforded pure ethyl trisyl ether (9 g, 54% yield), mp  $247$ – $248$  °C (sealed tube). Anal. Calcd for  $\text{C}_{12}\text{H}_{32}\text{OSi}_3$ : C, 52.03; H, 11.65. Found: C, 52.10; H, 11.56. The molecular weight was determined by vapor pressure osmometry in benzene: found 268 (calcd 277).

**Ethyl Trisyl Ether with HBr in Acetic Acid (Attempted).** A mixture of ethyl trisyl ether (10 g, 0.04 mol), 48% aqueous HBr (5.5 mL) and 60 mL of acetic acid was refluxed for 20 h in a 100 mL round-bottomed flask fitted with a water condenser. After this time, ca. 1 g of a white solid was visible and an additional 1 mL of 48% aqueous HBr was added prior to continued reflux for 56 h subsequent to removal of acetic acid by distillation, leaving a solid. Recrystallization from methanol prior to sublimation at  $150$  °C/ $0.1$  mmHg afforded a 71% recovery of ethyl trisyl ether, mp  $244$ – $248$  °C (sealed tube).

**Ethyl Trisyl Ether with  $\text{BCl}_3$  (Attempted).** A solution of ethyl trisyl ether (11.1 g, 0.04 mol) and  $\text{BCl}_3$  (0.06 mol) in 60 mL of methylene chloride was allowed to stand under nitrogen in a sealed vial (100 mL) at  $35$  °C for 18 h. Hydrolysis of the reaction mixture with 250 mL of ice-cold water was followed by the usual workup yielded a solid. Recrystallization from ethyl acetate/methanol prior to sublimation at  $135$  °C/ $1$  mmHg afforded pure ethyl trisyl ether (7.2 g, 65% recovery), mp  $245$ – $248$  °C (sealed tube).

**Ethyl Trisyl Ether with Iodotrimethylsilane (Attempted).** A stirred mixture of ethyl trisyl ether (10 g, 0.03 mol), chlorotrimethylsilane (3.6 g, 0.03 mol), and sodium iodide (5 g, 0.03 mol) in 50 mL of acetonitrile was refluxed under nitrogen for 12 h in a 100 mL round-bottomed flask fitted with a water condenser topped with a nitrogen inlet tube. The cooled reaction mixture was hydrolyzed with 150 mL of ice-cold water prior to extraction with 150 mL of ether. The organic layer was shaken with saturated aqueous  $\text{Na}_2\text{S}_2\text{O}_3$  (150 mL), washed twice with cold water (150 mL), and dried over molecular sieves, and the volatiles were removed by distillation. Recrystallization residue from 95% ethanol afforded an 80% recovery of ethyl trisyl ether, mp  $242$ – $245$  °C (sealed tube).

**Acknowledgment.** The National Institutes of Health (Grant No. 2 S06 GM08023) is gratefully acknowledged for financial support.

OM950085Q

# Synthesis and Characterization of a Phosphaalkyne-Bridged Pentairon Carbonyl Cluster. Crystal and Molecular Structure of $[\{Fe_3Se_2(CO)_8\}(\mu-PCBu^t)\{Fe_2Se(CO)_6\}]$

Pradeep Mathur\* and Md. Munkir Hossain

Department of Chemistry, Indian Institute of Technology, Powai, Bombay 400 076, India

Peter B. Hitchcock and John F. Nixon\*

School of Chemistry and Molecular Sciences, University of Sussex, Brighton BN1 9QJ, U.K.

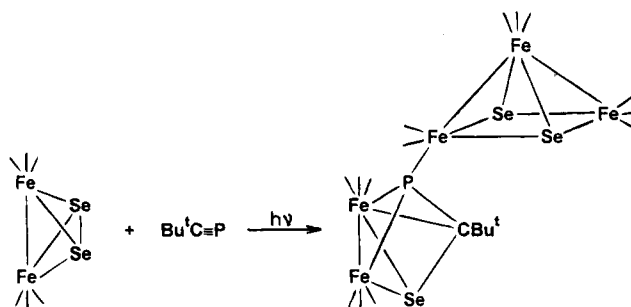
Received December 14, 1994<sup>⊗</sup>

**Summary:** The new cluster  $[\{Fe_3Se_2(CO)_8\}(\mu-PCBu^t)\{Fe_2Se(CO)_6\}]$  has been isolated in moderate yield from the photolytic reaction of  $[Fe_2(CO)_6(\mu-Se_2)]$  and the phosphaalkyne  $P\equiv CBu^t$ . Its structure has been established by single crystal X-ray diffraction methods: monoclinic,  $P2_1/c$  (No. 14),  $a = 9.378(1) \text{ \AA}$ ,  $b = 17.605(3) \text{ \AA}$ ,  $c = 18.631(2) \text{ \AA}$ ,  $\beta = 93.00(1)^\circ$ ,  $V = 3071.7 \text{ \AA}^3$ ,  $Z = 4$ ,  $R = 7.6\%$ ,  $R' = 6.5\%$ . The structure consists of a  $[Fe_3Se_2(CO)_8]$  unit and a  $[Fe_2Se(CO)_6(PCBu^t)]$  unit linked by the phosphorus lone pair electrons of the phosphaalkyne.

## Introduction

Transition metal clusters containing single atom ligands derived from several main group elements of the Periodic Table have been studied in detail.<sup>1–7</sup> Of the group 16 elements, sulfur has been the most extensively used for the purpose of cluster growth and cluster framework stabilization.<sup>8,9</sup> Recent studies on selenium- and tellurium-bridged cluster compounds have shown that the nature of the main group element can significantly influence both the structure and reactivity of the cluster.<sup>10–13</sup> We have previously investigated the activation of C≡C triple bonds of acetylenes by the Se–Se-bonded “butterfly” compound  $[Fe_2(CO)_6(\mu-Se_2)]$  and demonstrated the stepwise C≡C bond reduction.<sup>14,15</sup> These complexes can also be used for the synthesis of the new Se-bridged mixed-metal cluster  $[Mo_2Fe_2Cp_2Se_3(CO)_6]$ .<sup>16,17</sup>

## Scheme 1. Formation of $[\{Fe_3Se_2(CO)_8\}(\mu-PCBu^t)\{Fe_2Se(CO)_6\}]$



In view of the known similarity in ligating behavior of alkynes and phosphaalkynes,  $RC\equiv P$ ,<sup>18</sup> we have now extended our studies to the activation of the C≡P triple bond of the phosphaalkyne  $Bu^tC\equiv P$  by the  $[Fe_2(CO)_6(\mu-Se_2)]$  framework. Here we report the synthesis and characterization of the unusual cluster  $[\{Fe_3Se_2(CO)_8\}(\mu-PCBu^t)\{Fe_2Se(CO)_6\}]$ .

## Results and Discussion

When a mixture of  $[Fe_2(CO)_6(\mu-Se_2)]$  and  $Bu^tC\equiv P$  in hexane was photolyzed with ultraviolet light for 0.5 h, and the mixture was subjected to chromatographic workup, the new cluster  $[\{Fe_3Se_2(CO)_8\}(\mu-PCBu^t)\{Fe_2Se(CO)_6\}]$  was isolated (Scheme 1) and characterized by IR and <sup>1</sup>H NMR spectroscopy. The IR spectrum revealed the existence of only terminally-bonded carbonyl ligands, and the <sup>1</sup>H NMR spectrum showed a single peak for the  $Bu^t$  protons. Single crystals suitable for X-ray analysis were obtained from hexane at  $-4^\circ C$ . Its molecular structure is shown in Figure 1, and some important bond length and bond angle parameters are listed in Table 1.

The structure of  $[\{Fe_3Se_2(CO)_8\}(\mu-PCBu^t)\{Fe_2Se(CO)_6\}]$  can be described as consisting of both a  $Fe_3Se_2$  square pyramidal core and a  $Fe_2Se$  triangular unit linked by a  $Bu^tCP$  group which is  $\eta^1$ -bonded to one of the basal Fe atoms of the  $Fe_3Se_2$  unit and to both Fe atoms of the  $Fe_2Se$  unit. The C atom of the bridging phosphaalkyne is bonded to one Fe atom and the Se

- \* Abstract published in *Advance ACS Abstracts*, April 15, 1995.  
 (1) Whitmire, K. H. *J. Coord. Chem.* **1988**, *17*, 95.  
 (2) Roof, L. C.; Kolis, J. W. *Chem. Rev.* **1993**, *1037*.  
 (3) Compton, N. A.; Errington, R. J.; Norman, N. C. *Adv. Organomet. Chem.* **1990**, *31*, 91.  
 (4) Ansari, M. A.; Ibers, J. A. *Coord. Chem. Rev.* **1990**, *100*, 223.  
 (5) Layer, T. M.; Lewis, J.; Martin, A.; Raithby, P. R.; Wong, W. T. *J. Chem. Soc., Dalton Trans.* **1992**, 3411.  
 (6) Adams, R. D. In *The Chemistry of Metal Cluster Complexes*; Shriver, D. F., Kaesz, H. D., Adams, R. D., Eds.; VCH: New York, 1990; Chapter 3.  
 (7) Vahrenkamp, H. *Phil. Trans. R. Soc. Lond.* **1982**, *A308*, 17.  
 (8) Adams, R. D. *Polyhedron* **1985**, *4*, 2003.  
 (9) Adams, R. D.; Li, J.-C.; Wu, W. *J. Cluster Sci.* **1993**, *4*, 423 and references therein.  
 (10) Mathur, P.; Charkrabarty, D.; Mavunkal, I. J. *J. Cluster Sci.* **1993**, *4*, 351.  
 (11) Mathur, P.; Mavunkal, I. J.; Rheingold, A. L. *J. Chem. Soc., Chem. Commun.* **1989**, 382.  
 (12) Mathur, P.; Mavunkal, I. J.; Rugmini, V. *Inorg. Chem.* **1989**, *28*, 3616.  
 (13) Lesch, D. A.; Rauchfuss, T. B. *Organometallics* **1982**, *1*, 499.  
 (14) Mathur, P.; Hossain, Md. M. *Organometallics* **1993**, *12*, 2398.  
 (15) Mathur, P.; Hossain, Md. M.; Das, K.; Sinha, U. C. *J. Chem. Soc., Chem. Commun.* **1993**, 46.  
 (16) Mathur, P.; Hossain, Md. M.; Rheingold, A. L. *Organometallics* **1993**, *12*, 5029.

- (17) Mathur, P.; Hossain, Md. M.; Rheingold, A. L. *Organometallics* **1994**, *13*, 3909.  
 (18) Nixon, J. F. *Chem. Rev.* **1988**, *88*, 1327; *Chem. Ind.* **1993**, 404.

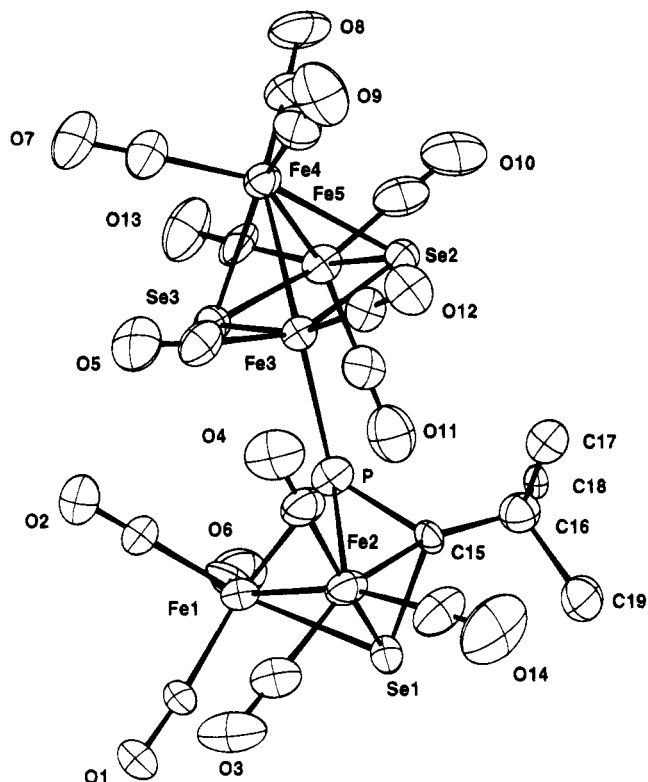


Figure 1. Molecular structure of  $[\{Fe_3Se_2(CO)_8\}(\mu-PCBu)_2]\{Fe_2Se(CO)_6\}$ , showing the atom-numbering scheme.

Table 1. Intramolecular Distances (Å) and Angles (deg) with Estimated Standard Deviations in Parentheses

(a) Bonds			
Se(1)–Fe(1)	2.379(4)	Se(1)–Fe(2)	2.350(3)
Se(1)–C(15)	1.93(2)	Se(2)–Se(3)	3.072(2)
Se(2)–Fe(3)	2.353(3)	Se(2)–Fe(4)	2.385(3)
Se(2)–Fe(5)	2.358(3)	Se(3)–Fe(3)	2.356(3)
Se(3)–Fe(4)	2.370(3)	Se(3)–Fe(5)	2.349(3)
Fe(1)–Fe(2)	2.690(4)	Fe(1)–P	2.319(5)
Fe(1)–C(1)	1.783(14)	Fe(1)–C(2)	1.78(2)
Fe(1)–C(6)	1.69(2)	Fe(2)–P	2.338(5)
Fe(2)–C(3)	1.80(2)	Fe(2)–C(4)	1.76(2)
Fe(2)–C(14)	1.83(2)	Fe(2)–C(15)	2.13(2)
Fe(3)–Fe(4)	2.646(3)	Fe(3)–P	2.195(5)
Fe(3)–C(5)	1.78(2)	Fe(3)–C(12)	1.736(15)
Fe(4)–Fe(5)	2.636(3)	Fe(4)–C(7)	1.80(2)
Fe(4)–C(8)	1.80(2)	Fe(4)–C(9)	1.79(2)
Fe(5)–C(10)	1.78(2)	Fe(5)–C(11)	1.76(2)
Fe(5)–C(13)	1.82(2)	P–C(15)	1.73(2)
(b) Angles			
Fe(1)–Se(1)–Fe(2)	69.3(1)	Fe(1)–Se(1)–C(15)	88.5(6)
Fe(2)–Se(1)–C(15)	58.8(6)	Se(3)–Se(2)–Fe(3)	49.34(6)
Se(3)–Se(2)–Fe(4)	49.56(6)	Se(3)–Se(2)–Fe(5)	49.13(7)
Fe(3)–Se(2)–Fe(4)	67.91(8)	Fe(3)–Se(2)–Fe(5)	98.07(9)
Fe(4)–Se(2)–Fe(5)	67.54(9)	Se(2)–Se(3)–Fe(3)	49.25(6)
Se(2)–Se(3)–Fe(4)	49.96(7)	Se(2)–Se(3)–Fe(5)	49.40(6)
Fe(3)–Se(3)–Fe(4)	68.09(8)	Fe(3)–Se(3)–Fe(5)	98.25(9)
Fe(4)–Se(3)–Fe(5)	67.93(8)	Se(1)–Fe(1)–Fe(2)	54.82(9)
Se(1)–Fe(1)–P	74.2(1)	Se(1)–Fe(1)–C(1)	97.9(5)
Se(1)–Fe(1)–C(2)	164.0(6)	Se(1)–Fe(1)–C(6)	101.5(8)
Fe(2)–Fe(1)–P	55.1(1)	Fe(2)–Fe(1)–C(1)	109.2(6)
Fe(2)–Fe(1)–C(2)	109.5(6)	Fe(2)–Fe(1)–C(6)	148.0(7)

atom of the  $Fe_2Se$  unit. In the  $Fe_3Se_2$  unit, the Fe atom which is bonded to the P atom has two terminal carbonyl groups bonded to it, and the remaining four Fe atoms of the whole structure each have three terminal carbonyl ligands bonded to them. The bond parameters of the  $Fe_3Se_2$  core are quite similar to the corresponding parameters in  $[Fe_3Se_2(CO)_9]$ .<sup>19</sup> The

Table 2. Crystallographic Data for the Complex

formula	$C_{19}H_9Fe_5O_{14}PSe_3$	$V, \text{Å}^3$	3071.7
fw	1008.4	$Z$	4
space group	$P2_1/c$	$D_{\text{calc}}, \text{g cm}^{-3}$	2.18
$a, \text{Å}$	9.378(1)	$\mu(\text{Mo K}\alpha), \text{cm}^{-1}$	59.4
$b, \text{Å}$	17.605(3)	$T, ^\circ\text{C}$	25
$c, \text{Å}$	18.631(2)	$\lambda, \text{cm}^{-1}$	0.7107
$\beta, \text{deg}$	93.00(1)	$R$	0.076

six-coordinate Fe atom of the  $Fe_2Se$  unit forms a shorter bond to the P atom (Fe(1)–P, 2.319(5) Å) than does the seven-coordinate Fe atom (Fe(2)–P, 2.338(5) Å). An opposite trend is observed between the bonding of these two Fe atoms and the Se atom; thus the six-coordinate Fe atom (Fe(1)–Se(1), 2.379(4) Å) forms a slightly longer bond than the seven-coordinate Fe atom (Fe(2)–Se(1), 2.350(3) Å).

When a hexane of  $[Fe_2(CO)_6(\mu-Se_2)]$  is photolyzed for 0.5 h in the absence of the phosphalkyne, formation of insoluble black material is observed, and after extraction and chromatographic workup, small quantities of  $[Fe_2(CO)_6(\mu-Se_2)]$  and  $[Fe_3(CO)_9(\mu-Se_2)]$  were obtained. The presence of phosphalkyne in the reaction medium thus serves to bridge these two species leading to the formation of  $[\{Fe_3Se_2(CO)_8\}(\mu-PCBu)_2]\{Fe_2Se(CO)_6\}$ . Similar ligating behavior of other novel cluster carbonyls derived from phosphalkynes has been previously reported by us in the synthesis of the polymetallic complexes  $[Mo_2(CO)_4(\eta^5-C_5H_5)_2(PCBu)_2M_xL_n]$ <sup>20</sup> ( $M_xL_n = [Os_3(CO)_{11}]$ ,<sup>20</sup>  $[Ru_3(CO)_{11}]$ ,<sup>20</sup>  $[PtCl_2(PR_3)]$ ,<sup>21</sup>  $[PdCl_2(PR_3)]$ ,<sup>21</sup>  $[Fe(CO)_4]$ ,<sup>22</sup> and  $[W(CO)_5]$ <sup>22</sup>).

## Experimental Section

**General Procedures.** All reactions and other manipulations were performed using Schlenk techniques under an inert atmosphere of argon. Solvents were deoxygenated immediately prior to use. Infrared spectra were recorded on a Nicolet 5DXB or Impact 400 FT spectrometer as hexane solutions in 0.1-mm pathlength NaCl cells. <sup>1</sup>H NMR spectra were carried out using a Carlo Erba automatic analyzer.  $[Fe_2(CO)_6(\mu-Se_2)]$ <sup>23,24</sup> and  $Bu^tC\equiv P$ <sup>25</sup> were prepared as reported in the literature.

**Preparation of  $[\{Fe_3Se_2(CO)_8\}(\mu-PCBu)_2]\{Fe_2Se(CO)_6\}$ .** A mixture of freshly prepared  $[Fe_2(CO)_6(\mu-Se_2)]$  (77 mg, 0.18 mmol) and 20  $\mu\text{L}$  of  $Bu^tC\equiv P$  in hexane solvent (150 mL) was photolyzed for 0.5 h. The color of the solution changed from orange to black. The solvent was removed *in vacuo*, and the residue was subjected to chromatographic workup using silica gel TLC plates. Using hexane as eluent, the following compounds were obtained, in order of elution: violet  $[Fe_3(CO)_9(\mu_3-Se)_2]$  (trace amount), orange  $[Fe_2(CO)_6(\mu-Se_2)]$  (trace amount), and dark green  $[\{Fe_3Se_2(CO)_8\}(\mu-PCBu)_2]\{Fe_2Se(CO)_6\}$  (29 mg, 17% based on Se). IR ( $\nu(\text{CO}), \text{cm}^{-1}$ ): 2082 (m), 2064 (s), 2045 (vs), 2034 (s), 2010 (s), 2001 (m). <sup>1</sup>H NMR:  $\delta$  1.29 (s). Mp: 101–3 °C. Anal. Calcd for  $C_{19}H_9Fe_5O_{14}PSe_3$ : C, 22.6; H, 0.89. Found: C, 22.7; H, 0.93.

**X-ray Structure Determination.** A summary of the crystal data is given in Table 2. A crystal (0.2 × 0.14 × 0.08 mm) was mounted on an Enraf-Nonius CAD 4 diffractometer.

(19) Dahl, L. F.; Sutton, P. W. *Inorg. Chem.* **1963**, *2*, 1067.

(20) Bartsch, R.; Hitchcock, P. B.; Meidine, M. F.; Nixon, J. F. *J. Organomet. Chem.* **1984**, *266*, C41.

(21) Meidine, M. F.; Meir, C. J.; Morton, S.; Nixon, J. F. *J. Organomet. Chem.* **1985**, *297*, 255.

(22) Hitchcock, P. B.; Meidine, M. F.; Nixon, J. F. *J. Organomet. Chem.* **1987**, *333*, 337.

(23) Mathur, P.; Hossain, Md. M. *Organometallics* **1993**, *12*, 2398.

(24) Mathur, P.; Chakrabarty, D.; Hossain, Md. M. R.; Rashid, R. S.; Rugmini, V.; Rheingold, A. L. *Inorg. Chem.* **1992**, *31*, 1106.

(25) Becker, G.; Gresser, G.; Uhl, W. *Z. Naturforsch.* **1981**, *36b*, 16.



Intensities were collected with monochromated Mo K $\alpha$  radiation ( $\mu = 59.4 \text{ cm}^{-1}$ ) in a  $\theta$ - $2\theta$  mode. A total of 7643 unique reflections were collected, and 2906 with  $|F^2| > 2\sigma(F^2)$  were used in the refinement. Structure analysis was by direct methods using SHELXS-86. Full matrix least squares refinement proceeded using Enraf-Nonius Mo1EN programs with non-H atoms isotropic. The Fe<sub>2</sub>Se moiety is disordered with 0.73 occupancy as shown in Figure 1 and 0.27 occupancy related by reflection through the P<sub>1</sub>Fe(2) and Se(1) plane. The final  $R$  value was 0.076 ( $R' = 0.065$ ), and the ORTEP drawing shows the non-H atoms as 20% thermal vibrational ellipsoids.

**Acknowledgment.** Financial assistance by the Royal Society of Chemistry to P.M. is gratefully acknowledged. J.F.N. thanks IPSERC for their continuing support of phosphalkyne chemistry.

**Supplementary Material Available:** Tables listing crystallographic structural details, complete fractional atomic coordinates and thermal parameters, bond distances and bond angles, and anisotropic thermal parameters (9 pages). Ordering information is given on any current masthead page.

OM940955O

# Stereoselective Pauson-Khand Reactions via the Chiral [(alkyne)Co<sub>2</sub>(CO)<sub>5</sub>{P(OMe)<sub>3</sub>}]

Hee-Jung Park, Bun Yeoul Lee, Youn Kyung Kang, and Young Keun Chung\*

Department of Chemistry and Center for Molecular Catalysis, College of Natural Sciences, Seoul National University, Seoul 151-742, Korea

Received December 28, 1994<sup>⊗</sup>

**Summary:** Dicobalt hexacarbonyl complexes of menthyl-substituted propargyl alcohol react with PR<sub>3</sub> (R = OMe, Ph) to form diastereomeric mixtures of complexes **3**. The isomeric complexes can be separated chromatographically. The isolated diastereomers can be used in the intra- and intermolecular Pauson-Khand reaction to give high yields of cyclopentenones with high diastereoselectivities or high enantioselectivities.

## Introduction

Among the transition-metal-mediated syntheses of cyclopentenones,<sup>1</sup> the Pauson-Khand reaction is the most powerful and popular. Thus there have been extensive studies of the Pauson-Khand reaction.<sup>2</sup> However, most of the reactions studied are not asymmetric. Recently asymmetric Pauson-Khand reactions were reported by several researchers.<sup>3,4</sup> One of them is based on the use of conventional chiral auxiliaries.<sup>3</sup> The other involves chirality transfer from another ligand, e.g., the optically active phosphorus donor.<sup>4</sup> Pauson et al.<sup>4</sup> reported the use of glyphos as an optically active

phosphine. When the glyphos reacted with Co<sub>2</sub>(CO)<sub>6</sub>-(HC≡CPh), two diastereomers were obtained in the ratio of 60:40 at 60 °C. Both diastereomers can be separated by preparative liquid chromatography. Thus the optically pure diastereomer gave the enantiomerically pure cyclopentenone derivative. However, the replacement of carbonyl by phosphine or phosphite ligands reduced the final yield or reduced the rate of reaction.<sup>5</sup> The yield was 22%–31%. In addition, the diastereomer was epimerized at high temperatures. Nicholas also reported<sup>6</sup> a partial isomerization of one diastereomer of (alkyne)Co<sub>2</sub>(CO)<sub>5</sub>(PPh<sub>3</sub>). Thus the epimerization is rather common. Recently, we reported<sup>7</sup> the promotion of the Pauson-Khand reaction in the mild reaction condition. Thus the use of promoters will solve the problems of low yield and epimerization. We investigated the asymmetric Pauson-Khand reaction by using the chiral (alkyne)Co<sub>2</sub>(CO)<sub>5</sub>L and amine N-oxide in THF/CH<sub>2</sub>Cl<sub>2</sub>. We herein report the stereoselective intra- and intermolecular Pauson-Khand reactions.

## Experimental Section

All reactions were conducted under nitrogen using standard Schlenk type flasks. Workup procedures were done in air. THF was freshly distilled from sodium benzophenone ketyl prior to use, and CH<sub>2</sub>Cl<sub>2</sub> was distilled over anhydrous P<sub>2</sub>O<sub>5</sub>. Hexane and ethyl acetate were used after simple distillation. Most organic compounds were purchased from Aldrich Chemical Co., and Co<sub>2</sub>(CO)<sub>8</sub> was purchased from Strem Chemical Co. Most chemicals were used as received. Anhydrous Me<sub>3</sub>NO was obtained from Me<sub>3</sub>NO dihydrates by azeotropic removal of water with benzene and subsequent sublimation. Thiol compound **13** used in this study was prepared from (–)-menthol according to the modified method.<sup>8</sup>

<sup>1</sup>H or <sup>13</sup>C NMR spectra were obtained with a Varian XL-200, an ARX 300, or a Bruker AMX-500 instrument. IR spectra were recorded on a Shimadzu IR-470 spectrophotometer (spectra measured as films on NaCl by evaporation of solvent). Mass spectra were recorded on a VG ZAB-E double-focusing mass spectrometer.

The procedure reported by Pauson<sup>9</sup> was employed for the preparation of **2** from **1**. The preparation of **3** was reported by McGlinchey et al.<sup>10</sup> However, they did not succeed in separating diastereomers. Thus we report the separation and physical properties of both diastereomers.

(5) Billington, D. C.; Helps, I. M.; Pauson, P. L.; Thomson, W. J. *Organomet. Chem.* **1988**, *354*, 233.

(6) Bradley, D. H.; Khan, M. A.; Nicholas, K. M. *Organometallics* **1989**, *8*, 554.

(7) Jeong, N.; Chung, Y. K.; Lee, B. Y.; Lee, S. H.; Yoo, S.-E. *Synlett* **1991**, 204. Chung, Y. K.; Lee, B. Y.; Jeong, N.; Hudecek, M.; Pauson, P. L. *Organometallics* **1993**, *12*, 220.

(8) Cooper, D. B.; Harrison, J. M.; Inch, T. D.; Lewis, G. J. *J. Chem. Soc., Perkin Trans. 1* **1974**, 1049.

(9) Dunn, J. A.; Pauson, P. L. *J. Organomet. Chem.* **1991**, *419*, 383.

(10) D'Agostino, M. F.; Frampton, C. S.; McGlinchey, M. J. *Organometallics* **1990**, *9*, 2972.

<sup>⊗</sup> Abstract published in *Advance ACS Abstracts*, May 15, 1995.

(1) Croudace, M. C.; Schore, N. E. *J. Org. Chem.* **1981**, *46*, 5357. Schore, N. E.; Croudace, M. C. *J. Org. Chem.* **1981**, *46*, 5436. Exon, C.; Magnus, P. *J. Am. Chem. Soc.* **1983**, *105*, 2477. Khand, I. U.; Knox, G. R.; Pauson, P. L.; Watts, W. E.; Foreman, M. I. *J. Chem. Soc., Perkin Trans. 1* **1973**, 977. Billington, D. C.; Willison, D. *Tetrahedron Lett.* **1984**, *25*, 4041. Knudsen, M. J.; Schore, N. E. *J. Org. Chem.* **1984**, *49*, 5025. Parshall, G. W.; Nugent, W. A.; Chan, D. M.-T.; Tam, W. *Pure Appl. Chem.* **1985**, *57*, 1809. Negishi, E.; Holmes, S. J.; Tour, J. M.; Miller, J. A. *J. Am. Chem. Soc.* **1985**, *107*, 2568. Negishi, E.; Cederbaum, F. E.; Takahashi, T. *Tetrahedron Lett.* **1986**, *27*, 2829. Buchwald, S. L.; Watson, B. T.; Huffman, J. C. *J. Am. Chem. Soc.* **1987**, *109*, 2544. Tamao, K.; Kobayashi, K.; Ito, Y. *J. Am. Chem. Soc.* **1988**, *110*, 1286. RajanBabu, T. V.; Nugent, W. A.; Taber, D. F.; Fagan, P. J. *J. Am. Chem. Soc.* **1988**, *110*, 7128. Negishi, E.; Holmes, S. J.; Tour, J. M.; Miller, J. A.; Cederbaum, F. E.; Swanson, D. R.; Takahashi, T. *J. Am. Chem. Soc.* **1989**, *111*, 3336. Buchwald, S. L.; Lum, R. T.; Fisher, R. A.; Davis, W. M. *J. Am. Chem. Soc.* **1989**, *111*, 9113. Hewlett, D. F.; Whitby, R. J. *J. Chem. Soc., Chem. Commun.* **1990**, 1684. Pearson, A. J.; Dubbert, R. A. *J. Chem. Soc., Chem. Commun.* **1991**, 202. Agnel, G.; Owczarczyk, Z.; Negishi, E. *Tetrahedron Lett.* **1992**, *33*, 1543. Grossman, R. B.; Buchwald, S. L. *J. Org. Chem.* **1992**, *57*, 5803. Berk, S. C.; Grossman, R. B.; Buchwald, S. L. *J. Am. Chem. Soc.* **1993**, *115*, 4912. Jeong, N.; Hwang, S. H.; Lee, Y.; Chung, Y. K. *J. Am. Chem. Soc.* **1994**, *116*, 3159. Lee, B. Y.; Chung, Y. K.; Jeong, N.; Hwang, S. H.; Lee, Y. *J. Am. Chem. Soc.* **1994**, *116*, 8793.

(2) Pauson, P. L.; Khand, I. U. *Ann. N.Y. Acad. Sci.* **1977**, *295*, 2. Pauson, P. L. *Tetrahedron* **1985**, *41*, 5855. Pauson, P. L. In *Organometallics in Organic Synthesis*; de Meijere, A., tom Dieck, H., Eds.; Springer-Verlag: Berlin, 1988; p 233–246. Schore, N. E. *Chem. Rev.* **1988**, *88*, 1081. Schore, N. E. *Organic Reactions*; John Wiley & Sons Inc.: New York, 1991; Vol. 40, p 1–90. Schore, N. E. In *Comprehensive Organic Synthesis*; Trost, B. M.; Fleming, I., Eds.; Pergamon Press: Oxford, U.K., 1991; Vol. 5, p 1037.

(3) Verdager, X.; Moyano, A.; Pericàs, M. A.; Riera, A.; Bernardes, V.; Greene, A. E.; Alvarez-Larena, A.; Piniella, J. F. *J. Am. Chem. Soc.* **1994**, *116*, 2153. Bernardes, V.; Verdager, X.; Kardos, N.; Riera, A.; Moyano, A.; Pericàs, M. A.; Greene, A. E. *Tetrahedron Lett.* **1994**, *35*, 575. Verdager, X.; Moyano, A.; Pericàs, M. A.; Riera, A.; Greene, A. E.; Piniella, J. F.; Alvarez-Larena, A. *J. Organomet. Chem.* **1992**, *433*, 305.

(4) Bladon, P.; Pauson, P. L.; Brunner, H.; Eder, R. *J. Organomet. Chem.* **1988**, *355*, 449.

**Separation of Diastereomers of 3.** A column (diameter, 2 cm) was packed with flash silica gel to a height of 15 cm. The column was washed with 100 mL of diethyl ether and then washed with 200 mL of hexane. Compound **3**, dissolved in 2–3 mL of hexane, was loaded and column chromatographed eluting with hexane. After column chromatography, we obtained the two diastereomers in the ratio of 1:1.

The spectral properties of the first-eluting diastereomer (**3a**):  $^1\text{H NMR}$  ( $\text{CDCl}_3$ )  $\delta$  5.50 (1 H, d, 3.4 Hz), 4.76 (1 H, dd, 12.8, 2.4 Hz), 4.40 (1 H, d, 12.8 Hz), 3.61 (9 H, d, 12.0 Hz), 3.18 (1 H, td, 10.4, 4.2 Hz), 2.39–2.31 (1 H, m), 2.11 (1 H, dm, 13.0 Hz), 1.68–1.18 (4 H, m), 1.03–0.81 (9 H, m), 0.77 (3 H, d, 6.8 Hz) ppm;  $^{13}\text{C NMR}$  ( $\text{CDCl}_3$ )  $\delta$  201.6, 90.06, 89.92, 78.79, 68.73, 68.57, 68.54, 51.69, 48.45, 40.42, 34.57, 31.56, 25.17, 23.19, 22.35, 20.93, 16.08 ppm.

The spectral properties of the second-eluting diastereomer (**3a'**):  $^1\text{H NMR}$  ( $\text{CDCl}_3$ )  $\delta$  5.53 (1 H, d, 3.4 Hz), 4.67 (1 H, d, 12.7 Hz), 4.47 (1 H, dd, 12.6, 1.7 Hz), 3.60 (9 H, d, 12.0 Hz), 3.18 (1 H, td, 10.5, 4.2 Hz), 2.34 (1 H, md, 7.2, 2.0 Hz), 2.12 (1 H, dm, 13.2 Hz), 1.68–1.18 (4 H, m), 1.07–0.81 (9 H, m), 0.75 (3 H, d, 6.8 Hz) ppm;  $^{13}\text{C NMR}$  ( $\text{CDCl}_3$ )  $\delta$  201.6, 90.10, 78.81, 68.61, 51.69, 51.62, 48.37, 40.42, 34.56, 31.60, 25.04, 23.09, 22.32, 21.01, 15.99 ppm.

**Reaction between 3a and Norbornene.** To a solution of **3a** (0.20 g, 0.35 mmol) and norbornene (0.16 g, 1.8 mmol) in  $\text{CH}_2\text{Cl}_2/\text{THF}$  (v/v, 1:1, 10 mL) was added  $\text{Me}_3\text{NO}$  (0.21 g, 2.8 mmol). The resulting solution was stirred at room temperature under  $\text{O}_2$  overnight. To remove excess  $\text{Me}_3\text{NO}$ , the reaction mixture was filtered on silica gel and then the filtrate was concentrated. The filtrate was column chromatographed on silica gel eluting with a mixture solvent of hexane/ethyl acetate (v/v, 10:1). The yield was 98%. IR (NaCl, neat) 1696, 1632  $\text{cm}^{-1}$ ; HRMS,  $m/z$ ,  $\text{M}^+$ , calcd 316.2394, obsd 316.2384;  $^1\text{H NMR}$  ( $\text{CDCl}_3$ )  $\delta$  7.38 (1 H, s), 4.35 (1 H, d, 14.2 Hz), 4.00 (1 H, d, 14.1 Hz), 3.12 (1 H, td, 10.4, 3.6 Hz), 2.63 (1 H, s), 2.39 (1 H, s), 2.20–2.11 (4 H, m), 1.67–1.54 (4 H, m), 1.35–1.22 (4 H, m), 1.05–0.82 (11 H, m), 0.77 (3 H, d, 6.8 Hz) ppm;  $^{13}\text{C NMR}$  ( $\text{CDCl}_3$ )  $\delta$  209.75, 159.74, 147.17, 79.96, 62.41, 54.36, 48.59, 48.15, 40.24, 38.88, 37.96, 34.49, 31.43, 31.11, 29.05, 28.34, 25.76, 23.44, 22.25, 20.83, 16.33 ppm.

**Reaction between 3a' and Norbornene.** A typical procedure was almost the same as the reaction between **3a** and norbornene. Compound **3a'** (0.21g, 0.36 mmol), norbornene (0.17 g, 1.8 mmol), and  $\text{Me}_3\text{NO}$  (0.22 g, 2.9 mmol) were used. The yield was 80%.  $^1\text{H NMR}$  ( $\text{CDCl}_3$ )  $\delta$  7.38 (1 H, s), 4.31 (1 H, d, 14.1 Hz), 4.04 (1 H, d, 14.1 Hz), 3.12 (1 H, td, 10.4, 3.8 Hz), 2.63 (1 H, s), 2.40 (1 H, s), 2.21–2.10 (4 H, m), 1.68–1.54 (4 H, m), 1.35–1.22 (4 H, m), 1.05–0.80 (11 H, m), 0.76 (3 H, d, 6.8 Hz) ppm;  $^{13}\text{C NMR}$  ( $\text{CDCl}_3$ )  $\delta$  209.75, 160.09, 147.12, 79.73, 62.03, 54.33, 48.54, 48.13, 40.28, 38.88, 37.96, 34.50, 31.46, 31.12, 29.03, 28.34, 25.74, 23.44, 22.26, 20.86, 16.33 ppm.

**Reaction between 3a and Norbornadiene.** Norbornadiene (0.61 mL, 5.8 mmol) and  $\text{Me}_3\text{NO}$  (0.69 g, 9.2 mmol) were added to the solution of **3a** (1.15 mmol) in  $\text{CH}_2\text{Cl}_2/\text{THF}$  (v/v, 1:1, 10 mL). After being stirred for 12 h at room temperature, the reaction mixture was filtered on silica gel to remove excess  $\text{Me}_3\text{NO}$  and then the filtrate was evaporated in vacuo. The filtrate was column chromatographed on silica gel eluting with a mixture solvent of hexane and ethyl acetate (v/v, 10:1). The yield was 90%. IR (NaCl) 1692, 1628  $\text{cm}^{-1}$ ; HRMS,  $m/z$ ,  $\text{M}^+$ , calcd 314.2238, obsd 314.2264.  $^1\text{H NMR}$  ( $\text{CDCl}_3$ )  $\delta$  7.36 (1 H, s), 6.21 (1 H, s), 6.12 (1 H, s), 4.25 (1 H, d, 14.1 Hz), 3.93 (1 H, d, 14.1 Hz), 3.05 (1 H, td, 10.5, 4.1 Hz), 2.84 (1 H, s), 2.70 (1 H, s), 2.63 (1 H, s), 2.25 (1 H, d, 4.0 Hz), 2.14 (1 H, m), 2.05 (1 H, d, 12.1 Hz), 1.56 (2 H, m), 1.31 (2 H, d, 9.3 Hz), 1.18 (2 H, d, 9.5 Hz), 0.93–0.76 (3 H, m), 0.84 (3 H, d, 8.1 Hz), 0.82 (3 H, d, 7.5 Hz), 0.70 (3 H, d, 7.2 Hz) ppm;  $^{13}\text{C NMR}$  ( $\text{CDCl}_3$ )  $\delta$  208.46, 159.66, 148.33, 138.38, 136.92, 79.91, 62.29, 52.99, 48.06, 43.44, 42.83, 41.19, 40.14, 34.41, 31.35, 25.67, 23.33, 22.21, 20.78, 16.26 ppm.

**Reaction between 3a' and Norbornadiene.** A typical procedure was almost the same as the reaction between **3a** and norbornene. When  $\text{CH}_2\text{Cl}_2$  was used as a solvent to compare the medium effect, the yield was 40%.  $^1\text{H NMR}$  ( $\text{CDCl}_3$ )  $\delta$  7.37 (1 H, d, 2.2 Hz), 6.22 (1 H, m), 6.13 (1 H, m), 4.23 (1 H, d, 14.1 Hz), 3.94 (1 H, d, 14.2 Hz), 3.05 (1 H, td, 10.6, 4.1 Hz), 2.80 (1 H, s), 2.70 (1 H, s), 2.60 (1 H, s), 2.25 (1 H, d, 4.9 Hz), 2.10 (1 H, m, 7.0, 2.7 Hz), 2.05 (1 H, d, 12.2 Hz), 1.60–1.50 (2 H, m), 1.32 (2 H, d, 9.4 Hz), 1.22–1.16 (2 H, m), 0.94–0.76 (3 H, m), 0.84 (3 H, d, 6.6 Hz), 0.83 (3 H, d, 7.1 Hz), 0.69 (3 H, d, 7.0 Hz) ppm;  $^{13}\text{C NMR}$  ( $\text{CDCl}_3$ )  $\delta$  208.50, 160.10, 148.37, 138.42, 137.01, 79.75, 61.94, 53.02, 48.09, 43.50, 42.89, 41.24, 40.25, 34.48, 31.45, 26.84, 25.72, 23.40, 22.25, 20.85, 16.29 ppm.

**Syntheses of Compounds 7, 8, and 9.** Typical reaction: compound **3a** or **3a'** (0.286 g, 0.50 mmol) was dissolved in 10 mL of diethyl ether. To the ether solution was added  $\text{HBF}_4 \cdot \text{OEt}_2$  (0.37 mL, 2.5 mmol) at 0 °C. While stirring for 1 h, red solids were precipitated. The red precipitates were filtered by using a cannula, washed three times with diethyl ether (10 mL  $\times$  3), and then redissolved in 5 mL of THF. Allyl alcohol (0.17 mL, 2.5 mmol) in 10 mL of THF was added to the reddish THF solution. After stirring for 1 h, water (50 mL) and ethyl acetate (50 mL) were poured into the reaction mixture. The ethyl acetate layer was separated and column chromatographed on silica gel eluting with a mixture of hexane and ethyl acetate (v/v, 10:1). The product (**4**, 90%) was reacted further. To a solution of **4** in a solvent mixture of  $\text{CH}_2\text{Cl}_2$  and THF (v/v, 1:1, 10 mL) was added  $\text{Me}_3\text{NO}$  (0.37 g, 4 mmol). The resulting solution was stirred for 1 h under oxygen. After column chromatography on silica gel eluting with a mixture of hexane and ethyl acetate (v/v, 2:1), **7** was isolated in 80% yield. Compound **7** is a known compound. Thus we only confirmed the formation of **7** by checking its  $^1\text{H NMR}$  spectrum.

**Characterization of 4:** IR (NaCl) 2060, 2003, 1992  $\text{cm}^{-1}$ ;  $^1\text{H NMR}$  ( $\text{CDCl}_3$ )  $\delta$  5.86 (m, 1 H), 5.48 (d, 3.2 Hz, 1 H), 5.25 (dd, 17.3, 1.7 Hz, 1 H), 5.15 (dd, 11.4, 1.7 Hz), 4.58 (d, 13.5 Hz, 1 H), 4.49 (d, 13.5 Hz, 1 H), 4.06 (td, 5.31, 1.22 Hz, 2 H), 3.54 (d, 12 Hz, 9 H) ppm; HRMS,  $m/z$ ,  $\text{M}^+ - 2\text{CO}$ , calcd 421.9376, obsd 421.9379.

$^1\text{H NMR}$  ( $\text{CDCl}_3$ ) spectrum of **7**:  $\delta$  6.06 (1 H, s), 4.65 (1 H, d, 16.0 Hz), 4.50 (1 H, d, 16.0 Hz), 4.31 (1 H, t, 6.1 Hz), 3.27–3.23 (2 H, m), 2.63 (1 H, dd, 17.7, 6.1 Hz), 2.14 (1 H, d, 17.4 Hz) ppm.

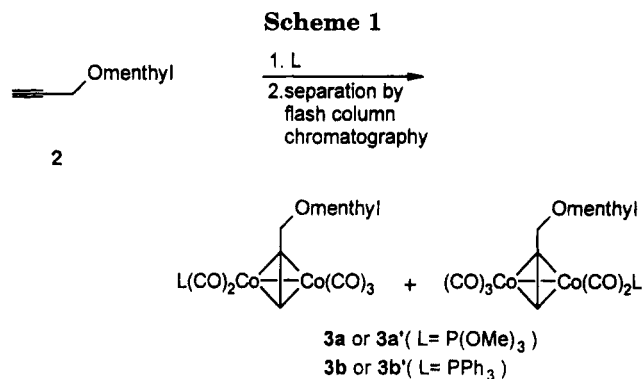
In the same way as the synthesis of compounds **4** and **7**, compounds **5** and **8** were obtained in 80% and 65% yields, respectively.

**Characterization of 5:** IR (NaCl) 2064, 2006, 1991  $\text{cm}^{-1}$ ;  $^1\text{H NMR}$  ( $\text{CDCl}_3$ )  $\delta$  7.36–7.29 (m, 5 H), 5.75 (m, 2 H), 5.51 (d, 3.17 Hz, 2 H), 4.51 (s, 2 H), 4.17 (m, 2 H), 4.11 (d, 4.1 Hz, 2 H), 3.59 (d, 12 Hz, 9 H) ppm; HRMS,  $m/z$ ,  $\text{M}^+ - \text{Co}_2(\text{CO})_5\text{P}(\text{OMe})_3$ , calcd 216.1150, obsd 216.1170.

**Characterization of 8:** IR (NaCl) 1699  $\text{cm}^{-1}$ ;  $^1\text{H NMR}$  ( $\text{CDCl}_3$ )  $\delta$  7.39–7.25 (5 H, m), 6.04 (1 H, d, 1.7 Hz), 4.72–4.37 (4 H, m), 4.28 (1 H, t, 7.3 Hz), 3.66 (1 H, dd, 9.5, 4.4 Hz), 3.50 (1 H, d, 7.3 Hz), 3.43 (1 H, d, 9.5 Hz), 3.68–3.35 (1 H, m), 3.09–2.99 (1 H, m) ppm;  $^{13}\text{C NMR}$  ( $\text{CDCl}_3$ )  $\delta$  208.58, 184.76, 137.40, 128.32, 127.72, 127.65, 123.11, 73.13, 68.20, 68.02, 65.62, 49.47, 48.77 ppm; HRMS,  $m/z$ ,  $\text{M}^+$ , calcd 244.1095, obsd 244.1128.

In the same way as the synthesis of compounds **4** and **7**, compounds **6** and **9** were obtained in 95% and 86% yields, respectively.

**Characterization of 6:** IR (NaCl) 2063, 2005, 1991  $\text{cm}^{-1}$ ;  $^1\text{H NMR}$  ( $\text{CDCl}_3$ )  $\delta$  7.39–7.19 (m, 5 H), 5.97–5.79 (m, 1 H), 5.58 (d, 3.4 Hz, 1 H), 5.20 (dd, 18, 1.46 Hz, 1 H), 5.13 (dd, 8, 1.46 Hz, 1 H), 3.89 (d, 13.8 Hz, 1 H), 3.85 (s, 2 H), 3.82 (d, 13.8 Hz, 1 H), 3.54 (d, 12 Hz, 9 H), 3.35 (dd, 14, 5.61 Hz, 1 H), 3.08 (dd, 14, 7.1 Hz, 1 H) ppm; HRMS,  $m/z$ ,  $\text{M}^+ - \text{CO}$ , calcd 538.9954, obsd 539.0096.



Characterization of **9**: IR (NaCl) 1705, 1638 cm<sup>-1</sup>; <sup>1</sup>H NMR (CDCl<sub>3</sub>) δ 7.33–7.25 (5 H, m), 5.90 (1 H, s), 3.96 (1 H, d, 17.9 Hz), 3.85 (1 H, d, 13.0 Hz), 3.69 (1 H, d, 13.0 Hz), 3.34 (1 H, t, 7.6 Hz), 3.26 (1 H, m), 3.15 (1 H, d, 17.8 Hz), 2.57 (1 H, dd, 17.6, 6.3 Hz), 2.11 (1 H, dd, 17.6, 3.6 Hz), 2.04 (1 H, dd, 10.7, 8.3 Hz) ppm; <sup>13</sup>C NMR (CDCl<sub>3</sub>) δ 209.46, 186.24, 138.11, 128.60, 128.37, 127.23, 124.29, 59.93, 58.07, 53.15, 45.70, 40.21 ppm; HRMS, *m/z*, M<sup>+</sup>, calcd 213.1150, obsd 213.1111.

**Reaction between 7 and Chiral Thiol 13.** Compound **7** was reacted with chiral thiol **13** (3 equiv) and Bu<sub>4</sub>NF (0.1 equiv) in THF. The reaction mixture was stirred for 3 h. After removal of the solvent, the residue was column chromatographed on silica gel eluting with a mixture of hexane and ethyl acetate (v/v, 5:1). The unreacted thiol was recovered, and the product was isolated in 70% yield. When we took <sup>1</sup>H NMR spectra (500 MHz) for the chiral compounds, we could confirm the stereoselective formation of one diastereomer with 90% *ee* (the diastereomer ratio was 95:5). We took the *de* as the *ee* value of the chiral bicyclic enone compounds. HRMS, *m/z*, M<sup>+</sup>, calcd 296.1810, obsd 296.1801.

<sup>1</sup>H NMR spectrum of **10** (major isomer) (CDCl<sub>3</sub>): δ 4.14 (1 H, t, 8.8 Hz), 4.02 (1 H, d, 8.9 Hz), 3.86 (1 H, d, 8.9 Hz), 3.60 (1 H, dd, 9.2, 5.6 Hz), 3.21 (1 H, d, 2.9 Hz), 2.82–2.77 (1 H, m), 2.72 (1 H, dd, 18.5, 1.7 Hz), 2.71 (1 H, d, 18.7 Hz), 2.59 (1 H, d, 18.7 Hz), 2.26 (1 H, dd, 18.5, 2.4 Hz), 2.18–1.98 (1 H, m), 1.78–1.65 (2 H, m), 1.65–1.57 (1 H, m), 1.34–1.24 (2 H, m), 1.17–1.08 (2 H, m), 0.92–0.83 (10 H, m) ppm.

**Reaction between 8 and Chiral Thiol 13.** In the same way as the synthesis of **10**, compound **11** was obtained in 70% yield with 80% *ee* (the diastereomer ratio was 90:10). HRMS, *m/z*, M<sup>+</sup>, calcd 416.2385, obsd 416.2376.

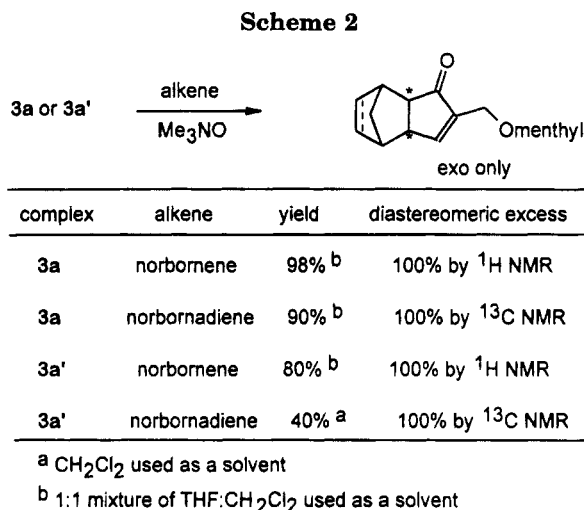
<sup>1</sup>H NMR spectrum of **11** (major isomer) (CDCl<sub>3</sub>): δ 7.35–7.26 (5 H, m), 4.51 (1 H, d, 15.1 Hz), 4.49 (1 H, d, 15.1 Hz), 4.20 (1 H, dd, 9.0, 6.1 Hz), 3.92 (1 H, d, 9.6 Hz), 3.84 (1 H, dd, 9.0, 2.1 Hz), 3.83 (1 H, d, 9.6 Hz), 3.71 (1 H, d, 1.4 Hz), 3.70 (1 H, s), 3.26 (1 H, s), 2.89–2.84 (1 H, m), 2.76 (1 H, d, 3.2 Hz), 2.43 (1 H, q, 6.9 Hz), 2.03–1.92 (1 H, m), 1.82 (1 H, dq, 14.4, 2.9 Hz), 1.76–1.66 (3 H, m), 1.32–1.03 (4 H, m), 0.93–0.82 (10 H, m) ppm.

**Reaction between 9 and Chiral Thiol 13.** In the same way as the synthesis of **10**, compound **12** was obtained quantitatively with 92% *ee* (the diastereomer ratio was 96:4). HRMS, *m/z*, M<sup>+</sup> – menthyl, calcd 246.0952, obsd 246.0911.

<sup>1</sup>H NMR spectrum of **12** (major isomer) (CDCl<sub>3</sub>): δ 7.32–7.22 (5 H, m), 3.64 (1 H, d, 13.4 Hz), 3.58 (1 H, d, 13.4 Hz), 3.21 (1 H, s), 3.00 (1 H, d, 9.1 Hz), 2.64 (1 H, d, 9.1 Hz), 2.75–2.59 (5 H, m), 2.22 (1 H, d, 15.7 Hz), 2.08–1.97 (1 H, m), 1.78–1.59 (4 H, m), 1.32–1.03 (4 H, m), 0.91–0.84 (10 H, m) ppm.

## Results and Discussion

As shown in Scheme 1, treatment of Co<sub>2</sub>(CO)<sub>8</sub> with (–)-menthyl propargyl ether followed by replacement of carbonyl by phosphine or phosphite generates the alkyne complexes **3** in good yields. Flash column chromatography of **3** enables separation of the two



diastereomers, **3a** (the first eluting, L = P(OMe)<sub>3</sub>) and **3a'** (the second eluting, L = P(OMe)<sub>3</sub>) (or **3b** and **3b'**; L = PPh<sub>3</sub>), in equal amounts. Thus we can obtain diastereomerically pure cobalt complexes. The diastereomers are dark-red crystalline compounds and are configurationally stable for several weeks in a freezer.

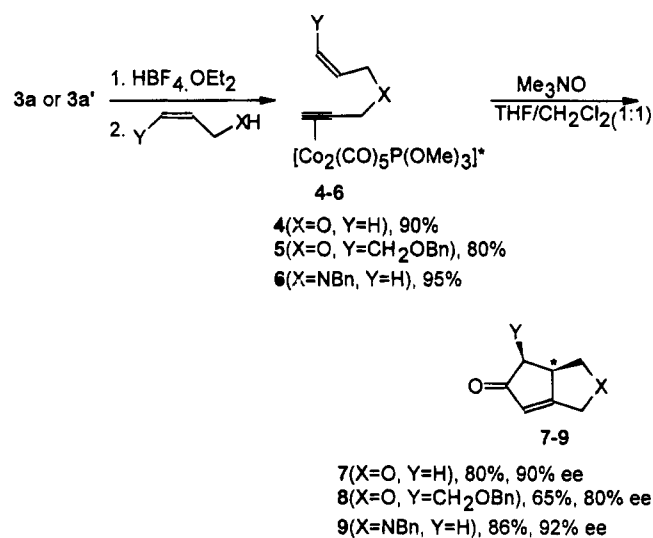
To test the diastereoselectivity in the intermolecular Pauson–Khand reaction, **3b** or **3b'** was reacted with norbornene in the presence of Me<sub>3</sub>NO in CH<sub>2</sub>Cl<sub>2</sub> (Scheme 2). However, the rate of the reaction was slow. After 2 days, 70% of the expected product was obtained with 100% diastereoselectivity. The use of Me<sub>3</sub>NO as a promoter retards the epimerization of the cobalt compound and enables the reaction to take place even in mild reaction conditions. When the reaction was carried with **3a** or **3a'** in the presence of Me<sub>3</sub>NO in CH<sub>2</sub>Cl<sub>2</sub>/THF (v/v, 1:1) (Scheme 2), the reaction time was shortened to 20 h and the yield was improved to 85%–98%. According to the analysis of <sup>1</sup>H and <sup>13</sup>C NMR spectra of the products from each diastereomer, the reaction was almost completely diastereoselective. Thus the reaction produced an exo compound with 100% diastereoselectivities. However, when the reaction of ((–)-menthyl propargyl ether)Co<sub>2</sub>(CO)<sub>6</sub> with norbornadiene in the presence of Me<sub>3</sub>NO was carried out, the diastereomeric mixtures of exo and endo product were obtained in 67% and 19% yields, respectively. Thus, we surmise that the diastereoselection mainly arises from the presence of a chiral cluster core. Krafft et al. found<sup>11</sup> that most of the enyne substrates reacted moderately faster in THF/CH<sub>2</sub>Cl<sub>2</sub> than in CH<sub>2</sub>Cl<sub>2</sub> alone. They explained that the role of the coordinating solvent was similar to the role of the tethered heteroatom. Thus the change of reaction medium and the use of Me<sub>3</sub>NO enable the reaction to occur in high yields with high diastereoselectivities. When **3a** or **3a'** was reacted with norbornadiene in the same reaction conditions as above, the expected exo compound was obtained in 85% yield with 100% diastereoselectivity.

To test the enantioselectivity in the intramolecular Pauson–Khand reaction, compounds **4**, **5**, and **6** were synthesized from **3a** or **3a'** using Nicholas's reaction<sup>12</sup> (Scheme 3). Compounds **4**, **5**, and **6** were treated with

(11) Krafft, M. E.; Scott, I. L.; Romero, R. H.; Feibelmann, S.; Van Pelt, C. E. *J. Am. Chem. Soc.* **1993**, *115*, 7199.

(12) Nicholas, K. M. *Acc. Chem. Res.* **1987**, *20*, 207. Stuart, J. G.; Nicholas, K. M. *Synthesis* **1989**, 6, 454. Montaña, A. M.; Nicholas, K. M. *J. Org. Chem.* **1990**, *55*, 1569.

## Scheme 3

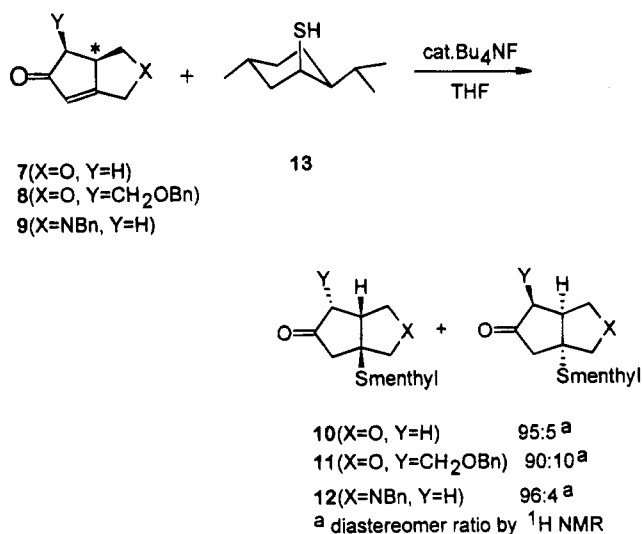


Me<sub>3</sub>NO in CH<sub>2</sub>Cl<sub>2</sub>/THF (v/v, 1:1). After reaction, bicyclic products **7**, **8**, and **9** were obtained in high yields. When CH<sub>2</sub>Cl<sub>2</sub> was used as a reaction medium, compounds **7**, **8**, and **9** were obtained in 70%, 34%, and 50% yields, respectively. Thus the choice of the reaction medium (CH<sub>2</sub>Cl<sub>2</sub>/THF, v/v, 1:1) was critical to the yield of the reaction and shortened the reaction time to less than 1 hr. Compared to **7** and **9**, compound **8** was a less effective substrate. When we used **3b** or **3b'** instead of **3a** or **3a'**, the corresponding **7**, **8**, and **9** were obtained in poor yields (ca. 15%).

To obtain the *ee* values, at first we took <sup>1</sup>H NMR spectra of compounds **7**, **8**, and **9** with a chiral shift reagent Eu(hfc)<sub>3</sub>. However, the chiral shift reagent did not induce any different chemical shifts for protons in different environments. Thus we used a chiral thiol as a chiral derivatizing reagent to convert an enantiomeric mixture to a pair of diastereomers.

Compounds **7**, **8**, and **9** were treated with chiral thiol **13**, which was derived from (–)-menthol (Scheme 4).<sup>13</sup> In the presence of a catalytic amount of Bu<sub>4</sub>NF, the thiol

## Scheme 4



undergoes smooth conjugate addition to α,β-unsaturated carbonyl compounds. Thus, for each bicyclic enone, we obtained the conjugate addition products, **10**, **11**, and **12**. The *ee* values were calculated by the inspection of <sup>1</sup>H NMR spectra of conjugated addition products. The *ee* values for **10**, **11**, and **12** were 90%, 80%, and 92%, respectively.

In conclusion, we have demonstrated that the inter- and intramolecular Pauson–Khand reaction can be carried out with high stereoselectivities using chiral (alkyne)Co<sub>2</sub>(CO)<sub>5</sub>P(OMe)<sub>3</sub> and Me<sub>3</sub>NO in CH<sub>2</sub>Cl<sub>2</sub>/THF (v/v, 1:1). We conjecture that the diastereoselection mainly arises from the presence of a chiral cluster core.

**Acknowledgment.** We are thankful to the Ministry of Education and Center for Molecular Catalysis.

OM9409938

(13) Kuwajima, I.; Murofushi, T.; Nakamura, E. *Synthesis* **1976**, 602.



**Table 1. Reduction of Functionalized Chlorosilanes with LDMAN Followed by Trapping with Me<sub>3</sub>SiCl<sup>a</sup>**

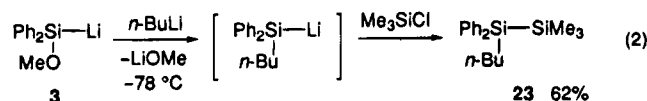
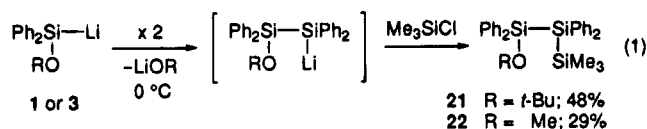
entry	chlorosilane	conditions	silyllithiums	trapping product, yield (%) <sup>b,c</sup>
1	( <i>t</i> -BuO)Ph <sub>2</sub> SiCl ( <b>7</b> )	-78 °C, 15 min	( <i>t</i> -BuO)Ph <sub>2</sub> SiLi ( <b>1</b> )	( <i>t</i> -BuO)Ph <sub>2</sub> SiSiMe <sub>3</sub> ( <b>13</b> ), 81 <sup>d</sup>
2	( <i>t</i> -BuO)Ph <sub>2</sub> SiCl ( <b>7</b> )	-78 °C, 15 min <sup>e</sup>	( <i>t</i> -BuO)Ph <sub>2</sub> SiLi ( <b>1</b> )	( <i>t</i> -BuO)Ph <sub>2</sub> SiSiMe <sub>3</sub> ( <b>13</b> ), 67 <sup>d</sup>
3	( <i>i</i> -PrO)Ph <sub>2</sub> SiCl ( <b>8</b> )	-78 °C, 15 min	( <i>i</i> -PrO)Ph <sub>2</sub> SiLi ( <b>2</b> )	( <i>i</i> -PrO)Ph <sub>2</sub> SiSiMe <sub>3</sub> ( <b>14</b> ), 46
4	(MeO)Ph <sub>2</sub> SiCl ( <b>9</b> )	-78 °C, 15 min	(MeO)Ph <sub>2</sub> SiLi ( <b>3</b> )	(MeO)Ph <sub>2</sub> SiSiMe <sub>3</sub> ( <b>15</b> ), 77
5	( <i>t</i> -BuO) <sub>2</sub> PhSiCl ( <b>10</b> )	-50 °C, 1 h	( <i>t</i> -BuO) <sub>2</sub> PhSiLi ( <b>4</b> )	( <i>t</i> -BuO) <sub>2</sub> PhSiSiMe <sub>3</sub> ( <b>16</b> ), 93
6	(Et <sub>2</sub> N)Ph <sub>2</sub> SiCl ( <b>11</b> )	-78 °C, 15 min	(Et <sub>2</sub> N)Ph <sub>2</sub> SiLi ( <b>5</b> )	(Et <sub>2</sub> N)Ph <sub>2</sub> SiSiMe <sub>3</sub> ( <b>17</b> ), 58
7	(Et <sub>2</sub> N)Ph <sub>2</sub> SiCl ( <b>11</b> )	-50 °C, 1 h	(Et <sub>2</sub> N)Ph <sub>2</sub> SiLi ( <b>5</b> )	(Et <sub>2</sub> N)Ph <sub>2</sub> SiSiMe <sub>3</sub> ( <b>17</b> ), 82
8	HPh <sub>2</sub> SiCl ( <b>12</b> )	-50 °C, 1 h	HPh <sub>2</sub> SiLi ( <b>6</b> )	HPh <sub>2</sub> SiSiMe <sub>3</sub> ( <b>18</b> ), 40 <sup>d,f</sup>
9	(Me <sub>3</sub> Si)Ph <sub>2</sub> SiCl ( <b>19</b> )	-78 °C, 15 min <sup>g</sup>		[(Me <sub>3</sub> Si)Ph <sub>2</sub> Si] <sub>2</sub> ( <b>20</b> ), 52 <sup>d,h</sup>

<sup>a</sup> Unless otherwise stated, an excess amount of LDMAN (4.5 equiv) was used. <sup>b</sup> The reaction mixture was subjected to the reversed phase column chromatography to remove the resulting 1-(dimethylamino)naphthalene. <sup>c</sup> The yields were estimated by GLC analysis, unless otherwise stated. <sup>d</sup> The reaction mixture was washed with 1 M hydrochloric acid followed by extraction with Et<sub>2</sub>O to remove 1-(dimethylamino)naphthalene. <sup>e</sup> LDMAN (2.2 equiv). <sup>f</sup> The yield was estimated by <sup>1</sup>H NMR analysis. <sup>g</sup> No silyllithium was formed. <sup>h</sup> Isolated yield.

order of the yields did not reflect directly the bulkiness of the alkoxy groups. Preparation of (dialkoxysilyl)lithium (*t*-BuO)<sub>2</sub>PhSiLi (**4**) required the higher temperature (-50 °C) (entry 5). No reduction occurred at -78 °C, and the starting chlorosilane **10** was recovered. The (aminosilyl)lithium (Et<sub>2</sub>N)Ph<sub>2</sub>SiLi (**5**) was also prepared in good but somewhat lower yield (82%) at -50 °C (entry 7) than that obtained by reduction of the chlorosilane **11** with lithium metal (98%).<sup>2</sup> (Hydrosilyl)lithium HPh<sub>2</sub>SiLi (**6**) was obtained in moderate yield (40%) (entry 8); the yield is, however, higher than that obtained by the Gilman's procedure (11%).<sup>9</sup>

Reduction of a disilanyl chloride (Me<sub>3</sub>Si)Ph<sub>2</sub>SiCl (**19**) gave the homocoupling tetrasilane [(Me<sub>3</sub>Si)Ph<sub>2</sub>Si]<sub>2</sub> (**20**) in 52% yield without detection of trapping products of the corresponding (disilanyl)lithium (entry 9).<sup>10</sup> Attempted reduction of methylchlorosilane analogs XMe<sub>2</sub>SiCl (X = Me, *t*-BuO, and Et<sub>2</sub>N) afforded neither silyllithiums nor homocoupling disilanes.<sup>11</sup>

As reported previously,<sup>1</sup> (*t*-BuO)Ph<sub>2</sub>SiLi (**1**) underwent self-condensation at 0 °C for 2 h to give, after trapping with Me<sub>3</sub>SiCl, trisilane **21** (48% yield) via a (β-alkoxydisilanyl)lithium in addition to disilane **13** (25% yield) (eq 1). The methoxy analog (MeO)Ph<sub>2</sub>SiLi (**3**) also underwent self-condensation similarly but more rapidly at 0 °C within 10 min to give trisilane (MeO)Ph<sub>2</sub>Si-Ph<sub>2</sub>Si-SiMe<sub>3</sub> (**22**) in 29% yield together with disilane **15** in 9% yield (eq 1). The methoxy derivative **3** also underwent butylation with *n*-BuLi even at -78 °C within 30 min to afford *n*-BuPh<sub>2</sub>Si-SiMe<sub>3</sub> (**23**) in 62% yield after trapping with Me<sub>3</sub>SiCl (eq 2). Thus, **3** exhibits both nucleophilicity and electrophilicity even at -78 °C.



(9) Gilman, H.; Steudel, W. *Chem. Ind. (London)* **1959**, 1094.

(10) For an example of homocoupling of a chlorosilane with lithium naphthalene: Stüger, H. *J. Organomet. Chem.* **1993**, 458, 1.

(11) Reduction of Me<sub>3</sub>SiCl and (Et<sub>2</sub>N)Me<sub>2</sub>SiCl with lithium metal gave coupling products Me<sub>3</sub>Si-SiMe<sub>3</sub> and [(Et<sub>2</sub>N)Me<sub>2</sub>Si]<sub>2</sub>, respectively: (a) Seitz, D. E.; Ferreira, L. *Synth Commun.* **1979**, 9, 451. (b) Tamao, K.; Kawachi, A.; Ito, Y. *Organometallics* **1993**, 12, 580.

The (dialkoxysilyl)lithium (*t*-BuO)<sub>2</sub>PhSiLi (**4**) is more stable than (monoalkoxysilyl)lithiums **1**–**3**. When the solution of **4**, prepared at -50 °C, was warmed to 0 °C followed by trapping with Me<sub>3</sub>SiCl after 2 h, we obtained the simply trapped disilane **16** in 76% yield. The expected self-condensation product (*t*-BuO)<sub>2</sub>PhSi-(*t*-BuO)PhSi-SiMe<sub>3</sub> was not detected even after a longer reaction time was employed. In addition, **4** did not undergo butylation with *n*-BuLi at 0 °C for 2 h to give here again **16** in only 73% yield after trapping with Me<sub>3</sub>SiCl.

Thus we have developed the new method for preparation of (alkoxy(phenyl)silyl)-, (amino(phenyl)silyl)-, and (hydro(phenyl)silyl)lithiums by reduction of the corresponding chlorosilanes with LDMAN at low temperatures. The successful preparation of primary and secondary (alkoxysilyl)lithiums and (dialkoxysilyl)lithium may shed new light on the silylenoid chemistry. Further investigation is now under study.

## Experimental Section

**General Comments.** <sup>1</sup>H (270 MHz), <sup>13</sup>C (67.94 MHz), and <sup>29</sup>Si (53.67 MHz) NMR spectra were recorded on a JEOL EX-270 spectrometer. <sup>1</sup>H and <sup>13</sup>C chemical shifts are referenced to internal benzene-*d*<sub>6</sub> (<sup>1</sup>H δ 7.200 and <sup>13</sup>C δ 128.00). <sup>29</sup>Si chemical shifts are referenced to internal tetramethylsilane (0 ppm). The <sup>29</sup>Si NMR spectra were observed in unlocked mode at -100 °C for **1**. Although the spectrometer was unlocked during the acquisition, the field was stable and no significant field shift was observed. For NMR measurements, silyllithium **1** was prepared in THF as described in the experimental procedure and the resulting solution was transferred to an NMR sample tube via a Teflon tube under an argon atmosphere. Mass spectra were measured at 70 eV on a JEOL JMS-DX300 mass spectrometer equipped with a JMA-3500 data-processing system. Melting points were measured with a Yanaco-MP-S3 apparatus and were uncorrected. The elemental analyses were performed at the Microanalysis Division of Institute for Chemical Research, Kyoto University: Analytical samples were purified by preparative GLC, preparative HPLC, or recrystallization. Analytical and preparative GLC were performed on a Shimadzu GC-4B gas chromatograph equipped with a 3-m or 1-m column packed with 30% Silicone DC550 on Celite 545.

(Diethylamino)diphenylchlorosilane was prepared by the same method as described in the literature.<sup>12</sup> Diphenylchlorosilane was purchased from Shin-etsu Chemical Co., Ltd., and distilled under reduced pressure before use. 1-(Dimethylamino)naphthalene was purchased from Wako Pure Chemical

(12) Tamao, K.; Kawachi, A.; Nakagawa, Y.; Ito, Y. *J. Organomet. Chem.* **1994**, 473, 29.



Industries and distilled under reduced pressure. Trimethylchlorosilane was treated with sodium that was cut under nitrogen to remove the dissolving HCl, and the supernatant was used. *n*-Butyllithium in hexane and granular lithium were purchased from Wako Pure Chemical Industries and Chemetall Gesellschaft, respectively. THF was distilled under nitrogen from sodium benzophenone ketyl. *tert*-Butyl alcohol, isopropyl alcohol, triethylamine, and carbon tetrachloride were distilled from calcium hydride. Methanol was distilled from magnesium methoxide. 4-(Dimethylamino)pyridine and palladium chloride were commercially available and used without further purification. All reactions were carried out under an argon atmosphere.

**Preparation of Starting Materials (Functionalized Chlorosilanes).** **Bis(*tert*-butoxy)phenylchlorosilane (10).** To a mixture of phenyltrichlorosilane (8.00 mL, 50.0 mmol), triethylamine (15.3 mL, 110 mmol), and 4-(dimethylamino)pyridine (305 mg, 2.5 mmol) in THF (100 mL) was added a solution of *tert*-butyl alcohol (10.4 mL, 110 mmol) in THF (10 mL) over 15 min at 0 °C. The mixture was stirred at room temperature for 6 h. The mixture was diluted with hexane (ca. 100 mL), and the salts were filtered with suction. The filtrate was concentrated, and the residue was distilled through a short column (85–91 °C/0.60 mmHg) to give **10** (9.50 g, 66% yield) as a colorless oil. <sup>1</sup>H NMR (C<sub>6</sub>D<sub>6</sub>): δ 1.368 (s, 18H), 7.200–7.226 (m, 3H), 7.936–7.972 (m, 2H). <sup>13</sup>C NMR (C<sub>6</sub>D<sub>6</sub>): δ 31.56, 75.76, 128.05, 130.62, 134.38, 135.57. MS: *m/e* 288 (M<sup>+</sup> + 2, 2), 286 (M<sup>+</sup>, 2), 273 (M<sup>+</sup> + 2 - Me, 26), 271 (M<sup>+</sup> - Me, 63), 217 (27), 215 (76), 159 (28), 157 (81), 57 (*t*-Bu<sup>+</sup>, 100). Anal. Calcd for C<sub>14</sub>H<sub>23</sub>O<sub>2</sub>SiCl: C, 58.62; H, 8.08. Found: C, 58.61; H, 8.32.

**(*tert*-Butoxy)diphenylchlorosilane (7).** This compound<sup>1</sup> was prepared from diphenyldichlorosilane and *tert*-butyl alcohol in 76% yield by essentially the same method as described above.

**(Isopropoxy)diphenylchlorosilane (8).** Isopropyl alcohol (3.83 mL, 50.0 mmol) was added to diphenyldichlorosilane (10.4 mL, 50.0 mmol) at 0 °C. Dry nitrogen gas was bubbled through the mixture at 0 °C for 3 h and then at room temperature for 4 h. The mixture was distilled through a short column (121–129 °C/0.7 mmHg) to give **8** (11.9 g, <86% yield) as a colorless oil with small amounts of impurities. <sup>1</sup>H NMR (C<sub>6</sub>D<sub>6</sub>): δ 1.171 (d, *J* = 6.2 Hz, 6H), 4.303 (septet, *J* = 6.2 Hz, 1H), 7.153–7.200 (m, 6H), 7.814–7.862 (m, 4H). <sup>13</sup>C NMR (C<sub>6</sub>D<sub>6</sub>): δ 25.27, 67.57, 128.29, 131.09, 134.81, 135.48. MS: *m/e* 278 (M<sup>+</sup> + 2, 5), 276 (M<sup>+</sup>, 14), 261 (M<sup>+</sup> - Me, 9), 241 (M<sup>+</sup> - Cl, 6), 217 (M<sup>+</sup> - *i*-PrO, 100), 198 (51), 181 (22), 157 (98). Anal. Calcd for C<sub>15</sub>H<sub>17</sub>OSiCl: C, 65.08; H, 6.19. Found: C, 65.49; H, 6.40.

**(Methoxy)diphenylchlorosilane (9).** To a mixture of diphenylchlorosilane (4.31 g, 19.7 mmol) and triethylamine (3.57 mL, 25.6 mmol) in hexane (80 mL) was added a mixture of methyl alcohol (1.04 mL, 25.6 mmol) in hexane (4 mL) over 5 min at -40 °C. The mixture was stirred at -40 °C for 3 h and warmed to the ambient temperature. The mixture was diluted with hexane (ca. 50 mL), and the salts were filtered with suction. The filtrate was concentrated, and the residue was distilled through a short column (85–94 °C/0.40 mmHg) to give (methoxy)diphenylsilane (3.29 g, 78% yield) as a colorless oil. A solution of the (methoxy)diphenylsilane (3.29 g, 15.3 mL) in carbon tetrachloride (5.0 mL) was added to a mixture of palladium chloride (17.3 mg, 9.76 × 10<sup>-2</sup> mmol) and carbon tetrachloride (10 mL) at room temperature over 1 h. After being stirred for 2 h, the mixture was concentrated, diluted with hexane (10 mL), and filtered. The filtrate was concentrated, and the residue was distilled through a short column (119–121 °C/1.50 mmHg) to give **9** (2.53 g, 97% purity by GLC, 67% yield) as a colorless oil. <sup>1</sup>H NMR (C<sub>6</sub>D<sub>6</sub>): δ 3.458 (s, 3H), 7.123–7.173 (m, 6H), 7.764–7.800 (m, 4H). <sup>13</sup>C NMR (C<sub>6</sub>D<sub>6</sub>): δ 51.15, 128.38, 131.25, 134.76, 135.31. MS: *m/e* 250

(M<sup>+</sup> + 2, 7), 248 (M<sup>+</sup>, 14), 199 (21), 171 (19), 153 (100). Anal. Calcd for C<sub>13</sub>H<sub>13</sub>OSiCl: C, 62.76; H, 5.27. Found: C, 62.80; H, 5.42.

**1-Chloro-1,1-diphenyl-2,2,2-trimethyldisilane (19).** This compound was prepared in 83% overall yield by a similar method as described in the literature.<sup>2</sup> The spectral data were identical with the literature data.<sup>13</sup>

**Typical Procedure for Reduction of Chlorosilane with LDMAN: Synthesis of [Bis(*tert*-butoxy)phenylsilyl]lithium (4) and Trapping as 1,1-Bis(*tert*-butoxy)-1-phenyl-2,2,2-trimethyldisilane (16).** To a suspension of granular Li (33 mg, 4.8 mg-atom) in THF (4.5 mL) was added 1-(dimethylamino)naphthalene (0.78 mL, 4.8 mmol) at room temperature. The green color appeared after 15 min, and then the mixture was cooled to -50 °C. A solution of LDMAN was completely formed by vigorous stirring at the same temperature for 6 h. Bis(*tert*-butoxy)phenylchlorosilane (**10**) (301 mg, 1.1 mmol) in THF (2.0 mL) was added over 9 min to the LDMAN solution at -50 °C. After the solution stirred for 1 h, Me<sub>3</sub>SiCl (0.66 mL, 5.2 mmol) was added to the silyllithium solution at -50 °C. After being stirred for 10 min, the mixture was warmed to the ambient temperature. The volatile materials were evaporated under reduced pressure. The residue was diluted with hexane (10 mL), filtered, and evaporated. The residue was subjected to reverse-phase column chromatography (Wakogel LP-40C18, 30 mL) with CH<sub>3</sub>CN as eluent to separate the resulting 1-(dimethylamino)naphthalene (*R<sub>f</sub>* = 0.58) and to afford crude **16** (555 mg) (*R<sub>f</sub>* = 0.40) together with uncharacterized impurities. The yield was estimated by means of GLC analysis (93%): Eicosane was used as internal standard. The pure sample was obtained as a colorless oil by preparative GLC. <sup>1</sup>H NMR (C<sub>6</sub>D<sub>6</sub>): δ 0.291 (s, 9H), 1.371 (s, 18H), 7.254–7.361 (m, 3H), 7.933–7.967 (m, 2H). <sup>13</sup>C NMR (C<sub>6</sub>D<sub>6</sub>): δ -1.02, 32.37, 73.34, 127.87, 129.35, 134.61, 140.97. MS: *m/e* 324 (M<sup>+</sup>, 0.5), 309 (M<sup>+</sup> - Me, 7), 251 (5), 211 (89), 139 (100). Anal. Calcd for C<sub>17</sub>H<sub>32</sub>O<sub>2</sub>Si<sub>2</sub>: C, 62.90; H, 9.94. Found: C, 62.67; H, 9.83.

**1,2-Bis(*tert*-butoxy)-1,1,2,2-tetraphenyldisilane.** The pure sample was obtained as a colorless solid by recrystallization from hexane, mp: 167.8–168.8 °C. <sup>1</sup>H NMR (C<sub>6</sub>D<sub>6</sub>): δ 1.312 (s, 18H), 7.188–7.200 (m, 12H), 7.872–7.920 (m, 8H). <sup>13</sup>C NMR (C<sub>6</sub>D<sub>6</sub>): δ 32.26, 74.52, 127.78, 129.62, 136.23, 138.22. MS: *m/e* 510 (M<sup>+</sup>, 0.1), 495 (M<sup>+</sup> - Me, 0.4), 437 (M<sup>+</sup> - *t*-BuO, 0.7), 397 (100), 319 (65), 199 (99), 181 (21). Anal. Calcd for C<sub>32</sub>H<sub>38</sub>O<sub>2</sub>Si<sub>2</sub>: C, 75.24; H, 7.50. Found: C, 75.21; H, 7.54.

**1-(*tert*-Butoxy)-1,1-diphenyl-2,2,2-trimethyldisilane (13).** This compound<sup>1</sup> was obtained in 81% yield (GLC) by essentially the same method as described above.

**1-(Isopropoxy)-1,1-diphenyl-2,2,2-trimethyldisilane (14).** The pure sample was obtained as a colorless oil by preparative GLC. <sup>1</sup>H NMR (C<sub>6</sub>D<sub>6</sub>): δ 0.283 (s, 9H), 1.163 (d, *J* = 6.3 Hz, 6H), 4.108 (septet, *J* = 6.3 Hz, 1H), 7.229–7.274 (m, 3H), 7.753–7.789 (m, 2H). <sup>13</sup>C NMR (C<sub>6</sub>D<sub>6</sub>): δ -1.22, 25.97, 66.83, 128.20, 129.71, 135.17, 137.85. MS: *m/e* 299 (M<sup>+</sup> - Me, 0.4), 271 (M<sup>+</sup> - *i*-Pr, 9), 255 (M<sup>+</sup> - *i*-PrO, 6), 241 (M<sup>+</sup> - Me<sub>3</sub>Si, 23), 199 (100), 181 (25). Anal. Calcd for C<sub>18</sub>H<sub>26</sub>O<sub>2</sub>Si<sub>2</sub>: C, 68.73; H, 8.33. Found: C, 68.50; H, 8.16.

**1-(Methoxy)-1,1-diphenyl-2,2,2-trimethyldisilane (15).** The pure sample was obtained as a colorless oil by preparative GLC. <sup>1</sup>H NMR (C<sub>6</sub>D<sub>6</sub>): δ 0.259 (s, 9H), 3.472 (s, 3H), 7.246–7.272 (m, 6H), 7.717–7.752 (m, 4H). <sup>13</sup>C NMR (C<sub>6</sub>D<sub>6</sub>): δ -1.40, 51.90, 128.31, 129.81, 134.99, 136.73. MS: *m/e* 286 (M<sup>+</sup>, 2), 271 (M<sup>+</sup> - Me, 100), 255 (M<sup>+</sup> - MeO, 5), 183 (68). Anal. Calcd for C<sub>16</sub>H<sub>22</sub>O<sub>2</sub>Si<sub>2</sub>: C, 67.07; H, 7.74. Found: C, 67.10; H, 7.86.

**1-(Diethylamino)-1,1-diphenyl-2,2,2-trimethyldisilane (17).** This compound has been reported.<sup>2</sup>

**Synthesis of (Hydrodiphenylsilyl)lithium (6) and Trapping as 1-Hydro-1,1-diphenyl-2,2,2-trimethyldisilane (18).** To a solution of LDMAN in THF (2.8 mL), which was prepared

(13) Ishikawa, M.; Fuchikami, T.; Kumada, M. *J. Organomet. Chem.* **1976**, *118*, 139.

from granular Li (20 mg, 2.8 mg-atom) and 1-(dimethylamino)naphthalene (0.47 mL, 2.8 mol), was added **12** (0.12 mL, 0.63 mmol) in THF (2.0 mL) at  $-50\text{ }^{\circ}\text{C}$  over 5 min. After the silyllithium solution was stirred for 1 h,  $\text{Me}_3\text{SiCl}$  (0.40 mL, 3.1 mmol) was added at  $-50\text{ }^{\circ}\text{C}$ . After stirring for 10 min, the mixture was warmed to the ambient temperature. After being cooled to  $0\text{ }^{\circ}\text{C}$ , 1 M hydrochloric acid (10 mL) was poured into the reaction mixture, which was extracted with  $\text{Et}_2\text{O}$  (10 mL  $\times$  3). The combined organic layer was washed with 1 M hydrochloric acid (10 mL),  $\text{H}_2\text{O}$  (10 mL), and brine (10 mL) and dried over  $\text{Na}_2\text{SO}_4$ . The solution was concentrated in vacuo to yield crude **18**. The yield was estimated by means of  $^1\text{H}$  NMR analysis (40%): Mesitylene was used as internal standard. The pure sample was obtained as a colorless oil by preparative GLC. The spectral data were identical with those of the literature.<sup>13</sup>

**Attempted Synthesis of a (Disilyl)lithium from 19: Formation of 2,2,3,3-Tetraphenyl-1,1,1,4,4,4-hexamethyltetrasilane (20).** To a solution of LDMAN in THF (2.4 mL), which was prepared from granular Li (17 mg, 2.5 mg-atom) and 1-(dimethylamino)naphthalene (0.40 mL, 2.5 mol), was added **19** (159 mg, 0.55 mmol) in THF (2.0 mL) at  $-78\text{ }^{\circ}\text{C}$  over 10 min. After the solution was stirred for 15 min,  $\text{Me}_3\text{SiCl}$  (0.34 mL, 2.7 mmol) was added at  $-78\text{ }^{\circ}\text{C}$ . After stirring for 10 min, the mixture was warmed to the ambient temperature. Usual workup as described above afforded crude **20**. Recrystallization from hexane gave **20** as a colorless solid (52% yield), mp:  $269\text{--}270\text{ }^{\circ}\text{C}$  (in a sealed capillary under atmospheric pressure). Sublimation point: about  $150\text{ }^{\circ}\text{C}$ .  $^1\text{H}$  NMR ( $\text{C}_6\text{D}_6$ ):  $\delta$  0.143 (s, 18H), 7.172–7.200 (m, 12H), 7.713–7.748 (m, 8H).  $^{13}\text{C}$  NMR ( $\text{C}_6\text{D}_6$ ):  $\delta$   $-0.32$ , 128.22, 128.92, 136.14, 137.06. MS:  $m/e$  510 ( $\text{M}^+$ , 16), 495 ( $\text{M}^+ - \text{Me}$ , 5), 437 ( $\text{M}^+ - \text{Me}_3\text{Si}$ , 12), 360 (89), 255 ( $\text{Me}_3\text{Si} - \text{Ph}_2\text{Si}^+$ , 87), 135 (100). Anal. Calcd for  $\text{C}_{30}\text{H}_{38}\text{Si}_4$ : C, 70.52; H, 7.50. Found: C, 70.34; H, 7.57.

**Self-Condensation of [(Methoxy)diphenylsilyl]lithium (3): Formation of 1-(Methoxy)-1,1,2,2-tetraphenyl-3,3,3-trimethyltrisilane (22).** A solution of **3** in THF (4.5 mL), which was prepared at  $-78\text{ }^{\circ}\text{C}$  from **9** (160 mg, 0.62 mmol), granular Li (19 mg, 2.7 mg-atom), and 1-(dimethylamino)naphthalene (0.45 mL, 2.7 mol), was warmed to  $0\text{ }^{\circ}\text{C}$ . After 10 min,  $\text{Me}_3\text{SiCl}$  (3.0 mmol, 0.38 mL) was added to the solution. After stirring for 20 min, the reaction mixture was warmed to the ambient temperature. The reaction mixture was evaporated, diluted with hexane, and filtered. The filtrate was concentrated to give a mixture of **22** and **15**. The yield of **15** was estimated by GLC analysis (9%): Docosane was used as internal standard. The mixture was subjected to reverse-phase column chromatography (Wakogel LP-40C18, 30 mL) with  $\text{CH}_3\text{CN}$  as eluent to separate the resulting 1-(dimethylamino)naphthalene ( $R_f = 0.58$ ) and to afford crude **22** (115 mg,  $R_f = 0.45$ ), followed by HPLC with hexane/AcOEt (10/1) as eluent to yield **22** (42 mg, 29% yield) as a colorless solid, mp:  $70.0\text{--}70.5\text{ }^{\circ}\text{C}$ .  $^1\text{H}$  NMR ( $\text{C}_6\text{D}_6$ ):  $\delta$  0.256 (s, 9H), 3.494 (s, 3H), 7.149–7.200 (m, 12H), 7.684–7.719 (m, 4H), 7.713–7.808 (m, 4H).  $^{13}\text{C}$  NMR ( $\text{C}_6\text{D}_6$ ):  $\delta$   $-0.55$ , 52.22, 128.18, 128.34, 128.92, 129.98, 135.26, 135.49, 136.59, 136.90. MS:  $m/e$  468 ( $\text{M}^+$ , 27), 453 ( $\text{M}^+ - \text{Me}$ , 45), 395 ( $\text{M}^+ - \text{Me}_3\text{Si}$ , 8), 364 (96), 255 ( $\text{Me}_3\text{Si} - \text{Ph}_2\text{Si}^+$ , 20), 213 ( $(\text{MeO})\text{Ph}_2\text{Si}^+$ , 100). Anal. Calcd for  $\text{C}_{28}\text{H}_{32}\text{OSi}_3$ : C, 71.74; H, 6.88. Found: C, 71.83, H, 6.88.

**1-(tert-Butoxy)-1,1,2,2-tetraphenyl-3,3,3-trimethyltrisilane (21).** This compound<sup>1</sup> was obtained in 48% yield as a mixture with **13** (25% GLC yield) by essentially the same method as described above. The yield was estimated from the relative intensity of  $^1\text{H}$  NMR spectra to the disilane.

**Reaction of 3 with *n*-Butyllithium: Formation of 1-*n*-Butyl-1,1-diphenyl-2,2,2-trimethylidisilane (23).** To a solution of **3** in THF (5.0 mL), which was prepared from (methoxy)diphenylchlorosilane (0.66 mmol), granular Li (3.0 mg-atom), and 1-(dimethylamino)naphthalene (3.0 mmol), was added *n*-BuLi in hexane (2.1 mL, 3.3 mmol) at  $-78\text{ }^{\circ}\text{C}$ . After the solution was stirred at that temperature for 30 min,  $\text{Me}_3\text{SiCl}$  (0.87 mL, 6.9 mmol) was added. The reaction mixture was stirred at  $-78\text{ }^{\circ}\text{C}$  for 20 min and warmed to the ambient temperature. An aliquot of 1 M hydrochloric acid (10 mL) was poured into the reaction mixture, and the mixture was extracted with  $\text{Et}_2\text{O}$  (10 mL  $\times$  3). The combined organic layer was washed with 1 M hydrochloric acid (10 mL  $\times$  2),  $\text{H}_2\text{O}$  (10 mL), and brine (10 mL) and dried over  $\text{MgSO}_4$ . After filtration, the filtrate was concentrated and subjected to silica gel column chromatography with hexane as eluent, followed by HPLC with hexane as eluent to afford **23** (128 mg, 62% yield). The spectral and analytical data have been reported.<sup>1</sup>

**Attempted Self-Condensation of 4.** A solution of **4** in THF (5.0 mL), which was prepared at  $-50\text{ }^{\circ}\text{C}$  from **10** (182 mg, 0.63 mmol), granular Li (20 mg, 2.9 mg-atom), and 1-(dimethylamino)naphthalene (0.48 mL, 2.9 mmol), was warmed to  $0\text{ }^{\circ}\text{C}$ . After 2 h,  $\text{Me}_3\text{SiCl}$  (0.41 mL, 3.2 mmol) was added to the solution. After stirring for 10 min, the reaction mixture was warmed to the ambient temperature. The reaction mixture was evaporated, diluted with hexane, filtered, and condensed under reduced pressure. No self-condensation product (*t*-BuO) $_2$ PhSi–(*t*-BuO)PhSi–SiMe $_3$  was detected in the residue by  $^1\text{H}$  NMR analysis. The residue was subjected to reverse-phase column chromatography (Wakogel LP-40C18, 20 mL) with  $\text{CH}_3\text{CN}$  as eluent to separate the resulting 1-(dimethylamino)naphthalene ( $R_f = 0.58$ ) and to afford crude **16** (197 mg) ( $R_f = 0.40$ ) together with uncharacterized impurities. The yield was estimated by means of GLC analysis (76%): Eicosane was used as internal standard.

**Attempted Reaction of 4 with *n*-Butyllithium.** A solution of **4** in THF (3.3 mL), which was prepared at  $-50\text{ }^{\circ}\text{C}$  from **10** (151 mg, 0.53 mmol), granular Li (16 mg, 2.3 mg-atom), and 1-(dimethylamino)naphthalene (0.38 mL, 2.3 mmol), was added to a solution of *n*-BuLi in hexane (2.5 mL, 4.2 mmol) and tetramethylethylenediamine (0.64 mL, 4.2 mmol) in THF (2.0 mL) at  $0\text{ }^{\circ}\text{C}$  over 2 min via a Teflon tube. After the solution was stirred at  $0\text{ }^{\circ}\text{C}$  for 2 h,  $\text{Me}_3\text{SiCl}$  (0.9 mL, 7.2 mmol) was added. The reaction mixture was stirred at  $0\text{ }^{\circ}\text{C}$  for 20 min and warmed to the ambient temperature. The reaction mixture was evaporated, diluted with hexane, filtered, and condensed under reduced pressure. Butylation products (*t*-BuO)(*n*-Bu)PhSi–SiMe $_3$  and (*n*-Bu) $_2$ PhSi–SiMe $_3$  were not detected in the residue by  $^1\text{H}$  NMR analysis. The residue was subjected to reverse-phase column chromatography (Wakogel LP-40C18, 20 mL) with  $\text{CH}_3\text{CN}$  as eluent to separate the resulting 1-(dimethylamino)naphthalene ( $R_f = 0.58$ ) and to afford crude **16** (215 mg) ( $R_f = 0.40$ ) together with uncharacterized impurities. The yield was estimated by means of GLC analysis (73%): Eicosane was used as internal standard.

**Acknowledgment.** We thank the Ministry of Education, Science, and Culture, Japan, for a Grant-in-Aid for Scientific Research (No. 06750886). We also thank Prof. M. Ishikawa, Hiroshima University, for instruction of preparation of chlorosilanes from hydrosilanes with  $\text{CCl}_4/\text{PdCl}_2$ . Thanks are also due to Shin-etsu Chemical Co., Ltd., for a gift of some chlorosilanes.

OM950205U

# Synthesis and Reactivity of Silylboranes

John D. Buynak\* and Bolin Geng

Department of Chemistry, Southern Methodist University, Dallas, Texas 75275

Received January 31, 1995\*

**Summary:** Several representative silylboranes, including *B*-(phenyldimethylsilyl)catecholborane (**7**), were prepared and their reactivity explored. The reaction of silylboranes with either vinylolithium or lithium acetylide generated the corresponding silylborates which rearrange upon treatment with  $I_2$ , producing the vinylsilane and silyl acetylide, respectively. The reaction of **7** with ethyl diazoacetate yielded ethyl (phenyldimethylsilyl)acetate upon hydrolysis.

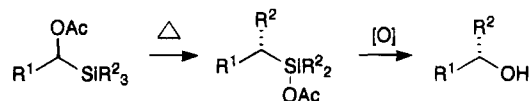
## Introduction

The first silylboranes were synthesized in 1960.<sup>1</sup> The preparation of compounds containing an Si–B bond has been briefly summarized.<sup>2</sup> Despite the relatively long history of silylboranes, few systematic studies of their reactivity are available. The most extensive studies were performed by Nöth, who prepared B–Si compounds which contain an (electronically shielding) B–N bond and described some of their chemistry.<sup>3</sup>

Silyl(mono)boranes are most commonly prepared by reaction of silyl anions with boron halides. However, the reaction is severely limited due to the ease with which the resultant silylboranes add an additional equivalent of the silicon nucleophile to form the corresponding anionic tetracoordinated borate. Strategies for overcoming this side reaction involve either sterically or electronically shielding the boron toward further reactivity. Very recently, a transition-metal-mediated instance of B–Si bond formation has been reported<sup>4</sup> as has the formation of a Bi–Si bond by the reaction of a phosphorus-complexed (and, therefore, electronically shielded) boryl anion with a silyl halide.<sup>5</sup>

We recently reported studies on the thermal rearrangements of  $\alpha$ -acyloxysilanes and the synthetic utility of such rearrangements in the preparation of chiral compounds.<sup>6</sup> Our ongoing research on the preparation and reactions of chiral organosilicon compounds<sup>7</sup> involved us in a search for new methods for the formation of the carbon–silicon bond. In our previous studies, C–Si bonds were usually formed by (a) reactions of carbanions with silyl halides or (b) reaction of silyl anions with organohalides. This methodology is inconvenient since both carbanions and silyl anions are

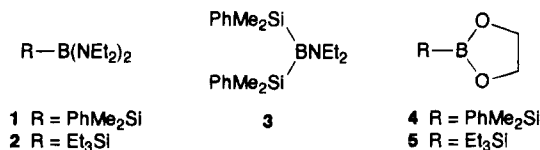
relatively intolerant of other intramolecular functionality. Also, many silylmetallics can be difficult to prepare in high yield and deteriorate upon prolonged storage. Our experience with organoboron compounds led us to wonder if compounds with direct bonds between boron and silicon would react with typical organic functionality (such as C=O or C=C) leading to the formation of new carbon–silicon bonds. We thus decided to explore the potential of silylboranes as silyl-transfer reagents.



## Results and Discussion

**Synthesis.** Our initial investigation into the preparation of silylboranes began with an attempt to react phenyldimethylsilyllithium with (+)-*B*-chlorodiisopinocampheylborane<sup>8</sup> (DIP chloride). While a reaction appeared to occur, the resultant solution, when reacted with benzaldehyde, produced only benzyl alcohol. Presumably this occurred from hydride transfer from the pinene ligand (analogous to the reaction of DIP–Cl itself with carbonyl compounds). The reaction mixture failed, however, to reduce acetophenone. Analysis of the crude reaction by <sup>11</sup>B NMR indicated the formation of a new compound with chemical shift of  $\delta = 1.2$  ppm, more appropriate for a borate than the desired borane.

We then decided to employ the more established methods of Nöth in the preparation of these compounds. The reaction of  $\text{PhMe}_2\text{SiLi}$  with  $(\text{Et}_2\text{N})_2\text{BCl}$ <sup>9</sup> in cyclohexane afforded silylborane **1** in good yield. Similarly, silyl borane **2** was obtained when  $\text{Et}_3\text{SiLi}$ <sup>10</sup> was used. If  $\text{Cl}_2\text{BNET}_2$  was reacted with 2 equiv of  $\text{PhMe}_2\text{SiLi}$ , the bis(phenyldimethylsilyl)borane **3** was obtained. As observed by Nöth, compounds **1** and **2** are easily derivatized to compounds **4** and **5**, respectively, by reaction with ethylene glycol in  $\text{CH}_2\text{Cl}_2$ .



The catechol derivatives of borane itself are known to have enhanced (hydroborating) reactivity relative to the analogous ethylene glycol derivatives.<sup>11</sup> We thus

\* Abstract published in *Advance ACS Abstracts*, May 15, 1995.

(1) (a) Seyferth, D.; Kogler, H. P. *J. Inorg. Nucl. Chem.* **1960**, *15*, 99. (b) Cowley, A. H.; Sisler, H. H.; Ryschkewitach, G. E. *J. Am. Chem. Soc.* **1960**, *82*, 501.

(2) Molloy, K. C. In *Inorganic Reactions and Methods*; Zuckerman, J. J., Hagan, A. P., Eds.; VCH Publishers, Inc.: 1989; Vol. 10, Section 5.3.7, pp 209–213.

(3) Biffar, W.; Nöth, H.; Schwerthoffer, R. *Liebigs Ann. Chem.* **1981**, 2067–2080.

(4) Jiang, Q.; Carroll, P. J.; Berry, D. H. *Organometallics* **1993**, *12*, 177.

(5) Blumenthal, A.; Bissinger, P.; Schmidaur, H. *J. Organomet. Chem.* **1993**, *462*, 107.

(6) Buynak, J. D.; Strickland, J. B.; Lamb, G. W.; Khasnis, D.; Modi, S.; Williams, D.; Zhang, H. *J. Org. Chem.* **1991**, *56*, 7076–7083.

(7) Buynak, J. D.; Geng, B.; Uang, S.; Strickland, J. B. *Tetrahedron Lett.* **1994**, *35*, 985–988.

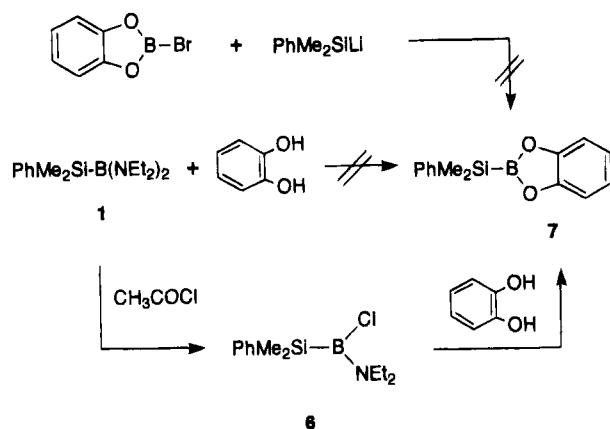
(8) Chandrasekharan, J.; Ramachandran, P. V.; Brown, H. C. *J. Org. Chem.* **1985**, *50*, 5448.

(9) Chavant, P. Y.; Vautier, M. *J. Organomet. Chem.* **1993**, *455*, 37.

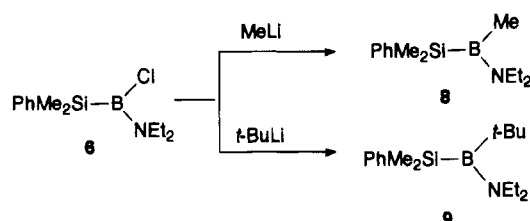
(10) Vyazankin, N. S.; Razuvaev, G. A.; Gladyshev, E. N.; Korneva, S. P. *J. Organomet. Chem.* **1967**, *7*, 353.

(11) (a) Brown, H. C. *Organic Synthesis via Boranes*; John Wiley and Sons: New York, 1975; p 44. (b) Brown, H. C.; Gupta, S. K. *J. Am. Chem. Soc.* **1971**, *93*, 1816.

Scheme 1



Scheme 2



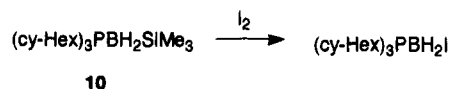
decided to prepare the previously unknown catecholborosilane, **7**, and to explore its chemistry. The direct synthesis of silylcatecholborane **7** using phenyldimethylsilyllithium with  $B$ -bromocatecholborane was not successful, once again probably due to the formation of tetracoordinated borates. Attempted direct reaction of either **1** or **2** with catechol (under a variety of conditions) also did not produce catecholborane **7** (or its triethylsilyl analog). While searching for conditions to remove the organoamine from borane, it was discovered that reaction of **1** with acetyl chloride cleanly produces chloroborane **6**. Compound **6** was found to react with catechol to generate catecholborane **7** (see Scheme 1).

As shown in Scheme 2, compound **6** could be used to produce other  $B$ -silyl- $B$ -(diethylamino)boranes by nucleophilic displacement of the chlorine. Unfortunately all attempts to remove the last diethylamine group from either **6**, **8**, or **9** failed.

We reasoned that the preparation of new members of this class of compounds would be made easier if we could generate a silylboron hydride, such as  $\text{R}_3\text{SiBH}_2$ , which could be used as a hydroborating agent. Attempts to prepare a silylboron hydride by ligand exchange of **1**, **3**, or **4** with borane dimethyl sulfide complex or direct reduction of these compounds with lithium aluminum hydride did not succeed. The major isolable product from such reactions was dimethylphenylsilane. No  $B$ -O or  $B$ -N bond reduced products were observed.

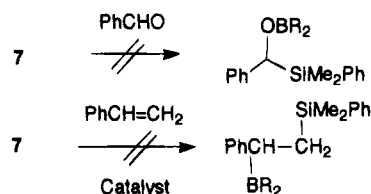
A recent report<sup>12</sup> of the preparation of tricyclohexylphosphine-complexed (trimethylsilyl)boron hydride **10** led us to prepare this compound and explore the potential for liberating the uncomplexed silylborane,  $\text{Me}_3\text{SiBH}_2$ . As described in the literature, the complexed silylborane is extremely stable, allowing its purification by column chromatography on silica gel.

Scheme 3



Bestmann<sup>13</sup> has reported the removal of a boron-complexed triphenylphosphine by reaction with methyl iodide. However, no reaction occurred on treatment of **10** with either methyl iodide or methyl tosylate. In an attempt to thermally liberate  $\text{Me}_3\text{SiBH}_2$ , **10** was heated (under vacuum) with an external flame while trapping all volatiles. Instead of liberating the free silylborane, only trimethylsilane ( $\text{Me}_3\text{SiH}$ ) was isolated. The  $\text{Si-B}$  bond was cleaved by iodine (Scheme 3), but **10** was inert toward reaction with nucleophiles such as tetrabutylammonium fluoride, vinylolithium, and triethylamine as well as toward electrophilic organic functionalities, such as aldehydes.

**Reactivity.** We had initially hoped that silylboranes would have enhanced reactivity (relative to alkylboranes, for example) leading to facile transfer of silicon to organic molecules. We had in particular hoped that such compounds would react with aldehydes and ketones (as shown below)



leading to (after hydrolysis) secondary and tertiary  $\alpha$ -hydroxysilanes. Unfortunately, both compounds **4** and **7** were inert in the presence of aldehydes and ketones, even at elevated temperatures. Secondly, we had hopes that catecholsilylborane **7** would undergo borosilylation of double bonds, either by itself or in the presence of catalysts. Once again, we were impressed by the inert nature of this compound in the presence of alkenes and alkynes, even in the presence of catalysts such as Wilkinson's catalyst.

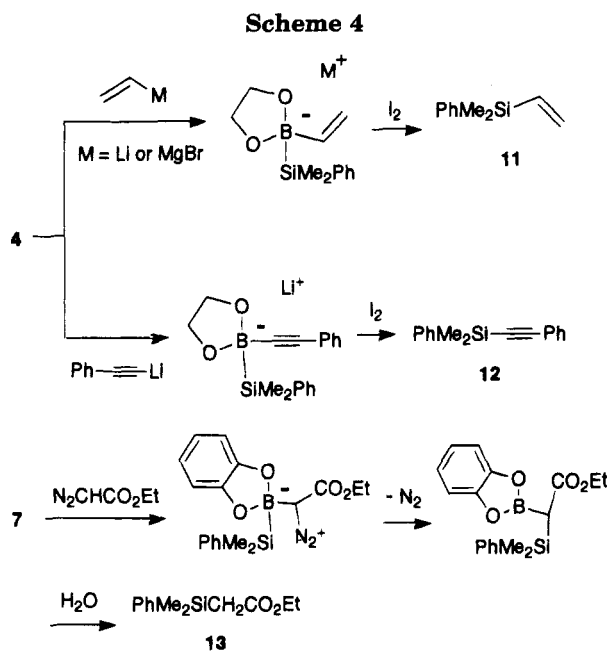
Many extremely useful transformations of boron-carbon bonds involve rearrangements of deliberately formed four-coordinate anionic organoborates.<sup>14</sup> In a suitable substituted organoborate, a 1,2-intramolecular migration can be induced by the presence or generation of an electron-deficient center  $\alpha$  to the boron. As a further extension of the analogy between  $B$ -Si and  $B$ -C, we desired to know if a similar transformation (with migration of silicon) was possible for silylborates.

As shown below, the silylborane **4** was treated with either vinylolithium or vinylmagnesium bromide to form the corresponding silyl borate. This borate was then reacted with iodine to form dimethylphenylvinylsilane, **11**. Similarly, the reaction of **4** with lithium phenylacetylide, and subsequent treatment with iodine, produced dimethylphenylsilylphenylacetylide **12**. Silylborane **7** reacted with ethyl diazoacetate yielding silyl substituted acetate **13** (Scheme 4). The intermediate borate formed by the reaction of **4** and lithium phenyl-

(13) Bestmann, H. J.; Roder, T.; Suhs, K. *Chem. Ber.* **1988**, *121*, 1509.

(14) Pelter, A.; Smith, K.; Brown, H. C. *Borane Reagents*; Academic Press: New York, 1988.

(12) Blumenthal, A.; Bissinger, P.; Schmidbaur, H. *J. Organomet. Chem.* **1993**, *462*, 107.



acetylide did not react with other electrophiles such as MeI, Me<sub>3</sub>SiCl, Me<sub>3</sub>SnCl, Bu<sub>3</sub>SnCl, CH<sub>3</sub>COCl, (MeO)<sub>2</sub>SO<sub>2</sub>, PhSeCl, and MeOTf.

### Conclusion

The chemistry of the Si–B bond of silylboranes and silylborates is most closely analogous to the chemistry of the C–B bond of organoboranes. No (silylboration) process analogous to hydroboration (of either alkenes or carbonyls) was discovered. Like the alkyl groups of organoborates, the silicon of silylborates can migrate to an adjacent electron-deficient center.

### Experimental Section

**General Procedures.** All reactions were performed under an atmosphere of argon using standard vacuum line techniques. <sup>1</sup>H, <sup>13</sup>C, and <sup>11</sup>B NMR spectra were obtained on a Bruker WP200SY spectrometer. Mass spectral data were obtained by the EI technique from Midwest Center for Mass Spectrometry at the University of Nebraska–Lincoln. Elemental analyses were performed by E+R Microanalytical Laboratory, Inc., Corona, NY. TLC was performed on Merck 0.2-mm Kieselgel 60 F254 silica-coated plates. The compounds were identified in one of the following manners: UV (254 nm) and phosphomolybdic acid spray reagent. Flash chromatography was performed in thick-walled glass columns using Merck 0.040–0.063-mm Kieselgel 60 silica gel. The glassware used in the reactions described below was oven- or flame-dried and was cooled under argon. The chromatography solvents were distilled from CaH<sub>2</sub> before use. All additional solvents were obtained from Aldrich in Sure-Seal bottles. Anhydrous reagents were used as received from Aldrich unless otherwise noted.

**PhMe<sub>2</sub>SiB(NEt<sub>2</sub>)<sub>2</sub> (1).** To a solution of bis(diethylamino)-boron chloride<sup>15</sup> (17.6 g, 92 mmol) in 100 mL of cyclohexane was added a solution of phenyldimethylsilyllithium in THF (0.8 M, 115 mL) at 0 °C via cannula (leaving behind most excess lithium). After addition, the brown reaction mixture was stirred overnight at room temperature. The precipitate was filtered under argon, and the yellow solution was concentrated *in vacuo*. Vacuum distillation of the residue produced

24.5 g (92%) of **1** as a slightly yellow liquid: bp 105–110 °C/0.2 mm Hg. <sup>1</sup>H NMR (CDCl<sub>3</sub>): δ 0.33 (s, 6H), 0.99 (t, *J* = 7.0 Hz, 12 H), 3.01 (q, *J* = 7.0 Hz, 8 H), 7.4–7.7 (m, 5 H). <sup>13</sup>C NMR (C<sub>6</sub>D<sub>6</sub>): δ 1.40 (q), 16.93 (q), 43.17 (t), 135.78, 132.71, 129.62, 126.48. <sup>11</sup>B NMR (C<sub>6</sub>D<sub>6</sub>): δ 36.5. Anal. Calcd for C<sub>16</sub>H<sub>31</sub>BN<sub>2</sub>Si: C, 66.20; H, 10.76; N, 9.65. Found: C, 66.25; H, 10.58; N, 9.47.

**Et<sub>3</sub>SiB(NEt<sub>2</sub>)<sub>2</sub> (2).** This compound was prepared as described for **1** using triethylsilyllithium<sup>16</sup> (84%): bp 89–92 °C/0.2 mm Hg. <sup>1</sup>H NMR (C<sub>6</sub>D<sub>6</sub>): δ 0.81 (q, *J* = 7.9 Hz, 6 H), 1.01 (t, *J* = 7.9 Hz, 12 H), 1.16 (t, *J* = 7.9 Hz, 9 H), 3.03 (q, *J* = 7.9 Hz, 8 H). <sup>13</sup>C NMR (CDCl<sub>3</sub>): δ 5.71, 8.66, 15.62, 42.30. <sup>11</sup>B NMR (CDCl<sub>3</sub>): δ 36.7. Anal. Calcd for C<sub>14</sub>H<sub>35</sub>BN<sub>2</sub>Si: C, 62.21; H, 13.04; N, 10.36. Found: C, 62.11; H, 12.91; N, 10.06.

**(PhMe<sub>2</sub>Si)<sub>2</sub>BNEt<sub>2</sub> (3).** This compound was prepared as described for **1** using 2 equiv of phenyldimethylsilyllithium and (diethylamino)boron dichloride (22%).<sup>17</sup> <sup>1</sup>H NMR (C<sub>6</sub>D<sub>6</sub>): δ 0.45 (s, 12 H), 0.85 (t, *J* = 7.0 Hz, 6 H), 3.20 (q, *J* = 7.0 Hz, 4 H), 7.2–7.8 (m, 10 H). <sup>13</sup>C NMR (C<sub>6</sub>D<sub>6</sub>): δ 0.32, 16.86, 50.35, 128.27, 133.32, 134.33, 143.17. <sup>11</sup>B NMR (C<sub>6</sub>D<sub>6</sub>): δ 55.7.

**PhMe<sub>2</sub>SiB(OCH<sub>2</sub>)<sub>2</sub> (4).** To a solution of **1** (8.74 g, 30.1 mmol) in 50 mL of CH<sub>2</sub>Cl<sub>2</sub> was added ethylene glycol (1.87 g, 30.1 mmol) slowly by syringe at room temperature. After addition, the slightly yellow solution was stirred for 1 h. Concentration and distillation gave 4.3 g of **4** (69%): bp 95–100 °C/0.5 mm Hg. <sup>1</sup>H NMR (C<sub>6</sub>D<sub>6</sub>): δ 0.48 (s, 6 H), 3.53 (s, 4 H), 7.2–7.9 (m, 5 H). <sup>11</sup>B NMR (C<sub>6</sub>D<sub>6</sub>): δ 34.3. HRMS. Calcd for C<sub>9</sub>H<sub>12</sub>BO<sub>2</sub>Si (M – CH<sub>3</sub>) 191.0700, found 191.0703.

**Et<sub>3</sub>SiB(OCH<sub>2</sub>)<sub>2</sub> (5).** This compound was prepared as described for **4** using **2** (47%). <sup>1</sup>H NMR (C<sub>6</sub>D<sub>6</sub>): δ 0.80 (q, *J* = 7.8 Hz, 6 H), 1.15 (t, *J* = 7.8 Hz, 9 H), 3.65 (s, 4 H). <sup>11</sup>B NMR (C<sub>6</sub>D<sub>6</sub>): δ 34.5.

**PhMe<sub>2</sub>SiBCl(NEt<sub>2</sub>) (6).** To a solution of **1** (15.1 g, 52 mmol) in 60 mL of diethyl ether was added acetyl chloride (5.2 g, 67 mmol) at 0 °C. After addition, the clear solution was stirred for 30 min at room temperature. Concentration and vacuum distillation produced 11.4 g of **6** (86%): bp 108–110 °C/1.0 mm Hg. <sup>1</sup>H NMR (C<sub>6</sub>D<sub>6</sub>): δ 0.55 (d, *J* = 0.5 Hz, 6 H), 0.75 (t, *J* = 7.0 Hz, 3 H), 0.97 (t, *J* = 7.0 Hz, 3 H), 2.90 (q, *J* = 7.0 Hz, 2 H), 3.15 (q, *J* = 7.0 Hz, 2 H), 7.2–7.5 (m, 5 H). <sup>13</sup>C NMR (C<sub>6</sub>D<sub>6</sub>): δ –1.8, 15.2, 15.9, 43.0, 46.0, 128.1, 128.8, 134.2, 140.0. <sup>11</sup>B NMR (C<sub>6</sub>D<sub>6</sub>): δ 40.7. Anal. Calcd for C<sub>12</sub>H<sub>21</sub>BClNSi: C, 56.83; H, 8.34; N, 5.52. Found: C, 56.70; H, 8.29; N, 5.71.

**PhMe<sub>2</sub>SiBMe(NEt<sub>2</sub>) (8).** To a solution of **6** (3.3 g, 13.0 mmol) in 20 mL of diethyl ether was added methylmagnesium chloride (3 M, 6.5 mL, 19.5 mmol) at room temperature. After 24 h of stirring, the suspension was centrifuged (3000 RPM). Concentration and distillation of the supernatant gave **8** (1.7 g, 58%) as a colorless oil: bp 95 °C/1.0 mm Hg. <sup>1</sup>H NMR (C<sub>6</sub>D<sub>6</sub>): δ 0.46 (s, 6 H), 0.64 (s, 3 H), 0.85 (t, *J* = 7.0 Hz, 3 H), 0.90 (t, *J* = 7.0 Hz, 3 H), 2.9 (q, *J* = 7.0 Hz, 2 H), 3.1 (q, *J* = 7.0 Hz, 2 H), 7.2–7.8 (m, 5 H). <sup>13</sup>C NMR (CDCl<sub>3</sub>): δ –1.33, 15.96, 16.51, 42.68, 48.36, 127.54, 133.05, 133.94, 142.78. <sup>11</sup>B NMR (C<sub>6</sub>D<sub>6</sub>): δ 49.1. Anal. Calcd for C<sub>13</sub>H<sub>24</sub>BNSi: C, 66.95; H, 10.37; N, 6.01. Found: C, 66.84; H, 10.24; N, 5.83.

**PhMe<sub>2</sub>SiB(NEt<sub>2</sub>)-*t*-Bu (9).** To an ice-cooled solution of **6** (2.1 g, 8.3 mmol) in 10 mL of cyclohexane was added *tert*-butyllithium (1.7 M, 6.0 mL, 10.2 mmol). After 24 h of stirring at room temperature, the suspension was centrifuged (3000 RPM). Concentration and distillation of the supernatant gave **9** (1.53 g, 67%) as a colorless oil: bp 125 °C/0.9 mm Hg. <sup>1</sup>H NMR (C<sub>6</sub>D<sub>6</sub>): δ 0.55 (s, 6 H), 0.76 (t, *J* = 7.0 Hz, 3 H), 0.95 (t, *J* = 7.0 Hz, 3 H), 1.25 (s, 9 H), 3.1 (m, 4 H), 7.1–7.7 (m, 5 H). <sup>13</sup>C NMR (C<sub>6</sub>D<sub>6</sub>): δ 2.89, 16.27, 30.48, 42.93, 48.45, 126.91, 128.23, 133.98, 144.80. <sup>11</sup>B NMR (C<sub>6</sub>D<sub>6</sub>): δ 50.0. Anal. Calcd for C<sub>16</sub>H<sub>30</sub>BNSi: C, 69.80; H, 10.98; N, 5.09. Found: C, 69.80; H, 10.93; N, 4.89.

(16) Vyazankin, N. S.; Razuvaev, G. A.; Gladyshev, E. N.; Korneva, S. P. *J. Organomet. Chem.* **1967**, *7*, 353.

(17) Bestmann, H. J.; Roder, T.; Suhs, K. *Chem. Ber.* **1988**, *121*, 1509.

(15) Nöth, H. In *Progress in Boron Chemistry*; Pergamon Press: Oxford, U.K., 1970; Vol. 3, p 281.

**B-(Phenyldimethylsilyl)catecholborane (7).** To a solution of **1** (7.32 g, 25.2 mmol) in 45 mL of cyclohexane was added dropwise acetyl chloride (1.98 g, 25.2 mmol) slowly at room temperature. After 20 min of stirring, the cloudy solution became clear (slightly yellow). NMR showed the silylborane chloride **6** was formed quantitatively after 1 h. Solid catechol (2.77 g, 25.2 mmol) was added under stream of argon, and then the reaction was stirred for 3 h at room temperature. The reaction mixture was transferred to a large, dry, septum-capped test tube and centrifuged at 3000 RPM for 5 min to separate the diethylamine·HCl salt. The supernatant was transferred to a flask. After concentration and distillation, 4.4 g of **7** was obtained as an oil (69%): bp 115–120 °C/0.4 mm Hg.  $^1\text{H}$  NMR ( $\text{C}_6\text{D}_6$ ):  $\delta$  0.50 (s, 6 H), 6.8–7.8 (m, 9 H).  $^{11}\text{B}$  NMR ( $\text{C}_6\text{D}_6$ ):  $\delta$  34.4. Anal. Calcd for  $\text{C}_{14}\text{H}_{15}\text{BO}_2\text{Si}$ : C, 66.16; H, 5.95. Found: C, 66.07; H, 6.04.

**Reaction of 4 with Vinylmagnesium Bromide.** To a solution of **4** (1.0 g, 4.85 mmol) in 5 mL of THF at 0 °C was added dropwise vinylmagnesium bromide (6.0 mL, 1 M, 6.0 mmol). After 15 h of stirring at room temperature, a solution of  $\text{I}_2$  (2.46 g, 9.7 mmol) in 5 mL of THF was added and then stirred for 6 h. The crude reaction mixture was diluted into 50 mL of pentane and washed with saturated  $\text{Na}_2\text{S}_2\text{O}_3$  (2 × 20 mL) and water (3 × 30 mL). The combined organic layers were dried ( $\text{Na}_2\text{SO}_4$ ) and concentrated. The colorless oil was purified by flash chromatography using pentane as eluant ( $R_f$  = 0.8). A 250 mg amount of colorless volatile oil **11**<sup>18</sup> was obtained (33%).  $^1\text{H}$  NMR ( $\text{C}_6\text{D}_6$ ):  $\delta$  0.31 (s, 6 H), 5.6–6.4 (ABX, 12 lines, 3 H), 7.2–7.7 (m, 5 H).  $^{13}\text{C}$  NMR ( $\text{CDCl}_3$ ):  $\delta$  -2.87, 127.76, 128.99, 132.79, 133.82, 137.96, 138.38. IR ( $\text{CCl}_4$ ): 1595, 1547, 1248, 1111, 1090  $\text{cm}^{-1}$ . The  $^1\text{H}$  NMR,  $^{13}\text{C}$  NMR, and IR were identical with material we independently prepared by the direct addition of vinylmagnesium bromide to phenyldimethylchlorosilane. This reaction could also be performed by using silylborane **4** and vinylolithium.

**Reaction of 4 with Lithium Phenylacetylide.** To a solution of **4** (1.0 g, 4.85 mmol) in 10 mL of THF was added dropwise lithium phenylacetylide (4.85 mL, 1 M in THF, 4.85

mmol) at 0 °C. After 2.5 h of stirring, the reaction was treated with a solution of  $\text{I}_2$  (1.23 g, 4.85 mmol) in 5 mL of THF. The stirring was continued for 1 h, and then the reaction mixture was diluted with 50 mL of diethyl ether and washed with saturated  $\text{NaHSO}_3$  solution (2 × 30 mL). The combined organic layers were dried ( $\text{Na}_2\text{SO}_4$ ) and concentrated *in vacuo*. Preparative TLC using pure hexane as eluent ( $R_f$  = 0.6) produced 720 mg (63%) of dimethylphenylsilyl phenyl acetylene **12**.<sup>19</sup>  $^1\text{H}$  NMR ( $\text{C}_6\text{D}_6$ ):  $\delta$  0.52 (s, 6 H), 6.8–7.9 (m, 10 H).  $^{13}\text{C}$  NMR ( $\text{CDCl}_3$ ):  $\delta$  -0.78, 91.98, 106.88, 122.93, 127.88, 128.14, 128.61, 129.38, 131.94, 133.65, 136.85. IR (liquid film) 2156.4, 1589.7, 1483.9, 1425.8, 1250.5, 1108.8  $\text{cm}^{-1}$ . The  $^1\text{H}$  NMR,  $^{13}\text{C}$  NMR, and IR are identical with that of dimethylphenylsilyl phenyl acetylene prepared by the direct addition of lithium phenylacetylide to phenyldimethylchlorosilane.

**Reaction of 7 with Ethyl Diazoacetate.** To a solution of **7** (117 mg, 0.46 mmol) in 11 mL of THF was added dropwise ethyl diazoacetate (48  $\mu\text{L}$ , 0.46 mmol) at 0 °C. After 3 h of stirring, 5 mL of water was added and the reaction was stirred for 30 min. Then the product was extracted with pentane. The organic layer was dried ( $\text{Na}_2\text{SO}_4$ ) and concentrated *in vacuo*. After preparative TLC separation using ether–hexane (9:1) as eluent, 61 mg (60%) of ethyl dimethylphenylsilylacetate,<sup>20</sup> **13**, was obtained.  $^1\text{H}$  NMR ( $\text{C}_6\text{D}_6$ ):  $\delta$  0.33 (s, 6 H), 0.93 (t,  $J$  = 7.6 Hz, 3 H), 2.03 (s, 2 H), 3.96 (q,  $J$  = 7.6 Hz, 2 H), 7.1–7.6 (m, 5 H).  $^{13}\text{C}$  NMR ( $\text{CDCl}_3$ ):  $\delta$  -2.78, 14.34, 26.29, 59.93, 127.84, 129.42, 133.48, 136.93, 172.49.

**Acknowledgment.** We thank the Robert A. Welch Foundation for the support of this work. We are also indebted to the Chemistry Department of Southern Methodist University for providing use of the high-field NMR and on-line literature searching.

OM950079U

(19) Jun, C. H.; Crabtree, R. H. *J. Organomet. Chem.* **1993**, *447*, 177.

(20) Danilkina, L. P.; Dorokhova, O. V.; Slobodin, Ya. M. *Zh. Obshch. Khim.* **1975**, *45*, 2677; *Russ. J. Gen. Chem. (Engl. Transl.)* **1975**, 2640.

(18) Fleming, I.; Newton, T. W.; Roessler, F. *J. Chem. Soc., Perkin Trans. 1* **1981**, 2527.

# Molecular Structure of Monomeric (Pentamethylcyclopentadienyl)aluminum(I) by Gas-Phase Electron Diffraction

Arne Haaland,<sup>\*,†</sup> Kjell-Gunnar Martinsen,<sup>†</sup> Sergey A. Shlykov,<sup>†,§</sup>  
Hans Vidar Volden,<sup>†</sup> Carsten Dohmeier,<sup>‡</sup> and Hansgeorg Schnöckel<sup>\*,‡</sup>

Department of Chemistry, University of Oslo, Box 1033, Blindern, N-0315 Oslo, Norway,  
and Institute for Inorganic Chemistry, University of Karlsruhe, Box 6980,  
D-76128 Karlsruhe, Germany

Received February 27, 1995<sup>©</sup>

**Summary:** Gas-phase electron diffraction data of Cp\*Al = (C<sub>5</sub>Me<sub>5</sub>)Al, Me = CH<sub>3</sub>, recorded with reservoir and nozzle temperatures of 139 ± 4 °C, show that the gas consists of monomeric (η<sup>5</sup>-Cp\*)Al units. Least-squares refinements of a molecular model of C<sub>5v</sub> symmetry yield the bond distances Al-C = 238.8(7), C-C(endocyclic) = 141.4(5), and C-C(exocyclic) = 152.9(5) pm and a perpendicular metal-to-ring distance of 206.3(9) pm.

The synthesis of the first molecular compound of monovalent aluminum which is stable at normal temperatures, (pentamethylcyclopentadienyl)aluminum or Cp\*Al, was reported by Schnöckel *et al.* in 1991.<sup>1</sup> The compound is tetrameric in the solid state. Room temperature X-ray crystallography shows that the tetramer consists of a tetrahedral Al<sub>4</sub> core. Each Al atom is η<sup>5</sup>-bonded to a terminal Cp\* ring in such a manner that the ring plane is parallel to the opposite Al<sub>3</sub> face of the tetrahedron.<sup>1</sup>

The <sup>27</sup>Al NMR spectrum of Cp\*Al in toluene at temperatures ranging from -80 to 25 °C consists of one sharp line at -80.7 ppm.<sup>2</sup> This line was assigned to the tetramer [Cp\*<sub>4</sub>Al<sub>4</sub>] by comparison with the shifts obtained for monomeric Cp\*Al, CpAl, and [Cp<sub>4</sub>Al<sub>4</sub>] by *ab initio* calculations with the gauge-including atomic orbital method at the dzp MP2 level.<sup>3</sup> Increasing the temperature above 30 °C led to reversible changes in the <sup>27</sup>Al NMR spectrum: A second line appears at -149 ppm. This line, which was assigned to monomeric Cp\*Al, became more intense as the temperature increased, while the peak assigned to the tetramer became less intense. Analyses of the variation of the intensities of the two lines with temperature yielded an estimate of 150 ± 20 kJ mol<sup>-1</sup> for the dissociation enthalpy of the tetramer in toluene.<sup>2-4</sup>

Cp\*Al appears to be thermally stable for infinite periods at room temperature but decomposes at temperatures above 100 °C. When a solution of Cp\*Al in

toluene was kept at 100 °C, finely divided aluminum metal became visible after some 24 h.<sup>2</sup> After 20 days at 100 °C the sample was completely decomposed. The decomposition products were pentamethylcyclopentadiene or Cp\*H, metallic aluminum, and nonvolatile organometallic Al(III) compounds which were not characterized.<sup>2</sup>

Cp\*Al may be sublimed with insignificant decomposition at about 140 °C, but at higher temperatures the rate of decomposition becomes prohibitive.<sup>2</sup> On the basis of the mass spectra and the intensity of the gas-phase electron diffraction pattern we estimate that the vapor pressure at 140 °C is about 0.05 Torr. This pressure is 2 or 3 orders of magnitudes below the pushing pressures normally used for the collection of gas-phase electron diffraction data.<sup>5,6</sup>

The intensity of the electron diffraction pattern is determined by the intensity of the primary beam, the concentration of the gas (mol L<sup>-1</sup>) in the scattering region, and the scattering power of the molecular species to be investigated. The scattering power of a molecule is proportional to the sum of the squares of the nuclear charges of the constituent atoms, ΣZ<sub>i</sub><sup>2</sup>. The concentration of the gas density in the scattering region is determined by the pushing pressure, which in turn is limited by the vapor pressure of the solid or liquid sample. Over the past years we have found that a primary beam intensity of about 50 nA combined with a pushing pressure between 0.5 and 5 Torr provides excellent conditions for the recording of electron diffraction data of organometallic compounds on our Balzers Eldigraph KDG 2 unit.<sup>7,8</sup>

Recently we have modified our instrument to allow us to increase the intensity of the primary beam: The magnetic lens, which in the original design was placed at a distance of 55 cm from the filament, was replaced by a new and slightly modified lens at about 22 cm from the electron-emitting filament. This modification allows the utilization of a greater fraction of the electrons emerging from the electrostatic focusing device and increases the primary beam current by 1 order of

<sup>†</sup> University of Oslo.

<sup>‡</sup> University of Karlsruhe.

<sup>§</sup> Present address: Ivanovo State Academy of Chemistry and Technology, Department of Physics, Engelsa Ave., Ivanovo 153460, Russia.

<sup>©</sup> Abstract published in *Advance ACS Abstracts*, May 15, 1995.

(1) Dohmeier, C.; Robl, C.; Tacke, M.; Schnöckel, H. *Angew. Chem., Int. Ed. Engl.* **1991**, *30*, 564-565.

(2) Dohmeier, C. Ph.D. Thesis, Ludwig-Maximilians-Universität München, München, Germany, 1994.

(3) Gauss, J.; Schneider, U.; Ahlrichs, R.; Dohmeier, C.; Schnöckel, H. *J. Am. Chem. Soc.* **1993**, *115*, 2402-2408.

(4) Roesky and co-workers, who prepared Cp\*Al by another route, found only one line, corresponding to the tetramer, in the <sup>27</sup>Al NMR spectrum in deuterated benzene in the temperature range 40-78 °C: Schulz, S.; Roesky, H. W.; Koch, H. J.; Sheldrick, G. M.; Stalke, D.; Kuhn, A. *Angew. Chem., Int. Ed. Engl.* **1993**, *32*, 1729-1731.

(5) Ebsworth, E. A. V.; Rankin, D. W. H.; Cradock, S. *Structural Methods in Inorganic Chemistry*, Blackwell, Oxford, U.K., 1987; pp 304-315.

(6) Hargittai, I. Gas-Phase Electron Diffraction In *Accurate Molecular Structures*; Domenicano, A., Hargittai, I., Eds.; Oxford University Press: Oxford, U.K., 1992; p 95-125.

(7) Zeil, W.; Haase, J.; Wegmann, L. *Z. Instrumentenk.* **1966**, *74*, 84-88.

(8) Bastiansen, O.; Graber, R.; Wegmann, L. *Balzers High Vacuum Report* **1969**, *25*, 1-8.



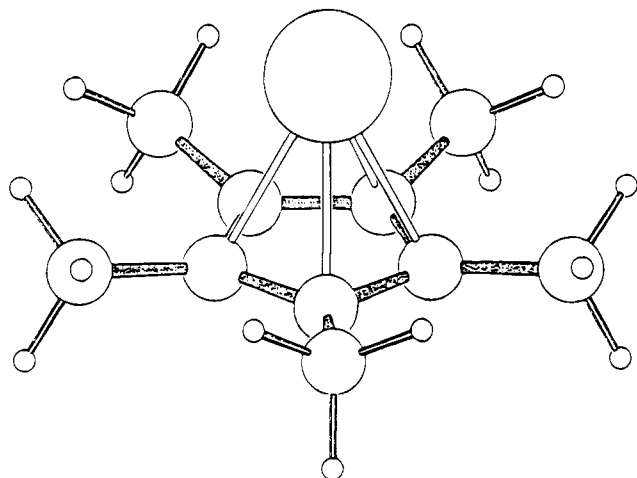


**Figure 1.** Molecular model (Pluton<sup>13</sup>) of ( $\eta^5$ -Cp\*)Al. Molecular symmetry,  $C_{5v}$ .

magnitude to a maximum value of about 1500 nA. With a primary beam current of this magnitude we were able to record the scattering pattern of Cp\*Al with a reservoir and nozzle temperature of  $139 \pm 4$  °C.

Crystalline Cp\*Al was synthesised from solvated AlCl<sub>3</sub> and Cp\*<sub>2</sub>Mg as described in ref 9. The NMR spectra in toluene contained no peaks indicating the presence of Cp\*H or other impurities. Gas-phase electron diffraction data were recorded with a metal inlet system. Exposures were made with nozzle-to-photographic plate distances of about 50 and 25 cm; structure refinements were based on data from four plates from the 50 cm set and three plates from the 25 cm set. The plates were photometered and the data processed by a program written by T. G. Strand. Atomic scattering factors were taken from ref 10. Backgrounds were drawn as least-squares-adjusted seventh (50 cm) or eighth (25 cm) degree polynomials to the difference between total experimental and calculated molecular intensity curves. Molecular structure refinements were carried out with the program KCED26, which was written by G. Gundersen, S. Samdal, H. M. Seip, and T. G. Strand.

Structure refinements were based on a molecular model of  $C_{5v}$  symmetry as shown in Figure 1. Methyl groups were assumed to have  $C_{3v}$  symmetry with the symmetry axes coinciding with the exocyclic C(Cp)–C(Me) bonds. The orientation of the methyl groups is such that one C–H bond points away from the metal as indicated in the figure. The molecular geometry is then determined by six independent parameters, e.g. the endocyclic C(Cp)–C(Cp) and the exocyclic C(Cp)–C(Me) bond distances, the Al–C and C–H bond distances, the valence angle  $\angle$ CCH and the angle between the exocyclic CC bonds and the ring plane which we denote by  $\angle$ C<sub>5</sub>,C–C and define as positive when the bonds are bent towards the metal atom. Several refinements showed that the magnitude obtained for  $\angle$ C<sub>5</sub>,C–C is independent of the orientation of the methyl groups. Since information on the vibrational spectrum of monomeric Cp\*Al is missing, shrinkage corrections were neglected.

(9) Dohmeier, C.; Loos, D.; Robl, C.; Schnöckel, H.; Fenske, D. *J. Organomet. Chem.* **1993**, *448*, 5–8.

(10) Bonham, R. A.; Schäfer, L. Complex Scattering Factors for the Diffraction of Electrons by Gases. In *International Tables for X-Ray Crystallography*; Ibers, J. A., Hamilton, W. C., Eds.; Kynoch Press: Birmingham, U.K., 1974; Vol. 4.

**Table 1.** Interatomic Distances ( $r_a$ ), Root Mean Square Vibrational Amplitudes ( $l$ ), and Valence Angles in (Cp\*)Al, and Mole Fraction of the Pentamethylcyclopentadiene, Cp\*H, Impurity<sup>a</sup>

	$r_a$	$l$
Al–C	238.8(7)	12(1)
C(Cp)–C(Cp)	141.4(5)	3.2(15) <sup>b</sup>
C(Cp)–C(Me)	152.9(6)	3.7(15) <sup>b</sup>
C–H	111.0(6)	8.4(5)
nonbonded distances		
Al–C(Me)	327(2)	22(4)
C(Cp)–C(Cp)	221(1)	[5.8]
C(Cp)–C(Me)	262(1)	5.9(8)
C(Cp)–C(Me)	377(1)	8.8(6)
C(Me)–C(Me)	320(1)	[13.1]
C(Me)–C(Me)	518(1)	14(1)
$h$	206.3(8)	
$\angle$ CCH	112.3(6)	
$\angle$ C <sub>5</sub> ,C–C	5(2)	
$\chi$ (Cp*H) (%)	7(3)	27(3)
$R$ factors <sup>c</sup> (%)	2.2 (50 cm)	8.6 (25 cm)

<sup>a</sup> Distances and vibrational amplitudes in pm, angles in degrees. Estimated standard deviations in parentheses in units of the last digit. <sup>b</sup> These vibrational amplitudes were refined with constant difference. <sup>c</sup>  $R = [\sum w(I_{\text{obs}} - I_{\text{calcd}})^2 / \sum w(I_{\text{obs}})^2]^{1/2}$ ; total, 2.9%.

Exploratory refinements showed that the gas-phase electron diffraction data were incompatible with a gas consisting of ( $\eta$ -Cp\*)Al only. Since the data had been collected at a temperature at which Cp\*Al is known to suffer some thermal decomposition, and since the only volatile decomposition product was Cp\*H,<sup>2</sup> we then attempted to refine the mole fraction of such an impurity along with the structure parameters of Cp\*Al. Cp\*H has never been studied by gas-phase electron diffraction. A molecular model was therefore constructed from the known molecular structure of the bicyclic compound Cp\*<sub>2</sub> by breaking the bond between the rings and adding a hydrogen atom.<sup>11</sup>

Separate refinements of the intensity data obtained with nozzle-to-plate distances of 50 and 25 cm indicated that, while the mole fraction of Cp\*H in the former was about  $\chi$ (Cp\*H) = 0.10, the mole fraction in the latter (which required longer exposure times) was about 0.30. The KCED26 program does not allow simultaneous refinement of different impurity mole fractions for different parts of the data. The 25 cm intensities data were therefore amended by subtraction of calculated intensity for Cp\*H until the two data sets yielded equivalent values for  $\chi$ (Cp\*H).

The intensity data recorded with a nozzle-to-photographic plate distance of 25 cm are normally of poorer quality than the data recorded with a distance of 50 cm, and the present study is no exception. Structure refinements were therefore carried out with unit weight for the 50 cm data and a weight of  $W = 0.2$  for the 25 cm data: this weighting scheme yielded square error sums,  $\sum W(I_{\text{obs}} - I_{\text{calcd}})^2$ , of about equal magnitude for the two data sets.

The final refinements involved the six independent structure parameters of Cp\*Al, 12 root mean square vibrational amplitudes,  $l$ , and the mole fraction of the impurity,  $\chi$ (Cp\*H). The best values are listed in Table 1. Since the refinements were carried out with diagonal weight matrices, the estimated standard deviations

(11) Blom, R. *Acta Chem. Scand., Ser. A* **1988**, *42*, 445–453.

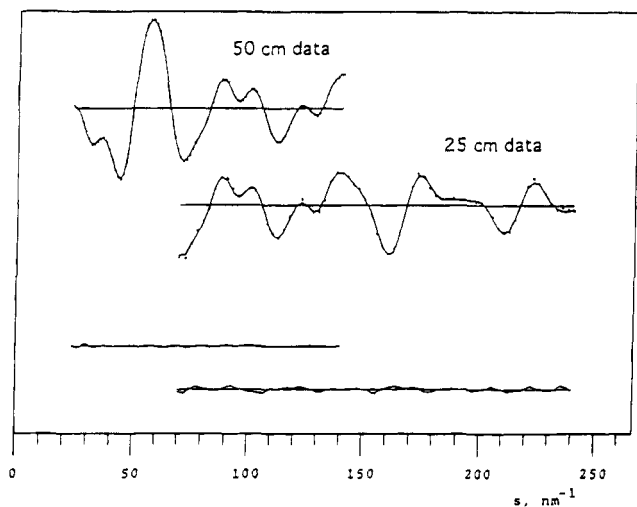


**Figure 2.** Experimental (···) and calculated (—) modified molecular intensity curves for  $(\eta^5\text{-Cp}^*)\text{Al}$ . The vertical scale is arbitrary. The experimental intensities obtained with a nozzle-to-photographic plate distance of about 25 cm have been amended by subtraction of molecular intensity calculated for pentamethylcyclopentadiene to reduce the level of this impurity to that found in the 50 cm data. See text. Difference curves are shown at the bottom of the figure.

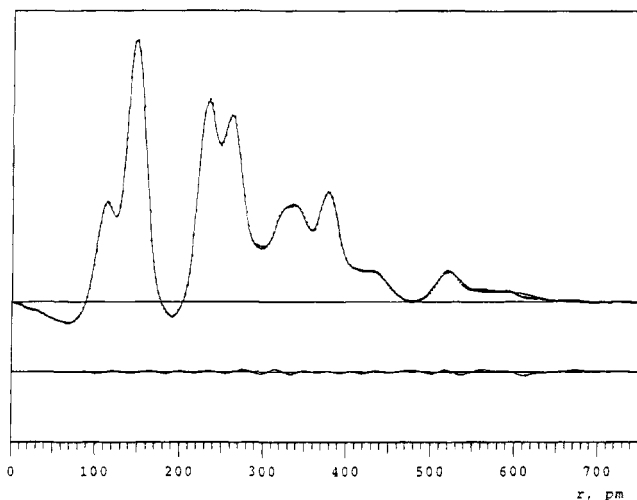


**Figure 3.** Experimental (···) and calculated (—) radial distribution curves of  $(\eta^5\text{-Cp}^*)\text{Al}$ . The vertical scale is arbitrary. Difference curve is shown at the bottom of the figure. Artificial damping constant,  $k = 25 \text{ pm}^2$ .

listed in the table have been multiplied by a factor of 3.0 to include the added uncertainty due to data correlation<sup>12</sup> and our modeling of the structure of  $\text{Cp}^*\text{H}$ . The parameter  $\angle\text{C}_5\text{-C-C}$  may be particularly sensitive to errors in the modeling of  $\text{Cp}^*\text{H}$ , the estimated standard deviation of this parameter was therefore, somewhat arbitrarily, further increased from  $0.7^\circ$  to  $2^\circ$ . Experimental and calculated intensity curves and radial distribution curves are compared in Figures 2 and 3, respectively.

Least-squares refinements were carried out on two more molecular models differing from the model in Figure 1 in the orientation of the methyl groups: another model of  $C_{5v}$  symmetry in which all methyl

groups had been rotated  $180^\circ$  from their original positions in the Figure and a model of  $C_5$  symmetry in which they had been rotated  $90^\circ$ . Refinement of these models yielded slightly, but not significantly, poorer agreement between observed and calculated intensities. We conclude that the data contain insufficient information to allow us to determine the equilibrium orientation of the methyl groups.

The Al atom is the heaviest atom in the molecule, and the terms representing the five Al-C(Cp) bond distances at 239 pm and the five nonbonded Al- -C(Me) distances at 327 pm are the largest terms in the molecular intensity curve along with the terms representing the nonbonded distances C(Cp)- -C(Me) at 262 and 377 pm. The good agreement between experimental and calculated curves obtained for a  $C_{5v}$  model shows that the five Al-C bond distances must be equal or nearly equal: If the metal atom in  $\text{Cp}^*\text{Al}$  was  $\eta^1$ -bonded to the ring, the peak representing the five Al-C bond distances would split into one peak at about 197 pm representing the Al-C  $\sigma$ -bond distance, and two peaks, each representing two nonbonded Al- -C(Cp) distances, at about 280 and 360 pm. The nonbonded Al- -C(Me) peak at 327 pm would be split in a similar manner. Such a model is clearly incompatible with the gas-phase electron diffraction data.

This study shows that the break up of the tetramer in the gas phase leads to monomeric  $(\eta\text{-Cp}^*)\text{Al}$  and lends indirect support to the conclusions reached in the  $^{27}\text{Al}$  NMR studies described above.

Comparison of structure parameters are complicated by the fact that the monomer and tetramer structures have been determined in different phases and by different methods. In particular, bond distances obtained by X-ray crystallography at room temperature are expected to be systematically shortened unless corrected for thermal motion. It nevertheless appears likely that the perpendicular metal-to-ring distance  $h$  is about 3 pm shorter in the tetramer than in the monomer: The values obtained for  $h$  in the crystal range from 199.7 to 203.2 pm with a mean value of 201.5 pm<sup>1</sup>, while the gas-phase value is 206.3(8) pm.

The bonding radii of monovalent metals Al, Ga, or In are generally larger than the single-bond radii of the trivalent metals. Thus the bond distances in the gaseous monomeric monochlorides AlCl, GaCl, and InCl are 213, 220, and 240 pm, respectively, while the bond distances in the gaseous monomeric trichlorides are 207, 211, and 229 pm, respectively.<sup>14</sup> The difference has been rationalized as a hybridization effect: The pair of nonbonding electrons in the monochlorides are assumed to occupy the valence shell  $s$  atomic orbital. This leaves a pure  $p$  AO for formation of the M-Cl bonding MO. The two-center bonding MOs in the trichlorides, on the other hand, are constructed from  $sp^2$  hybrid orbitals on the metal atom. The increased  $s$ -character is expected to lead to a better overlap with the ligand AO and to a shorter bond.<sup>15</sup> If real, the observed shortening of the metal to ring distance in  $[\text{AlCp}^*]_4$  as compared to  $\text{AlCp}^*$

(12) Seip, H. M.; Strand, T. G.; Stølevik, R. *Chem. Phys. Lett.* **1969**, *3*, 617-623.

(13) Spek, A. L. The "Euclid" Package. In *Computational Crystallography*; Sayre, D., Ed.; Clarendon: Oxford, U.K., 1982.

(14) Haaland, A.; Hammel, A.; Martinsen, K.-G.; Tremmel, J.; Volden, H. V. *J. Chem. Soc., Dalton Trans.* **1992**, 2209-2214.

(15) The bond energies of the monochlorides are, however, lower than the mean bond energies of the trichlorides. See ref 14 for a discussion.

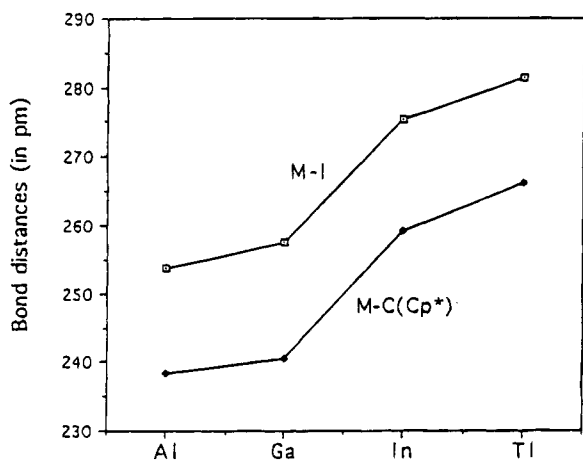


**Figure 4.** M-I bond distances in the gaseous monomeric monoiodides and M-C bond distances in gaseous ( $\eta^5$ -Cp\*)M, M = Al, Ga, In, and Tl.

may, in a similar manner, be due to increased s-character of the  $a_1$  hybrid AO pointing toward the ring center.

The bond distances in the Cp\* ligand are in reasonable agreement with those obtained by structure optimization of Cp\*Al at the dzp MP2 level, but the

experimental perpendicular metal-to-ring distance is 7 pm greater than calculated.<sup>3</sup>

In Figure 4 we compare the M-C bond distances in gaseous monomeric Cp\*Al, Cp\*Ga,<sup>16</sup> Ga-C = 240.5(4) pm, Cp\*In,<sup>17</sup> In-C = 259.2(4) pm, and Cp\*Tl,<sup>18</sup> Tl-C = 266.3(5) pm, with the M-I bond distances in the gaseous monoiodides, Al-I = 253.7, Ga-I = 257.5, In-I = 275.4, and Tl-I = 281.4 pm.<sup>19</sup> The similarity of the M-C and M-I bond distance curves suggest that both M-C and M-I bond distances are primarily determined by the size of the metal atom.

**Acknowledgment.** We are grateful to the VISTA program of STATOIL and the Norwegian Academy for Science and Letters for financial support.

OM9501586

(16) Haaland, A.; Martinsen, K.-G.; Volden, H. V.; Loos, D.; Schnöckel, H. *Acta. Chem. Scand.* **1994**, *48*, 172-174.

(17) Beachley, O. T., Jr.; Blom, R.; Churchill, M. R.; Faegri, K.; Fettinger, J. C.; Pazik, J. C.; Victoriano, L. *Organometallics* **1989**, *8*, 346-356.

(18) Blom, R.; Werner, H.; Wolf, J. *J. Organomet. Chem.* **1988**, *354*, 293-299.

(19) Huber, K. P.; Herzberg, G. *Molecular Spectra and Molecular Structure*; Van Nostrand: New York, 1979; Vol. 4.

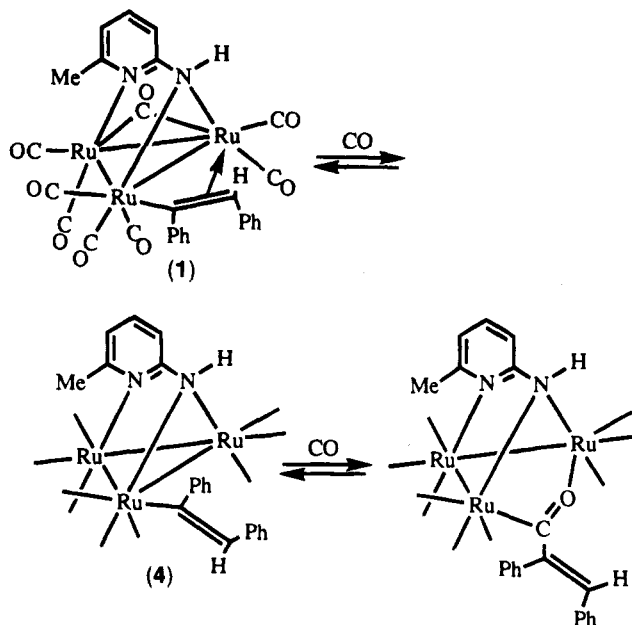
# Additions and Corrections

1994, Volume 13

**Javier A. Cabeza,\* José M. Fernández-Colinas, Angela Llamazares, Víctor Riera, Santiago García-Granda, and Juan F. Van der Maelen:** Carbonyl Clusters as Homogeneous Catalysts. Kinetic and Molecular Aspects of the Hydrogenation of Diphenylacetylene Promoted by an Alkenyl-Bridged Triruthenium Cluster Complex.

Page 4352. The  $\eta^1$ -alkenyl derivative  $[\text{Ru}_3(\mu_3\text{-ampy})(\eta^1\text{-PhC=CHPh})(\text{CO})_9]$  (4) is not the final product of the reaction of  $[\text{Ru}_3(\mu_3\text{-ampy})(\mu\text{-PhC=CHPh})(\text{CO})_8]$  (1) with carbon monoxide, but just a possible (unobserved) intermediate. The final product of this reaction is the  $\mu\text{-}\alpha,\beta$ -diphenylpropenoyl derivative  $[\text{Ru}_3(\mu_3\text{-ampy})(\mu\text{-O=CCPh=CHPh})(\text{CO})_9]$ <sup>1</sup> (Scheme 1). Although this compound is only stable in solution under a CO atmosphere, it has now been characterized by its <sup>13</sup>C NMR spectrum and by reactivity studies. Its <sup>13</sup>C NMR spectrum ( $\text{CD}_2\text{Cl}_2$ ,  $-70^\circ\text{C}$ ) contains a resonance at 301.4 ppm (acyl carbon) which was initially overlooked.  $\alpha$ -Phenylcinnamaldehyde and  $\alpha$ -phenylcinnamyl alcohol (GC-MS identification) are produced when a CO-saturated solution of this cluster in dichloromethane is treated with  $[\text{PPN}][\text{BH}_4]$ .

Scheme 1



We are very grateful to Dr. Guy Lavigne for his comments and suggestions.

(1) Nombel, P.; Lugan, N.; Mulla, F.; Lavigne, G. *Organometallics* 1994, 13, 4673.

OM9502392